

INTERNATIONAL SYMPOSIUM on
ADVANCED ENGINEERING & APPLIED MANAGEMENT
– 40th ANNIVERSARY in HIGHER EDUCATION (1970-2010)
4 – 5 November, 2010, Hunedoara, ROMANIA



INTERNATIONAL SYMPOSIUM
on
ADVANCED ENGINEERING
& APPLIED MANAGEMENT
– 40th ANNIVERSARY
in HIGHER EDUCATION
(1970-2010)



PROGRAM

Hunedoara, ROMANIA
4 - 5 November, 2010

ORGANIZERS:

UNIVERSITY POLITEHNICA TIMISOARA,



FACULTY OF ENGINEERING HUNEDOARA



**GENERAL ASSOCIATION OF THE ROMANIAN ENGINEERS (AGIR)
– Branch of HUNEDOARA**



with logistical support of:

**ANNALS OF FACULTY ENGINEERING HUNEDOARA
– INTERNATIONAL JOURNAL OF ENGINEERING**



and

ACTA TECHNICA CORVINIENSIS – BULLETIN OF ENGINEERING



SCIENTIFIC COMMITTEE

Prof. dr. eng. **Teodor HEPUT**
– dean of the Faculty of Engineering – Hunedoara

Prof. dr. **Stefan MAKSAY**
– scientific secretary of the Faculty of Engineering – Hunedoara

Prof. dr. eng. **Francisc WEBER**
– head of General Association of the Romanian Engineers
(AGIR) – branch of Hunedoara

Assoc. Prof. dr. eng. **Ana Virginia SOCALICI**
– vice-dean of Faculty of Engineering – Hunedoara

Assoc. Prof. dr. eng. **Caius PĂNOIU**
– vice-dean of Faculty of Engineering – Hunedoara

Assoc. Prof. dr. eng. **Sorin DEACONU**
– head of Electrical Engineering
& Industrial Informatics Department

Assoc. Prof. dr. eng. **Lucia VILCEANU**
– head of Engineering & Management Department

Assoc. Prof. dr. eng. **Manuela PĂNOIU**
– head of Life-Long Education Department

Assoc. Prof. dr. eng. **Imre KISS**
– Romanian Foundry Technical Association (ATTR)
– branch of Hunedoara



ORGANIZING COMMITTEE

Lect. ec. dr. eng. **Vasile ALEXA**
– coordinator of organizing activities,
Faculty of Engineering – Hunedoara

Lect. dr. eng. **Sorin RAȚIU**
– coordinator of organizing activities,
Faculty of Engineering – Hunedoara

Lect. dr. eng. **Vasile George CIOATĂ**
– coordinator of organizing activities,
Faculty of Engineering – Hunedoara

SECRETARY OFFICE



UNIVERSITY POLITEHNICA TIMIȘOARA
FACULTY OF ENGINEERING - HUNEDOARA
5, REVOLUTIEI, 331128, HUNEDOARA
phone: + 40 254 207522; fax: + 40 254 207501
e-mail: symposium@fih.upt.ro



INTERNATIONAL SYMPOSIUM on
ADVANCED ENGINEERING & APPLIED MANAGEMENT
- 40th ANNIVERSARY in HIGHER EDUCATION
(1970-2010)
4 - 5 November, 2010,
Hunedoara, ROMANIA

SCHEDULE OF EVENTS

1ST DAY, Thursday,
4th November, 2010

- 08.00 - 10.00 Welcoming of guests and registration of participants - in the Hall of the Faculty of Engineering - Hunedoara
- 10.00 - 11.00 Opening Ceremony - in the Amphitheatre of the Faculty of Engineering - Hunedoara
- Plenary Lecture # 1
Ioan ROMULUS
THE HISTORY OF IRON MAKING AT HUNEDOARA - ESSENTIAL ELEMENT FOR FOUNDING AN HIGHLY EDUCATION INSTITUTE
- Plenary Lecture # 2
Ioan ILCA
DEFFICIENCY OF SCIENCE AND TECHNIQUE ASSIMILATION
- Plenary Lecture # 3
Teodor HEPUT
FACULTY OF ENGINEERING HUNEDOARA - 40th ANNIVERSARY in HIGHER EDUCATION (1970-2010)
- Plenary Lecture # 4
Iulian RIPOSAN, Mihai CHISAMERA, Stelian STAN
GRAPHITE NUCLEATION IN GREY CAST IRON - A REVIEW
- 11.00 - 11.30 Coffee break - in the Halls and in the Amphitheatres of the Faculty of Engineering - Hunedoara
- 11.30 - 12.00 Setting of posters by sections - in the Halls and in the Amphitheatres of the Faculty
- 12.00 - 14.00 Presentations and debates by sections - in the Faculty's Amphitheatres
- 14.00 - 16.00 Lunch - at Restaurant of Hotel Maier, Hunedoara
- 16.00 - 19.00 Debates by sections - in the Faculty's Amphitheatres
- 19.00 Festive dinner - at Restaurant Ciuperca, Hunedoara

**2ND DAY, Friday,
5th November, 2010**

- 08.00 - 10.00 Breakfast - at the Faculty's Restaurant
- 10.00 - 12.30 Presentations and debates by sections and posters - in the Halls and in the Faculty's Amphitheatres
- 12.30 - 13.00 Coffee break - in the Halls and in the Amphitheatres of the Faculty of Engineering - Hunedoara
- 13.00 - 14.00 Final debates and Closing Ceremony - in the Faculty's Amphitheatre



SYMPOSIUM TOPICS

SECTION S01.

MATERIALS SCIENCE & ENGINEERING

SECTION S02.

ELECTRICAL ENGINEERING & INFORMATICS

SECTION S03.

MECHANICAL ENGINEERING & DESIGN

SECTION S04.

MANAGEMENT IMPLEMENT POLICIES & STRATEGIES

SECTION S05.

ENVIRONMENTAL ENGINEERING & ECOLOGY

ISBN 978-973-0-09340-7

SECTION S01. **MATERIALS SCIENCE & ENGINEERING**

PROGRAM SCHEDULE:

1ST DAY, Thursday,
4th November, 2010

- 11.30 - 12.00 Setting of posters by sections - in the Halls and in the Amphitheatres of the Faculty
- 12.00 - 14.00 Presentations and debates by sections - in the Faculty's Amphitheatres
- 16.00 - 19.00 Debates by sections - in the Faculty's Amphitheatres

2ND DAY, Friday,
5th November, 2010

- 10.00 - 12.30 Presentations and debates by sections and posters - in the Halls and in the Faculty's Amphitheatres

PROGRAM of PRESENTED PAPERS **(oral presentations and posters):**

No. crt.	Authors Surname & NAME TITLE OF PRESENTED PAPERS
S1-01.	Ana SOCALICI, Constantin ANDRONACHE, Teodor HEPUT RESEARCHS REGARDING THE QUALITY OF THE STEEL USED FOR MAKING ROLLING STOCK COMPONENTS
S1-02.	Violeta OANCEA, Nicolae CONSTANTIN, Cristian DOBRESCU RESEARCH REGARDING THE PHYSICAL AND CHEMICAL CHARACTERISTICS OF PRE-REDUCED IRON ORES AND THE ANALYSIS OF THE POSSIBILITIES OF THEIR USE IN THE IRON AND STEEL ELABORATING PROCESS
S1-03.	Violeta OANCEA, Nicolae CONSTANTIN, Cristian DOBRESCU RESEARCH ON THE POSSIBILITIES OF IMPROVING THE PRODUCTIN OF CAST IRON IN THE FIRST MERGER BY IMPROVING FLOW GAS PHASE IN THE BLAST FURNACE
S1-04.	Ioan MILOSAN STUDIES AND RESEARCHES ON THE DETERMINATION OF KINETIC AND THERMODYNAMIC PARAMETERS OF AN ADI
S1-05.	Maria NICOLAE, Irina VÎLCIU, Emanuela-Daniela STOICA RESEARCH ON THE MECHANISM OF DAMAGE LINE BRICKS IN THE SLAG LF
S1-06.	Victor BUDĂU, Sebastian DUMA HARDNESS AND STRUCTURAL ASPECTS OF THE HEAT - TREATED HS 18-0-1 STEEL

- S1-07. Erika ARDELEAN, Florin DRĂGOI, Marius ARDELEAN, Teodor HEPUT
WAYS OF INCREASING THE PURITY OF THE STEELS THROUGH SLAGS, IN
THE ELABORATION OF THE AGGREGATE
- S1-08. Claudiu CONSTANTIN, Alina MIHAIU, Nicolae CONSTANTIN
MATHEMATICAL MODEL ON THE CORRELATION OF THE COMBUSTION 'S
ZONE PARAMETERS IN CASE OF USING DIFFERENT AUXILIARY
COMBUSTIBLES
- S1-09. Nicolae CONSTANTIN, Cristian DOBRESCU, Raluca PETRACHE
ALTERNATIVE IRON MAKING TECHNOLOGIES
- S1-10. Alina MIHAIU, Claudiu CONSTANTIN, Cristian DOBRESCU
SOME COMPUTATIONS REGARDING THE DIRECT REDUCTION OF THE IRON
ORES
- S1-11. Vasile PUȚAN, Adriana PUȚAN
DESULPHURATION OF STEEL WITH SYNTHETIC SLAG WITH ADDITION OF
TITANIUM OXIDE
- S1-12. Mihaela FLORI, Bernard GRUZZA, Luc BIDEUX, Guillaume MONIER,
Christine ROBERT-GOUMET, Jean-Pierre CHERRE, Daniela MILOȘTEAN
INFLUENCE OF MICROSTRUCTURE DEFECTS ON THE PROPERTIES OF
42CrMo4 NITRIDED STEEL
- S1-13. Monika Erika POPA
RESEARCH AND SIMULATION OF THE SOLIDIFICATION FRONT AT THE
CONTINUOUS CAST HALF-FINISHED PRODUCT
- S1-14. Simon JITIAN
OBTAINING THE ABSORPTION SPECTRA OF SILICON FROM THE IR
REFLECTANCE SPECTRA RECORDED AT TWO ANGLES
- S1-15. Miriam MATÚŠOVÁ, Erika HRUŠKOVÁ, Angela JAVOROVÁ
MATERIAL FLOW STRATEGY BY SOFTWARE WITNESS
- S1-16. Imre TIMÁR, Péter KONCZ, Ferenc WÉBER, Csaba BALÁZSI
STRUCTURAL PROPERTIES OF NANO- STEEL POWDERS PREPARED BY
POWDER METALLURGY
- S1-17. Martina KUSÁ, Miriam MATÚŠOVÁ, Marcela CHARBULOVÁ
OPTIMALISATION METHOD OF MATERIAL FLOW AT MANUFACTURING
PROCESS
- S1-18. Ioan MĂRGINEAN, Irina Varvara ANTON, Crenguța Manuela PÂRVULESCU
VIBRATION TECHNIQUE - AN IMPROVEMENT SOLUTION FOR QUALITY OF
CAST METALLIC MATERIALS
- S1-19. Ioan ILCA
DEFFICIENCY OF SCIENCE AND TECHNIQUE ASSIMILATION

- S1-20. Monika Erika POPA, Gabriela Cornelia MIHUȚ
EXPERIMENTS REGARDING THE THERMICAL REGIME IN THE CONTINUOUS
CASTING PROCESS
- S1-21. Vasile PUȚAN, Ana JOSAN, Adriana PUȚAN
HEAT LOSS FLUXES FROM STEEL MELT TO DIFFERENT BOUNDARY REGIONS
OF A LADLE
- S1-22. Peter KOŠŤÁL, Andrea MUDRIKOVÁ
USE OF E-LEARNING AND VIRTUAL LABORATORY TO AUTOMATION
TEACHING
- S1-23. Štefan NIŽNÍK, Ondrej MILKOVIČ, Svätoboj LONGAUER
METALLURGICAL TWO-STEP PRODUCING METHOD OF FE NANOPARTICLES
- S1-24. Ioan MĂRGINEAN, Bogdan-Alexandru VERDEȘ,
Crenguța Manuela PÎRVULESCU
RESEARCH REGARDING THE EFFECT OF ALLOYS VIBRATION ON MICRO-
AND MACROBLISTER FROM CASTED PARTS
- S1-25. Eugen Mihai CRIȘAN, Teodor HEPUT
INFLUENCE OF BASIC ADDITIVE ON THE QUALITY OF PELLETS
- S1-26. I. MARGINEAN I., V. MIREA, B. FLOREA, L. MARGINEAN
MACRO-MICRO-NANO COMPOSITE MATERIALS
- S1-27. Ana JOSAN
THE ANALYSIS OF CASTING DEFECTS RECORDED IN THE METALLURGICAL
ENTERPRISES
- S1-28. Gabriela MIHUȚ, Erika POPA
ANALYSIS UPON INFLUENCE OF THE ALLOY ELEMENTS OVER THE
MECHANICAL CHARACTERISTICS OF THE HIGH RESISTENT STEEL WITH
HELP OF MATHEMATICAL MODELS
- S1-29. Lucia VÎLCEANU
THE INFLUENCE OF THE LOCAL COMPRESSION EFFECT ABOUT THE
WORKING LIFE OF THE COMPONENT WIRES IN A WIRE-ROPE
- S1-30. Sorina Gabriela ȘERBAN, Maria Laura STRUGARIU
DETERMINATION OF PARAMETERS INVOLVED IN TRANSFORMING THE
IDEAL GAS, USING MICROSOFT ACCESS
- S1-31. Ana JOSAN, Vasile PUȚAN, Sorin RAȚIU
THE OPTIMIZATION OF MANUFACTURING PROCESS OF A PART CAST
STEEL FOR QUALITY ASSURANCE
- S1-32. Teodor HEPUT, Erika ARDELEAN, Ana SOCALICI, Marius ARDELEAN
EXPERIMENTS AND RESULTS REGARDING THE USE OF FOAMED SLAGS AT
THE STEEL ELABORATION IN ELECTRIC ARC FURNACES

- S1-33. Marius ARDELEAN, Erika ARDELEAN, Teodor HEPUȚ, Ana SOCALICI
ESTABLISHING THE MAIN TECHNOLOGICAL PARAMETERS OF INDUCTION
SURFACE HARDENING FOR SHAFT PARTS TYPE
- S1-34. Daniela MILOȘTEAN, Mihaela FLORI
AN OVERVIEW ON THE SEMISOLID STATE PROCESSING OF STEEL
- S1-35. Adrian GAVANESCU
REFINING OF STEEL BY USING SYNTHETIC SLAG
- S1-36. Rodica ISTRATE, Manfred SCHMITT, Jens APFEL, Ioan ILCA
EFFICIENCY OF MAINTENANCE IN STEEL MAKING INDUSTRY
- S1-37. Iulian RIPOSAN, Mihai CHISAMERA, Stelian STAN
GRAPHITE NUCLEATION IN GREY CAST IRON - A REVIEW
- S1-38. I. HULKA, D. UȚU, V.A. ȘERBAN
MICRO-SCALE SLIDING WEAR BEHAVIOR OF HVOF SPRAYED WC-Co(Cr)
- S1-39. Doina PETRE
THE INFLUENCE OF THE TECHNOLOGICAL CONDITIONS UPON THE
TENACITY OF SOME ALL PURPOSE STEELS
- S1-40. Doina Elena PETRE, Adriana PUTAN
THE IMPROVEMENT OF RESISTANCE CHARACTERISTICS OF STEELS
THROUGH COLD PLASTIC DEFORMATION
- S1-41. Miron BUZDUGA, Adriana COMȘA, Radu BUZDUGA
RESEARCHES PERFORMED IN VIEW OF OBTAINED REFRACTORIES
PRODUCTS
- S1-42. Adriana COMȘA, Miron BUZDUGA, Radu BUZDUGA
RESEARCHES PERFORMED IN VIEW OF OBTAINED REFRACTORIES
PRODUCTS MONOLITHIC REFRACTORIES PRODUCTS
- S1-43. G. E. BADEA, P. CRET, M. LOLEA, A. SETEL
STUDIES OF CARBON STEEL CORROSION IN ATMOSPHERIC CONDITIONS



INTERNATIONAL SYMPOSIUM on
ADVANCED ENGINEERING & APPLIED MANAGEMENT
- 40th ANNIVERSARY in HIGHER EDUCATION
(1970-2010)
4 - 5 November, 2010,
Hunedoara, ROMANIA

SECTION S02. **ELECTRICAL ENGINEERING & INFORMATICS**

PROGRAM SCHEDULE:

1ST DAY, Thursday,
4th November, 2010

- 11.30 - 12.00 Setting of posters by sections - in the Halls and in the Amphitheatres of the Faculty
- 12.00 - 14.00 Presentations and debates by sections - in the Faculty's Amphitheatres
- 16.00 - 19.00 Debates by sections - in the Faculty's Amphitheatres

2ND DAY, Friday,
5th November, 2010

- 10.00 - 12.30 Presentations and debates by sections and posters - in the Halls and in the Faculty's Amphitheatres

PROGRAM of PRESENTED PAPERS **(oral presentations and posters):**

No. crt.	Authors Surname & NAME TITLE OF PRESENTED PAPERS
S2-01.	Caius PANOIU, Manuela PANOIU, Raluca ROB PROGRAMMABLE GAIN AMPLIFIER USING PARALLEL PORT CONTROLLING
S2-02.	Ion COPACI, Bogdan TĂŃĂSOIU ON THE DYNAMIC EXPERIMENTAL DETERMINATION OF THE CHARACTERISTICS OF SHOCK INSULATORS
S2-03.	Gelu Ovidiu TIRIAN, Camelia BRETOTEAN-PINCA, Cristian CHIONCEL, Sergiu MEZINESCU INDUSTRIAL IMPLEMENTATION OF THE PREDICTION, DETECTION, AND CRACK REMOVAL SYSTEM OF CONTINUOUS CASTING
S2-04.	Adrian DANILA THE DYNAMIC MODEL OF THE CAPACITOR-RUN TWO-PHASE INDUCTION MOTOR - A VARIATIONAL APPROACH
S2-05.	Anca IORDAN, Manuela PĂŃOIU DESIGN OF AN EDUCATIONAL INFORMATICS SYSTEM FOR THE STUDY OF THE EUCLIDIAN VECTORS USING UML DIAGRAMS
S2-06.	Susana ARAD, Marius MARCU, Dragos PASCULESCU, Codrut PETRILEAN ASPECTS OF THE ELECTRIC ARC FURNACE CONTROL

- S2-07. Raluca ROB, Caius PANOIU, Manuela PANOIU, Anca IORDAN
SIGNAL GENERATOR DESIGNED IN LabVIEW PROGRAM
- S2-08. Corina Daniela CUNȚAN, Ioan BACIU, Manuela PĂNOIU,
Gabriel Nicolae POPA
DIGITAL CONTROL MODES OF THE SEMI-CONTROLLED THREE-PHASED
RECTIFIERS
- S2-09. Adrian DANILA, Gabriela PAVEL, Radu MERA
A STUDY OF THE PARAMETER ESTIMATION OF THE SINGLE/TWO-PHASE
INDUCTION MACHINES
- S2-10. Cornelia Victoria ANGHEL
CONNECTING PC VIA WIRELESS NETWORK PERFORMANCE OF EQUIPMENT
- S2-11. Diana Alina BISTRIAN, Mihaela OSACI, Marcel TOPOR
SOLUTIONS TO ACCELERATE MATLAB PROGRAMS WITH GPU COMPUTING
- S2-12. Manuela PĂNOIU, Caius PĂNOIU, Anca IORDAN, Cosmina ILLES
SOFTWARE PACKAGE FOR ANALYSIS THE PERFORMANCES OF
BACKPROPAGATION NEURAL NETWORKS TRAINING ALGORITHM
- S2-13. Diana Alina BISTRIAN, Mihaela OSACI, Marcel TOPOR
NUMERICAL INVESTIGATION OF SWIRLING FLOWS STABILITY USING
MATLAB DISTRIBUTED COMPUTING SERVER ON A WINDOWS OPERATING
SYSTEM ENVIRONMENT
- S2-14. Stela RUSU-ANGHEL, Lucian GHERMAN, Sergiu MEZINESCU
USING THE MATLAB-SIMULINK SIMULATION FOR OPERATING ACTIVE
FILTERS ORDERED BY DIGITAL SIGNAL PROCESSOR (DSP)
- S2-15. Stela RUSU-ANGHEL, Lucian GHERMAN, Sergiu MEZINESCU
MANAGEMENT FLOW CONTROL ROTOR INDUCTION MACHINE USING
FUZZY REGULATORS
- S2-16. Ion COPACI, Aurelia TĂNĂSOIU
THE REDUCTION OF THE ACCELERATION LEVELS CONVEYED TO THE
FREIGHT HAULED ON CARRIAGES FITTED WITH LONG-RUN BUFFERS
- S2-17. Lucian GHERMAN, Stela RUSU-ANGHEL, Sergiu MEZINESCU
USING DSP TO ORDER ACTIVE FILTERS
- S2-18. Rastislav PIRNÍK, Ján HALGAŠ, Martin ČAPKA
NON-INVASIVE MONITORING OF CALM TRAFFIC
- S2-19. Martin VESTENICKÝ, Peter VESTENICKÝ, Martin VACULÍK,
Mária FRANEKOVÁ
SENSOR NETWORK FOR VEHICLES TRANSPORTING DANGEROUS GOODS
- S2-20. Martin VYSOCKÝ, Pavol LIPTAI, Zuzana FARKAŠOVSKÁ
ACOUSTIC QUALITY OF ELECTROMOTOR

- S2-21. Anjan KUMAR KUNDU, Bijoy BANDYOPADHYAY, Sugata SANYAL
A MICROWAVE IMAGING AND ENHANCEMENT TECHNIQUE FROM NOISY SYNTHETIC DATA
- S2-22. Pavel DRABEK, Martin PITTERMANN
CALCULATION OF INTERHARMONICS OF POWER ELECTRONIC CONVERTERS - USING OF HARMONIC ANALYSIS
- S2-23. Cornelia Victoria ANGHEL
DATA SECURITY IN WIRELESS NETWORKS
- S2-24. Corina Maria DINIȘ, Angela IAGĂR, Corina Daniela CUNȚAN, Gabriel Nicolae POPA
STUDY OF THE VOLTAGE RESONANCE IN ELECTRIC CIRCUITS
- S2-25. Gelu Ovidiu TIRIAN, Camelia BRETOTEAN - PINCA, Marcel TOPOR
SIMULATION OF NEURAL AND FUZZY SYSTEM TO PREDICT, DETECT AND ELIMINATE CRACKS IN CONTINUOUS CASTING
- S2-26. Mihaela OSACI, Ioana Sonia DRAGAN, Iulia TRIPA
STUDIES ABOUT MAGNETIC HYPERTHERMIA WITH SUPERPARAMAGNETIC NANOPARTICLES
- S2-27. Zsolt Csaba JOHANYÁK, Kálmán Milán BOLLA
DEVELOPMENT OF A TOOLBOX SUPPORTING FUZZY CALCULATIONS
- S2-28. Mária FRANEKOVÁ, Karol RÁSTOČNÝ, Aleš JANOTA, Peter CHRTIANSKY
SAFETY ANALYSIS OF CRYPTOGRAPHY MECHANISMS USED IN GSM FOR RAILWAY
- S2-29. Tibor MORAVČÍK, Emília BUBENÍKOVÁ, Ludmila MUZIKÁŘOVÁ
DETECTION OF DETERMINED EYE FEATURES IN DIGITAL IMAGE
- S2-30. Pavel DRABEK
APPLICATION OF THE SIC COMPONENTS IN POWER ELECTRONICS
- S2-31. Ioan BACIU, Corina Daniela CUNȚAN, Sorin DEACONU, Angela IAGĂR
THE STUDY OF QUALITY INDICATORS OF ELECTRICAL ENERGY IN ELECTRICAL RAILWAY TRANSPORT
- S2-32. Iosif POPA, Gabriel Nicolae POPA, Sorin Ioan DEACONU
THE SIZING OF THE BRANCH THREE-PHASE LOW VOLTAGE POWER LINES THROUGH SUPERPOSITION METHOD
- S2-33. Radovan HOLUBEK, Matuš VLÁŠEK
PLC PROGRAMMING IN LABORATORY OF PRODUCTION SYSTEM PROGRAM CONTROL
- S2-34. Tihomir LATINOVIC, Sorin DEACONU, Milosav DJURDJEVIC, Mirko DOBRNJAC
THE BASICS OF DESIGNING CONTROLLERS FOR INDUSTRIAL ROBOTS (EG. ROBOTS ABB IRB 2000)

- S2-35. István MATIJEVICS
REAL AND REMOTE LABORATORIES IN EDUCATION
- S2-36. Gabriel Nicolae POPA, Sorin Ioan DEACONU,
Iosif POPA, Corina Maria DINIȘ
NEW TRENDS IN DETECTION OF BACK-CORONA DISCHARGES IN PLATE-
TYPE ELECTROSTATIC PRECIPITATORS
- S2-37. Constantin OPREA, Cristian BARZ
CONTRIBUTION TO AUTOMATE REGULATION AFTER
THE SPEED OF ACTIONS WITH ASYNCHRONIZED SYNCHRONOUS MOTOR
- S2-38. Cristian BARZ, Constantin OPREA
STUDY OF ELECTROMAGNETIC FIELD IN CLAW-POLES ALTERNATOR
- S2-39. Sorin Ioan DEACONU, Lucian Nicolae TUTELEA,
Gabriel Nicolae POPA, Tihomir LATINOVIĆ
ARTIFICIAL LOADING FOR ROTATING ELECTRIC MACHINES
- S2-40. Gyula MESTER
CONTRIBUTION TO THE SIMULATION OF BIPED ROBOT USING 19-DOF
- S2-41. Angela IAGĂR, Gabriel Nicolae POPA, Corina Maria DINIȘ
STUDY UPON THE THERMAL FIELD FROM A RESISTANCE OVEN
- S2-42. Ionel MUSCALAGIU, Manuela PANOIU, Diana MUSCALAGIU, Anca IORDAN
THE IMPLEMENTATION OF THE MULTI-ROBOT EXPLORATION PROBLEM IN
DisCSP-NetLogo
- S2-43. Adela BERDIE, Mihaela OSACI, Robert RAICH, Daniela CRISTEA
THE COMPONENTISATION EFFICIENCY IN REALIZING A WD ABAP PROJECT



INTERNATIONAL SYMPOSIUM on
ADVANCED ENGINEERING & APPLIED MANAGEMENT
- 40th ANNIVERSARY in HIGHER EDUCATION
(1970-2010)
4 - 5 November, 2010,
Hunedoara, ROMANIA

SECTION S03. **MECHANICAL ENGINEERING & DESIGN**

PROGRAM SCHEDULE:

1ST DAY, Thursday,

4th November, 2010

- 11.30 - 12.00 Setting of posters by sections - in the Halls and in the Amphitheatres of the Faculty
- 12.00 - 14.00 Presentations and debates by sections - in the Faculty's Amphitheatres
- 16.00 - 19.00 Debates by sections - in the Faculty's Amphitheatres

2ND DAY, Friday,

5th November, 2010

- 10.00 - 12.30 Presentations and debates by sections and posters - in the Halls and in the Faculty's Amphitheatres

PROGRAM of PRESENTED PAPERS **(oral presentations and posters):**

No. crt.	Authors Surname & NAME TITLE OF PRESENTED PAPERS
S3-01.	Camelia PINCA -BRETOTEAN, Gelu-Ovidiu TIRIAN, Diana BISTRIAN, Gladiola CHEȚE DIMENSIONAL MATHEMATICAL MODEL TO OPTIMIZE THE PROCESSING MECHANISM OF TRANSLATIONAL ROTATING MOTION
S3-02.	Mihaiela ILIESCU, Marian LAZĂR, Victor GRIGORE RESEARCHES ON TRUE PULSE LASER MICRO-WELDING
S3-03.	Carmen Inge ALIC, Cristina Carmen MIKLOS, Imre Zsolt MIKLOS FINITE ELEMENT ANALYSIS OF A SEAT BELT BUCKLE DEVICE
S3-04.	Amalia Ana DASCĂL, Daniel CARAULEANU WHEELS AUTO MODELING USING FINITE ELEMENT METHOD
S3-05.	Paolo BOSCARIOL EXPERIMENTAL VALIDATION OF A SPECIAL STATE OBSERVER FOR A CLASS OF FLEXIBLE LINK MECHANISMS
S3-06.	Albano LANZUTTI SMOOTH TRAJECTORY PLANNING ALGORITHMS FOR INDUSTRIAL ROBOTS: AN EXPERIMENTAL EVALUATION

- S3-07. Aurelia TĂNĂSOIU, Stelian OLARU
ON THE LIFETIME OF RAILWAY VEHICLE BEARING STRUCTURES AND COMPONENTS
- S3-08. Corneliu BIRTOK-BĂNEASĂ, Sorin Aurel RAȚIU, Claudiu Alin BERTEAN
THE STUDY OF INFLOW IMPROVEMENT IN SPARK ENGINES BY USING NEW CONCEPTS OF AIR FILTERS
- S3-09. Veronica ARGESANU, Imre-Albert FARKAS, Ioan LAZA, Mihaela JULA
SEALING DESIGN IN MACHINE BUILDING
- S3-10. Renato VIDONI
A MULTI AGENT ROBOTIC SYSTEM FOR SIMULATION AND CONTROL OF A MANUFACTURING PROCESS
- S3-11. József SÁROSI
ACCURATE POSITIONING OF HUMANOID UPPER ARM
- S3-12. Iosif DUMITRESCU, Dumitru JULA, Vilhelm ITU
STUDY OF IMPROVEMENT OF ROTATION MECHANISM BALL OF EsRc-1400 ROTOR EXCAVATOR
- S3-13. Adina BUDIUL BERGHIAN, Teodor VASIU, Amalia DASCĂL
KINETIC AND STATIC ANALYSIS AT LOADED RUNNING OF MECHANISMS OF PARALLEL GANG SHEARS' TYPE ASSIGNED FOR CUTTING THE METALLURGICAL PRODUCTS
- S3-14. Ion Silviu BOROZAN, Veronica ARGESANU, Raul Miklos KULCSAR, Ioan LAZA
ABOUT THE TENSIONING OF THE BELT DRIVES
- S3-15. Cristina Carmen MIKLOS, Imre Zsolt MIKLOS, Carmen Inge ALIC
COMPUTER AIDED ANALYSIS OF A DIFFERENTIAL GEAR WITH SIMPLE SATELLITE
- S3-16. Camelia PINCA -BRETOTEAN, Gelu-Ovidiu TIRIAN
CONSIDERATIONS ON THERMAL FATIGUE INTERNAL COMBUSTION ENGINES
- S3-17. Dinu DRĂGAN, Mircea Cristian ARNĂUTU, Nicușor Laurențiu ZAHARIA, Ion SIMION
2100 HP DIESEL ELECTRICAL LOCOMOTIVE RUNNING TEST
- S3-18. Mihaela JULA, Raul KULCSAR, Ionut BOROZAN, Imre-Albert FARKAS
STRUCTURAL AND FUNCTIONAL PARTICULARITIES AS A CRITERION FOR THE DESIGN OF TANGENTIAL BELT DRIVE
- S3-19. Sebastian DUMA, Mihaela POPESCU, Cosmin LOCOVEI
STUDIES REGARDING THE ACQUIREMENT OF HARDNESS STANDARD BLOCKS FOR TRANSMITTING THE VICKERS HARDNESS SCALE 200...800 HV₁

- S3-20. Lubomír ŠOOŠ
NEW METHODOLOGY CALCULATIONS OF RADIAL STIFFNESS NODAL POINTS SPINDLE MACHINE TOOL
- S3-21. Paolo BOSCARIOL, Alessandro GASPARETTO, Albano LANZUTTI, Renato VIDONI, Vanni ZANOTTO
NEUMESY: A SPECIAL ROBOT FOR NEUROSURGERY
- S3-22. Přemysl MATOUŠEK
ADAPTIVE CONTROL OF PNEUMATIC SERVOMECHANISM
- S3-23. Todor BAČKALIĆ, Maša BUKUROV
MODELLING OF THE SHIP LOCKING PROCESS IN THE ZONE OF SHIP LOCK WITH TWO PARALLEL CHAMBERS
- S3-24. József SÁROSI
INVESTIGATION OF POSITIONING OF FLUID MUSCLE ACTUATOR UNDER VARIABLE TEMPERATURE
- S3-25. Ala'a M. DARWISH
STABILIZATION OF EMPTY UNDERGROUND CIRCULAR STORAGE TANKS AGAINST UPLIFTING UNDERGROUND WATER FORCES
- S3-26. Gergely DEZSŐ, Gyula VARGA, Ferenc SZIGETI
INVESTIGATION THE CORRELATION BETWEEN TECHNOLOGICAL PARAMETERS AND THE WEAR IN CASE OF DRILLING WITH MINIMAL LUBRICATION
- S3-27. Jarmila ORAVCOVÁ, František LACKO, Peter KOŠŤÁL
DEVIATIONS OF WORKPIECE CLAMPING AS FACTOR HAVING INFLUENCE ON ACCURACY OF A SURFACE MACHINED
- S3-28. Tamás ENDRÓDY, Adrián SZÓNYI
ANALYSING THE 2-7 DOF HUMANOID ROBOT ARM CONSTRUCTIONS AND THE POSSIBILITIES OF CONTROLLING/LEARNING THEIR MOVEMENTS
- S3-29. Flavius Lucian PATER, Ludovic Dan LEMLE
A DYNAMIC PROCESS MODEL BASED ON A FUNCTIONAL EQUATION
- S3-30. Flavius Lucian PATER, Liana Rodica PATER
A DYNAMIC PROCESS MODEL BASED ON A FUNCTIONAL EQUATION
- S3-31. Amalia Ana DASCĂL, Adina BUDIUL BERGHIAN
FOR MEASURING AN AMENDMENT DUROMETER BRINELL HARDNESS AT HOT
- S3-32. Siniša KUZMANOVIĆ, Milan RACKOV
THE INFLUENCE OF AXIAL LOAD AT OUTPUT SHAFT OF UNIVERSAL WORM AND HELICAL-WORM GEAR UNITS ON THEIR THERMAL POWER CAPACITY
- S3-33. Krassimir E. GEORGIEV
ADVANCED DESIGN OF MECHATRONIC WORKSTATIONS FOR TECHNOLOGICAL CONTACT OPERATIONS

- S3-34. Juraj HUDÁK, Miroslav TOMÁŠ
ANALYSIS OF FORCES IN DEEP DRAWING PROCESS
- S3-35. Peter KOŠTÁL, Imre KISS, Petar KERAK
THE INTELLIGENT FIXTURE AT FLEXIBLE MANUFACTURING
- S3-36. Miroslava KOŠTÁLOVÁ
ASSEMBLING AND VERIFICATION DESIGN CORRECTNESS OF PRESS TOOLS
BY HELP OF SYSTEM CATIA
- S3-37. Pavol ČEKAN, Anh NGUYEN THE, Ervin LUMNITZER
APPLICATION OPPORTUNITIES VIBRATION ANALYSERS
- S3-38. Adalbert KOVÁCS
THE LAGRANGE INTERPOLATION FORMULA FOR ANALYZING FLUID
MOVEMENT IN NETWORK PROFILES
- S3-39. Diana STOICA
DISCRETE ASYMPTOTIC BEHAVIORS OF STOCHASTIC SKEW-EVOLUTION
SEMIFLOWS IN HILBERT SPACES
- S3-40. Nicușor Laurențiu ZAHARIA, Tiberiu Ștefan MĂNESCU,
Mihaela Dorica ȘTROIA, Tiberiu MĂNESCU jr.
DYNAMIC COEFFICIENT DETERMINATION AT A TANK WAGON
- S3-41. Ștefan MAKSAY, Diana STOICA
CONSIDERATIONS ON THE RECTANGLE TRUNCATED BIDIMENSIONAL
NORMAL MODELING
- S3-42. Ludovic Dan LEMLE, Tudor BÎNZAR, Lucian Flavius PATER,
Valentina BALASOIU
RIESZ-DUNFORD REPRESENTATION THEOREM FOR UNIFORMLY
CONTINUOUS SEMIGROUPS
- S3-43. Imre Zsolt MIKLOS, Carmen Inge ALIC, Cristina Carmen MIKLOS
INDEXING DEVICE WITH SPHERICAL ELEMENTS (BALLS)
- S3-44. Teodor VASIU, Adina BUDIUL-BERGHIAN
THE PORTABLE GRINDERS BLACK& DECKER RELIABILITY DETERMINATION
- S3-45. Carmen Inge ALIC, Sorin Aurel RAȚIU, Vasile ALEXA,
Cristina Carmen MIKLOS, Imre Zsolt MIKLOS
CREATE OF INTERACTIVE LEARNING RESOURCES STRUCTURED IN
DATABASE, FOR THE ACQUISITION OF KNOWLEDGE AND SKILLS IN THE
WELDING FIELD
- S3-46. Vasile ALEXA, Sorin Aurel RAȚIU, Carmen Inge ALIC
DESIGN AND IMPEMENTATION FOR AN INFORMATICS APLICATION TO
WORKING-OUT THE MIG-MAG WELDING TECHNOLOGY
- S3-47. Georgeta Emilia MOCUȚA, Mihaela POPESCU, Ioan Danuț DAN
THE BEST WAY OF WORKING SPACE ROBOT WHICH EQUIPS A FLEXIBLE
MANUFACTURING CELL COMPONENT OF WELDED IN RAIL FIELD

- S3-48. Tamás ENDRÓDY
UNFOLDING THE CONVEX POLYHEDRONS TO A CONNECTED NON-
OVERLAPPING POLYGON (PREPARING TOOLS FOR CREATIVE PROOF OF
THE DÜRER'S CONJECTURE)
- S3-49. Vasile George CIOATA, Imre KISS
SIMULATION SOLIDIFICATION PROCESS OF THE PIECES OBTAINED
THROUGH DIE FORGING IN THE SEMISOLID STATE
- S3-50. Vasile George CIOATA, Imre KISS
DETERMINING THE CONTACT FORCES BETWEEN THE WORKPIECE AND
FIXTURE USING THE FINITE ELEMENT METHOD
- S3-51. L. MIHON, A. NEGOTESCU, A. TOKAR, D. OSTOIA
MOTOR AND VEHICLE OPTIMIZATION PROCESS MODELING BY USING THE
AVL CRUISE IN STANDARD APPLICATIONS
- S3-52. Siby ABRAHAM, Imre KISS, Sugata SANYAL, Mukund SANGLIKAR
STEEPEST ASCENT HILL CLIMBING FOR A MATHEMATICAL PROBLEM



INTERNATIONAL SYMPOSIUM on
ADVANCED ENGINEERING & APPLIED MANAGEMENT
- 40th ANNIVERSARY in HIGHER EDUCATION
(1970-2010)
4 - 5 November, 2010,
Hunedoara, ROMANIA

SECTION S04. **MANAGEMENT IMPLEMENT POLICIES & STRATEGIES**

PROGRAM SCHEDULE:

1ST DAY, Thursday,
4th November, 2010

- 11.30 - 12.00 Setting of posters by sections - in the Halls and in the Amphitheatres of the Faculty
- 12.00 - 14.00 Presentations and debates by sections - in the Faculty's Amphitheatres
- 16.00 - 19.00 Debates by sections - in the Faculty's Amphitheatres

2ND DAY, Friday,
5th November, 2010

- 10.00 - 12.30 Presentations and debates by sections and posters - in the Halls and in the Faculty's Amphitheatres

PROGRAM of PRESENTED PAPERS **(oral presentations and posters):**

No. crt.	Authors Surname & NAME TITLE OF PRESENTED PAPERS
S4-01.	Carmen HĂRĂU MIGRATION AND REMITTANCES - CASE STUDY ON ROMANIA
S4-02.	Gladiola C. CHETE, Ioana. A. STĂNESCU DECISION MAKING AND BUSINESS INTELLIGENCE SOLUTIONS
S4-03.	Natalia-Cernica BUZGĂU IMPLEMENTATION OF TOTAL PRODUCTIVE MAINTENANCE
S4-04.	Natalia-Cernica BUZGĂU RELIABILITY-CENTERED MAINTENANCE (RCM)
S4-05.	Árpád FERENCZ, Márta NÓTÁRI ROLE OF RURAL DEVELOPMENT IN THE PRODUCTION OF THE HUNGARIAN TRADITIONAL HORTICULTURAL PRODUCTS
S4-06.	Márta NÓTÁRI, Árpád FERENCZ THE CENTRAL AND THE LOCAL SYSTEMS OF RURAL DEVELOPMENT IN THE REGION MANAGEMENT
S4-07.	M. RAHMOUNI, M.N. LAKHOVA PROPOSAL OF THE INTEGRATION OF THE METHODS SADT AND GRAI IN THE ENTERPRISE

- S4-08. M.N. LAKHOUA
USING METHODS AND APPROACHES IN IS PLANNING AND REQUIREMENTS ANALYSIS
- S4-09. Zoltán BÁTORI, Tamás HARTVÁNYI
DEVELOPMENT OF FORECASTING SYSTEMS
- S4-10. Csaba TÁPLER
INVENTORY LEVEL REDUCTION BY INSERTING UNPACKING STATIONS IN PRODUCTION SUPPLY PROCESS
- S4-11. Ioan MILOSAN
STUDIES ABOUT THE TOTAL QUALITY MANAGEMENT CONCEPT
- S4-12. Jan MÖLLER, Ulrich J. SCHÖDEL, Christian SCHÖDEL
MID-SIZE COMPANIES AND LOGISTIC IN THE CHALLENGE OF GLOBALIZATION
- S4-13. Ulrich J. SCHÖDEL, Christian SCHÖDEL, Jan MÖLLER, Miroslav BADIDA
ECONOMIC ASPECTS OF THE DEVELOPMENT OF ENVIRONMENTAL PROTECTION
- S4-14. Christian SCHÖDEL, Ulrich SCHÖDEL, Jan MÖLLER, Ervin LUMNITZER
DETERMINING FACTORS INFLUENCING PRODUCTION SITE RELOCATION
- S4-15. Ferenc BAGLYAS, Gábor SUGATAGI
MULTIVARIATE ANALYSIS IN A WINE MARKET RESEARCH IN HUNGARY
- S4-16. Abdelnaser OMRAN, Imre KISS
FACTORS INFLUENCING COST OVERRUNS ON CONSTRUCTION PROJECTS
- S4-17. Mohammed Salleh HAMDAD, Abdelnaser OMRAN,
Abdul Hamid Kadir PAKIR
IDENTIFYING WAYS TO IMPROVE PRODUCTIVITY AT THE CONSTRUCTION INDUSTRY
- S4-18. Ferenc BAGLYAS
CONSUMER ATTITUDES TO GLOBAL GRAPE VARIETIES VERSUS HUNGARICUM VARIETIES IN THE SOUTH-ALFÖLD REGION
- S4-19. M. KATA, Z. AIGNER, P. SZABÓ-RÉVÉSZ, Z. SZABADAI, Á. GYÉRESI
RESEARCH COOPERATION BETWEEN THE UNIVERSITY OF TIMISOARA AND THE UNIVERSITY OF SZEGED
- S4-20. Eva BATEŠKOVÁ, Martina NOVÁKOVÁ, Tibor KRENICKÝ
TRANSFORMATION OF STN STANDARDS TO EN ISO STANDARDS IN THE FIELD OF ENGINEERING
- S4-21. Abdul Aziz HUSSIN, Abdelnaser OMRAN
IMPLICATION OF NON-COMPLETION PROJECTS IN MALAYSIA

- S4-22. Eva MATIJEVIC
APPLICATION OF PROJECT MANAGER METHODOLOGY IN PREPARING OF
THESIS
- S4-23. Mihaela POPESCU
DIRECTIONS TO APPROACH ERGONOMICS ISSUES IN WELDING
- S4-24. Mihaela POPA, Florin BUCUR
STUDY REGARDING COSTILL METHOD EFFICIENCY IN TRAINING OF SEMI-
FUND RUNNERS
- S4-25. Georgeta Emilia MOCUTA, Ioana IONEL, Mihaela TILINCĂ,
Luisa Isabela DUNGAN
ENGINEERING TRAINING SUPPORT THROUGH PRACTICE
- S4-26. Keil REINER, Tamás HARTVÁNYI, Péter NÉMETH
RELIABILITY-THEORETICAL APPROACHES TO ORGANIZATION OF
RESOURCE-LIMITED INFRASTRUCTURE CHARGES
- S4-27. Vasile ALEXA, Imre KISS
METHOD FOR CREATING AND MAINTAINING AN HIGHLY PERFORMING
SPACE AT THE WORKPLACE
- S4-28. Mihaela POPA, Grigore CONSTANTIN
SPORTS MARKETING MIX IN THE CONTEXT OF TRADITIONAL MIX
MARKETING



INTERNATIONAL SYMPOSIUM on
ADVANCED ENGINEERING & APPLIED MANAGEMENT
- 40th ANNIVERSARY in HIGHER EDUCATION
(1970-2010)
4 - 5 November, 2010,
Hunedoara, ROMANIA

SECTION S05. **ENVIRONMENTAL ENGINEERING & ECOLOGY**

PROGRAM SCHEDULE:

1ST DAY, Thursday,

4th November, 2010

- 11.30 - 12.00 Setting of posters by sections - in the Halls and in the Amphitheatres of the Faculty
- 12.00 - 14.00 Presentations and debates by sections - in the Faculty's Amphitheatres
- 16.00 - 19.00 Debates by sections - in the Faculty's Amphitheatres

2ND DAY, Friday,

5th November, 2010

- 10.00 - 12.30 Presentations and debates by sections and posters - in the Halls and in the Faculty's Amphitheatres

PROGRAM of PRESENTED PAPERS **(oral presentations and posters):**

No. crt.	Authors Surname & NAME TITLE OF PRESENTED PAPERS
S5-01.	Marius ARDELEAN, Teodor HEPUȚ, Erika ARDELEAN, Ana SOCALICI HIGH PRODUCTIVITY INSTALLATION FOR THE RECOVERY OF WASTE BY BRIQUETTING OF POWDER
S5-02.	Irina VÎLCIU, Maria NICOLAE, Emanuela-Daniela STOICA DIFFRACTOMETRIC ANALYSE OF STEEL SLAGS VIEWING THEIR USE FOR ROAD CONSTRUCTION
S5-03.	Adina Milena TATAR ATMOSPHERIC POLLUTION IN AREA CAREER GARLA
S5-04.	Avram NICOLAE, Ionel BORS, Cristian PREDESCU, Maria NICOLAE, Mirela SOHACIU, Ecaterina MATEI ELEMENTS OF METALLURGICAL ECONOMY
S5-05.	Aleksandar DVORNIC, Maja DJOGO Mirjana VOJINOVIC - MILORADOV, Goran VUJIC BIOLOGICAL AND CHEMICAL OXYGEN DEMAND AS INDICATORS OF ORGANIC POLLUTION OF LEACHATE AND PIEZOMETRIC WATER FROM SEMI CONTROLLED, NON SANITARY LANDFILL IN NOVI SAD, SERBIA
S5-06.	Zsuzsanna H.HORVÁTH, Cecília HODÚR ANALYSIS OF COLOUR CHARACTERISTICS OF PAPRIKA POWDER WITH DIFFERENT OIL CONTENT

- S5-07. Richard LADANYI
OPTIMISATION OF SELECTIVE WASTE COLLECTION ROUTES ON THE BASIS OF GEOGRAPHICAL INFORMATION SYSTEM (GIS)
- S5-08. Adina Milena TATAR
AIR POLLUTION IN THE AREA OF COAL DEPOSITS OF SE ROVINARI. RISK ASSESSMENT
- S5-09. Imre DÉKÁNY
TITANIUM DIOXIDE AND GOLD NANOPARICLES FOR ENVIRONMENTAL AND BIOLOGICAL APPLICATION
- S5-10. Ana SOCALICI, Erika ARDELEAN, Marius ARDELEAN, Teodor HEPUT
RESEARCHS REGARDING THE PELETIZING PROCESS OF FEROUS PULVEROUS WASTE
- S5-11. Monika BILOVÁ, Ervin LUMNITZER
DETERMINATION OF POROUS MATERIALS' ACOUSTICAL PARAMETERS
- S5-12. Vania RANGELOVA, Antonia PANDELOVA, Nikolai STOYANOV
INHIBITOR MULTIENZYME BIOSENSOR SYSTEM IN DYNAMIC MODE - PHOSPHATE MEASUREMENT
- S5-13. Erika ARDELEAN, Teodor HEPUT, Marius ARDELEAN, Ana SOCALICI
CAPITALIZATION OF POWDERY WASTE THAT CONTAINING IRON AND BASIC OXIDES UNDER BRIQUETTES FORM
- S5-14. Beata HRICOVÁ, Henrieta NAKATOVÁ
POSSIBILITIES OF APPLICATIONS OF TOOLS FOR ECODESIGN IN VARIOUS STAGES OF DESIGN PROCESS
- S5-15. Marek MORAVEC, Ervin LUMNITZER, Katarína LUKÁČOVÁ
APPLICATION OF ACOUSTIC CAMERA FOR MACHINE NOISE VISUALISATION AND DIAGNOSTIC
- S5-16. Sorina Gabriela ȘERBAN, Maria Laura STRUGARIU
RESEARCH ON WATER QUALITY IN THE CITY HATEG
- S5-17. Lenka RUSINOVÁ, Lenka MAGULÁKOVÁ, Jana POLAČEKOVA
THE POTENTIAL OF WIND ENERGY AND ITS USAGE IN THE CONDITIONS OF THE SLOVAK REPUBLIC
- S5-18. Miriama PIŇOSOVIÁ, Pavol LIPTAI, Ervin LUMNITZER
NOISE AND ITS SOURCES FOR THE REDUCTION IN WORK ENVIRONMENT
- S5-19. Sándor BESZÉDES, Nora PAP, Eva PONGRACZ,
Riitta L. KEISKKI, Cecilia HODÚR
DEVELOPMENT OF MEMBRANE WASTEWATER PURIFICATION PROCESS FOR MEAT INDUSTRY SME'S
- S5-20. Abdelnaser OMRAN, Abdelsalam O. GEBRIL
STUDY OF HOUSEHOLD ATTITUDE TOWARD RECYCLING OF SOLID WASTES: A CASE STUDY

- S5-21. Katarína KORÁLOVÁ
ENVIRONMENTAL ASPECTS SAFETY RISKS
- S5-22. Katarína LUKÁČOVÁ, Miroslav BADIDA, Marek MORAVEC
GENERAL PROCESS HOW TO ASSESS EXPOSURE TO SOLID AEROSOL IN
WORKING ENVIRONMENT
- S5-23. Lenka MAGULÁKOVÁ, Lenka RUSINOVA, Ladislav BARTKO
POSSIBILITY OF USAGE A NONSTANDARD SOURCES FOR WIND ENERGY
- S5-24. Zsuzsa FARKAS, Péter LÉVAL
GROWING GREENHOUSE CUT FLOWER IN HYDRO-CULTURE
- S5-25. Andra PREDESCU, Ecaterina MATEI, Andrei PREDESCU, Bogdan STROE
METHODS FOR RECOVERY AND RE-USE OF SLUDGE RESULTED FROM
WASTE WATER TREATMENT
- S5-26. Siniša BIKIĆ, Maša BUKUROV, Dušan UZELAC,
Slobodan TAŠIN, Marko ĐURĐEVIĆ
TESTING OF FILTER NOZZLE BY COLUMN
- S5-27. Dan CONSTANTINESCU, Mirela SOHACIU
ENERGY AND METAL SAVING IN THE HEATING FURNACES MEANS A
CLEANER ENVIRONMENT
- S5-28. Georgeta Emilia MOCUȚA
Promotion OF PASSENGER rail transport as a friendly solution TO
ENVIRONMENT



INTERNATIONAL SYMPOSIUM on
ADVANCED ENGINEERING & APPLIED MANAGEMENT
- 40th ANNIVERSARY in HIGHER EDUCATION
(1970-2010)
4 - 5 November, 2010,
Hunedoara, ROMANIA







UNIVERSITY POLITEHNICA TIMIȘOARA
FACULTY OF ENGINEERING - HUNEDOARA
5, REVOLUTIEI, 331128, HUNEDOARA
phone: + 40 254 207522; fax: + 40 254 207501
e-mail: symposium@fih.upt.ro



INTERNATIONAL SYMPOSIUM on
ADVANCED ENGINEERING & APPLIED MANAGEMENT
- 40th ANNIVERSARY in HIGHER EDUCATION
(1970-2010)
4 - 5 November, 2010,
Hunedoara, ROMANIA



RESEARCHS REGARDING THE QUALITY OF THE STEEL USED FOR MAKING ROLLING STOCK COMPONENTS

^{1,3} UNIVERSITY POLITEHNICA OF TIMISOARA, FACULTY OF ENGINEERING - HUNEDOARA

² ROMANIAN MINISTRY OF TRANSPORTS

ABSTRACT:

The work presents the manner of settlement of the specific problems of steel ingot cast in a smooth cylinder format and its use as semi-finished product, compatible with the manufacturing of monoblock wheels, under the quality conditions thereof imposed by the manufacturing regulations. By means of the proposed research and experiments we intend to get to know the specific characteristics of the ingot and the optimization thereof in order to satisfy the quality requirements imposed on the products (monoblock wheels). During the manufacturing of wheels the chemical composition and the gas content (hydrogen, nitrogen, oxygen) are to a large extent the decisive elements regarding the obtaining of the main characteristics of the wheels corroborated with the hot deformation of the cast semi-finished product and the adequate thermal treatment. The main physical and mechanical characteristics established for the wheels are: resistance to rupture; yield point; elastic limit; elongation; rupture resistance or energy upon shock bending; strength; K1C tenacity.

KEYWORDS:

steel, quality, monoblock wheel, rolling stock

1. INTRODUCTION

Various flow sheets are used, around the world, for the manufacturing of monoblock railroad wheels, which use as raw material semi-finished goods cut from ingots or blooms.

The casting process for the steel wheels is constantly improved, which ensures an increase of the quality and efficiency of their production.

In Romania the manufacturing of monoblock railroad wheels is 35 years old in the former Factory of Axles and Bogies of Balș, which is currently called SC Subansambluri de Material Rulant – SA.

For the manufacturing of monoblock railroad wheels we have the following main technological processes: the obtaining of the starting semi-finished product which includes – the manufacturing of the steel, the casting of the ingots, the potential rolling of the blooms, the division of the ingots or blooms; the forging of the wheels which includes: the heating of the bars resulting from the division of the ingots or blooms, the actual forging with its stages (stamping, rolling, forming – calibration, perforation of the central hole in the hub), the cooling of the forged wheels; the thermal treatment of the wheels; the mechanical processing of the wheels which is usually performed in most of the cases in two stages, namely before and after the thermal treatment of the wheels.

2. METHODOLOGY AND DISCUSSION

Starting from the obtaining of the starting semi-finished product, we can very well say that until the manufacturing of an almost ideal semi-finished product, obtained by computer assisted development in duplex or triplex system continuously cast conjugate aggregates, certain improvements can be obtained even with the current equipment: a chemical and structural

homogeneity of the ingots; advanced purity regarding the non-metallic inclusions as well as the gases; economic format of semi-finished product.

The following shortcomings must be noted regarding the manufacturing of the liquid steel and the casting of the ingots: the full development of the steel in electric-arc furnaces is uneconomical, and the quality of the steel is not fully satisfying, due to the chemical and thermal inhomogeneity, the high content of endogenous inclusions and gas.

For the performed researches, objectives were established which could harmonize the influences of certain ingot technological manufacturing – casting factors upon the behavior of the semi-finished obtained product in the process of plastic deformation and upon the physical – mechanical characteristics of the manufactured wheels.

For the manufacturing of the monoblock railroad wheels high quality carbon steels are used and only in few cases attempts have been made regarding the use of alloy construction steels.

During the manufacturing of wheels the chemical composition and the gas content (hydrogen, nitrogen, oxygen) are to a large extent the decisive elements regarding the obtaining of the main characteristics of the wheels corroborated with the hot deformation of the cast semi-finished product and the adequate thermal treatment. The main physical and mechanical characteristics established for the wheels are: resistance to rupture; yield point; elastic limit; elongation; rupture resistance or energy upon shock bending; strength; K1C tenacity.

Experimental data obtained on the influence of chemical composition on the characteristics of resistance were processed in MATLAB computer program results are presented in graphical and analytical.

Regression equations are hyper surfaces:

$$R_{p02} = -2182,1605 \cdot C^2 + 1683,4169 \cdot Mn^2 - 810861,048 \cdot P^2 - 3686,2945 \cdot C \cdot Mn - 43612,0459 \cdot Mn \cdot P + 182628,5699 \cdot P \cdot C + 2189,3056 \cdot C + 426,6009 \cdot Mn - 47302,4451 \cdot P - 346,8306; \quad R^2 = 0,8753 \quad (1)$$

$$R_m = -1058,2742 \cdot C^2 + 517,8169 \cdot Mn^2 - 212838,9859 \cdot P^2 - 851,711 \cdot C \cdot Mn - 15326,9006 \cdot Mn \cdot P + 54597,7285 \cdot P \cdot C + 985,0177 \cdot C - 17,1633 \cdot Mn - 13266,2739 \cdot P - 89,5498; \quad R^2 = 0,8307 \quad (2)$$

Because these hyper surfaces can be represented in space with four dimensions, was used to replace, in succession, independent variables with each of its average value. Surface regression obtained and the contour lines are shown in Fig.1-6.

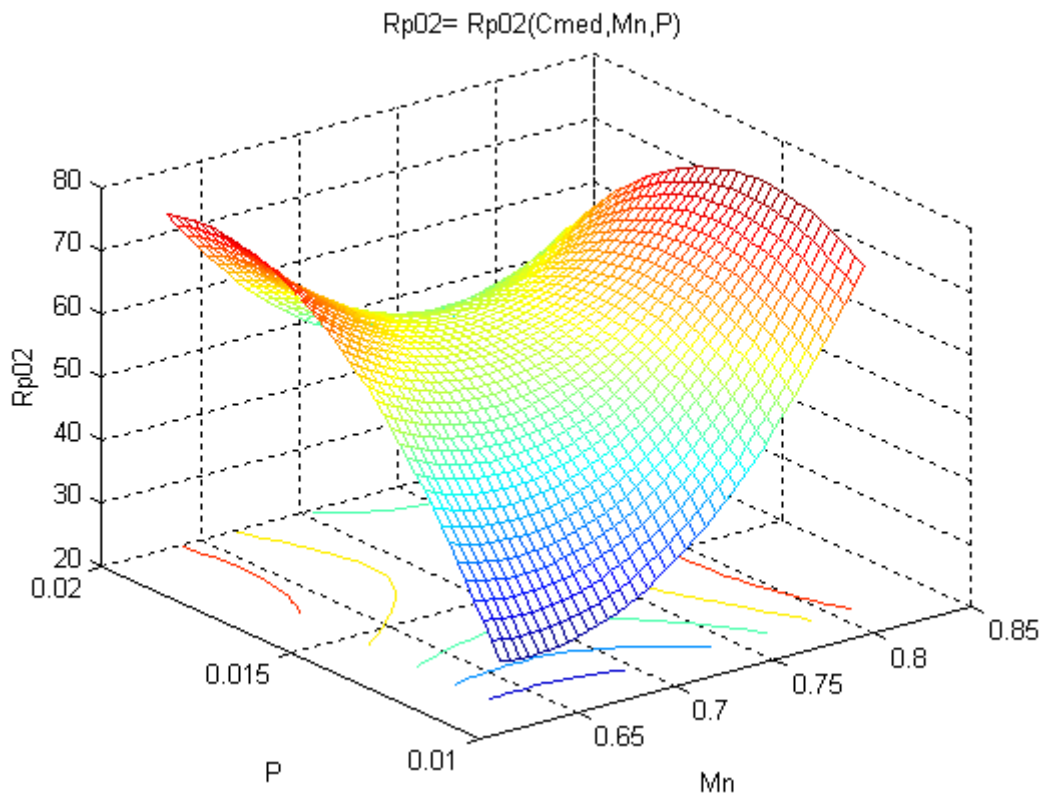


Fig.1. $R_{p0,2} = f(C_{med}, Mn, P)$

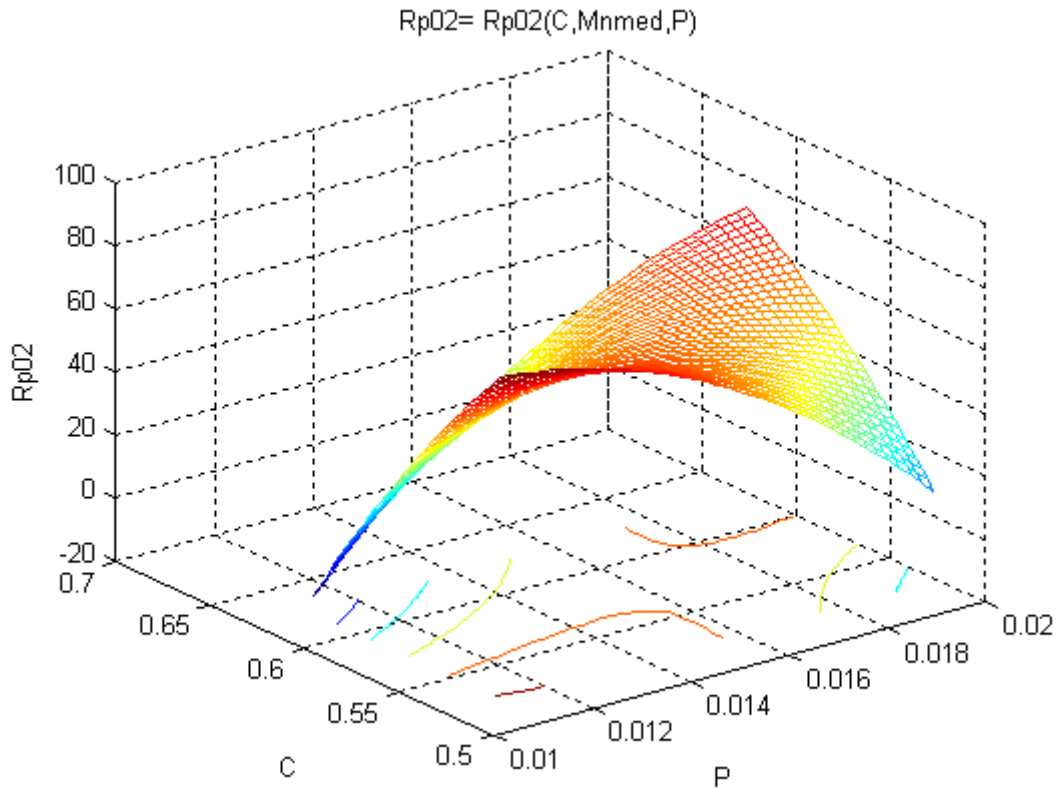


Fig.2. $R_{p0,2} = f(C, Mn_{med}, P)$

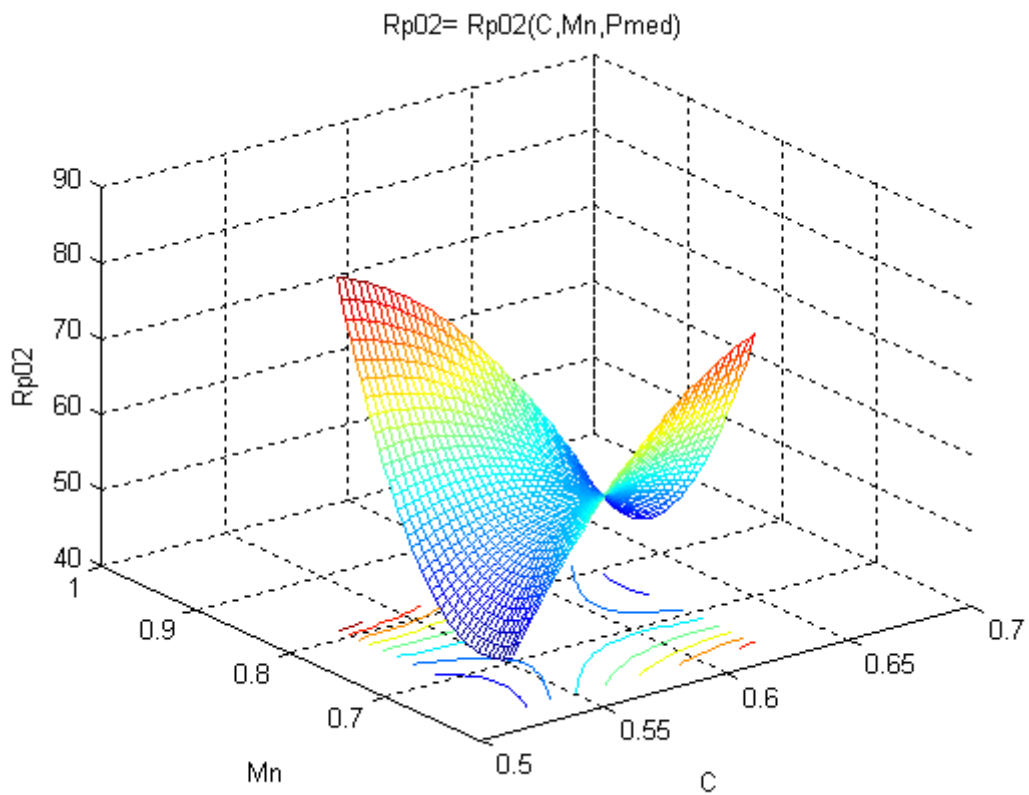


Fig.3. $R_{p0,2} = f(C, Mn, P_{med})$

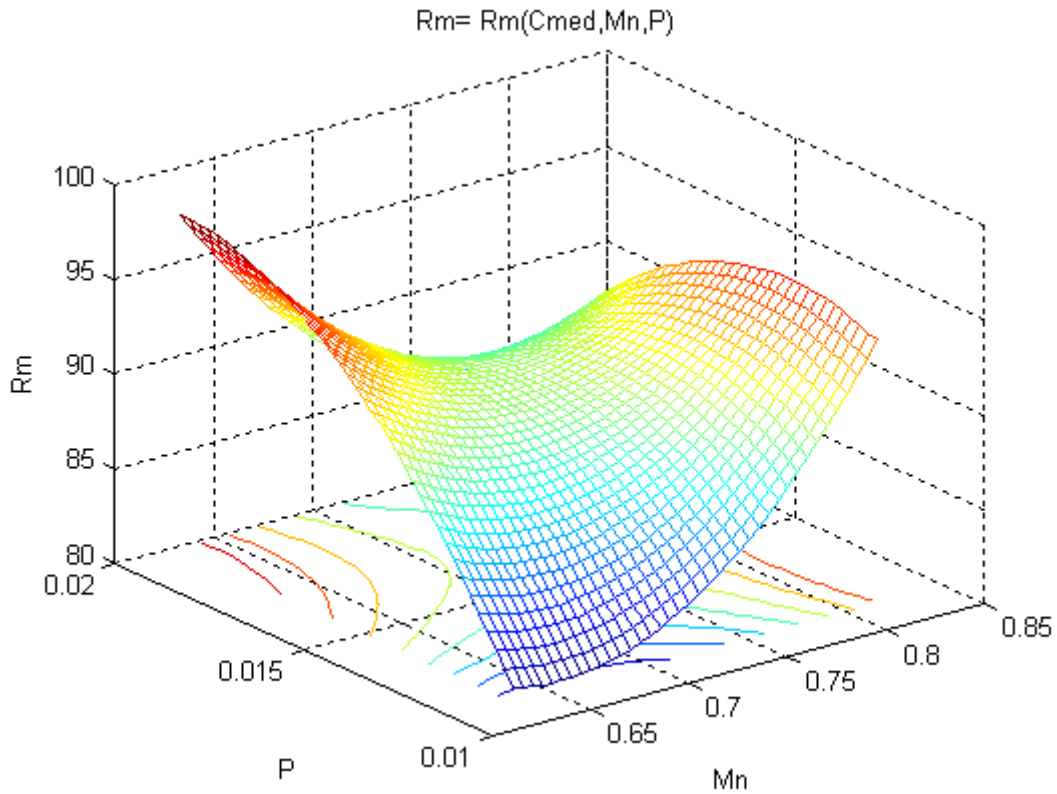


Fig.4. $R_m = f(C_{med}, Mn, P)$

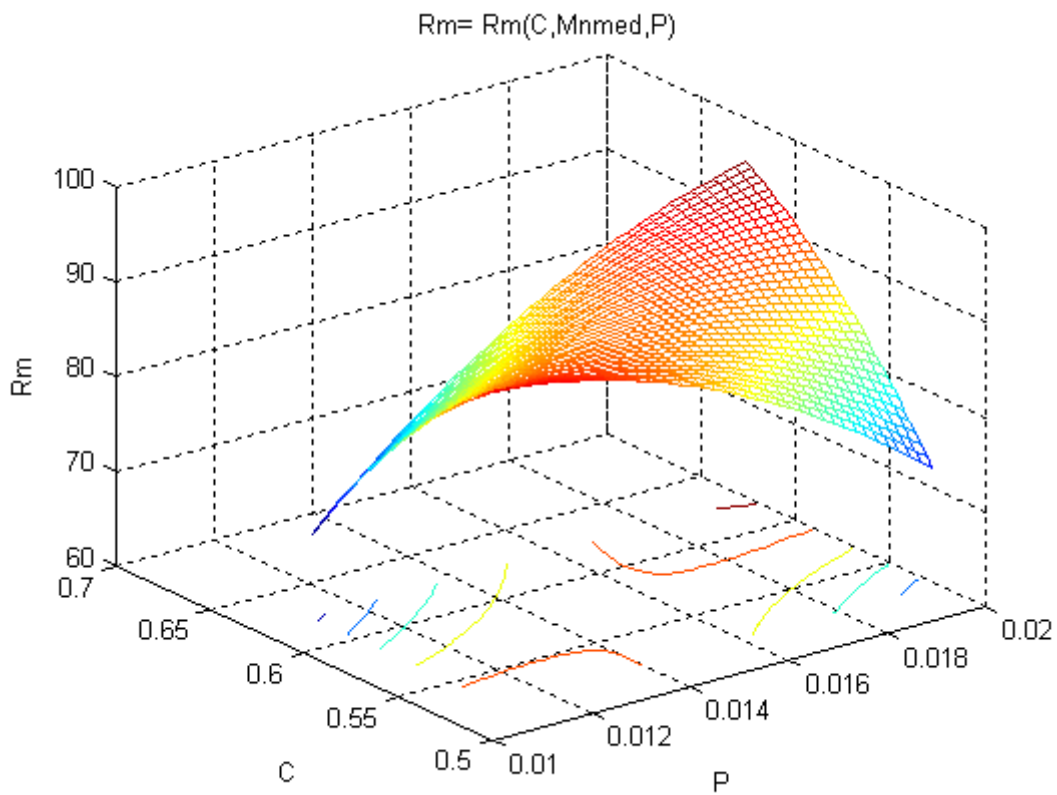


Fig.5. $R_m = f(C, Mn_{med}, P)$

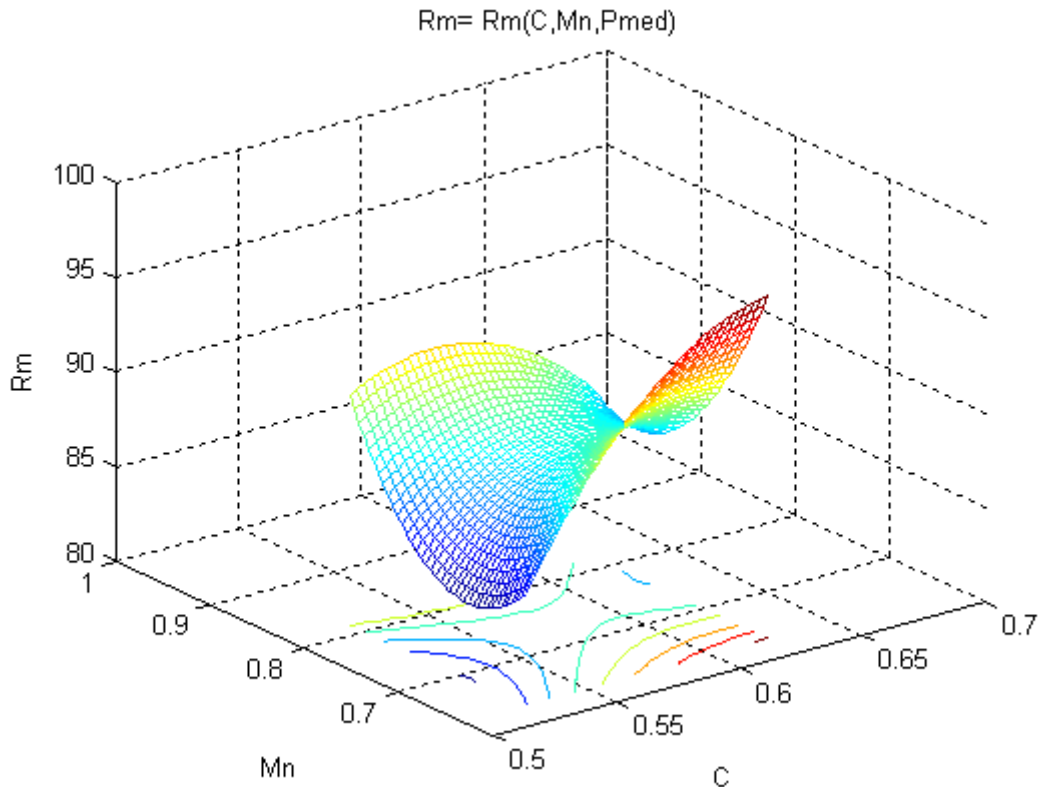


Fig.6. $R_m = f(C, Mn, P_{med})$

Surface regression equations for the mechanical strength are:

$$R_{p02}C_{med} = 1683,4169 \cdot Mn^2 - 810861,048 \cdot P^2 - 43612,0459 \cdot Mn \cdot P - 1698,0452 \cdot Mn + 57958,0215 \cdot P + 190,1026 \quad (3)$$

$$R_{p02}Mn_{med} = - 810861,048 \cdot P^2 - 2182,1605 \cdot C^2 + 182628,5699 \cdot P \cdot C - 79040,1203 \cdot P - 493,3114 \cdot C + 855,1341 \quad (4)$$

$$R_{p02}P_{med} = - 2182,1605 \cdot C^2 + 1683,4169 \cdot Mn^2 - 3686,2945 \cdot C \cdot Mn + 5177,7731 \cdot C - 287,0508 \cdot Mn - 1337,9938 \quad (5)$$

$$R_mC_{med} = 517,8169 \cdot Mn^2 - 212838,9859 \cdot P^2 - 15326,9006 \cdot Mn \cdot P - 508,0585 \cdot Mn + 18201,8715 \cdot P + 126,6252 \quad (6)$$

$$R_mMn_{med} = - 212838,9859 \cdot P^2 - 1058,2742 \cdot C^2 + 54597,7285 \cdot P \cdot C - 24420,0774 \cdot P + 365,2044 \cdot C + 172,1891 \quad (7)$$

$$R_mP_{med} = - 1058,2742 \cdot C^2 + 517,8169 \cdot Mn^2 - 851,711 \cdot C \cdot Mn + 1878,4351 \cdot C - 267,9671 \cdot Mn - 363,6258 \quad (8)$$

3. CONCLUSIONS

From the analysis of the data processed in a graphic and analytical form a series of conclusions can be drawn:

- ❖ the increase of the resistance to traction and of the yield point with the increase of the carbon content is due on the one hand to the increase of the pearlite ratio in the structure, constituent with superior values for these characteristics, and on the other hand due to the favorable action of the carbon upon the deoxidation and desulphuration process;
- ❖ manganese as element which is present in almost all steels dissolves in iron and forms solid solutions increasing their resistance. On the other hand, the manganese from the steel also has

a deoxidation and desulphuration role, which can be noticed in the improved resistance characteristics;

- ❖ regarding the silicon, it dissolves in ferrite increasing its resistance and toughness. At the same time, the silicon is also a deoxidizing agent with a great deoxidation power having the capacity to calm the steel completely and as a consequence decreases progressively the oxygen content of the steel, element which has a negative influence upon quality;
- ❖ in the analyzed steels phosphorous is present in very small concentrations and therefore it causes no negative effects, on the contrary when dissolved in iron it leads to the formation of mixed crystals which in their turn determine an increase of the toughness of the steel. The existing phosphorous content of the analyzed steel does not create the risk of the formation of a ternary eutectic $Fe_3P - Fe - C$ with a melting temperature of $953^{\circ}C$ which would cause the cracking of the ingot upon its processing due to the plastic deformation;
- ❖ regarding the sulphur content a decrease of the values for resistance to concentrations of more than 0.018% was found. Regarding the range of 0.011-0.018% we can say that its negative influence is insignificant. We believe that for values between 0.018 and 0.022% an inhomogeneity may exist regarding the distribution of the sulphur in the structure of the ingot, which may influence its characteristics;

Further research shall be performed in order to establish certain complex dependence relations, namely the data will be processed with the Matlab software by analyzing the influence of three independent factors (C, Mn, Si) upon the independent parameters (tensile resistance, yield point etc) and based on the obtained results we will be able to establish an optimal chemical composition. Moreover, we will also have in view the establishing of the dependence relations for other characteristics: toughness, resilience, elongation, as well as the gases content of the steel (a very important aspect for the steels destined for the manufacturing of rolling stock components).

REFERENCES

- [1.] BUTNARU, I., GEANTĂ, V., Tehnologii speciale de elaborare și rafinare a oțelurilor, Bucharest Polytechnic University Lithography, 1993.
- [2.] VACU, S., ș.a., Elaborarea oțelurilor aliate, vol.I and vol II, Tehnică Publishing House, Bucharest, 1980.
- [3.] NICA, GHE., SOCALICI, A., ARDELEAN, E., HEDUȚ, T., Tehnologii pentru îmbunătățirea calității oțelului, Mirton Publishing House, Timisoara, 2003.





RESEARCH REGARDING THE PHYSICAL AND CHEMICAL CHARACTERISTICS OF PRE-REDUCED IRON ORES AND THE ANALYSIS OF THE POSSIBILITIES OF THEIR USE IN THE IRON AND STEEL ELABORATING PROCESS

^{1, 2, 3} UNIVERSITY "POLITEHNICA" OF BUCHAREST, ROMANIA

ABSTRACT:

Taking into consideration the complexity of the traditional iron and steel elaborating methods that demand the existence of ore preparation plants, cookery, etc. moreover the deficit of coking coals and iron scrap it is necessary to search new possibilities of modifying the existent technologies or replacing them by new methods. One option regarding this way represents the use of sponge iron obtained by direct reduction of iron ores or prepared into the iron and steel elaborating process.

Considering the high materials and energy consumption and environment pollution in the traditional iron and steel elaborating methods our paper's aim is to analyze the opportunity and the possibilities of obtaining the iron and steel by non-conventional technologies.

Our paper presents the results obtained from direct reducing of iron ores and our conclusions resulted from statistic analysis of obtained data by correlating the initial characteristics of the ores and qualitative characteristics of the pre-reduced product.

KEYWORDS:

pre-reduced iron ores, iron sponge

1. INTRODUCTION

Taking into consideration the complexity of the traditional iron and steel elaborating methods that demand the existence of ore preparation plants, cookery, etc. moreover the deficit of coking coals and iron scrap it is necessary to search new possibilities of modifying the existent technologies or replacing them by new methods. One option this way represents the use of sponge iron obtained by direct reduction of iron ores or prepared into the iron and steel elaborating process.

Considering the high materials and energy consumption and environment pollution in the traditional iron and steel elaborating methods our paper's aim is to analyse the opportunity and the possibilities of obtaining the iron and steel by non-conventional technologies.

Our paper presents the results obtained from direct reducing of iron ores and our conclusions result from statistic analysis of obtained data by correlating the initial characteristics of the ores and qualitative characteristics of the pre-reduced product.

2. OBTAINING PRE-REDUCED MATERIALS AND THEIR PHYSICAL AND CHEMICAL CHARACTERISTICS RESEARCH

We conducted the research in the laboratories of University "Politehnica" of Bucharest, the Ferrous Department. We established the experiments conditions starting from the initial granule size and composition of the ores, agglomerates and pellets. For the pre-reduced product, we established the reducing degree, the softening and melting temperature, the mechanical resistance and we found the correlation between the initial physical and chemical characteristics of the ores and the final characteristics of the pre-reduced material.

The ore's reduction is made in a reactor pipe with 140 mm diameter and 1000 mm length, made from stainless steel, which has in its inferior half chamotte spheres in order to heat the reducing gas. The ore sample is introduced into a net wire cylinder with the capacity of 1-3 kg of iron ore. The reactor pipe's heating is realized into a furnace having vertical bars 95) that can assure temperatures of about 80-100°C (the transformer's power is 25 kVA). The reducing gas (H₂-99.5%) flows from the cylinder through the purifying vessels filled with mineral cotton, H₂SO₄ and CaCl₂. The hydrogen flow is measured and registered.

The determination of the removed oxygen quantity is made by continuous weighting of the reactor cylinder with the scales, and the temperature is measured with a platinum-platinum-rhodium couple. The methodology of the experiments is: the sample weigh: 1 kg, the sample's granule size, varies between 5 and 30 mm, temperature: 800-900°C, the process period: 45 min, the specific H₂ flow: 0,7 l/min. g O₂ in the sample.

The pre-reduced material is mainly characterized by the following parameters:

- the reducing degree – represents the percentage of oxygen from the iron oxides being removed in reducing process:

$$RD = \frac{O_{2\text{removed}}}{O_{2\text{initial}}} \cdot 100[\%], \quad (1)$$

- the reducing velocity – represents the medium velocity of the oxygen removal from the iron oxides:

$$RV = \frac{O_{2\text{removed}}}{\text{proc. period}} [\% / \text{min.}], \quad (2)$$

The pre-reduced sample (0, 5 kg and granule size over 5 mm) is maintained inside for 3 minutes (90 rotations). The crushed material is then screened on 5 mm and 1 mm screens, establishing the following parameters:

- the crushing index (C) – represents the 1-5 mm fraction (in percents);
- the dusting index (DI) – represents the 0-1 mm fraction (in percents);
- the degradation index (D) – represents the ratio between the crushing index for the material after (C_{a.r.}) and before (C_{b.r.}) reduction : D = C_{a.r.}/ C_{b.r.}

In Table 1 we present the experiment conditions and the results obtained at the pre-reduction of 10 sorts of iron ores previously agglomerated.

Table 1. Ore reduction experiments

Sampl. no.	Ore characteristics				Experiment conditions			Reduction characteristics		Resistance in hollow roll	
	Fe (%)	FeO (%)	CaO/SiO ₂	Granule Size (mm)	Time (min)	H ₂ flow (l H ₂ /min)	Temp. (° C)	RD (%)	RV (%O /min)	Re duced	Not re duced
1	51.75	8.4	1.26	5-10	45	0.0690	825	49.42	1.10	61	82
2	49.82	8.85	1.41	5-10	45	0.0698	810	63.82	1.42	53	65
3	51.79	13.18	1.20	5-10	45	0.0713	840	43.41	1.96	69	94
4	53.09	7.49	1.32	10-20	45	0.0699	835	57.02	1.28	56	76
5	52.48	12.74	1.23	10-20	45	0.0701	840	45.07	1.00	71	91
6	53.59	10.54	1.71	10-20	45	0.0698	825	64.23	1.43	46	88
7	53.01	10.37	1.02	5-20	45	0.0700	835	39.41	0.83	79	94
8	54.68	8.30	1.12	5-20	45	0.0700	840	42.20	0.94	73	92
9	53.27	7.77	1.30	10-30	45	0.0698	840	59.18	1.32	66	80
10	43.50	8.60	1.80	10-30	45	0.0700	835	62.19	1.38	51	93
11	48.6	10.18	1.20	5-10	46	0.072	870	50.74	1.10	78	88
12	48.7	9.32	1.35	5-10	46	0.067	860	40.20	0.87	76	88
13	51.5	10.00	1.31	5-10	46	0.064	830	50.05	1.09	66	83.8
14	51.98	8.03	1.35	5-10	45	0.070	834	59.40	1.32	79.8	86.2
15	50.47	10.32	1.35	5-10	46	0.072	818	48.82	1.06	68	85.7
16	48.6	10.18	1.20	10-20	46	0.073	855	63.45	1.38	66	90
17	48.7	9.30	1.35	10-20	46	0.068	878	65.32	1.41	68	87
18	51.5	10.00	1.31	10-20	46	0.067	830	54.81	1.19	50	80
19	51.98	8.03	1.35	10-20	45	0.071	838	63.14	1.40	64	75.5
20	50.47	10.32	1.35	10-20	46	0.072	818	48.82	1.06	68	85.7
21	48.6	10.18	1.20	10-20	46	0.072	878	56.1	1.21	70	72
22	48.7	9.32	1.35	10-30	46	0.069	885	52.74	1.15	69	86
23	51.5	10.00	1.31	10-30	46	0.069	825	57.20	1.24	42	59.6
24	51.98	8.03	1.35	10-30	45	0.070	843	57.05	1.27	69	78.7
25	48.6	10.18	1.20	10-30	46	0.072	870	48.74	1.08	73	87
26	48.7	9.32	1.35	unsorted	46	0.072	888	38.74	0.84	71	87
27	51.98	8.03	1.35	unsorted	45	0.071	841	57.53	1.27	69	78
28	50.47	10.32	1.35	unsorted	46	0.069	815	56.14	1.22	44	73.9

Analyzing the data from Table 1 we can conclude:

- generally, an optimal reduction degree can be obtained from granule size of about 15 – 25 mm;
- the easiest reducible materials are the ferrous ones with the basicity.
- $B = \text{CaO}/\text{SiO}_2$ between 1.35 and 1.7; a medium reducibility is reached by the samples with $B = 1.2 - 1.35$ and the samples with $B \leq 1.2$ being more difficult to reduce;

The tests we made shown that the higher is the reduction degree the higher is the crushing degree. Because pre-reduced materials obtained by reducing the iron ores (crude or prepared) are used in the blast furnace or the electric arc furnace, replacing the iron scrap, it is very important to know the behavior of these materials during the heating – the correlation between the reducing degree and their melting and softening temperatures. That is why we tested the softening of these materials. The plant we used to run these tests is presented in Figure 1.

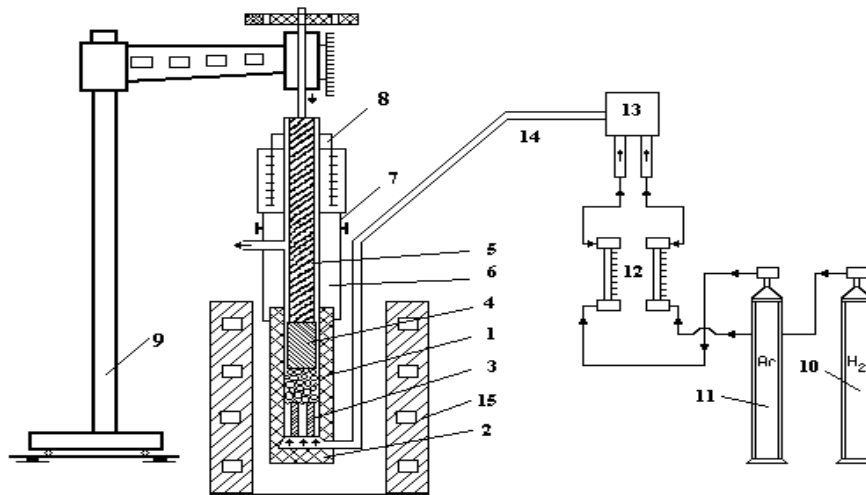


Figure 1. The experiment plant

- 1- graphite crucible; 2- gas distributor; 3- intermediary plate; 4 – piston; 5 – rod; 6 – graphite support; 7 – seal device; 8 – piston support; 9 – fixed support; 10 – H₂ cylinder; 11 – reducing gas cylinder; 12 – measuring device; 13 – gas mixer; 14 – gas pipe; 15 – induction electric furnace

Table 2. Data on the melting and softening characteristics of the agglomerates used in Romania

Sampl. no.	Chemical composition							Reduction degree (%)	Characteristics temperatures		
	FeO (%)	SiO ₂ (%)	CaO (%)	MgO (%)	Al ₂ O ₃ (%)	Fe (%)	B		T _{cz} (°C)	T _{mch} (°C)	ΔT (°C)
1	1.26	13.72	25.53	3.28	4.11	39.53	1.86	58.44	1010	1230	220
2	1.53	13.9	24.74	1.86	1.40	42.03	1.78	62.50	765	1240	475
3	3.11	13.75	24.71	1.29	2.16	41.18	1.79	70.00	1080	1320	240
4	6.59	10.28	26.16	3.72	0.28	43.65	2.54	68.00	1010	1330	220
5	8.52	10.60	24.73	3.40	1.76	43.13	2.33	69.80	1000	1330	330
6	7.40	11.05	23.56	5.45	1.96	43.18	2.13	70.35	980	1375	395
7	4.51	12.96	24.63	0.72	1.56	47.49	1.90	69.80	980	1210	230
8	10.56	12.64	24.11	2.80	3.06	44.26	1.90	53.60	1025	1240	215
9	3.64	11.10	24.37	4.74	1.89	44.94	2.10	54.64	1100	1270	170
10	3.94	10.08	24.72	2.49	0.21	44.98	2.45	58.50	1100	1250	150
11	8.60	10.38	20.35	1.57	0.31	46.81	1.95	56.51	1020	1240	220
12	8.20	9.52	17.12	2.75	3.49	48.77	1.79	50.57	1100	1360	260
13	19.90	7.00	14.43	3.00	1.90	51.79	2.06	60.84	1190	1365	175
14	16.24	8.08	16.25	2.15	3.64	52.36	2.01	50.53	1180	1295	115
15	19.93	7.93	16.00	0.87	4.72	49.84	2.01	58.00	960	1090	130
16	25.93	6.43	11.60	2.96	0.86	58.51	1.78	78.80	1170	1380	210
17	8.20	9.52	17.18	2.75	3.49	48.77	1.79	68.92	1155	1330	175
18	8.26	7.70	11.86	2.25	6.62	53.72	1.54	75.77	1160	1420	260

The experiment results are presented in Table 2. The experiments consisted of:

- ❖ from the crushed and screened material, we took a 3-5 mm fraction in samples of 240-310g;
- ❖ we heated the sample with 50-60°/minute;
- ❖ starting at 750°C we blew argon with 6.5-7.5 l/min., and at 900°C we blew hydrogen with 8 l/min. For 8 minutes, so we could reach reducing degrees of about 50-78%;
- ❖ we measured the temperatures every 3 min. and since the piston moved every 2 minutes;
- ❖ we determined the softening temperature when the piston moved firstly and the melting temperature when the piston movement as half the sample's height.

3. ECONOMICAL AND TECHNOLOGICAL CONSIDERATIONS ON THE USE OF PRE-REDUCED PRODUCTS IN IRON AND STEEL ELABORATING PROCESS

The pre-reduced materials obtained from solid reduction of iron ores (crude or prepared) can be used as raw material in the blast furnace charge with important economic effects.

Economies that can be obtained by using 1000 kg pre-reduced ore vary between 1 and 34 Euros for a pre-reducing degree of about 70%.

Pre-reducing the materials before using them in the furnace is a method that permits also the amelioration of the structure of the used combustibles (coke, etc.).

The economy obtained at the blast furnace, even in conditions of high energy consumption, covers completely the expenses from the pre-reducing process.

To study the possibilities of using the pre-reduced materials in electric arc furnace as iron sponge with different metallization degrees we made experiments on a 500 kg furnace in which the iron sponge was used 33, 55, and 79,100% of the charge.

We found out that using of iron sponge leads to a reduction of about 20% of the elaborating period and considerable diminish of manufacturing expenses.

4. CONCLUSIONS

Because they are very important we will mention these conclusions:

- ❖ the agglomerate's granule size doesn't have a notable influence on the "cohesive zone", that's why the recommended granule size (15-20 mm) which can assure a good permeability, can also assure the forming of an appropriate "cohesive zone";
- ❖ the chemical composition of the agglomerate influences the position and especially the width of "cohesive zone".

So, the rise of the MgO contents determines the rise of melting and softening temperatures and a lower position of the "cohesive zone" (i.e. positive influence). Also the rise of the MgO contents determines a higher difference between the melting and softening temperatures and rise the width of the "cohesive zone" (i.e. negative influence).

The necessary value for this parameter can be established following the influence of B on the "cohesive zone" and on charge's permeability in the granular zone. An optional value for B has to assure a goon mechanical resistance and an appropriate reducibility of the pre-reduced agglomerate.

From the experiments conducted on this last subject we conclude that the optimal value for B is 1.5 – 1.6. This value also assures a favorable influence on the "cohesive zone" that permits us to recommend the use of agglomerate with $B = 1.5 - 1.6$ in the blast furnace charge.

The laboratory research conducted on a large number of samples leaded us to the conclusion that the reduction degree of the iron oxides has the most important influence on the softening and melting of the agglomerate.

This influence due to the forming in the agglomerate granules of the metallic iron structures that assures a high permeability of the agglomerate layer in plastic state.

We can observe that the melting temperatures rise for a reduction degree over 58%. The same influence but less important manifests on the softening temperature.

REFERENCES

- [1.] N. CONSTANTIN, "Intensificarea proceselor din furnale prin perfectionarea circulatiei gazelor in vederea cresterii productivitatii si a economiei de cocs metalurgic si energie", Doctor Thesis, Bucharest, 1994.
- [2.] N. CONSTANTIN, "Ingineria producerii fontei in furnal", Ed. PRINTECH ", Bucharest, 2002.
- [3.] N. CONSTANTIN, C. PREDESCU, and M. JURA, "Cercetari pe model matematic asupra zonei coezive la furnale" International conference -Hunedoara 12-13 oct. 1995, pag. 18-26.
- [4.] N. CONSTANTIN, C. PREDESCU, and M. JURA, "Informatising management of blast furnace processes."București - International Symposium - "Traditions and perspectives in Romanian school of metallurgy." 25 - 26 oct. 1996, pag. 328-336.





¹. Violeta OANCEA, ². Nicolae CONSTANTIN, ³. Cristian DOBRESCU

RESEARCH ON THE POSSIBILITIES OF IMPROVING THE PRODUCTIN OF CAST IRON IN THE FIRST MERGER BY IMPROVING FLOW GAS PHASE IN THE BLAST FURNACE

^{1, 2, 3}. UNIVERSITY "POLITEHNICA" OF BUCHAREST, ROMANIA

ABSTRACT:

Because the cast iron-making blast furnace is a complex process of mass and energy transfer between solid and gas phase with reduced character, improving operating parameters can be achieved by improving gas flow in the blast furnace.

Obtaining an optimal permeability of the column of materials allow optimum circulation of a gaseous phase, using its entire reducing potential.

It is thus possible to increase utilization efficiency of useful volume thus increasing productivity.

This paper aims to study the permeability of different mixtures which can form the blast furnace load and propose optimal ratio between their weights.

KEYWORDS:

blast furnace, optimal permeability, mass and energy transfer

1. INTRODUCTION

Many research works as well as the practical operation of the blast furnaces have shown close correlation between the regime of operation of furnace and gas flow through solid materials in the tank column.

Thus the conclusion reached that gas can flow through the furnace in unit time through unit area of section, substantially influence the blast furnace productivity.

The blast furnace productivity decreases proportionally with increasing unevenness degree in the flow of gas, also an increase in specific consumption of coke due to improper use the reduction character of gaseous phase.

So it can't achieve an economic function of blast furnace without achieving optimal distribution of gas tank and consequently good contact of phases which are entering in reaction physics-chemical processes occurring in the blast furnace.

This favorable distribution of gases can be achieved by measures taken at the charge part of the blast furnace (the unit load size, the load schedule, the load level).

2. METHODOLOGY

In a column of infinite load as expanse volumes it can obtain a uniform distribution of the gases regardless of the size filling bodies particles. Instead in a limited load column as dimensions, the gases flowing depends on the ratio between (d) diameter of granules that are forming the load and (D) diameter of column, at high values of ratio d / D ascertaining a powerful peripheral gas circulation due to the higher value of the voids volume near the column walls.

But in a blast furnace, the flow of gas is influenced by the movement of cargo particles which facilitates the appearance of free spaces between these.

The tendency to form free spaces is larger to loads composed by large irregularly shaped pieces. From geometrical a reason at the spherical particles is accomplished the best possibility of charge particles movement.

In terms of the reduction process, small pieces behave better. Therefore it is seen mostly a better performance of the blast furnace when the pieces of agglomerate ores are smaller or when using pellets.

This leads on the one hand to a better performance of the blast furnace due to the gases uniform distribution on section by free spaces uniformly distributed without preferred corridors, but also may lead to a higher pressure loss to the equal flow of gases which are crossing the blast furnace because the pressure loss increases with decreasing of the particles diameter

The pressure loss per unit length depends on the gas flow speeds, the physical characteristics of these, the shape, the size and the settlement method of the filling bodies.

For dimensionless representation of the pressure loss it is used the relation between the dimensionless resistance coefficient ψ and Reynolds number: $\psi = f(Re)$

These two indices have been defined by M. Brauer as follows:

$$\Psi = \frac{\varepsilon^3}{1 - \varepsilon} \cdot \frac{d}{\rho w^2} \cdot \frac{\Delta p}{H}, \quad \text{and} \quad Re = \frac{1}{1 - \varepsilon} \cdot \frac{w \cdot d}{\nu}$$

where: ε - the goals factor in the column load; d - the diameter of filling bodies [m]; ρ - the gases density that flows through the load [kg/m³]; ν - the kinematic viscosity of gases [m²/s]; w - the speed of gases flow in the empty column [m/s]; H - the height column of load [m];

The loss of pressure has already been measured in a variety of materials. Most researches have been limited to the monogranulare materials and only few bigranulare materials such as the type of materials introduced into the blast furnace.

3. ANALYSES/ RESULTS

This paper aims to present the results and conclusions drawn for experiments with components materials of blast furnaces load from Romania.

The experiments dealt with determining the permeability of columns consisting of coke material, agglomerated, pellets but for comparison term and artificial load consisting by glass beads with diameter close to the pellets.

It has been followed the possibility of obtaining an optimum permeability for a column with similar load to that of cargo tank blast furnace, with the ultimate goal of increasing the intensity of operation by improving the gases flow through the blast furnace tank.

Experiments were conducted in the laboratory of Metallurgy of Cast Iron, Siderurgy Department from University "Politehnica" of Bucharest. The experimental installation is shown schematically in Figure 1.

The installation comprises a cylindrical container (1) with the height of 1.35 m and 0.35 m in diameter, provided at the top with a state gas valve for measuring the gas pressure after it passes through the granular load from the column (2). The cylinder is closed with a conical cap fitted with a gas discharge pipe (3). In the lower area there is a filler cap for draining of installation (4). Under the filling area is another one of pressure equalization (5). It consists of a cylindrical tube provided at both ends with flares of extending and tightens. Here there is a flare connected to measure the gases pressure in the entry of column load (6). The cylinder is fed with gas (air) through a pipe fitted with a valve for regulating the gas flow (7). The flow measurement is made with a measurement diaphragm (8). Gas supply (air) is made through a motor-blower group.

The experimental dates and a series of mathematical results of statistical processing are presented in Tables 1 and 2.

In the table 2 there are presented the linear correlations between pressure loss $y = \Delta p$ in [mmH₂O] and flow of air blown into the column $x = Q_a$ in [m³/h] of the form $y = f(x)$. For all 19th experiments were drawn simple linear correlations which can be accepted considering the correlation of coefficient values y_{xy} higher than 0.9. Grouping favorable studied cases and drawing lines in the same rectangular coordinates some important conclusions are obtained.

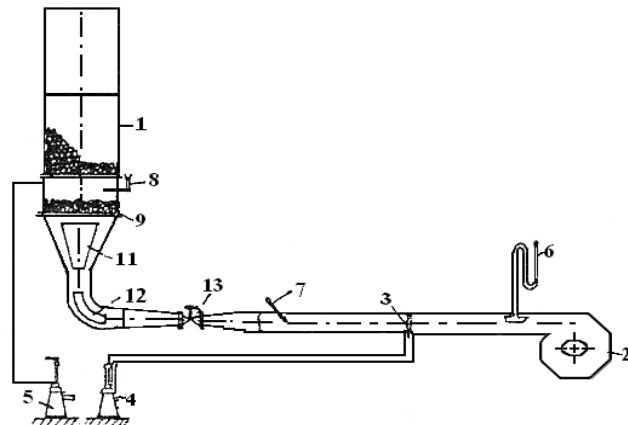


Figure 1. The experimental installation

Table 1.

Exp No	Load	Type of load	Average diameter[m]	Equivalent diameter[m]	Goals coefficient(ϵ)
1	1/1 balls	layer	0.019	0.019	0.371
2	1/1 pellets	layer	0.012	0.012	0.387
3	1/1 agglomerates	layer	0.03	0.03	0.417
4	1/1 coke	layer	0.04	0.04	0.478
5	1/3 balls+2/3 aggl.	mixture	-	0.022	0.380
6	1/3 balls+2/3 aggl.	layer	0.19/0.03	0.022	0.371/0.417
7	2/3 balls+1/3 aggl.	mixture	-	0.0179	0.378
8	2/3 balls+1/3 aggl.	layer	0.19/0.03	0.0179	0.371/0.417
9	1/3 pellets+2/3 balls	mixture	-	0.0158	0.35
10	1/3 pellets+2/3 balls	layer	0.012/0.019	0.0158	0.387/0.371
11	2/3 pellets+1/3 balls	mixture	-	0.0168	0.27
12	2/3 pellets+1/3 balls	layer	0.012/0.019	0.0168	0.387/0.371
13	1/3 balls+2/3 coke	mixture	-	0.029	0.40
14	1/3 balls+2/3 coke	layer	0.019/0.04	0.029	0.371/0.478
15	2/3 balls+1/3 coke	mixture	-	0.023	0.39
16	1/3 coke+2/3 aggl.	mixture	-	0.0186	0.39
17	1/3 coke+2/3 aggl.	layer	0.045/0.016	0.0186	0.478/0.395
18	1/3 coke+2/3 aggl.	mixture	-	0.0248	0.40
19	1/3 coke+2/3 aggl.	layer	0.04/0.021	0.0248	0.465/0.405

The dependences $\Delta p = f(Q_a)$, $y = f(x)$

Table 2.

Exp No	Eq $\Delta p=f(Q_a)$	Y_{xy}	The slope of line
1	$Y=1.542X-74.10$	0.970	57.03
2	$Y=1.570x-39.15$	0.976	57.50
3	$Y=0.887x-39.15$	0.966	41.57
4	$Y=1.208x-64.21$	0.969	50.38
5	$Y=1.134x-56.26$	0.960	48.59
6	$Y=1.035x-52.95$	0.965	45.98
7	$Y=1.614x-73.78$	0.978	58.12
8	$Y=1.294x-55.42$	0.981	52.30
9	$Y=2.188x-80.46$	0.975	65.43
10	$Y=2.474x-116.84$	0.965	67.99
11	$Y=2.577x-121.48$	0.968	68.79
12	$Y=2.010x-85.52$	0.969	63.54
13	$Y=1.442x-75.012$	0.969	55.26
14	$Y=1.396x-79.75$	0.966	54.38
15	$Y=1.596x-75.59$	0.969	57.93
16	$Y=1.151x-53.03$	0.970	41.73
17	$Y=0.892x-40.12$	0.977	49.01
18	$Y=1.027x-50.449$	0.951	45.76
19	$Y=0.789x-36.97$	0.945	38.27

4. CONCLUSIONS

Among the conclusions of the conducted research can be mentioned:

- ❖ The loads consisting of two granules size with small diameter d_k and large diameter d_g can represent the conditions from modern blast furnaces in which the load basically consists of agglomerates and coke, well grinded and loaded in granulate limits prescribed. In the case of loads formed by granules with two dimensions, the permeability varies according to how the load is made of in distinct layers or homogenous mixtures.
- ❖ confirming the experiments of Fomas, the coefficient of goals mixture (ϵ_m) passes through a minimum at about 28-30% large granules in mixture, the values of ϵ_m decrease in the same time with the diameters ratio d_k/d_g ;
- ❖ it is observed that regardless of the blowing air speed in the column, the pressure loss is greater at homogeneous mixtures than at loads in separate layers;
- ❖ the value of medium goals coefficient (ϵ_m) decreases proportionally with the size difference between the diameters of components (this value is best shown by these experiments (16 and 18));
- ❖ the coefficient values of goals for monogranular loads are different by the type of material. It can be noticed that at the same mixture of two different diameters the goals coefficient is not the same for different proportion participation of those two types of granules, (exp 9, 11).

- ❖ looking at the correlations $y = f(x)$ that means $\Delta p = f(Q)$, presented in Table 2, it can be observed the increase of Δp with Q_a for all experimental situations;
- ❖ for the mixtures made of the same type of granules the increasing of Δp with Q_a is more emphasized by the time the increasing of small granules proportion in the load (which is visible following the lines slope α in Table 2;
- ❖ for the same type of bigranulare loads the increase of Δp with Q_a is more emphasized for mixtures than for loads in separate layers;
- ❖ for the monogranulare loads the increase of Δp with Q_a is faster for loads with a smaller coefficient of goals.

As the gas flow through the furnace load, uniform and without fault in the descending column of material, requires minimal pressure loss, indicates that the upper area of the furnace (the granular area) there are advantageous to use the loads of granules of equal size between them, and the charging to be done in layers, each layer comprising granules of the same diameter.

From the technological point of view regarding the behavior of materials from the blast furnace load and in the other areas of the blast furnace it is necessary the existence of a certain ratio different from the value 1 between areas of agglomerate granulation and of the coke, the value of this ratio being 0.35 to 0.40.

REFERENCES:

- [1.] N. Constantin, "Intensificarea proceselor din furnale prin perfectionarea circulatiei gazelor in vederea cresterii productivitatii si a economiei de cocs metalurgic si energie", Doctor Thesis, Bucharest, 1994.
- [2.] N. Constantin, "Ingineria producerii fontei in furnal", Ed. PRINTECH", Bucharest, 2002.
- [3.] Nicolae CONSTANTIN: "Tratat de stiinta si Ingineria Materialelor vol 2 "Bazele teoretice si ingineria obtinerii materialelor metalice" Editura AGIR 2007,cap 5, pag.642-757 , ISBN 978-973-720-064-0, ISBN-978-973-720-162-1.
- [4.] Cezar NECȘULESCU, Edmond BERCEANU, Nicolae CONSTANTIN: "Îndrumar de prelucrare a datelor experimentale utilizând teoria probabilităților și statistica matematică" - tipărit Universitatea "Politehnica" București, 1993
- [5.] Nicolae CONSTANTIN, Victor GEANTĂ, Bogdan NICULAE, Radu ȘTEFĂNOIU: "Modelarea matematică și conducerea informatizată a proceselor din metalurgia extractivă feroasă." - tipărit Universitatea "Politehnica" București, 1997





¹ Ioan MILOSAN

STUDIES AND RESEARCHES ON THE DETERMINATION OF KINETIC AND THERMODYNAMIC PARAMETERS OF AN ADI

¹ TRANSILVANIA UNIVERSITY OF BRASOV, ROMANIA

ABSTRACT:

The paper presents an application for calculating the kinetics and thermodynamics parameters in the case of a phase transformation in solid state in A.D.I. S.G. grade. It is pointed out the influence of some factors (the temperature and the maintained time at the isothermal level) on the phase transformation and properties in the studied cast iron.

KEYWORDS:

A.D.I., phase transformation, kinetics, thermodynamics

1. INTRODUCTION

A wide range of properties can be obtained in these material components owing to changes in proportions of the major phases present in the microstructure: bainitic ferrite, high carbon austenite and graphite nodules. Martensite, ferrite, iron carbides and other alloy carbides may also be present.

Spheroidal graphite cast iron can be heat treated to produce Austempered Ductile Iron (A.D.I.). Recent studies have shown that, this material have excellent mechanical properties. The combination of high strength and high toughness achieved by A.D.I. suggests the engineering use of this material will continue to expand [1, 2].

The kinetics of austenitization of S.G. Cast Iron, was described by the Johnson-Mehl-Avrami equation and for the determination of the activation energy "Q", it was used the Arrhenius equation.

2. METHODOLOGY

The studied cast iron has the following chemical composition (% in weight): 3.85% C; 2.16% Si; 0.42 % Mn; 0.012%P; 0.0036%S; 0.076%Mg; 0.40% Ni; 0.39%Cu.

This cast iron was made in an induction furnace. Nodular changes were obtained with the "In mold" methods, with the help of prealloy FeSiCuMg.

The parameters of the heat treatment done were the following: the austenizing temperature, $T_A = 900$ [°C]; the maintained time at austenizing temperature, $\tau_A = 30$ [min]; the temperature at isothermal level, $T_{iz} = 380$ and 400 [°C]; the maintained time at the isothermal level, $\tau_{iz} = 1; 2; 5; 10; 20; 30; 40$ and 50 [min].

All these 2 experimental lots A ($T_{iz} = 380^\circ$ C) and B ($T_{iz} = 400^\circ$ C) were performed at isothermal maintenance in salt-bath, being the cooling after the isothermal maintenance was done in air.

From this material, 15 typical HB test specimens was done ($\phi 20 \times 50$ mm) and after the heat treating, it was determined the results of HB. The aim of the experiments is to determine the hardness (HB) at the isothermal temperature.

3. RESULTS

For the study of the phase transformation kinetics, it was used the first stage of the bainitic reaction [3]:

$$\gamma \rightarrow (\alpha) + (\gamma) \quad (1)$$

where: γ - metastable austenite; (α) - bainitic ferrite; (γ) - austenite enriched in carbon

In this researches work it was used the methods of the variation's hardness analyse function of the time at the isothermal level (τ_{iz}), considering that this values are depended from the proportion of the transformed fraction " $X(t)$ ". It was utilised the expression:

$$X(t) = \frac{H_0 - H(t)}{H_0 - H_f}, [\%] \quad (2)$$

where: $X(t)$ – the transformed fraction;

H_0 – initial hardness, corresponding $\tau_{iz} = 1$ min;

H_t – hardness obtained after a maintaining time (t) at the isothermal level, [%];

H_f – final hardness, corresponding at the maintaining time at the isothermal level, which are considered as a final time for the first stage of transformation of the bainitic reaction.

The experimental values of the hardness are presented in table 1.

Table 1. The experimental values of hardness, for various T_{iz} and τ_{iz}

T_{iz} , [°C]	τ_{iz} , [min]	Hardness, [HB]		
		H_0	H_f	$H(t)$
380	1	493	302	493
	2			464
	5			415
	10			375
	20			363
	30			354
	40			325
	50			302
400	1	438	295	438
	2			393
	5			354
	10			333
	20			325
	30			311
	40			295

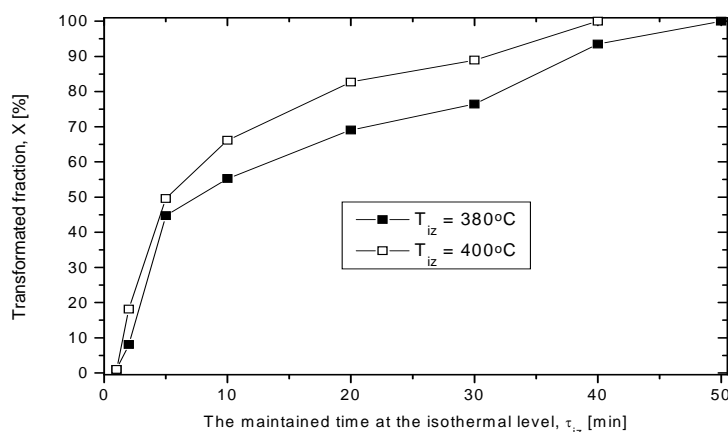


Fig. 1 Transformed fraction curves at $T_{iz} = 380$ and 400°C , for different maintaining time, τ_{iz} , at the isothermal level.

In order to determine "k" and "n", the natural logarithmic expression was used:

$$\log [-\log (1-X)] = (n \log k + \log \log e) + n \log t \quad (4)$$

The plot of " $\log [-\log (1-X)]$ " against " $\log t$ " in the isothermal temperature range $380-400^\circ\text{C}$ [3], for the isothermal maintaining time range 1 – 40 minutes, is shown in figure 2 and 3.

The obtained equations from the linear regression adjustment are:

$$Y_{380} = -4.32559 + 1.33043 \cdot X, R^2 = 0.95; \quad (5)$$

$$Y_{400} = -4.27583 + 1.37189 \cdot X, R^2 = 0.95; \quad (6)$$

Values of "n" and "k" determined from the slopes and intercepts of the linear regression lines are listed in table 2.

In figure 1 is represented the sigmoidal solid curves of the austenitic transformation during the bainite reaction.

Like the transformation fraction curves have sigmoidal shape, it was used the "Johnson-Mehl-Avrami" equation n [3]:

$$X(t) = 1 - \exp(-k t^n) \quad (3)$$

where:

$X(t)$ - the transformed fraction;

k - rate constant dependent on temperature;

n - exponent of the reaction.

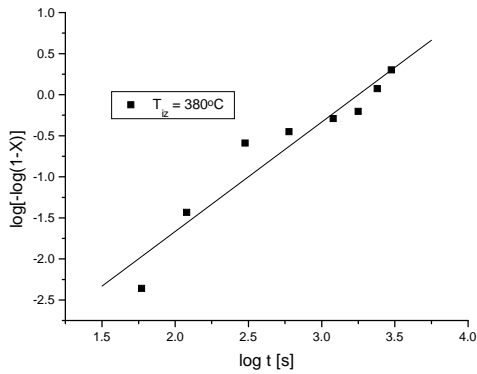


Fig. 2 The plot of “log[-log(1-X)] against “log t” in the isothermal temperature 380°C.

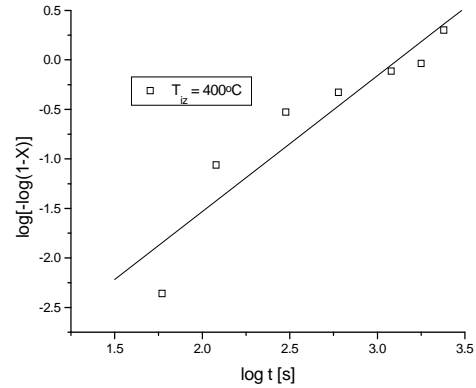


Fig. 3 The plot of “log[-log(1-X)] against “log t” in the isothermal temperature 400°C.

Table 2: Values of “n” and “k” for the formation of bainite

Lot	T _{iz} [°C]	n	k [1 / s]
A	380	1.33	1.05 x 10 ⁻³
B	400	1.37	1.40 x 10 ⁻³

According to Liu [3], if the “n” exponent is between 1 and 2.3 the transformation is interfacial controlled.

At the same maintaining time in the isothermal level, the transformation process is different in the each maintaining isothermal temperatures. The bainitic reaction rate “k” increases when the isothermal temperature increases from 380 to 400° C.

For the determination of the activation energy “Q”, it was used the Arrhenius equation:

$$k = A e^{-Q/RT}; [1/\text{min}] \quad (7)$$

where: k - constant rate dependent on temperature [1/s];

Q - activation energy [J /mol];

T - temperature [K]

R - gas constant 8.31 [J/mol.K]

A - constant dependent on frequency[1/s].

In order to determine “Q” and “A”, the natural logarithmic expression of eqn. (7) was used:

$$\log k = - \log e \frac{Q}{R} \frac{1}{T} + \log A \quad (8)$$

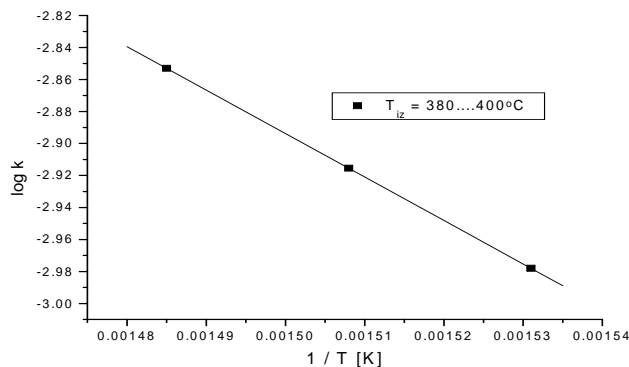


Fig. 4 Linear transform of the Arrhenius equation for the studied S.G. cast iron for T_{iz} = 380 and 400°C.

The plot of “log k” against “1/T” in the isothermal temperature range 380 - 400°C, for the isothermal maintaining time range 1 – 50 minutes, is shown in figure 4.

The equation of the linear regression is:

$$Y_{380 - 400} = - 1.18233 - 2717.3913 \cdot X, \quad R^2 = - 0.99; \quad (9)$$

Values of “Q” and “A” determined from the slope and intercept of the linear regression line are:

$$Q = 52029.891 [J/mol] \text{ and}$$

$$A = 0.0065 [1/s]$$

The activation energy of isothermal transformation are the same numerical

order like the values obtained in the technical specialty literature [2, 3].

From the linear regression, it was observed that the value of activation energy increases with the increasing of the maintaining temperature, from 380 to 400° C.

4. CONCLUSION

The isothermal bainitic transformation in a Ni-Cu S.G. cast iron was studied in the temperature range of 380-400° C and with maintaining time between 1-50 minutes. The main results are summarized as follows:

- a) The kinetics of austenitization of S.G. cast iron, can be described by an Johnson-Mehl-Avrami equation.
- b) The reaction exponent “n”= 1.33 – 1.37 and the transformation is interface controlled.
- c) The bainitic reaction rate "k" increases with increasing isothermal temperature from 380 to 400°C.
- d) The activation energy of isothermal transformation was 52030 [J/mol]
- e) The constant dependent on frequency was: 0.0065 [1/s]

REFERENCES

- [1.] D. Simon: ADI- a new material for the automotive engineer, Foundry Trade J., No. 2, p. 66-67, 1996.
- [2.] I. Miloşan: Some Aspects About Mo-Ni-Cu Low-Alloy S.G. Cast Iron Type A.D.I, Metalurgia International, No. 4, p. 54-55, 2008.
- [3.] Y.C. Liu, J.M. Schissler, J.P. Chabout, H. Vettters: Study of The Structural Evolution of Austempered Ductile Iron (ADI) during Tempering at 360°C”, Metallurgical Science & Tech. No. 13 p. 12-16, 1995



RESEARCH ON THE MECHANISM OF DAMAGE LINE BRICKS IN THE SLAG LF

^{1,3} POLITEHNICA UNIVERSITY BUCHAREST, ROMANIA

² ECOLOGICAL UNIVERSITY OF BUCHAREST, ROMANIA

ABSTRACT:

This paper proposed to analyze, based on fundamental known, the slag influence generated on LF process on the ladle refractory. In this purpose were studied the refractory destruction mechanisms used on LF, the slag quality, quality refractory and the slag influence on refractory especially because of the interactions between them, definitely elements for steel quality and also for the refractory endurance.

KEYWORDS:

refractory, interaction slag-refractory

1. INTRODUCTION

The main wear mechanisms of the refractory ladle slag line are chemical corrosion and mechanical erosion due to stirring of the steel bath. Chemical potential difference between the refractory and the slag under high temperature conditions is driving force for chemical wear mechanism. Destruction process depends on many variables: temperature, refractory composition, slag thickness, slag composition and stirring degree.

The objective of this paper is to analysis of the interaction between LF bricks steel ladle in contact with slag. In this purpose were determined the slag characteristics on the hot face brick, the slag and the refractory interaction carried out by optical and electronic microscopy (SEM) and X-ray diffraction.

2. THE STUDY

The study was carried out on scrapped brick from LF installation from Calarasi, the brick is part of the steel ladle refractory lining slag level. Determined proprieties for the studied brick are in the following table 1.

Tabel 1. Properties of bricks used at slag level

Apparent density (g/cm ³)	2,95
Apparent porosity (%)	4,8
Apparent density after heating at 1150 °C	2,87
Apparent porosity after heating at 1150 °C	11,2
Mechanical strength (MPa)	30

The slag deposited thickness on the refractory brick varies between 3-6 mm (fig.1).

The bricks appearance is shown in Figure 1 and in figure 2 is presented the bricks appearance after removal of an important part of slag layer deposited.

Tabel.2. LF slag chemical composition deposited on hot face brick

CaO	MgO	Al ₂ O ₃	SiO ₂	SO ₃	Fe ₂ O ₃	CoO	TiO ₂	MnO	Cr ₂ O ₃	P ₂ O ₅
30,14	29,54	10,43	2,95	1,31	0,16	0,33	0,12	0,08	0,05	0,05
Ca	Mg	Al	Si	S	Fe	Co	Ti	Mn	Cr	
25,64	15,45	5,14	1,36	0,59	1,06	0,34	0,01	0,08	0,05	



Fig.1. Deposited slag on brick after its used in LF



Fig.2. Interface between slag layer and brick

Tabelul 3.LF slag chemical composition

CaO	Al ₂ O ₃	SiO ₂	MgO	FeO	MnO	Cr ₂ O ₃	P ₂ O ₅	TiO ₂	S	K ₂ O	Na ₂ O
56,47	30,92	6,47	3,73	0,62	0,11	0	0,02	0,34	1,2	0,02	0,07
57,03	32,03	4,92	3,83	0,52	0,08	0	0,01	0,26	1,2	0,02	0,06
58,28	31,13	4,44	4,08	0,39	0,06	0	0,02	0,38	1,2	0,01	0,06

The removed slag was analyzed chemical and structural. The results are in table 3. Slag layer shows pores and two different layers (Fig. 3). These layers contain phases and micro structural aspects of different chemical compositions.

- ❖ First layer has 2.2 mm thickness and it is composed from dendrites crystals of magnesium oxide, iron oxide, iron and calcium aluminates and calcium silico-aluminates. All these are immersed in a matrix of calcium aluminates.
- ❖ The second layer has 3 mm thickness and it is composed of magnesium crystals damaged by iron and manganese alumino-silicates crystals with different contents of calcium, iron and titanium, calcium aluminates - magnesium - iron and calcium silicate crystals.



Fig.3. Two of slag layers

3. INTERACTION SLAG AND BRICK GRAIN

At the interface between slag and brick MgO grains were found torn from brick and immersed in slag. Distribution of elements in this area is shown in Figure 4. Corrosion can be observed due to the interaction between the iron grains oxide and magnesium oxide. Slag penetrates the silicate sinters grains network and melt intragranular silicates. This interaction speeds the lower temperature phase formed and facilitates separation from crystal.

Slag- brick martix

Micro structural analysis reveals the decarburization process of the brick matrix in contact with slag (Fig. 5). Interface slag-brick is shown in Figure 6. In the brick matrix there are formed spinal crystals. Also, crystals were identified calcium silicate in the brick matrix.

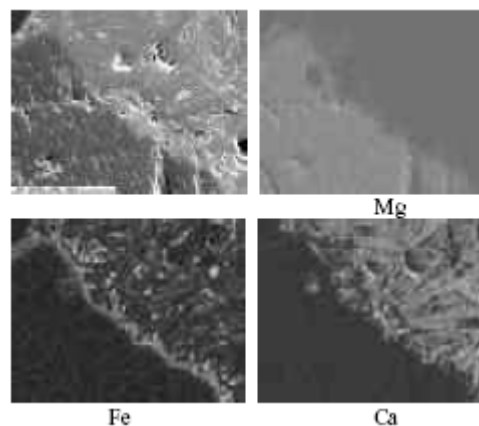


Fig.4. Indirectly Corrosion of MgO grains

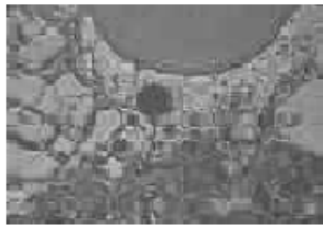


Fig. 5. Decarburization slag matrix and interface

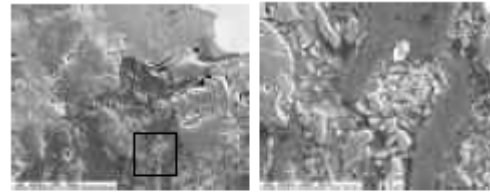
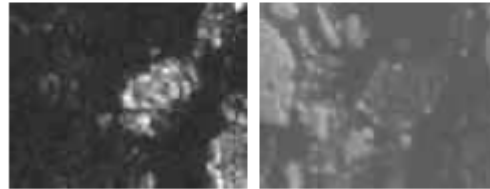


Fig. 6. Distribution of elements in hot brick surface



3. ANALISES, DISCUSSIONS, APPROCHES and INTERPRETATIONS

The first slag layer is composed on calcium aluminates matrix with melting temperature at 1400 °C and different crystals:

- ❖ calcium alumina and iron alumina, with softening temperature at 1336 °C (equilibrium phase diagram for the system $Al_2O_3 - CaO - FeO$);
- ❖ Calcium and aluminum silicates with softening temperature of 1380 oC (equilibrium phase diagram for the system $Al_2O_3 - CaO - SiO_2$ Fig. 7);
- ❖ MgO dendrites.

The chemical composition of the first slag layer is shown in Figure 6. This chart show that the slag is completely liquid at 1600 °C, and therefore, it is not saturated endanger. First layer of liquid slag is not saturated with MgO and at 1600 oC.



Fig. 7. Phase equilibrium diagram of the system $Al_2O_3-CaO-SiO_2$

The second layer is composed from adhered slag stickled to the brick, this layer contains a higher level than the first layer of iron oxide slag. He probably comes mainly from the pot slag before the LF treatment. Also, the second slag layer has a lower content of calcium oxide than the first layer of slag. The second layer of slag is composed of calcium aluminates matrix and different types of crystals:

- ❖ calcium, titanium, and iron silicates and aluminum with different contents of these elements with melting point at 1400-1500 °C;
- ❖ calcium silicates and aluminum with melting temperature at 1450 °C (fig. 7 diagram of phase equilibrium in the system $Al_2O_3 - CaO - SiO_2$);
- ❖ different contents alumina of calcium, magnesium and iron;
- ❖ MgO crystals attacked with iron oxide first and then the manganese oxide and calcium oxide.

This mechanism is the result of iron elements, manganese and calcium existing in the slag that runs the fastest in the refractory material to form the corresponding reaction products. The chemical composition of the second layer is shown in Figure 8. This slag is saturated with magnesium oxide at 1600 °C.

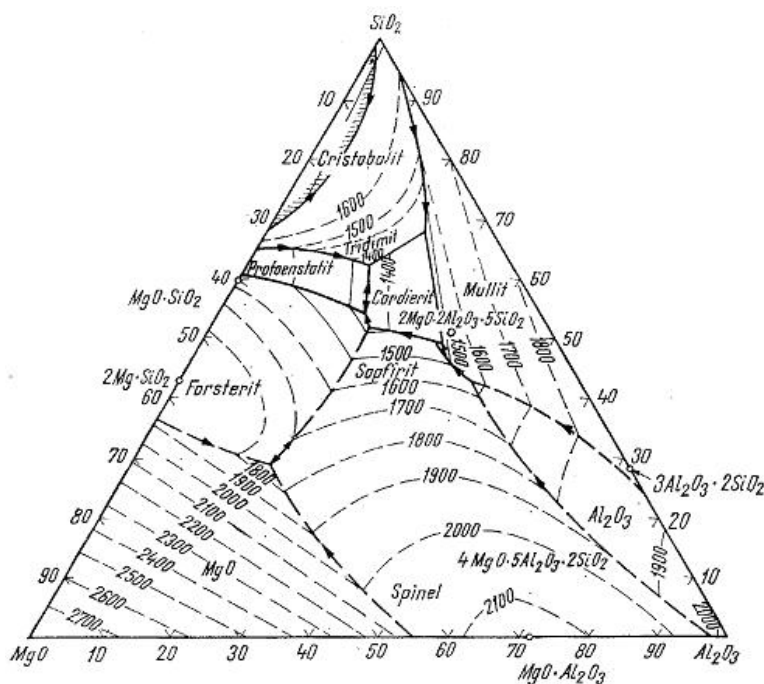
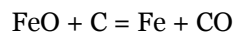


Fig. 8. Phase equilibrium diagram of the system $MgO-SiO_2-Al_2O_3$ temperature. It is well known that this conditions are the main cause of corrosions and bricklayer destructions;

- ❖ The second slag layer is saturated with MgO but contains a high level of iron content. This oxide in growth the slag fluidity-broke the silicate network from the brick and allow the matrix decarburization , thus :



Graphite oxidation growths bricks porosity, allowing slag penetration in the system, following periclase grains dispersion in slag. Review mechanisms identified are: graphite oxidation, slag penetration into matrix and around MgO grains and finally MgO grains dissolution into slag. More over, iron spread in MgO grain and allows MgO slag molder. This new phase decrease the MgO grains refractory and also delay speed destroy of refractory material. This mechanism leads indirect MgO grain dissolution.

4. CONCLUSIONS

The study of brick out off used was carried out through optical and electronic microscopy (SEM) and EDS analysis, allowed identification of slag- brick adherence characteristics, refractory wear mechanism and the microstructural changes inside the brick.

The slag on the brick hot face is composed of two different layers.. Aceste straturi conțin aspecte microstructurale distincte și faze cu compoziții chimice diferite. Both layers are aggressive to the refractory material lining.

- ❖ The first slag layer is not saturated with magnesium oxide and it is completely liquid at the process

REFERENCES

- [1.] A. Nicolae s.a. - Materiale ceramice refractare pentru instalații termotehnologice, Ed. Fair Parteners, București, 1999.
- [2.] P. Bartha et.al. – Heavy ceramic shaped materials, process for the production thereof and the thereof, United States Patent , nr. 4,775,648 oct.4.1988.
- [3.] G. Yuasa, et.al. - Refining Practice and Application of the Ladle Furnace (LF) Process în Japan, Transactions of the Iron and Steel Institute of Japan, vol, 24, no.5(1984), pp 412-418.
- [4.] P.G. Jonsson, L. Jonsson, D. Sighed – Viscosities of LF slag and their impact on ladle refining, ISIJ International, 1997, vol.37, no.5, pp 484-491.
- [5.] Z. Adolf, i. Husar, P. Suchanezk - Investigation of the influence of the melt slag regime in a ladle furnace on the cleanliness of the steel, Materiali in tehnologije / Materials and technology 41 (2007) 4, 185–188
- [6.] L.Mihok, K. Seilerova, M. Frohlichova - Influence of Steel Cleanliness by Ladle Furnace Processes, Materials Science, vol. 11, no. 4. 2005,pp 320-323.
- [7.] P..S. Fredriksson - Thermodynamic studies of FeO-containing slags and their impact on ladle refining process. VII International Conference on Molten Slags Fluxes and Salts, The South African Institute of Mining and Metallurgy, 2004, pp 285-292.
- [8.] K.C. Mills, E.D. Hondros, L.Yushu - Interfacial phenomena in high temperature processes, Journal of materials Science 40, 2005, pp 2403-2409.
- [9.] Silvia Camelli, Marcelo Labadie-Analysis of the wear mechanism of $MgO-C$ slag line bricks for seel ladles.49. Internationales Feuerfest-Kolloquium 2006, pp 30-34.

¹Victor BUDĂU, ²Sebastian DUMA

HARDNESS AND STRUCTURAL ASPECTS OF THE HEAT – TREATED HS 18-0-1 STEEL

¹⁻². UNIVERSITY "POLITEHNICA" OF TIMIȘOARA, FACULTY OF MECHANICS, TIMIȘOARA, ROMANIA

ABSTRACT:

High speed machining requires tools from special materials (rich alloyed steel, cermet materials etc.). In the category of high alloyed tool steels the important are high-speed steels. To obtain the corresponding operating characteristics they must be heat treated to show comparative features with ordinary steel. The paper presents the heat treatment and the structural characteristics and hardness analysis of HS 18-0-1 high-speed steel used to manufacture tools for cutting with high speed.

KEYWORDS:

HS 18-0-1 steel, annealing, quenching, tempering, ferroxylation, X-rays diffraction

1. INTRODUCTION

It's known that for cutting with high speed tools from high-speed steel are used. Compared with other tool steels these allow increased cutting speed of 2-4 times and ensure an increase of 10-30 times tool durability owing to high heat stability up to 600 – 620 °C [1, 4].

Achieving these performance is possible only after secondary quenching heat treatment followed by tempering which shows some features of carbon tool steels.

Based on these considerations, in the paper, the features of heat treatment and structural characteristics and hardness analysis of HS 18-0-1 high-speed steel are shown.

2. PREPARATION OF SAMPLES AND APPLIED HEAT TREATMENT

HS 18-0-1 steel (symbolization as EN ISO 4957) is a rich alloyed steel for tools, from high-speed steel category (symbolization as STAS with Rp3). Chemical composition of this steel is: C = 0.7 – 0.8 %; W = 17.5 – 18.5 %; Mo = max 0.6 %, V = 1 – 1.2 %; Cr = 3.8 – 4.5 %.

Φ 20 x 15 mm specimens were made from forged bars, and were subjected to heat treatment. The heat treatment cyclogram is shown in figure 1.

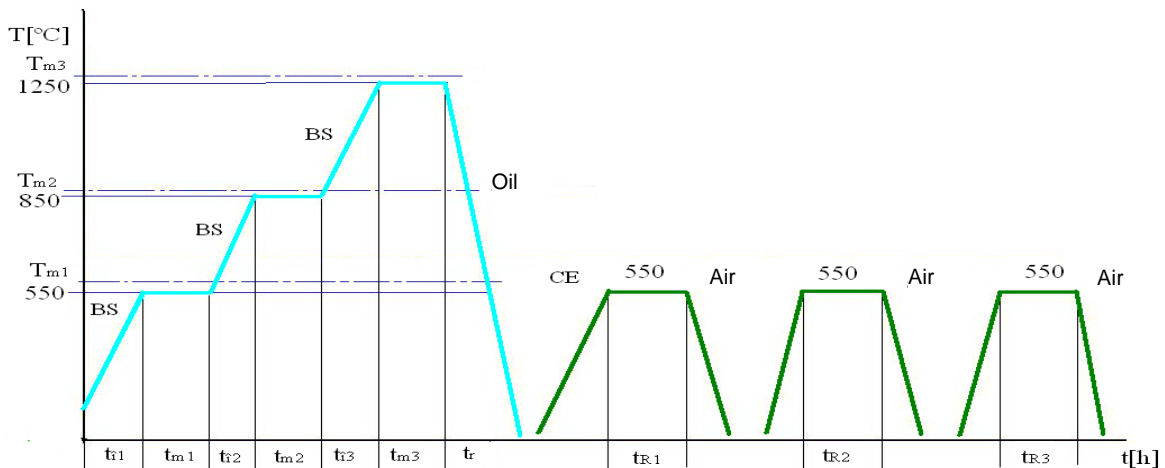


Figure 1. The cyclogram of the secondary heat treatment applied on the HS 18-0-1 steel

The transformations suffered by the material are as follows:

HEATING TRANSFORMATIONS

The heating for austenitization in order to quench high speed steels is made at high temperatures (1200- 1300°C). This ensures that a large quantity of carbides are decomposed and dissolved in austenite enriching it, and after cooling enriching the martensite [2,4].

These temperatures are much higher than the eutectoid temperatures of carbon steel used for tools. The components of the alloy (which are α -gene) increase the temperatures of critical points A_{c1} and A_{c3} forming carbides and reducing the susceptibility of overheating the austenite, reflected by its granulation (the susceptibility of overheating the austenite increases with the increase of dissolved carbon).

QUENCHING TRANSFORMATIONS

Because of the high austeniting temperatures, carbon and alloy components that lower the martensitic transformation point M_s , the austenite becomes stable and exists for a longer time, preventing it from fully transforming into martensite, leading to residual austenite. Thus, quenched high speed steels contain residual austenite, un-dissolved carbides and a small quantity of martensite. The presence of residual austenite in the structure prevents the reaching of a maximum hardness after quenching.

TEMPERING TRANSFORMATIONS

During the tempering process the diffusion intensifies because of the heating, resulting in a loss of hardness at about 300°C after carbon separation. Continuing with the heating process the diffusion of the iron and alloy components is favoured resulting in the precipitation of granular carbides that endow the structure with greater hardness. Thus, the austenite has a lower concentration of carbon and alloy elements, leading to an increase of temperature for martensitic transformation points, enabling the transformation of residual austenite in tempering martensite connected with an increase in hardness. The maximum hardness is obtained at 550°C and is called “secondary hardness” [1,2,3,4].

3. METALLOGRAPHIC, OPTICAL, ELECTRON, WITH X-RAY DIFFRACTION ANALYSIS AND HARDNESS MEASUREMENTS

After secondary heat treatment (as figure 1), the specimens were metallographic prepared and analysed by optical, electron microscopy and with X-ray, using equipment existing in the Chair of Materials Science and Welding - Timisoara (UPT – Mechanical Faculty).

In figure 1 is shown the microstructure (optical microscopy) of the specimen, which is in forged and annealed state, and in figure 3 is the corresponding X-ray diffraction spectrum.

It is noted that the structure in annealed state is formed by fine sorbite that includes primary and secondary carbides. The arrangement of carbides in strings is due to the forging.

In figure 4 is shown the microstructure (optical microscopy) of the specimen which is in quenched state. It is noted that the structure in quenched state is formed by austenite (polyhedral shape), undissolved carbides with a quantity of martensite. The diffractogram of this specimen (figure 5) confirms the microscopic analysis.

If the aim is to reduce the quantity of residual austenite before the high tempering treatment, the application of treatment at negative temperatures is required. [1],[4].

To draw attention of transformations from tempering process at 550 °C, especially the precipitations of fine carbides with globular shape, the quenching and tempering specimen at 550 °C was examined by electron microscopy (X 4000).

In figure 6 is shown the microstructure (electron microscopy) of the quenching and tempering specimen in three rounds of one hour at 550°C, and in figure 7 shows the resulting diffractogram.

It is noted that the structure is formed by fine martensite (Hardenită tempering martensite) and fine carbides.

Thus, the residual austenite that exists in a very low percentage even in annealed status grows in quenched status and totally transforms after tempering 2.

In order to ensure corrosion protection recommended application of termochemical ferroxated treatment.

Ferroxation was performed after the second tempering by introducing the specimen into a retort at a temperature of 350°C for 20 minutes. Steam was then introduced at a pressure of 1,2 atm continuing up to 550°C and one hour in the presence of steam. The opening of the retort follows and the cooling of the specimen at 100°C and after this, the final cooling in oil at 50°C.

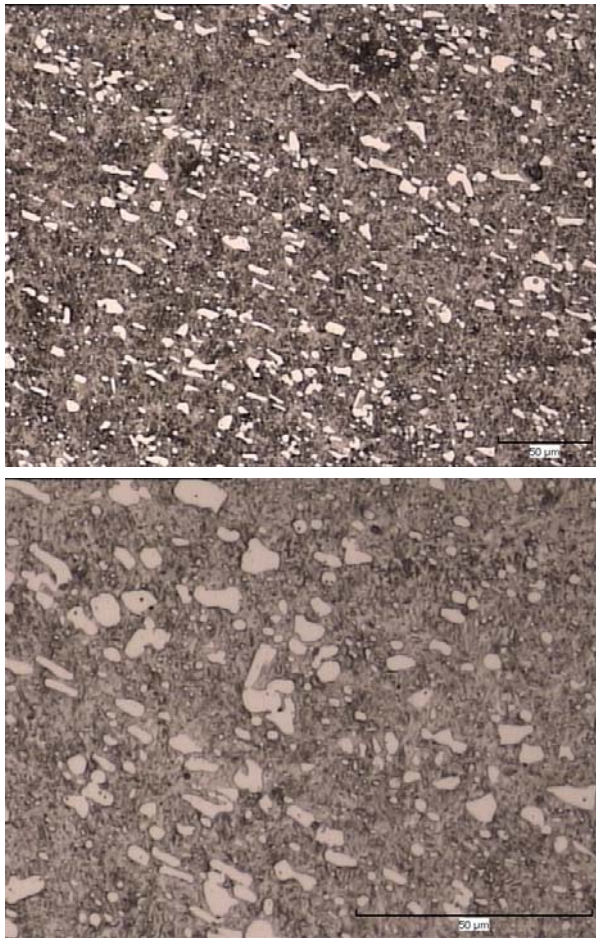


Figure 2. . HS 18 – o – 1 steel – forged + annealed (Sorbite and, primary and secondary carbides)

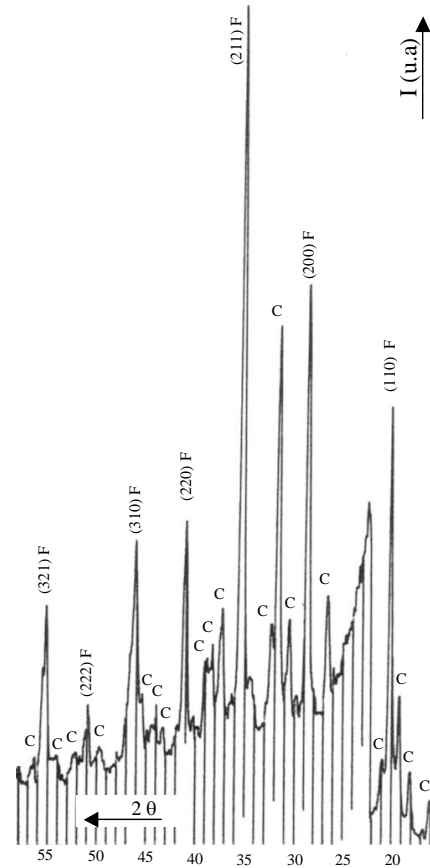


Figure 3: The diffractogram of the annealed status. (F-ferrite, C - Fe_3W_3C carbides).

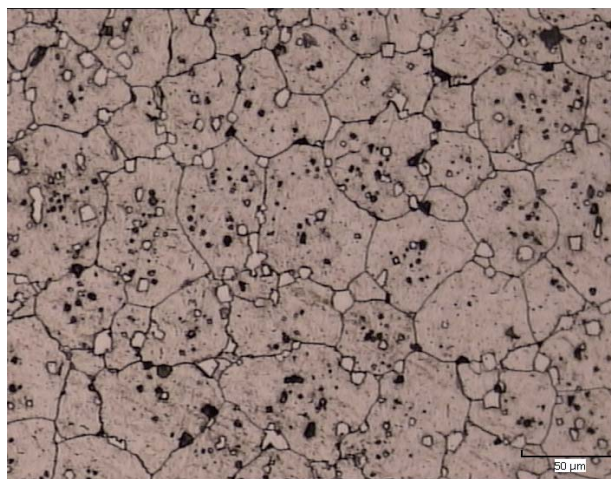


Figure 4. HS 18-0-1 steel - quenched

Figure 8 presents the diffractogram of the ferroxated state. Structure is formed out of tempering martensite, Fe_3W_3C carbides and iron oxides Fe_3O_4 majoritary and Fe_2O_3 minority.

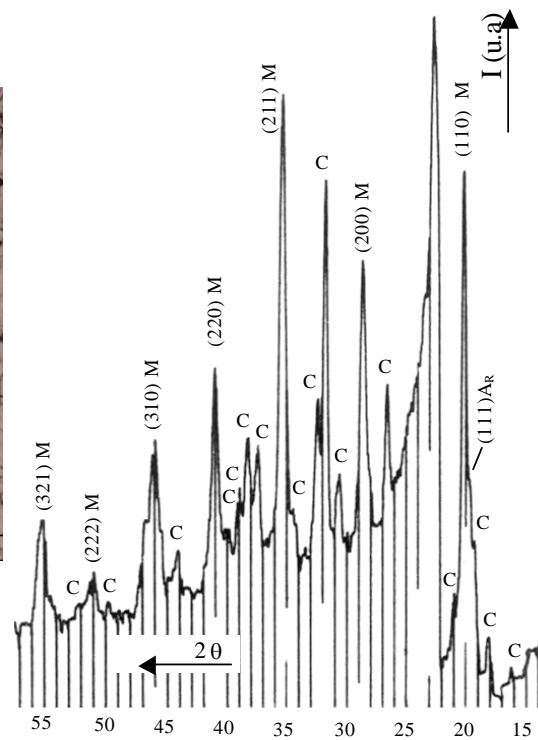


Figure 5: The diffractogram of the quenched status (M-quenching martensite, A_R - residue austenite, C- Fe_3W_3C carbides).

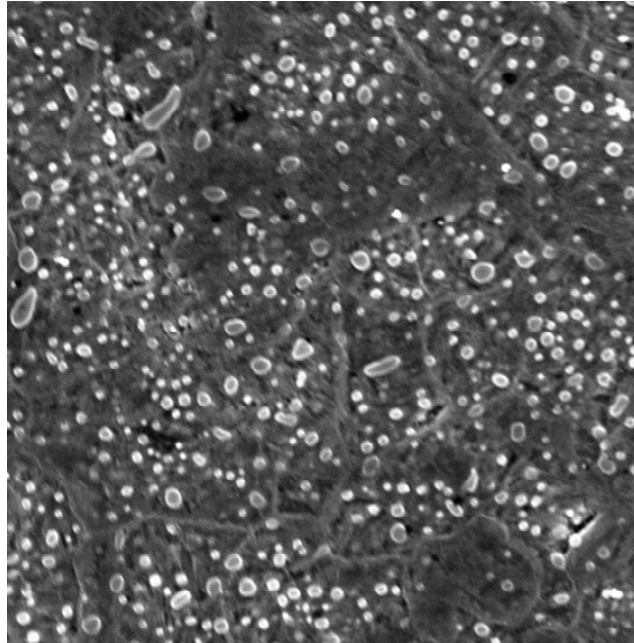


Figure 6. HS 18-0-1 quenched and tempered at 550 °C (x4000)

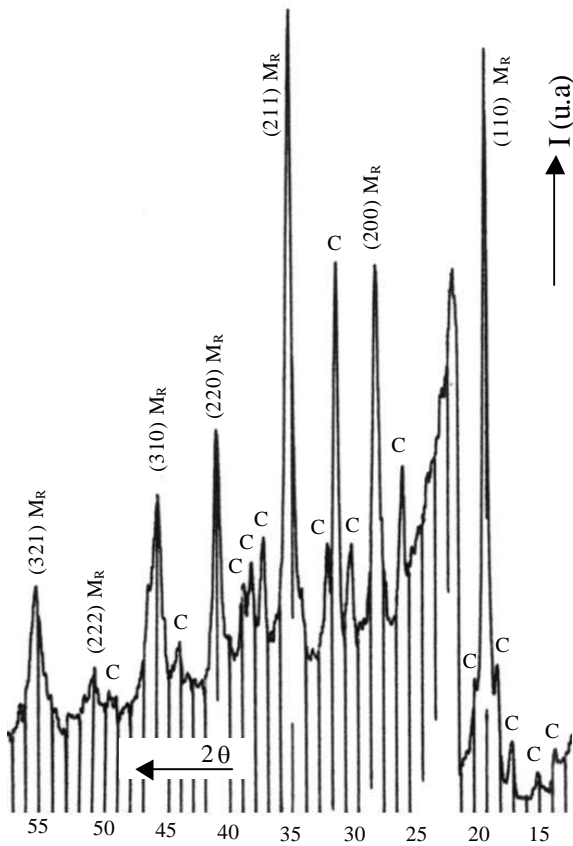


Figure 7: The diffractogram of the status, after tempering₃ (M_R tempering martensite, C - Fe_3W_3C carbides).

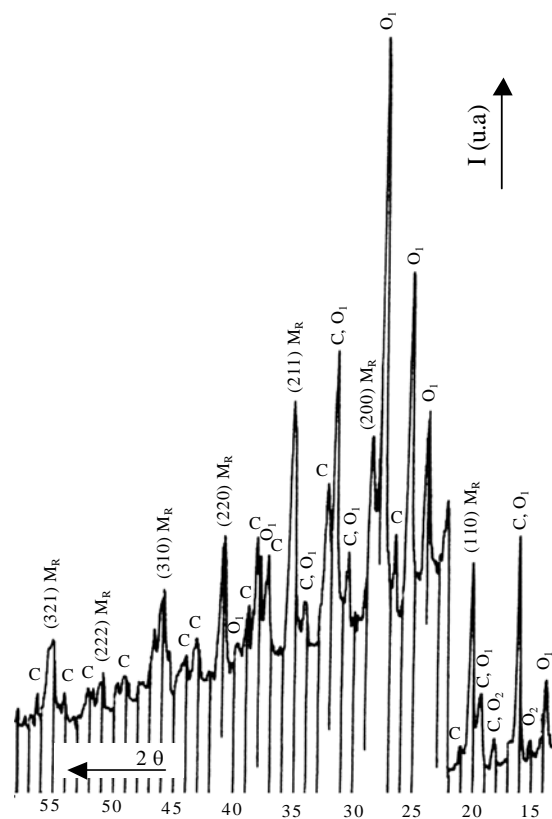


Figure 8: The diffractogram of the ferroxidated state (M_R tempering martensite, C - Fe_3W_3C carbides, O_1 - Fe_3O_4 oxide, O_2 - Fe_2O_3 oxide).

For all specimens hardness measurements was performed (Rockwell Method HRC) and the obtained values were presented in Table 1. It is noted that the hardness values are in close correlation with microscopic analysis and certifies the previously presented phenomena. Hardness after multiple tempering is higher than the quenching, phenomenon known as secondary hardness and this must be exploited when using high-speed steel to manufacture cutting tools.

Table 1. Hardness measurements

No.	Material	Status of thermal treatment	HRC hardness in 3 points	HRC hardness, average
1	HS 18-0-1	Forged + annealed	32, 35, 31	32,66
2	HS 18-0-1	Quenched	61, 62, 61.5	61,66
3	HS 18-0-1	Quenched and tempered at 550 °C	62.5, 64, 63	63,16
4	HS 18-0-1	Quenched + tempered at 550 °C and ferroxated	65, 63, 62.7	63,56

4. CONCLUSIONS

- ❖ HS 18-0-1 heat-treated steel by step-quenching (salts bath), with oil cooling and tempering in three rounds of one hour at 550 °C, ensure an uniform, hard and very thermally stable structure formed by fine tempering martensite and carbides of alloys elements.
- ❖ For aggressive environments, cutting tools executed from HS 18-0-1 high-speed steel, a final corrosion protection treatment is recommended.
- ❖ In special situations, when the active elements of the high-speed steel tool are strongly requested, for prolonging their service life up to three times, a coating with titanium nitride may be used.

REFERENCES

- [1.] Budău, V., Crăciunescu, C.M.: Studiul Materialelor. Ghid individual pentru lucrări de laborator. Editura Mirton, Timișoara, 1998
- [2.] Duma, S., Popescu, M.: The influence of thermic and thermochemical treatment on the structural characteristics and hardness on drills fabricated from HS 18-0-1 steel, Proceedings, Annual Session of Scientific Papers, "IMT Oradea – 2010", pp. 3.37, ISBN: 978-606-10-0128-6
- [3.] Liță, M.: Metode de investigație în știința materialelor, Editura Politehnica, 2009, ISBN 978-606-554-023-1
- [4.] Mitelea, I., Budau, V.: Studiul metalelor, Indreptar tehnic, Editura Facla, Timișoara 1987
- [5.] *** Metals Handbook, Ninth Edition, Vol. 9., Metallography and Microstructures, 1985







WAYS OF INCREASING THE PURITY OF THE STEELS THROUGH SLAGS, IN THE ELABORATION OF THE AGGREGATE

^{1,3,4} UNIVERSITY POLITEHNICA OF TIMISOARA, FACULTY OF ENGINEERING FROM HUNEDOARA

² ARCELORMITTAL SA HUNEDOARA, ROMANIA

ABSTRACT:

The purity of the steels, respectively the increase in their quality begins in the elaboration of the aggregate when, in addition to an appropriate load, the production should flow properly. This requires respecting the steel making technology, taking into account the specificity of the elaboration of the aggregate, the steel brand and the purity requirements required in the standards and / or by the beneficiary. The paper presents some correlations between the slag characteristics at the end of the melting process and the content of harmful elements (P, S).

KEYWORDS:

Steel, melting slag, EBT electric arc furnace, purity, dephosphoration, desulphuration

1. INTRODUCTION

Slag is a secondary product in the process of making steel, but the quality of the steel depends on the slag quality, because all the development processes depend on exchanges between metal bath and slag and between the atmosphere and metal bath through slag. If slag supplies the bath with the oxygen for purification processes and is able to retain the reaction products leaving the metal bath, if there are reactions in the slag that favors the reduction of oxides of alloying elements (Cr, Mn, etc.) then the steel will be of superior quality.

The slag, being at the steel surface, can be easily processed during development, so one should act on its characteristics to lead the process in the desired direction.

To do this, one should know the composition, liquid slag structure, physical properties and their physicochemical properties as well as the operational methods by which they may change during the production of steel. [1,2]

2. METHODOLOGY AND DISCUSSION

To analyze the influence of the slag on the steel purity, we analyzed the chemical composition of melting slags which result in the development of the pipe steel, the production taking place in an electric arc furnace EBT type of 100t capacity, data are presented in Table 1.

With these data we calculated the index of basicity (using equation 1 [2.3]), slag viscosity (according to the relation 2 [2.3]) and distribution reports of undesirable elements P and S:

$L_p = \frac{(P_2 O_5)}{[P]}$, respectively $L_s = \frac{(S)}{[S]}$ [3,4] the data being presented in tab.2.

$$p = \frac{(CaO)}{(SiO_2)} \quad (1)$$

$$\eta = -0,0509 \cdot (SiO_2) + 0,0178 \cdot (CaO) - 0,022 \cdot (MnO) - 0,0455 \cdot (Al_2O_3) - 0,0165 \cdot (FeO) + 0,0322 \cdot (Fe_2O_3) + 0,0201 \cdot (MgO) - 23,2 \cdot (S) + 1,17 \cdot (P_2O_5) + 1,88 \quad (2)$$

Table 1. Slags chemical composition, [%]

	Elements, [%]											
	S	Al ₂ O ₃	CaO	Cr ₂ O ₃	Fe ₂ O ₃	K ₂ O	MgO	MnO	Na ₂ O	P ₂ O ₅	SiO ₂	TiO ₂
1	0.133	2.53	31.36	1.19	33.07	0.004	7.52	8.56	0.084	0.589	13.11	0.25
2	0.134	5.06	34.03	1.02	27.92	0.002	7.13	9.24	0.076	0.509	13.36	0.25
3	0.153	4.27	33.48	1.02	26.21	0.001	7.97	9.19	0.072	0.537	15.21	0.27
4	0.107	3.18	32.70	1.31	34.97	0.002	7.06	7.78	0.082	0.476	11.72	0.21
5	0.098	2.95	29.55	1.09	43.37	0.001	7.00	6.47	0.091	0.372	8.72	0.17
6	0.159	3.66	36.95	1.12	29.28	0.001	7.83	7.24	0.069	0.460	11.26	0.22
7	0.145	4.14	31.78	1.26	31.35	0.008	7.58	8.75	0.091	0.513	14.28	0.27
8	0.072	1.98	23.52	1.12	46.82	0.009	8.39	7.01	0.121	0.324	11.01	0.18
9	0.168	3.20	30.52	1.15	36.13	0.004	6.46	8.05	0.095	0.430	14.05	0.25
10	0.089	2.99	30.24	1.11	35.38	0.006	7.34	7.75	0.096	0.445	13.83	0.24
11	0.069	3.43	30.71	0.90	32.58	0.001	9.53	7.50	0.079	0.417	13.28	0.24
12	0.092	2.27	32.37	0.99	33.48	0.001	8.48	7.86	0.085	0.440	13.12	0.25
13	0.098	2.28	30.39	0.96	37.95	0.007	7.06	6.94	0.092	0.435	12.63	0.26
14	0.116	3.52	29.25	0.97	41.92	0.006	6.57	6.46	0.086	0.410	10.64	0.23
15	0.072	3.99	29.98	1.00	35.31	0.003	7.48	8.14	0.085	0.423	13.00	0.26
16	0.133	4.59	34.13	0.93	27.55	0.007	7.41	8.75	0.074	0.427	14.39	0.31
17	0.065	1.53	24.92	0.93	49.32	0.004	5.92	6.31	0.102	0.349	10.63	0.19
18	0.097	2.37	32.48	1.07	33.90	0.004	9.11	7.08	0.071	0.453	13.02	0.26
19	0.089	2.08	30.06	0.99	36.99	0.002	8.69	6.86	0.080	0.446	11.80	0.26
20	0.045	3.07	23.87	1.48	43.85	0.005	9.52	7.39	0.106	0.468	9.78	0.24
21	0.061	3.59	28.64	1.47	33.73	0.010	8.48	7.97	0.085	0.561	12.20	0.27
22	0.053	3.58	27.23	1.34	33.44	0.009	8.54	7.77	0.092	0.558	12.51	0.29
23	0.051	2.50	27.45	1.42	36.54	0.006	11.60	7.87	0.086	0.540	11.97	0.27
24	0.048	3.43	24.65	1.26	41.55	0.017	8.81	7.03	0.107	0.467	11.82	0.25
25	0.047	2.09	27.05	1.53	35.12	0.016	12.07	8.26	0.094	0.473	13.14	0.27

Table 2. Indicators calculated based on the chemical composition of slag.

No.	$L_P = \frac{(P_2O_5)}{[P]}$	$L_S = \frac{(S)}{[S]}$	$p = \frac{(CaO)}{(SiO_2)}$	η
1	39.30	1.74	2.26	1.61
2	41.10	2.13	1.72	1.65
3	51.44	2.91	3.26	0.49
4	49.78	2.69	3.48	0.62
5	57.38	3.61	2.88	0.75
6	52.00	2.56	3.40	0.69
7	54.33	2.12	2.78	0.57
8	32.20	1.67	1.99	1.66
9	46.00	2.05	1.82	1.20
10	45.22	3.00	3.21	0.76
11	41.50	2.26	2.25	1.15
12	41.10	1.75	1.97	1.58
13	34.20	1.82	2.28	1.29
14	51.22	2.79	2.28	1.12
15	33.40	1.36	1.76	1.78
16	49.56	2.35	2.06	0.68
17	36.60	1.89	2.23	1.51
18	43.80	2.21	2.38	0.90
19	34.60	1.56	2.43	0.63
20	51.00	1.93	1.88	1.34
21	33.00	1.28	1.88	2.15
22	37.46	1.58	2.11	0.95
23	52.90	2.50	1.84	0.62
24	62.70	3.67	3.62	0.22
25	36.00	1.10	1.60	2.40

- With these data we performed the following dependency graphs and analysis, as follows:
- ❖ in figure 1 the histogram of the variation of slag basicity is shown. It can be seen that in 64% of data the basicity is more than two, which means that there are concerns from the oven to ensure optimal conditions of dephosphoration and prevents the absorption of the hydrogen in the metal bath;

- ❖ the variation of the slag viscosity is shown in figure 2, depending on the temperature of melting metal bath. The dependence is similar to that shown in figure 1 (inversely);
- ❖ the same dependency is shown in figure 3 – the variation of the slag viscosity depending on its basicity;
- ❖ instead, analyzing the dependencies between the distribution reports for P, respectively S depending on the bath temperature it can be observed that the dependence is directly proportional, the removal of these elements being driven by rising the temperature. The difference lies in the value of the distribution reports: to report the distribution of P values were calculated between $L_P = 32.2$ to 62.7 (figure 4) but to report the distribution of S the values were calculated much lower: $L_S = 1.1$ to 3.67 (figure 5).

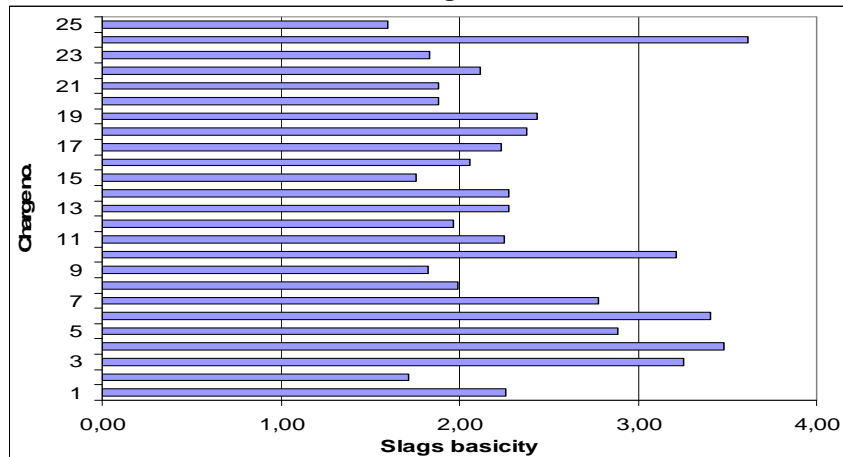


Fig.1. The basicity of the steel plants slag.

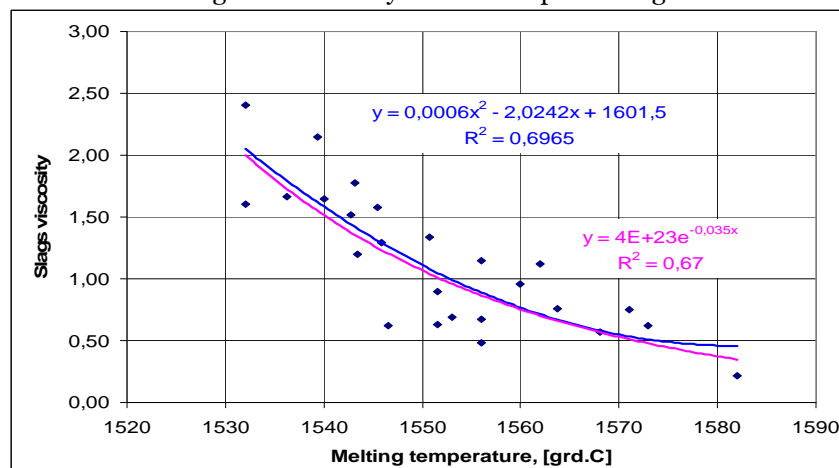


Fig.2. The dependence between the slag viscosity and the temperature of the metal bath.

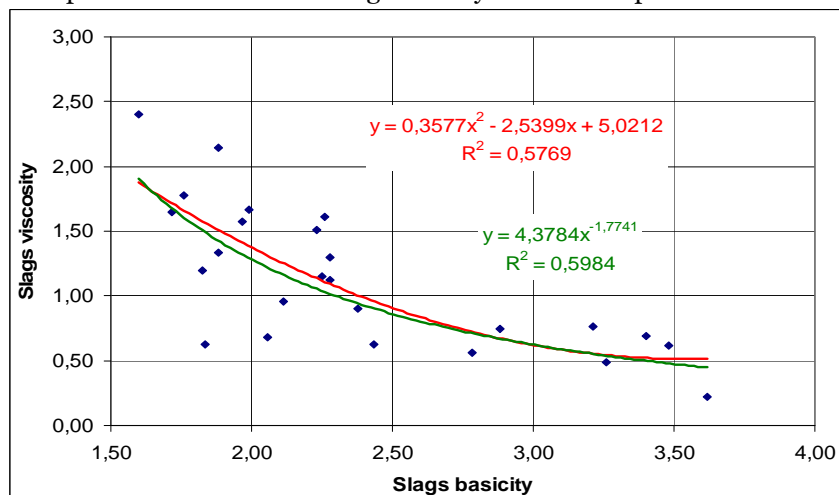


Fig.3. The variation of the viscosity depending on the slag basicity.

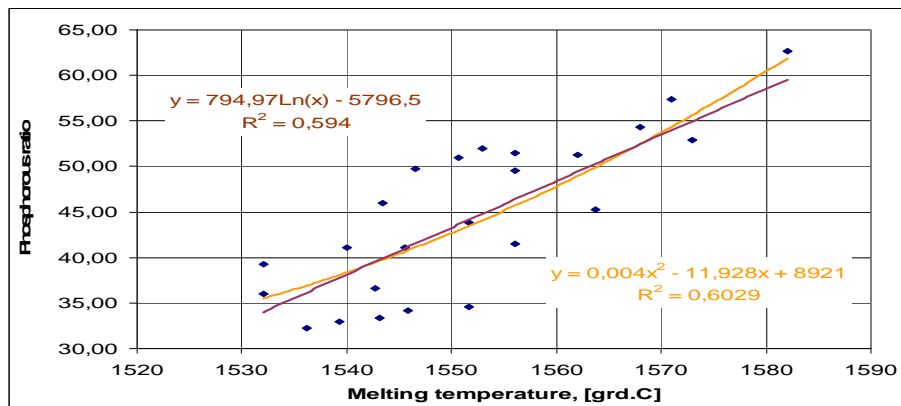


Fig 4. The dependence between the distribution report of the phosphorus between the slag and the metal bath and respectively the temperature of the bath.

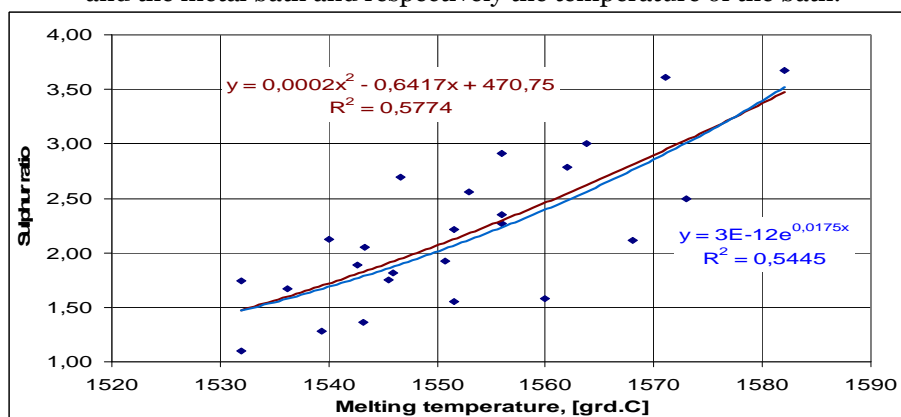


Fig 5. The dependence between the distribution report of the sulfur between the slag and the metal bath and respectively the temperature of the bath.

3. CONCLUSIONS

As a result of analyzing the literature and data from industrial practice, the following conclusions were presented:

- ❖ to increase the quality of the steel, the quality of the load should be the appropriate one;
- ❖ in what concerns the unwanted elements in the P it is known that the dephosphoration occurs at the end of the melting process. In industrial practice, P removal from the oven (by slag) is a continuous and constant over the last melting tip loading. At the end of melting, P contents are within the limits required by standards;
- ❖ S content decreases only at higher than 1620°C temperatures. We can observe an increase of S content compared to the sample in the melting process, due to melting of the amount of iron brought in the load (which places in the oven a high content of S) or by introducing petroleum coke (also with high S). Advanced desulphuration is achieved in the ladle during secondary treatment;
- ❖ In terms of hydrogen content at slag basicity $P > 2.1$, it is not absorbed into the metal bath. In industrial practice, basicity is adjusted by introducing lime calcined lumps containing approx. 98% CaO, dolomite reduction (by approx. 40% MgO and 58% CaO). Not to be neglected is the crushed magnesite inserted into the last tipper (1000 - 1100 kg/charge) for both protection of the refractory masonry and for basicity correction.

REFERENCES

- [1.] Geantă, V., Pumnea, C., Tehnologii speciale de elaborare și rafinare a oțelului, Ed. Universității Politehnica București, 1993.
- [2.] Oprea, F., Taloi, D., Constantin, I., Roman, R., Teoria proceselor metalurgice, Editura Didactică și Pedagogică, București, 1978.
- [3.] Tripșa, I., Pumnea C., Retopirea și rafinarea oțelurilor, Editura Tehnică, București, 1984.
- [4.] Nica, Ghe., Socalici, A., Ardelean, E., Heput. T., Tehnologii pentru îmbunătățirea calității oțelului, Ed. Mirton, Timișoara, 2003.



MATHEMATICAL MODEL ON THE CORRELATION OF THE COMBUSTION`S ZONE PARAMETERS IN CASE OF USING DIFFERENT AUXILIARY COMBUSTIBLES

^{1, 2, 3} UNIVERSITY "POLITEHNICA" OF BUCHAREST, ROMANIA

ABSTRACT:

The physical and chemical processes that are developing in the combustion zone of the blast furnace depend on many physical and metallurgical parameters, such as: blast air flow, oxygen content in blast air, humidity, pressure and blast air flow temperature.

The presented mathematical model establishes the correlation between blow parameters mentioned before and a performance function that is set to reflect precisely the development of the physical and chemical processes in the combustion zone of the blast furnace in case of using various auxiliary combustibles. This performance function is the theoretical temperature of the oxidant zone.

The establishment of the model equations was made starting from the functional real data of 1000 m³ blast furnaces.

KEYWORDS:

using different auxiliary combustibles

1. INTRODUCTION

The mathematical models established by many scientific research works make possible the computers assisted management of some stages of the pig iron manufacturing processes in blast furnace. They establish the correlation between the important parameters of processes and the choice performance functions selected to show the development of physical and chemical processes from blast furnace in the case of using auxiliary combustibles. This performance function for the presented model is the theoretical temperature of oxidant zone in blast furnace.

The establishment of the mathematical model starts from the presented model is the theoretical temperature of oxidant zone in blast furnace.

The mathematical model uses as enter variable or resulting variable the specifically consumption of the metallurgical coke (the physical coke – "without water coke").

A basis of the model is represented by the combustion zone thermal balance.

For an optimal function of blast furnace the theoretical temperature in this zone is accepted to be 1800...2000°C.

2. THE THEORETICAL AND CALCULATION PRESUMPTIONS OF THE MATHEMATICAL MODEL

The mathematical model proposed in the present scientific research work supposes the establishment of some correlations between the blow air parameters.

These parameters could enter or exit variables the other entire dependent.

The establishment of the mathematical models equations has been made starting up from the real function data of blast furnaces. As starting data for the calculation was proposed the following specifically consumptions:

- ❖ the metallurgical physical coke (the technical coke - "without water coke") - K_{ti} - as enter variable of the model with 400...600 kg/t values and K_{etr} as exit variable;
- ❖ the tar - D_t - as enter variable of the model with 0...5000 kg/h values and D_{et} as exit variable;

- ❖ the methane gas – M_{gi} – as enter variable of the model with 0...9000 Nm³/h values and M_{ge} as exit variable;
- ❖ the pitch liquid fuel – D_{pl} – as enter variable of the model with 0...5000 kg/h values and D_{epl} as exit variable.

Concerning the practical manage of pig iron manufacturing for tar methane gas and pitch liquid fuels it operates with hour flow and the mathematical model uses as enter variables the values of D_t , M_{gj} , and D_{pl} . In the same time, the mathematical model gives the relations to transform the hour flows in specifically consumption T_i , M_j , P_{li} . The exit variables of the mathematical model expressed in hour flows in specifically consumption T_i , M_j , P_{li} . The exit variables of the mathematical model expressed in hour flows are in this case the following: T_e , M_e , P_{le} .

The theoretical temperature from combustion zone T_{tez} is initially presented in mathematical model as exit variable, but after that it serves as enter variable with technological optimal value 2123K.

The values for specifically heat of the constant pressure by blow air and water vapors of blow air (h_a , h_w) are known, and for the specifically heat of the obtained gas in combustion zone (h_g) can be used in the initial calculation the value 0, 35. For other calculations the value is:

$$h_g = 0,311 + 0,208 T_{tez} \cdot 10^{-4}, \text{ [kcal/kg}\cdot\text{K]}, \quad (1)$$

The chemical composition used in calculation for the tar is:

$$C_{free} = 55\%, C_{(CS_2)} = 0, 2\%, C_{total} = 55, 2\%, CH_4 = 13, 6\%, C_2H_2 = 28, 8\%, W = 5\% \text{ (among } 5...20\%).$$

The chemical composition used in calculation for the pitch liquid fuel is:

$$C_{free} = 43\%, C_{(CS_2)} = 0, 2\%, C_{total} = 43, 2\%, CH_4 = 15\%, C_2H_2 = 16\%, W = 5\% \text{ (among } 5...20\%).$$

For the substitution index of coke by methane gas is used in calculation the value $I_{kmg} = 1$, obtained by pig iron making real data in blast furnace with 1000 m³ volume in different periods.

For the substitution index of coke by tar and pitch liquid fuel in concordance with data on specialty studies [1, 2] are used the values $I_{kt} = 0, 87$ and $I_{kpl} = 1, 04$.

The adopted values for this index can be modified by the subsequent functionally data of blast furnace.

3. THE MATHEMATICAL MODELS EQUATIONS

3.1. The hour production of pig iron

$$P_{hp} = \frac{Q_p \cdot n_{bu}}{24}, \text{ [pig iron t/h]}, \quad (2)$$

3.2. The specific consumption of the tar, methane gas and pitch liquid fuel

$$T_i = \frac{D_t}{P_{hp}}, \text{ [Kg/t]}, \quad (3)$$

$$M_i = \frac{M_{gij}}{P_{hp}}, \text{ [Nm}^3\text{ CH}_4\text{/t]}, \quad (4)$$

$$P_{li} = \frac{D_{pl}}{P_{hp}}, \text{ [kg/t]}, \quad (5)$$

3.3. The specific consumption of the technical coke

$$K_{th} = K_t \cdot P_{hp}, \text{ [kg/h]}, \quad (6)$$

3.4. The technical coke substituted by auxiliary combustibles

To determine the substitution index of coke by the tar is used the relation:

$$I_{kt} = 1,184 - 0,0191W_{tr} - 0,577 \cdot 10^{-3}S_{tr} + 0, 56 \cdot 10^{-5}W_t \cdot S_t, \text{ [kg/kg]}, \quad (7)$$

For substitution index of the coke by methane gas and pitch liquid fuel are used the values $I_{km} = 1$, $I_{kpl} = 1, 04$.

The substituted quantity of the technical coke by auxiliary combustibles is:

$$K_{ts} = I_{kt} \cdot T_i + M_i + 1,04P_{li}, \text{ [kg/t]}, \quad (8)$$

3.5. The technical coke specific consumption

In case of using auxiliary combustibles T_i , M_j , P_{li} the technical coke consumption will be:

$$K_{tr} = K_{ti} - K_{ts}, \text{ [kg/B.U]}, \quad (9)$$

3.6. The technical coke quantity in burden unity

$$K_{tbu} = K_{tr} \cdot Q_p, \text{ [kg/B.U]}, \quad (10)$$

3.7. The technological coke quantity in burden unity

$$K_{thbu} = \frac{100 \cdot K_{tbu}}{100 - W_{kt}}, \text{ [kg/B.U]}, \quad (11)$$

- W_{kt} represents the humidity of the technological coke.

Using the results given by the mathematical model of burden calculation the mass and the heat balances presented in other scientific research work [3] K_{ti} can be determined by the following mode:

$$K_{ti} = K_t + M, \text{ [kg/t]}, \quad (12)$$

A true correlation between the present mathematical model and [3] can lead to the equality:

$$K_{tbu} = K_{ti}, \quad (13)$$

3.8. The necessary combustion oxygen quantity

From the processing of the pig iron making real data in blast furnace with a volume of 1000 m³ and in correlation with the data presented by the specialty literature [4,5] it can be considered that approximately 68% of carbons coke burns in crucible (in front nozzle surface) will be:

$$C_b = 0,068 \cdot C_k \cdot K_{tr}, \text{ [kg/t]}, \quad (14)$$

- C_k represents the percentage content of free carbon out of coke.

The carbon quantity burnt in front nozzle surface in one hour time is:

$$C_{bh} = C_b \cdot P_{hp}, \text{ [kg/h]}, \quad (15)$$

The auxiliary combustible quantities burnt in one hour time in crucible reported at 1 kg C_{bh} are:

$$T_{rc} = \frac{D_t}{C_{bh}}, \text{ [kg tar/kg C]}, \quad (16)$$

$$M_{rc} = \frac{M_{gl}}{C_{bh}}, \text{ [Nm}^3 \text{ CH}_4\text{/kg C]}, \quad (17)$$

$$P_{lrc} = \frac{D_{pl}}{C_{bh}}, \text{ [kg pl/kg C]}, \quad (18)$$

The necessary oxygen for burning in front nozzle surface in case of using the quantities T_{rc} , M_{rc} , P_{lrc} is:

$$Q_{2nec} = 0,933 + 0,85T_{rc} + 0,5M_{rc} + 0,61P_{lrc}, \text{ [Nm}^3 \text{ O}_2\text{/kg C]}, \quad (19)$$

Considering the percentage content of oxygen in blow air O_2 among 21...30%, the necessary volume of blow air for burning will be:

$$V_a = 1,15 \cdot \frac{100 \cdot O_{2nec}}{O_2}, \text{ [Nm}^3 \text{ air/kg C]}, \quad (20)$$

The blow air hour flows necessary for burning 1 kg C out of coke:

$$Q_a = V_a \cdot C_{bh}, \text{ [Nm}^3 \text{ air/h]}, \quad (21)$$

This quantity represents the theoretical necessary of blow air for burning in blast furnace crucible and the quantity differs from the real quantity that considers all the casualties in air transport network.

3.9. The obtained quantity of gas in the combustion zone

The obtained carbon monoxide volume in combustion zone:

$$V_{CO} = 1,867 + M_{rc} + 1,75T_{rc} + 1,28P_{lrc}, \text{ [Nm}^3 \text{ CO/kg C]}, \quad (22)$$

The obtained hydrogen volume in combustion zone:

$$V_{H_2} = 0,01V_a + 2M_{rc} + 0,62T_{rc} + 0,52P_{lrc}, \text{ [Nm}^3 \text{ H}_2\text{/kg C]}, \quad (23)$$

The obtained nitrogen volume in combustion zone:

$$V_{N_2} = V_a \cdot (0,99 - 0,01O_2), \text{ [Nm}^3 \text{ N}_2\text{/kg C]}, \quad (24)$$

The obtained gas volume in combustion zone:

$$V_g = V_{CO} + V_{H_2} + V_{N_2}, \text{ [Nm}^3\text{/Kg C]}, \quad (25)$$

The obtained hour gas quantity in combustion zone:

$$v_{gh} = V_g \cdot C_{bh}, \text{ [Nm}^3\text{/h]}, \quad (26)$$

3.10. Objective function of present model and correlation between the blows parameters

“The theoretical temperature of combustion zone”: using the heat zone balance (heat balance at combustion zone of blast furnace) is obtained the following relation for the objective function of the present mathematical model:

$$T_{tez(e)} = \{2340 + 1583, 24T_{rc} + 439M_{rc} + 1120, 94P_{lrc} + v_a [(h_a + 0, 01\varphi \cdot h_w) \cdot t_a - 25, 8\varphi]\} / (h_g \cdot v_g), \text{ [}^\circ\text{C]}, \quad (27)$$

- φ , t_a represents the humidity and the temperature of blow air in [%] and [$^\circ\text{C}$].

“Correlation between blow parameters in crucible of the blast furnace”:

- Correlation $K_{eth} = f$ (other blow parameters):

$$K_{eth} = \{v_{gh} \cdot T_{tez} \cdot h_g - 1583, 24Dt - 439M_{gj} - 1150, 94Dpl - Q_a [(h_a + 0, 01\varphi \cdot h_w) \cdot t_a - 25, 8\varphi]\} / (15, 91 \cdot C_k), \text{ [kg/h]}, \quad (28)$$

- Specific consumption of technical coke:

$$K_{etr} = \frac{K_{th}}{P_{hp}}, \text{ [kg/t]}, \quad (29)$$

- Correlation $D_{et} = f$ (other blow parameters):

$$D_{et} = \{v_{gh} \cdot T_{tez} \cdot h_g - 15,91C_k \cdot K_{th} \cdot P_{hp} - 439M_{gi} - 1120, 94D_{pl} - Q_a [(h_a + 0, 01\varphi \cdot h_w) \cdot t_a - 25, 8\varphi]\} / 1583, 24, \text{ [kg/h]}, \quad (30)$$

- Correlation $D_{epI} = f$ (other blow parameters):

$$D_{epI} = \{v_{gh} \cdot T_{tez} \cdot h_g - 15,91C_k \cdot K_{th} \cdot P_{hp} - 439M_{gi} - 1583, 24D_t - Q_a [(h_a + 0, 01\varphi \cdot h_w) \cdot t_a - 25, 8\varphi]\} / 1120, 94, \text{ [kg/h]}, \quad (31)$$

- Correlation $M_{ge} = f$ (other blow parameters):

$$M_{ge} = \{v_{gh} \cdot T_{tez} \cdot h_g - 15,91C_k \cdot K_{th} \cdot P_{hp} - 1583D_{dt} - 1120, 94D_{pl} - Q_a [(h_a + 0, 01\varphi \cdot h_w) \cdot t_a - 25, 8\varphi]\} / 439, \text{ [Nm}^3/\text{h]}, \quad (32)$$

- Correlation $Q_{ea} = f$ (other blow parameters):

$$Q_{ea} = \{v_{gh} \cdot T_{tez} \cdot h_g - 15,91C_k \cdot K_{th} \cdot P_{hp} - 1583D_{dt} - 1120, 94D_{pl} - 439M_{gi}\} / (h_a + 0, 01\varphi \cdot h_w) \cdot t_a - 25, 8\varphi, \text{ [Nm}^3/\text{h]}, \quad (33)$$

- Correlation $D_{eO_2} = f$ (other blow parameters):

$$D_{eO_2} = 0,0135Q_a \cdot O_2 - 0,284Q_a, \text{ [Nm}^3/\text{h]}, \quad (34)$$

$$O_{2(e)} = \frac{100 - O_{2nec} \cdot C_{bh}}{Q_a}, \text{ [%]}, \quad (35)$$

Correlation $t_{a(e)} = f$ (other blow parameters):

$$t_{a(e)} = (v_g \cdot T_{tez} \cdot h_g - 15,91C_k \cdot K_{th} \cdot P_{hp} - 1583D_t - 1120, 94D_{pl} - 439M_{gi} + 25,8\varphi \cdot Q_a) / (h_a + 0,01\varphi \cdot h_w) \cdot Q_a, \text{ [}^\circ\text{C]}, \quad (36)$$

4. CONCLUSIONS

The mathematical model presented in this scientific research work can use for the computers assisted management for all processes that are developed in the blast furnace crucible combustion zone in case of using varied auxiliary combustibles.

For this reason, first of all the process simulation has been made using this model.

During the process simulation are obtained results that can be confirmed by the blast furnace real function. In certain real situations, the results of the mathematical model are not totally confirmed, in that case the models equations must being improved by adoption at the real pig iron making conditions (for these are introduce the corrections index).

It is obtained a mathematical model that shows obviously the carry on of all the processes in the blast furnace combustion zone. It can be obtained the automatically manage of the pig iron making and remarkable material and energy economy.

REFERENCES:

- [1.] N. CONSTANTIN, D. IONIȚĂ, A. SEMENESCU, C. V. SEMENESCU: „Analytical methods for blast furnace ironmaking optimization by optimal correlation of coke rate with blowing parameters in the raceway”, *Metalurgia* nr.6/2003, pag. 5 – 12.
- [2.] N. CONSTANTIN: „Blast furnace process intensification by gas circulation improvement, in order to ensure productivity growth and energy and metallurgical coke economy”, Doctor Thesis, Bucharest, 1994
- [3.] N. CONSTANTIN, D. IONIȚĂ, A. SEMENESCU, C. V. SEMENESCU, M. COSTACHE: „Efficiency of blast furnace making by computer-assisted of this process”, *Metalurgia*, nr.7, 2003, pag. 17 – 28
- [4.] N. CONSTANTIN: „Nonconventional process for production of ferrous materials”, “PRINTECH” Publishing House, Bucharest, 2002
- [5.] N. CONSTANTIN: „Blast furnace iron making engineering”, “PRINTECH” Publishing House, Bucharest, 2002
- [6.] N. CONSTANTIN: „Replacement of natural gas in the blast furnace by injected steam in the raceway area”, *Metalurgia*, nr.11 - 12, 1991, Romania





ALTERNATIVE IRON MAKING TECHNOLOGIES

^{1, 2, 3} UNIVERSITY "POLITEHNICA" OF BUCHAREST, ROMANIA

ABSTRACT:

The paper presents few aspects concerning the implementation of alternative iron making technologies in Romania. A few reasons are analyzed for the apparition and development of such technologies in the world steel market competition. The presence of alternative iron making technologies will be a benefit for metallurgic, economic, social and environmental reasons and a plus for EU adhesion.

The preliminary researches made using wastes from chemical and metallurgical industries are encouraging for developing alternative iron making pilot plants.

KEYWORDS:

alternative iron making technologies

1. INTRODUCTION

The steel industry has been greatly restructured, is much more competitive and is going through a technological revolution driven by capital requirements, shortages in raw materials such as coke and low residual scrap, environmental concerns and very important customer demands. It is very important to know if production technologies are still appropriate in present and which are the new processes that have to be developed in order to meet the future needs of steel market 1, 2, 3 and 4. The steel manufacturing process is highly capital intensive in relationship to the added value to the input materials. Direct iron making using coals and iron ores directly will eliminate the need for coking coals, coke making and agglomeration and address the need to reduce capital and environmental concerns 2, 3.

Society continues to press the industry to reduce emissions and recycle more waste materials. Consequently, processes that recycle blast furnace and steel making dust and have lower emissions than conventional coke making and sintering must be developed.

Customers will continue to require improved properties and quicker and more reliable delivery of steel at a good value relative to competitive materials. Development of a technique allowing coal and ore to be directly transformed into base iron solid/liquid products will enhance the flexibility and reliability of steel industry in order to maintain its competitive position. For industrialized areas such as the US, Japan and Europe a coal based and low capital cost process must be developed 1 and 4.

2. IRON MAKING ALTERNATIVE TECHNOLOGIES

It is well known that the quality of the main raw materials for EAF plants – scrap – has deteriorated during recent years. Scrap becomes more and more polluted by metallic tramp elements and organic compounds; this requires improved cleaning and sorting of scrap, by physical and chemical treatments. If the scrap quality is insufficient for achieving the required steel properties, virgin iron has to be added to the metallic charge. This addition can be hot metal, cold pig iron or direct reduced iron in order to improve the quality of products because they are tramp elements free 1, 4. Another reason for developing iron making alternative technologies is the possibility of wastes recycling as raw materials. Waste recycling processes will reduce the environmental impact of waste disposal. Minimizing plant waste/by-products (by in-works recycling) and valorizing them (by the use of slag in agriculture or civil engineering) are other important objectives including the ecological one.

In recent years, many alternative iron making processes have been proposed and developed to replace the conventional iron making process – the blast furnace process. Blast furnaces have played a major part in pig iron production because of their high heat and gas utilization efficiency, mass production. In present blast furnace processes have some unavoidable problems, environmental pollution by the coke plants, lower production flexibility and high degree of raw materials preparations.

The alternative iron making process may be required to satisfy the criteria such as the use of different coals, simplified material preparation, metal with little impurities, independent process steps, closed energy system, efficient pollution control and no waste generation. They also may have a higher productivity per unit volume than a blast furnace and the capital cost seems to be significantly lower than the conventional process 1, 2 and 4.

Until now, the Corex process was the most fully developed, which uses lump ore, pellets or sinter, as well as lumpy coal as raw materials, producing 300,000 tons of pig iron annually without any problems. In this process, coal is charged into the melter- gasifier reactor and is combusted to CO and H₂ to produce the heat to melt the iron pellets. Then the off-gas is used to reduce iron ore to more than 90% metallization in the shaft-type prereduce. The other smelting reduction processes presently under development throughout the world use ore fines and coal fines as feedstock in order to avoid as well the coking operation and the agglomeration of iron ores. They generally consist of two superposed reactors: a prereduction vessel and a smelting vessel. None of these processes (Hismelt, Dios, CCF and Circofer) has out passed the pilot and demonstration stage in spite of the considerable amount of research funds already invested. In view of the risks and costs inherent to developments it is questionable when they will reach industrial maturity 1, 4.

The direct reduction processes which today are in commercial use - Midrex, Hyl, Fior – produce about 20-25 million tones DRI (direct reduced iron) per annum, which is a rather small amount compared to the roughly 200-220 million tones of steel per annum produced by the EAF in the world.

3. FERROUS WASTES – RAW MATERIALS FOR ALTERNATIVE IRON MAKING

An efficient way to decrease the cost of raw materials and to meet the environmental requirements is to use alternative technologies for iron and steel making. For the alternative technologies the costs of raw materials and preparation is not so high especially if they are by-products from own or related industries. The environment protection is double, directly because the waste will be recycled in-works and not land filled and indirectly because the natural resources will be preserved.

In the world ferrous metallurgy around 75-80% of wastes are recycled. Unfortunately in the same time in Romania only 40-45 % of them are recycled. There are a lot of problems concerning collection, transportation, storage and recycling of all kinds of wastes from metallurgical and chemical industries. Subsequent problems with maintenance and extension of landfills are expected 1, 3 and 4.

In ferrous metallurgy an important part of the wastes are from blast furnaces (flue dust and sludge), sinter plants (dust and fines) and from EAF's and LD converters (dust and slurry). These kinds of wastes are very fine dusts from electrical dust collectors, wet gas cleaner secondary dedusting system.

Another category of by-products are cinder, mill scales, oily sludge, grinding swarfs. All this iron sources and moreover cheapest iron ore which is not suitable for blast furnace can be used for alternative iron making processes. Pyrite ashes are chemical by-products form sulphuric acid fabrication which could have great importance for ferrous metallurgy because of their high content in iron.

In Romania these kinds of wastes were land filled and the environment was damaged in that area (Valea Călugărească, Turnu Măgurele and Năvodari). The pyrite ashes are very light and in dust presentation (average diameter is 50µm). Land filling with this waste has lead to severe environmental impact on air, soil and surface and underground water in extended areas than landfills. It is creating a much polluted environment in plant proximity and affects also their own equipments and control devices, moreover agricultural areas are unproductive.

All types of low cost carbon bearing materials such as medium and low volatile coals, coke fines, coke breeze, graphite, pet coke, ground electrodes and toner can be used as reductants.

Taking into account the above mentioned reasons and the existence of such kind of wastes suitable for recycling Romania has to initiate projects in the alternative iron making area. This will be a good step for both steel industry and the environment.

Moreover, it will enhance the level of integration in the European Union.

4. EXPERIMENTS

Direct reduction processes are widely known alternatives for the blast furnace route to iron manufacture. In direct reduction rotary kilns, the solid reductant serves the purpose of both fuels and reducing agent.

In order to make estimation about using pyrite ashes and blast furnace dust like raw materials for a direct reduction process some preliminary experiments have been conducted.

For direct reduction experimental heats a lab scale rotary furnace with 2kW electrical resistance was used (figure 1). Internal space has a cylindrical shape with 200mm diameter and 350mm length. The raw materials chemical compositions used for the experimental heats are presented in table 1. The reduction and combustion agent was fine coal (87,5% carbon, 1% sulphur, 11% ash, 1,5% volatile) with dimension between 0 - 5mm.



Figure 1. Rotary furnace for direct reduction

(figure 1). Internal space has a cylindrical shape with 200mm diameter and 350mm length. The raw materials chemical compositions used for the experimental heats are presented in table 1. The reduction and combustion agent was fine coal (87,5% carbon, 1% sulphur, 11% ash, 1,5% volatile) with dimension between 0 - 5mm.

Table 1. Chemical composition of raw materials (%)

Raw material	Fe	Mn	SiO ₂	CaO	MgO	Cu	Pb	Zn	K	As	Al ₂ O ₃
Blast furnace dust	41,2	1,03	9,28	9,76	1,8	0,01	0,2	0,86	0,14	-	0,05
Pyrite ash Valea Călugărească 1	51,4	-	6,8	-	-	0,46	0,53	1,13	-	0,01	-
Pyrite ash Valea Călugărească 2	53,5	-	7,0	-	-	0,5	0,5	1,1	-	0,6	-
Pyrite ash Turnu Măgurele	51	-	6	-	-	0,35	0,25	0,4	-	0,25	-
Pyrite ash Năvodari	53	-	5	-	-	0,5	0,3	1,1	-	0,4	-

The raw materials (dusts and coal fines) were introduced in the rotary furnace together with a dispersion agent. This agent consists in 10-12 mm diameter wear resistant ceramic balls. Around 1, 5 kg ceramic balls were introduced. The role of the dispersion agent was to mix the charge increasing the reaction area, initiating the direct reduction process and preventing floating of coal on the raw materials. The types of charge and experimental conditions are depicted in table 2. The temperature was measured with a Pt/Pt-10%Rh thermocouple coupled with a digitally display device. In order to melt the obtained iron base powder a Tammann furnace was used. The samples of iron base powder from each charge were melted at 1700°C in 10-15 minutes, in reductive atmosphere in graphite or alumina crucibles.

Table 2. Experimental conditions

Sample	Charge	Temp., °C	Reaction time (min)
1	1 Kg, blast furnace dust + 0,3 Kg coal fines	900	30
2	1Kg pyrite ash Valea Călugărească 1+ 0,3 Kg coal fines	920	30
3	1 Kg pyrite ash Valea Călugărească 2 + 0,3Kg coal fines	940	30
4	1 Kg pyrite ash Turnu Măgurele + 0,3 Kg coal fines	820	30
5	1 Kg, pyrite ash Năvodari + 0,3 Kg coal fines	880	30

5. RESULTS

The products resulted from direct reduction process were: iron base powder, combustion gas, sterile. The iron base powder was separated from sterile with a permanent magnet. The analysis of combustion gases shown that they contain around 70-75% CO.

The resulted iron base powders from each charge were chemically analyzed. For iron base powder the metallization degree was establish with this formula:

$$M = \frac{Fe_{met}}{Fe_{tot}} \cdot 100 ,$$

Fe_{met} – metallic iron%, Fe_{tot} – total iron%

The results are depicted in table 3.

After melting iron base powder in a Tammann furnace, the crucibles were quenched and the slag and the metal phases were separated, weighted and analyzed. The results for the metallic phase are depicted in table 4.

Table 3. Chemical composition of iron base powder

Sample	Fe total	Fe metal	M, %	Cu	Pb	Zn	As
1	56,08	50,55	90,1				
2	61,8	55,87	90,4	0,37	0,18	2,05	0,09
3	60,55	56,3	93	0,32	0,72	0,97	0,09
4	55,97	41,4	74	0,31	0,07	0,86	0,07
5	63,29	55	86,9	0,34	0,06	2,08	0,05

Table 4 – Chemical composition of metallic phase

Nr	Metallic sample from:	C %	Mn %	Si %	S %	P %	Fe %
1	Blast furnace dust	4,00	0,62	2,30	0,074	0,135	92,87
2	Pyrite ash Valea Călugărească 1	3,25	0,60	2,75	0,054	0,141	
3	Pyrite ash Valea Călugărească 2	3,30	0,55	2,84	0,047	0,148	
4	Pyrite ash Turnu Măgurele	3,40	0,25	3,04	0,0281	0,146	93,13
5	Pyrite ash Năvodari	2,90	0,22	1,89	0,0136	0,108	94,86

After the melting of the obtained powder bath it is rich in iron, around 85-95%, and also with carbon that is necessary to eliminating the gases and nonmetallic inclusions. The contents of sulphur and phosphorus are not bigger than an usual pig iron as well as those of mangan and silicium.

6. COMMENTS

The iron base powder resulted from direct reduction can be used in steel making (powder injection in EAF, after briquetting as scrap substitute in LD, induction furnace, EAF), or raw material for ductile cast iron or other cast iron qualities.

The sensible heat of directly reduced iron can be utilized by hot charging in the above mentioned melting facility in order to increase the efficiency of the method.

The forecast of the authors to obtain a metallization degree of 85-90% was reached. But, the scale of the rotary lab furnace had a negative influence on direct reduction processes. For industrial scale we predict a metallization degree of 95% in 1/2 hour.

The forecast for energy consumption in industrial scale plant is around 2,2 Gcal/tFe under the present values 3,5-3,9 Gcal/tFe in other direct reduction processes. Future work has to take into account the recovery of other wastes (EAF, LD, and mill scale etc) and poor iron ore. Moreover topics concerning for example influence of raw material average diameter on reduction degree, slag basicity after melting, removal of sulphur and phosphorous, avoidance of ash sticking on the refractory walls and dispersion agent (balls) should be analyzed. In order to enhance the level of research and to propose a new alternative efficient direct reduction technique is necessary also to improve the experimental device: charge-discharge technique, gas energy recovery, pollution control and continuity of the process.

Efficient recycling metallurgical and chemical industries wastes and waste management are important topics in the European Union.

Taking into account the quantities of these kinds of wastes Romania should solve the problem by developing projects in the alternative iron making and steel making area. According to preliminary researches carried out this is very possible without big financial efforts.

The advantages of direct reduction processes are: using of waste from chemical and metallurgical industry and unmaking coal, small quantities of electrical energy, easy preparation of raw materials, small plants very flexible for different raw materials, high level of environment protection, minimization of land filling of wastes/by-products, saving natural raw materials utilizations.

Implementing at large scale this kind of technologies offers the steel industry flexibility and a chance to decrease the costs of products in the frame of environmental friendly processes.

REFERENCES

- [1.] N Constantin: „Procedee neconvenționale de obtinere a materialelor metalice feroase.” tipărit Editura PRINTECH București, 2002
- [2.] N. Constantin, M. Nicolae, V. Geantă and I. Butnariu: „Procese și tehnologii alternative în siderurgie.” Ed. Fundația Metalurgia Română, 1997, ISBN 973-98314-0-0
- [3.] N. Constantin, V. Geantă, M. Nicolae: „Procedee neconvenționale de reducere a minereurilor feroase.” tipărit Universitatea "Politehnica" București, 1995
- [4.] N. Constantin, V. Geantă, B. Niculae, R. Ștefănoiu: „Modelarea matematică și conducerea informatizată a proceselor din metalurgia extractivă feroasă.” - tipărit Universitatea "Politehnica" București, 1997



¹: Alina MIHAIU, ²: Claudiu CONSTANTIN, ³: Cristian DOBRESCU

SOME COMPUTATIONS REGARDING THE DIRECT REDUCTION OF THE IRON ORES

^{1, 2, 3}: UNIVERSITY "POLITEHNICA" OF BUCHAREST, ROMANIA

ABSTRACT:

In this paper, we present a technological solution to reduce the iron ores and specifically the zunder, broken in small pieces, in fluidized bed, where the energetically source and simultaneously, reducing thermal agent, is coal, eventually associated to another gaseous or liquid fuel, without use of technical oxygen; the forming of CO and heat are obtained by the oxidation of the coal and hydrogen from the fuel, by making use of the oxygen contained in the initial raw material.

KEYWORDS:

iron ores, zunder, small pieces, fluidised bed

1. INTRODUCTION

The nowadays technologies of cast obtaining starting from coal ores, subdued, before being introduced into the blast furnace, to some agglomeration and coking operations, use the furnace as the main elaboration aggregate. It is well known that in Romania the furnace departments are endowed with medium and big blast furnaces, having 1000...3500 m³.

Because of the lower demand of cast into the internal consumption, a series of furnaces has been closed, and those which still run are forced to work very slowly, registering small productivities, big materials and energy consumptions, resulting implicitly big production costs for the elaborated cast.

Because of the binding coal deficit and of the iron ores of a good metallurgical quality, the first fusion cast quantities necessary to the steel elaboration or to the cast pieces moulding are more and more difficult to ensure. Corroborated to the scrap iron deficit, this problem creates considerable difficulties to the steel producers. Thus, it imposes an alternative technology which allows the obtaining of the unconventional energo - technological resources from ferrous and coals wastes with small granulation which will be used as scrap iron substitute into the steel elaboration aggregates.

All over the world, the industrial implemented technologies allow the iron sponge obtaining from ball ore, reduced at Fe by a decelerator, usually gaseous (Hyl, Midrex, Wiberg, Purofer methods), from small ores reduced in layer fluidized by a gaseous decelerator (H₂, CO, H₂+CO) (Novalfer, Nu-Yron, H-Yron) or from balls ores and balls solid decelerator into circular furnaces (SLRN, Krupp - Renn).

The cast is directly obtained from coal and ores as a result of some alternative technologies (Corex, Kawasaki and Midrex) which suppose investments costs heavily supported by the economic agents from Romania, even in the conditions of some eventual associations.

Those being the conditions, the unconventional technology proposed by this research works allows the iron sponge obtaining with a high metallization degree, and afterwards, by its melting, the cast obtaining directly from small iron ores and from small coal into a main aggregate as a rotary tube furnace type where the dispensor mass, the thermic agent and the heat changer are represented by metallic or ceramic granules heated beforehand at about 1300°C into an aggregate which uses as an energetically fluid a re-circulated gas from its own process of fabrication.

Through the processes efficient leading they can obtain unconventional energo-technological resources having a high metallization degree used as scrap iron substitute by the steel producers.

It is necessary to mention that in Romania this technology is 100% original. So far there are no research units having such kind of preoccupations.

The proposed technology realizes with minimum technological and economical costs a very good scrap iron substitute, starting with the capitalization of some fine ferrous sub-products found as stored wastes.

2. EXPERIMENTS

2.1. Some theoretical considerations

One considers a raw material, formed by: 76 % FeO, 17 % Fe₃O₄, 2 % Fe₂O₃ and 5 % SiO₂. The content of Fe in the raw material will be: $76 \frac{56}{56+16} + 17 \frac{3 \cdot 56}{3 \cdot 56 + 4 \cdot 16} + 2 \frac{2 \cdot 56}{2 \cdot 56 + 3 \cdot 16} = 59.1 + 12.3 + 1.4 = 72.8\%$.

The oxygen extracted by a complete reduction is: $76 \frac{16}{72} + 17 \frac{64}{232} + 2 \frac{48}{160} = 16.9 + 4.7 + 0.6 = 22.2\%$ (SiO₂ is not reduced).

The consumption of raw material is: $\frac{1}{0.728} = 1.374$ t / t Fe, from which one extract 1.374 x 0.222 = 0.305 t O₂/t Fe, theoretically refound, at 1050°C, in 73.1 % CO and 26.9% CO₂, and practically in 75 % CO and 25 % CO₂. 1Nm³ from this mixture contains 0.75 x 0.5 + 0.25 x 1.0 = 0.625 Nm³ O₂/Nm³ = $0.625 \frac{32}{22.414} = 0.8923$ kg O₂/Nm³ and $\frac{12}{22.414} = 0.5354$ kgC/Nm³.

From reduction, it will result 305/0.8923 = 342 Nm³/tFe and one consume 342 x 0.5354 = 183.1 kgC/t Fe.

The heat ceded by the carbon refound in the gaseous mixture is: 0.25 x 8.140 + 0.75 x 2.452 = 3.874 kcal / kg C = 0.7093 Gcal/t Fe.

The consumption of heat for the ore reduction is 0.76 x 1150.5 + 0.17 x 1583 + 0.02 x 1758 = 1178.7 kcal/kg Fe = 1.179 Gcal/t Fe. The carbon necessary to deoxidations has an energetic share of 183.1 x 8140 x 10⁻⁶ = 1.490 Gcal/t Fe.

The surplus is equal to 1.490 – 1.179 = 0.311 Gcal/tFe and it is consumed in the heat dissipations, in the drying of raw material (with 5 % water) and the coal drying (with 15 % water) and in the evacuation of the substances emerged with some sensible heat.

The burning of the reducing gaseous combustible fuel is made with 1.1 x 0.75 x 0.5 / 0.21 = 1.964 Nm³ air/Nm³ mixture (with air excess of 10 %) and yields 1.000 (CO₂) + 0.79 x 1.964 (N₂) + 1.964 x 0.21 – 0.75 x 0.5 (O₂) = 2.589 Nm³ burning gas for any Nm³ gaseous mixture, with 38.6 % CO₂, 59.9 % N₂ and 1.5 % O₂.

In the focus-tubes, the gaseous mixture cedes 8.140 - 3.874 = 4.266 kcal/kg C = 4.266 x 0.5354 kcal / Nm³_n mixt. = 2.283 kcal / Nm³ gas.mixt. (= 0.75 x 68.220 / 22.414, as control).

For the gaseous mixture (75% CO și 25 % CO₂), at 1050°C, C_p = 0.75 x 0.339 + 0.25 x 0.530 = 0.387 kcal / Nm³K, and at 950°C, C_p = 0.75 x 0.336 + 0.25 x 0.522 = 0.382.

The gas of complete burning, with 10% air excess, have C_p at 1200°C, which represents the temperature at the emergence from the focus-tubes, of 0.386 x 0.541 + 0.599 x 0.339 + 0.015 x 0.358 = 0.417 kcal/Nm³K, and at 150°C (at the evacuation from exchangers), of 0.386 x 0.416 + 0.500 x 0.311 + 0.015 x 0.317 = 0.352 kcal/ Nm³K.

In order to avoid the gluing of the iron particles and faillit between them, at 1050°C= the temperature in the reactor in fluidised bed, one recirculates in reactor a mass of dust (silica, alumina, silicium carbide etc.), with a relatively high refractoritaty and such that, associated with the sterile from the ore and with the coal ash, totalize about 50% massic și 120% volumic in comparison with the iron.

2.2. A short description of the proposed solution

The raw material and the coal, both at a granulation under 1...2 mm, are introduced in a reactor with fluidised bed, at a flow of gas formed at 600...1050°C, recirculated in the proportion required by bed; the energy necessary for the continuity of the endothermic processes of the deoxidation is assured by the focus-tubes, where the gaseous fuel, coming from the space of reduction, is burnt with air preheated at 1000°C by the combustion gas collected from the focus-tubes.

The temperature in reactor is about 1050°C, in the case of use of coal only and sensibly diminished if this is associated with the gaseous fuel; the reactor operates at a pressure up to 10 bars (limited by the pressure of the gaseous fuel). If the raw material is particularly FeO, as in the case of zunder, considered in subchapter 2. 1, then one gets an excedent of gas, greater if less coal is used.

Due to the reduction of the iron ore in solid phase, the iron carburation is less than 0.8 %, much better than in the case of the liquid pig iron. In the case of iron ores having much sterile, the iron and sterile evacuation are made under the Curie point, thus allowing the sterile elimination by magnetic separation. As advantages of the technology, one mention: the possibility of iron ore reduction with inferior coal and waste coke, the consumption of fuel being smaller in comparison with the actual technologies, including the COREX procedure, diminishing the production of the „ gas export”.

Another important point is that no technical oxygen is used, being enough the oxygen from raw material. Due to the intensification of the heat and mass transfer, the plants applying the technology will be compact and cheap.

In what follows, we present as an example, the main components of a plant which yields 3 t/h iron, from the raw material initially considered, in subchapter 2. 1.

The iron ore from a silo enters the plant, being mixed up with coal; the mixture enters a preheater, then a reactor, organized as fluidised bed, where it takes place the reduction of the oxides from ore, with C, CO, H₂; in order to proceed the endothermic reactions, the heat consumption is recovered by burning gaseous fuel in the focus-tubes.

The reactor has a cylindrical construction, with a vertical axle, having the interior diameter about 3000 mm and the interior height of the fluidised bed of 1700 mm and that total of 3000 m, with walls in refractory concrete, plating with corindonic plates for max. 1300°C. The focus-tubes will have the diameter 120 mm, the length 2400 mm and the wall thickness about 10 mm, being carried-out of vibrated casting alumina.

The ore heater is vertical and has as a shape of truncated cone, with 9 fluidised beds in series, with a total height of about 3000 mm and the inferior diameter 1100 mm and that superior 2500 mm; the maximum interior pressure is 0.8 manometric bars at the inferior part, the construction of the heater being carried-out of usual materials for 900°C. The deoxidated ore is evacuated by a hook-up and cooled.

The ore cooler is similar to the ore heater, having the pressure at the inferior part of 1.5 manometric bars and at the superior one of 0.8 manometric bars, for max. 1100°C.

The circulation of nitrogen (in fact air with the oxygen retained by a small share of carbon), with the flow of 4200 Nm³ /h, is assured by a compressor with a flow 1.7 m³/s which compress it at 1.6 bars, by consuming max. 100 kW.

The plant also includes a compressor which compresses 0.8 m³/s gaseous combustible mixture at max. 80°C, from 3 to 3, 5 manometric bars and is mounted in a metallic precinct, where a pressure of 3 bars is setting up; the consumed power is only 5 kW. There also is an air ventilator for 800 m³ / h and 150 mm water spout (CA), trained by a motor of 1 kW; one also needs an exhaustor for the burning gas, for 1300 m³ /h at max. 200°C and 200 mm water spout, trained by a motor having an installed power of 3 kW (that consumed being of 1.2 kW).

The plant also includes two metallic silos, each 50 m², one for ore and another for coal, raised at about 14 m height.

The specific consumption of heat is about 1.55 Gcal / t Fe and it is recovered exclusively by the carbon from coal; one can also use of small coke, coke dust or coke of oil with an acceptable content of sulphur. One can also use any liquid or gaseous fuel , replacing partially or even totally the coal , remarking that , on a hand , the temperature of reduction decreases and , on the other hand , the production of excedentary gaseous combustible increases.

In order to avoid any glueings of the particles of iron ore in evolution, we have above underlined some sure measures and cautions.

The plant is highly ecological: indeed, the component CO circulates by airtight pipes only, the gas evacuated in atmosphere result after a complete combustion, without CO, NO_x or dioxins (by an air excess 20 % and by burning at favourable temperatures).

The plant can be carried-out with materials of current use.

3. RESULTS

In order to simplify the thermic and mass balances, one considers that the dried raw material and the coal (only dried C) are introduced in the plant together with 500 kg sterile per any tone of iron. One admits that the drying of the iron ore and coal takes place in the reactor (water is benefic, by the dissociation and reassociation in reactor, with the catalytic effects of the transient H₂, which proceed from some water molecules and is reformed in others; in fact, H₂ and H₂O spreads through the ore easier than CO and CO₂). The temperature of reduction descends towards 800°C, with a metallization degree over 99 % and, by replacing the coal with liquid and/ or gaseous fuel, which massively generates H₂ in reactor, the temperature could descend to 570°C. But one

encounters the disadvantage of producing some excedentary gaseous combustibile, which cannot be available in the plant and must be exported.

In what follows, we present the thermic balance and the mass balance on the components of a plant which produces 1 t iron, under the above mentioned hypothesis:

Component	kg	Nm ³	°C	kcal
1. COOLER OF REDUCED ORE				
Inputs				
- Reduced ore=iron +sterile	1069	-	1050	199796
- Ash + sterile	431	-	1050	126714
- Nitrogen	-	965	100	30012
TOTAL				356522
Outputs				
- Reduced ore	1069	-	200	29290
- Ash + sterile	431	-	200	17240
- Nitrogen	-	965	950	304361
- Dissipations				5631
TOTAL				356522
2. PREHEATER OF THE COMBURENT AIR				
Inputs				
- Burning gases	-	569	1200	284728
- Air	-	672	0	0
TOTAL				284728
Outputs				
- Air	-	672	1100	251328
- Burning gases	-	569	150	30043
- Dissipations				3357
TOTAL				284728
3. PREHEATER OF NITROGEN WITH BURNING GASES				
Inputs				
- Burning gases	-	316	1200	158126
- Nitrogen	-	413	100	12844
TOTAL				170970
Outputs				
- Burning gases	-	316	200	22752
- Nitrogen	-	413	1050	145273
- Dissipations				2945
TOTAL				170970
4. PREHEATER OF ORE AND COAL				
Inputs				
- Nitrogen from 1	-	965	950	304361
- Nitrogen from 3	-	413	1050	145273
- Ore	1374	-	0	0
- Carbon	183.1	-	0	0
- Ash	150	-	0	
- Recirculated sterile	281	-	200	11240
TOTAL				460874
Outputs				
- Nitrogen	-	1378	100	42856
- Iron ore	1374	-	880	263588
- Coal	183.1	-	880	53172
- Ash + recirc.sterile	431	-	880	92924
- Dissipations				8334
TOTAL				460874
5. THE PLANT OF REDUCTION (REACTOR)				
Inputs				
- Iron ore	1374	-	880	263588
- Coal – sensible heat	183.1	-	880	53172
- Coal- potential energy	(183.1)	-	880	1490434
- Ash + recirc.sterile	431	-	880	92924
- Gas. mixt. –sensible heat	-	283	1050	113511
- Gas. mixt. – potent.heat	-	(283)		646089
- Preheated air	-	672	1100	251328
TOTAL				2911046

	Outputs			
- Heat for reduction	-	-	1050	1179000
- Reduced ore	1069	-		
- Ash + sterile	431	-	1050	199796
- Gas. mixt. – sensible heat	heat -	342	1050	126714
- Gas. mixt. potent heat	-	342		137176
- Supplem. cooling of the recirc. gas. mixture	-	700		780786
- Burning gases	-	885	1200	23450
- Dissipations				21270
TOTAL				2911046

4. DISCUSSION

The nitrogen from the system of ore heating - cooling is formed in some minutes after the air introduction, which loses the oxygen retained by a part of the carbon from the heater of ore and coal.

The carbon imposed by deoxidations brings more heat than the plant consumes and this implies the production of that excedentary gaseous combustible (59 % Nm³ / t Fe = 0.16 Gcal / t Fe, hence over 10 % of the coal contribution), however about 10 times less than the COREX technology. One also mentions that the final iron will contain only 0.5 % = 5 kg C / t Fe, due to the ore reduction in solid phase (in liquid phase this content would be at least 4 %).

From the above balances, it follows that the specific consumption of carbon is 183.1 kg / t Fe, imposed by the deoxidations, but including the production of the excedentary gaseous combustible; adding the carburization of the final iron, all lead to a specific consumption of 1.52 Gcal / t Fe = 6.36 GJ / t Fe. The above mentioned excedent is less than 60 Nm³ / t Fe.

The total energy entered the plant is:

$$E = 183.1 \times 8140 \text{ kcal} = 1490434 \text{ kcal} \approx 6240 \text{ MJ} .$$

The dissipations of all 5 components included in the above balances cumulate: $\delta = 5631 + 3357 + 2945 + 8334 + 21270 = 41537 \text{ kcal} \approx 174 \text{ MJ}$ (representing about 3% of E).

Other losses are, according the above balances the following: the supplementary cooling (from the component 5 – the reactor): 23450 kcal; the burning gas (from 2): 30043 kcal; the burning gas (from 3): 22752 kcal; the ash+ sterile (from 1): 17240 kcal; the reduced ore (= iron + sterile from 1): 29290 kcal and finally, the excedent of sensible heat (from 5): 137176 – 113511 = 23665 kcal. All these totalize:

$$\lambda = 146440 \text{ kcal} \approx 613 \text{ MJ} \text{ (representing about 10 \% of E).}$$

The energetic efficiency of the plant is:

$$1 - (\delta + \lambda) / E = 1 - (174 + 613) / 6240 \approx 0.874 = 87.4 \text{ \%} .$$

This is superior to many similar technologies. Moreover, the above presented technology could be improved in many points: the useful cooling of the excedentary gaseous combustible (for instance, to heat the raw material and the coal), the sell of this excedent, the use of the sensible heat to produce hot water.

5. CONCLUSIONS

The implementation at the industrial level of the unconventional technology proposed by the present research paper, offers new and profitable adaptation possibilities without high costs of the Romanian metallurgy to the international economic situation imperatives.

From the multiple offered advantages it mentions the following:

- ❖ the reduction of the un-oxidization processes lasting from at least 20 hours to 0,5 hours;
- ❖ the direct utilization of the ore powder, eliminating the granulation;
- ❖ the capitalization of the pyretic ashes and the dusty ores;
- ❖ the capitalization of the waste chalk obtaining an acceptable quality lime and a carbon dioxide of high purity having multiple utilizations;
- ❖ the cheapness under 70% of the obtained iron, provided in granules;
- ❖ the utilization of the non-binding coal instead of the coke;
- ❖ there is no necessary another type of energy;
- ❖ the charge preparation is not so expensive as in blast-furnaces case;
- ❖ small units of production permit the easy adaptation at diverse requests.

REFERENCES:

- [1.] COREX, a revolution in iron making, Voest Alpine Industrie, 2001.
- [2.] C.STĂNĂȘILĂ, N. CONSTANTIN, O. STĂNĂȘILĂ – O posibilitate de reducere directă a minereurilor de fier, Conf. Naț. de Metalurgie , 2006.
- [3.] C. STĂNĂȘILĂ, N. CONSTANTIN, O. STĂNĂȘILĂ – New technology on coal drying, Metal. Intern, vol.11, nr. 1, 34-38, 2006.





¹Vasile PUȚAN, ²Adriana PUȚAN

DESULPHURATION OF STEEL WITH SYNTHETIC SLAG WITH ADDITION OF TITANIUM OXIDE

^{1,2} UNIVERSITY "POLITEHNICA" TIMIȘOARA, FACULTY OF ENGINEERING OF HUNEDOARA, ROMANIA

ABSTRACT:

In the practice of deoxidation with synthetic slag, we usually use the slag from the binary systems: CaO-Al₂O₃, CaO-TiO₂ and CaO-CaF₂ or from the ternary systems: CaO-SiO₂-Al₂O₃ and CaO-CaF₂-Al₂O₃. According to the literature, the best results were obtained with synthetic slag from the binary system CaO-Al₂O₃ (50-52% CaO and 38-42% Al₂O₃).

The paper presents the results of laboratory experiments on steel desulphurisation with slag from the system CaO-SiO₂-TiO₂.

To determine the influence, on the desulphurisation process, of the titanium oxide added in calcium aluminate slag, we experimented, in the laboratory phase, the steel treatment with a mechanical mixture consisting of lime, aluminous slag and slag obtained from the titanium making process through the aluminothermic technology.

During the research, we aimed to establish correlation equations between the sulphur distribution coefficient and the slag components (CaO, Al₂O₃, TiO₂, FeO, MgO and MnO). The data obtained in the experiments were processed in Excel and MATLAB programs, resulting simple or multiple correlation equations, which allowed the elucidation of some physical-chemical phenomena specific to the desulphurisation processes.

KEYWORDS:

steel, deoxidation, desulphuration, synthetic slag

1. GENERAL CONSIDERATIONS

In case of electric steel works, the sulphur reaches in the steel bay from the metallic charge and from adding's. Because the sulphur content of these sources cannot be lowered below certain limits, the elaboration process must be so developed to perform an advanced desulphuration, both in the oven and in the casting ladle. During the last years, it is more and more manifested the tendency to perform the desulphuration outside the elaboration aggregates (desulphuration with synthetic cinders under vacuum, with reactive powders injection), obtaining this way important energy saving, deoxidizers and desulphurants, as well as an productivity increase [1,2].

The steel refining with liquid slag or various powder mixtures of synthetic slag is based on the intensification of the unwanted impurities (sulphur, non-metallic suspensions & oxygen) passage from the liquid steel in the slag, mainly by diffusion, or partly through the entrainment of some suspensions by settling the synthetic slag particles found in the treated steel bath. The synthetic slag can be also obtained by adding mechanical mixture directly in the casting ladle; in this case, for compensating the cooling of the steel in the casting ladle due to the addition of materials (melting and superheating), the steel temperature should be at least 20-40°C higher than the normal one. In the practice of deoxidation with synthetic slag, we usually use slag that correspond to the binary systems CaO-Al₂O₃, CaO-TiO₂ and CaO-CaF₂, or to the ternary systems CaO-SiO₂-Al₂O₃ and CaO-CaF₂-Al₂O₃. According to the literature, the best results were obtained with synthetic slag that corresponds to the binary system CaO-Al₂O₃, containing 50-52% CaO and 38-42% Al₂O₃.

The viscosity of the synthetic slag has significant influence on the development of physical and chemical processes during the treatment of the liquid steel, interfering with significant weight on the emulsifying capacity of slag. The increase of the slag viscosity from 0.15 to 0.45 Ns/m² (from

1.5 to 4.5 Poise) determines the decrease with approx. 30% of the steel-slag interaction surface. Such increasing of the calcium aluminate slag viscosity can be seen when its temperature is decreasing (for example, from 1600°C to 1470°C). Therefore, it is very important to ensure, during processing the steel with liquid slag, the optimum thermal regime specific to the chosen slag type and to realise its convenient fluidity (viscosity).

The viscosity of the synthetic slag is also influenced by other components; it increases significantly with the increasing of the SiO₂ content, while MgO contents up to 8% are favourable. At temperatures higher than 1500°C, the viscosity is slightly decreasing when adding TiO₂ in the calcium aluminate slag.

2. LABORATORY EXPERIMENTS

To determine the influence, on the desulphurisation process, of the addition of titanium oxide in the calcium aluminate slag, we performed laboratory experiments, i.e. we treated the slag with liquid synthetic slag obtained by melting the mixture consisting of limestone, aluminate slag and slag obtained from the titanium making process through the aluminothermic technology.

The steel melting was carried out in an induction furnace of 10 kg capacity and the slag melting was carried out in a crucible furnace, both existent in the "METALLIC MELTS" laboratory of the Engineering Faculty of Hunedoara.

The charge to be melted consisted of steel samples (samples of steel for tubes, taken from the casting ladle before the LF treatment, i.e. before introducing the steel in the LF).

To form the liquid synthetic slag, we melted in the crucible furnace a mechanical mixture consisting of limestone, calcium aluminate slag (from melting the aluminium scrap) and slag obtained from the titanium making process through the aluminothermic technology. The steel quantity obtained was 10 kg/heat, and the addition of liquid slag was 3% (300 g/heat). The synthetic slag was added directly in the casting ladle; so, the slag reached the ladle before the steel, ensuring a good mix between the two melts. To determine the sulphur distribution coefficient, we took steel and slag samples before and after the treatment, to find the sulphur content and the chemical composition. We also measured the steel and slag temperature before and after the treatment.

3. RESULTS OBTAINED FROM PROCESSING THE EXPERIMENTAL DATA

By processing the data obtained in the laboratory phase, we obtained equations of correlation between the chemical composition of the synthetic slag and the sulphur distribution coefficient (L.S). The data were processed in Excel and MATLAB programs, the results being presented hereunder, in graphical and analytical forms.

In Fig. 1, we can see that a TiO₂ content increase up to 5-6% leads to the increasing of the L.S., fact explicable, from a technological point of view, through to the positive influence of the titanium oxide on the slag fluidity, especially at temperatures above 1500°C. Therefore, we recommend contents of 3-6% TiO₂ in the refining slag.

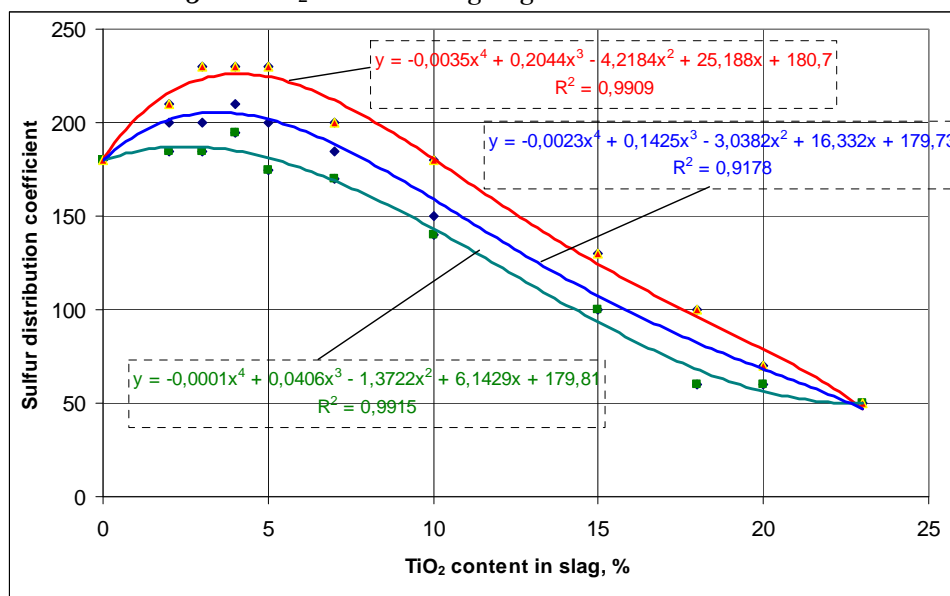


Fig.1 The variation of the sulphur distribution coefficient versus the TiO₂ content in slag

The graphical representation presented in Fig. 1 shows that the higher values for the L.S. (230-250) were obtained for a CaO content of 52 -54%. According to the data presented in the literature [2] the minimum viscosity of the slag that corresponds to the CaO – Al₂O₃ system is obtained for contents of approx. 56% CaO, which confirms the results obtained for the slag used in our experiments. The CaO contents higher than 55%, determine the decreasing of the L.S. values, because the slag viscosity is increasing. Having in view that, in industrial conditions, there are frequent deviations from the above mentioned range of chemical composition, we recommend contents of 52-56% CaO.

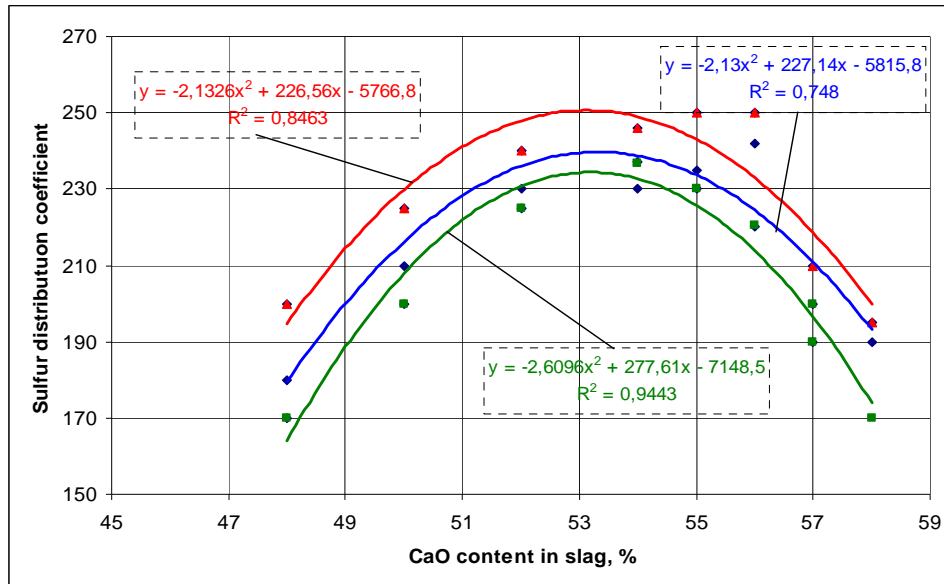


Fig.2 The variation of the sulphur distribution coefficient versus the CaO content in slag

Analysing the graphical representation presented in Fig.3, we can see a variation in the L.S. depending on the Al₂O₃ content, similar to the variation depending on the CaO content in slag. The maximum L.S. value was obtained at 34–37% Al₂O₃. The increasing of the aluminium oxide content up to values that vary between the above mentioned limits is due to the decreasing of the slag viscosity and, in consequence, the intensification of the sulphur diffusion in the slag bath. The increasing of the Al₂O₃ content beyond the above mentioned limits determines the decreasing of the L.S. values, as a consequence of the slag viscosity increasing. We recommend contents of 33-37% Al₂O₃ in slag.

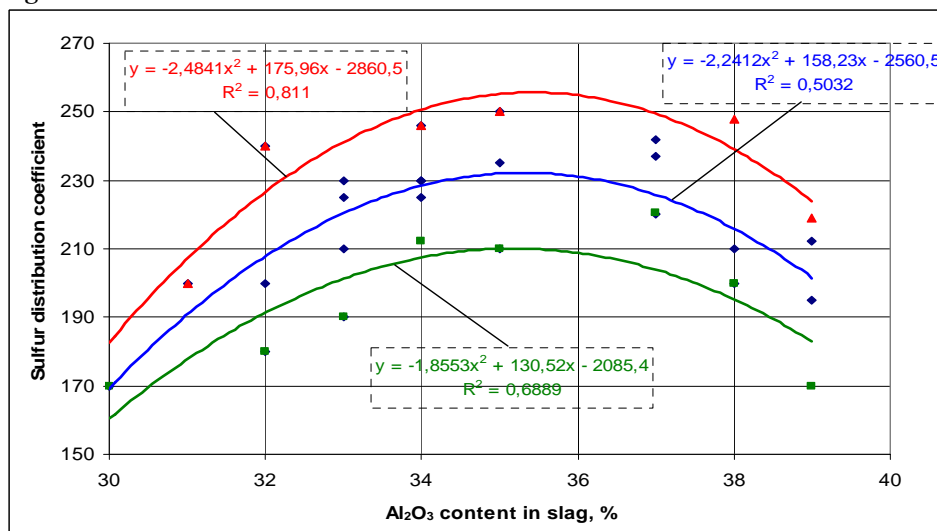
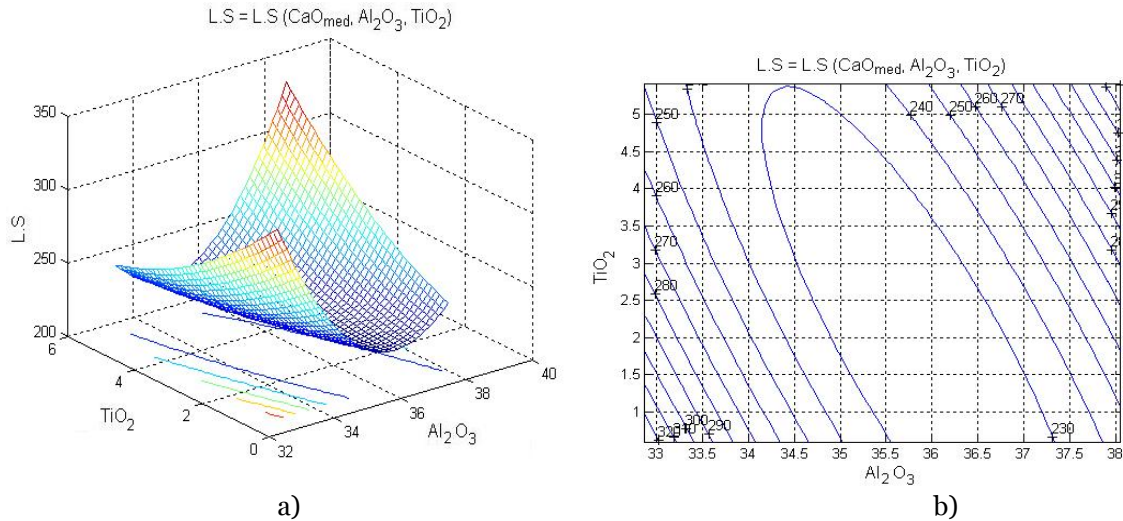
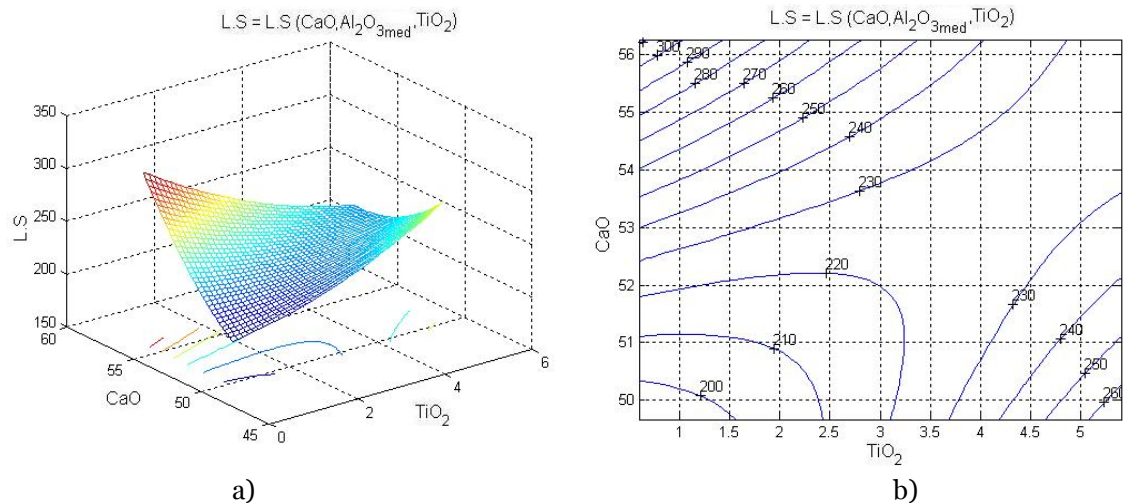


Fig.3 The variation of the sulphur distribution coefficient versus the Al₂O₃ content in slag

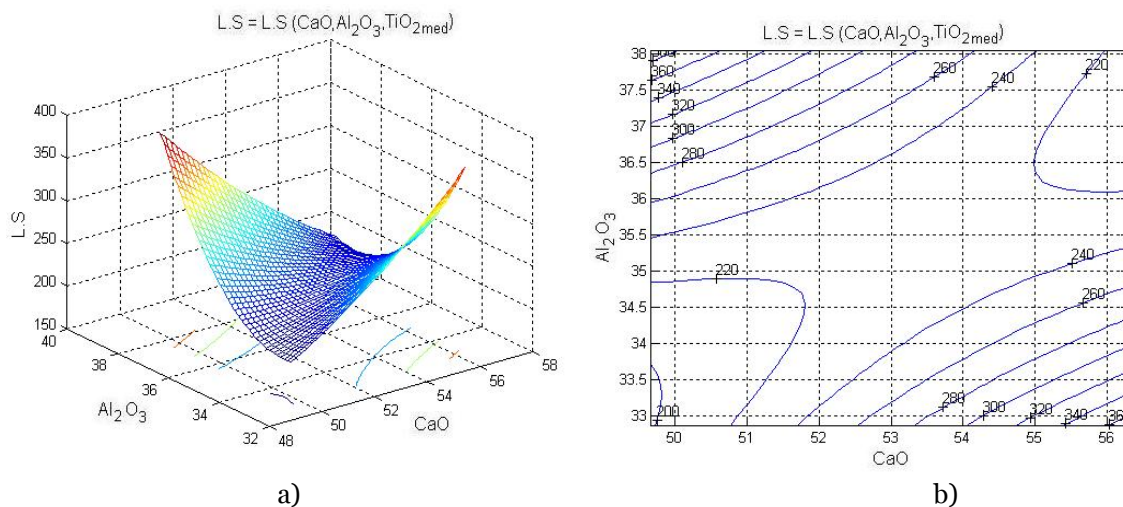
By processing the data in the MATLAB program, we obtained multiple correlation equations and, by graphically represented them, we obtained the correlation surfaces. To establish the optimum chemical composition range, we analysed the regression surfaces for finding the value of the L.S., desirable above the average value obtained from the data afferent to the analysed heats.



a) b)
 Fig.4 The variation of the sulphur distribution coefficient (L.S) versus the TiO₂ and Al₂O₃ content in slag: a) surface; b) contour lines



a) b)
 Fig.5 The variation of the sulphur distribution coefficient (L.S) versus the TiO₂ and CaO content in slag: a) surface; b) contour lines



a) b)
 Fig.6 The variation of the sulphur distribution coefficient (L.S) versus the CaO and Al₂O₃ content in slag: a) surface; b) contour lines

4. CONCLUSIONS

Based on the experiments, on the results obtained from data processing and on the technical analysis of these data, we concluded the followings:

- From a technological point of view, the slag types used in our experiments met our needs, mainly due to their adequate fluidity;
- The chemical composition of the slag has a significant influence on the L.S., either indirectly, due to the viscosity, or directly, due to the affinity of the oxide cautions to the sulphur anions;
- We consider that it is possible to obtain very good results in the desulphurisation process by using synthetic slag having the following chemical composition: $\text{CaO} = 48 - 55\%$; $\text{Al}_2\text{O}_3 = 40 - 45\%$; $\text{SiO}_2 = \text{maximum } 3.0\%$; $\text{MgO} = \text{maximum } 3\%$ and $\text{FeO} = \text{maximum } 1\%$
- Based on the results obtained during the laboratory phase, we believe that good results can be achieved under industrial conditions, too. So, we propose to perform such experiments in a future stage.

REFERENCES:

- [1.] VACU, S., ș.a., Elaborarea oțelurilor aliate vol. I, Ed. Tehnică, București, 1980.
- [2.] VACU, S., ș.a., Elaborarea oțelurilor aliate vol. II, Ed. Tehnică, București, 1980.
- [3.] TRIPȘA, I. PUMNEA, C., Dezoxidarea oțelurilor, Ed. Tehnică, București, 1981.
- [4.] HEPUȚ, T., ARDELEAN, E., KISS, I., Some influence of the viscosity of synthetic slags used in continuous steel casting. Revista de Metalurgia 41(3), Madrid, 2005.
- [5.] HEPUȚ, T., ARDELEAN, E., SOCALICI, A., MAKSAY, ST. GĂVĂNESCU, A., Steel desulphurization with synthetic slag, Revista de Metalurgia 43(3), Madrid, 2007.







¹Mihaela FLORI, ²Bernard GRUZZA, ²Luc BIDEUX, ²Guillaume MONIER,
²Christine ROBERT-GOUMET, ³Jean-Pierre CHERRE, ¹Daniela MILOȘTEAN

INFLUENCE OF MICROSTRUCTURE DEFECTS ON THE PROPERTIES OF 42CrMo4 NITRIDED STEEL

¹"POLITEHNICA" UNIVERSITY OF TIMISOARA, FACULTY OF ENGINEERING HUNEDOARA, ROMANIA

²LASMEA, UMR CNRS 6602, BLAISE PASCAL UNIVERSITY, CLERMONT-FERRAND, FRANCE

³LABORATOIRE DE GENIE CHIMIQUE ET BIOCHIMIQUE, BLAISE PASCAL UNIVERSITY, FRANCE

ABSTRACT:

Metallographic and chemical analyses were done in order to determine the influence of microstructure defects on the hardness of 42CrMo4 steel plasma nitrided in industrial conditions. By means of light microscopy carried out after Picral reagent etching it was revealed the steel sample microstructure presenting defects as segregation bands, probably formed during the elaboration stage of the steel. The Electron Probe MicroAnalysis (EPMA) technique was used for nitrogen and iron concentrations measurements, while HV_{0.3} hardness tests were done for the steel properties determination. Tests were made as vertical profiles and as individual measurements in the nitrided layer and in zones presenting defects, respectively.

KEYWORDS: Plasma nitriding; 42CrMo4 steel; Segregation bands; Picral etching; Light microscopy; Electron Probe MicroAnalysis (EPMA); Hardness measurements

1. INTRODUCTION

Although the behavior of quenched and tempered structural steels treated through plasma nitriding is much discussed in the literature, one may notice that the nitrided layer analysis concerns mainly the resistance to fatigue [1-3], to corrosion [4] or to wear [5]. Also, the microstructural analysis of the nitrided layer is turned on its thickness and nature of the constituent phases obtained by varying the treatment conditions (proportion and nature of the nitriding gases, treatment duration and temperature) [6]. However, there are not well delineated the studies on the defects existing in bulk material (i.e. segregation bands resulted in the solidification stage of the steel ingot) and their influence on the structure and mechanical properties of the nitrided structural steels.

It is known that all elements accompanying iron in low alloyed steels (chromium, manganese, sulfur, phosphorus) participates more or less to dendritic segregation during solidification, this phenomenon being more intense as the steel is rich in carbon. These elements influence the steel structure by forming longitudinal heterogeneities (named "segregation bands" or "microstructural banding"). In references [7, 8] are presented detailed reviews concerning the origins of the chemical segregation, its effects on the solidification structure and its influence on the properties of carbon and alloy steels. Also, reference [9] contains a literature overview on the microsegregation models which describe the alloys solidification phenomenon. The characteristic features of microstructural banding may be observed better by light microscopy after etching with Picral metallographic reagent [10, 11]. After etching, the steel structure appears as adjacent light and dark bands which are oriented in the rolling or forging direction. The non-uniform distribution of some of the alloying elements in the steel structure depends mostly on the austenite grain size and on the cooling rate during solidification [12].

The aim of this article is to study the influence of the banded structure on the mechanical properties of 42CrMo4 steel, plasma nitrided in industrial conditions. In order to evaluate the banded structure we have etched the steel sample with 4% Picral reagent and observed it by light microscopy. In completion with hardness measurements, EPMA chemical analysis and imaging are used.

2. EXPERIMENTAL AND ANALYSIS DETAILS

2.1. SAMPLE PREPARATION

In this study we have used a cylindrical piece (~25 mm diameter and ~10 mm thickness) of 42CrMo4 steel grade whose chemical composition (in wt%) was identified by spark spectroscopy as: 0.43%C, 0.33%Si, 0.78%Mn, 1.02%Cr, 0.17%Mo, 0.1%Cu, 0.11%Ni, 0.02%P and 0.02%S.

In order to obtain the martensitic structure needed for nitriding, the piece was subjected to a heat treatment consisting in: austenitization at 850 °C during 30 min. then water quenching and tempering at 650 °C for 30 min. with further slow cooling in air. Next, the piece was degreased with trichloretilene and introduced in a Nitron-10 industrial furnace for a conventional plasma nitriding treatment. The working parameters were: pressure of 10^{-2} mbar, applied voltage of 750 V, temperature of 530 °C and maintenance duration of 10 h. The nitriding atmosphere was obtained by ammonia thermal dissociation in 75% H_2 and 25% N_2 , this mixture being introduced in the furnace with a debit of about 20 l/h. At the end of the treatment, the piece was furnace cooled.

Further, the nitrided piece was cut along a diameter into two samples, so all the analyses could be made in the cross-section. After mounting in resin, the two samples were subjected to a metallographic preparation consisted in grinding with SiC papers (having different granulations from 120 to 2500), followed by polishing with diamond (3 μ m size) and finally by fine polishing with an alumina suspension (0.05 μ m size).

One sample (sample A) was used for microstructure observations and hardness measurements, while the other one (sample B) was used for the EPMA analysis. Sample A was etched with the Picral reagent, prepared with 4% picric acid in etilic alcohol and a few drops of benzalkonium chloride. Immersion was made at room temperature for 30 s, followed by ethanol rinsing and drying with hot air. As observed by light microscopy, etching with this metallographic reagent revealed very well the microstructure by differential color etching: the carbides and the metallurgical segregations were darkened, while the iron nitrides remained white.

2.2. DETAILS OF THE ANALYSIS TECHNIQUES

Microstructure observations were done with an Olympus BX60M light microscope.

The hardness was determined with a Mitutoyo Vickers instrument using a ~3 N force ($HV_{0.3}$). Results were obtained as a vertical profile with depth and as individual point measurements in the zones where it was observed the presence of defects (segregation bands).

The chemical analysis was made with a Cameca SX100 electron probe microanalyser (EPMA) employing five wavelength-dispersive spectrometers. Before being analyzed the sample was plated with a graphite layer under vacuum. The experiments were done with the following parameters of the incident electron beam: intensity of 15 nA and accelerating voltage of 10 kV. As standard samples for Fe and N concentration determinations it was used pure iron and BN, respectively.

Also, the EPMA technique permits, besides the chemical analysis, the imaging of the sample surface, so one may better interpret the experimental results. In an EPMA image the brightness (or contrast) of an area is proportional to the backscattered electrons intensity (of the incident beam) depending on the atomic number of the elements present in the sample. So, atoms having high atomic number backscatter the incident electrons strongly and give a bright area in the EPMA image, while atoms with low atomic number give a dark one [13]. Thus, in metallurgical research, using the EPMA technique to study the segregation phenomenon in steels is probably the most important application [13].

3. RESULTS AND DISCUSSIONS

3.1. METALLOGRAPHIC EXAMINATION

The light micrographs obtained in the cross-section of the steel sample plasma nitrided at 530 °C during 10 h are shown in Fig.1.a-d. For the metallographic etching it was used 4% Picral reagent. At low magnification (Fig.1.a) one may observe very well the banded structure. The bands that were etched darkly indicate a zone rich in alloying elements as Mn and Cr [14]. The distance between two successive segregation bands was estimated at about 50 μ m.

Also, etching with Picral reagent permitted identification of the diffusion zone which is formed by two regions: one, situated immediately under the surface, which was darkened and another one which was colored in lighter shades, being positioned under the first one (Fig.1.a). The thickness of the diffusion zone is estimated at about 0.3 mm.

The compound layer (“white layer”) formed on the surface of the steel sample during nitriding may be observed at higher magnification in Fig.1.b. This layer has a thickness of ~3.8 μ m.

In the diffusion zone the nitride precipitations appear as white dots at the grain boundaries (some are marked by the arrows in Fig.1.c). Also, in steel bulk one may recognize the tempered martensite features (Fig.1.d). Immediately after the microstructure observations, the sample was used for the hardness measurements and observed once more by light microscopy.

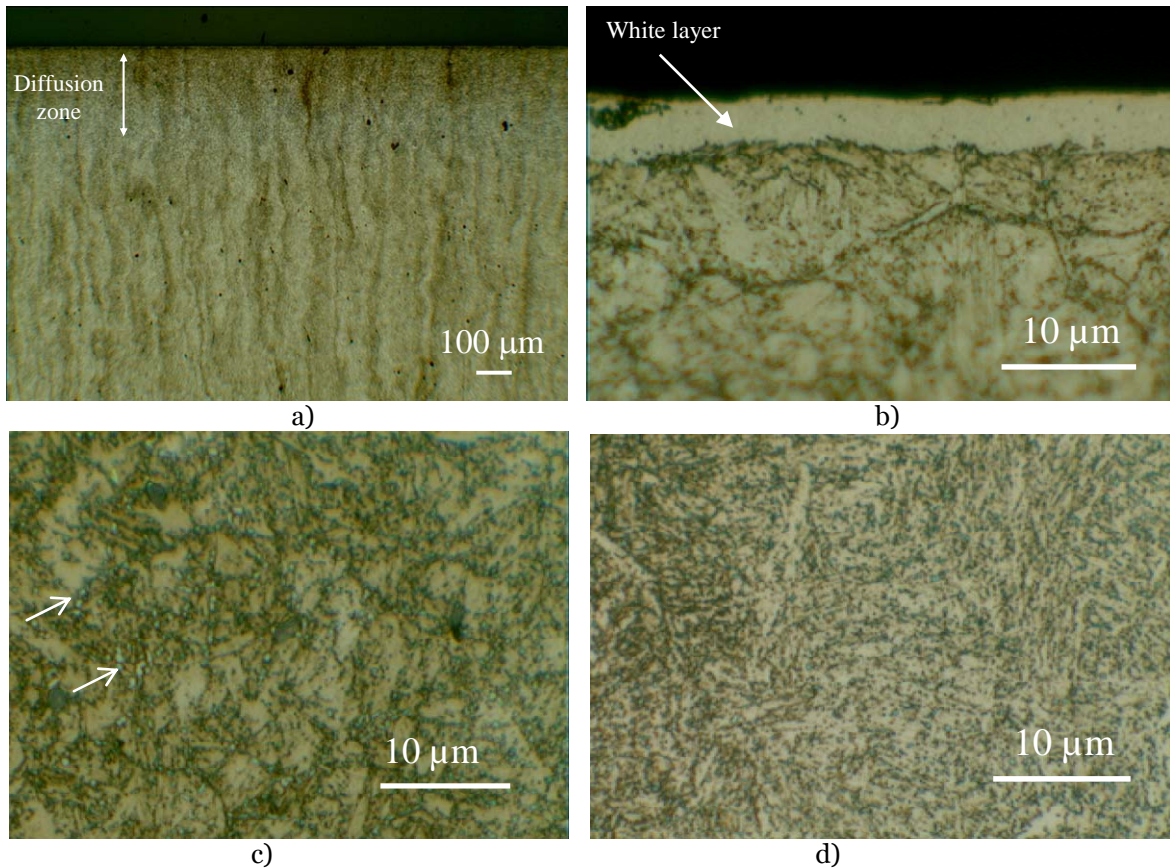


Figure 1. Cross-section micrographs of the nitrided steel sample after 4% Picral etching: low (a) and high magnification, near surface (b), in the diffusion zone (c) and in bulk (d).

3.2. HARDNESS MEASUREMENTS

A vertical hardness profile was measured in the cross-section of the nitrided sample on a length of about 1 mm. The distance between prints was kept approximately constant at 0.1 mm. A light micrograph of the analyzed zone is presented in Fig.2.a, and the variation of the hardness with depth (corresponding to the profile from Fig.2.a), is presented in Fig.2.b.

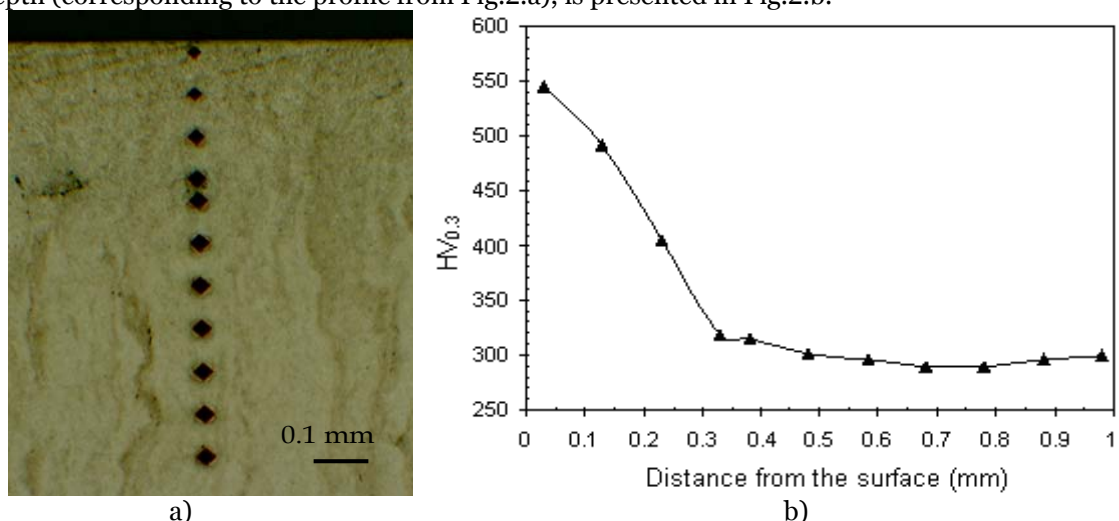


Figure 2. Light micrograph of the hardness prints distribution – 4% Picral etching (a) and the variation of the obtained values with depth (b).

As a general view, the $HV_{0.3}$ measured values taken in depth indicate a continuous decrease, which is characteristic to a nitrided structure. The uniformity of the values suggests that in vertical direction the segregations have not a great influence on the hardness probably because the experiments were done in a zone between two segregation bands (the diagonal of the prints being estimated at about $30 \mu\text{m}$).

By nitriding the steel sample surface hardness has increased by ~1.8 times with respect to the bulk, up to ~550 HV (Fig.2.b). From Fig.2.b one may estimate the diffusion zone thickness at about 0.32 mm, value close to that identified by the light microscopy observations (see Fig.1.a). Next, up to 1 mm in depth, the hardness values are maintained in a constant range around 300 HV (the bulk hardness). In the diffusion zone, the hardness is increased due to nitrogen incorporation which may be found as dissolved in the solid solution and as nitride precipitations [15]. It is known that only 0.1 wt% of nitrogen dissolved in the steel ferritic matrix during nitriding gives an important increase of hardness [15].

Moreover, to complete this study we have done nine punctual hardness measurements in the zones with (prints 3 up to 7) and without segregations (prints 1, 2, 8 and 9) in the bulk of the steel sample. Micrographs of the prints are shown in Fig.3.a-c, while in Tab.1 are given the print diagonals and the corresponding HV_{0.3} values.

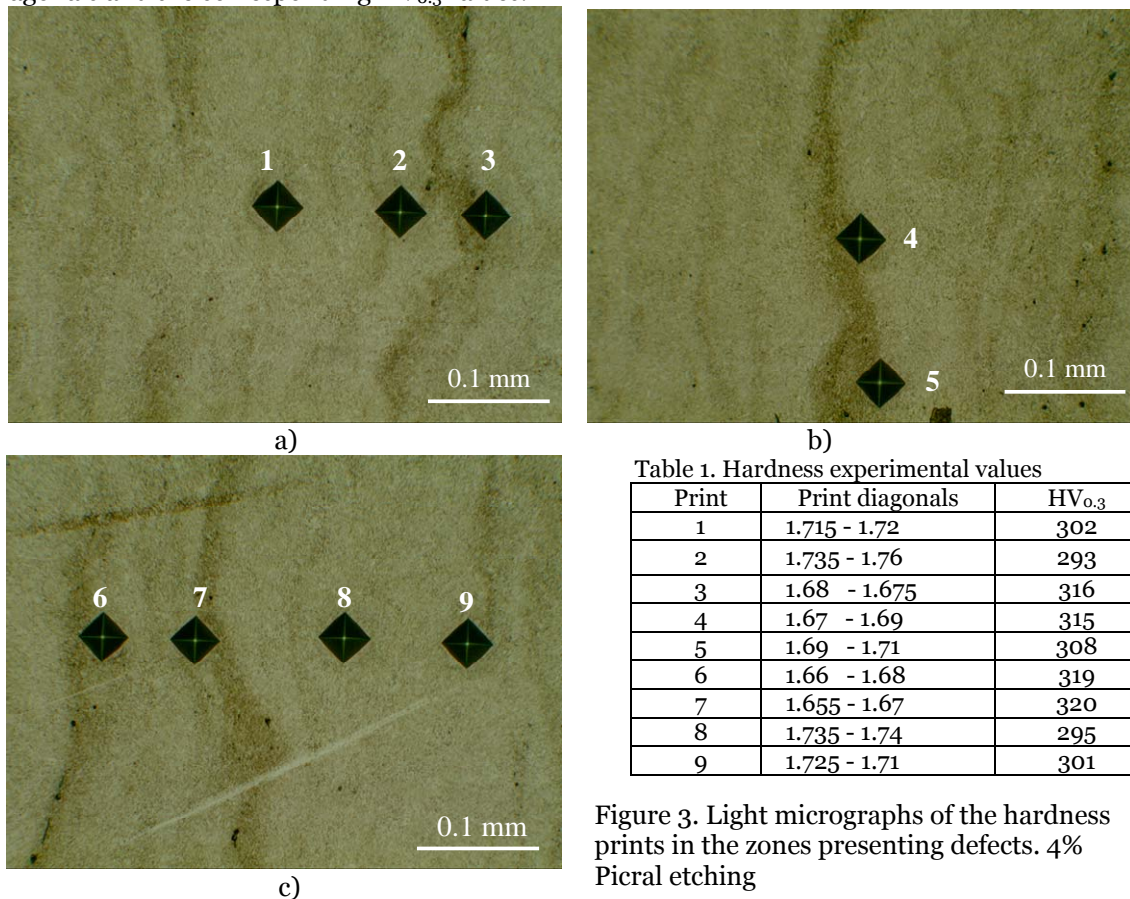


Figure 3. Light micrographs of the hardness prints in the zones presenting defects. 4% Picral etching

It is obvious a correlation between the presence of segregations and the hardness values. So, in the zones presenting defects (prints 3 up to 7), the average hardness is 315.6 HV_{0.3}, while in the others zones (prints 1, 2, 8 and 9), the average value of the hardness is 297.7 HV_{0.3}.

3.3. EPMA RESULTS

In Fig.4. are given: an EPMA image showing the path of incident electron beam in the analyzed area (indicated by the arrow in Fig.4.a) and the obtained atomic concentrations with depth (Fig.4.b). The nitrogen and iron concentration profiles in depth were determined from the surface of the sample through the compound layer and the transition zone to the diffusion layer, on a length of ~15 μm. As estimated from the EPMA image (Fig.4.a), in the analyzed zone the compound layer has a thickness of about 4.8 μm, but on the average this layer has a thickness close to 3.6 μm.

At the steel sample surface, in the compound layer, the presence of about 20% nitrogen and 80% iron suggest the presence of the γ'-Fe₄N nitride (Fig.4.b). In depth, up to ~5 μm, these proportions are changing toward lesser nitrogen but much iron content. The iron surplus is detected probably from the steel sample structure, this indicating a discontinuity (mixture) in the compound layer.

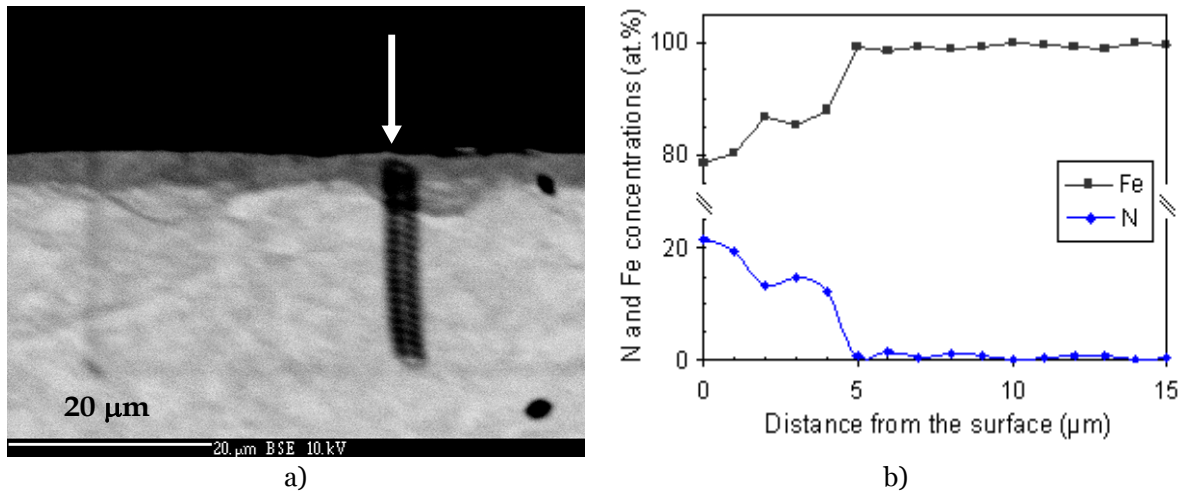


Figure 4. EPMA image showing the path of incident electron beam in the compound and diffusion layers (a) and the obtained atomic concentrations with depth (b).

Also, as shown in the EPMA image presented Fig.5 and taken in the diffusion layer, the nitrided steel sample structure appears inhomogeneous (with zones of different contrast). So, by the brightness, the analyzed area may be divided into two zones, a bright and a dark one (Zone A and B, respectively in Fig.5), bounded by a white dot line.

Further, we have measured the nitrogen and iron concentrations (in at.%) in different points in the analyzed zone, the results being presented in Tab.2. The three experimental points (from 1 to 3) where marked on the EPMA image during the measurements by the apparatus (Fig.5). The first experimental point (1) is situated at about 15 μm from surface and the position of the other points (2 and 3) was arbitrary chosen by the contrast of the zone. Thus, experiments 1 and 3 were done in the bright zone, while experiment 2, in the dark one.

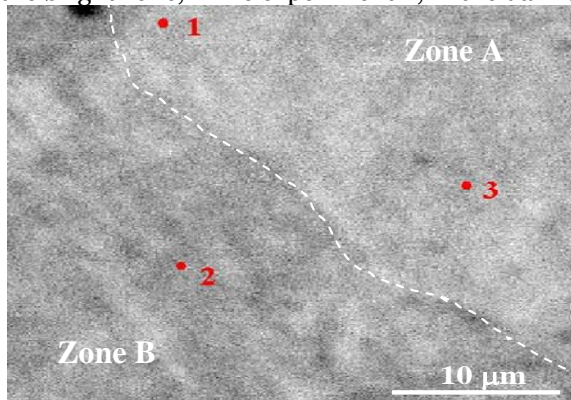


Table 2. Atomic concentrations determined in different points in the diffusion layer

Point	N (at.%)	Fe (at.%)	Zone
1	2.0795	97.9205	A - bright
2	0.8707	99.1293	B - dark
3	1.7101	98.2899	A - bright
4*	0.2799	99.7201	bright, at ~50 μm from surface
5*	0	100	bright, at ~350 μm from surface

*Not marked in Fig. 5.

Figure 5. EPMA image showing three experimental points taken in the diffusion layer

If the sample structure heterogeneity would be due to the nitriding treatment, in Zone A one would expect a nitrogen poor zone, while in Zone B, a nitrogen rich zone. Analyzing the experimental values from Tab.2 one may conclude that this assumption is not sustained because of the lesser nitrogen content obtained in experiment 2 versus experiments 1 and 3. So, the steel sample structure heterogeneity was formed before nitriding, probably during its solidification stage and the limit between Zone A and B may be probably assigned to a segregation band limit.

In Zone A, the nitrogen content maybe detected from the nitride precipitates, whose presence was already identified in the diffusion layer by the light microscopy (Fig.1.c). In Zone B the contrast is probably due to the presence of elements such as chromium, manganese, sulfur and phosphorus which have a smaller atomic number than iron and which segregate at the grain boundaries during the solidification period of the steel [14-16]. Also, in the bright zones situated more in depth (experiments 4 and 5- Tab.2), the nitrogen content decrease up to 0 because here the nitriding treatment effects are not visible.

4. CONCLUSIONS

A 42CrMo4 steel sample plasma nitrided in industrial conditions was used to study the correlation between the microstructure defects and the mechanical properties. The microstructural defects (i.e. segregations bands resulted in the solidification stage of the steel) were revealed by

light microscopy after 4% Picral reagent etching. The distance between two successive segregation bands was estimated at about 50 μm .

Also, the hardness measurements ($\text{HV}_{0.3}$) and the EPMA chemical analysis performed both in the nitrided layer and in the zones with defects, showed the following:

- ❖ The hardness profile, taken with depth from the steel sample surface, correspond to a nitrided structure and the uniformity of the values suggests that in vertical direction the segregations have not a great influence probably because the experiments were done between two segregation bands;
- ❖ The difference between the average hardness values measured in the zones with and without segregations is of only $\sim 18 \text{ HV}_{0.3}$ points;
- ❖ The nitrogen and iron concentration profiles indicate the presence of the $\gamma\text{-Fe}_4\text{N}$ nitride on the surface of the steel sample;
- ❖ The chemical analysis made in zones of the diffusion layer which appeared bright or dark in the EPMA backscattered electrons image showed an inhomogeneous structure due to the presence of segregations.

Acknowledgement

The authors would like to acknowledge Mr. Jean Luc DEVIDAL for the EPMA tests at "Magma et Volcan" Laboratory (UMR 6524), Blaise Pascal University, Clermont-Ferrand, France.

REFERENCES

- [1.] M.A. Terres, H. Sidhom, A.C. Larbi, H.P. Lieurade, Tenue en fatigue flexion d'un acier nitrué, *Ann. Chim. Sci. Mat.* 28 (2003) 25-41.
- [2.] K. Genel, M. Demirkol, T. Gulmez, Corrosion fatigue behaviour of ion nitrided AISI 4140 steel, *Mater. Sci. Eng. A* 288 (2000) 91–100.
- [3.] A. Celik, S. Karadeniz, Improvement of the fatigue strength of AISI 4140 steel by an ion nitriding process, *Surf. Coat. Technol.* 72 (1995) 169-173.
- [4.] A. Alasaran, F. Yildiz, A. Celik, Effects of post-aging on wear and corrosion properties of nitrided AISI 4140 steel, *Surf. Coat. Technol.* 201 (2006) 3147–3154.
- [5.] B. Podgornik, J. Vižintin, O. Wänstrand, M. Larsson, S. Hogmark, H. Ronkainen, K. Holmberg, Tribological properties of plasma nitrided and hard coated AISI 4140 steel, *Wear* 249 (2001) 254–259.
- [6.] P. Corengia, T.G. Ybarra, C. Moinaa, A. Cabo, E. Broitman, Microstructural and topographical studies of DC-pulsed plasma nitrided AISI 4140 low-alloy steel, *Surf. Coat. Technol.* 200 (2005) 2391–2397.
- [7.] G. Krauss, Solidification, Segregation, and Banding in Carbon and Alloy Steels, *Metall. Mater. Trans. B* 34/6 (2003) 781-792.
- [8.] J.D. Verhoeven, A Review of Microsegregation Induced Banding Phenomena in Steels, *J. Mat. Eng. Perf. JMEPEG* 9 (2000) 286-296.
- [9.] X. Tong, C. Beckermann, A diffusion boundary layer model of microsegregation, *J. Crystal Growth* 187 (1998) 289-302.
- [10.] L.E. Samuels, *Light Microscopy of Carbon Steels*, ASM International, Materials Park, OH, ISBN 0-87170-655-5, 1999.
- [11.] B.L. Bramfitt, A. O. Benscoter, *Metallographer's guide: practices and procedures for irons and steels*, ASM International (OH), ISBN-13: 9780871707482, 2002.
- [12.] D. Chae, D.A. Koss, A.L. Wilson, P.R. Howell, The effect of microstructural banding on failure initiation of HY-100 steel, *Metall. Mater. Trans. A* 31 (2000) 995-1005.
- [13.] J.A. Belk, A.L. Davidies, *Electron Microscopy and Microanalysis of Metals*, Elsevier Publishing Co. Ltd., London, 1968, pp. 151 and pp. 219.
- [14.] Z. Sterjovski, D.P. Dunne, D.G. Carr, S. Ambrose, The Effect of Cold Work and Fracture Surface Splitting on the Charpy Impact Toughness of Quenched and Tempered Steels, *ISIJ International* 44/6 (2004) 1114–1120.
- [15.] S.R. Hosseini, F. Ashrafizadeh, Accurate measurement and evaluation of the nitrogen depth profile in plasma nitrided iron, *Vacuum* 83 (2009) 1174-1178.
- [16.] T.F. Majka, D. K. Matlock, G. Krauss, Development of microstructural banding in low-alloy steel with simulated Mn segregation, *Metall. Mater. Trans. A* 33 (2002) 1627-1637
- [17.] A.C. Stauffer, D.A. Koss, J.B. McKirgan, Microstructural banding and failure of a stainless steel, *Metall. Mater. Trans. A* 35 (2004) 1317-1324





¹: Moniĳa Eriĳa POPA

RESEARCH AND SIMULATION OF THE SOLIDIFICATION FRONT AT THE CONTINUOUS CAST HALF-FINISHED PRODUCT

¹: UNIVERSITY POLITEHNICA OF TIMISOARA, FACULTY OF ENGINEERING FROM HUNEDOARA, ROMANIA

ABSTRACT:

This section is divided with discreet element structure. Using these experiments is made graphical dependents of temperature in some different point from surface crust to center of half-product, and also solidification speed for S235. Primordial method for the decrease of the superheat of the steel of the crystallizer, consist in the introduction of consumable micro-coolers, which can be exterior or internal. The mathematical molding of the solidification and cooling phenomenon of continuously cast half-products, presented the in afterwards, is based on the mathematical description of phenomenon.

KEYWORDS: steel, micro-coolers addition, continuous casting, experiments, simulations

1. INTRODUCTION

The main task of the continuous cast is improved of continuous cast steel quality. In order to assured the solidification conditions imposed by the steel chemical composition must be synchronize a numerous technological factors the most important be the steel chemical composition, the casting temperature and speed of drawing. Primordial method for the decrease of the superheat of the steel of the crystallizer, consist in the introduction of consumable micro-coolers, which can be exterior or internal. The exterior micro-coolers can be prepared out of the system and entered the crystallizer, and the internal micro-coolers are constituted from steels crusts, immediate format in the core of the half-products, on the water cooled surfaces. The outside micro-coolers can be entered in the liquid steel below different forms: small shots, granules or particles, draw-bars, wire, tube, etc.

The addition of micro-coolers in crystallizer drives to the growth of the zone of the echi-axial crystals, diminish the degree of superheat and reduce the axial porosity. The mathematical molding of the solidification and cooling phenomenon of the solidification and cooling phenomenon of continuously cast half-products, presented the in afterward, is based on the mathematical description of phenomenon. This solution problem is, practically, the heat solving equation in of nom-steady regime. For defined the heat conduction between half-product and crystallizer is necessary the cognition of initial conditions, the variation law of the heat flux between half-product – crystallizer – and the flux between crystallizer – cooling water. Some conditions are can easy schematized, other only that drive to systems of which equations can be solved on analytic path.

2. METHODOLOGY

The computer program is written in C++ and works under Win32. For the graphic interface the program uses Microsoft Foundation Classes, a class library that encloses the functional character of the standard programming interface Windows API – Application Program Interface. The 3D graphs are realized with the Windows implementation of OpenGL specification (Open Graphics Library). For implementation of an algorithm of the above described model we need the following initial data: ambient temperature, casting temperature, initial temperature of the crystallizer, number of nodes from half-finished product and from crystallizer with respect to both

axes, values of thermal conductivity for steel and copper function of temperature, values of enthalpy for steel and copper function of temperature. In case of steel this functional dependence need to include fusion latent heat; tapping condition of half-finished product from equipment; stopping condition of the algorithm. This could be: manual stopping, after a given time period at a specified minimum, average, or maximum temperature of the half-finished product, maximum variation of enthalpy at an iteration.

3. DISCUSSION

The simulation is realized for a half-finished product $\Phi 270$ mm made of steel OL37-2K, according to the SREN 1025 standard. The data are: the ambient temperature 20 °C, the casting temperature 1550 °C, the convection constant $K=15$. For configuration of specific dates for every steel grade, using the main interface (figure 1).



Figure 1. The main window of the program

The simulation of the continuously cast half-products is effectuated in the case of 1% consumable micro-coolers introduced in crystallizer. The simulation is effectuated just for the primary and secondary cooling and not for the entire line of cast installation. Thus is explained the great values of the temperature of steel in the interior of the half-products (the middle layers) but which we diminish the feather below the value of the temperature solidus up to the moment which in the half-products is uttered. With the number of knots of digitization in major (both the crystallizer and the half-products) and the maximum the variation of in an enthalpy in single iteration is less, the real time of simulation is major. The run of the program can be interrupted all moments, but with the mention as be start from same moment of time but must run the program from beginning. For illustrate the operation of the program, we accomplished captures of the screen to different moments of times, from which can obtain some information concerning the temperatures in the cast equipment, the real and simulated times.

The temperatures are indicated by the mean of a colored gradient, having the values: red for casting temperature, blue for ambient temperature and green for their average. Any intermediary temperature is a combination of these. A first obtained dependence is represented by temperature variation of the half-finished product function of time (figure 2). The distribution of the discredited points is also presented.

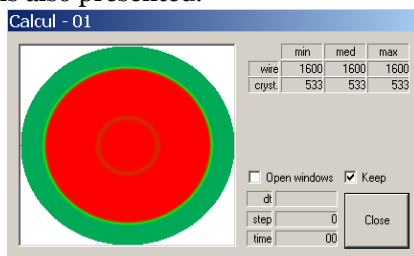


Figure 2. The dialog window at 1s (simulated time) at the moment of the micro-coolers introduces

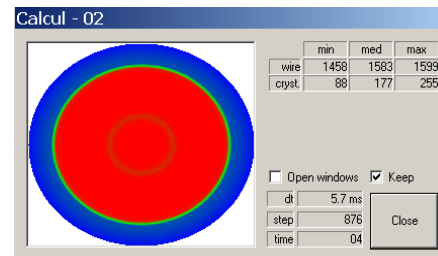


Figure 3. The dialog window at 2s

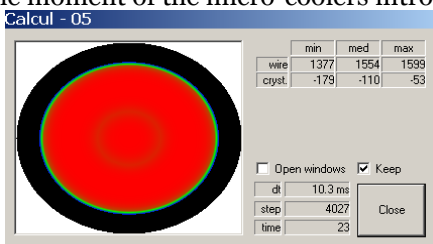


Figure 4. The dialog window at 5s

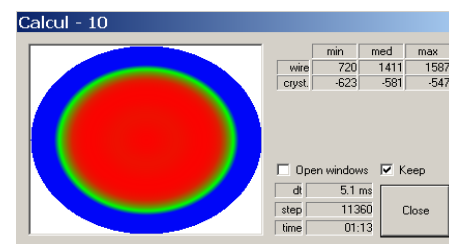


Figure 5. The dialog window at 10s

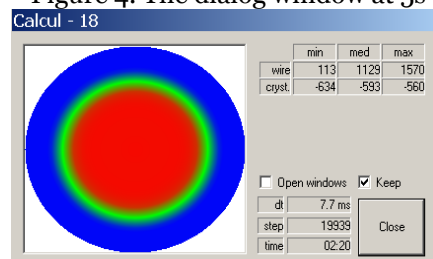


Figure 6. The dialog window at 18s

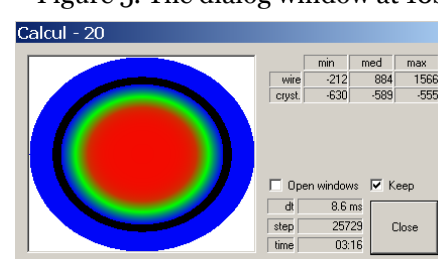


Figure 7. The dialog window at 20s

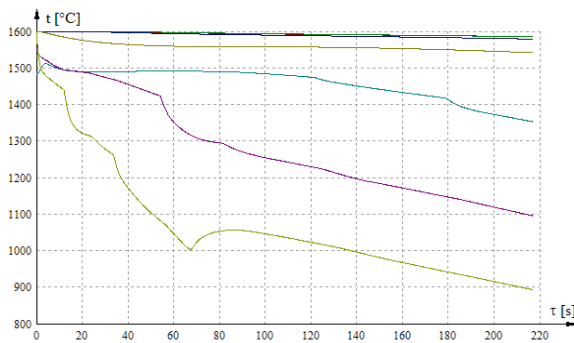


Figure 8. The temperature variation function of time (10%, 25% and 100% from the cast line)

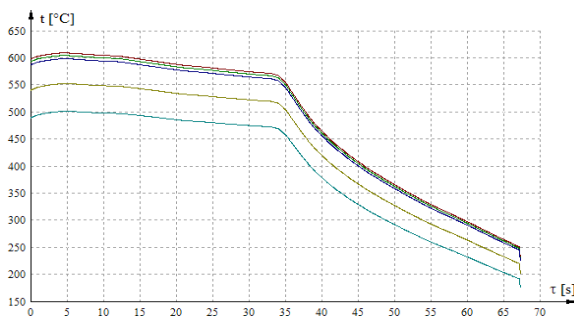


Figure 9. The temperature variation in the crystallizer, function of time (1%, 5%, 10%, 50% and 100% from crystallizer)

In figure 10 the cumulate diagram of the temperature are presented. It is observed the two cooling zone, respectively the primary cooling (when varied both the temperature in crystallizer and the cast line), and the secondary cooling (when only the cast line temperature is present). It was obtained variation type for the solidification speed function of time. It refers to a solidification speed calculated between two consecutive iterations, fact that partially explain the oscillating aspect of the curves (figure 11).

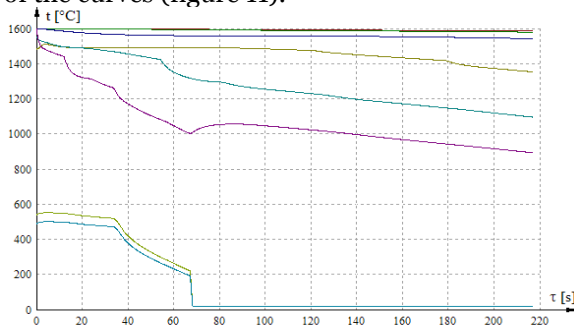


Figure 10. The temperature variation in the crystallizer and the cast line

At time moment, when it took place the driving out of considered surface from crystallizer, it took place an increasing of temperature in the superior layers of the half-finished product (with approximately 100 °C in the exterior and with 35...50 °C in different points of the surface). This increasing of the temperature is due to the lack of cooling of the wire immediately after the driving out from crystallizer to the first ring of secondary cooling. After this moment the cooling and the solidification of the wire took place normally, the recorded temperatures corresponding to the measured ones. It needs to be specified that the simulation was realized just for primary and secondary cooling not for the entire running of the wire in the equipment. This explains steel's high temperature values in the interior of the half-finished product (middle layers), but they are decreasing under the solidus temperature value until the cutting of the half-finished product.

As regards the temperatures distribution in the crystallizer (which take over the heat transferred by the half-finished product and transfer it to the cooling water), it is presented in figure 9. In this case to be presented also the position of the discredited points.

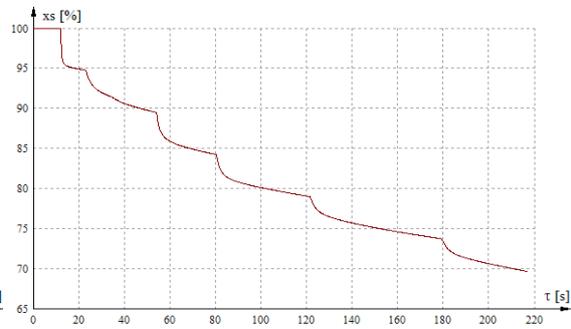


Figure 11. The solidification front (100%=surface of the cast line)

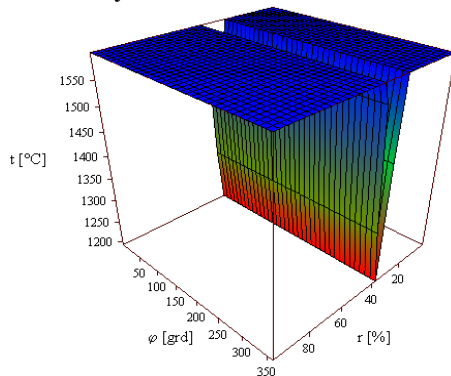


Figure 12. The thermal field at 1s after the micro-coolers addition

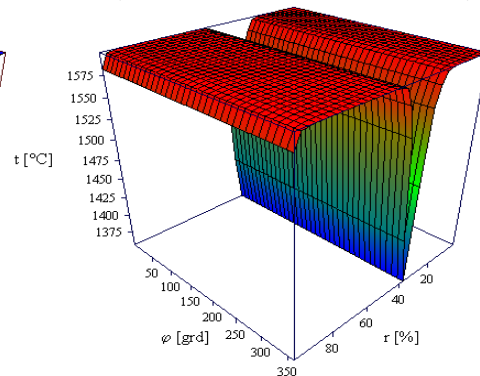


Figure 13. The thermal field at 2s after the micro-coolers addition

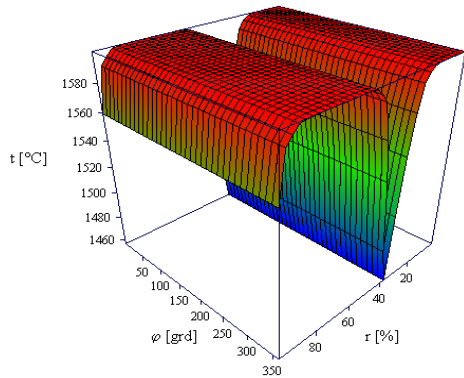


Figure 14. The thermal field at 5s after the micro-coolers addition

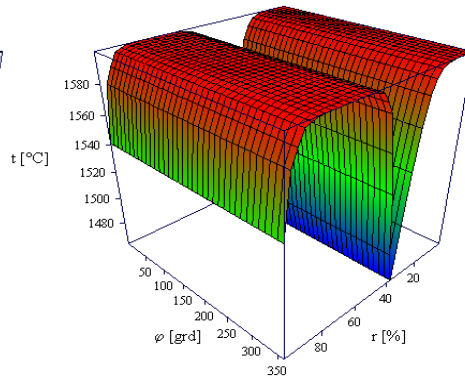


Figure 15. The thermal field at 10s after the micro-coolers addition

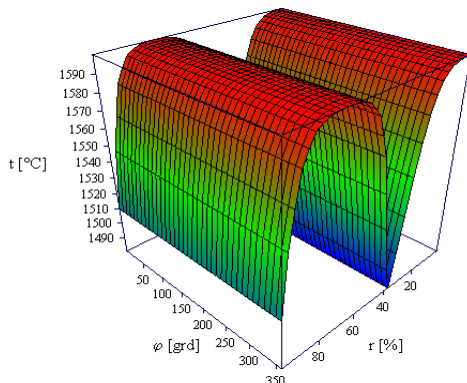


Figure 16. The thermal field at 18s after the micro-coolers addition

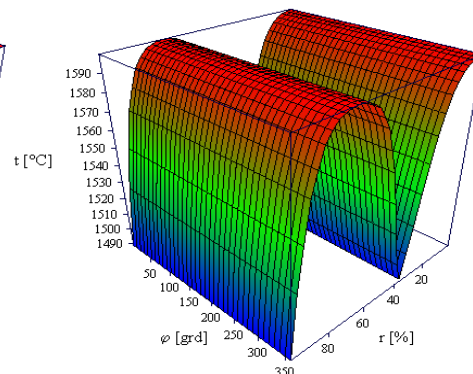


Figure 17. The thermal field at 20s after the micro-coolers addition

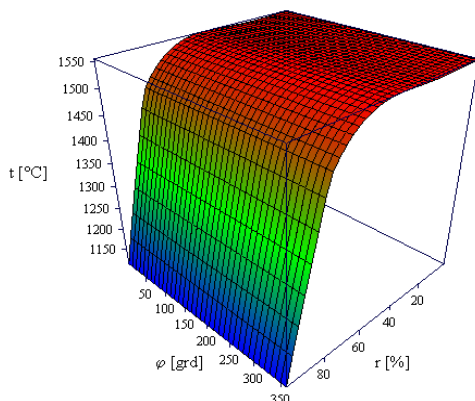


Figure 18. The thermal field in half-product ($\Phi 270$ mm), in time (at simulation's end)

Another type of temperature distribution, when the half-finished product is droved out from secondary cooling zone, it is presented in figure 12...figure 17, at 1s, 2s, 5s, 10s, 18s and 20s, after introduced the micro-coolers. The figure 18 presents the thermal field in the half-product in the end of the simulated time. The obtained regression surfaces corresponded from a quarter from the half-product section is like similarly of the other parts of the section. From the point of view of the temperature values, the half-product surface is the first cooled section, and the core is the most slowly cooled part.

4. CONCLUSIONS

Analyzing the graphical dependences from the performed researches, based on literature review data

and from own experimental work it results the following conclusions:

- ❖ The results obtained by simulation with presented program being similar with practical data;
- ❖ In every diagram there diagram there are observed a temperature leap or a solidification speed leap after approximately 60s from the beginning of the casting (from a totally 220s simulation time), respectively immediately after the driving out from the crystallizer of the considered section, leap caused by the impossibility of elimination of a heat flux from the half-finished product interior;
- ❖ It is observed a numerous crystallizing centers, uniform distributed;
- ❖ Also, it is observed an appreciate difference between the liquid steel temperature and the steel temperature from immediate proximity of micro-coolers;
- ❖ The indurations advances consisted standardized it a temperatures of first in of the minute after the administration of micro-coolers;
- ❖ After precinct a minute from the administration micro-coolers don't else notices significant differences what in looks the variation of the temperature of the in mass of steel;

- ❖ Through the addition of micro-coolers is obtained adjustment of the temperature of the in of the crystallizer depending on the quality and quantity of micro-coolers.

The chosen time interval represent the time in which the unsteady heat transfer process is approximate with a steady process. From this reasons as well as the characteristics of the real process are far from that of a steady one, the iteration period should be smaller. The proposed algorithm can be used for the analysis of both stationary and moving solidification problems in which phase change occurs at a specific temperature. An integrated understanding of heat transfer during solidification, friction/lubrication at solid-liquid interface, high temperature properties of the solidifying shell etc. is necessary to control the continuous casting process.

REFERENCES

- [1.] Popa Monika Erika – Cercetări privind procesele fizico-chimico-metalurgice ce au loc la interfețele cristalizor-zgură-oțel lichid asupra oțelului turnat continuu, Teza de doctorat, Ed. Politehnica 2009
- [2.] Hepuț T., Kiss I., Popa E., Ardelean E., Ardelean M. - Research and experiments regarding the quality of continuous cast steel- Scientific Conference Research And Development Of Mechanical Elements And Systems Jahorina – Irmes, Sarajevo, 2002, BOSNIA, Pp 349...354
- [3.] Popa E., Kiss I., Mihut G. - Researches regarding the quality of the continous cast semi-finished products- Management Of Manufacturing Systems MMS-2008 – 3rd Conference With International Participation, Presov, SLOVAKIA, 187...190 ISBN: 978 – 80 – 553 – 0069 – 6
- [4.] Popa E., Kiss I. -“ Mathematical modelling of the thermal regime in the continous casting process- Tinerii Si Cercetarea”, Al VII-Lea Simpozion International – Resita, 2005, ISSN 1453 – 7394
- [5.] Popa M. E., Kiss I., Danciu A. - The thermal regime in the continuous casting process– in mathematical interpretations - Annals of Faculty of Engineering Hunedoara, 2005, Tome III, Fasc 3, Pp 235...242, ISSN 1584 – 2673
- [6.] Popa E., Kiss I. - Mathematical Modelling Of The Thermal Regime In The Continous Casting Process - Analele Universității “Eftimie Murgu” Reșița, 2005, Pp 231-237, ISSN 1453 – 7394
- [7.] Popa E., Kiss I., Danciu A. - Research Of Experiments Regarding The Influence Of Casting Parameters Upon The Surface Temperature Of The Continous Caste Semiproduct. - Annals Of Oradea University, Fascicle Of Management And Technological Engineering, 2005, CD, ISSN 1583 – 0691



¹Simon JITIAN

OBTAINING THE ABSORPTION SPECTRA OF SILICON FROM THE IR REFLECTANCE SPECTRA RECORDED AT TWO ANGLES

¹UNIVERSITY „POLITEHNICA” OF TIMIȘOARA, FACULTY OF ENGINEERING HUNEDOARA, ROMANIA

ABSTRACT:

This paper presents an analytical method for obtaining optical constants \bar{n} and \bar{k} , which define the complex refractive index $\tilde{n} = \bar{n} - i\bar{k}$ of solid absorbent materials. From specular reflectance, IR spectra recorded at two different incidence angles φ_01 and φ_02 the reflectances R are measured, using unpolarized radiation. [1].

KEYWORDS:

optical constants, two angles IR reflectance spectra, refractive index spectra

1. INTRODUCTION

The reflection of a plane polarized monochromatic radiation on the boundary of two different optical media is expressed by the Fresnel complex reflection coefficient $\tilde{r} = r \cdot \exp(i\delta)$. Two reflection coefficients \tilde{r}_s and \tilde{r}_p are defined for two components of plane polarized radiation with the electric field vector located perpendicular and parallel to the plane of incidence, respectively.

The square modulus of the complex reflection coefficient is the reflectance (or the reflectivity) $R_s = \tilde{r}_s \cdot \tilde{r}_s^*$ or $R_p = \tilde{r}_p \cdot \tilde{r}_p^*$. In the first approximation we can consider the reflectance for natural radiation to be the arithmetic mean of the two components R_s and R_p :

$$R = \frac{R_s + R_p}{2} \quad (1)$$

If we consider that the two components in incident radiation do not have equal weight, we can introduce a parameter S whose value is between $S = 0$ for the radiation polarized parallel to the incidence plane ($R = R_p$) and $S = \infty$ for the radiation polarized perpendicular to the incidence plane ($R = R_s$) [2]. S is defined as the ratio between the intensity of light polarized perpendicular to the plane of incidence and the parallel polarized one reaching the detector:

$$S = \frac{R_s^o}{R_p^o} \quad (2)$$

where: R_s^o and R_p^o are the perpendicular and parallel components that were measured.

The reflectance can be expressed by:

$$R = \frac{S}{S+1} R_s + \frac{1}{S+1} R_p \quad (3)$$

The reflection coefficients \tilde{r} and the reflectance R depend on the relative complex refractive index of refractive and incidence medium, respectively:

$$\tilde{n} = \frac{\tilde{n}_1}{n_0} = \bar{n} - i\bar{k} \quad (4)$$

according to relations:

$$\tilde{r}_s = |\tilde{r}_s| \exp(i\theta_s) = \frac{\cos \varphi_o - \tilde{n} \cos \tilde{\varphi}}{\cos \varphi_o + \tilde{n} \cos \tilde{\varphi}} \quad (5)$$

$$\tilde{r}_p = |\tilde{r}_p| \exp(i\theta_p) = \frac{\tilde{n} \cos \varphi_o - \cos \tilde{\varphi}}{\tilde{n} \cos \varphi_o + \cos \tilde{\varphi}} = -\tilde{r}_s \frac{\tilde{n} \cos \tilde{\varphi} - \sin \varphi_o \tan^2 \varphi_o}{\tilde{n} \cos \tilde{\varphi} + \sin \varphi_o \tan^2 \varphi_o} \quad (6)$$

where $\tilde{\varphi}$ is the complex refractive angle, from Snell refraction law:

$$\sin \varphi_o = \tilde{n} \sin \tilde{\varphi} \quad (7)$$

A single measurement of the reflectance at a certain frequency is insufficient to determine the two optical constants \bar{n} and \bar{k} . Several methods that use at least two experimental values of measurable physical quantities corresponding to reflection [3] are known. Usually, they use graphical methods since the optical constants \bar{n} and \bar{k} can not be explicitly expressed from the reflectance expressions [4]

2. MODEL DETAILS

We present an analytical method, using some approximations, to obtain reflectance spectra $\bar{k} = f(\tilde{\nu})$ and $\bar{n} = f(\tilde{\nu})$ from the reflectance spectra $R = f(\tilde{\nu})$ recorded at two different incidence angles, using non-polarized radiation [5,6].

For two different incidence angles φ_{01} and φ_{02} the refraction law is written:

$$\sin \varphi_{01} = \tilde{n} \sin \tilde{\varphi}_1 \quad \text{and} \quad \sin \varphi_{02} = \tilde{n} \sin \tilde{\varphi}_2 \quad (8)$$

By writing equation (3) for the two angles of incidence, we obtain the system of equations:

$$S \cdot R_{s1} + R_{p1} - (S + 1) \cdot R_1 = 0 \quad (9)$$

$$S \cdot R_{s2} + R_{p2} - (S + 1) \cdot R_2 = 0 \quad (10)$$

If in relations (5) and (6) we introduce the notations:

$$\tilde{n} \cos \tilde{\varphi}_1 = X - i \cdot Y \quad \text{and} \quad \tilde{n} \cos \tilde{\varphi}_2 = U - i \cdot Z \quad (11)$$

then the reflectances for two polarization states corresponding to the two different incidence angles, are:

$$R_{s1} = \frac{(X - \cos \varphi_{01})^2 + Y^2}{(X + \cos \varphi_{01})^2 + Y^2} \quad \text{and} \quad R_{s2} = \frac{(U - \cos \varphi_{02})^2 + Z^2}{(U + \cos \varphi_{02})^2 + Z^2} \quad (12)$$

respectively:

$$R_{p1} = R_{s1} \frac{(X - \sin \varphi_{01} \tan \varphi_{01})^2 + Y^2}{(X + \sin \varphi_{01} \tan \varphi_{01})^2 + Y^2} \quad \text{and} \quad R_{p2} = R_{s2} \frac{(U - \sin \varphi_{02} \tan \varphi_{02})^2 + Z^2}{(U + \sin \varphi_{02} \tan \varphi_{02})^2 + Z^2} \quad (13)$$

X, Y, U and Z depend on the complex refractive index according to the relations:

$$\tilde{n}^2 = (X - i \cdot Y)^2 + \sin^2 \varphi_{01} \quad ; \quad \tilde{n}^2 = (U - i \cdot Z)^2 + \sin^2 \varphi_{02} \quad (14)$$

By equating the right side of each relationship (12) we get:

$$XY - UZ = 0 \quad (15)$$

$$X^2 + Z^2 - Y^2 - U^2 + \sin^2 \varphi_{01} - \sin^2 \varphi_{02} = 0 \quad (16)$$

The nonlinear system of equations (9), (10), (15) & (16) leads to optical constants \bar{n} and \bar{k} .

3. RESULTS AND DISCUSSION

To illustrate this method silicon was chosen. The refractive index values for this material are well known and stressed in the reference literature [9,10,11].

In order to obtain the optical constants \bar{n} and \bar{k} of silicon we used specular reflectance IR spectra. The spectra were recorded with a UR20 spectrograph, using non-polarized radiation. For IR radiation incident on the sample, the proportion of the plane polarized component, perpendicular to the plane of incidence, is 63% which corresponds to the parameter of equation (3) $S = 1.7$.

Figure 1 presents the IR reflectance specular spectra of silicon recorded at two incidence angles 20 and 55 degrees respectively.

To obtain optical constants \bar{n} and \bar{k} from reflectance spectra we used our own computer program in MATLAB language, calling a routine for solving systems of nonlinear equations. To do this, first we wrote the nonlinear system of equations (9), (10) (15) and (16) to canonical form.

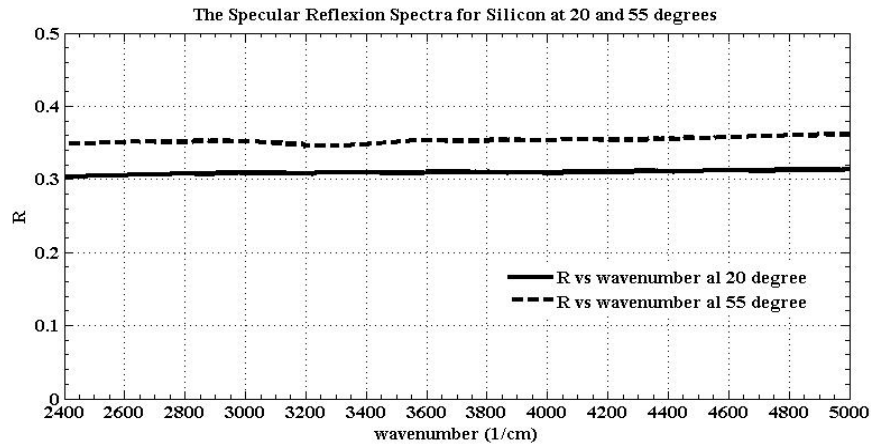


Fig. 1. The reflectance specular spectra of silicon recorded at two incidence angles, using non-polarized light

To find the solution of the nonlinear equations system it is very important to choose the correct test-solution to resolve the routine. For this, we started from the value $X = U = 3.4$ and $Y = Z = 0$ since it is known from reference literature that in the spectral range examined $n \cong 3.4$ and $k=0$ for silicon [9, 10, 11]. In (14) the contribution of the second term on the right is small, so $X = U = n = 3.4$ and $Y = Z = k = 0$.

The refractive index \tilde{n} and optical constants \bar{n} and \bar{k} respectively are calculated from equation (14) based on X and Y values obtained by solving the nonlinear equations system.

Figure 2 shows the refractive index spectrum of silicon obtained from specular reflectance spectra recorded at two incidence angles 20 and 55 degrees.

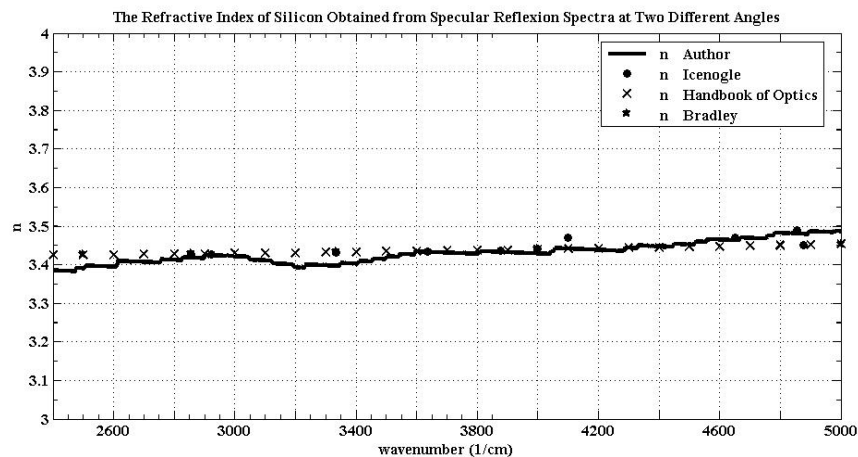


Fig. 2. The refractive index of silicon obtained from the specular reflectance spectra at two different incidence angles: 20° and 55°

The refractive index spectrum obtained by processing the silicon specular reflectance spectra are in very good agreement with the corresponding data from the reference literature, as can be noticed in Figure 2. The absorption index \bar{k} values are equal to zero over the whole spectral range analyzed, in agreement with literature data.

4. CONCLUSIONS

The specular external reflection spectra recorded at two or more different incidence angles can be used to determine the refractive index and absorption index spectra corresponding to solid materials.

When the radiation used to record the spectra is non-polarized or partially polarized it is important to know the contribution of the two components R_s and R_p in the incident radiation.

It is important to choose the correct initial solutions to start the routine for solving nonlinear equations system. The start solutions of the program for solving nonlinear equations system can be based on values of X and U close to $\bar{n} = 3.4$. The initial values of Y and Z should be close to $\bar{k} = 0$.

The values of the optical constants \bar{n} and \bar{k} obtained by the method are in agreement with the corresponding values reported in the reference literature.

REFERENCES

- [1.] S. Jitian și I. Bratu, Stud.Univ. Babeș-Bolyai, Phys., **31(2)**, p.30 (1986)
- [2.] Crawford Bryce Jr., „Measurements of Optical Constants in the Infrared by ATR”, in Advances in Infrared and Raman Spectroscopy, R.J.H. Clark and R.E. Hester eds., Heyden-London, (1978)
- [3.] E. Kawate, Measurement Science Review, **5 (3)**,(2005)
- [4.] A.Vasicek, „Tables of Determination of Optical Constants from the Intensities of Reflected Light”, Nakladatelstvi Ceskoslovenske Akademie Ved., Praga, (1964)
- [5.] S. Jitian, Teză de doctorat, Cluj-Napoca, (1987)
- [6.] S.Jitian, Analele Univ. Oradea, (1994), p. 74-78
- [7.] J. Fahrenfort, Spectrochim. Acta,**17**, p.698, (1961)
- [8.] W.R. Hunter, Journal of the Optical Society of America, **55**, (10), p.1197, (1965)
- [9.] - Handbook of Optics, 3rd edition, Vol. 4. McGraw-Hill, (2009)
- [10.] H. W. Icenogle, B. C. Platt, and W. L. Wolfe, "Refractive indexes and temperature coefficients of germanium and silicon" Appl. Opt. **15**(10), pp. 2348-2351, (1976),
- [11.] S. Khedim, A. Chiali, B. Benyoucef and N.E. Chabane Sari, Revue des Energies Renouvelables ICRESD-07, Tlemcen, pp. 337 – 341, (2007)





¹Miriam MATÚŠOVÁ, ²Erika HRUŠKOVÁ, ³Angela JAVOROVÁ

MATERIAL FLOW STRATEGY BY SOFTWARE WITNESS

¹⁻³SLOVAK UNIVERSITY OF TECHNOLOGY IN BRATISLAVA, FACULTY OF MATERIALS SCIENCE AND TECHNOLOGY IN TRNAVA, INSTITUTE OF PRODUCTION SYSTEMS AND APPLIED MECHANICS, DEPARTMENT OF TECHNOLOGICAL DEVICES AND SYSTEMS, SLOVAKIA

ABSTRACT:

Resolving of material flows is actual term in present. It brings a lot of problems with layout of particular devices as elements of manufacturing process according to required and defined technology. In present time are suitable software tools for improving of transport, manipulation and storage systems. The simulation of these three systems relation is realized support CA systems to optimal whole technological processes. In this case this problem is solved by simulation software Witness used in Institute of Manufacturing Systems and Applied Mechanics of our faculty.

KEYWORDS:

production system, manufacturing, material flow, layout optimizing

1. INTRODUCTION

Predictive simulation technology is attracted of specialists in many fields. Competitiveness retention and raising the level of services required by organizations constantly change. It is necessary to verify the possibility of planned systems and find successful solutions under conditions of strict monitoring costs. Requirements to change technology or business processes, however, entail some risk.

2. SIMULATION

The simulation model is a dynamic model in which there are phenomena of the same order as the system modeling. Simulation methods obtain solutions to some transformation of values that have been learned from observing the model run (run program). The simulation model provides results based on information collected from the changes in the model over time.

Contribution of simulation methods in the field of operational research is particularly in facilitating the work of dynamic and complicated probability ties. As far as the achievement of the goal to create an analytically solvable model, it is necessary to prioritize. Such a model adequately reflects the essential reality site. This model is usually more general (simulation methods provide results only in numerical form) and to construct and less expensive solutions. In addition, simulation methods are appropriate for assessing the number option than to solve problems that lie in finding optimal solutions to large sets or even an infinite number of elements. With the growing complexity of systems that need to be rationally designed and managed will need to increase the use of simulation methods.

3. SIMULATION MODELS AS TOOL TO OPTIMIZE THE MATERIAL FLOW

There are mostly used in practice following types of simulation:

- ❖ dynamic simulation and physical systems (differential equations, finite element method, etc.)
- ❖ discrete event simulation systems (network theory front, etc.)
- ❖ simulation aimed at training people (air simulators and trainers, simulators and other operator).

Using simulation to solve the various proposals for optimization of production lines and several systems in different industries to track:

- ❖ verification of the new designed production line operations, a comparison of the old organization to the proposed production control system based on KANBAN,
- ❖ the design of optimal production batch subject to a lot of clock and production of products,
- ❖ the optimization of the number of workers in the system, the allocation of operations jobs.

4. PROCESS SIMULATION SOFTWARE

WITNESS - is successful program to simulate the production, maintenance and logistics processes. It is used for interactive model creation, creation of modular structures, interactive experimentation, working with CAD / CAM applications and information systems, creating a single optimization module, 3D visualization - virtual reality module. Other administration routes of the Witness:

- ❖ modern methods implementation of production management,
- ❖ the identification and removal of bottlenecks,
- ❖ optimal allocation of production and logistics units, material flow analysis,
- ❖ the prediction of the operational interventions consequences.

Application Witness simulation program can be realized in the order:

- ❖ the choice of components,
- ❖ manufacturing process technology,
- ❖ the choice of machines,
- ❖ making production variations,
- ❖ comparison of the designed variations,
- ❖ selecting of an acceptable variant.

Technological process of production

In the technological process of product manufacture is necessary to ensure selection of appropriate means of production, namely:

- ❖ products production and production volume,
- ❖ determination of the technological processing structures and methods,
- ❖ technology and organizational structure of production, especially mass, production specified, degree of automation and flexibility,
- ❖ technology equipment - machines and devices, tools and products,
- ❖ handling equipment,
- ❖ control equipment. [3]

The choice of machine

The most important factor in machines classification is a kind of manufacturing plant production. This classification determined the concept of machine technology and automation. [2]

Classification systems of production machines recognize:

- ❖ universal production machines,
- ❖ specialized production machinery,
- ❖ special-purpose ,
- ❖ numerically controlled machine,
- ❖ numerically controlled manufacturing centers,
- ❖ numerically controlled machines for automated manufacturing systems.[1, 4]

Development of production variants

At this stage, to shape the overall concept of technology production. Detail degree of technology depends on whether the choice of production facilities does:

- ❖ for the compilation of the existing technological process in production,
- ❖ technological solutions to project a new or upgraded, respectively modernized production,
- ❖ reconstruction of production facilities.

It is possible to proceed in various ways to create proposals for production. One is the analysis of material flow in production. In Fig. 1 shows the analysis of material flow through production line graphical display.

Different variants of the production lines can be designed using the following symbols, depending on the technological process of manufacturing the product. Comparison of original and newly proposed material flow in production:

Symbol	classification activities
○	technological operation
□	control
→	transport, handling of material
D	break, downtime sorting
▽	storage
X	loading, unloading
⊥	weighing
⬡	packaging

Fig. 1 Symbols illustrated activities

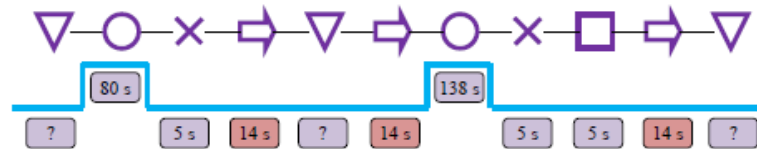


Fig.2 Production line variant by symbols

5. SIMULATION OF THE VARIANTS

Simulation of material flow production lines is shown in Fig. 3.

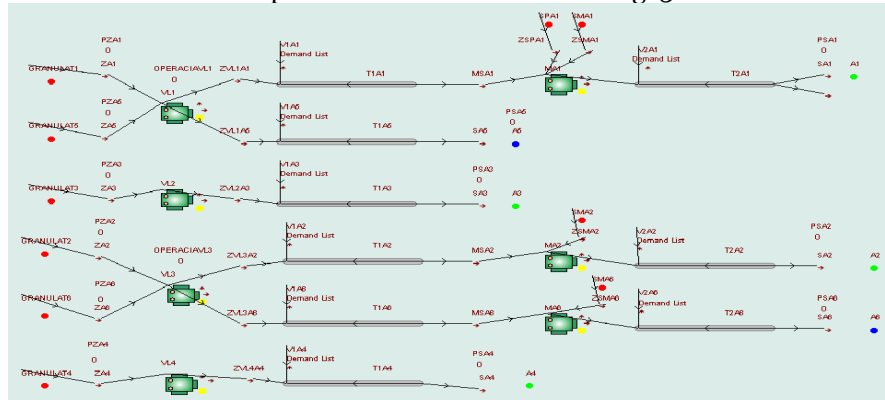


Fig. 3 Example of production lines simulation



Fig. 4 Graph operation of machines and devices during the simulation

6. GRAPHICAL SIMULATION OUTPUT OF MACHINERY AND DEVICES

The simulation software generates statistics on the performance of machines and devices after a simulation of the production line. In this case, the witness was used.

Based on the above chart it is possible to achieve productivity gains and to address the increasing efficiency of machines. The solution is to reduce downtime and streamlining manufacturing process technology for finishing. It is necessary to increase the number of inspectors who would ensure the continuity of material flow in quality control. This eliminates the accumulation of technology stocks.

7. CONCLUSION

Any proposal for a perfect relocation of production lines and the subsequent operation of the production system is still subject to further change. They are caused by innovation of products on the market, qualitative and quantitative requirements of the customer etc. Therefore, the production system in operation there may be changes in the parameters of the production system, which, depending on time may decrease, unchanged, or rise. Simulation of the production system is a tool to select from a large number of possible solutions. The simulation is to select the optimal variant. By choosing this option should be to optimize the production system. An appropriate choice of the optimal solution and the result of a rationalization of the project are dependent primarily on a thorough analysis of the production system and production program.

ACKNOWLEDGEMENT:

This paper was created thanks to project supported by European Union concrete Operational program RESEARCH and DEVELOPMENT (Appeal OPVaV-2009/2.2/03-SORO) named **Manufacture technical level and control effectiveness increase in the field of plastics component production**. Faculty of Material Science and Technology of Slovak University of Technology in Trnava is realized this project in cooperation with HANIL E-HWA AUTOMOTIVE SLOVAKIA s.r.o. in Považská Bystrica in Slovakia.

The main aim of cooperated project is increasing of manufacture technical level and of control effectiveness in the field of plastics component production with three specific project aims:

- ❖ Building of laboratory for construction and tool simulation for processing of plastics components,
- ❖ Material flow and production planning optimalization,
- ❖ Mechanisation and automation as a tooling for elimination of bad human factor influence to the manufacture quality.

This article was created with the support of the
OP Research and development for the project
**Manufacture technical level and control effectiveness increase in
the field of plastics component**
ITMS 26220220094,
co-financing from the resources of European Regional Development
Fund.



Support research activities
in Slovakia/
Project is co-financing
from resources EU



REFERENCES

- [1] Danišová, N., Zvolenský, R.: Intelligent manipulating and transport systems. In: International Doctoral Seminar 2007: Proceeding. 13-16 May, 2007, Smolenice. - Trnava : AlumniPress, 2007. - ISBN 978-80-8096-011-7. - pg. 34-38
- [2] Horváth, Štefan - Danišová, Nina: Power elements of flexible manufacturing and assembling systems. In: International Doctoral Seminar 2008 : Proceedings. Smolenice, May 18-20, 2008. - Trnava : AlumniPress, 2008. - ISBN 978-80-8096-058-2. - pg. 130-136
- [3] Horváth, Štefan - Javorová, Angela: Planning and design production system organizational structures and procedures. In: Annals of Faculty of Engineering Hunedoara - Journal of Engineering. - ISSN 1584-2673. - Tom VIII, Fasc 3 (2010), s. 331-335
- [4] Javorová, Angela - Matúšová, Miriam: Automated assembly system design with help of computer aided system. In: Annals of The Faculty of Engineering Hunedoara. - ISSN 1584-2665. - Tom VII, Fasc. 2 (2009), s. 43-48
- [5] Mudriková, Andrea - Hrušková, Erika - Velíšek, Karol: Logistics of material flow in flexible manufacturing and assembly cell. - registered in ISI Proceedings. In: Annals of DAAAM and Proceedings of DAAAM Symposium. - ISSN 1726-9679. - Vol. 19, No.1. Annals of DAAAM for 2008 & Proceedings of the 19th International DAAAM Symposium "Intelligent Manufacturing & Automation: Focus on Next Generation of Intelligent Systems and Solutions", 22-25th October 2008, Trnava, Slovakia. - Viedeň : DAAAM International Vienna, 2008. - ISBN 978-3-901509-68-1, s. 0919-0920
- [6] Mudriková, Andrea - Košťál, Peter - Velíšek, Karol: Material and information flow in flexible manufacturing cell. - registered in ISI Proceedings. In: Annals of DAAAM and Proceedings of DAAAM Symposium. - ISSN 1726-9679. - Vol. 18, No.1. Annals of DAAAM for 2007 & Proceedings of the 18th International DAAAM Symposium "Intelligent Manufacturing & Automation: Focus on Creativity, Responsibility, and Ethics of Engineers" : Croatia, Zadar 24-27th October 2007 (2007). - Viedeň : DAAAM International Vienna. - ISBN 3-901509-58-5, s. 485-486
- [7] Pecháček, František - Charbulová, Marcela: Stavebnicové upínacie systémy. Modular fixture systems. In: Strojárstvo - Strojírenství. - ISSN 1335-2938. - Roč. 12, č. 9 (2008), 191/5-192/5





STRUCTURAL PROPERTIES OF NANO- STEEL POWDERS PREPARED BY POWDER METALLURGY

¹ UNIVERSITY OF PANNONIA, EGYETEM U. 10, 8200 VESZPRÉM, HUNGARY

² RESEARCH INSTITUTE FOR TECHNICAL PHYSICS AND MATERIALS SCIENCE, HUNGARIAN ACADEMY OF SCIENCES, KONKOLY-THEGE M. ÚT 29-33, 1121 BUDAPEST, HUNGARY

ABSTRACT:

In this paper, the first results of preparation and structural characterization of the nanostructured strengthened steels are presented. The samples were prepared by powder technology. A high energy milling process at different parameters has been applied to strengthened steel powder production. The high efficient attrition mills are on the basis of this work assuring grains with nanostructure. Powder samples were investigated by scanning electron microscopy (SEM). The structural changes during milling steps have been described. It was demonstrated that 4 hours milling in wet atmosphere are enough to realize steel powders with nano dimensions.

KEYWORDS:

nanostructured strengthened steels, powder technology, scanning electron microscopy (SEM)

1. INTRODUCTION

Oxide dispersion strengthened (ODS) FMS are promising materials with a potential to be used at elevated temperatures due to the addition of extremely thermally stable oxide particle dispersion into the austenitic or martensitic matrix. ODS steels show high-strength at high-temperatures [1]. Oxide-dispersion-strengthened steels have attracted attention for advanced nuclear power plants applications such as fast and fusion reactors, because of their superior high temperature mechanical properties [2, 3]. ODS steels are being developed and investigated for nuclear fission and fusion applications in Japan [4, 5], Europe [6, 7] and the United States [8, 9].

Powder metallurgy of stainless steel (PM SS) components constitutes an important and growing segment of the PM industry. The PM processing provide a feasible and economic manu-facturing of au-stenitic stainless steels components with complex shape and advantages such as good dimensional precision, high surface finish and good mechanical properties [10 – 14]. The production of oxide dispersion- strengthened steel involves many processes, such as mechanical alloying, degassing, canning, hot extrusion, and heat treatments. In the procedures, the hot extrusion process strongly affects precipitation behavior of oxide particles and their dispersion. [15]. Fundamental studies concerning optimization of mechanical milling (MM) processing as well as effects of alloying elements on the high-temperature mechanical strength had been carried out in cooperation with fabrication vendors [16].

In this work, the structural and morphological properties of nanostructured ODS steel powders prepared by powder metallurgy methods are presented.

2. THE STUDY

An efficient dispersion of ODS steels will be achieved by employing a high efficient milling process, namely the attritor milling (Figure 1). In this paper the wet coating process of fine ceramic particles is proposed by the help of mechano-chemical processes assured by attrition milling. In the case of our model experiments, for some of the powder mixtures a high efficient attritor mill (DMQ-07 Union Process) was employed. This apparatus allowed a high rotation speed (2000-2800 rpm)

and a contamination free mixing process, because of stainless steel parts (tank, arm, balls) as in Figure 1.

Based on our former observations the attritor mill has more advantages to conventional planetary mill. In the wet process, the attritor may work at higher speeds as 3000 rpm in comparison to planetary mill, 500 rpm. The delta discs employed in the attritor, as well as the small media 0.1- 1 mm assure a very efficient dispersion. The commercial austenitic powder (Hoganas 316L) were milled by attritor for 1, 2, 3, 4 and 5 hours in propanol (wet milling).

Morphology and microstructure of the powder and sintered steels were studied by scanning electron microscope (Zeiss-SMT LEO 1540 XB and Jeol JSM-25-SIII).

3. ANALYSES, DISSCUSIONS, APPROACHES AND INTERPRETATIONS

Structural characterization of starting austenitic steel powder was performed by scanning electron microscopy (Figure 2). Austenitic sample consisted of globular particles. The average size of particles is 50 – 100 μm . The composition of starting austenitic powder is Fe and 0,02% C, 13% Ni, 16,8% Cr, 0,85% Si, 0,20%O, 0,04% N and 2,2% Mo.

The powder structure after 1 hour milling showed considerable differences to starting powder. The forms of austenitic particles are globular. Their average size is lower, about 80 μm (Figure 3a). The structural investigations demonstrated the existence of small grain in few micrometer ranges among globular grains (Figure 3b).

Figure 4 showed the morphology of austenitic sample after 2 hours milling time. The average size of globular particle is about 60 μm . 1 hour intensive high efficient milling decreased the particle size about 15 – 20 μm . The shape of grains has not changed.



Figure 1. Horizontal high efficient attritor mill

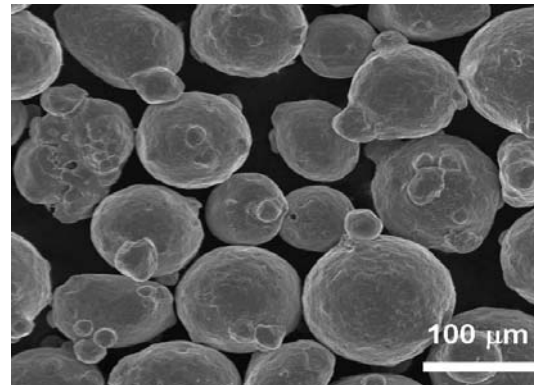
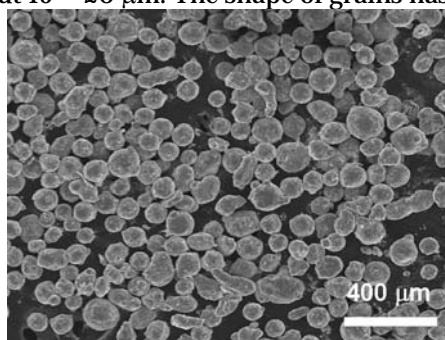
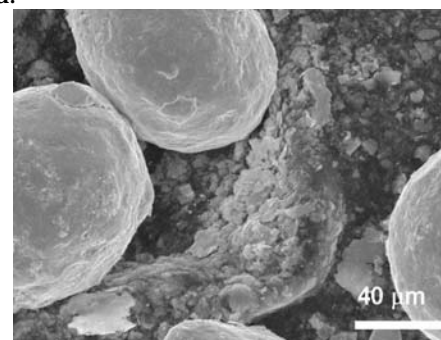


Figure 2. SEM image of starting commercial austenitic powder

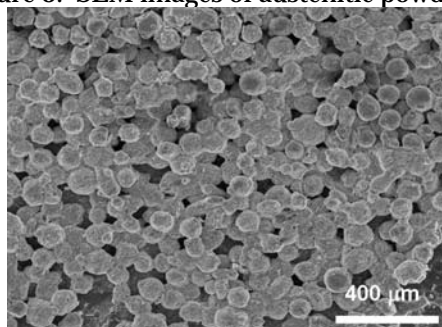


a)

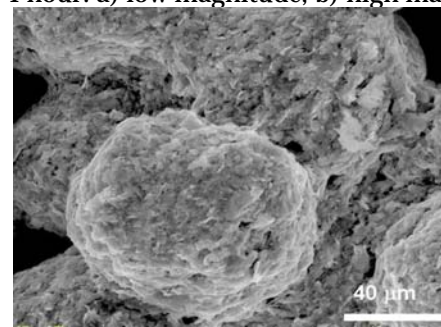


b)

Figure 3. SEM images of austenitic powder milled for 1 hour. a) low magnitude, b) high magnitude



a)



b)

Figure 4. SEM images of austenitic powder milled for 2 hour. a) low magnitude, b) high magnitude

The next 1 hour milling time (3 hours) decreased the particle size about $10\ \mu\text{m}$ as shown the Figure 5a. The parts of particles are globular, but the SEM investigation proved the developing of particles with rough surface (Figure 5b). This disintegration effect is on the basis of the evaluation of nanoparticles.

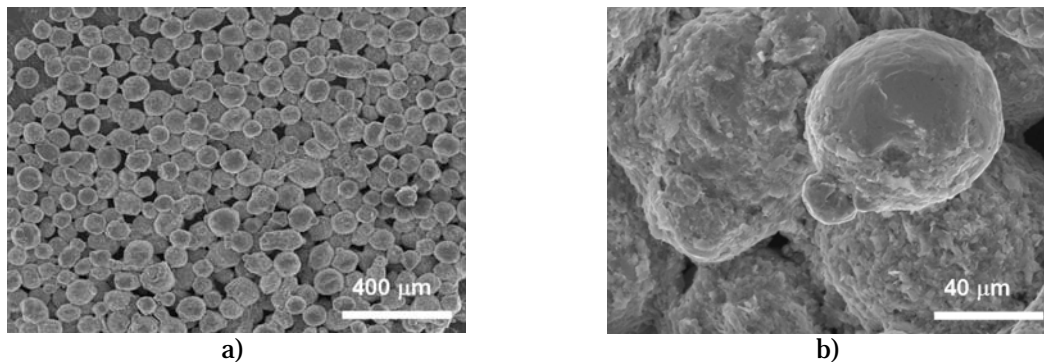


Figure 5. SEM images of austenitic powder milled for 3 hour. a) low magnitude, b) high magnitude

After 4 hours wet milling, the structure showed the drastically change in morphology. The sample consisted of very small austenitic grains with lamellar structure and of few $80\ \mu\text{m}$ size globular particles (Figure 6a). The average size of lamellar particles in one dimension is nanometer range, their length is few micrometers (Figure 6b).

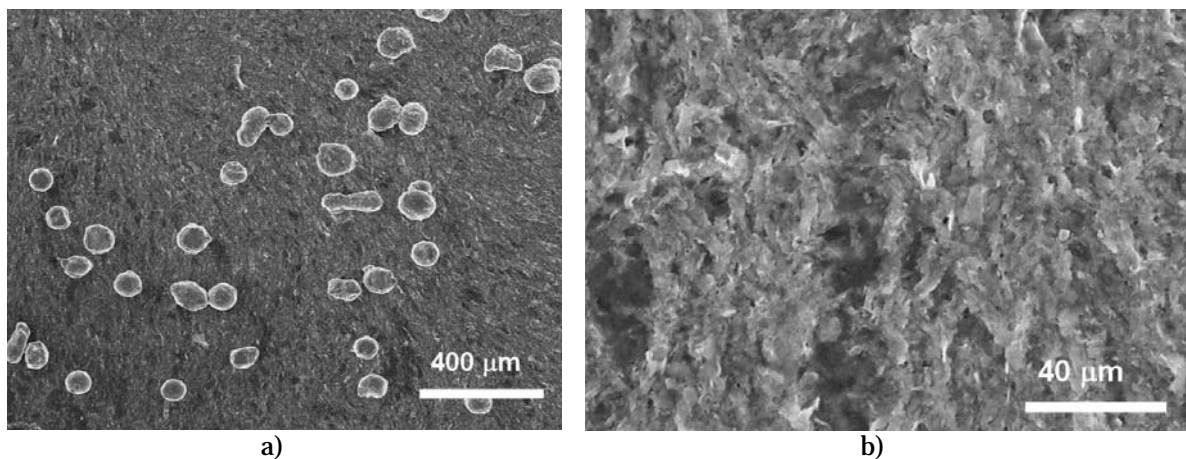


Figure 6. SEM images of austenitic powder milled for 4 hour. a) low magnitude, b) high magnitude

The final nanostructure was achieved after 5 hours milling time (Figure 7a). The sample consisted from very thin lamellar particles, the existing of larger grains is not shown. Figure 7b show the very fine austenitic structure.

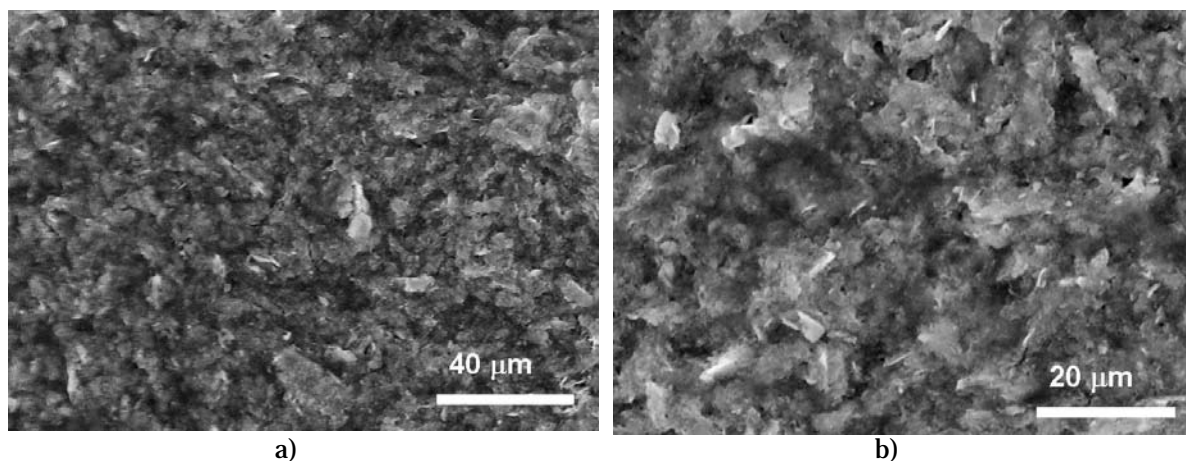


Figure 7. SEM images of austenitic powder milled for 5 hour. a) low magnitude, b) high magnitude

4. CONCLUSIONS

In this paper, the first results of preparation and structural characterization of the strengthened nanostructured steels prepared by the powder technology is presented. A high energy wet milling process in propanol for 1, 2, 3, 4 and 5 hours milling time has been applied to strengthened steel powder production. The structural changes have been observed. The average size of starting commercial austenitic powder was about 100 μm . The particle size of nanometer range in was achieved after 4 milling hours.

The help in the preparation of this work is gratefully acknowledged to Gy. Babócs, P., V. Varga, A. Petrik, L. Illés. Special thanks to Dr. Á. Horváth (AEKI). This work is supported by TÁMOP 4.2.2-08/1-2008-0016 project.

REFERENCES

- [1.] A. Kimura, T. Sawai, K. Shiba, et al. Nucl. Fusion 43 (2003) 1246.
- [2.] J.J. Huet, Powder Metall. 10 (1967) 208.
- [3.] J.J. Huet, V. Leroy, Nucl. Tech. 24 (November, 1974) 216.
- [4.] S. Ukai, T. Nishida, H. Okada, T. Okuda, et al., J. Nucl. Sci. Technol. 34 (1997) 256.
- [5.] S. Ukai, T. Yoshitake, S. Mizuta, et al., J. Nucl. Sci. Technol. 36 (1999) 710.
- [6.] A. Alamo, J. Decours, M. Pigoury, C. Foucher, Structural Applications of Mechanical Alloying, ASM International, Materials Park, OH, 1990.
- [7.] A. Alamo, H. Regle, G. Pons, L.L. Bechade, Mater. Sci. Forum 88–90 (1992) 183.
- [8.] D.K. Mukhopadhyay, F.H. Froes, D.S. Gelles, J. Nucl. Mater. 258–263 (1998) 1209.
- [9.] M.K. Miller, E.A. Kenik, K.F. Russell, et. al., Mater. Sci. Eng. A 353 (2003) 140
- [10.] F. Borgioli, E. Galvanetto, T. Bacci, et al., Surf. Coat. Technol. 149 (2002) 192–197.
- [11.] O. Sandberg, L. Jönson, Advances in Powder Metallurgy, Adv. Mater. Process. 12 (2003) 37–42.
- [12.] P. Lindskog, The future of ferrous PM in Europe, Powder Metall. 47 (2004) 6–9.
- [13.] Koszor O, Horváth A, Weber F, Balázsi K, Gillemot F, Horvath M, Fényi B, Balázsi Cs, KEY ENG MAT 409: pp. 237-243. (2009)
- [14.] H. Sakasegawa et al. / Journal of Alloys and Compounds 452 (2008) 2–6
- [15.] T. Okuda, S. Nomura, et al., Proc. Symp. Sponsored by the TMS Powder Metallurgy Committee, Indiana, 1989, p. 195.





¹ Martina KUSÁ, ² Miriam MATÚŠOVÁ, ³ Marcela CHARBULOVÁ

OPTIMALISATION METHOD OF MATERIAL FLOW AT MANUFACTURING PROCESS

¹⁻³ SLOVAK UNIVERSITY OF TECHNOLOGY, FACULTY OF MATERIALS SCIENCE AND TECHNOLOGY,
INSTITUTE OF PRODUCTION SYSTEMS AND APPLIED MECHANICS, TRNAVA, SLOVAKIA

ABSTRACT:

A today trend in manufacturing is characterized by production broadening, innovation cycle shortening, and products having new shape, material and functions. The production strategy focused to time needs change from traditional functional production structure to production by flexible manufacturing cells and lines. Production by automated manufacturing system (AMS) is a most important manufacturing philosophy in last years.

KEYWORDS:

production system, manufacturing, material flow, layout optimizing

1. INTRODUCTION

This paper was created thanks to project Operational program RESEARCH and DEVELOPMENT (OPVaV-2009/2.2/03-SORO) number ITMS 26220220094 named „Manufacture technical level and control effectiveness increase in the field of plastics component production“. Faculty of Material Science and Technology of Slovak University of Technology in Trnava is realized this project in cooperation with HANIL E-HWA AUTOMOTIVE SLOVAKIA s.r.o. in Považská Bystrica in Slovakia.

The main target of project is a manufacturing and control processes effectivity increasing at plastics parts production process. Goal of effectivity increasing is competitiveness increasing at automotive manufacturing market by knowledge and technology transfer and joined research and development activities between industrial and academic sphere.

This project is covered by the category of applied research. It is focused to planed research for new knowledges and skills acquirement for new plastic component development (tools for plastics molding), processes (new processes in manufacturing) and significant quality increasing of existing products (existing tools and processes optimizing).

Rationalization of production system allows elimination of negative influences on production costs and product price. Rationalization projects starts with data acquisition followed by analysis and evaluation of data. Once aims of rationalization are clearly defined a new production system or innovative production process is designed. Designed changes cannot be implemented during production of the factory, because effectiveness of proposed alternatives is not guaranteed. Due to this reason, simulation of proposed alternatives using various simulation computer programs gains on importance. Simulation is a suitable tool for elimination of imperfections in production process. Furthermore, it allows searching for possibilities of increasing effectiveness of production as well as for problems, which may interfere with continuous production cycle of a factory.

Main aim of rationalization projects is an improvement of production processes and prevention from losses and wasting of all possible kinds of production resources (material, energy, production area, production time, production facilities, etc.), this all from material purchase from supplier to dispatch of finalized products to customer at all workstations as in case of production preparation so as during production itself.

2. LAYOUT OPTIMIZATION

Principle of systematic application of logical thinking during solution of difficult issues and elimination of losses and wasting during production process is aimed predominately at 4 essential areas:

1. Minimization of stock size and supply and release of financial resources and also lowering the logistics expenditures for storage, manipulation, etc.
2. Constant improvement of all activities of logical chain: suppliers – product – customer (lowering the production costs, shortening the production time, improvement of work environment, etc.)
3. Concentrate attention at sites, which are decisive for quality, competitiveness, perspective, productivity, costs, etc.
4. Optimize system of material and information flows – eliminate losses, which may cause irregularity or overload of production, complexity of material flows, downtime caused by organization imperfections, etc..

Solving the optimization of production requires detailed information about whole production process. Because technological procedure of production is given, it is possible to adjust material and data flow. Fig. 1 shows former structure of material flow through production. Aim was to provide continuous production process in automotive area of Hanil company.

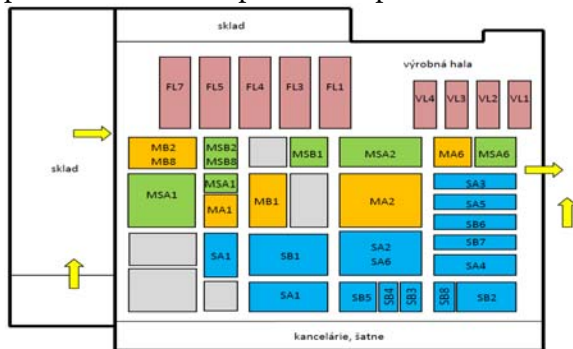


Fig. 1 Former layout of the company workshop

Wastage is present at each workshop, but it is possible to identify and solve it using 5S method, which is suitable for production and service oriented organizations. Applying the 5S method allows achieving an improvement and simplification of material flow, machine layout and stock.

Other benefits are:

- ❖ Quality, productivity and safety improvement
- ❖ Better company culture, people attitude, less apathy
- ❖ Improved work environment.

Method of 5S is under development and nowadays sixth S is also defined, know as safety. Reason is to realize all improvements at workplace in such manner, that employees are not endangered. Apart of this, it put emphasis on availability and unambiguous identification of all safety devices. The aim is to prevent from danger during work and limit occupational accident to a minimum possible.

The aim of material flow projection is solution of:

- ❖ Minimization of transport, manipulation and storage
- ❖ Simplification of system to minimum – minimum consumption of expenses and time □ solution of important relationships,
- ❖ Workplaces and capacities – incorrectly designed capacity causes unevenly distributed material flow, stock accumulation, necessity of inter-stocks and buffers and additional manipulation activities,
- ❖ Information flow and control system – correct control of inputs of production tasks, synchronization of purchase, production and dispatch, coordination of system of production control with transportation system,
- ❖ All components of the production system have to be designed in mutual relations and it is ideal if all are verified before installation using simulation model.

Solving the given material flow requires specification of the aim of innovation of a given material flow.

The proposal of the layout of production lines is solved as a combination of concerned layout (according to a number of products declared in PQ diagram) and technological layout (consideration of a technology of injection and technology of forming). In the frame of detailed design were relocated beginnings MT on production facilities in order to eliminate intersection of MT directly in front of production facilities. In fact this change counts only

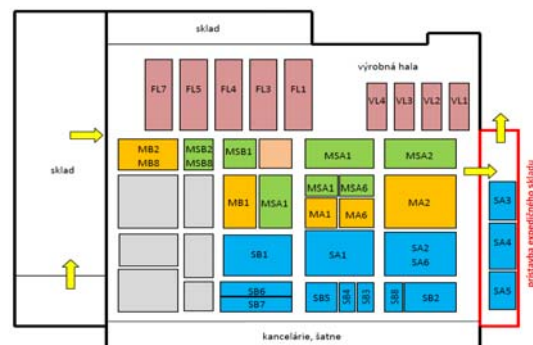


Fig.2 Innovation of the workshop

for location of the product, which undergoes technological operation. Combination of products in the frame of one production facility remains with respect to the available capacity unchanged. Respecting the MT proposal, the layout of stocks is realized close to dispatch, taking into account space required for expedition trolleys. Distribution of a part of trolleys with finalized products is realized in proposed annex building of dispatch stock with dimension of 10 × 70 meters.

Simulation of the proposed change is possible to avoid unavailing losses during ineffective trials related with application of innovations. During simulation is required to fulfill production plan, which is documented in the form of a table.

Fig. 3 shows production plan, which is compared with values of outputs after the simulation is completed.

SOFT TRIM				MAREC				ROK 2010								
sk. B	VÝROBOK	počet ks v aute	ED 5DV	ED WGN	ED 3DV	KM	EL	počet aut	celkom ks/mesiac	ED 5DV	ED WGN	ED 3DV	KM	EL	počet aut	celkom ks/rok
1.	LUGGAGE SIDE S	2	4 550	3 900	1 150			9 600	19200	50 600	43 400	12 300			106 300	212600
2.	FLOOR CARPET FRT	1	4 550	3 900	1 150	2 200		11 800	11800	50 600	43 400	12 300	33 700		140 000	140000
3.	LUGGAGE CVR MAT	1	4 550		1 150			5 700	5700	50 600		12 300			62 900	62900
4.	LUGGAGE CVR BORD	1	4 550		1 150			5 700	5700	50 600		12 300			62 900	62900
5.	C/SELF	1	4 550		1 150			5 700	5700	50 600		12 300			62 900	62900
6.	LUGGAGE CVR"G CTR	1		3 900				3 900	3900		43 400				43 400	43400
7.	LUGGAGE CVR"G FRT	1		3 900				3 900	3900		43 400				43 400	43400
8.	FLOOR CARPET RR	1				2 200		2 200	2200				33 700		33 700	33700

Fig. 3 Production plan

Figure 4 depicts simulation of SOFT TRIM component production in HANIL company and partial tables with outputs from simulation.

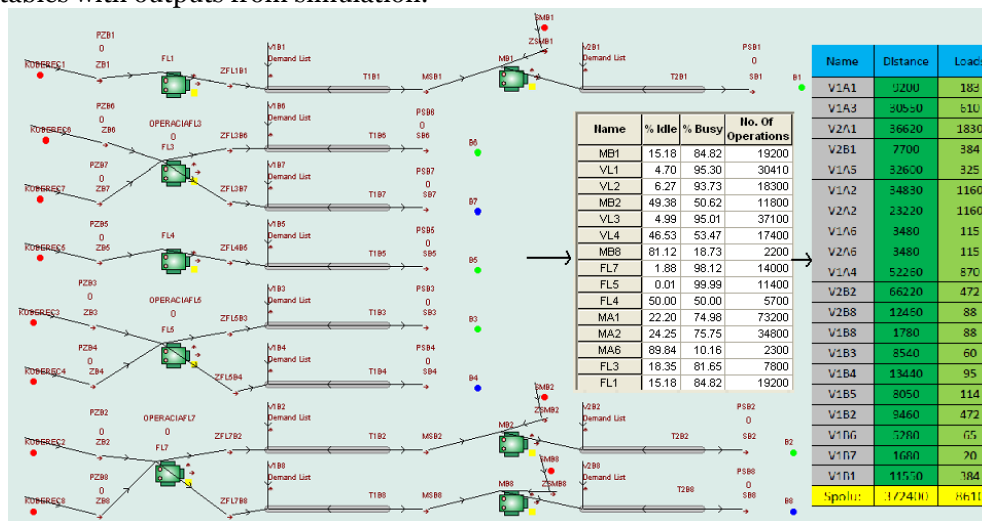


Fig.4 Simulation of innovation of workshop layout

3. CONCLUSIONS

Proposal of new layout of production lines is adjusted for current capacity of production with aim to optimize material flows. Application of proposed solution is in fact possible to realize during full production process, because it counts mostly for relocation of dispatch trolleys. Relocation of those trolleys would be effective after finishing the building of dispatch hall at current dispatch site. Building the dispatch hall would not affect production process, what is benefit of the proposed solution. Expected time required for building up the dispatch hall with dimensions of 10×70 meters is approximately one month. After finalizing the hall, zones required for different types of trolleys would be calculated and subsequently labeled zones for stock areas, service areas and transportation paths. After the trolleys relocation and clear out the spaces, workplaces for assembly would be relocated. This procedure would affect the production process significantly. This change would be implemented during weekends using internal employees of the company, predominately. Implementation of all changes is expected to last approximately two months. From economic point of view, most significant impact would have an investment into the new stock for distribution logistics. Expenses related with relocation of workplaces are negligible and could be realized also during full production. When comparing this investment with shortening transportation time between workplaces, return on investment is expected in few months. From the long term point of view and considering ambitions of the company, which are aimed at increasing volume of production, the investment into dispatch stock is in short term range necessity. Other advantage of building the dispatch stock is simplification of production process and establishment of space for dispatch trolleys with finalized products.

This article was created with the support of the
OP Research and development for the project
**Manufacture technical level and control effectiveness increase in
the field of plastics component**
ITMS 26220220094,
co-financing from the resources of European Regional Development
Fund.



Support research activities
in Slovakia/
Project is co-financing
from resources EU



REFERENCES

- [1] Danišová, N. - Zvolenský, R.: Intelligent manipulating and transport systems. In: International Doctoral Seminar 2007 : Proceeding. 13-16 May, 2007, Smolenice. - Trnava : AlumniPress, 2007. - ISBN 978-80-8096-011-7. - pg. 34-38
- [2] Horváth, Š. - Danišová, N.: Power elements of flexible manufacturing and assembling systems. In: International Doctoral Seminar 2008 : Proceedings. Smolenice, May 18-20, 2008. - Trnava : AlumniPress, 2008. - ISBN 978-80-8096-058-2. - pg. 130-136
- [3] Hrušková, Erika - Holubek, Radovan - Velíšek, Karol: The possibilities of increasing the flexibility of intelligent assembly cell. In: 10th Biennial Conference on Engineering Systems Design and Analysis (ESDA2010) : Turkey, Istanbul, July 12-14, 2010. - : ASME, 2010. - ISBN 978-0-7918-3877-8. - S. 1-10
- [4] Mudriková, Andrea - Hrušková, Erika - Velíšek, Karol: Logistics of material flow in flexible manufacturing and assembly cell. - registrovaný v ISI Proceedings. In: Annals of DAAAM and Proceedings of DAAAM Symposium. - ISSN 1726-9679. - Vol. 19, No.1. Annals of DAAAM for 2008 & Proceedings of the 19th International DAAAM Symposium "Intelligent Manufacturing & Automation: Focus on Next Generation of Intelligent Systems and Solutions", 22-25th October 2008, Trnava, Slovakia. - Viedeň : DAAAM International Vienna, 2008. - ISBN 978-3-901509-68-1, s. 0919-0920
- [5] Mudriková, Andrea - Košťál, Peter - Velíšek, Karol: Material and information flow in flexible manufacturing cell. - registrovaný v ISI Proceedings. In: Annals of DAAAM and Proceedings of DAAAM Symposium. - ISSN 1726-9679. - Vol. 18, No.1. Annals of DAAAM for 2007 & Proceedings of the 18th International DAAAM Symposium "Intelligent Manufacturing & Automation: Focus on Creativity, Responsibility, and Ethics of Engineers" : Croatia, Zadar 24-27th October 2007 (2007). - Viedeň : DAAAM International Vienna. - ISBN 3-901509-58-5, s. 485-486
- [6] Pecháček, F.; Charbulová, M.: Stavebnicové upínacie systémy. Modular fixture systems. In: Strojárstvo - Strojírenství. - ISSN 1335-2938. - Roč. 12, č. 9 (2008), 191/5-192/5
- [7] Velíšek, Karol - Javorová, Angela - Košťál, Peter: Flexible assembly and manufacturing cell. In: Academic Journal of Manufacturing Engineering. - ISSN 1583-7904. - Vol. 5, No. 2 (2007), s. 141-144



VIBRATION TECHNIQUE – AN IMPROVEMENT SOLUTION FOR QUALITY OF CAST METALLIC MATERIALS

¹⁻²UNIVERSITY POLITEHNICA BUCHAREST, ROMANIA

ABSTRACT:

The influence of purifying processes by metallic melts degassing and refinement it is not a recent technological news. The processes of local undercooling, nucleation, crystallization and solidification of metallic melts represent a future technical solution in quality increase of castings. The work presents the results of some reasearch experiments in this field.

KEYWORDS:

undercooling, nucleation, crystallization, metallic melts, castings

1. INTRODUCTION

High and low frequency mechanical oscillations, sonic and ultrasonic vibrations respectively, may form only in elastic continuous medium, and general acoustic laws are available also in the ultrasonic vibrations range.

Mechanical vibrations or sonic and ultrasonic vibrations convey by progressive particles movement of the medium, melt alloy respectively, and due to this particles will come back in the initial position.

Due to the inertia and elasticity of the liquid alloy, particles continue to oscillate around the equilibrium position, even after vibrations stop, but with a damped movement. If the oscillation direction of the particles is parallel with the propagation direction of the wave, waves are called longitudinal waves and the interference is made in the propagation direction, namely the particles movement $X(t)$ in the system which oscillate according to the harmonic oscillations, is parallel with normal \vec{n} to the waves surface.

Propagation speed of longitudinal elastic waves in solid medium is expressed by the square root of the elastic modulus and density ratio, with the Newton relation [1]:

$$v = \sqrt{\frac{E}{\rho}} \quad (1)$$

where: v is propagation speed of waves [m/s];

E – elastic modulus [N/mm²];

ρ – density of the medium [kg/m³].

If we considerate the fact that oscillations are produced adiabatically, namely the variation speed of pressure is so high that the heat exchange between the near layers can be neglect, the propagation speed of mechanical oscillations in elastic liquid mediums is given by the relation:

$$v = \sqrt{\frac{1}{\rho \cdot K}} \quad (2)$$

ρ is desity of the medium [kg/m³];

K – adiabatic compression of the medium.

$$K = \frac{1}{\chi \cdot p} \quad (3)$$

χ - specific heats ratio varying with number of atoms in the molecule;
 p - alloys pressure at a given moment [Pa].

For gases, elastic modulus has to be replaced with pressure. Because of rapid progressive dilatations and compressions, the local temperatures have variations which can not be balanced by heat exchanges. These compressions and dilatations have adiabatic feature.

If we multiply the pressure with the specific heats ratio, the propagation speed of longitudinal waves will be expressed by relation:

$$v = \sqrt{\frac{p}{\rho} \cdot \chi} \quad (4)$$

Knowing the value of $\chi = 1.66$ for monoatomic gases, 1.4 for biatomic gases and 1.33 for triatomic gases, thus we can calculate the speed v .

Relation (4) gives the possibility to calculate the speed, at a given temperature t , when temperature t_0 is known and pressure stays unchanged.

Knowing that density varies with temperature by the relation:

$$\rho_t = \frac{\rho_0}{1 + \alpha \cdot \Delta t} \quad (5)$$

results:

$$v = \sqrt{\frac{p \cdot (1 + \alpha \cdot \Delta t)}{\rho_0}} \cdot \chi \quad (6)$$

and thus:

$$v_t = v_0 \sqrt{1 + \alpha \Delta t} \quad (7)$$

In conclusion: speed of the elastic longitudinal waves for gases, increase proportionally with the square root of dilatation binomial [1].

In real conditions of solidification, pressures may reach values of dozens of atmospheres and may substantially influence on the reordering of the insoluble impurities and crystalline structure formation of metals.

Crystallization pressure p is the maximum possible for a given undercooling of the growing surface, calculable with relation:

$$p = - \frac{\Delta T \cdot L}{T \cdot V_0} \quad (8)$$

where: ΔT is alloy undercooling [K];

L – latent heat of alloy crystallization [J/kg];

T – absolute temperature [K];

V_0 – molecule volume in crystal lattice [m³/kmol].

At high undercoolings appear many centres of crystallization embedding all impurities. At low undercooling, crystals grow in dendritic form, and impurities are also embedded by the growth of branches I and II type.

Analysis of the thermophysical conditions of crystallization pressure development shows that it has a peculiar role in ingots and castings solidification. To identify the influence rate of different parameters on the movement process or impurities embedding, we will show how forces influence in the area of stranger particles for the alloy in solidification progress (fig.1).

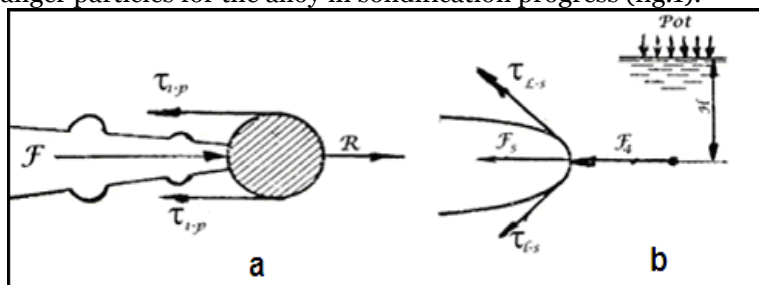


Fig.1. Representation of forces action in area of stranger particles in the liquid alloy
 a) interaction with particle; b) exceeding the ferrosstatic pressure

Force of crystallization pressure of the crystal acts on the particle being able to move in the alloy with crystallization speed. Forces of interphasic tensions inbetween impurities and liquid

alloy stand up to this movement ($\Gamma_{\sigma} = \pi \cdot r \cdot \sigma_{l-p}$), and movement hydrodynamical resistance of spherical surface in the alloy is:

$$\Gamma_s = C_r \cdot \rho \cdot \frac{v_{\text{crist}}^2}{2} \cdot \pi \cdot r^2 \quad (9)$$

Equilibrium conditions of forces are:

$$\frac{\Delta T \cdot L}{T \cdot V} = \pi \cdot r \cdot \sigma_{l-p} + C_r \cdot \rho \cdot \frac{v_{\text{crist}}^2}{2} \cdot \pi \cdot r^2 \quad (10)$$

where: C_r is the resistance coefficient.

Knowing the crystallization speed v_{crist} and ΔT we can determine the tolerable radius of the inclusion which is going to be separated by the crystallization pressure inside the casting, where after that it will be able to curdle and float to the surface.

It has been determined that during crystallization process of the alloy it may appear some ferrosstatic pressures same as alloy hydrodynamical resistance itself. This assumption is real, since the dendrites growth (according to the literature) it takes place with the speed $v_{\text{crist}} = 1000$ mm/min. In some conditions, the growth speed can be much more increased.

Analysing the scheme for this case in fig.1.b, it results that following forces acts on the growing crystal:

- 1) Force of ferrosstatic pressure

$$F_f = p_{\text{at}} + \gamma \cdot H \quad (11)$$

where: p_{at} is atmospheric pressure [N/m²];

H - height of metal layer above the crystal [m];

γ – alloy specific weight [N/m³].

- 2) Force of hydrodynamic resistance

$$F_s = C_f \cdot \rho \cdot \frac{R^2}{2} \cdot \pi \cdot r^2 \quad (12)$$

- 3) Capillary forces of moistening

$$F_{\sigma} = \pi \cdot \sigma_{l-s} \quad (13)$$

σ_{l-s} – interphasic force at alloy-crystal limit.

Based on these equations it might be assumed:

$F > F_f + F_s + F_{\sigma}$ crystal growth can take place;

$F < F_f + F_s + F_{\sigma}$ crystal growth is arrested or interrupted;

$F = F_f + F_s + F_{\sigma}$ it appears the optimum crystallization speed;

$$v_{\text{crist}} = \frac{1}{r} \cdot \sqrt{\frac{2}{C_f \cdot \pi \cdot \rho} \left(\frac{\Delta T \cdot L}{T \cdot V} - \pi \cdot r \cdot \sigma_{l-s} \right)} \quad (14)$$

Fact that at the liquid – mould contact at the beginning of crystallization, the undercooling ($\Delta T = 150 - 200^{\circ}\text{C}$) and real speed of crystallization doesn't exceed 25–30 mm/min in the first minute, leads to the idea that beside the thermophysical conditions, crystallization is also influenced by hydrodynamic ones. This fact is proven by lower dimensions of crystalline grains from the inferior levels of the ingot which solidify under the influence of some high ferrosstatic pressures.

2. METHODOLOGY

Greatest effects of ultrasonic cavitation are those observed in the metals crystallization process. The kinetics of this process it can be characterized by the nucleation rate (number of crystallization centers “n” which appears on the volume unit in the time unit) and linear growth speed “c” of crystals. More higher the nucleation speed and lower the growth speed is, more finer the grains structure will be.

Number of grains is determined by relation:

$$N = \sqrt{\frac{n^3}{c^3}} \quad (15)$$

Granular structure with fine grains randomly oriented with about same size in any direction, indicates a macroscopic isotropic and relatively homogeneous material, with good properties from

technological point of view. Undercooling degree influences both the kinetics of crystallization and structure, and formed crystals configuration. For high values of crystalline undercooling, crystals grow without attaining a regular shape and get a branched dendritic form, which reduces significantly the resistance of material.

The cavitation will appear in ultrasonic melts, if the acoustic pressure exceeds a specific value (table 1) feature to every metal. Usually, there are favoured the incipient conditions and cavitation bubbles in the melts, because they easily saturate with different gases, dissolved in melts volume, and their different solubility degree eases the formation of undissolved gas supply of nucleation centers of cavitation.

Cavitation process, generate shock waves of high intensity in the melts, nearby the crystallization front (if we consider the factors which produce the break of and dispersion of growing crystals, as a strong local perturbation source of homogeneity and melts thermodynamical equilibrium respectively).

Table 1. Values of P_t and P_c for some metallic materials

Material	Threshold power P_t [W]	Inceipient power of cavitation [W]
Aluminium	400	400
Bismuth	60	50
Cadmium	400	-
Lead	250	200
Antimony	300	300
Tin	350	250
Zinc	500	-

Effects role of cavitation in fine granular structure formation of metals appear when it exists a correlation between ultrasonic threshold power $P_{t \text{ required}}$ for important structure modifications and power P_c at which cavitation will start to appear into the melt. For cadmium and zinc cases, when cavitation appears at much more higher powers (over 400) given to that required for obtaining a fine structure, it results that cavitation has no effect for obtaining a fine granular structure.

Cavitation influence on crystallization process it can be explained by the fact that pulsatile cavitation bubbles appear in the melt, whose volumes suddenly increase in semiperiod of expansion and liquid evaporation takes place inside the bubble. Increase of evaporation and bubble volume leads to a decrease of temperature inside of it. If temperature reaches below the equilibrium one, melt gets into an undercooled state at bubble wall and it might appear a crystallization center. In the next stage, when bubble breakage takes place, the crystal just formed it detaches the bubble wall due to the difference between liquid speed and that of the solid phase, and shock wave generated by the implosion of bubble will throw the crystalline nucleus into the melt mass.

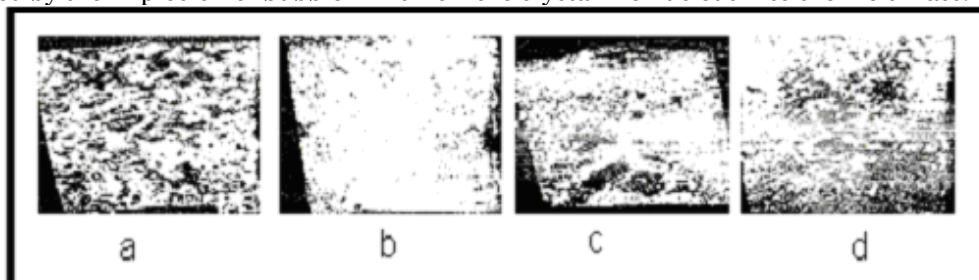


Fig.2. Structure of bismuth ultrasonic vacuum processed samples:

- a) reference ingot; b) processed ingot at atmospheric pressure; c) at pressure of 10^{-3} mmHg;
 d) at pressure of $1,5 \cdot 10^{-3}$ mmHg.

Another explication is based on shock wave generation during cavitation bubble breakage.

Efficiency of ultrasonic depends on the capacity of ultrasound to penetrate the melt volume and the capacity of crystallization process. Penetration of ultrasound into the melt is determined by the acoustic joint made between the acoustic radiator and melt, and in its turn, this joint is function of interfacial tension on the radiator – melt separation surface and the melt viscosity. Cavitation effects has a significant role, leading to the substantial improvement of mechanical and technological properties of materials.

Fluxes of metallic melt mass which move along the solidification limit with high speed and form low pressure areas, can generate hydrodynamic cavitation. By decreasing absolute pressure (below the critical one), in this area will appear gas bubbles or cavitation bubbles, filled with vapours. Their movement from low pressure areas leads to bubbles destruction (breakage), this

being accompanied by the immediate increase of pressure and temperature and destroys the solidification front.

Pressures reached in the moment of gas bubbles disintegration in liquid may be considerable (see table 2). Maximum cavitation pressure is in the center of bubble, and at a distance of $l = 2r$ it decreases with more than two times. Therefore, cavitation caverns in narrow bands form are close to the damaged solid surface.

Table 2. Pressure value in the moment of gas bubbles disintegration in liquid

Initial radius of the bubble r_0 [mm]	Radius in the breakage moment r [mm]	Maximum pressure in the breakage moment P_{max} [MPa]	Pressure at distance: $l = 2r$ [mm]
40	0.64	220	-
40	0.017	2500	200
40	0.006	25000	1000
1,27	0.012	6700	350
1,27	0.00371	58200	800

Cavitation caverns form in those discharged points of melt volume at solidification limit, where tensions stress which acts on the liquid, exceed bonding forces between its molecules. In this case, fracture strength reaches 150MPa as a result of the hydrophobic solid particles and insoluble gases presence into the melt.

Cavitation tendency is determined with dimensional criteria named critical number of cavitation:

$$Q_k = \frac{P - P_n}{\rho \cdot \frac{v}{2}} \quad (16)$$

unde: v flux speed [W/m^2]; ρ – density of molten mass [kg/m^3].

Cavitation develops in conditions when cavitation number $Q_k < 0,35 \dots 1$. Base parameter which influences the development process of cavitation is flux speed, which determines the value of static pressure at solidification limit. Its value is equal with the sum of surrounding static pressures, $P_o = 0.1MPa$ and dynamic ones:

$$P = P_o + \rho \frac{v^2}{2} \quad (17)$$

A.D.Pernik established the relationship between cavitation and Reynolds criteria value, relating to predominant influence on cavitation processes of kinetic speed of medium. Accepting the known condition that cavitation caverns form predominantly while crossing solid surfaces, he proposed the following function for cavitations number determination:

$$Q_k = 2 \cdot \frac{P - P_n}{\rho \cdot v^2} \approx Re^{0,282} \quad (18)$$

where: P is the absolute external pressure [N/m^2];

P_n – elasticity (pressure) of saturated vapours of liquid [N/m^2];

v – kinetic speed of liquid [m/s].

Cavitation centers are solid particles which exist in molten mass, gases bubbles, non-metallic inclusions. Cavitation bubbles appear more intensive close to the crystallization front surface, which has crystals peaks coming out from different caverns and cracks, filled with gas.

In the elastic forces field, two compression and dilatation zones can be distinguished (see fig.3) by longitudinal formed wave, with maximum values [1].

To obtain high cavitation pressures which determine crystals destruction, molten mass must have a smaller possible diameter of dispersed particles and gas bubbles. Usually, molten mass is subjected to degassing and refining during ultrasonic processing. Use of physical modelling for studying processes of cavitation caverns appearance allowed to obtain the following results:

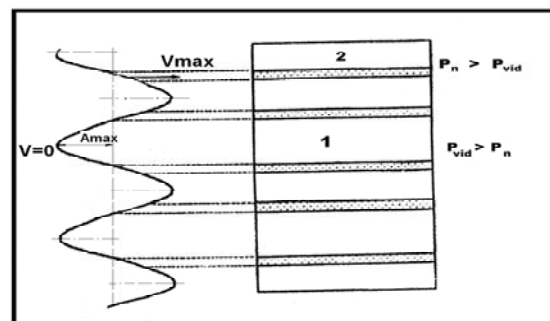


Fig. 3. Distribution of elastic wave in molten liquid mass: 1 – compression zone; 2 – dilatation zone

1. gas bubbles move inbetween growing crystal by alloy solidification without external actions;
2. for average and high speeds, the limit of solidification is covered by small gas bubbles which can form cavitation centers by superposition of elastic waves;
3. at temper crystallization speed and high gas content in alloy, big gas bubbles are emitted at solidification limit whose radius is bigger than critical one. These can generate centers for development of cavitational processes, but they remain in casting (as gas inclusions) or they leave the liquid mass.

Researching of a considerable quantity of crystalline structure obtained by high frequency vibrations, allowed to establish the influence of frequency and amplitude on solidification processes. Quantity of bubbles which appears in a second in 1cm³ of metal can be determined by I.R.Zeldovici equation:

$$J = A \cdot e^{-\frac{W}{RT}} \quad (19)$$

where: A is a constant equal for all liquids 10³¹[m³/s];

W – mechanical work required for bubble formation with radius r [J]

$$W = 4 \cdot \pi \cdot r^2 \cdot \sigma + \pi \cdot r^3 \cdot \gamma - \frac{4}{3} \pi \cdot r^3 \cdot P \quad (20)$$

P – pressure inside the bubble, equal in equilibrium existence of its external vibration pressure P_{vib} [N/m²].

From propagation theory of elastic waves it is known that vibration pressure value (without considering atmospheric pressure) depends on frequency and oscillations amplitude:

$$P_{vib} = \rho \cdot A \cdot \omega^2 \cdot \sin \omega t \quad (21)$$

Forces which determined formation and destruction of caverns at vibrations, represent continuous high frequency oscillations with high amplitude. So, it can be concluded that modidying the base parameters of elastic wave and vibrations regimes, it can control the crystalline structure of alloys.

In fig.4. it is presented schematically the movement of gas bubble (with the pressure inside equal with saturated vapours pressure P_n) along the peak of crystal. Its kinetic speed is equal with local speed of flux which depends on relief of solidification limit.

At undersonic speeds, calculated value of pressure for cavitation bubble destruction reaches 3·10⁵MPa (practically, these pressures reaches values of 220...400MPa).

At a relative low distance of the breakage center, this pressure decreases more than 10 times. Distance from breakage point to the destroyed surface of crystal depends on the initial dimension of gas bubble. More bigger it is, more time will take to break and transportation time of cavern to destruction surface [1].

After Relley data, breakage timp is:

$$\tau = 0,9146 \cdot r_0 \cdot \sqrt{\rho/P_\infty} \quad (22)$$

where: r₀ is initial radius of bubble [mm];

P_∞ – pressure into the flux of medium [N/m²];

ρ – density of medium [kg/m³].

The biggest caverns break close to the crystal surface.

Gas content has a great influence on saturated vapours pressure in cavitational medium. At a high gases content which diffuses into the cavern, the force of shock wave decreases at its disintegration. This is explained by that a part of the gas which is in cavern absorbs part of destruction energy, because it is consumed at gas compression.

3. DISCUSSIONS/RESULTS/ANALYSES

Waves propagate in a limited space and they always have two phases: of compression in waves maximum values (where amplitude has maximum value, and kinetic speed is zero) and

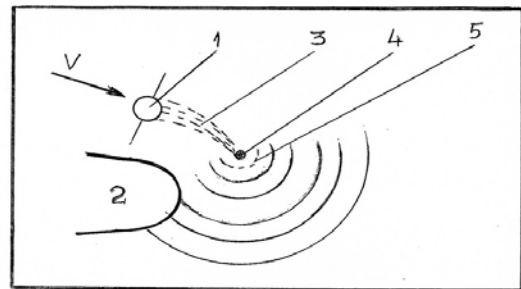


Fig. 4. Propagation scheme of shock wave obtained by cavitational bubble breakage close to the crystal peak: 1) bubble; 2) crystal; 3) pressure increase in flow direction; 4) breakage point; 5) shock wave determined by bubbles breakage

discharging in the center of oscillations (where the kinetic speed has maximum value, and wave deviation from average position is zero).

Kinetic speed of the medium is calculated by wave propagation:

$$v = A \cdot \omega \cdot \cos \omega \tau; \quad v_{\max} = A \cdot \omega \quad (23)$$

where: v is kinetic speed of the medium [m/s];

A – amplitude of vibration [10^{-3} m];

ω – frequency of vibration [Hz];

τ – time of system to move from maximum value to the center position [s].

Limited use of vibration of metallic alloys work is explained by contradictory data about the vibration action mechanism on solidifying metal. Causes of vibration influence on crystalline structure are explained by different authors by following factors:

- 1) mechanical damage of crystallization front under the strong elastic waves action and generation of complementary crystallization centers;
- 2) appearance of undercoolings grown in periodical dilatation ranges of molten mass and increase of existent additions activity, by which are created the conditions to increase the appearance speed of crystallization centers;
- 3) surface tension reduction between phases and the viscosity of molten mass, which eases the movement process of atoms from liquid phase in solid one by crystallization centers formation;
- 4) acceleration of thermocapillary mass transportation of elements from the space between the dendrites ramifications.

Microstructure of the sample obtained without vibration is presented in fig.5.a. Characteristic elements can be observed: columnar and equiaxed crystal, shrinkage, inferior cone formed by individual crystals precipitation zones. Obtained sample by vibration action in crystallization period has a different macrostructure than the control sample fig.5.b.

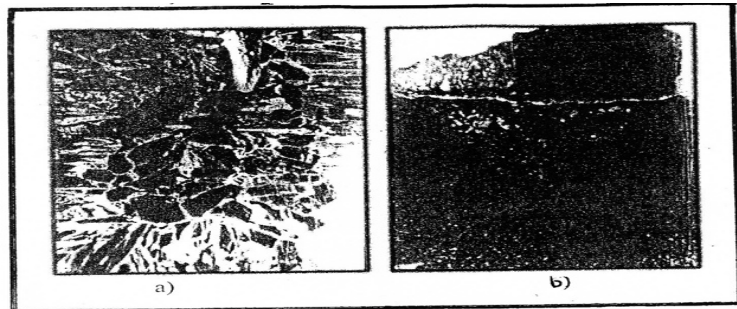


Fig. 5. Aspect of microstructure in a salol sample
 a) without vibration ; b) after vibration

Practically, the zone of columnar crystals disappeared and equiaxed crystals zone increased properly and determined a ragging of grains and increased concentration. This fact indicates a more compacted configuration of crystalline structure in the sample under elastic oscillation action.

In fig.6.a are presented the typical diagrams recorded during the crystallization process of samples without vibration, and fig.6.b shows the diagrams by vibration action with a frequency of 94Hz and amplitude 1mm. OA sector corresponds to the thermostatic period of molten mass, and AB corresponds to the cooling period. At the beginning moment of crystallization latent heat of phase transformation is released, and thus, it is explained the bounce of temperature of BC sector. CD sector corresponds to the cooling of solid phase.

Comparative analysis of crystallization process diagrams (thermograms) of ingot in control experiments and by the vibration action indicates that vibration in beginning state of process (AB sector) contributes to temperature equalization in the whole volume of sample. It influences the heat transfer rate from molten mass to cooled chamber. Vibration also influences maximum undercooling of molten mass, which can be seen from the placing of points B comparison (fig. 6. a and b). It can be seen that rapidly increase of temperature starts simultaneous in the whole samples volume by vibration, and without vibration, the beginning of this increase of temperature it is unequal for different portions of molten mass. Following section explains the decrease of columnar zone thickness, which has been determined in practice. Temperature growth speed in portion BC (fig.6) is unequal without elastic oscillations application and by the vibration action.

By vibration, temperature reaches a certain minimum value, increase suddenly, and temperature increase takes place slower during control experiments, and when it reaches a certain value, it increases again (CD sector).

In fig.7. it is presented the dependence cooling rate of molten mass with vibration frequency. Increase of cooling rate in elastic oscillations field it is caused by intensive movements of molten mass in crystallization chamber and by the increase of heat transfer coefficient from the molten superheated mass to the wall of crystallizer. Its value it is proportional with kinetic speed of molten mass ($\alpha = A \cdot W^{0.8}$), and increase of oscillations frequency contributes to increase of this speed. In

fig.8. it's been highlighted the dependence of maximum undercooling with elastic oscilations frequency. It can be noticed that an oscilations frequency takes place, which leads to the decrease of maximum undercooling zone of molten mass (hatched section). In fig.9. appear the dependences of structural features (grains dimensions) of ingots with vibrations frequency at constant amplitude of oscilations equal with $10^{-3}m$. Maximum (1) and minimum (2) dimension decreases with the increase of frequency up to 40 Hz. Variation of frequency from 50 up to 4500 Hz didn't indicate any minimal differences in ingots structure.

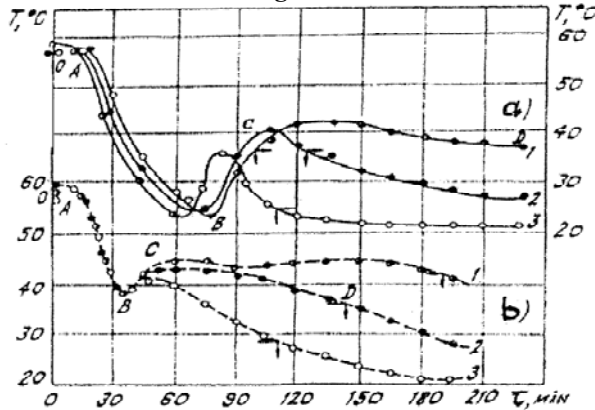


Fig.6. Diagrama solidificării probei de salol: a) fără vibrație; b) cu

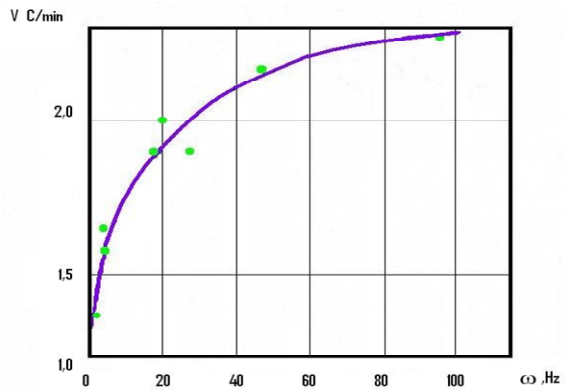


Fig.7. Dependența vitezei de răcire a masei topite funcție de frecvența vibrației

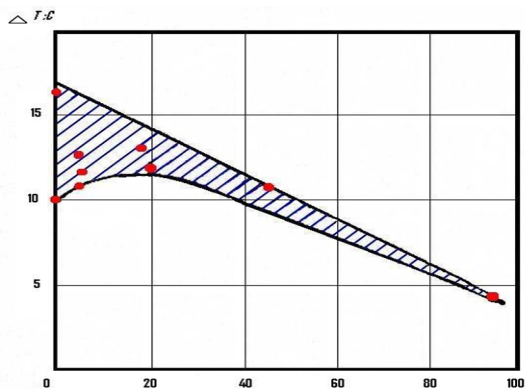


Fig.8. Dependence of molten mass undercooling with elastic oscilations frequency

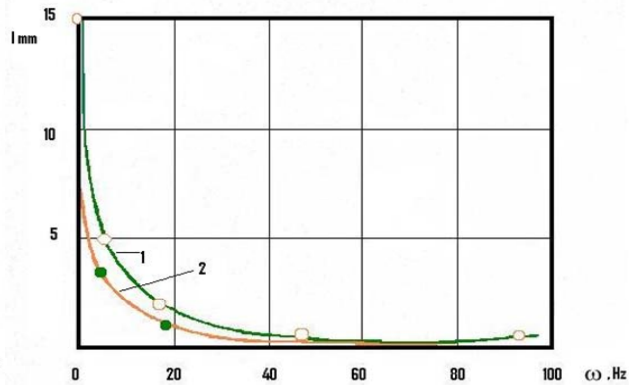


Fig.9. Dependence of crystalline grains dimensions with vibration frequency (at constant amplitude) : 1 – maximum dimension of grains ; 2 – minimum dimension of grains

4. CONCLUSIONS

Main effect of forced oscilations is the movement of waves by pressure and depression which alternates forcing the cyclic movement of alloy mass, with formation of extra crystallization centers and dendrites fragmentation.

Vibration leads to breakage of secondary branches of dendritic crystals. Increase of pressure by 105 times in liquid due to the cavitation carvens implosion, contributes to formation of new crystallization centers. Undissolved impurities may become sites for crystallization nuclei. The greatest finishing is given by vibration with circular amplitude in horizontal plan, but it can be used forms of different dimensions. Once frequency value increase, number of equiaxed grains increases and decreases the number of columnar crystals. At vibration with frequency of 100 Hz, the value of angle ω formed between surface of solidification front and vertical axe of casting has the value of $\omega > 120^\circ$, which means that it forms an open concentrated shrinkage, with small height, which can lead to a reduction of feeder by 50%.

Once the amplitude increases, it increases the proportion of equiaxed crystals and decrease the columnar ones. Alloy vibration during all the solidification time, leads to the decrease of grains by about three times. Influence of mechanical vibrations at metals casting are characterized by:

- ❖ increase of undercooling degree by increase of alloy - mould heat transfer;
- ❖ creating new nuclei for fragmentation of forming solid phase;
- ❖ activity of crystallization surfaces;

- ❖ at high solidification rates and small temperature gradient it appear nuclei in whole casting section, when the mould can continuously remove the crystallization latent heat;
- ❖ mechanical vibrations decrease the thermal gradient and increase the solidification rate favouring endogenous growth;
- ❖ the decrease of distance between dendritic branches leads to shorter time of homogenization thermal treatment;
- ❖ materials with fine grains are recommended as materials subjected to plastic deformation;
- ❖ improvement of properties results from the fine distribution of microporosity and secondary phases during blocking the dislocations at grains borders;
- ❖ columnar crystals zone can be eliminated for non-ferrous materials: Al, Cu, Sn, Zn, etc. And especially for their alloys (bronzes, brass);
- ❖ mechanical vibrations influence the interphase surface tension (solid – liquid) by decreasing it, which leads to the decrease of minimum radius of nuclei from which they can't melt anymore but develops.

REFERENCES

1. PĂRVULESCU C. - Cercetări privind influența vibrației asupra solidificării aliajelor turnate în piese; Teză de doctorat, UPB 2010.
2. ȘUȘU Cătălin - Contribuții la îmbunătățirea calității topiturilor unor aliaje de aluminiu destinate turnării pieselor. Teză de doctorat, Universitatea Tehnică din Cluj-Napoca, 2008.
3. CĂMUI C. - Studii și cercetări privind efectul acțiunilor fizice ale energiei vibrațiilor de joasă frecvență asupra cuprului în momentul turnării și solidificării în semifabricate; lucrare de absolvire cursuri post universitare, București 1991.
4. MĂRGINEAN L. - Studii și cercetări privitoare la realizarea unor compozite ceramo-metalice. Teză de doctorat, Universitatea Tehnică din Cluj-Napoca, 2007.
5. POP Alin Mihai - Cercetări asupra tehnologiilor și materialelor moderne pentru confecționarea garniturilor de model. Teză de doctorat, Universitatea TRANSILVANIA din Brașov , 2009.





¹Ioan ILCA

DEFFICIENCY OF SCIENCE AND TECHNIQUE ASSIMILATION

¹FACULTY OF ENGINEERING HUNEDOARA, ROMANIA
Member of ROMANIAN SCIENCE AND TECHNIQUE ACADEMY

ABSTRACT:

Assimilation in production of acquirement of science and new technique is the most important motor of development. Romania must improve step by step organizational systems, in view to develop the science, to improve the material basis, to grow the quality level and to increase the productivity in science researches, to reduce the gap in science, between our country and UE.

KEYWORDS:

acquirement of science, new technique, productivity, production, scientist

1. INTRODUCTION

Is very known that the main indicator of national economy progress is labor productivity and productivity increase is possible with implementation of technical progress and science conquest.

If the rate of productivity decrease, is necessary to cast about for deficiencies of science and technique assimilation.

Based on Romanian statistics, we can observe that in the past the labor productivity was around 13 %, after this was stagnation, and now is dramatically decrease. Is clear that the assimilation of science and technique are not properly and because of this I want to discuss the break down of new technique assimilation.

Is known, that in Romanian Industry, the assimilation of science and techniques novelties are very slow and difficult to be done. In Romanian language we use for it the word “introducere= introduction”; introduction of new technique, introduction of science realization, etc”. The word “introduction” in Romania language have the understanding of a difficult process take in place with environment resistance and we used this word for many years without observation of un careless condition of new technique assimilation. When we will pass from this to “acquirement of new technique” will be created the normal conditions for assimilation process.

2. CONDITIONS FOR NEW TECHNIQUE AND SCIENCE ASSIMILATION

My personal experiences for many years in this field show those are necessary to be fulfilling some conditions, we name those and will analyze the possibility to be fulfill.

First conditions: Assimilation of new technique – artless say, industry to learn to do what he never does until now.

This assimilation is necessary to grow into a learning process, mandatory sustain of pedagogical procedures used in case of new learning's. To want to learn, is the most important condition, when we communicate knowledge's to the students. In case of our Industry we have questions: Our industry wants all the times, willingly, get into new technique? Are we created conditions for convince our industry of needed new technical assimilation?

Admittedly, to appear this wish, we must create adequate material and ethic conditions. Our industry must create adequate conditions in which, our industry, our Commercial Companies, to be interested in new technologies, those must fill the necessity, and the profitableness, and that acquirement of new technologies represent progress.

The second condition: Satisfactoriness, basic level of knowledge's for learning peoples. We can't teach for example "Theory of Plastic Deformation in case of metallic materials" to the students who don't know "Superior Mathematics". Who learn new things must have a adequate technical preparation for clear understanding of new technique.

The third condition: very known in pedagogy is – Don't overload the student in learning process. Each Company, each industrial plant, can assimilate during an year, a limited quantity of new things, even the peoples are properly prepare and have the desire to improve. In Romania, happen frequently, when new companies start to manufacture some products, she starts to be overload with new tasks. Is important to don't forget that industry, like people, have a limited capacity to acquire the new.

The fourth condition: in learning process, must be created the adequate material conditions.

To educate, a person or a company, only with internal material resources, is not possible.

Higher education needs a proper material base, adequate at his purpose. Simple say: we must allotment sufficient of funds, for learning process.

The necessity of those four conditions, is easier to understand and make them happen is also easier.

The fifth condition not saw evident and considerable difficult to be achieve, is: in educational process is imperious necessary to have/ elaborate an analytical learning program.

Practical, for new science and technique acquirement is necessary to have a proper, detailed action plan in view to achieve the request results.

In our case, usual, the attention is low, and often the educational process is made haphazard, without thinking about the necessity of an even simple action plan.

There is a dilemma, when the action plan is made by scientist, inventor, or research institute, they don't take in consideration the particularities of production process. When the action plan is made by the companies are not taken in consideration specific tasks of new technologies. The result action plans contain a lot of imperfections. How to solve this dilemma? The life shows us that there are engineers with capabilities to cover both parts of the issue, they are not sowing many, and we must find and promote this kind of specialists in new science and technique acquires teams. As rule we must include the applicable idea that new science and technique acquires in practical, industrial process to be done based on a proper action plan.

The seventh and last condition, under my opinion is applied to the scientist. Where are students, is necessary to have teachers. If the new technique creators, is scientist, inventor, or research institute, must be directly interested in practical implementation of new technology. Are they? There is a link between the scientists and companies?

We will analyze now, only the case when the "teacher" is scientist.

Under our legislation, the teacher who is also scientist, concern oneself about implementation of new technology, is not pay for this. In Romania the collaboration between the teachers/scientist from Technical Universities and industrial sector is consider gratuitously activity.

Normally the teacher who is also scientist, make this work from his conviction, but is must to have an proper working environment, to be social recognize and the state must appreciate his cooperation with industrial activity. The State institutions, like Ministries', don't have a proper attitude in case of recognize of this special work and this are not good for the relations between students and teachers.

Many times are considered if a edict was emitted, in view to a technology assimilation, the process of acquirement of new technique was done. The acquirement of new technique and technology is not only an administrative activity, sure by administration activity is establish the amount, financing elements and number of peoples, but this important and special activity of acquirement of new technologies is based on the good communication between the magister and his disciple, on the interest of this in achievement of proper results and on a proper Action plan.

3. COMPARISON OF SCIENCE ACTIVITIES IN ROMANIA, EUROPEAN COMMUNITY AND THE WORLD

I want to open a new subject: Is sufficient the infusion bring by our science in national economy progress? The efficiency of scientist work is satisfactory?

To answer to this question is important to compare some of the elements of our scientific activities with similar activities from the states of European Community.

Research activity is one of the most actual points in political agenda of European Community. In accordance with EUROSTAT – European Statistics Office, in 2009, the allowance for Research and Development was 1.84% from GDP, in Europe, compare with 3.2 % in Japan and 2.7 % in USA.

Inside European Community the allowance have significant variations: for example in Sweden – was 3.82 % and Finland – 3.45 % from GDP, opposite was the allowance in Cyprus - 0.42 % and Bulgaria – 0.48 % from GDP.

In Romania the allowance in 2009 was 0.46 % from GDP, the most amount from public founds, $\frac{1}{4}$ from this amount was ensure by private sector, and Attention!, only 0.02 % from outside founds.

This was the situation in 2009, but now in 2010 the allowance for Research and Development in Romania is 0.19 % from GDP, we considered this” dangerous”, taken in consideration that European Union target is 3 % from GDP – part of Lisbon Strategy for economical and competitively enlargement.

Making a analysis of allowance for Research and Development in Japan, SUA and UE, we can see that a large part of this have the destination research for acquirement of science and new technique in production, or like we preferred to say “researches with applicative theme”.

In last 10 years, statistical based, in SUA was draw in more than 53000 scientists, most of them younger scientists, out of which 30000 engineers, 14000 physicians and 9000 other kind of scientists, that means more than 5000 specialists per year.

If we consider 500 younger graduates per year per University, that means that minimum 10 University from Europe prepare free of charge specialists for SUA, but the American’s take only the best elements – cream of 50 Universities. This situation alarmed the Royal British Society, who named a special committee to analyze the exodus of youngest scientist and propose action plans for stopped this impoverishment of British science. The conclusion was that England and Germany however, pay to their good scientist a big amount, American’s pay double. But the payment is not the only reason; the committee establishes that the most attractive is the science development conditions create in SUA.

We must say that in last period the gap in science, between our country and UE, increase, that means a big need to find solutions and founds for elimination of this gap. If in next future years the Romanian scientist productivity will not be improved, if we will not improved the acquirement of science and new technique in production, then the assignment to come up with the European developed states, will failed. But, if we used with determination and intelligence the experience we have in education organization, scientifically research and in industry, than the gap will means only a passing episode.

We must improve step by step organizational systems, in view to develop the science, to improve the material basis, to grow the quality level and to increase the productivity in science researches.

4. CONCLUSIONS

We, scientist from Romania, must be preoccupied with all seriousness about this new provocation. We are the avant-garde of Scientist Institution of the Country, and due to this we are responsible, more than other people, from development of our science and acquirement of science and new technique in production.

REFERENCES

- [1.] Irina, St. – Dezvoltarea infrastructurii de cercetare-dezvoltare (CD) a intreprinderilor cu sprijinul finantarilor europene, Tehnica si Tehnologie, Editura Tehnica Maria, nr. 6, 2009, Bucuresti
- [2.] EVZ Special – Cercetarea romaneasca are probleme de “marketing”, EVZ, nr. 5781, 2009, Bucuresti



¹Monika Erika POPA, ²Gabriela Cornelia MIHUT

EXPERIMENTS REGARDING THE THERMICAL REGIME IN THE CONTINUOUS CASTING PROCESS

¹⁻² UNIVERSITY POLITEHNICA OF TIMISOARA, FACULTY OF ENGINEERING FROM HUNEDOARA, ROMANIA

ABSTRACT:

Continuous casting is one of the prominent methods of production of casts. Effective design and operation of continuous casting machines needs complete analysis of the continuous casting process. In this paper the basic principles of continuous casting and its heat transfer analysis using the finite element method are presented. In the analysis phase change is assumed to take place at constant temperature. A front tracking algorithm has been developed to predict the position of the solidification front at each step. Finally, examples that are solved by the proposed algorithm are discussed. The results show that there is a good agreement between the method developed in this work and other previously reported works.

KEYWORDS:

steel, micro-coolers addition, continuous casting, experiments, simulations

1. INTRODUCTION

In the continuous casting process, illustrated in figure 1, molten metal is poured from the ladle into the tundish and then through a submerged entry nozzle into a mould cavity. The mould is water-cooled so that enough heat is extracted to solidify a shell of sufficient thickness.

The shell is withdrawn from the bottom of the mould at a "casting speed" that matches the inflow of metal, so that the process ideally operates at steady state. Below the mould, water is sprayed to further extract heat from the strand surface, and the strand eventually becomes fully solid when it reaches the "metallurgical length".

Solidification begins in the mould, and continues through the different zones of cooling while the strand is continuously withdrawn at the casting speed. Finally, the solidified strand is straightened, cut, and then discharged for intermediate storage or hot charged for finished rolling.

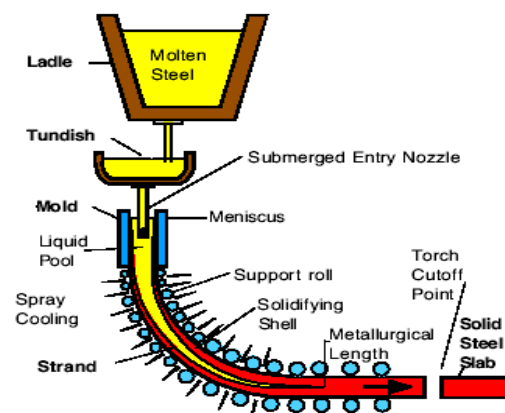
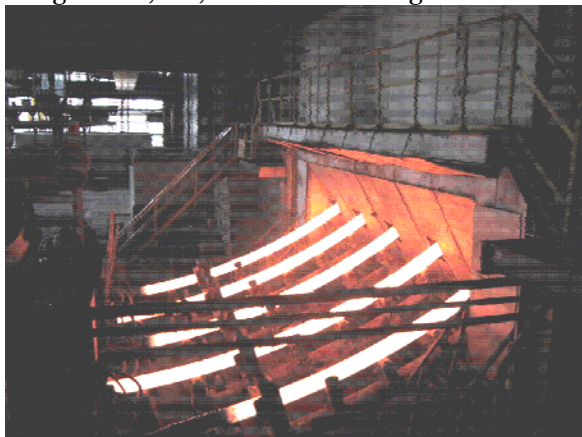


Figure 1. Schematic representation of the continuous casting process

To start a cast, the bottom of the mould is sealed by a steel dummy bar. This bar prevents liquid metal from flowing out of the mould and the solidifying shell until a fully solidified strand

section is obtained. The liquid poured into the mould is partially solidified in the mould, producing a strand with a solid outer shell and a liquid core. In this primary cooling area, once the steel shell has a sufficient thickness, the partially solidified strand will be withdrawn out of the mould along with the dummy bar at the casting speed. Liquid metal continues to pour into the mould to replenish the withdrawn metal at an equal rate. Upon exiting the mould, the strand enters a roller containment section and secondary cooling chamber in which the solidifying strand is sprayed with water, or a combination of water and air (referred to as "air-mist") to promote solidification. Once the strand is fully solidified and has passed through the straightened, the dummy bar is disconnected, removed and stored.

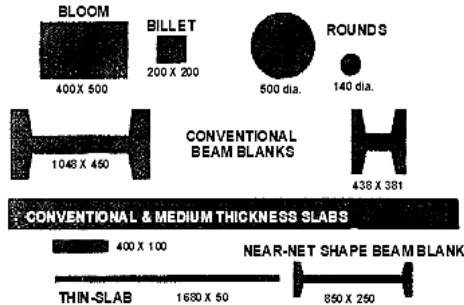


Figure 2. Continuously cast sections

Depending on the design of the casting machine, the as-cast products of the continuous cast process are slabs, blooms, billets, or beam blanks. The cross sections of these products are shown in Figure 2. Billets have cast section sizes up to about 200 mm square. Bloom section sizes typically range from approximately 200 mm to 400 mm by 600 mm. Round billets include diameters of approximately 140 mm to 500 mm. Slab castings range in thickness from 50 mm to 400 mm, and over 2500 mm wide. The aspect ratio (width-to-thickness ratio) is used to determine the dividing line between blooms and slabs. An aspect ratio of 2.5:1 or greater constitutes an as-cast product referred to as a slab.

2. METHODOLOGY

By its nature, continuous casting is primarily a heat-extraction process. The conversion molten metal into a solid semi-finished shape involves the removal of the following forms of heat: superheat from the liquid entering the mould from the tundish. The latent heat of fusion at the solidification front as liquid is transformed solid, and finally the sensible heat (cooling below the solidus temperature) from the solid shell.

These heats are extracted by a combination of the following heat-transfer mechanisms: convection in the liquid pool heat conduction down temperature gradients in the solid shell from the solidification front to the colder outside surface of the cast, and external heat transfer by radiation, conduction and convection to surroundings. Also not less important is heat transfer before the molten metal is poured into the mould. For instance, in the casting of steel, heat transfer is important before the steel enters the mould because control of superheat in the molten steel is vital to the attainment of a predominantly equiaxed structure and good internal quality. Thus, conduction of heat into ladle and tundish linings, the preheat of these vessels, convection of the molten steel and heat losses to the surroundings also play an important role in continuous casting.

Because heat transfer is the major phenomenon occurring in continuous casting, it is also the limiting factor in the operation of a casting machine. The distance from the meniscus to the cut-off stand should be greater than the metallurgical length, which is dependent on the rate of heat conduction through the solid shell and of heat extraction from the outside surface, in order to avoid cutting into a liquid core. Thus, the casting speed must be limited to allow sufficient time for the heat of solidification to be extracted from the strand.

Heat transfer not only limits maximum productivity but also profoundly influences cast quality, particularly with respect to the formation of surface and internal cracks. In part, this is because metals expand and contract during periods of heating or cooling. That is, sudden changes in the temperature gradient through the solid shell, resulting from abrupt changes in surface heat extraction, causes differential thermal expansion and the generation of tensile strains.

Depending on the magnitude of the strain relative to the strain-to-fracture of the metal and the proximity of the strain to the solidification front, cracks may form in the solid shell. The rate of heat extraction also influences the ability of the shell to withstand the bulging force due to the ferostatic pressure owing to the effect of temperature on the mechanical properties of the metal. Therefore, heat transfer analysis of the continuous casting process should not be overlooked in the design and operation of a continuous casting machine.

3. DISCUSSION

The importance of mathematical modeling of the continuous casting process can be seen in situations where the following are necessary.

- ❖ Simulation of an existing casting machine with a view to learning more about its operation;

- ❖ Prediction of effects of a change in a casting parameter on the performance of an operating caster;
- ❖ Design of new casting machines.

In particular, most process engineers are probably interested in the effect of increasing the casting speed on machine operation as higher output is sought to match planned or existing production capacity. Do changes then need to be made to the mould length, spray system, and position of the cut-off strand? Another area of interest to the process engineer is the minimization of internal cracks such as halfway or centerline cracks. These points are discussed in this section to show the importance of a mathematical model, based on heat-transfer principles, in adjusting casting conditions and improving overall machine performance.

Increasing the casting speed will have the effect of decreasing the time that the strand spends in the mould and spray zones, and also of increasing the depth of the liquid pool. Looking first at the mould, a decrease in the mould dwell time will result in a thinner shell at the bottom of the mould. Since this may increase the danger of break-outs, an increase in the mould length should be considered. Here the mathematical model can assist us since it can calculate the shell thickness for different casting speeds and mould lengths.

Halfway or midway cracks are the result of reheating of the surface of the strand due to a sudden reduction in the rate of surface heat extraction as the strand moves into the secondary cooling zone. So, if the spray system is to be altered to avoid midway cracks, reheating of the surface of the strand must be minimized as much as is practicable. How can this be achieved? A mathematical model can give part of the answer. For example, if the surface temperature distribution to be maintained through the sprays is specified, the mathematical model can provide the spray heat-flux distribution that is required to achieve it. The following basic assumptions were made during the formulation of the mathematical model:

- ❖ The continuous casting process is steady state.
- ❖ A round billet is considered and radial symmetry assumed.
- ❖ Energy dissipation due to internal friction in the liquid state is neglected.
- ❖ The melt free surface is assumed to be covered with a protective slag layer, through which negligible heat is assumed to be lost.

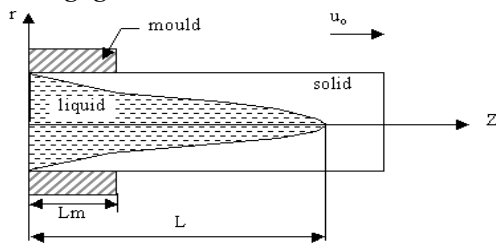


Figure 3. R-Z coordinates attached to mould

The governing equation for the heat transfer analysis of continuous casting is:

$$\rho c \left(\frac{\partial T}{\partial t} + V \cdot \nabla T \right) = \nabla \cdot (k \nabla T) \quad (1)$$

Taking the above assumptions into account, the governing equation will be reduced to:

$$\rho c u \frac{\partial T}{\partial z} = \frac{\partial}{\partial z} \left(k \frac{\partial T}{\partial z} \right) + \frac{1}{r} \frac{\partial}{\partial r} \left(kr \frac{\partial T}{\partial r} \right) \quad (2)$$

The axial heat conduction is negligible compared to that convected due to the bulk motion of the moving

strand. Thus, heat conduction is important solely in the radial direction. Under this condition the governing equation becomes:

$$\rho c u \frac{\partial T}{\partial z} = \frac{1}{r} \frac{\partial}{\partial r} \left(kr \frac{\partial T}{\partial r} \right) \quad (3)$$

The boundary conditions are:

$$\text{At the meniscus/free surface } (z = 0, 0 < r < R), T = T_p \quad (4)$$

At the billet surface:

$$q_s = -k \frac{\partial T}{\partial r} \quad \text{or} \quad h(T - T_\infty) = -k \frac{\partial T}{\partial r} \quad (5)$$

At the center due to axis symmetry ($r = 0$ and $0 \leq z \leq L$):

$$\frac{\partial T}{\partial r} = 0 \quad (6)$$

At the liquid-solid interface ($r = r_i$ and $0 \leq z \leq L$): $T = T_m$;

$$\left(k \frac{\partial T}{\partial r} \right)_l + \left(k \frac{\partial T}{\partial r} \right)_s = \rho Q_L \frac{dr_i}{dt} \quad (7)$$

4. CONCLUSIONS

A one dimensional solidification problem was solved for a slab-like region of water with initial temperature of 10 °C when a temperature of -20 °C is applied on the outer surface shown in

Figure 4. The slab was modeled by using 20 two-node linear elements, 10 for the liquid part and 10 for the solid part. As solidification progresses, the mesh on the water is compressed and on the ice side is expanded;

The continuous casting process is introduced. One and two dimensional heat transfer analyses of the process are discussed. Results showed that such mathematical analysis of the process can help to control and optimize the process and to investigate the consequences of parameter changes without the safety and cost limitations of in-plant experiments.

The proposed algorithm can be used for the analysis of both stationary and moving solidification problems in which phase change occurs at a specific temperature.

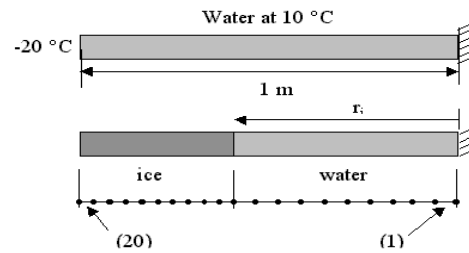


Figure 4. Modeling of the one dimensional problem

REFERENCES

- [1.] Choudhary, K. and Mazumdar, Dipak, "Mathematical modeling of fluid flow, heat transfer and solidification phenomena in continuous casting of steel", Steel Research, 66, No. 5, 1995
- [2.] Popa, E., Kiss I., Danciu A. "Research and experiments the influence of casting parameters upon the surface temperature of the continuous cast semi-products", Annals of the Oradea University, România 2005
- [3.] Popa, E., Mihuț G. "Simulation of the continuously cast semi-products in the case of introduction of consumable microcoolers, KOD 2008 Conference, Novi Sad, Serbia





¹Vasile PUȚAN, ²Ana JOSAN ³Adriana PUȚAN

HEAT LOSS FLUXES FROM STEEL MELT TO DIFFERENT BOUNDARY REGIONS OF A LADLE

¹⁻³ UNIVERSITY “POLITEHNICA” TIMIȘOARA, FACULTY OF ENGINEERING OF HUNEDOARA, ROMANIA

ABSTRACT:

One of the important outputs of the heat conduction model is the heat loss flux from steel melt to different heat transfer regions of a ladle. These papers present examples of the predicted heat loss fluxes to different heat transfer regions of mid-aged 105-tonne steel ladles lined with alumina and spinel as working refractory in walls. The heat loss fluxes to different ladle heat transfer regions, except for the top free surface, generally exhibit exponential decay with time.

KEYWORDS:

steel ladle, numerical simulation, CFD, fluid flow, heat loss

1. GENERAL CONSIDERATIONS

In modern steelmaking throughout the world, continuous casting (CC) is the dominating process for producing semi-finished steel products (billets, blooms and slabs). However, the CC process requires a strict control on the temperature of liquid steel in the tundish. Further, the tundish temperature is influenced considerably by the temperature of teeming steel streams coming from the ladles. Therefore, it would be of practical importance to predict the teeming stream temperature as a parameter for further prediction and control of the steel temperature in tundishes.

Three numerical models were developed. Firstly, a one-dimensional (1D) numerical model for simulating heat conduction in ladle wall, bottom and top slag layer for the whole ladle operation cycle was established. This model was used for predicting steel ladle heat loss fluxes. Secondly, using the predicted heat loss fluxes as thermal boundary conditions, a two-dimensional (2D) CFD numerical model was developed for simulating natural convection flow in steel ladles during holding. Thirdly, a three-dimensional (3D) CFD model was also developed for simulating fluid dynamics in steel ladles with drainage flows during teeming. The 3D CFD model was used for predicting the teeming stream temperatures.

In the present parameter numerical experiments, two types of 105-tonne steel ladles were investigated: the one lined with alumina as working refractory in wall, the other lined with spinel as the working refractory in wall. Other lining materials were the same for both types of ladles. Totally 18 simulation cases are performed for the two types of steel ladles lined with alumina and spinel, respectively. Table 1 gives the parameter of numerical experiments.

Table 1. Parameter of numerical experiments

Simulation case No. *	Hot-face temperature [°C]	Slag thickness ** [mm]	Holding time [min]	Teeming rate*** [t/min]	
A1	S1	1000	83	30	2,816
A2	S2	1000	55	20	2,488
A3	S3	1000	28	10	2,229
A4	S4	800	55	30	2,229
A5	S5	800	28	20	2,816
A6	S6	800	83	10	2,488
A7	S7	600	28	30	2,488
A8	S8	600	83	20	2,229
A9	S9	600	55	10	2,816

* “A” refers to alumina ladles and “S” refers to spinel ladles

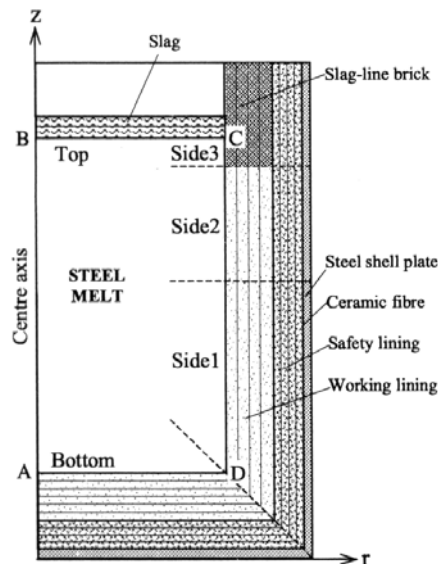
** The slag thickness of 28, 55 and 83 mm corresponds, respectively, to 500, 1000 and 1500 kg slag

*** The teeming rates are calculated based on 105 tonne liquid steel drained for 38, 43 and 48 minutes, respectively.

2. SIMULATION METHODS

The mathematical models used in this work for carrying out numerical experiments were established in two computer software environments. The one is a special-purpose computer program, TEMPSIM [1], for only simulating heat transfer in steel ladles. The other is a general-purpose CFD modelling computer code, ADINA-F (Automatic Dynamic Incremental Nonlinear Analysis). The former numerically solves the heat conduction equation for ladle wall, bottom and top slag layer, while the latter numerically solves the Navier-Stokes type momentum, energy and turbulence equation group for the steel melt bounded by ladle wall, bottom and top slag layer.

TEMPSIM assumes the heat conduction is either in radial direction through ladle wall or in axial direction through ladle bottom and top slag layer. Accordingly, it was used to establish the 1D heat conduction model described previously (Fig. 1). This heat conduction numerical model was applied in this work for predicting heat loss fluxes. Figure 2a schematically illustrates the computation domain with grid lines defined by the heat conduction model. Note that the computation domain used by the model excludes the region marked with "ABCD" standing for the steel bath. Moreover, in this computation domain, five heat transfer regions named as "Bottom", "Top", "Side1", "Side2" and "Side3" are further defined, (Fig. 2a). The region "Bottom" is the interface between steel melt and bottom lining; the region "Top" is the interface between steel melt and top slag layer; the regions "Side1", "Side2" and "Side3" are, respectively, the interfaces between steel melt and sidewall lining at different levels.



(a) 1D heat conduction model

Fig.1. Computation domains defined in the numerical models

With all these numerical models available, a three-step modelling strategy was employed in the present work in which,

- the 1D heat conduction model was first implemented to the wall, bottom and top slag layer in steel ladles to provide the thermal boundary conditions (e.g., heat loss fluxes) to the 2D and 3D CFD models; then,
- the 2D CFD model was applied to simulate natural convection in the ladles and to provide the initial conditions (velocity and temperature profiles) to the 3D CFD model; and, finally,
- the 3D CFD model was executed to simulate fluid flow and heat transfer in the ladles with drainage flows during teeming and to predict the teeming stream temperatures. This three-step modelling methodology was applied to each simulation case listed in Table 1.

Table 2. Thermal-physical properties of lining materials used in numerical simulations [2]

Lining material	Density [kg/m ³]	Heat conductivity [W/m °C]					Heat capacity [J/kg °C]				
		200 °C	600 °C	1000 °C	1400 °C	1600 °C	200 °C	600 °C	1000 °C	1400 °C	1600 °C
Ceramic fibre	80	0,02	0,03	0,04	0,04	0,04	850	1000	1100	1200	1200
Chamotte	2100	1,56	1,65	1,76	1,87	1,87	860	977	1084	1200	1200
Slag line brick	3110	4,00	2,60	2,09	2,00	2,00	1010	1194	1280	1368	1419
80%Al ₂ O ₃	2900	2,15	2,00	1,84	1,74	1,65	850	1030	1125	1180	1200
Spinel (10 % C)	3000	7,40	7,40	7,40	7,40	7,40	850	1030	1125	1180	1200
Bottom mass	2750	1,00	1,30	1,50	1,70	1,80	850	1030	1125	1180	1200
Slag scull	3648	3,91	3,46	3,41	3,08	2,99	840	993	1073	1120	1137

3. SIMULATION CONDITION

In steel plant, the steel ladles are operated in the following cycle: tapping (from electric furnace EBT) → ladle furnace LF → continuous casting CC → ladle maintenance → transfer to EBT or to preheating station → tapping. The liquid steel held in ladles goes through LF treatment where

the steel is homogenized by argon bubbling and its temperature is adjusted to 1570 - 1590°C. After that, the liquid steel is transported to the CC station and cast into slabs. The time lapse between the end of LF treatment and the start of teeming is around 10-30 minutes, which is defined as the holding time in this work.

Since the ladles to be simulated are mid-aged, which means that they have normally been in operation for more than 30 heats, quasi-steady thermal states have more likely been reached in the ladle linings.

Numerical experiment cases are executed under the following conditions (Table 1):

- ❖ after the end of teeming, all the ladles without preheating are directly transported to the EBT and prepared for tapping;
- ❖ just before the start of tapping, the average hot-face temperatures, weighted by the areas of heat transfer regions (Fig. 2a), are set at 600°C, 800°C and 1000°C, respectively, by manipulating the cooling time of the ladles after teeming and before receiving the next heat;
- ❖ all heats of liquid steel (105 tonne) together with different amounts of slag (500 kg, 1000 kg and 1500 kg) are tapped from EBT into the ladles during 5 minutes and have the same tap-end temperature of 1675°C;
- ❖ 25 minutes after tapping, the ladles are covered with a refractory lid for 30 minutes corresponding to the period of LF treatment;
- ❖ at the end of LF treatment, all heats of liquid steel are homogeneous and have the same temperature, 1580°C;
- ❖ the holding periods, i.e., the duration of steel melt held in the ladles after LF treatment/homogenization and before the start of teeming, are 10 min, 20 min and 30 min, respectively; and, finally,
- ❖ the teeming time is designed to be 38 min, 43 min and 48 min corresponding to teeming rates of 2.816 tonne/min, 2.488 tonne/min and 2.229 tonne/min, respectively.

In addition, the conditions (5) to (7) are also used in CFD simulations of the same ladles during holding and teeming periods.

4. SIMULATION RESULT

One of the important outputs of the heat conduction model is the heat loss flux from steel melt to different heat transfer regions of a ladle. Figures 2 and 3 illustrate, respectively, examples of the predicted heat loss fluxes to different heat transfer regions (Fig. 1) of mid-aged 105-tonne steel ladles lined with alumina and spinel as working refractory in walls. The simulation conditions follow cases No. A5 and S5 in Table 1 for both types of steel ladles. It can be seen from both figures that the heat loss fluxes to different ladle heat transfer regions, except for the top free surface, generally exhibit exponential decay with time. A comparison between the two figures shows that the alumina ladle loses more heat per unit area and time to the top region of the wall (Side3), which is slag-line brick having greater heat conductivity than alumina, (Fig. 2a and Table 2); while the spinel ladle loses most heat per unit area and time to the lower regions (Side1 and Side2) of the wall. This difference is not surprising, because spinel (mixed with 10% graphite) is much more conductive than alumina and slag-line brick (Table 2).

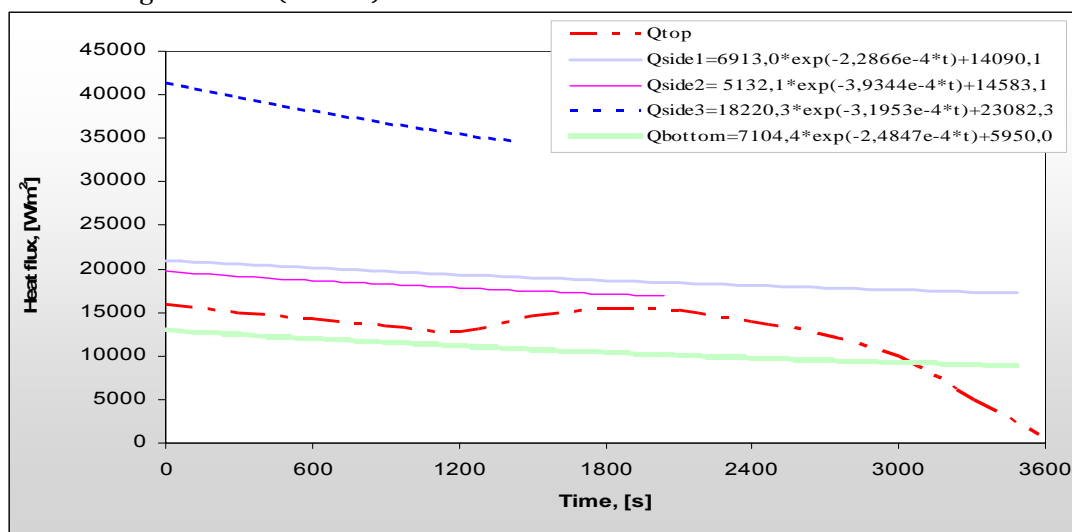


Fig.2. Predicted heat loss fluxes to different region of a mid-aged 105-tone steel ladle with alumina as working refractory in wall

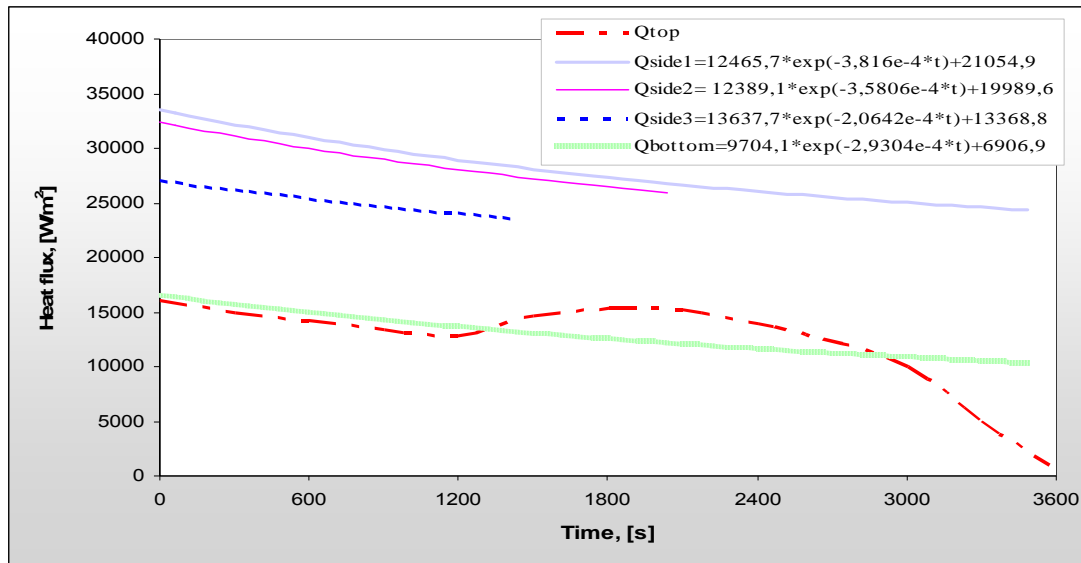


Fig.3. Predicted heat loss fluxes to different region of a mid-aged 105-tonne steel ladle with spinel as working refractory in wall

6. CONCLUSIONS

The influences of some important parameters on fluid flow and heat transfer in steel ladles during holding and teeming, which are normally inconvenient or impossible to examine directly using experimental methods, have been studied by means of mathematical modelling through performing numerical experiments. In this work, a three-step modelling strategy for the numerical experiments has been adopted. Two types of mid-aged 105-tonne production steel ladles, lined with alumina and spinel in walls, have been investigated, respectively. The following conclusions can be drawn from the present parameter numerical simulation studies.

It can be deduced that local heat losses from top and bottom regions of the steel bath to nearby boundaries will play a decisive role in affecting the top and bottom temperatures (hence the extent of thermal stratification). Generally, for the same bulk-cooling rate, larger heat fluxes to ladle bottom and lower section of sidewall (resulting in further lowered bottom temperatures) will lead to a greater extent of thermal stratification than uniformly distributed heat fluxes; while larger heat fluxes to top slag layer and upper section of sidewall (resulting in lowered top temperatures) may lead to smaller extent of thermal stratification than uniformly distributed heat fluxes.

REFERENCES:

- [1] Fredman T. P., Scand. J. Metall., Vol. 29, 2000, pp. 232-258.
- [2] Kitamura M., Kawasaki S., Kawai S., Kawai K. and Miyake K., Trans. Iron Steel Inst. Jpn., Vol.23,1983,pp. B165.
- [3] Minion R. L. and Leckie C. F., Steelmaking Conference Proceedings, Vol. 69, 1986, Iron and Steel Society, Washington, U.S.A., pp. 335-343.
- [4.] Olika Bekele, "Simulation of Ladle Lining and Steel Temperature in Secondary Steelmaking", Licentiate Thesis, 1992, Lulea University of Technology, Sweden.





¹ Peter KOŠTÁL, ² Andrea MUDRIKOVÁ

USE OF E-LEARNING AND VIRTUAL LABORATORY TO AUTOMATION TEACHING

¹⁻² SLOVAK UNIVERSITY OF TECHNOLOGY, FACULTY OF MATERIALS SCIENCE AND TECHNOLOGY,
INSTITUTE OF PRODUCTION SYSTEMS AND APPLIED MECHANICS, TRNAVA, SLOVAKIA

ABSTRACT:

In this paper is described the main ideas of national project "KEGA 3/7131/09 – Laboratory of production system program control". This project is focused to build of virtual laboratory and supplemental e-learning documents for several studying subject at our institute. This virtual laboratory serve for teaching automatic control principles and programming in flexible production via various control modes often used in the technical practice. In this laboratory there are applied real elements of control systems. By means of these laboratory students as future graduates of technical university can acquire and improve occupational competences demanded by actual labor market.

KEYWORDS:

virtual laboratory, e-learning, production system, automation

1. INTRODUCTION

Within the grant project KEGA being solved in the Institute of Production Systems and Applied Mechanics, STU Bratislava, in years 2009-2011, we endeavor to acquire and improve abilities and skills which employers expect graduates of technical universities to have in present circumstances.

Intent of this project is to create a laboratory for program control of production systems by pneumatics and a suitable teaching system supporting key and occupational competencies, abilities and skills of technical university students which at the same time would reveal strong point's and weak spots of their preparation for practice. In this paper we wish to present targets of this grant mission and its expected merit.

To achieve project goals it is necessary to revise curriculum and to use such teaching forms and methods that enable to exceed the scope of cognitive knowledge of scientific disciplines and professions that means to develop key competencies of students. These gain extraordinary significance not only for the personal development but also in term of lifelong education and employability of technical university graduates.

The present time brings along the need of superior education providing for:

- ❖ Ability to make decisions,
- ❖ Solve problems,
- ❖ Work with information,
- ❖ Ability to learn – lifelong education,
- ❖ Computer literacy,
- ❖ Communicative skills even in foreign languages,
- ❖ Self-activity and self-responsibility

Rapid changes put higher and higher demands on people nowadays. Obtained professional knowledge is out of date after a shorter and shorter time. Professional knowledge includes areas of „general basic knowledge and knowledge specific for particular major“.

This one is usually obtained cognitively and stored in the left brain hemisphere. However, in the area of electronics and technology, changes will be more frequent.

Key competencies should help us deal with professional knowledge with aim to solve the problems. Competencies with focus on one particular situation are quickly out of date or totally useless.

„Key competencies have longer lifetime than professional qualification. That’s why these are the basis for the next learning“

Key competencies can be understood as a complex of universal abilities exceeding the boundaries of specific professional knowledge and abilities. They express abilities of people to behave adequately to a specific situation.

Working in virtual laboratory will develop and strengthen computer literacy, so important on the present and even more important in future as we presume and last but not least will absolutely support acquisition of other key and occupational competencies of our university graduates.

Graduates will acquire the needed skills, experience and knowledge of production system controlling design methodology. They can simulate functions of designed devices. For simulation a specialized software will be installed on our intranet. By this software we can supervise every part of the designed control system. This control system includes only real industrial parts (PLC, stepper driver, servo driver, sensors, etc.).

By object-lessons and connection with practice we want to increase value of our graduates at the labour market.

2. PROJECT TARGET AND IMPLEMENTATION

The Project target includes building of virtual laboratory for program control systems. That laboratory is instrumental to teaching architecture principles of pneumatic and electro-pneumatic and program control systems and to verification of these systems’ functions by simulations.

Students gain experience of working with real industrial parts and the learning process is more effective. The goal is to make the pedagogical process more attractive for students in several studying subjects e.g. :

- ❖ Automation and mechanization,
- ❖ Theory of automates,
- ❖ Production systems,
- ❖ Production systems operation,
- ❖ Production and manipulation devices programming,

Students learning in this planned laboratory will acquire necessary skills and will acquaint themselves with generation methodology of several systems (pneumatic, electro-pneumatic, and electric ones) what will markedly increase their value at the labour market. The Fig. 1 presents the mentioned virtual laboratory.

Creation of virtual pneumatic or electro-pneumatic program control systems requires both individual work and decision making and cooperation including discussion on simulation of the proposed control circuit (Fig. 2).



Fig. 1: View to virtual laboratory

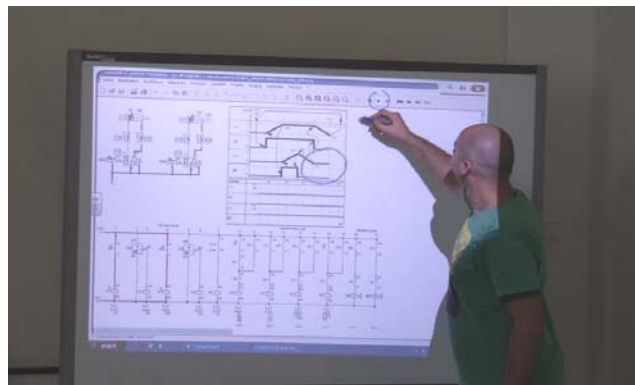


Fig. 2: Discussion about an electro-pneumatic scheme

By this laboratory students will obtain an opportunity to prepare assignments and projects of various subjects applying pneumatic and electro-pneumatic control systems and get ready for the real problem solving in practice. Thereby they also get a practice so important for employers. It widely develops and strengthens their technical occupational competencies and also their key competencies.

Within the project there will be developed study e-learning materials (manuals, methods, examples,...) and made available on Internet which will enable effective working in the laboratory and serve as a basis for further development of knowledge and skills of our students.

3. E-LEARNING

Traditional learning design is indicative of the learning field's reluctance to change. In spite of advances in neuroscience, collaborative technology, and globalized business climate, learning is still largely based on design theories created during the early 1900's to 1960's. The environment in which we are immersed has changed. Media and technology has changed. The social environment has been altered. The world has become networked and connected. In this environment of colossal change, the design methodologies used to foster learning remain strangely outdated – created for a time and need which no longer exist. Learning Development Cycle (LDC) is a learning design model to bridge the gap between design approaches and knowledge needs of academic and corporate learners.

Much of LDC is rooted in more traditional design structures. We are currently still in the beginning stages of societal and technological alterations. The model is intended to simply open doors to new design approaches, while maintaining aspects from previous models that still serve learners. More developed (connectivist-centric models) will be required as we move forward. LDC is a transitory design approach, bridging traditional design and beginning to embrace internet-era design.

Different types of learning exist. Learning happens in a variety of ways – from courses, conversations, life experiences, personal thought, or working on a project. Each different type of learning requires a different design process (as the object of the design differs depending on learning type). LDC presents four broad learning categories: transmission, acquisition, emergence, and accretion. These categories will be discussed in greater detail in this paper.

Learning today has moved beyond courses (courses serve a static knowledge field). As a result, course-based ID is not as useful for designing alternative modes of learning. The more rapidly knowledge and information climates change, the greater the need for responsive dynamic models.

E-Learning – phenomena of education of the 21st century. It is astounding by its extensiveness, attracts by huge amounts of technical resources, and affects nearly all areas of human gnosis. The reason is time and change velocity in daily life of all of us. One option is to apply electronic education – e-Learning in our lifelong education. Education is one of the most important life priorities for us but also for the modern society.

Electronic learning or e-learning (sometimes written as elearning) has various definitions. E-learning is facilitated and supported via information and communications technology (ICT).

The American Society for Training and Development (ASTD) defines e-learning as a broad set of applications and processes which include web-based learning, computer-based learning, virtual classrooms, and digital. Much of this is delivered via the Internet, intranets, audio- and videotape, satellite broadcast, interactive TV, and CD-ROM. The definition of e-learning varies depending on the organization and how it is used but basically it involves electronic means of communication, education, and training.

Many terms have been used to define e-learning in the past. For example web-based training, computer-based training or web-based learning, and online learning are a few synonymous terms that have over the last few years been labelled as e-learning. Each of this implies a "just-in-time" instructional and learning approach.

Regardless of the definition you chose to use, designers, developers, and implementers make or break the instructional courses and tools. E-learning is simply a medium for delivering learning and like any other medium, it has its advantages and disadvantages. E-learning covers a wide array of activities from supported learning, to blended or hybrid learning (the combination of traditional and e-learning practices), to learning that occurs 100% online.

Sound e-learning is founded on instructional design principles, pedagogical elements that take into account learning theories. Given its nature, online distance education is well matched with e-learning and flexible learning but is also used for in-class teaching and blended learning.

4. E-LEARNING IN VIRTUAL LABORATORY

If we look at e-learning as at efficient utilization of information technologies in educational process then it actually means new opportunities that can be used in education.

E-learning is a solution designed for education, however education conceived in full context. It is not limited to education of students only but is in a broad sense a method of information sharing and passing within lifelong education that is a necessity especially for technicians.

In contrast to classical information systems dealing especially with information sharing and a possibility to find information necessary in proper time; e-learning lays a big stress on method of representation. Nowadays it is not enough only to acquire correct information in due time but it

also is necessary to understand it fully and see it in context. And just e-learning supports these abilities.

E-education as a progressive teaching form opens many new opportunities. This form can be used in all formal education grades and also in lifelong education

E-Learning effectively measures every course by means of testing objects and control systems. It enables to set up desired goals without prejudice (e.g. student must answer correctly to test questions verifying his/her actual knowledge of studied subject after taking in the course). E-Learning gives immediately available information on individual students, how many points they achieved, how much time they spent in individual course parts, how they answered questions. Equally simply E-Learning evaluates statistically fruitfulness of individual courses and thereby identifies courses to be revised. Likewise E-Learning brings new forms of communication and cooperation among students and between students and lectors which would be inconceivable without using information technologies.

E-Learning turns teaching into an addressed, individual, interactive and interesting process integrated with daily life of students.

E-learning means a process which describes and solves creation, distribution, managing and feedback realization of the pedagogical process by computers and network. These applications contain simulations, multimedia, combinations of text and graphics, audio, video and electronically testing of students. Every student can choose individual form of study that is suitable for him. E-learning is a high quality extension of existing possibilities of study.

The virtual laboratory applies a combination of classical way of teaching and e-Learning courses.

E-Learning turns teaching into an addressed, individual, interactive and interesting process integrated with daily life of students.

For working in the virtual laboratory of pneumatics and electro-pneumatics we use software environment FluidSIM that is one of many software enabling to set up various pneumatic and electro-pneumatic control circuits as well as to verify their function by simulation of these control circuits. Fig. 3

Software FluidSIM was compiled by the company FESTO and serves the purpose of control simulation of pneumatic and electro-pneumatic circuits.

Step by step students learn creation principle of pneumatic and electro-pneumatic control circuits by means of e-Learning materials and with participation of a lector. On the basis of e-Learning courses they pass step by step through creation principles of control circuits at first, thereafter through verification by simulation of control circuit function. Control circuit diagram can be seen in Fig. 4.

Work of students in the virtual laboratory is a part of e-Learning courses where they can create their own pneumatic and electro-pneumatic control circuits for control of specific equipment and thereafter verify its reliable function via simulation.

5. CONCLUSIONS

We have “learning centers” and “training departments” – treating learning as if it were a compartment or corporate activity in which we sometimes engage, rather than a constant, ongoing process – a thread through the fabric of daily activities. Learning is a thread that runs through all of life. We do not belong only in corporate training rooms. The act of learning is ongoing and constant.

An organization’s ability to adapt is important to ongoing survival (even innovation, if you will). But the adaptation must be of a particular type. It must be progressive, ongoing, punctuated with periodic bursts (the transformation), but many about a progressive, but not overly reactionary trends to what is going on in the larger learning landscape. Few organizations will be positioned to

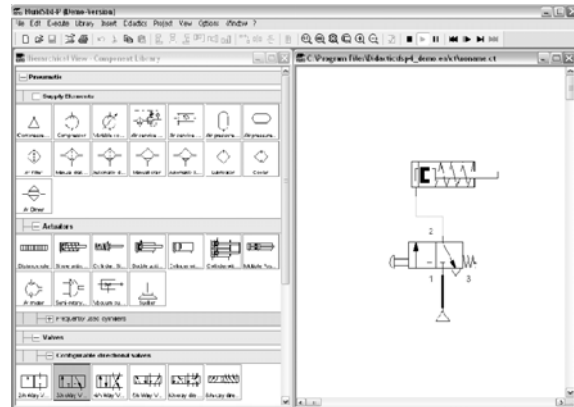


Fig. 3: FluidSIM workbench

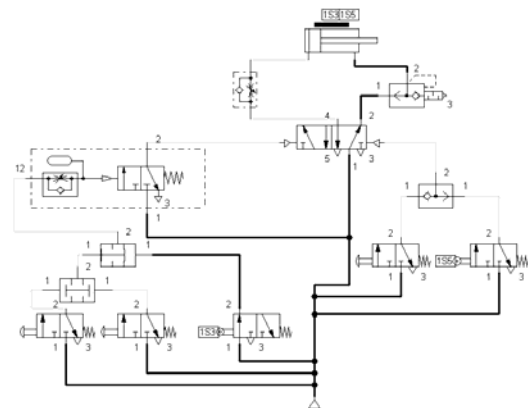


Fig. 4: Circuit scheme in FluidSIM

adopt wholesales the ideas I've presented. To do so would damage many elements of the system continuing to work well. But to survive, all organizations need to embrace experimentation – an ongoing “blood in the corporate veins” type of experimentation. Policy-induced change can be effective, but most often, if we follow the lessons of evolving organisms, developing corporate competence progressively is the best approach for long-term sustained change.

The needs of continual learning, often tightly linked to work, required a new approach and model. LDC has been designed to create an alternative, less-linear view of learning. Learning is the intent of any development activity – communities, courses, networks, or ecology. Selecting the most appropriate design approach will assure greater a more positive and valuable experience for the learner.

ACKNOWLEDGMENT

This paper was created thanks to the national grant KEGA 3/7131/09 – Laboratory of production system program control

REFERENCES

- [1] Rusková, Dagmar, Cagaňová, Dagmar 1997, Needs analysis, In: IATEFL. Proceedings of the Teacher Training Symposium. Teacher Training in a Climate of Change. – Bratislava, Univerzita Komenského v Bratislave., - ISBN 80-88901-08-1. - S. 87-94
- [2] Mudriková, Andrea - Charbulová, Marcela: Virtual laboratory for pneumatic and electropneumatic as a tool for increasing efficiency of teaching technical academic fields. In: AMO 2008 : 8th international conference on advanced manufacturing operations. Bulgaria, Kranevo, 18-20 June 2008. - Sofia : DMT Product, 2008. - S. 115-118
- [3] Holubek, Radovan - Horváth, Štefan - Velíšek, Karol: Increased effective education pneumatic and electropneumatic at virtual laboratory. In: Annals of DAAAM and Proceedings of DAAAM Symposium. - ISSN 1726-9679. - Vol. 20, No. 1 Annals of DAAAM for 2009 & Proceedings of the 20th international DAAAM symposium "Intelligent manufacturing & automation: Focus on theory, practice and education" 25 - 28th November 2009, Vienna, Austria. - Vienna : DAAAM International Vienna, 2009. - ISBN 978-3-901509-70-4, s. 0193-0194
- [4] Matúšová, Miriam - Hrušková, Erika - Košťál, Peter: Spatial arrangement of information and power flows in pneumatics and electro pneumatics laboratory. In: Annals of MTeM for 2009 & Proceedings of the 9th International Conference Modern Technologies in Manufacturing : 8th - 10th October 2009, Cluj-Napoca, Romania. - Cluj-Napoca : Technical University of Cluj-Napoca, 2009. - ISBN 973-7937-07-04. - S. 169-172
- [5] Bílik, Jozef - Kapustová, Mária - Košťálová, Miroslava: Zvýšenie teoretickej a praktickej pripravenosti absolventov študijného programu tvárnenie pre súčasnú prax. (Increasing of theoretical and practical readiness of graduates in studying subject forming for today praxis) In: Inovatívne postupy výučby výrobných technológií na univerzitnom stupni štúdia: Zborník vedeckých príspevkov, vydaný pri príležitosti ukončenia projektu KEGA 3/5209/07 s názvom "Podpora výučby výrobných technológií formou virtuálnych exkurzií". - Zvolen : Technická univerzita vo Zvolene, 2009. - ISBN 978-80-228-2050-9. - S. 7-10
- [6] Mudriková, Andrea - Košťál, Peter - Matúšová, Miriam: Building of a production system program control laboratory. In: Annals of DAAAM and Proceedings of DAAAM Symposium. - ISSN 1726-9679. - Vol. 20, No. 1 Annals of DAAAM for 2009 & Proceedings of the 20th international DAAAM symposium "Intelligent manufacturing & automation: Focus on theory, practice and education" 25 - 28th November 2009, Vienna, Austria. - Vienna : DAAAM International Vienna, 2009. - ISBN 978-3-901509-70-4, s. 0603-0604





¹. Štefan NIŽNÍK, ². Ondrej MILKOVIČ, Svätoboj LONGAUER

METALLURGICAL TWO-STEP PRODUCING METHOD OF FE NANOPARTICLES

¹. TECHNICAL UNIVERSITY OF KOŠICE, FACULTY OF METALLURGY, KOŠICE, SLOVAKIA

ABSTRACT:

Submitted paper is dealt with preparation of iron based nanoparticles and marginally also cobalt nanoparticles through precipitation from solid solution of age-hardenable alloys and their subsequent insulation by electrochemical or chemical resolution of matrix. The simplest system is Cu-matrix in which Fe resp. Co as elements are precipitated in form of coherent particles γ -Fe,Co. These particles are changed at plastic deformation or at extraction and insulation by martensitic transformation on α -Fe, Co. For purposes of nanoparticles precipitation from solid solution there is performed the targeted heat treatment consisting of solution annealing, quenching and precipitation annealing. The size of nanoparticles is regulated by heat treatment of chosen material according to the required procedure. The volume of separated nanoparticles is proportional to the time of dissolution and to the potentiostatic mode according to applied potential-dynamic curves. The quality and material characteristics of nanoparticles was controlled by the methods of TEM, x - ray analysis and measurement of magnetic properties.

KEYWORDS:

Fe nanoparticles, precipitation, electrochemical dissolution, characteristics

1. INTRODUCTION

At present time the nanoparticles are produced by intricate sophisticated techniques e.g. laser-induced pyrolysis, laser evaporation and condensation, plasma torch synthesis, deposition from colloidal solutions, reduction from aqueous solutions, crystallization from amorphous solid phase, etc. from which neither one reckons with precipitation of nanoparticles from crystalline solid phase. At the same time almost each of the appointed technologies is complicated and from views of investment and also operating cost is considerably demanding. When techniques producing free metallic nanoparticles are used, the particles are usually covered by oxides with thickness depending on technique [1,2].

Method for nanoparticles preparation presented in this work consists of the aimed heat treatment of basic material where nanoparticles are formed by controlling precipitation from solid solution and the production is reposed on insulation or extraction of nanoparticles by electrochemical eventually chemical way. So, the largeness of nanoparticles in the range 3 – 1000 nm is intentionally regulated by metallurgical heat treatment of chosen material according to the required procedure. Quantity of separated nanoparticles is straight-proportioned to the time of solution and to the potentiostatic mode. According to [3] the amount of Fe nanoparticles electrochemically separated from Cu matrix is 0,024 μ g from the plane 0,5 cm² within 30 min and are stored in n-hexane. Besides, preliminary experiments with Cu-Fe material system show that extracted Fe particles are either oxidless or only with small not dangerous oxide layer.

It is a matter-of-course, the supposed method allow to production also of nanowires by creating their shape through the thermo-mechanical treatment or through the separation of regular rod-shaped Fe particles from eutectoid or eutectic alloys. The idea as well as the procedure of nanoparticles separation are safekeeping by two patents [4,5]. As a very significant factor from the point of view of exploitability of nanoparticles prepared by „metallurgical“ method there is high

quality of particles appreciated by size and shape homogeneity as well as their structure. It's utilizable in the medical applications [6-7].

Electrochemical isolation consists of the matrix solution in the selected solvent during which the nanoparticles are at least ~ 100 mV more ingenuous and their corrosion potential is more positive towards the metal potential of the basal matrix. During the solution process of the matrix, the particles hold their stability and keep their consistency in solution. In some alloyed systems it is sufficient to use a chemical solution of the matrix for favourable insulation of particles, so as not to come to attacking of the particles [3].

2. EXPERIMENTAL METHODS

For the operation of presented method of nanoparticles preparation the model alloy system Cu-Fe was chosen, which marks out max solubility of Fe in Cu solid solution $\varepsilon 4\%$ at 1096°C . With decreasing temperature the solubility of iron in solid solution is falling down to zero at room temperature.

Copper wire with diameter 10 mm and chemical composition 1,88 % Fe, 0,015 % P, 0,08 % Zn a 0,05 % B was submitted to the dissolving annealing at $1000^\circ\text{C} / 12$ hod and was quenched into cold water. In order to precipitate the spheroid Fe nanoparticles, the samples were annealed at the temperature of $600^\circ\text{C} / 30$ min, 1, 12 and 24 hours, and quenched into cold water.

Producing of Fe nanoparticles was design by electrochemical dissolution of copper matrix in aqueous solution as well as etching solution by potentiostatic mode. Labor technique was followed: Pt electrode as auxiliary; SCE (saturated calomel electrode) as reference; specimen as anode. Computer controls the potentiostat fixed on a defined value. The dissolving conditions are appropriate at the potentiostatic mode of -250 mV (SCE) in ammonia solution.

The morphology and distribution of particles and the state of substructure and interphase boundary were monitored by optical and transmission electron microscopy TEM by electronic microscope JEM 2000 FX and JSM 35 CF with microanalytical Link 860. Results of electron-microscopic observation will be evaluated by statistical methods.

3. RESULTS AND DISCUSSION

Morphology and distribution of the Fe particles were studied by means of carbon replica technique by TEM. After precipitation annealing, soft precipitate consisting of regular globular particles was found within the samples. The information about its control is very important for obtaining the specific dimension of particles by consumer order especially for medical applications. The distribution function is time invariant during the steady-state precipitation annealing. This reason is a good condition for preparing the smaller (one domain) particles, because the smaller precipitates are assigned the smaller dispersion.

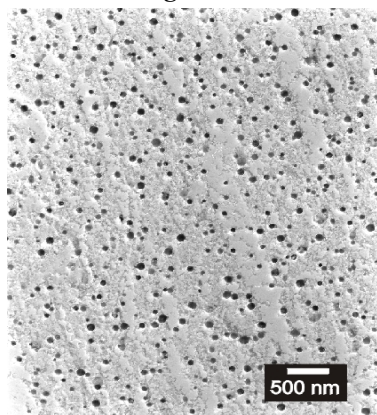


Fig. 1 Extracted Fe precipitates from Cu matrix

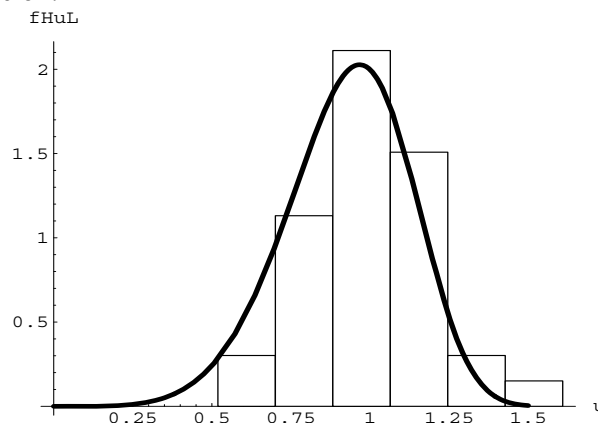


Fig. 2 The size distribution of Fe precipitates aged at 973 K for $86,4\text{ ks}$

The regular spherical particles with extraordinary homogeneous distribution can be observed in the Fig. 1. According to the expectation, the increase of annealing time resulted in growth of particles. The range size of particles after annealing 12 hours moves between $18 - 22$ nm. Fe particles after 24 hrs of annealing had the dimension $\approx 26 - 32$ nm. In all cases, the distribution of particles was statistically equable in whole volume of samples and the particles had globular shape [8].

Quantity of isolated nanoparticles is directly proportional to time of dissolution in potentiostatic mode. The amount of 0,024 mg Fe spherical nanoparticles were separated from the surface 0,5 cm² in 20 ml electrolyte at potentiostatic mode -250 mV (SCE) for 30 min.

Characterization of Fe nanoparticles after their insulation from Cu matrix is documented in Fig. 3. Measuring of the nanoparticles radiuses was shown a good agreement with the mean precipitate radius after precipitation annealing. This confirms that precipitates are not dissolution in the electrolyte.

TEM micrograph of nanoparticles diffraction is shown in Fig. 4. The core-shell structure can be shown with the dark core end the light shell. Shel thickness is around 3 – 4 nm at mean diameter of nanoparticles 10 – 21 nm. Fig. 5 presents the selection electron diffraction. The straight pattern of α -Fe phase and two diffusive rings corresponding to 2 line ferrihydrite.

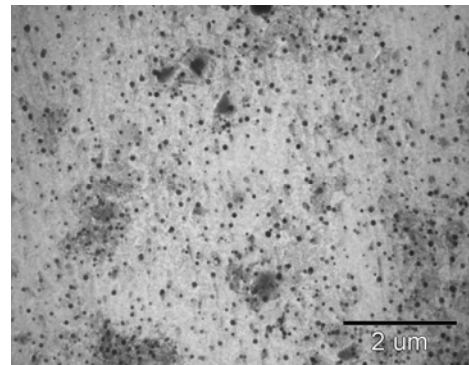


Fig. 3 Insulated nanoparticles after matrix dissolution

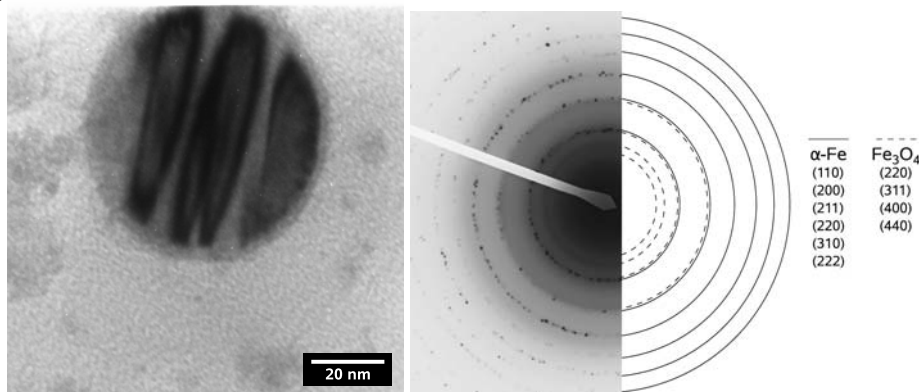


Fig. 4 TEM micrograph of insulated Fe nanoparticles

Fig. 5 Selection electron diffraction of nanoparticles

Characteristics of the magnetic properties of nanoparticles was determined by measuring the temperature dependence of magnetization in the magnetic field (FC) and without magnetic field (ZFC) and also from measurements of magnetic hysteresis loops at different temperatures.

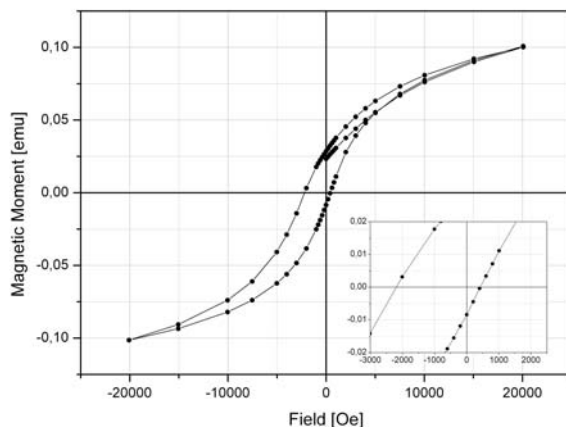


Fig. 5 Magnetic hysteresis loop at 2 K

Measurements of magnetic properties of Fe nanoparticles with a mean radius of 27.7 nm from the dependence of magnetic moment on the temperature not confirmed the superparamagnetic behavior of these particles. At produced nanoparticles with mean radius of 10 nm was found the blocking temperature ($T_b = 65$ K), which characterizes the behavior of superparamagnetic particles above this temperature. This justifies the fact that the presented method of nanoparticles production can be used for applications which require phenomenon of superparamagnetism (medicine: magnetic resonance imaging, medicament carrier).

4. CONCLUSIONS

1. After choosing experimental treatment of precipitation annealing at 600 °C/0,5, 1, 12, 24 hours, the statistically regular distribution of precipitate was obtained in the volume of samples. There were the particles with globular shape, which dimensions grew by annealing time from 4,5 to 32 nm.

2. The advantages of this method consists of possibilities to control the size and shape of nanoparticles in a narrow range tolerance with relative accuracy 5 nm by heat treatment at min financial costs of the production facilities.
3. The amount of Fe nanoparticles separated from the surface of 0,5 cm² for 30 min is 0,024 mg. The particles are not dissolved during the dissolution process of the matrix and the particles don't change their chemical composition.
4. Nanoparticles with mean radius of 10 nm have the blocking temperature (T_b = 65 K), which characterizes the behavior of superparamagnetic properties above this temperature, what can be used for applications in medicine.

ACKNOWLEDGEMENTS

The autors would like to acknowledge the support of Scientific Grant Agency of the Ministry of Education of the Slovak Republic for its financial contribution to the project No.1/4138/07 „Magnetic nanopartricles for medical and technical applications“.

LITERATURE

- [1] Schmid, G.: Nanoparticles, Wihley-VCH Verlag GmbH & Co. KgaA, 2004.
- [2] Jönsson, B., J., at al.: Oxidation states and magnetism of Fe nanoparticles prepared by a laser evaporation technique. In: Journal of Application Physics, 1996, č. 79.
- [3] Milkovič, O., Halama, M., Longauer, S., Nižník, Š.:Preparation mode of Fe nanoparticles, Acta Met. Slovaca, 13, 2007, 694.
- [4] Milkovič, O., Halama, M., Nižník, Š.: Spôsob výroby feromagnetických Fe nanočastic elektrochemickou separáciou, Zn. spisu: PP 0087 – 2005, zaregistrovaná 29.7.2005,
- [5] Longauer, S., Nižník, Š.: Spôsob prípravy a izolácie nanočastic z tuhej fázy, Zn.spisu: PP0088 – 2005, zaregistrovaná 29.7.2005
- [6] Wang, Y., C., et al.: The preparation, surface modification, and characterization of mettalic γ -Fe nanoparticles. In: Material science and engineering B, 1999, č. 60, s. 223- 226.
- [7] Salata, O.V.: Applications of Nanoparticles in biology and medicine, Journal of Nanobiotechnology, 2, 2004.
- [8] Hirata, V. M. L. et al.: Ostwald ripening of γ -Fe precipitates in Cu-1,5 at. % Fe alloy. In Scripta Metallurgia et Materialia, č. 31, 1994, s. 2.
- [9] Timko, M., et al.: Czechoslovak Journal of Physics 54, Part 2 Suppl. D., 2004, s. 599-606.
- [10] Bansmann, J., et al.: Materials Science and Engineering C 19, 2002, s. 305-310.
- [11] Martin, J., I., et al.: Journal of Magnetism and Magnetic Materials 256, 2003, s. 449-501.
- [12] Konerecká, M., et al.: Journal of Magnetism and Magnetic Materials 293, 2005, s. 271-276.



RESEARCH REGARDING THE EFFECT OF ALLOYS VIBRATION ON MICRO- AND MACROBLISTER FROM CASTED PARTS

^{1,2} UNIVERSITY POLITEHNICA BUCHAREST, ROMANIA

³ TECHNICAL COLLEGE "MEDIA" BUCHAREST, ROMANIA

ABSTRACT:

Compacting casted parts and reducing the blister on the solidification of alloys are equally interests in improving the quality, characteristics and reducing manufacturing costs by increasing the removal result index from blister compaction.

Theoretical and experimental research conducted by the authors has lead to obtain beneficial results in this respect. This paper presents the results and conclusions drawn from this research.

KEYWORDS:

Alloys, quality, manufacturing costs

1. INTRODUCTION

The structure and physical-mechanical characteristics of a casted metal material are influenced by its density and compactness.

At the alloys solidification it can occur discontinuities, due to the shrinkage phenomenon, characteristic of most alloys and to the pronounced decrease in solubility of gases in the melt, at crystallization temperature.

2. THE STUDY

Obtaining a compact metal material is provided if the v speed of the alloy penetration into capillary channels of the biphasic zone is equal to the contraction speed v_{contr} . [1]

$$v_{\text{contr}} = \alpha \cdot m \cdot R \quad [\text{m/s}] \quad (1)$$

where: α - contraction coefficient of the alloy at solidification;

m - ratio between the liquid mass volume from the biphasic zone and this zone's volume;

R - rate of occurrence of solid phase [m/s].

In ordinary conditions, the v speed is expressed as such:

$$v = \frac{r^2}{8\eta} \cdot \frac{P_e + P_m - P_g + \frac{2\sigma}{r} \cos \theta}{l}, \quad [\text{m/s}] \quad (2)$$

where: r - radius of the capillary channel [m]; P_e - external pressure [Pa]; P_m - metalostatic pressure [Pa]; P_g - channel gases pressure [Pa]; σ - superficial tension of the alloy [N/m]; θ - wetting angle [rad]; η - dynamic viscosity of the alloy [Pa · s]; l - length of penetration of the alloy in capillary channels [m].

From the equality of the two speeds $v=v_{\text{contr}}$ results:

$$\frac{r^2}{8\eta} \cdot \frac{P_e + P_m - P_g + \frac{2\sigma}{r} \cdot \cos \theta}{l} = \alpha \cdot m \cdot R \quad (3)$$

from where:

$$l = \frac{r^2 \left(P_e + P_m - P_g + \frac{2\sigma}{r} \cdot \cos \theta \right)}{8\eta \cdot \alpha \cdot m \cdot R} \quad (4)$$

Mechanical oscillations decreases the superficial tension σ at the liquid-solid interface wetting angle θ and imprints the alloy a maximum initial speed $v_i = A\omega$.

Mechanical vibrations action produces in the biphasic zone a dendrite fragmentation, reducing the length of capillary channels to be covered by the liquid alloy to fill the gaps caused by shrinkage and increase the speed of the liquid alloy flow in these areas, improving supply conditions in micro-cavities.

Also, vibrations determine a macro-blister concentration and a reduction of the porosity in the hot spots, an effect explained by increasing the melt flow.

Mechanical vibrations applied in liquid metal alloys introduce new forces that determine changes in the macrostructure and macro-blister of the casted parts.

The size, shape and position of micro-blister can be determined theoretically by plotting isotherms of solidification in the walls of the casted parts.

Macro-blister is located in those areas of the wall where the liquid alloy solidifies last and alone. Macro-blister consists of one or more concentrated cavities in clearly defined areas, they result from the solidification of large volumes of liquid alloy. Macro-blisters are called as well concentrated blisters. [2]The alloy layers that isolate the blisters between them and cover them in the top part are called decks.

The main macro-blister is found in the upper part to the casted part compared with the casting position, while the secondary macro-blister is found in the lower part or in hot spots in the thermal axis zone.

Macro-blister is determined using technological evidence, while micro-blister by applying methods of flaw (X or gamma rays) or by determining the density of samples cut from the casted part wall.

The volume, shape and position of the macro-blister and micro-blister in the walls of the casted parts are influenced by several factors which at their turn depend on the technological nature of the alloy, the nature of the mold, the casting conditions and the casted part geometry.

The total volume of the blister is:

$$V_r = V_{MR} + V_{mr} \quad (5)$$

in which: V_{MR} - the macro-blister volume; V_{mr} - micro-blister volume.

The factors which influence the blister are the following:

- ❖ alloy's nature;
- ❖ form's nature;
- ❖ casted part geometry;
- ❖ casting conditions.[3]

Avoiding the process of developing a micro-blister is impossible, but the routing of the contraction process in order to obtain a macro-blister with as smaller as possible volume and with an optimum distribution in the part's wall is possible.

3. ANALISES, DISCUSIONS, APPROACHES and INTERPRETATIONS

The development of the alloy was made in a crucible furnace, heated by burning a natural gas flame. After melting, the temperature was increased and maintained at 800°C.

For casting and solidification of the samples were used metal forms.



Fig. 1. Alloy's solidification



Fig. 2 Extraction of vibrated samples from the mold

Among physical properties, density is directly related to the development process and represent the unit volume's mass.

From the performed measurements performed we can remember the following:

- ❖ sample casted from non-vibrated alloy, solidified in outdoor air; (O)
- ❖ sample casted in non-vibrated alloy, solidified under the influence of vibration after casting until solidification; (V)
- ❖ sample casted from alloy vibrated in pot, solidified without vibration (O')
- ❖ sample casted from alloy vibrated in pot, solidified under the influence of vibration after casting until solidification. (VV)[4]

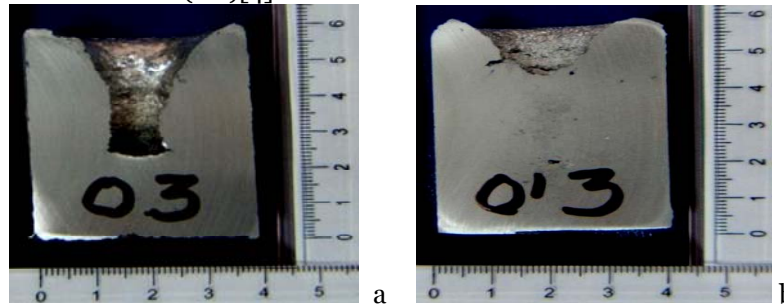


Fig. 3 Blister aspect for different situations
 a- non-vibrated; b- the vibration of melted alloy (only in pot, before casting)

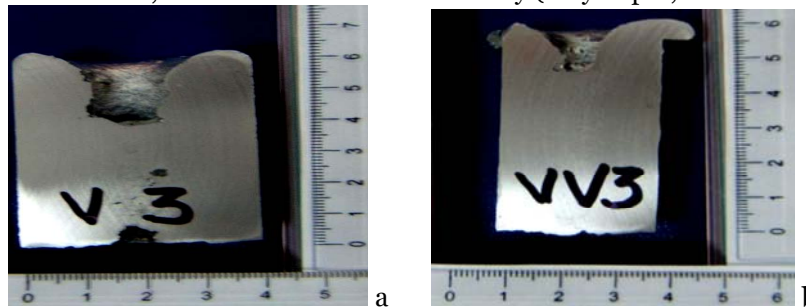


Fig. 4 Examples of section blisters
 a- solidified under the influence of vibration after casting until solidification; b- vibrating the alloy in the pot and during casting until solidification.

Vibrations determine macro-blister concentration, a decrease of porosity from the liquid alloy, to manage the formation processes and structure compacting with small crystals which present the best physical and mechanical characteristics, including increased density of casted alloys with those advantages. Measurement results are presented in Table 1 for an aluminum alloy type ATSi12.5 Mg0.25.

Table 1. The measurements results on non-vibrated, vibrated samples

No.	Sample	Sample mass [g]	Volume [cm ³]	Density [g/cm ³]	Density increase thought vibrating [%]
1	O	30,9044	11,6	2,66	-
2	V	31,9044	11,4	2,79	4,88
3	VV	30,8544	10,9	2,83	6,39

Mechanical properties are also determined by the macrostructure because of the existence of chemical heterogeneity, crystalline or mechanical or discontinuities that play the role of power and micro-concentrators, by size, crystal form, nature and morphology of structural constituents.

Table 2 shows the values obtained by carrying out systematic evidence of resistance to fracture, yield, and elongation at break for the four types of casting:

- ❖ casting in gravitational field (O);
- ❖ casting after the liquid alloy vibrating in the mold (O');
- ❖ vibrating after casting in the mold until solidification (V);
- ❖ sample from the liquid alloy vibrated in the pot casted in the mold and vibrated until solidification (VV). [4]

Following research which refers to treating metal melts with mechanical vibrations, highlighting the fact that they have positively influenced the structure obtained after solidification and on mechanical properties, in the sense that it improves them. The values obtained are much higher than those obtained in the classical variant.

Table 2. Values for tensile strength, yield, elongation, weakening the fracture toughness for the cast alloy AlSi12.5Mg0.25 of samples realized during research

No.	Sample type	R _m [MPa]	R _{p0.2} [MPa]	A _u [%]	Z [%]	HB [MPa]	Observations
R1	O1	170	102	3,5	2	87,5	Un-worked sample
R2	O2	176	101	3	2,04	88,6	The split inclusions 0.5 mm
R3	O3	175	103	3,2	2,2	87,3	
R4	O/1	185	111	4,2	5,8	89,3	Un-worked sample inclusions in the area from feeder
R5	O/2	93,8	-	-	-	-	Defect in structure, blister with a diameter of 1.5 mm
R6	O/3	186	112	5	-	90,6	
R7	V1	295	162	4,4	3	105	
R8	V2	296	162	4	2,7	104,3	
R9	V3	295	160	3,9	2,7	106,3	
R10	V4	294	170	3,9	-	103,1	
R11	V5	294	165			103,2	
R12	VV1	150	-	-	-	-	Defect in structure
R13	VV2	295	147	5,6	3	99,3	
R14	VV3	294	145	4,2	1,5	98,6	
R15	VV4	290	150	2,1	2,1	97,2	
R16	VV5	285	151	4	2,8	97,3	Turning diameter of 50 mm, sample in the thermal axis

The mechanisms by which these vibrations act on the liquid phase during solidification and melting are complex. [5] Explanation and understanding of these mechanisms is of great theoretical and especially practical importance, allowing us to define appropriate technology for treatment of melt with vibrations.

Figure 5 shows the variation of the degassed alloy hardness under the influence of vibration (50Hz) in the casting pot. It is noted that though gas elimination was achieved a material compaction, evidenced by increasing the hardness by about 5 percent compared with the gross alloy.[6]

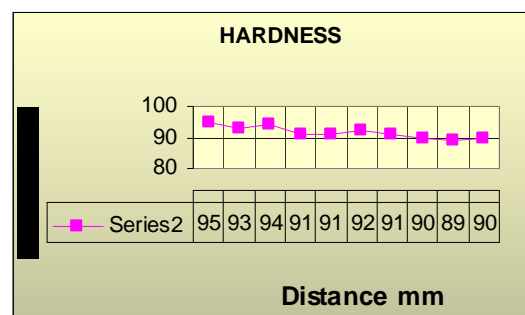


Fig. 5 HB-hardness variation on the radius for alloy AlSiMg vibrating pot, gravitational casting for the ϕ 20mm disc, sample O'2

4. CONCLUSIONS

The contour analysis of the contraction gap leads to the conclusion that under the natural action of vibration is reduced the blister depth and its lower part is rounded.

For the alloys with high contraction, prone to cracking, it was observed that due to mechanical vibrations the micro-blisters decrease reducing axial porosity.

Under the influence of mechanical vibration decreases the total volume of macro-blister and focuses on the superior side, reducing the volume of liquid alloy for feeders.

The main favorable technological effects obtained by applying physical-mechanical treatments, consisting of increasing compactness and improving the structure of castes parts.

It also finds a sharp increase in hardness values by 25 percent compared to a gravity cast alloy (static), a slight decrease in the hardness towards the thermal axe, at the same diameters or different diameters of the samples a longer vibrating time leads to chopped microstructures and higher hardness values.

REFERENCES

- [1.] BAUM B.A., TIAGUNOV G. B. - Protessa litiia, Moskova 1992
- [2.] CĂMUI C. - Studii și cercetări privind efectul acțiunilor fizice ale energiei vibrațiilor de joasă frecvență asupra cuprului în momentul turnării și solidificării în semifabricate; lucrare de absolvire cursului post universitare, București 1991
- [3.] MĂRGINEAN I., VELICU Șt. - Procedee speciale și neconvenționale în turnătorii, vol. I și II. Ed. BREN, București 2002
- [4.] PĂRVULESCU C.-Cercetări privind influența vibrației asupra solidificării aliajelor turnate în piese; Teză de doctorat, UPB 2010
- [5.] POP M.A.-Cercetări asupra tehnologiilor și materialelor moderne pentru confecționarea garniturilor de model; Teza de doctorat, UT Brașov 2009
- [6.] ȘUȘU C.-Contribuții la îmbunătățirea calității topiturilor unor aliaje de aluminiu destinate turnării pieselor; Teză de doctorat, UT Cluj-Napoca 2008.



¹Eugen Mihai CRIȘAN, ²Teodor HEPUT

INFLUENCE OF BASIC ADDITIVE ON THE QUALITY OF PELLETS

¹ UNIVERSITY "POLITEHNICA" TIMIȘOARA, FACULTY OF ENGINEERING HUNEDOARA, ROMANIA

ABSTRACT:

Besides the humidity, the granulometric composition and the specific surface of the pelleted material, the compressive strength of the pellets is also influenced by some additions with binding proprieties (bentonite, lime, limestone, dolomite, etc.). During the hardening process, these additions form a resistant slag that contributes to the binding of the granules of ferrous raw materials and, finally, to the increasing of the compressive strength of the pellets.

To determine the influence of the addition of lime and dolomite on the compressive strength of pellets, we performed a series of experiments in the laboratory phase, consisting of the production of pellets based on various recipes, by adding bentonite & lime or bentonite & dolomite.

During the research, we aimed to establish correlations between the compressive strength of pellets and the additions of water, bentonite, lime or dolomite. The data obtained in the experiments were processed in MATLAB programs, resulting simple or multiple correlation equations. Based on these equations, we could establish the optimum addition of materials with basic character.

KEYWORDS:

pellet, compressive strength, lime, dolomite, iron oxide, calcium oxide

1. INTRODUCTION

Besides the humidity, the granulometric composition and the specific surface of the pelleted material, the compressive strength of the pellets is also influenced by some additions with binding proprieties (bentonite, lime, limestone, dolomite, etc.). During the hardening process, these additions form a resistant slag that contributes to the binding of the granules of ferrous raw materials and, finally, to the increasing of the compressive strength of the pellets.

When using the lime as additive, simultaneously with the hardening process can appear various chemical combinations between the iron oxide and the calcium oxide, obtaining calcium ferrites, or between the iron oxide, silica and lime, obtaining calcium and iron silicates. In case of CaO additive in excess and basicity ration up to 1.8, we obtain calcium diferrite, $2\text{CaO}\cdot\text{Fe}_2\text{O}_3$, which becomes friable in case of reduction at low temperatures.

When using dolomite as basic additive, the formation of calcium diferrite is avoided mostly due to the reduction of the CaO content. From the reaction between CaO and SiO_2 that takes place in the gangue of the pelleted raw material, it results calcium silicates of CaOSiO_2 or 2CaOSiO_2 types, which ensure a good binding of the material during the low temperature reduction process.

The use of additives for increasing the resistance of the pellets should be made respecting an optimal proportion, this being the subject of the present research.

2. LABORATORY EXPERIMENTS

The experiments regarding the producing of pellets were performed in the laboratory "Energy and raw material base in industry", at the Engineering Faculty of Hunedoara. This laboratory is endowed with the installations required for producing pellets (volumetric ranking device, mixing drum, pellet making machine and hardening installation). The compression resistance has been determined by using the tension-compression test machine found in the "Strength of materials" laboratory of the faculty. The raw material used to produce pellets consisted

of steel plant dust and red mud (resulted from alumina production). The compositions are presented in Table 1. We produced two sets of pellets, each set consisting of 3 lots.

Table 1

Set	Lot	Set	Lot	Remarks
A	A1 with 1% lime	B	B1 with 1.5% dolomite	In each set, the addition of bentonite ranged between 0 and 1% (i.e. 0%; 0.5% and 1%), and the addition of water ranged between 7.5 and 11.5%, (i.e. 7.5%, 9.5% and 11.5%)
	A2 with 3% lime		B2 with 3.5 dolomite	
	A3 with 5% lime		B3 with 5% dolomite	

The weight of the pellet batch was 2 kg (ferrous raw material, bentonite, lime/dolomite). The hardening of the pellets respected the combustion diagram of hematite ferrous materials. From each batch, we selected three pellets to determine their compression resistance. To establish the correlations, we took into account the average value.

3. RESULTS OBTAINED FROM PROCESSING THE EXPERIMENTAL DATA

By processing the data obtained in the laboratory phase, we obtained equations of correlation between the binder additives & water (considered as independent parameters) and the pellet compression resistance (considered as dependent parameter). The data were processed in MATLAB programs, the results being presented hereunder, in graphical and analytical forms.

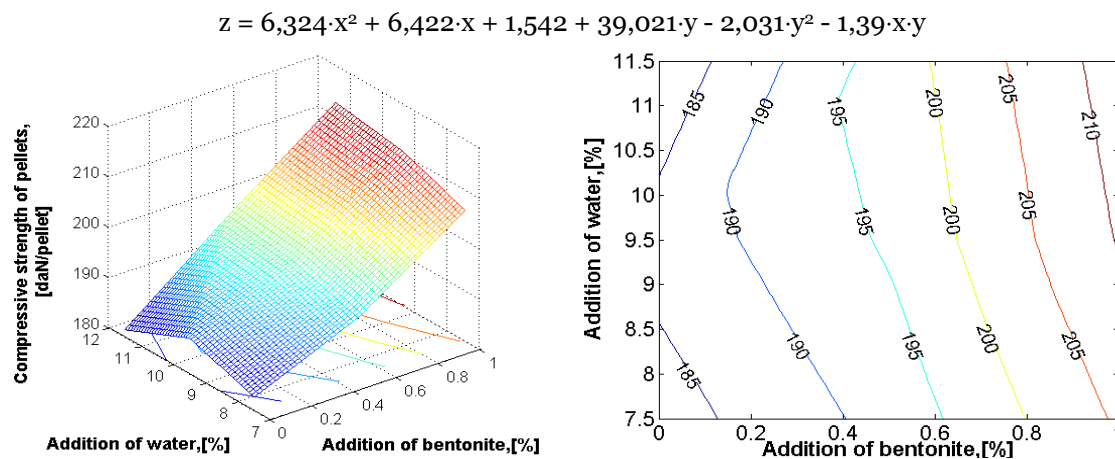


Fig.1. Variation of compressive strength of pellets to a concentration of 1% lime
 (x- addition of bentonite [%], y- addition of water [%],
 z- compressive strength of pellets, [daN/ pellet])

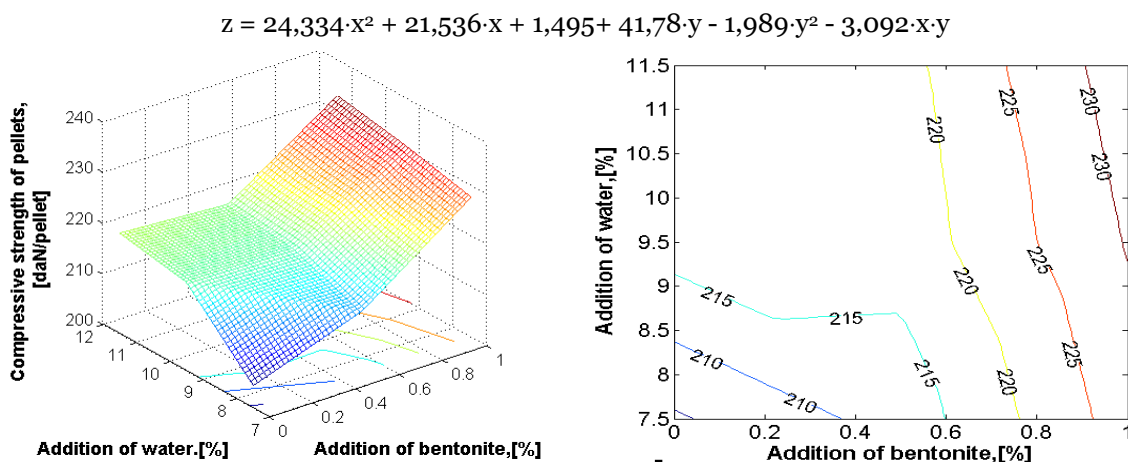


Fig.2. Variation of compressive strength of pellets to a concentration of 3% lime
 (x- addition of bentonite [%], y- addition of water [%],
 z- compressive strength of pellets, [daN/ pellet])

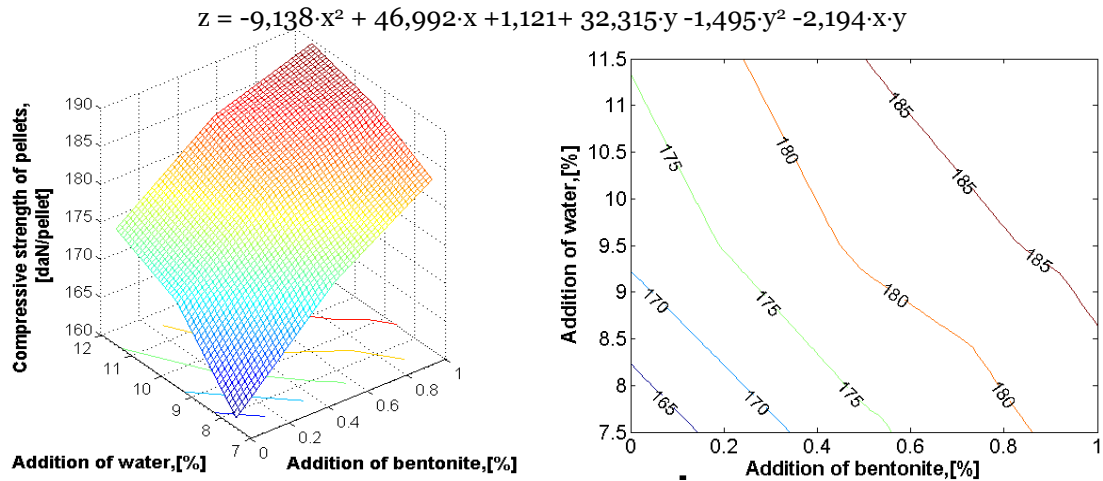


Fig.3. Variation of compressive strength of pellets to a concentration of 5% lime
 (x- addition of bentonite [%], y- addition of water [%],
 z- compressive strength of pellets, [daN/ pellet])

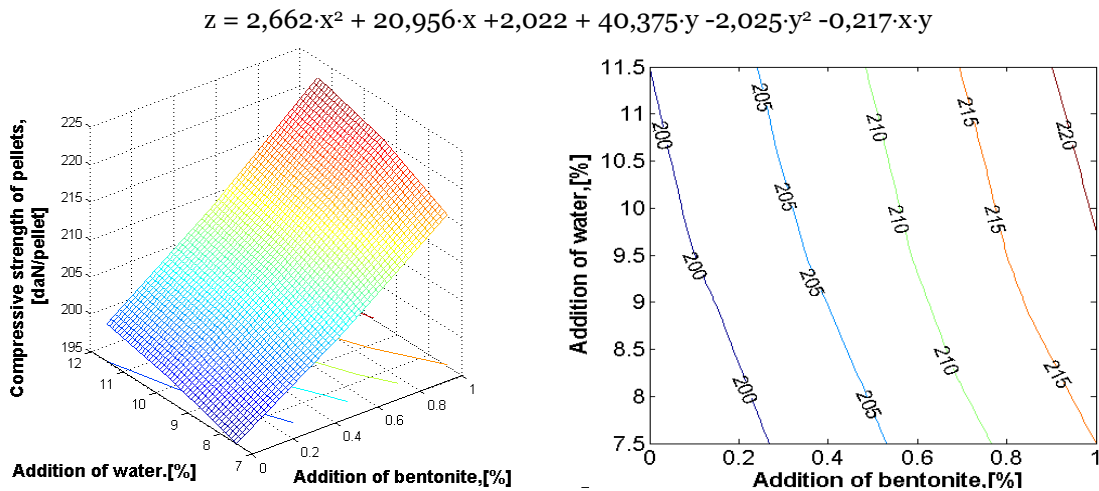


Fig.4. Variation of compressive strength of pellets to a concentration of 1.5% dolomite
 (x- addition of bentonite [%], y- addition of water [%],
 z- compressive strength of pellets, [daN/ pellet])

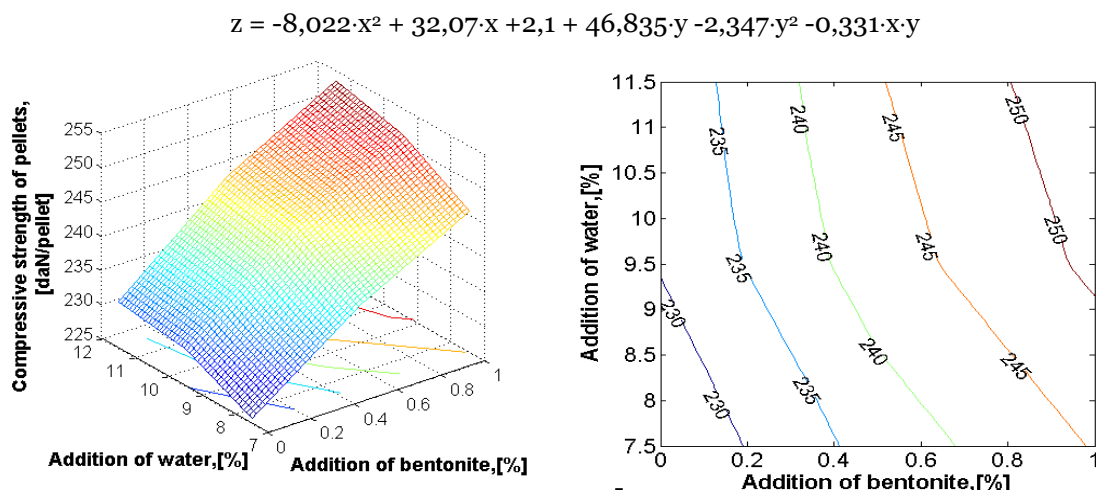


Fig.5. Variation of compressive strength of pellets to a concentration of 3.5% dolomite
 (x- addition of bentonite [%], y- addition of water [%],
 z- compressive strength of pellets, [daN/ pellet])

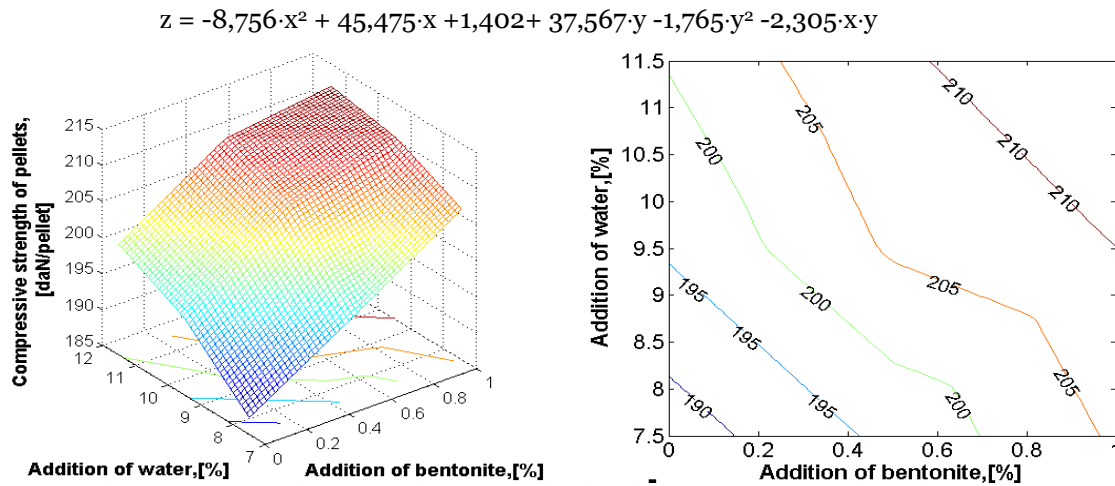


Fig.6. Variation of compressive strength of pellets to a concentration of 6% dolomite
 (x- addition of bentonite [%], y- addition of water [%],
 z- compressive strength of pellets, [daN/ pellet])

Analysing these correlations, we could establish the optimum domains for the flux, bentonite and water additions, in order to obtain higher pellet compression resistance values in case of flux addition.

4. CONCLUSIONS

Based on the experiments, on the results obtained from data processing and on the technical analysis of these data, the following conclusions resulted, in a nutshell:

- ❖ the two types of ferrous wastes (steel plant dust and red mud), both resulted from metallurgical processes, can be processed through pelleting. This means they can be used in the iron & steel industry;
- ❖ it is advisable to add 1% bentonite and 10-11% water, the upper limit corresponding to the higher limit of the added flux;
- ❖ by processing these wastes and transforming them in pellets fit to be used as raw or auxiliary materials in the iron & steel industry, the areas currently covered by them can be given back to nature, contributing in this way to the greening of the environment.

BIBLIOGRAPHY

- [1.] Project nr.31-098/2007 with title Prevention and fighting pollution in the steelmaking, energetic and mining industrial areas through the recycling of small-size and powdery wastes, Program 4 "Parteneriate in domeniul prioritare" 2007-2013.
- [2.] Heput Teodor, Constantin Nicolae, Socalici Ana, Ardelean Marius, Ardelean Erika, Researchs regarding recycling of small-size and powdery ferrous wastes existing in Hunedoara area, Symposium Generation, prevention and processing of pollutant emissions in industrial environment, Bucuresti, 12-13 iunie 2009.
- [3.] Ardelean Erika, Ardelean Marius, Socalici Ana, Heput Teodor, Josan Ana, Researches in laboratory phases regarding to capitalization of ferrous pulverous waste in pellets, International Conference of Metallurgy and Materials Science, Bucuresti, 2008.
- [4.] Heput Teodor, Socalici Ana, Ardelean Erika, Ardelean Marius, Environment ecological process in Hunedoara area through reinsertion in economic circuit of scrap and pulverous waste, Annals of the Faculty of Engineering Hunedoara - Journal of Engineering, VII(3), pp. 293-298, 2009





MACRO-MICRO-NANO COMPOSITE MATERIALS

¹⁻³. POLITEHNICA UNIVERSITY OF BUCHAREST, ROMANIA

⁴. TECHNICAL UNIVERSITY OF CLUJ NAPOCA, ROMANIA

ABSTRACT:

Metal or ceramic composites with reinforced metal or ceramic materials consist the future for material class. The paper proposes to present the results and the conclusions of a few researches in this field.

KEYWORDS:

composite, nano-composite, metallic materials

1. INTRODUCTION

Mixture of several components, whose properties complement each other, resulting in a material with properties superior to those specific to each component part, defines the composite material.

Delineate the difficulties arising in composite materials based on the idea (often used as an objection) that, practically, almost any material is a composite material are extremely rare because no impurities, no defects, alloying elements or not impregnated, coated, treated superficially covered. The distinction is harder to do if their material is taken into account the atomic and molecular scale.

Depending on the structure of materials can be classified as :

- a) crystalline materials:
 - ❖ polycrystalline (ferrous and nonferrous alloys);
 - ❖ crystal (metals, oxides, carbides, nitrides, semiconductor and optoelectronics)
 - ❖ Microcrystalline (alloys subjected to heat treatment such as hardening);
- b) semicrystalline (polymer);
- c) amorphous and glassy materials (metallic and nonmetallic);
- d) composite materials:
 - ❖ Each component dispersed;
 - ❖ Pressed powder aggregate;
 - ❖ Associated material, obtained by surface coating with metallic or nonmetallic substances;
 - ❖ Layered (obtained by assembling successive or simultaneous).

The superiority of composite materials compared to conventional materials, resulting in Figure 1.1, which is the ratio of tensile strength and density with temperature.

As shown, metal matrix composites are superior to conventional ones, but with lower properties of ceramic composites.

Resistance-temperature composite materials, corrosion or oxidation is determined primarily by the nature of the matrix. In general, the matrix is deformable composite material, having a lower strength than the composite material. Matrix choice is based on the purpose and the possibility of producing composites. Components operating at high temperatures should not occur expansion differences between the matrix and dispersed component (if metal or alloy cermet). In case of major mechanical stress, modulus reinforcement material must be greater than the matrix material to provide load transfer between components. A very strong adhesion between the composite constituents favor this transfer, leading to increased fragility.

Concerns about the world in terms of technology, have led to technologies shaping next generation of ceramic-metal composite materials:

- ❖ by polyphasic sintering process (or cosinterizare) under load or no load;
- ❖ by impregnating the porous ceramic with molten metal mass;
- ❖ by deposit of very fine particles (nano) on various supports (metal, ceramic composite were even) by electrodeposition method, the adsorption, diffusion, thermochemical treatments, etc.. In-depth analysis of processes, it is found that any of the methods used to manufacture composite aggregates and other processes specific phenomena. The result is a composite manufacturing process engineer pluricomplex with specific physical, chemical, thermal, electrical.

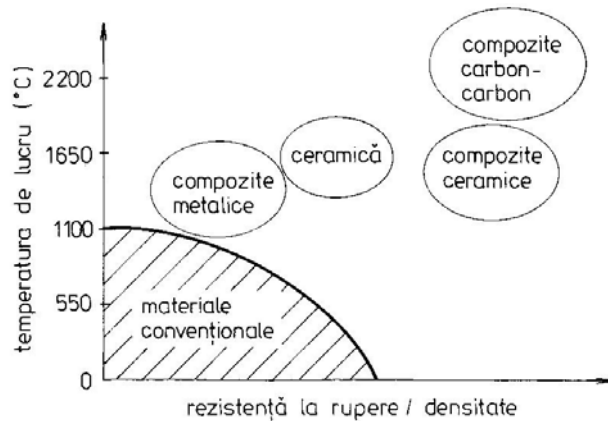


Fig. 1.1 The place they occupy between the composites materials resistant to high temperatures

In theory composites seem to be two basic models, namely, model Naidich Weyl respectively. Principle schemes for the two models are presented in figures 1.2 and 1.3. Due to the high polarizabilității of oxygen anions and their large size compared with metal cations, can be considered in accordance with Weyl's model that the surface oxide layer is a double-anion, figure 1.2.

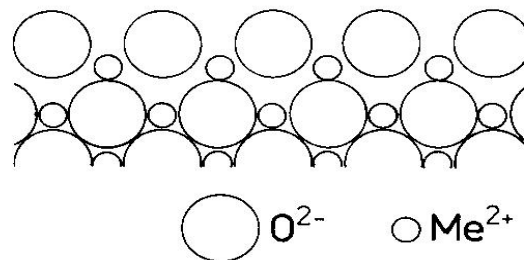


Fig. 1.2 The surface structure of the Weyl phase ceramic-metal oxides

In the absence of oxygen in the bath metal compound $Me^{2+}O^{2-}$ formation involves the deployment of a reaction:

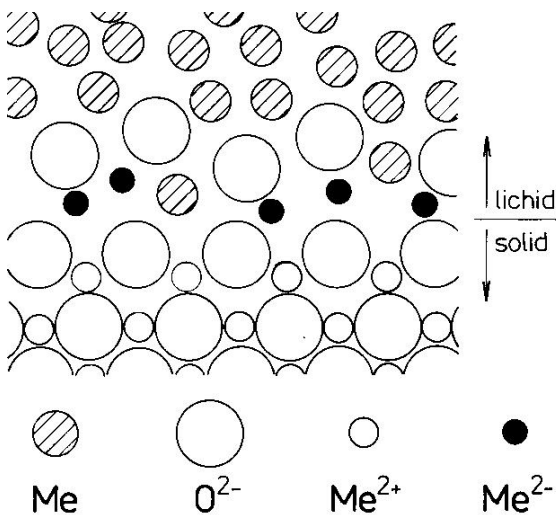


Fig. 1.3 Naidich's model for liquid metal-oxide ceramic interface

Chemical interaction contribution to the adhesion energy increases with increased production of free energy of reaction (1.1), thus increasing the liquid metal affinity for oxygen. Naidich's model - Fig. 1.3, on the situation in which the metal bath is dissolved oxygen. It forms a compound with the metal surrounding $Me^{2+}O^{2-}$, which is adsorbed at the interface due to electrostatic attraction forces of Me^{2+} cation and the anion layer, the surface oxide paticle.

The increased metal affinity for oxygen, the solubility of the compound $Me^{2+}O^{2-}$ drops and activity at the interface increases. For sufficiently high oxygen content in the melt formed a continuous layer of metal oxide to the substrate surface. Adhesion energy is approximately equal to the energy required to destroy the ionic bonds between the two oxides.

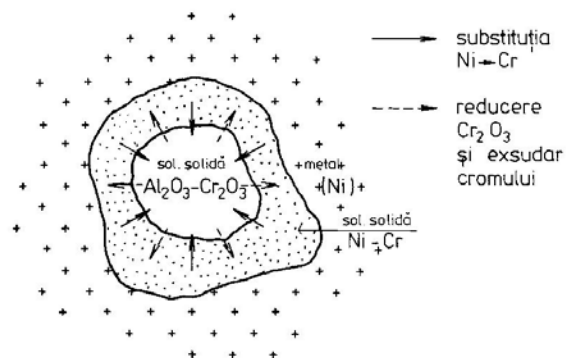


Fig. 1.4 The scheme links the formation mechanism of solid solution

Active metals forming strong links with ceramic materials, making them usable for metal or alloy elements. Customize these models for making ceramic-metal composite is presented in figures 1.4 and 1.5.

Figure 1.4 is represented schematically by the solid solution formation of connections, Cr_2O_3 , reduction occurs, followed by the appearance of metallic chromium exudate, or substitution unoxidised metal chromium and chromium metal-forming solution (in this example nickel-chromium).

Another link between the formation mechanism involves the formation of a cermet components spinels intermediate phases, as in the case of cermet (Fe, Ni, Co) - Al_2O_3 .

Figure 1.5 is represented schematically by the phase spinels link formation mechanism.

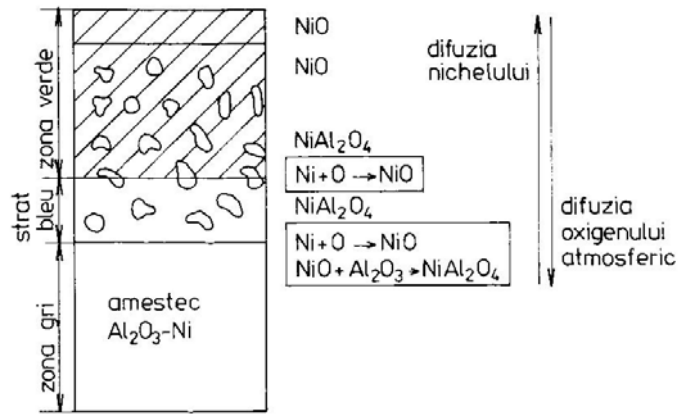


Fig. 1.5 Formation mechanism of the phase diagram link spinels

2. EXPERIMENTAL RESEARCH RESULTS

Distribution of aluminum in the ceramic composite made by impregnating aluminum can highlight thin section due to metal opacity, it appeared black on photomicrography.

Aluminum content throughout the ceramic wall thickness is not uniform. Entering the ceramic mass takes place only until a certain depth, and its amount decreases from the periphery inwards (fig. 1.6, 1.7, 1.8).

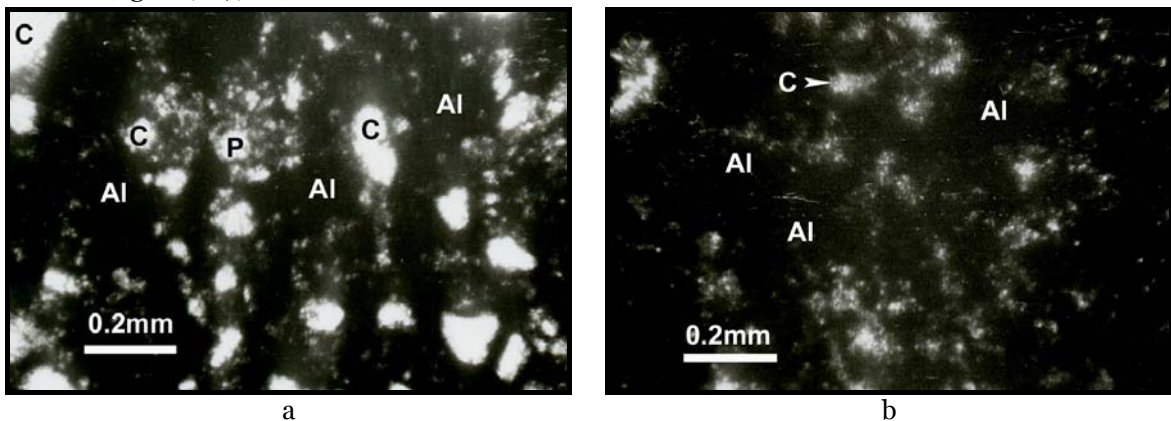


Fig. 1.6. Composite - ceramic-aluminum product R1 + Al (transmission polarizing microscopy). Microcrystalline structure consisting of an opaque metal mass (Al) ceramic relics occur \pm matrix composed of tiny pores (P) (see b). Most clastelor are represented by corundum (C). The texture is compact. a) The exterior of the composite - 1N; b) central area of the composite - 1N

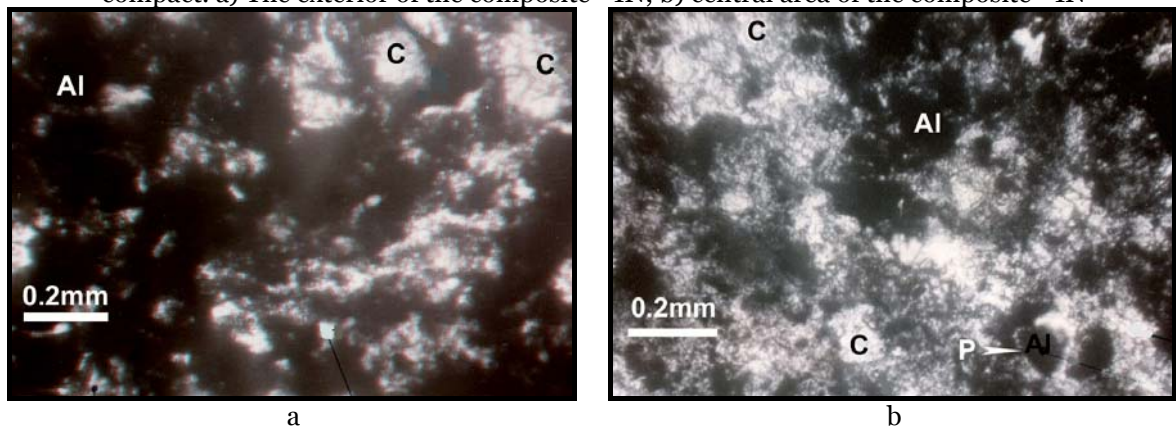


Fig. 1.7. Composite - ceramic-aluminum product R2 + Al (transmission polarizing microscopy). Microcrystalline structure consisting of an opaque metal mass (Al) occur relict crystals formed ceramic matrix \pm sometimes with pores (P) (see b). Most clastelor are represented by corundum (C). The texture is compact. a) The exterior of the composite - 1N; b) intermediate zone of the composite - 1N

Microscopically the mass is noted ceramic aluminum penetration through the pores open and total or partial substitution of mineral phases that contain silicon (mull, quartz, vitreous mass).

Marginal area of the composite structure is microcrystalline, consisting of an opaque mass, a uniform, which contains rare relics of corundum (Fig. 1.6a, 1.7a).

Composition, the interior wall mass content is remarkable decrease opaque (metal) and ceramic mass relics increase the structure and composition can be recognized (Fig. 1.6b, 1.7b, 1.8, and b).

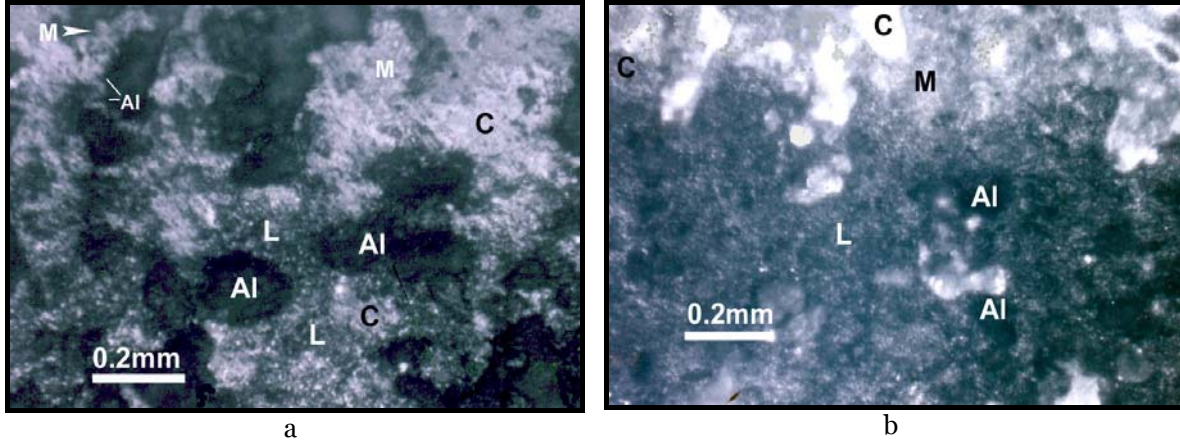


Fig. 1.8. Composite - ceramic-aluminum product R2 + Al (transmission polarizing microscopy).

Microcrystalline structure consisting of an opaque metal mass (Al) ceramic relics occur in aggregates of crystals formed and the matrix (L). Most clastelors are represented by corundum (C), reporting to mull (M). The texture is compact. a) The term close to the center. Observe the unit mull corrosion by aluminum (top left) - 1N; b) central area of the composite - 1N

Metallographic microscopy study of the structure allowed the predominantly metallic phases. Metallographic preparations were made from all sorts of evidence: impregnated with aluminum, nickel and copper. Microphotographs were conducted on samples and free of damage caused by chemical attack (Fig. 1.9 and 1.10)



Fig. 1.9. Table R1 ceramic impregnated with copper zone of transition between the coated and impregnated; 250X

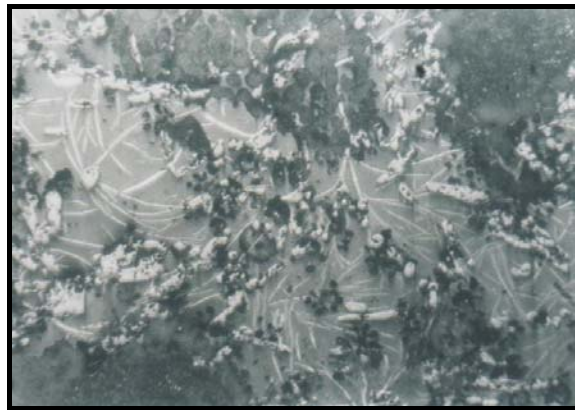
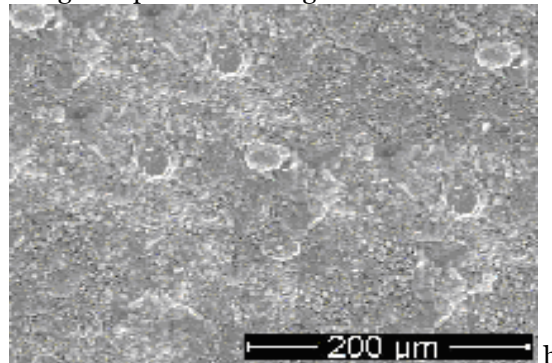
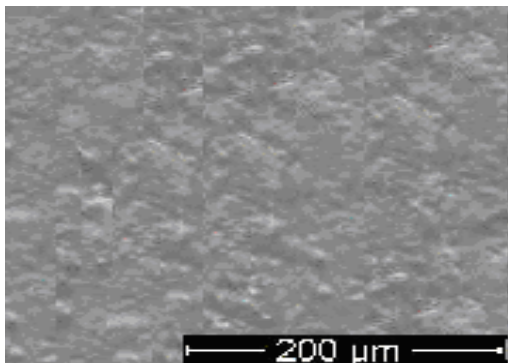


Fig. 1.10. Sample appeal $FeCl_3+HCl$ chemical mass-R1 ceramic impregnated with Cu, marginal zone; 250X

SEM microstructures surface for Cu- Mo coatings are presented in fig.1.11.



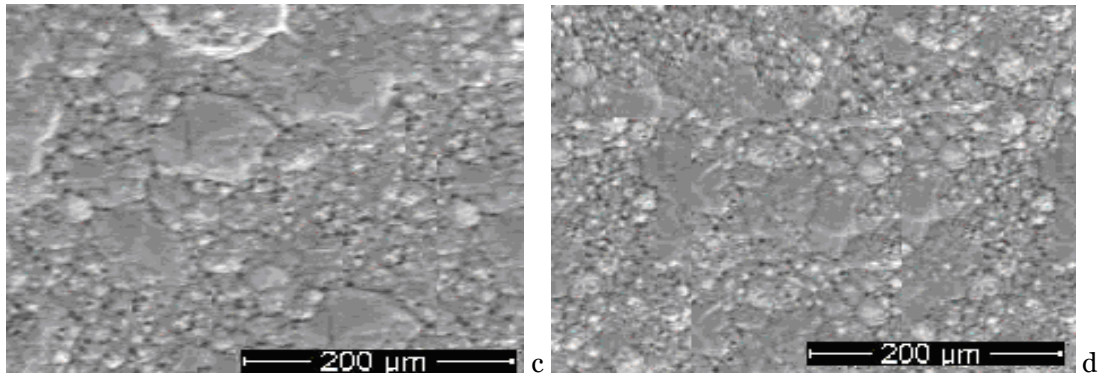


Fig. 1.11. SEM surface microstructures for Cu-Mo coatings size $3\mu\text{m}$, 90min, 500rpm, $i=1,5\text{ A/dm}^2$: a) pure b) Cu-Mo, 20g / L, c) Cu-Mo 40g / L, d) Cu-Mo, 60g / L, magnification x 500

3. CONCLUSIONS

From the figure for nano-composites made by electro-deposition, our analysis reveals their fine structure.

Metallographic microscopy study of the structure allowed the predominantly metallic phases highlighting the fact that metal has penetrated into the pores of the ceramic material.

REFERENCES

- [1.] Banea, Valentina, Surdeanu, T., Turos, Maria, Noi tendințe de utilizare a ceramicii tehnice în industria românească, *Lucrări ale Conferinței de Știința și Ingineria Materialelor CONSILOX – VII, Vol.I, 11-13 sep. 1996, p.116-122.*
- [2.] Iancau, V. *Materiale metalice compozite si tratamentele lor termice*, Ed. Dacia Cluj-Napoca, ISBN 973-35-07-96-2, 1999.
- [3.] Marginean L. *Studii și cercetări privitoare la realizarea unor compozite ceramo-metalice*. Teză de doctorat, Universitatea Tehnică din Cluj-Napoca, 2007.
- [4.] Pop Alin-Mihai. *Cercetări asupra tehnologiilor și materialelor moderne pentru confecționarea garniturilor de model*. Teză de doctorat, Universitatea TRANSILVANIA din Brașov , 2009.
- [5.] Fodor Liliana. *Cercetări privind realizarea unor depuneri de straturi superficiale compozite armate cu nanoparticule*. Teză de doctorat, Universitatea Tehnică din Cluj-Napoca, 2010.
- [6.] Orac Lucica. *Materiale compozite cu proprietăți speciale*. Universitatea „Dunărea de Jos” din Galați, România; Univesitatea de Arhitectură și Construcții Kiev, Ucraina, 2009.



¹Ana JOSAN

THE ANALYSIS OF CASTING DEFECTS RECORDED IN THE METALLURGICAL ENTERPRISES

¹ UNIVERSITY POLITEHNICA OF TIMISOARA, FACULTY OF ENGINEERING FROM HUNEDOARA, ROMANIA

ABSTRACT:

This paper presents the range of types and sizes of castings in a foundry, that The Foundry Criscior Brad. Are presented percentage, the types of defects recorded in technological practice (in elaboration, moulding, casting), and the possibilities of preventing their occurrence.

KEYWORDS:

Casting, defects, foundry, casting pieces

1. INTRODUCTION

The Foundry Crişcior Brad is a foundry small and medium-sized pieces. In this foundry, it casting a wide range of pieces, both in terms of material and dimensions of (fig.1).

Thus, in terms of material casted are obtained castings of:

- ❖ austenitic manganese steel
- ❖ carbon steel
- ❖ Low-alloy steel with manganese and chromium
- ❖ Grey iron
- ❖ Non-ferrous alloys.

Foundry typo-dimensional range includes castings such as presented in Table 1.

Table 1.

- swing hammers	- 4,5 kg
- wear plates	- 6,5 kg
- grills	- 7,3 ...9,7 kg
- Wheels Drive	- 25 kg
- Wheels shaft	- 30 kg
- cylinders	- 70 kg
- racks	- 100 kg
- roller support	- 18 kg
- Train bandages	- 270 kg
- pump housings	- 100...150 kg
- rotor	- 120 kg



Figure 1. Castings from Foundry Criscior Brad.

2. METHODOLOGY AND DISCUSSION

Performed the qualitative analysis of a batch of steel castings in Foundries Criscior Brad, be found that of 360 castings, 47 pcs. had casting defects (fig. 2).

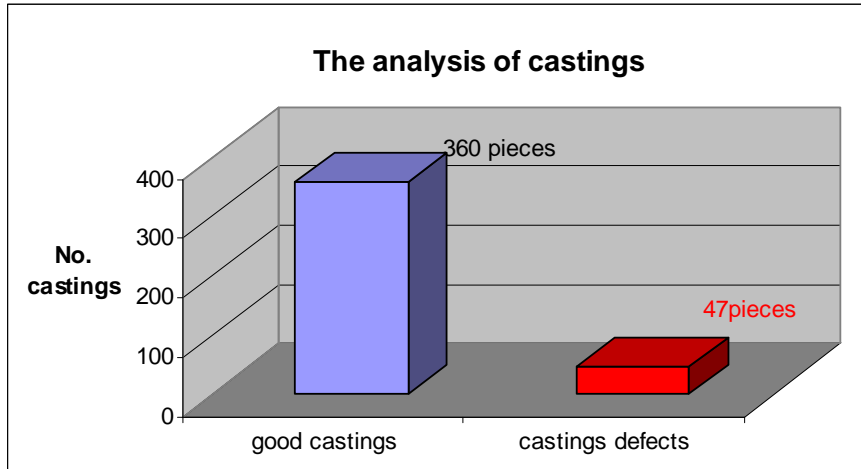


Figure 2. The analysis of castings.

Given the casting technology, and the statements made in industrial practice, can state that most common defects (of all defect castings) leading to the rejecting of them are [1, 2, 3]:

- inclusions (G 131) și adherences (D 221) rate of 7,74%; in fig. 3 are presented types of adherences appeared in steel casts;



Figure 3. Castings presenting non-metallic inclusions and adherences. Cavities, micro-cavities and pores (B 311) appeared at a rate of 3,59%;



Figure 4. Casting presenting micro-cavities and pores.

- fissures or cracks (C 221) rate of 1,67%;



Figure 5. Castings presenting fissures.

- Inadequate chemical composition - is a defect which, because standards stipulated in the chemical composition leads, definitely, to the rejecting of castings;
- Inadequate hardness – is a defect which, because the elaborating technology is not respected leads, definitely, to the rejecting of castings.

3. CONCLUSIONS

The share of defects registered in the period that were analyzed is shown in fig. 6

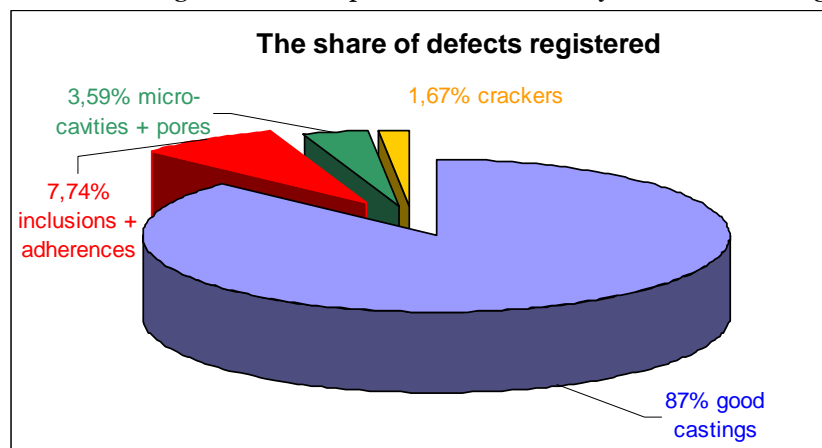


Figure 6. The share of defects registered in industrial practice.

Preventing the occurrence of failures presented in this paper, can be done only through strict compliance of their manufacturing technology, as well as by a good disciplined technology. Thus, for the avoidance of defects described above, should be taken following measures [3, 4]:

- ❖ strictly respecting their elaborating technology of the liquid alloy;
- ❖ correct Choosing choice of moulding technology;
- ❖ correct Choosing of moulding materials (sand, binders);
- ❖ correct execution of moulds;
- ❖ respecting the alloy casting parameters;
- ❖ respecting the thermal treatment diagrams applied castings;
- ❖ correct rapping of moulds.

REFERENCES

- [1.] Ștefănescu, C., Tehnologii de executare a pieselor prin turnare, Ed. Tehnică, București, 1981.
- [2.] Istrate, C., Toboc, P., Controlul de calitate și remanierea defectelor pieselor turnate, București, E.D.P., 1981.
- [3.] * * *, Atlas internațional al defectelor de turnare, Ed. Tehnică, București, 1977;
- [4.] Josan, A., Tehnologia formării și turnării aliajelor, Ed. Politehnica, Timișoara, 2002.





¹ Gabriela MIHUȚ, ² Erika POPA

ANALYSIS UPON INFLUENCE OF THE ALLOY ELEMENTS OVER THE MECHANICAL CHARACTERISTICS OF THE HIGH RESISTENT STEEL WITH HELP OF MATHEMATICAL MODELS

¹⁻² UNIVERSITY "POLITEHNICA" TIMIȘOARA, ENGINEERING FACULTY FROM HUNEDOARA, ROMANIA

ABSTRACT:

In this paper we suggest a mathematical shaping of the influence of the main alloy elements over the mechanical characteristics of steel type 15VMoCr14X. It has been noticed that the alloy elements increase the tensile strength, but differently: Cr, Mo and V increase the resistance of ferrite less than Si, Mn and Ni. Si, Mn and Mo very much decrease the resilience of ferrite, more than Ni and Cr do. The increase of the alloy content over 1.2% leads to a sudden fall of the resilience. The exception of this rule is nickel that both increases the resilience of ferrite and decreases the transition temperature.

KEYWORDS:

alloyed steels, tensile strength, mathematical shaping

1. INTRODUCTION

In the alloyed industrial steels, the alloy elements are to be found under many forms: solid solutions (dissolved in ferrite), chemical compounds (carbides) as alloyed cementite and special carbides, inter-metallic compounds with iron or with each other, sulfides and other non-metal inclusions, in free state, under the form of dispersed particles in the steel.

Many alloy elements, holding higher affinity with carbon than iron, dissolve in cementite, being capable of forming both alloyed cementite and special carbides. The elements situated at the left of iron in the periodical system of elements (Cr, Mn, Mo, V, etc.) form carbides. The elements that hold higher affinity with oxygen than iron form oxides. When processing steel, as a result of the oxidation process, the oxides Al_2O_3 , V_2O_5 and SiO_2 can be formed. The alloy elements that hold higher affinity with sulphur than iron form sulphides (MnS, etc.). The alloy elements increase the tensile strength, but differently: Cr, Mo and V increase the resistance of ferrite less than Si, Mn and Ni. Si, Mn and Mo very much decrease the resilience of ferrite, more than Ni and Cr do.

Chromium is an alpha favouring element that, when over 12%, determines the disappearance of the γ - α range. It dissolves both Fe_α and Fe_γ , forming especially simple and double carbides, when the carbon content is sufficient. The chromium-based carbides have a higher thermal stability and it is necessary for the austenitic transformation to be made at high temperatures, as well as a long maintenance so that hardening can be possible. The hypoeutectic chromium alloyed steel types have a reduced hardenability because they always contain a bigger quantity of proeutectic ferrite.

Chromium is characterized by high temper and by the fact that it forms stable carbides that give steel high resistance to wear and makes it suitable for steel cutting. The hardening of alloyed steel is accompanied by a certain loss of its resilience and elongation per unit length. For increasing the resilience and the elongation per unit without decreasing the temper too much, nickel is added in the chemical composition of steel.

Chromium determines an increase in the steel hardening, being the third most used element, after manganese and silicon, the most used chromium alloyed steel types being the perlitic ones. We can say that:

- ❖ a chromium content lower than 1% favours the steel hardening;
- ❖ a chromium content of 1-3% increases the resistance to hydrogen under pressure and favours the nitrification process;
- ❖ as the chromium content increases, the steel becomes more and more resistant to oxidation and corrosion;
- ❖ a chromium content higher than 30% determines steel to become infusible;
- ❖ chromium increases the temper and the resistance to wear but decreases the resilience (tenacity).

Molybdenum is an alpha-favouring element, just like chromium, but weaker than silicon. The austenite range of steel is restrained in the presence of molybdenum, becoming closed at concentrations higher than 2% Mo, raising the eutectic transformation temperature and moving it when the carbon content is lower. Dissolved in ferrite, molybdenum hardens it and increases its resistance to creep.

Molybdenum is twice more carbide-favouring than wolfram and its diffusion speed in austenite is four times higher. This property, that determines a better homogeneity when in hot condition, determines a better machinability and tenacity of medium-carbon steel and high-carbon steel but also a higher sensitivity to the thermal treatment and decarburization. Molybdenum very much lowers the martensitic transformation temperature (M_s), to 1.5% Mo, and decreases the softening tendency when tempering of the hardened steel types, even when the Mo content is only 0.2%.

When tempering the molybdenum alloyed steel types, it takes place a finely dispersed precipitation of some constituents similar to carbides that cancel the tempering brittleness effect, the steel types with 0.5% Mo content not having this effect anymore. Usually, molybdenum is used as an alloy element along with other elements, at processing the alloyed steel types.

2. THE RESULTS OF THE EXPERIMENTS

The chemical composition of type 15VMoCr14X steel is shown in Table no.1 and the requested values of the mechanical characteristics, compared to those obtained as a result of laboratory tests, are shown in Table no. 2.

Table 1

Chemical composition, %	C	Si	Mn	P	S	Cr	Mo	V	Cu	Ni
Requested	0.12- 0.18	Max. 0.20	0.8- 1.10	Max. 0.02	Max. 0.015	1.25- 1.50	0.80-1.00	0.20-0.30	Max. 0.16	Max. 0.30
Obtained	0.18	0.09	0.86	0.006	0.015	1.50	0.92	0.30	Max. 0.16	-

Table 2

Mechanical characteristics	$R_{p0.2}$ N/mm ²	R_m N/mm ²	A_5 %	WU_5 J	KCU_5 J/cm ²	$R_1 \cdot 10^{-7}$ N/mm ²
Requested	930	1080-1280	10	39	80	500
Longitudinally	1153-1170	1240-1238	17.5-15	54.8-55.8	140-152	550
Transversally	1148-1152	1230-1240	15.75-17.5	47.1-48.1	72-50	510

For the statistical and mathematical analysis, there were used 50 industrial batches.

The average values and the average square aberration of the variables are:

C	0.16385	0.022374
Cr	1.4554	0.076195
Mo	0.86115	0.014365
R_m	1173.1	57.189

Next, there are shown the results of the multidimensional processing of experimental data. For that purpose, we searched for a method of moulding the dependent variables depending on the independent variables x, y, z :

$$u = c_1 \cdot x^2 + c_2 \cdot y^2 + c_3 \cdot z^2 + c_4 \cdot x \cdot y + c_5 \cdot y \cdot z + c_6 \cdot z \cdot x + c_7 \cdot x + c_8 \cdot y + c_9 \cdot z + c_{10} \quad (1)$$

The optimal form of moulding, studied on a sample of 50 batches is given by the equations:

$$R_m = -1.73e + 004 \cdot C - 4511 \cdot Cr^2 - 4.07e + 004 \cdot Mo^2 + 1.078e + 004 \cdot C \cdot Cr + 2.113e + 004 \cdot Cr \cdot Mo - 4.668e + 004 \cdot Mo \cdot C + 3.063e + 004 \cdot C - 7307 \cdot Cr + 4.691e + 004 \cdot Mo - 1.582e + 004 \quad (2)$$

where the correlation coefficient is: $r = 0.75898492451823$ (3)

and the aberration from the regression surface is: $s = 37.23642463369599$ (4)

This surface from the four dimensional space allows a maximum point having the following co-ordinates:

$$C = 0.2592; Cr = 1.277; Mo = 0.7591; R_m = 1281 \quad (5)$$

3. CONCLUSIONS

The behaviour of these hypersurfaces in the vicinity of the point where three independent variables take their average value can be studied only tabular (for example, table no.3), by attributing values to the independent variables on spheres concentric to the studied point. Because this surface cannot be represented in the three-dimensional space, the independent variables were successively replaced with their average values.

Table 3

No.	Chemical composition [%]			The tensile strength Rm, [N/mm ²]
	Cr	Mo	C	
1.	1.51	0.86	0.14	1160
2.	1.48	0.87	0.15	1235
3.	1.48	0.88	0.16	1203
4.	1.48	0.86	0.17	1204
5.	1.35	0.86	0.18	1200

This is how the following equations were obtained.

$$Rm_{Cmed} = -4511 \cdot Cr^2 - 4.07e + 004 \cdot Mo^2 + 2.113e + 004 \cdot Cr \cdot Mo - 554 \cdot Cr + 3.926e + 004 \cdot Mo - 1.127e + 004 \quad (6)$$

$$Rm_{Crmed} = -4.07e + 004 \cdot Mo^2 - 1.73e + 004 \cdot C^2 - 4.668e + 004 \cdot Mo \cdot C + 7.765e + 004 \cdot Mo + 4.632e + 004 \cdot C - 3.601e + 004 \quad (7)$$

$$Rm_{Momed} = -1.73e + 004 \cdot C^2 - 4511 \cdot Cr^2 + 1.078e + 004 \cdot C \cdot Cr - 9573 \cdot C + 1.089e + 004 \cdot Cr - 5614 \quad (8)$$

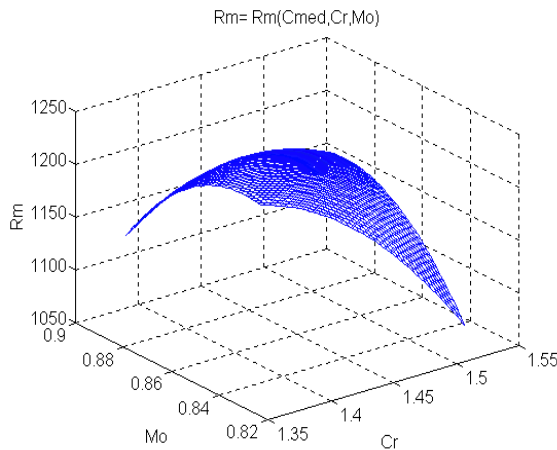


Figure 1. The surface
Rm = Rm(C_{med}, Cr, Mo)

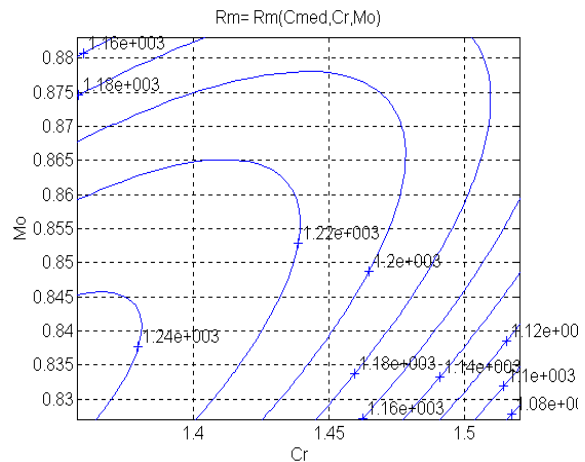


Figure 2. The level curves of distribution
Rm = Rm(C_{med}, Cr, Mo)

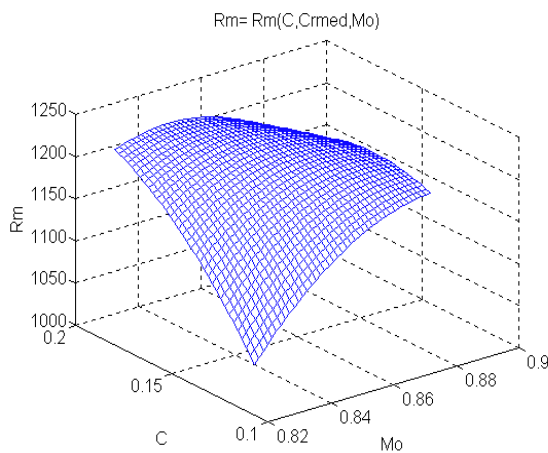


Figure 3. The surface
Rm = Rm(C, Cr_{med}, Mo)

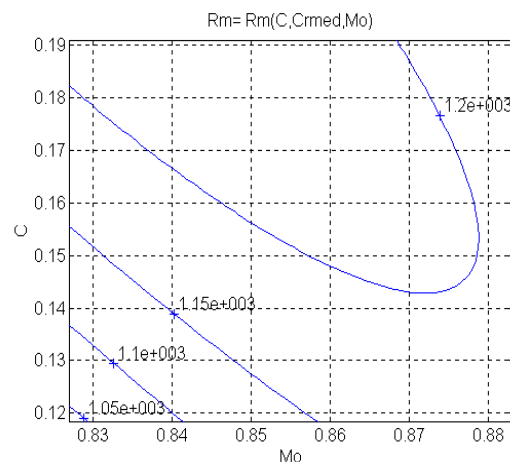


Figure 4. The level curves of distribution
Rm = Rm(C, Cr_{med}, Mo)

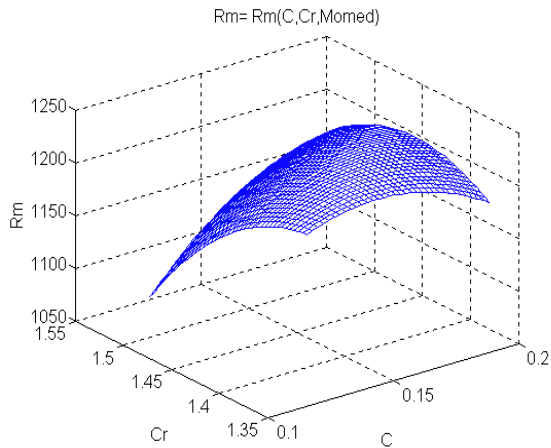


Figure 5. The surface $R_m = R_m(C, Cr, Mo_{med})$

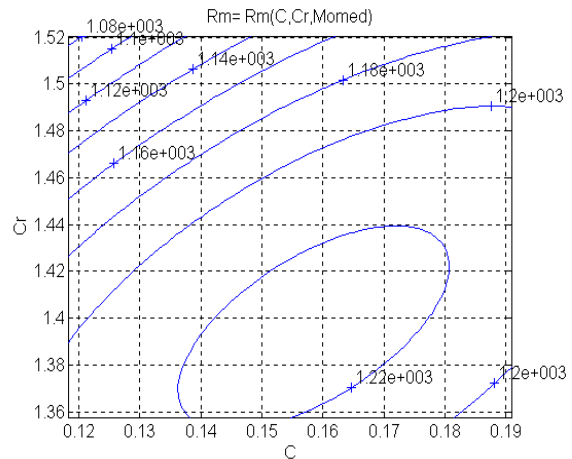


Figure 6. The level curves of distribution $R_m = R_m(C, Cr, Mo_{med})$

These surfaces, belonging to the three-dimensional space, can be represented and, therefore, interpreted by technologists. The surfaces are represented in fig. 1, 3 and 5. For a more correct quantitative analysis, in fig. 2, 4 and 6, there were represented the corresponding level lines, resulting the following conclusions: in the case of $C = C_{med}$, R_m allows a maximum for $Mo = 0.86\%$ and $Cr = 1.5\%$, and minimum values for $Mo = 0.84\%$ and a maximum Cr ; in the case of $Cr = Cr_{med}$, a maximum can be noticed in the area where $Mo = 0.84\%$ and $C = 0.14\%$; when $Mo = Mo_{med}$, there can be noticed a maximum of R_m for $Cr = 1.47\%$ and C is maximum, the minimum value being reached when Cr is maximum and $C = 0.13\%$.

Knowing these level curves allows the correlation of the values of the two independent variables so that R_m be obtained in between the requested limits.

REFERENCES

- [1.] Taloy - Optimizarea proceselor metalurgice, E.D.P. București, 1982.
- [2.] Maksay, Șt. - Matematici speciale, Editura „Politehnica” Timișoara, 2001.
- [3.] Vacu, S., ș.a. - Elaborarea oțelurilor aliate, vol.I, E.T. București, 1980





¹ Lucia VÎLCEANU

THE INFLUENCE OF THE LOCAL COMPRESSION EFFECT ABOUT THE WORKING LIFE OF THE COMPONENT WIRES IN A WIRE-ROPE

¹ FACULTY OF ENGINEERING HUNEDOARA, ROMANIA

ABSTRACT:

Steel ropes are important elements for the functioning of the machineries and of the equipment for transportation: mineral-drawing installations, boring plants, cranes, elevators, excavators, funiculars. Examining the wires of an out-of work steel rope, they noticed that the local compression stress in between the wires had such high values that it produced an impression on the wire in the contact area. The contact stress appears between the wires of the same rope strand, of two adjacent rope strands and between the wires and the rope take-up roller.

The paper shows the research regarding the induced and deforming stress at the moment of contact between wires and the traction cable take-up roller. The results will be used to calculate the fatigue crack propagation and to estimate the steel rope working life.

KEYWORDS:

contact pressure, working life, finite element method, stress-strain state, numerical analysis

1. INTRODUCTION

The wire ropes' durability, equated with the service life of the wire ropes, is determined to some extent by their appropriate choice and their rational exploitation. Using the best types of steel ropes, in different industrial areas, finding better ways for improving their quality and their exploitation conditions, will lead to the increase of their durability, the safety of the exploitation and to the achieving of great savings for the industry. These savings may come from the reduction of the rope consumption, thus from the reduction of quality steel consumption and from the cutting of break times in production, necessary for replacement of used ropes. During operation we encounter a supervised behaviour of the ropes because terms for replacing used ropes are always followed and the quality of the wire components is periodically checked. Withdrawing the rope from exploitation is operated when one or more of the following conditions are fulfilled:

- ❖ ropes reaching their service life, evaluated in tones-kilometres or kilometres- time in connection with the weight per meter of cable.
- ❖ reaching a certain number of broken wires per cable pace.
- ❖ the decrease of the safety coefficient of the cable at a certain value, the decrease of the real laceration force of the cable and diminishing of the number of bents until the breaking of the wires settles at the regular control testing. If during one of these current tests 25% of the wire components do not fit the standards, the cable is quashed.
- ❖ if during a macroscopic examination the deterioration of a strand is found, the breaking of the wires on a certain section is accelerating or an accentuated wear is found in one of its areas due to rust and corrosion.

During the examination of the wires that make up an out of order cable, evidence was found that the request of local compression between wires had such high values that a print appeared on the wire on the contact area. Contact requests appear among wires of the same strand, among wires belonging to bordered strands and among wires and the cable winding reel. The parameters involved in the evaluation of the voltage state and wear, belonging to wires in contact, may refer to: the geometry of contact elements, the statistic and tribology of the contact, mechanical

characteristics of the materials, operating factors. These parameters possess a simultaneously influence during contact, conditioning and influencing each other, which leads to a mingling of the result of their action.

2. METHODOLOGY

The estimation of the real stresses in the cross-section of the wire rope is very difficult because the wires are placed under different angles reported to the axes. There are subjected not only to traction, but also to bending and torsion. So, the state of stress in the wires is very sophisticated after the wiring manufacturing process. According to the hypothesis which fundament the strength calculus, the mechanical loads in the wires of a wire rope are considered as statically loads type Saint-Venant: traction, bending and secondary bending because of the support of a wire to other two adjacent wires, respectively the static contact loading type Hertz or Steuermann. *The classical contact theory between elastic bodies proposed by Hertz* (Fig.1), which did not take into account the non-linear aspects of every contact problem, is comparatively presented with *Steuermann's and Panton's theories* for the contact under a straight common line, typically for the contact between an external and an internal cylinder surfaces.

A comparison between the results obtained by Steuermann and Hertz (Fig.2) leads to the following conclusion: when the ratio $\frac{q}{E(R_2 - R_1)}$ increase, the difference between the results (according to the above mentioned theories) also increases. Anyway, there is a relative good agreement between the results for contact angles less than 20°.

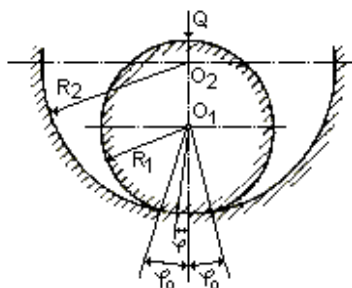


Fig.1. Contact between a cylinder and a cylinder cavity

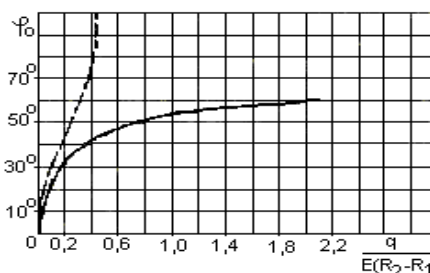


Fig.2. Comparison between Steuermann's and Hertz's results

For the particular case when the two cylinders are manufactured from the same material, E. Panton proposed the following approximate formula:

$$Q(\varphi) = \frac{Q}{R_1 (\sin \varphi_0 \cos \varphi_0 + \varphi_0)} \cos \varphi \quad (1)$$

There is presented in Fig.3 the distribution $Q(\varphi)$ for three values of the contact angle: $\varphi_0 = 30^\circ$, 50° and 60° according to Panton's (non-continuous line) and Steuermann's theories (continuous line). It may be observed in Fig.3 that the results according to the above mentioned two theories are in a perfect agreement when increasing the contact angle φ_0 .

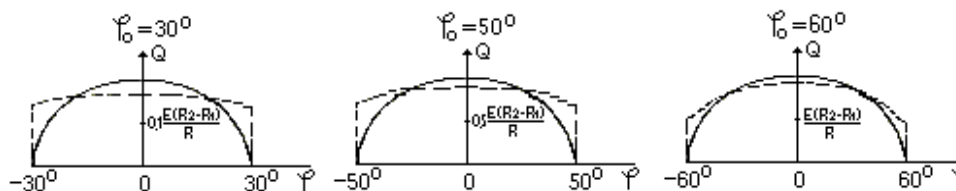


Fig.3. The distribution $Q(\varphi)$ according to Panton's (non-continuous line) and Steuermann's theories (continuous line)

The purpose of the *experimental research by photoelasticity* about the state of stress in the component wires of a wire rope consist in the estimation of the percentage deviations of the contact stress calculated values according with Hertz's, Panton's and Steuermann's theories in comparison with the real values of the stresses. This type of experimental research would ease the choice of the best relation depending on the size of the contact angle φ_0 . In terms of contact problems, the location of the maximum tangential stresses is associated with the initiation and propagation points of several cracks, which require the accurately determining of the voltage spectrum in the immediate vicinity of the contact area.

In view of the photoelastic analysis were made two discs having the diameters of 15 and 20 mm and concave surfaces with beams of 26; 20,1 and 15,15 mm. They were made out of optical

active and translucent materials. For the achieving of the isochrones photos an installation with two polaroids was used. The polaroids consisted of \varnothing 150 mm of monochromatic light produced by a bulb with downloads of sodium vapours. This installation is part of the endowment of The Laboratory of Strength of Materials from the Mechanical Engineering Faculty belonging to Polytechnic University of Timisoara (Fig.4).

A specimen was made for the calibration of the photoelastic material. This specimen was tested during a pure bending thus determining the photoelastic constant of the material $\sigma_0 = 2,65$ MPa, with a 6 mm thickness. During the tests the goal was not to induce contact requests which could lead to plastically strains. The tests ensured the reproductively of the results, reproductively checked by the lack of residual stress state in the parts after the download, a fact easy found in polarized light.



Fig. 4. The isochrones photos for $R_1/R_2 = 0,58$ at $q=74,21$ N/mm, the higher level of isochrone $n=8$ φ_0

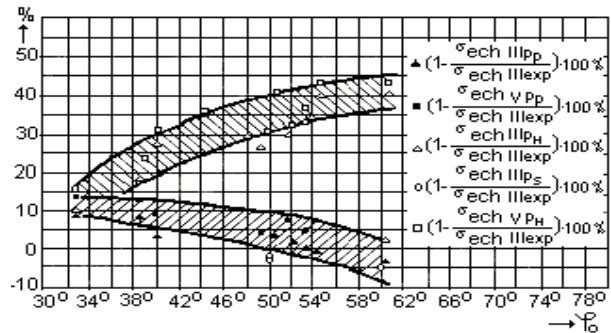


Fig.5. The deviation variation of theoretical results from the experimental tests depending on the contact angle for two contacts $R_1/R_2 = 0,58$ and $R_1/R_2 = 0,75$

The Fig.5 diagram represents the deviation variation of results from the experimental ones depending on the contact angle φ_0 for the two contacts $R_1/R_2 = 0,58$ and $R_1/R_2 = 0,75$ where Hertz's hypothesis is not valid.

From this representation results the fact that the values σ_{ech} calculated after Panton and Steuermann are grouped in an area of deviation of (+10%...-5%), while when using Hertz's formulas they leads to deviations of approximately (+15%) at $\varphi_0 = 33^\circ$ up to approximately (+40%) at $\varphi_0 = 60,5^\circ$.

This percentage error of the results decreases with the rising of the application and with the rising of the maximum order of the isochrones, up to a stresses value of approximately 10 MPa. This leads to an increase due to the value of variation of the elasticity modulus reaching an error of 10% at 20 MPa. This error is introduced by the asymmetry request wich couldn't be completely eradicated. The error is compensated by the average between the readings of the isochrone's order from the two edges of the contact area.

The *fatigue alternant loading* is the main reason of the degradation of the wire ropes. The results of the compression contact fatigue tests, performed on the Nădășan-Boleanțu testing machine placed in the Laboratory of Strength of Materials from the Mechanical Engineering Faculty, are plotted in a diagram (Fig.6) which expresses the dependence between the life-time of a wire with a 1 mm diameter versus the compression contact stress.

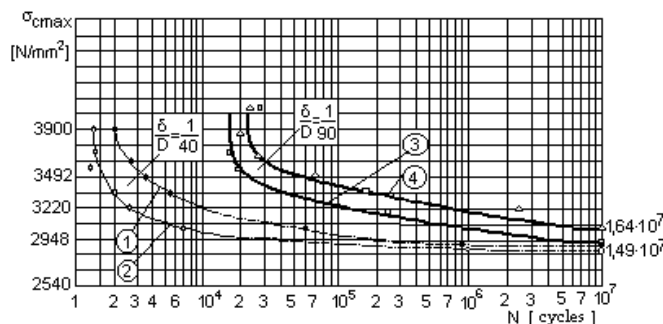


Fig.6. The results of wires fatigue testing on NB machine

A statistical analysis according to the log-normal distribution law has been performed.

The value of the life-time of the wires belonging to a traction wire rope obtained after the linearization of the distribution curve is in a perfect agreement with the life-times indicated in the special references when the wire rope considered as an element with a restricted life-time because of the typical working conditions.

The *finite element numerical analysis about the local compression effect* is the solution for the contact problem between two wires with different or same diameters in contact. Also the contact problem between an external and an internal cylinder shape bodies (Fig.7) has been analyzed by

using a hybrid technique considering the contact without friction for all the cases which have been presented above.

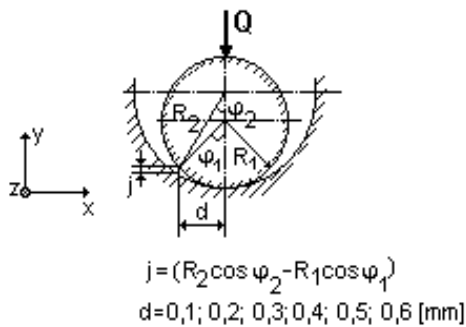


Fig. 7. The objective geometry

From the analysis of the graphical processing of the results we can reach the following conclusions:

- ❖ The equivalent von Mises stress σ_{VM} [N/mm²] has a maximum value in the center of the contact surface, decreasing to its extremities;
- ❖ The tangential stress τ_{xy} [N/mm²] is zero in the center of the contact surface, where the triaxial compression appears [1]. The maximum value of the tangential stress corresponds to the value of the half-breadth of the contact surface $b = 0,0545$ mm, decreasing to its extremities;
- ❖ The vertical movement is greatest possible in the middle of the contact surface, situation that can be visualized by representing the deforming state by bands of equal movement on the deformed position of the cylinder (Fig.9).

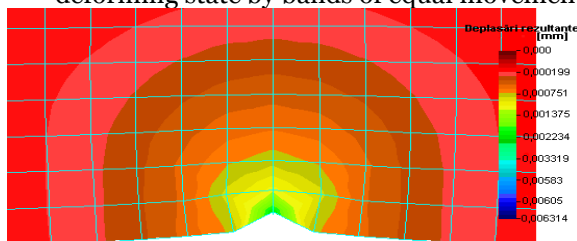


Fig. 9. The resultant displacements [mm] for the cylinder of radius $R_1 = 0,625$ mm, case of loading $Q = 45$ N

phenomenon because of the maximum σ_y stresses which are perpendicular on the contact area has been analyzed after the loading fatigue block (Fig.10) has been imposed ($\sigma_{y\max}$ - in function of the number of cycles). After the running on of the software, the cumulative degradation coefficient for every loading step and the total cumulative degradation coefficient have been performed.

During this program the fatigue limit curve (Fig.6-curve 1) for an alternative-symmetrical loading cycle of a non-torsion wire, bent on a segment lacking a channel and with the diameter of 40 mm, was used.

The calculus performs the link between state of stress in wires produced by the request of contact compression and of the wires' working life belonging to the steel wire ropes which are subjected to multiple and different requests encountered during the functioning of the operating wire ropes.

At first the meshing of two wires with same diameters in contact and the calculus model has been performed. After the running on of the software, all the components of stress and deformation tensors have been performed for 9 equal representation steps in function of the maximum and the minimum variation limits of stresses and deformations (Fig.8). Results are presented as special tables and diagrams about the stress and deformation fields. It can be observed that the state of stress and deformation is similar for every two adjacent wires in contact.

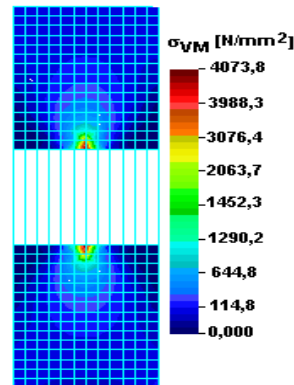


Fig. 8. The equivalent von Mises stress σ_{VM} [N/mm²] for the considered stress model, case of loading $Q = 45$ N

that can be visualized by representing the deforming state by bands of equal movement on the deformed position of the cylinder (Fig.9).

The analysis about the life-time of the component wires of a steel wire rope by finite element numerical analysis presents the opportunities to use dedicated software, which is typical for the analysis of the behavior of wires under variable loading as well for the life-time estimation. The finite element numerical analysis of the degradation of the wires because of an alternant loading has been performed for the contact between two wires with same diameters of 1,25 mm, for 9 loading cases. The fatigue

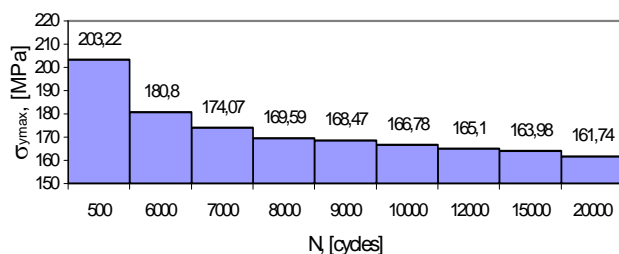


Fig.10. Loading fatigue block $\sigma_{y\max} - N$

3. CONCLUSIONS

The static processing of the results coming from the fatigue attempt along with the contact compression of wires on the NB testing machine, accepting a normal distribution of life-time, provided that the values of wire's life-time obtained after the lining of the distribution right are fitting in the range of accredited values by specialists in the market.

The paper also presents the numerical modeling with the finite elements of the contact request between a cylindrical surface and a concave one, achieved in order to visualize the state of displacements and stresses.

The finite elements numerical analysis of degradations which appear inside the steel wire ropes because they are subjected at variable loading was performed in order to obtain the cumulative degradation coefficient for every loading step.

REFERENCES

- [1.] Babeu, T. – The Basic Theory for Resistance of Materials, Mirton Publishing House, Timisoara, 1998
- [2.] Faur, N., Dumitru, I. – Finite differences and finite elements in resistance of materials, Mirton Publishing House, Timisoara, 1997
- [3.] Ghita, E. – Resistance and working life at solid bodies' contact, Mirton Publishing House, Timisoara, 2000
- [4.] Tudor, A. – The real contact of friction surfaces, Romanian Academy Publishing House, Bucharest, 1990
- [5.] Vilceanu, L. – Resistance and working life at steel wire ropes in contact, Mirton Publishing House, Timisoara, 2003





¹Sorina Gabriela ȘERBAN, ²Maria Laura STRUGARIU

DETERMINATION OF PARAMETERS INVOLVED IN TRANSFORMING THE IDEAL GAS, USING MICROSOFT ACCESS

¹⁻² UNIVERSITY POLITEHNICA OF TIMISOARA, FACULTY OF ENGINEERING FROM HUNEDOARA, ROMANIA

ABSTRACT:

A transformation is a sequence of states through which a thermodynamic system when its parameters vary from baseline values to those in the final state. All thermodynamic properties at a time system is the system state. State parameters are all measurable physical quantities that characterize the unique thermodynamic state of the system. A substance is characterized, as we know, the state variables: pressure, volume, temperature, etc.. At a certain amount of substance, these three variables are a well established interdependence of thermal equation of state.

To ease the study of gases have made some considerations that lead to a relatively simple model study. These so-called ideal gas, the molecules are considered material points, and the interaction forces between molecules are void. It is obvious that this case can not be met in practice, but the considerations made on this system can be extended with some corrections and within certain limits, the real gas.

The application is done using Microsoft Access and was made for students to be able to easily own knowledge about the transformations simple ideal gas of this gas. Students can calculate and make conclusions can be drawn, however this program is not meant to replace the teacher but to offer a tool to study in classes, the theory that parties are not very many. The menu is affordable, intuitive and helpful. For a better understanding of the application is structured in four parts.

KEYWORDS:

transformation isobar, izocoră transformation, isothermal transformation, the parameters of state, Microsoft Access

1. INTRODUCTION

Following the experiences with the constant volume gas thermometer was found that at very low pressures, tending to zero, all gases tend to behave the same way. Based on these considerations the notion of ideal gas.

Ideal gas is a homogeneous and isotropic gas whose molecules have their own volume and between them there is no interaction forces.

Ideal gas is a theoretical concept, it does not actually exist, but all gases tend to behave as the ideal gas (using the same law) when their pressure tends towards zero, as in this case, the volume of gas is very busy compared with the volume of the molecules (which becomes negligible), and greatly increase the distances between molecules and the forces of interaction between them also become negligible.

In 1661 Boyle Mariotte discovered in 1679 and experimentally verified and confirmed exactly that for an ideal gas in all possible states of an isothermal, the product of pressure and volume is constant, ie:

$$(p \cdot V)_{T=const} = const.$$

For any two states 1 and 2 of the same isotherm:

$$(p_1 \cdot V_1)_{T=const} = (p_2 \cdot V_2)_{T=const}.$$

In 1790 Charles found experimentally that if a given amount m of ideal gas occupies a constant volume when the pressure is proportional to the temperature, so their ratio is constant:

$$\left(\frac{P}{T}\right)_{V=const} = const$$

For any two states that occupy the same volume of gas:

$$\left(\frac{P_1}{T_1}\right)_{V=const} = \left(\frac{P_2}{T_2}\right)_{V=const} = const$$

In 1802 Gay-Lussac has shown that the volume of an ideal gas maintained at constant pressure varies linearly with temperature:

$$V = V_0 + V_0 \cdot \gamma \cdot (t - t_0)$$

where: $\gamma [1/^\circ C]$ = volumetric expansion coefficient of ideal gas;

$V_0 [m^3]$ = gas volume at the reference temperature t_0 .

$$\gamma = \frac{1}{273,15} \left[\frac{m^3}{m^3 \cdot ^\circ C} \right] \text{ or } \left[\frac{1}{^\circ C} \right]$$

For any two states 1 and 2 volume ratio is:

$$\left(\frac{V_1}{T_1}\right)_{p=const} = \left(\frac{V_2}{T_2}\right)_{p=const}$$

2. DESIGN AND IMPLEMENT APPLICATION

Data was stored in an Access database type, called ChimUniv. As an Access database type it includes all the items needed for the application: data tables, forms, query requests, reports, macros, modules.

Today there are applications that do not have a graphical interface through which to access the program options. Therefore, it was developed and implemented a main interface that allows accessing various options of the application, using the mouse and keyboard. The main interface has the following layout:



Fig.1. Main Menu

It is noted that there are several command buttons, labeled, to be used to select various options of the program. The main menu contains a summary of this application, and skills that they need to learn the student until the end of time.

For a better understanding of the application is structured in four parts, each with several components:

- ❖ Isothermal transformation: definition, graphical representation,
- ❖ Isobar transformation: definition, graphical representation,
- ❖ Transforming izocoră: definition, graphical representation,
- ❖ Ideal gas law applied problems.

Figure 2 is the transformation of the isotherm shape and includes a summary of Boyle-Mariotte law and is made in the same way as the other two forms (Fig.3 and Fig.4).

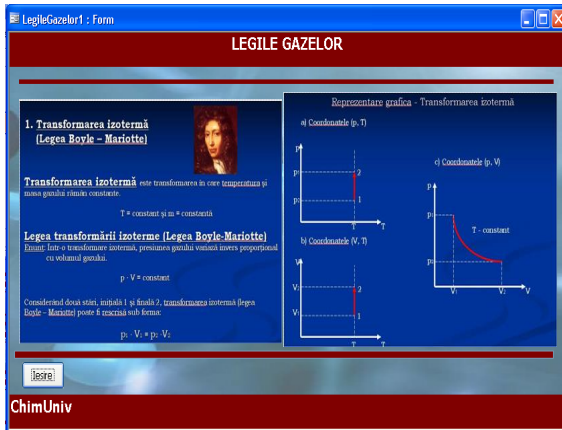


Fig.2. Isothermal transformation

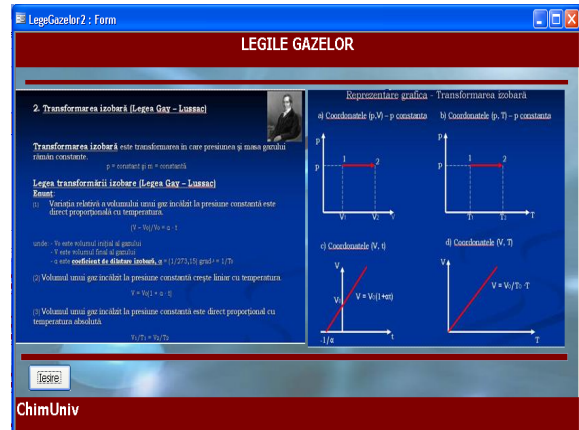


Fig.3. Transforming isobar

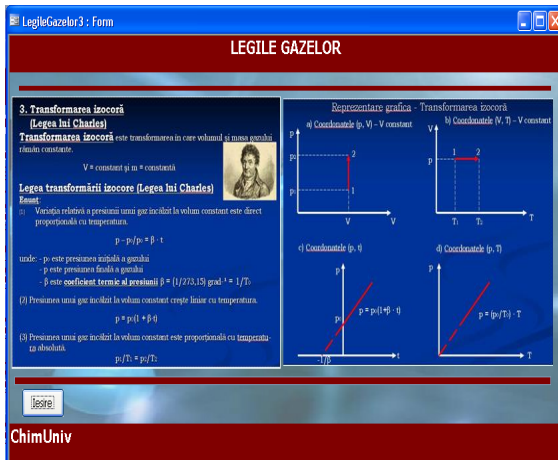


Fig.3. Transforming izocoră

Gas Laws form includes all three transformations, and moreover appears Van der Waals equation and the Clapeyron-Mendelev equation. By activating buttons , will open the forms that will present an example of application to each law separately. Clapeyron-Mendelev equation in the case is five examples of problems.

Each application / problem has boxes where the student will enter data in the problem statement will be executed transformations and the application will calculate what the problem is required. Each form has a pressing „Clear” button that will clear the boxes and other data can be entered and a button”to exit” out of the application.

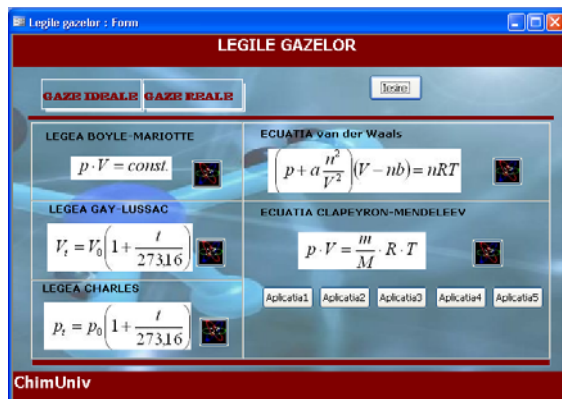


Fig.4. Forma_ Gas Laws

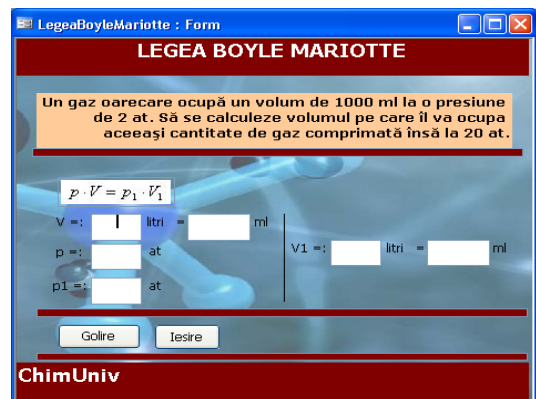


Fig.5. Application _ Boyle Mariotte Law

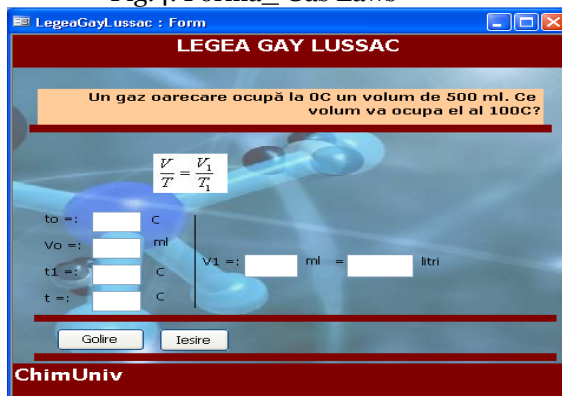


Fig.6. Application _ Gay Lussac Law

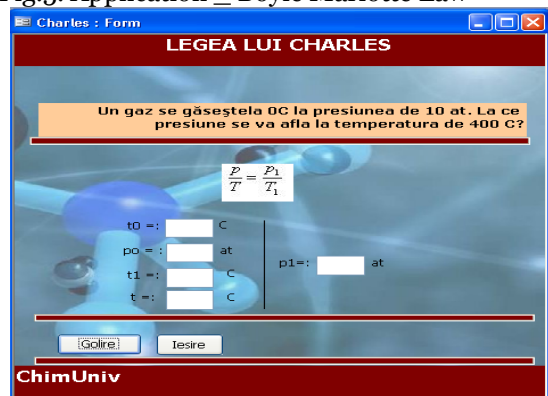


Fig.7. Application _ Charles Law

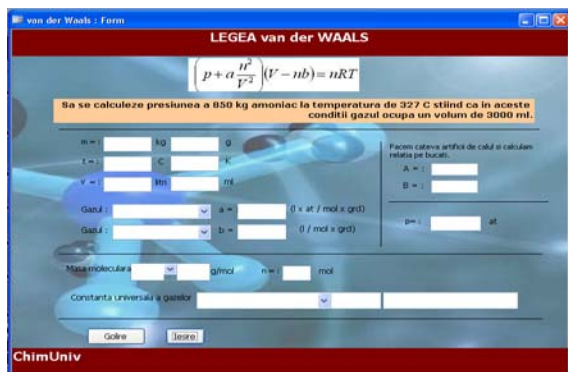


Fig.8. Application _ van der Waals Law

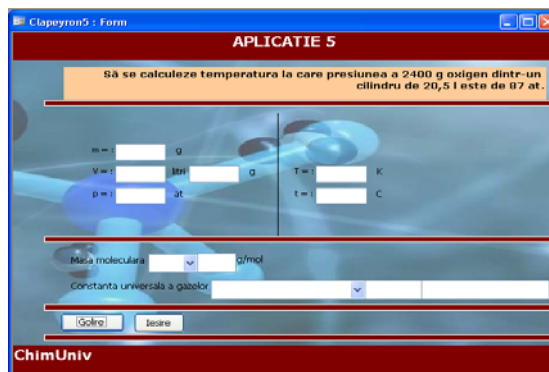


Fig.9. Application _ Mendeleev Clapeyron Equation

Submitted application can run on the following conditions: - the existence of a computing system, Pentium I 200 MHz at least 32 MRAM available - there is a Windows operating system and Office 2003 package.

It can be converted and Office 97, if this software is available.

Experimental data processing by computer is faster, more complete, attractive and can help increase motivation and interest of students to study Chemistry.

4. CONCLUSION

Feedback provided by participants (pupils, students), underlines the strong impact that the use of educational software can play in teaching and learning chemistry. Such applications are considered as an alternative to the real experiment and a means to improve understanding by learners of abstract concepts.

They may increase the motivation of students to learn and to engage their interest in making science topics. Clearly, the attractiveness is enhanced lessons, the teacher is the best choice in joining the virtual real experiment.

Using educational software will increase the competence and creativity, increasing the average educational attainment and higher to increase the knowledge base of students, and generally to increase the use of information technologies in various fields activity.

Development of educational software, with the pupils / students is one way to attract those who are less interested in Chemistry.

I must mention that this application is part of my doctoral thesis (still unfinished at this point), which includes a number of such applications developed with Microsoft Access and others.

ChimUniv system development aimed at creating an easy to use for both learners, but perhaps especially for teachers, given that a very large extent, success depends on the availability of this in a manner that Such educational programs more attractive. Feedback is always assured.

The point at which we started in implementing this system was that the information could greatly facilitate the study of chemistry in school and university, this is because, using the computer can accumulate knowledge in a more intuitive and more attractive.

Bibliography

- [1.] Eleonora Neacșu, Bazele termotehnicii, Litografia Institutului Politehnic „Traian Vuia”, Timișoara 1990
- [2.] Mădărășan, T, Bălan, M., Termodinamică tehnică – Editura Sincron, Cluj Napoca 1999.
- [3.] Atkins P.W., Trapp C.A., Exerciții și probleme rezolvate de chimie-fizică, Editura Tehnică, București 1997
- [4.] Florescu Vasile, Baze de date – fundamente teoretice și practice Editura Infomega, București 2002
- [5.] Eduard Koller, Monica Roșculeț, Programare în Access 97 ,Teora, București 2002
- [6.] Sorina Șerban, Referat Nr.3 - Stadiul actual și tendințe în cercetările privind sistemele de instruire asistată de calculator, Universitatea “Politehnica” Timișoara,2006



¹ Ana JOSAN, ² Vasile PUȚAN, ³ Sorin RAȚIU

THE OPTIMIZATION OF MANUFACTURING PROCESS OF A PART CAST STEEL FOR QUALITY ASSURANCE

¹⁻³. UNIVERSITY POLITEHNICA OF TIMISOARA, FACULTY OF ENGINEERING FROM HUNEDOARA, ROMANIA

ABSTRACT:

This paper presents a critical analysis of a part manufacturing technology low alloy steel castings T35Mn14. Technology deficiencies are presented and the measures in order to optimize the technology.

KEYWORDS:

Castings, defects, foundry, armors, molding

1. INTRODUCTION

Generally, the admitted rejectings registered for castings in a foundry should be within the range 4 ... 5%.

A particular case of castings obtained at The Foundry Criscior Brad and which particular aspects is the casting called *Armor* (fig. 1).

This armor is a steel casting T35Mn14 (low alloy steel castings) and represents the active part of a large spiral classifier (ϕ 2000 x 6000 mm), used in mining, the classifying of materials.

The spiral classifier has two propellers, and for each propeller is need 120 pcs. armor, so that an order of a classifier is needed the casting of 240 armors.

This piece is relatively small scale, i.e. 800 x 180 mm, , weighing 19 kg and low alloy cast steel castings, *T35M14*, whose chemical composition is as follows: C = 0,33...3,38%; Mn = 1,30...1,50%; Si = 0,30...0,50%; Cr = 0,50...0,70%; P = max 0,035%; S = max 0,035% [1].

2. METHODOLOGY AND DISCUSSION

Industrial practice has shown that, for casting analyzed, registered rejecting for the 120 armors is about 11%, respectively 13 rejecting castings (fig. 2, 3).

Following the critical analysis of the molding-casting technology of casting *Armor* and to decrease the percentage of rejecting registered in industrial practice, is necessary to optimize the manufacturing process of casting under study.

Thus, the current molding-casting technologies were identified these deficiencies:

- ❖ Use wooden models lead to material consumption lead to a higher consumption of material.
- ❖ High manual labour the processing of inner holes
- ❖ Appearance of the defect called *corner blister* (*B 122*) in the interior angles [3]
- ❖ High percentage of rejects due to improper use molding batch.

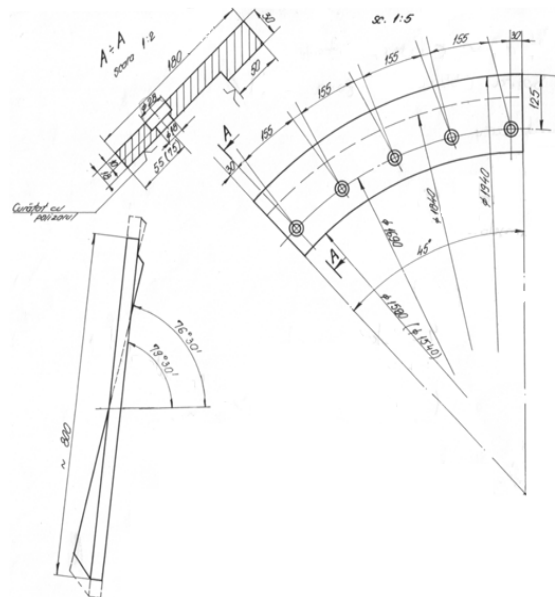


Figure 1. The armor - finished piece design

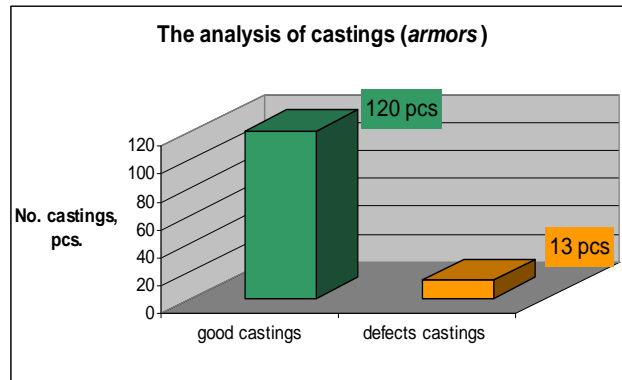


Figure 2. The analysis of castings

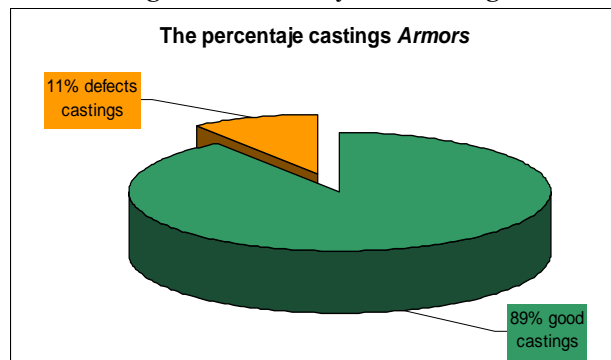


Figure 3. The share of defects registered at casting for casting studied



Figure 4. The metal model of casting *Armor*

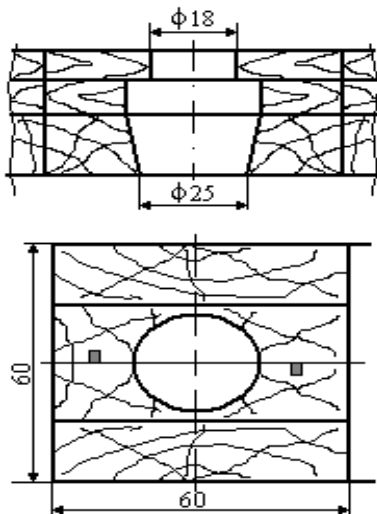


Figure 5. Core boxes.

In order to optimization the obtaining technology of casting studied (armored) shall take the following measures [2, 3, 4, 5, 6]:

1. replacing wooden model of a metal model (model is chosen for making aluminum alloy) (fig.4):
2. Obtaining molded cores in core boxes (Core boxes are made of wood and will produce five cores while). Core dimensions are made in core boxes are presented in Fig. 5, 6.



Figure 6. Mould cores made to obtain the holes of the casting *Armor* and fitting them into the mold.

- using the interior cooler and proper execution of the connections to the joint walls at right angles; the cooler for the casting studied (fig. 7), are made of same material as the alloy that is casting and has the form of a bar, with dimensions 20x10 mm.

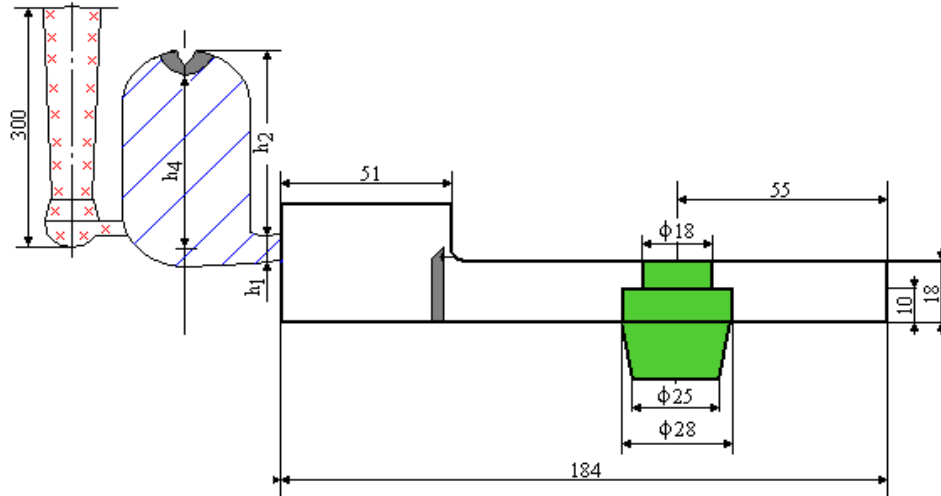


Figure 7. Apply the cooler interior and outline the connection radius.

- changing the moulding technology with two types of moulding batch (filling and model) and adoption of molding technology based with a mixture of sodium silicate.

The best method of prevention of the occurrence of defects registered at moulding is to ensure a high quality of moulding mixture for steel castings, because much of the defects is due to the way of realization of the mould.

Thus, by examining the 13 rejecting castings, results the following (fig. 8):

- ❖ 6 pcs. presented a large amount of nonmetallic inclusions and adherences, because inadequate quality of the moulding batch ;
- ❖ 4 pcs. presented a internal holes, both intercrystalline and intracrystalline (shrink pores, blisters, corner blisters, micro-shrinkages hole);
- ❖ 3 pcs. presented the cracks, crusts.

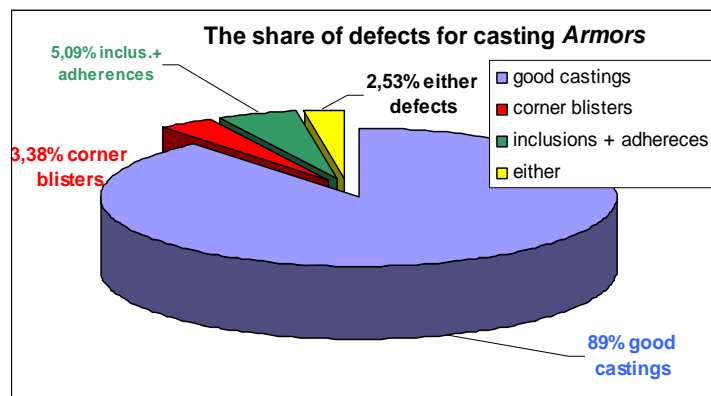


Figure 8. The share of defects registered for casting *Armor*.

3. CONCLUSIONS

The two mould parts, before assembly, are presented fig. 9 and the casting studied, mounted on spiral classifier is presented in figure fig. 10.



Figure 9. The mould parts (upper and lower), before assembly for casting.



Figure 10. The armor mounted on spiral classifier

Change the current moulding-casting technology a landmark analysis involves changing costs of obtaining its.

Thus:

- ❖ The total value of materials used in elaborating-moulding, a labour and a production price for the two technologies are presented in fig. 11.
- ❖ Even if the consumption of materials has increased significantly (12%), the following diagram is noted that, in improved technology, the price has dropped by approx. 7%

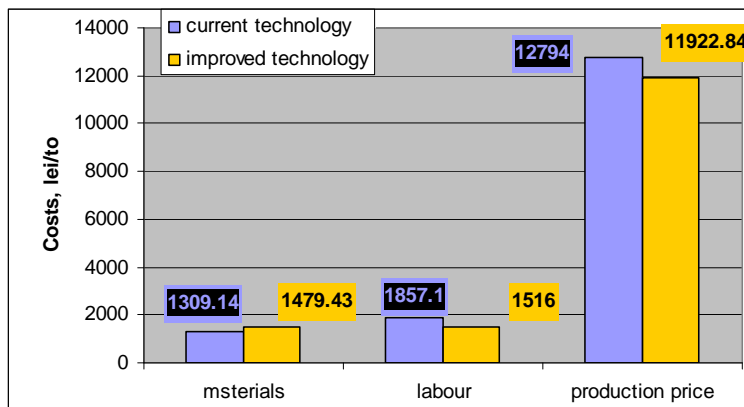


Figure 11.

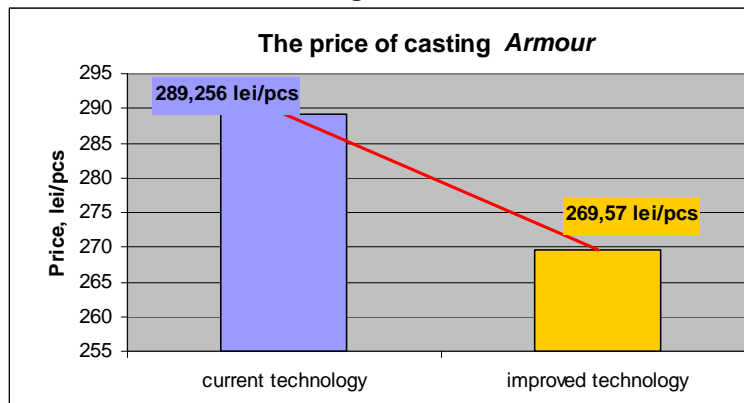


Figure 12.

- ❖ percentage of reject has decrease after the application of new technology with 5,5%
- ❖ the durability of the metal model is about 10 times higher than the wood, and dimensional accuracy is ensured when using metal models.

REFERENCES

- [1.] STAS 1773-76, Oțeluri slab aliate, turnate în piese.
- [2.] Ștefănescu, C., Tehnologii de executare a pieselor prin turnare, Ed. Tehnică, București, 1981
- [3.] * * * Atlas internațional al defectelor de turnare, Ed. Tehnică, București, 1977.
- [4.] Ștefănescu, Cl, Cosneanu, C., Sisteme de amestecuri de formare pentru turnătorii, București, Ed. Tehnică, 1989
- [5.] Josan, A., Tehnologia formării și turnării aliajelor, Ed. Politehnica, Timișoara, 2002.
- [6.] Socalici, A., Ardelean, E., Ardelean, M., Hepuț T., Josan, A. – Turnarea și solidificarea oțelului, Ed. Cerami, Iași, 2007

EXPERIMENTS AND RESULTS REGARDING THE USE OF FOAMED SLAGS AT THE STEEL ELABORATION IN ELECTRIC ARC FURNACES

¹⁻⁴UNIV. POLITEHNICA OF TIMISOARA, FACULTY OF ENGINEERING – HUNEDOARA, ROMANIA

ABSTRACT:

In paper is presented a synthesis of results obtained of authors regarding to reinsertion in the economic circuit of scrap and pulverous waste existing in Hunedoara area.

Through these capitalization of wastes in the iron and steel industry I done substantial economies in cost-price of final product, on aside, and but the other side are in progress an ecological process of environment Hunedoara area through give back of occupied surfaces with these waste to the natural frame.

KEYWORDS: Pulverous wastes, briquette, steel plant dust, agglomeration-blast furnace sludge, lime dust

1. INTRODUCTION

Use of steelworks dust from steel production or as a mechanical mixture or as micropellets (even pellets) as a slag foaming agent to believe that technology is the optimal solution for the use of these wastes. Simultaneous processing of waste containing iron powder and waste containing carbon powder to obtain a product suitable for use in various stages of technological flux led to the development process of obtaining a product called CARBOFER ®.

Data from literature and those obtained from their experiments, CARBOFER recommended as a substitute for the official site of slag foaming in electric arc furnaces, no influence chemical composition of steel and slag.

2. THE STUDY

In order to achieve phase laboratory experiments, we collected samples from several sections powdery waste of ArcelorMittal steel platform and storage ponds, being collected representative samples of the following types of waste: electric steelworks dust; - scale and dump the dross; the agglomeration, blast furnace dust (sludge agglomeration-blast); lime powder. Each waste sample was subjected to the operation of mixing (the homogenization was processed drum). Evaluating the quality of waste powder, determinations were made of physicochemical characteristics, namely: chemical composition and size. Experiments on the production site CARBOFER were conducted in the laboratory energy and raw materials base of the Faculty of Engineering of Hunedoara.

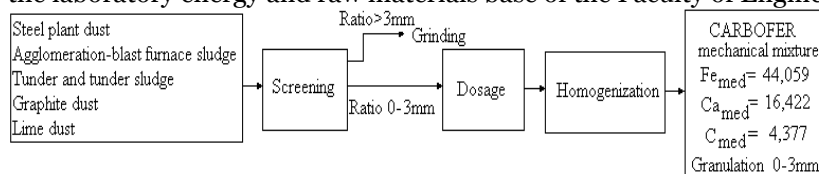


Fig.1. CARBOFER mechanical mixture flux

CARBOFER production powdery mixture flux, processing took place after the technological shown in Figure 1, Figure 2 is presented in such a recipe. I experienced a total of 10 recipes with chemical composition in Table 1. Also, for those recipes we determined size composition, presented in tabular and graphic tab.2 in fig.3



Fig.2. Example CARBOFER mechanical mixture

Tab.1. The chemical composition of the mixture mechanically CARBOFER

Recipes no.	The chemical composition, [%]										
	SiO ₂	FeO	Fe ₂ O ₃	P ₂ O ₅	S	C	Al ₂ O ₃	CaO	MgO	MnO	other oxide
R1	4,65	4,88	39,93	0,10	0,56	23,55	3,72	9,13	1,11	1,22	11,14
R2	4,25	4,97	43,82	0,09	0,50	22,67	3,36	7,75	1,00	1,24	10,36
R3	3,86	5,05	47,70	0,09	0,44	21,78	3,00	6,36	0,88	1,26	9,58
R4	3,47	4,96	51,74	0,09	0,39	17,96	2,64	7,87	0,81	1,40	8,66
R5	3,07	5,04	55,67	0,09	0,33	17,07	2,28	6,49	0,70	1,43	7,84
R6	2,67	5,13	59,57	0,08	0,28	16,19	1,92	5,11	0,58	1,45	7,04
R7	2,29	5,10	63,51	0,08	0,22	13,34	1,56	5,65	0,50	1,54	6,21
R8	1,89	5,18	67,44	0,08	0,17	12,46	1,20	4,27	0,38	1,57	5,39
R9	1,50	5,14	71,44	0,08	0,11	9,61	0,84	4,81	0,29	1,67	4,51
R10	1,50	5,22	72,30	0,08	0,11	9,61	0,83	3,85	0,28	1,67	4,55

Tab.2. Product classification CARBOFER granulometric class.

Recipes nr.	Granulometric class, [mm] / Share, [%]						
	3,0-1,0	1,0-0,75	0,75-0,45	0,45-0,315	0,315-0,25	0,25-0,18	0,18-0
R1	6,325	39,975	24,93	14,75	6,135	4,25	3,635
R2	10,625	37,2	24,433	14,083	6,031	4,221	3,407
R3	14,925	34,425	23,936	13,416	5,927	4,192	3,179
R4	14,7	30,795	24,485	15,807	6,358	4,485	3,37
R5	17,22	28,23	24,65	15,96	6,252	4,52	3,168
R6	20,63	25,56	24,484	15,703	6,147	4,523	2,953
R7	23,99	21,97	23,912	16,118	6,402	4,634	2,974
R8	26,51	19,405	24,077	16,271	6,296	4,669	2,772
R9	27,2	16,13	24,498	17,916	6,548	4,876	2,832
R10	28,09	16,175	24,325	17,239	6,54	4,865	2,766

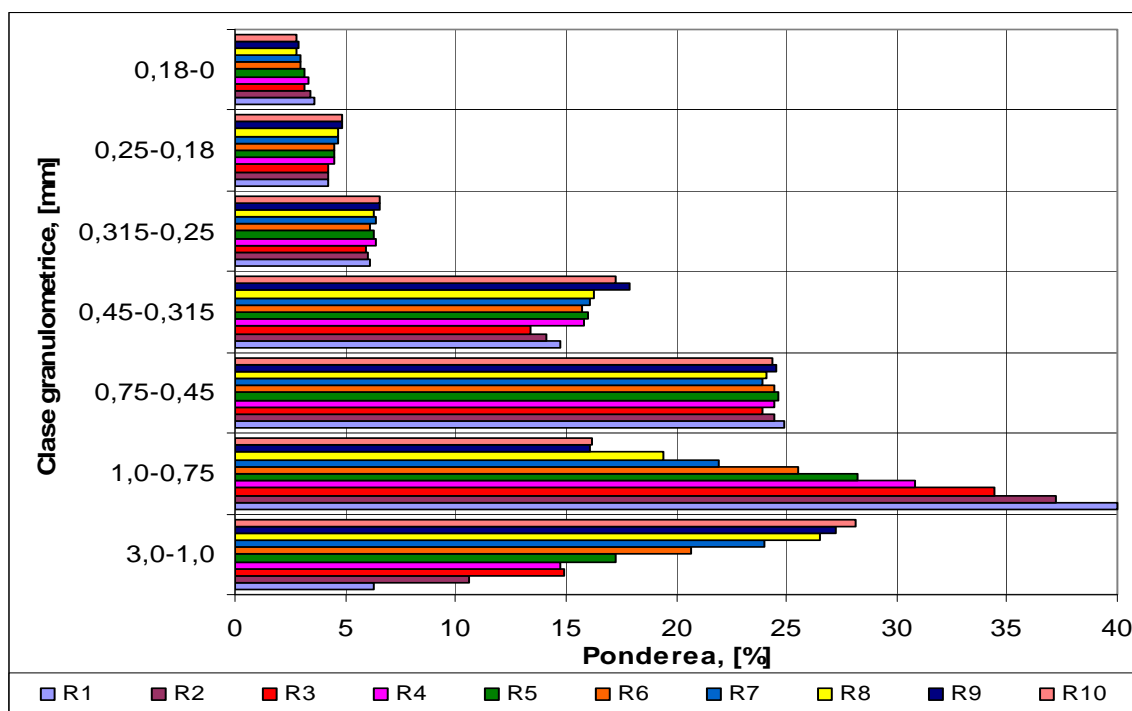


Fig.3. Product classification CARBOFER granulometric class.

3. DISCUSSIONS

CARBOFER product - mix engineer, the first stage, we sampled from the 10 recipes tested in laboratory conditions, samples were analyzed at SC CCPPR SA Alba Iulia.

For each recipe there was a quantity of 2kg of powdered mechanical mixture, which was melted in an induction furnace melts Metal fitted Laboratory of the Faculty of Engineering of Hunedoara. After having analyzed the behavior of each recipe were chosen as representative recipes R1 and R5 (to continue industrial experiments), obtained by using various waste materials both ferrous and addition chemistry of recipes (calculated and determined) is tab.3 presented.

Bulk density was determined only for the two recipes are selected for subsequent experiments, results are presented in tab.4

Tab.3. Chemical composition of tested recipes industrial.

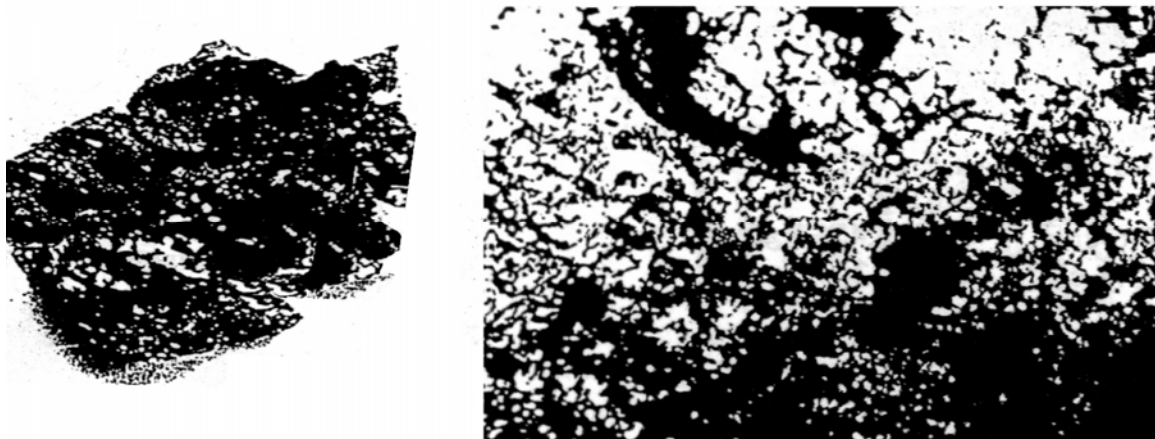
Recipea nr.	Chemical composition, [%]										
	SiO ₂	FeO	Fe ₂ O ₃	P ₂ O ₅	S	C	Al ₂ O ₃	CaO	MgO	MnO	alți oxizi
calculated											
R1	4,65	4,88	39,93	0,10	0,56	23,55	3,72	9,13	1,11	1,22	11,14
R5	3,07	5,04	55,67	0,09	0,33	17,07	2,28	6,49	0,70	1,43	7,84
determined											
R1	4,72	-	40,07	-	-	-	3,81	9,52	1,23	-	16,43
R5	3,22	-	52,68	-	-	-	2,67	7,14	0,71	-	15,7

Tab.4. CARBOFER product bulk density, mechanical mixture.

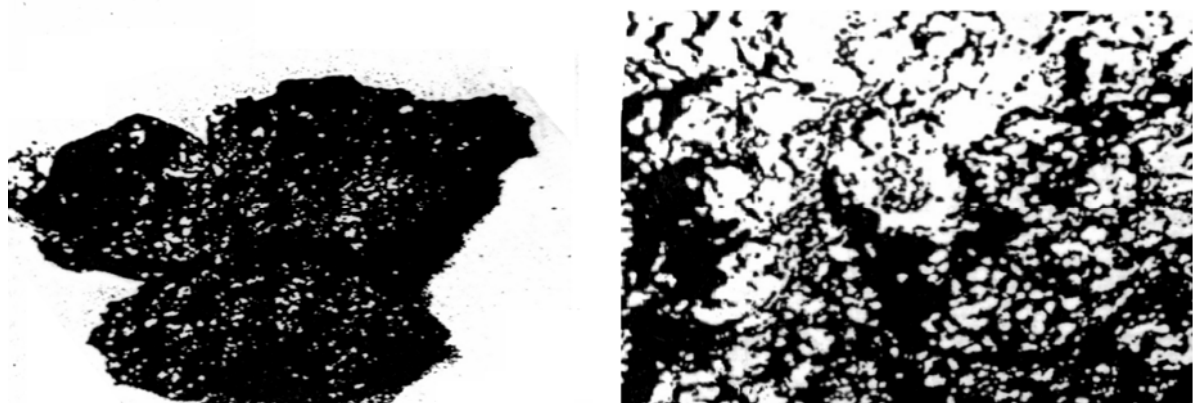
Density, [kg/dm ³]	Recipe no.	
	R1	R5
	0,8854	1,1150

To determine the foaming capacity, slag samples taken were investigated in terms of macroscopic and microscopic appearance.

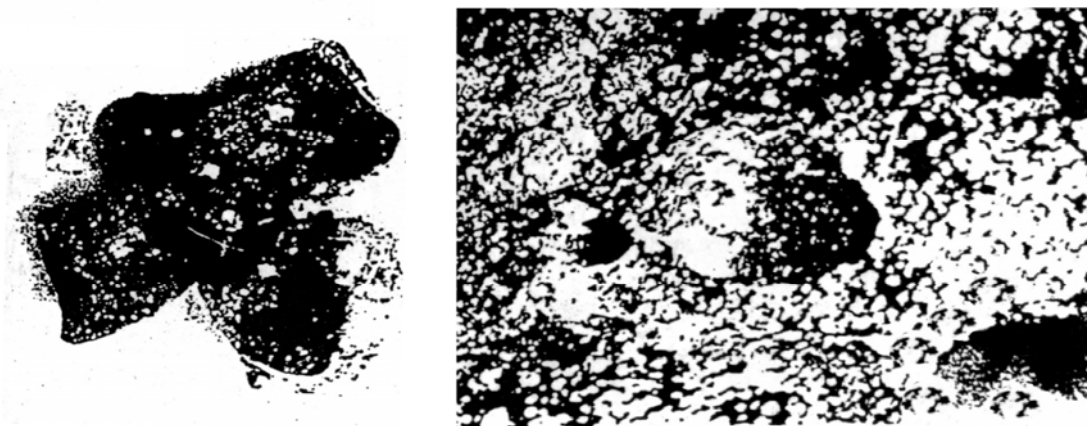
The analysis was done by examining the macroscopic appearance of virtual samples and conducting clay-sized photographs (Fig. 4 and 5), all recipes slag formed is uniform porosity and the pores are smaller (especially in cases where the height of the slag foaming was smaller and less intense) respectively standard slag (fig.6).



Size
 Macroscopic appearance-slag
 Fig.4. The physical characteristics of slag and addition of product standard CARBOFER (R1).
 x10
 Microscopic appearance-slag



Size
 Macroscopic appearance-slag
 Fig. 5. The physical characteristics of slag and addition of product standard CARBOFER (R5).
 x10
 Microscopic appearance-slag



Size
Macroscopic appearance-slag
x10
Microscopic appearance-slag
Fig. 6. The physical characteristics of standard slag

4. CONCLUSIONS

Experiments performed revealed that the product CARBOFER added a foaming slag with good capacity, leading to foaming phenomenon. There was a difference in the intensity of the two products CARBOFER frothing; foaming is more intensive use after the first prescription product.

Product CARBOFER use as a substitute for the usual agents of slag foaming in electric arc furnace has both an environmental benefit and economic one. Environmental benefits are shown by a significant reduction in environmental pollution, namely by increasing recovery of waste powder and reducing these waste storage facilities. The economic advantage is the immediate transfer of costs for waste disposal in the UK which are between £ 30-57 / t waste stored to other destinations.

ACKNOWLEDGMENT

The researches do the object of Research Project no.31-098/2007, with title Prevention and fighting pollution in the steelmaking, energetic and mining industrial areas through the recycling of small-size and powdery wastes, financed by National Center of Program Management, project managed by Prof.dr.ing. Teodor Hepuț.

REFERENCES

- [1.] Nicolae, M., ș.a., Dezvoltare durabilă în siderurgie prin valorificarea materialelor secundare, Ed. Printech, București, 2004.
- [2.] Constantin, N., Procedee neconvenționale de obținere a materialelor feroase, Editura Printech București, 2002.
- [3.] Dobrovici, D., Hățărascu, O., Șoit-Vizante I., Intensificarea proceselor din furnal, Ed. Tehnică, București, 1983
- [4.] Ilie, A., Cercetări privind valorificarea superioară a materialelor pulverulente din siderurgie, Teză de doctorat, Conducător științific: Prof.dr.ing. Dragomir I., București, 1999.
- [5.] Borza, I., Popoiu, Ghe., Coican A., Tehnologia elaborării fontei, Litografia Timișoara, 1983.
- [6.] Hepuț, T., ș.a., Prevenirea și combaterea poluării în zonele industriale siderurgice, energetice și miniere prin reciclarea deșeurilor mărunte și pulverulente, Contract de cercetare nr.31-098/2007, beneficiar: CNMP, parteneri: CEMS București, SC CCPPR SA Alba Iulia





ESTABLISHING THE MAIN TECHNOLOGICAL PARAMETERS OF INDUCTION SURFACE HARDENING FOR SHAFT PARTS TYPE

¹ UNIV.POLITEHNICA OF TIMISOARA, FACULTY OF ENGINEERING FROM HUNEDOARA, ROMANIA

ABSTRACT:

Induction heating is a particular process which uses electromagnetic fields for heating conductive materials (steel, copper, brass, aluminium).

The main difference from a traditional heating process is the location of heat sources which are distributed inside the work-piece. For this reason the induction heating process is very fast and controllable. Depending on the frequency used the heating can be superficial (induction surface hardening) or deep in the piece (forging, heat treatment etc.).

The main advantages of this technology are: high production rate due to the high specific power delivered to the work-piece, high automation of the process, precise repeatability of treated pieces, in-line installation, low floor space needed, controllability of temperature with high precision, avoiding of deformation of pieces especially in surface hardening, primary energy saving, safe and clean work ambient for employees.

There are a lot of applications where induction heating is used in different industries: melting of metals, heat treatments (hardening, tempering, annealing), forging, hot rolling, surface hardening, cold crucible melting, welding, pre-heating, dry-coating, special applications. All these applications get benefits from the suitable characteristics of this technology.

In this paper is presented the determination of the technological parameters for superficial hardening of axel pieces type made from 41Cr4 and 54CrMo4 steel. This technological parameters is optimum heating temperature, heating time and adequate cooling method for obtains a higher hardness.

KEYWORDS:

induction heating, hardness, heating temperature

1. INTRODUCTION

Surface hardening is a local heat treatment, which is applied to obtain a martensitic structure on the surface of pieces, to the depths between tenths of a millimetres up to 5-10 mm. Surface hardening is done by heating at high speed of the surface layer of products to a temperature in the austenitic range, shortly maintain and rapid cooling at rates higher than the critical quenching speed.

After applying surface hardening results duplex pieces, with hardened outer layer, resistant to wear and fatigue with plastic and tenacious core, resistant to other types of service loads: bending, shock, twisting. In addition, the compressive stress in the hardened layer increases resistance than alternating loads. However, for the combination of features, surface hardening must be applied to semi-hard steel with carbon content between 0.3% and 0.65%.

Given the specific heating conditions, heating temperature decreases rapidly from the surface to the center of product. As a result, only a very thin layer over the surface are heating upper the A_{C3} point and presents after the rapid cooling a complete quenching structure (martensitic), but with different degrees of overheating. Next layer heated between A_{C1} and A_{C3} , becomes an incomplete hardened layer, which makes the transition to the initial structure (feature the core).

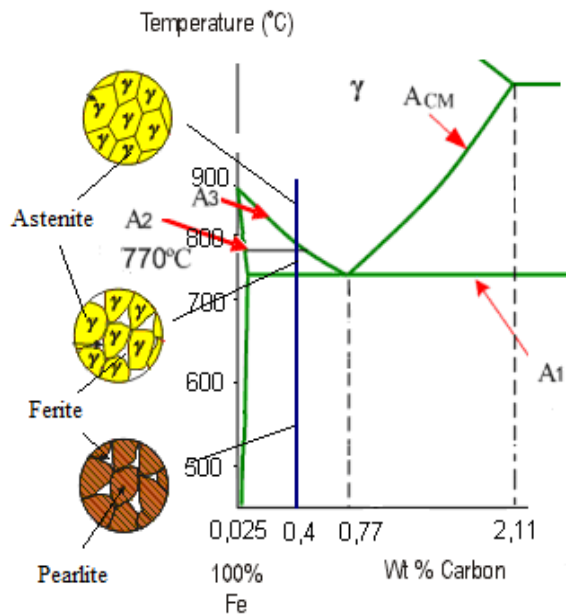


Fig.1. Fe-Fe₃C diagram, steel area

This change occurs because the magnetic permeability decreases suddenly at reach and overcome the Curie point temperature (770° C). In figure 2 is presented some pieces with different hardening depth.

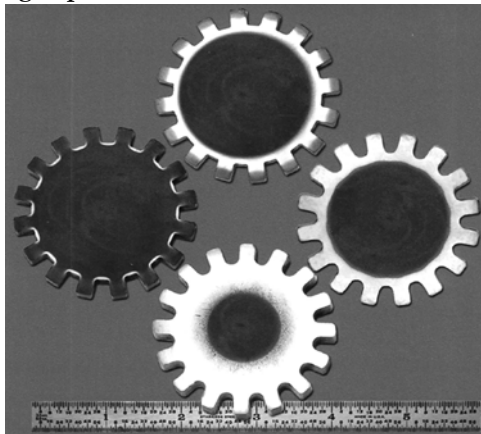


Fig. 2. Some pieces with different hardening depth depending of generator power, frequency and maintained time in inductor

2. THE STUDY

For practice work of this surface hardening process is requires the following steps: - choosing the power and frequency AC generator;

- ❖ choose the method of heating and cooling;
- ❖ the choice of working parameters.

Special attention is given to steel. The charge is made that preliminary tests, should be possible have the average chemical composition presented in standard and and have average hardenability to lower limit of the hardenability band.

Current charge used in the production process must then be reasonably restricted in terms of chemical composition, purity, austenitic grain and hardenability, otherwise there is risk of deviations in treatment results from batch to batch of products.

Of particular importance for the results of inductive quench and subsequent their reproducibility is the initial structure, namely heat treatment earlier surface hardening. Ferrito-pearlitic structures (rolling, annealing and normalizing) give a good response to induction surface hardening, with uniform and smooth as possible condition.

In conclusion, for high frequency current heating, the initial structure of the problem assumes a special importance because it usually is accompanied by an extremely high heating rate

The final thickness of hardened layer depends not only completely during heating, but also the time of the finish action of heat source and start cooling, period during which the temperature distribution changes in the product section.

Depth current penetration in the superficial layer and finally hardened layer depth depends on frequency of induced current is determined by the relation:

$$\delta = 5,03 \cdot 10^3 \sqrt{\frac{\rho}{\mu \cdot f}}, [\text{cm}]$$

where: ρ - receptivity of steel, cm;
 μ – relative magnetic permeability of steel;
 f - current frequency, Hz.

For steel the current penetration depth is determined by the formula:

$$\delta = \frac{14,1}{\sqrt{f}}, [\text{cm}] \text{ at } 15^\circ\text{C}$$

$$\delta = \frac{200}{\sqrt{f}}, [\text{cm}] \text{ at } 800^\circ\text{C}.$$

and, accordingly, change phase and diffusion processes are limited here within extremely small. The greater dispersion of steel structural components, the solid solution is formed faster and faster the diffusion process completes, which contributes to the uniformity of composition. In figure 3 and 4 is presented a microstructure of steel pieces before and after the induction surface hardening.

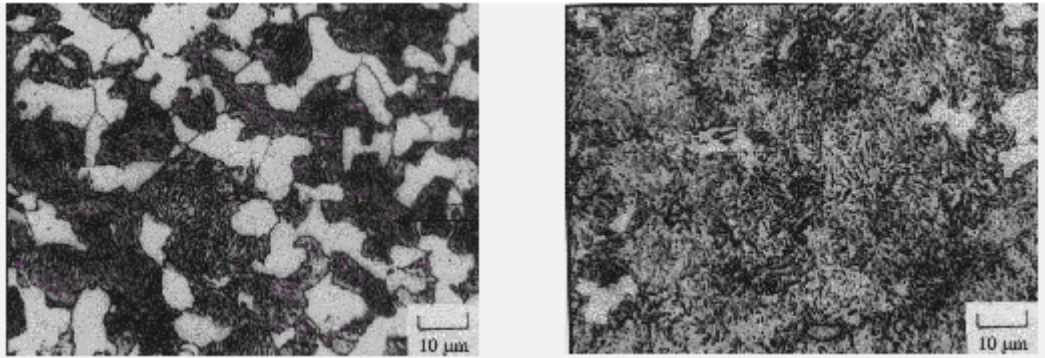


Fig.3. Steel microstructure 1C45 (AISI 1045) before and after the induction surface hardening

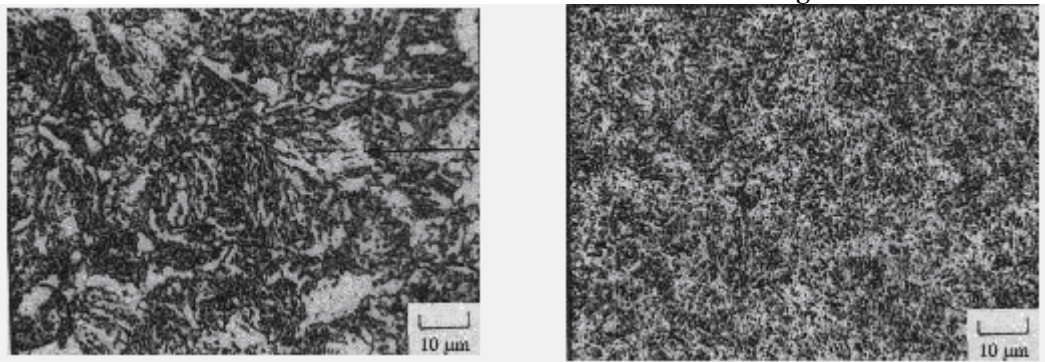


Fig.4. Steel microstructure 42CrMo4 (AISI 4140) before and after the induction surface hardening

It appears that the induction heating is desirable that the initial structure to be sorbite or perlite, where results the different quench depths:

- ❖ steel microstructure dependent mostly on temperature and speed of induction heating, the higher the heating rate is higher, the layer structure of hardened steel will be fine;
- ❖ it is desirable that the initial structure of steel is therefore required to provide good properties for core, i.e. resistance;
- ❖ initial structure should favours changes in solid state and there lead to a favourable state and to eliminate the soft layer (ferrite network and transition layer).

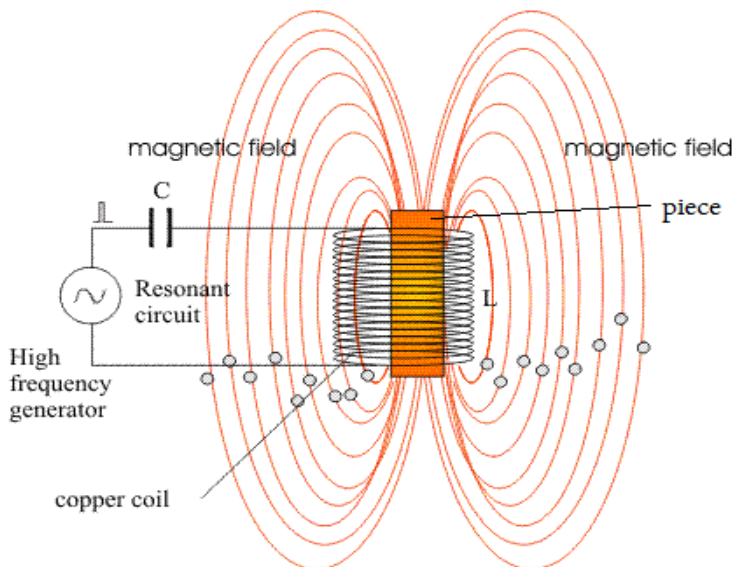


Fig.5 Work principle for induction heating

A surface hardening equipment, fig.5 is composed of high-frequency generator and tempering machine, whose construction depends on the geometry of surface hardening of parts subject. Also in this picture is presented work principle for induction heating.

3. DISCUSSIONS

Experiments were conducted in the laboratories of the Faculty of Engineering Hunedoara. For experiments have been used a specialized facility for surface induction hardening (type CTC100K15 compact frequency converter), T200 FLIR thermal imager, a

radiation pyrometer ST88 PLUS and a metallographic microscope type Krüss Optronic. Medium frequency power converter converts the medium frequency power used of induction heating. All parts of converter, both as external power is cooled with water. It is recommended for reducing the cost of cooling water, the water recirculation and cooling in a heat exchanger.

Power circuit of converter is a parallel resonant LC circuit provided with of inductive and capacitive compensation composed from inductor and hot work pieces. Power circuit includes tempering transformer, shown in the figure below, and also is presented the inductor who are used in experiments.



Fig.6 . Tempering transformer and inductor

Quenching transformer is shown in figure 6, is provided with multiple entries, depending on the inductor used. If heating is not correct (too long heating time) is needed to move to other transformer connections tempering ($\Phi 30$ mm inductor, transformer coupled 4:1; piece $\Phi 19$ mm diameter).

For a better control of temperature as was preferred measurements of temperature using thermographic cameras that allows real-time continuous measurement of pieces temperature in inductor with sufficiently high precision. The following figure shows how the pieces temperature was measured.

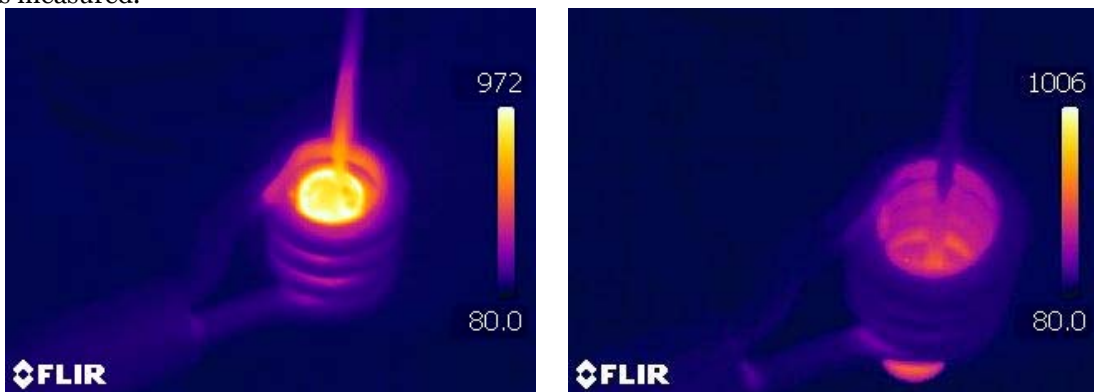


Fig. 7. Temperature of pieces measured with thermographic cameras

For experiments we used two sets pieces, consisting of 4 pieces made of steel 41Cr4 improvement, and 6 pieces of steel made from 34CrMo4. The specimens have dimensions $\Phi 19$ mm diameter, length 26 m

In order to conduct experiments, it was measured the sample temperature maintained in the inductor, while the power generator was kept constant at 60% and 70% of rated generator power. Please note that attempts to measure temperature and using a radiation pyrometer, but measurement errors occurred because of how the piece is heated (inside the ring inductor with multiple coil). All the pieces were quenched in water, and the hardness was measured in several points on the surface.

4. CONCLUSIONS

Since the experiments were conducted using the methodology described above, were measured hardness at three points on the surface of samples by Rockwell method, and the values obtained are presented in the following tables.

Tab.1 Hardness for pieces from 34CrMo4 steel

Pieces	Temperature	Hardness			Time	Power
	°C	HRC	HRC	HRC	s	%
1	910	52,5	50	52	9,1	70
2	920	53	55	50	11,3	60
3	880	49	46	48,5	10,2	60
4	1002	54	55	51	10,5	70
5	980	57	54	54	9,2	70
6	930	49,5	50	50	11,5	60

Tab.2 Hardness for piceses from 41Cr4 steel

Pieces	Temperature	Hardness			Time	Power
	°C	HRC	HRC	HRC	s	%
1	840	53	54	47	9,8	60
2	1010	65	61	61,5	10,7	70
3	972	59	60,5	65	9,1	70
4	980	56,5	59	60,5	12,3	60

In the first phase, a macroscopic analysis of surface was studied of the two cut samples in order to reveal the penetration depth of the hardened layer. These samples are presented in the following figures on the right is highlighted hardened layer, for 41Cr4 steel.



Fig. 8 Microstructure for pieces made from 41Cr4 steel

Hardened layer depth, is about 4 mm for specimens of steel and approximately 3.5 mm for specimens of steel. Are normal differences between hardened layer depth and hardness differences because steel 41Cr4 steel has a greater hardenability as 34CrMo4 steel (higher carbon content and boron contains increases hardenability).

The sample thus prepared was studied with metallographic microscope, as shown in the following figures some of the photos microstructures obtained. It just shows the microstructure of the steel sample 41Cr4 with different orders of magnitude.

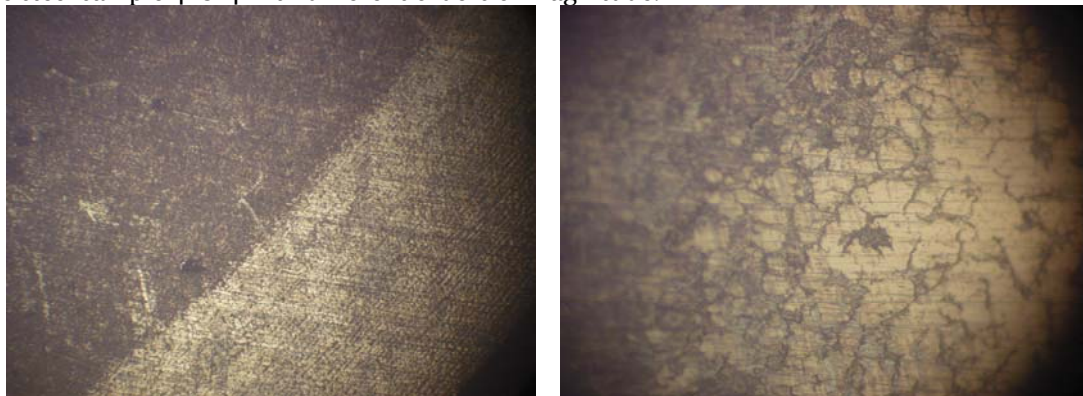


Fig.9 Microstructure of transition zone hardned-unhardned at magnitude 140x – left and 350x – right, for 41Cr4 steel

In figure 10 and 11 is presented dependences between hardness of pieces and heating temperature for booth of steel quality.

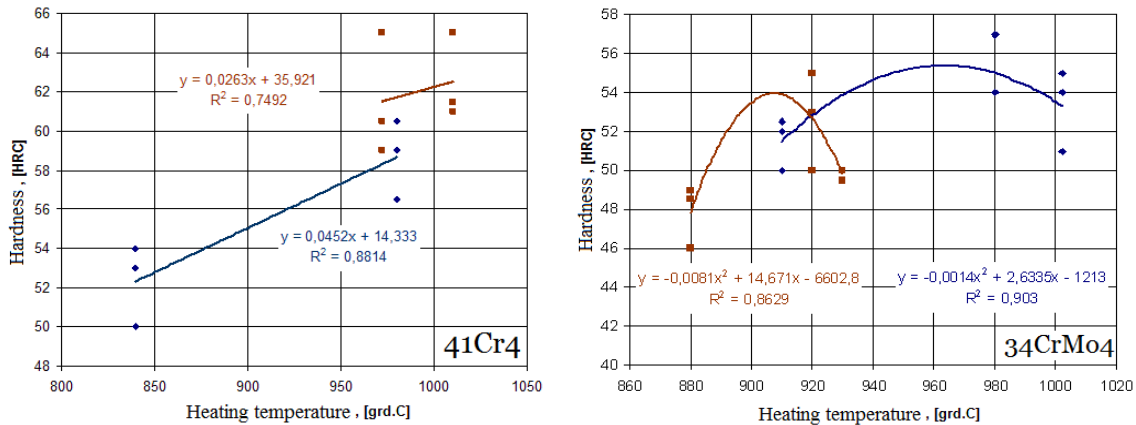


Fig.10 Hardness variation for pieces in case of 60% and 70% nominal power of generator.

In the case of 34CrMo4 steel data (which are in greater number) can be traced and a spatial dependence, in this case the hardness depending on temperature and time heating. This kind of variance of hardness is built in the statistical analysis program.

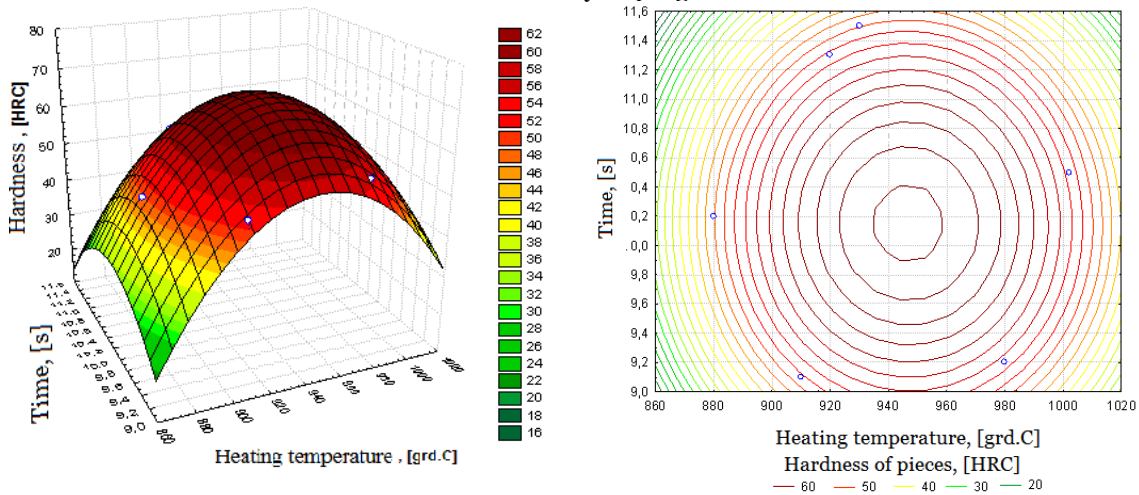


Fig.11. Hardness variation for pieces made from 34CrMo4 steel, cumulative value

In figure 11 is added also the contour graph which provide more suggestive of dependence that exists between the three parameters.

Thus, studying the previous charts are recommended for heating the steel 41Cr4 temperature range 950...1000°C to obtain a hardness of about 58... 62 HRC, while the equipment is above to 60-70% of maximum power (9 ... 10.5 kW).

For steel 34CrMo4, we recommend heating at 940 ... 980°C to obtain hardness values of 52...56 HRC, under the same power condition. In addition, in this case it may recommend duration of heating time to be 9.8 ... 10.6 seconds.

In both cases it is noted that the heating temperature for quenching is recommended to be much higher, with 120 ... 150 °C than classical austenitic temperature (which for these two steels is 840 ... 860 °C), due to this high-speed heating.

REFERENCES

- [1.] Carțis I. Gh., - Tratamente termice, Editura Facla, Timișoara, 1982.
- [2.] Ardelean M., Prejban I., Mihut G. - Tratamente termice, calcule tehnologice, Editura Cerami, Iași, 2007.
- [3.] Anghel F. - Metode și procedee tehnologice, volumul II - Tehnologii moderne, Editura Printech, Bucuresti 2006.
- [4.] *** Documentație tehnică instalație compactă de încălzire prin inducție tip CTC 100K15, AAGES Targu Mures.



¹Daniela MILOȘTEAN, ¹Mihaela FLORI

AN OVERVIEW ON THE SEMISOLID STATE PROCESSING OF STEEL

¹ FACULTY OF ENGINEERING HUNEDOARA, UNIVERSITY "POLITEHNICA" TIMISOARA, ROMANIA

ABSTRACT:

The high melting point alloys such as steels are difficult to process in semisolid state due to high temperature needed for processing. Owing to the obvious advantages of this new technology comparative with the conventional manufacturing technologies, many studies try to resolve the technological problems and to offer the possibility of a profitable commercial exploitation.

This article emphasizes the importance of solid fraction in semisolid state processing technology and exposes the main steel grades investigated and presented in the literature. Also are presented the methods to obtain precursory material for thixoforming and the materials used for die manufacturing needed in this new process.

KEYWORDS: steel, semisolid state, solid fraction, thixoforming, die material

1. INTRODUCTION

Topics as decreasing manufacturing costs and increasing the quality of the final products draw attention to many production engineers. Thus, the development of new technologies as *semisolid state processing* (known as SSP) becomes necessary.

Semisolid processing of alloys was initiated at the beginning of the 70's at MIT (Massachusetts Institute of Technology) [1,2]. At the basis of this new technology are the experiments realized by David Spencer *et al.* on Sn-15Pb alloy where he obtained a semisolid suspension with thixotropic characteristics by mechanical stirring [3].

Semisolid metal forming is realized at temperatures between liquidus and solidus lines, when in the alloy exist about 40-60% solid fraction [4]. In this range, if the microstructure of the alloy is globular it manifests a property named thixotropy. This term was introduced by Peterfi in 1927 to define the property of slurry which become fluid when is agitated and to thicken when resting [5]. Thus, this interesting property of semisolid alloys with globular structure made possible the invention of a new technology that offers several advantages over the conventional casting, forging, etc, such as porosity reduction, lower forming temperatures, improved flow properties, reduced process force, near net shape forming, better mechanical properties, etc. [6]. The most known SSP technologies are: *thixoforming* and *rheocasting* used for aluminum and other alloys, respectively *thixomolding* and *rheomolding* especially for magnesium alloys [7]. Thixoforming consist in obtaining parts in final shape from semisolid slurries with globular structure achieved by heating the semi-finished product with non-dendritical structure. If the shaping takes place in an open die the process is called thixocasting and if the shaping is realized in a close die, is called thixoforging. Rheocasting is actually the process of forming in the semisolid state direct from cooling melt, without the need for using of a globular structure semi-finish product [3].

This article presents an overview on the most studied steels processed in semisolid state; it also refers on the methods used to obtain precursor material for thixoforming and on the most suitable materials for die manufacturing.

2. THE IMPORTANCE OF SOLID FRACTION IN SSP

The solid fraction is one of the most important parameters that affect principally the viscosity of the semisolid slurry. It can be calculated using a simple phase diagram (fig.1) and level rule. In

fig. 1 is presented the phase diagram of a binary alloy, together with microstructures obtained by casting (fig.1.a) and by thixoforming (fig.1.b) of X210CrW12 steel. So, for simple binary eutectic alloys that melt and solidify under equilibrium condition (assuming that the liquidus and solidus line are linear), the weight of solid fraction f_s at a given processing temperature T is given by [8,9]:

$$f_S^{ech} = \frac{(T_M - T) - m_L \cdot c_0}{(T_M - T) \cdot (1 - k)} \quad (1)$$

where T_M is the melting point of the pure solvent, m_L is the slope of the liquidus line, c_0 is the alloy composition and k is the partition coefficient of the alloy.

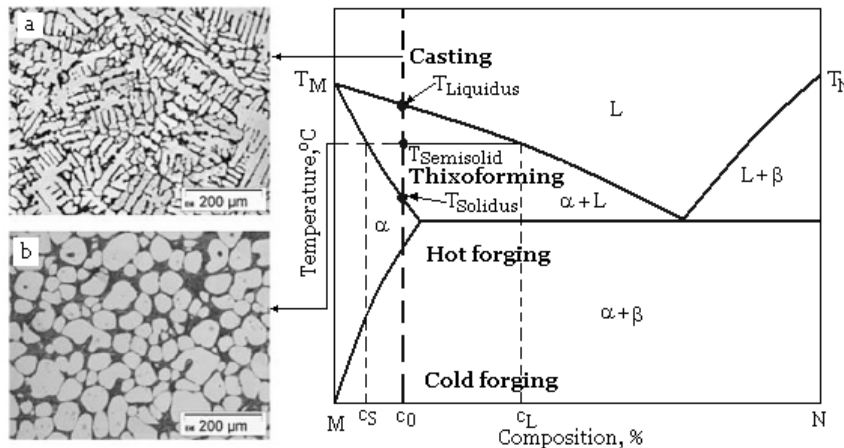


Fig.1. Schematic representation of the thixoforming area in a simple phase diagram and the corresponding microstructure (a-dendritic, b-globular) for X210CrW12 steel [10]

Under fast solidification condition, when occurs a complete diffusion in the liquid and no diffusion in the solid phase (maximum microsegregation) the weight of solid fraction f_s at a given processing temperature T is given by Scheil equation [8,9]:

$$f_S^{Sch} = 1 - \left(\frac{T_M - T}{T_M - T_L} \right)^{\frac{1}{1-k}} \quad (2)$$

where T_L is the liquidus temperature of the alloy.

The steel grades processed in semisolid state are selected according to few criteria:

- ❖ the material must have a wide solidification range ($T_L - T_S$). Usually the methods used to determine the semisolid range are Differential Thermal Analysis-DTA (fig.2), Differential Scanning Calorimetry-DSC and thermodynamic data [9];
- ❖ the temperature processing interval when in the alloy exist 40-60% solid fraction f_s must be sufficiently large;
- ❖ the volume of solid fraction must not be sensitive to temperature variations specially in the range with 40-60% solid fraction [4,8].

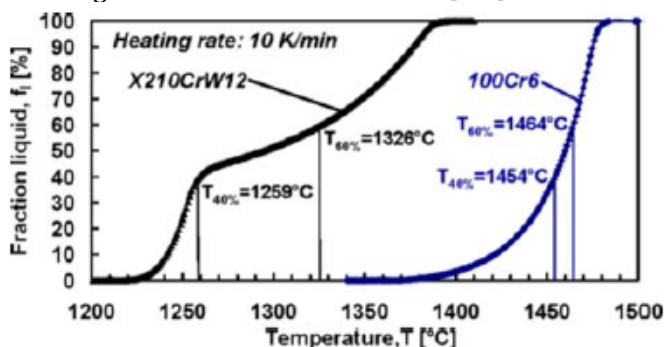


Fig.2. The variation of the liquid fraction versus temperature obtained by DTA [11]

It can be seen in fig.2 that the X210CrW12 steel has a temperature processing range (40-60% f_s) of 67°C while for 100Cr6 steel the interval is only of 10°C. Hence for the second steel grade it is necessary a very strict temperature control [11].

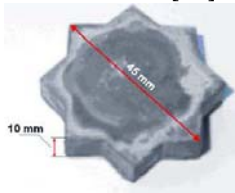
So, the slurry temperature influences the solid fraction with direct consequences on the viscosity which indicate the capability of a material to fill a mold and determines the force necessary for deformation and flow of materials [2].

3. STEEL GRADE SELECTED FOR THE SSP

It should be noted that semi-solid processing bases were established by studying low melting point alloys such as aluminum and magnesium alloys used for the most parts that are now

commercialized. So far, the SSP technology was not applied on industrial scale for high melting point alloys such as steels [12-14], but over time have been done researches on several steel grades that are more likely to be processed by this new technology (tab.1).

Table 1. An overview on the steel grades processed in semisolid state

	<p>Process – Thixocasting Year - 2004 Reference – [15]</p>  <p>Thixocasted steel part</p>	<p>Process –Thixo-extrusion Year – 2009 Reference – [16]</p>  <p>Extruded bars</p>
X210CrW12 (AISI D6)	<p>Process –Thixo-extrusion Year – 2009 Reference –[17]</p>  <p>Extruded bars. Left: view of a cut segment, right: cross-section</p>	<p>Process – Thixocasting Year - 2009 Reference – [18]</p>  <p>Thixocast sample</p>
	<p>Process – Rheoforging Year – 2005 Reference – [11]</p>  <p>Part obtain through rheoforging</p>	<p>Process – Thixocasting Year – 2010 Reference – [19]</p>  <p>Thixocast samples</p>
100Cr6	<p>Process - Thixoforging Year – 2010 Reference – [20]</p>  <p>Part obtain through thixoforging</p>	
	<p>Process – Thixoforging Year – 1993 Reference – [1]</p>  <p>M2 tool steel thixoforged parts</p>	<p>Process – Thixoforging Year – 2010 Reference – [14]</p>
M2	<p>Process - Rheo-rolling Year – 2003 Reference – [21]</p>	<p>Process - Rheo-rolling Year – 2008 Reference – [6]</p>
60Si2Mn	<p>Process - Rheo-rolling Year – 2003 Reference – [22]</p>	<p>Process - Rheo-rolling Year – 2008 Reference – [6]</p>
1Cr18Ni9Ti	<p>Process – Rheo-rolling Year – 2005 Reference – [23]</p>  <p>Rheo-rolled product</p>	
T12		

UHCS

Process - Rheocasting
Year – 2006
Reference – [24]

Process - Thixoforging
Year – 2005
HP9/4/30 Reference – [25]



Thixoforged fingers from a slug

At the University of Science and Technology Beijing, China, a research group have focused the studies on the rheo-rolling process and developed a device for semisolid steel preparation and rolling. The steel grades used in their investigation are principally: 60Si2Mn, 1Cr18Ni9Ti and T12 [6,21-23,26]. Results showed that semi-solid slurry obtained through electromagnetic stirring, of the steel grades 60Si2Mn and 1Cr18Ni9Ti, can be rolled successfully. They observed that for 1Cr18Ni9Ti stainless steel the strength of the plate rheo-rolled is increased compared to that of the conventionally repeated hot-rolled plate, but the elongation is decreased [22]. For 60Si2Mn spring steel rheo-rolled the rupture strength and elongation are lower than that of traditionally repeated hot-rolled plate [21]. Also, through rheo-rolling at different solid fraction, with increasing the solid fraction the mechanical properties (rupture strength and elongation) of semisolid rolled products become better [6]. T12 high carbon steel (1,2%C) was investigated only in terms of microstructure [23].

The Institute of Metal Forming, RWTH Aachen University of Technology, from Germany is another research center interested of the SSP technology. G. Hirt and his team investigated two different process routes for semi-solid precursor material preparation subsequently forged in semisolid state. The 100Cr6 steel grade was chosen for investigation because of the various application possibilities, and the X210CrW12 steel for his good suitability for microstructure studies. They concluded that the preliminary semisolid forging and rheoforging trials for both steels grade predict the high potential of the process [11].

The study realized by W. Püttgen et al. on the two steel grades mentioned above, describe the phase formation during rapid cooling from semisolid state. They have shown that the microstructure in the as-quenched state does not reflect the condition from semisolid state, and therefore is not possible a metallographic evaluation of the liquid fraction [12].

In the work carried out at the University of Sheffield a research group has demonstrated the feasibility of HP9/4/30 steel thixoforging having prior microsegregated microstructure [25].

The steel grades M2 [14], X210CrW12 [18] and 100Cr6 [19] are also investigated at the Institute of Metallurgy and Materials Science of the Polish Academy of Science, Krakow.

Even if semisolid forming of steel is more difficult to be realized compared with that of low melting point alloys there is a progress made so far in this domain and exists the possibility of industrial scale implementation.

4. METHODS USED TO OBTAIN SEMISOLID PRECURSORY MATERIAL

A successful thixoforging process requires precursory material with a unique microstructure in which the solid particles are spheroidal. This material has a thixotropic behavior in semisolid state and it can be obtained in several ways as were published in the literature [7,27].

The usual routes used to produce the steel feedstock material for thixoforging are: electromagnetic stirring (fig.3), spray forming-Osprey (fig.4) and SIMA-Strain Induced Melt Activated. For low melting point alloys besides the above mentioned methods there are other techniques of obtaining raw material for thixoforging as: mechanical stirring [28], casting at liquidus temperature (the UBE new rheocasting process is based on this principle) [27], the new MIT process [27], etc.

The *electromagnetic stirring* process was developed in the USA and consists in breaking the dendrites during solidification due to the rotating electromagnetic fields within the continuous casting crystalliser and in forming of an alloy with a nondendritic structure under the shape of a rosette [7,29]. This method is used both in the semisolid processing of low and high melting point alloys (60Si2Mn, 1CrNi9Ti [6,21,22]).

In the *SIMA process* the alloy which has been previously hot-worked is heated so recrystallisation take place before partial melting; so the liquid penetrates the grain boundaries and leads to a fine globular microstructure [27,30].

In the *OSPRAY process* the melted metal passes through a nozzle and encounters an inert gas at a high pressure. The liquid metal is sprayed by the high pressure gas as micrometric drops which

cool down with a high speed while being in the air. While the bigger drops remain intact and the smaller ones are solidified during spraying, those having intermediary dimensions become semisolid (fig.4). Liquid and semisolid drops with a high liquid fraction spread upon impact, while the solid and semisolid drops with a high solid fraction get fragmented. So the resulted structure contains fine and spherical grains [27].

In 1993 Kapranos and his colleagues [1] have investigated two distinct routes (RAP and Ospray) used to produce the feedstock for M2 tool steel thixoforging. Both methods have proved to be viable for production of precursory material for tool steel thixoforging.

Recently feedstock material (M2 tool steel) obtained by Ospray method was thixoformed and the results show that the hardness value recorded a significant increase [14].

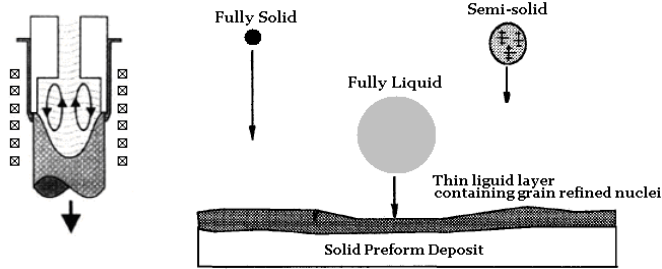


Fig.3. Electromagnetic stirring [29] Fig.4. The Osprey process [1]

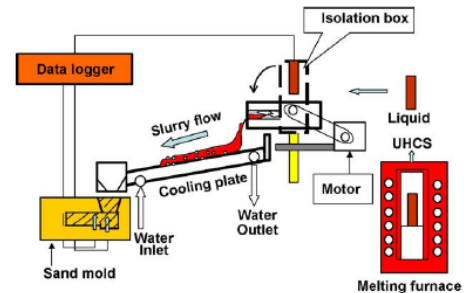


Fig.5. The cooling plate technique [24]

The “rheo” routes (rheocasting, rheoforging, rheo-rolling, rheoextrusion) does not require semi-finished products with globular structure, because in this type of process the melted material is subjected to different techniques (electromagnetic stirring [21-23], mechanical vibration [31], cooling slope technique - fig.5 - [24,32], etc.) in order to obtain in the semisolid interval a globular solid fraction in a liquid matrix.

Ultra-high carbon steel (UHCS) with 1,49%C processed in semisolid state by the cooling plate technique gave good results in terms of the mechanical properties compared with the conventional casting [24].

Because the rheo-route does not require a semi-finished product with a globular structure as a starting material there are lower energy costs and thus from this point of view this route is preferable.

5. DIE MATERIALS

One of the biggest problems which appear at the semisolid state processing of steel is finding an appropriate die material. This is due to the high temperature at which the process takes place. The searched material must have properties like: resistance at high temperatures, thermal shock resistance, good wear and corrosion resistance [33], durability in exploitation, low coefficient of thermal expansion [34], etc. In this condition the materials appropriated for thixoforming die are principally dense ceramic materials, laser treated steels or others alloys (Inconel 617, Satellite 6, CrNiCo).

Recently, S. Muenstermann et al. developed a self-heating ceramic tool for the semi-solid extrusion of steel (X210CrW12) under near-isothermal conditions. The ceramic material used for the die is high-purity alumina (Al_2O_3). Results showed that this new concept allows isothermal thixoextrusion of the steel. Also they investigated the behavior of the alumina die regarding wear and corrosion resistance. The conclusion was that by applying the self-heating tool concept the ceramic dies have excellent corrosion and wear resistance, and regarding the chemical interaction between tool and the work material, alumina dies are not decomposed in the steel thixoextrusion process, leaving the work piece unaffected [17,33].

Another potential tool material for steel semisolid forming is silicone nitride (Si_3N_4) thanks to its high strength and excellent thermal shock resistance at 300-400°C [35]. The non-oxide ceramics materials (Si_3N_4) are susceptible to oxidation and corrosion while oxide ceramics (Al_2O_3) exhibit significant lower mechanical properties and poor thermal shock resistance [35]. Despite these properties unfavorable for a die material used in semisolid processing of steel, S. Muenstermann and R. Telle developed two new tool concept strategies based on the benefits of the both materials (high strength of non-oxide ceramics materials and excellent corrosion resistance of oxide ceramics) [35]. A schematic view of the tool concept strategies for thixoforming dies is given in fig.6.

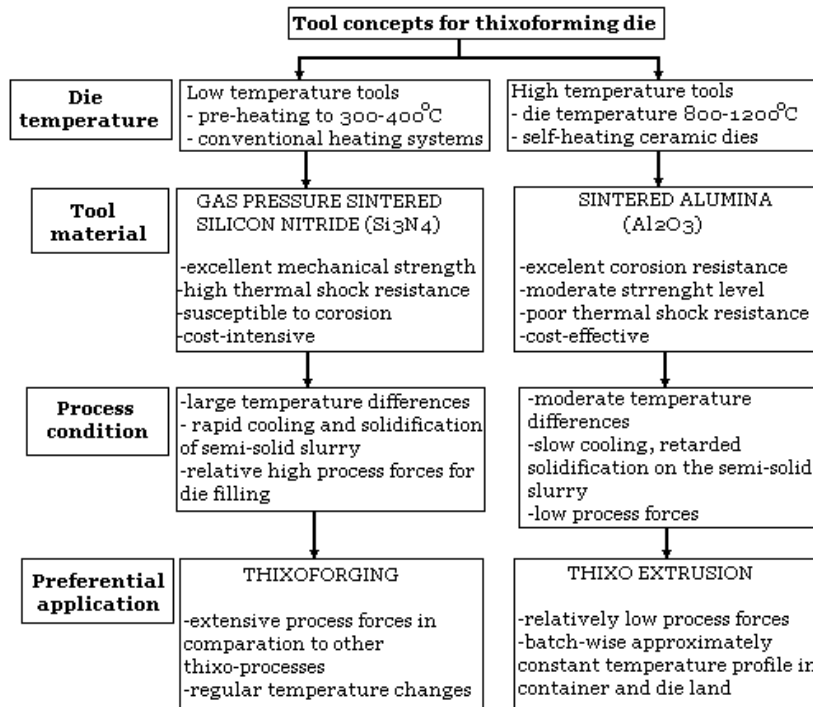


Fig.6. Tool concept strategies for steel thixoforming die [35]

These two strategies developed by S. Muenstermann and R. Telle for the thixoforging and thixoextrusion of steel using silicon nitride and respectively alumina die were experimented and the results were promising.

Regarding the die final price, it was concluded that the alumina tool costs (raw material, production and investment costs) are lower compared with the non-oxide ceramics [33].

Y. Birol [34] tested the CrNiCo die material alloy and used it in the steel thixoforming process. By comparing the thermophysical properties and the thermal fatigue behavior of CrNiCo alloy with the X38CrMoV5 steel used in manufacture of conventional forging dies, it was concluded that the first one can be a viable die material.

Other alloys (Inconel 617, Satellite 6) were investigated as die materials and subjected to high temperature abrasive wear testing and compared to the X32CrMoV33 hot work tool steel (used in conventional hot forging of steel parts). At 625°C, the wear resistance (represented by weight loss) and the surface hardness of the tool steel is better compared to the alloys, while at 750°C the results are superior for the alloys [36]. From the point of view of service life, Inconel 617 and Satellite 6 alloys presented few and shallow cracks after 5000 thermal cycling while X32CrMoV33 steel resisted only 1500 cycles [37].

Also, by laser glazing of tool steel (AISI H13) dies, the initial results showed a large increase in hardness value for the surface layer, but the temperature working limit was only of ~600°C. So the results are unsatisfactory for thixoforming of steel (where the die cavity surface reaches 700-750°C only for a few seconds [34,38]) and this steel could be used as die material for non-ferrous semisolid forming [39,40].

The investigations realized so far on die materials are encouraging, but just now it wasn't found a material that meets all requirements necessary for large scale use.

6. CONCLUSIONS

Analyzing the literature studies it may be concluded that the semisolid processing has many advantages over traditional technologies and has already been applied to industrial production of magnesium and aluminum alloys. In recent years, steel semisolid processing also drew attention, the results on applying this technology being encouraging with high melting point alloys. Also finding an appropriate die material with a good durability in exploitation is yet under investigation, but the research made so far are promising.

REFERENCES

- [1.] P. Kapranos, D.H. Kirkwood and C.M. Sellars, Semi-solid processing of tool steel, *Journal de Physique IV, Colloque C7, supplement au Journal de Physique III*, Vol. 3 (1993)
- [2.] O. Lashkari, R. Ghomashchi, The implication of rheology in semi-solid metal processes: An overview, *Journal of Materials Processing Technology*, Vol. 182 (2007) 229–240
- [3.] M.C. Flemings, Semi-solid forming: the process and the path forward, *Metallurgical Science and Technology*, Vol. 18 (2) (2000)
- [4.] D.I. Ulenhaut et al., Structure and properties of a hypoeutectic chromium steel processed in the semi-solid state, *Acta Materialia*, Vol. 54 (2006) 2727-2734
- [5.] F. Czerwinski, The Basics of Modern Semi-Solid Metal Processing, *JOM*, Vol. 58 (6) (2006) 17-20
- [6.] R. Song, Y. Kang and A. Zhao, Semi-solid rolling process of steel strip, *Journal of Materials Processing Technology* Vol. 198 (2008) 291-299
- [7.] Z. Fan, Semisolid metal processing, *International Materials Reviews*, Vol. 47 (2) (2002)
- [8.] E. Tzimas, A. Zavaliangos, *Materials Selection for Semisolid Processing*, *Materials and Manufacturing Processes*, Vol.14 (1999)
- [9.] E. Tzimas, A. Zavaliangos, Evaluation of volume fraction of solid in alloys formed by semisolid processing, *Journal of Materials Science*, Vol. 35 (2000) 5319-5329
- [10.] H. Stankova et al., Influence of thixoforming on structure development of the tool steel, 12th International Research/Expert Conference "Trends in the Development of Machinery and Associated Technology" TMT 2008, Istanbul, Turkey
- [11.] G. Hirt et al., Semi-Solid Forging of 100Cr6 and X210CrW12 Steel, *CIRP Annals – Manufacturing Technology*, Vol. 54, Issue 1 (2005) 257-260
- [12.] W. Püttgen et al., On the microstructure formation in chromium steels rapidly cooled from the semisolid state, *Acta Materialia*, Vol. 55 (2007) 1033-1042
- [13.] R. Kopp et al., Forming and joining of commercial steel grades in the semi-solid state, *Journal of Materials Processing Technology* 130-131 (2002) 562–568
- [14.] J. Dutkiewicz et al., Thixoforming of spray formed M2 tool steel, *International Journal of Material Forming* Vol. 3, Suppl.1 (2010) 755 – 758, DOI 10.1007/s12289-010-0880-3
- [15.] H. Bramann et al., Casting of a cold work steel alloy in semi-solid state, *Journal of Materials Processing Technology* 155-156 (2004) 1357-1364
- [16.] F. Knauf, R. Baadjou and G. Hirt, Analysis of semi-solid extrusion products made of steel alloy X210CrW12, *International Journal of Material Forming*, Vol. 2, Suppl. 1 (2009) 733-736 DOI 10.1007/s12289-009-0426-8
- [17.] S. Muenstermann et al., Semi-solid extrusion of steel grade X210CrW12 under isothermal conditions using ceramic dies, *Journal of Materials Processing Technology* 209 (2009) 3640–3649
- [18.] J. Dutkiewicz et al., Thixoforming technology of high carbon X210CrW12 steel, *International Journal of Material Forming* Vol. 2, Suppl. 1: 753 – 756 (2009), DOI 10.1007/s12289-009-0558-x
- [19.] L. Rogal et al., Characteristics of 100Cr6 bearing steel after thixoforming process performed with prototype device, *Trans. Nonferrous Met. Soc. China* 20 (2010) 1033-1036
- [20.] K. P. Solek et al., Characterization of thixoforming process of 100Cr6 steel, *Trans. Nonferrous Met. Soc. China* 20 (2010) 916-920
- [21.] W. Mao et al., Slurry Preparation and Rolling of Semi-Solid 60Si2Mn Spring Steel, *Journal of Material Science and Technology*, Vol. 19, No. 6 (2003)
- [22.] W. Mao et al., Semi-solid slurry preparation and rolling of 1Cr18Ni9Ti stainless steel, *Journal of University of Science and Technology Beijing*, Vol. 10, No.6 (2003)
- [23.] J.G. Li et al., Microstructural morphology of the semi-solid high carbon steel T12 before and after rheo-rolling, *Journal of University of Science and Technology Beijing*, Vol. 12, No. 2 (2005)
- [24.] M. Ramadan et al., Semi-solid processing of ultrahigh-carbon steel castings, *Material Science and Engineering A* 430 (2006) 285-291
- [25.] M.Z. Omar et al., Thixoforming of a high performance HP9/4/30 steel, *Materials Science and Engineering A* 395 (2005) 53-61
- [26.] R. Song et al., Investigation of the Microstructure of Rolled Semi-Solid Steel, *Journal of Materials Sciences and Technology*, Vol. 18, No. 3, (2002)
- [27.] H.V. Atkinson, Modelling the semisolid processing of metallic alloys, *Progress in Materials Science*, No. 50 (2005) 341-412
- [28.] M. Modigell, J. Koke, Time-Dependent Rheological Properties of Semisolid Metal Alloys, *Mechanics of Time-Dependent Materials* 3 (1999) 15-30

- [29.] D. Stoica, I. Ilca, Reflection regarding the obtaining of precursor material at semisolid state processing, Scientific Bulletin of the „Politehnica” University of Timisoara, Transaction of Mechanics, Editura Politehnica, Timișoara, ISSN 1224-6077, Tom 52(66), Fasc. 8, (2007) 43-48
- [30.] J.-Y. Li et al., Microstructural evolution and flow stress of semi-solid type 304 stainless steel, Journal of Materials Processing Technology, 161 (2005) 396-406
- [31.] D. Miloștean, M. Flori, Experimental research in pilot phase regarding the semisolid state processing of steel, Annals of the Faculty of Engineering Hunedoara, Mirton Publishing House, Timisoara, ISSN 1584-2673, Tome VII, Fascicule 3, (2009) 383-385
- [32.] B. Amin-Ahmadi, H. Aashuri, Semisolid structure for M2 high speed steel prepared by cooling slope, Journal of Materials Processing Technology, 210 (2010) 1632-1635
- [33.] S. Muenstermann, R. Telle, Wear and corrosion resistance of alumina dies for isothermal semi-solid processing of steel, Wear 267 (2009) 1566–1573
- [34.] Y. Birol, Testing of a novel CrNiCo alloy for tooling application in semi-solid processing of steel, International Journal of Material Forming (2010) 3:65–70, DOI 10.1007/s12289-009-0418-8
- [35.] S. Muenstermann, R. Telle, Ceramic tool concepts for the semi-solid processing of steel alloys, Mat.-wiss. u. Werkstofftech., Vol. 37, No. 4 (2006)
- [36.] Y. Birol, High-temperature abrasive wear testing of potential tool materials for thixoforming of steel, Tribology International 43 (2010) 2222-2230
- [37.] Y. Birol, Ni- and Co-based superalloys as potential tool materials for thixoforming of steel, International Journal of Material Forming, Vol. 3, Suppl. 1 (2010) 739-742
- [38.] A. Rassili et al., X38CrMoV5 hot-work tool steel as tool material for thixoforming of steel: Numerical and experimental evaluation, Trans. Nonferrous Met. Soc. China 20 (2010) 713-718
- [39.] D. Brabazon et al., Glazing of tool dies for semi-solid steel forming, International Journal of Material Forming, Vol. 2, Suppl. 1 (2008) 985-988, DOI 10.1007/s12289-008-0223-9
- [40.] S.N. Aqida et al., Thermal stability of laser treated die material for semi-solid material forming, International Journal of Material Forming, Vol. 2, Suppl. 1 (2009) 761-764





¹ Adrian GĂVĂNESCU

REFINING OF STEEL BY USING SYNTHETIC SLAG

¹ UNIVERSITY POLITEHNICA OF TIMISOARA, FACULTY OF ENGINEERING FROM HUNEDOARA, ROMANIA

ABSTRACT:

Treating the liquid steel with synthetic slag in the casting ladle is an efficient and relatively cheap method of reducing the non-metal inclusion content by reducing the sulphur and oxygen content. The synthetic slag used in the experiments corresponds to the CaO - Al₂O₃ system, which ensures, by their composition, the extraction of sulphur and oxygen from the liquid steel, based on Nernst's repartition law. The method also has the advantage of being applicable in all the processing technologies. The paper presents the results and conclusions of the laboratory experiments regarding treatment of steel with various composition synthetic slags.

KEYWORDS:

synthetic slag, steel, desulphurization, deoxidation

1. INTRODUCTION

The essence of the process of using synthetic slag consists in making a contact on a large surface between the melted steel and a slag having a composition selected to ensure an advanced steel deoxidation and desulphurization.

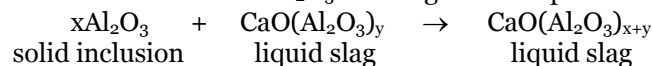
The disadvantages of diffusion (extraction) deoxidation are removed by this procedure as it is made by emulsifying the steel with the slag (which does not contain CaC₂) and the process is very fast (10 to 12 minutes) [1].

The admixture represents 2 – 4 % of the liquid steel quantity in case of using solid synthetic slag and 3 – 6% in case of using melted slag.

It was proved by practice that the most effective slag are the ones from the systems CaO – Al₂O₃, CaO – Al₂O₃ – CaF₂, CaO – Al₂O₃ – CaF₂ + NaF.

Compositions of some slag on the market are presented in Table 1 [2]. The composition of these slag can be modified according to the requirements of the users in the metallurgic industry.

The used calcium-aluminate synthetic slag are liquid at work temperature and they participate not only in the deoxidation process (by oxygen diffusion), but also in the removal of inclusions they come in contact with. When solid Al₂O₃ inclusions come into contact with CaO – Al₂O₃ liquid slag, the alumina inclusions are absorbed and form liquid calcium-aluminates which are richer in Al₂O₃. The reaction between Al₂O₃ and slag can be represented as follows:



Beside the deoxidation effect, the synthetic slag, mainly the ones with a high content of CaO, due to their increased basic capacity and fluidity, high dispersion and contact surface increase capacity ensure favourable conditions for advanced desulphurization of steel.

Table 1. Synthetic slag available on the market

	CaO(%)	Al ₂ O ₃ (%)	SiO ₂ (%)	CaF ₂ (%)	MgO(%)	Na ₂ O(%)	FeO(%)
1.	72-77	0-2	19-24	2-4	-	0,5-1,5	-
2.	75-80	12-15	0,7-1,5	4-6	-	-	-
3.	17-20	63-68	< 4	-	7-10	-	-
4.	70	15	0,9	-	2,5	-	0,5
5.	50	42	2	-	1,5	-	1,5

2. DISCUSSIONS

Laboratory experiments were conducted to verify the efficiency of synthetic slag deoxidation and desulphurization capacity. Experiments consisted in melting in a Tamann furnace steel samples with the next composition (Table 2)

Table 2. Compositions of steel before the treatment

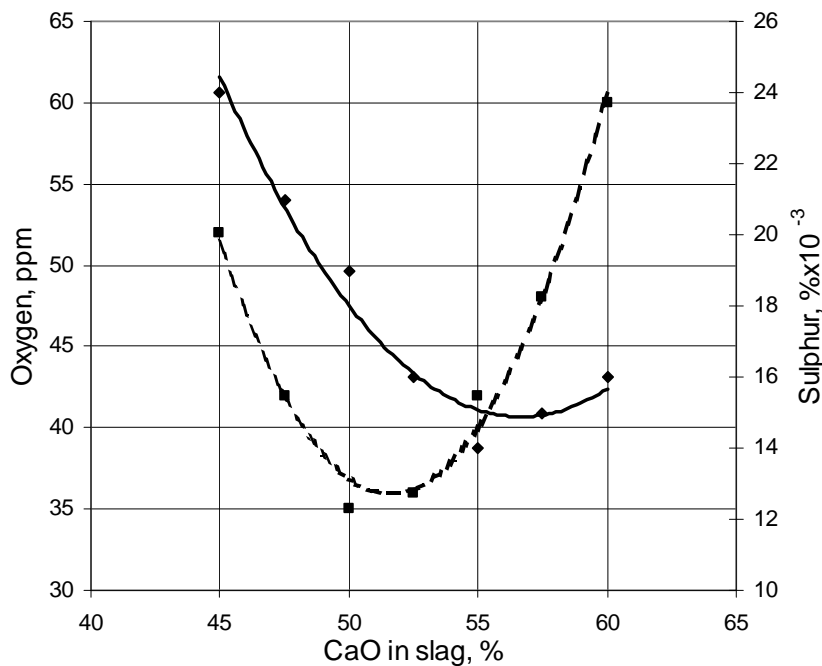
C [%]	Mn [%]	Si [%]	P [%]	S [%]	O _{total} [p.p.m.]
0.34	0.56	0.28	0.031	0.030	78

A quantity of 4 kg of steel was melted for each determination of oxygen and sulphur content after a treatment under 80 grams synthetic slag for 10 minutes. The compositions of the synthetic slag and the results of the oxygen and sulphur content measurements after treatment are shown in Table 3 and in Figure 1.

The dependence between slag compositions and oxygen and sulphur contents of steel after treatment is:

$$[O] = 0,3524 \cdot (CaO)^2 - 36,386 \cdot (CaO) + 975,19 \quad R^2 = 0,98 \quad (1)$$

$$[S] = 0,0705 \cdot (CaO)^2 - 7,9857 \cdot (CaO) + 241,1 \quad R^2 = 0,96 \quad (2)$$



oxygen (—◆—) and sulphur (---■---) after treatment

Fig. 1. Influence of slag compositions to oxygen and sulphur contents of steel

Table 3. Contents of oxygen and sulphur before and after treatment

	Slag compositions[%]		Oxygen [ppm]		Sulphur [%x10 ⁻³]	
	CaO	Al ₂ O ₃	before	after	before	after
1	45,0	55,0	30	24	78	52
2	47,5	52,5	30	21	78	42
3	50,0	50,0	30	19	78	35
4	52,5	47,5	30	16	78	36
5	55,0	45,0	30	14	78	42
6	57,5	42,5	30	15	78	48
7	60,0	40,0	30	16	78	60

In conclusion, calcium-aluminate solid synthetic slag, with a content of CaO between 51 ... 56% will ensure a removal of about half of initial quantity of sulphur and oxygen from treated steel.

For establishing the regression equations between the quantities of synthetic slag and final contents of oxygen and sulphur were made experiments using different quantities of slag, with a duration of 10 minutes.

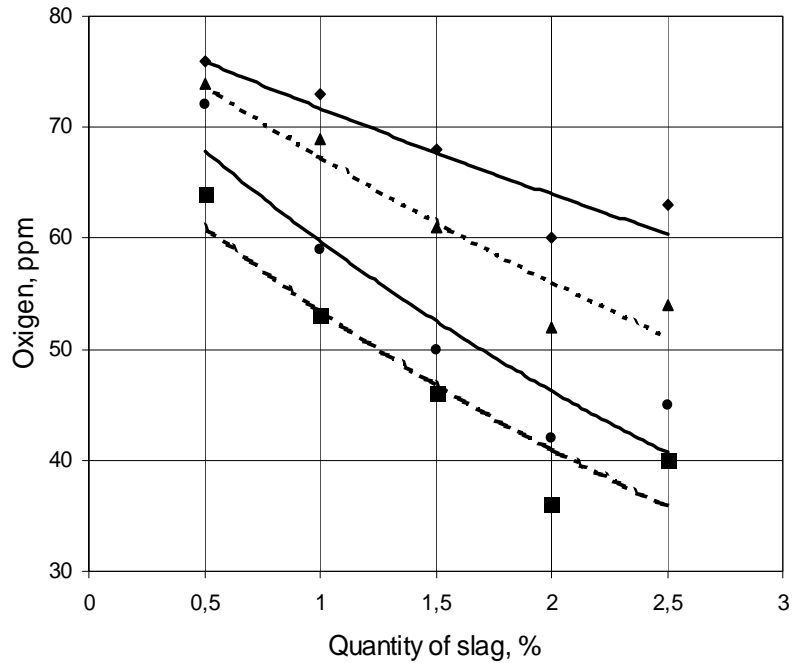
Dependence between the oxygen and sulphur contents of steel after treatment and the quantity of synthetic slag is:

$$[O] = a \cdot e^{-bQ} \quad (3)$$

$$[S] = c \cdot e^{-dQ} \quad (4)$$

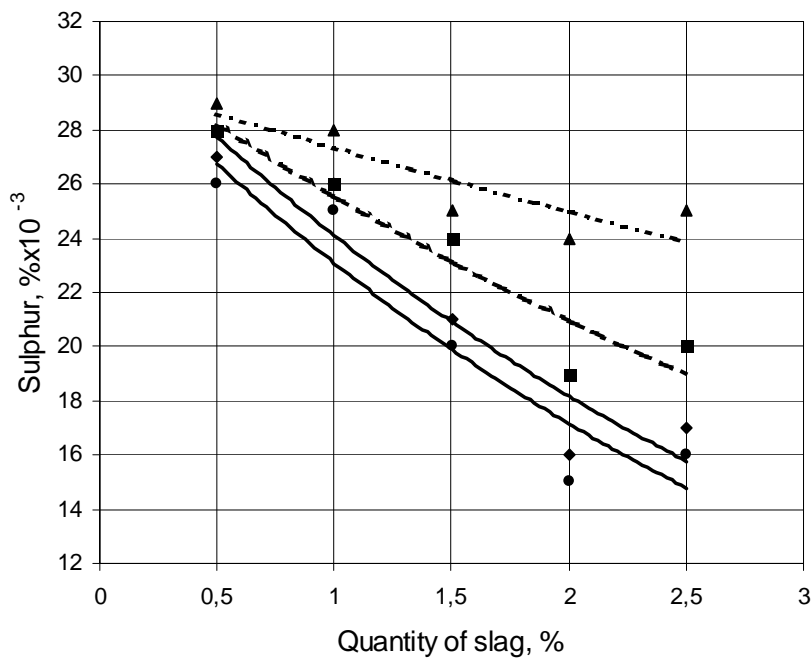
and is presented in table 4 and in figures 2 and 3.

Quantity of synthetic slag Q is in percent from the quantity of steel and the high values of correlation coefficient shows tide interdependency between the oxygen and sulphur contents of steel, after treatment and the quantity of synthetic slag.



CaO-Al₂O₂ slag with: — ▲ — 45% CaO — ■ — 50% CaO — • — 55% CaO — ◆ — 60% CaO

Fig. 2. Influence of slag quantity to oxygen contents of steel



CaO-Al₂O₂ slag with: — ▲ — 45% CaO — ■ — 50% CaO — • — 55% CaO — ◆ — 60% CaO

Fig.3. Influence of slag quantity to sulphur contents of steel

Table 4. Dependence between the oxygen and sulphur contents of steel after treatment and the quantity of synthetic slag - Q [% from steel quantity]

Slag composition		Oxygene [ppm]			Sulphur [%x10 ⁻³]		
CaO [%]	MgO [%]	Coefficient of ecuation		Coeff. of correlation R ²	Coefficient of ecuation		Coeff. of correlation R ²
		a	b		c	d	
45	55	80,783	0,1826	0,9002	29,915	0,0902	0,7596
50	50	69,961	0,2654	0,8495	31,115	0,1973	0,8739
55	45	76,786	0,9141	0,9141	30,797	0,3027	0,9229
60	40	80,401	0,1143	0,8406	31,947	0,2822	0,8756

For establishing the regression equations between the duration of treatment τ and final contents of oxygen and sulphur were made experiments using 80 grams of synthetic slag (representing 2% from the steel quantity) with different contents.

Dependence between the oxygen and sulphur contents of steel after treatment and the duration of treatment is:

$$[O] = a \cdot e^{-b\tau} \quad (5)$$

$$[S] = c \cdot e^{-d\tau} \quad (6)$$

and is presented in table 5 and in figures 4 and 5.

Table 5. Dependence between the oxygen and sulphur contents of steel after treatment and the duration of treatment with synthetic slag - τ [minutes]

Slag composition		Oxygene [ppm]			Sulphur [%x10 ⁻³]		
CaO [%]	MgO [%]	Coefficient of ecuation		Coefficient of correlation R ²	Coefficient of ecuation		Coefficient of correlation R ²
		a	b		c	d	
45	55	70,088	0,0272	0,8974	30,152	0,0183	0,8647
50	50	60,625	0,0477	0,8219	28,031	0,0340	0,8084
55	45	70,335	0,0518	0,8539	27,492	0,0582	0,8450
60	40	70,469	0,0140	0,9043	28,237	0,0490	0,8937

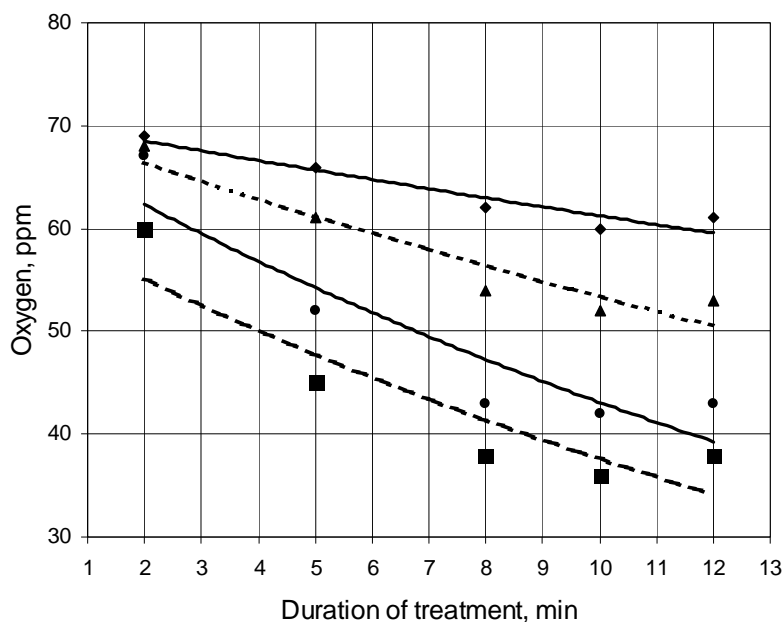


Fig.4. Influence of treatment duration to oxygen contents of steel

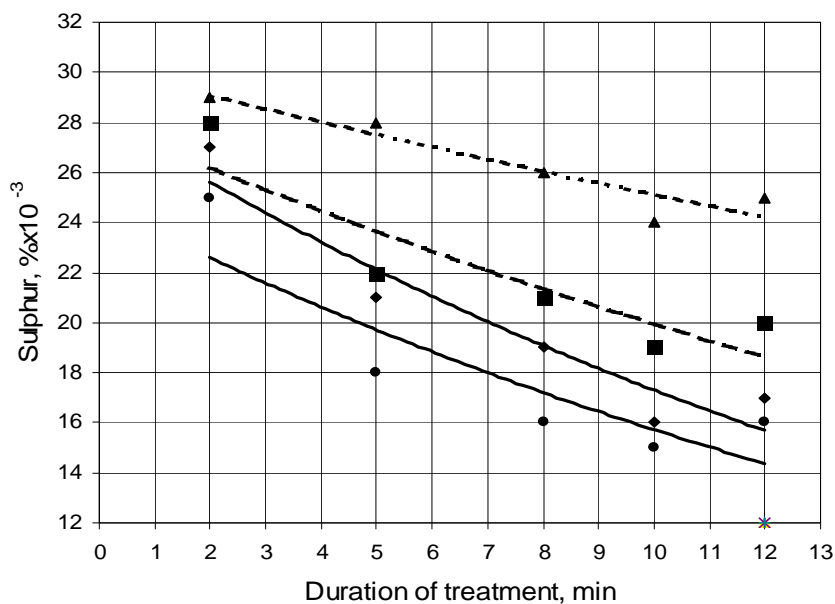


Fig.5. Influence of treatment duration to sulphur contents of steel

CaO-Al₂O₃ slag with:

— ▲ — 45% CaO ; — ■ — 50% CaO ; — ● — 55% CaO ; — ◆ — 60% CaO

The equations which describe the dependency between the oxygen and sulphur contents of steel, after treatment and duration of treatment are either exponential or lineal, but both ensure the increasing of the deoxidation and desulphurization process, through increasing treatment duration (τ is in minutes).

3. CONCLUSIONS

The following conclusions can be drawn regarding the deoxidation and desulphurization effect of synthetic slag:

- ❖ the optimal contents of CaO from calcium – aluminate slag is situated between 50 ... 55%, richer in CaO ensuring a better desulphurization of steel;
- ❖ the contents of oxygen and sulphur are decreasing exponentially with increasing of slag quantity, a quantity of solid slag representing 1,5 ... 2 % from steel is optimal, using a bigger quantity is not justified because it raise melting problems;
- ❖ the optimal duration of treatment is 8 ... 10 min., an increasing is not justified because it causes an excessive coldness of liquid steel;
- ❖ the steel treatment with synthetic slag can be considered as the most accessible and safe method to effectively improve the qualities of regular steels, having positive economic effects by reducing the duration of furnace processing and decreasing the ferro-alloy consumption.

REFERENCES

- [1.] I.Dragomir, Teoria proceselor siderurgice, Editura didactică și pedagogică, București, 1985.
- [2.] A.Cubero, J. Molinero, C. Bertrand, Secondary steelmaking synthetic slags for ultra clean steel production, in Proceedings of the 5th International Conference on clean steel, Balatonfured, Ungaria, June 1997, pp. 140-150
- [3.] A. Găvănescu, Effects of synthetic slag steel treatment, in Proceedings of the National Conference on metallurgy and materials science, București, Sept. 2001, pp. 96-101
- [4.] A. Găvănescu, G. Nica, Experiments and results regarding the refining of steel by synthetic slag treatment, in Proceedings – Istrazivanje i razvoj mašinskih elementa i sistema IRMES – Jahorina Sarajevo, Sept. 2002, pp. 409-414





EFFICIENCY OF MAINTENANCE IN STEEL MAKING INDUSTRY

¹⁻³. BADISCHE STHAL ENGINEERING GMBH, GERMANY

⁴. MEMBER OF ROMANIAN SCIENCE AND TECHNIQUE ACADEMY, FACULTY OF ENGINEERING HUNEDOARA, ROMANIA

ABSTRACT:

Efficient maintenance brings efficient energy consumption and efficient environmental work of the steel making equipments. Maintenance is a real partner for profit.

BSE – Badische Stahl Engineering - “Best practice” tools give to the Steel Making Companies, the possibility to know where their “maintenance efficiency” is located compared to others in the industry.

KEYWORDS:

Maintenance; Effectiveness; Efficiency; Best practice; Steel making industry.

1. INTRODUCTION

The steel making industry, steel represent in Romania a very important part of GDP. In this industry branch the crisis appear to be at the final. In August 2010 as compared to August 2009 gross industrial production index increased by 5.7% due to the production increase in electricity, gas, steam and air conditioning supply sector (+8.5%) and in manufacturing (+6.2%). The industrial branches which especially determinate the increases of the manufacturing gross index were: Metallurgy (+27.0%).

Steel production in Romania belongs to the international owners – more than 95 % and the international trend of the steel making industry is also apprehend in Romania.

In steel making industry the volume and the costs of production are very important for a profitable activity. It is important to see the whole picture to make the right decisions and to follow the right strategy. In our conception there are two options:

Focus on direct costs:

- ❖ Limited market
- ❖ Low sales prices
- ❖ Low contribution margin per ton
- ❖ Cost saving (expenditures) is crucial
- ❖ Indirect costs are in this situation not that important because additional output would only increase stock level and bind capital
- ❖ In this case it is possible to increase the risk of delays, while less money is spent for maintenance activities

Focus on indirect costs:

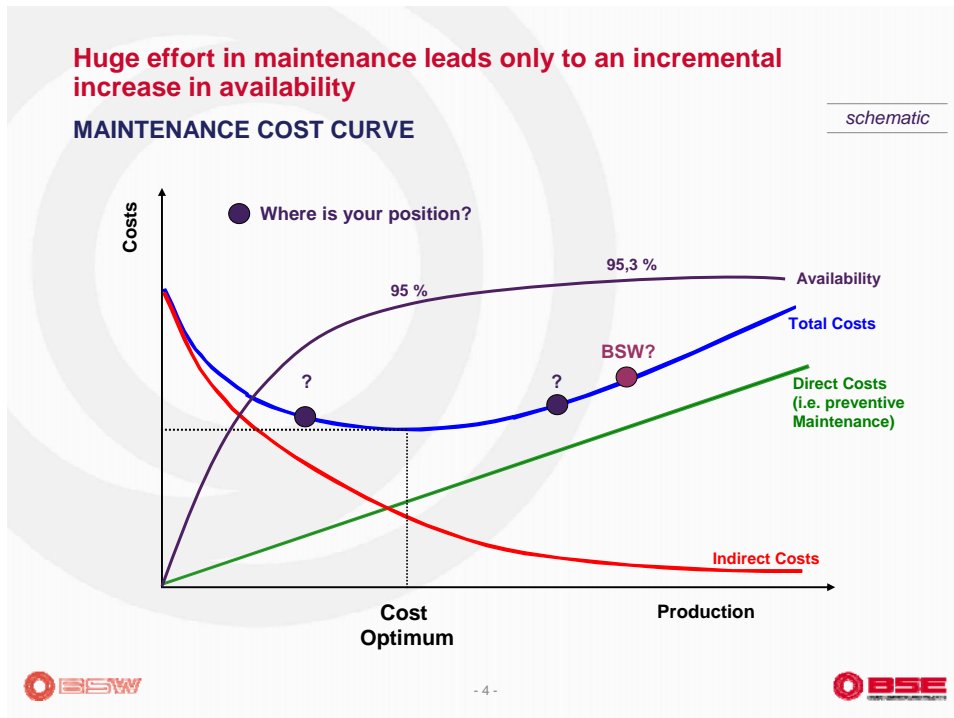
- ❖ Strong market demand
- ❖ Attractive sales prices
- ❖ High contribution margin per ton
- ❖ High availability and operation time required to meet market demand
- ❖ Focus on time, spend more for direct maintenance cost in order to reduce indirect cost
- ❖ Achieved additional contribution margin is higher, than expenditure for maintenance

Maintenance is operational partner for efficiency; especial in Steel making industry, operational should recognize the benefits of working together with maintenance, as a supportive team to reduce unplanned breakdowns, to increase equipment effectiveness, and to reduce overall maintenance costs.

The future capable company has a firm understanding of physical asset management and maintenance process and its important role. It recognizes the contribution of maintenance to total operations' success and profitability. Effective maintenance and physical asset management are closely linked to success and profitability.

The Steel making Companies must analyze and find the most efficient maintenance process.

BSE developed a concept named "Best practice". Best Practice Study covers very important aspects of successful steel operations and the main indicator is "Total operational efficiency". Maintenance efficiency is one of the component, analyze by us in this paper. Maintenance is forever.



2. MCM – MAINTENANCE COST MANAGEMENT

BSW – Badische Stahlwerke GmbH, is one of the most productive Mini Mill in the world; few years before the maintenance cost start to increase continuously, like contra-measure BSW communicate this issue to BSE specialists and after proper researches in the plant come MCM concept. Was analyze all the components of Maintenance costs: Material costs, contractors, own maintenance, etc. Was also analyzing the saving possibilities, risk estimation and major issues concerning maintenance at BSW in a full year (2005).

	Site issues	Results
Integration of production team	<ul style="list-style-type: none"> -Too little integration of production team into maintenance processes -Lower responsibility and less care for equipment by operator -Unconscious handling -Strong wear 	High costs for maintenance and spares parts
Capacity balance	<ul style="list-style-type: none"> -Strong separation between the sectors, although the activities are not that different -The need of employees were counted for each sector -Free capacities between the ranges are not used -Experiences of sectors are not exchanged 	More contracting
Shift work	<ul style="list-style-type: none"> -70 % of the BSW maintenance employees work in the 5-shift-System (112 of 162) -Shift work is primarily risk insurance. -The effectiveness of standard works is smaller. -No comprehensive job planning -Only absolutely necessary work is done, other jobs shifted to dayshift or shutdown day 	More contracting

Results three points to starting from:

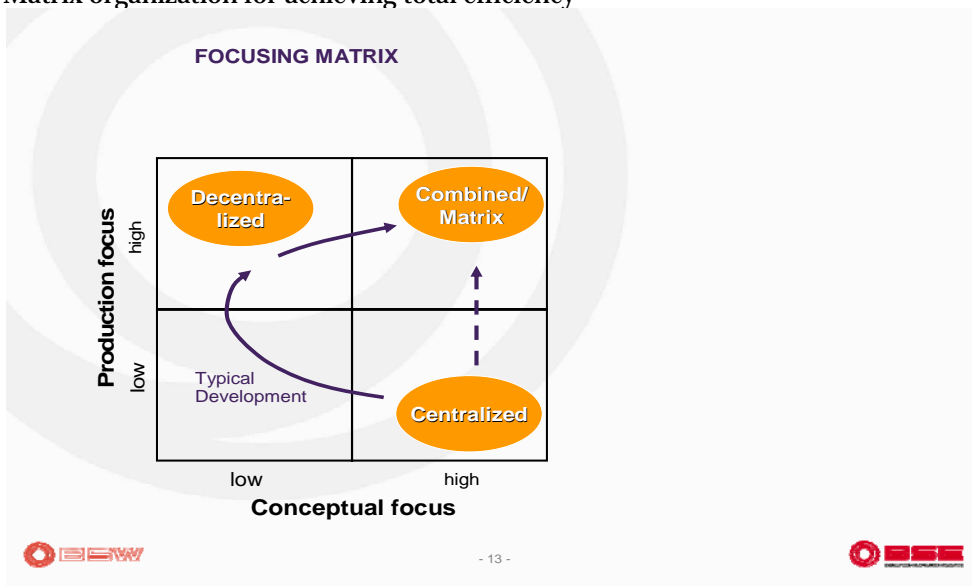
- ❖ Material costs
- ❖ Contractors
- ❖ Own maintenance

Possible solutions of the maintenance optimisation can be represented by side condition for solution:

- ❖ Adapt the maintenance to the changed conditions
- ❖ Engage the production stronger
- ❖ Improve the work scheduling
- ❖ Create capacities in the own maintenance
- ❖ Make a comprehensive common strategy possible
- ❖ Reduce contracting significantly
- ❖ Offer a high work quality and improvement potential with spare part repairs

An optimum maintenance organization must be adapted to the individual situation of a mini mill

- ❖ Centralized maintenance for building up skills and knowledge
- ❖ Decentralized maintenance for pushing productivity
- ❖ Matrix organization for achieving total efficiency



Action plan:

1. Appropriate maintenance strategy to be establish

In general three different maintenance strategies exist

- **Breakdown strategy (run to failure)**
- **Condition based preventive maintenance (exchange after inspection)**
- **Time based preventive maintenance (exchange after fixed period of time)**

Depending on the impact on production, an appropriate strategy needs to be applied, together with other important tools: 5 “S” – House quipping and Continuous improvement concept.

2. Detailed down day planning and appropriate coordination during execution are factors for efficiency

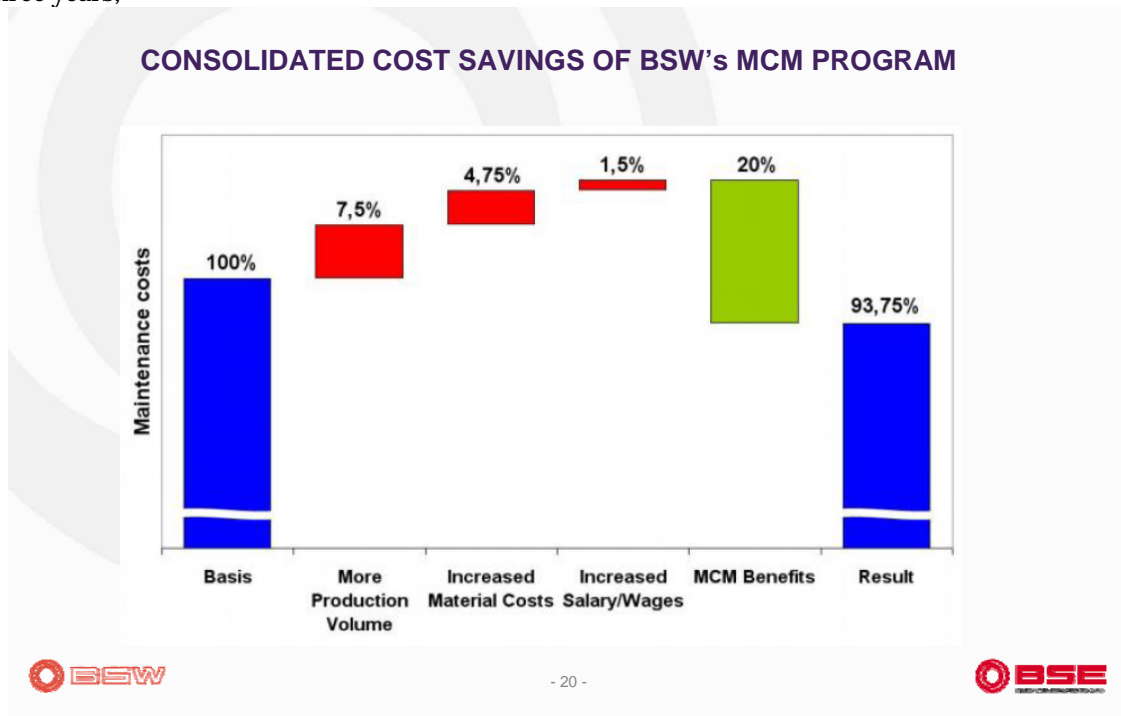
3. A detailed and comprehensive delay reporting is the base for continuous optimization

PROCESS MONITORING – DELAY REPORTING

- Reporting covers the
 - recording of production delays (production loss)
 - recording of equipment problems (no production loss)
- Equipment problems must not be identical with production delays.
- Not every equipment problem causes a production delay.
- Therefore it is important to analyze the combination of production records and maintenance records.
- Production and maintenance reports should be computerized and should use a code system based on a common categorization of equipment. This allows quick evaluation.

3. RESULTS OF MCM

After MCM implementation at BSW, considerable savings could already be realized within three years,



Can maintenance efficiency be measured?

The tool name: “Best practice” was developing by BSE.

The BSE Best Practice Study covers every important aspect of steel making and helps to determine the Company position in the industry.

a). Background Best Practice Study

- The Best Practice Study compares steel plants and rolling mills from all over the world in order to find the best performers, e.g. per region or steel quality.
- It is possible to carry out an overall benchmark, and also to study the details and compare consumption figures or cost on a detailed level (e.g. kWh per ton...).
- Our customers can position themselves within this framework in order to benchmark their performance with the industry and also to identify potentials for future improvement.
- Selected Key Performance Indicators (KPI's) are used for the comparison

b). Holistic approach through four different areas:

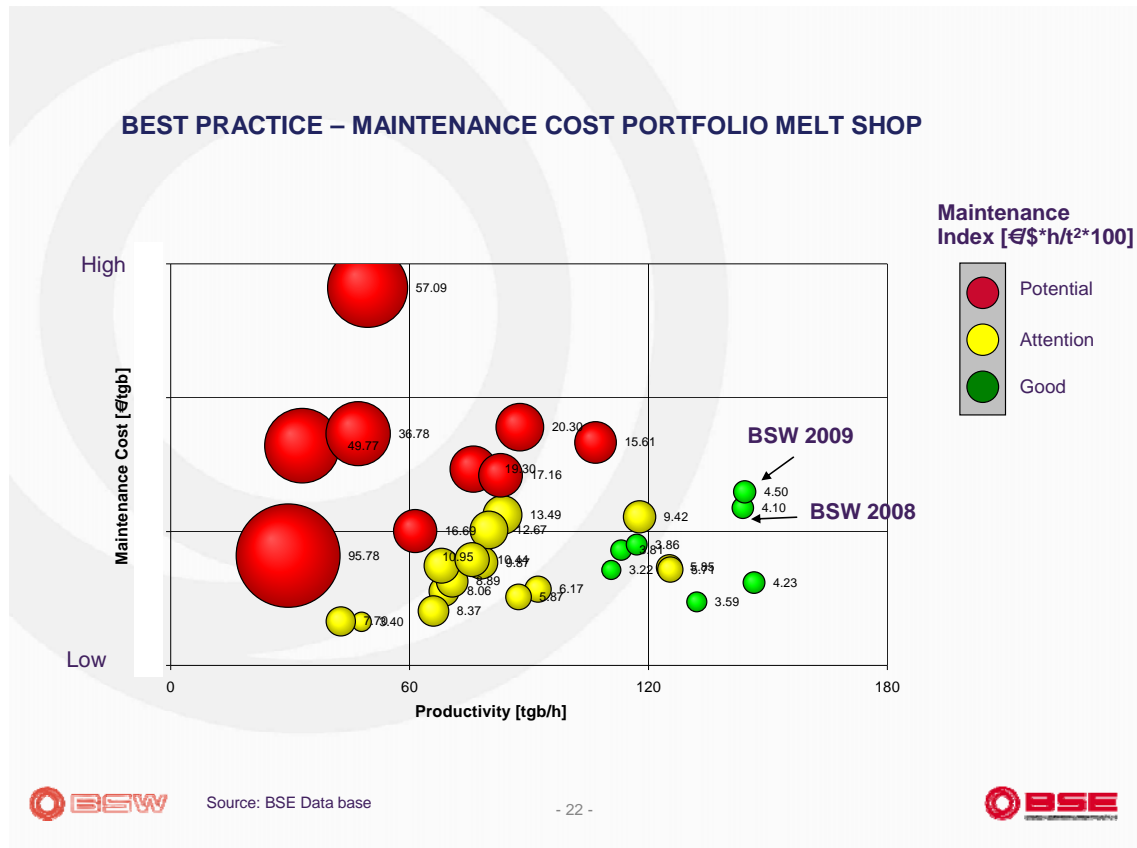
- Productivity Management
- Cost Management
- People Management
- Environmental Management

c). Identification of Best Performers per grade or region

d). Determination of position within industry and identification of potentials for further improvement

In our case, to measure and compare the maintenance efficiency and effectiveness, we try to find a correlation between the maintenance efforts by means of money and the productivity in tones per hour. The size of the bubbles represents the maintenance index itself. Green bubbles are good, red bubbles are bad.

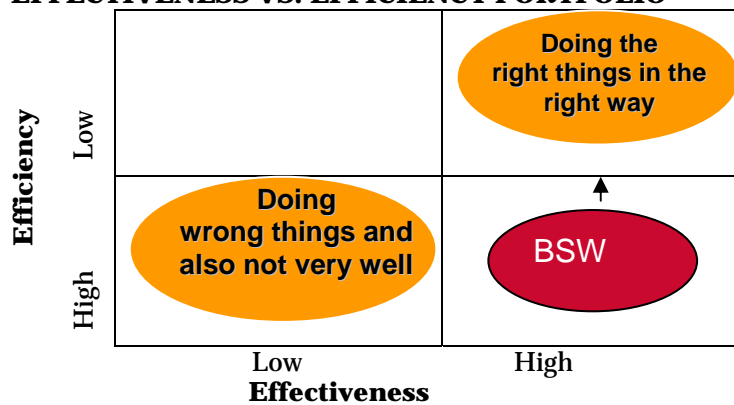
Efficient maintenance is represented by low costs and high output. But high output also allows higher absolute maintenance costs. This graph should give the customer an indication where his own maintenance efficiency is located compared to others in the industry.



4. CONCLUSIONS

Effectiveness comes before efficiency, but the goal is “doing the right things in the right way”

EFFECTIVENESS VS. EFFICIENCY PORTFOLIO



If you want to know where your position in the industry is, you can apply to Best practice, free of charge – “bestpractice@bse-kehl.de”

REFERENCES

1. Reiner Hageman - Efficiency in maintenance - 4” International Mini-Mill symposium “We SEE the future” April 25 to April 28, 2010 in Schluchsee / Germany.
2. *** The future Capable Company – Maintenance Life Cycle Engineering Inc. 2002.
3. BSE – Best practice in the steel industry, framework for Mini Mills - 2010
4. www.bse-kehl.de





¹Iulian RIPOSAN, ²Mihai CHISAMERA, ³Stelian STAN

GRAPHITE NUCLEATION IN GREY CAST IRON – A REVIEW

¹⁻³.POLITEHNICA UNIVERSITY OF BUCHAREST, BUCHAREST, ROMANIA

ABSTRACT:

A three-stage model for the nucleation of graphite in grey irons has been proposed. Stage 1 involves formation of small oxide-based sites (usually less than 2.0 μm) in the melt. Stage 2 involved precipitation of complex (Mn,X)S compounds (usually less than 5.0 μm) nucleated by stage 1 micro-inclusions. Finally in stage 3 graphite nucleates on the sides of the (Mn,X)S compounds which have low crystallographic misfit with graphite. Three groups of elements are important to sustain this sequence for effective graphite nucleation. These are strong deoxidizing elements, such as Al and Zr, to form a high count of very small stage 1 micro-inclusions; Mn and S to sustain MnS type sulphide formation; and inoculating elements which act in the first stage and/or in the second stage of the graphite nucleation sequence. Inoculating elements improve the capability of (Mn,X)S compounds to nucleate graphite. In inoculated irons the (Mn,X)S compounds are more complex. They have a lower Mn/S ratio and higher capability to nucleate graphite, especially when preconditioning/inoculating elements contribute with a high count of effective stage 1 particles.

KEYWORDS:

Grey iron; Graphite nuclei; Graphite nucleation model; Inoculation; Preconditioning; Oxides; Sulphides





¹I. HULKA, ²D. UȚU, ³V.A. ȘERBAN

MICRO-SCALE SLIDING WEAR BEHAVIOR OF HVOF SPRAYED WC-Co(Cr)

¹⁻³DEPARTMENT OF MATERIALS AND WELDING SCIENCE, "POLITEHNICA" UNIVERSITY OF TIMIȘOARA, ROMANIA

ABSTRACT:

The paper presents the investigations of the sliding wear behavior of two different thermal sprayed cermet coatings. WC-Co and WC-CoCr powders were HVOF sprayed on a C45 steel substrate using an ID Cool Flow gun. Scanning electron microscopy (SEM) and X-Ray Diffraction (XRD) were performed in order to investigate the coatings morphology as well as the phase modification achieved through the HVOF spraying process. Tribological tests concerning the sliding wear behavior of the tested materials were performed using the pin-on-disk method.

KEYWORDS: sliding wear behavior, thermal sprayed cermet coatings

1. INTRODUCTION

In industries, mechanical components have to operate under severe conditions such as high load, speed or temperature and hostile chemical environments. Usually, various surface treatments have been used in order to improve the surface characteristics. Such treatments are: ion implantation, laser nitriding alloying, physical vapor and thermal spraying deposition etc [1].

Thermal spray coatings are becoming increasingly used as surface engineering option to resist corrosive and sliding wear and as thermal barriers in many industries [2]. Thermal spraying involves projection of powders particles into a high temperature flame, produced by igniting hydrogen, oxygen and kerosene, where they are melted and accelerated on the substrate surface. The resulted coatings are formed by the immediate solidification of the molten droplets on the substrate surface of lower temperature where they form splats.

High velocity oxygen fuel (HVOF) is a thermal spraying method which allows spraying of coatings with advanced and often unique properties. Therefore the process has been used in numerous advanced applications and has become very popular over the last two decades [3].

One of the great advantages of the HVOF process is the higher velocity reached by the particles and the low temperatures involved which minimizes any potentially damaging effect to the coating and substrate [4].

Wear protection is an important application field of HVOF sprayed coatings. HVOF technology has improved over the years and now provides coatings with better compaction and low chemical decomposition, especially for WC- based cermet coatings [5].

It is known that high velocity oxy-fuel (HVOF) spraying provides superior results than any other thermal spraying technology by manufacturing cermet coatings, because of the gas velocity and lower flame temperature [6]. A cermet is a composite material composed of ceramic and metallic materials which have the optimal properties as high temperature resistance, high hardness and the ability to undergo plastic deformation.

WC- based coatings are deposited not only on originally manufactured components but also on worn areas of used components for repair purpose. The use of WC based thermal spray coatings has been increasing in several areas due to their potentially high erosion and sliding wear resistance.

The present work investigates the sliding wear behavior of the obtained coatings deposited on C45 specimens using an HVOF gun and as feedstock WC-Co 86 14 and WC-CoCr 86 10 4 micro powders.

2. EXPERIMENTAL PROCEDURE

The substrate used in this study was rectangular C45 still plates with dimensions of 50x50mm which were thoroughly sand-blasted with electrocorindon in order to enhance the binding force between the substrate and the deposited coating. After the grinding process the samples were cleaned with acetone.

The feedstock material used in the study were WC based cermet powders, respectively WC-Co 86 14 and WC-CoCr 86 10 4 micro powders.

The morphology of the powder and of the sprayed samples has been characterized by scanning electron microscopy (SEM) and X-Ray diffraction (XRD) using a $\text{Cu-K}\alpha$ radiation.

The sliding wear resistance was determined using the pin-on-disk method by calculating the variation of the wear track depth with the applied load.

The normal load applied of the ball (WC-Co with a 6 mm diameter) was 10 N, relative velocity between the ball and surface was $v = 20$ cm/s, and the testing distance 1000 m (the trajectory was a circle with a radius of 5.4 mm). The relative humidity was 65 %.

3 RESULTS AND DISCUSSIONS

3.1 Coating morphology

The morphology of the used powder is shown in the SEM micrographs from figure 1. The powder particles are spherical having the size between $-45+15$ μm .

Figure 2 and 3 presents the SEM micrographs of the HVOF sprayed coatings at different magnification (x 500 and x 2000). The thickness of the obtained coatings was about 200 μm .

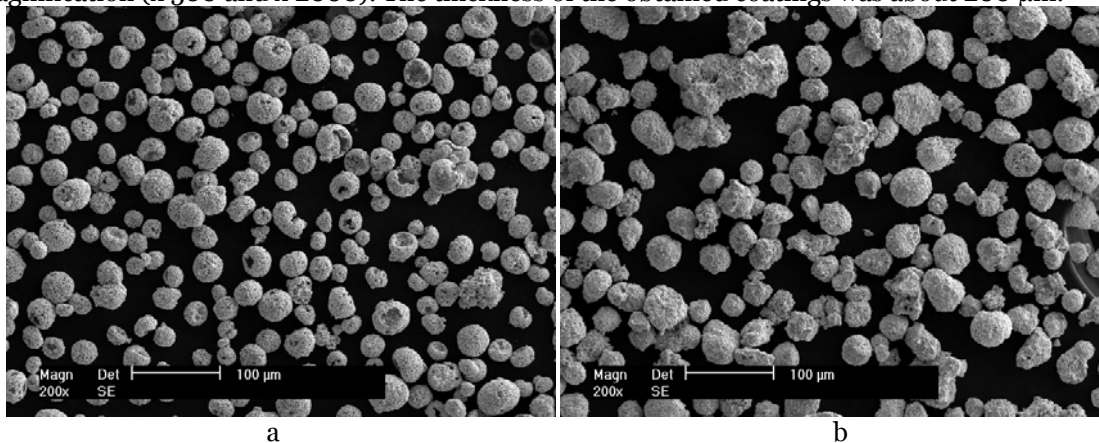


Fig. 1: SEM micrographs of the WC Co (a) and WC CoCr (b) powder

In both cases one may observe a good adhesion between the coating and substrate (Fig.2a and 3a). Comparing the SEM images at higher magnitudes (Fig.2b and 3b) both HVOF sprayed coatings present a certain degree of porosity respectively of internal oxidation.

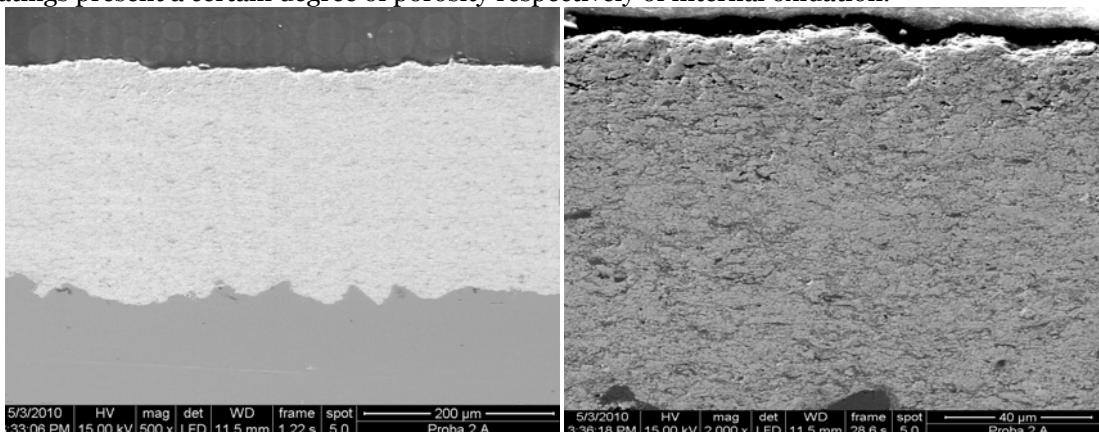


Fig. 2 SEM micrographs of the WC Co coatings

The XRD patterns of the WC-Co(Cr) sprayed coatings are similar, no transformation of the WC-phase into W_2C -phase occurred during the deposition process (figure 4). However one may see a broad signal corresponding to the WC_{1-x} -phase, which indicates a light decarburization of the WC-phase.

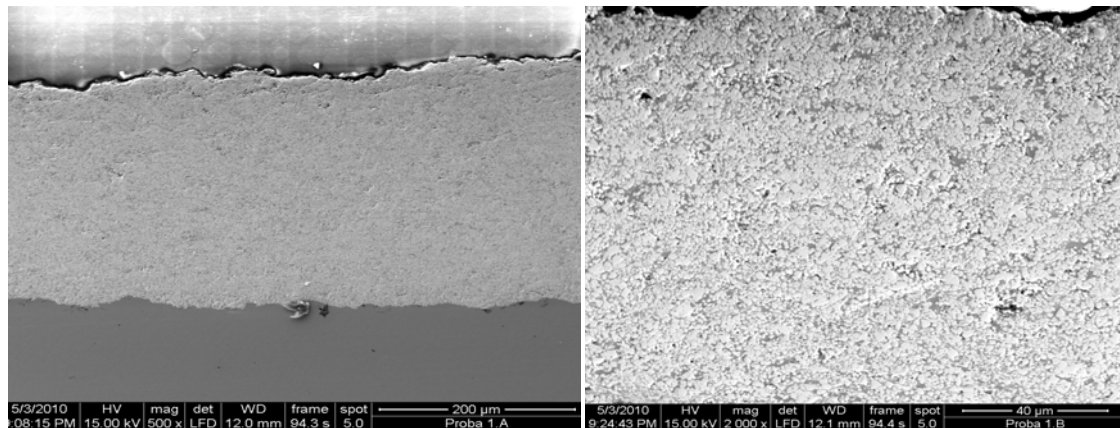


Fig. 3 SEM micrographs of the WC CoCr coatings

The Co- and CoCr-phases corresponding to the metallic matrix were not identified by XRD-measurements due to its low content in the chemical composition.

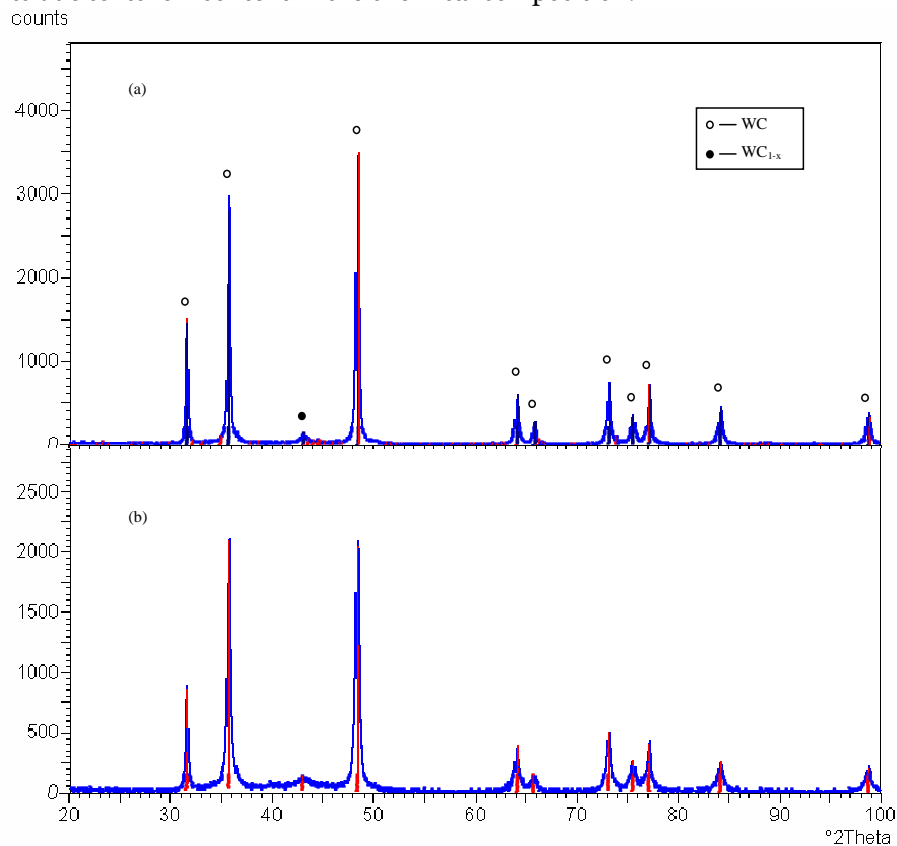


Fig. 4 X-ray diffraction patterns of sprayed coatings (a) WC-Co coating, (b) WC-CoCr coatings

3.2 Wear resistance tests

The pin on disk tests indicated that sliding wear resistance of the deposited coatings was different. The results are summarized in table 1 and the sliding wear rates histograms are shown in figure 5.

Comparing the obtaining result it can be seen that the material loss in case of WC Co was higher in comparison with the WC CoCr coatings. The phenomenon can be explained by the fact that addition of Cr to WC-Co improves binding of the metallic matrix with the WC grains and provides better wear resistant coating.

Table 1 Wear rate of the coatings.

Coating	Wear rate*10 ⁻⁷ [mm ³ /N/m]
WC-Co	51.71
WC-CoCr	39.21

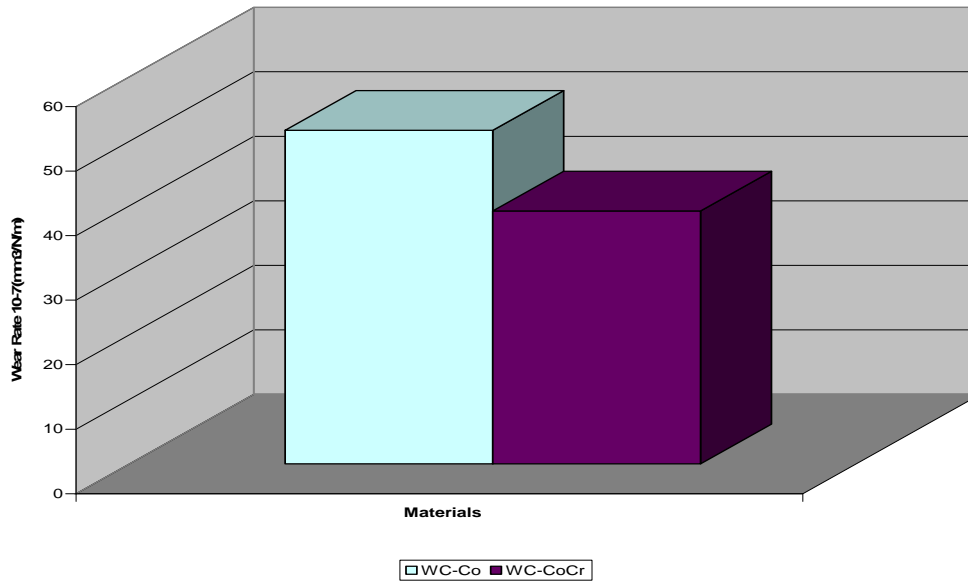


Fig. 5 Sliding wear rates of the tested samples

4. CONCLUSIONS

Different HVOF coatings using WC-Co and WC-CoCr powders have been deposited onto the surface of a C45 steel substrate. The sliding wear resistance of the both coatings was analyzed using the pin on disk method.

Analyzing the obtaining results it was found that WC-Co coating has a higher wear rate in comparison with the WC-CoCr. This phenomenon can be explained by the fact that addition of Cr to WC-Co improves binding of the metallic matrix with the WC grains and provides better wear resistant coating.

In conclusion it can be said that WC-CoCr is considered to be a potential wear resistant coating material as compared to WC-Co coating.

ACKNOWLEDGEMENT

This work was partially supported by the strategic grant POSDRU 2009 project ID 50783 of the Ministry of Labor, Family and Social Protection, Romania, co-financed by the European Social Fund – Investing in People.

REFERENCES

- [1.] Prince M, Gopalakrishnan P, Duraiselvam Muthukannan, More Satish D, Naveen R, Natarajan S. : *Study of Dry Sliding Wear of Plasma Sprayed Mo-Ni/Cr - Ti-6Al-4V Tribo Pair*, European Journal of Scientific Research, ISSN 1450-216X Vol.37 No.1, 2009, pp.41-48;
- [2.] Hodgkiss T, Neville A.: *An analysis of environmental factors affecting corrosion behavior of thermal spray cermet coatings*, Proceedings of the 15th International Thermal Spray Conference, May 2009, Nice, France, pp. 25-29;
- [3.] Klaus E. Schneider, Vladimir Belashchenko, M. Dratwinski, S. Siegmann, Alexander Zagorski: *Thermal Spraying for Power Generation Components*, WILEY-VCH Verlag, GmbH & Co. KGaA, Weinheim, 2006;
- [4.] T. Sudaprasert, P.H. Schipway, D.G. McCartney: *Sliding wear behavior of HVOF sprayed WC-Co coatings deposited with both gas-fuelled and liquid fuelled system*, Wear, Vol. 255, 2003, pp. 943-949;
- [5.] V. A. D. Souza, A. Neville: *Corrosion and synergy in a WC-CoCr HVOF thermal spray coating – understanding their role in erosion-corrosion degradation*, Wear, Vol. 559, pp. 171-190;
- [6.] V.A. Serban, C. Codrean, D. Utu, I. Hulka: *Obtaining of High Performance WC-CoCr CermetCoatings. Alternative Ecological Spraying Methods at Reduced Power Levels*, The 3rd WSEAS International Conference on LANDSCAPE ARCHITECTURE, Timisoara, Romania, October 21-23, 2010;





¹Doina PETRE

THE INFLUENCE OF ELABORATION CONDITIONS UPON THE TENACITY OF SOME ALL PURPOSE STEELS

¹ UNIVERSITY POLITEHNICA OF TIMISOARA, FACULTY OF ENGINEERING FROM HUNEDOARA, ROMANIA

ABSTRACT:

The paper introduces the relationships established between the elaboration conditions (e.i. the chemical composition and the quieting degree) and the level of cold plastic deformation the one part, and the tenacity of some all-purpose steels. The conclusions define the maximum admitted level of deformation in order to preserve an acceptable tenacity of steel, as well as the compulsory content in aluminum left in the steel which can guarantee a minimum level of tenacity.

KEYWORDS:

steel, aluminium, tenacity

1. INTRODUCTION

Since all-purpose steels may be looked for in certain fields and be subject to particular conditions of mechanical shock strains, we did some experiments meant to establish correlations between the chemical composition and the degree of deformation on the one part, and the shock break energy on the other part.

2. EXPERIMENTS

The shock break energy can only be determined on 10mm-side test bars, according to the standards in use. In order to place the notch of the test bar in the least favorable part of the rolled section, respectively in the center, we decided to carry on the experiments on test bars 25 mm long. We considered it important to have the root of the notch in the center of the rolled section, as the central part is most influenced by hardening in the case of round samples deformed between parallel plane surfaces. Structurally, too, the central part is the most segregated one.

In order to establish the influence of the chemical composition and the quieting degree upon tenacity, for steels having a carbon content of up to 0.35%, we tested rolled sections from six steel charges, all of them quieted with silicon, three of them being alloyed with Al (0.027 - 0.05%).

Rolled sections of 35 to 40 mm were turned into samples 25mm diameter, which were subjected to cold plastic deformations.

The tests aimed at determining the dynamic characteristics by shock-bending of U and V-notched test bars.

Since the reference literature mentions as a basic influential factor for steel tenacity the size of the real and inherited austenitic grain, the annealing temperature was 925°C, corresponding to the standard temperature for determining the hereditary austenitic granulation.

After annealing and turning, the samples were kept at room temperature for 72 hours, in order to eliminate all the remnant strains.

The test bars used for determining the shock-break energy were processed to a diameter of 25mm and a length of 60mm, then cold plastic deformed by pressing on 30 kN, 50 kN, 60 kN and 70 kN force generators.

The samples used for shock bending tests were made both of deformed test bars and the blank assay, so that the notch root corresponds to the central area of the rolled section, deformed or not deformed.

The test was performed with a Charpy pendulum hammer, with a direct reading of the break energy in J.

For the identification of the samples and test rods, we established, before the thermal treatment, a marking code based on the steel chemical composition, which was preserved during all tests and which corresponds to a charge and a bar out of which all the samples and test bars with the respective mark have been made. Although the number of tests is reduced by using this procedure, for research purposes it is very efficient, as it eliminates the influence, of temperature, hot deformation, cooling rate after rolling, of area segregation in the ingot, etc.

Table 1 presents the chemical compositions of the charges under analysis.

Table 1. The chemical composition of the charges under analysis

Steel grade	Sample mark	Chemical composition, %								
		C	Mn	Si	P	S	Cr	Ni	Cu	Al
OL321k	1	0.10	0.40	0.25	0.017	0.015	0.05	0.05	0.08	0.005
OL341k	2	0.13	0.34	0.25	0.045	0.014	0.07	0.15	0.30	0.006
OL371k	3	0.17	0.58	0.23	0.042	0.023	0.10	0.07	0.13	0.005
OLC20	4	0.20	0.58	0.34	0.045	0.020	0.16	0.12	0.21	0.030
OLC25	5	0.25	0.70	0.27	0.027	0.016	0.07	0.06	0.09	0.050
OLC30	6	0.33	0.73	0.26	0.040	0.020	0.08	0.06	0.09	0.027

The analysis of the data under question leads to the conclusion that the steels we used belong to the carbon quieted steels, with different contents in aluminum, charges 1-3 with a low aluminum content, which determined a rough austenitic granulation (under 5), and charges 4-6, with a content in aluminum higher than 0.02 %, ensuring a fine austenitic granulation (5-8).

Before the shock break test, we underwent Vickers HV₅ hardness tests, the values obtained on both the blank assay and the deformed samples being given in Table 2.

Table 2. The (HV₅) hardnesses of test rods for shock break tests

Sample mark	% C	HV ₅ hardness				
		Deforming force, x 10 ⁴ N				
		0	30	50	60	70
1	0,10	144	155	151	162	152
2	0,13	146	152	167	-	-
3	0,17	150	158	167	180	174
4	0,20	144	150	165	-	-
5	0,25	152	140	160	178	-
6	0,33	156	158	168	168	-

The table given above presents the results obtained under different deforming forces, for test bars having the same dimensions, namely 25 mm diameter and 60 mm length.

The next table presents the deformation degrees obtained by applying different deforming forces, expressed both by the deformation degree of the section ϵ_s and by the unitary deformation degree ϵ_u .

Table 3. The deformation degree of samples undergoing the shock break test

Sample mark	%C	Deforming force, x 10 ⁴ N							
		30		50		60		70	
		ϵ_s	ϵ_u	ϵ_s	ϵ_u	ϵ_s	ϵ_u	ϵ_s	ϵ_u
1	0,10	3.6	10.5	11.2	21.5	14.5	25.5	18.4	30.0
2	0,13	3.0	9.0	9.7	19.0	-	-	-	-
3	0,17	2.5	7.5	7.9	17.0	11.3	21.6	14.9	26.0
4	0,20	2.6	8.0	7.6	16.5	-	-	-	-
5	0,25	1.4	5.5	6.5	15.1	10.0	20.0	-	-
6	0,33	1.5	5.7	5.5	13.3	9.2	18.7	-	-

The break energy obtained on Charpy V test rods under the pendulum hammer having the energy of 30 daJ is given in table 4.

Table 4. The break energy for the shock bending test

Sample mark	%C	%Al	Compression force, x 10 ⁴ N				
			0	30	50	60	70
1	0,10	0,005	183	22	17	7	10
2	0,13	0,006	138	46	11	-	-
3	0,17	0,005	118	11	9	9	6
4	0,20	0,030	125	135	101	-	-
5	0,25	0,050	127	122	97	97	-
6	0,33	0,027	96	50	98	94	-

It is to be noticed that with shock bending, there is a grouping of the values of the break energy, with respect to the contents in aluminum. Thus:

- ❖ with charges 1 - 3 , where the Al content is 0.005 - 0.006%, the break energy is much below the one in charges 4 - 6 where the Al content is above 0.027%. With charges 1 - 3, the break energy diminishes at a rapid rate even for slight deformation degrees, of 2.5 - 3.0 %, the 15 J brittleness level (accepted for semi-quieted steels) being attained only by the steel with 0.10%C for a deformation of 11%. For the steel with 0.17%C, the brittle fracture is attained even for deformation degrees of 2.5% and for the 0.13%C steel, the deformation should be over 3%;
- ❖ for fine-grained quieted steels, the brittleness level admitted in the reference literature is 29 J and in the case of the steels from charges 4 - 6 , even for deformation degrees of 10 % and contents in carbon of 0.33 % the break energy is above 90 J. With these steels, the decrease in the break energy values is less influenced by the degree of deformation when the content in carbon increases, than in the case of rough austenitic granulation steels.

In order to bring into relief the influence of the connection radius of the notch upon the break energy, we made Charpy U and V test rods out of charge 4. Table 5 presents the comparative results of these tests.

Table 5. Comparative data regarding the values obtained in testing U Charpy and V Charpy tests of the same steel grade

Deformation degree %	Break energy			
	KV J	KU J	KCU J/cm ²	KCU' J/cm ²
0	125	136	170	139
2,6	135	130	163	146
7,6	101	130	163	120

As charge 4 is a steel with fine austenitic granulation, it belongs to the group of high tenacity steels, the values obtained for the break energy ranging within 100 - 136 J, for both the plastic deformed samples and for the non-deformed one.

The break energy of the Charpy V samples show a decrease for the deformation degrees of 7.6 % as compared to the value corresponding to a 2.6% deformation degree, while for the Charpy U samples tenacity is practically maintained at the same level. By comparing the resilience values determined experimentally to those of standard STAS R 10025 - 75 we will find higher real values than those given in table 2 of the above-mentioned standards.

Thus, in order to obtain high tenacities for deformation degrees above 10%, with steels having a carbon content of up to 0.35%, it is compulsory to have an aluminum addition during steel elaboration, so that the rolled sections should preserve an aluminum level of at least 0.025%. In the case of steels with content in aluminum of about 0.005%, the steel is brittle even for low deformation forces, in the range of 3 - 5 %.

3. CONCLUSIONS

- ❖ the break energy for quieted all-purpose construction steels decreases abruptly while cold plastic deforming, the decrease being more accented when the content in carbon is higher. Practically, the quieted steels grade OL 32, OL 34, OL 37 k can not guarantee the tenacity expressed by the break energy of 27J at environment temperature;
- ❖ with steels OL 37 kf, OL 42 kf and OLC 20, OLC 25, OLC 35, with a content in aluminum per product of at least 0.020% the break energy of at least 27J can be guaranteed even for deformation degrees of up to 20 %.

As a conclusion, we suggest as a method of increasing the resistance characteristics by about 30%, the cold plastic deformation by compressing (rolling) to a deformation degree of up to 15%, and if a minimum tenacity level is requested, the steels have to be quieted complementarily, by addition of aluminum, ensuring a minimum aluminum level per product of 0.020 %.

REFERENCES

- [1.] Cazimirovici, E. Teoria deformării plastice, Editura didactică și pedagogică, București, 1981
- [2.] Drăgan, I., Ilca, I., Badea, S., Cazimirovici, E. -Tehnologia de formării plastice, Editura didactică și pedagogică, București, 1979
- [3.] *** Metals Handbook - Proprieties and Selection, Iron and Steel, vol. I ASM, Ohio, 1978
- [4.] Szacinski, A.M., Thompson, P.E. - Comparison of effect on material properties on growth of wrinkles in sheet metal during forming and their removal, Materials Science and Technology, mart. 1991





THE IMPROVEMENT OF RESISTANCE CHARACTERISTICS OF STEELS THROUGH COLD PLASTIC DEFORMATION

¹⁻². UNIVERSITY POLITEHNICA OF TIMISOARA, FACULTY OF ENGINEERING FROM HUNEDOARA, ROMANIA

ABSTRACT:

The application of a pressing along the generatrix for some steel laminates for general use, with diameters between 6-16 mm, leads to ensuring an important improvement of resistance characteristics, especially the flow limit.

KEYWORDS:

plastic, cold, deformation

1. INTRODUCTION

The following paper shows the results obtained through the application of the mentioned procedure as well as the optimum domain of chemical composition and deformation degrees, in order to get an optimum correlation between the resistance and plastic characteristics of steels. Steels which are the main objective of the presented study, are part of the categories of round wire of laminated steel and concrete steel laminated in heat, with chemical composition like steels for general use for construction (less type OL70), quality carbon steels for heat treatments aimed at machines manufacture and concrete laminated steel at heat with periodical or smooth / fine profile

2. EXPERIMENTS

The utilization characteristics of these steels, and especially flow limit (apparent Re_H or technical $Rp_{0,2}$) and tenacity, are influenced by a complex of factors including the chemical composition and deoxidation practices used for elaboration, the regime of temperatures and the deformation degree in lamination, the width of the products.

Regarding the mechanical characteristics of these products the following mentions must be made:

- the contain of carbon through influencing the pearlite/ferrite proportion and the contain of manganese through the alloying effect of ferrite, are the main controlling factors to reach the guaranteed resistance characteristics. The structure modifications that ensure the improvement of resistance characteristics have adverse effect on plastic characteristics
- the majority of products of general use steel are delivered in hot deformation status. Once the width of the product increases – as an effect of temperature increase at the end of lamination and decrease of cooling speed, at the same chemical composition, the wider products have less resistance characteristics than thinner products.

I chose the concrete irons as a first application of the studied procedure because:

- ❖ they are the steels with a contain of carbon within the limits of the theoretical interval;
- ❖ on of the compulsory characteristics at the reception of these steels is floe limit, on which the pressing by generatrix has an absolute influence;
- ❖ they are not very pretentious form a dimensional point of view;
- ❖ can substantially increase sales value if delivered with higher resistance characteristics;
- ❖ the require restrictions for chemical composition, more precisely the limitation of contains of alloying elements (calculus relations for CE), and thus the value of resistance characteristics cannot be influenced through alloying.

For the research regarding the influence of plastic deformation at cold through the application of force on generators over the resistance characteristics of carbon not-alloyed steels, we used wire samples 6 mm diameter, with lengths between 500 and 1500mm. The wire was taken

from the heart of wire in order to avoid the results be influenced by the way of cooling of wire (eventually not uniform) and in order to ensure very similar conditions at trials.

The samples taken on plastic deformation at cold and determination of characteristics, were used as such, without any preliminary pre-work, in order to reproduce very accurately and application of this process directly on industrial products.

The steel charge that were used for quasi-industrial trials have carbon contains between the limits 0,07-0,14%. The chemical composition of the studies charges is shown in table 1.

Table 1. Chemical compositions of experimental charges

Charge	Chemical composition, %								
	C	Mn	Si	S	P	Cr	Ni	Cu	Al
1	0,07	0,32	0,01	0,030	0,016	0,06	0,07	0,07	-
2	0,11	0,50	0,01	0,045	0,020	0,08	0,06	0,12	-
3	0,09	0,53	0,01	0,028	0,016	0,06	0,09	0,12	-
4	0,07	0,34	0,01	0,030	0,018	0,10	0,10	0,15	-
5	0,14	0,53	0,22	0,030	0,017	0,06	0,06	0,09	0,007
6	0,09	0,37	0,22	0,043	0,015	0,08	0,06	0,09	0,006
7	0,08	0,46	0,01	0,040	0,016	0,07	0,10	0,10	-

Six samples were taken out of each charge, out of which one is the etalon sample (E) and the others (1,2,3,4,5) were exposed to cold deformation on generatrix with different deformation degrees. The deformation degree was determined using the following relation $\varepsilon = \frac{d_0 - d}{d_0} \cdot 100$

in which ε represents the degree of deformation [%], d_0 – the initial diameter of the sample, [mm] and d – the final diameter of the sample [mm].

The study undertaken before, using a deformation through pressing on generatrix for steel products with diameters between 6 and 8 mm, showed the fact that it is possible to obtain a significant growth of resistance characteristics and especially flow limit (proportion $R_{p0,2}/R_m=0,70-0,98$) when relatively small degrees of deformation are applied (table 2).

Table 2. Mechanical characteristics of deforming samples

Nr. crt.	Sample	$\varepsilon, \%$	Mechanical characteristics				Increase $R_{p0,2}, \%$	Increase $R_m, \%$	$R_m/R_{p0,2}$	$R_{p0,2}/R_m$
			Z, %	A, %	$R_{p0,2}, N/mm^2$	$R_m, N/mm^2$				
1.A	E.1	-	74,68	23,3	265	353	-	-	1,33	0,75
	1.1	4,92	68,68	20,5	310	385	16,98	8,96	1,24	0,80
	2.1	18,03	60,89	14,4	440	455	66,03	25,76	1,03	0,96
	3.1	26,23	64,69	15,8	482	493	81,88	39,20	1,02	0,97
	4.1	29,51	65,60	14,8	507	520	91,32	46,76	1,02	0,98
	5.1	34,43	56,54	10,7	528	537	99,24	51,52	1,01	0,99

The aim was to experiment the same procedure on industrial products with bigger diameters.

In order to do this, samples were taken from steels out of the current production, from steel charges with different chemical compositions and different dimensions of the laminated products.

The samples had lengths between 500-1500 mm. the samples used for trials were collected so that the results of the application of deformation not to be influenced by the cooling way and in order to ensure initial conditions as similar as possible.

The samples exposed to plastic cold deformations and determinations of characteristics were used as such, without any preliminary influence, in order to obtain a very accurate reproduction of this procedure directly on industrial products.

After cold deformation on generatrix, from each charge, some samples were taken in order to determine the mechanical characteristics. Samples were debited at 150mm, according to the prescriptions.

The steel charges that were used for the second set of trials have carbon contains between the limits 0.07-0.22%.

After an analysis of the presented data, it comes out that like in the case of wider industrial products, the effect of plastic deformation by pressing on generatrix shows especially on flow limit that registers the higher growth rates till deformation degrees of aprox. 30%, after which the growth rate of, flow limit decreases.

The conclusions that can be drowned from the analysis of the presented data, are:

- ❖ the plastic cold deformation process by pressing on generatrix applied to industrial products of wire with medium diameter between 6-8 mm and laminated products with width between 12-

25 mm, made of steels with less carbon contain, are applied without any difficulty, steels presenting a weak resistance to deformation

- ❖ the influence on resistance characteristics is very strong starting even from low deformation degrees (aprox. 12%)
- ❖ the growth rate of resistance characteristics is high, till deformation degree of cca. 30%, after which the continuing application of deformation on generators does not lead anymore to high growth of resistance.
- ❖ the biggest influence is on flow limit, that registers substantial increases, reaching values similar to those of resistance to breaking for the same type of steels.
- ❖ the proportion $R_{p0,2}/R_m$ increases very much, which constitutes a criteria for determination of steel quality for concrete, which reaches values of cca. 0.99.

In order to set up the technological conditions of the plastic deformation by pressing on generatrix, the data obtained from the experiment in the lab and industrial trials was studied. The analysis of data was based on statistical-mathematical methods, using specific calculus programs.

In order to obtain the correlation between the technological factors that influence the plastic deformation, more precisely the chemical composition of steel and the deformation degree applied, the MATLAB program was used.

We considered 48 sets of data that include the chemical composition of steel, the value of the proportion C/Mn, the value of the reduction degree, applied, as well as determined values flow limit, resistance to breaking, and the calculated value for the proportion $R_{p0,2}/R_m$.

For each correlation the medium values of the parameters, the correlation coefficient, standard exception from the regression area, and the values of the stationary point (minimum, maximum or medium) are presented. In the following lines, based on the analyzed data, the variation areas obtained and the diagrams of level curves, one can set the technological conditions, respectively the chemical composition and deformation degree which leads to the best correlation with the mechanical characteristics of resistance of the deformed products.

During the experiments it was observed that the substantial influence of the deformation by pression on generatrix process is on flow limit that registers very high growth at relatively low deformation degrees. Therefore, in the following lines we present the variation areas of flow limit $R_{p0,2}$, as well as the variations of the proportion $R_{p0,2}/R_m$, function of independent parameters mentioned before.

The analyzed data are $R_{p0,2}$ like an dependent parameter and C, C/Mn, ϵ like independent parameters .

The variation limits of the variables are:

$$C_{\min} = 0,07\% - C_{\max} = 0,22 \%; (C/Mn)_{\min} = 0,17 - (C/Mn)_{\max} = 0,35; \epsilon_{\min} = 0 - \epsilon_{\max} = 38\%;$$

$$R_{p0,2\min} = 255 - R_{p0,2\max} = 623$$

The equation of the hiper-surface of regression is:

$$R_{p0,2} = 5064 * C^2 - 5295 * (C/Mn)^2 - 0,1725 * \epsilon^2 - 5595 * C * C/Mn - 1,945 * C/Mn * \epsilon + 5,866 * \epsilon * C + 3274 * C + 3606 * C/Mn + 13,75 * \epsilon \quad (1)$$

The correlation coefficient for this hypersurface is $r=0,98$, standard exemption from the regression surface is $s=21,13$, and the coordinated of the maximum point are; $C = 0,2319$; $C/Mn = 0,2103$; $\epsilon = 42,62$; $R_{p0,2} = 649,5$.

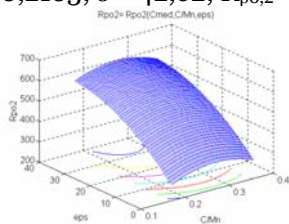


Figure 1. The $R_{p0,2} = R_{p0,2}(C_{med}, C/Mn, \epsilon)$ distribution and level curves

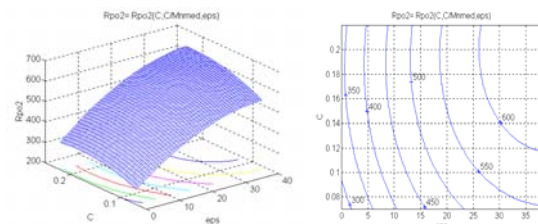


Figure 2. The $R_{p0,2} = R_{p0,2}(C, C/Mn_{med}, \epsilon)$ distribution and level curves

Due to the fact that these hypersurfaces cannot be represented in a tridimensional space, I chose the successive replacement of an independent variable with its medium value, getting to surfaces that can be represented in the tridimensional space and can be interpreted from the technological point of view.

Therefore, we obtain the surfaces that are the object of the following study. Associated to the surfaces we have the level curves for each value of the presented characteristics. Based on these analyses, one can set the maximum level of deformation by pressing on generatrix, that can ensure simultaneously with the increase of resistance of steels and a convenient behavior while processed.

The influence of chemical composition and degree of deformation over the flow limit is highlighted through the regression surface represented by the equation:

$$R_{p0,2} = - 5295 * (C/Mn)^2 - 0,1725 * \varepsilon^2 - 1,945 * C/Mn * \varepsilon + 2858 * C/Mn + 14,54 * \varepsilon - 55,1 \text{ (for } C=C_{med} \text{)} \quad (2)$$

The dependency between the value of flow limit, value C/Mn and the degree of reduction if a constant carbon contain and equal with the medium level on charge is considered, presented by figures 1.a and 1.b is the normal one, technological, in the sense that its value increases continuously with the increase of C/Mn and E, on one hand due to the hardness effect of the two elements and on the other, due to hardness induced by the increasing reduction degrees.

3. CONCLUSIONS

The undertaken analysis through mathematical methods of the obtained data, under the conditions of a plastic deformation at cold on generators, with deformation by pressing on generatrix degrees varying between 2- 40%, highlights the fact that in order to obtain increase of resistance, which would not affect the behavior during processing of steels, one must consider a series of measures such as:

- ❖ the carbon contain must be kept under 0,25%, and Mn contain must be kept at the technological limit necessary for carbon not-alloyed steels, respectively under 0,8%.
- ❖ the proportion C/Mn must be kept within the interval 0,2-0,3, so that the value of the flow limit and the proportion $R_{p0,2}/R_m$ can be maintained within the technologically admitted limits.
- ❖ the data shown before highlight the fact that the described process can be applied without any problems directly on industrial products, without a preliminary preparation, getting to important increases of the resistance characteristics.

REFERENCES

- [1.] Petre Doina Elena- Metode de crestere a capacitatii de rezistenta a laminatelor din otel prin modificari microstructurale- Teza de doctorat, Timisoara 2002
- [2.] Dieter, E.G. -Metalurgie mecanica, Editura Tehnica, Bucuresti, 1970





¹Miron BUZDUGA, ²Adriana COMȘA, ³Radu BUZDUGA

RESEARCH IN ORDER TO OBTAIN SPECIAL FIRE BRICK PRODUCTS

¹⁻³FIRE BRIKS RESEARCH, DESIGNING, AND PRODUCTION CENTER, SC CCPPR SA ALBA IULIA, ROMANIA

ABSTRACT:

The purpose of the present paper was obtaining special fire brick products for the metallurgy industry, through a forming and casting method without using clay binder. The laboratory trials have led to finding some compositions used to fire brick products of superior quality from superaluminum chamotte (with over 85 % Al_2O_3) and tabular alumina (with about 98,5 % Al_2O_3).

KEYWORDS:

fire brick products, metallurgy

1. INTRODUCTION

The present theme has imposed itself due to the development and modernizing technologies in ferrous metallurgy and metallurgy in general led to extremely severe demandings on fire brick products used in various equipments and aggregates.

For silicon-aluminum fire brick products (the system SiO_2 - Al_2O_3) the condition for quality increase has meant obtaining products with a high alumina (Al_2O_3).

Initially the silico-aluminum refractory products were made from refractory clay, natural silicates of alumina, with a maximum percentage of 38-40% Al_2O_3 . Later on, there have been made aluminum refractory products with a content of 45-60 % Al_2O_3 , refractory products with 60-75% Al_2O_3 , mullitico-corrundum products with 75-90 % Al_2O_3 and corrundum products with 90-95 % Al_2O_3 . The path to follow was to ennoble the chamottes from refractory clay with incinerated alumina, with higher and higher proportions, together with the alteration of burning parameters (temperature, time etc.). In all the cases though, although the chamotte increased in quality, the binder used in forming remained the same refractory clay, natural raw material with impurities, which did not allow the increasing of Al_2O_3 content in the final product over a certain limit.

To achieve this goal SC CCPPR SA Alba Iulia has studied, produced and patented (BI A/00491), a chemical binder to provide a good binding of the refractory material, but, at the same time, as low as possible impurification of the refractory matrix with foreign, potentially damaging ions.

As testing products in industrial conditions we have chosen the following:

- ❖ special masonry products from the bottom of the casting ladle – ensemble of bubbling inert gases,
- ❖ tubes for the distribution of cast iron in shapes and shells,
- ❖ special holders for the electric resistances of the treatment furnaces,
- ❖ briks and burner bloks for metallurgic industry etc.

2. PRELIMINARY LABORATORY WORK

The raw materials used were high purity tabular alumina and super-alumina chamotte, available on the market. Their properties are presented in Table 1.

The binder used was the one produced by SC CCPPR SA, with the technical characteristics presented in Figure 2.

Tabel 1

Characteristics	Chamotte S68 A	Tabular alumina
Chemical composition :		
Al ₂ O ₃ ,min, %	99.65	70.04
Fe ₂ O ₃ ,max, %	0.04	0.98
Granulometric spectrum		
Residue on the 3,2 mm screen , %	1	
Residue on the 2,5 mm screen, %	14	
Residue on the 1,25 mm screen, %	56	
Residue in the 0,50 mm screen, %	13	
Residue on the 0,50 mm screen, %	16	100

Table 2

Characteristics	Chemical binder
pH	2,5
Density, g/cm ³	1,25

The strenghtner used was magnesium oxide with 98% MgO, chemically detected.

Based on these raw material we made slurries from super-aluminnum chamotte, and, separately, from tabular alumina.

The procedure we used was identical, in both cases, the difference was only in the percentage of solid and liquid materials we used in the production recipe.

2.1. Preparing slurry from aluminum chamotte

There have been prepared two different granulometric recipes to determine the optimum type of packing the chamotte and tabulat alimina in order to get the best omogenity of the casting material, and implicitly the best physico-mechanical characteristics of the end product.

The recipes are as follows, in tables 3 and 4.

Table 3

Receipe	Chamotte SA68A 0-3,2 mm granulation, %	Chamotte SA68A under 0,06 mm granulation, %
R1	55	45
R2	50	50

Table 4

Ingredients	R3	R4
Tabular alumina 8-14	35	
Tabular alumina 14-28	10	
Tabular alumina -325	55	100

The dosage of the ingredients has been gravimetric for the solid materials, and volumetric for the binding solution.

The following recipes have been used:

Table 4

Ingredients	R1	R2	R3	R4
Granulated SA68A chamotte, %	x	y		
Fine SA68A chamotte, %	x	y		
Tabular alumina in granules			z	
Intermediate tabular alumina			z	
Fine tabular alumina			z	w
Chemical binder	x	y	z	w
Strenghtener	x	y	z	w

The casting mix has been prepared in a 10 l ladle with an agitating device with propeller. The order of the preparing steps was as follows:

1. We put the binding solution into the agitating ladle.
2. As wvestarted the agitator the refractory unit, with fine granulation, then the granulated one have been introduced, stirring for about 3 min.
3. After mixing the refractory unit with the binder, the strenghetner has been added, constantly stirring, until the best mix of the casting mass.

4. After the agitator was stopped the slurry was casted in cube shapes, with 80 mm angle sides, and cylinders with 50 mm diameter and 50 mm high.
5. After about 80-90 min. the material was solid enough to allow decasing and manipulation in safe conditions for the test pieces which have been dried and sintered, and physico-mechanically tested.

Without being able to establish precise relationships over various factors, we could see that the coagulation interval, and, respectively of paste hardening within the shapes, is influenced by:

- External parameters:

- ✓ Temperature of the environment
- ✓ Mixing time
- ✓ Agitator speed.

- Internal parameters:

- ✓ Solid material granulation, chiefly the specific contact surface between the solid and the liquid binder.
- ✓ Liquid (binder) concentration and quantity in the mass.

2.2. Characterization of produced compositions

From the casting paste – slurries, cubic test pieces, with 80 mm angle sides, and cylindrical ones, with 50 mm diameter there have been cast.

To shape the test pieces, the shapes have been set on a vibrating table and filled with casting slurry. The vibration carried on during the filling with material, and 60 more seconds after that. Then the shapes have been transferred on a fixed table and let still, so that the material got harden.

After hardening inside the shapes, which took from a few minutes to two hours, depending on the recipe, preparation conditions and environmental factors, the products have been decased and let to dry for 24 hours. After that they have been introduced in the drying stove, at 120°C for another 8 hours.

In all the cases, the dried products have been introduced in the chamber furnace of S.C.CCPR S.A. Alba Iulia on a burning diagram for refractory products of 60A type, for 24 hours at maximum temperature of 1520 - 1550°C.

When out of the furnace the tests have been submitted to various laboratory tests, to determine their quality.

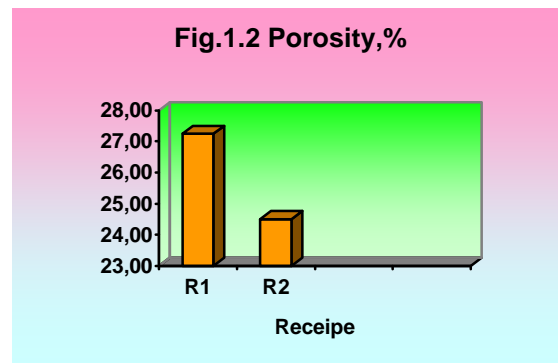
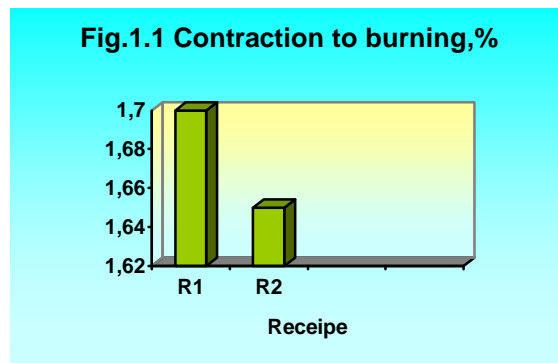
2.3. Characterization of produced compositions

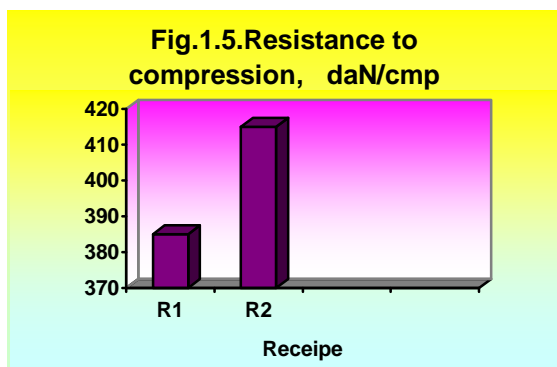
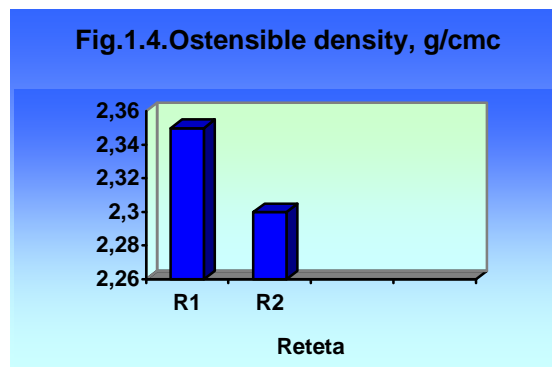
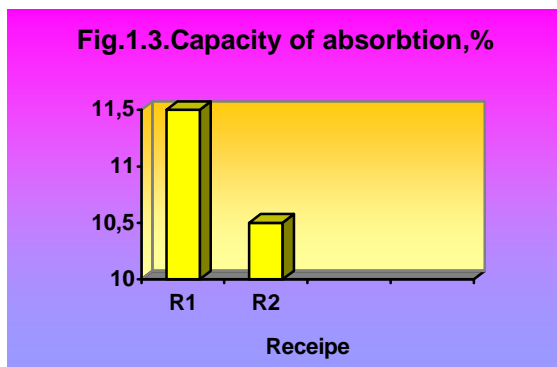
2.3.1. Characterization of compositions from aluminum chamotte

Determinations of porosity and resistance to compression have been performed on the two recipes of slurry from aluminum chamotte SA68A, with different solid granulation. There have also been performed measurements of contraction (after burning) to better appreciate the degree of compacting of products after sintering. The results are as follows, in table 5 and in fig.1-5

Table 5

Determination	Recipe 1	Recipe 2
Contraction, %	1,5-2,2 average 1,7%	1,2-2,1 average 1,65
Ostensible porosity, %	26,5-28	24-25
Absorbion capacity, %	11,0-12,0	10-11
Ostensible density, g/cm ³	2,35	2,30
Resistance to compression, daN/cm ²	343-415 average 385	400-420 average 415





We can see from the results that the two recipes have quite similar final characteristics, with a compaction slightly better for recipe 2, (with finer granulation), which means that both recipes might be used, depending on the dimensions of the pieces we need to produce.

Otherwise, we need to consider the thermo-mechanical and thermo-chemical characteristics of the products for metallurgic industry. Those can be determinantly influenced by the granulation of the refractory material, regardless of its binding manner.

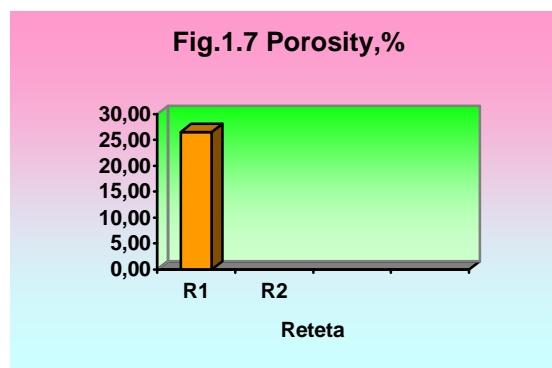
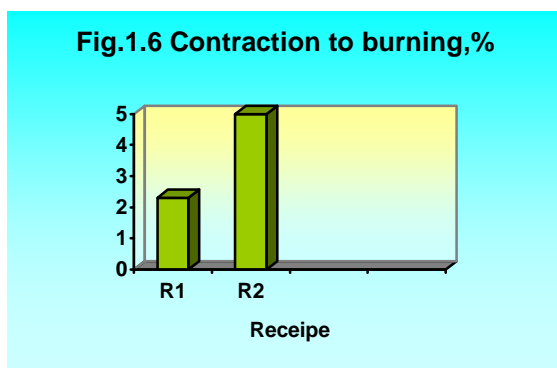
Anyhow, the basic physico-mechanical properties (porosity, resistance to compression, etc.) do not differ from the properties of classical products, shaped by pressing, with clay binder.

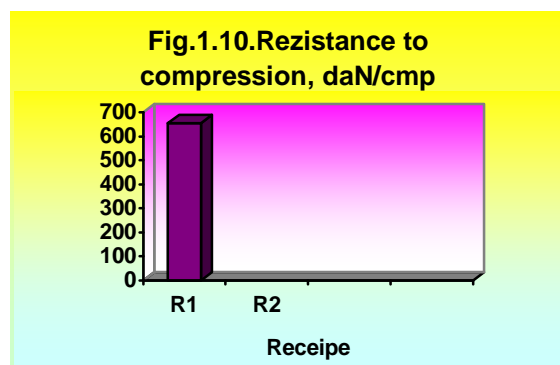
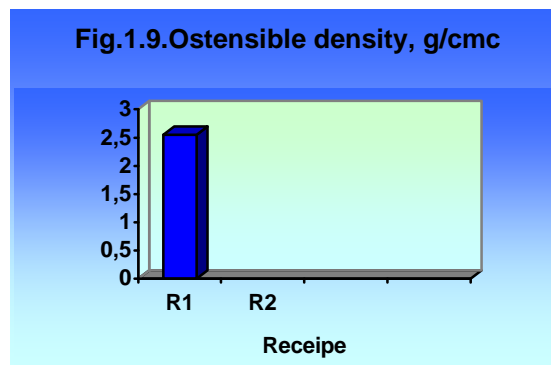
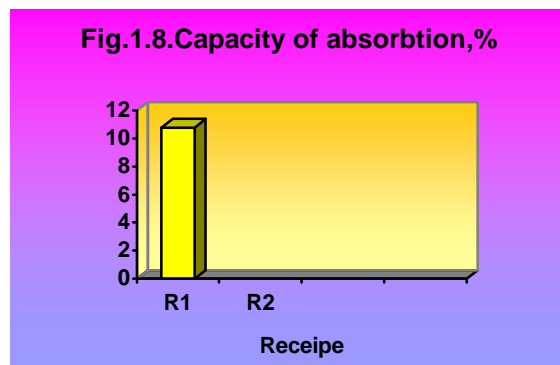
2.3.2. Characterization of compositions from tabular alumina

The results of determinations of contraction to burning, ostensible density, absorption, ostensible porosity and resistance to compression are shown in table 6.

Table 6

Determination	Recipe 3	Recipe 4
Contraction, %	1,9-2,6 average 2,3	4,0-5,8 average 5,0
Ostensible porosity, %	23-28 average 26,5	-
Absorption capacity, %	8,2-11,8 average 10,8	-
Ostensible density, g/cm ³	2,41-2,82 average 2,55	-
Resistance to compression, daN/cm ²	650-666 average 655	-





For the tests in the recipe with 100% fine tabular alumina we did not perform any characteristic determination, because the contractions after burning were much to high, both in their absolute value and variation interval, which led to the conclusion that from this kind of casting paste we can not get refractory products within the dimensional allowed tolerance for metallurgic industry.

The tests from the first recipe, with different tabular alumina granulations have presented acceptable values so that we could recommend their use in various industrial areas of metalurgy.

Considering the results, the laboratory work have proven that there is the possibility of producing cast refractory products without using clay binder in metallurgic industry, products that are able to meet quality requirements for different purposes.

REFERENCES / BIBLIOGRAPHY

- [1.] Goleanu, M. Buzduga, N. Constantin, A. Comsa, M. Butu Effects of Additives on the Sintering Process of Al₂O₃-based Ceramic Materials 2nd International Congress on Ceramics, Verona, 29 iun-4 iul 2008-3-P-38
- [2.] Aurica Goleanu, Miron Buzduga, Adriana Comsa, Radu Buzduga Design of cordierite-mullite refractory material by using recycling grog International Conference B.EN.A - Management and sustainable Marine Development, iul 2008
- [3.] Heput Teodor. Buzduga Miron, Maksay Ștefan, Osaci Mihaela Study on the syntetic flux viscosity used at the continuous casting 11 International Research/Expert Conference Trend in the Development of Machinery and Associated Technologies, TMT 2007, Hammamet, Tunisia ISBN 9958-617-30-7
- [4.] Ștefan Mircea Utilajul și tehnologia produselor refractare și abrazive, Ed. Didactică și Pedagogică - București - 1980
- [5.] I. Teoreanu; N. Ciocea Lianți, mase și betoane refractare, Ed. Tehnică - București - 1977
- [6.] I. Teoreanu și colab Bazele fizico-chimice ale întăririi lianților anorganici, Ed. Didactică și Pedagogică - București - 1972
- [7.] H.C. Emblem, J.R. Walters Barbotină gelificabilă - Patent nr. 1546208/23.05.1979-Zirconal Processes Ltd. - Anglia



¹: Adriana COMȘA, ²: Miron BUZDUGA, ³: Radu BUZDUGA

MONOLITIC FIRE BRICK PRODUCTS

¹⁻³: FIRE BRIKS RESEARCH, DESIGNING, AND PRODUCTION CENTER, SC CCPPR SA ALBA IULIA, ROMANIA

ABSTRACT:

The paper comprises data regarding the monolithic fire brick products, the main characteristics of LCC and ULCC concretes, as well as the influence of certain additives on these characteristics and the advantages of using these concretes in metallurgy.

KEYWORDS:

fire brick products, concretes, additives, metallurgy

1. INTRODUCTION

Classification of refractory concretes according to ISO/DIS 1927-1:2008 is as follows presented (Figure 1).

Concluding the above, the content of cement in these concretes is presented in Figure 2.

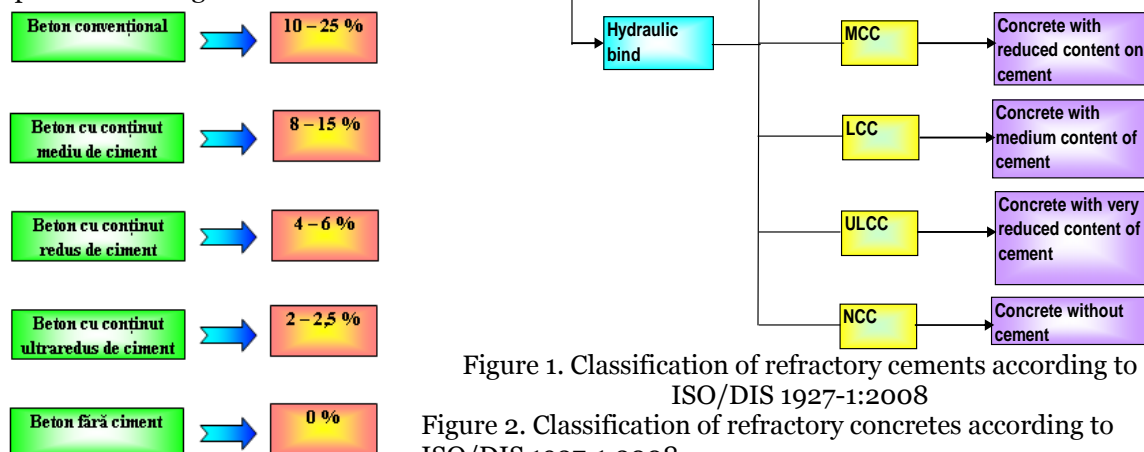


Figure 1. Classification of refractory cements according to ISO/DIS 1927-1:2008

Figure 2. Classification of refractory concretes according to ISO/DIS 1927-1:2008

1.1. Concretes with low and very low content of cement

In Romania, although the low cement concretes have been studied even since 1980, those have not been used in mass production. That is due to the fact that low cement concretes are more demanding and sensitive on first heating.

The production of low cement refractory concretes is based on using additives with advanced grinding gauge, due to the fact that in a casting mix, the density obtained with a classic granulometric distribution is limited to the hollows between the grains, which are filled with excess water during processing.

In figure 3 there is a graphic representation of the dependency of calcium oxide of the cement content, both for an ordinary concrete, and for a reduced cement one.

In Figure 4 there is a graphic representation of the compression resistance on the temperature. As it can be well seen, for an intermediate temperature (800 - 1000°C) the mechanical resistance of ordinary concretes is much lower than that of low cement concretes.

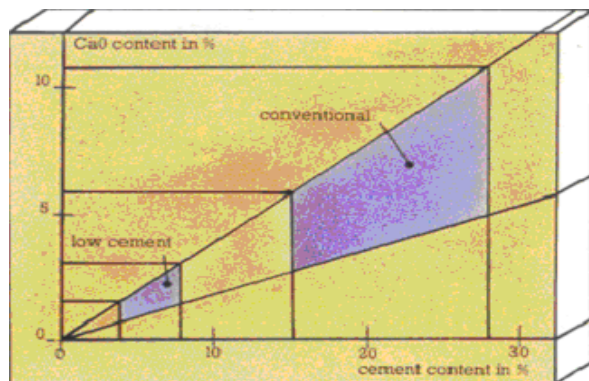


Figure 3. Dependency of CaO on the cement content

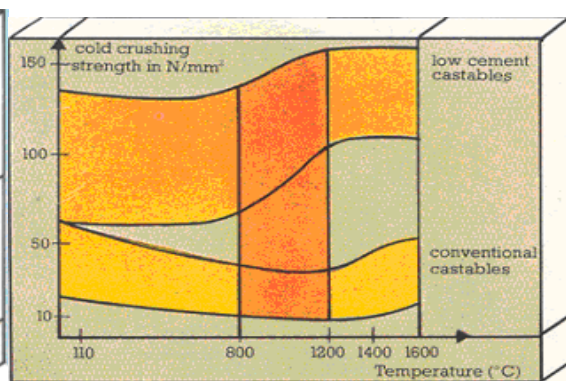


Figure 4. Dependency of temperature resistance on the temperature

The main feature that isolates concretes with low and very low content of hydraulic binder from other types of cement is the presence of very fine components. This very fine material replaces part of the cement content in the conventional concrete.

In table no.1.1 we present the influence of LCC concrete properties varying with its components.

Table 1.

Components of LCC	Properties influence
Refractory aggregate	Capacity of absorption, ostensible density, thermal conductivity, range of temperature of utilization
Super aluminum cement	Rheological properties – capacity of processing by casting, vibration, flowing, mechanical resistance
Dispersing agents	The tixotropy of the mixture
Reactive oxides (Al_2O_3 , SiO_2 , MgO , Cr_2O_3 , TiO_2)	Flowing, volumic stability, ostensible density, resistance to abrasion
Granulometric distribution Relation between grains >1 mm and fine fraction <1 mm	The work: - torcretation – adherence - casting – homogenous flow Homogenous structure

The production of concretes with low content of hydraulic binder is made by casting – vibration, either within the shapes, thus resulting in prefabs, or directly, at the very place used by the beneficiary, using encasements after that being treated until the maximum temperature, following a diagram, according to the quality of the concrete.

1.2. The main characteristics of LCC and ULCC refractory concretes

The classical concretes are generally characterized by the content of Al_2O_3 , which reflects both their refractivity and other physical properties. Regarding the concrete with low content of cement (LCC) and very low content of cement (ULCC) the content of Al_2O_3 is no longer enough for this characterization, other oxides (with smaller percentage of participation) having a great influence on the physico-chemical characteristics.

In table 2 the main oxides in LCC and ULCC concretes are presented, compared to a classical concrete, with the same content of Al_2O_3 and tabular alumina aggregate.

Table 2.

The main oxides	Classical concretes	Concrete with low cement	Concrete with very low cement
The aggregate	Tabular alumina	Tabular alumina	Tabular alumina
Al_2O_3 , %	90	90	88
CaO, %	5	1,1	0,3
SiO_2 , %	2,8	4,0	7,5
Fe_2O_3 , %	1,0	0,15	0,1

The high content of SiO_2 of LCC and ULCC concretes comes, in this case, from the ultrafine powders. In case of using other aggregates (chamotte, bauxite etc.) the content of SiO_2 can be higher to Al_2O_3 content's detriment.

Through the dosage of ultrafine powders an optimum percentage of SiO_2 , can be achieved, which is important because the bending resistance at temperature and the softening temperature of

LCC and ULCC concretes depend of the percentage of anortit formed with calcium aluminates at 1350°C (Figure 5), and the one of ULCC depends on the content of mulit formed with Al₂O₃ at 1300°C (Figure 6).

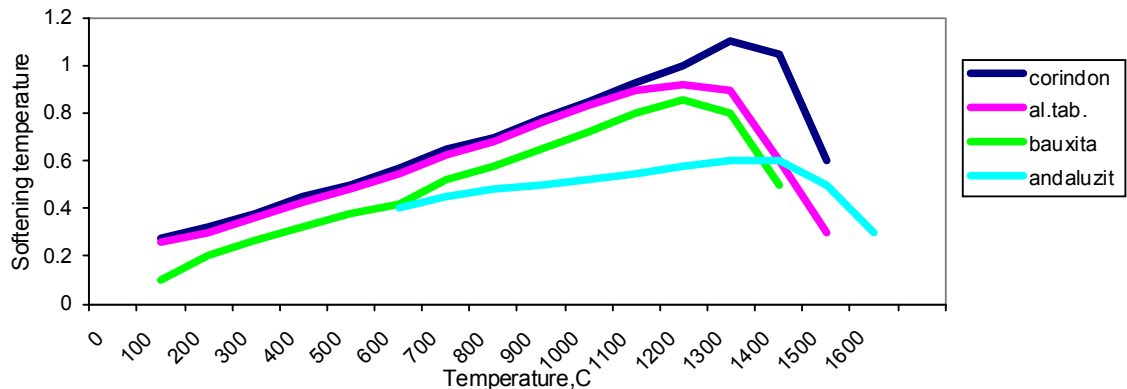


Figure 5. Softening temperature of burned LCC concrete, with various aggregates: 1 – corindon, 2 – 2 tabular alumina, 3 – bauxite, 4 – andalusite

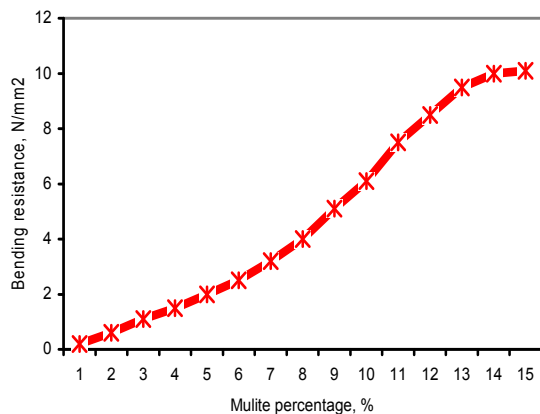


Figure 6. Influence of mulite percentage on the bending resistance at 1500°C of burned ULCC concretes

The ratios of CaO and Fe₂O₃ coming from cement, respectively the impurities of the aggregate, influence the bending resistance and corosion resistance of concretes. Due to the small percentage of CaO and Fe₂O₃, LCC and ULCC concretes have, compared to classical concretes, a higher resistance to chemical corosion, sometimes even better than burned shaped products.

All the classical concretes present, around the critical temperatures, (300 - 1200°C) a drop in mechanical resistance, wich can go up to 75% from the initial resistance, and which is provoked by dehydration of hydroaluminates of calcium, and successive transformations they endure until the beginning of sintering.

In case of LCC and ULCC concretes, instead of this dropping resistance there is a constant increasing, because, due to the presence of tripoliphosphate of aluminum the preponderance of gellic phase is insured, within the compact structure formed by the aggregate and the ultrafine powders, and wich, with the increasing temperature, crystallize forming gibbsit și boehemit. Because of this, the dehydration of crystalline hydrates can not cause, in low temperatures area, up to 500 - 600°C, the policondensation of phosphates coming from the reaction of sodium tripoliphosphate compounds, which fights the drop of resistance due to phase transformations and mentains its values on an ascending curve, until CA și CA₂ appear, when a new increase occurs.

Although at the temperature of 1000°C all the compounds are completly dehydrated, and CA și CA₂ are formed, the increase of mechanical resistance is mentained through the double phosphates of calcium and potasium chrystalization and sodium salts until the beginning of sintering, when the increase of the resistance is high.

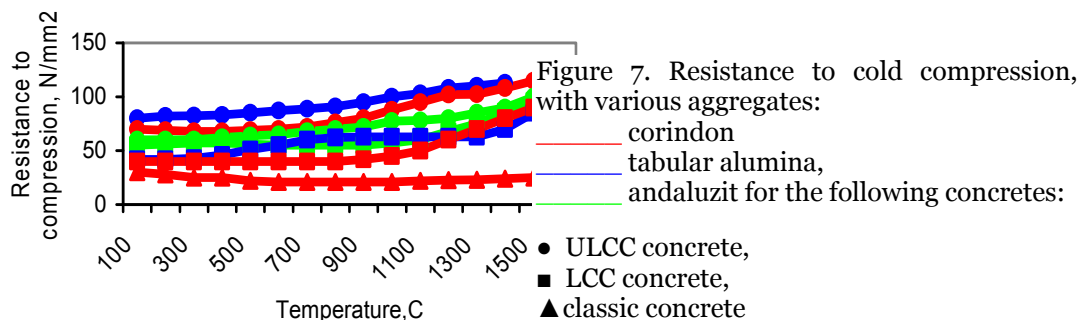


Figure 7. Resistance to cold compression, with various aggregates: corindon, tabular alumina, andaluzit for the following concretes:

● ULCC concrete,
 ■ LCC concrete,
 ▲ classic concrete

The variation of resistance to compression in low temperature after burning at various temperatures, of both classical concrete and LCC și ULCC concretes with various aggregates, is shown in figure 7.

There can be seen that the values of resistance to compression of LCC concrete up to 1300°C are similar to the ones of burned shaped products and far better than in the case of classical concrete. The curves for ULCC concrete show that, regardless of the aggregate, its resistance to compression is much higher than LCC, or classical concretes, or burned shaped products. Resistance to bending in heat is also increased compared to burned shaped products and classical concrete (figure 8).

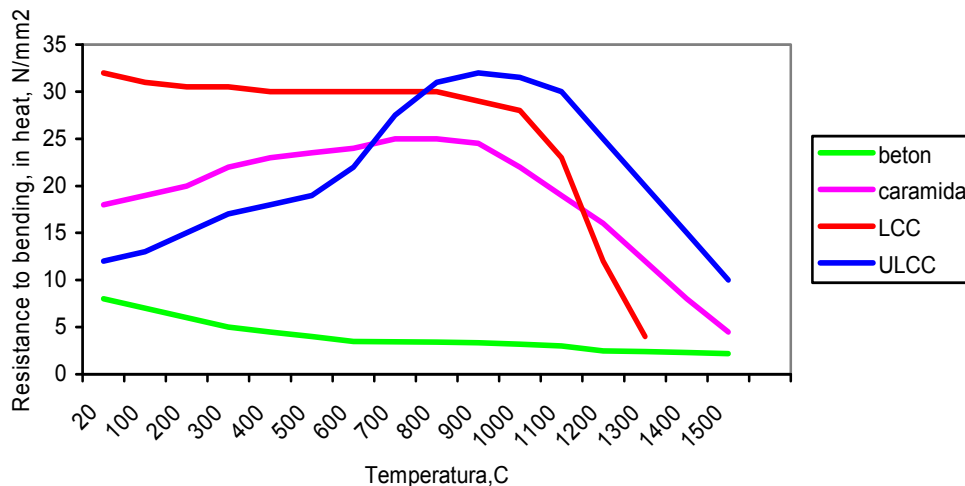


Figure 8. Resistance to bending in heat:

1 – concrete, 2 – brick, 3 – LCC concrete, 4 – ULCC concrete corindonic aggregates

A great influence on heat resistance is due to the mult quantity formed in the process, as well as the drop of CaO percentage in the concrete (Figure 9).

Due to the high values of mechanical resistance, internal tensions and pores distribution, LCC and ULCC concretes have a better impact resistance than classical concretes and burned shaped products, reaching over 50 heading-cooling cycles, when the aggregate is corindonic or tabular alumina.

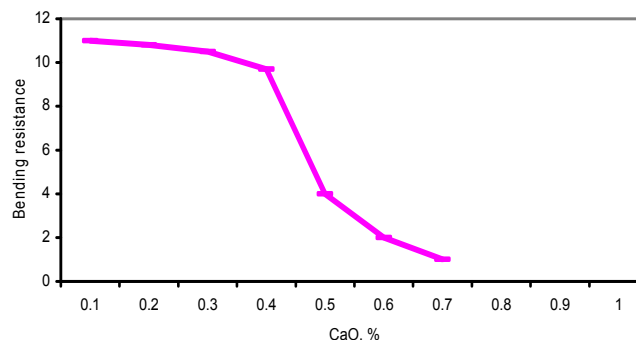


Figure 9. Influence of CaO ratio on the bending resistance at 1500 C, of a burned ULCC concrete

2. GRANULOMETRIC DISTRIBUTION

Producing dense refractory concretes, of high quality, Realizarea unor betoane refractare dense, de calitate superioară este determinată atât de puritatea chimică a componentilor, de dozajul acestora cât și de compoziția granulometrică a amestecului prin care se urmărește să se obțină o compactitate cât mai mare.

By pursuing the granulosity we reach to get as much compactness as possible. This characteristic generally depends both on the distribution, and the shape of the grains. Compounds of aggregates of splintery shape sometimes have a double surface compared to those spheric, thus needing more water to be prepared. To get a high resistance to bending, the rough surfaces of the grains are more advantageous than the smooth ones. The rate of fine aggregate from refractory concretes must be higher than that of ordinary concretes, because they are more profitable to the purpose and provide a relief of sintering process between the aggregate and the cement. The maximum dimension of the aggregate enclosed in refractory concretes is mainly determined by the section of the pieces to be made; it does not have to be bigger than 1/4 - 1/5 from the minimum dimension of the concrete piece. In common practice there are not used aggregates with a higher diameter than 40 mm. In the case of corindon aggregates the maximum dimension reaches just 10 mm.

To obtain maximum capacity of concretes the granulation of the compound needs to approach the ideal curves established by Fuller - Bolomey. In Figure 10 we can see the ideal granulation, in volumes, for the aggregates used for refractory concrete. Establishing the granular distribution according to the maximum section of the concrete piece, the dosages between the aggregate and concrete will be of 3-4,5 volumes of aggregate for a volume of cement.

The maximum dimension of the granules, mm

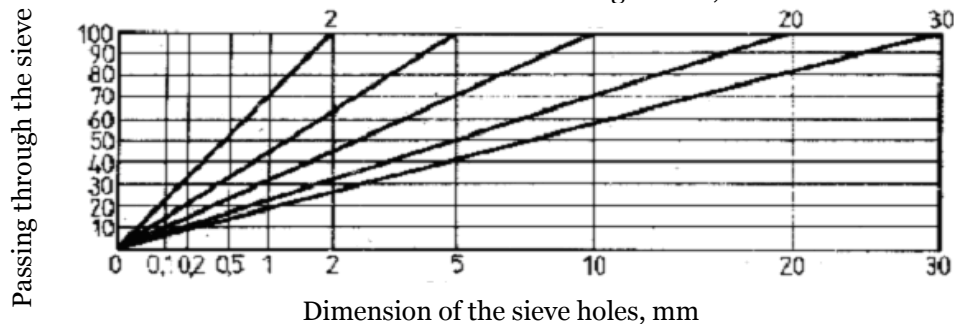


Figure 10. Ideal granularity, in volumes, for refractory aggregates used in refractory concretes

The granulometric distribution of refractory distribution can also be established through the following formulae:

$$y = 100 \cdot \sqrt{d/D}$$

Fuller's formula

$$y = A + (100 - A) \cdot \sqrt{d/D}$$

Bolomey's formula

$$y = 100 \cdot \left(\frac{d}{D}\right)^n$$

Gummel's formula

where: d – dimension of particles

D – maximum dimension dimensiunea of particles

A – coefficient, according to the type of aggregate, A = 8 – 12

n – coefficient, n = 0.2-0.4 – 0.3-0.5. For Gummel n = 0.1 – 1

Granule, peste 1 mm

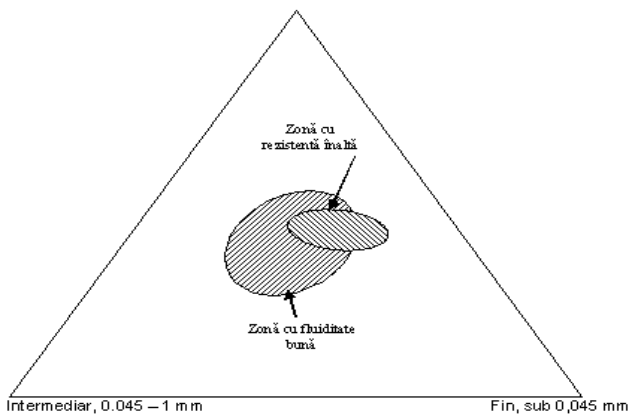


Figure 11. Areas of fluidity of granular compounds

- ❖ 30-45% fine (with no intermediary ratio) lead to good compacticities and low contractions;
- ❖ compositions with 70-80% granules have a good resistance to mechanical impact;
- ❖ compositions with fine ratio, or with granules (provided that the different granular components have the same contraction when burned) lead to a reduced permeability.

3. POROSITY

One of the most important properties of concretes is the ostensible porosity. This gives indications on the resistance to impact, corrosion and infiltration. One of the most important properties of the concretes is the ostensible porosity. This gives indications on the resistance to impact, corrosion and infiltration. According to the place we use the concretes, the ostensible porosity needs to be controlled, to provide the infiltration of melt metal, and, implicitly, the corrosion. The lower ostensible density of tabular alumina is due to the small pores (closed) (<10μm), which do not allow the infiltration of slag, but improve considerably the resistance to impact of the aggregate.

Tabular alumina has a high chemical purity ($Al_2O_3 > 99,4\%$), which improves the resistance to usage for concretes for trenches.

Classic refractory concretes, due to the high content of cement, have, when raw, an ostensible porosity around 9 – 10%. When the content of cement is higher, the ostensible porosity when raw, decreases. This porosity increases during heating, due to dehydration and phase transformations of calcium hydro-silicates, reaching a maximum of 30-35% and dropping then to 23-26% as ceramic conection and sintering occur.

Both LCC and ULCC concretes, although the cement content is reduced, have a reduced porosity, when raw around 6-9%. This is due to filling the intergranular spaces with very fine ratios of powders, the micropores still remained being filled with gelly phase. We have to mention that the ostensible density of LCC and ULCC concretes is high particularly because of that, reaching up to 3-3,2 g/cm³ (according to the nature of the refractory aggregate and temperature). With the increase of temperature LCC and ULCC concretes have a small increase of porosity, compared to ordinary concretes, reaching to max. 14-18% (Figure 14).

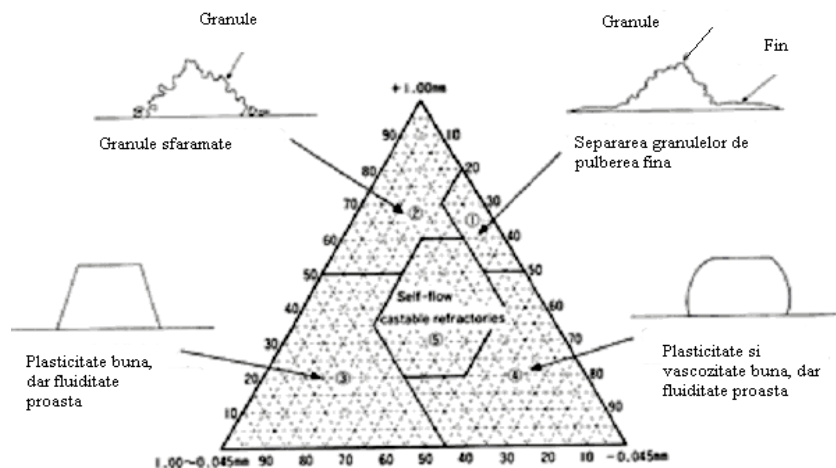


Figure 12. Influence of the dimension of particles on fluidity

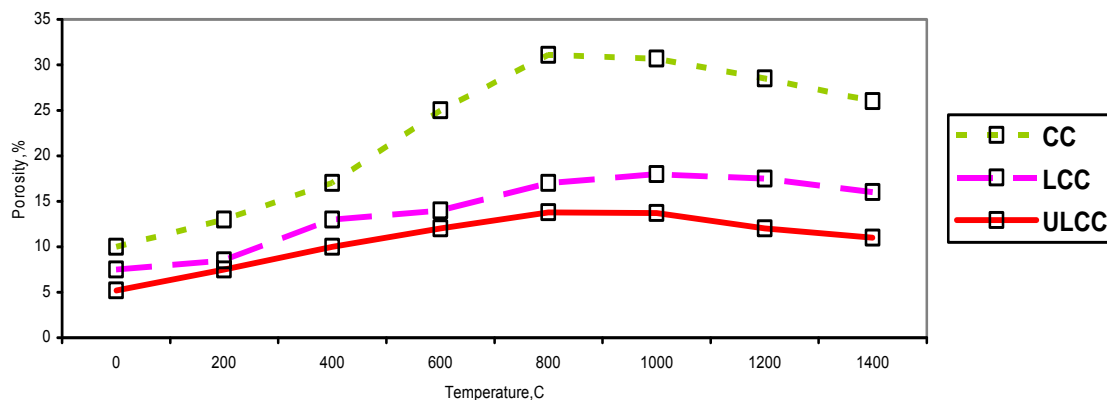


Figure 14. Porosity according to temperature for:

- 1 – classic concrete, 2 – LCC concrete, 3 – ULCC concrete with tabular alumina aggregate

This is due to the small ratio of hydration water in LCC and ULCC concretes compared to classic concrete, and the preponderance of gellic phase which increases very little the porosity, with the increase of temperature, through the transformations that occur. Thus, LCC concrete has a porosity of 11-14%, which is a far better porosity compared to classical concretes - 25-27%.

The permeability of concretes depends mostly on the size of the pores and less on the total content of pores. In classic concretes, even if after heating the porosity is high until 800°C, the porosity is very low. Over this temperature the permeability increases, due to the increase in crystals, fact that leads to the decrease of internal specific intern surface, and to intern structural changes of dehydrated product of cement.

For temperatures over 1000°C, the permeability of classic concrete reaches the values of other refractory materials. The same thing happens in case of LCC and ULCC concretes, but with smaller values in the area of low temperatures. Over 800°C, the permeability of concretes increases considerably, as at temperatures of 1200-1300°C its value can be compared to a classic concrete.

The low values of permeability to gass of LCC and ULCC concretes, until 800°C lead to the need to carefully choose the heating speed for the vaporization of water, unless special additives are used. Over 800°C the heating speed can be increased without the risk of explosions.

4. EXPANSION – CONTRACTION

During the heating of a classic concrete, especially at first burning, a series of contractions and expansions occur, initially provoked by dehydration and phase changing's of the cement and the expansion – contraction of sinterized cement – aggregate system. Up to 1000°C the expansion of concrete is reversible, the concrete not having yet being made a ceramic connection.

Over 1000°C, and, especially from 1200°C up, due to ceramic conection and sintering of concrete, irreversible changes occur in the dimensions which firstly expand, and when the temperature reaches the refractarity limit of the concrete, or overcomes the temperature of aggregate burning, contract. The contractions occur mainly in chamotte aggregate concretes, when the heating temperature of the concrete reaches and overcomes the burning temperature of the chamotte. The well burned chamotte has, though, small contractions. Unlike the chamotte, the corindonic or tabular alumina aggregates expand continuously almost to the limit of refractarity, when contraction begins.

When cooling, the irreversible expansion or contraction reached at the maximum heating temperature, will contract over or under the initial dimensions, the values ranging between +1,5 and -0,6%. At a new heating, the concrete will reversibly expand to the maximum temperature of the first irreversible heating, which will be the value of maximum expansion for the next heating.

Within LCC and ULCC concretes the contraction determined by the low ratio of cement is compensated by the expansion of ultra-fine powders, making a neutral system for LCC, while for ULCC the trend is towards expansion. Thus, for LCC the variation of dimensions will be given by the expansion-contraction of the aggregate, which, when corindonic or tabular alumina, begins expansion at 1200°C keeping linearly increasing, and when chamotte, will have a reversible expansion, followed, at 1200-1300°C by a contraction (which is partially compensated by the expansion of ultra-fine powders of SiO₂ at the transformation of α-quartz in tridimit around 873°C), reaching, at the maximum temperature of concrete usage (about 1350°C) aproximately - 0,3%.

Usage of corindonic or tabular alumina aggregates is not justified unless LCC concrete for high temperatures. In this case the concrete will have an almost continuous expansion, until a maximum of +0,8 - -1% .

Unlike the LCC, in ULCC concrete, the tendency to expand occurs regardless of the aggregate we use. When using the chamotte, at a temperature of usage for the ULCC concrete of 1600°C the mulit formed from 1300°C contracts, its contraction giving final expansions of up to +0,4%. For corindonic or tabular alumina aggregates values of expansion of +0,9 ... +1,26% at temperatures of 1600-1700°C occur.

In these conditions, the expansion gaps of LCC concrete clothings must be very carefully dimensioned, taking into consideration the fact that the values presented above are obtained in laboratory where the samples are heated on all their facets. In common practice we must take into consideration values of 70-90% from the theoretical value of expansion. Contraction gaps in the clothings are compulsory, regardless of the concrete or aggregate type.

For LCC concrete with chamotte aggregates these gaps are superficial for low volumes, but for higher values, we need to provide the expansion gaps with dimensions according to the medium reversible expansion factor. This has values ranging from 40·10⁻⁶/°C to 6·10⁻⁶/°C. Even if the concrete contracts under initial dimensions, the contraction occurred after the concrete had expanded.

Similarly, we calculate the expansion gaps for chamotte aggregate ULCC concrete.

Table 4.

Characteristics	Ttype of concrete	Aggregate,%Al ₂ O ₃				
		Chamotte 44-46	Andaluzit 59-61	Chamotte 69-71	Corrindon 91-93	Tabular alumina 98-98,5
Refractoriness	Classic concrete	1460	1500	1670	1820	1850
	LCC concrete	1760	1790	1870	1930	2000
	ULCC concrete	1760	1800	1870	1950	2000
Maximum temperature of use	Classic concrete	1300	1400	1520	1750	1800
	LCC concrete	1550	1560	1600	1800	1900
	ULCC concrete	1600	1650	1650	1800	1900

5. REFRACTORINESS

Using superaluminum cements, the classic refractory concretes will have a variation of refractoriness due not only to the type of aggregate but also to its proportion within the compound.

Both LCC and ULCC concretes, due to their low or very low content of cement and high proportion of aggregate and ultra-fine powders, have higher refractoriness than classic concretes with the same type of aggregate. We need to mention that LCC concrete is refractory just in case of replacing the ultra-fine powders of SiO_2 with Cr_2O_3 or Al_2O_3 . From economic reasons we recommend the use of LCC concrete at temperatures of 1350°C , over this temperature ULCC concrete being the best solution. In table 4 there can be seen the values of refractoriness for different types of concretes.

REFERENCES / BIBLIOGRAPHY

- [1.] Adriana Mioara Comșa, Maria Nicolae, Applications of refractory concretes with low hydraulic binder content, *Metalurgia International*, 8 (2008) 5-7, ISSN 1582 – 2214
- [2.] Adriana Mioara Comșa, Nicolae Avram, Dima Adrian Refractory linings realized from refractory concretes with low hydraulic binder content, *Metalurgia International*, 9 (2008) 9-14, ISSN 1582 – 2214
- [3.] Adriana Mioara Comșa, Buzduga Miron, Constantin Nicolae, Aurica Goleanu, Buzduga Radu, Monolithic refractory for metallurgy, *Metalurgia International*, Special issue nr.3 (2008) 71-72, ISSN 1582 - 2214
- [4.] ISO/DIS 1927-1:2008 Unshaped refractory materials — Part 1:Introduction and classification
- [5.] Drd.ing. Buzduga Miron, Drd.ing. Comșa Adriana , Mase monolitice cu conținut redus de liant hidraulic, *Scientific Bulletin of the Politehnica University of Timișoara*, Tom 52(66), 2007; ISSN 1224-6077
- [6.] Catalog ALCAN 2007
- [7.] Albinas GAILIUS, Dangyras ŽUKAUSKAS Optimisation of the Aggregates Composition in Concrete, ISSN 1392–1320 *Materials Science (MEDŽIAGOTYRA)*. Vol. 12, No. 1. 2006, Lithuania
- [8.] Abilio P. Silva, Ana M. Segadães, Tessaleno C. Devezas Particle Distribution Design in a Self-Flow Alumina Refractory Castable Without Cemente *Advances in Science and Technology* Vol. 45 (2006) pp. 2260-2265
- [9.] L Lipan, A Comsa Studiu C 2080 RELANSIN - Tehnologie ecologica de fabricare a betoanelor refractare cu continut redus de liant hidraulic, 2005
- [10.] Myhre, B. Microsilica in Refractory Castables – How Does Microsilica Quality Influence Performance? 9-th Biennial Worldwide Congress on Refractories 2005: pp. 191 – 195.
- [11.] I.Teoreanu, N. Ciontea Tehnologia produselor ceramice si refractare, Vol. II, Editura Tehnica, Bucuresti, 1985, p. 37-49, 125-135.
- [12.] xI. Teoreanu, N. Ciocea, A. Barbulescu, N. Ciontea Tehnologia produselor ceramice si refractare, Vol. I, Editura Tehnica, Bucuresti, 1985, p. 109-117, 121-122
- [13.] N.Deică, Utilizarea rațională a produselor refractare, Editura Tehnică, 1982
- [14.] R. Abramovici Materii prime ceramice, Editura Institutului Politehnic “Traian Vuia”, Timisoara, 1974, p. 369-375.
- [15.] Konopický,K Materiale refractare, Centrul de documentare și publicații tehnice al Industriei Metalurgice, 1970





STUDIES OF CARBON STEEL CORROSION IN ATMOSPHERIC CONDITIONS

^{1,3}. FACULTY OF ENERGY ENGINEERING, UNIVERSITY OF ORADEA

^{2,4}. CENTER OF TECHNOLOGICAL TRANSFER, UNIVERSITY OF ORADEA

ABSTRACT:

One of the most frequently corrosion type is the atmospheric corrosion. Carbon steel behaviour at atmospheric corrosion is presented on base of the literature data study. This has been reported to account for more failures in terms of cost and tonnage than any other type. About 80% from all degradations produced by corrosion in the metallic constructions are due to the atmospheric corrosion. The atmospheric conditions for corrosion are very complex and the corrosion rates vary in function of geographic zone, of season and daily time. The complexity of the atmosphere, as corrosion environment, results from atmosphere composition and from presence of some factors as pollutants, temperature, humidity, wind speed and direction, etc. These variables make meaningful results from laboratory experiments very difficult to obtain. The object of this work is to outline the principles that govern atmospheric corrosion of the carbon steel – the construction material with the largest application – how is influenced his corrosion rate by the atmospheric variables and that are the corresponding corrosion products

KEYWORDS:

carbon steel, atmospheric corrosion

1. INTRODUCTION

One of the most frequently corrosion type is the atmospheric corrosion. This has been reported to account for more failures in terms of cost and tonnage than any other type. About 80% from all degradations produced by corrosion in the metallic constructions are due to the atmospheric corrosion. The atmospheric conditions for corrosion are very complex and the corrosion rates vary in function of geographic zone, of season and daily time. The complexity of the atmosphere, as corrosion environment, results from atmosphere composition and from presence of some factors as pollutants, temperature, humidity, wind speed and direction, etc. [1]. These variables make meaningful results from laboratory experiments very difficult to obtain.

The atmospheric corrosion is conveniently classified in three [2, 3] types: (1) *dry oxidation*, (2) *damp corrosion* and (3) *wet corrosion*. *Dry oxidation* takes place in the atmosphere with all metals that have a negative free energy of oxide formation. For metals forming non-porous oxides, the films rapidly reach a limiting thickness since ion diffusion through the oxide lattice is extremely slow at ambient temperatures, and at the limiting thickness, the oxide films on metals are invisible. For certain metals and alloys, these films confer remarkable protection on the substrate, e.g. stainless steel, titanium and chromium. *The damp and wet atmospheric corrosion* are characterized by the presence of a thin, invisible film of electrolyte solution on the metal surface (damp type) or by visible deposits of dew, rain, sea-spray etc. (wet type). In these categories may be placed the rusting of iron and steel, 'white rusting' of zinc (wet type) and the formation of patina on copper and its alloys (both types).

The corrosion products may be soluble or insoluble. Usually, those insoluble reduce the corrosion rate by isolating the substrate from the corrosive environment. Less commonly, they may stimulate corrosion by offering little physical protection while retaining moisture in contact with the metal surface for long periods. The soluble products may increase corrosion rates.

The severity of atmospheric corrosion depends on the environment type [4, 5]: *rural, urban, industrial, marine* and *combined*.

The *rural* atmosphere generally the least corrosive and normally does not contains chemical pollutants. The principal corrosive agents are moisture, oxygen and carbon dioxide.

The *urban* atmosphere is similar to the rural type in that there is little industrial activity. Additional contaminants are of the SO_x and NO_x variety, from motor vehicle and domestic fuel emissions.

The *industrial* atmospheres are associated with heavy industrial processing facilities and can contain sulphur dioxide, chlorides, phosphates and nitrate.

The *marine* atmospheres are usually highly corrosive, due to the presence of chlorides, and corrosivity tends to be significantly dependent on wind direction, wind speed and distance from the coast.

The object of this work is to outline the principles that govern atmospheric corrosion of the carbon steel – the construction material with the largest application – how is influenced his corrosion rate by the atmospheric variables and that are the corresponding corrosion products.

2. CORROSION PRINCIPLES OF CARBON STEEL IN ATMOSPHERE

A fundamental requirement for electrochemical corrosion process is the presence of an electrolyte. This film 'invisible' electrolyte tends to form on metallic surfaces under atmospheric exposure conditions after certain critical humidity level is reached. The critical humidity level is not constant and depends on the corroding material, the tendency of corrosion products and surface deposits to adsorb moisture, and the presence of atmospheric pollutants. For iron, the relative critical humidity is 60% in atmosphere free of sulphur dioxide.

In absence of the pollutants, in an atmosphere with relative humidity of least 70%, the carbon steel corrodes with formatting in time of Fe(OH)₂, after the electrochemical mechanism [6], conform to the reactions:

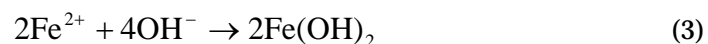
Anodic reaction:



Cathodic reaction:



The products of these reactions combine forming ferrous hydroxide – a compound insoluble at neutral pH – that deposits on the metal surface:



In presence of the oxygen, the ferrous hydroxide oxidizes and forms the rust.

If oxygen from the atmosphere diffuses through the electrolyte film to the metal surface, a diffusion-limiting current density should apply. It has been shown that a diffusion transport mechanism for oxygen is applicable only to an electrolyte-layer of approximately of 30 μm and under strictly isothermal conditions [3]. The predicted theoretical limiting current density of oxygen reduction in an electrolyte-layer of 30 μm significantly exceeds the practical observations on atmospheric corrosion rates. Therefore, the overall rates of the atmospheric corrosion are likely to be controlled not by the cathodic oxygen reduction process, but rather by the anodic reaction(s).

In the presence of gaseous air pollutants, other reduction reactions, involving ozone, sulphur dioxide and nitrogen species have to be considered [7]. It be noted that corrosive contaminant concentrations can reach relatively high values in the thin electrolyte films, especially under conditions of alternate wetting and drying.

2. THE ROLE OF THE IMPORTANT VARIABLES IN ATMOSPHERIC CORROSION OF CRBON STEEL.

Humidity. From the above theory, it should be apparent that presence of electrolyte on the corroding surface (time of wetness) is a key parameter, directly determining the duration of the electrochemical corrosion process. This variable is a complex one, since all the means of formation and evaporation of an electrolyte solution on a metal surface must be considered.

The time of wetness is strongly dependent on the critical relative humidity. The relative humidity of the air varies in large limits, in function of geographic zone, of season and daily time.

Apart from the primary humidity, associated with clean surfaces, secondary and tertiary critical humidity levels may be created by hygroscopic corrosion products and capillary condensation of moisture in corrosion products, respectively. A capillary condensation mechanism may also account for electrolyte formation in microscopic surface cracks and the metal surface-dust

particle interface. Other sources of surface electrolyte include chemical condensation (by chloride, sulphates and carbonates), adsorbed molecular water layers, and direct moisture precipitation (ocean spray, dew, rain).

Temperature. The effect of temperature on the atmospheric corrosion rates is quite complex. An increase in temperature will tend to stimulate corrosive attack by increasing the rate of electrochemical reactions and diffusion processes. For a constant humidity level, the increase in temperature would lead to a higher corrosion rate. However, raising the temperature will, generally, lead to a decrease in relative humidity and more rapid evaporation of the surface electrolyte. When the time of wetness is reduced in this manner, the overall corrosion rate tends to diminish.

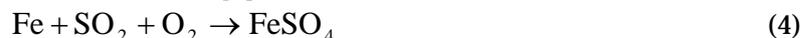
For closed air spaces, it has been pointed out that the increase in relative humidity associated with a drop in temperature has an overriding effect on corrosion rate [8]. This implies that simple air conditioning that decreases the temperature without additional dehumidification will accelerate atmospheric corrosion damage. An important factor in corrosion favouring is the continue oscillations of temperature.

For atmospheric corrosion of metals, the extreme temperatures do not an important role.

Atmospheric contaminants. The electrolyte film that forms on metallic surface contains various compounds resulted from the atmospheric pollutants. Karlson *et al* [9] observed a severe corrosion of steel if in atmosphere there are sulphur dioxide (SO₂) or alkaline chlorides (in principal NaCl).

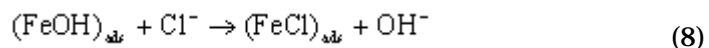
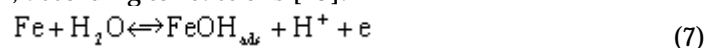
Sulphur dioxide. SO₂, a product of combustion of fossil fuels containing sulphur, play an important role in atmospheric corrosion in urban and industrial atmospheres. For all metals, SO₂ appears to be selectively adsorbed from the atmosphere, less so for aluminium than for other metals, and for rusty steel it is almost quantitatively adsorbed even from dry air at 0°C [2]. Under humid conditions sulphuric acid is formed, the oxidation of SO₂ to SO₃ being catalysed by metals and by metallic oxides.

For non-ferrous metals, SO₂ is consumed in the corrosion reaction whereas in the rusting of iron and steel it is considered [2] that ferrous sulphate is hydrolysed to form oxides and thus the sulphuric acid is regenerated. Sulphur dioxide thus acts as catalyst such that one SO₄²⁻ ion can catalyse the dissolution of more 100 atoms of iron [2]. The reactions can be summarized as follows:



The high solubility of SO₂ (of 1300 times more soluble than O₂ in water) [2] would make it a more effective cathodic reactant than dissolved oxygen even though its concentration in the atmosphere is comparatively small.

Chlorides. The corrosion rates of the carbon steel increase in marine atmosphere due to its salinity [3]. Apart from enhanced surface electrolyte formation by hygroscopic salts such as NaCl and MgCl₂, direct participation of chloride ions in the electrochemical corrosion reactions is also likely. In case of the ferrous metals, chloride anions are known to compete with hydroxyl ions, to combine with ferrous cations produced in the anodic reaction. In the case of hydroxyl ions, stable passivating species tend to be produced. In contrast, iron chloride complexes are soluble, resulting in further stimulation of corrosive attack, according to reactions [10]:



Other atmospheric contaminants, related to industrial emissions in specific microclimates are: hydrogen sulphide, hydrogen chloride, and chlorine that can intensify atmospheric corrosion damage. Hydrogen sulphide is known to be extremely corrosive producing Hydrogen Embrittlement Corrosion of alloys [11]. The corrosive effects of gaseous chlorine and hydrogen chloride in presence of moisture tend to be stronger than those of chloride salts anions because of the acidic character of the former species.

The deposition of solid matter from atmosphere can have a significant effect on atmospheric corrosion rates, particularly in the initial stages. Such deposits can stimulate the atmospheric attack by three mechanisms: (1) reduction in the critical humidity levels by hygroscopic action; (2) the provision of anions, stimulating metal dissolution and (3) microgalvanic effects by deposits more

noble than the corroding metal (carbonaceous deposits deserve special mention in this context) and by different aeration, so it shows in Fig. 1.

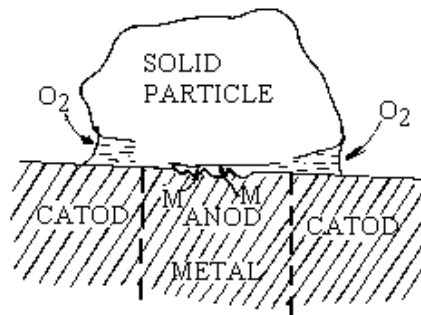


Figure 1 – Corrosion in centre of a surface covered by a solid particle

4. THE CORROSION PRODUCTS FORMED ON CARBON STEEL IN ATMOSPHERIC CORROSION

In presence of oxygen the ferrous hydroxide (reaction 3) oxidizes forming the rust. The iron corrosion products, the rust, have complex composition.

Hiller [12] given a scheme (figure 2) that shows the principal crystalline components of the rust and possible way of their formatting.

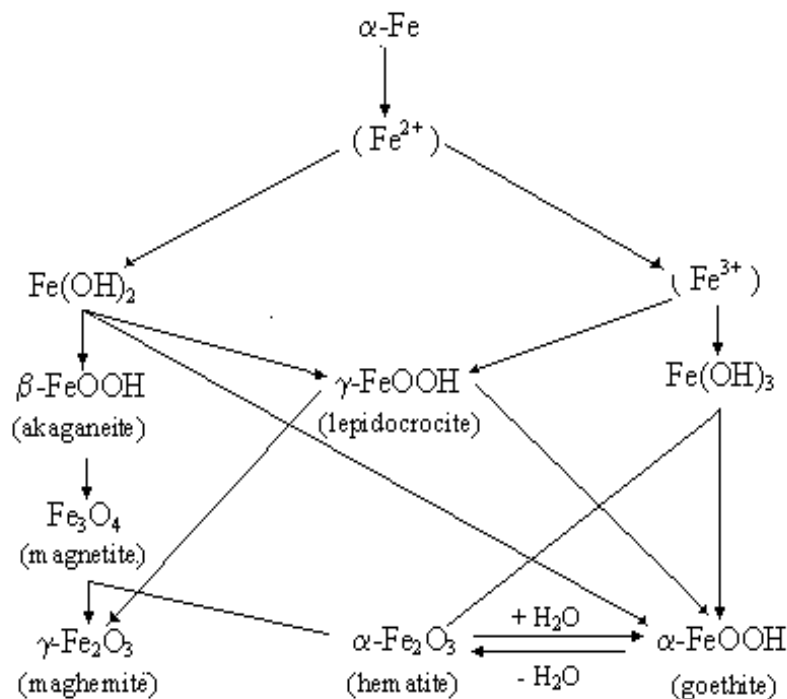
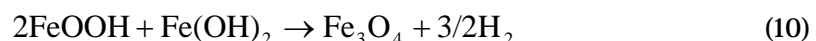


Figure 2 – Hiller scheme for the iron rust compounds [12]

In the first phase of the steel rusting forms $\text{Fe}(\text{OH})_2$, which it oxidizes suddenly forming *lepidocrocite* ($\gamma\text{-FeOOH}$), a crystalline phase with rhombic structure. In function of water presence or absence, this isomerises in *goethite* ($\alpha\text{-FeOOH}$), with rhombic structure also. If the corrosion rate is low, a part of lepidocrocite it transforms in *maghemite* ($\gamma\text{-Fe}_2\text{O}_3$), having a cubic structure.

Akaganeite ($\beta\text{-FeOOH}$), with tetragonal structure, it forms in the environments with high chlorides content. After Keller [13] akaganeite is the most unstable oxihydrate formed at corrosion steel. In humidity conditions this it transforms in *magnetite* (Fe_3O_4), having cubic structure. After Hiller [12] magnetite it forms only in direct contact with metal surface and in presence of a high humidity. This compound does not appear in the incipient phases of rusting; it is a product that forms in time from akaganeite, conform to the reaction:

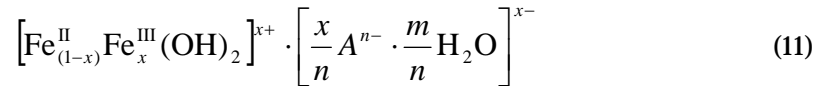


Another oxihydroxide of iron, *crystallite* (δ -FeOOH), having a hexagonal structure, it forms especially in the atmosphere with low humidity [14]. This can find and in the amorphous state – *ferroxite*.

After K.A. van Oeceron [15] the most important compounds of the rust are oxihydroxides of iron and magnetite.

In presence of the pollutants and in the incipient stages of the carbon steel corrosion, sometimes, forms on metal surface the, so called 'green rust' [16-20].

Green rust is a mixture of hydroxide-salts of Fe(II, III) with formulae:



This has a structure in which the iron hydroxide layers with positive charge alternate with negative charged anion layers and with water molecules, leading to a hexagonal symmetry. The green rust is classified [21] in two types:

- ❖ green rust I, in which A^{n-} are anions with planar structure, as Cl^- ;
- ❖ green rust II, in which A^{n-} are anions with three-dimensional structure, as, sulphate, carbonate, etc.

The change in corrosion rate with time varies markedly for different metals due to the differing degrees of protection conferred by the corrosion products. The behaviour of steel is conditioned by the alloying elements present for any given environment. Thus the decrease in corrosion rate with time for carbon steel is very much slower than for low-alloy steel. This can attributed to the much more compact nature of the rust formed on the latter type.

5. CONCLUSIONS

The atmospheric corrosion, the most frequently corrosion type of the carbon steel takes place in presence of the humidity surface layer after the electrochemical corrosion mechanism. The principal parameters that determine the corrosion rate are: humidity temperature and presence of pollutants as sulphur dioxide and chloride ions. The carbon steel corrosion products – the rust – have a complex composition, being formatted of various iron oxides and oxihydroxides types.

REFERENCES

- [1.] X. Naixin, L. Zao, C. Ding, C. Zhang, R.Li and Q. Zhong, *Corrosion Science*, 2002, 44
- [2.] L.L. Shreir, R.A. Jarman and G.T. Burstein (eds), *Corrosion*. Vol. 1: Metal/Environment reactions, Third Edition, Butterworth Heinemann, Oxford, 1994, Reprinted 2000, p. 2.2
- [3.] P.R.Roberge, *Handbooh of Corrosion Engineering*, McGraw-Hill, USA, 1999, p. 58-69.
- [4.] S. Szed, *Emirates Journal for Engineering Research*, 2006, 11 (1), 1-24.
- [5.] J.R. Vilche, F.E. Varela, G. Acuna, E.N. Codaro, B.M. Rosales, A. Fernandez, G. Moreina, *Corrosion Science*, 1995, 37 (7), 941-961.
- [6.] T. Badea, M. Popa, M. Nicola, *Coroziunea și ingineria coroziunii*, Ed. Academiei Române, 2002, București, p. 101
- [7.] S. Oesch and M. Faller, *Corrosion Science*, 1997, 39 (9), 1505-1530.
- [8.] S. Sharp, *Materials Performance*, 1990, 29 (12), 43-48.
- [9.] A. Karlsson, P.J. Moller and J. Vagn, *Corrosion Science*, 1990, 30 (2, 3), 153-158.
- [10.] N.G. Smart, M. Gamboa, J. O'M. Bockris, J. Aldeco, *Corrosion. Science*, 1993, 34, 759.
- [11.] G.E.Badea, P.Cret, T.Badea, *Proceedings of the 7th International Conference URB-CORR: Study and Control of Corrosion in the Perspective of Sustainable Development of Urban Distribution Grids*, June 25-27, 2008, Baile Felix, Romania, PRINTECH Printhouse Bucharest, 2008, 266-271.
- [12.] J. Hiller, *Werkstoffe und Korrosion*, 1966, 11, p.943-995.
- [13.] P. Keller, idem, 1969, 11, p. 943-950
- [14.] A.M.G. Pacheco, M. Teixeira, M. Ferreira, *British Corrosion Journal*, 1990, 25 (1), 19-25.
- [15.] K.A. van Oeceron, *Korrosionsschutz durch Beschichtungsstoffe*, Carl Hauser Verlag, Munchen, Wien, 1980, Band I, Band II, p. 35-54.
- [16.] Ph. Refait, O. Benali, M. Abdelmoula, J. M. R. Genin, *Corrosion Science*, 2003, 45 (8), p. 2435-2449.
- [17.] L. Legrand, G. Sagon, S. Lecompte, A. Choausse, R. Messina, *Corr. Sci.*, 2001, 43 (9), 1739-1749.
- [18.] Ph. Refait, J.B. Memet, C. Bon, R. Sabot, J.M.R. Genin, *Corr. Sci.*, 2003, 45 (4), 833-845.

- [19.] A. Gehin, C. Ruby, M. Abdelmoula, O. Benali at. Al. Solode State Science, 2002, 4, 61-66.
[20.] C. Ruby, A. Gehin, M. Abdelmoula, J.M.R. Genin, J.P. Jolivet, Solide State Science, 2003, 5, 1055-1062.
[21.] S.H. Drissi, Ph. Refait, M. Abdelmoula, J. M. R. Genin, Corrosion Science, 1995, 37 (12), 2025-2041.



¹Caius PANOIU, ²Manuela PANOIU, ³Raluca ROB

PROGRAMMABLE GAIN AMPLIFIER USING PARALLEL PORT CONTROLLING

¹⁻³. ELECTRICAL ENGINEERING AND INDUSTRIAL INFORMATICS DEPARTMENT, UNIVERSITY POLITEHNICA TIMISOARA, FACULTY OF ENGINEERING HUNEDOARA, HUNEDOARA, ROMANIA

ABSTRACT:

This paper presents a way to realize a programmable gain amplifier that can be software controlled using parallel port. The controlling scheme is made in LabVIEW, which permits visualisation of the both input and output of the amplifier and also gain control using parallel port.

KEYWORDS:

Programmable gain amplifier, parallel port, spectral characteristic

1. INTRODUCTION

Realizing a programmable gain amplifier is a difficult problem, especially if the purpose is obtaining a huge number of regulation steps and a good accuracy. In case of this amplifier, the controlling gain implies 255 equal steps, using a digital to analogue converter, whose reference current can be adjusted by controlling the digital inputs using parallel port.

2. METHODOLOGY

The application can acquire a signal using a real generator using the analogical inputs of the data acquisition board NI – 6221 [1]. This signal can be followed on a virtual oscilloscope display built in LabVIEW. As well, the input signal is added with a continuous signal in order to obtain a unipolar reference signal for digital analogue converter. Gain control can be made controlling digital inputs of the converter using parallel port. Block scheme of the application is represented in figure 1.

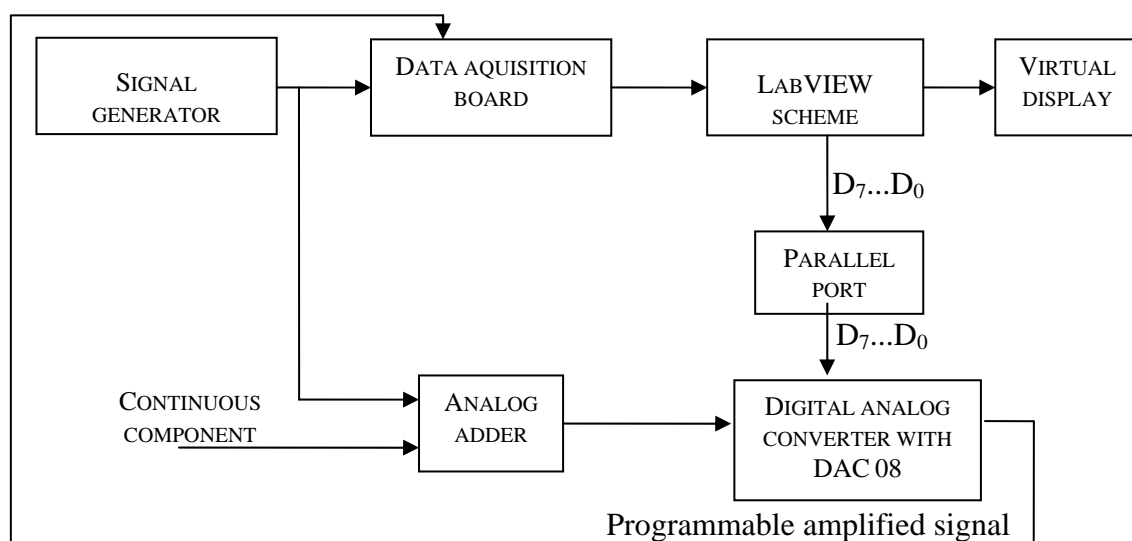


Fig.1. Block scheme of the application

In order to build a programmable gain amplifier of the input signal, the authors used an analogical adder realized with an operational amplifier $\mu A741$, like in figure 2. The output of the $\mu A741$ is connected at the reference input of a digital analogical converter with DAC 08.

LabVIEW scheme is completing with a $D_7...D_0$ byte generating system [4], byte that is sent on data lines of the parallel port using 378h address. This byte becomes digital input signal for DAC 08. In this way, according with the byte value, there can be obtained different values for the output current of the converter [5]. The analogical output represents the acquired signal from the signal generator and programmable amplified by the present application. This signal can be followed on the virtual oscilloscope display if it is connected to an analogical input of data acquisition board.

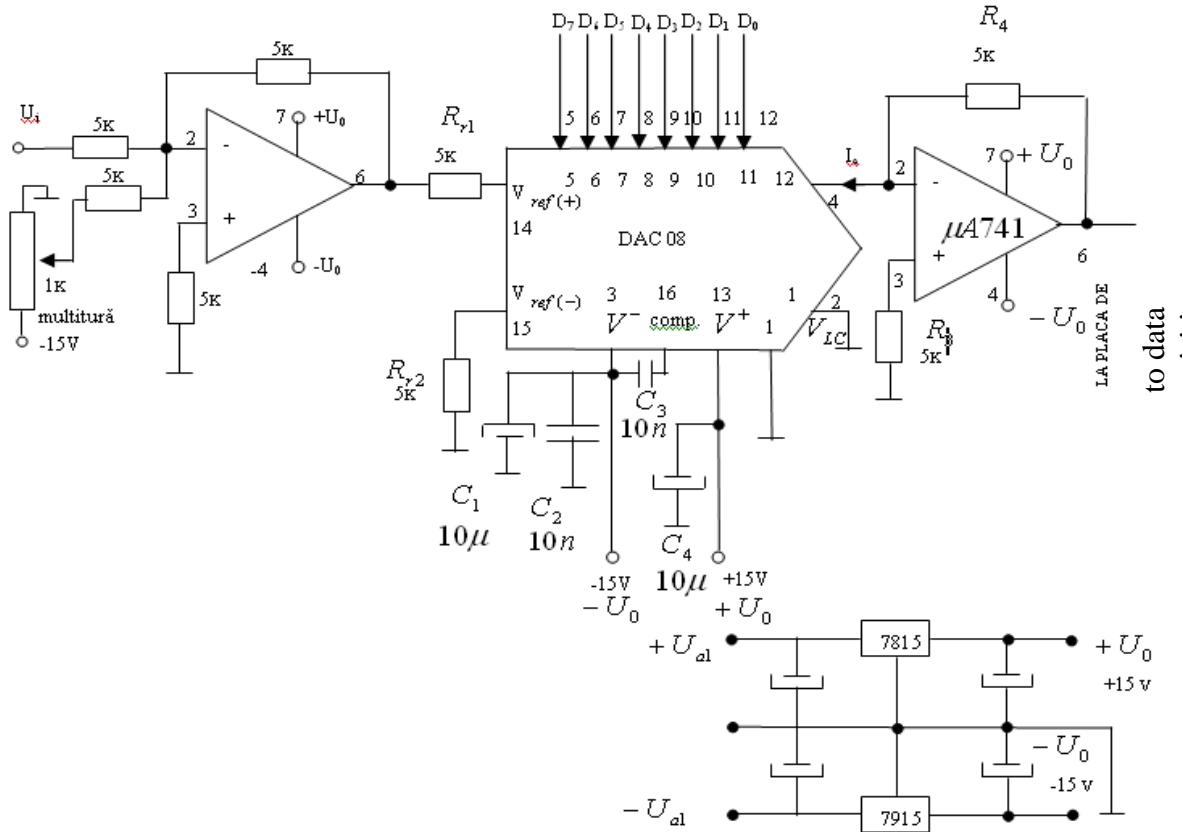


Fig.2. Electronic scheme of the application

Data acquisition board NI-6221

This application is realized using data acquisition board National Instruments NI – 6221, presented in figure 3.

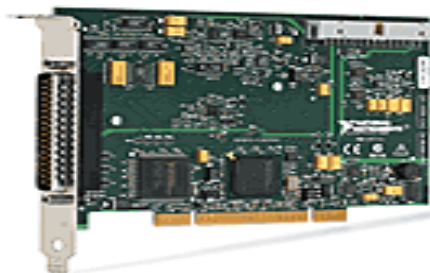


Fig.3. Data acquisition board PCI-6221.

Characteristics:

- ❖ 16 analogical inputs, 250 kS/s, resolution 16 bits
- ❖ 2 analogical outputs, 833 kS/s, resolution 16 bits
- ❖ 10 digital I/O compatible TTL
- ❖ 2 counter/timers on 32 bits
- ❖ Digital trigger
- ❖ Compatibility with Windows (2000/NT/XP), Linux and Mac OS X
- ❖ Integration with software components LabVIEW, CVI, Measurement Studio for Visual Studio NET.

Table 1. PCI-6221 Pins signification

AI 0	68	34	AI 8
AI GND	67	33	AI 1
AI 9	66	32	AI GND
AI 2	65	31	AI 10
AI GND	64	30	AI 3
AI 11	63	29	AI GND
AI SENSE	62	28	AI 4
AI 12	61	27	AI GND
AI 5	60	26	AI 13
AI GND	59	25	AI 6
AI 14	58	24	AI GND
AI 7	57	23	AI 15
AI GND	56	22	AO 0
AO GND	55	21	AO 1
AO GND	54	20	NC
D GND	53	19	P0.4
P0.0	52	18	D GND
P0.5	51	17	P0.1
D GND	50	16	P0.6
P0.2	49	15	D GND
P0.7	48	14	+5V
P0.3	47	13	D GND
PFI 11/P2.3	46	12	D GND
PFI 10/P2.2	45	11	PFI 0/P1.0
D GND	44	10	PFI 1/P1.1
PFI 2/P1.2	43	9	D GND
PFI 3/P1.3	42	8	+5V
PFI 4/P1.4	41	7	D GND
PFI 13/P2.5	40	6	PFI 5/P1.5
PFI 15/P2.7	39	5	PFI 6/P1.6
PFI 7/P1.7	38	4	D GND
PFI 8/P2.0	37	3	PFI 9/P2.1
D GND	36	2	PFI 12/P2.4
D GND	35	1	PFI 14/P2.6

3. DISCUSSION LabVIEW implementation

Control elements are rotary buttons, pushing buttons, circular dial and other input devices.

This paper is an oscilloscope application that is structured on two channels. Using NI-6221 data acquisition board, to each channel it can be provided a signal from a real generator. Different types of signal could be chosen depending on the generator capacity. Through LabVIEW program, there can be set the amplitude and the vertically position independently, like in figure 4. For these, there are used *Knob* control buttons [2].

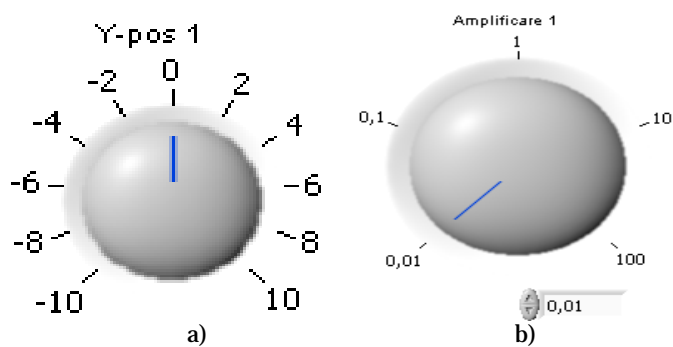


Fig. 4. The electric scheme
 a) Button for controlling the vertically position,
 b) Button for controlling the amplification

The number of the acquired samples can be controlled using a control button placed on Front Panel.

In order to acquire signals on two different channels, there is using *DAQ Assistant* block that can determine the number of employed channels, sampling rate, amplitude, error, etc. For separating the desired channels, there is using *Trigger and Gate* block. With *Multiply* and *Add*, the user can control the amplitude and the vertically position.

For spectral analysis of the acquired signals in frequency domain, it is using *Spectral Measurements* block.

Time base scheme of the indicator display is presented in figure 6.

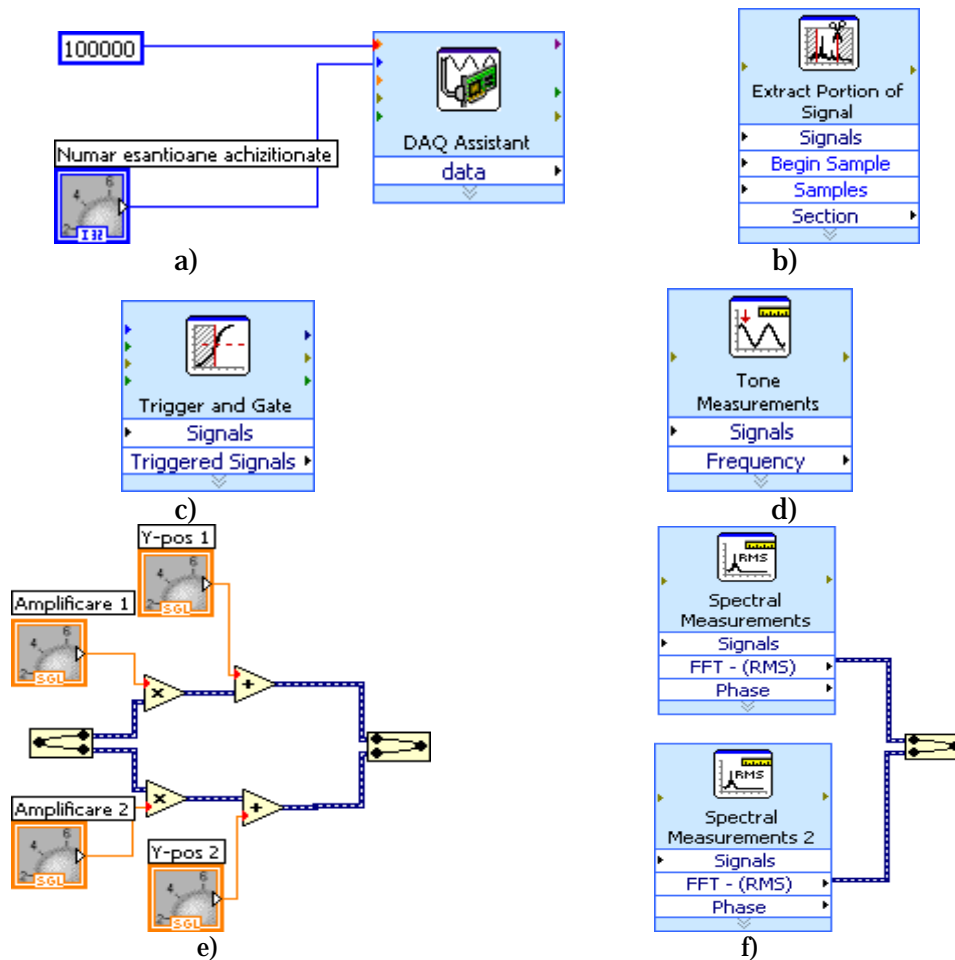


Fig. 5. a) DAQ Assistant, b) Extract Portion of Signal, c) Trigger and Gate, d) Tone Measurements, e) Mathematical blocks Multiply and Add, f) Spectral Measurements.

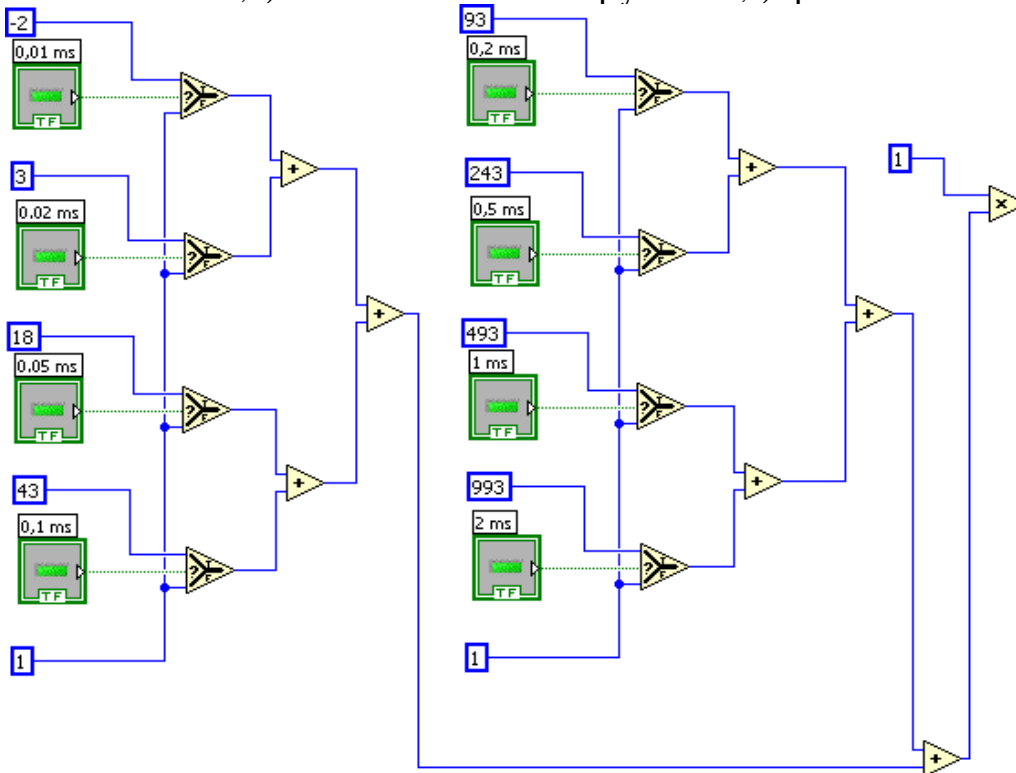


Fig. 6. Time base

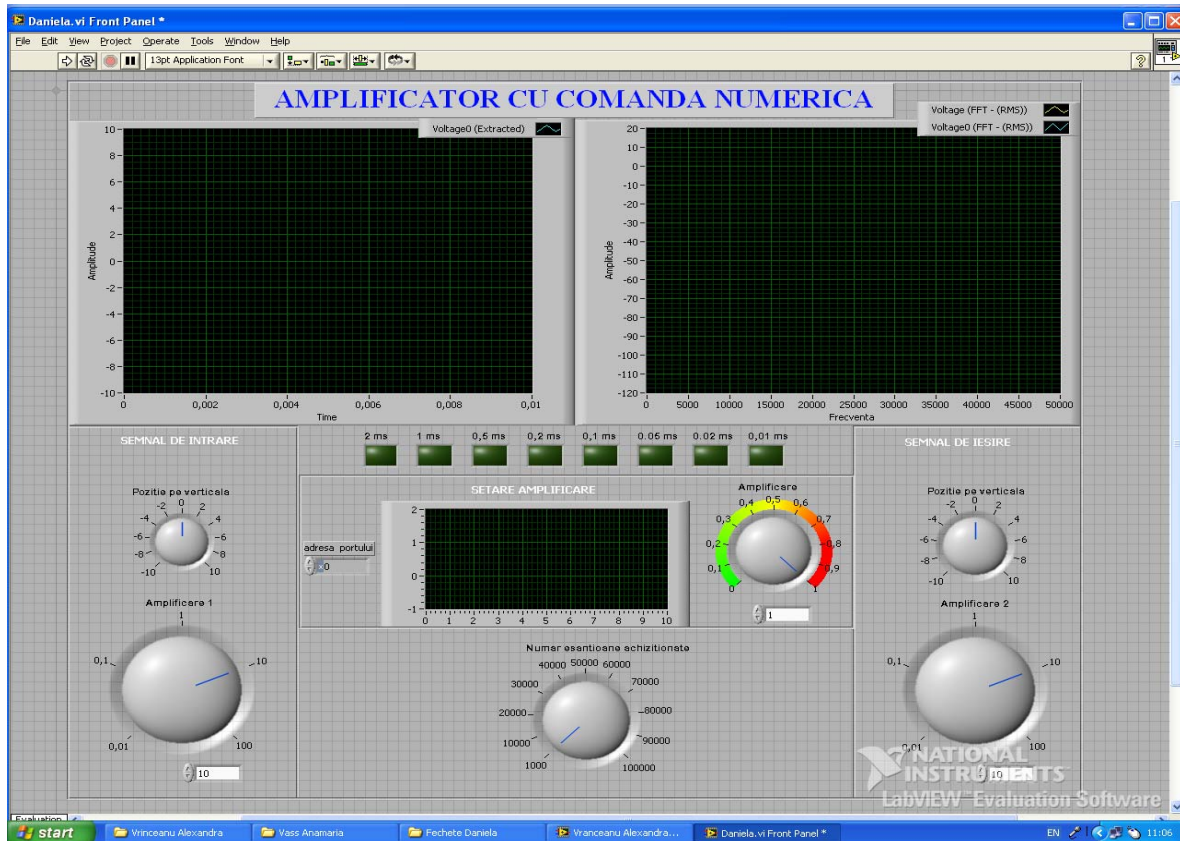


Fig. 7. Front panel of the application

The assumed signals according with the electrical scheme can be viewed on a display indicator placed on Front Panel [3] (two channels). On the first display can be viewed signals in time domain, on the second can be viewed signals in frequency domain, like in figure 7.

4. CONCLUSIONS

The programmable gain of the amplifier solves the accuracy problem, because realizing a high number of voltage steps, which represents a difficult problem. The application permits the input and output signals to be viewed on virtual displays in order the amplitude and vertically position to be adjusted.

REFERENCES

- [1.] Liviu Toma, *Sisteme de achiziții de date*, Editura de Vest, Timișoara, 1998.
- [2.] Francis Cotet, Octavian Ciobanu, *Bazele programării în LabVIEW*, Editura Matrix Rom București, 1998.
- [3.] <http://www.ctanm.pub.ro/academic/labview/Tutorial.htm>
- [4.] MIRCEA POPA, *SISTEME CU MICROPROCESOARE*, EDITURA ORIZONTURI UNIVERSITARE, TIMIȘOARA, 2003.
- [5.] POPA M, MARCU M, *PORTURILE PARALEL ȘI SERIE ALE CALCULATORULUI PC*, EDITURA ORIZONTURI UNIVERSITARE, TIMIȘOARA, 2001.







¹Ion COPACI, ²Bogdan TĂNĂSOIU

ON THE DYNAMIC EXPERIMENTAL DETERMINATION OF THE CHARACTERISTICS OF SHOCK INSULATORS

¹ UNIVERSITY "AUREL VLAICU" ARAD, ROMANIA

² REMARUL „16 FEBRUARIE” CLUJ-NAPOCA, ROMANIA

ABSTRACT:

The paper presents and compares two methods for establishing the dynamic characteristics of shock insulators and underlines the authenticity and scientific validity of the method of collision testing in specialized stands.

The paper also contains the experimental results obtained for a shock insulator with elastomer type elastic elements, together with a series of conclusions that regard the equipping of shock insulators with a high capacity for storing and dissipating potential deformation energy, as well as the importance of the 2β energy characteristic for the collision process.

KEYWORDS: shock insulators, potential deformation energy, buffers, transmitted forces

1. INTRODUCTION

The shock caused by collision [2] leads to the transmission of forces and accelerations that can determine unwanted consequences on the resistance structures, equipment, passengers and freight transported by railway vehicles.

In order to reduce the transmitted forces and accelerations and, consequently, the unwanted consequences of the shock, railway vehicles are equipped with shock insulators. The capacity of the shock insulators to store potential deformation energy, described by the 2β energy coefficient [1], directly influences the magnitude of the forces and accelerations transmitted to the vehicles, the level of the potential energy $(1 - 2\beta)E_p$ received by the vehicles, as well as the effects caused by the shock during the collision process. Therefore, during the design and execution of railway vehicles, there is a tendency to increase the storage capacity for potential deformation energy of shock insulators in order to reduce the levels of the forces and accelerations transmitted to the vehicles during the collision.

In regard to the use of railway vehicles there is a tendency to increase travel velocities, reduce the formation times of trains as well as increase the axle load. Consequently, the forces and accelerations transmitted to the vehicles as a result of collisions reach relatively high values that need to be considered during the conception, design and execution of railway vehicles.

2. DETERMINING THE DYNAMIC CHARACTERISTICS OF SHOCK INSULATORS EXPERIMENTALLY

Initially, the characteristic dynamic diagrams were obtained under the action of the shock caused by the free fall of a weight (ram), with a well determined mass, from different launching heights, on the buffer or central coupling dampener affixed to a rigid plane [2].

This adopted system differs significantly from the mechanical system encountered in the use of railway vehicles, specifically the one formed by the masses of the two cars separated by shock insulators, system which has a longitudinal freedom of motion.

The excitation function (system entry), specifically the momentum "mv" of the ram mass is applied through the buffer or central coupling dampener to a plane with a theoretically infinite mass. Thus, time variations of the force and contraction of the buffer or central coupling dampener

are obtained, as response functions to the applied excitation, particular to the used mechanical system and different from those of the real system.

Consequently, through the use of this method, characteristic dynamic diagrams are obtained that can not lead to a correct qualitative appreciation of the shock insulator, resulting in erroneous dynamic characteristics.

Through the experimental determination process for the characteristic dynamic diagrams involving the falling ram we have established the diagram in figure 1 for a central coupling dampener type S-2V-90, used by the railway administrations of the former USSR countries. In figure 2 we have represented the characteristic dynamic diagram of the same type of dampener, determined by colliding two railway cars, each with a mass of $\approx 92t$, at a collision velocity of 6,0km/h. The following observations can be made:

- ❖ the variation of the force as a function of contraction differs substantially. In the case of the diagram in figure 1 sudden increases of the force appear, followed by decreases. In the case of the diagram in figure 2, the evolution is approximately linear up to a contraction of $\approx 75mm$;
- ❖ the stored potential deformation energy and the dissipation coefficient η for the same maximum contraction $D_{max}=85mm$ have higher values for the collision, $We=30,4KJ$, $\eta=0,88$, than in the situation of the falling ram, when $We=21,8KJ$, $\eta=0,63$.

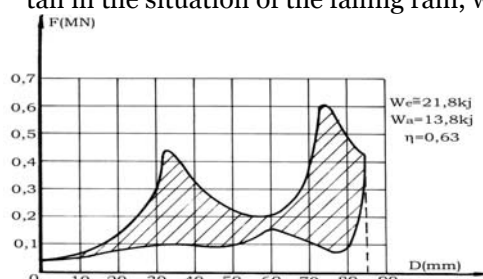


Fig.1

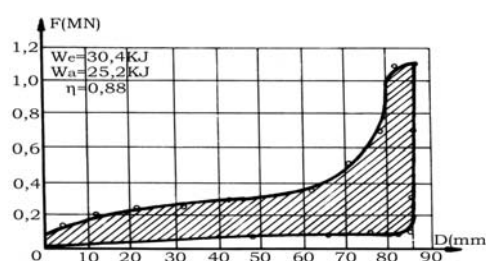


Fig. 2

Thus, significant differences are observed in regards to the obtained dynamic characteristics, which categorically imposes the option for determining the characteristic dynamic diagram for the shock insulators through the collision method.

3. FORCES TRANSMITTED TO THE VEHICLES DURING THE COLLISION

A series of authors have tried to theoretically establish mathematical expressions for the forces and accelerations transmitted to the vehicles during the collision process.

The general case of the collision of two railway cars is considered. The colliding car, with mass m_1 and velocity v_1 , interacts with a collided car, with mass m_2 and velocity v_2 , where $v_1 > v_2$. The cars are equipped with shock insulators (buffers or central coupling insulators).

During the collision process, part of the kinetic energy of the vehicles is transformed into potential deformation energy that is maximal at time t_{12} when the vehicles travel at the same velocity v_{12} . The expression for the potential deformation energy E_p is:

$$E_p = \frac{m_1 m_2}{m_1 + m_2} \frac{(v_1 - v_2)^2}{2} = \frac{m_1 m_2}{m_1 + m_2} \frac{v^2}{2} \quad (1)$$

where: m_1 – mass of the colliding car; m_2 – mass of the collided car; v – relative velocity between vehicles (collision velocity).

The energy factor that characterizes the efficiency of shock insulators is 2β , which represents the ratio between potential deformation energy stored by the shock insulators, W_e , and the total potential energy, which includes the potential energy stored by the elastic elements that represent the bearing structures, the elastic elements that form the suspension of the vehicle, the equipment and the existing load (freight, passengers):

$$2\beta = W_e / E_p \quad (2)$$

The theoretical expressions of the transmitted force established previously can be used only under the condition that the vehicles are equipped with shock insulators that show a linear variation between force and contraction, consequently we propose the following relations.

Railway vehicles can be equipped with shock insulators whose elastic elements show a nonlinear variation between force and contraction [2], [3].

In the case of a collision between two vehicles of the same type, with $m_1 = m_2 = m$, $K_{T1} = K_{T2} = K_T$, $p_1 = p_2 = p$, and $\beta_1 = \beta_2 = \beta$, the expression of the transmitted force becomes:

$$F_{max} = (v_1 - v_2) \sqrt{\frac{m}{4} 2\beta \frac{K_T}{p}} \quad (3)$$

where:

- ❖ $p = f(v)$ is the plenitude coefficient and represents the ratio between the stored potential deformation energy and the product between the maximum transmitted force and the maximum contraction of the shock insulator;
- ❖ $K_T = f(v)$ is the convetional rigidity of the shock insulator (buffer) and represents the ratio between the maximum transmitted force and the maximum contraction of the shock insulator.

4. EXPERIMENTAL DETERMINATIONS

During the testing, the colliding car, launched from the inclined plane of the testing stand, collided at various velocities the standing, unbraked, collided car sitting on the level part of the stand. The used cars, colliding and collided, were 4 axle freight cars, loaded with uniform materials (sand, gravel, broken rock, etc.) up to a total mass of 80t/car. The colliding car was equipped with category A buffers and the collided car with category C buffers (studied with elastomer elastic element).

For each shock caused by the collision of the vehicles, during the collision process the following parameters were determined experimentally:

- ❖ collision velocity v ;
- ❖ forces transmitted through the buffers $F_1(t)$, $F_2(t)$;
- ❖ contraction of the dampener of the collided car $D_1(t)$, $D_2(t)$.

Tables 1 and 2 show the experimental results obtained during the testing conducted.

The adnotations made in the tables represent:

- ❖ F_{total} – force transmitted during collision;
- ❖ $F_{med} = \frac{F_1 + F_2}{2}$ - average force transmitted through the buffer;
- ❖ $D_{med} = \frac{D_1 + D_2}{2}$ - average buffer contraction;
- ❖ W_{e1} , W_{e2} – potential deformation energy stored by the buffers of the collided vehicle (category C);
- ❖ W_{a1} , W_{a2} - potential deformation energy dissipated by the buffers of the collided vehicle (category C);
- ❖ η_1 , η_2 – energy coefficients for the dissipation of potential deformation energy of the shock insulators: $\eta_1 = \frac{W_{a1}}{W_{e1}}$ and $\eta_2 = \frac{W_{a2}}{W_{e2}}$;
- ❖ $W_{emed} = \frac{W_{e1} + W_{e2}}{2}$ - average potential deformation energy stored by the category C buffers.

Table 1

V [km/h]	F ₁ [MN]	F ₂ [MN]	F _{total} [MN]	F _{med} [MN]	D ₁ [mm]	D ₂ [mm]	D _{med} [mm]
8,4	0,564	0,551	1,115	0,557	48,1		48,85
9,6	0,627	0,628	1,255	0,627	60	65,9	62,95
10,7	0,652	0,718	1,37	0,685	65,9	70,4	68,15
12,7	0,852	0,872	1,724	0,862	74,1	77,8	75,95
13,9	0,952	1,026	1,978	0,989	75,6	80,7	78,15
14,7	1,09	1,038	2,128	1,064	77	78,5	77,75
16	1,215	1,217	2,432	1,216	89	90,1	89,55

Table 2

V [km/h]	W _{e1} [KJ]	W _{a1} [KJ]	η_1	W _{e2} [KJ]	W _{a2} [KJ]	η_2	W _{e med} [kJ]
8,4	15,1	13,4	0,887	15,3	14,3	0,934	15,2
9,6	23,4	20,5	0,876	25,5	22,5	0,882	24,45
10,7	28,6	24,7	0,863	31,6	28,1	0,889	30,1
12,7	38,8	34,6	0,892	41,8	37,8	0,904	40,3
13,9	46,5	41,6	0,995	48,7	45,4	0,932	47,6
14,7	48,5	43,6	0,9	51,8	48,8	0,94	50,15
16	70,5	65,5	0,93	74,5	69,7	0,93	72,5

Figures 3, 4, 5 and 6 show the diagrams of the force transmitted through the buffers as a function of the buffer contraction, together with the energy characteristics for the collisions at the marked velocities.

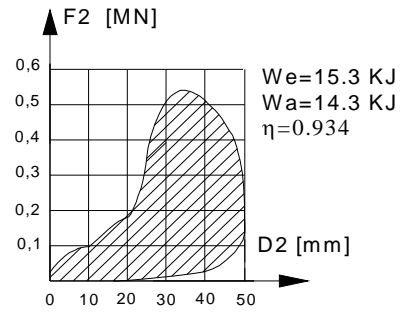
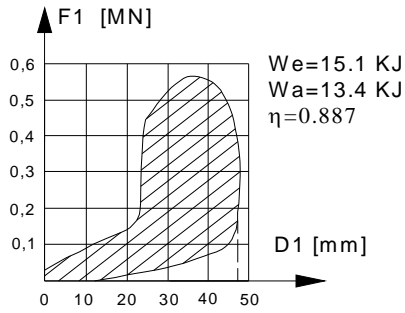


Fig. 3 $V = 8,4$ Km/h

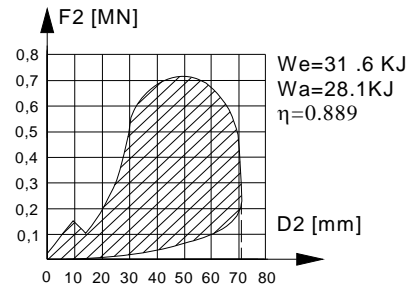
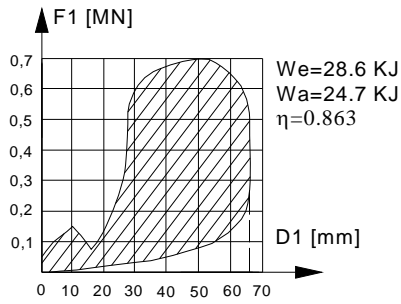


Fig. 4 $V = 10,7$ Km/h

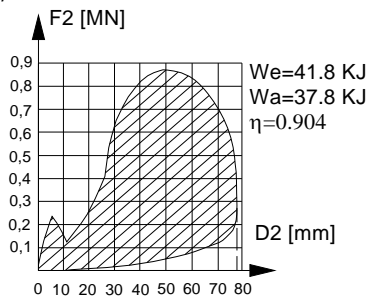
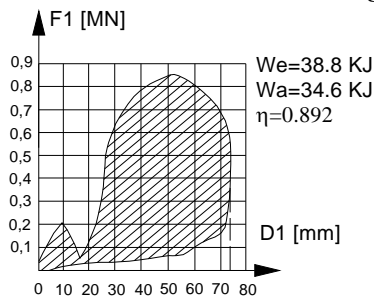


Fig. 5 $V = 12,7$ Km/h

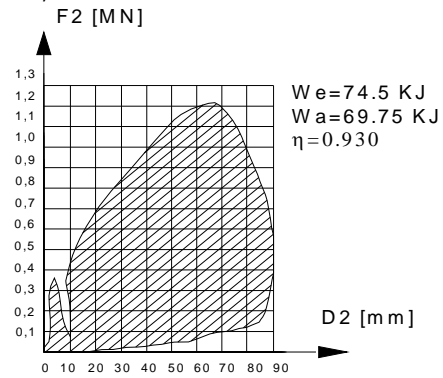
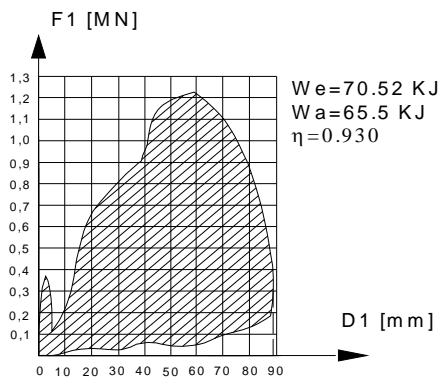


Fig. 6 $V = 16$ Km/h

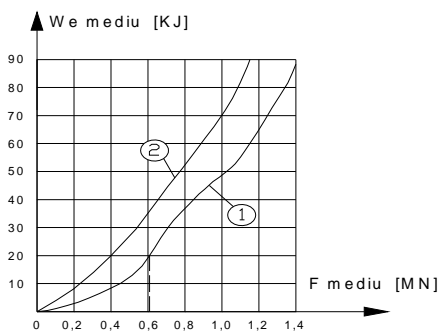


Fig. 7

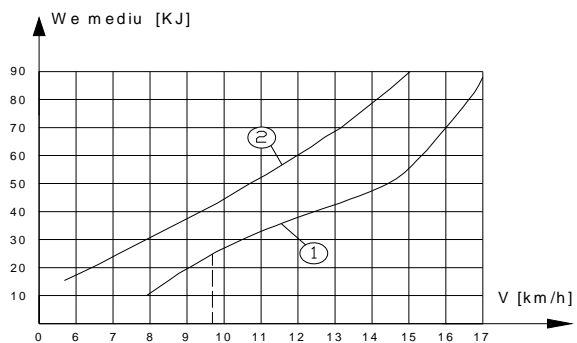


Fig. 8

Figures 7 and 8 show the variations of the average stored potential deformation energy of the category C buffers, as a function of the average force transmitted through the buffers and the collision velocity (curves 1). In the diagrams the same variations are shown for a category C buffer with a RINGFEDER type elastic element connected in parallel with a hydraulic dampener of own design (curves 2).

5. CONCLUSIONS

In order to establish the dynamic characteristics of the shock insulators (buffers, central coupling dampeners, long displacement dampeners), the method of the collision is imposed, which offers the real characteristics. Following the analysis of the experimental results for a force of under 1,3MN and a collision velocity above the velocity of 15Km/h, the studied buffers store potential deformation energy above 70KJ and consequently they can be classified as being category C according to UIC 526 -1 in accordance to the type of testing conducted.

REFERENCES

- [1.] Copaci I., Trif E. ș.a. „Aplicarea metodei tensometrice pentru calcularea forței transmise și a lucrului mecanic înmagazinat de amortizoarele de șoc în timpul tamponării”. Revista Transporturilor și Telecomunicațiilor nr. 3 la al II-lea Simpozion Național de Tensometrie cu participare internațională , Cluj Napoca – 1980, pg.33-39 .
- [2.] Sebesan I., Copaci I., „Teoria sistemelor elastice la vehiculele feroviare”, Editura Matrix Rom Bucuresti – 2008.
- [3.] Tănăsioiu Aurelia, Copaci Ion, „Study on the Sock caused by Collision of Railway Vehicles”, International Journal of Mechanics, ISSN 1998-4448, pag. 67-76, www.naun.org/journals/mechanics.







¹Gelu Ovidiu TIRIAN, ²Camelia BRETOTEAN-PINCA,
³Cristian CHIONCEL, ⁴Sergiu MEZINESCU

INDUSTRIAL IMPLEMENTATION OF THE PREDICTION, DETECTION, AND CRACK REMOVAL SYSTEM OF CONTINUOUS CASTING

^{1,2,4} UNIVERSITY POLITEHNICA OF TIMISOARA, FACULTY OF ENGINEERING FROM HUNEDOARA, ROMANIA
³ UNIVERSITY „EFTIMIE MURGU”, RESITA, ROMANIA

ABSTRACT:

The paper presents the industrial FDS deployment of crack prediction and elimination, and also an adaptive system to eliminate slipping between the semi-finished and pulling rollers (FAS), when the FDS casting speed performs any corrections.

KEYWORDS:

Continuous casting, implementation, crack, slip

1. INTRODUCTION

Continuous casting facilities are currently managed by automated systems organized several hierarchical levels [3].

Control systems ensure the right working algorithms required by an appropriate system working – both technologically and generally speaking –, and also in case of classical systems based on PID numerical controller [7]. Usually, there are no measures for crack prediction, thus rejects results from the process (in terms of tenth of tones of steel). In such case, working staff changes the working methods of the installation, based on internal instructions.

The casting programmer is not appropriate and that has important economical implications. Worldwide, there is research [1], [2], [4], [5] who might lead to already-made crack detection (inside the crystallizing apparatus) and damaged goods. Currently used methods do not entirely eliminate the cracks.

In [6], [8], it is proposed a number of original solutions allowing the complete crack rejection from the cast material, outside the crystallizing apparatus. Therefore, we have designed a neural network [6] allowing us to detect any primary crack, by a thorough predictive analysis of the information received from a thermo-couple matrix [7]. Information is used by a system based on fuzzy logics [8], which enables corrections of the casting speed and of the cooling water flow. Since this method does not lead to a complete crack rejection (although specialized literature refers to correcting the casting speed alone, in addition to that we have proposed to change the cooling water flow as well), we have adopted a new predictive principle who diminishes any possible cracking. Thus, the fuzzy system [8] analyzes a number of characteristic measurements and, although the neural network [6] has not yet acknowledged any crack, but it considers they may occur they perform casting speed corrections and cooling water flow occurs. Certainly, the solution we have proposed also implies a more complex fuzzy controller, using two sets of distinct set of rules.

Because crack disposal system produces speed corrections they are applied as a step; it was necessary to analyze any potential slipping between the bars and poured pick rollers (this slip happens when the casting starts, but then is not important). To remove the slide, which may adversely affect the speed adjustment, we designed an adaptive fuzzy system [9]. This crack prediction and elimination fuzzy system software was implemented on a development board then, it was tested in the plant.

2. METHODOLOGY DISCUSSION

To validate industrial principles and methods of prediction and elimination of cracks, attempts have been implemented in a real continuous casting plant, in operation, fig. 1. Since it is an operating plant, implementation was accomplished without significant disruption of the production process, which would immediately lead to unacceptable economic loss to the firm.



Fig. 1. Real continuous casting plant

Major subassemblies of the installation and key operating parameters when the tests have been performed are presented in figure 2., in a print-screen of the process management system.

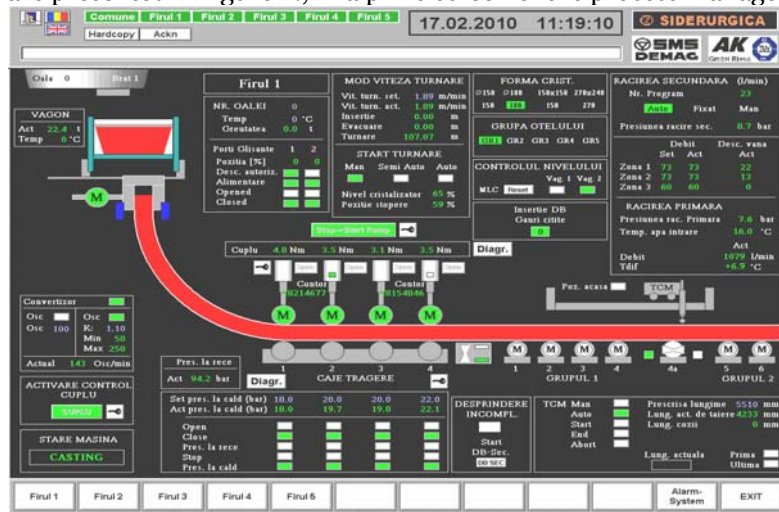


Fig.2. Continuous casting facility – print-screen of the industrial process management system

This was implemented under the FDS industrial cracks prediction and elimination adaptive system to eliminate slipping between semi finished-drawing rollers (FAS). Conditions in which attempts were made were very strict, with minimum disruption process and assistance of specialized hardware.

Implementing solutions within the industrial plant consisted mainly in the following:

Two plates full development were purchased, including related software.

A. On one plate we implemented ADF cracks prediction and elimination system, and on the other plate the adaptive system to eliminate slipping (FAS). Since the software implementation is performed in C-language, related programs were designed.

B. Specialists have introduced these systems in driving continuous casting process.

C. Technological parameters were performed during the casting: up to 1042 o'clock, cooling water flow was very high, the casting speed reached its average values, temperature distributor was high, the technological risk was high, and FDS considered a risk of cracks large enough; when we did a very small correction of cooling water flow rate and a large correction of the casting speed, which is 1.6 m/min. At 1043 o'clock, the distributor temperature was lower and become small. FDS noticed a decrease in the risk of a rupture, dictating a low speed correction, fig.3. Accordingly, the casting speed increased to 2 m/min. Following the rules, the first situation corresponds to rule 207, and the second to rule 205. From fig.3, recorded directly from the process, we conclude that FDS interpreted correctly the situations encountered and dictate related remedies.

D. To check the operation of the FAS, there were also a series of tests. Its implementation was carried out by specialists of the beneficiary, in accordance with their internal rules.

All the records presented were taken directly from the production control system. Implementation agreement with the FDS and the FAS has been very difficult, since this is private property multifunction with a continuous casting line in current production. This agreement was achieved and supported by business professionals of the company because research conducted by them was considered very interesting and useful, but they wanted a confirmation of their practice.

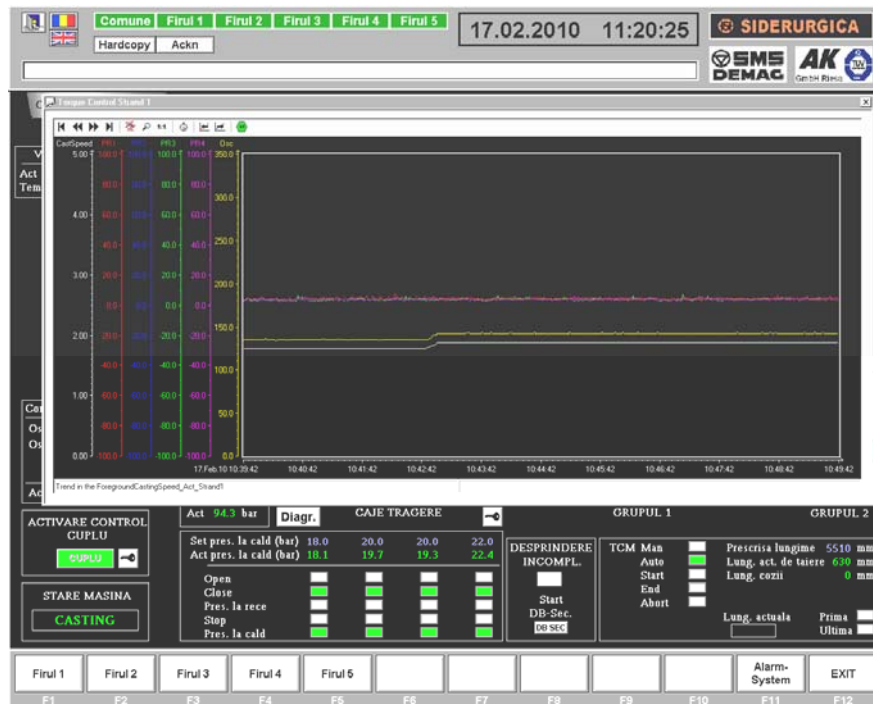


Fig.3. Evolution of casting speed to decrease the risk of a rupture



Fig.4. Variation of active wheel speed without FAS action

Initially, the FAS was no longer used. At 1030 o'clock, it required an increase in casting speed from 1-2 m/min. In fig.4 we see that there is an increase in active roll (with a small override for growth approximately 8 seconds). Because of this fast growth there is a slip between the roll and the cast material. Passive wheel speed changes as in fig.5, and lasts for 48 seconds, which is very

much. At 1036 o'clock, the phenomena repeated in reverse order (we ordered a decreasing of the speed drawing). It was confirmed that in case slipping occurs more often the effective time of casting speed change.

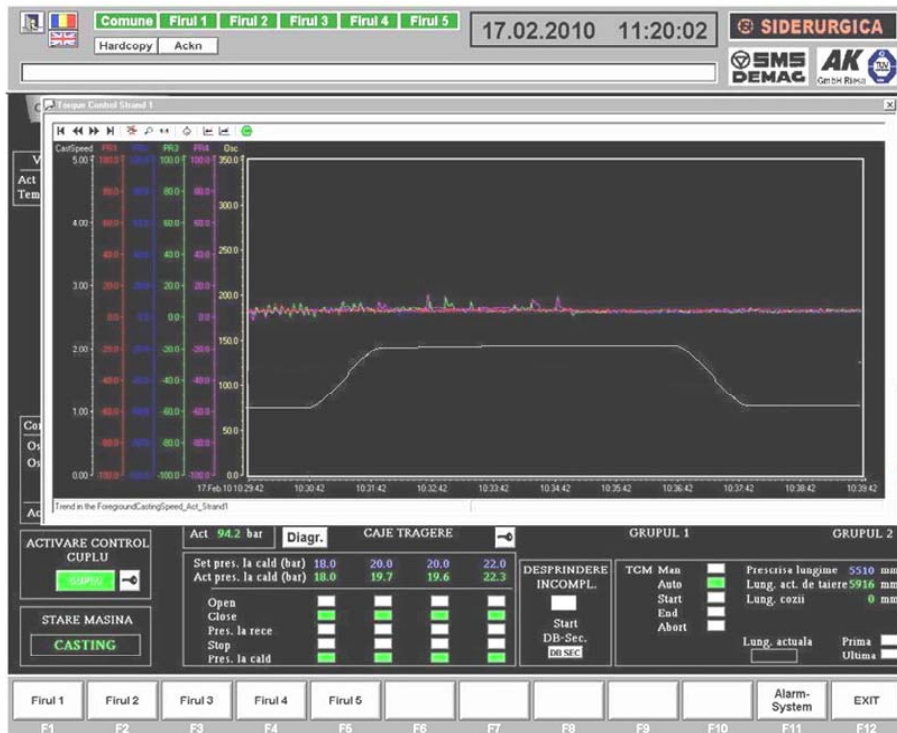


Fig.5. Variation of passive wheel speed without FAS action

Next, we put API into service. At 1041 o'clock we ordered to increase again the speed of 1-2 m/min, fig.6. Note that now the active drawing roller speed varies slowly (rise time approximately 18 seconds) and bar cast speed increase without sliding fig.7 in 18 seconds. In conclusion it appears that FAS acted under rule base.



Fig.6. Active wheel speed variation when FAS is in running

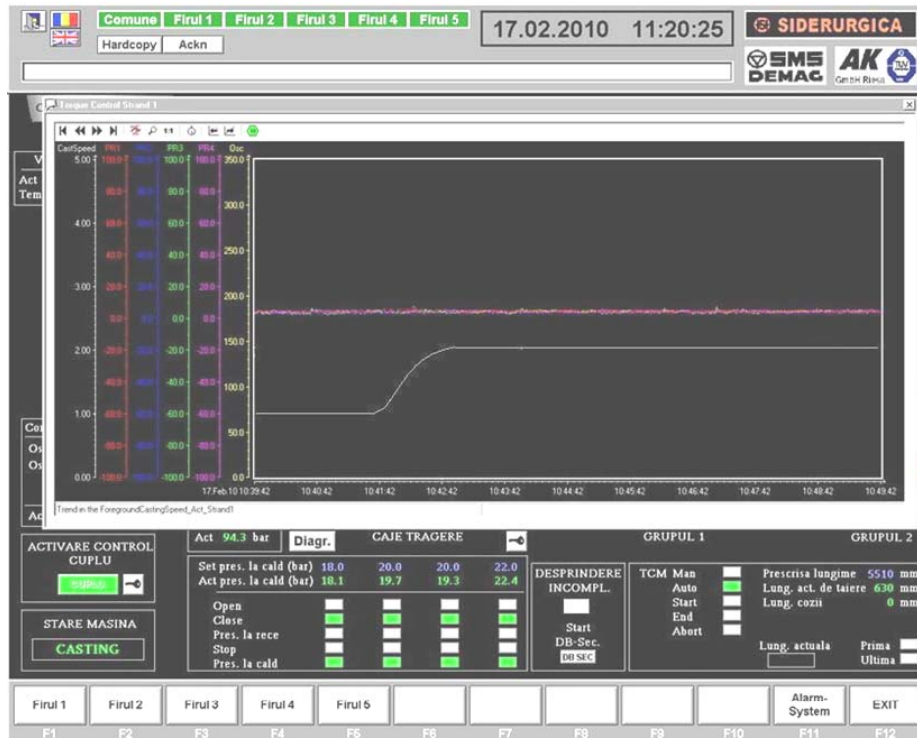


Fig.7. Variation passive roller speed when FAS is in running

3. CONCLUSIONS

We implemented an industrial FDS for crack prediction and elimination adaptive system to eliminate slipping semi-finished - roller drawing (FAS). Following implementation of the FDS and the FAS industry have achieved very good results, which led both to eliminate cracks and to eliminate slipping semi-finished - drawing roll.

REFERENCES

- [1.] J. Adamy - *Device for Early Detection of run-out in continuous casting*, United States Patent, No.5, 904.202, Date of Patent May 18 (1999).
- [2.] C. Avila, Y. Tsuji - *Crack width prediction of RC structures by Artificial Neural Networks, Adaptive and Natural Computing Algorithms*, Springer Vienna, pg.92-95, 12.dec. (2005).
- [3.] S. Bouhouche, et. all - *Quality Monitoring Using Principal Component Analysis and Fuzzy Logic. Application in Continuous Casting Process*, American Journal of Applied Science (AJAS), 4 (9), ISSN: 1546-9239, 2007, pp.637-644.
- [4.] T. Nakamura, K. Kazuho - *Breakout Prediction System in the continuous casting process*, the United States Patent, No.5, 548.520, Date of Patent Aug. 20 (1996).
 5. F.P. Pleschiutchnugg - *Method and apparatus for the early recognition of ruptures in the continuous casting of steel a year with Oscillating Mold*, United States Patent, No. US 6,179,041 B1 Date of Patent Jan. 30 (2001).
- [5.] G.O. Tirian - *Neural system for detecting cracks in the wire of the continuous casting*, 12th International Research/Expert Conference, Trends in the Development of Machinery and Associated Technology, pp 649-652 Istanbul, Turkey, August 2008.
- [6.] G.O. Tirian, S. Anghel S., M. Pănoiu, C. Pinca-Bretotean - *Control of the Continuous Casting Process Using Neural Networks*, Proceedings of the 13th WSEAS International. Conference on Computers, Rhodes Island, Greece, July 23-25, ISSN :1790-5109, ISBN :978-960-474, 099-4, 2009, pp.199-204.

- [7.] G.O. Tirian, O. Prostean, S. Anghel, Pinca B. C, D.Cristea - *Fuzzy Control System for Implementing the cracks During the continuous casting*, Annals of DAAAM & Proceedings of the 20th International Symposium DAAAM, Volume 20, No.1, ISSN 1726-9679, ISBN 978-3-901509-70-4, pp 1661-1662, 25-28th November 2009, Vienna, Austria.
- [8.] G.O Tirian, G. Prostean, S. Rusu-Anghel, D. Cristea et. all - *Adaptive control system of continuous casting process based on the fuzzy logic mechanism* - IEEE International Joint Conferences on Computational Cybernetics, ICC3 and Technical Informatics CONTI 2010, May 27-29, Timisoara, ISBN: 978-1-4244-7431-8, pp.379-382, 2010.





¹Adrian DANILA

THE DYNAMIC MODEL OF THE CAPACITOR-RUN TWO-PHASE INDUCTION MOTOR - A VARIATIONAL APPROACH

¹ TRANSYLVANIA UNIVERSITY OF BRASOV, ROMANIA

ABSTRACT:

The dynamic models of the three-phase electric machines are obtained within the classical approach with the direct- and quadrature-axis theory via two transformations of the dynamic set of equations, i.e. the Park and Clarke transformations. Several assumptions such as no magnetic saturation, no space-harmonics are used for simplification purposes. The variational method also called the Euler-Lagrange method is another approach for modeling the dynamic behaviour of the electric machines that relates to the physical energy of the drive. The Euler-Lagrange models are more suitable than the two-axis theory models when magnetic saturation or/and space harmonics are to be taken into account. In this paper, an analysis of the coarse start-up of a capacitor-run two-phase induction motor based on the variational approach is presented. The core of this approach is the Lagrangian of the system i.e. a real function describing the dynamic behaviour of the system, [1], [2]. The basics of this approach and its main characteristics are discussed into the first chapter. In the second chapter of the paper an expression for the Lagrangian for the capacitor-run two-phase induction motor is introduced. In the third chapter, the evolution with time of the values of the Lagrangian's components is detailed. The discussion is based on a set of experimental data and a dedicated software application. The results of the analysis show that the variation approach may provide not only basic information such as the values of the induced currents, but can also give additional information about the stability of the drive. The conclusions and further developments are presented in the last chapter of the paper.

KEYWORDS:

three-phase electric machines, variation approach

1. INTRODUCTION

The dynamic models of systems are representations such as functions, sets of differential equations and so that allow estimations on the outputs based on input measurements. There are two basic ways to determine the dynamic models of a given system (1) either using explanatory theories or (2) with input and output measurements and system identification algorithms.

In the basic approach, the dynamic models of the electric drives are obtained with the direct and quadrature-axis theory tailored to the specific class of the electric machine and power converter. The implementation of the direct and quadrature-axis theory provide models that allow estimating system's response in the time domain, [3]. The estimate's consistency is affected by the accuracy of the measurements and the consistency of the parameters' estimates. With the space vector definition, the time domain model of the machine may be transformed into the complex representation. The complex representation of the electric machine model provides the easiest way to transform the dynamic model from one reference coordinate system to another. In addition, in the complex representation the command of the three-phase inverters can be handled in the most appropriate manner.

With the notations generally accepted in the literature, index 1 for the stator and index 2 for the rotor, the dynamic set of equations in complex representation is as follows, [3].

$$\underline{u}_1 = R_1 \cdot \underline{i}_1 + \frac{d\Psi_1}{dt} \quad \text{voltage equation – stator,} \quad (1)$$

$$0 = R_2 \cdot \underline{i}_2 + \frac{d\Psi_2}{dt} + j \cdot \Psi_2 \cdot \frac{d\gamma}{dt} \quad \text{voltage equation – rotor,} \quad (2)$$

$$\Psi_1 = L_1 \cdot \underline{i}_1 + L_h \cdot \underline{i}_2 \quad \text{flux linkages equation – stator,} \quad (3)$$

$$\Psi_2 = L_1 \cdot \underline{i}_1 + L_h \cdot \underline{i}_2 \quad \text{flux linkages equation – rotor,} \quad (4)$$

$$M_{el} = \frac{3}{2} \cdot p \cdot \text{Im}(\Psi_2 \cdot \underline{i}_2^*) = \frac{J}{p} \cdot \frac{d\gamma}{dt} + M_w \quad \text{torque equation.} \quad (5)$$

Another approach issued from the quantum electro-dynamic theory relates to the Lagrangian function of the system represented as a function of two sets of generalized coordinates [1] as follows.

$$\text{- the first is a set of complex numbers } q^c = (q_1, \dots, q_{2n^c}) \text{ with } 2 \cdot n^c = \overline{0, n} \text{ and} \quad (6)$$

$$\text{- the second, a set of real numbers } q^r = (q_{2n^c}, \dots, q_n) \text{ with } n^r = n - n^c. \quad (7)$$

The Lagrangian is a real-value and analytic function of complex variables, $L(q^c, q^{c*}, q^r, \dot{q}^c, \dot{q}^{c*}, \dot{q}^r)$ related to the dynamic set of equations by the Euler-Lagrange equations on the following form.

$$\frac{d}{dt} \left(\frac{\partial L}{\partial \dot{q}_k} \right) = \frac{\partial L}{\partial q_k} + S_k, \quad k = \overline{0, n} \quad (8)$$

where the S_k -terms correspond to the non-conservative energy exchanges with the environment.

For the electrical drives, the dynamic set of equations, in variational form is as follows, [2].

$$\frac{d}{dt} \left(\frac{\partial L}{\partial \dot{\gamma}} \right) - \frac{\partial L}{\partial \gamma} = -M_w \quad \text{torque equation,} \quad (9)$$

$$2 \cdot \frac{d}{dt} \left(\frac{\partial L}{\partial \dot{i}_1^*} \right) - \frac{\partial L}{\partial i_1} = \underline{u}_1 - R_1 \cdot \underline{i}_1 \quad \text{voltage equation - stator} \quad (10)$$

$$2 \cdot \frac{d}{dt} \left(\frac{\partial L}{\partial \dot{i}_2^*} \right) - \frac{\partial L}{\partial i_2} = -R_2 \cdot \underline{i}_2 \quad \text{voltage equation - rotor} \quad (11)$$

2. METHODOLOGY

The stator of the capacitor-run, two-phase induction machine has two distributed windings, the main and the auxiliary windings. The axes of these windings are located at 90 electrical degrees with respect to the air gap of the machine. The numbers of turns of these windings usually differ. The main winding is supplied directly from the grid whereas the auxiliary winding is supplied through a capacitor from the grid to produce the quadrature current component.

The rotor is symmetrical and similar to the rotor of the squirrel-cage three-phase induction machine. Due to these features, the stator produces an elliptic magnetic motion field into the air gap, [4].

The dynamic set of equations in complex representation with the stator asymmetry taken into account will be as follows.

$$\underline{u}_{S1} = R_{1m} \cdot \underline{i}_{S1} + \frac{d\Psi_{S1}}{dt} - R_{1a} \cdot \underline{i}_{S1}^* \quad \text{voltage equation – stator} \quad (12)$$

$$0 = R_2 \cdot \underline{i}_{R1} + \frac{d\Psi_{R1}}{dt} + j \cdot \Psi_{R1} \cdot \frac{d\gamma}{dt} \quad \text{voltage equation - rotor} \quad (13)$$

$$\Psi_{S1} = L_{hm} \cdot (1 + \sigma_1) \cdot \underline{i}_{S1} + L_{hm} \cdot \underline{i}_{R1} - L_{ha} \cdot \underline{i}_{S1}^* - L_{ha} \cdot \underline{i}_{R1}^* \quad \text{flux linkage equation - stator} \quad (14)$$

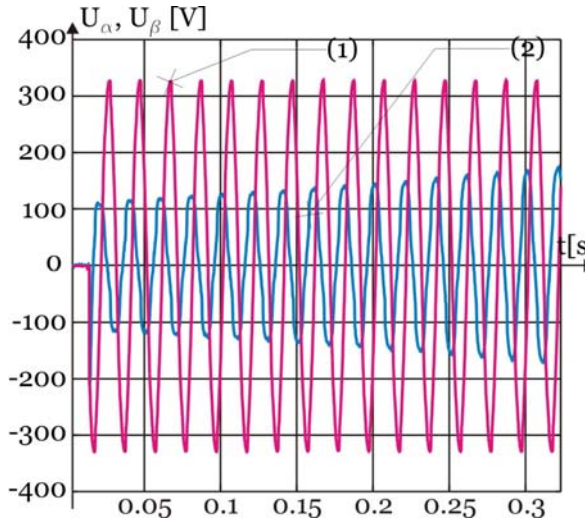


Figure 1: the input supply voltages at the motor terminals; (1) – the main winding supply voltage and (2) – the auxiliary winding supply voltage.

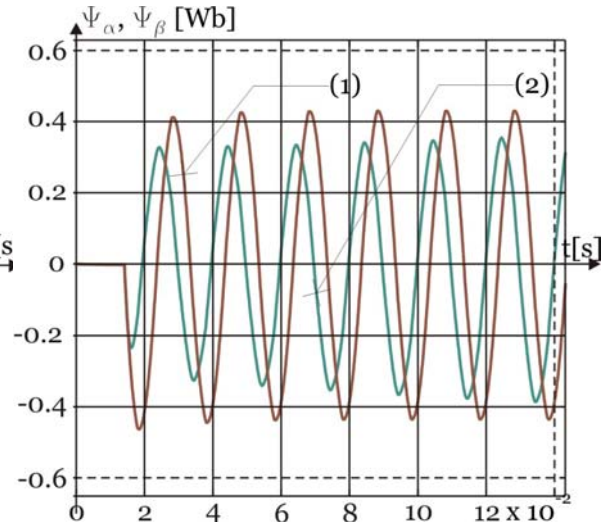


Figure 2: the components of the flux linkages within the air gap; (1) – the direct component and (2) – the quadrature component.

$$\underline{\Psi}'_{R1} = L_{hm} \cdot (1 + \sigma_2) \cdot \dot{i}_{R1} + L_{hm} \cdot \dot{i}_{S1} - L_{ha} \cdot \dot{i}_{S1}^* - L_{ha} \cdot \dot{i}_{R1}^* \quad \text{flux linkage equation - rotor} \quad (15)$$

$$M_{el} = p \cdot \text{Im} \left(L_{hm} \cdot \dot{i}_{S1} \cdot \dot{i}_{R1}^* - L_{ha} \cdot \dot{i}_{S1}^* \cdot \dot{i}_{R1} - L_{ha} \cdot (\dot{i}_{R1}^*)^2 \right) \quad \text{torque equation} \quad (16)$$

The magnetizing inductances over the two axes of magnetic asymmetry of the stator are given by the following expressions.

$$L_{hm} = \frac{L_{h\alpha} + L_{h\beta}}{2}, \quad \text{and} \quad L_{ha} = \frac{L_{h\alpha} - L_{h\beta}}{2} \quad \text{respectively.} \quad (17)$$

We introduce the Lagrangian of the run-capacitor induction machine as follows.

$$\begin{aligned} \mathcal{L}(\gamma, \dot{\gamma}, \dot{i}_{R2}, \dot{i}_{R2}^*, \dot{i}_{S1}, \dot{i}_{S1}^*) &= \mathcal{L}_{mec} + \mathcal{L}_{mag} \\ &= \frac{J}{2} \cdot \dot{\gamma}^2 + \frac{L_{hm}}{2} \cdot \left| \dot{i}_{S1} + \dot{i}_{R2} \cdot e^{j\gamma} \right|^2 - \frac{1}{4} \cdot L_{ha} \cdot \left[\left(\dot{i}_{S1} + \dot{i}_{R2} \cdot e^{j\gamma} \right)^2 + \left(\dot{i}_{S1}^* + \dot{i}_{R2}^* \cdot e^{-j\gamma} \right)^2 \right] + \\ &+ \frac{L_{\sigma 1}}{2} \cdot \left| \dot{i}_{S1} \right|^2 + \frac{L_{\sigma 1}}{2} \cdot \left| \dot{i}_{R2} \right|^2 \end{aligned} \quad (18)$$

With the magnetic fluxes given by the expressions:

$$\underline{\Psi}_{S1} = 2 \cdot \frac{\partial \mathcal{L}}{\partial \dot{i}_{S1}^*} \quad (19)$$

$$\underline{\Psi}_{R1} = 2 \cdot \frac{\partial \mathcal{L}}{\partial \dot{i}_{R1}^*}. \quad (20)$$

As seen from the notation (18), the magnetic Lagrangian has four components. An evaluation of the variation of these components at the coarse start-up of the capacitor-run induction machine is subsequently analysed.

3. DISSCUSSIONS/RESULTS/ANALYSES

The motor under the investigation was of MSP311 type. The nominal parameters of the motor are given in Table 1.

Table 1: The Nominal Parameters of the MSP311 Motor

Denomination	Rated supply voltage	Rated frequency	Rated angular speed	Number of pair poles	Capacitance
Units	[V]	[Hz]	[rpm]	[-]	[μF]
Value	220	50	2820/420	1/6	14

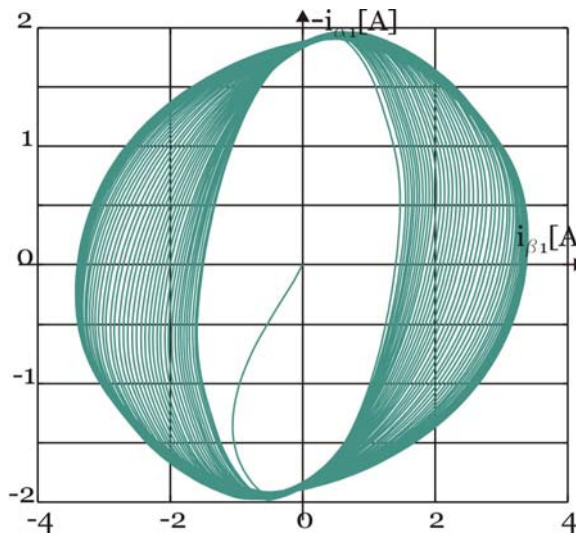


Figure 3: The space vector of the stator currents at coarse, no-load start-up.

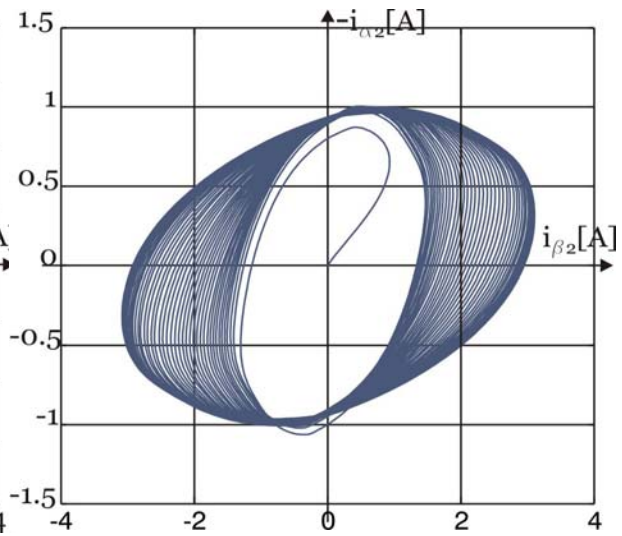


Figure 4: the estimated space vector of the rotor currents at coarse, no-load start-up.

The electrical and magnetic parameters of the motor had been earlier determined by direct measurements for the stator windings or had been computed through the FEM method for inductances, [5]. The results are presented in Table 2.

Table 2. The Electrical and Mechanical Parameters of the MSP311 Motor

Denomination	Stator resistance d/q axis	Stator self-inductance d/q axis	Mutual inductance d/q axis	Rotor resistance	Rotor self-inductance
Units	[Ω]	[H]	[H]	[Ω]	[H]
Value	20,8/57,5	0,358/0,665	0,275/0,504	17,0	0,523

The values were defined as follows.

- excitation values:

$$\underline{u}_{S1}, M_w$$

- state values:

$$\underline{\Psi}_{S1}, \underline{\Psi}_{R1}, \omega$$

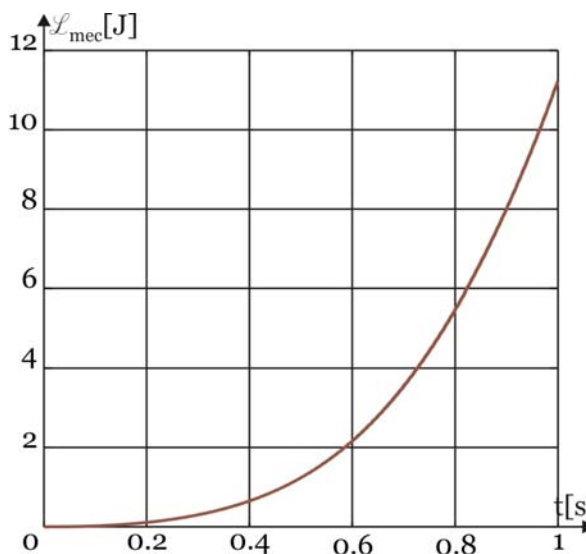


Figure 5: the mechanical component of the Lagrangian at coarse start-up.

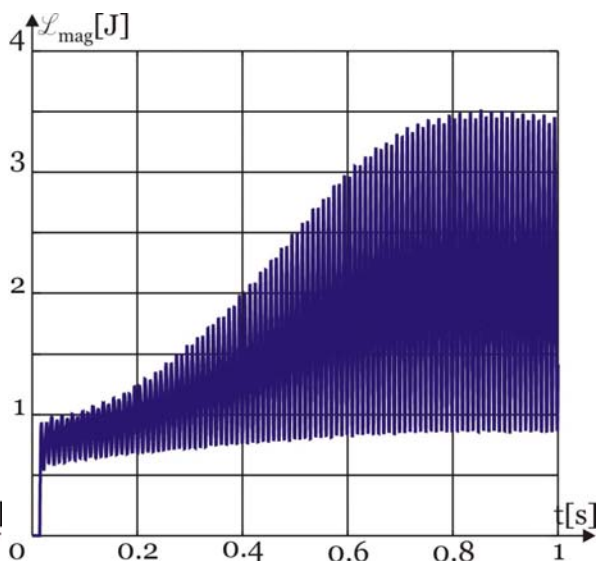


Figure 6: the magnetic Lagrangian at coarse start-up.

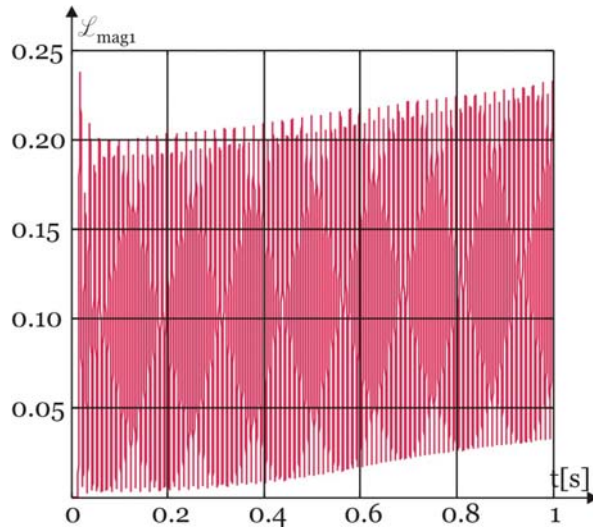


Figure 7: the symmetrical magnetizing component of the Lagrangian at coarse start-up.

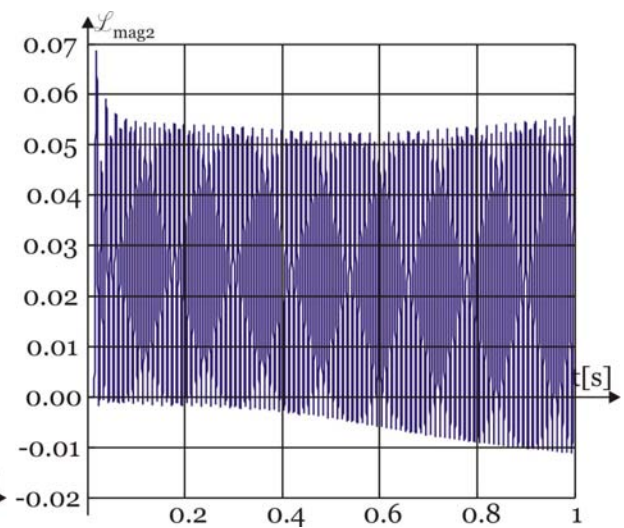


Figure 8: the asymmetrical magnetizing component of the Lagrangian at coarse start-up.

The supply voltage components were acquired on a dedicated test-band with a computer-aided measurement system. The state values and the Lagrangian were determined through a dedicated Matlab application. The dynamic model used to estimate the rotor currents and fluxes was the flux model of the machine issued from the equations set (1) to (5).

The supply voltages dependencies with time and the components of the flux linkages within the air gap of the machine are presented in Figure 1 and Figure 2.

The space vectors of the stator and rotor currents are presented in Figures 3 and 4, respectively.

As shown in Figure 1, the auxiliary voltage increased to the steady state magnitude with a time constant of about 0.6 seconds. The magnetic motion field (mmf) into the air gap of the machine was highly elliptic during the start-up. In the steady-state operation the mmf became almost circular, Figures 3 and 4. However, in direct operation of the machine, the shape of the mmf is dependent on the load. Therefore, in direct operation, the efficiency of the machine cannot be optimized. To optimize the efficiency, an electronically controlled voltage supply must be added to the drive.

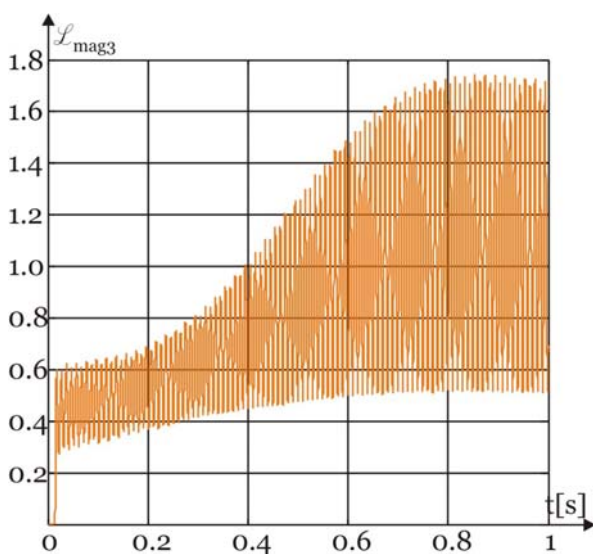


Figure 9: the symmetrical leakage magnetic component of the Lagrangian at coarse start-up

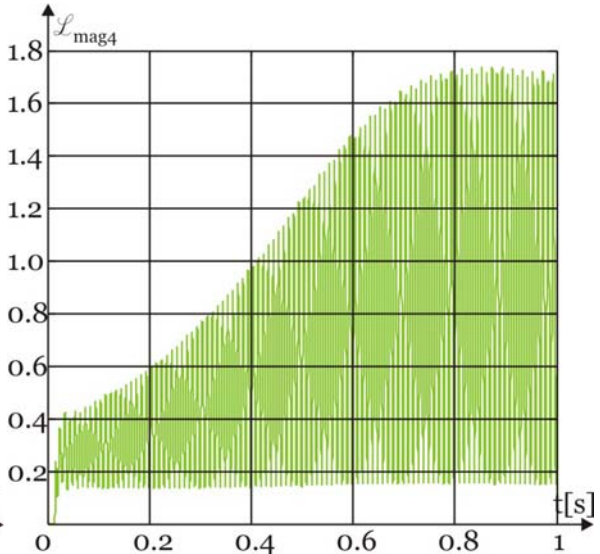


Figure 10: the asymmetrical leakage magnetic component of the Lagrangian at coarse start-up

In figures 5 and 6 the mechanical and the magnetic components of the Lagrangian are depicted. The mechanical Lagrangian represents the kinetic energy of the drive. The experiment was performed at no-load operation of the drive therefore the angular speed increased proportional with time. The magnetic Lagrangian takes into account the total amount of the magnetic energy into the machine. As seen from the plot, at the beginning of the process the magnetic circuitry of the machine was not magnetized. Therefore the start-up took some time until reaching the steady-state operation. This phenomenon is similar with the coarse start-up of the DC-shunt machine. The components of the magnetic Lagrangian are presented in Figures 7 to 10. As seen from the plots, the magnitude of the magnetizing components of the Lagrangian both symmetrical and asymmetrical parts are almost unchanged during the start-up process. However, the two magnitudes of the leakage components of the Lagrangian increase during the process. The maximum magnitude is achieved near the synchronous angular speed before the steady-state regime of the drive. In addition, the leakage components of the Lagrangian are much greater in comparison with the previous two components of the Lagrangian.

4. CONCLUSIONS/FURTHER PROPOSALS

In this paper, the variation of the Lagrangian of a capacitor-run two-phase induction motor during the coarse start-up of the drive has been investigated. The investigation proved an interesting similarity between the coarse start-up of the capacitor-run two-phase induction motor and the coarse start-up of the DC-shunt machine. As for the DC-shunt machine, the capacitor-run two-phase induction motor is not suitable for fast tracking servo-drives due to its large time constants.

The analysis also proved that the magnetic component of the Lagrangian has four components. The information regarding the dynamics of the start-up is mainly contained into the two leakage components of the Lagrangian. Because the Lagrangian and its components may not be measured through direct transducers, in the on-line applications, a digital signal processor should be used. Further developments consist in the use of the drive's Lagrangian to produce the command law for the drive system.

REFERENCES

- [1.] D. Basic, F. Malrait, and P. Rouchon, Euler-Lagrange Models With Complex Currents of Three-Phase Electrical Machines and Observability Issues, IEEE Transactions on Automatic Control, Vol.55, No.1, 2010, pp. 212-217
- [2.] I. Boldea and S. A. Nasar, The Induction Machine Handbook, CRC Press, 2002
- [3.] G. Henneberger, Electrical Machines II. Dynamic Behavior, Converter Supply and Control, Aachen University, 2002
- [4.] S. Bala, Dynamics of Single/Two Phase Induction Motors, University of Wisconsin-Madison, 2004
- [5.] A. Danila, I. Margineanu, R. Campeanu, C. Suciu, I. Boian, The Optimization of the Single/Two Phase Induction Motor Start-Up with Electronically Switched Capacitor, 2008 IEEE International Conference on Automation, Quality and Testing, Robotics. Proceedings – Tome III pp 450-454





DESIGN OF AN EDUCATIONAL INFORMATICS SYSTEM FOR THE STUDY OF THE EUCLIDIAN VECTORS USING UML DIAGRAMS

¹⁻² TECHNICAL UNIVERSITY OF TIMISOARA, ENGINEERING FACULTY OF HUNEDOARA, ROMANIA

ABSTRACT:

The informative society needs important changes in educational programs. The informational techniques needs a reconsideration of the learning process, of the programs, manuals structures, a reconsideration of the methods and organization forms of the didactic activities, taking into account the computer assisted instruction and self instruction. This paper presents the necessary stages in implementing an informatics system used for the study of euclidian vectors. The modeling of the system is achieved through specific UML diagrams representing the stages of analysis, design and implementation, the system thus being described in a clear and concise manner.

KEYWORDS:

Educational Software, Java, Vector, Distance Education, UML

1. INTRODUCTION

In the condition of informatics society whose principal source in the social-economic development is to produce and consumption the information, the complex and fast knowledge of the reality for rational, opportune, effective decisions is a desideratum which generate the necessity to form some superior level habituation in information manage for the whole population. The computers and their programs offer to the users powerful capabilities for the information manipulation: image and text visualize on the screen which can be manipulate later; memory storage of an important quantity of information, his accessing and selection of a part of them; possibility to realize a great volume of computation; possibility of equipment control and fast decisions; Computer Based Training [1].

This facilities offer to the microcomputers higher educational capabilities versus other technologies used in education and provide learning controlled based on many parameters: intellectual aptitude, level of knowledge, abilities, rhythm of work.

2. COMPUTER BASED TRAINING AS A DIDACTIC METHOD

The informatics society makes sensitive modification in education programs. In this scope, the school must prepare programmers, maintenance technicians, etc. In the same time it is necessary that the teacher make ready to use the computer in education process.

These informational techniques impose to reorganize the contents of the education process, of the programs, course books and manuals, to reconsider the methods and organization forms of didactic activities, which follow to be center on individualization of the teaching process [2].

The programmed teaching consist in information presentation in small units, logic structured, units that compose a program, the teaching program. The user will have possibility that after each sequence to have a knowledge about the measure of understanding the give information. The programmed teaching method organize the didactic action applying the cybernetic principles to the teaching-learning-evaluating activities level, considering like a complex and dynamic system, composed as an elements ensemble and inter-relations and develop his personal principles valid on the strategic level in any cybernetic organization form of teaching.

On the other hand, programmed teaching assumes some principles which the teaching program must respect [3]:

- ❖ The small steps principle consists in progressive penetration, from simple to complex, in a subject content which logic divided in simple units series lead to minimal knowledge, which later will form an ensemble. This principle regards the subject division in contents/information units that give to user the chance to succeed in his teaching activities;
- ❖ The principle of personal rhythm of study regard mannerism observance and capitalization of each user of the program which will be able to make the sequences of knowledge learning or control, in a personal rhythm appropriate to his psycho-intellectual development, without time limits. The user can progress in the program only if he accomplished the respective sequence requirement;
- ❖ The active participation principle, or active behavior, regard user effort trend into selection, understanding and applying the necessary information in elaboration of a correct answer. On each step the user is liable to an active participation to resolve the step job;
- ❖ The principle of inverse connection, regard positive or negative inputs of user competence, refer to the success or breakdown in task performed;
- ❖ The immediate and directly control of the task work precision with the possibility to progression to the next sequence, in case of success;
- ❖ The repetition principle, based to the fact that the programs are based on return to the users initial knowledge.

The combined programming interposes the linear and branch sequence according to teaching necessities.

After linear and branch programming the computer aided generative teaching has appear, where the exercises are gradually present, with different difficulty steps and answers on the students questions.

The expert system consists of self-teaching training programs, tutorial strategies, and the usage of natural language, mixed initiative and some complex representation of knowledge usage [4]. The computer based programmed teaching realize learning process with a inputs flow – the command, an executive controlled system, an output flux – control and a control system functions which correct measure establish.

In such a system have tree stages of teacher perceive: teaching, evaluating and the feedback loop closing, the computer being present in all of tree stages.

3. UML

Unified Modeling Language (UML) is a standardized general-purpose modeling language in the field of software engineering [5]. UML includes a set of graphical notation techniques to create abstract models of specific systems.

The Unified Modeling Language (UML) is an open method used to specify, visualize, construct and document the artifacts of an object-oriented software-intensive system under development. UML offers a standard way to write a system's blueprints, including conceptual components such as: actors, business processes, system's components and activities, as well as concrete things such as: programming language statements, database schemas and reusable software components.

UML combines the best practice from data modeling concepts such as entity relationship diagrams, business modeling (work flow), object modeling and component modeling. It can be used with all processes, throughout the software development life cycle, and across different implementation technologies. UML has succeeded the concepts of the Booch method, the Object-modeling technique (OMT) and Object-oriented software engineering (OOSE) by fusing them into a single, common and widely usable modeling language. It is very important to distinguish between the UML model and the set of diagrams of a system. A diagram is a partial graphical representation of a system's model. The model also contains a "semantic backplane" – documentation such as written use cases that drive the model elements and diagrams.

UML diagrams represent two different views of a system model [6]:

- ❖ Static view: Emphasizes the static structure of the system using objects, attributes, operations and relationships. The structural view includes class diagrams and composite structure diagrams.
- ❖ Dynamic view: Emphasizes the dynamic behavior of the system by showing collaborations among objects and changes to the internal states of objects. This view includes sequence diagrams, activity diagrams and state machine diagrams.

UML models can be exchanged among UML tools by using the XMI interchange format.

4. DEVELOPMENT STAGES OF THE EDUCATIONAL INFORMATICS SYSTEM

4.1. System's analysis

Using the UML modeling language, the analysis of an informatics system consists in drawing the use case and activity diagrams [7]. The software utility ArgoUML [8] was used to construct the diagrams.

The informatics system will be described in a clear and concise manner by representation of the use-cases. Each case describes the interaction between the user and the system. The use case diagram is represented in figure 1.

The presented diagram defines the system's domain, allowing visualization of the size and scope of the whole developing process. It contains:

- ❖ an actor - the user who represents the external entity with which the system interacts;
- ❖ six use cases describing the functionality of the system;
- ❖ relationships between the user and use cases (association relationships) and the relationships between use cases (generalization relationships).

For each use-case in the diagram presented earlier an activity diagram is constructed. Each diagram will specify the processes and algorithms that are behind the use cases studied. Activity diagrams [9] are represented by nodes (with partitions and branches) or conditional blocks (with decisions). The activity diagrams are used to visualize, specify, build and document dynamic issues related to the informatics system processes. They focus on flow control seeking the transition, in a certain order, from one activity to another.

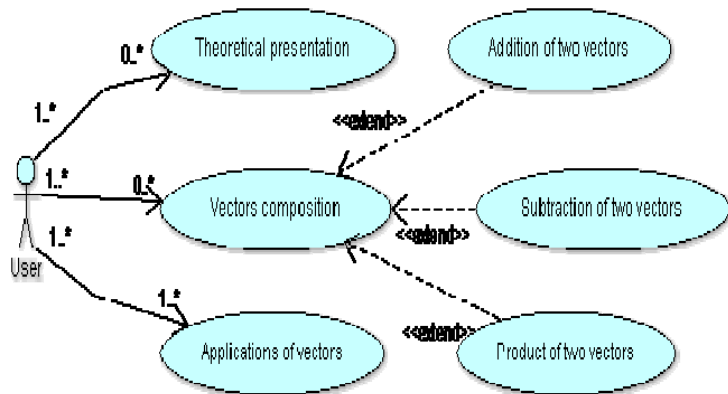


Figure 1 Use-cases Diagram

4.2. System's designing

Conceptual modeling [10] allows the identification of the most important concepts for the system. Since classes are concepts, the following two diagrams present the classes that will be used in the project.

Figure 2 presents the inheritance and achievement relationships used. It may be noted that all attributes and methods of the *Applet* class will apply to the derived class *Forta*, which implements two interfaces, *Runnable* and *ActionListener*.

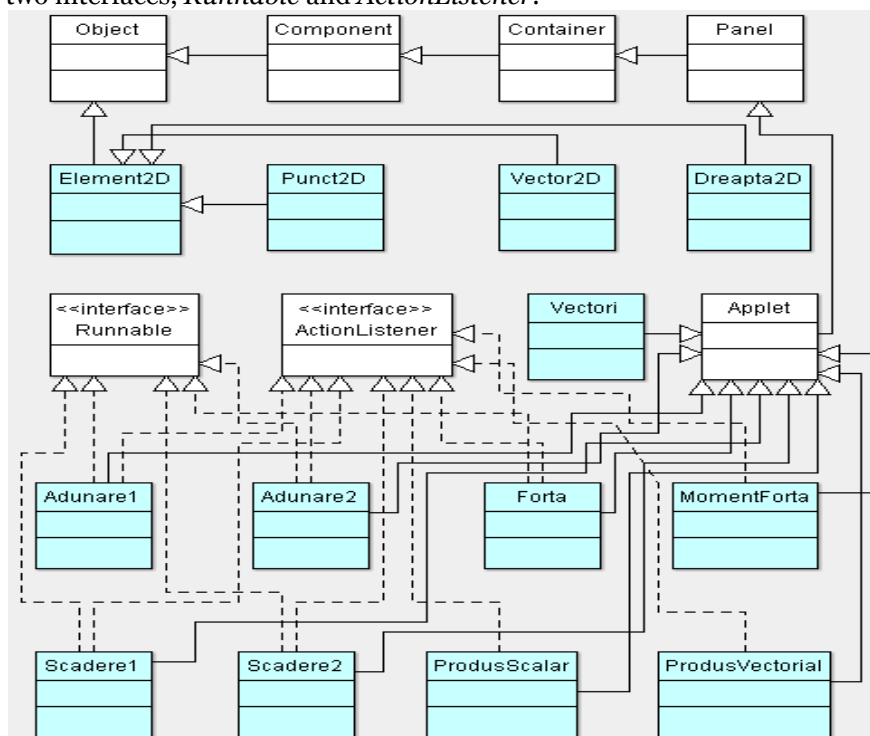


Figure 2 Class Diagram: the inheritance and achievement relationships

The composition relationships that exist between instances of the classes in the architecture are shown in figure 3. The difference of the composition relationship, with respect to aggregation, is that the instance of the whole could not exist without part objects. When looking at figure 3 one can see that a type *Vectori* instance consists of two *Punct2D* type items, one *Vector2D* object type, one *Dreapta2D* object type, five *JButton* object type and five *JTextField* object type. In such a relationship it is possible for an object to belong to several instances of a whole. For example object type *Vector2D* belongs to *Vectori*, *Adunare1*, *Adunare2*, *Scadere1*, *Scadere2*, *ProdusScalar*, *ProdusVectorial*, *MomentForta* and *Forta* type instances.

Both class diagrams shown contain specific classes to the application as well as existing classes and interfaces from Java.

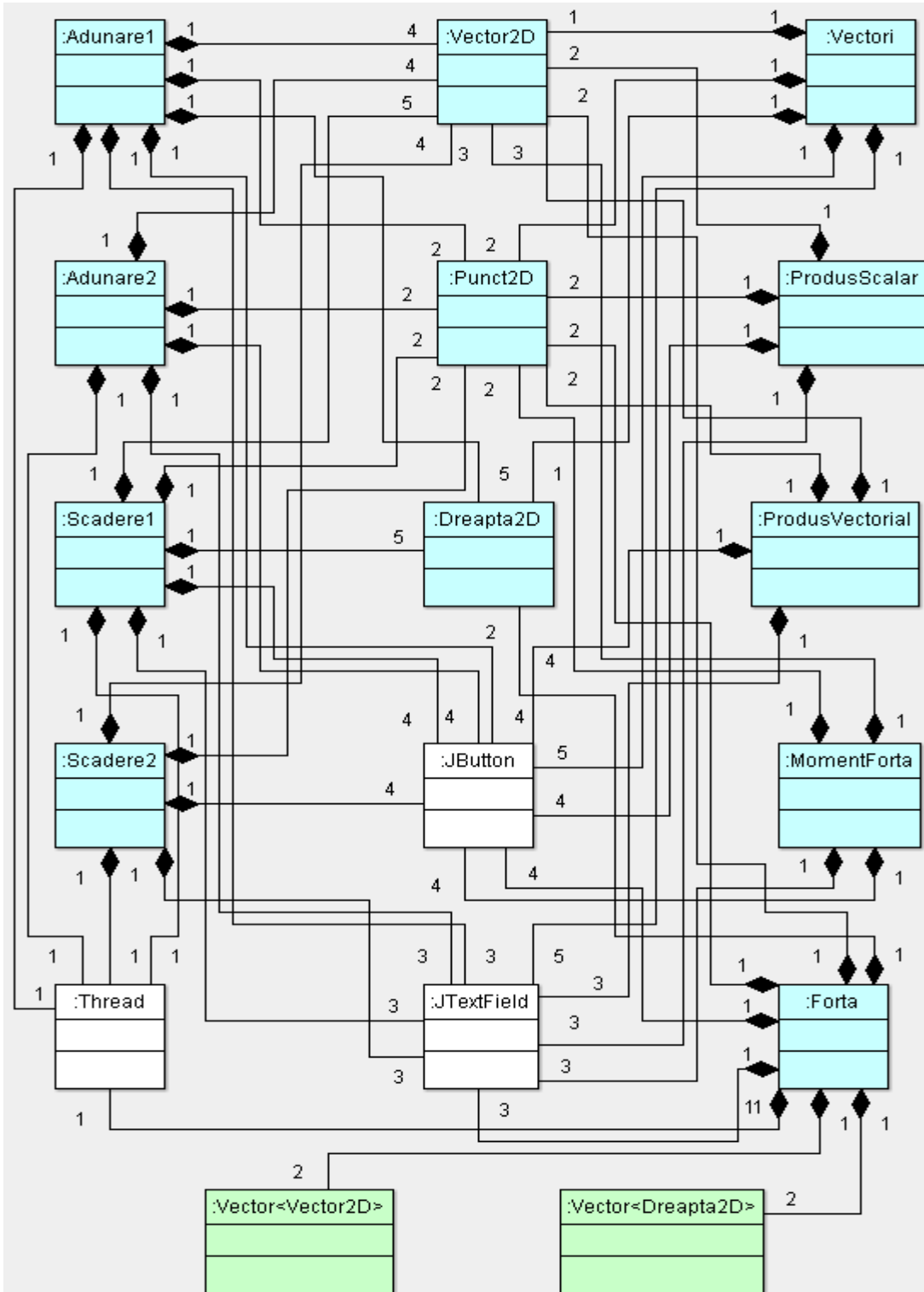


Figure 3 Class Diagram: The composition relationships

4.3. System's implementation

The component diagram [11] allows the visualization of the module in which the system is broken into and the dependencies between modules. The component diagram emphasis on physical software components (files, libraries, executables) and not on logic components, such as packages.

The diagram in figure 4 describes the collection of components that all together provide functionality for the educational informatics system.

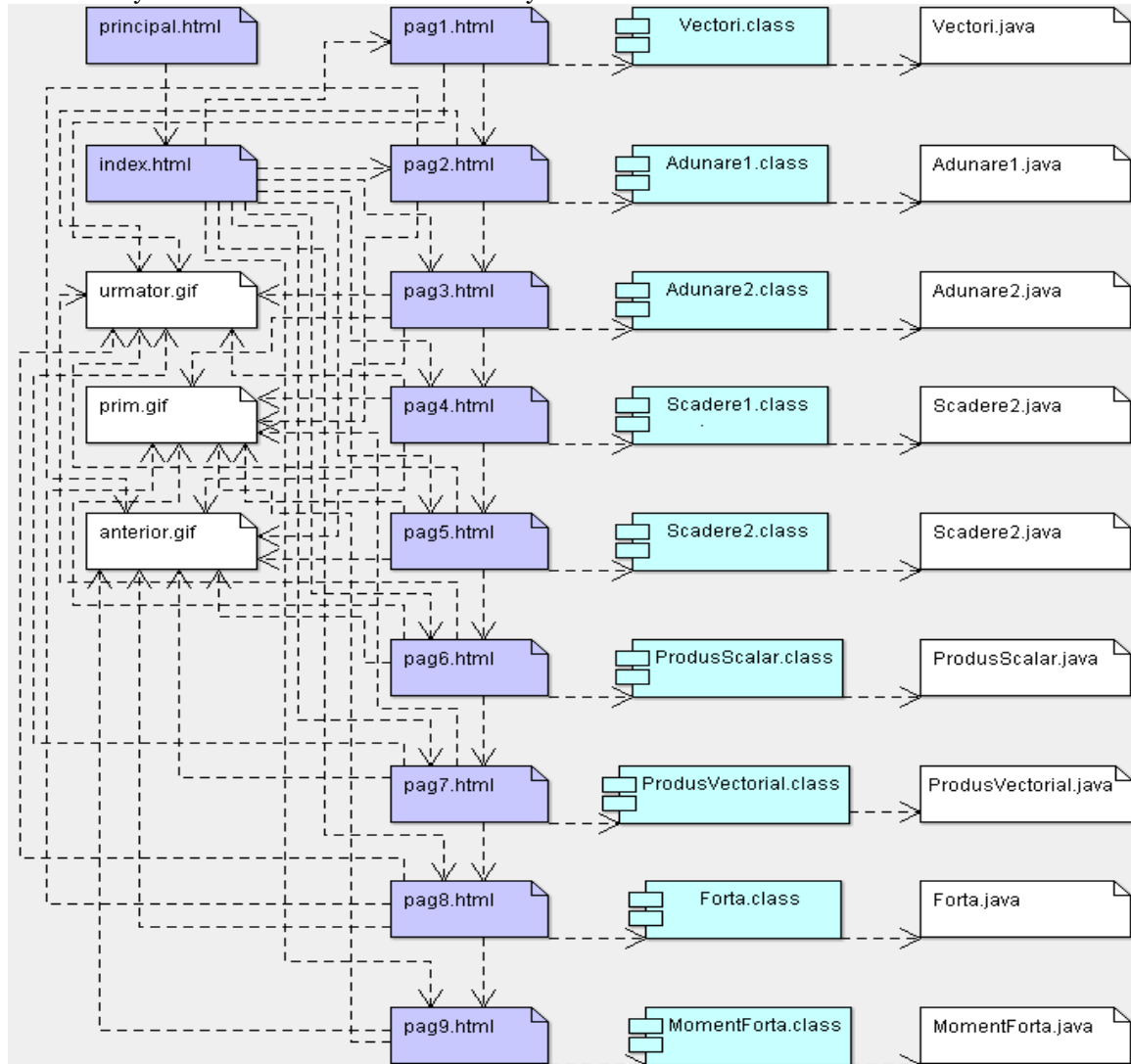


Figure 4 Component Diagram

5. USER INTERFACE

The educational informatics system is accomplished using the Java programming language [12]. The main page of the application contains buttons for selecting the following options: addition of two vectors using the parallelogram rule and the triangle rule (figure 5), subtraction of two vectors using the parallelogram rule and the triangle rule (figure 6), scalar product of two vectors, cross product of two vectors, total forces what reacts on a material point (figure 7) and force momentum in rapport with a point. The method of the class *Adunare2* which draw the addition of two vectors is presented forwards:

```
public void run() { pas=3;
    for (int k=9;k>=0;k--) {double x,y,x1,y1;
        x=k/(double)10*v2.getOrigine().getX()+ (1-k/(double)10)*v1.getExtremitate().getX();
        y=k/(double)10*v2.getOrigine().getY()+ (1-k/(double)10)*v1.getExtremitate().getY();
        O=new Punct2D(x,y);
        x1=v1.getExtremitate().getX()+ (v2.getExtremitate().getX()-v2.getOrigine().getX());
        y1=v1.getExtremitate().getY()+ (v2.getExtremitate().getY()-v2.getOrigine().getY());
        x=k/(double)10*v2.getExtremitate().getX()+ (1-k/(double)10)*x1;
```

```

y=k/(double)10*v2.getExtremitate().getY()+v2.getOrigine().getY();
E=new Punct2D(x,y); O.setId("O2"); E.setId("E2"); vaux=new Vector2D(O,E);
repaint(); pause(300); } pas=4; double x1,y1;
x1=v1.getExtremitate().getX()-v2.getOrigine().getX();
y1=v1.getExtremitate().getY()+v2.getExtremitate().getY()-v2.getOrigine().getY();
E=new Punct2D(x1,y1); E.setId("E"); suma=new Vector2D(v1.getOrigine(),E);
String s1="O("+String.format("%.1f",suma.getOrigine().getX())+"";
s1+=String.format("%.1f",suma.getOrigine().getY())+"";
s1+="E("+String.format("%.1f",suma.getExtremitate().getX())+"";
s1+=String.format("%.1f",suma.getExtremitate().getY())+"";
s1+="p="+String.format("%.1f",suma.get_p());
s1+="q="+String.format("%.1f",suma.get_q());
t3.setText(s1); repaint(); pause(300); }
    
```

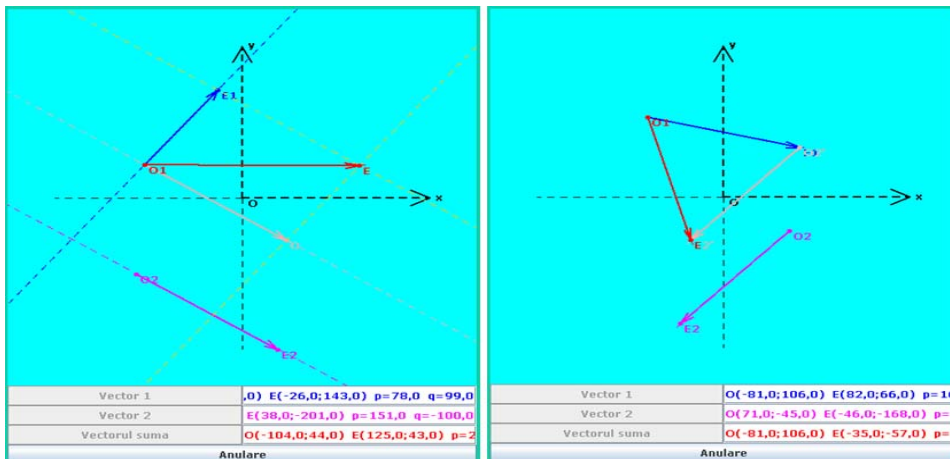


Figure 5. Addition of two vectors using the parallelogram rule and the triangle rule

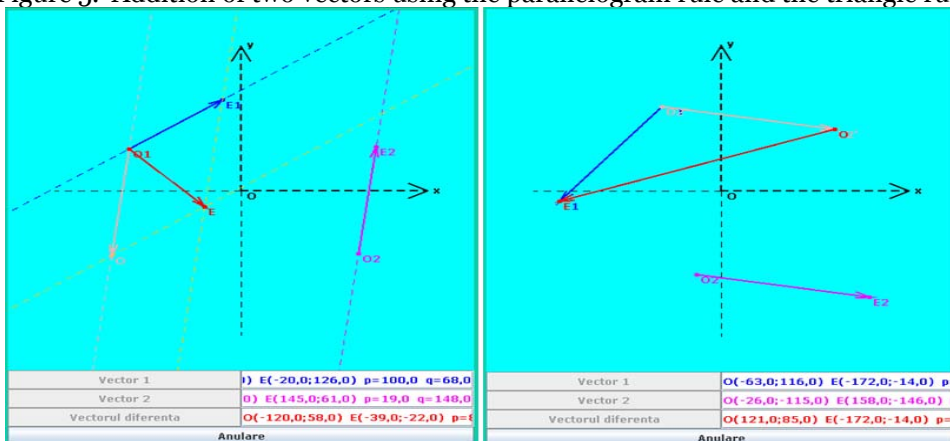


Figure 6. Subtraction of two vectors using the parallelogram rule and the triangle rule

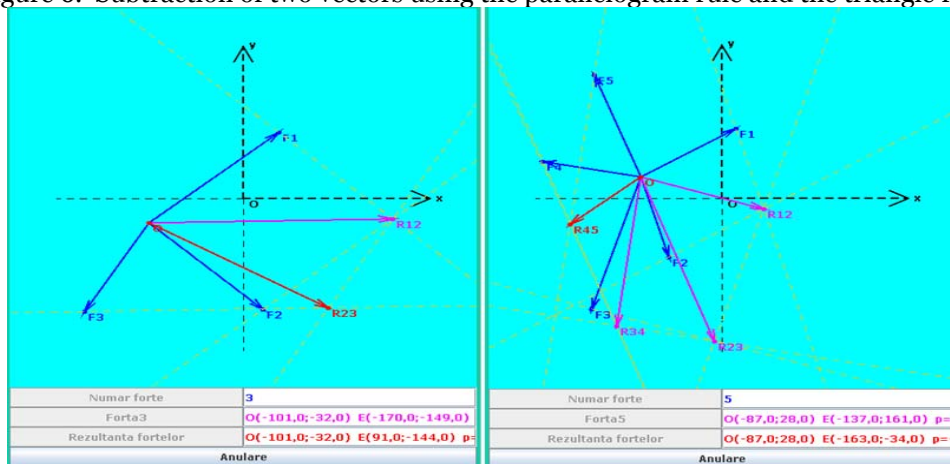


Figure 7. Total forces what reacts on a material point

6. CONCLUSIONS

Through the diagram representation all three phases: analysis, design and implementation, the educational informatics system has been described in a clear and concise manner. The use of the UML modeling language for the creation of the diagrams is characterized by rigorous syntactic, rich semantic and visual modeling support.

The diagrams were made using a new approach, multidisciplinary of the informatics application, encompassing both modern pedagogy methods and discipline-specific components. The link between teaching activities and scientific goals and objectives was established through the development of the new methods and the assimilation of new ways, capable of enhancing school performance, enabling students to acquire the knowledge and techniques required and apply them in optimum conditions.

REFERENCES

- [1.] A. Adăscăliței, *Instruire asistată de calculator. Didactica informatica*, Editura Polirom, 2007
- [2.] D. Glusac, D. Radosav, D. Karuovic, D. Ivin, *Pedagogical and Didactic-Methodical Aspects of E-learning*, 6th WSEAS International Conference on E-ACTIVITIES, Tenerife, Spania, 2007, pp. 67-75
- [3.] I. Negret-Dobridor, I. Panișoara, *Știința învățării. De la teorie la practică*, Editura Polirom, 2005
- [4.] I. Nicola, *Tratat de pedagogie școlară*, Editura Aramis, 2003
- [5.] G. Booch, J. Rumbaugh, I. Jacobson, *The Unified Modeling Language User Guide*, Addison Wesley, 1999
- [6.] M. Fowler, K. Scott, *UML Distilled: A Brief Guide to the Standard Object Modeling Language*, Addison Wesley, Readings MA, USA, 2000
- [7.] D. Bocu, *Inițiere în modelarea orientată obiect a sistemelor soft utilizând UML*, Editura Albastră, Cluj-Napoca, 2002
- [8.] <http://argouml.tigris.org>
- [9.] J. Odell, *Advanced Object Oriented Analysis & Design using UML*, Cambridge University Press, 1998
- [10.] J. Rumbaugh, I. Jacobson, G. Booch, *The Unified Modeling Language Reference Manual*, Addison Wesley, 1999
- [11.] D. Bocu, *Modelare orientată obiect cu UML*, Editura Albastră, Cluj-Napoca, 2006
- [12.] S. Tănasă, C. Olaru, S. Andrei, *Java de la 0 la expert*, Polirom Press, Iasi, 2007







ASPECTS OF THE ELECTRIC ARC FURNACE CONTROL

¹⁻⁴UNIVERSITY OF PETROSANI, ROMANIA

ABSTRACT:

Operating mode of electric arc furnace is influenced by a series of disturbances. These perturbations lead to growth of specific energy consumption and decrease in total electric oven We addressed the mathematical modeling of electric arc furnace (EAF) by analysis of related technological processes and the possibility of using simulation software model arc furnace as part of the grid. Mathematical modeling of electric arc furnace related processes (EAF) in order to optimize functional and technological performance of this complex aggregate has the direct positive consequences reducing specific consumption of electricity in steel development with about 15%, simultaneously obtaining a high quality steels electricity produced.

KEYWORDS:

electric arc furnace, energy consumption, modeling, optimize, control

1. INTRODUCTION

Electric arc furnaces (EAFs) are widely used in steelmaking and in smelting of nonferrous metals. Typical EAFs operate at power levels from 10MW to 100MW. The power level is directly related to production throughput, so it is important to control the EAF at the highest possible average power with a low variance to avoid breaker trips under current surge conditions. For efficient power control, good dynamic models of EAFs are required [2]. Melting metal in electric arc furnaces is based on the amount of heat developed in the arc and transmitted by radiation burden. Arc burning between solid electrodes and liquid (molten metal) in an ionized gaseous medium is the presence of an appropriate voltage [1].

Furnaces for steel development are generally three phase AC. Arcs are established between the electrodes and melt, representing oven with a consumer phase Y connection with isolated neutral. The three phase arc, unlike the single phase, has the advantage of load balancing supply network. In the system three- phases with the isolation of neutral, represented by arc furnace, the re-ignition of arc to one of three phase occurs more rapidly than for a single-phase arc, due to increasing pressure on this phase which contributes to increased stability of the arc combustion.

During operation of electric arc furnace, so that the power developed in the arc should have imposed, it is necessary that the distance between electrodes and solid or molten metal bath is kept constant. This distance and arc length is required so the voltage and current in the arc, the temperature and degree of ionization of the melting area.

The power indicators of the arc furnaces depend heavily on the current of arc. The variations are caused by current fluctuation in operating state. The dynamic characteristic V-I depends on the rapid variation of AC, which is not followed closely by voltage, especially at small currents due to thermal persistency of the arc-over which is reflected by different voltage in the same value of the current in arc [3].

2. ELECTRIC ARC FURNACE MODELLING

The notable contribution to EAF modeling was made by Morales et al [7]. An initial contribution was the study of the slag foaming where extensive slag data was collected and analyzed; the practical benefits of slag foaming by reduced electrical consumption and improved yield were reported from continued use a foaming on a plant [8].

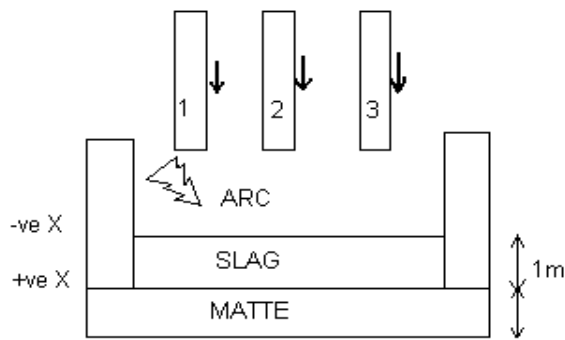


Fig. 1: Physical Model of EAF

The arc furnace model employs non-linear differential equations¹ as opposed to the traditional piecewise linear method resulting in more accurate and realistic simulation.

Arcing is a phenomenon that occurs when the electrodes are moved above the slag. As the electrode approaches the slag, current begins to jump from the electrode to the slag, creating electric arcs. Depending on the magnitude of the input voltages of the electrodes, the arcing distance can vary. Usually, arcing occurs in a region within centimeters of the slag (approximately 10- 15cm). Therefore, the EAF model must take into account the instances when x_1, x_2, x_3 are negative (i.e. the electrodes are suspended above the slag). The factors that affect the arc furnace operation are the melting or refining materials, the electrode position, the electrode arm control scheme and supply system voltage and impedance. Thus, the description of an arc furnace load depends on the following items: arc voltage, arc current and arc length (which is determined by the position of electrode).

In general, the different methods for arc furnace modeling may be classified into the "time domain" and "frequency domain" methods [6]. The electric arc furnace is a highly variable non-linear load, which according to some studies, possesses what is described as a chaotic pattern.

Voltage flicker is a stochastic and time varying phenomenon that causes variation in voltage root mean square in the frequency range (0.5-25 Hz) [6]. To generate the dynamic behavior of the arc furnace using different models, the slope of the V-I curve should be changed as a sinusoidal function. Since the electrical arc is a nonlinear and time varying phenomenon, description of its behavior in the time domain is easier than in the frequency domain. Let " l " be the arc length, A and B are the coefficients from experimental formula, then

$$v_{at} = A + B \cdot l \quad (1)$$

where, v_{at} reflects the arc furnace operating condition.

Time domain methods are the basic methods for flicker study in electrical arc furnaces.

Time domain methods can be classified into V-I Characteristic (VIC), and Equivalent Circuit Methods (ECM) [6]. The arc resistance in the case of sinusoidal variation is defined as: the ECM methods can be obtained from arc operation; the periodic variation of arc voltage and the resistance that arc shows can be used to develop the arc furnace model [1]. Too much simplification in developing the model may affect the accuracy of the model.

The dynamic load models consider periodic change of the arc resistance about the value given for each model. The electric arc furnace model was studied as a part of the electrical network as depicted in Figure 2. In a simulated attempt to reduce voltage flicker, the size of the STATCOM (the converter solution for reliable and stable grids) in the network was varied, while the size of the capacitors and parameters of

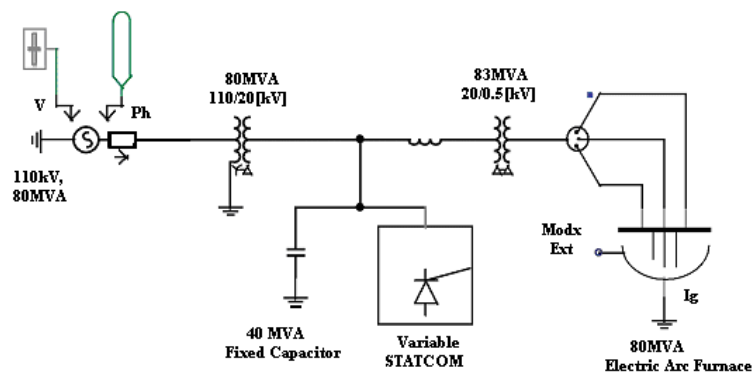


Fig. 2: Electric Arc Furnace System

the arc furnace remained fixed. The function of static compensator provides reactive power compensation to solve industrial system voltage fluctuation.

AC arc furnaces are a major source of grid disturbances. The frequent interruption of the arc leads to strong voltage fluctuations and unbalance between phases too. The converters operate as a 64 MVar STATCOM on the grid supplying the furnace. It is possible to compensate the unbalanced load with the single phase control of the STATCOM and at the same time, supply the required reactive power to stabilize the grid voltage. In normal operation the mean value of current unbalance without operating converter was 8.6%. With the STATCOMs in operation the unbalance is reduced by a factor of nearly four.

Mathematical modeling of processes related to EAF electric arc furnace in order to optimize functional and technological performance of this complex aggregate was based on the following principles [10]: the analogy, the concepts and principles of hierarchically. According to these principles for developing mathematical models to go through stages:

- ❖ Identify target shape. This step has to satisfy the purpose and objectives of the system, while ensuring their compatibility;
- ❖ Defining criteria of efficiency, it is a correct step conditioned by defining objectives optimization solutions enable system and modeling;
- ❖ Develop options based on accesses of realistic solutions, effective and originals;
- ❖ Assessment of scenarios depending on efficiency criteria established;
- ❖ Fixing the final solution based on comparative analysis of various solutions of modeling.

These require detailed and accurate knowledge of the technological process optimization and implicitly to all installations and components of them and involve the need for develop a hierarchical models system in order to framework of decision and coordination of interactive subsystems shown like in Figure 3.

Application of specific mathematical models to optimize the operation of arc furnaces, particularly the mathematical model to conduct the effectively melting MCT and the mathematical model of load preheating MPI (including the mathematical model for calculating the design of recovery burners related to preheating MPAR). The main component of furnace processes modeling EAF is the FO aim function of the system. Given the fact that the study related to technological processes EAF is responsible for obtaining high quality steel, the modeling system aim function FO is the quality/cost relation; the responsible model for maximizing the efficiency of the whole system and the aim function is *Max FO*. Operative management of melting COT is done by mathematical models to calculate the load MCI and the mathematical model to conduct the effectively melting MCT. The modeling of the designed system for technological processes from EAF is composed of subsystems that describe the algorithm of the aggregate modeling. The mathematical model for calculating the design of recovery burners related to preheating MPAR has the positive consequence reducing specific consumption of electricity in steel elaboration with about 15%, simultaneously obtaining a high quality of steels and is directly correlated to MPI.

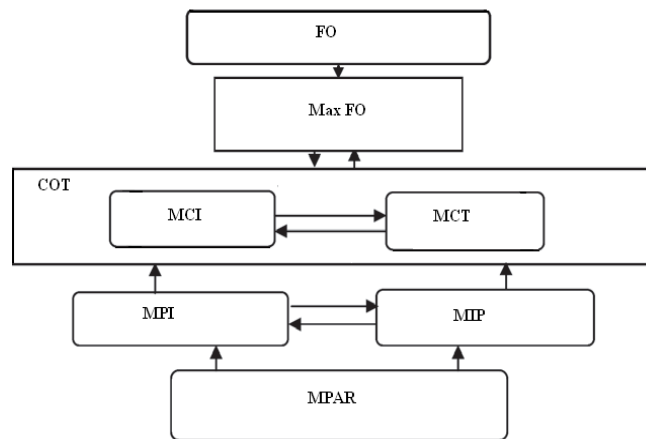


Fig. 3: Sequence algorithm modeling aggregate

The modeling system aim function FO is the quality/cost relation; the responsible model for maximizing the efficiency of the whole system and the aim function is *Max FO*.

Operative management of melting COT is done by mathematical models to calculate the load MCI and the mathematical model to conduct the effectively melting MCT. The modeling of the designed system for technological processes from EAF is composed of subsystems that describe the algorithm of the aggregate modeling. The mathematical model for calculating the design of recovery burners related to preheating MPAR has the positive consequence reducing specific consumption of electricity in steel elaboration with about 15%, simultaneously obtaining a high quality of steels and is directly correlated to MPI.

3. ELECTRIC ARC FURNANCE CONTROL

In order to maintain the arc length constant of the electric arc furnace, a control system for the electrode position according to the arc impedance is used. The automat system must rapidly change the position of the electrodes (1.5 ... 3 seconds) if a disturbance action sets up, therefore the time constants of the system components must be minimized. On three-phases electric furnaces, each electrode has its own control installation [9].

Whatever the electrodes' mode of action in automatic systems is, impedance Z_c is used as a parameter set furnace, Eq. (2), the ratio between the supply voltage $U = k_2 U_a$ (or a proportional size to the arc voltage measured with a voltage transformer or directly at the terminals of the arc) and the arc current $I = k_3 I_a$, (or a proportional size with the arc current measured with a current transformer) [9].

$$Z = k_1 \cdot Z_c = \frac{k_2 \cdot U_a}{k_3 \cdot I_a} \quad (2)$$

For a certain adjusted value of the impedance Z_0 results a deviation ΔU_0 like in Eq (3) and the result of the comparison, the U_0 parameter, is transmitted to the controller which acts on the execution element (continual flow motor, three-phase induction motor or hydraulic operation shaft) and determines the transition of the electrodes in order to delete the difference and so, to re-establish the required value of the arc impedance.

$$\Delta U_0 = U_a - Z_0 \cdot I_a \quad (3)$$

The deletion of the automatic temperature control drawbacks, for example that at some stages of the technological process one can stock the furnace with energy of up to plus or minus 15% in relation to the optimal one, can be obtained by the use of on-line conduct systems and temperature control.

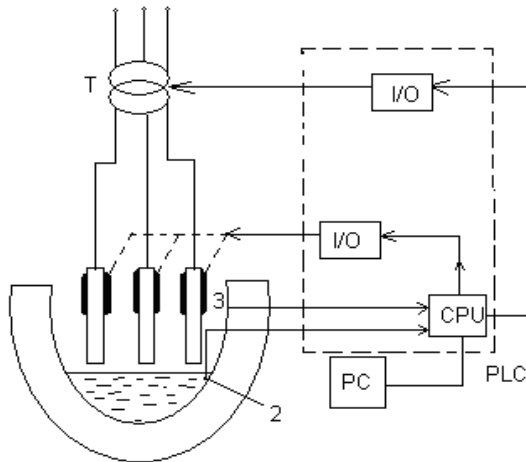


Fig. 4: Control system of power electric on arc furnace

The regulation and control scheme of the arc furnace through a logical programmable controller PLC is described in Figure 4.

PLC is robust and compact devices specially created to monitor and control some automation parameters. With their use various automation schemes can be implemented of medium complexity. Initially they were designed to implement binary control functions: combinational logical functions and automate programmable (control sequence). Hence there had been added more continuously adaptive control functions, communication features and functions for viewing and storing the

collected data. With output interfaces, PLC controls various elements of digital performance (two-position). Outputs are usually voltaic isolated from the logical aspect to allow linkage of greater value voltages or currents and to protect the logical aspect of any accidental over-voltages. Depending on the building of PLC, there can be repeater contact, power transistor or thyristor type outputs.

LG Industrial Systems has introduced the range programmable controllers (PLC), GLOFA-GM series for medium and large applications which can use here.

Automatic system is to ensure as far as possible to optimum functioning furnace, quickly remove those disturbances.

Electrodes position adjustment is made regarding furnace current which receives information about heating regime using the programming logic controller PLC. The controller commands by the central processing unit power regulators which provide the amount of set energy for each stage of technological process.

The controller receives technological tasks (electrical parameters, metal temperature) from the programming device on Windows- Based Programmer and bases on them it establishes the necessary power and controls its insertion in the furnace through the power regulator. The controller may also perform other functions on the introduction of materials, oxygen and to optimize the process.

One of the main objectives of the three-electrode Electric Arc Furnace simulator study is to have the electrodes maintain constant power consumption. This is achieved by moving the electrodes to a given depth, obtaining the desired resistances (conductance), which leads to a constant power consumption. Identification system block diagram is shown in Figure 5.

The dynamic behavior is based on the arc length variations. The nonlinear and time varying characteristic of the arc length cause changes in arc resistance and so the slope of the V-I characteristic [6].

To attain this goal, the open-loop system described in the previous section must be closed in order to create an error signal. The control principle is accomplished by minimizing this error signal with specific controllers. For this system, although the power is to remain constant, since the power magnitudes are scalar multiples of the electrode currents, controlling the current will lead to power control as well. A feedback loop has now been added to the output of the open loop system.

The output currents are fed back into the negative port of an adder block, where they are combined with the initial step responses representing the desired current. The difference between the desired current and output current is then fed into a PID controller set appropriately to transform a current magnitude to a percent error. This percent error orders the hydraulic actuators to open the valves such that a new resistance sets the corresponding currents to converge to the desired currents.

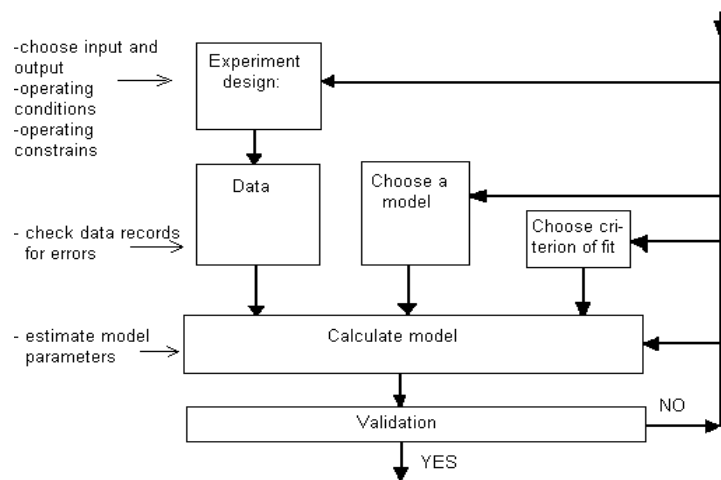


Fig. 5. The system identification loop

4. CONCLUSIONS

Application of specific mathematical models to optimize the operation of arc furnaces, particularly the mathematical model to conduct the effectively melting MCT and the mathematical model of load preheating MPI (including the mathematical model for calculating the design of recovery burners related to preheating MPAR).

The mathematical model for calculating the design of recovery burners related to preheating MPAR has the positive consequence reducing specific consumption of electricity in steel elaboration with about 15%, simultaneously obtaining a high quality of steels and is directly correlated to MPI.

The deletion of the automatic temperature control drawbacks, for example that at some stages of the technological process one can stock the furnace with energy of up to plus or minus 15% in relation to the optimal one, can be obtained by the use of on-line conduct systems and temperature control.

The regulation and control scheme of the arc furnace through a logical programmable controller PLC was proposed. Finally, a feedback loop was introduced to create a closed-loop system. The input step functions now represent the desired current to control the power.

REFERENCES

- [1.] S. Arad, Electrotehnologii. Utilizarea energiei electrice in industrie. Focus Publishing, Petrosani 2009.
- [2.] B. Boulet, V. Vaculik and G. Wong, "Control of High-Power Non-Ferrous Smelting Furnaces", IEEE Canadian Review, 1997.
- [3.] D. Comşa, L. Pantelimon, Electrotehnie, Didactical and Pedagogical Publishing House, Bucureşti, 1979.
- [4.] D. Comşa, S. Darie, „Măsurarea mărimilor şi parametrilor cuptoarelor electrice cu arc”, Energetica, 7(6), 1976, pp.289-294.
- [5.] Cz. Flueraşu, C. Ionescu and C. Flueraşu, "Numerical Simulation of Over voltages Occurring at the Virtual Chopping of Currents in Electric Arc Furnaces", Proc. of Int. Conf in Electro Heating Equipment, Sibiu, 1991.
- [6.] M. A. Golkar, M. Tavakoli Bina and S. Meschi, „A Novel Method of Electrical Arc Furnace Modeling for Flicker Study”, Proc of Int. Conf. on Renewable Energies and Power Quality, ICREPQ'07, 2007
- [7.] R.D. Morales, et al. „A mathematical simulator for the EAF steelmaking process using direct reduced iron”. ISIJ International vol 41(5), 2001, pp 426-435..
- [8.] L.P. Rathaba,.. „Model Fitting for Electric Furnace Refining”, M. Eng. Thesis, University of Pretoria, 2004
- [9.] A. Saimac, E. Roşu, et al. Utilizarea energiei electrice în metalurgie, Didactical and Pedagogical Publishing House, Bucureşti, 1980
- [10.] A. Ioana, A. Nicolae, et al Conducerea optimala a cuptoarelor cu arc electric, Fair Partners Publishing, Bucuresti, 2002.



SIGNAL GENERATOR DESIGNED IN LabVIEW PROGRAM

¹⁻⁴ ELECTRICAL ENGINEERING AND INDUSTRIAL INFORMATICS DEPARTMENT, UNIVERSITY POLITEHNICA TIMISOARA,
FACULTY OF ENGINEERING HUNEDOARA, HUNEDOARA, ROMANIA

ABSTRACT:

In this paper the authors present a virtual signal generator that contains two independent channels. It was chosen the LabVIEW Tool for designing the generator, because it permits a practical graphical interface with the user. The generated signals can be visualized using the indicated displays of the virtual instrument, as on a real oscilloscope using a data acquisition board.

KEYWORDS:

Signal generator, Noise signal, Spectral analysis

1. INTRODUCTION

Signal generators are electric devices that are used as time variable voltage sources with a specified waveform and adjustable amplitude and frequency. These instruments are used in electrical laboratory at controlling, adjusting, measuring the electrical signals.

2. LABVIEW IMPLEMENTATION OF THE SIGNAL GENERATOR

INPUT DATA

The parameters of generated signals can be introduced in program using appropriate control elements: rotary buttons, pushing buttons, circular dial.

The signal generator is designed using two independent channels. Generated signals can be sinusoidal, rectangular, triangular, slope, continuous component. Input parameters: offset, frequency, amplitude and phase can be introduced using numeric control elements described in figure 1.

Signal selection can be made using two inputs multiplexers.

BLOCK DIAGRAM

The elements from block diagram that introduce the input data are presented in figure 2. In order to obtain different types of signals, the electric scheme contains *Simulate Signal* blocks that can be set to generate the desired signal.

The electric scheme can realize signal reversing operations, half wave and full wave rectification. Full wave rectification is done using *modulus* mathematical block [3]. Half wave rectification is made according with the following principle: signal is reversing, the result is subtracting from the full wave rectificated signal. The obtained signal is a half wave rectificated signal and amplified twice. The result is divided by 2, and the final signal represents the half wave rectificated signal (figure 3).

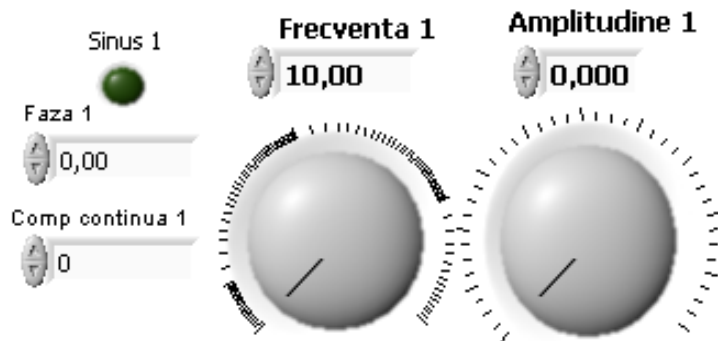


Fig.1. Numeric control elements

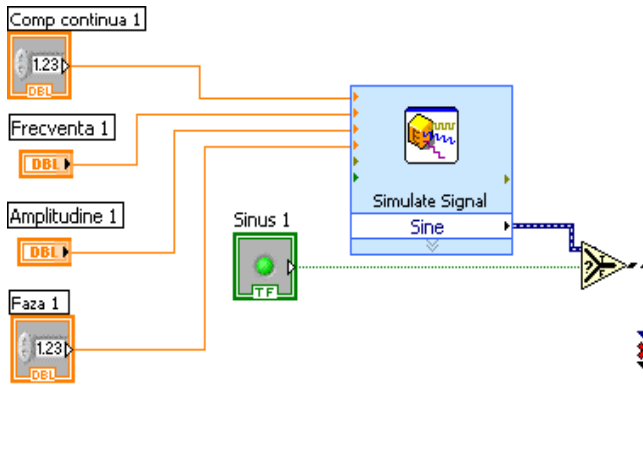


Fig.2 Simulate signal block

Each signal can be viewed with noise. The noise level can be adjusted. There were chosen the following noise types: Uniform, Gaussian, Periodic random, Bernoulli, MLS Sequence, Gamma, Poisson, and Binomial.

Noise signals are generated using *Simulate Signal* blocks set with *Numeric* and *Boolean* control elements [2].

In order to obtain a continuous functioning, all elements of electric scheme are introduced in a *While* structure. Loop condition represents the *Stop* button placed on Front Panel.

Time base scheme of the indicator display is presented in figure 4.

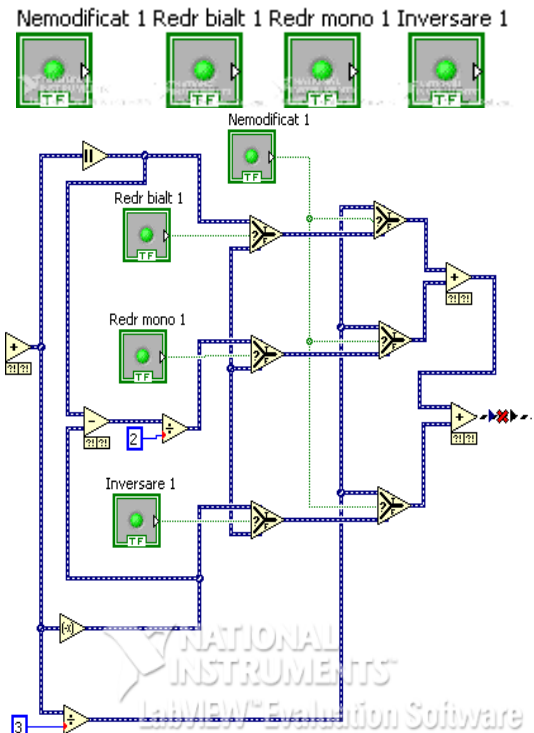


Fig.3. Rectification scheme

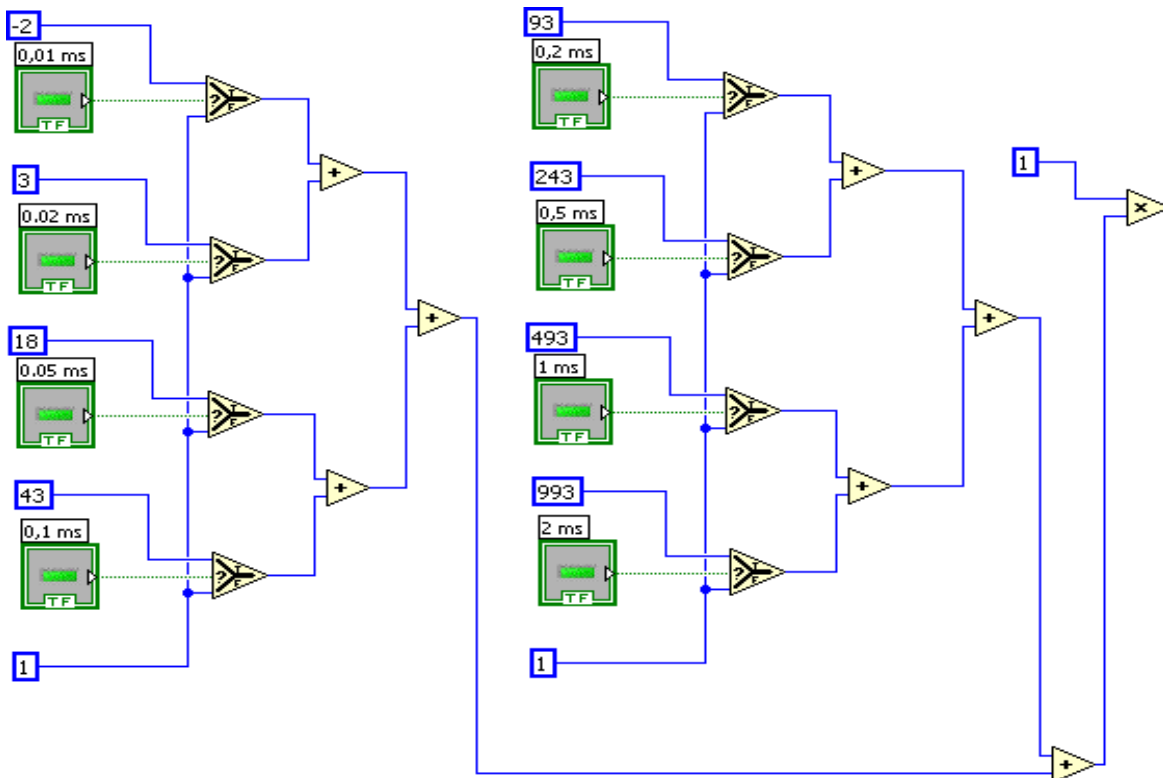


Fig.4. Time base.

The signals can be followed on a real oscilloscope display if it is connected to an analog input of data acquisition board, like NI-6221 (figure 5).

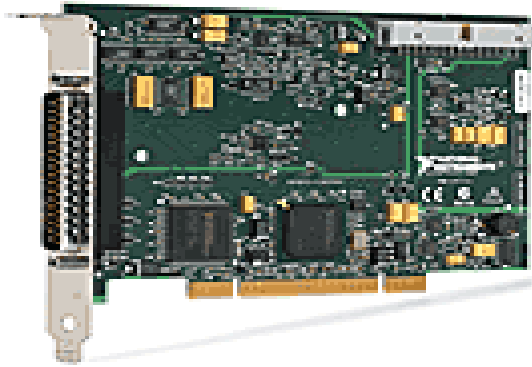


Fig.5. Data acquisition board PCI-6221.

Characteristics:

- ❖ 16 analog inputs, 250kS/s, resolution 16 bits
- ❖ 2 analog outputs, 833kS/s, resolution 16 bits
- ❖ 10 digital I/O compatible TTL
- ❖ 2 counter/timers on 32 bits
- ❖ digital trigger
- ❖ compatibility with Windows (2000/NT/XP), Linux
- ❖ integration with software components LabVIEW, CVI, Measurement Studio for Visual Studio NET

Figure 6 presents the front panel of the application.

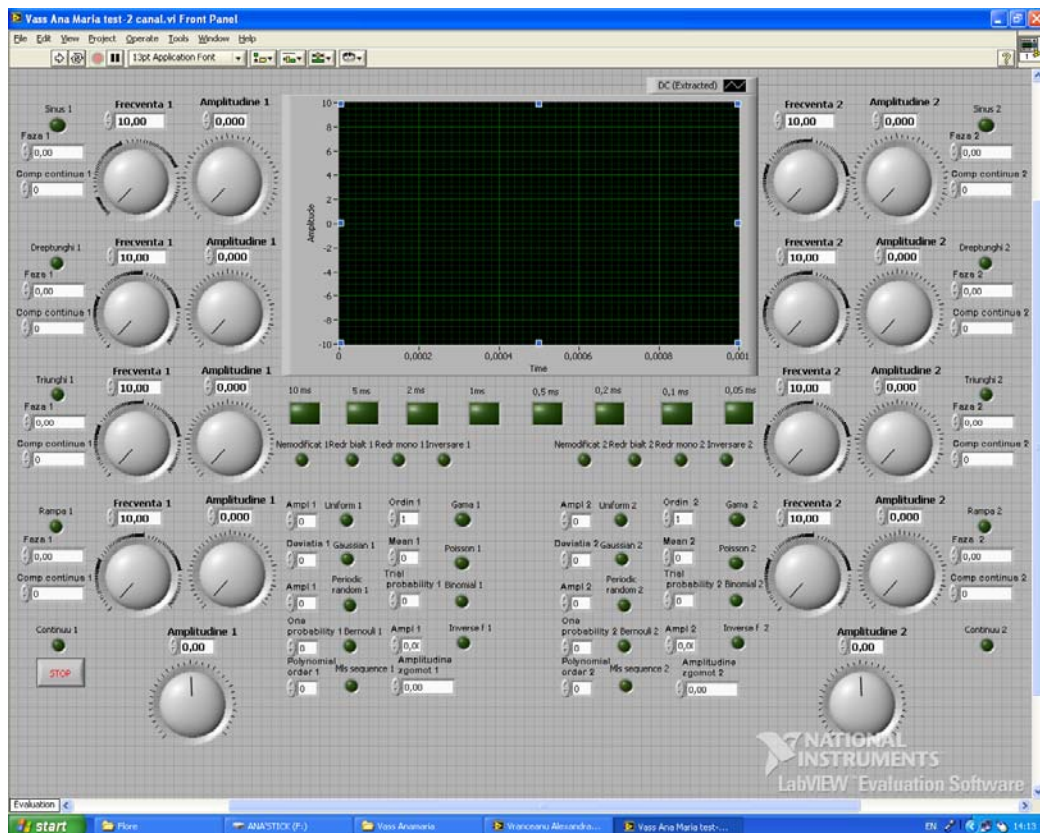


Fig.5. Front panel of the application

3. CONCLUSIONS

This application becomes very useful in electrical laboratories, because it is a virtual instrument that simulates a real oscilloscope on two independent channels. In this way there can be simulated different types of signals that can be viewed on the virtual display. Using a data acquisition board [1], these virtual signals can be transformed in real voltage signals.

REFERENCES

- [1.] Liviu Toma, *Sisteme de achiziție de date*, Editura de Vest Timișoara, 1998
- [2.] Francis Cottet, Octavian Ciobanu, *Bazele programării în LabVIEW*, Editura Matrix ROM București, 1998
- [3.] <http://www.ctanm.pub.ro/academic/labview/Tutorial.htm>





DIGITAL CONTROL MODES OF THE SEMI-CONTROLLED THREE-PHASED RECTIFIERS

¹⁻⁴ UNIVERSITY POLITEHNICA TIMIȘOARA, FACULTY OF ENGINEERING HUNEDOARA, ELECTRICAL ENGINEERING AND INDUSTRIAL INFORMATICS DEPARTMENT, ROMANIA

ABSTRACT:

In this work is presenting an interface circuit between a PC and a semi-controlled three-phased rectifier. The circuit performs a numerical-analogue conversion using a CAN followed by a current-voltage conversion and a galvanic separation using opto-couplers that enter into a linearity circuit with the operational amplifiers. The output voltage is used to control the impulse forming circuits for the thyristor grids.

KEYWORDS: parallel port, numerical-analogue converter, opto-coupler, process control, power systems control, hybrid systems

1. INTRODUCTION

The numerical management of the industrial processes acquired today new valencies, both following the evolution of the management concept, and especially following the large scale evolution of the integrated circuits technology (LSI) and on very large scale (VLSI) of the microprocessors, microcomputers and minicomputers. Thus, the modern concepts regarding the process management, materialized in large classes of adjusting and management algorithms, become operational and efficient following the development of the hardware instructions and the microprocessors on which are implemented with special performances.

The progress obtained in the field of interface systems with the industrial processes, of the data acquisition systems, of conversion and primary processing, as well as of the drive systems allowed the extension of the fields of utilization numerical computation technique in the management of the industrial processes.

Taking into account the processes' diversity, their complexity degree, the performance requirements imposed by the management systems, the knowledge level of them, there have been developed and implemented structures of management systems with different complexity degrees compatible both with relatively simple problems regarding the processes' numeric adjustment and with complex problems of the process management by global performance criteria.

2. WORK'S PRESENTATION

2.1. Semi-controlled three-phased rectifying bridge

The application diagram is presented in fig. 1.[1]

The three-phase bridge is formed by the diodes D_1, D_2, D_3 and thyristors Th_1, Th_2, Th_3 .

Between phases R, S, T there is a phase difference of 120° . The current through R_L is closing successively by Th_3 and D_2 then by Th_2 and D_1 and, finally, by Th_1 and D_3 . The circuits β AA 145 having the terminals 16 connected together and the same control voltage in the terminal 8, they open the thyristors at the same conduction angle (considered against each of the three grid voltages).

The ignition impulses will be identical as duration but dephased in time by 6,66 ms (corresponding to the 120°). Under load, it appears a voltage of which shape is strongly dependent by the value of the conduction angle φ .

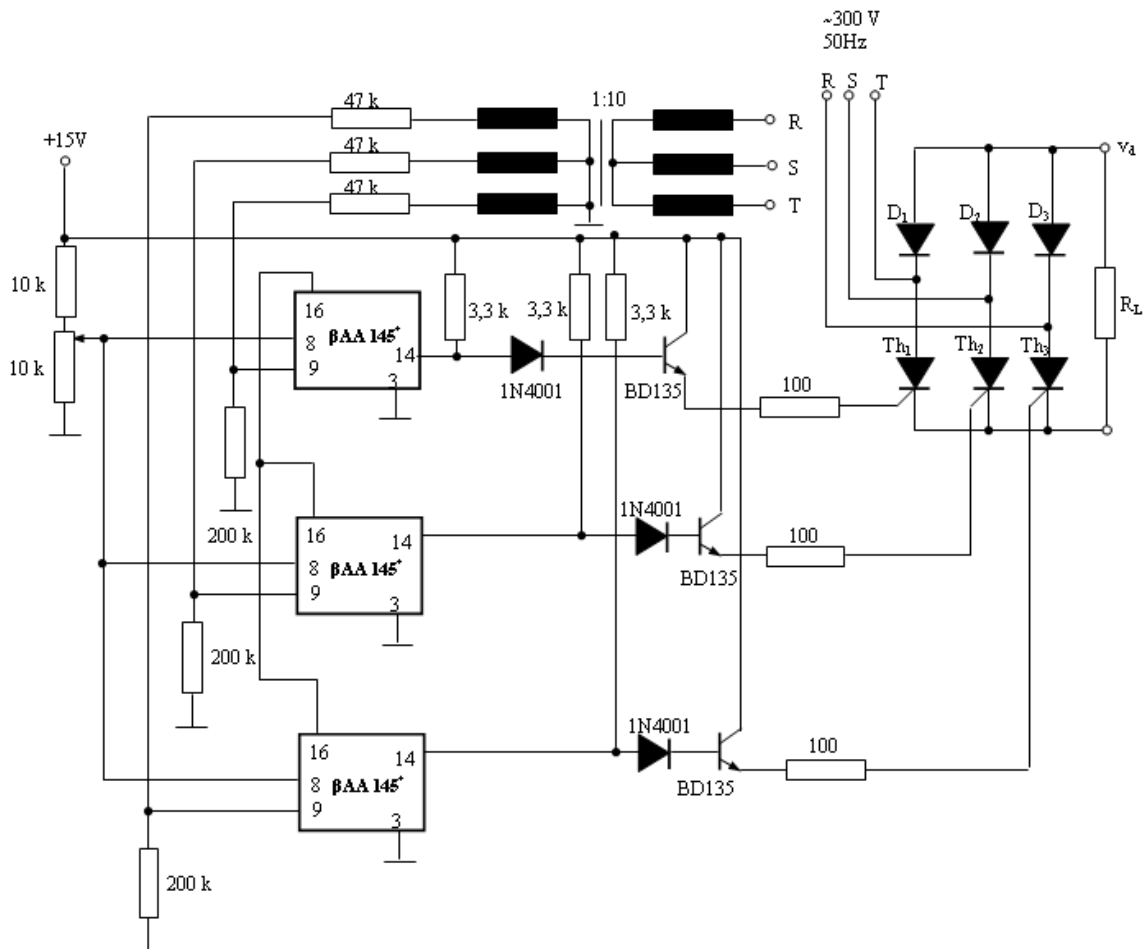


Fig. 1. The electric diagram of three-phase control of a semi-controlled bridge

The average value of the rectified voltage in case of a rectifier with m phases becomes:

$$U_{do} = 2 \frac{m}{2\pi} \int_0^{\pi/m} \sqrt{2} U_2 \cos \omega t d(\omega t) = \sqrt{2} U_2 \frac{\sin \pi / m}{\pi / m}, \quad (1)$$

where U_2 is the effective value of the voltage in the transformer's secondary; the index „o” featuring the situation of an ideal rectifier.

The above relation is valid for $m = 2, 3, \dots$

$$\text{For } m \rightarrow \infty, \lim_{m \rightarrow \infty} U_{do} = \sqrt{2} U_2.$$

The effective value of the rectified voltage is calculated as follows:

$$U_{d0ef} = \sqrt{2 \frac{m}{\pi} \int_0^{\pi/m} (\sqrt{2} U_2 \cos \omega t)^2 d(\omega t)} \quad (2)$$

obtaining the expression:

$$U_{d0ef} = \sqrt{\frac{m U_2^2}{\pi} \left| \omega t + \frac{\sin \omega t}{2} \right|_0^{\pi/m}} = U_2 \sqrt{1 + \frac{m}{2\pi} \sin \frac{2\pi}{m}}. \quad (3)$$

$$\text{When } m \rightarrow \infty, \lim_{m \rightarrow \infty} U_{d0ef} = \sqrt{2} U_2.$$

An important issue arisen in case of the power application is to insure the protection of the controlled active element (thyristor, triac) against the possible accidents related to the malfunction of the reaction loop that has to ensure the on-load power stabilization. The integrated circuit $\beta AA 145$ that ensures the control can „interpret” this accident as a decrease of the power under load and as consequence to generate ignition impulses with increasing conduction angle, increasing unjustified the on-load power and putting in thermal destruction danger the controlled thyristor or triac.

The same effect can have also an accident in the cooling circuit of the radiator of a power thyristor, of which heat resistance has increased and which, therefore, can not dissipate anymore the calculated maximum power.

For such accidents there are protection schemes, separated by the reaction loop of stabilizing the on-load power, that acts at the level of the thyristor's gate, blocking it when the temperature of the controlled active element's radiator decreases a certain value.

In case when the blocking is made directly on the thyristor's gate, then must be manipulated big currents, which makes that the sensitivity of the protection circuit (in case it's a circuit not too complex) to be small. Therefore, the thyristors' integrated control circuits are provided with a terminal with blocking priority of the ignition impulses. The circuit has a high sensitivity because it works at small currents (characteristic to an integrated circuit).

Terminal 6 of the circuit β AA 145 is the terminal with blocking priority. When terminal 6 is „put" to the supply voltage (e.g. short-circuited with terminal 7) the impulse generation on both outputs is inhibited. In normal operation within the time interval passed from the null impulse generation until the appearance of the ignition impulse, the input impedance on terminal 6 is very high (there are only blocked junctions).

Any application diagram that uses terminal 6 for blocking the ignition impulses should respect this condition. If this condition is not taken into account, is possible to appear abandoned ignition impulses.

The circuit β AA 145 is destined most exclusively to the on-phase control of the thyristors' (triacs') ignition. The increasing complexity of the thyristors' control circuits made that their monolithic achievement to be very attractive, as proven also by the great number of integrated circuits destined to the thyristors' and triacs' cocontrol.

In principle, the priming of a thyristor can be achieved with a circuit extremely simple. Utilization of a complex circuit or an integrated circuit is justified when is desired not only the thyristor's priming but also the control of the dissipated power in the anode circuit.

From the priming achievement's viewpoint, all the existent integrated circuits are identical: they supply current impulses (positive or negative) necessary to the control on the thyristor's grid. However, the circuits are distinguished as regards the control mode of the power dissipated in the thyristor's anode circuit's load. As result, hereby the expression „thyristors' control" refers to the control of the power from the load circuit. From this viewpoint, there are three control modes offered by the integrated circuits [1]:

- (a) control through phase;
- (b) control through zero with constant reference in time;
- (c) control through zero with lineary variable reference in time.

2.2. The numerical-analogue conversion principle

There will be used balanced codes to present the the numerical information because they have the advantage of a natural expression and are compatible with the numerical calculation circuits. In case of such a code, a figure from a number has both the semnificance of its value itself, and the balance due to the position within the number. The numerical-analogue conversion assumes the transformation of the value and proportion of the number's figures into a corresponding analogue measure.

Is considered a binary integer of N bits, as [2]:

$$\overline{B_{N-1}B_{N-2}\dots B_{i-1}\dots B_1B_0} = \sum_{i=1}^{N-1} B_i 2^i \quad (4)$$

The figure B_{i-1} has the position i starting with the less significant bit (LSB) and has the balance 2^{i-1} , which means that the balance increases from right to left, the most significant bit (MSB) having the balance 2^{N-1} . The previous remarks are valid also for subunit binary numbers of N bits [2]:

$$\overline{B_1B_2\dots B_i\dots B_{N-1}B_N} = \sum_{i=1}^N \frac{B_i}{2^i}, \quad (5)$$

One can notice that the numerical-analogue conversion process is similar with the transformation procedure of a number from the binary numeration system, in the decimal numeration system, in this case to each binary figure "1" being associated a certain value of an electric measure (current or voltage) which is summed-up proportionally according to the rank that occupies within the numerical representation (for the figure "0" is associated the value zero of the same electric measure). Modification of the figures' balance with factors under form $1/2^i$ suggests a simple solution to achieve the balancing operation. This would be the utilization of some divisor

resistive grids, with more nodes, having between successive nodes the division ratio of 1/2. The resistances corresponding to the binary figures are introduced in the circuit when the associated binary figure is 1 or are disconnected in contrary case, by means of some electronic switches. The most usual types of grids are the ones with balanced resistances and with resistances $R - 2R$ [3]. The electronic switches can be achieved with bipolar transistors or with transistors with field effect.

In the great converters family, the integrated circuit β DAC-08, 8-bit converter, occupies a position of industrial standard [4]. The circuit has a precision of 0,19% sufficient for the usual industrial applications. Being a speed circuit (set-up time of 100 ns order) can be used for data acquisition for the control of the industrial processes and numerical processing.

The circuit has two current outputs noted I_0 and \bar{I}_0 . These currents have the property that their sum is constant and equal with $\frac{255}{256} I_{REF}$, where I_{REF} is the current imposed from exterior.

Thus, depending on the logical configuration, at the inputs B_1, \dots, B_8 is obtained a current I_0 proportional with the numerical value of the binary word formed by the eight bits.

The maximum value at the current output I_0 is obtained when all the currents I_k are switched in this output.

$$I_0 = \sum_{k=1}^8 I_k = I_{REF} \sum_{k=1}^8 1/2^k = \frac{255}{256} I_{REF} \quad (6)$$

The current I_{REF} is supplied from exterior by means of a current generator or from a voltage generator, V_{REF} , and a resistance, R_{REF} , that determines the current's value:

$$I_{REF} = \frac{V_{REF}}{R_{REF}} \quad (7)$$

The output current's conversion into voltage, maintaining a small value for the set-up time is very difficult. The end-scale current for β DAC 08 is set-up in 100 ns [1]. At output can be attached a load resistance in order to obtain an output voltage between 0 and -10 V.

Due to this time constant (RC), the conversion current/voltage is achieved usually with the diagram presented in fig. 2 [1]. The response time is limited now by the set-up time and by the value of the operational amplifier's slew-rate.

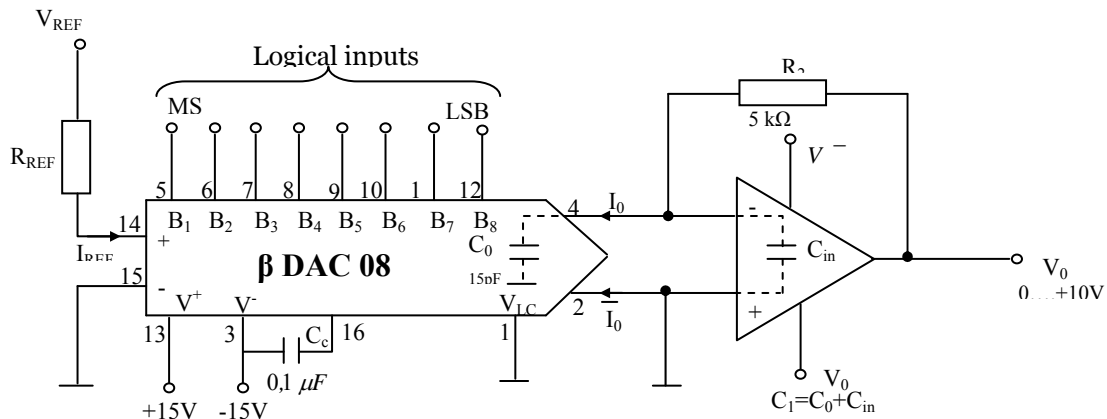


Fig.2. Electric diagram with current-voltage convertor at output

2.3. Galvanic insulation circuit

The process interfaces ensure the junction between the the computing system and the managed process, and as result should be taken safety measures in such way that the damaging of a component of the managed process (including transducers, execution elements) to not cause the damaging of the computing system [3]. Among the protection techniques used in such situations is also the galvanic insulation between the computer's and process' circuits.

The galvanic insulation consists in elimination of any direct electric connection between the computer's circuits and the ones corresponding the process. This is achieved usually electromagnetically (with transformers and relays), optically (with opto-couplers or optical insulators) and capacitive (with capacitive barriers).

Utilization of galvanic insulation in the acquisition and management systems ensure the protection of the system and the operator, reducing the noise and rejection of common mode voltages, especially of the ones caused by the mass loops.

The diagram of the galvanic separation circuit is the one from fig.3.

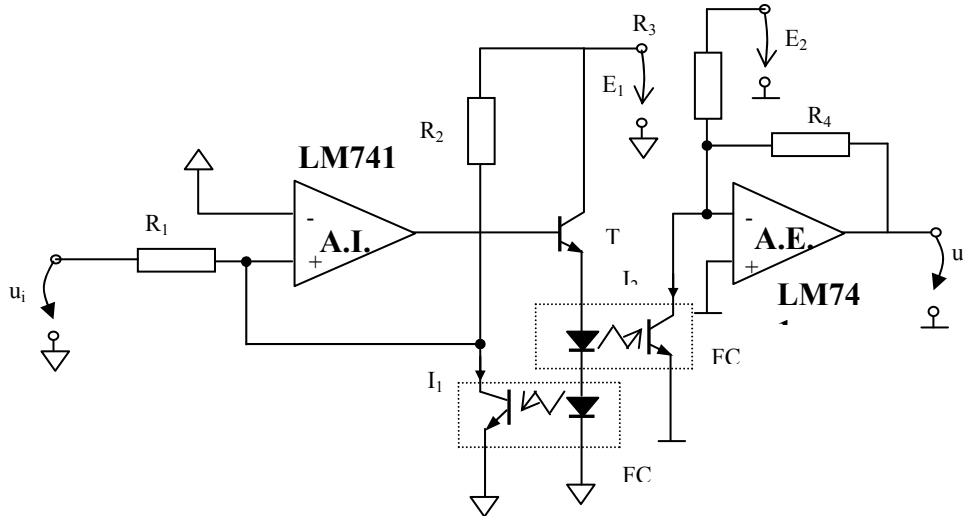


Fig. 3. The galvanic separation circuit

The transfer function of the insulation amplifier is made based on the hypothesis regarding the identity of the characteristics of the two photo-couplers [3].

$$I_1 = \frac{u_i}{R_1} + \frac{E_1}{R_2} \quad (8)$$

$$I_2 = \frac{u_o}{R_4} + \frac{E_2}{R_3} \quad (9)$$

where I_1 and I_2 represent the collector currents corresponding to the two photo-transistors. Because the diodes are connected in serial, it results that $I_1 = I_2$ resulting the transfer function of the insulation amplifier:

$$u_o = \frac{R_4}{R_1} u_i + R_4 \left(\frac{E_1}{R_2} - \frac{E_2}{R_3} \right) \quad (10)$$

It's determined that this transfer function is linear and independent by the photo-couplers' characteristics, with the condition regarding the identity of the two photo-couplers' characteristics.

2.4. Programming of the parallel port

The parallel port is used at the computer's communication with the peripheral equipments and for monitoring of different processes by PC [4].

The standardized connector of the parallel port is of D type, mother, with 25 pins [5].

The pin's number is the number inscribed on the connector in front of each pin. "In" represents the data transfer from peripheric to the port, and "Out" from the port to peripheric.

At the pins 1, 11, 14, 17 the signal is reversed by the hardware board and the pins from 18 to 25 represent the mass. Presentation of the parallel port's pins (fig. 4).

3. EXPERIMENTAL RESULTS

Following the experimental verifications, the output voltages from the numerical analogue converter block were noted U_{ies1} and respectively the galvanic separation circuit U_{ies2} , for the input measures between 0 – 255. The measured values are recorded in table 1.

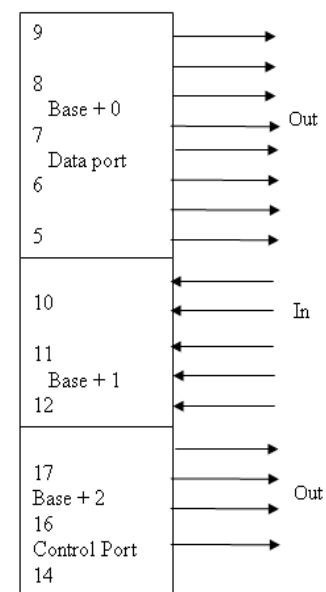


Fig. 4. Parallel Port

Table 1 Output voltages CNA and for control of rectifying block

Input	U _{ies1}	U _{ies2}
0	1,1mV	300 mV
10	194 mV	590 mV
25	480 mV	1,15 V
50	969 mV	1,7V
75	1,45 V	2,54 V
100	1,94 V	3,08 V
125	2,42 V	3,89 V
150	2,91 V	4,49 V
175	3,41 V	5,21 V
200	3,9 V	5,8 V
225	4,38 V	6,52 V
250	4,87 V	7,11 V
255	4,96 V	7,24 V

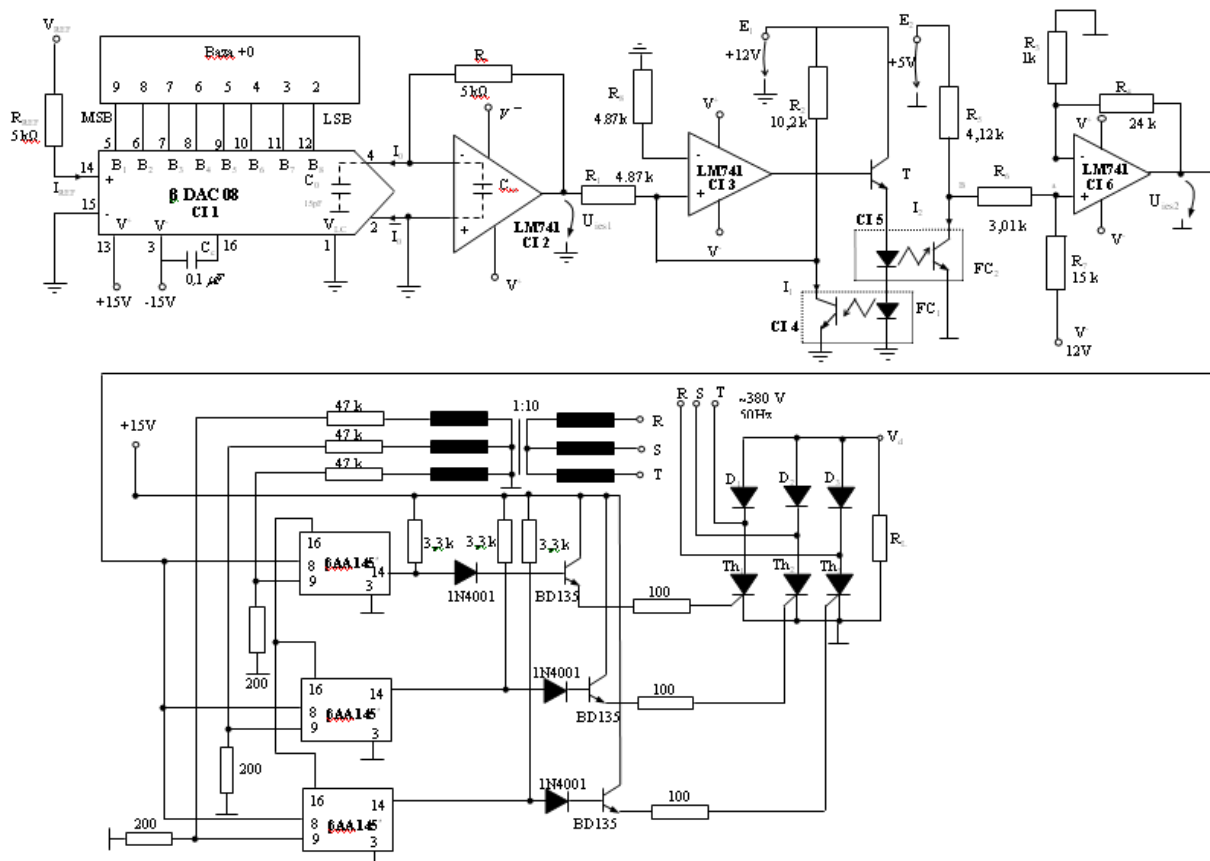


Fig. 5 Diagram of the three-phased rectifier's control interface

The control circuit represents in fact an interface between a computer and a three-phased power rectifier (fig. 5) that operates linearly on the entire variation scale of the numerical sequence on 8 bits (0-255). The program that allows to obtain at the parallel port the numerical sequence is achieved in C++ [6][7].

The thyristors of the rectifying bridge are independently controlled each by an integrated circuit β AA 145 specialized in thyristors controll, of which synchronization is achieved through a three-phased transformer with the transformation factor 1:10, directly from the voltage of the supply system.

The control impulse is the one related to the positive alternance corresponding to each phase of the supply system.

Further, the obtained impulse is amplified in current by means of the medium power transistors of BD 135 type and which allow the direct connection to the thyristor grids of the rectifying bridge, without being necessary an additional galvanic separation circuit.

4. CONCLUSIONS

Analyzing the experimental data from table 1 one can notice a linear operation of each block in part, respectively of the conversion circuit, as well as of the galvanic separation circuit. The control circuit allows obtaining at output, directly proportional with a numerical value introduced from the keyboard, a maximum value that does not exceed 8 V, which represents also the maximum input voltage for the circuit β AA 145 which is the impulse former for the thyristors of the semicontrolled rectifying bridge.

Following the performed experiments was found that for the numerical values 0-10 as input in the control circuit is obtained a neglectable voltage at the rectifying bridge's output, which means that the thyristors are practically not controlled.

By introducing of a reaction loop can be obtained the adjustment of the output voltage automatically by bringing of a part from the output voltage tensiunea de ieşire to the computing system which determines the optimal control value.

REFERENCES

- [1.] Bodea M., Vătăşescu A., Linear integrated circuits. Manual of utilization vol. IV, Technical Publishing House, Bucharest, 1985.
- [2.] Toma L., Acquisition systems and numerical processing of signals, Western Publishing House, Timișoara, 1996;
- [3.] Ignea A., Electric measurement of non-electric measures, Western Publishing House, Timișoara, 1996;
- [4.] Popa M., Systems with microprocessors, "University Horizons" Publishing House, Timișoara, 2003;
- [5.] Cristea D., Pănoiu C., Interfaces and peripherals, "Mirton" Publishing House, Timișoara, 2007;
- [6.] Jordan A., Pănoiu M., Object-oriented programming. C++ Language. Laboratory guide, "Mirton" Publishing House, Timișoara, 2007;
- [7.] Popovici D., Popovici I., C++ Object-oriented technology. Applications. "Teora" Publishing House, Bucharest, 2002.







¹Adrian DANILA, ¹Gabriela PAVEL, ¹Radu MERA

A STUDY OF THE PARAMETER ESTIMATION OF THE SINGLE/TWO-PHASE INDUCTION MACHINES

¹⁻²TRANSYLVANIA UNIVERSITY OF BRASOV, ROMANIA

ABSTRACT:

A key point in simulation and control of the electrical drives is the accuracy of the available dynamic model. Especially for the squirrel-cage induction machines, the exact determination of the rotor's parameters i.e. resistances and inductances is not a straightforward task because these parameters cannot be determined through direct measurements during the drive's operation. Several techniques are used to obtain estimates for the machine's parameters as well as to obtain estimates for the process parameters such as flux-linkages components. Among these techniques, the observer-based methods are widely used in control engineering. The finite elements methods (FEM) are commonly used in design. In this work, the authors implemented both methods to determine the process parameters for a given single/two-phase induction machine. To validate the estimations, the results were compared with the measurements.

KEYWORDS:

electrical drives, simulation and control, finite elements methods, measurements

1. INTRODUCTION

The on-line estimation of the process parameters is essential in the adaptive control of the variable- parameters systems but also for the constant-parameters systems in the presence of stochastic disturbances, such are the electrical drives destined to the control of speed and position.

In particular, the sensor-less estimation of the rotor's position is of major interest due to (1) the low cost implementation and (2) the increased maintenance issued from the elimination of the speed or position transducers. In addition, the on-line estimation of the process parameters allow the direct torque control and the implementation of advanced control algorithms such as the slider-mode control.

In this approach, the deterministic Luenberger's observer may be used to the angular speed reconstruction of the induction machine's rotor based on the measurements or estimated values of the torque and rotor's position. The Bocker's observer allows the reconstruction of the electromagnetic field's components based on the phase-voltages and currents, and the angular speed at the machine's shaft. In the same context, there are two applications of the extended Kalman filter that allow estimating the time constant of the rotor in presence of disturbances [1].

The typical applications of these algorithms are the control laws for the command of the three-phase inverters into the speed and position control of the induction machines electrical drives. Despite that from the theoretical point of view, the state observers are asymptotical stable, the convergence – and the estimate accuracy – depend on the accuracy of the parameters of the motor and finally on the electrical and mechanical parameters of the machine.

Because not all parameters of the machine may be determinate through direct measurements, numerical methods, based on the machine's geometry are often used, [2]. The commonly used approach is the use of the finite differences method, the finite elements method, integrals methods the frontier's elements methods. The field analysis allows determining the process parameters in the same manner as the observer-based methods and in addition the model's parameters or the physical parameters may also be determined.

Based on this idea, the paper presents an implementation of a state observer with the separation of the fast variables, the Pietrzak-David algorithm,[1], in comparison with the implementation of the FEM method to estimate the stator flux-linkages components within an single/two-phase induction machine.

2. METHODOLOGY

2.1. The Implementation of the FEM method to compute the inductances and the magnetic fluxes within the single/two-phase induction machine

The basis of the FEM method, [3] is the transformation of the solution of the electromagnetic potential, ψ into a linear combination of coordinate functions $\psi = \sum_{k=1}^n \alpha_k \cdot \varphi_k$. The unknown

coefficients, $\alpha_k, k = \overline{1, n}$ result from a minimisation of the energetic functional associated to the field $F(\psi)$. There are various software applications that allow the FEM implementation to analyse the electromagnetic field both at low and high frequencies. In this paper, the Ansoft-Maxwell SV environment was used for the 2D analysis of the electrical machine, [4].

2.2. The Implementation of the Pietrzak-David State Estimator, [1]

The dynamic model of the induction machine is represented into a coordinate reference system related to the magnetic motion field as shown in the expressions below.

$$\frac{d}{dt} \begin{bmatrix} \Psi_{1d} \\ \Psi_{1q} \\ i_{1d} \\ i_{1q} \end{bmatrix} = \begin{bmatrix} 0 & \omega_e & -R_1 & 0 \\ -\omega_1 & 0 & 0 & -R_1 \\ \frac{R_2'}{\sigma \cdot L_2 \cdot L_1} & \frac{\omega}{\sigma \cdot L_1} & -\frac{1}{\sigma} \cdot \left(\frac{R_1}{L_1} + \frac{R_2'}{L_2} \right) & \omega_1 - \omega_2 \\ \frac{\omega}{\sigma \cdot L_1} & \frac{R_2'}{\sigma \cdot L_2 \cdot L_1} & -\omega_1 + \omega_2 & -\frac{1}{\sigma} \cdot \left(\frac{R_1}{L_1} + \frac{R_2'}{L_2} \right) \end{bmatrix} \cdot \begin{bmatrix} \Psi_{1d} \\ \Psi_{1q} \\ i_{1d} \\ i_{1q} \end{bmatrix} + \begin{bmatrix} 1 & 0 \\ 0 & 1 \\ \frac{1}{\sigma \cdot L_1} & 0 \\ 0 & \frac{1}{\sigma \cdot L_1} \end{bmatrix} \cdot \begin{bmatrix} V_{1d} \\ V_{1q} \end{bmatrix} \quad (1)$$

The time constants of the drive may be grouped into three categories as follows.

- | | | |
|---|---------------------------|------------|
| 1 | very slow time constants: | mechanical |
| 2 | slow time constants: | magnetic |
| 3 | fast time constants: | electrical |

After eliminating the variations of the variables associated to the very slow and slow time constants, the dynamic model of the induction machine may be reduced to a second-order linear system as shown in the expressions below.

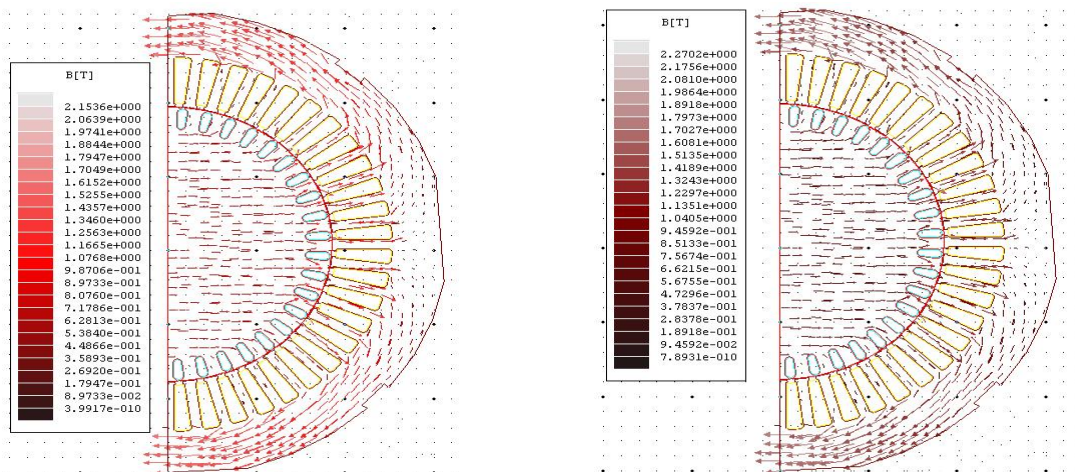


Figure 1: The spectra of the magnetic field determined with the FEM method; to the left - the (Od) axis component, to the right – the (Oq) axis component.

$$\begin{cases} \frac{d\mathbf{Y}_1}{dt} = \mathbf{A} \cdot \mathbf{Y}_1 + \mathbf{B} \cdot \mathbf{U}_1 \\ \mathbf{X}_1 = \mathbf{C} \cdot \mathbf{Y}_1 + \mathbf{D} \cdot \mathbf{U}_1 \end{cases} \quad (2)$$

where the significance of the matrices is given in expressions (3) to (6).

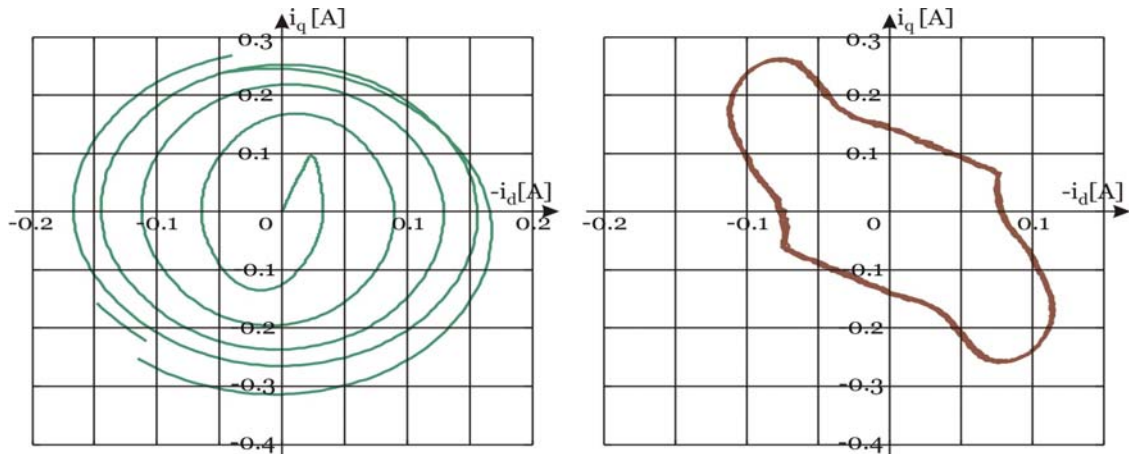


Figure 2: The loci of the stator currents space-vector, estimated values- to the left and measured values – to the right.

$$\mathbf{A} = \begin{bmatrix} -\frac{1}{T_1 + T_2} & \omega_1 - \omega \cdot \frac{T_2}{T_1 + T_2} \\ -\left(\omega_1 - \omega \cdot \frac{T_2}{T_1 + T_2}\right) & -\frac{1}{T_1 + T_2} \end{bmatrix} \quad T_1 = \frac{L_1}{R_1}, T_2 = \frac{L_2'}{R_2'} \quad (3)$$

$$\mathbf{B} = \frac{T_1}{T_1 + T_2} \cdot \begin{bmatrix} 1 & 0 \\ 0 & 1 \end{bmatrix} \quad (4)$$

$$\mathbf{C} = \frac{T_1}{T_1 + T_2} \cdot \begin{bmatrix} 1 & \omega \cdot T_2 \\ -\omega \cdot T_2 & 1 \end{bmatrix} \quad (5)$$

$$\mathbf{D} = \frac{T_1}{T_1 + T_2} \cdot \begin{bmatrix} T_2 & 0 \\ 0 & T_2 \end{bmatrix} \quad (6)$$

Input variables

$$\begin{bmatrix} v_{1d} & v_{1q} \end{bmatrix}^T$$

Output variables

$$\begin{bmatrix} i_{1d} & i_{1q} \end{bmatrix}^T$$

State variables

$$\begin{bmatrix} \Psi_{1d} & \Psi_{1q} \end{bmatrix}^T$$

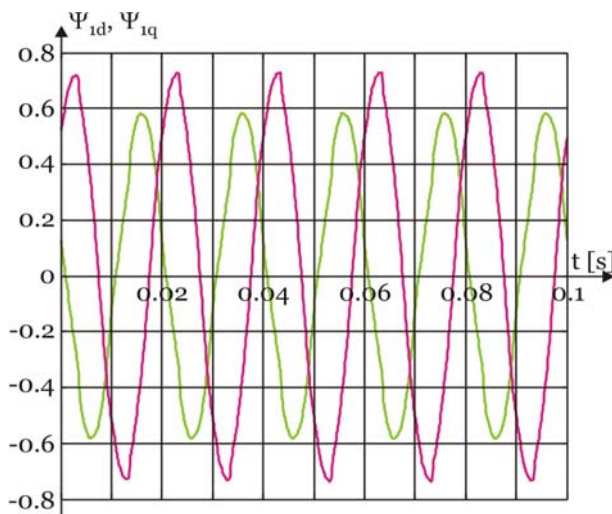


Figure 3: time-dependencies of the estimated flux components.

The Luenberger observer reconstructs the flux-linkage components based on the measurements of the input and output variables. Then the estimations are corrected in closed-loop with a term $K \cdot (i_{1d} - \hat{i}_{1d})$ where the gain is determined with a Kalman filter.

3. DISSCUSIONS/RESULTS/ANALYSES

The motor under the investigation was a MSP311 type. The nominal parameters of the motor are given in Table 1.

3.1. The determination of the flux-linkage components with the FEM method

In Figure 1 the spectra of the magnetic field components are presented, [4]. The spectra have been determinate within the MAXWELL SV software environment and a geometrical representation of the cross-section of the machine.

The computations performed with the field calculator give the following values for the self inductances of the stator: $L_{1d} = 0,665 H$ and $L_{1q} = 0,358 H$. A remark issued at the implementation of the method is that the estimate is dependent on the values of the magnetic permeability of the on the magnetization curve. If an experimental determination of the magnetization curve is not available the estimation will be performed carefully and several data sets shell be used to increase the accuracy of the estimate.

Table 1: The Nominal Parameters of the MSP311 Motor

Denomination	Rated supply voltage	Rated frequency	Rated angular speed	Number of pair poles	Capacitor
Units	[V]	[Hz]	[rpm]	[-]	[μF]
Value	220	50	2820/420	1/6	14

3.2. The determination of the magnetic flux with state observers

The measurements used within the observer's implementation are presented in [4]. The implementation of the state observer is associated to the model in notation (2). The loci of the stator currents space-vector, estimated values and measured values are depicted in Figure 2.

From the analysis follows that the estimator cannot describe the non-linearity effects into the model but the information about the magnitude of the variables is conserved. The time-dependencies of the estimated flux components are presented in Figure 3.

4. CONCLUSIONS/FURTHER PROPOSALS

In this paper, the implementation of two different methods – the FEM method and an observer-based method - for the magnetic field components estimation is presented. The model under investigation was a single/two-phase capacitor-run induction machine.

The FEM method is widely used at the design level; the state observer is implemented in the adaptive control. From the analysis above, both methods provide

REFERENCES

- [1.] G. GRELLET and G. CLERC, Actionneurs électriques. Principes/Modèles/Commande, Eyrolles, 2000
- [2.] A. NICOLAIDE, Bazele Fizice ale Electrotehnicii, Scrisul Românesc, 1983
- [3.] GH. MÎNDRU, M.M. RĂDULESCU, Analiza numerică a câmpului electromagnetic, Editura Dacia, 1986
- [4.] A. DANILA, I.MARGINEANU, R. CAMPEANU, C. SUCIU, I. BOIAN, The Optimization of the Single/Two Phase Induction Motor Start-Up with Electronically Switched Capacitor, 2008 IEEE International Conference on Automation, Quality and Testing, Robotics. Proceedings – Tome III pp 450-454



¹Cornelia Victoria ANGHEL

CONNECTING PC VIA WIRELESS NETWORK PERFORMANCE OF EQUIPMENT

¹ EFTIMIE MUTGU UNIVERSITY OF REȘIȚA, FACULTY OF ENGINEERING,
COMPUTER SCIENCE DEPARTMENT, REȘIȚA, ROMÂNIA

ABSTRACT:

Increasing popularity of wireless networks has led to a rapid decrease in the price of wireless devices along with a marked improvement in their technical performance. A wireless network infrastructure can now be achieved with much lower costs than a traditional cable. In this way, there are prerequisites to achieve cheap and easy Internet access local communities, with all the benefits resulting. Access to information is a source of global network.

KEYWORDS:

computers, Wireless Network, drivers

1. INTRODUCTION

Increasing popularity of wireless networks has led to a rapid decrease in the price of wireless devices along with a marked improvement in their technical performance.

A wireless network infrastructure can now be achieved with much lower costs than a traditional cable. In this way, there are prerequisites to achieve cheap and easy Internet access local communities, with all the benefits resulting.

2. METHODOLOGY

2.1. Connecting the Device

Before installing the Router, please make sure your broadband service provided by your ISP is available. If there is any problem, please contact with your ISP. After that, please install the Router according to the following steps. Don't forget to pull out the power plug and keep your hands dry.

1. Locate an optimum location for the Router. The best place is usually near the center of the area in which your PC will be wirelessly connected. The place had better accord with the Installation Environment Requirements.
2. Adjust the direction of the antenna. Normally, upright is a good direction.
3. Connect the PC(s) and each Switch/Hub in your LAN to the LAN Ports on the router.
4. (If you have the wireless NIC and want to use wireless function, you can skip this step.)
5. Connect the DSL/Cable Modem to the WAN port on the router.

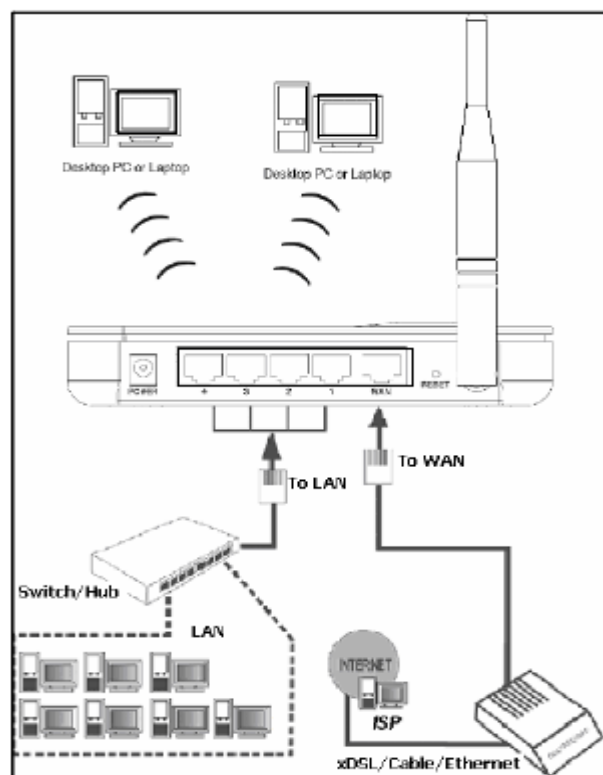


Figure 1. Hardware Installation of the Router

6. Connect the AC power adapter to the AC power socket on the router, and the other end into an electrical outlet. The router will start to work automatically.
7. Power on your PC and Cable/DSL Modem.

2.2. Configure our PC

Our PC needs a network adapter. You may directly connect your adapter to the Router, or you may connect your adapter to a Hub/Switch, and then connect the Hub/Switch to the Router.

Follow the instructions below to configure a computer running Windows XP to be a DHCP client.

1. From the **Start** menu on your desktop, go to **Settings**, and then click on Network Connections.
2. In the **Network Connections** window, right-click on LAN (Local Area Connection), then click Properties.
3. In the **General** tab of **Internet Protocol (TCP/IP) Properties** menu, highlight Internet Protocol (TCP/IP) under “This connection uses the following items:” by clicking on it once. Click on the Properties button.
4. Select “Obtain an IP address automatically” by clicking the radio-button. Click OK.

2.3. Configure the IP address manually

1. 1. Open TCP/IP Properties of the LAN card in our PC, enter the IP address. Now, we can run the Ping command in the command prompt to verify the network connection between your PC and the Router.
2. 2. Open a command prompt, From the Start menu on your desktop, select run tab, type **cmd** in the field, and complete the numbers of *ping* on the screen that appears, and then press Enter.

If the connection between our PC and the Router is correct the LEDs of LAN port which link to on the device and LEDs on our PC's adapter should be lit.

3. PERFORMANT EQUIPMENTS FOR CONNECTING PC VIA WIRELESS NETWORK

3.1. 1W AMPLIFIER 1000MW WIRELESS 6DBI

Art equipment that allows us to receive signals wirelessly at distances up to 3,000 meters and 5,000 meters in urban areas without major obstacles.

Increase signal reception power of over 5 times!

It is compatible with all types of laptop.

BGN 2.4 GHz wireless adapter, antenna 6dBi, MIMO technology, 100Mbps, notebook support

Compatible with IEEE 802.11n draft 3.0 wireless 802.11a/b/g Standards

- ❖ 2.4GHz frequency band, MIMO (Multiple Input Multiple Output)
- ❖ Complies with Universal Serial Bus Rev. 2.0 Specifications TX
- ❖ High speed transfer data rate up to 150 Mbps
- ❖ High speed transfer data rate up to 300 RX Mbps
- ❖ Supports WPS by S / W
- ❖ Supports Wireless Data Encryption with 64/128-bit WEP, WPA, WPA2, TKIP, AES.
- ❖ Wide Range coverage
- ❖ Compliant with FCC Part 15.247 for U.S., ETS 300 328 for Europe
- ❖ Supports drivers for Windows 2000, XP 32/64, Vista 32/64, Linux (2.4.x/2.6.x), Mac (10.4.x/10.5.x) Power PC & PC

3.2. DIRECTIONAL WLAN ANTENNA (2.4GHz, 17 dB)

This model has thus having a high resistance grounding surge caused by storms and lightning. The antenna is small and is easily installed on the roof or balcon, not special support required, it can be used in access-point and the client (please make sure you have plugged into the equipment, otherwise it will be necessary cables and adapters). It can operate in both polarization (horizontal or vertical) depending on how it is mounted

Most often, vertical polarization antenna is used in this way it can be changed by rotating the 90° antenna. The radiator can be unscrewed and no position can be changed. If the antenna must operate with a sectorial antenna, it has to be put in horizontal position as in the picture below.



Figure 2. Directional WLAN Antenna

4. RESULTS

The results are detailed in the graphic representation:

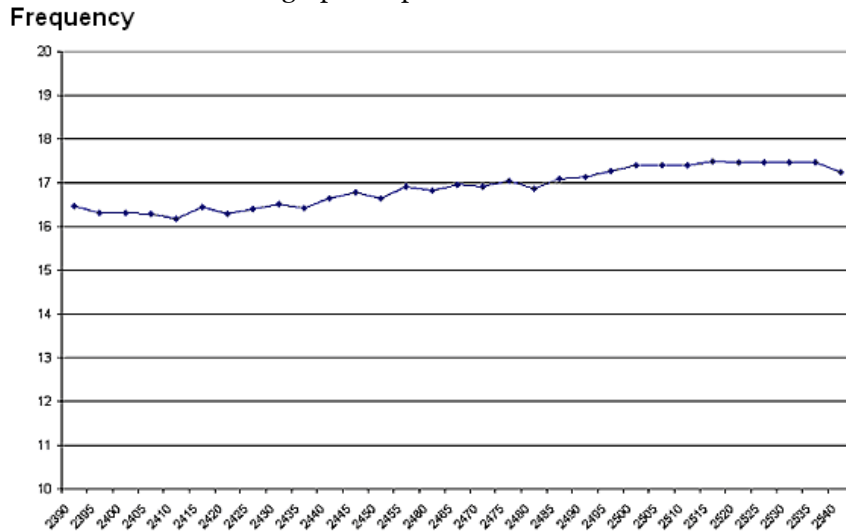


Figure 3. The graphic representation

Features horizontally

Characteristics of vertically

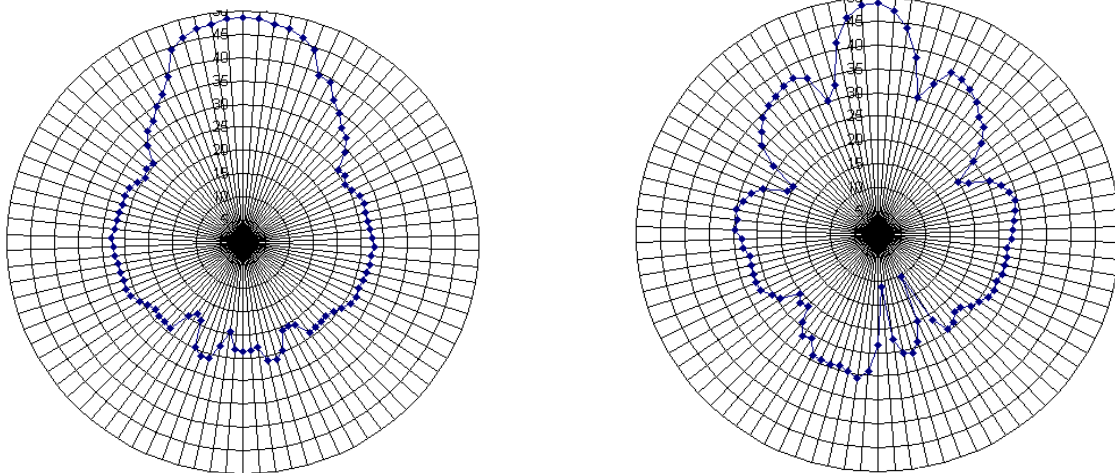


Figure 4. The representation of horizontally and vertically characteristics.

The specifications and characteristics are presented in Table 1.

Table1: Specifications and characteristics

Name	Directional WLAN Anthen
Gain	17dB
Band	2390-2540 MHz
Polarization	V / H
Report of the wave state. (VSWR)	<1.9
Report front / rear	25 dB
Half power beam - H	30 °
Half power beam - E	15 °
Impedance	50 ohms
Connector	N-socket (female)
Size	450 x 390 x 285 mm
Mounting Diameter	35-40mm

5. CONCLUSIONS

Wireless computer networks are intended for applications where cable installation is not possible or where necessary to terminal mobility.

The performance equipments presented in this article allows our PC to receive signals wirelessly at distances up to 3,000 meters and 5,000 meters in urban areas without major obstacles.

REFERENCES

- [1.] Anghel, C.V. – „Considerații privind conectarea la o rețea Wireless securizată” Al XII-lea Simpozion Internațional “Tinerii și Cercetarea Multidisciplinară”, 11-12 noiembrie, Timișoara, 2010
- [2.] Dixit, R. Prasad (eds.), Wireless IP and Building the Mobile Internet, Artech House, 2003
- [3.] M. Mallick, Mobile and Wireless Design Essentials, Ed. John Wiley & Sons, 2003
- [4.] Tanenbaum A. - Rețele de calculatoare (ediția a patra), Ed. Byblos, Tg.Mureș, 2003
- [5.] Raab S. et al. - Mobile IP Technology and Applications, Cisco Press, 2005





SOLUTIONS TO ACCELERATE MATLAB PROGRAMS WITH GPU COMPUTING

¹⁻³. "POLITEHNICA" UNIVERSITY OF TIMISOARA, FACULTY OF ENGINEERING OF HUNEDOARA, DEPARTMENT OF ELECTRICAL ENGINEERING AND INDUSTRIAL INFORMATICS, ROMANIA

ABSTRACT:

The present paper presents recent advances in computational technology using the computational power offered by modern graphic processing units (GPUs). The technology is applied in Matlab scientific computations. Two different software solutions are evaluated and compared in order to reveal the main features and particularities from the point of view of a scientific computation user. The benefits and the drawbacks of this new technology are pointed out.

KEYWORDS:

CUDA technology, GPU computing, accelerating algorithms

1. INTRODUCTION

Over the past few years, graphics processing units (GPUs) have advanced at an astonishing rate and gained significant popularity as powerful tools for high performance computing (HPC). A GPU is a highly parallel computing device designed for the task of graphics rendering. However, the GPU has evolved in recent years to become a more general processor, allowing users to flexibly program certain aspects of the GPU to facilitate sophisticated graphics effects and even scientific applications. In general, the GPU has become a powerful device for the execution of data-parallel, arithmetic (versus memory) intensive applications in which the same operations are carried out on many elements of data in parallel. Example applications include the iterative solution of PDEs, video processing, machine learning, and 3D medical imaging.

The design philosophy of the GPUs has historically been motivated by the fast growing video game industry that exerts tremendous economic pressure for the ability to perform massive numbers of floating point calculations in advanced games. Therefore, the design goal for GPU vendors is to look for ways to maximize the chip area and power budget dedicated to floating point calculations. The general philosophy for GPU design is to optimize for the execution of massive number of threads. The hardware takes advantage of a large number of execution threads to find work to do when some of them are waiting for long-latency memory accesses, minimizing the control logic required for each execution thread. Small cache memories are provided to help control the bandwidth requirements of these applications so that multiple threads that access the same memory data do not need to all go to DRAM. As a result, much more chip area is dedicated to the floating-point calculations.

CUDA stands for **Compute Unified Device Architecture** and is a software architecture and API geared towards the utilization of the GPU as a computing device rather than a graphics rendering device. The CUDA software includes a GPU device driver, a runtime system that serves as an abstraction over the driver, and also runtime libraries that CUDA applications may link to in order to provide GPU-enabled FFT and BLAS support, among others. CUDA also includes a compiler tool chain which provides extensions onto the C/C++ languages for the construction of GPU applications. While programming the GPU with the CUDA tool chain, the GPU is viewed as a coprocessor to the CPU, or host, which orchestrates the executions carried out by the GPU as needed. In order to utilize the GPU to its fullest potential, the CPU must minimize data communication with the GPU, due to limited bus bandwidth, and maximize data parallelism in the

tasks given to the GPU to maximize usage of GPU processors. Though the GPU can be viewed as capable of executing a large number of general threads in parallel, GPU programming is still typically accomplished through the specification of kernels which operate across an array of data elements. These kernels are limited in their length and the amount of local memory they use. The potential bottlenecks involved in computing with the GPU include memory allocation, memory transfer, and kernel execution. In the ideal case, each of these tasks is done sparingly to ensure that minimal overhead is accrued over the lifetime of an application.

The CUDA software stack is composed of several layers: a hardware driver, an application programming interface (API) and its runtime, and two higher-level mathematical libraries of common usage, CUFFT (The Fast Fourier Transform implementation) and CUBLAS (Basic Linear Algebra Subprograms implementation).

The Fast Fourier Transform is a divide-and conquer algorithm for efficiently computing discrete Fourier transform of complex or real-valued data sets. CUFFT is the CUDA FFT library that provides a simple interface for computing parallel FFT on an NVIDIA GPU. It allows users to leverage the floating-point power and parallelism of the GPU without having to develop a custom GPU-based FFT implementation.

Implementation of the Basic Linear Algebra Subprograms on top of CUDA driver provides the interface for parallel computation of basic models of matrix and vector objects in GPU memory space, filling objects with data, calling sequence of CUBLAS functions, retrieving data from GPU, creating and destroying objects in GPU space, writing data to and retrieving data from objects.

The hardware has been designed to support lightweight driver and runtime layers, resulting in high performance. When programmed through CUDA, the GPU is viewed as a compute device capable of executing a very high number of threads in parallel. It operates as a coprocessor to the main CPU, or host. In other words, compute intensive portions of applications running on the host are off-loaded onto the device. CUDA has hierarchical and non-unified memory access and both the host and the device maintain their own DRAM, referred to as host memory and device memory, respectively. One can copy data from one DRAM to the other through optimized API calls that utilize the device's high-speed Direct Memory Access (DMA) engines [1].

There are two ways to speed up the solver by CUDA:

- ❖ keeping at least the spirit of the current algorithm, and
- ❖ developing a totally new algorithm considering the new architecture.

We chose for the work presented in this report the first alternative believing that the second one is quite timely.

To keep the current algorithm, we partially-modified the algorithm without changing its underlying paradigm, implementing it in CUDA, and then porting it to Matlab. Although CUDA is a new architecture, there is a large amount of related work in the academic and a few in industrial scales. However, they have mostly not been applied to the field of equation solvers. Reference [2] reports a practice on CG solver.

2. SOLUTIONS FOR USING GPUS IN SCIENTIFIC COMPUTING

Finding parallelism in a program has been a challenge for at least the past twenty years of research in parallelism, and is still one today. But with the arrival of GPU chips capable of executing many instructions in parallel, available to average users, it become even more important to be able to utilize this power so that the end-users of computers can benefit from it and not only elite or research members.

Languages should evolve and low-level languages like C are not well suited for programming complex parallel tasks. It is a necessity to give to programmers new tools to effectively develop parallel program while reducing the need of a full parallelism comprehension and good knowledge of the underlying architecture. Matlab [3] is a high-level language with a powerful matrix-based system. It is often used for easy prototyping in early development stages because it relieves the programmer of many details like memory management and has an impressive library of built-in many matrix functions. Hence, it is a useful tool for many simulation domains like fluid mechanics, biology or mechanical engineering, especially for people whose first domain of competence is not computer science and are programmers by necessity.

There already exist different ways to speed up the computation of Matlab programs using GPUs, including several third-party toolboxes. Some options available, all built on top of the Compute Unified Device Architecture (CUDA) developed and provided by NVIDIA to access its GPUs will be presented in forthcoming sections.

2.1 GPUMAT LIBRARY

GPUmat is a freeware library, in a more advanced state than GPUlib, so memory management on the GPU is automated, even if data movements still need to be explicit. This is done through the

addition of a new type of variables, GPUsingle, which makes use of GPU memory transparent for users. Deletion of unused variables is taken care of by a garbage collector so as not to clobber the GPU memory. This is important as data processed by GPUs tend to be very big since computations are based on data-parallelism. The use of this new type allows Matlab functions to be overloaded so that either the GPUmat or the original Matlab function is called depending on the type of the arguments.

The start command for GPUmat library *GPUstart* generate the following output in Matlab command window

```
>> GPUstart
Copyright gp-you.org. GPUmat is distributed as Freeware.
By using GPUmat, you accept all the terms and conditions
specified in the license.txt file.
Please send any suggestion or bug report to gp-you@gp-you.org.
Starting GPU
There is 1 device supporting CUDA
CUDA Driver Version:      2.30
CUDA Runtime Version:    2.30
Device 0: "GeForce 9500 GT"
  CUDA Capability Major revision number:    1
  CUDA Capability Minor revision number:    1
  Total amount of global memory:    1073414144 bytes
  Number of multiprocessors:        4
  Number of cores:                  32
  - CUDA compute capability 1.1
...done
- Loading module EXAMPLES_CODEOPT
- Loading module EXAMPLES_NUMERICS
-> numerics11.cubin
- Loading module NUMERICS
-> numerics11.cubin
```

GPUmat enables Matlab code to run on the Graphical Processing Unit. The following is a summary of GPUmat most important features:

- ❖ GPU computational power can be easily accessed from Matlab without any GPU knowledge.
- ❖ Matlab code is directly executed on the GPU. The execution is transparent to the user.
- ❖ GPUmat speeds up Matlab functions by using the GPU multi-processor architecture.
- ❖ Existing Matlab code can be ported and executed on GPUs with few modifications.
- ❖ GPU resources are accessed using Matlab scripting language. The fast code prying capability of the scripting language is combined with the fast code execution on the GPU.
- ❖ GPUmat can be used as a Source Development Kit to create new functions and extend the library functionality.
- ❖ GPU operations can be easily recorded into new functions using the GPUmat compiler.

The following example presents the computational solution of the wave equation using the discrete Fast Fourier Transform. Consider the variable coefficient wave equation

$$\frac{du}{dt} + c(x) \frac{du}{dx} = 0, \quad c(x) = 0.3 + \cos^3(x-1), \quad (1)$$

for $x \in [0, 2\pi], t > 0$, with periodic boundary conditions. As an initial condition we take $u(x, 0) = \exp(-100(x-1)^2)$. This function is not mathematically periodic, but it is so close to zero at the ends of the interval that it can be regarded as periodic in practice.

In the first case the process is based on a CPU computation (Program 1), while in the second case the solving is executed using the GPU unit (Program 2). The *fft* function was realized using GPU instructions with the help of GPUmat library.

Comparative with the GPU results, the CPU results have a better accuracy (Figure 1), while the computation using the GPUmat *fft* function introduced the occurrence of spurious dispersion. In Figure 2 can be noticed that the algorithm loses its stability with oscillations that will grow exponentially and swamp the solution. The code requires another corrections to increase the accuracy.

Program 1.

```

clc;clear all;
tic;
N = 128; h = 2*pi/N; x = h*(1:N); t = 0; dt = h/4;
c = 0.3 + cos(x-1).^3;
v = exp(-100*(x-1).^2); vold = exp(-100*(x-.2*dt-1).^2);
tmax = 8; tplot = .15; clf, drawnow
plotgap = round(tplot/dt); dt = tplot/plotgap;
nplots = round(tmax/tplot);
data = [v; zeros(nplots,N)]; tdata = t;
for i = 1:nplots
for n = 1:plotgap
t = t+dt;
v_hat = fft(v);
w_hat = 1i*[0:N/2-1 0 -N/2+1:-1] .* v_hat;
w = real(ifft(w_hat));
vnew = vold - 2*dt*c.*w; vold = v; v = vnew;
end
data(i+1,:) = v; tdata = [tdata; t];
end
waterfall(x,tdata,data), view(10,70), colormap([0 0 0])
axis([0 2*pi 0 tmax 0 5]), ylabel t, xlabel u, grid off; toc
    
```

Program 2.

```

clc;clear all;
tic;
N = 128; h = 2*pi/N; x = h*(1:N); t = 0; dt = h/4;
c = 0.3 + cos(x-1).^3;
v = exp(-100*(x-1).^2); vold = exp(-100*(x-.2*dt-1).^2);
tmax = 8; tplot = .15; clf, drawnow
plotgap = round(tplot/dt); dt = tplot/plotgap;
nplots = round(tmax/tplot);
vGPU=GPUsingle(v); % transfer variable v to GPU memory
data = [v; zeros(nplots,N)]; tdata = t;
for i = 1:nplots
for n = 1:plotgap
t = t+dt;
v_hatGPU = fft(vGPU); % perform Fast Fourier Transform on GPU
v_hat = single(v_hatGPU); % copy v_hat in CPU memory
w_hat = 1i*[0:N/2-1 0 -N/2+1:-1] .* v_hat;
w_hatGPU=GPUsingle(w_hat); % transfer variable w_hatGPU to GPU memory
wGPU = real(ifft(w_hatGPU)); % perform Inverse Fast Fourier Transform on GPU
w = single(wGPU); % copy w in CPU memory
vnew = vold - 2*dt*c.*w; vold = v; v = vnew;
end
data(i+1,:) = v; tdata = [tdata; t];
end
waterfall(x,tdata,data), view(10,70), colormap([0 0 0])
axis([0 2*pi 0 tmax 0 5]), ylabel t, xlabel u, grid off
toc
    
```

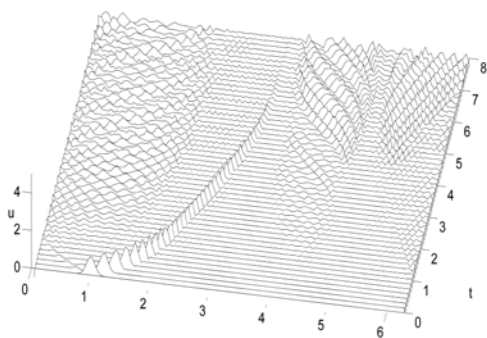


Figure 1. Program 1 output: solution of the wave equation (1) computed on CPU.

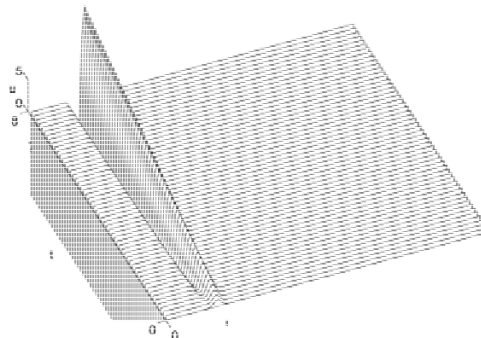


Figure 2. Program 2 output: solution of the wave equation (1) computed using GPUmat- algorithm loses its stability

2.2. JACKET PLATFORM FOR GPU COMPUTING WITH MATLAB

Jacket is a software platform designed for engineers, scientists, and analysts who want maximum application performance, minimum programming difficulty and maximum leverage of available technical computing resources, including laptops, desktops, servers, clusters and the Cloud. Jacket provides a middleware approach to GPU programming, with MATLAB as the fronted point of interaction for the user [4]. MATLAB with millions of users worldwide is the platform of choice for engineers and scientists alike, for rapid algorithm prototyping. MATLAB is an extensible interactive programming environment for numerical analysis built on a vector language called M. The M-language, like other vector languages, provides users with a high-level interface at which operations may be specified over large sets of data at once making the expression of data-parallel algorithms natural. M is also dynamically typed, adheres to pass-by-value semantics, and is integrated into a well developed interpreted environment. With these characteristics, M has proven to be a powerful, user-friendly language. Using Jacket, the M-language and MATLAB transparently adapt to GPU computing. Unlike other GPU solutions, Jacket provides GPU computation and graphics ability from a language which is inherently parallel and interpreted, thereby providing a standard, extensible, and simple method of programming for the GPU in an already proven rapid prototyping environment. Jacket adds few GPU-specific data types to MATLAB with overloaded operators and entire CPU-bound MATLAB programs can be converted into GPU-enabled programs through as little as adding a 'g' prefix onto memory allocation commands. Otherwise, the user interacts with MATLAB as they normally would either from the command line or when running scripts.

Changing the data type allows the user to tap into the GPUs tremendous computational power. All standard data types are supported, including real and complex versions of singles, doubles, and integers. CUDA-capable GPUs of all types are supported. For instance, NVIDIA's Fermi-based Tesla C2050 contains 448 cores that are now fully accessible with Jacket, but those with lesser budget can also run Jacket on GeForce and Quadro GPUs.

Performance tests were performed on a desktop configuration of dual core CPU and Windows 2010 64 bite operating environment, using Matlab 2010a with Jacket v1.4. The GPU used is CUDA enabled GeForce 9500 GT with CUDA drivers.

Let us considered again the wave equation (1) with the CPU computed solution depicted in Figure 1. Program 3 represents the modified Jacket code for solving the wave equation (1) using the Fast Fourier Transform on Graphic Processing Unit.

Program 3.

```

clc;clear
tic;
N = 128; h = 2*pi/N; xx=1:N; % CPU variables
x = h*xx; t = 0; hCPU=h; % CPU variables
dt = hCPU/4;
c = 0.2 + cos(x+1).^2 + sin(x+1).^2; % CPU variable
%c = 0.3 + cos(x-1).^3;
v = exp(-100*(x-1).^2); % CPU variable
vold = exp(-100*(x-.2*dt-1).^2); %CPU variable
tmax = 8; tplot = .15; clf, drawnow
plotgap = round(tplot/dt); dt = tplot/plotgap;
nplots = round(tmax/tplot);
data = [v; zeros(nplots,N)];
tdata = t;
nplots=gsingle(nplots); %transfer variable on GPU
plotgap=gsingle(plotgap); % transfer variable on GPU dt=gsingle(dt); % transfer
variable on GPU
data=gsingle(data); % transfer variable on GPU
for i = 1:nplots
for n = 1:plotgap
t = t+dt;
v_hat = fft(v); % perform FFT on GPU
w_hat = 1i*[0:N/2-1 0 -N/2+1:-1].*v_hat;
w = real(iff(w_hat)); % perform IFFT on GPU
vnew = vold - 2*dt*c.*w; vold = v; v = vnew;
end
data(i+1,:) = v; tdata = [tdata; t];
end
x=single(x);tdata=single(tdata);data=single(data); % transfer variables back to CPU
waterfall(x,tdata,data), view(10,70), colormap([0 0 0])
axis([0 2*pi 0 tmax 0 5]), ylabel t, xlabel u, grid off; toc
    
```

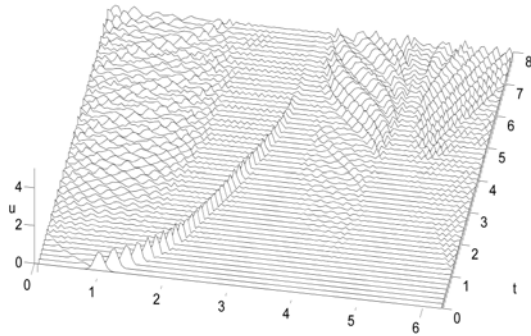


Figure 3 Program 3 output: solution of the wave equation (1) computed on GPU with Jacket v1.4.

Figure 3 shows the output of the Program 3. It can be noticed no difference between the output of the CPU code presented in Figure 1.

3. LIMITATIONS IN EXISTING ACCELERATION SOLUTIONS

Jacket provides an extensive list of Matlab functions with their state of support, ranging from “fully supported,” meaning that they should work in any situation authorized by the original Matlab function, to “not supported,” which cannot be used with *gsingle* arguments and there is no plan to support them in the immediate future.

The number of supported functions is much bigger in Jacket than in GPUmat at the time of this writing. Because of no dynamic matrices with Jacket, hence the assignment

$$\text{data} = [\text{v}; \text{zeros}(\text{nplots}, \text{N})];$$

is not valid as computed on GPU, it was necessary a two-way directional transfer of variables between the GPU and the CPU for the source Program 3. This increases the elapsed time, despite of the performance improvement obtained by using the GPU processing. In Table 1 a comparison between the CPU computation time of the wave equation (1) and the GPU computation time of the same is presented.

Table 1 Comparison between the computation time of the wave equation, on CPU and GPU.

Elapsed time of computation on CPU	Elapsed time of computation on GPU
0.883485	1.539880

Since our GPU works only with single precision floats, hence gives a less precise calculations, the conclusion is that this technology is not mature enough to be used effortlessly by the average user.

4. CONCLUSION

Some reasons for which Jacket is not suitable for development of our stability investigation algorithms are the facts that Jacket are a rather limited functions for matrix operations (for example *diag(M)* *diagonal scaling* is not supported), there is no eigenvalue solver supported by Jacket (as *qz factorization for generalized eigenvalue problems* is not currently supported, *eigs largest eigenvalues and eigenvectors of matrix* are unsupported), except some trials, these being insufficient for a generalized eigenvalue problem, at the time being.

That is the reason that most applications will use both CPUs and GPUs, executing the sequential parts on the CPU and numeric intensive parts on the GPUs. This induces a significant overhead of memory transfers between the host CPU and the GPU. In general, the overhead of time spent in sending data to the GPU and bringing it back neutralizes any performance benefit obtained by computing on the GPU.

REFERENCES

- [1.] NVIDIA CUDA development team: NVIDIA CUDA Compute Unified Device Architecture Programming Guide, NVIDIA corporation, 2007.
- [2.] Wiggers, W.A., Bakker, V., Kokkeler, A.B.J., Smit, G.J.M., Implementing the conjugate gradient algorithm on multi-core systems, *IEEE International Symposium on System-on-Chip*, Finland, 2007.
- [3.] <http://www.mathworks.com>
- [4.] Jacket v1.4 *Getting Started Guide*, <http://www.accelereyes.com/>





SOFTWARE PACKAGE FOR ANALYSIS THE PERFORMANCES OF BACKPROPAGATION NEURAL NETWORKS TRAINING ALGORITHM

¹⁻⁴ UNIVERSITY POLITEHNICA TIMISOARA, FACULTY OF ENGINEERING HUNEDOARA,
ELECTRICAL ENGINEERING AND INDUSTRIAL INFORMATICS DEPARTMENT, ROMANIA

ABSTRACT:

In this paper we present a software package use to analysis the performances of backpropagation neural networks training algorithm. It was analyze the dependency of performances with the learning rate of the algorithm. The software was implemented in Java language. The software was designed with the aim of offering a very easy-to-use user interface. It can be use as an educational tool for teach the basic concepts of backpropagation neural networks.

KEYWORDS:

neural networks, Java, learning algorithm, backpropagation algorithm

1. INTRODUCTION

Artificial neural networks (ANNs) are tools that have proved to be valuable to solve complex problems in many different application fields of science and technology [1, 2]. As a result, it is increasingly usual to find notions of neural networks included in the curricula of many Engineering studies [1].

Neural networks are interdisciplinary and have been used extensively in various fields ranging from electrical engineering to computer science from biology to image processing. Neural networks can solve prediction, estimation, classification, clustering, forecasting, control and decision making problems accurately and quickly [2].

Studying and researching neural networks, results the mathematical nature and underlying complexity. For this reason many students find the neural networks behavior difficult [9]. Moreover, neural networks are dynamic systems, which evolve in time, especially during their design and training phases. For engineering students, the most important is to understand this dynamic nature, and the real utility and operation of neural networks. Classroom-based teaching, books, and lecture notes are not sufficient to transmit this kind of knowledge [1].

Neural Networks have ability to learn from its environment and improve the performance through learning. The procedure used to selflearning process of an NN is called a learning algorithm. Some important application areas of neural networks are: Engineering and industrial applications, Business and financial applications, Medical applications. Some engineering and industrial applications are [2]: control, monitoring and modeling; process engineering; technical diagnosis; nondestructive testing; power systems; robotics; transportation; telecommunications; remote sensing; image processing.

The use of neural networks offers the many useful properties and capabilities [2]: nonlinearity; adaptivity; contextual information; fault tolerance; uniformity of analysis and design; neurobiological analogy.

In this paper is described an educational software useful for a better understanding the basic concepts of backpropagation neural networks and their training algorithm.

2. THE INFORMATICS SYSTEM DESIGN AND IMPLEMENTATION

The application was implemented in Java using NetBeans platform. The graphical user interface for this application is presented in figure 1. Using main menu for the application you could select the main options that are available.

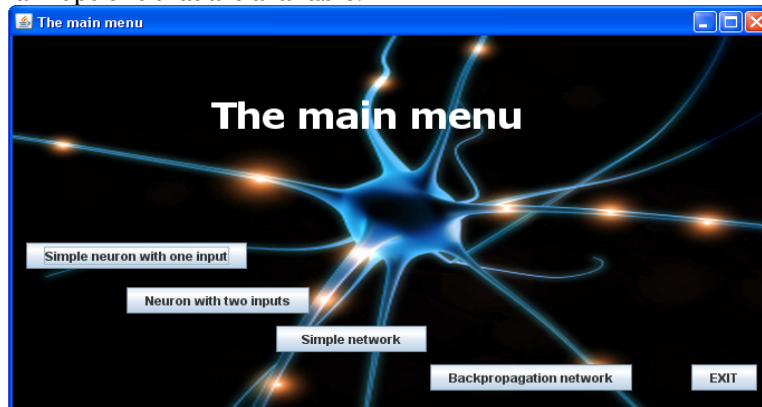


Fig. 1 The main menu of the application

The first and second options present the principle of the simplest artificial neuron operating. The simplest model of artificial neuron is represented by a nonlinear limiting or threshold element which excites if their inputs activation, fig. 2.

In according to threshold-logic units model each of continuous-valued input signals shall represent the electrical activity on the corresponding input line, or alternatively, the momentary frequency of neural impulses delivered by another neuron to this input.

The output frequency y is approximated by a function

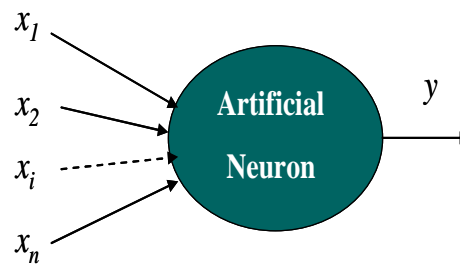


Fig. 2 The simplest model of the artificial neuron

$$y = c \cdot f\left(\sum_i x_i w_i - \theta\right), \quad (1)$$

where $f()$ is the Heaviside function:

$$f(\cdot) = \begin{cases} 1, & \text{for positive argument} \\ 0, & \text{for negative or zero argument} \end{cases} \quad (2)$$

The principle of a single input neuron operating is present in fig. 3a and in fig. 3 b the principle of multiple inputs neuron operating.

In both these windows it can be separately select the input, the threshold, the weight and the activation function.

For implement this software package it was design a Java class, Neuron, was implemented. This Java class was use in all modules of the package software.

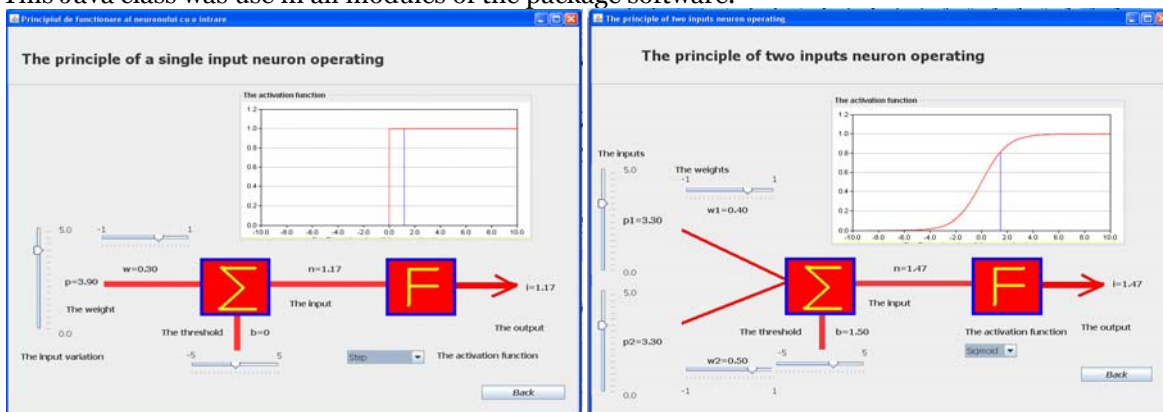


Fig. 3. a) The principle of a single input neuron operating
 b) The principle of two inputs neuron operating

The “Simple network” option is design in order to analyze a simple neural network operating mode. Like the other two previous options it can be separately select the input, the threshold, the weight and the activation function for each neuron.

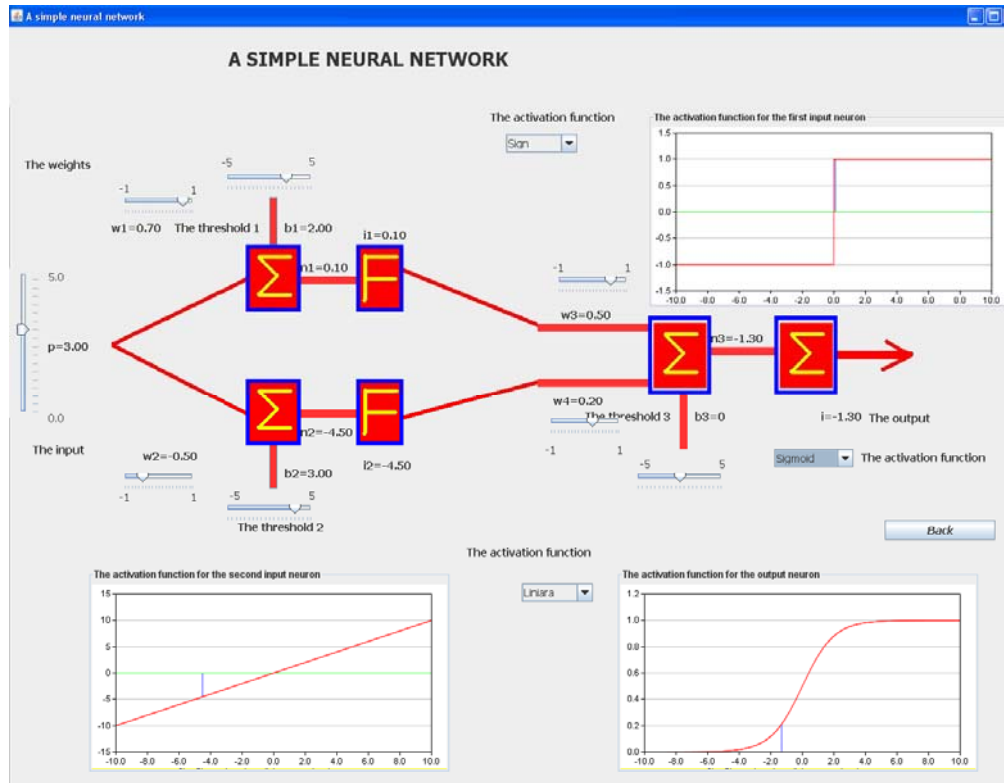


Fig. 4. The principle of a simple neural network operating

The last option of the software package is design in order to study the backpropagation network and the training algorithm for this network.

A BackPropagation network consists of at least three layers of units: an input layer, at least one intermediate hidden layer, and an output layer (see Figure 5) Typically, units are connected in a feed-forward fashion with input units fully connected to units in the hidden layer and hidden units fully connected to units in the output layer. When a BackPropagation network is cycled, an input pattern is propagated forward to the output units through the intervening input-to-hidden and hidden-to-output weights [3].

With BackPropagation networks, learning occurs during a training phase in which each input pattern in a training set is applied to the input units and then propagated forward. The pattern of activation arriving at the output layer is then compared with the correct (associated) output pattern to calculate an error signal. The error signal for each such target output pattern is then back propagated from the outputs to the inputs in order to appropriately adjust the weights in each layer of the network.

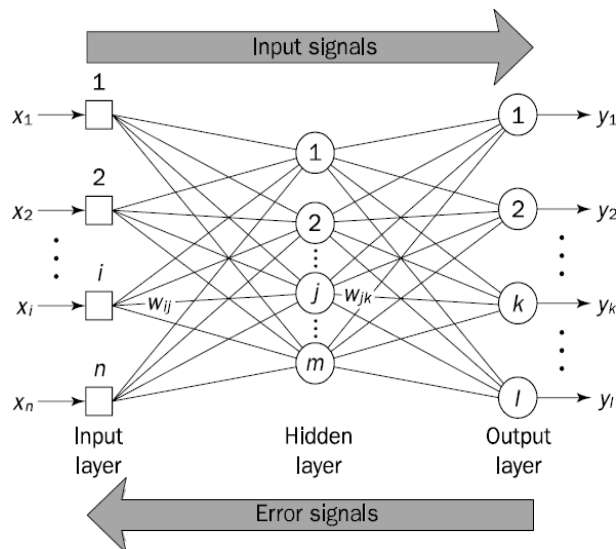


Fig. 5 A three layer backpropagation network

After a BackPropagation network has learned the correct classification for a set of inputs, it can be tested on a second set of inputs to see how well it classifies untrained patterns. Thus, an important consideration in applying BackPropagation learning is how well the network generalizes [3]. Backpropagation, or propagation of error, is a common method of teaching artificial neural networks how to perform a given task [4]. The backpropagation algorithm is:

Step 1. Initialisation.

Set all the weights and threshold levels of the network to random numbers uniformly distributed inside a small range[5], typically $(-2.4/F_i, 2.4/F_i)$, where F_i is the total number of inputs of neuron i ;

Step 2. Activation

Activate the back-propagation neural network by applying inputs $x_1(p), x_2(p), \dots, x_n(p)$, and desired outputs $y_{d,1}(p), y_{d,2}(p), \dots, y_{d,n}(p)$,

(a) Calculate the actual outputs of the neurons in the hidden layer:

$$y_j(p) = \text{sigmoid} \left[\sum_{i=1}^n x_i(p) \cdot w_{ij}(p) - \theta_j \right] \quad (3)$$

(b) Calculate the actual outputs of the neurons in the output layer

$$y_k(p) = \text{sigmoid} \left[\sum_{j=1}^m x_{jk}(p) \cdot w_{jk}(p) - \theta_k \right] \quad (4)$$

Step 3: Weight training

Update the weights in the back-propagation network propagating backward the errors associated with output neurons.

(a) Calculate the error gradient for the neurons in the output layer

$$\delta_k(p) = y_k(p) \cdot [1 - y_k(p)] \cdot e_k(p) \quad (5)$$

(b) Calculate the weight corrections

$$\Delta w_{jk}(p) = \alpha \cdot y_j(p) \cdot \delta_k(p) \quad (6)$$

Update the weights at the output neurons

$$w_{jk}(p+1) = w_{jk}(p) + \Delta w_{jk}(p) \quad (7)$$

(c) Calculate the error gradient for the neurons in the hidden layer

$$\delta_j(p) = y_j(p) \cdot [1 - y_j(p)] \cdot \sum_{k=1}^1 \delta_k(p) \cdot w_{jk}(p) \quad (8)$$

Calculate the weight corrections and update the weights at the hidden neurons

Step 4: Iteration

Increase iteration p by one, go back to Step 2 and repeat the process until the selected error criterion is satisfied.

In fig. 6 is show the graphical user interface for training algorithm. As can see, it can be selected some options, the learning rate, the number of training cycles and the logical function for approximation.

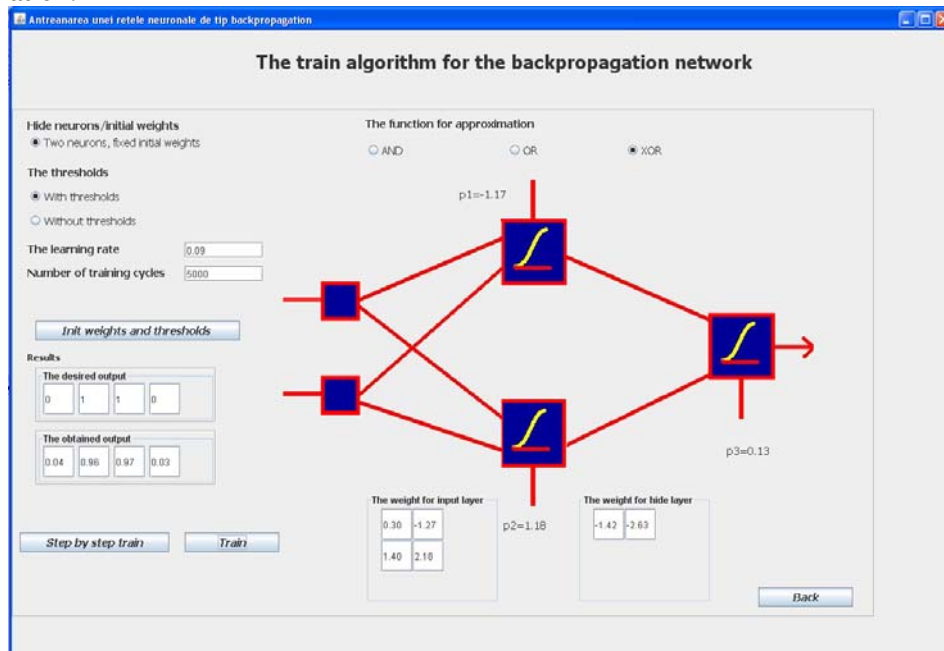


Fig. 6 Training a backpropagation network for logical function approximation

In the figures 7, 8 and 9 are the results of a study that show the dependency of mean square error to the learning rate for 500, 3000 and 5000 training cycles.

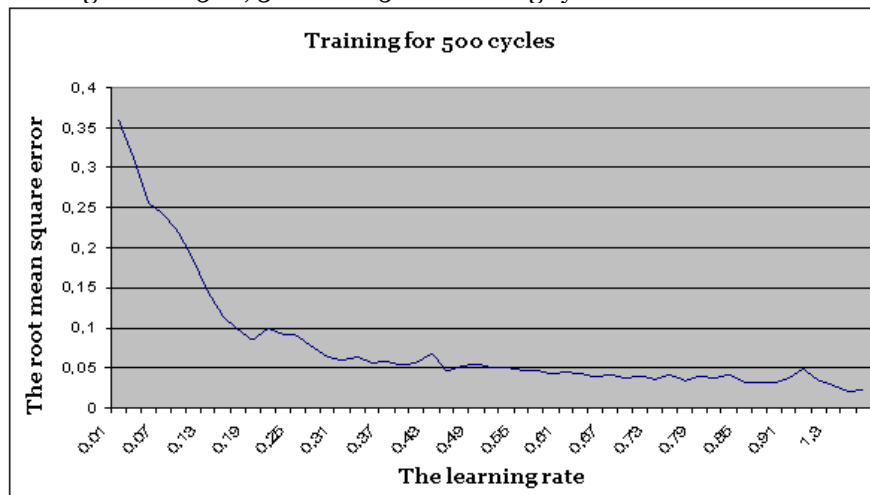


Fig. 7. The dependency of mean square error to the learning rate for 500 cycles

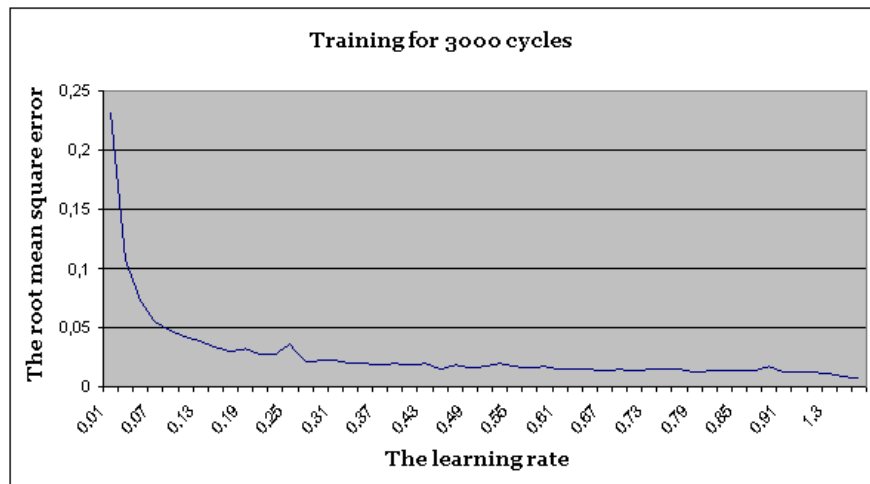


Fig. 8. The dependency of mean square error to the learning rate for 3000 cycles

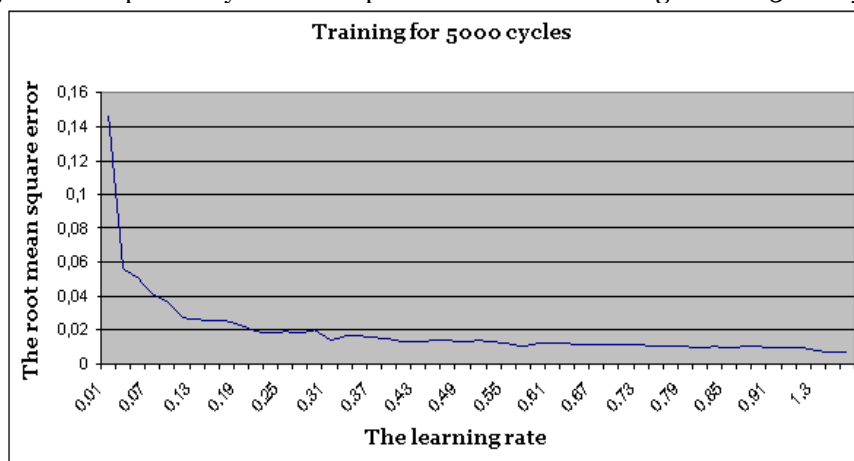


Fig. 9. The dependency of mean square error to the learning rate for 5000 cycles

3. CONCLUSIONS

In this paper an interactive software package was describe. The software can be use as a educational tool for a better understand of neural networks especially of backpropagation neural networks. It was also present some results of running the backpropagation algorithm and the dependency of mean square error to the learning rate of the algorithm. Using object oriented design and Java language allowed us to ease extendibility for the software.

REFERENCES

- [1.] Emilio Garcia Rosello , Jose B. Garcia Perez-Schofield, Jacinto Gonzalez Dacosta, Manuel Perez-Cota, Neuro-Lab: A Highly Reusable Software-Based Environment to Teach Artificial Neural Networks, Computer Application in Engineering Education, vol 11, Issue 2, pp 93-102, 2003
- [2.] Aybars Ugur, Ahmet Cumhur Kinaci , A Web-Based Tool For Teaching Neural Network Concepts, Computer Application in Engineering Education, Volume 18, Issue 3, pages 449–457, September 2010
- [3.] <http://www.itee.uq.edu.au/~cogs2010/cmc/chapters/BackProp/>
- [4.] <http://en.wikipedia.org/wiki/Backpropagation>
- [5.] Michael Negnevitsky - Artificial Intelligence A Guide to Intelligent Systems, editura Addison-Wesley,2005





NUMERICAL INVESTIGATION OF SWIRLING FLOWS STABILITY USING MATLAB DISTRIBUTED COMPUTING SERVER ON A WINDOWS OPERATING SYSTEM ENVIRONMENT

¹⁻³. "POLITEHNICA" UNIVERSITY OF TIMISOARA, FACULTY OF ENGINEERING OF HUNEDOARA, DEPARTMENT OF ELECTRICAL ENGINEERING AND INDUSTRIAL INFORMATICS, ROMANIA

ABSTRACT:

This paper presents an evaluation of the parallel processing for meshless algorithm for solving Navier-Stokes problems in fluid dynamics. The fluid dynamics existing solvers take use of finite element methods which are cumbersome and very exhaustive in computational resources. Meshless algorithms uses a different approaches using high level eigenvalue solvers. In order to evaluate the parallel processing performance, a cluster using Matlab development environment was build. Using the Matlab parallel and distributed toolbox it was possible to perform a profiling of the algorithm and to observe the eventual bottlenecks and flaws of the algorithm. Using this approach we obtained a very effective tool for processing the numerical stability investigation of the swirling flow in the Francis hydropower turbine.

KEYWORDS:

Cluster technology, parallel computational algorithms, fluid dynamics spatial stability, swirling flow, meshless method

1. CONSIDERATIONS ABOUT PARALLEL COMPUTING

Parallel programming and the design of efficient parallel programs have been well established in high-performance, scientific computing for many years. The simulation of scientific problems is an important area in natural and engineering sciences of growing importance. More precise simulations or the simulations of larger problems need greater and greater computing power and memory space. In the last decades, high-performance research included new developments in parallel hardware and software technologies [1-4] and a steady progress in parallel high-performance computing can be observed. Popular examples are simulations of weather forecast based on complex mathematical models involving partial differential equations or crash simulations from car industry based on finite element methods [5].

Other examples include drug design and computer graphics applications for film and advertising industry [6]. Depending on the specific application, computer simulation is the main method to obtain the desired result or it is used to replace or enhance physical experiments. A typical example for the first application area is weather forecast where the future development in the atmosphere has to be predicted, which can only be obtained by simulations [7]. In the second application area, computer simulations are used to obtain results that are more precise than results from practical experiments or that can be performed with less financial effort. An example is the use of simulations to determine the air resistance of vehicles [8]. Compared to a classical wind tunnel experiment, a computer simulation can give more precise results because the relative movement of the vehicle in relation to the ground can be included in the simulation. This is not possible in the wind tunnel, since the vehicle cannot be moved. Crash tests of vehicles are an obvious example where computer simulations can be performed with less financial effort.

Computer simulations often require a large computational effort. A low performance of the computer system used can restrict the simulations and the accuracy of the results obtained significantly. In particular, using a high-performance system allows larger simulations which lead to better results. Therefore, parallel computers have often been used to perform computer simulations. Today, cluster systems built up from server nodes are widely available and are now often used for parallel simulations. To use parallel computers or cluster systems, the computations to be performed must be partitioned into several parts which are assigned to the parallel resources for execution. These computation parts should be independent of each other, and the algorithm performed must provide enough independent computations to be suitable for a parallel execution. This is normally the case for scientific simulations. To obtain a parallel program, the algorithm must be formulated in a suitable programming language. Parallel execution is often controlled by specific runtime libraries or compiler directives which are added to a standard programming language like C, Fortran, or Java [9-13].

MATLAB [14] is currently the dominant language of technical computing with approximately one million users worldwide, many of whom can benefit from the increased power offered by widely available multicore processors and multinode computing clusters. MATLAB is also an ideal environment for learning about parallel computing, allowing the user to focus on parallel algorithms instead of the details of the implementation.

Higham & Higham [15] and Moler [16] offer an introduction to MATLAB in their surveys. In [17] Jeremy Kepner introduces the theory, algorithmic notation, and an „under the hood" view of distributed array programming. He discusses metrics for evaluating performance and coding of a parallel program. A selected survey of parallel application analysis techniques are presented in this book, with a particular emphasis on how the examples used in the book relate to many wider application domains. In [18], Rauber and Runger take up the new development in processor architecture by giving a detailed description of important parallel programming techniques that are necessary for developing efficient programs for multicore processors as well as for parallel cluster systems or supercomputers. Both shared and distributed address space architectures are covered.

Parallel programming is an important aspect of high-performance scientific computing but it used to be a niche within the entire field of hardware and software products. However, more recently parallel programming has left this niche and will become the mainstream of software development techniques due to a radical change in hardware technology. Major chip manufacturers have started to produce processors with several power efficient computing units on one chip, which have an independent control and can access the same memory concurrently. Normally, the term core is used for single computing units and the term multicore [19, 20] is used for the entire processor having several cores. Thus, using multicore processors makes each desktop computer a small parallel system. The technological development toward multicore processors was forced by physical reasons, since the clock speed of chips with more and more transistors cannot be increased at the previous rate without overheating. Multicore architectures in the form of single multicore processors, shared memory systems of several multicore processors, or clusters of multicore processors with a hierarchical interconnection network will have a large impact on software development. In 2009, dual-core and quad-core processors are standard for normal desktop computers, and chip manufacturers have already announced the introduction of oct-core processors for 2010. It can be predicted from Moore's law [21] that the number of cores per processor chip will double every 18–24 months. According to a report of Intel, in 2015 a typical processor chip will likely consist of dozens up to hundreds of cores where a part of the cores will be dedicated to specific purposes like network management, encryption and decryption, or graphics [22].

As computational fluid dynamics (CFD) matures so rise the expectations of what it can or should deliver. Practitioners and designers are no longer content with qualitative statements on trends, but judge the utility and value of CFD by its ability to provide quantitatively accurate predictions for property fields and engineering parameters derived therefrom. In the extreme, theoretical fluid dynamicists expect fully-resolved simulations of turbulence to provide fundamental information on turbulence mechanics of greater accuracy and detail than can be derived from the most sophisticated experimental techniques.

In computational fluid dynamics, several software packages solving either the Euler or the Navier-Stokes equations around complex geometries have been developed and are currently used by aircraft or engine manufacturers. The use of unstructured meshes is one of the most efficient ways to solve complex problems, because they allow high flexibility in specifying a geometry. The possibility of using the modern parallel machines even for unstructured mesh based codes implies the necessity of dealing with two problems: the first one lies on the strategies and algorithms which can be used for the partitioning of the grid and the mapping of the subdomains among the

processors; the second one is related to the structure of the code, which has to be designed in such a way that the features of the modern parallel machines are fully exploited.

The first efficient implementation of a 2D unstructured flow solver on MIMD parallel computers was presented by Venkatakrishnan et al [23] in 1992: they demonstrated that a good supercomputer performance can be reached and that a careful implementation of the message passing routines is a critical point, even for an explicit code. In 1995, Lanteri [24] developed a parallel version of an industrial code based on a mixed finite element/finite volume method. The parallelization strategy combines mesh partitioning and message passing programming model: basically, the same old serial code is going to be executed within every subdomain. Modifications occurred in the main loop in order to take into account the assembly phases of the subdomain results.

The literature on these topics can be considered exhaustive for two-dimensional applications and parallel machines of the old generation. The same cannot be said for three-dimensional complex flows and for the new machines in terms of optimization of the performances and assessment of algorithms and techniques (i.e. [25-28]).

2. CLUSTER CONFIGURATION

In this paper we have build and tested a small scale cluster based on a Matlab Parallel Processing Toolbox. Using the internal cluster manager from Matlab we were able to evaluate the algorithm behaviour using a distributed process. In this situations we have perform the profiling and we have noticed a speed increase of the algorithm compared to a single computer run. The cluster was conceived using homogenous hardware

Dell Optiplex 755

Intel(R) Core(TM)2 Duo CPU, 2.66GHz 1.97 GHz, 1.95 GB of RAM

MATLAB Distributed Computing Server (MDCS) is a toolbox that lets users solve computationally and data-intensive problems by executing MATLAB and Simulink based applications on a computer cluster.

For numerical investigation of swirling flows stability, a Windows operating system cluster was configured in Computer Aided Mathematics and Numerical Analysis Laboratory of the Engineering Faculty of Hunedoara (Figure 1).



Figure 1. Computer Aided Mathematics and Numerical Analysis Laboratory at the Engineering Faculty of Hunedoara.

The first step to set up the cluster configuration was to install the MDCS on a node called the head node. The license manager was also installed on the head node. After performing this installation, the MDCS was installed on the other cluster nodes, called worker nodes. Figure 2 shows the installations that was performed on our MDCS cluster nodes.

The MDCS service must be running on all machines being used for job managers or workers. This service manages the job manager and worker processes. One of the major tasks of the MDCS service is to recover job manager and worker sessions after a system crash, so that jobs and tasks are not lost as a result of such accidents. To run the MDCS, the license manager must be running on the head node.

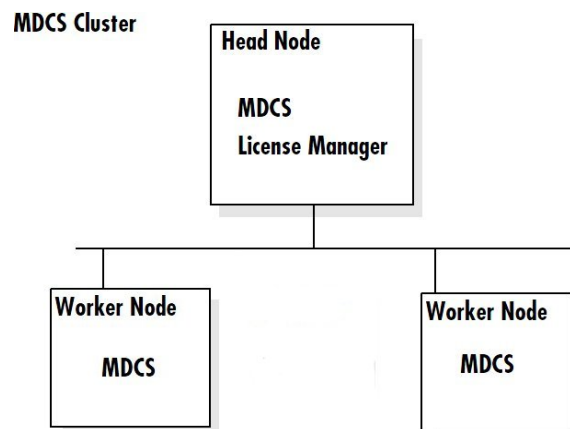


Figure 2. MDCS cluster with local access configuration.

We made sure the license manager was running by performing a Status Enquiry. The next step in configuring the cluster was to start the job manager and workers. From the Admin Center, the setup and monitoring utility for the Matlab Distributed Computing Server, we select the list of the hosts in the text box. When Admin Center completed the update, the listing looked like the following Figure 3.

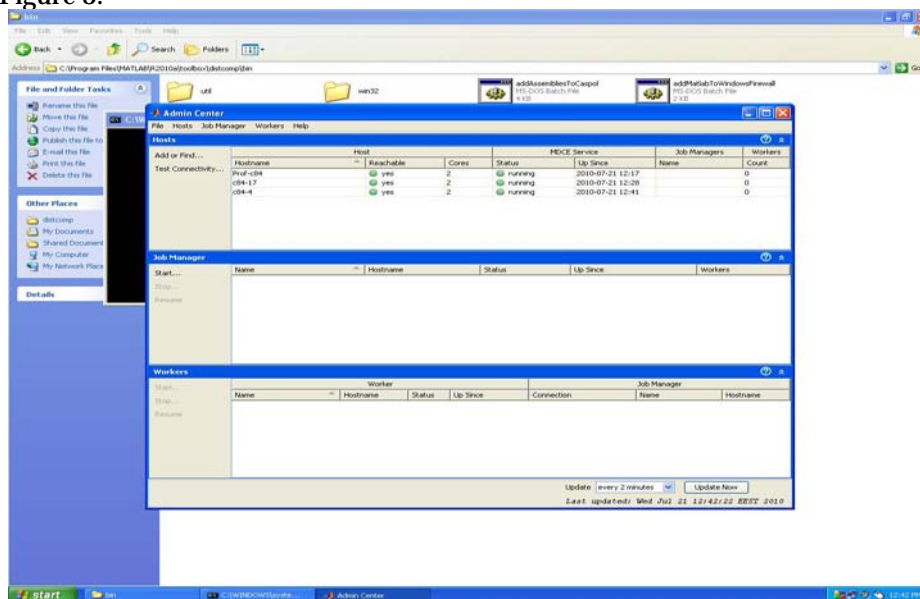


Figure 3. Nodes added in the configuration of the cluster.

At this point, the connectivity between nodes was tested. This assures that the cluster can perform the necessary communications for running MDCS processes. After the cluster configuration was completed, a job manager have been started using the Job Manager module. In the Start Workers dialog box, we specify the number of workers to start on each host, a value that cannot exceed the total number of licenses we have. A number of two workers was set for each host. The Connectivity Testing dialog box shows the results of the last test, reported in Figure 4.

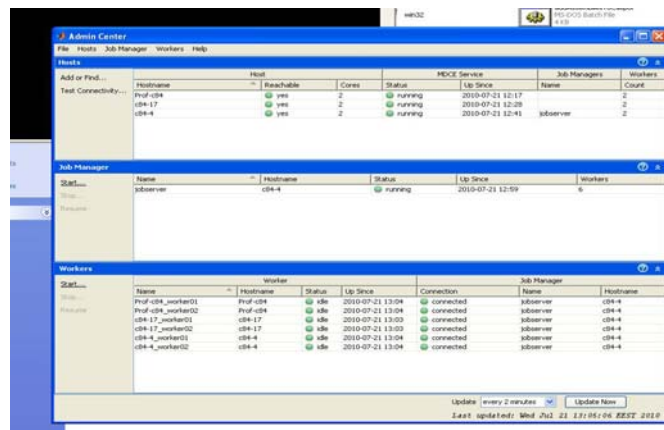


Figure 4. The connectivity test of the configuration of the cluster passed.

3. PARALLEL AND DISTRIBUTED INVESTIGATION OF THE VORTEX ROPE MODEL

The helical vortex breakdown (also known as precessing vortex rope) is a self-induced instability of a swirling flow, encountered in the draft tube cone of hydraulic Francis turbines operated far from the best efficiency. Figure 5 shows the axial and the swirl velocity profiles of the vortex rope model used in our stability analysis.

Let us define the eigenvalue problem governing the hydrodynamic stability in operator formulation

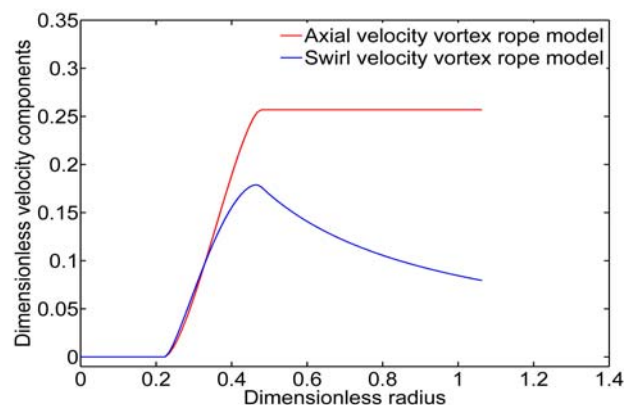


Figure 5 Axial and circumferential velocity profiles.

$$(kL^{[k]} + \omega L^{[\omega]} + L)\mathbf{u} = 0, \quad \mathbf{u} = (F \quad G \quad H \quad P)^T \quad (1)$$

where

$$L^{[k]} = \begin{pmatrix} r & 0 & 0 & 0 \\ 0 & U & 0 & 0 \\ 0 & 0 & rU & 0 \\ U & 0 & 0 & 1 \end{pmatrix}, \quad L^{[\omega]} = \begin{pmatrix} 0 & 0 & 0 & 0 \\ 0 & -1 & 0 & 0 \\ 0 & 0 & -r & 0 \\ -1 & 0 & 0 & 0 \end{pmatrix}, \quad L = \begin{pmatrix} 0 & 1+d_r & -m & 0 \\ 0 & mW/r & 2W/r & -d_r \\ 0 & W+rdW/dr & mW & m \\ mW/r & dU/dr & 0 & 0 \end{pmatrix} \quad (2)$$

The boundary relations are translated into equations that complete the computational model and can be transposed as

$$\sum_1^N (-1)^{k+1} g_k = \sum_1^N (-1)^{k+1} h_k = 0, \quad (3)$$

$$f_2 \frac{2}{r_{\max}} + \sum_{\substack{3 \\ k \text{ odd}}}^N f_k \frac{2(k-1)}{r_{\max}} \left[\sum_{\substack{2 \\ r=k-1 \\ k \text{ even}}} (-2) \right] + \sum_{\substack{4 \\ k \text{ even}}}^N f_k \frac{2(k-1)}{r_{\max}} \left[\sum_{\substack{2 \\ r=k-1 \\ k \text{ odd}}} 2+1 \right] = 0, \quad (4)$$

$$p_2 \frac{2}{r_{\max}} + \sum_{\substack{3 \\ k \text{ odd}}}^N p_k \frac{2(k-1)}{r_{\max}} \left[\sum_{\substack{2 \\ r=k-1 \\ k \text{ even}}} (-2) \right] + \sum_{\substack{4 \\ k \text{ even}}}^N p_k \frac{2(k-1)}{r_{\max}} \left[\sum_{\substack{2 \\ r=k-1 \\ k \text{ odd}}} 2+1 \right] = 0, \quad (5)$$

$$\frac{2W_{r_{\max}}}{r_{\max}} \sum_1^N h_k - p_2 \frac{2}{r_{\max}} - \sum_{\substack{3 \\ k \text{ odd}}}^N p_k \frac{2(k-1)}{r_{\max}} \left[\sum_{\substack{2 \\ r=k-1 \\ k \text{ even}}} 2 \right] - \sum_{\substack{4 \\ k \text{ even}}}^N p_k \frac{2(k-1)}{r_{\max}} \left[\sum_{\substack{2 \\ r=k-1 \\ k \text{ odd}}} 2+1 \right] = 0, \quad (6)$$

$$\sum_1^N g_k = 0, \quad (kU_{r_{\max}} - \omega) \sum_1^N h_k = 0, \quad k \left(U_{r_{\max}} \sum_1^N f_k + \sum_1^N p_k \right) - \omega \sum_1^N f_k = 0. \quad (7)$$

The numerical investigation employed both the positive and the negative modes. Let us define by the critical frequency that temporal frequency corresponding to a maximum growth rate for a given mode number. The numerical results are summarized in Table 1.

Table 1 The critical frequency and the maximum growth rates obtained for the investigated modes

Mode m	-3	-2	-1	0	1	2	3
Critical Frequency	0.1	0.3	0.3	0.3	0.3	0.3	0.35
Maximum Growth Rate	14.129	11.947	6.932	0.043	0.544	0.535	0.395

Figure 6 presents the three dimensional map of the growth rate as function of the frequency and mode number and the density map of the growth rate. The negative modes present an amplitude increase depending on the mode number. However, these amplitude growth rates increase linear up to a frequency of 0.25 both for the positive and the negative modes.

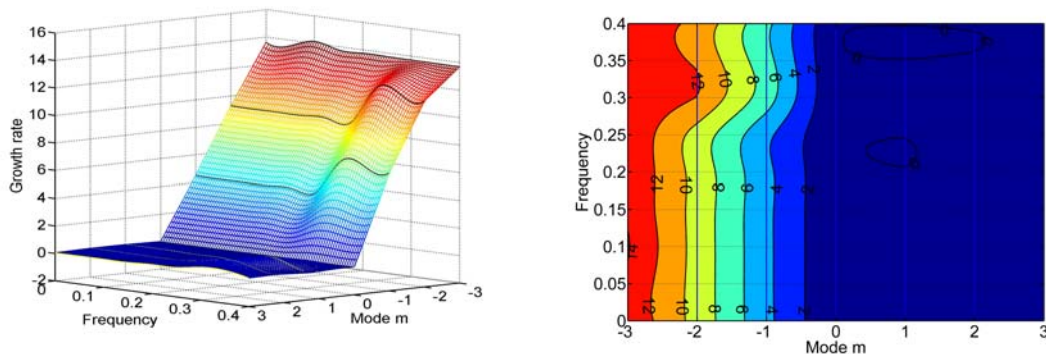


Figure 6. Plot of the growth rate as function of frequency and mode (left) and density map (right).

The convergence behavior of the collocation algorithm for $m = -1$ case is reported in Table 2 on few cluster configurations with six, four and two labs, respectively. It is noticeable that the time increase is relevant when the numerical experiments run on four labs configuration instead of 2 labs configuration. The time increase becomes irrelevant when the number of cluster nodes is increased at six labs, thus the conclusion that the cluster has no need to be extended for numerical improvements of our stability analysis.

Table 2. Elapsed time (in seconds) of the numerical computation for mode $m = -1$, on three cluster configurations.

N	Critical frequency	Elapsed time on 2 labs	Elapsed time on 4 labs	Elapsed time on 6 labs
5	0.25	1.463658	0.196285	0.211601
6	0.1	1.569234	0.225536	0.193199
8	0.1	1.584621	0.210344	0.222434
10	0.25	1.611874	0.328014	0.341408
12	0.3	1.632951	0.345925	0.360558
16	0.3	1.751369	0.431654	0.431196
17	0.3	1.836951	0.460168	0.451093
19	0.3	1.854693	0.519268	0.524420
29	0.3	2.234852	1.005637	1.015383
32	0.3	2.672955	1.479596	1.448778
37	0.3	2.895647	1.682333	1.726657
40	0.3	3.269854	2.064365	2.087408
46	0.3	4.125965	2.942432	2.948638
61	0.3	8.264985	6.453132	6.318485

4. CONCLUSION

The cluster technology represents the state of the art in computational technology. This extends the limit imposed by the single computer analysis, reducing in a large manner the amount of time required for solving complex mathematical models. Using a rather usual hardware (desktop PCs) it is possible to obtain a significant acceleration of the computation process. However, the acceleration depends on the algorithm structure and it is necessary to perform a profiling of the solving process (that means to analyze carefully the behavior of the computational process- the number of steps required, the mathematical operations involved, the size of matrix variables) in order to avoid the eventual bottlenecks in the algorithm.

REFERENCES

- [1.] Culler, D.E., Singh, J.P., Gupta, A., Parallel Computer Architecture: A Hardware Software Approach, Morgan Kaufmann, San Francisco, 1999.
- [2.] Conway, M.E., A Multiprocessor System Design, In Proceedings of the AFIPS 1963 Fall Joint Computer Conference, volume 24, pages 139–146, Spartan Books, New York, 1963.
- [3.] Chin, A., Complexity Models for All-Purpose Parallel Computation, In Lectures on Parallel Computation, chapter 14. Cambridge University Press, Cambridge, 1993.
- [4.] Bertsekas, D.P., Tsitsiklis, J.N., Parallel and Distributed Computation, Athena Scientific, Nashua, 1997.
- [5.] Braess, D., Finite Elements, 3rd edition, Cambridge University Press, Cambridge, 2007.
- [6.] Krikelis, A., Parallel Multimedia Computing, Parallel Computational Fluid Dynamics Recent Developments and Advances Using Parallel Computers, Elsevier Science B.V., 1998.
- [7.] Gulzow, V., Diehl, T., Foelkel, F., About the Parallelization of Climate Models, Parallel Computing: Fundamentals, Applications and New Directions, Elsevier Science B.V., 1998.
- [8.] Reid, J., Supalov, A., Thole, C.A., PARASOL Interface to New Parallel Solvers for Industrial Applications, Parallel Computing: Fundamentals, Applications and New Directions, Elsevier Science B.V., 1998.
- [9.] Allen, R., Kennedy, K., Optimizing Compilers for Modern Architectures, Morgan Kaufmann, San Francisco, 2002.
- [10.] Bishop, P., Warren, N., JavaSpaces in Practice, Addison Wesley, Reading, 2002.
- [11.] Bodin, F., Beckmann, P., Gannon, D.B., Narayana, S., Yang, S., Distributed C++: Basic Ideas for an Object Parallel Language. In Proceedings of the Supercomputing'91 Conference, pages 273–282, 1991.
- [12.] Dongarra, J., Performance of various Computers using Standard Linear Equations Software in Fortran Environment. Technical Report CS-89–85, Computer Science Department, University of Tennessee, Knoxville, 1990.
- [13.] Kennedy, K., Koelbel, C., Zima, H., The Rise and Fall of High Performance Fortran: An Historical Object Lesson. In HOPL III: Proceedings of the Third ACM SIGPLAN Conference on History of Programming Languages, pages 7–1–7–22, ACM, New York, 2007.

- [14.] www.mathworks.com
- [15.] Higham, D.J., Higham, N.J., MATLAB Guide, Second Edition, SIAM, Philadelphia, 2005.
- [16.] Moler, C., Numerical Computing with MATLAB, SIAM, Philadelphia, 2004.
- [17.] Kepner, J., Parallel MATLAB for Multicore and Multinode Computers, SIAM, Philadelphia, ISBN 978-0-898716-73-3, 2009.
- [18.] Rauber, T., Runger, G., Parallel Programming for Multicore and Cluster Systems, Springer-Verlag Berlin Heidelberg, ISBN 978-3-642-04817-3, 2010.
- [19.] Jaja, J., An Introduction to Parallel Algorithms, Addison-Wesley, New York, 1992.
- [20.] Lenoski, D.E., Weber, W., Scalable Shared-Memory Multiprocessing, Morgan Kaufmann, San Francisco, 1995.
- [21.] Koch, G., Discovering Multi-core: Extending the Benefits of Moore's Law, Intel White Paper, Technology@Intel Magazine, 2005.
- [22.] Kuck, D., Platform 2015 Software-Enabling Innovation in Parallelism for the Next Decade, Intel White Paper, Technology@Intel Magazine, 2005.
- [23.] Venkatakrisnan, V., Simon, H.D., Barth, T., A MIMD implementation of a parallel Euler solver for unstructured grids, The J. of Supercomputing 6, pp. 117-137, 1992.
- [24.] Lanteri, S., Parallel solutions of Three-Dimensional compressible flows', INRIA, Rapport de recherche n. 2594, June 1995.
- [25.] Diurno, W.G., Higher Order Solution of the Compressible Viscous Flows Arising in Aerothermodynamics Using a Finite Element Method, Proc. AIDAA Congress, Roma (Italy), 11-15 September 1995.
- [26.] Barth, T.J., Aspects of Unstructured Grids and Finite-Volume Solvers for the Euler and Navier Stokes Equations, VKI - AGARD R 787, 1992.
- [27.] Peraire, J., Peiro, J., Morgan, K., Multigrid Solution of the 3-D Compressible Euler Equations on Unstructured Tetrahedral grids, Int. J. Num. Meth. in Engin. 36, 1993.
- [28.] Bucchignani, E., Diurno, W.G., Parallel computation of inviscid 3D flows with unstructured domain partitioning: performances on SGI-Power Challenge Supercomputer, Parallel Computing: Fundamentals, Applications and New Directions Elsevier Science B.V., 1998.





¹ Stela RUSU-ANGHEL, ² Lucian GHERMAN, ⁵Sergiu MEZINESCU

USING THE MATLAB-SIMULINK SIMULATION FOR OPERATING ACTIVE FILTERS ORDERED BY DIGITAL SIGNAL PROCESSOR (DSP)

¹⁻⁵ UNIVERSITY POLITEHNICA OF TIMISOARA, FACULTY OF ENGINEERING FROM HUNEDOARA, ROMANIA

ABSTRACT:

The paper proposes the use of a DSP family ADMC330 several ways to control an active filter. It is made available as filter simulation in Matlab-Simulink environment, and the results confirm the effectiveness of the filter.

KEYWORDS:

DSP family, simulation, Matlab-Simulink

1. INTRODUCTION

Figure 1.1. is a schematic diagram of a DSP controlled active filter. The R_p resistors are denoted preloading the filter capacitor C , necessary to limit the current drawn from the converter to the mains connection.

Signals from voltage / current transducers are taken through LEM type, and block 'Adaptation Signals' are made in the range of 0.3 - 3.2 V analog converters acceptable entry - digital. To order using a digital converter evaluation board CMDA signal processor 330 - control processor specifically designed for electric cars.

ADMC330 microprocessor family is part of the signal processor (DSP) which operates fixed-point math calculations. It's characteristics is recommended for high performance control of electrical drives. Among these we mention below the most important:

- ❖ 20 MHz clock frequency;
- ❖ Seven analog inputs for external signal acquisition;
- ❖ Data acquisition synchronized with the PWM signal;
- ❖ Control signal generator for PWM voltage inverter (Pulse width modulation in - pulse width modulation)
- ❖ Programmer detection dead time and minimum pulse;
- ❖ Minimum inverter frequency 2.5 kHz;
- ❖ Maximum inverter frequency 25 kHz;
- ❖ Generator for the space vector control inverter;
- ❖ Program counter and address two generators;
- ❖ Two 8-bit timers for PWM generation;
- ❖ Eight ports of entry and exit;
- ❖ Implementation of 20 MIPS (million instructions per second);

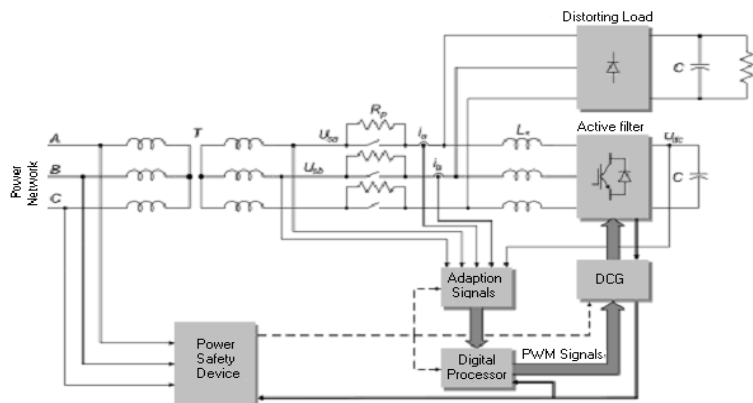


Fig. 1.1. Schematic diagram

- ❖ Arithmetic logic unit for executing mathematical calculations;
- ❖ Mathematical operands displacement unit;
- ❖ 50 ns instruction cycle time;
- ❖ Type 16-bit timer watchdog to reset the DSP;
- ❖ Two synchronous serial ports;
- ❖ 2k x 24 bit program memory and data RAM 1k x 16 bits;
- ❖ 2k x 24 bit program memory ROM.

The flexibility of the internal structure ADMC330 signal processor, allow for the following operations in a machine cycle (50 ns)

- ❖ Generating new program addresses;
- ❖ Taking the next instruction stack;
- ❖ Achieving two data moves;
- ❖ Loading two data pointers with addresses;
- ❖ Performing a calculation operation.

The processor can also independently control the peripherals that are fitted, so while it may do the following:

- ❖ Generation of three PWM signals for inverter;
- ❖ Generation of the two auxiliary PWM signals generators;
- ❖ The acquisition of four analog channels;
- ❖ Control of eight digital input / output pin;
- ❖ Decrementing timer control program (Watchdog).

ADMC330 processor includes internal memory as we have seen, so the 2K monitor ROM program is to interface with a PC UART for serial communication interface, boot loader, mathematical tables to implement the following functions: sine, cosine, tangent and inverse tangent, logarithm and inverse logarithm, square root, inverse function, divide unsigned, transformations from Cartesian to polar marker, functions for interpolation.

2. SOFTWARE SIMULATION SYSTEM USING MATLAB-SIMULINK

Four schemes were carried out using both types of construction, with and without feedback loop, for three-phase voltage sources but nonlinear loads balanced (neutral wireless). The first two schemes will be presented using real-time Fourier analysis of the currents on each phase.

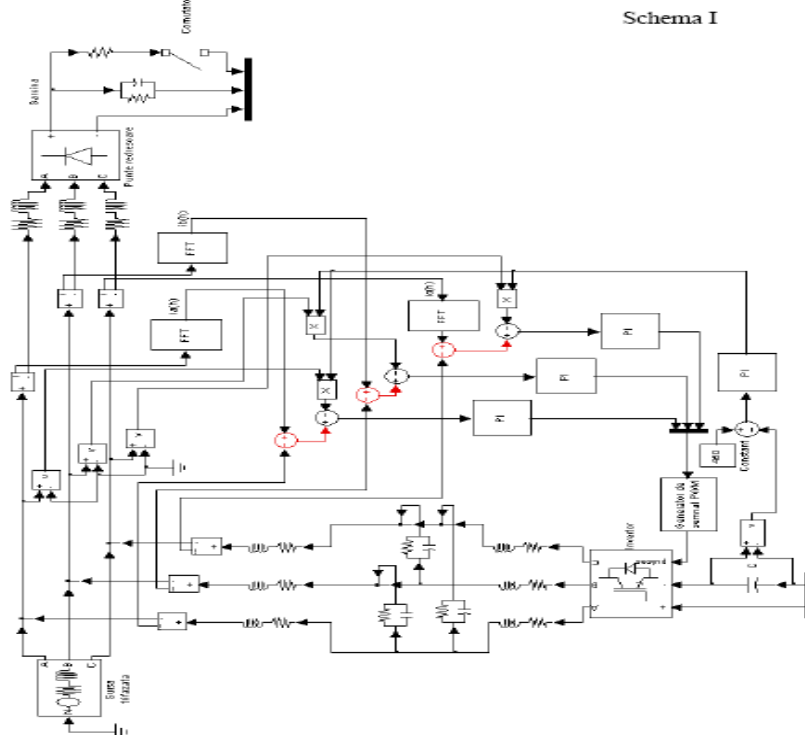


Fig. 2.1. FFT alternative work schedule

Fourier transform is calculated using the fastest FFT algorithm. By Fourier analysis of the currents on each phase has succeeded in its breakdown of its component harmonics. Recomposed signal using only the higher order harmonics (less than first harmonic), it is a signal that will be

introduced in the network with the sign reversed. So the grid will run a first harmonic signal. This method is applied to the first scheme.

A second solution is to calculate only the fundamental harmonic is then subtracted from the total current network to produce the higher harmonic current is given by the opposite sign is the reference active filters. Such an approach is adopted in the sliding mode option, which is shown in diagram two.

In the following we present diagrams made for each model calculation and simulation results obtained.

FFT block in the current decomposition of its component harmonics. Computer program called the block "MATLAB Function" allows the extraction of harmonics first. IFFT block recomposed signal using only higher order harmonics, resulting in a signal that will be introduced in the network with the sign reversed.

Below are the results obtained by simulation.

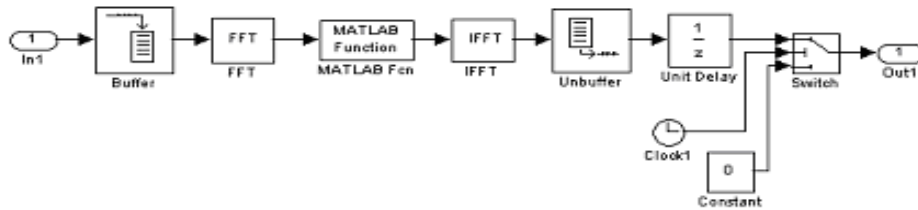


Fig. 2.2. FFT block

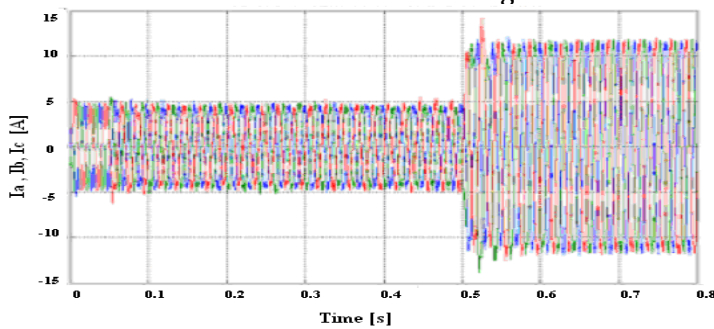


Fig. 2.3. The mains currents

In Fig 2.3 the currents are presented mains throughout the simulation period. In the interval (0 - 0.1) current network is not filtered, at time 0.1 comes into the active filter. 0.5 At the burden is doubled.

In Fig. 2.4 phase currents are given power to the system without active filter. It can be seen as their harmonic due to the presence of higher order harmonics.

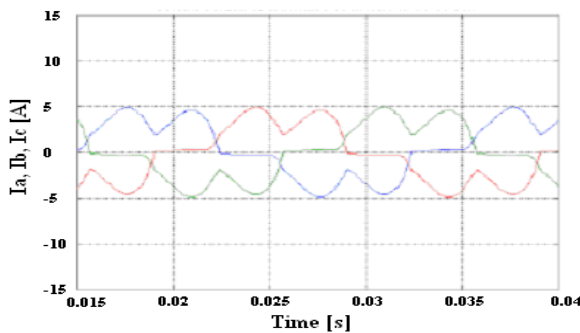


Fig. 2.4. The mains currents without filter

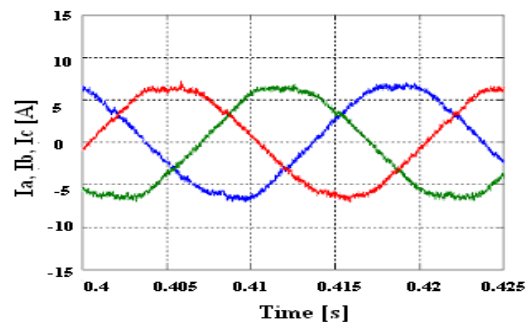


Fig. 2.5. The mains currents active filter

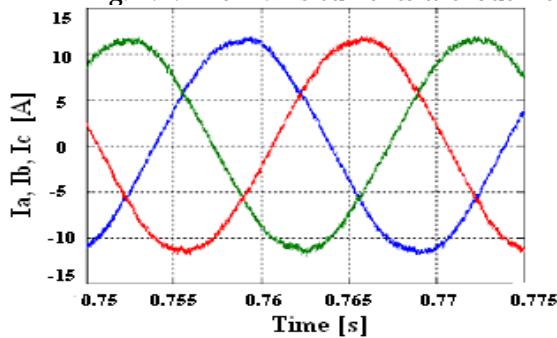


Fig. 2.6. Power supply currents for

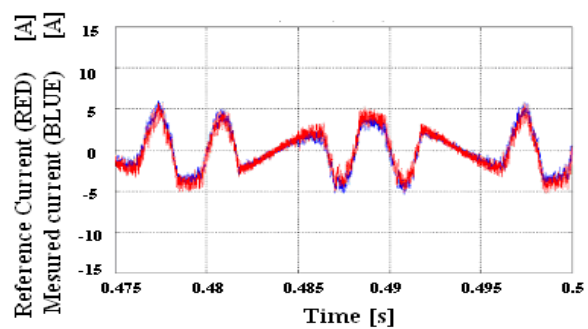


Fig. 2.7. Current compensation the double burden

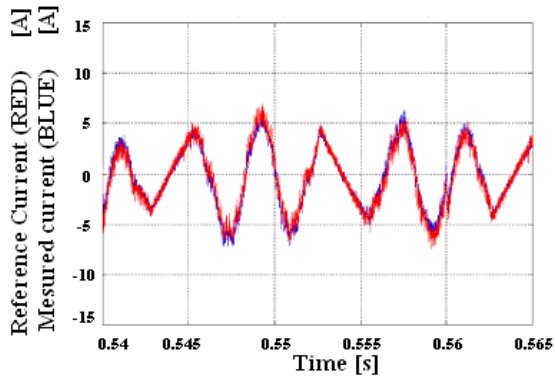


Fig. 2.8. Current produced by the active filter compensation

From Fig. 2.5 can be observed that with the arrival of an active filter, three-phase currents are sinusoidal mains.

In Fig. 2.6 we presents three mains currents, the active filter for a dual task.

In Figures 2.7 , 2.8 and 2.9, the reference current (red) are harmonics with opposite sign that must be placed on the network. The blue is injected currents in inverter network.

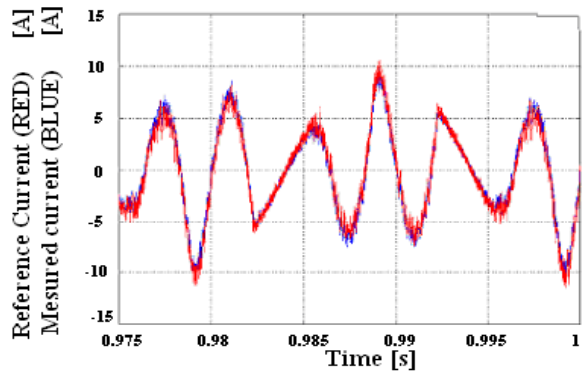


Fig. 2.9. Curent double load compensation

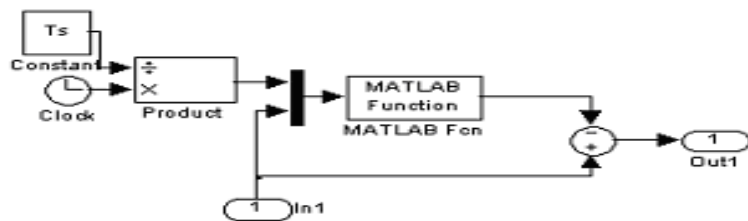


Fig.2.10. Sliding FFT block

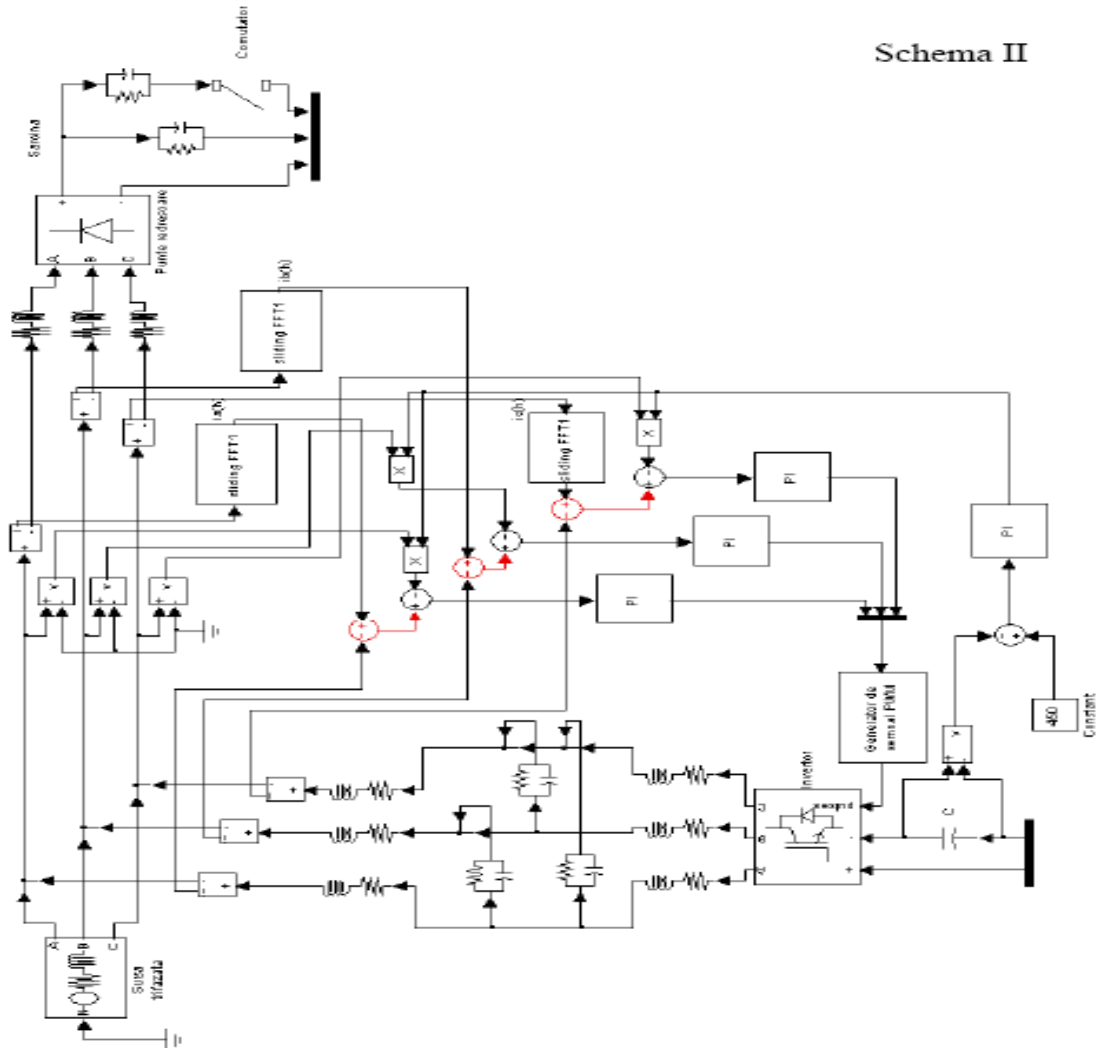


Fig. 2.11. Alternative work schedule with sliding FFT mode

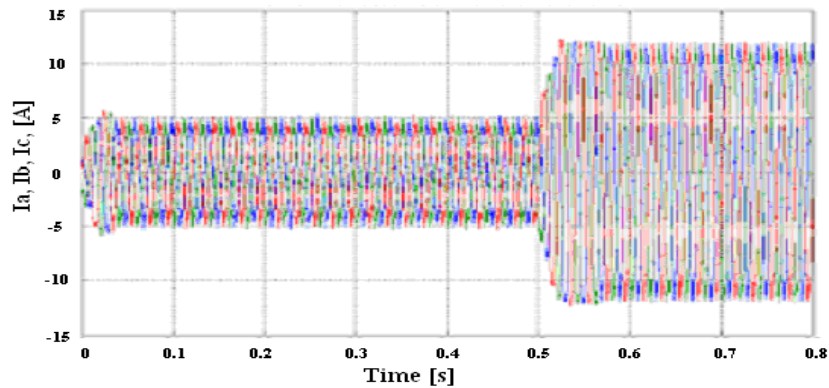


Fig. 2.12. The mains currents throughout the simulation time

Extract the first harmonic sliding FFT block which then decreased the current network consists of harmonics resulting in a higher power.

In the following we present scheme for model calculation carried in variant sliding mode.

In Fig. 2.12. currents are presented mains throughout the simulation period. Results obtained from simulation with the sliding mode method are similar to those obtained in the FFT version. The only notable difference is that there is an increasing burden smooth current growth.

Unfortunately, this method has the disadvantage that it requires real-time applications using DSP with large memory. This leads to the impossibility of using cheap DSP having more than one Kb of RAM. In this case we propose another solution that enables the calculation based on the fundamental harmonic active and reactive power (by averaging the instantaneous value).

In the following experimental results will be presented.

On the basis of this technique is that transfers of active and reactive power defined as the product of the fundamental harmonic voltage and currents is real only on the first harmonic current harmonic currents rest do not give power. Unfortunately, in some applications the source voltage contains higher harmonics. For this reason the calculation of power is no longer used that tension, but tension given by a PLL circuit realized by software and implemented on a DSP which provides as output a sinusoidal signal in phase with the fundamental harmonic amplitude equal to unity. This signal is subtracted from the total current network to produce the higher harmonics given the current reference is changed in sign of active filter.

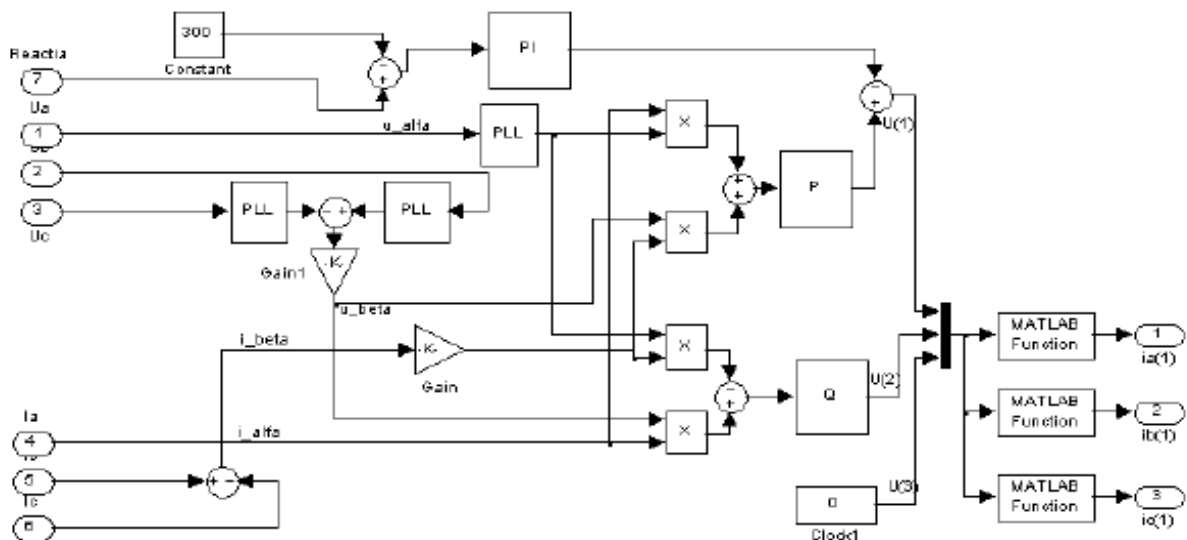


Fig. 2.13. PQ Building

In this block currents and voltages are introduced in three phases. Calculate the first-order harmonic currents. They will then be subtracted from a signal resulting network consists of higher order harmonics to be introduced into the network with the sign reversed.

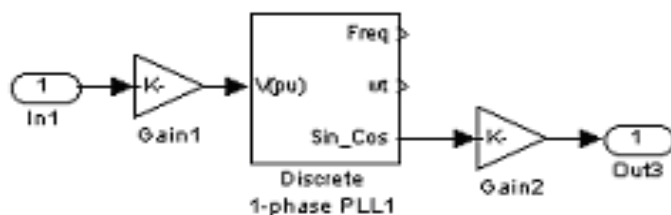


Fig. 2.14. PLL block

In Fig. 2.14. PLL block is presented which provides as output a sinusoidal signal in phase with the fundamental harmonic amplitude equal to unity.

Have been developed for this model two types of construction, with and without feedback loop. In the following we present schemes for the two models made constructive and results obtained from simulation. The former alternative presented feedback loop variant.

Results will be presented in the following experimental. In Fig.2.17 currents are presented mains throughout the simulation period. Note that at time 0.3 with a double load variation occurs due to sudden changes in voltage on the load current, the variation is shown in the figure below. This surge current limiter can be removed from power.

Block P-Q is presented in Fig. 2.13. The difference between the two modes of constructive notice is observed in the manner of placing the measure voltages and currents in relation to the inverter, and how the taxation of reference.

Figures 2.19, 2.20 and 2.21 are shown the three phase currents at different moments in time simulation.

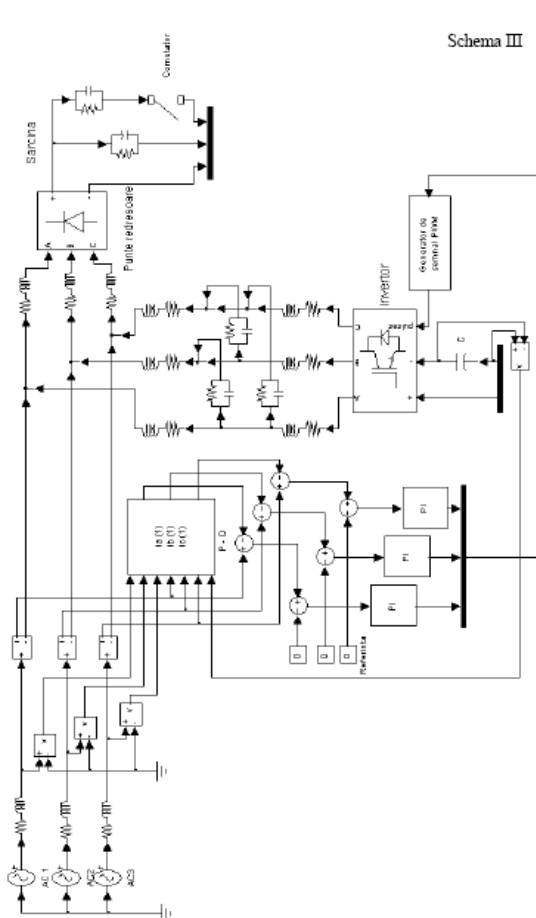


Fig. 2.15. Alternative work schedule PQ-loop response

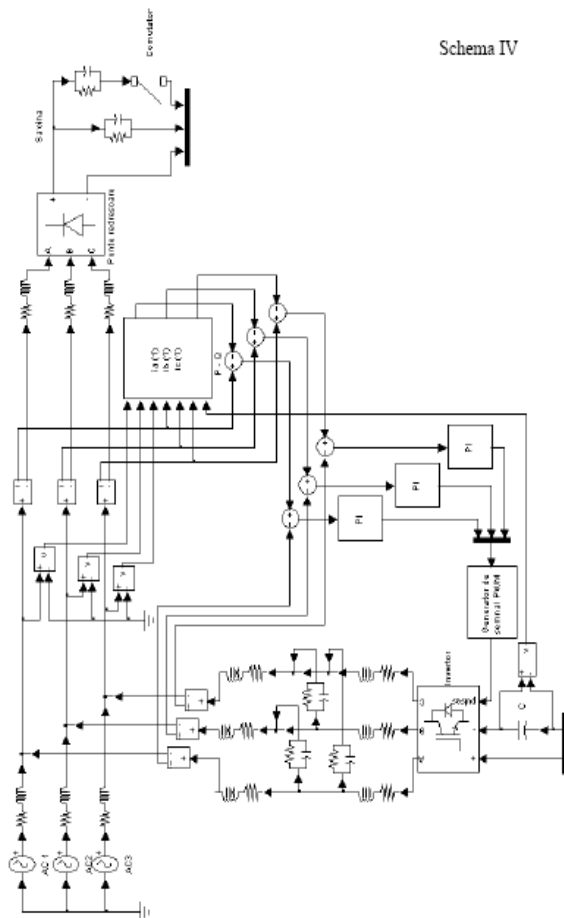


Fig. 2.16. PQ alternative work schedule without feedback loop

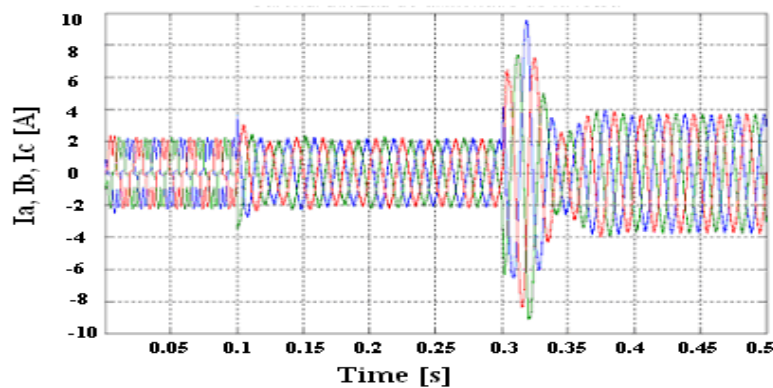


Fig. 2.17. Mains currents throughout the simulation time

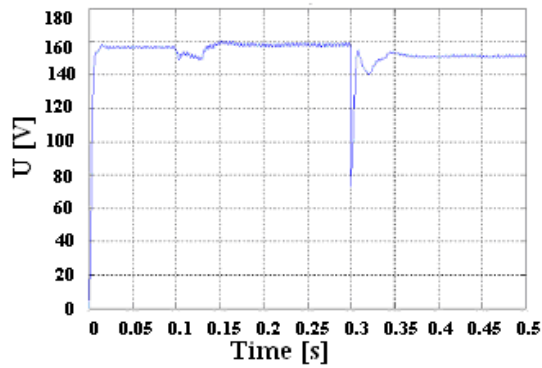


Fig. 2.18. Voltage on the load the mains supply without active filter

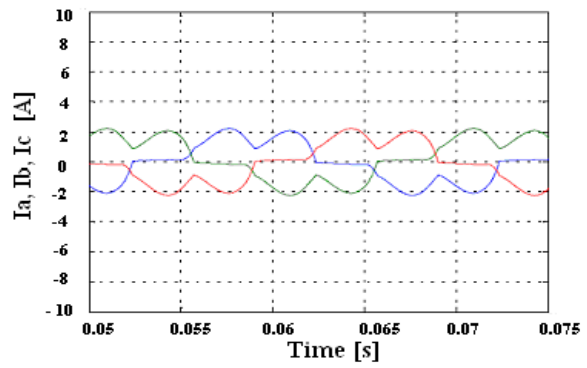


Fig. 2.19 Three-phase currents from the mains supply without active filter

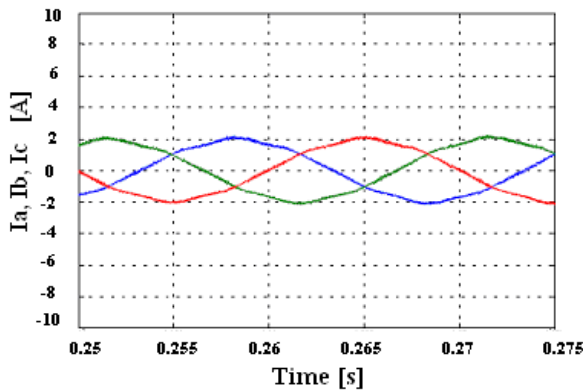


Fig. 2.20. Phase currents from the power network with active filter

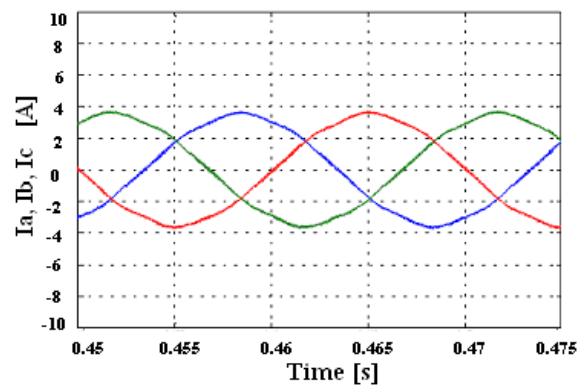


Fig. 2.21 Three-phase currents from the mains supply for dual task

In the following we present the results obtained from simulation for this type of construction.

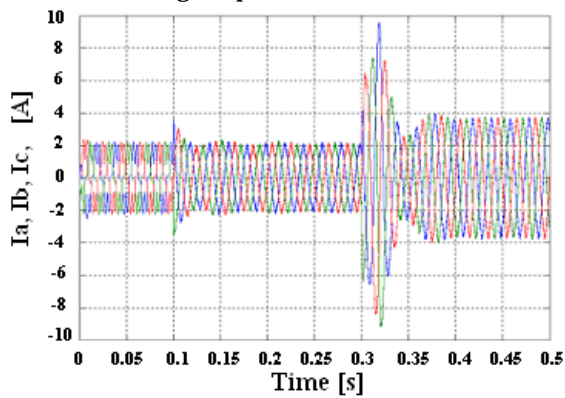


Fig. 2.22 Three-phase currents from the power supply throughout the simulation time

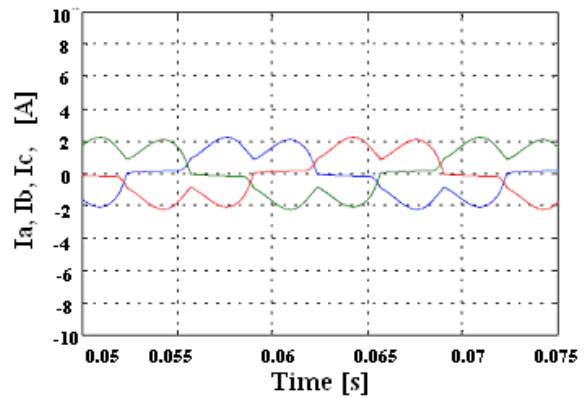


Fig. 2.23. Phase currents from the power network without active filter

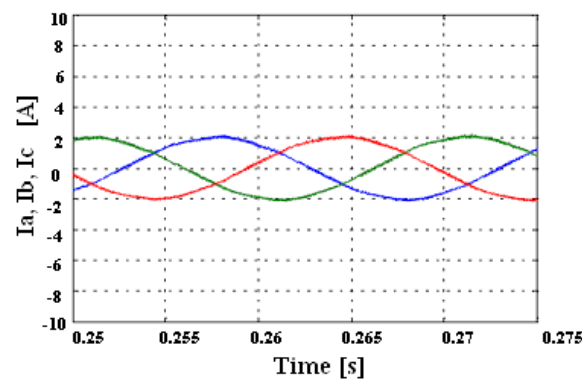


Fig. 2.24 three-phase currents mains an active filter

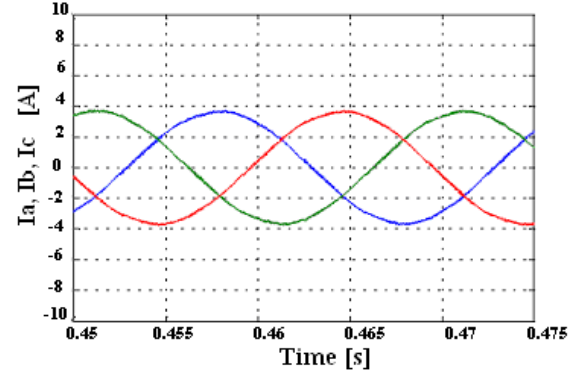


Fig. 2.25. Phase currents from the mains supply for dual task

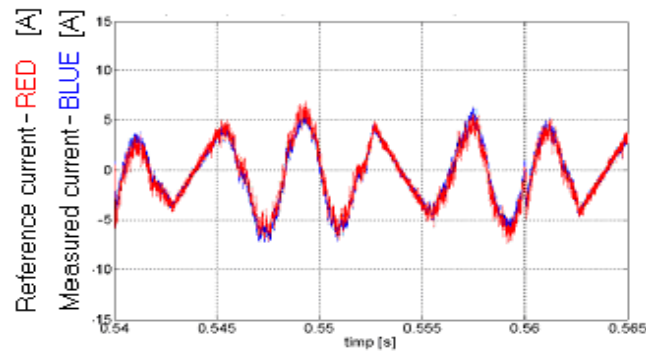


Fig. 2.26. Compensation current produced from the active phase of growth after pregnancy

3. CONCLUSIONS

This paper presents four schemes using both types of construction, with and without feedback loop, for three-phase voltage sources but balanced nonlinear load (no neutral wire). The first two schemes use a calculation method based on real-time Fourier analysis of the currents on each phase. The other two schemes propose another solution that enables the calculation based on the fundamental harmonic active and reactive power (by averaging the instantaneous value). Simulation of these schemes was done in Matlab-Simulink environment. In all cases observed sharp decrease distorting effect caused by pregnancy. Using sliding mode version requires use of a DSP but need large memory.

REFERENCES

- [1.] Gelu-Ovidiu Tirian, Stela Rusu-Anghel – Automatizarea Proceselor Continue, Editura Mirton, Timisoara, 2008
- [2.] Anghel Stela, Tirian Gelu-Ovidiu – Teoria Sistemelor si Reglaj Automat, Aplicatii in Matlab, Editura Mirton, Timisoara, 2007
- [3.] Task Force on Harmonics Modeling and Simulation, IEEE PES Harmonic Working Group: „Characteristics and Modeling of Harmonic Sources – Power Electronic Devices”, IEEE Trans on Power Delivery, Vol 16, No 4, october 2004, pp. 791-800.



¹ Stela RUSU-ANGHEL, ² Lucian GHERMAN, ⁵Sergiu MEZINESCU

MANAGEMENT FLOW CONTROL ROTOR INDUCTION MACHINE USING FUZZY REGULATORS

¹⁻⁵ UNIVERSITY POLITEHNICA OF TIMISOARA, FACULTY OF ENGINEERING FROM HUNEDOARA, ROMANIA

ABSTRACT:

Commands based on static characteristics of induction motor inevitably produce a number of undesirable effects on the dynamic behavior of the engine. These disadvantages can be partially eliminated by appealing to the orientation control strategy flow. The paper proposes the use of fuzzy controllers for rotor flow and electromagnetic torque, and simulation in Matlab-Simulink them. The results show that using fuzzy controllers compared with conventional methods allow a quick start and a small error rate in both task and goal.

KEYWORDS:

fuzzy controllers, Matlab-Simulink, induction motor

1. INTRODUCTION

Perturbations introduced by the inverter are most stator voltage and stator flow so. Instead, the rotor flow does not vary depending on the stator current with a time constant T_r so great. Vector diagram in Figure 1.1 describes the principle of rotor flow orientation with respect. Also the rotor flow estimation and adjustment can be made with a larger sampling period than the average of Stroke inverter.

So after the rotor flow orientation allows us to combine the requirements in terms of rapidity and computing performance. In addition to orientation relative to the rotor flow, allows decoupling of flow and electromagnetic torque regulation.

Ψ_r rotor flow vectors and stator current is moving at the speed of the mobile coordinate system ω_s synchronism. It is found that the flow vector is in phase with the real component of stator current phasor $i_{s\alpha}$ and therefore is out of phase by 90 degrees from the imaginary component $i_{s\beta}$.

Also, the rotor flow is purely real ($\underline{\Psi}_r = \Psi_{r\alpha}, \Psi_{r\beta} = 0$) in mobile reference system. $I_{s\alpha}$ real component of current flow while producing so imaginary component $i_{s\beta}$ produce electromagnetic torque. Because of this dynamic coupling of the engine components are independent in terms of operation. Flow and torque can also be ordered individually.

In Figure 1.2 is a circuit schematic diagram of power, control and control of a controlled induction motor rotor relative to the flow. Logic control signals, but ($i = 1 \dots 6$) are determined from the adjustment phase currents. In principle, adjusting the phase currents are made just like the current order - variable stator frequency. Phase current shape is determined by the block (6) by making measurements $i_{s\alpha}$ and $i_{s\beta}$ mobile reference system fixed reference system with stator frequency f_s estimated.

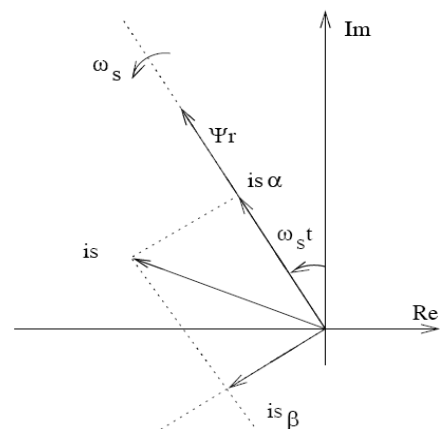


Figure 1.1. Vector diagram in mobile reference system command oriented in relation to the flow rotor

Numerical simulation was done in Matlab - Simulink using real data of a 133Hz engine. The mathematical model of rotor flow control the orientation is shown in Figure 2.3., And the induction motor model used in this type of order is shown in Figure 2.2.

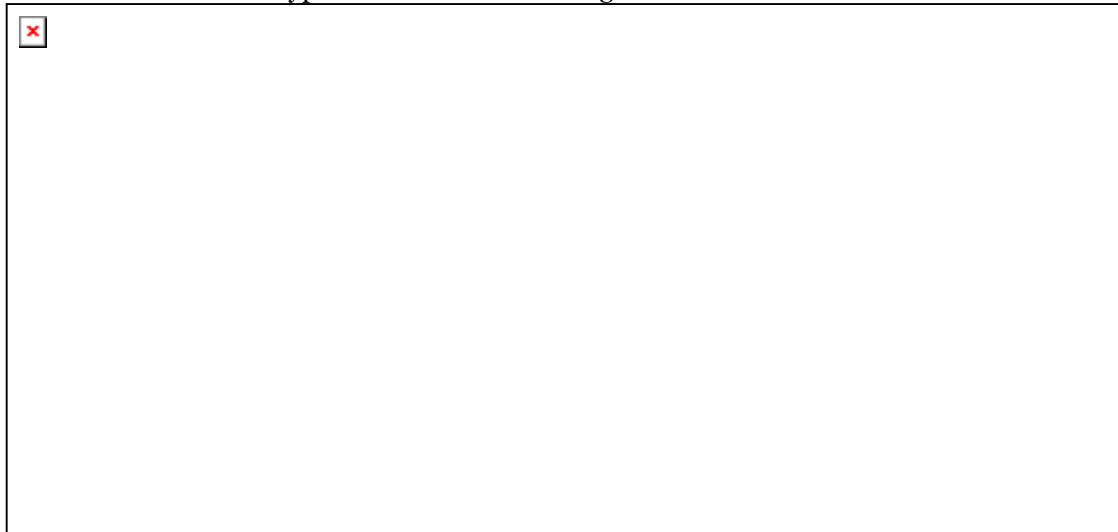


Figure. 2.2. The Matlab Simulink controlled induction motor after the flow rotor oriented

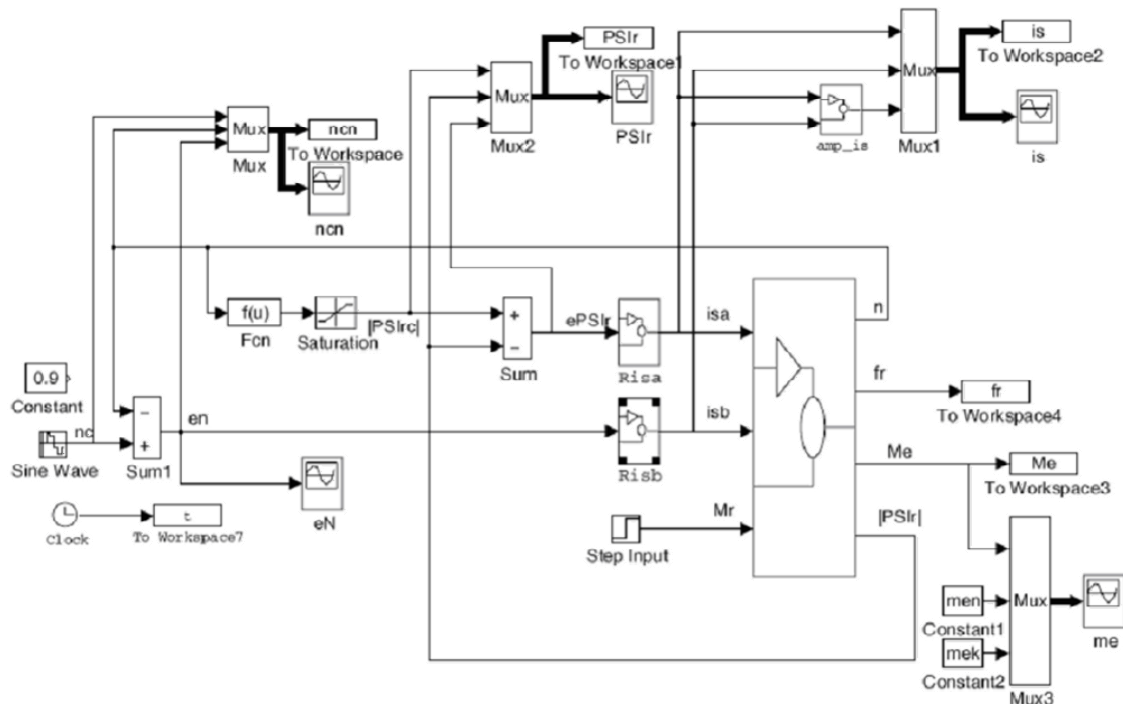


Figure 2.3 .. The Matlab Simulink-controlled induction motor rotor flow oriented by using fuzzy controllers

Obtained speed at the exit block that models the asynchronous motor (Figure 1.4.) Block is applied to determine the rotor flow imposed, which is then limited to the nominal value of rotor flow. Using the rotor flow modulus value obtained in the block that models the asynchronous motor and the rotor flow value imposed by loss of control error to determine the rotor flow will apply fuzzy controller that will calculate the real component of stator current i_{sa} , which would apply to model induction motor.

I_{sb} imaginary component of stator current is determined by the second fuzzy controller based on speed error.

3. DESIGNING FUZZY CONTROLLERS

3.1. FUZZY REGULATOR FOR FLOW ROTOR

Ψ_r rotor flow is controlled by the real component of stator current i_{sa} . The block diagram of this controller is shown in Figure 3.1.

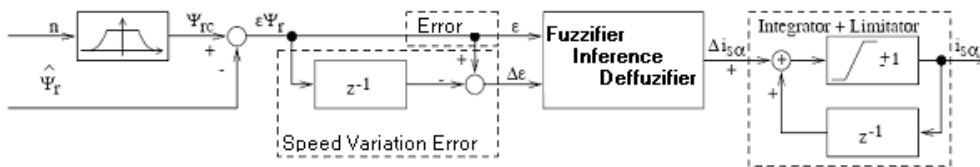


Figure 3.1. Block diagram of fuzzy controller to control flow rotor oriented control after the flow rotor

Ψ_r rotor flow current value is taken from the induction motor model, but in practice it can be determined the stator currents depending on the stage. Rotor flow Ψ_{rc} prescribed value is determined using the rotational speed, not based on static characteristics. The estimated value of rotor flow is calculated.

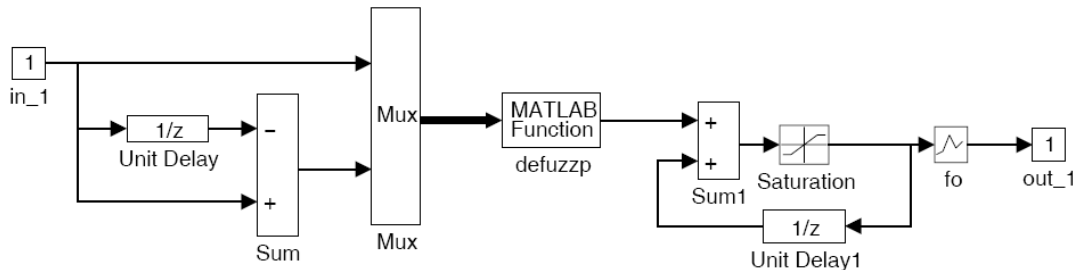


Figure 3.2. Matlab-Simulink model of the fuzzy controller for the rotor flow

Time delay is equal to sampling period $TE = 0.001$ s. Sampling period was chosen so that a sufficient number of samples to control the rotor flow following engine speed. The sampling period should not be confused with the sampling period to generate the inverter control pulses, the period must be much smaller ($\sim 500 \mu s$) to have a sufficient number of points to generate the stator current frequency.

Numerical variables $\epsilon\Psi_r$ and $\Delta\epsilon\Psi_r$ fuzzy variables are converted into speech presented fig.3.3 universal and triangular membership functions.

Each universes of discourse is divided into seven fuzzy sets according to a k^n : NL = Negative Large, NM = Negative Medium, NS = Negative Small, ZE = Zero, PS = Positive Small, PM = Positive Medium, PL = Positive Large. The coefficient k is chosen in the range (0.1 - 1.0). Variables $\epsilon\Psi_r$ and $\Delta\epsilon\Psi_r$ inference are processed using the 49 (7×7) rules, type If ... then ..., shown in Figure 3.4., using the min / max.

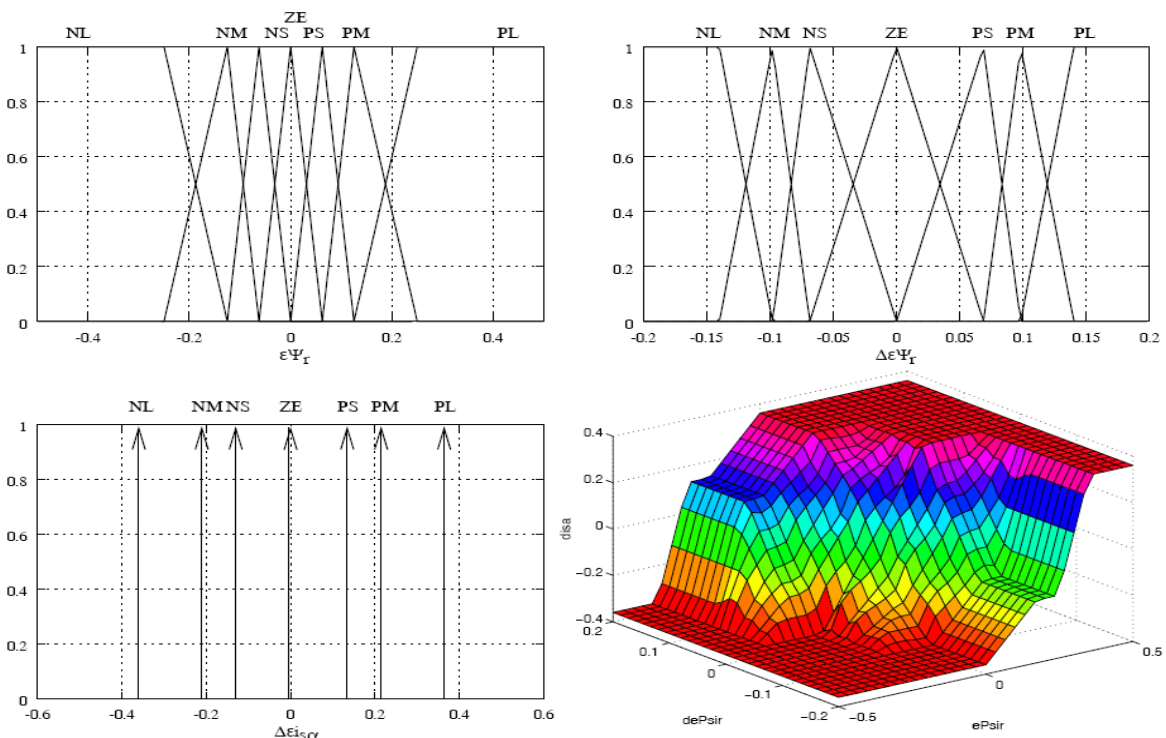


Fig. 3.3. The inputs $\epsilon\Psi_r$ and $\Delta\epsilon\Psi_r$; the output $\Delta i_s \alpha$ and the command surface of fuzzy controller proposed

For defuzzification centroid method was used. Command area of fuzzy controller is presented in Figure 3.3.

		$\Delta \varepsilon \Psi_r$						
$\Delta i_{s\alpha}$		NL	NM	NS	ZE	PS	PM	PL
NL		NL	NL	NL	NL	NL	NL	NL
NM		NL	NL	NL	NL	NM	NS	PS
NS		NL	NL	NL	NL	NM	NS	PS
ZE		NL	NM	NS	ZE	PS	PM	PL
PS		NS	PS	PM	PL	PL	PL	PL
PM		NS	PS	PM	PL	PL	PL	PL
PL		PL	PL	PL	PL	PL	PL	PL

Figure 3.4. Table of proposed rules of fuzzy controller

3.2. FUZZY REGULATOR FOR ELECTROMAGNETIC TORQUE

Electromagnetic torque and rotational velocity is controlled by imaginary component of stator current $i_{s\beta}$. The proposed controller error as input rotational speed, and speed variation ε_n this error $\Delta \varepsilon_n$. Error rate is obtained by the difference between the prescribed speed, n_c , and the actual value of rotor speed n - Matlab Simulink model of this controller is shown in Figure 3.5.

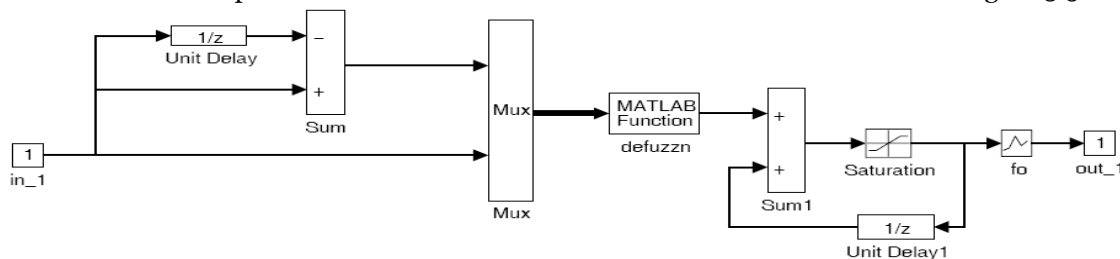


Figure 3.5. Matlab-Simulink model of the electromagnetic torque fuzzy controller

Time delay is equal to sampling period $T_E = 0.001$. Sampling period was chosen so that a sufficient number of samples to control and track engine speed.

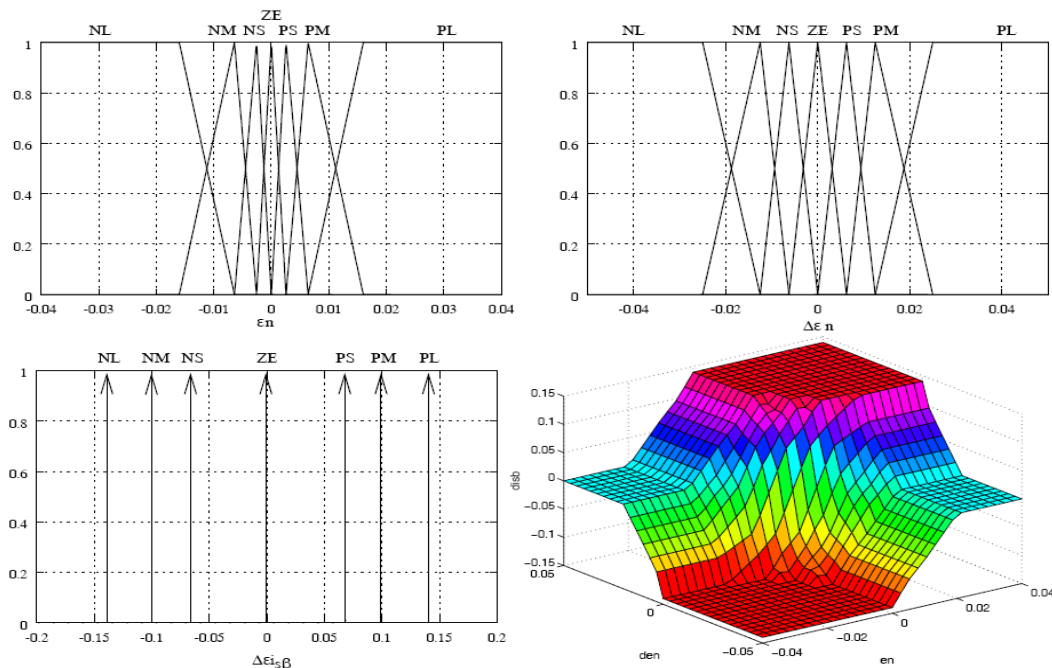


Figure 3.6. The inputs ε_n and $\Delta \varepsilon_n$; output $\Delta i_{s\beta}$ and control surface fuzzy controller proposed

Numerical variables $\varepsilon \Psi_n$ and $\Delta \varepsilon \Psi_n$ fuzzy variables are converted into speech presented fig.3.6 universes and triangular membership functions. Each universe of discourse is divided into seven fuzzy sets according to a k^n : NL = Negative Large, NM = Negative Medium, NS = Negative Small, ZE = Zero, PS = Positive Small, PM = Positive Medium, PL = Positive Large. The coefficient k is chosen in the range (0.1 - 1.0).

After optimization of the system were determined universes of speech and sharing factor k of the law in language degrees. ε_n variable universes of discourse is $[-0.04 \div 0.04]$, the variable is $\Delta \varepsilon_n$

$[-0.05 \div 0.05]$, and the output is $\Delta i_{s\beta}$ $[-0.2 \div 0.2]$. For entry ε_n factor $k = 0.4$ for entry $\Delta \varepsilon_n$ factor $k = 0.5$ and $k = 0.7$ exit $\Delta i_{s\beta}$ factor.

		$\Delta \varepsilon_n$						
		NL	NM	NS	ZE	PS	PM	PL
ε_n	NL	NL	NL	NL	NL	NM	NS	ZE
	NM	NL	NL	NL	NM	NS	ZE	PS
	NS	NL	NL	NM	NS	ZE	PS	PM
	ZE	NL	NM	NS	ZE	PS	PM	PL
	PS	NM	NS	ZE	PS	PM	PL	PL
	PM	NS	ZE	PS	PM	PL	PL	PL
	PL	ZE	PS	PM	PL	PL	PL	PL

Figure 3.7. Fuzzy inference table of the controller proposed by the engine. For defuzzification centroid method was used. Fuzzy control surface of the controller is presented in Figure 3.6.

Variables ε_n and $\Delta \varepsilon_n$ inference are processed using 49 (7 x 7) rules, type If ... then ..., shown in Figure 3.7., using the min / max.

Table rules underlying fuzzy speed regulator is shown in Figure 3.7 has been determined using the following logic: if the component of stator current imagination, $i_{s\beta}$, it will grow and grow me electromagnetic torque generated

4. RESULTS NUMERICAL SIMULATION

To simulate the operation of induction motor rotor flow controlled by using two independent fuzzy controllers for the rotor flow and electromagnetic torque respectively, was done in Matlab. For numerical integration of differential equations resulting system was used Runge-Kutta algorithm of order 5. For simulation we use a 133 engine Hz/160W.

The mathematical model implemented in Matlab Simulink-Target Order of the rotor flow is shown in Figure 2.1. At the current fed induction motor stator variable in Figure 2.2. And the two fuzzy controllers used to control rotor flow and electromagnetic torque are shown in Figure 3.1. and Fig.3.2

Speed, n , and rotor flow $|\Psi_r|$ obtained from the induction motor model is applied to the two control loops, the rotor flow and electromagnetic torque. Rotor flow imposed Ψ_{rc} is calculated based on the actual rotor speed. Since rotor flow is dependent only real component of stator current, i_{sa} , the fuzzy controller will only control the rotor flow I_{sa} . Also, because the electromagnetic torque depends only on the imaginary part of the stator current, $i_{s\beta}$, then the controller will only control the electromagnetic torque $i_{s\beta}$.

To study the static behavior and response to the step signal of the current controlled induction motor with rotor flow orientation after two tests were performed. These tests, which are part of the first set of tests, consisting in imposing a constant speed $n_c = 0.9$ [pu], and the first engine test was considered void start ($M_r = 0$) at $t = 0.5s$ and applying a torque resistant equal to the nominal torque ($M_r = m_{en}$). For the second test was also considered imposing a constant speed $n_c = 0.9$ [p.u.], but starting the engine in charge ($M_r = m_{men}$) and at $t = 0.5s$ resistant torque cancellation. Graph of the main parameters can be simulated in Figure 4.1 follow.

In Fig. 4.1. prescribed speed is presented charts, still, the rotor speed, n , electromagnetic torque, m_e , speed error, ε_n , the rotor flow modulus, $|\Psi_r|$ and stator current (i_{sa} real component, imaginary component and module $i_{s\beta} |i_s|$ the first set of tests. From these graphs you can see a great variation in the behavior of the prescribed speed gear so the engine speed error in the gap, and with the engine load.

The transitional arrangement is very short settling speed prescribed in 0.14 and up, without a long-harmonic regime. Study the dynamic regime controlled induction motor operation in the stator current with rotor flow orientation was made after the imposition of a speed, yet, to form sinusoidal amplitude 0.2 [p.u.] and the frequency of 6Hz. Frequency was chosen maximum speed acceleration imposed.

Otherwise that is approximately equal to the maximum acceleration that the engine can have rated load. For the first test of this set of tests, Fig 4.2 we considered to start in goal, ($M_r = 0$), and applying a torque at $t = 0.5s$ electromagnetic torque is equal to the nominal resistance, and for the second test, Fig 4.3. , To start the task ($M_r = m_{en}$) and at $t = 0.5s$, strong torque cancellation.

From the study of dynamic graphics system (Figure 4.4.) shows that using fuzzy controllers to get a quick start and a small error rate in both task and goal.

The principle of command guidance after the rotor flow using fuzzy proposed to impose independent stator current components, compared with the methods described above, and leads to obtain very good results both in steady and dynamic conditions.

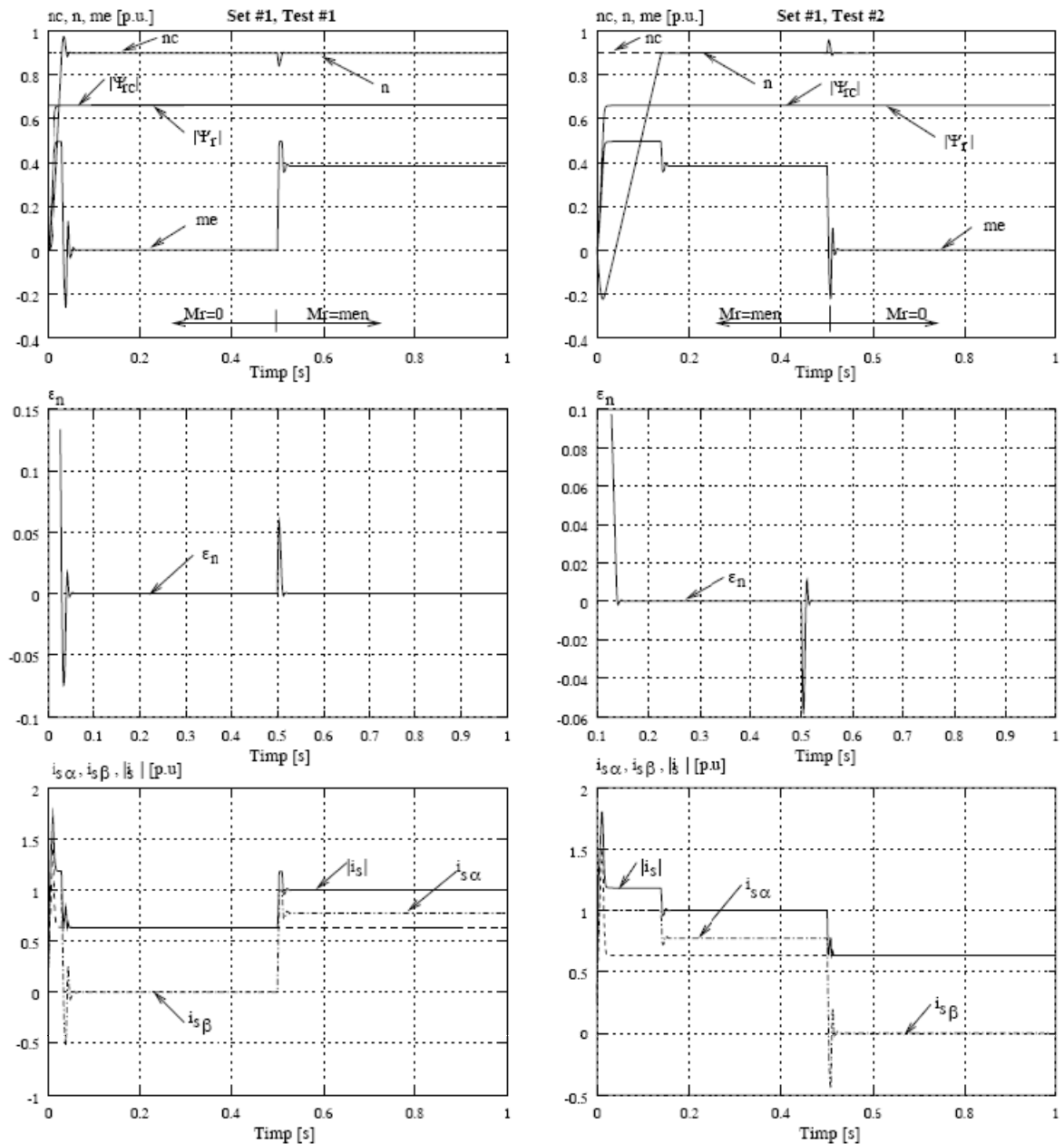


Fig. 4.1 . Speed n electromagnetic torque me , rotor flow module $|\Psi_r|$, ϵ_n speed error and stator current (real part $i_{s\alpha}$, $i_{s\beta}$ imaginary component and module i_s) the first set of tests

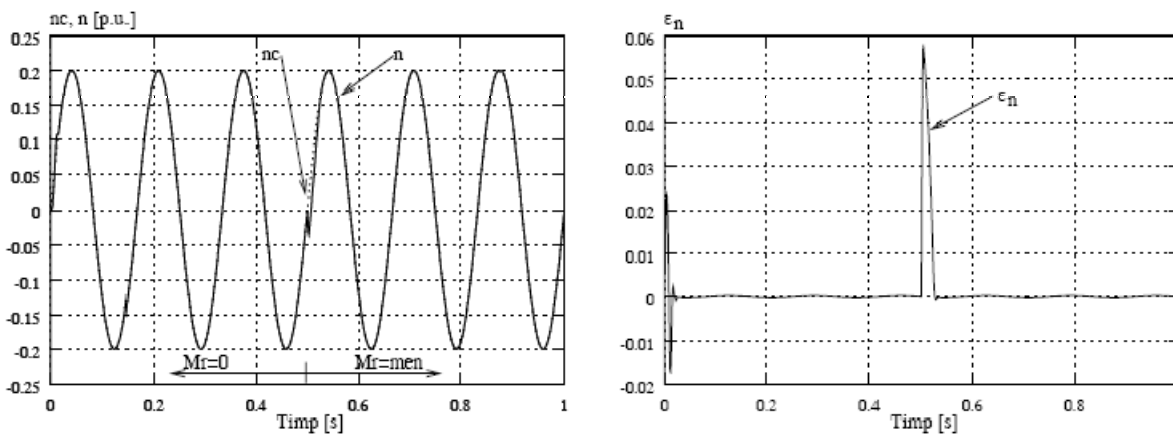


Fig. 4.2. Rotor speed n , rpm still imposed, and the speed error ϵ_n 1 test 2 test kit.

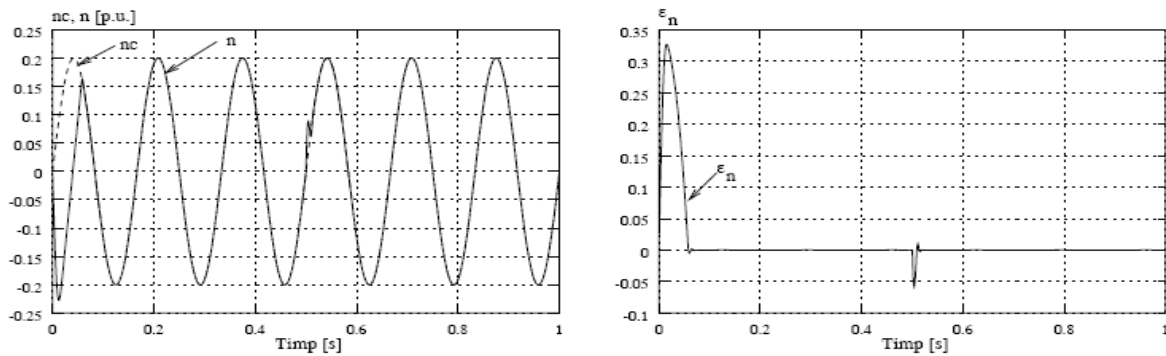


Fig. 4.3. Rotor speed n , rpm still imposed, and the speed error ϵ_n Test 2 of 2 set of tests.

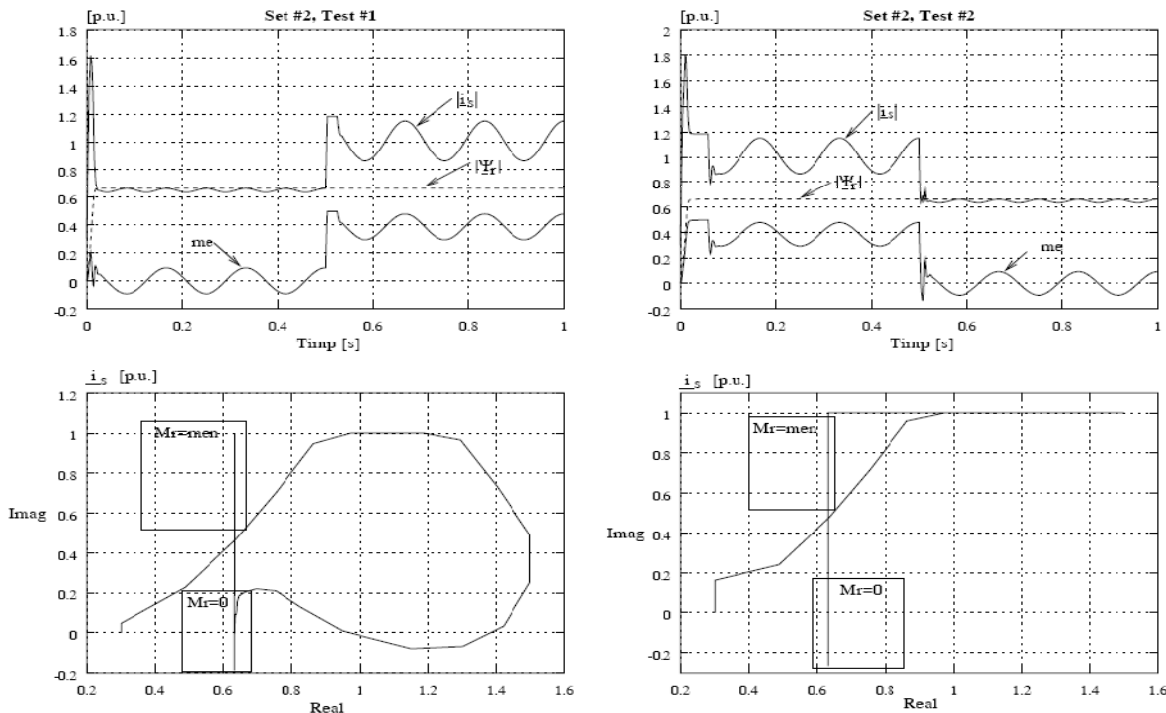


Fig. 4.4. Variation of stator current phasor module, $|i_s|$, is the stator current phasor, the rotor flow phasor module, $|\Psi_r|$ and electromagnetic torque, me 2 test kit.

5. CONCLUSIONS

It can highlight the following conclusions: asynchronous motor is a nonlinear system described by a 7-order differential equations with variable parameters, the inverter, the control algorithm and the limitations imposed on the hysteresis, inter switching times is also a powerful nonlinear, speed control motors, control methods studied impugn regulators with variable coefficients depending on the operating point of engine controllers to drive motors implementation requires knowledge of how real operating parameters, and their evolution, the parameters may vary The magnetic circuit saturation and / or temperature, quality tuning fuzzy actually requires a wider range of motion controllers used in applications for robotics, machine tools, transportation, etc.

REFERENCES

- [1.] Gelu-Ovidiu Tirian, Stela Rusu-Anghel – Automatizarea Proceselor Continue, Editura Mirton, Timisoara, 2008
- [2.] Anghel Stela, Tirian Gelu-Ovidiu – Teoria Sistemelor si Reglaj Automat, Aplicatii in Matlab, Editura Mirton, Timisoara, 2007
- [3.] Peter Vas. Electrical machines and Drives – a Space – Vector Theory Approach, Volume 25 of Monographs in electrica land Electronical Engineering. Oxford science Publications, Walton Street, Oxford OX2 6DP, 1992.
- [4.] Fariba Moghaddam Butzberg. Etude et Comparaison de Differentes Strategies de Reglage et de Commande de Servomoteurs Asynchrones. These no. 1414 pour l’obtention du grande de docteurs sciences techniques, Ecole polytechnique federale de Lausanne, Department d’Electricite, 1995.

¹Ion COPACI, ²Aurelia TĂNĂSOIU

THE REDUCTION OF THE ACCELERATION LEVELS CONVEYED TO THE FREIGHT HAULED ON CARRIAGES FITTED WITH LONG-RUN BUFFERS

¹⁻² UNIVERSITATEA "AUREL VLAICU" ARAD, ROMANIA

ABSTRACT:

The current trend towards the increase of speeds in the railway traffic and the ever growing gain weight on the axles has brought about a series of special problems concerning the impact stress which occurs at collision.

In order to isolate the shock that occurs longitudinally, the rail vehicles are fitted with shock dampers:

- ❖ Buffers or main coupling dampers
- ❖ Long-rung buffers fitted on the platform wagons, meant as an additional safety measure for the goods loaded on the storage platform

Long-rung buffers fitted on the platform wagons are reducing the level of the longitudinal acceleration.

KEYWORDS: shock, collision, long-run damper, acceleration, contraction, mobile longeron, storage platform, mobile covering

1. INTRODUCTION

The collision of the rail vehicles takes place under shunting conditions while the carriages are being coupled and during traffic following the start-ups and brakings of the set of cars.

The stress produced at the collision of the rail vehicles generates the transmission of certain forces and accelerations of considerable value that convey acceleration to the goods hauled. This acceleration, in its turn, may jeopardize their integrity and their anchoring, fixing and packing systems.

Fig. 1 shows Rijmmns- 600, a 4-axle platform wagon fitted with a long-run buffer fixed on a 76-350 mm OLEO INTERNATIONAL mobile longeron .

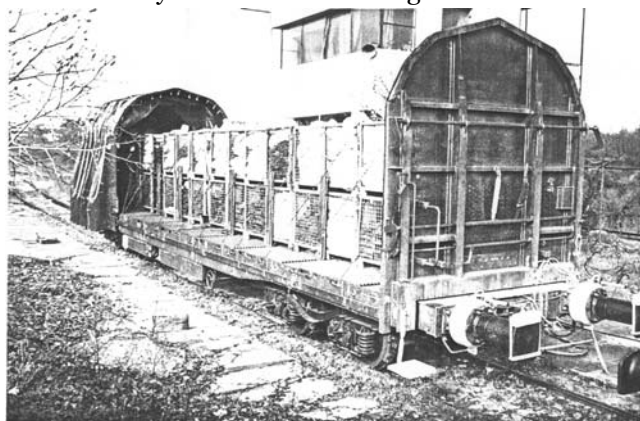


Fig. 1

2. COLLISION TEST

Fig. 2 shows the way in which damper (1) is fixed, in between the mobile longeron and the storage platform, as well as the mounting of force cell (2) that determines the force conveyed through damping.

The collided wagon was loaded with pellets and small products in two different variants:

- ❖ Variant 1: a half-load for a tare weight of 56,960 kg ;
- ❖ Variant 2: a total load for a tare weight of 90,000 kg;

The colliding wagon was a gondola car loaded with sand at a tare weight of 80 t., fitted with A category buffers in keeping with UIC 526-1. During the tests the following parameters were determined as response functions of the collided car:

- ❖ $F_1; F_2$ [kN] – the forces conveyed through the buffers of the car;
- ❖ D_1, D_2 [mm] – the contraction of the buffers;
- ❖ F_L [kN] – the force conveyed by the mobile longeron to the long-run buffer;
- ❖ D_L [mm] – the contraction of the long-run buffer;
- ❖ a_s [g] – the acceleration imparted to the undercarriage on which the hauled goods are fixed;
- ❖ a_L [g] – the acceleration of the longeron;

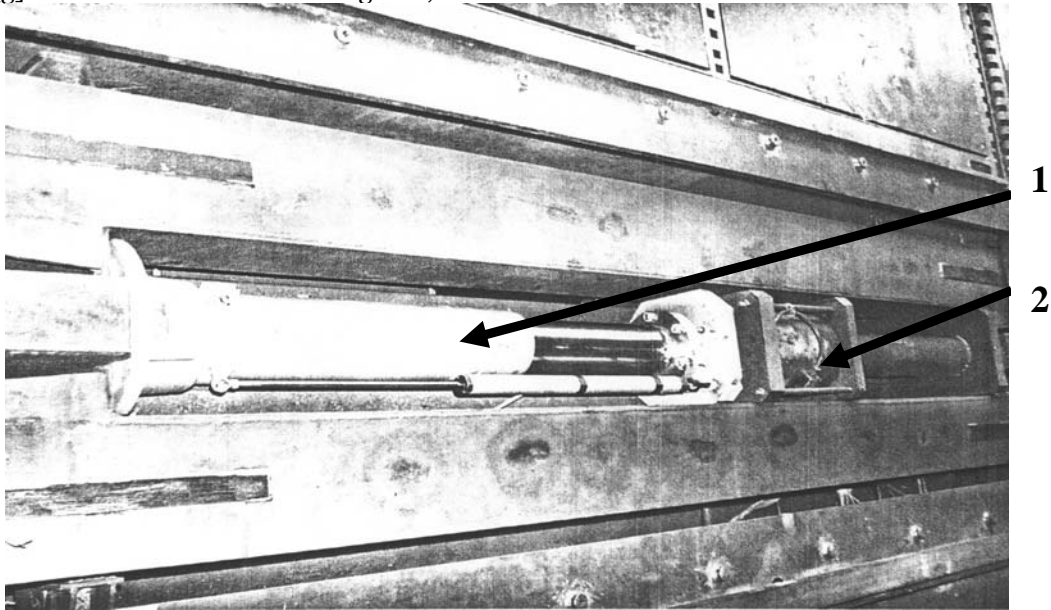


Fig. 2

The colliding car was launched from an incline and it collided into the tested car which was lined up at various collision speeds. The results of the collision tests are shown in Tabel no.1

The analysis of the results for the second collision variant ($V= 11.68$ km/h), shows that the collision process lasts 0.75 s. By the integration of the curve of the undercarriage acceleration as a function of time, we determined the evolution of the speed correlated with time during the process of collision, as shown in Fig. 3. The evolution in time of the undercarriage acceleration as is illustrated in Fig. 4.

Tabel no. 1

Parametri masurati	Vagon tara 56.960 kg								Vagon tara 90.000 kg					
	Viteza (km/h)													
	7,1	8,12	8,93	8,91	8,95	10,16	10,84	11,61	12	8,29	8,95	10,22	10,87	11,68
F_1 (kN)	118	142	158	158	158	190	208	229	241	152	168	199	211	238
F_2 (kN)	106	129	152	153	151	186	199	224	235	142	158	194	207	232
F_L (kN)	219	282	340	345	347	427	472	534	565	346	390	486	499	570
D_1 (mm)	32	38	40	41	41	48	51	56	59	35	38	46	50	55
D_2 (mm)	27	32	32	35	35	41	46	49	53	27	31	37	44	49
D_L (mm)	289	312	318	318	317	329	336	340	340	337	340	347	350	350
a_s (g)	0,67	0,86	0,92	0,92	0,92	1,44	1,63	1,67	1,74	0,65	0,7	0,95	1,05	1,22
a_p (g)	0,72	0,83	0,93	0,91	0,94	1,43	1,5	1,55	1,62	0,69	0,75	0,85	0,98	1,14
a_L (g)	4,13	4,54	4,69	4,67	4,65	6,17	6,58	6,68	6,92	5,09	5,3	6,13	6,44	6,95

The figure shows speeds at time $t=0$, the start –up of collision and at time $t= 0.75$ s, the end of collision. We have to point out also time $t_{1,2} = 0.27$ s, the moment when the process of turning the kinetic energies of the masses taking part in the collision into stored potential strain energy came to an end and the masses of the vehicles were running at the same speed.

Making up the energetic balance for the collision of the car having a tare weight of 90,000 kg at a speed of $V= 11.68$ km/h, we concluded the following:

- ❖ the strain energy stored by the shock dampers is $W_e = 180.46$ kJ , so that the potential strain energy stored in by the resistance structures of the vehicles and the freight becomes $W_{v+i} = 43.32$ kJ;
- ❖ the strain energy dispersed by the shock dampers is $W_a = 139.44$ kJ and consequently the strain energy dispersed by the resistance structures of the vehicles and the freight becomes $W_{v+i} = 22,26$ kJ.

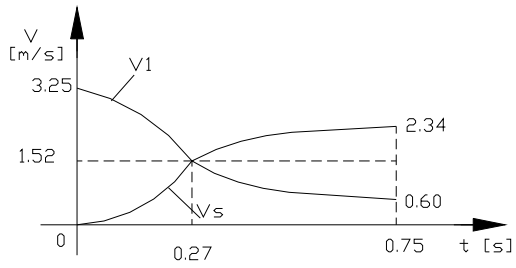


Fig. 3

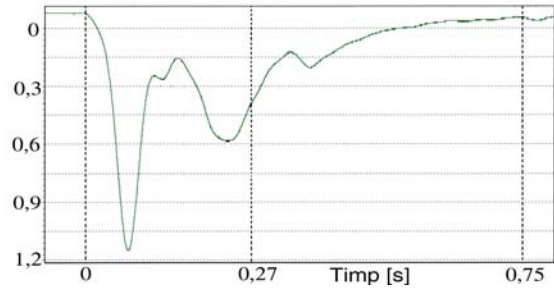


Fig. 4

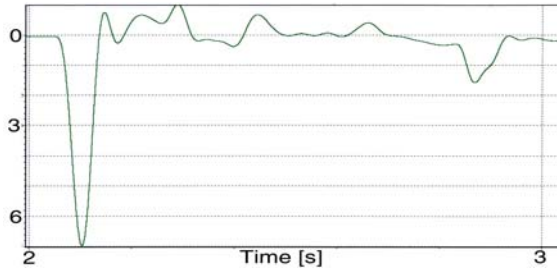


Fig. 5

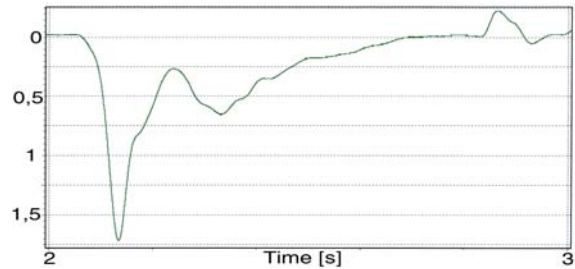


Fig. 6

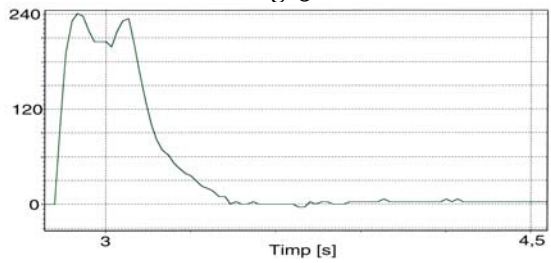


Fig. 7

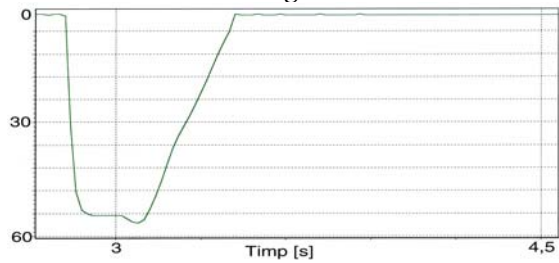


Fig. 9

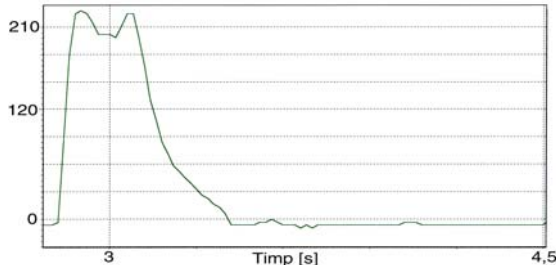


Fig. 8

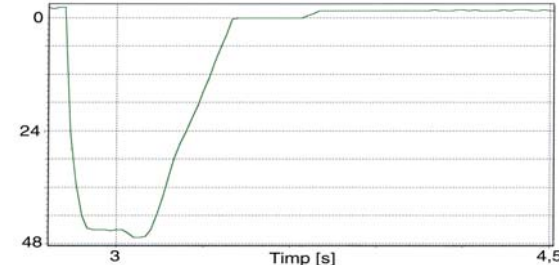


Fig. 10

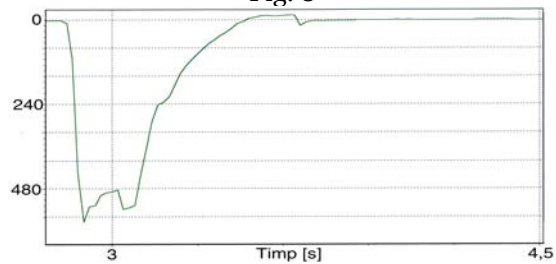


Fig. 11

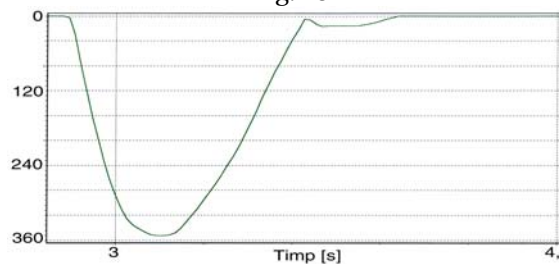


Fig. 12

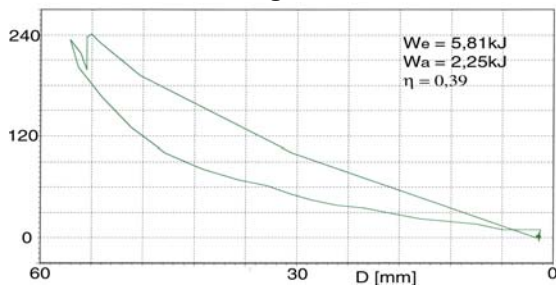


Fig. 13

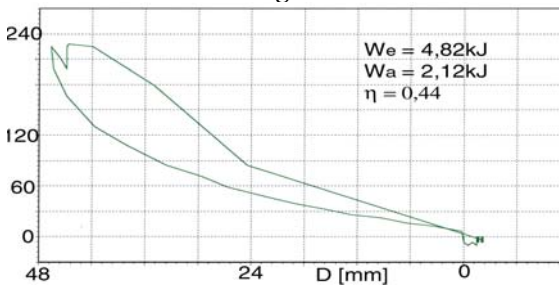


Fig. 14

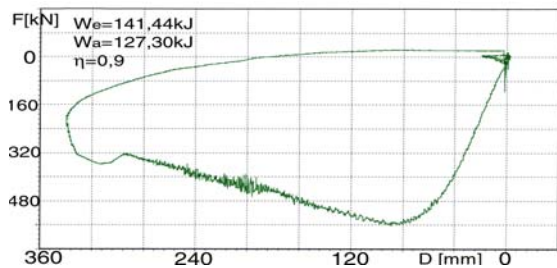


Fig. 15

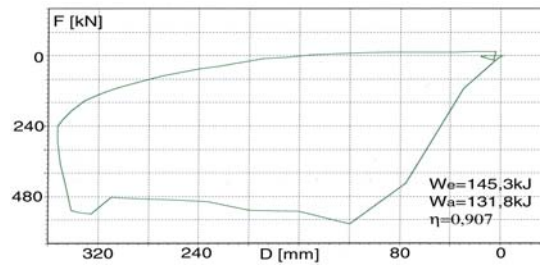


Fig. 16

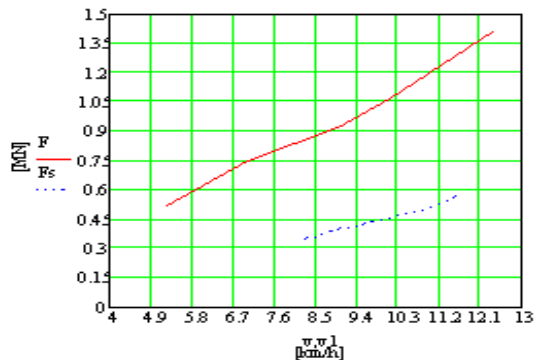


Fig. 17

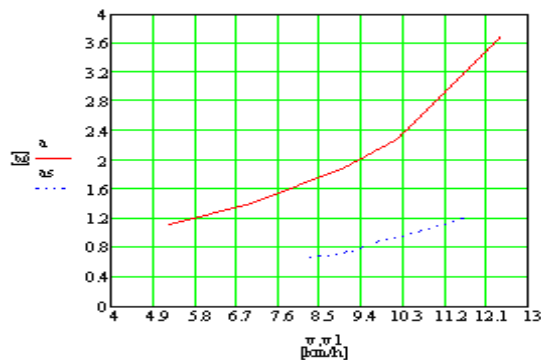


Fig. 18

Fig. 5 and 6 shows the variation of the mobile longeron acceleration and that of the undercarriage in variant 1 of collision at a speed of 12 km/h.

Fig. 7, 8, 9, 10 show F_1 ; F_2 ; D_1 ; D_2 correlated with time in variant 2 of collision at a speed of 11.68 km/h. Fig. 11 and 12 show F_L , D_L correlated with time in the same variant of collision. Fig. 13, 14 and 16 show the graphs characteristic for buffer 1; buffer 2 and the long-run damper in collision variant 2. Fig. 15 shows the characteristic of the long-run damper in collision variant 1.

Fig.17, 18 illustrate the variation of the forces conveyed and of the acceleration of the car undercarriages in the following situations:

- ❖ collision of 80 t → 90 t cars fitted with buffers of category C (full line graph);
- ❖ collision variant 2 of a 80 t car → 90 t car fitted with long-run dampers.

3. CONCLUSION

The utilization of long-run dampers leads to a significant reduction of the level of forces conveyed, of the accelerations imparted to the cars and of the potential and dispersed energies which apply to the resistance structures of the cars and freight hauled. Fig. 17 and 18 show that the conveyed forces decrease approx. with 60 %, while the accelerations imparted with approx. 50 % as compared to a collision in which the cars are fitted with buffers of category C – 70kJ, buffers which have the highest capacity of energy storage.

REFERENCES

- [1.] UIC 529- Amortizori hidrodinamici de cursă lungă- 1998
- [2.] Cyril M. Harris, Charles E. Crede – Shock and Vibration Handbook – McGraw Hill Book Company – New York 1961
- [3.] Louis – Marie Cleon, Henri Lagneau – Physique du choc et accidentologie, Revue generale des chemins de fer, November 1993
- [4.] Tyrell D., Severson K., Perlman A. – Single Passenger Rail Car Impact Test Volume I: Overview and Selected Results, US Department of Transportation, Federal Railroad Administration, March 2000
- [5.] Severson K., Tyrell D., Perlman A. – Single Passenger Rail Collision Test: Analysis of structural Measurements, ASME Winter Annual Meeting 2000
- [6.] Severson K. – Development of Collision Dynamics Models to Estimate the Result of Full-scale Rail Vehicle Impact Tests, Tufts University Master's Thesis, November 2000



USING DSP TO ORDER ACTIVE FILTERS

¹⁻⁴ UNIVERSITY POLITEHNICA OF TIMISOARA, FACULTY OF ENGINEERING FROM HUNEDOARA, ROMANIA

ABSTRACT:

This deformed system power supply networks of different consumers is increasingly common. At European level there are rules limiting factors distorting the values strict enough. This goal can be achieved using active harmonic filters. The present paper shows how to control such an active filter using a digital signal processor (DSP) DSP family of 56 F805.

KEYWORDS:

DSP family, digital signal processor, active harmonic filters

1. INTRODUCTION

1.1. P-Q-N METHOD TO ORDER ACTIVE FILTERS.

If sinusoidal supply voltage, active power and reactive mediated network is taken from the first harmonic. Since it is not perfectly sinusoidal voltage using a PLL circuit which generates a fundamental voltage in phase with equal amplitude but of unity.

Active power is calculated using this voltage and reactive power $p = 3 \cdot U \cdot I \cdot \cos\varphi$, where $q = 3 \cdot U \cdot I \cdot \sin\varphi$ is the phase angle between voltage and current fundamental harmonic. This technique called "generalized theory of instantaneous reactive power in three phase circuits" or "PQ theory" was developed in [2]. Change the coordinates from A, B, C in $\alpha, \beta, 0$ for three-phase voltages and currents:

$$\begin{bmatrix} u_{\alpha} \\ u_{\beta} \\ u_0 \end{bmatrix} = \sqrt{\frac{2}{3}} \cdot \begin{bmatrix} 1 & -\frac{1}{2} & -\frac{1}{2} \\ 0 & \frac{\sqrt{3}}{2} & -\frac{\sqrt{3}}{2} \\ \frac{1}{\sqrt{2}} & \frac{1}{\sqrt{2}} & \frac{1}{\sqrt{2}} \end{bmatrix} \cdot \begin{bmatrix} u_a \\ u_b \\ u_c \end{bmatrix} \quad (1.1)$$

and reverse:

$$\begin{bmatrix} i_{\alpha} \\ i_{\beta} \\ i_0 \end{bmatrix} = \sqrt{\frac{2}{3}} \cdot \begin{bmatrix} 1 & -\frac{1}{2} & -\frac{1}{2} \\ 0 & \frac{\sqrt{3}}{2} & -\frac{\sqrt{3}}{2} \\ \frac{1}{\sqrt{2}} & \frac{1}{\sqrt{2}} & \frac{1}{\sqrt{2}} \end{bmatrix} \cdot \begin{bmatrix} i_a \\ i_b \\ i_c \end{bmatrix} \quad (1.2)$$

can be obtained:

$$p = u_{\alpha} \cdot i_{\alpha} + u_{\beta} \cdot i_{\beta} \quad - \text{Instantaneous active power}$$

$$q = u_{\beta} \cdot i_{\alpha} - u_{\alpha} \cdot i_{\beta} \quad - \text{Instantaneous reactive power} \quad (1.3)$$

$$n = u_0 \cdot i_0 \quad - \text{Instantaneous homopolar power}$$

To improve the performance of this method and to simplify calculations, instead of the three instantaneous voltages will use three generators PLL output which will produce three sinusoidal signals of amplitude and phase of a fundamental supply voltage (this assumption is valid only in the absence of even harmonics).

To call these virtual voltage: $1A(1)$, $1B(1)$, $1C(a)$ and corresponding powers:

$$\begin{bmatrix} p_1 \\ q_1 \\ n_1 \end{bmatrix} = \begin{bmatrix} 1_\alpha^{(1)} & 1_\beta^{(1)} & 0 \\ 1_\beta^{(1)} & -1_\alpha^{(1)} & 0 \\ 0 & 0 & 1_0^{(1)} \end{bmatrix} \cdot \begin{bmatrix} i_\alpha \\ i_\beta \\ i_n \end{bmatrix} \quad (1.4)$$

Calculating the average value of this power and knowing that for basic fundamental virtual voltage just currents averaged can give a average value different by zero, we can write:

$$\begin{bmatrix} P \\ Q \\ N \end{bmatrix} = \begin{bmatrix} \frac{1}{T} \int_0^T (1_\alpha^{(1)} \cdot i_\alpha^{(1)} + 1_\beta^{(1)} \cdot i_\beta^{(1)}) dt \\ \frac{1}{T} \int_0^T (-1_\alpha^{(1)} \cdot i_\beta^{(1)} + 1_\beta^{(1)} \cdot i_\alpha^{(1)}) dt \\ \frac{1}{T} \int_0^T (1_0^{(1)} \cdot i_0^{(1)}) dt \end{bmatrix} \quad (1.5)$$

By reversing the relationship (1.5) can be obtained fundamentally load currents $i_\alpha(1)$, $i_\beta(1)$,

$$\begin{bmatrix} i_\alpha^{(1)} \\ i_\beta^{(1)} \end{bmatrix} = \begin{bmatrix} i_\alpha^{(1)} & i_\beta^{(1)} \\ i_\beta^{(1)} & -i_\alpha^{(1)} \end{bmatrix} \cdot \begin{bmatrix} P - N \\ Q \end{bmatrix} \quad (1.6)$$

Respective reference currents of active filter i_{AH}^* , i_{BH}^* , i_{CH}^* if SFFT site.

If we do not have the neutral wire to calculate the instantaneous active power and instantaneous reactive power we use (1.7).

$$\begin{bmatrix} p \\ q \end{bmatrix} = \begin{bmatrix} u_\alpha & u_\beta \\ u_\beta & -u_\alpha \end{bmatrix} \cdot \begin{bmatrix} i_\alpha \\ i_\beta \end{bmatrix} \quad (1.7)$$

This solution enables the calculation based on the fundamental harmonic active and reactive power (through mediation instantaneous value). On the basis of this technique lies that transfer of active and reactive power defined as the product of the fundamental harmonic voltage and currents is real only on the first harmonic current harmonics current remaining power fail.

Unfortunately, in some applications the source voltage contains higher harmonics. For this reason the calculation of power no longer use this tension, but tension time achieved by a PLL circuit implemented on a DSP software and providing an output sinusoidal signal in phase with the fundamental harmonic and amplitude equal to unity. This signal is subtracted from the total current network and thus obtain higher current harmonics which are given by reference to the sign change of active filter.

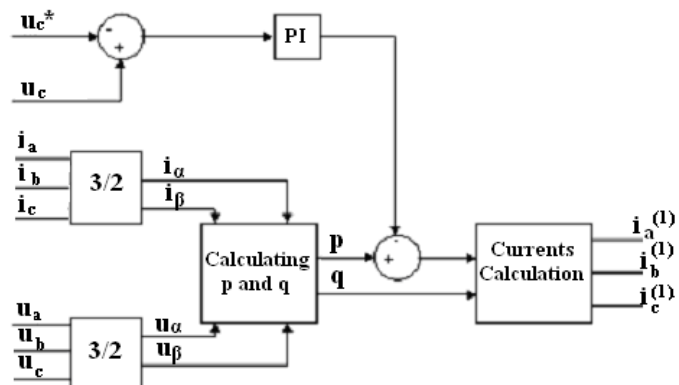


Fig. 1.1. Order active filter with instantaneous power control

1.2. THE FFT AND SFFT METHOD TO ORDER ACTIVE FILTERS.

It is known that a periodic signal can be decomposed into spectral components whose frequency is a multiple of the fundamental frequency. These components are known as harmonic components. A periodic signal can be represented by a Fourier series:

$$V(t) = \frac{1}{2} a_0 + \sum_{k=1}^n (a_k \cdot \cos k\omega t + b_k \cdot \sin k\omega t) \quad (1.8)$$

where $1/2 \cdot a_0$ is the DC component of the signal.

Coefficients a_k and b_k of the series can be defined as:

$$a_0 = \frac{2}{T} \int_t^{t+T} v(t) dt \quad (1.9)$$

$$a_k = \frac{2}{T} \int_t^{t+T} v(t) \cos(k\omega t) dt \quad (1.10)$$

$$b_k = \frac{2}{T} \int_t^{t+T} v(t) \sin(k\omega t) dt \quad (1.11)$$

The two coefficients a_k and b_k are the amplitudes of spectral components of order k . There is the possibility of formulating such a Fourier series:

$$V(t) = \frac{1}{2} a_0 + \sum_{k=1}^n A_k \cdot \cos(k\omega t - \phi_k) \quad (1.12)$$

where A_k represents the signal amplitude and ϕ_k represents the signal phase.

We define two such values:

$$A_k = \sqrt{a_k^2 + b_k^2} \quad ; \quad \phi_k = \arctan \frac{b_k}{a_k} \quad (1.13)$$

Fourier transform is calculated using the fastest FFT algorithm. By Fourier analysis of the currents on each phase has succeeded in its breakdown of its component harmonics. Recompose signal using only the higher order harmonics (less than first harmonic), a clear signal that the network will be introduced with the sign reversed. So that the grid will run a first harmonic signal.

A second solution is to calculate only the fundamental harmonic is then subtracted from the total current network and thus obtain higher current harmonics which are given by reference to the sign change of active filter. This method is used in sliding mode option.

2. ORDER AND DATA ACQUISITION SYSTEM WITH DIGITAL SIGNAL FROM DSP56 F805 FAMILY PROCESSOR

Signal processor is part of the family DSP56800 and belongs to class 16-bit processor, the fixed-point, manufactured by Motorola, is the most complex family. It includes all the necessary peripherals and control procurement system in real time. Calculation speed is very high, tens of millions of instructions per second (MIPS), which allows implementation of sophisticated algorithms.

CPU power signal is enhanced by the existence of a very strong package of software development (SDK - System Development Kit) that allows you to write algorithms in high level languages without a significant increase in computing time. Besides software development environment, the processor comes with a hardware development board, which facilitates much effort to implement the control scheme.

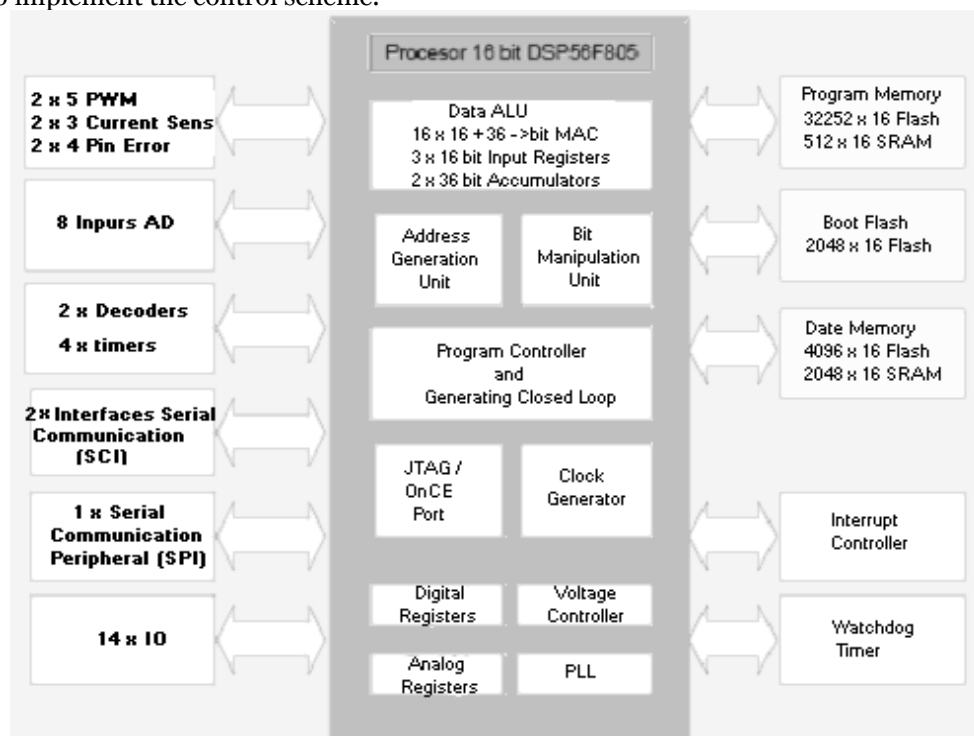


Fig.2.1. The principle scheme DSP56F805

Essential characteristics of the digital signal processor are listed below. Schematic diagram of the component blocks is presented in Fig. 2.1 .

The processor is built on a modified Harvard architecture, with three execution units, able to carry up to six instructions per cycle, or three memory locations to access data or programs, simultaneously. It can execute 40 million instructions per second (MIPS) at a frequency of 80Mhz internal work.

Internal features DSP (core) - site can be grouped as follows:

- ❖ 16x16 36-bit - parallel multiplier accumulator (MAC) in a single cycle
 - ❖ Implementation of hardware DO loops and REP
 - ❖ Three internal address bus and an external
 - ❖ Four internal data bus and an external
 - ❖ Parallel instruction set with unique addressing modes
 - ❖ Instruction set compatible with that of microcontrollers
 - ❖ Two 36-bit accumulators, including extension of mark
 - ❖ 16-bit bidirectional shifter
 - ❖ Internal memory
 - ❖ 32,252 words on 16-bit program memory (FLASH)
 - ❖ 512 words 16-bit program memory (RAM)
 - ❖ 2k words 16-bit data memory (RAM)
 - ❖ 4k words 16-bit data memory (FLASH)
 - ❖ 2k words 16-bit boot memory (FLASH)
 - ❖ Possible memory expansion Up to 64k program and 64k data
 - ❖ JTAG interface for debugging programs / OnCETM
- Peripherals embedded in DSP56F805 are:
- ❖ Second PWM signal generating modules, each with 6 outputs, three inputs of sense of current four error inputs, generating PWM dead time
 - ❖ Two 12-bit digital analog converters with parallel conversion and 2x4 input multiplexed, the port be synchronized with the PWM module
 - ❖ Two quadrature decoders, each with four entries
 - ❖ Two hours dedicated
 - ❖ Two serial communication interface (SCI)
 - ❖ Serial peripheral interface (SPI)
 - ❖ Two dedicated external interruptions
 - ❖ CAN 2.0 A / B (Controller Area Network)
 - ❖ 14 output ports of entry for general use; 18 ports multiplexed
 - ❖ Programmable PLL
 - ❖ Internal voltage regulators for digital and analog circuits to reduce cost
 - ❖ Supports standby and stop
 - ❖ Manufactured in CMOS technology (5V), supports digital TTL inputs
 - ❖ Single power supply 3.3 V

PWM pulse generation block provides considerable flexibility in configuration. It has the following characteristics:

- ❖ Three pairs of complementary pulse generation channels, or six channels independent
- ❖ Dead time insertion software
- ❖ Current status or via pulse correction software
- ❖ Polarity control to arm up or down inverter
- ❖ Resolution 15-bit pulse setting
- ❖ Programmable protection fault condition

Digital analog converters provide optimum control algorithm necessary. Is it possible to plan how to read their policy. Is the input voltage between 0 and 3.3V. Offset can be set for each channel, and maximum or minimum allowable to digital output. ADC units can work synchronized with the PWM unit. As the PWM generation unit, this unit is assigned its own disruption. Conversion during the 8 channels in the U.S. is 5.5 mode simultaneously.

DSP56F805EVM development board features:

DSP56F805EVM development board is built to facilitate the development of specific applications DSP56F805 signal processor. These include: electric drive applications, remote communications, modems, automatic telephone response, optical cameras. The plate is designed so that the user can easily run and debug programs and data on the host computer. This is done through JTAG interface / OnCETM - which allows software debugging and modification of various internal registers of the processor in real time.

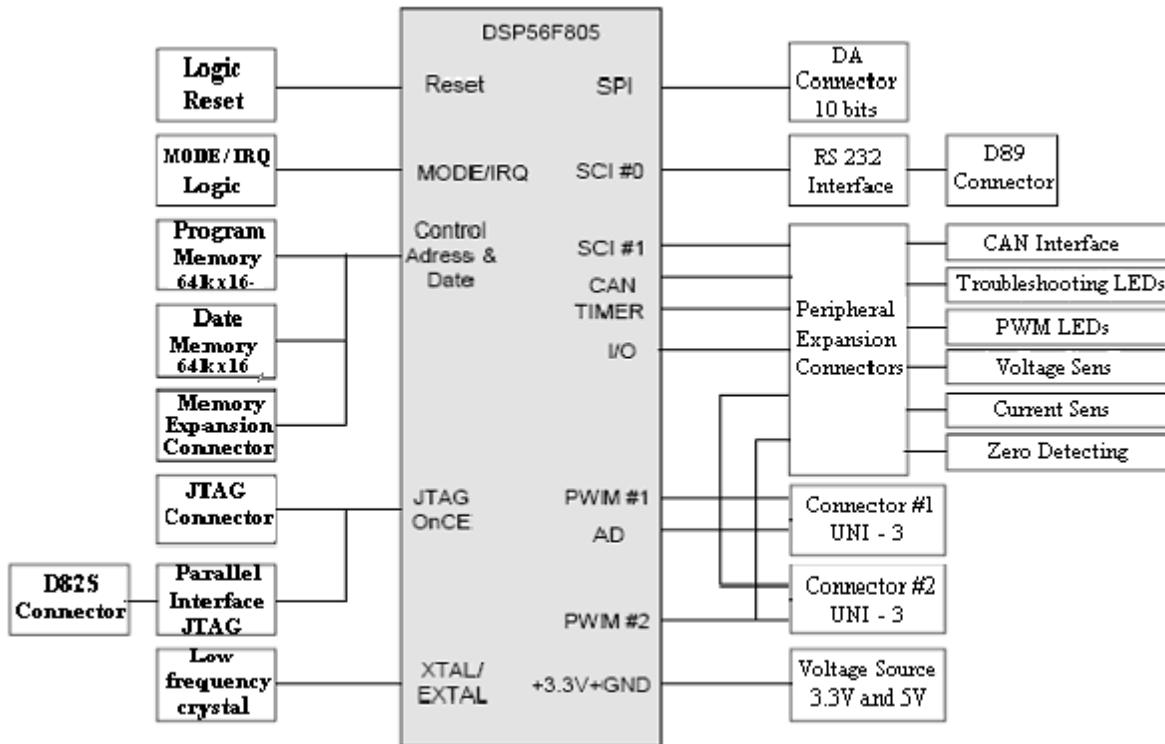


Fig.2.2. Block diagram of DSP56F805EVM

Hardware development can also be very easy, user can connect with existing system in November peripherals, and disconnect peripherals that are not necessary. For this special plugs are designed for specific ports and control and communication applications. Block diagram is shown in Figure 2.2.

The main components of plaque development are described below:

- ❖ DSP56F805 signal processor internal working frequency 80Mhz
- ❖ Rapid static external memory (FSRAM) with the following configuration
- ❖ 64k x 16 program memory 70Mhz
- ❖ 64k x 16 70Mhz data memory
- ❖ Analog digital converter with four channels 10-bit SPI interface
- ❖ Frequency oscillator to generate the DSP 8Mhz
- ❖ JTAG connector for debugging programs
- ❖ SCI interface for connection to a host processor
- ❖ 1Mbps CAN interface for fast communication
- ❖ UNI interface - 3 for engine control, I / O specific
- ❖ Connectors for I / O General purpose
- ❖ LED - sites for debugging programs
- ❖ LED - sites for PWM outputs
- ❖ Disruptions associated external buttons
- ❖ Buttons RESET and I / O
- ❖ Power source of 3.3V and 5V

Development board is connected via serial and parallel interfaces to the host computer (DB9 DB25 connectors respectively) connector UNI - 3 # 1 inverter and analog acquisition board.

Characteristics of software development:

Motorola offers a wide range of tools for generating and debugging code. Besides these there is a business application developed by Metrowerks particular signal processor produced by Motorola, CodeWarrior. This software includes a C + + compiler, a macro assembler, a librarian, and editor of links, all with an easy to use graphical interface Tools for debugging and system integration including a simulator and a method of assessment.

For ease of software development DSP56F805 processor is a package of routines and specialized functions (Development System Kit). Package software development (SDK) contains predefined control peripheral functions (DSP routines PWM, ADC, etc.), electrical drives functions (Clarke, Park, etc.). C compiler generates machine code in a very efficient way, enabling this rapid development and implementation of control algorithms.

All these applications use for communication with the board JTAG/OnCETM interface development and parallel interfaces, existing host computer.

Manner of application development:

Complexity need to be controlled requires work in phases, with several intermediate stages of development. Simulators existence much easier the implementation effort, assessing system responses to control algorithms. After estimation follows the actual implementation of programs on the processor, while testing them if the values do not depend on the stand have a corresponding dynamic. It can even control the reaction test on samples of data obtained from simulations made in advance, without providing any service bench.

The final phase is starting to stand algorithm implemented, the acquisition of control variables and comparing them with values obtained by simulation.

Phase I - Simulation

Control algorithm is simulated in Simulink - Matlab, so the model should be implemented as close as possible to reality. The results are analyzed, and extrapolated to the real case, eliminating possible simplifying assumptions made in the simulation. If the solution is convenient pass to the next stage.

Phase II - Implementation of the DSP algorithm

Write control program for the DSP. Using both C language and assembly language-specific processor, the compiler is used with CodeWarrior SDK package. Along the way, to create intermediate steps to test the algorithm - partial results of the control is highlighted with embedded debugger (to view specific areas of memory, CPU registers), or towards the end, when appropriate, values are saved in memory card development on the host computer's hard disk using the communication program (TTY.exe). If the results are similar, it's case to move to the next stage.

Phase III - Implementing the algorithm on bench

The program is developed in the previous phase test bench. At the end of the test are saved and the data acquired control with communication program. These are viewed in Matlab and compared with those obtained by simulation. If the results are similar, the development application is deemed complete.

3. DEDICATED PROGRAMME FOR DSP56F805 PVM TYPE OF ORDER INVERTER ACTIVE FILTERS

```
#include <stdio.h>
#include "805registers.h"
void init_PWM(void);
void init_PORTB(void);
void intr_PWM(void);
int contor=0;
int var=0;
int test=0;
void main(void)
{
  init_PWM();
  init_PORTB();
  // set PWM_reload interrupt vector
  asm {
    move #S0076,r0          // PWMA_reload interrupt vector adress
    move #Se9c8,a          // JSR
    movem a,p:(ro)+
    move #intr_PWM,a       // 3 means no address, no there is value
    movem a,p:(ro)+
  };

  // PWM values
  *gpr14 = 0 x 7000;        // set level 7 for PWM_reload
  *pwmctl1 = 0 x 50e0;     // divide by 8 and 6 in6! ----->25 Hz
                          // PWM Channel 0 Value Reg.
  *pwmval0 = 0 x 4000;    // PWM Channel 1 Value Reg.
  /*pwmval1 = 0 x 0fa0;   // PWM Channel 2 Value Reg.
  *pwmval2 = 0 x 4000;    // PWM Channel 3 Value Reg.
  /*pwmval3 = 0 x 0fa0;   // PWM Channel 4 Value Reg.
  *pwmval4 = 0 x 4000;    // PWM Channel 5 Value Reg.
  /*pwmval5 = 0 x 0fa0;
  // enable all interrupts
  *ipr = 0 x fe12;
```

```

// Enable maskable (Level 0) interrupts
asm {bfclr #S0002,X:S0e00};
// set LDOK; 0e00 ----->pwmctl
asm {bfset #S0002,X:S0e00};
//set PWM_Enable; 0e00 ----->pwmctl
asm {bfset #S0001,X:S0e00};
while (1)
{
    test++;
    // if (test>20) goto stop;
};
stop;
asm { bfset #S0001,X:S0e00} ;
while (1)
{
    test++;
    // if (test>20) goto stop;
};
stop;

asm {bfclr #S0001,X:S0e00} ; // desable PWM
}
// ISR -----> PWM_reload
void intr_PWM (void)
{
asm{ bfclr #S0010,X:S0e00 } ; // Interrupt acknowledge; 0e00 ----->pwmctl
*ipr = 0 x 0000; // disable all external interrupts
// test++; //timp
var++;
if (var>0)
{
    var = 0;
    contor++;
    if(contor>8) contor=;
    *pbdr = contor;
};
*ipr = 0 x fe12; // enable all interrupts
asm (bfcl #S0200, sr); // Enable maskable (Level 0) interrupts
}
//initializare PORTB ca port de iesire
void init_PORTB(void)
{
    *pbiar = 0 x 0000;
    *pbien = 0 x 0000;
    *pbipol = 0 x 0000;
    *pbiesr = 0 x 0000;
    *pbper = 0 x 0000;
    *pbddr = 0 x ffff;
}
void init_PWM(void)
{
    pwmctl = 0 x 0000; //PWM Control Reg.
    pwmfct1 = 0 x 0000; //PWM Control Reg.
    pwmfsa = 0 x 0000; //PWM Fault Status & Acknowledge Reg.
    pwmout = 0 x 8000; //PWM Output Control Reg.
    pwmcnt = 0 x 0000; //PWM Counter Reg.
    pwmcn = 0 x 7fff; //PWM Counter Modulo Reg.
    pwmval0 = 0 x 0000; //PWM Channel 0 Value Reg.
    pwmval1 = 0 x 0000; //PWM Channel 1 Value Reg.
    pwmval2 = 0 x 0000; //PWM Channel 2 Value Reg.
    pwmval3 = 0 x 0000; //PWM Channel 3 Value Reg.
    pwmval4 = 0 x 0000; //PWM Channel 4 Value Reg.
    pwmval5 = 0 x 0000; //PWM Channel 5 Value Reg.
    pwmdeadtm = 0 x 002f; //PWM Deadtime Reg.
    pwmdismap1 = 0 x 0000; //PWM Disable Mapping Register 1
    pwmdismap2 = 0 x 0000; //PWM Disable Mapping Register 2
    pwmcfg = 0 x 0000; //PWM Config Register
    pwmccr = 0 x 0000; //PWM Channel Control Register.
    pwmport = 0 x 0000; //PWM Port Reg.
}
    
```

4. CONCLUSIONS

In this paper we presented the general principles used in order active filters. On the basis of a program designed to drive filters through DSP56F805.

REFERENCES

- [1.] Abellan, A. Benavent, J. M. (2001). "A New Combined Control Method for Shunt Active Filters applied to Four-Wire Power Systems", EPE 2001 – Graz
- [2.] Afonso, J. Couto, C. Martines, J. (2000) "Active Filter with Control Based on the p-q Theory", IEEE Industrial Electronics Society Newsletter, Vol. 47, No. 3
- [3.] Aredes, M. Watanabe, E. H. (1995) "New Control Algorithms for Series and Shunt Three-phase Four-Wire Active Power Filters", IEEE Transaction on Power Delivery, Vol. 10, No. 3
- [4.] Fujita, H. Akagi, H. (1998). "The Unified Power Quality Conditioner: The Integration of Series and Shunt-Active Filters", IEEE Transactions on Power Electronics, Vol. 13, No. 2





¹Rastislav PIRNÍK, ²Ján HALGAŠ, ³Martin ČAPKA

NON-INVASIVE MONITORING OF CALM TRAFFIC

¹⁻³ UNIVERSITY OF ŽILINA, FACULTY OF ELECTRICAL ENGINEERING,
DEPARTMENT OF CONTROL AND INFORMATION SYSTEMS, ŽILINA, SLOVAKIA

ABSTRACT:

This paper deals with the use of video detection to identify the occupancy of a parking place from image information. The video detection comes in handy for cases of large and indented car parks. Suitably mounted camera can cover large area and software can locate from its images occupied places. The whole video detection system interprets the situation at car park and information about free parking places could be displayed on navigation panels guiding the drivers to the nearest free places. An added value for the management is the real-time video overview about the situation.

KEYWORDS:

car park occupancy, car park management, video detection, object tracking, calm traffic

1. INTRODUCTION

Today, the frequently discussed problem is how to detect the occupancy of parking places at institutions, park-and-ride areas, shopping centres etc. If there is a way of reliable detection of occupancy of parking place, it could be used for many commercial and security applications as well. Targeting this domain, there was realised a project “Non-invasive monitoring of calm traffic”. It solves the problem of recognition of occupancy of parking places at the University of Žilina by using the video detection.

2. ESTIMATION OF CAR PARK OCCUPANCY RATE.

Every kind of car park has its own limited capacity of parking places given by areal possibilities. Already all accessing roads can be considered as a part of the car park system. Depending on many factors, the information about occupied parking places can differ from the real situation. This could lead to misinformation of drivers searching for a parking place. So an early and advisable consideration that the car park is full can prevent the ineffective navigation. The estimation of the maximum rate of occupancy to declare the car park as full depends on type, complexity, area and many other criteria. Generally there are hints helping to estimate the moment to declare the car park as full:

- ❖ To gain information about vehicles routing from/to car park
- ❖ To use zone detection and zone navigation in cases of complex car parks
- ❖ To use time zones during the day with different upper limits to declare the car park as full
- ❖ To leave a gap to take into accounts some critical situations (fire, police, ambulance, guests, etc.)
- ❖ To take into account the capacity and characteristics of car park

3. METHODS FOR OBJECT DETECTION AND TRACING

The content of every image (regardless if standalone or in a video sequence) can be divided into several levels of abstraction hierarchy [4]. The first one consists of pixels, elementary parts of every digital image, containing information about brightness or colours. The next level is aimed at features as edges, corners, curves, areas, etc. The upper level of abstraction combines and interprets this information as objects and their attributes. The top level uses concepts of processing and

analyzing of images similar to human perception. These methods couple individual objects and define relations between them. The process of detection of an object in video sequence includes the step of catching its occurrence and locating it as accurate as possible in individual frames for further processing. The principle of tracking the object is generally based on processing the detected changes of its location, size, and shape in consecutive frames. Basic methods used to detect objects:

- ❖ Detection of objects based on their features
- ❖ Detection based on shape
- ❖ Detection based on colour information
- ❖ Detection based on pattern matching
- ❖ Motion detection

4. CAMERA POSITION

The position of a camera is important to effectively use its images. Therefore this fact has to be taken into account for every car park individually when using a video detection system. There are generally following two rules:

- ❖ place the camera to cover most parking places
- ❖ place the camera to minimize overlapping of objects (e.g. van vs. sport car)

In our case there were two possible views:

1. To shoot our experimental car park lengthwise, where all parking places were covered. But the problem was the height the camera to be placed (see Figure 1b). The farthest objects were overlapped. It is important to keep the ratio between the height h and length d as great as possible to reach higher point of view (Figure 1a)
2. To shoot the experimental car park broad wise, where the ratio was more suitable. Though the angle of view of the camera in this position was limited (Figure 2 - not all parking places were covered) it was sufficient to verify our algorithm to detect the occupancy of a parking place.

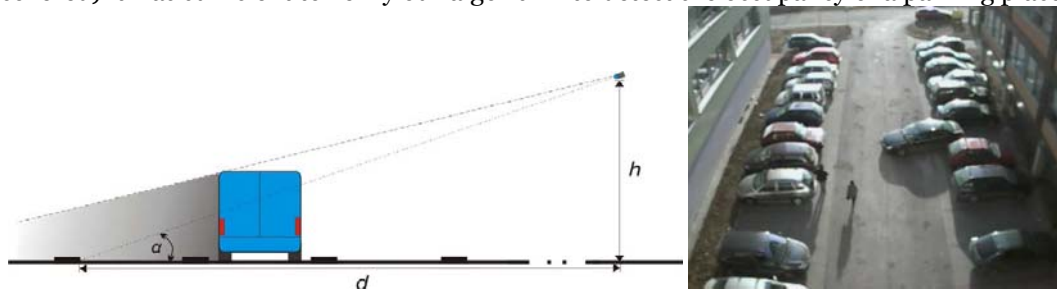


Figure 1. a) Overlapping the parking place by a vehicle, b) general view

5. STRUCTURE AND DESCRIPTION OF THE PROGRAMM

The program implements methods of detection of object based on its motion and colour information. It was written in the C++ language using the “OpenCV” – a library for computer vision. The source code was written according to the specification given in [1]. The structure of the application is explained in following text.

Definition of Region of interest - ROI

There are defined three ROI for each parking place. Two of them are used to gain relevant data (Figure 2: blue, the narrower ROI1, the wider ROI2). The ROI3 is used to visually inform about the occupancy of a parking place (Figure 2: green=free, red=occupied). For every ROI are defined four basic pixel values of its position in the frame: top, left, width and height.

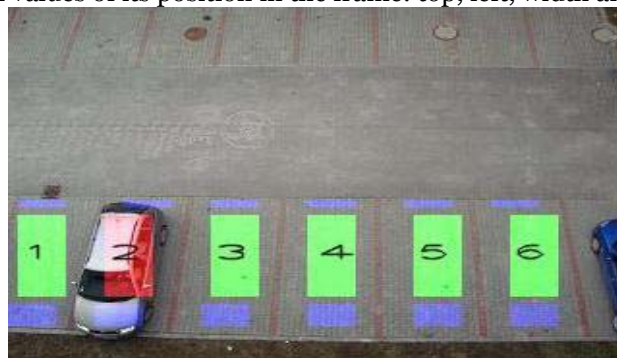


Figure 2. Example of ROI placement for parking places

Detection of moving object

For the proper run of the application it is important to accurately designate the moving objects and to interpret their impact on the parking place. Therefore the following schema illustrates the most important part of the application (Figure 3).

Block of initialization of variables

Definition and initialization of variables used during the application run for storing data

Block of getting image

The reading of image data into variables. There are three alternatives of getting the image data:

- ❖ Reading the video from connected camera (integrated webcam, camera connected through supported interfaces)
- ❖ Reading the video directly from a local storage in AVI format
- ❖ Reading the image directly from a local storage as a simple file

Block of conversion

Because of further processing, here takes the conversion from colour to greyscale place

Block R1

Because there is nothing before to compare with the first image, the application stores it in a variable to compare it with the next one.

Block of computation of changes

Computation of data changes takes place. Figure 4 shows us an example of detected changes in two consecutive frames.

Threshold block

The value of change for each pixel varies in range from 0 to 255. Processing such data structure would be complicated. Therefore a transformation to binary values is needed. It is important to set properly the threshold value [2]. The following example shows the presence of a shadow as an unwanted element when setting the threshold too low. The threshold value has to remove the artefacts and to preserve the best compactness of pixels of the moving object. The threshold value was estimated experimentally (Figure 5).

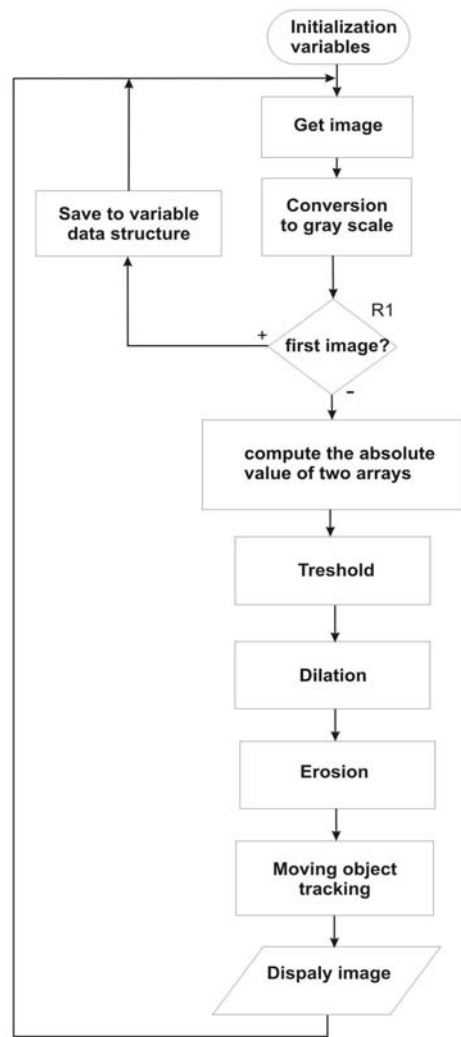


Figure 3. Block diagram of detection of a moving object



Figure 4. Example of comparing two consecutive frames in time of 0,5s

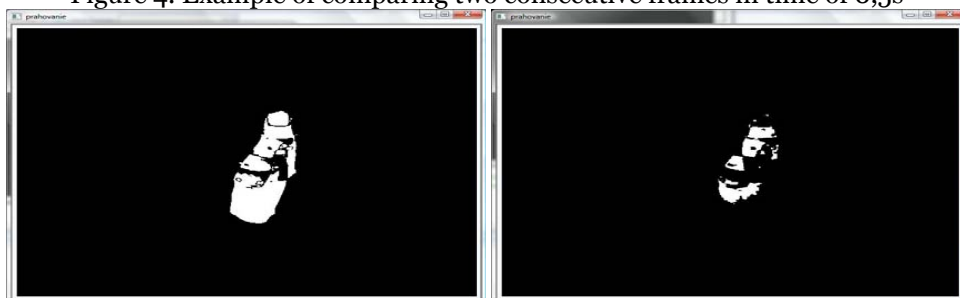


Figure 5. Example of using the threshold (values: left 35, right 80)

Blocks of dilatation and erosion

Even after an ideal threshold, the information about changed pixels will be insufficient to locate the moving object as a whole. To overcome this, several morphological transformations are used [3], [5]. The goal can be reached by their appropriate combination and properly set structural elements. All pixels of a moving object will be then compact. The modified binary image matches the moving object. In this state, there is no problem to find the object (Figure 6).

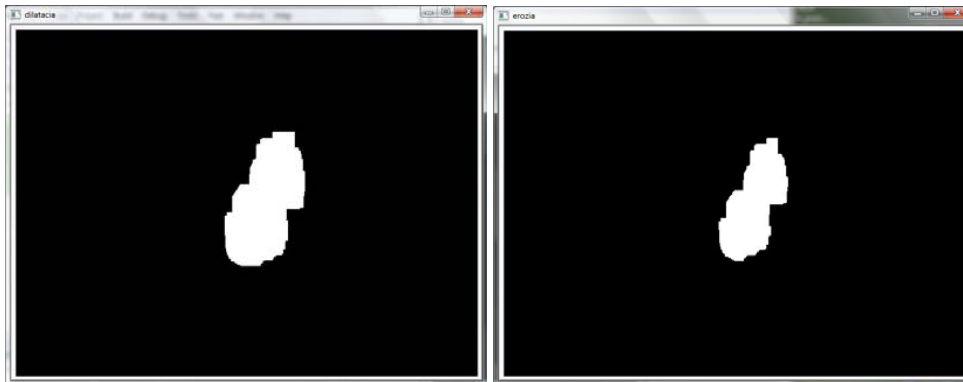


Figure 6. Example of an image dilatation (left) followed by erosion (right)

Block of moving object detection

Using mentioned modifications we can locate moving objects by finding their borders after the erosion step. The application gains data about the binary object and stores them. Based on the saved data as well, we can detect and display the moving object in actual frame to demonstrate this way the process we described.

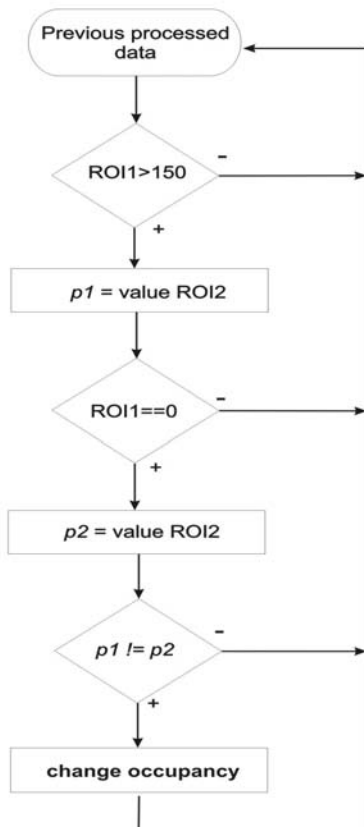


Figure 8. Algorithm of occupancy changes

proved at the car park of university (Figure 9, 10). The proper evaluation of parking place occupancy was only influenced by vehicles moving too fast.



Figure 7. Example of visual location of an object

The visual location of an object is done by a function drawing a rectangle around it (Figure 7). There are some limitations on accuracy according to the speed limits and refresh rate.

Evaluation of parking place occupancy

If required data for evaluation of occupancy are available (detected motion of an object in ROI1 and colour information from ROI2), the application is driven by the algorithm of evaluating changes of parking place occupancy (Figure 8.).

6. CONCLUSION

There was proposed an algorithm for evaluation of parking place occupancy by joining two methods of object detection. The algorithm is resistant to influence of weather conditions and walking pedestrians on car park. It is based on attributes of objects (speed and size of vehicles) that need to be detected. The functionality of the application was



Figure 9. Filling of parking places



Figure 10. Freeing of parking places

ACKNOWLEDGEMENT

This paper was supported by the operation program “Research and development” of ASFEU-Agency within the frame of the project “Nové metódy merania fyzikálnych dynamických parametrov a interakcií motorových vozidiel, dopravného prúdu a vozovky”. ITMS 26220220089 OPVaV-2009/2.2/03-SORO co financed by European fond of regional development. “We support research activities in Slovakia / The project is co financed by EU”.

REFERENCES:

- [1.] HALGAŠ, J., *Riadiaci videodetekčný parkovací systém*: diplomová práca. Žilina: Žilinská univerzita v Žiline, 2010. 45s.
- [2.] HUDEC, R., *Snímanie obrazu*, vysokoškolská učebnica, EDIS, August 2008, 150 strán, ISBN 978-80-8070-880-1.
- [3.] R. HUDEC, M. BENČO: Systém automatickej identifikácie dopravných priestupkov, Medzinárodná konferencia „Research in Telecommunication Technology 2006“, Part II. pp. 133-136, September 11th - 13th 2006, Nové Město na Moravě, Czech Republic, ISBN 80-214-3243-8.
- [4.] JURÍŠICA, L. - HUBINSKÝ, P. - KNOT, J. *Detekcia a sledovanie objektov*. In *AT&P journal*. [online]. 2005, číslo 6. www.atpjournal.sk/casopisy/atp_05/pdf/atp-2005-06-69.pdf
- [5.] P. LUKÁČ, M. BENČO, R. HUDEC, Z. DUBCOVÁ: Color image segmentation for retrieval in large image-databases, TRANSCOM 2009, pp. 113-116, Žilina, Slovakia. ISBN 978-80-554-0039-6.





SENSOR NETWORK FOR VEHICLES TRANSPORTING DANGEROUS GOODS

^{1, 3} UNIVERSITY OF ŽILINA, FACULTY OF ELECTRICAL ENGINEERING,
DEPARTMENT OF TELECOMMUNICATIONS AND MULTIMEDIA, ŽILINA, SLOVAKIA
^{2, 4} UNIVERSITY OF ŽILINA, FACULTY OF ELECTRICAL ENGINEERING,
DEPARTMENT OF CONTROL AND INFORMATION SYSTEMS, ŽILINA, SLOVAKIA

ABSTRACT:

The described sensor network has been designed to enable real-time monitoring of dangerous goods status during transport. The network is based on well known CAN bus which is widely used in automotive industry. The sensors measure temperature, LPG concentration, vehicle inclination and pressure. Status of the sensor is transferred via OBU into monitoring centre by GSM network.

KEYWORDS:

Sensor, LPG, inclination, temperature, pressure, CAN bus, on-board unit

1. INTRODUCTION

The dangerous good transport by road network is everyday threat for population and environment close roads which are being used for these transports. Despite of respecting of all regulations there always exists possibility of technical failures, crashes and malfunctions. For elimination of these risks an information system for the monitoring of the dangerous good transport has been developed. This system uses standard communication technologies GPS, GSM/GPRS and CAN (Controller Area Network). The whole project of dangerous goods transport monitoring was solved as a part of the project CONNECT [1] which was funded by the European Commission.

The sensor network for vehicles transporting dangerous goods has been designed to monitor selected parameters of the dangerous goods during transport. Conception of the sensor network is open to enable flexible selection of number and types of the sensor units. For connection to the vehicle OBU (On Board Unit) a standard industrial CAN bus has been selected. CAN bus is often being used in automotive industry for its robustness, resistance against the external environment and fault management [7]. Topology of designed sensor network is shown in Fig. 1.

2. CONCEPTION OF THE SENSOR UNITS

Because standard types of analog or digital sensor elements have not direct CAN bus interface the conception of intelligent sensor units has been selected. Every sensor is equipped with its own microcomputer which performs several functions: communication, diagnostic and data processing. During the design steps of sensor network the reliability and autodiagnostic properties have been emphasized [6]. The microcomputer of sensor unit periodically checks the checksums of program memory and configuration memory. Next diagnostic mechanism built in sensor unit is self test of used sensor elements. The simple sensor elements (contacts, temperature sensor etc.) are doubled and the microcomputer compares if both elements give similar data in the predefined tolerance field. All sensor units have the same block diagram which is in Fig. 2. Except for the sensor element the unit contains microcomputer with CAN bus support and driver of CAN physical

layer. The sensor unit has linear DC stabilizer for supplying of electronic circuits. The current consumption is from 50 to 80 mA in dependence on the sensor type.

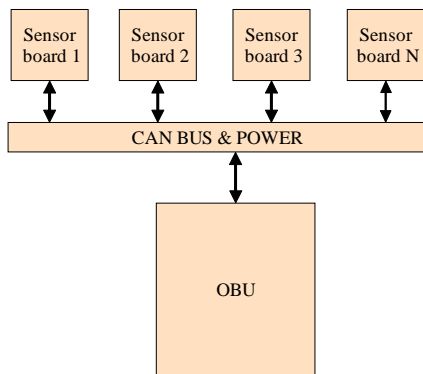


Figure 1. Interconnection of the sensor network

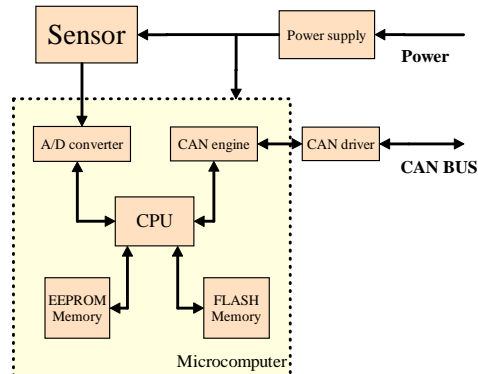


Figure 2. Block diagram of sensor unit

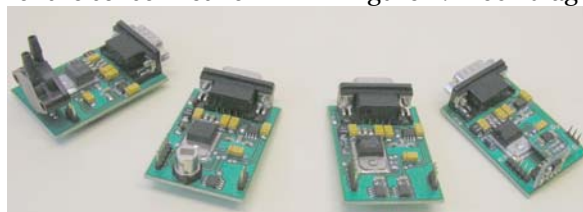


Figure 3. Functional samples of sensor units

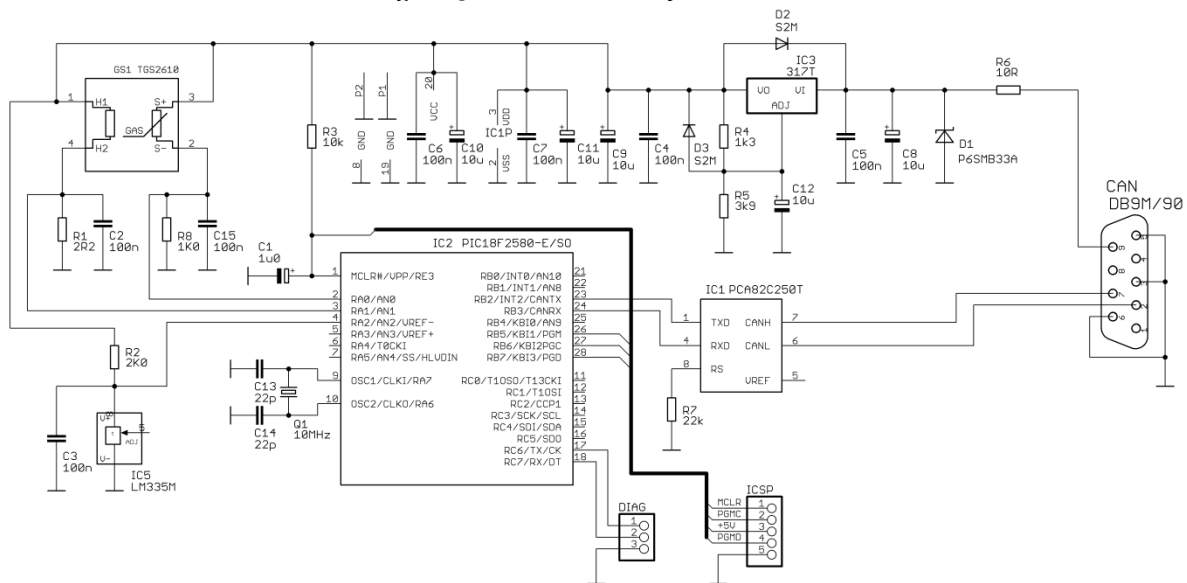


Figure 4. Schematic diagram of LPG sensor unit

For verification of selected conception these functional samples of sensor units have been designed and produced:

- ❖ Temperature sensor unit
- ❖ Gas detector unit (LPG)
- ❖ Unit for measurement of vehicle inclination and detection of overturning
- ❖ Unit for measurement of absolute or relative pressure of transported medium.

All four samples of sensor units are shown in Fig. 3, detailed schematic diagram of LPG concentration sensor is shown in Fig. 4 and detail of the vehicle inclination sensor is in Fig. 5.

Physical communication medium of vehicle sensor network is created by STP cable of category 5e which is mostly being used in local area networks. The cable has suitable impedance and wire cross section. One pair is used for data communication and next pair is used for powering of sensor elements. Other two pairs are not used. Connectors used in functional samples and their pinning are compliant with specification [2]. In case of real usage in vehicle environment more suitable cable and connectors will be chosen.

3. FIRMWARE OF THE SENSOR UNITS

Firmware of the sensor unit consists of several key parts which enable to perform all required functions. These functions are defined as follows:

- ❖ Initialization of sensor unit i. e. definition of input and output ports of microcomputer, initialization of A/D converter, CAN engine, interrupt system and loading of calibration constants.
- ❖ Autodiagnostic of the sensor unit consists from test of microcomputer [4] and test of sensor elements. The test of microcomputer is the same for all kinds of sensor units. During this test the checksums of program (FLASH) memory and configuration (EEPROM) memory are computed and compared with predefined values which are stored at the last addresses of program memory and configuration memory. The test of sensor element depends on the type of sensors. Temperature sensors are tested by comparison of values from two identical sensors placed close together. The test result is positive if absolute value of difference of both temperatures is less than predefined constant. Accelerometers and pressure sensors have self test mechanisms integrated and they can be activated by a logical signal from microcomputer. After activation of self test known value is added to sensor output voltage and the test result is positive if this voltage increase is registered by microcomputer. The LPG sensor is tested by monitoring of heating DC current which must be in predefined interval.
- ❖ Data processing - the sensor elements provide analog signals which are digitalized by 10 bit A/D converter built in the microcomputer. The sampling rate in all sensor units has been set to 8 kHz. This value is sufficient for processing signal spectrum generated by used sensors. In the next step the sampled signals are digitally filtered by averaging filter with length of 8 samples and decimated by ratio 1:8 because the computational power of used microcomputer is limited. From preprocessed signal the value of observed quantity is calculated in accordance with mathematical formulae given for sensor elements. For example, gas concentration (in ppm) can be calculated from these equations:

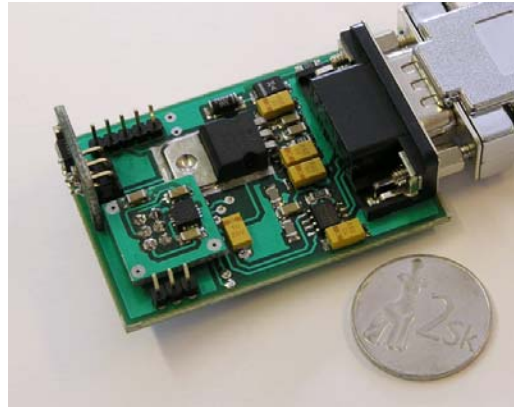


Figure 5. Detail of vehicle inclination sensor unit

$$C = 10^{-\frac{105 \cdot \frac{R_{S20}}{R_8}}{\alpha}} \quad (1)$$

$$R_{S20} = \frac{R_8}{T_{C1} \cdot R_{MEAS} + T_{C2}} \quad (2)$$

$$R_S = R_8 \cdot \frac{1004 - RES_{AD}}{RES_{AD}} \quad (3)$$

where α , K , T_{C1} , T_{C2} are specific constants for given type of gas sensor (Table 1), R_0 is sensor resistance at gas concentration 1800 ppm and temperature 20 °C, R_S is sensor resistance before temperature compensation, R_{S20} is sensor resistance after temperature compensation (2), R_8 is 1 kΩ resistor in series with the sensor (see Fig. 4) and RES_{AD} is the result of A/D conversion. The calculations are performed in the space of integer numbers. In the calculation process the compensation and calibration data are taken into account. If the result values exceed the boundary values an alarm message is sent into the OBU.

- ❖ The communication with the OBU is on the physical and data link layers performed by the CAN bus controller which is integrated into the microcomputer. The CAN controller after proper configuration performs all needed communication functions without CPU intervention. For communication on the application layer a simple protocol has been designed. The role of the CPU is to read and write data and configuration registers of the CAN controller, evaluation of its status, receiving of commands from the OBU and sending responses or alarms to the OBU.

4. COMMUNICATION PROTOCOL ON THE APPLICATION LAYER

A simple communication protocol has been designed for communication between sensor units and the OBU. Standardized application protocols working on the CAN bus (CANOpen, DeviceNet) have not been used for their complexity. The protocol is based on command – answer principle. Protocol data units are transferred by using standard data frames with 8 octet data field

in accordance to CAN 2.0A specification [3]. The PDU structure is given in the Table 2. The CAN message identifier (11 bits) is used to address group of sensor units which measure the same quantity (000H – OBU, 010H – inclination sensors, 020H – pressure sensors, 030H – gas sensors, 040H – temperature sensors). The sensor unit uses CAN filter to select only the messages relevant for its group. The whole sensor network is addressed by message with identifier 000H. Individual sensors can be addressed on the application layer by the 16 bits sensor unit number SENS_NBR.

The command, answer or alarm is identified by the CMD_ID/ANS_ID field (Table 3).

Table 1. The Constants for LPG Sensor FIGARO TGS2610

α	K	T_{C1}	T_{C2}	R_0
0.5413	57.82	-0.02	1.4	1.46 k Ω

Command parameters or measured values are transferred in the fields VAL₁_L – VAL₀_H. If longer message must be fragmented the field MES_NBR gives number of fragments (4 bits) and fragment order (4 bits). An example of communication shows Fig. 6.

Table 2. Structure of The PDU

ID	D ₀	D ₁	D ₂	D ₃	D ₄	D ₅	D ₆	D ₇
SENS_I D	CMD_ID/ ANS_ID	MES_NBR	SENS_NBR_ L	SENS_NBR_ H	VAL_1_L	VAL_1_H	VAL_0_ L	VAL_0_ H

Table 3. Definition of Commands, Answers and Alarms

CMD_ID/ ANS_ID	TYPE	Description
00H	CMD	Get sensor unique identifier
01H	ANS	Number of sensor unit
02H	CMD	Set number of sensor unit
04H	CMD	Get sensor unit status
05H	ANS	Sensor unit status
06H	CMD	Get actual sensor data
07H	ANS	Actual sensor data
08H	CMD	Set sensor limit value
0AH	CMD	Get sensor limit value
0BH	ANS	Sensor limit value
0DH	ALM	Upper limit exceeded
0FH	ALM	Lower limit exceeded
11H	ALM	Sensor error
12H	CMD	Sensor reset
13H	ANS	OK
15H	ANS	Error

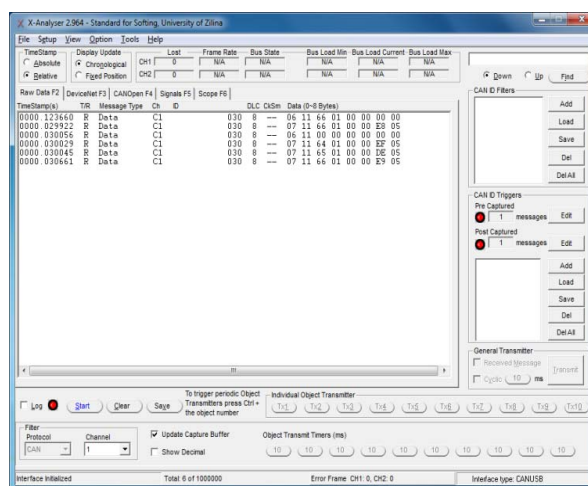


Figure 6. Snapshot of CAN protocol analyzer

Example of communication among the OBU and the sensor units shows the measurement of LPG concentration. Three gas sensors with identification numbers SENS_NBR 0164H, 0165H and 0166H respectively have been used and they have been placed into environment with LPG concentration approximately 1500 ppm. The first two lines in Fig. 6 show communication between the OBU and the sensor with number 0166H which returned value 05E8H (1512 ppm), the third line shows multicast communication from the OBU to the sensors (SENS_NBR=0000H). Last three lines are answers from all three sensor units, respectively.

5. CONCLUSION

The project CONNECT [1] solved in domain 4 (Traveler Information Services) and in its subdomain 4.9 problems of creation “Dangerous goods monitoring and information system.” At present a new project EasyWay [5] continues in solving of similar themes focused on intelligent transport systems.

The described design of the sensor network is an integral part of the subdomain 4.9 system solution. For the test purposes three sets of OBUs and sensor networks have been manufactured. The tests have been performed on the territory of north Slovakia by staff of Transport Research Institute, Inc. and University of Žilina. Results of the tests prove full functionality of manufactured OBU prototypes, sensor networks and real time data transfer into the monitoring centre. Next development will be focused on design of new sensor units, for example “black box” for road traffic accident analysis.

In addition to the technical development of the information system for dangerous good transport monitoring the questions about standardization and legislative are interested, for example the standardization of sensors in vehicles, integration of the various functions into the OBU, the international cooperation on dangerous good monitoring etc.

ACKNOWLEDGMENT

This work was created as a part of solution of international project “Coordination and Stimulation of Innovative ITS Activities in Central and Eastern European Countries – CONNECT“, TEN-T Programme EC. Project number: Addition no. 3 to Contract no. 472/VÚD 2002.

This work has been supported by the Grant Agency VEGA of the Slovak REPUBLIC, grant No. 1/0023/08 “Theoretical Apparatus for Risk Analysis and Risk Evaluation of Transport Telematic Systems.”

REFERENCES

- [1] CONNECT, Co-ordination and Stimulation of Innovative ITS Activities in Central and Eastern European Countries. [online]. URL <<http://www.connect-project.org/>>
- [2] CiA 303-1 DR V1.7: CANopen additional specification – Part 1: Cabling and connector pin assignment
- [3] CAN specification, Version 2.0. Robert Bosch GmbH. 1991. [online] URL <<http://www.semiconductors.bosch.de/pdf/can2spec.pdf>>
- [4] HOTTMAR, V., SCHWARTZ, L., TRSTENSKÝ, D.: End User Box for Interactive Cable Television. IEEE Transactions on Consumer Electronics, May 2007, volume 53, number 2, pp. 412-416, ISSN 0098-3063
- [5] EasyWay. [online]. URL <<http://www.easyway-its.eu/>>
- [6] ZOLOTOVÁ, I., LANDRYOVÁ, L.: Knowledge model Integrated in SCADA/HMI System for Failure Process Prediction. WSEAS Transaction on Circuits and Systems, Issue 4, Volume 4, April 2005, pp. 309-318, ISSN 1109-2734
- [7] BALOG, R., BÉLAY, I., DORNER, J., DRAHOŠ, P.: Industrial Communications. Slovak Technical University, Bratislava, 2001, ISBN 80-227-1600-6 (in slovak)





¹Martin VYSOCKÝ, ²Pavol LIPTAI, ³Zuzana FARKAŠOVSKÁ

ACOUSTIC QUALITY OF ELECTROMOTOR

¹⁻³ TECHNICAL UNIVERSITY IN KOŠICE, FACULTY OF MECHANICAL ENGINEERING, DEPARTMENT OF ENVIRONMENTAL STUDIES AND INFORMATION ENGINEERING, KOŠICE, SLOVAKIA

ABSTRACT:

Article trial above all about acoustic quality of products, then relationship between source and recipient of noise. Concrete oneself dealt one of major sources a noise near appliance and it is a noise of electromotor. Electromotor is able to cause unfavourably on man and there are several criterion that are in this article designated. Modification on given spoil whether position of electromotor is able improve acoustic quality of products.

KEYWORDS:

electromotor, acoustic quality of products, appliance

1. INTRODUCTION

On introduction this contributions is needed to say, what this is in fact acoustic quality of products and why it is important for presentation. Noise us round everywhere about, at home, in the streets, in work, in industries, transport etc. But a noise we can to find on appliance too, whether already is going about fridge, washing machine or mixer and when is more friendly for man, thereby we can to talk about higher acoustic quality of products. It doesn't need to be quite eliminated, even though is this most ideal solution, but be enough, as far as is possible identify and partly lower.

2. ACOUSTIC QUALITY OF PRODUCTS

Designers make choices regarding structure, materials and components in a product. The tools they use should allow them to anticipate the effect of these choices on sound quality. This discussion recounts the role of psychoacoustics in product design and product acceptability and notes the results of that work in metrics for sound quality and consumer/ user perceptions about the product. [1]

Sounds of assistance can be displeased, but also can be luck to. Every engineer should be take note of product by managerial views, because analysis of acoustic signal, humane perception, design and coast-benefit analysis to general profit too are criterion for quality assurance of products. Responsibilities designer, whether manager is propose and try quality of products, remove limitations still during testing products and take to high-class product on market. All these products are before application on market testing and feigned. Important factor for arbitration qualities of products is department psychoacoustics.

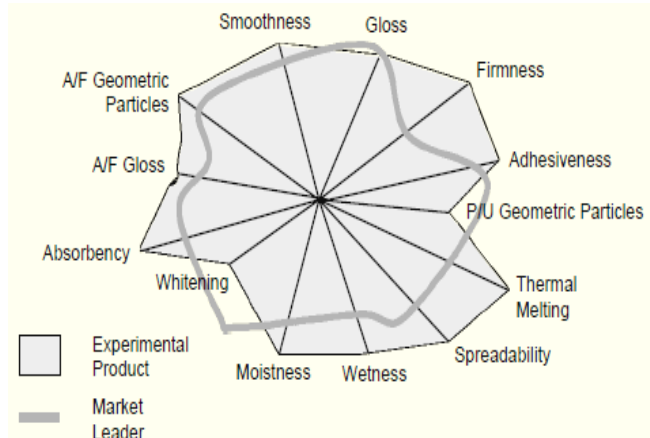


Figure 1. Sensory profiles of two skin care products [2]

Psychoacoustics is science or study that is dealt thereby, how given product perceive single man, and then centre his acoustic receptors on surroundings extraditing sound whether noise. Main aid of psychoacoustics is alternate testing, where people are asked to reception various sound, then are testing and there are additionally producing specific performance chart about sound. Industries use near for training experts a panel or "sensory profiles" (Figure 1.).[2]

3. SOURCES OF NOISE ELECTROMOTOR

Electromotor we can classify as one of major source of transmission sound from appliance and it is needed more closely present of this problem. Electromotor is machine, wherein is electric energy turn on kinetic energy revolving sections of electromotor, rotor. Electromotores utilize physical phenomenon electromagnetics, but there have been motores bottom on by other electromechanical phenomenon e.g . electrostatics, piezoelectric phenomenon and below. Every electromotor is unloaded from duo basic sections - statically boot immobile sections - stator, and mobile sections (usually spinning) rotor. (Figure 2.).

Between general sources of noise in electromotor belong:

- ❖ Unbalance of electromotor,
- ❖ Bearing of electromotor,
- ❖ Commutators,
- ❖ Aerosound (scoring on rotor).
 - a) Unbalance of electromotor

Concerning noise electromotor by his unbalance, is this narrowly linear just with vibration of rotor in electromotor, then given noise is doing single vibrations, it is unbalance rotor. We can to say, that unbalance is one from source judder.

Judder are considered as very suitable operating parameter, by that is possible assess AF - audio frequency dynamic construction sequence cases. On creation of vibration in construction sections of electromotor is sharing different sorts of source vibration, mainly recollection unbalance and further mechanical clearance of mounting, resonance of construction, abnormal wear bearing or snap small shovel rotor.

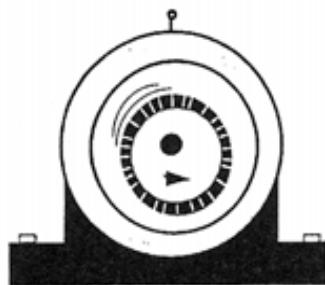
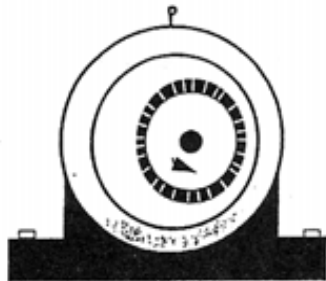


Figure 3. Drive vibrations in electromotor [6]

b) Bearing of electromotor

On part of electromotor in appliance are bearing, that are be instrumental to placing rotor in electromotor (Figure 4.). They are next possible of cause noise of electromotor and thanks for bearing is raising life of electromotor and products or appliance too.

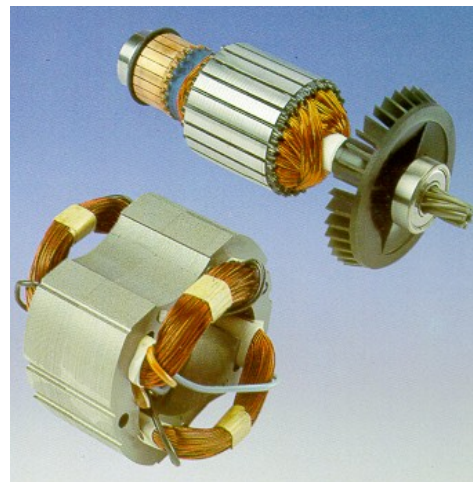


Figure 2. Electromotor of appliance

Suitable cap for creation exciting vibration in the working condition machinery is half-round placing rotor and stator of electromotor (Figure 3.). Inaccuracy production rigger ganglion (rotor - bearing - stator) and his consistent working resort influence mutual dynamic eccentricity to excitement vibration. [6].



Figure 4. Bearing of electromotor for appliance Source: <http://www.okokchina.com>

Good and effective diagnostics is able to prevent crash and meaningly to lower repair for costs. Providing electromotor allows timely revelation "inadmissible" technical conditions bearing with exchange bearing in optimally time in several tenth euro without serious after-effects or damage prominent sections of electromotor. If electromotor isn't monitoring, is able to come about disintegration of bearing, in pursuance of st. (under working arrangements) is rotary part aggravating stator and resort to destruction winding or to deformation mechanical sections and in extremeness case to complete destruction of electromotor. [4]

c) Commutators

Commutators (Figure 5.) create conductive half-ring uncross isolating layer. Every commutator is connected with one end of reel and act motion of rotation included with cateterisation. Brushes invariable one's position, and are conductivity connection with district and source. Commutator and brushes still baffle whereupon is reel turn on drowe energy. This machinery we are talking about electromotor.[5]



Figure 5. Commutator

Good commutation lead the way assumption of correct functions commutator to dress. Below concept commutation is understand complex march in reel winding rotor, that are near turning curl grind from influence one's pole below another pole. Near this change is through the medium commutator changing direction flow in reel. Volts every commutating reel, in who is turn direction flow, arrive together toward connecting briefly over brushes and lamella of commutator. [5]

d) Aerodynamic noise of electromotor

Tone noise is editing providing, when flow over blown space too. It's infliction shift of backward whirls, that are stroke on border wall and further are throw back about additional walls. Flow further and form new maelstroms (Figure 6.).

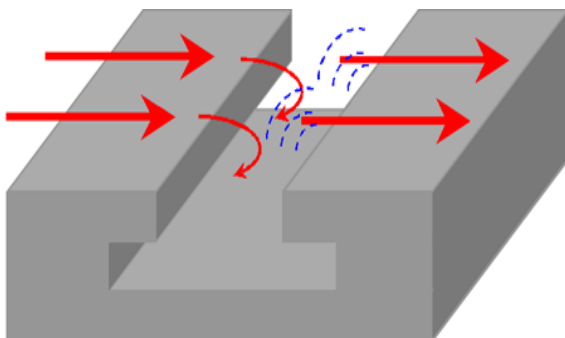


Figure 6. Flowinf of sound in hollow spaces [3]

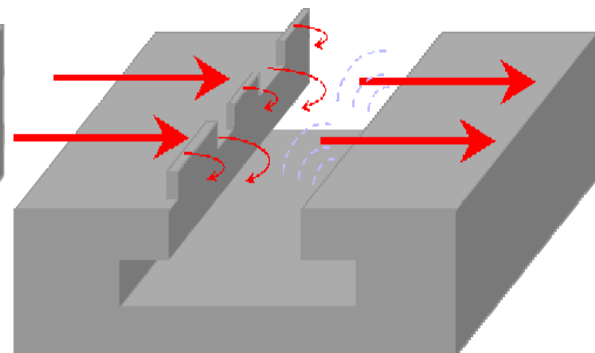


Figure 7. Measure for cut-down aerodynamic noise in hollow spaces [3]

Flowing acoustic coupling can be cut-down additional groove on front edge of sections walls (Figure 7.).

As a result is turbulence with different length weight and thereby creation small constructive sound of windy. In the last analysis is concerned the same thought, in to have be near falling noise around cylindral surface sections electromotor.[3]

4. CONCLUSION

This article apprised reader not only with acoustic quality of products and main sources of noise in electromotor for appliances too, but also abets possibilities of improvements acoustic qualities of products, then possibility noise reduction on electromotor.

Acknowledgement

This paper was supported by projects APVV-0176-071/0453/08 and KEGA 3/7426/09.

REFERENCES

- [1.] B. G. Churcher and A. J. King, "The Performance of Noise Meters in Terms of the Primary Standard," Journal of the Institute of Electrical Engineers, (London) Vol 81, pp 59-90, 1937.
- [2.] H. Fletcher and J. A. Munson, "Loudness, Its Definition, Measurement, and Calculation," Journal of the Acoustical Society of America, Vol. 5, pp 82-108, 1933.
- [3.] Aerodynamic noise electric motor: Available online 10.09.2010 on <http://www.diracdelta.co.uk/science/source/a/e/aerodynamic%20noise/source.html>
- [4.] Bearing of electromotor: Available online 15.09.2010 on http://www.atpjournal.sk/casopisy/atp_09/pdf/atp-2009-06-16.pdf
- [5.] Commutators: Available online 08.09.2010 on <http://lazo.czechian.net/elektrika/dynamo.htm>
- [6.] Unbalance of electromotor: Available online 26.09.2010 on <http://web.tuke.sk/fvtpo/casopis/pdf07/3-str-75-78.pdf>





A MICROWAVE IMAGING AND ENHANCEMENT TECHNIQUE FROM NOISY SYNTHETIC DATA

¹⁻². INSTITUTE OF RADIOPHYSICS & ELECTRONICS, UNIVERSITY OF CALCUTTA, KOLKATA, INDIA.

³ TATA INSTITUTE OF FUNDAMENTAL RESEARCH, INDIA

ABSTRACT:

An inverse iterative algorithm for microwave imaging based on moment method solution is presented here. The iterative scheme has been developed on constrained optimization technique and is certain to converge. Different mesh size for the model has been used here to overcome the Inverse Crime. The synthetic data at the receivers is contaminated with different percentage of noise. The ill-posedness of the problem is solved by Levenberg - Marquardt method. The algorithm is applied to synthetic data and the reconstructed image is then further enhanced through the Image enhancement technique.

KEYWORDS: Microwave Tomography, Levenberg-Marquardt Method, Inverse crime, Percentage noise, Image Adjustment

1. INTRODUCTION

For the last few decades, microwave tomography techniques for biomedical applications have been received increasing interest. Intensive studies in this field able to give an efficient solution to quantitative imaging. We had proposed several algorithms [1-2] which though reconstructed the image without any misfit, yet the mesh size remains the same both in the forward and the inverse problem leading to inverse crime. This paper represents an iterative algorithm based on Levenberg-Marquardt regularization technique with necessary considerations to avoid inverse crime. The reconstructed image is then undergone through image enhancement mechanisms to minimize the noise.

2. THE STUDY

During the past 20 years, immense research has been carried out in microwave tomography to quantitatively reconstruct the complex permittivity distribution of the biological media. Standard spectral diffraction tomography [3-7] which has been investigated with application to microwaves, prove to be very fast and capable of producing reconstructions with good quantitative accuracy for small contrast objects.

Yet it is subjected to various limitations, including the artifacts due to the diffraction effects in strongly inhomogeneous media where Born or Rytov approximations are not valid [8-9]. Several approaches based on moment methods [10-12] have, in past, been explored rigorously, but the stability depends on the measurement accuracy due to ill-conditioning of the matrix. Also the convergence depends on the contrast of the objective.

In recent years, multiplicative regularized contrast source inversion method is applied to microwave biomedical applications [13-14]. The inversion method is fully iterative and avoids solving any forward problem in each iterative step.

In our earlier works [15-16], we had suggested quasi-ray optic SIRT-style algorithms for microwave imaging. In those first generation algorithms it was assumed that only those cells situated within the beamwidth of the transmitter radiation pattern, would effectively contribute to the field at the end of a ray. Those linear and nonlinear algorithms did not reconstruct the image quantitatively to the extent which could be considered to be clinically important.

The earlier algorithms proposed by us [1-2] which, though reconstructed the image without any misfit, yet the same mesh size for both in the forward and the inverse problem leading to inverse crime. This paper represents an iterative algorithm with necessary considerations to avoid inverse crime.

3. ANALYSIS, DISCUSSIONS, APPROACHES AND INTERPRETATIONS

3.1. Forward problem

The forward problem has already been discussed in details in our previous work [2]. A cylindrical object of arbitrary cross section is considered here which is characterized by a complex permittivity distribution $\varepsilon(x,y)$. An electromagnetic wave radiated from an open-ended waveguide is used here for the illumination. The incident electric field E^{inc} is parallel to the axis of the cylinder.

The expression for the total electric field E is

$$\vec{E} = \vec{E}^{inc} + \vec{E}^s \quad (1)$$

where E_s represents the scattered field which is generated by the equivalent electric current radiating in free space.

The total electric field can be calculated with an integral representation

$$\vec{E}(x, y) = \vec{E}^{inc}(x, y) + \int_s \int_s (x, y) G(x, y; x', y') d x' d y' \quad (2)$$

where the Green's function can be given by

$$G(x, y; x', y') = -\frac{j}{4} H_0^2 \left(k \sqrt{(x-x')^2 + (y-y')^2} \right) \quad (3)$$

Here (x, y) and (x', y') are the observation and source points respectively.

The solution of the forward problem are carried out by moment method [17] using pulse-basis function and point matching technique. The synthetic data at the receivers is then contaminated with different percentage of noise as our main objective is to reconstruct the numerical model under noisy conditions.

3.2. Inverse problem

The aim of the inverse problem is to find a stable solution for permittivity distribution ε^* which minimizes the squared error output at the receivers i.e.

$$\|E(\varepsilon) - e\|_2^2 \quad (4)$$

where $e \in C^n$, the n electric fields we measure at receiver points,

$E: C^m \rightarrow C^n$, a function mapping the complex permittivity distribution with degrees of freedom into a set of n approximate electric field observations, and also $\varepsilon \in C^m$, the complex permittivity distributions with m degrees of freedom.

The Levenberg-Marquardt regularization technique for the minimization of the (4) leads to an iterative solution

$$\varepsilon_{i+1} = \varepsilon_i + \Delta \varepsilon_i \quad (5)$$

where ε_{k+1} is the permittivity distribution at the $k+1$ th iteration.

$\Delta \varepsilon$ can be written as

$$\Delta \varepsilon = (E'(\varepsilon)^\dagger E'(\varepsilon) + \lambda I)^{-1} E'(\varepsilon)^\dagger (E(\varepsilon) - e) \quad (6)$$

where E' is the Jacobian matrix, \dagger denotes the conjugate transpose, λ is a monotonically decreasing regularization parameter, I is the identity matrix, $E(\varepsilon)$ is the calculated electric fields at the receivers.

3.3. Numerical Model

To test our algorithm, we have considered the following model as shown in Figure 1.

It is a high contrast square biological object $9.6 \text{ cm} \times 9.6 \text{ cm}$ consisting of muscle and bone having complex dielectric constants $50-j23$ and $8-j1.2$ respectively at a frequency of 1 GHz. The object is kept immersed in saline water having complex dielectric constant $76-j40$.

The target is illuminated with TE fields radiating from an open ended dielectric filled wave guide having sinusoidal aperture field distribution. The transmitter is moved along four mutually orthogonal directions. For each of the transmitter positions along a particular transmitting plane, the received fields at eighteen locations in the other three orthogonal planes were measured theoretically at a frequency of 1 GHz.

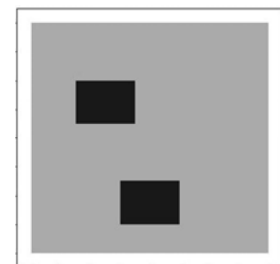


Figure 1. Numerical model

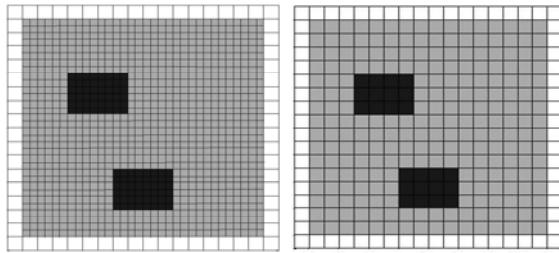


Figure 2. Meshes used to overcome the inverse crime (a) Mesh used in forward problem (b). Mesh used in inverse problem

Different meshes are used to overcome the inverse problem as shown in figure 2. The finer mesh is used in the forward problem (Figure 2(a)) whereas the inverse solver uses the coarse mesh (Figure 2 (b)).

In case of forward problem, the rectangular model is divided into 1024 square cells of dimension 0.3cm X 0.3cm and the saline water region is divided into 32 cells of dimension 0.6cm X 0.6cm. During the inverse problem, the rectangular model together with saline water region is divided into 324 equal

square cells $0.6 \text{ cm} \times 0.6 \text{ cm}$. The measurement set contains 288 independent data.

During the iterative reconstruction, the complex permittivity values of the cells filled up with saline water were assumed to be known, thus rendering the problem of estimating the complex dielectric constants of the remaining 256 cells.

3.4. RESULTS AND DISCUSSIONS

To apply the reconstruction algorithm, it was initially assumed that the biological medium is filled up with muscle only. The received fields at different receiver locations were computed for each transmitter position. The only priori information we have used in our algorithm is that the real part of the complex dielectric constant cannot be negative and the imaginary part cannot be positive. The iteration is stopped when the 2-norm error output is of the order of 10^{-4} .

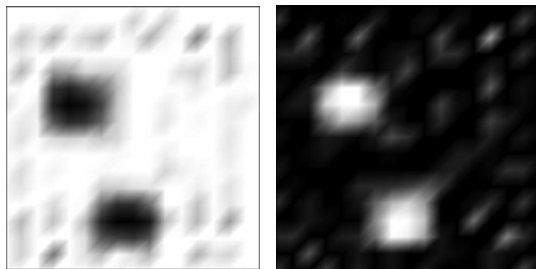


Figure 3. Reconstructed model with 1%noise (a) Real part (b) Imaginary part

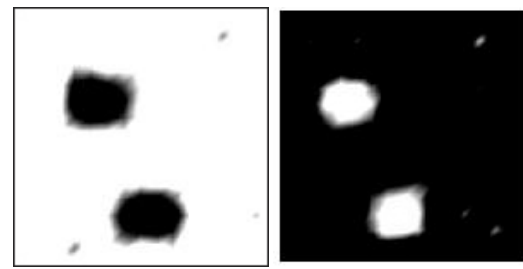


Figure 4. Reconstructed model with 1%noise after using image adjustment technique (a) Real part (b) Imaginary part

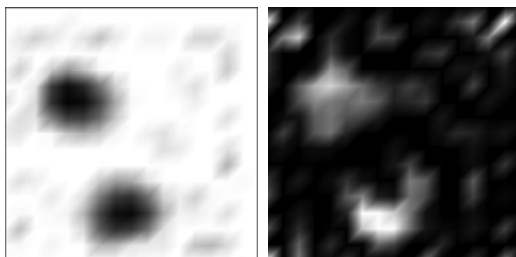


Figure 5. Reconstructed model with 2%noise (a) Real part (b) Imaginary part

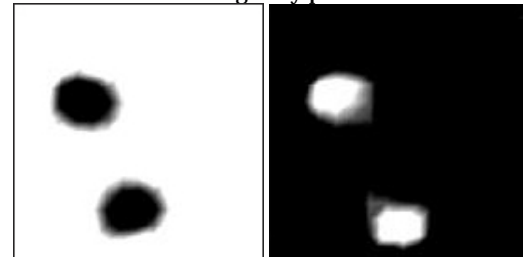


Figure 6. Reconstructed model with 2%noise after using image adjustment technique (a) Real part (b) Imaginary part

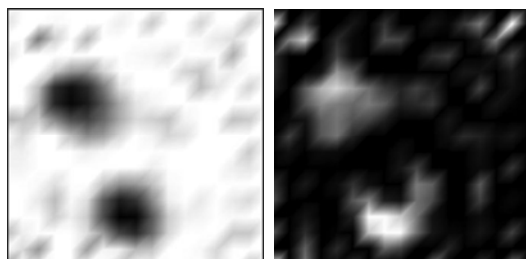


Figure 7. Reconstructed model with 5%noise (a) Real part (b) Imaginary part

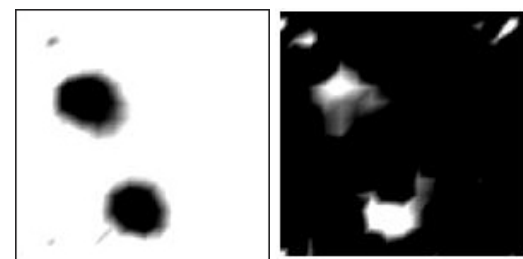


Figure 8. Reconstructed model with 5%noise after using image adjustment technique (a) Real part (b) Imaginary part

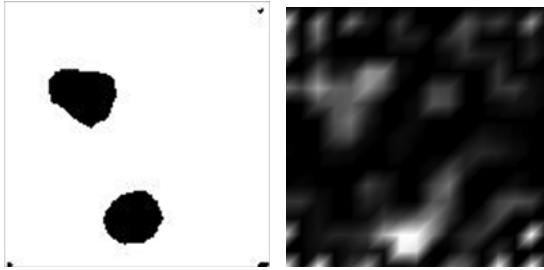


Figure 9. Reconstructed model with 10%noise (a) Real part (b) Imaginary part

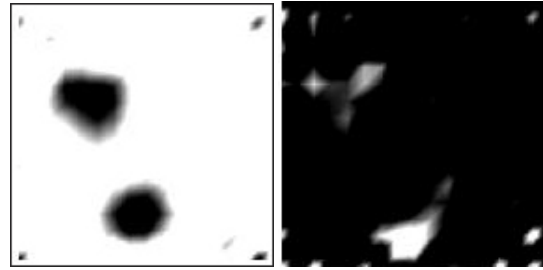


Figure 10. Reconstructed model with 10%noise after using image adjustment technique (a) Real part (b) Imaginary part

The reconstructed models for different percent of noise in the synthetic data are then undergone through image enhancement filter in particular through the histogram equalization technique to have an improved quality of reconstructed model in terms of noise. The figures 3 to 10 display the reconstructed models for different percent of noise and their enhancement in quality after using the Image adjustment technique.

4. CONCLUSIONS

Thus using the different mesh sizes in the forward and reverse problem, the inverse crime has been avoided in this proposed algorithm. Also the clarity of the reconstructed images for different percentage of noise has been improved through Image adjustment technique. This work can be further extended by incorporating different other regularization techniques along with other image enhancement techniques for a comparative study.

REFERENCES

- [1.] A.K.KUNDU, B.BANDYOPADHYAY "Reconstruction Algorithm for Microwave Tomography Using Iterative Regularized Gauss-Newton Method", International Conference on Computer and devices for Communication (CODEC 06), Kolkata, India, 2006
- [2.] B.BANDYOPADHYAY, A.KUNDU, and A.N.DATTA, "An Iterative Algorithm for Microwave Tomography Using Levenberg-Marquardt Regularization Technique", Ind J Pure & Appl Physics, 43, 649 – 653, 2005
- [3.] ADAMS F M & ANDERSON A P, Inst Elec Eng Proc-H, Microwaves, Opt, Antennas, 129(1982)83.
- [4.] BOLOMEY J C, IZADNEGAHDAR A, JOFRE L, PICHOT C , PERONNET G & SOLAIMANI M, IEEE Trans Microwave Theory Tech, 30(1982)1998.
- [5.] BOLOMEY J C & PICHOT C, Int J Imag Syst Tech, 1(1990) 119.
- [6.] DEVANEY A J, IEEE Trans Biomed Engg, 30(1983)377.
- [7.] RIUS J M, FERANDO M., JOFRE L & BROQUETAS A, Electron Lett, 23(1987)564
- [8.] SLANEY M., KAK A C & LARSEN L E , IEEE Trans Microwave Theory Tech, 32(1984)860.
- [9.] BOLOMEY J C, PICHOT C & GABORIAUD G, Radio Sci, 26(1991)541.
- [10.] NEY M N, SMITH A M & STUCLY S S, IEEE Trans Med Imaging, 3(1984) 155.
- [11.] WANG Y M. & CHEW W C , Int J Imag Syst Tech, 1(1989)100.
- [12.] CAORSI S, GAGNANI G L & PASTORINO M, IEEE Trans Microwave Theory Tech, 38(1990) 981.
- [13.] P.M. VAN DEN BERG and A. ABUBAKAR, "Contrast source inversion method: State of Art". Progress in Electromagnetics Research, PIER 34, 189-218, 2001
- [14.] ARIA ABUBAKAR, PETER M. VAN DEN BERG and JORDI J. MALLORQUI "Imaging of Biomedical data Using a Multiplicative Regularized Contrast Source Inversion method" IEEE transactions on Microwave theory and Techniqes. Vol. 50, No. 7, July 2002
- [15.] A.N. DATTA, and B. BANDYOPADHYAY, "An SIRT style reconstruction algorithm for microwave tomography", IEEE Trans. Biomed. Engg., vol 32, pp 719-723, 1985
- [16.] A.N. DATTA, and B. BANDYOPADHYAY, "Non-linear extension of moment method solution for microwave tomography", Proc. IEEE. vol. , pp.604 - 605, 1986.
- [17.] J.H. RICHMOND, "Scattering by a dielectric cylinder of arbitrary cross- section shape," IEEE Trans. Antennas and Propagation, vol. 13, No. 3, 334-341, 1965



¹ Pavel DRABEK, ² Martin PITTERMANN

CALCULATION OF INTERHARMONICS OF POWER ELECTRONIC CONVERTERS – USING OF HARMONIC ANALYSIS

¹⁻². UNIVERSITY OF WEST BOHEMIA IN PILSEN, FACULTY OF ELECTRICAL ENGINEERING,
DEPT. OF ELECTROMECHANICS AND POWER ELECTRONICS, CZECH REPUBLIC

ABSTRACT:

Paper deals with problems of using Fourier progression for harmonic analysis of unfavourable effects in power grid made by power semiconductor converters. Detailed theoretical analyze has been made and useful mathematical equations for interharmonics calculation were derived. Several simulations and experimental measurements for analytical calculation verification have been realized.

KEYWORDS:

Fourier Series, EMC, Harmonic Analysis, Interharmonics, Power Converters

1. INTRODUCTION

The power quality is primarily influenced by the electric appliances connected to the power grid. If a linear load such as resistive heater is connected to the power grid, the resulting current will be a sine wave and, therefore, only the fundamental frequency will be introduced. However, if the load is non-linear, drawing short pulses of current within each cycle, the current shape will be distorted (non-sinusoidal) and higher frequency current components (e.g. characteristic and non-characteristic harmonics, interharmonics – see Fig.1 and 2) will occur in the frequency spectrum of phase current.

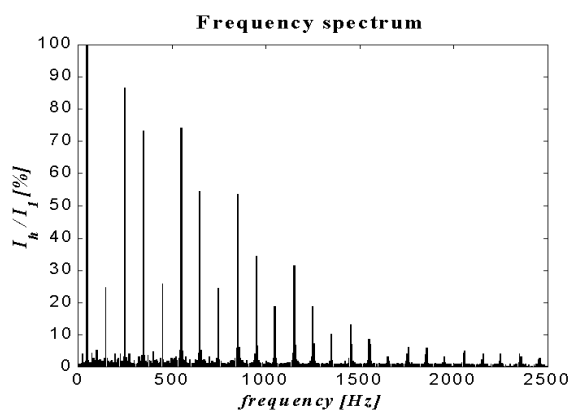


Figure 1. Frequency spectrum of phase current taken by uncontrolled 3phase bridge rectifier (e.g. frequency converter)

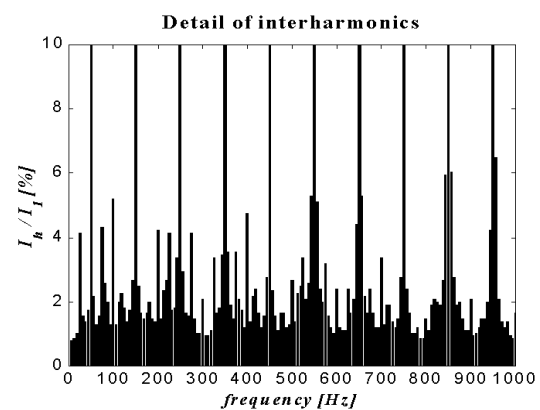


Figure 2. Detail of frequency spectrum of phase current with focus on interharmonic components (defined below)

Thus, the resulting current will be composed of the fundamental and higher frequency components. These frequency components are transferred to the power grid, where they can cause distortion of supply voltage, disturbance of connected equipment (e.g. ripple control devices, compensation units), etc [1,2].

This paper looks mainly at the problem how to calculate these harmonic components. According to standards the low-frequency interference is considered on a frequency range 2.5 kHz and the frequency components can be defined as follows:

- Harmonic $f = h \cdot f_1$ where h is an integer > 0
- DC $f = 0$ Hz ($f = h \cdot f_1$ where $h = 0$)
- Interharmonic $f \neq h \cdot f_1$ where h is an integer > 0
- Sub-harmonic $f > 0$ Hz and $f < f_1$

Where f_1 is the fundamental power system frequency (50 Hz).

2. HARMONIC ANALYSIS

For calculation of the frequency components in the power grid we can use Fourier progression which is defined for periodical functions. We can show its use at the following example of taken phase current of the 3-phase uncontrolled diode rectifier (see Fig.3). The typical waveform of a taken phase current under ideal operating conditions (symmetrical power supply, ideal power semiconductor devices, indefinite short circuit power etc.) is shown in Fig.4. The non-sinusoidal waveform of a phase current creates higher frequency current components. For the harmonic components calculation of phase current it is necessary to simplify the phase current wave as is shown in Fig.4.

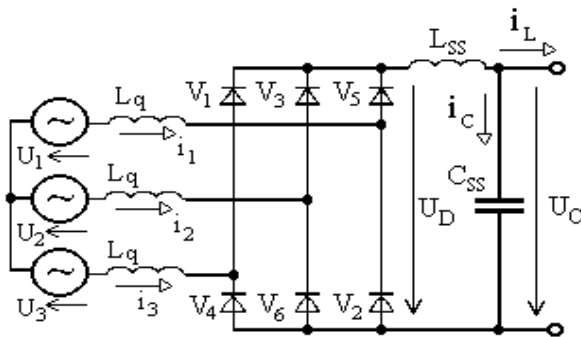


Figure 3. Three-phase bridge rectifier configuration

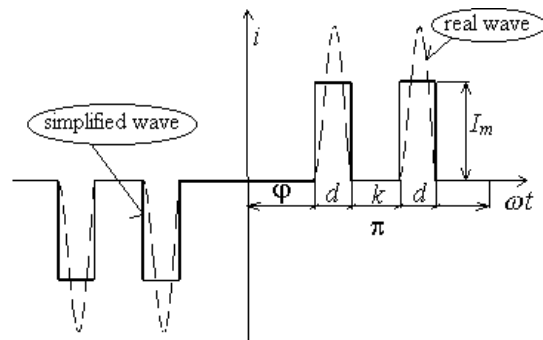


Figure 4. Real and simplified phase current wave

Amplitude I_m is constituted so that the area of both currents will be identical for the same parameter d (where d is a diode conduction time). From the figure it is obvious that used simplification is rough in commensurate with the value of parameter d . The error of used simplification decreases with the decreasing of parameter d and for small value d corresponds to reality.

Using the well-known quotation for Fourier analysis [1,3] we can calculate coefficients a_h and b_h :

$$f(t) = \frac{a_0}{2} + \sum_{h=1}^{\infty} [a_h \cos(h\omega t) + b_h \sin(h\omega t)]. \quad (1)$$

For Fourier coefficients valid:

$$a_0 = \frac{2}{T} \int_0^T f(t) dt, \quad a_h = \frac{2}{T} \int_0^T f(t) \cos(h\omega t) dt, \quad b_h = \frac{2}{T} \int_0^T f(t) \sin(h\omega t) dt, \quad h=1,2,\dots$$

Since the current waveform from Fig.4 is symmetrical odd function, coefficients a_h are zero and we can solve coefficients b_h only:

$$b_h = \frac{2}{\pi} \int_0^{\pi} i_f(\omega t) \sin(h\omega t) d\omega t \quad (2)$$

After editing we will get:

$$b_h = -\frac{4I_m}{h\pi} \left[\sin\left(\frac{hk}{2}\right) - \sin\left(\frac{hk}{2} + hd\right) \right] \cdot \sin\left(\frac{h\pi}{2}\right)$$

For symmetrical power network is valid $d+k=600$ and relation (2) we can convert to:

$$b_h = \frac{8I_m}{h\pi} \cdot \sin\frac{hd}{2} \cdot \cos\frac{h\pi}{6} \cdot \sin\frac{h\pi}{2} \quad (3)$$

The Back expression of current i by Fourier progression is:

$$i_f(\omega t) = \sum_{h=1}^{\infty} \frac{8I_m}{h\pi} \sin \frac{hd}{2} \cdot \sin \frac{h\pi}{2} \cdot \cos \frac{h\pi}{6} \cdot \sin(h\omega t) \quad (4)$$

For higher current harmonics amplitudes is valid:

$$I_h = \frac{1}{h} I_1 \cdot \frac{\sin \frac{hd}{2}}{\sin \frac{d}{2}} \quad (5)$$

where

$$I_1 = \frac{8I_{fm}}{\pi} \cdot \sin \frac{d}{2} \cdot \cos \frac{\pi}{6} = 2,205 \cdot I_{fm} \cdot \sin \frac{d}{2}$$

When we use the relation (4), we find out that only harmonics of a definite order (5., 7., 11., 13. etc.) will appear on a frequency spectrum. These harmonic orders are called characteristic harmonics and their amplitudes are solved by an equation (5) so-called "1 over h rule". Under real conditions, unbalanced power source - amplitude or phase non-symmetry, the considered problem becomes more complicated and in the frequency spectrum we can find also non-characteristic components. In contrast to characteristic harmonics for calculation amplitudes of non-characteristic harmonics we can not use equation (5) and we have to apply numerical Fourier analysis (DFT or FFT). Power source non-symmetry causes distortion of phase currents and drift of basic harmonic wave of phase current against phase voltage [2,3,4,5].

Excepting characteristic and non-characteristic harmonics discussed in the previous paragraph, we can also find interharmonic components in frequency spectrum of consumed current (see Figure 1). The interharmonics occur as a consequence of dynamic changes of circuit parameters (power supply voltage dips, load variation etc.). The interharmonic current magnitudes are relatively small in comparison with characteristic and non-characteristic harmonic components, but they may impact the proper function of neighbouring appliances (e.g. interference of ripple control and tuned filters). However frequency of the interharmonic is not integer multiple of the fundamental grid frequency 50Hz, therefore we cannot use standard Fourier quotations (1). For an explanation occurrence of the frequency components in the power grid it is necessary to derive new multipurpose quotations which allow calculating interharmonic components.

If function $f(t)$ is defined and integrable in the close interval $\langle -l, l \rangle$ so valid $f \in L(-l, l)$:

$$f(t) = \frac{1}{2} a_0 + \sum_{n=1}^{+\infty} \left(a_n \cos \frac{n\pi\omega t}{l} + b_n \sin \frac{n\pi\omega t}{l} \right) \quad (6)$$

For Fourier coefficients valid:

$$a_n = \frac{1}{l} \int_{-l}^l f(t) \cos \frac{n\pi\omega t}{l} d\omega t \quad (n = 0, 1, 2, \dots) ,$$

$$b_n = \frac{1}{l} \int_{-l}^l f(t) \sin \frac{n\pi\omega t}{l} d\omega t \quad (n = 1, 2, \dots) \quad (7)$$

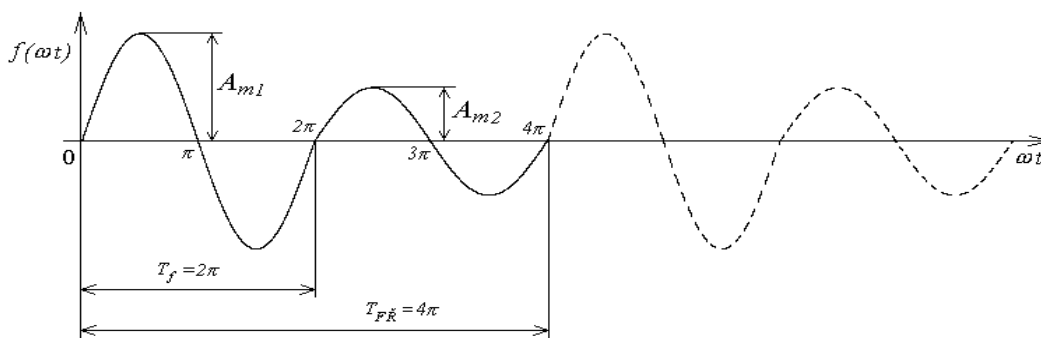


Figure 5. Harmonic waveform of function $f(\omega t)$ for interharmonic components analysis

For the function waveform in the Fig. 5 valid following coefficients calculation:

$$a_h = -\frac{(A_{m1} - A_{m2})4}{(h-2)(h+2)\pi}$$

for $h \neq 2$ and $h = 1, 3, 5, 7, \dots$

$$b_2 = \frac{2\pi A_{m1} + 2\pi A_{m2}}{4\pi} = \frac{A_{m1} + A_{m2}}{2} \tag{8}$$

Other coefficients b_h are zero.

Now it is necessary to verify these new equations (6-8) for interharmonics calculating, we make harmonic analysis of periodical function in Fig.5 with period $T_f=2\pi$ (50Hz). It changes amplitude each period from value A_{m1} to A_{m2} and so on. From the function behaviour it is evident, that Fourier progression of the function have double period $T_{FR}=4\pi$ (25Hz).

In relation to difference between function period and Fourier progression period we can expect relation between frequency of first harmonic of time function f_1 and frequency of first harmonic of Fourier progression time function f_{FR1} :

$$f_1 = \frac{1}{T_f} = \frac{1}{2\pi}, \quad f_{FR1} = \frac{1}{T_{FR}} = \frac{1}{4\pi} \Rightarrow f_1 = 2 f_{FR1} \tag{9}$$

Therefore we can expect frequency components as multiple of 25 Hz although the function waveform has period 50 Hz as shown in Figures 6-8 (frequency component 50 Hz is 100% and it is second component in the figures).

3. SIMULATION AND EXPERIMENTAL RESULTS

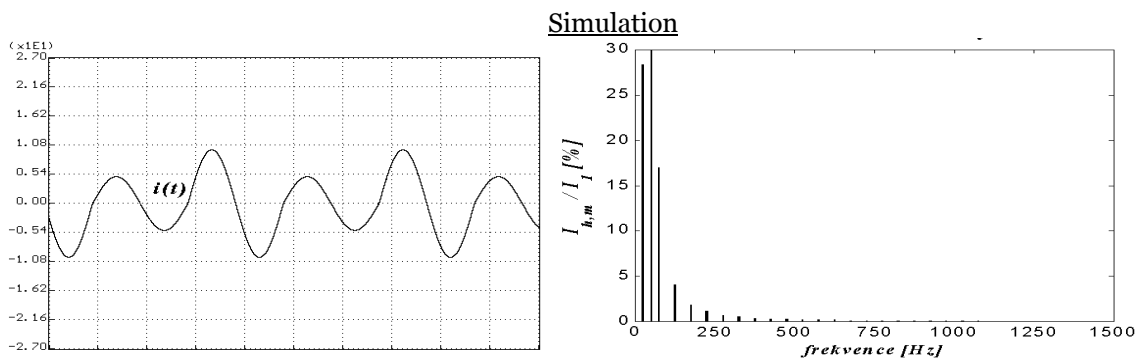


Figure 6. Simulation results of function waveform harmonic analysis

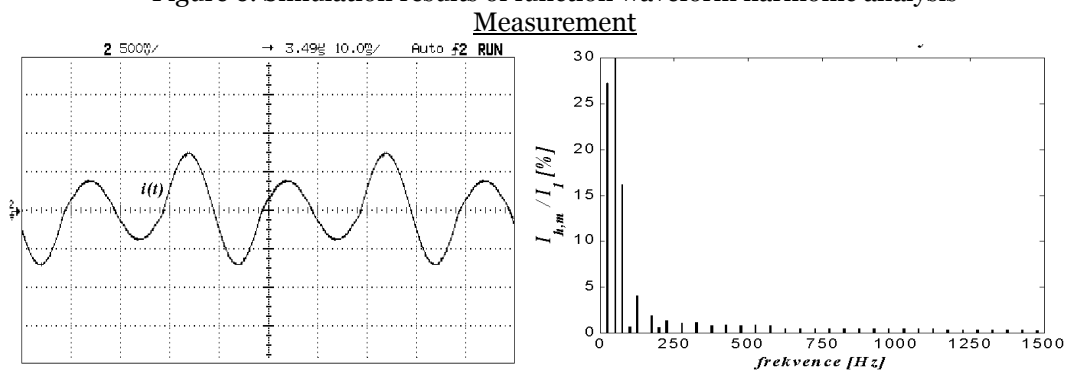


Figure 7. Measurement results of function waveform harmonic analysis

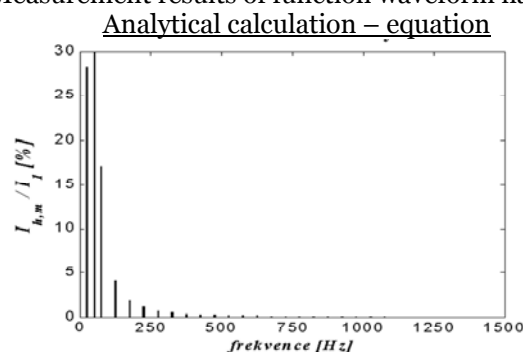


Figure 8. Measurement results of function waveform harmonic analysis

4. CONCLUSION

Detailed theoretical analyze has been made and useful mathematical equations for interharmonics calculation were derived. Several simulations and experimental measurements for analytical calculation verification have been realized. Results from simulation and measuring confirm that frequency of first harmonic of time function f_1 and frequency of first harmonic of Fourier progression time function fFR_1 should not be the same thing.

ACKNOWLEDGMENT

This research work has been made within research project of Czech Science Foundation No. GACR 102/09/1164.

REFERENCES / BIBLIOGRAPHY

- [1] Bauta, M., Grötzbach, M., "Noncharacteristic Line Harmonics of AC/DC Converters with High DC Current Ripple," In: 8th IEEE-ICHQP, Athens, Proc. Vol. II, pp. 755-760, 1998.
- [2] Drábek, Pavel; Kůs, Václav. EMC Issues of Power Electronic Converters. In IEEE SYMPOSIUM EMC 2009. Austin: IEEE, 2009. s. 296-301. ISBN: 978-1-4244-4267-6.
- [3] Drábek, P., Peroutka, Z.: Electromagnetic Compatibility Issues of Variable Speed Drives. In: IEEE SYMPOSIUM on Electromagnetic Compatibility 2002. Minneapolis, Minnesota, USA 2002, pp. 308-313
- [4] KŮS, V.; PEROUTKA, Z.; DRÁBEK, P. Non-characteristic harmonics and interharmonics of power electronic converters. In 18th International conference and exhibition on electricity distribution. Turin: IEE, 2005. p. 1-5.
- [5] KŮS, V.; DRÁBEK, P.; FOŘT, J.; PITTERMANN, M. Harmonic currents of frequency converters with voltage source inverters. In International 15 symposium Micromachines and servosystems. Warszawa : Wydawnictwo Książkowe Instytutu Elektrotechniki, 2006. s. 45-50. ISBN 83-922095-1-6.
- [6] DRÁBEK, P.: Harmonic analysis use for investigation of semiconductors converters EMC. Transcom 2007, Žilina 2007.
- [7] Drábek, P.: EMC issues of controlled rectifiers. In 2007 European Conference on Power Electronics and Applications. Piscataway: IEEE, 2007. s. 4801-4807. ISBN: 978-90-75815-11-5.







¹ Cornelia Victoria ANGHEL

DATA SECURITY IN WIRELESS NETWORKS

¹ EFTIMIE MUTGU UNIVERSITY OF REȘIȚA, FACULTY OF ENGINEERING,
COMPUTER SCIENCE DEPARTMENT, REȘIȚA, ROMÂNIA

ABSTRACT:

Wireless networks are relatively less secure than wired network because of easier access of unauthorized persons in coverage areas of access points. There is implicit in the implementation of wireless networks, different barriers that form the so-called basic security of wireless networks, which prevents unintended access of foreigners network in the coverage of an access point.

Security barriers (basic security) protocols have been provided in Wi-Fi networks provide a relatively low level of security of these networks, which has slowed development somewhat.

KEYWORDS:

Wireless Network, data security, Mac Filtering, WEP, WAN

1. INTRODUCTION

Wireless networks are relatively less secure than wired network because of easier access of unauthorized persons in coverage areas of access points. There is implicit in the implementation of wireless networks, different barriers that form the so-called basic security of wireless networks, which prevents unintended access of foreigners network in the coverage of an access point.

Security barriers (basic security) protocols have been provided in Wi-Fi networks provide a relatively low level of security of these networks, which has slowed development somewhat.

In June 2004, was adopted 802.11i standard which improves Wireless network security.

Basic security of wireless networks is ensured by the following features implemented:

- ❖ SSID (Service Set Identifiers);
- ❖ WEP (Wired Equivalent Privacy);
- ❖ Address validation MAC (Media Access Control).

SSID is a code that defines membership of a particular wireless access point. All wireless devices that will communicate on a network must have its own SSID, set the same value as the value of SSID access point to achieve connectivity.

Normally the access point transmits its SSID every few seconds. This mode can be stopped so that an unauthorized person can not automatically find the SSID and the access point. But since the SSID is included in any sequence of wireless beacons, it is easy for a hacker equipped with monitoring equipment to discover and bind the value network.

WEP can be used to improve ongoing problem SSID transmission by encrypting traffic between wireless clients and access point. This is accomplished by an authentication with a key (shared-key authentication). Wireless client access point transmits a challenge that he must return it encrypted. If the access point can decrypt the client's response, the key is valid proof that it possesses and is entitled to join the network. WEP encryption has two options - to 64-bit key or 128-bit.

WEP does not provide much security. Hacker equipped with monitoring equipment can receive and record first challenge away from the access point and then answer the customer's encrypted on the basis of processing can determine the key that can then be used to join the network.

Checking the MAC address. It can enhance network security, if the network administrator is using MAC address filtering, in the access point is configured with the MAC addresses of clients are granted network access.

Unfortunately, even this method does not provide much security.

A hacker can record footage from traffic and, after analysis, can extract a MAC address that can then be used to join the network.

2. METHODOLOGY

Wireless MAC Filtering is the simplest method for limiting access in a Wireless Network.

Only wireless equipment, who has been previously, registered MAC address of the router or Access Point can connect to wireless network.

SSID Hiding (Wireless Broadcast SSID Disabled) is a method for limiting unauthorized access to a wireless network.

Securing the network can be done with WEP or WPA.

- ❖ **WEP** (Wired Equivalent Protection) is an encryption method:
 - using 64 bits (10 hexa characters) or 128 bits (26 hexa characters). Hexa characters are: 0-9 and A - F
 - authentication: Open or Shared Key Now the 64-bit WEP encryption can be cracked in minutes, and the 128 bits in a few hours, using public applications.
- ❖ **WPA-PSK** (WPA Preshared Key or WPA-Personal) is a much safety method such as WEP.
- ❖ **WPA2** is the safest encryption method is an improved version of WPA method.

Also, those encryptions (WPA and WPA2) can be broken if the password contains fewer characters or a word found in the dictionary. To break this encryption makes it impossible to use long passwords, randomly generated.

3. ANALYSES

We use the TL-WR340G/TL-WR340GD 54Mbps Wireless Router. This router provides dedicated solution for Small Office/Home Office (SOHO) networks. With our network all connected, our local wired or wireless network can share Internet access, files and fun for multiple PC's through one ISP account. In addition, this device supports Bridge mode which can make two AP's communicate with each other wirelessly.

There are three submenus under the Wireless menu (shown in Figure 1): **Wireless Settings**, **MAC Filtering** and **Wireless Statistics**. Click any of them, and we should be able to configure the corresponding function. The detailed explanations for each submenu are provided below.

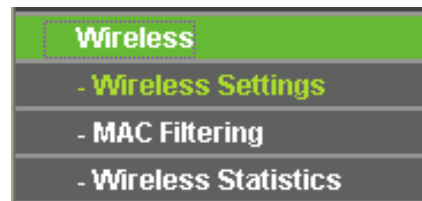


Figure 1. Wireless menu

SSID - Enter a value of up to 32 characters. The same name (SSID) must be assigned to all wireless devices in our network. The default SSID is TP-LINK, but it is recommended strongly that we change our networks name (SSID) to a different value. This value is case-sensitive. For example, *TP-LINK* is NOT the same as *tp-link*.

Region - Select our region from the pull-down list. This field specifies the region where the wireless function of the router can be used. It may be illegal to use the wireless function of the router in a region other than one of those specified in this field. If the country or region is not listed, we can contact the assistance.

The default region is United States. When we select our local region from the pull-down list, we click the **Save** button, then the Note Dialog appears. Then we click OK.

Channel - This field determines which operating frequency will be used. It is not necessary to change the wireless channel unless we notice interference problems with another nearby access point.

Mode - Select the desired wireless mode. The options are:

- ❖ **54Mbps (802.11g)** - Both 802.11g and 802.11b wireless stations can connect to the router.
- ❖ **11Mbps (802.11b)** - Only 802.11b wireless stations can connect to the router.

Enable Wireless Router Radio - The wireless radio of this Router can be enabled or disabled to allow wireless stations access. If enabled, wireless stations will be able to access the router. Otherwise, wireless stations will not be able to access.

Enable SSID Broadcast - If we select the **Enable SSID Broadcast** checkbox, the Wireless Router SSID will broadcast its name (SSID) on the air.

Enable Bridges - If we select the **Enable Bridges** checkbox, we can input MAC address of other AP's to communicate with them wirelessly in Bridge mode.

MAC of AP (1-6): Input the MAC address of the AP which we want to communicate with. There are six entries can be configured.

The AP's can communicate with each other in Bridge mode unless they know each other's MAC address. For example, if the router whose MAC address is 00-13-56-A8-9E-1A wants to communicate with an AP whose MAC address is 00-13-56-A8-9E-1B in Bridge mode, we should do as following:

Enable Wireless Security – The wireless security function can be enabled or disabled. If disabled, the wireless stations will be able to connect the router without encryption. It is recommended strongly that we choose this option to encrypt our wireless network. The encryption settings are described below.

Security Type - We can select one of the following authentication types:

- ❖ **WEP** - Select WEP authentication type based on 802.11 authentications.
- ❖ **WPA-PSK/WPA2-PSK** - Select WPA/WPA2 authentication type based on pre-shared passphrase.
- ❖ **WPA /WPA2** - Select WPA/WPA2 authentication type based on Radius Server.

Security Options - We can select one of the following Security options:

When we select **WEP** for authentication type we can select the following authentication options:

- ❖ **Automatic** - Select Shared Key or Open System authentication type automatically based on the wireless station request.
- ❖ **Shared Key** - Select 802.11 Shared Key authentication.
- ❖ **Open System** - Select 802.11 Open System authentication.

When we select **WPA-PSK/WPA2-PSK** for authentication type we can select **Automatic, WPA –PSK** or **WPA2-PSK** as authentication options. When we select **WPA/WPA2** as an authentication type we can select **Automatic WPA** or **WPA2** as authentication option.

WEP Key Format - We can select **ASCII** or **Hexadecimal** format. ASCII Code Format stands for any combination of keyboard characters in the specified length. Hexadecimal format stands for any combination of hexadecimal digits (0-9, a-f, A-F) in the specified length.

WEP Key settings - Select which of the four keys will be used and enter the matching WEP key information for our network in the selected key radio button. These values must be identical on all wireless stations in our network.

Key Type - We can select the WEP key length (**64-bit**, or **128-bit**, or **152-bit**) for encryption. "Disabled" means the WEP key entry is invalid.

- ❖ For **64-bit** encryption - we can enter 10 hexadecimal digits (any combination of 0-9, a-f, A-F, zero key is not permitted) or 5 ASCII characters.
- ❖ For **128-bit** encryption - we can enter 26 hexadecimal digits (any combination of 0-9, a-f, A-F, zero key is not permitted) or 13 ASCII characters.
- ❖ For **152-bit** encryption - we can enter 32 hexadecimal digits (any combination of 0-9, a-f, A-F, zero key is not permitted) or 16 ASCII characters.

Encryption - When we select **WPA-PSK/WPA2-PSK** or **WPA/WPA2** for **Security Type** we can select **Automatic, TKIP** or **AES** as **Encryptions**.

The Wireless MAC Address Filtering feature allows we to control wireless stations accessing the router, which depend on the station's MAC addresses.

MAC Address - The wireless station's MAC address that we want to access.

Status - The status of this entry either **Enabled** or **Disabled**.

Privilege - Select the privileges for this entry. We may select one of the following **Allow / Deny**.

Description - A simple description of the wireless station.

First, we must decide whether the unspecified wireless stations can access the router or not. If we desire that the unspecified wireless stations can access the router, please select the radio button **Allow the stations not specified by any enabled entries in the list to access**, otherwise, select the radio button **Deny the stations not specified by any enabled entries in the list to access**.

Figure 2. Add or Modify Wireless MAC Address Filtering entry

To Add a Wireless MAC Address filtering entry, click the **Add New...** button. The "**Add or Modify Wireless MAC Address Filtering entry**" page will appear, shown in Figure 2.

4. CONCLUSIONS

The article presents some aspects about the router configuration on a safety wireless network by Mac Address Filtering. An example used use the TL-WR340G/TL-WR340GD 54Mbps Wireless Router, is detailed. This router provides dedicated solution for Small Office or Home Office (SOHO) networks.

REFERENCES

- [1.] Anghel, C.V. – „*Considerații privind conectarea la o rețea Wireless securizată*” Al XII-lea Simpozion Internațional “Tinerii și Cercetarea Multidisciplinară”, 11-12 noiembrie, Timișoara, 2010
- [2.] Dixit, R. Prasad (eds.), *Wireless IP and Building the Mobile Internet*, Artech House, 2003
- [3.] M. Mallick, *Mobile and Wireless Design Essentials*, Ed. John Wiley & Sons, 2003



¹ Corina Maria DINIȘ, ² Angela IAGĂR,
³ Corina Daniela CUNȚAN, ⁴ Gabriel Nicolae POPA

STUDY OF THE VOLTAGE RESONANCE IN ELECTRIC CIRCUITS

¹⁻⁴ UNIVERSITY POLITEHNICA TIMIȘOARA, FACULTY OF ENGINEERING HUNEDOARA, ROMANIA

ABSTRACT:

This work is presenting the study of the voltage resonance in the a.c. R-L-C series circuits, as well as the practical implications of this phenomenon in electrotechnics.

In order to verify the voltage resonance phenomena by simulation, there have been achieved applications using the programs EWB -Multisim 9 and LabVIEW 7.1.

KEYWORDS:

Voltage resonance, R-L-C series circuit, variable frequency, variable inductivity, variable capacity

1. INTRODUCTION

The voltage resonance takes place in the R-L-C series circuit supplied by the alternate voltage $u(t) = U\sqrt{2} \sin \omega t$, when the reactive power absorbed by the circuit at the terminals is null $Q=0$, e.g. when is obtained a null phase-difference ($\varphi=0$) between the voltage applied to the circuit and the absorbed current's intensity. In this case, the inductive reactance X_L becomes equal with the capacitive reactance X_C . This equality is obtained either by modifying the inductance L or capacity C , or by supplying the circuit with a voltage of variable frequency.

The resonance condition can be obtained:

- ❖ at pulsation's, respectively supply voltage frequency's variation, keeping constant the inductance L and capacity C :

$$\omega_r = \frac{1}{\sqrt{LC}} \text{ respectively } f_r = \frac{1}{2\pi\sqrt{LC}}, \omega_r \text{ and}$$

f_r being called pulsation, respectively resonance frequency;

- ❖ at inductance's variation, supplying the circuit from a fix frequency source and keeping constant the capacity C : $L_r = \frac{1}{\omega^2 C}$, L_r being called resonance inductance;

at capacity's variation, supplying the circuit from a fix frequency source and keeping constant the inductance L : $C_r = \frac{1}{\omega^2 L}$, C_r being called resonance capacity.

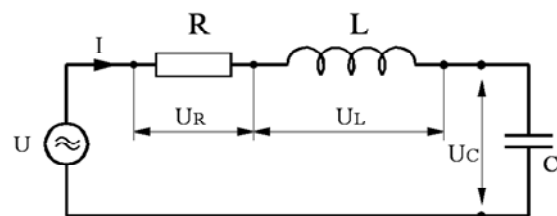


Fig. 1 R-L-C series A.C. circuit

2. PROBLEM STUDY

In case of a R-L-C series circuit operating in permanent sinusoidal regime, in resonance conditions, is obtained:

- the complex impedance of the R-L-C series circuit is:

$$\underline{Z} = R + j \cdot (X_L - X_C) \tag{1}$$

- having the module $Z = \sqrt{R^2 + (X_L - X_C)^2}$. (2)

According to the Ohm's Law, the current from circuit is:

$$\underline{I} = \frac{\underline{U}}{\underline{Z}} = \frac{\underline{U}}{R + j(X_L - X_C)} \quad (3)$$

- The current's effective value is determined by the relation:

$$I = \frac{U}{\sqrt{R^2 + (X_L - X_C)^2}} = \frac{U}{\sqrt{R^2 + \left(\omega L - \frac{1}{\omega C}\right)^2}} \quad (4)$$

- The phase-difference between current and voltage is given by the relation:

$$\operatorname{tg}\varphi = \frac{X_L - X_C}{R} = \frac{\omega L - \frac{1}{\omega C}}{R} \quad (5)$$

$$\varphi = \operatorname{arctg}\left(\frac{U_L - U_C}{U_R}\right) = \operatorname{arctg}\left(\frac{X_L - X_C}{R}\right) \quad (6)$$

- At resonance, $X_L = X_C$, and the current through the circuit is reaching the maximum value:

$$I_{\text{rez}} = \frac{U}{R} \quad (7)$$

During the experiment, the R-L-C series circuit could be found in the following situations: $X_L > X_C$ (inductive character, fig. 2.1); $X_L = X_C$ (voltage resonance, fig. 2.2); $X_L < X_C$ (capacitive character, fig. 2.3).

The phase diagrams of voltages and currents for the three cases are presented in the following figures:

For the circuit in fig.1, the variation of impedance Z , resistance R and reactance X_L and X_C , as well as the phase-difference angle φ between the voltage applied at the circuit's terminals and the current through the circuit are presented in fig. 3.

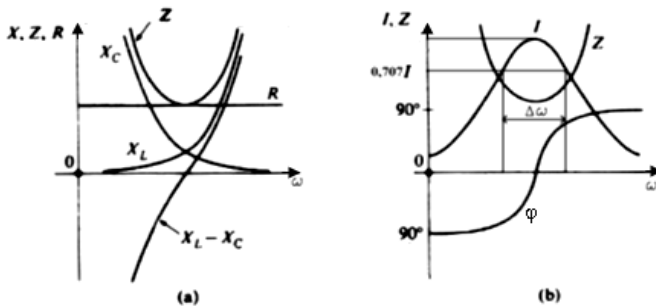
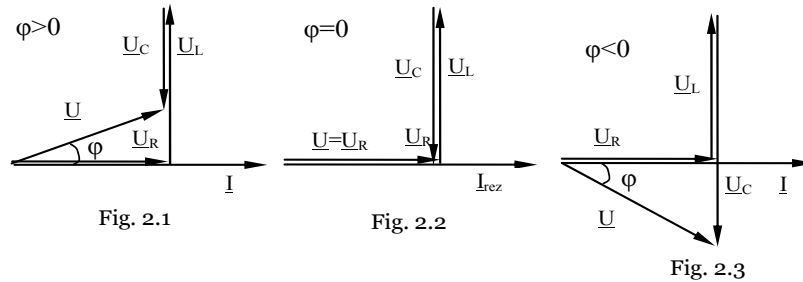


Fig. 3

We notice that at the resonance frequency (pulsation), the circuit's impedance is minimum and equal with R , and the current is maximum:

$$I_{\text{rez}} = I_0 = \frac{U}{R}$$

The voltage drops U_L and U_C are equal and in phase opposition, and they can be much higher than the supply voltage, reason for which the resonance in the R-L-C series circuit is also called *voltage resonance*.

3. APPLICATIONS ACHIEVED IN MULTISIM 9 FOR THE VOLTAGE RESONANCE STUDY

For the study of the R-L-C series circuit's operation, there have been achieved the applications from figure 4, 6 and 8. The circuit components are linear and constant or variable (constant resistor, variable coil, variable capacitor). This allows us to analyze the circuit's operation at inductivity, respectively variable capacity.

The applications emphasize the phenomena of voltage resonance achieved by one of the three ways:

- ❖ inductivity variation
- ❖ capacity variation
- ❖ frequency variation

Further, are presented the circuits implemented in simulations with Multisim 9 for verifying the voltage resonance in the R-L-C series single-phased A.C. circuits de c.a. The circuits' resonance moment is emphasized aslo by means of oscilloscope, on which screen being noticed the two voltage and current signals, which are in phase.

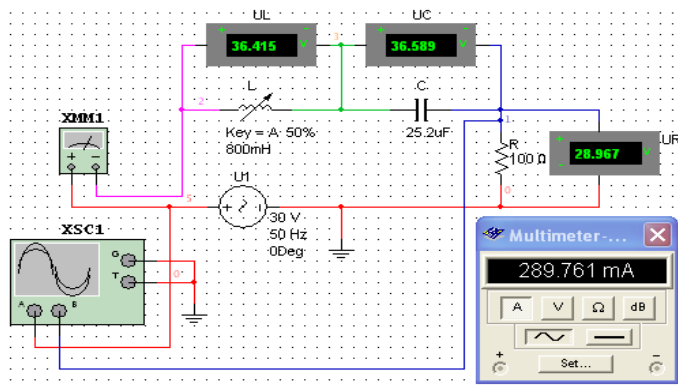


Fig. 4

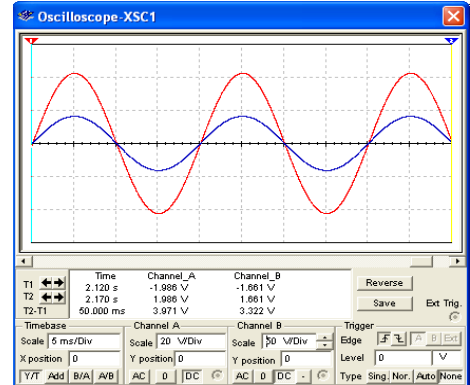


Fig. 5

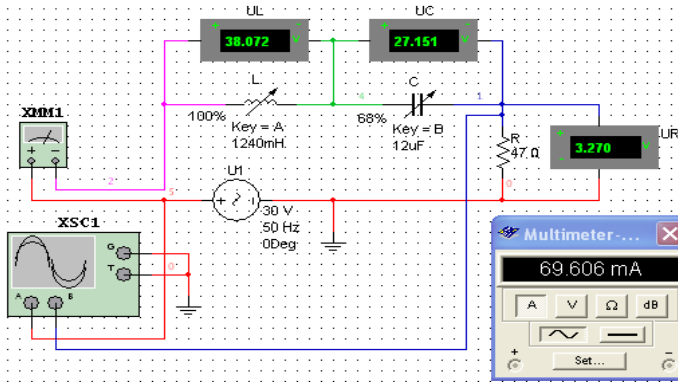


Fig. 6

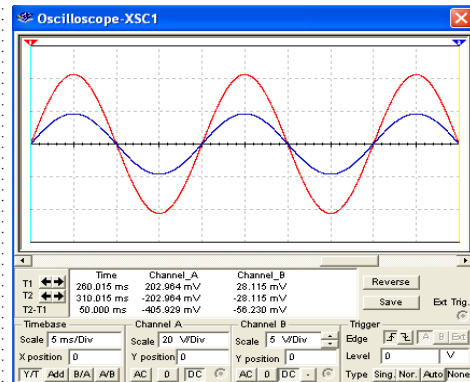


Fig. 7

In fig. 8, the supply source is a signal generator, to which can be modified both the amplitude and the frequency of the circuit's supply voltage, which allows us the analysis of its operation at variable frequency.

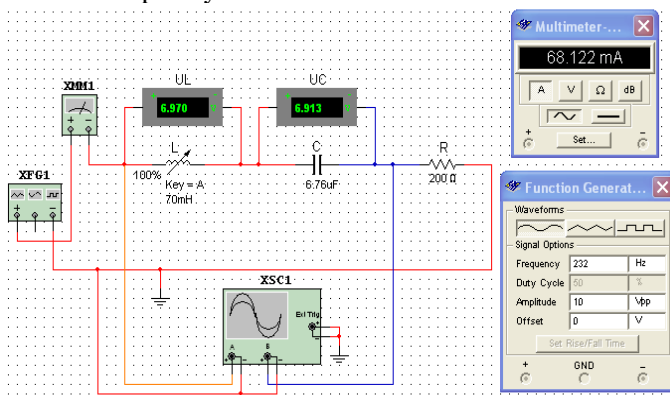


Fig. 8

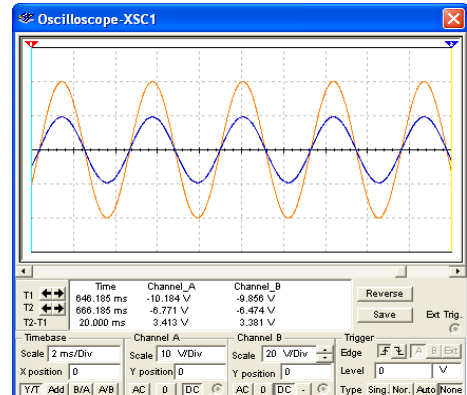


Fig. 9

4. EXPERIMENTAL RESULTS

For the circuits from fig. 4, 6 and 8 were obtained the experimental results presented in tables 1, 2 and 3.

Table 1. RLC series circuit at variable inductivity

L, [mH]	I, [mA]	U _R , [V]	U _L , [V]	U _C , [V]
100 %	184,819	18,482	46,454	23,339
90 %	208,537	20,847	47,160	26,332
80 %	234,931	23,485	47,243	29,665
70 %	261,307	26,130	45,980	33,006
60 %	281,988	28,190	42,534	35,607
50 %	289,761	28,976	36,427	36,6
40 %	281,181	28,118	28,285	35,507
30 %	260,026	25,996	19,622	32,836
20 %	233,537	23,353	11,768	29,499
10 %	207,237	20,723	5,260	26,177

where $L_{max} = 800$ mH (100%)

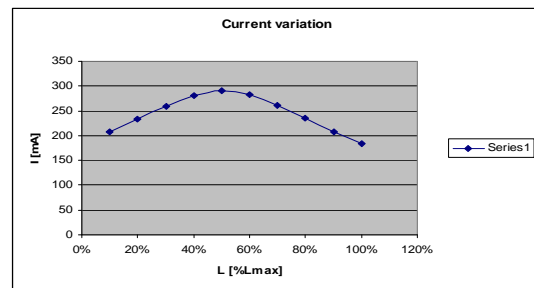


Fig. 10

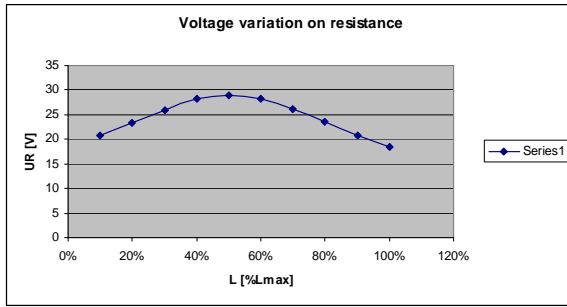


Fig. 11

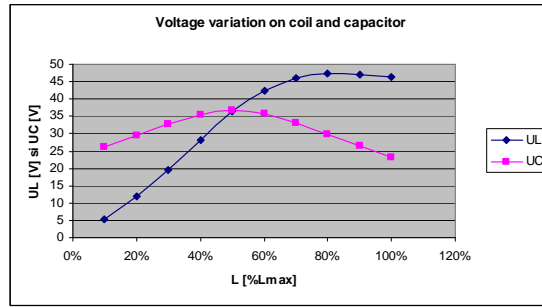


Fig. 12

Table 2. RLC series circuit at variable capacity

C, [μ F]	I, [mA]	U_R , [V]	U_L , [V]	U_C , [V]
100 %	66,882	3,143	36,571	17,736
90 %	67,982	3,195	37,183	20,029
80 %	68,985	3,242	37,732	22,873
70 %	69,585	3,269	38,048	26,361
68 %	69,606	3,271	38,072	27,142
60 %	69,093	3,247	37,791	30,545
50 %	66,155	3,108	36,175	35,095
40 %	58,762	2,762	32,140	38,956
30 %	45,723	2,149	25,009	40,416
20 %	29,093	1,367	15,912	38,572
10 %	13,022	0,612	7,123	34,541

where $C_{max} = 12 \mu\text{F}$ (100%)

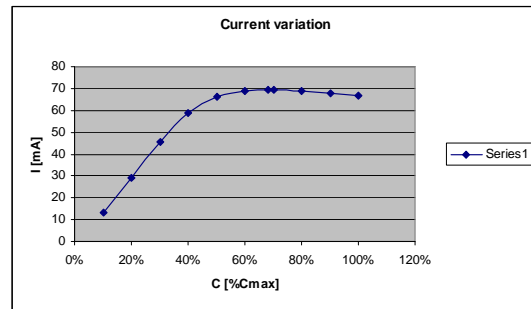


Fig. 13

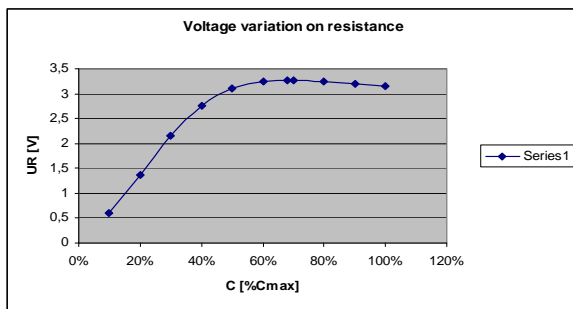


Fig. 14

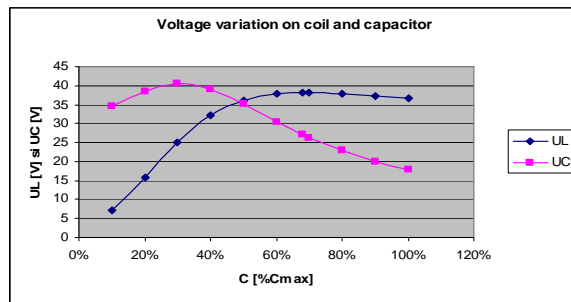


Fig. 15

Table 3. RLC series circuit at variable frequency

f, [Hz]	I, [mA]	U_R , [V]	U_L , [V]	U_C , [V]
150	62,394	12,478	4,144	9,793
170	65,125	13,025	4,894	9,019
190	66,872	13,374	5,611	8,286
210	67,817	13,563	6,285	7,603
230	68,122	13,624	6,911	6,973
232	68,123	13,624	6,971	6,913
240	68,08	13,615	7,205	6,678
260	67,68	13,536	7,757	6,128
280	66,948	13,389	8,26	5,629
300	65,97	13,194	8,719	5,177

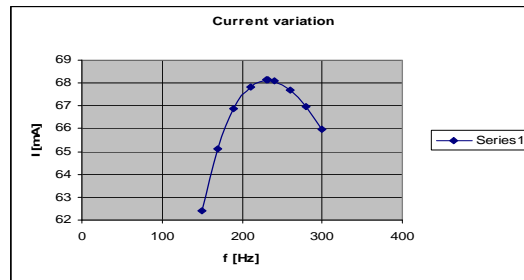


Fig. 16

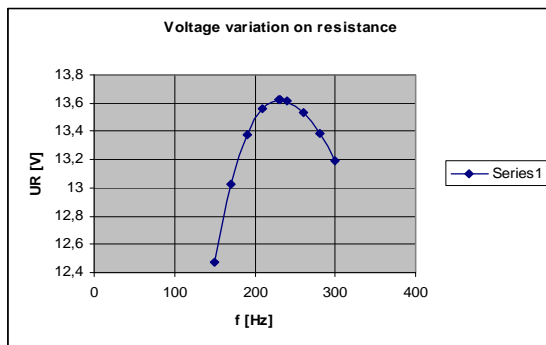


Fig. 17

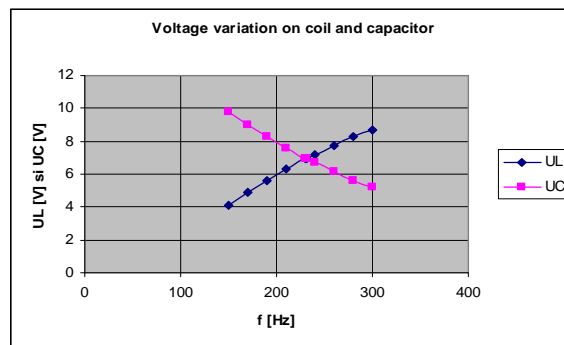


Fig. 18

5. APPLICATION LABVIEW 7.1 FOR THE VOLTAGE RESONANCE'S STUDY

For a thoroughly study of the voltage resonance phenomena, it's been achieved the application with the front pannel presented in fig.19 and fig.20.

The front pannel is organized on three zones:

- ❖ supply zone (voltage with variable effective value and frequency)
- ❖ circuit components zone (variable resistance, inductivity, capacity)
- ❖ display and visualizing zone (digital indicators, oscilloscope).

The application allows:

- ❖ modification of the supply voltage effective value within [0 ; 220] V
- ❖ modification of the supply voltage frequency within [0 ; 10000] Hz
- ❖ modification of the circuit components' parameters:
 - resistance – within [0 ; 200] Ω
 - inductivity – within [0 ; 1240] mH
 - capacity – within [0 ; 25,2] μF
- ❖ selection of the variable parameter (frequency, inductivity, capacity) depending on which are analyzed certain measures and against which is emphasized the resonance;
- ❖ visualizing variation graphics of certain measures depending on the selected variable parameter:
 - effective values of the supply voltage and the voltage on resistance;
 - voltages on inductivity and capacity;
 - impedance
 - current's intensity
 - active power
 - phase-difference between the supply voltage and current;
 - selecting the measures visualized at a certain moment;
 - possibility to use some cursors which, fixed on a certain point of a wave form, should indicate its coordinate;
- ❖ displaying of some important values of certain parameters, respectively electric measures:
 - variable parameter's value for which the resonance is obtained
 - impedance at resonance
 - current intensity's effective value at resonance
 - effective values of voltages on resistance, inductivity and capacity at resonance
 - maximums of the effective values of voltages on inductivity and capacity
 - active power at resonance.

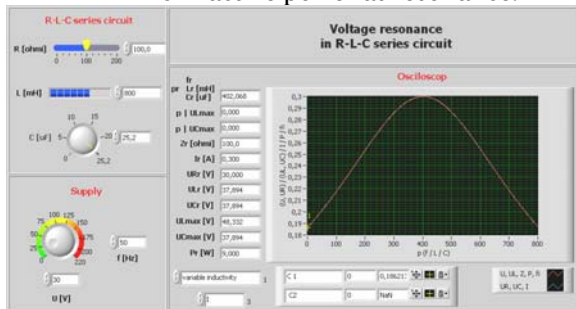


Fig. 19 Study of the voltage resonance in R-L-C series circuit at variation of the coil's inductivity –front panel

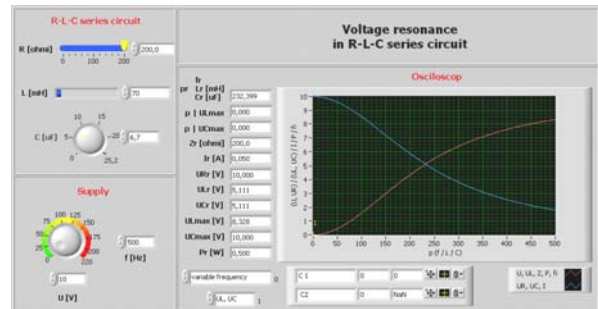


Fig. 20 Study of the voltage resonance in R-L-C series circuit at variation of the frequency – front panel

The application's block diagram is presented in fig.21. The values of the parameters set at a given moment are transformed in step-type, respectively ramp-type signals (in case of the ones against which is made the graphic representation), obtaining this way a set of values for the respective parameters, corresponding to the variation interval of the variable parameter (frequency, inductivity, capacity).

For calculating the pulsation, reactances, impedance, voltage drops, power and phase difference are used „formula”-type blocks.

For selecting the parameter against which is made the circuit's analysis, as well as for selecting the visualized graphics, at a given moment, are used „Case” structures, inside which are made the suitable operations.

For detecting the minimum or maximum values of certain analyzed measures, which correspond the resonance, are used dedicated subprograms from the functions library of the programming environment.

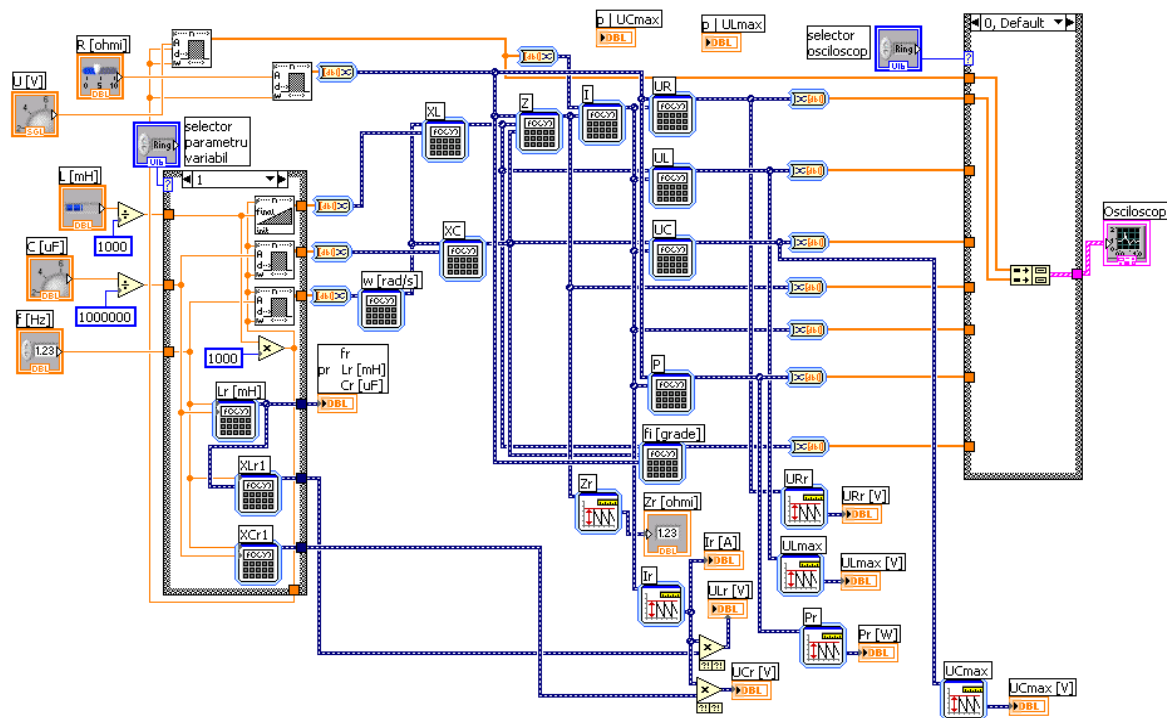


Fig. 21 Study of the voltage resonance in R-L-C series circuit – block diagram

6. CONCLUSIONS

In conclusion, in resonance regime:

- ❖ the (real) impedance, equal with the circuit's resistance, has minimum value,
- ❖ the power factor is maximum,
- ❖ the voltage on resistance has maximum value,
- ❖ the current, in phase with the voltage, has maximum value,
- ❖ the voltage on coil and capacitor are equal in effective values, and of contrary sign, and can exceed the voltage applied to the circuit, e.g. in the circuit appear *over voltages*. From this reason, the series resonance is also called voltage resonance.

The main advantage provided by the simulation program Electronic Workbench – Multisim 9 consists in high flexibility as regards the modification of the analyzed electric circuits' structure and their operation regimes, fact that allows an analysis and a diagnose of those circuits within a much more reduced time interval, than the case when these would be physically achieved, allowing in addition a facile storage and in large quantities of the information about the circuit's operation in different implementation versions.

To be noticed the time savings and the possibility of further processing of data, especially of graphic dependencies for different measures, by means of the Electronic Workbench – Multisim 9 program.

Utilization of the simulation program Electronic Workbench – Multisim 9 in the university educational activity, at disciplines with electric and electronic profile, allows the educational process to become more attractive, providing the students a large perspective in their professional training.

LABVIEW was materialized into a versatile development environment, based, mainly, on the advantages of graphic programming, in detriment of the traditional one.

Combining the special features of the LabView environment with the computing power and high flexibility of the current generation computers, can be implemented powerful instruments for the analysis of some systems from various activity fields.

The significant obtained advantages (the created unit is very powerful from the calculations viewpoint, easy to use – due to the friendly graphic interface, easy to configure and a much lower price compared with the classic testing system) indicate the fact that the virtual instrumentation represents an adequate solution for implementation of some complex testing systems, reliable and, not the least, advantageous from financial viewpoint.

The present and future measuring systems cannot be conceived without virtual instruments, that should replace the actual dedicated measuring devices and instruments.

REFERENCES

- [1.] C.M. Diniş, A. Iağăr, C.D. Cunţan, Fundaments of electric and electronic engineering, Experimental themes, Politehnica Publishing House, Timişoara, 2009.
- [2.] E. Cazacu, I. Nemoianu, a.o., Special issues about electric circuits theory, Elements of theory and applications, Vol. 1 and Vol. 2, MatrixRom Publishing House, Bucharest, 2005.
- [3.] H. Gavrilă, Electrotechnics and electric Equipments, Vol. I, Didactic and Pedagogic Publishing House, RA, Bucharest, 1993.
- [4.] A. Saimac, C. Cruceru, Electrotechnics, Didactic and Pedagogic Publishing House, Bucharest, 1981.
- [5.] * * * – Electronics Workbench/ Multisim 9 – User's guide.
- [6.] V. M. Popa, Electrotechnics' Basics, Alma Mater Publishing House, Sibiu, 2002.
- [7.] Mariana Milici, Concepts of electric circuits theory – Signals. Laws, theorems and analysis methods, MatrixRom Publishing House, Bucharest, 2005.
- [8.] Mariana Milici, Electric circuits – Sinusoidal and particular operation regimes, MatrixRom Publishing House, Bucharest, 2005.
- [9.] Cottet Francis, Ciobanu Octavian, Programming bases in LabVIEW, Matrix Rom Publishing House, Bucharest, 1998.
- [10.] M. Dobriceanu, Introduction in virtual instrumentation and LabView, Universitaria Publishing House, Craiova, 2005.
- [11.] M.V. Drăgoi, Data acquisition-distribution systems, Programming bases in LabVIEW, Transilvania University Publishing House from Braşov, 2001.
- [12.] V. Dogaru-Ulieru, ş.a., Aplicatii LabVIEW in measurements, Ed.CONPHYS, Rm. Vâlcea, 2002.
- [13.] * * * NI , LabVIEW Basic Introduction, Manual Course.
- [14.] Gabriel Gorghiu, Applications of virtual instrumentation in education, Bibliotheca Publishing House, Targoviste, 2007







SIMULATION OF NEURAL AND FUZZY SYSTEM TO PREDICT, DETECT AND ELIMINATE CRACKS IN CONTINUOUS CASTING

¹⁻³. UNIVERSITY POLITEHNICA OF TIMISOARA, FACULTY OF ENGINEERING FROM HUNEDOARA, ROMANIA

ABSTRACT:

This paper work present Simulink implementation of a neural and a fuzzy system for prediction, detection and rejection of cracks in continuous casting processes. The neural and fuzzy system is made up by a neural network used for fissures detection and a fuzzy controller for predicting and rejecting them, who uses the signal from neural network and a part of data in the process to correct the casting speed and the primary cooling water.

KEYWORDS:

Neural system, fuzzy controller, control, crack

1. INTRODUCTION

Control systems [3] ensure the right working algorithms required by an appropriate system working– both technologically and generally speaking –, and also in case of classical systems based on PID numerical controller. Usually, there are no measures for crack prediction, thus rejects results from the process (in terms of tenth of tones of steel). In such case, working staff changes the working methods of the installation, based on internal instructions. The casting programmer is not appropriate and that has important economical implications [4].

Worldwide, there is research [1], [2], [5], [6], [7] who might lead to already-made crack detection (inside the crystallizing apparatus) and damaged goods. Currently used methods do not entirely eliminate the cracks; they are effective only if some features are being accomplished (crack detection at both exits of the crystallizing apparatus, a pretty slow phenomenon feature as far as the cracking correction is concerned etc.).

In [8], [9], [10], it is proposed a number of original solutions allowing the complete crack rejection from the cast material, outside the crystallizing apparatus. Therefore, it is designed a neural network [8] allowing us to detect any primary crack, by a thorough predictive analysis of the information received from a thermo-couple matrix. Information is used by a system based on fuzzy logics [10], which enables corrections of the casting speed and of the cooling water flow. Since this method does not lead to a complete crack rejection (although specialized literature refers to correcting the casting speed alone, in addition to that we have proposed to change the cooling water flow as well), we have adopted a new predictive principle who diminishes any possible cracking. Thus, the fuzzy system [10] analyzes a number of characteristic measurements and, although the neural network [8] has not yet acknowledged any crack, but it considers they may occur they perform casting speed corrections and cooling water flow occurs. Certainly, the solution we have proposed also implies a more complex fuzzy controller, using two sets of distinct set of rules [10].

2. METHODOLOGY AND DISCUSSION

A. System description

To review the functioning of neural and fuzzy systems, we carry out the simulation in a Matlab-Simulink environment. Scheme implementation is given in fig.1.

Block temperature data generation

In principle, we used recordings of the unfolding process. The best solution is to use two separate sets, one normal and one in case there is a crack. To switch between the two sets of data,

we use a switch - control implemented in Simulink - Stateflow. Depending on a given parameter to the entry of this block, it switches between the two sets of data (1 - with crack, 0 – no crack). Block "CT Temperature" operate successively (every 120 s), the data "0" or "1", which basically makes the crack to occur or not. All data are memorized in „look-up data” tables.

Neural data processing block

We are able to identify any fissure if using data received from the 48 thermocouples mounted in 12 rows and 4 columns (on one side of the crystallizing apparatus). For each thermocouple, a dynamic neural network processes 10 consecutive temperature values. Any data received from a dynamic network is then processed by a space network who analyzes the values received from the two adjacent thermocouples. The input size value of such space networks (0 or 1) is introduced into a logical SAU (OR) block [9].

Figure 2 describes the connection amongst two dynamic networks and of a space network for data processing from two adjacent thermocouples.

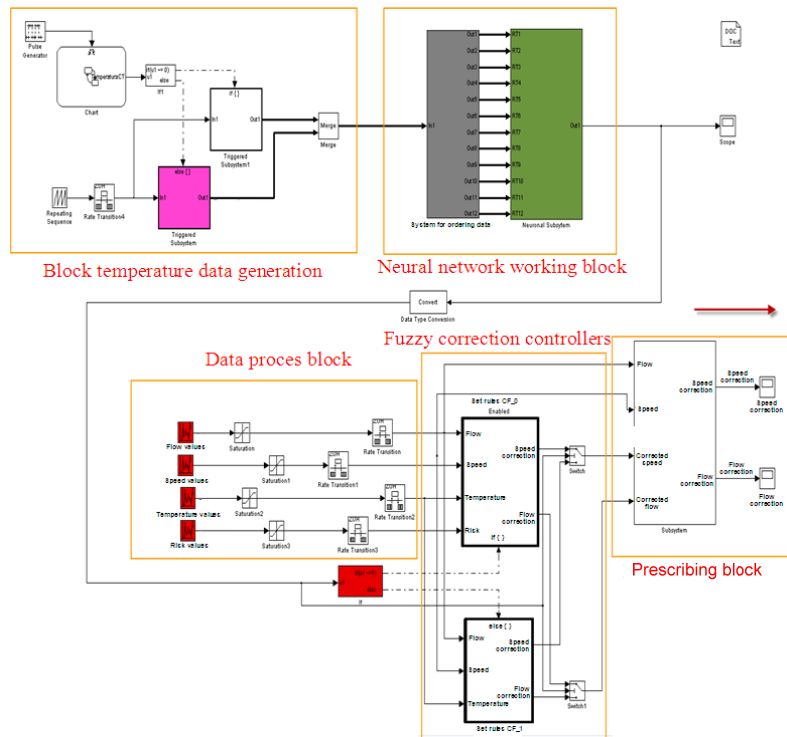


Fig. 1. Implementation in Matlab - Simulink of system

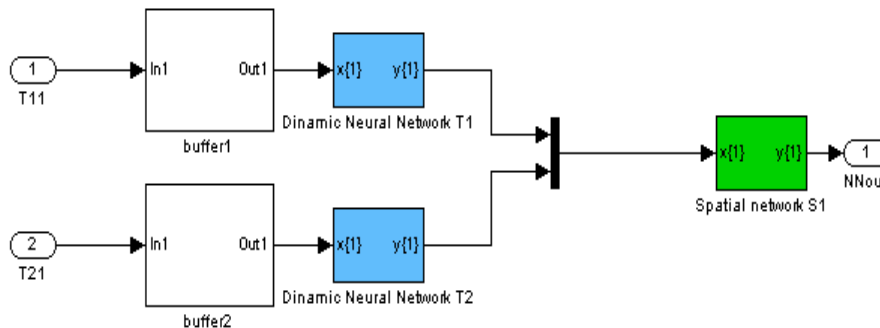


Fig. 2. Connecting two dynamic networks to space network for data processing from two thermocouples

According to the results of the logical SAU operation (we have analyzed output values of the space networks), when leaving the neural block we get a 0-value (there is no primary crack), and a 1-value (there is a primary crack).

Fuzzy Controller (RG-F)

According to the value of the output value of the neural network, RG-F starts two different base sets: a corresponding base in case there are no cracks for „0” (225 rules), and a corresponding base in case there are some primary cracks (75 rules) [7]. The first set has four entries (casting speed, primary cooling water flow, distributor temperature, and technological risk). They are all read from the process (in real situations).

We have used the „Process data block” to simulate it. The „technological risk” parameter is not necessary for the second set of rules, because its value is the highest since we have already detected some cracks. The two outputs of the RG-F (p_v - correction of speed, and p_q - correction of flow), are used for the limitation block [10]. Figure 3 describes the implementation of RG-F “0”, and in figure 4. we describe the implementation of RG-F “1” in the environment Matlab-Simulink.

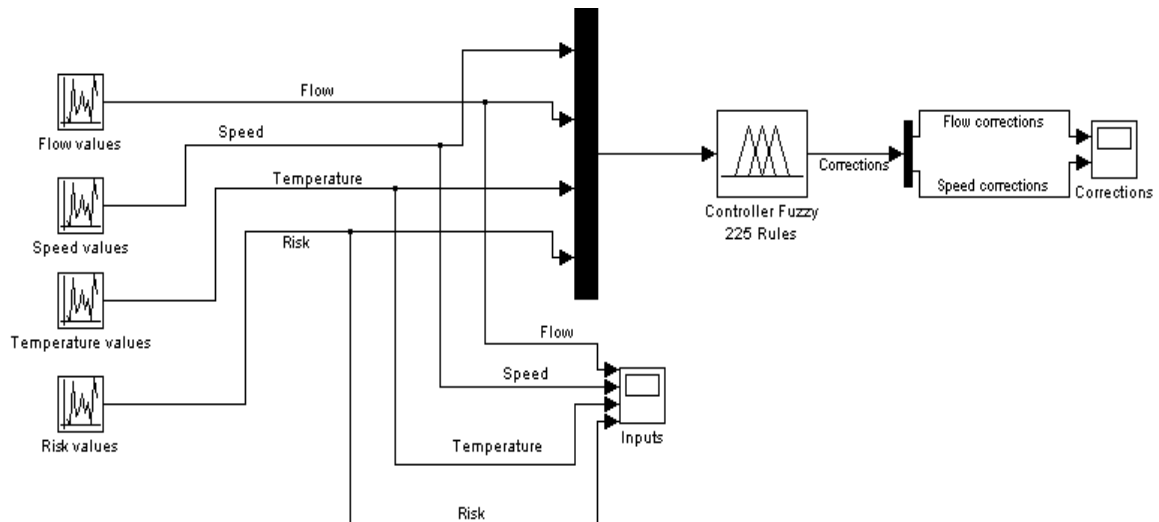


Fig. 3. Implementation in Matlab - Simulink to RG-F with basic rules "0"

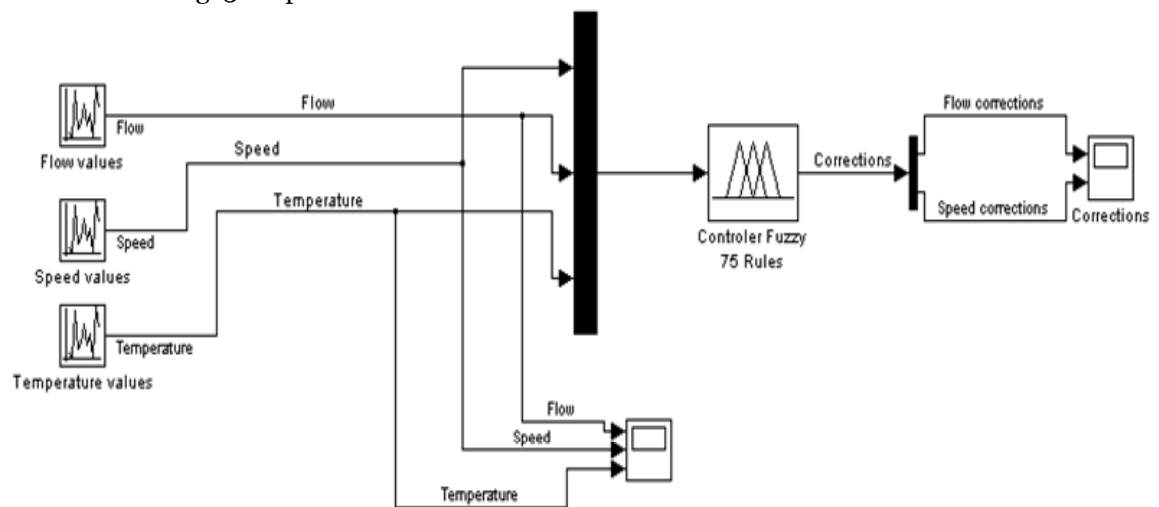


Fig. 4. Simulink implementation of the RG-F with basic rules "1"

Block prescribing

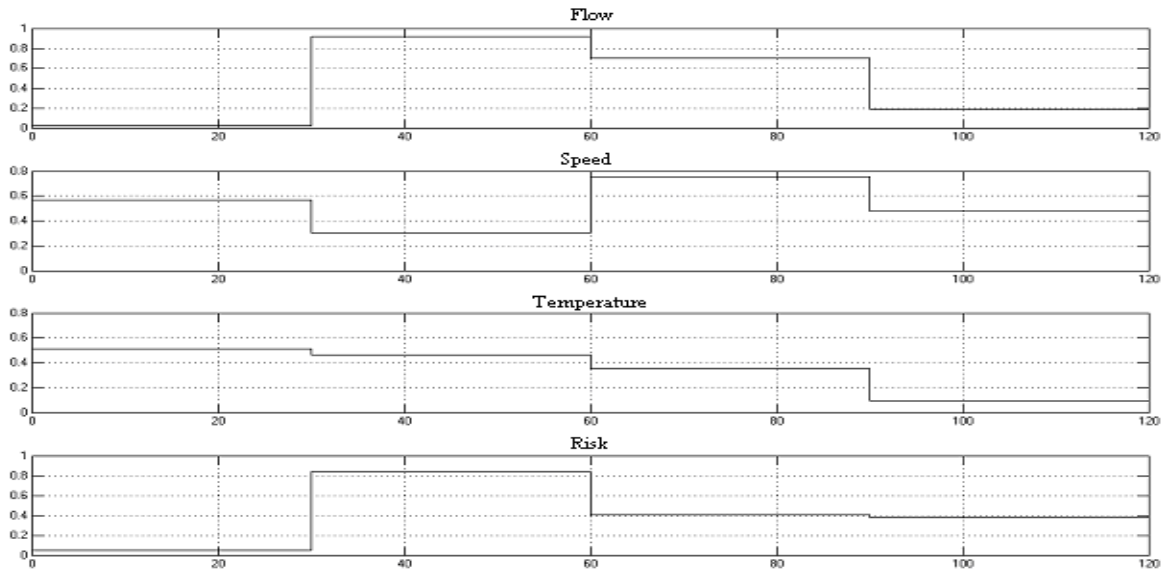
Block prescribing is replacing the values required for speed and flow (v^* , q^*), from the installation of automation existing in their new corrected values v_c , q_c , resulting in RG-F outputs. For simulation, the values v^* and q^* were considered equal to those measured sizes of the process (from "Block data processing").

B. Validation of simulated system operation

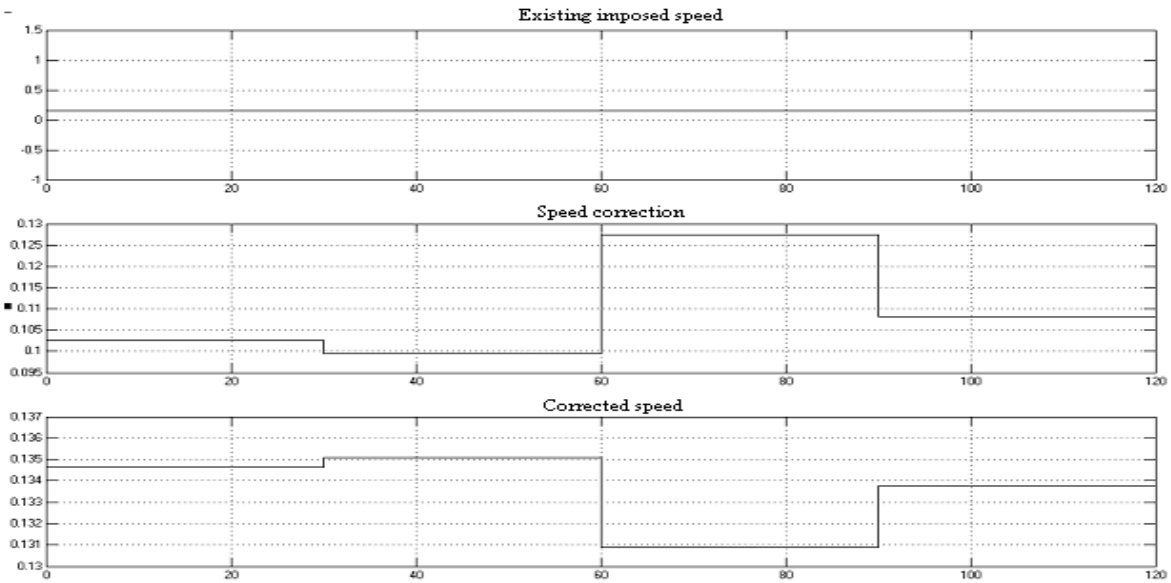
For validation of simulated system operation, for the entry fissures detection neural network we have applied two different sets of data measured during the current process and stored in tables. One of the sets refers to the situation when there are no cracks and the other one in case there is a crack. Neural network outputs reach 0 and 1 value and they show the network works correctly and it has detected the crack (in case they occur).

For each of the two cases generated at RG-F input, there are several input values (flow, speed, temperature, risk – if the neural network has produced a „0” output – there are no cracks or flow, speed, temperature; - if the neural network has produced an "1" output value – there are primary cracks). These values are described in figures 5. and 6. : a) – time variation (120 seconds) of RG-F input values; b) – speed correction and new speed values; c) – flow correction and new flow values.

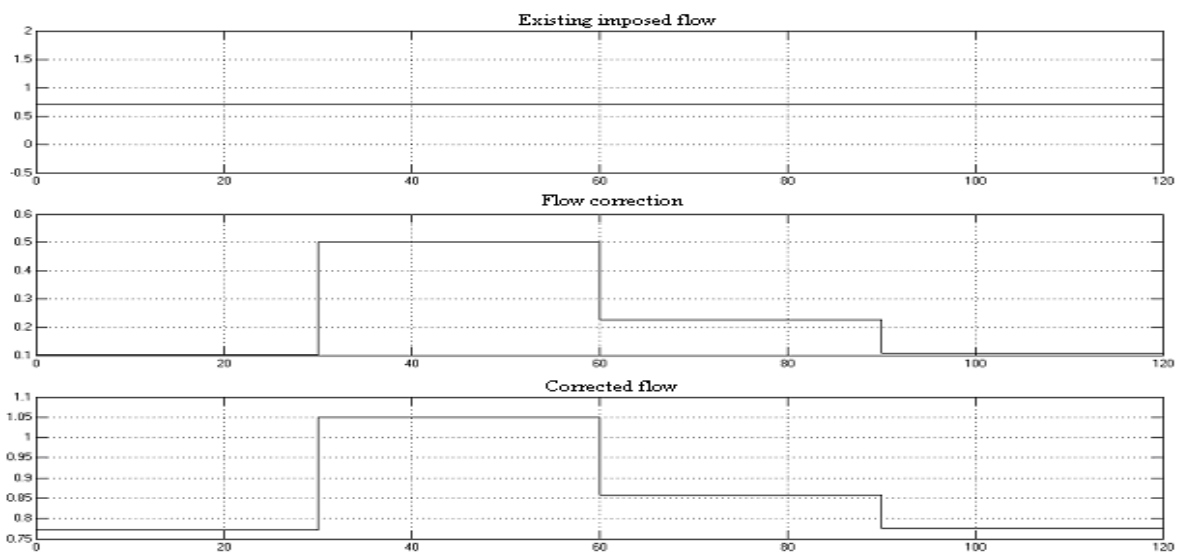
Figure 5. describes the situation during the first 30 simulation seconds, when the cooling water flow is low, the casting speed is low, the temperature inside the crystallizing apparatus is high, and the technological risk is low. Speed correction is very low, hence required casting speed is almost unchanged. During the next simulation 30 seconds, the technological risk increases, the fuzzy controller causes speed correction, and also avoids any crack (casting speed decreases). During the whole time, cooling water flow increases significantly. We can see that the other two simulation rounds are similar.



a) RG-F Input Data

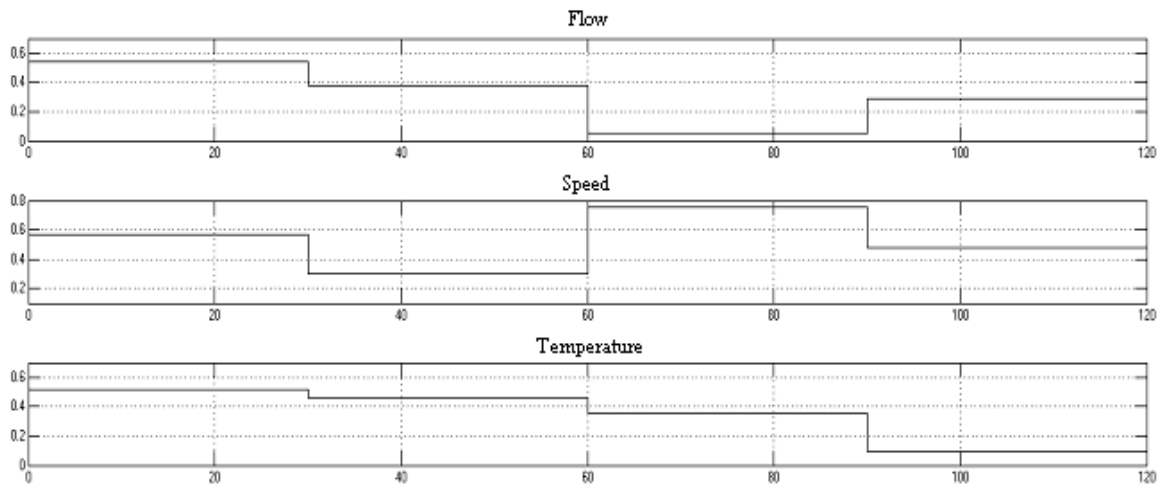


b) Output data – speed

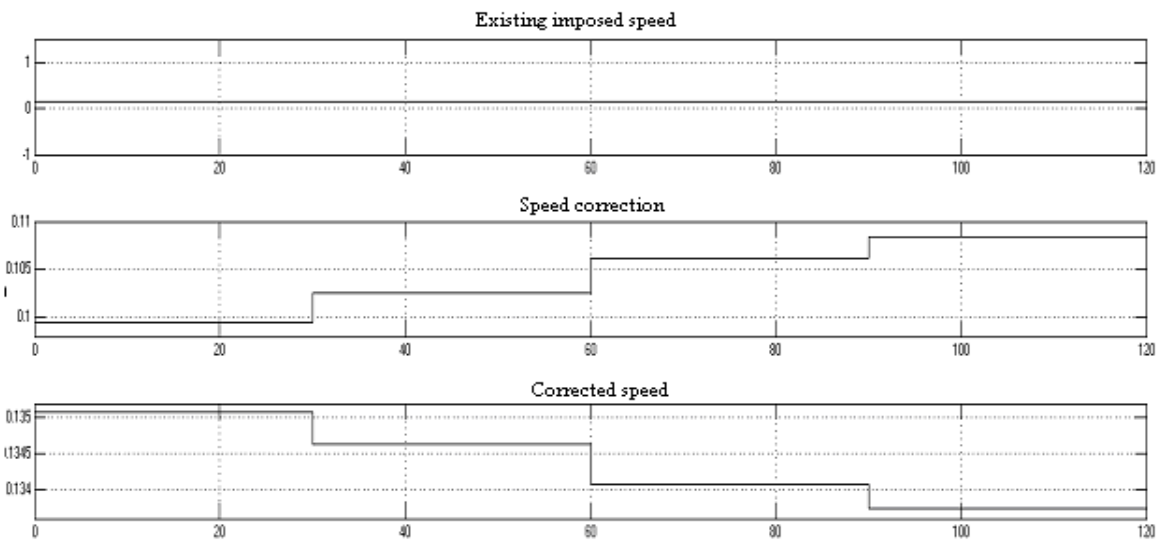


c) Output data - flow

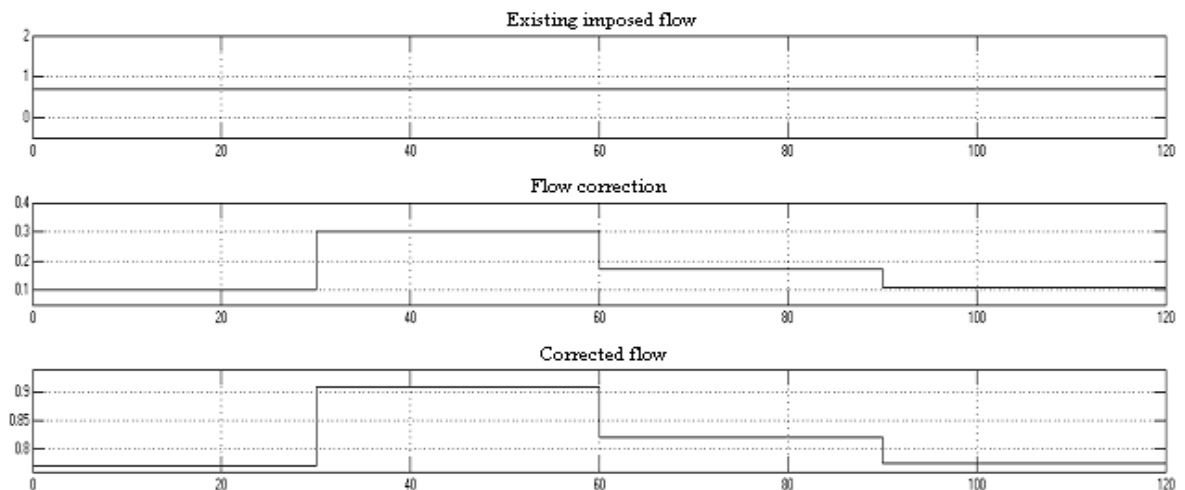
Fig. 5. RG-F Validation (RN=0)



a) RG-F input data



b) Output data – speed



c) Output data - flow

Fig. 6. RG-F validation (RN = 1)

When analyzing all cases described in figures 5. and 6, we draw the following conclusions:

- ❖ RG-F analyzes the input values and elaborates speed corrections and water flow correctly, according to two base sets connected to each output of the neural network;

❖ Fore-writing block corrects all required values for speed and flow, according to RG-F outputs.

By simulating in Matlab-Simulink, we have proved that all solutions are correct – predicting, detecting, and rejecting any crack during continuous casting. Such simulation is made for performing a check out on the fuzzy system. During operation, all size values do not change so fast, hence some input values combinations are not that predictable. Once the system is implemented, the rules referring to such situations could be eliminated.

3. CONCLUSIONS

We have performed a Matlab-Simulink simulation of the entire system. Considering this aspect, we have designed the simulation design and designed input sign generators, a neural network, a fuzzy regulator, and the fore-writing block for speed and flow values. When using this method, we have been able to use several input data sets, and the design has correctly generated all output values, acknowledging the whole system.

REFERENCES

- [1.] J. Adamy - Device for early detection of run-out in continuous casting, United States Patent, No.5, 904,202, Date of Patent 18 may (1999).
- [2.] C. Avila , Y. Tsuji, - Crack width prediction of RC structures by Artificial neural networks, Adaptive and Natural Computing Algorithms, Springer Viena, pg.92-95, 12.dec.(2005).
- [3.] S. Bouhouche, et. all - Quality Monitoring Using Principal Component Analysis and Fuzzy Logic. Application in Continuous Casting Process, American Journal of Applied Science (AJAS), 4(9), ISSN: 1546-9239, 2007, pp.637-644.
- [4.] Drainkov, et. all. - An Introduction to Fuzzy Control, Springer-Verlag, Berlin, 1993.
- [5.] L. Herbert Gilles, J. Shipman - Method and apparatus for controlling heat removal by varying casting speed, United States Patent, No.4,235,276, Date of Patent 25 nov. (1980).
- [6.] T. Nakamura, K. Kazuho - Breakout prediction system in a continuous casting process, United States Patent, No.5, 548,520, Date of Patent 20 august (1996).
- [7.] F.P. Pleschiutschnugg, - Method and apparatus for the early recognition of ruptures in continuous casting of steel with an oscillating mold, United States Patent, No.US 6,179,041 B1, Date of Patent 30 jan.(2001).
- [8.] G.O.Tirian, - Neural system for detecting cracks in the wire of the continuous casting, 12th International Research/Expert Conference–Trends in the Development of Machinery and Associated Technology, pp. 649-652 Istanbul, Turkey, August 2008.
- [9.] G.O. Tirian, S. Anghel, M.Pănoiu, C.Pinca-Bretotean - Control of the continuous casting process using neural networks, Proceedings of the 13th WSEAS International. Conference on Computers, Rodos Island, Greece, July 23-25, ISSN:1790-5109, ISBN:978-960-474-099-4, 2009, pp.199-204.
- [10.] G.O.Tirian, O. Prostean, S. Rusu-Anghel, Pinca B. C, D.Cristea - Fuzzy system for implementing the cracks control during the continuous casting, Annals of DAAAM & Proceedings of the 20th International DAAAM Symposium, Volume 20, No.1, ISSN 1726-9679, ISBN 978-3-901509-70-4, pp.1661-1662, 25-28th November 2009, Vienna, Austria.



¹Mihaela OSACI, ²Ioana Sonia DRAGAN, ³Iulia TRIPA

STUDIES ABOUT MAGNETIC HYPERTHERMIA WITH SUPERPARAMAGNETIC NANOPARTICLES

¹POLITEHNICA UNIVERSITY OF TIMISOARA, HUNEDOARA ENGINEERING FACULTY, ROMANIA

²SCHOOL GROUP TELECOMMUNICATIONS AND PUBLIC WORKS HUNEDOARA, ROMANIA

³HIGH SCHOOL TEACHERS "SABIN DRAGOI" DEVA, ROMANIA

ABSTRACT:

The hyperthermias, as an alternative choice for the cancer therapy, are more and more interesting for many researches. When applying the hyperthermia, the cancerous cells are destroyed by increasing their temperature. The idea of using superparamagnetic nanoparticles in hyperthermia is up-to-date, because it offers the possibility of direct inoculation in the target places of the human body, where they remain locally by applying a magnetic field. If the magnetic field is radio-frequency alternating, the magnetic losses that lead to temperature increase are caused by the Neel relaxation processes. The matrix where they are dispersed and the physical properties of the nanoparticles have a crucial importance in the magnetic hyperthermia applications. In this article, we undertake to realise a analytic study about specific absorption rate behavior that characterise the heating in hyperthermia.

KEYWORDS:

magnetic hyperthermia, superparamagnetic nanoparticles, specific absorption rate

1. INTRODUCTION

Electromagnetic (EM) radiation is a fundamental tool in cancer therapy [1], extensively used for both diagnostics and therapy. Physical interactions between EM waves and living matter can be very different depending on the portion of the electromagnetic spectrum considered. A variety of clinical tools have been established in physical medicine based on direct emission and detection of EM waves such as x-ray radiography, computer tomography scanning (CT scan) and gamma-ray radiotherapy from radioactive isotopes. Many other techniques rely on indirect uses of EM radiation such as positron-emission tomography (PET), magnetic resonance imaging (MRI), and microwave hyperthermia (MWH). In fig. 1 [1] it present a frequency ranges for some of the most used diagnostic/therapy equipments (MFH = Magnetic Fluid Hyperthermia, MRI = Magnetic Resonance Imaging). B. The respective main physical mechanisms at each frequency range. Also shown in (C) is the common nomenclature for the electromagnetic waves at each region: RF = radiofrequency; MW = microwaves; IR = infrared; Vis = visible; UV = ultraviolet and X-Ray.

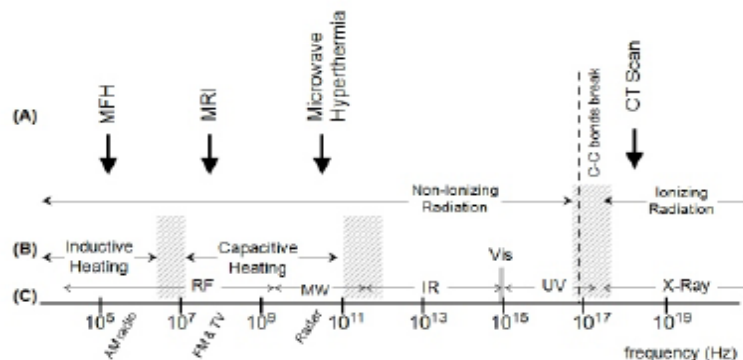


Fig 1.

2. METHODOLOGY

The hyperthermia in oncology consists of increasing the temperature of the cancerous tumours in order to destroy them [3,4,5], and can be used concurrently with other therapeutic techniques, as chemotherapy or radiotherapy. Lately, the magnetic hyperthermia attracted more and more interest [2, 6, 7, 8, 9, 10 ...], being one of the basic subjects debated at the International Conference of Magnetism that took place, during 26th-31st July 2009, in Karlsruhe, Germany. As a ground rule, the magnetic germs or particles are inoculated directly in the tumour zone. Under the action of the alternative magnetic field, the magnetic particles can generate heat via four different mechanisms [9, 10, 11]:

- 1) generation of the Foucault currents in conductor materials;
- 2) losses through hysteresis;
- 3) losses through Neel magnetic relaxation in superparamagnetic nanoparticle systems;
- 4) losses through Brown magnetic relaxation Brown in the nanoparticle systems found in slimy suspensions.

The mechanism of producing Foucault currents in conductor materials in a time-variable magnetic field is governed by the electromagnetic induction law. Through this mechanism, a significant heating effect is obtained if the material is under an alternative magnetic field. An example of hyperthermia that uses this method is the inoculation of acicular copper particles in the tumour zone, followed by their excitation in a radiofrequency magnetic field. The significant losses through hysteresis are characteristic to the ferromagnetic materials. But, the usage of this mechanism in hyperthermia is problematical [11] due to the temperature control in a quite limited domain (41-48 °C). A solution can be the usage of certain materials that have their Curie points around the heating temperature (41-48 °C), but it's very difficult to find such materials due to their chemistry [11]. A less traumatic solution consists of using an "intelligent" polymer-base ferrogel.

In case of mono-domain particles, where there are no domain walls, when the particles are immersed into a solid matrix or when dispersed particle systems are in high frequency magnetic fields, the inversion of the particle magnetization is realised through the rotation of the particle, and these rotation processes cause losses due to the Neel relaxation processes. In case the magnetic particles are in a liquid matrix, if the frequency of the excitation magnetic field is not too high, the particles tend to rotate until they reach a minimum energy position. These rotation processes lead to losses due to the Brown relaxation.

The measure that characterize the efficiency of the transformation of these losses, via those four mechanisms described above, it is known in the literature as the *specific absorption rate* (SAR), and it is defined as the absorbed power per the mass unit of the tumour material, at a given strength of the excitation magnetic field.

The SAR amplitude is given by

$$\text{SAR} = A \cdot f \quad (1)$$

where A is the specific area of the hysteresis loop (i.e. specific losses) at the frequency and magnetic field at which the experiment is conducted.

Recent experimental researches [12] showed that, at a given amplitude of the excitation field, at the same frequency, the specific absorption rate is higher in case of using superparamagnetic nanoparticles in radiofrequency fields. These observations, and the fact that the magnetic nanoparticles can be more easily inoculated in the tumour, explain the interest for using them in the magnetic hyperthermia.

To calculate A and interpret hyperthermia experiments, two models -valid in different regimes- can be used. First, when the applied magnetic field is small compared to the saturation field of the NPs, the linear response theory can be used. In this case [12],[13],[14], the hysteresis loop is an ellipse of area [12]:

$$A = \frac{\pi \mu_0 H_{\max}^2}{\rho} \cdot \chi''(f), \quad (2)$$

$$\chi'' = \frac{\mu_0 M_s^2 V}{3 k_B T} \cdot \left(\frac{f \tau_N}{1 + (f \tau_N)^2} \right) \quad (3)$$

M_s is the saturation magnetization, ρ the density of the material (for magnetite 8300 kg/m³).

$$\tau_N = \tau_0 \exp\left(\frac{KV}{k_B T}\right) \quad (4)$$

is the Néel relaxation time, and τ_0 the interwell relaxation time. The linear theory is suitable to interpret hyperthermia experiments on superparamagnetic NPs, since the rather weak magnetic field used (generally up to 30 mT) is far from the saturation field of the NPs.

If we consider Brown relaxation time:

$$\tau_B = \frac{3\eta V_H}{k_B T}, \quad (5)$$

where η is the liquid matrix dynamic viscosity coefficient, V_H is hydrodynamic magnetic nanoparticles volume, in eq. 1 and 2 τ_N becomes total relaxation time $\tau = \tau_N + \tau_B$.

3. DISCUSSION

The most studied superparamagnetic nanoparticles for hyperthermia are those of magnetite, due to their very low toxicity. To be possible to be used in hyperthermia, the magnetic nanoparticles are coated with a carbon layer, to make them biocompatible, and immersed in dextran [15] or polymers (for example, polyvinyl alcohol [16]), to make them biodegradable. For a better penetration of the nanoparticles in the cancerous cells, they are coated with a bioactive compound, as antibodies or proteins [15].

Jennifer L. Phillips, in the paper “A Topical Review of Magnetic Fluid Hyperthermia”, available online on the Internet network, describes the possibility of using magnetic fluids in hyperthermia. The superparamagnetic nanoparticles are dispersed in water or hydrocarbon with neutral pH and physiological salinity. The resulted ferrofluid is directly injected in the tumour and a radiofrequency magnetic field is applied.

If the problem of the magnetic nanoparticle inoculation in the tumour zone is rather solved, there are no complex studies to clearly present the relation between the physical properties of the nanoparticle systems and their thermal efficiency in the hyperthermia therapy, or the modality to control the thermal efficiency by controlling the physical properties in a way that implies low costs and small technological efforts.

The heating capacity of a magnetic material or electromagnetic device is quantified through the specific absorption power rate (SAR), defined as the amount of energy converted into heat per time and mass. In terms of the usual experiments and parameters for magnetic colloids, the loss power per gram of Fe₃O₄ is obtained from the heating curves within the initial T temperature rising interval through the definition [1] where c_s is the sample heat capacity, defined as a mass-weighted mean value for a given concentration of magnetic material, calculated as

$$SAR = c_s \frac{\Delta T}{\Delta t} \cdot \frac{1}{m_{mag}} \quad (6)$$

$$c_s = \frac{m_{mag} c_{mag} + m_l c_l}{m_{mag} + m_l} \quad (7)$$

with c_{mag} , m_{mag} and c_l , m_l being the specific heat capacities and masses of magnetic material and liquid carrier, respectively.

The study we performed on spherical magnetite nanoparticles with specific heat capacities $c_{mag} = 0.67$ J/gK, mass $m_{mag} = 1$ g and diameter 9 nm in water with mass 5 mg and specific heat capacity $c_l = 4.18$ J/gK and dynamic viscosity coefficient $\eta = 0.633 \cdot 10^{-3}$ Ns/m². The physical properties of the magnetite nanoparticles is: saturation magnetization $M_s = 4.7 \cdot 10^5$ A/m and effective anisotropy constant $K = 1900$ J/m³. Initially we consider the system temperature 37.5 degrees Celsius. We believe that the maximum intensity alternating magnetic field applied is between 100 mT 1mT's frequency range between 10kHz and 100 kHz. In first phase we study how depend SAR of frequency and maximum magnetic intensity of magnetic field applied. Result is present in fig. 2, 3.

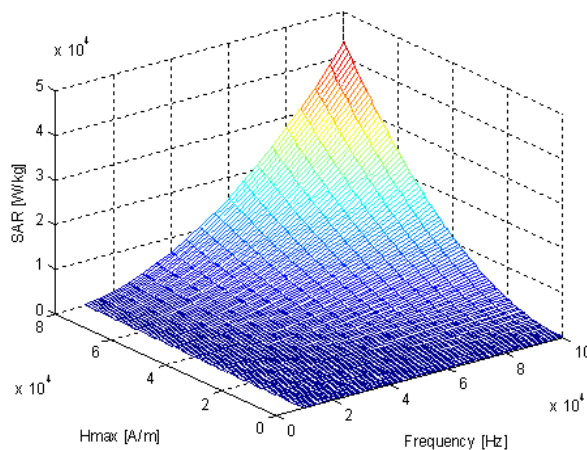


Fig.2

From Fig. 2.3 Note that SAR increases with increasing frequency and amplitude of applied magnetic field.

In Figure 3 is seen as keeping the value constant amplitude magnetic field intensity, it can get a SAR increase if applied field frequency increases.

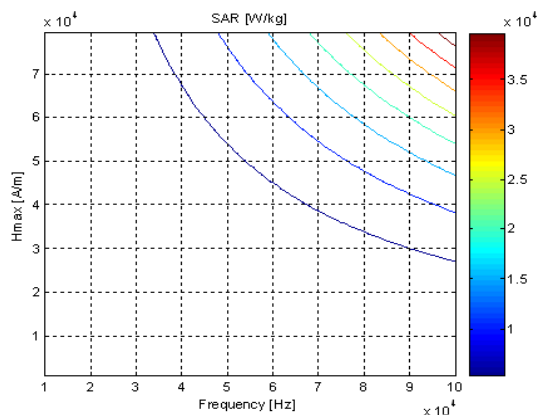


Fig. 3

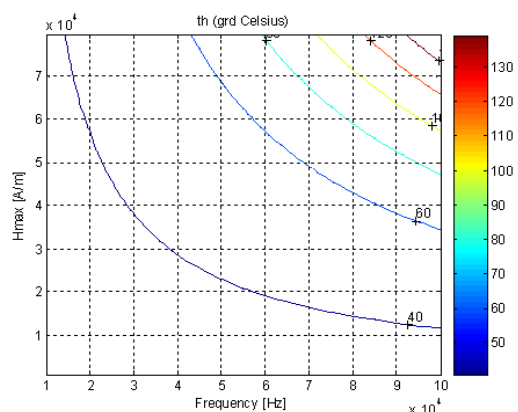


Fig. 5

applied and frequency of magnetic field, influence the temperature in the tumour zone and, in the same time, to obtain a theoretical tool for controlling the temperature in the magnetic hyperthermia by controlling this physical properties.

Then we study how depend the temperature growth of of frequency and maxim magnetic intensity of magnetic field applied. Result is present in fig.4,5.

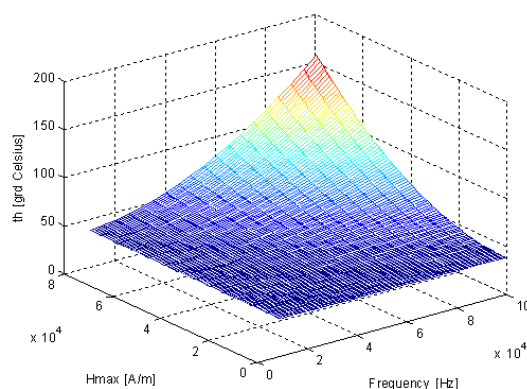


Fig. 4

From Fig. 4.5 Note that the tumor tissue temperature increases with increasing frequency and amplitude of applied magnetic field.

In Figure 5 is observed as a nursery for the temperature ment units when working in weak magnetic fields should work at high frequencies.

4. CONCLUSIONS

In this article, we realise a analytical study that implies the analysis how certain physical properties that maxim intensity of magnetic field

REFERENCES

- [1.] <http://esm.neel.cnrs.fr/2007-cluj/abs/Ibarra2-abs.pdf>
- [2.] Y.Akin, I.M. Obaidat, B. Issa, Y. Haik, Cryst. Res. Technol., 44, no.4, 388-390
- [3.] P. Wust, B. Hildebrandt, G. Sreenivasa, B. Rau, J. Gellermann, H. Riess, R. Felix, and P. M. Schlag, Lancet Oncol. 3, 487 (2002).
- [4.] C. C. Vernon, J. W. Hand, S. B. Field, D. Machin, J. B. Whaley, J. van der Zee, W. L. J. van Putten, G. C. van Rhoon, J. D. P. van Dijk, D. G. Gonzalez, F. F. Liu, P. Goodman, and M. Sherar, Int. J. Rad. Oncol. Biol. Phys. 35, 73 (1996).
- [5.] J. J. W. Lagendijk, Phys. Med. Biol. 45, R61 (2000).
- [6.] M. Kawashita, Y. Iwahashi, T. Kokubo, T. Yao, S. Hamada, and T. Shinjo, J. Ceram. Soc. Jpn. 112, 373 (2004).
- [7.] S. Deger, K. Taymoorian, D. Boehmer, T. Schink, J. Roigas, A. H. Wille, V. Budach, K. D. Wernecke, and S. A. Loening, Europ. Urol. 45, 574 (2004).
- [8.] S. Mornet, S. Vasseur, F. Grasset, and E. Duguet, J. Mat. Chem. 14, 2161 (2004).
- [9.] Q. A Pankhurst, J. Connolly, S. K. Jones and J. Dobson, J. Phys. D 36, R167 (2003).
- [10.] R. Hergt, W. Andra, "Magnetic Hyperthermia and Thermoablation" in "Magnetism in Medicine", Eds. W. Andra and H. Nowak, Second Edition (Wiley-VCH Verlag 2006).
- [11.] Proc. First Intl. Bioengg. Conf., F.K. Fuss, S.L. Chia, S.S. Venkatraman, S.M. Krishnan and B. Schmidt (eds.), Singapore, p.69 (2004).
- [12.] M. Zeisberger et al., J. Magn. Magn. Mater. **311**, 92 (2007)
- [13.] R. Hergt et al., J. Magn. Magn. Mater. **270**, 345 (2004)
- [14.] X. Wang, H. Gu and Z. Yang, J. Magn. Magn. Mater. **293**, 334 (2005)
- [15.] Gruttner C., Rudershausen S. and Teller J. (2001) "Improved properties of magnetic particles by combination of different polymer materials as particle matrix", J. Magn. Magn. Mat. Vol. 225 (1-2), pp. 1-7
- [16.] Pardoe H., Chua-anusorn W., St Pierre T.G. and Dobson J. (2001) "Structural and magnetic properties of nanoscale iron oxide particles synthesized in the presence of dextran or polyvinyl alcohol", J. Magn. Magn. Mat. Vol. 225 (1-2), pp. 41-46



¹ Zsolt Csaba JOHANYÁK, ² Kálmán Milán BOLLA

DEVELOPMENT OF A TOOLBOX SUPPORTING FUZZY CALCULATIONS

^{1,2}KALMÁR SÁNDOR INSTITUTE OF INFORMATION TECHNOLOGIES,
KECSKEMÉT COLLEGE, KECSKEMÉT, HUNGARY

ABSTRACT:

Alpha-cut based calculations are widely used in fuzzy arithmetic and fuzzy rule interpolation based reasoning. One of the key issues of the successful development of these applications is the availability of a toolbox that makes possible the quick and efficient calculation of the α -cuts' endpoints. In this paper, after reviewing some basic theoretical concepts, we present the methods of the α -cut calculation in case of the most used membership function types. The presented methods were also implemented in C# in form of a dynamic link library, which is easy useable in every .NET or traditional Windows or Linux targeting software applications.

KEYWORDS:

α -cut calculation, fuzzy set, toolbox

1. INTRODUCTION

Fuzzy sets can be seen as an extension of the traditional set concept. In case of a crisp (traditional) set (A) every x element of a universe of discourse X can be evaluated only two-way, either as part of the set ($x \in A$) or as not belonging to the set ($x \notin A$). Contrary to this all-or-nothing approach the fuzzy concept [11] makes possible a more colorful interpretation of boundaries. It allows the expression of the membership's measure not only by 0 and 1 but also by any value of the unit interval.

The fuzzy approach has been successfully applied in several areas of the science and the everyday life. Thus has been emerged the fuzzy arithmetic (e.g. [2],[3]) and one can find many practical applications in the field of control (e.g. [9],[4]) or fuzzy modeling of processes and systems (e.g. [6]). A huge amount of these applications does the computations α -cut wise based on Zadeh's extension principle [3]. One of the key issues of the successful practical application is the availability of a toolbox that supports the auxiliary calculations, i.e. the quick and efficient determination of the α -cuts.

In this paper, after reviewing some important theoretical concepts, we present the α -cuts' calculation methods for the most often used membership function types. The methods being presented were also implemented in C# in form of a dynamic link library, which is easy useable in every .NET or traditional Windows or Linux targeting software applications.

2. FUZZY SETS AND RELATED CONCEPTS

In this section we review briefly some concepts and definitions that are strongly related to the α -cut calculation and its applications.

Universe of discourse. Notation: X or U .

The universe of discourse is a crisp (traditional) set, also called domain, from which the members of a fuzzy set are taken. For example the set of the real numbers (\mathcal{R}) can be an universe of discourse.

Fuzzy set. Notation: capital roman letter, e.g. A .

The fuzzy set can be seen as an extension of the traditional set concept. While in case of the crisp sets each member of the universe of discourse can be tagged squarely as member of the set or outsider, in case of fuzzy sets one can assign a membership level as well.

Membership function. Notation: μ_A .

The function $\mu_A : X \rightarrow [0,1]$ expresses in which measure the members of the universe X belong to the fuzzy set A .

Normal fuzzy set.

The fuzzy set A is considered normal if $\exists x \in X$, for which $\mu_A(x) = 1$.

α -cut. Notation: $[A]_\alpha$.

The α -cut of a fuzzy set (A) is a crisp set that is defined by

$$[A]_\alpha = \{x \in X \mid \mu_A(x) \geq \alpha; \alpha \in (0, 1]\} = [\underline{a}_\alpha, \bar{a}_\alpha], \quad (1)$$

where $\underline{a}_\alpha = \inf\{ [A]_\alpha \}$ and $\bar{a}_\alpha = \sup\{ [A]_\alpha \}$ are the lower respective upper endpoints of the α -cut.

Convex fuzzy set.

A fuzzy set (A) is convex when all of its α -cuts are convex sets

$$\mu_A(\lambda x_1 + (1 - \lambda)x_2) \geq \min[\mu_A(x_1), \mu_A(x_2)] \quad \forall x_1, x_2 \in \mathfrak{R}^2, \lambda \in [0, 1]. \quad (2)$$

Support. Notation: $\text{supp}(A)$ or $[A]_{0+}$.

The support of a fuzzy set is defined by

$$\text{supp}(A) = \{x \in X \mid \mu_A(x) > 0\}. \quad (3)$$

Core. Notation: $\text{core}(A)$.

The core of a fuzzy set is crisp set that contains those elements of X for which the membership function takes its maximum value

$$\text{core}(A) = \{x \in X \mid \mu_A(x) = \max(\mu_A(x))\}. \quad (4)$$

Compact fuzzy set.

A fuzzy set (A) is compact when its support is bounded, i.e. $\exists x_1, x_2 \in X$, $\text{supp}(A) \subset [x_1, x_2]$.

Fuzzy number.

A fuzzy set A ($\mu_A : \mathfrak{R} \rightarrow [0, 1]$) is a fuzzy number when fulfills the following requirements [2].

- ❖ The set is convex and normal.
- ❖ The membership function is at least piece-wise continuous.
- ❖ The set is compact on \mathfrak{R} .

Reference point. Notation: $RP(A)$

The reference point of a fuzzy set (A) is that element of X , which is in one or more aspects characteristic to the position of A . The reference point is used by several fuzzy methods (e.g. fuzzy rule interpolation based inference techniques) for the characterization of a set's position. Although there are several options for its selection, usually the center point of the set's core is applied for this task [1].

Left/Right flank.

The point $\{RP(A), \mu_A(RP(A))\}$ divides the membership function (set shape) into two parts called left and right flanks of the set.

3. ALPHA-CUT COMPUTATION

Several fuzzy methods use the set's left and right flanks separately for the calculations; furthermore in several cases one needs different α -cuts in case of the two flanks. In order to satisfy this need our toolbox calculates and handles separately the lower and upper endpoints of the cuts. The calculation methods were developed for the most frequently applied convex membership function types, which are the singleton, the triangle, the trapezoidal, the piece-wise linear, the bell-shaped (Gauss), and the LR type.

3.1. SINGLETON TYPE MEMBERSHIP FUNCTION

The α -cut computation is the simplest in case of the singleton type fuzzy sets (see figure 1.a), because one needs to know only the value of the parameter a . Here the membership function is described by

$$\mu_{\text{Singleton}}(x; a) = \begin{cases} 0 & x \neq a \\ 1 & x = a \end{cases} \quad (5)$$

All cut endpoints are identical with the value a .

3.2. TRIANGLE SHAPED, TRAPEZOIDAL AND CONVEX PIECE-WISE LINEAR TYPE MEMBERSHIP FUNCTIONS

In case of triangle shaped, trapezoidal and convex piece-wise linear type membership functions the α -cut computations are similar, thus we discuss these cases together. First of all let us give a brief description of the formulas used for their calculation. We can describe the triangle shaped membership function (see Fig. 1.b) by

$$\mu_{triangle}(x; a, b, c) = \max\left(\min\left(\frac{x-a}{b-a}, \frac{c-x}{c-b}\right), 0\right), \quad (6)$$

where the parameters a , b , and c define the break-points of the shape. Similarly the trapezoidal type membership function (see Fig. 1.c) is defined by

$$\mu_{trapezoid}(x; a, b, c, d) = \max\left(\min\left(\frac{x-a}{b-a}, 1, \frac{d-x}{d-c}\right), 0\right), \quad (7)$$

where the parameters a , b , c , and d define the break-points of the shape. The i^{th} line segment of a convex piece-wise linear membership function (Figure 1.d) is given by

$$\mu_{pwl}(x; p_i, p_{i+1}) = \mu_{p_i} + (x - x_{p_i}) \cdot \frac{\mu_{p_{i+1}} - \mu_{p_i}}{x_{p_{i+1}} - x_{p_i}}, \quad x \in [x_{p_i}, x_{p_{i+1}}]. \quad (8)$$

where $p_i = \{x_i, \mu_i\}$ and $p_{i+1} = \{x_{i+1}, \mu_{i+1}\}$ are the bounding points of the line segment.

In case of the membership function types (6)-(8) the computation of the α -cuts is based on similar triangles. A third point is assigned to the two endpoints of the line segment (Fig. 2) in order to form a rectangular triangle. p_i and p_{i+1} are adjacent points where the x and μ values (co-ordinates) are known. The sides of the triangle can be calculated by their help.

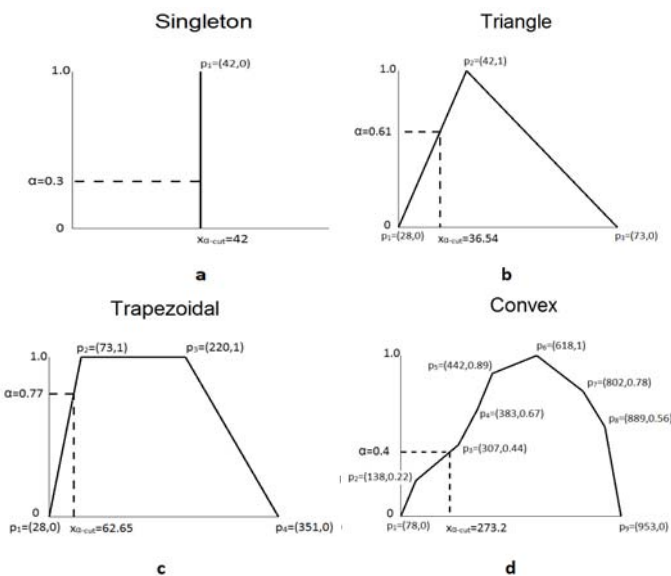


Figure 1 Singleton (a), triangle shaped (b), trapezoidal (c), convex piece-wise linear (d) membership functions and the lower endpoints of their α -cuts

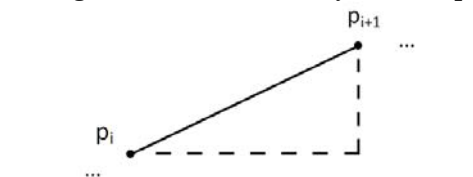


Figure 2. The i^{th} linear segment of the set shape

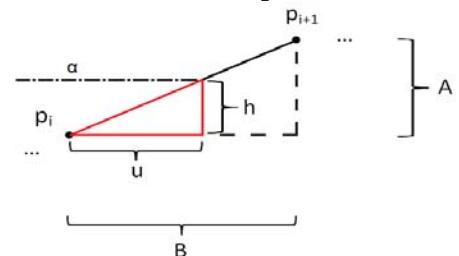


Figure 3. Similar triangles

The determination of a left endpoint of an α -cut is shown in Fig. 3 (the computation of the right endpoint is similar). The figure also shows that the α -cut creates a new triangle. The two existent triangles are similar ones. Their most important feature is that the corresponding sides are in the same ratio. The α -cut computation becomes straightforward owing to this feature.

Fig. 3 shows that the two known sides of the first triangle are A and B . The corresponding sides of the triangle created by the α -cut are h and u , where the size of h is known. Our task is to determine u . In case of the α -cut's left endpoint the x co-ordinate of p_i plus the size of u give the endpoint we are looking for (in case of the α -cut's right endpoint u is subtracted from the abscissa of the p_{i+1} point). For the computation of u the following equations are used.

$$\frac{A}{h} = \frac{B}{u} \quad (9)$$

$$u = \frac{B \cdot h}{A} \quad (10)$$

3.3. SMOOTH MEMBERSHIP FUNCTIONS

In case of smooth membership functions (e.g. Gaussian, LR, etc) the α -cut computations are similar, thus we discuss these cases also together. An example of a Gaussian type membership function is shown in Fig. 4. It is calculated by the formula:

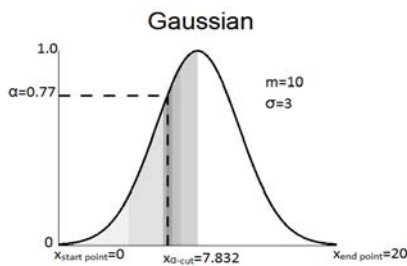


Figure 4 Gauss type membership function and the lower endpoint of its α -cut

$$\mu_{Gauss}(x; \sigma, m) = e^{-\frac{(x-m)^2}{2\sigma^2}}, \quad x \in [x_{start}, x_{end}] \quad (11)$$

where σ is the variance and m is the expected value, and x_{start} , x_{end} are the lower respective upper bounds of the partition.

One calculates the LR function by

$$\mu_{LR}(x; \alpha, \beta, c) = \begin{cases} \max\left(0, 1 - \left(\frac{c-x}{\alpha}\right)^2\right) & x < c \\ e^{-\left|\frac{x-c}{\beta}\right|^3} & x \geq c \end{cases}, \quad x \in [x_{start}, x_{end}]. \quad (12)$$

Here we use the bisection method for the calculation of the endpoints of the cuts. After bisecting an interval, one calculates the membership value for the resulted abscissa value (x) using the equation (11) or (12). One continues the search in that half interval which contains the demanded α -value. Fig. 4 illustrate the steps of the algorithm. After each bisection one chooses the darker half interval containing the α value. The stopping condition of this method is the execution of 100 iterations, which usually provides a sufficiently good approximation.

4. CONCLUSIONS

The presented calculation methods were implemented in C# in form of a dynamic link library (DLL). The lower and upper endpoints of the α -cuts can be calculated by calling the *AlphaCut* method. It takes as parameters the membership function type (we defined an enumeration type for this purpose), the actual parameters of the shape, two array containing the α -levels for which the lower and upper cut-endpoints have to be calculated, as well as two references for the two arrays in which the results will be returned.

We applied the toolbox successfully in course of the development of the software support for a fuzzy arithmetic based student evaluation method (FUSBE) [5], as well as in course of the implementation of an α -cut based fuzzy rule interpolation method called LESFRI [7].

Further research plans include the consideration of other possible quicker algorithms for the calculation of the α -cuts in case of smooth membership function types.

REFERENCES

- [1] Baranyi, P., Kóczy, L. T. and Gedeon, T. D.: A Generalized Concept for Fuzzy Rule Interpolation, in IEEE Transaction on Fuzzy Systems, Vol. 12, No. 6, 2004, pp 820-837.
- [2] Fodor, J., and Bede, B.: Arithmetics with fuzzy numbers: a comparative overview, in Proceedings of the 4th Slovakian-Hungarian Joint Symposium on Applied Machine Intelligence (SAMI 2006), Herlany, Slovakia, 2006, pp. 54-68.
- [3] Hanss, M.: Applied Fuzzy Arithmetic. An Introduction with Engineering Applications, Springer, Berlin, 2005.
- [4] Hladek, D., Vascak, J., Sincak, P.: Multi-Robot Control System For Pursuit-Evasion Problem; Journal of Electrical Engineering, Vol. 60, No. 3, 2009, pp. 143-14.
- [5] Johanyák, Z.C.: Fuzzy set theory based student evaluation, Proceedings of IJCCI 2009 - International Joint Conference on Computational Intelligence, 5-7 October, Funchal-Madeira, Portugal, pp. 53-58.
- [6] Johanyák, Z.C., Ádámné, M.A.: Fuzzy Modeling of the Relation between Components of Thermoplastic Composites and their Mechanical Properties, Proc. of the 5th Int. Symp. on Appl. Comp. Int. and Informatics, 2009, Timisoara, Romania, pp. 481-486.
- [7] Johanyák, Z. C., Kovács, S.: Fuzzy Rule Interpolation by the Least Squares Method, 7th Int. Symp. of Hung. Res. on Comp. Int. (HUCI 2006). 2006 Budapest, pp. 495-506.
- [8] Klir, G. J. and Folger, T. A.: Fuzzy Sets , Uncertainty, and Information, Prentice-Hall International Inc., Binghamton, 1988.
- [9] Precup, R.E. Doboli, S., Preitl, S.: Stability analysis and development of a class of fuzzy systems. Engineering Appl. of Art. Int., vol. 13, no. 3, June 2000., pp. 237-247.
- [10] Škrjanc, I., Blažič, S., Oblak, S., Richalet, J.: An approach to predictive control of multivariable time-delayed plant: Stability and design issues, ISA Transactions, vol. 43, no. 4, Oct. 2004, pp. 585-595.
- [11] Zadeh, L. A.: Fuzzy Sets, in Information and Control, Vol. 8, 1965, pp. 338-353.



SAFETY ANALYSIS OF CRYPTOGRAPHY MECHANISMS USED IN GSM FOR RAILWAY

^{1,2,3} UNIVERSITY OF ŽILINA, FACULTY OF ELECTRICAL ENGINEERING, DEPARTMENT OF CONTROL AND INFORMATION SYSTEMS, ŽILINA, SLOVAKIA

⁴ TEMPEST, A. S., GBC IV, GALVANIHO 17/B, 821 04 BRATISLAVA, SLOVAKIA

ABSTRACT:

The paper deals with problems related to safety analysis of cryptography mechanisms that are applied in the GSM-R system. Within introduction the authors briefly describe necessary background and position of the GSM-R and Euroradio in the European Train Control System. To ensure required safety level, in the context of OSI Reference Model an additional safety layer must be implemented consisting of two sub-layers: Euroradio Safety Layer and Safety Application Interface. The authors address only the former when paying attention to safety analysis of cryptographic mechanisms applied. To demonstrate and verify some of theoretical findings, an experimental part has been involved to show results of the particular attack to the DES algorithm, in this case an attack based on the birthday paradox realised via UML.

KEYWORDS:

safety-related communication, Euroradio, GSM-R, cryptoanalysis, block cipher, CBC-MAC, 3-DES

1. INTRODUCTION

Any railway infrastructure operator operating in the Central Europe area should endeavour to modernize trans-European corridor lines as fast as possible, with the highest investment priority. Requirement for corridors modernization results from a need to provide the best quality of railway infrastructure respecting both technological and legislative bases according to the latest technologies and European standards.

To fulfil really this requirement means to implement the European Train Control System (ETCS) as a part of the European Rail Traffic Management System (ERTMS) [1] that has been developed since early 90-ties of the 20th century. The main objective of the ERTMS programme is to design a standardized European rail system, common for all EU countries, which will make possible movement of trains equipped with the ETCS wherever within the European railway network. Based on the track-side ERTMS/ETCS equipment the ETCS may be built on one of three basic application levels L1, L2 and L3 [2]. For the ETCS level L2 and higher the technical solution also must inevitably comprise the Global System for Mobile Communications – Railway (GSM-R) which provides radio information transmission between a stationary and mobile part of the ETCS system.

The GSM-R network, as a technological base for open communication system in the railway transport was chosen and specified within the EIRENE and MORANE projects solved under the auspices of the International Union of Railways (UIC). The project EIRENE led to specification of system and functional requirements representing a fundamental interoperability frame for mobile radio communication at lines of the European conventional railway system according to TSI CCS (Technical Specifications for Interoperability Control-Command and Signalling). The final documents [3] and [4] define a set of requirements to the railway radio communication system. The GSM-R system specification results from a technological platform of digital public cell radiophone GSM system extended for specific requirements of railways and properties required from the

professional radio system dedicated to railway operation. From the topology point of view, the GSM-R system is a line system, unlike the public GSM system with an area topology. The GSM-R cells are typically overlapped, sometimes up to a half cell; due to ability to serve a mobile station MS reliably at any place. Assumed velocities within the GSM-R network are up to 350 km/h and frequency bands reserved for data transmission are „uplink“ (876 – 880 MHz) and „downlink“ (921 – 925 MHz).

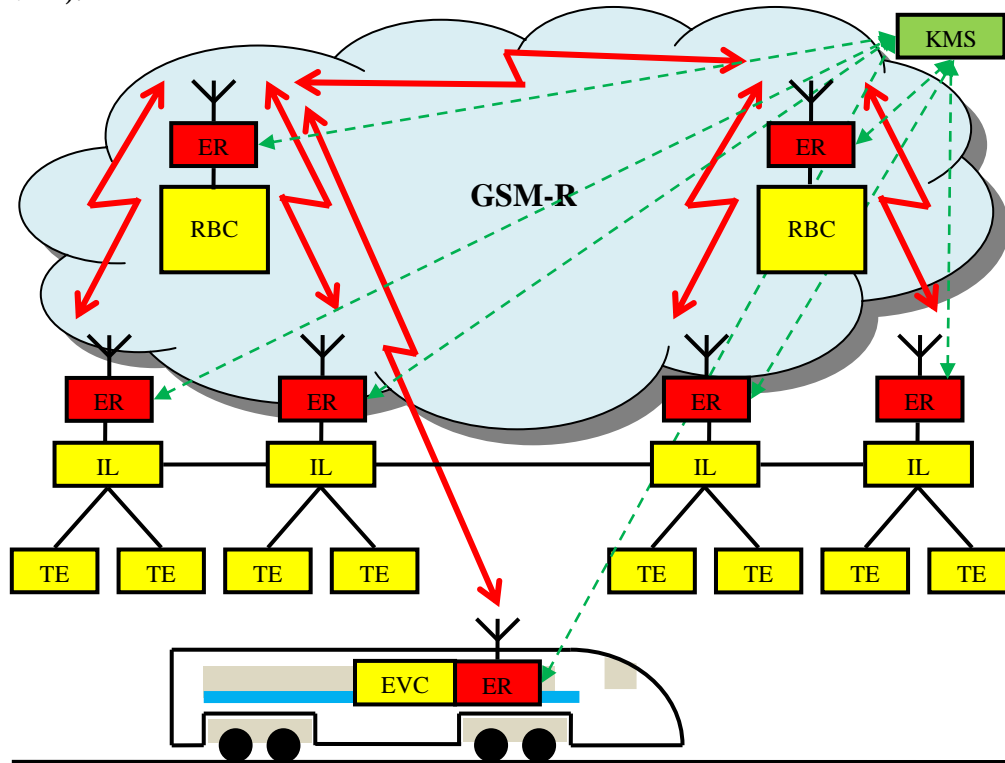


Figure 1. Localisation of GSM-R and ER systems in ETCS architecture

Figure 1 shows usage of the GSM-R system within the ETCS L2. Information needed for railway traffic control (train position, vacancy of track sections, etc.) obtained from Trackside Elements (TE) is concentrated to classical railway interlocking and signalling systems (IL) and from there transmitted via EuroRadio (ER) system and the GSM–R communication network. On the base of that information the Radio-Block Centre (RBC) transmits move permissions to individual trains together with other information, again using EuroRadio (ER) and the GSM-R communication network. A train sends backward information on its position and other train data to RBC. All functions related to supervision and controls of train velocity are performed by the central European Vital Computer (EVC) located on board the locomotive. EuroRadio needs a key management system (KMS) due to management of keys used in cryptographic algorithms.

2. SAFETY OF GSM-R NETWORK

Since the GSM-R transmission system is classified to open transmission systems (classes 6 and 7 according to [5]) it is necessary to assess risk of unauthorised access and consider all threads listed in the standard [5]. According to [5] messages transmitted by ETCS system correspond to the message model of A1 type utilizing the secure cryptographic code with a secret key. Communication between system components is based on layer principle and meets standardised demands for safety-related communication. Additional safety-related layer, added to standard layers of the Open System Interconnection Reference Model (RM OSI) is formed by two sub-layers:

- ❖ EuroRadio Safety Layer (EuroRadio SL) [6];
- ❖ Safety Application Interface (SAI) [7].

Within the RM OSI they are integrated above transport layer, having an adaptation layer between them. Figure 2 shows a reference structure of the message for functional specification of interface between trackside subsystems A and B. EuroRadio Safety Layer is responsible for secure data transmission which implies protection against threats such as corruption, masking or inserting a message, establishment and release of secure communication link together with error handling. Among secure procedures of the layer there are procedures ensuring message authentication and integrity during transmission. They are realized with the help of the cryptographic technique MAC

(Message Authentication Code) which is a function of the message M and the shared key K_c , when applying operation of ciphering C . The formal notation of MAC calculation is:

$$MAC = C_{K_c}(M). \quad (1)$$

MAC is calculated both at the side of transmitter which adds it to the message being sent, and the side of receiver which verifies coincidence of received and self-calculated authentication codes.

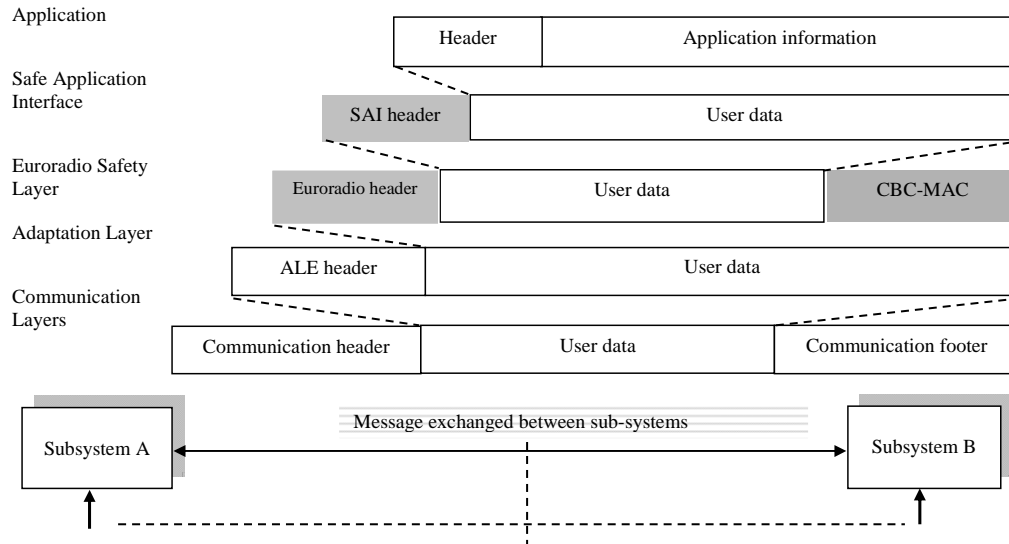


Figure 2. Reference structure of the message

If the codes are equivalent it may be assumed the message has not been corrupted (message integrity), and the message has been sent by the original sender because no one else shares the secret key. To increase safety of procedure for MAC calculation in Euroradio Safety Layer the chained mode of Cipher Block Chaining MAC (CBC-MAC) is used together with the algorithm Triple-DES in EDE mode (Encryption – Decryption - Encryption), also known as a Triple Data Encryption Algorithm (TDEA) defined in ANSI X9.52 [8]. Another safety procedure of the Euroradio SL is procedure for peer entity authentication, which also uses the algorithms CBC-MAC and Triple-DES. In addition to mutual authentication of communicating partner entities the procedure also outputs the session key K_s . The paper only contains a detailed analysis of the Euroradio SL.

3. SAFETY ANALYSIS OF CRYPTOGRAPHY MECHANISMS IN EURORADIO SL

Fundamental requirement of the cryptosystem applied in Euroradio is that implemented cryptographic mechanisms must be able to resist cryptoanalytic attacks during the whole life-cycle of the system. To make assessment of safety and effectiveness of applied cryptographic algorithm those cryptoanalysis methods may be used that are based on complexity theory. Computationally complexity of the algorithm can be determined on the base of asymptotic complexity describing how behaviour of the algorithm changes in dependence on the size of n input data. Operation complexity is usually notated O (called Landau notation or Bachmann-Landau notation) and is a function of input data $O(f(n))$ [9]. It is a limit description of the function curve, so called asymptotic upper limit of the magnitude MG of the function $f(n)$ expressed by other (usually simpler) function $g(n)$. Computation complexity is usually determined by three parameters: space S , time T , and data D .

Algorithm optimisation is then related to minimisation of one out of these three parameters. Algorithms applied in computer science most often have one of the following complexities (m is a real number, $m > 1$):

- ❖ Linear complexity: $O(n)$
- ❖ Logarithmic – linear complexity: $O(n \cdot \log n)$
- ❖ Polynomial complexity: $O(n^m)$
- ❖ Exponential complexity: $O(m^n)$
- ❖ Combinatorial complexity: $O(n!)$

The fastest algorithms are considered algorithms with linear, logarithmic-linear or polynomial complexities, algorithms with exponential or combinatorial complexities are realizable in real-time only for low number of inputs n .

Safety analysis of cryptographic algorithms used to secure GSM-R communication via Euroradio system must be concentrated on safety assessment of the CBC-MAC algorithm based on Triple-DES, which is applied within the Euroradio SL.

As inputs to safety procedure of CBC-MAC calculation based on Triple-DES the following entities can be seen: the session key K_S with sub-keys K_1, K_2, K_3 , message M and cryptographic key K_C shared by transmitter with the source address S_A and receiver with destination address D_A . Addresses S_A and D_A represent entities of the ETCS (e.g. RBC and EVC).

Safety procedure of CBC-MAC calculation in the Euroradio SL can be described in the following way:

1. A flag is set to the value log. 0 in the case of communication initiator (transmitter) or the value log. 1 in the case of respondent (receiver).
2. Destination address D_A is added to beginning of the message: $D_A _ M$ (the symbol „_“ represents concatenation).
3. A length of the chain $D_A _ M$ (denoted as d , in the form of two octets added ahead the chain: $d _ D_A _ M$).
4. If a length of the chain $d _ D_A _ M$ in bits is not a multiple of 64 (block size), at the end of the message padding p is added: $d _ D_A _ M _ p$.
5. The authentication code MAC is calculated from the chain $d _ D_A _ M _ p$ and the shared key K_C using the chained mode CBC-MAC based on symmetric Triple-DES cipher which can be written in the following way: $MAC(M) = CBC-MAC(K_C, d _ D_A _ M _ p)$.

Let the session key consists of three parts of the same length (64 bits) $K_C = (K_1, K_2, K_3)$ with the total length 192 bits, including parity bits (every eighth bit). Let data chain (message) consists of bit blocks $X_1, X_2, X_3, \dots, X_q$. Every block has a size of 64 bits. Encryption function E is a ciphering operation of the DES algorithm in the basic mode, which performs ciphering of data chain with use of the key K_i for $i = 1, 2, 3$, and decryption E^{-1} is decryption operation of the DES algorithm. Then individual parts of the key are applied when creating the authentication code MAC in the CBC operation mode for data chain parts X_i using the formula (2). Result of the iteration procedure is $H_q = CBC-MAC(M)$.

$$\begin{aligned} H_0 &= 0, \\ H_i &= E(K_1, H_{i-1} \oplus X_i); i=1,2,\dots,q-1, \\ H_q &= E(K_3, E^{-1}(K_2, E(K_1, H_{q-1} \oplus X_q))). \end{aligned} \tag{2}$$

From the cryptanalytic view, calculation of the authentication code in the chained CBC-MAC mode of the cryptographic Euroradio protocol implies several essential facts:

- ❖ 192 bit key K_S is used sliced to 3 equally long parts K_1, K_2, K_3 , while every eighth bit of the key is the parity bit.
- ❖ Function $E(K,P)$ represents encryption of input P by the block cipher DES with a key K . Function $E^{-1}(K,C)$ is decryption of the C by the cipher DES with a key K . Thus input to procedure is divided to 64 bit blocks X_1, X_2, \dots, X_q .
- ❖ Message M is extended using a prefix „ $d \mid D_A$ “, where d is a length of the chain „ $D_A \mid M$ “ in octets, and p is padding of the last block X_q to the size 64 bits.
- ❖ Hash function CBC-MAC is initialised by zero initialisation vector (IV), formula (2).
- ❖ The first $q-1$ steps of the procedure represent a simple DES cipher in a chained CBC mode.
- ❖ The last step q is a cipher Triple-DES in so called EDE mode (Encryption - Decryption - Encryption) only.

It is apparent that using the Triple-DES or DES algorithms in a chained mode (multiple operation mode) increases safety of the DES algorithm but what also should be considered is the fact that in the formula (2) the simple DES is used in $q-1$ steps.

Quite a lot of cryptanalytic works have been published, describing theoretical attacks to the DES, faster than brute force attack with computing complexity $O(2^{56})$. There are known several attacks to all 16 rounds of the DES cipher (there are also attacks to the reduced version of the cipher having less than 16 rounds of calculation). There are known attacks based on differential cryptanalysis [10] and linear cryptanalysis [11]. It seems that so called Davies attack [12] is very efficient, based on assumption of knowledge of a certain number of pairs of input and output data that can be used for determining so called empirical distribution of certain characteristics. In this way several bits of the key may be found, the rest of them can be detected using a brute force attack. For 2^{52} known pairs of input and output data it is possible to determine 24 bits of the key with probability of success about 53%.

Usage of the TDEA or DES algorithms in a chained mode (multiple operation mode) increases safety of the DES algorithm. However, as shown in [13], theoretical power of the algorithm is only $O(2^{84})$ at 228 known encrypted data, or $O(2^{112})$ at the use of meet-in-the-middle

attack which is under present conditions, permanently growing computing capabilities and in certain applications sufficient only for several coming years. The National Institute of Standard Technology (NIST) confirmed the Triple-DES as a cipher applicable concurrently with the AES for sensitive government data till 2030 year [14]). Meet-in-the-middle attack is a standard technique for cryptanalysis of the TDEA algorithm, in principle it is similar to a birthday paradox.

In an experimental part of the paper there is realization of an attack based on the birthday paradox which reduces the power of the key by the square root of the key size. This attack can also be extended to the DES applied in a multiple operation mode with an initialisation vector. Then for m multiple mode of the cipher the computing complexity $O(2^{m.k/2})$ is assumed at $2^{k/2}$ known encrypted data, if used in combination with the meet-in-the-middle attack.

Supposed that a head (prefix) of the message (input data) A with a larger number of bits than a key is known, every message has it the same (on each occasion encrypted with a different key), it is possible to obtain one of the keys through this attack (actual for a certain modification of the algorithm) as early as for $2^{k/2}$ messages, where k is size of the encryption key. Let l is a number of casually chosen keys K , which will be used to encrypt a head of the message A and result will be inserted to the table as a pair $[E(K, A), K]$, while encryption result $E(K, A)$ will be an index of the table and K its value. Let's choose a number of obtained encrypted messages n , which will be used to extract encrypted head C . On each occasion when a message is received we can have a look into a table whether C is obtained or not. If yes the value for this row of table is the used encryption key. Another possibility is using two tables and analysing an encrypted message without pre-calculation of casually encrypted heads. Probability of finding one of n used keys is expressed by the formula (3).

$$P_S = 1 - (1 - l \cdot 2^{-k})^n = 1 - \left(1 - \frac{1}{2^k/l}\right)^n \geq 1 - e^{-l \cdot n / 2^k} \quad (3)$$

If $l \cdot n \geq 2^k$, probability of finding the key P_S is high (e.g. $l = 2^{k/2}$, $n = 2^{k/2}$). So under given circumstances (known prefix of the message, pre-calculation with casually chosen keys, searching in the table with a constant time) theoretical power of the DES algorithm is only $O(2^{28})$ at 2^{28} known encrypted data. This attack may also be extended to the DES applied in a multiple operation mode with the initialisation vector. Then for the m multiple mode of cipher there is assumed computing complexity $O(2^{m.k/2})$ at $2^{k/2}$ known encrypted data, if used in combination with meet-in-the-middle attacks.

4. EXPERIMENTAL VERIFICATION

Within the experimental verification a simple software application has been developed making possible to verify success of a birthday attack to the DES cipher with effective size of the key 56 bits. For this purpose the Unified Modeling Language UML 2.0 has been used supported by the Enterprise Architect 6.0 tool. A chosen development tool for Java has been Oracle JDeveloper 10.1.3.3. The application has been primarily designed as a console-based with opportunity for later GUI implementation. Logging is solved through the *log4j* frame. Running scripts with pre-set parameters have been written in the shell script. Class diagram of the model is shown in Figure 3. Package of cryptographic attacks *pch.crypto.attack* contains the following trends necessary for the attack realization:

- ❖ **ACryptoAttack** – abstract class creating an implementation frame for particular tasks, requires implementation of the method `doAttack()` from the descendent class returning instance of the class `AttackInfo`. Further there are methods implemented for writing to so called log (listing directed to file or to console, depending on configuration *log4j*) and to the standard system console.
- ❖ **BirthdayAttack** – implementing class of the birthday attack. Besides the overload method `doAttack(*)` performing one realization of attack set according to the class attributes, it also contains the overload method `doAttacks(*)` performing a chosen number of attacks and returning instance of the class `AttackStats`. This class is also the target class for running application from the console, so it contains the method `main(String[])`.
- ❖ **HalfSecureRandom** – descendant of the standard class of the language `java.security.SecureRandom`, covers the method `nextBytes(byte[])` to return a mirror symmetrical field of pseudorandom generated bytes.
- ❖ **Routines** – a class of accessory statistic methods.

The package of processing (statistic) data from attacks *pch.crypto.stat* contains classes for saving mentioned data (beans) and their processing:

- ❖ **AttackInfo** – a class with attributes containing data about the course and result of the attack.
- ❖ **AttackStats** – a class with attributes containing statistic data obtained from several attacks.

❖ **AttackStatCollector** – a class containing a container for collectivisation of instances AttackInfo and a method calculateStats() for processing of obtained data and creating the instance AttackStats.

The birthday attack according to variant with the use of two indexed tables without pre-calculation would need 2.2^{28} records (memory places) and the same number of encryptions for successful finding of the first key with high probability provided that within the application simulation of obtaining messages with different keys is also considered. Obviously time needed for writing and lookup in tables must also be calculated. Such large tables (either as objects in the operation memory or database) are practically unrealizable on the current hardware (the laptop HP Compaq nx7300 with two-core processor Intel Centrino Duo with clock frequency 2 GHz and operation memory 2 GB, frequency 997 MHz has been available), especially if feasibility is considered from statistic point of view, that is repeated running of the application with the same input parameters. Therefore it was necessary to reduce complexity of the task and thus decreasing effective size of the key. The simplest solution is to decrease effective size of the key to half so that cryptographic keys are generated in mirror symmetry (in bytes – to avoid problem with parity bites), so if n is a length of the key, the byte b_i is identical with the byte b_{n-i} for $i = 0, \dots, n-1$. Then the size of necessary tables (and thus also computing complexity) should be on average $2^{14} = 16384$ records for the successful attack.

Experimental results are summarized in Table 1. Expected probability of success P_S has been calculated according to the formula (3), $k = 28$, $l = n = k / 2$. Probability of successful experiment P_S^* is determined by the empirical formula as a proportion of successful and whole realisations of the experiment.

Table 1. Results of verification of the birthday attack to the modified cipher DES

Characteristics	Maximum number of attempts of the 2nd realisation			
	2^{12}	2^{13}	2^{14}	2^{15}
Number of realizations	1000	1000	1000	1000
Number of successful realizations	68	226	639	984
Number of unsuccessful realizations	932	774	361	16
Effective size of the key k [bit]	28	28	28	28
Probability of success P_S^*	0,068	0,226	0,639	0,984
Expected P_S	0,061	0,221	0,632	0,982
Average number of attempts	3949,888	7228,148	10811,649	11353,897
Average time of attack realization [s]	0,077	0,147	0,234	0,282

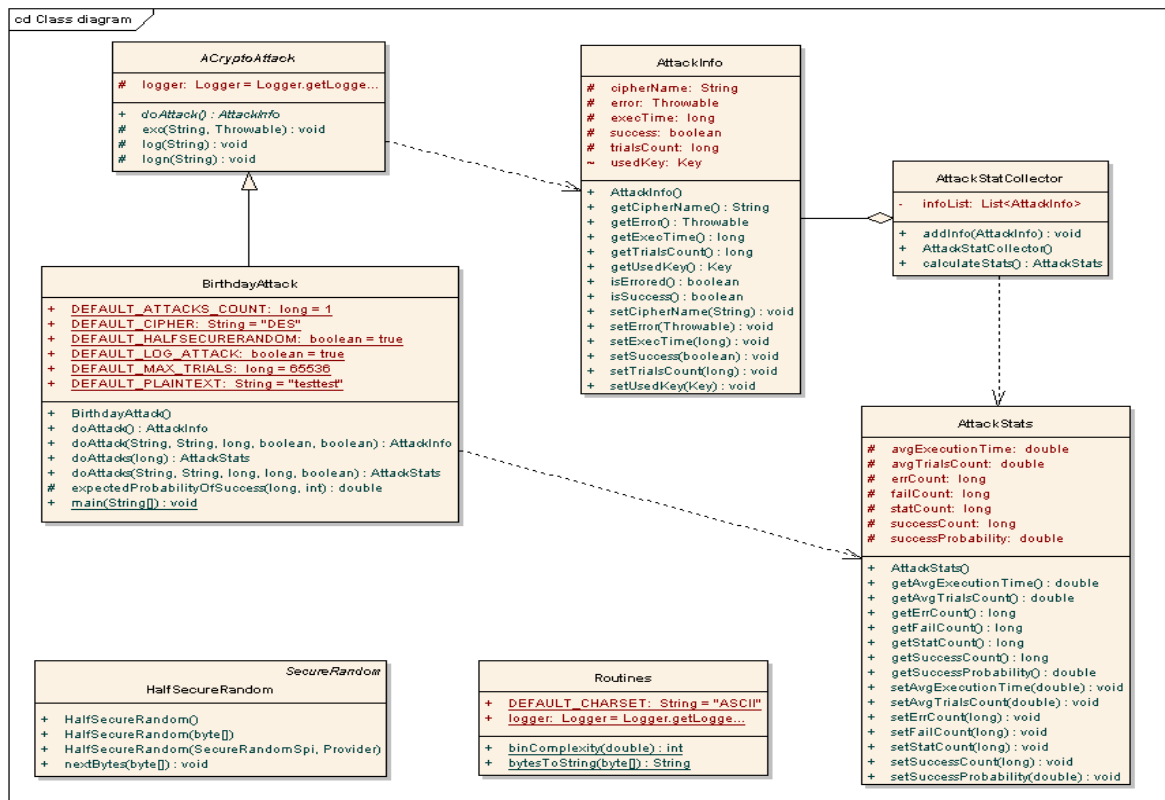


Figure 3. Class diagram of the application BirthdayAttack

On the base of experimental results we can state that theoretical assumes of the birthday attack have been successfully verified for the block cipher with intentionally decreased cryptographic power. On the other side it is necessary to emphasize that possibility of practical realization of such a type of attack in real cryptosystem is extremely low. However, the birthday paradox has been successfully used and applied in different types of theoretical considerations and as we can see it is also applicable for construction of cryptanalytic attack.

5. CONCLUSIONS

Safety of the Euroradio SL communication, particularly algorithms CBC-MAC and associated power of encryption of the authentication key, may be theoretically lower than expected.

Operation modes have been projected to reduce propagation of bit errors, they better overlay certain characteristics of input data and protect against attacks with chosen input data (chosen plaintext). Obviously higher safety of operation modes against cryptanalytic attacks has been assumed. However, theoretical safety is the same in comparison with simple encryption (usage of the key with the same length). Potential shortcomings of the safety procedure MAC may lead to disclosure of the session key. Then it should be mentioned that cryptographic power of the first q -1 steps of the chained CBC-MAC applied in the Euroradio SL is not higher than it is in the case of a simple DES algorithm usage.

Mentioned shortcomings may be improved in several ways. For example the DES cipher or 3-DES could be substituted with the AES cipher which features higher safety limits, higher flexibility of use and higher software efficiency. What's more modifications of safety mechanisms would be minimal. Size of the block would increase to 128 bits and one 192 bit key would be used. Another alternative of how to increase safety of the authentication procedure MAC based on the Triple-DES is to use a proper triple cascade code, for example CBC|CBC|CBC⁻¹ [15].

Acknowledgements

This paper was supported by the scientific grant agency VEGA, grant No. VEGA-1/0023/08 "Theoretical apparatus for risk analysis and risk evaluation of transport telematic systems".

REFERENCES

- [1.] <http://www.ertms.com>
- [2.] ZAHRADNÍK, J., RÁSTOČNÝ, K.: Safety of Railway Interlocking Systems. (in Slovak), EDIS Zilina, 2006, ISBN 80-8070-546-1.
- [3.] UIC EIRENE SRS: System requirements specification. 2006, PSA167D006-15.
- [4.] UIC EIRENE FRS: Functional requirements specification. 2006, PSA167D005-7.
- [5.] EN 501 59-2: Railway applications: Communication, signalling, and processing systems. Part 2: Safety-related communication in open transmission systems, 2001.
- [6.] Subset-037: Euroradio FIS. 2005, v 2.3.0
- [7.] FIS SAI: Safe Application Service. 2002, v 8.0, SI/TRK/UP/2.
- [8.] ANSI X9.52: Triple Data Encryption Algorithm Modes of Operation.
- [9.] <http://www.cs.cas.cz/portal/AlgoMath/MathematicalAnalysis/Inequalities/BachmannLandauNotation.htm>
- [10.] BIHAM, E., SHAMIR, A.: Differential Cryptanalysis of the Data Encryption Standard. Springer-Verlag, 1993, ISBN 3-540-97930-1.
- [11.] MATSUI, M.: Linear Cryptanalysis Method for DES Cipher. Advances in Cryptology – EUROCRYPT'93, In: Lecture Notes in Computer Science, Vol. 765, Springer-Verlag, 1993, p. 386-397, ISBN 3-540-57600-2.
- [12.] BIHAM, E., BIRYUKOV, A.: An Improvement of Davies' Attack on DES. Advances in Cryptology – EUROCRYPT'94, In: Lecture Notes in Computer Science, Vol. 950, Springer, 1995, p. 461-467, ISBN 3-540-60176-7.
- [13.] BIHAM, E.: How to Forge DES-Encrypted Messages in 228 Steps. In: Technical Report, Department of Computer Science, Technion, Haifa, Israel, 1996, CS 884.
- [14.] NIST SP 800-67: Recommendation for the Triple Data Encryption Algorithm (TDEA) Block Cipher. 2004, v 1.0.0.
- [15.] BIHAM, E.: Cryptanalysis of Multiple Modes of Operation. In: Technical Report, Department of Computer Science, Technion, Haifa, Israel, 1994, CS 0833.





¹Tibor MORAVČÍK, ²Emília BUBENÍKOVÁ, ³Ľudmila MUZIKÁŘOVÁ

DETECTION OF DETERMINED EYE FEATURES IN DIGITAL IMAGE

¹⁻³UNIVERSITY OF ŽILINA, FACULTY OF ELECTRICAL ENGINEERING,
DEPARTMENT OF CONTROL AND INFORMATION SYSTEMS, ŽILINA, SLOVAKIA

ABSTRACT:

This paper deals with problem of digital image processing, mainly with localisation of determined interest objects. As application area the eye localisation in a frame of video-sequence has been chosen with continuing in iris and pupil detection. The article contains a theoretical part, with preview of frequently used methods and reasoning of concrete methods selection. The next part presents the actual experiment realised via computing environment MATLAB. In paper conclusion the acquired results are summarised and commented.

KEYWORDS:

Digital image processing, localisation of interest objects, features of human eye, iris, pupil, circular Hough transform, threshold, MATLAB, Image Processing toolbox

1. INTRODUCTION

The localization of interest objects presents the important task of image analysis. At first, for eye image analysis it is necessary to detect the exact eye position, then its main parts and its parameters, e.g. the pupil, the iris, the eyelids, the border of the eyes. This information is used in different applications: monitoring of eye movement, iris extraction for biometrical identification purpose etc. According to the winking frequency it is possible to ascertain driver vigilance, too. In all listed cases several advisable methods of image processing are applied, which afford an opportunity to detect and to locate the interest areas in static image or video-sequence frame. For detection the typical features of eye and of its parts are used, which afford an opportunity to differentiate the particular objects. The resolution of input image is an important factor, which limits the choice of adequate methods. The resolution of eye image for its analysis has a fundamental influence on its precision. Some methods can not be used due to low image resolution because of insufficient details. Generally, image analysis deals with compromise between processing reliability and required processing time. The lower resolution is often used for acceleration of detection process, for working in real time with frames of video-sequence. In these cases the eye area is acquired from the face image cut-out. In the frames of face in resolution 640x480 cut-out of the eye can represent too small part of the frame.

2. LOCALISATION OF HUMAN EYE AND DETECTION OF ITS PARTS

2.1. Features of human eye

The most significant feature in the eye is the iris with a large variety of colours. The iris is the annular part between the pupil and the sclera. Iris and pupil can be taken approximately as non-concentric circles. Apart from these features, the eye has two additional features – the upper and lower eyelid. The ring of the iris might not be completely visible even if the eye is in its normal state, because its top and bottom part are often covered by eyelids and eyelashes. Pupil size varies depending on the light conditions and it is darker than the rest of the eye, even in brown or dark eyes. Sclera is the white visible portion of the eyeball. At a glance with unaided eye, it is the brightest part in the eye region, which directly surrounds the iris. The radius of iris can be defined

by the anthropometric measures approximately as $1/6$ of the length of the eye. The next constraint for iris detection is that the directions of the edge gradient and the normal to the annulus should not differ more than $\pi/6$. The iris is always darker than the sclera no matter what colour it is. In this way the edge of the iris is relatively easy to detect as the set of points that are disposed on a circle. In Fig. 1 are shown all main features in the human eye.

2.2. Methods for localization of eyes

Eyes can be generally localized from face image in two ways. Either is first detected face or eyes are detected from whole image, with using active infrared (IR) based approaches or image-based passive approaches. Eye detection based on active remote IR illumination is a simple effective approach which relies on an active IR light source to produce the dark or bright pupil effects. This method is not widely used, because in many real applications the face images are not IR illuminated. This paper only focuses on the image-based passive methods, which do not affect the input image. In our application we are detecting position of eyes in two steps, the first is locating face to extract eye regions and the second is eye detection from eye window. The face detection problem has been faced up with different approaches: neural network, principal components, independent components, skin colour based methods etc.

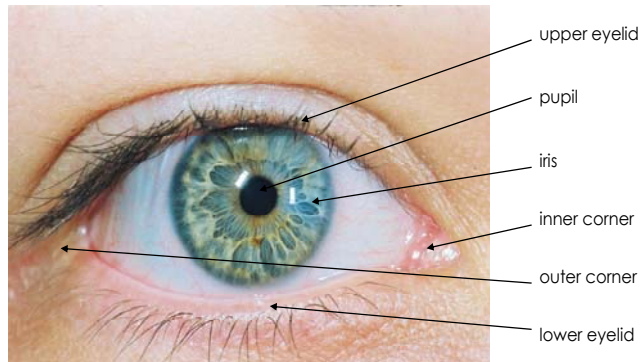


Figure 1. Eye features

We used the method Viola – Jones [1] where face is detected in image with using of AdaBoost classifiers. The image-based passive methods can be classified into three categories. First, template based method, secondly is feature based method and the third is the appearance based method [2]. In the template based method, a generic eye model, based on the eye shape, is designed first. Template matching is then used to search the image for the eyes. While this method can detect eyes accurately, it is normally time-consuming. The appearance based method detects eyes based on their photometric appearance. For this method is needed a large amount of data, representing the eyes of different subjects in different conditions for training classifiers (e. g. neural network or the support vector machine). Feature based methods use for detecting the characteristics of eyes such as contrast difference between iris, pupil and sclera and their edges. This method has a problem with low contrast images. In [3] circular Hough transform is used to detect the iris border where both centre and radius are estimated simultaneously. In some approaches, the iris radius is supposed to be known or limited to a set of expected values.

2.3. Detecting of eye features

The main objective of our work is to detect features such as iris and pupil boundary in eye region. Many distinct approaches have been proposed in this area. [4] Integrodifferential operator is introduced in [5] to find both the iris inner and outer borders. This operator is sensible to the specular spot reflection of non diffused artificial light. Wildes [6] uses for iris segmentation binary edge map followed by circular Hough transform. Liam et al. [7] have proposed a simple threshold method with function maximisation to obtain iris inner and outer borders. Another approach [16] is finding approximate pupil centre as minimum value of the summation of intensity along each row and each column. Then it is applying Canny edge detection and Hough transformation for detection of exact pupil centre. Also morphologic operators, Laplacian or Gaussian operator for edge detection with median filter can be applied to obtain iris borders [2].

In order to locate eye corners, one general approach is utilization of deformable templates [2] which requires a good initialization for correct work, and another common approach is projection functions [9]. Lastly, the proposed methods for eyelids can be classified under two groups: using deformable contour models or curve fitting [2].

In our work we focus on detecting iris and pupil as features of eye. From all approaches mentioned above, we chose circular Hough transform for detecting circles of iris. Hough transform is a very precise technique which can be used to isolate features of a particular shape within an image.

3. APPLICATION OF SELECTED METHODS

In our application we acquire the eye areas proportionally from face dimension. Moreover, these larger areas contain the eye image background too. This background is necessary to be eliminated, than we can work only with the area, which responds to the eye. For distinguishing the

objects from background and for the precise eye localisation we used combination of the image segmentation methods, thresholding and edge-based methods. Before using these methods, pre-processing is applied to image for improving the details and adjust the contrast differences. We use histogram equalization, Gamma correction to improve its contrast and brightness and median filter to eliminate the noise [10].

Thresholding is the transformation of an input image f to an output binary image g as follows:

$$g(i, j) = 1 \quad \text{for } f(i, j) \geq T, \quad (1)$$

$$= 0 \quad \text{for } f(i, j) < T,$$

where T is the threshold. Since the eye borders are markedly darker, applying adequate threshold allows dividing the background [11]. An example of thresholding method on eye region image is shown in Fig. 2. The result is a binary image with the brightest part of image, which is sclera.

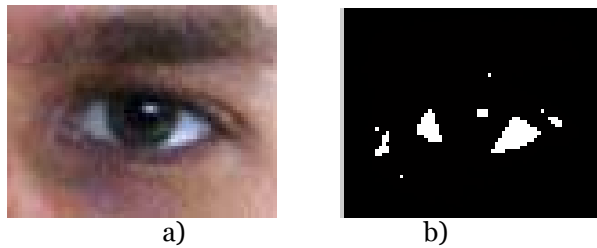


Figure 2: a) Original image, b) segmented image

The threshold is added with horizontal and vertical projection [9]. We used variance projection function (VPF) rather than integral (IPF) because variance projection better reflects the difference in image. It is defined with

$$\sigma_H^2(y) = \frac{1}{w} \sum_{i=1..w} [I(x_i, y) - H(y)]^2, \quad (2)$$

where $H(y)$ is the mean value for the line y , calculated as:

$$H(y) = \frac{1}{w} \sum_{i=1..w} I(x_i, y), \quad (3)$$

where y is the number of the line, w is the width of the image. With horizontal projection we can determine height of the eye opening. The vertical projection is realised likewise (2), but we don't observe the changes in the rows but in columns.

Thresholds in both normalized projections Fig. 3 a), c) are evaluated based on mean and standard deviation of each function. Green lines represent limitation from horizontal projection while the red ones the limitation from vertical projection. Result from region cropping is on Fig. 3 b). Disadvantage of this method is that the presence of any other significant objects such as glasses or some mark on skin in the eye region affects projection function.

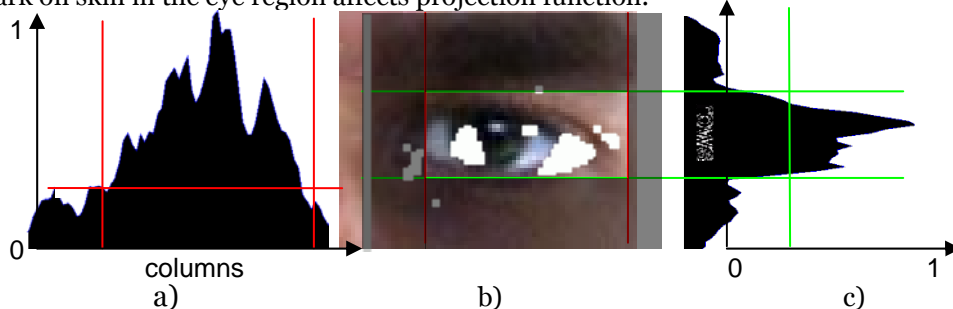


Figure 3: a) vertical projection, b) result from variance projection function, c) horizontal projection

For the purpose of eye and background segmentation, the Skin-Tone Segmentation method is often used. The skin-tone has specific colour-ranges that distinguish between the colours of the inner parts for eye. Human skin colours can be mapped into one of quadric plane on Cb-Cr chrominance space. But it is necessary to have a colour image in such case.

3.1. Circular Hough transform for iris detection

Having selected the more accurately the region of the eye, the next step is iris detection. For this purpose we used circular Hough transform (CHT), since the iris is nearly circular. The pupil of the eye is plotted as the circle centre and the circular shape of the iris is located and drawn as the circle parameter with its specific radius from the circle centre. As a first, Hough transform is applied to whole eye region, to detect iris. When both centre and radius of iris is detected, then the pupil circle inside iris is localized.

This technique detects imperfect instances of objects within a certain class of shapes by a voting procedure. This voting procedure is carried out in a parameter space, from which object candidates are obtained as local maxima in an accumulator space [3].

The result of Hough transform is an accumulation array in which the higher values represent areas with the occurrence of circles in image with specific radius.

In many cases an edge detector can be used as a pre-processing stage, to obtain image points or image pixels that are on the desired curve in the image space.

Our algorithm is based on the gradient field of the input gray-scale image. A thresholding on the gradient magnitude is performed before the voting process of the Circular Hough transform to remove the 'uniform intensity' image background from the voting process. Thus pixels with gradient magnitudes smaller than gradient threshold are not considered in the computation.

It is not possible to know the exact diameter of the iris, since people can have different iris dimensions and also the system has to manage variable distances between people and the camera. For this reason a range [minimum_radius, maximum_radius] is set to tackle different iris radius. These values are estimated from ratio of iris size to eye width (1/6) mentioned in 2.1. But larger range of radius results in more computational time and memory consumption.

The main advantage of the Hough transform technique is its tolerance to the gaps in feature boundary descriptions and that it is relatively unaffected by image noise.

The circular Hough transform is almost identical to the Hough transform for lines, but it uses the parametric form for a circle:

$$\begin{aligned} x &= x_0 + r \cos \Theta, \\ y &= y_0 + r \sin \Theta, \end{aligned} \quad (4)$$

where x_0, y_0 is the coordinate of the circle centre, r is the radius of the circle. When the θ varies from 0 to 360° , a complete circle of radius r is generated.

Gradient of image

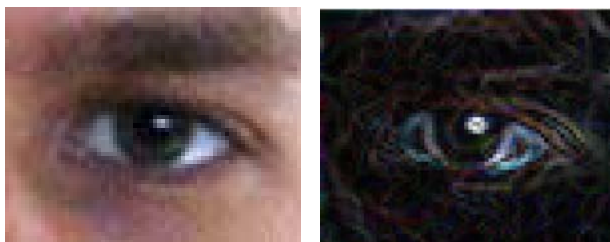
To build the accumulation array it is necessary to compute the gradient (5) and the gradient magnitude (6) of the selected eye region (Fig. 4). It is the first derivative of 2D image. The gradient follows the changes in gray level in direction x and y [12]. Gradient $\nabla I[m, n]$ of image in direction x and y is defined as:

$$\nabla I = \frac{\partial I}{\partial x} \vec{i}_x + \frac{\partial I}{\partial y} \vec{i}_y = (h_x \otimes I) \vec{i}_x + (h_y \otimes I) \vec{i}_y, \quad (5)$$

where \vec{i}_x and \vec{i}_y are unit vectors in the horizontal and vertical direction, h_x horizontal derivative and h_y vertical derivative.

Gradient magnitude:

$$|\nabla I| = \sqrt{(h_x \otimes I)^2 + (h_y \otimes I)^2}, \quad (6)$$

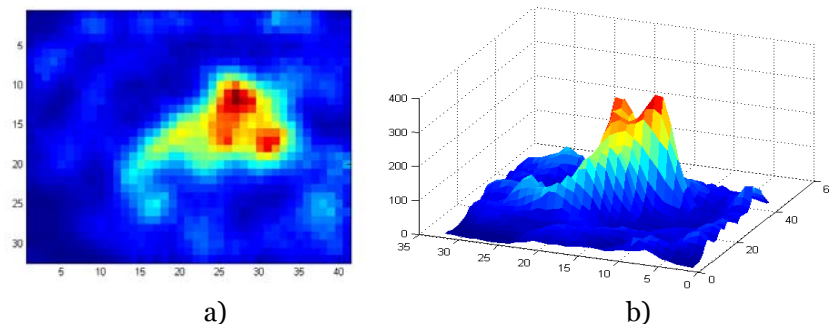


a) Original image, b) gradient magnitude of image

For pixels whose gradient magnitudes are larger than the given threshold, the linear indices, as well as the subscripts are created. The accumulation array of the image consists of the gradient magnitude of the image and its linear indices as

$$A = \text{accumarray}(\text{subs}, \text{val});$$

Accumarray is created by an A array, accumulating elements of the vector val (gradient magnitude) using the subscript in subs (linear indices). Each row of the m-by-n matrix subs defines an N-dimensional subscript into the output A. Each element of val has a corresponding row in subs. Finally the locating of local maxima in the accumulation array is executed (Fig. 5).



a) 2D representation, b) 3D representation

3.2. Experimental results

All methods and algorithms have been implemented in programming environment Matlab, using function from Signal and Image processing toolbox. Input images have been taken from video sequence with resolution 640x480 pixels captured with common web camera.

The set of tested images has contained approximately one hundred video frames from few different people. After face detection, the eye region was cropped for next analysis. One eye region had resolution about 80x80 pixels with some surroundings and the segmented real eye size is only about 50x25 pixels. For its correct function, the CHT Algorithm requires an input image sized 32x32 pixels as a minimum, thus it is necessary to adjust the segmented eye region to this dimension.

Experiments were carried out to test the accuracy of CHT algorithm in iris, using many variations of parameters and input images. For pupil detection, the algorithm is searching for the circle with the smallest average intensity inside localized iris.

Pupil detection requires elimination of reflections on eye; this is done with fill in the brightest parts inside localized iris boundary. In Fig. 6 are presented the examples of testing set of left eye images in many variations of eye gaze and states of eye opening.

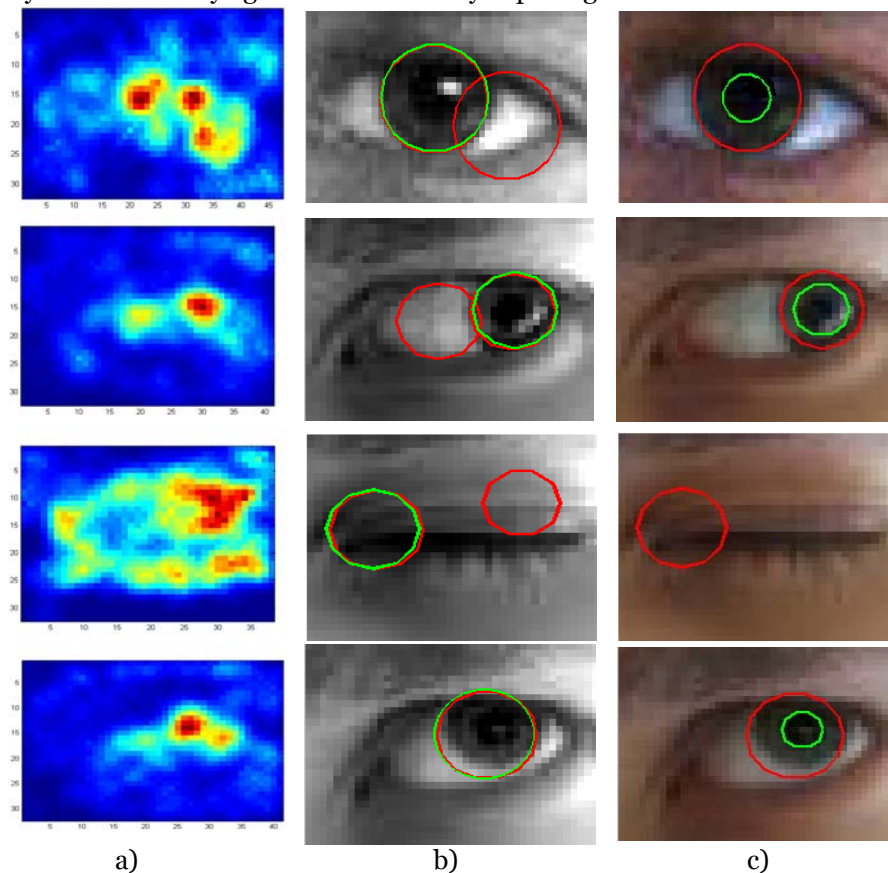


Figure 6: a) CHT accumulation array, b) CHT candidates to iris, c) result of iris and pupil detection

4. CONCLUSION

The circular Hough transform (CHT) is very reliable and for a small browsing area it is a fast method for iris detection. This conclusion is valid for our concrete experiment, where the circular object with small resolution has been used. If the iris position in the direction towards the eye corner, its precision is slightly worse, due to the loss of circle configuration of the iris, compared with centre position. In this case it is necessary to expand the range of an expected radius. For evaluation and selection from more candidate circles, except local maximum criteria of accumulated area, the darkness criterion of candidate area has been added. This combination helps to eliminate the error detection in some cases. The detection failed only if the opening of eye was not sufficient. For closed eye the dark area in eye corner was detected as iris area. In this case it is necessary to use other methods to evaluate the iris colour.

ACKNOWLEDGEMENT

This work has been supported by the Grant Agency VEGA of the Slovak Republic, grant No. 1/0023/08 "Theoretical apparatus for risk analysis and risk evaluation of transport telematic systems".

REFERENCES

- [1.] VIOLA, P. – JONES, M.: Robust Real-Time Face Detection, International Journal of Computer Vision 57(2), 2004, ISSN 0920-5691.
- [2.] ŠONKA M. – HLAVÁČ V. - BOYLE R.: Image Processing, Analysis and Machine Vision. Thomson, Toronto, 2008, ISBN 978-0-495-24428-7.
- [3.] BALLARD, D. H.: Generalizing the Hough transform to detect arbitrary shapes, Rochester, USA, 1980, ISBN 0-934613-33-8.
- [4.] SOMNATH, D. - DEBASIS, S.: An Efficient Approach for Pupil Detection in Iris Images, 15th International Conference on Advanced Computing and Communications, 2007, ISBN 0-7695-3059-1.
- [5.] DAUGMAN, J. G.: High confidence visual recognition of persons by a test of statistical independence. IEEE Trans. Pattern Analysis and Machine Intelligence, 1993, 15, (11), pp. 1148–1161, ISSN 0162-8828.
- [6.] WILDES, R. P.: Iris Recognition: An Emerging Biometric Technology. Proceeding of the IEEE, 85(9):1348–1363, Sep 1997, ISSN 0018-9219.
- [7.] LIAM, L. - CHEKIMA, A. - FAN, L. - DARGHAM, J.: Iris recognition using self-organizing neural network. IEEE, 2002 Student Conf. On Research and Developing Systems, Malaysia, 2002, pp. 169–172, ISBN 0-7803-7565-3.
- [8.] MA, L. - TAN, T. - WANG, Y., - ZHANG, D.: Efficient Iris Recognition by Characterizing Key Local Variations. IEEE Trans. on Image Processing, 13(6):739–750, 2004, ISSN 1057-7149.
- [9.] FENG, G.C. - YUEN, P.C.: Variance projection function and its application to eye detection for human face recognition, International Journal of Computer Vision. 19 (1998) 899–906, ISSN 0167-8655.
- [10.] LUKÁČ, P. – BENČO, M. – HUDEC, R. – DUBCOVÁ, Z.: Color image segmentation for retrieval in large image databases, Conference Transcom 2009, 22-24, Žilina, June 2009, ISBN 978-80-554-0059-6.
- [11.] MORAVČÍK, T.: Image Segmentation in Programming Environment MATLAB. OWD 2009, Poland, ISBN 83-922242-5-6.
- [12.] WAN MOHD KHAIROSAFAIZAL, W. M.– NOR'AINI, A. J.: Eyes Detection in Facial Images using Circular Hough Transform, International Colloquium on Signal Processing & Its Applications, Kuala Lumpur, 2009, ISBN 978-1-4244-4151-8.



¹Pavel DRABEK

APPLICATION OF THE SiC COMPONENTS IN POWER ELECTRONICS

¹UNIVERSITY OF WEST BOHEMIA IN PILSEN, FACULTY OF ELECTRICAL ENGINEERING,
DEPT. OF ELECTROMECHANICS AND POWER ELECTRONICS, CZECH REPUBLIC

ABSTRACT:

This paper presents research motivated by industrial demand for using power semiconductor devices based on SiC (Silicon Carbide). The paper deals with possibility of SiC devices application in traction vehicles. The main attention has been given to the topology of 3-phase voltage-source inverter with free-wheeling SiC schottky diode and 1-phase traction converter with middle frequency converter for auxiliary drives. The theoretical conclusions and simulation results are compared with experimental measurements on laboratory model with rated power of 2kVA

KEYWORDS: Silicon Carbide, Traction application, Power semiconductor device, Hybrid power integration, Electric vehicle

1. INTRODUCTION

Power semiconductor devices based on the SiC substrate is coming more and more popular with increasing development of the power electronics. Due to the advantageous qualities discovered at the SiC this material becomes very interesting object for research and development and subsequent using in the all sorts of applications where bigger and bigger exigencies on efficiency, magnitudes, weight and impact on surroundings are set.

2. SiC PROPERTIES

Crystals of SiC have analogical crystalline structure as diamond and therefore they belong among the hardest known materials, in the Moh's scale of the hardness they reach levels 9-10. Primarily SiC finds use as material called "Carborundum" and it used to exploit for grinding and polishing. Later it was used in the fire-resistant fireclay brickworks and heating shells for industry furnaces or in the composite materials.

With development of the electrotechnics the semiconductor features of SiC were detected and it started to add to the semiconductor substrate of blue shining LED diodes, later in the high shining diodes and in the last few years it has also started to assert in the field of the power electronics.

3. COMPARISON OF THE SiC WITH OTHER MATERIALS

SiC has several unique properties, which make SiC very interesting object for research and development, mainly in the area of high voltage applications. Fig.1 shows these features in comparison with commonly used semiconductor materials (Gallium Arsenide and Silicon).

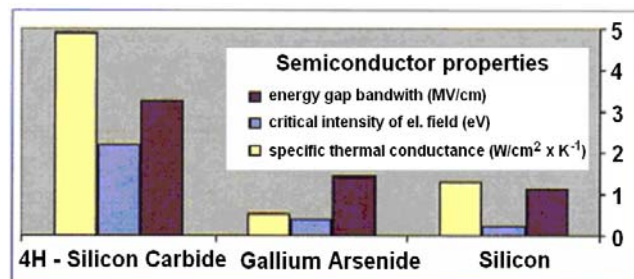


Figure 1. Comparison of individual semiconductor features[3]

4. PRACTICAL USING OF THE SiC

Meantime SiC diodes are the most used devices based on the Silicon Carbide. They are used in many applications. Blocking (freewheeling) diodes in the PFC applications has been the first example of using and it is still frequently used. Rectifying and freewheeling diodes in the switching sources and freewheeling diodes in voltage inverters or active switching rectifiers are the next using of SiC. Further we will discuss possibility of other devices based on the SiC:

At the first we will compare two version of classical 3-phase VSI (see Fig. 2).

The first version of VSI is mounted by classical silicon IGBTs as shown in Fig.3 in left part. The “hybrid” combination of silicon IGBTs and SiC Schottky freewheeling diodes present the second version of VSI (Fig. 3 in right part).

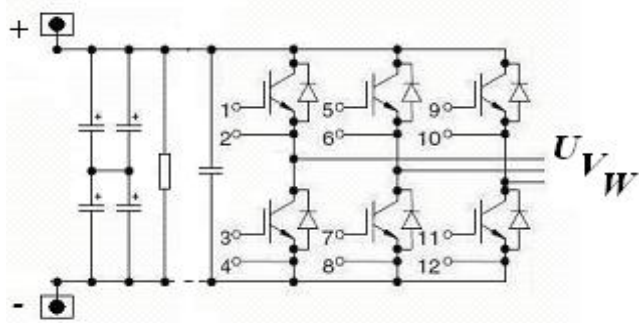


Figure 2. Topology of VSI

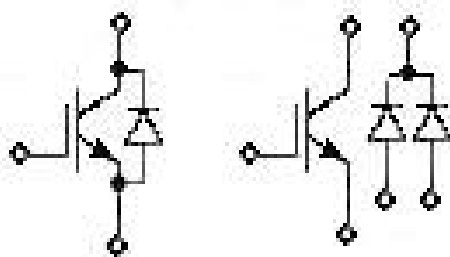


Figure 3. Detailed scheme of used semiconductor devices for VSI

The main advantage of SiC presents following figures 4 and 5 and it is coming-out from Schottky diode properties. The current waveform of silicon diode in the first version of VSI is shown in Fig. 4 and you can clearly see the classical recovering current area.

Against this fact the SiC Schottky diode has very positive waveform of recovering current area (Fig. 5) which is diametrically lower than at Si diode. This is advantage of Schottky structure and SiC material are able produce high voltage Schottky diodes and that is reason of such wave. The double SiC diode module from CREE is used.

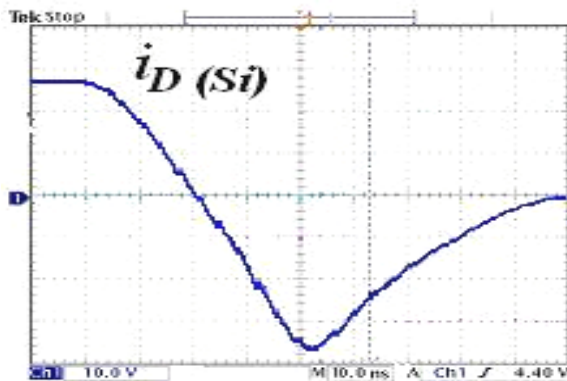


Figure 4. Current waveform of the ultrafast soft recovery epitaxial silicon diode

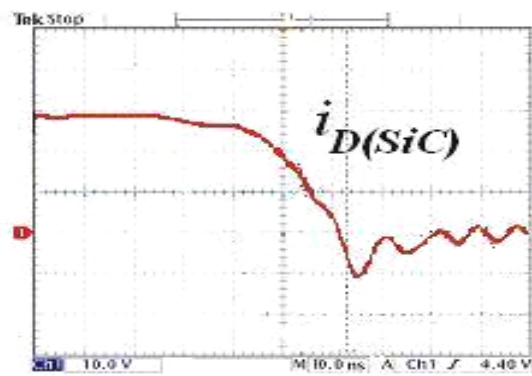


Figure 5. Current waveform of the SiC Schottky diode (produced by CREE as shown in Fig..9)

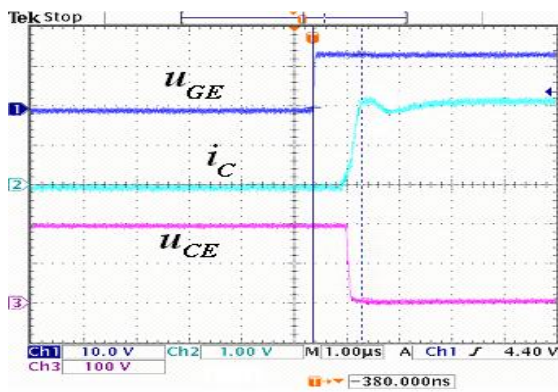


Figure 6. Start up of the hybrid VSI version

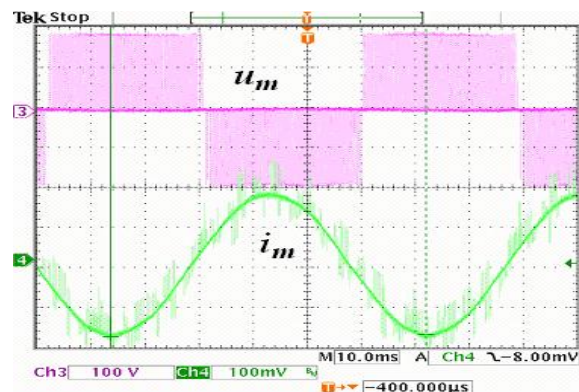


Figure 7. Principal scheme of device J-FET (cascade)

Experimental example of star up of the hybrid VSI version presents Fig. 6. It is evident that using of SiC freewheeling diode has positive influence on current overshoot of collector current of IGBT transistor. The testing has been provided under lower supply voltage 200V according to the used devices of 600V range (available free samples).

Typical output waveforms of VSI (line to line voltage U_M and phase current I_M) are shown in Fig. 7.

Fig. 8 – Fig. 11 present photos of experimental prototypes of VSI with classical Si IGBTs and hybrid version with Si IGBTs and SiC Schottky diodes.

The hybrid version enables use 5-time higher switching frequency under the same conditions as standard topology with silicon IGBT transistors. It is done by expressively lower losses of SiC schottky diodes (Fig.5). For comparison of the appropriate running condition and losses we have used measuring of circuits values and steady-state temperature of the heat sink.

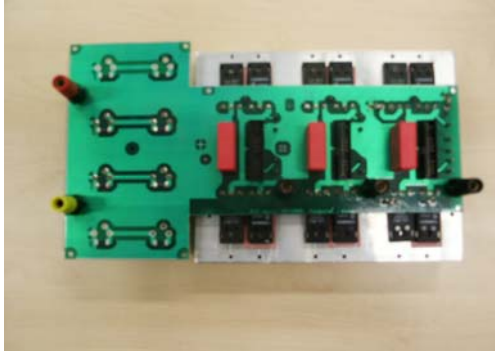


Figure 8. Prototype of hybrid VSI



Figure 9. Detail of hybrid VSI devices

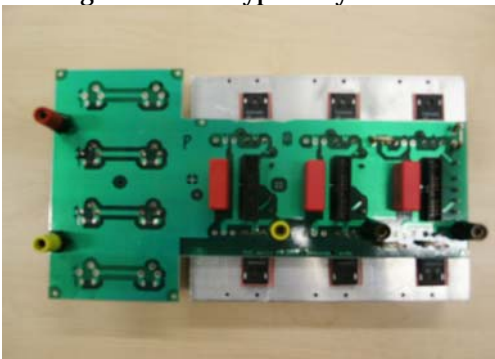


Figure 10. Prototype of VSI with classical IGBTs



Figure 11. Detail of VSI with classical device

The single phase traction converter for auxiliary drives is the second presented application of SiC (Fig. 12). The auxiliary drive converter presents galvanic insulation VSI for auxiliary drives. The input part is directly connected to the DC bus line of main traction converter, it means 1500 V or 3000 V according to the traction vehicle topology. Due to the voltage level the number of serial connections of input 1f VSI has to be placed. Input 1f VSIs fed the middle-frequency transformer (MFT) and the standard diode bridge rectifier with SiC is connected on the MFT output. The key is in the using of high switching frequency up to 100 kHz to decrease of weight of auxiliary drive transformer. Output diode rectifier supply DC bus line where several of VSI + auxiliary drives are connected.

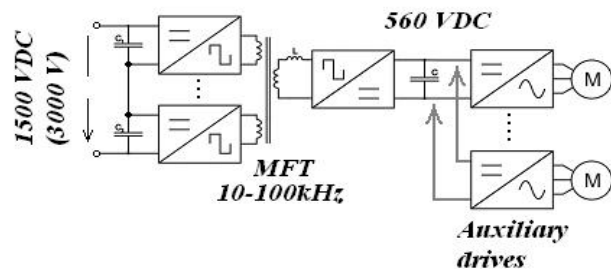


Figure 12. Principal scheme of auxiliary drives traction converter

Fig. 13 presents experimental results of steady state waveforms of MFT voltage and current (output values of input VSI as well). It is evident from the picture that the switching frequency is only 10kHz. This is fact of VSI design with IGBTs and control circuit based on the DSP TEXAS 2812, both aspects limited available switching frequency with reasonable rated power (DSP: A-D converters limited monitoring of analog values, IGBTs limited ratio between switching frequency and reasonable rated power).

The next step is in a new design of the input single phase VSI based on power MOSFETs (to increase switching frequency with reasonable rated power) and mainly using of superior control system based on analog circuits (analog operational amplifiers) to achieve 100kHz switching frequency.

5. CONCLUSION

This paper presents research motivated by industrial demand for using power semiconductor devices based on SiC. The main attention has been given to the topology of 3-phase voltage-source inverter with free-wheeling SiC schottky diode and comparing with topology with classical Si IGBTs. The 5-times increasing of switching frequency with the same losses is the main advantage of this hybrid structure. The second mentioned structure is 1-phase traction converter with middle frequency converter for auxiliary drives. Using SiC diodes in the secondary bridge rectifier brings opportunity to use high switching frequency approximately 50-100kHz. Proposed converter runs at 10kHz according to used devices and control system based on DSP Texas 2812 (problem with conversion speed of standard A-D converters).

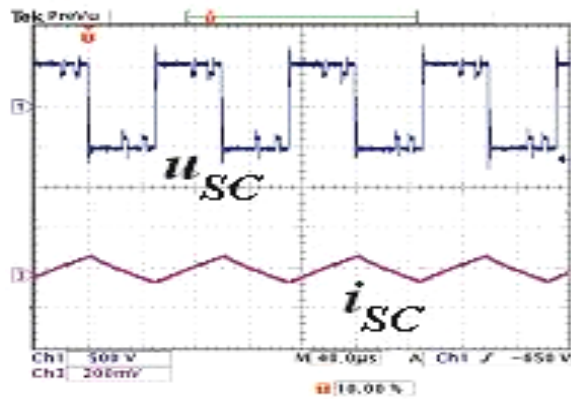


Figure 13. Steady state of voltage and current of MFT, rated power 2kVA

ACKNOWLEDGMENT

This research work has been made within research project of Czech Science Foundation No. GACR 102/09/1164.

REFERENCES / BIBLIOGRAPHY

- [1] Dahlquist, F. - Frank, W. and Deboy, G. SiC diodes improve boost converter. vyd. Infineon technologies, 2004, 3s, SiC Diodes Improve Boost Converters (PEE 4-04).pdf
- [2] Richmond, J. – Hodge, S. and Palmour, J. Silicon carbide power application and roadmap. Publ. Cree inc, 2004, 4s, SiC Power Appl. and Devices Roadmap (PEE 7-04).pdf
- [3] Friedrichs, P. – Rupp, R. Silicon Carbide Power Devices - Current Developments and Potential Applications. EPE 2005. ISBN : 90-75815-08-5.
- [4] Hruška, M. Application of Silicon Carbide in the power electronics. Publ. in UWB in Pilsen, 2006, 21s.
- [5] Kapels, H et. al. A revolutionary step towards energy saving power Electronic systems. vyd. Infineon technologies AG, 2001, 5s, SiC- PFC Inf. - SiC Schottky Diode - Revolutionary Step to Energy Saving.pdf
- [6] Technical documentation, CoolMOS Power transistor – SPW35N60C3. publ. Infineon technologies, 2005, 11s, SPW35N60C3_Rev.2.4.pdf
- [7] Technical documentation, SiC diode – SDT12S60. publ. Infineon technologies, 2002, 8s, 1-SDT12S60.pdf





THE STUDY OF QUALITY INDICATORS OF ELECTRICAL ENERGY IN ELECTRICAL RAILWAY TRANSPORT

¹⁻⁴ UNIVERSITY POLITEHNICA TIMIȘOARA, FACULTY OF ENGINEERING OF HUNEDOARA,
ELECTRICAL ENGINEERING AND INDUSTRIAL INFORMATICS DEPARTMENT, ROMANIA

ABSTRACT:

In this work is presenting the study of the electric current's parameters and characteristics, obtained by means of an electric power's quality analyzer. The measurements were made into an AC railway electric traction substation of 27 kV, during more hours, being registered momentary and average values. The data acquired with the electric power's quality analyzer were registered into a computing system, for their further analysis. In order to achieve the adaption between the analyzer's input measures and the traction line's values, the measurements were made in the secondaries of the voltage and current transformers existent in the traction substation.

KEYWORDS: electric power's quality, active power, reactive power, apparent power, harmonic distortion factor, power factor, electric power's quality analyzer

1. INTRODUCTION

The three-phased systems were conceived and achieved to operate in symmetric balanced regimes. In these regimes, all the component elements: generators, transformers, lines and consumers present identical circuit parameters on each phase, and the currents' and voltages' systems in any section are symmetric. If one of the grid's or consumer's elements gets out-of-balance, the regime becomes non-symmetric and the current and voltage systems are losing their symmetry.

The most unfavorable consequence of the voltage unbalance is the circulation of some additional current component (negative and zero) that lead to additional losses, parasite couples at AC electric motors, wear increase, etc.

A prime cause of the unbalances comes from the grid elements: i.e. the non-symmetric space disposition of the aerial electric lines' conductors is translated by impedance differences for the grid's phases, being in this way a source for unbalances. A transposition of the aerial lines' conductors allows, however, the reduction of this unbalance up to the level it becomes negligible. The main cause for non-symmetries is the consumers' supply, great part of them being unbalanced, single-phased and connected between two phases of the grid, or between a phase and null.

The most important unbalances are produced by the high-power industrial single-phased consumers, connected to the medium or high voltage electric grids, e.g: transformation stations for supplying the railway electric traction, welding installations, single-phased electric furnaces, etc.

The non-symmetries provoked by these loads are accompanied most of the times also by other forms of perturbations: harmonics, voltage shocks, voltage holes, etc.

The effects of the current unbalances, indicated by the appearance of the negative and zero sequence components, lead to the increase of longitudinal losses of power and active energy in electric grids. [1]

2. WORK'S PRESENTATION

Conditions for quantities analysis of the harmonic components in the structure of a signal are [58],[71]:

a) *Harmonic level* – is the ratio, expressed as a percentage of the effective amount of harmonics considered (F_k) and the effective value of the fundamental F_1

$$\gamma_K = \frac{F_k}{F_1} \cdot 100 [\%] \quad (1)$$

b) *The deforming residue* – represent wave that is obtained from the given wave when is eliminated fundamental harmonic

$$F_d = \sqrt{F^2 - F_1^2} \quad (2)$$

c) *Global distortion coefficient (non-sinusoidal shape)* – is defined as the ratio, expressed as a percentage of the effective value of deforming residue and the one of fundamental.

$$d = \frac{F_d}{\sqrt{F^2 - F_0^2}} = \frac{\sqrt{\sum_{k=2}^{\infty} F_k^2}}{\sqrt{\sum_{k=1}^{\infty} F_k^2}} \cong \frac{\sqrt{\sum_{k=2}^{\infty} F_k^2}}{F_1} \cdot 100 [\%] \quad (3)$$

a) Total harmonic distortion, is defined similarly to global distortion coefficient except that the overall distortion is taken into account the first 50 harmonics

$$THD = \sqrt{\sum_{k=2}^{50} \left(\frac{F_k}{F_1} \right)^2} \cdot 100 [\%] \quad (4)$$

b) Partially weighted harmonic distortion introduced to ensure that when increased rank, descending harmonic and relationship is defined by

$$THD_P = \sqrt{\sum_{k=2}^{50} k \cdot \left(\frac{F_k}{F_1} \right)^2} \cdot 100 [\%] \quad (5)$$

c) The deformation coefficient of non-sinusoidal periodic wave, ΔF has the expression

$$\Delta F = \frac{|a - b|}{c} \cdot 100 [\%] \quad (6)$$

where:

- ❖ a represent y-coordinate of the curve representative for the given periodic wave;
- ❖ b represent y-coordinate of the curve representative for the fundamental harmonic of the given wave, corresponding to the same x-coordinate as for “a”;
- ❖ c represent curve amplitude representative for the fundamental harmonic. Determinations of the current harmonics, as well as the THD factor, are made with a three-phased energy analyzer which allows the computing of these parameters according to the following relations.

RMS values for voltage and current:

$$V_{rms}(i) = \sqrt{\frac{1}{N} \cdot \sum_{n=0}^N V(i, n)^2} \quad (7)$$

where: N represent the number of samples for the acquisition time;

V_{rms} single RMS voltage $i + 1$ phase; $V_{avg}[i] = V_{rms}[i]$

$$U_{rms}(i) = \sqrt{\frac{1}{N} \cdot \sum_{n=0}^N U(i, n)^2} \quad (8)$$

where: U_{rms} compound RMS voltage $i + 1$ phase $U_{avg}(i) = U_{rms}(i)$

$$Arms(i) = \sqrt{\frac{1}{N} \cdot \sum_{n=0}^N A(i, n)^2} \quad (9)$$

where: $Arms(i)$ - Effective current phase $i + 1$; $A_{avg}(i) = Arms(i)$

Computing of harmonic:

By FFT (16 bits) 1024 samples on 4 cycles without windowing (CEI 1000 – 4-7). From real and imaginary parts, each bin computed on each phase V_{harm} , U_{harm} and A_{harm} in proportion to the fundamental value and the angles V_{ph} , U_{ph} , and A_{ph} between each bin and the fundamental.

This computing is done by the following principle:

$$\text{Module in } \% : \text{mod}_k = \frac{c_k}{c_1} \times 100$$

angle in degree: $\theta_k = \arctan\left(\frac{a_k}{b_k}\right)$

$$\text{With } \begin{cases} c_k = |b_k + ja_k| = \sqrt{a_k^2 + b_k^2} \\ b_k = \frac{1}{512} \sum_{s=0}^{1024} F_s \times \sin\left(\frac{k\pi}{512} s + \theta_k\right) \\ a_k = \frac{1}{512} \sum_{s=0}^{1024} F_s \times \cos\left(\frac{k\pi}{512} s + \theta_k\right) \\ c_o = \frac{1}{1024} \sum_{s=0}^{1024} F_s \end{cases} \quad (10)$$

c_k is the amplitude of frequency $f_k = \frac{k}{4} f_1$, F_s is sampled signal, c_o is the DC component, k is the ordinal number (spectral bin).

Computing of the distortion factor (DF):

There are computed two global values that give the relative quantity of harmonics: total harmonic distortion (THD) against the fundamental and the distortion factor (DF) and DF against the effective value (RMS).[2]

$$V_{thd}(i) = \frac{\sqrt{\frac{1}{2} \sum_{n=2}^{50} V_{harm}(i, n)^2}}{V_{harm}(i)} \quad U_{thd}(i) = \frac{\sqrt{\frac{1}{2} \sum_{n=2}^{50} U_{harm}(i, n)^2}}{U_{harm}(i)}$$

$$A_{thd}(i) = \frac{\sqrt{\frac{1}{2} \sum_{n=2}^{50} A_{harm}(i, n)^2}}{A_{harm}(i)} \quad (11)$$

$$V_{dr}(i) = \frac{\sqrt{\frac{1}{2} \sum_{n=2}^{50} V_{harm}(i, n)^2}}{V_{rms}(i)} ; U_{dr}(i) = \frac{\sqrt{\frac{1}{2} \sum_{n=2}^{50} U_{harm}(i, n)^2}}{U_{rms}(i)} \quad A_{df}(i) = \frac{\sqrt{\frac{1}{2} \sum_{n=2}^{50} A_{harm}(i, n)^2}}{A_{rms}(i)} \quad (12)$$

Multiplying the voltage's harmonics factor with the current's harmonics factor, results the power's harmonics factor. Differentiating the voltage's harmonic phase angle with the current's harmonic phase angle, results the power's phase angle.

- different ratios

$$PF(i) = \frac{W(i)}{VA(i)} \text{ power factor, phase } i + 1$$

Cosinus angle between the voltage's fundamental and the phase current $i + 1$

$$\cos[\theta(i)] = \frac{\sum_{n=0}^{N-1} VF(i, n) \cdot AF(i, n)}{\sqrt{\sum_{n=0}^{N-1} VF(i, n)^2} \cdot \sqrt{\sum_{n=0}^{N-1} AF(i, n)^2}} \quad (13)$$

Total power factor of various types of energy

$$PF_3 = \frac{PF(0) + PF(1) + PF(2)}{3} \quad (14)$$

Active energy consumed $i + 1$ phase;

$$Wh(o, i) = \sum_{T_{int}} \frac{W(i)}{3600} \quad (15)$$

Reactive inductive energy consumed $i + 1$ phase;

$$VARhL(o, i) = \sum_{T_{int}} \frac{VAR(i)}{3600} \text{ for } VAR(i) \geq 0 \quad (16)$$

Reactive capacitive energy consumed $i + 1$ phase.

$$VARhC(o, i) = \sum_{T_{int}} \frac{VAR(i)}{3600} \text{ for } VAR(i) \leq 0 \quad (17)$$

The measurements were made in the traction station CFR Deva, by means of the electric power quality's analyzer CA 8334B. During the data acquisition it was caught a passing from one supply transformer to another power factor or distortion factor. Further is presented the variation form of the line voltage and current at a given moment (Fig. 1). One can notice a reduced modification in the voltage form, and a pronounced one in the current's variation form.

Variation of the power factor's measures PF (Fig. 2), of the voltage's harmonic distortion factor V_{thd} (Fig. 3) and of the current's harmonic distortion factor I_{thd} (Fig. 4) is presented during the entire acquisition period, where from can be determined the fluctuation of the determined measures, fluctuation that leads to distortions in the general power supply grid [3].

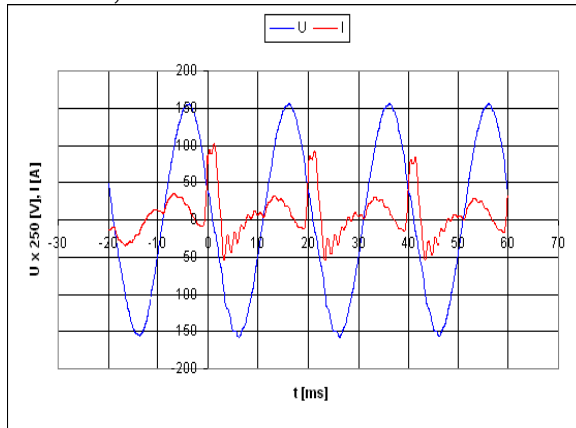


Figure 1 Variation form U, I

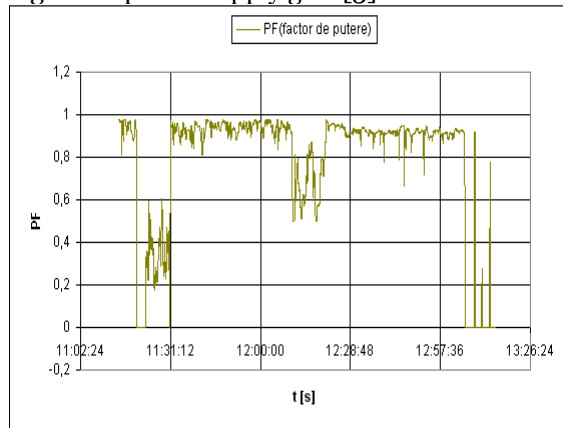


Figure 2 Power factor

Depending on these obtained values, can be designed diverse compensation systems of the perturbations introduced in the grid [4][5].

Within the AC electric traction of 50Hz with DC motors and implicitly with converters [6], was obtained a harmonic distortion factor of the voltage (Fig. 5), relatively reduced, of 4,5% in conditions of a normal traffic, and the values of the voltage harmonics are also reduced.

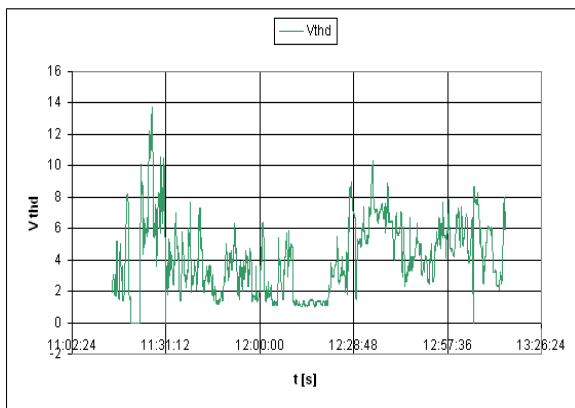


Figure 3 Voltage's harmonic distortion factor

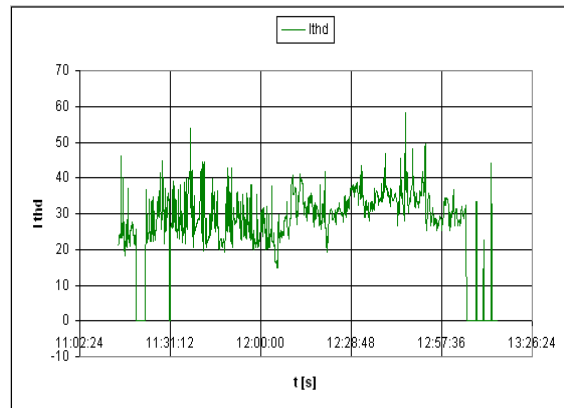


Figure 4 The current's harmonic distortion factor

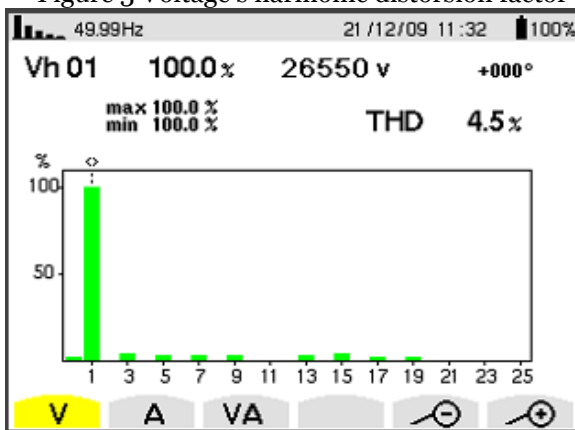


Figure 5 Values of the voltage harmonics

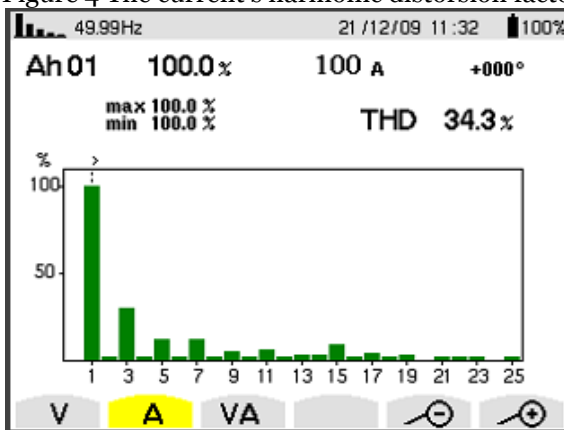


Figure 6 Values of the current harmonics

For the current harmonics (Fig. 6) things are changed, we have high THD of 34,3% and harmonics' individual values also high, up to 25% from the fundamental harmonic, that should be eliminated.

For eliminating the current harmonics, can be introduced passive filters of LC type [4][5], that should eliminate the low-rank harmonics, and for the superior rank ones it can be used the solution of the active power filter, which cannot be connected on the locomotive but only in the traction station. Dimensioning of the passive filters (for the harmonics 3,5,7 can be made on the minimum reactive power criteria, thus being possible to reduce the reactive power consumption [1].

The LC-type filters use coils with variable inductivity by modifying the iron core's penetration depth inside the copper winding. By modifying the inductance, it is modified the LC circuit's tuning frequency, influencing the current absorbed from the power supply system, both as value and shape. For the computing of L and C elements, it was chosen the minimum reactive power criteria.

For each current harmonic that is possible to be introduced is used such a resonant circuit. The elements of each filter are dimensioned in such way that for the resonance frequency that coincides with the respective current harmonic frequency result impedance very small.

$$Z_k = k \omega_1 L - \frac{1}{k \cdot \omega_1 \cdot C} \quad (18)$$

where: Z_k is the equivalent impedance of the resonant circuit for the harmonic of k order (the equivalent resistance of the coil of capacitors and electric connection elements were neglected).

ω_1 = fundamental current pulsation.

Pulsation:

$$\omega_k = k \omega_1 = \frac{k}{\sqrt{LC}} \quad (19)$$

is quite the resonance pulsation of LC circuit.

Usually, the absorbing filters are installed for the harmonics with the highest amplitudes, which correspond in general to the low order of harmonic.

Designing of filters' inductivity and capacity is made by applying of some algorithms that could be differentiated first depending on the filters' role from the viewpoint of reactive power compensation on the fundamental. All the resonant circuits will have capacitive character on the fundamental's frequency, so they will produce, no matter what, a capacitive transversal compensation of the network.

Even though this is a rare solution, it could be taken into account in boundary situations when the deformant regime in current is very pronounced. Even the reactive power compensation is not a primary objective, the filter will generate in the grid reactive power on fundamental. Therefore, the filter's dimensioning criteria, more specifically of the capacity from its componency, is to minimize the installed capacitive reactive power (which, beside a minimum cost of the battery, leads to a minimum influence on the active power circulation in the grid):

$$Q_c = Q_{cmin} \quad (20)$$

This reactive power will have two components corresponding to the two above mentioned currents, the current corresponding to the fundamental and the current corresponding to harmonic k on which the resonance is taking place:

$$Q_c = Q_{c1} + Q_{ck} = U_c^2 \cdot \omega_1 \cdot C + \frac{I_k^2}{k \cdot \omega_1 \cdot C} \quad (21)$$

where: Q_{c1} - reactive power supplied by the filter's capacitor on fundamental;

Q_{ck} - reactive power supplied by the filter's capacitor on k harmonic;

U_c - voltage at the capacitor's terminals;

I_k - harmonic current that follows to be filtered.

Making the partial derivate depending on the capacity of the installed capacitive reactive power equation and canceling it, we obtain the equation of the filter's capacity:

$$C = \sqrt{\frac{1}{k}} \frac{I_k (k^2 - 1)}{U_c \cdot \omega_1 \cdot k^2} \quad (22)$$

The L filter's coil inductivity is determined from the resonance condition of the filter's LC:

$$L = \frac{1}{\omega_k^2 C} = \frac{1}{k^2 \cdot \omega_1^2 \cdot C} \quad (23)$$

By introducing of such resonant filters on the odd harmonic frequencies, we can study the influence on each filter in part, as well as the effect of many filters connected in parallel. Beside the

amplitude value, is aimed also the phase-difference introduced by each harmonic against the fundamental.

Will be analyzed the current harmonics for three different loading situations of the generator, respectively three values for the slide potentiometer, at three different supply voltages [1][7][8].

3. CONCLUSIONS

From the analysis of the obtained graphics, can be seen the need to reduce the existent perturbations in the grid. Introduction of the passive filters beside the active filter only reduces the harmonics' values, without having a major influence upon the reactive power and especially upon the non-symmetry of the supply system. The passive filters can be connected either on the locomotive, or in substation, their dimensioning being specific to each case in part. The non-symmetries introduced in the grid by the single-phased supply of the railway electric traction system can be reduced only in the traction substation; therefore we must act on more plans simultaneously to obtain satisfactory results regarding the reduction of the perturbations induced in the supply grid.

For a better study is needed to examine the variation form of voltage and current on the train in case of normal traction. Depending on the results obtained can find appropriate ways to compensate harmonic regime.

REFERENCES

- [1.] Adrian Buta, Adrian Pană, Symmetrization of the Electric Distribution Grids' Load, „University Horizons”, Timișoara, 2000.
- [2.] C.A. 8334B, Three Phase Power Quality Analyser, Chauvin Arnaud, France, 2007.
- [3.] Steimel A., Electric Traction Motive-Power and Energy Supply. Basics and Practical Experience, Oldenbourg Industrie GmbH, 2008.
- [4.] Pănoiu, M., Pănoiu, C., Osaci, M., Muscalagiu, I., Simulation result about harmonics filtering using measurement of some electrical items in electrical installation on UHP EAF, WSEAS Transactions on Circuits and Systems 7 (1), pp. 22-31, ian 2008;
- [5.] Angela Iagar, Gabriel Nicolae Popa, Ioan Șora, Analysis of electromagnetic pollution produced by line frequency coreless induction furnaces, Wseas Transactions on Systems, January 2009, volume 8, Issue 1, ISSN 1109-2777;
- [6.] Corneliu Botan, Vasile Horga, Florin Ostafi, Marcel Ratoi, Minimum Energy and Minimum Time Control of Electrical Drive Systems, WSEAS Transactions on Power Systems, Issue 4, Volume 3, April 2008, ISSN: 1790-5060.
- [7.] Pănoiu M, Pănoiu C, Osaci M, Muscalagiu I. Simulation result about harmonics filtering for improving the functioning regime of the UHP EAF, Proceedings of the 7th Wseas International Conference on Signal Processing, Computational Geometry and Artificial Vision (iscgav'-07), aug 24-26, 2007 Vouliagmeni, GREECE. Pages: 71-76;
- [8.] Alan k. Wallace, Rene Spee, The Effects of Motor Parameters on the Performance of Brushless d.c. Drives, IEEE Transactions on Power Electronics, vol.5, no.1, January 1990;



THE SIZING OF THE BRANCH THREE-PHASE LOW VOLTAGE POWER LINES THROUGH SUPERPOSITION METHOD

¹⁻³DEPARTMENT OF ELECTROTECHNICAL ENGINEERING AND INDUSTRIAL INFORMATICS, FACULTY OF ENGINEERING HUNEDOARA, POLITECHNICA UNIVERSITY TIMIȘOARA, ROMANIA

ABSTRACT:

Traditionally, the main and branch three-phase distribution lines are dimensioned by the minimum conductor-material volume method or that of the moments method.

The paper introduces a new method of designing the power distribution lines. Its advantage consists in the fact that it is simple and easy to apply. It is based on the superposition method used in solving the three-phase electric circuits.

KEYWORDS:

sizing, three-phase distribution lines, superposition method

1. INTRODUCTION

Usually, the branch three-phase low voltage distribution power lines can be size by the admissible maximum voltage drop method, the minimum conductor material volume method and the moments' method [1,2,3,4]. These methods can be use easy, when is not necessary the admissible maximum current correction by a specify cross-section, depending on duty type of the consumer. If is necessary to use this correction, the sizing of the branch three-phase power lines is made simple, through superposition method propose in this paper. This method consists in compute of simple power lines cross-section that composes the complex branch power lines through the admissible maximum voltage drop method. For the common cross-section lines, these are compute like sum of the determinate cross-section for every line partly.

The paper gives an example of sizing the branch three-phase low voltage power lines through superposition method.

2. METHODOLOGY. THE SIZING OF THE BRANCH THREE-PHASE POWER LINES THROUGH SUPERPOSITION METHOD

It is consider the general case for a simple branch power line (fig.1) that supplies n three-phase inductions motors. Each motor works in intermittent periodical duty with the different relative duty cycles, DA_i ($i = 1,2,\dots,n$). These motors have the powers P_{ci} [W] ($i = 1,2,\dots,n$). First time, is calculate the currents I_{ci} [A] for every n motors:

$$I_{ci} = \frac{P_{ci}}{\sqrt{3} \cdot U_{ln} \cdot \eta_{ci} \cdot \cos \varphi_{ci}} \text{ [A]} \quad (1)$$

In this relation U_{ln} [V] is the line rated voltage, η_{ci} [-] is the efficiency, and $\cos \varphi_{ci}$ [-] is the power factor for every motors.

The branch line is decomposing in n simple branch lines (fig.2), every line will be calculated with the admissible maximum voltage drop method. The lengths L_i of the simple lines, in that case, become:

$$L_i = l_0 + l_i, i = 1,2,\dots,n \quad (2)$$

Will be size the simple lines from fig.2 that compose the branch line from fig.1. For this reason it is approximate compute the reactive voltage drop for every line:

$$\Delta U_{lri} = \sqrt{3} \cdot X_i \cdot I_{ci} \sqrt{1 - \cos^2 \varphi_{ci}} \text{ [V]}, i=1,2,\dots,n \quad (3)$$

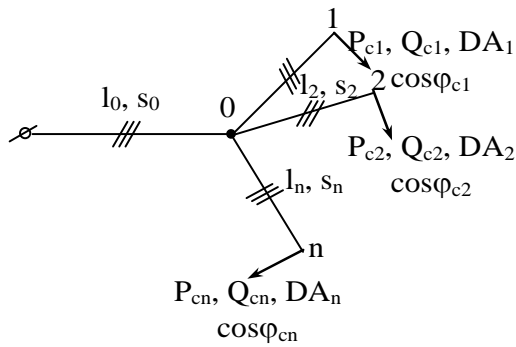


Figure.1 The branch three-phase power lines that feeds with electric energy n consumers

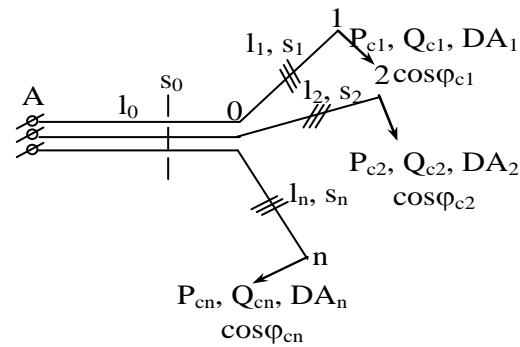


Figure.2 Decomposition of the branch three-phase power lines from figure 1 in n simple power lines

The reactances X_i [Ω] for every simple line are compute with:

$$X_i = 2\pi \cdot f \cdot L_{01} \cdot (l_0 + l_i) \quad (4)$$

In this relation L_{01} [H/m] is the specific line inductance, for underground cable, in the first phase it is calculated with [1]:

$$\begin{aligned} L_{01} &= (2.6 \dots 3.2) \cdot 10^{-7} \text{ [H/m]}, \text{ for underground cable with } U_{ln} \leq 15 \text{ kV} \\ L_{01} &= (3.2 \dots 3.9) \cdot 10^{-7} \text{ [H/m]}, \text{ for underground cable with } U_{ln} > 15 \text{ kV} \end{aligned} \quad (5)$$

For overhead line the specify reactance is estimate with: $X_{01} = 0.4 \cdot 10^{-3}$ [Ω /m].

In this case:

$$X_i = X_{01} \cdot (l_0 + l_i) \text{ [}\Omega\text{]} \quad i = 1, 2, \dots, n \quad (6)$$

The total active voltage drop for n simple lines, it is calculate with:

$$\Delta U_{lmax} = \frac{\Delta U_1 [\%]}{100} \cdot U_{ln} \text{ [V]} \quad (7)$$

For motors $\Delta U_1 [\%] = 5$.

Now it computes the active voltage drops for n simple lines:

$$\Delta U_{lai} = \Delta U_{lmax} - \Delta U_{lri} \text{ [V]} \quad i = 1 \dots n \quad (8)$$

Using the admissible maximum voltage criterion, the simple three-phase cross-sections are calculated with:

$$s_i = \frac{\sqrt{3} \cdot \rho \cdot I_{ci} \cdot \cos \varphi_{ci}}{\Delta U_{lai}} \cdot (l_0 + l_i) \quad (9)$$

Afterwards, it is choose for lines normalized cross-sections s_{ni} , by an immediate superior value ($s_{ni} \geq s_i$).

The choose cross-sections are further performed to warm check of the conductors. For this, the admissible maximum current I_{max} [A] from the tables [3,5], depending on real temperature θ_{02} [$^{\circ}$ C] and on duty cycle of the motor:

$$I'_{max} = c_0 \cdot c_1 \cdot I_{max} \quad (10)$$

The temperature correction coefficient c_0 of admissible maximum current is calculated with [4]:

$$c_0 = \sqrt{\frac{\theta_{max} - \theta_{02}}{\theta_{max} - \theta_{01}}} \quad (11)$$

Here, θ_{max} [$^{\circ}$ C] is the admissible maximum temperature of conductor insulation, and θ_{01} [$^{\circ}$ C] is temperature for the maximum value of current I_{max} .

The correction coefficient c_1 of maximum current depending on duty cycle and it is calculated with [3]:

$$c_1 = \frac{0.875}{\sqrt{DA}}; \quad c_1 = 0.875 \cdot \sqrt{\frac{t_c}{t_f}} \quad (12)$$

The relative duty cycle DA it is compute with:

$$DA = \frac{t_f}{t_f + t_p}; \quad DA = \frac{t_f}{t_c} \quad (13)$$

where t_f [s] is a work time of motor, t_p [s] is pause time of motor and t_c [s] is cycle time:

$$t_c = t_f + t_p \quad (14)$$

The motors feed with electric energy through branch line work in intermittent periodical duty if the maximum time cycle is by 10 minutes and the work time of motor is by 4 minutes. For copper conductors with cross-sections under 10 [mm²] and for aluminium conductors with cross-section under 16 [mm²], $c_1=1$ both in intermittent periodical duty and in permanent duty.

The line cross-sections will not warm, if are valid the relations:

$$I_{ci} \leq I_{\max i}, \quad i = 1, 2, \dots, n \quad (15)$$

After will find the normalized cross-sections s_{ni} , $i = 1, 2, \dots, n$ of simple three-phase line, it can be calculating the main cross-section line:

$$s_0 = s_{n1} + s_{n2} + \dots + s_{nn}; \quad s_0 = \sum_{i=1}^n s_{ni} \quad (16)$$

After that, are calculate the voltage drop when the motors are start for the line from fig.1. It is consider that one motors start and the other work at rated values. These voltage drops are calculated with:

$$\begin{aligned} \Delta U_{p1} = & \sqrt{3} \left[R_{010} \cdot l_0 \cdot \left(k_{p1} \cdot I_{c1} \cdot \cos \varphi_{c1} + \sum_{i=2}^n I_{ci} \cdot \cos \varphi_{ci} \right) + \right. \\ & + R_{011} \cdot l_1 \cdot k_{p1} \cdot I_{c1} \cdot \cos \varphi_{c1} + X_{010} \cdot l_0 \cdot \left(k_{p1} \cdot I_{c1} \cdot \sin \varphi_{c1} + \right. \\ & \left. \left. + \sum_{i=2}^n I_{ci} \cdot \sin \varphi_{ci} \right) + X_{011} \cdot l_1 \cdot k_{p1} \cdot I_{c1} \cdot \sin \varphi_{c1} \right] \end{aligned} \quad (17)$$

$$\begin{aligned} \Delta U_{p2} = & \sqrt{3} \left[R_{010} \cdot l_0 \cdot \left(I_{c1} \cdot \cos \varphi_{c1} + k_{p2} \cdot I_{c2} \cdot \cos \varphi_{c2} + \right. \right. \\ & \left. \left. + \sum_{i=3}^n I_{ci} \cdot \cos \varphi_{ci} \right) + R_{012} \cdot l_2 \cdot k_{p2} \cdot I_{c2} \cdot \cos \varphi_{c2} + \right. \\ & \left. + X_{010} \cdot l_0 \cdot \left(I_{c1} \cdot \sin \varphi_{c1} + k_{p2} \cdot I_{c2} \cdot \sin \varphi_{c2} + \sum_{i=3}^n I_{ci} \cdot \sin \varphi_{ci} \right) + \right. \\ & \left. + X_{012} \cdot l_2 \cdot k_{p2} \cdot I_{c2} \cdot \sin \varphi_{c2} \right] \end{aligned} \quad (18)$$

...

$$\begin{aligned} \Delta U_{pn} = & \sqrt{3} \left[R_{010} \cdot l_0 \cdot \left(k_{pn} \cdot I_{cn} \cdot \cos \varphi_{cn} + \sum_{i=1}^{n-1} I_{ci} \cdot \cos \varphi_{ci} \right) + \right. \\ & + R_{01n} \cdot l_n \cdot k_{pn} \cdot I_{cn} \cdot \cos \varphi_{cn} + X_{010} \cdot l_0 \cdot \left(k_{pn} \cdot I_{cn} \cdot \sin \varphi_{cn} + \right. \\ & \left. \left. + \sum_{i=1}^{n-1} I_{ci} \cdot \sin \varphi_{ci} \right) + X_{01n} \cdot l_n \cdot k_{pn} \cdot I_{cn} \cdot \sin \varphi_{cn} \right] \end{aligned} \quad (19)$$

The cross-sections have been chosen, when are true the relations:

$$\Delta U_{pi} \leq \Delta U_{p \max} = \frac{12}{100} U_{ln} \quad (i=1, 2, \dots, n) \quad (20)$$

In relations (17), (18), (19), R_{010} , R_{011} , ..., R_{01n} , X_{010} , X_{011} , ..., X_{01n} are the specific resistances and reactances for main line and for the lines with cross-sections s_{n0} , s_{n1} , s_{n2} , ..., s_{nn} . Can be determining with accuracy the voltage drops on branch simple line when the motor works at rated values:

$$\Delta U_{l1} = \sqrt{3} \cdot \left(R_{010} \cdot l_0 \cdot \sum_{i=1}^n I_{ci} \cdot \cos \varphi_{ci} + R_{011} \cdot l_1 \cdot I_{c1} \cdot \cos \varphi_{c1} + X_{010} \cdot l_0 \cdot \sum_{i=1}^n I_{ci} \cdot \sin \varphi_{ci} + X_{011} \cdot l_1 \cdot I_{c1} \cdot \sin \varphi_{c1} \right) \quad (21)$$

$$\begin{aligned} \Delta U_{l2} = & \sqrt{3} \cdot \left(R_{010} \cdot l_0 \cdot \sum_{i=1}^n I_{ci} \cdot \cos \varphi_{ci} + R_{012} \cdot l_2 \cdot I_{c2} \cdot \cos \varphi_{c2} + \right. \\ & \left. + X_{010} \cdot l_0 \cdot \sum_{i=1}^n I_{ci} \cdot \sin \varphi_{ci} + X_{012} \cdot l_2 \cdot I_{c2} \cdot \sin \varphi_{c2} \right) \end{aligned} \quad (22)$$

...

$$\Delta U_{ln} = \sqrt{3} \cdot \left(R_{010} \cdot l_0 \cdot \sum_{i=1}^n I_{ci} \cdot \cos \varphi_{ci} + R_{01n} \cdot l_n \cdot I_{cn} \cdot \cos \varphi_{cn} + X_{010} \cdot l_0 \cdot \sum_{i=1}^n I_{ci} \cdot \sin \varphi_{ci} + X_{01n} \cdot l_n \cdot I_{cn} \cdot \sin \varphi_{cn} \right) \quad (23)$$

In these relations:

$$\sin \varphi_{ci} = \sqrt{1 - \cos^2 \varphi_{ci}}, \quad i = 1, 2, \dots, n \quad (24)$$

These voltage drops are calculate on the following ways $l_0 - l_1$ (21), $l_0 - l_2$ (22) and $l_0 - l_n$ (23). The calculate voltage drops with relations (21), (22), (23) must be under admissible maximum voltage from (7).

3. DISCUSSION. EXAMPLE OF SIZING THE BRANCH THREE-PHASE POWER LINES WITH SUPERPOSITION METHOD

It is supposed the size of the branch three-phase power line (presented in fig.1) made from appearance cable with plastic insulator that has copper conductors ($\rho=0.017 \Omega\text{-mm}^2/\text{m}$), through feed three motors (three-phase inductions motors M_1 , M_2 , and M_3), that work in intermittent periodical duty ($t_{f1} = 200\text{s}$, $t_{c1} = 420\text{s}$, $t_{f2} = 180\text{s}$, $t_{c2} = 460\text{s}$, $t_{f3} = 230\text{s}$, $t_{c3} = 560\text{s}$), which characteristics are present in table 1. In the same table gives the relative duty cycle for these three motors determine with relation (13).

Table 1: The motors characteristics feed through main line and relative duty cycle

Motor symbols	P_{ci} [kW]	η_{ci} [%]	$\cos\phi_{ci}$	U_{ln} [V]	$k_{pi} \frac{l_{pi}}{t_{ci}}$	DA_i (13)
M_1	37	90	0.855	380	7	0.476
M_2	15	88	0.845	380	7	0.391
M_3	18.5	89	0.845	380	7	0.411

The medium temperature that are place the line is $\theta_{o2} = +16 \text{ }^\circ\text{C}$ ($\theta_{max} = 70 \text{ }^\circ\text{C}$). The line parts have the following lengths $l_0 = 30 \text{ m}$, $l_1 = 60 \text{ m}$, $l_2 = 50 \text{ m}$, and $l_3 = 70 \text{ m}$. The admissible maximum currents for different cross-sections on warm criterion are presented in table 2.

Table 2: The admissible maximum currents for different cross-sections, for copper appearance cable, with plastic isolation at $\theta_{o1} = +25 \text{ }^\circ\text{C}$ temperature

$s[\text{mm}^2]$	2.5	4	6	10	16	25	35	50	70	95	120	150
$I_{max}[\text{A}]$	25	34	44	60	80	105	130	160	200	245	285	325

For the line sizing are use data from table 3. The compute results of main line through superposition method are present in tables 4.a, b, c and d.

Table 3: The specify values resistors and reactances for copper armoured cable, up to 1kV

$s[\text{mm}^2]$	2.5	4	6	10	16	25	35
$R_{oii}[\Omega/\text{km}]$	7.54	4.71	3.14	1.88	1.17	0.75	0.53
$X_{oii}[\Omega/\text{km}]$	0.098	0.095	0.090	0.073	0.068	0.066	0.064

$s[\text{mm}^2]$	50	70	95	120	150	185	240
$R_{oii}[\Omega/\text{km}]$	0.37	0.26	0.198	0.157	0.125	0.101	0.078
$X_{oii}[\Omega/\text{km}]$	0.063	0.06	0.060	0.059	0.058	0.056	0.054

Table 4.a

Com- pute values	I_{ci} [A] (1)	l_0+l_i [m] (2)	ΔU_{lri} [V] (3)	X_L [Ω] (4)	L_{o1} [H/ m] (5)	ΔU_{lmax} [V] (7)	ΔU_{lai} [V] (8)	S_i [mm^2] (9)	S_{ni} [mm^2] (10)	S_o [mm^2] (11)
1	73.05	90	0.48	0.0074	2.61· 10 ⁻⁷	19	18.52	8.94	10	20
2	30.65	80	0.19	0.0066			18.81	3.24	4	
3	37.37	100	0.28	0.0082			18.72	4.97	6	

Table 4.b

	c_θ [-] (11)	c_l [-] (12)	I_{maxi} [A] (Table 2)	I'_{maxi} [A] (10)	S_{ni} chose [mm^2] (13)
0	1.095	1.325	105	152.34	25
1		1.268	60	83.34	10
2		1.400	34	37.25	4
3		1.365	44	48.2	6

Table 4.c

Computer values	ΔU_{pmax} [V] (20)	ΔU_{pi} [V] (17),(18), (19)	$\sin\phi_{ci}$ [-] (24)	R_{oii} [Ω/km] table 3	X_{oii} [Ω/km] table 3	R_{o10} [Ω/km] table 3	X_{o10} [Ω/km] table 3
1	45.6	110.48	0.519	1.88	0.073	0.75	0.066
2		96.44	0.535	4.71	0.095		
3		98.41	0.535	3.14	0.09		

Table 4.d

Computer values	S_{n1} [mm ²]	S_{n2} [mm ²]	S_{n3} [mm ²]	S_{no} [mm ²]	R_{oii} [Ω/km] table 3	X_{oii} [Ω/km] table 3	ΔU_{pi} [V] (17)... (19)	ΔU_1 [V] (21)... (23)
	Increase until the inequality (20) is true							
0	35	10	16	50	0.37	0.063	-	-
1					0.53	0.064	36.4	6.24
2					1.88	0.073	40.2	6.87
3					1.17	0.068	39.1	7.19

To compute the line voltage drop when the motors starting, the equations system (17), (18), (19), was simplify for the branch line that feeds with electric energy three motors.

From table 4.a for cross-sections: $s_{no} = 25 \text{ mm}^2$, $s_{n1} = 10 \text{ mm}^2$, $s_{n2} = 4 \text{ mm}^2$, and $s_{n3} = 6 \text{ mm}^2$, the voltage drops when motors M_2 and M_3 are starting, overtakes the admissible maximum values. These cross-sections increase step by step until the inequality (20) is true.

The final values of branch line cross-sections are present in table 4.d. For these cross-sections, with relations (21),(22),(23) (that was simplify for branch power line with three lines), was compute the total voltage drops when the motors work at rated values. These are smaller than admissible maximum voltage drop $\Delta U_{lmax} = 19 \text{ V}$.

4. CONCLUSIONS

The superposition method use to sizing the branch three-phase power lines is to decomposition the lines in a number of simple lines that are equal with the consumer number that are feed with electric energy. This method it is simple and easy to apply and it is useful to sizing lines that are supply motors that work in intermittent periodical duty. The superposition method is an economical sizing for electric power lines. This method may be applied, also, to sizing complex three-phase power lines with different configuration: the branches, the mains, the complexes, the lines that are supply from two or many feed point, and so on.

REFERENCES

- [1.] D. Comşa and other, Proiectarea instalațiilor electrice industriale, Editura Didactică și Pedagogică, București, 1976.
- [2.] N. Gheorghin, Aparate și rețele electrice, Editura Didactică și Pedagogică, București, 1971.
- [3.] T. Ionescu, O. Pop, Ingineria sistemelor de distribuție a energiei electrice, Editura Tehnică, București, 1998.
- [4.] M. Păsculescu and other, Instalații electrice miniere, Editura Tehnică, București, 1988.
- [5.] I. Popa, G.N.Popa, Instalații electrice, vol.I, Editura Mirton, Timișoara, 2000.
- [6.] G.N.Popa, I. Popa, Instalații electrice, Editura Mirton, Timișoara, 2005.







¹Radovan HOLUBEK, ²Matuš VLÁŠEK

PLC PROGRAMMING IN LABORATORY OF PRODUCTION SYSTEM PROGRAM CONTROL

¹⁻² SLOVAK UNIVERSITY OF TECHNOLOGY, FACULTY OF MATERIALS SCIENCE AND TECHNOLOGY,
INSTITUTE OF PRODUCTION SYSTEMS AND APPLIED MECHANICS, TRNAVA, SLOVAKIA

ABSTRACT:

Currently, the emphasis on improving the effectiveness of automation in industry. One of the base parts for automation is control devices such as different PLC systems and programming environments. This programming environment for PLC system use in laboratory of production system program control. Base for the control of real output per axis manipulator, a schemes is possible in the virtual software followed by simulated and tuning errors. Thus the scheme is then verified recorded in PLC control and prepared to manage the various movements of the manipulator.

KEYWORDS:

PLC systems, manipulator, automation, sensor, virtual laboratory

1. INTRODUCTION

Within the solution of KEGA grant task, which is being solved at the Institute of Production systems and Applied Mechanics STU Bratislava in years 2009-2011, there is an opportunity to develop the abilities and skills that employers usually expect from the graduates of technical universities. The main goal of this project is to create a virtual laboratory of manufacturing devices programming control and build a suitable system of teaching that will support the creation and consolidation of professional key competences. The result presents both virtual programming PLC with a feedback simulation and checking the graduates' skills that would support their preparing for practice and whole-life education. The demands on graduates' skills and their job market preparedness are deeply analyzed.

2. PRINCIPLE OF PROGRAMMABLE LOGIC CONTROLLER OPERATION

Operation of PLC – the program stored in memory periodically evaluates input signals and set the output.

Using PLC – PLC is used in machine tools, material handling, automated assembly, and in many other industrial applications.

2.1 Preparation of PLC and its structure, types of input and output units

The basic structure of the PLC:

2.1.1 Compact (Fixed Hardware Style)

This copy is cheap and is used more for simpler applications. Configuration variability is low with it. Usually have a limited number of digital inputs, digital outputs or analog input or output. Some compact PLCs also have the option to extend the variability of configurations using additional modules.

2.1.2 Modular (Modular Hardware Style)

It is suitable for demanding applications. This allows much more variable configuration. The basis of the frame (rack, chassis), which in its left is the resource. The rear frame is driven internal bus on which the connector module. Frame length varies according to the number of slots for insertion module (unit). As the first module from the right source plugins CPU (processor) and then followed by further input / output modules (I / O modules).

2.2 Function parts PLC:

CPU - central processing unit

- ❖ control all operations in the PLC,
- ❖ performs programmed sequence of instructions stored in memory,
- ❖ CPU can be implemented as a separate module that can add input and output circuits (ie, other modules).

Memory - into PLC memory is stored

- ❖ technology program management process,
- ❖ titles and operating system PLC.

Input and output circuits

- ❖ connecting PLC to sensors and actuators, where the galvanic separation of signals,
- ❖ A / C and C / A conversion of continuous variables (current, voltage, resistance),
- ❖ each input and output PLC has a (unique) address through which they can access it (write to it or read it).

Programming the device

- ❖ configuration and PLC programming [1].

Programmable logic controller PLC is a digital computer consisting of a programmable memory for internal instructions saving. It performs different specific functions such as logical, sequential, timing and start-stop functions by means of digital or analogue input and output modules. More simplified, PLC can be characterized as an industrial digital computer designed especially for controlling in the field of industry [2].

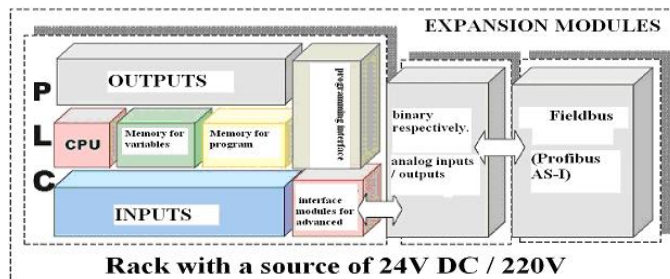
Type of PLC depends on the complexity of controlled technology. Choice of PLC type depends on the application in service. Small PLC is sufficient for plants with simple technological cycle. For automated production and assembly halls it is suitable to use big PLC mainly because of the possibility to extend it by input or output modules and communication interface integration.

Nano PLC and Micro PLC are used as substitutions for switching relay. They control devices like parking automata, manipulators, and machine tools. Their size is very similar to a relay. Small PLC, sometimes called SLC (small logic control), is suitable for plants where PLC performs independently. PLC usually contains an integrated pushbuttons package and an internal LCD display.

2.3 Fundamental structure of PLC systems

Fundamental structure of PLC systems is identical for any PLC (fig.1). Differences are mainly in other options of its expansion. PLC structure is composed of the following parts:

- ❖ power supply,
- ❖ control processor,
- ❖ inputs and outputs (binary, analogue),
- ❖ program memory, memory for variables,
- ❖ connector interface for program loading,
- ❖ other peripherals (floating battery, memory card, RTC, communication conductor bar).



Rack with a source of 24V DC / 220V

Fig. 1 Structural diagram of PLC

PLC Programming Alpha used in the laboratory of manufacturing devices programming control, is performed by assembling functional blocks of logic with the help of members [3].

3. PROGRAMMING METHOD

Controlling and programming of these devices is a very important field of study. For particular manipulator (Fig.2), we used PLC Alpha Controller for cycle automation.

3.1 The workplace of one purpose manipulator "Pick & Place"

The one purpose manipulator consists from pneumatics actuators and components and the

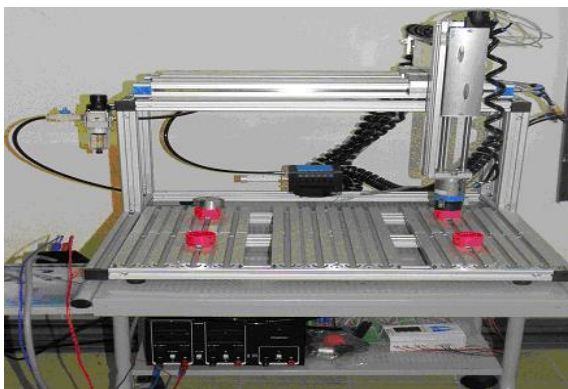


Fig. 2 Real construction „Pick and Place“manipulator controlled by PLC

main frame is realized out of aluminum profiles [4].

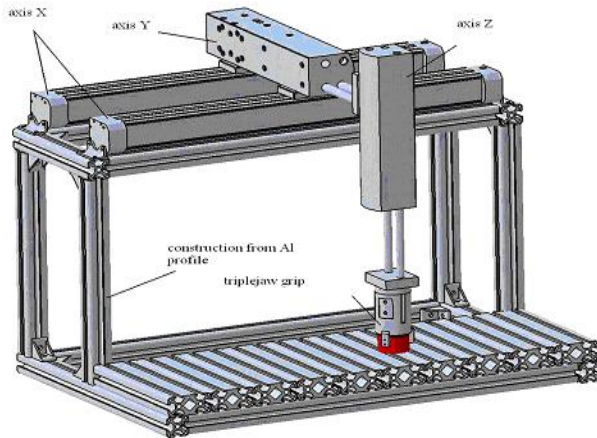


Fig. 3 Three-axis pneumatic „Pick and Place“ workstation design

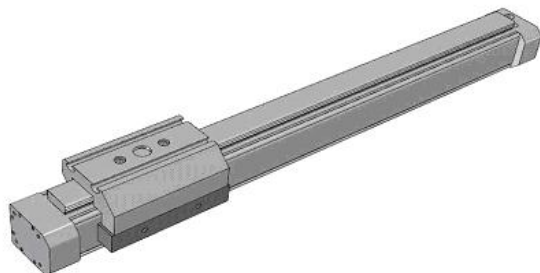


Fig. 4 The X - axis drive (direct pneumatic driver DGPL-25-350-PPV-A-GF-B)

3.1.1 The X - axis drive

The X-axis drive is marked as DGPL-25-350-PPV-A-GF-B. It is linear pneumatic actuator with plain bearing. .

- ❖ DGPL – linear actuator,
 - ❖ 25 – piston diameter [mm],
 - ❖ 350 – stroke [mm],
 - ❖ PPV – adjustable pneumatic absorbing of end positions,
 - ❖ A – magnetic proximity switch possibility,
 - ❖ GF – bead fixation,
 - ❖ B – actuator generation B
- Supplementary data:
- ❖ Synchronization principle by shape connection,
 - ❖ Position detection,
 - ❖ Work pressure (2 – 8 bar),
 - ❖ Double acting motion,
 - ❖ Work medium – filtered, oiled or no-oiled compressed air.

3.1.2 The Y - axis drive

The Y-axis drive is marked as HMPL-20-200-AI-VP-2A3. This actuator is one of type category of pneumatic actuated linear axes for assembly and manipulation equipment and devices. It is possible directly to combine between actuators and loads into axis systems and thereafter to complete into manipulators units “Pick & Place”. The category HMPL is included into modular technique for assembly and

manipulation HMT. It is supplemented this category by it in its construction size and utility mass to down direction. The horizontal axis with vertical axis HMPL creates system “Pick & Place”. It is optimized to stiffness, dynamics and function.

The main characteristics of this actuator are:

- ❖ HMPL – pneumatic linear axis,
- ❖ 20 – piston diameter [mm],
- ❖ 200 – stroke [mm],
- ❖ AI – absorbing of position,
- ❖ VP – armature plate desk,
- ❖ 2A3 –proximity switch position.

Supplementary data:

- ❖ Assembly position,
- ❖ Ball bearing,
- ❖ Work pressure – (4 - 8 bar),
- ❖ Double acting motion.

3.1.3 The Z - axis drive

The z-axis drive is marked as HMPL-16-160-AI-VP-2A3.

- ❖ HMPL – pneumatic lienar axis,
- ❖ 16 - piston diameter [mm],
- ❖ 160 – stroke [mm]
- ❖ AI – absorbing of position,

The actuator axis Z is one of type category as actuator axis Y. the different is only in piston diameter and stroke.

This PLC (Fig. 6) is able to process binary or analogue electric signals.

Programming can be realized either with using the buttons on the front panel or by PC (software Alpha-PCS-WIN-E). By reason of user accessibility, we use the programming language FBD (functional block diagram) for programming. Then we load the following into PLC Alpha by the real output implementation from the created program in given software. Pick and Place manipulator performs single moves on the ground of sensors which are installed on it [5].



Fig. 5: The Y- axis driver (linear pneumatic driver HMPL-20-200-AI-VP-2A3)

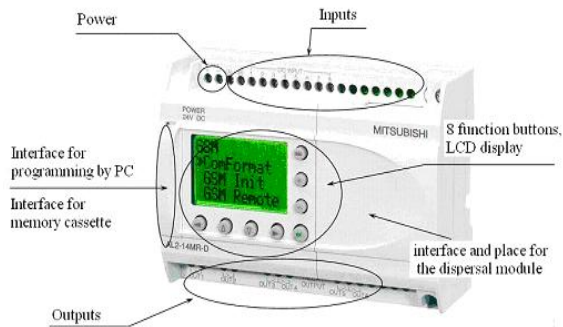


Fig. 6 Programming machine Mishubishi Alpha

Functional blocks are available for:

- ❖ simple and complex logical connections,
- ❖ attributes (parameters) setting,
- ❖ timers,
- ❖ visual display of notifications,
- ❖ analogue processing parameter settings (offset / gain).

Functional blocks – a program is created by joining of main components. They enable us to process the information gained from inputs, or other source, and on their ground (according to dependency of a given stored program) switch the corresponding outputs. It is possible to use 22 different functional blocks when compiling a program. These blocks are pre-programmed for performing of specific tasks and they can have different parameters (Fig. 7). Parameters can be changed where necessary [6].

FBD layout – place for positioning programming features (inputs, outputs, functional blocks, memory cells, or keys) during the programming process.

Binary value – variable type (input, output, and memory cell) can have only two states - 0 (Off) or 1 (On).

Analogue quantity – variable type has numeric value.

Program variables of different types can be edited or read by an open protocol. PC communication, utility panels communication or other PA is possible with the help of communication cable RS-232C. Created programs can be password protected. This type of security answers the purpose of programmer's copyright protection because so protected program cannot be copied any more.

4. CONCLUSION

At present it is very important to know the flexibility to enter into the controlling process at every moment of the automatic cycle manipulation, or technology operations. Therefore, we in our laboratory program of controlling manufacturing systems to teach students to interact. Whether it is the creation of a virtual program by PLC, but also a change in real time the parameters of input and output units.

Acknowledgement

This paper was created thanks to the national grant KEGA 3/7131/09 – Laboratory of production system program control

REFERENCES

- [1] ŽIDEK, K., MAXIM, V., Kurz programovateľných automatov - PLC. J. *INTERNETOVÝ ČASOPIS*, 2009, Vol. 1, č. 1, Bratislava: , 2009, www.oktagon.sk
- [2] VARGA G., DUDAS, I.: Intelligent Manufacturing System for Production of Helicoid Surfaces, Gep, Vol.: LI. No.: 09, 2000, pp.: 44-46

It is possible to program in two ways: direct programming or flexible programming. When we use direct programming, it is possible to programmed simplified commands with the help of pushbuttons. All performed changes will be shown on the display. Direct programming is mainly used for controlling and maintenance, eventually a small program change. Flexible programming is performed by interconnection of the functional blocks so they complete the automation task. It is possible to use up-to 200 functional blocks in one program and the individual functions can repeat arbitrarily often.

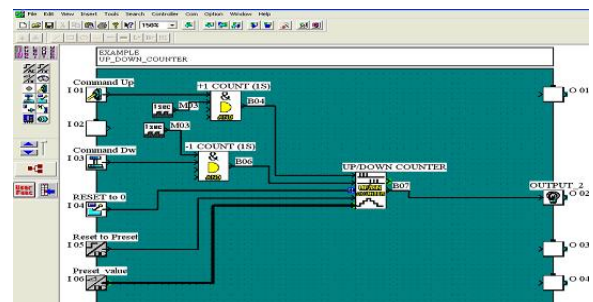


Fig. 7 Programming environment with functional blocks

- [3] DRSTVENŠEK, I., PAHOLE, I., KOVAČIČ, M., BALIČ, J. Intelligent interface in a flexible production environment. J. mater. process. technol. [Print ed.], 15. maj 2005, vol. 164-165, pp.1309-1316. <http://dx.doi.org/10.1016/j.jmatprotec.2005.02.074>
- [4] HORVÁTH, ŠTEFAN - RUŽAROVSKÝ, ROMAN - VELÍŠEK, KAROL: Flexible assembly system generation by CAD and PPS systems. In: Machine Design. - ISSN 1821-1259. - 2010 (2010), s. 269-272
- [5] DANIŠOVÁ, N., VELÍŠEK, K., KOŠTÁL, P.: Automated tool changing system in the intelligent manufacturing and assembly cell. In: ISCCC 2009: Proceedings of the 2009 International Symposium on Computing, Communication and Control, October 9-11, 2009, Singapore. - Singapore : International Association of Computer Science and Information Technology Press, 2009. - ISBN 978-9-8108-3815-7. - S. 1-8
- [6] JAVOROVÁ, A., HRUŠKOVÁ, E., MATUŠOVÁ, M.: Automated design of assembly system with computer aided system help. In: MMA 2009. Flexible Technologies: Proceedings. 10th international scientific conference. - Novi Sad, 9.-10.10. 2009. – Novi Sad: Faculty of Technical Sciences, 2009. - ISBN 978-86-7892-223-7. - S. 206-209







THE BASICS OF DESIGNING CONTROLLERS FOR INDUSTRIAL ROBOTS (EG. ROBOTS ABB IRB 2000)

^{1,3,4} FACULTY OF MECHANICAL ENGINEERING, UNIVERSITY IN BANJA LUKA, BOSNIA & HERZEGOVINA

²UNIVERSITY POLITEHNICA TIMISOARA, FACULTY OF ENGINEERING HUNEDOARA, ROMANIA

ABSTRACT:

The paper explains the basic aspects of designing controllers for an industrial robot control. Industrial robots are basically mechanical devices which, to a certain degree, replicate human motions. They are used whenever there is a need to reduce the danger to a human, provide more strength or accuracy than a human, or when continuous operation is required.

Most industrial robots are stationary, but some move throughout the workplace delivering materials and supplies. While we have the technical ability to produce human robots, industrial robots are actually quite simple devices.

Motions that we take for granted—picking up a something from the table, for instance—are considerably more difficult for a robot. Its mains characteristics of operation, degrees of freedom, etc. They are solved and the calculations developed to obtain the kinematics and dynamics. The accomplished test to each servomotors and the research about its operation.

Basically all industrial robot have a similarly control, because have a similarly actions.

KEYWORDS:

industrial robot control, designing controllers, basic aspects

1. INTRODUCTION

Robotics is a new field of modern technology that crosses traditional engineering boundaries. Understanding the robots and their applications requires knowledge of many areas of engineering, informatics, mechanic and mathematics. We need to know the dynamics, kinematics to control of the robot manipulator. Is the basic to the understanding of the robot operation?

An official definition of such a robot comes the Robot Institute of America (RIA): A robot is a reprogrammable, multifunctional manipulator designed to move material, parts, tools, or specialized devices through variable programmed motions for the performance of a variety of tasks.

In the Laboratory of Intelligent Systems in Faculty of Mechanical Engineering in Banja Luka we have a robot IRB 2000. This robot was starting for this study of design controller.

IRB 2000 is a six-axis robot with a large work volume and is primarily intended for arc welding and glueing/sealing.

The IRB 2000 is also suitable for applications such as assembly, water jet cutting, laser cutting, material handling and stud welding. The handling capacity is 10 kg and the very quick movements of the wrist axis are other important features for the intended applications. The S3 control system makes use of established features like soft keys, joystick and the robot language ARLA for simple and fast programming. The IRb 2000 is in its basic form equipped with an absolute measuring servo system. Another important factor is the interface capacity. The S3 controller has the ability to perform a communication in several different ways. These are digital or analogue I/Os and the serial computer link.

2. THE STUDY

A robot is the main component of a flexible production system (FPS). Other components of this system are machine tools, transport machines, control devices, and different auxiliary

elements. A flexible production system is an automatically operating production system that can be easily reprogrammed and adapted to manufacture different products.

Robot centered modules of FPS, called robot modules or robot systems are intended for specified technological operations like welding, surface coating, packaging, etc. The robot module includes one or more robots (with manipulators and control devices), pallets for details or products, auxiliary positioning, transport devices, etc.

Therefore, robot control means control of a complete robot module and a certain part of the production process. The control system has the whole electronic of the system and allows the external communications with peripheral equipment.

Fig. 1 shows main hardware and software components of the IRB2000 robot from ABB.

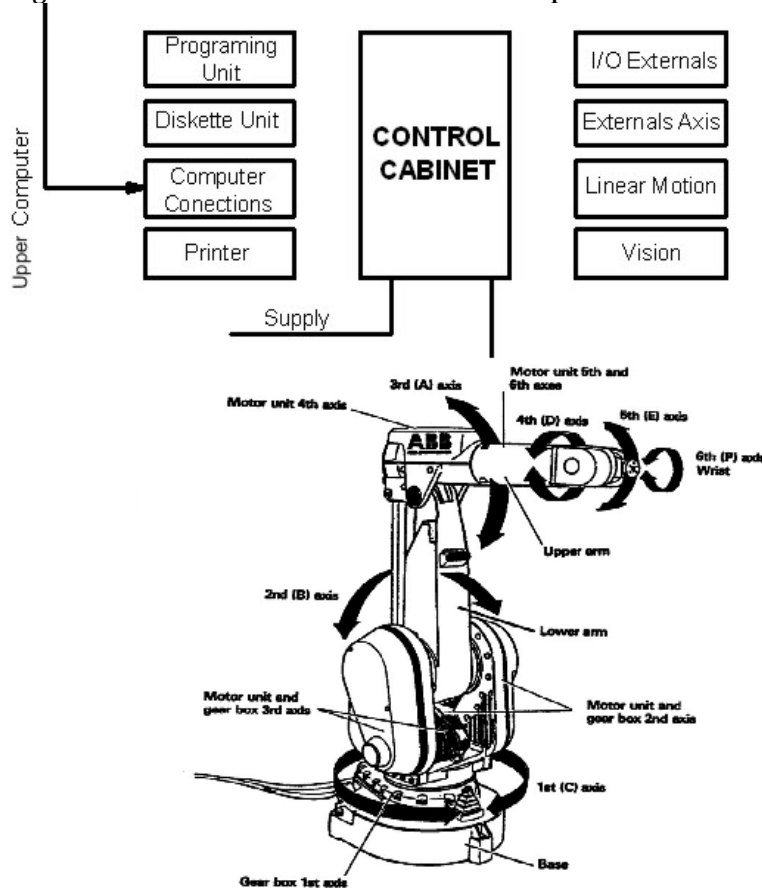


Fig. 1 main ABB IRB 2000 hardware and software components

The mechanical robot is provided with servomotors controlled, in each axes, the servo system have:

- ❖ Speedometer for the speed control.
- ❖ Resolver for the position control.
- ❖ Resolver for the absolute measurement system

The robot is equipped with brakes in each axes, is automatically brake in the emergency stops, power supply fails, or when the motors are disconnected of power supply.

The robot is equipped with brakes in each axes, is automatically brake in the emergency stops, power supply fails, or when the motors are disconnected of power supply. This brakes setting in stand by mode or totally disconnected. While the robot is running and still static the brakes activate automatically after three seconds (automatic operation) or after five seconds. The brakes can turn off manually one by one through of switches in the side of the robot.

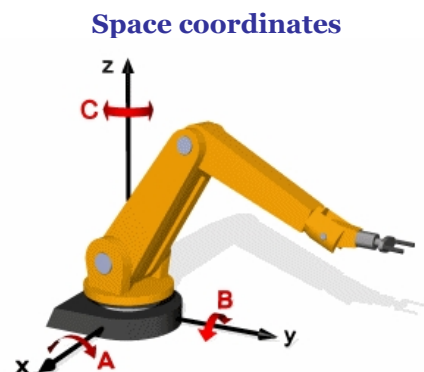
3. ANALISES, DISCUSSIONS, APPROACHES and INTERPRETATIONS

Industrial robots are all-purpose mechanical arms with a number of axes. Regarding movement cycle, route and angle its movements are programmable without mechanical intervention and where required also sensor guided. The mechanical arms are equipped with grippers, other tools and they achieve handling tasks and assembly works.

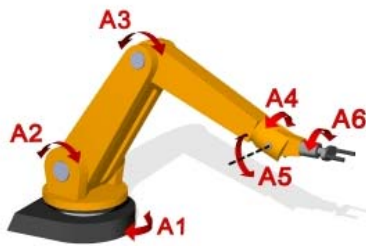
The path between the positions of robot can be executed in three different coordinate systems: rectangular coordinates, robot coordinates and modified rectangular coordinates.

Each one of the coordinate systems will produce a different path and are used according to the needs of speed, precision and direction. All can be activated through instructions in a robot program.

All the positions of the robot are expressed through the coordinates system that which describe the positions of the robot in the space. This system is setting to the base of the robot with plane X - Y in floor and the axis Z noting upward and concentric to the first rotation shaft.



Joint coordinates



The point of origin of the space coordinate system usually is located at the first axis of universal robots. In linear robots the point of origin is located at the intersection point of the three linear axes.

The angle and length description of the particular robot axes describe the orientation of the TCP explicitly. A polar insertion of the coordinates is best.

Gripper coordinates describe the orientation and position of the effector in space.

Workpiece coordinates



The zero point of the coordinate systems is located at the Tool-Center-Point (TCP) of the effector.

If a workpiece has to be processed in different positions, one can site a workpiece coordinate system into one corner of the workpiece.

IRB 2000 manipulates charges in a wide work area, with great rapidity and precision. This robot is particularly adapted for arc welding, application of adhesives and manipulation of materials, because its speed, wide work area and the inherent flexibility of the design of their 6 shafts. The admissible maximum load is of 10 Kg and depends on the distance to the center on the wrist.

Gripper coordinates



Table 1: Scopes of the robot's axis IRB 2000

Motion	Workspace	Max. Speed
Axis 1: Rotation	+180° -180°	115°/sec
Axis 2: Arm	+100° -100°	115°/sec
Axis 3: Arm	+60° -60°	115°/sec
Axis 4: Wrist	+200° -200°	280°/sec
Axis 5: Lurching	+120° -120°	300°/sec
Axis 6: Draft	+200° -200°	300°/sec

The set of points in the space that they can be reached by the extreme of the wrist of the robot constitute its workspace. Remain limited by the maximum angle or linear displacement that permits the joints and the length of the arms.

The movements and degrees of freedom of the robot IRB 2000 are described in table below:

The robot connections for tools and grippers have been designed as a modular system to achieve the best flexibility when accessories are selected. Component can be selected in various ways without limiting the robot working area. Compressed air as well as electrical signals are supplied to the tools via well integrated cabling. Tool exchange can be performed automatically. The exchanger provides a tool fixing plate free from play which allows supply of compressed air and electrical signals from the tools. Main components in the system are:

- ❖ Connection unit
- ❖ Swivel with cabling carrier
- ❖ Tool exchanger
- ❖ Slip ring
- ❖ Tool attachment
- ❖ Dual grippers
 - The modular design enables the unit to be offered in many variants.
 - Computer board contains four microprocessors.
- ❖ Main computer – for overall control
- ❖ Servo computer – for control of servo functions and robot movements
- ❖ Axis computer – for individual control of robot axes
- ❖ I/O computer – for control of communication with operators unit, peripheral equipment, host computer and floppy or cd disk
 - Safety board contains circuits for the personal safety functions
- ❖ Emergency stop
- ❖ Work hold
- ❖ Safety hold
 - Digital I/O boards have digital process communication up to 128 inputs and 128 outputs
 - Analogue I/O board has analogue process communication up to 4 inputs and 4 outputs

Combined I/O board has digital and analogue communication up to 16 digital inputs and 16 outputs + 2 analogue outputs

Control Board for external axes also we have communication via RS 232 interface with computer.

4. CONCLUSIONS

The control panel must to provide full communication with robot system. The emergency stop button and button for resetting the emergency stop function are salient buttons for reasons of safety. The control panel is designed for a demanding industrial environment.

The control panel must includes functions for:

- ❖ Selection of operation modes for the robot system, STANDBY (electronics powered, motor de-energized) and RUN (the entire robot system powered)
- ❖ Synchronization of the robot system
- ❖ Loading of programs from floppy disk or CD
- ❖ Start and stop of programmed operation
- ❖ Emergency stop and re-setting of emergency stop function
- ❖ Locking by key of the programming unit
- ❖ Separate LEDs or LCD for indicating emergency stop and fault status
- ❖ Remote control with joystick

The robot system can be controlled by sensors mounted on the robot or on the object. The robot system can store signal data from sensors , and used then for program. The robot system can receive digital, analog and asynchronics signal with RS232 or other interfaces from the outside computer.

Programming method are point to point method by:

- ❖ Interactive dialogue
- ❖ Manual running with joystick
- ❖ Off-line via terminal
- ❖ Connected with computer

REFERENCES

- [1.] Konukseven, E. L. & Abidi, A. (2004). Developmen of man machine interface software for an industrial robot. Proc. of 2004 IEEE Symposium on Virtual Environment, Human-Computer Interfaces and Measurement Systems, (VECIMS), pp. 49-53.
- [2.] Pires, Norberto: Industrial Robot Programming, Building Applications for the Factories of the Future. New York; Springer, 2006., 282 str.
- [3.] Lizenberger, Gudrun: World Robotics 2007 survey. Frankfurt; IFR Statistcal Department, 2007., URL: http://www.worldrobotics.org/downloads/20071023_Pressinfo_charts.pdf. (05.04.2008.).
- [4.] Lundqvist, Rasmus; Söreling, Tobias: New Interface for Rapid Feedback Control on ABB-Robots. Linköping; Linköping University, 2005., URL: <http://urn.kb.se/resolve?urn=urn:nbn:se:liu:diva-2762>. (20.03.2008.).
- [5.] Mihali, Raul C., Sobh, Tarek M., "The Formula One Tire Changing Robot (F1-T.C.R.)", accepted for publication in the Journal of Intelligent and Robotic Systems, April 1999
- [6.] Mark W. Spong, M. Vidysagar, "Robot dynamics and control"
- [7.] Dr.-ing. Gabriel Hernández López "El origen de la robótica industrial y su desarrollo" in InTech México Automatización pp. 16-22 Octubre-Diciembre 2008
- [8.] Reference Manual, ABB Robotics Products, 1993.
- [9.] Craig, J.J., "Introduction to Robotics, Mechanics and Control", 2[^] Edition, Addison-Wesley, 1989.
- [10.] Sciavicco, L., and Siciliano, B., "Modeling and Control of Robot Manipulators"-2[^]* Edition, McGraw-Hill, 1996





¹István MATIJEVICS

REAL AND REMOTE LABORATORIES IN EDUCATION

¹INSTITUTE OF INFORMATICS, UNIVERSITY OF SZEGED, HUNGARY

ABSTRACT:

One of the most important areas in the education of students is the laboratory realization of various technical subjects. The institutions are faced the burden of large numbers of students and the high costs of laboratory equipment and staff. In many cases, on top of the afore-mentioned problems comes the lack of space. The most appropriate solution is to develop a laboratory in a given place, this could in an industrial environment, as well, and then in real time establish access via the internet and with user interface and visualization enable two-way data exchange. This way only practice has to be organized, parameter setting, real time running can be achieved any given day or time, and from any location. The already established laboratories are capable of operating as distance laboratories if expanded with internet. At the Institute of Informatics of the University of Szeged the establishment of a distant laboratory has been started. This article shows the development of the server and user interface, and presents its use with a step motor. Since the web server is equipped with standard serial connection, it is suitable for connecting other laboratory instruments, as well, thus for the development of any further practices the internet part does not need to be designed again.

KEYWORDS: Remote control, distant laboratory, education of students

1. INTRODUCTION

It is important that students have experience with microcontrollers. These requirements give for a university with the challenge of establishing in the sufficient laboratory establishment. Other important factors are also the large number of students in the education process, the sometimes limited laboratory space and the financial possibility of the universities.

In an effective way we can use existing Embedded System Laboratory (LAN with PC-s) together with other techniques from the web (Internet) and microcontroller trainer boards. Solutions over the internet open the possibilities for the distance learning. Open source distance learning software gives for the lecturers and students the chance for the distance administration, literature access, rapid and constantly updating the materials, renovation and use of tests. Main standing-point in laboratory-making are the following points: low level investment, using extant pieces of equipment together with the improvement of educational effectiveness. Including trainer boards and the internet in the laboratories does not change the old functions of the Laboratory. This paper presents a project to enhance the embedded system education of students. Some courses provide preliminary knowledge for students who selected microcontroller/microprocessor based classes.

In some obligatory and eligible courses students involve the design and development of microcontroller based technologies, for example in Robotics, Autonomous systems and Mechatronics. These courses include both lecture and laboratory components. In some cases in other courses students do interdisciplinary projects, or diploma works, also using microcontroller applications. Interfacing techniques of embedded systems require some physical and also electrical knowledge from students in microcontroller – external equipment connections. Students must know some electrical laws of electrical engineering: common grounds, voltage/current limitations, noise shielding, timing (delaying) problems. Other courses deal with physical/electrical questions, but the experience is, that a course on microcontrollers needs to remind students of these basics.

Also, we do not forget the mechanical interfacing aspects, this field is always imperfect in educational process of students.

2. DISTANCE EDUCATION

Remote operation and control of the Embedded System Laboratory opens great potentials in distance learning. Educational institutes independent from geographical limitations (distributed laboratories) will integrate material and knowledge potentials into a virtual but very realistic form, a complete unit, in the common educational space. The interactive video link connects two or more laboratories, so the instructor from one laboratory guides all students in the common educational space. Students from far-away workstations can operate through the internet with various remote laboratory equipments 24 hours on 7 days a week. Integrated web-learning environments seem to become more and more accepted. Our College's remote course is basically the traditional one with the big difference that it is remotely accessible over the internet.

3. GENERAL DESCRIPTION OF THE SYSTEM

The general scheme of the application architecture is shown in Figure 1. In this system the software and hardware elements are split into two main blocks: local area (client side) where the user works, and remote area where the whole real system with control elements are located (Laboratory).

The elements of systems are:

- ❖ Local area: PC computer with Internet connection and HTTP 4.0 client application,
- ❖ Remote area: Internet connection, Web-server, Experimental board, real hardware (stepper motor) and image capture system.

The control software communication is RS 232 serial communication. End-user (client) can have access to the process and run step-motor application in real time using TCP/IP. The user can change different parameters: number of steps, direction (left or right) and RUN/STOP status.

4. WEB-BASED STEPPER MOTOR ACQUISITION AND CONTROL SYSTEM

The world-wide-web gives method for information transmission. The web enables the control of stepper motor systems from anywhere in the world. The Real system is shown in Figure 2, Lantronix web-server board, self-made experimental printed circuit and stepper motor.

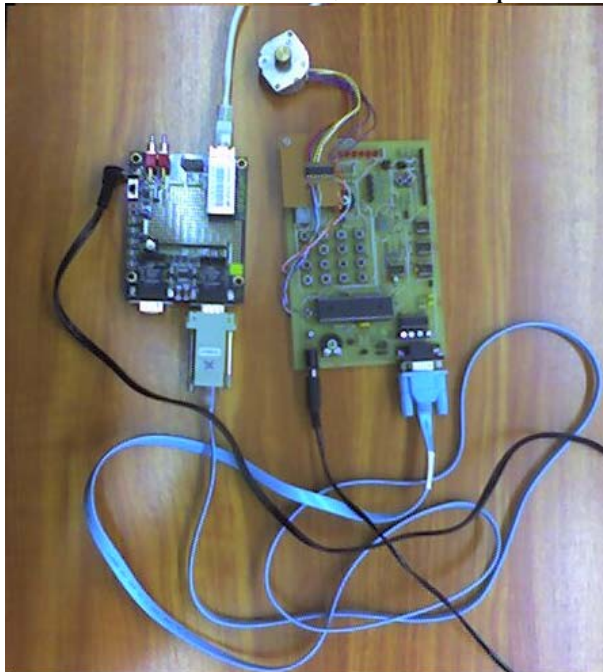


Fig.2. Real system

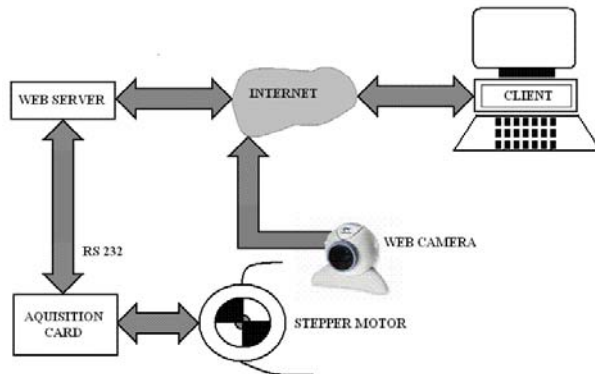


Fig.1. Schematic representation of the Distance Laboratory

The first step in the starting the process is to turning-on of the web-camera. After the typing of IP address from web-camera into the browsers address-line the D-Link server sends trough the internet to the client a window with **login** and **password** requirements (Figure 3).



Fig.3. Login into the camera

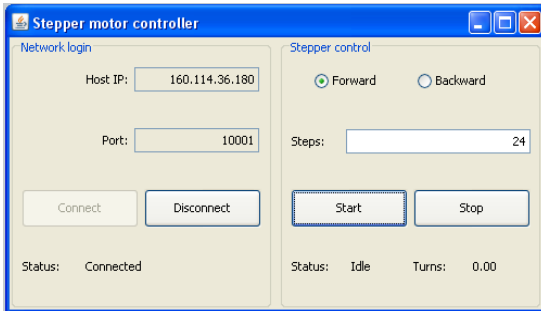


Fig.4. Control panel window on the client side

The web-server for the camera (D-Link) is integrated onto a circuit board that uses HTML.



Fig.5. Real laboratory system in browser using camera picture

The second step is starting the example software, written in Java environment. The Client side network login and stepper control window is shown in Figure 4. Lantronix web-server board needs IP address (160.114.36.180) and Port number (10001) and press the “Connect” button. The connection status is displayed on the bottom part of the window. In the right part of window, in this example there are two buttons for rotational direction (left or right), one stepper motor step is 15 degrees, so full rotation is 24 steps. All our activities are displayed in browser window (Figure 5).

5. COMPARATION OF TWO TECHNICS

In the next table there are some advantages and disadvantages of real and remote laboratories:

Table 1. – comparison of two types of laboratories (rel and remote)

Properties	Real laboratory	Remote laboratory
Contact with system in real work	High-efficiency, full real connection	Indirect relationship, partly real work (programming, parameters)
Delay	There is no immediate response	Internet and internal network-dependent
Financial investment	Great, all exercises should be constructed separately	Smaller, limited to a specific laboratory practices should be established
Other equipment	No	Servers, software and webcams
Student Access	Only under the supervision of a pre-specified times, at night, Sundays and holidays no	7 days in week, 24 hours in day
Supervision	One or more persons	No
Maintenance	Yes	yes
Contribution to the cooperation between the institutions	Limited, it still must be organized	Constant, to be jointly developed curricula should be standardized in the laboratories

6. CONCLUSION

This paper describes the first steps in building combined microcontroller/robotics distance laboratory for several courses in the teaching process of students via the Internet. Teaching microcontrollers for robotics and industry applications is feasible for compulsory courses as well as voluntary courses. This piece of laboratory equipment is also appropriate for other microcontroller applications. Applications of internet tools allow building very operative remote controlled laboratories for the teaching of mobile robots and industry control architecture.

REFERENCES

- [1.] Cheever E., Molter L.A., Maxwell BA, (2003) A Remote Wireless Sensing and Control Laboratory”. Proceedings of the 2003 American Society for Engineering Education Annual Conference & Exposition Copyright 2003, American Society for Engineering Education

- [2.] Puerto R., Jiménez L.M., Fernández Ó.R.C., Neco R., (2002) Remote Control Laboratory using MATLAB and SIMULINK: Application to a DC Motor Model, Dpto. Ingeniería de Sistemas Industriales, Universidad Miguel Hernandez, Elche (Alicante), 03202 Spain
- [3.] Ogot M., Elliot G., Glumac N., (2002) Hands-On Laboratory Experience via Remote Control: Jet Thrust Laboratory”, Proceedings of the 2002 American Society for Engineering Education Annual Conference & Exposition Copyright 2002, American Society for Engineering Education
- [4.] Saad M., Saliah-Hassane H., Hassan H., El-Guetiout Z., Cheriet M., (2001) A Synchronous Remote Accessing Control Laboratory on the Internet. International Conference on Engineering Education, August 6-10, 2001 Oslo, Norway, p.p. 8D1-30-33
- [5.] Ciubotariu C., Hancock G. (2004) Work in Progress – Virtual Laboratory with a Remote Control Instrumentation Component. 34th ASEE/IEEE Frontiers in Education Conference, October 20-23, Savannah, GA, p.p. T3C 18-19
- [6.] Mester Gy. (2006) Distance Learning in Robotics. Proceedings of the Third International Conference on Informatics, Educational Technology and New Media in Education, pp. 249-245, Sombor, Serbia.
- [7.] Kucsera P. (2007) Modular Industrial Mobile Robot Systems, Mobile Robot Docking. Proceedings of the XXV. Science in Practice, pp. 1-5, Schweinfurt, Germany.
- [8.] Böhning H., Keller J., Schiffmann W.. (2004) A combined virtual and remotely accessible microprocessor laboratory. In Proc. 11th Workshop on Computer Architecture Education (WCAE 2004), pages 136–141, June.
- [9.] Mester Gy., Pletl Sz.: Rugalmas robotok hibrid irányítása, Gép, IV. Évfolyam, 2004/6, 1-2 oldal, 2004.
- [10.] www.lantronix.com
- [11.] www.chipcad.com



NEW TRENDS IN DETECTION OF BACK-CORONA DISCHARGES IN PLATE-TYPE ELECTROSTATIC PRECIPITATORS

¹⁻⁴DEPARTMENT OF ELECTROTECHNICAL ENGINEERING AND INDUSTRIAL INFORMATICS, FACULTY OF ENGINEERING
HUNEDOARA, POLITECHNICA UNIVERSITY TIMIȘOARA, ROMANIA

ABSTRACT:

Current voltage characteristics are the main tool to control the operation of the ESP fields and to detect the back Corona.

The collecting efficiency of an ESP depends on the large number of parameters. An important parameter is the current emitted from the discharge electrodes and collecting plates. Generally, the higher secondary current the better are collecting performances. Some parameters, like back Corona discharges, high resistivity fly ash reduce the collecting performances of the ESP.

The paper presents some new methods detection of back-Corona discharges in plate-type electrostatic precipitators.

KEYWORDS:

electrostatic precipitators, negative Corona, back Corona discharge

1. INTRODUCTION

An important un-dust device is plate-type electrostatic precipitator (ESP). It is used in power plant, cement, steel and glass industries. In classical design, a d.c. high voltage (up to 100 kV) is used to generate the Corona effect through discharge wires. The electrons bombard the dust particles from the gas, and after a period of time the particles have negative charges, that are moved toward collecting plates, where the particles are collected [1].

In an ESP a negative applied voltage between a discharge wires (connected at negative polarity) and a collecting plates (connected at positive polarity) produce a negative Corona at discharge wires (fig.1).

The collecting high resistance dusts with ESP it is a not well resolved problem. The back-Corona phenomenon is specific for high resistance dust and consists in a series of micro-discharges between the particles from dust layer on the collecting plates. The current-voltage characteristics changes and decrease the efficiency of the ESP.

The back-corona is a non-linear phenomenon [2,3].

A method to determine the occurrence of back-Corona, in a section of ESP, is the measured the current-voltage (i-u) curve. It is important the slope of i-u curve: if the slope is infinite or negative, a back-Corona occurs in a section. The practical experience shows that the mean current depending on minimum value of the precipitator voltage is the better indication of back-Corona [4].

The new voltage control unit include back-Corona detector device. The old back-Corona detector device has the principle of slope of i-u curve. The main disadvantage of this method is that the power must be reduced to detect the back-Corona.

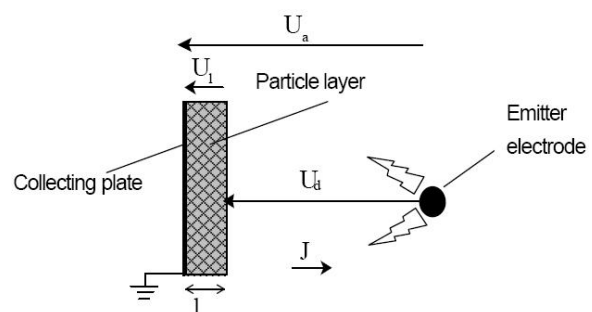


Fig.1. Principle of negative Corona discharge

Another method is based on the minimum value of the precipitator voltage, before and after a spark. If the minimum voltage after spark has higher value than the value before the spark, the back-Corona is detected. It is a better method than the first one. If it is not a spark, a blocking period is induced, when the thyristors are not fired. The current is measured before and after this blocking period of time.

2. METHODOLOGY

The back Corona effect occur when the particle of the dust has a very high resistivity, especially when is burning low quality coal in power plants, sinter plants, and cement plants. When the particulates have high resistivity, a voltage drop can develop on the layer on the collecting plates. If this voltage drop is high can occurs breakdown between discharge wires and the surface of the layer. A hole of dust results in the layer, on the collecting plates. The electric field increased near this hole (fig.2).

A strong positive field (instead negative field) occurs in the hole, which generates positive ions which neutralize the charged of the particles in the gas. The dust particles may have positive charged and they migrate towards discharge wires. The operation of the electrodes is upside down. This phenomenon (back Corona) is self perpetuating. Many holes occur on the dust layer on the collecting plates, dust particles will be attaching on the discharge wires. A voltage drop will be on the dust layer. Electrically, a high current occurs on the low voltage operation, and specify to back Corona, the rise current-voltage characteristic is different then fall current-voltage characteristic (fig.3) [5,6].

A positive back-Corona discharge occurs when the Corona discharge and layer resistivity are high (10^{10} - 10^{11} Ω ·cm). The positive ions from the dust layer drift towards the discharge wires and charged the dust particles with positive charges. The discharge wires become the collecting wires, but the total surface it is not large enough and the particles remain un-collected. The collecting efficiency of ESP drastically decreases.

Usually, the value of electric field in a dust layer is 10-20 kV/cm, and the value of electric field of air is 26 kV/cm.

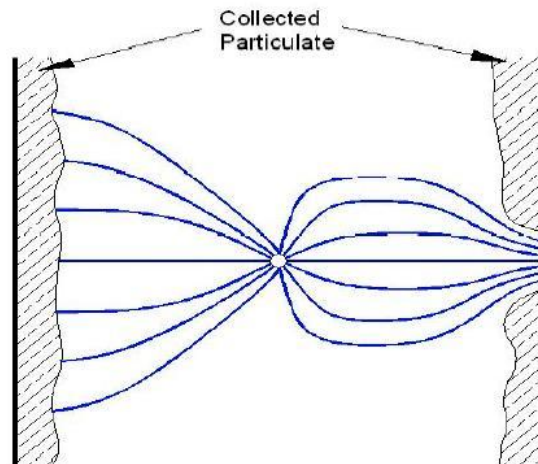


Fig.2. The back Corona between the electrodes

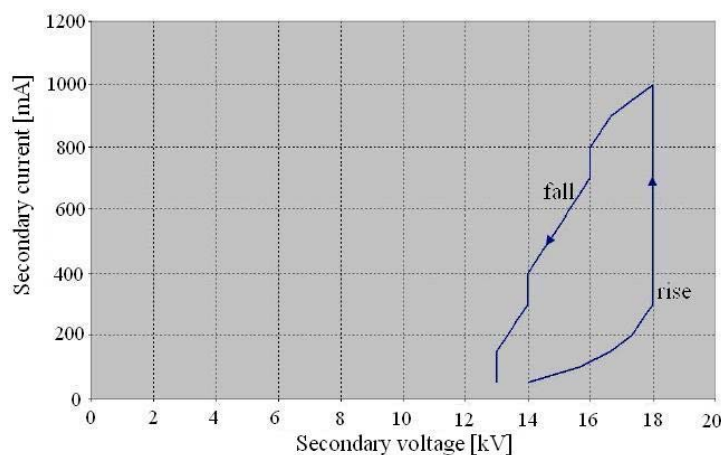


Fig.3. Secondary current as function of secondary voltage in case of back Corona discharges

The back Corona density J_b may be computed with:

$$J_b = k_b \cdot I^{0.4} \cdot (E_l - E_t)^2 \quad (1)$$

Where k_b is the power of the particle layer thickness, E_l is the average electric field in the layer, and E_t is the average electric threshold.

The average electric field in the layer depends on resistivity of the dust ρ , and current density J :

$$E_l = \rho \cdot J \quad (2)$$

In time, various methods have been proposed to detect the back Corona. The ratio between the peak and the mean value of the secondary voltage depends on the back Corona. Other electrical parameters that depend on back Corona are: power supply impedance, supply frequency, precipitator load characteristics.

A method is to inhibit the thyristors pulses for a period of time, and than applied pulses for a period of time t_1 . The controller monitors the effect of the decay voltage. In this period of time is analyzing the decay characteristics of the voltage. Back Corona is detected when is available the equation:

$$U_{ref} - U_{offset} > U_{decay} \quad (3)$$

where U_{ref} is a reference voltage in the non back Corona condition, U_{offset} is the offset voltage to determine the sensitivity of the detection and it is a controller parameter, and U_{decay} is a decay voltage that is measure Corona onset voltage. The secondary voltage is recorded after the time t_1 .

3. DISCUSSION

At operation of the ESP it is necessary to avoid the negative effects of the back Corona discharges.

In fig.4 are present the computed current-voltage characteristics for different dust resistivities. The dust thickness is 0.1 cm. The characteristics were made in a model ESP into laboratory [3].

For high resistance dust (over $1 \cdot 10^{11} \Omega \cdot \text{cm}$) the slope of i - u curve is infinite that indicates the back Corona discharges.

The dust resistivity strongly influences the current-voltage characteristics. The thickness of the dust modify the current-voltage characteristics. In fig.5 the dust resistivity is $6 \cdot 10^{10} \Omega \cdot \text{cm}$.

The thicknesses of dust layer increase the current from source. For high value of the voltage, the i - u curve is spreads. The computed and experimental characteristics are likewise.

In fig.6 is present a comparison of collecting efficiency, experimentally by different authors, depending on dust resistivity. Starting at a resistivity about $5 \cdot 10^{10} \Omega \cdot \text{cm}$ the efficiency drastically decreasing [4,7].

In the following figures are present current-voltage characteristics from the industrial ESP connected at a 600 MW coal burning boiler. The ESP has 5 fields, the first one and the last one are equipped with traditional d.c. power supply, while the other 3 fields have d.c. switching power supplies (with low voltage ripple $\pm 1\%$) [8].

The static current voltage characteristics (fig.7 and 8) have been measure with slowly speed increasing voltage.

The characteristics from fig.7 was made for a fly ash resistivity $7 \cdot 10^{10} \Omega \cdot \text{cm}$. Under approx. 28 kV, the characteristics are the same, and above this value, the current is higher for the characteristics with dust layer.

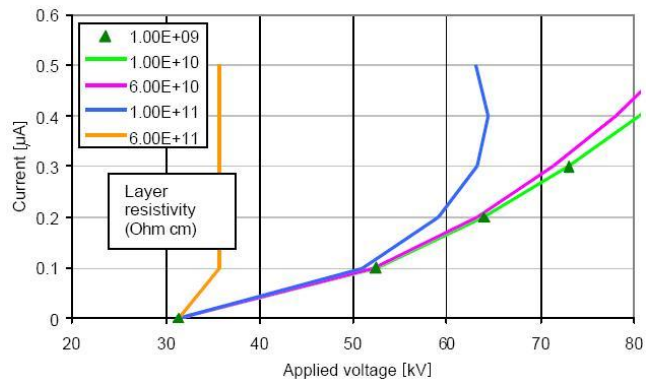


Fig.4. The current-voltage characteristics as function of dust resistivity

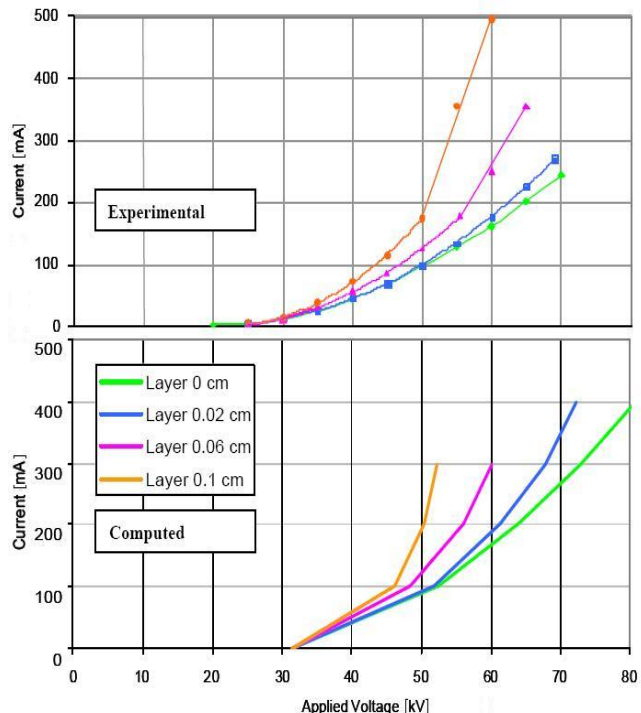


Fig.5. Computed and experimental current-voltage characteristics depending on dust particles thickness

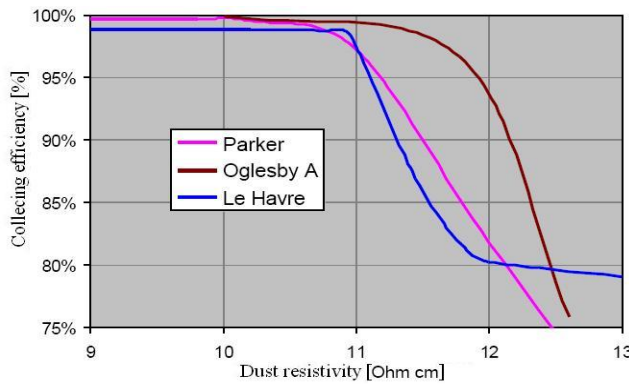


Fig.6. Collecting efficiency depending on dust resistivity

In fig.8 are present three current-voltage characteristics made from different fly ash resistivity: a. high value ($2 \cdot 10^{11} \Omega \cdot \text{cm}$), b. medium value ($7 \cdot 10^{10} \Omega \cdot \text{cm}$) and c. low value ($3 \cdot 10^9 \Omega \cdot \text{cm}$).

The presence of the back Corona can be made with dynamic (the voltage rise and fall rapidly) current voltage characteristics. The rise and the fall characteristics (the shape of „8”) identify the back Corona discharges.

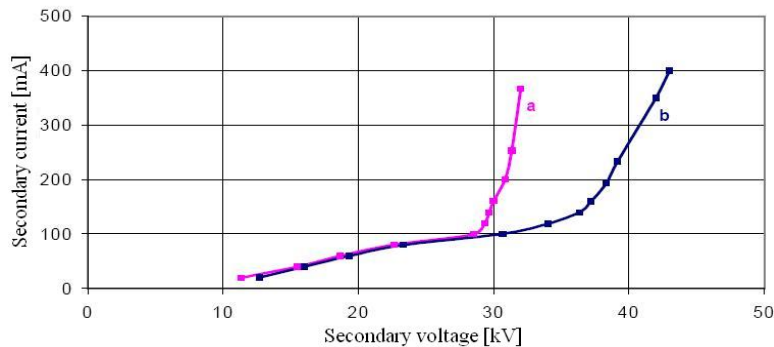


Fig.7. Current voltage characteristics: a. with dust layers; b. without dust layers on the collecting plates

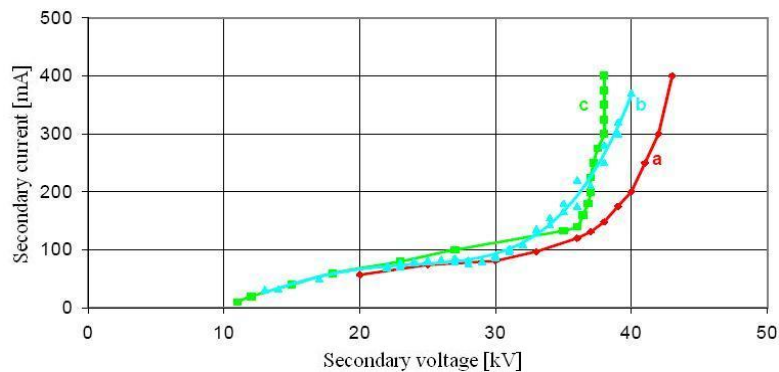


Fig.8. Current voltage characteristics: a. high, b. medium, c. low resistivity fly ash

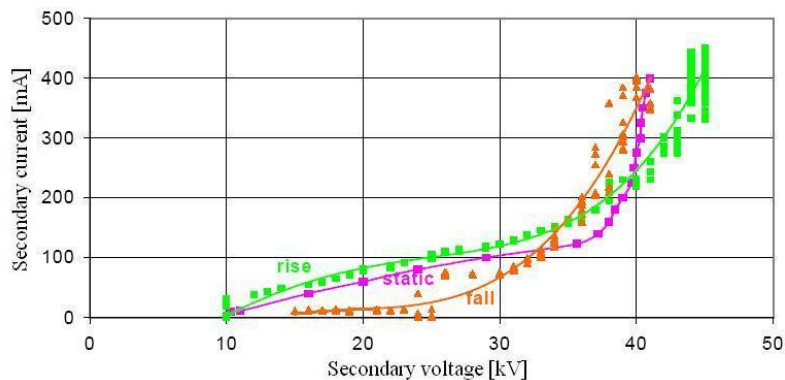


Fig.9. Dynamic current voltage characteristics: at fast rise voltage and at fast fall voltage

In fig.9, is present the dynamic current voltage characteristic for a high resistivity of the dust. For comparison, on the same graph is the static current voltage characteristic.

4. CONCLUSIONS

For an ESP that collects high resistivity dust the presence of back Corona discharges is inevitable problem. The negative resistance area from a current voltage characteristics (if the characteristics depending on minimum voltage) is a result of back Corona discharges. With modern control techniques and with adapted algorithm the back Corona may be detected.

The back-Corona phenomenon is diminish if is burn coal with better characteristics. Another solution to diminish back Corona discharges is to modify the dust resistivity by condition the flue gas (with sulphur and ammonia). Using another control technique, intermittent energisation or pulse energisation will be decreasing the back Corona discharges.

REFERENCES

- [1.] K. Huang – *Spark and its Effect on Electrostatic Precipitators*, the Xth International Conference on Electrostatic Precipitation (ICESP), Cairns, Queensland, Australia, july, 2006, no. 5B1, 12 pp.
- [2.] W. Wang, R. Li, F. Cao, A. Fang, S. Chen, A. Pei – *The Newest Research Results for Collection of High Specific Resistance Dusts with Electrostatics Precipitators*, the Xth International Conference on Electrostatic Precipitation (ICESP), Cairns, Queensland, Australia, july, 2006, no. 5B2, 11 pp.
- [3.] G. Bacchiega, I. Gallimberti, V. Arrondel, N. Caraman, M. Hamlil – *Back Corona Model for Prediction of ESP Efficiency and Voltage-Current Characteristics*, the Xth International Conference on Electrostatic Precipitation (ICESP), Cairns, Queensland, Australia, july, 2006, no. 3B3, 11 pp.
- [4.] K.R.Parker and other – *Applied Electrostatic Precipitation*, Chapman and Hall, Londra, U.K., 1997.
- [5.] J.M.Leach, S.J. Duddy – *The Development of an Algorithm for the Dynamic Adjustment of the Pulse Repetition Frequency for Minimising Back Corona in Electrostatic Precipitators*, the IXth International Conference on Electrostatic Precipitation (ICESP), Mpumalanga, South Africa, may 17-21, 2004, 9 pp.
- [6.] W. Weixue, F. Aimin, C. Feng – *The Newest Technical Results Capable of Remarkably Increasing ESP Efficiency*, the IXth International Conference on Electrostatic Precipitation (ICESP), Mpumalanga, South Africa, may 17-21, 2004, 10 pp.
- [7.] S. Oglesby, G. Nichols – *Electrostatic Precipitation*, Dekker, New York, U.S.A., 1978.
- [8.] G. Bacchiega, I. Gallimberti – *Static and Dynamic Back-Corona Characteristics*, the IXth International Conference on Electrostatic Precipitation (ICESP), Mpumalanga, South Africa, may 17-21, 2004, 11 pp.





¹Constantin OPREA, ²Cristian BARZ

CONTRIBUTION TO AUTOMATE REGULATION AFTER THE SPEED OF ACTIONS WITH ASYNCHRONIZED SYNCHRONOUS MOTOR

¹⁻² UNIVERSITY OF NORTH, FACULTY OF ENGINEERING BAIA MARE, ROMANIA

ABSTRACT:

The actions with asynchronous synchronous motor must assure every overload, which should not depend on the electric parameters of motor, in conditions in which the power of supply sources and mechanical robust allow this thing. At the same time the system of regulation must also assure the possibility of command the reactive power in such way as to maintain at an economical level impose. In this paper, we consider a synchronous motor with a symmetrical wind in stator, supplied from the network and a three-phase symmetrical wind of excitation, alimentated from a static converter with thyristor. The structural scheme of the motor and automate regulator for reactive moment and power; structures which have at basis the Park relations, following as on base of these structures to realize the system model.

KEYWORDS:

asynchronous synchronous motor, automate regulator, structural scheme

1. INTRODUCTION

The utilization of electric motors by direct current in actions, assure the system a high precision and rapidity for regulation of rotation speed at a pre-establish level, but it presents and a series of disadvantages as well. Because of this cause, it has tried the passing to actions with motors of alternative current without collector synchronous and asynchronous synchronous [1, 4].

In particular, the motors synchronous asynchronous (MSA) must not be less accurate than the ones of continuous current with regard to the quality of regulation, must assure any overload necessary to action without depending on the electric parameters of motor. One of the very important conditions imposed to this type of action consists of the fact that, the system of regulation must assure the possibility of command of the reactive power in such a way to maintain it at an economical level imposed.

2. THE FUNCTIONAL SCHEME OF SYSTEM REGULATION

By MSA we understand a synchronous motor with a symmetrical wind in the stator, alimentated from a network of alternative current and a wind bi- or tri- phased symmetrical of excitation alimentated from a static converter of frequency with thyristor (for example with direct link).

This system can be processed in the limits of a close system of automate regulation of the reactive moment and power of the motor, as in figure 1, where: 1 – MSA; 2 – transducers of rotor current; 3 – static

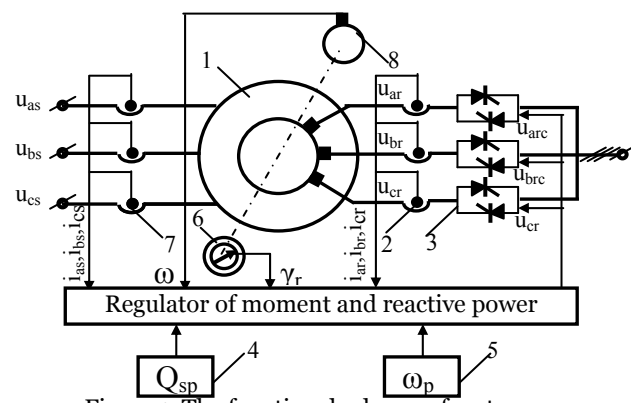


Figure 1. The functional scheme of system

reversible converter with thyristor; 4 – command sensor of reactive power; 5 – command sensor of rotation speed; 6 – angle transducer; 7 – transducers of stator current; 8 – tahogenerator.

Upon the regulator of reactive moment and power, activate the command signals after speed ω_p and after reactive power Q_{sp} , as well as the signals of stator currents, rotor currents, the angular position of rotors v_r and ω . Under the action of this signals, the regulator will process the command signals u_{arm} , u_{brm} , u_{crm} which activate at the entrance of the supply sources of rotor phases. The regulator of the reactive moment and power is synthesized in such a way that the system assures in stationary regime the maintaining of ω and Q at the given level, indifferent of the load at motor tree.

The system synthesis and analysis simplifying assumptions: at MSA with symmetrical three phases winds in stator and rotor are not be taken in consideration the iron losses and the change of saturation rank at this; the stator network supply is considered as infinite; the rotor supply sources are presumed to be electric generators without inertia, with electromotor tensions proportional with the entrance signal, that is: $U_{ar} = U_{arm}$, $U_{br} = U_{brm}$, $U_{cr} = U_{crm}$.

3. THE STRUCTURAL SCHEME OF MSA

Take into account the simplifying assumptions taking in to consideration a system of coordinates round synchronous after axes α, β [2, 3, 5], the functional ecuations of system can be written under the forms:

$$\begin{aligned} \frac{d\Psi_{as}}{dt} &= u_{as} + \omega_s \cdot \Psi_{\beta s} - r_s \cdot i_{as}; \\ \frac{d\Psi_{\beta s}}{dt} &= u_{\beta s} - \omega_s \cdot \Psi_{as} - r_s \cdot i_{\beta s}; \\ \frac{d\Psi_{ar}}{dt} &= u_{ar} + (\omega_s - \omega) \cdot \Psi_{\beta r} - r_r \cdot i_{ar} \quad (1) \quad \text{where:} \\ \frac{d\Psi_{\beta r}}{dt} &= u_{\beta r} - (\omega_s - \omega) \cdot \Psi_{ar} - r_r \cdot i_{\beta r} \\ \frac{d\omega}{dt} &= \frac{1}{J} (M_e - M_r) \end{aligned}$$

$$\begin{aligned} \Psi_{as} &= x_s \cdot i_{as} + x_m \cdot i_{ar}; \quad \Psi_{ar} = x_m \cdot i_{as} + x_r \cdot i_{ar}; \\ u_{as} &= U_{sm} = 1; \quad u_{\beta s} = 0; \quad u_{ar} = u_{arc}; \quad u_{\beta r} = u_{\beta rc}; \\ \Psi_{\beta s} &= x_s \cdot i_{\beta s} + x_m \cdot i_{\beta r}; \quad \Psi_{\beta r} = x_m \cdot i_{\beta s} + x_r \cdot i_{\beta r} \end{aligned} \quad (2)$$

The reactive power of stator circuits will be:

$$Q = u_{\beta s} \cdot i_{as} - u_{as} \cdot i_{\beta s} = -U_{sm} \cdot i_{\beta s} \quad (3)$$

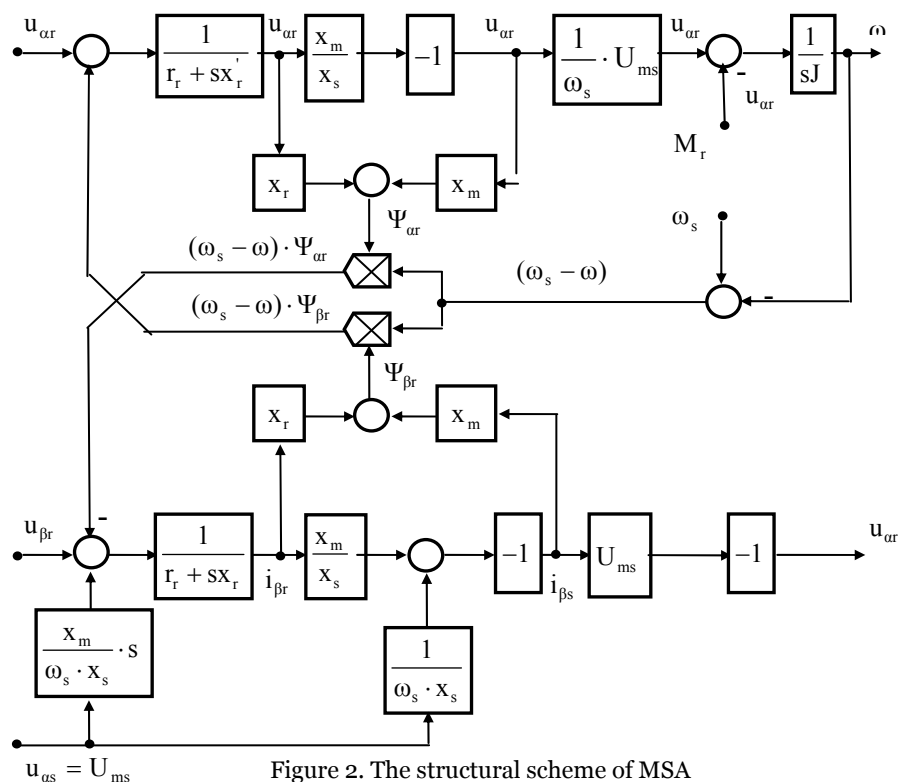


Figure 2. The structural scheme of MSA

With the specifications that in (1) all sizes are expressed in relative units. The variables on axes α , β are connected through:

$$\begin{aligned} i_{\alpha s} &= \frac{2}{3}[i_{as} \cdot \cos \omega_s t + i_{bs} \cdot \cos(\omega_s t - 2\pi/3) + i_{cs} \cdot \cos(\omega_s t + 2\pi/3)] \\ i_{\beta s} &= \frac{2}{3}[i_{as} \cdot \sin \omega_s t + i_{bs} \cdot \sin(\omega_s t - 2\pi/3) + i_{cs} \cdot \sin(\omega_s t + 2\pi/3)] \\ i_{\alpha r} &= \frac{2}{3}[i_{ar} \cdot \cos v_r + i_{br} \cdot \cos(v_r - 2\pi/3) + i_{cr} \cdot \cos(v_r + 2\pi/3)] \\ i_{\beta r} &= \frac{2}{3}[i_{ar} \cdot \sin v_r + i_{br} \cdot \sin(v_r - 2\pi/3) + i_{cr} \cdot \sin(v_r + 2\pi/3)] \end{aligned} \quad (4)$$

where v_r is the electric angle between the rotor axes and the coordinate system which turns synchronously.

The reverse pass towards the command tensions of rotor phases is made through the relations:

$$\begin{aligned} u_{ar} &= u_{arc} \cdot \cos v_r - u_{\beta rc} \cdot \sin v_r \\ u_{br} &= u_{arc} \cdot \cos(v_r - 2\pi/3) - u_{\beta rc} \cdot \sin(v_r - 2\pi/3) \\ u_{cr} &= u_{arc} \cdot \cos(v_r + 2\pi/3) - u_{\beta rc} \cdot \sin(v_r + 2\pi/3) \end{aligned} \quad (5)$$

The system (1) gives the possibility of constructing the scheme of structure MSA, represented in figure 2, observing that the structure contains some non-linear elements as well as a cross reaction created by the presence of the electromotor force of rotation in the stator and rotor circuit, as well as of the magnetic links of these circuits.

The structural scheme can be simplified considerably if the secondary links (by ord. II) are eliminated in particular admitting the elimination of active resistor R_s and a transistor process in statoric circuit. Under these conditions from (1) the fluxes can be determinate:

$$\Psi_{\beta s} = -\frac{1}{\omega_s} \cdot u_{\alpha s} = -\frac{1}{\omega_s} \cdot U_{sm} = -1; \quad \Psi_{\alpha s} = 0 \quad (6)$$

the electromagnetic moment becoming:

$$M_c = -\Psi_{\beta s} \cdot i_{\alpha s} = \frac{1}{\omega_s} \cdot U_{sm} \cdot i_{\alpha s} \quad (7)$$

4. THE STRUCTURAL SCHEME OF THE REGULATOR

As it was mention, the actions with MSA must present the characteristics at similar performance of action case with motors of direct current, carrying out at the same time the part of synchronous compensators as well. From this point of view, we must totally take into account the dynamic proprieties of the regulate object, it is indicated that the regulator be construct not in phase coordinates, but in synchronous coordinates α , β , taking into account (4) and (5).

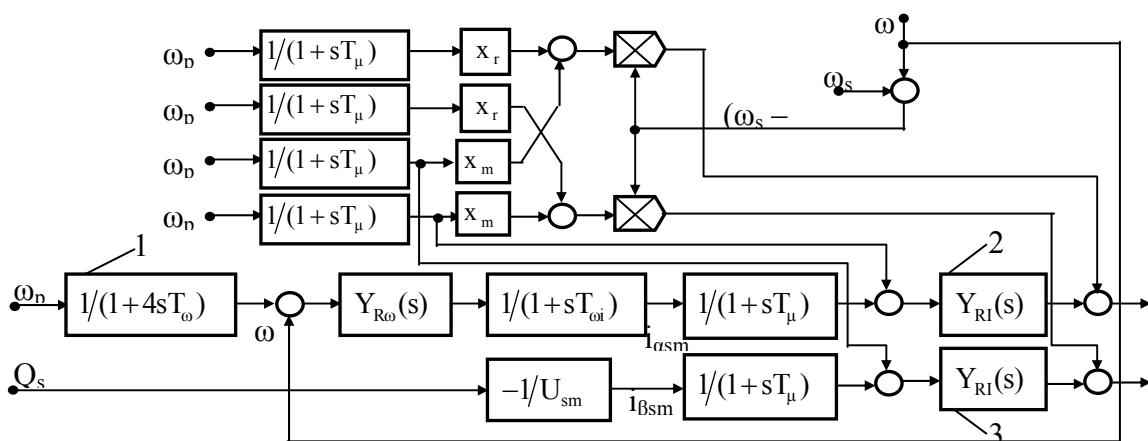


Figure 3. The structural scheme of regulator

From the structural scheme (figure 2), we can observe that, if in the regulator of reactive moment and power, the compensation condition of electromotive force of rotation at rotor is carried out $(\omega_s -)$ and $(\omega_s -)$. Then appears the possibility of separate regulation of active current $i_{\alpha s}$ (electromotive moment and ω) and reactive current $i_{\beta s}$ (power Q_s), with the help of voltage U_{ar} , $U_{\beta r}$. Thus, on the channel $U_{cr} - \omega$, the structure analyzed is analogous with the motor structure of direct current compensated and the regulation is subordinated to the method with series correction. So,

the regulator exit of speed represent the regulator entrance of current, and the motor moment is proportional with the regulator exit of speed.

On the channel $U_{br} - Q_s$, for the regulation it is enough to work only the current regulator.

Taking into account those presented based on figure 2, was obtained the structural scheme of the regulator of reactive moment and power of the MSA from figure 3, at the basis of the regulator synthesis being the general methods of synthesis subordinated to the regulation with series correction.

Through the supply of rotor winds from the static converter of frequency with thyristor, with direct link, the speed is regulated in the approximate limits $(1 \pm 0.3) \cdot \omega_s$. Beside, the speed regulator, in the structural scheme there appear another two regulators: 2 – regulator of active current and 3 – regulator of reactive current, at the regulator entrance 2 appears the command from the regulator exit of speed, again at the regulator entrance–3 it is applied the command of reactive power Q_{sm} .

The transfer functions of regulator are established starting from the optimum transfer functions of the regulation systems in close circuit [2, 6]. So, the transfer function of the current regulator can be give by:

$$Y_{RC}(s) = (r_{rech} + x_r') / 2 \cdot s \cdot T_\mu \quad (8)$$

where T_μ – represent the time constant of measurement filters and its chosen according to the necessary action speed of the regulation circuits of current.

In some cases [4] for increasing the fiability of frequency converters it is indicated that the entries of the regulator non-inertial reverse supplementary connection be introduced after the faze currents, through this the aspect of the transfer function is not modified, only an increase of the equivalent resistance being necessary to be introduced init. The transfer function of the speed regulator can be written under the following aspect, taking into consideration a regulation law PI:

$$Y_{R\omega}(s) = J \cdot (1 + 4 \cdot s \cdot T_\omega) / 8 \cdot s \cdot T_\omega^2 \quad (9)$$

where T_ω – time constant which characterizes the regulation loop of speed and in general $T_\omega \geq 2T_\mu$.

In the regulation, loop of speed a supplementary tuning filter can be introduced as well, whose time constant to be $T_{\omega i} = T_\omega - 2T_\mu$.

5. CONCLUSIONS

The establishing of structural scheme allows the model of electric actions with MSA, this model being made taking into account the machine-static converter assemble. The compensation of the electromotor tension of the rotor and the selection of the activating speeds of the regulation loop constitutes a special problem because it can lead to the worsening of the transitory processes and the apparition of oscillations. In the structural scheme, the compensation of the internal reverse reaction is presented after the rotation electromotor tension through the multiplication elements 4 and 5.

Since the results of the modelation on a red case are not finalized, then results will be presented in the future, taking into account [7] as well.

REFERENCES

- [1.] Boldea I., Parametrii maşinilor electrice, Ed. Academiei Române, Bucureşti, 1991.
- [2.] Botvinnik M., M., Asinhronizirovannaia sinhronnaia maşina, Gosenergoizdat, Moskva, 1960.
- [3.] Câmpeanu A., Introducere în dinamica maşinilor electrice de curent alternativ, Ed. Academiei Române, Bucureşti, 1998.
- [4.] 4. Ferraz, C.A.M.D., de Souza, C.R., Reluctance synchronous motor asynchronous operation, Electrical and Computer Engineering, 2002. IEEE CCECE 2002. Canadian Conference ,
- [5.] pg. 195 – 200, vol.1.
- [6.] Gayadhar Panda, Sidhartha Panda and Cemal Ardil , Automatic Generation Control of Interconnected Power System with Generation Rate Constraints by Hybrid Neuro Fuzzy Approach, World Academy of Science Engineering and Technology 52, pg. 543-548, 2009.
- [7.] Lebedev E., D., Neimark B., E., Upravlenie ventilnîmi elektropribodami postoiannovo toka, Moskva, 1970.
- [8.] Oprea C., Barz Cr., The contributions at modeling sincron machine trough utilization of Labview language, Buletinul Institutului Politehnic din Iaşi, Tom. XLVIII(LII), pg. 117-121, 2002.
- [9.] Soran I.F., Kisch D.O., Sîrbu G.M., Modelarea sistemelor de conversie a energiei, Editura ICPE, Bucureşti, 1998.



¹Cristian BARZ, ²Constantin OPREA

STUDY OF ELECTROMAGNETIC FIELD IN CLAW-POLES ALTERNATOR

¹⁻² UNIVERSITY OF NORTH, FACULTY OF ENGINEERING BAIA MARE, ROMANIA

ABSTRACT:

The paper presents the tridimensional analysis of electromagnetic field of an claw poles alternator, in whose construction has been used non-magnetic material, such aluminum, that form the rings in the rotor's structure. This structure aims to establish lower levels of saturation in the claw-pole of Lundell alternator. Reducing the level of saturation in the rotor, lead to reduction of the losses in hysteresis, the power will be exchangeable in the output of the machine, while achieving its growth the performances.

KEYWORDS:

3D analysis, claw-pole alternator, simulation, finite element method

1. INTRODUCTION

Due to the gradual replacement of hydraulic and mechanical organs of the auto vehicles with electrical devices, power demand in automobiles has greatly increased, where electricity plays a decisive role, the conventional vehicle generator (Lundell alternator) tends rapidly to the maximum that can charge.

The Lundell alternator is the most common power generation device used in cars. It is a wound-field three-phase synchronous generator containing an internal three-phase diode rectifier and voltage regulator. The rotor consists of a pair of stamped pole pieces (claw poles), secured around a cylindrical field winding. The field winding is driven from the voltage regulator via slip rings and carbon brushes. The output voltage of the alternator is maintained at about 14V DC, as this is the nominal charging voltage of a 12V lead-acid battery. The voltage is regulated at 14V by an internal controller that continuously samples the battery voltage and adjusts the field current accordingly.

Electromagnetic behavior of the alternator with claw-poles and its interaction with the bridge rectifier, the load and the vehicle power system is generally considered as a spatial-temporal feature. Thermal model was validated by comparing calculation of temperature distribution with the measured values. [1]

Some studies are based on the idea of increasing the power out and efficiency of the alternator, while maintaining the alternator operating point in the optimum zone. Theoretical expectations are compared with experimental results using a car alternator; the output power increases to 200% and significant improvement of efficiency are demonstrated at high speeds. [2]

Utilization of computational analysis allows for the substitution of expensive prototype construction at early design stages. Authentic simulations of the real machine behaviour require advanced component modelling.

Methods using numerical simulations based on finite elements are often used because permit a better precision performance of the devices. Using these methods can overcome all the surveys and the assumptions made to establish an analytical model often long and hard to build.

Analytical models allow preliminary design studies, so the numerical simulations as an opportunity to validate and refine solutions based on analytical methods.

Henneberger S.A, Damerdash S.A., Viorel S.A. investigated the electromagnetic and thermal phenomena of Lundell alternator using the finite element method.

Perreault's studies have investigated ways to extract more power from existing claw-pole alternators by using a rectifier switching system. Have also been proposed alternators driven by inverter, these can provide energy to a capacitive power factor and being able to extract about twice as much power from alternative to the low speeds.

Proposed solutions include also other types of electric machines: asynchronous machines, variable reluctance machines, synchronous machines with permanent magnet for surface and permanent magnet for interior: Boldea, Naidu, Liang, J.M. Miller s.a. The proposed alternators systems are expensive because the power electronics and the complex control. [3]

Schulte describes two approaches for calculating the mutual inductance between rotor and stator of the synchronous alternator with claw-poles about the claw shape. If the prototypes are available, mutual inductance can be calculated from the voltage measured at no load. Description of the mutual inductance obtained can be used to implement the circuit based on numerical simulations. [4]

2. NUMERICAL ANALYSIS OF THE ELECTROMAGNETIC FIELD - THE CONCEPT

The numerical analysis 3D by finite element method for the electromagnetic field produced by electric drives, is currently, in terms of reliability of results obtained, one of the most powerful means for analyzing the electromagnetic field, for determining the parameters of these complex structures, indifferent of the field shape or the existence or absence of some symmetry.

2.1. Formulation for the finite elements method

The software used in this paper is MagNet, 6.24.1 version, a product of Infolytica. Without many details, it will be still specified that for this software the general 3D formulation is based on the T-Ω method in which the magnetic field is represented as the sum of two parts: the gradient of a scalar potential and, in conductors, an additional vector field represented with vector-edge elements.

In a conducting medium, the equation to be solved is one in \vec{H} of the following form:

$$\nabla \times [\nabla \times \vec{H}] + \sigma \mu \frac{\partial \vec{H}}{\partial t} + \varepsilon \mu \frac{\partial^2 \vec{H}}{\partial t^2} = 0 \quad (1)$$

where $\vec{\mu}$ is magnetic permeability tensor, $\vec{\sigma}$ is electric conductivity tensor, $\vec{\varepsilon}$ is electric permittivity tensor and \vec{H} is magnetic field strength.

In a non-conducting medium, \vec{H} can be written as:

$$\vec{H} = -\nabla \psi + \vec{H}_s \quad (2)$$

where \vec{H}_s is any source field that satisfies $\nabla \times \vec{H}_s = \vec{J}_s$, where \vec{J}_s is the current density in an eventual stranded coil, and ψ -scalar potential. [6]

2.2. The Newton-Raphson method

Finite elements method is a numerical method based on the application of variation principles to solve equations with partial derivatives. In technique, was first developed to solve the problems of resistance material, its application to calculate electric and magnetic fields are relatively recent.

Finite element method is suitable for work with non-linear components such as electromagnets with materials ferromagnetic who manifest anisotropic phenomenon that and saturation.

Relationships formed between magnetic flux (B) and magnetic field (H) are generally nonlinear, over some materials present hysteresis, in "state" BH for a particular point in space and time depends on the previous magnetic values.

To extend the procedure for finite elements to include non-linear properties of materials are required a mathematical model to describe the properties of the material.

The software of field analysis used is based on the calculation method Newton Raphson who converges quickly, providing sufficient initial values. So, if $u^{(0)}$ is a matrix of values of the initial solution, $u^{(1)}$ can be write:

$$u^{(1)} = u^{(0)} + \delta u^{(0)} \quad (3)$$

where: $\delta u^{(0)}$ – matrix of errors values.

$$(K(u) - Q) = F(u) = 0 \quad (4)$$

where Q is independent by u , the factor F define in equation (4) can be extended from multidimensional Taylor series.

The simple iteration scheme (9) Newton Raphson, as illustrated in Figure 1. b), it may not converge if the initial assumptions are not close enough solution. For this reason, is usual in practice, to get the initials startup by completing several steps of iteration before applying Newton Raphson method

In Newton Raphson is essential that curves made it to be smooth, this allowing to be made a better estimation of derivatives. [5].

The treatment of nonlinearities with the Newton-Raphson method and application of finite element method to solve the problems of field, for every iteration, is currently the most used method of analysis of the magnetic field of rotating electrical machines.

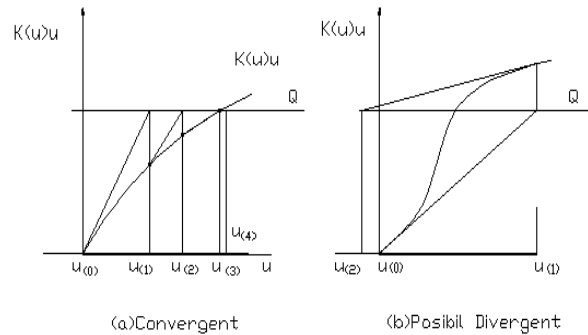


Fig. 1. Simple iteration scheme Newton-Raphson

3. THE REALIZATION OF NUMERICAL MODEL OF THE ALTERNATOR WITH CLAW-POLES

Complex construction of the alternator with claw poles, the existence of magnetic fields both radial and axial, the lack of symmetry plane-parallel magnetic field study require the car to be achieved through three-dimensional finite element numerical modeling.

It highlights sub domains characterized by different magnetic properties: magnetic core of the rotor (polar components as claws), axis machine made from the magnetic material, coil excitation, the stator magnetic core provided with notches in which are placed winding induced.

Starting from the model of alternator with claw-poles in the experimental study, and checking in the same time the geometric dimensions of its design, was performed three-dimensional model of the alternator to following the behavior of this. There are various studies related to various forms of cut or teeth geometry [3], we tried to make some options for changing them, to follow in the subsequent analysis of the influences on the electromagnetic field of alternative.

The program allows saving the models (Fig. 2) and retrieving of this for further modifications to the building with new data, which are made by environmental Magnet 6.11

```
CALL saveDocument("D:\doctorat\MODELE ALTERNATOR\scripturi\stator.mnte", infoMinimalModel)
Call getDocument().getView().addRotation(0, 45, 0)
Call getDocument().getView().addRotation(0, 0, 10)
Call getDocument().getView().addRotation(10, 0, 0)
Call getDocument().getView().rotateToAxis(infoPositiveZAxis)
Call getDocument().getView().rotateToAxis(infoPositiveXAxis)
CALL closeDocument()
msgbox("")
'deschidre fisier
CALL openDocument("D:\doctorat\MODELE ALTERNATOR\scripturi\stator.mnte")
'setarea unitatilor in milimetrii
Call getDocument().beginUndoGroup("Set Default Units", true)
Call getDocument().setDefaultLengthUnit("Millimeters")
Call getDocument().endUndoGroup()
'introducere dimensiuni
dim Rnext, Rrint, Rrdinte, Lrdinte, npoli, Rgheara, Lrbaza, Lgdinte, dist, Rbaza, Lrotor, g1z01
```

Fig. 2. The saving model

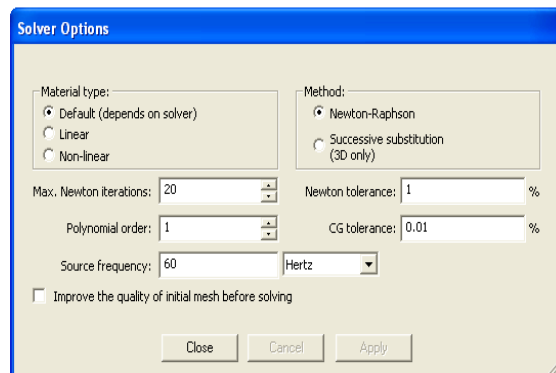


Fig. 3. The solver options

Accessing computing environment for the analysis magnet field define boundary conditions, the currents that cross both the involution stator and the rotor.

Magnet computing environment allows the choice of several ways of calculating the field, find the most used Newton Raphson method, and also choose the orders of the polynomial calculation. (Fig. 3)

Realizing some analysis of the shape and size of the volume of air surrounding the model alternator (Fig.4), brings us attention over some influence of that, on energy stored in the model.

By interpreting the results obtained in the analysis field (Fig. 5), can automatically change the input data to obtain a new constructive model to be analyzed.

It won a precious time with automatic model building constructively us needs another soft drawing a constructive model.

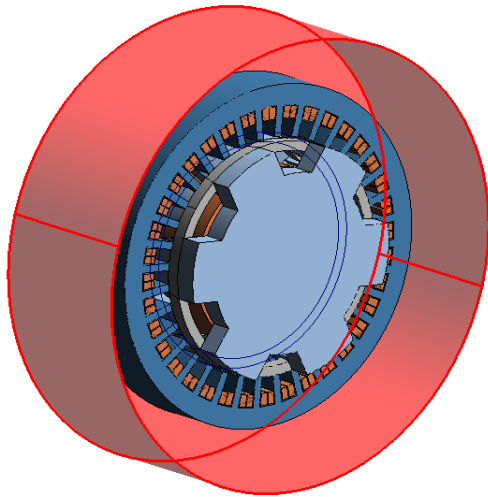


Fig. 4. The volume of air surrounding the alternator model

The uniform level of magnetic saturation in the whole magnetic circuit is usually required, but it is seen that the magnetic flux density in the claw-poles roots is significantly higher in comparison with other magnetic circuit components and areas.

The representation of the magnetic induction along the claw-poles as so on the axis claws, but also on its edges for different excitation currents is made in Fig. 6.

The construction and optimal sizes of the claw poles are required by their role to converting the axial flow produced by the excitation winding in radial flow in air gap.

Begin from the experimental data, in the tridimensional analysis of the alternator with claw poles, we can make comparisons with different configurations of the numerical model of the alternator.

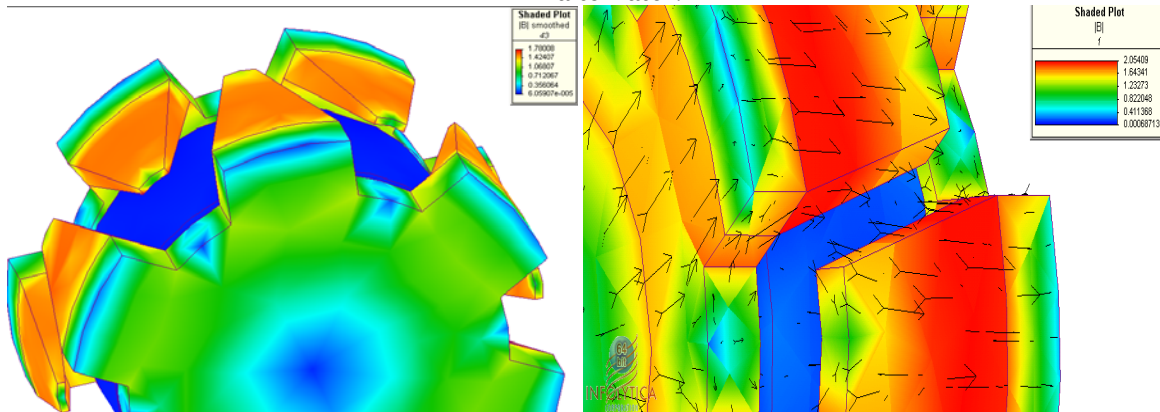


Fig. 5. The results obtained with Magnet 6.11

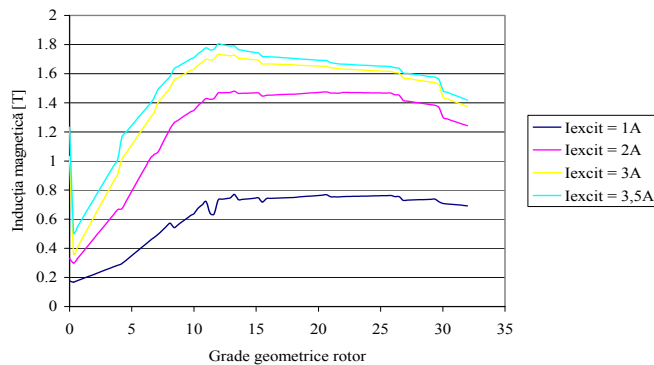


Fig. 6. The representation of the magnetic induction along the claw-poles.

Thus, we can observe how the inductance of the claw poles depends by the geometry and the nature of material from the rotor is achieved.

The uniform level of magnetic saturation in the whole magnetic circuit is usually required, but it is seen that the magnetic flux density in the claw-poles roots is significantly higher in comparison with other magnetic circuit areas and components. Improvement of claw-pole design is therefore advisable. On the other side, increasing the cross-section area of the claw-pole root causes reduction of exciting winding space.

The numerical analysis carried out covering two constructive variants of the rotor unit. The first variant considered involves a distribution of aluminum between the rotor claws, replacing the air gape with aluminum (Fig. 7. a.). The second consists in a ring shape build on the crown of the rotor to reduce the saturation level, but only space between the claws (Fig. 9. b.).

In Fig. 8. have represented the magnetic induction over along the claw pole for the cases: simple alternator, resulting from design and build the model studied, for the case when the air gap between the claws is replaced with aluminum, and, the case when the aluminum is used as the ring shape on the crown of the rotor, but only in free space of the claw.

It can be notice, an increase in saturation along the axis of claw pole in the first case, with the aluminum between the claws beside to the case of standard alternator.

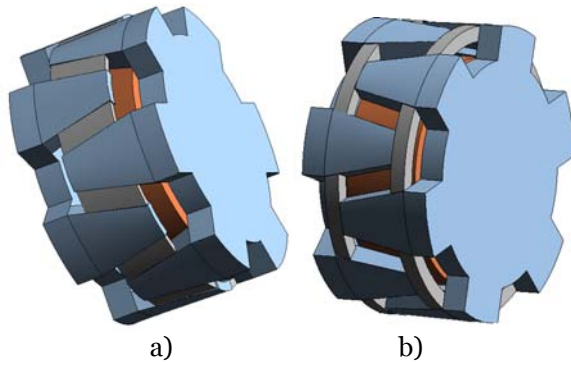


Fig. 7. The repartition of aluminum in the rotor structure of the alternator

Changing the magnetic circuit of the alternator is based on the perspective to optimization the results to be included in designing a prototype of the alternator with claw-poles.

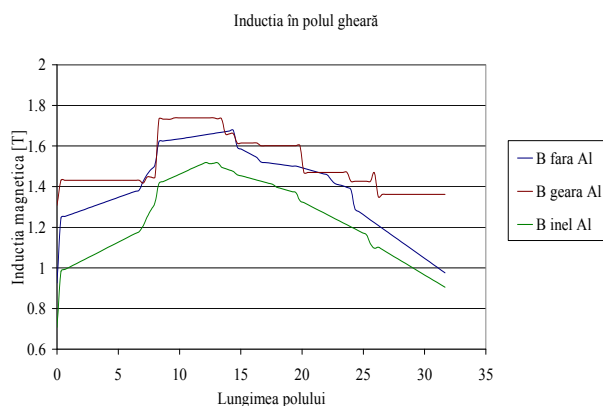


Fig. 8. The magnetic induction over along the claw-pole axis

interaction of aluminum segments enter into the construction of the rotor.

- ❖ The present paper deals with specific issues concerning modeling and numerical analysis of an alternator with claw-poles, with certain portions of nonmagnetic material (Al), using the finite element method.
- ❖ The introduction of the nonmagnetic materials in the rotor assemble as the rings shape on the rotor crowns, try to establish some lowest levels of the saturation in different parts of magnetic circuit (teeth, yokes) and to increase the useful power of the alternator.

In the second case study, however, is important the decrease of saturation by 15%, when the aluminum is in the shape of rings on the crown of the rotor. There is a sharp reduction in magnetic saturation in the aluminum zone, but the decreased saturation is present and to the claw pole tip (up to 5%), there is initial a lower saturation.

The results obtained from experimental measurements, from the aluminum version of the crown ring rotor, show us that reducing the saturation, are going to decrease the output power of the alternator with claw-poles.

4. CONCLUSIONS

The programs which realized field analysis based on the finite element method, come in help of the designer from the checks who can be make in usually time and with high precise, thus removing any errors made during in the design of electric machines, providing reached the designer intended purpose. These programs of analysis and verification ensure the safety of a proper design of the electric cars.

Numerical investigations carried out aimed at optimizing the machine design by reducing the magnetic saturation of the poles' alternator which is due to the

REFERENCES

- [1.] Sai Chun Tang, Member, IEEE, Thomas A. Keim, and David J. Perreault, Member, IEEE, „*Thermal Modeling of Lundell Alternators*”, IEEE TRANSACTIONS ON ENERGY CONVERSION, VOL. 20, NO. 1, MARCH 2005, pag 25
- [2.] Ceuca, E.; Joldes, R.; Olteanu, E „Simulation of automotive alternator - solution for increasing electrical power”. Automation, Quality and Testing, Robotics, 2006 IEEE International Conference on Volume 1, Issue , 25-28 May 2006 Page(s):292 – 297
- [3.] V. Comnac, M. Cernat, A. Mailat, J. Vittek, R. Rabinovici, „New 42 V Automotive Supply System Based on Conventional 14 V Alternator”, in Proceedings OPTIM 2008, Brasov, Romania, 22-24 May 2008, vol. II, pp. 271-276
- [4.] St. Schulte, K. Hameyer „Computation of the Mutual Inductance between Rotor and Stator of Synchronous Claw-Pole Alternators regarding Claw Chamfers”, Institute of Electrical Machines, RWTH Aachen University, Schinkelstr. 4 52056 Aachen Germany, 2005

- [5.] Barz C., Oprea C., Chiver O., „Modelig of Lundell alternator”, 6-th Japanese-Mediteranean Workshop on Applied Electromagnetic Engineering for Magnetic, Superconducting and Nano Materials, Bucuresti, 2009.
- [6.] O. Chiver, E. Micu si C. Barz, „Stator winding leakage inductances determination using finite elements method”, OPTIM 2008, Proceeding of the 11 th International Conference on Optimization of Electrical and Electronic Equipment, 22-23 May 2008, Braşov, IEEE XPLORE INSPEC, pag. 69-74





¹Sorin Ioan DEACONU¹⁾, ²Lucian Nicolae TUTELEA,
³Gabriel Nicolae POPA, ⁴Tihomir LATINOVIC

ARTIFICIAL LOADING FOR ROTATING ELECTRIC MACHINES

^{1,3} DEPARTMENT OF ELECTRICAL ENGINEERING AND INDUSTRIAL INFORMATICS,
FACULTY OF ENGINEERING HUNEDOARA, UNIVERSITY "POLITEHNICA" TIMISOARA, ROMANIA
² DEPARTMENT OF ELECTRICAL ENGINEERING, ELECTROTECHNICAL FACULTY,
UNIVERSITY "POLITEHNICA" TIMISOARA, ROMANIA
⁴ DEPARTMENT OF ROBOTICS, UNIVERSITY OF BANJA LUKA, BOSNIA & HERZEGOVINA

ABSTRACT:

The paper presents many methods to produce synthetic loading of rotating electric machines (induction, synchronous and DC) without load to the shaft using power converter. The required equipment is simple. Setting-up time is considerably reduced because it is not required to connect an external load to the machine's shaft. The range of r.m.s. current control is large beginning from no-load current to overload at rated speed and temperature, that the total losses in the machine can be identified by taking the average of the measured power over one cycle of synthetic loading of the machine.

KEYWORDS:

Ytterberg's method, DC machine, induction machine, synchronous machine, synthetic loading

1. INTRODUCTION

The machine temperature at full load represents an essential parameter of rotating electric machine. The conventional method is to produce the shaft's load using another electric machine. The cost of test equipment and setting-up procedure for mechanical coupling make the conventional method prohibitively expensive, especially for large machine or for high speed machine. Thermal test of vertical mounted machines is quite impossible due difficulties to fit the vertical load [1].

Hence, currently there is no cost-effective method of assessing the state of a machine on-site and whether or not it would be economically and environmentally beneficial to replace it. However, the regulations are not retrospective and so many poor performing machines will remain in service for many years to come. A method of evaluating the efficiency of machines currently in service to ascertain whether or not it should be replaced needs to be developed [2], [3], [4].

The dual frequency method was proposed in 1921 by Ytterberg [5] in order to produce synthetic loading of induction machine.

Now, using power converters several methods have been developed. Dynamic thermal loading [6], [7], [8], constant speed method [9], sweep frequency method [10] and also the dual frequency method [10], [11], [12], [13], [14], can be implemented using power converters.

2. THEORETICAL STUDY

The essence of the dual frequency method is to produce a supply voltage containing two distinct frequencies. This way, two magnetic fields are produced, rotating at different speeds. The shaft speed can not change quickly, so the machine is oscillating between motoring and regenerating. This way, the r.m.s. motor current is increased compared to the no-load current [1].

In Ytterberg's method the loading machine is supplied from two series three-phased symmetrical systems having different frequencies. One of the sources has a fixed frequency f_1

(frequency of the network's power supply) and is called "base source" and the other one has a variable frequency f_2 , usually less than f_1 , and it is called "auxiliary source". The emf's supply by the two sources can be written as:

$$u_1 = \sqrt{2} \cdot U_1 \cdot \sin \omega_1 t, \quad (1)$$

$$u_2 = \sqrt{2} \cdot U_2 \cdot \sin \omega_2 t. \quad (2)$$

Consequently, the resulting wave has amplitude modulated by a frequency equal to the difference between f_1 and f_2 . In the rotating rotor winding is induced a voltage with the frequency equal to the difference between the frequencies f_1 and f_2 . The interaction between rotor current and the rotating magnetic field in the core creates an electromagnetic torque which in a semi-period acts as an accelerating torque, while in the next semi-period acts as a generating torque, reducing the rotating speed of the rotor. In other words, in the first semi-period the machine absorbs active power from the source, while in the next semi-period it releases active power to the source. The resulting voltage has the following expression [15], [16]:

$$u(t) = \sqrt{2} \cdot U_1 \cdot \sin \omega_1 t + \sqrt{2} \cdot U_2 \cdot \sin \omega_2 t, \quad (3)$$

$$u(t) = \sqrt{2} \cdot (U_1 - U_2) \cdot \sin \omega_1 t + \sqrt{2} \cdot U_2 \cdot (\sin \omega_1 t + \sin \omega_2 t). \quad (4)$$

In figure 1 is presented the current in the machine's windings

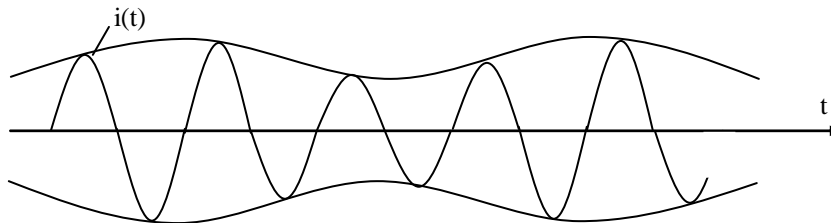


Fig. 1 The current $i(t)$ for synthetic charge loading

Further, we introduce the following notation:

$$\alpha = \omega_1 - \omega_2, \quad (5)$$

$$\beta = \frac{\omega_1 + \omega_2}{\omega_1 - \omega_2}, \quad (6)$$

$$\beta \cdot \alpha = \omega_1 + \omega_2. \quad (7)$$

By combining equations (5) and (6) results:

$$(\beta + 1) \cdot \alpha = 2\omega_1. \quad (8)$$

Thus equation (4) becomes:

$$u(t) = \sqrt{2} \cdot \left[(U_1 - U_2) + U_2 \cdot \cos \frac{\alpha t}{2} \right] \cdot \sin \frac{\alpha \beta}{2} \cdot t. \quad (9)$$

We can observe that this voltage varies periodically with the frequency ω_1 and is modulated with the frequency $\frac{\alpha}{2}$.

In dynamic thermal loading, the rotor's inertia moment will produce the electromechanical load during the acceleration and brake cycle. The induction machine will be repeatedly motor and generator. The average value of electromagnetic torque is close to zero, but not zero, in order to compensate the ventilation and mechanical losses. This method can be implemented as torque control or speed control.

In torque control implementation the reference will be a rectangle wave with a small positive offset. The amplitude of reference torque controls the stator and rotor load current. The offset value of reference torque controls the average value of speed. The average reference speed will be the rated speed in order to keep the same cooling conditions and mechanical loss as in conventional loading [1].

The internal air-gap voltage of an unloaded induction machine is very close in magnitude and phase angle to the applied armature voltage and no load current is small. As the machine becomes loaded, the load angle increases and a larger armature current is produced. The principle of equivalent loading is to increase the internal load angle without connecting any mechanical load onto the shaft. The inertia of the rotor acts as an energy storing device [17].

The constant speed method keeps the flux speed constant and changes only its amplitude. This method works in much the same way as a transformer in which the primary and secondary windings are magnetically coupled by varying flux magnitude. A small oscillating torque will be

produced due to interaction of rotor current and the resultant rotating flux. The rotor speed will be close to rated speed ensuring equivalent cooling conditions. In order to produce the flux magnitude oscillating around rated flux value a higher than rated voltage is necessary in DC link circuit [1].

The other method to produce artificial loading is the sweep frequency method [1], [9]. In this method the supply voltage of induction machine is the result of standard frequency modulation. This voltage, as in the two frequency method, produces a flux wave which varies both in magnitude and angular velocity.

For synchronous machines, there are two loading methods in artificial load: by sub-excitation or over-excitation, and active loading by passing repeatedly from the motor regime in generator regime.

The reactive loading presents the advantage that it only intervenes upon excitation, so it will be adjusted small powers. The synchronous machine can be reactively loaded by sub-excitation or over-excitation, according to the excitation currents I_{\min} and I_{\max} . These currents being different by the rated value, the condition to have the same losses distribution is not respected. The average heating of the excitation winding can be achieved if the machine passes periodically from a loading regime to the other.

Thus, during t_{sub} the current through excitation will have the value I_{\min} and during $T-t_{\text{sub}}$ will have the value I_{\max} . The period T will be chosen in such way that the duration of the transitory processes to be negligible against the duration of the stabilized process and sufficiently small compared with the thermal time constants of the machine.

The active loading is achieved by accelerating the machine in motor regime, than braking in generator regime. During loading, the machine's speed is oscillating around the rated speed. Loading is achieved by controlling the internal angle θ by means of a voltage inverter and a control system. The position of d-axis can be known either using a position transducer, or is estimated knowing the machine's parameters and the variation dynamics of currents and voltages.

The reactive loading can also be done by means of a voltage inverter that modifies the stator voltage (it increases it in the sub-excited regime and decreases it in over-excited regime in such way that the operation point at rated current to be within the stability field, respectively the excitation current to not reach to high values).

The synthetic on-load charging of the DC machines is achieved by producing an oscillating couple that has the average value approximately equal to zero and amplitude close to the rated value. This condition is met if the average couple developed in the machine equals the couple of mechanical losses produced when the machine operates at rated speed. For the DC machines with separate excitation, in derivation or with permanent magnets, the artificial load can be obtained by supplying from a 4-quadrant chopper or by connecting the machine between two branches of a three-phased inverter. Occurrence of some small errors in estimating the mechanical losses depending on speed is producing high deviations of the average speed. Is imposed the utilization of a speed regulator, and for speed's control can be used a speed transducer or a speed estimator.

At the DC machines with serial excitation is needed an additional voltage source, of reduced value and high currents, which during the test to supply separately the excitation and to have the possibility of voltage adjustment. Utilization of a single chopper for testing of some machines with much different voltages is possible by adapting the variator's supply voltage to the rated voltage of the tested machine, or only by adjusting the variator's output voltage. By using of a three-phased inverter, with the 3rd branch can be achieved the source in commutation for supplying the serial excitation winding.

3. DIAGRAMS FOR EXPERIMENTAL TESTS

A. Synthetic loading for induction machine. The first block diagram of the dual frequency method is presented in fig. 2. Autotransformer (AT) plays the role of the base source supplying the voltage with the constant frequency $f_1 = 50\text{Hz}$. Static frequency converter (SFC) supplies a voltage with variable amplitude and frequency f_2 , and plays the role of an auxiliary source which gives the power of the machine that can be loaded. Adapting block controls the level of the signals provided by the transducers to the input of the data acquisition system, which acquires analog signals and convert them to digital. The computing system compares the data received from the transducer to the default set of the loading machine and controls the change of the voltage sources' parameters until one obtains the default value of the artificial charge. The shunts play the role of current transducers.

In fig. 3 is presented another system for synthetic loading [17]. The driver motor D_0 is on the same shaft with generators G_1 and G_2 . Generator G_1 of system (1) is rated at the maximum power rating P_{\max} of the test rig (highest motor rating to be tested), and feeds the motor M_1 under test. The test motor could be either a wound rotor machine or a squirrel cage machine. Both the generator G_2

and the recovery machine M_2 of the system (2) are rated at P_{max} . If the field modulation of each generator is in opposition of phase, the power generated by each system is also in opposition of phase and, therefore, when one system absorbs power, the other generates it and vice-versa. By adjusting the magnitude of the excitation swing of generator G_2 , one can adjust the power exchange with system (2) to exactly match the power swing of system (1). When this equilibrium is reached, the driver motor D_0 needs to provide only the losses in all five machines. Driver D_0 is preferably a synchronous motor, but can be a DC motor or an induction motor with low slip. In the latter case, the motor would have to be slightly over rated in order to perform the test at close to synchronous speed. It's been shown that the optimal performance to reach full rated load is achieved with a 10 Hz modulation depth (55 to 65 Hz).

Fig. 4 presents the diagram of artificial loading using a single supply source. The static frequency converter (SFC) is supplied from the power system and is controlled by a computing system. The frequency converter supplies the induction machine with the free shaft. Before the start, in the computing system are introduced the prescribed values. Depending on the rated speed n_N , is chosen the maximum speed n_{max} and minimum speed n_{min} values. The values of voltage and current are controlled by the computer with the adapting block and transducers. The power delivered towards the SFC in the generating period is consumed by the broke resistance in the DC link of SFC. The speed can be adjusted until the rated value is obtained.

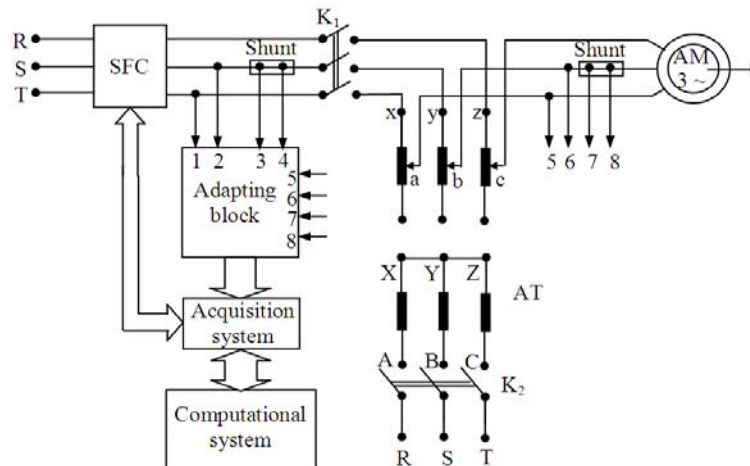


Fig. 2 The block diagram with autotransformer and static frequency converter

The power delivered towards the SFC in the generating period is consumed by the broke resistance in the DC link of SFC. The speed can be adjusted until the rated value is obtained.

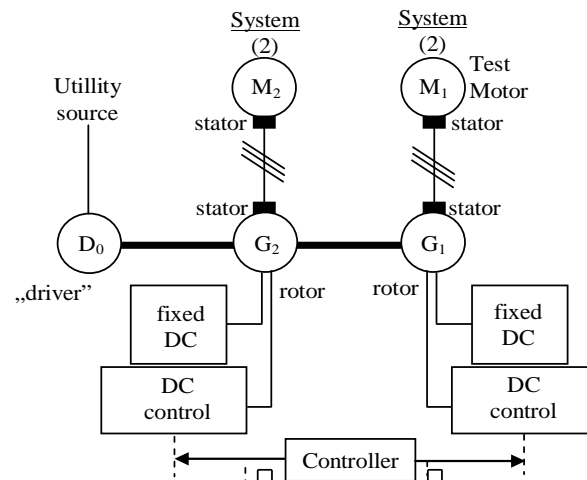


Fig.3 Diagram for large induction machines with no feedback into the power system

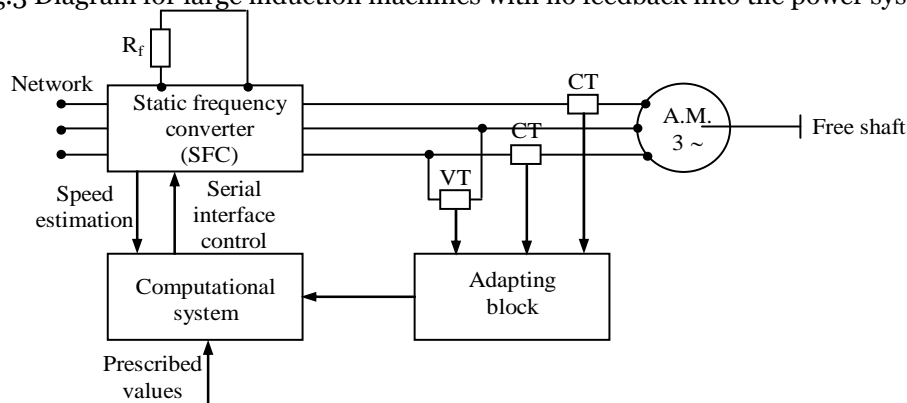


Fig. 4 Artificial loading of induction machine using a single supply source

B. Synthetic loading for synchronous machines

The diagram presented in fig. 5 allows the utilization of the synthetic charge of the synchronous machines (SM) both by using the reactive loading method and the active loading method. The AC/DC converter allows the excitation's supply both in sub-excited regime and in over-excited regime, and the static frequency converter (SFC) allows the modification of the voltage and stator frequency. The rotor position is obtained by means of a position transducer.

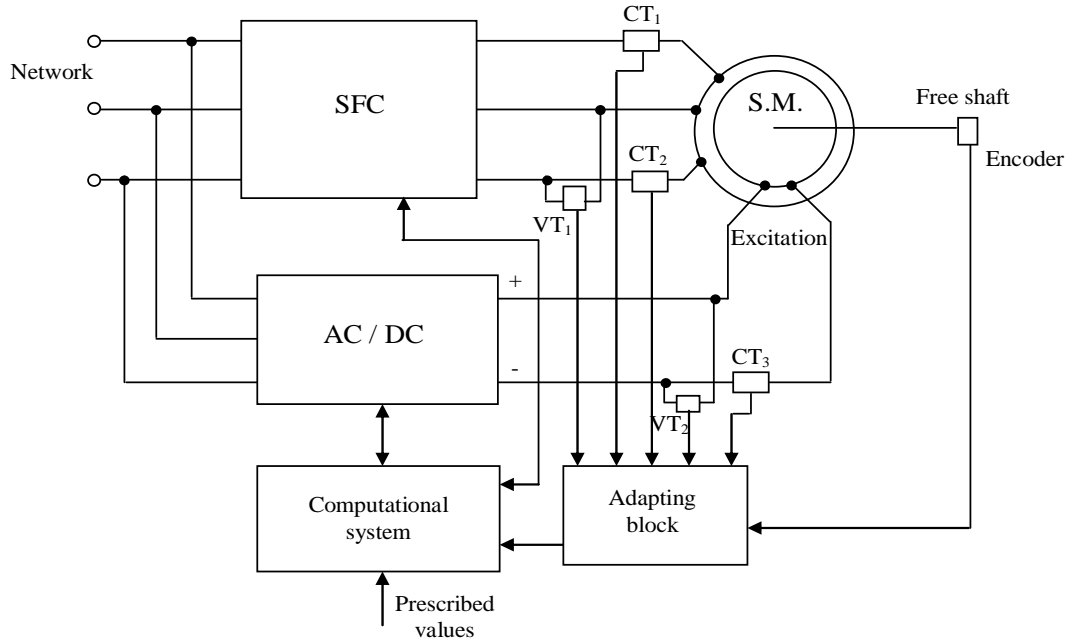


Fig.5 Reactive and active artificial loading for synchronous machines

C. Synthetic loading for DC machines

A synthetic on-load charging diagram of the DC machine using a 4-quadrant chopper is presented in fig. 6.

For a DC machine perfectly compensated, the induced voltage is directly proportional with speed. The proportionality factor between voltage and current is the flux produced by excitation which can be read from a table depending on the measured current.

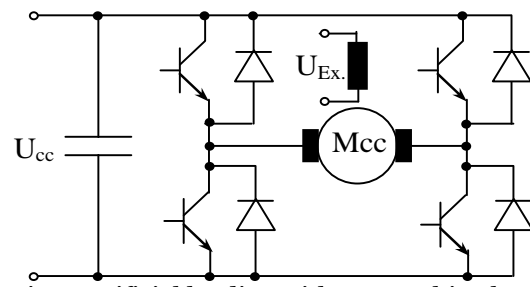


Fig.6 Artificial loading with DC machine by using 4Q chopper

4. EXPERIMENTAL RESULTS

The test machine was an induction motor with the following rated values: shaft power $P_N = 2,2 \text{ kW}$, voltage $U_N = 380 \text{ V}$, speed $n_N = 1420 \text{ rpm}$, current $I_N = 4,7 \text{ A}$, stator winding resistance $R_1 = 2,75 \Omega$, rotor winding $R_2 = 2,1 \Omega$ at 20°C and $R_1 = 3,7 \Omega$, $R_2 = 2,85 \Omega$ at 90°C . The temperature of the stator winding was measured using electrical sounders.

In table I we present the variation of the loading current, average speed, voltage and efficiency as a function of the source's frequency.

Table I

Frequency [Hz]	Average speed [rpm]	Voltage U[V]	Loading current I[A]	Efficiency [%]
45	1445	377,6	4,75	84,9
46	1450	378,2	4,73	85,2
47	1447	378,6	4,77	85,4
48	1453	379,1	4,8	85,6
49	1441	379,5	4,66	85,9
50	1420	380	4,68	86,2
51	1418	379,9	4,72	86,15
52	1425	380,2	4,71	86,0
53	1433	380,1	4,73	85,9
54	1435	380,3	4,74	85,7
55	1438	380	4,725	85,1

The final over-temperature on artificial loading was higher than for shaft loading and sinus supply by about 5°C (10 %) for windings and about 6°C (12 %) for core. The voltage supply from inverter source contains high harmonics which are increasing the core losses and copper losses.

The main problem identified during the experimental part was the need for a closed-loop control to maintain the constant ratings on the test motor and the matching power exchanged with the recovery system.

Further this, the variation of efficiency with auxiliary frequency is only small, namely 1% as shown in Table I. The friction and winding losses will only be marginally higher since the average speed during synthetic loading is near to the rated speed.

5. CONCLUSION

The artificial on-load testing of the rotating electric machines is a modern solution for the simple verification, low-cost, of parameters and characteristics. In the specialty literature is insisted more on testing the induction machines, but of great interest becomes the testing of the synchronous machines and DC machines, including the ones where the inductor field is produced with permanent magnets.

Synthetic loading, the two frequency method, dynamic thermal loading and the constant speed methods of evaluating the efficiency of electric machines has been confirmed, using computer modeling and simulation techniques, as accurate, and able to identify the total losses in the machine under test. Experimental results agree with the modeled synthetic loading and measured steady-state efficiencies.

REFERENCES

- [1.] I. Boldea, L. Tutelea and Klumpner C., "Artificial loading of induction machines: a review", Workshop on Electrical Machine's Parameters, Technical University of Cluj-Napoca, 26th of May, 2001, pp. 9-14.
- [2.] D.J. McKinnon and C. Grantham, "Experimental Confirmation of On-Site Efficiency Evaluation of Three-Phase Induction Motors using Synthetic Loading Techniques", Australasian Universities Power Engineering Conference AUPEC 2004, 26-29 September 2004, Brisbane, Australia, pp. 78-83.
- [3.] D. McKinnon, D. Seyoum and C. Grantham, "Novel dynamic model for a three-phase induction motor with iron loss and variable rotor parameter considerations", Journal of Electrical & Electronics Engineering, Australia, Vol. 22, No. 3, The Engineers Australia College of Electrical Engineers, 2003, pp. 219 - 225.
- [4.] D.J. McKinnon, D. Seyoum and C. Grantham, "Investigation of parameter characteristics for induction machine analysis and control", Conf. Proc. Of the Second International Conference on Power Electronics, Machines and Drives, (PEMD 2004), University of Edinburgh, UK, 31 Mar. – 2 Apr. 2004, pp. 320-325.
- [5.] A. Ytterberg, "Ny method for fullbelastning av elektriska maskiner utan drivmotor eller avlastningsmaskin", s.k. skakprov, Teknisk tidskrift, 1921, S42-44.
- [6.] P. Templin, M. Alacula, M. Gertmar, "Dynamic Thermal Loading of an inverter fed Induction Machine", IEEE /KTH Stockholm Power Tech. Conference, 1995, pp. 241-244.
- [7.] P. Lesage, M. Alacula, L. Gertmar, "The dynamic thermal loading of an induction machine", Record ENE'97 vol.2 pp. 520-525.
- [8.] C. Klumpner, I. Boldea, F. Blaabjerg, "Artificial loading of the induction motors using a matrix converter", Proceedings of PEMD London 2000, pp. 40-45.
- [9.] C. Grantham and M. Sheng, "The synthetic loading of three-phase induction motors using microprocessor controlled power electronics", Record IEEE Catalogue No. 95TH8025/1995, pp. 471-476.
- [10.] D.J. McKinnon and C. Grantham, "Modeling of synthetic loading for efficiency evaluation of three-phase induction motors", Proc. AUPEC 2003, Christchurch, New Zealand, 28 Sept. – 1 Oct. 2003.
- [11.] C. Grantham, "Full load testing of three phase induction motors without the use of a dynamometer" ICEMA, 14-16 September 1993 Adelaide Australia, pp. 147-152.
- [12.] S. Garvey, I. Kolak and M.T. Wright, "Aspect of mixed frequency testing for induction machines", Record of ICEM-1994, D14, Paris, France.
- [13.] I. Boldea, L. Tutelea and N. Muntean, "A new approach to inverter-fed mixed frequency testing of induction machines", Proc. Electromotion'97, Cluj-Napoca, Romania, pp. 82-87.
- [14.] L. Tutelea, I. Boldea, E. Ritchie, P. Sandholdt and F. Blaabjerg, "Thermal testing for inverter-fed induction machines using mixed frequency method", Proceedings of ICEM'98 Istanbul, vol.1, pp.248-253.
- [15.] M. Biriescu, "Testing elements of electric machines", Politechnica Publishing House, Timisoara, Romania, 1994 (in Romanian).
- [16.] S.I. Deaconu, G.N. Popa and L. Gherman, "Diagram for artificial charge loading of asynchronous machine and the study of the influence of the frequency change on the charge loading", Buletin of Politechnic Institute of Iasi, Tom XLVIII, Fasc. 5, 2002, pp. 127-130.
- [17.] J. Soltani, B. Szabados, and Gerry Hoolboom, "A New Synthetic Loading for Large Induction Machines With No Feedback Into the Power System" IEEE Transactions on Energy Conversion, Vol. 17, No. 3, September, 2002, pp. 1-7.



¹: Gyula MESTER

CONTRIBUTION TO THE SIMULATION OF BIPED ROBOT USING 19-DOF

¹: UNIVERSITY OF SZEGED, DEPARTMENT OF INFORMATICS, ROBOTICS LABORATORY, SZEGED, HUNGARY

ABSTRACT:

This paper presents contribution to the simulation of biped robot Kondo robot KHR-1HV using 19-DOF. Studies in the area of humanoid robotics have recently made a remarkable progress. The modeling of the Kondo KHR-1HV humanoid robot motion is analyzed. A kinematic scheme of a 19-DOF biped locomotion system is used in simulation. The simulation results in the Matlab /Simulink and Robotics Toolbox for Matlab/Simulink environment show the validity of the proposed method.

KEYWORDS: Modeling, dynamic model, Lagrangian dynamics simulation, biped locomotion, humanoid robot motion, Kondo robot KHR-1HV, 19-DOF, rigid segments, joints, bipedal walking, locomotion mechanism

1. INTRODUCTION

In recent years, there has been a growing interest in modeling, simulation and control of the humanoid robot motion. Currently many researches in robotics are dealing with different problems of humanoid robot motion. This paper deals with the simulation of biped robot Kondo robot KHR-1HV using 19-DOF.

The modeling of the Kondo humanoid robot motion is analyzed. The problem of bipedal motion is a very complex task. Studies in the area of humanoid robotics have recently made a remarkable progress.

The considered humanoid locomotion in this paper has 19-DOF. The simulation results in the Matlab/Simulink and Robotics Toolbox for Matlab/Simulink environment show the validity of the proposed method. The paper is organized as follows:

The paper is organized as follows:

- ❖ Section 1: Introduction.
- ❖ In Section 2 modeling of the Kondo robot motion is proposed.
- ❖ In Section 3 the simulation results of the Kondo humanoid robot motion are illustrated.
- ❖ Conclusions are given in Section 4.

2. MODELING OF THE KONDO ROBOT MOTION

The Kondo KHR-1HV humanoid robot's body consists of a number of rigid segments interconnected with joints. During the bipedal walking, some kinematic chains in their interaction with the unknown environment transform from open to closed type of kinematic chain.

The dynamic model of the locomotion mechanism of the robot in a vector form is:

$$(1) \quad \mathbf{H}(\mathbf{q})\ddot{\mathbf{q}} + \mathbf{h}(\mathbf{q}, \dot{\mathbf{q}}) = \boldsymbol{\tau} + \mathbf{J}^T(\mathbf{q})\mathbf{F}$$

where:

- $\mathbf{H}(\mathbf{q})$ – is the inertia matrix of the mechanism,
- \mathbf{h} – is the vector of centrifugal, Coriolis and gravitational moments,
- $\mathbf{J}(\mathbf{q})$ – is the Jacobian matrix of the system,
- \mathbf{q} – is the vector of the internal coordinates,
- \mathbf{F} – is the vector of external forces and moments,
- $\boldsymbol{\tau}$ – is the vector of the driving torques at the robot joints.

Biped locomotion of humanoid robots is a very complex process to modeling. The bipedal walking of the robot consists of several phases that are periodically repeated: single-support phases and double-support phases.

The dynamics of the locomotion mechanism can be expressed by the Lagrangian dynamics. Computed Torque Control method is applied for control of the humanoid robot motion. The widely-known method to generate a stable trajectory for a biped robot is based on the Zero-Moment-Point (ZMP) equation. The concept of Zero-Moment-Point was first introduced by Miomir Vukobratovic and has an essential role both in scientific research and practical applications of bipedal motion of humanoid robots. The Zero-Moment-Point is the center of pressure at the feet on the ground, and the moment applied by the ground about the ZMP is zero.

The considered humanoid locomotion mechanism used in simulation in this paper has 19-DOF. The scheme of a 19-DOF biped locomotion system, masses and dimensions of the biped Kondo KHR-1HV humanoid robot is presented in Fig. 1.

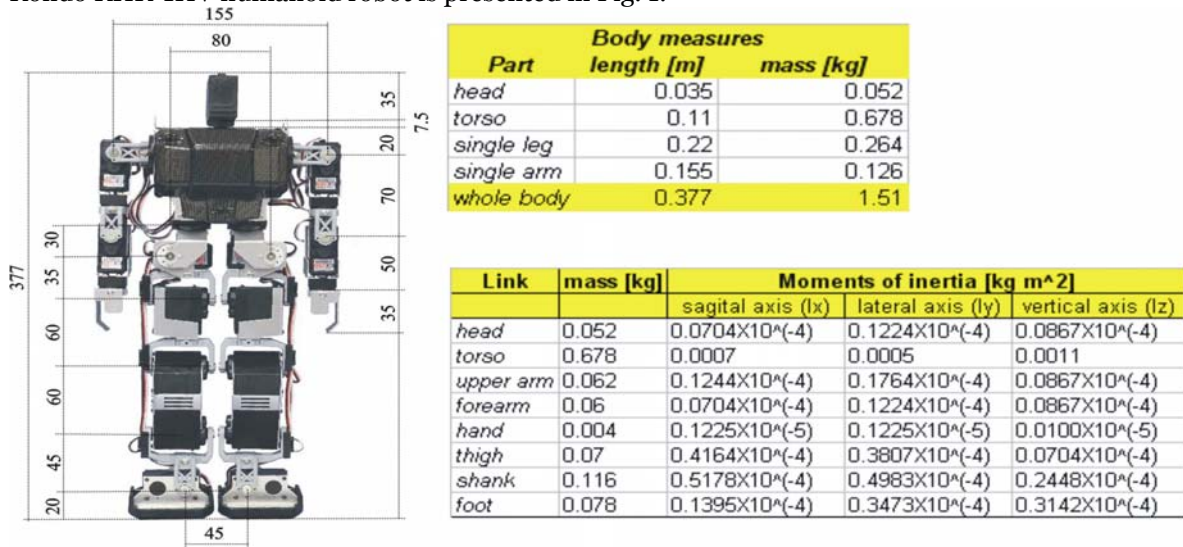


Fig.1. The Kondo KHR-1HV humanoid robot

3. SIMULATION RESULTS OF THE KONDO HUMANOID ROBOT MOTION

Simulation experiments are commonly used for the initial system analysis and control design while the experimental scalable tested system has to be used in the final phase of system evaluation and control verification. The obtained results and control architecture can be afterwards adapted to the different application of mobile robots. Based on this, the important task in system development is accurate and valuable modeling of the observed system.

Simulation of the humanoid robot motion was performed using Matlab/Simulink and Robotics toolbox for Matlab/Simulink. In the simulation the biped robot walks on a flat horizontal plane. The simulation time is 3 s. The results of the simulation of Kondo robot motion are shown in Fig. 2-6.

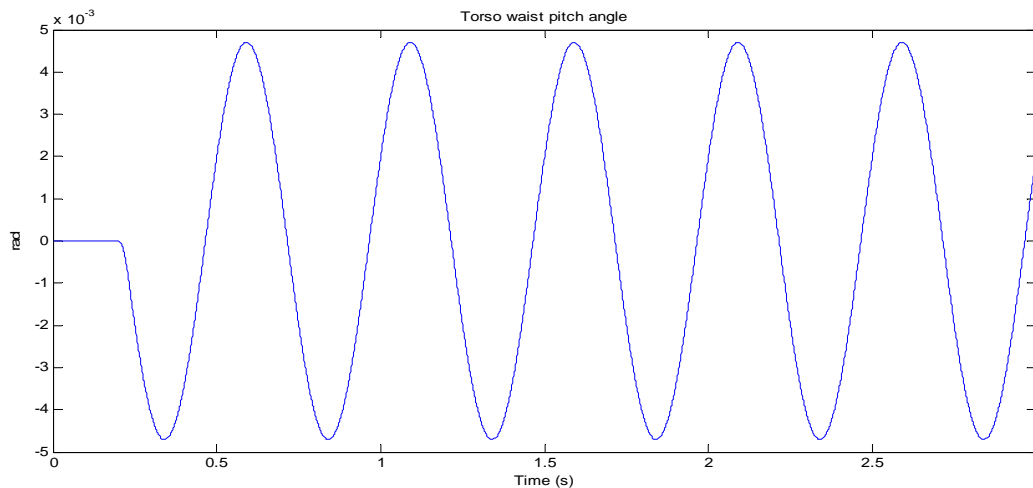


Fig.2. Torso waist pitch angle

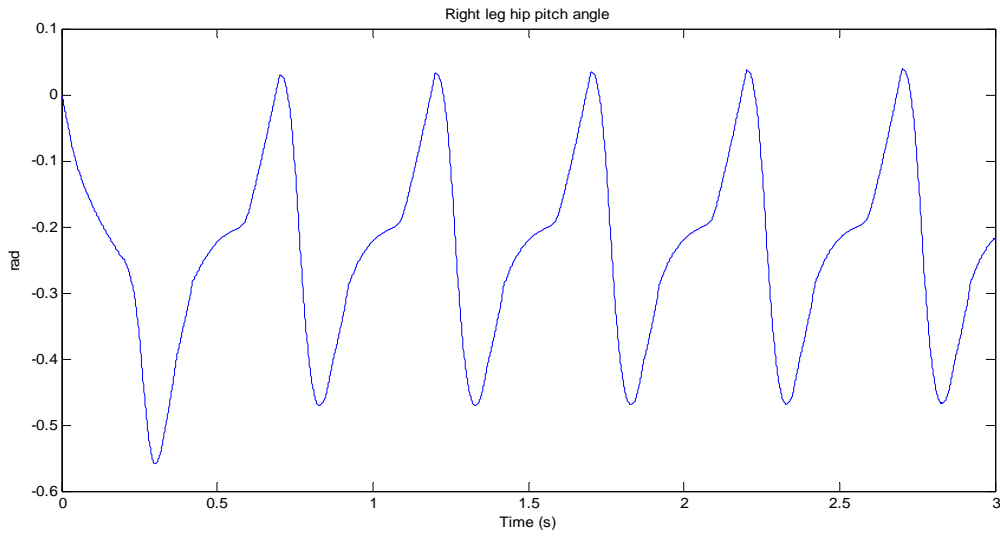


Fig.3. Right leg hip pitch angle

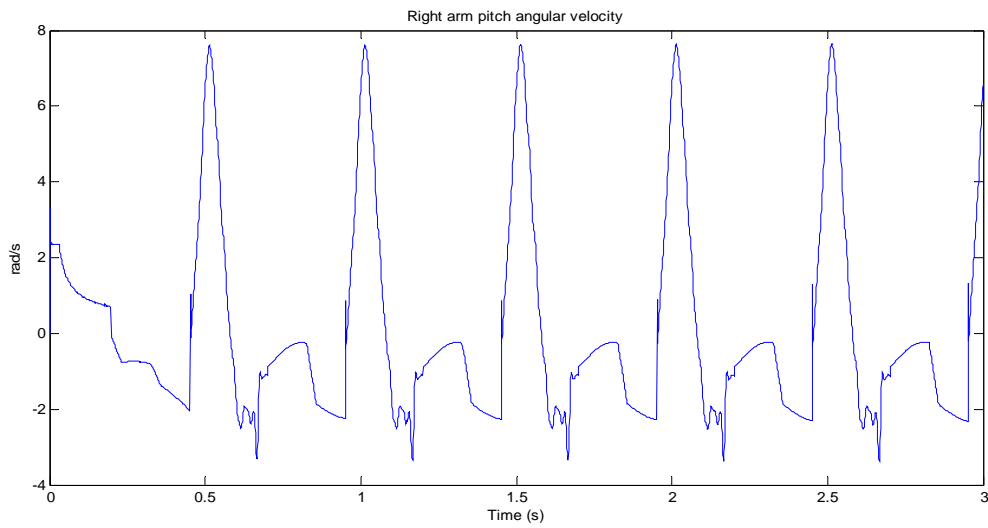


Fig.4. Right arm pitch angular velocity

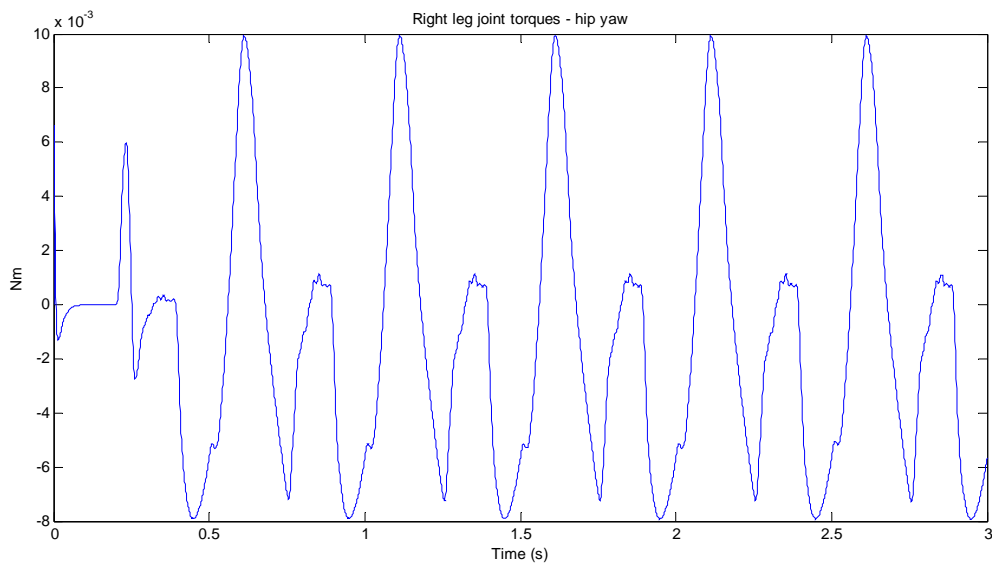


Fig.5. Right leg joint torques – hip yaw

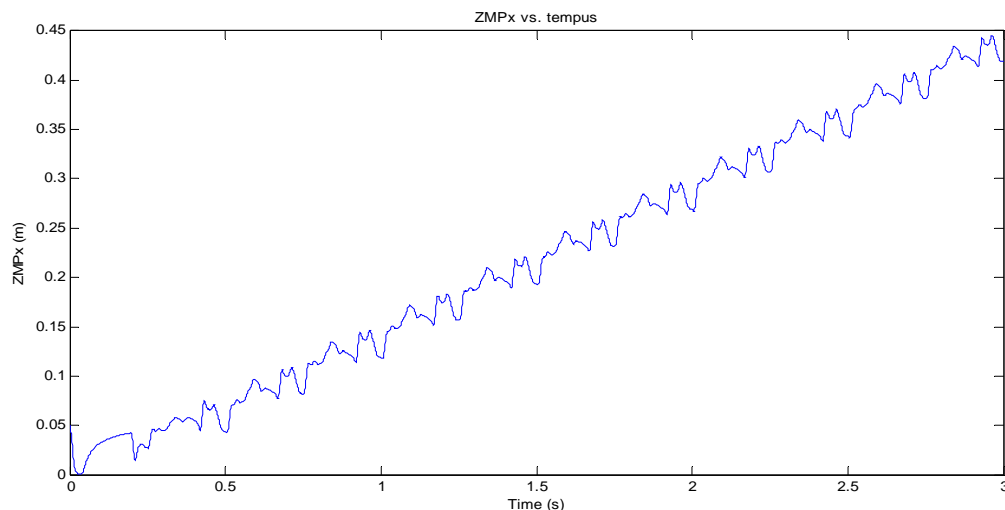


Fig.6. ZMP x trajectory

4. CONCLUSION

This paper will deal with the modeling and simulation of the autonomous motion of KONDO KHR-1HV humanoid robots. A scheme of a 19-DOF biped locomotion mechanism of the anthropomorphic structure is used. The simulation results in the Matlab/Simulink and Robotics Toolbox for Matlab/Simulink environment show the validity of the proposed method.

REFERENCES

- [1.] Vukobratović M. et al., Biped Locomotion-Dynamics, Stability, Control and Application, Springer Verlag, Berlin, Germany, 1990.
- [2.] S. Kajita, K. Tani, Experimental study of biped dynamic walking in the linear inverted pendulum mode. Proceedings of the IEEE International Conference on Robotics and Automation, pp. 2885-289, Nagoya, Japan, 1995.
- [3.] J. H. Park, K. D. Kim (1998) Biped robot walking using gravity-compensated inverted pendulum mode and computed torque control. Proceedings of the IEEE International Conference on Robotics and Automation, Leuven, Belgium, 1998.
- [4.] T. Furuta et al., Design and construction of a series of compact humanoid robots and development of biped walk control strategies. Robotics and Autonomous Systems, pp. 81-100, 2001.
- [5.] A.Rodić, D.Katić, M.Vukobratović, "The Connectionist Compensator for Advanced Integrated Road Vehicle Controller", International Journal Engineering & Automation Problems, vol.2, no.1, pp.27-39, 2001.
- [6.] A.Rodić, D.Katić, M.Vukobratović, "The Connectionist Compensator for Advanced Integrated Vehicle", Proceedings of the IEEE International Conference on Control Applications, Mexico City, Mexico, September 2001.
- [7.] A.Rodić, D.Katić, M.Vukobratović, "The Neural Compensator for Advanced Vehicle Controller", Proceedings of the 6. Workshop Application of Neural Networks in Electrotehnics - NEUREL'02, Belgrade, Yugoslavia, September 2002.
- [8.] D.Katić, A.Rodić, "Neural Control Techniques For Humanoid Robots", Proceedings of the 47. ETRAN Conference, Herceg-Novi, Serbia & Montenegro, June 2003, vol. 4, pp.386-389.
- [9.] A.Rodić, M. Vukobratović, M. Filipović, D. Katić, "Modelling and Simulation of Locomotion Mechanisms of Anthropomorphic Structure Using Contemporary software tools", Proceedings of the 47. ETRAN Conference, Herceg-Novi, Serbia & Montenegro, June 2003, Vol.4, pp.347-350.
- [10.] A.Rodić, D.Katić, M.Vukobratović, "The Advanced Vehicle Control Algorithm Using Neural Networks", Proceedings of the European Control Conference ECC 2003., Cambridge, UK, September 2003.
- [11.] J. H. Park, Fuzzy-Logic Zero-Moment-Point Trajectory Generation for Reduced Trunk Motions of Biped Robots. Fuzzy Sets and Systems 134, pp. 189-203, 2003.
- [12.] Vukobratović M., Rodić A.: Contribution to the Integrated Control of Artificial Human Gait. Proceedings of the SISO 2004, Symposium on Intelligent Systems, Subotica, Serbia, pp. 59-70, 2004.
- [13.] Vukobratović M, Potkonjak V, Rodić A (2004) Contribution to the Dynamic Study of Humanoid Robots Interacting with Dynamic Environment. Robotica. Vol. 22, pp. 439-447
- [14.] M.Filipović, A.Rodić, D.Katić, "An Analysis of Movement of Elastic Robotic System under the influence of environment dynamics", Proceedings of 29. HIPNEF 2004, Vranjačka Banja, Serbia & Montenegro, May 2004, pp.385-390.

- [15.] M.Filipović, D.Katić, A.Rodić, " An Analysis of Movement of the Flexible Robotic System in Horizontal Plane", Proceedings of the 7th DQM-2002 Dependability and Quality Management, Belgrade, Serbia & Montenegro, June 2004.
- [16.] M. Vukobratovic, V. Potkonjak, A. Rodic, "Contribution to the Dynamic Study of Humanoid Robots Interacting with Dynamic Environment", Robotica, CAMBRIDGE university press, United Kingdom, Vol. 22, pp. 439-447, 2004
- [17.] A. Rodić, D. Katić, "Intelligent Control of Road Vehicles by Implementation of Artificial neural Networks", Technics-Mechanic Engineering, No. 5/04, pp. 1-12, in Serbian, 2004
- [18.] M. Filipović, A. Rodić, D. Katić, "Motion Analysis of Elastic Robotic Systems Under Influence of Dynamic Environment", Proceedings of 29th symposium HIPNEF 2004, pp.385-390, Vrnjačka Banja, Serbia, May, 2004
- [19.] M. Filipović, D. Katić, A. Rodić, " Motion Analysis of Elastic Robotic Systems in Horizontal plane", Proceedings of the 7th DQM-2004 Dependability and Quality Management, Belgrade, Serbia & Montenegro, June, 2004
- [20.] M. Vukobratović, A. Rodić, "Contribution to the Integrated Control of Artificial Human Gait", Proceedings of 2nd Serbian-Hungarian Joint Symposium on Intelligent Systems, SISY 2004, pp. 59-70, Subotica, Serbia & Montenegro, 2004
- [21.] Metta G, Sandini G, et. all (2005) The RobotCub Project – an open framework for research in embodied cognition. Proc. of the 2005 IEEE-RAS Int. Conf. On Humanoid Robots
- [22.] K. Addi, D. Goeleven, A. Rodic, "Nonsmooth Mathematical Modelling and Numerical Simulation of a Spatial Vehicle Dynamics", *Zeitschrift für Angewandte Mathematik und Mechanik (ZAMM)*, Wiley-VCH Verlag GmbH & Co. KGaA - Weinheim, DOI 10.1002/zamm.200410235, pp. 1-25 (2005)
- [23.] A. Rodić, D. Katić, M. Filipović, "Control of Dynamic Balance and Trunk Posture of Humanoid Robots in Service Tasks", in Proceedings of 49th Conference on ETRAN, Vol. IV, pp. 347-350, Serbia & Montenegro, Budva, 2005
- [24.] Rodić A, Vukobratović M (2006) Control of Dynamic Balance of Biped Locomotion Mechanisms in Service Tasks Requiring Appropriate Trunk Postures. Engineering & Automation Problems. ISSN 0234-6206, Vol. 5, No. 1, pp. 4-22.
- [25.] D. Katić, A. Rodić, "Control Algorithm for Humanoid Robots Walking Based on Learning Structures", in Proceedings of 49th Conference on ETRAN, Vol. IV, pp. 355-358, Serbia & Montenegro, Budva, 2005
- [26.] A. Rodić, M. Vukobratović, "Intelligent Integrated Control of Vehicle Stability Characteristics", in Proceedings of EAEC2005 European Automotive Congress, Serbia & Montenegro, Belgrade, June, 2005
- [27.] A. Rodić, E. Schnieder, "Hybrid Model-Based – Knowledge-Based Control of Driver-Vehicle System Performances", in Proceedings of EAEC2005 European Automotive Congress, Serbia & Montenegro, Belgrade, 2005
- [28.] A. Rodić, "User Oriented Software Toolbox for Advance Modeling, Control Synthesis and Simulation of Automotive Systems", in Proceedings of EAEC2005 European Automotive Congress, Serbia & Montenegro, Belgrade, June, 2005
- [29.] A. Rodić, K. Addi, G. Dalleau, "Contribution to the Mathematical Modeling of Multi-point, Non-smooth Impact/Contact Dynamics of Human Gait", in Programme resume of the 6th International Conference AIMS 2006 "Dynamic Systems, Differential equations and Applications", pp. 101-102, University Poitiers, Poitiers, France, 2006
- [30.] K. Addi, G. Dalleau, A. Rodic, "Linear Complementarity Problem Formulation Used for Modeling of Impact/Contact Dynamics of Byped Locomotion Mechanisms", in Proceedings of ETRAN 2006, Belgrade, Serbia, 2006
- [31.] A. Rodic, M. Vukobratovic "Multi-feedback Dynamic Control of Byped Robots", in Proceedings of ETRAN 2006, Belgrade, Serbia, June, 2006
- [32.] Katić D, Rodić A, Vukobratović M (2007) Reinforcement Learning Control Algorithm for Humanoid Robot Walking. International Journal of Information & Systems Sciences. Vol.4, No.2, pp.256-267
- [33.] Vukobratović M, Rodić A (2007) Contribution to the Integrated Control of Biped Locomotion Mechanisms. International Journal of Humanoid Robotics. World Scientific Publishing Company. New Jersey, London, Singapore. Vol. 4, No. 1, pp. 49-95
- [34.] Gyula Mester: „ Bipedal Walking in Robots", Proceedings of the IV. Európai kihívások nemzetközi konferencia, pp. 703-707, Szeged, Hungary, 2007.
- [35.] A. Rodić, "Towards Sustainable Transport and Active Traffic Safety – Synthesis of Hazard Prevention Control System based on Modeling of Cognitive Driver Behavior", UNESCO Program – Education for All by 2015, 11th Education and Training Workshop, Belgrade, Serbia, 22th – 28th October, 2007
- [36.] Gyula Mester, „Lépegető humanoid robotok mozgástervezése", MTA, VMTT konferencia, pp.267-273, Novi Sad, Serbia, 2007.
- [37.] Gyula Mester, „Dynamic Modeling for a Walking Robot", Proceedings of the SIP 2008, 26th International Conference SCIENCE IN PRACTICE, pp.87-89, ISBN 978-953-6032-52-4, Osijek, Croatia, 2008.
- [38.] Mester Gyula, „Kétlábon járó robot modellezése", Informatika a felsőoktatásban 2008, Konferencia kiadvány, pp. 1-8, ISBN 978-963-473-129-0, Debrecen, 2008.
- [39.] Gyula Mester, „Simulation of Humanoid Robot Motion", Proceedings of The KANDÓ CONFERENCE, pp. 1-8, ISBN 978-963-7154-74-4, Budapest, 2008.

- [40.] Rodić A, Vukobratović M, Addi K, Dalleau G (2008) Contribution to the Modeling of Non-smooth, Multi-point Contact Dynamics of Biped Locomotion – Theory and Experiments., Robotica. CAMBRIDGE Univ. Press. Vol. 26, Issue, 02, pp. 157-175
- [41.] Katić D, Rodić A, Vukobratović M (2008) Hybrid Dynamic Control Algorithm For Humanoid Robots Based On Reinforcement Learning. Springer Journal of Intelligent and Robotic Systems. No.1, pp.3-30
- [42.] D. Katić, A. Rodić, "Intelligent Autonomous Locomotion of Humanoid Robots through Perception, Learning and Spatial Reasoning", in Proceedings of the ETRAN 2008, Subotica, Serbia, June, 2008
- [43.] A. Rodić, V. Potkonjak, "Towards Advanced Personal Robot Platform – Concept of Intelligent Service Robot of High Performances", in Proceedings of the ETRAN 2008, Subotica, Serbia, June, 2008
- [44.] A. Rodić, D. Katić, "Trajectory Prediction and Path Planning of Autonomous Biped Robots – Learning Locomotion and Fuzzy Reasoning", in Proceedings of the 9th Symposium on Network Applications in Electrical Engineering, Electrotechnic Faculty, Belgrade, Serbia, September, 25-27, 2008
- [45.] D.Katić, A.Rodić, "Dynamic Control Algorithm for Biped Walking Based on Policy Gradient Fuzzy Reinforcement Learning", in Proceedings of the 17th IFAC World Congress, Seoul, Republic of Korea, July 2008.
- [46.] D. Katić, A. Rodić, "Intelligent Autonomous Locomotion of Humanoid Robots through Perception, Learning and Spatial Reasoning", in Proceedings of the ETRAN 2008, Subotica, Serbia, June, 2008
- [47.] D.Katic, A.Rodic, M.Vukobratovic, "Reinforcement Learning Control Algorithm for Humanoid Robot Walking", International Journal of Information & Systems Sciences, Vol.4, No.2, pp.256-267, 2008.
- [48.] A. Rodić, D. Katić, "Trajectory Prediction and Path Planning of Autonomous Biped Robots – Learning Locomotion and Fuzzy Reasoning", in Proceedings of the 9th Symposium on Network Applications in Electrical Engineering, Electrotechnic Faculty, Belgrade, Serbia, September, 193-197, 2008
- [49.] D.Katic, A.Rodic, M.Vukobratovic, "Hybrid Dynamic Control Algorithm For Humanoid Robots Based On Reinforcement Learning", Journal of Intelligent and Robotic Systems, vol.51,No.1,pp.3-30, January 2008,
- [50.] Siciliano, Khatib editors, Springer Handbook of Robotics, Springer-Verlag Berlin Heidelberg, 2008.
- [51.] Gyula Mester, Aleksandar Rodic, "Autonomous Locomotion of Humanoid Robots in Presence of Mobile and Immobile Obstacles", Studies in Computational Intelligence, Towards Intelligent Engineering and Information Technology, pp. 279-293, ISBN 978-1-642-03736-8, Library of Congress: 2009933683, DOI 10.1007/978-3-642-03737-5-20, Springer, 2009.
- [52.] Aleksandar Rodić, Dusko Katić, Gyula Mester, "Ambient Intelligent Robot-Sensor Networks for Environmental Surveillance and Remote Sensing", Proceedings of the IEEE SISY 2009, pp. 39-44, IEEE Catalog Number: CFP0984C-CDR, ISBN: 978-1-4244-5349-8 Library of Congress: 2009909575, DOI 10.1109/SISY.2009.5291141, Subotica, Serbia, 2009.
- [53.] Web-page (2009) <http://world.honda.com/ASIMO/>
- [54.] Web-page (2009) <http://jp.fujitsu.com/group/labs/downloads/en/business/activities/acties-4/fujitsu-labs-robotics-005-en.pdf>
- [55.] Web-page (2009) http://www.sony.net/SonyInfo/News/Press_Archive/200312/03-060E/
- [56.] Rodic A (2009) Humanoid Robot Simulation Platform – HRSP. Matlab/Simulink Software Toolbox for Modeling, Simulation & Control of Biped Robots. Robotics Lab. Mihajlo Pupin Institute. <http://www.institutepupin.com/RnDProfile/ROBOTIKA/comprod.htm>.





STUDY UPON THE THERMAL FIELD FROM A RESISTANCE OVEN

¹⁻³POLITEHNICA UNIVERSITY TIMIȘOARA, FACULTY OF ENGINEERING HUNEDOARA, ROMANIA

ABSTRACT:

This work presents a study of the thermal field from an indirect resistance oven. Temperature acquisition was achieved with a Conrad Electronic data acquisition board and 8 integrated temperature sensors LM35DH. The utilized software, Ser10bit, allowed the data saving both as list of values and multi-graphics, for being further processed.

It's been analyzed the influence upon the thermal regime of the oven by its operation steps and heating period.

KEYWORDS:

indirect resistance oven, data acquisition system, thermal field

1. INTRODUCTION

The most used temperature sensors are currently the thermo-resistances, thermistors, thermocouples and integrated sensors.

For the temperature sensors, very important are the following features: sensitivity, reproductibility, low response time, linearity on an increasing range, rapid and easy mounting and inter-changeability [1-4].

In order to chose correctly the temperature sensor, should be analyzed: the temperature range in which it should operate, response time, sensitivity, precision for establishing the temperature, maximum temperature to which the sensors will be submitted, utilization time, if the determination is made with or without contact and, not the last, the costs, which are directly proportional with the sensor's precision and with its mounting mode [4, 7, 9].

The integrated temperature sensors (or IC - Integrated Circuit sensors) are precision ones, and easy to calibrate, being much used in digital applications for temperature measuring and control, because they produce an output signal proportional with temperature [1, 2].

The temperature sensors with semi-conductors have a high level of the output signal, but they cover a relatively limited temperature range [1, 2].

2. TEMPERATURE ACQUISITION SYSTEM FROM THE RESISTANCE OVEN

The temperature sensors used within experiments where of LM35DH type, in TO-46 capsule.

LM35DH is a very precise integrated sensor, of which output voltage varies linearly with the temperature measured in Celsius degrees, within -60°C and $+180^{\circ}\text{C}$; the sensor's sensitivity is $10\text{ mV}/^{\circ}\text{C}$. Is supplied by a continuous voltage within $4...30\text{ V}$, the current absorbed being below $60\text{ }\mu\text{A}$.

The temperature sensors from the LM35 series don't need external calibration or adjustment to ensure a typical precision of $\pm 1/4^{\circ}\text{C}$ at the chamber's temperature and $\pm 3/4^{\circ}\text{C}$ within the temperature range $-55...+150^{\circ}\text{C}$. The same sensors have low output impedance ($0,1\text{ W}$ for a load current of 1 mA), linear output, accurate calibration, and the interface to the reading or control circuits is achieved easily.

The output voltage expression is:

$$V_T = V_{T_0} \cdot \frac{T}{T_0}, \quad (1)$$

where V_{T_0} is the output voltage at temperature T_0 .

For measuring the temperature inside the resistance oven it was used a Conrad Electronic data acquisition board (fig. 1).

The module's supply can be achieved directly from PC (switch 82 Int) or externally from a 9 V d.c. source (switch 82 Ext by the supply between GND - ground and external UB +9 V).

Communication with the PC is made by serial interface, by duplex communication. Transmission is achieved on 16 bits out of which 12 are used for measuring, and 4 bits are used for the selected channel's address and the measurement type (unipolar or differential).



Fig. 1. Conrad Electronic data acquisition board

An analogue signal is unipolar at module's input, when the applied signal (within 0-5 V) is with the positive potential to a channel, and the negative potential is connected to ground. In this way can be measured 8 analogue signals.

An analogue signal is differential at module's input, when the signal is applied between two inputs (without using ground); in this way is measured the difference between the two signals. Thus, can be measured 4 analogue signals. The current absorbed by the module is 8mA to an impedance ≤ 1 k Ω .

The module's basic integrated circuit is LTC 1290 (CI 1, 12-bit converter A/D, precision 0,02%), which, in principle, has two base blocks: a multiplexer with 8 analogue channels (CH0, CH1, ..., CH7) and a 12-bit analogue-digital converter (CAN). Each of these two modules has a register, which establishes for the multiplexer what channel to read, and for CAN allows the serial data transfer towards the PC. The transfer is achieved based on the successive approximation principle.

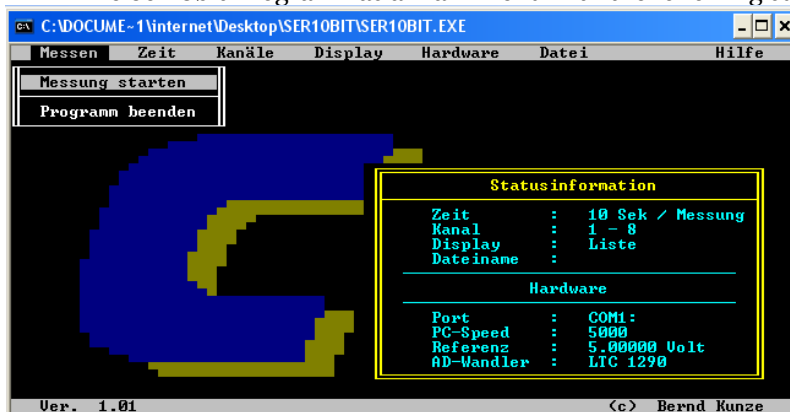
For operation, this circuit needs a supply source of proper precision and stability. In this purpose is used the integrated circuit LT 1021-5 (CI 4, with 0,05% accuracy) which is a precision stabilizer of 5 V.

Between the measurement part (the integrated circuit LTC 1290) and PC is ensured the separation of signals by means of the trigger-Schmitt inverter circuits (6 pcs.). These inverters are in the circuit 40106 (CI 3). The first inverter circuit (1-2) produces the tact of 300 Hz for the CAN's control, while the serial tact (shift clock) for introducing the command word and reading the measurement comes from PC.

Is used also a bi-stable (of D-type) of CMOS type, high speed, from the circuit 74C74 (CI 2). This integrated circuit has two D-type bi-stables, out of which is used only one.

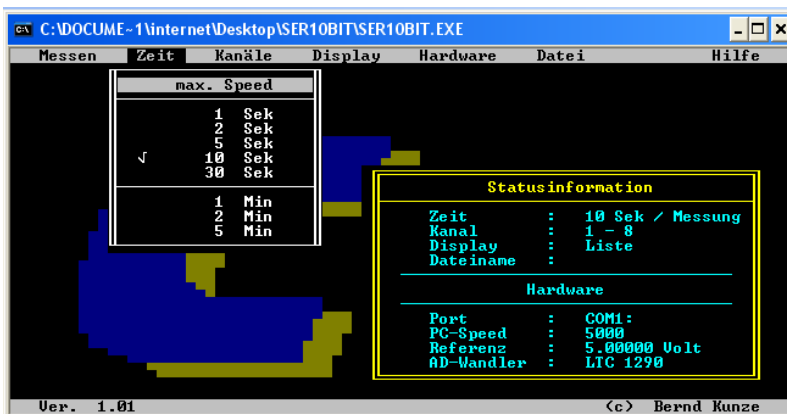
Within experiments, the acquisition board was connected to the serial interface RS 232 (with 9 poles) and by COM1 to a PC. The software used by PC was Ser10bit (achieved in Basic). Communication was achieved on the hexa-decimal addresses which are activated by the Basic INP and OUT controls.

The Ser10bit Program has a main menu with the following submenus:



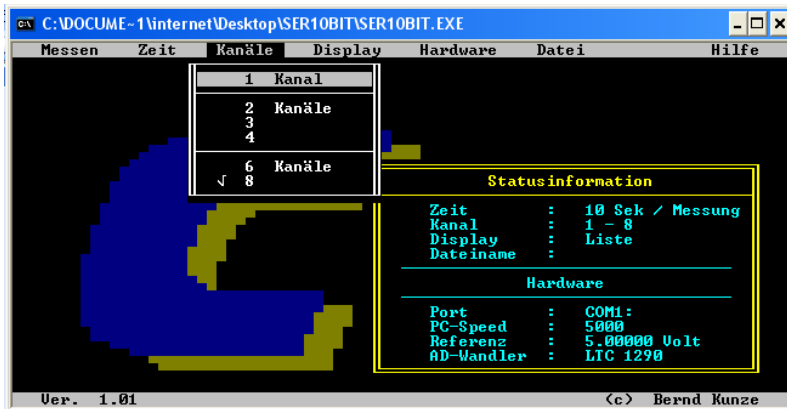
Submenu Measurements (Messen):

- Measurements achievement (Messung starten);
- Exit program (Programm beenden).



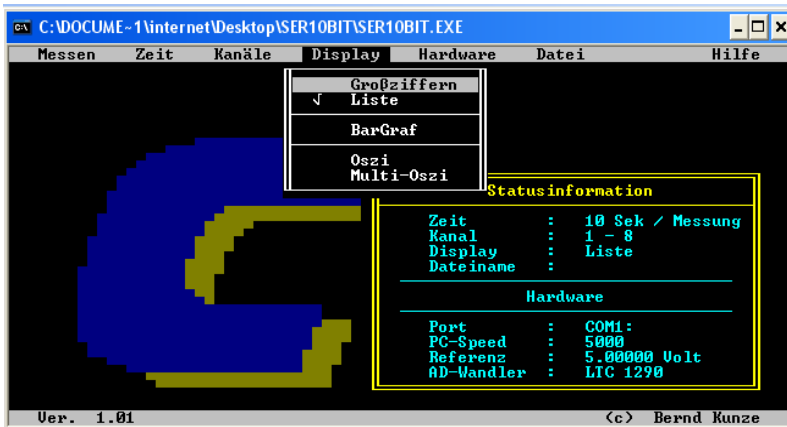
Submenu Sampling Speed (Zeit):

- maximum speed (max Speed);
- 1 s, 2 s, 5 s, 10 s, 30 s;
- 1 min, 2 min, 5 min.



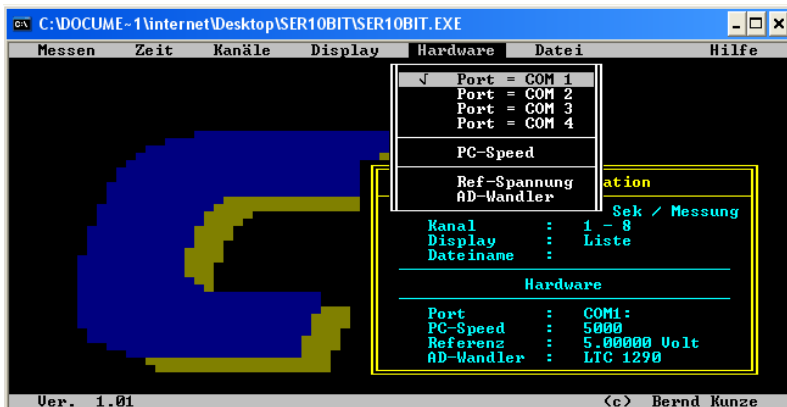
Submenu Number of Channels (Kanäle):

- 1, 2, 3, 4, 6, 8.



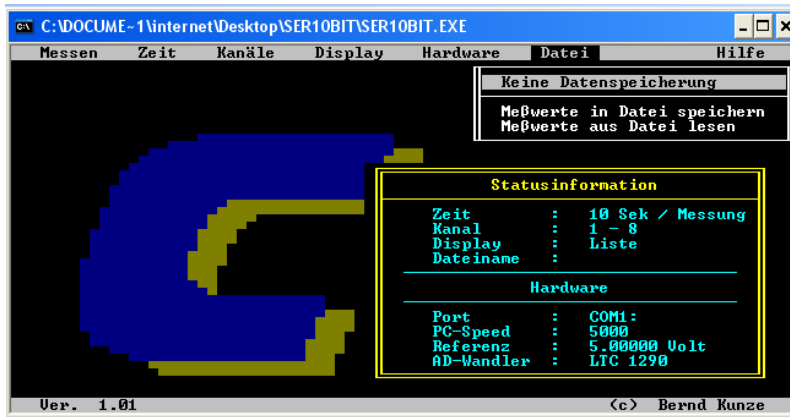
Submenu Display Mode (Display):

- Multimeter (Großziffern);
- Values List (Liste);
- Voltmeter Bar (Bargraf);
- Graphic (Oszi);
- More graphics (Multioszi).



Submenu Hardware:

- COM 1, COM 2, COM 3, COM 4;
- PC speed (PC speed): 0, 10, 20, 50, 100, 200, 500, 1000, 2000, 5000;
- reference voltage (Ref-Spannung) 5 V;
- CAN-type (AD-Wandler):
 LTC 1090 (conversion on 10 bit);
 LTC 1290 (conversion on 12 bit).



Submenu Data (Datei):

- No data (Keine Datenspeicherung);
- Creating a file for saving data (Meßwerte in Datei speichern);
- Opening a file already created (Meßwerte aus Datei lesen).

To the previously described submenus is added also the submenu **Help (Hilfe)**. Passing from one submenu to another is achieved only with the arrows from the keyboard. The files' extension is of *.mwt type.

3. EXPERIMENTS

Within the experiments was used a resistance oven, model KWS1015J-FB, with rated power of 1000 W and capacity of 15 l (fig. 2).

The oven is provided with 4 stainless heating elements that ensure 3 operation steps: all heating elements (or up-down), two heating elements in the upper part, or two heating elements in the lower part.

The oven's walls are made by two metallic layers (steel) separated by an air layer. The temperature from the oven can be adjusted within 90 - 230°C, and the operation time can be adjusted within 0 – 60 minutes. The oven is supplied from the single-phased voltage grid (220 V, 50 Hz).

In fig. 2 is presented the location of the sensors LM35DH inside the resistance oven. For supplying the temperature sensors it was used a stabilized voltage source (0 – 20 V). Position of the temperature sensors LM35DH (measured against the oven's bottom) is shown in table 1.

Within the experiments, the data acquisition was achieved on 8 channels, with a sampling period of 10 seconds.

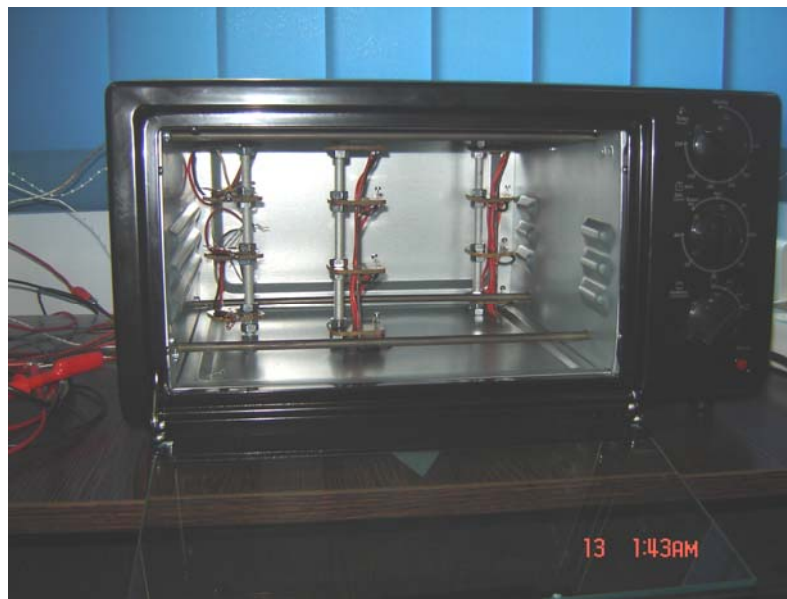


Fig. 2 Placing of the 8 sensors LM35DH inside the resistance oven

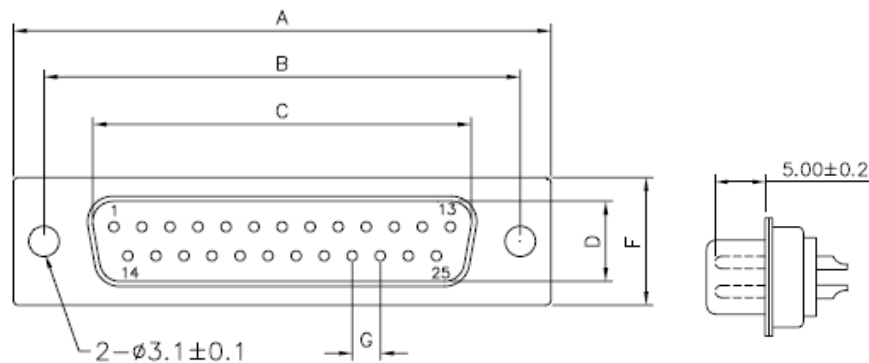


Fig. 3 Connector DB25.

Table 2 – Sensors location at connector DB25 and configuration of its pins

DB25 connector's pin	Pins' configuration
1, 2, 14	+5 V
12, 13, 25	GND
7	Sensor no. 8
8	Sensor no. 7
9	Sensor no. 6
10	Sensor no. 5
16	Sensor no. 1
17	Sensor no. 2
18	Sensor no. 3
19	Sensor no. 4

Table 1 – Position of temperature sensors LM35DH

Temperature Sensor	LM35DH Sensor's position
Sensor no. 1	Right (h1=15,5 cm)
Sensor no. 2	Right (h2=11,5 cm)
Sensor no. 3	Right (h3=6,5 cm)
Sensor no. 4	Right (h4=1,5 cm)
Sensor no. 5	Right (h5=16 cm)
Sensor no. 6	Right (h6=12 cm)
Sensor no. 7	Right (h7=7 cm)
Sensor no. 8	Right (h8=2 cm)

Table 3 – Pins' configuration on the strip from the data acquisition board

Strip's pin from the acquisition board	Acquisition board's channel	Temperature sensor
1	CH8	Sensor no. 1
2	CH7	Sensor no. 2
3	CH6	Sensor no. 3
4	CH5	Sensor no. 4
5	CH4	Sensor no. 5
6	CH3	Sensor no. 6
7	CH2	Sensor no. 7
8	CH1	Sensor no. 8
9	GND	

There have been analyzed the following cases:

- a. oven supplied on step II (2 resistances up): initial temperature $\theta_i = 27^\circ\text{C}$, adjusted temperature $\theta_r = 110^\circ\text{C}$, heating period $t_i = 60$ minutes;
- b. oven supplied on step I (2 resistances down): initial temperature $\theta_i = 27^\circ\text{C}$, adjusted temperature $\theta_r = 110^\circ\text{C}$, heating period $t_i = 60$ minutes;
- c. oven supplied on step III (4 resistances up-down): initial temperature $\theta_i = 27^\circ\text{C}$, adjusted temperature $\theta_r = 110^\circ\text{C}$, heating period $t_i = 30$ minutes, cooling period $t_r = 54$ minutes.

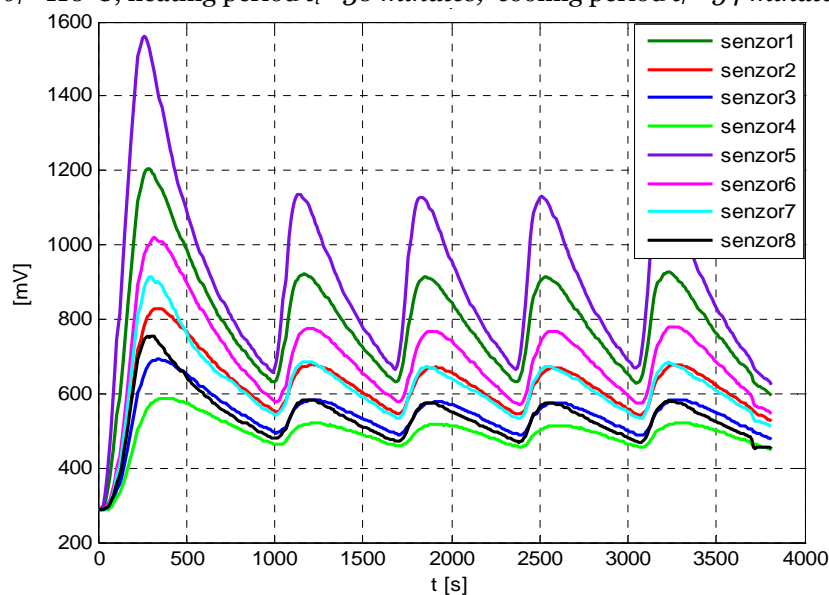


Fig. 4 Output voltages on sensors LM35DH in case a. Oven supplied on step II (2 resistances up), $\theta_r = 110^\circ\text{C}$, $\theta_i = 27^\circ\text{C}$, $t_i = 60$ min.

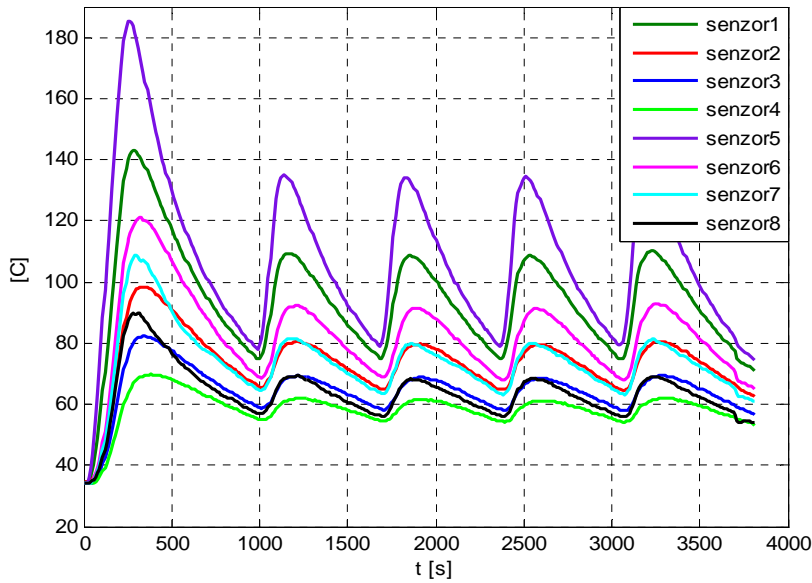


Fig. 5 Temperatures indicated by sensors LM35DH in case a. Oven supplied on step II (2 resistances up), $\theta_r = 110^\circ\text{C}$, $\theta_i = 27^\circ\text{C}$, $t_i = 60$ min.

Fig. 6 Output voltages on sensors LM35DH in case b. Oven supplied on step I (2 resistances down), $\theta_r = 110^\circ\text{C}$, $\theta_i = 27^\circ\text{C}$, $t_i = 60$ min.

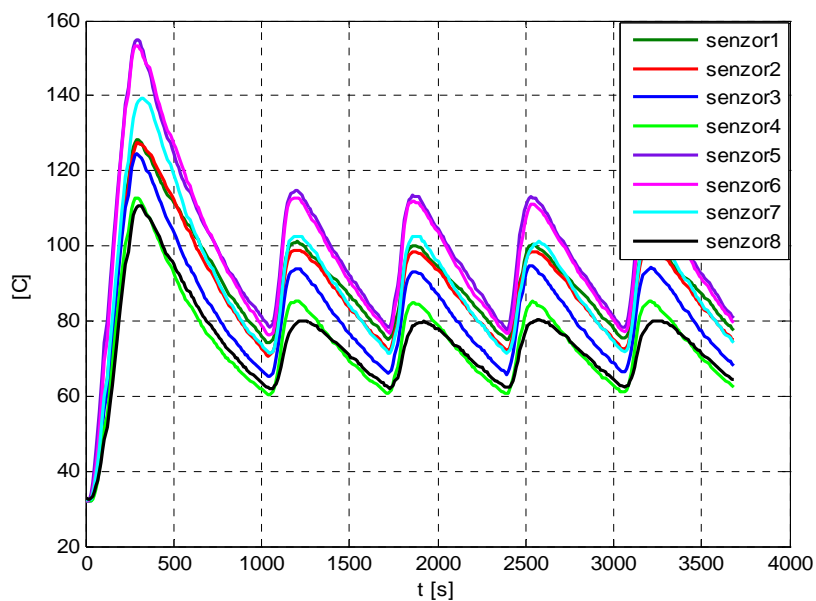
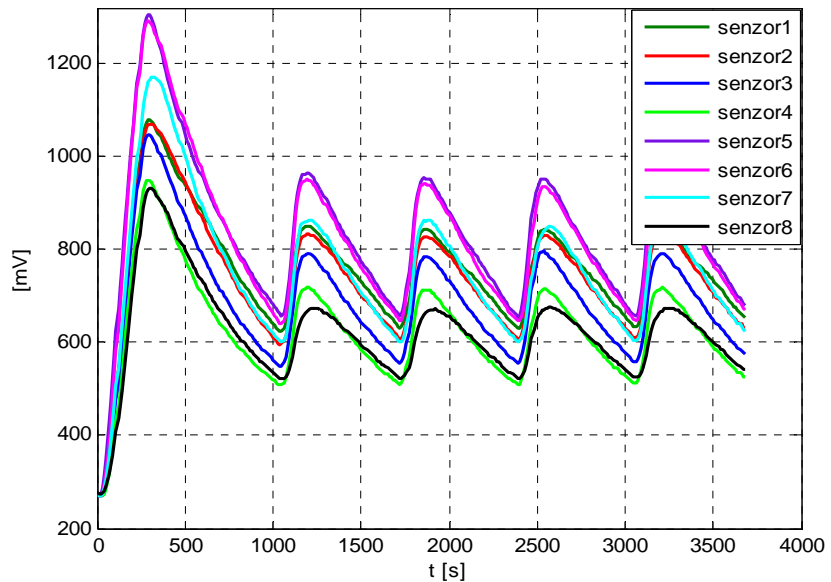


Fig. 7 Temperatures indicated by sensors LM35DH in case b. Oven supplied on step I (2 resistances down), $\theta_r = 110^\circ\text{C}$, $\theta_i = 27^\circ\text{C}$, $t_i = 60$ min.

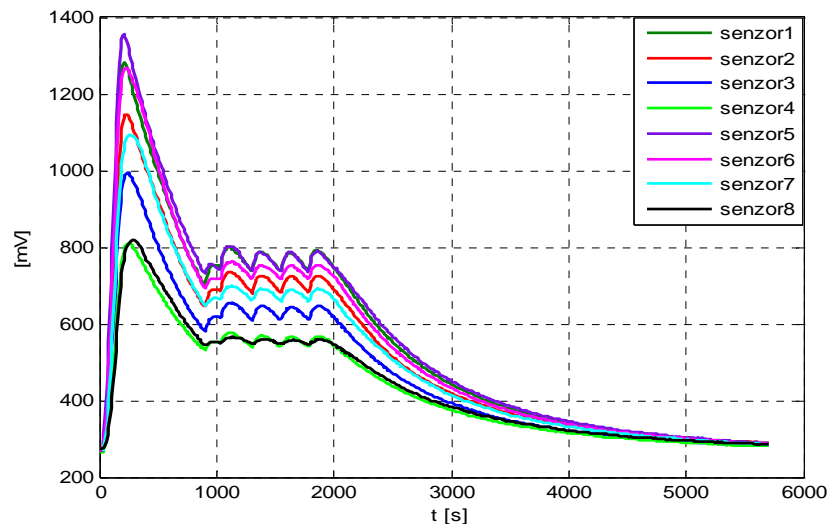


Fig. 8 Output voltages on sensors LM35DH in case c.

Oven supplied on step III (4 resistances up-down), $\theta_r = 110^\circ\text{C}$, $\theta_i = 27^\circ\text{C}$, $t_i = 30 \text{ min}$, $t_r = 54 \text{ min}$.

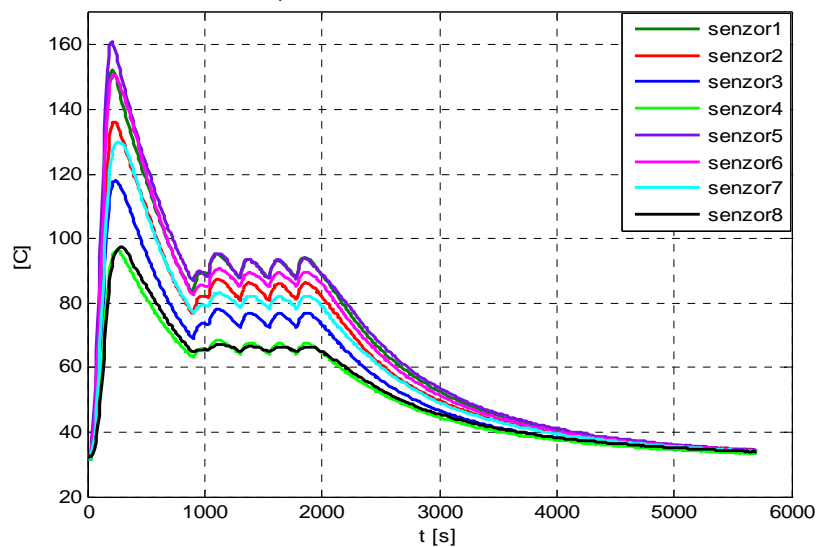


Fig. 9 Temperatures indicated by sensors LM35DH in case c.

Oven supplied on step III (4 resistances up-down), $\theta_r = 110^\circ\text{C}$, $\theta_i = 27^\circ\text{C}$, $t_i = 30 \text{ min}$, $t_r = 54 \text{ min}$.

4. CONCLUSIONS

In the first analyzed case is registered the greatest non-homogeneity of the temperature inside the oven, because the heat was transmitted from the resistances placed in the upper part of the oven.

The maximum temperature difference (120°C) between the upper part (sensor 5) and the lower one (sensor 4) of the oven's enclosure was recorded at $t=210 \text{ s}$. At this moment the temperature inside the oven has reached the maximum value (185°C), and then were disconnected the oven's resistances (by the bimetallic element), up to $t=1000 \text{ s}$; further, the heating's intermittent periodical regime had a cycle duration (connecting-disconnecting) $t_c=700 \text{ s}$.

Within $t=1000 \text{ s} \dots 3500 \text{ s}$ the up-down temperature difference inside the oven was 70°C , and in final, 25°C .

The temperature from the oven's enclosure had the maximum value in the area of sensor 5, placed in centre at maximum height ($h_5=16 \text{ cm}$). The temperature from the up-right corner (indicated by sensor 1, placed at height $h_1=15,5 \text{ cm}$) is lower than the one from centre (up) by approximately 15°C . Sensor 6, placed in centre at height $h_6=12 \text{ cm}$ indicates a higher temperature by approximately 12°C against sensor 2, placed on right side at a height of $11,5 \text{ cm}$.

Sensor 2 and sensor 7 (placed in centre, $h_7=7 \text{ cm}$) have indicated approximately the same temperature (the values max/min were $80^\circ\text{C}/65^\circ\text{C}$). Sensor 3 (placed on right side, $h_3=6,5 \text{ cm}$) and sensor 8 (placed in centre, $h_8=2 \text{ cm}$) have indicated approximately the same temperature

(values max/min: 70°C/58°C). The minimum temperature's value from the oven's enclosure was registered in the right-down corner (the temperature indicated by sensor 4 was within 55°C...65°C).

In the second case, the heat was transmitted from the resistances placed in the lower part of the oven, which determined a non-homogeneity of the oven temperature more reduced compared with the previous situation.

The maximum temperature difference between the upper part (sensor 5) and the lower one (sensor 4) of the oven's enclosure was of 45°C; within $t=1020$ s...3500 s the up-down temperature difference inside the oven was 35°C, and at the end of the recording period, it was 15°C.

After the first 1020 s the transient state disappears. The steady-state of the oven was intermittent periodic duty-type (with a cycle duration of $t_c=700$ s) in this case.

Sensors 5 and 6 (placed in centre at $h_5=16$ cm and $h_6=12$ cm) have indicated the same temperature (the values max/min being 115°C/78°C). Sensors 1, 2 (placed on right side at $h_1=15,5$ cm and $h_2=11,5$ cm) and sensor 7 (placed in centre, $h_7=7$ cm) have indicated the same temperature (the values max/min being 105°C/70°C).

Within $t=1020$ s...3500 s the max/min temperature values indicated by the other sensors were the following: sensor 3 - 95°C/65°C, sensor 4 - 85°C/60°C, sensor 8 - 80°C/63°C.

In the last case were supplied all the 4 resistors of the oven (up-down). This has determined a non-homogeneity of the temperature inside the oven much more reduced compared with the previous cases.

The maximum temperature difference (65°C) was registered at $t=210$ s; within $t=1000$ s...3000 s the up-down temperature difference inside the oven was 30°C, and at the end of the recording period, the temperature inside the oven was homogeneous.

In the first 210 seconds from the heating's beginning, the temperature inside the oven reached the maximum value (161°C), and then were disconnected the oven's resistances (by the bimetallic element), up to the moment in time $t=1020$ s; further, the heating intermittent periodic regime had a cycle duration (connecting-disconnecting) $t_c=250$ s.

After the first 1020 s the max/min temperatures indicated by sensors were: sensors 1 and 5 - 95°C/90°C, sensor 6 - 90°C/85°C, sensor 2 - 85°C/81°C, sensor 7 - 83°C/79°C, sensor 3 - 78°C/73°C, sensors 4 and 8 - 68°C/65°C. At supplying of all the oven's resistances (up-down) the variations max/min indicated by each sensor were much more reduced than the previous cases.

Is found that, to obtain a thermal field as uniform possible, is necessary to be supplied all the heating elements of the oven (up-down).

The thermal regime of the resistance oven is very much influenced by its operation steps (resistances up-down, or only resistances up, respectively down), but also by the heating duration (due to the bimetallic elements that adjust the temperature from the oven).

REFERENCES/BIBLIOGRAPHY

- [1.] Șt. Laurențiu, Temperature transducers (III). Semiconductor transducers, Conex Club Magazine, pp. 18-21 (October 2004).
- [2.] Șt. Laurențiu, Temperature transducers (I). Semiconductor transducers, Conex Club Magazine, pp. 12-16 (July-August 2004).
- [3.] A. Heler, Șt. Hărăguș, Transducers and measuring the non-electric measures, Politehnica University from Timișoara, 1997.
- [4.] V. Dolga, Sensors and transducers, Eurobit Publishing House, Timișoara, 1999.
- [5.] A. Ignea, Electric measurement of non-electric measures, Western Publishing House, Timișoara, 1996.
- [6.] N. M. Bârlea, Semiconductors, dielectrics and applications, Blue Publishing House, Cluj-Napoca, 2002.
- [7.] Monica-Anca Chita, Sensors and transducers, MatrixROM Publishing House, Bucharest, 2003.
- [8.] M. Saracin, Cristina Saracin, Electric and electronic measurements, MatrixROM Publishing House, Bucharest, 2003.
- [9.] M. Saracin, Cristina Saracin, Transducers. Interfaces. Data acquisition, MatrixROM Publishing House, Bucharest, 2010.
- [10.] D. Comșa, Industrial electrothermal installations, vol. I și II, Technical Publishing House, Bucharest, 1986.
- [11.] I. Șora, N. Golovanov et al, Electrothermal conversion and electrotechnologies vol 1 (in Romanian), Technical Publishing House, (Bucharest, Romania), 1997.
- [12.] 12. Marilena Ungureanu, M. Chindriș, I. Lungu, Utilisations of electric power, E.D.P. R.A. Bucharest, 1999.
- [13.] A. C. Metaxas, Foundations in Electroheat, A unified approach, John Wille&Sons Ltd, Baffins Lane, Chichester, West Sussex England, 1996.



THE IMPLEMENTATION OF THE MULTI-ROBOT EXPLORATION PROBLEM IN DisCSP-NetLogo

¹⁻⁴ UNIVERSITY „POLITEHNICA” OF TIMISOARA, FACULTY OF ENGINEERING OF HUNEDOARA, ROMANIA

ABSTRACT:

The implementation and evaluation of asynchronous search techniques can be done in any programming language allowing a distributed programming. Nevertheless, for the study of such techniques and for their evaluation, it is easier and more efficient to implement the techniques under certain distributed environments, such as NetLogo and are open-source. Recently, for evaluation of this algorithm it is used a multi-robot exploration problem. This problem is a natural application of Distributed Constraint Reasoning in which each robot is represented by an agent/variable; the different values for agents are the future directions they may move. The aim of this article is to introduce an model of study and evaluation for the asynchronous search techniques in NetLogo using a multi-robot exploration problem, model model calling DisCSP-NetLogo.

KEYWORDS: Artificial intelligence, distributed programming, constraints, agents

1. INTRODUCTION

The constraint programming is a model of the software technologies, used to describe and solve large classes of problems as, for instance, searching problems, combinatorial problems, planning problems, etc. A large variety of problems in the A.I field and other domains specific to computer sciences could be regarded as a special case of constraint programming. Lately, the A.I community showed a greater interest towards the distributed problems that are solvable through modeling by constraints and agents. The idea of sharing various parts of the problem between agents that act independently and that collaborate between them using messages, in the prospective of gaining the solution, proved itself useful, as it conducted to obtaining a new modeling type called Distributed Constraint Satisfaction Problem(DisCSP) [1][7],[8].

Many algorithms to solve Distributed Constraint Satisfaction Problems (DisCSP) have been introduced in the literature There exist complete asynchronous searching techniques for solving the DCSP, such as the ABT (Asynchronous Backtracking) and DisDB (Distributed Dynamic Backtracking) [1],[7],[8]. There is also the AWCS (Asynchronous Weak-Commitment Search) [7],[8] algorithm which records all the nogood values. The ABT algorithm has also been generalized by presenting a unifying framework, called ABT kernel [1]. From this kernel two major techniques ABT and DisDB can be obtained.

The evaluation of the asynchronous search techniques depends on at least two factors: the types of problems used at the evaluation and the units of measurement used. Each problem can be used with a certain efficiency of a certain technique, depending on the problem's difficulty. For the CSP modeling there were used some types of classic problems: the n queens problem, the graph coloring problems, uniform random binary or the SAT problem. These problems were taken over for the analysis of the DisCSP techniques in the distributed formulation in which the variables where taken over by agents. For these problems there are a few parameters that define them. The most important are the dimension of the problem and the density of the constraints graph associated to the DisCSP problem. There should be mentioned that the problem of the coloring of a graph and the randomly generated binary are the most suitable for the evaluation, because they allow different densities for the constraints graph and they have many direct applications in real practice.

Recently, for evaluation of this algorithm it is used a multi-robot exploration problem [2][3][4]. This problem is a natural application of Distributed Constraint Reasoning (DCR) in which each robot is represented by an agent/variable; the different values for agents are the future directions they may move. We will observe that using both classical and real world problem is interesting to obtain a better and more precise comparison.

The implementation of asynchronous search techniques based on distributed constraints can be done in any programming language allowing a distributed programming, such as Java, C, C++ or other. Nevertheless, for the study of such techniques, for their analysis and evaluation, it is easier and more efficient to implement the techniques under certain distributed environment, which offer various facilities, such as NetLogo [12], [9],[10],[11].

NetLogo, is a programmable modelling environment, which can be used for simulating certain natural and social phenomena. It offers a collection of complex modelling systems, developed in time. The models could give instructions to hundreds or thousands of independent agents which could all operate in parallel. NetLogo is the next generation in a series of modeling languages with agents that began with StarLogo [12]. It is an environment written entirely in Java, therefore it can be installed and activated on most of the important platforms (Windows, Unix).

The aim of this article is to introduce an model of study and evaluation for the asynchronous search techniques in NetLogo using a multi-robot exploration problem in [2][3], by extending the model in [5][6], model calling DisCSP-NetLogo. This model can be used in the study of agents behavior in several situations, like the priority order of the agents, the synchronous and asynchronous case, leading, therefore, to identifying possible enhancements of the performances of asynchronous search techniques. We extend the model in [5][6] with support for the problem a multi-robot exploration problem.

2 DisCSP FOR MULTI-ROBOT COORDINATION

2.1 Distributed Constraint Satisfaction Problems (DisCSP)

This paragraph presents some notions known from the IT literature related to the DCSP modeling [1][7][8].

Constraint satisfaction is a classical and powerful tool in artificial intelligence whose traditional applications concern planning, scheduling, placement, logistics and so on.

Definition 1.-CSP model. The model based on constraints CSP-Constraint Satisfaction Problem, existing for centralized architectures, consists in:

- ❖ n variables X_1, X_2, \dots, X_n , whose values are taken from finite, discrete domains D_1, D_2, \dots, D_n , respectively.
- ❖ a set of constraints on their values- C .

Solving a CSP requires to find for each variable x_i a value in D_i which is consistent with set of constraint C (i.e. which does not violate any constraint of C).

The concept of distributed CSP has been introduced to formalize and solve naturally distributed decision problems which generally deal with a set of data, shared out among many sites and whose centralization is often impossible.

Definition 2.-The DisCSP model. A problem of satisfying the distributed constraints (DisCSP) is a CSP, in which the variables and constraints are distributed among autonomous agents that communicate by transmitting, messages.

Formally, a DisCSP (X, D, C, A) is an extension of the triplet (X, D, C) where A is a finite set of agents $\{A_1, A_2, \dots, A_p\}$ in which each A_k ($1 \leq k \leq p$) owns a subset of X : X_{A_k} with $\bigcap_{A_k \in X_{A_k}} X_{A_k} = \emptyset$ and a

subset of C : C_{A_k} . From the point of view of agent A_k , variables of set X_{A_k} are called "owned variables" whereas the set $X \setminus X_{A_k}$ refers to the "foreign variables".

Most of algorithms to solve disCSP are distributed and asynchronous. To execute such algorithms, an agent has to be able to send messages to any other agents of its acquaintance set. As the algorithms are asynchronous, delays can occur when messages are exchanged through the communication network. For more details about DisCSP algorithms, readers can consult [1][7][8].

2.2 Modelling the multi-robot exploration problem as a DisCSP

Multi-robot systems (MRS) consist in a set of autonomous mobile robots which collaborate to perform a mission. This collaboration is allowed by communication abilities which usually rely on radio communication technologies. Among the applications of multi-robot system, the exploration of an unknown environment under communication constraint is a difficult problem [2][3][4]. In

such an application, it is consider robots with communication abilities and sensing abilities (like laser, sonar, camera).

To perform the exploration, the robots move toward the frontier between open space and unexplored area. In addition, robots have to collaborate to spread out on the ground (requirement to speed up the exploration and use less energy) and to keep in touch with each other (requirement to be able to exchange partial maps during the resolution and maintain a communication link with a control center). In [2][3][4] these two last requirements can be integrated into a coordination scheme as constraints of a DisCSP.

To express the multi-robot exploration as a distributed constraint satisfaction problem [2], [3] will be to discretize the space of actions of robots. The movement of a mobile robot is usually the result of a combination of lateral and longitudinal accelerations. To simplify in [2],[3] it consider 8 possible directions corresponding to the cardinal points of a compass: go to the north, go to the north-east, go to the east, go to the south-east, etc .

Each robot is considered as an agent and owns a variable to instantiate. This variable represents its next heading (in other words, the next direction to explore). The domain of each variable is composed with the 8 cardinal directions: {N,NE,E, SE, S, SW,W,NW}. The assignment of each variable has to satisfy two constraints:

- ❖ according to a direction, the future position of a robot does not have to break the connectivity of the network,
- ❖ according to a direction, the future position of a robot does not have to create overlapping with the sensor range of its neighbors.
- ❖ its future location allows to discover new unexplored areas.

Constraints can be summarized as follows in [2][3]. Thus, the requirement 1. can be expressed as a constraint defined by an inferiority test between two values: the distance between the future positions of the two robots and the communication range (Figure 1). The requirement 3. can be expressed as a specific ordering between the 8 cardinal positions such that the first cardinal position allows to have the lowest distance between the robot and the frontier, the second cardinal position allows to have the second lowest distance, etc. To enforce the efficiency of the exploration by reducing overlaps (requirement 2), we can also impose that the distance between the future positions of any two robots of A have to be superior to the sum of their sensor ranges[2][3].

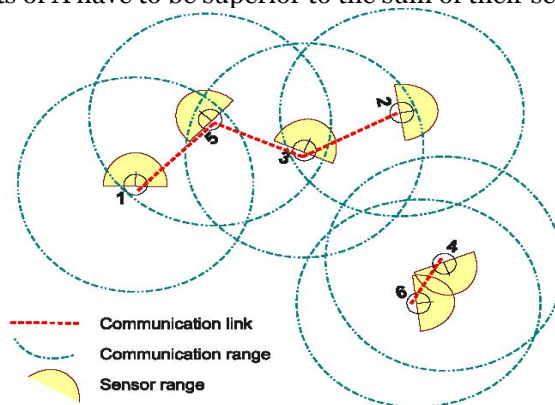


Figure 1: Connectivity constraint between two robots

This previous statement can be expressed as the following disCSP [2],[3]:

- ❖ $A = \{A_1, A_2, \dots, A_p\}$ denotes a fleet of p robots exploring an unknown environment and sharing a common map of already explored areas.
- ❖ $X = \{x_1, x_2, \dots, x_p\}$ is composed of variables storing the next heading of each robot of A .
- ❖ $D = \{\text{dom}(x_1), \dots, \text{dom}(x_p)\}$ with $\text{dom}(x_i)$ ($1 \leq i \leq p$) is the set of all 8 cardinal directions that a robot A_i can choose to plan its next movement. The domain is ordered by the following relation:

$$v_1 \leq v_2 \equiv \text{dist}(\text{fp}(A_i, v_1), \text{frontier}) < \text{dist}(\text{fp}(A_i, v_2), \text{frontier}) \text{ with } (v_1, v_2) \in \text{dom}(x_i).$$

- ❖ $C = C_1 \cup C_2$ where:

$$C1 = \{\forall A_i \in A, \exists A_j \in AR_{A_i}, \text{dist}(fp(A_i, x_i), fp(A_j, x_j)) < cr\}$$

$$C2 = \{\forall A_i \in A, \forall A_j \in A \setminus A_i, 2 sr < \text{dist}(fp(A_i, x_i), fp(A_j, x_j))\}$$

with:

- ❖ sr the sensor range of a robot;
- ❖ dist(p1, p2) the euclidian distance between the position p1 and the position p2 ;
- ❖ fp(A_i, x_i) the future position of A_i considering its future direction x_i and its current vector speed;
- ❖ cr the communication range of a robot.

To explore an unknown environment, the robots of set A have to periodically solve this DisCSP in order to be able to choose a heading compatible with the requirements previously introduced.

3. MODELING AND IMPLEMENTING OF THE MULTI-ROBOT EXPLORATION PROBLEM IN DisCSP-NetLogo

In this section we present a solution of modeling and implementation for the existing agents' process of execution in the case of the asynchronous search techniques for the multi-robot exploration problem in DisCSP-NetLogo. This solution, calling DisCSP-NetLogo will be extended with support for the evaluation of the performances of asynchronous search techniques using a multi-robot exploration problem in [2][3].

This modeling can also be used for evaluation of the asynchronous search techniques, such as those from the AWCS family [7][8], ABT family [1], DisDB [1]. Implementation examples for these techniques can be found on the site in [11].

The modeling of the agents' execution process will be structured on two levels, corresponding to the two stages of implementation.

The definition of the way in which asynchronous techniques will be programmed so that the agents will run concurrently and asynchronously will be the internal level of the model. The second level refers to the way of representing the NetLogo application. This is the exterior level. The first aspect will be treated and represented using turtle type objects. The second aspect refers to the way of interacting with the user, the user interface. Regarding that aspect, NetLogo offers patch type objects and various graphical controls.

3.1. Agents' simulation and initialization

First of all, the agents are represented by the breed type objects (those are of the turtles type). In there fig. 1 is presented the way the agents are defined together with the global data structures proprietary to the agents.

```

breeds [agents-robots]
globals [variables that simulate the memory shared by all the agents]
agent-robots-own [message-queue current-view nogoods messages-received_ok messages-
received_nogood total_distance the-neighbors nr_constraintc nr_cycles AgentC_Cost]
;message-queue contains the received messages.
;current-view is a list indexed on the agent's number, of the form [v0 v1 v2...]. vi = -1 if we don't
know the value o that agent or vi=1,8 ( the cardinal directions: {N,NE,E, SE, S, SW,W,NW}).
; nogoods is the list of inconsistent positions [0 1 1 0 ... ] where 0 is a good position, and 1 is
inconsistent.
; total_distance the total traveled distance by the robots
; nr_cycles -the number of cycles
; nr_constraintc - the number of constraints checked
; AgentC_Cost – a number of non-concurrent constraint checks
; messages-received_ok and messages-received_nogood are variables that count the
; number of ok and nogood messages received by an agent.
    
```

Figure 2. Agents' definition in the case of the multi-robot exploration problem

For the evaluation of the multi robot exploration problem in this paper we using the three classical metrics and the total traveled distance by the robots, from [4]:

- ❖ **the number of messages transmitted during the search:** messages-received_ok, messages-received_nogood, messages-received_removed, etc.
- ❖ **the number of cycles.** A cycle consists in the necessary activities that all the agents need in order to read the incoming messages, to execute their local calculations and send messages to the corresponding agents. This metrics allows evaluating the calculation of the global effort evaluation for a certain technique
- ❖ **the number of constraints checked.** The time complexity can be also evaluated by using the total number of constraints verified by each agent. There is a measurement of the global time consumed by the agents involved. It allows the evaluation of the local effort of each agent. The number of constraints verified by each agent can be monitored using the variables proprietary to each robots called **nr_constraintc**.
- ❖ **a number of non-concurrent constraint checks.** This can be done by introducing a variable proprietary to each agent, called AgentC-Cost. This will hold the number of the constraints concurrent for the agent. This value is sent to the agents to which it is connected through the messages. Each agent, when receiving a message that contains a value SenderC-Cost, will update its own monitor AgentC-Cost with the new value.
- ❖ **the total traveled distance by the robots.** This metric is specific to this application [4]. It makes it possible to evaluate if an algorithm is effective for mobile and located agents in an unknown environment. Indeed, it is not because an algorithm obtains a low number of cycles or a low number of messages which it is more adapted to obtain a coherent displacement of the robots.

3.2. Representation and manipulation of the messages

Any asynchronous search technique is based on the use by the agents of some messages for communicating various information needed for obtaining the solution. The manipulation of the messages supposes first of all message representation. This thing can be achieved in Netlogo by using some indexed lists. The way of representation of the main messages encountered at the asynchronous search techniques is presented as follows:

- ❖ (list "ok" agent-robot value agent_costs) – messages of the *ok* type; *value*= cardinal directions.
- ❖ (list "nogood" agent-robot current-view agent_costs) - messages of the *nogood* type;
- ❖ (list "addl" agent-robot₁ agent-robot₂ agent_costs)
- ❖ (list "removal" agent-robot₁ agent-robot₂ agent_costs)

3.3. Definition and representation of the environment

As concerning the interface part, it can be used for the graphical representation of the DCSP problem's objects (robots, obstacle etc) of the patch type. It is recommended to create an initialization procedure for the display surface where the agents' values will be displayed. For the case of the multi-robot exploration the representation of robots, links and obstacle is modeled asa a grid with a number de cells. Each cell can be empty, occupied by a robot or an obstacle, explored or unknown.

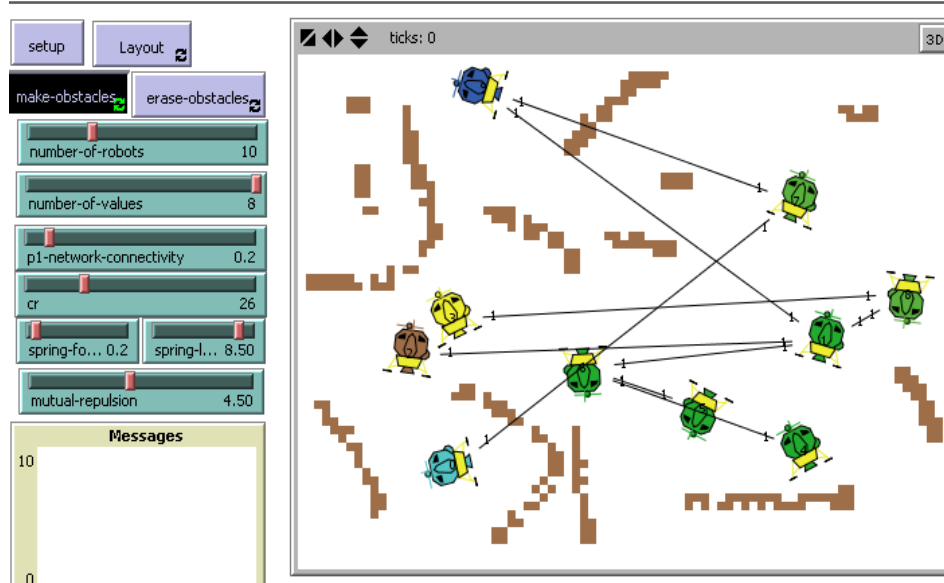


Figure 3. Representation of the environment in the case of the multi-robot exploration problem

To model the surface of the application are used objects of the *patches* type. Depending on the significance of those agents, they are represented on the NetLogo surface. In figure 3 are presented one way in NetLogo for representing the agents of the *robots* type. For this implementation we have considered environments with different levels of complexity depending on: number of obstacles, the size of the obstacles, the density of the obstacles, the minimum distance between two close obstacles.

3.4. Application initialization. "The main program" for the application

The initialization of the application supposes the building of agents and of the working surface for them. Usually, there are initialized the working context of the agent, the message queues, the variables that count the effort carried out by the agent. In figure 4 there are presented the two routines of the application initialization.

The working surface of the application should contain NetLogo objects through whom the parameters of each problem could be controlled: the number of agents, the density of the constraints graph, the number of colors. These objects allow the definition and monitoring of each problem parameters.

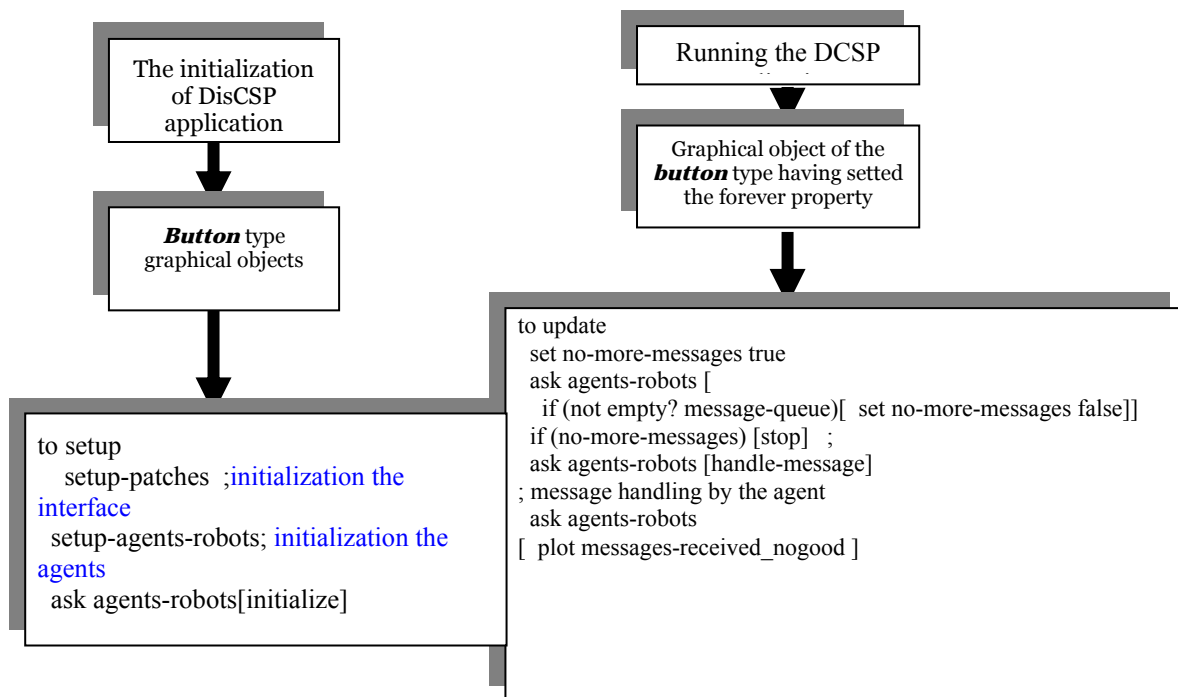


Fig. 4. Initialization and running of the DisCSP application

For the application running there is proposed the introduction of a graphical object of the *button* type and setting the forever property. That way, the attached code, in the form of a NetLogo procedure (that is applied on each agent) will run continuously, until emptying the message queues and reaching the stop command.

Another important observation is tied to attaching the graphical button to the *observer* [5][6]. The use of this solution allows obtaining a solution of implementation with synchronization of the agents' execution. In that case, the *observer* will be the one that will initiate the stopping of the DisCSP application execution. In this case the *update* procedure is attached and handled by the *observer*. These elements lead to the multi-agent system with synchronization of the agents execution. If it's desired to obtain a system with asynchronous operation, will be used the second method of detection, which supposes another *update* routine. That new *update* routine will be attached to a graphical object of the *button* type which is attached and handled by the turtle type agents[5][6].

In figure 5. there is captured an implementation of the AWCS for the multi-robot-exploration problem technique that uses the model presented. In figure 5 the update procedure is attached and handled by the observer. These elements lead to the multi-agent system with synchronization of the agents' execution.

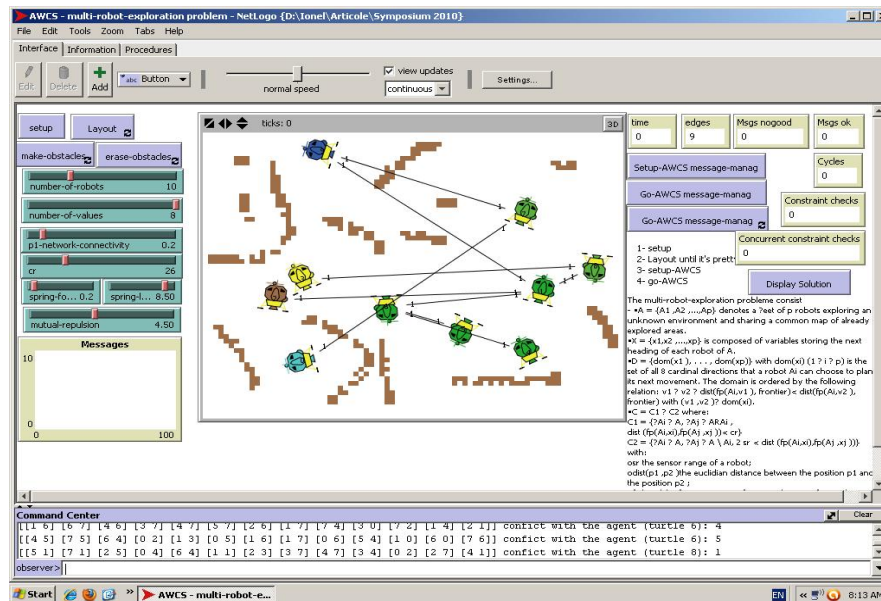


Fig 5. NetLogo implementation of the AWCS for the multi-robot-exploration problem

4. CONCLUSIONS

In this article was analysed the NetLogo environment with the purpose of building a general model of implementation and evaluation for the asynchronous techniques such as they could use the NetLogo environment as a basic simulator in the study of asynchronous search techniques.

In this paper is to introduce an model of study and evaluation for the asynchronous search techniques in NetLogo using a multi-robot exploration problem, by extending the old model, model calling DisCSP-NetLogo. This model can be used in the study of agents behavior in several situations, like the priority order of the agents, the synchronous and asynchronous case, leading, therefore, to identifying possible enhancements of the performances of asynchronous search techniques. We extend the old model in [5][6] with support for the problem a multi-robot exploration problem.

As a general conclusion, we think that the model we achieved can be used for the study and analysis of the asynchronous techniques, the model allowing their complete evaluation. Students can use the models on the site [11] to study, to understand the functioning of the asynchronous search techniques and, perhaps, to extend them.

REFERENCES

- [1.] C. Bessiere, I. Brito, A. Maestre, P. Meseguer, Asynchronous Backtracking without Adding Links: A New Member in the ABT Family. *Artificial Intelligence*, 161:7-24, 2005.
- [2.] A. Doniec, N. Bouraqadi, M. Defoort, V-T. Le, and S. Stinckwich. Distributed constraint reasoning applied to multi-robot exploration. In *21st International Conference on Tools with Artificial Intelligence (ICTAI)*, New Jersey, USA, 2009.
- [3.] A. Doniec, N. Bouraqadi, M. Defoort, V-T Le, and S. Stinckwich. Multi-robot exploration under communication constraint: a disCSP approach. In 5th National Conference on "Control Architecture of Robots", May 18-19, 2010 - Douai, FRANCE.
- [4.] Pierre Monier, A. Doniec, S. Piechowiak and R. Mandiau. Metrics for the evaluation of DisCSP: some experiments on multi-robot exploration. In 2010 IEEE/WIC/ACM International Conference on Web Intelligence and Intelligent Agent Technology, Canana, August, 2010.
- [5.] I. Muscalagiu, H. Jiang, H.E. Popa. "Implementation and evaluation model for the asynchronous techniques: from a synchronously distributed system to a asynchronous distributed system", in *Proceedings of the 8th International Symposium on Symbolic and Numeric Algorithms for Scientific Computing (SYNASC 2006)*, Timisoara, Romania, IEEE Computer Society Press, 2006, pp. (209-216).
- [6.] Muscalagiu, I., Iordan, A., Muscalagiu, D., Panoiu, M. Implementation and evaluation model with synchronization for the asynchronous search techniques. *Proceedings of the 13th WSEAS International Conference on Computers*, Rhodes Island, Greece, July 23-25, pg. 211-216, 2009.

- [7.] Yokoo M., E.H. Durfee, T. Ishida, K. Kuwabara (1998): *The distributed constraint satisfaction problem: formalization and algorithms*. IEEE Transactions on Knowledge and Data Engineering 10 (5).
- [8.] Yokoo Makoto (2001): *Distributed Constraint Satisfaction- Foundation of Cooperation in Multi-agent Systems*. Springer.
- [9.] MAS Netlogo Models-a. <http://jmvidal.cse.sc.edu/netlogomas/>
- [10.] MAS Netlogo Models-b. <http://ccl.northwestern.edu/netlogo/models/community>
- [11.] MAS Netlogo Models-c. <http://discsp-netlogo.fih.upt.ro/>
- [12.] Wilensky, U. *NetLogo itself: NetLogo*. <http://ccl.northwestern.edu/netlogo/>. Center for Connected Learning and Computer-Based Modeling, Northwestern University, IL, 1999



THE COMPONENTISATION EFFICIENCY IN REALIZING A WD ABAP PROJECT

¹⁻³POLITEHNICA UNIVERSITY OF TIMISOARA, ENGINEERING FACULTY OF HUNEDOARA, ROMANIA

⁴CELLENT AG, STUTTGART, GERMANY

ABSTRACT:

In this paper, we realised a study regarding the efficiency of using the componentisation technique with faceless component, in developing a Web Dynpro ABAP project. The componentisation is possible due to the architecture of the Model View Controller, the base of the Web Dynpro ABAP framework. According to the faceless componentisation technique, a Web Dynpro ABAP project is made of different components, the basic three components being: the *model* that contains the data model, the *view* component in charge with the visual part, and the *controller* component that links them and contains the testing web application. The realised case study was ordered by a company that offered the required support in selecting and recruiting the work force. The Web Dynpro ABAP application is realised with SAP NetWeaver Application Server ABAP 7.0 - trial version.

KEYWORDS:

integrated system, web programming, web dynpro ABAP application

1. WEB DYNPRO ABAP – CONCEPT AND ARCHITECTURE

The current standard for realising web applications in the ABAP environment is represented by the SAP NetWeaver concept, named *Web Dynpro*. This one is a framework integrated into the ABAP Workbench (SE80 transaction) that contains the required execution environment and the graphical development environment with special Web Dynpro tools.

The Web Dynpro architecture is based on the Web Dynpro component. The **Web Dynpro component** is the programmable and reusable entity which represents the „heart” of a Web Dynpro application [3]. It can be considered as a unilateral representation of its parts and can be executed only through a Web Dynpro application. The parts included into a Web Dynpro component are: *component Interface*, *component controller*, *component usage*, *window* and *view* (Fig.1) [4].

The *component interface* enables the component to interact with other components, being made of a visual part (interface view) and a programmable part (interface controller). The *component controller* is in charge with the data transfer and the links among the parts of the component. By defining a component reuse, then in a component can be used other components. The *View* is the part where a visual interface is defined to the user. To be able to be visualised, it must be integrated in a window. The *Window* is the container of views among which

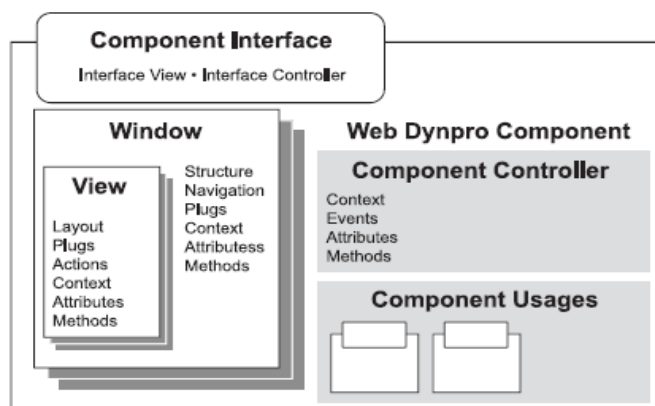


Fig.1 Parts of a Web Dynpro component [5]

the navigation is realised; it has an interface view uniquely associated and connected to the test application Web Dynpro.

This framework is realised according to the Model View Controller (MVC) paradigm. The MVC is an architectural model that divides the implementation of an application in three components: the *model* component, the *view* component and the *controller* component. The *model* component is in charge with data processing and returning the result to the controller; the *view* component is in charge only with the interface displayed to the user, and the *controller* component is in charge with the evaluation of the requests, sending data and instructions to the *model* component, and sending data to the *view* component. In principle, this *controller* component is in charge with the interaction between the *view* component and the *model* component (Fig. 2).

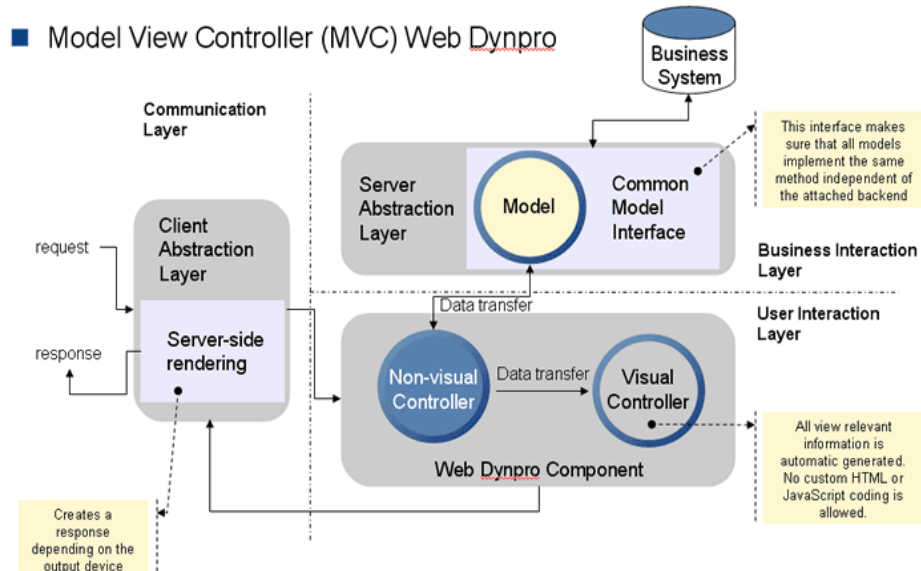


Fig.2 The architecture of the Web Dynpro framework [2]

With the Web Dynpro framework, we can develop user interfaces by using two techniques: declarative (when the interface structure is known before the execution) and dynamic (when the interface structure is partly known during the execution).

The client implementation can be defined for the web browser (Server-Side Rendering) and XML. The implementation of the metadata and the generation of HTML pages with integrated JavaScript functionalities are required for the web browser, and the implementation of XML is currently used for eCATT scenarios (extended Computer Aided Test Tool) and for client integration (*SP Smart Board*) [1].

Some of the advantages, offered by Web Dynpro in developing web applications, are [1], [3], [4]: possibility to use graphical tools, large offer of technologies, e.g. HTTP, HTML, CSS, XML and client-side scripts that are the base of each Web application, strictly separation between the data presentation and processing, possibility of using and reusing the components, easy modification of the application due to the tools it disposes of, possibility to access the data from the application context that remain intact even if the page is changing, automatic transportation of the data through data binding, automatic verification of the inputs, access to the user interface, totally integration in the ABAP development environment.

2. THE CONCEPT OF COMPONENTISATION WITH FACELESS COMPONENT

The componentisation is the concept used to structure a large project in Web Dynpro components. The componentisation technique is based on three such components: the *View* component, in charge with the data presentation to the user, the *Model* component, in charge with the logical part of data programming, and the *Controller* component, in charge with the link between the other two components – *Model* and *View*, the base of the project testing application.

The *View component* will integrate all the components included in the graphical part of the project, defining a usage for each one.

The *Model component* is a Web Dynpro component without graphical elements, i.e. without *window* and *view* (faceless). This component is used to realise the logical part and to structure the data used in the entire project. We can use a faceless component [4] for a componentised application if more than one component of the project uses the same data, and if we want to extend the project.

According to the programming paradigm *Model View Controller* of Web Dynpro ABAP, it is possible to detach the data model (the logical part of the project) from the visual part. This step requires a quite big programming effort, but ensures a high transparency and quality to the project. Through this process, the componentisation methods used in the project, which need to be visible throughout the project, are moved in the *Model* component controller, as interface methods.

The great win of the componentisation based on the design pattern *Model View Controller* is that the individual components of a project are interdependent, can be easily changed and extended, can be reused, the entire project being able to be extended and easily managed and, the last but not the least, we have to mention the possibility to use in common the data models.

3. THE COMPONENTISATION TECHNIQUE IN REALISING A WEB DYNPRO PROJECT

This technique has been implemented based on a case study realised for a company that wanted to put at the visitors' disposal information regarding the activity field, the services and the products of the company, and to offer the available working places to those people who wanted to join the company. The Web Dynpro ABAP application was realised on the *SAP NetWeaver AS ABAP 7.0* trial and consisted of Web Dynpro components.

The steps in realising a complex project, based on the faceless technology, are: realising the database, implementing and preparing the components to be linked in the componentisation structure, preparing the componentisation structure by realising the three components: view, model and controller, linking the components in the structure and detaching the model from the visual part. For realising the database, we need to create and link the tables in the DDIC data dictionary, by using the SE11 transaction (Fig. 3).

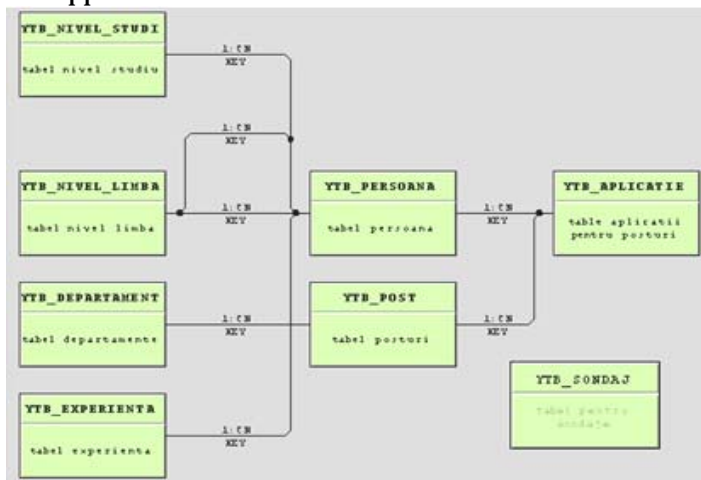


Fig. 3 Database table links

The diagram of componentisation with faceless component, used for this project, is presented in Fig. 4.

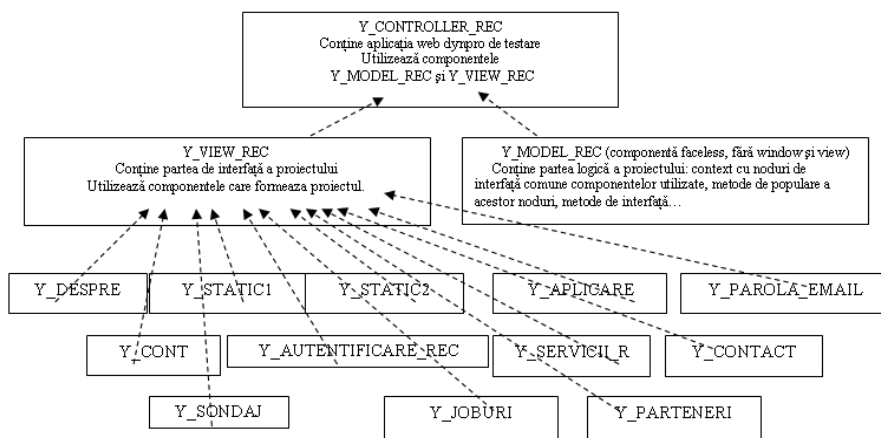


Fig.4 Diagram of componentisation with faceless component

The realisation of the project starts from the main *view* component that defines its components as usage, and realises the entire interface with the user. The data migration is made through direct external mapping. The *Model* or *faceless* component includes the logical part of the project: the common nodes of the components that compose the visual part, the methods of populating these nodes, the interface methods and other methods adequate for the *view* components [6].

Because the navigation from one page to another is the basic element of any web application, the windows of the components embedded into the main *View* component will define outputs

(outbound plugs) and inputs (inbound plugs) used to realise the navigation diagram . At the *view* level, the outputs will be linked with the inputs defined in the *window*. The link between the window inputs and outputs is logically realised, by using the interface event handler methods that correspond to the defined inputs.

The *Controller* component links the components *Model* and *View*, defining them as usage, to ensure the data traffic.

Regarding the separation of the data model from the visual part, in the *Model* component, besides the methods used to populate the interface nodes that correspond to the reused components, there are brought all the methods along with their afferent codes from the component controller of the used components which, even without navigation sequences, want to be visible in other components. The reused components will keep the name of the respective methods, but these methods will trigger only interface events. The controller component that links the components *View* and *Model* includes the event handler methods able to call these methods.

4. CONCLUSIONS

Web Dynpro is one of the top technologies used to realise high quality web applications, and the componentisation is the technique used to build web projects on the nowadays SAP platform. The faceless componentisation, as a technique based on the design of the *Model View Controller* pattern, enables the independence of the components along with their interchange and reuse and, in the same time, the easily extension of the project. Although this requires a greater programming effort, it offers a maximum win.

Comparing with other frameworks (e.g. Prado), where the physical creation of the file that runs the application and the interface file are required, the Web Dynpro applications need only the realisation of a component whose window will be attached to the user. The application structure is realised without writing a single line of code, and the interface with the user is a view built with view design elements and programmed according to the requirements.

In conclusion, the Web Dynpro framework is not a tool for creating presentation pages with much animation and sophisticated graphical elements, but for implementing and realising latest generation business applications.

REFERENCES

- [1.] Ulli Hoffmann, *Web Dynpro for ABAP*, Publishing House SAP Galileo Press, Bonn, Germania, 2007.
- [2.] SAP Developer Network (<http://sdn.sap.com>).
- [3.] SAP Portal - Help (<http://help.sap.com>).
- [4.] Web Dynpro for ABAP (WDA, WD4A, WDF4A), Release NW2004s SP8 (SAP AG Online Help 2006), available in electronic format (pdf) on Internet network.
- [5.] Ulli Hoffman, *Get started developing Web – native custom SAP application with Web Dynpro ABAP*, SAP Professional Jurnal, 2007.
- [6.] Web Dynpro ABAP Programming Guidelines (SAP AG 2006), available in electronic format (pdf) on Internet network.





¹ Camelia PINCA -BRETOTEAN, ² Gelu-Ovidiu TIRIAN,
³ Diana BISTRIAN, ⁴ Gladiola CHEȚE

DIMENSIONAL MATHEMATICAL MODEL TO OPTIMIZE THE PROCESSING MECHANISM OF TRANSLATIONAL ROTATING MOTION

¹ UNIVERSITY POLITEHNICA OF TIMISOARA, FACULTY OF ENGINEERING FROM HUNEDOARA, ROMANIA

ABSTRACT:

The paper realized the analysis of the mechanisms eccentric cam with point of contact, the constructiv and functional point of view, considering a mathematical model that allows a dimensional optimization. This paper reports the application of the Karush–Kuhn–Tucker method in the optimization process of a rotating cam dimensions. The problem was assessed both in analytical and numerical approaches.

KEYWORDS: Mechanism, cam, mathematical, model, dimensional, optimization

1. INTRODUCTION

Processing mechanisms of translational rotating motion are the cam and tachtet mechanisms, [1], [2]. They belong to the upper bucket mechanisms and consist of a driver shaped element called cam, which is designed to transmit motion to another element of translational or oscillation motion, called tachtet. Because movement can make any law by projecting properly any cam profile, these mechanisms are used in most areas of engineering (mechanical, textiles, fine mechanics, machine tools, internal combustion engines, and food engineering) which are necessary certain laws of motion technology or process required by mechanization and automation systems. It is recommended using these mechanisms because it has many advantages, such as: small dimensions, easy design, very good durability for complicated laws of motion, simple changes to the law of motion, relatively simple construction. The only disadvantage of these mechanisms is that superior coupling wear accidentally causing significant changes in the law of motion, noise, and vibration.

2. METHODOLOGY AND DISCUSSION

Rod push and cam mechanisms are part of the upper joints. They consist of a driver element having a profile, called cam and a driven element called rod push. The transmission from the driver element (cam) led to the component (rod push) is made by direct contact. This is a curve-shaped element, and it is well established and in close contact with the pusher motion. The pusher is made particularly by simple shapes: point-shaped planes, flat, circular (or roll), but may also have some curves and shapes. The laws of motion of the cam are usually those specific to the uniform movement, without acceleration. Standard laws of motion of pusher can be: linear, parabolic, co-sinusoidal, and sinusoidal; but there are also more complicated laws, such as power or exponential polynomials, etc. Because these mechanisms can perform any motion, by the appropriate design of the cam profile, they can be used in all engineering fields. Relative to the nature of the movement they are different: camshafts rotating basis related to the torque, the translational cam connected to the base by translational coupling, spinning translation cams, joint with a quadrilateral articulated rod. The pushers are the same: rotating (oscillating), translation or spinning translation [1], [2].

The main components of a cam mechanism and tachtet are presented in fig.1. These three elements are denoted by 1, 2, 3; there are also three couplings: the A-rotation, B-top rotation and translation, the C-translation, [1], [2].

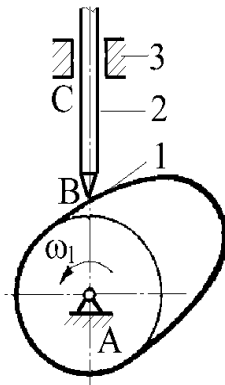


Fig.1 Components of cam mechanism with tachtet
 1-cam, 2-tachtet, 3-layer; A-rotation, B-upper phase of rotation and translation, C-translation.

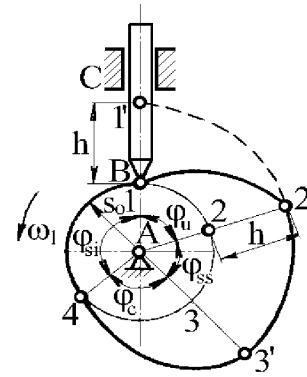


Fig.2 The phases of work of the cam mechanism with tachtet

A pusher moving from a position in a certain sense returns to the same position forming a kinematical cycle. This corresponds to a rotation of cam 360° .

The paper will analyze a cam mechanism and an eccentric translational tachtet (point), which will create a dimensional optimization.

Phases of working mechanism are described in fig.2. They are:

- ❖ U - the climbing phase, when the pusher moves away from the rotation axis of the cam;
- ❖ SS - the upper stationary phase, when the pusher reaches the higher peak;
- ❖ C - the descent phase is the phase when the pushes gets closer to the rotation axis of the cam; and the lower stationary phase, when the pusher reaches its highest value.

In case of mechanisms with tachtets reaching their highest values, the phase angle is the same with the cam angle.

If translational tip pushers, all operating parameters, established due to technological conditions are: h - the longest tachtet pathway; the pusher cam angles covered by certain movements executed in accordance with technological requirements, called phase angles. Two of the phase angles are required: first of all, to climb the phase angle pusher away from the rotation axis of the cam, and the downhill phase angle, when the pusher approaches the rotation axis of the cam. Angles corresponding to the stationary phase are called stationary phase angles:

- ❖ superior stationary phase angle, when the pusher is situated to the maximum distance from the cam axis;
- ❖ angle of stationary phase, when the pusher is situated closer from the cam axis.

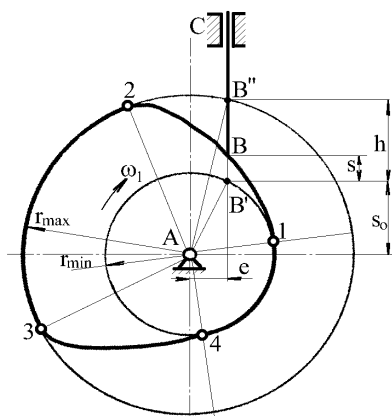


Fig. 3. The geometric parameters of the cam mechanism and eccentric tip translational tachtet

When climbing, stroke size and phase angle influences on the pressure angle a lot, which is an important functional parameter. Pressure angle is defined as an acute angle formed between the load direction pusher motor speed and direction point of application of this force, which is identical to the relationship between the cam and the tachtet.

Geometric parameters of cam mechanisms and eccentric tip translational tachtet are shown in fig. 3.

Geometrical parameters of this mechanism are:

- ❖ S_0 – the lowest distance from the contact point to the cam axis of rotation, measured on a parallel to the axis pusher;
- ❖ e - pusher eccentricity is the distance from the axis of rotation of the cam to the tachtet.

Regarding the latter, cam gauge is determined using relations (1) and (2):

$$r_{\min} = \sqrt{s_0^2 + e^2} \quad (1)$$

$$r_{\max} = \sqrt{(s_0 + h)^2 + e^2} \quad (2)$$

As shown in fig. 3 and equation (1), the cam minimum radius depends on e - the initial eccentricity and space. The calculation scheme to optimize the dimensions is shown in fig. 4.

The optimization problem is to minimize the radius “ r_0 ”. This is done in the presence of restrictions, which take account of maximum and minimum values of allowable pressure angles, the phase of lifting and lowering, respectively. Calculations were made following notations:

- S_1 - current area map of tachtet lifting phase;
- S_3 - space to exit.

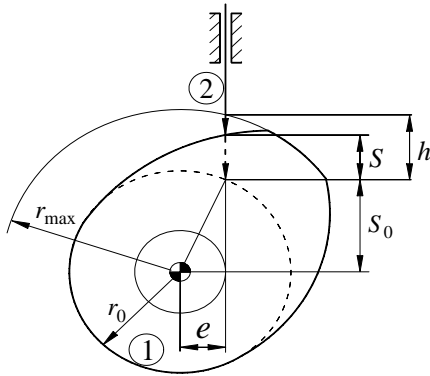


Fig. 4 Scheme of calculating the cam and tacket mechanisms

The objective function describing the problem under consideration is the form given in equation (5):

$$f(S_0, e) = S_0^2 + e^2 \quad (5)$$

We obtain restrictions optimization problem (6) and (7) from relations (3) and (4).

$$g_1 = \frac{dS_1}{d\varphi} - e - (S_0 + S_1)\tan(\alpha_{\max}) \leq 0; \quad (6)$$

$$g_2 = (S_0 + S_3)\tan(\alpha_{\min}) - \frac{dS_3}{d\varphi} + e \leq 0, \quad (7)$$

Karush–Kuhn–Tucker (KKT) conditions [4], generalize the Lagrange method for finding the extrema of a function subject to a family of constraints. While Lagrange multipliers consider only equality constraints, KKT conditions allow for general inequality constraints [3], [5]. In [6], for example, has implemented and tested a modified version that outperforms every other tested method in terms of efficiency, accuracy, and percentage of successful solutions, over a large number of test problems.

Considering the problem of finding the extreme of a multivariate function “ f ” subject to a family of constraints χ_i , $1 \leq i \leq m$, where χ_i are inequalities of the form $g_i \leq v_i$. Expressing the inequality constraints in the form $\chi_i \equiv g_i - v_i \leq 0$, the Lagrange function is defined as:

$$L(x, \mu) = f(x) + \sum_{1 \leq i \leq m} \mu_i (g_i(x) - v_i). \quad (8)$$

A point x^* is said to be feasible point if it satisfies all the inequality constraints. Assume the vector $x^* = (x_1^*, \dots, x_n^*)$ minimizes the continuous function f subject to the constraints $\chi_i \equiv g_i(x) - v_i \leq 0$, $1 \leq i \leq m$, than the vectors $(\nabla g_i(x^*))_{1 \leq i \leq m}$ are linearly dependent, or there exists a vector $\mu^* = (\mu_1^*, \dots, \mu_m^*)$ which is an optimal solution for the original optimization problem satisfying the following KKT conditions

$$\nabla L(\mu^*, x^*) = 0 \Leftrightarrow \left(\frac{\partial L}{\partial x_i}(x^*) = 0 \right)_{1 \leq i \leq n} \quad (9)$$

$$\mu^*(g_i(x^*) - v_i) = 0, \quad g_i(x^*) \leq v_i, \quad \mu_i \geq 0 \quad (10)$$

where ∇ is the gradient. The condition $\mu_i \geq 0$ implies non negative Lagrange multipliers and the relation $\mu^*(g_i(x^*) - v_i) = 0$ generates two cases

$$g_i(x^*) = v_i \quad (11)$$

$$g_i(x^*) < v_i \Rightarrow \mu_i = 0 \quad (12)$$

We consider the transmission function of growth (lifting) phase $S_1(\varphi) = h \sin(\varphi)$ and the transmission function of descending phase $S_3(\varphi) = h[1 - \sin(\varphi)]$, fig. 5.

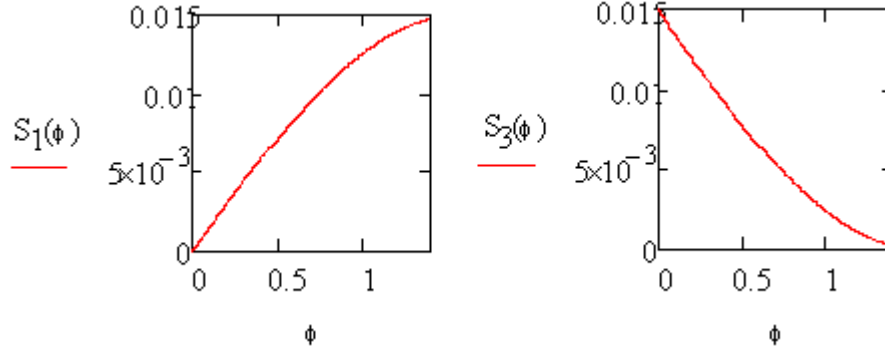


Fig. 5. The transmission function of lifting phase (left) and the transmission function of descending phase (right)

In the lifting phase, the tangent of the pressure angle must be less or equal then the tangent of the utmost pressure angle α_{\max} and in the descending phase the tangent of the pressure angle must be grater or equal than the tangent of the least pressure angle α_{\min} , leading to the inequalities:

$$\frac{dS_1}{d\varphi} - e \leq (S_0 + S_1) \tan(\alpha_{\max}) \quad \text{and} \quad \left. \frac{dS_1}{d\varphi} \right|_{\varphi=\varphi_1} - e = (S_0 + S_1) \tan(\alpha_{\max}) \quad (13)$$

$$\frac{dS_3}{d\varphi} - e \leq (S_0 + S_3) \tan(\alpha_{\min}) \quad \text{and} \quad \left. \frac{dS_3}{d\varphi} \right|_{\varphi=\varphi_3} - e = (S_0 + S_3) \tan(\alpha_{\min}) \quad (14)$$

We consider the objective function presented in relation (5) $f(S_0, e) = S_0^2 + e^2$, where e represents the eccentricity and S_0 is the initial space, which should be minimized subject to the following constraints:

$$\chi_1 \equiv h \cos(\varphi_1) - \tan(\alpha_{\max}) [S_0 + h \sin(\varphi_1)] - e \leq 0 \quad (15)$$

$$\chi_2 \equiv e + h \cos(\varphi_3) + \tan(\alpha_{\min}) [S_0 - h(\sin(\varphi_3) - 1)] \leq 0 \quad (16)$$

The KKT conditions state the following necessary conditions for a feasible point $x^* = (S_0^*, e^*, \varphi_1^*, \varphi_3^*)$ be a local optimal solution point:

$$\nabla f(x^*) + \sum_{i=1}^2 \mu_i \nabla \chi_i(x^*) = 0, \quad (17)$$

$$\chi_1(x^*) \leq 0, \quad \chi_2(x^*) \leq 0, \quad (18)$$

in terms of a Lagrangean function defined as follows:

$$L(S_0, e, \varphi_1, \varphi_3, \mu_1, \mu_2) = f(S_0, e) + \mu_1 \chi_1(S_0, e, \varphi_1, \varphi_3) + \mu_2 \chi_2(S_0, e, \varphi_1, \varphi_3) \quad (19)$$

The necessary conditions given by equation (17) can be restated in a compact formulation as $\nabla_x L(x^*, \mu^*) = 0$. We define the vectors:

$$\nabla f \equiv 2 \begin{bmatrix} S_0 \\ e \\ 0 \\ 0 \end{bmatrix}, \quad \tilde{\chi}(S_0, e, \varphi_1, \varphi_3) = \begin{bmatrix} \chi_1(S_0, e, \varphi_1, \varphi_3) \\ \chi_2(S_0, e, \varphi_1, \varphi_3) \end{bmatrix}, \quad \bar{H}(S_0, e, \varphi_1, \varphi_3) = \begin{bmatrix} \nabla \chi_1 \\ \nabla \chi_2 \end{bmatrix},$$

where:

$$\nabla \chi_1 \equiv \begin{bmatrix} -\tan(\alpha_{\max}) \\ -1 \\ -h \sin(\varphi_1) - h \cos(\varphi_1) \tan(\alpha_{\max}) \\ 0 \end{bmatrix}, \quad \nabla \chi_2 \equiv \begin{bmatrix} \tan(\alpha_{\min}) \\ 1 \\ 0 \\ -h \sin(\varphi_1) - h \cos(\varphi_1) \tan(\alpha_{\min}) \end{bmatrix}$$

The equations of the constrained optimization problem are translated in the following form:

$$\begin{aligned} \nabla f(x^*)^T + \bar{H}(x^*)^T \mu^* &= 0, \\ \tilde{\chi}(x^*)^T \mu^* &= 0, \\ \mu^* &\geq 0, \end{aligned} \tag{20}$$

with $x^* = (S_0^*, e^*, \varphi_1^*, \varphi_3^*)$ and $\mu^* = (\mu_1^*, \mu_2^*)$.

To resolve the optimization model for the mechanism considered these stages are known lifting height of the pusher:

$h = 0.015$ m – lifting height of the pusher;

$\varphi_1 = 80^\circ$ - angle of rotation of the cam corresponding lifting phase;

$\varphi_2 = 20^\circ$ - angle of rotation of the cam corresponding to the upper stationary phase;

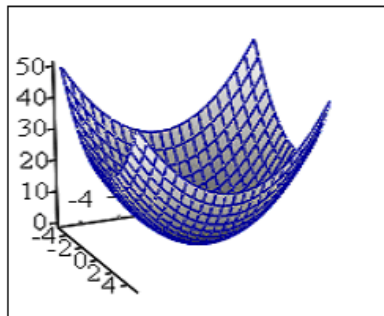
$\varphi_3 = 80^\circ$ - angle of rotation of the cam corresponding to the descendent phase;

- transmission function for the ascendent phase, sinusoidal;

- transmission function for the descendent phase, sinusoidal.

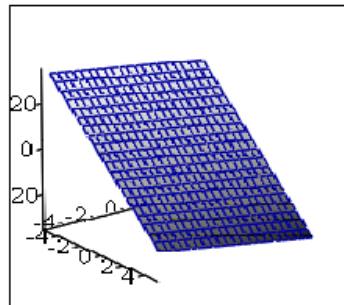
Starting the computation with the initial solution $S_0 = 0.02$, $e = 0.002$, $\varphi_1 = 0.6$, $\varphi_2 = 3.1$, $\mu_1 = \mu_2 = 0.1$, the feasible point is calculated as:

$$x^* = \begin{pmatrix} S_0^* = \mathbf{0.01398937243798}, \\ e^* = \mathbf{0.003998901367188}, \\ \varphi_1^* = \mathbf{1.599993896484375}, \\ \varphi_3^* = \mathbf{2.792587280273438} \end{pmatrix} \tag{21}$$



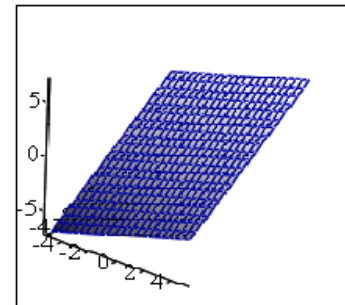
f

Fig. 6. The response surface of the objective function



x_1

Fig.7. The constrained planes for optimal angles $\chi_1(S_0, e, \varphi_1^*, \varphi_3^*)$ (left) and $\chi_2(S_0, e, \varphi_1^*, \varphi_3^*)$ (right)



x_2

The response surface determined by the objective function defined in (5) is depicted in fig. 6. Setting the optimal rotating angles to φ_1^* and φ_2^* respectively, the constrained surfaces become two constrained planes, which are presented in fig. 7.

3. CONCLUSIONS

This paper reports the application of the Karush–Kuhn–Tucker method in the optimization process of a rotating cam dimensions.

The problem was assessed both in analytical and numerical approaches. The mathematical states of the method is described and the Karush–Kuhn–Tucker conditions of the constrained optimization are translated into a structure containing the objective function, the matrix for the inequality constraints, lower and upper bounds for the feasible point. The strategy for numerically implementation was to transform the problem into an easier subproblem that can then be solved and used as the basis of an iterative process. By assuming that the bound constraints have been expressed as inequality constraints we obtained the subproblem by linearizing the nonlinear constraints.

REFERENCES

- [1.] Antonescu P., s.a., Mecanisme, Editura Printech București, 2000.
- [2.] Bratu I., Rus A., Mecanisme. Aplicații , Editura Universității din Oradea, 2003
- [3.] Conn A.R., Gould, Ph. L. Toint. "A Globally Convergent Augmented Lagrangian Pattern Search Algorithm for Optimization with General Constraints and Simple Bounds", SIAM Journal on Numerical Analysis, Volume 28, Number 2, pages 545–572, 1991.
- [4.] Lewis, R. M., Torczon V., "A Globally Convergent Augmented Lagrangian Pattern Search Algorithm for Optimization with General Constraints and Simple Bounds", SIAM Journal on Optimization, Volume 12, Number 4, pages 1075–1089, 2002.
- [5.] Malacaria P., Han Chen: Lagrange Multipliers and Maximum Information Leakage in Different Observational Models. In Proc. PLAS 2008, ACM.
- [6.] Schittkowski, K., "NLQPL: A FORTRAN-Subroutine Solving Constrained Nonlinear Programming Problems," Annals of Operations Research, Vol. 5, pp. 485-500, 1985.





¹Mihaiela ILIESCU, ²Marian LAZĂR, ³Victor GRIGORE

RESEARCHES ON TRUE PULSE LASER MICRO-WELDING

¹UNIVERSITY POLITEHNICA OF BUCHAREST, MANUFACTURING DEPARTMENT, ROMANIA

²⁻³S.C. OPTOELCTRONICA 2001, S.A., MĂGURELE, ROMANIA

ABSTRACT:

Microwelding represents an important machining method that, theoretically, requires special technological equipment. Also, the involved „working” parameters must be set to their appropriate values, depending on material’s type, workpiece’s thickness, welding’s required characteristics, etc. [2].

Some preliminary research results on Nd: YAG laser microwelding are going to be presented above, for some specific type materials (aluminium alloy, stainless steel, copper-zinc alloy), while the technological equipment is a „combination” of two already existing ones: Trumf laser and Isel CNC machine.

KEYWORDS:

microwelding, preliminary research results

1. INTRODUCTION

Laser Beam Machining (LBM) is highly used in top industrial fields (aerospace, nuclear), because of, both, tough characteristics of the involved materials and required machining complexity (high geometrical precision, such as x100 or, x 10 μm).

The applicability of this machining method is due to laser beam’s specific properties, such as: one direction; intensity; monochromatics; amplifying when passing through different environments, coherent light and high energy density.

Laser beam represents an „universal tool” used in micromachinig (welding, drilling, cutting, engraving, deposition, etc.) one of its important characteristics being the lack of direct physical contact tool – workpiece. As consequence, there are no machining forces on the workpiece and no wear of the tool [1]

When laser micromachinig ther is no absolute request for void equipment, thermal influenced zones can be neglected and thermal deformations are very small, while the machined materials can be tough, extra-tough or, fragile ones.

Microwelding represents an important machining method that, theoretically, requires special technological equipment. Also, the involved „working” parameters must be set to their appropriate values, depending on material’s type, workpiece’s thickness, welding’s required characteristics, etc. [2]. Some preliminary research results on Nd: YAG laser microwelding are going to be presented above, for some specific type materials (aluminium alloy, stainless steel, copper-zinc alloy), while the technological equipment is a „combination” of two already existing ones: Trumf laser and Isel CNC machine.

2. METHOD AND EQUIPMENT

When laser machinig, there has to be defined two important parameters [1]:

- spot diameter obtained in lens focus:

$$d_o = \frac{4}{\pi} \frac{f\lambda}{D} \quad [\mu\text{m}] \quad (1)$$

where: f is lens focal distance [mm]; D – lens opening [mm]; λ – wave length of emitted radiation [μm].

- power maximum density in lens focus.

$$W_p = \frac{P}{10^{-2} \lambda^2} \quad [\text{W}/\text{cm}^2] \quad (2)$$

where: P represents the power emitted by laser radiation [W].

There are also some other laser beam specific parameters that do influence the machining process, meaning:

- **power** – determines the penetration depth;
 - **power density / intensity** – is dependent on cross section of the laser beam;
 - **energy** – determines the volume of molten material and can be calculated by:
 → the product of power and laser – material interaction time,
- or
 → the product of power and pulse duration.

Laser (micro)machining is based on two main phenomena: material's melting and vaporisation when the laser beam impacts the work-piece surface by spot focusing. Each material has a specific value of density power when vaporisation starts, for example: alluminium – $W_{PS}=2 \times 10^5 \text{ W}/\text{cm}^2$, iron / steel – $W_{PS}=1,2 \times 10^5 \text{ W}/\text{cm}^2$ etc.

So, radiation penetration depth can be determined by:

$$h = v \cdot t_i \quad [\text{mm}] \quad (3)$$

where: v represents prelevation speed; t_i – pulse duration

$$h = v \cdot t_i \quad [\text{mm}] \quad (4)$$

This paper presents experimental results in laser microwelding, the equipment used being made of the following ones.

A. Laser central unit TruePulse 62 – see figure 1

This is a Nd: YAG laser type, that generates intense invisible radiations, with wavelength „close to” infrared radiations.

Some of its technical charactersitics, as mentioned by the producer, are presented in table 1.

Laser lenses can be used for radiation wavelength values from 1030 nm to 1064 nm.

Tabel 1 [4]

Characteristics	Values
- Radiation wave length	1064 nm
- Medium power	65 W
- Pulse minimum power	250 W
- Pulse maximum power	5000 W
- Pulse minimum duration	0,2 ms
- Pulse maximum duration	50 ms
- Pulse maximum energy	50 J
- Maximum frequency of pulse repetition	900 Hz
- Laser beam quality	8 mm mrad

B. Isel-automation machining systems [5] - systems made of three main components: isy CAM software, ProNC software and Flatbed or Euromod basic units.

An image of its basic unit – used in experiments can be seen in fig. 2.

3. EXPERIMENTS

There are many factors that do influence laser micro-welding process, some being: material's type, laser beam power density, pulse duration and shape, shielding gas etc.

Even the process is rather complex, it has many advantages, the main ones dealing with: welding materials with different physical – chemical properties; welding in hard accessible zones and positions – by laser beam focusing with lenses; or, by allowing its pass through medium that are transparent with respect to laser radiation wavelength, etc.



Fig.1 Laser optical unit True Pulse [4]



Fig.2 Isel Flatbed unit [5]

Mainly, there are two micro-welding principles, one is *conduction* (the heat source generated by laser beam absorption is localised on work-piece surface, where melting starts - see fig. 3) and the other is *penetration* (melting temperature is above evaporation value and so, into the metal it is generated an absorbent cavity full of ionized metallic gas - see fig. 4).

The experiments used penetration micro-welding so, high depth and very narrow welding belt could be obtained. The Nd:YAG laser was used in CW mode CW (continuous wave) . Images taken while micro-welding experiments are presented in fig. 5, 6 and 7 – there can be noticed both values of the laser beam parameters, and images of the welding belt of the work-piece.

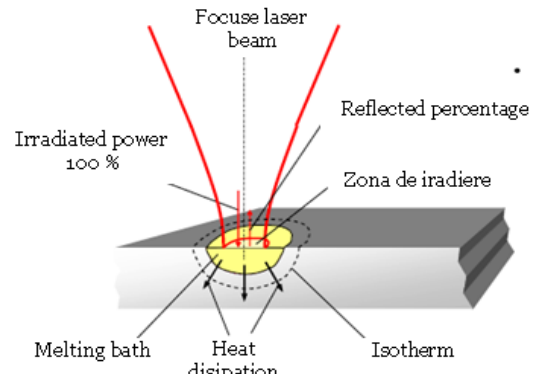
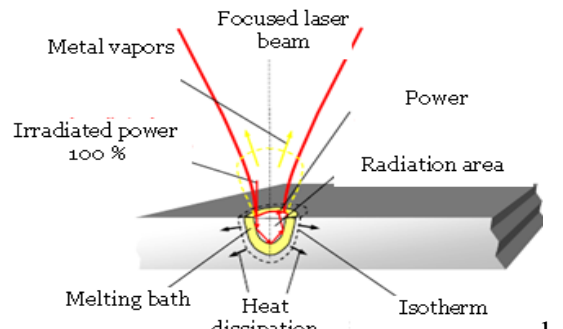
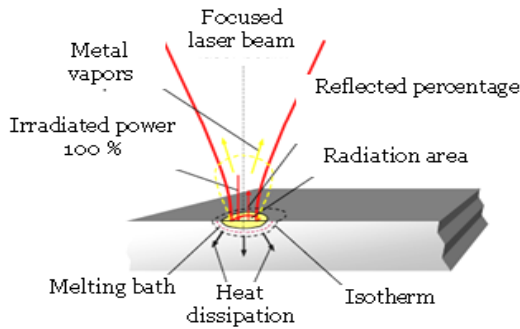


Fig. 3 Micro-welding by thermal conduction



a. b.

Fig. 4 Micro-welding by penetration



Fig. 5. Alluminum alloy micro-welding

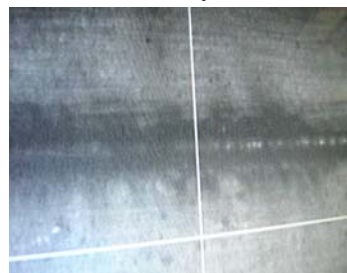
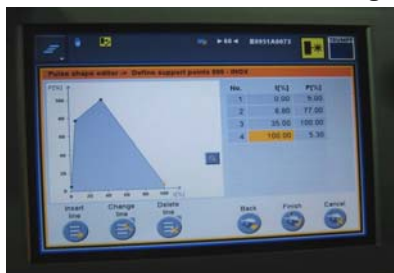


Fig. 6. Copper alloy micro-welding



Fig. 7. Stainless-steel micro-welding



Alluminum alloy welding belt width: 651 μm

Copper alloy welding belt width: 263 μm

Stainless steel welding belt width: 831 μm

Fig. 8. Microscope images of the welding belts

The results presented by this paper are part of the Research Project on Innovation no. 229/2008.- Advanced Micro-Technologies on Laser Machining

It has to be pointed out the fact that even some orientative values of laser beam parametrs in micro-welding are presented in specific references, if considering them exactly, no good results are obtained. So, it was necessary to make experiments with specific materials and existing equipment – and the results to be further used in industrial application.

The laser head (on TruePulse 62) is the one generating radiation (for micro-), and the CNC machine (Isel Flatbed) allows computer aided welding - on various complex trajectories and high precision (1 μm) [3].

Images of microscope checking on the welding belts width (that points out the micro- charactersitic) are presented in figure 8.

4. CONCLUSION

Laser Beam Machining is highly used in top indutrial fields. When machinig materials, welding is an important method.

Some orientative values of laser beam parametrs in micro-welding are presented in specific references, but, no good results are really obtained, if considering.

It was necessary to make experiments with specific materials and existing equipment – and the results are further used in industrial application.. The material testec were:alluminum alloy, copper alloy and stainless steel.

Further research must be developped – based on design of experiments and specific software so that, if possible, regression models of micro-welding parameters and welding belt's characteristics, to be obtained.

REFERENCES:

- [1.] Marinescu N., Nanu D., ș.a., „Procese de prelucrare cu fascicule și jeturi”, INOE, București, 2000, ISBN 973-98742-6-6 ;
- [2.] Yi Qin, „Micromanufacturing Engineering and Technology”, William Andrew Inc., USA, 2008
- [3.] Iliescu M., „Computer Aided Technolgies (CAD, CAM and CNC) Important Means in Developing an Innioative Machinig Force's Measuring Mevice”, Metalurgia International, no. 7/ /2010, ISSN 1582-2214
- [4.] www.us.trumpf.com, accessed, september, 2010
- [5.] www.isel.com, accessed, september, 2010





FINITE ELEMENT ANALYSIS OF A SEAT BELT BUCKLE DEVICE

¹⁻³. UNIVERSITY „POLITEHNICA” TIMIȘOARA, FACULTY OF ENGINEERING HUNEDOARA, ROMANIA

ABSTRACT:

In the last years, there has been rapid and extensive progress in automotive technologies. These technical advances include devices that provide increased protection for the occupants of the vehicle in case of crash and systems that allow drivers to avoid collisions, or at least to mitigate their severity. Integrated systems for restraining the occupant, used in automotive applications, have shown to improve the safety of the occupant and to decrease the risk of injury during impacts of motor vehicles.

Although safety belts and air bags are always been considered among the primary safety devices, today the seat belt system is widely regarded as being the most important element of safety equipment in a vehicle.

In the first section of this paper, the most important elements of the safety equipment in a vehicle are described. The second section presents the modeling, analysis and evaluation techniques for the Seat Belt Buckle Assembly strength, used in order to ensure the safety of the occupants in conditions of impact. Proper design of the seat belt buckle assembly is crucial, as in case the seat belt buckle assembly can not endure the load that was derived by the motion of an occupant during an impact, the seat belt system can not play the role of a restraining system anymore. In order to perform this analysis and evaluate the strength, we examine the effectiveness of a latch plate as component of the seat belt buckle assembly, using the finite element analysis method.

KEYWORDS:

safety device, safety belt system, seat belt buckle assembly, finite element analysis

1. INTRODUCTION AND CONTEXT

Vehicle crashworthiness and occupant safety remain among the most important and challenging design considerations in the automotive industry. In the recent years, there has been rapid and extensive progress in automotive technologies, especially with respect to electronic sensing and control systems, which allowed engineers to develop a wide range of "high-tech" safety systems. These include devices that provide increased crash protection for vehicle occupants, and systems that may allow drivers to avoid collisions or, at least, to mitigate their severity. Some of these systems, described in Fig.1, are available as standard equipment on new vehicles, while others involve additional costs, as part of specific and optional equipment packages on certain vehicle models.

The most important safety devices are considered today the Safety belts and Air bags (Fig.2) which save thousands of lives each year (for example, according to the reports [5], the use of seat belts in 2009 saved an estimated of 12,713 lives). The air bag is a proven and effective safety device, but it doesn't replace a seat belt. Air bags are designed to work only with seat belts, because if an occupant doesn't wear his seat belt, he could be thrown into a rapidly opening frontal air bag and a movement of such force could injure or kill him. Consequently, the seat belt system is widely regarded today as being the most important element of safety equipment in a vehicle. When used according to [1], seat belts are approximately 45% effective at preventing fatal injuries and 67% effective at preventing serious injuries. Moreover, nearly all safety experts agree that buckling up dramatically increases the chances of surviving an accident, and those seat belts reduce the risk of death for a front seat car occupant by about 50 percent.

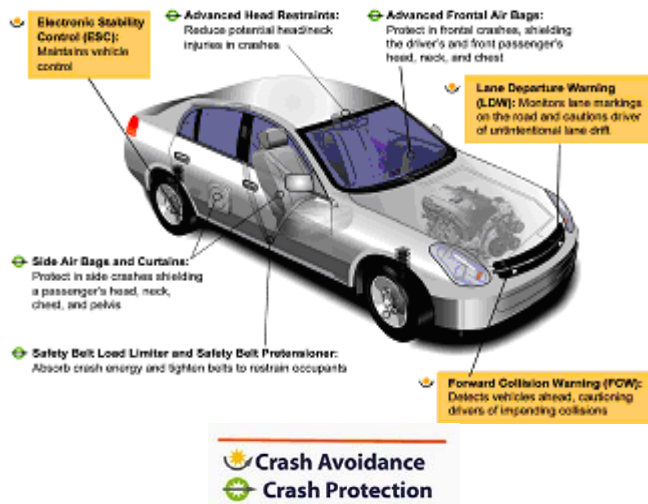


Fig.1 Safety technologies:

Crash Avoidance and Crash Protection

Despite this safety record, the performance of the belt systems is continuously being refined. Recent papers discuss the development of 4-point harnesses for use in production vehicles [2], [3], while devices such as pretensioners and belt load limiters [4] are becoming common features in contemporary vehicles.

The development and the evaluation of protection measures against the effects of accidents, require an accurate assessment of the operational behavior in the exploitation of safety systems, and involve a good knowledge of the tolerance of the human body, as well as its mechanical response to impact.

2. PRESENTATION OF THE STUDIED SAFETY BELT SYSTEM

2.1 Standard three-point safety belt system

The safety belt, also called seat belt, is part of an overall occupant restraint system. This is intended to reduce injuries by stopping the wearer from hitting hard interior elements of the vehicle or other passengers, respectively the so-called second impact [6], and by preventing the passenger from being thrown-out from the vehicle. A properly secured seat belt offers protection in head-on, side and rollover collisions, by securing in the life space of the vehicle. In fact, the belts system help spread out the energy of the moving body in a collision over the chest, pelvis, and shoulders.

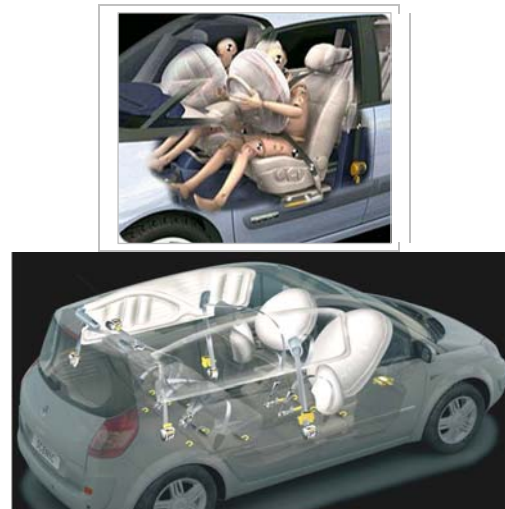


Fig.2 Safety belts and air bags

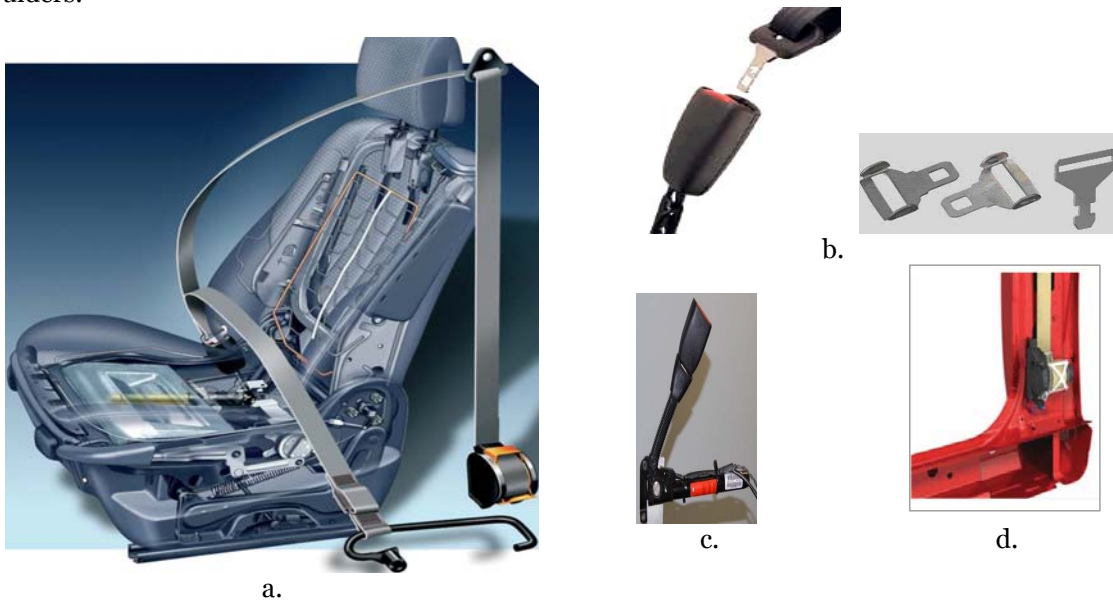


Fig.3. Standard three-point seat belt system and its components

The standard three-point belts shown in Fig. 3a, attaches to the car in three places, two mount near the rear of the seat bottom and one towards the top of the side pillar, offering a maximum of comfort and convenience. The seat-belt latch plate clips into a buckle Fig.3b, which in the front seats of cars is usually placed at the end of a stiff stalk. A pretensioner Fig.3c, and a

retractor device Fig.3d, are included as part of the safety belt system. In the event of an impact, the safety belt system is designed to grip the belt and not allow the occupant to travel forward any more than they already are.

The seat belt buckle assembly, Fig.3b, must be able to withstand extremely high loads during a crash, and at the same time it must be easy to open even when heavily loaded. Moreover, the buckle assembly must withstand high accelerations in all direction without opening. This feature is critical when the seatbelt system includes a pretensioner, as such a pyrotechnic device pulls rapidly the buckle in one direction towards the floor and then the pulling force suddenly switches in the other direction. (Fig.4)

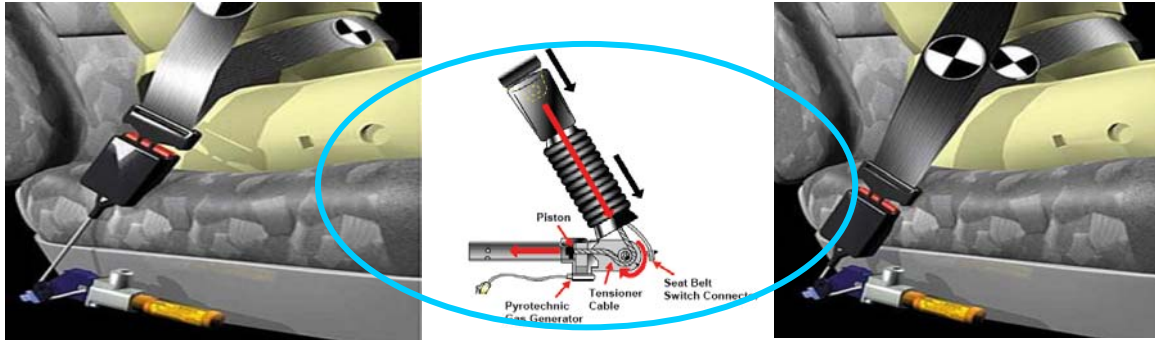


Fig.4 Functions and operating mode of a pyrotechnic pretensioner

2.2 Faulty Seat Belts

If the seat belt buckle can not endure the load that was derived by the motion of an occupant motion during a frontal impact, the seat belt can not do the role of a restraint system any more. Thus, proper strength of a seat belt buckle is essential in the case of a frontal impact.

In general, motor vehicle safety teams check the performance of their equipment to protect the occupant against unreasonable risk of accidents and of death or injury in an accident. In this context, a safety defect is defined as a problem that exists in a motor vehicle or in its equipments and that: poses a risk to motor vehicle safety; may exist in a group of vehicles of the same design or manufacture, or in items of equipment of the same type and manufacture.

Examples of defects considered safety-related to a vehicle occupant, are listed below:

- ❖ Critical vehicle components that break, fall apart, or separate from the vehicle, causing potential loss of vehicle control or injury to persons inside or outside the vehicle.
- ❖ Seats and/or seat backs that fail unexpectedly during normal use.
- ❖ Safety seats that contain defective safety belts, buckles, or components that create a risk of injury, not only in a vehicle crash but also in non-operational safety of a motor vehicle.
- ❖ Air bags that deploy under conditions for which they are not intended to deploy.

A typical auto crash is viewed as having “two collisions”: the “first collision” occurs when the vehicle impacts another vehicle or a fixed object; the “second collision” (following immediately, often after only milliseconds, the first collision) occurs when a vehicle occupant impacts the interior of the vehicle or is ejected and hits the ground (the literature notes also the existence of a “third impact”, between the internal organs and the frame of the body).

The purpose of a seat belt is to either prevent the second collision or to minimize its injury-producing potential. When it works properly, the seat belt is indisputably the most important safety device in an automobile, however when it works poorly or completely fails to work, the seat belt can cause serious injury and even death.

Seat belts can fail to restrain occupants due to both poor design and/or faulty manufacturing. Some of the more common defects include: Inertial unlatching & False latching, or/and the Failure of some component parts of the seat belt buckle. Consequently, the ways to unlatch a seat belt buckle in an accident, [7], can be: Overload; Inadvertent contact; False latch/Partial engagement; Inertial release. During a collision in such situations, the seat belt becomes unlatched and can allow the latch plate to pull out of the buckle. As a result, the occupant is essentially unbelted and unrestrained and, frequently, can be ejected from the car. If a seat belt system failure is suspected, the evidence that a seat belt failed because of design or manufacturing defects is often subtle and can be difficult to detect; since it is extremely difficult to prove that a seat belt failed without the physical evidence, it is important to preserve the failed seat belt system and to attach it to the technical expertise.

2.3 Presentation of the studied device

A safety belt buckle device, Fig.5a, is designed to coupling the seat belt that fixes to seat the occupant of the vehicle in order to limit its movement during a shock, and thus, during a strong deceleration, the occupant of a vehicle in motion is not projected in the moving direction as result

of the accumulated kinetic energy. Generally, the most current safety belts are equipped with buckles devices similar to those presented in Fig.5b and Fig.5c.

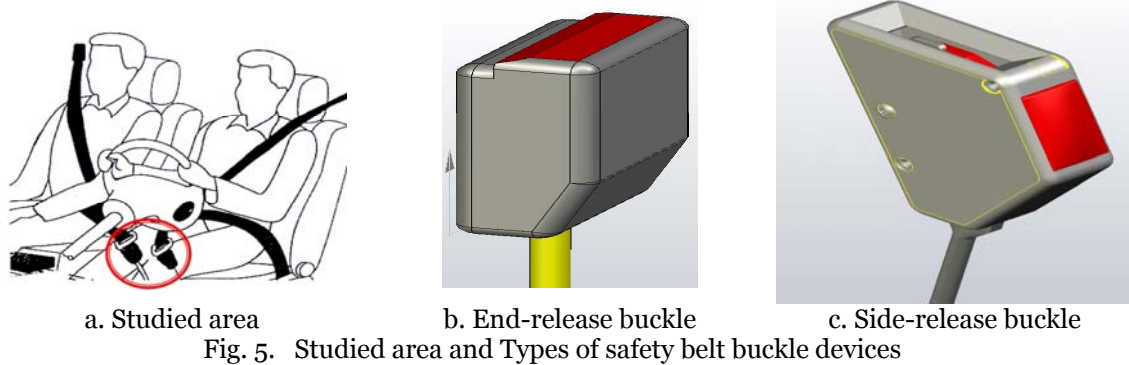


Fig. 5. Studied area and Types of safety belt buckle devices

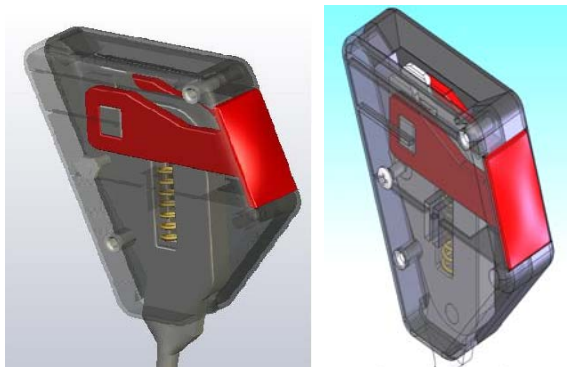


Fig.6. 3-D model of the studied coupling device

The 3D model of the studied coupling device (with side-release button) is shown in Fig.6.

2.4. Effort evaluation in pretensioned seat belt system

The static analysis of the cable–guide subassembly, Fig. 7a, followed by the solving of the equations equilibrium system (1), with $F_1=400$ daN and $F_2=300$ daN, give as result the forces in the belt system, $F=635$ daN. After the decomposition of this force, at A, C and E points, Fig.7b, we obtained the following values of forces:

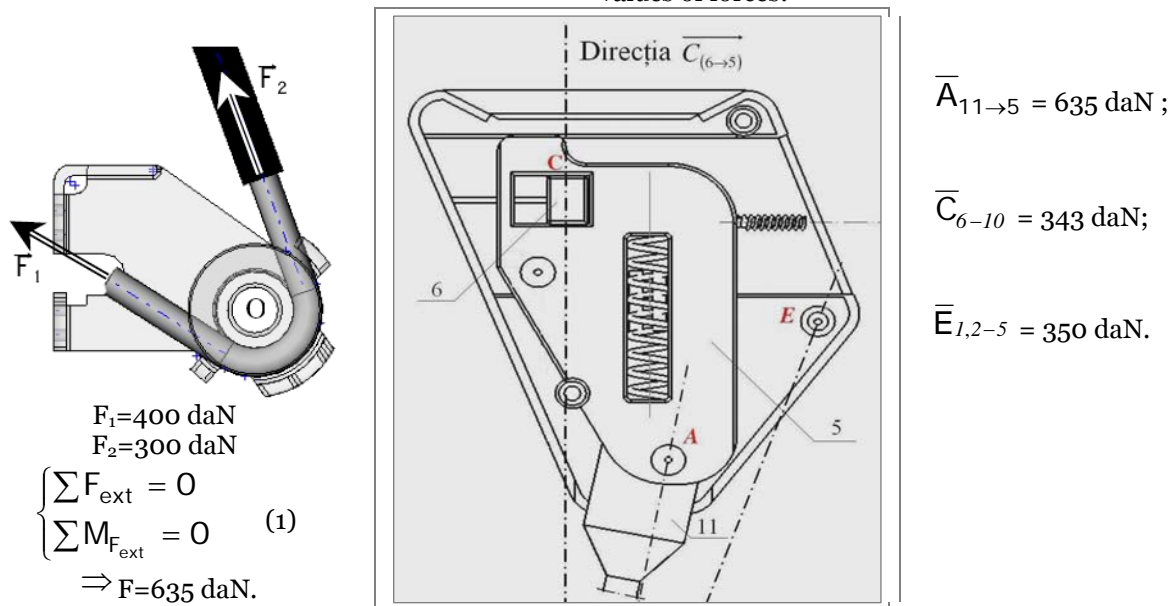


Fig.7. Evaluation of the resultant force in the safety belt system and its components

2.5 Finite Element Analysis of the buckle latch plate

The belt buckle assembly must have the capacity to transmit the forces being put on the system. In case one of its component parts, in particular the latch plate, can not endure the load that was derived by the motion of an occupant during an impact, the safety belt system can not play the role of a restraining system anymore.

Therefore, the latch plates of the seat belts, although have different designs being manufactured by different companies, are an important element of the system. The importance of this element lies in its own security and is related to assure the functional role of the safety belts systems.

- **Material Proprieties:** the analyzed latch plate is made of steel grade CK55 (corresponding to OLC 55 X, STAS 880), whose properties are listed in Table 1a and 1b.

Table 1a. Mechanical properties in the quenched and tempered condition (+QT)

Mechanical properties	Mechanical properties for the ruling sections (see prEN10083-1:2002, Annex A) with a diameter (d) or for flat products thickness (t) of		
	$d \leq 16\text{mm}$ $t \leq 8\text{mm}$	$16\text{mm} < d \leq 40\text{mm}$ $8\text{mm} < t \leq 20\text{mm}$	$40\text{mm} < d \leq 100\text{mm}$ $20\text{mm} < t \leq 60\text{mm}$
Re min. (MPa)	550	490	420
Rm (MPa)	800-950	750-900	700-850
A min. (%)	12	14	15
Z min. (%)	30	35	40
KV min. (J)	-	-	-

Table 1b. Mechanical properties in the normalized condition – (+N)

	Mechanical properties for products with a diameter (d) or, for flat products thickness (t) of		
	$d \leq 16\text{mm}$ $t \leq 16\text{mm}$	$16\text{mm} < d \leq 100\text{mm}$ $16\text{mm} < t \leq 100\text{mm}$	$100\text{mm} < d \leq 250\text{mm}$ $100\text{mm} < t \leq 250\text{mm}$
Re min. (MPa)	370	330	300
Rm min. (MPa)	680	640	620
A min. (%)	11	12	12

- **Geometric parameter and 3-D CAD model:** the geometry of the latch plate, shown in Fig.8, was based on these functional requirements and is in accordance with the configuration of the belt buckle.

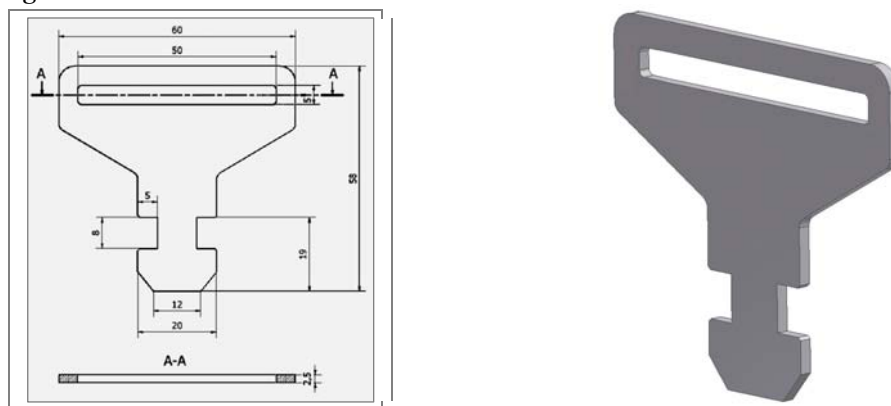


Fig.8. Geometric parameters and the 3-D model of the latch plate



Fig.9. Discretization (meshing) of the latch plate model

- **Finite Element Analysis of the latch plate**

The finite element analysis performed using Algor software, involved the following steps:

- ❖ Conception of the 3-D CAD model of the latch plate (or transfer to Algor a CAD model designed in another modeling tools/dedicated software/, like Inventor, Mechanical Desktop, SolidEdge, in .stp format file), for creating the 3D geometry of the part/assembly to perform FEA.
- ❖ Save of the 3D CAD geometry in neutral format like IGES, STEP etc. Though some of the FEA packages allow importing the CAD geometry directly from some of the 3D CAD packages.
- ❖ Start of FEA package and import the CAD geometry into the FEA package.
- ❖ Defining Material Properties: modulus of elasticity, Poisson ratio, etc.
- ❖ Defining the displacement boundary conditions (Fig.10) and applying the mechanical loads (Fig.11);
- ❖ Discretization (meshing) of the model (Fig.9);
- ❖ Performing of the finite element analysis, respectively obtaining the solution of the finite element matrix equations (solved for the unknown displacements, given material properties, forces, boundary conditions and mesh size);
- ❖ Analysis and interpretation of the FEA results (Fig.12), and conclusions drawn from the analysis.

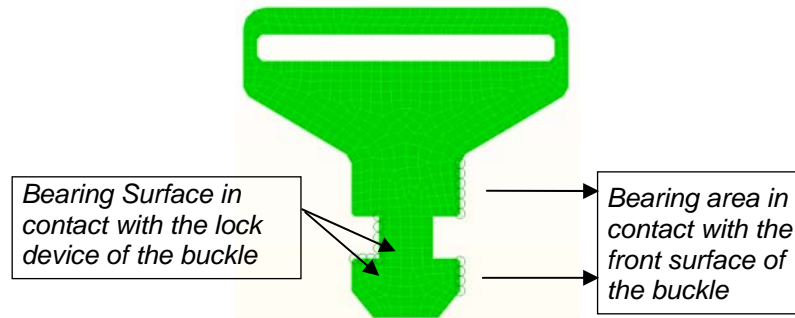


Fig.10. Boundary displacement constraint conditions

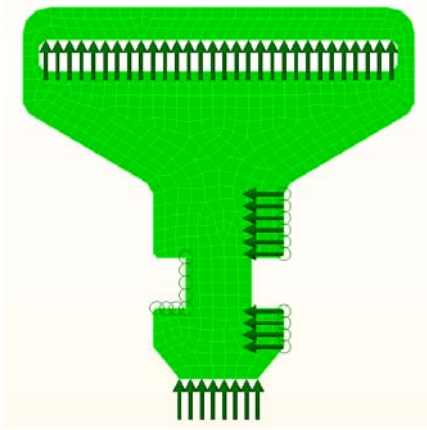


Fig.11. Applied of mechanical loads

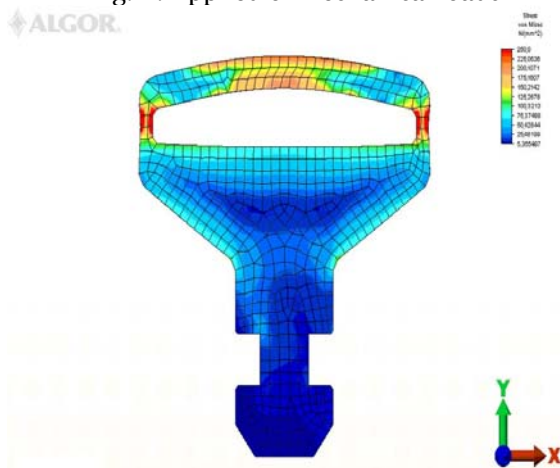


Fig.12. Finite Element Analysis of the safety belt latch plate. Distribution and values of Stress

3. INTERPRETATION AND CONCLUSIONS. FUTURES STUDIES

The CAD modeling and the Finite Element Analysis of the seat belt system (buckle assembly and latch plate), was carried out in order to verify the safety of the car occupants in impact conditions. The proper design of a seat belt buckle is essential for the situation of a frontal impact, because if the buckle assembly can not endure the load derived by an occupant motion during a frontal collision, the safety belt can not serve as functional restraint system.

The effectiveness of the component parts of the safety belt assembly was analyzed using the *Algor V Release* software, based on the Finite Element Method, and the results that we obtained reveal the correct design conception of the examined elements.

In our future studies, we are planning to do further development on the subject of analyzing the passive safety systems using FEA software. This work is motivated by the continuously increasing standards for protection measures against the effects of accidents. These require an accurate assessment of the operational behavior of the safety systems in exploitation, and involve a good knowledge of the tolerance of the human body, as well as its mechanical response to impact.

REFERENCES

- [1.] Transport, Infrastructure and Communities Portfolio/Government of Canada, www.tc.gc.ca
- [2.] High-Tech Vehicle Safety Systems. Canadian Association of Road Safety Professionals, <http://www.carsp.ca/page/111/400>
- [3.] National Highway Traffic Safety Administration, <http://www.nhtsa.gov/>
- [4.] Limiting performance analysis of a seat belt system with slack, Richard W. Kent, Sergey V. Purtsezoв, Walter D. Pilkey, International Journal of Impact Engineering 34-8 (2007) 1382–1395.
- [5.] Report/Lives Saved in 2009 by Restraint Use and Minimum Drinking Age Laws and Seat Belt Use in 2010 – Overall Results.
- [6.] <http://en.academic.ru/dic.nsf/enwiki/7248718>
- [7.] <http://www.vehiclesafetyfirm.com/cm/crashworthiness/diagnosing-seatbelt-use.pdf>
- [8.] http://www.algor.com/news_pub/tech_reports/2004/interpretingresults/
- [9.] Tichkiewitch, S. - Méthodologie et outils pour l'intégration dans la conception. "Conception et fabrication de produits mécaniques". Drăghici, G. și Brissaud, D.(coord) Ed.Eurobit, Timișoara, 1999



WHEELS AUTO MODELING USING FINITE ELEMENT METHOD

^{1,2}UNIVERSITY POLITEHNICA OF TIMISOARA, FACULTY ENGINEERING OF HUNEDOARA, ROMANIA

ABSTRACT:

The question always arises buying rims "steel or alloy wheels?". In addition to the rims look more appealing than those of alloy steel, there are technical reasons why it tends to use them: reduced weight, starting and braking, rigidity, rapid cooling. Although it can produce sheet steel or cast alloy wheels profile is adopted depending on the specifics of the construction vehicles and the stress faced by their wheels.

In this paper we studied the tensions that arise when a wheel is subjected to aerodynamic loading conditions, trying to play the best areas in which attention must be enhanced in order to prevent premature destruction. Using CATIA V5, we designed a concept of light and have undergone a finite element method using different forces and accelerations restrictions in areas where problems occur during use. Calculating the diagrams thus playing rim is observed when the material behavior is tensed and so we can correct the areas that present a danger of destruction.

At the end of the method could draw the conclusion which shows the success of the concept, but also design new technologies for observation and verification of parts or assemblies.

KEYWORDS:

wheels auto, finite element method, aluminum alloys, stress

1. INTRODUCTION

Although the design is changing rims, some classical models are still within the top preferences. Versions with 4 or 5 spokes or those with cross-spoke wheels are derived from racing cars. The conclusion is that it hides behind the form and function. The shape is derived from this calculation is to provide durability, low weight and hardness. On the other hand there and "trendy wheels" that change from one "season" to another. If these wheels to decide the importance of technical characteristics is the designer and engineer, [4]. Because these types of wheels have a relatively short life focuses on the methods of production as cheap and as fast. Unfortunately, to meet the above conditions, is unable to use the latest technology in the field. On the other hand, car manufacturers tend to include standard equipment alloy wheels. Since their invention in the '50s, alloy wheels have been used to improve machine performance.

In terms of material they are made, the wheels are magnesium alloy (the original version was produced) or aluminum alloy. The magnesium alloys are too fragile to be used on the streets. I'm pretty hard to maintain and limited in terms of resistance to harmful environmental factors. For example, the tendencies to oxidize magnesium have often varnished. Currently this type of wheels used on racing cars participating in such as Formula 1 races held in Indianapolis, etc.. which are continuously monitored by staff members. For normal use of the machines were designed aluminum alloy wheels having a greater resistance to common shocks from a road. They are made in different models, all weighing less than the steel version, [2].

2. METHODOLOGY

2.1. Jante alloy or steel?

When you think about when choosing a winter set of wheels to choose between alloy and steel wheels. Below we have listed some advantages and disadvantages to light:

Alloy wheels - is a plus in terms of aesthetics - have a very good precision manufacturing - are lighter than steel rims - have a greater strength and durability - helps to brake - Requires special care (especially in winter) to avoid damaging action skid materials, dust and mud;

Wheels of steel - Satisfy the requirements of drivers who want a winter set of wheels at the highest price - can be found in two types of finishes (black or metallic);

- Changing the layout is easy and relatively cheap by replacing the protective caps - are cheaper than alloy rims due to lower costs for materials and labor;

2.2. Influence rims

The question always arises buying rims "steel or alloy wheels?". In addition to the rims look more appealing than those of alloy steel, there are technical reasons why it tends to use them, fig. 1.



Fig.1. Appearance of some wheels

behaves tire mounted on it. This will, in turn, less malleable by the opposing forces of resistance acting on her great curves, which leads to a good response.

4. *Rapid cooling.* Due to high thermal conductivity property of the material they are made of alloy wheels to ensure rapid cooling of the wheel and brake components in their proximity.

2.3. Construction

In general running wheel disc pressed steel sheet, but in some cases logs are used and spoke cast or dragged in obtaining an adequate rigidity to the smallest weight. Merge wheel rim is made by welding, sheet metal disc by mechanical fasteners for spokes drawn, and if cast alloy wheels with lightweight wheels, disc and rim forming common body. Drive-wheel assembly is mounted on the hub with screws or bolts.

Configuration and rim profile is adopted depending on the specifics of the construction vehicles and the stress faced by their wheels.

Depending on constructive solutions adopted there are two types of wheels:

- ❖ wheels joints (fig.2.a) - used in the wheels of cars, light commercial vehicles, 4x2 wheeled steering wheels and engines of small power tractors;
- ❖ removable wheels with cylindrical or slightly conical profile (fig.2.b) - used wheels trucks, buses, vans and heavy wheels of large and medium power tractors.

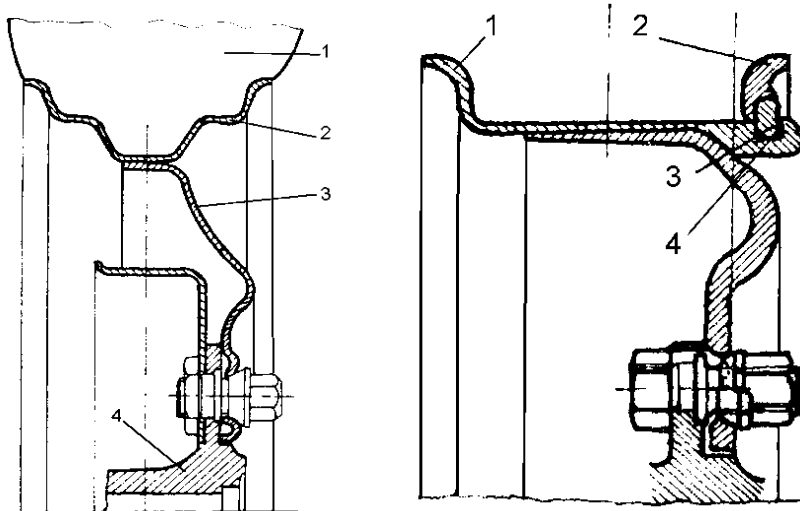


Fig.2. Constructive Solutions wheels

Joints with deep profile wheels have ears shoulder high profiled rim, providing a strong tire lateral stability. These buildings used tire edges are elastic and flexible, being allowed profiled rim mounting them directly.

If removable wheels, figure 2.b, less tapered profile, 5-15A taper creates the possibility of a better tire crosses. Installation is as simple as pushing the tire on the rim a border of fixed and removable border 2 fixation with flexible sealing ring 3 which is inserted into channel 4.

This construction allows easy mounting and dismounting tires and ensure takeover axial forces. For vehicles that are used for rear-wheel dual (double), disc wheel profile is designed to allow both wheels to the hub assembly, symmetrical about the plan to raise and support. If the rims for tubeless tires to be given to sealing surfaces must not show local irregularities or bulging, [1].

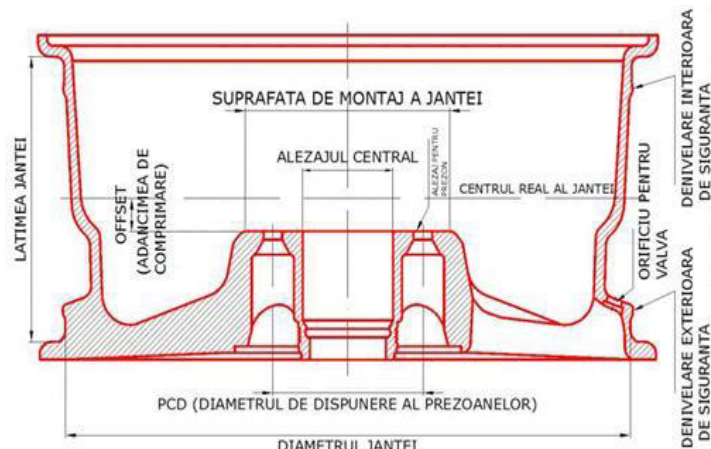


Fig.3. Elements of the rim

Symbolization. Ex. of symbolization: 5 1/2 J x 49 ET 14H2 = 5 1/2 inch rim width (inches), J = border rim shape feature point, x = rim in one piece, 14 = nominal rim diameter in inches (inches) H2 = rim profile; ET49 = depth Compression: 49mm;

2.4. Compatibility wheel / tire – oversize

Oversize rim and tire, was conceived to enhance performance and appearance of your vehicle. It is accomplished by fitting larger diameter wheels and tires compared to the lower height. It is envisaged that following these changes to keep the overall diameter of the wheel to a maximum difference of 3% compared to the initial diameter. This is important because variations larger diameters would lead to traction problems, and finally to a modified fuel consumption. Also, the cars equipped with computer-assisted braking some confusion could arise, leading to accelerated brake failure.

The rule for dimensioning:

- * Plus 1: Increase section width by 10 mm, reduces the appearance of 10 points. Increases rim diameter by 1 inch.
- * Plus 2: Increase section 20 mm, decreases aspect with 20 points. Increases rim diameter by 2 inches

2.5. Aided design in CATIA V5.

CATIA (Computer Aided Three Dimensional Interactive Applications) product of Dassault Systemes is currently one of the most widely used integrated CAD / CAM / CAE in the world, with applications in various fields, including: mechanical engineering, aerospace, shipbuilding, automotive, robotics, agricultural machinery, chemical, food and more. To version 5 is available since 1999, every new update is introduced new modules and functionality, while improving existing ones.

CATIA V5 is the top information technology design technologies such as machine building and construction industry in different parts. CATIA V5 is the cornerstone in the integration of people, tools, methods and resources in an enterprise. Its unique model Product/Process/Resources results in a truly collaborative work environment that enhances creativity and flow of information, the definition of 3D products and processes.

Using an intuitive interface and flexible CATIA Part Design module makes it possible to design three-dimensional sound of different pieces most often encountered in the design of mechanical products, as, with CATIA Sketcher, the other modules of the program. The module offers a highly productive working environment, each piece designed with a number of parameters, both in its use and in how CATIA Knowledge Advisor for parameterization and automatic creation of families of parts, a set of dependencies between parts, etc.

3. ANALYSES

FINITE ELEMENTS ANALYSIS METHOD WITH WHEELS FEM incorporating CAD programs contain special procedures that allow optimization optimization through automatic calculation of optimal values for some design parameters so as to satisfy a set of conditions imposed on an objective function, defined by the user. Also, the designer can always return to the

geometric shape of the structure, the material of which it will be made and, of course, the loads that will be covered in this stage of development where the structure is only a virtual model. The first step in addressing a new analysis is its choice of the [Insert], but, implicitly, the execution module, the type of static analysis (Static-house) is the default. As an immediate result, shaft specifications are added element 'Static Case ". The expansion element "Static Case" (press the mouse icon with the symbol "to his left), its elements are displayed: Restrictions (Restrains), loads (Loads) solutions (Static Case Solution) and sensors (Sensors). They have very important roles in finite element analysis. Of course, the early analysis, sub-items do not contain values, the user must set restrictions and tests for the program to calculate solutions CATIA and activate the sensors. For example may be given three tests, Deformed Meshes, Von Mises stress and the estimated local error. They can be active and/or off simultaneously, the result of the analysis being presented on the screen, [3].

3.1. Command Masses

In general, instruments masses Masses are based on distribution theory, used to model the characteristics of purely inertial system, representing scalar fields table, a certain intensity, applied the model to be analyzed in a single point on an edge or a surface it. (Fig. 3).

3.2. Command Restraints

Restrictions should be defined to represent a structural interface between the model and analyzed subassembly or assembly to which it belongs. If the model is not properly constrained, will result in many numerical problems (singularity) and finite element analysis could not be done. Clamp restriction model requires a one-piece module created a solid modeling program. (Fig. 4).

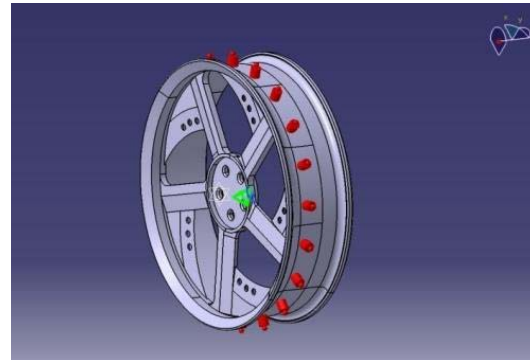


Fig. 3 Masses Order

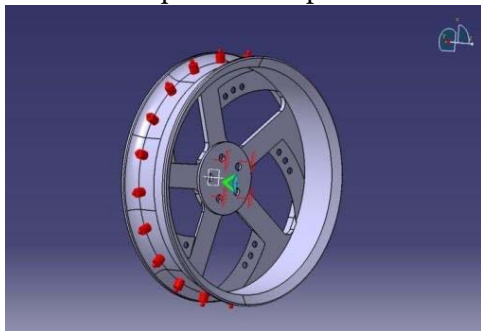


Fig.4.Order restraints

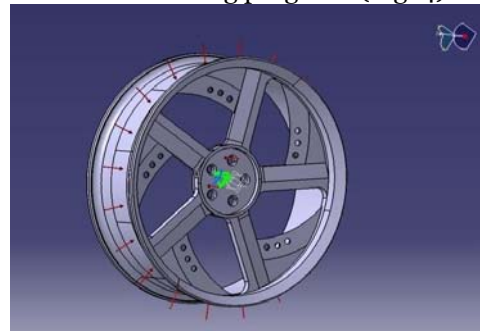


Fig.5 Pressure Control

3.3. Command Loads

Loads various instruments added load models will be analyzed by finite element method, essential step analysis process. These virtual loads simulating actual loads to which the model will be subjected during operation.

Pressure - this charge, expressed in N / m creates a uniform pressure applied on the given area so that the forces exerted directions are always perpendicular (Fig. 5).

Distributed Force - distributed forces are in fact equivalent static system with a resultant force of a real force, applied at a certain point of a model or virtual components (Fig. 6).

Acceleration - is concentrated loads type acceleration field (N/kg or m/s) with uniform intensity, applied in virtual models or parts examined (Fig. 7).

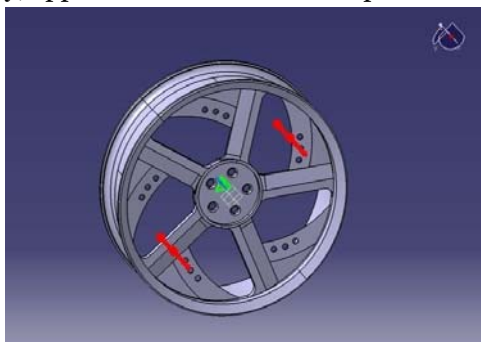


Fig.6 Distributed control force

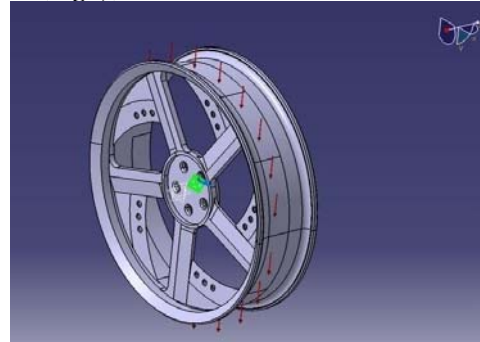


Fig.7 Aceleration command

4. CONCLUSIONS

Compute a tool meets the most important roles in the finite element analysis of a model: triggers this process, but only for the completely bound and showing loads. Thus, throughout the process, the user defines a set of parameters (material characteristics, limitations, strengths, etc.), Following the steps described above. Then, during calculation, the program transforms the conditions applied to interpret the model parameters, allowing users access to visual and numerical data.

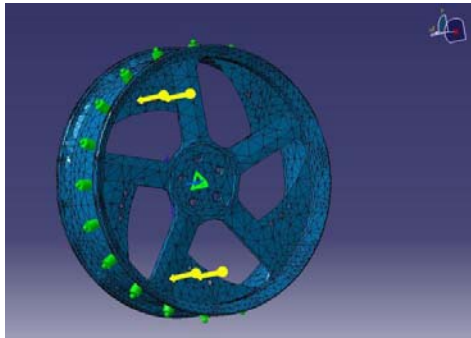


Fig.8. Deformation diagram Fig.8

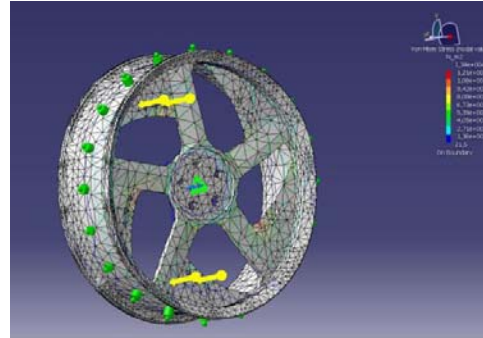


Fig.9 Von Mises Stress Diagram

Deformation - images provided by this tool are used to visualize the model analyzed in the distorted representation as a result of all the conditions imposed (material restriction loads) (Fig. 8). Von Misses Stress - images produced from the use of this tool shows Von Misses field model, representing in fact, a scalar field values derived from the volume density: strain energy and used to measure the tension created in the model (Fig. 9).

Displacement - tool is used to view the field trips (in mm) of network nodes as a result of the imposition of load restrictions and conditions on a model (Fig. 10).

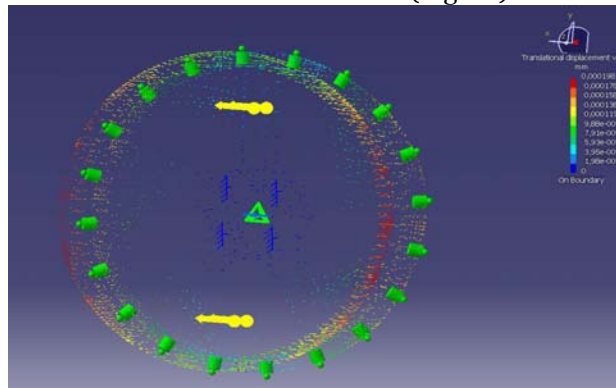


Fig.10 Diagram displacement



■ Zona 1 ■ Zona 2 ■ Zona 3 ■ Zona 4 ■ Zona 5 ■ Zona 6

Fig. 11 Air dispersion diagram

Following analysis, the program discretized surface nodes and 14 253 4807 rim type TE4 elements that were used to play Deformed Mesh diagram. Consider having a rim made of aluminum 2710kg/m³ density and temperature variation of 2.36 K.

Getting the number of nodes and elements to apply a single restriction supportive axis forces Fx-182 N, N-0 Fy and Fz-413N, 2591 ± 001kg loads on a total of 14,421 lines that compose the song, they an X-axis inertial de6 mm, 9 mm Z axis and Y axis 7mm.

Applying finite element program calculates a rigidity of 2.82 N on the curve track construction, restrictions imposed on a single area, the constraints are on one surface which is divided into a number of 258 points.

Applying energy of 1925 J-006's with the song being in balance, the program plays the Von Misses stress diagram (loading values in network nodes) after the following table:

Table 1. Finite element analysis result

Components	Force applied	Restrictions	Arrears	Size relative error
Fx (N)	5.1822e+001	-5.1822e+001	3.3040e-012	2.6954e-013
Fy (N)	2.0000e+000	-2.0000e+000	1.6995e-012	1.3864e-013
Fz (N)	-1.4131e-003	1.4131e-003	-1.0375e-011	8.4638e-013
Mx (N/m)	-1.6294e-001	1.6294e-001	-2.1683e-012	4.3130e-013
My (N/m)	3.7634e+000	-3.7634e+000	3.4395e-012	6.8415e-013
Mz (N/m)	-4.7306e-004	4.7306e-004	-4.0315e-013	8.0192e-014

Following tests carried out we sought the advice of corporations specializing in design and manufacturing of car wheels, which are PIAA Corporation (USA) and Enke Corporation (Japan), who helped design the tests based on which we performed. Their responses were:

PIAA Corporation - is a unique design with small defects in the layout STAS. Our tests show that a light produced by the initial appearance and size model for 17", 20", 21" inch would require producers of aluminum alloy. A problem would be hiding cover stud be bent in the wind very well so will lose the whole concept. Otherwise we want to congratulate you for design and design and wish you success in the future.

Enke Corporation - We are glad that you asked us to think and hope we can help. First we conducted a test I noticed that you made and I have attached chart to see the success of the rim. To explain the diagram as soon as possible: one is where the air has a very good aerodynamic curve, which means that the aerodynamic design point of view is correct, Area 2 is where the air is blocked so there will lose speed but that area is too small can be ignored. Instead hide stud should be done with great precision our advice a little curve max. 2-3 mm from the plane to remove the green rim.

This approach is useful for any product development needs of Class A-surfacing. CATIA V5 users can implement and practice the same technique, without adding any costly hardware. As a personal opinion I add, as a matter of fact, over time, the need to design a new model of the rim in a short period of time can be achieved only with computers, specialized software specifically with these dedicated engineers today.

REFERENCES:

- [1.] UNTARU, M., Dynamics of motor vehicles on wheels, Didactics and Pedagogic Publishing House, Bucharest, 1981.
- [2.] STOICESCU, AP, Design and drive performance cars, consumer, Technical Publishing House, Bucharest, 2007.
- [3.] GHIONEA, I.G., Assisted design in Catia V5. Theoretical and applications, Ed Bren, Bucharest, 2007.
- [4.] OPREAN, M., Modern car. Requirements, Constraints, Solutions, Romanian Academy Publishing House, Bucharest, 2003.
- [5.] DASCAL, A. Body and supporting structures for road vehicles, Publishing House Cermei, 2008.



¹Paolo BOSCARIOL

EXPERIMENTAL VALIDATION OF A SPECIAL STATE OBSERVER FOR A CLASS OF FLEXIBLE LINK MECHANISMS

¹ UNIVERSITY OF UDINE – DIEGM,
Udine, ITALY

ABSTRACT:

This paper presents an experimental validation of a state observer for flexible-link manipulators (FLM). The design of this observer is based on an accurate dynamic model of the mechanisms, able to take into account the coupled rigid-flexible dynamics of the system.

Experimental results on a single-link manipulator affected by gravity force show that the proposed observer achieves a good estimation of the plant dynamics even if the displacement signal is not measured. The evaluation of the performance is done experimentally by comparing the estimated elastic displacement with the measures obtained on the field.

KEYWORDS:

flexible-link manipulators (FLM), mechanisms, dynamic model

1. INTRODUCTION

Dynamics and control of flexible-link mechanisms are topics of a widespread interest in the scientific literature. From the 70's, a large number of papers have been published: Dwivedy [1] cites 433 works from 1975 to 2005 on the modeling of this class of mechanism and Benosman [2] cites 119 papers up to 2003. This popularity is motivated by several advantages of flexible-link manipulators over their rigid counterpart, such as lower weight, higher operative speed and reduced power consumption. Nevertheless, specific solutions in terms of control must be used to reach satisfactory performance, high accuracy and stability.

Model-based control strategy for flexible manipulators, such as [3,4,5] by the same Author or [6] and [7], just to mention some recent works, requires the use of state observers to estimate the evolution of the dynamics of the plant. The estimation of the dynamics of such plant is essential, since complexity of the motion would otherwise require the use of a very large number of sensors. In this case the proposed state-space observer requires the measure of only the angular position of the mechanism and the instant value of the torque applied to the mechanism, so it does not require the use of other sensor such as strain gauge bridges or accelerometers. For example in [8] a strain gauge bridge is adopted to measure the elastic deformation of a four links FLM.

The test bench is a single-link flexible mechanism affected by gravity force. The performance of the proposed Kalman state observer is evaluated experimentally. The estimation of the state of the plant is based only on the measure of the angular position of the hub and on the torque signal, thus reducing the effects of measures such as strain gauge signal which are usually affected by noise. The accuracy of such system is evaluated experimentally by comparing the estimated state with the measure of the elastic displacements performed by a strain gauge transducer.

2. THE STUDY

In this section the dynamic model of a flexible-link mechanism suggested by Giovagnoni [9] will be briefly explained. The choice of this formulation among the several proposed in the last 30 years has been motivated by the high grade of accuracy provided by this model, which has been proved several times, for example in [10,11].

The main characteristics of this model can be summarized in four points:

1. finite element (FEM) formulation
2. Equivalent Rigid-Link System (ERLS) formulation [12]
3. mutual dependence of the rigid and flexible motion
4. capability of describing mechanisms with an arbitrary number of flexible and rigid links

First, each flexible link of the mechanism is subdivided into several finite elements. Referring to the Figure 1 the following vectors, calculated in the global reference frame $\{X, Y, Z\}$, can be defined:

- \mathbf{r}_i and \mathbf{u}_i are the vectors of nodal position and nodal displacement in the i -th element of the ERLS
- \mathbf{p}_i is the position of a generic point inside the i -th element
- \mathbf{q} is the vector of generalized coordinates of the ERLS

The vectors defined so far are calculated in the global reference frame $\{X, Y, Z\}$. Applying the principle of virtual work:

$$\delta W^{elastic} + \delta W^{external} + \delta W^{inertia} = 0$$

the following relation can be stated:

$$\sum_i \int_{V_i} \delta \mathbf{p}_i^T \mathbf{p}_i \rho_i dw + \sum_i \int_{V_i} \delta \check{\mathbf{n}}_i^T \mathbf{D}_i \check{\mathbf{n}}_i dw = \sum_i \int_{V_i} \delta \mathbf{p}_i^T \mathbf{g} \rho dw + (\delta \mathbf{u}^T + \delta \mathbf{r}^T) \mathbf{F} \quad (1)$$

ε_i , \mathbf{D}_i , ρ_i and $\delta \varepsilon_i$ are the strain vector, the stress-strain matrix, the mass density of the i -th link and the virtual strains, respectively. \mathbf{F} is the vector of the external forces, including the gravity, whose acceleration vector is \mathbf{g} . Eq. 1 shows the virtual works of inertial, elastic and external forces, respectively.

From this equation, $\delta \mathbf{p}_i$ and $\check{\mathbf{p}}_i$ for a generic point in the i -th element are:

$$\begin{aligned} \delta \mathbf{p}_i &= \mathbf{R}_i \mathbf{N}_i \mathbf{T}_i \delta \mathbf{r}_i \\ \check{\mathbf{p}}_i &= \mathbf{R}_i \mathbf{N}_i \mathbf{T}_i + 2(\dot{\mathbf{R}}_i \mathbf{N}_i \mathbf{T}_i + \mathbf{R}_i \mathbf{N}_i \dot{\mathbf{T}}_i) \dot{\mathbf{u}}_i \end{aligned} \quad (2)$$

where \mathbf{T}_i is a matrix that describes the transformation from global-to local reference frame of the i -th element, \mathbf{R}_i is the local-to-global rotation matrix and \mathbf{N}_i is the shape function matrix. Taking $\mathbf{B}_i(x_i, y_i, z_i)$ as the strain-displacement matrix, the following relation holds:

$$\begin{aligned} \check{\mathbf{n}}_i &= \mathbf{B}_i \mathbf{T}_i \delta \mathbf{u}_i \\ \delta \check{\mathbf{n}}_i &= \mathbf{B}_i \delta \mathbf{T}_i \mathbf{u}_i + \mathbf{B}_i \mathbf{T}_i \delta \mathbf{u}_i \end{aligned} \quad (3)$$

Since nodal elastic virtual displacements ($\delta \mathbf{u}$) and nodal virtual displacements of the ERLS ($\delta \mathbf{r}$) are independent from each other, from the relations reported above the resulting equation describing the motion of the system is:

$$\begin{bmatrix} \mathbf{M} & \mathbf{MS} \\ \mathbf{S}^T \mathbf{M} & \mathbf{S}^T \mathbf{MS} \end{bmatrix} \begin{bmatrix} \ddot{\mathbf{u}} \\ \ddot{\mathbf{q}} \end{bmatrix} = \begin{bmatrix} \mathbf{f} \\ \mathbf{S}^T \mathbf{f} \end{bmatrix} \quad (4)$$

\mathbf{M} is the mass matrix of the whole system and \mathbf{S} is the sensitivity matrix for all the nodes. Vector $\mathbf{f} = \mathbf{f}(\mathbf{u}, \dot{\mathbf{u}}, \mathbf{q}, \dot{\mathbf{q}})$ accounts for all the forces affecting the system, including the gravity force. Adding a Rayleigh damping, the right-hand side of Eq. 4 becomes:

$$\begin{bmatrix} \mathbf{f} \\ \mathbf{S}^T \mathbf{f} \end{bmatrix} = \begin{bmatrix} -2\mathbf{M}_G - \alpha \mathbf{M} - \beta \mathbf{K} & -\mathbf{M} \dot{\mathbf{S}} & -\mathbf{K} \\ \mathbf{S}^T (-2\mathbf{M}_G - \alpha \mathbf{M}) & -\mathbf{S}^T \mathbf{M} \dot{\mathbf{S}} & 0 \end{bmatrix} \begin{bmatrix} \dot{\mathbf{u}} \\ \dot{\mathbf{q}} \\ \mathbf{u} \end{bmatrix} + \begin{bmatrix} \mathbf{M} & \mathbf{I} \\ \mathbf{S}^T \mathbf{M} & \mathbf{S}^T \end{bmatrix} \begin{bmatrix} \mathbf{g} \\ \mathbf{F} \end{bmatrix} \quad (5)$$

Matrix \mathbf{M}_G accounts for the Coriolis contribution, while \mathbf{K} is the stiffness matrix of the whole system. α and β are the two Rayleigh damping coefficients. System in (4) and (5) can be made solvable by forcing to zero as many elastic displacement as the generalized coordinates, in

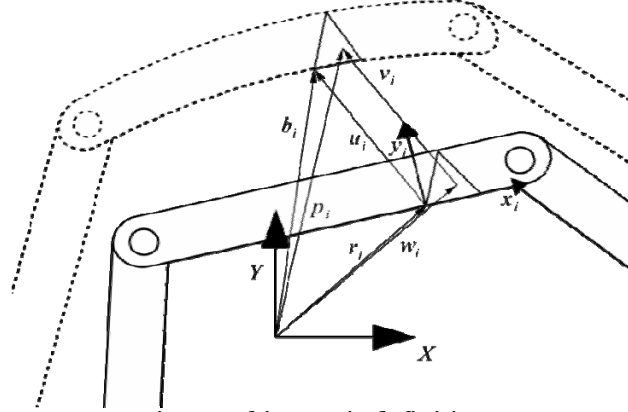


Figure 1: kinematic definitions

this way ERLS position is defined univocally. Therefore removing the displacement forced to zero from (4) and (5) gives:

$$\begin{bmatrix} \mathbf{M}_{in} & (\mathbf{MS})_{in} \\ (\mathbf{S}^T \mathbf{M})_{in} & \mathbf{S}^T \mathbf{MS} \end{bmatrix} \begin{bmatrix} \ddot{\mathbf{u}}_{in} \\ \ddot{\mathbf{q}} \end{bmatrix} = \begin{bmatrix} \mathbf{f}_{in} \\ \mathbf{S}^T \mathbf{f} \end{bmatrix} \quad (6)$$

The values of the accelerations can be computed at each step by solving the system in (6), while the values of velocities and displacements can be obtained by an appropriate integration scheme (e.g. the Runge-Kutta algorithm).

It is important to focus the attention on the size and the rank of the matrices involved in (6), and also to the choice of the general coordinates used in the ERLS definition. Otherwise it might happen that a singular configuration is encountered during the motion of the mechanism [9]. In this case, (6) cannot be solved.

3. ANALISES, DISCUSIONS, APPROACHES and INTERPRETATIONS

In the first part of this section the experimental setup and the test bench single-link flexible manipulator are briefly described. Then the equations and the design of the proposed state observer are introduced. In the last part of the section the experimental results of the observer used with a PID position control are shown and discussed.

3.1. EXPERIMENTAL SETUP

The plant used to evaluate the effectiveness of the proposed predictive control strategy is a single-link flexible mechanism. It is made by a long and thin steel rod, actuated by a brushless motor. No reduction gears are used, so one end of the link is rigidly coupled to the motor shaft. The flexible link can rotate on the vertical plane, so the mechanism dynamics is heavily affected by the gravity force. The structural and dynamic characteristics of the flexible rod can be found in Table 1. Owing to the overall dimensions, the mechanism has a limited movement range (around ± 25 [deg]) from the vertical position. The motion of the link is governed through an Indramat DKC-MKD brushless servo drive system. This drive is used as a torque generator, i.e. the instant value of the torque applied by the motor can be controlled by using an analog signal. Such a signal is supplied by a National Instruments PCI-6259 DAQ board, controlled by a Core 2 Quad PC.

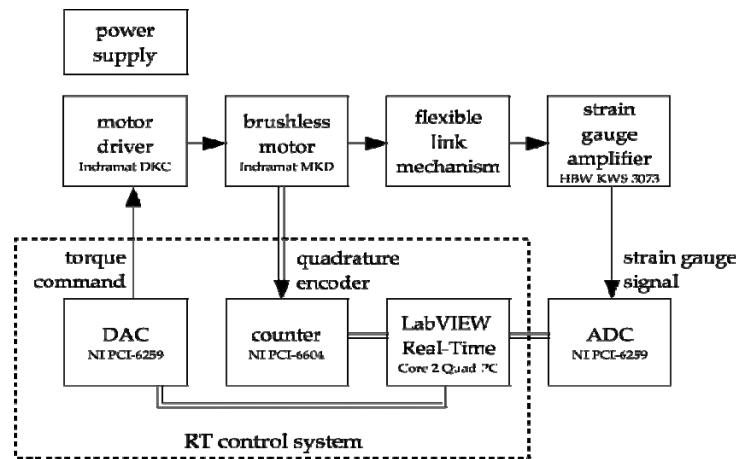


Figure 2: The experimental setup

Table 1: structural and dynamic characteristics of the flexible rod

	Symbol	Value
Young's modulus	E	230×10^9 [Pa]
Flexural stiffness	EJ	191.67 [Nm ⁴]
Beam width	a	1×10^{-2} [m]
Beam thickness	b	1×10^{-2} [m]
Mass/unit length	m	0.7880 [kg/m]
Flexible Link length	l	1.5 [m]
Strain sensor position	s	0.75 [m]
First Rayleigh damping constant	α	4.5×10^{-1} [s ⁻¹]
Second Rayleigh damping constant	β	4.2×10^{-5} [s ⁻¹]

The angular position is measured by a 4000 cpr quadrature encoder is read with a National Instruments PCI-6602 board. The strain gauge signal is measured with the same PCI-6259 board used to generate the torque reference signal, as it is visible in Figure 3. The data acquisition and the control software runs over the LabVIEW Real-Time OS.



Figure 3: The flexible-link mechanism used for experimental tests

The dynamic model can be described with a good accuracy it with four finite elements. This discretization is sufficient to describe accurately the first four modes of vibration: 23 Hz, 63 Hz, 124 Hz, 206 Hz. Higher order modes can be neglected as they have low energy and high damping values.

3.2. DESIGN OF THE STATE OBSERVER

Most model-based control strategies can be applied only when a measure of the whole state \mathbf{x} is available. In this application, there are only two measured values, so a state observer must be used. Here a Kalman asymptotic estimator has been chosen. An estimation of $\mathbf{x}(k)$ and $\mathbf{x}_m(k)$ (where $\mathbf{x}(k)$ is the state of the plant model and $\mathbf{x}_m(k)$ is the state of the measurement noise model) can be computed from the measured output $\mathbf{y}_m(k)$ as:

$$\begin{bmatrix} \hat{\mathbf{x}}(k|k) \\ \hat{\mathbf{x}}_m(k|k) \end{bmatrix} = \begin{bmatrix} \hat{\mathbf{x}}(k|k-1) \\ \hat{\mathbf{x}}_m(k|k-1) \end{bmatrix} + \mathbf{L}(\mathbf{y}_m(k) - \hat{\mathbf{y}}_m(k)) \quad (7)$$

$$\begin{bmatrix} \hat{\mathbf{x}}(k+1|k) \\ \hat{\mathbf{x}}_m(k+1|k) \end{bmatrix} = \begin{bmatrix} \mathbf{A}\hat{\mathbf{x}}(k|k) + \mathbf{B}\mathbf{z}(k) \\ \mathbf{A}_m\hat{\mathbf{x}}_m(k|k) \end{bmatrix}$$

$$\hat{\mathbf{y}}_m(k) = \mathbf{C}_m\hat{\mathbf{x}}(k|k-1)$$

The gain matrix \mathbf{L} has been designed by using Kalman filtering techniques (see Franklin et al. [13])

The design of both the estimator and the prediction model is based on a linear state-space model of the FLM which has been obtained by applying the linearization procedure developed by Gasparetto in [14] to Eq. (6). The resulting state-space model can be rewritten as:

$$\begin{cases} \dot{\mathbf{x}}(t) = \mathbf{A}\mathbf{x}(t) + \mathbf{B}\mathbf{z}(t) \\ \mathbf{y}(t) = \mathbf{C}\mathbf{x}(t) \end{cases} \quad (8)$$

where $\mathbf{A} \in \mathbb{R}^{[26] \times \mathbb{R}^{[26]}}$, $\mathbf{B} \in \mathbb{R}^{[26] \times \mathbb{R}^{[1]}}$, $\mathbf{C} \in \mathbb{R}^{[2] \times \mathbb{R}^{[26]}}$ are time-invariant matrices. The state vector \mathbf{x} includes all the nodal displacements and the angular position q , as well as their time derivatives:

$$\mathbf{x}(t) = [u_1, u_2, \dots, u_{13}, q, \dot{u}_1, \dot{u}_2, \dots, \dot{u}_{13}, \dot{q}]^T \quad (9)$$

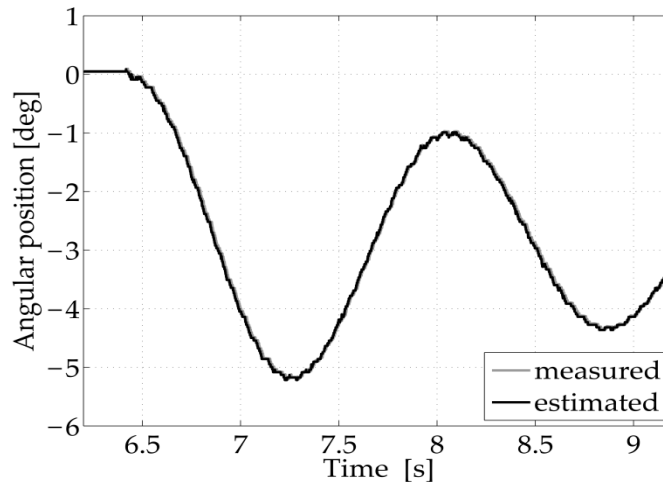


Figure 4: Experimental comparison of measured and estimated angular position

The output vector of the LTI system consists of two elements: $\mathbf{y}(t) = [u_6, q]^T$, being u_6 the rotational displacement at the midspan of the link. The input vector $\mathbf{z}(t)$ includes the torque applied to the link as single element.

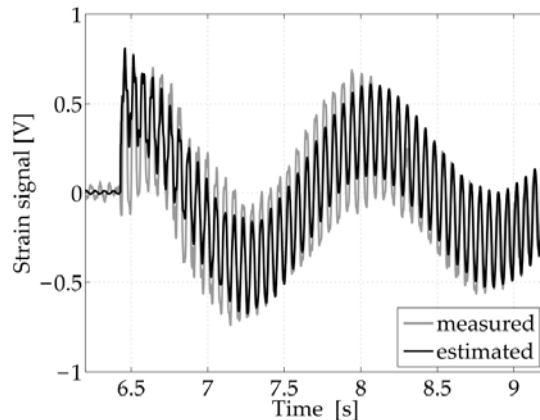


Figure 5: Experimental comparison of measured and estimated elastic displacement

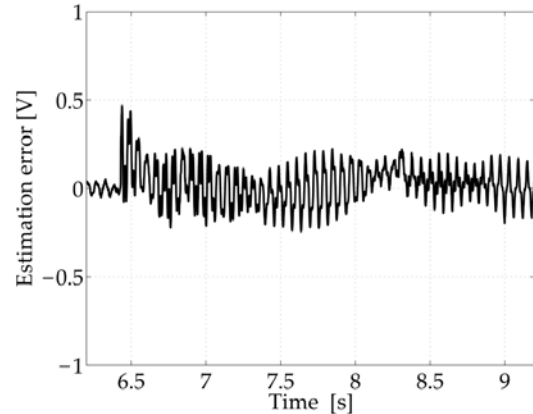


Figure 6: Elastic displacement: estimation error

A comparison of measured and estimated values of the link curvature is reported in Figures 3,4,5. As it can be seen, the value of the elastic displacement can be evaluated with a good accuracy. The angular position of the mechanism is controlled with a PID controller with gravity compensation. The block diagram of the closed-loop control system is provided in Figure 6.

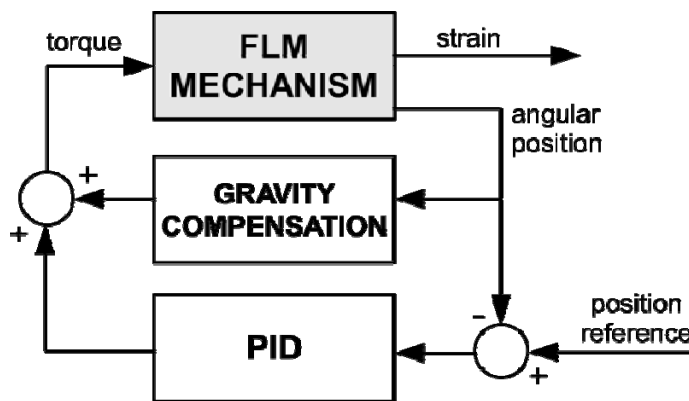


Figure 7: Block diagram of the closed-loop control system

It must be pointed out that the state observer has the availability of only the quadrature encoder signal and the nominal torque applied to the rod. In this way, the robustness of the closed-loop system can be improved, since the measure of the strain gauge signal is heavily affected by noise. Moreover, the reduced number of sensor make this control strategy suitable to most robotic manipulators for industrial use, since sensors such as accelerometers and strain gauge bridges are usually unavailable on these systems.

4. CONCLUSIONS

A state estimator for flexible-link mechanisms has been implemented and tested on a real single link mechanism. It has been proved experimentally that the state estimator used for all the experimental tests is capable of providing an accurate estimation of the plant dynamics with a very limited set of sensors. Such an estimator needs the measure of the angular position only and the torque applied by the brushless motor. For this reason, the proposed controller can be easily adapted to most of the industrial manipulators, which usually do not have sensors for measuring the elastic displacement of the links.

REFERENCES

- [1.] DWIVEDY, S., EBERHARD, P., 2006. Dynamic analysis of flexible manipulators, a literature review. *Mechanism and Machine Theory* 41 (7), 749–777. 17
- [2.] BENOSMAN, M., LE VEY, G., 2004. Control of flexible manipulators: A survey. *Robotica* 22 (05), 533–545.
- [3.] Boscarìol, P., Gasparetto, A., Zanotto, V., 14-17 April 2009. Vibration reduction in a flexible link mechanism through the synthesis of an mpc controller. In: *Proceedings of the 5th IEEE International Conference on Mechatronics (ICM2009)*. Malaga, Spain.

- [4.] Boscariol, P., Gasparetto, A., Zanotto, V., January 2010. Active position and vibration control of a flexible links mechanism using model-based predictive control. *Journal of Dynamic Systems, Measurement, and Control* 132.
- [5.] P. Boscariol, A. Gasparetto, V. Zanotto Model Predictive Control of a Flexible Links Mechanism *Journal of Intelligent and Robotic Systems: Volume 58, Issue 2 (2010), Page 125-147*
- [6.] Hassan, M., Dubay, R., Li, C., Wang, R., 2007. Active vibration control of a flexible one-link manipulator using a multivariable predictive controller. *Mechatronics* 17 (6), 311–323.
- [7.] Chalhoub, N., Kfoury, G., Bazzi, B., 2006. Design of robust controllers and a nonlinear observer for the control of a single-link flexible robotic manipulator. *Journal of Sound and Vibration* 291 (1-2), 437–461.
- [8.] R. Caracciolo, A. Gasparetto, A. Trevisani and V. Zanotto. On the Design of State Observers for Flexible Link Mechanisms. In *Proceedings of the 1st IASME International Conference on Advances in Mechanics and Mechatronics (483-144)*, Udine, Italy, March 2004
- [9.] Giovagnoni, M., 1994. A numerical and experimental analysis of a chain of flexible bodies. *Journal of Dynamic Systems, Measurement, and Control* 116, 73–80.
- [10.] Gasparetto, A., 2004. On the modeling of flexible-link planar mechanisms: experimental validation of an accurate dynamic model. *Journal of dynamic systems, measurement, and control* 126, 365.
- [11.] Caracciolo, R., Richiedei, D., Trevisani, A., Zanotto, V., 2005. Robust mixed norm position and vibration control of flexible link mechanisms. *Mechatronics* 15 (7), 767–791.
- [12.] Chang, L., Hamilton, J., 1991. The kinematics of robotic manipulators with flexible links using an equivalent rigid link system (ERLS) model. *Journal of Dynamic Systems, Measurement, and Control* 113, 48.
- [13.] Franklin, G., Workman, M., Powell, D., 1997. *Digital control of dynamic systems*. Addison-Wesley Longman Publishing Co., Inc. Boston, MA, USA.
- [14.] Gasparetto, A., 2001. Accurate modelling of a flexible-link planar mechanism by means of a linearized model in the state-space form for design of a vibration controller. *Journal of Sound and vibration* 240 (2), 241–262.





¹ Albano LANZUTTI

SMOOTH TRAJECTORY PLANNING ALGORITHMS FOR INDUSTRIAL ROBOTS: AN EXPERIMENTAL EVALUATION

¹ DIPARTIMENTO DI INGEGNERIA ELETTRICA, GESTIONALE E MECCANICA
UNIVERSITA' DI UDINE, UDINE - ITALY

ABSTRACT:

An analysis of the experimental results of a new method for smooth trajectory planning for robot manipulators is presented in this paper.

The technique is based on the minimization of an objective function that is composed of two terms: the first one is proportional to the trajectory execution time, the second one is proportional to the integral of the squared jerk. The need for a smooth trajectory and the need for a fast execution can be adjusted by changing the values of two constants that weigh the two terms. The trajectory execution time is not set *a priori* and the kinematic constraints on the robot motion are taken into account. Cubic splines and fifth-order B-splines are used to compose the overall trajectory.

Two different trajectory planning techniques (the first one minimizes the maximum absolute value of the jerk along the whole trajectory, while the second one ensures only the continuity of the position, velocity and acceleration values) have been implemented with the aim to compare the outcomes of the tests.

The described methods are applied to a 3-d.o.f. Cartesian robot and the experimental tests are carried out by using an accelerometer mounted on the manipulator end-effector.

KEYWORDS:

Trajectory planning, Smoothness, Time-jerk optimization, Experimental validation

1. INTRODUCTION

One of the most important current robotic industrial requirements is the estimation and the reduction of the manipulators vibrational phenomena. Indeed, the demand for increasing productivity through fast and high precision motion is growing, thus the designers are forced to reduce the masses of the robot structures, resulting in a loss of structural rigidity and an increase of flexibility affecting also the dynamic response of the system.

A proper calibration of the manipulator control system and a dedicated action on the trajectory planning phase [**Eroare! Fără sursă de referință.**] can be considered as a solution of the problem.

The trajectory planning is a fundamental issue for robotics applications and automation in general. At high operating speeds, required in many current tasks, the possibility to generate trajectories that satisfy specific targets and requirements is a basic step to ensure optimal results. Robotic movements and trajectories that have smoothness properties are becoming more widely used in modern applications. Indeed, the planning of trajectories with a bounded value of the jerk is an important target, since this allows to reach higher task execution speeds, reduce the excitation of the resonant frequencies of the manipulator structure and improve the tracking accuracy.

The analysis of the scientific literature shows that the trajectory planning problem is based on the optimization of some objective function or of some parameters. Criteria that are based on minimum execution time, minimum energy or actuator effort, minimum jerk or hybrid optimality approaches can be found.

With the aim to increase the productivity in the industrial sector, the first trajectory planning techniques proposed were the minimum-time algorithms. Starting from unconstrained problems [Eroare! Fără sursă de referință.], this type of optimization is recently evolved in minimum time algorithms under kinematic constraints (i.e. maximum values for velocity, acceleration and jerk) [Eroare! Fără sursă de referință.].

A second important criterion for trajectory planning is focused on the minimization of the actuator effort, i.e. the minimization of the energy required to the manipulator actuators [Eroare! Fără sursă de referință.]. If the energy consumption is minimized instead of the execution time, the effort of the actuators and the stresses of the manipulator are reduced, moreover the resulting trajectory is easier to track. This type of optimization is then preferable in applications with limited capacity of energy source.

Another type of trajectory planning algorithms are based on the optimization of the jerk along the whole length of the path [Eroare! Fără sursă de referință.-Eroare! Fără sursă de referință.]. If this technique is used, the excitation of the resonant frequencies of the mechanical system is reduced. Thus, the stresses to the actuators and to the robot structure are intrinsically reduced, and the tracking errors decrease.

As mentioned in the foregoing, starting from the fundamental optimization techniques above described, hybrid optimality approaches are implemented.

For instance, hybrid time-energy-optimal trajectory planning algorithms can be found in [Eroare! Fără sursă de referință.]. With the aim to reach the advantages of the jerk reduction in fast trajectories, hybrid time-jerk optimal techniques are proposed [Eroare! Fără sursă de referință.-Eroare! Fără sursă de referință.]. These algorithms are based on different primitives that are used to interpolate the path (e.g. trigonometric splines in [Eroare! Fără sursă de referință.], polynomials of fourth and fifth order in [Eroare! Fără sursă de referință.]) and different optimization procedures (e.g. genetic algorithms are used in [Eroare! Fără sursă de referință.], SQP algorithm in [Eroare! Fără sursă de referință.-Eroare! Fără sursă de referință.]).

One of the most popular algorithms for planning smooth trajectories is described in [Eroare! Fără sursă de referință.-Eroare! Fără sursă de referință.]. Based on interval analysis, this technique minimizes the absolute maximum value of the jerk along a trajectory whose execution time is known and set *a priori*. Cubic splines are used to interpolate the via-points of the path and the output of the algorithm is a set of time intervals that produces the lowest jerk peak.

A minimum time-jerk trajectory planning technique is presented in [Eroare! Fără sursă de referință.-Eroare! Fără sursă de referință.]. Two algorithms based upon a minimization of an objective function that takes into account the speed and the smooth of the trajectory are presented. More in detail, the objective function is composed of a term that is proportional to the total execution time and of a term that is proportional to the integral of the squared jerk along the path, both weighted by two parameters.

A method based on the objective function defined in [Eroare! Fără sursă de referință.-Eroare! Fără sursă de referință.]. and extended by considering also the power consumption of the actuating motors and the joints physical limits (so that the technique is a time-jerk-energy planning algorithm) is presented in [Eroare! Fără sursă de referință.].

In this paper, the two trajectory planning algorithms presented in [Eroare! Fără sursă de referință.-Eroare! Fără sursă de referință.]. are considered. Unlike most jerk-minimization techniques, this method does not require a trajectory execution time set *a priori*, and takes into account the robot motion constraints. Thus, one can define the upper bounds on the absolute values of velocity, acceleration and jerk for each robot joint. In order to demonstrate the benefits of the used algorithms (i.e. reduced mechanical stresses and reduced vibrational phenomena), the trajectories so planned are input to a 3-d.o.f. Cartesian robot and the vibrations of its arms during their movements are evaluated by using an accelerometer.

With the aim of evaluating the results obtained with the minimum time-jerk technique, both the method described in [Eroare! Fără sursă de referință.-Eroare! Fără sursă de referință.]. and a classical spline based planning algorithm have been implemented and experimentally tested on the Cartesian manipulator.

The paper is organized as follows : in section 2 the planning algorithms [Eroare! Fără sursă de referință.-Eroare! Fără sursă de referință.]. and [Eroare! Fără sursă de referință.-Eroare! Fără sursă de referință.]. and the main characteristics of the planning techniques under test are explained; the simulations and experimental results of the used techniques ,with a brief description of the experimental set-up, are analyzed in section 3.

2. THE TRAJECTORY PLANNING ALGORITHMS

2.1. MINIMUM TIME-JERK TRAJECTORY PLANNING ALGORITHM

The minimum time-jerk algorithm (described with many details in [Eroare! Fără sursă de referință.-Eroare! Fără sursă de referință.]) concerns trajectories *off-line* geometrically defined. Accordingly, a *path planner* at the top level generates the geometric paths (obstacle avoidance problems are solved at this level) as a sequence of nodes in the operative space which represent successive positions and orientations of the end-effector of the manipulator. The execution time of the planned trajectory is not set *a priori* (it is a result of the algorithm), and the upper bounds on velocity, acceleration and jerk (the kinematic constraints) are taken into account.

The generated trajectory is optimized in the sense of the best compromise between execution time and value of the jerk. In order to achieve this task, a hybrid objective function made of two terms having opposite effects is considered. The first term is proportional to the trajectory execution time, whereas the second term is proportional to the integral of the squared jerk. The two effects are weighted by the coefficients k_T and k_J respectively.

In order to represent the trajectories, two specific primitives are chosen.

The first primitive is a cubic spline (the algorithm is so called SPL3J) and the objective function is given by:

$$FOBJ = k_T \sum_{i=1}^{n-1} h_i + k_J \sum_{j=1}^N \sum_{i=1}^{n-1} \left[\frac{(\alpha_{j,i+1} - \alpha_{j,i})^2}{h_i} \right] \quad (1)$$

where $\alpha_{j,i}$ is the acceleration of the j -th joint at the i -th via-point, n is the number of the via-points of the path, N is the number of robot joints and h_i is the time interval between two via-points (for more details [Eroare! Fără sursă de referință.]).

The second primitive is a fifth-order B-spline, degree $p = 5$ and order $k = 2r = 6$, (the algorithm is so called BSPL5J) and the objective function is given by :

$$FOBJ = k_T \sum_{i=1}^{vp+1} h_i + k_J \sum_{j=1}^N \int_0^{t_f} \left(\sum_{k=1}^{n-2} CPJ_{j,k} \cdot N_{p-3,k}(t) \right)^2 dt \quad (2)$$

where vp is the number of via-points, $n+1$ is the number of control points ($n = vp + 2(r-1)$), $N_{i,p}(t)$ is the base function, $CPJ_{j,k}$ is the control point of the jerk and t_f is the total execution time of the trajectory (for more details [Eroare! Fără sursă de referință.]).

The solution of the optimization problem is a vector of time intervals h_i between two subsequent via-points that minimize the objective functions (1) or (2).

With a suitable choosing of the value of the two weights k_T and k_J , in both solver methods above described, a balance between speed and smoothness of the trajectory can be reached. The limit conditions are the minimum execution time (i.e. $k_J = 0$) and the minimum jerk value (i.e. $k_T = 0$). A criterion to make the choice of the two weights is reported in [Eroare! Fără sursă de referință.].

2.2. GLOBAL MINIMUM JERK TRAJECTORY PLANNING ALGORITHM

For a comparative analysis of the experimental results, the global minimum jerk trajectory planning algorithm (so called GMJ) presented in [Eroare! Fără sursă de referință.-Eroare! Fără sursă de referință.] has been implemented. In this technique, the execution time of the trajectory is set *a priori* and the manipulator kinematic constraints are not taken into account. Moreover, cubic splines are used to interpolate the sequence of points of the geometric path that is planned in *off-line* mode.

The algorithm can be summarized as follows.

If \mathbf{h} is the vector of the time intervals between two consecutive via-points, and defined $j_{k,i}(\mathbf{h})$ as the value of jerk of the i -th spline at the k -th joint, the optimization problem of the GMJ algorithm is :

$$\min_{\mathbf{h} \in \mathbb{R}^n} \max \{ |j_{k,i}(\mathbf{h})| : i = 1, \dots, n; k = 1, \dots, m \} \quad (3)$$

subject to:

$$\sum_{i=1}^n h_i = T \quad (4)$$

where n is the number of via-points, m is the number of robot joints and T is the trajectory execution time. The output of the algorithm is a set of time intervals h_i that minimizes the absolute maximum value of the jerk along the whole path.

2.3. COMPARATIVE ANALYSIS OF THE PLANNING TECHNIQUES PROPERTIES

With the aim of evaluating the trajectories obtained by running the three techniques above described (SPL3J, BSPL5J and GMJ), a fourth algorithm has been implemented. It is based on cubic splines (so as to ensure the continuity of position, velocity and acceleration values). The duration of the time intervals between two via-points is proportional to the trajectory execution time, that is set *a priori*, and the number of via-points (accordingly the algorithm is called PROP). The algorithm so implemented does not take into account the kinematic constraints of the manipulator. In Table I the main properties of the four algorithms are reported.

Table I : Main properties of the SPL3J, BSPL5J, GMJ and PROP algorithms

Algorithm	Primitive	Trajectory time	Optimization	Kinematic Constraints
SPL3J	cubic spline	calculated	jerk-time	Yes
BSPL5J	quintic B-spline	calculated	jerk-time	Yes
GMJ	cubic spline	imposed	max jerk	No
PROP	cubic spline	imposed		No

An important remark on the convergence time of the four techniques that have been used must be done: for all the tested trajectories, GMJ algorithm gives the solution after several hours, whereas SPL3J, BSPL5J and PROP algorithms take less than a minute to produce the solutions. This drawback is very important if, for example, the techniques will be used to plan trajectories for industrial applications where short times of solution are necessary.

4. EXPERIMENTAL EVALUATION OF VIBRATIONAL PHENOMENA

4.1. IMPLEMENTED TRAJECTORIES

Three different trajectories have been implemented in Matlab™ and then input to the Cartesian manipulator with the aim to test and validate the benefits of using smooth trajectory planning algorithms.

The target of the experimental tests is to compare the vibrational phenomena on the robot end-effector that are induced by the movements of its arms after applying the four techniques above described on the same geometric path. This means that the trajectories via-points and the execution time associated to each path are the same for each algorithm. In order to reach the second target, the three trajectories are first simulated with the SPL3J and BSPL5J (the values of k_T and k_J are set with the aim to get the same execution time) and the execution time so obtained is then input in the GMJ and PROP algorithms. In this way, with the same test starting conditions for the four techniques, a more strict evaluation of the vibrational phenomena can be conducted. The three trajectories are below described:

Trajectory #1 : the first path implements a pick-and-place movement. The k_T and k_J values are respectively 860 and 0.005 for SPL3J technique, 10 and 1 for BSPL5J and the execution time is 7.4 s. The via-points of the trajectory are reported in Table II and in Table III the simulated mean and maximum jerk values for each algorithm are included.

Table II : Trajectory #1 via-points

Via-points	X position [mm]	Y position [mm]	Z position [mm]
1	0	0	0
2	0	0	-170
3	10	12.9	-190
4	30	38.6	-200
5	175	225	-200
6	320	411.4	-200
7	340	437.1	-190
8	350	450	-170
9	350	450	0

Table III : Maximum and mean jerk values for the four algorithms

	max [mm/s ³]			mean [mm/s ³]		
	x	y	z	x	y	z
SPL3J	183.54	230.43	322.49	90.04	115.68	182.84
BSPL5J	178.90	231.13	376.55	74.90	96.16	178.77
GMJ	169.52	212.19	305.21	88.90	114.18	193.02
PROP	588.30	756.70	1105.20	264.32	340.06	533.65

Trajectory #2: the second example implements a “L-shaped” path. The k_T and k_J values are respectively 845 and 0.005 for SPL3J technique, 139 and 1 for BSPL5J and the execution time is 5 s. In Table IV the trajectory via-points are reported. For each technique, the simulated maximum and mean jerk values are shown in Table V.

Table IV : Trajectory #2 via-points

Via-points	X position [mm]	Y position [mm]	Z position [mm]
1	0	0	0
2	270	0	20
3	290	0	40
4	290	20	60
5	290	290	80

Table V : Maximum and mean jerk values for the four algorithms

	max [mm/s ³]			mean [mm/s ³]		
	x	y	z	x	y	z
SPL3J	531.75	532.01	195.93	278.86	278.22	84.96
BSPL5J	615.39	696.89	189.58	244.31	215.50	64.04
GMJ	511.99	524.35	184.15	273.33	293.09	56.49
PROP	1259.40	1259.20	34.60	474.02	473.92	23.04

Trajectory #3 : the last trajectory is a square with five via-points, whose sequence is reported in Table VI. The k_T and k_J values are respectively 1280 and 0.5 for SPL3J technique, 10 and 1 for BSPL5J and the execution time is 14.5 s.

The simulated maximum and mean jerk values for the four algorithms are reported in Table VII.

Table VI : Trajectory #3 via-points

Via-points	X position [mm]	Y position [mm]	Z position [mm]
1	10	10	0
2	330	10	0
3	330	330	-170
4	10	330	-170
5	10	10	0

As mentioned before, the SPL3J and BSPL5J algorithms optimize the trajectories in the sense of best trade-off between the execution time and the integral of the squared jerk, whereas the GMJ technique minimizes the absolute maximum value of the jerk along the path. Starting from these considerations, the lowest maximum values of the jerk and the lowest mean jerk values are expected if the GMJ and SPL3J/BSPL5J are used respectively.

Table VII : Mean jerk values for the four algorithms

	max [mm/s ³]			mean [mm/s ³]		
	x	y	z	x	y	z
SPL3J	68.96	61.95	32.91	35.39	32.38	17.26
BSPL5J	86.44	69.30	36.82	30.25	27.66	14.70
GMJ	49.42	57.28	30.43	32.35	34.11	18.12
PROP	82.59	82.59	43.88	38.87	38.87	20.65

If Tables III, V and VII are considered, it is possible to find a confirmation to the above anticipations: the GMJ algorithm provides the lowest maximum jerk values if compared with the other three techniques, while SPL3J and BSPL5J feature the lowest mean jerk values. Then, it is possible to verify that the PROP method is the worst in terms of both the mean and the maximum jerk values.

4.2. EXPERIMENTAL SET-UP

The experimental tests, aimed to evaluate the vibrational phenomena during the execution of the three trajectories planned with the four algorithms, are made on a Cartesian manipulator (Figure 1), controlled using a real time external controller.

The 3-d.o.f. manipulator has three prismatic joints, whose kinematic bounds are shown in Table VIII, a workspace of 500x600x500 mm (X, Y and Z) and an accuracy of 0.1 mm.

Table VIII : Kinematic bounds of the Cartesian manipulator

Joint	Kinematic Bounds		
	Velocity [mm/s]	Acceleration [mm/s ²]	Jerk [mm/s ³]
1	225	700	2400
2	225	700	2400
3	225	700	2400

The joints are actuated by means of brushless servo-motors, coupled with the robot arms by using a cogged belt and equipped with resolver position sensors. Each motor is linked to the transmission belt by a reduction gearhead.

An embedded multifunction board, the Sensoray S626, is used in order to realize a link between the manipulator and the external control loop.

The position real time controller is set up on an AMD Athlon(tm) XP 2400 (1.99 GHz with 480 MB of RAM memory) by means of the xPC Target™ toolbox of Matlab™.

In order to evaluate the vibrational phenomena of the robot during the movements of its arms induced by the planned trajectories, an uni-axial accelerometer is mounted on the end-effector. The device has a maximum value of acceleration of $\pm 5g$ and an accuracy of 1036 mV/g .

It is important to emphasize the fact that the evaluation of the vibrational phenomena is only focused on the performance of the four trajectory planning algorithms, since the performances of the real time controller are not considered as fundamentals for the experimental tests. Starting from this assumption, the only inputs that can be changed in a “simulated” industrial task are the trajectories parameters, in good accordance with the conditions found in industrial environments, where generally a user is not allowed to change the parameters of the machine controller.

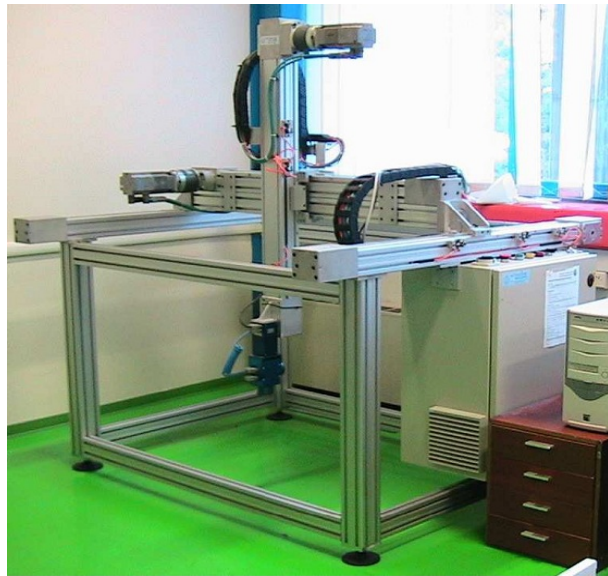


Figure 1 : Cartesian manipulator used for testing the trajectory planning algorithms

4.3. EVALUATION OF THE TRAJECTORIES SMOOTHNESS

The smoothness of the three trajectories planned with the four algorithms is experimental tested by means an accelerometer mounted on the robot end-effector. The direction used to measure the vibration of the manipulator has been chosen by taking into account the mean values of the simulated jerk along the path. By considering this assumption and the Tables III, V and VII, the X cartesian direction has been chosen for trajectories #2 and #3, whereas the Z cartesian direction has been chosen for trajectory #1.

In Table IX the mean values of the measured accelerations are reported. If the PROP values are considered as reference, a mean improvement of 36% is obtained if SPL3J and GMJ techniques are considered, a mean improvement of 31% is obtained if BSPL5J algorithm is used.

Table IX : Measured accelerations mean value

	Accelerations mean value [m/s^2]		
	SPL3J	BSPL5J	GMJ
Trajectory #1	0.12	0.12	0.13
Trajectory #2	0.40	0.43	0.37
Trajectory #3	0.48	0.55	0.47

The comparison between the four trajectory planning algorithms for all the paths implemented, confirms the effectiveness of the SPL3J, BSPL5J and GMJ techniques in reducing the vibrations if compared to the PROP method.

All the experimental tests demonstrate that the real behavior of the Cartesian manipulator is effectively represented by the simulations, since the simulated accelerations obtained by running the algorithms and input to the manipulator have a time course comparable with the accelerations measured by the accelerometer mounted on the end-effector. To confirm this, in Figures 2-5 a comparison between the simulated and the measured accelerations (for Trajectory #1) is reported.

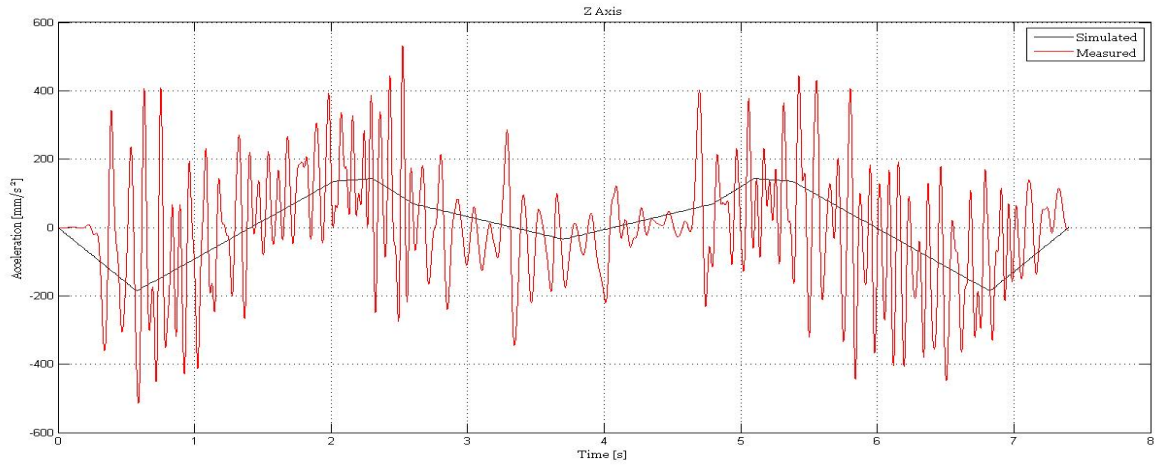


Figure 2 : Simulated vs. measured acceleration (Trajectory #1 - SPL3J)

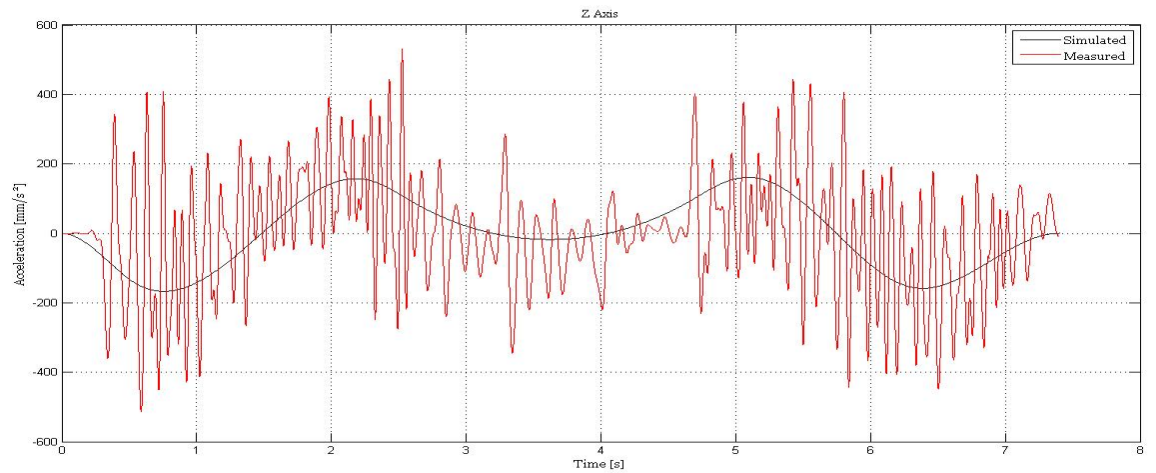


Figure 3 : Simulated vs. measured acceleration (Trajectory #1 - BSPL5J)

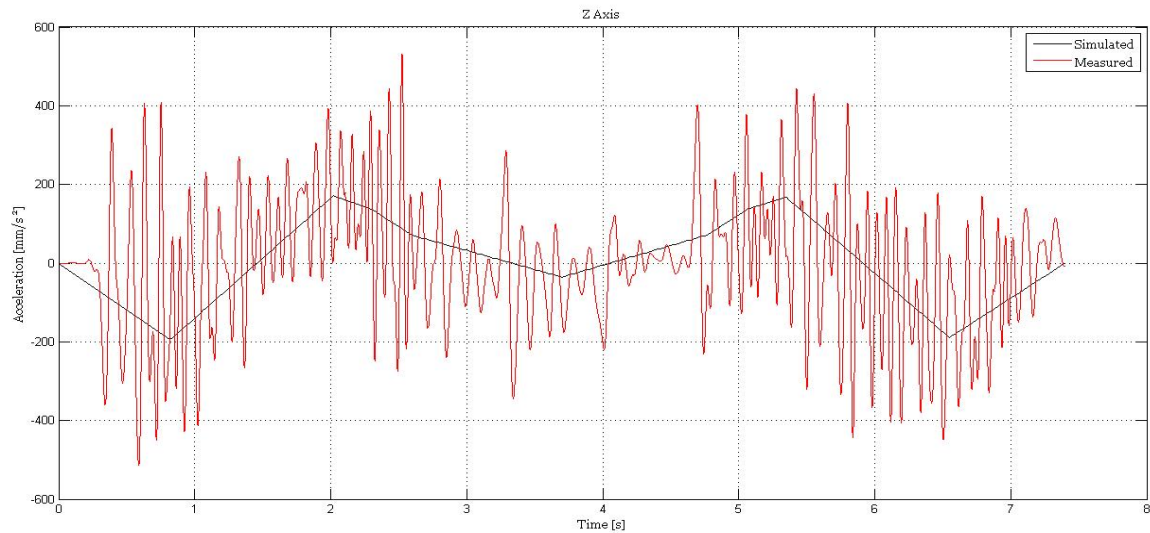


Figure 4 : Simulated vs. measured acceleration (Trajectory #1 - GMJ)

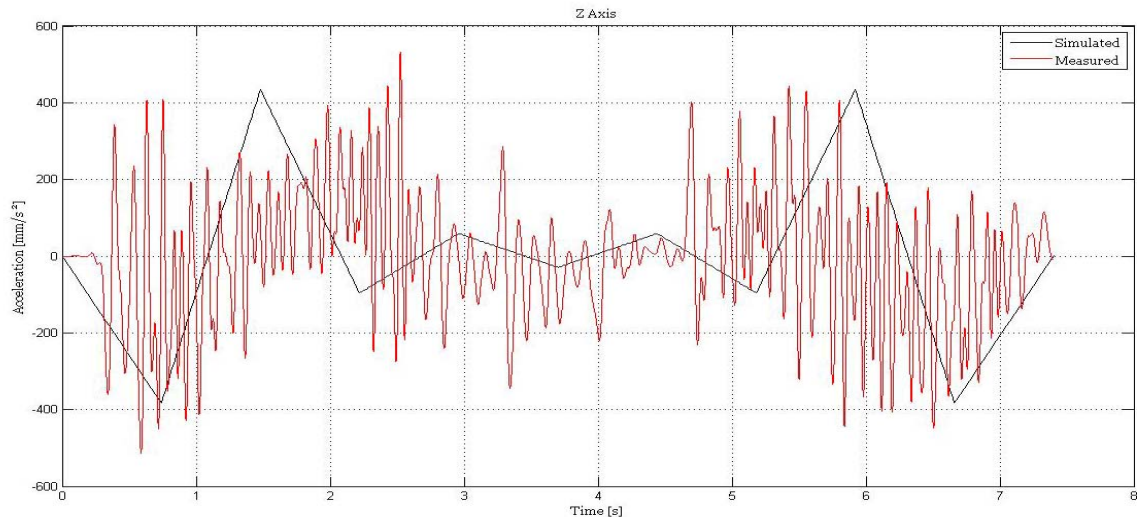


Figure 5 : Simulated vs. measured acceleration (Trajectory #1 - PROP)

5. CONCLUSIONS

In the present paper a minimum time-jerk trajectory planning technique has been experimental evaluated and validated. This method, that takes into account both the integral of the squared jerk along the trajectory and its execution time, is implemented by using two types of primitives : cubic splines (SPL3J) and fifth-order B-splines (BSPL5J). The kinematic constraints are considered in the optimization problem, and the execution time is not set *a priori*.

An accelerometer mounted on the robot end-effector has been used with the aim to measure the accelerations of the manipulator joints, in order to evaluate the vibrational phenomena of the Cartesian robot. Three test-trajectories have been implemented on a Cartesian manipulator and the experimental results have been compared with the results obtained with a global minimum jerk (GMJ) method, one of the most popular for planning smooth trajectories, and with a “classic” spline algorithm. The outcomes of the tests demonstrate the effectiveness of the smooth trajectory planning techniques, since the results prove the reductions of the vibrational phenomena of the robot arms during the trajectory execution.

REFERENCES

- [1.] T. BROGARDH, Present and future robot control development – An industrial perspective, *Annual Reviews in Control*, 31 (1) (2007), 69-79.
- [2.] A. PIAZZI and A. VISIOLI, Global minimum-time trajectory planning of mechanical manipulators using interval analysis, *International Journal of Control*, 71 (4) (1998), 631–652.
- [3.] K. JOONYOUNG, K. SUNG-RAK, K. SOO-JONG, K. DONG-HYEOK, A practical approach for minimum-time trajectory planning for industrial robots, *Industrial Robots : An International Journal*, 37 (1) (2010), 51–61.
- [4.] G. FIELD and Y. STEPANENKO, Iterative dynamic programming: an approach to minimum energy trajectory planning for robotic manipulators, *Proc. of the IEEE International Conference on Robotics and Automation*, 3 (1996), 2755–2760.
- [5.] A. PIAZZI, A. VISIOLI, An interval algorithm for minimum-jerk trajectory planning of robot manipulators, *Proceedings of the 36th Conference on Decision and Control*, (1997), 1924–1927.
- [6.] A. PIAZZI, A. VISIOLI, Global minimum-jerk trajectory planning of robot manipulators, *IEEE Transactions on Industrial Electronics*, 47 (1) (2000), 140–149.
- [7.] H.XU, J.ZHUANG, S.WANG and Z.ZHU, Global Time-Energy Optimal Planning of Robot Trajectories, *Proc. of the International Conference on Mechatronics and Automation*, (2009), 4034–4039.
- [8.] D. SIMON and C. ISIK, A trigonometric trajectory generator for robotic arms, *International Journal of Control*, 57 (3) (1993), 505–517.
- [9.] P. HUANG, Y. XU and B. LIANG, Global minimum-jerk trajectory planning of space manipulator, *International Journal of Control, Automation and Systems*, 4 (4) (2006), 405–413.
- [10.] K. PETRINEC and Z. KOVACIC, Trajectory planning algorithm based on the continuity of jerk, *Proc. of the 15th Mediterranean Conference on Control & Automation*, (2007).
- [11.] A. GASPARETTO and V. ZANOTTO, A new method for smooth trajectory planning of robot manipulators, *Mechanism and Machine Theory*, 42 (4) (2007), 455–471.

- [12.] A. GASPARETTO and V. ZANOTTO, A technique for time-jerk optimal planning of robot trajectories, *Robotics and Computer-Integrated Manufacturing*, 24 (3) (2008), 415–426.
- [13.] F. LOMBAI and G. SZEDERKENYI, Throwing motion generation using nonlinear optimization on a 6-degree-of-freedom robot manipulator, *Proc. of IEEE International Conference on Mechatronics*, (2009).
- [14.] A. GASPARETTO, A. LANZUTTI, R. VIDONI and V. ZANOTTO, Trajectory planning for manufacturing robots: algorithm definition and experimental results, *Proc. of ASME 2010 10th Biennial Conference on Engineering Systems Design and Analysis ESDA2010*, (2010).



¹Aurelia TĂNĂSOIU, ²Stelian OLARU

ON THE LIFETIME OF RAILWAY VEHICLE BEARING STRUCTURES AND COMPONENTS

¹⁻²UNIVERSITY "AUREL VLAICU" ARAD, ROMANIA

ABSTRACT:

The paper presents a study on the lifetime of railway vehicle bearing structure components. A lifetime calculation is presented on the basis of static strain and stress measurements. The calculation is then compared to the experimental results of fatigue tests and the ensuing conclusions are presented.

KEYWORDS:

strain, stress, lifetime, Wohler curves

1. INTRODUCTION

Gondola wagons are used for bulk goods, the carbody being formed by a metallic structure covered with sheet metal. During travel the lateral walls are heavily loaded such that a careful study is necessary for the resistance of the pillars that are part of the structure of the lateral walls.

The carbodies of gondola wagons contain two types of pillars within the structure of the lateral walls:

- ❖ Pillars fixed next to the pivot bearing beam;
- ❖ Pillars fixed next to the intermediary beams.

The strain and stress state was determined experimentally for two constructive options of the affixing of the pillars corresponding to the pivot bearing beam:

- a. Without welding between the lower frame and the lateral pillar;
- b. With welding between the lower frame and the lateral pillar.

The study aims to determine the optimal constructive option in regards to the resistance of the pillar joining with the chassis structure.

The testing was conducted on a number of 3 pillars (no. 1, 2, 3) without welding between the lower frame and the lateral pillar, and on a number of 2 pillars (no. 4, 5) with welding between the lower frame and the lateral pillar [1].

In order to conduct the testing, 5 pillars were manufactured such that they could be fixed to the testing device. The static testing were conducted on all 5 pillars in order to determine the strains and stresses.

2. EXPERIMENTAL STUDY OF THE LIFETIME

Analyzing the experimental results, it was observed that the maximum values of the stresses were measured at the points denoted by TER5 and TER6 (table 1), situated in an area that constitutes a remarkable stress concentrator.

The applied forces were determined experimentally with a force transducer with a measurement range of 0 – 10 tf, precision class 0,1 type C1 – HBM.

Table 1

Pillar no.	TER5 - σ [N/mm ²]			TER6 - σ [N/mm ²]		
	30kN	45kN	60kN	30kN	45kN	60kN
1	227	351	391	183	257	327
2	170	246	320	143	232	343
3	182	242	326	144	186	292
4	142	210	285	159	231	313
5	194	290	372	159	240	323

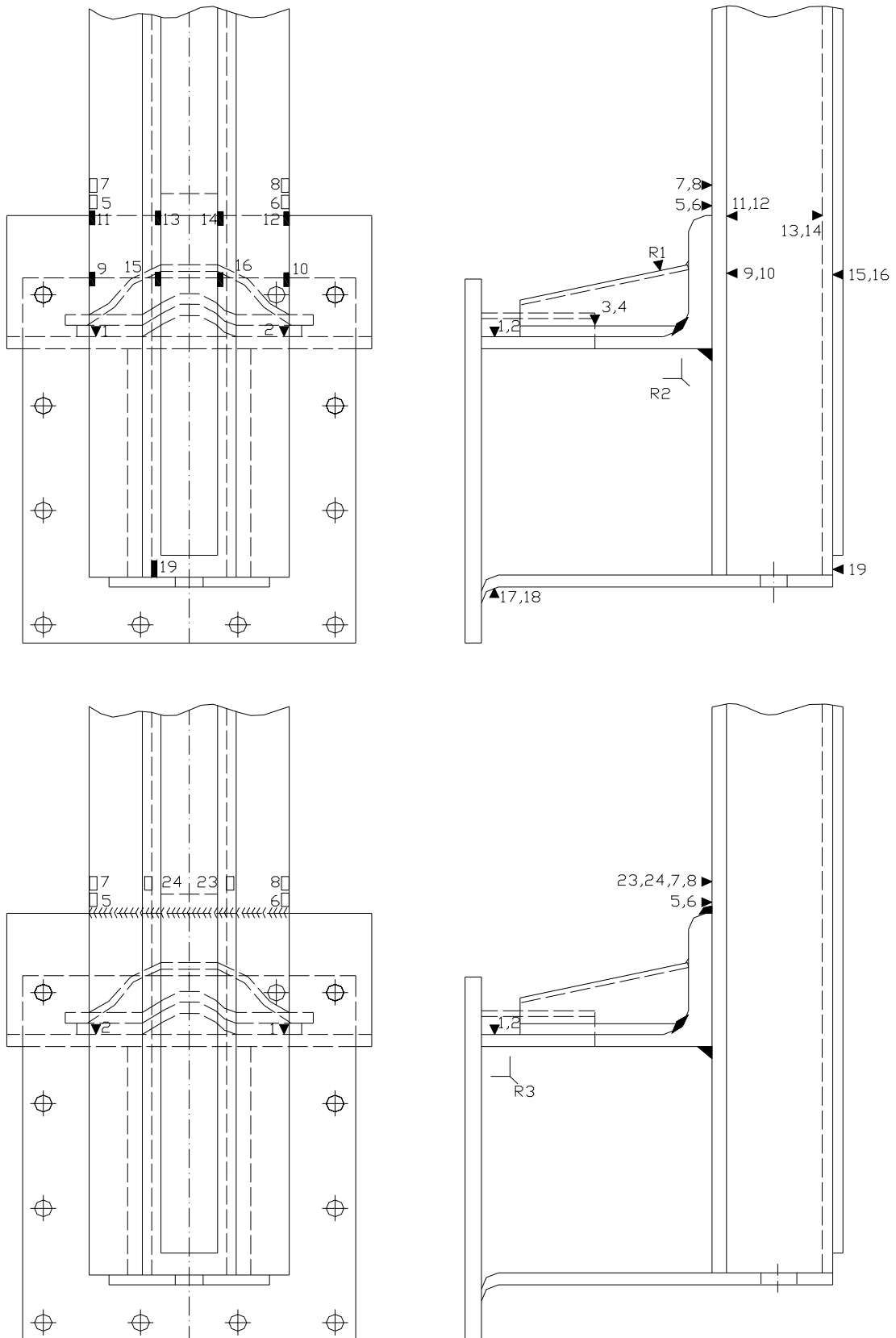


fig. 1a, 1b Placement of the electric resistive transducers

The estimation of the lifetime was done using the Wohler fatigue curves recommended by the UIC (European Railway Association) in report ERRI B12/Rp60 [4]. The curves are shown in figure 2 and table 2.

Table 2.

Concentration class	Log a		Fatigue stress [N/mm ²]
	m=3	m=5	
160	12,901	17,036	117
140	12,751	16,786	104
125	12,601	16,536	93
112	12,451	16,286	83
100	12,301	16,036	74
90	12,151	15,786	66
80	12,000	15,536	59
71	11,951	15,286	52
63	11,701	15,036	46
56	11,551	14,786	41
50	11,401	14,536	37
45	11,251	14,256	33
40	11,101	14,036	29
36	11,001	13,386	26

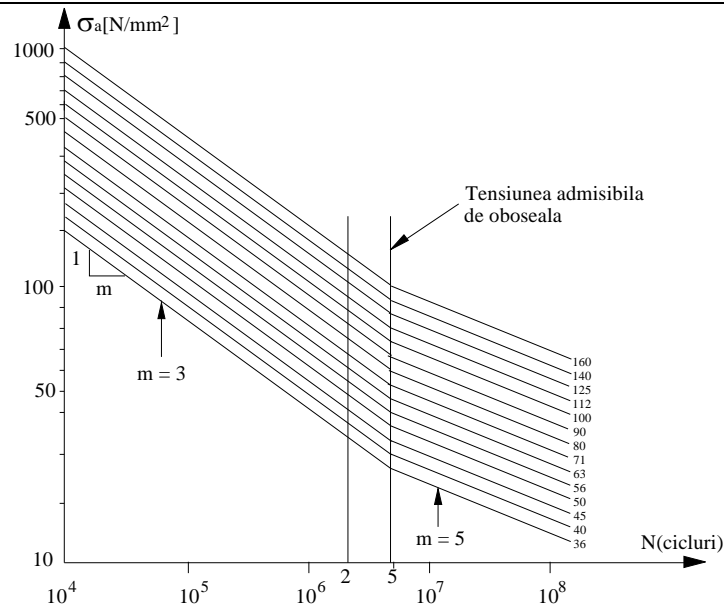


Figure 2.

Consequently, we have conducted the lifetime computation using adequate Wohler curves [2] and the stresses determined experimentally for a load cycle of ± 15 kN, hence resulting the number of predicted cycles until the appearance of the first crack (N_f) in the area of transducers TER5, TER6 as being those in table no. 3.

Table 3.

No.	Pillar no.	N_f
Pillars without welding between the lower frame and the lateral pillar		
1.	1	387.648
2.	2	223.606
3.	3	454.926
Pillars with welding between the lower frame and the lateral pillar		
4.	4	862.622
5.	5	564.952

3. EXPERIMENTAL FATIGUE TESTING

Fatigue testing was conducted on a stand adequate to the desired goal, applying each pillar dynamic forces within a load cycle $F_{med} = 45$ kN, $\Delta F = \pm 15$ kN and a frequency of 5,83 Hz. Throughout the trials, the time evolutions of the strains and stresses were followed closely.

The results of the lifetime estimation of each pillar for a dynamic exceedent $2\Delta\sigma$ corresponding to a load $\Delta F = \pm 15$ kN are shown in table 4.

Table 4.

Pillar no.	Nf estimated [cycles]	Nf exp. [cycles]	Nr exp. [cycles]
1	387.648	445.000	740.000
2	223.606	235.000	390.000
3	454.926	483.000	818.000
4	862.622	960.000	1.101.600
5	564.952	830.00	970.000

The tests determined the number of cycles applied until the appearance of the first crack, „Nf” and the number of cycles applied until complete failure „Nr”.

Figures 4 and 5 show the appearance of the fissure in the area of the stress concentrator, which was observed during the testing using the penetrating liquid method, together with the cracking or breaking manner of the pillar that have undergone fatigue testing.

During the trials it was observed that at points TER5 and TER6 the values of the stresses tend to decrease in value prior to the appearance of a crack due to the accentuated degradation of the material in the cracking section.

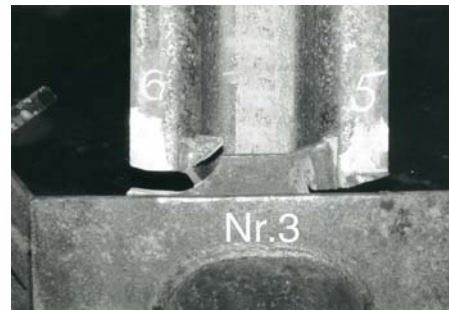


fig. 3



fig.4

4. CONCLUSIONS

Comparing the values for the estimated lifetime to the values of the lifetime up to the appearance of the first crack, a good accordance is observed between the calculated and experimental results. This fact further confirms the correct assessment of the concentration class of the TER5 and TER6 areas, and therefore the correct choice of the used Wohler curves.

From the analysis of the experimental results it is observed that the lifetime for the pillars with welding between the lower frame and the lateral pillar is approximately 100% higher than that of the pillars without welding between the lower frame and the lateral pillar. Consequently, the solution used for pillars nr. 4 and nr. 5 should be used in the fabrication process of the wagons.

It is appreciated that the lifetime observed, estimated and determined experimentally by fatigue testing for the considered loads, is consistent in relation to the resistance of the lateral wall structure under the conditions of wagon use over a time of at least 25 years.

REFERENCES

- [1.] Lășleanu A., Copaci I. ș.a. – „Încercări la oboseală la stâlpii laterali ai vagoanelor gondolă – export URSS” – lucrare cercetare C.C.S.I.T.V.A. Vagoane Arad 1990.
- [2.] Copaci Ion, Tănăsioiu Bogdan – *Durata de viața a elementelor elastice metalice, arcuri elicoidale folosite la suspensia vehiculelor feroviare*, Sesiunea de comunicări științifice cu participare internațională „Cercetare științifică și educație în forțele aeriene”, pag. 238 -245 AFASES – 2008 Brașov 16 – 17 mai.
- [3.] Aurelia Tanasoiu, Ion Copaci, Nicolae Ilias, Iosif Andras – Railway vehicle response to diferent testing scenarios and procedures, Al XVI-lea Seminar International de Stiinte Tehnice, “INTERPARTNER”23-29 sept. 2007, Alushta, Crimea, Ucraina.
- [4.] ERRI B12 RP 60 - „Test to demonstrate the strength of railway vehicles”, Utrecht, 1995





THE STUDY OF INFLOW IMPROVEMENT IN SPARK ENGINES BY USING NEW CONCEPTS OF AIR FILTERS

^{1,2,3} "POLITEHNICA" UNIVERSITY OF TIMISOARA, FACULTY OF ENGINEERING HUNEDOARA, ROMANIA

ABSTRACT:

The article presents an experimental study conducted in the laboratory of Internal Combustion Engines belonging to the Road Motor Vehicles specialization within the Polytechnic University of Timisoara, the Faculty of Engineering of Hunedoara.

The purpose of this experiment consists in testing two concepts of air filters, conceived and made by one of the authors, filters which have been awarded at numerous invention rooms, both inside the country and abroad.

At the basis of the experimental measurements there is a stand that contains a spark engine - and its afferent apparatuses – conceived by the authors, stand which allows the determination of the pressure field on the inflow track into the engine. A series of pressure plugs were made downstream the air filter, and measurements were performed at different operating drives of the engine positioned on the stand.

The experimental results have been processed and compared with the ones obtained during the operation of the classical filter engine, provided by the builder. When the new filters are installed, one can observe a genuine improvement of the pressure drive on the inflow track.

KEYWORDS:

Air filter, spark engine, the inverted super absorbing filter, pressure field

1. INTRODUCTION

The correct filtration of the air flowing inside the cylinders of the internal combustion engine is essential for preserving the good engine's operation in time. The obstruction of various impurities' admission from the atmospheric air significantly lowers the wearing-out of the engine's moving parts. Unfortunately, in addition to its air filtration function, the air filter displays a significant gas-dynamic resistance of the absorbed air. If the air filter is not periodically cleaned and the car runs frequently in a dusty area, both the absorption pressure p_a and the filling coefficient η_v are dramatically decreased.

Currently, on the market there are several constructive air filters versions, which differ according to the filtering principle:

- ❖ filters with filtering cell;
- ❖ inertia filters;
- ❖ combined filters.

These air filters have the following disadvantages:

- ❖ the presence of the filtering element inside the box induces an enhanced gas-dynamic resistance of the absorbed air (generating the phenomenon of insufficient absorption);
- ❖ storage of impurities inside the filter affects the self-cleaning feature of the filtering element;
- ❖ the filtering element can not be visualized and it has to be dismantled for the impurity level to be checked;
- ❖ incapacity of the air filter to significantly increase the speed of the absorbed air;
- ❖ incapacity of the air filter to cool the absorbed air;
- ❖ impossibility of the air filter to create a slight effect of overfeeding during the functioning of the engine.

2. DESCRIPTION OF EXPERIMENTAL STAND

The basis for experimental measurements represents a stand containing a 4-stroke spark engine with 4 vertical cylinders in line, with a camshaft in the engine block, Dacia make, model 810.99, with carburettor and the afferent equipment, which enables the pressure field to set on the engine intake route (figure 1). A series of pressure plugs have been made downstream the air filter, and measurements have been made for different operation regimes of the engine installed on the stand, as well as for different super absorbing filters designed and made by the authors.

The positioning of the pressure plugs on the engine intake route is illustrated in figure 2.

The measurements have been made for the idle engine regime and for different revolutions. The values of the relative pressures in the intake route points where the pressure plugs were mounted have been measured, as seen in figure 2. The TESTO 510 (0-100hPa) digital manometer shown in figure 3 was used.

Moreover, to simulate motor vehicle movement, the measurements were made with an air-blower present, placed in front of the cooling radiator of the engine installed on the stand.



Fig. 1. Bird's-eye view of the experimental stand



Fig. 2. Placement and numbering of the pressure plugs



Fig. 3. TESTO 510 digital manometer



Fig. 4. Stand trial of the original classic filter

Data for the intake system equipped with original classic filter (figure 4), super absorbing filter with internal diffuser (figure 5), and supple super absorbing filter (figure 6) have been prevailed.



a.



b.

Fig. 5. Super absorbing filter with internal diffuser: a – detail, b – mounted on the stand

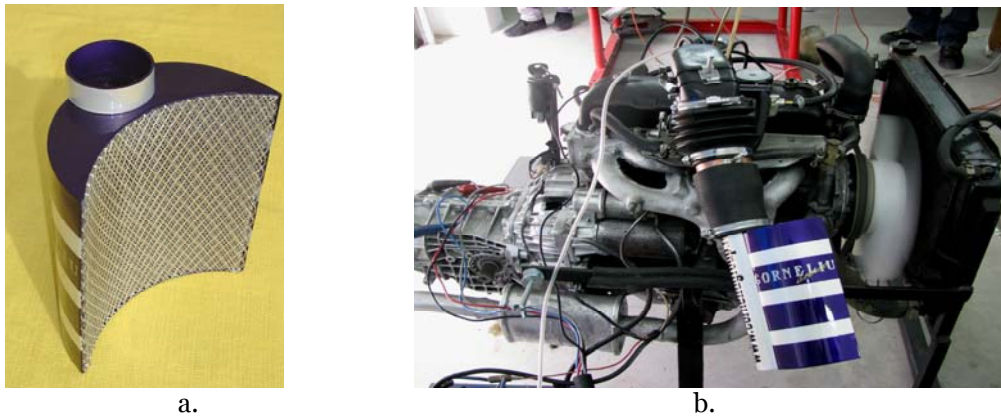


Fig. 6. Supple super absorbing filter: a – detail, b – mounted on the stand

3. RESULTS OF EXPERIMENTAL MEASUREMENTS

The results of the experimental measures for each concept are shown below, monitoring the pressure evolution for each plug, and then for each revolution, as well as the pressure distribution on the intake route up to the gallery entrance.

Due to the presence of pressure waves generated by the alternative movement of the pistons in the engine cylinders, and by the periodic opening and closure of the intake valves, the pressure values fluctuate on quite a wide range. Thus, after stabilizing the engine revolution, the (upper and lower) limit values of the pressures in the mounted plugs were registered and their average was calculated.

Original classic filter

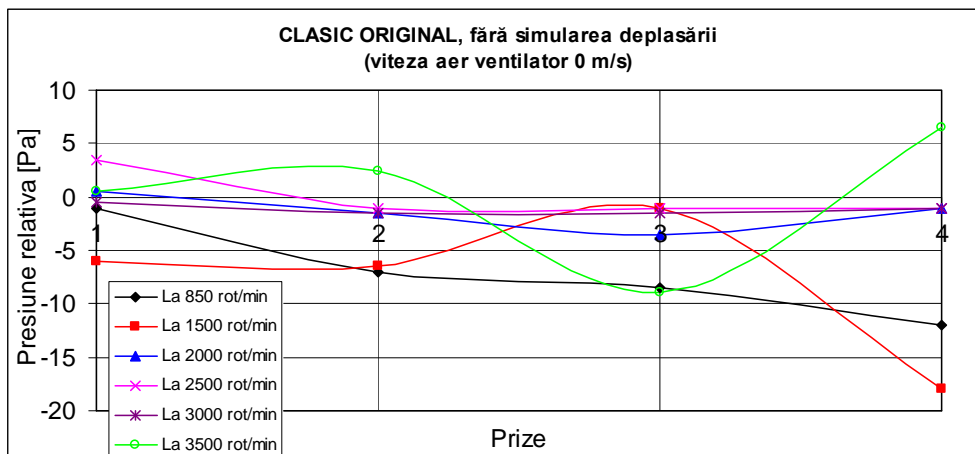


Fig. 7. Relative pressure variation along the intake route for each revolution, without movement simulation (0 m/s for air-blower air speed)

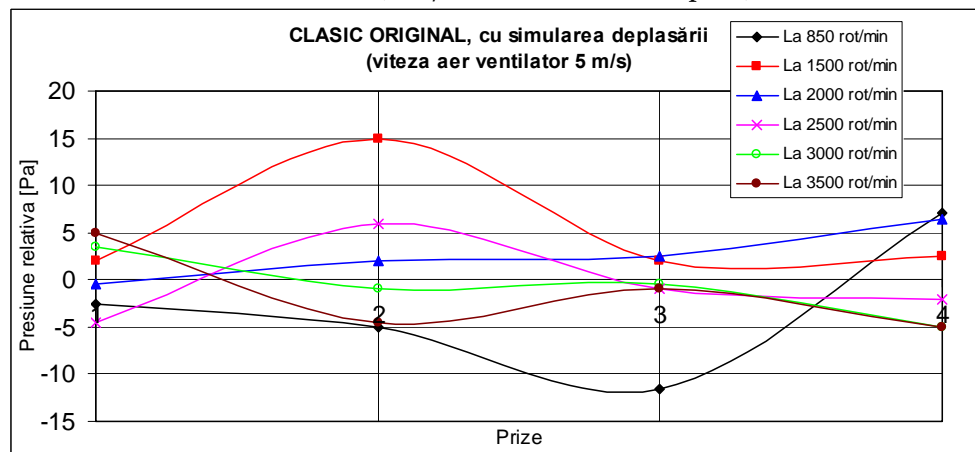


Fig. 8. Relative pressure variation along the intake route for each revolution, with movement simulation (5 m/s for air-blower air speed)

Super absorbing filter with internal diffuser

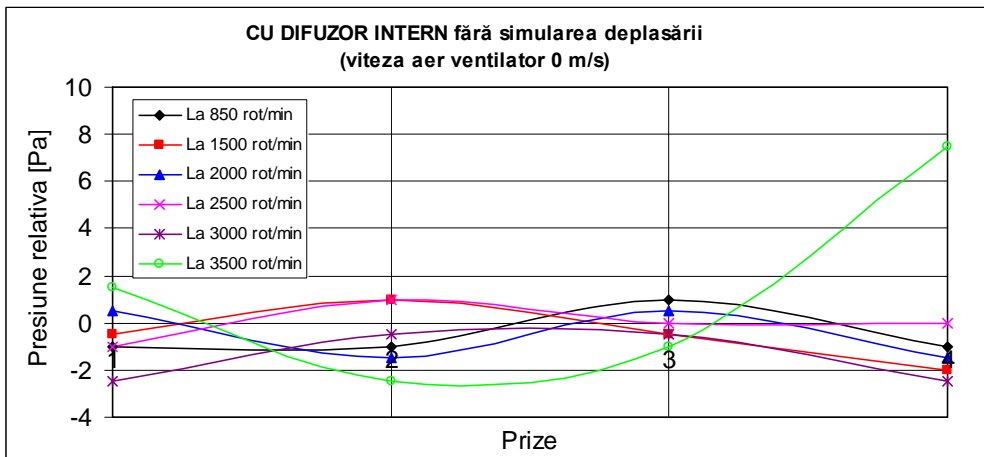


Fig. 9. Relative pressure variation along the intake route for each revolution, without movement simulation (0 m/s for air-blower air speed)

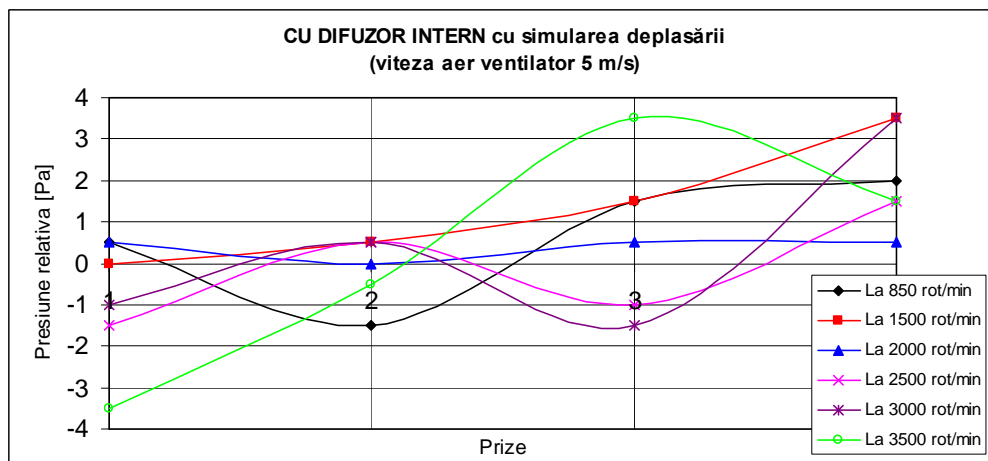


Fig. 10. Relative pressure variation along the intake route for each revolution, with movement simulation (5 m/s for air-blower air speed)

Supple super absorbing filter

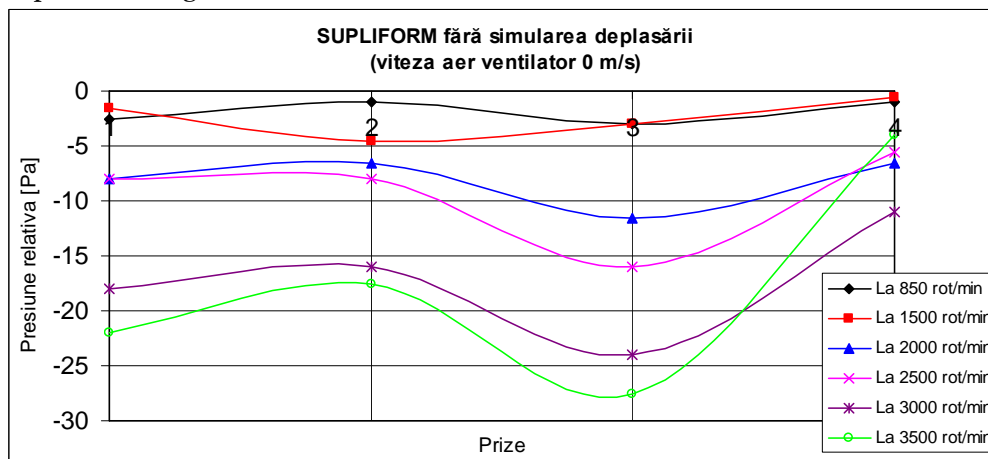


Fig. 11. Relative pressure variation along the intake route for each revolution, without movement simulation (0 m/s for air-blower air speed)

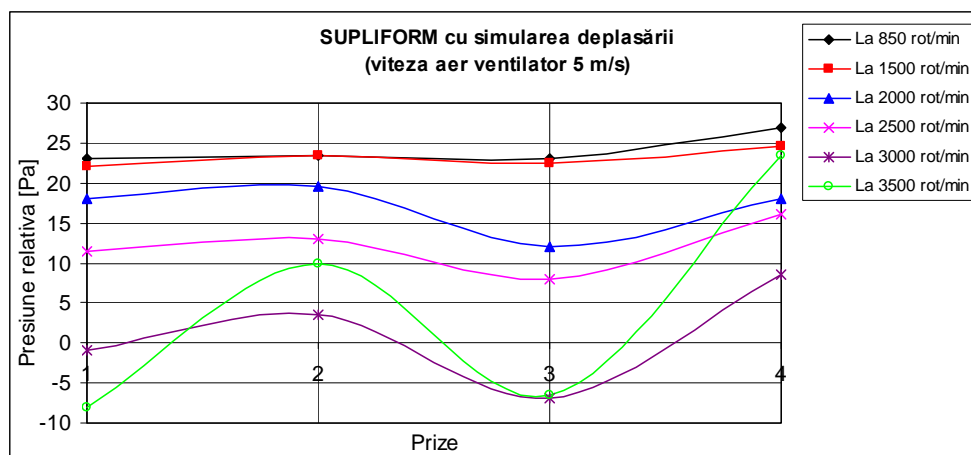


Fig. 12. Relative pressure variation along the intake route for each revolution, with movement simulation (5 m/s for air-blower air speed)

4. CONCLUSIONS

Monitoring the pressure evolution for each plug and for different engine revolutions, we can conclude the following:

- ❖ A slight overpressure effect produced by the super absorbing filter with internal diffuser along the entire revolution range, which is beneficial to the filling process;
- ❖ The overpressure effect is more evident for low revolutions for both filter concepts, and it diminishes as the revolution increases;
- ❖ The super absorbing filter with internal diffuser and the supple super absorbing one maintain the overpressure effect at high revolutions, too;
- ❖ The pressure fluctuation depending on the revolutions is less visible for the super absorbing filters with internal diffuser and broad area;
- ❖ Monitoring the pressure evolution on the intake route for different engine revolutions, one can see that for low revolutions the designed filters have a pressure fluctuation which is a lot weaker than the one induced by the original classic filter. For high revolutions the pressure evolution is somehow similar for all filters.

REFERENCES

- [1.] Birtok-Băneasă, C. – *Studii privind îmbunătățirea admisiei motoarelor cu ardere internă* – Proiect de diplomă 2010, coordonator: Șef lucrări dr.ing. Sorin RAȚIU, UNIVERSITATEA "POLITEHNICA" TIMIȘOARA, Facultatea de Inginerie Hunedoara;
- [2.] Birtok-Băneasă, C. – *Creșterea randamentului volumetric al m.a.i. prin valorificarea undelor de presiune pe traseul de admisie – SDTA* – Simpozion Științific studentesc, 22-23 mai 2009, HD-39-STUD, Hunedoara;
- [3.] Birtok-Băneasă, C. – *Stand experimental pentru măsurarea câmpurilor de presiuni într-un filtru de aer inversat* – Simpozion Științific studentesc, 23-24 mai 2008, HD-38-STUD, Hunedoara;
- [4.] Birtok-Băneasă, C. – *Noi concepte privind proiectarea filtrelor de aer pentru motoarele cu ardere internă*, Simpozion Științific studentesc, 18-19 mai 2007, HD-37-STUD, Hunedoara;
- [5.] McComb, W.D. – *Turbulența fluidelor*, Editura Tehnică, București, 1997 ;
- [6.] Rațiu, S., Mihon, L. – *Motoare cu ardere internă pentru autovehicule rutiere* – Procese și Caracteristici, Editura Mirton, Timișoara, 2008;
- [7.] Rațiu, S. – *Motoare cu ardere internă pentru autovehicule rutiere* - Procese și Caracteristici, Experimente de laborator, Editura Mirton, Timișoara, 2009;
- [8.] Rațiu, S. ș.a. – *New concepts in modeling air filters for internal combustion engines*, The 20th International DAAAM SYMPOSIUM, 25-28th November 2009, Vienna, Austria;
- [9.] www.corneliugroup.ro.





SEALING DESIGN IN MACHINE BUILDING

¹⁻⁴. UNIVERSITY "POLITEHNICA" TIMIȘOARA, FACULTY OF MECHANICS, TIMIȘOARA, ROMANIA

ABSTRACT:

The paper shows how the variation of the functional surfaces may be applied in the problem of design an area of sealing round a lid cover cork or similar object taking into interdependence form-function-technology. The proposed analysis method in the constructive generations of areas of sealing and the succession of analysis stages has the advantage of obtaining optimal types of the product which correspond to the purpose in the conditions of maximum economics.

The analysis criteria from technologic and behavior during using point of view has not been the object of the selection of the purpose types.

KEYWORDS:

machine building, sealing

1. GENERAL PROBLEMS REGARDING SEALS PROBLEMS – INTRODUCTIONS

The sealing are assemblies of machines parts, having the essential role to close as tight as possible a space that contains a pressurized environment as the separation of two or more pressurized environments that are under different pressures and also the air-tight protection of environments that contain lubricant against leakage or foreign objects.

A good operations sealing is an essential factor for the rehabilitate of the machines that use them. Because of that is necessary that all the sealing problems are well analyzed and resolved with all the implications even from the first concept of those machines, installations and device's.

From the point of view of the surface shape, sealing can be plane, conical and spiral. The quality of fixing sealing in the majority of cases depends not only on the type of rubber used but also of the surface geometry.

The gasket quality of sealing is in the majority cases in function not only the rubber mixture chosen but in the same measure with the geometry of surfaces.

The choice of the right seals a very difficult issue especially if the work conditions are not ordinary and must be based on the detailed knowledge of all the intervening factors.

The knowledge of the theoretical and practical aspects of the sealing process is slowed by the fact that for every type of sealing there is a basic principle of closing a gap. These principles which allowed the selection of the optimal fixing, try to explain the process of closing a gap for maintaining a certain pressure in a certain space, also to specify the contributing factors to this process that influence the loss of fluid through leakage from the gap.

The sealing process is influenced by the kind and shape of the fixing material used, and the properties of the sealed environment, excepting the phenomena occurring in the sealing gap.

So far a general theory regarding sealing that also explains its aspects has yet to be published. The process of sealing through direct contact link to the pressured gap that needs to be covered can be well defined by the pressure gradient dp/dl , parameters that define the allure of the pressure drop on the length of the gap curve.

2. THE SHAPE-FUNCTION-TECHNOLOGY INDUSTRIAL DESIGN

Following the steps to achieve a process, starting from the logical scheme (fig. 1) taking as its starting point two aspects of problem analysis one will reach the desired function formulation and the other maintaining the desired proprieties or performances, represent the set that can represent all the criteria for an optimal product.

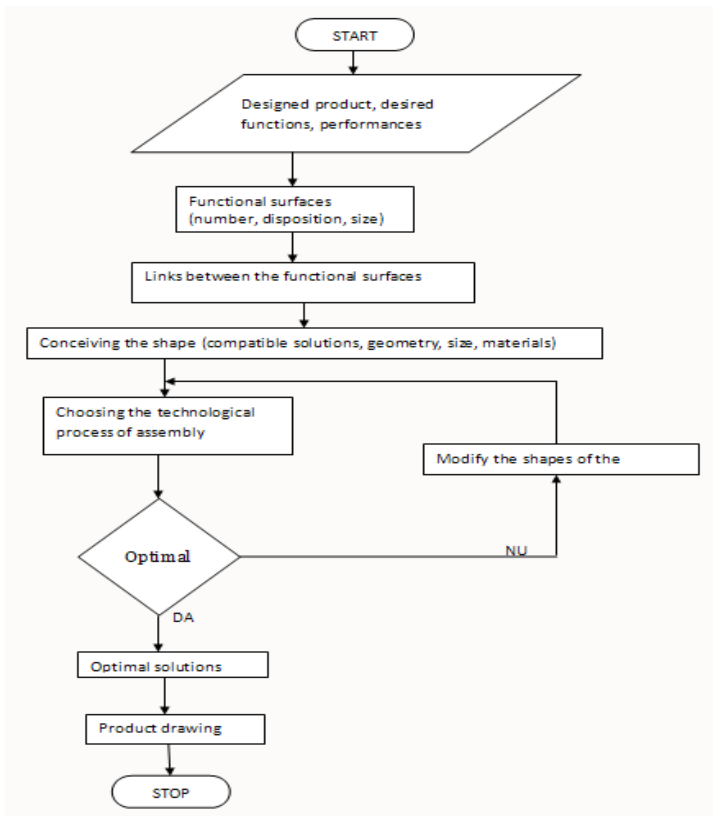


Fig. 1. Logical scheme

They are possible solutions for the sealing area. Varying structure, shape, materials, and choosing from the set of possible solutions after eliminating the possible imposed solutions, a set to match the desired optimal properties results.

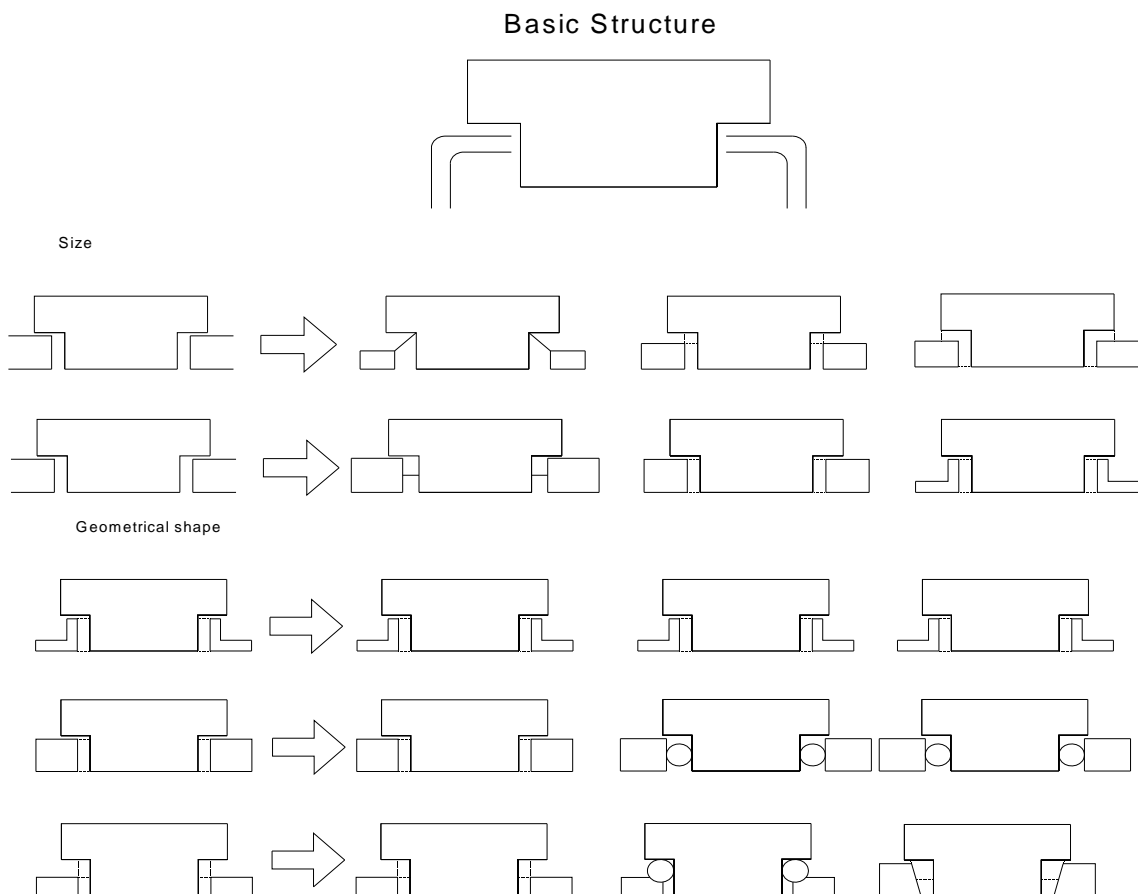
Starting from the variation of functional surfaces the sealing area can be designed for ducts, lids or similar parts. The issue is drawn in fig. 2

Examining the problem on the basis of variation of the four variable parameters can show the suggestion drawing from figure 2 and 3. These don't have to be seen as final solutions but only as types of solutions that need to ulterior be worked at in detail after. (Fig.4)

FUNCTIONAL SURFACES

Parameter variation:

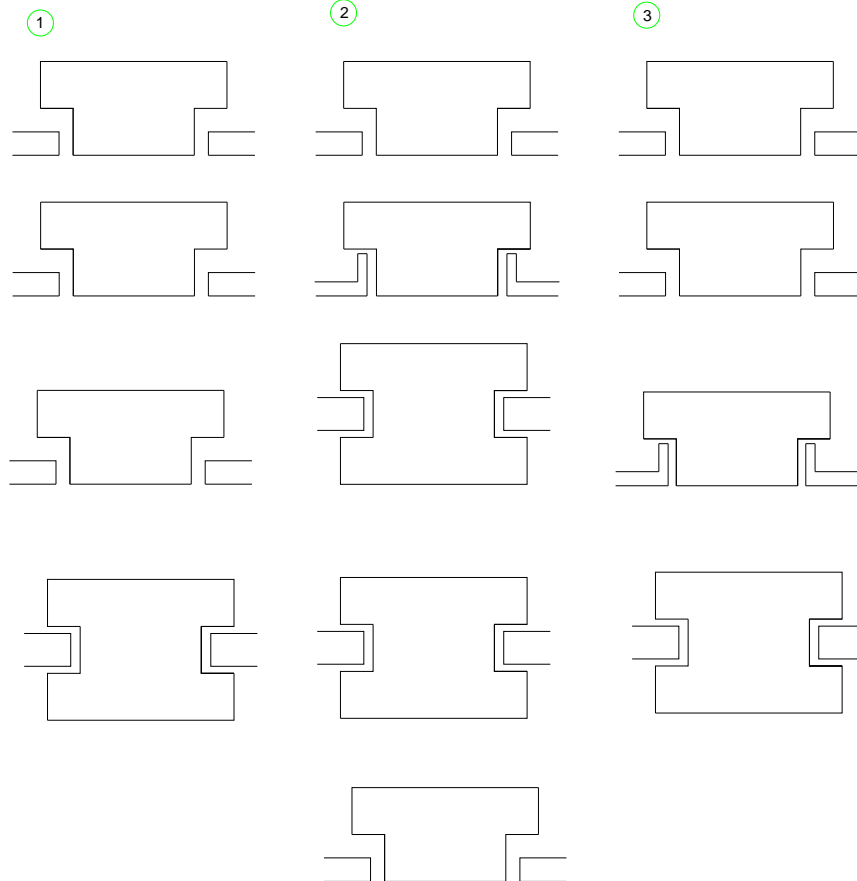
- Number
- Placement
- Size
- Geometrical shape



Number



Placement

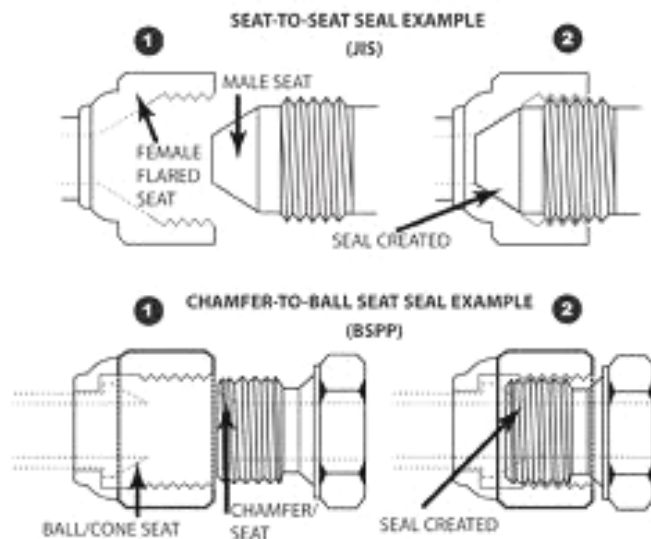


The parameter variation can be freely altered within the confines of the functionality of the surface. If one examines the whole array of solutions the evaluation of limits by individual parameters is required.

As general control of limitation it is necessary to examine the functional surfaces with both the highest and lowest use.

Such surfaces can be referred as minimal or maximal surfaces.

It is the choice of the designer to systematically apply the variation of principles or just apply the principle of maximal or minimal surface and adding few connections between the possibilities of the two cases. (Figure 5)



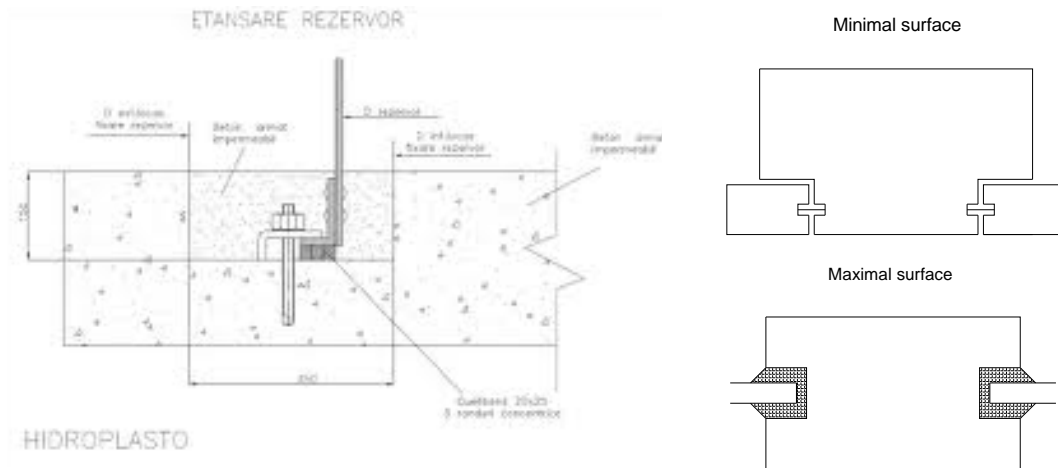


Fig. 5

Knowing the varieties, number, placement, shape and size is important in both cases. The number of solutions after every analysis is presented in figure 6.

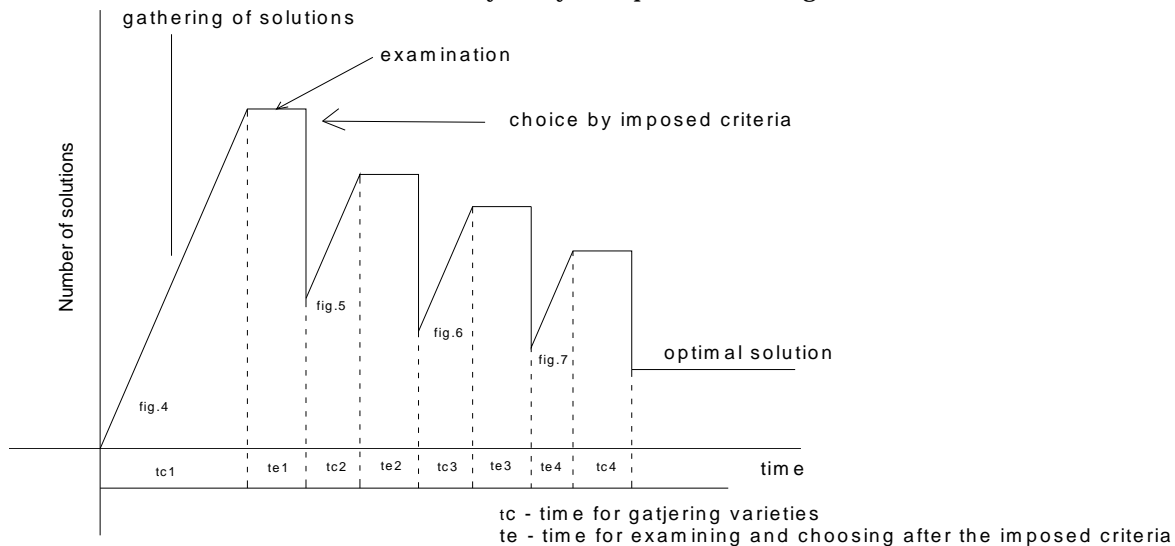


Fig. 6

The achievement of optimal varieties dependant of the domain of use results passing through the design stages presented in the paper.

3. CONCLUSION

The proposed analysis method in the constructive generations of areas of sealing and the succession of analysis stages has the advantage of obtaining optimal types of the product which correspond to the purpose in the conditions of maximum economics.

The analysis criteria from technologic and behavior during using point of view has not been the object of the selection of the purpose types.

REFERENCES

- [1.] Eskild, Tealve : - A short course in industrial design, Hermes-Butterworts, London, 1979.
- [2.] Cristea, V. s.a : - Etansari ET., Bucuresti, 1973.
- [3.] K. Prilutskii, D. N. Ivanov, E. I. Zamolotskaya, A. N. Bessonnyi and A. I. Prilutskii - Modeling methods for perfecting sealing units of piston compressors at the design stage, September, 2004.
- [4.] Fu Ying Zhang, Xi Mei Lu, Ping Wang, Qing Ping He, Efficiency-Reinforcement Design, Reciprocating Sealing Element, TRIZ Technology Evolution, August, 2009



¹ Renato VIDONI

A MULTI AGENT ROBOTIC SYSTEM FOR SIMULATION AND CONTROL OF A MANUFACTURING PROCESS

¹ DIPARTIMENTO DI INGEGNERIA ELETTRICA,
GESTIONALE E MECCANICA UNIVERSITA' DI UDINE, UDINE – ITALY

ABSTRACT:

In this work the multi-agent technology is exploited in order to develop a Multi-Agent Robotic System with the aim to simulate and control a production chain and lay the bases for the introduction of the agent technology into a manufacturing industrial process.

In particular, a simplified washing-machine production system has been studied and agentified. More in detail, automatic production, negotiation, supplying of pieces and management of the production have been considered.

The overall simplified system has been implemented by means of the JADE (Java Agent Development Environment) platform, compliant with the FIPA (Foundation for Intelligent Physical Agents) specifications, and extensively tested in order to prove the robustness and effectiveness of the approach. The developed simplified system has been conceived in order to be easily expandable, thanks to its modularity and structure, and ready to be upgraded.

KEYWORDS:

manufacturing process, assembly line, Multi-Agents, robots

1. INTRODUCTION

Reconfigurable and adaptive production systems, which can provide companies with the proper level of agility and effectiveness, are necessary in order to satisfy fast changes of customers' needs and demands.

Markets are highly competitive and push manufacturing systems from a mass production to a mass customization fashion. A reduction of the product life-cycles, short lead times and high utilization of resources without increasing the costs are the main targets to satisfy.

In order to comply with these requests, Just In Time (JIT) techniques that allow to reduce waste of time and resources are adopted. Thus, the market is becoming more and more mutable and changeable and new technologies have to be adopted in order to react and adapt in a fast manner.

Such premises do not allow a centralized production because a high amount of work and a low flexibility of the structure will occur. Hence, production means need to become reconfigurable and founded on autonomous and intelligent modules, which dynamically interact with each other for the achievement of local and global objectives. Production processes have to provide the required level of agility, i.e. the ability to success in a rapidly changing outer environment, and embed adaptivity attributes. Moreover, in a flexible production system the goals are also the time-to-market reduction, the raise of the productivity level and the cost reduction.

Autonomous and intelligent agents - an agent is a system situated in some environment and capable of autonomous action in this environment in order to meet its design objectives [1] -, that model the production by means of a decentralized control unit and are suitable for high uncertainty and error ratios, can be the answer. Indeed, differently from the Computer Integrated Manufacturing, there is no need of a centralized approach and a unique complex process manager; only the communication and negotiation phases between agents for the use and control of machinery, resources and materials are needed.

The main advantages of this technology and approach are:

1. Decentralized and distributed decision (i.e. each agent keeps decisions autonomously).
2. Modular structure (i.e. agents are independent).

Agents can be used and exploited for:

1. *Simulation.* Agent frameworks are extensively used where the interactions between different entities have to be studied;

2. *Management and control.* An effective control system has to show flexibility, fault tolerance, reusability and low costs. As underlined in [2], agent technology is suitable for effectively reacting to the production changing and high volumes production.

In the last decade, the *scientific community* has *contributed* to the development of techniques and applications of Multi-Agent systems (MAS [1,3]).

A Multi-Agent System (MAS) consists of a group of agents that can potentially interact with each other [3]. By exploiting this feature several advantages such as reliability and robustness, modularity and scalability, decentralization, time-dependency, adaptivity, concurrency, parallelism and dynamism [4,5] can be reached. Bussman in [6] shows how a Multi-Agent system matches the requirements for agile and fast reaction to sudden and unpredictable changes in production demands and is suitable for high volumes production.

In literature, many works that deal with MAS can be found (e.g. [2]; [7]; [8]; [9]; [10]) but agent concepts and techniques are rarely applied and practically adopted in industry. Only few applications and a small part of the available technology has been successfully applied and is currently on the market. How underlined in ([2]; [11]), many works do not specify the working environment or the production plant, focusing only on the definition of a general or theoretical model. Usually, MAS has been applied in order to simulate process flows or decision activities by developing demonstrators, industrial process and chain production simulators, and small system prototypes ([8]; [12]; [13]; [14]; [15]).

At today, industrial companies rarely use Multi-Agents mechatronic systems in production and management. Most of the works are only simulations ([2]; [11]; [16]) while successful working applications is low. Among these, the flexible and distributed MAS control of a ship equipment, the Rockwell Automation, Inc. "MAST" simulation tool for material-handling and the application of MAS for production planning of SkodaAuto cars [11] can be cited.

With the purpose of standardizing agent technologies for the interoperation of heterogeneous software agents, "the Foundation for Intelligent Physical Agents" (FIPA) has become an IEEE Computer Society standards organization and has developed specifications for permitting the creation of a set of shared rules. Thanks to this efforts on standardization, FIPA-OS (FIPA-Open Source), JADE (Java Agent Development Environment) and ZEUS agent platforms compliant to the FIPA rules and directives have been created. The JADE agent platform [17], based on Java, has been chosen in this attempt in order to implement the agents and deploy the multi-agent environment.

In this work, the intelligent agent techniques will be adopted in order to study and develop a distributed framework in order to simulate and control an industrial process like the washing machine chain production.

The target is to model and identify the production chain and to realize a Multi-Agent-Robotic-System (MARS) able to simulate and control a fully autonomous assembly process that works by means of the cooperation of software and robotic agents. Such physical robotic agents moves on the environment in order to comply with specific requests as transport and station restocking like in a real factory.

2. THE STUDY: WASHING-MACHINES CHAIN PRODUCTION

Industrial manufacturing, robotized and autonomous operations and washing-machines chain production are addressed in this work. These fields suit well with the agent technology and theories.

The main target is to develop a MARS (Multi Agent Robotic System) with a high degree of flexibility that can be exploited as the base for a future intelligent and automatic system able to control the full chain production. Such a chain can be viewed, in a simplified scheme, as a collection of working stations.

Each station is in charge to assembly one (or a set of) component and pass the piece at the following station where the next correct component has to be assembled.

Each station is furnished with a small store of components (i.e. local store) that, in order to not stop the production, has to be correctly supplied and refurnished. Thus, each station can be viewed as an agent that is autonomous and reactive. Moreover, autonomous agents or robotic

agents can be applied in order to consider and substitute the human work (i.e. a human that drives a forklift truck for supplying an order).

In practice, when the autonomous agent that represents the i -th station realizes that the local store has to be refurnished, searches a free autonomous robotic agent that can supply its request both in terms of material quantity and time. After a negotiation phase and the entrust of the task, the chosen autonomous robotic agent goes to the central store, loads the components and brings them to the calling station. Some agents can be used as traders and facilitators in order to manage the communication or settle the conflicts and some others can record the robot data in order to give information to the stations like a yellow page service.

In this attempt, some simplifications have been made but the developed framework is implemented in order to be modular and easily expanded. A sketch of the chosen scenario is shown in Fig. 1.

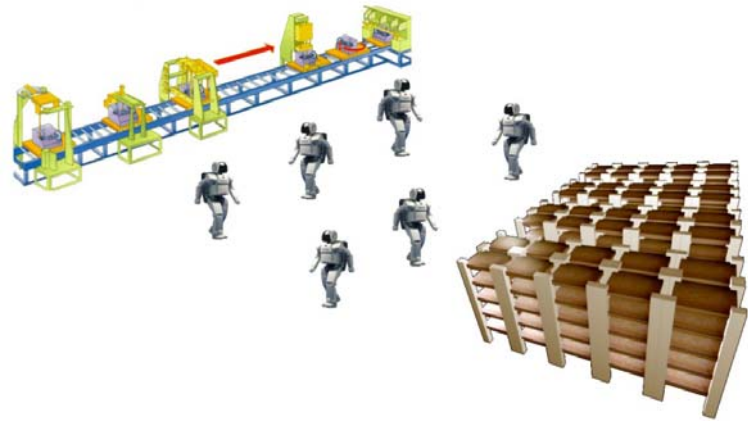


Fig. 1: Sketch of the scenario: assembly line, supply robots and main store

In this work the simplified supply chain has been modeled by means of four stations, each one in charge of assembly a specific part of the washing-machine:

- Station 1: motor and belt;
- Station 2: drum and washing tank ;
- Station 3: two bearings;
- Station 4: frame.

In a simplified view, the production follows the following operations:

- Station i , if the component is available in the local store, assembles the piece and, if Station $i+1$ is free, pushes forward the assembly; if Station i does not have the piece to be mounted, searches and calls an autonomous robotic agent in order to be re-furnished. If an autonomous robotic agent is free, it is charged/entrusted to go to the central store, keep the lacking components and refurnish the calling station.
- When Station i has sent the current assembly to the station $i+1$, its internal state is set on “free” and it is able to receive and manage another piece.

All the works and operations have to be carried out in a parallel and not sequential manner. The flow-chart of the simplified process is presented in Fig. 2.

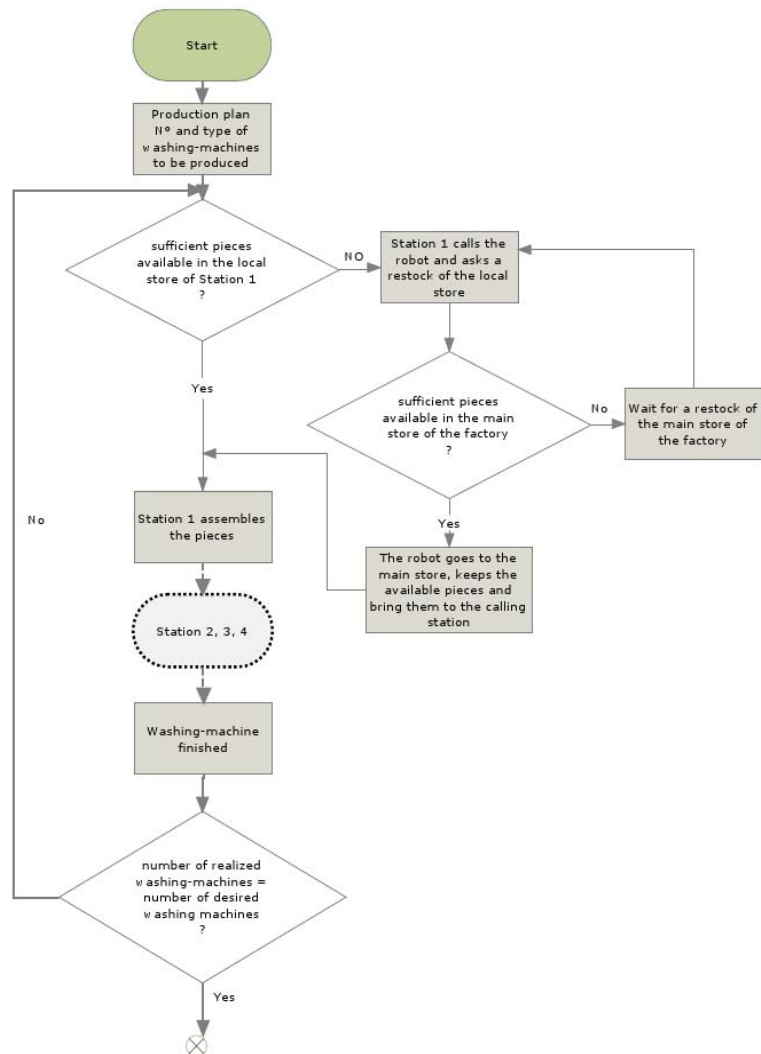


Fig. 2 : Flow-chart of the simplified process

3. THE MA(R)S SYSTEM

At least two kind of agents are necessary: one for the stations, *Station Agent*, and one for the autonomous robots, *Robot Agent*.

Moreover, a *Production Agent*, that is in charge to start and stop the process flow, and a *Supply agent*, that will manage and supply the main store when the stocks are ending, are necessary. Thus, by considering for sake of simplicity only one autonomous robotic agent, 7 agents are single out: 4 *Station Agents*, 1 *Production Agent*, 1 *Robot Agent* and 1 *Supply Agent*.

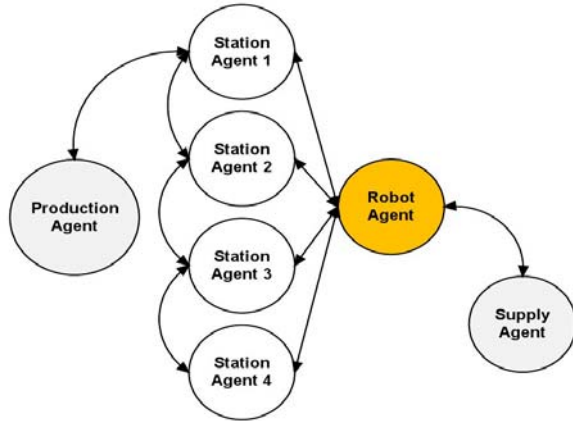


Fig. 3 : Agents of the framework

Inner this behavior, the *Station Agent 1*, i.e. the one related to the first station, is searched by means of a *CALL_FOR_PROPOSAL (CFP)*-message inner the *StationCommand* behavior.

If the *Production Agent* receives a *PROPOSE*-message, the *Station Agent 1* is ready to work; otherwise, if the replies are only *REFUSE*-messages, it means that there are no free agents or their name is not *Station Agent 1* and the behavior is repeated (general case). Within the *REFUSE-MESSAGE* the number of completed washing-machines is passed and, in the particular case of a number of completed pieces equal to the desired one, the production is completed.

If a *PROPOSE*-message is received, the *Production Agent* sends an *ACCEPT_PROPOSAL*-message with the current number of lacking washing-machines to the *Agent Station* that replied with a *PROPOSE*-message.

3.2 Station Agent

Each *Station Agent* has to know the number of available pieces in its local store, the part to assembly, how many and which *Robot Agents* and *Station Agents* are present in the framework and the name of the following station.

Each station has a certain number of available pieces in its local store and of elements that has to assembly (e.g. motor, bearings).

Moreover, each agent has to register itself into the *Directory Facilitator (DF)* that is a sort of “yellow page”, in order to be found.

For this class, six behaviors are implemented:

- *ResearchRequest*, cyclic.

This behavior waits the *CFP*-messages from both the *Production* and the other *Station Agents* and sends a *PROPOSE*-message if it is free and is the correct station. Otherwise, a *REFUSE*-message is sent.

- *ArrangeResearch*, cyclic

This behavior starts with the *ACCEPT_PROPOSAL*-message of the *Production Agent* and sends an *INFORM*-message to the calling agent.

- *ProductionResearchRobotAgent*, one-shot.

It is called inner the *ArrangeResearch* behavior. If the local store is not empty, the correct piece is assembled and the *SearchStationAgent* behavior is called. If the local store has few pieces or it is empty the *ExecutionResearch* behavior is called.

- *ExecutionResearch*, generic.

It asks the lacking components to a suitable *Robot Agent*.

- *SearchStationAgent*, oneshot.

It is similar to the cyclic behavior of the *Production Agent*. It calls the *StationbystationCommand* generic behavior.

- *StationbystationCommand*, generic.

If all works properly, the *Production Agent* calls *Station Agent 1* that, after its assembly task, calls *Station Agent 2* and so on. If a component to be mounted is ending, the related station calls the *Robot Agent* that negotiates the components with the *Supply Agent* (see Fig. 3).

3.1 Production Agent

The *Production Agent* starts the production and sets the number of washing-machines that has to be produced.

First of all, it continuously searches all the available *Station Agents* by means of a cyclic behavior.

Similar to the *CommandStation* behavior. The next station is searched in order to pass the current washing-machine to be assembled.

If the local store is empty, a *REQUEST-message* is sent to the *Robot Agents*. A first research of the available robots is made; after that the lacking piece is requested by means of a *CFP-message*.

The negotiation is based on the time requested to supply the local store. The request is repeated until when at least one robot replies positively.

3.3 Supply Agent

It has two cyclic behaviors:

- *SupplyRequest*, cyclic.

In this behavior the supply requests from the *Robot Agents* are evaluated.

In this first version of the framework the main store is considered as ideal and, thus, the reply is always a *PROPOSE-message*.

- *SupplyOrder*, cyclic.

With this behavior the supply requests are satisfied and an *INFORM-message* is sent to the calling *Robot Agent* when the operation is ended.

3.4 Robot Agent

Each *Robot Agent* is able to supply a certain number of pieces and is registered into the *DF* in order to make visible its services. Moreover it represents a real autonomous robotic system (e.g. AGV, forklift truck).

The implemented behaviors are:

- *RequestOffer*, cyclic.

This behavior is used in order to supply the *CFP-messages* of the *Station Agents*. If the requested components are available and the robot is able to fulfill the order, it replies with a *PROPOSE-message* with the estimated time for making the operation. Otherwise a *REFUSE-message* is sent.

- *SupplyOrder*, cyclic.

This behavior reacts when the *Agent Station* accepts the proposal; it makes the restocking and sends an *INFORM-message* when a successful delivery is done.

- *SearchSupplyAgent*, one-shot.

It searches a *Supply Agent* in order to satisfy the order. It calls the *SupplyOrder* behavior.

- *SupplyOrder*, generic.

Similar to *StationCommand* behavior.

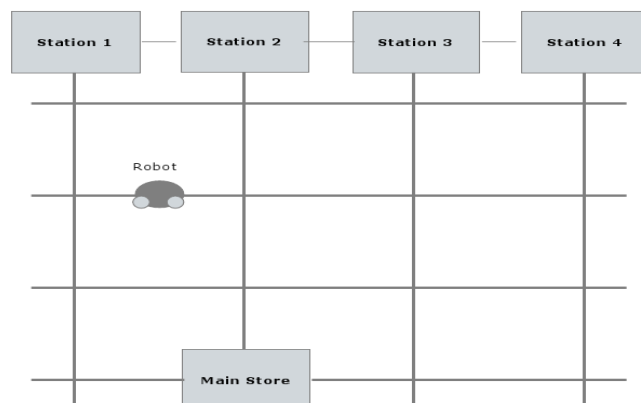
When a *Robot Agent* accepts a task, its state is set to “occupied” until when the requested components are not delivered.

In order to realize a framework that deals not only with software agents but also with physical agents, real robots have to be integrated into the framework. The software language, the communication channel and the physical sensors and actuators have to be set-up.

The hardware chosen in order to create a realistic simplified scenario is the *Lego Mindstorms NXT* shown in Fig. 4(a) [18].



(a)



(b)

Figura 4: the NXT robot (a) and the realized scenario (b)

This robot has been employed on a three wheeled (tricycle) configuration with two motors that control the two tractor wheels (see Fig.4(a)). The robot is equipped with different sensors. In particular, two classes of them have been used. Two light sensors have been installed and located at

the robot front in order to follow the chosen road and recognize the crosses. Indeed the travel area has been defined as a grid of roads to be followed. Also, an ultrasonic distance sensor has been included in the robotic system in order to evaluate if there are obstacles in a range between 10 and 15 cm. Java is the programming language that has been used to implement the overall system. In particular, in order to command and control the robot, the ICOMMAND API has been exploited and the leJOS firmware has been employed [18].

As depicted in Fig.4(b), the working stations are at the top while the main store is at the bottom of the plant. When a robot is called and accepts the work, it has to leave from the calling station or from the current position, go to the central store and come back to the calling station. For each station a predefined path can be used or a shortest path searching algorithm can be exploited. In order to communicate, send orders and receive information with the real robot, a Bluetooth-connection is established between the Robot Agent and the NXT.

The overall system has been implemented on an Intel Pentium Dual Core T3400 @ 2.16 Ghz, RAM 4 GB PC hardware and extensively tested in order to fix bugs or unwanted behaviors. Different production orders have been sent to the *Production Agent* in order to simulate a realistic production.

4. CONCLUSIONS

In this work a Multi-Agent Robotic System has been studied, defined and realized in order to lay the bases for the optimization and management of an industrial process by means of the theories based on the autonomous agents.

As a scenario, a washing-machine assembly line has been evaluated. Human operators that work in order to restock the local stores of each working station have been considered as autonomous (robotic) agents.

Each working station has been modeled as an agent, and a simplified agentification of the process has been made. The overall framework and agents have been realized by means of the JADE platform that follows the FIPA standards and a NXT robot has been integrated into the system in order to simulate in a realistic manner the motion of a robotic agent and the communication process into the real-environment.

Future work will cover the extension of the framework in order to consider the main store management and the integration of different robotic systems with high navigation, motion and handling capabilities.

REFERENCES

- [1.] Wooldridge, M. *An introduction to multiagent Systems*. Ed. JohnWiley & SonsLtd., Chichester, (2002).
- [2.] Caridi, M. and Cavalieri, S., (2004), *Multi-agent systems in production planning and control: an overview*, Production Planning & Control, 15:2, 106-118.
- [3.] Vlassis, N. *A concise introduction to multiagent systems and distributed artificial intelligence. Synthesis*, Lectures on Artificial Intelligence and Machine Learning. Morgan and Claypool Publishers. (2007).
- [4.] Elamy, A. H. *Perspectives in agent-based technology*. AgentLink News, Vol. 18 pp. 19-22. (2005).
- [5.] Parunak, H. V. D., (1998), *Practical and industrial applications of agent-based systems*. URL: <http://agents.umbc.edu/papers/apps98.pdf>.
- [6.] S. Bussmann, K. Schild, *An agent-based approach to the control of flexible production systems*, In Proc. of the 8th IEEE Int. Conf. on Emergent Technologies and Factory Automation (ETFA 2001) (2001), pp. 481-488.
- [7.] Hao, Q, Shen, W, Zhang, Z., (2005), *An Autonomous Agent Development Environment for Engineering Applications*, Int. J. of Advanced Engineering Informatics, 19(2):123-134.
- [8.] Hao, Q. and Shen, W., (2006), *An agent-based simulation of a JIT material handling system*, in IFIP Int. Federation for Information Processing, 220: 67-78, Information Technology for Balanced Manufacturing Systems, (Boston: Springer).
- [9.] Sayda, A.F., and Taylor, J.H., (2007), *Toward A Practical Multi-agent System for Integrated Control and Asset Management of Petroleum Production Facilities*, IEEE Int. Symposium on Intelligent Control (ISIC), Singapore, October 2007.
- [10.] Dangelmaier, W, Heidenreich, J, Pape, U, () *Supply Chain Management: A Multi-Agent System for Collaborative Production Planning*, Proc. Of the IEEE Int. Conf. on e-Technology, e-Commerce and e-Service, 2005. (EEE '05).

- [11.] Pechoucek, M., Marík, V., (2008), *Industrial deployment of multi-agent technologies: review and selected case studies*, Autonomous Agent and Multi-Agent Systems, 17:397–431.
- [12.] Albert, M., Längle, T., Wörn, H., Capobianco, M., Brighenti, A., (2003), *Multi-Agent Systems for Industrial Diagnostics*, Proceedings of 5th IFAC Symposium on Fault Detection, Supervision and Safety of Technical Processes 2003.
- [13.] Hallenborg, K., (2007), *Decentralized scheduling of baggage handling using multi-agent technologies*, in *Multiprocessor Scheduling: Theory and Applications*, ed. Levner, Dec. 2007, Tech Education and Publishing, Vienna, Austria
- [14.] Trullàs-Ledesma, J. and Ribas-Xirgo, L., (2008), *Integrating physical and software sub-systems in a manufacturing environment through agentification*, IX Workshop of Physical Agents 2008.
- [15.] Xiaohua Liu, Jie Lin, Feng Wang, (2009), *Simulation system of Production Scheduling Multi-Agent-Based*, 2009 World Congress on Computer Science and Inf. Eng.
- [16.] Burmeister, B., *Industrial Application of Agent Systems: Lessons Learned and Future Challenges*, L. Braubach et al. (Eds.): MATES 2009, LNAI 5774, pp. 1–3, 2009. © Springer-Verlag Berlin Heidelberg 2009.
- [17.] Bellifemine, F., Caire, G., Poggi, A., Rimassa, G. JADE: *A software framework for developing multiagent applications. Lessons learned*. Information & Software Technology, Vol. 50(1-2) pp. 10-21, 2008.
- [18.] leJOS, 2010. *Java for lego mindstorms*. Web available, <http://lejos.sourceforge.net>







¹ József SÁROSI

ACCURATE POSITIONING OF HUMANOID UPPER ARM

¹ FACULTY OF ENGINEERING, UNIVERSITY OF SZEGED, HUNGARY

ABSTRACT:

Several control ways have been applied to control different humanoid or robot arms, manipulators, prosthetic and therapy devices driven by pneumatic artificial muscles (PAMs). The early control methods were based on classical linear controllers and then some modern control strategies have been developed (e. g. adaptive controller, sliding-mode controller, fuzzy controller, neural network controller and others) ([1], [2] and [3]).

This paper presents a humanoid upper arm and discusses its positioning using sliding-mode control.

KEYWORDS:

humanoid or robot arms, pneumatic artificial muscles, sliding-mode control

1. INTRODUCTION

Nowadays, pneumatic actuators have been considered as a substitute of conventional motors because of its high power/weight and power/volume ratios. The newest type of pneumatic actuator the McKibben muscle possesses all advantages of traditional pneumatic actuators without the main drawback such as low power to weight ratio. The main disadvantages are connected with the accuracy of control and nonlinearities of pneumatic systems [4].

The behaviour and structures of PAMs are well described in literature ([5], [6] and [7]).

Many researchers have studied to generate easier model of PAM to overcome difficulty in control because of its nonlinearity, also some have tried to control robot using that model, but their studies are limited on simulation and their good performances are valid only being applied to simulation model. Physical implementation is more complicated problem [4].

Pneumatic artificial muscles show similarity to biological muscles, for this it's very effective to implement humanoid. The PAMs are one-way acting, we need two ones to generate bidirectional motion: one of them moves the load, the other one will act as a brake to stop the load at its desired position and the muscles have to change function to move the load in the opposite direction. This specific connection of the muscles to the load is generally named as an antagonistic setup.

The layout of this paper is as follows. Section 2 (The study) is devoted to display our test-bed and the LabVIEW program for positioning. Section 3 (Results and discussion) presents several experimental results. Finally, section 4 (Conclusions) gives the investigations we plan.

Fluid Muscles DMSP-10-250N-RM-RM (with inner diameter of 10 mm and initial length of 250 mm) produced by Festo company were selected for our newest study.

2. THE STUDY

In [8] and [9] can be found detailed descriptions of our test bed and former experimental results for positioning.

The newest setup for positioning a humanoid upper arm is shown in Figure 1. The PAMs were installed horizontally and can be controlled by MPYE-5-M5-010-B type proportional valve made by Festo.

Because of the difficulties caused by the nonlinear properties of pneumatic systems a LabVIEW based sliding mode control was designed. The purpose of positioning is to move the arm from a starting position to a desired position. With the use of sliding-mode control the positioning error can be minimized.

The positioning of the arm was measured with a BDF-6350-3-05-2500-65 type (produced by Balluff) rotary incremental encoder.

The signals from the encoder have to be acquired by the LabVIEW program so that they can be used by computer. The device is a NI 6251 card equipped with a PCI interface, to this a SCB 68 type I/O device has been attached with a special connecting cable, on the data acquisition card there are 16 16-bit analog inputs and two 16-bit analog outputs also there are 24 digital inputs and two 32-bit counters as well.

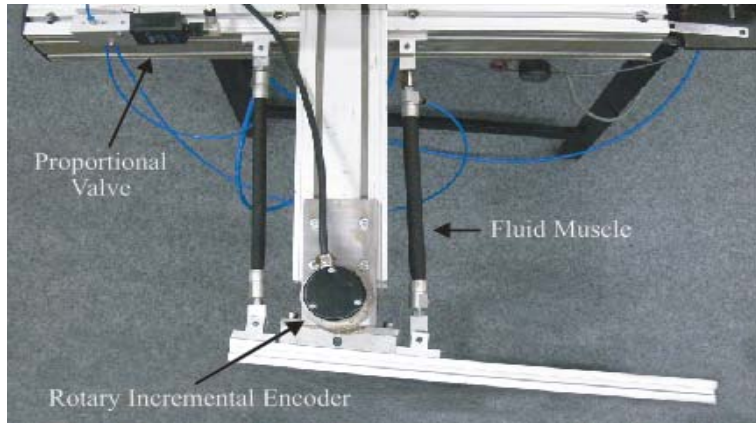


Figure 1. Experimental setup

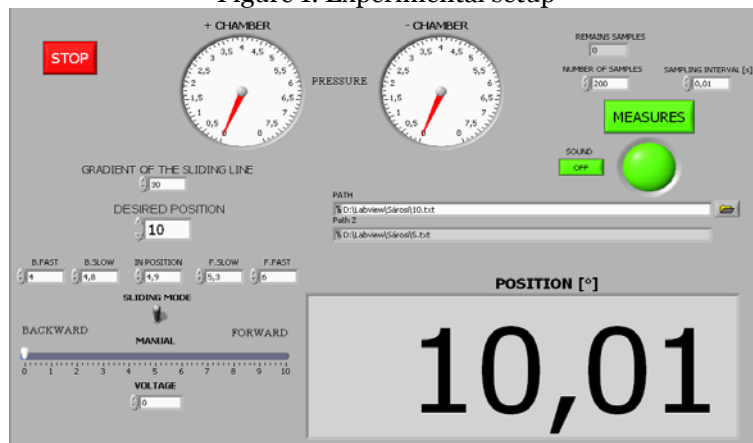


Figure 2 Front panel of LabVIEW program for positioning

The Figure 2 shows data acquisition and positioning that can be achieved in LabVIEW environment. Aside from the desired position the number of samples and the sampling time can also be set. The data can be saved into a text file.

3. RESULTS AND DISCUSSION

Positioning was first done in room temperature on the pressure of 6 bar. The desired positioning was set to 10° , the number of samples was set to 200, while the sampling rate was set to 10 ms, thus the measurement took 2 s. The quality of the positioning (overshoot, steady state error) can be manipulated with the slope of the sliding line. When choosing the slope of the sliding line the optimum between two concurrent properties must be found (speed, accuracy). The more smaller the slope the more faster the trajectory reaches the sliding line, but it will take longer to set. For the slope of the sliding line a value of 30 was set.

Figure 3 shows the positioning as a function of time. It took about 1 s for the position to reach the set value. To show the accuracy of positioning the area around the desired position has been magnified (Figure 4). It has been observed that the value of the steady state error is quite favorable, $0,04^\circ$.

The measurements were repeated in 20° position. The desired positioning was set to 20° , the number of samples was set to 200, while the sampling rate was set to 10 ms, thus the measurement took 2 s, and the slope of the sliding line a value of 30 was set. Figure 5 shows the positioning as a function of time. It took about 1,2 s for the position to reach the set value. To show the accuracy of positioning the area around the desired position has been magnified (Figure 6). This Figure shows the accuracy of positioning is within $0,04^\circ$.

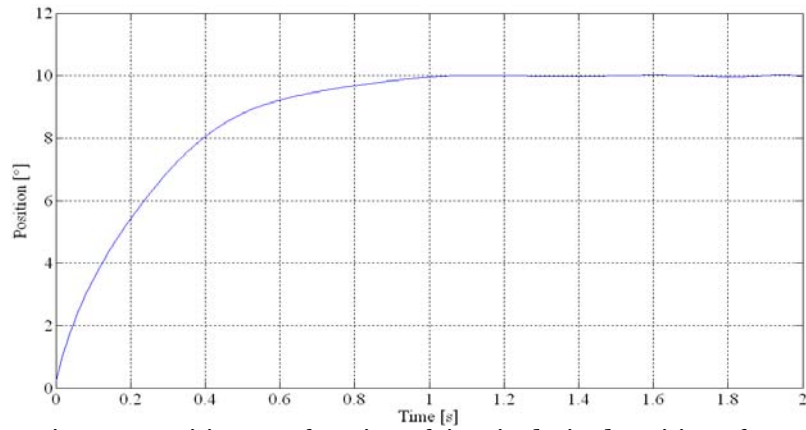


Figure 3. Position as a function of time in desired position of 10°

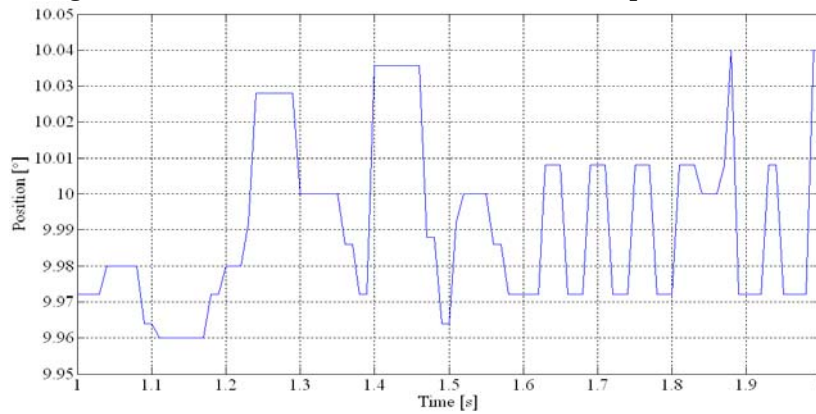


Figure 4. Position as a function of time in desired position of 10° (enlarged)

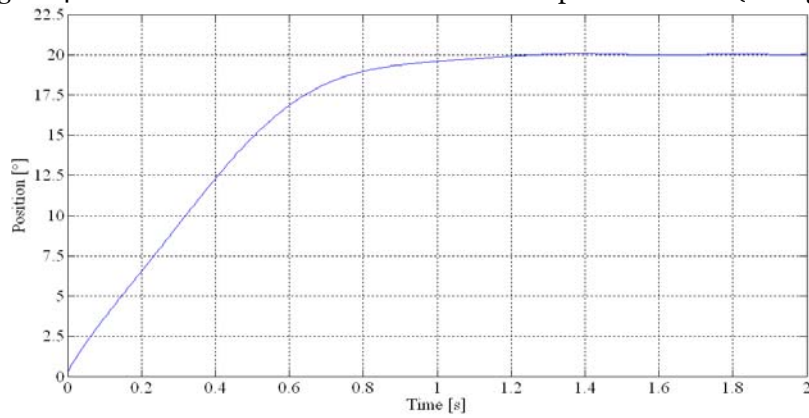


Figure 5. Position as a function of time in desired position of 20°

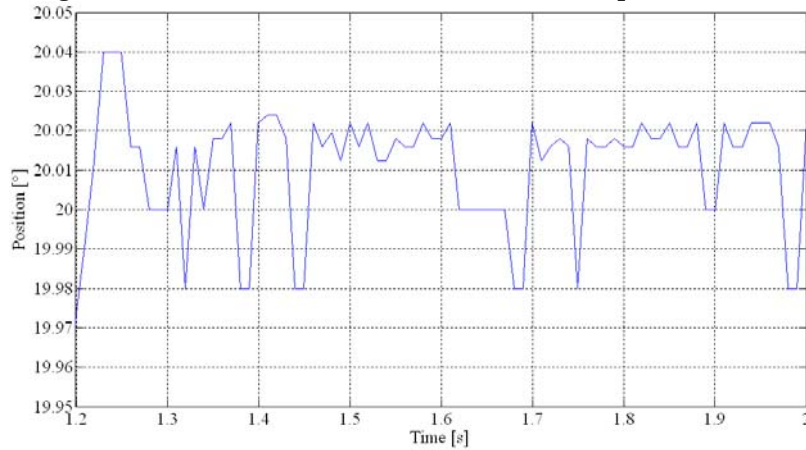


Figure 6. Position as a function of time in desired position of 20° (enlarged)

4. CONCLUSIONS

From these experiments we concluded is that the sliding-mode control can be used for precise robust control of positioning of a humanoid upper arm, for it is fast, robust to external interferences and the changing of internal parameters. Our plans include building a new arm with more muscles and more degrees of freedom for more complex movement and analyzing the data.

REFERENCES

- [1.] Caldwell, D. G., Medrano-Cerda, G. A. and Goodwin M. (1995): Control of pneumatic muscle actuators, IEEE Control System Magazine, Volume 15 (1), pp. 40-48.
- [2.] Situm, Z. and Herceg, Z. (2008): Design and control of a manipulator arm driven by pneumatic muscle actuators, 16th Mediterranean Conference on Control and Automation, Ajaccio, France, 25-27 June, 2008, pp. 926-931.
- [3.] Zhu, X., Tao, G., Yao, B. and Cao, J. (2008): Adaptive robust posture control of parallel manipulator driven by pneumatic muscles with redundancy, Mechatronics, IEEE/ASME Transactions on, Volume 13 (4), pp. 441-450.
- [4.] Choi T. Y., Kim J. J., and Lee J. J. (2006): An artificial pneumatic muscle control method on the limited space, SICE-ICASE International Joint Conference, Bexco, Busan, Korea, 18-21 October, 2006, pp. 4738-4743.
- [5.] Daerden, F. and Lefeber, D. (2002). Pneumatic artificial muscles: actuator for robotics and automation, European Journal of Mechanical and Environmental Engineering, Volume 47, pp. 10-21.
- [6.] Caldwell, D. G., Razak, A. and Goodwin, M. J. (1993): Braided pneumatic muscle actuators, Proceedings of the IFAC Conference on Intelligent Autonomous Vehicles, Southampton, United Kingdom, 18-21 April, 1993, pp. 507-512.
- [7.] Tondu, B. and Lopez, P. (2000): Modeling and control of McKibben artificial muscle robot actuator, IEEE Control System Magazine, Volume 20, pp. 15-38.
- [8.] Sárosi J., Gyeviki J., Szabó G. and Szendrő P. (2010): Laboratory Investigations of Fluid Muscles, International Journal of Engineering, Annals of Faculty of Engineering Hunedoara, 2010, Volume 8 (1), pp. 137-142.
- [9.] Sárosi J., Gyeviki J., Véha A. and Toman P. (2009): Accurate Position Control of PAM Actuator in LabVIEW Environment IEEE, 7th International Symposium on Intelligent Systems and Informatics, Subotica, Serbia, 25-26 September, 2009, pp. 301-305.



¹Iosif DUMITRESCU, ²Dumitru JULA, ⁵Vilhelm ITU

STUDY OF IMPROVEMENT OF ROTATION MECHANISM BALL OF EsRc-1400 ROTOR EXCAVATOR

^{1, 2, 3}UNIVERSITY OF PETROȘANI, ROMANIA

ABSTRACT:

The paper presents the study of the possibility of improvement of EsRc-1400 rotor excavator's rotation mechanism ball.

KEYWORDS:

EsRc-1400 Rotor, Rotation Mechanism Ball, Improvement

1. INTRODUCTION

Increasing mechanization of lignite strata and sterile rocks extraction from their stripping, involves modernization processes, as well as technological systems used in specific extraction conditions and technical refurbishing of quarries.

Lignite quarries in Romania are equipped with technological flows provided with rotor excavators, conveyer belts, dumping machines, depositing and additional machines, providing a theoretical capacity of 200 000 m³/h, and transportation and dumping of 300 000 m³/h, respectively.

In Romanian lignite quarries 99 rotor excavators are in use, 53 dumping machines, 584 conveyer belts summing up 325 km and other depositing and additional machines.

EsRc rotor excavator is the basic machine in the lignite quarries in our country, approximately 70% of the excavations' volume being done with this type of machine.

Fig. 1 shows an overall view of EsRc-1400 excavator where the rotation mechanism between the lower platform on the track and the upper part with the cutting part, the lifting mechanism and the related metal structure can be seen.

The upper platform of the excavator is positioned over the basic shaft and can rotate by the Ø 8650 mm support and rotation ball, and by two gears that match with a toothed wheel.

The toothed wheel and the lower rolling path of the ball are interlocked with the basic shaft, and the upper rolling path is interlocked with the rotating platform.

The platform rotation with all the upper structure leaning on it is made with the rotation mechanism.

2. DESIGN OF LONGITUDINAL BALL BEARING

Fig. 2 shows the overall solution for longitudinal ball bearings, which are the portent mobile structure that makes possible the rotation of the upper platform of the excavator as to the shaft and its handling mechanism, which stays fixed from a rotation point of view.

The lower rolling path, 3, made up of six segments fixed between them with bolts, is fixed, being mounted on the excavator shaft, and the upper rolling path, 10 fixed to the upper structure of the excavator, rotates along with it.



Fig. 1. Overall view of EsRc -1400 rotor excavator

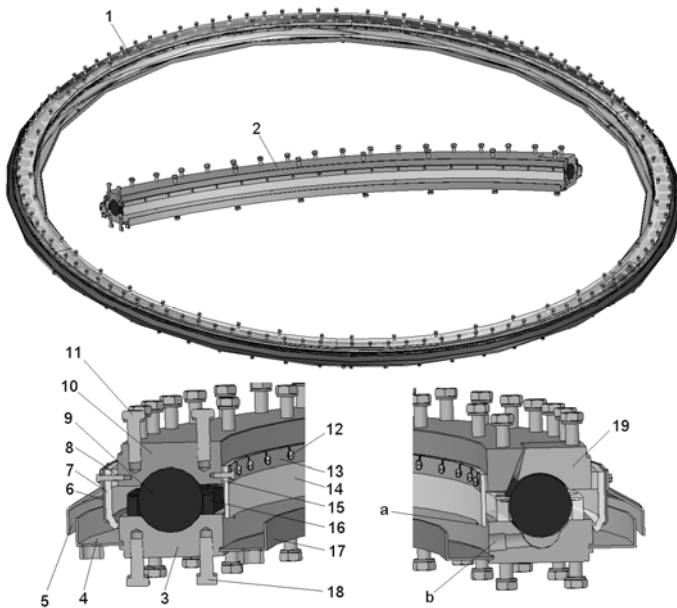


Fig. 2. Longitudinal ball bearing with 8650 rolling diameter

M12x1,5 holes on each segment to supply oil under pressure; b – a G1 ¼ hole on each segment to remove oil.

Construction details of a segment running track component are presented below in Figure 3.

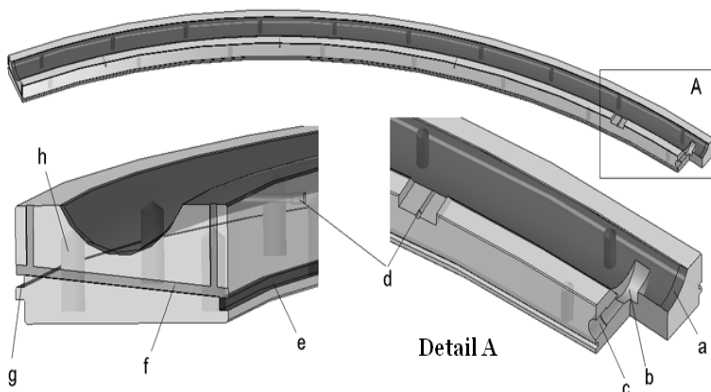


Fig. 3. Lower rolling path segment
 a – 1,5x20 mm cut at the end of the segment; b – collecting duct; c – G 1¼ ” hole for oil removal; d – 4 M12x1,5 holes for oil supply under pressure; e – duct for positioning the lower chute; f – 12x8 mm ducts for oil removal from cage greasing; g – duct for positioning outside duct; h – 16 M30x50/60 holes.

3. PROPOSALS TO IMPROVE THE DESIGN OF LONGITUDINAL BALL BEARING

Following the analysis of the pressure longitudinal ball bearing presented above, it results that both operation life and static load are improved by increasing the number of balls of the bearing, without modifications of the rolling path and ball sizes.

Fig. 4 shows the modified bearing with 143 balls, made up of: 1 – lower ring, made up of 6 segments; 2 – cage with 4 balls; 3 – cage with 3 balls; 4 – 150 mm diameter ball. The numbers of cages were maintained for this bearing (35+1), only that the 3 ball were transformed in 4 balls cages, and the cage with 4 balls in 3 balls cage.

Fig. 5 shows the variation of the operation life of the two design variants, with dotted line the 109 bearing.

This analysis was made because it assists in the execution of the 41MoCr11/STAS 791-80 alloyed steel rolling paths execution improvement and not steel for RUL2 bearings.

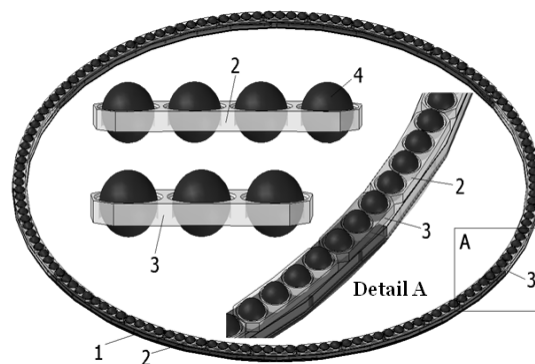


Fig. 4. Modified bearing with 143 balls

A solution was adopted by which the rolling paths are obtained from segments, due to the large sizes.

The marks in this figure mean: 1 – longitudinal ball bearing, 8650 mm rolling diameter, made up of six segments; 2 – rolling segment; 3 – lower rolling path segment, fixed; 4 – outside chute to collect greasing oil; 5 – baffle; 6 – outside sleeve doubling; 7 – outside sleeve; 8 – outside spacing ring; 9 – Ø150 mm ball, 109 pieces; 10 – mobile segment for upper rolling path; 11- M30x100 special screw with Grower nut, 207 pieces; 12 – M12x30 screw with safety washer; 13 – inside ring; 14 – inner sleeve; 15 – inside spacing ring; 16 – cage for 3 balls, 35 pieces and a cage for 4 balls; 17 – inside chute to collect greasing oil; 18 – M30x85 special screw with Grower washer, 108 pieces; 19 – inspection part, 2 pieces; a – four.

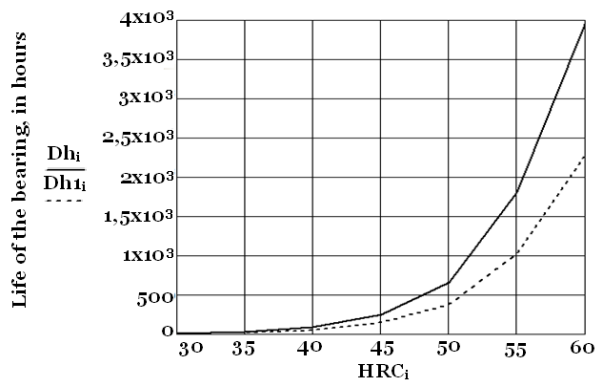


Fig. 5. Operation life variation module for the two longitudinal ball bearing constructive variants

The thermal treatment applied is superficial tempering of the rolling path, since on the opposite M30 end threaded holes required to mount the bearing on the metal structure of the excavator are executed.

As a result of superficial tampering, along the rolling path the hardness is uneven, leading to its uneven wear. Both for the axial bearing and for the toothed wheel cyclical change of the excavator position to the face is required, for an even wear of the rolling path segments, and of the toothed wheel segments, respectively.

Fig. 6 shows an improvement solution for the longitudinal ball bearing.

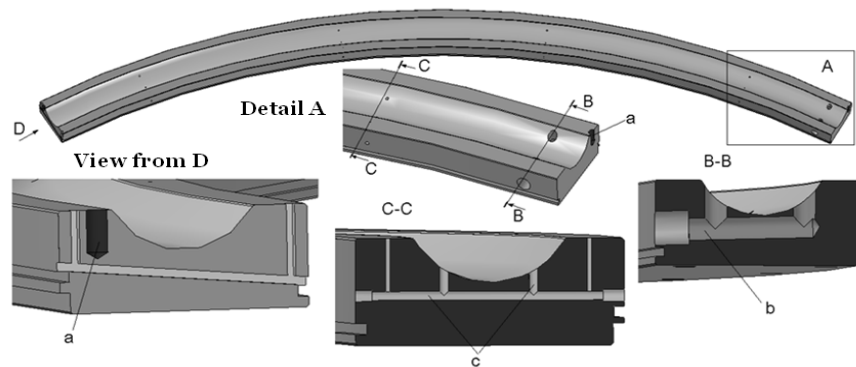


Fig. 6. Improvement solution of the lower rolling path segment

4. CONCLUSIONS

Increasing the number of balls with 34, from 109 to 143, an increase of the operation life is obtained by more than 70%. In absolute value it is 300 hours at 50 HRC hardness and reaches to 1650 hours at 60 HRC harness of the rolling path. From the above, it is required a thermal treatment of superficial tampering for a harness of more than 60 HRC and in a variation range along the rolling path as small as possible, for an even wear. The rolling paths are made from improved 41MoCr11/STAS 791-80 steel alloy and not RUL2 steel for bearings.

The design of the lower rolling path of the bearing can be improved by:

- ❖ removal of (1,5x20 mm) cuts at the end of the segments to have a continuous rolling path, without thresholds;
- ❖ bores at each end for $\Phi 20 \times 40$ mm dowel pin (a), in view of centring segments between them, a solution also found in the toothed wheel;
- ❖ modification of the oil collecting solution on the rolling path (b) in order to keep up continuity of the rolling path;
- ❖ improving solution for grease supply under pressure for the rolling path (c), with the possibility of supply on the outer or inner side and easy decongestion of grooves, with greasing of the friction surface between the cage and the lower ring.

According to literature, it is recommended to grease with consistent grease, due to the way the proofing is done, mineral oil under pressure is required, which should remove abrasive particles from the rolling path. For the future, a study can be done and tests for using a greasing system with consistent grease.

REFERENCES

- [1.] Găfițeanu, M. șa – Organe de mașini, vol. I și II, Editura Tehnică, București, 1981 și 1983.
- [2.] Muscă G. – Proiectarea asistată folosind Solid Edge, Editura Junimea, Iași, 2006.
- [3.] *** - Documentația tehnică a excavatorului cu rotor EsRc-1400.
- [4.] *** - Colecția de standarde de Organe de mașini, vol. I.b, I.c, Editura Tehnică, București, 1983.



¹Adina BUDIUL BERGHIAN, ²Teodor VASIU, ³Amalia DASCĂL

KINETIC AND STATIC ANALYSIS AT LOADED RUNNING OF MECHANISMS OF PARALLEL GANG SHEARS' TYPE ASSIGNED FOR CUTTING THE METALLURGICAL PRODUCTS

¹⁻³. UNIVERSITY "POLITEHNICA" TIMISOARA, FACULTY OF ENGINEERING HUNEDOARA, ROMANIA

ABSTRACT:

In this study is presented the kinetic and static analysis of shear type mechanisms for cutting metallurgical products at the mill train of the semi-finished steel products Rolling Mill No. 1 – S.F.1 of S.C. MITTAL STEEL S.A. HUNEDOARA, in conditions of disregarding the frictions existent in the kinetic couplings.

KEYWORDS:

mechanism, forces and moments of inertia forces, reaction

1. INTRODUCTION

The kinematical scheme for the mechanism of parallel gang shears assigned to cut metallurgical products is shown in Figure 1 and consists in: hand-hold 1, short driving rod 2, upper arm 3, long driving rod 4, lower arm 5 and upper slide 6. This type of mechanism works in phases i.e.: in the first phase is lowered the superior cutter up to the surface of the steel semi-finished product and then stopped and locked in this position moment when the inferior cutter, which performs the cutting of steel semi-finished product, starts to lift. After cutting has done the inferior cutter comes back to the initial position and then the upper arm is lifted in the initial position. All these movements are coordinated by the crankshaft, i.e. handhold 1 and are accomplished at a stroke of 360° of the handhold. From this reason, the kinetic analysis and kinetic and static analysis as well for this type of mechanism will be performed on phases of movement [1].

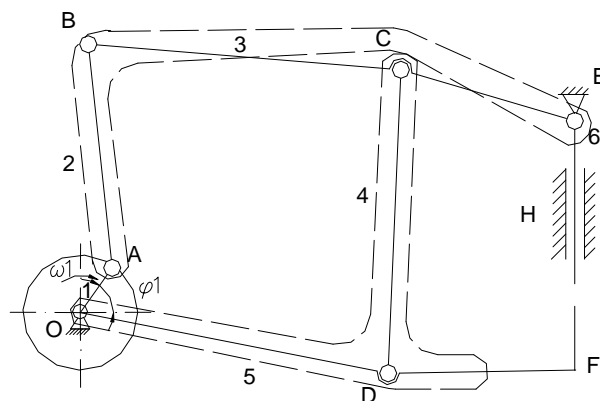


Figure 1. Kinetic Scheme of the 8000kN shear

2. KINETIC AND STATIC ANALYSIS OF THE DYAD ODC

2.1. Determination of the position for gravity centers of the elements to the dyad ODC

- long driving rod 4 (Figure 2).
- lower arm 5 (Figure 3)

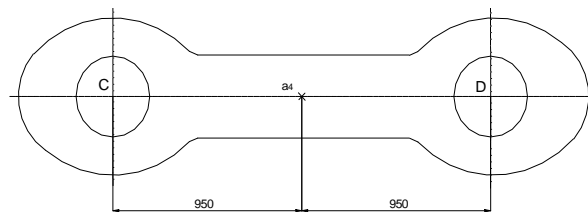


Figure 2. Gravity centre of the element (4) (long driving rod)

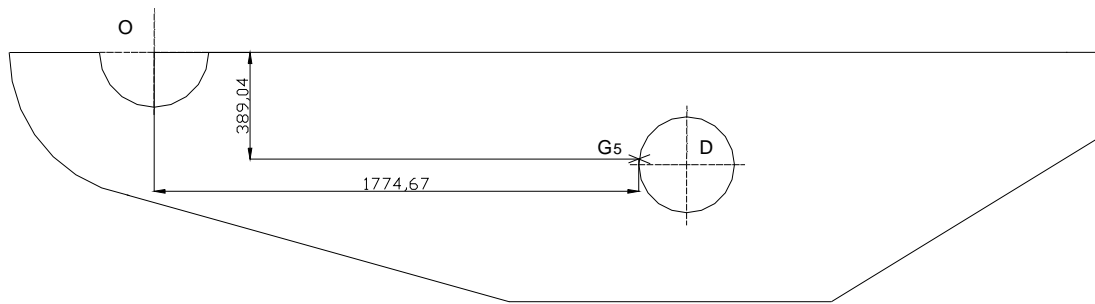


Figura 3. Gravity centre of the element (5) (lower arm)

2.2. The determination of the accelerations of the gravity centre and these directions

- accelerations of the gravity centre to the long driving rod (element4)[2]

$$a_{G_4C} = G_4 C \sqrt{\omega_4^4 + \varepsilon_4^2} \text{ the acceleration center } G_4 \text{ against the point C;} \quad (1)$$

$$\bar{a}_{G_4} = \bar{a}_C + \bar{a}_{G_4C}^n + \bar{a}_{G_4C}^t \Rightarrow$$

$$a_{G_4} = \sqrt{a_C^2 + a_{G_4C}^2 - 2a_C a_{G_4C} \cos s_4}, \text{ the acceleration center } G_4 \quad (2)$$

- accelerations of the gravity centre to the lower arm (element 5)

$$a_{G_5D} = G_5 D \sqrt{\omega_5^4 + \varepsilon_5^2} \text{ the acceleration center } G_5 \text{ against the point D;} \quad (3)$$

$$\bar{a}_{G_5} = \bar{a}_D + \bar{a}_{G_5D}^n + \bar{a}_{G_5D}^t \Rightarrow$$

$$a_{G_5} = \sqrt{a_D^2 + a_{G_5D}^2 - 2a_D a_{G_5D} \cos s_5}, \text{ the acceleration center } G_5 \quad (4)$$

The directions of the accelerations to the gravity centers G_4 respective G_5 and to the forces of inertia reacts on the elements (4) and (5) are determined from the polygon of the accelerations.

2.3 The calculus of the inertia forces and to the moments of the inertia forces reacts on the elements of the dyad ODC

The inertia forces and the moments of the inertia forces to the elements of the dyad ODC are caused with help of the relations [10], ($m_4=2543$ Kg, $m_5=8597$ Kg) [1]:

$$\begin{aligned} \bar{F}_{i5} &= -m_5 \bar{a}_{G_5} \\ \bar{F}_{i4} &= -m_4 \bar{a}_{G_4} \end{aligned} \quad (5)$$

$$\begin{cases} J_{G_4} = m_4 \frac{I_4^2}{12} \\ J_{G_5} = m_5 \frac{I_5^2}{12} \end{cases} \Rightarrow \begin{cases} \bar{M}_{i4} = -J_{G_4} \bar{\varepsilon}_4 \\ \bar{M}_{i5} = -J_{G_5} \bar{\varepsilon}_5 \end{cases}$$

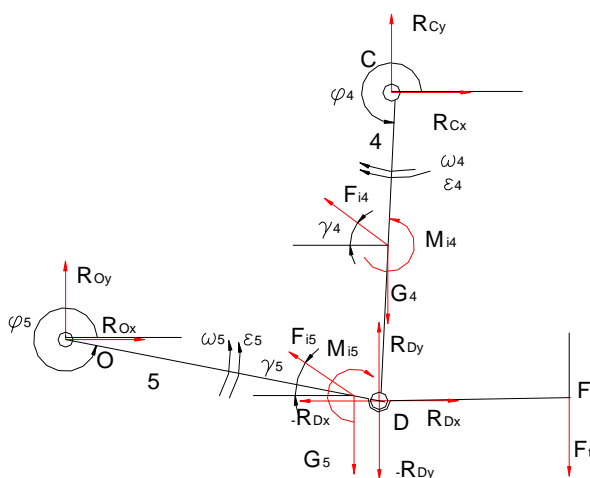


Figure 4. Loading Scheme of ODC dyad

2.4. Determination of reactions in kinetic couplings of dyad ODC without taking into account the frictions of kinetic couplings

Determination of reactions in couplings is performed having as base the loading scheme presented in Figure 4.

With the notations of figure 4. and in conditions when are known the weights of component elements (thus are known the weight forces too) can be written the following equations of equilibrium ($m_4=2543$; $m_5=8597$ Kg) [1].

$$\left\{ \begin{array}{l} \sum F_x(5) = 0 \Rightarrow R_{Ox} + R_{Dx} - F_{i5} \cos \gamma_5 = 0 \\ \sum F_y(5) = 0 \Rightarrow R_{Oy} + R_{Dy} - G_5 + F_{i5} \sin \gamma_5 - F_t = 0 \\ \sum F_x(4) = 0 \Rightarrow R_{Cx} - R_{Dx} - F_{i4} \cos \gamma_4 = 0 \\ \sum F_y(4) = 0 \Rightarrow R_{Cy} - R_{Dy} + F_{i4} \sin \gamma_4 - G_4 = 0 \\ \sum M_D(5) = 0 \Rightarrow -R_{Ox} I_5 \sin(360 - \varphi_5) - R_{Oy} I_5 \cos(360 - \varphi_5) - M_{i5} + G_5 Da_5 \cos(360 - \varphi_5) - \\ \quad - F_{i5} Da_5 \sin[\gamma_5 - (360 - \varphi_5)] - F_t DF = 0 \\ \sum M_D(4) = 0 \Rightarrow -R_{Cx} I_4 \sin(360 - \varphi_4) - R_{Cy} I_4 \cos(360 - \varphi_4) + M_{i4} - G_4 Ca_4 \cos(360 - \varphi_4) - \\ \quad - F_{i4} Ca_4 \sin(360 - \varphi_4 - \gamma_4) = 0 \end{array} \right. \quad (6)$$

in which: l_i -represent the loungers of kinematic elements; $-a_i$ represented the positions to the gravity centers of the elements in report with one from couples the marginal, their values the by-paths determinate in the previous paragraphs.

The unknown are $R_{Ox}; R_{Oy}; R_{Cx}; R_{Cy}; R_{Dx}; R_{Dy}$, and has been solved in MathCAD, and with solutions obtained can be calculated the values of reactions in couplings O, D, C:

$$\begin{aligned} R_O &= \sqrt{R_{Ox}^2 + R_{Oy}^2} \\ R_C &= \sqrt{R_{Cx}^2 + R_{Cy}^2} \\ R_D &= \sqrt{R_{Dx}^2 + R_{Dy}^2} \end{aligned} \quad (7)$$

Graphic representation of reaction variation in coupling C, without friction, depending on variation of handhold angle φ_1 is shown in Figure 5.

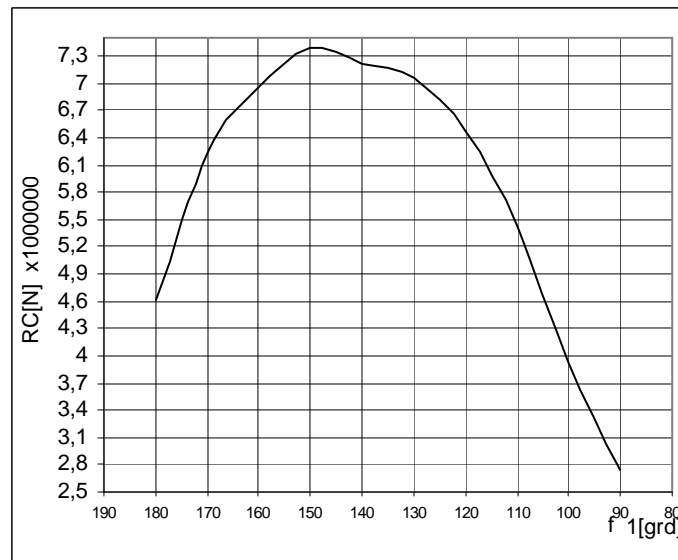


Figure 5. Variation of reaction in coupling C, without friction

3. Kinetic and static analysis of the dyad ABE

3.1. Determination of position for gravity centers of the elements to dyad ABE

-element (2) – short driving rod :

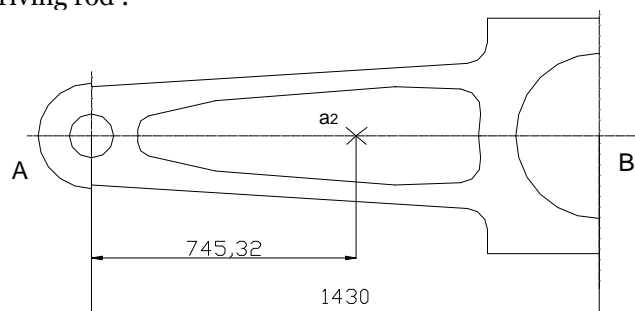


Figure 6. Gravity centre of the element (2) (short driving rod)

- element (3)- upper arm:

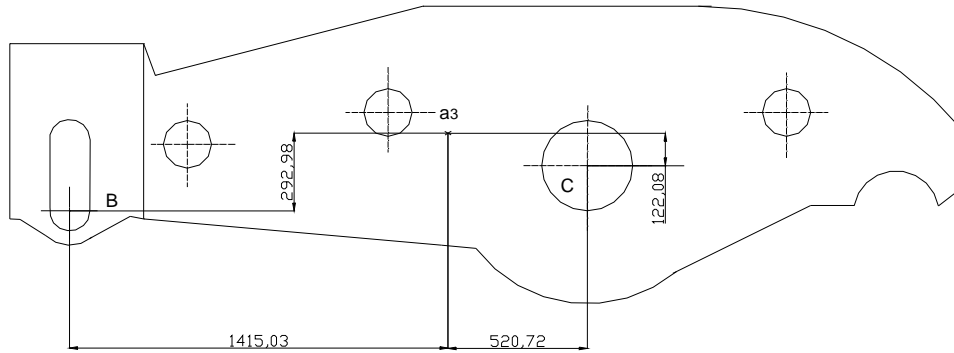


Figure 7. Gravity centre of the element (3) (upper arm)

3.2. The determination of the accelerations of the gravity centre and these directions

- accelerations of the gravity centre to the short driving rod

$$a_A = OA\omega_1^2, \text{ the acceleration of the point A;} \quad (8)$$

$$a_{G_2A} = G_2A\sqrt{\omega_2^4 + \varepsilon_2^2}, \text{ the acceleration center } G_2 \text{ against the point A} \quad (9)$$

$$\bar{a}_{G_2} = \bar{a}_A + \bar{a}_{G_2A}^n + \bar{a}_{G_2A}^t \Rightarrow$$

$$a_{G_2} = \sqrt{a_A^2 + a_{G_2A}^2 - 2a_A a_{G_2A} \cos s_2}, \text{ the acceleration center } G_2 \quad (10)$$

- accelerations of the gravity centre to the upper arm (element 3):

$$a_{G_3B} = G_3B\sqrt{\omega_3^4 + \varepsilon_3^2} \text{ the acceleration center } G_3 \text{ against the point B;} \quad (11)$$

$$\bar{a}_{G_3} = \bar{a}_B + \bar{a}_{G_3B}^n + \bar{a}_{G_3B}^t \Rightarrow$$

$$a_{G_3} = \sqrt{a_B^2 + a_{G_3B}^2 - 2a_B a_{G_3B} \cos s_3}, \text{ the acceleration center } G_3 \quad (12)$$

3.3. The calculus of the inertia forces and to the moments of the inertia forces reacts on the elements of the dyad ABE

The inertia forces and the moments of the inertia forces to the elements of the dyad ABE are caused with help of the relations ($m_2=425\text{Kg}$, $m_3=6\ 155\text{Kg}$):

$$\begin{aligned} \bar{F}_{i3} &= -m_3 \bar{a}_{G_3} \\ \bar{F}_{i2} &= -m_2 \bar{a}_{G_2} \\ \left. \begin{aligned} J_{G_2} &= m_2 \frac{l_2^2}{12} \\ J_{G_3} &= m_3 \frac{l_3^2}{12} \end{aligned} \right\} \Rightarrow \begin{cases} \bar{M}_{i2} = -J_{G_2} \bar{\varepsilon}_2 \\ \bar{M}_{i3} = -J_{G_3} \bar{\varepsilon}_3 \end{cases} \end{aligned} \quad (13)$$

3.4. Determination of reactions in kinetic couplings of dyad ABE without taking into account the frictions of kinetic couplings

Determination of reactions in couplings is performed having as base the loading scheme presented in Figure 8:

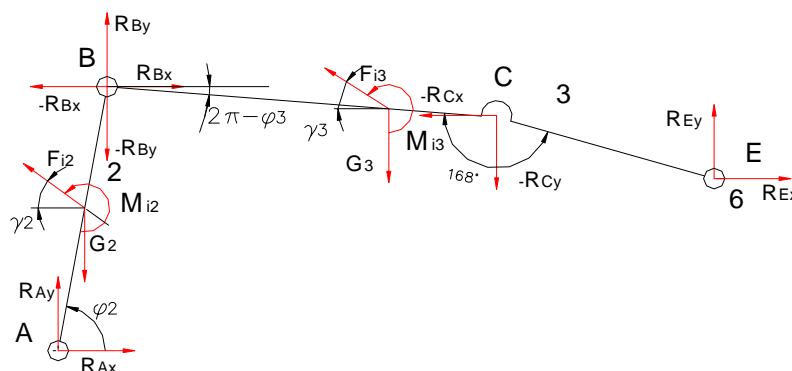


Figure 8. Loading Scheme of ABE dyad

With the notations of figure 13. and in conditions when are known the weights of component elements can be written the following equations of equilibrium: ($m_2=425$; $m_3=6155\text{Kg}$)[1]:

$$\left\{ \begin{array}{l} \sum F_x(2) = 0 \Rightarrow R_{Ax} + R_{Bx} - F_{i2} \cos \gamma_2 = 0 \\ \sum F_y(2) = 0 \Rightarrow R_{Ay} + R_{By} - G_2 + F_{i2} \sin \gamma_2 = 0 \\ \sum F_x(3) = 0 \Rightarrow -R_{Bx} - R_{Cx} + R_{Ex} - F_{i3} \cos \gamma_3 = 0 \\ \sum F_y(3) = 0 \Rightarrow -R_{By} - R_{Cy} + R_{Ey} + F_{i3} \sin \gamma_3 - G_3 = 0 \\ \sum M_B(2) = 0 \Rightarrow R_{Ax} l_2 \sin \varphi_2 - R_{Ay} l_2 \cos \varphi_2 + G_2 Ba_2 \cos \varphi_2 - F_{i2} Ba_2 \sin(180^\circ - \gamma_2 - \varphi_2) + \\ \quad + M_{i2} = 0 \\ \sum M_E(3) = 0 \Rightarrow -R_{Bx} l_3 \sin(360^\circ - \varphi_3 + 4^\circ) + R_{By} l_3 \cos(360^\circ - \varphi_3 + 4^\circ) + \\ \quad + M_{i3} + G_3 Ea_3 \cos(360^\circ - \varphi_3 + 8^\circ) - F_{i3} Ea_3 \sin[\gamma_3 - (360^\circ - \varphi_3) - 8^\circ] \\ \quad - R_{Cx} l'_3 \sin(\varphi_3 - \theta) + R_{Cy} l'_3 \cdot \cos(\varphi_3 - \theta) = 0 \end{array} \right. \quad (14)$$

The set of equations is a linear one with 6 equations and 6 unknown R_{Ax} ; R_{Ay} ; R_{Bx} ; R_{By} ; R_{Ex} ; R_{Ey} , and has been solved in MathCAD, and with solutions obtained can be calculated the values of reactions in couplings A; B; E:

$$\begin{aligned} R_A &= \sqrt{R_{Ax}^2 + R_{Ay}^2} \\ R_B &= \sqrt{R_{Bx}^2 + R_{By}^2} \\ R_E &= \sqrt{R_{Ex}^2 + R_{Ey}^2} \end{aligned} \quad (15)$$

Graphic representation of reaction variation in coupling E, without friction, depending on variation of handhold angle φ_1 is shown in Figure 9:

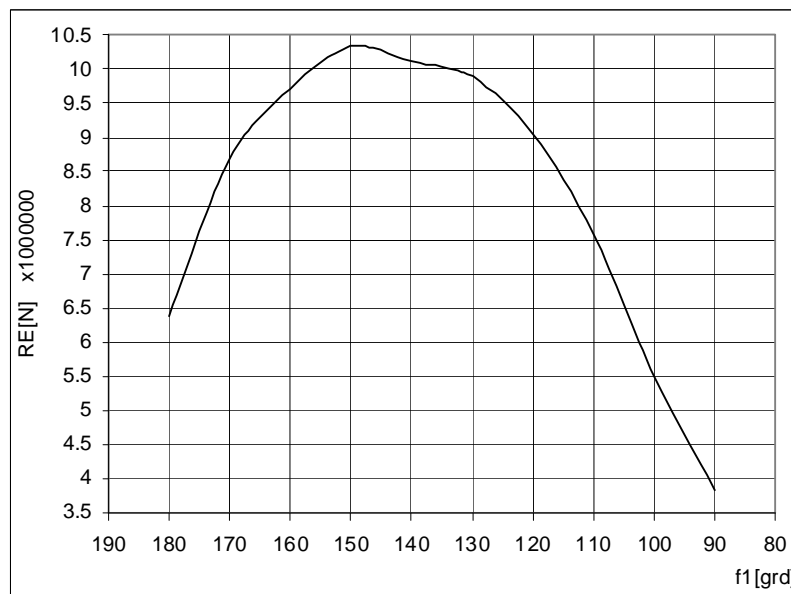


Figure 9. Variation of reaction in coupling E, without friction

4. CONCLUSIONS

The kinetic and static analysis of the mechanism of the guy scissors for cutting metallurgical products of 8000kN are accomplished without the taking in consider the frictions from couple kinematic for the case in which is cut (300x300) mm² metallurgical product, from OLC20, to a temperature of 970°C. The reactions from couples kinematic have the values maxims when the relativ deepness of penetrate to the knives in material is $\varepsilon= 04$.

BIBLIOGRAPHY

- [1.] Budiul, Berghian, A. "Contributions on reliability improvement of shear type mechanisms assigned to cut metallurgical products", PhD Thesis (Doctor's Degree).
- [2.] Conțiu, T.- "Culegere de probleme din Teoria mecanismelor și a mașinilor", Editura Tehnică, București, 1957;
- [3.] Handra Luca, V. Stoica, I. A.- "Introducere în teoria mecanismelor", Vol. I, II, Editura Dacia, Cluj Napoca, 1982;



ABOUT THE TENSIONING OF THE BELT DRIVES

¹⁻⁴. UNIVERSITY "POLITEHNICA" TIMIȘOARA, FACULTY OF MECHANICS, TIMIȘOARA, ROMANIA

ABSTRACT:

The intensity of the initial tensioning effort must be correlated with the belt drive tensioning system and with the maximum torque to be transmitted.

In the particular case of the constant tensioning of belt drives, this correlation is analyzed and there is recommended the appropriate control methods.

The automotive industry is in continuous expansion and the competition for timing belt drive requires high standards of manufacturing. As a result, the belt drive not only requires a strict correlation but also a high durability if not, the effects could be dramatic.

KEYWORDS:

automotive industry, manufacturing, standards, control methods

1. INTRODUCTION

Rational limits of the initial tensioning.

The pulling capacity, the mechanical efficiency and the fatigue durability of a belt drive are conditioned by the correct evaluation and conservation time of the tensioning.

The initial tension effort intensity must be correlated with the maximum transmitted torque and tensioning system of the drive.

In case of a transmitted power $K_t P$ [kW], by $z \geq 1$ number of parallel belts at a velocity v [m/s], the optimum level of tensioning results from the relation:

$$F_0^* = 10^3 (K_t P / vz / 2\varphi) \text{ [N]} \quad (1)$$

When setting –in repos state– the influence of the centrifugal forces that result in function must be compensated (not taking in consideration the elasticity of the drive-shaft system):

$$F_0 = F_0^* + m_1 v^2 \text{ [N]} \quad (2)$$

where: m_1 –belt linear weight

2. THE STUDY

Tension systems

The traction coefficient (Kutzbach invariant) from relation (1), defined as a proportion between the transmitted tangential force F_t and the double initial tensioning effort $2F_0$:

$$\varphi = F_t / 2F_0 \quad (-) \quad (3)$$

depends on the exact tensioning situation of the belt and the proportion between the active efforts in the branches:

$$m = F_1^* / F_2^* = \exp(\mu \beta_{gr}) \quad (-) \quad (4)$$

where: $\mu = \mu_0 / \sin(\alpha/2)$ –is the apparent friction coefficient (for $\alpha = 40^\circ$) at the V belts, and $\beta_{gr1} \leq \beta_1$ [rad] representing the minimum (active) slip angle on the pulley with $d_{p1} \leq d_{p2}$.

Based on the command and adjust mode of the forced contact between the conjugated surfaces of the pulley and belt, we have the following constructive solutions for permanent tensioning.

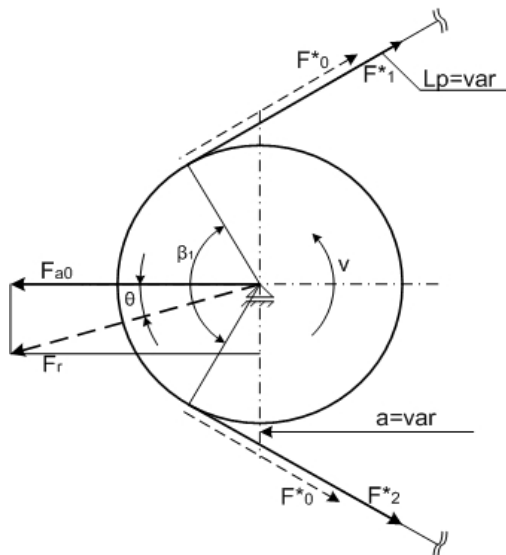


Fig. 1

The drive with $a = \text{constant}$, $L_p = \text{variable}$, tensioned by loading the driven side (pushed with a tightening pulley) exterior force F_{ac} , invariable in intensity and direction (Fig. 2).

The drive with $a, L_p = \text{variable}$ tensioned by loading of one of the shafts with an exterior force F_{ac} , invariable in intensity and guided by the centers' line (Fig. 1):

$$F_{ac} = 2F_0^* \sin(\beta_1/2) - (F_t/\varphi) \sin(\beta_1/2) \quad [\text{N}] \quad (5)$$

$$\varphi = (m-1)/(m+1) \quad [-]$$

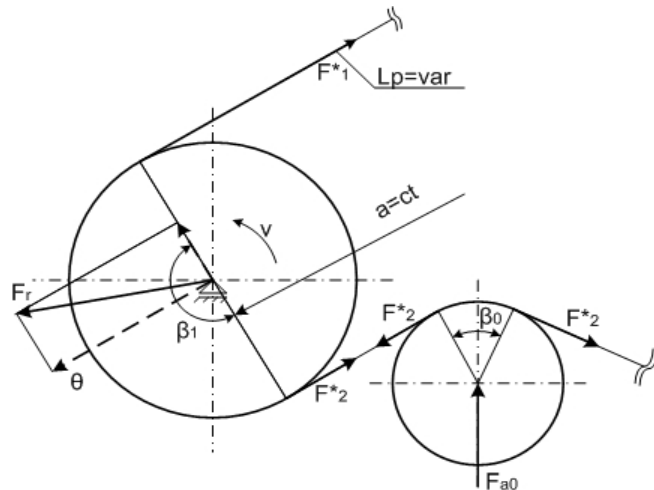


Fig. 2

$$F_{ac} = 2F_0^* \sin(\beta_0/2) = 2F_0^* \sin(\beta_0/2) \quad [\text{N}] \quad (6)$$

$$\varphi = (m-1)/2m \quad [-]$$

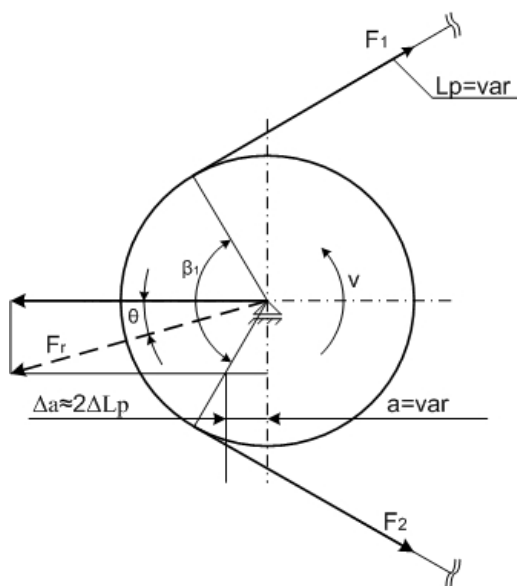


Fig. 3

Both methods accomplish the tensioning on the constructive way and, as a result, further operations of control and adjustment are no longer necessary.

The drive with $a, L_p = \text{constant}$, tensioned by forced fixing the belt with an initial elongation (Fig. 3):

$$\Delta L_p = \frac{F_0 L_p}{E_t A_c} = \frac{F_t L_p}{2\varphi E_t A_c} = \frac{m-1}{2\varphi c a k_\beta} \quad (-) \quad (7)$$

where, for L_p [mm], primitive length of the belt, $E_t A_c$ [N] traction rigidity; k_β represents the correction factor of the wrapping angle.

In this case, according to relations (1, 2, and 7) each belt must be tensioned when fixing it with the effort:

$$F_0 = 5c\varphi (K_r P / z v) (2.5 - k_\beta) / k_\beta + m_1 v^2 \quad [\text{N}] \quad (8)$$

3. ANALYSES, DISCUSSIONS, APPROACHES AND INTERPRETATIONS

The measurement of the fixing and in use tensioning effort

For the drives with $a, L_p = \text{constant}$, the initial tensioning effort can be measured indirectly in two distinctive ways:

The measurement of the fixing elongation Δl_0 [mm] of a belt segment, of initial length l_0 [mm], situated on one of the free sides of the drive (Fig. 4):

$$F_0 = (\Delta l_0 / l_0) A_c E_t \quad [\text{N}] \quad (9)$$

where: A_c [mm²] the belt's transversal section area; E_t [mm²] -the belt's equivalent elasticity module.

Examining the law of the propagation of errors (in the hypothesis of the use of a stress measuring device of first class precision) results that upon the precision of the measurement the determinant weight $\Delta E_t/E$.

$$\Delta F_0/F_0 = \pm [(\Delta l_0/l_0)] + (\Delta E_t/E_t) + (\Delta A_c/A_c) \cong \pm (\Delta E_t/E_t) \quad [-] \quad (9a)$$

Consequently, this measurement method may be used only if the experimental dependence load-strain $F(\Delta L)$ is known.

The measurement of the sag of the belt f_n [mm] produced by a control force F_n [N] applied normal on the middle of one of the branches opening l [mm] (Fig. 4).

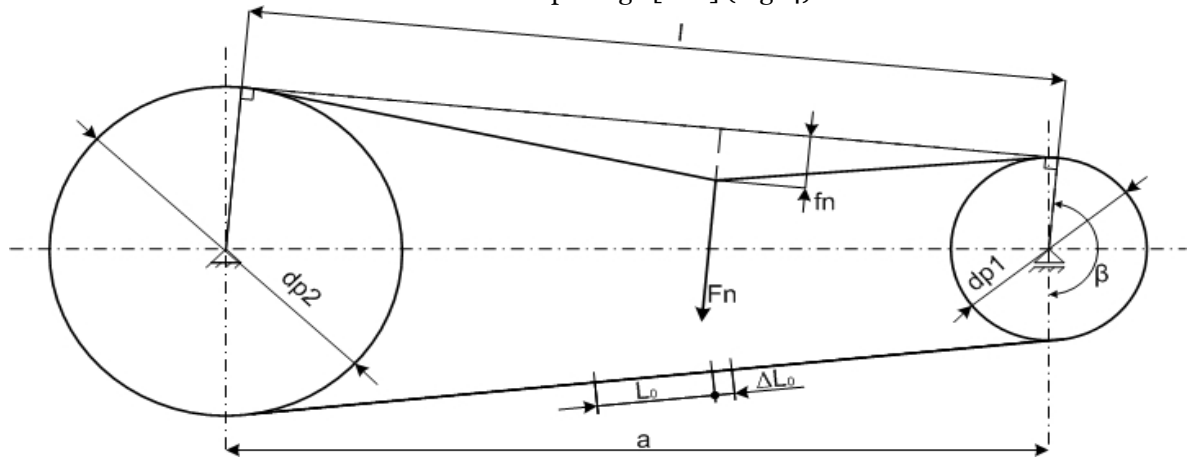


Fig. 4

The connection between control sizes f_n and F_n , the drive geometry and initial effort are shown in the following relation:

$$F_0 \cong F_n/4 (f_n/l) - 2A_c E_t (f_n/l)^2 (l/L_p) \quad [N] \quad (10)$$

where: $l = a \sin(\beta/2) \cong a \{1 - 0.125 [(d_{p2} - d_{p1})/a]^2\}$ [mm] is the length of the free side of the drive.

Perturbation analysis of the control force measurement shows the fact that the systematic errors can be minimized if $f_n/l \in [1/50; 1/100]$ (because $l/L_p < 1/2$ and $A_c E_t/F_0 \leq 100$)

$$\Delta F_0/F_0 = 2(f_n/l)^2 (l/L_p) A_c E_t/F_0 \leq 0.02 \quad [-] \quad (10a)$$

According to this theory there are recommended two alternatives:

a). Limitation of the f_n sag of the belt to the value $f_n = l/100$ [mm] (Gates method) in which the intensity of the control force is given by the relation:

$$F_n = [F_0 + 2A_c E_t (l/L_p)] 10^4 / 25 \quad [N] \quad (10b)$$

b). Fixation of the control force at the value $F_n \cong 0.5A_c$ [N] (Optibelt method) in which the proportioned arrow f_n/l must realize the relation 10.

First approximation is initialized at the value:

$$(f_n/l)^* = F_n / 4F_0 > (f_n/l)^* \quad [-] \quad (10c)$$

And by successive iterations the proportionate arrow (f_n/l) is obtained for which $\Delta F_0/F_0 \leq 0.01$.

The conduction law of measurement errors for both alternatives:

$$(\Delta F_0/F_0) \cong \pm (\Delta F_n/F_n + \Delta l/l + \Delta f_n/f_n) \cong \pm \Delta f_n/f_n \quad [-] \quad (10d)$$

As a result, at the measurement of the arrow the absolute error must be limited to the value:

$$\Delta f_m \in \pm (0.1; 0.5) \text{ mm.}$$

The Gates and Optibelt methods can be applied with any restrictions to any type of belt (round, flat or V). The belt's loosening imposes periodic control and correction of the initial tension by a conditioned program of endurance structure.

In case of a new belt the following stage control is recommended:

STAGE	o	I	II	III and the following
*Period of functioning	Installation (fixing)	0.5...5 hours	24...36 hours	500...1000 hours

*Inferior limits are accepted in case of a pronounced loosening!

4. CONCLUSIONS

The correct evaluation and periodic control of an initial tension are vital operations for the function of a belt drive in the projected parameters.

For the narrow V belts STAS 7192-81 specific parameters that complete the control and calculation of the initial tensioning have the following values:

Profile Parameter	SPZ	SPA	SPB	SPC
m_1 [kg/m]	0.066...0.07	0.12...0.13	0.17...0.21	0.32...0.38
A_c [mm ²]	53	89	153	279
$F_n = 0.5A_c$ [N]	25	50	75	125
$2A_c E_r \cdot 10^{-4}$ [N]*	15	20	26	41

*Chords by polyestheric fibres.

Outside the specifications according to the shafts parallelism and belt pulleys alignment the execution and exploitation documentary must contain the minimum recommendations regarding the appropriate tension effort intensity and the control method.

REFERENCES

- [1.] Gheorghiu, N., Transmisii prin curele trapezoidale- contributi la studiul teoretic si experimental al capacitatiide tractiune- Teza de doctorat, IPTV Timisoara, 1969/70.
- [2.] Gheorghiu, N., Ionescu, N., Argasanu, V., Sistematizarea controlului tensionarii initiale la transmisiile prin curele, PRASIC-Brasov, mai 1982.
- [3.] *** Antriebaentwurfshandbuch für Industriekeilriemen, Gates (Deutschland) GmbH.
- [4.] *** Berechnungsunterlagenbuch für Optibelt-Keilriemen mit Kevlar-Aufbau, Arntz-Optibelt KG.
- [5.] *** Blauri Schmalkeilriementriebe und Keilriementriebe-Groößenbestimmung Henn-Leistungen, A. Fr. Flender GmbH.
- [6.] www.syncrotech.eu
- [7.] www.gates.com
- [8.] www.optibelt.de



¹Cristina Carmen MIKLOS; ¹Imre Zsoft MIKLOS; ¹Carmen Inge ALIC

COMPUTER AIDED ANALYSIS OF A DIFFERENTIAL GEAR WITH SIMPLE SATELLITE

¹⁻³ UNIVERSITY POLITEHNICA OF TIMISOARA, FACULTY OF ENGINEERING FROM HUNEDOARA, ROMANIA

ABSTRACT:

In the present paper shows how to achieve structural and kinematic analysis of a differential gear with simple satellite, assisted by computer, using an application written in Matlab, based on the method of Willis. Differential gear with satellite is simply part of the chain of kinematic motion transmission from tilting mechanism from the Blooming type rolling trains.

KEYWORDS:

differential gear, planet gear, planet carrier, degree of mobility, kinematic analysis

1. INTRODUCTION

Differential gear who is studied in this paper is part of the handling - tilting mechanism, from the blooming type rolling train. Kinematical scheme of the handling - tilting mechanism is shown in figure 1.

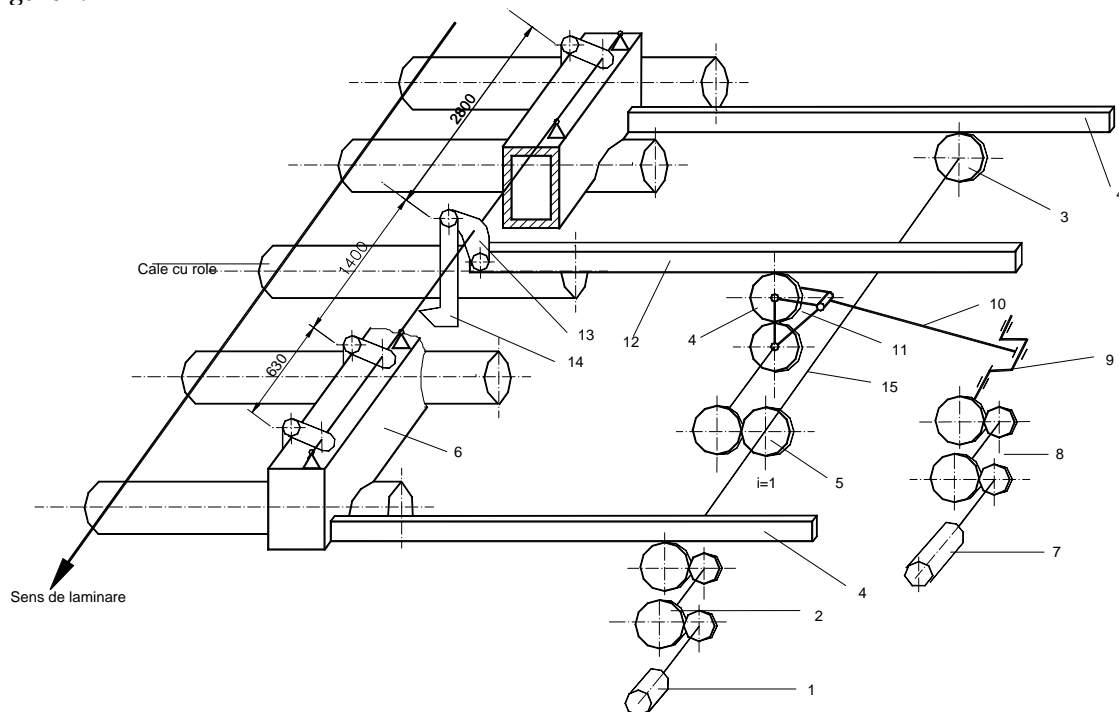


Fig.1. Kinematic scheme of the handling - tilting mechanism

From Figure 1 shows that the two mechanisms (handling and tilting) acting on interdependence. Handling mechanism is driven by electric motor (1), which through the gears (3) (pinion - rack) act handling ruler rods (4). It is noted that the rollover mechanism hooks (14) are mounted directly on handling ruler, so during the handling process they must move with them together, without performing the actual overthrow (hooks must remain stationary). This is ensured

by the gears train (5) that synchronizes the movement of the two mechanisms and through the differential gear (11) allows racks movement (12), together with handling ruler, so the rollover mechanism will remain stationary.

To achieve the overthrow blooms without there side move, of the handling drive motor is stopped by braking, and the differential gear drive motor is turned on. In this way is distributing movement on crankshaft (9) mounted on the gear output shaft (8), and through the connecting rod (10) at the housing differential gear (11), (which serves as a satellite port arm) impart him an oscillatory motion. By this motion, spur gear (4) (satellite) rotates clockwise and engage the tilting mechanism rack, which it gives a movement that allows the uplift hooks. Through a complete rotation of the mechanism tilting crankshaft is achieved also the uplift and descent their hooks.

2. ANALYSIS OF A DIFERENTIAL GEAR WITH SIMPLE SATELLITE

Geometric and kinematic input data's necessary for structural and kinematic analysis of the differential gear are taken from the tilting mechanism analysis results of the rolling train [4], [5].

Kinematic scheme of the differential gear who engages the tilting mechanism is shown in fig.2.

Differential gear is composed of central wheel **rc**, satellite **s**, planet carrier **b** (housing gear) and the rack **cr**. Central wheel and the satellite are cylindrical spur gear of the same size ($r = 378$ [mm]), and the same number of teeth $Z_c = Z_s = 18$, the modulus being $m = 42$ [mm].

Differential gear is considered a plan mechanism with number of family 3, has four moving parts (central wheel **rc**, satellite **s**, planet carrier **b** and rack **cr**), four kinematic lower joints on V class (three rotational and one translational - fig. 2) and two kinematic upper joints on IV class (the two points of engagement). Mechanism degree of mobility is:

$$M_3 = 3n - 2C_5 - C_4 = 3 \cdot 4 - 2 \cdot 4 - 1 \cdot 2 = 2$$

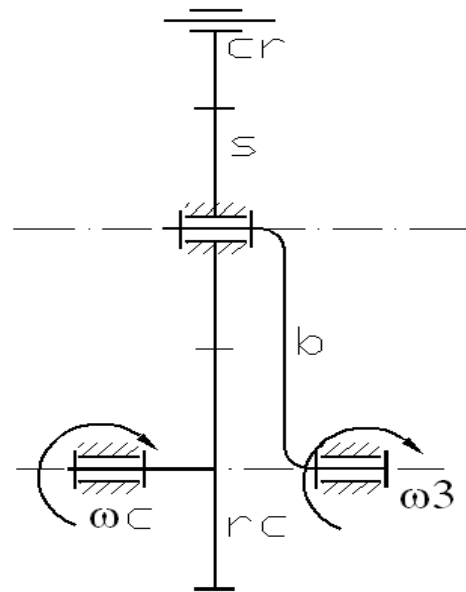


Fig.2. Differential gear kinematic scheme

With the conditions that the central wheel is braked (differential gear action time), the mechanism is reduced to three mobile elements (satellite **s**, planet carrier **b** and rack **cr**), three kinematic lower joints V class (two rotational and one translational - fig. 2) and two kinematic upper joints IV class. Mechanism degree of mobility is:

$$M_3 = 3n - 2C_5 - C_4 = 3 \cdot 3 - 2 \cdot 3 - 1 \cdot 2 = 2$$

and so the mechanism is a planetary mechanism.

Universal method for kinematic study of the differential gear and planetary gear is stop planet carrier method or Willis method. For the kinematic study the real mechanism need to turn into an equivalent mechanism with fixed axes, whose study is already known. In order to understand the problems easier is used a new scoring system for the transmission ratio, who has

three indices: i_{a-b}^b , where **i** is mechanism gear ratio, the higher index is fixed element to which motion is relate, in this case planet carrier **b**, and lower indices in order, are the driver element **a** and the driven element, **b**.

Stop planet carrier method is that the in imaginary mode to entire mechanism assembly is give an angular velocity $-\omega_3$ (or speed $-n_3$), opposite to the gear case angular velocity ω_3 (with planet carrier role) around its own rotational axis. In this way planet carrier (gear housing) will have zero angular velocity, planetary gear has become an ordinary gear, which can be studied by known methods.

$$i_{rc-cr}^b = \frac{\omega_c - \omega_3}{\omega_s - \omega_3} = -\frac{Z_s}{Z_c} = -1$$

During the tilting mechanism operating the central wheel is fixed ($\omega_c = 0$), so the angular velocity of the satellite will have the following value:

$$\frac{-\omega_3}{\omega_s - \omega_3} = -1 \Rightarrow \omega_s - \omega_3 = \omega_3 \Rightarrow \omega_s = 2 \cdot \omega_3$$

and the rack linear speed of movement will be:

$$V_{cr} = r \cdot \omega_s$$

The calculations above are provided from Răsturnător1000 program written in Matlab, and the angular velocity of the satellite according to the position angle φ_1 of the crank tilting mechanism is shown in fig. 3 [4].

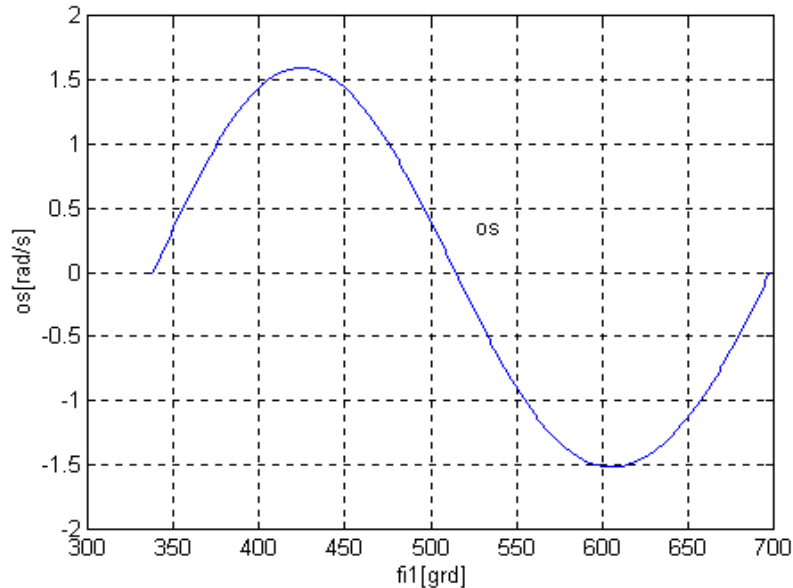


Fig.3. Satellite angular velocity

3. CONCLUSIONS

Differential gears with simple satellite structural and kinematic analysis, but also other types of construction, are achieved simply by applying the Willis method, and by using computer programs written in different programming languages. Before the kinematic analysis, according to fig.3 results a sinusoidal continuous variation of satellite angular velocity:

- satellite angular velocity from the differential gear ω_s is twice the gear case angular velocity with the conditions that during the tilting mechanism operating the central wheel is braked.
- angular speed ω_3 gear case varies between the following limits: 0,9 [rad/s] and 0,95 [rad/s].

REFERENCES

- [1.] GHINEA, M., FIREȚEANU, V., Matlab, calcul numeric, grafică, aplicații. Editura Teora București 1997.
- [2.] MANOLESCU, N., KOVÁCS, FR., Teoria mecanismelor și a mașinilor, Editura Didactică și Pedagogică, București, 1972
- [3.] MIKLOS, I. Zs., Mecanisme. Analiza mecanismelor, Editura Mirton Timișoara, 2005
- [4.] MIKLOS, I. Zs., Contribuții cu privire la îmbunătățirea performanțelor tehnologice ale mecanismelor de răsturnat la liniile de laminare, Teză de doctorat, Universitatea din Petroșani, 2001
- [5.] ZAMFIR, V., MIKLOS, I. Zs., The kinetostatic analysis of the tilting mechanism at the 1000 mm rolling train, UPT's Scientific Bulletin, Vol. 44(58), Fascicle 2, 1999
- [6.] * * * Instrucțiuni tehnologice pentru liniile de laminare Blooming 1300 și 1000 mm, Combinatul Siderurgic Hunedoara, Uzina nr.4 – Laminoare, Vol. II, 1983





¹ Camelia PINCA -BRETOTEAN, ² Gelu-Ovidiu TIRIAN

CONSIDERATIONS ON THERMAL FATIGUE INTERNAL COMBUSTION ENGINES

¹ UNIVERSITY POLITEHNICA OF TIMISOARA, FACULTY OF ENGINEERING FROM HUNEDOARA, ROMANIA

ABSTRACT:

This paper refers to the principle of thermal fatigue research on internal combustion engines, particularly for Dacia engine ignition engines.

Knowing the negative effects in case of any harm caused to the gears making up the internal combustion engines, in order to mitigate the causes of destruction caused by cracking, we must do some thorough, complex, theoretical, and experimental research on thermal fatigue, using new theoretical and experimental approaches. Research is done in three directions: to study the thermal component of part machineries, to study and perform experimental determination of variable fields of surface temperature of machine components, to perform experiments on thermal fatigue life samples subjected to different regimes of stress. The main objective of this paper is to solve complex problems of internal combustion engines by acquiring new, original, theoretical and experimental knowledge on the thermal fatigue phenomenon that occurs in part machinery enabling the transfer of heat from the combustion chamber to the cooling fluids for engines fitted to motor vehicles.

KEYWORDS:

Thermal, fatigue, internal, combustion, engine, cyclic

1. INTRODUCTION

Basic research on thermal fatigue of internal combustion engines is an important problem both from a theoretical or an experimental point of view, but also in economic terms.

Machine gears of motor vehicles participate in the working cycle. This cycle is characterized by temperature variations. Such variations are important for heat developed inside the combustion chamber and sent forwards to the cooling fluid. Thus, within certain parts of their gears, they create some temperature fields triggering cyclic tension. The rate of temperature change is very important in case of internal combustion engines fitted to motor vehicles; they create some variable and cyclical thermal fields up to a speed measured in seconds or even tenths of seconds, producing specific thermal fatigue cracks. These cracks appear after a certain number of thermal cycles; their number depends on the material machine gears are made of, as well as on the operating mode of the engine parameters. If the number of thermal cycles increases, it develops and increases heat exhaustion, and cause some specific surface cracks across the entire surface layer of the gears, negatively changing energy and economic indices of the engine.

Knowing the negative effects in case of any harm caused to the gears making up the internal combustion engines, in order to mitigate the causes of destruction caused by cracking, we must do some thorough, complex, theoretical, and experimental research on thermal fatigue, using new theoretical and experimental approaches. We must study and do important research on thermal fatigue, not only mitigating the raging crack, but also avoiding thermal shock, which is particularly dangerous during working of the engine. Classical methods of resistance calculation for machine gears inside internal combustion engines which are exposed to thermal fatigue do not consider the demands of certain items, which are caused by variations of temperature fields across the surface and within the surface layer. Such phenomena occur during the engine working, and it is being offset by increasing the allowable tension values.

Although scientific literature referring to the research on internal combustion engines is quite extensive, research do not refer particularly to the phenomenon of thermal fatigue within the superficial layer of fixed and mobile machine gear. The research of thermal fatigue of internal combustion engines, particularly of fixed and mobile machine gears, is less studied both on national and international level.

So far, there are no specialized publications covering thermal fatigue of internal combustion engines in detail, both theoretically and experimentally. Within the context of market economy, a new development in basic research of thermal fatigue of machine gear is necessary. This research should use the most modern and efficient solutions.

2. METHODOLOGY AND DISCUSSION

The main objective of this them of researches is to solve fundamental and complex problems of internal combustion engines by acquiring new, original, theoretical, and experimental knowledge on thermal fatigue occurring inside all machine gears that enable the transfer of heat from the combustion chamber to the cooling fluid inside internal combustion engines.

During internal combustion engines working, specific fatigue cracks appear within the surface layer of any item enabling the transfer of heat, and they grow slowly due to thermal cyclic variations of temperature fields, [1].

Thermal fatigue cracks appear on the surface and within the outside layers of the parts participating in the heat transfer. Thermal fatigue cracks specific that develops gradually because of cyclic temperature variations. These cracks appear and on the upper layers and on the surface of parts machineries (although in the most favorable operating conditions), limiting their use to situations which have negative effects on energy and economic indices of the engine[2],[3].

To study thermal fatigue of the organs that make up fixed and mobile internal combustion engines the following objectives must be achieved:

- ❖ to study the thermal behaviour of part machinery of vehicle engines participating in the transfer of heat from the combustion chamber cooling fluid during operation;
- ❖ to experimental and determine all variable fields and surface temperature of the upper layers of part machinery;
- ❖ to perform experimental research on fatigue resistance of samples subjected to different thermal regimes request.

The operation of an internal combustion engine is characterized by a set of values that define the operating system. The operating regime is defined by three fundamental dimensions: speed, load, and temperature characterizing the thermal regime of the engine. The thermal regime is the body temperature indicating the degree of enforcement mechanism for heating the engine. Thermal regime is indicated by the exhaust gas temperature " t_{ge} " or cooling fluid temperature " t_r " [2].

To achieve thermal regime we have built a trial bench to measure the temperature inside the combustion chamber and cylinder head wall temperature in the intake and exhaust valves, fig.1.



Fig.1 The experimental bench with ignition engine type Dacia

Experimental bench includes a Dacia spark ignition engine, with all related auxiliary facilities that allow normal functioning. The engine is mounted on a resistance structure which enables a rather good stiffness to the bench and eliminates engine vibration during operation, a phenomenon that would adversely affect experimental measurements.

The thermal study raises questions about [1], [2],[4], [5] how to: clarify the limit; evaluate heat passing through the pieces as part of the heat developed in the combustion chamber;

The main technical parameters considered for a thermal study of spark ignition engine are [1], [2], [4], [5]: gas temperature; pieces on the wall temperature chamber and the cooling fluid; heat transfer coefficient.

Of all these parameters, the temperature of the combustion chamber is necessary to determine how precisely it influences major heat transfer and thermal default application of part

machinery of the engine structure, both directly and through the coefficients of convection, radiation and conduction heat [1], [4]. Thus, the gas temperature in the engine combustion chamber is determined analytically and experimentally.

In terms of analytical research, gas temperature in the combustion chamber is determined based on the indicated chart, and the method involves choosing a number of sizes that varies a lot, which means obtaining the actual values who differ from the regular ones.

From the experimental point of view, gas temperature in the combustion chamber is determined by a chamber of thermo-vision, type T200 - the characteristics of the view field are of 25 x 19 mm focus distance, min 0.4 laser semi penetrating mm, 635 HM (red) laser wavelength, and 7.2 V ionic power battery. Following the transfer of heat from flue gases to the walls of the chamber, by convection and radiation transfer that occurs inside the internal combustion engines mechanical stress, thermal stresses appear in addition. Temperatures that vary over time in the combustion chamber are transmitted as oscillations to fixed and mobile part machinery composition engine. Heat taken from them during operation is transferred to a lesser extent during the gas engine fluid change. Depending on the quantity of heat generated by engine operation and the different thermal resistance which occur during heat transfer (thermal conductivity material, building sections, etc.), part machineries suffer from temperature fields. These fields are cyclic at very small intervals (seconds or tenths of seconds) and are responsible for the occurrence of thermal fatigue.

The reason why these varying temperature fields occur is explained as follows: during the intake stroke of a piston engine, the intake valve is open, and cool air intake cools off the intake drift; during the compression stroke both valves remain closed; at the beginning of the compression cylinder walls yield air heat. In the further compression, the phenomenon is reversed, heat flows from the compressed air cylinder walls during the discharge gas resulting from combustion exhaust valve opens, and exhaust gases warm up the gallery.

Determination of the variable temperature field is the second objective of further research on thermal fatigue. Their experimental determination is made by mounting thermocouples in the wall of Dacia engine cylinder head areas of intake and exhaust valves fig. 2.

Thus, we have created a succession plan that includes next steps:

- ❖ Removing the entire engine cylinder head;
- ❖ Appropriate training to detect areas where the cylinder head and the temperature difference is high;
- ❖ Drawing and making channels in areas to be fitted thermocouples;
- ❖ Performance and installation works were thermocouples;
- ❖ Fitting the so prepared engine cylinder head assembly;
- ❖ Check thermocouples mounting and connecting them to systems of data acquisition;
- ❖ Measuring and recording changes in temperature fields;
- ❖ Assessing and obtaining experimental determinations of temperature charts;
- ❖ Highlighting areas where thermal fatigue occurs.

Following the analytical calculations, we observed that the center axle of the valve is subject to cyclical variations in temperature, fig. 3.

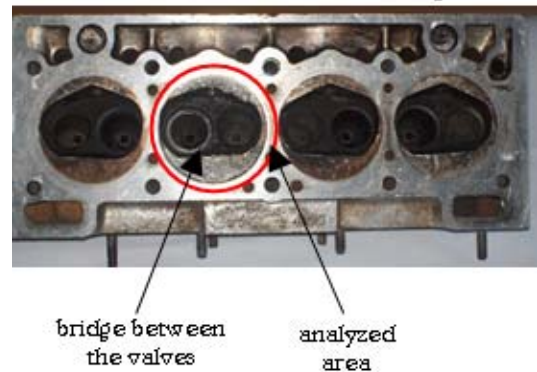


Fig.2 Studied area of Dacia engine cylinder head

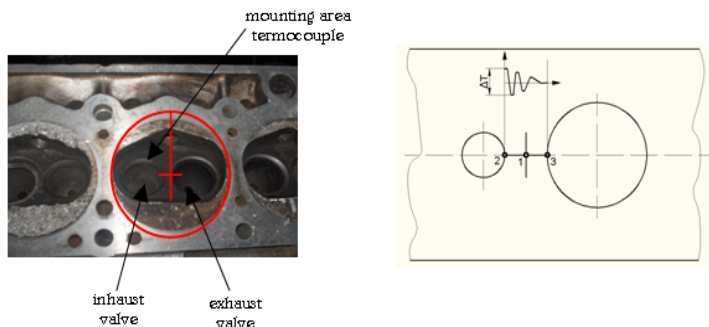


Fig.3 Location of the areas that appear schematized cyclical temperature changes

The center deck of valves - the zone is located in section 1 - the highest temperature occurs at the end of the combustion process. The highest temperature difference at the end of admission is between points 1 and 2, and between points 1 and 3 the difference still reaches the highest value at the end of the admission, but less than that between points 1 and 2. Temperature oscillation amplitude gets lower to reaching the cooling fluid. The highest amplitude of

these oscillations occurs during the engine operation in overload. The effect of these oscillations and the temperature difference is the appearance of thermal stress cracks generating specific thermal fatigue. This phenomenon is more pronounced inside spark ignition engine cylinder heads due to operation in very different thermal regimes. In general, engine parts fitted vehicles is more pronounced appearance of cracks due to operation in very different thermal regimes compared to engines operating in stable regimes, [2], [3].

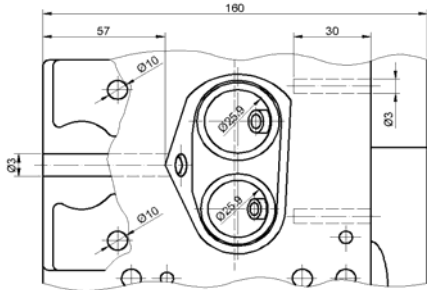


Fig.4 Position channels for mounting thermocouples

For sensing variable temperature fields were chosen thermocouple Pt, Rh-Pt, with a measuring domain of -50 ... 17500C, 0.01 mm diameter, and 6 V/oC by sensitivity. These thermocouples were installed near the outlet and inlet pipes and valves in the deck of under representation of fig. 4. These thermocouples are connected to a data acquisition system comprising a data acquisition card that allows recording data during engine operation. When using such a computer program experimental data are processed and converted into temperature charts. Through these diagrams temperature we are able to determine the evolution of thermal tensions causing thermal fatigue.

Further research will be done to study how thermal fatigue influence part machinery constituting the main engine, on an original design facility being registered by OSIM patent, No. A/00439/17.05.2010. This facility was originally designed for durability determinations in thermal fatigue tests as rings, made by hot rolled cylinders.

This facility suitable for experimental determination of thermal fatigue involves mounting some samples of various sizes and shapes on the main shaft of ignition engine, and which are subject to simultaneously heating in an oven at a temperature of 1000° C and cooled off in different environments. Samples are mounted tangentially on all generators of rigid disks mounted on the main axis of the plant. In fig. 5 we describe the intermediate and edgeways support discs provided with channels for assembling samples that may have cross-section shapes and sizes, and different lengths, but approximately equal sets.



Fig.5 Lateral and intermediate support discs provided with channels mounted on the main axis, prepared for sample mounting



Fig.6 Thermocouples crossed through the main axis of the facility to connect their data acquisition system



a - overview of the oven for sample heating



b - detail view of the oven profile



c - loop mounting resistors for electric sample heating

Fig.7 Oven to heat samples taken from fixed and mobile parts machinery of a ignition engine to determine thermal fatigue resistance

Thermocouples are mounted on two samples set opposite on the circumference of the supporting disc. These thermocouples response inertia correspond to thermal load cycle, whose conductors are rigid and sent to the reaming of the main shaft to the tension collector, and then to data acquisition system that allows simultaneous recording of temperature variations of experimental application. In Figure no. 6 we describe thermocouples that cross through the main axis to connect their facility data acquisition system. During experiments samples of different materials and quality are subject to cyclic thermal heating inside ovens and cooled off in different environments, fig.7 - carbonic snow, water, and air.

3. CONCLUSIONS

The main objective of the paper is determining the main directions and principles of experimental research work on thermal fatigue phenomenon that occurs in part machinery that participate in the transfer of heat from the combustion chamber to coolant engines fitted to motor vehicles.

Importance of carrying out such research derives from the fact that thermal fatigue of vehicles' engines is less studied both nationally and internationally. So far no specialized publications which deal in detail, theoretical and experimental thermal fatigue of internal combustion engines. Market economy requires a new development in fundamental research of thermal fatigue of motor part machinery, using the most modern and efficient worldwide technology solutions.

REFERENCES

- [1.] Bătașă N., Brânzaș P, Iancu A.- Determinarea câmpului de temperatură pentru piesele de autovehicule solicate termic, Metrologie aplicată, Nr.6,1970
- [2.] Botean A.I. – Studiul solicitărilor termomecanice în motoarele cu ardere internă utilizând metode moderne de cercetare – Raport final grant de cercetare, 2006
- [3.] metode moderne de cercetare – Raport final grant de cercetare, 2006
- [4.] Popa B., Bătașă N., Mădărășan T., Marinescu M.- Solicitarea termică în construcția de mașini, Ed. Tehnică, București, 1978
- [5.] Tănase P.- Teoria modelării proceselor termoenergetice, Ed. Evrika, Brăila, 1996
- [6.] Teborean I. – *Agenți termodinamici și mașini termice*, Editura Dacia, 1999





¹Dinu DRĂGAN, ²Mircea Cristian ARNĂUTU,
³Nicușor Laurențiu ZAHARIA, ⁴Ion SIMION

2100 HP DIESEL ELECTRICAL LOCOMOTIVE RUNNING TEST

¹ ROMANIAN RAILWAY AUTHORITY – AFER, 393 CALEA GRIVIȚEI, BUCHAREST, ROMANIA

ABSTRACT:

The diesel – electrical locomotives are used from Romanian freight operators to run trains where electrical locomotives can't run. At Romanian Railways, one of diesel locomotives is 2100 HP Sulzer diesel – electrical locomotives.

KEYWORDS:

strain gauge, experimental stress analysis, Hottinger

1. INTRODUCTION

The early diesel – electrical locomotives manufactured in Romania under Sulzer license had leaf type springs at secondary suspension. During time, the operators wasn't satisfied about leaf type springs so it was necessary a replacement with other types of spring. One of the solutions was using of rubber springs. Because the dimensions of the rubber springs are others than leaf springs the frame of the bogie was modified so it was necessary to perform an experimental stress analysis with strain gages. According to the Railway standards, the tests can performed on bench test or with locomotive in circulation with a method accepted at Romanian Railways. Because in Romania are only wagon/passenger cars bench test, it was necessary to develop the test method necessary for testing the locomotive's bogie. This paper presents the method which was use for testing.

Figure 1 and figure 2 illustrate the two types of secondary suspension (leaf springs and rubber springs).



Fig. 1: Bogie with leaf spring



Fig. 2: Bogie with rubber spring

2. TESTS

The tests were performed in two steps:

- ❖ static tests,
- ❖ dynamic tests.

During the static test, were recorded the static stress σ_{st} due the locomotive's body action on the bogies.

Recording of the stress variation (dynamic components of the stress) $\Delta\sigma_+$ and $\Delta\sigma_-$ were made during locomotive's circulation on 100 km/h speed. Based on values of $\Delta\sigma_+$ and $\Delta\sigma_-$ were calculated utmost values of the stress with the equations:

$$\sigma_{\max} = \sigma_{st} + \Delta\sigma_+ \quad (1)$$

$$\sigma_{\min} = \sigma_{st} + \Delta\sigma_- \quad (2)$$

The medium value of the stress results from the equation:

$$\sigma_m = \frac{\sigma_{\max} + \sigma_{\min}}{2} \quad (3)$$

The amplitude of the stress results from the equation:

$$\sigma_v = \frac{\sigma_{\max} - \sigma_{\min}}{2} \quad (4)$$

The σ_v values were comparative with the values from Goodman – Smith diagrams presented in annex F.3 of the report ERRI B12/RP17. The allowable condition is:

$$\sigma_v \leq \sigma_{vadm} \quad (5)$$

In the figure 3 is presented graphically how the tests were done.

The measurement points were located in the relevant areas of the modified bogie's frame.

The measurements were performed in 10 points. Hottinger LY11-10/120 strain gages were glued on the elements of the bogie with Hottinger Z70 adhesive. The strain gages were connected at measuring devices with cables.

The measurements were performed with Hottinger Centipede 100 Multipoint Measuring Unit (for the static tests) and Hottinger MGCplus (for the dynamic tests).

The measuring devices Centipede 100 and MGCplus were connected to a laptop computer. The acquisition software used was Catman 4.5 (an Hottinger product).

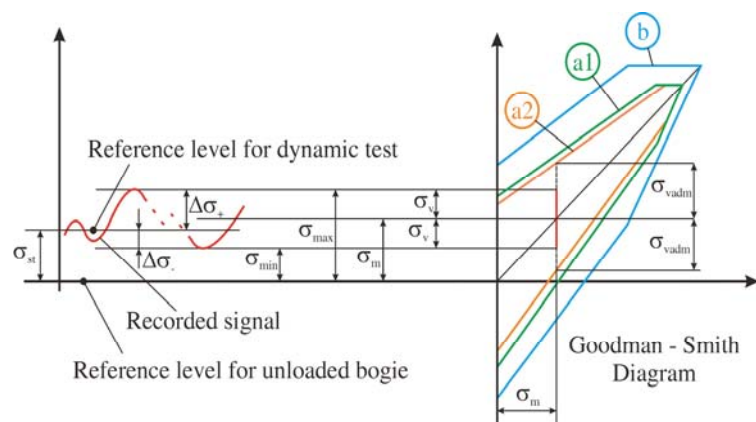


Fig. 3. Tests diagram

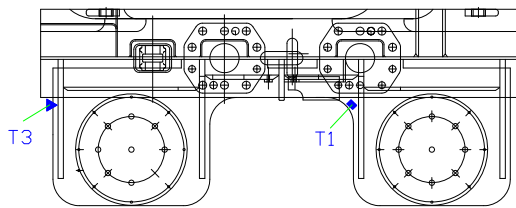


Fig. 4. Strain gauges T1 and T3

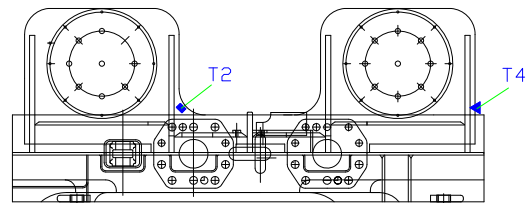


Fig. 5. Strain gauges T2 and T4

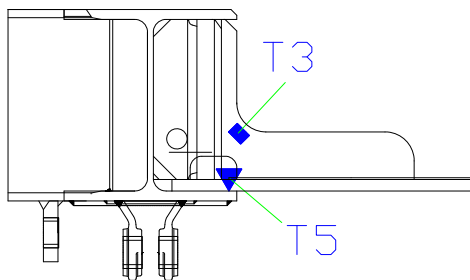


Fig. 6. Strain gauges T3 and T5

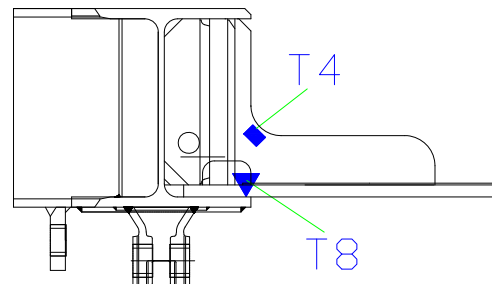


Fig. 7. Strain gauges T4 and T8

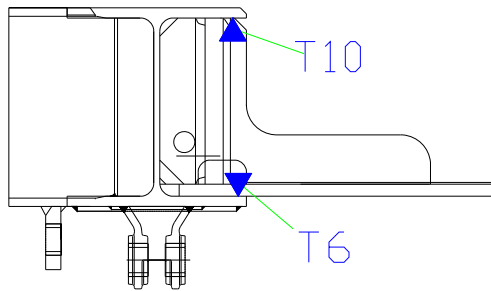


Fig. 8. Strain gauges T6 and T10

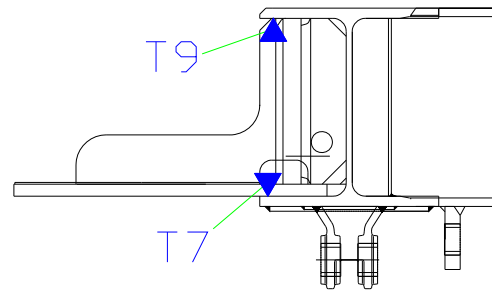


Fig. 9. Strain gauges T7 and T9

3. RESULTS

The dynamic diagrams of the measurement points are shown in figures 9÷14 (there are presented only the diagrams for the most stressed points static and dynamic).

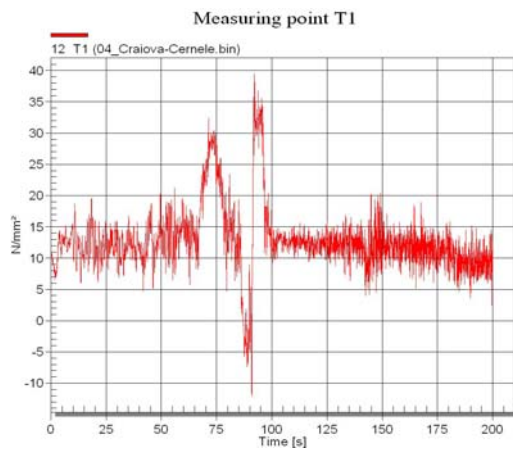


Fig. 10. T1 strain gauge stress

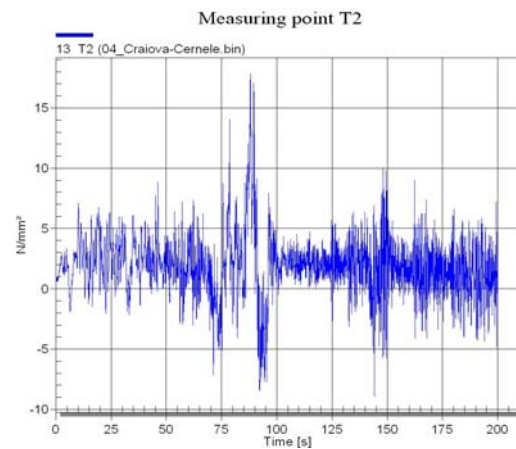


Fig. 11. T2 strain gauge stress

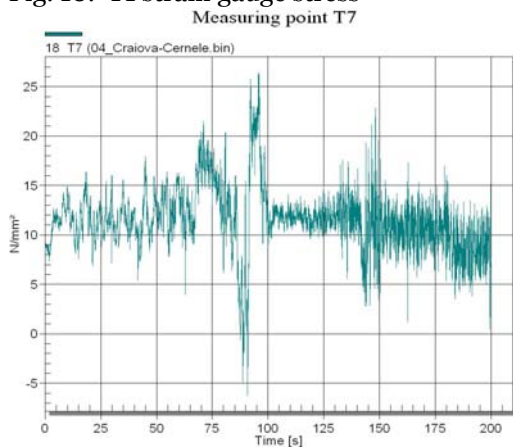


Fig. 12. T7 strain gauge stress

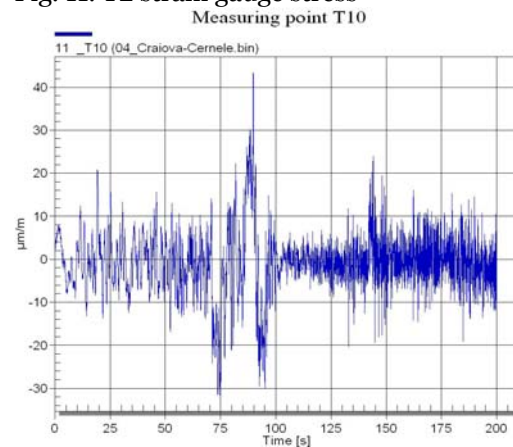


Fig. 13. T10 strain gauge stress

During the tests, the measuring tests were on curve “a2” and “a1” (from the Goodman – Smith diagram) – table 1.

Table 1: Position of the measuring points on Goodman - Smith diagram

SG	T1	T2	T3	T4	T5	T6	T7	T8	T9	T10
Curve	a2	a2	a2	a1	a2	a2	a2	a2	a2	a2

4. CONCLUSIONS

The results, was smaller than permissible stress, so we can concluded that the design solution used by manufacturer was good.

Based on test results, the designer can improve his design to increase the quality of the final product.

After the tests the new certification from the Railway Commission was obtain.

REFERENCES

- [1.] Mănescu T. Ș., Jiga G. G., Zaharia N. L., Bîtea C. V., Noțiuni fundamentale de rezistența materialelor și teoria elasticității, Editura „Eftimie Murgu”, ISBN 978-973-1906-67-6, Reșița, 2010
- [2.] Mănescu T. Ș., Jiga G. G., Zaharia N. L., Bîtea C. V., Noțiuni fundamentale de rezistența materialelor, Editura „Eftimie Murgu” Orizonturi tehnice, ISBN 973-8286-79-4, Reșița, 2008
- [3.] Mănescu T. Ș., Copaci I., Olaru S., Creangă F.Ș, Tensometria electrică rezistivă în cercetarea experimentală, Editura Mirton, ISBN 973-661-892-5, Timișoara, 2006
- [4.] Karl Hoffman: An Introduction to Measurement using Strain Gages, Hottinger Baldwin Messtechnik GmbH, Darmstadt, 2005
- [5.] Mănescu T. Ș., Zaharia N. L., Experimental Stress Analysis at a Diesel – Electrical Locomotive Frame Bogie, Structural Analysis Of Advanced Materials Proceedings, page 123, ISBN 978-2-9534804-0-5, Tarbes, Franța, 2009
- [6.] ***ERRI B12/RP17 – Programme des essais à faire subir aux wagons à châssis et superstructure en acier (aptes à recevoir l’attelage automatique de choc et traction) et à leurs bogie à châssis en acier, Utrecht, 1997



STRUCTURAL AND FUNCTIONAL PARTICULARITIES AS A CRITERION FOR THE DESIGN OF TANGENTIAL BELT DRIVE

¹⁻⁴ UNIVERSITY "POLITEHNICA" TIMIȘOARA, FACULTY OF MECHANICS, TIMIȘOARA, ROMANIA

ABSTRACT:

The tangential belt drive is a relatively inexpensive solution to increase productivity in the textile industry and it is made by assembling two friction transmissions with flexible elements into a functional hybrid system, namely an open flat belt drive with parallel shafts and velocity ratio $i=1$ as being the motor element for the actual tangential drive (reduced to the driving wheel), and the tangential transmission itself, consisting of the "n" consumers displayed cvasitangentially on one or both free sides of the flat belt drive (basic drive) being the driven element. The functionality of this drive is based on the friction force between the belt and driving pulley on one hand, and between the belt and the tangential pulleys on the other hand.

KEYWORDS: tangential belt drive, productivity

1. INTRODUCTION

Increasing productivity in the textile industry was made simultaneously in two ways:

- ❖ by increasing the processing speed;
- ❖ by increasing the number of processing stations which equips a single machine.

The simultaneous drive of the spindles of textile machinery requires the following additional conditions:

- ❖ the starting and the stopping of the spindles must be made simultaneously when starting or stopping the machinery;
- ❖ speed differences between two or more spindles to be within acceptable limits of the processing method (reflected by the uniformity of the produced wires in length and overall);
- ❖ stopping and starting a post should not affect the operation of the other posts;
- ❖ low cost.

These requirements have led to the emergence of a new transmission, the tangential drive which is a speed amplifier and uses a flat belt with both sides active.

The tangential drive is strictly applied in the textile industry, spinning machinery, twisting, texturing, elastic wrapping etc. and, more recently, in mail sorting.

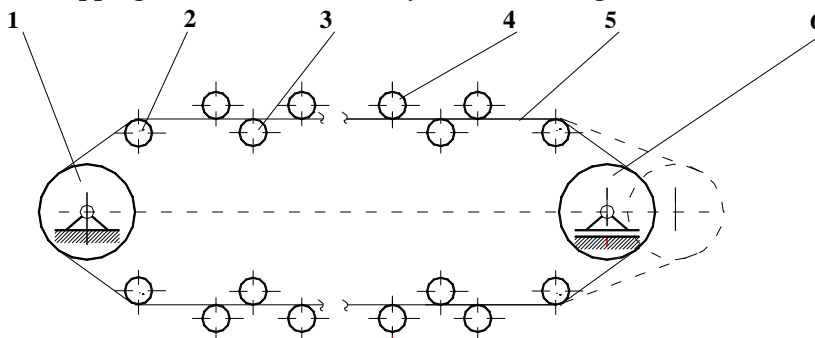


Fig.1a. 1. driving pulley; 2. deviation pulley; 3. pressure pulley; 4. tangential pulley;
5. tangential belt; 6. deviation (free) pulley.

It is made by assembling two friction drives with flexible elements into a functional hybrid system, namely (fig.1a):

- ❖ an open flat belt drive with parallel shafts and velocity ratio $i=1$ as being the motor element for the actual tangential drive
- ❖ the tangential drive itself, consisting of the "n" consumers displayed cvasitangentially on one or both free sides of the flat belt drive, being the driven element.
- ❖ in the same direction and having the velocity ratio $i=1$. On its free sides there are disposed the driven tangential pulleys. The deviation pulley rotates free and doesn't transmit energy.

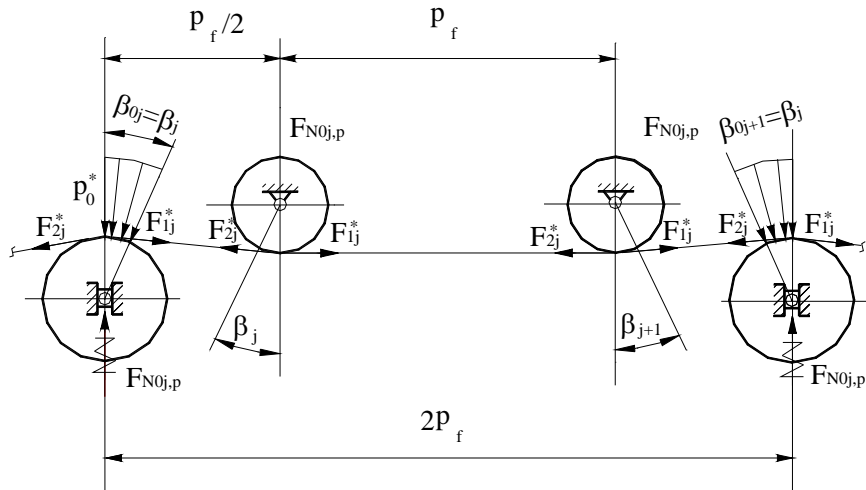


Fig.1b

The over all size of the drive and the tensioning of the belt is determined by this construction. The dimensions of the drive are established in two steps:

- a. the pulley diameter of the flat belt drive can be calculated by using one of the quasi empiric relations [1]:

$$\begin{aligned} d &\gg c_d (k_A P_m / \omega_m)^{1/3} \quad [\text{mm}] \in \{d_1\}_{STAS} \\ d_1 &\gg (d_{min}/h)_a \cdot h \quad [\text{mm}] \in \{d_1\}_{STAS} \end{aligned} \quad (1)$$

The option must satisfy the obvious equality:

$$\omega_m \cdot d_1 = \omega_f \cdot d_f \quad (2)$$

where:

ω_f [rad/s] - angular velocity;

d_f [mm] – tangential pulley diameter (sizes required by the process and by construction/ design).

If equality (1) is not satisfied, parameters ω_m and d_1 are changed within rational limits (engine change or introducing an additional drive between the engine and the primary transmission).

- b. The distance between the $d_{1,2}$ pulley axes of the primary transmission is evaluated from the following:

$$a \cong [n' + (2 \dots 3)] p_f + d_1 \quad (3)$$

by : $n' = n$ or $n' = 0,5 n$ –it is expressed the number of the tangential pulleys disposed entirely to a side or divided on both of the free sides (of useful length $l \cong n' \cdot p_f$).

p_f [mm] is the optimal distance between two successive tangential pulleys (step) and it is set by the textile machine manufacturer according to its type, processed wire and processing technology;

- c. Whereas the pressure pulleys have a diameter $d_p \geq d_f$, the step p_f and the distance between axes will be adjusted in the second approximation thus setting the actual drive overall dimensions;

- d. The geometrical sizes being established and given the flat configuration of the twin transmission (see fig.1a), it is established graphically or analytically the primitive length of the belt (L_p) and the wrapping angle on the driving pulley (β_1).

2. TANGENTIAL BELT DRIVE TENSIONING. RATIONAL LIMITS OF THE INITIAL TENSION

To achieve the friction force necessary for the energy transfer, the two drives will be tensioned individually, namely: the flat belt drive is permanently tensioned with a and $L_p =$ variable; (fig.3) and the tangential belt drive itself will also be permanently tensioned with spring or, more rarely, roller locked (fig.3).

The first step is the stretching of the belt and takes place when the tangential pulleys are moved off. It must create the operating conditions of the whole drive. The force of initial tension is installed like in open belt drives with parallel shafts rotating in the same direction, with variable center distance, and corresponds to the total peripheral force to be transmitted by the driving pulley (fig.2).

The second step also involves two different stages:

- ❖ bringing the tangential pulleys into contact with the belt;
- ❖ the realization of an angle of contact on the tangential pulleys and providing for a permanent belt tension irrespective of its stretching by help of idler pulleys. A lamellar spring device ensures pressure of idlers on the belt (fig.3).

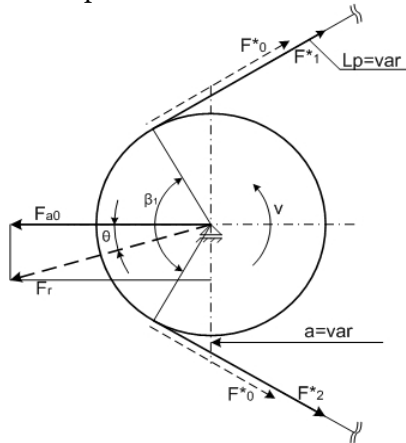


Fig.2

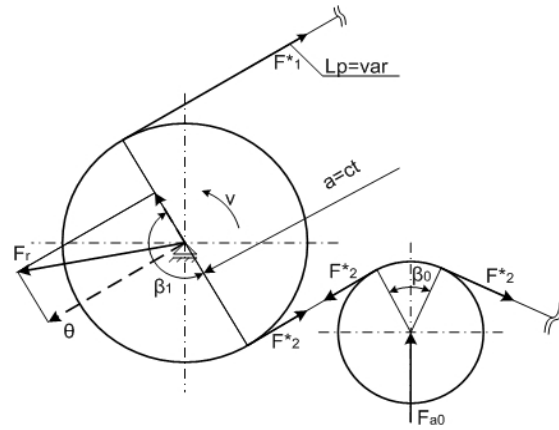


Fig.3

3. ANALISES, DISCUSSIONS, APPROACHES and INTERPRETATIONS

a. The pulling capacity, efficiency and fatigue resistance of a belt drive are conditioned by a proper assessment and by the conservation in time of the stretching.

The force of initial tension is installed like in open belt drives with parallel shafts rotating in the same direction, with variable center distance, and corresponds to the total peripheral force to be transmitted by the driving pulley. On the driving pulley (1) Fig.1 the wrap angle $\beta > 30^\circ$ corresponds to the case of classical belt drive studied by the specialized literature. Thus, the tensioning force is for the real values of the power and torque transmitted by a spindle on a textile machine [1];

$$P_m = c_1 \sum_{j=1}^n P_j \cong c_1 \cdot n \cdot P_j \quad (4)$$

$$F_t = \sum_{j=1}^n F_{tj}; F_{tj} = \frac{2T_j}{d_j}; T_j = \frac{P_j}{\omega_j}$$

b. The actual tangential drive is achieved likely a belt drive $a = ct$, $L_p = var$ strained by loading the conducted side of the drive (with an idler) with an external force having a invariable intensity and direction (fig. 3). The wrap angle on the tangential pulley (4) tends to zero as in friction drives when friction is of coulombian nature. In this case the Euler formula loses its validity. Pressure of the idler on the belt is recommended in the catalogues of Habasit and VIS tangential belt firms from the formulae:

$$F_{N0j,f} = 2.5 \cdot \frac{F_t}{n} \quad (\text{Habasit}) \quad (5)$$

$$F_{N0j,f} = 2.2 \cdot \frac{F_t}{n} \quad (\text{VIS}) \quad (6)$$

where:

F_t = peripheral force for the entire machine;

n = number of operating members.

As we can see, these formulae do not contain explicitly the coefficient of friction.

4. CONCLUSIONS

The overall size of a tangential belt drive is determined especially by the technological process. The tangential pulleys have a very small wrap angle ($\beta_j < 5^\circ$) that introduced in the Euler's formulae the relations are losing their validity. This low value of the wrap angle β_j of the belt on the tangential pulley (fig.1) allows us to describe the proper tangential belt drive with equations specific to cylindrical friction drives, that is, following the coulombian friction model. In this case, the higher the coefficient of friction, the lower is the pressing force on the belt corresponding to the tangential consumer (the spindle of the textile machine

REFERENCES

1. Jula M, Mădăras About the Necessary Pressing Force in Tangential Belt Drives., Buletinul științific al Universității „Politehnica” din Timișoara seria Mecanica, Tom 49(63), Fascicola 2, 2004.
2. *** Catalog VIS
3. *** Catalog Habalsit



¹ Sebastian DUMA, ²Mihaela POPESCU, ³Cosmin LOCOVEI

STUDIES REGARDING THE ACQUIREMENT OF HARDNESS STANDARD BLOCKS FOR TRANSMITTING THE VICKERS HARDNESS SCALE 200...800 HV₁

¹ UNIVERSITY "POLITEHNICA" TIMIȘOARA, FACULTY OF MECHANICS, ROMANIA

ABSTRACT:

Abstract: In the present work the conditions that the hardness standard blocks must comply with are briefly presented in order to materialize the Vickers scales HV₁. Starting from these conditions the accent is placed on choosing the material, the primary and secondary treatment applied in order to comply with the imposed metrological requirements for the hardness standard blocks.

KEYWORDS:

Vickers, scales, hardness standard blocks, hardness testing

1. INTRODUCTION

The hardness standard blocks are measures with unique value. These are materializations of standardized hardness points. They are used to verify periodically the hardness determining devices, being a very important constituent of a high quality product.

2. THE STUDY - CONDITIONS IMPOSED BY THE VICKERS HARDNESS STANDARD BLOCKS

The test consists of the applying on the part a diamond penetrator with an F force and a given time, which has a pyramidal shape with a square base and with the angle between 2 sides of 136°

At the Vickers test, the hardness characteristics is a plastic one that is determined with the ratio between the applied force F and the lateral surface of the remnant track – figure 1.

The hardness standard blocks are made out of steel or metals and non-ferrous alloys with a homogenous and stable structure, as to ensure the uniformity and stability in time of the hardness.

Irregularities such as cracks, pores or non-metallic inclusions are not accepted. Grain size has to be fine and uniform.

The base surfaces of the hardness standard blocks must be:

- ❖ flat and parallel
- ❖ finely rectified
- ❖ without corrosion spots, scratches or other imperfections that might influence the hardness tests.

The hardness standard blocks must have a high uniformity of the hardness on the testing surface. The uniformity of the hardness is given by the fidelity error that must not cross a specified value. The maximum value accepted for the fidelity error depends on the method of hardness testing, the hardness scale, the hardness interval and the precision class. For the scales analysed in the present work the uniformity of the hardness must be high, $e_f \leq 1\%$.

For the Vickers method the error is calculated as following:

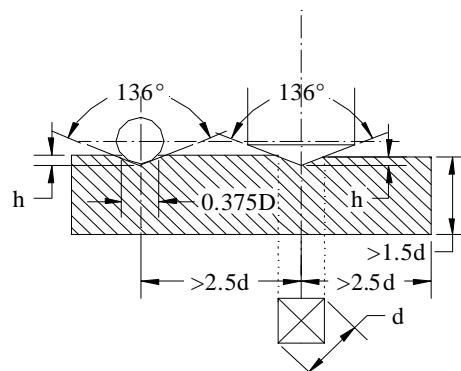


Figure 1. The Vickers test

$$e_f = \frac{R}{\bar{d}} \cdot 100 \text{ [%]} \quad (1),$$

where

amplitude $R = d_{\max} - d_{\min}$

d_{\max} – the maximum average diagonal obtained at the measuring of every indent made at calibration.

d_{\min} – the minimum average diagonal obtained at the measuring of every indent made at calibration.

$\bar{d} = \frac{1}{n} \sum_{i=1}^n d_i$ (2) - the average of the n indents from where the periodical hardness is calculated

$d = \frac{d_I + d_-}{2}$ (3)- average indent diagonal

d_I, d_- - the diagonals of a print

3. ANALISES, DISCUSIONS APPROACHES AND INTERPRETATIONS EXPERIMENTAL RESULTS

The material chosen for experimentations is 100Cr6 steel (RUL 1). From previous experiments [1], [3], results that the analysed material may have a homogenous structure that ensures the uniformity and stability in time of the hardness. One of the primary conditions is the supplementary refinement of the steel by remelting with a void spring (RAV) and electrical remelting under cinder (REZ) and primary thermic treatment (annealing of globulization).

The chemical composition of the samples, after elaboration, is presented in table 1.

Table 1 The chemical composition of the sample's material

C [%]	Mn [%]	Si [%]	Cr [%]	P [%]	S [%]	Ni [%]
1,00	0,33	0,29	1,6	0,014	0,006	0,12

The whole experimental lot was quenched at 840°C, temperature obtained as optimum after previous experiments [3]. After this, the subzero treatment is applied (-183°). After the treatment each sample is metallographically prepared and structurally analysed, using electron microscopy and X-rays diffraction. The structure is homogenous in section and formed out of fine martensite, remnant carbides from initial status – globulisation, small carbides and uniformity spread and small quantities of residue austenite.

The hardness oh the samples is too high (approx 835HV₁) for a Vickers 200...800 HV₁ scale materialization.

Table 2 The results of the measuring of twenty samples of about 200, 250, 440 and 760 HV₁

No.	Material; Thermic treatment	Average diagonal \bar{d} , μm	Hardness HV ₁	Fidelity error ef, %
1	100Cr6 Globulized	95.12	205	0.36
2		95.20	205	0.50
3		94.82	206	0.46
4		96.44	200	0.46
5		93.94	210	0.98
6	100Cr6 Quenched + Tempered at 700 °C	87.37	243	0.93
7		85.20	255	0.20
8		85.36	254	0.56
9		85.27	253	0.17
10		85.07	257	0.19
11	100Cr6 Quenched + Tempered at 400 °C	64.66	443	0.72
12		65.39	434	0.76
13		62.96	467	0.18
14		65.38	434	0.70
15		65.17	436	0.21
16	100Cr6 Quenched + Tempered at 160 °C	48.85	757	0.81
17		49.52	739	0.67
18		49.03	760	0.26
19		49.83	742	0.91
20		48.41	792	0.70

In order, to obtain a softer material, tenacious (with a sorbitic or a pearlitic globular structure), the tempering treatment has been applied right after quenching [2], [4]. The tempering temperatures experimented were 160, 400, 700 °C. After tempering, the Vickers HV₁ hardness has been determined for all tempered samples and for the samples that have not been treated with the secondary treatment. The sclerometrical determining was made by the calibration device for Vickers hardness determining currently in the endowment of the National Institute of Metrology.

In order, to confer the nominal hardness and to have the possibility to calculate the fidelity error, on each sample the hardness was measured in five points. In the following tables the experimental results are presented for the samples that led to acquiring a hardness of approx. 200, 250, 440 and 760 HV₁.

In table 2 the results of the measuring are presented for twenty samples of about 200, 250, 440 and 760 HV₁.

It is observed that all the samples are proper for the hardness standard blocks performing. (hardness uniformity is between the specified limits).

Each sample was metallographically prepared and structurally analysed using electron microscopy and X-rays diffraction.

In figure 2 a part ($2\theta = 31...39$) of the diffraction spectrum is presented for the sample tempered at 700, 400°C and the sample globulized.

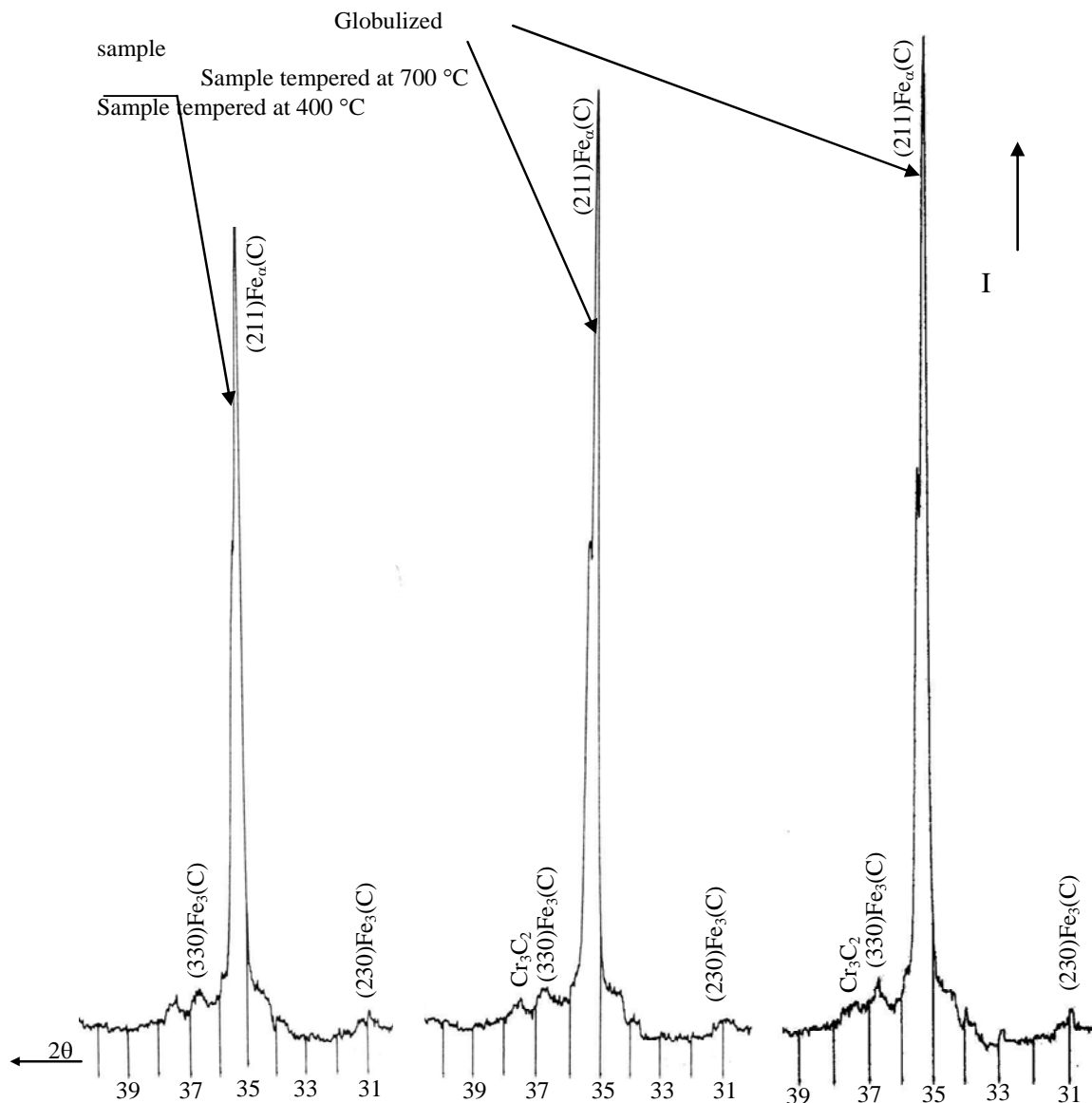


Figure 2. Part of the diffraction spectrum for samples tempered at 700°, 400° C and for the globulized sample

The structures obtained from electron microscopy are presented in figures 3, 4 and 5.

Analysing the resulting hardness values, X-rays diffractions and microstructures it can be observed that the growth of the tempering temperature is the bigger the carbide particles are and the lower internal tensions which leads to a decrease of the hardness.

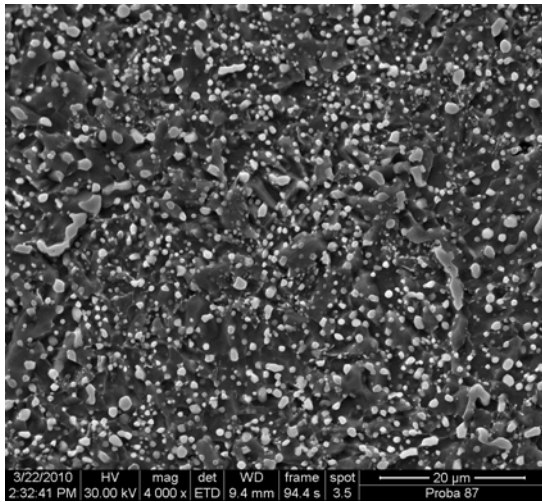


Figure 3. Microstructure of the annealed material (4000 X)

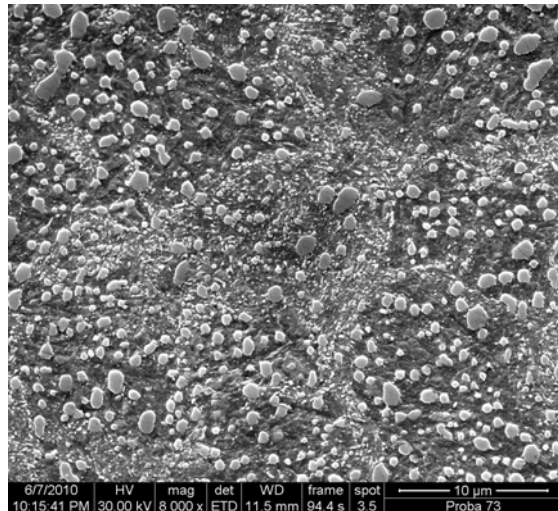


Figure 4. Structural aspect of the material after the tempering at 700 °C (8000 X)

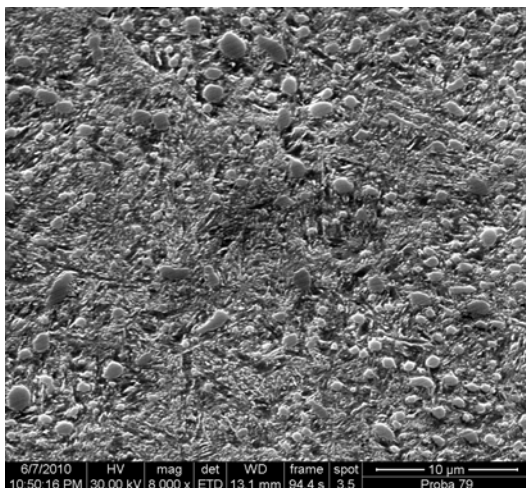


Figure 5. Structural aspect of the material after the tempering at 400 °C (8000 X)

4. CONCLUSIONS

To comply with the requirements of uniformity and stability in time imposed to the hardness standard blocks, some conditions must be respected. The most important are:

- using a premium quality steel, supplementary refined and received with high strictness bar by bar;
- the correct appliance of the primary and secondary thermic treatment (in this case: globulisations + quenching + subzero treating + tempering).

The appropriate elaboration of the 100Cr6 and the primary treatment following by quenching and subzero treating gives a uniformity and stability in time of the properties (especially hardness). The value of the hardness is established with the tempering treatment.

REFERENCES

- [1] Duma. S.: *Studies regarding the acquirement of hardness standard blocks for transmitting the Knoop hardness scale 275...577 HK_{0.2} and Brinell 416...589HBW 5/750* – Scientific Bulletin of the “POLITEHNICA” University of Timisoara, 2009, Tom 54(68) Fasc. 3, ISSN :1224-6077;
- [2] Hazotte. A. (ed.): - *Solid State Transformation and Heat Treatment*. Wiley-VCH, Weinheim 2004, ISBN-10: 352731007X, ISBN-13: 9783527310074;
- [3] Popescu, M., Duma, S., Locovei, C.: Experimental research concerning structural and hardness stability of 100Cr6 steel machine parts, 10th International Conference “Research and Development in Mechanical Industry” RaDMI 2010, 16 - 19. September 2010, Donji Milanovac, Serbia, ISBN 978-86-6075-018-3;
- [4] Serban, V.A., Răduță, A.: *Știința și Ingineria Materialelor*, Editura Politehnica, Timișoara, 2010, ISBN: 978-606-554-044-6.

¹ Ľubomír ŠOOŠ

NEW METHODOLOGY CALCULATIONS OF RADIAL STIFFNESS NODAL POINTS SPINDLE MACHINE TOOL

¹ SLOVAK TECHNICAL UNIVERSITY IN BRATISLAVA
FACULTY OF MECHANICAL ENGINEERING, BRATISLAVA, SLOVAKIA

ABSTRACT:

Spindle - bearings system of the machine tools play a major role in the fulfilling the required working accuracy and productivity. The number of spindles supported on angular contact ball bearings is increasing proportionally with increasing demands on the machine tool quality. It is caused by the fact that these spindle bearings in various combinations can to reach sufficient radial and axial stiffness and revolving frequency of the spindle-bearing system. The complex analysis stiffness of nodal points is difficult and complicate. In this paper is introduced as well simplified mathematical apparatus for evaluation of radial stiffness bearing knot.

KEYWORDS:

Spindle, Bearing, Machine Tools, Stiffness

1. INTRODUCTION

The number of spindles supported on angular contact ball bearings is increasing proportionally with increasing demands on the machine tool quality. It is caused by the fact that these bearings can be arranged in various combinations to create bearing arrangements which can be enabling to eliminate radial and also axial loads. The possibility of variation of the number of bearings, preload value, bearings dimensions and contact angle of bearings used in bearing arrangements create wide spectrum of combination to reach sufficient radial stiffness and revolving frequency of the spindle-bearing system, (Fig.1). The sufficient stiffness and revolving frequency of headstock are necessary criteria for reaching demanding manufacturing precision and machine tool productivity.

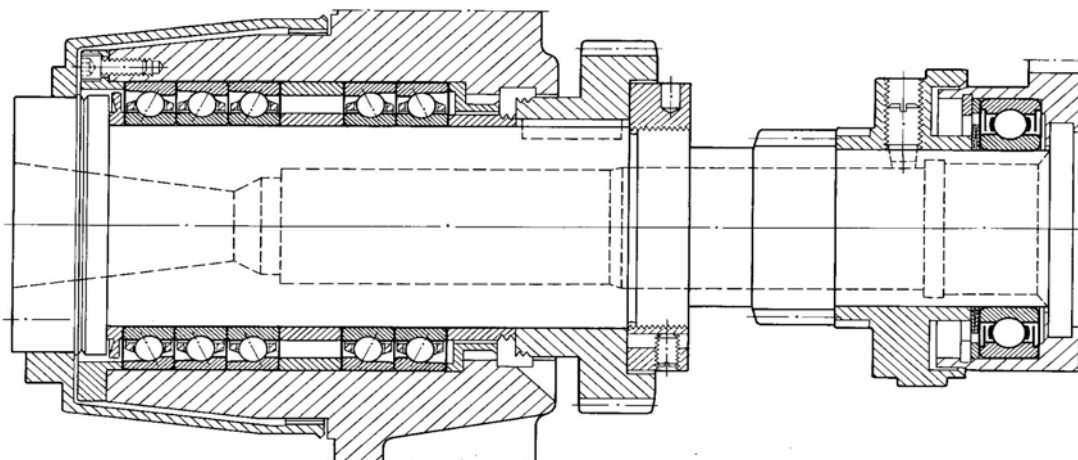


Figure 1: Horizontal machining centre, Thyssen-Hüller Hille GmbH , Germany
Work nodal – 3x71914 ACGB/P4 - 2x71914 ACGB/P4, Opposite side– 6011-2Z

$$\delta_j = l_{rj} - l_p = \sqrt{[l_z \cdot \sin(\alpha_z) + \delta_p]^2 + [l_z \cdot \cos(\alpha_z) + \delta_{r0} \cdot \cos(j \cdot \gamma)]^2} - l_p \quad (5)$$

$$\cos(\alpha_j) = \frac{l_z \cdot \cos(\alpha_z) + \delta_{r0} \cdot \cos(j \cdot \gamma)}{\sqrt{[l_z \cdot \sin(\alpha_z) + \delta_p]^2 + [l_z \cdot \cos(\alpha_z) + \delta_{r0} \cdot \cos(j \cdot \gamma)]^2}} \quad (6)$$

By loading the pre-stressed bearing by radial force is distance between center of balls $O_A O_{ip}$ constant, (Fig.1 b, c).

$$l_p \cdot \sin(\alpha_p) = l_{rj} \cdot \sin(\alpha_{rj}) = konst. \quad (7)$$

The dependence between the deformation of the j-th ball and the top ball can be determined by the relation

$$\delta_j = \delta_0 \cdot \cos(j \cdot \gamma) \quad (8)$$

By derivation of the equation (4) we get

$$\frac{d F_{r1}}{d \delta_0} = i \cdot \sum_{j=0}^z \left[\frac{d P_j}{d \delta_j} \cdot \cos(\alpha_j) - P_j \cdot \sin(\alpha_j) \cdot \frac{d \alpha_j}{d \delta_j} \right] \cdot \frac{d \alpha_j}{d \delta_0} \cdot \cos(j \cdot \gamma) \quad (9)$$

The unknown derivatives in equation (9) can be calculated by derivation/simplification of the relations (1), (7), (8).

$$\frac{d P_j}{d \delta_j} = \frac{3}{2} k_s^{2/3} P_j^{1/3} \quad (10)$$

$$\frac{d \alpha_j}{d \delta_j} = - \frac{tg(\alpha_j)}{l_{rj}} \quad (11)$$

$$\frac{d \delta_j}{d \delta_0} = \cos(j \cdot \gamma) \quad (12)$$

The dependence of the contact deformation and radial displacement, Fig. 1, can be determined from the relation

$$\frac{d \delta_0}{d \delta_{r0}} = \left(\frac{d \delta_j}{d \delta_0} \right)^{-1} \cdot \frac{d \delta_j}{d \delta_{r0}} \quad (13)$$

where $\frac{d \delta_j}{d \delta_{r0}}$ is calculated from the equation (5)

by inserting equations (14) and (12) into equation (13)

$$\frac{d \delta_j}{d \delta_{r0}} = \frac{1}{2} \cdot \frac{2(l_z \cos \alpha_z + \delta_{r0} \cos(j \cdot \gamma)) \cos(j \cdot \gamma)}{\sqrt{(l_z \cos \alpha_z + \delta_{r0} \cos(j \cdot \gamma))^2 + (l_z \sin \alpha_z + \delta_p)^2}} = \cos \alpha_j \cos(j \cdot \gamma) \quad (14)$$

$$\frac{d \delta_0}{d \delta_{r0}} = \frac{1}{\cos(j \cdot \gamma)} \cdot \cos(\alpha_j) \cos(j \cdot \gamma) = \cos(\alpha_j) \quad (15)$$

After inserting equations (15) and (9) into equation (3) we will get the resulting relation for the stiffness of a pre-stressed nodal point with directionally-arranged bearings.

$$C_r = i \cdot \sum_{j=0}^z \left[\frac{3}{2} k_s^{2/3} P_j^{1/3} \cdot \cos^2(\alpha_j) + P_j \cdot \frac{\sin^2(\alpha_j)}{l_{rj}} \right] \cdot \cos^2(j \cdot \gamma) \quad (16)$$

2.3 The stiffness of nodal point with bearings arranged according to the shape

When calculating the nodal point with bearings arranged according to the shape we divide the nodal point into part "1" and part "2" (Fig.1), with the same orientation of contact angles -nodes as directionally-arranged bearings, and the stiffness of the parts will be calculated as follows:

$$C_{r1} = i_1 \cdot \sum_{j=0}^z \left[\frac{3}{2} k_s^{2/3} P_j^{1/3} \cdot \cos^2(\alpha_{1j}) + P_j \cdot \frac{\sin^2(\alpha_{1j})}{l_{r1j}} \right] \cdot \cos^2(j \cdot \gamma) \quad (17a)$$

$$C_{r2} = i_2 \cdot \sum_{j=0}^z \left[\frac{3}{2} \cdot k_s^{2/3} \cdot P_j^{1/3} \cdot \cos^2(\alpha_{2j}) + P_j \cdot \frac{\sin^2(\alpha_{2j})}{l_{r2j}} \right] \cdot \cos^2(j \cdot \gamma) \quad (17b)$$

for Fig. 1: numbers of balls: $i_1 = 3$, $i_2 = 2$, contact angles $\alpha_1 = \alpha_2 = 25^\circ$
 By their subsequent addition we determine the total stiffness of the nodal point with

$$C_r = C_{r1} + C_{r2} \quad (18)$$

In order to optimize the stiffness and load-bearing capacity for determined technological conditions, the manufacturers of machine tools have come out with a new, non-traditional solution of nodal points. By diminishing the contact angle of the bearing in Part 2, the axial stiffness of the nodal point is partially decreased, but at the same time the value of the radial stiffness and boundary axial load is increased.

2.4 Approximate calculation of stiffness

When evaluating the overall stiffness of a spindle, the designer must take into account the approximate calculation of the stiffness of the nodal points.

If all the rollers are loaded, and their number is more than 2 per bearing [4], the following equation can be applied:

$$\sum_{j=0}^z \cos^2(j \cdot \gamma) = \frac{z}{2} \quad (19)$$

If the bearing angle is loaded only in an axial direction by the pre-stressing force, then the load on the rollers is constant around the whole circumference and can be expressed, for the particular parts of the nodal point [8], in the form

$$P_{1j} = \frac{F_p}{i_1 \cdot z \cdot \sin(\alpha_{p1})}; P_{2j} = \frac{F_p}{i_2 \cdot z \cdot \sin(\alpha_{p2})} \quad (20)$$

The magnitude of the contact angles of spindle bearings is not greater than 26 degrees. In that case the value of the second expression in equations (17a) and (17b) is negligible.

Taking into consideration these assumptions, we will get the relationship for the approximate calculation of the radial stiffness of a bearing angle with directionally placed bearings.

$$C_r = \frac{3 \cdot 10^{-3}}{4} \cdot z^{2/3} \cdot k_s^{2/3} \cdot i^{2/3} \cdot F_p^{1/3} \cdot \frac{\cos^2(\alpha)}{\sin^{1/3}(\alpha)} \quad (21)$$

and with bearings arranged according to shape:

$$C_r = \frac{3 \cdot 10^{-3}}{4} \cdot z^{2/3} \cdot k_s^{2/3} \cdot i_1^{2/3} \cdot F_p^{1/3} \cdot \frac{\cos^2(\alpha_1)}{\sin^{1/3}(\alpha_1)} \cdot \left[1 + \frac{i_2^{2/3} \cdot \cos^2(\alpha_2) \cdot \sin^{1/3}(\alpha_1)}{i_1^{2/3} \cdot \cos^2(\alpha_1) \cdot \sin^{1/3}(\alpha_2)} \right] \quad (22)$$

where the approximate value of the deformation constant is $k_s = \sqrt{1,25 \cdot d_w}$, d_w – diameter of balls.

The pre-stressing value “ F_p ” can be calculated according to the standard STN 02 46 15. Some foreign manufacturers (fy SKF, FAG, SNFA ...) publish this value in their catalogues. The number of balls “ z ” and diameters of balls “ d_w ” of some types of bearings are quoted in literature, e.g. [7].

3. VERIFICATION OF MEASURED AND CALCULATED VALUES

The results obtained according to this mathematical model were compared with the values measured by means of the experimental device shown in Fig 3. This device was used to measure the deformation characteristics of nodal points with different combinations of arrangement, pre-stressing values, contact angles, loads and revolution frequencies. This new equation (22) for middle stiffness of the bearing arrangement “ C_r ” calculation was experimental verified, [1], [5], [6].

At Fig. 3 we have been compared experimental measure stiffness, exactly theoretical and middle calculated radial stiffness of the bearing arrangement B7216 AATB P4 O UL. Results are very good. At zero frequencies the values of radial stiffness are experimental higher than theoretical values, Fig.3. The dependence of stiffness on loading has a digressive (decreasing) course. The decrease is nearly linear, until a certain critical force “ F_{kr} ”, at this point the least-loaded roller becomes unloaded. The deformation characteristic of the nodal point is influenced by the type of flange. The direction and gradation of the stiffness change under the given operation conditions depend on their construction.

At Fig. 4 and Fig. 5 is experimental stand for messing radial and axial stiffness.

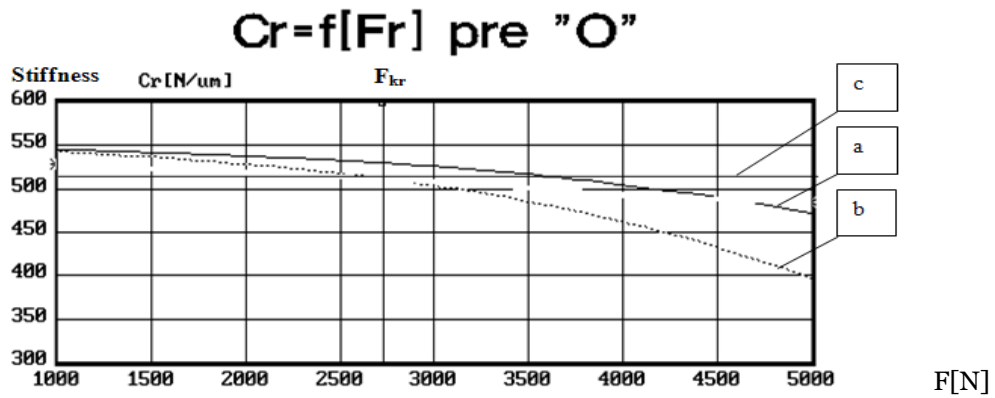


Figure 3 Radial stiffness of the bearing arrangement B7216 AATB P4 O UL,
 a - experimental, b – exactly theoretical, c – middle theoretical

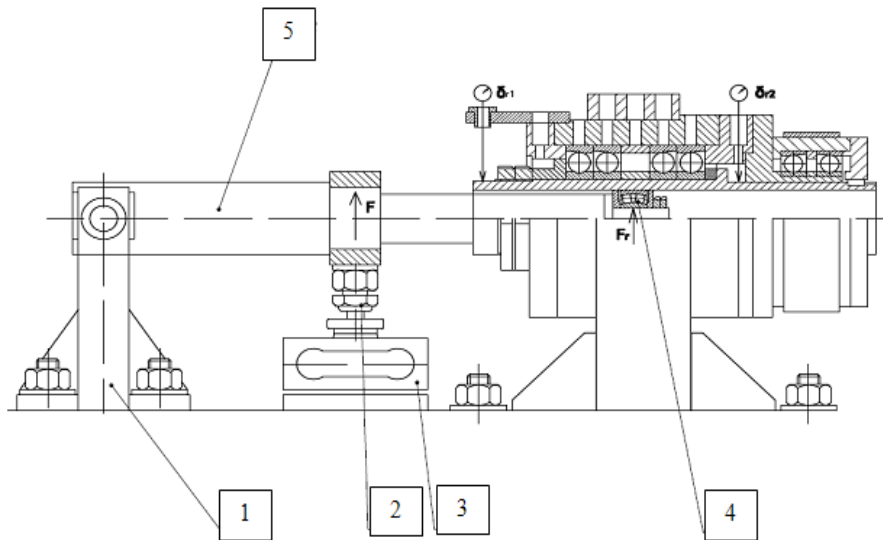


Figure 4 Cut of experimental stand, 1- holder, 2- to retighten screw, 3- dynamometer, 4- force bearing, 5- force arm

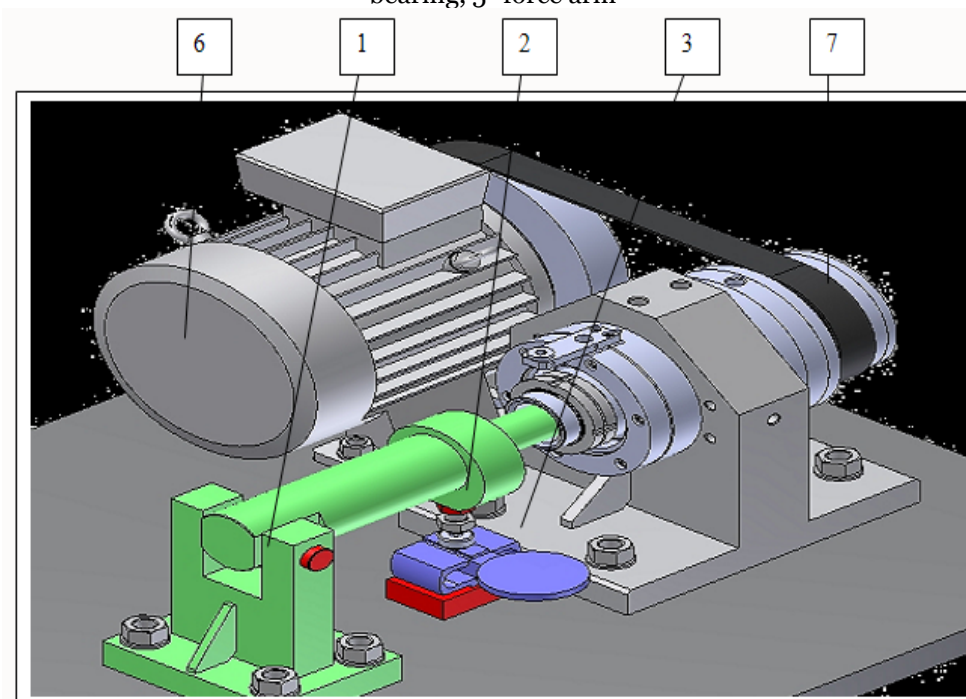


Figure 5.3D model of experimental stand, 1- holder, 2- to retighten screw, 3- dynamometer, 4- force bearing, 5- force arm, 6- drive, 7- Poly V belt

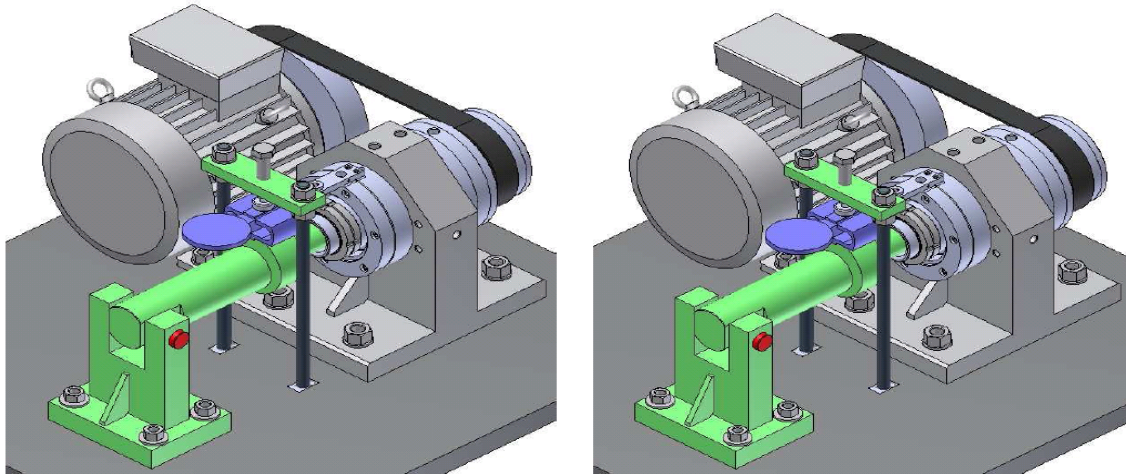


Figure 6. Different decisions measuring radial stiffness bearing knot

4. SUMMARY

In this paper are presented the regulations for selection and calculation of the radial stiffness of nodal points composed of radial ball bearings with beveled contact. The resulting radial stiffness of spindle nodes is a function of various factors. Its calculation, considering the operation conditions of the node, is quite complicated, and cannot be accomplished without the use of computer technologies.

The research results show that the change of the radial stiffness of pre-stressed nodes is relatively small at zero revolution frequencies, in dependence on loading, and can be mineralized.

In this field the results of the precise and the approximate mathematical model are practically equal. From the preceding it follows that in a preliminary design of mounting, a simplified mathematical model for calculating the stiffness of nodal points can be used, as derived in this article.

This contribution has arisen in assistances financial resources project KEGA nr. 3/7216/09.

LITERATURE

- [1.] Šooš, L.: Statika ložiskových uzlov vretien obrábacích strojov. [Kandidátska dizertačná práca]. STU Bratislava. 1992, 140 s.
- [2.] Harris, T.A.: Rolling Bearing Analysis. New York - London - Sydney, 1966, 481s.
- [3.] Balmont, V.B. - Russkich, S.P.: Rasčet radialnoj žestkosti radialno - upornogo podšipnika. Trudy instituta. M., Specinformcentr VNIPPa, 69, 1978, č.1, s..93 - 107.
- [4.] Kovalev, M.P.- Narodeckij, M.Z.: Rasčet vysokotočnych šarikopodšipnikov. 2 vyd. Moskva, Mašinostroenie 1980. 279s.
- [5.] Šooš, L.: Quality of design engineering: case of machine tools headstock. In: Quality Festival 2008 : 2nd International quality conference. - Kragujevac, May 13-15, 2008. - Kragujevac : University in Kragujevac, 2008. - ISBN 978-86-86663-25-2.
- [6.] Lavorčík, L.- Šooš, L.- Zoň, J.: Applied Software Technology of Designing a Bearing Housing Fitted with Rolling Bearing Arrangement. In... "ICED 91". Zurich, August, 1991, s.1228 -1233.





¹Paolo BOSCARIOL, ²Alessandro GASPARETTO,
³Albano LANZUTTI, ⁴Renato VIDONI, ⁵Vanni ZANOTTO

NEUMESY: A SPECIAL ROBOT FOR NEUROSURGERY

¹⁻⁵ UNIVERSITY OF UDINE – DIEGM. VIA DELLE SCIENZE 208, 33100 UDINE, ITALY

ABSTRACT:

In the last years a large number of new surgical devices have been developed so as to improve the operation outcomes and reduce the patient's trauma. Nevertheless the dexterity and accuracy required in positioning the surgical devices are often unreachable if the surgeons are not assisted by a suitable system. From a kinematic point of view, the robot must reach any target position in the patient's body being less invasive as possible with respect to the surgeon's workspace. In order to meet such requirements a suitable design of the robot kinematics is needed. This paper presents the kinematic design of a special robot for neurosurgical operations, named NEUMESY (NEUrosurgical MEchatronic SYstem).

NEUMESY is a six joints serial manipulator whose kinematic structure lets the robot to adapt to different patient's positions while minimizing the overall dimensions. Owing to the usual symmetry of a surgical tool, the kinematic dimension of the neurosurgical task is five, being given by one point and one direction on the space. Therefore the NEUMESY is kinematically redundant, leaving an extra DOF to the surgeon to choose a suitable robot configuration which minimally limits his movements during the surgical operations. The link lengths have been optimized in order to maximize the robot workspace with respect to the surgical task, while minimizing the links static deformations.

KEYWORDS: surgical devices, kinematic design, special robot, neurosurgical operations, NEUMESY

1. INTRODUCTION

The initial experimentation of robotic systems in surgery was undertaken during the early 1980s [6,7,3], and it basically consisted of adapting the industrial robot technologies already in existence. In the last decade, there has been a growing awareness, within the medical community, of the benefits offered by using robots in various surgical tasks. Traditional surgery involves making large incisions to access the part of a patient's body that needs to be operated on. Minimally Invasive Surgery (MIS), on the other hand, is a cost-effective alternative to open surgery. Basically, the same operations are performed using instruments designed to enter the body cavity through several tiny incisions, rather than a single large one. By eliminating large incisions, trauma to the body, post-operative pain, and the length of hospital stay are significantly reduced.

However, new problems connected to the use of robots in surgery have arisen, since there is no direct contact with the patient. For this reason, it is necessary to develop suitable tactile sensors to provide surgeons with the perception of directly operating on the patient. Such a result can be achieved by using force feedback systems, in which the force applied to patient's tissue is fed back to a robotic device (haptic master) directly operated by the surgeon.

We can categorize surgical robots based on their different roles during surgical treatment [4,5] Passive robots only serve as a tool-holding device once directed to the desired position. Semiactive devices perform the operation under direct human control. Active devices are under computer control and automatically perform certain interventions. Moreover, the surgical robot can have different levels of autonomy. To be specific, systems that are able to perform fully automated procedures are called autonomous. On the other hand, when the surgeon completely controls every single motion of the robot, this is called a tele-operated system or a master-slave system. Medical robotics has found fruitful ground especially in neurosurgical applications, owing to the accuracy required by the high functional density of the central nervous system [6,11,9].

In past decades, several different robotic neurosurgical devices have been created. A comprehensive survey can be found in [4]. In particular, in the 1980s Benabid and colleagues [1,2] experimented with an early precursor to the robot marketed as Neuromate [5] (Renishaw Mayfield, UK). Today's robot projects focus on three major areas of improvement [4]:

- ❖ increasing the overall accuracy of the classical stereotactic systems
- ❖ increasing the added-value of the equipment
- ❖ enhancing the capabilities of the surgeon

The Mechatronics Research Group (composed of researches of the University of Padova, University of Udine and University of Trieste, Italy) [10] with the assistance of the Neurosurgical Department of the University of Florence [11] has developed two master-slave robotic systems for minimally-invasive neurosurgical operations. The first robot (Figure 1), named LANS (Linear Actuator for Neuro Surgery) has been conceived specifically to perform biopsies and neurosurgical interventions by means of a miniaturized x-ray source (the PRS, Photon Radiosurgery System, by Carl Zeiss), whose emitting tip must be placed accurately inside the patient's brain tissues [12,13]. The LANS robotic system is composed of a haptic master module, operated by the surgeon, and a slave mechatronic module moving a PRS probe, or a biopsy needle, along a predefined emission axis in accordance with the master position imposed by the surgeon. In order to orient the LANS along the established emission axis, a NeuroMate robot is employed in a frame-based configuration which ensures the highest possible accuracy. The system has been designed assuming that during the surgical operation only the LANS (which is very accurate, and provides the surgeon with force feedback) is in active mode while the NeuroMate is powered off. This allows overcoming much of the problems associated with the complex nature of this surgical therapy. Moreover, very precise and repeatable movements of the biopsy needle and of the x-ray source can be obtained, thus improving the overall intervention outcomes.

DAANS (Double Action Actuator for NeuroSurgery, [14]) is the second robot (Figure 2) carried out by Mechatronics research group. The aim of the system is to provide another degree of freedom to the PRS source about the emission axis. The system allows extending the therapy with PRS also to irregular shape tumorous lesions, by integrating translation and spin movements of the source.

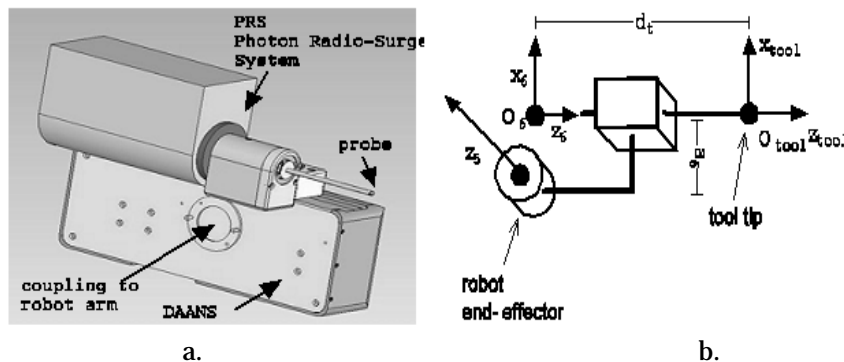


Fig. 2 (a) The DAANS actuator and the PRS x-ray source
 (b) Simplified kinematic structure of the DAANS

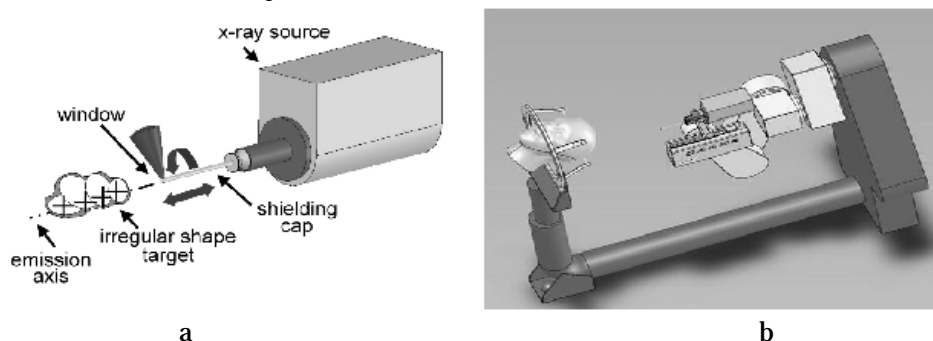


Figure 4: (a) PRS and shielding caps (b) NEUROMATE and DAANS

Indeed, single isocenter radiosurgery procedures produce nearly spherical isodose distributions. In order to avoid unacceptable dose delivery to non target tissues, the high-dose region must be shaped to fit individual targets. The high-dose region can be manipulated into a variety of shapes that closely conform to a tumour shape by means of shielding caps and multiple targets dose delivery.

The caps are placed on the probe of the x-ray source as in Figure 4(a). Nevertheless, LANS and DAANS limit the NeuroMate mobility, owing to their geometrical dimension, which can interfere with the robot arm movements (Figure 4(b)). In this manner the NeuroMate workspace is reduced and some tool configuration are not reachable [12-14].

This paper presents the results of a preliminary analysis on the kinematic structure of a new surgical robot, named NEUMESY. The robot is able to maximize the performances of the therapy by means of the DAANS and PRS, increasing the workspace of the overall robotic system and allowing all possible tool configurations on the patient's head to be reached.

2. THE STUDY

Introducing a robot in an operating room must fulfil some elementary rules. From a kinematics point of view two type of constraints can be taken: medical requirements and robotics requirements [15].

2.1 Medical requirements:

For sterilization reasons no non-medical equipment must be closer than a fixed distance from the operating site. Thus the robot must collide neither with the patient, nor with the medical staff, nor with the surgical tools [15]. The requirement becomes quite complex in the frame-based applications, where the stereotactic frame (the mechanical structure the patient's head is fixed on) interferes with the robot movements. In order to satisfy this requirement, it is useful to define a virtual sphere (Figure 6) including the patient's head and the stereotactic frame. The robot must neither cross nor touch this sphere. The radius of the sphere depends on the stereotactic frame dimensions, while the center is on the patient's head. Moreover, the robot must minimally limit the surgeon's movements during the operation. To this end, the surgeon must be able to choose a suitable robot configuration for each tool position and the robot must adapt its workspace to the surgeon's requirements, which may change during the surgical task.

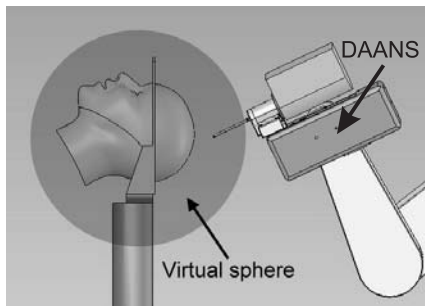


Fig. 6 The virtual sphere includes the patient's head and the stereotactic frame

2.2 Robotics requirements:

The robotics constraints concern the structure of the NEUMESY in order to satisfy the above medical constraints. The preliminary choice considers the robot kinematic structure. The advantages of a serial robot if compared to a parallel one are due to the larger workspace and the higher dexterity and manipulability. On the other hand a parallel manipulator is stiffer allowing higher accuracy in the tool positioning. According to the medical constraints, the robot has to be able to avoid the virtual sphere and it must minimally limit the surgeon's movements. Therefore, the solution adopted consists in a serial structure.

Nevertheless this choice requires a links length optimization so as to maximize both the workspace and the stiffness of the robot.

Moreover, since the neurosurgical tools have usually an axial symmetry, only two spatial points on the patient's head have to be stated by the surgeons. The first one is the Target Point (TP), the center of the cerebral lesion where the tool has to be placed, while the second one, is the Entry Point (EP), the hole through which the surgical instruments go into the skull. EP and TP state the Line of Action (LoA) along which the tools should be moved (Figure 7). Since the surgical operation fixes only five constraints on the space, a five DoF manipulator should be sufficient to a neurosurgical operation, nevertheless, a further DOF yields the kinematic redundancy which allows infinite configuration for the same surgical task, letting the surgeon choose the suitable one.

3. ANALISES, DISCUSSIONS, APPROACHES and INTERPRETATIONS

3.1 Robot kinematics

The structure of the designed robot and its Denavit-Hartenberg description are displayed in Figure 7 and in Table 1, respectively. The first prismatic joint allows the robot to adapt to the patient's vertical position and change the robot configuration according to the surgeon requirements. The next three revolute joints form a spherical wrist whose position reduces the load and the elastic displacements on the robot links. Finally, two revolute joints allow orienting the end-effector while keeping the robot outside of the virtual sphere.

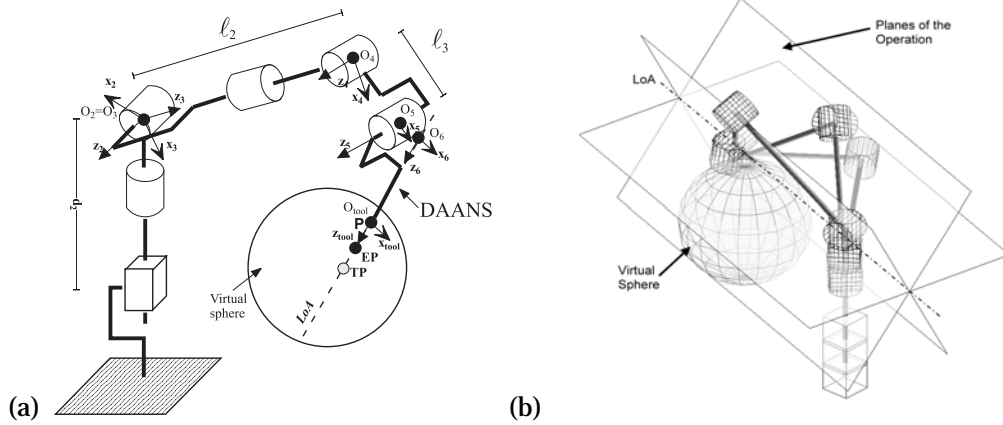


Fig. 7 (a) The NEUMESY, the DAANS and the virtual sphere (b) Three robot configurations for the same TP and LoA

The robot features six DoFs while the kinematic dimension of the neurosurgical task is five, being given by one point and one direction on the space. Therefore the NEUMESY is kinematically redundant. As stated above, the redundancy can be used by the surgeon to choose a suitable robot configuration which minimally interferes with his movements. Indeed, the origins $O_2 \div O_6$ belong to the same plane on the sheaf (of planes) defined by the LoA. The plane is arbitrary but fixes the robot configuration and the constraints on the surgeon's movements. By choosing a different plane, the space required by the robot for the surgical operation changes and the surgeon's movement could be easier (Figure 8). The solution of the robot inverse kinematic will be presented in the next section

3.2 Solution of the inverse kinematic

For sake of simplicity, let \mathbf{T}_i be the matrix ${}^{i-1}\mathbf{T}_i$, as well as $\mathbf{R}_i = {}^{i-1}\mathbf{R}_i$ the rotation matrix from the frame i to the frame $i-1$ and $\mathbf{p}_i = {}^{i-1}\mathbf{p}_i$ the origin of the frame i referred to the frame $i-1$. The inverse kinematic problem can be expressed as

$${}^0\mathbf{T}_6 = \check{\mathbf{T}}^6 \mathbf{T}_{tool}^{-1} =: \mathbf{T} = \begin{bmatrix} \mathbf{s} & \mathbf{n} & \mathbf{a} & \mathbf{p} \\ 0 & 0 & 0 & 1 \end{bmatrix} \quad (1)$$

where $\check{\mathbf{T}} = \begin{bmatrix} \check{\mathbf{s}} & \check{\mathbf{n}} & \check{\mathbf{a}} & \check{\mathbf{p}} \\ 0 & 0 & 0 & 1 \end{bmatrix}$

Equation (1) can be rearranged as

$${}^2\mathbf{T}_6 = \mathbf{Q}_1 \quad (2)$$

where: ${}^2\mathbf{T}_6 = \mathbf{T}_3 \mathbf{T}_4 \mathbf{T}_5 \mathbf{T}_6$ and $\mathbf{Q}_1 = ({}^0\mathbf{T}_2)^{-1} \mathbf{T}$

Table 1 Denavit-Hartenberg parameters of the NEUMESY

i	${}^{i-1}\mathbf{T}_i$	σ_i	α_i	a_i	θ_i	d_i
1	${}^0\mathbf{T}_1$	1	0	0	0	q_1
2	${}^1\mathbf{T}_2$	0	$\frac{\pi}{2}$	0	q_2	d_2
3	${}^2\mathbf{T}_3$	0	$-\frac{\pi}{2}$	0	q_3	0
4	${}^3\mathbf{T}_4$	0	$\frac{\pi}{2}$	0	q_4	ℓ_2
5	${}^4\mathbf{T}_5$	0	0	ℓ_3	q_5	0
6	${}^5\mathbf{T}_6$	0	$\frac{\pi}{2}$	a_6	q_6	0
	${}^6\mathbf{T}_{tool}$	1	0	0	0	d_t

Equation (2) can be rewritten as:

$$\mathbf{T}_3 \mathbf{T}_4 \mathbf{T}_5 \mathbf{T}_6 = ({}^0\mathbf{T}_2)^{-1} \mathbf{T} (\mathbf{A}_6)^{-1} \quad (3)$$

Where: $\mathbf{T}_6 = \begin{pmatrix} \mathbf{R}_6 & \mathbf{0} \\ \mathbf{0}^T & 1 \end{pmatrix}$ and $\mathbf{A}_6 = \begin{pmatrix} 1 & 0 & 0 & a_6 \\ 0 & 0 & -1 & 0 \\ 0 & 1 & 0 & 0 \\ 0 & 0 & 0 & 1 \end{pmatrix}$

Comparing to each other the left and the right sides of (3), the following equations must hold:

$$\begin{aligned} \bar{\mathbf{a}} &= \mathbf{R}_3 \mathbf{R}_4 \mathbf{R}_5 \mathbf{R}_6 \mathbf{z} \\ \bar{\mathbf{p}} &= \mathbf{R}_3 \mathbf{R}_4 \mathbf{p}_5 + \mathbf{R}_3 \mathbf{p}_4 \end{aligned} \quad (4)$$

where $\bar{\mathbf{a}}$ and $\bar{\mathbf{p}}$ are defined by: $({}^0\mathbf{T}_2)^{-1} \mathbf{T}(\mathbf{A}_6)^{-1} = \begin{pmatrix} \bar{\mathbf{s}} & \bar{\mathbf{n}} & \bar{\mathbf{a}} & \bar{\mathbf{p}} \\ 0 & 0 & 0 & 1 \end{pmatrix}$

and $\mathbf{z} = [0, 0, 1]^T$. Equations (4) can be further transformed into:

$$\begin{aligned} \mathbf{R}_4^{-1} \mathbf{R}_3^{-1} \bar{\mathbf{a}} &= \mathbf{R}_5 \mathbf{z} \\ \mathbf{R}_4^{-1} \mathbf{R}_3^{-1} \bar{\mathbf{p}} &= \bar{\mathbf{p}}_5 + \mathbf{R}_4^{-1} \bar{\mathbf{p}}_4 \end{aligned} \quad (5)$$

After multiplying left and right sides to each other of the equations (5), it is possible to write:

$$\bar{\mathbf{p}} \cdot \bar{\mathbf{a}} = \bar{\mathbf{p}}_5 \cdot (\mathbf{R}_5 \mathbf{z}) + (\mathbf{R}_4^{-1} \bar{\mathbf{p}}_4) \cdot (\mathbf{R}_5 \mathbf{z}) \quad (6)$$

where the right side of (6) is zero, since the vectors therein involved are orthogonal. Therefore from (6) the value of the q_1 can be determined, since the projection of $\bar{\mathbf{p}}$ into $\bar{\mathbf{a}}$ depends only on this

joint variable. In particular: $q_1 = -\frac{d_1 \bar{\mathbf{a}} \cdot \bar{\mathbf{n}} + a_6 \bar{\mathbf{s}} \cdot \bar{\mathbf{n}} - \bar{\mathbf{p}} \cdot \bar{\mathbf{n}}}{\bar{n}_z} - d_2 q$. When $\bar{n}_z = 0$ the z_0 -axis belongs

to the operation plane. In this case, if the target point belongs to robot workspace, there are infinite solutions for q_1 . Taking into account the module of $\bar{\mathbf{p}}$, there is:

$$\bar{\mathbf{p}} \cdot \bar{\mathbf{p}} = \mathbf{p}_4 \cdot \mathbf{p}_4 + \mathbf{p}_5 \cdot \mathbf{p}_5 + 2(\mathbf{R}_4 \mathbf{p}_5) \cdot \mathbf{p}_4 \quad (7)$$

the left side of (7) being noted, since the module of $\bar{\mathbf{p}}$ depends only on joint variable q_1 . In this way the value of q_5 can be determined from (7):

$$\sin q_5 = \frac{\bar{\mathbf{p}} \cdot \bar{\mathbf{p}} - \ell_2^2 - \ell_3^2}{2\ell_2 \ell_3} \quad (8)$$

The equation (1) can be rearranged as ${}^1\mathbf{T}_5 = \mathbf{Q}_2$, where ${}^1\mathbf{T}_5 = \mathbf{T}_2 \mathbf{T}_3 \mathbf{T}_4 \mathbf{T}_5$ and $\mathbf{Q}_2 = \mathbf{T}_1^{-1} \mathbf{T} \mathbf{T}_6^{-1}$. Considering the new vectors:

$$\begin{aligned} \tilde{\mathbf{s}} &= \mathbf{R}_2 \mathbf{R}_3 \mathbf{R}_4 \mathbf{R}_5 \mathbf{x} \\ \tilde{\mathbf{p}} &= \mathbf{R}_2 \mathbf{R}_3 \mathbf{R}_4 \mathbf{p}_4 + \mathbf{R}_2 \mathbf{R}_3 \mathbf{p}_4 + \mathbf{p}_2 \end{aligned} \quad (9)$$

where $\tilde{\mathbf{a}}$ and $\tilde{\mathbf{p}}$ are defined by: $\mathbf{T}_1^{-1} \mathbf{T} \mathbf{T}_6^{-1} = \begin{pmatrix} \tilde{\mathbf{s}} & \tilde{\mathbf{n}} & \tilde{\mathbf{a}} & \tilde{\mathbf{p}} \\ 0 & 0 & 0 & 1 \end{pmatrix}$ and $\mathbf{x} = [1, 0, 0]^T$, rearranging (9) as

$$\begin{aligned} (\mathbf{R}_2 \mathbf{R}_3)^{-1} \tilde{\mathbf{s}} &= \mathbf{R}_4 \mathbf{R}_5 \mathbf{x} \\ (\mathbf{R}_2 \mathbf{R}_3)^{-1} (\tilde{\mathbf{p}} - \mathbf{p}_2) &= \mathbf{R}_4 \mathbf{p}_5 + \mathbf{p}_4 \end{aligned}$$

and operating as in (5) it is possible to write:

$$(\tilde{\mathbf{p}} - \mathbf{p}_2) \cdot \tilde{\mathbf{s}} = \mathbf{p}_5 \cdot (\mathbf{R}_5 \mathbf{x}) + (\mathbf{R}_4^{-1} \mathbf{p}_4) \cdot (\mathbf{R}_5 \mathbf{x}) \quad (10)$$

The left side of (10) depends only on joint variable q_6 , while the right side is known, once q_1 and q_5 have been calculated. In this way (10) can be expressed in the form: $A c_6 + B s_6 = C$,

$$A = a_6 \tilde{\mathbf{s}} \cdot \tilde{\mathbf{s}} + d_1 \tilde{\mathbf{s}} \cdot \tilde{\mathbf{a}} - \tilde{\mathbf{s}} \cdot \tilde{\mathbf{p}} + \tilde{s}_z q_1$$

where $B = a_6 \tilde{\mathbf{s}} \cdot \tilde{\mathbf{a}} + d_1 \tilde{\mathbf{s}} \cdot \tilde{\mathbf{s}} - \tilde{\mathbf{s}} \cdot \tilde{\mathbf{p}} - \tilde{a}_z q_1$

$$C = -(\ell_3 + \ell_2 s_5)$$

The solutions are: $q_6 = \text{atan2}(\pm\sqrt{A^2 + B^2 - C^2}, C) - \text{atan2}(B, A)$.

Equation (1) can be rearranged as: ${}^1\mathbf{T}_5 = \mathbf{Q}_3$

where ${}^1\mathbf{T}_5 = \mathbf{T}_2\mathbf{T}_3\mathbf{T}_4\mathbf{T}_5$, $\mathbf{Q}_3 = \mathbf{T}_1^{-1} \mathbf{T} \mathbf{T}_6^{-1} \mathbf{A}_5^{-1}$, $\mathbf{T}_5 = \begin{pmatrix} \mathbf{R}_5 & \mathbf{0} \\ \mathbf{0}^T & 1 \end{pmatrix}$ and $\mathbf{A}_5 = \begin{pmatrix} \ell_3 & \\ \mathbf{I}_3 & \mathbf{0} \\ \mathbf{0}^T & 1 \end{pmatrix}$

Considering the vectors:

$$\hat{\mathbf{a}} = \mathbf{R}_2\mathbf{R}_3\mathbf{R}_4\mathbf{R}_5\mathbf{z} \tag{11}$$

$$\hat{\mathbf{p}} = \mathbf{R}_2\mathbf{R}_3\mathbf{p}_4 + \mathbf{p}_2$$

where $\hat{\mathbf{a}}$ and $\hat{\mathbf{p}}$ are defined by $\mathbf{Q}_3 = \begin{pmatrix} \hat{\mathbf{s}} & \hat{\mathbf{n}} & \hat{\mathbf{a}} & \hat{\mathbf{p}} \\ 0 & 0 & 0 & 1 \end{pmatrix}$ and rearranging as above, it is possible to write:

$$\mathbf{R}_2^{-1}\hat{\mathbf{a}} = \mathbf{R}_3\mathbf{R}_4\mathbf{R}_5\mathbf{z} \tag{12}$$

$$\mathbf{R}_2^{-1}(\hat{\mathbf{p}} - \mathbf{p}_2) = \mathbf{R}_3\mathbf{p}_4 \tag{13}$$

From the projection of the equation (13) along $\mathbf{y} = [0, 1, 0]^T$, the value of c_3 can be determined as $c_3 = \frac{-d_2 + \hat{p}_z}{\ell_2}$ where $\hat{p}_z = (-\tilde{a}_z)d_t + \tilde{p}_z - q_1 - \tilde{a}_z\ell_3s_6 - a_6\tilde{s}_z - c_6\ell_3\tilde{s}_z$ while from

the projection of the equation (13) along \mathbf{z} , it is possible to write $\hat{p}_y c_2 = \hat{p}_x s_2$ where

$$\hat{p}_x = \tilde{p}_x - \tilde{a}_x(d_t + \ell_3s_6) - (a_6 + c_6\ell_3)\tilde{s}_x$$

$$\hat{p}_y = \tilde{p}_y - \tilde{a}_y(d_t + \ell_3s_6) - (a_6 + c_6\ell_3)\tilde{s}_y$$

In this way: $q_2 = \text{atan2}(\hat{p}_x, \hat{p}_y) + k\pi$ with $k = 0, 1$

Finally, projecting (12) along \mathbf{z} , the value of c_4 is determined as: $c_4 = \hat{a}_x s_2 - \hat{a}_y c_2$, where $\hat{a}_x = \tilde{n}_x$ and $\hat{a}_y = \tilde{n}_y$. Therefore: $q_4 = \text{atan2}(c_4, \pm\sqrt{1 - c_4^2})$. There are four solutions for each pose defined by the matrix \tilde{T} , which mainly differ to each other on the elbow configuration. During the surgical operation only the DAANS is in active mode while the NEUMESY is powered off. Therefore the requirement on the accuracy on the tool positioning concerns only the robot in the static configuration. At the same time, for safety reasons, the contacts between the robot and the virtual sphere have to be avoided.

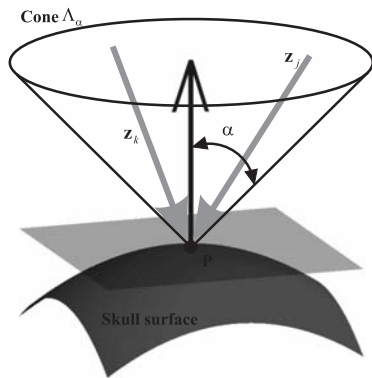


Figure 9. Cone Λ_α

The link lengths affect both the accuracy and the robot workspace owing to the NEUMESY kinematic structure and have to be appropriately chosen in order to satisfy the requirements stated above. The requirement on the robot workspace can be described by a reachability index which gives information about the number of points on the patient's skull being achievable along each desired tool configuration.

Let the skull surface S be discretized into N points \mathbf{P}_i and the desired tool orientations at \mathbf{P}_i be described by all the vectors \mathbf{z}_k internal to the cone $\Lambda_\alpha(\mathbf{P}_i)$ with vertex at \mathbf{P}_i , angle α and axis

coincident with the normal to the skull surface in \mathbf{P}_i (Figure 9). Moreover, let the function $\text{IK}(\mathbf{P}, \mathbf{z})$ calculate the number of solutions for the inverse kinematic problem:

$$\begin{cases} \mathbf{P}_{tool} = \mathbf{P} \\ \mathbf{z}_{tool} = \mathbf{z} \end{cases}$$

subject to the constraint that all the robot links are external to the virtual sphere. The reachability index can be defined as:

$$\Phi_{\ell_2, \ell_3} = \frac{1}{N} \sum_{i=1}^N \Theta_{\alpha}(\mathbf{P}_i), \quad \mathbf{P}_i \in S$$

where the function Θ_{α} returns 1 if, for each vector \mathbf{z}_k belonging to the cone $\Lambda_{\alpha}(\mathbf{P}_i)$, the function $\text{IK}(\mathbf{P}, \mathbf{z})$ is nonzero. The function Θ_{α} returns 0 otherwise. The index Φ_{ℓ_2, ℓ_3} achieves the maximum (i.e. 1) when every point $\mathbf{P}_i \in S$ is reachable along any direction internal to its cone $\Lambda_{\alpha}(\mathbf{P}_i)$.

Table 2 Parameters employed in the optimization problem

Parameter	Value
d_2	450 mm
a_6	55 mm
d_t	100 mm
q_1	$\in [0, 1200 \text{ mm}]$
$q_i, i = 2..6$	$\in [-170^{\circ}, +170^{\circ}]$
α	$\frac{7}{18} \pi$
R	250 mm
\mathbf{C}	$[500 \text{ mm}, 0, 800 \text{ mm}]^T$

In order to maximize the robot workspace, the skull surface is taken coincident with the virtual sphere. Therefore the generic point can be described as $\mathbf{P}_i = R[\cos \varphi_i \cos \theta_i, \cos \varphi_i \sin \theta_i, \sin \varphi_i]^T$ where R is the radius of the virtual sphere and φ_i and θ_i are the polar angles of the point. The angle α is chosen coherently with the tool orientation allowed during a neurosurgical task. A suitable value is $\alpha = 70^{\circ}$.

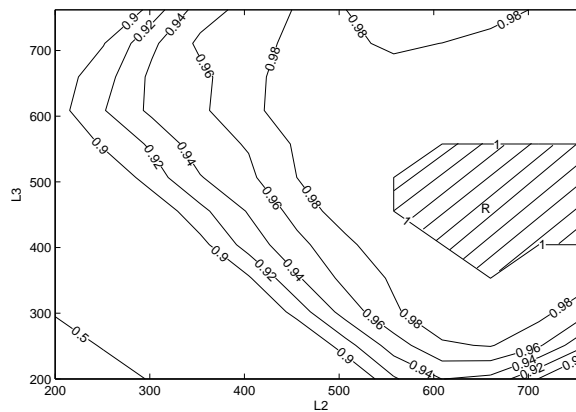


Figure 10: Level curves of Φ_{ℓ_2, ℓ_3} when the robot parameters of Table 2 are assumed

Figure 10 shows the level curves for Φ_{ℓ_2, ℓ_3} as a function of the link lengths ℓ_2 and ℓ_3 for the robot parameters in Table 2. It can be noticed that the index value is maximum inside the region R , while outside of this region $\Phi_{\ell_2, \ell_3} < 1$, which means that some tool configurations are not reachable by the robot.

Since both the index Φ_{ℓ_2, ℓ_3} and the arm stiffness depend on the link lengths, a suitable optimization problem must be defined so as to maximize the robot workspace while keeping the position errors, due to the links deformations, to a minimum. The optimization problem can be stated as:

$$\begin{aligned} \max_{\ell_2, \ell_3 > 0} \quad & \frac{1}{(\ell_2 + \ell_3)^3} \\ \text{s.t.} \quad & \Phi_{\ell_2, \ell_3} = 1 \\ & \mathbf{P} \in \mathbf{S} \quad \ell_2, \ell_3 > 0 \end{aligned}$$

where the cube at the denominator of the objective function takes into account the fact that the link stiffness at the end point is inversely proportional to the cube of link length. With reference to the values of Table 2, the maximum is reached at $\ell_2 = 660 \text{ mm}$ and $\ell_3 = 355 \text{ mm}$.

In order to highlight the performances of the NEUMESY for the chosen ℓ_2 and ℓ_3 values, let the function Θ_α be modified in $\bar{\Theta}_\alpha(\mathbf{P}_i)$, so that it returns not only a boolean value (0 or 1) but the mean number of solutions for each tool configuration defined by $\mathbf{P}_i \in \mathbf{S}$ and $\mathbf{z}_k \in \Lambda_\alpha(\mathbf{P}_i)$:

$$\bar{\Theta}_\alpha(\mathbf{P}_i) = \frac{1}{M} \sum_{\substack{\mathbf{z}_k \in \Lambda_\alpha(\mathbf{P}_i) \\ k=1..M}} \text{IK}(\mathbf{P}_i, \mathbf{z}_k)$$

Figure 11 shows the $\bar{\Theta}_\alpha(\mathbf{P}_i)$ function for the values in Table 2. It can be noticed that there are on average more than ten admissible solutions for each tool configuration.

In order to have a clearer idea of the robot performances, it is convenient to give a spatial representation of the $\bar{\Theta}_\alpha(\mathbf{P}_i)$ index, by introducing a suitable surface $S_{\bar{\Theta}_\alpha}$ defined as:

$$S_{\bar{\Theta}_\alpha} = \{ \mathbf{x} \in \mathbb{R}^3 \mid \mathbf{x} = \frac{1}{R} \bar{\Theta}_\alpha(\mathbf{P}) \mathbf{P}, \mathbf{P} \in \mathbf{S} \}$$

where R is the radius of \mathbf{S} .

Figure 12 shows the projections of the $S_{\bar{\Theta}_\alpha}$ on the three principal planes. It can be noticed that the highest performances are achieved on the lateral sides of the virtual sphere, where there is the largest number of configurations allowing the robot to avoid the virtual sphere

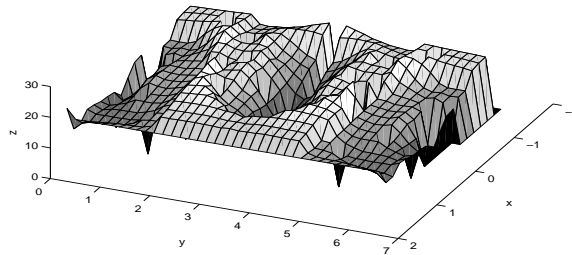


Figure 11: Performance index $\bar{\Theta}_\alpha(\mathbf{P}_i)$

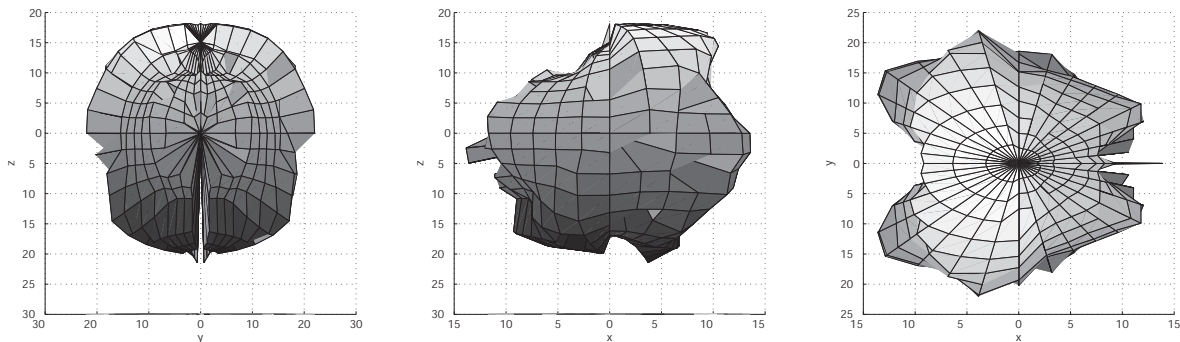


Figure 12: Projections of $S_{\bar{\Theta}_\alpha}$ on the cartesian planes

4. CONCLUSION

In this paper a new robot for neurosurgery is presented. The robot, named NEUMESY, is a six joints serial manipulator designed as positioning device for a neurosurgical actuator previously built by our research group, able to move a low energy x-ray source for the treatment of cerebral lesions. The redundancy respect to the surgical task (5 DoFs, being given by one point and one direction on the space) gives an extra DoF allowing the surgeon to choose the suitable robot configuration which reduces the space required by the robot and maximizes the safety, keeping the robot links away from the patient's head.

The solution of the non-trivial inverse kinematic problem is produced and a kinematic simulator has been carried out in order to analyze the performances of the robot.

Finally, the links length has been optimized in order to satisfy the workspace requirements fixed by the neurosurgical task and reduce the static deformations of the robot arm.

Future works consist in the study of the trajectory planning using the benefits taken by the redundancy so as to limit the link vibrations and deformations during the surgical task.

REFERENCES

- [1] Benabid AL, Cinquin P, Lavalée S, Le Bas JF, Demongeot J, de Rougemont J. Computer-driven robot for stereotactic surgery connected to CT scan and magnetic resonance imaging. Technological design and preliminary results. *Appl Neurophysiol* 1987;50:153-154.
- [2] Benabid AL, Lavalée S, Hoffmann D, Demongeot J, Danel F. Potential use of robots in endoscopic neurosurgery. *Acta Neurochir Suppl (Wien)* 1992;54:93-97
- [3] Faust R.A. *Robotics in Surgery: History, Current and Future Applications*. Nova Science Publishers, New York, 2007
- [4] Haidegger T., L. Kovacs, G Fordos, Z. Benyo, P. Kazanzides. Future Trends in Robotic Neurosurgery. Proc. of 14th Nordic-Baltic Conf. on Biomedical Engineering and Medical Physics, 2008
- [5] Haidegger, T. Tian Xia Kazanzides, P. Accuracy improvement of a neurosurgical robot system In Proc. Of BioRob 2008. 2nd IEEE RAS and EMBS Int. Conf. on Biomedical Robotics and Biomechatronics, 19-22 Oct. 2008, 836-841
- [6] Kwoh Y.S., J. Hou, E.A. Jonckheere and S. Hayati A previous termrobotnext term with improved absolute positioning accuracy for CT guided stereotactic brain previous termsurgery. *IEEE Trans Biomed Eng* 35 (1988), pp. 153-160.
- [8] McBeth P, Deon F. Louw M.D., Peter R. Rizun B.A.Sc.a and Garnette R. Sutherland M.D. Contact Information Robotics in neurosurgery. *The American Journal of Surgery*, Volume 188, Issue 4, Supplement 1, October 2004, Pages 68-75
- [8] Nathoo N., Cavusoglu MC, Vogelbaum MA, Barnett GH. In touch with robotics: neurosurgery for the future. *Neurosurgery*. 2005 Mar;56(3):421-33
- [9] Zamorano L, Li Q, Jain S, Kaur G. Robotics in neurosurgery: state of the art and future technological challenges. *Int J Med Robot*. 2004 Jun;1(1):7-22.
- [10] <http://www.mechatronics.it>
- [11] <http://www.neurochirurgiafirenze.it>
- [12] G. Rosati, A. Rossi, and V. Zanotto Lans: a haptic system for minimally invasive radio-surgery *International Journal of Mechanics and Control*, 4(2):45U50, 2003
- [13] A. Rossi, A. Trevisani, and V. Zanotto A telerobotic haptic system for minimally invasive stereotactic neurosurgery *Int. J. Medical Robotics and Computer Assisted Surgery*, Robotic Publications Ltd.,1(2):64-75, 2005
- [14] A.Rossi, A.Gasparetto, A.Trevisani, and V.Zanotto A robotic approach to stereotacticradio-surgery Proc. Of the 7th Biennial *ASME Conference Engineering Systems Design and Analysis*, Manchester, UK, 19-22 July, 2004.
- [15] Duchemin, G. Poignet, P. Dombre, E. Peirrot, F. LIRMM SCALPP: A 6-. dof robot with a non-spherical wrist for surgical applications *Advances in Robot Kinematics*, Kluwer Academic Publisher, 2000, 165-174





¹ Přemysl MATOUŠEK

ADAPTIVE CONTROL OF PNEUMATIC SERVOMECHANISM

¹ TECHNICAL UNIVERSITY OF LIBEREC, FACULTY OF MECHANICAL ENGINEERING,
DEPARTMENT OF APPLIED CYBERNETICS, LIBEREC, CZECH REPUBLIC

ABSTRACT:

The pneumatic positional servomechanism is highly non - linear system and that is why its identification and control is more exacting than at hydraulic or electric servomechanisms. To be able to reach a better control process it is not enough only to identify the system and than set the parameters of the controller but the system also has to be identified continuously and simultaneously with the identification of the parameters of the controller which have to be re - set depending on the achieved mathematical model. This article briefly describes the two main parts that constitute an adaptive control. The first part describes a design of an optimal structure of mathematical model that allows the continuous identification. The second part describes a design of an adaptive space-state controller whereby the adaptive control is implemented.

KEYWORDS:

pneumatic system; identification; model; state – space

1. INTRODUCTION

The pneumatic servomechanism is a non - linear and integral system. The air is a gas characterized by its compressibility, concurrently the passive resistances arise during the motion of the piston, and these resistances cause the non - linearity. This is why it is not effective to take several measurements, identify the system and set the parameters of the controller on the basis of the resultant mathematical model, because at each motion of the piston we get different parameters of the mathematical model. And the controller adjusted to a concrete mathematical model would not control exactly. Thus the system has to be identified continuously to get the most accurate mathematical model that is corresponding to the given state of the system. At the same time it is necessary to re - set the parameters of the controller, depending on the achieved mathematical model. The pneumatic system and the wiring of the components is shown in figure 1.

2. PNEUMATIC SYSTEM

Pneumatic positional servomechanism consists of the cylinder with one - side piston rod with maximal stroke 960mm, proportional directional valve MPYE-5-1/8-HF-010-B, proportional pressure regulator VPPM-6L-L-1-618-0L10H-A4P-S1C1 and pressure regulator HEE-D-MINI-24 with the filter LF-D-5M-MINI. The position of the piston rod is measured by means the linear displacement encoder with the 1000mm measurement length.

The feeding is realized by the power supply 24V/2A. This voltage serves for feeding the pressure regulator, proportional pressure regulator and proportional directional valve and it is also regulated to 10V voltage, by which the linear displacement encoder is supplied. This displacement encoder is connected with the piston of the pneumatic drive. The voltage on the slider appropriate to the position of the piston is applied to connector block SCB - 68 of the data acquisition card, its analog inputs and outputs are from the range of 0 - 10V.

The air from the compressor is brought to the input of the pressure regulator, through which the air supply to the whole system is switched on or off. The pressure regulator is switched on by the 24V and to be able to switch it on by the digital output of the data acquisition card (5V), the

signal convert from 5V to 24V has to be ensured. This convert is ensured by the switching transistor.

Constant pressure in the system is ensured by means of proportional pressure regulator. This regulator is controlled by the 0 - 10V voltage, where 1V equals to 1bar. As the analog output of the data acquisition card is in the range of 0 - 10V, the proportional pressure regulator is controlled straight by the means of output voltage of the card. This is how the air regulation to the required constant pressure is ensured.

When the air pressure is set to the required value, the air is brought to the input of the proportional directional valve. The motion of the slide valve is also controlled by the 0 - 10V voltage because the proportional directional valve is connected in the same way as the proportional pressure regulator. The system further contains of two DMP 331 pressure sensors that measure the running pressure over and below the piston and they also generate the flow signal in the range of 4 – 20mA. To be able to connect the sensors to the data acquisition card two I/U converters are used. They bring the current signal to 0 – 10V voltage.

The data acquisition card is a part of the control system PXI - 1042Q and an external connector block SCB - 68 is attached to it. PXI system communicates with the PC by means of Ethernet interface and LabView software is used to the control of the system. Simplified electrical scheme is shown in the figure 2.

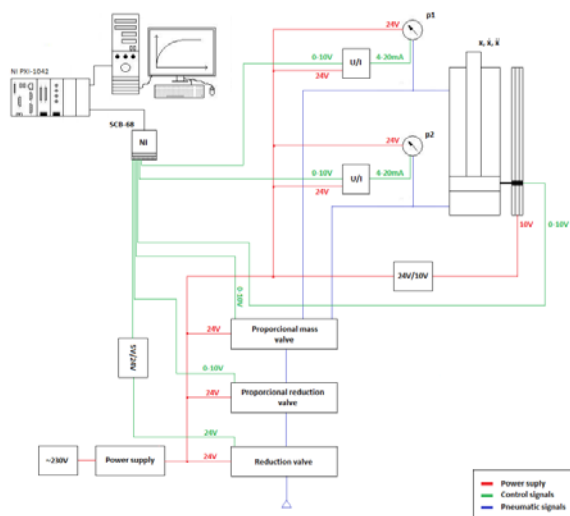


Figure 1: Pneumatic system

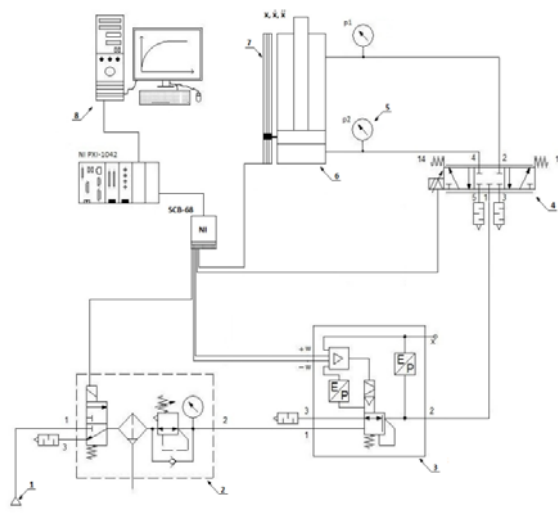


Figure 2: Simplified circuit

(1 – compressor, 2 – pressure regulator, 3 – proportional pressure regulator, 4 – proportional directional valve, 5 – pressure sensors, 6 - cylinder with one - sided piston rod, 7 - linear displacement encoder, 8 – control system)

3. IDENTIFICATION OF PNEUMATIC SYSTEM

To be able to realize the online identification of the pneumatic positional servomechanism, it is necessary to determine the order of the numerator and denominator of the system transfer. The system transfer was set by jumps in voltage excitation of various voltages, when the response of the system was recorded into the folder and was later identified in Matlab programme according to the quadratic criterion:

$$J_2 = \int [y(t) - y_m(t)]^2 dt = \sum [y(t) - y_m(t)]^2 \quad (1)$$

where $y(t)$ is the output of the system, $y_m(t)$ is the response of the model of the system.

The identification was realized with different structures of the model, when the most accurate transfer was achieved with the structures of the model in form:

$$G_1(s) = \frac{b_0}{a_2 s^2 + a_1 s}, G_2(s) = \frac{b_2 s + b_0}{a_2 s^2 + a_1 s + a_0}, G_3(s) = \frac{b_2 s + b_0}{a_4 s^4 + a_3 s^3 + a_2 s^2 + a_1 s} \quad (2, 3, 4)$$

where $a_4 - a_1$ are the coefficients of the numerator of the system transfer, $b_2 - b_0$ are the coefficients of the denominator of the system transfer.

In figure 3 there is the response of the pneumatic system for pressures of 3, 4 and 5 bars with the step change $U = 4,6V$ voltage on the proportional directional valve and then in the figure 4 there is the progress of the system response $y_m(t)$ and the comparison of the mathematical models $G_1(s)$, $G_2(s)$ and $G_3(s)$ for pressure of 4 bar at this jump.

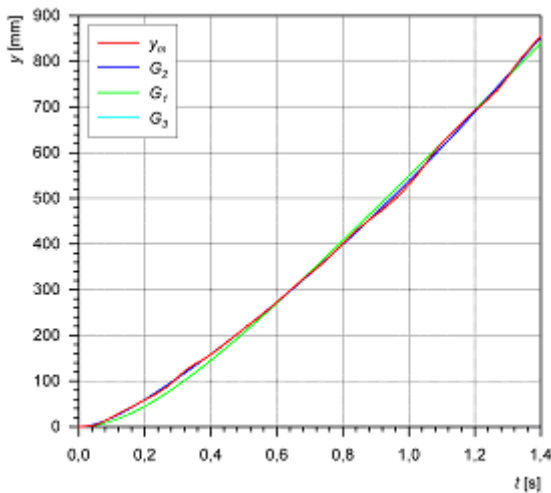


Figure 3: Response of the pneumatic system at 3, 4 and 5 bar pressures

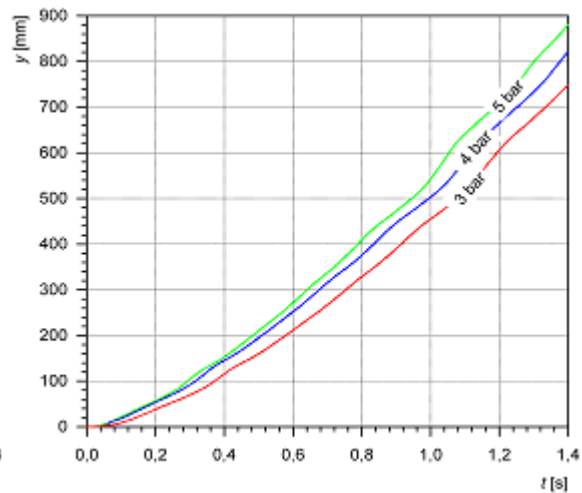


Figure 4: Comparison of the models $G_1(s)$, $G_2(s)$, $G_3(s)$

In the figure 4 there is noticeable that the differences among the models $G_1(s)$, $G_2(s)$, $G_3(s)$ of the pneumatic system are minimal, but on the more detailed investigation it is clear that the transfer $G_2(s)$ reaches the most accurate reset and this is why it was finally chosen for the online identification of the system. It is needful to convert this transfer from the continuous to the discrete area to be able to realize the project of model structure, the convert from continuous to the discrete area was implemented by the Matlab software.

The model for online identification was chosen from three kinds, model ARX, ARMAX and Box - Jenkins. Model Box - Jenkins cannot be used for this identification, because its error differs from an order over against ARX and ARMAX models. The structure of ARX and ARMAX models results from the structure of discrete transfer that was achieved by the convert of the continuous model to the discrete model. Structure ARX model is used in $[3 \ 3 \ 1]$ form, structure of ARMAX model in $[3 \ 1 \ 3 \ 1]$ form, where the difference equations are set by equation 5 and 6. The difference between the error of the ARX and ARMAX models during the identification of the system is nearly insignificant and it is shown in the figure 6. Finally, the ARX model was chosen for the online identification.

The signal from the linear displacement encoder is filtered, because it is extensively noisy. Kalman filter with the polynomials degree of 3 and number of samples 8 is used for the filtration. The comparison of the progress of the output signal ARX model with the structure that is defined by equation 6 and a measured signal $y_m(t)$ is shown in the figure 5.

$$(1 + a_1 z^{-1} + a_2 z^{-2} + a_3 z^{-3})y(k) = (b_1 z^{-1} + b_2 z^{-2} + b_3 z^{-3})u(k) + e(k) \quad (4)$$

$$(1 + a_1 z^{-1} + a_2 z^{-2} + a_3 z^{-3})y(k) = (b_1 z^{-1} + b_2 z^{-2} + b_3 z^{-3})u(k) + (1 + c_1 z^{-1})e(k) \quad (5)$$

where $a_3 - a_1$, $b_3 - b_1$, c_1 are coefficients of the difference equations of ARX and ARMAX models, $u(k)$ is exciting signal, $y(k)$ the output of the model and $e(k)$ the error of the model.

In the figure 5 it is obvious, that the response of the pneumatic system $y_m(t)$ is nearly identical with the output of the ARX model and the error arising during the identification reaches at most 3,7mm and so it can be neglected during the next calculations.

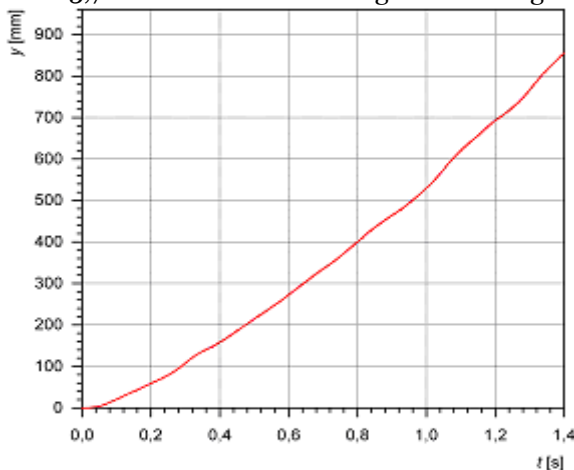


Figure 5: Identification of the system by ARX model

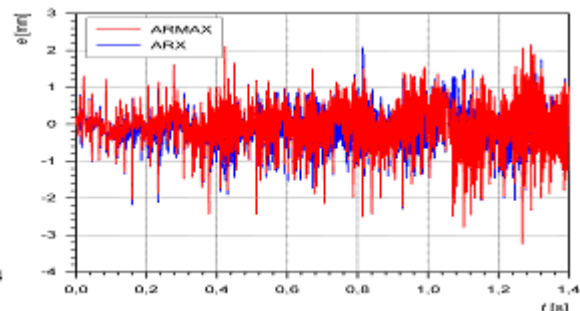


Figure 6: Difference of ARX and ARMAX models

4. STATE DESCRIPTIONS

The pneumatic system is regulated by the adaptive LQ controller, hence the discrete transfer of the ARX model has to be converted to state - space form (7). This conversion resides is based on the compilation of the state matrixes, when the observable canonical form was chosen for the state description. This canonical form reconstructs the response of the pneumatic system $y_m(k)$. The state vector consists of three state variables $x_1(k)$, $x_2(k)$, $x_3(k)$.

$$G(s) = \frac{b_2s^2 + b_1s + b_0}{a_3s^3 + a_2s^2 + a_1s + a_0} \quad \rightarrow \quad \begin{cases} x(k+1) = Mx(k) + Nu(k) \\ y(k) = Cx(k) + Du(k) \end{cases} \quad (6.7)$$

where $x(k)$ is the state vector [n, 1], $u(k)$ is the input vector [p, 1], $y(k)$ is the output vector, M is the state matrix [n,n], N is the input matrix [n, p], C is the output matrix [1, n], D is the feedforward matrix [1, 1].

4.1 REDUCED ORDER OBSERVER

The state vector consists of three variables where the first one is the measured response of the pneumatic system $y_m(k)$. The response of this system (position of the piston rod of the pneumatic cylinder) is measured by the linear displacement encoder and so it is not necessary to observe the variable $x_1(k)$ of the state vector. The two rest variables $x_2(k)$, $x_3(k)$ of the state vector are observed (8, 9). Not a full – state observer but the reduced order observer (designed by D.G. Luenberger) is used for the observation of the state vector.

$$\begin{bmatrix} x_1(k+1) \\ x_2(k+1) \\ x_3(k+1) \end{bmatrix} = \begin{bmatrix} y_m(k+1) \\ x_{z1}(k+1) \\ x_{z2}(k+1) \end{bmatrix} = \begin{bmatrix} M_{11} & M_{12} & M_{13} \\ M_{21} & M_{22} & M_{23} \\ M_{31} & M_{32} & M_{33} \end{bmatrix} \begin{bmatrix} y_m(k) \\ x_{z1}(k) \\ x_{z2}(k) \end{bmatrix} + \begin{bmatrix} N_1 \\ N_2 \\ N_3 \end{bmatrix} u(k) \quad (8)$$

$$y(k) = [C_1 \quad C_2 \quad C_3] \begin{bmatrix} y_m(k) \\ x_{z1}(k) \\ x_{z2}(k) \end{bmatrix} + Du(k) \quad (9)$$

During the project of the observer it is necessary to select the eigenvalues so that the error of the observe converges to zero. The dynamic qualities of the error of the observe are given by the eigenvalues $\lambda_{1,2}$, that's why the eigenvalues of the designed observer are zero. The observer was designed on the basis of equations 10, 11, 12, 13, 14 where $\hat{x}_z(k)$ is the estimate $\hat{x}_z(k)$.

$$\hat{x}_z(k+1) = M_z \hat{x}_z(k) + H_z y_m(k) + N_z u(k) \quad (10)$$

$$\hat{x}_z(k) = \hat{x}_z(k) + Q y_m(k) \quad (11)$$

$$M_z = F - QG \quad (12)$$

$$H_z = H - QM_{11} \quad Q = G + Q \quad | \quad FC \quad (13)$$

$$N_z = K - QN_{11} \quad (14)$$

where $H = \begin{bmatrix} M_{21} \\ M_{31} \end{bmatrix}$, $K = \begin{bmatrix} N_{21} \\ N_{31} \end{bmatrix}$, $F = \begin{bmatrix} M_{22} & M_{23} \\ M_{32} & M_{33} \end{bmatrix}$, $G = [M_{12} \quad M_{13}]$.

The process of the state vector of the designed observer at jump in voltage $U = 4,6V$ on the proportional directional valve is shown in the figure 7.

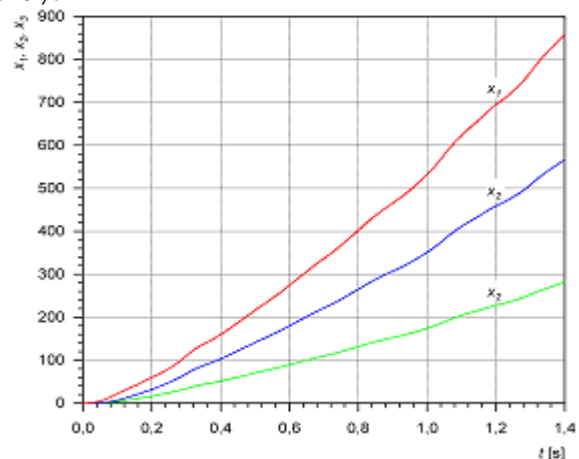
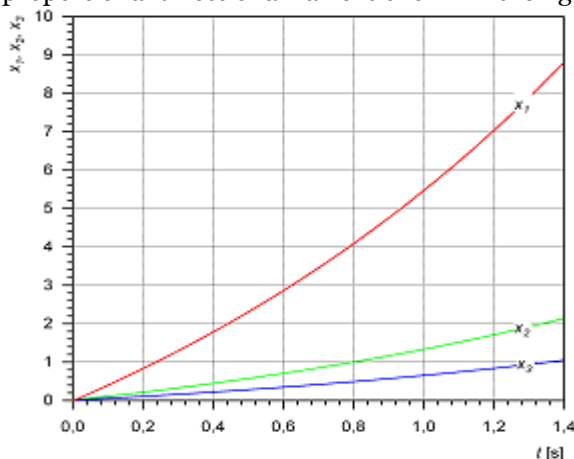


Figure 7: Simulation of the process of the state vector Figure 8: Real process of the state vector

In the figure 8 we can see the real process of the state vector of the designed observer. The calculation of the observer comes from the online identification of the pneumatic system by the ARX model. In each period of sampling we obtain new coefficients of the convert of the system. These coefficients are used for the construction of the new state matrixes that are necessary for the calculation of the state vector.

4.2 LQ CONTROLLER

The regulation of the piston position of the pneumatic system in the state space is implemented by means of LQ controller that is quadratically optimal for the linear systems. The controller minimizes the quadratic criterion for the discrete systems in the equation:

$$J(u(k)) = \sum_{k=0}^{N-1} (x^T(k) Q x(k) + u^T(k) R u(k)) + x^T(N) P x(N) \quad (15)$$

where Q is a positive - definite Hermitian or real symmetric matrix, R is a positive - definite or real symmetric matrix.

For the calculation of LQ controller that regulates the position of the piston we used simplified quadratic criterion in this equation:

$$J(u(k)) = \sum_{k=0}^{N-1} (x^T(k) Q x(k) + u^T(k) R u(k)) \quad (16)$$

where Q is a positive - semidefinite Hermitian or real symmetric matrix, R is a positive - semidefinite or real symmetric matrix.

The calculation of LQ controller comes from Riccati equation, when the condition of matrixes convergence $V = V(k+1)$ is kept:

$$V = Q + M^T V M - M^T V N (R + N^T S N)^{-1} N^T V M \quad (17)$$

and the resultant increase of the feedback of the state LQ controller is defined by this relation:

$$K = [R + N^T V N]^{-1} N^T V M \quad (18)$$

Our LQ controller should also equalize the influence of the constant failure and should follow the jump in voltage of the control quantity, so it is necessary to place a digital adder into the circuit. This adder increases the order of the system and the equation 8, 9 changes to form:

$$\begin{bmatrix} x(k+1) \\ x_4(k+1) \end{bmatrix} = \begin{bmatrix} M & 0 \\ CM & E \end{bmatrix} \begin{bmatrix} x(k) \\ x_4(k) \end{bmatrix} + \begin{bmatrix} N \\ CN \end{bmatrix} u(k) \quad (19)$$

$$y(k) = [C \quad 0] \begin{bmatrix} x(k) \\ x_4(k) \end{bmatrix} \quad (20)$$

where $x(k)$ is the state vector of variables $x_1(k)$, $x_2(k)$, $x_3(k)$ and $x_4(k)$ is the state variable that arised, because the adder was added to the system.

In the figures 9 and 10 there we can see the simulation of the regulation of the pneumatic system with the reduced order observer and LQ controller with the 0,2 m/s jump change of speed.

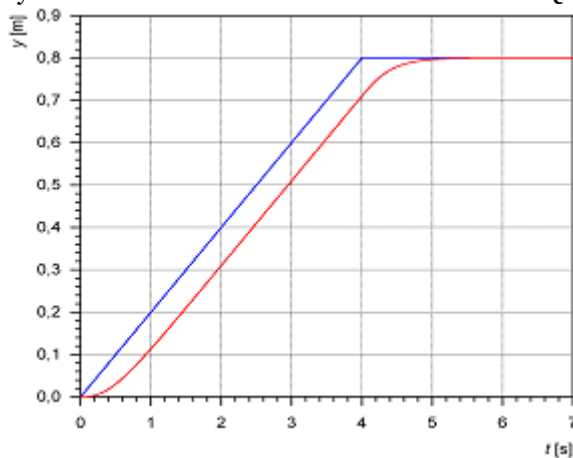


Figure 9: Simulated process of position

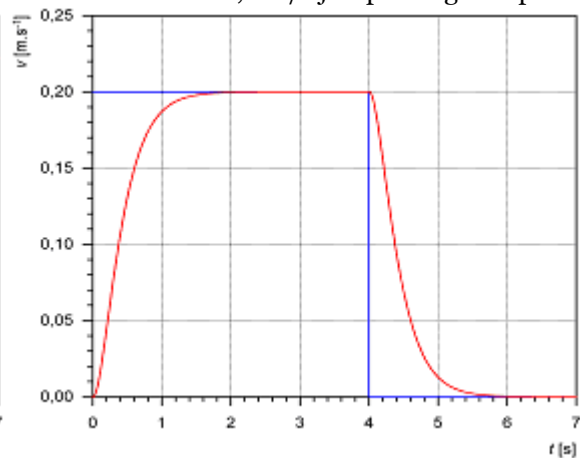


Figure 10: Simulated process of speed

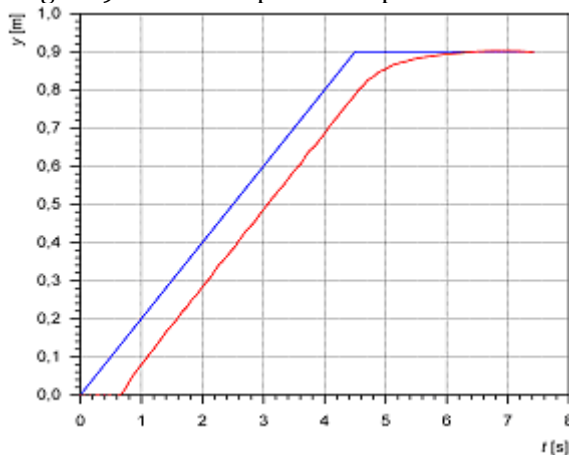


Figure 11: Real process of position

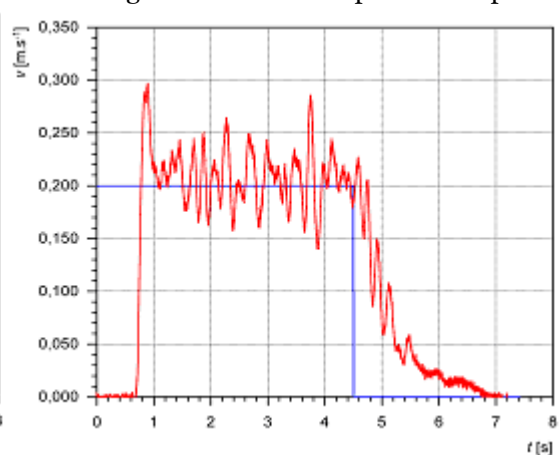


Figure 12: Real process of speed

In the figures 11 and 12 we can see the process of the regulation by means of LQ controller on the real pneumatic system to the speed step 0,2 m/s. During the regulation of the piston position at first the system is identified by ARX model. Then the state description of the system is made. As soon as the state matrixes are made the actual value of the state vector is calculated. The parameters of LQ controller are re - calculated after the completion of the calculation of the state vector. The output of LQ controller (an action interference) is observed on the directional valve.

5. RESULTS

The differences between the simulation and the real process of the regulation are evident from the figures 9 and 11. The differences between the smooth process of the simulation and the real process are caused mainly by the compressibility of the air and the passive resistances that have to be overcome during the motion of the piston. The passive resistances are also caused by the linear displacement encoder at which the stronger passive resistances arise in some places of the stroke. These resistances are probably caused by twisting the rod that connects the slider of the sensor with the end of the pneumatic piston inside the sensor case.

During the regulation by means of the state controller it is necessary to set the matrixes of weight coefficients accurately. If these matrixes are not set accurately the piston of pneumatic cylinder passes the required position at a high speed and after then it started to move to the required position at a low speed. When the matrix is set incorrectly the second most often behaviour of the piston occurs. It moves slowly to the required position from the beginning of setting the position. Another problem that we face at the pneumatic servomechanism is keeping the stable position. If we let the pneumatic servomechanism in a rest for a while, the air leakage occurs due to the untightness. This leakage deflects the piston from the equilibrium position so that the controller vibrates the piston around the required position.

The position at this pneumatic servomechanism is controlled only by means of the positional feedback and the LQ controller. At the hydraulic servomechanisms not only the positional feedback with the P controller is used for the control, but also the internal speed feedback with PI controller. We would like to eliminate an uneven speed of the piston motion of the pneumatic cylinder with the help of installation of the speed feedback as we can see it at hydraulic servomechanisms. Regulation of the position and the speed should not be implemented by the cascade connection of P and PI controllers but by two state LQ controllers that would be connected in cascade.

REFERENCES

- [1] Strejc, V.: *Stavová teorie lineárního diskrétního řízení*. Academia, Praha 1978
- [2] Modrlák, O.: *Úvod do diskrétní parametrické identifikace*. Skripta Liberec, 2004
- [3] Modrlák, O.: *Základy analýzy a syntézy ve stavovém prostoru*. Skripta Liberec, 2004
- [4] Balátě, J.: *Automatické řízení*. BEN-Technická literatura, Praha 2003





¹ Todor BAČKALIĆ, ² Maša BUKUROV

MODELLING OF THE SHIP LOCKING PROCESS IN THE ZONE OF SHIP LOCK WITH TWO PARALLEL CHAMBERS

¹ FACULTY OF TECHNICAL SCIENCES, UNIVERSITY OF NOVI SAD, NOVI SAD, SERBIA

ABSTRACT:

Being aware of the waterway capacity, as a substantial characteristic of each traffic way, has a great importance to authorities that perform control and regulation of the vessel traffic. In specific real conditions and situations, for the purpose of the vessel traffic control, it is necessary to know specified limits of traffic density, which depends on corresponding parameters of observed system (ship lock zone). The vessel traffic control in the zone of ship lock is a complex system that is made of numerous subsystems. Determination of subsystems and their external and internal connections is conducted according to analysis of a real system. Simulation model is developed according to the analyzed model of vessel traffic process. Developed simulation model contain data on vessels which have passed through the observed system in defined time interval. Also, it contains statistic data on number of vessels and delays due to waiting queues for locking. An application of this model is possible in all cases of the waterway capacity determination by varying numerical data. Obtained results may be used as a planning and decision-making support in the process of the vessel traffic control in the zone of ship lock with two parallel chambers.

KEYWORDS:

ship lock, navigation, simulation, model

1. INTRODUCTION

Capacity is one of the most important characteristics of transportation systems. In analysis of traffic flows, the capacity should be distinguished from the traffic density. Capacity of the waterway is the maximal amount of cargo per time unit (day, month, and navigation period) for specific technical characteristics of waterway and fleet, as well as appropriated type of traffic organization. The waterway capacity can be measured according to two parameters: the amount of cargo per time unit (as a basic parameter) and the number of vessels per time unit (which is often applied in a real system).

The growth of traffic density on waterways initiated research of capacity determination and how to increase it. Each traffic system is complex system. Capacity determination of such system requires complex analysis of present state and existing problems, as well as possibilities to solve them. Magnitude of the waterway capacity, as a substantial characteristic of each traffic way, has a great importance for institutions and services that perform control and regulation of vessel traffic. Analytical methods for waterway capacity determination give average values of capacity [5]. In specific real situations, besides the vessel traffic safety [6], activities in vessel traffic control and decision-making processes require knowledge of traffic density limits, which depend on parameters of observed system.

Being aware of the capacity of certain waterway requires preliminary determination of influential factors and their effect on capacity quantity. Technological process of navigation is defined according to connections between elements and changes of the system state during navigation. After that follows model development and realization of simulation experiments. The capacity of the most difficult section of observed waterway determines capacity of the waterway as a

whole. It is possible to establish upper limit (maximal value) of waterway capacity as a whole by comparison of particular waterway section capacities, i.e. “bottle necks” based on capacity. When the traffic density on observed waterway reaches the limit values under certain technical and exploitation conditions, it is necessary to determine the waterway capacity for changed mode of exploitation (i.e. for changed technical characteristics and/or mode of exploitation). Some authors [9], [7] most attention give to determination of the ship lock capacity and its impact on the vessel traffic.

While studying problem of waterway capacity it is necessary to set apart natural and artificial sections of waterways. Natural waterways and canals can be divided into sectors: navigable sections and those that include objects on waterway (ship locks, inclined plane, boat lifts or other).

2. ORGANIZATION OF TRAFFIC AND TECHNOLOGICAL PROCESS OF NAVIGATION

The traffic organization on the waterway is represented by set of rules and activities for the control of navigation in the waterway, in order to perform rational utilization of waterway capacity and reduce time delays of vessels, with respect to existing navigational rules and the safety level of navigation. The traffic organization on the waterway or the section of waterway depends on [1]:

- ❖ technical and exploitation characteristics of the waterway and objects on the waterway
- ❖ technical and exploitation characteristics of fleet
- ❖ traffic density
- ❖ number of different types of vessels in fleet
- ❖ priority of specific vessels
- ❖ hydrological and meteorological conditions.

Each organization scheme is characterized by certain technological process of navigation (ship passing process or ship locking process). Also, for a certain type (scheme) of the vessel traffic organization there are different technological processes of navigation depending on vessel characteristics.

Technological process of navigation is presented by set of activities with defined phase change schedule. The phases are influenced by specific factors and limited by duration of time necessary to accomplish certain activity. Technological process of navigation depends on:

- an appropriate traffic organization scheme
- traffic density
- priority of vessels
- navigation conditions on the waterway
- technical and exploitation characteristics of objects on the waterway
- technical and exploitation characteristics of fleet
- hydrological and meteorological conditions.

There are following groups of technological processes depending on exploitation conditions on waterways' sections:

- technological process of navigation in two-way navigation sections
- technological process of navigation in one-way navigation sections
- technological process of navigation in zones of ship locks.

2.1. ORGANIZATION OF TRAFFIC IN THE ZONE OF SHIP LOCK

Organization of traffic on the waterway in the zone of ship lock, i.e. organization of ship locking process, is a compromise between the rational utilization of ship lock and reduction of vessels' delays in the zone of ship lock.

Organization of the vessel traffic on the waterway in the zone of ship lock depends on:

- number of locks (one or two parallel)
- number of lock chambers (one, two or more chambers in a row)
- way of ship locking process (one direction or both directions)
- technical characteristics of locks and approach canals
- traffic density
- technical characteristics of a fleet
- number of different types of vessels in a fleet
- priority level for certain vessels
- hydrological and meteorological conditions.

The factors listed above indicate a variety of organization ways, i.e. ability to determine a large number of traffic organization schemes, which depend on the degree of importance assigned to particular criterion.

From the standpoint of traffic organization and traffic density, there are three different types of navigation: free, restricted and regulated navigation [1]. The highest level is automated navigation (automated guidance). The navigation in two-way section corresponds to type of free navigation, since only restrictions in navigation are maximal allowed speed and distance between two vessels from the same direction. In other hand, navigation in a ship lock zone corresponds to type of regulated navigation.

During the ship locking process vessel changes position in real space and ship lock goes through certain phases, or states. Traffic organization scheme in a ship lock zone is influenced by adopted organization type. The technological process of the ship locking is analysed as a complex process in order to more clearly noticed specificity and mutual dependence between the state change of locks and movement of vessels. Long waiting of vessels at the entrance and vessels amassing must not be permitted.

2.2. THE TECHNOLOGICAL PROCESS IN THE ZONE OF SHIP LOCK

The technological process of ship locking is divided into two main subsets:

- from the aspect of ship lock
- from the aspect of vessels.

Phases, which ship lock and vessel go through during locking process, are defined by operations which must be executed. Duration of operations depends on several factors: the state of technical equipment, hydrologic and weather conditions, number and type of locked vessels, the intensity of the flow of requests for ship locking (traffic density) and other.

The technological process of ship locking was analyzed as a complex system. It consists of different phases through which pass: only vessels, only ship lock and phases for both - vessels and ship lock. Also, there are certain activities of the control of the ship locking process. Phases are represented by following activity flows:

- flow of vessel activities (ships and compositions),
- flow of ship lock activities (with or without vessels in the lock chamber),
- flow of control activities during the ship locking process.

Technological processes of ship locking can be classified according to:

- type and technical - exploitation characteristics of ship lock, approach canals and lock pools
- technical -exploitation characteristics of vessels
- organization mode of ship locking process.

From the standpoint of the ship locking process, according to the technical-exploitation characteristics, there are following systems:

- one lock (with one, two or more lock chambers in a row)
- two parallel locks (with one, two or more lock chambers in a row).

Technological processes of ship locking can be distinguished from the aspect of locking mode: one lock - one direction and one lock - both directions.

Depending on the technical-exploitation characteristics of the fleet and the locks, or possible number of vessels in the lock chamber during one cycle, there are following relationships between the lock and technological processes of ship locking:

- one lock chamber - one vessel (relevant)
- one lock chamber - one composition (relevant)
- one lock chamber - many vessels and compositions.

Taking into account assigned priority technological processes can be classified as:

- all vessels and compositions have equal priority, i.e. ship locking process without priority
- different priority levels for certain ships and compositions, i.e. ship locking process with priorities.

Table 1. Criteria for the classification of technological processes of ship locking

Type of the technological process of ship locking	Number of ship lock rows (1 or 2)	Number of lock chambers in a row (1, 2, ..., n)	Number of vessels in a lock chamber (1, 2, ..., m)	Ship lock is assigned to one or to both directions (one=1, both=2)	Number of ship priority levels (1, 2, ..., p)
11121	1	1	1	2	1
11122	1	1	1	2	2
...
22m21	2	2	m	2	1
...
2 nm 2 p	2	n	m	2	p

Depending on the classification criterions above there are a lot of ship locks systems with the appropriate technological processes of ship locking (Table 1).

3. TECHNOLOGICAL PROCESS OF THE SHIP LOCKING IN THE ZONE OF SHIP LOCK SYSTEM WITH TWO PARALLEL LOCKS FOR BOTH DIRECTIONS

Technological process of the system with two parallel locks with two chambers in a row for more vessels in one cycle will be presented in the following schemes. Both locks are designed for both directions, giving greater importance to reduction of vessels delays in the ship lock zone (type 22m21, part marked in Table 1).

In Figure 1 are presented connections between segments of the technological process of navigation in the zone of a system.

In Figure 2 are presented activities of vessels at both levels (arrivals from the lower and upper level). In Figure 3 are presented some lock activities at ship locking process. In the Figures 4 and 5 are presented some activities of the ship lock control centre.

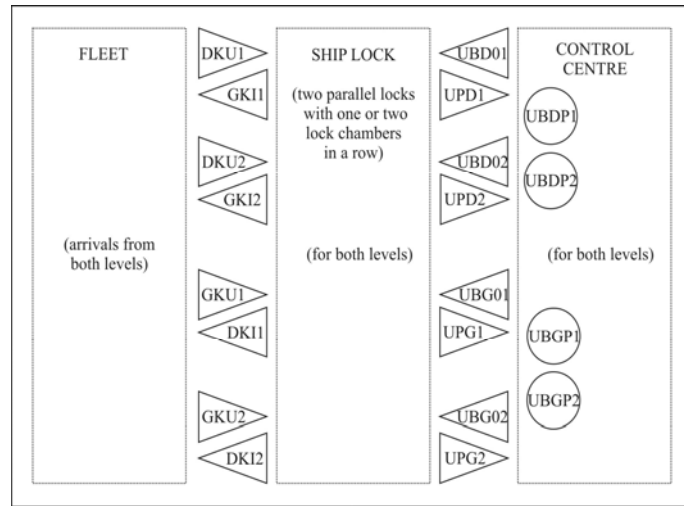


Figure 1. Connections between segments of the technological process in the ship lock zone

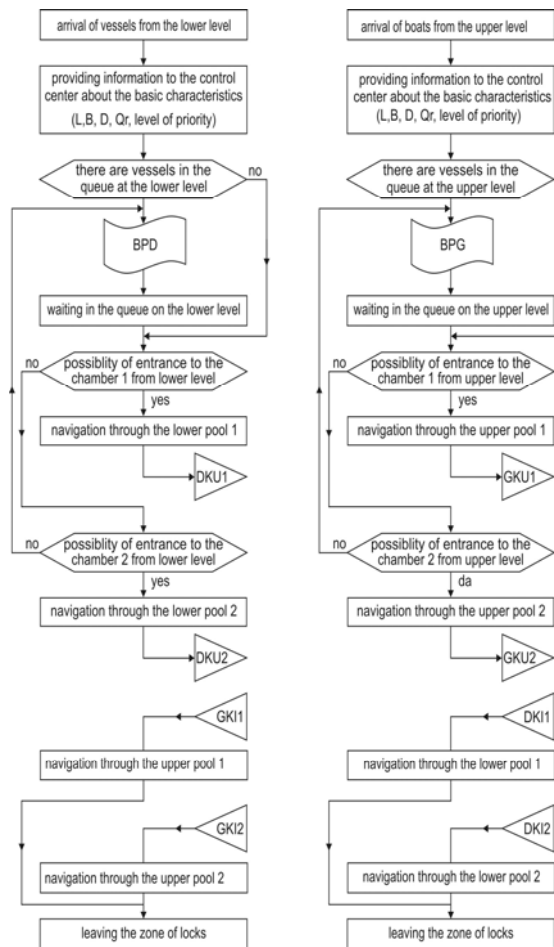


Figure 2. Activities of vessels at both levels

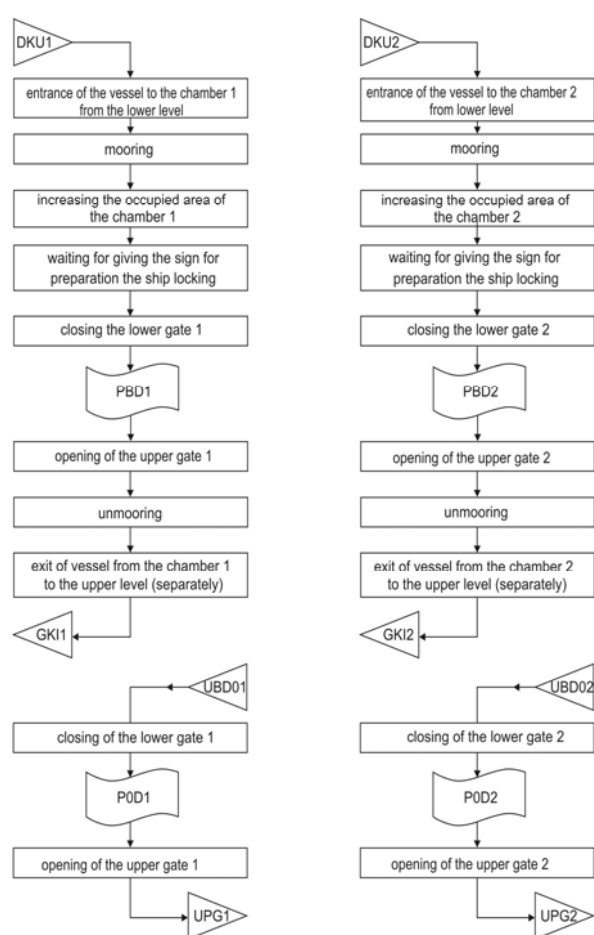


Figure 3. Ship lock activities at ship locking process (from lower to upper level)

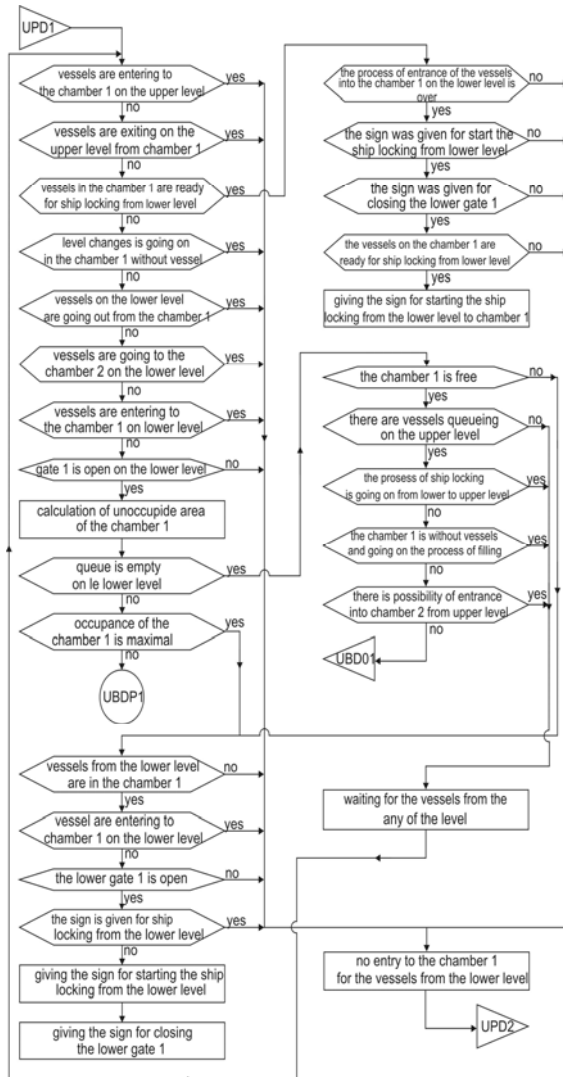


Figure 4. Activities of the ship lock control centre (locking from lower to upper level – lock1)

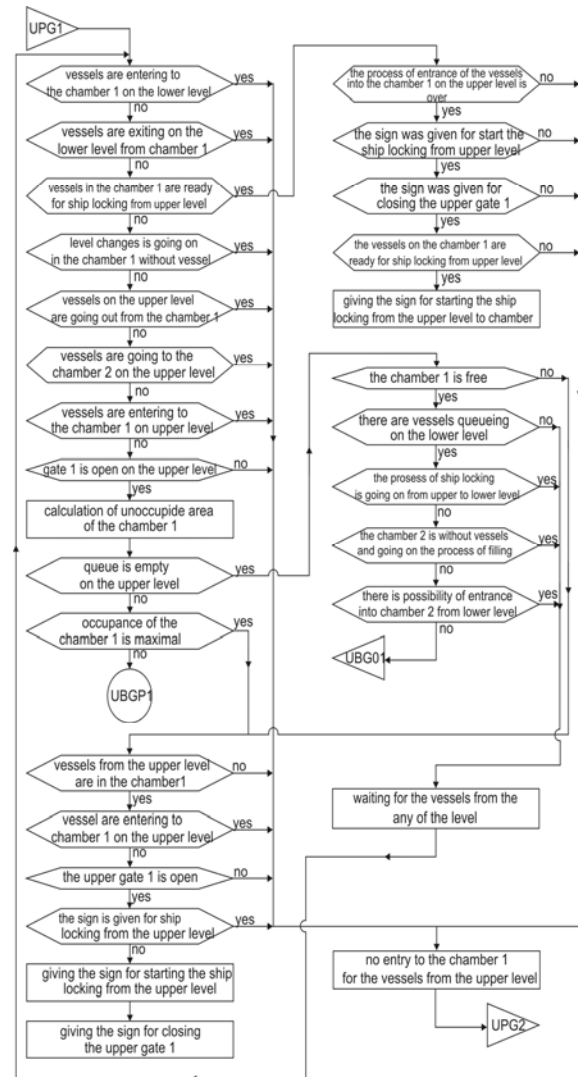


Figure 5. Activities of the ship lock control centre (locking from upper to lower level – lock1)

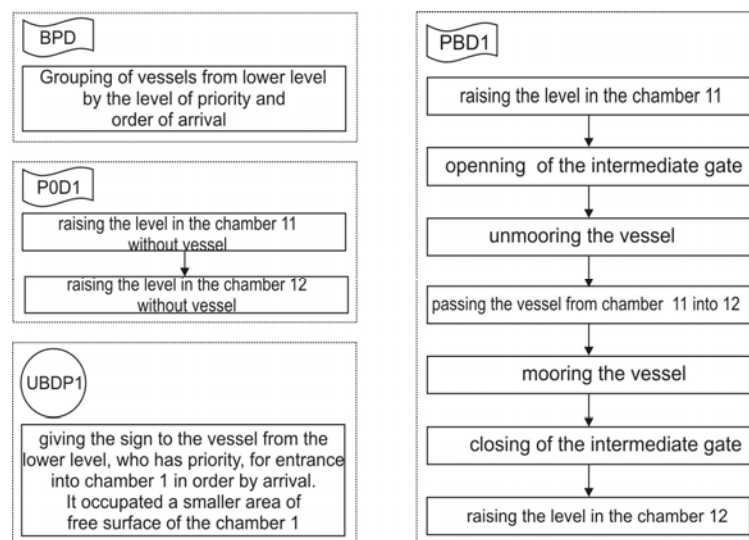


Figure 6. Description of some activities in the ship lock process

4. SIMULATION MODEL

4.1. DESCRIPTION OF THE SIMULATION MODEL

The developed simulation model is composed of nine sub-models:

- sub-model 1 - the ship locking process for vessels from the lower level
- sub-model 2 - the ship locking process for vessels from the upper level
- sub-model 3 - the control process of the ship lock 1 during locking from the lower level
- sub-model 4 - the control process of the ship lock 2 during locking from the lower level
- sub-model 5 - the control process of the ship lock 1 during locking from the upper level
- sub-model 6 - the control process of the ship lock 2 during locking from the upper level
- sub-model 7 – the control process of grouping of vessels in the queue at the lower level, depending on: the priority level, the order of arrival and area size ($L \times B$) that occupy the vessel in the lock chamber
- sub-model 8 - the control process of grouping of vessels in the queue at the upper level, depending on: the priority level, the order of arrival and area size ($L \times B$) that occupy the vessel in the lock chamber
- sub-model 9 - time sub-model (timer).

Ship locks are static elements in sub-models 1, 2, 3 and 4, while vessels are dynamic elements in sub-models 1 and 2. Control actions are dynamic elements in sub-models 3, 4, 5 and 6. In sub-models 7 and 8, control actions are dynamic elements, while queues (if were formed) are static elements.

Sub-model 1 is the locking process of vessels from the lower level to the upper level. It includes all operations and delays of vessels and locks from the moment vessel entrance into the ship lock zone at the lower level.

Sub-model 2 is the locking process of vessels from the upper level to the lower level. It includes all operations and delays of vessels and locks from the moment vessel entrance into the ship lock zone at the upper level.

Sub-models 3 and 4 describe control processes of ship locks 1 and 2 during locking from the lower level and include:

- control of vessels' entering in ship locks 1 and 2 from the lower level
- water level change in ship locks 1 and 2 without vessels, in cases when there is no queue at the lower level, lower gates 1 or 2 are opened, while vessels at the upper level wait in the queue.

Sub-models 5 and 6 describe control processes of ship locks 1 and 2 during locking from the upper level and include:

- control of vessels' entering in ship locks 1 and 2 from the upper level
- water level change in ship locks 1 and 2 without vessels, in cases when there is no queue at the upper level, upper gates 1 or 2 are opened, while vessels at the lower level wait in the queue.

Sub-models 7 and 8 describe control processes of vessels re-grouping in the queues at the lower and upper levels. Re-grouping depends on: priority level, order of arrival and area size ($L \times B$) which vessel occupies in the lock chamber. Sub-model 9 represents the duration of the simulation experiment.

4.2. EVALUATION OF THE SIMULATION MODEL

Evaluation of the developed simulation model included determination of the model validity and the model testing [2], [3]. Determination of the model validity was done up to the level of predictability. Predictive model validity is a stricter level of evaluation that is related to the model ability to be used to predict the situations that are not observed and studied on the real systems. That level was tested with simulation experiments. In the simulation experiments the traffic density was altered in both directions and system reactions were observed.

The model testing was done from the beginning of the real system modelling and includes:

- application of specialized language (GPSS) to realize the simulation program
- validity and accuracy testing of the simulation model (verification of static and dynamic properties of the model)
- correctness testing of the model to generate different distributions of input variables and system parameters.

Control of the simulation model has determined if there is a match between behaviour of program and model. The developed simulation model completely fulfils presented requirements and criteria, and such can be used in simulation experiments for capacity determination and change in density of traffic on certain real system.

5. CONCLUSION

Navigation in ship lock zones, as a part of system of navigation on inland waterways, apart other things, is characterized by limited capacity and the need to use information-control systems. Capacity presents one of the most important characteristic of each waterway, especially ship lock. The organization of traffic on the observed real system has significant influence on the capacity.

The developed simulation model of the technological process of ship locking gives a number of data, like vessel delays, transit times, resource utilizations, number of vessels in queues and others. The developed model can be applied to planning of vessel traffic control, since they give a possibility of choice of traffic organization that depends on certain conditions. Connections between elements of technological process in presented models have been copied from real system. This allows variation in densities and distribution of all incoming vessels' flows, as well as changes of technical characteristics of ship lock and vessels.

Application of developed simulation models is applicable for planning and decision making in ship locking control. Also, they can be applied to define type of organization of ship locking process. It is possible to do almost unlimited number of simulation experiments. More important, the model's fidelity enables to predict conditions for any future scenarios of interest (e.g., under increasing traffic volumes), and to answer various other "what-if" questions [8].

High-fidelity simulation models of ship locking process consisting of the entire vessel classes as well as level of priority, weather and waters conditions can be easily developed. Significant extensions of model can be made by adding new segments. Such extended simulation model includes the following: application of control rules, ability to monitor the influence of large vessels on waterway capacity.

Also, further research should focus on problems how to define optimal density of traffic for given conditions. To solve this problem it is necessary to introduce the term "level of service" (as a qualitative measure). Determination of the optimal density requires application of certain optimization methods in order to achieve certain levels of service with defined conditions and relevant parameters.

REFERENCES

- [1] Bačkalić, T.: Traffic control on artificial waterways with limited dimensions as function of their capacity, (in Serbian), PhD thesis, University of Novi Sad, Serbia, 2001
- [2] Biles, W.E., Sasso, D., Bilbrey, J.K.: Integration of simulation and geographic information systems: modeling traffic flow in inland waterways, Proceedings of the 36th conference on Winter simulation, ISBN:0-7803-8786-4, Washington D.C., USA, December 2004
- [3] Bush, A., Biles, W.E., DePuy, G. W.: Iterative optimization and simulation of barge traffic on an inland waterway, Proceedings of the 35th conference on Winter simulation, ISBN: 0-7803-8132-7, New Orleans, Louisiana, USA, December 2003.
- [4] Filipowicz, W.: Vessel Traffic Control Problems, Journal of Navigation, ISSN: 0373-4633, The Royal Institute of Navigation, Vol. 57, No. 1, 2004, pp. 15-24
- [5] Griffiths, J.D.: Queueing at the Suez Canal, The Journal of the Operational Research Society, Palgrave Macmillan Journals on behalf of the Operational Research Society, Vol. 46, No. 11 (Nov., 1995), pp. 1299-1309
- [6] Ince A.N., Topuz E.: Modelling and simulation for safe and efficient navigation in narrow waterways, Journal of Navigation, ISSN: 0373-4633, The Royal Institute of Navigation, Cambridge University Press, Vol. 57, No. 1, 2004, pp. 53-71.
- [7] Ramanathan, V., Schonfeld, P.: Approximate Delays Caused by Lock Service Interruptions, Transportation Research Record 1430, Jan. 1994, pp. 41-49
- [8] Smith, L.D., Sweeney, D.C., Campbell, J.F.: A simulation model to evaluate decision rules for lock operations on the Upper Mississippi river, Proceedings of 40th Hawaii International Conference on Systems Science (HICSS-40 2007) Waikoloa, HI, USA, 3-6 January 2007
- [9] Wang, S.L., Schonfeld, P.: Demand Elasticity and Benefit Measurement in a Waterway Simulation Model, Transportation Research Record: Journal of the Transportation Research Board, Transportation Research Board of the National Academies, ISSN: 0361-1981, Volume 2033 / 2007, pp. 53-61, 2008



¹ József SÁROSI

INVESTIGATION OF POSITIONING OF FLUID MUSCLE ACTUATOR UNDER VARIABLE TEMPERATURE

¹ FACULTY OF ENGINEERING, UNIVERSITY OF SZEGED, HUNGARY

ABSTRACT:

Some researchers have mentioned that temperature creates an important part in the accuracy of positioning of pneumatic artificial muscles (PAMs). However, in literature investigations for measuring temperature inside and outside the PAMs have not been found. This paper presents our robust motion control of these muscle actuators under different temperatures using sliding-mode control.

KEYWORDS:

muscle actuators, variable temperature

1. INTRODUCTION

The working principle of the pneumatic artificial muscles is well described in literature ([1], [2], [3], [4], [5] and [6]).

There are a lot of advantages of these muscles like the high strength, good power-weight ratio, low price, little maintenance needed, great compliance, compactness, inherent safety and usage in rough environments. However, problems with the control of the highly nonlinear pneumatic systems have prevented their widespread use [7]. For this, a fast and robust control necessary to achieve the desired motion. Several control ways have been applied to control different humanoid or robot arms, manipulators, prosthetic and therapy devices driven by pneumatic artificial muscles. The early control methods were based on classical linear controllers and then some modern control strategies have been developed (e. g. adaptive controller, sliding-mode controller, fuzzy controller, neural network controller and others) [8].

The layout of this paper is as follows. Section 2 (The study) is devoted to display our test-bed and the LabVIEW programs. Section 3 (Results and discussion) presents several experimental results. Finally, section 4 (Conclusions) gives the investigations we plan.

Fluid Muscles DMSP-10-250N-RM-RM (with inner diameter of 10 mm and initial length of 250 mm) produced by Festo company were selected for our newest study.

2. THE STUDY

A good background of our test bed and former experimental results of positioning can be found in [9] and [10].

The PAMs were installed horizontally and can be controlled by MPYE-5-M5-010-B type proportional valve made by Festo. Our robust position control method based on sliding-mode control. The linear displacement of the actuator was measured using a LINIMIK MSA 320 type linear incremental encoder with 0,01 mm resolution.

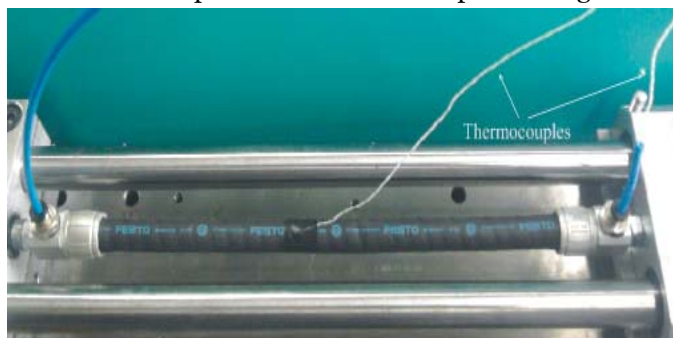


Figure 1. Muscle with two thermocouples

To measure temperature inside and outside the muscle the test-bed was completed two thermocouples type K (Figure 1). Figure 2 shows the block diagram of this positioning system with proportional valve.

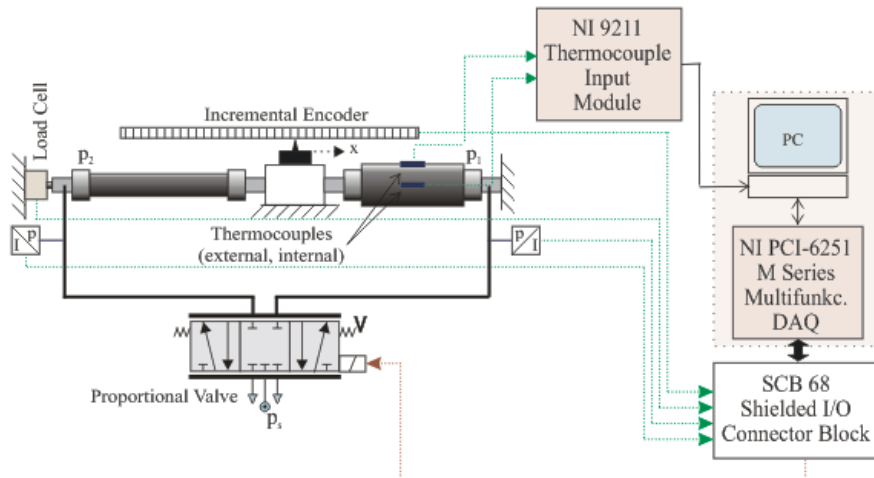


Figure 2. Block diagram of positioning system with proportional valve

The Figure 3 shows data acquisition and positioning that can be achieved in LabVIEW environment. Aside from the desired position the number of samples and the sampling time can also be set. The data can be saved into a text file.

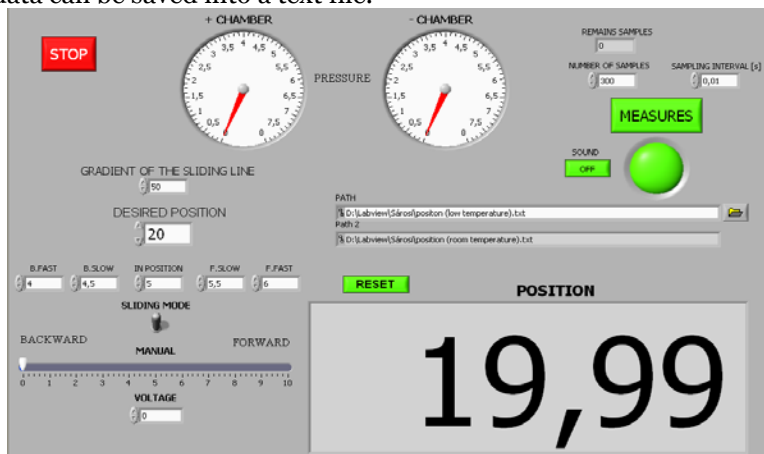


Figure 3 Front panel of LabVIEW program for positioning

The Figure 4 shows the front panel of the LabVIEW program created for temperature measurement. Here the number of samples and sampling time can also be set. During the periodic and automatic working of the muscles the contraction and rate of release can be adjusted with the frequency of the sine wave. The temperature inside and on the surface of the muscle can be read on the indicators on the screen also it is shown as a number. The measured results are saved in a text file for later processing.

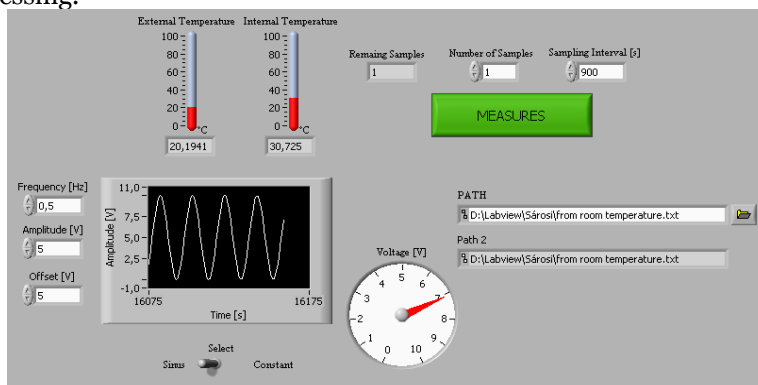


Figure 4. Front panel of LabVIEW program for measuring temperature

3. RESULTS AND DISCUSSION

Positioning was first done in room temperature on the pressure of 6 bar. The desired positioning was set to 20 mm, the number of samples was set to 300, while the sampling rate was set to 10 ms, thus the measurement took 3 s.

Figure 5 shows the positioning as a function of time. It took about 1,85 s for the position to reach the set value. To show the accuracy of positioning the area around the desired position has been magnified (Figure 6). This Figure shows the accuracy of positioning is within 0,01 mm.

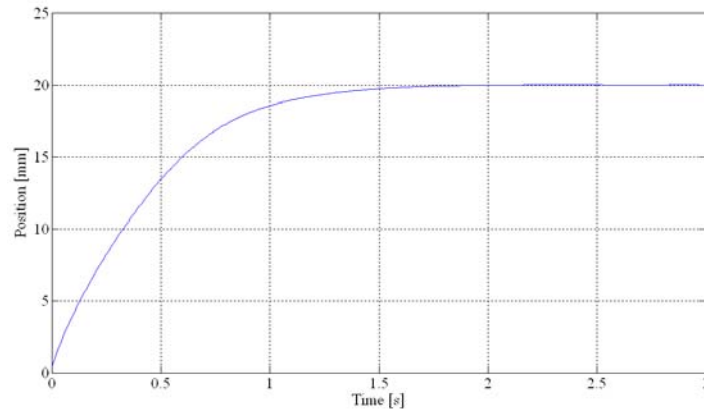


Figure 5. Position as a function of time

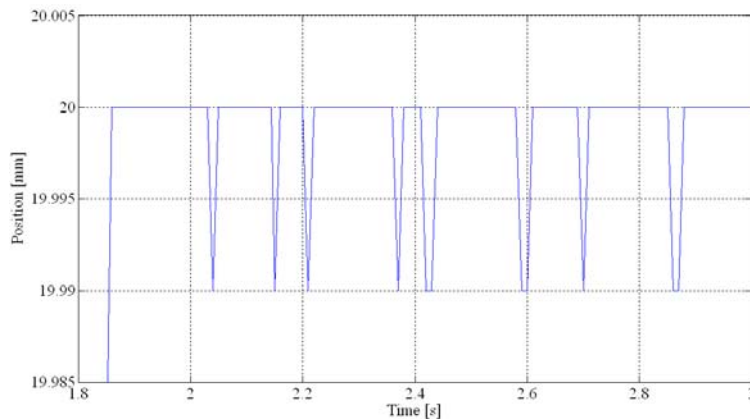


Figure 6. Position as a function of time (enlarged)

The periodic working of the muscles was achieved with a 0,5 Hz frequency sine wave. The measurement took 900 s during which the sampling time was 0,25 s, the acquired data is shown in Figure 7. While the surface temperature reached about 28 °C, the internal temperature oscillated a lot during contraction and release, for this reason a spline approximation was used for the internal temperature (Figure 8).

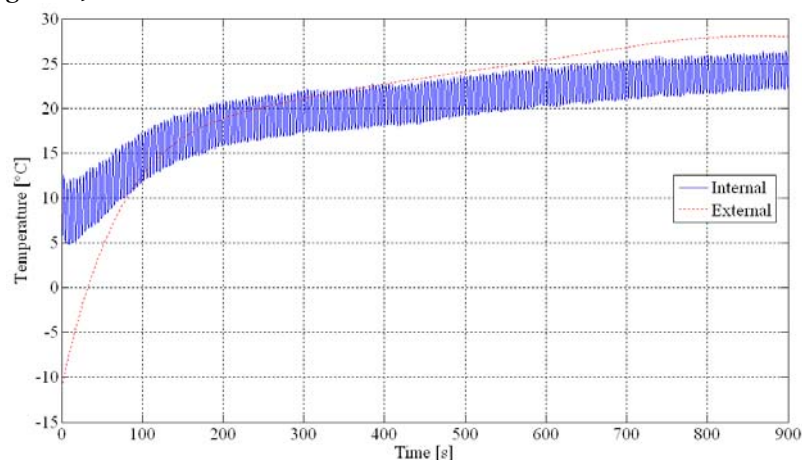


Figure 7. Temperature as a function of time

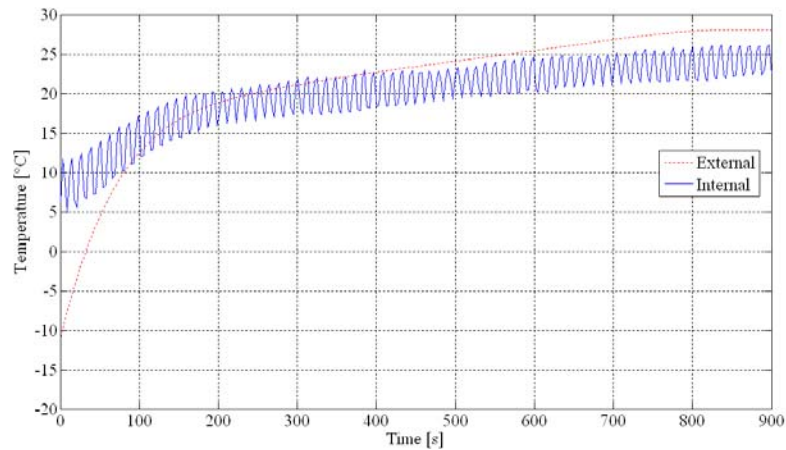


Figure 8. Temperature as a function of time with spline interpolation for internal temperature

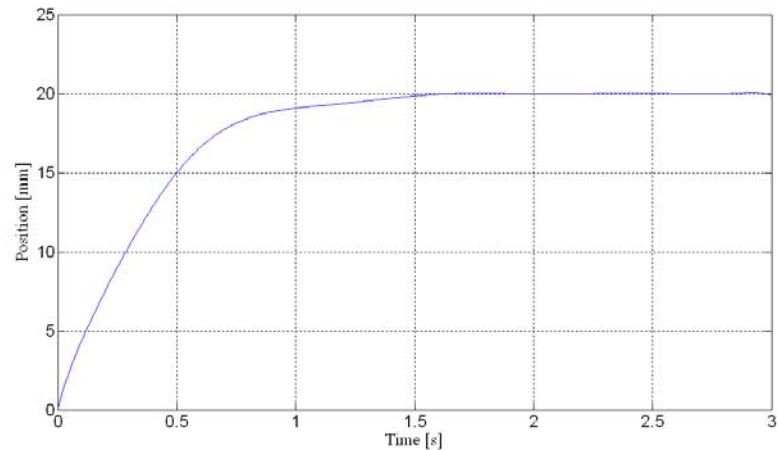


Figure 9. Position as a function of time after work cycle

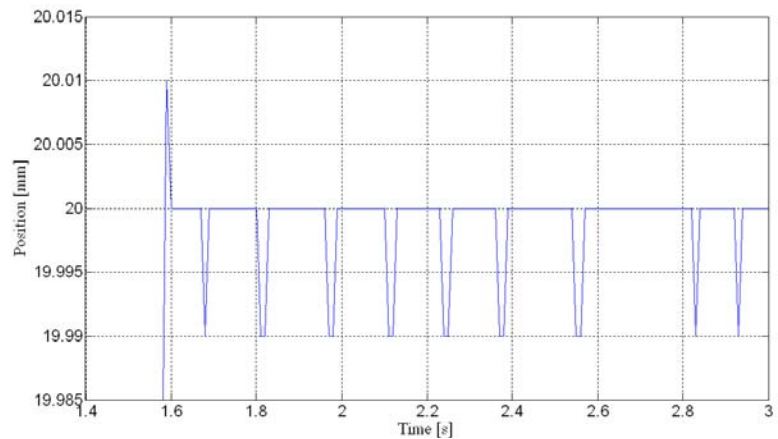


Figure 10. Position as a function of time (enlarged) after work cycle

After a constant temperature was reached positioning was measured on the pressure of 6 bar, too. The result of it is shown in Figure 9. It shows the desired position was reached within 1,6 s. To show the accuracy of positioning the area around the desired position has been magnified (Figure 10.). The accuracy of positioning remained within 0,01 mm.

4. CONCLUSIONS

From these measurements the conclusion is that the sliding-mode control is rather robust for accurate positioning and the accuracy and time of positioning is more favorable at higher temperature. We plan these investigations will be repeated with different muscles.

REFERENCES

- [1.] Daerden, F. (1999): Conception and realization of pleated artificial muscles and their use as compliant actuation elements, PhD Dissertation, Vrije Universiteit Brussel, Faculteit Toegepaste Wetenschappen Vakgroep Werktuigkunde, pp. 5-33.
- [2.] Daerden, F. and Lefeber, D. (2002): Pneumatic artificial muscles: actuator for robotics and automation, European Journal of Mechanical and Environmental Engineering, Volume 47, pp. 10-21.
- [3.] Caldwell, D. G., Razak, A. and Goodwin, M. J. (1993): Braided pneumatic muscle actuators, Proceedings of the IFAC Conference on Intelligent Autonomous Vehicles, Southampton, United Kingdom, 18-21 April, 1993, pp. 507-512.
- [4.] Balara, M. and Petík, A. (2004): The properties of the actuators with pneumatic artificial muscles, Journal of Cybernetics and Informatics, Volume 4, pp. 1-15.
- [5.] Chou, C. P. and Hannaford, B. (1996): Measurement and modeling of McKibben pneumatic artificial muscles, IEEE Transactions on Robotics and Automation, Volume 12 (1), pp. 90-102.
- [6.] Tondu, B. and Lopez, P. (2000): Modeling and control of McKibben artificial muscle robot actuator, IEEE Control System Magazine, Volume 20, pp. 15-38.
- [7.] Caldwell, D. G., Medrano-Cerda, G. A. and Goodwin M. (1995): Control of pneumatic muscle actuators, IEEE Control System Magazine, Volume 15 (1), pp. 40-48.
- [8.] Situm, Z. and Herceg, Z. (2008): Design and control of a manipulator arm driven by pneumatic muscle actuators, 16th Mediterranean Conference on Control and Automation, Ajaccio, France, 25-27 June, 2008, pp. 926-931.
- [9.] Sárosi J., Gyevikí J., Szabó G. and Szendrő P. (2010): Laboratory Investigations of Fluid Muscles, International Journal of Engineering, Annals of Faculty of Engineering Hunedoara, 2010, Volume 8 (1), pp. 137-142.
- [10.] Sárosi J., Gyevikí J., Véha A. and Toman P. (2009): Accurate Position Control of PAM Actuator in LabVIEW Environment IEEE, 7th International Symposium on Intelligent Systems and Informatics, Subotica, Serbia, 25-26 September, 2009, pp. 301-305.







¹: Ala'a M. DARWISH

STABILIZATION OF EMPTY UNDERGROUND CIRCULAR STORAGE TANKS AGAINST UPLIFTING UNDERGROUND WATER FORCES

¹DEPARTMENT OF BUILDING AND CONSTRUCTION ENGINEERING,
UNIVERSITY OF TECHNOLOGY, BAGHDAD, IRAQ

ABSTRACT:

Circular swimming pools or, in general, underground tanks can be mobilized due to two coincide factors: the first is when they are emptied for maintenance, while the second factor is when underground water level rises up to be close to the natural ground surface.

Under such circumstances an underground circular tank will be subjected to a buoyancy force equal to the weight of the displaced underground water minus the weight of the tank.

In this research eleven prototype models were tested to simulate the mentioned case. The base diameter of each model was different than the other, with an increment of 1cm each time. Water head required to float each model was recorded.

Test result shows that: Stabilizing of an empty underground circular tank can be reached by extending it's base diameter.

Finally, the equation of calculating the required base extension was derived.

KEYWORDS:

circular tank, swimming pool, underground tank, buoyancy, stabilization, state-of-the art design approach

1. INTRODUCTION

During a maintenance process for a circular reinforced concrete swimming pool, it was found that there were some visible cracks along its circumference. These cracks were situated exactly between the pool walls and its surrounding shoulders. Moreover, after excavating few holes in the burying soil around the pool in order to fix its piping system, it was noticed that there were some movements/ disorientations in the piping fittings which had made the maintenance process a bit more complicated.

After verifying the mentioned case a complete analysis was done to find the cause of these engineering defects. The analysis result indicated that the pool was suffering from a noticeable amount of uplifting buoyancy force due to the rising of the surrounding water table level.

Going through the literature of the subject, it was found that; no concern had been paid to fix a swimming pool against uplifting pressure. This might be due to their shallow depth, normally 2 to 4 meters, in addition to the rare condition of the augmentation of buoyancy forces.

Taking the general case of deeper buried circular tanks (actually cylindrical tanks), it was found that some tanks are based upon reinforced concrete piles which can resist the calculated uplifting forces (Westbrook 1984). But, "Piles penetrating into a stratum having a confined hydrostatic head will be subjected to uplift, possibly sufficient to raise them from their end bearing. Seepage around piles in un-watered excavation may reduce skin friction to less than the hydrostatic uplift", (Chellis 1992). While (Darwish 2008) had complained about using piled foundation for this

purpose arguing that “Even if the piles are not lifted up, they are still subjected to repetitive high tensile stresses. These tensile stresses may be greater than the pile’s concrete tensile strength and cracks near the pile heads can be expected. Crack formation across the entire cross section of a pile head will lead to an increasing tendency for corrosion of its reinforcing steel. Usually, sub-soil can support an underground tank without using any pile, because it is overburdened by the weight of the excavated soil which is normally greater than the weight of the filled tank. But if the tank becomes empty, during the rise of the underground water level, such soil even if it is hard as rocky soil can do little to resist tank floatation”.

(Darwish 2008) had also solved the problem of anchoring empty underground storage rectangular tanks against underground- water-induced floatation by using two parabolic profile cables passing through the long side walls of a tank and anchored to sub-grade soil at their ends. While this solution is appropriate for rectangular and square cross-section underground tanks, it is not so for underground cylindrical tanks.

To study the case of unstable pools and, in general, underground circular tanks, prototypes of a steel circular tank with variable base diameters were used to simulate the case and to find a reasonable solution. The solution was based upon finding a balancing weight which can counter the net uplifting buoyancy forces. By changing the diameter of the prototype tank base, it was found that: with each increment of base extension there was an increase of the water head required to float the tank. Contentment was reached that the weight of the surrounding soil situated directly, as a ring of soil, over the tank base extension can manage to counter the net buoyancy force tending to lift the buried tank.

In spite of the complication of each case due to the variable water head height, the shape of the slipping surface, friction between the tank walls and the surrounding submerged/non-submerged soil and the length of the base extension, an equation was derived to calculate the required length of the base extension which can stabilize any tank with an average safety factor of +17%.

2. EXPERIMENTAL WORK

2.1 Materials

2.1.1 Transparent square plastic container having the dimensions of 50cm×50cm and a depth of 20cm.

2.1.2 Clean sand with the following properties:

- Specific weight = 2.61
- Dry density = 1.8 gm/cm³
- Wet density = 1.42 gm/cm³
- Submerged density = 0.42 gm/cm³
- Angle of repose = 35°

2.1.3 Four water inlets to the container, one on each side, to discharge a controllable amount of water near the inner face of the container base, see Fig.1.

2.1.4 Four measuring stickers, one on each corner of the container.

2.1.5 A changeable base cylindrical steel pan having an outer diameter of 20cm, depth of 10cm, and a wall/ base thickness of 1mm. Its weight was 732gm.

2.1.6 Variable Steel bases, all with a thickness of 1mm, were used through the test. Their diameters start from 20cm to 30cm with an increment of 1cm. The first four columns of Table -1 show Notations, diameters and weights of the pan and its different bases.

2.1.7 Two dial gauges were attached to indicate any upward movement in the level of the buried pan.

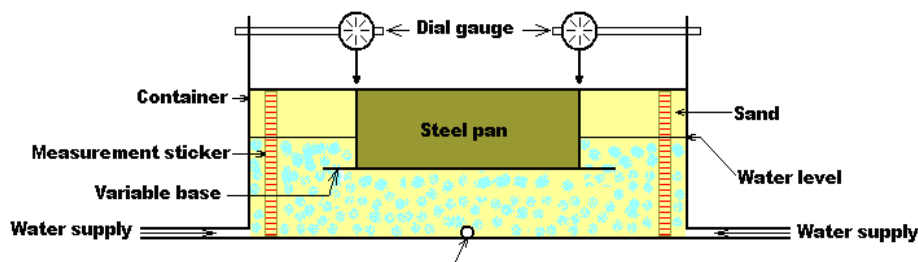


Fig.1 Testing device

2.2 Testing procedure

The container was filled with wet sand for half of its depth, the cylindrical steel pan #0 was placed on the sand and then the container was completely filled with wet sand. Water was allowed to seep slowly through the four inlets with a rising speed of 10cm/h. This rate was chosen to let the water surface to be at the same level all over the area of the container and to facilitate recording the rise of water by the four measuring stickers that were placed at the four inner sides of the container. Zero level was fixed at 10cm above the level of the inner face of the base. Mean value of water level was considered in the next calculations. Two dial gauges were attached to the container walls to measure any perpendicular movement might occur in the level of the steel pan.

The following observations were noted:

- ❖ The cylindrical pan was stable in its place until the height of water recorded 3.7cm. Suddenly, the pan was lifted and it continued to rise directly with the increase of water level.
- ❖ The same test was repeated using pan #1 which had a base extension of 1cm instead of pan #0 with no base extension to monitor the effect of increasing the diameter of the base of a buried tank on its stability against floating. After supplying the container with the same rate of water through the four water inlets, the steel pan remained stable until the level of water reached 4.3cm, then the pan started to rise and it continued to move upward directly with the rise of water level.
- ❖ The same procedure was repeated with pans #2, #3 and #10 on turn. The results are listed in table-1. It shows the theoretical water head required to lift the weight of each pan with respect to the actual recorded head of water.

Table -1 Theoretical and Actual head of water required to mobilize each pan

Notation	Base diameter (cm)	Weight (gm)	Theoretical head (cm)*	Actual head of water (cm)
Pan #0	20	732	2.33	3.7
#1	21	758	2.41	4.3
#2	22	784	2.50	5.3
#3	23	812	2.58	6.0
#4	24	841	2.68	6.8
#5	25	871	2.77	7.5
#6	26	902	2.87	8.1
#7	27	935	3.00	8.6
#8	28	968	3.10	9.1
#9	29	1003	3.20	9.6
#10	30	1040	3.30	10.0

* Only the weight of the pan was considered.

3. RESULTS & COMMENTS

One of the well known principles is that: the water floating force equals the weight of the displaced water by a submerged body. By applying this concept to pan #0, with no base extension, it indicates that a water level of 2.33cm is enough to push it up, but during the test the pan remained stable when water level reached this point. Pan #0 started to move up only when water level reached 3.7cm. The mentioned difference means that an extra force is required to lift the empty pan. The explanation is simply that the pan was not free to float and the extra force was required to overcome the friction between the outer surface of the pan's wall and the surrounding sand, see Fig.2-a.

Repeating the same testing procedure but with pan #10, with a base of 30cm diameter, the pan remained stable until the water level reached 10cm in depth. Taking into account that the displaced water was approximately the same for the two pans #0 and #10, in other word the required uplifting force should be very close, but test results showed that this is not true. The main difference between the two pans was the extended base of pan #10. This extension showed that it was active in stabilizing pan #10 against floating. It required $(10-3.7 = 6.3\text{cm})$ of an extra head of water to initialize its upward movement. While pan #0 required an extra force to overcome the friction between the outer surface of the pan's wall and the surrounding sand, pan #10 did not require such extra force because there was no direct slipping between the pan's wall and the surrounding sand. Actually, the base extension had shifted the slip surface away from the pan's wall, see Fig.2-b.

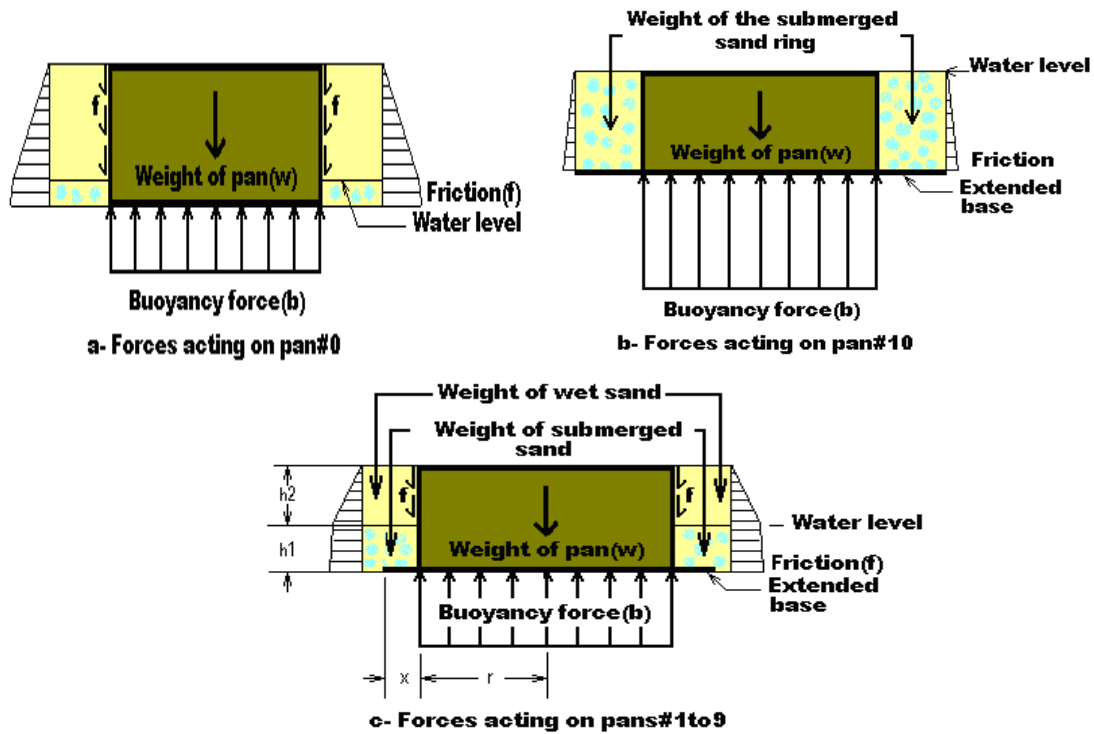


Fig.2 Forces distribution on testing pans

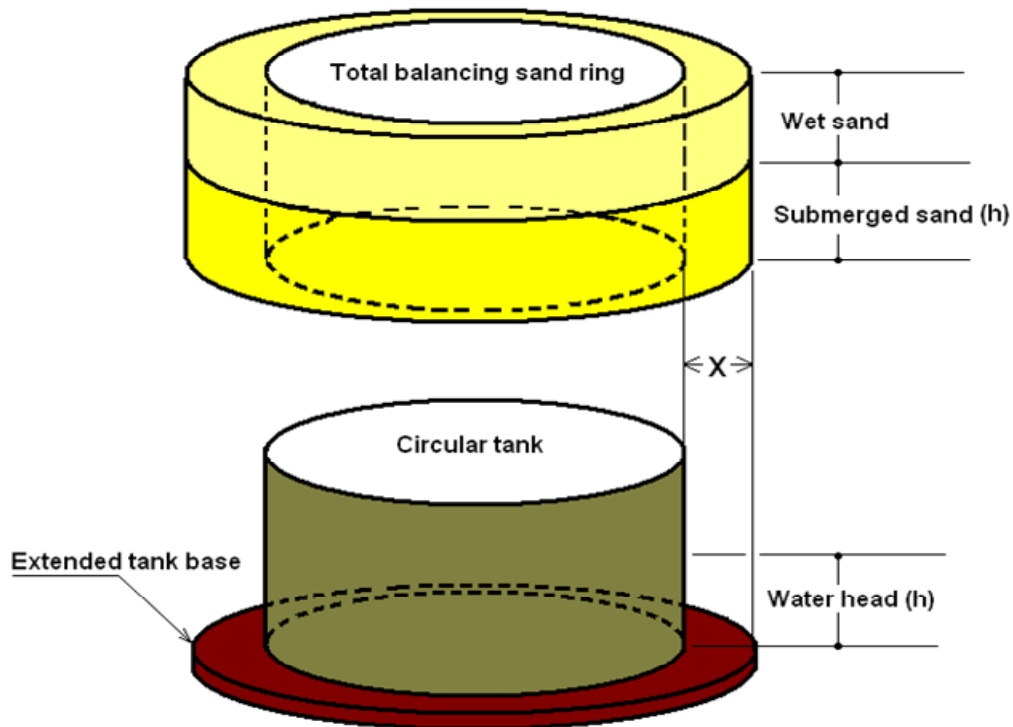


Fig.3 The balancing sand ring

By calculating the weight of the submerged ring of sand around the pan, see Fig.3, which was situated directly over the base extension, a hollow 10cm high cylinder with an interior diameter of 20cm and an exterior diameter of 30cm, it was found that it's weight equals:

$$(15^2 - 10^2) \times \pi \times 10 \times 0.42 = 1650 \text{ gm}$$

While the uplifting force of the extra head of water equals:

$$10^2 \times \pi \times 6.3 = 1980 \text{ gm}$$

By reducing the difference of weight between the two pans (1040-732= 308gm), the net extra uplifting force will be:

$$1980 - 308 = 1672\text{gm}$$

The difference between the weights of the surrounding submerged sand ring and the net uplifting force is equal to:

$$1672 - 1650 = 22\text{gm}$$

This force was required to overcome the friction between the submerged sand particles along the slip surface. It is worth to compare between that force and the force required to overcome the friction in the case of pan #0 which was equal to:

$$10^2 \times \pi \times (3.7 - 2.33) = 430\text{gm}$$

It is clear that, pan #0 required an extra uplifting force of 430gm to overcome friction compared to 22gm required by pan #10 for the same purpose, that is justified due to the decrease of friction coefficient by the effect of submerging.

During the test, the procedure was repeated using different pans with a base extension increment of 0.5cm each time as mentioned in table-1, pan#1 with a base extension of 0.5cm to pan#9 with a base extension of 4.5cm. The mean level of water head required to mobilize each pan was recorded and listed in table-1.

It should be noted that these nine pans were different in boundary conditions than pans#0
, while pan#0 was mobilized immediately after overcoming the soil friction with its walls and pan#10 was mobilized after it was surrounded completely by submerged sand, in the case of these nine pans, see Fig.-2-c, there were the following factors influencing their bouncy:

- ❖ Generation of a mechanical resistance for floating due to the base extension.
- ❖ The surrounding soil was partially submerged.
- ❖ The slip surfaces were started from the end of the base extension upwards.
- ❖ The slip surface was not identical around each pan; it came close to the upper part of the pan's wall from one side and shifted away from another side. In other word no specific slip surface angle could be defined.

A further calculation was done for each case based upon the bouncy force minus both of the weight of the pan and the weight of the composite, submerged& non-submerged, soil ring with a base equal to the extension of the base. Percentage of the actual extra water heads are shown in table-2.

Table-2 Percentage of the difference between actual/ theoretical floating water head

Notation	Weight of stabilizing soil ring (gm)	Equivalent head (cm)	Theoretical head (cm)	Total required head (cm)	Actual Water head (cm)	Head difference percentage %
Pan #0	0000	0.00	2.33	2.33	3.7	+58%
#1	0320	1.00	2.41	3.41	4.3	+26%
#2	0543	1.73	2.50	4.23	5.3	+25%
#3	0820	2.61	2.58	5.19	6.0	+16%
#4	1023	3.25	2.68	5.93	6.8	+15%
#5	1185	3.77	2.77	6.54	7.5	+15%
#6	1323	4.21	2.87	7.08	8.1	+14%
#7	1448	4.61	3.00	7.61	8.6	+13%
#8	1538	4.90	3.10	8.00	9.1	+14%
#9	1594	5.07	3.20	8.27	9.6	+16%
#10	1650	5.25	3.30	8.55	10.0	+17%
						Σ = +17%*

*Pan #0 was not included.

Excluding pan#0 with no base extension, the average actual water head required to mobilize the rest of pans having different base extensions is +17% greater than the theoretical required head, with a minimum of +13% for pan#7. As mentioned earlier, this increment is required to overcome friction forces which have different surface modes. Due to the accuracy in calculating buoyancy forces and all the weights of the pans and the surrounding soil rings, it could be concluded that protecting an underground circular tank against flotation can be done by adapting a weight of submerged/ non-submerged soil ring equal to the buoyancy force minus the weight of the pan/ tank. According to the required weight of the soil ring the length of the extension(x), see Fig.2-c, in any underground tank base can be determined by the following equation. This solution can guarantee an average safety factor of +17%:

$$V\gamma_w - w = \{(r + x)^2\pi - r^2\pi\}h_1\gamma_{sub} + \{(r + x)^2\pi - r^2\pi\}h_2\gamma_s$$

where: V = Volume of tank

γ_w = Density of water

w = Weight of tank

r = Outside diameter of the tank

x = Length of the tank's base extension

h_1 = Underground water head measured from tank base level

γ_{sub} = Submerged soil density

h_2 = Height between soil top surface and underground water level

γ_s = Density of soil

The simplified form of the above equation can be written as follows:

$$2rx + x^2 = \frac{V\gamma_w - w}{\pi(h_1\gamma_{sub} + h_2\gamma_s)}$$

4. CONCLUSIONS

The following points can be concluded:

- ❖ Circular underground tanks are subjected to floating due to buoyancy forces created by the rise of water table level.
- ❖ Circular underground tanks constructed in soils having high water table levels should be stabilized against uplifting.
- ❖ Increasing the diameter of the base of an underground tank can increase its stability against floating.
- ❖ The required increment in the radius of the base of an underground circular tank can be safely taken equal to the thickness of a surrounding soil ring having a submerged/ non submerged weight, according to the highest expected underground water level, equal to the buoyancy force minus the weight of the tank.
- ❖ The mathematical derived equation for calculating the required base extension x is given as follows:

$$2rx + x^2 = \frac{V\gamma_w - w}{\pi(h_1\gamma_{sub} + h_2\gamma_s)}$$

REFERENCES

- [1.] Chellis, R.D. (1992). Foundation Engineering, Chapter 7, McGraw-HILL Book Company, USA.
- [2.] Darwish, A.M. "Anchoring of empty underground tanks against underground-water-induced floatation by using arched cable system", The IES Journal Part A: Civil & Structural Engineering, Vol. 1, No. 3, The Institution of Engineers, Singapore, August 2008.
- [3.] Westbrook, R. (1984). Structural Engineering Design in Practice, 1st ed, Longman Inc., New York, USA.





¹Gergely DEZSŐ, ²Gyula VARGA, ¹Ferenc SZIGETI

INVESTIGATION THE CORRELATION BETWEEN TECHNOLOGICAL PARAMETERS AND THE WEAR IN CASE OF DRILLING WITH MINIMAL LUBRICATION

¹COLLEGE OF NYÍREGYHÁZA, 4400, NYÍREGYHÁZA, HUNGARY

²UNIVERSITY OF MISKOLC, 3515, MISKOLC, HUNGARY

ABSTRACT:

College of Nyíregyháza and University of Miskolc has a common research project on environmentally conscious technologies. In the work published in this paper our purpose was to investigate the effects of technological parameters on the process of drilling and tool wear under outer minimal lubrication conditions.

Method of factorial experiment planning was applied for evaluation of experimental results. Relationships were determined between technological parameters and measured tool wears.

Physical model of twist drill was developed for calculating stress state and compare results with experimental wear measurements. This model shows good agreement with experiments and gives account of places of highest strain.

In this paper we demonstrate a formula describing the corner wear ($V_{B_{\text{corner}}}$) and flank wear ($V_{B_{\text{flank}}}$) as function of three quantity: feed (f), length of drilling (L_0) and volume of the lubricant (V_{oil}).

KEYWORDS:

environmentally technologies, parameters, drilling, tool wear, minimal lubrication conditions

1. INTRODUCTION

The stress and temperature distribution in the tool during the drilling process basically influences the lifetime of the drill and the rentability of machining by its effect to wear and vibrational state. That's why complex investigation of drill by experimental way and modelling is reasonable for it allows of determining relationship between tool wear, thermal state and stress state.

Finite element modelling of the twist drill was performed assuming minimal volume lubrication circumstances. We took into account that practical realization the principle of minimizing the environmental pollution in the European Union gradually got into the foreground even in production engineering [1, 2, 3, 9].

2. AIM OF EXPERIMENTS

Aim of our investigations was to develop a model for relationship between the wear and stress state of the twist drill, being suited for determining most loaded areas during the drillin process.

We used factorial experiment design for evaluating our experimental results on minimal lubrication drilling, so that we determine relationship between technological parameters of drilling and wear values.

In the modelling experimental data were used as input parameters.

We applied experiences of Department of Production Engineering at University of Miskolc when designing our experiments [4].

3. CIRCUMSTANCES OF EXPERIMENTS

At our experiments we used the following circumstances:

Machine tool: Universal milling machine, type: MU-250

Adjusted parameters:

Revolution number of main spindle: $n = 2250 \text{ rev/min}$,

Feeds: $f = 0,18 \text{ mm/rev}$ and $f = 0,35 \text{ mm/rev}$

Cutting speed: $v_c = 72,06 \text{ m/min}$

Cutting tool: twist drill (with right hand side flute) having inner cooling channels ($\varnothing 10,2$ K20 Gühring WRDG DIN 6537)

diameter: $\varnothing 10,2 \text{ mm}$,

material and coating: K20 carbide (monolith) twist drill with TiAlN coating.

Specimen material: cast iron, (EN-GJL-200 (MSZ EN 1561))

length of the holes: 30 mm,

Lubrication equipment: „NOGA MINI COOL”

Adjusted volumes: $\dot{V}_{oil} = 0 \text{ cm}^3/h$, $\dot{V}_{oil} = 10 \text{ cm}^3/h$, and $\dot{V}_{oil} = 28 \text{ cm}^3/h$.

Oil: OMV cut XU (without chlorine).

Realization of minimum volume of lubrication was done by outer admission of the lubricants to the superficies of the twist drill by vaporizer type „NOGA MINI COOL” (we controlled two different volume per hour values: $\dot{V}_{oil} = 10 \text{ cm}^3/h$ and $\dot{V}_{oil} = 28 \text{ cm}^3/h$). Furthermore we have elaborated our experiments without using any coolants or lubricants. This was the dry machining, that is the dry drilling.

4. EVALUATION OF MEASURED WEAR RESULTS

Each measurement was repeated at least three times when the same parameter setup during executing our experiments. The evaluation was done by using mathematic statistics.

For characterisation of wear of the twist drill we have chosen the corner wear (VB_{Corner}) and flank wear (VB_{Flank}) [5, 6, 7]. The flank wear was measured on the direction radius at 3,5 mm from centre line on the main cutting edge, wear width into the direction of flank. By using of Factorial Experiment Design 12 experiments were elaborated (Table 1.).

The result of the experiments can be seen on Figure 1 and 2 for the values of corner and flank wear when the volume of coolants and lubricants were $\dot{V}_{oil} = 10 \text{ cm}^3/h$, $\dot{V}_{oil} = 28 \text{ cm}^3/h$, and for dry drilling.

On the figures can be seen that the wear of the twist drill was smaller at the case of higher value of coolants and lubricants ($\dot{V}_{oil} = 28 \text{ cm}^3/h$).

Table 1. Codes of specimen and technological and experimental data applied

Number	Feed, f , mm/ford	Length of drilling, L_0 , m	Oil volume, \dot{V}_{oil} , cm^3/h
1	0,18	0,03	0,0
2	0,35	0,03	0,0
3	0,18	30,0	0,0
4	0,35	30,0	0,0
5	0,18	0,03	10,0
6	0,35	0,03	10,0
7	0,18	30,0	10,0
8	0,35	30,0	10,0
9	0,18	0,03	28,0
10	0,35	0,03	28,0
11	0,18	30,0	28,0
12	0,35	30,0	28,0

The evaluations of the experiments were done by the full Factorial Experiment Design. Equations (2) and (3) valid when the drilling length varies in between $L_0 = 5 \text{ m}$ and $L_0 = 30 \text{ m}$, the volume of coolants and lubricants from $\dot{V}_{oil} = 10 \text{ cm}^3/h$ till $\dot{V}_{oil} = 28 \text{ cm}^3/h$, and the feed from $f = 0,18 \text{ mm/rev}$ till $f = 0,35 \text{ mm/rev}$.

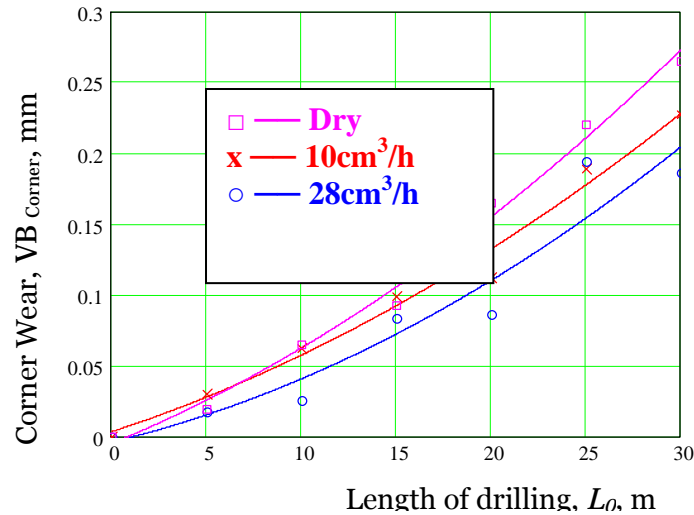


Figure 1. VB_{Corner} - Measured values of corner wear,

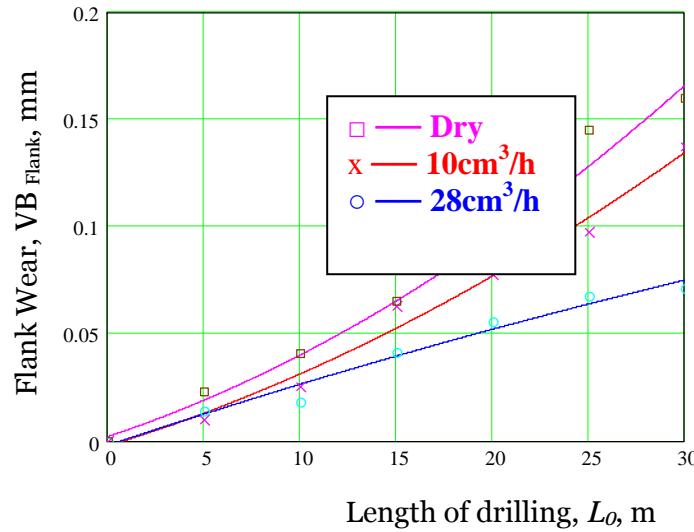


Figure 2. VB_{Flank} - Measured values of corner wear,

$$VB_{Corner} = k_0^{Corner} + k_1^{Corner} f + k_2^{Corner} L_0 + k_3^{Corner} \dot{V}_{oil} + k_{12}^{Corner} f \cdot L_0 + k_{13}^{Corner} f \cdot \dot{V}_{oil} + k_{23}^{Corner} L_0 \cdot \dot{V}_{oil} + k_{123}^{Corner} f \cdot L_0 \cdot \dot{V}_{oil} \quad (2)$$

$$\begin{aligned} k_0^{Corner} &= -0.0146 & k_1^{Corner} &= 0.031 \\ k_2^{Corner} &= 5.789 \cdot 10^{-3} & k_3^{Corner} &= 2.118 \cdot 10^{-4} \\ k_{12}^{Corner} &= 6.85 \cdot 10^{-3} & k_{13}^{Corner} &= -2.288 \cdot 10^{-3} \\ k_{23}^{Corner} &= -1.41 \cdot 10^{-4} & k_{123}^{Corner} &= 3.268 \cdot 10^{-4} \end{aligned}$$

$$VB_{Flank} = k_0^{Flank} + k_1^{Flank} f + k_2^{Flank} L_0 + k_3^{Flank} \dot{V}_{oil} + k_{12}^{Flank} f \cdot L_0 + k_{13}^{Flank} f \cdot \dot{V}_{oil} + k_{23}^{Flank} L_0 \cdot \dot{V}_{oil} + k_{123}^{Flank} f \cdot L_0 \cdot \dot{V}_{oil} \quad (3)$$

$$\begin{aligned} k_0^{Flank} &= -2.686 \cdot 10^{-3} & k_1^{Flank} &= -0.04 \\ k_2^{Flank} &= 3.065 \cdot 10^{-3} & k_3^{Flank} &= 2.804 \cdot 10^{-4} \\ k_{12}^{Flank} &= 8.575 \cdot 10^{-3} & k_{13}^{Flank} &= 8.497 \cdot 10^{-4} \\ k_{23}^{Flank} &= -9.007 \cdot 10^{-5} & k_{123}^{Flank} &= -1.046 \cdot 10^{-4} \end{aligned}$$

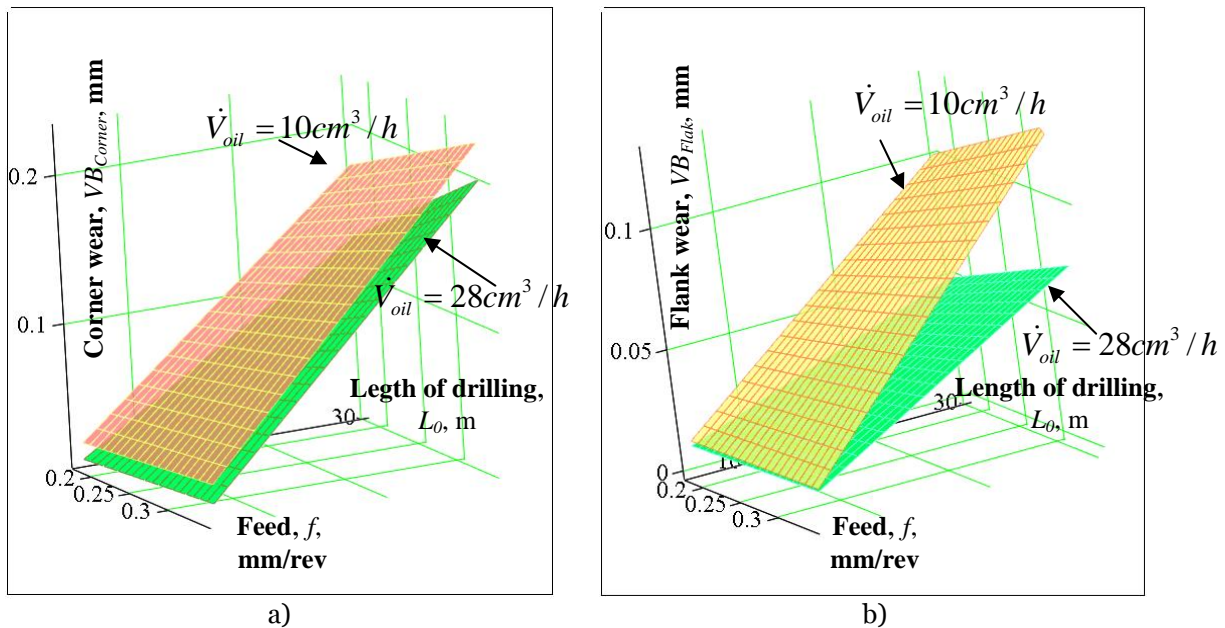


Figure 3. Measured wear values of twist drill, a) corner wear, b) flank wear

5. MODELING

The thermal- and stress state of the drill was investigated by physical modelling. Our goal was to describe a model, which is simple as much as possible and stands in good accordance with observed wear picture.

The cutting force acting on edges was set as equal to the feed force per edge [8]. Material properties were of the K20 hard metal data.

We performed calculation for the sharp and the partly worn state of the tool. The worn state was modelled by rounding of the edges with 0,1mm and 0,2mm radii. The gradient of the stress far from the top in the drill was negligible, that's why we studied only 20mm long working part of the drill. So we avoided the superfluously large number of finite elements, and we managed to refine the mesh where it was necessary, i.e. where the gradient of physical quantities was large.

In our calculations both known mesh refinement methods were applied. The adaptive h refinement made the mesh denser where the target function changed rapidly, this decreasing the error of the finite element approximation. In our case, this resulted in refinement around edges and corners. The other method for improving the finite element mesh was the p-refinement, which increased the range of polynomial basis functions without changing of the original mesh, so making the approximating function much more flexible where the gradient of the target function was large. The software used realized these two types of refinement in two separate steps. Mechanical stress was used as target function for mesh refinement.

Finite element meshes of sharp and two worn drills are shown in Figures 4 and 5. Figure 4 demonstrates the finite element mesh and stress results for the sharp twist drill, Figure 5 shows the shape of a worn twist drill when the effect of the wear is represented by radius 0,1mm.

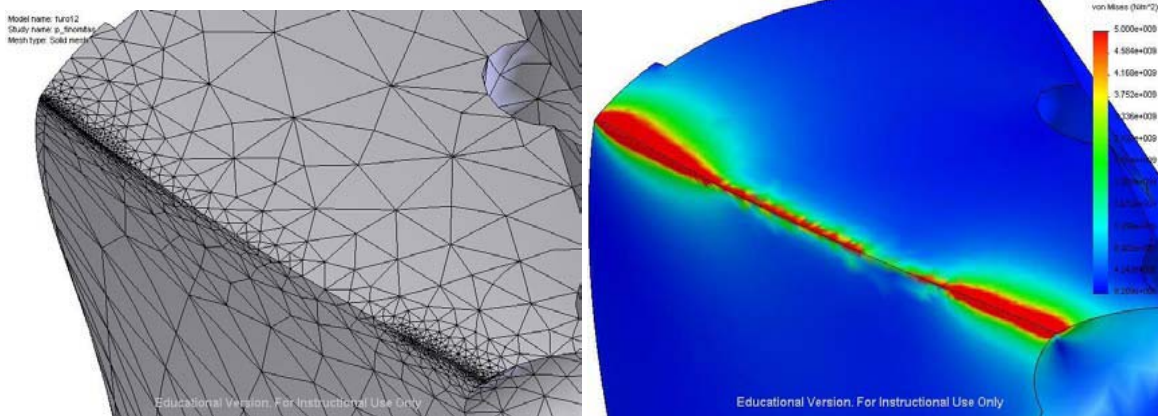


Figure 4. Mesh and stress state of sharp twist drill

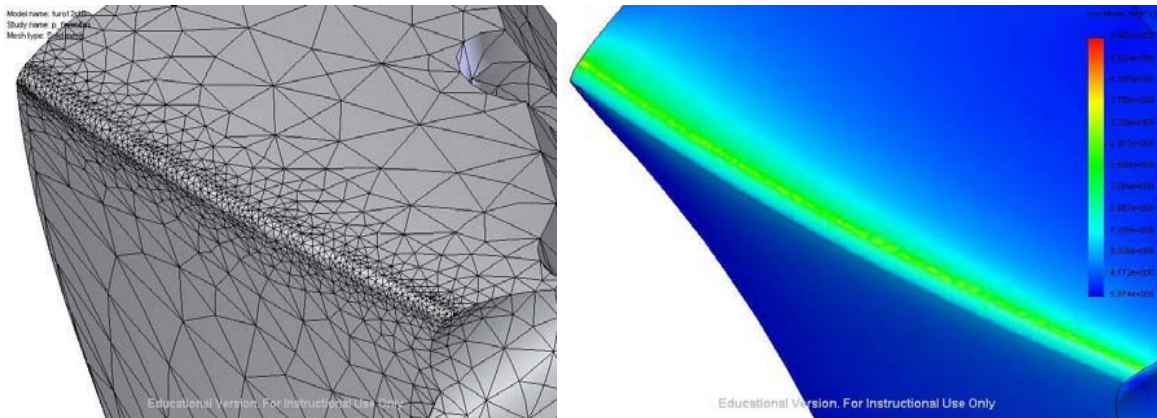


Figure 5. Mesh and stress state of the worn twist drill

6. CONCLUSIONS

This paper gave some remarks of successful implementation of dry and different near dry machining and for different experimental parameters.

- ❖ Formulas are derived by means of factorial experiment design describing the corner wear (VB_{Corner}) and the flank wear (VB_{Flank}) as function of three quantities: feed (f), length of drilling (L_o) and volume of the lubricant (V_{oil}).
- ❖ The feed of the twist drill and the applied volume of coolants and lubricants have significant effects to the wear of the twist drill.
- ❖ At the case of using similar volumes of coolants and lubricants, the measured values of flank wears (VB_{Flank}) were always smaller than the values of corner wears (VB_{Corner}).
- ❖ Modelling showed that wear changes significantly the stress state.
- ❖ In the first short period of drilling the maximum of the stress is at the chisel edge.
- ❖ Then as the wear increases, the stress distribution has been significantly changed spreading along the edge.

ACKNOWLEDGEMENTS

This work was supported as preferred research in 2010 by Scientific Committee of College of Nyíregyháza.

REFERENCES

- [1.] WEINERT, K.: Trockenbearbeitung und Minimalschmierung. Springer Verlag Berlin 2000.
- [2.] IGAZ, J., PINTÉR J., KODÁCSY J.: Minimálkenés. Gépgyártás XLVII. évf. 2007. 4.sz pp.: 22-31
- [3.] KODÁCSY J., - NYÍRI J.: A fúrési folyamat összehasonlító vizsgálata különböző hűtés- kenési eljárásokkal. Gépgyártás XLVII. évf. 2007. 2-3.sz pp.: 27-29
- [4.] DUDÁS, I., VARGA GY., CSERMELY, T., TOLVAJ, I. Umweltgerechte Zerspanungstechnik - Reduzierung und Ersatz von Fertigungshilfsstoffen beim Bohren (STD - 2EC jelű, ERB CIPACT 930167 témaszámú), Európai Közösség által finanszírozott kutatási projekt, Miskolci Egyetem, Gépgyártástechnológiai Tanszék, 4. Jelentés, 1995, pp.: 27.
- [5.] VARGA, GY., DUDAS, I.: Modelling and Examinations of Environmentally Friendly Machining Processes, Proceedings of the 9th International Research/Expert Conference on Trends in the Development of Machinery and Associated Technology, TMT 2005, Antalya, Turkey, 26-30 September, 2005. pp.: 121-124. ISBN: 9958-617-28-5.
- [6.] KANAI, M., KANDA, Y: Statistical Characteristics of Drill Wear, and Drill Life for the Standardized Performance Tests, Annals of the CIRP, 1978, Vol. 27, No. 1, pp.: 61-66
- [7.] SZIGETI, F., VARGA, GY., PÉTER, L., SZÁZVAI, A.: Examination of outer and inner lubrication with minimum volume of lubricants when drilling of grey cast iron, Proceedings of the 7th International Multidisciplinary Conference, Baia Mare, Romania, 2007. p. 687-93,
- [8.] DUDÁS I.: Gépgyártástechnológia I., A gépgyártástechnológia alapjai, Műszaki Kiadó, 2004, pp.583. ISBN 963 16 4030 2
- [9.] DUDÁS, I.: Gépgyártástechnológia III. Miskolci Egyetemi Kiadó, Miskolc, 2003. p. 539.





¹: Jarmila ORAVCOVÁ, ²: František LACKO, ³: Peter KOŠTÁL

DEVIATIONS OF WORKPIECE CLAMPING AS FACTOR HAVING INFLUENCE ON ACCURACY OF A SURFACE MACHINED

¹⁻³: SLOVAK UNIVERSITY OF TECHNOLOGY, FACULTY OF MATERIALS SCIENCE AND TECHNOLOGY,
INSTITUTE OF PRODUCTION SYSTEMS AND APPLIED MECHANICS, TRNAVA, SLOVAKIA

ABSTRACT:

The paper deals with some questions regarding workpiece clamping in fixtures from the point of view of production inaccuracies. These inaccuracies consist of deviation of medium economical accuracy, deviation of seating and deviation of the fixture. The final achievable workpiece accuracy depends on the components of the mentioned deviations. The paper describes influence of the support point choice on deviation extend of the surface machined. Way for workpiece seating deviation calculation is given in the paper when the workpiece seats on various supporting points.

KEYWORDS:

seating deviation, non-identity deviation, clamping deviation, basic positioning surface, basic dimensional surface, supporting element

1. INTRODUCTION

We usually meet great amount of products different in shape and in their dimensions within engineering production praxis. The requirements on workpiece accuracy, and such way also on workpiece seating are permanently higher. For that reason it is important to appreciate suitability of the clamping equipment design for each actual case. Among various factors influencing the final achievable accuracy of the surface machined belong primary inaccuracies brought into production process.

2. DEVIATIONS INFLUENCE ON DIMENSIONAL ACCURACY OF THE SURFACE MACHINED

Various requirements concerning accuracy of the individual surfaces machined are set by designer for components production. Possibility to achieve the required dimensional accuracy for the concrete component depends on more factors. The important factor having influence on accuracy of the surface machined is way of workpiece positioning and its clamping in fixture. Another factor is the accuracy of fixture positioning within machine tool. The accuracy of the final dimension also depends on values of cutting parameters chosen for machining, on stiffness of the entire system and on accuracy of mutual position between tool and workpiece. The said factors generate great amount of deviations, which can be divided into following three deviation groups:

- ❖ deviation of medium economical accuracy \mathbf{s} ,
- ❖ seating deviation $\boldsymbol{\varepsilon}$,
- ❖ fixture device deviation $\boldsymbol{\varepsilon}_p$

The required dimension accuracy \mathbf{v} given by dimension tolerance \mathbf{T}_v prescribed in drawing is stipulated by the formula:

$$T_v \geq \sqrt{\boldsymbol{\varepsilon}^2 + \mathbf{s}^2} + \boldsymbol{\varepsilon}_p \quad (1)$$

Value of the deviation of medium economical accuracy \mathbf{s} is usually obtained by practical experiences and is elaborated for individual technological machining techniques of various

surfaces. Requirement for economical production is considered within this deviation, because to close tolerances can cause inadequately high production costs connected with surface machined and to cause increase of the final product price.

So as to find out the deviation of the fixture device ε_p for the concrete workpiece it is to find out the individual components which are part of the total deviation. The deviation of the fixture device consists of sum of the clamping deviation ε_{py} , the deviation of fixture positioning within machine tool ε_{po} , the deviation of tool adjustment ε_{pn} and of the dividing device deviation ε_{pd} . So value of the fixture device deviation can be calculated as:

$$\varepsilon_p = \varepsilon_{py} + \varepsilon_{po} + \varepsilon_{pn} + \varepsilon_{pd} \quad (2)$$

The seating deviation is to be taken as:

$$\varepsilon = \varepsilon_n + \varepsilon_s \quad (3)$$

where

ε_s - means the deviation (value) by which the produced dimension is modified as influence of workpiece seating through support surface,

ε_n - means the non-identity deviation of the basic positioning surface against basic dimensional surface, when it is to be taken as:

$$\varepsilon_n = \sum_{i=1}^n T_{zi} \cos \beta_i \quad (4)$$

where

T_{zi} - means tolerance of the distance between positioning and basic dimensional surface

$\cos \beta_i$ - means angle between perpendicular line of the positioning surface and perpendicular line of the surface machined.

3. SUPPORTING ELEMENT INFLUENCE ON DEVIATION OF THE DIMENSION PRODUCED

An important decision step is choice of the clamping and positioning surfaces of the workpiece. In the end, this step influences achievement of the required dimensional accuracy of the surface machined. It is to take into consideration the basic dimensional surface, i.e. the surface from which the distance required machined surface is given on the drawing, when making decision, which surface should be taken as positioning surface.

The most common cases of workpiece seating in the fixture are when the positioning workpiece surface is:

- ❖ plane,
- ❖ external cylindrical surface,
- ❖ cylindrical opening.

When a prismatic component is positioned on two parallel stepped planes (Fig. 1), the deviation of supporting elements ε_e occurs because of allowed workpiece inaccuracies and because of shape of fixture supporting elements. The component of the deviation ε_e into direction of the dimension produced is ε_s . In this case means:

$$\varepsilon_s = L_1 \tan \varepsilon_e \quad (5)$$

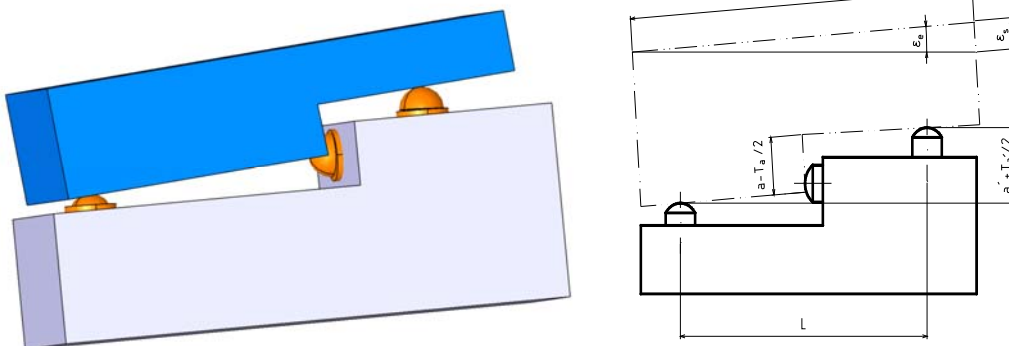


Fig. 1 Prismatic component on two parallel stepped planes

When positioning is made through cylindrical opening, the line contact between supporting elements and workpiece comes into existence. Value of the deviation ε_s is given as:

$$\varepsilon_s = \varepsilon_e = \Delta + T_d + T_d' \quad (6)$$

When a cylindrical surface is positioned in a prismatic support, the supporting contact is made through two straight lines. The value of the deviation ε_s depends on the dimensional basis. The said basis can be axis of the positioning surface or creating line of the rotary profile (Fig.2). For the first mentioned case means:

$$\varepsilon_s = \frac{T_d \cos \gamma}{2 \sin \frac{\alpha}{2}} \quad (7)$$

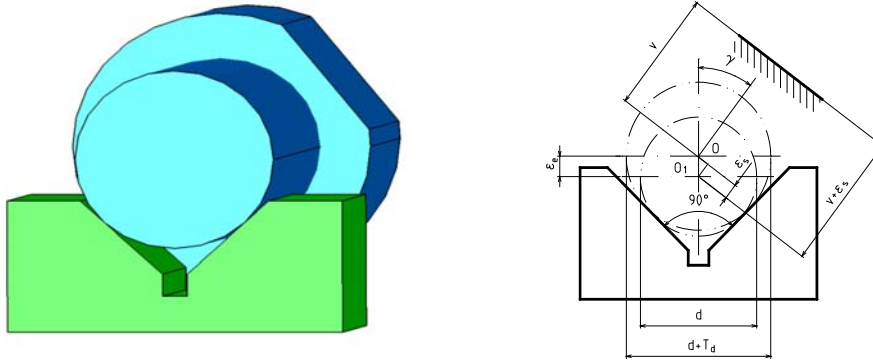


Fig. 2 Cylindrical surface in a prismatic support, when basis the axis is

The influence of the maximal deviation of machined surface distance on the surface angle of inclination and on choice of the basic dimensional surface is shown on workpiece positioned in prism. The results are summarised in the table 1.

Table 1

Positioning deviation ε_{\max} for $\phi 40h8$ and prism angel $\alpha=90^\circ$ [mm]			
Inclination angle of the surface machined γ	Basic dimensional surface		
	More distanced creating line of the positioning surface	Axis of the positioning surface	Les distanced creating line of the positioning surface
0°	0,008077	0,027577	0,047077
15°	0,007137	0,026637	0,046137
30°	0,004382	0,023882	0,043382
45°	0,000000	0,019500	0,039000
60°	0,005711	0,013788	0,033288

4. CONCLUSION

The proper design and construction of some clamping or fixing devices is not so simple task. Such equipment should meet many various requirements, which can influence its proper function an utilization. That is why it is to take into consideration and to analyze which requirements are the most important ones and in this connection decide which deviations should be minimalised primary.

Acknowledges

OPVaV-2008/2.2/01-SORO – 26220220055 – Laboratory of flexible manufacturing systems with robotized manipulation supported by no drawing production

This article was created with the support of the
 OP Research and development for the project
**Laboratory of flexible manufacturing systems with robotized
 manipulation supported by no drawing production**
 ITMS 26220220055,
 co-financing from the resources of European Regional Development
 Fund.



Support research activities
 in Slovakia/
 Project is co-financing
 from resources EU



REFERENCES

- [1.] Charbulová, Marcela - Mudriková, Andrea - Danišová, Nina: Fixture devices for production systems. - Vega č. 1/0163/10. In: AMO Conference. - ISSN 1313-4264. - 10. International conference, 27 - 29 June 2010 AMO 10, 27 June - 01 July 2010 CEEPUS (2010), s. 1-6
- [2.] Charbulová, Marcela - Mudriková, Andrea: Clamping Devices for Intelligent Production Systems. In: AMO Conference. - ISSN 1313-4264. - Vol. 3. 9. International Conference Advanced Materials and Operations : Scientific Reports. Project CII-BG-0203-02-0809 CEEPES. Bulgaria, Kranevo 24-28 June 2009. - Sofia : Technical University of Sofia, 2009, s. 597-601
- [3.] Charbulová, Marcela: Modular clamping systems. In: Annals of Faculty of Engineering Hunedoara - Journal of Engineering. - ISSN 1584-2673. - Tom V, Fasc 3 (2007), s. 49-54
- [4.] Košťál, Peter - Velíšek, Karol - Zvolenský, Radovan: Intelligent Clamping Fixture in General. In: Lecture Notes in Computer Science. - ISSN 0302-9743. - Vol. 5315 : Intelligent Robotics and Applications. First International Conference, ICIRA 2008, Wuhan, China, October 15-17, 2008. Part II (2008). - ISBN 978-3-540-88516-0, s. 459-465
- [5.] Košťál, Peter - Velíšek, Karol: Flexible manufacturing cell 's clamping fixture. In: Proceedings of the 9th Biennial ASME Conference on Engineering Systems Design and Analysis (ESDA2008) : Haifa, Israel, 7.-9.7.2008. - : ASME, 2008. - ISBN 0-7918-3827-7. - CD Rom
- [6.] Matúšová, Miriam - Hrušková, Erika: Element selection algorithm of modular fixture system. In: Annals of Faculty of Engineering Hunedoara - Journal of Engineering. - ISSN 1584-2673. - Tom V, Fasc 3 (2007), s. 36-40
- [7.] Matúšová, Miriam - Javorová, Angela: Modular clamping fixtures design for unrotary workpieces. In: Annals of Faculty of Engineering Hunedoara - Journal of Engineering. - ISSN 1584-2673. - Tom VI, Fasc 3 (2008), s. 128-130
- [8.] Mudriková, Andrea - Hrušková, Erika - Horváth, Štefan: Areas in flexible manufacturing-assembly cell. - článok vyšiel v časopise: Annals of Faculty of Engineering Hunedoara - Journal of Engineering, ISSN 1584-2673, Tome VI, Fascicule 3, 2008, str. 123-127. In: Scientific Bulletin. - ISSN 1224-3264. - Vol. XXII (2008), s. 293-298
- [9.] Mudriková, Andrea - Velíšek, Karol - Košťál, Peter: Clamping fixtures used for intelligent assembly systems. In: ISCCC 2009 : Proceedings of the 2009 International Symposium on Computing, Communication and Control, October 9-11, 2009, Singapore. - Singapore : International Association of Computer Science and Information Technology Press, 2009. - ISBN 978-9-8108-3815-7. - S. 9-15
- [10.] Oravcová, Jarmila - Košťál, Peter - Riečičiarová, Eva: Active parts of clamping devices. In: Annals of The Faculty of Engineering Hunedoara. - ISSN 1584-2665. - Tom VIII, Fas. 1 (2010), s. 235-236
- [11.] Velíšek, Karol - Košťál, Peter - Zvolenský, Radovan: Clamping Fixtures for Intelligent Cell Manufacturing. In: Lecture Notes in Computer Science. - ISSN 0302-9743. - Vol. 5315 : Intelligent Robotics and Applications. First International Conference, ICIRA 2008, Wuhan, China, October 15-17, 2008. Part II (2008). - ISBN 978-3-540-88516-0, s. 966-972





¹Tamás ENDRŐDY, ²Adrián SZŐNYI

ANALYSING THE 2-7 DOF HUMANOID ROBOT ARM CONSTRUCTIONS AND THE POSSIBILITIES OF CONTROLLING/LEARNING THEIR MOVEMENTS

¹ UNIVERSITY SZENT ISTVÁN & UNIVERSITY OF SZEGED, HUNGARY

² FACULTY OF MECHANICAL ENGINEERING OF TECHNICAL AND ECONOMICAL UNIVERSITY OF BUDAPEST, HUNGARY

ABSTRACT:

Previously the authors mainly dealt with the construction and modelling of **2 DOF** (Degree of Freedom) and 2 links Humanoid robot arms which were operated in agonist-antagonist mode by 2 pairs of **PAM** (Pneumatic Artificial Muscle) elements to a target point in plane. The presented constructions were modelled and controlled by modifying the angles between shoulder-upper arm (α_{uo}) at the shoulder and between the upper arm-forearm (β_{fo}) at elbow artificial articulations. The kinematic systems fairly determine the trajectories of their structure joints, thus if the trajectory and derivatives are given - generally an inverse dynamic task has to be solved.

This lecture deals with the construction of **2-7 DOF** and **3-4 links** robot arms modelling and comparing to each other their advantages-disadvantages. The authors operate the links of the robot arm with the flexor-extensor agonistic-antagonistic pairs of **PAM** elements, also developed and analysed adaptive/learning algorithms for them.

By developing the humanoid robot arm constructions – modelling and mimicking the very complex structured and controlled human arm one can be successful only by significantly simplifying the structures of the human muscles, tendons, articulations and bones. Similarly one can be successful in guiding and learning the limbs' movements if we make simplifications in modelling the functionalities of the human brain.

KEYWORDS:

Humanoid robot arm, kinematic constructions, **PAM**, controlling movements, Folium model, tripod

1. INTRODUCTION

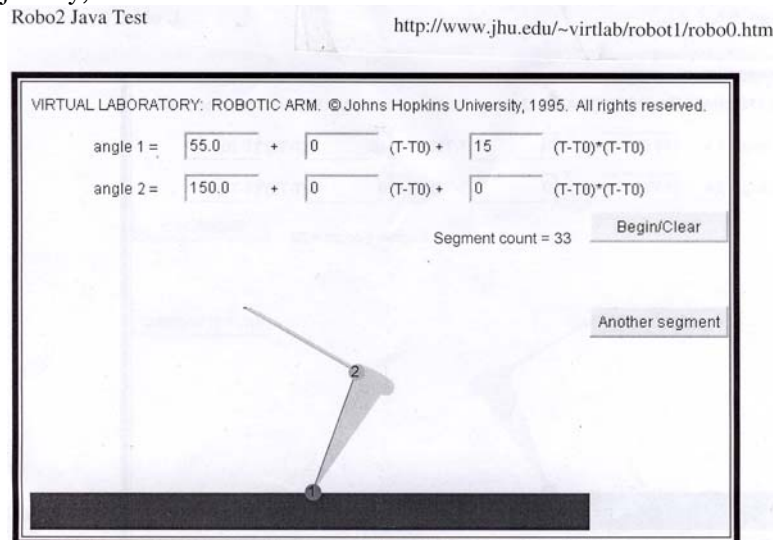
After some experiences having the manageable working points for any agonist-antagonistic pair of **PAM** (Pneumatic Artificial Muscle) elements, automatic/crude and adaptive/heuristic models have been made for driving the artificial wrist articulation of the robot arm through efficient series of points (line/arc segments) to the target point by harmonically controlling the flexor and extensor pneumatic muscles of the upper- and forearm [1.], [3.], [4.].

The punctiform considered elbow articulation can move on a circle with radius $R=I_{\text{upper arm}}$ and centre S_o (shoulder) of a **2 DOF** humanoid robot arm; while the wrist point is guiding from a starting point to the plane target point by modifying the angles between shoulder-upper arm (α_{uo}) at the shoulder and between the upper arm-forearm (β_{fo}) at elbow artificial articulations. The punctiform wrist can move on any given trajectory inside a semicircle with radius $R=I_{\text{upper arm}} + I_{\text{upper arm}}$ and S_o centre by series of generated short lines/circle arcs up to the target point. Thus the wrist can go round arbitrary obstacles in plane.

Instead of the more expensive stepping-motor and servo-motor actuators the angle-measuring sensors, mass flow rate valve and on-off proportional pressure valves were used which were programmable by the height or number of electronic pulses. The electronic pulses-pressure steps controlling mode was chosen by agonist-antagonist operated **PAM** elements. Thus the human brain controlled flexor-extensor muscles were mimicked in the **pulses-steps** operating mode. A complex controlling equipment and its virtual models were developed with crude and

adaptive/heuristic learning algorithms for controlling the movement trajectories of the wrist of the robot arm [3.].

There are many publications with agonist-antagonist pairs of **PAM** elements controlled by stepping-motors and servo-motor actuators e.g. at the Robot-laboratory of the Johns Hopkins University [5.], where they can also solve the guiding process from a starting wrist-point to the target-point in a plane, modifying the **angle1** and **angle2** by **a**, **b** and **c** parametres defining the position, velocity and acceleration by given functions. This example can also show the difficulties in controlling the punctiform wrist articulation via a given trajectory and its derivatives (**Picture 1**). This example gave a test and learning task possibilities following a given trajectory and its derivatives in the case of using stepping-motors. One can give 3 parametres for the position, velocity and acceleration -using the $(T-T_0)$ time slice every time- to go to the target point by changing the angles at the “shoulder” and the “elbow”. The task is more difficult if one would like to follow a trajectory, etc.



Picture 1. A test example: one can practice and learn how he can follow a given trajectory with its derivatives by giving 3 parametres and using the $(T-T_0)$ time slice every time

The humanoid robot arm generally has shoulder, elbow, wrist artificial articulations and -at the other end of the hand- a holder modellizing the human articulations and fingers/thumb.

It is well-known that the humanoid robot can possess more than **1 DOF** at any articulation by the artificial bones and muscles of its kinematic systems. Any way at the industrial robot generally every link/tag has only **1 DOF**.

Thus **at the shoulder** -as at an origo- one can realise **1, 2 or 3 flexing DOF the upper arm around x,y and z axes**, besides sometimes it has a **1 twisting DOF** around the axe of the upper arm;

- ❖ at other end of the upper arm -**at the elbow** origo articulation- one can realise **1 flexing DOF for the forearm** around the perpendicular axe to the upper arm, besides it can have **1 twisting DOF around the axe of the forearm** (around the radius);
- ❖ at wrist **1 flexing DOF** for the hand around the perpendicular axe to the forearm;
- ❖ finally at the other end of the hand there is a holder by the thumb and the fingers, but this later one can be operated by other typed tools, not by PAM elements.

These twisting DOFs can be operated and analysed separately from the other flexing DOFs at the shoulder, elbow and wrist. In the case of 3 DOF flexing around parallel axes it can lose the unambiguous trajectory moving of the hand's holder point from starting to target point.

This lecture mainly deals with constructing 3 or more DOF kinematic systems, humanoid robot arms, their virtual models and their guiding/learning movements. Our basic motivation was that we should define several kinds of kinematic (mechanical) constructions without building up them but their virtual model could be operated for the given tasks and could be tested ([3.]; see also: Balara, M. et al., (2004), [6.]; Fagg, A. H., et al., 1999, [7.]).

Having designed these robot arm constructions (and all of their parts) kinematically we gave the adequate constraints in every artificial articulation in order to be able to assemble the whole robot arm afterwards. **Thus every motion type, controlling and/or learning their typical movements should be studied/analysed without building up all of our constructions** to spare a lot of time, money and material.

2. ROBOT ARM CONSTRUCTIONS

The artificial shoulder articulation can be modelized by a ball-and-socket joint (spherical joint) or 3 cylindrical flexing joints and 1 twisting joint around the upper arm-axe.

The elbow can be modelized by 1 cylindrical flexing joint.

Finally the artificial wrist can be realised virtually by 1 cylindrical flexing joint and 1 other twisting joint around the forearm-axe which operates the forearm and hand equally. Keeping the notations for the artificial articulations' angles at shoulder (α) and at elbow (β), we can choose (γ) at wrist for the angle between the axes of the hand and forearm. Thus, at the beginning of the movements to guard the unambiguous solution, one can transform the arm's holder point by ($\Delta\gamma = 0$), that is the forearm and the hand will move together. One can move the **Inventor-made virtual robot arm models** directly and also by **VBA Macro program**. So, this lecture deals with guiding and controlling movement-strategies in the following cases:

- ❖ guiding the wrist or holder point of the robot arm from a starting to the target point,
- ❖ guiding the wrist/holder point movements via given trajectory and its derivatives.

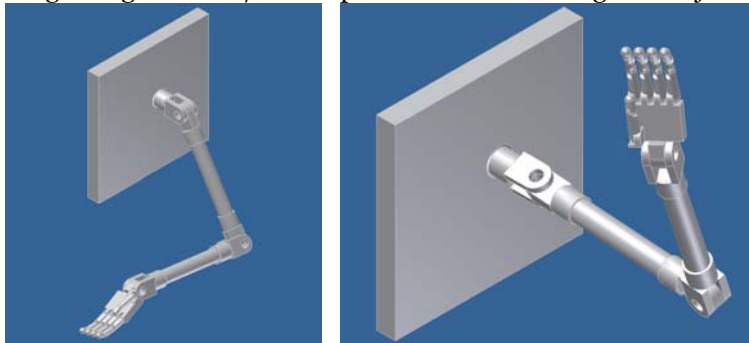


Figure 1. A 6 DOF humanoid robot arm in two characteristic states

There are some moving/controlling strategies but all of them can be characterised by a kind of inverse dynamic controlling process. The Figure 1 shows a 6 DOF robot arm which was analysed by object oriented VBA Macro programs, too. We tested its movements step by step at some given trajectories. In this robot arm we wanted to modelize **1-1**

flexing DOF by cylindrical joints at the shoulder, elbow and wrist artificial articulations.

Figure 2 shows a **5 DOF** humanoid robot arm (which had not flexing DOF at the wrist, that is $\Delta\gamma = 0$) in two characteristic states: at the starting state of its wrist and at end state with its wrist at the target point of a plane.

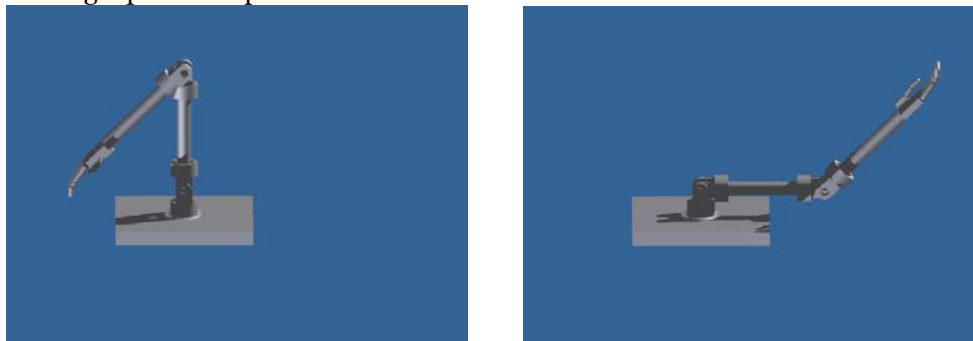


Figure 2. A **5 DOF** robot arm with **Angle1** and **Angle2** parametres at the shoulder and elbow articulations were identified for the control VBA Macro program

The controlling Macro program is the following:

```

Sub Move()
Dim AssemblyDocument As AssemblyDocument
Dim Angle1Param, Angle2Param As Parameter
Dim AssCompDef As AssemblyComponentDefinition
Dim CY1 As Integer
Set AssemblyDocument = ThisApplication.ActiveDocument
Set AssCompDef = AssemblyDocument.ComponentDefinition
Set Angle1Param = AssCompDef.Parameters.Item("Angle1")
Set Angle2Param = AssCompDef.Parameters.Item("Angle2")
For CY1 = 1 To 45
Angle1Param.Value = 90 / 180 * 3.14 - 2 * CY1 / 180 * 3.14
AssemblyDocument.Update
Angle2Param.Value = 45 / 180 * 3.14 + 2 * CY1 / 180 * 3.14
AssemblyDocument.Update
Next
End Sub
    
```

Figure 2 shows how these Inventor made kinematic models could be controlled by identifying the **I.1.** (constraint) = **Angle1** and the **II.1.** (constraint) = **Angle2** parameters of this **5 DOF** robot arm after modified them by the above VBA macro program. We can see the results only for the Angle1 and Angle2 parameters. We also mention that only **2 flexing DOF** must be used out of the **3 flexing DOF** around the same (parallel) direction axes to preserve the unambiguous solution. In the **6 DOF** case the **3rd one** at the wrist, e. g. the **III.1.** (flexing constraint) has to be fixed at the first motion step. At the shoulder and wrist articulations **1-1 twisting DOF** (**I.2.** and **II.2.** constraints) can be realised around the axes of the links (actual pieces of the arm), the twisting angles are addable sum. At the shoulder we can use **1 other flexing DOF** by a cylindrical joint (**I.3.** constraint) to realise the **3rd DOF** at the shoulder. But it is more useful if one has a **7 DOF** robot arm with **3 flexing DOF** around the **x,y** and **z** axes besides the **1 twisted DOF** around the axe of the upper arm at the shoulder.

There are some other applications of the robot arms: e.g. Figure 3 shows a virtual kinematic model (**5 DOF** Reha-robot arm) for rehabilitating movements for somebody who has arm, muscles, tendons, articulations, but after a stroke or spinal/cerebral injury needs motion-rehabilitation by a kind of robot control. This model was also tested with some VBA macro programs by circular moving steps for any planar target points.

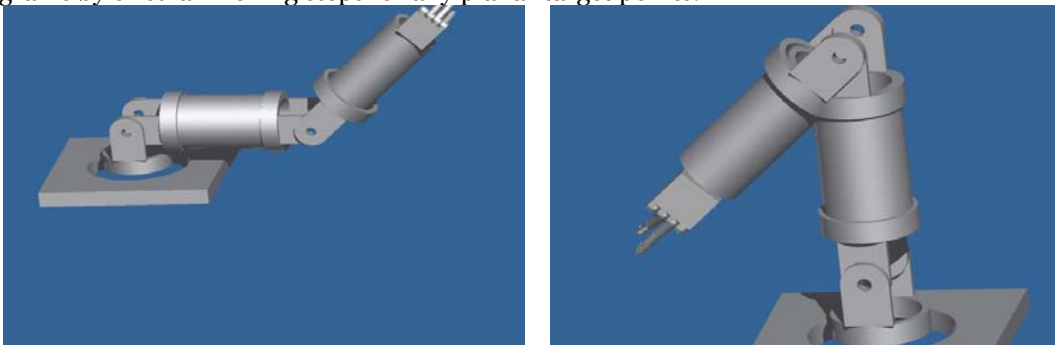


Figure 3. This Reha-robot arm also can be controlled by the same VBA Macro program

Figure 4 shows two experimental arm-prosthesis constructions: **4 DOF** prosthesis for replacing the upper and forearm and the other one with **3 DOF** for a person who partially lost this upper arm, too.

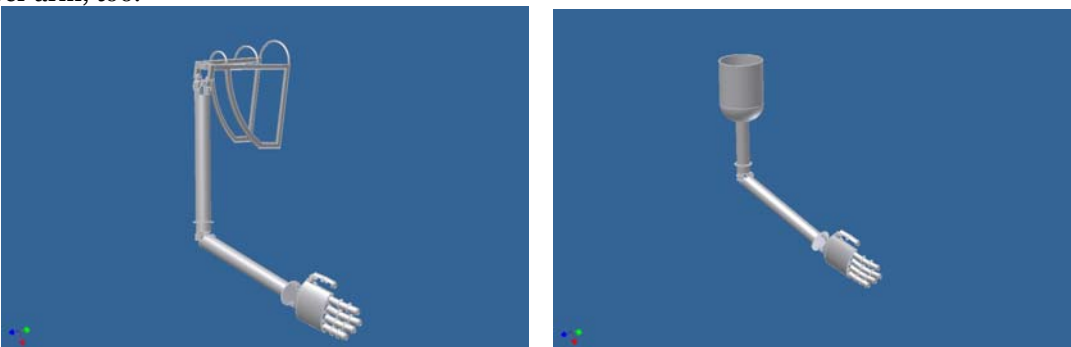
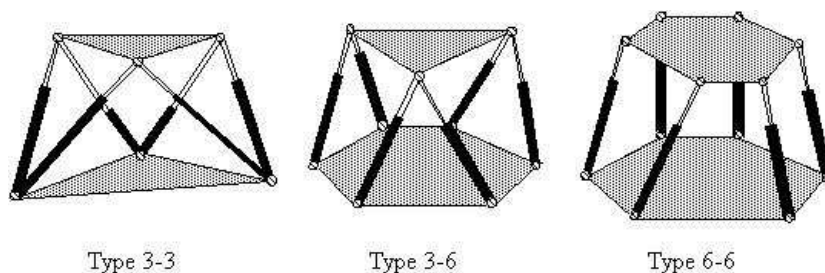


Figure 4 There are a **4 DOF** and another **3 DOF** prosthesis analysed

3. APPLICATION STEWART-PLATFORM STRUCTURE DEVELOPING A 3 DOF ROBOT ARM ARTICULATION

The *Stewart-platform* (known as 'hexapod' too) has **6 DOF**, and it has high payload-to-weight ratio (alike PAMs) since the payload is carried by several links in parallel (Ronen Ben-Horin, 1996, [14.]). Generally it is used as a base of the motion in the flight or automobile simulators, too (Picture 2).

We can similarly use a **3 DOF** tripod PAM controlled structure as a more simple variation of Stewart-platform. This



Picture 2. Examples for the Stewart-platform 'hexapod'

compact kinematic structure is analogue the **3 DOF** spherical joint at the artificial shoulder articulation of the **6 or 7 DOF** controlled by **PAMs** humanoid robot arms analysed above. It can replace the **2 or 3 flexing/twisting DOF** articulation with **2 or 3** cylindrical joints or **1** spherical joint.

Picture 3 shows the developed tripod-platform virtual model flexing/twisting around **x, y** and **z axes** in **CCW (+)** and **CW (-)** directions, which shows also its efficiency.

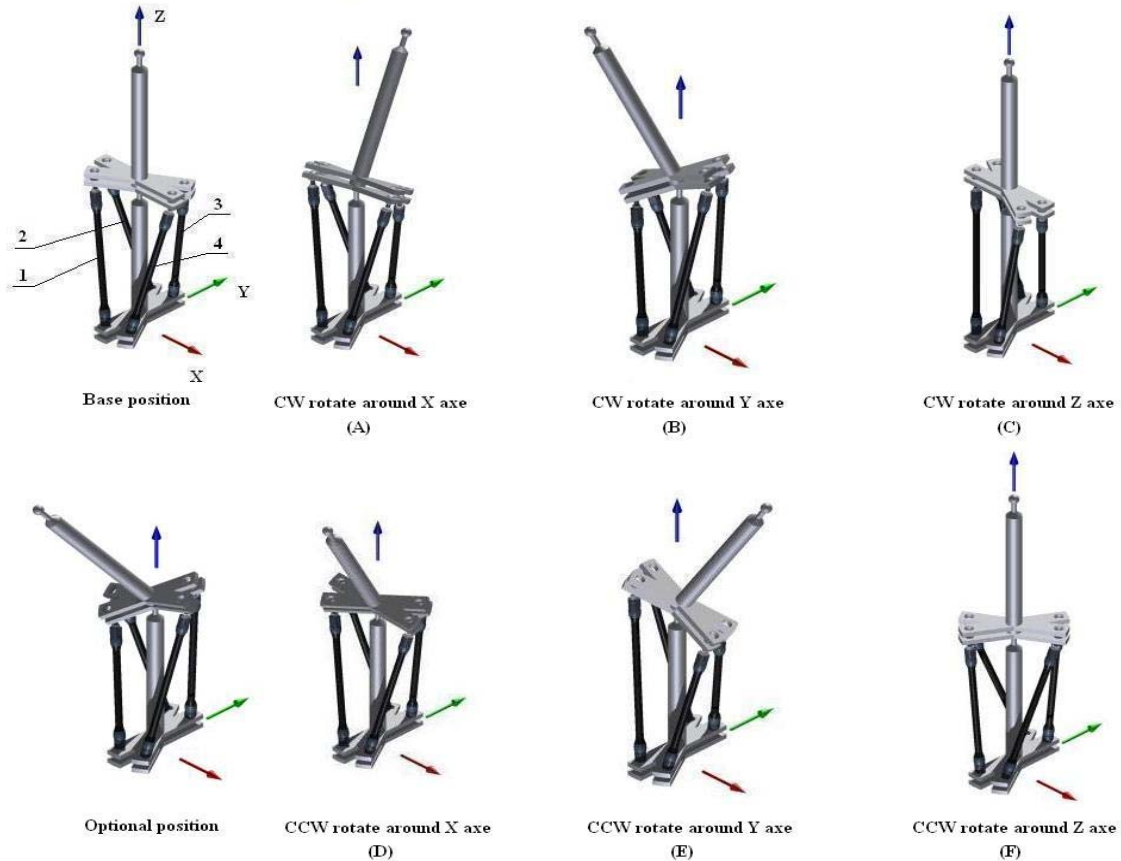


Figure 5. The basic solution of the developed **Stewart** tripod-platform by **PAM** actuators

This Table 1 shows the logical conditions with **C=contraction** and **L=lengthening** the named **PAM** elements for operating the rotation of the platform around the **x,y** and **z axes**. The main information which comes from this table, is that the structure **does not need 4 PAM** elements for moving the platform in 3 different ways -for having **3** different **flexing/twisting DOF**. If any one of this table-rows will be cleared, all the columns will be different. This means that three PAM could give constraints for the **3 flexing/twisting DOF** structure. The reason why it is better using **4** muscles here is that during the motions all the agonistic-antagonistic PAM elements have a twin/pairing element which gives more stability and balance for this developed tripod Stewart-type platform. The even-number of muscles give the easier way to solve the inverse kinematic task, too. Thus all the muscles need to be supported by another one operating in flexor or extensor mode. Many researches progressed this agonistic-antagonistic habit and finally used positioning by muscle pairs. The precise positioning is possible by using the sliding mode with the chosen PAM elements (Chin-I Huang et al., 1998, [11.]; and [3.]; [4.]; [2.]; [15.]).

Table 1 The state-table of the basic motions of this Stewart tripod-platform

PAM	Motion					
	A	B	C	D	E	F
1	L	C	L	C	L	C
2	C	C	C	L	L	L
3	C	L	L	L	C	C
4	L	L	C	C	C	L

4. MOVING-STRATEGIES FOR 2-7 DOF ROBOT ARM

The authors would like to expound some fundamental robot arm moving-strategies which can solve inverse dynamic controlling programming task but we analysed only the unambiguous flexing DOF cases:

- ❖ 1st possibility: One can determine the inverse transformation (more generally inverse Jakobi) $T_{j i} = T_{ij}^{-1}$ matrix which is simple enough to apply, but only in the 2 DOF cases and besides when only the starting and the target point are given for the robot arm holding point. If the trajectory is also given, we must apply the inverse transformation matrix for $P_i(x_i, y_i, z_i)$ points backward from the target point up to the starting point- densely enough (n-times) along the trajectory. But first we can choose the 2 DOFs (articulations/links) which are most important in the task to solve. In this method we can get a lot of difficulties even in the 2 DOF cases also if we have to solve the task with given 1st and 2nd derivatives of the trajectories and/or the robot arm possesses not only (parallel) flexing DOFs. To solve this task, e. g. the object oriented Inventor VBA Macro programming system is suitable for this aim: writing the controlling program.
- ❖ 2nd possibility: We can use the **Inventor CAD system** itself to produce the inverse dynamic programs to control movement-steps: by defining the “trajectory-rail/track” (for the robot arm holder point) as a continuous polyline which consists of any number of lines/arcs, segments with equal tangents between them constraint; otherwise we can use the so-called transitional constraint between the cylindrical/spherical holder (virtually) and a series of surface-pairs producing the composed trajectory. One can store data in a table at **n** pieces of the trajectory before the robot arm has to go along these $P_i(x_i, y_i, z_i)$ connecting points, the angles (α_i, β_i) of the shoulder and the elbow articulations for these places. That is the angles (α_i, β_i) will be needed in the expected applications to control the robot arm along the given trajectory from the starting to the target point.
- ❖ 3rd possibility: We can design/make also adaptive/heuristic control programs **considering the given trajectory and the position-errors in every i-th steps** between the starting and the target point Endrődy T. et al., 2009, [1.]. These adaptive control algorithms could be added with a kind of heuristic learning and/or remembering possibilities and if the adaptive/heuristic learning control algorithms do not work (e.g. stopped further of the target point, one must use a kind of direct/crude algorithm to finish the process going to the target point. There are some direct and heuristic/adaptive moving algorithms on the **Figure 6** and **Figure 7**.

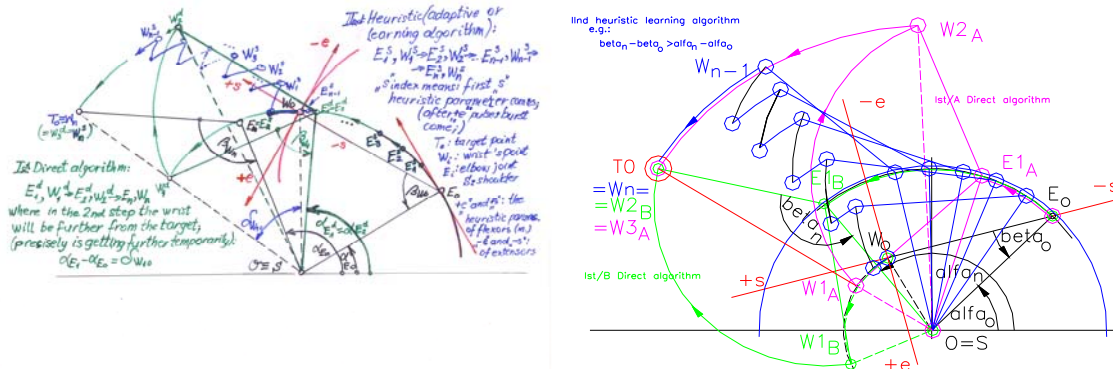


Figure 6 Direct and heuristic algorithms for controlling PAM elements of the upper- and forearm by electronic pulses controlled pneumatic valves

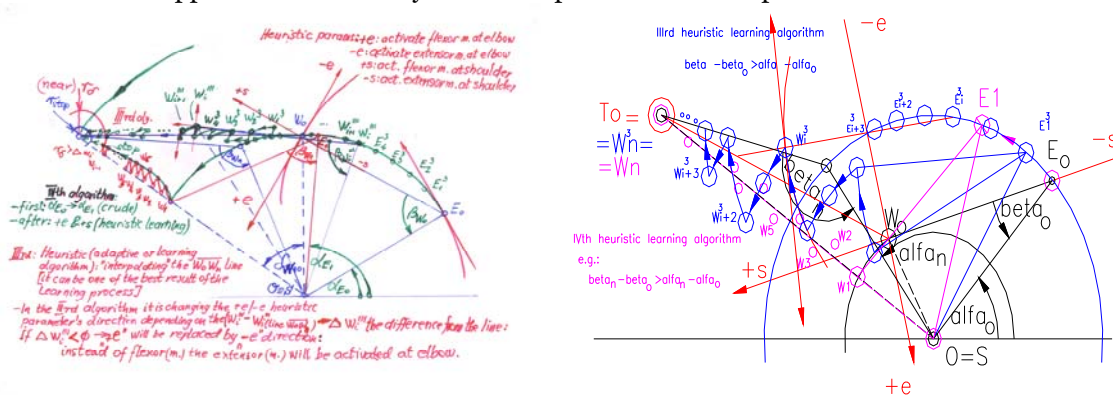


Figure 7. Two further more effective heuristic/learning controlling algorithms

In every controlled step the errors between the expected and the actual arrived i-th point of the trajectory can be corrected for the following experiences. For this aim the actual difference can be analysed between the wanted and the actual wrist/holder point supplementing the predicted

deviation of the holder position of the robot arm to produce better and better controlling program (Fagg, A. H., 1997, [9.]).

- ❖ 4th possibility: One can use Stewart typed tripod platform or other planarly actuated parallel robot construction for replacing e.g. a **3 DOF** spherical joint at the shoulder artificial articulation (see Figure 5). At this type solution one can enjoy the kinematic and dynamic advantages of the parallel robot constructions, which are the following:
 - higher payload-to weight ratio (alike PAM elements) in the consequence of the payload is carried here by several link in parallel,
 - higher accuracy without cumulative joint error,
 - simpler dynamic of the inverse dynamic equations, etc. (Ronem Ben-Horin, et al., 1996, [14.]).
- ❖ 5th and the best possibility (but can be entirely realised only in the future):

The best controlling system for humanoid robot arm (upper arm-forearm-hand) could mime the human brain neuronal networks' controlling process for the muscles, tendons and bones of the human limbs by a neural network e.g. the MLPNN structure with an inverse dynamic model and artificial muscle PAM elements (see: Ahn, K.A. and Anh, H. P. H. (2009), [8.]).

According to our present knowledge the required limbs' conscious movements are controlled first of all by motor cortex' nuclei given commands via the spinal cords' efferent neuronal networks.

The eyes and visual cortex' neuronal networks watch the movements of the arm's articulations along the wanted trajectory. The visual system generates error-series along the trajectory between the actual and required positions, velocity, accelerate (Figure 8). This schema came from Smagt, van der P. (1998, [12.]) and it was added by the authors. Besides from the periphery, the neuronal network of Cerebellaris folium/folia gets information by the afferent fibres about the state of the tones and positions of the muscles, tendons, articulations and bones. Thus the nervous system can predict the position, error of the positions, the tensil forces and moments/torques, too. The Cerebral Motor-cortex nuclei can give the main commands for the muscles in cosequence of the actual learned knowledge made by the Cerebellar Folioms' networks. The learning process based the perceived and predicted position, velocity and acceleration errors during all of the motions. This is a very complex process, thus only the main information paths could be emphasized here.

The cerebellum has homogenous folium-structures and deep nuclei for connecting other parts of the brain. The folium-networks have special "inverse neuronal structures", as Prof. J. Szentágothai said: it is similar to an organist who presses all the keys except the one which gives the sounds (Szentágothai, J., 1977, [13.]). Thus every folium can control by its inverse structure the agonistic-antagonistic and synergic mode operated muscles in an adequate way, because as well-known, the limbs and the articulations of the arm **need inverse dynamic control**. Besides the cerebellar folium-neuronal-structures can learn from the sensed and predicted positions, parameters of the limbs for the sophisticated movements. The "output" Purkinje neurons of folium bring inhibiting distributed commands via the cerebellar deep nuclei for spinal cord and via thalamus nuclei for cortex, so the folium-structures have very effective fluencies in controlling and learning the sophisticated movements of the arm. We developed a new controlling/learning neural system flowchart (Figure 10) which hopefully can use the advantages of the Folium's inverse structure to operate efficiently the needed inverse dynamic control process [16.]).

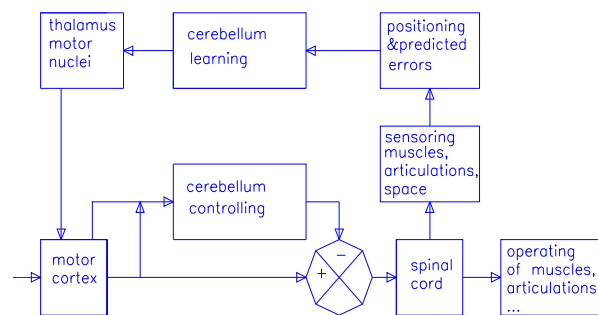
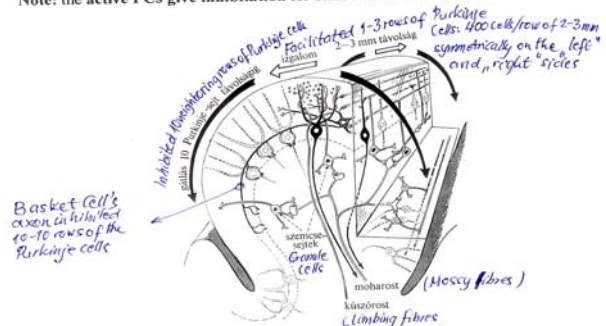


Figure 8. Controlling the human limbs' motion by the Motor cortex, Cerebellaris folium/folia and Spinal cord

Output 1: the 1-3 rows of activated Purkinje Cells by Granular Cells (Parallel Fibres) with 10-10 rows of their neighbouring inhibited PCs by Basket Cells and
 Output 2: the individually activated 1-1 Purkinje Cells by Climbing Fibres
 Note: the active PCs give inhibition for other nucleus of the brain



Input 1: Moss Fibres (Moha Rostok) for activating 1-3 rows of Purkinje Cells
 Input 2: Climbing Fibres (Kúszó Rostok) for activating 1-1 PC individually

Figure 9. The main neuronal network of a typical Cerebellaris Folium by Pr. Szentágothai, J.

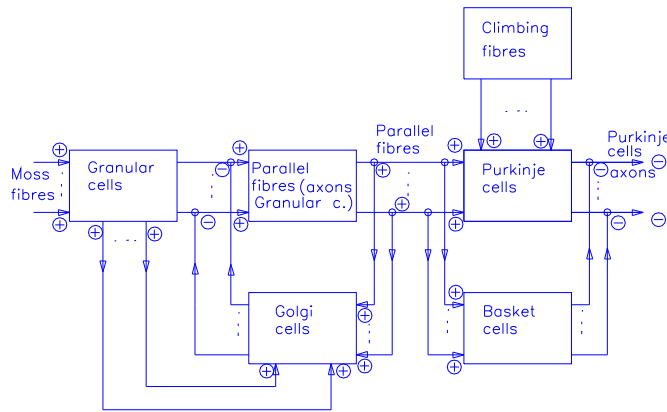


Figure 10. The neural model of the folium with feed-back and feed-forward control possibilities

5. CONTROLLING THE ROBOT ARM'S CIRCULAR STEPS BY PAM ELEMENTS

Till now we have not analysed how the robot arm-links can be moved along an arc separately/one-by-one and together along a kind of bowed trajectory in the case of **2 flexing DOF** arm by the **PAM** elements. These **PAM** elements can contract linearly in different extent. The **PAMs** operate only in one direction (pulling) so it must be used together with its agonist or antagonistic pair, similarly to the muscles in the human body. Last

years we made a few test-bed constructions to analyse its highly nonlinear character (e. g. F [N], Δl [mm] and p [bar, Pa]), its other important parameters: its exact longitudinal (± 0.01 mm) sliding control process and defined maximal contractions (e. g. ± 10 %). After fixing the angle domain (e. g. $0-90^\circ$) at every flexing articulation for moving a link of the robot arm, one can define (for the rotational torque) the measures of the actual force-arm [mm], the point of application of the force and the direction line of the force, that is the fixing places of the artificial muscle elements. One of the main problems at any **2 DOF** robot arm-controlling process is how the given trajectory function of the holder point can be interpolated by little arcs from the starting point up to the target point (see: the **Figure 6** and **Figure 7**, or more detailed: the publication [3.]). First we have to find better and better interpolating by arcs „in second order” for α_i and β_i at the elbow and the shoulder articulations. Then at any movement strategies controlling algorithms mentioned, it is more simple to map the α_i , β_i [$^\circ$] angles to the controlled contractions of the agonistic-antagonistic pairs of **PAM** elements at the shoulder and elbow artificial articulations.

6. CONCLUSIONS

The earlier cerebellar models demonstrated the possibilities of the role of the folium in solving the inverse dynamic control tasks of the robot arm movements. The main possibility came by the Purkinje cells generated inhibitory output.

One must take into consideration that the new light mass-weight artificial muscles (**PAMs**) changed the traditional robot control methods. Recently large contradictions came between the earlier cerebellum models and understanding its role in the motor cortex-cerebellum-spinal cord neuronal networks for the controlling and learning processes of the human limbs' movements. It seems more important to define inverse and forward models, too. We ought to modellize not only the motor apparatus, sensory organs but also the external world from which the actual movement controlling tasks come. The mimesis of the cerebellum could get more attention in present-day research.

REFERENCES

- [1.] T. Endrődy, J. Gyeviski, J. Sárosi and Adrián Szőnyi, Constructions of humanoid robot arm, controlling and learning the movements of their joints, Synergy 2009 Conference, Gödöllő, Hungary, 30 August - 3 September, 2009, p 6
- [2.] Sárosi, J., Gyeviski, J., Endrődy, T., Szabó, G. and Szendrő, P. (2009), Characteristics of the pneumatic artificial muscles, Synergy2009 Conference, Gödöllő, Hungary, 30 August - 3 September, 2009, p 6
- [3.] Endrődy, T., Gyeviski, J., Sárosi, J., Véha, A., and Toman, P. (2008), Automatic and learning model of a planar humanoid robot arm controlled by 2 pairs of antagonistic PAMs moving to a target, ICoSTAF, Szeged, Hungary, 5-6 November, 2008, pp. 367-375
- [4.] Toman, P., Gyeviski, J., Endrődy, T., Sárosi, J. and Véha, A. (2008), Design and fabrication of a test-bed aimed for experiment with pneumatic artificial muscle, International Conference on Science and Technique in the Agri-food Business, Szeged, Hungary, 5-6 November, 2008, pp. 361-366

- [5.] <http://www.jhu.edu/~virtlab/robot1/robo0.htm>, Johns Hopkins University's Robot-laboratory, 1995
- [6.] Balara, M. and Petík, A. (2004), The properties of the actuators with pneumatic artificial muscles, Journal of Cybernetics and Informatics, Volume 4, pp. 1-15.
- [7.] Fagg, A. H., Barto, A.G., Zelevinsky, L. (Univ. of Massach., Dep. of Comp. Sci), Houk, J.C., Northwestern Univ., Dep. of Physio.: Using Crude Corrective Movements to Learn Accurate Motor Programs for Reaching, 1999, pp.20-24
- [8.] Ahn, K. A. and Anh, H. P. H. (2009), Design and implementation of an adaptive recurrent neural networks (ARNN) controller of the pneumatic artificial muscle (PAM) manipulator, pp.1-13.
- [9.] Fagg, A. H., Zelevinsky, L., Barto, A. G. and Houk, J. C. (1997), Using Crude Corrective Movements to Learn Accurate Motor Programs for Reaching, Ch 6, NIPS*97 Workshop, 1997, pp. 20-24.
- [10.] M. Kawato Hikoridai, (1997), Multiple Internal Models in the Cerebellum, Ch5, NIPS*97 Workshop, 1997, pp. 17-19.
- [11.] Chin-I Huang, Chih-Fu Chang, Ming-Yi Yu, Li-Chen Fu, Sliding-Mode Tracking Control of the Stewart Platform, 1998, p. 8
- [12.] Smagt, van der P. (1998), Cerebellar control of robot arms, Inst. of Robotics and System Dynamics German Aerospace Center/DLR, Connection Science 10, pp.301-320.
- [13.] Szentágothai, J. (1977), Funkcionális anatómia (Functional anatomy), Medicina publish., pp. 206-212., pp. 1426-1439., pp. 1484-1490.
- [14.] Ronen Ben-Horin, Moshe Shoham and Shlomo Djerassi, Kinematics, Dynamics and construction of a planarly actuated parallel robot, Dep. of Mechanical Engineering Technion – Israel Institute of Technology, Haifa, 1996, p.2
- [15.] P. Tomán, J. Gyeviki, T. Endrődý, J. Sárosi, A. Véhá, Z. Szabó (2009), Sliding mode control of a robot arm driven by pneumatic muscle actuators, Journal of Engineering Annals of Faculty of Engineering Hunedoara, Tome VII (year 2009), Fascicule 4, (ISSN 1584-2665), pp.95-100
- [16.] T. Endrődý: Developing product and prototype in integrated CAD/CAM system by application of complex modelling, effective communication, data- and knowledge base, PhD Dissertation, Eötvös Loránd University Budapest, Faculty of Informatics, Budapest, 2005, p. 174







¹Flavius Lucian PATER, ²Ludovic Dan LEMLE

A DYNAMIC PROCESS MODEL BASED ON A FUNCTIONAL EQUATION

¹ UNIVERSITY "POLITEHNICA" TIMIȘOARA, DEPARTMENT OF MATHEMATICS, ROMÂNIA

² UNIVERSITY "POLITEHNICA" TIMIȘOARA, FACULTY OF ENGINEERING HUNEDOARA, ROMÂNIA

ABSTRACT:

In this paper, we present some new and original proofs of known results related with unitary operators acting on $B(H^2)$ algebra.

A.M.S.(2010) Subject Classification: 47A20

KEYWORDS:

reproducing kernel, multipliers algebra, anti-unitary operator, polar decomposition

1. INTRODUCTION

First, let us remind some of the results well known in the literature.

Definition 1.1 We define the Bergman's space $H^2(B_d)$ such that

$$H^2(B_d) = \{ f \text{ analytic} \mid \int_{B_d} |f(z)|^2 dm(z) < \infty \}$$

where m represents a Lebesgue measure on B_d .

Theorem 1.2 Let H a Hilbert space, then an operator $T \in B(H)$ is of rank 1 if and only if there exist $\eta \in H$ such that

$$T(\xi) = (\xi \otimes \overline{\eta})(\xi) = \langle \xi, \eta \rangle \xi, \quad (\forall) \xi \in H.$$

Definition 1.3 For any operator $T \in B(H)$ given by

$$T = \sum_{k=1}^N x_k \otimes y_k$$

for N fixed and $x_k, y_k \in H$ with $(x_k \otimes y_k)u = \langle u, x_k \rangle y_k$, we put associated the $\tau(T) = \sum_{k=1}^N \langle x_k, y_k \rangle$. The linear form τ is called **trace**.

Proposition 1.4 We have $\tau(T) = \sum_{j \geq 1} \langle T e_j, e_j \rangle$ for any orthonormal base

$(e_j)_{j \geq 1}$ in H . Moreover, if $R \in B(H)$, we have $\tau(TR) = \tau(RT)$

Let B_d be the unit ball from the complex space \mathbf{C}^d , $d = 1, 2, \dots$ i.e.

$$B_d = \{ z = (z_1, z_2, \dots, z_d) \in \mathbf{C}^d : \|z\| < 1 \},$$

where by $\|z\|$ we denoted the usual norm associated of inner product from \mathbf{C}^d :

$$\|z\|^2 = |z_1|^2 + |z_2|^2 + \dots + |z_d|^2$$

Let P be the algebra of all holomorphic polynomials f . Each $f \in P$ have an expending in a Taylor series of form

$$f(z) = a_0 + a_1 z_1 + \dots + a_n z_n$$

and we can define the norme $\|f\|$ for this polynomial as the norm in l^2 there sequence of Taylor coefficients.

$$(1.1) \quad \|f\|^2 = |a_0|^2 + |a_1|^2 + \dots + |a_n|^2$$

We consider the case $d > 1$ and we denote by P the algebra of all complex holomorphic polynomials f which depends of $z = (z_1, z_2, \dots, z_d)$. Each polynomial f has a unique expansion in a finite series

$$(1.2) \quad f(z) = f_0(z) + f_1(z) + \dots + f_n(z),$$

where f_k is the homogeneous polynomial of degree k .

Now, we'll introduce a seminorm on P . Let be the homogeneous polynomial of degree k :

$$f(z) = \sum a_{i_1 \dots i_d} z_1^{i_1} \dots z_d^{i_d}$$

where the degree of f is given by $\max(i_1 + \dots + i_d)$.

Let $E = \mathbf{C}^d$ be the linear space over \mathbf{C} of dimension d having the inner product:

$$\langle z, w \rangle = z_1 \bar{w}_1 + z_2 \bar{w}_2 + \dots + z_d \bar{w}_d.$$

We build the following spaces $E^{\otimes k}$ thus:

$$E^{\otimes 0} = \mathbf{C}$$

$$E^{\otimes 1} = E$$

...

$$E^{\otimes k} = \underbrace{E \otimes E \otimes \dots \otimes E}_k = \{ \varphi : E' \times \dots \times E' \mapsto \mathbf{C} \}$$

where E' is duality space of E . We have

$$E^k = \{ \varphi \in E^{\otimes k} : \varphi(f_{\tau(1)}, f_{\tau(2)}, \dots, f_{\tau(k)}) = \varphi(f_1, \dots, f_k), (\forall) f_i \in E', i = 1, \dots, k \},$$

where $\tau \in S_k$ and S_k is the group of permutation.

First, we'll prove that the elements of H^2 can be identified with the elements of the symmetric Fock space over E , $F_+(E) = E^{\otimes 0} \oplus E^{\otimes 1} \oplus E^{\otimes 2} \oplus \dots$, the sum from the right member denoting an infinite direct sum of Hilbert spaces (see [1], [3]). Also, related work was done by ([2], [4], [5], [6], [7]).

Proposition 1.5. For each $f \in P$, let $Jf \in F_+(E)$, (see [1]).

$$Jf = (\xi_0, \xi_1, \dots)$$

Where the sequence $\{\xi_k\}_k$ is the Taylor coefficients for $k \leq n$ and for $k > n$, $\xi_k = 0$. Then J is a unique extension at an antiunitary operator from H^2 at $F_+(E)$.

Proposition 1.6. Each element from H^2 may be considered like an analytic function in B_d , having the following form:

$$f(z) = \sum_{k=0}^n \langle z^k, \xi_k \rangle, \quad z = (z_1, \dots, z_d) \in B_d$$

where the norm $\|\cdot\|$ from H^2 is given by $\|f\|^2 = \sum_k \|\xi_k\|^2 < \infty$. Such function satisfies the

following increasing condition

$$|f(z)| \leq \frac{\|f\|}{\sqrt{1 - \|z\|^2}},$$

for any $z \in B_d$.

2. ON SOME UNITARY REPRESENTATIONS ON $B(H^2)$ ALGEBRA

Proposition 2.1. Let A be a closed, normed $B(H^2)$ sub-algebra, generated by the multiplication operators $M_f, f \in P$.

Each element of A is a multiplication operator M_f for any $f \in M$, which is extending continuously to the closed unit ball \bar{B}_d and there exists a natural homeomorphism from \bar{B}_d to the space $\sigma(A)$ of all complex homeomorphisms of A , $x \rightarrow w_x$, defined by

$$w_x(M_f) = f(x), \quad \|x\| \leq 1$$

For each $f \in M$ we have

$$\lim_{n \rightarrow \infty} \|M_f^n\|^{1/n} = \sup_{\|x\| \leq 1} |f(x)|$$

Proof. As the application $f \in M \rightarrow M_f \in B(H^2)$ is a isometric representation of the multipliers algebra on H^2 which carries the unit of M in the unit from $B(H^2)$, is enough to work on M . That means to consider A the closure in M of the polynomial algebra, practically needing to identify the space of maximal ideals.

Due to the inequality $\|f\|_\infty \leq \|f\|_M$ from proposition 1.6, one can deduce that for every polynomial f and any $x \in \mathbf{C}^d$ satisfying $\|x\| \leq 1$, we have

$$|f(x)| \leq \sup_{z \in B_d} |f(z)| = \|f\|_\infty \leq \|f\|_M$$

This implies there exist a unique complex homomorphism $w_x \in A$, satisfying:

$$w_x(f) = f(x), (\forall) f \in P$$

For all $g \in A$ we have now a continuous natural extension \tilde{g} of g to the closed unit ball by putting

$$\tilde{g}(x) = w_x(g), \|x\| \leq 1$$

$x \rightarrow w_x$ is a continuous application of the unit ball \mathbf{C}^d on its image from $\sigma(A)$. In order to show its surjectivity, let w be an element of $\sigma(A)$. Then $(\forall) y \in \mathbf{C}^d$ we can consider the linear functional

$$\hat{y}(z) = \langle z, y \rangle, z \in \mathbf{C}^d$$

The application $y \rightarrow \hat{y}$ is an anti-linear application of \mathbf{C}^d onto the space of linear functionals of P and we have $\|\hat{y}\|_M \leq \|y\|$. Indeed suppose $y \neq 0$. Then the linear function

$$u(x) = \hat{y} / \|y\| = \langle x, y \rangle / \|y\|$$

belongs to the coordinate system of \mathbf{C}^d . Proposition 1.9 implies $\|u\|_M \leq 1$, hence $\|\hat{y}\|_M \leq \|y\|$. So $y \rightarrow w(\hat{y})$ defines an antilinear functional on \mathbf{C}^d satisfying

$$|w(\hat{y})| \leq \|\hat{y}\|_M \leq \|y\|, (\forall) y \in \mathbf{C}^d$$

It follows there exist a unique vector x in the unit ball of \mathbf{C}^d such that

$$w(\hat{y}) = \langle x, y \rangle, y \in \mathbf{C}^d$$

Hence, $w(f) = w_x(f)$ for each linear functional f . As w and w_x are continuous unitary homeomorphisms of A , as P is the algebra generated by the linear functions and by constants and as P is dense in A it can be deduced that $w = w_x$ and so we've identified the maximal ideals space of A with the closure of the unit ball of \mathbf{C}^d . From the elementary theory of commutative Banach algebras we deduce that for every $f \in A$,

$$\lim_{n \rightarrow \infty} \|f^n\|_M^{1/n} = r(f) = \sup \{ |w(f)| : w \in \sigma(A) \} = \sup \{ |\tilde{f}(x)| : \|x\| \leq 1 \} = \|f\|_\infty$$

q.e.d.

The d – shift considered as d – tuple of multiplication operators onto H^2 is not always convenient for calculations. We'll need the following equivalent definition of (S_1, \dots, S_d) as being operators „created” on the symmetric Fock space $F_+(E)$.

Proposition 2.2 *Let e_1, \dots, e_d be an orthonormal base for a Hilbert space E of dimension d . Define the operators A_1, \dots, A_d on $F_+(E)$ by*

$$A_i \xi = e_i \otimes \xi, \xi \in F_+(E)$$

where by $e_i \otimes \xi$ denote the projection of $e_i \otimes \xi \in F(E)$ onto the symmetric subspace $F_+(E)$. Let z_1, \dots, z_d an orthogonal system of coordinates $z_i(x) = \langle x, e_i \rangle, 1 \leq i \leq d$. Then it exists an unique unitary operator $W : H^2 \rightarrow F_+(E)$ such that $W(1) = 1$ and

$$(2.1) \quad w(z_{i_1}, \dots, z_{i_n}) = e_{i_1} \otimes \dots \otimes e_{i_n}, n \geq 1, i_k \in \{1, 2, \dots, d\}$$

In particular, the d – tuple of operators (A_1, \dots, A_d) is unitary equivalent with the d – shift.

Proof. For any $x \in E$ satisfying $\|x\| < 1$ define an element $v_x \in F_+(E)$ by

$$v_x = 1 \oplus x \oplus x^2 \oplus x^3 \oplus \dots$$

It is obvious that $\|v_x\|^2 = (1 - \langle x, x \rangle)^{-1}$ for $\|x\|, \|y\| < 1$ and more general

$$\langle v_x, v_y \rangle = (1 - \langle x, y \rangle)^{-1}, \|x\|, \|y\| < 1$$

We deduced this using $\langle z^k, w^k \rangle_{E^k} = \langle z, w \rangle_{E^k}$. $F_+(E)$ is generated by the set $\{v_x : \|x\| < 1\}$. Let $\{u_x : \|x\| < 1\}$ the set of H^2 functions definite in 1.11 and let $*$ the canonical conjugation unique on E defined by $e_i^* = e_i$, as

$$(a_1 e_1 + \dots + a_d e_d)^* = \bar{a}_1 e_1 + \dots + \bar{a}_d e_d$$

then, we have

$$\langle u_x, u_y \rangle = (1 - \langle y, x \rangle)^{-1} = (1 - \langle x^*, y^* \rangle)^{-1} = \langle v_{x^*}, v_{y^*} \rangle$$

For any x, y from the unit open ball of E . By Proposition 2.1 [3] there exists an unique unitary operator $W : H^2 \rightarrow F_+(E)$ such that $W(u_x) = v_{x^*}, \|x\| < 1$. $W(1) = W(u_0) = v_0 = 1$. Let $x \in E, \|x\| \leq 1$

and let f_x be the linear functional on E defined $f_x(z) = \langle z, x \rangle$. We have $\|f_x\|_{H^2} \leq 1$ and from that $\|f_x^n\|_{H^2} \leq 1$ for $n=0,1,2,\dots$. Hence for any $0 \leq r < 1$ and any $z \in B_d$ we have

$$u_{rx}(z) = (1 - \langle z, rx \rangle)^{-1} = \sum_{n=0}^{\infty} r^n \langle z, x \rangle^n = \sum_{n=0}^{\infty} r^n f_x^n(z) \in H^2$$

Similarly $v_{rx^*} = \sum_{n=0}^{\infty} r^n (x^*)^n \in F_+(E)$.

Taking $W(u_{rx}) = v_{rx^*}$ and comparing the coefficients of r^n , we obtain

$$W(f_x^n) = (x^*)^n, \text{ for } n=0, 1, \dots$$

It can be deduced that

$$(2.2) \quad W(f_{x_1}, \dots, f_{x_n}) = x_1^* x_2^* \dots x_n^*$$

For any $x_1, x_2, \dots, x_n \in E$. Indeed, by putting

$$(2.3) \quad \begin{aligned} L(x_1, x_2, \dots, x_n) &= W(f_{x_1}, \dots, f_{x_n}) \\ R(x_1, x_2, \dots, x_n) &= x_1^* x_2^* \dots x_n^* \end{aligned}$$

for $x_1, x_2, \dots, x_n \in E$, it can be observed that L and R are symmetric n – antilinear applications which are equal when $x_1 = x_2 = \dots = x_n \in B_d$. Hence $L = R$ and (2.1) is true. (2.2) is obtained by taking $x_k = e_{i_k}$ in (2.3).

(2.2) obviously implies $WS_i = A_i W$ for $i=1..d$ so the d – tuples (S_1, \dots, S_d) and (A_1, \dots, A_d) are unitary equivalent.

REFERENCES

- [1.] Arveson, W. (1997). Subalgebras of C^* - algebras III; multivariable operator Theory (preprint).
- [2.] Coburn, L.A. (1973). Singular integral operators and Toeplitz operators on odd spheres, Ind. Univ. Math J 23, 433-439.
- [3.] Pater, F., Juratoni, A., Bundău, O.(2008). O., On some reproducing kernel property for C^d orthonormal basis. Bulletin for Applied Computer Mathematics, B.A.M., ISSN 0133-3526, Hungary.
- [4.] Popescu, G. (1991). Von Neumann inequality for $(B(H)^n)_1$, Math Scand 68, 292-304.
- [5.] Rudin, W. (1976). Principles of Mathematical Analysis, 3rd edition, McGraw Hill.
- [6.] Segal, I.E. (1956). Tensor algebras over Hilbert spaces, Trans. Amer. Math. Soc, 106 –134.
- [7.] Sz-Nagy, B. and Foias, C. (1970). Harmonic analysis of operators on Hilbert spaces, American Elsevier, New York.





¹Flavius Lucian PATER, ²Liana Rodica PATER

A DYNAMIC PROCESS MODEL BASED ON A FUNCTIONAL EQUATION

¹ UNIVERSITY "POLITEHNICA" TIMIȘOARA, DEPARTMENT OF MATHEMATICS, ROMÂNIA

² "TIBISCUS" UNIVERSITY OF TIMIȘOARA, FACULTY OF ECONOMICAL SCIENCES, ROMÂNIA

ABSTRACT:

In this article is presented a new approach to some fundamental techniques of solving dynamic programming problems with the use of functional equations.

A.M.S.(2010) Subject Classification: 37J99

KEYWORDS:

dynamic programming, optimum, recurrence, resources, activity

1. INTRODUCTION

Dinamic programming represents a group of techniques and methods of optimization which helps solving large categories of problems of the form:

$$(1) \quad \max R(x_1, x_2, \dots, x_n) = g_1(x_1) + g_2(x_2) + \dots + g_n(x_n)$$

with the restrictions:

$$(2) \quad x_1 + x_2 + \dots + x_1 + \dots + x_n = Z$$
$$x_i \geq 0$$

knowing that g_1, g_2, \dots, g_n are mostly exponential type functions:

$$(3) \quad g(x) = A + Be^{-cx}$$

This mathematical theory treats especially the resources usage problem (people, materials, machines, etc.) with the purpose of their optimal recovery (see [1, 6, 8, 9]).

The notions used in dinamic programming are the following:

- ❖ *resources*: any means or reserves that can be mobilized and employed in order to achieve a productive activity;
- ❖ *activity*: any possible use of a resource;
- ❖ *profit*: partially or wholly the result obtained by the use of resources.
Profit can be measured with different units but by convention it is assumed that:
 - ❖ profits are measured with the same unit of measurement in all activities;
 - ❖ an activity-profit resource allocation is independent of all other activities;
 - ❖ total profit obtained in the end is the sum of individual profits of the business.
- ❖ Other important concepts are:
 - ❖ *utility-function*: function of the type $g(x)$ mentioned above and which is measured by size of profit made in relation to the resources allocated;
 - ❖ *target-function*: function of the type $R(x_1, x_2, \dots, x_n)$ (see [1]), which is the total amount of profit that can be achieved by allocating resources;
 - ❖ *restrictions*: functions as those of (2) and limiting the use of resources;
 - ❖ *allocation*: the allocation of resources in a given activity.

Of course, within optimization issues you may encounter different types of functions R (respectively g) which are required to be maximized (or minimized), as appropriate.

2. A DYNAMIC PROCESS MODEL

In the case of "regular" functions, the optimization process takes place in a possible domain, which is bounded by restrictions, so the most commonly used technique is based on Lagrange

multipliers, which we will denote by λ (see [7]). Assuming that the functions g_i in (1) are also regular functions, we form an auxiliary function $S(\lambda; X)$ as follows:

$$(4) \quad S(\lambda; x_1, x_2, \dots, x_n) = g_1(x_1) + g_2(x_2) + \dots + g_n(x_n) - \lambda (x_1 + x_2 + \dots + x_1 + \dots + x_n - Z)$$

In this way we've included the first restriction from (2) in (1) and we've obtained a problem without restrictions. Because g_i are regular functions, obtaining the optimum is done by imposing the condition:

$$(5) \quad \frac{\partial S(\lambda, X)}{\partial x_i} = 0$$

where $x \in E_n$. In this way we get equations of the form:

$$(6) \quad g'_i(x_i) - \lambda = 0 \quad (i=1, 2, \dots, n)$$

Solving the above equation depending on λ :

$$(7) \quad x_i = h_i(\lambda)$$

we determine λ by replacing all x_i values in (2) with their coresspondents from (6):

$$(8) \quad h_1(\lambda) + h_2(\lambda) + \dots + h_n(\lambda) = Z$$

from where λ could be easily obtained, which will allow us to immediately find the values x_i , by using relations like (6).

As an example suppose we have a quadratic programming problem which asks the following:

$$(9) \quad \max R(X) = a_1 x_1^2 + a_2 x_2^2 + \dots + a_n x_n^2$$

where $a_i > 0$, and satisfies :

$$(10) \quad x_1 + x_2 + \dots + x_1 + \dots + x_n = Z$$

$$x_i \geq 0$$

The auxiliary function S has the form:

$$(11) \quad S(\lambda; X) = a_1 x_1^2 + a_2 x_2^2 + \dots + a_n x_n^2 - \lambda (x_1 + x_2 + \dots + x_1 + \dots + x_n - Z)$$

Deriving $S(X)$ with respect to x_i we'll obtain:

$$(12) \quad \frac{\partial S(\lambda, X)}{\partial x_i} = 2 \cdot a_i \cdot x_i - \lambda$$

And by writing according to (5):

$$(13) \quad 2 \cdot a_i \cdot x_i - \lambda = 0$$

hence (14) $2 \cdot a_i \cdot x_i = \lambda$ and in consequence

$$(15) \quad x_i = \frac{\lambda}{2 \cdot a_i}$$

Replacing (15) in (10) it results:

$$(16) \quad \sum_{i=1}^n \frac{\lambda}{2 \cdot a_i} = Z \text{ or } \frac{\lambda}{2} \sum_{i=1}^n \frac{1}{a_i} = Z \text{ so that } \lambda = \frac{2 \cdot Z}{\sum_{i=1}^n \frac{1}{a_i}} \text{ and}$$

$$(17) \quad x_i = \frac{Z / a_i}{\sum_{i=1}^n \frac{1}{a_i}} .$$

This allows us to find the maximum value of R :

$$(18) \quad R = \sum_{i=1}^n a_i x_i^2 = \frac{Z^2}{\sum_{i=1}^n \frac{1}{a_i}}$$

Unfortunately the method described above cannot be used for the general case. Because of this there were introduced new research methods and mathematical techniques, our original method, subject of this article, being one of them. In this way, solving the particular problem of maximizing the function:

$$(19) \quad R(X) - g_1(x_1) + g_2(x_2) + \dots + g_n(x_n), \quad X \in E_n,$$

inside the real domain delimited by:

$$(20) \quad \sum_{i=1}^n x_i - Z,$$

$$x_i \geq 0$$

means to approach a series of allocation processes, where n can take any positive, integer value and x_i any non-negative value. The allocation process is done by passing from one activity to another so

it has a dynamic character. If the maximum of $R(x)$ depends on n and Z , then the dependence will become clearer if we introduce a series of functions $f_n(Z)$ defined as follows:

$$(21) \quad \begin{aligned} n &= 1, 2, 3, \dots \text{ (integers)} \\ Z &\geq 0, \\ f_n(Z) &= \max_{x_i} R(x_1, x_2, \dots, x_n), \\ x_i &\geq 0, \sum_{i=1}^n x_i = Z \end{aligned}$$

The third relation in (21) could be interpreted by defining $f_n(Z)$ as the maximum value of the realized profit. This is done by allocating most conveniently the total resources Z to all the n activities. It is important to notice though that sometimes the functions $f_n(Z)$ take some particular values. Hence, if there isn't any resource allocation, respectively $Z=0$ and $x_i=0$ then $f_n(0)=0$, ($n=1, 2, 3, \dots$), which is, in fact, a consequence of $g_i(0)=0$. But if $n=1$, that means $R(Z)=g_1(Z)$, so $f_1(Z)=g_1(Z)$.

If $f_n(Z)$ is the maximum profit that can be obtained by dividing Z optimally to n activities, then as a consequence we could say that $f_{n-1}(Z_1)$ is the maximum profit that can be obtained by dividing the resource Z_1 optimally to $n-1$ activities. Between $f_n(Z)$ and $f_{n-1}(Z_1)$ there exists a recurrence which can be emphasized as follows:

Suppose a resource x_n is spread to activity n such that

$$(22) \quad 0 \leq x_n \leq Z.$$

But according to (22), x_n can take any integer value between 0 and Z . Suppose now, x_n is a random value, constant for the moment, which satisfies the condition (22). In this way the available resource quantity to be spread to the other $n-1$ activities is:

$$(23) \quad Z_1 = Z - x_n$$

If we accept that $f_{n-1}(Z_1)$ has the significance given above, then we can write:

$$(24) \quad R(Z) = g_n(x_n) + f_{n-1}(Z_1),$$

Which is equivalent with writing:

$$(25) \quad R(Z) = g_n(x_n) + f_{n-1}(Z - x_n)$$

In order to obtain the maximum value $R(Z)$ can take, meaning $f_n(Z)$, it will be assumed that x_n take all possible values between 0 and Z , then considering that value for which $R(Z)$ is maximum, this being equivalent with writing:

$$(26) \quad \max R(Z) = f_n(Z) = \max_{0 \leq x_n \leq Z} [g_n(x_n) + f_{n-1}(Z - x_n)]$$

In this way we can obtain the basic functional equation from dynamic programming that could be completely formulated as below:

$$(27) \quad f_n(Z) = \max_{0 \leq x_n \leq Z} [g_n(x_n) + f_{n-1}(Z - x_n)]$$

$$\begin{aligned} &\text{for } n=2, 3, \dots \\ &\text{when } Z \geq 0 \\ &\text{and } f_1(Z) = g_1(Z) \end{aligned}$$

3. CONCLUSIONS

The relations (27) leads to the optimality principle which can be presented as follows:

An optimal policy has the property that whatever the initial state and the initial decision, the resulting decisions (available at the moment) must constitute an optimal policy regarding the state implied by the first decision. At this point, some conclusions can be drawn:

- ❖ The optimization process has a decision character because at each step, a new decision has to be made regarding the next steps.
- ❖ The optimization process has a sequential character, meaning it takes place in a number of steps.
- ❖ The optimization process has a economic policy character (optimal policy) because is being realized based on a strategy with the ultimate goal the optimum economical result.

One can observe, though, the first relation in (27) is a recurrence relation which is in the same time a teoretical method used to obtain the series $\{f_n(Z)\}$ inductively, once $f_1(Z)$ is know. It is obvious that $f_1(Z)$ determines $f_2(Z)$, then $f_2(Z)$ leads to $f_3(Z)$ and so on. From here one can conclude that the optimization process using the dynamic programming method is defined by analyzing descendingly the n -th activity towards the first one then is resolved going ascendingly from the first one to the last one.

REFERENCES

- [1.] Bell P., C., Newson E., F. (1992). Statistics for business, The Scientific Press, San Francisco.
- [2.] Boldur Gh., Rațiu-Suciu Camelia, Ciobanu Gh., Stancu I. (1975). Cercetare operațională cu aplicații în economie, ASE, București.
- [3.] Boldur-Lățescu, Gh., Săcuiu I., Țigănescu E. (1979). Cercetarea operațională cu aplicații în economie, E. D. P., București.
- [4.] Leontief W. (1970). Analiza input-output, Ed. Științifică, București.
- [5.] Mendenhall W., Reinmuth J., E., Beaver R., Duhan D. (1986) Statistics for management and economics, Duxbury Press, Boston.
- [6.] Popa H., L., Străuți G., Vasu M., Pater F. (2001). Managementul și ingineria sistemelor de producție, Ed. Politehnica, Timișoara.
- [7.] Rafiroiu M. (1980). Modele ale cercetării operaționale aplicate în construcții, Ed. Tehnică, București.
- [8.] Rațiu-Suciu C. (1997). Modelarea și simulare proceselor economice, E. D. P., București.
- [9.] Turban E., Meredith J. (1991). Fundamentals of Management Science, Irwin, Boston.



¹Amalia Ana DASCĂL, ²Adina BUDIUL BERGHIAN

FOR MEASURING AN AMENDMENT DUROMETER BRINELL HARDNESS AT HOT

^{1,2}UNIVERSITY POLITEHNICA OF TIMISOARA, FACULTY ENGINEERING OF HUNEDOARA, ROMANIA

ABSTRACT:

The paper presents the theoretical studies and experimental results obtained from the mechanical attempts of hardness at heat, made on a Brinell hardmeter, using original heating precincts of the test-bars. Thermal-resistant steel types had been used for testing, which practically are submitted at high functional temperatures. Therefore, the precincts and the annex elements as well as the obtained results are shown. They can be applied practically in order to determine the life length of component parts made of this steel.

KEYWORDS:

mechanical test, Brinell hardness, heat chamber, high temperature

1. INTRODUCTION

When choosing a method for testing hardness at high temperatures should take into account a number of reasons, such as: if the surface resistance element can be explored by traces of hardness, the nature of the material under test, the field likely hardness, precision sought the test medium heat (heating chamber, control system and keep warm).

It should be noted that, until now, high temperature hardness tests are not covered by national or European regulations. Few research found in literature, [1], aimed at establishing correlations between characteristics of hardness, high temperature and other mechanical properties of material produced at the same temperatures (eg. correlation between hardness and tensile strength and resilience to high temperatures). Appropriate test methods Brinell and Vickers methods rather than dynamic methods. Brinell and Vickers methods are used can be used to design devices that adapt to a normal oven (chamber) heating.

Of static methods for determining hardness at high temperatures may be used as durometer Brinell method allows selection of a specific task using a touch and penetrated by a certain diameter, thereby realizing different values of the degree of demand.

In establishing the test parameters and specimen dimensions were considered in data requirements [3]. Given the recommendations set out and acknowledging that hardness steels studied at high temperatures may be more than 150 but greater than $HB\ d \leq 6\text{ mm}$ and $\leq 150\text{ HB}$, the average diameter of the footprint adopt d diameter ball Steel $a \geq 2,5 \cdot 6 = 12\text{ mm}$, $b \geq 4 \cdot 6 = 24\text{ mm}$, $D = 10\text{ mm}$ resulting to minimum thickness of the specimen $s_{\min} = 8\text{ mm}$ (Table A.1. of [3]). Using this geometry and considering that it made three prints for each high temperature test, samples were taken for dimensions of $L \times l \times s = 60 \times 40 \times 10$.

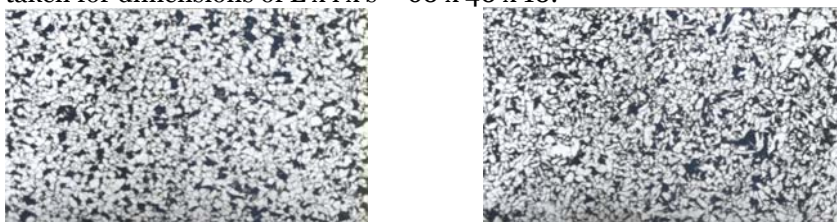


Fig.2. OLT35K and OLT 45K steel structures and the delivery status

The samples were analyzed for hardness in terms of metallographic, the state of delivery, and then after heat treatment and initial structures are shown in Figure 1, the marks of steel that have been performed hardness tests at high temperatures. Nital reagent used was 2%, and samples were studied at a magnification of 100 times.

Metallographic study showed that OLT 35k steel (left) has a structure with grain perlite ferito real-scoring 7-6 according to SR ISO 643-93, and the sample of OLT 45K (left) has a slightly heterogeneous structure ferito-perlite (islands have large grains). Structures correspond to the normative status of delivery specified in the manufacturer of the metal.

2. METHODOLOGY

According to literature [1], the main requirement to carry out proper test under conditions of high temperature hardness is equal between the test sample temperature and temperature head penetrator.

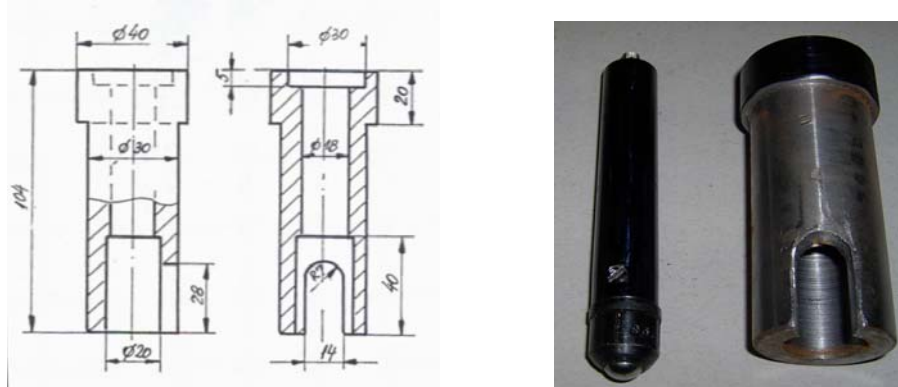


Figure 1. Variants penetrator rod extending rod and heat protection for flat

In order to perform Brinell hardness test was performed by heating specimens in a chamber that was adjusted to a pH durometer - C-02/02. The principle scheme is shown in enclosure made [9]. Temperature samples on site and hence temperature is adjusted by computer.

To ensure equality and head penetrator specimen temperature (in our case - steel ball) was used variant penetrator execution of an extension rod and to achieve thermal protection of the rods, through an appropriate head bush durometer Brinell.

These variations are shown in Figure 2 and Figure 1. Within the thermal protective sleeve were placed rings of asbestos, which provides thermal protection and sealing the area between the working chamber and head load Brinell apparatus.

3. RESULTS

The paper presents experimental tests on two brands of heat-resistant steel, the kind used in making steam pipes, namely: OLT 35k and OLT45K.



Figure 2. Lot samples OLT 35k, unused material, tested at high temperatures

Normalized specimens were tested at room temperature and at elevated temperatures up to 500°C. In Figure 2 are 35k specimens of OLT and in Figure 3, specimens of OLT 45K, where hardness tests at high temperatures: 20°C, 100°C, 200°C, 300°C, 400°C, 500°C.

After the samples were tested was conducted to measure two perpendicular diameters of each finger, and average diameter was calculated from tables [3] resulted Brinell hardness value.

4. CONCLUSIONS

The results of measurements, calculated values of hardness and size are presented in Tables 1 and 2, for each brand of steel.

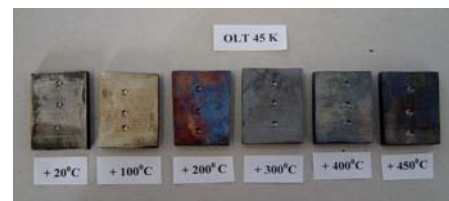


Figure 3. Lot samples OLT 45K, unused material, tested at high temperatures

The hardness values listed in tables were drawn curves of hardness variation depending on test temperature for each brand of steel, shown in Fig.3

The data obtained for hardness tests and analysis of the graph in Fig. 5 it is noted that the tested steels, the toughness shows a similar variation in tensile breaking strength R_m , Brinell hardness increases with increasing temperature up to 200°C, then begins to decline.

Table 1. Brinell hardness at high temperatures, steel 35k OLT, after normalization

Nr. crt.	Temperature test [°C]	Diameter, [mm]				Media	Brinell hardness, [HBS]			
		Footprint			Media		Footprint			Media
		1	2	3			1	2	3	
1	+20	d ₁	5,14	5,18	5,16	5,18	134	132	133	132
		d ₂	5,18	5,22	5,20		132	130	131	
		d _m	5,16	5,20	5,18		133	131	132	
2	+100	d ₁	4,71	4,67	4,69	4,676	162	165	164	164,33
		d ₂	4,73	4,61	4,65		161	170	167	
		d _m	4,72	4,64	4,67		161	167	165	
3	+200	d ₁	4,54	4,51	4,61	4,533	175	178	170	176
		d ₂	4,48	4,52	4,55		180	177	174	
		d _m	4,51	4,51	4,58		178	178	172	
4	+300	d ₁	4,78	4,80	4,76	4,765	157	156	158	158
		d ₂	4,75	4,78	4,74		159	157	161	
		d _m	4,476	4,79	4,74		158	156	160	
5	+400	d ₁	4,92	4,86	4,98	4,923	148	152	144	147,66
		d ₂	4,95	4,90	4,93		146	149	147	
		d _m	4,935	4,88	4,955		147	150	146	
6	+450	d ₁	5,17	5,17	5,18	5,156	133	133	132	133,66
		d ₂	5,14	5,10	5,20		134	137	131	
		d _m	5,15	5,13	5,19		134	135	132	

Brinell hardness at high temperatures, OLT 45K steel, after normalization

Nr. crt.	Temperature test [°C]	d	Diameter, [mm]			Media	Brinell hardness, [HBS]			Media
			Footprint				Footprint			
			1	2	3		1	2	3	
1	+20	d ₁	5,25	5,24	5,30	5,263	128	129	126	127,66
		d ₂	5,25	5,28	5,26		128	127	128	
		d _m	5,25	5,26	5,28		128	128	127	
2	+100	d ₁	4,65	4,82	4,79	4,705	167	154	156	162,66
		d ₂	4,57	4,71	4,69		173	162	164	
		d _m	4,61	4,76	4,74		170	158	160	
3	+200	d ₁	4,52	4,47	4,46	4,520	177	181	182	177
		d ₂	4,58	4,56	4,54		172	174	175	
		d _m	4,55	4,51	4,50		174	178	179	
4	+300	d ₁	4,73	4,75	4,73	4,738	161	159	161	160,33
		d ₂	4,76	4,63	4,78		158	164	157	
		d _m	4,745	4,71	4,755		160	162	159	
5	+400	d ₁	4,92	4,92	5,05	4,94	148	148	140	146,33
		d ₂	4,90	4,92	4,94		149	148	146	
		d _m	4,91	4,92	4,99		148	148	143	
6	+450	d ₁	5,34	5,22	5,21	5,245	124	130	130	128,66
		d ₂	5,30	5,20	5,20		126	131	131	
		d _m	5,32	5,21	5,205		125	130	131	

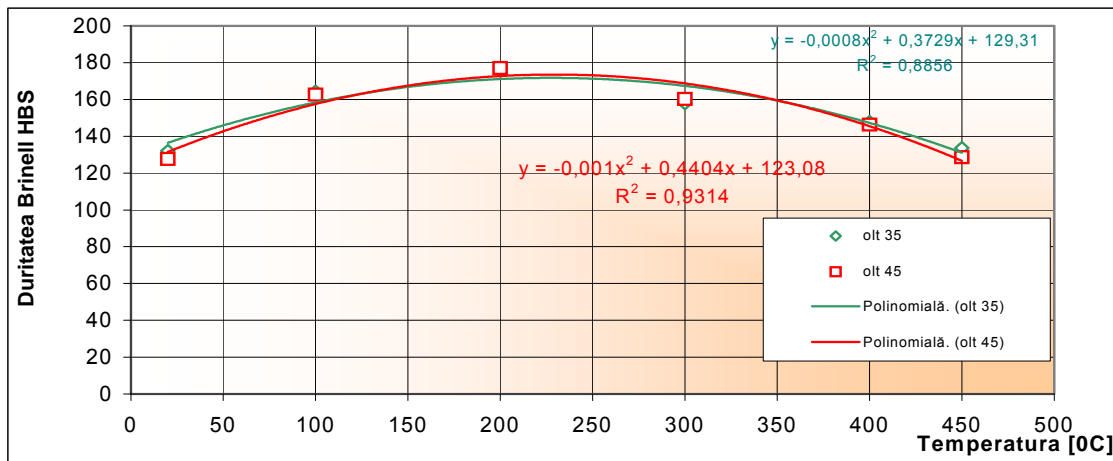


Fig.3. Variation curves of hardness versus temperature, for steels tested

This makes us conclude that one can determine the tensile breaking strength of steel, knowing its toughness and vice versa. Moreover, the literature gives relations between the two features.

REFERENCES

- [1.] Borzdík, AM, Methods goriaceh mehaniceschih ispitanii metallov, Moscow, 1962.
- [2.] Weber, F., Strength of materials, laboratory guide, Mirton Publishing House, Timisoara, 2000.
- [3.] SR EN 10003-1:1997, Metallic materials. Brinell hardness test. Part 1: Test method.
- [4.] Marchidan, DI Ciopec, M., Temperature - steps, methods and instruments, Scientific and Encyclopedic Publishing House, Bucharest, 1977.
- [5.] Mocanu, R.D., and others, Testing materials, vol. I. Destructive testing of metals, Technical Publishing House, Bucharest, 1982.
- [6.] Nădășan, st., Etc., tests and analysis of metals, Technical Publishing House, Bucharest, 1965.
- [7.] Rășănescu, I., Transfer phenomena, Didactic and Pedagogic Publishing House, Bucharest, 1984.
- [8.] Dascăl, A., Contribution to study the behavior of steels at elevated temperatures, PhD thesis, Timisoara, 2004.
- [9.] Dascăl, A., Behaviour of steel hardness test baking at high temperatures, Annals of the Faculty of Engineering of Hunedoara, Tom IV, Fasc.3, 2002.





^{1, 2} Siniša KUZMANOVIĆ, ² Milan RACKOV

THE INFLUENCE OF AXIAL LOAD AT OUTPUT SHAFT OF UNIVERSAL WORM AND HELICAL-WORM GEAR UNITS ON THEIR THERMAL POWER CAPACITY

^{1, 2} UNIVERSITY OF NOVI SAD, FACULTY OF TECHNICAL SCIENCES, SERBIA.

ABSTRACT:

Universal worm and helical-worm gear units are among the mechanisms that operate with a relatively low level of efficiency for which their thermal power capacity is paid extremely high attention. Value of thermal power limit for gearboxes with free input shaft is particularly defined in the catalogue, enabling their correct choice, i.e. enables the timely assessment of the needs of taking certain procedures in order to overcome problems that may arise due to excessive heating of reducers. Thermal power capacity of motor gear reducer is taken into account when defining a range, i.e. when combining (connecting) the motor and gearbox which is made according to the catalogue, so that the problem is not noticeable to the customer. Today, in an era of tough competition, it is necessary to consider the impact of external overhung and axial loads applied to output shaft on the thermal power capacity of gearbox, so that it could be eventually taken into account when gear reducer is selected. This paper deals with the problem of reducing of thermal power capacity of gearboxes due to external loads of output shaft, i.e. it deals with additional heating due to increased power loss in the bearings. At the end it is concluded (as expected) that the effect of those loads is negligible and there is no need to take them into account when selecting the gear unit, because it does not achieve any effect.

KEYWORDS:

worm and helical-worm gear units, thermal power capacity

1. INTRODUCTION

When choosing a universal worm and helical-worm gear reducer, service factor is selected from the catalogs of almost all manufacturers of gearboxes according to the service nature (uniform, medium and heavy), operating time during a day (0 to 24 hours), starting frequency – number starting during an hour (from 0 upwards), ambient temperature, the effective operating of reducer in an hour (so called ED factor), permissive overhung and axial loads of the output shaft (and input shaft for gear reducers with solid shaft) and thermal power capacity, accounting that the electric motor drives gearbox. However, when the large overhung and axial loads are applied, in this case only axial load on the output shaft, it comes to additional heat generating of gear reducer and thus reducing its thermal capacity. This can cause excessive heating of gear unit (usually above 80°C, or even 100°C), which may, mainly due to changes in size, have bad influence on their operating. Therefore, in this paper it is necessary to consider the influence of external axial load on the thermal capacity of the worm and helical-worm gear unit and, perhaps, suggest ways to not occur problems due to excessive heating of gearbox.

2. THE AIM OF THE STUDY

The main objective of this paper is to point out the importance of thermal capacity of worm and helical-worm gear units, as well as the influence of the external axial load on the output shaft to the value of this capacity.

3. PROBLEM INTERPRETATIONS

Universal worm and helical-worm gear units can be delivered with motor or with free input shaft. If they are delivered with electric motors, they can be delivered with special motors, so called geared motors, or with standard (IEC) motors. What electric motors will be used depends on the attitude of the manufacturers company as well as specific demands of the customer [1].

If gear units are delivered with free input shaft, they can have usual solid input shaft and with IEC motors interface.

Large manufacturers usually use special motors, which are characterized by special flanges, special diameters of output shafts, stronger bearings and better sealing solution, so they have a number of advantages (easier, cheaper and more compact design, the possibility of achieving higher gear ratios, greater permitted force of the motor shaft and better tightness). Since they are buying large quantities of such motors, they get them quickly and at almost a price of standard motors, so that this procedure is completely payable to manufacturer. In addition, these manufacturers usually have their own factory of electric motors, so that they do not have practically this problem.

Small and medium manufacturers of gear units usually use standard IEC motors, although it is not the rule, mainly because of lower cost and short delivery time, and all the benefits of special motors they try to compensate by suitable way of installing motor to the gear unit. Since it is difficult to make up a lot of advantages of special motor, in practice there are different construction solutions of installing gear unit with standard IEC motors that are directly, or with IEC motors interface, connected for the housing of gear unit.

Gear units with standard IEC motors are delivered by large manufacturers, who use special geared motors, especially when customers require. For example, when customer wants to install motors on purchased gear units by himself. It is usually case when they think they can do cheaper or faster service of their motors, or in case of export of gear units in the country, where there are factories of electric motors, which wants with a large taxes on motors to protect their products from foreign competition, and customers are payable to buy electric motors, so they buy gear units with free input shaft motor, usually, with IEC motors interface, which allow them much easier and more secure mounting IEC motors, so that there is no possibility to install motor incorrectly.

Regardless of the type of the applied electric motor, it must consider that power losses originated in the gearbox must be delivered to the surroundings [1]:

$$P_L = P_{in}(1-\eta) = Q \leq Q_o = \alpha A \Delta\Theta \quad (1)$$

where: P_L – losses in the gearbox,

P_{in} – input power of gear reducer,

η – efficiency of gear reducer,

Q – heat flux caused by originated losses,

Q_o – maximum heat flux that can be transmitted to the ambient,

α – coefficient of heat transmission,

A – the surface area of housing of gear reducer that can exchange heat,

$\Delta\Theta$ – temperature difference, where $\Delta\Theta = \Theta - \Theta_o$,

where: Θ – the temperature of surface of reducer

housing, usually it is considered that maximum

temperature is $\Theta = 80...100^\circ\text{C}$ [1] and Θ_o –

temperature of ambient where the gearbox operates.

From equation (1) it follows that the value of the

thermal power capacity (P_Q) is [3]

$$P_{in} \leq P_Q = \frac{\alpha A \Delta\Theta}{1-\eta} \quad (2)$$

This means that thermal power limit is the greatest power in the input at which, in a permanent operating, obtained losses in the gearbox can be transferred around without excessive heating of gear reducer (Fig.1).

It should take into account that the speed of heating depends exclusively on operating regime, input power, thermal inertia of gear reducer (of its mass) and selected cooling method. So, when choosing gear, among other requirements it must be met the following condition: $P_{in} \leq P_Q$.

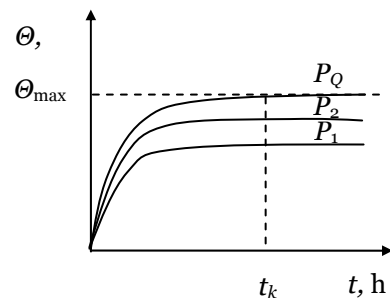


Figure 1. Graphical review of heating gear reducers depending on the input power (where t – time of heating, t_k – critical time when maximum permissible temperature is achieved (Θ_{max}), Θ – temperature of the gearbox housing, P – input power of gearbox)

When developing a catalog of geared motor, i.e. when the manufacturers compose the assembly of driving and gear unit (geared motor), they concern to fulfill this condition, and they account that the normal temperature of outside air is $\theta_o = 20^\circ\text{C}$. When gear reducer operates at higher ambient temperatures, the value of thermal power capacity is corrected by special coefficient.

However, when selecting gearbox with free input shaft, the customers are referred by manufacturers (in their catalogs) to detailed procedure of gearbox selection, so that problem must be considered by customers (designers) that make procedure for gearbox installation, in order to avoid possible accidents that may occur in the overheated gearboxes.

4. DESCRIPTION OF WAYS OF SOLVING PROBLEMS

When selecting gear reducer with free input shaft, it must be provided:

$$T_N \geq T_{out} f_B \quad (3)$$

where: T_N – nominal torque,

T_{out} – output torque,

f_B – minimum value of the service factor.

When selecting motor gear reducer it is indirectly defined by service factors [2, 4, 5]

$$f_{Bperm} \geq f_B \quad (4)$$

where: f_{Bperm} – permissive value of service factors given in the catalogs for each motor power, speed and size of reducer (it is determined by expression $f_{Bperm} = T_N / T_{out}$),

f_B – service factor defined according to the type of loading, operating time in hours during a day, the number of cycles during an hour, the ambient temperature, the effective operative duration during an hour and, eventually, the desired life of gearbox.

So, the choice of gear reducer with solid input shaft is based on its load torque (T_N), or motor service factor (equat.5), as well as the permissive values of radial ($F_{Ri perm}$) and axial ($F_{Ai perm}$) loads of the free input shaft of gearbox (for gearboxes with solid input shaft) and radial ($F_{Ro perm}$) and axial ($F_{Ao perm}$) loads of the output shaft (for both types of gear units), Fig.2.

Additionally, the choice of gear reducer is also based on thermal capacity (equation 2), where it should take into account that thermal capacity depends on the ambient temperature, as well as on the size (and sometimes the shape and position of mounting) of gear reducer. Its values can be obtained as a table or a diagram (Fig.3).

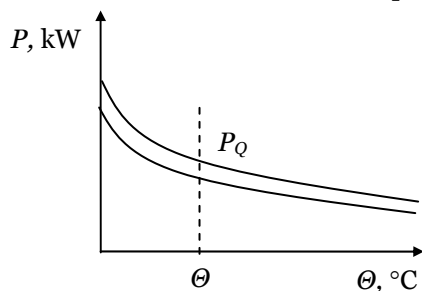


Figure 3. Graphic display of thermal capacity for particular size of gear reducer

so that today insulation material of class F is installed in motors (which allow their heating up to 150°C). Of course, the fan of electric motor does not allow reaching this temperature, but certainly because of higher temperatures of motor it comes to a stronger heating of gear unit, especially if the motor has bigger number of starting during an hour, and particularly if it is a motor with a brake which additionally heats the reducer.

Manufacturers of gear reducers are aware of this problem and take into account the thermal capacity of their gearboxes and try to increase it. They usually manage this by increasing the surface area of housing (i.e. by placing ribs on the surface of housing of gear unit), or by increasing the coefficient of heat transmission by defining of such forms of housing that will provide better air circulation around it, which is driven by a fan of electric motor (this is only applied for geared motor), or by placing a special fan (by manufacturers) on the worm shaft of worm and helical-worm gear reducer.

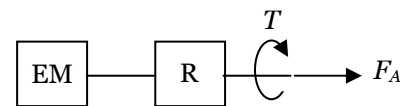


Figure 2. Schematic review of a loading of the output shaft of geared motor (EM – electric motor, R – reducer, F_A – axial load)

Thermal capacity is a little different for geared motor and gear reducer with solid shaft (with classic input or with input for IEC motors), because the fan of electric motor of geared reducer provides some greater air circulation and thus better cooling of reducer, while, due to the heating of electric motor, gearbox is subjected to somewhat larger heating from the motor. Sometimes these cooling and heating quantities can be canceled, and sometimes unfortunately not, so they should be separately shown in the diagram (or table).

In order to reduce the production cost of electric motors, it is going on a maximum reduction of material consumption, which causes faster heating of the motor,

Operating regime of gear units has also major impact on their thermal capacity. For example, service nature, operating time and number of starting can strongly affect on the heating and thus the thermal capacity of gear reducer. Especially different combinations of these parameters can strongly affect on the heating which is considered by service factor. The calculation of their actual impact is quite complex and can not be accurately described by mathematics, but very accurate values can be obtained by concrete measurements.

In the case that condition is not satisfied (equation 2), it is necessary to adopt a larger (stronger) gearbox, with a larger surface area participating in the exchange of heat, or it is need to use the system for cooling oil. For smaller sizes of gear reducers it is cheaper to select larger gearbox, while in medium and large size of reducer it is rational to use oil cooling system. The system consists of filter, circulating pumps, overflow and several classic valves, piping and heat exchanger with fan and electric motors.

The existence of an external axial load on the output shaft, which permissive limit values can be found in the catalogs of manufacturers of gear reducers, causes additional load of bearings of gearbox and the occurrence of additional friction in them (whose approximate value amounts $F_{\mu A} = \mu F_{Aperm}$ – friction in the bearing due to the external axial force) and it causes additional heating of gear unit. Since there is no additional overhung load, bearing will be subjected to maximum permissive axial force according to the catalog.

Additional losses of power in the bearing (P_L) can be calculated by the equation:

$$P_L = 1.05 \times 10^{-4} M n \quad (5)$$

where: n – number of revolution of output shaft, min^{-1}

M – total frictional moment of bearing

Total frictional moment of bearing (M) depends on several frictional moments as follows:

$$M = M_0 + M_1 + M_2 + M_3 \quad (6)$$

where: M_0 – load independent frictional moment, Nmm

M_1 – load-dependent frictional moment, Nmm

M_2 – axial load-dependent frictional moment, Nmm

M_3 – frictional moment of seals, Nmm

The frictional moment (M_0) is not influenced by bearing load but by the hydrodynamic losses in the lubricant and depends on the viscosity and quantity of the lubricant and also the rolling velocity. It dominates in high-speed, lightly loaded bearings and is calculated using:

$$M_0 = 10^{-7} f_0 (\nu n)^{2/3} d_m^3 \quad (7)$$

if $\nu n \geq 2000$ or using

$$M_0 = 160 \times 10^{-7} f_0 d_m^3 \quad (8)$$

if $\nu n < 2000$, where: d_m – mean diameter of bearing (for particular bearing $d_m = 0.5(d + D) = 0.5(30 + 72) = 51$ mm)

f_0 – a factor depending on bearing type and lubrication (for particular bearing $f_0 = 1$)

ν – kinematic viscosity of the lubricant at the operating temperature, mm^2/s (for operating temperature $\Theta = 40^\circ\text{C}$)

The load dependent frictional moment (M_1) arises from elastic deformations and partial sliding in the contacts and predominates in slowly rotating, heavily loaded bearings. It can be calculated from:

$$M_1 = f_1 P_1 d_m \quad (9)$$

where:

f_1 – a factor depending on bearing type and load

$$\text{for particular bearing and load: } f_1 = (0.0006 \dots 0.0009) \left(\frac{F_{Rperm}}{C_0} \right)^{0.55} \quad (10)$$

P_1 – the load determining the frictional moment, N, for particular bearing and load:

$$P_1 = 3 F_{Aperm} - 0.1 F_{Rperm} = 3 F_{Aperm} (F_{Rperm} = 0) \quad (11)$$

Frictional moment (M_2) which depends mostly on the axial load can be calculated as follows:

$$M_2 = f_2 F_{Aperm} d_m \quad (12)$$

where: f_2 – a factor depending on bearing design and lubrication (for particular bearing design and lubrication $f_2 = 0.006$)

The frictional moment (M_3) of the seals for a sealed bearing can be estimated and for particular bearing it is calculated as $M_3 = 18$ Nmm.

For a smaller size of gear reducer (with shaft height $h = 80$ mm) orientation values of frictional moments and additional losses of power in worm and helical-worm reducer are calculated and shown in Table. 1.

Table 1. Results of calculation of a typical worm gear reducer without a fan with shaft height 80 mm

Thermal capacity – P_Q , W	1500	920	280
Permissible axial force of output shaft – F_{Aperm} , N	5520	7800	7800
Speed ratio – u	5.4	26	79
Revolution number of output shaft – n , min ⁻¹	259	54	18
Load independent frictional moment – M_0 , Nmm	7.66	6.7	6.07
Load-dependent frictional moment – M_1 , Nmm	289.14	494.14	494.14
Axial load-dependent frictional moment – M_2 , Nmm	1689.12	2386.8	2386.8
Frictional moment of seals – M_3 , Nmm	18	18	18
Total frictional moment of bearing – M , Nmm	2003.92	2905.63	2905.01
Additional power losses in gear reducer – P_L , W	54.5	16.47	5.49
Percent ratio of power losses – $\frac{P_L}{P_Q} \cdot 100$, %	3.63	1.79	1.96

Based on carried out calculation it follows that the additional power losses in the gearbox, with the maximum permissible axial load of the output shaft, amounts about up to 3.63%. For lower speed ratio, power loss is less, not bigger than 2%. The power loss is bigger than only overhung load subjects the output shaft, but it is not so high and many manufacturers of gear reducer completely ignore it. When making the instruction for selecting gearbox, manufacturers of gear reducers, ignore the influence of external loads on the thermal capacity of gear unit and thus considerably simplify their selection of gear reducer.

5. CONCLUSION

Based on the conducted analysis it can be seen that the external axial loads of the output shaft of worm and helical-worm gear reducers have a small influence on the change of thermal capacity, usually about 2%, or for higher output speed up to 3.6%. Therefore, manufacturers of gear reducers ignore it with a full right, i.e. they do not take external forces into account when selecting gearbox and do not make correction in thermal capacity. This power loss would be more important for higher transmitted power with high output speed, when this 3.6% power loss is not negligible value, but it is a very rare case.

REFERENCES

- [1] KUZMANOVIĆ, S., *Universal Gear Reducers with Cylindrical Gears*, University of Novi Sad, Faculty of Technical Sciences, Novi Sad, 2009. (in Serbian)
- [2] Catalog SEW Eurodrive, Movimot Gearmotors, Edition 04/2004
- [3] SKF General Catalogue, 2007
- [4] Catalog Nord, Constant speeds, G1000/2008, Getriebebau Nord, Hamburg
- [5] Catalog Siemens, Flender Gear Units, Catalog MD 20.1-2009







¹Krassimir E. GEORGIEV

ADVANCED DESIGN OF MECHATRONIC WORKSTATIONS FOR TECHNOLOGICAL CONTACT OPERATIONS

¹BULGARIAN ACADEMY OF SCIENCE, INSTITUTE OF MECHANICS,
MECHATRONIC SYSTEMS DEPARTMENT, SOFIA, BULGARIA

ABSTRACT:

The objective of this paper is to outline the necessity of understanding vertical and horizontal system integration in advanced mechatronic systems. A Methodology, theoretical aspects and some practical results of creating and research of distributed mechatronic environment are presented, based on robotic assembly systems and 3D virtual models. A global algorithm for simulation and advanced design is presented as well.

KEYWORDS:

advanced mechatronic systems, system integration, global algorithm, simulation

1. INTRODUCTION

The flexibility of a mechatronic system can be obtained either by making its mechanical and electronic part as universal as possible or by constructing a large set of simple models which will be interchanged whenever the task of the system changes. In the latter case the mechanical and electronic structure of the system can be tailored exactly to the needs of the task at hand.

In both cases the control of such system is implemented in software. The software should be structured as a library of procedures and functions possibly concurrent, which will be used as software blocks for construction of the control system.

Virtual product models, together with adapted development methods and processes are the key to an integrated view of development, manufacturing and usage of products as they promise a significant increase of efficiency, quality and flexibility of product development.

For ROBOTIC and MECHATRONIC systems the coupling of subsystems could be realized on three different levels – physical modeling, mathematical modeling and behavioral modeling. At physical description and modeling a system is represented by physical models, for example as a multibody system, containing rigid bodies, joints and coupling force elements. The mathematical description and modeling is a representation of a system by mathematical equations which can be derived from the physical model description, e.g. the equations of motion of a multibody system.

The simulation results of the mathematical model description are considered as the behavioral model description - the trajectories of position and velocity of the bodies. Then coupling of models in the behavioral model description is referred to as simulator coupling, modular modeling and simulation or virtual assembly of them. The simulation of the global system is realized by time discrete linker and scheduler which combines the inputs and outputs of the corresponding subsystems and establishes communication between the subsystems to discrete time instants. Therefore it is possible to use different software packages for each subsystem and then to link the solvers together. Now the general modeling and design of MS may be presented in form with respective levels of task simulation and planning (distributed mechatronic environment). The modular description of systems allows for independent and parallel modeling of the internal dynamics of each subsystem. The inputs and outputs of the physical model are also physical quantities such as forces or motion of the bodies.

Here the main goal is to present a modular –block concept, mechatronic approach and 3D virtual environment for real time computer control, complex simulation and interactive user's design solutions of mechatronic (robotic) systems for contact operations.

2. DESIGN APPROACH AND MODELING OF DESIGN ALTERNATIVES

The full dynamic model is presented in previous author's publications and here we shortly note that, the models derived, based on the Lagrange's equations have the advantage that they are in closed form concerning the geometrical, inertial and functional parameters of the mechanical system. The joint reactions are excluded and considering the immense computational power of today's computers one can successfully explore various aspects of the dynamic modeling of the robotized system. This enables us to carry out dynamic synthesis of the technological movements and to build a strategy for dynamic behavior. Based on the derived equations we can compute the appropriate joint torque of the regional structure of the assembly robot, considering the predefined generalized coordinates $q_i = q_i(t)$ and the finite increments of the generalized coordinates $o_i = |q(t_i) - q(t_i - 1)|$, in order to minimize to total system energy and power consumption. Using MATLAB and Solid Works environments, we can derive effective solutions for the corresponding parameters m_i, l_i, h_i, J_{sk}^i as well as get results applicable in the practice in order to achieve higher velocities and minimal duration of the technological assembly.

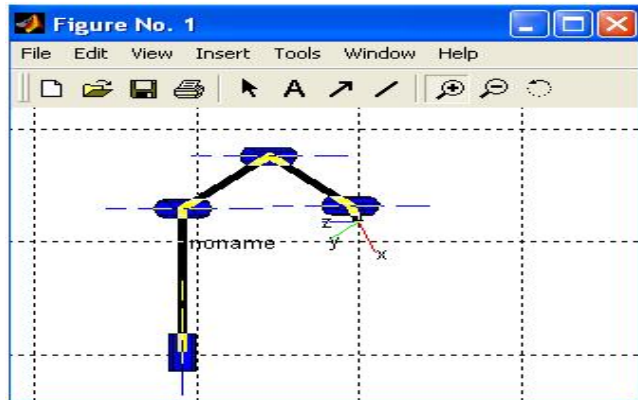


Fig. 1. Matlab simulation of robotic regional structure

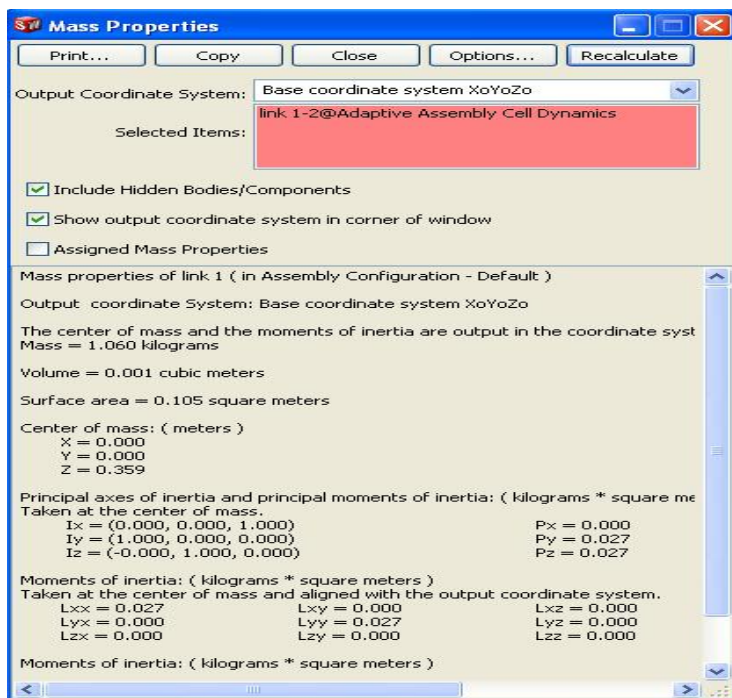


Fig.2. Solid works simulation of mass/inertia properties of robot links

is why it was necessary to validate the results. For this purpose a mathematical kinematic computer model was built and researched using Matlab v6 combined with the specialized software toolbox Robotics Toolbox. The kinematic model was introduced using Denavit-Hartenberg convention. The direct and inverse kinematics was solved and the results were exported to the 3D robot model. Based on respective simulations we obtain the following results: at lower values of angular velocity of driving shaft and higher spring stiffness the driving robot torques are extremely low and the influence of initial contact between the assembled details is minimal. This fact is

Using the original author's idea of designing the system from modular structures with 3R active joints and adaptive sockets (accommodating the concept of local dynamic compliance), we are able to combine higher speed, thus obtaining solutions to the extremely difficult assembly tasks of prismatic details without chamfers. After the virtual 3D model is built (using Solid Works environment) it is possible to conduct various simulations. This enables us to research the model, carry out different scenarios to see what will be the behavior of the real adaptive assembly cell. The results from the kinematic simulations are presented further in the paper. However the question of the validity of the model is always open. Even in the user's guide of the simulation product is written that one shouldn't rely solely on the obtained results. That

confirming at the investigation of robot joint reactions at the computer simulations. The ultimate purpose is to achieve a system performance superior to what can be achieved by traditional development and design cycle. The author's idea follows this approach and mechatronics principles to close the open kinematic chains, using control and information loops. Then is possible to estimate different parameters of RS, to compliance them and to achieve complex properties: Adaptively, reconfigurable structure, energy efficiency and high performance.

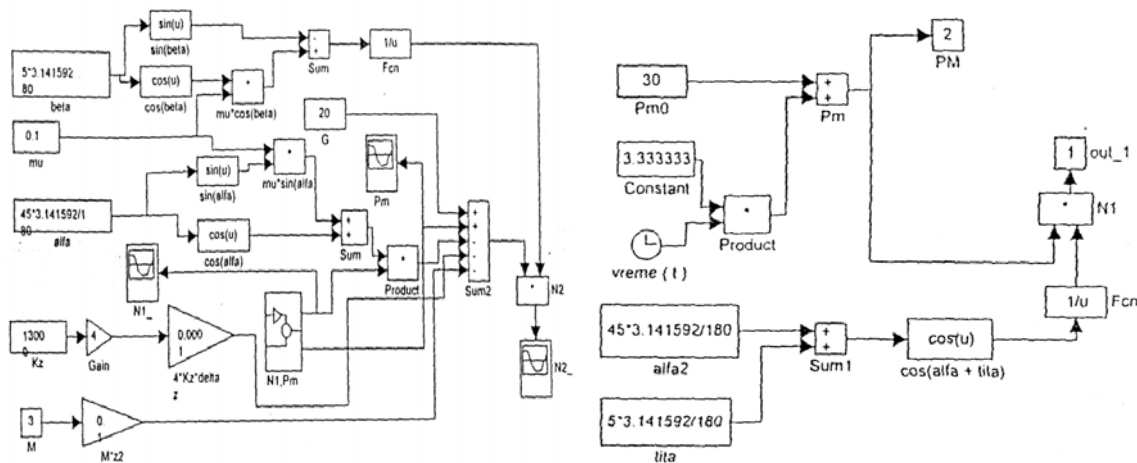


Fig.3 Simulink modeling of contact stages, during adaptive assembly

Therefore for the 6 R robotic structure the axis models are represented with the modules (blocks)- controller, motor, gearbox (including gear elasticity, damping and bearing friction) and mechanical part. The calculated parameters are involved in the 3D kinematic model of the robotic system, using Solid Works 2005 - Cosmos Motion 2005. It is also possible to simulate the space contact at the adaptive assembly, using appropriate data of materials and dry friction forces. The respectively modular component of distributed mechatronic environment is shown on fig 4.

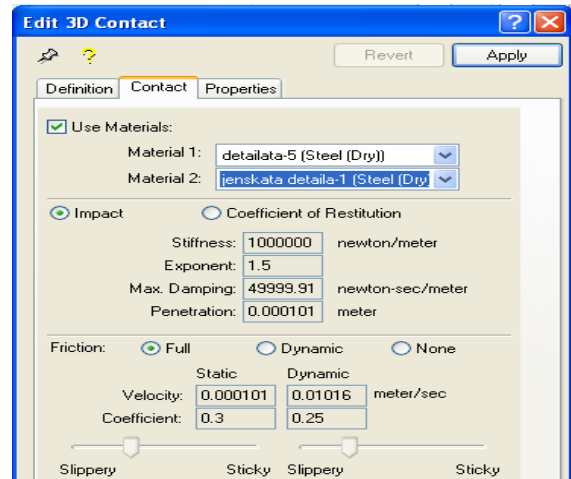


Fig 4 .Module of 3D contact interaction

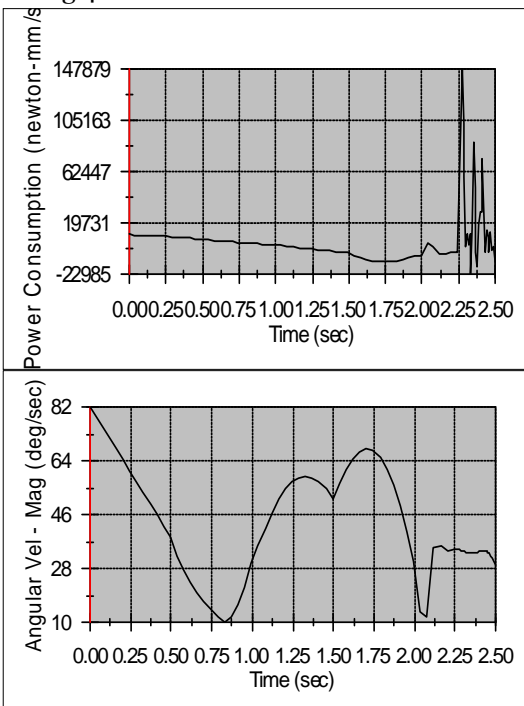


Fig. 5. Power consumption and angular joint velocity

The mechatronic environment consists of different number modular components and mechatronics procedures. Each procedure consists of 5 steps:

- ❖ Initial synthesis of 3D kinematical models
- ❖ Preliminary metrical synthesis
- ❖ Preliminary synthesis of control functions, direct and inverse dynamic tasks
- ❖ Using multivariant analysis and varying the important characteristics to obtain optimal design of building modules
- ❖ Final synthesis of the control functions (optimization) accounting for the full dynamic models

The full process of modeling and design we denote as synthesis by using analysis.

The modular component structure of environment supports a rapid exchangeability of models and allows spreading out modeling tasks and skills to different researchers in order to achieve sophisticated integration of capable models, reduce

developing time and costs. The given examples show both the necessity for applying a mechatronic design and simulation environment. This way the feasibility of highly complex systems can be studied by the combined efforts of numerical computation, simulation and CAD design (fig.5,6,7) . Effective system modeling needs of distributed simulation environment and respective subfunctions and subconfigurations F^i_j, C^i_j (fig.7), concerning to database of different components: Sockets, actuators sensors, controllers, etc.

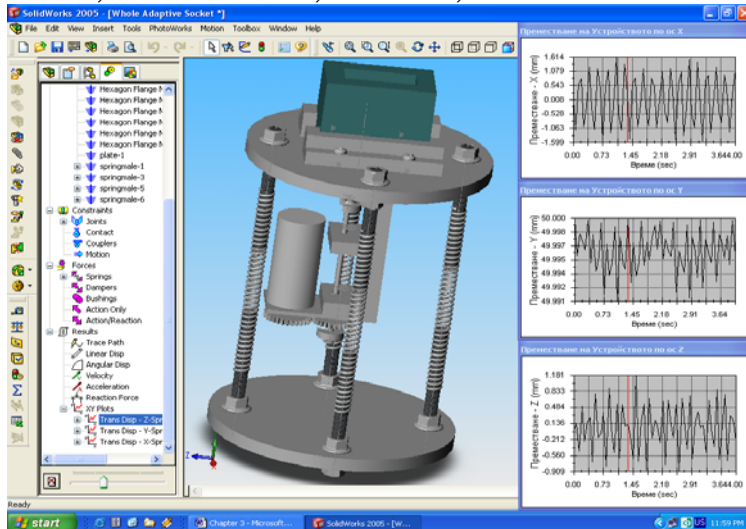


Fig.6 Modelling and simulation of adaptive assembly socket

In accordance with the above mentioned principles a virtual model of an adaptive assembly socket is realized and it is further more developed to a whole. The three dimensional model of the device is built using Solid Works 2005 environment assuming that all main dimensions of the real model are exactly reproduced. The correct construction and mating of all the details in the assembly allows us to create a virtual assembled model of the adaptive assembly socket and a family sockets.

Furthermore a 3D model of a whole robotized unit is developed. The goal is to

investigate and research the process of adaptive assembly using the developed devices. There have been various simulations with different parameters of local micro motion.

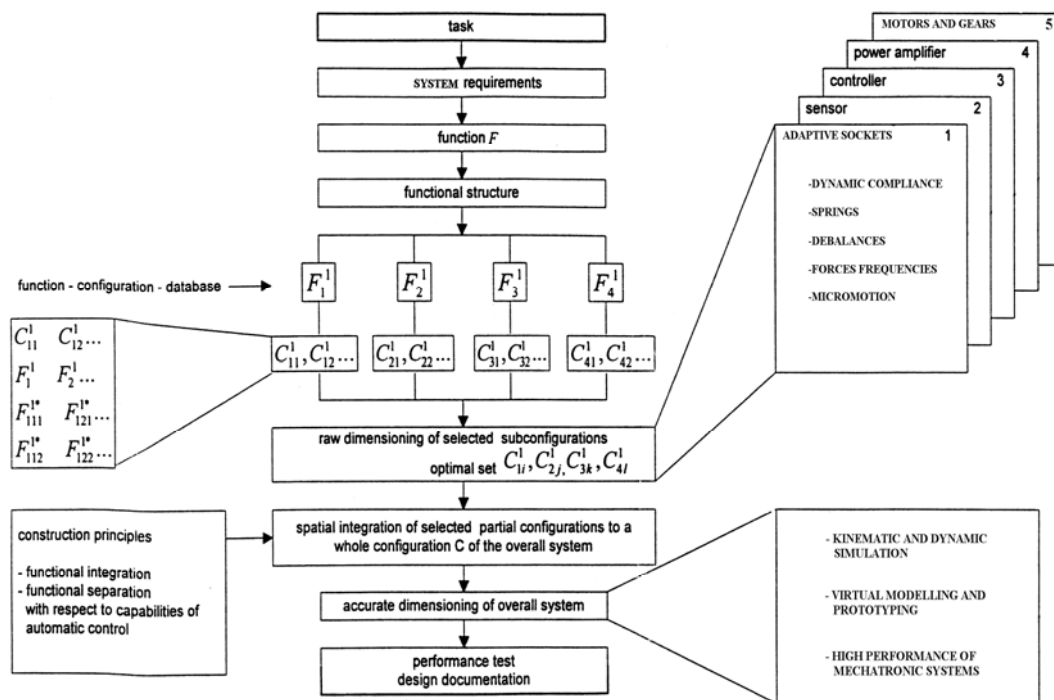


Fig.7. Design and simulation algorithm
 (subfunctions and subconfigurations of complex robotic system)

Based on this methodology and interactive mechatronic environment, a real structure and solutions of adaptive robotic system are obtained. Real positioning accuracy and speed are improved, more than 15 % and the development time reduced more than 40%. Emphasis has been put on lightweight design and simulation, reconfiguration and different controller solutions. A raw draft of a controller or topological optimization can already be done with quite simple mathematical descriptions at an early stage of development. The model development can be performed in steps and adding of sensors will not affecting the modeling procedure of the submodel. The massive computational resources now available make it possible to treat the full

parametric description of a much more general class of robotic units, so the researcher can think much more freely of generic design and control strategies which should lead to a maximum level of productivity of new ideas and technology evaluated by complete simulations. The next step is to use elaborate ways of modeling and description methods to cover all subtasks of this system in an integrative matter.

3. SENSOR BASED TASKS- MODELING AND SIMULATION

Let us first summarize the similarities and differences between non-contact sensor based tasks and force based tasks.

The task-function approach applies to both problems. The implementation of a control law involves two levels:

- ❖ High level consist of specifying the task to be performed and of choosing the vector of signals to be regulated in order to fulfill the user's objectives (choice of so called task function)
- ❖ Low level consists of writing and computing a control law (actuator torques):

$$T = M(q)\ddot{q} + N(q, \dot{q}, t), \dim(q) = \dim(M) = n \quad (1)$$

where: T is the vector of applied actuator torques; M is the kinematic energy matrix; N gathers gravity, coriolis, centrifugal and friction forces; q, \dot{q} - constitute the natural state vector of the system.

It may be shown that an efficient way to specify the objective that researcher wishes to reach with the robot consists of defining an output n-dimensional function e (q,t), called task to be regulated to zero during a time interval [0,T], starting from initial position q₀. A realistic approach to practical design and simulation of control laws is suggested in the form:

$$T = -K\hat{M} \left(\frac{\partial \hat{e}}{\partial q} \right)^{-1} G \left(\mu \underline{D} e + \frac{\partial \hat{e}}{\partial q} \dot{q} + \frac{\partial \hat{e}}{\partial t} \right) + \hat{N} - \hat{M} \left(\frac{\partial \hat{e}}{\partial q} \right)^{-1} \quad (2)$$

where: symbol ^ points out that models (approximations, estimates) are used instead of the true terms. In this general expression all the terms except μ , \underline{D} , \underline{G} are allowed to be functions of q and t (here f comes from the difference of e, \underline{G} and \underline{D} are positive matrices; K and μ are positive scalars, all to be tuned by the researcher). Some terms (\hat{M} , \hat{N}) depend mainly on the used robots, while others also depend on the considered tasks, sampling period of the control laws. The performance of the feedback control loops is very sensitive to the sampling rates and propagation delays between measurements and control emission. Their value must be guaranteed in order to tune the gains of the loop.

At the equilibrium i.e. in the absence of motion the model reduces to:

$$T_{eq} = G(q_{eq}) + T_c = G(q_{eq}) + J^T(q_{eq})F_{eq} \quad (3)$$

where: J is the Jacobian matrix associated with the gripper. The differences between two classes of tasks – contact and noncontact come in part, from the physical characteristics of real contacts. For example – friction forces have to be modeled so as to estimate their contribution to the measured contact force. Then we may say that virtual contacts are easier to control than real contacts (assembly, grinding and polishing). Some knowledge of the interaction matrix is needed in the case of non-contact sensors and in both cases fine control of sensor-based tasks may require the use of dedicated estimation algorithms. Problem solutions very commonly rely on decomposition into smaller more easily understood solutions, ie the braking down of a problem into soluble parts. The whole process of investigation and creation can be represented in the form of splitting, effectively component solutions and integration after that via electronical (information) means. Physical integration is possible as well, for example intelligent actuators with sensors and etc.

4 . CONCLUSIONS

- ❖ To improve the reliability of Complex robotic systems ,make them faster and reduce the costs we have to use mechatronic environment for design and investigation,
- ❖ mechatronic modular-parameric approach to the horizontal and vertical integration and CAD integrated solutions (3D solutions)
- ❖ Sensor based control via aggregation of sensor data
- ❖ Virtual prototyping of mechanics and control via iterative mechatronic procedures (including so called hardware in the loop simulations)

This is perhaps the most efficient and modern way to the creation and application of High-performance intelligent manufacturing systems in the industry.

REFERENCES

- [1.] ISSI T., Mechatronics , Moscow, 1988 (in Russian).
- [2.] HONEKAMP R.et al., Structuring approach for complex mechatronic systems, Proceedings of ISATA, Florenz, VI.1997.
- [3.] GEORGIEV Kr., Robotic systems for adaptive assembly, D.Sc.Thesis, 2003, 278 p., Sofia, BAS.
- [4.] GEORGIEV Kr., Mechatronic assembly system with reconfiguration, Journal of Technical .Ideas, BAS, Sofia, 2005,(1).
- [5.] HOLLERBACH J., Kinematics and dynamics for control in "Robotics Science", MIT,Cambridge, 1989.
- [6.] GALABOV V., Synthesis of mechanisms for robotics ,Sofia ,TU edition ,1992 ,263 pages
- [7.] PAVLOV V., Design of industrial robots, Sofia, 1993, 207 pages.
- [8.] GEORGIEV K., Hybrid mechatronic systems for adaptive assembly and welding , Cd Proceedings of 12th international symposium MECHATRONIKA 2009 , ISBN 978-80-8075-209-5 ,Slovakia, 2009
- [9.] GEORGIEV K., Accuracy analysis of MICR positioning robotic systems, Proceedings of 7th International Conference on Biomechanics, Mechatronics and Robotics, Lepaya-Latvia, May 2010) , pp 59-63, ISBN 978-9934-10-027-7
- [10.] GEORGIEV K, Synthesis and analysis of hybrid mechatronic systems for contact tasks, Proceedings of 13th international symposium MECHATRONIKA 2010, Slovakia, pp. 62-66
- [11.] GEORGIEV K., KOTEV V., TIANKOV T, Callibration methodology for micro-nano robotic systems, Proceedings of 13th international symposium MECHATRONIKA 2010, Slovakia, Tr. Teplice, 2010, pp. 67-70, Proceedings registered at IEEE Xplore. DVD: (ISBN 978-80-8075-451-8; CFP1057K-DVD)PRINT: (ISBN 978-80-8075-457-0





¹ Juraj HUDÁK, ² Miroslav TOMÁŠ

ANALYSIS OF FORCES IN DEEP DRAWING PROCESS

¹ DEPARTMENT OF TECHNOLOGIES AND MATERIALS, TECHNICAL UNIVERSITY OF KOŠICE,
FACULTY OF MECHANICAL ENGINEERING, KOŠICE, SLOVAKIA

ABSTRACT:

Presented contribution deals with force parameters research (drawing and blankholding) in deep-drawing process of flat bottomed cylindrical cup. Experimental research was realised using steel sheets for enamelling KOSMALT produced by U.S.Steel Košice, Ltd. Deep drawing process of this steel is complicated due to contradictory requests from the view of steel structure: good drawability and good enameling. At the present, there are new ways how to ensure requested properties from both views [6].

KEYWORDS: force parameters, research, deep-drawing processes

1. INTRODUCTION

Production of pressings is realized using forming machines, which ones act by force onto initial blank through forming die. Therefore they change its initial flat shape onto semi-finished or final product. Forming processes force parameters knows enable to technologists – forming processes designers and forming machines designers to dimension forming machine and forming die components. Besides, experimental research of forming forces allows process optimization, because they are complicated multi-factors systems. [1,2,3,5].

There are two types of sensors used in the field of force parameters research of deep-drawing processes – mechanical and electrical [3,4]. Experimental research of forces in deep-drawing processes is based on principle of non-electrical parameters measurement by electric way. Force parameters measurement (drawing and blankholding), is realized through elastic deformation element – dynamometer, which one is equipped by 4 tensometric sensors connected to Wheatston's bridge.

Experimental research of forces in deep-drawing processes is long-time realized in the Department of technologies and materials. In the past there was used measuring and monitoring system created by dynamometers (drawing and blankholding), voltage stabilizer, tensometric apparatus UM 131 and oscillograph for forces recording in force-time coordinates. Necessity of computer processing measured values required innovation of measured and monitoring system, where tensometric apparatus was developed and produced by INSPECT, Ltd. This tensometric apparatus has three canals for force recording and 1 canal for path recording and allows researching not only force-time relations, but also force-path relations.

Presented contribution deals with force parameters research (drawing and blankholding) in deep-drawing process of flat bottomed cylindrical cup. Experimental research was realised using steel sheets for enamelling KOSMALT produced by U.S.Steel Košice, Ltd. Deep drawing process of this steel is complicated due to contradictory requests from the view of steel structure: good drawability and good enameling. At the present, there are new ways how to ensure requested properties from both views [6].

2. METHODS OF EXPERIMENTAL WORK

Experimental measuring system

Research of forces in deep-drawing process was realised using with experimental measuring system machine-die-pressing consists subsystems:

1. double action hydraulic press Fritz Müller BZE 100
2. experimental drawing die with blankholder
3. pressing
4. measuring and monitoring subsystem for forces recording

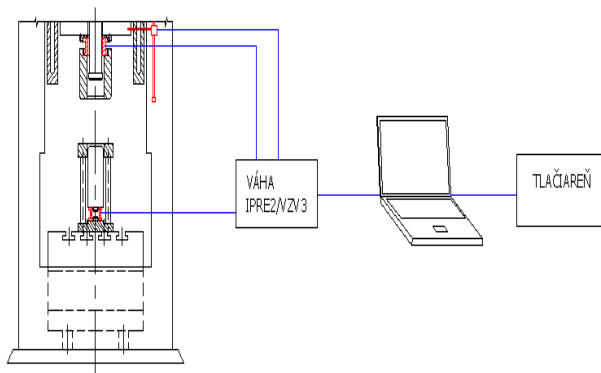


Fig. 1 Scheme of experimental measuring system.
 Cup, experimental material and experimental forming die

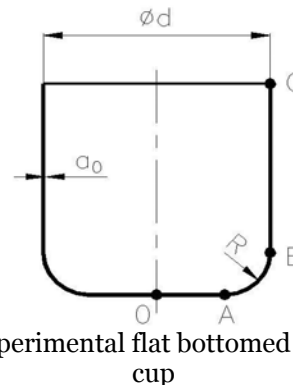


Fig. 2 Experimental flat bottomed cylindrical cup

2). These cups were deep-drawn in experimental drawing die with blankholder (punch diameter $\varnothing 73,5$ mm, die diameter $\varnothing 76$ mm, punch radius $r_p = 5$ mm, die radius $r_t = 6$ mm). Drawing of pressings with outside diameter $\varnothing 76$ mm were realised from initial blank diameters $\varnothing 125$ mm, $\varnothing 134$ mm, $\varnothing 139$ mm a $\varnothing 145$ mm.

As an experimental material there was used cold rolled drawing quality steel sheet for enamelling KOSMALT 190.21 with thickness 0,8 mm produced by U.S.Steel Košice, Ltd. Directional values of mechanical properties, normal anisotropy ratio and strainhardening exponent are shown in Table 1.

Table 1 Material formability values of KOSMALT 190.21, $a_0=0,8$ mm

direction [°]	$R_{p0,2}$ [MPa]	R_m [MPa]	A_{80} [%]	r	r_m	Δr	n	n_m	Δn
0°	181	287	44,7	1,910	1,802	0,727	0,203	0,212	-0,006
45°	186	304	38,2	1,438					
90°	183	289	44,7	2,422					

Drawing punch and die of experimental modelling die were fastened onto press ram first and on press bed last mentioned by blankholder and drawing dynamometers. Blankholding force in drawing process was implied by rods to which act drawing cushion placed in the press bed. Blankholder dynamometer, fastened onto drawing die in the press ram, records overall force, drawing dynamometer records drawing force only. Final blankholding force is then calculated as a difference between overall force and drawing force. Path reader was placed in the left press shoe, where press ram movement was transferred onto slider movement of digital ruler SD-60.

Measuring subsystem for scanning and recording of drawing forces

Measuring subsystem for drawing forces recording consists:

1. dynamometers - drawing and blankholding (Fig. 3a)
2. path reader – digital ruler Mitutoyo SD-60 (Fig. 3b)
3. tensometric apparatus IPRE2/VZV3 (Fig. 3c)
4. notebook PC – Pentium III (Fig. 3c)
5. joining cables CANNON 9F/9M and RS232 cable

Tensometric apparatus (called weighing-machine by producer) IPRE2/VZV3 is set to continuous force measurement (weighting) and synchronised path reading from digital ruler SD-60. Electronics allows from 1 to 3 dynamometers reading and path reading. Also shows measured values of each dynamometer or path reader on display. It is also possible to set required sensor on display and set sampling frequency by which are measured and recorded data send to PC. Communication between tensometric apparatus and PC is realised through RS232 interface and apparatus is connected to PC by serial port. Data are send to PC in text file in ASCII code and allows simple importing to Excel. All communication and data sending is realised by Hyperterminal, which is standard part of MS Windows operating systems.



Fig. 3 Components of measuring subsystem for recording forming forces
 a) – drawing force dynamometer, b) path reader Mitutoyo SD-60,
 c) tensometric apparatus IPRE2/VZV3 interconnected with PC

3. REACHED RESULTS AND INTERPRETATION

Graphic courses of drawing and blankholding forces at deep-drawing of flat bottomed cylindrical cup without failure are shown in Fig. 4 to Fig. 6 for each initial blank diameter. Graphic course of drawing and blankholding forces at deep-drawing of flat bottomed cylindrical cup from initial diameter where broken cup occurs is shown in Fig. 7

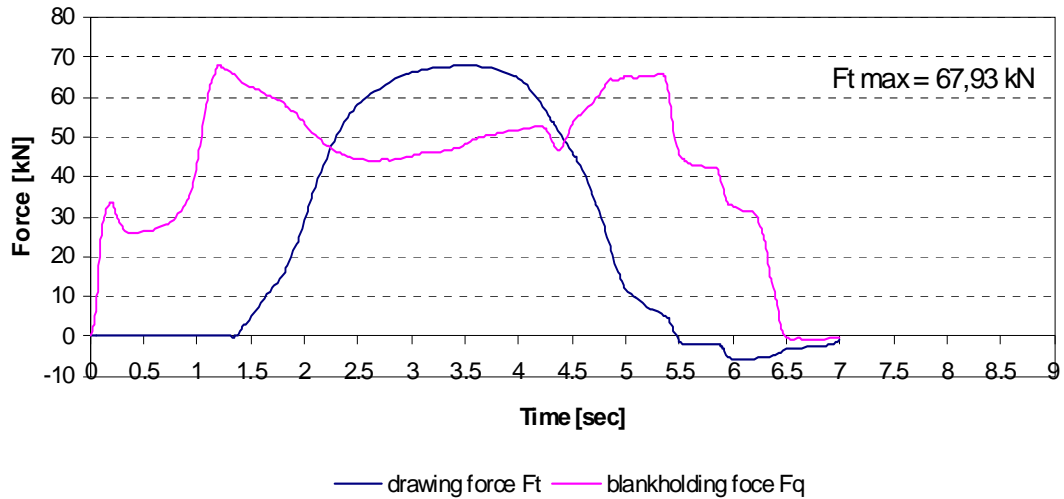


Fig. 4 Course of drawing and blankholding forces, $D_o = 125$ mm, $m = 0,608$

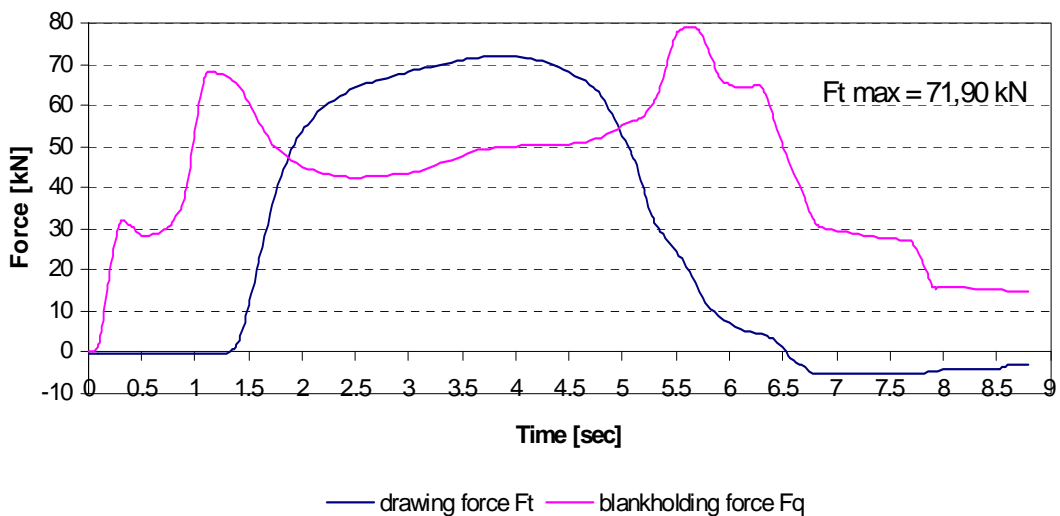


Fig. 5 Course of drawing and blankholding forces, $D_o = 134$ mm, $m = 0,567$

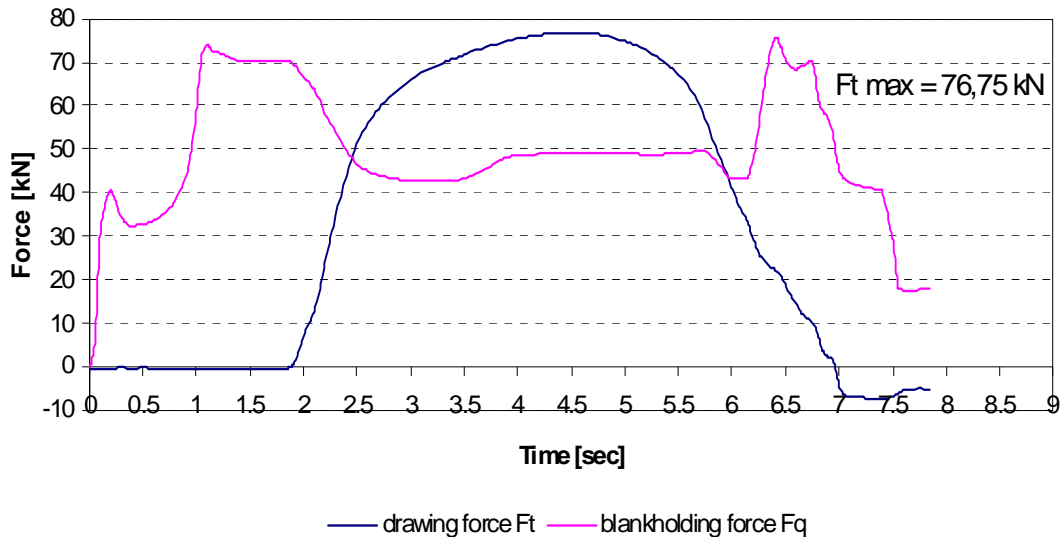


Fig. 6 Course of drawing and blankholding forces, $D_o = 139$ mm, $m = 0,547$

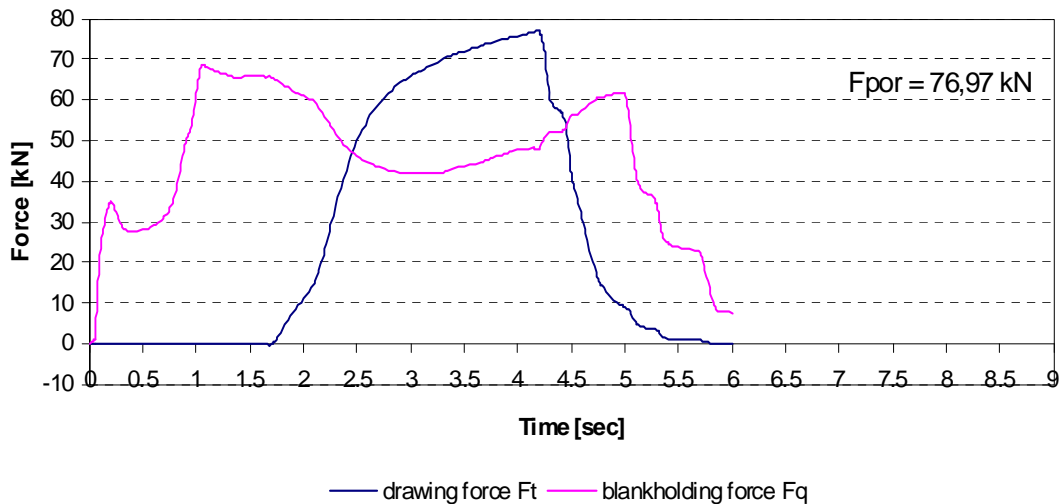


Fig. 7 Course of drawing and blankholding forces at cup breaking $D_o = 145$ mm, $m = 0,524$

Courses of drawing force at deep-drawing of flat bottomed cylindrical cup without flange from initial blanks, where no cup breaking occurs are typical for limit drawing case – drawing from flange. Drawing force increases rapidly at first stage next grows up slowly until drawing force maximum and then decreased. There is clearly seen maximum drawing force increasing with drawing ratio m decreasing. The area below drawing force line also increases. As a limit drawing ratio could be considered here drawing ratio $m = 0,547$ because of maximal drawing force ($F_t \text{ max} = 76,75$ kN) is nearly to cup breaking force ($F_{por} = 76,97$ kN). Limit drawing ratio was observed at deep-drawing of initial blank diameter $D_o = 139$ mm, while cup breaking force was reached at deep drawing of initial blank $D_o = 145$ mm, where drawing ratio is $m = 0,524$.

Course of blankholding force has a dynamic character at the first stage, when blankholding touch down the drawing die. After rising up to 70 kN approx. drawing process begins and blankholding force decreases rapidly. Blankholding force decreasing could be explained as a response of press hydraulic system to press ram force movement, but there is also blankholding area decreasing due to drawing-in to die. Blankholding is then stabilised on 50 kN approx. When maximal drawing force is reached and is decreased, blankholding force increased again to initial value and next drops down after cup is drawn.

Dynamical processes at the beginning and at the end of cup drawing presents response of used machine, where there was used double action hydraulic press Fritz Müller BZE 100 equipped with drawing cushion placed in the press bed. Deep-drawing was realised using Vantol S lubricant.

Course of drawing and blankholding force at deep-drawing process when cup broke shows the same character in the first stages, as it is in deep-drawing of unbroken cup. After maximum drawing force is reached, drawing force sharply decreased. Maximum drawing force is called cup breaking force in this case. Cup breaks at the bottom to cup wall transition – at the cup radius, whereby bottom is tear off from cup wall.

4. CONCLUSIONS

From realised experiments follows:

1. course of drawing force at flat bottomed cylindrical cup without flange deep drawing process with blankholder respond to limit drawing case of deep-drawing from flange,
2. decreasing the drawing ratio caused maximal drawing force growth until cup breaking force,
3. course of blankholding force has a dynamic character at the start and at the end of deep-drawing with stabilized course when cup is drawn. This dynamic character represents response of press hydraulic system on deep-drawing process.

Realised measuring subsystem for drawing and blankholding forces recording allows realising power parameters research of deep-drawing process in dependence force-time with sampling frequency up to $0,01 \text{ s}^{-1}$. When path reader Mitutoyo SD-60 is used also, sampling frequency decreased up to $0,1 \text{ s}^{-1}$, what suit to static processes only. For that reason we consider to buy path reader with sampling frequency up to $0,01 \text{ s}^{-1}$, but also modification of tensometric apparatus is needed.

The advantage of measuring and monitoring subsystem is possibility to use it on whatever machine. The main restriction is the maximal allowed loading of used dynamometers, over crossing which leads to its plastic deformation.

The matter of this contribution is a part research project APVV-0629-06 [7], which is solved on Department of technologies and materials, Faculty of Mechanical Engineering, Technical university of Košice.

REFERENCES

- [1] BLAŠČÍK, F. – POLÁK, K.: Teória tvárnenia. Alfa Bratislava, 1987
- [2] SPIŠÁK, E. – BEŇO, J. – TOMÁŠ, M. – VINÁŠ, J.: Teória konvenčných technológií. TU v Košiciach, Strojnícka fakulta: 2009, 162 s. ISBN 978-80-553-0201-0
- [3] BAČA, J. – BÍLIK, J. – ŽATKOVIČ, J.: Experimentálne metódy v tvárnení. Bratislava, Vydavateľstvo STU Bratislava, 2000
- [4] KLEMENTEV, I. – KYŠA, R: Elektrické meranie mechanických veličín, ALFA Bratislava, 1990
- [5] BÍLIK, J. – BALÁŽOVÁ, M. – KRŠIAKOVÁ, L.: Vlastnosti a tvárnosť plechov z ocele DP 450. Kovárenství, září 2010/38, s. 45-48, ISSN 1213-9289
- [6] NIŽNÍK, Š. – ZAVACKÝ, M. – JANÁK, G. – FURMAN, L.: Nové možnosti tvorby vodíkových pascí v hlbokotlačných IF oceľových plechoch určených pre smaltovanie. Acta Metallurgica Slovaca, roč. 13, č. 3 (2007), s. 336-344, ISSN 1335-1532
- [7] SPIŠÁK, E. a kol.: Dizajn moderne koncipovaných ocelí na základe charakteristík lisovateľnosti. APVV-0629-06







¹ Peter KOŠTÁL, ² Imre KISS, ³ Petar KERAK

THE INTELLIGENT FIXTURE AT FLEXIBLE MANUFACTURING

¹ SLOVAK UNIVERSITY OF TECHNOLOGY, FACULTY OF MATERIALS SCIENCE AND TECHNOLOGY,
INSTITUTE OF PRODUCTION SYSTEMS AND APPLIED MECHANICS, TRNAVA, SLOVAKIA

² UNIVERSITY POLITEHNICA TIMISOARA, FACULTY OF ENGINEERING HUNEDOARA, HUNEDOARA, ROMANIA

ABSTRACT:

Development of new generation production machines and systems demand that they are equipped by adequate fixture devices. These fixture devices are developed with machine together, to don't decrease their production facilities and their time and performance utilizations. Efficiency of fixture device in automatized production systems underlie using efficiency of entire production systems. The majority of actual production is small or middle batch character. Thence, using of flexible production systems has lot of advantages. Their new generation fixture devices different from classical fixtures not only by design but also by its properties.

KEYWORDS:

intelligent fixture, flexible manufacturing, clamping, intelligent manufacturing

1. INTRODUCTION

Before 70th years of last centuries the mass production respond to basic requirements of market, but after this get started consumer affect the market. The producer must adapt to consumers requests and get started production of some variants of its products. This changeover has significant impact to mass production. Producers who can produce the wild range variants of its product have domination at market.

This trend in production continues to present time. Today market is characterized by strategy of consumer's individualization. This strategy is oriented to consumer's requests. Consumers want new products and time has a fundamental task to its satisfaction. The production was broadened, innovation cycle is shortened, the products have new shape, material and functions. At this strategy the traditional understand of costs lost in importance. Most important is a time and improving is its shortening. The production strategy focused to time need change from traditional functional production structure to production by flexible manufacturing cells and lines. Production by flexible cells (FMS) is a most important manufacturing philosophy in last years. This philosophy is based on similarity:

- ❖ similarity of manufactured parts,
- ❖ similarity of process plans.

Recognize the similarity of manufactured parts allow grouping them to groups by machines required to its manufacturing. By manufacturing of this group of parts we achieve economical effect near to mass production.

The manufacturing cell is an open manufacturing unit with transparent manufacturing processes. Flexible manufacturing cells represent a today trend to manufacturing innovations and productivity increasing.

The clamping fixture provides clamping of workpiece on machine desk, so as the workpiece have the right position toward a tool. This position must be retaining in machining time too.

Fixture using increasing the production quality, the productivity and decreasing the production costs. In some cases are fixtures using necessary. The fixture design is dependent on the

batches of production. In small batches we use the fixtures designed from modular system and in large batches we can use the dedicated fixtures.

The clamping fixture providing these basic functions:

- ❖ workpiece positioning on the desk of machine,
- ❖ to prevent of workpiece deformation when cutting and clamping forces are acting,
- ❖ tool support (in some cases).

These functions are provided by positioning, clamping and supporting elements (active elements) of fixture. These elements can be placed on standalone unit or on some units or can be mounted to machine or some its part.

Automated technological system must ensure required product quality by their properties and parameters without human action. Consequently all subsystems automated technological systems are participated to provide for required quality with different but function dependent deals. For automated technological system production quality requirement assurance are needed correct decomposition functions between individual subsystems ATS, their time and position synchronization. In this process are needed respect dynamic shows and compatibility bilateral inputs and outputs of technological process in ATS.

2. FLEXIBLE MANUFACTURING

The flexible manufacturing cells are characterized by high level of manufacturing process automation. They are used mainly in middle batch production (500 – 2000 pieces of products) and for middle products range (5 – 100 types of products).

The supplementary devices are used mainly to manipulation with workpieces and tools:

- ❖ workpiece storage and device for workpiece changing,
- ❖ storage, controlling and changing of tools,
- ❖ quality control.

A part of complex automated manufacturing process is an automation of technological process control, automated transportation, handling, feeding, interchange of workpieces, tools and automated waste cleaner. There are many technological sites existing, which match given requirements. Besides obvious computer techniques for controlling the manufacturing machines, automatically working bins, loaders, conveyors, manipulators and industrial robots are implemented step by step. As industrial production is growing constantly, besides implementing of the classical automated means, which were mentioned above, manufacturing systems with intelligent control are being installed.

Exploitation of automated manufacturing systems is conditional by effectiveness of all subsystems, from which is the automated manufacturing system created. All subsystems are often developed together with certain automated system, not to decrease parameters of whole system.

3. INTELLIGENT CLAMPING FIXTURE AT GENERAL

The majority of actual production is small or middle batch character. Thence, using of flexible production systems for these types of production has a lot of advantages. The flexible production systems must has a flexible clamping fixtures too. This new generation fixture devices different from classical fixtures not only by design but also by its properties.

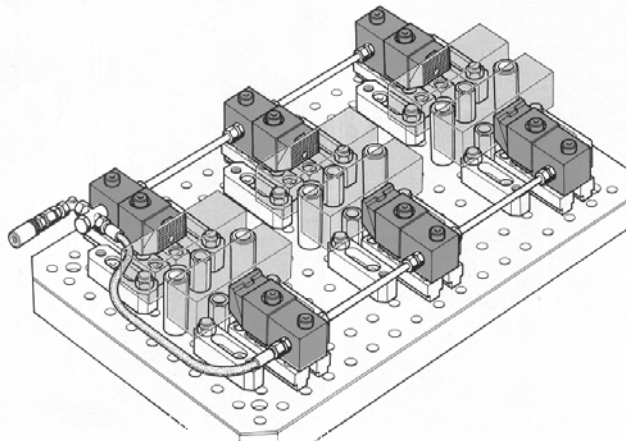


Fig. 1: Hydraulically operated clamping fixture

In standard production are mechanical peripheries (for example fixtures) controlled and monitored by operators. In automated production must these mechanical peripheries working in automated mode too. It means, that they must have not only own driving mechanism (hydraulic, pneumatic, electrical), but must have control and monitoring units too. The examples of hydraulic controlled clamping mechanism is at Fig. 1.

In time of working cycle these devices working automatically, without operator intervention and cooperate with other devices of production system.

During a automated work cycle are control and monitoring execute by sensors. The control based on sensors and controlled driving mechanism is base conditions for intelligent clamping fixture realize.

These intelligent clamping fixtures apart from the base functions provide same “intelligent” functions too:

- ❖ control of forces and torques acting to workpiece,
- ❖ monitoring of clamping operations and particular elements of fixture by sensors,
- ❖ other purpose oriented functions as clamping jaw change, or change of industrial robots end effectors

The aims of force and torque controlling are increasing of clamping operations reliability, decrease of workpiece deformation and decrease of workpiece surface damage possibility.

The clamping forces are proportional to pressure in pneumatic or hydraulic cylinder. This means, that we can monitor the clamping forces by monitoring of pressure in the cylinder. For pressure monitoring are used pressure sensors on base of tenzometers. For exact measure of clamping forces we can use force sensors build in clamping jaws.

The monitoring of clamping operations and particular elements of fixture enable the continuous diagnostic of clamping system. In base of this diagnostics can predict the possible future damages of fixture and we can disposal them before come the dropout in production, or ensue the bigger damage on the fixture system, tools or workpiece.

4. INTELLIGENT CLAMPING FIXTURE DESIGN

At our department is under realization the intelligent clamping fixture for flexible manufacturing cell. The basic condition to this clamping fixture is fellows:

- ❖ clamped workpiece has dimensions up to 60 mm,
- ❖ this fixture must be operated pneumatically (simply to change the clamping force by pressure),
- ❖ possibility of clamping jigs change,
- ❖ this fixture must give information to control system about:
 - air pressure,
 - position of clamping jigs (open or closed),
 - workpiece occurrence in clamping space,
 - clamping jig occurrence at jig holder,

When we will equip the clamping fixture by sensors, we achieve to capability collaboration between clamping fixture and flexible manufacturing cell.

The moving of clamping jigs holder are solved by pneumatic cylinders. Synchronization of this moving are realized by gears. Position of clamping jigs can be detected by magnetic sensors on side of fixture body. The position of clamping jig holder is detected by two magnetic sensors on side of fixture body.

The CAD model of our intelligent clamping fixture is shown in Fig. 2. These clamping fixtures can be used in a various field of small batch production:

- ❖ clamping for NC, CNC machines,
- ❖ clamping for robotized production,
- ❖ clamping for measure systems,
- ❖ clamping for special automatized operations.

5. CONCLUSION

The cell manufacturing become in last years one of most important manufacturing type. This conception is based on relation between manufacturing cell – workpiece. Flexible manufacturing cells allows manufacturing the small numbers of part from huge range of types and achieve good economical effects near by large batch or mass production. The manufacturing cells structure has

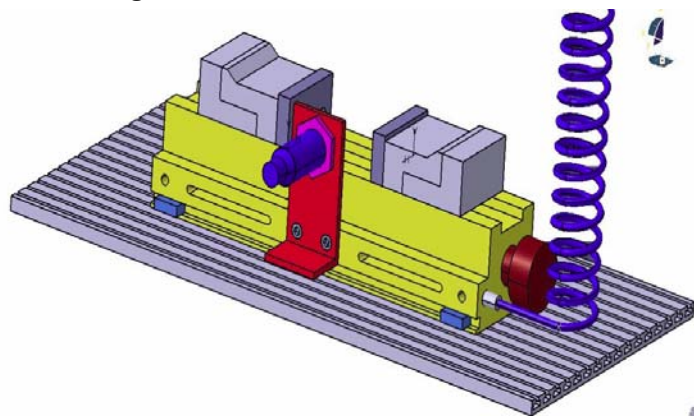


Fig. 2: CAD model of clamping fixture equipped by sensors

connected the machines and save the production time, space and production costs too. Function of machines is coordinated and the material flow can be quick.

Use of intelligent fixtures helps increase reliability of manufacturing operations. Production with intelligent fixtures is more flexible. These fixtures are more expensive and more complex as classical fixtures, because has own automated clamping, positioning, control and monitoring units.

The intelligent devices helps prevent the production disorders in automated production systems.

Application of intelligent fixtures eliminates the hard manual works. Also can save manpowers and increase the productivity.

The aim advantage of intelligent fixture using is their capability reacts to production program exchange. Adaptability of these systems is base of higher generation of automation.

Acknowledgment:

This paper was created thanks to the national grants: VEGA 1/0163/10 – Clamping fixtures in intelligent production systems

REFERENCES

- [1.] Danišová, Nina: Application of intelligent manufacturing system in the flexible assembly cell. In: Annals of Faculty of Engineering Hunedoara - Journal of Engineering. - ISSN 1584-2673. - Tom V, Fasc 3 (2007), s. 41-45
- [2.] Charbulová, Marcela: Modular clamping systems. In: Annals of Faculty of Engineering Hunedoara - Journal of Engineering. - ISSN 1584-2673. - Tom V, Fasc 3 (2007), s. 49-54
- [3.] Košťál, Peter - Velíšek, Karol - Zvolenský, Radovan: Intelligent Clamping Fixture in General. In: Lecture Notes in Computer Science. - ISSN 0302-9743. - Vol. 5315: Intelligent Robotics and Applications. First International Conference, ICIRA 2008, Wuhan, China, October 15-17, 2008. Part II (2008). - ISBN 978-3-540-88516-0, s. 459-465
- [4.] Matúšová, Miriam - Javorová, Angela: Modular clamping fixtures design for unrotary workpieces. In: Annals of Faculty of Engineering Hunedoara - Journal of Engineering. - ISSN 1584-2673. - Tom VI, Fasc 3 (2008), s. 128-130
- [5.] Mudriková, Andrea - Hrušková, Erika - Horváth, Štefan: Areas in flexible manufacturing-assembly cell. - článok vyšiel v časopise: Annals of Faculty of Engineering Hunedoara - Journal of Engineering, ISSN 1584-2673, Tome VI, Fascicule 3, 2008, str. 123-127. In: Scientific Bulletin. - ISSN 1224-3264. - Vol. XXII (2008), s. 293-298
- [6.] Mudriková, Andrea - Hrušková, Erika - Velíšek, Karol: Logistics of material flow in flexible manufacturing and assembly cell. - registered in ISI Proceedings. In: Annals of DAAAM and Proceedings of DAAAM Symposium. - ISSN 1726-9679. - Vol. 19, No.1. Annals of DAAAM for 2008 & Proceedings of the 19th International DAAAM Symposium "Intelligent Manufacturing & Automation: Focus on Next Generation of Intelligent Systems and Solutions", 22-25th October 2008, Trnava, Slovakia. - Vienna : DAAAM International Vienna, 2008. - ISBN 978-3-901509-68-1, s. 0919-0920
- [7.] Mudriková, Andrea - Velíšek, Karol - Košťál, Peter: Clamping fixtures used for intelligent assembly systems. In: ISCCC 2009: Proceedings of the 2009 International Symposium on Computing, Communication and Control, October 9-11, 2009, Singapore. - Singapore: International Association of Computer Science and Information Technology Press, 2009. - ISBN 978-9-8108-3815-7. - S. 9-15
- [8.] Velíšek, Karol - Košťál, Peter - Zvolenský, Radovan: Clamping Fixtures for Intelligent Cell Manufacturing. In: Lecture Notes in Computer Science. - ISSN 0302-9743. - Vol. 5315: Intelligent Robotics and Applications. First International Conference, ICIRA 2008, Wuhan, China, October 15-17, 2008. Part II (2008). - ISBN 978-3-540-88516-0, s. 966-972





¹Miroslava KOŠTÁLOVÁ

ASSEMBLING AND VERIFICATION DESIGN CORRECTNESS OF PRESS TOOLS BY HELP OF SYSTEM CATIA

¹ SLOVAK UNIVERSITY OF TECHNOLOGY IN BRATISLAVA, FACULTY OF MATERIALS SCIENCE AND TECHNOLOGY,
INSTITUTE OF PRODUCTION TECHNOLOGIES, DEPARTMENT OF FORMING, SLOVAKIA

ABSTRACT:

The paper deals with application of CATIA software in press tools construction for sheet metal forming. For development trends is characteristic utilization of scientific research in area of technological forming method with output on optimization, standardization and normalization. Software CATIA enables creation of catalogue of pressed parts, parametric creation of pressed tools, quickly design of required press tool and verification of correctness press tool design.

KEYWORDS:

combination press tool, verification, designing, kinematics

1. INTRODUCTION

Information technologies are means, which provides help to users in concrete disciplines in determination of optimal problems solving out of possible variants. In the area suggestion and construction of new products means set of informative technologies in the first place abbreviation of development period and possibility of complex product description in term of its geometry and mechanical properties. Information about tool acquired on base the creation of 3D models is more complex than 2D drawing documentation. It is possible to use 3D dates in the preparation area and it makes possible consecutive immediate interconnection construction with production. It is first of all qualitative and it is quite principled change to the development of new product. It is characteristics for developments trends application results of scientific research in the area CA technology in designing of tools with output on optimization, standardization and normalization of segments and constructive groups of tools. It makes possible to apply standardization of constructive tools systems and consecutive quick design ground of tool, with the correspondent complement of functional parts. The tools for sheet metal forming in term of construction are very individual, production of each of pressed part requires dedicated tool.

Resource at tools construction is job description of production, it essentially influence on selection of operational and constructive parts of stamping dies, for design of tool are necessary construction-technological calculus, choice of suitable type of tool is realized on base request of automation.

2. FEATURE OF PRESS TOOL MODELLING BY SOFTWARE CATIA

The base for suggestion of press tool is computer model, which is created in development places of work. At data transmission between various places of work with the same system is secured full compatibility and transmission of various parameters, technological oriented entity and alike. CAD software have function for recovery of random damaged dates.

The main reasons, which guide to decide to use 3D system in construction works:

- ❖ enhancement of productivity in construction works
- ❖ reduce of mistakes in documentation
- ❖ improve documentation, especially bigger clearness at using of axonometric views, which are easy deduced from 3D model

- ❖ parametrization of each components, tools.
- ❖ the check is rises on models, not on drawing
- ❖ consistent structure of assemblies
- ❖ excessively effective tool to eliminating crashes

The possibilities of tools construction by software CATIA:

- ❖ construction of tool with possibility of its next modification
- ❖ creation of standard tool by part choosing from several modular systems (HASCO, FIBRO, RABOURDIN, STEINEL)
- ❖ creation own database of tools, components,
- ❖ catalogization of constituent components
- ❖ creation of full parametric model

3. SOLUTION OF CHOSEN TYPE OF TOOL

Technical characterization of press tool

The basic parameter for design type of tool was request of mass production of pressing, with designation as bottom. It was suggested combination press die that realizes operations blanking and drawing for one press stroke. According number of pressed parts of the same sort manufactured for one stroke it belongs in category of single-impession tools. In term of construction it is tool with guide by help of pins and guide bushings. Sheet strip will be used as semiproduct that will be manually put in tool on stepper backstop and back guiding pins. After first stroke is strip manually by operator moved and positioned on stepper backstop. Finished pressing is at the same time ejected through front chute in prepared container at shifting of strip. The scrap is removed in form of remains of strip, which operator put to palette after processing of last piece.

Operating characteristic of tool

- ❖ by type of feeding and collating of semiproduct - tool with manual feeding
- ❖ by type of pressing removal - tool with backward pressing displacement and its self-acting removal
- ❖ by type removal of scratch - removed in form strip remnant or strap

Solution of tool kinematics

On the fig. 1 is start of kinematics tool motion, when is tool in top dead centre. Than top part of tool moves down and after 30 mm it occurs touch of stripper with material and next after one mm occurs touch between cutting punch and material. Stripper is compressed through springs. The cutting punch stepwise intrudes into material and after cut compresses cutting punch blankholder and by consecutive compression draws bottom until achievement of bottom died center, when the tool returns into its initial position. End of tool motion is on the fig. 2.

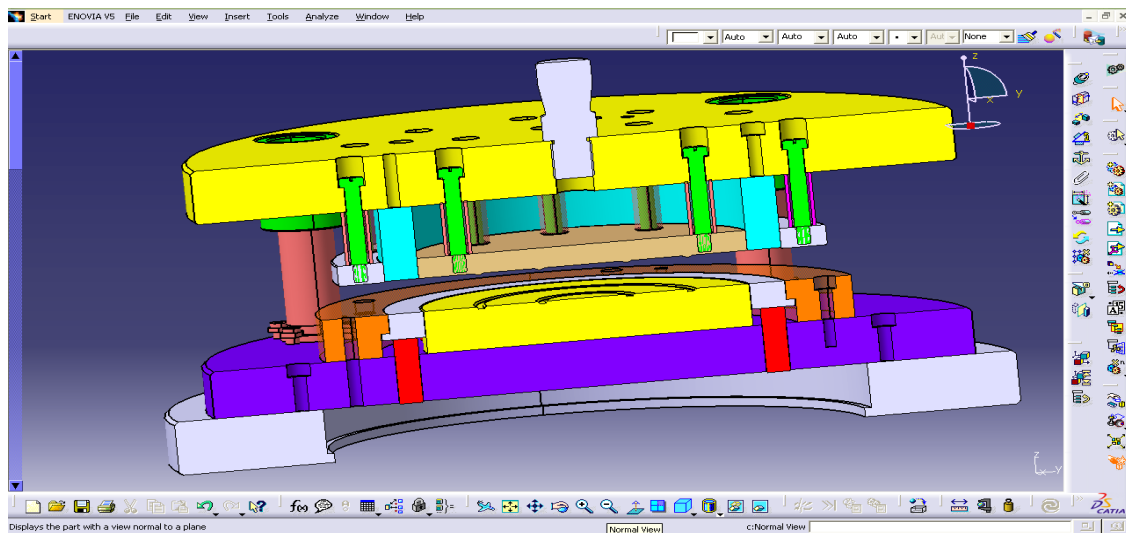


Figure 1 The press tool at start of motion

It was possible to trace tool motion from top die center to bottom die center after simulation running. It was utilized for description tool kinematics module Digital Mockup.

The module has appliances for design and control of digital prototype of press tool and for simulation of its functionality, it draws possible kinematics collision.

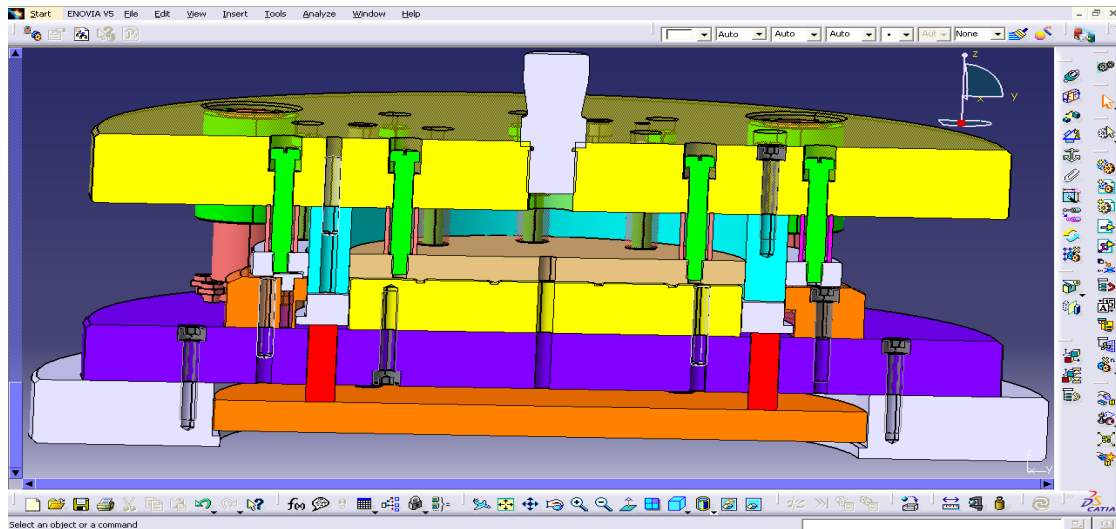


Figure 2 The press tool at end of motion

Verification of technologic parts of tool by help of analysis

It was required from constructional aspect allowance between cutting punch and stripper 0,5 mm. This request was checked by collision analyze, which establishes collision between components, eventually touch of components. On the fig. 3 is displayed contact between cutting punch and stripper with orange color, and at table on the right side is value of clearance equal 0 mm. The analyze mention on necessity of dimensions modification.

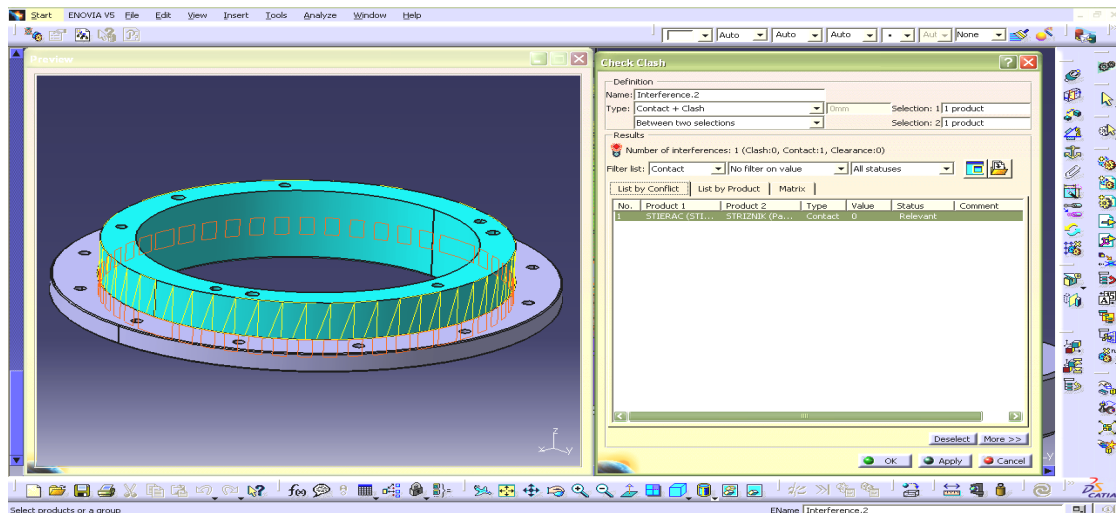


Figure 3 Contact representations between cutting punch and stripper

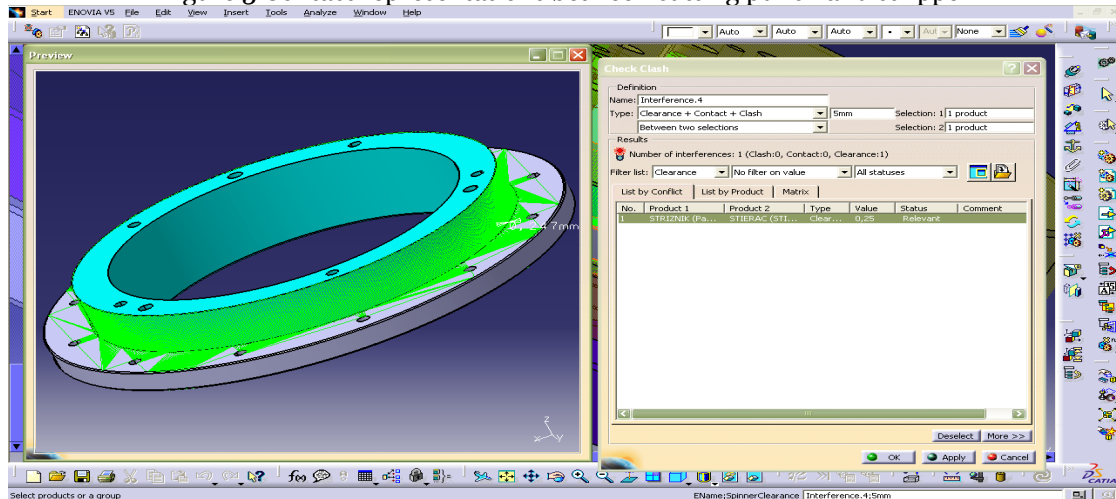


Figure 4 Allowance representation between cutting punch and stripper

Analysis of overhangs is on fig. 4. It results from analyze, that value of allowance corresponds to required value, in due window is value 0,25 mm and status Relevant, the allowance is displayed by green color. For creating analyze of overhangs and various collisions it was used modules Compute a Clash and Compute Clearance.

4. CONCLUSION

In respect of demand production of various shapes of pressed parts, the press tool represents very often the complicated kinematics system. By help of specialized functions of CATIA software constructor can in whichever state of production to analyze kinematics functions and to search possible clashes. It is possible to move with kinematics parts of tool and to check false clashes between various parts. The tool is possible to check by dynamic section by moveable plane and so it is possible quickly control 2D section. After verification precision of digital model it is possible automatic generation of NC programs for production. Such manner is saved time and material in preliminary stage of feeding production.

ACKNOWLEDGEMENTS

The paper was created with thanks of national grant VEGA 1/0060/08

REFERENCES

- [1] KURIC, I., Košturiak, J., Janáč, A., Peterka, J., Marcinčin, J. Počítačom podporované systémy v strojárstve. Žilina : EDIS, 2002, s. 11-39 ISBN 80-7100-948-2
- [2] POLÁK, K. Strihanie. Bratislava, SVTL 1967
- [3] ZEMAN K. Přípravky, obrábecí a tváreční nástroje. Nástroje pro tváření., Praha: ČVUT 1988
- [4] KAPUSTOVÁ, M. – BÍLIK, J. Využitie výpočtovej techniky v oblasti tvárnenia. In Trendy technického vzdelávani 2000, Olomouc, s. 161-164
- [5] KOŠTÁL, Peter - Mudriková, Andrea: Material flow in flexible manufacturing and assembly. In Computing and Solutions in Manufacturing Engineering, September 25-27, 2008, Brasov, Romania. In: Academic Journal of Manufacturing Engineering. - ISSN 1583-7904. - Supplement, Issue 1 (2008), s. 185-191
- [6] KOŠTÁL, Peter - Mudriková, Andrea: Uniwersalny system produkcyjny z wykorzystaniem komputerowo sterowanych urzadzeń. In: Nowoczesne, niezawodne i bezpieczne systemy mechanizacyjne dla górnictwa. - Gliwice : Centrum Mechanizacji Górnictwa KOMAG, 2008. - ISBN 978-83-60708-23-1. - S. 429-437
- [7] KOŠTÁLOVÁ, Miroslava - Kapustová, Mária: Designing variable parts of shearing tools by help of computer technique. In: Scientific Bulletin. - ISSN 1224-3264. - Vol. XXI / nadát. International Multidisciplinary Conference. 7th. Baia Mare, Romania, May 17-18, 2007 (2007). - Baia Mare : North University of Baia Mare, s. 359-362
- [8] KOŠTÁLOVÁ, Miroslava - Kapustová, Mária: Model construction of tools for sheet metal forming. In: KOD 2006 : Zbornik radova / nadát. Simpozijum sa medunarodnim učešcem. 4. Konstruisanje, oblikovanje i dizajn. Palic, 30-31. maj 2006. - Novi Sad : Fakultet tehničkih nauka, 2006. - ISBN 86-85211-92-1. - S. 271-272
- [9] KOŠTÁLOVÁ, Miroslava: Suitable forming tools types for robotized workplace. In: RaDMI 2006 : Proceedings on CD-ROM / nadát. International Conference. Budva, Montenegro, 13-17.Sept. 2006. - Trstenik : High Technical Mechanical School of Trstenik, 2006. - ISBN 86-83803-21-X. - S. 1-5
- [10] KOŠTÁLOVÁ, Miroslava: Designing variable parts of forming tools. Modelovanie variabilných častí tvárniacich nástrojov. In: CO-MAT-TECH 2006. 14. medzinárodná vedecká konerencia (Trnava, 19.-20.10.2006). - Bratislava : STU v Bratislave, 2006. - ISBN 80-227-2472-6. - S. 576-579
- [11] KOŠTÁLOVÁ, Miroslava: Model construction of shearing tools. In: CO-MAT-TECH 2005 : Proceedings/ International Scientific Conference, 13th, Trnava, Slovak Republic ,20-21 October 2005. - Bratislava : STU v Bratislave, 2005. - ISBN 80-227-2286-3. - S. 578-581





¹ Pavol ČEKAN, ²Anh NGUYEN THE, ³Ervin LUMNITZER

APPLICATION OPPORTUNITIES VIBRATION ANALYSERS

¹⁻³ TECHNICAL UNIVERSITY IN KOŠICE, FACULTY OF MECHANICAL ENGINEERING, DEPARTMENT OF ENVIRONMENTAL STUDIES AND INFORMATION ENGINEERING, KOŠICE, SLOVAKIA

ABSTRACT:

This contribution dwell on apportionment accelerometer to categories. Characteristic any choises class accelerometers and allocation baseline allegation for choice adequate type. Alternative correct arection accelerometers in alone process of metering vibes.

KEYWORDS:

accelerometer, signal, vibration, sensor

1. EXORDIUM

At the present time quality of environment human is constantly invade whereby several factors, which negatively effects arrogate in large criterion also vibes. We know, that vibes let us say vibration in common is move physical system, which over deviation get back always into the stability location. Fot all that for metering vibes most often use as electromechanical converter of mechanical vibration on electrical signal (analyzer), which works on principle Newton´s intensity canon and piezoelectrical effect. By piezoelectrical effect is intensity on output directly in proportion to power and acceleration vibes, result from also name analyser – accelerometer.

2. ALLOTMENT ANALYSERS OF ACCELERATION VIBRATION (ACCELEROMETS)

Accelerometer is apparatus, which mete vibrations or acceleration in move compages (construction, parts of machines tec.). Intensity induce vibes or change move (acceleration) affect on substance analyse, which then compress piezoelectrical element generating electrical charge commensurable to compression. Because is electrical charge commensurable to intensity and substance of analyzer is constant, is so electrical charge also commensurable to acceleration.

Analyzers mechanic vibration (accelerometers) by principle activity we can separate on:

- ❖ **Active (generatorical)**, which are generic on their output electrical module e.g. piezoelectricaland electrodynamical;
- ❖ **Passive, exigent of power energy**, which are modulation of any electrical modulate, or parameter of electrical circuit.

From these two basic groups analysers are used most often on metering of vibes:

- ❖ Piezoelectric (PE),
- ❖ Piezoelectrical with inbuilt electronic (IEPE),
- ❖ Piezorezistive (PR),
- ❖ Capacitive (VC). [3]

3. CHARACTERISTIC SOME CHOICES TYPES OF ANALYSERS

On the basis listed above knowledges, opportunites use analysers and their technical parameters we can characteristic following types:

- a) Model 7251A piezoelectric accelerometer IEPE

The Endevco model 7251A is a small piezoelectric accelerometer with integral electronics is shown on figure 1, designed specifically for measuring vibration on most structures. The unit is

hermetically sealed against environment contamination, offers high output sensitivity, and wide bandwidth. This new light weight (10.5 gm) design effectively minimizes mass loading effects.



Figure 1. Piezoelectric accelerometer IEPE model 7251A

The model 7251A features Endevco's Piezite type P-8 crystal element, operating in annular shear mode, which exhibits low base strain sensitivity and excellent output stability over time. This accelerometer incorporates an internal hybrid signal conditioner in a two-wire system, which transmits its low impedance voltage output through the same cable that supplies the constant current power. Signal ground is connected to outer case of the unit and, when used with the supplied isolated mounting screw, it is electrically isolated from ground. The centrally located mounting bolt permits 360° cable orientation, a very desirable feature in many applications. A model number suffix indicates sensitivity in mV/g ; i.e., 7251A-10 features output sensitivity of 10 mV/g .
 Tablet 1. usher specification hereof scanner. [2]

Tablet 1. Specification [2]

Sensitivity (typical)	-10; 10 mV/g -100;100 nV/g
Frequency response (± 1 dB)	2 to 10 000Hz
Shock limit	5000g pk
Temperature range	-67° F to + 257° F (-55 °C to +125 °C)
Weight	10,5 grams (0,37 oz)
Mounting	Insulated mounting screw or adhesive

b) Model 7264G Piezoresistive accelerometer

The Endevco model 7264G is a very low mass piezoresistive accelerometer (figure 2) weighing only 1.4 gram. This accelerometer is designed for crash testing, rough road testing and similar applications that require minimal mass loading and a broad frequency response. This accelerometer meets SAEJ211 and SAEJ2570 specifications for instrumentation for impact testing. It is equivalent in form and fit to the Endevco model 7264C-2K in that the location of the center of seismic mass is the same.



Figure 2 Piezoresistive accelerometer model 7264G.

The model 7264G utilizes a unique and advanced micromachined sensor which includes integral mechanical stops and damping. This monolithic sensor offers improved ruggedness, stability and reliability over previous designs. The model 7264G has suitable damping to minimize phase shift over the useful frequency range and attenuate resonance. With a frequency response

extending down to dc (steady state acceleration), this accelerometer is ideal for measuring long duration transient shocks.

This accelerometer has a two active arm full bridge circuit with two fixed resistors to facilitate shunt calibration. Full scale output is 400 mV with 10 Vdc excitation. It is also available with less than 1% transverse sensitivity ("T" option) and less than ± 25 mV zero measured output ("Z" option).
 Tablet 2. usher specification hereof scanner. [2]

Tablet 2. Specification [2]

Sensitivity	(at 100 Hz & 10 g) (min/typ/max) mV/g 0.15/0.20/0.30
Frequency response Hz	($\pm 2.5\%$ max, ref. 100 Hz) 0 to 2000 ($\pm 4.0\%$ max, ref. 100 Hz) 0 to 4000
Transverse sensitivity %	max 3 (1 optional)
Thermal sensitivity shift (max)	From +10 °C to +30 °C %/° C typ ± 0.06 From +50 °F to +86 °F %/° F typ ± 0.1

c) Acceleration Sensor AS – 020

The acceleration sensor AS-020 is used for measurement of vibration acceleration. Acceleration sensors operate in accordance with the piezo-electric compression principle (see figure 3).



Figure 3
Acceleration sensor
AS-020

Inside the sensor, a spring/mass damping system is formed by a piezo-ceramic disk and an internal sensor mass. When introducing vibrations into this system, the mass exerts an alternating force on the ceramic disk, and due to the piezo-electric effect, electric charges are caused which are proportional to acceleration. An integrated charge amplifier increases the output signal to a usable signal level. Table 3 usher specification hereof scanner.[1]

Tablet 3. Specification [1]

Transmission factor	100 $mV/g \pm 5\%$ 10,2 $mV/m/s^2 \pm 5\%$
Sensitivity deviation due to Temperature	- 22 °C - 3 % + 22 °C 0 % + 65 °C + 2,5 % + 120 °C + 5,5 %
Measuring range	$\pm 80 g$ (UB = -24 V...-30 V) $\pm 40 g$ (UB = -20 V) $\pm 20 g$ (UB = -18 V)
Frequency range	4 ... 10 000 Hz ($\pm 0,5 dB$) 1,5 ... 15 000 Hz ($\pm 3 dB$)

4. EXAMPLES INSTALLATION OF ACCELEROMETER IN THE PROCESS OF METERING VIBES

Accelerometer we can install by six methods in the seriaty duality to accomplish results of metering (see figure 4).:

- The mechanical screw (needs a preparations on all kinds catch are mostly in accessories accelerometers, sometime their is advisable specify in the order) (see figure 4a);
- The electric isolate screw (this metod we apply if we get signal, although the measure point is not energizing) (see figure 4b);
- The gripping by parametral magnet (this is the simplest gripping and is use in normal metering most useles) (see figure 4c);
- The affixion of sensor with bee-wax (see figure 4e) or with fast toughen glue (see figure 4d);
- The metering to screw by hand sonde (see figure 4f).

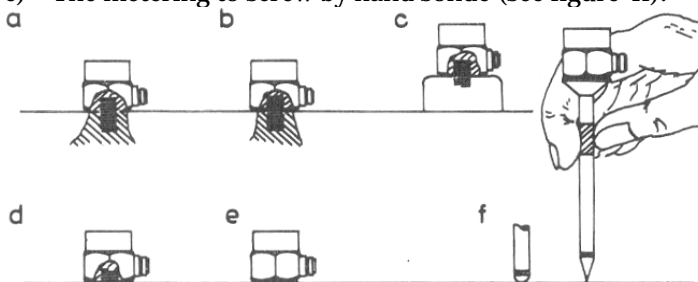


Figure 4 The style of gripping accelerometer. a – gripp by steel screw, b – gripp by electric isolate screw on isolate plate, c – gripp by permanent magnet, d – affix by the fast-gel glue, e – affix by bee-wax, f – screw by hand sonde with various types of tip

On (figure 5) is schematic exemples odvise installation of accelerometer and cable in process metering vibes.

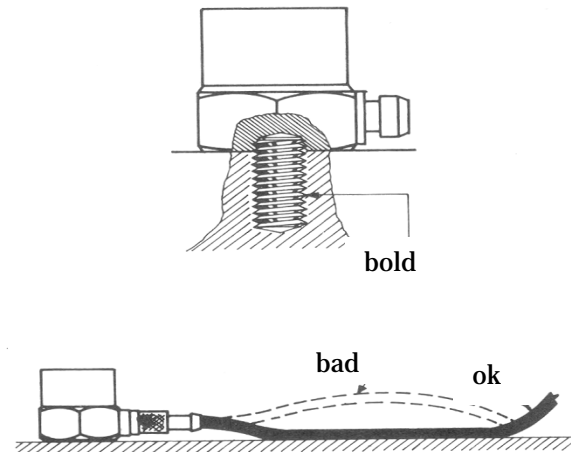


Figure 5 The instal accelerometer and cable at measure of vives

On measure of vives is important deliberate all positive requests at choice the favourable type soft sensor. Basal request, important especially on measuring of vives easiest objevte is, that substanciality used sensor could not affected the vives of measure point. On normal valuation is valid one princip, that sensor must by minimal 10 times easier as measure object and at the same time is necessary by care on the places, which have small consistence.[3]

5. CONCLUSION

The vives as well as another factors are inseparatable component of environment for human. Summarize is therefore necessarily accentuate importace of measure vife as negative factor of environment. Provide full elimination or cut down negative effects of vives and contribute for upgrade of environment for human.

Acknowledgement

This paper was supported by projects KEGA 3/7426/09 Creation of didactic details and publishing of university textbook „Physical factors of environment - valuation and assessment" for main field 2nd and 3rd level of study environmental focused studying programs.

REFERENCES

- [1.] Brüel&Kjaer Vibro [citing 2010-10-1]. Available on internet: <<http://www.bkvbros.com>>.
- [2.] Endevco [citing 2010-10-1]. Available on internet: <<http://www.endevco.com>>.
- [3.] ZAJAC, Jozef – TOMAŠVIČ, Peter – STAŠ, Anton: Znižovanie hluku a vibrácií v strojárskych prevádzkach: Bratislava: ALFA, 1990. 224 s. ISBN 80-05-00674-8



copyright © University Politehnica Timisoara,
Faculty of Engineering Hunedoara,
5, Revolutiei, 331128, Hunedoara,
ROMANIA
www.fih.upt.ro



¹ Adalbert KOVÁCS

THE LAGRANGE INTERPOLATION FORMULA FOR ANALYZING FLUID MOVEMENT IN NETWORK PROFILES

¹UNIVERSITY "POLITEHNICA" OF TIMISOARA, DEPT. OF MATHEMATICS, TIMIȘOARA, ROMANIA

ABSTRACT:

The paper presents two calculus algorithms for the study of the compressible fluid's stationary movement through profile grids on an axial-symmetric flow-surface. The first method is based on an iterative formula developed by the authors to calculate the complex conjugate velocity (using the CVBEM algorithm). The second method solves the fundamental integral equation in real values by a priori building up the velocity potential's integral equation (BEM method). In this case it is presented the necessity of using the Lagrangian interpolation formula through five points for the calculation of the derivatives of the velocity potential. In both cases the consecutive approximations can be organized simultaneously or successive with respect to parameters ζ (fluid's density) and h (thickness variation of fluid stratum).

KEYWORDS: hydrodynamic networks, boundary element method, Lagrange interpolation, complex velocity, velocity potential, Fredholme integral equation

1. INTRODUCTION

We study the direct problem from the hydrodynamics of networks for the stationary subsonic movement of the compressible fluid through profile grids on an axial-symmetric flow-surface, in variable thickness of stratum.

The movement is completely defined by the following equations [6]:

- ❖ Continuity equation for the compressible fluid:

$$\operatorname{div}(\zeta \cdot h \cdot \bar{v}) = 0 \quad (1)$$

- ❖ Potential (irrational) movement equation:

$$\operatorname{rot} \bar{v} = 0 \quad (2)$$

- ❖ Characteristic equation of state of compressible fluid:

$$\zeta = \zeta(p) \quad (3)$$

where:

- ζ and p are the fluid's density and pressure, respectively;
- \bar{v} is the fluid's absolute velocity;
- h is a function of the thickness variation of fluid stratum.

Additionally to equations (1), (2), (3), while studying the direct problem, the following boundary value conditions are also considered:

- The upstream and downstream velocities ($\vec{V}_{1\infty}$ and $\vec{V}_{2\infty}$, respectively) of the fluid are considered to be known;
- The relative velocity on a flow-surface, thus also on the base profile L_0 , is a tangential velocity.

The transport velocity \vec{u} is tangent to the circle that contains the current point of L_0 . Hence, the considered flow-surface is a flow-surface for the absolute motion, thus we have:

$$(\vec{v} \cdot \vec{n})|_{L_0} = (\vec{w} + \vec{u}) \cdot \vec{n}|_{L_0} = (\vec{w} \cdot \vec{n})|_{L_0} = 0 \quad (4)$$

where: - \vec{n} is the normal versor to the flow-surface;

- \vec{w} is the fluid's relative velocity.

- c. For ensuring unique solution, it is assumed that in the motion without detachments an equivalent condition with the Jukovski-Ciaplighin hypothesis is fulfilled, e.g. the equality of velocities in two points A' and A'' symmetrically situated on the trailing edge, thus we have [6]:

$$|\vec{v}_{A'}| = |\vec{v}_{A''}| \quad (5)$$

2. PREZENTING THE PROBLEM. THE COMPLEX VELOCITY OF MOVEMENT

The fundamental equations from the CVBEM method [3] in the problem of the compressible fluid's movement on a axial-symmetric flow–surface, in variable thickness of stratum are [6, 7, 8]:

$$\begin{aligned} \bar{w}(z) &= \bar{V}_m + \int_{L_0} H(z, \xi) \bar{w}(\xi) d\xi + i \iint_{D_0^-} H(z, \xi) \hat{q}(\xi) d\xi d\eta \\ F(z) &= \bar{V}_m \cdot z + \Gamma \cdot G(z, \xi_A) + \int_{L_0} H(z, \xi) F(\xi) d\xi + i \iint_{D_0^-} G(z, \xi) \hat{q}(\xi) d\xi d\eta \end{aligned} \quad (6)$$

where: $\bar{w}(z) = v_x - iv_y$ – is the complex conjugate velocity of motion; $F(z) = \varphi + i\psi$ is the complex potential of motion, where φ is the velocity potential and ψ is the flow rate function; A – is a fixed point on the base profile L_0 ; t – is the grid step; Γ – is the circulation around L_0 ;

$\bar{V}_m = \frac{1}{2}(\bar{V}_{1\infty} + \bar{V}_{2\infty})$ – is the asymptotic mean velocity;

$$\begin{aligned} H(z, \xi) &= \frac{1}{2it} \operatorname{ctg} \frac{\pi}{t} (z - \xi) \\ G(z, \xi) &= \frac{1}{2\pi i} \ln \sin \frac{\pi}{t} (z - \xi) \\ \hat{q}(\xi) &= 2 \frac{\partial \bar{w}}{\partial \xi} = - \left(v_x \frac{\partial \ln p^*}{\partial \xi} - v_y \frac{\partial \ln p^*}{\partial \eta} \right), p^* = \frac{\zeta \cdot h}{\zeta_0}, \\ v_x &= \frac{\partial \varphi}{\partial x} = \frac{1}{p^*} \frac{\partial \psi}{\partial y}, \\ v_y &= \frac{\partial \varphi}{\partial y} = - \frac{1}{p^*} \frac{\partial \psi}{\partial x} \end{aligned} \quad (7)$$

$$D_0^- \text{ – bounded simple convex domain, defined as: } D_0^- : \left[-\frac{t}{2} \langle \xi \langle \frac{t}{2}, - \left(t + \frac{l}{2} \right) \rangle \eta \langle \frac{t}{2}, \frac{l}{2} \rangle \right] \quad (8)$$

where l – is the projection of L_0 profile's frame on the Oy axis.

Based on the results of [5], [6] in the practical calculus of the complex conjugate velocity $\bar{w}(z)$, given by (6), the following iteration formula can be applied:

$$\bar{w}(z) = \bar{V}_m + \bar{w}_0^{(n)}(z) + \bar{w}_{\Delta q^*}^{(n-1)}, \quad n = 1, 2, \dots \quad (9)$$

where: $\bar{w}_0^{(n)}(z) = \frac{1}{2it} \int_{L_0} \bar{w}^{(n)}(\xi) \cdot H(z, \xi) d\xi$

$$\begin{aligned} \bar{w}_{\Delta q^*}^{(n-1)} &= i \iint_{D_0^-} \Delta q^{*(n-1)} \cdot H(z, \xi) d\xi d\eta \\ \Delta q^{*(n-1)}(\xi) &= -\Delta v_x^{(n-1)} \frac{\partial \ln p^{*(n-1)}}{\partial \xi} - \Delta v_y^{(n-1)} \frac{\partial \ln p^{*(n-1)}}{\partial \eta} \\ p^{*(n-1)} &= \frac{(\zeta \cdot h)^{(n-1)}}{\zeta_0} \end{aligned} \quad (10)$$

$$\zeta^{(n-1)} = \zeta_0 \left(1 - \frac{k-1}{2} \frac{(\bar{w}^{(n-1)})^2}{c_0^2} \right)^{\frac{1}{k-1}}, \text{ where } k \text{ is the adiabatic constant}$$

$$|\bar{w}^{(n-1)}|^2 = (v_x^{(n-1)})^2 + (v_y^{(n-1)})^2$$

c_0 – is the sound velocity

The successive approximation methods can be applied on (9) simultaneously over ζ and h , or successively over ζ and h . In the first approximation step it is assumed that $\zeta = \zeta_0 = \text{const.}$ and $h = \text{const.}$, hence $q^{*(0)}(\xi) = \Delta q^{*(0)}(\xi) = 0$, and (6) is solved without the double integral. For the velocity $\bar{w}^{(1)}(z) = v_x^{(1)} - iw_y^{(1)}$ thus obtained it is possible to determine $\zeta^{(1)}, p^{*(1)}$. Next, $\Delta q^{*(1)}$ is calculated, and $\bar{w}^{(1)}$, is obtained from (10). Furthermore, we proceed similarly with the second approximation step, etc. Another possibility for solving the fundamental equations (6) is given by the BEM method [6], i.e. solving the equations in real variables, using the results of [7]. For doing so, we consider the integral equation of the complex potential $F(z) = \varphi + i\psi$, and transform it into an integral equation with real variables, i.e. we build the integral equation of the velocity potential $\varphi(x, y)$.

3. THE LAGRANGE INTERPOLATION POLYNOMIAL IN DETERMINING THE VELOCITY POTENTIAL OF MOVEMENT

3.1. The Lagrange Interpolation Polynomial

The problem of constructing a continuously defined function from given discrete data is unavoidable whenever one wishes to manipulate the data in a way that requires information not included explicitly in the data. The relatively easiest and in many applications often most desired approach to solve the problem is *interpolation* [2], where an approximating function is constructed in such a way as to agree perfectly with the usually unknown original function at the given measurement points. In the practical application of the finite calculus of the problem of interpolation is the following: given the values of the function for a finite set of arguments, to determine the value of the function for some intermediate argument [2].

A chronological overview of the developments in interpolation theory, from the earliest times to the present date could be found in. In this section we focus our attention on the theory of the *lagrange interpolation polynomial* [2], since, as we have already mentioned in the proof of proposition 3.3, its usage arises also in our calculus algorithm for the study of the compressible fluid's stationary movement through profile grids on an axial-symmetric flow-surface in variable thickness of stratum.

The problem of interpolation consists in the following [2: Given the values y_i corresponding to $x_i, i = 0, 1, 2, \dots, n$, a function $f(x)$ of the continuous variable x is to be determined which satisfies the equation:

$$y_i = f(x_i) \text{ for } i = 0, 1, 2, \dots, n \quad (11)$$

and finally $f(x)$ corresponding to $x = x'$ is required. (i.e. x' different from $x_i, i = \overline{1, n}$.)

In the absence of further knowledge as to the nature of the function this problem is, in the general case, indeterminate, since the values of the arguments other than those given can obviously assigned arbitrarily.

If, however, certain analytic properties of the function be given, it is often possible to assign limits to the error committed in calculating the function from values given for a limited set of arguments. For example, when the function is known to be representable by a polynomial of degree n , the value for any argument is completely determinate when the values for $n + 1$ distinct arguments are given.

Consider the function $f : [x_0, x_n] \rightarrow R$ given by the following table of values [2]:

$$\begin{array}{c|cccc} x_k & x_0 & x_1 & \dots & x_n \\ \hline f(x_k) & f(x_0) & f(x_1) & \dots & f(x_n) \end{array}$$

x_k are called *interpolation nodes*, and they are not necessary equally distanced from each other. We seek to find a polynomial $P(x)$ of degree n that approximates the function $f(x)$ in the interpolation nodes, i.e.:

$$f(x_k) = P(x_k); k = 0, 1, 2, \dots, n \quad (12)$$

The **Lagrange interpolation method** finds such a polynomial without solving the system (12).

Theorem 3.1. Lagrange Interpolating Polynomial

The Lagrange interpolating polynomial is the polynomial of degree n that passes through $(n + 1)$ points $y_0 = f(x_0), y_1 = f(x_1), \dots, y_n = f(x_n)$. It is given by the relation ([2]):

$$P(x) = \sum_{j=0}^n P_j(x) \quad (13)$$

where:

$$P_j(x) = y_j \prod_{k=0, k \neq j}^n \frac{x - x_k}{x_j - x_k} \quad (14)$$

Written explicitly:

$$P(x) = \frac{(x - x_1)(x - x_2) \dots (x - x_n)}{(x_0 - x_1)(x_0 - x_2) \dots (x_0 - x_n)} y_0 + \frac{(x - x_0)(x - x_2) \dots (x - x_n)}{(x_1 - x_0)(x_1 - x_2) \dots (x_1 - x_n)} y_1 + \frac{(x - x_0)(x - x_1) \dots (x - x_{n-1})}{(x_n - x_0)(x_n - x_1) \dots (x_n - x_{n-1})} y_n \quad (15)$$

For illustrating the usability of the Lagrange interpolation method through five points for our calculus algorithm for the study of the compressible fluid's stationary movement through profile grids on an axial-symmetric flow-surface in variable thickness of stratum, namely, for calculating the tangential velocity $v_\tau = \frac{d\varphi}{ds}$ (see section 3, proposition 3.3, equation (24)).

3.2. Solving the Integral Equation of Velocity Potential

Our purpose is to solve the fundamental equations (6) (obtained from the CVBEM method) using (BEM) in real variables. For doing so, we consider the fundamental integral-equation of the complex potential $F(z) = \varphi + i\psi$ and transform it into an integral equation with real variables, i.e. we build the integral equation of the velocity potential $\varphi(s)$ ($\psi(s)$ is the flow rate function).

Theorem 3.2. [6], [8] *In the subsonic motion of the compressible fluid through the profile grid, on an axial-symmetric flow-surface, in variable thickness of stratum, the velocity potential $\varphi(s)$, $s \in L_0$ is the solution of the integral equation (16):*

$$\varphi(s) + \int_{L_0} \varphi(\sigma) \frac{dM(s, \sigma)}{d\sigma} d\sigma = b(s) + \iint_{D_0^*} \bar{q}(\sigma) N(s, \sigma) d\xi d\eta \quad (16)$$

where:

$s(x_0, y_0)$ and $\sigma(\xi, \eta)$ are the curvilinear coordinates of the fixed point A on the L_0 base profile;

$$b(s) = 2(x_0 V_{mx} + y_0 V_{my}) + \Gamma M(s, \sigma_A) + \int_{L_0} [\psi(s) - \psi(\sigma)] \frac{dN}{d\sigma} d\sigma$$

$$M(z_0, \zeta) = \frac{1}{\pi} \operatorname{arctg} \frac{th \frac{\pi}{t} (\eta - y_0)}{tg \frac{\pi}{t} (\xi - x_0)} \quad (17)$$

$$N(z_0, \zeta) = \frac{1}{\pi} \ln \sqrt{\frac{1}{2} \left[ch \frac{2\pi}{t} (\eta - y_0) - \cos \frac{2\pi}{t} (\xi - x_0) \right]}$$

V_{mx}, V_{my} - are the components of the asymptotic mean velocity v_m .

Proposition 3.1. [7],[8] *In the case of an axial-subsonic movement of a perfect and compressible fluid through profile grids, the flow rate function is determined from the boundary condition (6):*

$$\psi(s) = u_0 \cdot \int_0^s p^*(s) \left(\frac{R}{R_0} \right) ds, \quad u_0 = \omega R_0, \quad (18)$$

where: ω is the angular rotation velocity of the profile grid; R_0 defines the origin of the axis system related to the turbine's axis.

Equation (16) is an integro-differential equation. In this section, we will show a possibility of solving this equation applying the *method of successive approximation* (the iteration method), using also the result from [6] about the order of the term containing the double integral expression:

$$\varphi_{\bar{q}}(s) = \iint_{D_0^*} \bar{q}(\sigma) N(s, \sigma) d\xi d\eta \quad (19)$$

Proposition 3.2. [6], [8] *In the case of the subsonic movement of the compressible fluid through the profile grid on an axial-symmetric flow-surface, in variable thickness of stratum, the integral equation of the velocity potential $\varphi : D_0^* \rightarrow \mathfrak{R}$ is solvable by applying the method of*

successive approximations w.r.t. the parameter $p^ = \frac{\zeta \cdot h}{\zeta_0}$.*

Proof. For isentropic processes, by the Bernoulli–equation, we obtain:

$$\zeta = \zeta_0 \left(1 - \frac{\gamma - 1}{2} \frac{v^2}{c_0^2} \right)^{\frac{1}{\gamma - 1}}, v^2 = v_\tau^2 + v_n^2, v_\tau = \frac{d\varphi}{ds}, v_n = \frac{1}{p^*} \frac{d\psi}{ds} \quad (20)$$

where: γ is the adiabatic constant; c_0 is the sound velocity in the zero velocity point; v_τ and v_n are, respectively, the tangential and normal velocities on L_0 .

In the first approximation it is assumed that $\zeta = \zeta_0 = \text{constant}$ and $p^* = p^{*(0)} = \text{constant}$. Thus, from (7), it results that $q^{(0)}(\sigma) = 0$. Hence, in the integral equation (4) the double integral (19) is neglected and results the following Fredholme integral equation of second type, with continuous nucleus:

$$\varphi^I(s) + \int_{L_0} \varphi^I(s) \frac{dM(s, \sigma)}{d\sigma} d\sigma = b^I(s) \quad (21)$$

From solving equation (21) we obtain φ^I , and furthermore from (18), (20), (24) ψ^I, ζ^I are obtained. Finally, using the relation:

$$p^* = \frac{\zeta \cdot h}{\zeta_0}, \quad \tilde{q}(\sigma) = -\text{grad}\varphi \cdot \text{grad}\ln p^* \quad (22)$$

a p^{*I} and $\tilde{q}^I(\sigma)$ are determined.

In the second iteration $p^* = p^{*I}$ is assumed and for the determination of $\varphi^{II}(s)$ the following Fredholme integral equation of second type, with continuous nucleus, will be solved:

$$\varphi^{II}(s) + \int_{L_0} \varphi^{II}(\sigma) \frac{dM(s, \sigma)}{d\sigma} d\sigma = b^{II}(s) + \iint_{D_0^-} q^I(\sigma) N(s, \sigma) d\xi d\eta \quad (23)$$

where a φ^I and $b^{II}(s)$ are previously calculated from (18) and (17), respectively.

From solving equation (23), we obtain φ^{II} . Furthermore, from (18), (20), (24) and (22) $\psi^{II}, \zeta^{II}, p^{*II}$ and $\tilde{q}^{II}(\sigma)$ are obtained, respectively. Next, the third approximation might be done by assuming $p^* = p^{*II}$, and so on.

Proposition 3.3. [7], [8] *Having given the values of the velocity potential on each element of the L_0 profile's division, the tangential velocity v_τ may be calculated in each division element of the L_0 basic profile's boundary by the formula, given by the Lagrange interpolation method through five points:*

$$v_{\tilde{a}} = \frac{d\varphi}{ds}(s_i) = \frac{2}{3\Delta s_i} (\varphi_{i+2} - \varphi_{i-2}) - \frac{1}{12\Delta s_i} (\varphi_{i+4} - \varphi_{i-4})$$

$$h = \Delta s_i = s_{i+1} - s_{i-1}, \quad (24)$$

$$i = 1, 3, 5, \dots, 2n - 1,$$

where n denotes the number of division elements and by s_i we refer to the i^{th} element of the division of L_0 .

To ensure the practical functionality of proposition 3.2, i.e. to indicate the solving method of the Fredholme integral equation of second type obtained in each approximation step (equation (18), (23)), let us formulate and prove two more propositions.

Based on the results obtained by employing the interpolation formula through five points (24), we further determine the velocities $v_{\tilde{a}}$ and with the size of the complex velocity w_i . Using such obtained values, in [8] we give an efficient algorithm for deriving the fluid's complex velocity through profile grids.

4. CONCLUSION

We have shown some practical aspects of the usage of the calculus algorithm for the study of the compressible fluid's stationary movement through profile grids, on an axial–symmetric flow–surface, in variable thickness of stratum, namely :

- ❖ the usage of the boundary element method with real values;
- ❖ the applicability of the successive approximation method w.r.t. the parameters ζ (fluid's density) and h (thickness variation of fluid stratum) for solving the integral equation of the velocity potential;
- ❖ the usage of the Lagrangian interpolation formula through five points for calculating the derivatives of the velocity potential.

Regarding practical applicability of our algorithm, our plans for the near future are:

- ❖ make more test cases w.r.t. several input (geometrical and hydrodynamical) values of the velocity potentials taken from practical experiments involving profile grids;
- ❖ study the possibility of applying the algorithm (i.e. the approximation methods) for the calculation of other fluid-characteristics.

REFERENCES

- [1] P. Benerji and R. Butterfield: The Boundary Element Method in Applied Sciences (in Russian), MIR, Moskow, 1984.
- [2] B. P. Demidovici and I. A. Maron: The Mathematical Basis of Numeric Calculus (in Russian). Nauka, Moskow, 1970.
- [3] T.V. Hromadka II: The Complex variable boudary element method. Springer Verlag, Berlin, 1984.
- [4] A. Kovács: Boundary element method for analyzing fluids movements in network profiles, Proc. of 8th Int. Symposium of Hungarian Researches on Computational Intelligence and Informatics, Budapest, Hungary, Nov. 15-17, 2007, pp. 139-150.
- [5] A. Kovács: Über die Stabilierung und Bestimmung einer Iterationsformel für einen konexen unendlichen Bereich. Proc. of the 8th Symposium of Mathematics and its Applications, Timisoara, Romania, Nov. 4-7, 1999, pp. 88-92.
- [6] A. Kovács: Mathematische Modelle in der Hydrodynamik der Profiligitters. Monographical Bookles in Applied and Computer Mathematics PAMM, Budapest, MB-19, 2001.
- [7] A. Kovács and L. Kovács: The Lagrange Interpolation Formula in Determining the Fluid's Velocity Potential through Profile Grids. Bulletins for Applied Mathematics, Proc. of 2005 PAMM's Annual Central Meeting T.CVII/2005, Nr.2252, Balatonalmádi, Hungary, May 26-29, 2005, pp. 126-135.
- [8] A. Kovács and L. Kovács: On the Calculus Algorithm of the Fluid's Velocity Potentials Through Profile Grids. Annals of the Faculty of Engineering Hunedoara-Journal of Engineering, Tome VII, Fasciule 3, pp. 232-237.
- [9] G. V. Viktorov and I. V. Vutchikova: The Calculus of Fuid-Flow through Profile Grids on an Axial-Symmetric Flow-Surface with Variable Thickness of Stratum (in Russian), Izd. ANSSSR, MJG, vol. 5, 1969, pp. 96-102.
- [10] G. N. Poloji: The Theory and Applications of P-analytic and (P,Q)-analytic Functions (in Russian). Nauka Dumka, Kiev, 1973.



¹Diana STOICA

DISCRETE ASYMPTOTIC BEHAVIORS OF STOCHASTIC SKEW-EVOLUTION SEMIFLOWS IN HILBERT SPACES

¹UNIVERSITY "POLITEHNICA" TIMISOARA, FACULTY OF ENGINEERING OF HUNEDOARA, ROMANIA

ABSTRACT:

The paper presents the properties of exponential stability and instability in mean square for discrete stochastic skew-evolution semiflows in Hilbert spaces. Some characterizations which generalize classic results obtained in deterministic case are also provided.

KEYWORDS:

Discrete stochastic skew-evolution semiflows, stability and instability in mean square

1. INTRODUCTION

In this article we consider the stochastic skew-evolution semiflows, which can be considered a generalization of skew-product introduced by Arnold L. in [1], and present the properties of discrete exponential stability.

The problem of existence of stochastic cocycle over the stochastic semiflows is presented in many papers (see [2], [3], [6] and [8]).

Some of the results for uniform asymptotic behaviors in mean square of stochastic cocycles generated by stochastic differential equations was studied in the papers of D. Stoica [11,12].

We considered H a real Hilbert space. Let $B(H)$ be a Banach space of all linear and bounded maps $A : H \rightarrow H$. We denote the sets $T = \{(m, n) \in \mathbb{N}^2, m \geq n \geq 0\}$.

Assume $(\Omega, \mathfrak{F}, P)$ is a complete probability space with a normal filter $\{\mathfrak{F}_t\}_{t \geq 0}$, i.e. \mathfrak{F}_0 contains the null sets in \mathfrak{F} and $\mathfrak{F}_t = \bigcap_{s > t} \mathfrak{F}_s$, for all $t \geq 0$, and let us consider a real valued $\{\mathfrak{F}_t\}$ -Wiener process $\{W(t)\}, t \geq 0$.

Let be $F : [0, T] \times \Omega \rightarrow H$ a stochastic process, and then $E(F) = \int_{\Omega} F(\Omega) dP(\omega)$ represent the mean of stochastic process F , where P is the probability measure. If $F \in C([0, T], L^2(\Omega, H))$

$$\text{then } \int_0^T E \|F(t)\|^2 dt = E \int_0^T \|F(t)\|^2 dt.$$

For an process Wiener $W(t)$ in rapport with the filter $\{\mathfrak{F}_t\}$ we have

$$E \left\| \int_0^T F(t) dw(t) \right\|^2 = E \int_0^T \|F(t)\|^2 dt.$$

Definition 1. Let be H a Hilbert space. A discrete stochastic semiflow on H is a random field $\varphi : (T \times \Omega, B(H) \times \mathfrak{F}) \rightarrow (\Omega, \mathfrak{F})$ satisfying the following properties:

- (1) $\varphi(n, n, \omega) = \omega$, for all $n \geq 0$ and $\omega \in \Omega$;
- (2) $\varphi(m, n, \varphi(n, p, \omega)) = \varphi(m, p, \omega)$, $\forall (m, n), (n, p) \in T, \forall \omega \in \Omega$.

Definition 2. A discrete stochastic cocycles on H , over an discrete stochastic semiflow $\varphi : (T \times \Omega, B(H) \times \mathfrak{F}) \rightarrow (\Omega, \mathfrak{F})$, is a random field $\Phi : (T \times \Omega, B(H) \times \mathfrak{F} \times B(H)) \rightarrow L(H)$, with the following properties:

- (1) $\Phi(n, n, \omega) = I$, (Identity operator on H), $\forall n \geq N$, and $\omega \in \Omega$,
 (2) $\Phi(m, n, \varphi(n, p, \omega))\Phi(n, p, \omega) = \Phi(m, p, \omega)$, $\forall (m, n), (n, p) \in T$, and $\omega \in \Omega$.

Definition 3. The mapping $\Theta : T \times Y \rightarrow Y$, defined by

$$\Theta(m, n, \omega, x) = (\varphi(m, n, \omega), \Phi(m, n, \omega)x)$$

where $Y = \Omega \times H$ is called the discrete stochastic skew-evolution semiflow on Y , and we denoted by $\Theta = (\varphi, \Phi)$.

Example 1. Let $\Theta_0(m, \omega, x) = (\varphi_0(m, \omega), \Phi_0(m, \omega)x)$ be the discrete skew-product of the metric discrete dynamical system $\varphi_0(m, \cdot)$, $\forall m \in \mathbb{N}$ on Ω , generated by de Wiener shift, introduced by Arnold in [1]. Then the mapping $\Theta = (\varphi, \Phi)$, defined by

$$\begin{aligned} \varphi(m, n, \omega) &= \varphi_0(m - n, \omega) \\ \Phi(m, n, \omega) &= \Phi_0(m - n, \omega), \quad \forall (m, n) \in T, \omega \in \Omega. \end{aligned}$$

is a discrete stochastic skew-evolution semiflow, which generalizes the notation of classical discrete skew-product, considered by Arnold L. in [1].

A typical example of discrete skew-evolution semiflow is generated by the solution operator at time $t = n$ for a stochastic linear differential equation.

2. UNIFORMLY EXPONENTIALLY STABILITY AND INSTABILITY IN MEAN SQUARE

In this section we give the integral characterizations of uniform exponential stability and instability in mean square of discrete stochastic skew-evolution semiflows in Hilbert spaces. The main results are generalizations of the characterizations obtained in deterministic case, and presented of many authors including the papers [4], [9] and [10].

Definition 5. The discrete stochastic skew-evolution semiflow Θ is said to be uniformly exponentially stable in mean square if for some positive random variables $N(\omega) \geq 1, a(\omega) \in (0,1)$ one has

$$E \|\Phi(m, p, \omega)x\|^2 \leq N(\omega)a(\omega)^{m-n} E \|\Phi(n, p, \omega)x\|^2, \quad (1)$$

for all $(m, n), (n, p) \in T, (x, \omega) \in Y$.

Definition 6. The discrete stochastic skew-evolution semiflow Θ is said to be uniformly exponentially instable in mean square if for some positive random variables $N(\omega) \geq 1, a(\omega) \in (0,1)$ one has

$$N(\omega)a(\omega)^{m-n} E \|\Phi(m, p, \omega)x\|^2 \geq E \|\Phi(n, p, \omega)x\|^2, \quad (2)$$

for all $(m, n), (n, p) \in T, (x, \omega) \in Y$.

Theorem 7. Let be $\Theta = (\varphi, \Phi)$ a discrete stochastic skew-evolution semiflow. Then $\Theta = (\varphi, \Phi)$ is uniformly exponentially stable in mean square if and only if there are random variables $D(\omega) \geq 0$, such that:

$$\sum_{k=n+1}^{\infty} E \|\Phi(k, p, \omega)x\|^2 \leq D(\omega) E \|\Phi(n, p, \omega)x\|^2, \quad (3)$$

for all $(n, p) \in T, (x, \omega) \in Y$.

Proof. Necessity. Let be a discrete stochastic skew-evolution semiflow $\Theta = (\varphi, \Phi)$ uniformly exponentially stable in mean square. Then, for $N(\omega) \geq 1, a(\omega) \in (0,1)$ we have from Definition 5, that

$$E \|\Phi(m, p, \omega)x\|^2 \leq N(\omega)a(\omega)^{m-n} E \|\Phi(n, p, \omega)x\|^2,$$

for all $(m, n), (n, p) \in T, (x, \omega) \in Y$. Write this relationship for $k = n + 1, n + 2, \dots, L$ and then we sum these relations member with member and we have:

$$\sum_{k=n+1}^L E \|\Phi(k, p, \omega)x\|^2 \leq N(\omega) \sum_{k=n+1}^L a(\omega)^{m-n} E \|\Phi(n, p, \omega)x\|^2 \text{ for all } (n, p) \in T, (x, \omega) \in Y.$$

Passing to the limit for $L \rightarrow \infty$ and we obtained

$$\sum_{k=n+1}^{\infty} E \|\Phi(k, p, \omega)x\|^2 \leq D(\omega) E \|\Phi(n, p, \omega)x\|^2$$

where $D(\omega) = N(\omega) \frac{a(\omega)}{1-a(\omega)}$, for all $(n, p) \in T, (x, \omega) \in Y$.

Sufficiency. For $(n, p) \in T$ and $(x, \omega) \in Y$ we denote by $S_{n+1} = \sum_{k=n+1}^{\infty} E \|\Phi(k, p, \omega)x\|^2$

and from hypothesis we have

$$E \|\Phi(m, p, \omega)x\|^2 \leq S_m \leq \left(\frac{D(\omega)}{D(\omega)+1}\right)^{m-n-1} S_{n+1} \leq \left(\frac{D(\omega)}{D(\omega)+1}\right)^{m-n} (D(\omega)+1) E \|\Phi(n, p, \omega)x\|^2$$

for all $(m, n), (n, p) \in T, (x, \omega) \in Y$. So we have the relation

$$E \|\Phi(m, p, \omega)x\|^2 \leq N(\omega)a(\omega)^{m-n} E \|\Phi(n, p, \omega)x\|^2,$$

where $N(\omega) = \frac{D(\omega)}{D(\omega)+1}$, and $a(\omega) = \max\{1, (D(\omega)+1)\}$, for all

$(m, n), (n, p) \in T, (x, \omega) \in Y$, and we obtain that the discrete stochastic skew-evolution semiflow $\Theta = (\varphi, \Phi)$ is uniformly exponentially stable in mean square.

Theorem 8. Let be $\Theta = (\varphi, \Phi)$ a discrete stochastic skew-evolution semiflow. Then $\Theta = (\varphi, \Phi)$ is uniformly exponentially instable in mean square if and only if there are random variables $D(\omega) \geq 1$, such that:

$$\sum_{k=0}^n E \|\Phi(k, p, \omega)x\|^2 \leq D(\omega) E \|\Phi(n, p, \omega)x\|^2, \quad (4)$$

for all $(n, p) \in T, (x, \omega) \in Y$.

Proof. Necessity. Let be a discrete stochastic skew-evolution semiflow $\Theta = (\varphi, \Phi)$ uniformly exponentially instable in mean square. Then, for $N(\omega) \geq 1, a(\omega) \in (0,1)$ we have from Definition 6, that

$$N(\omega)a(\omega)^{m-n} E \|\Phi(m, p, \omega)x\|^2 \geq E \|\Phi(n, p, \omega)x\|^2,$$

for all $(m, n), (n, p) \in T, (x, \omega) \in Y$. Write this relationship for $k = \overline{0, n}$ and then we sum these relations member with member and we have:

$$\sum_{k=0}^n E \|\Phi(k, p, \omega)x\|^2 \leq N(\omega) \sum_{k=0}^n a(\omega)^{n-k} E \|\Phi(n, p, \omega)x\|^2 \leq D(\omega) E \|\Phi(n, p, \omega)x\|^2 \quad \text{for all}$$

$(n, p) \in T, (x, \omega) \in Y$, where $D(\omega) = \max\left\{2, \frac{N(\omega)}{1-a(\omega)}\right\}$ and we obtain the relation (4).

Sufficiency. For $(n, p) \in T$ and $(x, \omega) \in Y$ we denote by $S_m = \sum_{k=0}^m E \|\Phi(k, p, \omega)x\|^2$ and

from relation (4) we obtain

$$\left(\frac{D(\omega)}{D(\omega)-1}\right)^{m-n} S_n \leq S_m \quad \text{for all } (m, n) \in T, (x, \omega) \in Y$$

From this relation we obtain

$$\left(\frac{D(\omega)}{D(\omega)-1}\right)^{m-n} E \|\Phi(n, p, \omega)x\|^2 \leq D(\omega) E \|\Phi(m, p, \omega)x\|^2,$$

and if we denote $N(\omega) = D(\omega)$, and $a(\omega) = \frac{D(\omega) - 1}{D(\omega)}$, for all $(m, n), (n, p) \in T$, $(x, \omega) \in Y$, and

we obtain that the discrete stochastic skew-evolution semiflow $\Theta = (\varphi, \Phi)$ is uniformly exponentially instable in mean square.

REFERENCES

- [1.] L. Arnold, Stochastic Differential Equations: Theory and Applications, New York: Wiley, (1972)
- [2.] A. Bensoussan, F. Flandoli, Stochastic inertial manifold, Stochastic Rep. 53 (1995), no. 1-2, 13–39.
- [3.] F. Flandoli, Stochastic flows for non-linear second-order parabolic SPDE, Ann. Probab. 24 (1996), no. 2, 547–558.
- [4.] M. Megan, A. L. Sasu, and B. Sasu, On uniform exponential stability of linear skew-product semiflows in Banach spaces, Bulletin of the Belgian Mathematical Society - Simon Stevin, 9 (2002) 143–154.
- [5.] M. Megan, C. Stoica, On Uniform Exponential Trichotomy of Evolution Operators in Banach Spaces, Integral Equations and Operator Theory, 60 (2008) 499–506.
- [6.] S. E. A. Mohammed, T. Zhang, H. Zhao, The stable manifold theorem for semilinear stochastic evolution equations and stochastic partial differential equations, Memoirs of the A.M.S., 196(917) (2008)
- [7.] G. Da Prato, J. Zabczyk, Stochastic Equations in infinite dimensions, University Press, Cambridge, 1992.
- [8.] Skorohod, A.V., Random linear operators, Riedel, 1984.
- [9.] C. Stoica, M. Megan, Discrete Asymptotic Behaviors for Skew-Evolution Semiflows on Banach Spaces, arXiv:0808.0378v2 [math.CA].
- [10.] V.M. Ungureanu, Representations of mild solutions of time-varying linear stochastic equations and the exponential stability of periodic systems, Electronic Journal of Qualitative Theory of Differential Equations 4 (2004), 1–22.
- [11.] D. Stoica, Exponential stability for stochastic cocycle, Ann. Tiberiu Popoviciu Semin. Funct. Equ. Approx. Convexity, 7 (2009), 111–118
- [12.] D. Stoica, Uniform exponential dichotomy of stochastic cocycles, Stochastic Process. Appl., 12(2010), 1920–1928



¹Nicușor Laurențiu ZAHARIA, ²Tiberiu Ștefan MĂNESCU,
³Mihaela Dorica STROIA, ⁴Tiberiu MĂNESCU jr.

DYNAMIC COEFFICIENT DETERMINATION AT A TANK WAGON

¹ ROMANIAN RAILWAY AUTHORITY – AFER, 393 CALEA GRIVIȚEI, BUCHAREST, ROMANIA
²⁻⁴ “EFTIMIE MURGU” UNIVERSITY REȘIȚA, 1-4 TRAIAN VUIA SQUARE, REȘIȚA, ROMANIA

ABSTRACT:

The tank wagons are widely used by railway freight operators to load and transport products like oil, gases, crude oil, mineral and vegetal oils, acids, alcohol, bitumen, water etc.

KEYWORDS:

dynamic coefficient, tank wagon, strain gages, rosettes, experimental stress analysis

1. INTRODUCTION

This paper present determination of dynamic coefficient based on the stress analysis results, of the strength structure of a tank wagon designed for chemical/mineral products. Before the tank wagon was allowed to circulate a series of tests had to be carried out, among which stress analysis, in accordance with international standards, as follows:

- ❖ EN 12663 – Structural requirements of railway vehicle bodies;
- ❖ UIC leaflet 577 (UIC = Union Internationale des Chemins de fer);
- ❖ ERRI B12/RP17 report (ERRI = European Rail Research Institute).

The tests which are presented in this paper were performed at Romanian Railway Authority – AFER on Stress Analysis Bench Test (fig. 1) and at Railway Test Centre Făurei (fig. 2).



Fig. 1. The tank wagon on AFER's Stress Analysis Bench Test



Fig. 2. Railway Test Centre Făurei

2. TESTS AND MEASURING POINTS

The following tests were performed in accordance with the above mentioned standards:

- A. Static (Stress Analysis Bench Test):
 1. 2 MN compressive force at buffer level (CT);
 2. 2 MN compressive force at coupler level (CA);
 3. 1.5 MN compressive force below buffer (CT50);
 4. 0.4 MN compressive force applied diagonally at buffer level (CD);

5. 1 MN tensile force in coupler area (TA);
6. tank load under pressure (SV);
7. lifting at one end of the vehicle (RID);
8. lifting the whole vehicle (RID4).
- B. dynamic (Railway Test Centre Făurei):
9. impact tests (T).

Horizontal loads (A1...A5) were applied at one end of the wagon by means of hydraulic cylinders. The other end of the wagon was leaned at buffer level, coupler level respectively. The vertical load (A6) was obtained by water filling at nominal capacity. The A7 test was performed by lifting the loaded wagon from under the buffer beam until the adjacent bogie got off the railways, with the other bogie still leaned. The A8 load was obtained by fully lifting the wagon from under its lateral support. Combination of horizontal forces with vertical loads were performed.

In figure 3 is show how the forces were applied in case of compressive force at buffers level combined with vertical load.

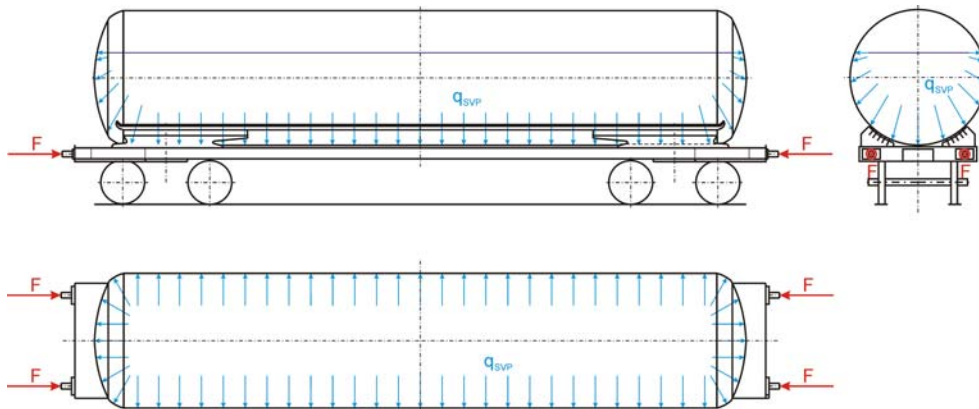


Fig. 3. Compressive force at buffers level combined with vertical load

Table 1. Static tests limits [N/mm²]

		Welding free area	Welding area
Horizontal loads (σ_{aH})		355	309
Vertical load (σ_{aV1})	Class A	277	
	Class B	150	
	Class C	133	
	Class D	110	
Vertical load (σ_{aV2})		182	166

Static tests allowable limits are shown in table 1.

The dynamic (shock) tests were performed by ramming the tank wagon, stationary on horizontal straight railways, and a wagon set up according to ERRI B12/RP17, launched down a slope (fig. 4 , fig. 5 and fig. 6).

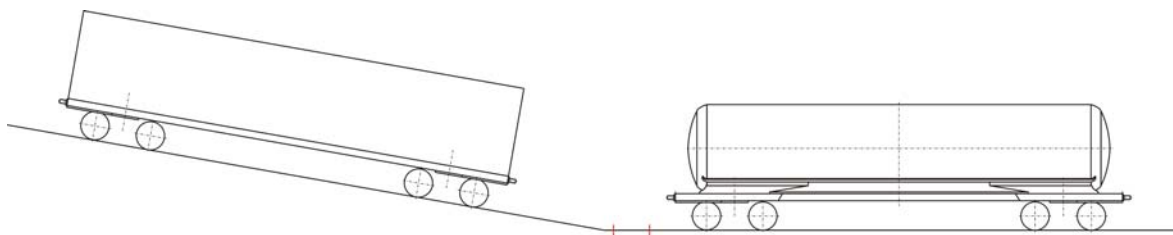


Fig. 4. Dynamic tests at Railway Test Centre Făurei



Fig. 5. The tested wagon and the ramming wagon



Fig. 6. The tested wagon and the laboratory coach

The test was performed in two stages:

1. Ten shocks at speeds growing until the sum of the forces against the two buffers reached 2.5 MN, while monitoring the relationship between the forces and the speed;
2. Another 20 shocks at the speed corresponding to 2.5 MN, namely 13.5 km/h, while recording the cumulative residual strains ϵ_{rc} and the maximum stress values as shown in figure 7.

The ram forces $F_1+F_2=F$ were measured with load cells located under the buffers, as shown in figure 11.



Fig. 7. The residual strains



Fig. 8. Load cell mounted under the buffer

The speeds were determined by taking into account the time it took the first axle of the moving wagon to run the distance of 1 m between reference points a and b (fig. 4).

Acceptance criteria:

- ❖ cumulative residual strains ϵ_{rc} on shock completion should be less than 2,000 $\mu\text{m}/\text{m}$;
- ❖ ϵ_{rc} should become steady after 30 shocks;
- ❖ the wagon equipment should remain operational.

The measurement points were located in the relevant load areas, which are:

- ❖ the chassis;
- ❖ the cradle (connection between the chassis and the tank);
- ❖ the tank.

The measurements were performed at 67 measurement points, out of which 12 rosettes. The following devices and material was used: Hottinger CENTIPEDE, MGCplus, LY11-10/120 strain gauges, RY91-6/120 (0° - 45° - 90°) rosettes and Z70 bonding material, all of them produced by HBM. The diagrams of the measurement point location on the frame and the tank are shown in figure 9 and 10.

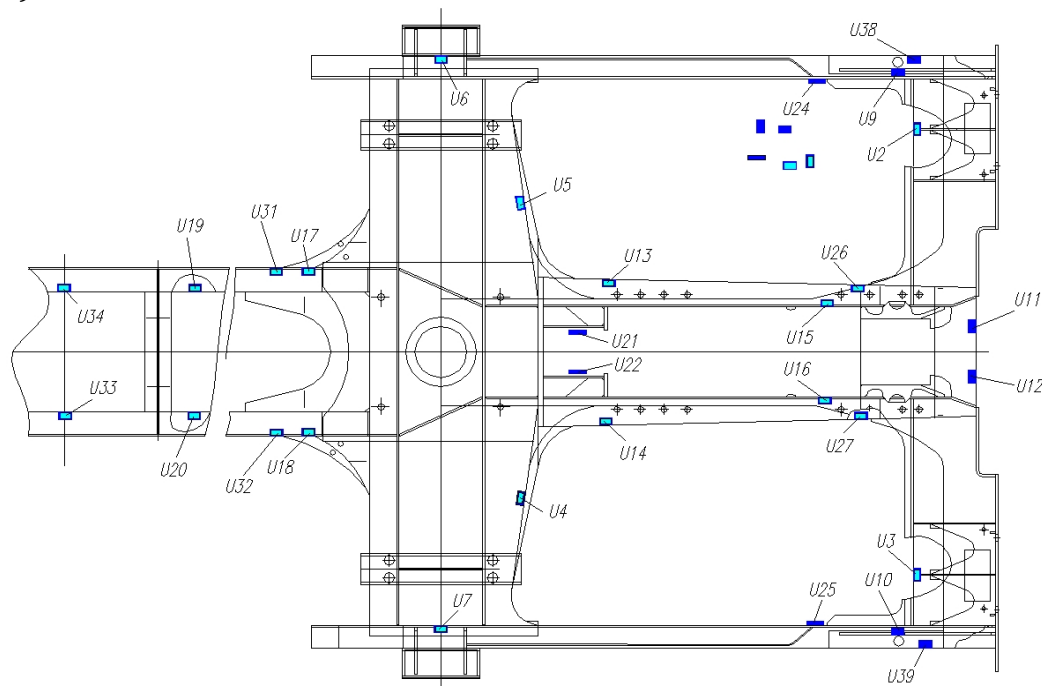


Fig. 9. Measuring points on chassis

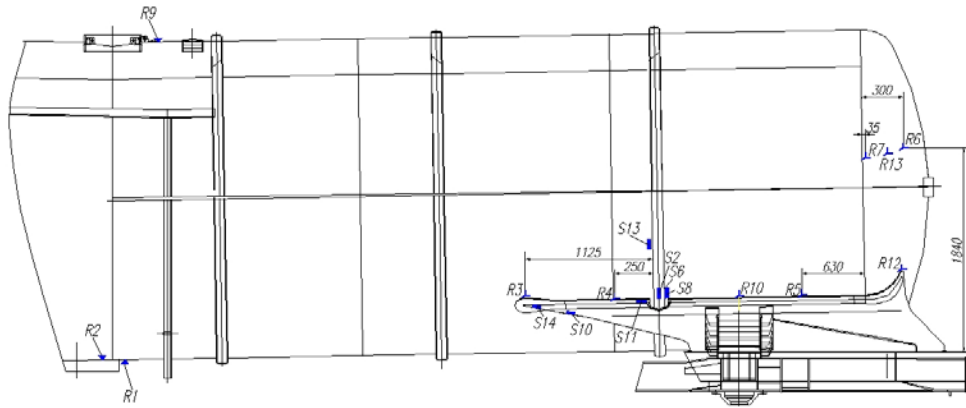


Fig. 10. Measuring points on tank and cradle

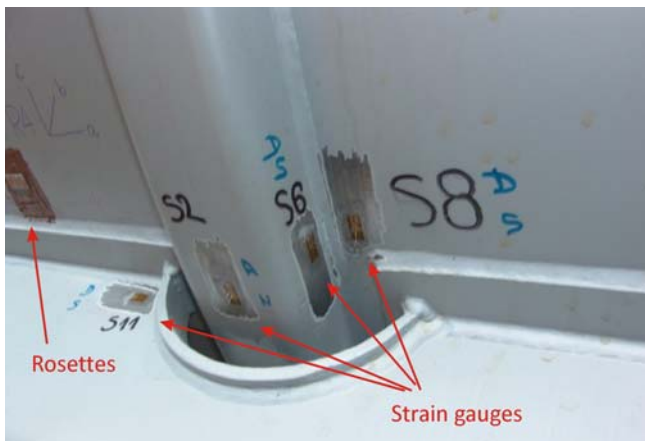


Fig. 10. Measuring points - strain gauges and rosettes (photo)

3. RESULTS

For the static tests, the measured stress was below the limits in table 1 except the following:

- ❖ During tests A1 and A3, the limit was exceeded by 3.7 % at measurement point U2; at the symmetrical measurement point U3 the measured stress was 291 N/mm², respectively 279 N/mm², less than σ_{aH} , which indicates that the accepted limit was exceeded because of asymmetrical load application;
- ❖ During test A1, at rosette R8 a specific strain ϵ_1 was measured, which exceeded the accepted limit by 4.9%

The highest cumulative residual strains ϵ_{rc} , during dynamic test, were found at measurement points U2, U3, located on the buffer beam, behind the buffers, and S2. The measured values were: $\epsilon_{rc,U2}=776 \mu\text{m/m}$, $\epsilon_{rc,U3}=821 \mu\text{m/m}$ and $\epsilon_{rc,S2}=-577 \mu\text{m/m}$.

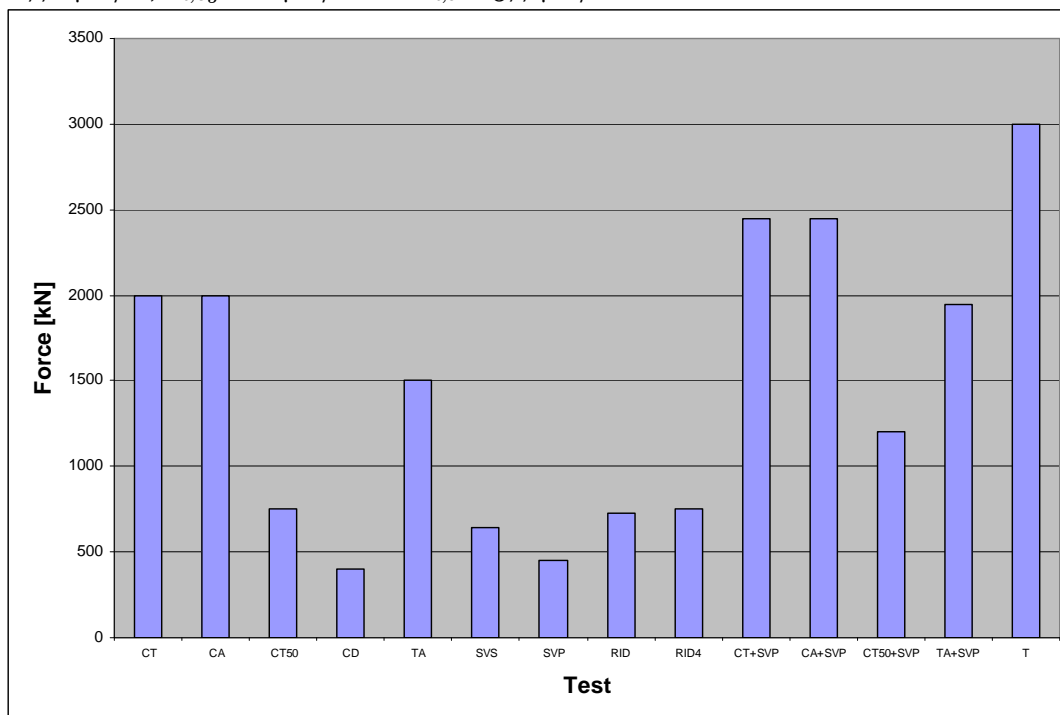


Fig. 11. The results for all test

The number of measuring points used at dynamic test is smaller than those used at static test, because of limited number of channels of measuring devices. One of choosing criteria is based on results of combined horizontal force at buffers level combined with vertical load (CT+SVS). This static test, simulate (because of buffer forces) dynamic (shock at ramming at wagons sorting) or quasi-static forces on buffers during circulation.

In figure 11, are presented the results (stress in N/mm²) for the tank wagon for entire test program.

The results grouped on main tank elements – chassis (U), cradle (C), tank (R) for CT+SVS and T test are presented in figure 12 and 13.

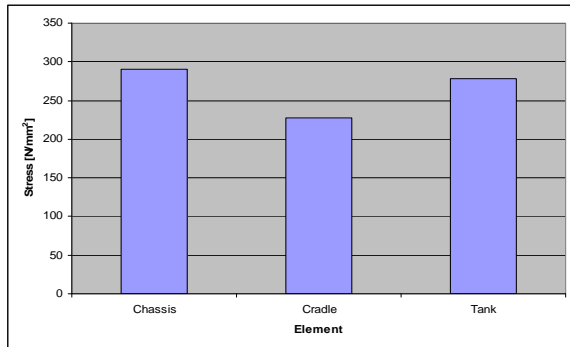


Fig. 12. The results at CT+SVS test

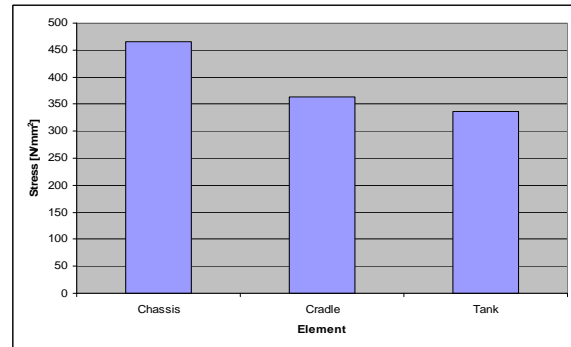


Fig. 13. The results at T test

Based on dynamic shock test results an evaluation of dynamic coefficient (by reference to CT+SVS test) – figure 14. Dynamic forces appear because of accelerations, vertical oscillatory movement of the wagon etc. From figure 14, the maximum stress at chassis level, is at U3 measuring point witch is glued behind the buffer. On the cradle, the maximum stress is at S2 measuring point witch is glued on one of tank’s reinforcing ring. The maximum stress on the tank is at rosettes R3 witch is glued on the front of the tank

From expression $F_{dynamic} = \Psi \cdot F_{static}$, where Ψ is the dynamic coefficient. According to some authors, $\Psi = 1,3$.

The maximum value of the dynamic coefficient is 5,13 at rosettes R13 and the minimum value is 1,07 at S9 strain gauge.

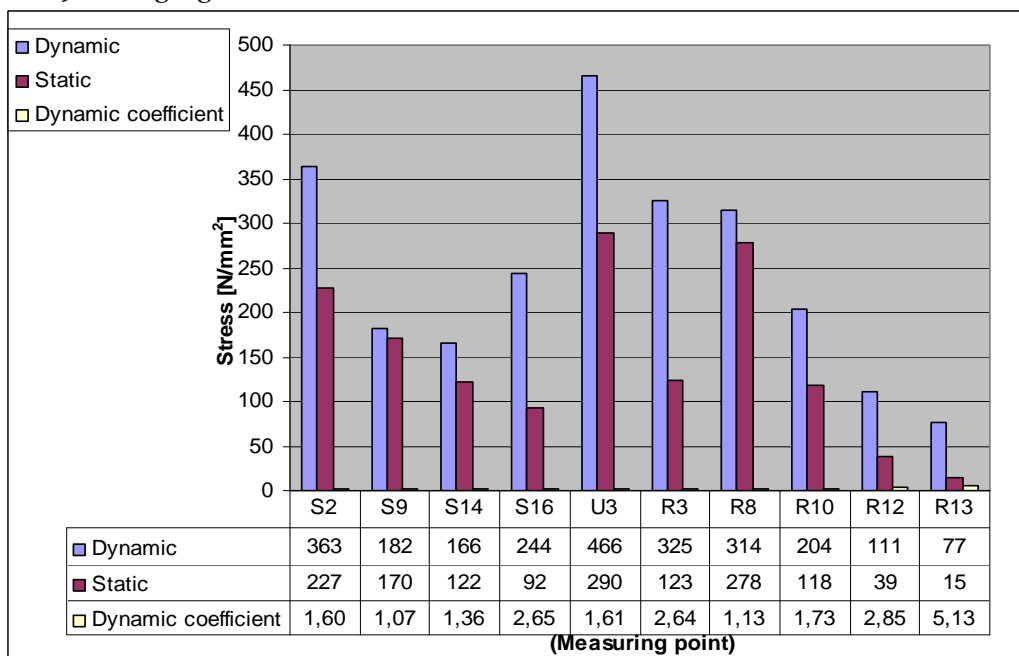


Fig. 14. Dynamic coefficient

The figure 14 show larger values of dynamic coefficient than 1,3 value, during a test witch simulate a real condition service of the tank wagon, but the dynamic coefficient it is not an evaluation condition of the wagon’s conformity with reference documents. More, according to some UIC (International Railway Union) studies, the ramming speed is smaller than 10 km/h while the maximum ramming test speed was 13,5 km/h.

4. CONCLUSIONS

After the test, based on Testing Report from experimental stress analysis and other tests the tank wagon was certificate to circulate on European Railways (the client of the tank wagon was from Western Europe).

REFERENCES

- [1.] Zaharia N. L., Contribuții privind optimizarea structurilor portante ale vagoanelor cisternă de cale ferată în vederea creșterii sarcinii pe osie și micșorarea tarei vehiculelor – teză de doctorat, conducător științific prof. dr. eur. ing. Mănescu T. Ș., Universitatea „Eftimie Murgu” Reșița, 2010
- [2.] Mănescu T. Ș., Jiğa G. G., Zaharia N. L., Bîtea C. V., Noțiuni fundamentale de rezistența materialelor și teoria elasticității, Editura „Eftimie Murgu”, ISBN 978-973-1906-67-6, Reșița, 2010
- [3.] Mănescu T. Ș., Jiğa G. G., Zaharia N. L., Bîtea C. V., Noțiuni fundamentale de rezistența materialelor, Editura „Eftimie Murgu” Orizonturi tehnice, ISBN 973-8286-79-4, Reșița, 2008
- [4.] Mănescu T. Ș., Copaci I., Olaru S., Creangă F.Ș., Tensometria electrică rezistivă în cercetarea experimentală, Editura Mirton, ISBN 973-661-892-5, Timișoara, 2006
- [5.] Karl Hoffman: An Introduction to Measurement using Strain Gages, Hottinger Baldwin Messtechnik GmbH, Darmstadt, 2005
- [6.] Simion I., Melinte F., N. L. Zaharia, The Application Of Electrical Strain Gages For Stress Analysis On A Tank Wagon, 24th Danubia-Adria Symposium on Developments in Experimental Mechanics, pag. 183÷185, ISBN 978-973-739-456-9, Sibiu, 2007
- [7.] ***EN 12663 – Structural requirements of railway vehicle bodies, 2000
- [8.] ***UIC leaflet 577 – Sollicitations des wagons, 2004
- [9.] ***ERRI B12/RP17 – Programme des essais à faire subir aux wagons à châssis et superstructure en acier (aptés à recevoir l’attelage automatique de choc et traction) et à leurs bogie à châssis en acier, Utrecht, 1997





¹Ștefan MAKSAY, ²Diana STOICA

CONSIDERATIONS ON THE RECTANGLE TRUNCATED BIDIMENSIONAL NORMAL MODELING

^{1,2} UNIVERSITY "POLITEHNICA" TIMISOARA, FACULTY OF ENGINEERING HUNEDOARA, ROMANIA

ABSTRACT:

In this article, which generalizes the paper [1], we started from the expression of the classic normal distribution density with two variables, we made a few considerations about the process of experimental data, by means of the distribution density that generalizes the bidimensional classical normal law. The bidimensional distribution densities are rectangle truncated [2], obviously keeping the properties of a density. The new expressions of the density, having one or more extra parameters, can better approximate the experimental data.

A.M.S.(2000) Subject Classification: 35B15; 00A71;

KEYWORDS:

Modeling truncated, normal distribution density, coefficient of correlation

1. INTRODUCTION

In this article, which generalizes the paper [1], we started from the expression of the classic normal distribution density with two variables [3], we made a few considerations about the process of experimental data, by means of the distribution density that generalizes the bidimensional classical normal law. Thus, we further on present a few distinct modeling variants.

The first two expressions for the distribution density will introduce one, respectively two parameters, fact that permits an optimal modeling of the experimental data.

This article proposes to model the experimental data presented in the next table, which shows the coordinates of points in the space with three dimensions, where the first two lines represent the independent variables x and y , and the tree lines represent the dependent variable u .

	1	2	3	4	5	6	7	8	9	10	11	12	13	14	15	
var =	1	0.483	1.06	1.144	1.389	1.574	1.605	1.891	2.039	2.501	2.606	2.728	2.776	2.824	2.887	3.973
	2	2.093	2.132	2.153	2.227	2.38	2.706	2.782	3.002	3.083	3.107	3.67	3.836	4.071	4.329	4.514
	3	0.03	0.064	0.073	0.105	0.18	0.196	0.231	0.229	0.229	0.215	0.149	0.1	0.084	0.05	0.02

Further on we note

$$\begin{aligned} mx &:= \text{mean}(x) & my &:= \text{mean}(y) & mu &:= \text{mean}(u), \\ sx &:= \text{stdev}(x) & sy &:= \text{stdev}(y) & su &:= \text{stdev}(u), \end{aligned}$$

where *mean* and *stdev* represent the mean value and respectively the standard deviation of the corresponding variable. For the given measurements, we have

$$\begin{aligned} mx &= 2.0986 & my &= 3.0724 & mu &= 0.1304 \\ sx &= 0.8795 & sy &= 0.8042 & su &= 0.0748 \end{aligned}$$

Note by $f_{clas}(x,y)$ the classic normal distribution density with two variables [3]

$$f_{clas}(x,y) := \frac{1}{2 \cdot \pi \cdot sx \cdot sy} \cdot \exp \left[\frac{-1}{2} \cdot \left[\frac{(x - mx)^2}{sx^2} + \frac{(y - my)^2}{sy^2} \right] \right] \quad (1)$$

2. PRACTICAL CASE

Instead of the classic distribution density (1) we consider the function:

$$ftrunc1(x, y, cx, cy) = \begin{cases} K \cdot \frac{1}{2\pi \cdot sx \cdot sy} \exp\left[-\frac{1}{2} \cdot \left[\frac{(x - mx)^2}{sx^2} + \frac{(y - my)^2}{sy^2}\right]\right], & (|x - mx| < cx \cdot sx) \wedge (|y - my| < cy \cdot sy) \\ 0, & \text{in rest} \end{cases} \quad (2)$$

where K , cx and cy are positives constants.

For the function $ftrunc1$ to be a distribution density we impose the conditions

$$ftrunc1(x, y, cx, cy) \geq 0 \quad \text{and} \quad \int_{-\infty}^{\infty} \int_{-\infty}^{\infty} ftrunc1(x, y, cx, cy) dx dy = 1,$$

hence results the value for K

$$K := \frac{1}{\int_{mx-cx \cdot sx}^{mx+cx \cdot sx} \int_{my-cy \cdot sy}^{my+cy \cdot sy} \text{if} \left[(|x - mx| < cx \cdot sx) \wedge (|y - my| < cy \cdot sy), \frac{1}{2\pi \cdot sx \cdot sy} \cdot \exp\left[-\frac{1}{2} \cdot \left[\frac{(x - mx)^2}{sx^2} + \frac{(y - my)^2}{sy^2}\right]\right], 0 \right] dy dx}$$

We remark the fact that for $cx \rightarrow \infty$ and $cy \rightarrow \infty$, the function $ftrunc1(x, y, cx, cy)$ coincides with the function $fclas(x, y)$.

The constants cx and cy will be determined by imposing the condition of minimizing the sum of the difference squares between of the value of theoretic function $ftrunc1(x, y, cx, cy)$ and experimental value of independent variable u , that is we minimize the function $F(cx, cy)$

$$F(cx, cy) := \sum_{i=1}^n (ftrunc1(x_i, y_i, cx, cy) - u_i)^2$$

In order to achieve this, we will use the next program, written in language MathCAD.

```

ORIGIN ≡ 1
x := (0.4829 1.0601 1.1437 1.3885 1.574 1.6049 1.8914 2.0392 2.5008 2.6057 2.7279 2.776 2.824 2.8866 3.9726)
y := (2.0933 2.1323 2.1534 2.2267 2.3801 2.7062 2.7818 3.0022 3.0829 3.1074 3.6696 3.836 4.0711 4.3291 4.5142)
u := (0.03 0.0639 0.0733 0.1055 0.1802 0.1956 0.2314 0.2294 0.2288 0.2149 0.1492 0.1003 0.0836 0.0501 0.02)
x := xT          y := yT          u := uT
n := length(x)    i := 1..n        nrdivx:= 5    nrdivy:= 7
dxi := 1          dx := 2.
dyi := 1          dy := 3
prog1 :=
px ← nrdivx
py ← nrdivy
for j ∈ 1..px + 1
    cx_j ← dxi + (j - 1) · (dx - dxi) / px
    for k ∈ 1..py + 1
        cy_k ← dyi + (k - 1) · (dy - dyi) / py
        K ← 1 / (∫_{mx-cx_j·sx}^{mx+cx_j·sx} ∫_{my-cy_k·sy}^{my+cy_k·sy} if[[[(x - mx)² < (cx_j·sx)²] ∧ [(y - my)² < (cy_k·sy)²]], fclas(x, y), 0] dy dx)
        fCT_j,k ← ∑_{i=1}^n [if[[[(x_i - mx)² < (cx_j·sx)²] ∧ [(y_i - my)² < (cy_k·sy)²]], K · fclas(x_i, y_i), 0] - u_i]²
    fmin ← min(fCT)
    for j ∈ 1..px + 1
        for k ∈ 1..py + 1
            indx ← j
            indy ← k
            break if (fCT_j,k - fmin) = 0
        break if (fCT_j,k - fmin) = 0
    [cx_j cy_k fCT (indx indy fmin)]
prog1 = (2 1.8571 {6,8} {1,3})
    
```

$$\begin{aligned}
 cxf &:= \text{prog1}_{1,1} & cxf &= 2 \\
 cyf &:= \text{prog1}_{1,2} & cyf &= 1.8571 \\
 fCT &:= \text{prog1}_{1,3} \\
 (\text{indx } \text{indy } \text{fmin}) &:= \text{prog1}_{1,4} \\
 \text{prog1}_{1,4} &= (6 \ 4 \ 2.477 \times 10^{-3}) \\
 \text{indx} &= 6 & \text{indy} &= 4 & \text{fmin} &= 2.477 \times 10^{-3} \\
 fCT - \text{fmin} &= \begin{pmatrix} 0.2904 & 0.1436 & 0.0864 & 0.0623 & 0.0512 & 0.046 & 0.0436 & 0.0425 \\ 0.1823 & 0.0708 & 0.0341 & 0.0203 & 0.0143 & 0.0117 & 0.0105 & 9.9963 \times 10^{-3} \\ 0.1283 & 0.0399 & 0.0152 & 7.3245 \times 10^{-3} & 4.353 \times 10^{-3} & 3.1694 \times 10^{-3} & 2.6787 \times 10^{-3} & 2.4737 \times 10^{-3} \\ 0.0993 & 0.0248 & 7.1072 \times 10^{-3} & 2.6071 \times 10^{-3} & 1.3245 \times 10^{-3} & 9.7519 \times 10^{-4} & 8.8255 \times 10^{-4} & 8.5732 \times 10^{-4} \\ 0.0831 & 0.017 & 3.5837 \times 10^{-3} & 1.1204 \times 10^{-3} & 8.4481 \times 10^{-4} & 9.9182 \times 10^{-4} & 1.1357 \times 10^{-3} & 1.2172 \times 10^{-3} \\ 0.0737 & 0.012 & 1.2018 \times 10^{-3} & 0 & 3.4867 \times 10^{-4} & 8.0354 \times 10^{-4} & 1.0942 \times 10^{-3} & 1.2419 \times 10^{-3} \end{pmatrix}
 \end{aligned}$$

Substituting these values of cx and cy in expression of $ftrunc1(x,y,cx,cy)$ leads to the expression of the truncated distribution density of first form that approximate better the experimental data.

Thus, the graphs of the classic and truncated distribution density, for the given experimental values, are shown in Figure 1 and respectively in Figure 2.

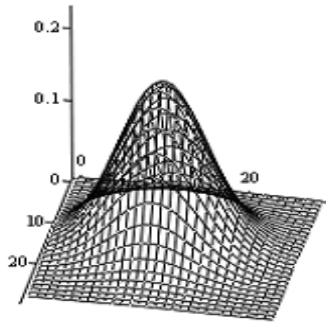


Figure 1. The classical distribution density

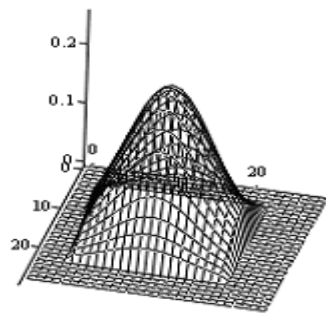


Figure 2. The truncated distribution density $ftrunc1(x,y,cx,cy)$

The correlation coefficients corresponding of the two modeling's are

$$\begin{aligned}
 r_{clas} &:= \sqrt{1 - \frac{\sum_i (u_i - f_{clas}(x_i, y_i))^2}{\sum_i (u_i - \text{mean}(u))^2}} & r_{clas} &= 0.9631 \\
 r_{trunc1} &:= \sqrt{1 - \frac{\sum_i (u_i - f_{trunc1}(x_i, y_i, cxf, cyf))^2}{\sum_i (u_i - \text{mean}(u))^2}} & r_{trunc1} &= 0.9852
 \end{aligned}$$

The values of dependent variable u , of the distribution density f_{clas} , f_{trunc1} in the points (x_i, y_i) are given, comparatively, in the next table.

$$\begin{aligned}
 f_{clas_i} &:= f_{clas}(x_i, y_i) & f_{trunc1_i} &:= f_{trunc1}(x_i, y_i, cxf, cyf) \\
 vb &:= \text{augmen}(x, y, u, f_{clas}, f_{trunc1})^T
 \end{aligned}$$

	1	2	3	4	5	6	7	8	9	10	11	12	13	14	15
1	0.4829	1.0601	1.1437	1.3885	1.574	1.6049	1.8914	2.0392	2.5008	2.6057	2.7279	2.776	2.824	2.8866	3.9726
2	2.0933	2.1323	2.1534	2.2267	2.3801	2.7062	2.7818	3.0022	3.0829	3.1074	3.6696	3.836	4.0711	4.3291	4.5142
3	0.03	0.0639	0.0733	0.1055	0.1802	0.1956	0.2314	0.2294	0.2288	0.2149	0.1492	0.1003	0.0836	0.0501	0.02
4	0.0198	0.0566	0.065	0.0934	0.13	0.1733	0.205	0.2236	0.2026	0.1904	0.1322	0.1066	0.0741	0.0444	0.0110 ⁻³
5	0.0222	0.0633	0.0727	0.1045	0.1454	0.1938	0.2293	0.2501	0.2267	0.2129	0.1479	0.1192	0.0828	0.0497	0

The distribution rate function $F_{clas}(x,y)$ is given by

$$F_{clas}(x, y) = \int_{-\infty}^x \int_{-\infty}^y f_{clas}(u, v) dv du .$$

The rate of the truncated distribution functions is

$$F_{trunc1}(x, y, cx, cy) = \int_{-\infty}^x \int_{-\infty}^y f_{trunc1}(u, v, cx, cy) dv du .$$

Using the following program, we showed in Figure 5 the function F_{trunc1} and in Figure 6 the corresponding contours lines.

nrn := 15

k := 1..nrn $xv_k := (\min(x) - 1) + \frac{(\max(x) + 1) - (\min(x) - 1)}{nrn - 1} \cdot (k - 1)$

h := 1..nrn $yv_h := (\min(y) - 1) + \frac{(\max(y) + 1) - (\min(y) - 1)}{nrn - 1} \cdot (h - 1)$

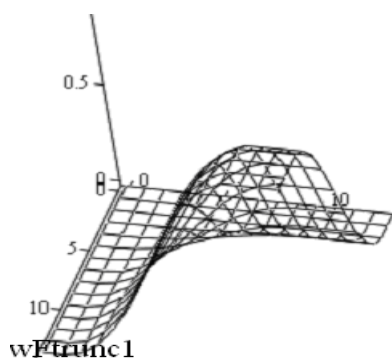


Figure 5. The truncated distribution function F_{trunc1}

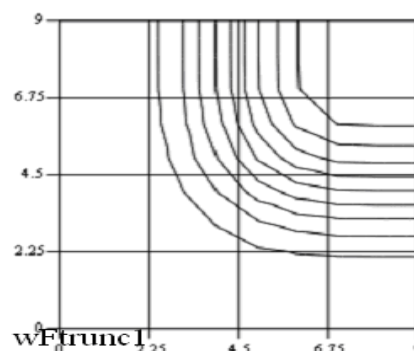


Figure 6. The contour lines of the truncate distribution function F_{trunc1}

Inserting the notations

$$F_{clas_i} := F_{clas}(x_i, y_i), \quad F_{trunc1_i} := F_{trunc1}(x_i, y_i, cx_i, cy_i),$$

$$vb := \text{augmen}(F_{clas}, F_{trunc1})^T,$$

the constants that appear as having been previously determined, results the distribution of the values of distribution functions in points corresponding to the experimental system point.

	1	2	3	4	5	6	7	8	9	10	11	12	13	14	15	
vb=	1	54·10 ⁻³	0.0134	0.0165	0.0295	0.0519	0.0904	0.143	0.2161	0.3373	0.367	0.5817	0.6389	0.7024	0.7587	0.9393
	2	43·10 ⁻⁴	71·10 ⁻³	0.0123	0.024	0.0461	0.0866	0.1406	0.2184	0.3461	0.3776	0.6121	0.6746	0.7441	0.8056	0.9948

3. CONCLUSIONS

We notice that, for the experimental data presented in the paper, the optimal modeling is given by the distribution density $f_{trunc1}(x,y,cx,cy)$ ($r_{trunc1} = 0.9852$).

This modeling are better than the non-truncated modeling $f_{clas}(x,y)$ ($r_{clas} = 0.9631$).

In the practical case these results show us, that is more advantage to use the truncated modeling, because the classical modeling is the practical case of these.

REFERENCES

- [1.] Șt. Maksay, D. Stoica – Considerations on Modeling Some Distribution Laws, Applied Mathematics and Computation, Volume 175, Issue 1, 1 April 2006, Pages 238-246;
- [2.] Johnson, A.C. (2001), "On the Truncated Normal Distribution: Characteristics of Singly- and Doubly-truncated Populations of Application in Management Science," PhD. Dissertation, Stuart Graduate School of Business, Illinois Institute of Technology, Illinois.
- [3.] Șt. Maksay, D. Stoica – Calculul probabilităților, Editura Politehnica, Timișoara, 2005;



RIESZ-DUNFORD REPRESENTATION THEOREM FOR UNIFORMLY CONTINUOUS SEMIGROUPS

¹ UNIVERSITY "POLITEHNICA" TIMIȘOARA, FACULTY OF ENGINEERING HUNEDOARA, ROMÂNIA

²⁻³ UNIVERSITY "POLITEHNICA" TIMIȘOARA, DEPARTMENT OF MATHEMATICS, ROMÂNIA

⁴ NATIONAL COLLEGE OF INFORMATICS "TRAIAN LALESCU" HUNEDOARA, ROMANIA

ABSTRACT:

This note presents a Riesz-Dunford type representation and a Bromwich type representation for uniformly continuous semigroups on a Banach space.

A.M.S.(2010) Subject Classification: 47D03.

KEYWORDS:

uniformly continuous semigroups, Riesz-Dunford representation, Bromwich representation

1. INTRODUCTION

Let E be a complex Banach space. We denote by $B(E)$ the Banach algebra of bounded linear operators on E . For a closed linear operator A , not necessarily bounded, with domain $D(A)$ in the space E , denote by $\rho(A)$ and $R(\cdot, A)$ the resolvent set of A and the resolvent of A , respectively.

The family of operators $\{T(t)\}_{t \geq 0} \subset B(E)$ is said to be a *semigroup of bounded linear operators on E* if

- (i) $T(0) = I$ (I is the identity operator on E);
- (ii) $T(t+s) = T(t)T(s)$ for all $t, s \geq 0$ (the semigroup property).

The semigroup $\{T(t)\}_{t \geq 0} \subset B(E)$ is said to be *uniformly continuous* if $t \mapsto T(t)$ is continuous on $[0, \infty)$ in the uniform operator topology. Due to semigroup property this is equivalent to

$$\lim_{t \downarrow 0} \|T(t) - I\| = 0.$$

The most important object associated to a C_0 -semigroup $\{T(t)\}_{t \geq 0}$ is its infinitesimal generator. The linear operator A defined by

$$D(A) = \left\{ x \in E : \lim_{t \downarrow 0} \frac{T(t)x - x}{t} \text{ exists} \right\}$$

and

$$Ax = \lim_{t \downarrow 0} \frac{T(t)x - x}{t}, \quad \forall x \in D(A)$$

is the *infinitesimal generator* of the semigroup $\{T(t)\}_{t \geq 0}$. Clearly the operator $A : D(A) \subseteq E \rightarrow E$ is linear but not necessarily bounded unless $D(A)$ is all of E . Nathan [4] and Yosida [7] proved that the infinitesimal generator of a semigroup is a bounded linear operator in E if and only if the semigroup is uniformly continuous. For more information about C_0 -semigroup we refer to Davies [1], Hille and Phillips [2], Pazy [5], Yosida [8] and the references therein.

This paper is dedicated to the problem of representing the semigroup $\{T(t)\}_{t \geq 0}$ in terms of its infinitesimal generator. We can obtain the semigroup from the resolvent of the generator A by inverting the Laplace transform. Similar results for C_0 -semigroups were presented in Lemle and Jiang [3].

2. RIESZ-DUNFORD'S TYPE REPRESENTATIONS

In this section we give a Riesz-Dunford's type representation for uniformly continuous semigroups. For this purpose we use a special class of Jordan's curves for a bounded linear operator defined by Reghiş and Babescu [6].

2.1. Definition. A Jordan closed smooth curve which surround $\sigma(A)$ is said to be A -spectral if it is homotope to a circle C_r of radius $r > \|A\|$ centered at the origin.

We have:

2.2. Theorem. Let A be the infinitesimal generator of the uniformly continuous semigroup $\{T(t)\}_{t \geq 0}$. If Γ_A is an A -spectral curve then

$$T(t) = \frac{1}{2\pi i} \int_{\Gamma_A} e^{\lambda t} R(\lambda; A) d\lambda \quad , \quad \forall t \geq 0.$$

Proof. Let Γ_A be an A -spectral curve. Then Γ_A is homotope to the circle C_r of radius $r > \|A\|$ centered at the origin. We have:

$$\frac{1}{2\pi i} \int_{\Gamma_A} e^{\lambda t} R(\lambda; A) d\lambda = \frac{1}{2\pi i} \int_{C_r} e^{\lambda t} R(\lambda; A) d\lambda \quad , \quad \forall t \geq 0.$$

But the serie

$$R(\lambda; A) = \sum_{n=0}^{\infty} \frac{A^n}{\lambda^{n+1}}$$

converges uniformly for λ on compacts set of $\{\lambda \in C : |\lambda| > \|A\|\}$, particularly on circle C_r . Then

$$\frac{1}{2\pi i} \int_{C_r} e^{\lambda t} R(\lambda; A) d\lambda = \frac{1}{2\pi i} \int_{C_r} e^{\lambda t} \sum_{n=0}^{\infty} \frac{A^n}{\lambda^{n+1}} d\lambda = \sum_{n=0}^{\infty} \frac{1}{2\pi i} \int_{C_r} \frac{e^{\lambda t}}{\lambda^{n+1}} d\lambda A^n.$$

Using the identities

$$\frac{1}{2\pi i} \int_{C_r} \frac{e^{\lambda t}}{\lambda^{n+1}} d\lambda = \frac{t^n}{n!} \quad , \quad \forall n \in N,$$

we conclude that

$$\frac{1}{2\pi i} \int_{\Gamma_A} e^{\lambda t} R(\lambda; A) d\lambda = \sum_{n=0}^{\infty} \frac{t^n A^n}{n!} = T(t) \quad , \quad \forall t \geq 0. \blacksquare$$

3. BROMWICH'S TYPE REPRESENTATION

Next theorem gives Bromwich's type representation theorem for uniformly continuous semigroups.

3.1. Theorem. Let A be the infinitesimal generator of a C_0 -semigroup $\{T(t)\}_{t \geq 0}$. If $a > \|A\|$, then

$$T(t) = \frac{1}{2\pi i} \int_{a-i\infty}^{a+i\infty} e^{zt} R(z; A) dz$$

and the integral converges uniformly for t in bounded intervals.

Proof. Let $a > \|A\|$. For $R > 2a$ we consider Jordan's closed smooth curve

$$\Gamma_R = \Gamma'_R \cup \Gamma''_R$$

where

$$\Gamma'_R = \{a + i\tau : \tau \in [-R, R]\}$$

and

$$\Gamma''_R = \left\{ a + R(\cos \varphi + i \sin \varphi) : \varphi \in \left[\frac{\pi}{2}, \frac{3\pi}{2} \right] \right\}$$

For $z \in \Gamma'_R$ we have

$$|z| = |a + i\tau| > a > \|A\|$$

and for $z \in \Gamma''_R$ we find

$|z| = |a + R(\cos \varphi + i \sin \varphi)| = |a - [-R(\cos \varphi + i \sin \varphi)]| \geq |a - R| > \|A\|$. Therefore from $z \in \Gamma_R$ it follows $z \in \rho(A)$. Moreover, Γ_R is homotop to the circle C of radius $R-a$ centered at the origin.

Then Γ_R is an A-spectral curve and from theorem 2.2 it follows that

$$T(t) = \frac{1}{2\pi i} \int_{\Gamma_R} e^{zt} R(z; A) dz \quad , \quad \forall t \geq 0$$

for every $R > 2a$. If we denote

$$I'_t(R) = \frac{1}{2\pi i} \int_{\Gamma'_R} e^{zt} R(z; A) dz$$

and

$$I''_t(R) = \frac{1}{2\pi i} \int_{\Gamma''_R} e^{zt} R(z; A) dz$$

we can see that $T(t) = I'_t(R) + I''_t(R)$, $\forall t \geq 0$.

Next we show that

$$\lim_{R \rightarrow \infty} \frac{1}{2\pi i} \int_{\Gamma''_R} e^{zt} R(z; A) dz = 0$$

uniformly for t in bounded intervals. To this end we use the serie

$$R(z; A) = \sum_{n=0}^{\infty} \frac{A^n}{z^{n+1}}$$

which converges uniformly for z on compacts set of $\{z \in C : |z| > \|A\|\}$, particularly on Γ''_R . For every $R > 2a$ and every $t \geq 0$ we have

$$\begin{aligned} I''_t(R) &= \sum_{n=0}^{\infty} \left(\frac{1}{2\pi i} \int_{\Gamma''_R} \frac{e^{zt}}{z^{n+1}} A^n dz \right) = \\ &= \left(\frac{1}{2\pi i} \int_{\Gamma''_R} \frac{e^{zt}}{z} dz \right) I + \sum_{n=1}^{\infty} \left(\frac{1}{2\pi i} \int_{\Gamma''_R} \frac{e^{zt}}{z^{n+1}} dz \right) A^n \end{aligned}$$

We consider

$$A_t(R) = \left(\frac{1}{2\pi i} \int_{\Gamma''_R} \frac{e^{zt}}{z} dz \right) I$$

and

$$B_t(R) = \sum_{n=1}^{\infty} \left(\frac{1}{2\pi i} \int_{\Gamma''_R} \frac{e^{zt}}{z^{n+1}} dz \right) A^n$$

Changing variables to

$$z = a + R(\cos \varphi + i \sin \varphi) \quad , \quad \varphi \in \left[\frac{\pi}{2}, \frac{3\pi}{2} \right]$$

we obtain

$$\begin{aligned} A_t(R) &= \left[\frac{1}{2\pi i} \int_{\frac{\pi}{2}}^{\frac{3\pi}{2}} \frac{e^{t(a+R \cos \varphi + i \sin \varphi)}}{z} R(-\sin \varphi + i \cos \varphi) d\varphi \right] I = \\ &= \left[\frac{R}{2\pi} e^{ta} \int_{\frac{\pi}{2}}^{\frac{3\pi}{2}} e^{tR \cos \varphi} e^{itR \sin \varphi} \frac{1}{z} (\cos \varphi + i \sin \varphi) d\varphi \right] I \end{aligned}$$

from where one deduce that

$$\begin{aligned} \|A_t(R)\| &\leq \frac{R}{2\pi} e^{ta} \int_{\frac{\pi}{2}}^{\frac{3\pi}{2}} e^{tR \cos \varphi} \left\| e^{itR \sin \varphi} \right\| \frac{1}{|z|} |\cos \varphi + i \sin \varphi| d\varphi \leq \\ &\leq \frac{R}{2\pi} e^{ta} \int_{\frac{\pi}{2}}^{\frac{3\pi}{2}} e^{tR \cos \varphi} \frac{1}{R-a} d\varphi \leq \frac{1}{2\pi} \frac{R}{R-a} \int_{\frac{\pi}{2}}^{\frac{3\pi}{2}} e^{tR \cos \varphi} d\varphi \end{aligned}$$

since for $z \in \Gamma''_R$ we have

$$|z| = |a + R(\cos \varphi + i \sin \varphi)| > R - a$$

therefore

$$\frac{1}{|z|} < \frac{R}{R-a}.$$

Consider $0 < t_1 < t_2$ and $t \in [t_1, t_2]$. From the inequality $R > 2a$, it follows that $2R - 2a > R$ and therefore

$$\frac{R}{R-a} < 2.$$

Consequently

$$\|A_t(R)\| \leq \frac{1}{\pi} e^{ta} \int_{\frac{\pi}{2}}^{\frac{3\pi}{2}} e^{tR \cos \varphi} d\varphi \leq \frac{1}{\pi} e^{t_2 a} \int_{\frac{\pi}{2}}^{\frac{3\pi}{2}} e^{t_1 R \cos \varphi} d\varphi$$

But for every $\varphi \in \left[\frac{\pi}{2}, \frac{3\pi}{2} \right]$ one obtain $e^{t_1 R \cos \varphi} \leq 1$ and we have

$$\lim_{R \rightarrow \infty} e^{t_1 R \cos \varphi} = 0.$$

By Lebesgue's bounded convergences theorem it follows

$$\lim_{R \rightarrow \infty} \int_{\frac{\pi}{2}}^{\frac{3\pi}{2}} e^{t_1 R \cos \varphi} d\varphi = 0$$

so we deduce that

$$\lim_{R \rightarrow \infty} A_t(R) = 0$$

and the limit is uniform for $t \in [t_1, t_2]$.

We consider now the integral

$$B_t(R) = \sum_{n=1}^{\infty} \left(\frac{1}{2\pi i} \int_{\Gamma_R^n} \frac{e^{zt}}{z^{n+1}} dz \right) A^n$$

For every $t \in [t_1, t_2]$ and $R > 2a$ we have

$$e^{tR \cos \varphi} \leq 1, \quad \forall \varphi \in \left[\frac{\pi}{2}, \frac{3\pi}{2} \right],$$

so that

$$\left| \int_{\Gamma_R^n} \frac{e^{zt}}{z^{n+1}} dz \right| \leq \frac{R e^{ta}}{(R-a)^{n+1}} \int_{\frac{\pi}{2}}^{\frac{3\pi}{2}} e^{tR \cos \varphi} d\varphi \leq \pi e^{ta} \frac{R}{(R-a)^{n+1}}$$

Since $R > 2a > a + \|A\|$, it follows

$$\|B_t(R)\| \leq \sum_{n=1}^{\infty} \frac{\|A\|^n}{2\pi} \left| \int_{\Gamma_R^n} \frac{e^{zt}}{z^{n+1}} dz \right| \leq \frac{e^{ta}}{2} \frac{R}{R-a} \sum_{n=1}^{\infty} \left(\frac{\|A\|}{R-a} \right)^n$$

and because

$$\frac{\|A\|}{R-a} < 1$$

one deduce that

$$\|B_t(R)\| \leq e^{ta} \frac{\|A\|}{2} \frac{R}{R-a} \frac{1}{R-a-\|A\|}.$$

Consequently

$$\lim_{R \rightarrow \infty} B_t(R) = 0$$

and the limit is uniform for $t \in [t_1, t_2]$.

Then we have

$$\lim_{R \rightarrow \infty} I''(R) = 0$$

uniformly for $t \in [t_1, t_2]$ from where we conclude that

$$T(t) = \lim_{R \rightarrow \infty} \frac{1}{2\pi i} \int_{\Gamma_R} e^{zt} R(z; A) dz = \frac{1}{2\pi i} \int_{a-i\infty}^{a+i\infty} e^{zt} R(z; A) dz$$

and the integral converges uniformly for $t \in [t_1, t_2]$. ■

REFERENCES

- [1.] Davies, E.B. (1980). *One-parameter semigroups*. Academic Press.
- [2.] Hille, E. and Phillips, R.S. (1957). *Functional Analysis and Semi-Groups*. A.M.S. Providence.
- [3.] Lemle, L.D., Jiang, Y. (2007). Bromwich's type representation for semigroups of linear operators, *The Cyprus Journal of Sciences*, Vol. 5, 107-125.
- [4.] Nathan, D.S. (1935). One parameter semigroups of transformations in abstract vector spaces, *Duke Math. J.*, 518-526.
- [5.] Pazy, A. (1983). *Semigroups of Linear Operators and Applications to Partial Differential Equations*. Springer Verlag.
- [6.] Reghiş, M. and Babescu, Gh. (1980). Cosine and sine functions valued in Banach algebras, *Analele Univ. Timișoara*, Vol. 1, 83-92.
- [7.] Yosida, K. (1936). On the group embedded in the metrical complete ring, *Japan J. Math.*, 7-26.
- [8.] Yosida, K. (1967). *Functional Analysis*. Springer Verlag.



¹Imre Zsolt MIKLOS; ²Carmen Inge ALIC; ³Cristina Carmen MIKLOS

INDEXING DEVICE WITH SPHERICAL ELEMENTS (BALLS)

¹⁻³ UNIVERSITY POLITEHNICA OF TIMISOARA, FACULTY OF ENGINEERING FROM HUNEDOARA, ROMANIA

ABSTRACT:

In the present paper it's present an indexing device used to protect the blooms tilting mechanisms on rolling train, the modeling and its CAD using Autodesk Inventor Professional, respectively that experimental tests on a laboratory model of the device together with the results analyzes in table and graphically form.

KEYWORDS:

Tilting mechanism, indexing device, experimental trials

1. INTRODUCTION

The proposed device is used to protect the tilting mechanisms from the blooming type rolling train if accidental increase the force from the main tilting rod.

The main rod of the tilting mechanism is a sword-sheath construction; the combination of the two components is accomplished by two bolts, which are designed to break when the force exceeds a value determined by design. The proposed protection device works on the principle of indexing systems with balls, is adaptable to the tilting mechanism rod and serves to eliminate the time when the rolling train not work to change the broken bolts with new ones. Principle sketch of the protection device with balls is shown in fig. 1.

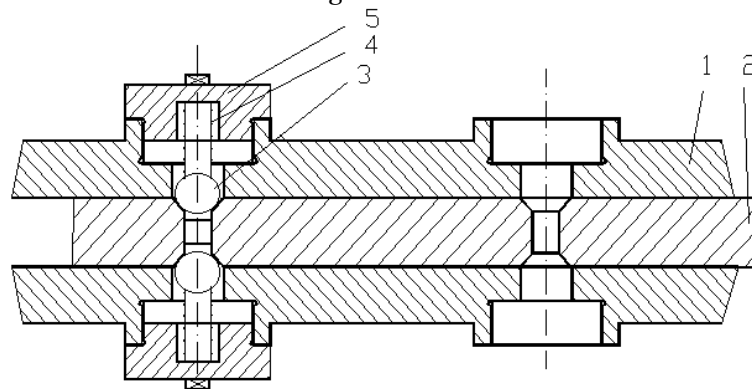


Fig. 1. Protection device with spherical elements. 1 - rod sheath; 2 - sword rod; 3 - spherical locking element (ball); 4 - compression spring; 5 - screw cap

Instead each shear bolt will be mounted a pair of spherical locking elements (balls).

If the force of the rod tilting mechanism exceeds (accidentally) the operation mode corresponding value, the balls from the device construction are retracting in space from the sheath rod, compressing the springs. In a new cycle of the tilting mechanism, in the conditions when the causes that led to accidental increased of the force from rod mechanism stops, the springs will push the balls back into the tapered channels from the sword rod, and the mechanism will still function normally, without the rolling train to be stopped, respectively the rolling process stopped.

Taking into account that the connecting rod's critical force (the spring's pressing force) is very big and because the spring's space is limited (for a little deformation), is recommended to use compression ring springs, which satisfy the conditions below.

2. INDEXING DEVICE DESIGN

The dynamic analysis of the tilting mechanism from the rolling train 1000 mm found that the maximum force (to break the bolts) of the rod mechanism is:

$$F = 475000 \text{ [N]}$$

As noted in the bibliography, for designing the indexing device, the calculation force that this device need to give up, is obtained by amplifying the regime force system with a safety factor from the biggest force in the rod $K_F = 1,116$. So, the calculation force that triggers the locking device with spherical bodies is:

$$F_{\max} = K_F \cdot F = 1,116 \cdot 475000 = 530100 \text{ [N]}$$

Calculation scheme for ball device design is shown in fig. 2.

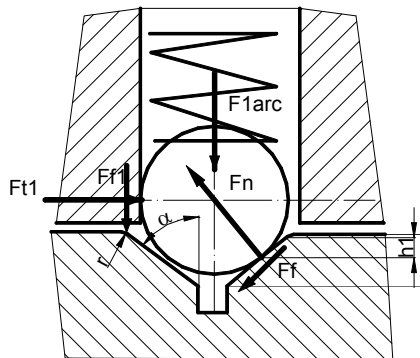


Fig. 2. Indexing device calculation scheme

In order to design the protection device with ball, the constructive choose the following sizes:

- ❖ trapezoidal channel opening semiangle, $\alpha=30-50$ degrees
- ❖ ball diameter, depending on indexing device dimension, $d_b = 40-50$ [mm]
- ❖ trapezoidal channel depth, $h = (0,2...0,5)d_b$
- ❖ trapezoidal channel connection radius, $r \leq 0,5d_b$
- ❖ load uneven distribution coefficient between the ball and lock body, $\lambda=0,8$
- ❖ Initial deflection for spring assembly, $\delta_1 = 18$ [mm]
- ❖ coefficient of friction $\mu_0 = 0,15$
- ❖ longitudinal MOE $E = 215000$ [Mpa]
- ❖ admissible strength at the balls contact load $\sigma_{ak} = 5000$ [Mpa]

Then calculate the following sizes:

- spring preloaded force: $F_{1arc} = \frac{F_{\max}}{2} \left[(1 - \mu_0^2) \operatorname{tg} \alpha + 2 \mu_0 \right]$

- spring stiffness: $k_a \leq \frac{F_{1arc}}{\delta_1}$

- normal force between the balls and trapezoidal channel: $F_n = \frac{F_{1arc}}{\lambda} \left[(1 - \mu_0^2) \sin \alpha + 2 \mu_0 \cos \alpha \right]$

- resistance to balls contact load: $\sigma_{kmax} = 0,633 \sqrt{\frac{F_n E^2}{d_b^2}} \leq \sigma_{ak}$

The above calculations are performed using a computer program written in Visual Basic. Program work interface is shown in fig. 3, together with calculated values displayed (including sizes for ring springs).

Based on the above calculated sizes, automatic protection device with balls was modelled 3D, in Autodesk Inventor Professional program. In fig. 4 presents the model photo-realistic images.

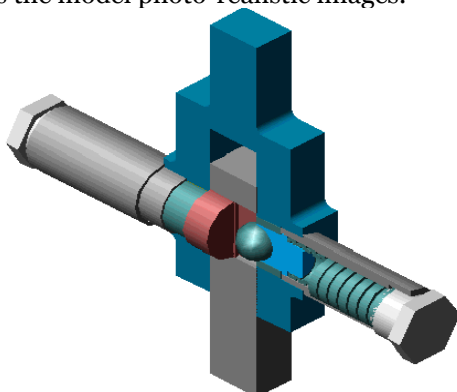


Fig. 4. 3D model indexing device

Rezultate Calcul arc inelar Inchiide

Elemente necesare proiectării

- Unghiul canalului trapezoidal: 30 - 50 grd
- diametrul bilei 40 - 50 mm
- Coefficientul de frecare bilă - canal
- Coefficientul repartiției neuniforme a sarcinii
- Modulul de elasticitate longitudinal [daN/mmp]
- Rezistența admisibilă la solicitarea de contact [daN/mmp]
- Forța de regim din bilă

Mărimi calculate sistem de indexare

Mărim	Valoare
Forța de comprimare arc F1arc [daN]	6397,69
Rigiditatea arcului ka [daN/mm]	58,31
Forța normală Fn1 [daN]	1600,22
Raza de racordare canal r [mm]	5,4
Adâncime canal h [mm]	18
Et unitar strivire [daN/mmp]	421,71

Dimensiuni arc inelar

Dimensiuni arc	Valoare
Inclinarea tetelor alfa [grd]	14
Unghiul de frecare [grd]	7
Înălțimea inelelor [mm]	16,59667
sem [mm]	4,375
sim [mm]	2,92
se	6,44
sfe [mm]	2,31
si [mm]	4,99
sfi [mm]	1,53
Numar inele z	21
Dm [mm]	50
Di [mm]	44,16
De [mm]	58,75
Lung. arc blocat [mm]	187,7088
Lung arc liber Lo [mm]	205,7088
Sageata elementara fo [mm]	0,9332322

Fig. 3. Program interface

3. EXPERIMENTAL TESTS ON INDEXING DEVICE

In order to follow the behavior of the indexing device with spherical locking elements whose design and model were presented in paragraph 2, because of rod big dimensions where this system adapts, has been designed and implemented a small dimensions model to be tested under laboratory conditions.

Active elements of the device experimental model with nominal dimensions respectively how to make a contact between trapezoidal channel - ball - ball guide element are presented in fig. 5.

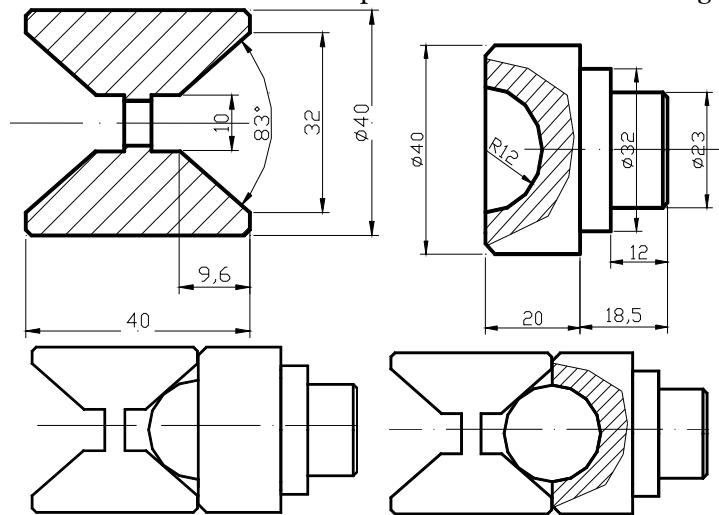


Fig. 5. Active elements geometric dimensions

According to fig.5 trapezoidal channel angle is $\alpha = 83/2 = 41,5$ degrees, which is within the range 30-50 degrees, and ball diameter is 24 mm.

The fig. 6 picture presents the active elements of the developed device model.



Fig. 6. Active elements of the indexing device

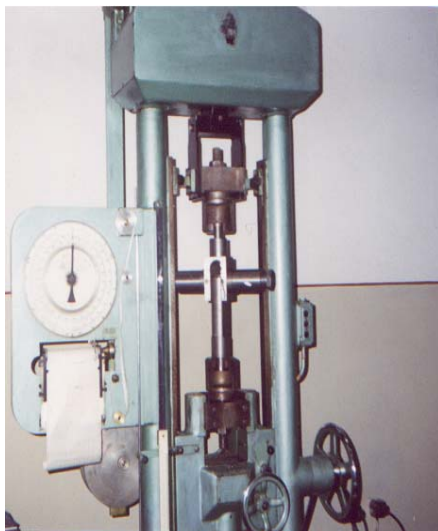


Fig. 7. Experimental tests on experimental model

As a compression spring, for pressing the balls in trapezoidal channels, to the indexing device experimental model studied, does used compression springs, know their calibration curves.

Experimental tests on experimental model of protection device with balls, where made on the universal test machine, according to fig. 7.

Table 1 Arc 1 $C_1 = 3,82$ [N/mm]

f[mm]	3	6	9	15	18
	4	7,5	11	19	24
	3,5	8	12	18,75	23,6
	4	7,75	12,5	20	23
Fmediu[daN]	3,833333	7,75	11,833333	19,25	23,533333
Farc [daN]	1,2	2,4	3,4	5,8	6,8
F [daN]	3,83	7,75	11,83	19,25	23,53

The experimental tests will pursue a dependency between the preload force of coil springs and the force where device with balls will trigger (read on the test machine dial).

Compression springs preload force, will result from their calibration graphs based on their deformation, determined as the multiplication of the turns number of cover and their thread pitch ($p = 1,5$ [mm]).

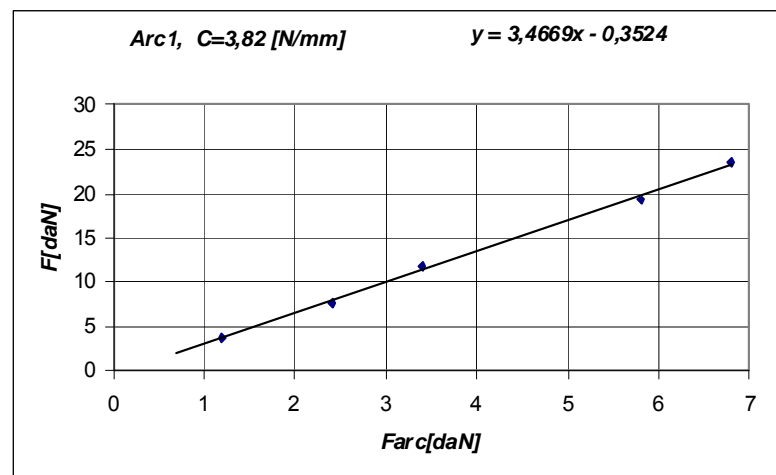


Fig. 8. Trigger force variation of the indexing device

The experimental results are processed into tables and graphics, and an example is shown in table 1 and fig. 8.

4. CONCLUSIONS

Indexing device with balls was bring under stress tension, aiming determining the dependence between the force where the system gives up (read on the test machine dial) and the preload force of the spring coil (determined from their calibration graphs).

We used three pairs of compression springs, different stiffness, respectively $C_1 = 3,82$ [N/mm], $C_2 = 11,25$ [N/mm] and $C_3 = 6,56$ [N/mm].

The construction of the device with spherical locking elements was used two balls with a 24 mm diameter and a tronconical channel with 83 degrees opening angle and a depth of 9.6 mm.

Analyzing the results of experimental tests on an experimental model of ball device, it can say the following conclusions:

- The model on small-scale of indexing device with spherical locking elements work correctly for all three pairs of springs used.
- In the tests it was found a linear increase of the force when the ball device gives up, in relation to the spring's preload force.
- For springs pairs with different stiffness, on the same preload force, the force at which the indexing device with balls starts increases with the spring stiffness.
- The force value in which the device with balls starts, depends on trapezoidal channel dimensions, decreasing with the increasing its angle.

REFERENCES

- [1.] Burchard, B., ș.a., Secrete AutoCAD 14, Editura Teora București 1998
- [2.] Cioată, V., Miklos, I. Zs., Proiectare asistată de calculator cu Autodesk Inventor, Editura Mirton, Timișoara, 2009
- [3.] Drăghici, I., ș.a., Indrumar de proiectare în construcția de mașini, Vol. I,II Editura Tehnică București, 1981.
- [4.] Kelly, J., Utilizare, Microsoft Excel 97, Editura Teora, București, 1998.
- [5.] Miklos I. ZS., Cioată, V., Desenare 2D cu AutoCAD 2002, Editura Mirton Timișoara, 2003
- [6.] Miklos, I. ZS., Contribuții privind îmbunătățirea performanțelor tehnologice ale mecanismelor de răsturnat blumuri la liniile de laminare, Teză de doctorat, Universitatea din Petroșani, 2001.



THE PORTABLE GRINDERS BLACK& DECKER RELIABILITY DETERMINATION

^{1,2} FACULTY OF ENGINEERING HUNEDOARA, ROMANIA

ABSTRACT:

In this work is represented the assessment method to real reliability of electromechanic entities. The practical example is done for a tipo - dimensional portable grinder. The example needs illustrated the interpretation of experimental date (looking the operation/breakdown of grinders) statistically analyzed.

KEYWORDS: reliability, statistical analysis, portable grinders

1. INTRODUCTION

The determination real reliability by portable grinders is done abaft the research of their behavior in exploitation. Were, drew up a program of follow the operation of a breakdown number of seventeen grinders Black& Decker. This program contains the acquet moment of each grinder, who tallies with the first moment of utilization the entity, the breakdown moment and entrance in service and in latter, the duration of maintenance activities. The systematized data are right truncated because pursuit grinders stop after first period of operation and reestablishment. Certainly that the study till be much more former if the studios entities be can be seed on whole their duration of life. This thing presupposes a tight cooperation between provider and user, carry don't always he is obtained on the measure of our desires.

2. METHODOLOGY

For determination the real reliability of portable grinders, the values of their times of good operation were entered in a specialized software, WEIBULL++6 (figure 3. 1), who permits the quick settlement depending on repartition most fit the case, with a coefficient of correlation Rho or ρ .

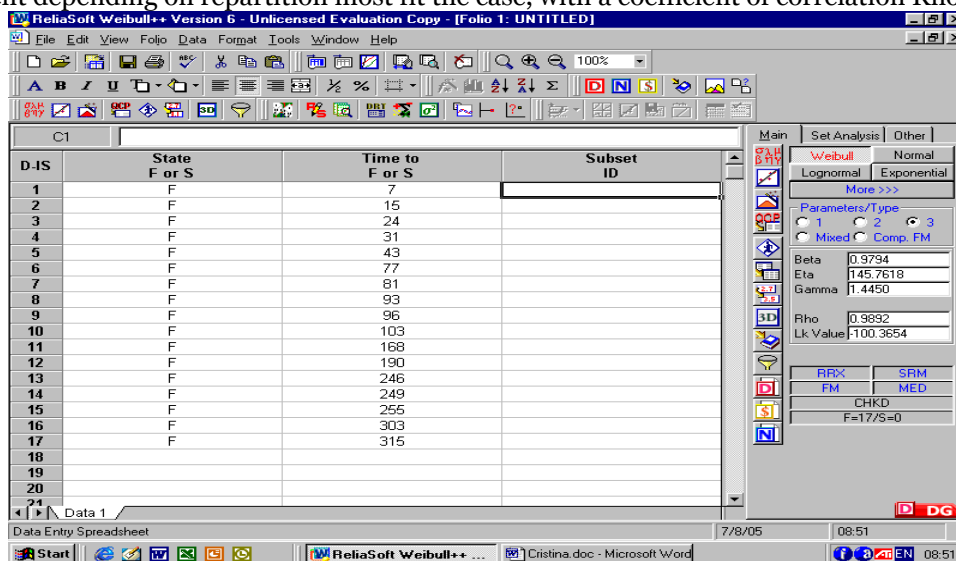
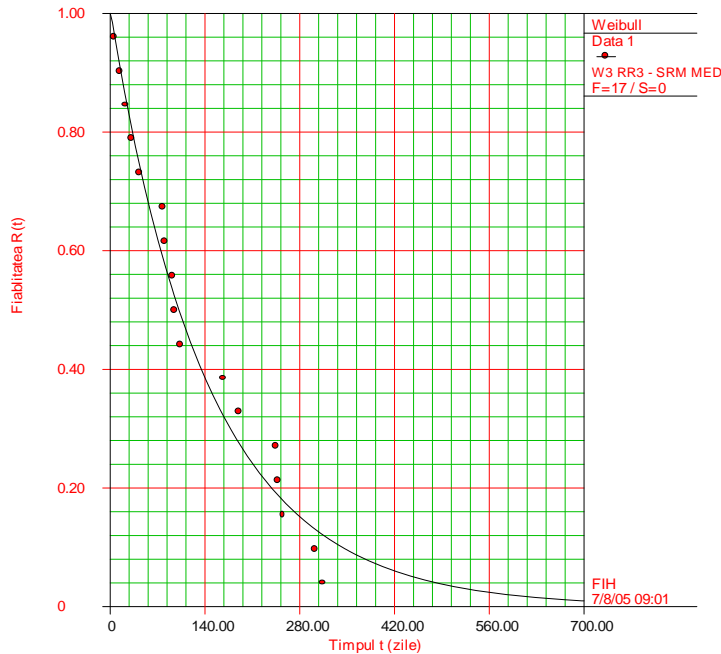


Fig.1. Time of good operation

For the present case, the distribution law of portable grinders functioning is Weibull with three parameters $\beta = 0,9794$, $\eta = 145,7618$ and $\gamma = 1,4450$. The correlation coefficient is 0,9892. Accordingly these laws the mean time between failures is

$$MTBF = \eta \Gamma\left(\frac{1}{\beta} + 1\right) = 145,7618 \times \Gamma(2,021) = 145,7618 \times 1 = 145,7618 \text{ days,}$$

ReliaSoft's Weibull++ 6.0 - www.Weibull.com



$\beta=0.9794, \eta=145.7618, \gamma=1.4450, \rho=0.9892$

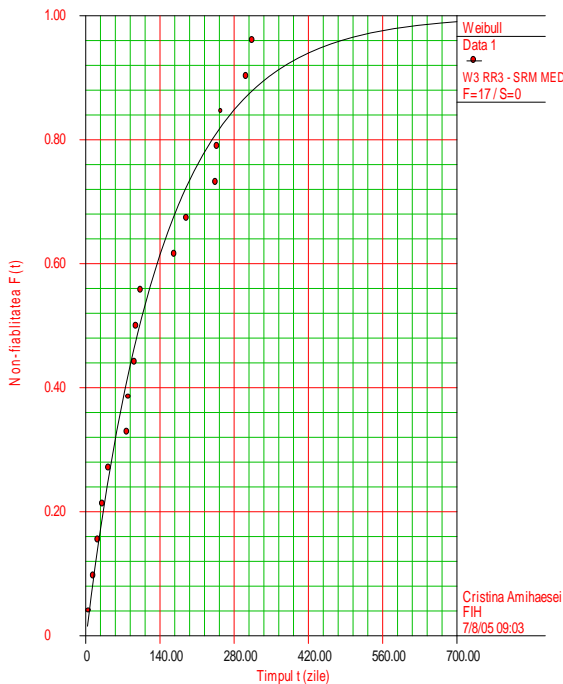
Fig. 3.2 Reliability depending on time

in which $\Gamma(x)$ is the Eulerian integral of second kind.

The β value, gated closer to 1 indicated the fact that the abrasive discs with all as the new, there are in the natural period of life. This thing show that the entities are submissive of a proper running in to producer. The positive γ value show that no faultiness appears in the exploitation of grinders giddap of 1,445 days.

The program WEIBULL+ + 6 permits curve-plotting depending on the time of reliability (fig.3.2), percentile (non-reliability) (fig.3.3), density of probability (fig.3.4) and failure rate (fig.3.5), as well as the correlation among the parameters of Weibull law, materialized through the zone with probability of 95% (fig.3.6) and the function Likelihood (fig.3.7).

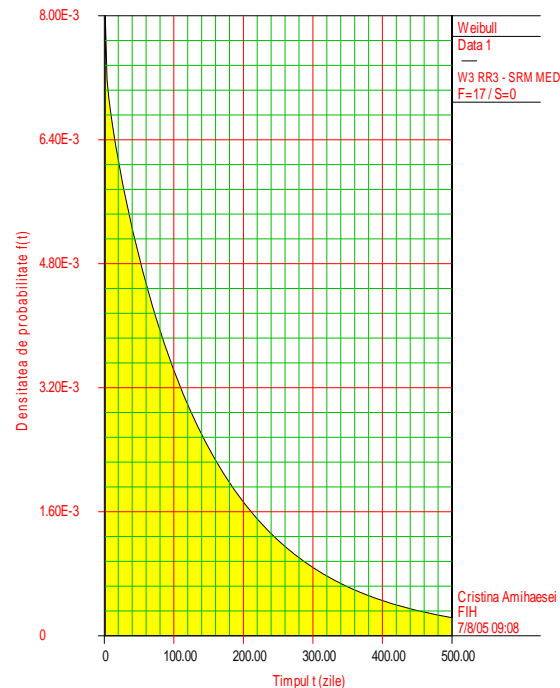
ReliaSoft's Weibull++ 6.0 - www.Weibull.com



$\beta=0.9794, \eta=145.7618, \gamma=1.4450, \rho=0.9892$

Fig. 3.3 The percentile depending on time

ReliaSoft's Weibull++ 6.0 - www.Weibull.com

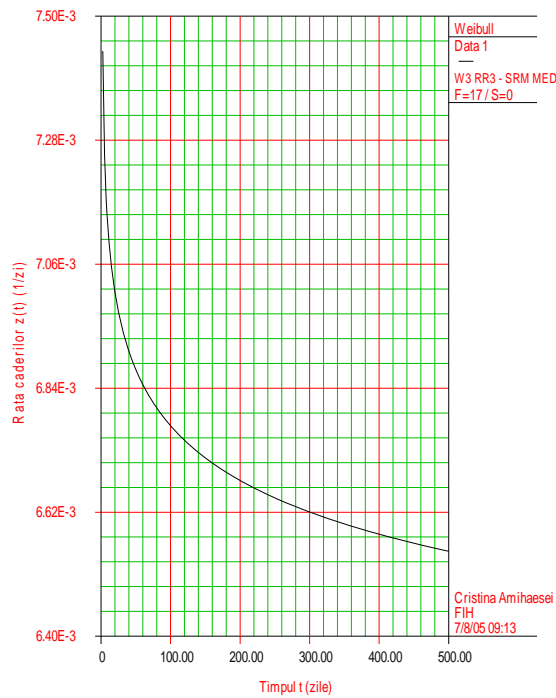


$\beta=0.9794, \eta=145.7618, \gamma=1.4450, \rho=0.9892$

Fig. 3.4. The density of probability depending on time

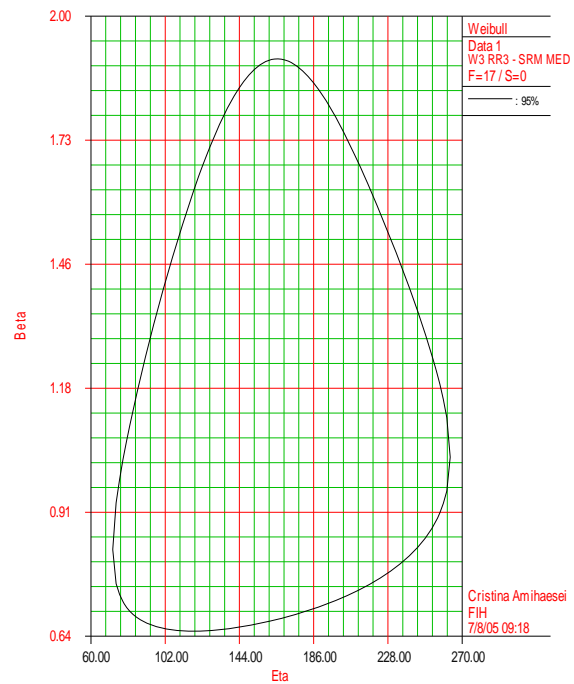
ReliaSoft's Weibull++ 6.0 - www.Weibull.com

ReliaSoft's Weibull++ 6.0 - www.Weibull.com



$\beta=0.9794, \eta=145.7618, \gamma=1.4450, \rho=0.9892$

Fig. 3.5 The failure rate depending on time



$\beta=0.9794, \eta=145.7618, \gamma=1.4450, \rho=0.9892$

Fig. 3.6 Values β și η with 95% probability

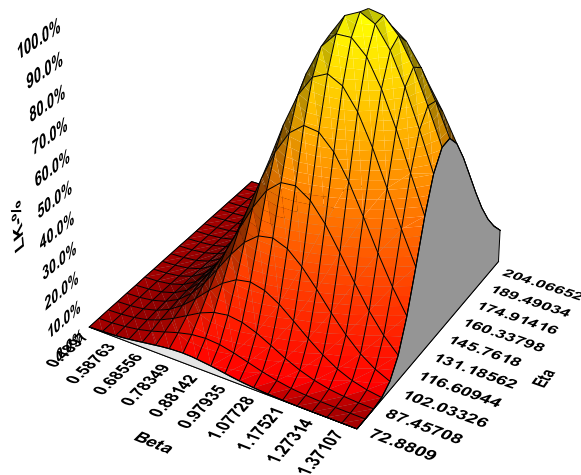


Fig. 3.7. Likelihood function

3. CONCLUSION

Consisted that, figure 3.5, as a starter, failure rate has relative erect values, specify operate of a new entities. He follows a quick diminution, what show that the regime of natural life is installed relatively quick. This thing is strengthened also be β value. Reduce bold the failure rate, specifies the electric components and electronic, is waited directing to the ascertainments concerning the out of order nature of by hand grinder.

The electric defects of portable grinders reduce significantly (fig.3.2) the reliability still of their working setting, what does as the period of established guarantee of producer to is attenuate properly.

REFERENCES

1. Baron, T., ș.a., Calitate și fiabilitate - manual practic, vol. 1 și 2, Editura Tehnică, București, 1988.
2. Budiul-Berghian, A., Contribuții privind îmbunătățirea fiabilității mecanismelor tip foarfece pentru debitat produse metalurgice, Teză de doctorat, Petroșani, 2007.
3. Mihoc Gh., Muja A., Diatcu E., Bazele matematice ale teoriei fiabilității, Editura Dacia, Cluj-Napoca, 1976.
4. Niculesc, D., Calitate, fiabilitate, mentenanță, A. M. C., vol. 18-19, Editura Tehnică, București, 1975.
5. Roman, I., Determinarea indicatorilor de fiabilitate, în Calitatea producției și metrologie, nr. 1, 1974.
6. Vasiu T., Fiabilitatea sistemelor electromecanice, Editura Bibliofor, Deva, 2000.





¹ Carmen Inge ALIC, ² Sorin Aurel RAȚIU, ³ Vasile ALEXA,
⁴ Cristina Carmen MIKLOS, ⁵ Imre Zsolt MIKLOS

CRÉATION DE RESSOURCES PÉDAGOGIQUES INTERACTIVES ORGANISÉES EN BASE DE DONNÉES, POUR DES APPRENTISSAGES EN SOUDAGE

¹ UNIVERSITY „POLITEHNICA” TIMIȘOARA, FACULTY OF ENGINEERING HUNEDOARA, ROMANIA

ABSTRACT:

Create of interactive learning resources structured in database, for the acquisition of knowledge and skills in the welding field

This publication aims to expose the collaborative work and the experiences of our project team in order to design and implement a training tool in the welding domain, which includes interactive educational resources organized into a database. The training tool is currently in developing progress under a two years European project, funded by the LLP/Lifelong Learning Program/Sectorial Program Leonardo da Vinci/Partnerships. The transnational project team consists of four partner organizations, of which AFPA– Lyon, France, ensures the coordination of the project, and *Universitatea „POLITEHNICA” Timisoara-Facultatea de Inginerie Hunedoara*, Romania, the *Institut de Soudure-Paris*, France, and *Le FOREM-Bruxelles/Charleroi*, Belgium, are the partners.

The goal of the project is to design a more attractive multimedia training content, with multimodal character (accessible on keywords-based consultation, or in training route mode), which will contribute to the development of personal and professional autonomy of the employees, students and European people in training and further training activities in welding domain, since the practitioner level until the welding engineer.

This publication was developed to promote the visibility of the project and its progress, and is dedicated, also, to the intent of dissemination and exploitation of the project results.

KEYWORDS:

collaborative work, European project, training resources, welding training

1. CONTEXTE ET MOTIVATION

Dans de nombreux pays de l'Europe, les métiers du soudage font aujourd'hui l'objet d'une définition qui varie considérablement selon l'activité et le type de production réalisée (unitaire ou en série, en entreprise ou sur chantier). Ainsi, pour une partie de l'industrie, il s'agit avant tout d'un métier très spécialisé ; pour l'autre partie du secteur, être soudeur impose une polyvalence et de multiples compétences qui se rapprochent de celles du chaudronnier ou du tuyauteur. De tels éléments contribuent à l'existence d'un marché de l'emploi « éclaté », en pleine évolution au sein des différents pays, distinguant nettement les salariés spécialisés de ceux à qui il est demandé d'être poly-compétents, autonomes et capables de réaliser un travail depuis sa conception jusqu'à sa réalisation. Cet élargissement des tâches, qui s'accroît de plus en plus et impose une mobilité accrue des personnes, entraîne des difficultés de recrutement pour les entreprises, argumentée à la fois par des exigences de qualité de production et la recherche de profils plus ou moins qualifiés, selon les tâches.

Si l'unique réponse fournie reste à ce jour le recours massif aux entreprises de travail temporaire, ces dernières dans leur travail de placement offrent généralement un personnel dont le niveau de formation se limite au passage des licences autorisant le travail du soudage. Cela ne permet pas toujours l'ouverture vers de nouvelles perspectives de production et n'encourage pas non plus une possible réorganisation du travail vers des profils d'exécution. Aussi qu'elle s'adresse à

des soudeurs spécialisés, de « simples » soudeurs ou tout autres praticiens, tantôt sédentarisés, tantôt mobiles, la formation reste l'une des clés d'adaptation à l'évolution technique, technologique et organisationnelle des métiers liés au domaine du soudage.

Problématique généralement commune aux pays européennes, la formation en soudage devrait donc faire l'objet d'un projet permettant de réfléchir ensemble à la modernisation des ressources formatives existantes, et travailler à sa mise en œuvre pour:

- ❖ Former selon des modes diversifiés à différents niveaux d'emploi dans les métiers du soudage;
- ❖ Répondre aux besoins en main d'œuvre qualifiée des entreprises et les aider dans leur développement et leur conquête de nouveaux marchés, en formant des salariés capables d'autonomie et de réflexion sur le travail;
- ❖ Accompagner et faciliter la transmission des savoirs au sein même des entreprises ;
- ❖ Fixer une partie de la main d'œuvre tentée par des secteurs plus attractifs ;
- ❖ Apporter un outil de formation adapté aux contraintes (recrutement, compétitivité, formation) des entreprises en termes de flexibilité et de souplesse d'utilisation ;
- ❖ Doter d'un outil moderne de formation au soudage à la fois les entreprises et les principaux opérateurs de formation au soudage en Europe ;

Dans le contexte décrit, au sein des organismes de formation on compte aujourd'hui d'un nombre important de ressources formatives attachées à l'apprentissage des gestes et techniques des métiers du soudage. L'essentiel de ces ressources mises à la disposition des personnes en formation, reste principalement constitué de textes et d'images fixes, n'autorisant que peu d'interactivité entre l'utilisateur et les ressources. L'utilisation de l'interactivité sous forme de navigation ou de recherche d'information, reste souvent limitée aux liens internes attachés à des diaporamas réalisés par les personnels enseignants, et si certaines de ces ressources font l'objet d'une animation par l'intégration d'images vidéos, elles sont à la fois peu nombreuses et peu attractives. L'évolution des techniques de soudage, la diversification des contextes d'application, l'exigence de compétences, ainsi que la demande croissante de souplesse au sein de la formation intégrée au travail imposent la nécessité d'une modernisation et/ou d'adaptation des ressources formatives existantes.

2. OBJECTIFS DU PROJET. ÉTAPES ET APPROCHES. ACTIVITÉS.

Les activités du projet ont les objectifs suivants :

- Construire un cadre d'échange et de coopération entre des acteurs de la formation soudage en Europe, Fig.1 ;



Fig.1. Le projet de partenariat - Cadre européenne d'échange et de coopération entre des acteurs de la formation soudage

- Offrir aux partenaires la possibilité de moderniser et d'harmoniser leurs patrimoines de ressources de formation au soudage (Fig.2) ;

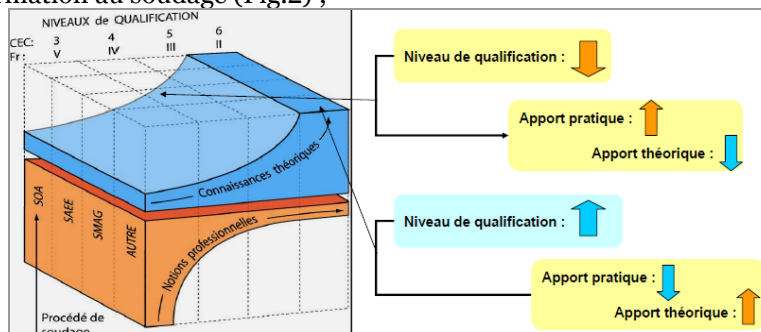


Fig.2 Construction du parcours de formation en intégrant la logique ECVET - "European Credit for Vocational Education and Training".

- Concevoir et proposer un support plus attractif de contenus de formation (multimédia), au caractère multimodal (accès en consultation sur mots clé ou en mode parcours de formation), Fig.3, et qui puisse contribuer au développement de l'autonomie personnelle et professionnelle des salariés, des étudiants et des personnes en formation soudage en Europe, depuis le niveau praticien jusqu'à l'ingénieur soudage ;



Fig.3. Contenus de formation au caractère multimodal, accès en mode « parcours de formation » ou en mode « consultation par mots clé »

- Rapprocher formation et lieux de travail en proposant à des utilisateurs de pays différents (formateurs, enseignants, responsable d'atelier, chef d'entreprise, etc.) un outil évolutif de consultation et d'utilisation de ressources en soudage, Fig.4.



Fig. 4. a. Principe d'utilisation global du support de contenus de formation multimédia, au caractère multimodal ; b. Scénario d'apprentissage

L'outil de formation en cours d'être réalisé, se différencie des environnements virtuels et autres simulateurs en soudage, en le sens qu'il offre des fonctionnalités différentes, principalement ouvertes sur l'acquisition des connaissances, concepts et techniques nécessaires à l'activité, suivant des niveaux de pratiques différenciés, et qu'il n'est pas orienté sur l'acquisition d'habiletés psychomotrices pour une maîtrise de la manipulation des outils de soudage. Les principaux sujets traités sont : Procédés de soudage ; Rappel d'électricité et de physique ; Métaux d'apport ; Accessoires de soudage ; Environnement de la zone de travail ; Mise en service ; Maintenance ; Réglages de base en soudage ; Influence des paramètres ; Contrôle ; Hygiène, sécurité et développement durable ; Traitement des défauts.

L'approche adoptée afin de mettre en oeuvre le projet va de l'ingénierie pédagogique jusqu'au test en situation réelle et comprend la conception, la réalisation, la validation et

l'évaluation. Ces principales étapes se décomposent en plusieurs étapes durant lesquelles chaque partenaire, compte tenu de ses spécificités et de son degré d'expertise lié à l'apprentissage du soudage, a une part à prendre et donc des tâches à réaliser, [1].

- La première étape des activités a permis aux partenaires de se positionner sur un même niveau de connaissance concernant les objectifs et les modalités de déroulement du projet, et a été consacrée à un travail de *collecte*, de *sélection* et d'*harmonisation* des contenus de formation existants et susceptibles de nourrir l'outil interactif mis en projet;

- La seconde étape, a été de *structurer* les contenus d'apprentissage retenus en *unités indépendantes* (granularisation) répondant à des acquisitions de connaissances et de compétences suivant différents niveaux fixés (opérateur – Technicien - Ingénieur). Cette étape a abouti à la présentation de progressions pédagogiques d'utilisation souple, complète ou partielle et différenciées suivant les niveaux d'emplois retenus ; Fig.5.

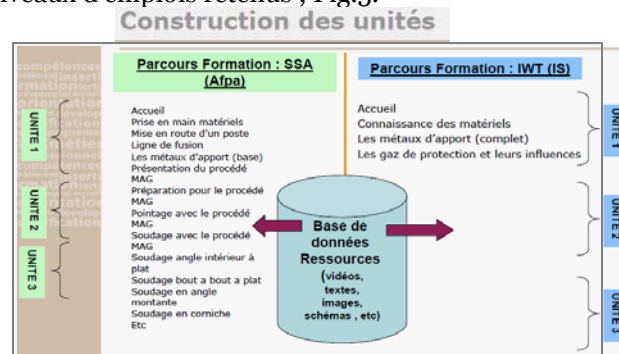


Fig.5. Construction des unités de l'outil évolutif de ressources en soudage

- La troisième étape a eu pour objectifs la *scénarisation des contenus* choisis et structurés en progressions, Fig.6. Elle s'est accompagnée d'une phase *d'essais et d'adaptation* de la méthode auprès des différents environnements représentatifs des partenaires (entreprises, centres de formation, d'enseignement) qui a permis *l'ajustement, l'harmonisation et la stabilisation* en matière de format des scénarii intégrés à la future borne interactive.

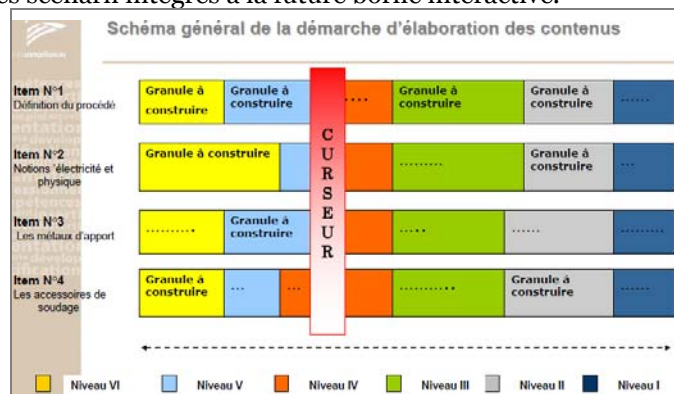


Fig.6. Structuration et de scénarisation des contenus de formation en soudage

- Une quatrième étape a pour objectif de *définir* puis *choisir* les *modalités et moyens techniques* de mise en place de l'outil interactif (modalités pédagogiques, formats multimédias, traduction, etc.) et intégrera une démarche d'assurance qualité.

- La cinquième étape favorisera la mise en œuvre par *expérimentation* de la nouvelle solution de formation finalisée et organisera la *mesure de ses effets*.

3. RÉPARTITION DES TÂCHES. COOPÉRATION ET COMMUNICATION

La répartition des tâches entre les organismes participants assure l'implication active de tous les partenaires et, selon les compétences requises, prévue que chaque partenaire contribue à des degrés différents aux travaux à réaliser. Ainsi :

- L'AFPA (Fig.7a), entité à vocation nationale sur le champ de la formation et de la certification, en complément de sa connaissance des publics en formation, dispose d'une expérience importante dans la pédagogie adaptée aux formations des professionnels qualifiés en soudage. En possédant à ce titre une expertise en matière d'environnement pédagogique et d'outils didactiques, elle assure la coordination du programme d'actions et contribue prioritairement aux étapes de conception et de réalisation de l'outil par l'apport d'un patrimoine ressources et par son expertise en matière d'ingénierie pédagogique.

- L'Institut de Soudure (Fig.7c), outre sa renommée nationale et internationale sur le champ de la formation et de la certification des professionnels d'entreprises, des niveaux soudeurs jusqu'aux niveaux ingénieurs, dispose d'une grande expertise en recherche et développement industriels en soudage, ainsi que dans la conception et le développement de supports et d'outils pédagogiques. A ce titre, il apporte une contribution soutenue à chacune des étapes, allant de la conception à l'évaluation du produit de formation réalisé. Ses compétences en matière de veille normative et documentaire favorisent la mise en place de l'outil au caractère à la fois actualisé et évolutif, et participe à la démarche qualité contenue dans le projet.

- Le FOREM (Fig.7d), outre l'adaptation et l'insertion des travailleurs et des demandeurs d'emploi sur le marché du travail (aide au repérage des compétences et conseils aux dispositifs de recrutement) justifie une très bonne connaissance des entreprises et de leurs besoins en qualifications liées au soudage. A ce titre, son implication dans l'évaluation et la dissémination auprès d'entreprises du produit de formation réalisé, favorisera l'expérimentation et l'exploitation de ce dernier et permettra les ajustements et modifications nécessaires à sa finalisation, tout en facilitant la mesure des effets constatés.



Fig.7. Les organismes participants à la répartition des tâches du projet de partenariat

- L'Université Polytechnique de Timisoara et la Faculté d'Ingénierie d'Hunedoara (Fig.7b), par leur expertise en recherche, contribuent à la fois à la modélisation de l'outil de formation et aux stratégies argumentatives qui accompagnent un système d'apprentissage interactif. L'apport du travail universitaire permette dans la phase de réalisation, un approfondissement des éléments de réalité virtuelle attachés à l'apprentissage proposé par le nouvel outil interactif, qu'il s'agisse des phases d'apprentissage ou encore de phases d'évaluation. Sa participation à la phase de conception est envisagée pour ce qui concerne les ressources de formation affectées au niveau ingénieur.

Afin d'assurer la cohérence dans la conduite du projet et de permettre un partage optimal des informations relatives aux travaux, chaque partenaire, malgré une répartition préalable des tâches, participe à l'ensemble des étapes constitutives de la démarche, et apporte sa contribution par la présence de son référent ou des acteurs repérés pour leur expertise dans le projet. Afin de pouvoir s'assurer d'une plus large possibilité d'expérimentation, donc d'évaluation de l'outil créé, la cinquième étape aura un caractère transverse et mobilisera l'ensemble des partenaires et les contextes d'activité qu'ils représentent. Cela va permettre une évaluation plus juste et va offrir une ouverture en termes de communication externe et de dissémination du produit.

L'un des objectifs majeurs de ce projet est de réaliser un outil commun de formation au soudage, en établissant une collaboration renforcée entre les partenaires. A ce titre, et afin de pouvoir engager efficacement un travail de réflexion et de conception du support de formation, l'équipe a trouvé opportun de mettre en place une organisation collégiale basée sur le partage à la fois des informations, des expériences vécues et des travaux à réalisés. Les partenaires, disposant tous d'outils de communication modernes (site Web, systèmes de messagerie, de vidéoconférences, etc.), l'outil privilégié a été l'Internet, avec toutes les possibilités d'échanges de données. De plus, en qualité de coordonnateur, l'AFPA a déployé l'infrastructure nécessaire à la mise en place d'un outil collaboratif, la *Plateforme informatique "BRIS"*, Fig.8, organisée autour de la technologie *Share Point* de Microsoft.

Les nombreuses fonctionnalités de cette plateforme, applicables au projet, permettent : l'utilisation par les partenaires d'espaces de travail pour la création ; la révision ou la publication de documents de formation attachés au soudage; une gestion plus efficace du projet à l'aide du modèle de liste de tâches; la coordination du travail d'équipe à l'aide des calendriers partagés, des alertes et des notifications ; un renforcement de la communication entre partenaires à l'aide des fonctionnalités de présence et de messagerie instantanée.

Afin de solidifier la communication interne autour du projet, l'utilisation régulière de conférences téléphoniques et de plus, à partir du juin 2010, de vidéoconférences, Fig.8b, la rencontre des référents au sein des réunions du comité de pilotage, comme l'invitation des acteurs (personnels et apprenants) de chaque organisme aux différents groupes de travail, ont renforcé la garantie d'une bonne coopération et d'une circulation des informations efficace.

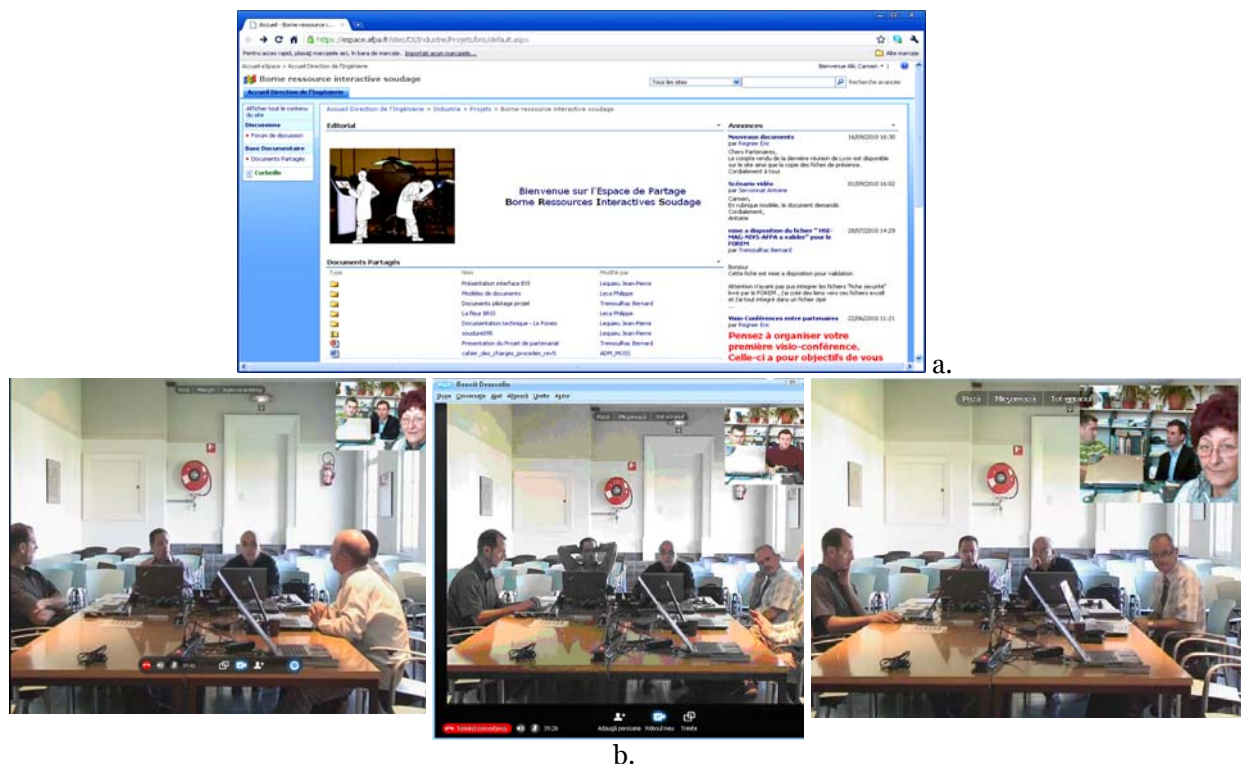


Fig.8. a. Plateforme informatique collaborative (technologie *Share Point*);
 b. Vidéoconférence Bruxelles-Paris-Hunedoara, Group de travail, oct.2010

4. IMPACT ET VALEUR AJOUTÉ EUROPÉENNE

L'intérêt de la mise en œuvre du projet réside dans la possibilité pour les apprenants d'accéder à un processus d'apprentissage du soudage individualisé, dynamique et adapté. La mise au point de ce support interactif reprenant l'ensemble des connaissances, gestes et techniques du soudage constitue un guide des pratiques et d'apprentissage spécialement conçu pour les professionnels de l'activité. En leur offrant la possibilité d'un développement des compétences par un accroissement de l'attractivité de la formation proposée, il est possible d'envisager une amélioration de la compétitivité de ces praticiens, leur permettant par là même de faire valoir en entreprises, comme sur le marché du travail, leur capacité d'insertion et d'adaptation aux exigences économiques, technologiques et techniques.

De leurs cotés, les partenaires sont demandeurs d'aide à la mise en place d'une nouvelle ingénierie et/ou d'une nouvelle méthodologie d'apprentissage des gestes et techniques en soudage. En privilégiant la recherche d'une solution innovante, et en proposant une approche pédagogique originale à un niveau européen, les organismes partenaires pourront mettre à profit dans leurs activités (Formation, Enseignement, Insertion) l'expertise combinée issue du projet, et renforceront ainsi leur efficacité en matière de demandes d'amélioration des compétences en soudage. Également, en développant un tel projet, chaque partenaire renforce sa dimension réseau au niveau européen et promeut la coopération en matière d'assurance qualité dans le domaine des apprentissages, et de la formation au soudage, en particulier.

5. PERTINENCE PAR RAPPORT AUX OBJECTIFS DU PROGRAMME LEONARDO da VINCI

Le projet de partenariat répond à l'objectif d'améliorer la qualité des partenariats et d'accroître le volume de coopérations entre les organismes proposant des offres d'éducation et de formation, les entreprises, les partenaires sociaux et tous acteurs pertinents de la formation professionnelle dans toute l'Europe. (LEO- Objectif 2). Les mesures et activités envisagées pour répondre aux objectifs fixés sont de deux ordres: *stratégique et opérationnel*.

- *Stratégique*, par l'organisation des séminaires : Réunissant principalement les membres du Comité de Pilotage formé des référents nommés pour le projet, le calendrier prévoit tout au long de la durée du projet (2 ans) une réunion trimestrielle, alternativement chez les différents partenaires (Lyon, Bruxelles, Hunedoara, Paris). Chaque séminaire serve de point étape et permette à la fois le suivi et la coordination des travaux, ainsi que la prévision des recadrages et réajustements

nécessaires à la bonne progression du projet. L'ensemble des informations de ces séminaires traitées est diffusé par le biais de la *Plateforme collaborative*.

- *Opérationnel*, par la mise en place localement ou transnationalement des étapes identifiées : Des temps de regroupement (travail communs), des temps d'échanges entre les équipes de chaque organisme partenaire, ainsi que des temps de travail autonomes, pleinement intégrés aux activités de chacun des partenaires. Les équipes participantes assurent la responsabilité globale de la qualité technique du produit à réaliser.

- Les temps d'échanges sont consacrés à la fois aux réalisations à produire et au partage des informations entre les équipes, en bénéficiant de la *Plateforme collaborative* qui permettent de : gérer le cycle de vie des documents ; créer et contrôler leurs propres espaces de travail ; afficher les relations entre les tâches et l'état du projet ; coordonner le travail d'équipe à l'aide des calendriers partagés ; communiquer avec l'ensemble des « adhérents » au projet.

- Les temps de regroupement, réunissent les personnels mandatés par chaque organisme partenaire qui, en fonction de la répartition des tâches, se regroupent indépendamment en des séminaires afin d'analyser, confronter et mettre en œuvre les réalisations attendues par le projet. On utilise ces temps aussi pour associer des apprenants (étudiants, stagiaires, salariés) suivant la nature des tâches à réaliser.

En répondant aux objectifs opérationnels du programme Leonardo da Vinci, les principaux thèmes du partenariat sont : le développement de contenus et de concepts communs dans le domaine de l'*EFP (Tpc-13)*, et l'adaptation des compétences nécessaires sur le marché du travail. Le domaine pédagogique et de formation, selon les *VET fields*, est « *540-Industrie et Développement au sens large* ».

6. ÉVALUATION

La méthode utilisée pour évaluer la réalisation des objectifs du partenariat et les moyens qui l'accompagnent, permette la récupération constante des informations liées à la vie du projet, l'identification des bonnes pratiques ainsi que le recensement des productions telles que décrites dans les attendus du projet. Le coordonnateur (AFPA), ainsi que les partenaires, mettent en œuvre une organisation dynamique et un processus permanent de suivi du projet :

- Réalisation et communication des *planifications de travail* qui suivent les réunions de comité de pilotage à l'ensemble des équipes partenaires ;

- *Echanges réguliers* d'informations liées au projet entre le coordonnateur et les différents organismes partenaires par l'intermédiaire du référent nommé (lien direct par la plateforme collaborative) ;

- *Consultation régulière* des éléments d'échange et de travail mis en partage sur la plateforme collaborative ;

- *Invitation* de participants externes lors de certains comités de pilotage (participants aux groupes de travaux, bénéficiaires concernés par le projet ou invités des organismes) ;

- Responsabilisation des partenaires dans l'évaluation des résultats obtenus par la mise en place sur la plateforme collaborative de *questionnaires de suivi* (documents harmonisés) ;

- Établissement de *rapports* (initial, intermédiaire et final), reprenant : les principales réalisations (points forts, points faibles, opportunités, menaces qui prévalent pendant la mise en œuvre du projet ; conclusions et recommandations en vue de favoriser la réalisation des effets durant la période restant à couvrir.

7. INTÉGRATION AUX ACTIVITÉS PÉDAGOGIQUES OU AUX AUTRES ACTIVITÉS EN COURS

Pour les organismes partenaires dont l'activité repose principalement sur l'enseignement et la formation professionnelle (*AFPA, IS, UPT/FIH*), les tâches nécessaires à la mise en œuvre du projet ont été directement intégrées aux activités de chacune des structures. Ainsi, les travaux relevant de la phase de conception et de réalisation du projet sont conduits par des personnels dont les compétences et l'expertise en ingénierie de formation, en pédagogie et en recherche s'expriment quotidiennement dans les activités dont ils ont la charge. Ils réalisent régulièrement : des temps de travail consacrés au projet ; des sollicitations auprès des centres d'enseignement et de formations recevant des publics en formation soudage pour des confrontations régulières au produit en cours de construction (soit pour des expérimentations, soit pour des évaluations ponctuelles des réalisations en cours). Pour ce qui est de la phase de mise au format multimédia des ressources ordonnées, ce temps de travail associe plus spécialement l'université par la conduite d'encadrants qualifiés (enseignants-chercheurs et étudiants impliqués dans la recherche sur les applications multimédias). L'intégration des activités du projet aux enseignements proposés par le cursus des

étudiants de l'Université Polytechnique et de sa Faculté d'Ingénieurs de Hunedoara serve, également, de support à des travaux pratiques.

Comme pour les organismes de formation et d'enseignement, *Le FOREM*, par les sollicitations exprimées auprès des entreprises pour évaluation et validation du produit développé, intègre à ses activités habituelles celles relevant du projet. On envisage ainsi, en fin de programme, un travail d'expérimentation et d'exploitation des résultats qui associerait, sur des bassins d'emplois identifiés par *Le FOREM*, salariés comme demandeurs d'emploi pour une utilisation de l'outil en vue de se former au soudage suivant des niveaux de besoins différenciés. Le suivi de telles activités nécessitera un travail de programmation et de suivi intégrés aux activités habituelles.

8. FINANCEMENT EUROPÉEN. PERSONNEL IMPLIQUÉ. RÉSULTATS

Les organismes participants ont choisi le type de partenariat qui correspond le mieux au plan de travail pour toute la durée de 2 ans, «LEO- 24 M» (nombre min. de 24 mobilités sortantes/partenaire, effectués durant la période contractuelle). Le montant des subventions obtenues variable d'un pays à l'autre, est le maximal : 25.000 Euro pour chaque des partenaires français et roumain, et 20.000 Euro pour le partenaire belge (95 000 Euro/total projet). Le nombre de personnels impliqués dans les activités du partenariat a été établi à 4 pour chacun des organismes participants. La description détaillée des résultats attendus ainsi que les dates afférentes, sont inscrits dans les documents [1], [3], [4], [5].

9. DIFFUSION ET EXPLOITATION DES RÉSULTATS. CONCLUSIONS

Ces activités se réalisent mettant en œuvre le "*Plan de diffusion et exploitation des résultats*", élaboré au niveau transnational, ainsi qu'au niveau de chaque partenaire. La cohérence des activités de diffusion est facilitée par l'utilisation de la *Plateforme collaborative*, qui assure que l'ensemble des acteurs impliqués bénéficie d'un même niveau d'information sur les avancées et les résultats. Ils mettent à profit ces informations pour en informer leur environnement professionnel, et la mise en lien avec un certain nombre d'entreprises pour l'évaluation et la validation du produit de formation, participe également à la diffusion des résultats par l'intermédiaire des organismes partenaires.

Le projet rapproche formation et lieux de travail, en proposant à des utilisateurs de pays différents un outil évolutif de consultation et d'utilisation de ressources en soudage. A son fin, le projet mettra à la disposition des acteurs de formation en soudage un support plus attractif de contenus de formation, qui contribuera au développement de l'autonomie personnelle et professionnelle des salariés, des étudiants et des personnes en formation soudage en Europe. L'intérêt de la mise en œuvre du projet réside dans la possibilité pour les apprenants d'accéder à un processus d'apprentissage du soudage individualisé, dynamique et adapté. Le développement des compétences par un accroissement de l'attractivité de la formation, envisage une amélioration de la compétitivité de ces praticiens, leur permettant par là même de faire valoir en entreprises, comme sur le marché du travail, leur capacité d'insertion et d'adaptation aux exigences économiques, technologiques et techniques.

A la suite de ce projet, il est envisagé d'exploiter plus largement les résultats obtenus, en établissant un plan de transfert auprès d'autres organismes et établissements traitant de l'apprentissage du soudage, ceci vers des pays européens concernés par le champ traité. Ce transfert pourrait se traduire par la mise en œuvre d'une mesure de transfert d'innovation Leonardo, ayant pour objet la mise en place d'un projet de coopération basé sur la dimension innovante de l'outil élaboré.

REFERENCES/RÉFÉRENCES

- [1] Document Candidature. Programme Éducation et Formation Tout au Long de la Vie/EFTLV. Partenariat Leonardo da Vinci 2009, Janvier 2009.
- [2] Pacht documente "Reuniune de informare privind implementarea Proiectelor de Parteneriat Leonardo da Vinci", ANPCDEFP, București, octombrie 2009.
- [3] Synoptique du projet Leonardo - Soudage. Équipe BRIS, Lyon, Décembre 2009.
- [4] Projet LdV-Partenariats. Partage des tâches -Équipe BRIS, Lyon, Février 2010.
- [5] Proiect LLP-LdV/PAR/2009/RO/003. Plan de implementare la nivel local. Februarie 2010
- [6] Cahier des charges - Procédés de soudage. Équipe BRIS, Janvier, 2010.
- [7] Pacht Documente Proiect LLP-LdV/PAR/2009/RO/003 pentru "Reuniune coordonatori de proiecte LdV". Timișoara, aprilie 2010.
- [8] Proiect LLP-LdV/PAR/2009/RO/003. Raport de progres intermediar și Anexe. Iunie, 2010.



Vasile ALEXA¹, Sorin Aurel RAȚIU¹, Carmen Inge ALIC¹

DESIGN AND IMPLEMENTATION FOR AN INFORMATICS APPLICATION TO WORKING-OUT THE MIG-MAG WELDING TECHNOLOGY

¹UNIVERSITY POLITEHNICA OF TIMISOARA, FACULTY OF ENGINEERING FROM HUNEDOARA, ROMANIA

ABSTRACT:

This paper work presents the technology development for welding in MIG-MAG shielding gas environment and a new calculation methodology for major welding parameters using an informatics application.

KEYWORDS:

welding, Mig-Mag, informatics, software

1. INTRODUCTION

The information system is a coherently structured assembly, made of electronic computing and communication equipments, software, processes, automated and manual procedures, used as automatic data processing tool within a field of activity.

The designing and developing of computer systems is appropriate in new IT systems, or for developing, upgrading or maintaining the existing ones.

In case of designing, the information system development team must carry out the following successive modelling processes [5], [6]:

- ❖ information modelling that provides the critical description of the existing system and defines the functional requirements measured by the objectives to be met by the new information system;
- ❖ conceptual modelling that describes the structure and functional solution of the new system to meet in the best possible conditions the required objectives, independent of computer, operating system or data management system;
- ❖ technical or detailed modelling that implies the transformation of the functional solution into an operational solution on a particular type of computer and data management system.

In database applications, the tables are updated by means of specialized models, called forms, which provide:

- ❖ end-user *friendly interface*, achieved through various controls (buttons, text boxes, etc.) or other embedded graphics;
- ❖ *simultaneous updating* of multiple tables through subforms;
- ❖ *validation rules in addition* to those defined in the tables.

2. THE MIG-MAG WELDING PROCEDURE

Welding in protective environment is the generic term for all the welding processes in which the weld pool and the metal transferred into it are protected, by a shielding gas, against the action of the atmosphere. The arc between the electrode and work piece burns visible.

The processes of welding in shielding gas environment can be classified according to the type of electrode, shielding gas and the electric arc protection used.

A first classification can be done by electrode type[1], [2]. Thus, the processes can be divided into non-fusible electrode processes and fusible electrode processes.

The non-fusible electrode – or „permanent” – is made of tungsten, and that's why this procedure is called *gas-shielded arc welding with a non-fusible electrode*.

In case of fuse welding electrode, this is simultaneously one of the electric arc poles, and filler. It has the same chemical composition or very close to that of base material. This procedure is called *gas-shielded arc welding with a fusible electrode*.

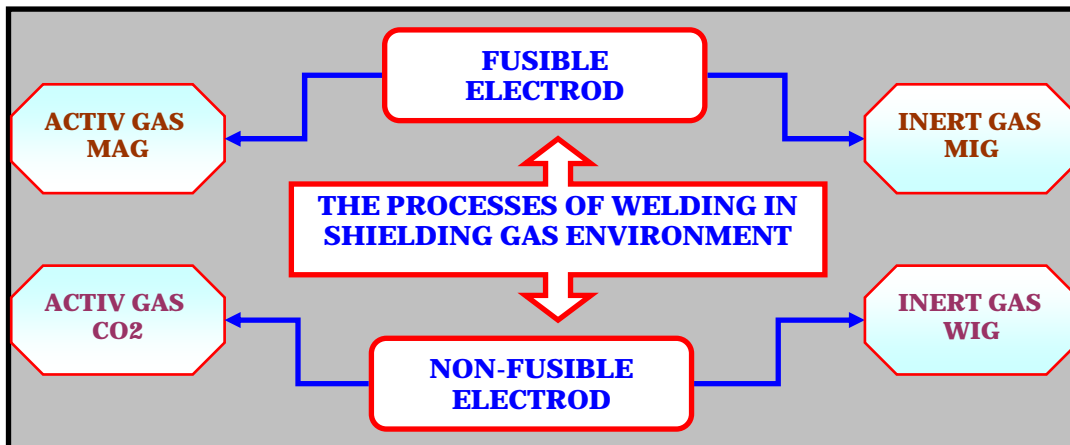


Fig. 1. The processes of welding in shielding gas environment

These two categories can be differentiated by the shielding gas they use [1].

In the process of welding in shielding gas environment with non-fusible electrode, there are used inert or noble gases. The term "inert" comes from Greek and means "indifferent" or „slow in reaction". Among the noble gases available, for welding in inert gas environment with fusible electrode (WIG) there are mainly used argon or helium, or mixtures thereof.

In the process of welding in shielding gas environment with fusible electrode, there are used either inert or active gases. Therefore, we make the distinction between *welding in an inert gas environment with fusible electrode* (MIG) and *welding in an active gas environment with fusible electrode* (MAG).

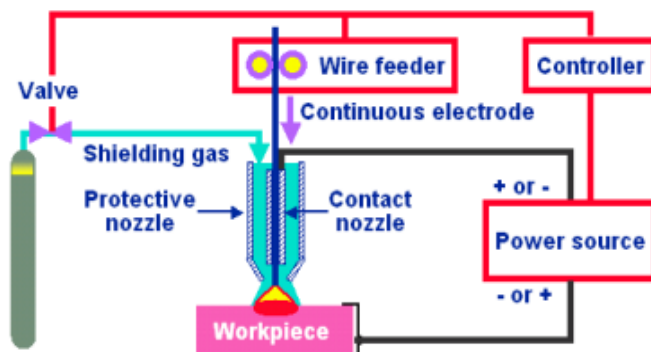


Fig. 2. MIG / MAG welding process

Another distinction is made depending on the type of shielding gas used, i.e. between the MAGM welding, where there are used mixtures of argon-based gasses with addition of active components, as CO₂ and O₂ (also known as *GMMA* = "gas-mixture metal arc" welding), and the MAGC welding, where it is used technical carbon dioxide, CO₂, (also known as *GMA-CO2*).

3. TECHNOLOGY DEVELOPMENT FOR WELDING IN MIG/MAG SHIELDING GAS ENVIRONMENT

Classically, this technology involves the following stages [4], figure 3:

- ❖ presentation of backlash shape and establishing the actual sizes;
- ❖ choice of welding materials;
- ❖ calculation of parameters and welding technology;
- ❖ tabulation.

The first stage, *presentation of backlash shape and establishing the actual sizes*, figure 5, will be based on the following features [3]:

- ❖ reduced diameter of the electrode wire;
- ❖ lack of coating material;
- ❖ high current densities.



Fig. 3. User interface

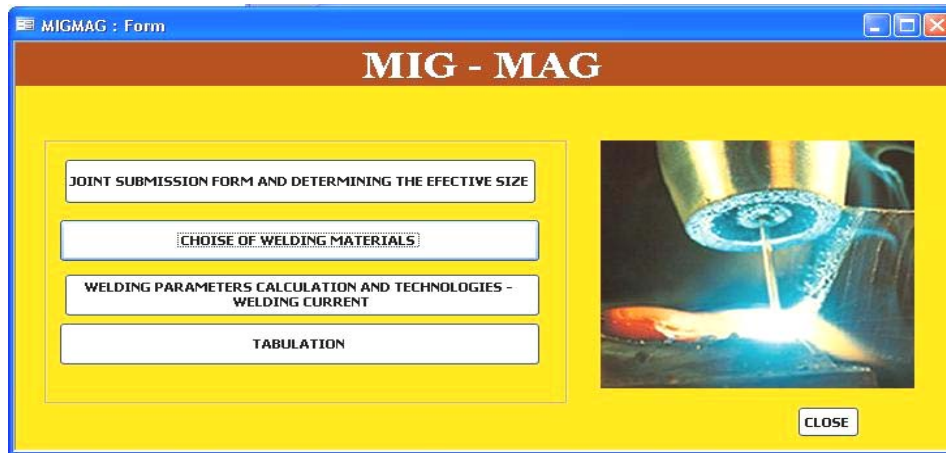


Fig. 4. MIG / MAG welding technologies

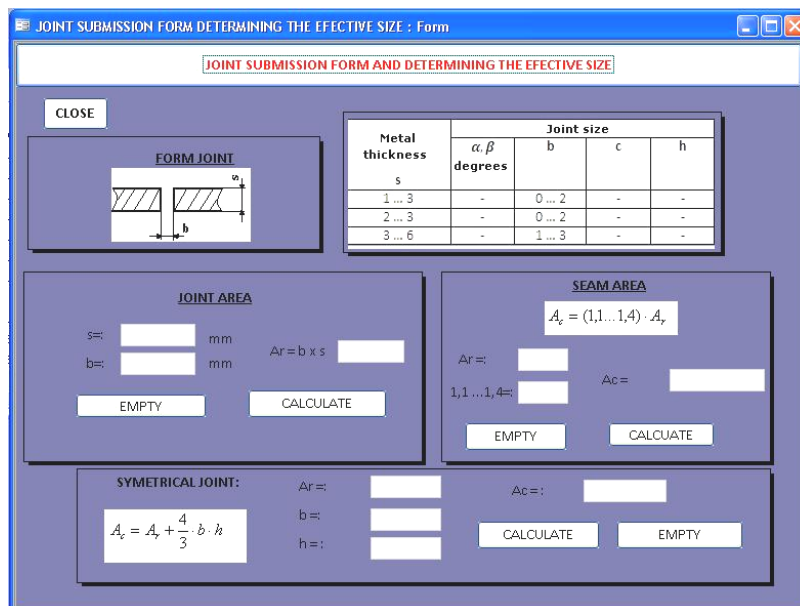


Fig. 5. Joint submission form and determining the effective size

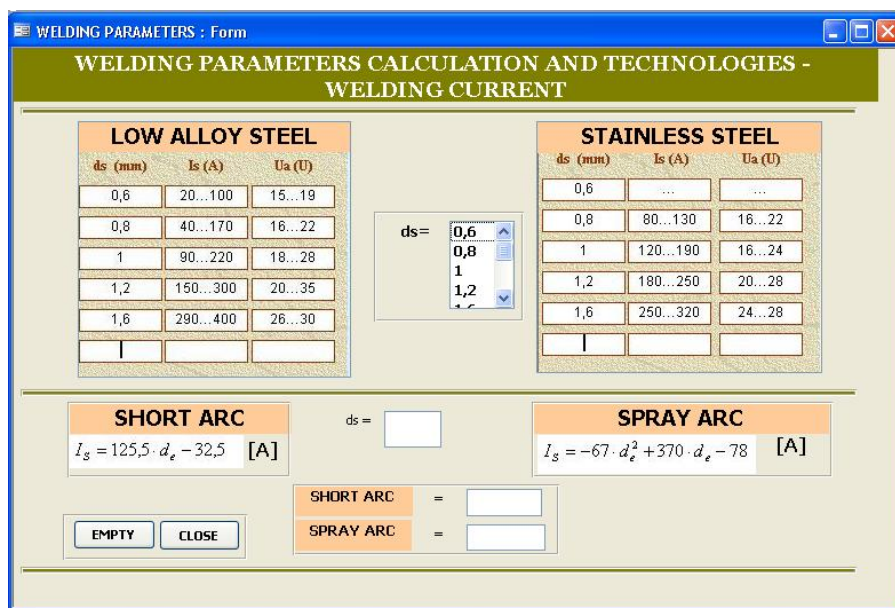


Fig. 6. Strength of the welding current

The inadequately chosen of backlash sizes and the mismatch of technological welding parameters can lead to malfunctions, as follows:

- ❖ puncture and drainage of molten metal material at the root;
- ❖ electrode wire passing among components without arc ignition, or its discontinuation;
- ❖ lack of penetration at the root;
- ❖ root unmelting.

The second stage, *choice of welding materials*, includes:

- ❖ choosing the wire brand and shielding gas;
- ❖ establishing the electrode wire diameter;
- ❖ determining the number of passes;
- ❖ arrangement of passes.

The third stage, *calculation of parameters and welding technology*, aims to establish, figure 6:

- ❖ the welding variance;
- ❖ free length of electrode wire;
- ❖ current amperage;
- ❖ spring tension

The first form of application is called *Interface* and allows the launching of the other options of the application, figure 3.

The program requires data entry in the afferent fields. Then, by pressing the button „CALCULATE”, the requested result is automatically displayed.

4. CONCLUSIONS

This type of information system enables the development of welding technology automatically, saving time, because the engineer disposes of a comprehensive database, from where he extracts the values of the imposed welding parameters.

So, the values of the other parameters are going to be calculated based on the extracted values, through an intuitive and friendly interface.

REFERENCES

- [1.] M. Burcă, S. Negoiteasa – Sudarea MIG/MAG, Editura SUDURA Timișoara, ediția a 2- a, 2004.
- [2.] G., Aichele, 116 Reguli de sudare în mediu de gaz protector, Editura Sudura, Timișoara, 1999.
- [3.] N. I., Trif, Automatizarea proceselor de sudare, Tom V, Vol. 2, Enciclopedie de Sudură, Editura Lux Libris, Brașov, 1996.
- [4.] *** Colecția de standarde comentate, Editura Sudura, Timișoara, 2000-2005.
- [5.] P., Norton, ș.a , Microsoft Office 2000 Editura Teora, București, 2003.
- [6.] J., Habracken, Microsoft Access 2002 pentru începători Editura Teora, București, 2003.





THE BEST WAY OF WORKING SPACE ROBOT WHICH EQUIPS A FLEXIBLE MANUFACTURING CELL COMPONENT OF WELDED IN RAIL FIELD

¹⁻²POLITEHNICA UNIVERSITY OF TIMISOARA, ROMANIA

³. SOCIETATEA NAȚIONALĂ TRANSPORT FEROVIAȚ MARFĂ, "CFR MARFA"-SA SUCURSALA TIMISOARA, ROMANIA

ABSTRACT:

The industrial robot acts on its operating space under different shapes, namely by manipulating parts, by executing processing technological operations, by measuring specific parameters of products or even of the operating space etc.

Many applications and functions performed by a robot reveal an essential characteristic, namely their versatility.

Studying the movement of a robot consists of a single well-defined problem but a collection of several problems that are more or less than one other option. Exemplification was performed using MSC NASTRAN program.

KEYWORDS:

industrial robot, operating space, movement of a robot, exemplification

1. INTRODUCTION

The industrial robot acts on its operating space under different shapes, namely by manipulating parts, by executing processing technological operations, by measuring specific parameters of products or even of the operating space etc.

Many applications and functions performed by a robot reveal an essential characteristic, namely their versatility.

Versatility defined as the robot's physical ability to perform various functions and to take various actions in a given technological application is closely related to the structure and mechanical ability of the robot, which in turn determines the configuration of the robot workspace.

Since the workspace of a robot has geometry depending on components and structure of its mechanisms, in this space the characteristic point of the robot must execute motions on trajectories imposed by obstacles to avoid collision. In a first analysis of a robot working space should not be dealt with "obstacles" and can be utilized. "Obstacles" are operating in the area of warehouses or other exhaust retrofit devices of flexible robotic cell in which all components must interact.

Trajectory through "obstacles" can be chosen so that we can avoid collisions with maximum probability.

2. THE STUDY

Studying the movement of a robot consists of a single well-defined problem but a collection of several problems that are more or less than one other option.

The robot is becoming a more autonomous mechanical system that increases the need for automatic trajectory planning in its development.

The simplest planning problem assumes that the robot is only moving object in space which does not possess dynamic properties thus avoiding temporal problems.

It also considers that the robot does not come into contact with surrounding objects, thus avoiding problems of mechanical interaction.

These considerations turn the physical planning problem into a purely geometric problem.

Furthermore it is considered that the robot is only moving rigid solid which is limited only by the obstacles.

With these simplifications the basic problem of planning robot trajectories can be formulated as follows:

- ❖ let's consider A a single solid or rigid (robot) that moves in a Euclidean space W, called workspace, represented by R^n , $n = 2$ or 3 ; it's movement is not limited by any restriction on kinematics.
- ❖ let's consider B_1, \dots, B_q fixed rigid objects (obstacles) distributed in well defined positions in working space W;
- ❖ knowing the position and orientation, at baseline, the robot, and final finishing position and orientation of this workspace W, generate a path specifying a continuous sequence of positions and orientations of A starting from the initial configuration (position and orientation), avoiding the contact with obstacles B_j and finishing in the final configuration (position and orientation) final;
- ❖ if such a path does not exist, "error" must be reported.

It is obvious that although the basic planning problem is super simplified it is still a difficult problem with many solutions and direct extensions to more complicated issues.

Objectively mobile object (the robot the characteristic point) in such a matter is referred to in the literature as "flying objects".

The basic problem involves the robot path planning through exactly the trajectory generated by the planner. It is also assumed that both the geometry and robotics as well as obstacles positions are known with precision. In reality no planning problem meets these assumptions. Moreover, they control their robots and geometric patterns are not precise. Since the robot has no a priori information about the desktop, it must be based on runtime its sensory system for recording information necessary to achieve the task. It must work in exploring space and solve the problem of planning in the presence of uncertainties.

The problem is to calculate the trajectory generation based on data received from the motion planner sizes order to ensure passage of the robot through the established points.

Generation of movement can be made directly in the space coordinates kinematics couplings, or operational area.

Navigation strategy refers to determining how (methods) to move the robot according to the type of task performed.

Modelling space implies establishing navigation maps in the considered space.

Modelling methods known in literature are [1-5]:

- ❖ uniform grid method;
- ❖ tree method;
- ❖ heterogeneous grid method;
- ❖ convex polygon method;
- ❖ method of crossing points.

Evolution of the robot in the workspace imposes the statement that the space of configurations SC is intrinsically independent of the choice of reference systems SA and SW.

Trajectory planning problem in the presence of obstacles can be expressed as: given a workspace populated with obstacles known through their borders, and by moving objects, must determine a path without collisions with obstacles in bringing mobile objects in the final initial configuration.

The problem can be approached in two ways global or local, hence the two types of planning methods: global and local.

Application of global methods require complete knowledge of the working space "in advance", modelling proper clearance, research and selection of all possible paths of a certain trajectories corresponding to a minimum cost criterion. Such a method guarantees the existence or absence of a solution. Also global planning methods can be easily adapted to the off-line programming.

Applying a local method requires partial knowledge of the workspace.

Such a method does not guarantee reaching the final configuration, but the advantage of good real-time adjustments.

In both cases, solving the planning problem involves solving geometric problems (pure geometry) or combine geometry with kinematics and/or dynamics.

In such situations often are used the results of algorithmic geometry.

In general the application of planning methods must meet certain restrictions such as: the safest way, the shortest path, etc.

3. ANALYSES, DISCUSSIONS, APPROACHES AND INTERPRETATIONS

Analyzing the best methods in place of the theoretical and the application can highlight the road map method, exact cell decomposition method and the potential field method. Of these potential field method treats the robot represented as a point in configuration space, that as a particle under the influence of an artificial potential field U whose local variations reflects "structure" of the free space.

Potential function is defined as the amount of free space on an attractive potential, which attracts the robot toward the final configuration, and a repulsive potential, which removes the robot from obstacles.

The method was originally developed as an "on line" method to avoid collisions to be applied when there is no model of obstacles, in advance, but they may refer to during the execution of movement. In particular, the procedure can lock in a local minimum of potential function.

This deficiency can be corrected by calculating the finite element method applied to study a potential field.

Starting from the potential field finite element method we propose, as an effective tool for the analysis of optimum road space of the robot.

Thus we suggest that the workspace of a robot to be modelled as a homogenous body which is dependent on structure geometry of components and obstacles.

In this space to work tasks the robot must go through the obstacles imposed trajectories which it has to avoid.

The road through the obstacles can be chosen so that to avoid the maximum probability collisions. If we accept that two neighbouring obstacles behave as two sources of the same physical stationary field and consider that the moving of the characteristic point is carried on the same potential trajectory as that of the resulting field we can select a family of trajectories corresponding to a certain field potential in a given interval.

In the application illustrated in Figure 1 the working space was modelled as a homogeneous body with known thermal characteristics.

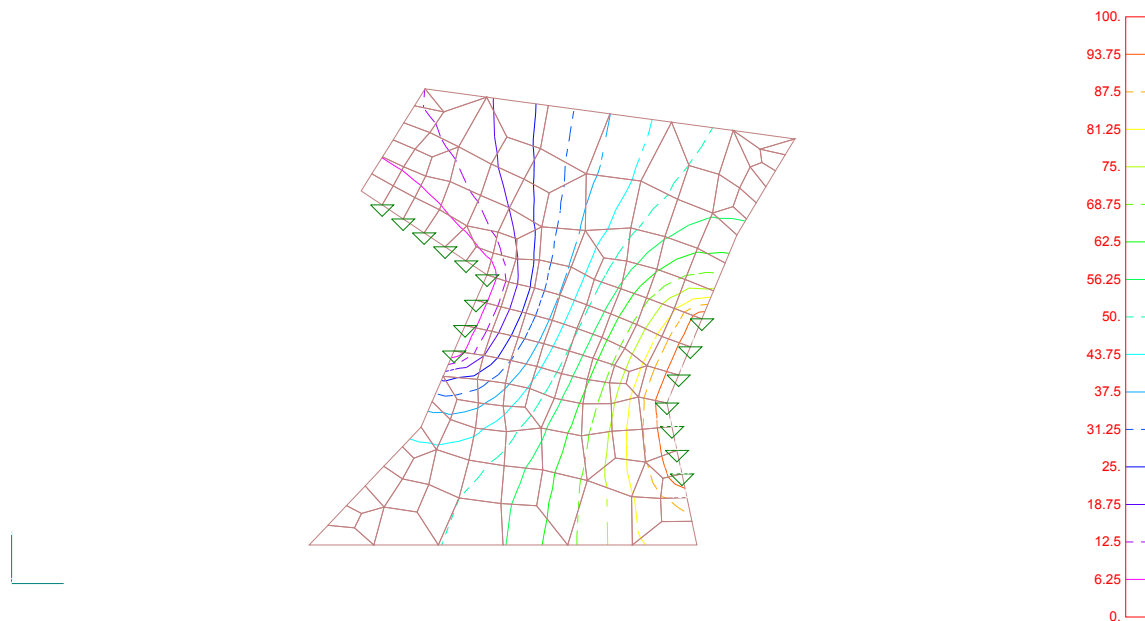


Figure 1 Thermal analysis of a working space modelled as homogeneous body found in a field where the heat source hot / cold data are boundaries of obstacles.

Obstacles are considered as being „hot" or "cold" areas/sources on the boundary of the considered working space as being an homogenous body on which a thermal field is applied from the hot/cold sources (modelled obstacles).

Applying the finite element method analysis facility on the thermal model workspace the outcome is isothermal surfaces. From these areas we can define curves obtained by modelling which can be trajectories of the characteristic point.

Using the family of isothermal surfaces in the average temperature (resulting from thermal finite element analysis) on this can reside optimum trajectories to be passed.

So configurations libraries can be built-up for the working space and trajectories to pass, respectively located on the average temperature isothermal surface.

Illustrated in Figure 1 is a workspace of a robot modelled as homogeneous body found in a field where heat sources hot / cold data are borders of the obstacles that need to avoid in his motion.

Thermal finite element analysis on the isothermal model gives us the results. The treaty was exemplified in the plan but can be generalized in three-dimensional space. Most times one of the 3D motion parameters can be imposed by the kinematics couplings which controls programming. Applications can be treated and depending on who is involved in the process robot. The most complex situation is found in welding rail vehicle structures.

4. CONCLUSIONS

A key issue in the field of industrial robots operation (i.e. programming the optimal path of motion) enjoys the benefits of programs devoted to finite element analysis to allow for applying the "potential field method" as an analysis of a stationary thermal field.

Exemplification was performed using MSC NASTRAN program.

REFERENCES

1. Gârbea D., Analiză cu elemente finite Editura Tehnică București 1990
2. Hubner H. K., "Metoda Elementului Finit Pentru Ingineri" Departamentul de inginerie mecanică, Laboratorul de cercetări Genenral Motors, Wiley-Interscience, John Wiley&Sons, New York, London, Sydney, Toronto, 1990
3. Pires, J. N, Loureiro, A., Bölmjsjo, G., Welding Robots - Technology, System Issues and Application, 1st Edition., 2006, XVIII, 180 p. 88 illus., Hardcover, ISBN: 978-1-85233-953-1
4. Staicu, S., Liu, X-J., Wang, J., Inverse dynamics of the HALF parallel manipulator with revolute actuators, Nonlinear Dynamics, Springer, 50, 1-2, pp. 1-12, 2007
5. Staicu,S., Zhang, D., A novel dynamic modelling approach for parallel mechanisms analysis,Robotics and Computer-Integrated Manufacturing, Elsevier, 24, 1, pp. 167-172, 2008





¹ Tamás ENDRÓDY

UNFOLDING THE CONVEX POLYHEDRONS TO A CONNECTED NON-OVERLAPPING POLYGON (PREPARING TOOLS FOR CREATIVE PROOF OF THE DÜRER'S CONJECTURE)

¹ CAD EXPERT, FORMER SCIENTIFIC ADVISOR UNIVERSITY OF SZEGED, HUNGARY
and SZENT ISTVÁN UNIVERSITY, HUNGARY

ABSTRACT:

Albrecht Dürer published his conjecture around 1525: "All the polyhedrons can be unfolded by their suitable cutting edges to a plane so that we can receive a joined polygon-mesh with non-overlapping faces". The author of this article is dealing basically with the suitable positioning of cutting edges for unfolding the convex polyhedrons to a plane, coding the polygon received and its modelling surface. His aim is to give tools for proving Dürer's conjecture and/or to prepare a creative proof for the essential categories of the convex polyhedrons. The notion of the finite convex polyhedrons has a very large set of solids from tetrahedrons to the arbitrarily complicated polyhedrons —covered by $p \geq 3$ sided convex polygons— which have 1 less and less or nil symmetrics. In the case of the analysed finite convex polyhedrons 2 polygons meet in each edge, in their peak $q \geq 3$ pieces of polygons meet where the angle is $\alpha_p < 360^\circ$ in consequence of convexity, otherwise it can be degraded to a plane and can become infinitely big, which was formerly excluded.

The BREP model, an augmented structure of the "Winged edge model" for unfolding the convex polyhedrons and the spherical mosaic/ellipsoid ordered to the polyhedron can help us several times, which can be gained by the projected polyhedron-peaks from an internal point to an external sphere surface which has only mutual points (min.2) with the polyhedron.

The author developed a special complete induction method of the "Winged edge model" for preparing a creative proof of the Dürer's conjecture.

KEYWORDS: Dürer's Conjecture, convex polyhedrons, spherical mosaic/ellipsoid



¹Vasile George CIOATA, ²Imre KISS

SIMULATION OF SOLIDIFICATION PROCESS OF THE PIECES OBTAINED THROUGH DIE FORGING IN SEMI-SOLID STATE

¹UNIVERSITY "POLITEHNICA" TIMISOARA, FACULTY ENGINEERING HUNEDOARA,

²UNIVERSITY "POLITEHNICA" TIMISOARA, FACULTY ENGINEERING HUNEDOARA

ABSTRACT:

In paper is presented some considerations regarding the semi-solid processing of alloys and is presented a new variant of the Rheocasting method. Because the simulation of solidification process has become an important tool for semi-solid processing, in paper is developed a simulation model, developed by means of the finite analysis program Ansys V.6.1, which allows the analysis of the thermal phenomenon. To validate the simulation model, the results is compared with experimental results and is observed slight differences between these, which means that the suggested simulation model can be used with sufficient precision for the analysis of the thermal phenomenon within the process of die-forging in semi-solid state.

KEYWORDS: thixoforming, semi-solid state, solidification, finite element method, heat transfer

1. INTRODUCTION

The basic principle of processing in a semi-solid state consists in obtaining the pieces during the solidification stage of the alloy. Along this time interval, part of the material is still liquid, while other parts are entirely solid. In order to have a thixotropic behavior, the solid phase has to consist in spheroidal (globular) particles, coated in liquid material. This special microstructure can be obtained by rigorous (mechanical, electromagnetic, etc.) mixing during solidification.

The semi-solid state processing knows, generally, two-development route: thixoforming route and rheocasting route.

Thixoforming is the general used term for described of the obtained process of the final parts from the semi-solid state materials, with a help of the metallic dies/forms and the top die. If the part is obtained in a metallic closed form, the method is called thixocasting, and if the part is obtained in a open die, is called thixoforging.

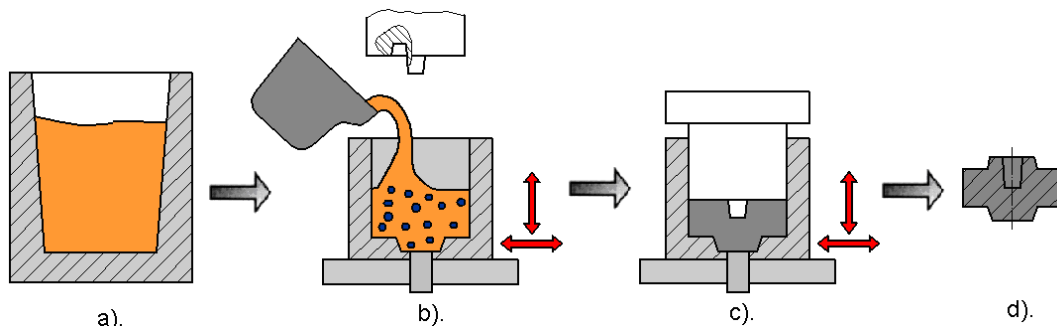


Fig. 1 – Diagram of the new NRC variant [2]

a). alloy elaboration; b). alloy casting into the mould and the obtaining of a structure with thixotropic behavior; c). the formation proper, under vibrations; d). the finished piece

The Rheocasting is other route for development of the processing in the semi-solid state. It is used, still from beginning of the researches like as the technology for obtaining of the material with non-dendrite microstructure for ulterior processing through thixoforming. In 1996, is developed a new rheocasting (NRC) process, which was patented by UBE Industries Ltd. In November 2000, the authors mention this new method in the *Diecasting World* magazine [1].

A variant of the Rheocasting method is presented in [2]. This variant involves the following processing stages: alloy elaboration, feeding the mould with it and mechanically agitating the material by vibration, in order to obtain a structure with a thixotropic behavior (the solid phase has to consist of spheroidal particles coated by the liquid phase) and the formation proper as a result of vibrations. Figure 1 shows a diagram of this variant and points out to the main stages of processing. The red arrows symbolize the mechanical agitation of the metal and mold, by vibration.

2. SIMULATION OF SOLIDIFICATION PROCESS BY FINITE ELEMENT METHOD

2.1. Preliminary

The solidification process is complex in nature and the simulation of such process is required in industry before it is actually undertaken. Finite element method is used to simulate the heat transfer process accompanying the solidification process.

We further introduce a simulation model, developed by means of the finite analysis program Ansys V.6.1, which allows the analysis of the process behavior under the conditions of a variation of the feeding temperature of the mould and of the mould preheating temperature.

By means of this method we managed to determine the temperature field inside the processed alloy, as well as inside the punch mould, during the forging process in a semi-solid state, at certain points. The alloy is poured into the mold in a liquid state, with temperature higher than melting temperature; it solidifies in the range of solidification, followed by cooling.

In order to further validate the simulation model, the points under consideration, used for measuring the temperature, correspond to the position of the thermocouples mounted on the experimental installation, as given in detail in [2]. Their positions are given in figure 2; to be mentioned that they are related to the origin (0,0) of the XOY coordinate system.

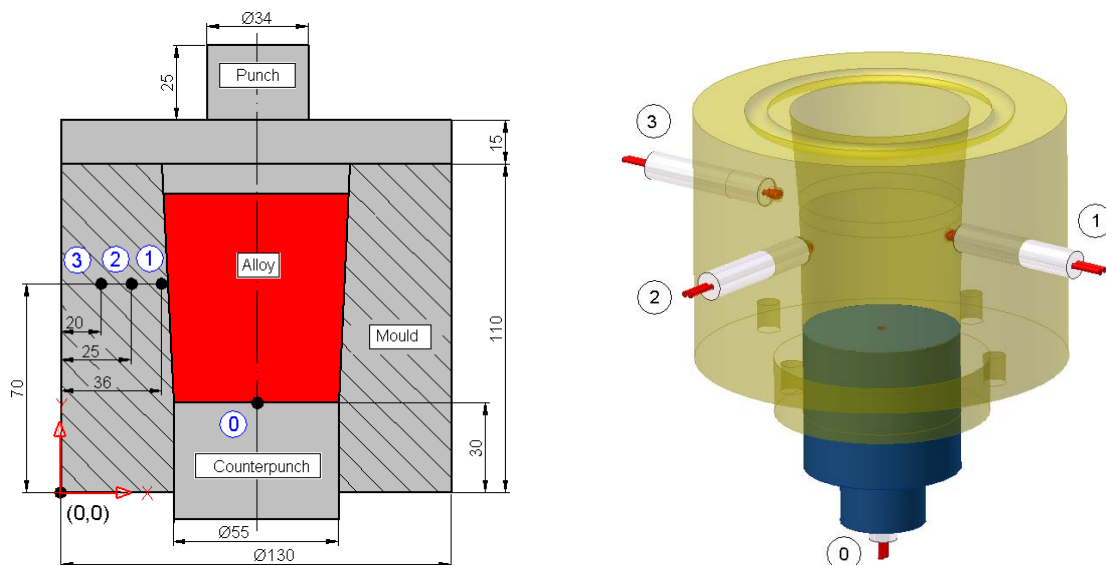


Fig. 2 – Location of thermocouples

After that, it traces the curves $T=f(t)$ (temperature vs. time) for points 0, 1, 2 and 3 for comparison with experimental results.

2.2. Model development

The problem can be modeled in the two-dimensional space, considering the cross section containing the symmetry axis, through the ensemble mould-alloy-punch-counter-punch. Considering the dimensions given in figures 2 and 3, the geometrical model needed by the analysis is obtained by means of the intrinsic modeler of the software, the modeling stages being shown in figure 4.

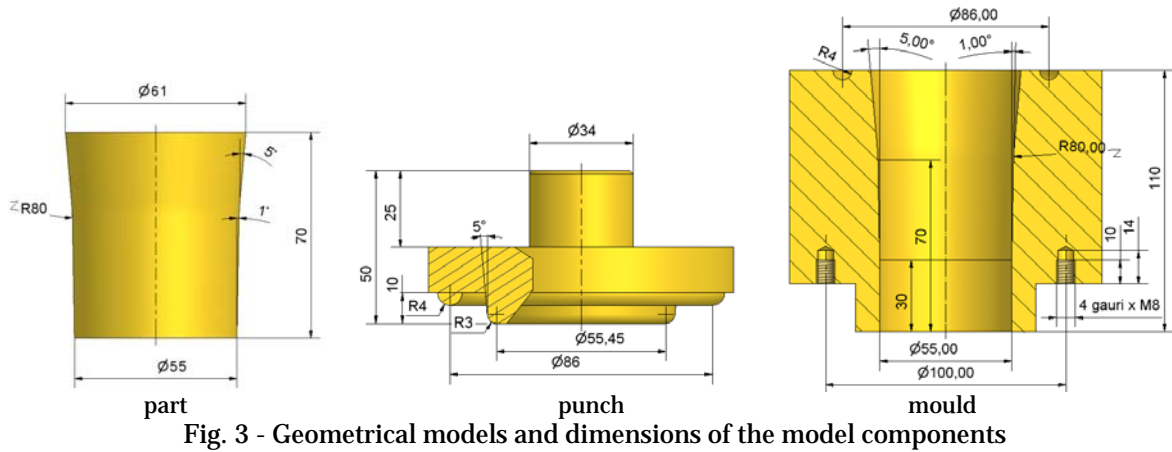


Fig. 3 - Geometrical models and dimensions of the model components

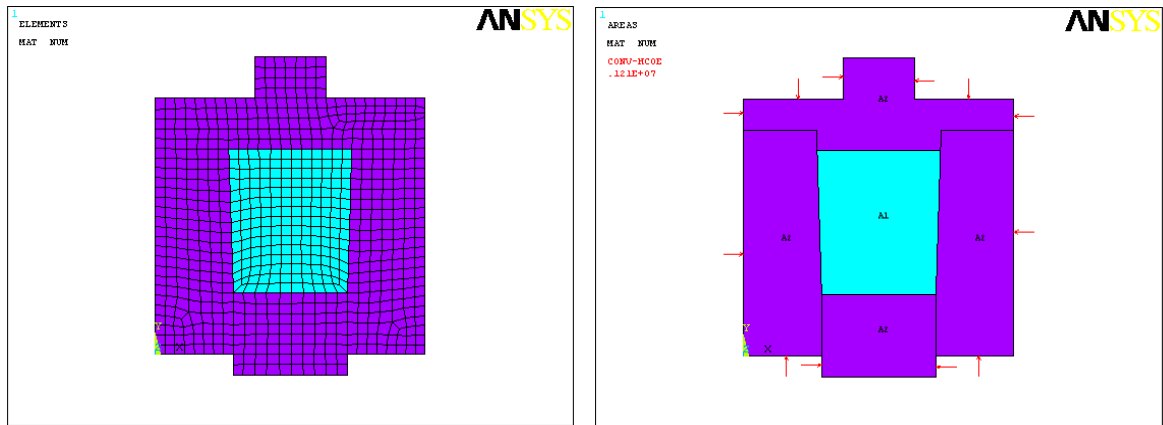


Fig. 4 – Stages of obtaining the geometrical model

For the given analysis, we chose as element of the discretization network, the element type PLANE 55, which is specific to the stationary or transitory thermal analysis, in a two-dimensional plane. At the moment of generating the finite element network we also assigned the corresponding material characteristics.

The materials and their properties are given in table 1 and in figures 5 and 6.

Table 1 – The materials properties

	Material	Density, kg/m ³	Specific heat, J/kg·C	Thermal conductivity, W/mC	Enthalpy, kJ/g
Alloy	AlSi7Mg0,38	2230	1300	As in fig. 5	As in fig.6
Mould, punch and counterpunch	Steel	8000	500	As in fig. 5	-

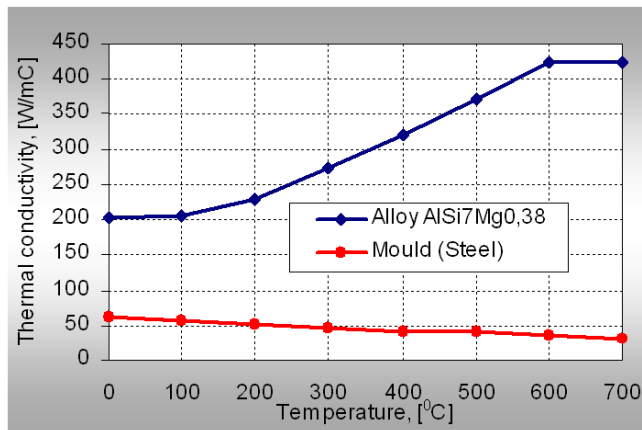


Fig. 5 – Thermal conductivity of the materials

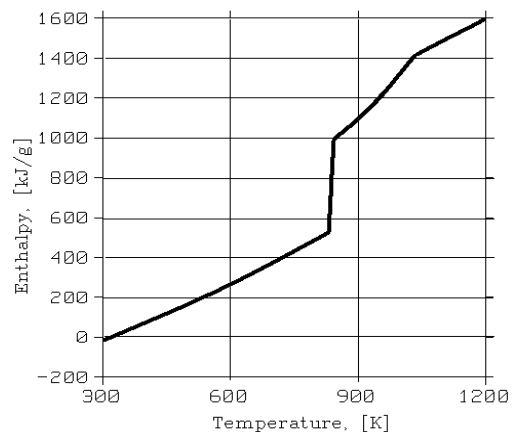


Fig. 6 – The dependency enthalpy – temperature for the alloy AlSi7Mg0,38

The heat transfer between the mould and the environment is done by free convection. This is materialized by the application of certain contour conditions along the lines that make the outer contour of the geometrical model (fig. 4). The parameters of the condition are: the convection coefficient is 12,30 W/m².C and the room temperature is: 25°C.

The alloy is cast into the mould in a liquid state, at a higher temperature than the melting one, and it solidifies during the solidification interval, after which it cools down.

The temperature of the alloy and of the mould/punch is time-dependent, so the analysis will be a transitory (non-stationary) one. The chosen analysis time was 300 seconds and the step, 1 second. The initial analysis conditions are:

- The nodes corresponding to the alloy at the initial moment have all the temperature of 630 °C;
- The nodes corresponding to the mould, punch and counterpunch, at the initial moment, have all the temperature of 100 °C.

2.3. Results

After the analysis proper (processing) has been done, in the post-process stage one can visualize the temperature fields inside the alloy and mould, at various moments, as shown in figures 7...10.

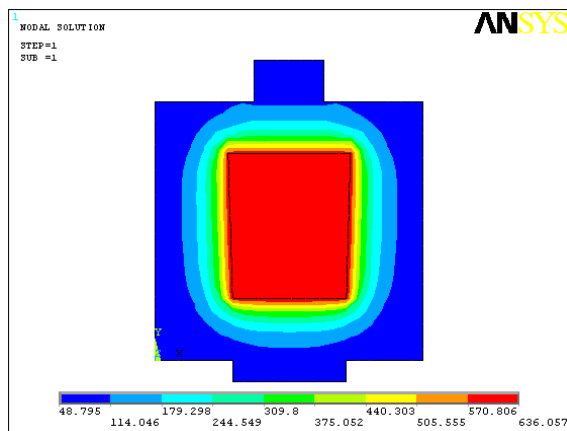


Fig. 7 – The temperature field at moment t=1s

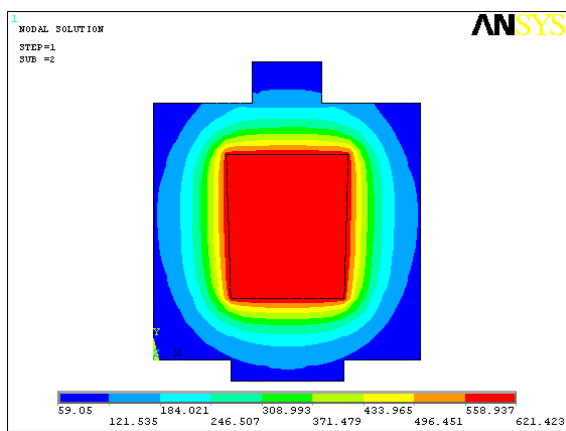


Fig. 8 – The temperature field at moment t=2s

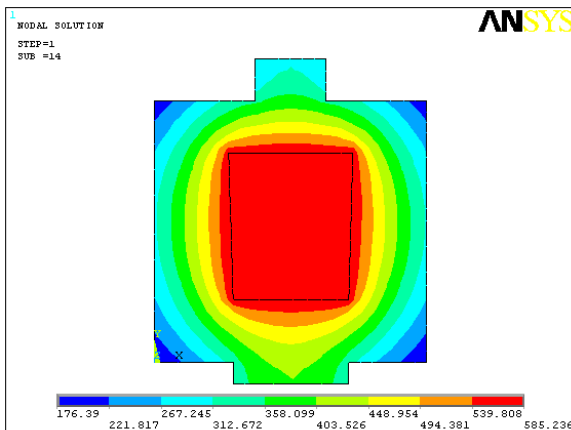


Fig. 9 – The temperature field at moment t=14s

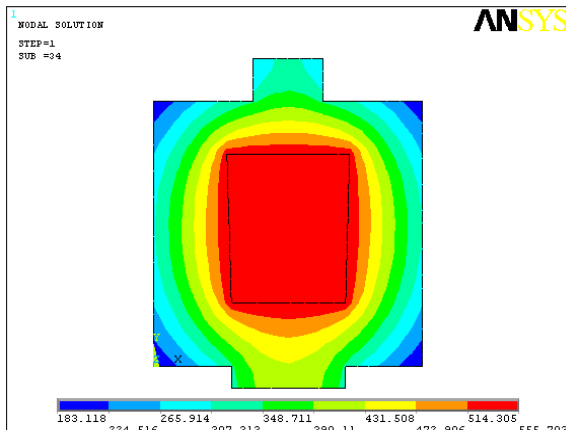


Fig. 10 – The temperature field at moment t=34s

At the same time, one can visualize the evolution of the solidification front inside the piece, at various moments. Thus, in figure 10 we give the evolution of temperature inside the piece and mould, from the casting of the alloy, up to the moment of complete solidification of the piece.

In order to determine the temperatures at the points of interest, at specific times, we identified the node corresponding to the location points of the thermocouples and we defined the variables marked as 0, 1, 2 and 3.

We plotted the curves $T=T(t)$ (temperature depending on time) for points 0, 1, 2 and 3 in order to obtain a comparison with the experimental results.

Temperature variation at the points of interest is given in figure 12. The shape of the curves resembles a lot that of the curves obtained during the experiments.

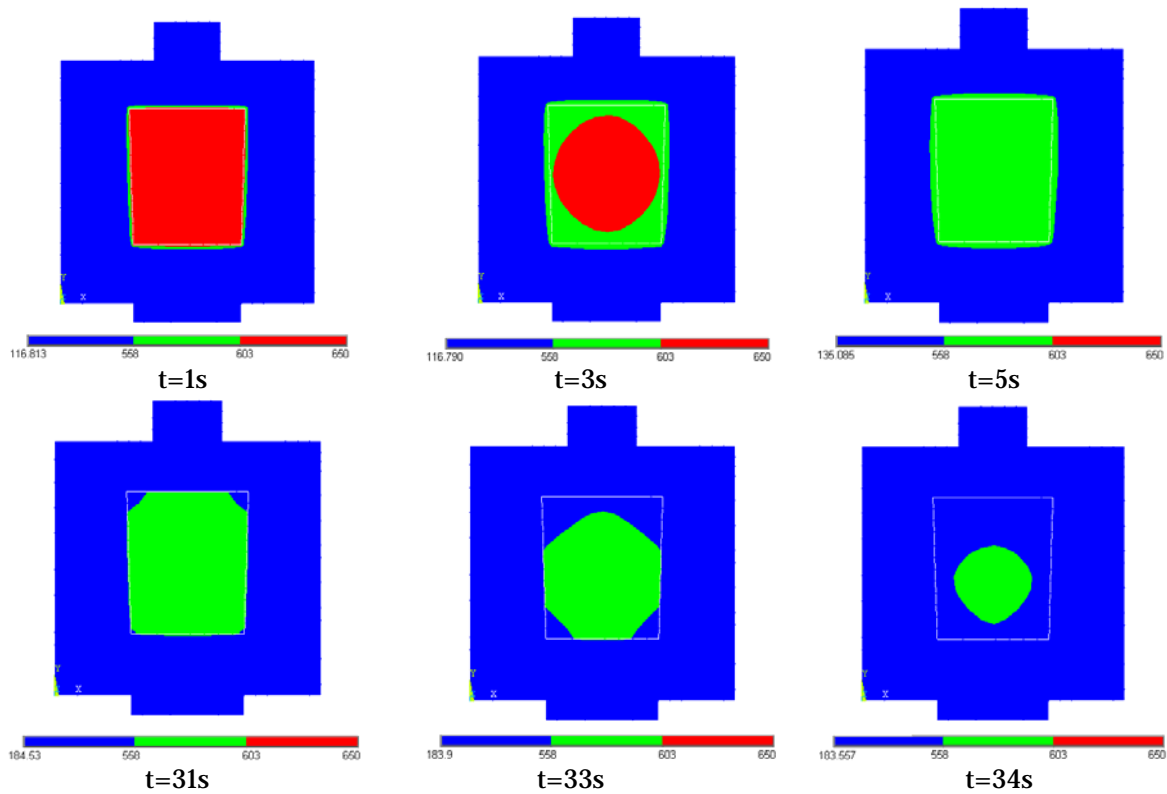


Fig. 11 – The evolution of the solidification front inside the piece

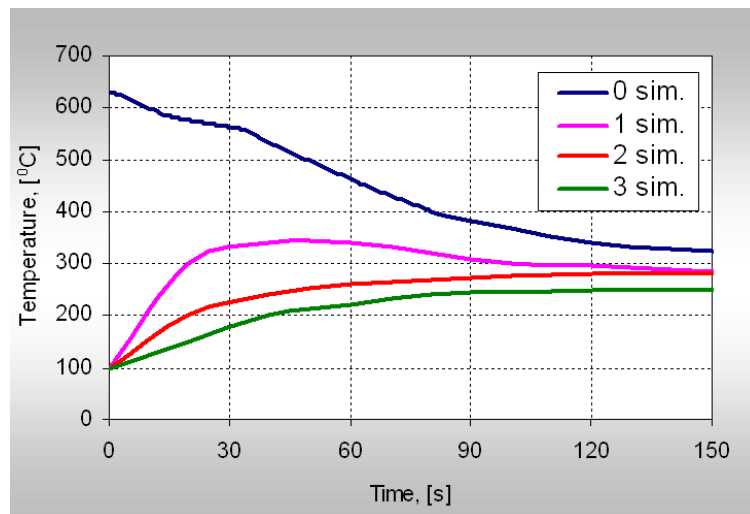


Fig. 12 – The piece cooling curve (0 sim.) and the mould heating curves (1 sim., 2 sim., 3 sim.), obtained by simulation under conditions: $T_T=630^{\circ}\text{C}$, $T_{OM}=100^{\circ}\text{C}$

The moulding times under various processing situations can be obtained by detailing the cooling curves $T=T(t)$ obtained during the temperature interval T_T-T_S .

3. VALIDATION OF THE SIMULATION MODEL

In order to compare the experimental data with those resulted from simulation, we created the graphical representation given in figure 13, where we showed, in the same diagram, the dependencies $T=T(t)$ – corresponding to points 0, 1, 2 and 3 – obtained experimentally and, respectively, by simulation.

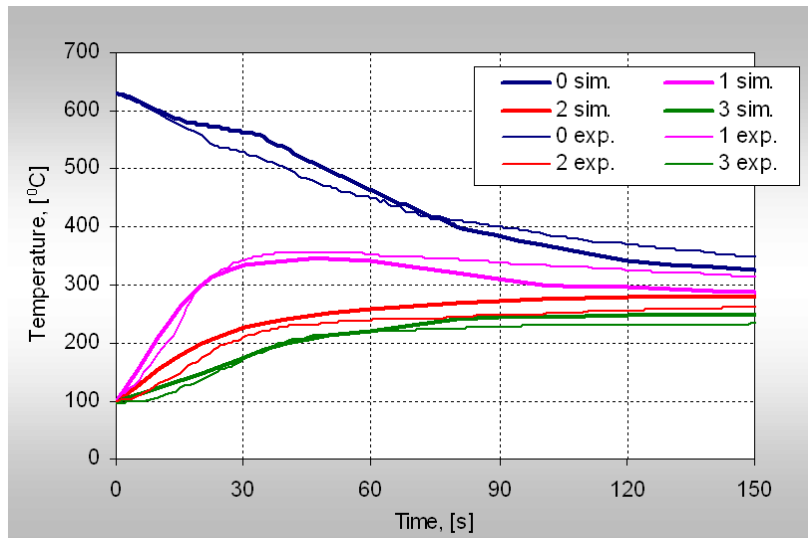


Fig. 13 – Comparison between the experimental results and the ones obtained by simulation, under conditions $T_T=630^{\circ}\text{C}$, $T_{OM}=100^{\circ}\text{C}$

One can notice really slight differences between the results to be compared, which means that the suggested simulation model can be used with sufficient precision for the analysis of the thermal phenomenon within the process of forging in a semi-solid state.

REFERENCES

- [1.] KAUFMANN, H., et all, New Rheocasting: a novel approach to semi-solid casting, Diecasting World, November 2000, 14 -17
- [2.] CIOATA, V. G., Studii si cercetari privind matritarea metalelor si aliajelor in stare semilichida (Studies and researchs on die forging of the metals and alloys in the semi-solid state), Doctorate Thesis, Timișoara "Politehnica" University, 2004, p. 6-7, 83-84, 123-132
- [3.] KIRKWOOD, D. H., et.all, Semi-solid Processing of Alloys, Springer, 2010
- [4.] HIRT, G., KOPP, R., Thixoforming. Semi-solid Metal Processing, Wiley VCH, 2009





¹Vasile George CIOATA, ²Imre KISS

DETERMINING THE CONTACT FORCES BETWEEN THE WORKPIECE AND FIXTURE USING THE FINITE ELEMENT METHOD

¹UNIVERSITY "POLITEHNICA" TIMISOARA, FACULTY ENGINEERING HUNEDOARA,

²UNIVERSITY "POLITEHNICA" TIMISOARA, FACULTY ENGINEERING HUNEDOARA

ABSTRACT: During clamping operations and machining, the forces which act on the workpiece (weight, inertial forces and moments, cutting forces and moments, clamping forces) cause the contact forces between the locators and the workpiece. Because of these contact forces, elastic deformations appear in the contact area between the locators and the workpiece, deformations which are a source of machining errors. If the values of the contact forces is big, these can cause plastic deformations which leads to the destruction of the workpiece in the contact area. Also, the very small values of the contact forces can cause the slipping of the workpiece on the locators or even the loss of the contact between the workpiece and the locators compromising the orientation scheme. Therefore, the evaluation of the contact forces between the workpiece and the locators is an important stage in the design process of the binding devices. In this paper work there is presented an example of using the finite element method in order to determine the contact forces for a real situation of processing.

KEYWORDS: fixture, workpiece, contact force, locators, clamping elements, finite element method

1. INTRODUCTION

In order to execute the different processing operations, the workpiece must be installed in the fixture or directly on the tool-machine in a certain position in comparison with the cutting tool. The installation of a workpiece has two functional phases: the orientation and the clamping. These two phases can be executed successively with orientation elements and clamping elements, or simultaneously, with an auto centered device.

The orientation of a workpiece is the operation which establishes a strictly determined position of the workpiece in comparison with the edges and the trajectory of the cutting tool. An object in the three-dimensional space disposes of six degrees of freedom: three translations through the length of the axes and three rotations around the axes of an orthogonal system of axes. In order to ensure a unique position for the workpiece in comparison with a XYZ axes system, all the six degrees of freedom must be bound. The orientation notion has to be related to the technological system adjusted to the dimension and to the serial production.

During the workpiece's processing action, the workpiece's position has to be maintained, that means that the orientation scheme must be preserved, which corresponds to the clamping phase. Clamping means applying on the workpiece which is oriented on the locators, a clamping forces system built to make the orientation scheme and preserve it during the processing. This forces system must achieve the contact between workpieces and locators and maintain it during the processing, assuring at the same times a maximum rigidity for the workpiece-device system, which has to remove or diminish the vibrations.

In order to determine the clamping force, the most detrimental situations must be considered, even though these situations are unlikely to occur. For example, for a milling device we must consider the next possible situations: milling towards or against the advance, milling with a cylindrical mill or a cylindrical-frontal mill, milling towards the device's locators or in the opposite way, technological indiscipline. Clamping forces are calculated using the workpiece equilibrium under the influence of the forces which act on it (weight, inertial forces and moments, cutting forces and moments) or using the rigidity of the locators and clamping elements of the workpiece.

2. THE CALCULATION OF THE CONTACT FORCES

During clamping operations and machining, the forces which act on the workpiece (weight, inertial forces and moments, cutting forces and moments, clamping forces) cause the contact forces between the locators and the workpiece. Because of these contact forces, elastic deformations appear in the contact area between the locators and the workpiece, deformations which are a source of machining errors. If the values of the contact forces is big, these can cause plastic deformations which leads to the destruction of the workpiece in the contact area.

Also, the very small values of the contact forces can cause the slipping of the workpiece on the locators or even the loss of the contact between the workpiece and the locators compromising the orientation scheme.

Therefore, the evaluation of the contact forces between the workpiece and the locators is an important stage in the design process of the binding devices.

For the fixture design practice, the evaluation of the contact forces between the elements of the workpiece-fixture system is very important because their size is not constant during the processing of the workpiece, depending on the cutting forces and moments, which have a variable feature and a position and direction which vary during the processing.

To the design of the devices for processing of the workpieces, the extreme values of the contact forces are important. The maximum and minimum values of the contact forces are determined according to the next reasons [1, 2]:

- The maximum contact force, $f_{c \max}$: the maximum value of the contact pressure (Hertz pressure, p_{\max}) is

$$p_{\max} = 3\tau_{\max},$$

where τ_{\max} is the maximum shear stress. And the indentation will appear when:

$$\tau_{\max} = \frac{\sigma_y}{2},$$

where σ_y is the yield stress of the workpiece material.

Therefore

$$p_{\max} = 1,5\sigma_y.$$

The maximum contact force for locators with a plane contact surface is

$$f_{c \max} = p_{\max} \cdot \pi a^2 = 1,5\sigma_y \cdot \pi a^2,$$

where a is the radius of the contact area.

- The minimum contact force, $f_{c \min}$. The contact forces must be bigger than this value, to prevent the workpiece from slipping on the locators or lose contact with it. To prevent the loss of the contact between the workpiece and the locators the contact force must be bigger than zero. To prevent the slipping of the workpiece, this condition is required:

$$\sqrt{q_x^2 + q_y^3} \leq \mu \cdot f_{c \min},$$

from where the minimum value of the contact force comes out:

$$f_{c \min} \geq \frac{\sqrt{q_x^2 + q_y^3}}{\mu}$$

where q_x and q_y are components on the x and y directions of the tangential forces which act in the contact area and μ is the static friction coefficient between the workpiece and the locators.

3. EVALUATION OF THE CONTACT FORCES WITH THE FINITE ELEMENT METHOD

A quick calculus of the contact forces which appear between the locators and the workpiece to be processed can be made using the finite element method.

Forwards it is presented an example of application of this method for a practical situation of machining.

Considered the machining of a prismatic workpiece into a device formed by 6 locators emplaced in three reciprocal perpendicular planes-which allow locking the workpiece's 6 DOFs- and two clamping systems C1 and C2 (Fig. 2). It is necessary milling a feature to 25 ± 0.002 mm and 12 ± 0.002 mm dimensions, measured from the AC edge. The workpiece is made of aluminum, with the sizes: $220 \times 122 \times 112$ mm, with the density 2700 kg/m³, Young's modulus $E_p = 70$ GPa and Poisson's ratio $\nu_p = 0.334$. The locators and the clamping elements have plane surfaces, the diameter is 18 mm and are made of hardened steel with $E = 207$ GPa and $\nu_p = 0.292$. Clamping forces of 640 N and 690 N

are applied simultaneously by clamp C1 and clamp C2. The static friction coefficient is assumed to be 0.25 between the workpiece and fixture elements.

The cutting force's constituents and torque used in milling the considered feature are estimated to be $F_x=131$ N, $F_y=232$ N, $F_z=55$ N and $M=2.77$ N·m as in Fig. 1.

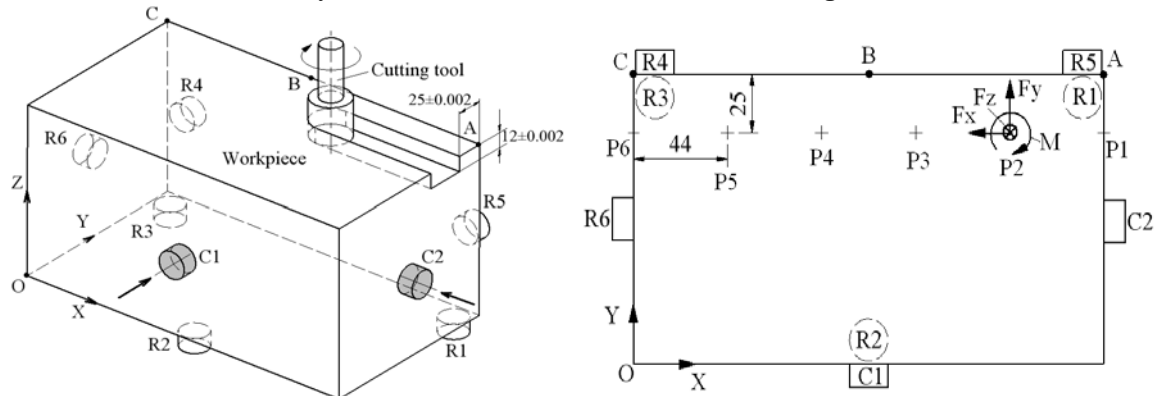


Fig. 1. Scheme of workpiece-fixture system [3]

The coordinates of the locators, of the clamping elements and the application points of the cutting force and moment, related to the OXYZ system are presented in table 1.

Table 1

Coordinates	Locators						Clamps		Points					
	R1	R2	R3	R4	R5	R6	C1	C2	P1	P2	P3	P4	P5	P6
X [mm]	210	110	10	10	210	0	110	220	220	176	132	88	44	0
Y [mm]	112	10	112	122	122	61	0	61	97	97	97	97	97	97
Z [mm]	0	0	0	56	56	56	56	56	0	0	0	0	0	0

4. MODEL DEVELOPMENT

The solid model of the system chosen to be analyzed was realized in Autodesk Inventor Professional and then transferred in Ansys Version 11.0 for the FEA analysis. All the elements of the system have been modeled as isotropic elastic bodies. The locators and the fixture tips have cylindrical shape, the contact surface is plane and has circular shape with the area assumed to be 254 mm². The 10-node tetrahedral element Solid92 was used to mesh all solid bodies. Contact between the workpiece and fixture was simulated using the quadratic surface-to-surface contact elements Target170 and Conta174. A constant static coefficient of friction was used to establish contact properties at the interfaces. To simulate the locators being rigidly fixed in place, the surface of each locator tip opposite to the contact was restrained in all three translational degrees of freedom. In order to simulate the clamping force, there have been applied single forces over the surface of both fixture elements, in opposite contact.

In order to determine the contact forces which appear during the processing, the cutting force and moment were applied in 6 equidistant points (P1,..., P6) on the top surface of the workpiece, at a distance of 25 mm from the AC edge.

5. RESULTS

The contact forces between locators and workpiece were determined for each loading situation. Contact forces between the workpiece and the locators were also determined after applying the clamping forces, before the processing, their values are presented in table 2.

Table 2

	Locators					
	R1	R2	R3	R4	R5	R6
Contact forces [N]	11,88	33,1	19,81	217,16	178,69	411,25

The diagrams in fig 2, which present the variation of the contact forces between the locators and the workpiece during the processing, were drawn. The contact forces which appear during the processing are not constant; these have values which depend on the cutting tool position. The extreme values of the contact forces were represented with a discontinued line; these define the recommended area where the contact forces must be situated.

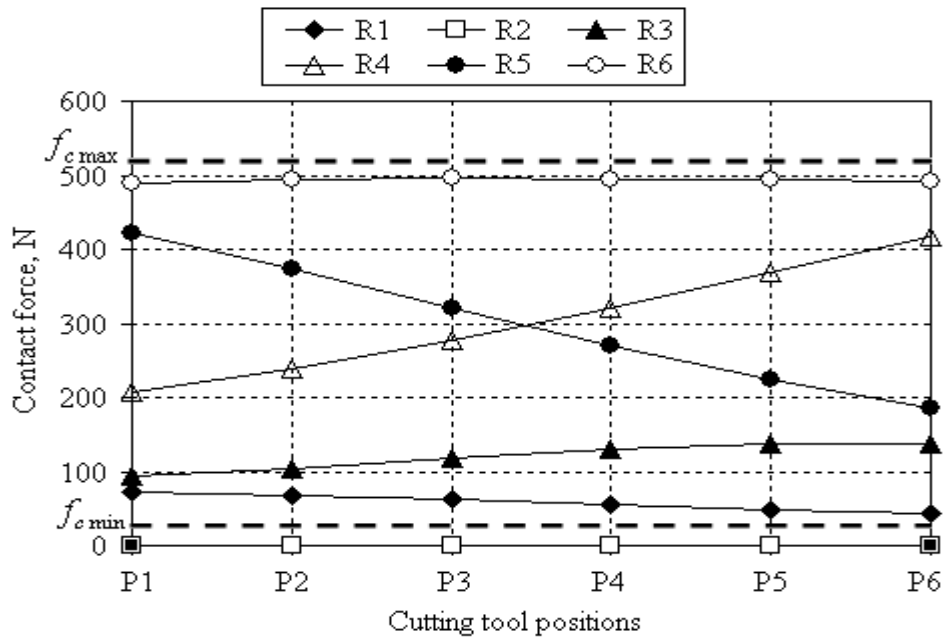


Fig. 2. Contact forces

A value of the contact force which is outside the defined area causes either the instability of the workpiece on the locators, like the case of the contact force between locator R1 and the workpiece, or the destruction of the workpiece in the contact area because of the plastic deformations.

REFERENCES

- [1.] JONHSON, K. L., Contact mechanics, Cambridge University Press, Cambridge, 1987
- [2.] SANCHEZ, H. T., ESTREMS, M., FAURA, F., Fixturing analysis methods for calculating the contact load distribution and the valid clamping regions in machining processes, Int J Adv Manuf Technol, (2006) 29: 426–435
- [3.] CIOATĂ, V. G., Determining the machining error due to workpiece - fixture system deformation using the finite element method, Annals of DAAAM for 2008 & Proceeding of The 19th International DAAAM Symposium "Intelligent Manufacturing & Automation: Focus on Next Generation of Intelligent Systems and Solutions", Published by DAAAM International, Vienna, 2008, 127-128.
- [4.] RONG, Y., ZHU, Y., Computer-aided fixture design. Dekker, New York, NY, 1999
- [5.] KOŠTÁL, P., VĚLIŠEK, K., ZVOLENSKÝ, R., Intelligent Clamping Fixture in General, In: Lecture Notes in Computer Science. - ISSN 0302-9743. - Vol. 5315 : Intelligent Robotics and Applications. First International Conference, ICIRA 2008, Wuhan, China, October 15-17, 2008. v Part II (2008). - ISBN 978-3-540-88516-0, p. 459-465



MOTOR AND VEHICLE OPTIMIZATION PROCESS MODELING BY USING THE AVL CRUISE IN STANDARD APPLICATIONS

¹⁻⁴. „POLITEHNICA” UNIVERSITY OF TIMISOARA, ROMANIA

ABSTRACT:

AVL CRUISE is used to perform simulation and analysis of the vehicle propulsion system. It is designed to develop and optimize low-emission engines, power trains and sophisticated engine control systems, cooling systems and transmissions. CRUISE allows modeling the entire optimization process for motor and vehicle in standard applications, such as fuel consumption reduction, acceleration tests, full load tests, traction diagrams and calculation of thermal, mechanical, electrical and control system parameters. In the paper are presented results obtained for a regular simulation of road vehicle behaviour in working conditions.

KEYWORDS: Simulations, vehicle propulsion system

1. INTRODUCTION

CRUISE allows the simulation of vehicle driving performance, fuel consumption and emissions. This concept can be used for modeling all vehicle configurations with scalable fidelity. This approach allows the reuse of models or sub-systems in different optimization phases of a process in order to improve vehicle performances.

The engine operation optimization is done by calculating and optimizing fuel consumption and emissions, road performances (acceleration and deceleration), transmission ratios, braking performances, in order to determine the load for resistance and vibration calculation.

CRUISE allows modeling existing vehicles and new vehicle concepts with single or double traction (cars, trucks, motorcycles, etc) (Fig. 1).

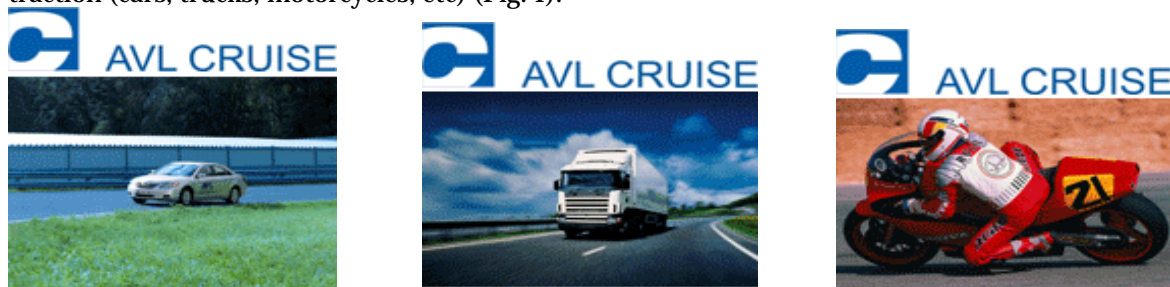


Fig. 1. Vehicle types that can be modeled with AVL CRUISE

AVL CRUISE simulation platform vehicle emphasizes:

- ❖ Optimization of vehicle and vehicle components (fuel economy, vehicle performance);
- ❖ Extensive range of vehicles and possible propulsion configurations;
- ❖ Assessment of new vehicle concepts (i.e., hybrid, electric vehicles, fuel cells);
- ❖ Transitory propulsion effects analysis;
- ❖ Design of vehicle thermal management systems;
- ❖ Smart driving module to reproduce the real vehicle behavior.

2. CALCULATION POSSIBILITIES

The software enables simple or mixed kinematic calculation (dynamic modeling) to study low frequencies, vibrations occurred during vehicle running, the axis torque (power shaft or rear and front axles).

Calculations can be made in quasi-stationary regime or allow the engine real cycle simulation, where the throttle shutter position can be controlled.

The calculation allows the following:

- ❖ Fuel consumption and emissions determination under the next driving conditions:
 - *Running cycle* – for driving, a simulated speed profile is imposed to the vehicle. Driving conditions are specified: runway slope, wind speed, the rolling friction coefficient, etc. Speed profile data can be entered as time and distance dependent values.
 - *Cruise* - running on a real route can be simulated. Speed profile based on distance is defined as the maximum speed that cannot be overtaken. Additional maximum values for acceleration and deceleration can be defined. These values can be used by the driver, but does not interact with the maximum load when the speed profile is suddenly changed.
 - *Constant speed* - involves running in all gears.
- ❖ Driving performances determination consists of acceleration behavior calculation which indicates the increase of performances and traction force, by following (Fig.2):
 - Running at constant speed;
 - Performances increase;
 - Acceleration at full load;
 - Maximum traction force;
 - Vehicle handling.

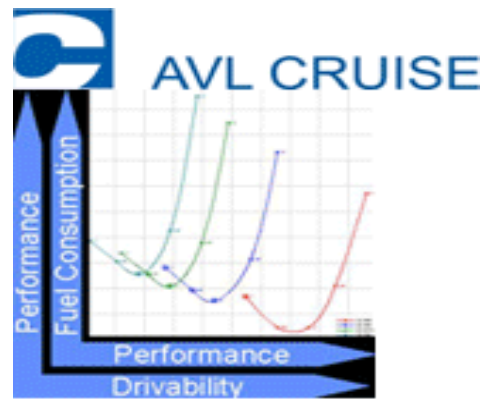


Fig. 2 Fuel consumption, performances and vehicle handling efficiency

CRUISE provides interfaces with MATLAB and Simulink through a DLL created by Real-Time Workshop or through a MATLAB API. The MATLAB API interface enables the user to run Simulink in the background and use scopes as well as variable time step integration methods.

Simulink is an environment for multidomain simulation and Model-Based Design for dynamic and embedded systems.

3. SYSTEM AND SUB-SYSTEM STRUCTURE

Components and their connections can be grouped into sub-systems and can be activated or deactivated so that side-bar configurations of active sub-system can be defined.

All systems contain the same systems; they differ only by their activation status. The structure of the systems/sub-systems and their activation status is shown in the navigation tree and also in the side-bar systems section of the vehicle modeler (Fig. 3, Fig.4). Correlations between AVL Cruise interface and other programs are very easy and allow too modify and interact all the time in the modelling process. A lot of parameters can be easily monitorized through the interfaces, either AVL Cruise or the other program that waork together with (Fig.5).

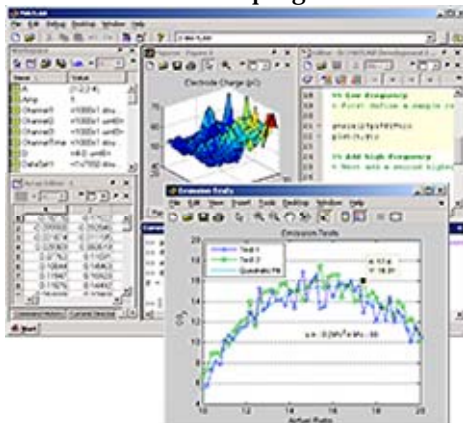


Fig. 3. MATLAB Interface

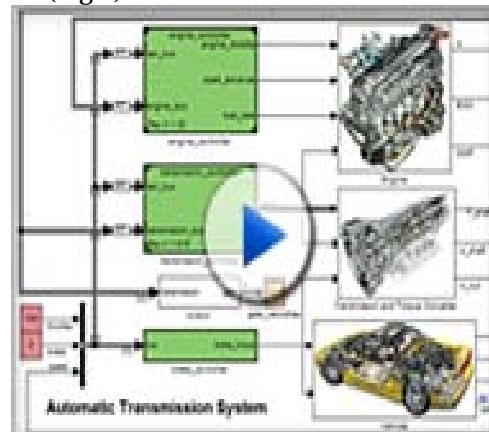


Fig. 4. Simulink simulation environment

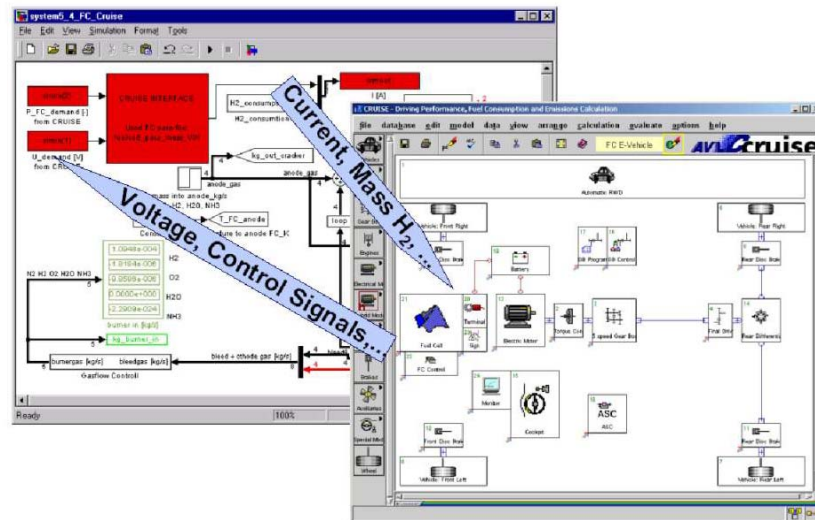


Fig.5. Direct correlation between AVL Cruise Interface and Matlab/Simulink environment

4. ANALYSIS AND SIMULATION RESULTS

The technical data of a BMW 535i E28 vehicle having above 200000 km run and 11 PTI were used for simulation.

After selecting Vehicle in the Main Window, it can be chosen between the following power train configurations: general, manual standard or automatic standard.

For Vehicle Modeling the components are organized into component groups and they can simply be dragged and dropped onto the working area, where they can be linked together to represent the desired power train configuration (Fig.6).

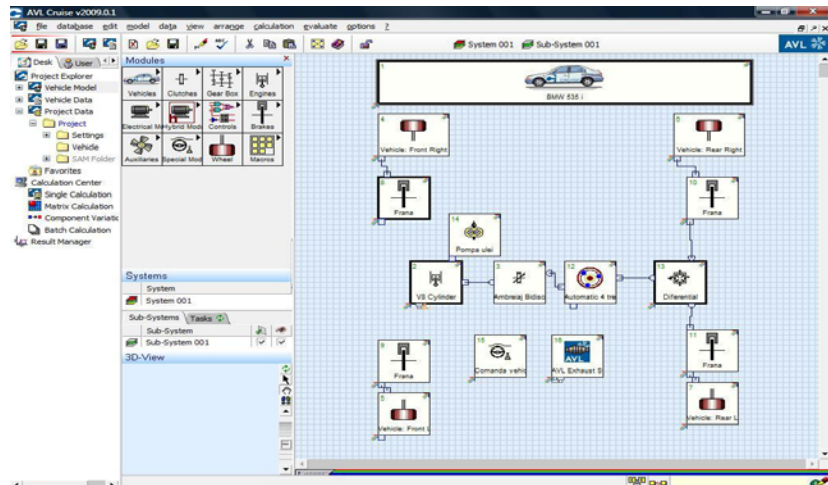


Fig. 6. Vehicle Modeler View

Each component contains the Properties option as is shown in Fig. 7. The calculation can be influenced in the Properties window. With these settings it is also possible to run a calculation with minimal input data (i.e., in prototype phase), as the input fields of the unavailable data can be switched off.

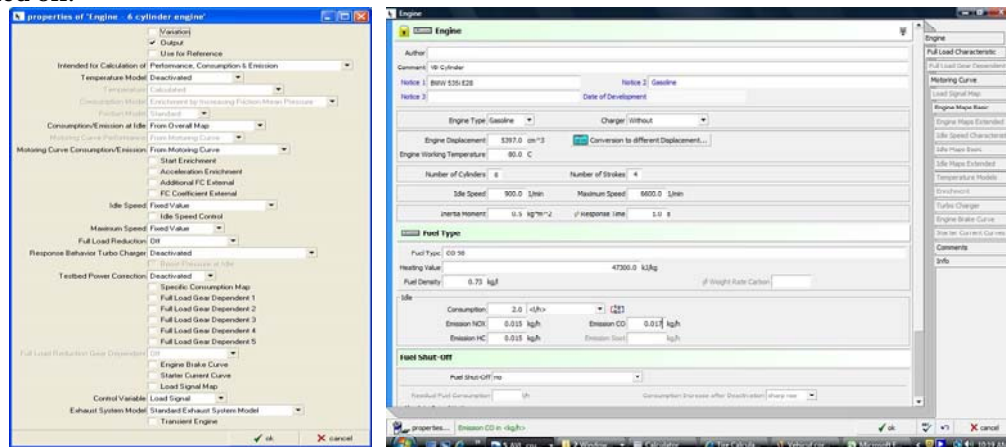


Fig. 7. Engine Properties

After simulation there were obtained: load characteristic (Fig. 8), torque characteristic (Fig. 9) and their dependence in 3D representation (Fig. 10), and also the fuel consumption variation (Fig.11).

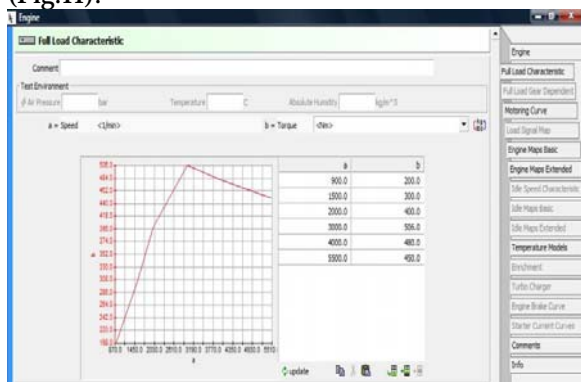


Fig. 8 Load Characteristic

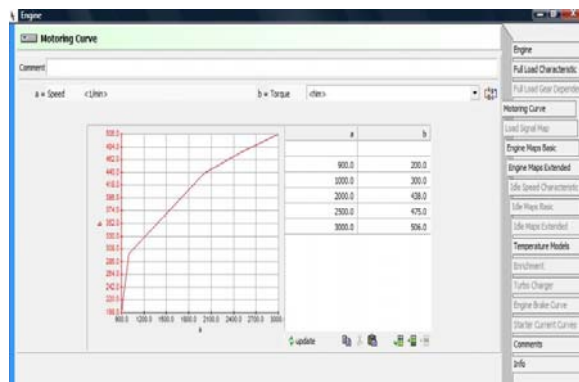


Fig. 9 Torque Characteristic

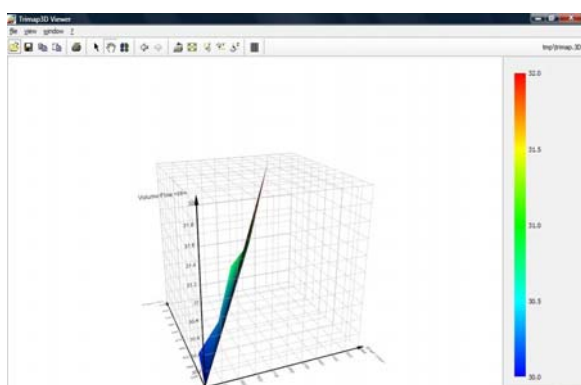


Fig. 10 Engine characteristics in 3D Representation

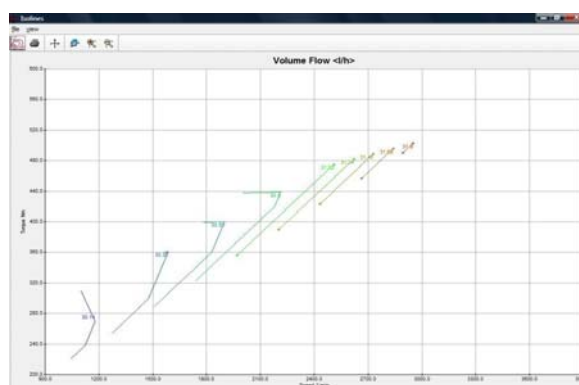


Fig. 11 Fuel Consumption Variation versus Engine Torque and Speed

5. CONCLUSIONS

CRUISE allows the calculation of driving performance, fuel consumption and emissions, the various driving cycle evaluation (i.e., FTP72, ECE-R15, HDC), traction curves, acceleration, maximum speed, hill climbing ability, etc.

The characteristics include the modular concept, the implementation of vehicle simulation, elastic shafts torsion and engine cold start.

Its modularity enables modeling of vehicles running on the basis of the available modules (engine, gearbox, clutch, etc.) as well as novel concepts achievement such as hybrid cars or cars with several engines.

CRUISE enables the characteristic curves and maps interactive modification. The data is represented in a graph and table form at the same time. Modifications are possible in either of these representations. Data map can be directly introduced or can be read from ASCII files. The application of arithmetic functions on certain single points or the entire curve is possible.

REFERENCES

- [1.] Gillespie, T.D., Fundamentals of Vehicle Dynamics, SAE International, 1992
- [2.] AVL CRUISE v.2009, Technical Documentation
- [3.] http://www.mathworks.com/products/connections/product_detail/product_35685.html
- [4.] http://www.figes.com.tr/carmaker/dokuman/CarMaker_0702.pdf





¹Siby ABRAHAM, ²Imre KISS, ³Sugata SANYAL, ⁴Mukund SANGLIKAR

STEEPEST ASCENT HILL CLIMBING FOR A MATHEMATICAL PROBLEM

¹ DEPT. OF MATHS & STATS, G. N. KHALSA COLLEGE, UNIVERSITY OF MUMBAI, MUMBAI, INDIA

² DEPT. OF ENG & MANAGEMENT, FACULTY OF ENGINEERING HUNEDOARA,
UNIVERSITY POLITEHNICA TIMISOARA, ROMANIA

³ SCHOOL TECH & COMP SC, TATA INST. OF FUNDAMENTAL RESEARCH, MUMBAI, INDIA

⁴ DEPT. OF MATHEMATICS, MITHIBAI COLLEGE, UNIVERSITY OF MUMBAI, MUMBAI, INDIA

ABSTRACT:

The paper proposes artificial intelligence technique called hill climbing to find numerical solutions of Diophantine Equations. Such equations are important as they have many applications in fields like public key cryptography, integer factorization, algebraic curves, projective curves and data dependency in super computers. Importantly, it has been proved that there is no general method to find solutions of such equations. This paper is an attempt to find numerical solutions of Diophantine equations using steepest ascent version of Hill Climbing. The method, which uses tree representation to depict possible solutions of Diophantine equations, adopts a novel methodology to generate successors. The heuristic function used help to make the process of finding solution as a minimization process. The work illustrates the effectiveness of the proposed methodology using a class of Diophantine equations given by $a_1 \cdot x_1^{p_1} + a_2 \cdot x_2^{p_2} + \dots + a_n \cdot x_n^{p_n} = N$ where a_i and N are integers. The experimental results validate that the procedure proposed is successful in finding solutions of Diophantine Equations with sufficiently large powers and large number of variables.

KEYWORDS:

artificial intelligence technique, hill climbing, Diophantine Equations

1. INTRODUCTION

A Diophantine Equation [Cohen 2007] [Rossen 1987] [Zuckerman 1980] is a polynomial equation, given by

$$f(a_1, a_2, \dots, a_n, x_1, x_2, \dots, x_n) = N \quad (1)$$

where a_i and N are integers. These equations, which were initially studied in detail by third century BC Alexandrian Mathematician Diophantus [Bashmakova 1997] [Bag 1979], have many different types. The simplest ones are the linear equations given by:

$$ax_1 + bx_2 = c \quad (2)$$

The equations of the form

$$x_1^2 + x_2^2 = x_3^2 \quad (3)$$

are important as they give solutions, which are Pythagorean triplets. In 1665, French Mathematician Fermat popularized such equations by famously stating that equations of the form

$$x_1^n + x_2^n = x_3^n \quad (4)$$

have no solutions for $n > 2$, though the world had to wait till 1994 for an actual proof, which used elliptic curves [Shirali & Yogananda 2003]. An elliptic curve (Stroeker and Tzanakis, 1994; Poonen, 2000) is a particular type of Diophantine equation given by

$$y^2 = x^3 + ax + b, \quad (5)$$

where a and b are rational numbers and the right hand side of the equation (5) are given to have distinct roots. There are many such important equations in the collection of Diophantine equations.

Diophantine equations are used extensively in many fields. Elliptic curve based public key cryptosystems [Lin CH 1995][Laih CS 1997] [Koblitz 1984] offer better security provisions

comparing with other cryptosystems. The performance of super computers can be enhanced by parallelizing compilers to check the problem of data usage which can be reduced to characterization of a Diophantine equation [Zhiyu 1989]. Computable economics [Velu 2004] uses decision problems like Diophantine equations to propose a change in the market equilibrium conditions instead of the conventional parameters. Integer factorization [Knuth 1997] uses Diophantine equations in the process of breaking down a composite number into smaller non-trivial divisors. Diophantine equations are also used in other areas like algebraic curves [Ponnen 2000], projective curves [Brown & Myres 2002] [Stroecker & Tzanakis 1994] and theoretical computer science [Ibarra 2004][Guarari 1982]. These application areas make Diophantine equations an important domain not just in the realm of Mathematics but in other fields too.

Though Diophantine equations have a great historical background and have been used in many areas, there does not exist a general method to find solutions of such equations [Davis 1992] [Matiyasevich 1993]. Then, finding numerical solutions to such equations is the only next way out. This is a tough task as the computing complexity involved in such a process is quite high. In this regard, applying artificial intelligence techniques, which are known for maneuvering huge search space, is significant. Literature talks about few attempts to find numerical solutions of Diophantine equations using hard computing and soft computing techniques of Artificial Intelligence. Abraham and Sanglikar [Abraham and Sanglikar 2001] used basic genetic operators like mutation, inversion and crossover [Michalewicz 1992] to find numeric solutions of some elementary equations. They [Abraham and Sanglikar 2007 a] later used a procedure called 'host parasite co-evolution' [Hills 1992] [Paredis 1996][Wiegand 2003] in a typical genetic algorithm to find numerical solutions. They also proposed [Abraham and Sanglikar 2007 b] a unique evolutionary and co-evolutionary [Rosin and Belew 1997] computing method to find numerical solutions of such equations. Joya et al [Joya et al., 1991] used higher order Hopfield neural networks to find solutions of Diophantine equations. Abraham and Sanglikar [Abraham and Sanglikar 2008] offered simulated annealing as a possible strategy to find solutions of these equations. Abraham et al [Abraham et al 2010] discussed in detail a particle swarm optimization based method to find numerical solutions of such equations. In addition to these methods based on soft computing, literature also mentions A * search based hard computing mechanism as a possible alternative to find numerical solutions of these equations [Abraham and Sanglikar 2009]. Hard computing methods are significant as they try to explore as many candidate solutions as possible in a systematic way unlike soft computing, which uses randomness in the process and hence risks of 'slipping away' the solutions on the way.

This paper proposes hill climbing as a hard computing artificial intelligence technique to find numerical solutions of Diophantine equations. Hill Climbing is a local search [Russel & Norwig 2003] technique. It starts with an initial solution and steadily and gradually generates neighboring successor solutions. If the neighboring state is better than the current state, we make the neighboring state the current state. The whole process can be taken as an optimization process [Lugar 2006]. There are different variants of hill climbing. They are simple hill climbing, steepest hill climbing, stochastic hill climbing and random restart hill climbing. The paper uses steepest ascent version of the hill climbing to find numerical solution of Diophantine equations. In steepest hill climbing all successor nodes are probed and compared for its relevance and then the best amongst them is taken as the successor node. This results in having an exhaustive local search and identification of the best possible successor of a given node at any instant of time.

2. HILL-DOES Methodology

The system developed to find numerical solutions of Diophantine equations using Hill climbing is based on the Steepest Ascent version of Hill Climbing and is called HILL-DOES. It uses a system of equations given by

$$a_1 \cdot x_1^{p_1} + a_2 \cdot x_2^{p_2} + \dots + a_n \cdot x_n^{p_n} = N \quad (6)$$

where a_i and N are integers, for demonstrating the effectiveness of the system proposed.

2.1 Representation

The possible solutions of the Diophantine equation (6) are represented by a tree whose nodes are taken as n -vectors given by (x_1, x_2, \dots, x_n) . The procedure starts with an initial solution, given to be $(1, 1, 1, \dots, 1)$ and uses two queues in its construction. The first queue, which is called PROBE-Q, is used to store the nodes, which have been probed. The second queue, which is referred as NOPROBE-Q, is used to store the nodes, which have been generated but not better than the current node. These two queues help to separate the generated nodes into two distinct classes – 'probed nodes' and 'not-probed nodes'.

2.2 Successor nodes

Successor nodes of the current node are generated in HILL-DOES using specially defined production rules. The production rules applied are given by:

$$(x_1, x_2, \dots, x_i, \dots, x_n) \rightarrow (x_1, x_2, \dots, x_{i+1}, \dots, x_n) \text{ for } i=1, 2, \dots, n \quad (7)$$

These production rules help to generate all possible nodes in the vicinity of the current node. Hill climbing, being a local search technique, needs to explore all possible nodes within the neighborhood of the current node. The successor nodes generated in this way, take care of this requirement of the search strategy.

2.3 Heuristic function

The heuristic function used to evaluate the effectiveness of a node $(x_1, x_2, x_3, \dots, x_n)$ in the search process is given by

$$H(x_1, x_2, \dots, x_n) = N - (a_1x_1^{p1} + a_2x_2^{p2} + a_3x_3^{p3} + \dots + a_nx_n^{pn}) \quad (8)$$

Since the objective of the procedure is to find numerical solutions of equation (6), the problem reduces to find a vector given by (x_1, x_2, \dots, x_n) with $H(x_1, x_2, \dots, x_n) = 0$. The value of 'H' shows how far is a given node away from the goal node. Lower the value of 'H', closer is the node to the solution. However, the negative value of 'H' requires some extra care to make the search process on track. Whenever H value becomes negative, the proposed procedure does not expand the corresponding node even if that has better heuristic function value compared to others. Instead, the node with the next better heuristic function value is expanded and the process is continued. In other words, the nodes having negative H values are replaced with the better nodes from the NO-PROBEQ.

2.4 Backtracking

It is possible to have a current node, with all its successor nodes having inferior heuristic values in comparison with that of the current node. Steepest ascent hill climbing always demands having better nodes as successor nodes to continue the procedure. This drawback of hill climbing is overcome in the procedure by incorporating a strategy of backtracking. As per this, when the procedure fails to produce better nodes as successor nodes, it leaves the current node and goes back or backtracks to the previous best node generated. Then, the exploration process resumes from that node and the process of traversing through the tree in another path is followed. It is quite possible that during the search process, the procedure might hit on such inferior successor nodes on a regular basis. At these instances, the procedure is continued with backtracking at each and every instance. This way an unhindered search procedure is guaranteed always in HILL-DOES.

2.5 Algorithm

The basic steepest ascent hill climbing algorithm is slightly restructured to be acquainted with the constraints of Diophantine equations. The algorithm used in HILL-DOES is explained in the following lines.

- Step1:** Initialize node, which is usually $(1, 1, \dots, 1)$. Evaluate it.
Put it in the PROBE-Q.
- Step2:** If PROBE-Q is empty, then stop.
- Step3:** Pick first node from PROBE-Q. Label it as current node: C-Node.
- Step4:** If C-Node is the goal node then return C-Node as a solution.
(Goal state is reached when $H(x_1, x_2, \dots, x_n) = 0$)
- Step5:** If C-Node is not a goal node, check whether $H(x_1, x_2, \dots, x_n) > 0$
 - a) If yes, generate successors of C-Node and evaluate them.
 - b) If no, Go to step 2.
- Step6:** Compare successors of C-node and the better node amongst them.
Store the remaining nodes in the NOPROBE-Q.
 - a) If the better node is better than C-Node and if it has not been probed before, then make it C-Node. If it has been probed, then pick the first element from NOPROBE-Q and make it as the C-Node. Put C-Node in the PROBE-Q.
 - b) If the better node is not better than C-Node, then pick the first element from the NOPROBE-Q, make it as the C-Node and put in PROBE-Q. If NOPROBE-Q is empty, then do nothing.

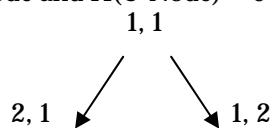
Step6: Go to step 2.

The algorithm as it is used in HILL-DOES is illustrated using a simple Diophantine Equation given by $x_1^2 + x_2^2 = 100$. The initial node is $(1, 1)$ and $H(1, 1) = 100 - (1^2 + 1^2) = 98$.

Step1: Put $(1, 1)$ in PROBE-Q.

Step3: C-Node = $(1,1)$.

Step5: Since it is not a goal node and $H(\text{C-Node}) = 98 > 0$, generate Successors of it.



Step6: Both $(2,1)$ and $(1, 2)$ have the same heuristic function value 95. So, choose any one say $(2,1)$. Put $(2,1)$ in PROBE-Q and $(1, 2)$ in NOPROBE-Q. Generate children of $(2,1)$.

Since the heuristic value of node (3, 1) is 90, which is better than the heuristic value 92 of the node (2, 2) and 95 of (2, 1) we select (3, 1) as the next node to be expanded. Continue this process of generating successors and identifying the best amongst them to be C- Node, which is illustrated in figure 1. If the process gets stuck in not finding a better successor, back track to the previous node and continue the process of exploration until a node with heuristic function value zero is generated. Such a node will be the solution of the given Diophantine equation.

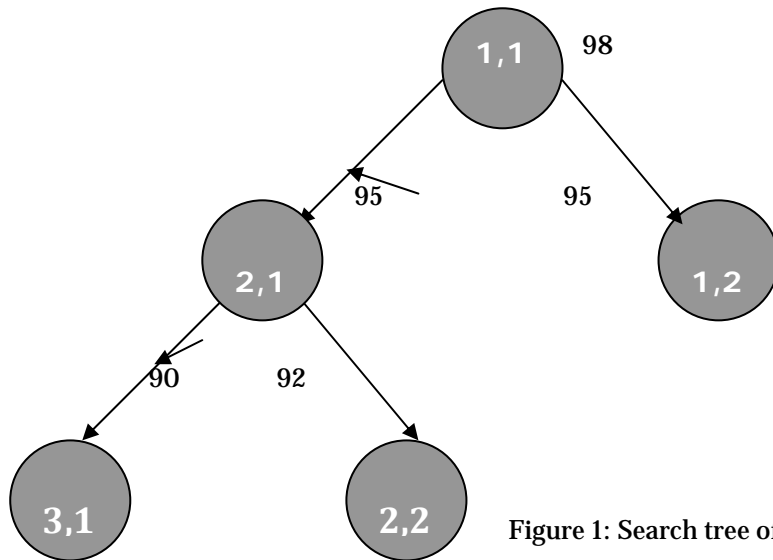


Figure 1: Search tree of $x_1^2 + x_2^2 = 100$

3. ANALYSIS, DISCUSSION AND INTERPRETATION

The procedure discussed in HILL-DOES has been implemented in Java. The user supplies the details of the equation like number of variables involved, coefficients, powers and the value of N. The experimental results have been analyzed and discussed in the following sections.

3.1 Nodes Generated

Figure 2 shows the nodes generated by HILL-DOES for an elementary equation $x_1^2 + x_2^2 = 149$, before finding the first solution (10,4). The process generated 68 nodes during the search process. The figure shows the steady search of the process in the search space. Figure 3 demonstrates the convergence of heuristic function values of the nodes generated in the same demonstration. Initially, there is a sudden reduction of heuristic function values and once the process becomes mature, there is a directed approach towards the value zero, finally resulting in the solution.

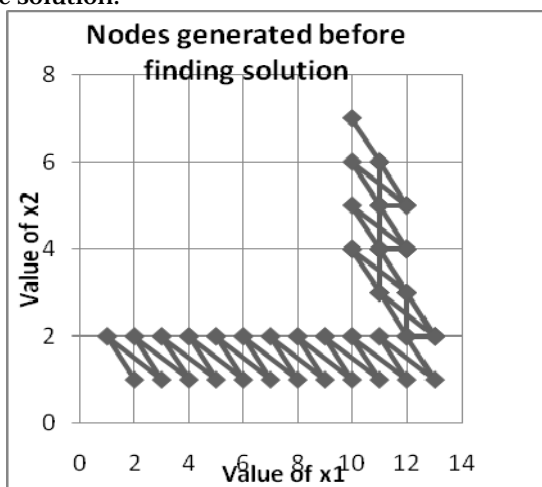


Figure 2: Nodes generated during the search

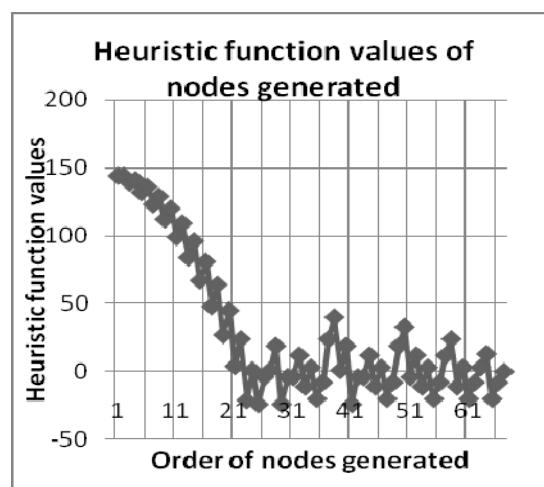


Figure 3: Heuristic function values of nodes

3.2 Results on equations with varying degrees

Table 1 demonstrates the results obtained when the system was run for different Diophantine equations with varying values for the degrees. It shows that irrespective of reasonably large values for degrees and higher values of N, the system could give solutions within a smaller number of iterations. This points out that those large values of N do not affect the efficiency of the system. In addition, the comparatively lesser number of iterations only consumed for finding the solutions also validate the effectiveness of the system in finding solutions of Diophantine equations with larger value of N.

Table 1: Results on equations with varying degrees

No	Diophantine Equation	Degree of equation	Solution found	Iterations
1	$x_1^2 + x_2^2 = 625$	2	24,7	29
2	$x_1^3 + x_2^3 = 1008$	3	10, 2	10
3	$x_1^4 + x_2^4 = 1921$	4	6, 5	9
4	$x_1^5 + x_2^5 = 19932$	5	7, 5	10
5	$x_1^6 + x_2^6 = 47385$	6	6, 3	7
6	$x_1^7 + x_2^7 = 4799353$	7	9, 4	11
7	$x_1^8 + x_2^8 = 16777472$	8	8, 2	8
8	$x_1^9 + x_2^9 = 1000019683$	9	10, 3	11
9	$x_1^{10} + x_2^{10} = 1356217073$	10	8, 7	13

3.3 Results on equations with varying number of variables

Table 2 shows the results obtained when HILL-DOES was run on Diophantine equations with varying number of variables. This shows that the system provides solutions even when the number of variables is competitively high.

Table 2: Results on equations with varying number of variables

No	Diophantine Equation	Degree of equation	Solution found	Iteration required
1	$x_1^2 + x_2^2 = 149$	2	10, 7	34
2	$x_1^2 + x_2^2 + x_3^2 = 230$	3	15, 2, 1	15
3	$x_1^2 + x_2^2 + \dots + x_4^2 = 295$	4	17, 2, 1, 1	17
4	$x_1^2 + x_2^2 + \dots + x_5^2 = 325$	5	17, 1, 1, 3, 5	22
5	$x_1^2 + x_2^2 + \dots + x_6^2 = 420$	6	20, 1, 1, 1, 1, 4	22
6	$x_1^2 + x_2^2 + \dots + x_7^2 = 450$	7	21, 2, 1, 1, 1, 1	21
7	$x_1^2 + x_2^2 + \dots + x_8^2 = 590$	8	23, 2, 1, 1, 1, 1, 2, 7	86
8	$x_1^2 + x_2^2 + \dots + x_9^2 = 720$	9	26, 2, 1, 1, 1, 2, 2, 2, 5	42
9	$x_1^2 + x_2^2 + \dots + x_{10}^2 = 956$	10	30, 2, 1, 1, 1, 1, 2, 2, 2, 6	48

4. CONCLUSION

The paper presents steepest ascent hill climbing search based procedure to find numerical solution of Diophantine equations. Local optimum points were tackled by resorting to backtracking as and when the procedure hit on such local optimum points. The experimental results showed that the technique work fine for Diophantine equations of varied types. However, the solutions generated, especially when the number of variables is large, have the tendency to have the coordinates closely placed. Further enhancement to the work is directed at addressing this issue.

REFERENCE

- [1.] [Abraham & Sanglikar 2001]: Abraham, S and Sanglikar, M; 'Diophantine equation solver-a genetic algorithm application', Mathematical Colloquium Journal, Vol. 15, No 3, pp 16-20, 2001.
- [2.] [Abraham & Sanglikar 2007a]: Abraham, S and Sanglikar, M; 'Nature's way of avoiding premature convergence: a case study of Diophantine equations', Proceedings of the International Conference on Advances in Mathematics: Historical Developments and Engineering Applications, Pantnagar, Uttarakhand, India, 19–22 December, pp 182, 2007.
- [3.] [Abraham & Sanglikar 2007b]: Abraham, S and Sanglikar, M; 'Finding solution to a hard problem: an evolutionary and co-evolutionary approach' Proceedings of the International Conference on Soft Computing and Intelligent Systems, Jabalpur, India, 27–29 December, pp 262-267, 2007.
- [4.] [Abraham & Sanglikar 2008]: Abraham, S and Sanglikar, M; 'Finding numerical solution to a Diophantine equation: simulated annealing as a viable search strategy', Proceedings of the International Conference on Mathematical Sciences, United Arab Emirates University, Al Ain, UAE, 3–6, pp 319, March, 2008.
- [5.] [Abraham & Sanglikar 2009]: Abraham, S and Sanglikar, M; 'A* search for a challenging problem', Proceedings of the 3rd Internl Confer.on Maths and Computer Science, Loyola College, Chennai, 5th–6th January, pp 453-457, 2009.

- [6.] [Abraham et al 2010]: Abraham, S; Sanyal, S and Sanglikar, M; 'Particle Swarm Optimization based Diophantine Equation Solver', International Journal of Bio-inspired Computation, Vol 2, No 2, pp 100-114, 2010.
- [7.] [Bag 1979]: Bag A K; 'Mathematics in ancient and medieval India', Chaukhambha Orientalia, Delhi, 1979.
- [8.] [Bashmakova 1997]: Bashmakova et al; 'Diophantus and Diophantine Equations, Mathematical Association of America, 1997.
- [9.] [Brown & Myers 2002]: Brown, E. and Myers, B; 'Elliptic curves from Model to Diophantus and Back', The Mathematical Association of America Monthly, August–September, Vol. 109, pp.639–649, 2002.
- [10.] [Cohen 2007]: Cohen, H; Number Theory, Vol. I: Tools and Diophantine Equations and Vol. II: Analytic and Modern Tools, Springer-Verlag, pp. 239- 240, 2007.
- [11.] [Davis 1982]: Davis, M; 'Hilbert's tenth problem is unsolvable', Computability and Unsolvability, Appendix 2, 1999-235, Dover, New York, 1982.
- [12.] [Guarari 1982]: Guarari, E.M; 'Two way counter machines and Diophantine equations', Journal of ACM, Vol. 29, No. 3, 1982.
- [13.] [Hills 1992]: Hills, W.D; 'Co-evolving parasites improve simulated evolution as an optimization procedure', Artificial Life, Addison Wesley, Vol. 2, 1992.
- [14.] [Ibarra et al. 2004]: Ibarra, O.H. et al; 'On two way FA with monotone counters and quadratic Diophantine equations', Theoretical Computer Science, Vol. 312, pp.2–3, 2004.
- [15.] [Joya et al 1991]: Joya et al; 'Application of Higher order Hopfield neural networks to the solution of Diophantine equation', Lect. Notes in Comp Sc. Vol.540, Springer, 1991.
- [16.] [Knuth D 1997]: Knuth, D; 'The Art of Computer Programming, Volume 2: Semi-numerical Algorithms', Third Edition, Addison-Wesley, 1997.
- [17.] [Koblitz 1984]: Koblitz, N; Introduction to Elliptic Curves and Modular Forms, Springer, 1984.
- [18.] [Laih. et al., 1997]: Laih, C.S. et al; 'Cryptanalysis of Diophantine equation oriented public key cryptosystem', IEEE Transactions on Computers, April, Vol. 46, 1997.
- [19.] [Lin et al. 1995]: Lin, C.H. et al 'A new public-key cipher system based upon Diophantine equations', IEEE Transactions on Computers, January, Vol. 44, 1995.
- [20.] [Luger 2006]: Luger, G.L; Artificial Intelligence: Structures and Strategies for Complex Problem Solving, 4e Pearson Education, 2006.
- [21.] [Matiyasevich 1993]: Matiyasevich, Y.V; Hilbert's Tenth Problem, MIT press, 1993.
- [22.] [Michalewicz 1992]: Michalewicz, Z; GA + Data Structures = Evaluation Programs, Springer Verlag, 1992.
- [23.] [Paredis, J. 1996]: Paredis, J; 'Co-evolutionary computation', Artificial Life Journal, Vol. 2, No. 3, 1996.
- [24.] [Poonen 2000]: Poonen, B; 'Computing rational points on curves', Proceedings of the Millennial Conference on Number Theory, 21–26 May, University of Illinois at Urbana-Champaign, 2000.
- [25.] [Rosin & Belew 1997]: Rosin, C.D. and Belew, R.K; 'New methods for competitive co-evolution', Evolutionary Computation, Vol. 5, No. 1, pp.1–29, 1997.
- [26.] [Rossen, K. 1987]: Rossen, K; Elementary Number Theory and its Applications, Addison, 1987.
- [27.] [Russell & Norwig 2003]: Russell, S. and Norwig, P; Artificial Intelligence– A Modern Approach, 2nd ed., Pearson, 2003.
- [28.] [Shirali & Yogananda 2003]: Shirali, S. and Yogananda, C.S; 'Fermat's last theorem: a theorem at last', Number Theory: Echoes From Resonance, University Press, 2003.
- [29.] [Stroecker & Tzanakis 1994]: Stroecker & Tzanakis; "Solving elliptic Diophantine equations by estimating linear forms in elliptic logarithms, Acta Arithmetica, Vol. 67, No. 2, 1994.
- [30.] [Velu 2000]: Velu Pillai K; Computable Economics: The Arne Memorial Lecture Series, Oxford University Press, 2000.
- [31.] [Wiegand 2003]: Wiegand, P; 'An analysis of cooperative co-evolutionary algorithms', PhD dissertation, George Mason University, 2003.
- [32.] [Zhiyu 1989]: Zhiyu, S., Li, Z., Yew, P.C. 'An empirical study on array subscripts and data dependencies', CSRD Report 840, August, 1989.
- [33.] [Zuckerman 1980]: Zuckerman; An Introduction to the theory of numbers', 3rd ed., Wiley, 1980.





¹ Carmen HĂRĂU

MIGRATION AND REMITTANCES – CASE STUDY ON ROMANIA

¹UNIVERSITY POLITEHNICA TIMISOARA, FACULTY OF ENGINEERING HUNEDOARA, ROMANIA

ABSTRACT:

One of the most studied topics of each time in economics refers to the economic growth of a country and what causes it. There have been developed different theories throughout time and there have been questioned different possible relations between the growth rate and different variables. A highly debated causality refers to migration, remittances and growth, therefore, in this context, through this paper it is analysed the impact of remittances upon Romania's economy. The subject discussed is a very present-day issue that Romania is facing, so it is important to determine both the short-term and the long-term effects of the phenomenon. The paper builds mathematical models for testing the correlation between the growths of Romania (measured as GDP/capita).

KEYWORDS:

Migration, remittances, GDP/capita, growth, Romania, emigrants, foreign direct investments

1. INTRODUCTION

In the past couple of years migration has become a very hot topic of debate and analysis, as it is an ever growing component of contemporary society. It is considered a factor for stimulating global markets but also an instrument for regulating imbalances on the regional and local labour markets. Work related migration is today the most dynamic form of circulation.

One of the main positive consequences of international migration refers to remittances, financial transfers to the senders' country of origin, which are often seen as a compensation for the brain drain phenomenon and human capital outflow. Remittances increase the country's income from external sources and, as a result, not only does the living standard of the recipients grow but so does the level of local economic development, through consumption and investment. However, there isn't a consensus concerning their contribution to economic growth and new job creation.

In what concerns Romania, the transition period following 1990 led to significant restructuring, mainly throughout industrial markets. One can go as far as the disappearance of some industrial branches, bankruptcies and an overall destabilisation process for the country's economy in general. Financial problems led to a mass migration to countries like Italy or Spain. Temporary jobs abroad can be considered an adaptive strategy for almost 100% of Romanians. Once visas for EU entry were eliminated, labour related migration became one of the most important phenomena for social change in the country.

As for remittances, Romania is in the worldwide top ten and in the top at European level concerning the money sent by Romanians working abroad according to a UNDP (United Nations Development Programme) report of human development. Still, in the past 2 years remittances have significantly dropped for different reasons. As such this article sets out to estimate the impact of this decrease.

2. METHODOLOGY AND DISCUSSION

2.1. FIRST STEPS – HOW THE PHENOMENON STARTED TO SPREAD

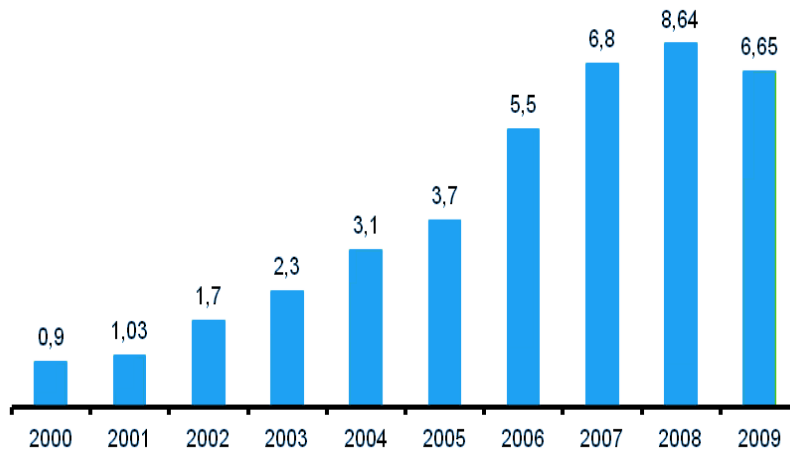
Migration has multiple causes, but the main one relates to the desire for financial comfort, and this is possible through emigration due to international wage differences. Other reasons wide spread in the Romanian society are the need for professional statement, the desire to provide a

bright future for children or just young people characteristic need for independence. The real number of the Romanian population that chose the path of migration at this time is not known. Figures and official records say that almost 900,000 people left. The data provided by a study done by Romanian Academic Society[2], quotes the International Labour Organization which states that "approximately 47% of Romanians who work abroad have not had legal forms of employment(2004)".

Italian and Romanian authorities estimate more than 2,000,000 Romanian immigrants. The fact is that in Italy, even if the exact numbers are not known, Romanians are first among legal immigrants (a total of 555,997 persons). The number of illegal immigrants is not known but it is estimated that it would only be around 1.5 million.

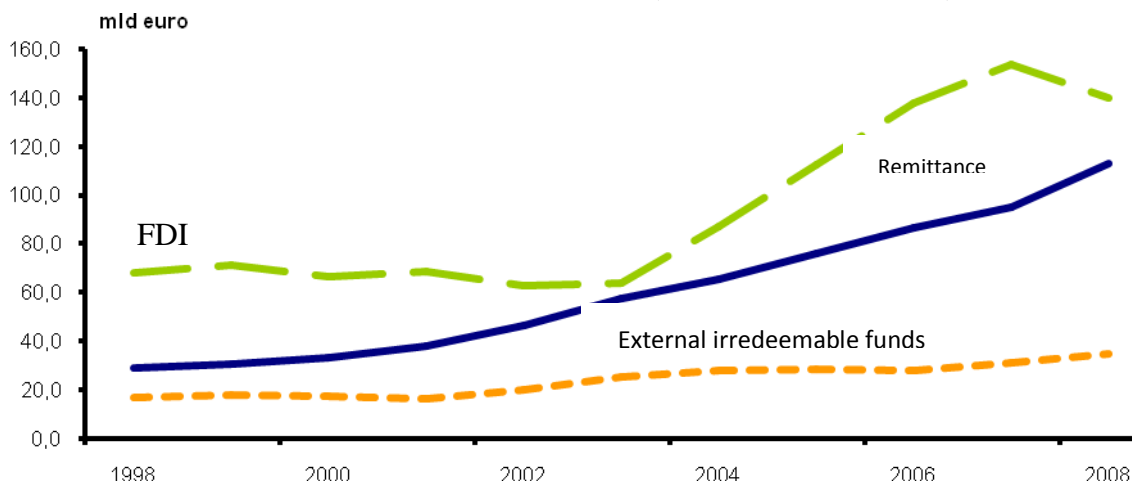
Romanian migrants, although neglected by the authorities, are becoming more potential agents of development. Their private transfers (remittances) increased significantly to 0.9 billion Euros in 2000, from 1.03 billion in 2001 to 5.5 billion Euros in 2006 and 6.65 billion in 2009. The peak was reached in 2008 with a value of EUR 8.64 billion (see Chart 1). Such transfers tend to exceed the volume of foreign investments in 2007, at around 7.1 billion Euros (according to National Bank). Better managed labour migration would stimulate social development concerning personal, family and community levels, leading to a reduced rate of unemployment and poverty.

In this chart we can easily see the evolution of remittances from 2000 until the year 2009. In the year 2009 there was a decrease in remittances due to the financial crisis. Estimates show a strong decrease in 2010. In this context, the most important question that arises is what will be the effect of a decrease in remittances on the Romanian economy on the short, medium and long term. There are no relevant studies to indicate those aspects which make this question a difficult problem to quantify.



Source: National Bank of Romania

Chart 1. The evolution of direct transfers (remittances in billion lei)



Note: The graph is computed at global level and it shows the external private funds that are sent to this countries

Source: Migrant remittances to developing countries[3]

Chart 2. External funding in developing countries

In Chart 2 we find an overview of the migratory phenomenon, which highlights the magnitude of the phenomenon at a global level. Developing countries are those that contribute most, with a rate of 87% of international migration, mainly because of poverty and low living standards. This chart is very relevant to link the main incoming funds in a country, i.e. non-reimbursable external funds, foreign direct investment and remittances. As can be seen from the chart, the level of remittances between 2003 and 2008 was very close to the level foreign direct investment, which means that the importance of remittances has increased dramatically in recent years.

The main cause for remittances is empathy, but the reasons behind these transfers can be classified thus:

- ❖ *endogenous* - those pertaining to migrants themselves, given an empathic attitude toward family and close ones back home. The level depends on the type of migration: temporary or permanent, migrant education and skills, etc)
- ❖ *exogenous* - those pertaining to the external environment, such as security in the transmission of funds, a reduction or cancellation concerning transfer charges, the geographical distribution of migrants and between differences in GDP between the country of origin and destination.

2.2. THE EFFECTS OF MIGRATION AND REMITTANCES

It's hard to find a phenomenon that can produce a more complex set of economic effects than migration on the countries from which people migrate. As remittances are the most visible result of migration, we take two independent phenomena. The image below illustrates the main economic impacts of migration and remittances, emphasizing the positive and negative effects (Figure 1)

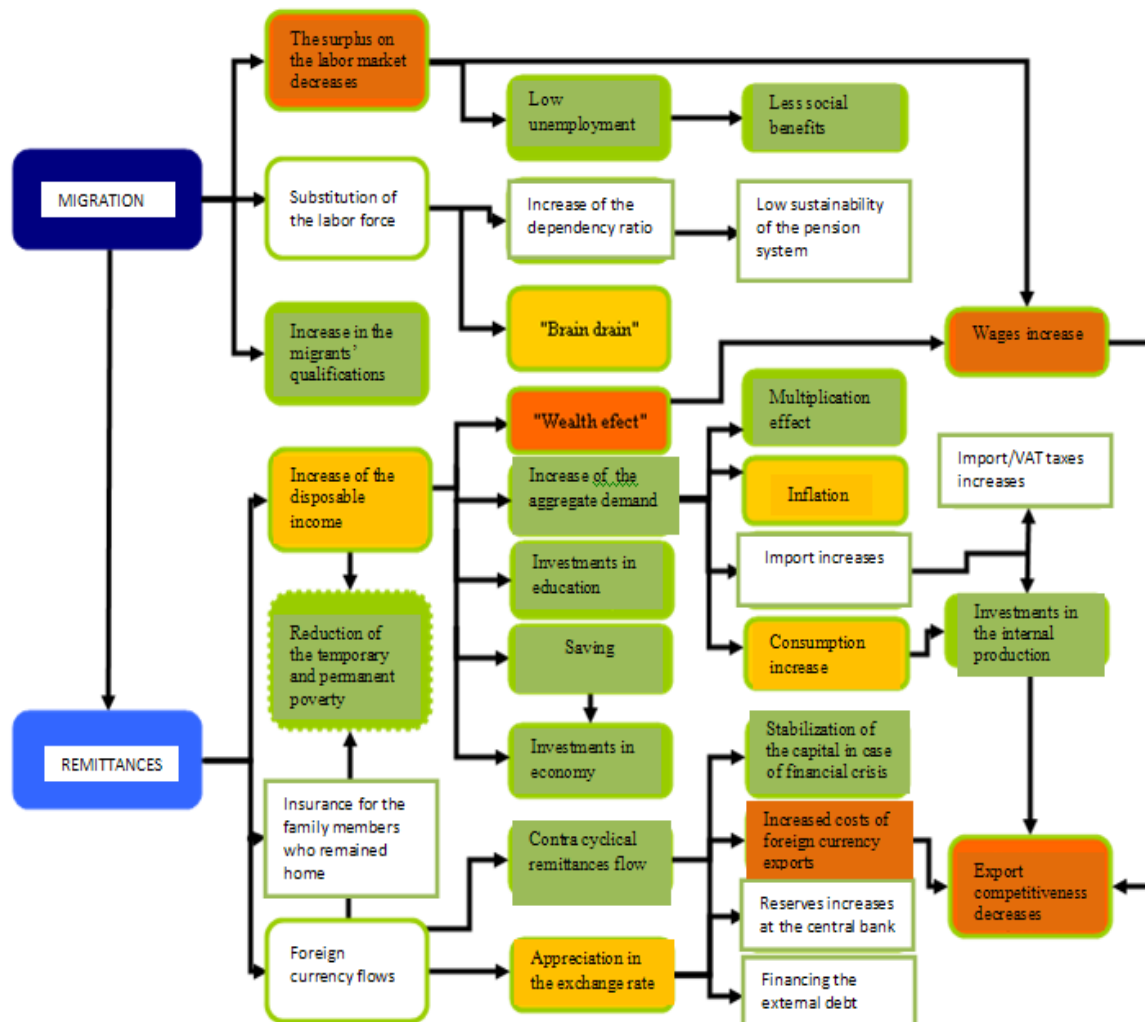


Figure 1. The economic effects of migration and remittances on the economy

Note: Green indicates the positive effects and orange the negative effects. Yellow represents the debatable elements in the branch literature.

Source: Alexandru Culiuc[4]

As observed in the graph presented above (Figures 1), remittances represent the second largest source of external financing after foreign direct investment (FDI) in the economy. Without this revenue, Romania's current account deficit would have been 21% by the end of 2008 instead of 16%. These remittances cover a shortfall of income, basic daily needs, ensure access to services, increase the standard of living and are believed to support growth in the country of origin of the worker. With the increase in imports generated by a consumer supported by remittances, and increased state budget revenues through import duties and taxes on consumption. At the same time, rising real interest rates and thus lowering the value of public debt, lower unemployment and hence the state-supported social services, benefit the country of origin of migrants.

Corresponding to the above, we can say that remittances are desirable in an economy and undoubtedly, remittances lead to a short-term positive impact by filling the needs of households participating in the scheme. The effects are further propagated in the economy through the multiplication effect - a large part of remittances is used to purchase goods and services. Three studies from different countries identify the values of this multiplier, ranging from 1.24 (Bangladesh - Stahl and Habib[5]) 1) to 3.2 (study from Mexico - and Taylor Adelman[6]).

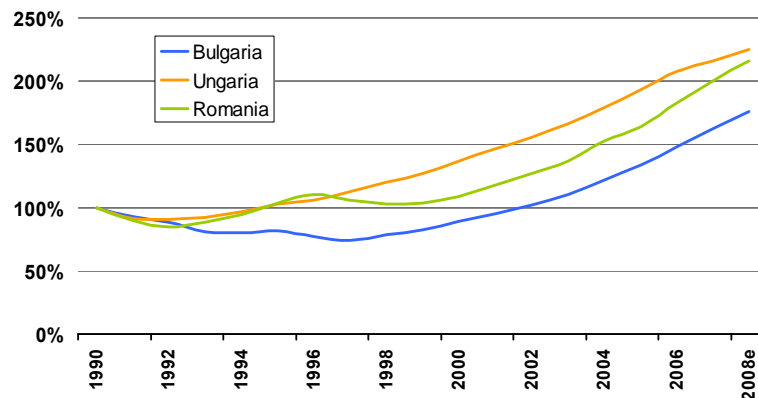
Looking at the long-term contribution of remittances to economic growth we find conflicting opinions in literature. As these foreign funds increase, officials record levels, and the academic community fails to reach a consensus on the long-term impact of remittances on the economy and its development. The link between remittances and economic development has been a constant topic of debate in recent decades between migration researchers. While some authors and organizations say that it has a positive impact by developing regions of origin, other researchers are more sceptical. In principle, if we consider the brain drain, migration process is one that adjusts itself. If we take a region that has a surplus labour market, it will undergo a migration process until the market in that region will reach equilibrium.

However, there are a substantial number of disadvantages produced by high remittances, such as: feeding inflation, reduced interest in work on behalf of the beneficiaries, the social impact on family members remaining in the country of origin. In 2005, 9% of all households in an independent study declared that they have at least one family member abroad. In 2007 around 14% of all households in Romania had migratory experience.

3. REMITTANCES AND ECONOMIC GROWTH

One way to assess the growth of a country is to measure the progress of GDP per capita. The chart below shows the comparative evolution of the indicator in Romania, Hungary and Bulgaria over the 1990 – 2008 period.

According to the graph above, we can say with certainty that the transition to a market economy had a positive effect on Romania's economic growth. But the question is how much did remittances contribute to this growth? Remittances help to influence the economy, and hence economic growth, through several channels of influence. An indicator that is part of GDP, and is influenced by direct transfers, is household consumption.

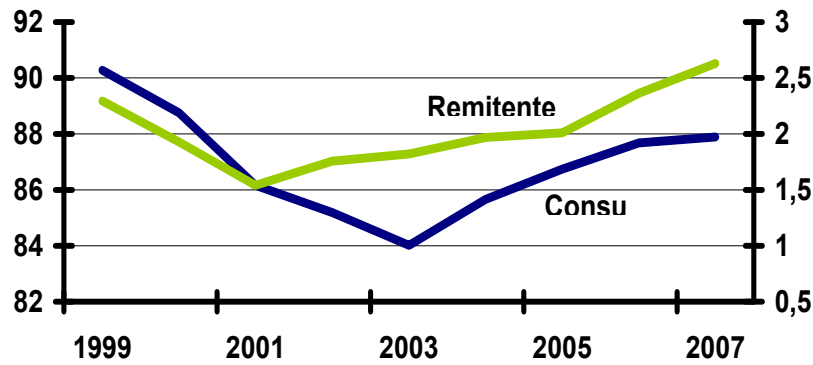


Source: IMF
 Chart 3. GDP per capita PPC (1990=100%)

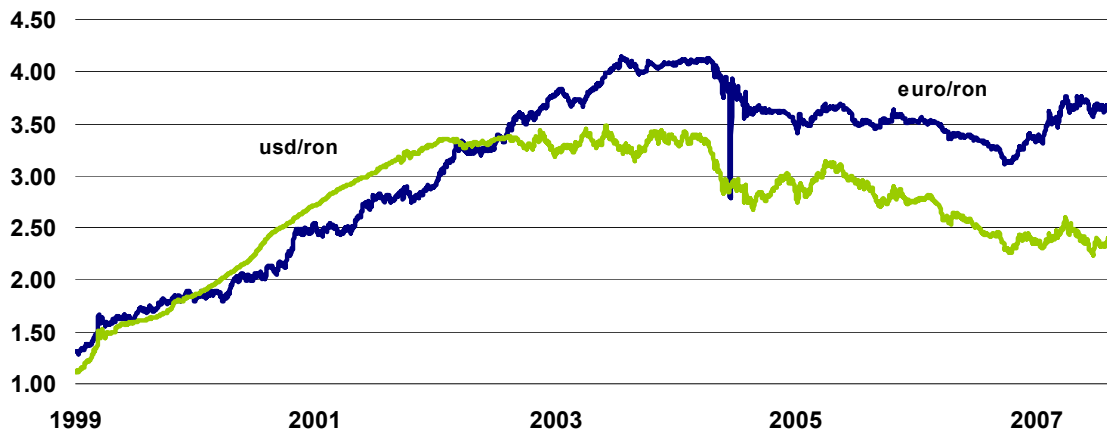
Increased consumption can directly affect the economy because a high aggregate demand stimulates domestic production. Thus, the economy grows. But we cannot speak for the large demand made on the basis of imports.

“Dutch disease” is another issue closely related to imports and exports which also takes the form through currency appreciation. The leu appreciated in the period 2004-2008, depreciating in 2009 and then stabilizing. Thus, one can say that the national currency follows the remittances trend, but we cannot say with certainty that this assessment is an effect caused by remittances.

In what follows, I tried to highlight the link between remittances and GDP per capita, using annual data over the period 1990-2006 for remittances, GDP per capita, FDI and the number of migrants. All the following correlations and regressions are made using the EVIEWS 5 statistical package.



Source: IMF
Chart 4 Evolution of consumption and remittances (real values)



Source: National Bank of Romania
Chart 5. The evolution of the exchange rate

In the first instance, I made the chart below to illustrate the direct relationship between remittances and GDP per capita. As far as it can be seen, it would seem that there is a direct linear correlation between the two variables.

Through the simple univariate regression, using the method of least squares we obtained the data found in the table below. These data reinforce the assumption that between GDP per capita and remittances there is a direct linear correlation. The high R-squared (0.9325) shows how much variation can be explained by variation of GDP/capita by remittances and zero values for samples and F-statistic indicates the validity of the model and that the two coefficients are statistically significant.

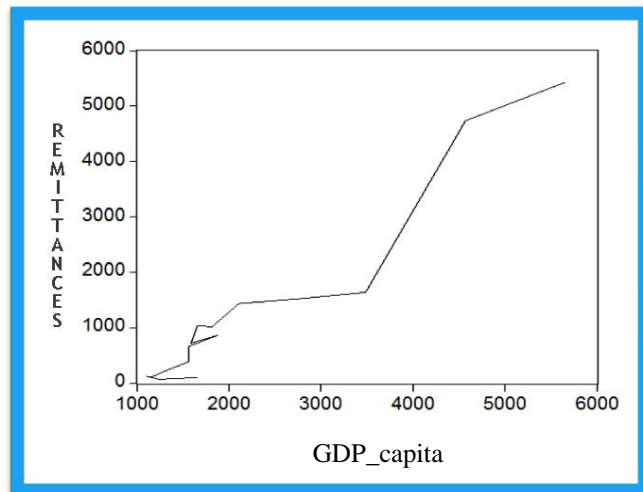


Chart 6 Correlation between GDP/capita and remittances

By slightly complicating the model, we want to see how much of the growth is due to remittances, foreign direct investment, namely the number of emigrants. For this, we used a multivariate regression, with GDP per capita as dependant variable and FDI and the number of migrants as independent variables.

It is noted that the parameter is statistically significant number for only 10% level of significance, but for $\alpha = 0.05$, this is not statistically significant. In this model, the greatest influence on economic growth is due to, as expected, foreign direct investment. The influence of the number of immigrants is very low.

Table 1. Univariate simple regression between GDP per capita and remittances
 Dependent Variable: GDP_CAPITA
 Method: Least Squares
 Sample: 1990 2006
 Included observations: 17

Variable	Coefficient	Std. Error	t-Statistic	Prob.
REMITTANCES	0.795212	0.055205	14.40459	0.0000
C	1187.173	106.4590	11.15146	0.0000
R-squared	0.932582	Mean dependent var		2154.437
Adjusted R-squared	0.928087	S.D. dependent var		1270.151
S.E. of regression	340.6104	Akaike info criterion		14.60949
Sum squared resid	1740232.	Schwarz criterion		14.70751
Log likelihood	-122.1806	F-statistic		207.4921
Durbin-Watson stat	1.871687	Prob(F-statistic)		0.000000

Table 2 Multivariate regression between GDP per capita and remittances, FDI and number of emigrants

Dependent Variable: GDP_CAPITA
 Method: Least Squares
 Date: 04/16/10 Time: 03:41
 Sample: 1990 2006
 Included observations: 17

Variable	Coefficient	Std. Error	t-Statistic	Prob.
REMITTANC	0.491389	0.112900	4.352437	0.0008
FDI	4.190867	1.327508	3.156943	0.0076
EMIGRANTS	0.006020	0.003390	1.776025	0.0991
C	1017.110	127.5061	7.976951	0.0000
R-squared	0.964627	Mean dependent var		2154.437
Adjusted R-squared	0.956464	S.D. dependent var		1270.151
S.E. of regression	265.0217	Akaike info criterion		14.19982
Sum squared resid	913074.2	Schwarz criterion		14.39587
Log likelihood	-116.6985	F-statistic		118.1696
Durbin-Watson stat	1.323489	Prob(F-statistic)		0.000000

Trying to improve the model, we removed the number of migrants from the variables. We obtained a model that explains the GDP per capita variable proportion of 95.6%, both parameters being statistically significant for a significance level of $\alpha = 0.05$.

Table 3. Multivariate regression between GDP per capita, remittances and FDI
 Dependent Variable: GDP_CAPITA
 Method: Least Squares
 Sample: 1990 2006
 Included observations: 17

Variable	Coefficient	Std. Error	t-Statistic	Prob.
REMITTANCES	0.488657	0.121264	4.029700	0.0012
FDI	3.859385	1.411826	2.733611	0.0162
C	1189.265	88.98187	13.36525	0.0000
R-squared	0.956044	Mean dependent var		2154.437
Adjusted R-squared	0.949764	S.D. dependent var		1270.151
S.E. of regression	284.6826	Akaike info criterion		14.29941
Sum squared resid	1134619.	Schwarz criterion		14.44645
Log likelihood	-118.5450	F-statistic		152.2497
Durbin-Watson stat	1.222042	Prob(F-statistic)		0.000000

4. CONCLUSIONS

There are many studies on migration and remittances, but most of them deal with the short-term effects of these phenomena. There is a long debate regarding long-term effects and conflicting results in different places.

In my opinion, through a rigorous economic analysis we could establish long-term effects of remittances at the local level, but generalising the results for all countries is extremely difficult if not impossible, due to differences that occur from country to country .

In the present study, it was tested if there is a link between the amount of remittances and GDP per capita and calculated its power and sense of connection. There were also taken into account two other factors, FDI and the number of migrants. The result is that in Romania, for the set of data from the period 1990-2006, FDI and remittances strongly influence the value of GDP per capita, whereas the impact of the number of migrants is not significant. Since the estimated relationship between GDP per capita and remittances is direct and linear in the period following the decrease of remittances, we can expect a decrease in GDP/capita to a certain extent due to reduced remittances.

In the short term, reduced remittances will lead to a lower level of consumption, leading to a decrease in state revenue (lower import duties and taxes on consumption). There are also chances of an increased budget deficit, which is not desirable, especially taking into consideration external debt, which should cover it. However, on the long term, with the decrease in remittances, inflation is no longer threatened if the other conditions remain the same.

As with any economic process, there is a trade-off between short and long term even between different phenomena such as inflation and unemployment characterized by the Phillips curve. What matters, ultimately, is achieving a balanced state, identifying the optimal level for both long term and short-term ones.

In conclusion, I believe that a certain level of remittances is good for any developing economy, but when this level is exceeded and constantly becomes higher, it can become a risky phenomenon on the long term.

ANNEX

The data used for the regression can be found in the tables bellow and was taken from the National Institute of Statistics, Eurostat and IMF websites.

Obs	PIB/CAPITA (\$)	REMITTANCES (mil \$)	FDI MIL LEI PRICES 1990	EMIGRANTS (no. people)
1990	1650.330	102.0000	0.000000	96929.00
1991	1244.200	69.00000	1.750000	44160.00
1992	1100.980	122.0000	4.270000	31152.00
1993	1158.480	116.0000	3.750000	18446.00
1994	1322.980	234.0000	6.290000	17146.00
1995	1564.180	392.0000	7.200000	25675.00
1996	1562.880	613.0000	9.340000	21526.00
1997	1564.510	662.0000	8.470000	19945.00
1998	1871.550	858.0000	6.930000	17536.00
1999	1584.840	722.0000	9.270000	12594.00
2000	1650.970	1024.000	124.3700	14753.00
2001	1815.500	1019.000	149.9000	9921.000
2002	2101.740	1437.000	126.9800	8154.000
2003	2736.970	1517.000	170.9300	10673.00
2004	3481.200	1640.550	256.6700	13082.00
2005	4568.880	4733.000	306.2800	10938.00
2006	5645.240	5417.564	440.8700	14197.00

REFERENCES

- [1.] Ratha Dilip (2003), „Worker Remittances: An Important and Stable Source of External Development Finance”, in *Global Development Finance: Striving for Stability in Development Finance*, Washington, DC: International Monetary Fund
- [2.] Analysis and Prognosis Report, edited by Romanian Academic Society
- [3.] Global development finance – edited by World Bank, International Monetary Fund – balance of payments
- [4.] Integrating migration and remittances into a development strategy. The case of Moldova, Alexandru Culuic, 2006.

- [5.] The Impact of Overseas Workers' Remittances on Indigenous Industries: Evidence from Bangladesh, The Developing Economies, Stahl and Habib, 1989.
- [6.] Is structural adjustment with a human face possible? The case of Mexico, Journal of Development Studies, Adelman si Taylor, 1992.
- [7.] İnsan Tunali, "Rationality of Migration", International Economic Review, Vol. 41, No. 4 (Nov., 2000), pp. 893-920, Published by: Blackwell Publishing for the Economics Department of the University of Pennsylvania and Institute of Social and Economic Research -- Osaka University
- [8.] World Investments Report 2009, Transnational Cooperation, Agricultural Production and Development, United Nations, New York and Geneva, 2009
- [9.] www.bnr.ro
- [10.] www.insse.ro
- [11.] ec.europa.eu/eurostat
- [12.] www.imf.org





¹Gladiola C. CHEȚE, ²Ioana. A. STĂNESCU

DECISION MAKING AND BUSINESS INTELLIGENCE SOLUTIONS

¹UNIVERSITY POLITEHNICA OF TIMISOARA, FACULTY OF ENGINEERING FROM HUNEDOARA, ROMANIA

²RESEARCH INSTITUTE FOR ARTIFICIAL INTELLIGENCE, ROMANIAN ACADEMY, ROMANIA

ABSTRACT:

Good decision making is as important in the working world as it is in the rest of our lives. Every day a number of decisions must be made that determine the direction and efficiency of the organizations we work for. Decisions are made concerning production, marketing, and personnel. Decisions are made affecting costs, sales, and margins. The key to organizational success is to make good choices. This paper highlights the relevance of business intelligence solutions within an effective decision making process. Business intelligence is not just technology, nor is it just practices and methods. It is more a combination of the best of both the business world and the technical world – using advanced algorithms and data management techniques to better implement the way a business works. The authors aim to provide a knowledge base for the decision maker to determine the value of integrating these kinds of technologies into the company and to offer a clear explanation of the utility of this technology.

KEYWORDS: business analysis, decision support, dashboard

1. INTRODUCTION

Most real life problems are complex and multi-facet, and involve many criteria in the decision making process. Automated tools and systems for decision support are always in demand. Business intelligence is a window to the dynamics of a business. It reveals the performance, operational efficiencies, and untapped opportunities. Business intelligence (BI) is a set of technologies and processes that allows people at all levels of an organization to access, interact with and analyse data to manage the business, improve performance, discover opportunities, and operate efficiently (Loshin, 2003; Howson, 2007).

Used effectively, business intelligence allows organizations to improve performance. Business performance is measured by a number of financial indicators such as revenue, margin, profitability, cost to serve, and so on (Larson, 2008). In marketing, performance gains may be achieved by improving response rate for particular campaigns by identifying characteristics of more responsive customers. Eliminating ineffective campaigns saves companies millions of euros each year.

Business intelligence allows companies to boost revenues by cross-selling products to existing customers. Accounting personnel may use BI to reduce the aging of accounts receivable by identifying late-paying customers. In manufacturing, BI facilitates gap analysis to understand why certain plants operate more efficiently than others. In all these instances, accessing data is a necessary first step. However, improving performance also requires people's interaction to analyse the data and to determine the actions that will bring about improvement.

This paper underlines the importance of considering business intelligence tools as a solution that transforms the mountains of raw data within an organization into valuable information that is understandable and useful to decision makers. The authors focus on the benefits of multidimensional analysis and on the competitive advantage that intelligent technologies can bring to businesses and detail on the impact of BI solutions for both executive and operational personnel. The paper considers at the same time the current limitations of business intelligence solutions and also the fact that measuring the business impact of business intelligence can be difficult as improvements in performance are attributable to factors beyond business intelligence.

2. BUSINESS VALUE THROUGH BUSINESS INTELLIGENCE

An effective decision makes the difference between the success and the failure of an organization. The key ingredients necessary for making effective decisions can be summarized as follows (Larson, 2008):

- ❖ determine a set of goals to work towards;
- ❖ define ways to measure whether a chosen course is moving towards or away from those goals; and
- ❖ provide the information based on those measures to the decision maker in a timely manner.

Information technology (IT) plays a significant role in our business life, making everything more connected, faster, mobile, potentially more efficient, and at the same time more demanding for the average users (Stănescu & Chețe, 2009; Turban et. al, 2010). The latest IT developments include business intelligence tools that aim to enhance the decision making process on all the levels of a company and allow employees to improve their overall performance in their daily work.

2.1 Business success through BI Tools

Business intelligence means different things to different people. To one businessperson, business intelligence means market research; to another person, accessing a static report; others will use terms such as business analytics or decision support. In its most basic sense, business intelligence provides managers information to know what is going on in the business. Without business intelligence managers may talk about how they are “flying blind” with no insight until quarterly financial numbers are published. With business intelligence, information is accessible on a timelier and more flexible basis to provide a view of:

- ❖ how sales are tracking in various regions and by various product lines;
- ❖ if expenses are on plan or running over budget;
- ❖ if warehouse capacities are at optimal levels;
- ❖ if sales pipelines are where they should be.

Business intelligence does not address only to managers, and cuts across all functions and all industries. BI interacts with any employee of a company and beyond to customers and suppliers (Moss & Atre, 2003). When any particular metric is not where it should be, business intelligence allows users to explore the underlying details to determine why metrics are off target and to take action to improve the situation. In the past, if managers monitored the business via paper-based reports, they had no flexibility to explore why the business was operating a certain way.

For example, many companies use BI to monitor expenses to ensure costs do not exceed budgets, rather than waiting until the close of the quarter to discover that excessive expenses have reduced profitability, timely access to expense data allows managers first to identify which business unit is over budget and then to take immediate action to reduce overtime pay or travel expenses, or to defer purchases (Vercellis, 2009).

Successful BI initiatives provide businesspeople with the information they need to do their jobs more effectively and they result in (Vitt et. al, 2002; Howson, 2007):

- ❖ Increased profitability;
- ❖ Decreased costs;
- ❖ Improved customer relationship management (CRM); and
- ❖ Decreased risk.

These goals can be achieved when the BI technologies available to organizations are used to positively impact organizational behaviour. The success of BI initiative depends on the level of technology acceptance among the employees of a company and is built upon a long-term strategy. No matter how complex a BI solution is, it is still up to the people to use it. The employees need to become aware of the impact that BI tool can have on their work and gradually integrate them in their activity.

2.2 BI Solutions in Practice

Business intelligence tools provide monitoring, performance analysis and effective business planning by providing a tool for rapid data access, while the time saved can be used to identify solutions and act on the data obtained.

2.2.1 The Executive Director

The Executive Director of a company must ensure that employees are aligned with the business strategy, must be able to analyse the regular progress in comparison with the business objectives and must be able to easily and continuously monitor performance at the company level.

Companies currently develop an annual plan because the development a plan on a shorter interval of time is proving too costly and complex. Executive Directors must assume the role of a guide to other decision makers so that they can effectively carry out their work, be responsible for their work, in relation to the general objectives of the company.

BI Solutions allows the Executive Directors to:

- ❖ **Align business operations at the company level:** The detailed overview, the updated dashboard and scorecards allow users to align their actions with strategic objectives. All users can learn about the business and developers can collaborate more effectively using analysis and detailed contextual information obtained on the basis of structured and unstructured information.
- ❖ **Support responsibility:** Users may assume responsibility for the results of an evaluation sheet, drawing the responsibility and organization-wide alignment.

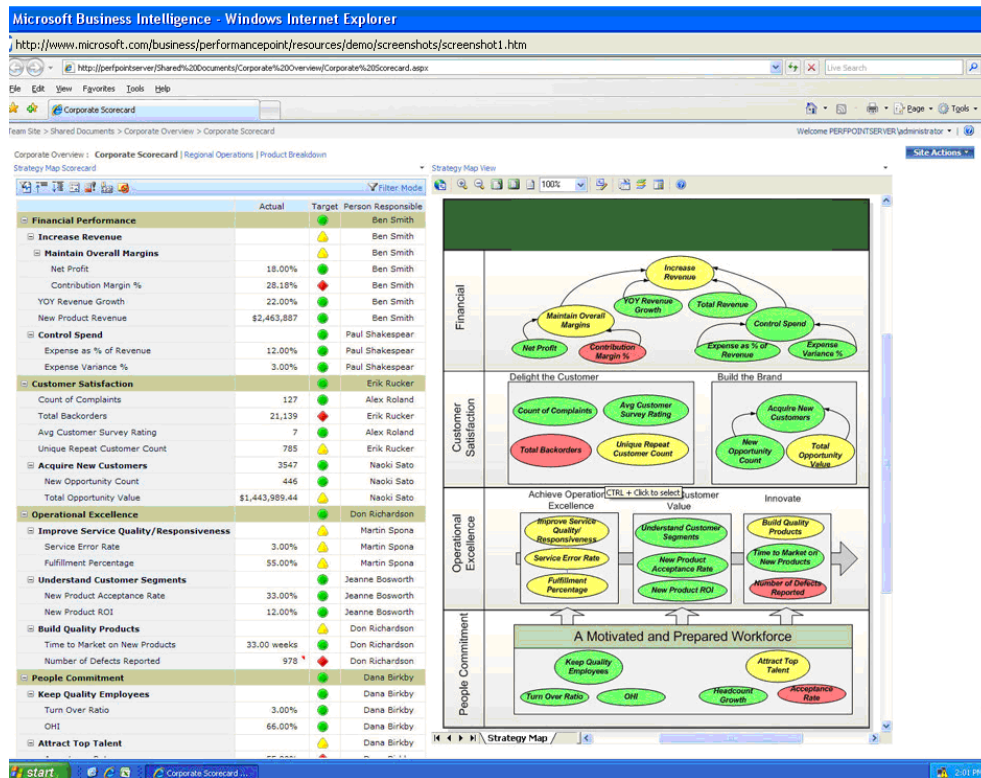


Figure 1. The integration of financial intelligence mechanisms

2.2.2 The Financial Manager

The activity undertaken within a company is based on many financial data. This makes the quality and continuity of data extremely important. The financial manager must be able to rely on the information used is accurate and can be used in internal and external reports. Currently, reports are done mostly manually, consuming time and present the risk of presenting wrong data.

The implementation of a BI solution provides access to regular updates of the performance indicators monitored by financial managers, helping them to respond promptly to a changing business environment and allowing the decision makers on the last hierarchical level to take effective decisions.

The financial manager can:

- ❖ **Monitor, analyse and plan using an integrated solution:** Evaluation sheets and KPIs reflect changes to the planning, budgeting and forecasting, which occur in real time by helping policy makers to understand the levers of business operation, challenges and opportunities.
- ❖ **Integration of advanced solutions for financial intelligence:** BI solutions provide mechanisms to ensure the consolidation and standardization of business logic, including foreign exchange for various currencies, intercompany agreements and allocations on multiple levels. The product also allows customization of business rules, calculations and assumptions.
- ❖ **Obtaining a full picture of business:** Users can easily integrate information from multiple sources (internal and external) and multiple versions of planning and budgets in a single plane to facilitate analysis and reporting.
- ❖ **Support the consistency of the performance management process:** Real-time calculations and business rules managed at server level allow users to manage processes and consistent data allows them to simplify multiple budgets. Data entry forms, workflow, data transmission, approval, templates and other forms facilitate the standardization of planning, budgeting and forecasting processes.

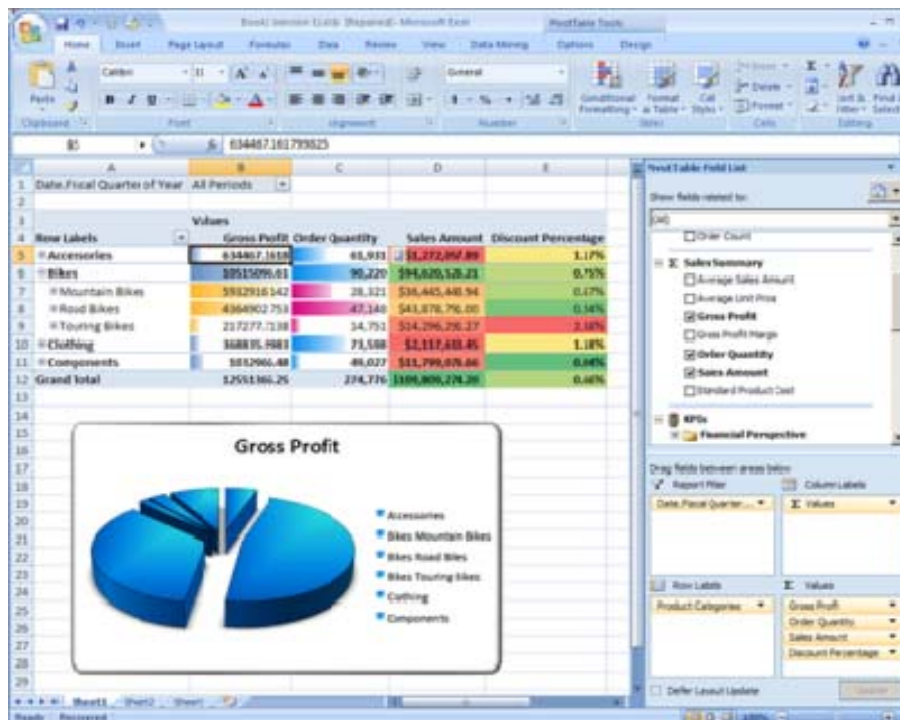


Figure 2. Ad-Hoc Reporting with Microsoft Excel and OLAP

2.2.3 The Analyst

The analysts support the planning process within a company and are those who analyse data in order to identify ways in which efficiency can be improved. The analysts need an easy to use tool that allows them to spend less time on collecting data and more time on analysing them. By using BI solution, analysts can:

- ❖ Obtain very detailed data: Users can obtain data with a high level of detail, from which they can make better decisions faster.
- ❖ Carry out complex analysis: BI solutions enable data acquisition from multiple sources and prepare them to be used in different contexts, facilitating data mining and analysis of the causes that drew decreases or increases in performance.
- ❖ Perform predictive analysis: Users can access data mining models from the SQL Server, enabling them to develop forecasts and analyze trends.
- ❖ Model different scenarios: Users can build and can replicate the business model to implement different scenarios and methodologies, such as analysis of "what if" and modelling to maximize the profit.

2.3 How BI provides business value

The business intelligence infrastructure allows the implementation of business information on a secure, scalable, qualitative platform and allows a company to (Stănescu & Ștefan, 2010; Kimball & Ross, 2010):

- ❖ benefit of data integration facilities. The SQL Server 2005 Integration Services (SSIS) carry out the full integration, transformation and synthesis of large volumes of data at high speeds.
- ❖ **develop complex analytical models that can be included in business applications.** Data search capabilities and online analytical processing (OLAP) of the SQL Server 2005 Analysis Services make searching for data more accessible in an environment with enhanced security.
- ❖ **develop comprehensive and complete reporting solution.** Using SQL Server 2005 Reporting Services it is possible to create, manage and deliver both traditional printed reports and also Web-based, interactive reports.
- ❖ **use the relational database engine, which is scalable and secure.** The relational database management system, SQL Server 2005, sustains performance improvement and support for structured and unstructured XML data, as well as verified performance and availability.
- ❖ **use a rich and familiar development environment.** The integration with Microsoft Visual Studio 2005 provides developers with a platform that enables productive development and secured collaboration solutions

3. CONCLUSIONS

The key to win in the Information Age is making decisions that are consistently better and faster than the competition. Business intelligence is an approach to managing business that is dedicated to providing competitive advantage through the execution of fact-based decision making. This paper presents the business intelligence technology as a mean to achieve this goal by applying a decision-making cycle of analysing information, gaining insight, taking action, and measuring results. The authors underline the fact that technology enables business intelligence, but it is the people that interpret and act on the information. Business intelligence it is not only about the technology, but also about creativity, culture, and whether people view information technology as a critical asset.

The implementation of today's information management is limited to providing mostly analysis of financial data and such approaches do not cover the area of knowledge management systems. The authors aim to extend their research and identify solutions that facilitate real-time availability of know-how in desktop and merging mobile environments.

REFERENCES

- [1.] Larson, B. (2008). *Delivering Business Intelligence with Microsoft SQL Server 2008*, McGraw-Hill Osborne Media.
- [2.] Loshin, D. (2003). *Business Intelligence: The Savvy Manager's Guide (The Savvy Manager's Guides)*, Morgan Kaufmann.
- [3.] Howson, C. (2007). *Successful Business Intelligence: Secrets to Making BI a Killer App*, McGraw-Hill Osborne Media.
- [4.] Kimball R. & Ross, M. (2010). *The Kimball Group Reader: Relentlessly Practical Tools for Data Warehousing and Business Intelligence*, Wiley.
- [5.] Moss, L. & Atre, S. (2003). *Business Intelligence Roadmap: The Complete Project Lifecycle for Decision-Support Applications*, Addison-Wesley Professional.
- [6.] Stănescu I.A. & Chete G.C. (2009). *Knowledge Enriched Decisional Environments*, published in the ISI proceedings of the 15th International Scientific Conference "Knowledge Based Organization" – KBO, Sibiu, Romania, November 28-29, 2009.
- [7.] Stănescu I.A. & Ștefan A. (2010). *Web-Based Knowledge-Driven Decision Support Systems*, published in the ISI proceedings of the 12th LSS Symposium, Large Scale Systems: Theory and Applications, Villeneuve d'Ascq, France, July 11-14, 2010.
- [8.] Turban, E., Sharda R., Delen D. & King, D. (2010). *Business Intelligence*, Prentice Hall.
- [9.] Vercellis, C. (2009). *Business Intelligence: Data Mining and Optimization for Decision Making*, Wiley.
- [10.] Vitt E., Luckevich M. & Misner S. (2002). *Business Intelligence: Making Better Decisions Faster*, Microsoft Press.







¹ Natalia-Cernica BUZGĂU

IMPLEMENTATION OF TOTAL PRODUCTIVE MAINTENANCE

¹ S.C. REVA S.A. SIMERIA, ROMANIA

ABSTRACT:

Total Productive Maintenance (TPM) is a system of maintenance covering the entire life of the equipment in every division including planning, manufacturing and maintenance. Because of its targeted achievement to increase productivity out of the equipment, the term Total Productive Maintenance is sometimes known as Total Productivity Management.

KEYWORDS:

Maintenance, TPM, equipments, productivity

1. INTRODUCTION

In modern day manufacturing and service industries, improved quality of products and services increasingly depend on the features and conditions of organizations' equipment and facilities. In the late 70's, there was heavy snow in Sapporo, the northern-most island of Japan. Because the workers could not get to work, Matsushita's vacuum cleaner factory stood still. Mr. Matsushita thought, „Can we not rely on our workers for production?” A year later, the first unmanned-factory in the world was born. As the production relied 100% on equipment, Total Productive Maintenance became mandatory. Today, there are many similar examples such as Fujitsu-Fanuc, the world's most advanced unmanned-factory, which uses reliable computer controllers for manufacturing automation. Likewise super-computers run 24 hours a day all over the world to provide uninterrupted services to the banking, finance, air-flight, hotel, tourist, telecommunication and other service industries. However, this would not be possible without Total Productive Maintenance.

Total Productive Maintenance is a program for fundamental improvement that involves the entire human resources. When implemented fully, Total Productive Maintenance dramatically improves productivity and quality and reduces costs. As automation and labor-saving equipments take production activities away from humans, the condition of production and office equipments increasingly affects output quality, cost, delivery, health and safety, and employee morale. In a typical factory, however, many pieces of equipment are poorly maintained. Neglected equipment results in chronic losses and time wasted on finding and treating the causes.

Both operations and maintenance departments should accept responsibility of keeping equipments in good conditions. To eliminate the waste and losses hidden in a typical factory environment, we must acknowledge the central role of workers in managing the production process. No matter how thoroughly plants are automated or how many robots are installed, people are ultimately responsible for equipment operation and maintenance. Every aspect of a machine's performance, whether good or bad, can be traced back to a human act or omission. Therefore no matter how advanced the technology is, people play a key role in maintaining the optimum performance of the equipment.

When company employees accept this point of view, they will see the advantage of building quality into equipment and building an environment that prevents equipment and tools from generating production or quality problems. This company-wide team-based effort is the heart of Total Productive Maintenance. It represents a dramatic change from the traditional „I make-you fix” attitude that so often divides workers. Through Total Productive Maintenance, everyone cooperates to maintain equipment the company depends on for survival and ultimately for

profitability. The goal of Total Productive Maintenance is to increase the productivity of plant and equipments. Consequently, maximized output will be achieved through the effort of minimizing input-improving and maintaining equipments at optimal levels to reduce its life cycle cost.

2. THE STUDY

The Japan Institute of Plant Maintenance runs the annual Productive Maintenance Excellence Award and they provide a checklist for companies applying for the award. There are 10 main items in the checklist:

- a. Policy and objectives of Total Productive Maintenance.
- b. Organization and operation.
- c. Small-group activities and autonomous maintenance.
- d. Training.
- e. Equipment maintenance.
- f. Planning and management.
- g. Equipment investment plans and maintenance prevention.
- h. Production volumes, scheduling, quality and cost.
- i. Safety, sanitation and environmental conservation.
- j. Results and assessments.

How to Implement the Total Productive Maintenance:

- a. Element losses based on project teams organized by the production, maintenance, and plant-engineering departments.
- b. Planned maintenance carried out by the maintenance department.
- c. Autonomous maintenance carried out by the production department in seven steps.
 - Step 1: Initial cleaning
 - Step 2: Actions to address the causes and effects of dust and dirt
 - Step 3: Cleaning and lubrication standards
 - Step 4: General inspection training
 - Step 5: Autonomous inspection
 - Step 6: Workplace organization standards
 - Step 7: Full implementation of autonomous maintenance
- d. Preventive engineering carried out mainly by the plant-engineering department.
- e. Easy-to-manufacture product design carried out mainly by the product design department.
- f. Education and training to support the above activities.

Total Productive Maintenance can be successful in achieving significant results only with universal cooperation among all constituents involved with the six activities listed above. Once a decision has been made to initiate Total Productive Maintenance, company and factory leadership should promote all six of these activities despite excuses that may come from various quarters.

Through these activities, the company can gradually eliminate the losses, establish a more effective relationship between operators and machines, and maintain equipment in the best possible condition.

The continuous request that managers provide better customer service, improve space comfort, supply reliable mechanical and electrical energy performance, and to do so at no more cost than last year's operating budget. Overall, this fresh look at how building operation and maintenance is done is a very good idea.

Today's economic and competitive environment requires that industry sustain full production capabilities and minimize capital investment. From the maintenance perspective, this means finding ways to maximize equipment reliability and up time, and extend plant and equipment life through cost effective maintenance. To achieve these objectives, industry must move away from the traditional reactive maintenance mode and move to proactive maintenance and management philosophies. Maintenance processes that fully address the program and technical concerns of maintenance must be adopted and the process must realize the value of integration, engineering, planning and quality. Such change requires a complete shift in the maintenance approach. Total Productive Maintenance is such an approach.

Total Productive Maintenance is based on the premise that effective maintenance requires that the elements of maintenance be defined, operational and interactive. The phases and concepts to implement the Total Productive Maintenance in a dependent or independent maintenance facility (figure 1).

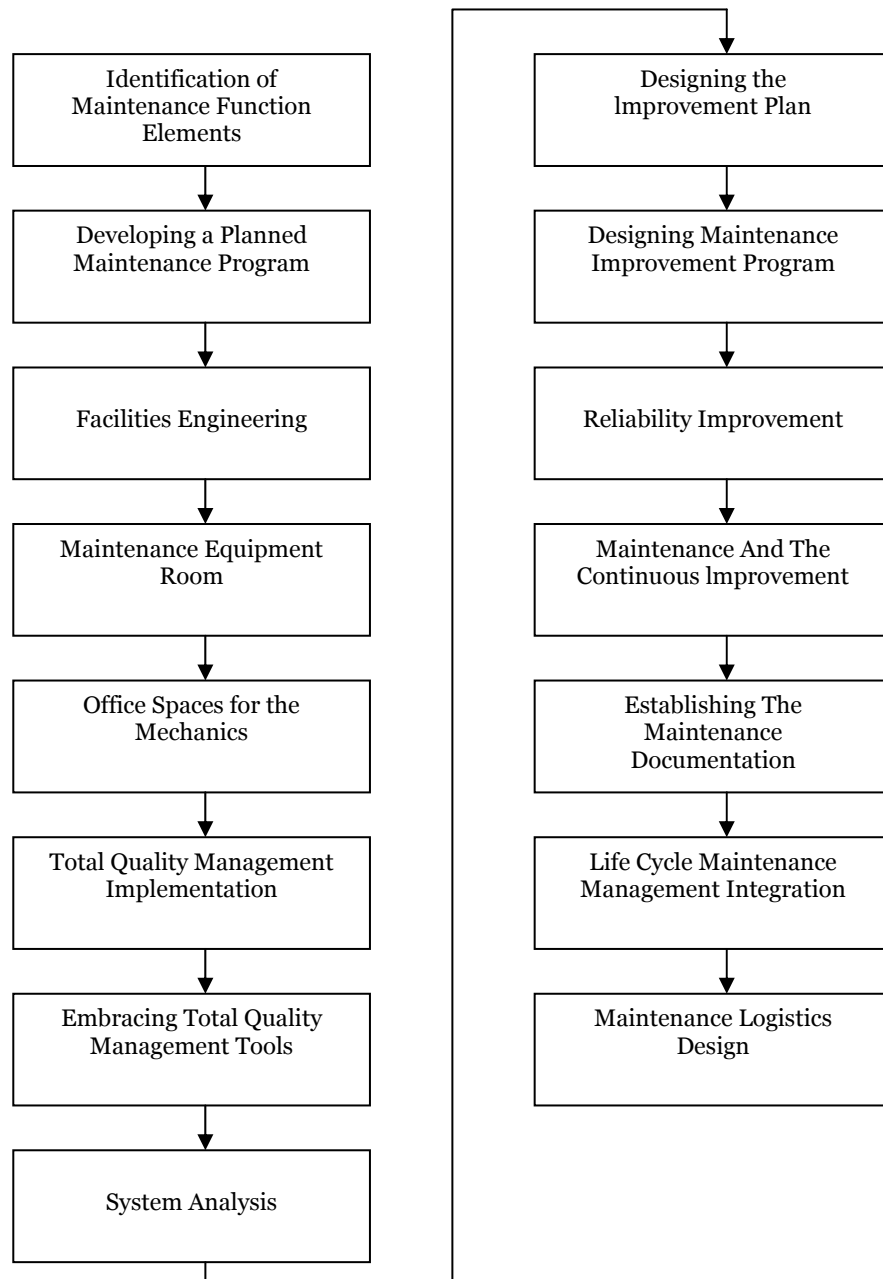


Figure 1. Total Productive Maintenance Implementation Phases

One of the difficulties in implementing TPM as a methodology is that it takes a considerable number of years. The time taken depends on the size of the organization. There is no quick way for implementing TPM. This is contradictory to the traditional management improvement strategies. Following are the other difficulties faced in TPM implementation:

- ❖ Typically people show strong resistance to change.
- ❖ Many people treat it just another „Program of the month” without paying any focus and also doubt about the effectiveness.
- ❖ Not sufficient resources (people, money, time, etc.) and assistance provided.
- ❖ Insufficient understanding of the methodology and philosophy by middle management.
- ❖ TPM is not a „quick fix” approach, it involve cultural change to the ways we do things.
- ❖ Departmental barrier existing within Business Unit.
- ❖ Many people considered TPM activities as additional work/threat.

3. CONCLUSIONS

Total Productive Maintenance is a maintenance and management philosophy that advocates planning all maintenance (i.e., preventive, predictive, corrective and inactive) and the control of quality in maintenance. It is a concept that addresses both programmatic and technical concerns of maintenance and considers maintenance an integrated function rather than a specific activity. Today, with competition in industry at an all time high, TPM may be the only thing that stands between success and total failure for some companies. It has been proven to be a program that works. It can be adapted to work not only in industrial plants, but also in construction, building maintenance, transportation, and in a variety of other situations. Employees must be educated and convinced that TPM is not just another „Program of the month” and that management is totally committed to the program and the extended time frame necessary for full implementation. If everyone involved in a TPM program does his or her part, an unusually high rate of return compared to resources invested may be expected.

REFERENCES

- [1.] Hartmann, Edward, Maintenance Management, Norcross, Georgia, Industrial Engineering and Management Press, pp3-239, 1987.
- [2.] Maggard, Bill N., P.E., TPM That Works, Allision Park, PA, TPM Press, Inc., pp7-123, 1992.
- [3.] Moubray John, Maintenance Management - A New Paradigm, Maintenance, Volume, 11, n° 1, 1996.
- [4.] Niebel, Benjamin W., Engineering Maintenance Management, New York, N.Y., Marcel Dekker, Inc., pp 123-197, 1985.
- [5.] Robinson, Charles J., Ginder, Andrew P., Implementing TPM, Productivity Press, Portland Oregon, 1995.
- [5.] http://www.plant-maintenance.com/maintenance_articles_tpm.shtml.
- [6.] <http://www.maintenanceresources.com>.
- [7.] <http://www.reliabilityweb.com>.





¹ Natalia-Cernica BUZGĂU

RELIABILITY-CENTERED MAINTENANCE (RCM)

¹ S.C. REVA S.A. SIMERIA, ROMANIA

ABSTRACT:

RCM is a common sense approach for achieving reliability. It is the best known proven method for developing a preventive maintenance (PM) program for any type of plant or facility. RCM is defined as a set of tasks generated on the basis of a systematic evaluation that are used to develop or optimize a maintenance program. RCM incorporates decision logic to ascertain the safety and operational consequences of failures and identifies the mechanisms responsible for those failures.

KEYWORDS:

RCM, PM, evaluation

1. INTRODUCTION

Due to a competitive environment, many companies are required to reduce their overall costs while maintaining the value and reliability of their assets. The use of Reliability-Centred Maintenance, RCM, can help organisations to develop a systematic maintenance programme, meeting these requirements in a cost-effective manner. RCM basically combines different techniques and tools in a systematic approach to manage risks as a basis for maintenance decisions. However, a long-term approach may be difficult to manage since it involves many people. Although RCM is an organised common sense approach to improvements of preventive maintenance, it still represents a very new and revolutionary idea for many people.

When introducing RCM with the aim of changing the overall way of working with maintenance in the organisation, i.e. on a full-scale basis, a long-term introduction approach should preferably be used. In several cases organisations have experienced severe difficulties when introducing RCM on a full-scale basis. Some of the reason are technical in nature, but the majority are managerial obstacles.

2. THE STUDY

F. Stanley Nowlan and Howard F. Heap, at the United Airlines under the Department of Defence, in US, established the concept „Reliability-Centered Maintenance”, RCM, in 1978. The principles of RCM arose from a rigorous examination of certain questions that were often taken for granted (Nowlan & Heap, 1978):

- ❖ How does a failure occur?
- ❖ What are its consequences?
- ❖ What good can preventive maintenance do?

The RCM method can be described in four unique features, see e.g. Smith (1992) and Anderson & Neri (1990):

- Preserve functions.
- Identify failure modes that can defeat the functions.
- Prioritise function need, via the failure modes.
- Select only applicable and effective preventive maintenance tasks.

Moubray (1997) defines RCM in two ways:

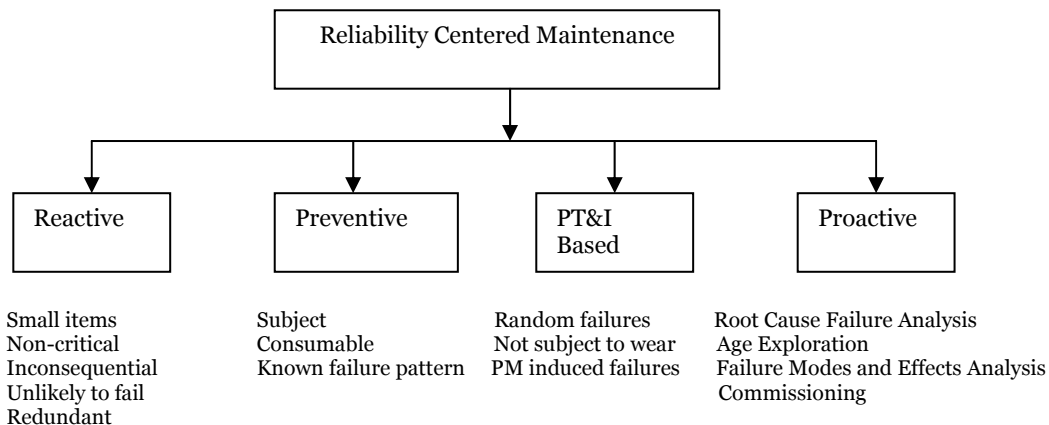
- 1) „A process used to determine the maintenance requirements of any physical asset in its operating context”;
- 2) „A process used to determine what must be done to ensure that any physical asset continues to do whatever its users want it to do in its present operating context”.

Another definition is „A systematic approach for identifying effective and efficient preventive maintenance tasks for items in accordance with a specific set of procedures and for establishing intervals between maintenance tasks” (IEC 60300-3-11, 1999).

The RCM analysis carefully considers and answers the following questions:

- What does the system or equipment do; what are its functions?
- What functional failures are likely to occur?
- What are the likely consequences of these functional failures?
- What can be done to reduce the probability of the failure, identify the onset of failure, or reduce the consequences of the failure?

Reliability-Centered Maintenance (RCM) integrates Preventive Maintenance (PM), Predictive Testing and Inspection (PT&I), Repair (also called reactive maintenance), and Proactive Maintenance to increase the probability that a machine or component will function in the required manner over its design life-cycle with a minimum amount of maintenance and downtime. These principal maintenance strategies, rather than being applied independently, are optimally integrated to take advantage of their respective strengths, and maximize facility and equipment reliability while minimizing life-cycle costs. The goal of this approach is to reduce the Life-Cycle Cost (LCC) of a facility to a minimum while continuing to allow the facility to function as intended with required reliability and availability. The basic application of each strategy is shown in figure 1:



The goal of an effective maintenance organization is to provide the required system performance at the lowest cost. This means that the maintenance approach must be based upon a clear understanding of failure at each of the system levels. System components can be degraded or even failed and still not cause a system failure. The role of the maintenance and operations (M&O) staff is to recognize the margin to failure, estimate the time of failure, and pre-plan required repairs in order to minimize the Mean Time to Repair (MTTR) and associated downtime in order to achieve the maximum Overall Equipment Effectiveness within budgetary constraints.

The benefits and advantages of using RCM are several and have an impact on operations, safety, logistics, configuration and administration (Smith, 1993). Some of the benefits are tangible and others are intangible. Examples of potential benefits of using RCM:

- ❖ Cross-discipline utilisation of knowledge;
- ❖ Traceability of decisions;
- ❖ A broader and more attractive way of working;
- ❖ More condition monitoring;
- ❖ More systematic maintenance;
- ❖ More comprehensive documentation;
- ❖ Fewer maintenance hours;
- ❖ Improved operational feedback;
- ❖ Higher quality maintenance plans;
- ❖ Better availability of maintenance history;
- ❖ Significant reductions in preventive maintenance costs while maintaining or even improving the availability of the systems;
- ❖ Less corrective maintenance;
- ❖ Establish an uniform and consistent approach asset maintenance across the company;
- ❖ Improved understanding between representatives of the operations and maintenance functions;
- ❖ Improved operating performance;

- ❖ Improved plant reliability;
- ❖ Improved availability;
- ❖ Greater safety;
- ❖ Maintenance optimisation;
- ❖ Greater staff motivation;
- ❖ Educational capabilities.

Examination of the RCM benefits reveals that their effects can be grouped into five categories (Bowler & Leonard, 1994a):

- ❖ Reduced maintenance activity;
- ❖ Improved maintenance management systems;
- ❖ Improved productivity;
- ❖ Greater safety and environmental integrity;
- ❖ Other benefits.

It should be noted that several of the benefits can belong to more than one category. According to Johnston (2002), benefits of RCM can usually be traced back to two broad categories:

- ❖ Risk reduction;
- ❖ Cost savings.

Full benefit of RCM can only be achieved when we have access to reliability data for the items being analysed, when considering the optimising of preventive maintenance intervals. The operating organisation must be prepared to collect and respond to real data throughout the operating life of the equipment (Nowlan & Heap, 1978; Vatn et al., 1996).

The primary RCM principles are:

- ❖ RCM is Function Oriented
- ❖ RCM is System Focused
- ❖ RCM is Reliability Centered
- ❖ RCM Acknowledges Design Limitations
- ❖ RCM is Driven by Safety, Security, and Economics
- ❖ RCM Defines Failure as "Any Unsatisfactory Condition"
- ❖ RCM Uses a Logic Tree to Screen Maintenance Tasks
- ❖ RCM Tasks Must Be Applicable
- ❖ RCM Tasks Must Be Effective
- ❖ RCM Acknowledges Three Types of Maintenance Tasks
- ❖ RCM is a Living System.

RCM is applicable to:

- Where large, complex equipment is used
- Where equipment failures pose significant economic, safety or environmental risk:
 - ❖ aero/astro industries;
 - ❖ navy;
 - ❖ utility companies;
 - ❖ offshore industry;
 - ❖ manufacturing process.

Instituting an RCM Program depend on:

- ❖ Nature of the business;
- ❖ Risks posed by equipment failure;
- ❖ State of the existing maintenance program.

3. CONCLUSIONS

RCM in its purest form is a resource hungry process that should only be applied to the most critical of assets. The results from the process if performed properly and coupled with assessment of historical failures will produce efficient and effective maintenance strategies, but this will be at the expense of a significant amount of time for plant staff and the project analyst.

RCM yields results very quickly; most organisations can complete an RCM review on existing equipment and achieve substantial benefits in a matter of months. It is also an ideal approach for determining the maintenance requirements of new equipment of all kinds. When applied correctly, it transforms both the maintenance requirements themselves and the way in which the maintenance function as a whole is perceived.

REFERENCES

- [1.] Anderson, R. T. and Neri, L., Reliability-Centered Maintenance, University Press, Great Britain, Cambridge, 1990.
- [2.] Bowler, D. J. And Leonard, R., Economic considerations underlying the adoption of Reliability-Centered Maintenance. Proceedings of Life Management of Power Plants, Edinburgh, UK, pp. 14-20, 1994a.
- [3.] IEC 60300-3-11, Dependability Management – Part 3-11: Application Guide – Reliability Centered Maintenance. Standard IEC 60300-3-11:1999, International Electrotechnical Commission, Geneva, 1999.
- [4.] Johnston, D. C., Measuring RCM implementation. Proceedings of The IEEE Annual Reliability and Maintainability Symposium, Seattle, WA, pp. 511-515, 2002.
- [5.] Moubray, John, Reliability-Centered Maintenance II, Industrial Press, New York, NY, April 1997.
- [6.] Nowlan, F. Stanley and Heap, Howard F., Reliability Centered Maintenance, Dolby Access Press, 1978.
- [7.] Smith, Anthony M., Reliability-Centered Maintenance, McGraw Hill, New York, NY, September, 1992.
- [8.] Vatn, J., Hokstad, P. and Bodsberg, L., An overall model for maintenance optimisation. Reliability Engineering and System Safety, Vol. 51, No. 3, pp. 241-257, 1996.
- [9.] <http://www.wbdg.org>.
- [10.] <http://reliabilityweb.com>.





¹ Árpád FERENCZ, ² Márta NÓTÁRI

ROLE OF RURAL DEVELOPMENT IN THE PRODUCTION OF THE HUNGARIAN TRADITIONAL HORTICULTURAL PRODUCTS

¹⁻² DEPARTMENT OF ECONOMICS AND RURAL DEVELOPMENT COLLEGE OF KECSKEMÉT, HUNGARY

ABSTRACT:

Union and their development is not controlled by strict quota systems. In Hungary a lot of unique products of excellent quality are produced. Here in this essay we would like to find the answer to the question how the two significant products of the southern part of the Great Hungarian Plain can provide the families with the income that they can live on. We aim at the economical examination of the cucumber grown in Méhkerék and asparagus of Homok. To do this we will apply the so called Standard Gross Margin. The agriculture of the states of the European Union is measured with the help of this method. It can also help us in the future to decide whether the different farms belonging to families are economically viable in Hungary.

KEYWORDS:

unique products, SGM of cucumber and asparagus

1. INTRODUCTION

We would like to find the answer to the question how some significant products of Hungary can provide the families with the income that they can live on. I aim at the economical examination of the asparagus, the cucumber. To do this I will apply the so called Standard Gross Margin. The agriculture of the states of the European Union is measured with the help of this method. It can also help us in the future to decide whether the different farms belonging to families are economically viable in Hungary. I make suggestions regarding the sizes of the area, which would be required to provide a livelihood for a Hungarian family. Agriculture has been and probably will be a significant branch in the south part of the Great Plain in the future as well. Besides the mass products and in many cases instead of them when forming the agricultural structure, this region has to pay more attention to the branches that were important in the past (Berde, 2000). Hungarian experts who are famous in foreign countries as well deal with these branches and they provide excellent products (Juhász et al., 2006). The rules referring to these products are more liberal in the market places of the European Union and their development is not controlled by strict quota systems.

2. MATERIAL AND METHOD

2.1. THE STANDARD GROSS MARGIN (SGM)

Our calculations were carried out with the help of a method worked out and applied in the European Union. In the European Union the agricultural enterprises have been regularly assessed (since 1966) and comparative data have been given to the decision-making organisations of the Union. Because of the number and the variations of the enterprises more than one form of measuring was applied such as the territory of the factory, the number of the employees, the number of the animals bred and the price of the products sold. As it was experienced the

achievement of the agriculture in a state could not have been defined by these forms of measuring and by the combination of them. Similar to this they were not sufficient to determine the economic size of an enterprise and to compare the different factories from economic aspect (Kovács, 2001). The unified classification system (the economy typology) was accepted in 1978 that pays attention to two aspects, the type of farming (the structure of production) and the size of the economy. In order to define the economic size the Standard Gross Margin (SGM) was worked out (Kovács et.al., 1999). The natural data referring to the structure of the factory cannot say anything about the achievement of the agriculture of a country and they are not good for economic comparing. The size of the factory is defined the best of all by the potential profitable capacity which equals with the total standard gross margin (SGM) of the particular factory -which is the same as the added value (Agriculture in the European Union 2001, European Commission).

2.2. THE CALCULATION OF THE STANDARD GROSS MARGIN

According to the regulations of the European Union, in cultivation of plants the costs of the seeds, the propagation, the artificial fertilizers, the insecticides, the heating, the irrigation, the processing, the classification, the packing, the insurance and other variable costs that are connected with the particular production activity have to be taken into consideration among the direct variable expenses. The indirect variable costs are also defined. The variable expenses in connection with the machines belonging to the factory (such as fuel, lubricants, repairing costs) are listed here. These two groups together mean the variable costs of the economy (Hajduné et.al., 2008). It does not include the costs of amortization and the rent of the agricultural land. This method takes into consideration every wages and their complementary costs as constant expenses without paying attention to whether they were paid to the owner of the farm or to a family member or to an employee. The amortization costs of the tangible assets, the rent of the agricultural land and the general costs are referred to as constant expenses.

The SGM₁ and SGM₂ index numbers can be calculated on the basis of the relations mentioned above.

SGM₁ = sales – direct variable cost (direct material costs)

SGM₂ = sales – direct variable cost – indirect variable cost (the direct material costs and the direct costs of machine work are deducted from the sales).

The SGM₂ index number is in fact the gross income.

2.3. THE NECESSITY OF LIVE LABOUR

The basis of the economy producing unique Hungarian products is to deal with growing plants that assure the costs of living for a long time; can be easily produced in the south of the Great Hungarian Plain, can be easily sold in the market and can be produced by own live labour.

The necessity of live labour has to be determined especially in the harvesting and the selling period. It can be calculated on the basis of detailed producing technology. In this essay we determine the area that a family can cultivate on its own – without employing workers seasonally. If we take a family with four members we calculate with three manpower units. In our earlier research the working days and working hours in cultivation of plants were defined. These data are essential to calculate the necessity of live labour especially when we plan the working peak. In the harvest phase we calculate with 7-10 working hours per manpower units a day. The family can perform 200-250 hours every ten days.

3. RESULTS AND DISCUSSION

3.1. THE ECONOMIC ASSESSMENT OF THE CUCUMBER GROWN

The training system for growing cucumber assures bigger quantities and better quality comparing to the plough-land cultivation. The cost of it is 3600-4400 euro per hectare that does not include the farmer's labour. This system can be planned for ten years and can be applied when growing tomatoes as well. A particularity of growing cucumbers intensively is that the size of the desired product is in inverse relation to its yield and average price. The yield is lower if we pick cucumbers every day which are 1cm-3cm, 2cm-5cm and 3cm-6cm big and their price is higher. In the model we plan to pick 3cm-6cm and 6cm-9cm big cucumbers every two days.

From among the direct variable expenses the costs of artificial and organic fertilizers, pesticides, plants, irrigation and other variable costs were calculated in our project. The direct variable cost of the cucumbers grown on family farms with the help of training system and irrigation is 600 euro per hectare. In our technology 800 euro per hectare variable cost was calculated taking into consideration the running and the repairing costs of the machines of own

property. The total variable cost in a year (1.400 euro) was compared to the probable income. The yield can reach 80 tons per hectare in the south of the Great Hungarian Plain if irrigation is applied. The 0,24 euro/kg average price could assure the farm a 19.200 euro income. We must not forget about the fact that such an intensive planting culture requires 800 euro costs per hectare at the beginning taking only an average data. This cost cannot be taken into consideration among the expenses (according to the terminology of the European Nations). Similarly to this the salary cannot be deducted although the application of live labour is the highest in case of growing plants in the fields. $SGM_1 = 19.200 \text{ euro income} - 600 \text{ euro direct variable cost} = 18.600 \text{ euro/year/hectare}$. $SGM_2 = 19.200 \text{ euro income} - 600 \text{ euro direct variable cost} - 800 \text{ euro indirect variable cost} = 17.800 \text{ euro / year / hectare}$. The need for live labour is the greatest first when planting starts. If own labour is used, the work can be finished in time. The next peak of work appears during harvest when 540 working hours of live labour per hectares are needed. Taking into consideration the number of the working hours, one family can manage 0.51-hectare-post system area without employing working seasonally. The area that can be cultivated by the family on average assures only 9.076 euro SGM.

3.2. THE ECONOMIC ASSESSMENT OF THE ASPARAGUS

The basis of the production is the asparagus plantation, which has a good effect on the farming. After planting there are three or four years without harvest but the field must be cultivated although there is no income and no other plants can be grown meanwhile to utilize the area. The cost of plantation and cultivation is 8.0000 euro in the proportion of 85+5+5+5 every year. Besides this 1600 working hours are needed. The factor cost of one hectare is 10.400 -12.000 euro. The length of the period when there is harvest is 6-8 years. The accountable depreciation is 15% a year. During this period the quantity of the yield is not the same: in the first two or three years it is growing, then it is stagnating for two or three years and after that it is decreasing. In this model we calculate with the yield of a stagnating year. The variable cost of the enterprise is encumbered with almost 220 euro per hectare. This includes the costs of the materials, the artificial and organic fertilizers, the pesticides, the packing and the processing. The indirect variable cost of the farm – according to our survey - is 170 which give a result of a total 400 euro variable cost. In the south of the Great Hungarian Plain – taking into consideration the areas not abounding in nutrients – we can calculate with a five- tonne average yield per hectare.

The distribution must be calculated with care with a 16 euro/kg - average price. The income is 8.000 euro per hectare. The biggest peak of work appears during the harvest. Taking into consideration the number of working hours 0.97 hectare of asparagus plantation ripening at the same time can be accomplished without employing workers for this season.

$SGM_1 = 8.000 \text{ euro income} - 220 \text{ euro direct variable cost} = 7.780 \text{ euro / year / hectare}$

$SGM_2 = 8.000 \text{ euro income} - 220 \text{ euro direct variable cost} - 170 \text{ euro indirect variable cost} = 7.610 \text{ euro / hectare/ year}$.

The SGM_2 for a 0.97 hectare is 7.390 euro.

4. CONCLUSIONS

4.1. THE BREAD WINNING CAPACITY OF THE CUCUMBER IN HUNGARY

In order to get the income expected the cucumber should be grown with the help of post system on a 0.72 hectare big area. On such a big area other workers have to be employed during the harvest period for 540 working hours. The cost of it is 780 euro.

This kind of cucumber growing makes it possible for the family to make ends meet. On the basis of the significant export, the market for the cucumber can be said to be steady. The income depends on the Hungarian sale ring and the processing. The cost of introducing the post system is high but the income of the first year can cover this cost on a successful farm.

4.2. THE BREAD WINNING CAPACITY OF THE ASPARAGUS GROWN IN HUNGARY

In order to get the income expected the pale asparagus should be grown on a 1.66 hectare big area. On such a big area other workers have to be employed during the harvest period for 469 working hours. The cost of it is 680 euro. The kinds of the asparagus make it possible for the family to make ends meet. On the basis of the significant export, the market for the asparagus can be said to be steady. The income depends on the Hungarian sale ring. Because of the frost in late spring it is not recommended to base the whole income of the farm on the asparagus. Other recommended products can be the ones the harvesting time of which not the beginning of April is or the middle of June.

REFERENCES

- [1.] Agriculture in the European Union 2001, European Commission.
- [2.] Berde, Cs (2000): Changes of Approaches to Management Functions in Agriculture. Zbornik, Vedeckych Prac, Nitra p. 217-222.
- [3.] Juhász, Cs.-Berde, Cs. (2006): Synchronisational problems in organisational motivation in agriculture. Studies in Agricultural Economics. No. 104. p. 129-142.
- [4.] Hajdu I-né- Nótári M. (2008): Fogyasztói attitűdök vizsgálata a hungarikum jellegű kertészeti- és élelmiszeripari termékek piacán. Acta Oeconomica Kaposvariensis 2008. No.1. p. 25-32.
- [5.] Kovács G.-Keszthelyi Sz.(1999):A teszüzemek 1998.évi gazdálkodásának eredményei, AKII Füzetek,1.
- [6.] Kovács G. (2001). Mérethatárok és lefedettség, Magyar Mezőgazdaság XII. p. 12.





¹ Márta NÓTÁRI, ² Árpád FERENCZ

THE CENTRAL AND THE LOCAL SYSTEMS OF RURAL DEVELOPMENT IN THE REGION MANAGEMENT

¹⁻² DEPARTMENT OF ECONOMICS AND RURAL DEVELOPMENT COLLEGE OF KECSKEMÉT, HUNGARY

ABSTRACT:

The sustainability is strongly connected to the conception of Food Sovereignty, which became an everyday issue again in the last years among the people dealing with agriculture. Considering the philosophy of the movement, the farmers have a right to produce local food, and the consumers have a right to decide by whom and how produced provisions intend to buy. In our research we examined the attitude of the consumers toward the natural foodstuff. The tools of the marketing have a role in the positioning of these products.

KEYWORDS:

region marketing, rural development

1. INTRODUCTION

Regional marketing is a new concept, which is not widely known in Hungary, there are only very few and limited experiences with it. It is a total of all the activities and at the same time a way of thinking, the aim of which is to take a product to the customers very efficiently (Berács, 2006). The task of regional marketing is to explore the competitive assets and attractions of a region, to help the realization of the plans in order to support achieving the goals of economic and community life. In the South Great Plain Region several top-quality products are made and these products are Hungarian specialties (Piskóti, 2006). In this immense competition an image formed about a country, a part of a country or about a region has a considerable influence on the decision of customers – both on the national and international market.

2. MATERIAL AND METHODS

Region marketing is barely known in Hungary and we have only limited experience in connection with its Hungarian applications. Region marketing is by all means part of marketing. It is a mixture of such activities which purpose is to effectively channel products to the customers. It must be considered, that there is a strong competition in satisfying consumer demand. Main goal of region marketing is to help discovering the competitiveness and charm of the region in order to reach multilateral development-, economic- and life-conduct objectives. Being a member of the European Union, it is vital for Hungary that its food industry could reserve its traditional role. Numerous high-quality, special products are produced in the South Great Plain Region. Farming experience – gained throughout centuries - resulted in special, unique products representing national values

Europeanisation is about opening up political, economic, geographic and social space. This is being carried out through the reduction of a wide range of traditional protection mechanisms of these spaces. The process serves the interests of the *economic centre*, the market, international capital and multinational companies. Nationally or regionally specific rules and regulations currently represent obstacles for the free movement of people, goods and capital (Camagni, 1995). Business needs to have *access* to local and regional economies. To achieve this, generally accepted

regulations and policies, to ensure the necessary conditions (stability, proper relations, common technical standards, etc.), are needed. The European Union, the *political centre* of Europe, can be seen as a central organisation, which can design, negotiate and enforce these conditions. The continuously growing common regulations on markets, trade, safety, environment and different aspects of production, aim to provide for the access required by the *economic centre* (Picchi, 1994).

3. RESULTS AND DISCUSSION

3.1. REGION MARKETING IN THE REGION OF DÉL-ALFÖLD OF HUNGARY

The contradiction of the present time is the “global-local paradox”. While global competition is intensifying, more and more companies have been concentrating in one region, where the local environment provides appropriate conditions for production. The reason of that is that among the advantages of the association, the advantages coming from a local environment secure increasing revenue levels.

In the Region of Dél-Alföld, the image was created in a way that it reflects the characteristics of the countryside, the atmosphere of the land, values of local people and history and traditions of the region. The region possesses a number of good quality agricultural products that have great prospects for the future. The positive image of the regions enhances the identity of local communities that assist them in finding their interest locally.

The figure 1 shows the aspects of situation survey basing marketing strategy.

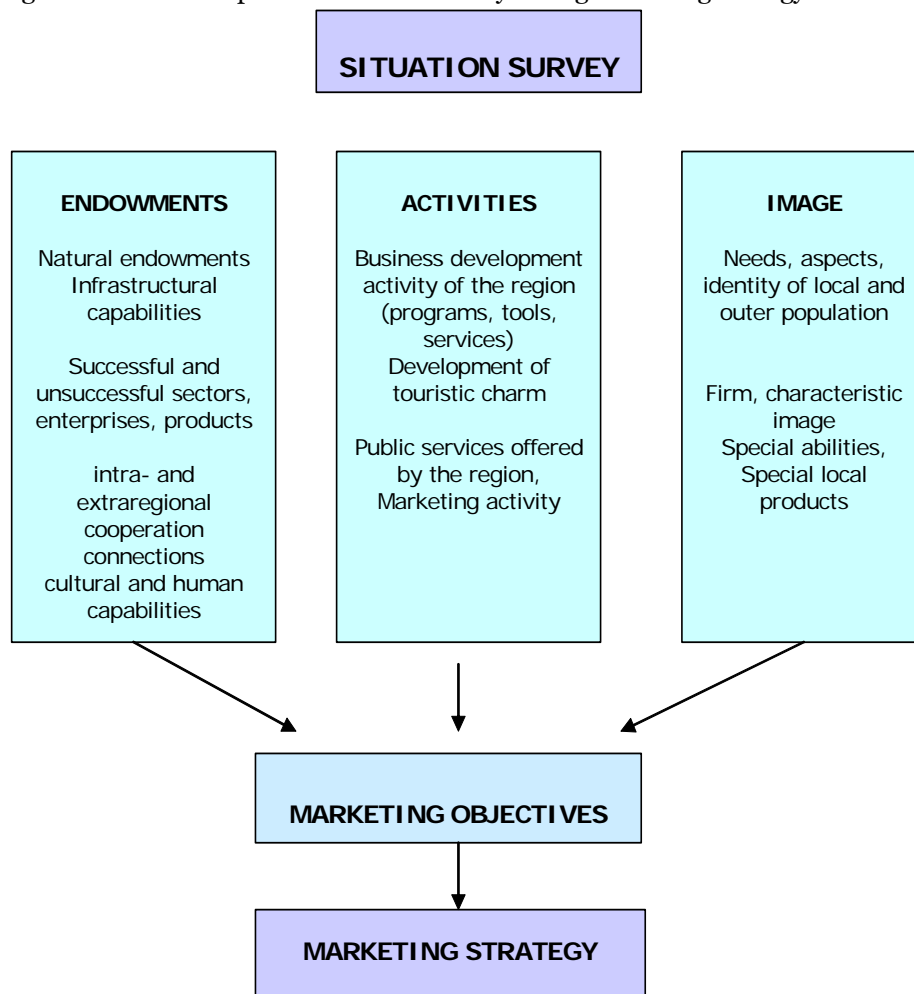


Figure 1. The aspects of situation survey basing marketing strategy

3.2. THE CENTRAL AND THE LOCAL SYSTEM OF RURAL DEVELOPMENT

One type could be called the central administrative system of rural development, based on fundamentally top-down interventions of the political centre (Gusztáv, 2005). It comprises such elements as: European and domestic policies; centrally redistributed resources; institutional networks; skills, technical and procedural knowledge of various level bureaucrats; strategic

development plans. It has a formalised and institutionalised character. It is based on written rules, established procedures and controlled by bureaucratic institutions. It uses external resources for intervention, usually works with a very narrow flow of information, with high transaction costs and aims at quantifiable results. At the same time it can have a large scope and embrace higher level or long term strategic objectives, which are above short term economic rationality (Amin et al., 1994). The other type could be called the local heuristic system of rural development, based on essentially endogenous, bottom-up processes (Ray, 2001). It comprises such elements as: local economic, political and social actors; local development plans; social networks and kinship relations; local authorities, innovative individuals, development associations and partnerships as well as the development skills and experiences of these local actors (Gusztáv, 2005). Although it builds upon local resources, rural values and synergistic effects of multiple activities, it often needs external finance and encouragement: financial resources, technical assistance, mediation, expert knowledge, etc. (Terluin, 2003).

3.3. SWOT ANALYSIS OF THE REGION

Strengths of the region:

- ❖ Role of agriculture is dominant in the Region, the food industry is competitive even by international comparison;
- ❖ Number of sunshine hours is very high and the average yearly temperature is also amongst the highest in Hungary;
- ❖ Number of tertiary educational-, research- and cultural centers is outstanding in national comparison.
- ❖ Many famous firms with high level of professional culture and brands connected to them works in the Region.
- ❖ There are a number of unique, excellent quality traditional product, which are unambiguously characteristic to the region.

Weaknesses:

- ❖ The GDP per capita has remained unchangedly below the national average in the past years;
- ❖ Quality and quantity of transportation infrastructure is insufficient;
- ❖ Proportion of foreign capital is lower than the national average;
- ❖ Many small regions of the Region belong to the group of small regions currently being in critical position.

Threats:

- ❖ Regional effects of the EU's Agricultural Policy;
- ❖ Appropriate environmental protection agreements and cooperations wouldn't be signed with the neighbouring countries;
- ❖ Sharpening competition between the domestic region and the regions of neighbouring countries.

Possibilities:

- ❖ Growth of the role of euroregional organizations;
- ❖ Affirmation of the South-Western European gate role with the reconciliation of the Balkanic situation;
- ❖ Change in consumer preferences;
- ❖ Positive international image of certain kinds of foods;
- ❖ Demand for unique, special provincial products.

4. CONCLUSION

Material and immaterial products which are manufactured in, and are representative exclusively to the Region should be supported practically in regional cooperation. Beside measurable economic profits the following advantages can be achieved:

- ❖ conservation of traditions and cultural heritage, strengthening the idea of belonging to the same community among the people living in the region;
- ❖ forming the peculiar image in the competition among the regions and in the accelerating globalization processes of our days.

It can be expected only as a result of a long-term, coordinated marketing strategy that the image of South Great Plain Region becomes widely known and attractive. One precondition of this is that the Region should successfully represent the selected image and to develop a positive affection for its special local products. This affection could be formed inside the region by positive local-patriotism, while outside the region with the sympathetic and valuable features.

This is important because the South Great Plain Region has its competitors by now – certain domestic and neighbouring country regions. In the future, the enhancement and specialization of the competition between regions could be expected. The South Great Plain Region only has its chance to effectively join the domestic and international competition if conscious preparations and image-forming takes place.

REFERENCES

- [1.] Amin, A. Thrift, N. (1994): Globalisation, Institutions, and Regional Development in Europe Oxford University Press
- [2.] Berács J. (2002): Nemzeti imázs és versenylőny. Marketing és menedzsment, No.1 p. 8-11.
- [3.] Camagni, R. (1995): Global network and local milieu: Towards a theory of economic space in: Conti, S. Malecki, E. and Oinas, P. (eds) The industrial enterprise and its environment: spatial perspective Avebury, Aldershot
- [4.] Nemes, G. (2005): Disintegration, the reason for policy failure – an analytical model of integrated rural development. Hungarian Academy of Sciences – Institute of Economics. ESRS XXI Congress, WG8 – Keszthely
- [5.] Picchi, A. (1994): The relation between central and local powers as context for endogenous development, in. Van der Ploeg, D.J. and Long, A. (eds)
- [6.] Piskóti (2006): Régió- és település marketing. KJK Kerszöv Kiadó Budapest, p.31-41.
- [7.] Ray, C. (2001) Culture Economies – A perspective on local rural development in Europe CRE Press, University of Newcastle upon Tyne
- [8.] Terluin, I.J. (2003): Differences in economic development in rural regions of advanced countries: an overview and critical analysis of theories, Journal of Rural Studies 19, 327-344



¹. M. RAHMOUNI, ² M.N. LAKHOUA

PROPOSAL OF THE INTEGRATION OF THE METHODS SADT AND GRAI IN THE ENTERPRISE

¹. ESSTT, 5 AVENUE TAHA HUSSEIN MONTFLEURY 1008, TUNISIA

². ISSAT DE MATEUR, ROUTE DE TABARKA, MATEUR 7030, TUNISIA

LABORATORY OF ANALYSIS AND COMMAND OF SYSTEMS, ENIT, TUNISIA

ABSTRACT:

The restructuring of enterprises constitutes a complex process allying various points of view that the conventional approaches don't manage to satisfy. Indeed, the restructuring of enterprises cannot be achieved only according to a global approach of analysis. In order to contribute to the restructuring of an enterprise, we present a proposal of the integration of two systemic methods: SADT and GRAI. In fact, we interest in this paper to the use of the global approach that allows us to act not only on the organisation and the management system of the enterprise but also on its information system.

KEYWORDS:

Enterprise modelling, Global approach, Systemic methods, SADT, GRAI

1. INTRODUCTION

The system approach enables us to analysis the complex process elements as components of a whole in reciprocal dependence relation. Its field of survey doesn't limit itself to the mechanisation of the thought. In fact, the systemic analysis is a methodology that organises knowledge to optimise an action. The objective of a system approach is to schematise a complex process, to lead to a modelling that enables to act on it, after we understand its architecture and its dynamic structure [1] [2].

The systemic analysis has for role to define the general strategy of the modelling survey to achieve. This strategy must enables to fix a way that specifies the limits of the modelling while defining the borders of the system to model and to specify among the data that are really exchanged between the different components of the system those that the modelling will cover [3][4].

Because of the complexity of activities of the enterprise and the interdependence of its various functions, its restructuring cannot achieve itself only according to a global approach of analysis based on the use of systemic methods [5] [6].

The use of systemic and participative approach facilitates the adoption of the strategy of restructuring of enterprises. It is therefore necessary to adopt a scientific gait based not only on the structured analysis but also on the modelling technique that will act not only on the organisation and the management system of the enterprise but also on its information system (See Figure 1).

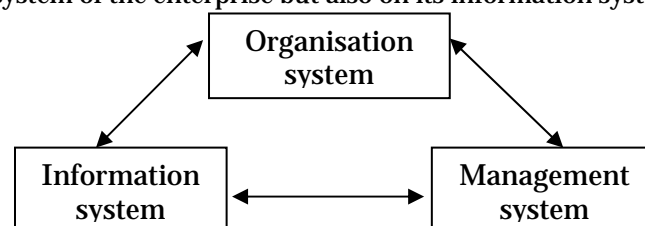


Figure 1- Representation of the enterprise

The principal objectives waited of the analysis of a system of the enterprise are: to offer a support of communication between operators of the system; to lead to a tool of performance analysis and to incline a tool of help to the decision making.

The object of this work is to propose a global approach based on the use of two systemic methods SADT (Structured Analysis Design Techniques) [7] [8] and GRAI (Graphes et Réseaux d'Activités Inter-reliés) [9] [10] enabling to reach the aimed objectives. This approach requires a new and suitable tools conceptualization that would be used by the various actors in the enterprise.

2. REVIEW ON PARTICIPATIVE METHODS

There are many methods that have been used to enhance participation in Information System (IS) planning and requirements analysis. We review some methods here because we think them to be fairly representative of the general kinds of methods in use. The methods include Delphi, focus groups, SADT, OOPP method, multiple criteria decision-making (MCDM), total quality management (TQM) and GRAI.

The objective of the Delphi method is to acquire and aggregate knowledge from multiple experts so that participants can find a consensus solution to a problem [11].

A second distinct method is focus groups (or focused group interviews). This method relies on team or group dynamics to generate as many ideas as possible. Focus groups been used for decades by marketing researchers to understand customer product preferences [12].

MCDM views requirements gathering and analysis as a problem requiring individual interviews. Analysts using MCDM focus primarily on analysis of the collected data to reveal users' requirements, rather than on resolving or negotiating ambiguities. The objective is to find an optimal solution for the problem of conflicting values and objectives, where the problem is modelled as a set of quantitative values requiring optimization [13].

TQM is a way to include the customer in development process, to improve product quality. In a TQM project, data gathering for customers needs, i.e., requirements elicitation may be done with QFD [14].

The SADT method represent attempts to apply the concept of focus groups specifically to information systems planning, eliciting data from groups of stakeholders or organizational teams [15]. They are characterized by their use of predetermined roles for group/team members and the use of graphically structured diagrams. SADT enables capturing of a proposed system's functions and data flows among the functions.

The OOPP method also referred to as Logical Framework Approach (LFA), is a structured meeting process [16]. This approach seeks to identify the major current problems using cause-effect analysis and search for the best strategy to alleviate those identified problems. OOPP method has become the standard for the International Development Project Design. Team Technologies have continued to refine the approach into TeamUP.

3. PRESENTATION OF THE METHODS SADT AND GRAI

In this part, we present two methods of enterprise modelling [17-20] SADT and GRAI that we propose to use for restructuring approach of the enterprise.

3.1 SADT method

The SADT method [7] represent attempts to apply the concept of focus groups specifically to information systems planning, eliciting data from groups of stakeholders or organizational teams. SADT is characterized by the use of predetermined roles for group/team members and the use of graphically structured diagrams. It enables capturing of proposed system's functions and data flows among the functions.

SADT, which was designed by Ross in the 1970s, was originally destined for software engineering but rapidly other areas of application were found, such as aeronautic, production management, etc.

SADT is a standard tool used in designing computer integrated manufacturing systems, including flexible manufacturing systems [8]. Although SADT does not need any specific supporting tools, several computer programs implementing SADT methodology have been developed. One of them is Design: IDEF, which implements IDEF0 method. SADT: IDEF0 represents activity oriented modelling approach (See Figure 2).

IDEF0 representation of a manufacturing system consists of an ordered set of boxes representing activities performed by the system. The activity may be a decision-making, information conversion, or material conversion activity. The inputs are those items which are transformed by the activity; the output is the result of the activity. The conditions and rules describing the manner in which the activity is performed are represented by control arrows. The

mechanism represents resources (machines, computers, operators, etc.) used when performing the activity.

The boxes called ICOM's input-control-output-mechanisms are hierarchically decomposed. At the top of the hierarchy, the overall purpose of the system is shown, which is then decomposed into components-subactivities [15]. The decomposition process continues until there is sufficient detail to serve the purpose of the model builder. SADT: IDEF0 models ensure consistency of the overall modelled system at each level of the decomposition. Unfortunately, they are static, i.e. they exclusively represent system activities and their interrelationships, but they do not show directly logical and time dependencies between them. SADT defines an activation as the way a function operates when it is 'triggered' by the arrival of some of its controls and inputs to generate some of its outputs. Thus, for any particular activation, not all possible controls and inputs are used and not all possible outputs are produced. Activation rules are made up of a box number, a unique activation identifier, preconditions and postconditions.

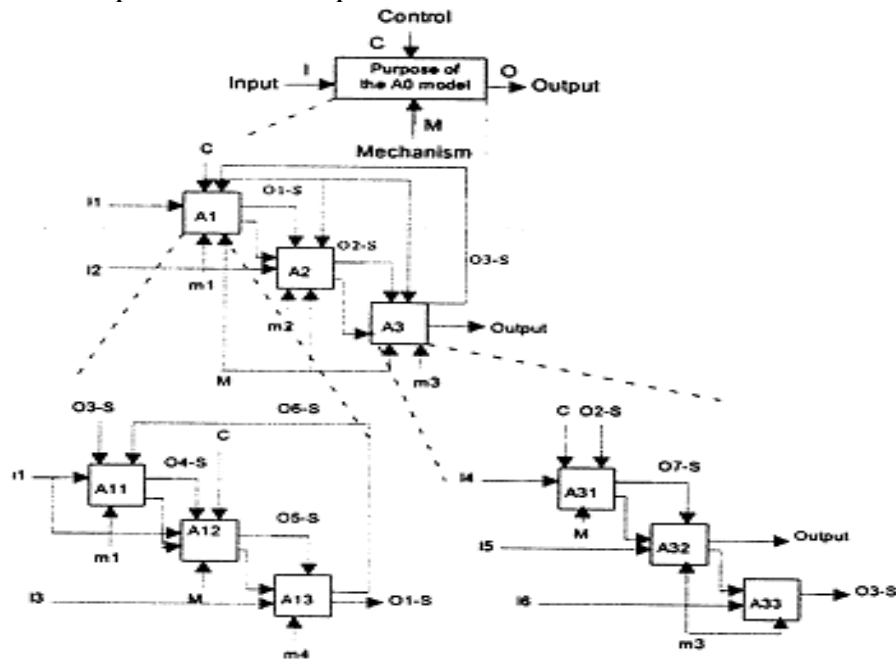


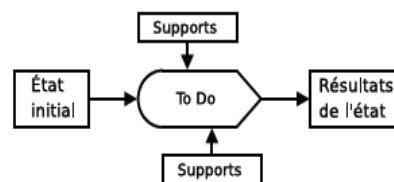
Figure 2- Top-down, modular and hierarchical decomposition of SADT method

3.2 GRAI method

Developed by the laboratory for automation and production at the university of Bordeaux-France since 1970's [9]. Before developing the GRAI method, some existing works had been reviewed, notably SADT method. It was found that the decisional aspects were not very well taken into account in these methods. So, it was important for the GRAI method particularly to deal with the decisional aspects of manufacturing systems. Based on the GRAI models, two formalisms were developed to model the macro decision structure and the micro decision center; the GRAI grid and the GRAI nets. A structured approach was defined to show how to apply the method (See Figure 3).

		Fonction j	
Horizon i		CD ij	
Période i			

Grille GRAI



Réseau GRAI

Figure 3- Formalism of the GRAI method

Another work performed at the GRAI laboratory was the extension of the GRAI method to GRAI-GIM (GRAI Integrated Methodology) [10].

GIM is composed of the following elements:

- ❖ GRAI conceptual model: a representation of basic concepts of a manufacturing system decomposed into three sub-systems: physical system, decision and information system.

- ❖ GIM modeling framework (RA) with three dimensions: views, life cycle, and abstraction level.
- ❖ GIM structured approach: guide to show how to perform analysis and design of the manufacturing system in three main phases: analysis, user-oriented design, and technical-oriented design.
- ❖ GIM modeling formalisms (languages): GRAI grid and GRAI nets for decision system modeling, IDEF0 and stock/resource for physical system modeling, ER for information system modeling, IDEF0 for functional system modeling.

The GRAI model is a reference through which various elements of real world can be identified. The macro conceptual model is used to express one's perception and ideas on the manufacturing system which is decomposed into a decision subsystem, an information subsystem and a physical subsystem. Particularly within the decision subsystem one finds a hierarchical decision structure composed of decision centres. Decision centres are connected by a decision frame (objectives, variables, constraints and criteria for decision making). The operating system is an interface between the decision system and the physical system. The micro conceptual model is used to represent the internal elements and structure of the decision centre.

GRAI-GIM contains a user-oriented method and a technically-oriented one. The user-oriented method transforms user requirements into user specification in terms of function, information, decisions and resources. The technically-oriented method transforms the user specification into technical specifications in terms of information and manufacturing technology components and the organization. The technical specification must allow the implementer to choose (buy, commission, or develop) all the components needed to implement the system. A computerized support tool known as CAGIM (Computer Aided GIM) is being developed at the GRAI Laboratory within the framework of the IMPACS project on Unix systems with X-Windows, to support the GRAI-GIM method.

4. METHODOLOGICAL INTEGRATION OF THE TWO METHODS

In order to establish a global approach for the restructuring of the enterprise (See Figure 4), it's necessary to proceed first of all to the instruction of the situation with the decision-makers according to a Brainstorming gait; thereafter, we exploit an analysis of the existing led by a support committees constituted to this effect. This analysis will be driven according to a participative gait while associating the various structures of an enterprise and while adopting an environment of Quality. It is necessary to organize different production workshops. These workshops are organized implying very well collectively all concerned by the various functions assigned in enterprise, either of a manner dedicated to a specific function.

1st stage: Functional model

The modeling oriented functions consist in describing processes of the enterprise. They must be capable to show interactions between these processes and to proceed to a decomposition of functions or activities.

In the first stage, we proceed to the functional modelling of the organisation that is not other than the exam of the situation of the enterprise in order to better understand its working. This stage enables us to decompose the system of the enterprise in a hierarchical manner in order to lead it in to elementary situations.

The first type of workshops enables to first of all to identify basis functions of an enterprise; it also enables to identify participants to the dedicated workshops and to establish a first work planning. Thereafter, it is during these workshops that various validations and various adjustments will be made and this thanks to the phenomenon of synergism of group and complementarities of functions.

The dedicated workshops enable to exploit the appraisal of People Resources to describe by a logical and hierarchical manner the various activities of every function. We exploit the formalism of SADT method which represent a general method that tries to encourage the communication between claimants and users, on the one hand, inventors and producers, on the other hand.

2nd stage: Informational model

The architecture of information is composed not only of a combination of structures fixed but also of objects that have some short life cycles.

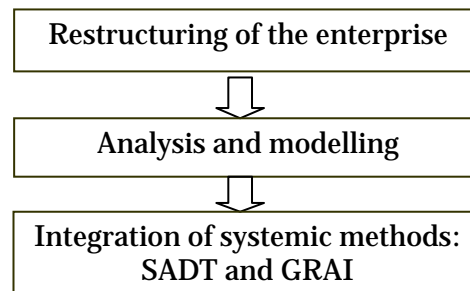


Figure 4- Systemic analysis of System Organisation

Methods of modelling are destined to model the information system of the enterprise. They permit to assure the circulation of information in the enterprise concerning processes, functions, resources, the organization...

Once functions and activities of every function have been identified, the following stage of the methodology proposed consists in analyzing the informational environment of these activities using the SADT method.

The performances of a system as complex it depends especially on the performance of its information system. This is why the development of the information system of the enterprise and the efficiency of its exploitability is important. It enables to adapt constraints of measure and collection of information to those of treatment and exploitation.

The modelling of the information system of the enterprise offers the tools of analysis and help to the decision making. These elements contribute to illuminate the decision or merely to encourage the consistency between the evolution of the process, objectives and the system of values to the service of which one is placed.

3rd stage: Decisional model

This stage aims the detailed description of decisions to take in a very definite time horizon and according to activities. In fact, the decision is about an interfacing between the strategy and the operation in the enterprise.

We propose to use the GRAI method. In fact, the GRAI modelling is the only existing modelling that proposes a representation of decisional structure of the enterprise. This representation is important to detect incoherencies in the coordination and the synchronization of decision makings and in the dynamics of evolution of the enterprise. Then, we propose to adopt the three element of this approach: models of reference, formalisms of modelling and structured approaches.

5. CONCLUSION

The process of modelling of the enterprise is a methodological gait well structured aiming the representation of an enterprise while developing models or languages of modelling and with contribution of all actors of the enterprise to arrive to a well identified finality.

A proposal of the integration of two systemic methods SADT and GRAI is presented in this paper in order to contribute to the restructuring of the enterprise. This approach is developed according to three essential stages: functional model, informational model and decisional model of the organisation system of the enterprise.

REFERENCES

- [1.] Melese J., (1990) « Approches systémiques des organisations », Editions d'organisation, p. 43, Paris, France.
- [2.] Landry M., Banville C., (2000) « Caractéristiques et balises d'évaluation de la recherche systémique », *Revue Tunisienne des Sciences de Gestion*, vol.2, N°1.
- [3.] Larvet P., (1994) « Analyse des systèmes : de l'approche fonctionnelle à l'approche objet », InterEditions, Paris.
- [4.] Sticklen J., William E., (1991) « Functional Reasoning and Functional Modelling », *IEEE Expert: Intelligent Systems and Their Applications*, p. 20-21.
- [5.] Vautier J.F., (1999) « Méthodes systémiques appliquées aux facteurs humains », *Techniques de l'ingénieur, traité Génie industriel*.
- [6.] Lakhoua M.N, (2008) « Analyse systémique d'un environnement de production en vue d'implanter un système d'information : étude de cas d'un silo de stockage des céréales », Thèse, ENIT, Tunisie.
- [7.] Jaulent P., (1989) « SADT un langage pour communiquer », IGL Technology, Eyrolles, Paris.
- [8.] Jaulent P., (1992), « Génie logiciel les méthodes : SADT, SA, E-A, SA-RT... », Armand Colin, Paris, France.
- [9.] Roboam M. (1993), La méthode GRAI. Principes, outils, démarche et pratique, Teknea.
- [10.] Doumeings G. (1984), La méthode GRAI, Thèse d'Etat, Université de Bordeaux I.
- [11.] R.M. Roth, W.C.I. Wood (1990) A Delphi approach to acquiring knowledge from single and multiple experts, in: Proceedings of the 1990 ACM SIGBDP Conference on Trends and Directions in Expert Systems.

- [12.] M. Parent, R.B. Gallupe, W.D. Salisbury and J.M. Handelman (2000), Knowledge creation in focus groups: can group technologies help? *Information & Management* 38 (1), pp. 47–58.
- [13.] H.K. Jain, M.R. Tanniru and B. Fazlollahi (1991), MCDM approach for generating and evaluating alternatives in requirement analysis, *Information Systems Research* 2 (3), pp. 223–239.
- [14.] A.C. Stylianou, R.L. Kumar and M.J. Khouja (1997), A Total Quality Management-based systems development process, *The DataBase for Advances in Information Systems* 28 (3), pp. 59–71.
- [15.] K. Schoman, D.T. Ross (1977), Structured analysis for requirements definition, *IEEE Transaction on Software Engineering* 3 (1), pp. 6–15.
- [16.] LFA (1999), *Handbook for objectives-oriented planning*. Norad. Fourth edition.
- [17.] Vernadat, F. (1996). *Entreprise modeling and integration*. England: T.J Press Ltd, Padstow.
- [18.] A.Errasti, (2008). Engineer to order supply chain improvement based on the GRAI meta-model. *Entreprise interoperability III*. London. pp. 524-531.
- [19.] Talbi I A., (2002). Analyse de l'entreprise dans une démarche d'intégration. *Journal Européen des Systèmes Automatisés*, 33.
- [20.] Andrew P. Sage, W. B. (2009). *Handbook of system engineering and management*. USA.





¹ M.N. LAKHOUA

USING METHODS AND APPROACHES IN IS PLANNING AND REQUIREMENTS ANALYSIS

¹ ISSAT DE MATEUR, ROUTE DE TABARKA, MATEUR 7030, TUNISIA
LABORATORY OF ANALYSIS AND COMMAND OF SYSTEMS, ENIT, TUNISIA

ABSTRACT:

After a presentation of different methods and approaches used to enhance participation in Information System (IS) planning and requirements analysis, we present the Logical Framework Approach (LFA) also referred to as Objectives Oriented Project Planning (OOPP) and how to refine it into TeamUP. In fact, the OOPP method constitutes a tool of a global systemic modelling enabling to analysis a complex situation by a hierarchically decomposition until reaching an elementary level allowing an operational planning. Some applications of the OOPP method in Tunisia are presented.

KEYWORDS:

Strategic Planning, OOPP method, Problem tree, Objective tree

1. INTRODUCTION

The purpose of this paper is to introduce the different methods and approaches used to enhance participation in Information System (IS) planning and requirements analysis. We review some methods and approaches here because we think them to be fairly representative of the general kinds of methods and approaches in use. The methods include Delphi, focus groups, Structured Analysis Design Technique (SADT), multiple criteria decision-making (MCDM), and total quality management (TQM) and the approaches include Future Search, Open space, SWOT (Strengths, Weaknesses, Opportunities and Threats) and ZOPP/OOPP/LFA. These different approaches are in use to define the strategic objectives.

The objective of the Delphi method [1] is to acquire and aggregate knowledge from multiple experts so that participants can find a consensus solution to a problem.

A second distinct method is focus groups (or focused group interviews) [2]. This method relies on team or group dynamics to generate as many ideas as possible. Focus groups been used for decades by marketing researchers to understand customer product preferences

MCDM [3] views requirements gathering and analysis as a problem requiring individual interviews. Analysts using MCDM focus primarily on analysis of the collected data to reveal users' requirements, rather than on resolving or negotiating ambiguities. The objective is to find an optimal solution for the problem of conflicting values and objectives, where the problem is modeled as a set of quantitative values requiring optimization.

TQM is a way to include the customer in development process, to improve product quality. In a TQM project, data gathering for customers needs, i.e., requirements elicitation may be done with QFD [4].

The SADT method [5] represent attempts to apply the concept of focus groups specifically to information systems planning, eliciting data from groups of stakeholders or organizational teams. They are characterized by their use of predetermined roles for group/team members and the use of graphically structured diagrams. SADT enables capturing of a proposed system's functions and data flows among the functions.

The approaches of strategic planning have some principles in common: a belief that the future can be changed and is not pre-destined and a belief that the whole system, which is all significant stakeholders, should be involved in the process of defining the desired future.

The approaches differ in several ways and each has its strengths and weaknesses. For example, the focus on present problems and problem analysis found in the LFA (Logical Framework Approach) [6] can lead to groups getting bogged down in the negative feelings of persistent problems or in trying to apportion blame for the problems to a particular part of the organization. This is often not conducive to resolving the situation. However, there are occasions where it is vital to identify the cause of a problem if a cure for that problem is to be found.

In practice, combinations of these approaches may be used. For example, the initial step might be a future search conference to define the strategic objectives. The second step might be to use part of the LFA approach to examine alternative strategies to achieve those objectives and to produce the detailed plans and to test their validity.

Future search is a structured planning meeting that makes possible actions once thought beyond reach in large, diverse groups. These include projects and programs based on new forms of cooperation devised by participants. This approach is popular in non-business communities. In future search the emphasis is to “leap forward” in time to identify the desired future condition and work back to find ways to reach that situation.

Open space was a precursor to future search. It is far less structured than most other methods. There is no preset agenda other than the topic previously agreed to and the time allotted to the meeting. There are no planned panel discussions and no plenary sessions. The agenda is created through the facilitator inviting everyone present to nominate issues that he or she feels strongly about and is prepared to take responsibility for.

The approach SWOT is popular in business environments. It seeks to identify what the organization is currently doing well (Strengths), what it is not doing well (Weaknesses), what market conditions can be exploited to advantage (Opportunities) and what factors, internal and external can derail the organization’s efforts (Threats).

This paper can be loosely divided into three parts. First, we present the strategic planning, and we present the issues involved in defining the strategic objectives. In order to deal with these issues, we present the case study of the Logical Framework Approach (LFA). The last section concludes the article, presenting likely some attempts to refine the LFA approach.

2. PRESENTATION OF STRATEGIC PLANNING

Strategic, or long term planning, is an attempt to shape the future. This implies that some vision of the desired future has to be formulated. Strategic planning therefore starts by seeking to define this vision [6]. The current approach to strategic planning assumes that it will be a collaborative process, rather than one person deciding what the vision and goals should be. The strategic plan will define a small number, usually less than ten, of strategic objectives, which, if they are met will result in achieving the goal of the group or organization.

Organizations plan strategically with a number of expectations for example:

- ❖ To increase their probability of survival.
- ❖ To improve their competitive position.
- ❖ To increase their market share.
- ❖ To plan mergers and acquisitions.
- ❖ To help the organization better manage the effects of external forces.
- ❖ To motivate key people within the organization.
- ❖ To plan a quantum leap to a new phase of company growth.
- ❖ To plan for renewal and to consider to a new direction for the organization.

The planning process is the sequence of steps the group go through to produce the plan [7].
For example:

- ❖ Articulate the core values of the planning group.
- ❖ Develop a mission statement.
- ❖ Develop a vision statement.
- ❖ Determine the strategic objectives.
- ❖ Define the main activities and responsibilities.
- ❖ Disseminate and implement the plan.
- ❖ Monitor results and amend the plan as required.

The essential features of a process are:

- ❖ There are several steps; each step will involve a number of activities.
- ❖ All steps must be executed.
- ❖ The steps must be executed in the correct order.
- ❖ If the order is incorrect, or if any step is compromised, all following steps of the process will be compromised.

3. LOGICAL FRAMEWORK APPROACH (LFA)

The Logical Framework Approach (LFA), also referred to as Objectives Oriented Project Planning (OOPP) and in German as Ziel Orientierte Projek Planung (ZOPP) [8][9][10] is a structured meeting process. This approach seeks to identify the major current problems using cause-effect analysis and search for the best strategy to alleviate those identified problems.

The two terms Logical Framework (Logframe) and the LFA are sometimes confused. The LogFrame is a document; the LFA is a project design methodology.

The logical framework document is a 4 column by 4 row matrix. The cells of the matrix contain text that succinctly describes the most important features of a project. If the correct process was used to develop the content of the logframe, the document will reveal the quality of the design and make flaws readily apparent.

We might note that one common misuse of the logframe is to design the project first and attempt to “fill in” the logical framework matrix as an after thought. This defeats the whole purpose of the logical framework and the design methodology.

There is a logical connection between the cells of the matrix. The logic that connects the cells in the left most columns is referred to as the vertical logic; the logic that connects the remaining three columns is referred to as the horizontal logic. The vertical logic is the hierarchy of objectives of the project. The horizontal logic is rather more involved. For a given level of objective (equivalent to a horizontal row of cells) the horizontal logic describes:

- How the achievement of the objective will be measured or verified.
- How this information will be obtained.
- What are the external factors that could prevent the project manager and staff from achieving the next level objective?

3.1. Design methodology of LFA

The design methodology of LFA is a rigorous process, which if used as intended by the creators will impose a logical discipline on the project design team [11]. If the process is used with integrity the result will be a high quality project design. The method is not without its limitations, but most of these can be avoided with careful use of ancillary techniques. Many things can go wrong in the implementation phase of a project, but if the design is flawed, implementation starts with a severe handicap.

The first few steps of LFA are [12][13]: situation analysis; stakeholder analysis; problems analysis.

The document of “**Situation Analysis**” describes the situation surrounding the problem. The source could be a feasibility study, a pre-appraisal report, or be a compilation done specifically for the project design workshop. Typically, the document describes the problem situation in detail, identifies the stakeholders and describes the effects of the problems on them.

The stage of “**Stakeholder or Participation Analysis**” is an analysis of the people, groups, or organizations that may influence or be influenced by the problem or a potential solution to the problem. This is the first step to understanding the problem. We might say, without people or interest groups there would be no problem. So to understand the problem, we must first understand the stakeholders. The objectives of this step are to reveal and discuss the interest and expectations of persons and groups that are important to the success of the project.

If there is no agreement between participants on the statement of the problem, it is unlikely there will be agreement on the solution. This stage of “**Problem Analysis**” therefore seeks to get consensus on the detailed aspects of the problem [8]. The first procedure in problem analysis is brainstorming. All participants are invited to write their problem ideas on small cards. The participants may write as many cards as they wish. The participants group the cards or look for cause-effect relationship between the themes on the cards by arranging the cards to form a problem tree (Fig.1).

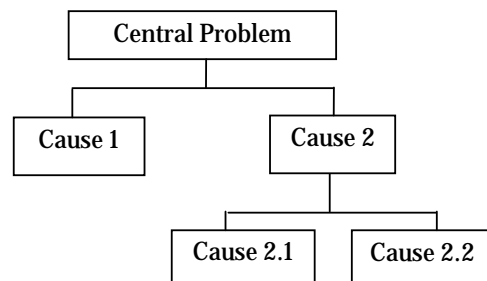


Fig. 1 - Problem tree

In the step of “**Objectives Analysis**” the problem statements are converted into objective statements and if possible into an objective tree (Fig.2). Just as the problem tree shows cause-effect relationships, the objective tree shows means-end relationships [14] [15]. The means-end relationships show the means by which the project can achieve the desired ends or future desirable conditions. Frequently there are many possible areas that could be the focus of an “intervention” or development project. The next step addresses those choices.

The objective tree usually shows the large number of possible strategies or means-end links that could contribute to a solution to the problem. Since there will be a limit to the resources that can be applied to the project, it is necessary for the participants to examine these alternatives and select the most promising strategy. This step is called “**Alternatives Analysis**”. After selection of the decision criteria, these are applied in order to select one or more means-end chains to become the set of objectives that will form the project strategy.

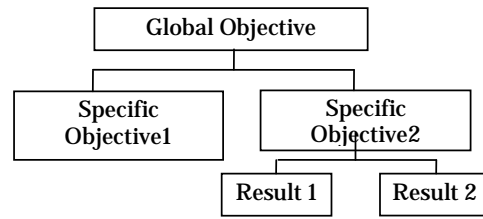


Fig.2- Objective tree

After defining the objectives and specifying how they will be measured (OVIs) and where and how that information will be found (MOVs) we get to the detailed planning phase: “**Activities Planning**”. We determine what activities are required to achieve each objective. It is tempting to say; always start at the situation analysis stage, and from there determine who are the stakeholders.

3.2. Logical framework document

The Logical Framework as a document (Tab.1) is deceptively simple. There are 16 cells in a 4 column by 4 row matrix. To provide the text in the cells of the logframe (sometimes called the project matrix) the project designers are asked to address and answer a number of questions which, on the surface seem self evident. However, articulating the answers to these apparently self evident questions exposes many unstated assumptions and hypotheses.

Tab.1- Logical framework document

Narrative Summary	OVI	MOV	External Factors (Assumptions)
Development Objective			
Immediate Objective			
Outputs (Results)			
Activities	Inputs		

The process of examining these unstated beliefs should cause them to be questioned more closely during the design of the project.

This examination often reveals that the assumptions and hypotheses are often questionable. If we test these assumptions and hypotheses and return the results of our work to the project design, we should produce a higher quality design [16][17].

The term Narrative Summary used to describe the text that “narrates” the objectives. It could have been given the title “Hierarchy of Objectives”, but this might be misleading because the bottom cell in the column is a summary of the activities.

The Objectively Verifiable Indicators (OVIs) are the measures, direct or indirect that will verify to what extent the objectives have been fulfilled. The term “objectively” implies that if these should be specified in a way that is independent of possible bias of the observer.

The Means of Verification (MOVs) are statements that specify source of the information for the measurements or verification specified in the indicators column. For example, will statistics from an external source be used for the verification or will project resources be used to gather the statistics.

The External Factors (Assumptions) are important events, conditions, or decisions which are necessarily outside the control of the project, but which must remain favorable for the project objective to be attained. The implication here is the design team has an obligation to consider what might derail their efforts and to plan responsibly to reduce that risk of “derailment”.

The Development Objective is the higher level objective that the project is expected to contribute to. The addition of the word “contribute” implies that this project alone is not expected to achieve the development objective. Other project’s immediate objectives are expected to also contribute.

The Immediate Objective is the effect which is expected to be achieved as the result of the project delivering the planned outputs. There is a tendency for this to be expressed in terms of the “change in behavior” of a group, or institution and the project outputs are expected to facilitate this change.

The Outputs are the “deliverables” the tangible results that the project management team should be able to guarantee delivering. The objective statements should specify the group or organization that will benefit. Outputs are delivered, usually on a certain date or dates.

The Activities have to be undertaken by the project to produce the outputs. The activities take time to perform. The Inputs are the resources that the project “consumes” in the course of undertaking the activities. Typically they will be human resources, money, materials, equipment, and time.

The “Vertical Logic” is the reasoning which connects the three levels of objectives in the matrix; the outputs, the purpose, and the goal. For example achievement of all the output level objectives should lead to achieving the purpose. Each of these links between the objectives is connected by hypotheses.

The “Horizontal Logic” has similar features to the vertical logic. In this case, the links between the levels of objectives are the items in the External Factors column. For example, if the project is successful in implementing all of the planned activities, we ask ourselves, what circumstances or decisions (outside the project's control) could prevent the delivery of the project outputs.

4. REFINING THE LFA INTO TEAMUP

The LFA approach has become the standard for International development project design. Team Technologies expert staff assisted in the original method development and has continued to refine the approach into TeamUP: the team-based Logical Framework method. In fact, Team Technologies has worked with numerous international aid organizations to implement its Project Cycle Management method organization-wide based upon the LFA.

TeamUP developed in the late 1980s by the World Bank's World Bank Institute and Team Technologies, uses the basic ZOPP method and then expands it. TeamUP assumes that the past and future are two different sources on which to draw when designing and implementing project related events [18].

ZOPP, mainly concerned with anticipating and avoiding problem situations, looks to the past to understand the present. TeamUP, concerned with problems and opportunities, looks to the past and the future to understand the possibilities that offer themselves to the present. Furthermore, TeamUP adds depth to basic problem identification and design features by encouraging teams to anticipate implementation arrangements and inform the quality of their designs with these realities.

TeamUP's twelve steps are arranged so that earlier steps help a team build identity and later steps help them take action [19][20]. These twelve basic steps are: Opening round; Clarify representation ; Set norms; Identify client; Review history; Define mission; Define deliverables and assumptions; Clarify work plan; Define roles and responsibilities; Define learning system; Establish budget; Implement and improve.

The latest software from Team Technologies, integrates the most popular, proven set of tools for international development planning and implementation into an easy-to-use, windows based software application supporting program portfolios and their associated project. The modules of the software include Program and Project Information, Stakeholder Analysis, Trees Analysis, Program and Project Structure, Conflict Analysis, Logical Framework, Schedule, Performance Tracker, Performance Budget.

5. USING THE OOPP METHOD IN TUNISIA

The OOPP method, widely used in the planning of complex projects, involves many operators and partners. In Tunisia, The OOPP method was used in Development projects financed by bilateral or multilateral co-operation mechanism (with Germany, Belgium, Canada, World bank,...), in upgrading different structures (Training and Employment through MANFORME project, Organization of the Tunis Mediterranean Games 2001,...) and in restructuring private and public enterprises.

An effort has been provided in order to bring improvements to this method [21]. This is how the OOPP method has been spread and a new MISDIP denomination (Method of Specification, Development and Implementation of Project) was adopted. The MISDIP method adopts the OOPP analysis and the complete it to specify the system of organization, to specify the system of information, and to contribute to its development and implementation.

In order to specify this information, information matrix (Fig.3) associated to OOPP analysis was defined enabling the determining of the relations between the activities or between the concerned structures identify the information sources, determine the manner in which the information is exploited [21].

In addition of the information matrix of the new MISDIP method as well as the different tools developed, the development of the organization chart constitutes an essential stage. Indeed, variants of the organization chart are elaborated according to the strategy of the enterprise while taking account of the hierarchy of entities and the balancing of stations according to their complexity. These variants constitute a tool the decision making.

N°	Code	Activity	If ₁	If ₂	If ₃	If ₄	If ₅	If ₆	If ₇	If ₈	If _n
1		A ₁	0	0	1	1					
2		A ₂		0	0		1	0			
3		A ₃	1	0	0	0		0	0	1	
4		A _n									

Fig.3. Information matrix associated to the OOPP analysis

6. CONCLUSION

In this paper, we presented different methods and approaches used to enhance participation in IS planning and requirements analysis and the different approaches in use to define the strategic objectives. Many attempts are presented in order to refine the LFA approach. The methods LFA and TeamUP are described and commented and some applications of the OOPP method in Tunisia are presented.

REFERENCES

- [1.] R.M. Roth, W.C.I. Wood and A Delphi approach to acquiring knowledge from single and multiple experts, in: Proceedings of the 1990 ACM SIGBDP Conference on Trends and Directions in Expert Systems, 1990.
- [2.] M. Parent, R.B. Gallupe, W.D. Salisbury and J.M. Handelman, Knowledge creation in focus groups. *Information & Management* 38 (1), 2000, pp. 47–58.
- [3.] H.K. Jain, M.R. Tanniru and B. Fazlollahi, MCDM approach for generating and evaluating alternatives in requirement analysis, *Information Systems Research* 2 (3), 1991, pp. 223–239.
- [4.] A.C. Stylianou, R.L. Kumar and M.J. Khouja, A Total Quality Management-based systems development process, *The DataBase for Advances in Information Systems* 28 (3), 1997, pp. 59–71.
- [5.] K. Schoman, D.T. Ross, Structured analysis for requirements definition, *IEEE Transaction on Software Engineering* 3 (1), 1977, pp. 6–15.
- [6.] Cracknell, B. Evaluating the Effectiveness of the Logical Framework System in Practice, *Project Appraisal*, 1989.
- [7.] Kensing F., Simonsen J, "Participatory design: issues and concerns. Computer Supported Cooperative Work", *The Journal of Collaborative Computing*, 7 (3/4), p.243-271, 1998.
- [8.] McLean D., Logical Framework in Research Planning and Evaluation, International Service of National Agricultural Research Working, Washington, 1988.
- [9.] GTZ, ZOPP: an Introduction to the Method, Eschborn, Germany 1988.
- [10.] GTZ, Methods and Instruments for Project Planning and Implementation, Eschborn, Germany 1991.
- [11.] Administration Générale de la Coopération au Développement, Manuel pour l'application de la «Planification des Interventions Par Objectifs (PIPO)», 2ème Edition, Bruxelles 1991.
- [12.] Walter EM., Introduction à la méthode de Planification des Projets par Objectifs, Rapport de l'atelier de formation REFA, Maroc 1998.
- [13.] Killich S., TeamUp, a software-technical support-tool, businesses of the future, Aachen, 2002.
- [14.] Killich S., Luczak H., Support of Interorganizational Cooperation via TeamUp at Internet-Based Tool for Work Groups, Work With Display Units, Proceedings of the 6th internationally Scientific Conference, Berchtesgaden, May 22-25, Berlin 2002.
- [15.] Killich, S., Fahrenkrug C., Intercompany Cooperations smaller and middle Businesses in the automobile-supply-industry, VDI-Verlag, Düsseldorf 2002.
- [16.] Luczak H., Nölle T., Kabel D., "Benchmark of team-performance in the Product development: use a model-was based tool", *Ergonomia*, Stuttgart 2003.
- [17.] Weissenbach, M., Killich S., TeamUp: An Internet based tool to the support cooperation, VDI-Verlag, Düsseldorf, 2002.
- [18.] Team Technologies, LogFrame R&D Software and User Manual, Virginia, 1991.
- [19.] P. Gu and Y. Zhang, OOPPS: an object-oriented process planning system, *Computers & Industrial Engineering*, Volume 26, Issue 4, October 1994, Pages 709-731.
- [20.] Peffers K. and Ture Tunanen T, Planning for IS applications: a practical, information theoretical method and case study in mobile financial services, *Information & Management*, Volume 42, Issue 3, March 2005, pp 483-501.
- [21.] Annabi M., PIPO étendue : Méthode Intégrée de Spécification, de Développement et d'Implémentation de Projet (MISDIP), STA 2003, Sousse, 21-23 déc. 2003.





¹ Zoltán BÁTORI, ² Tamás HARTVÁNYI

DEVELOPMENT OF FORECASTING SYSTEMS

¹⁻² ÓBUDA UNIVERSITY, KELETI KÁROLY FACULTY OF BUSINESS AND MANAGEMENT,
INSTITUTE OF ENTERPRISE MANAGEMENT, HUNGARY

ABSTRACT:

In this paper we demonstrate a detailed overview of the history of forecasting software applications over the past decades, concentrating especially on the interaction between hardware and software. Additionally we present a framework by describing important developments of forecasting techniques in terms of hardware and software environments. We then focus on the application areas of forecasting software modules in business and planning environments which are often partially automated due to the large number of time series involved. Finally we make some suggestions about in which direction forecasting software should be improved.

KEYWORDS:

forecasting software applications, detailed overview

1. INTRODUCTION: THE HISTORY OF COMPUTER DEVELOPMENT AND FORECASTING METHODS

The history of forecasting and time series methods began in the 17th century when numbers of sunspots and price indices were analyzed by scientists. However, the practical use of statistical techniques has been made possible by the invention of computers in the 1950s.

At the beginning, the use of computers for forecasting was limited by inadequate processor speed, random access memory and disk space. In the 1960s, forecasting was capable to analyze short and isolated series, collected in flat files, and processed by batch runs using Hollerith cards on mainframes. In these days programming was mainly done in Assembler and FORTRAN under a variety of different and largely incompatible operating systems.

The introduction of OS/360 in 1967 as a scalable operating system for IBM mainframes resulted rapid migration between hardware platforms, simplifying the movement of programs. It was developed by IBM (Brooks, 1974) with the intention of creating programs that could be run on IBM computers of different sizes. Prior to the development of OS/360, operating systems were only designed for individual computer architectures. With the arrival of the system, software could finally be moved from one computer to another.

The appearance of UNIX in 1969 resulted in the development of portable software for smaller systems. The introduction of personal computers such as IBM PCs and Apple Macintoshes in the first years of the 1980s allowed the use of computers at everywhere, independent of mainframes.

Many advances in computer science had an influence on forecasting. The continuous increase of processor performance, memory and disk space allowed scientists to deal with larger data sets and more complex algorithms. Later cathode-ray terminals supported the design and use of interactive applications with their character user interfaces (CUI), screen reports, and graphs. This development occurred in the 1970s, when a lot of mainframe management information systems and manufacturing resource-planning systems appeared on the market. The next step to graphical user interfaces (GUI) in the 1980s changed the software environment, as allowed a much larger community to use forecasting software.

Application software also changed in the 1960s, when forecasting methods were individually programmed using either Assembler or FORTRAN. This allowed later the selective use of new techniques such as smoothing or complex techniques such as Box-Jenkins models. Several

statistical and econometric software systems were developed in the 1970s. In the meanwhile, material replenishment systems, which focused on inventories and production, were developed independently of the statistical forecasting tools. Later these became the roots of enterprise resource planning (ERP) and management information systems (MIS). This is important because this difference has never been closed entirely. Only in recent years have the data produced by ERP systems been used as input data into forecasting software.

Databases were developed simultaneously. At the beginning, data was collected manually and stored on punched cards, or transferred to text files on disks and tapes. While this remained the primary method of data input into statistical systems for a long years, transaction and planning data were migrated to database management systems (DBMS) quite quickly. The development process started from hierarchical and network databases in the 1970s to relational database systems in the 1980s, enhanced by object-oriented DBMS in the 1990s. The last two resulted in the object-relational database systems used these days. Within business planning, data processing was often replaced by PC-based spreadsheets, which were saved and modified on local PCs. This separation of local planning data and centralized transaction data still can be detected today, often resulting in problems of consistency and concurrency of the database. In a further step, the integration of database systems and transaction systems happened. With the constant increase of available data, databases moved on to data warehouses, offering also a wide range of tools for extraction (on-line analytical processing, OLAP), visualization, and analysis, including predictive data mining techniques.

2. DEVELOPMENT PERIODS OF FORECASTING SOFTWARE

While computer development was evolutionary, the development of forecasting software can be categorized into periods. These are:

- Period I.: Mainframe forecasting software
- Period II.: PC and workstation forecasting software
- Period III.: Process-oriented and highly integrative forecasting software

2.1. Period I.: Mainframe forecasting

Mainframe software, either in batch or timesharing mode, dominated forecasting software in Period I. However, some very popular programs took quite a while to offer even basic forecasting features. For example, SPSS surprisingly had no forecasting functionality until it added the „Trends” module in 1994. On the other hand, SAS/ETS was first released in 1980.

In industry, commercial firms devoted to forecasting for industrial clients did so with mainframe computing capabilities. The main packages offered were DAMSEL, TROLL, AUTOBJ, B34S, and TSP were available not only to industry but also to academical use.

Prior to this time, microcomputers had been the domain of computer programmers, primarily because of the lack of application software. The first popular spreadsheet package, Visicalc, turned the microcomputer into an effective business application. Lotus 1-2-3, released in 1982, offered the combination of spreadsheet, presentation graphics, and simple database functionality to for the PC. However, there was no forecasting in this field in Period I. There were two main reasons for this. First, the lack of solid compilers. Second, mainframe packages could not be moved directly to the PC, as the PC was still not powerful enough. Only some parts of the mainframe software could be used on a PC version, and even then it should have to be rewritten in BASIC instead of the original FORTRAN.

2.2. Period II.a: IBM PC and forecasting packages

By 1985, the succesful IBM PC and its clones had been around long enough that forecasting software was available. By 1989, more than one hundred software forecasting packages were available for the PC (Rycroft, 1994).

In this period, universities also began to move away from mainframes, setting up PC laboratories. For industrial companies, the situation was slightly different. Corporate IT departments, in order to controlling the mainframe, had long dictated computer use. Every single department could buy and use a PC, and they didn't need the IT department to approve the purchase or maintain the computer. For such departments, the PC had become effective enough to work in large scale forecasting, for example for production and inventory purposes.

However this decentralization generated new problems. Different organizational units might track the same data but maintain them differently, or use different numbers to represent the same facts. Therefore, the databases would also produce conflicting data, and different forecasts too. The PC was at this stage just a batch engine, it was capable of only to produce forecasts for large numbers of items, and then write these forecasts to a file. It was still not good enough to do this work interactively.

The wide spread of standalone PCs produced its own urgent need. These PCs might solve the problems of individual organizational units, but they did nothing to improve the flow of information between these units. The persons making the forecasts for production had no idea how many parts were in inventory. Solving this incompleteness would be up to Enterprise Resource Planning (ERP) systems.

2.3. Period II.b: modern PCs and forecasting software

The Intel 486 processor appeared in the market 1989, and the class of forecasting problems for which mainframes were necessary become much smaller. The capabilities of forecasting software had reached a stage where even persons with no technical training could benefit from methods that previously had required technical training and support. After this, given just a univariate time series, a program could determine which method best suited the data (for example exponential smoothing or ARIMA) and then optimize the parameters for the chosen model. The importance of this advance was that people could work out very good forecasts without consulting an expert. However for these forecasts to be good, they also needed reliable data. In this period, each department maintained its own database and each database had to be updated individually, so multiple databases could not be updated from the same source. Consequently, in these databases there were conflicting information and could not serve the entire organization. ERP vendors such as ORACLE, SAP and People- Soft realized the opportunity, connecting the disparate computers and databases via a client/server architecture. However, it required many years before this task was completed.

2.4. Period III.: PC and client/server architectures with forecast software

After ERP systems has been implemented, with all the data flowing back and forth, forecasts were completely missing from them and were often made with Excel 6, if at all (Sanders, Manrodt, 2002). Forecasting methodology has made great developments (Chatfield, 1996), but the pace at which these advances have been included into software were not fast enough. As far as industrial software is concerned, ERP vendors can't produce forecasting software. The solution was the integration of existing forecasting software with the ERP systems.

3. DEVELOPMENT OF FORECASTING SYSTEM FOR BUSINESS AND OPERATIONAL PLANNERS

3.1. Business and operational planning

Business planning repeated on a regular basis, often with the creation of a monthly sales plan. Accordingly, the sales plan is the basis for marketing plans, purchase and production decisions or investment planning. A sales plan differs from an operational plan in that it addresses a higher level of aggregation in terms of both time and product, and is expressed in revenues rather than volume. Business planning forecasts are usually worked out on a monthly, quarterly or annual basis for product groups (instead of products), brands, and different business units such as sales regions. The average forecasting horizon usually ranges from 1 to 5 years.

Production and logistic decisions are supported by an operational plan. The main aspects of these plans come from the company's supply chain:

- ❖ demand plan,
- ❖ inventory plan,
- ❖ transport or distribution plan,
- ❖ replenishment plan,
- ❖ production plan,
- ❖ maintenance plan, and
- ❖ collaborative plans.

For operational planning, forecasting programs are used to calculate future demand per stockkeeping-unit (SKU) on a daily, weekly or monthly basis. For example in energy planning, forecasts are required by the hour and at 15 minute intervals. In general, forecasts at the SKU-level needed for a large number of items, very often in the thousands, and these items are usually grouped into a product hierarchy, by distribution channels and by sales regions. When numerous items must be forecasted on a frequent regular basis, the uses of pre-defined or automatic forecasting techniques are critical. Forecasting systems must not only meet organizational requirements for accuracy but also for processing speed and robustness (Hartványi, Nagy, 2009).

The difference between business planning and operational planning depends on the way a firm organizes its planning processes. Ideally, a forecasting system should integrate both elements into a consistent set of plans. This is not easy for many companies today, where we find separation more often than integration. In operational planning, the forecast time interval is short and often not more than 6 weeks. These forecasts heavily affect decisions on the production levels per line, lot sizes, transportation schedules, and the purchasing of materials for particular time periods. In

business planning forecasting the number of time series is usually low, allowing individual inspection and modification by the planner. On the other hand, in operational planning the number of time series is huge, which severely limits the possibility of individual inspection and modification. So automatic procedures for forecast calculation are necessary.

Additionally, business planners are usually less experienced in forecasting techniques than in the functional areas of the business, such as marketing, finance and accounting. For operational planners it is the same, because they are often engineers or business administrators with a detailed knowledge of the logistical and technical processes, but with limited knowledge with forecasting methodologies.

3.2. Forecasting system for business and operational planners

Although forecasting libraries in FORTRAN and Assembler were used from the 1960s, but their use was very limited. Practically this meant that, sales plans were still set up on paper. Very slowly, larger companies began to implement these routines for business planning. However, these routines only provided forecasts, without any integration to other systems. To calculate forecasts, batch runs had to be programmed and intervention in the forecasting process itself (for example alteration of parameters) was not possible. While an analyst concentrating on forecasting a few series has enough time to try out different forecasting models to improve forecast accuracy, the time needed for an operational planner with a much larger number of series was too much. Therefore, they used only basic, standard models within the business forecasting process. As a result, forecasting accuracy was usually poor. It took a long period of time for companies to implement forecasting for business planning and even longer for operational planning.

In simple batch processing systems, the user could not interact with the software as it was described. This deficiency was remedied by the introduction of line-oriented terminals, which allowed the software to ask the user for his input during the different processing steps. For example, a seasonal decomposition could be calculated before deciding whether to apply seasonal or nonseasonal forecasting models.

With the appearance of character-based user interfaces the user could move the cursor all over the monitor, and enter instructions without following a prescribed sequence. This was the first time the planner could make technique selections by setting all parameters simultaneously on the same screen before starting the forecast calculation.

The first software products that allowed business planners to interact closely with the forecasting process appeared in the 1970s. These offered simple planning methods such as administration of time series, aggregation and disaggregation of series, planning screens, report generators, and functions to modify data and produce simple graphs.

Simultaneous progress was being available in data base programs (for example dBase) and spreadsheet systems. These, along with rapidly increasing hardware capabilities, offered major advances in forecasting software including parameter optimization (optimizing smoothing constants in exponential smoothing), multi-level forecasting for product and geographic hierarchies, data and forecast overrides, and so on.

Graphical elements, interfaces to databases, spreadsheets, external data sources, numerically and statistically robust methods, and simple automatic algorithms for the selection and specification of forecasting models were now common tools of business forecasting software. Not surprisingly, awareness of forecasting program tools grew rapidly, although the majority of companies at the end of the 20th century still used spreadsheets to develop sales plans.

Most recently, with the emergence of computing networks and intranets, participants in the forecasting process who were located at different sites could more readily collaborate with each other, particularly on sales plans. Collaborative forecasting capabilities were implemented into systems such as Demand Solutions, Futurmaster and Futurcast.

The difference between business planning and operational planning was now disappearing. Softwares such as Peer Planner and Logol could be used to calculate forecasts at the product level for operational planning, as well as at the product-group level for business planning. The emphasis in such softwares was not on the planning process but on the forecasting engine. However, the use of methodologically sophisticated forecasting softwares strongly linked to production scheduling, transport planning, inventory and purchasing was unknown in the past. After a long period of time the main obstacles were the missing interfaces between the forecasting and the production planning components.

The first commercial forecasting softwares, like IMPACT, were simply operational forecasting and replenishment systems, providing SKU forecasts. However, product-level forecasts were needed to support production scheduling and material replenishment. As a result, simple forecasting models were included in production planning systems, including BAAN, i2, Peoplesoft and SAP/ R3 (Fandel et. al., 1998). In comparison to the business forecasting softwares, these

operational systems (SAP/R3, mySAP) incorporated only simple methods such as trend curves, elements of exponential smoothing and tracking signals. Standard techniques, such as probability-based prediction intervals and out-of-sample evaluations, were not implemented. This difference was partially closed by the end of the 1990s. SAP for example developed an application called APO, where forecasting methods and sophisticated optimization routines augment the simpler functions included in SAP/R3. Still, sophisticated modeling such as the automatic Box–Jenkins systems as implemented in Autobox and SCA-Expert, as well as rule based forecasting (Collopy, Armstrong, 1993), have not developed into operational planning.

3.3. The future of forecasting systems for business and operational planners

The most business and operational planners focusing on similar data, mainly sales figures. Sales effects at both the product and group levels have common origins, such as seasonality, trading days, and promotions, so it would seem that the same forecasting methods could be applied. On the other hand, there are significant differences. While a business planner focuses on forecasting a small number of aggregated series and makes effort to provide detailed explanations and reporting, operational planners have to keep their attention across a large number of series and frequent forecast rounds. So the operational planner can intend much less time to the specific features of the data and the forecast models, and seeks to automate the forecast process as much as possible.

Future challenge is to integrate the business and operational planning components in one application. First of all DBMS interfaces are required, just as they are made by analysts. However, for rolling planning systems it is not so important to have many interfaces. Instead, a stable, solid and fast interface to the transaction database or online data warehouse needed. Obviously this technique is simplified (and cheaper) if little or no interface programming is required. The reliability and online synchronization of the forecasting database with the actual enterprise database are the most important factors here.

Additionally, in supply chains of consumer products bullwhip effects often occur, which can be described as an increase in variability as fluctuations move up the supply chain. This means that retailers directly detect the customer demand without much variation while inventory and reorder levels fluctuate considerably across their supply chain. An possible method to handling this problem is the introduction of collaborative planning and forecasting replenishment (CPFR) and vendor managed inventory (VMI) applications. Because these forecasting processes involve several organizations of the supply chain, the software must come with a standard interface by which data can be exchanged. Some companies have developed standards regulating the data exchange processes, as well as the data structures and contents. For example, a standard for exchanging information within the German consumer goods industry has been worked out by the Centrale für Coorganisation (CCG, 2002). Standardization of supply chain management processes is also began, according to the Supply Chain Council (2004), which developed the „Supply Chain Operations Reference”. More and more SCM vendors follow this process architecture, so forecasting system vendors will also have to pay attention to it.

There is a special problem with truncated supply chains which quite common in practice. In the case of a surplus demand, most systems usually do not archive the actual demand but only the actual sales, so that only sales data can be used for forecasting. Consequently all forecasting techniques, with the exception of subjective approaches, generate biased forecasts which lag behind real demand. Another frequent problem which sometimes happens in practice is that sales data are archived on the day of invoicing which often does not fall on the day of shipment. Shipment being relevant for production and logistics scheduling. Such problems cannot be solved by methodological inventions but only by correct database structures. Nevertheless, application and database vendors should set up solutions to save this information jointly with the time series to be forecasted to allow more detailed analysis and to make the application suitable for future methodological enhancements.

Additionally, when implementing special effects like advertising and calendar events, modeling is still often on a case-specific base requiring user interaction, for example by setting up a distributed lag structure for the advertising effect. With the huge number of time series in planning, some of the techniques indicated above (pre-defined effect profiles and lag specifications) should be run automatically and over hierarchies. Manual modification must be limited to a small number, requiring the use of some kind of effect prorating or automatic modeling.

Error prone procedures can only be used if exceptions will be caught by trap mechanisms. Unfortunately there are still many softwares that are not able to detect and handle numerical errors (such as overflow and insufficient data) suitably. Furthermore there are still wellknown and widely sold softwares where the forecasting methodology is limited to a small number of trend curves and exponential smoothing methods.

While many methods usually work satisfactorily for some longer series, especially on a monthly base for short time intervals, the increased application of high frequency data needs the incorporation of causal effects. Unfortunately, current softwares do not offer a well established but simple methodology. As a result, most planners are forced to limit their forecasting repertoire to techniques which do not take causal effects into account.

Forecasting systems has been designed as standalone applications focusing on model selection for obtaining accurate forecasts. The forecast software vendors invest little in the processing of the forecasts for important decisions such as those involved in inventory replenishment and production scheduling. Moreover, many of them do not offer interfaces to other information systems.

An important deficiency of planning systems is the lack of attention paid to the theoretical basis of modeling, and therefore to the measurement of uncertainty in the forecasts. Without measures of uncertainty, the forecasts are not directly useable to replenishment and scheduling decisions. If, for example, forecast error distributions were computed and passed on to ERP software, forecast uncertainty could be involved into the computing of lot sizes and replenishment levels and intervals.

It is expected that forecast method selection should not be based simply on forecast error metrics but also on the costs of forecast errors in terms of replenishment decisions (Gardner, 2004). For example, the frequency of out-of-stock occurrences resulting from a certain method should suggest the need to change to a different method, as should excessive inventory costs. The required feedback between the forecast and the decision is not resolved in planning softwares. The problem is aggravated by the concentration on point forecasts in optimization routines for production scheduling. Consequently they fail to provide the capabilities of modern forecasting methodologies to measure uncertainty.

In production systems, the number of out-of-stock situations are often tracked by key-performance indicators (KPI). Most KPI-systems do not include reliable indicators of forecast errors, the difference of forecasts from actual demand. While recording signals have been around since the 1960s, these metrics are more often found in planning system than in forecasting system. Sometimes statistical metrics can be found in systems with a primary focus on planning, but the majority of advanced planning systems only give non-statistical alerts. From a business point of view, out-of-stock percentages and excess stock are useful, but these statistics are hardly used for reporting forecast accuracy. For the last static and dynamic forecast simulations are suggested, but their availability in integrated planning and forecasting softwares is not common.

4. CONCLUSIONS

Only a few forecasting systems offer state-of-the-art functionality. Too many softwares rely on outdated techniques. Examples are non-optimized smoothing parameters, poor initialization in exponential smoothing, erroneous formulas for computing safety stocks, graphs with inefficient time scales, lack of capability for forecast adjustments, aggregation of individual item forecasts and prorating of aggregate forecasts, as well as erroneous prediction intervals. Forecasting vendors need to upgrade to incorporate more recent methods.

Many new techniques in forecasting are not included into forecasting software within a reasonable time. Software vendors usually have to wait to see which new methods stand the test of time, but these methods are tend toward the simpler ones. If a scientist wishes to apply a new method, he must duplicate the effort of the inventor, as he must rewrite code that already has been written once. This is not the right way for science to progress. By given the choice between programming a difficult method and a simple method, many researchers will choose the simple method, because it is easier. So these are the easily programmable methods that get used in applied journals.

Software vendors concentrate to new techniques face an additional obstacle. They discover that a new technique has become popular in the applied literature, and then try to write their own code for the proposed forecasting model. Often they must make educated guidance about the details of the algorithm that were publicated in the article. Moreover, testing new techniques is even more difficult than it should be because inventors of the methods were not required to create an archive of the data used. Sometimes it is impossible for the developer to decide that his version of the program gives the same answer as the inventor's published results.

So while hardware processes are much faster, software advances are lagging behind. In order to test a new method, the developers and researchers have to program the code from the start. In the age of the internet, there is no reason not to record the data and the code used as the basis for an article. Imagine how easy it would be for a researcher to compare two or three different techniques if he did not have to program each one from the beginning.

We believe that development in forecasting needs forecasting methodology to be closely linked to the available data and to the environment in which business decisions are made. We would require much closer integration between the information offered by forecasting and the use of this information in optimization and decision-making.

REFERENCES

- [1.] Brooks, P. (1974). The mythical man-month. Reading, Massachusetts Addison-Wesley
- [2.] CCG (2002). Der Weg zum erfolgreichen supply chain management. Köln Centrale für Coorganisation
- [3.] Chatfield, C. (1996). Forecasting in the 1990s. The Statistician
- [4.] Collopy, F., Armstrong, S. (1993). Rule-based forecasting: Development of an expert system approach to combining time series extrapolations. Management Science
- [5.] Fandel, G., Francois, P.(1998). PPS- und integrierte betriebliche Softwaresysteme. Grundlagen, Methoden, marktanalyse. Berlin, Springer
- [6.] Gardner, S. (2004). Exponential smoothing: The state of the art: Part II. Paper presented at the ISF 2004, San Antonio
- [7.] Hartványi, T., Nagy, V. (2009): In-sourcing Model for Food Storage and Forwarding. Acta Technica Jaurinensis, Series Logistica. Vol. 2. No. 3.
- [8.] Rycroft, S. (1994). Microcomputer software of interest to forecasters in comparative review, International Journal of Forecasting
- [9.] Sanders, R., Manrodt, B. (2002). Forecasting software in practice: Use, satisfaction, and performance. Interfaces
- [10.] Supply Chain Council (2004). Supply chain operations reference model (SCOR) 6.1. www.supply-chain.org







¹ Csaba TÁPLER

INVENTORY LEVEL REDUCTION BY INSERTING UNPACKING STATIONS IN PRODUCTION SUPPLY PROCESS

¹ FACULTY OF LOGISTICS AND FORWARDING, SZÉCHENYI ISTVÁN UNIVERSITY, GYŐR, HUNGARY

ABSTRACT:

This paper deals with questions of production supply of assembly plants. It is a general aim to resolve the trade-off between production supply service level and engrossed component stock level in production. On the one hand by pumping components to production in larger portions supply processes become simpler and quicker. On the other hand large portions cause high level of component stock. By inserting unpacking stations between warehouse and production lines, optimal system can be achieved. With the help of computer simulation software a model a single-stage kanban controlled production supply system was modeled where production lines receive components directly from warehouse. After that we simulated the effects of establishing unpacking stations that distribute components for production lines and determined the inventory level reduction.

KEYWORDS:

Production, inventory level, unpacking station, simulation

1. INTRODUCTION

New trends of manufacturing systems concentrating fully on perfect customer fulfillment (e.g.: MCM - Mass Customized Production) emerged in the previous decades. Manufacturers are facing with the problem that mass production should be run according to diverse claims. Because of diversity large lots are split into smaller ones which results in set up time increase; which of course results in decrease of production capacity and increase of costs. In order to find optimal solution of these kinds of trade-offs several methods, philosophies exist. In this paper we deal with a narrow problem which is a decrease factor of production costs that affect the mentioned trade-off at kanban system supplied manufacturers. The size of packaging units delivered from warehouse to production firmly influences inventory level and cost. In order to minimize this inventory level by unpacking packaging units into smaller ones may be one possibility. During our research we used logistic simulation software to validate the assumptions.

2. REVIEW OF KANBAN PRODUCTION SUPPLY SYSTEMS

Kanban originates from the Japan word “card”. Several researches were made in this topic Junior and Filho gives a broad overview of kanban features [9].

In production systems cards, empty boxes or digital signals indicates the consumption of production processes. Kanbans usually contain part number, lot number, part description, location, destination, quantity, lot quantity, and other additional information.

Reaching a pre-defined inventory level – e. g.: certain number of empty boxes accumulates at an inventory buffer – starts the supply process; inventories are filled with kanban quantity. By kanban philosophy WIP (work in process) level can be decreased drastically since only the used up quantity is ordered from warehouse or partner. However packaging unit quantity, size and material handling circumstances – e.g.: lead time - often strongly determine kanban batch size and affect

WIP level. Also safety factor is built in the system; these are the causes why zero inventory level can not be achieved in manufacturing practice. The schematic figure of kanban material flow is illustrated on Fig. 1.

Just in time (JIT) manufacturing systems produce according to production schedule, which is generated by ERP (enterprise resource planning) systems based on customer orders. Purchase orders and incoming deliveries fit to production schedule; the right product is delivered/produced at the right time. According to Chan the most appropriate tool for supporting JIT manufacturing is kanban [3].

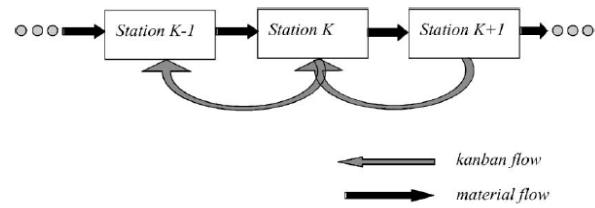


Fig. 1. Mechanism of the material and message flow in a Pull-type manufacturing system [3]

Sharma and Agrawal established a simulation model in order to aid control policy selection; their simulation result showed that in case of manufacturing systems the most preferred control policy is kanban [15]. Simulation is widely used to investigate features of manufacturing systems or whole supply chains applying kanban control policy – e.g.: [5],[6],[10],[13],[21]. Also applications of mathematical models confirm advantages of kanban [20].

The kanban size has a prior importance on determining in-process inventory level. The number of kanbans can be calculated with Toyota's formula [3], [4], [8] in Eq. 1.

$$n = \frac{d_a \cdot (t_w + t_{pc}) \cdot s}{k} \quad (1)$$

where d_a means the average consumption of the particle during given period, t_w means the waste and waiting times, t_{pc} means the processing time, s is a safety factor, k is the quantity of kanban packaging unit, kanban box or container.

The demand of a production line is a stochastic value, methods to calculate variability of production lines exist [7]. Also optimal planning methods support demand estimation [14],[11].

An approach for determining the optimal location of inventory control points in serial production systems with pull control has been presented by Askin and Krishnan [2].

The trade-offs between optimal base stock levels, numbers of kanbans, and planned supply lead times are demonstrated by Liberopoulos and Koukoumialos [10]. When designing single-stage kanban system the main parameters are the workstation production capacity and processing rate, utilization factor of the system, number of servers in the system, and the ordering rate of raw material [1]. However kanban systems are getting more and more complicated Sarker and Balan indicate that the issues of raw material orders, WIP inventory and finished goods setups (batch sizing) have to be considered together rather than separately in order to minimize the total cost of the inventory system [13].

In adaptive kanban systems the number of kanbans changes according to the consumption and inventory level [17], [19]. The design of adaptive systems is supported by mathematical models (Genetic algorithm, Simulated annealing-based heuristics) [16], [17].

3. BUILDING SIMULATION MODEL

During our research we have collected production data from electronic assembly company that used single stage kanban system. In this case operations on products are taken by only one single work center; material movement between work centers is not present.

In our research the current kanban system is compared with a modified system:

I. The current is a simple single-stage shop-floor kanban system in which raw materials are delivered from warehouse to work centers in the package provided by vendor. This means fix, non-optimal kanban number and quantities.

I. In the other version unpacking station is applied. We assume that by applying unpacking station inventory level would decrease smaller buffers at work centers and in warehouse is needed.

At many cases it is not recommended to unpack packaging units without proper identification process, because it would damage product traceability. This is problem is especially present at participants of automotive, industry, machinery, food industry, etc. If the connection between new package and the parent package is registered traceability is feasible.

We examined 5 raw materials used at 3 work stations. This survey is an initiative investigation to a broad company research; in the future this simulation model will be expanded to most problematic material. There is a company directive regarding raw material inventories namely the inventory located at shop-floor should not exceed inventory level enough for half an hour production. Of course if packaging unit quantity exceeds this half an hour inventory level, it can not

be achieved. Considering this the installation of unpacking stations is not a possibility but compulsory.

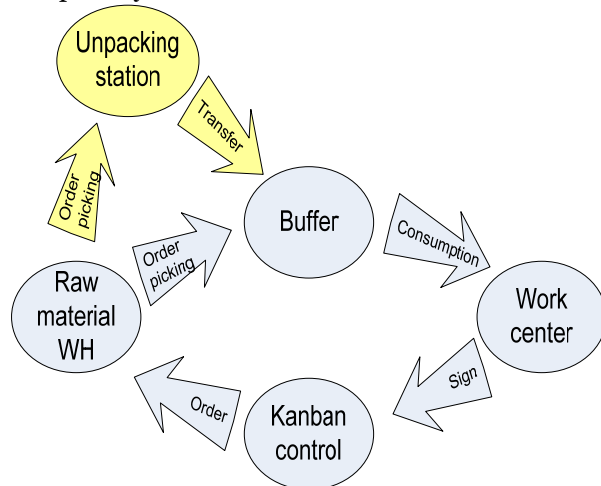


Fig. 1. Simple scheme of manufacturing system

Fig.1. shows the schematic model of current manufacturing system and manufacturing system installed with unpacking station. At each work center maximum 2 packaging units can be present, one with whole quantity and one in process. At the point when the whole packaging unit is opened a new kanban is forwarded to the warehouse, the order is picked and delivered to the work center.

Basic input data of the model are the followings:

- N_{RM} : quantity of raw centers
- Q_{PU} : Packaging unit material per finished good, retrieved form BOM list
- T_{CWC} : Cycle times of work quantities
- T_{CP} : Cycle time of picking process

The numeric data used for simulation are demonstrated in table 1. The size of packaging units are determined by the vendors, the company has some influence on it during the product and packaging design phase. The packaging unit quantity is usually size dependent. For example Part_05 is a larger box that is why the packaging unit quantity is only 10. Naturally in case of smaller kanban quantities more picking cycles should be made and higher kanban number should be determined and also unpacking would not have significance in the simulation. Based on simulation results the kanban number of Part_05 at Work center 01 is 3 so the maximum number of packaging units can be 12 (11 whole and 1 in use).

Table. 1. Input parameters of simulation

Work center	Part_01	Part_02	Part_03	Part_04	Part_05	Throughput of production line (pcs/min)	Cycle time (sec/pcs)
Work center 01	0	0	0	4	2	2	33
Work center 02	5	0	2	12	0	1	74
Work center 03	0	1	6	0	1	2	55
Quantity of packaging unit (pcs)	300	25	1000	300	10		

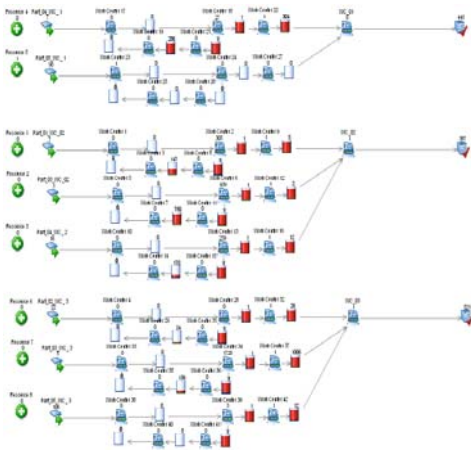


Fig. 2. Graphics of simulation model

The picking process lasts at about 300 sec with normal distribution, the material handling between buffer and production process is negligible, it is contained in the processing cycle time of the production line. The operators have some extra time to unload buffers without setting back production.

The simulation was made by Simul8 software, the graphics of the model is represented on Fig. 2. In the first part of the simulation the material flow of units separately in reality picking cart is used, this negligence is not significant considering inventory relations.

4. SIMULATION RESULTS

A. Current single-stage kanban manufacturing supply control

After running model described in previously the inventory quantities engaged at work centers was collected (Table II.), which values were compared to results of improved system.

It is a common problem at kanban systems that kanban orders are put on when packaging unit consumption starts,

Table 2. Results of simulation of current system

	WC_01	WC_02	WC_03	Total
Part_01		449		449
Part_02			39	39
Part_03		1553	1513	3066
Part_04	425	456		881
Part_05	54		17	71

since the inventory in one single packaging unit may cover several day long production (e.g.: tiny screws, microchip, micro compounds for SMT – Surface Mount Technology or other typical fields.

B. Two-stage kanban manufacturing supply control with unpacking station.

The material flow between the raw material warehouse is interrupted with unpacking. However unpacking is not worth in all cases of packaging units. Table III. indicates that in cases of Part_02, Part_04 and Part_05 packaging unit is smaller than consumption during 30 minutes, which is the company directive, so unpacking has no advantage.

In case of Part_01 the suggested modified packaging quantity is 150 (enough for 37 minutes), it is recommended to use rounded quantities when unpacking is made by operators and not by machine.

Table 3. Raw material consumption during 30 minutes

	Part_01	Part_02	Part_03	Part_04	Part_05
WC_01	0	0	0	220	110
WC_02	121	0	48	291	0
WC_03	0	56	338	0	56
Consumption in 30 min	121	56	386	510	166
Packaging unit quantity	300	25	1000	300	10
Number of kanbans	1	3	1	2	17

The situation is a bit complicated in case of Part_03. The packaging unit quantity is 1000 pieces; the total consumption during 30 minutes is 386. The problem is that the consumption

Table 4. Results of simulation of modified system

	WC_01	WC_02	WC_03	Buffer	Total
Part_01		229		183	412
Part_02			39		39
Part_03		731	753	823	2307
Part_04	425	456			881
Part_05	54		17		71

difference between Work center 02 and Work center 03 is significant. In practice it is often too complicated to distinguish packaging quantities according to destination. Sometimes even adding information to each raw material is a very hard task. We took the simpler case when a common quantity is defined for both work places; 400 pieces. Although the inventory level will cover 44 minutes at Work center 03 and 310 minutes at Work center 02 least developed informatics system is capable handling this version.

By installing unpacking stations the shop-floor inventory of raw materials involved in unpacking decreased significantly. In case of Part_01 the decrease was 8,2% at Part_03 the decrease was 24,8%.

Considering kanban quantities the inventory of unpack station buffer is relatively low. (Part_01: 183, Part_03: 823). The unpacking station coherences were demonstrated in this paper through a simple example, in practice much more production lines and raw materials are usually included. It can be assumed that the average inventory in the unpack station buffer would increase in a low rate as more work centers are included.

5. CONCLUSION

During the research single-stage kanban system was investigated at a electronic assembly-type manufacturing system. Two versions were examined: one without another with unpacking station. We assumed that the inventory level can be decrease radically in case of the second version; the aim was to determine the extent of this decrease.

After installing unpacking station the work centers stopped ordering separately from raw material warehouse, they ordered from unpacking station. Previously for example in case of Part_03 in the moment of delivering new packaging unit to work stations 4 packaging units were reserved in production.

As the result of this the main buffer of unpacked materials evolved at the unpacking station, the kanban quantities between the work centers and the unpacking station decreased. Smaller kanban quantities resulted smaller in-process inventory level, significant cost savings can be achieved by unpacking stations. The advantages come out especially at relatively large packaging unit quantities and high value products. The rate of cost saving can reach 25-30 % of the engaged inventory.

However we have to mention that unpacking may have disadvantages; it may damage or weaken traceability features. The other additional drawback is the extra information handling constraint and extra material handling processes may occur.

Further researches focus on the material flow intensity in case of different type of supply control policies. By installing unpacking stations the material movement tasks also change this way

the utilization of resources modifies. Unpacking is an extra handling process, the deliveries from unpacking station to production lines should be solved a different way. It is not that obvious which version is the more cost-, and time effective, if unpacking stations cause a growth in material handling intensity than we are facing a new trade-off – for which simulation is an effective tool to investigate.

REFERENCES

- [1] Al-Tahat, M. D.; Mukattash, A. M.: Design and analysis of production control scheme for Kanban-based JIT environment, *Journal of the Franklin Institute* 343 (2006) 521–531
- [2] Askin, R. G.; Krishnan, S.: Defining Inventory Control Points in Multiproduct, Stochastic Pull Systems, *International Journal of Production Economics* (2009)
- [3] Chan, F.T.S.: Effect of kanban size on just-in-time manufacturing systems, *Journal of Materials Processing Technology* 116 (2001)
- [4] Co, H. C.; Sharafali, M.: Overplanning factor in Toyota's formula for computing the number of kanban, *IIE Trans*, 29 (5) (1997) 409-415
- [5] Donner, R.; Scholz-Reiter B.; Hinrichs, U.: Nonlinear characterization of the performance of production and logistics networks, *Journal of Manufacturing Systems*, 2009
- [6] Hao, Q.; Shen, W.: Implementing a hybrid simulation model for a Kanban-based material handling system, *Robotics and Computer-Integrated Manufacturing* 24 (2008) 635–646
- [7] He, X. F.; Wu, S.; Li, Q. L.: Production variability of production lines, *International Journal of Production Economics* 107 (2007) 78–87
- [8] Huang, C. C.; Kusiak, A.: Overview of kanban systems, *International Journal of Computer Integrated Manufacturing* 9 (10) (1996) 169-189
- [9] Junior, M., L.; Filho, M. G.: Variations of the kanban system: Literature review and classification, *International Journal of Production Economics* 125 (2010) 13–21
- [10] Liberopoulos, G.; Koukoumialos, S.: Optimal models for a multi-stage supply chain system controlled by kanban under just-in-time philosophy, *International Journal of Production Economics* 96 (2005) 213–232
- [11] Mascolo, M. D.: Analysis of a synchronization station for the performance evaluation of a kanban system with a general arrival process of demands, *European Journal of Operational Research* 89 (1996) 147-163
- [12] Pettersen, J.A.; Segerstedt, A.: Restricted work-in-process: A study of differences between Kanban and CONWIP, *Int. International Journal of Production Economics* 118 (2009) 199–207
- [13] Sarker, B. R.; Chidambaram, V. B.: Operations planning for a multi-stage kanban system, *European Journal of Operational Research* 112 (1999) 284-303
- [14] Sarker, B.R.; Diponegoro, A.: Optimal production plans and shipment schedules in a supply-chain system with multiple suppliers and multiple buyers, *European Journal of Operational Research* 194 (2009) 753–773
- [15] Sharma, S.; Agrawal, N.: Selection of a pull production control policy under different demand situations for a manufacturing system by AHP-algorithm, *Computers & Operations Research* 36 (2009) 1622-1632
- [16] Shahabudeen, P.; Gopinath, R.; Krishnaiah, K.: Design of bi-criteria kanban system using simulated annealing technique, *Computers and Industrial Engineering* 41 (2002) 355-370
- [17] Shahabudeen, P.; Sivakumar, G. D.: Algorithm for the design of single-stage adaptive kanban system, *Computers & Industrial Engineering* 54 (2008) 800–820
- [18] Takahashi, K.; Nakamura, N.: Decentralized reactive Kanban system, *European Journal of Operational Research* 139 (2002) 262–276
- [19] Tardif, V.; Maaseidvaag, L.: An adaptive approach to controlling kanban systems, *European Journal of Operational Research* 132 (2001) 411-424
- [20] Wang, S.; Sarker, B. R.: Optimal models for a multi-stage supply chain system controlled by kanban under just-in-time philosophy, *European Journal of Operational Research* 172 (2006) 179–200
- [21] Hartványi, Tamás and Nagy, Zoltán András, Logisztikai „trade-off” a transzkontinentális ellátási láncokban, *Logisztikai Évkönyv, Magyar Logisztikai Egyesület*, 2007.





¹ Ioan MILOSAN

STUDIES ABOUT THE TOTAL QUALITY MANAGEMENT CONCEPT

¹ TRANSILVANIA UNIVERSITY OF BRASOV, ROMANIA

ABSTRACT:

The paper presents some fundamentals aspects about the Total Quality Management (TQM) concept. In is pointed out the representative models: Oakland, SOHAL, three dimensional and also some representative areas of TQM interest

KEYWORDS:

quality, management, TQM, models, areas of interest

1. INTRODUCTION

Total Quality Management is an organizational strategy founded on the idea that performance in achieving a quality education is achieved only through involvement with the perseverance of the entire organization in improving processes permanently. The objective is to increase the efficiency and effectiveness in satisfying the customers.

The concept of Total Quality Management (Total Quality Management - TQM) has been proposed by Dr. Edwards Deming in 1940 but its use started in 1985 with the takeover by American principles of working in Japanese industry:

- ❖ focus on process improvement permanent, so that processes are visible, repeatable and measurable;
- ❖ focus on analyzing and eliminating undesirable effects of production processes;
- ❖ consideration of how the users use products in order to improve product;
- ❖ expanding beyond concerns of product management.

TQM is a description of culture, attitude and organization of a company that strives to provide clients with products and services that meet their needs and expectations. This culture involves all the processes as the company did so well in the first, zero defects, zero waste.

The concept of quality has undergone several stages, adapting to every level of technology and market requirements. Thus, gradually, the selection of finished class performance has been replaced by statistical control of quality parts on-stream, then to extend the process, becoming, through the concept of quality an important factor in delivering products and services.

Charge on a gate of which are increasingly a concern for quality led to the appearance TQM as a full definition concept which has a dimension in time correlate thus competing with the concept and simultaneous engineering.

2. METHODOLOGY

To successfully implemented TQM organization should focus on 6 key elements:

1. CONFIDENCE;
2. TRAINING;
3. TEAMWORK;
4. LEADERSHIP;
5. RECOGNITION;
6. COMMUNICATION

1. CONFIDENCE – It is a result of integrity and ethics of the organization without trust cannot be built within the work of TQM. The trust helps the full participation of all employees.

Allows every employee empowerment which leads to involvement and engagement. Allow decisions to be made at levels closest to the problem, encourages risk taking individual and continuous improvement to help ensure that everyone on measurement indicators is made to accuse employees.

Trust is essential to ensure customer satisfaction and is one that builds a climate of cooperation essential for TQM.

Ethics – It is discipline which transposes each situation in terms of good or bad. Has two components represented the organization's ethics and individual ethics.

Organizational Ethics establishes a code of ethics guidelines emphasize that you should join all the employees when operating. Ethics include the individual opinion of what is right and what is bad.

Integrity - honesty involved, morals, values, honesty, sincerity and support with facts. It is important that expects and deserves to get the client (internal or external). As opposed to the integrity of character have duplicity. In a duplicity atmosphere, TQM cannot work.

2. TRAINING – Training is very important for employees to be very productive. Supervisors are responsible for implementing TQM in their departments and to spread the philosophy of TQM among employees operate.

Training of employees who need to refer to interpersonal skills, the ability to work as a team, techniques for solving, the ability to make decisions, performance analysis in order to improve the work, understanding the business is located. You have to be trained to become more efficient and more effective.

3. TEAMWORK – To be successful in business teamwork is an essential element of TQM, with the team can find solutions faster and better to the problems that occur in the organization. Teams can provide improvement of processes and activities.

The teams people feel more comfortable to highlight problems that may occur and may receive help from colleagues to find and implement solutions. There are mainly three types of teams that TQM organizations have:

- a. Quality improvement teams. Temporary teams created in order to analyze the problems that appear or reappear, often are established for periods of 3-12 months.
- b. Teams to solve problems. Intended to solve certain problems and to identify the true root causes. Usually they have a duration of life between one week and three months.
- c. Work Teams. These are small working groups comprised of skilled workers who share the same tasks and responsibilities.

These teams use concepts such as: employee involvement, self leadership, quality circles. These teams meet one or two hours per week.

4. LEADERSHIP – Probably the most important element of TQM. Appears everywhere in organization.

Leadership in TQM means that the manager must have the vision to inspire, to trace the strategic directions that would be understood and implemented by all employees that will lead subordinates. For TQM to be successful in business supervisor must be dedicated leadership subordinates. A leader must understand the TQM, believe in his principles and to demonstrate this fact by faith every day. Supervisor to ensure that strategies, philosophies, values and goals are transmitted down the organization in order to provide focus, clarity and direction.

A key factor is that TQM must be introduced and led by management at the highest level. Personal involvement and commitment is absolutely necessary from the top management in determining values and goals for all levels in line with company objectives and define the systems, methods and measurable indicators to achieve these goals.

5. COMMUNICATION – is one that unites all these concepts. This acts as a vital link between all elements of TQM. Communication is there a common understanding of the ideas so that it emits and the one who receives them.

TQM success is conditioned by the communication between all members of the organization, suppliers and customers. Superiors should create and maintain channels of communication through which to receive and transmit information about TQM processes.

Sharing of accurate information is vital.

For a credible communication is absolutely necessary that the message be clear that the interpretation of receptor to be in the sense in which the broadcaster has intentionally.

6. RECOGNITION – This is the last element of the system, it should be given both for and suggestions for performance, both for teams and individuals.

Employees shall endeavor to obtain recognition for themselves and for their teams. Detection and recognition of individual contribution is the most important duty that each supervisor has.

Then when people recognized the merits of producing major changes in terms of self respect, productivity, quality and quantity of effort for each task.

Recognition is the greatest impact when it is close can be a reward or just a message from top management.

3. RESULTS

It was proposed several models for the representation of TQM, in accordance with definitions given by different researchers.

Model Oakland (1989) proposes that TQM representation of a pyramid in the supply chain to customer-supplier of quality systems, tools of statistical quality control method of teamwork. These are integrated to support communication by stimulating the cultivation of a new industrial crops and immediate employment of all managerial structures.

The model focuses on meeting customer requirements in the external and the internal (which is translated by satisfying the requirements of any recipient of services or track the flow of production), the firm commitment to quality that has to start from the high level of management and should be reflected until the last level. This commitment is found both in quality investments for the specific field of activity, and by increasing the risk taken in an effort to get success.

A good quality management system covers all major aspects of business such as management, conception, design, materials, manufacturing processes, qualifications, distribution of products and services.

TQM requires a continuing review of compliance with agreed standards of clients and performance tracking tools with statistical control of processes.

The "team work" model involves promoting the idea of continuous and sustained improvement, and implementation in the organization.

Model SOHAL (1989) suggests that quality improvement continues to come from an integrated approach to quality control action plans at various operations during the business cycle.

The principal elements of the model are:

- ❖ focusing the customer: the objective of all of the organization should improve the quality of processes and services delivered.
- ❖ engage management to build a culture and an environment of quality, expressed by changing attitudes and expectations and supported by the measurement and quality control.
- ❖ total staff participation from the base to the peak, the problems associated with understanding the processes in the sense of moral responsibility and membership.
- ❖ use of statistical techniques for analysis of correlated data and to solve various problems.
- ❖ a systematic process of solving problems using the cycle execution-check-action-and concentration items on clients business process.

Three dimensional model proposed by Price and Gaskill. This model is to:

- ❖ the size of products and services, and the degree to which a customer is satisfied with our products and services;
- ❖ personal dimension and the degree to which a customer is satisfied relationship with the organization providing personnel;
- ❖ size processes and the degree to which the supplier is satisfied with the internal working processes, which are used to develop products and services provided to the client.

The three dimensions are considered together and reflect the organization and request that it can evaluate, analyze and can only improve business.

In terms of scope of TQM, there are implementations in the different areas are:

- ❖ protection of health education and research;
- ❖ government agencies;
- ❖ the environment;
- ❖ banks;
- ❖ manufacturing.

The difficulties encountered in implementing TQM come most often from:

- ❖ lack of sufficient involvement of top management;
- ❖ resistance to change;
- ❖ insufficient training and education;
- ❖ the poor communication;
- ❖ lack of resources, high costs.

For the enterprise stimulation and implementation of the TQM, the European Foundation for Quality Management (EFQM) has developed starting with 1991, European Quality Award – EQA.

Developing this reward system, was achieved with the help of European Organization for Quality and European Commission.

The pressure of new conditions in the world economy, globalization of market demand orientation and relaxation dynamics of technology and resources, orientation and expectations of customers, forcing the application of appropriate managerial concepts, this being a condition of competitiveness

By entering the European Quality Award, is meant by the European Foundation for Quality Management (EFQM) the stimulation and implementation of the TQM.

4. CONCLUSION

TQM refers to an integrated approach by management to focus all functions and levels of an organization on quality and continuous improvement.

Over the years TQM has become very important for improving a firm's process capabilities in order to achieve fit and sustain competitive advantages. TQM focuses on encouraging a continuous flow of incremental improvements from the bottom of the organization's hierarchy.

TQM is not a complete solution formula as viewed by many – formulas cannot solve managerial problems, but a lasting commitment to the process of continuous improvement.

REFERENCES

- [1.] Oakland, I.S.: Total Quality Management, Heinemann Professional, UK, 1989, p. 25-37.
- [2.] Lakhe, R.R., Mohanty, R.P.: Understanding TQM, Production Planning and Control, 1994, 5, p. 426-431.
- [3.] Tobin, L. M.: The New Quality Landscape = TQM, International Journal of Systems Management, 1990, 41, p. 10-14.
- [4.] Maxim, E.: The Quality Management, Sedcom Libris, Iasi, 1996, p. 58-64.
- [5.] Stancu, I.: Total Quality Management, Cartea Universitara, Bucuresti, 2004, 120-125.



MID-SIZE COMPANIES AND LOGISTIC IN THE CHALLENGE OF GLOBALIZATION

¹⁻³TECHNICAL UNIVERSITY IN KOŠICE, FACULTY OF MECHANICAL ENGINEERING,
DEPARTMENT OF ENVIRONMENTAL STUDIES AND INFORMATION ENGINEERING, KOŠICE, SLOVAKIA

ABSTRACT:

The publication is about the relationship between midsize technical companies and logistic and about the challenges they face during the growing globalization.

KEYWORDS:

Globalization, Business succession, Technical, Small and mid sized companies

1. CURRENT SITUATION

Midsize companies and Logistic are nowadays in a special relationship. With some of the mid size company's it appears logistic is still an unknown word. Other business in contrast glances with some fabulous logistic invents. The core of the Europe logistic industries is marked of middle size companies with some global players among them. Logistic products from midsize companies are well demanded by global company's which can be seen as a prove that a lot of logistic know how must be embodied with these kind of family driven company's.

Today more and more midsize companies do business with Europe and some of them even with the whole world. With continuously growth and increasing international business the economic meaning of logistic for the companies have with grown. A lot of them nowadays own high tech logistic systems and processes. Although in the matter of globalisation these Adjustments sound evident, some of them are still representing the old fashion way and stick to historical traditions. Backwardness would rather be the right expression to that kind of behaviour.

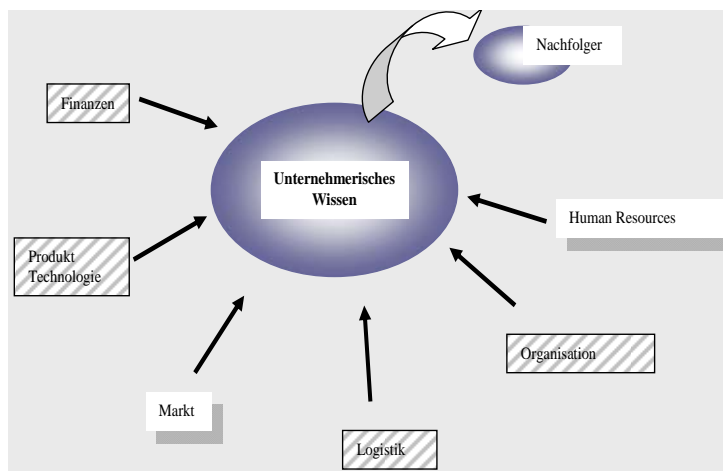


Table 1

Knowing that change is coming bring up the questions where does it come from is obvious. To explain it is necessary to rethink about the overall meaning of logistic in terms of their economic meaning. The Area of logistic accomplishes and constructs the preconditions for our working economy and therewith must be seen as the heart and nerve centre for globalisation all over the world. In order to respond in an appropriate way to this kind of new responsibility it is mandatory to investigate and double check

without restriction all of the previous basic principles and system concepts. A cardinal challenge especially for owner of for mid size company who likes to stick to traditions and the old way of leading a company not acknowledging the alteration. Potential successors who are already facing the complex business succession have to acknowledge very soon that adjusting the company's

logistic for the future is a important additional task in the overall challenge of business succession. It's up to them to distinguish which direction and steps need to be taken to adjust logistic alignments in order to be competitive for tomorrow's world.

Only knowing that change is coming is certainly not enough to have the own logistic department prepared for the requirements of tomorrow. It is essential to know from which direction the logistical adjustments of the next century will come and how do they look like. Below facts should be taken into consideration:

2. ASSUMPTIONS

Political changes and the opening of European borders have accelerated the globalisation development and cause in a worldwide business extension. Hence the work share become spacious and therefore the range of good transport all kind of carrier increased.

- ❖ Decentralised Logistic systems become more and more important. The principal of Just in Time (JIT) brings every production to the challenge of on time driving and optimisation of material and goods.
- ❖ The nowadays necessary strategies of internationality of midsized company's require a worldwide procurement and organisation.
- ❖ The World Wide Web based e-commerce caused radical change of economy and therewith lead to new challenges in logistically handling of Internet based orders.
- ❖ The general trend of reduction of manufacturing penetration in production leads to an significant increase of suppliers which on the other hand create new dependencies young entrepreneurs have to take into account.

3. CONCLUSION

This enumeration could be continued arbitrary. This argument show very clear that especially mid size companies are with logistic industry involved face huge challenges and require a much higher flexibility compared with company owner who are not affected by logistical globalisation changes. The already tough defiance of succeeding business succession will make this even more complex and difficult to resolve. An early start with a well prepared business succession plan becomes more fundamental than ever.

REFERENCES

- [1] BEUMER, C.:Logistik im Mittelstand- Best Practices- Strategien für den Erfolg. 2008
- [2] BADIDA, M. - LUMNITZER, E. – ROMÁNOVÁ, M.: The application of recycled materials for products that provide noise reduction in living and working environment, 2006Acta Acustica united with Acustica | Vol. 92, suppl. 1, p. 108
- [2] BILIOVÁ, M – LUMNITZER E. Comparison of measurement methods for acoustical parameters determination of sound absorbers In: AEI '2010: International Conference on Applied Electrical Engineering and Informatics: September, Italy, 2009.
- [3] DELFMANN, W.: WIMMER Thomas, Strukturwandel in der Logistik, 2010





ECONOMIC ASPECTS OF THE DEVELOPMENT OF ENVIRONMENTAL PROTECTION

¹⁻⁴TECHNICAL UNIVERSITY IN KOŠICE, FACULTY OF MECHANICAL ENGINEERING,
DEPARTMENT OF ENVIRONMENTAL STUDIES AND INFORMATION ENGINEERING, KOŠICE, SLOVAKIA

ABSTRACT:

The following publication gives an overview Economic of the development of environmental protection.

The impact of motorization, CO₂ emissions and various fuels – fossil as well as biomass based fuels is given – are discussed in brief showing the need for future developments

KEYWORDS:

Environmental protection, CO₂ emissions, Industry and customer

1. INTRODUCTION

Environmental protection is a term meaning the entirety of all measures for the protection of the environment, with the aim to maintain the natural basis of live for all creatures by ensuring a functioning balance of nature. The term has become popular only in the last 40 years.

The need to limit or minimise the impact of technical progress to the environment increases with the same speed as the increasing desire for comfort and the increase of world population, both of which is connected with increasing need for energy.

Environmental protection focuses on individual components of the environment, such as the climate, the soil, water and air, as well as on their interactions. Further, damage to the environment caused by human impact in the past shall be corrected.

In the past years, the focus has shifted mainly to energy generation, which is predominantly due to the climate change and to the popular opinion that global warming has been caused by the increasing CO₂ contents in the air. This background implicates that it is necessary to turn away from using fossil fuels. As an aside, such turning away may be also desirable in order to secure supply.

The replacement of the fuels commonly used to date by alternative fuels, for the purposes of CO₂ reduction, will be possible and reasonable only if a whole series of requirements is met.

Significant investments will be required in basically all the steps of production, distribution and consumption, even if every action is taken to adjust all their features of the alternative fuels to the fuels used by now.

The environmental requirements do not only have a huge impact on energy generation in industry and society. Environmental protection has generally great influence on everyday life and placed high demands on research, development and infrastructure.

However, the economic aspect is very important. In the following, the requirements, influencing factors and effects of environmental protection are presented from the economic point of view, on the example of operating supplies.

Does environmental protection “pay off” after all?

2. COST REVIEW – THE “VALUE” OF ENVIRONMENTAL PROTECTION

Any reduction of environmental pollution, be it due to CO₂ emissions or other types of pollution, is desirable.

For many decades, the emphasis was placed on the function of machines; emissions were rather treated as an orphan. However, discussions about environmental pollution, particularly those in the USA, have led to a change of mind. For example, in California, air pollution was at some times so severe that the smog massively impaired sight and contributed to health concerns. Already in December 1952, thousands of people died in London from stagnant air pollution caused by heating with coal.

At the latest at those times, people started to reflect about ways how to reduce such emissions. In the late 70-ies and 80-ies, for the first time, exhaust catalysers were installed in vehicles powered by petrol, which was also supported by the government. Minor increases in fuel consumption were tolerated for the good of less unburned hydrocarbons and carbon monoxide being emitted.

The important question when implementing environmental protection measures is, what costs will incur and how much, for example, the emission on a ton CO₂ may cost the national economy. Only the answer to that question can tell whether it will “pay off” to support so-called “climate-friendly” renewable energies or to further the reduction of fuel consumption and motivate vehicle owners to retrofit emission-reducing means, or to even purchase new, more economic vehicles.

But how can we assess what taxes are appropriate on fuel and other sources of energy? By now, the taxes were determined based on the estimated damage to the environment and to public health, for which the general public must pay the costs. However, the costs and the benefits of environmental protection are vaguely defined.

The [German] Federal Environmental Agency has now issued the recommendation, as for ensuing damage to the climate, to establish a cost rate of €70 / ton of CO₂ in all areas of application. The limits are set at €20 to €280 per ton. This background allows for further considerations.

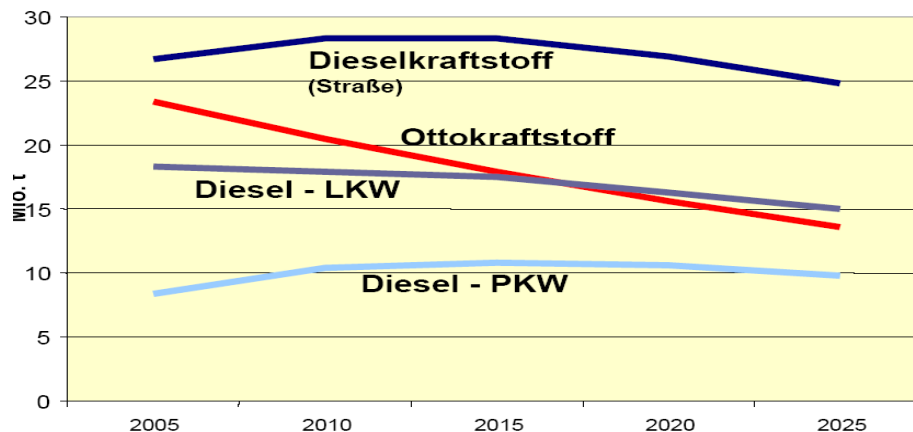
3. FUEL CONSUMPTION AND VEHICLE NUMBERS IN GERMANY

The total number of vehicles in Germany is approximately 50 million, divided into 41 million cars, a quarter of which is equipped with diesel engines, 4.5 million trucks and buses, and the rest being other vehicles.

The consumption of diesel fuel in Germany is about 30 million tons p.a., whereas petrol accounts for about 22 million tons p.a.

Approximately 150 million tons of emitted CO₂ are the result of motor traffic.

Inlandsabsatz Otto- und Dieselkraftstoff



Title	Domestic Sales of Petrol and Diesel Fuel
Dieselkraftstoff	Diesel Fuel
Ottokraftstoff	Petrol
Diesel-LKW	Diesel Trucks
Diesel-PKW	Diesel Cars

4. ECONOMIC REFLECTION ABOUT CO₂ EMISSIONS

For the reflection below, the assumption is made that a car has a lifetime of 150,000 km and emits an average of 200 g CO₂/km.

Based on the set €70/ton CO₂, this results in the emission of 30 tons of CO₂ over the lifetime of the vehicle and in total costs of € 2,100.

A 10% reduction of the consumption would reduce the CO₂ costs to € 1,890, which corresponds to a reduction by € 210 over the lifetime of the vehicle. For the operator, the costs for reducing the consumption would be approximately € 1,500 or 1ct/km.

Accordingly, halving the CO₂ emission - which, realistically, can be achieved only in the long term - would result in potential CO₂ savings worth € 1,050 per vehicle, which then could be reinvested into the development of the vehicles. With 1 million vehicles, this would correspond to 1 billion euro in “costs” over the assumed lifetime of 150,000 km per vehicle that could be invested into further development. This is a significant amount, which would certainly make a lot of development work possible.

A 10% decrease in diesel fuel consumption, corresponding to 3 million, would mean a reduction by approximately 9 million tons CO₂. With € 70/ton, this would lead to a cost reduction of € 630 million.

Promoting the installation of the particle filter in only 10% of the existing diesel-fuelled vehicles – i.e. in 1 million vehicles – would result in the payment of 330 million Euro incentives. This, again, corresponds to the costs for 4.7 million tons CO₂ and is therefore, mathematically, equal to the reduction of the consumption of approximately 1.5 million tons diesel fuel. Finally, this would correspond to a 5% reduction in the annual diesel consumption.

When looking at the 22 million tons of petrol for the 30 million vehicles with petrol engine, a 10% reduction of the consumption would correspond to a cost reduction of 154 million Euros, which is a background that provides sufficient scope for justifying sales-promoting measures and, as it was done with the scrappage premium, to also implement it. However, the scrappage premium need to be also viewed from the aspect involving the processing of many tons of raw materials and the energy input required for such production. After all, over 20% of emissions are generated during the production of the vehicle – as compared to the lifetime of the vehicle.

Summa summarum, however, considering other factors such as the energy consumption in the production of new vehicles, it can be said that a reduction of CO₂ emissions is and will remain a worthy goal.

5. REQUIREMENTS TO FUELS

For the evaluation of the quality of fuels as they are being generally used for combustion engines and especially in vehicles, specifications are applied that have been developed and established by consumers, manufacturers and public authorities over a long period of time.

Any developments within the industry are based on those specifications and, therefore, the use of fuels with different specifications will cause extensive changes in development and also in usage.

For the products demonstrated and specified in detail above, an infrastructure has been created over many decades which cover all the necessary steps from the exploration and production, refining, storage and distribution, in order to facilitate and secure the continuous supply of large numbers of vehicles.

The development of a different system on the basis of alternative fuels, for environmental reasons, extensive efforts will have to be made, connected with accordingly large economic effects.

Fuels Based on Fossil Raw Materials Customary by Now

The given specifications of currently customary fuels represent the current minimum requirements. Changes can be expected from the further development of combustion engines considering the reduction of emissions.

Thanks to modern engine and fuel developments, consumption is reduced and this results in lower CO₂ emissions. However, it must be examined to what degree necessary modifications of the production process may result in smaller output and, in turn, again cause higher energy consumption.

Therefore, energy balances should be set up for the desired improvements.

The costs for adjusting the by now customary production and distribution system for fuels generated from fossil raw materials should be reflected in the budget with a lower amount than the construction of new production and distribution plants. The situation will be different after a complete switch to alternative products.

Fossil Fuels with Reduced CO₂ Emission

A reduction of CO₂ emissions on the basis of fossil raw materials, as another option, can be achieved only if the by now customary hydrocarbons with C-values of about 8 to 20 are replaced by lower-grade hydrocarbons with C-values such as 1 (methane) or 3 or 4 (propane/butane).

This is being done in different ways in different countries, by powering vehicles with natural gas (Compressed Natural Gas CNG) or petroleum gas (Liquefied Petroleum Gas LPG). In these cases, the CO₂ emission is simply reduced, because more hydrogen is available, as compared to carbon, for the combustion required to generate energy.

Similar reductions of the CO₂ emission are, from the start, also ensured when fuels are produced and combusted on the basis of renewable raw materials.

The costs for switching to hydrocarbons with lower C-values, which means basically to gas, requires not only plant modifications in the production and refining facilities as well as in the distribution channels, but also adjustments in vehicle components.

6. RENEWABLE RAW MATERIALS

The generation of these raw materials is, by principle, based on the photochemical reaction in plants, also called photosynthesis.

Products generated on this basis will, by principle, contain compounds with higher C-values; however, they have the advantage that they process carbon from the CO₂ contained in the air and, therefore, when combusted, they do not emit more CO₂ than had been extracted from air at an earlier point in time. In such cases, we speak of CO₂-neutral behaviour. However, this approach does not consider the comparison between the time when the raw material was generated, and the time of its later combustion.

Ways to Utilise Renewable Raw Materials

By principle, fuels from renewable materials can be produced according to consumer demand; with that, the advantages and disadvantages always have to be weighed.

Advantages and Disadvantages of the Use of Agricultural Basic Products

Opposed to the benefit of renewable raw materials from agriculture, is a series of disadvantages the largest part of which, however, can be eliminated by means of the corresponding investments and creation of infrastructure. The time factor cannot be neglected, either, as it is clear that these are long-term measures.

Utilising Sun, Wind and Water Power

The requirement to generate energy without any release of CO₂ can be met if sun energy or its daughter elements, wind and water energy, are transformed into electricity. Provided there are suitable storage media, this energy, generated entirely without CO₂, can be then used for transport and traffic.

Sun power plants, as they have been put up already, focus sun beams on piping systems and heat up the working fluids contained therein which, in turn, overheat water by means of heat exchangers. The generated steam can power steam turbines in the usual manner which, in turn, power generators for electricity production. However, the storage of electric energy generated this way and ensuring its retrieval or usage on demand, still constitutes a problem. This also applies to wind and water power plants with their direct energy generation. Batteries for the storage of very large volumes of electricity are not available yet. A solution to this problem could be the generation and storage of hydrogen H₂.

Electric Vehicles

At this place, reference shall be made to electric vehicles which are powered without CO₂ production and also require CO₂-free generation of electricity.

The transformation of sun, wind and water energy into electricity, as described above, is particularly important in this context.

7. ADJUSTMENT OF INDUSTRY AND CONSUMER

Automotive Industry

The switch from the by now customary fossil fuels to alternative fuels, in order to reduce CO₂, will cause further developments in the automotive industry.

Despite of the already advanced state of technology, especially the application of electric drives, and there especially energy storage, still requires further extensive development.

Transportation Industry

The transportation industry, in particular the heavy goods traffic by trucks, will not be able to profit from the developments towards CO₂-reduced operation to the same extent as the car industry does, as the development of electrically powered trucks in particular is still in its infancy.

However, as it is also the case for all diesel-powered vehicles, the operation with bio fuels can be relatively easily implemented, and is therefore worthwhile. The connected costs are reasonable.

Fuel Production

Large efforts will be required for setting up production of the same extent as currently exists for fossil fuels. A general question that arises is the availability of renewable raw materials, as some of them are foods, too, as we all know, which means that opposed interests need to be met.

Infrastructure

With regards to infrastructure, the existing infrastructure can be used for the application of bio fuels, too. However, it must be considered that, beside the storage and filling possibilities for the by date customary fuels, the same infrastructure must be created for additional fuels, which is connected with costs.

Transport and Distribution

The transport and the distribution can be secured via the existing distribution channels without any major investments, as these facilities require modernisation in regular intervals anyway.

Agricultural Production Capacity

Cultivation Areas, Crop Yield, Environment

Cultivation areas are just as limited as is the yield per hectare. For example, replacing 30 million tons of diesel fuel by methyl ester of rapeseed (bio diesel), with a yield of approximately 1,550 l/ha (about 1,350 kg/ha), equals to a required area of more than 20 million hectare of area to be cultivated. With an agricultural area of “only” 17 million ha in Germany, this is basically impossible.

Assumed that only 10% of the agricultural area would be used for bio diesel crops, this could not cover more than 8% of the demand.

This does not even yet consider the environmental impact of cropping, harvesting and production, as the cultivation of productive land is again connected with CO₂ emissions.

In the case of bio ethanol, the situation is similar, despite of the higher yield per hectare, as the so-called fuel equivalent is significantly lower and it must be accounted for an increase of about 40% in fuel consumption.

8. CONCLUSION

The traffic and transportation sector in Germany needs more than 50 million tons of fuel.

From these more than 50 million tons of fuel, realistically, not more than 5% can be covered by biological products from agricultural production in Germany.

While traffic is responsible for about 20% of CO₂ emissions, fuel production based on agriculture can contribute only to an insignificant extent to their reduction. Such contribution to the CO₂ reduction is very desirable, for reasons of eco-political considerations and decisions. All possible ways to reduce CO₂ emissions must be utilised, in order to reach the goal of falling 20% below the values of CO₂ emissions in the year 1990, which is a value that has been determined by the European Parliament within the frame of the climate package.

Therefore, it is imperative to exploit other sources of energy for traffic and transport. In principle, the only available source is sun energy, which in turn produces electric power and, with that, must and can provide power for vehicles.

A realistic calculation of the investments required for this new area is probably not yet possible. However, irrespective of economic aspects, the reduction of CO₂ emissions is desirable no matter what the case may be.

Acknowledgement

This paper was supported by projects APVV-0176-071/0453/08 and KEGA 3/7426/09.

REFERENCES

- [1.] Biokraftstoffe Basisdaten Deutschland, Bundesministerium für Ernährung, Landwirtschaft und Verbraucherschutz Oktober 2009
- [2.] Volkswagen AG, Golf V Hintergrundbericht
- [3.] Methodenkonvention zur Schätzung externer Kosten am Beispiel Energie und Verkehr. Umweltbundesamt April 2007
- [4.] Magazin für Menschen mit Energie 2/2008, Stadtwerke Bochum, Herne, Witten
- [5.] Buch der Synergie, Achmed A. W. Khammas, S. C 4 31
- [6.] Jörn Altmann: Umweltpolitik, Daten, Fakten, Konzepte für die Praxis. Stuttgart, 1997, ISBN 3-8252-1958-5

- [7.] Beck IPCC Report 2007
- [8.] Klaus Georg Binder: Grundzüge der Umweltökonomie. München 1999, ISBN 3, 8006-2232-7
- [9.] Energie und Umwelt 4. Symposium der deutschen Akademien der Wissenschaften, Springer Verlag 2000
- [10.] Alfred Endres: Umweltökonomie. 3., vollst. überarbeitete u. wesentlich erweiterte Auflage. Stuttgart 2007, ISBN 978-3-17-019721-3
- [11.] Bruno S. Frey.: Umweltökonomie. 3., erw. Auflage. Göttingen 1992, ISBN 3-525-33581-4
- [12.] Franz Jaeger: Natur und Wirtschaft. Ökonomische Grundlagen einer Politik des qualitativen Wachstums. Chur/Zürich 1993, ISBN 3-7253-0405-X
- [13.] Rainer Marggraf/Sabine Streb: Ökonomische Bewertung der natürlichen Umwelt. Theorie, politische Bedeutung, ethische Diskussion. Spektrum, Heidelberg / Berlin 1997, ISBN 3-86025-206-2
- [14.] www.wikipedia.de





DETERMINING FACTORS INFLUENCING PRODUCTION SITE RELOCATION

¹⁻⁴TECHNICAL UNIVERSITY OF KOŠICE, FACULTY OF MECHANICAL ENGINEERING, SLOVAKIA

ABSTRACT:

The following publication gives an introduction concerning the discussions concerning the relocation abroad of automotive industry.

This paper shall give the basic information explaining the way to find out about influences of different aspects.

KEYWORDS:

Politics, automotive industry, labour cost, emission regulations

1. INTRODUCTION

The relocation of industrial production facilities is based on the assumption that the relocation will result in lower costs for a given product. Not only is the wage differential between two production centres decisive in this respect, but also the varying environmental legislation in different regions and countries. In the final analysis, the actual decision to buy is highly dependent upon the purchase price. The customer is at pains to buy the supposedly cheapest product. Despite the availability of these cheap products and the social acceptability of buying them, wage increases are being demanded to increase purchasing power, e.g. by the United Services Union (VERDI) in Germany. Employers argue on the other hand, that raising wages could make a relocation of the production facilities to a foreign country unavoidable.

2. AN ATTEMPT AT AN OBJECTIVE ASSESSMENT OF THE DETERMINING FACTORS FOR PRODUCTION RELOCATION

Considering the vehicle in its totality, from manufacture to recycling, it is the operation of the vehicle that is responsible for the greatest share of emissions. One may conclude from this that the greatest potential for the reduction of emissions is the optimisation of vehicles in terms of the consumption and clean burning of fuel. The fraction of emissions due to the production of the vehicle is so large that an easing of restrictions (e.g. by relocating to emergent economic regions) would have a significant impact on the material balance sheet. A relocation of the power unit production to countries with lower environmental constraints would only have a very slight effect on the overall product cost of a vehicle. As mentioned above, there are four variables in this sector, which affect the choice of production centre location and therefore also on the total emissions.

3. DIFFERENCES IN THE COST OF LABOUR AS A DETERMINING FACTOR IN THE SELECTION OF A PRODUCTION LOCATION

As demonstrated in Section 1.1, the first factor to be considered is represented by wage differences. The following overview of how the cost of labour can vary within the European Union will serve to put this in context.

The image above shows significant wage differences even within Europe. What may be required in this context, at a later date, is an evaluation relative to the country specific environmental directives. But a decision on this will be postponed until after the international analysis.

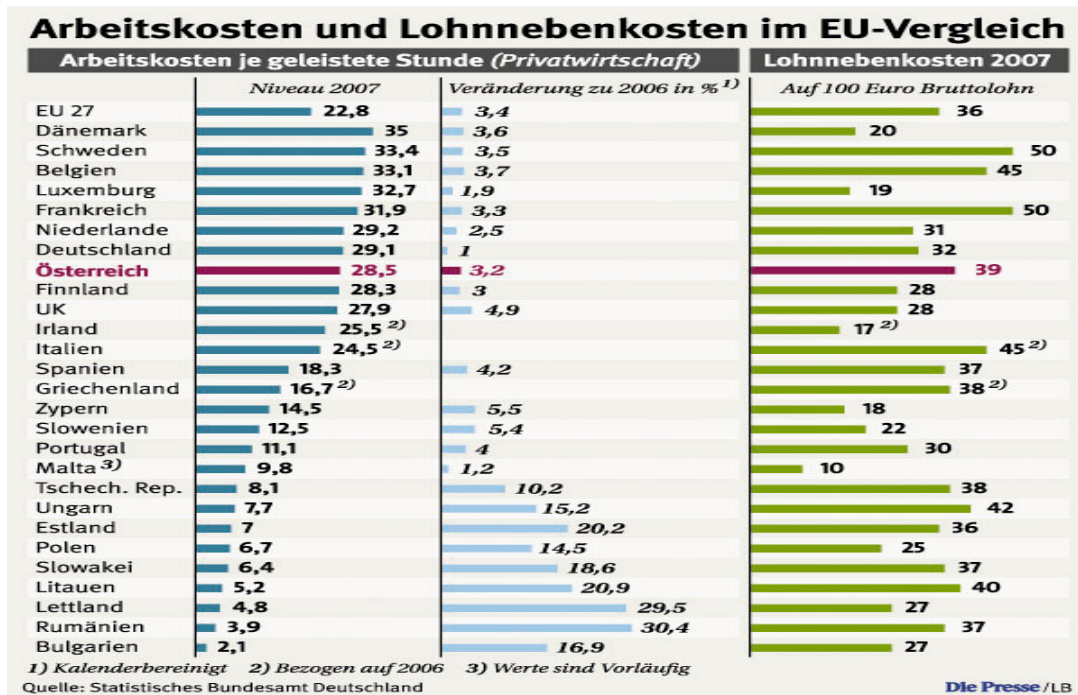


Figure 1: Source Euro per hour

Of more interest in this context are the fundamental differences per professional category. The chart below shows a comparison between Germany and China in terms of various level of qualification. This shows clearly that the wages differ in the unskilled labour category by a factor of 15 and by a factor of 3 in the high qualification bracket. It is understandable from this perspective that businesses view simple tasks falling within the domain of unskilled labour as attractive candidates for relocation to emergent economic regions.

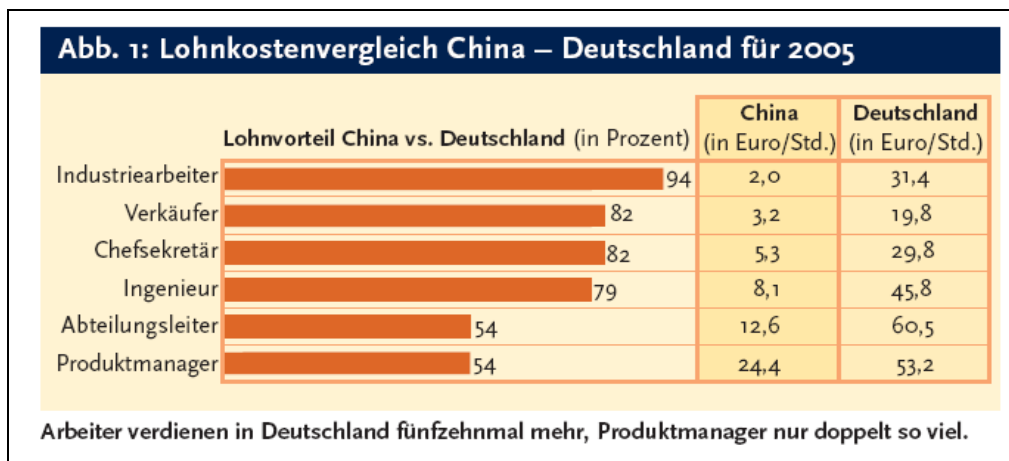


Figure 2 Source²

The following figure further breaks down the industrial worker's wage differential and shows the cost of labour in China, Mexico, Russia, Thailand and India next to that of the industrialised countries.

Two aspects are worthy of note in this context. The cost of labour for industrial workers in Germany are almost forty times higher than in India, whilst in China, Russia and India wages have increased by 12 to 15 percent within a single year. But as wages in Germany increased by ten percent at the same time, there has been virtually no change in terms of percentages and none at all in real terms. Nevertheless, the high wage increases in the boom regions China and India indicate that further high rates of increase can be expected in the coming years. These increases could mean that the absolute difference decreases thereby making relocation less interesting. It requires a more in-depth analysis to determine exactly what difference in hourly wages is required to reduce the attractiveness of emergent economies.

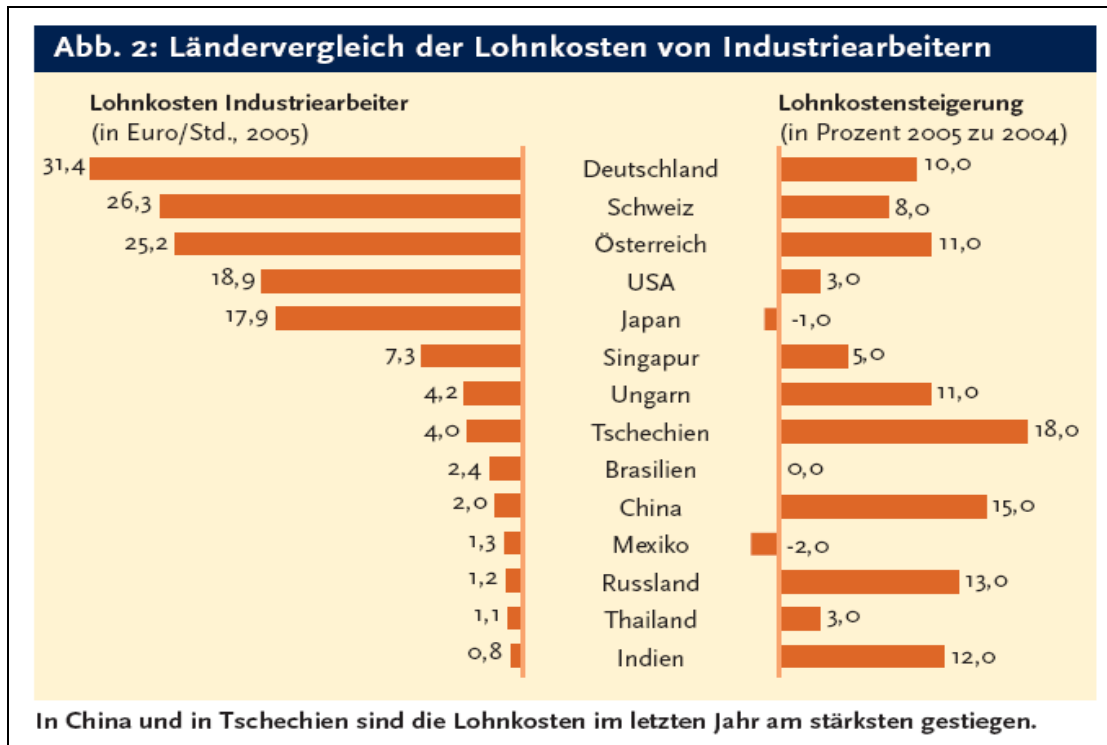


Figure 3 Source³

4. POWER AND LOGISTICS COSTS AS DETERMINING FACTORS IN THE SELECTION OF A PRODUCTION SITE LOCATION

One consideration in terms of relocating production facilities to emergent economic regions is the cost of component transportation. This includes finished products, e.g. toys as well as ancillary components such as circuit boards or other plastic parts for automobile manufacture. Transport costs are taken into consideration when deciding whether or not to relocate a production centre.

Wage costs are one element of transport cost, which have already been covered in Section 3.1. Another element is transport infrastructure as well as the related energy costs. Even if the cost of energy for transportation only constitutes a small fraction of the overall cost of transport and the cost of transport itself is only one small part of the cost of production, a variation in the cost of energy is relevant to the consideration of the overall cost of production. These energy costs are also reflected within the overall scope of production and have been ignored in the current model, as energy costs are similar throughout the world. The only variable in this context is in the level of taxation. Only the cost of energy for transportation can work against a business trend towards relocating and therefore represents a key variable. The graph below shows the historical development of the cost of crude oil.

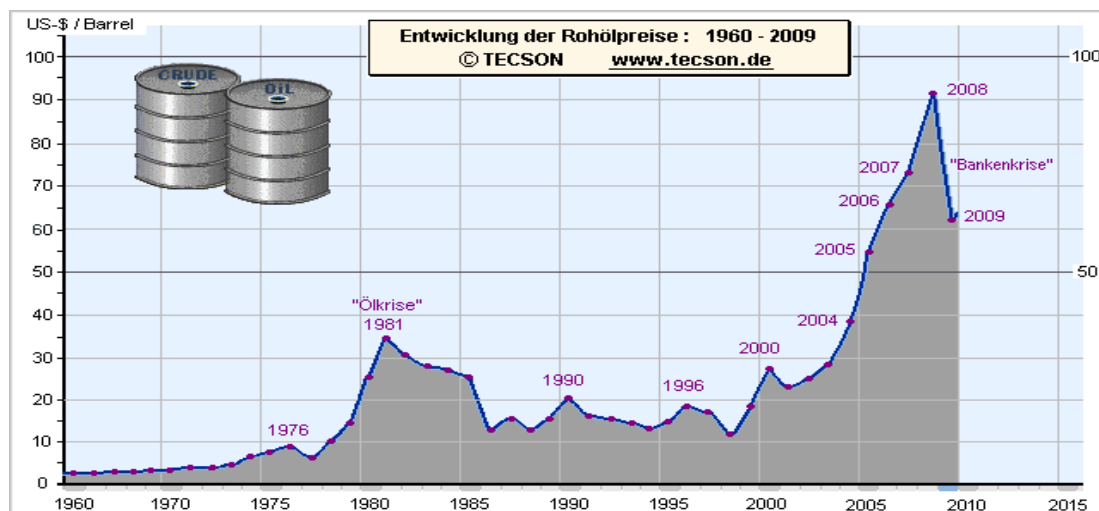


Figure 4 Source⁴

The energy cost variations, as a variable, will be of relevance to the overall model from a historical perspective, as the intention is to verify the mathematical model to be developed on the basis of the history of the various determining factors.

5. ENVIRONMENT PROTECTION COSTS AS A DETERMINING FACTOR IN THE SELECTION OF A PRODUCTION LOCATION

Environmental protection costs in this context means those costs that are necessary within a given country to meet the stipulations of the country in question. For example these can be environmental constraints on exhaust air, wastewater filtration and cleaning, noise restrictions, building regulations for production facilities including lighting, social institutions etc. The following image, designed to enable a comparison between countries, is the result of previous research. The basic data from this graph cannot be used in the mathematical model but does give an indication of the development of CO₂ on a per region basis and also of the changes over a 15 year period.

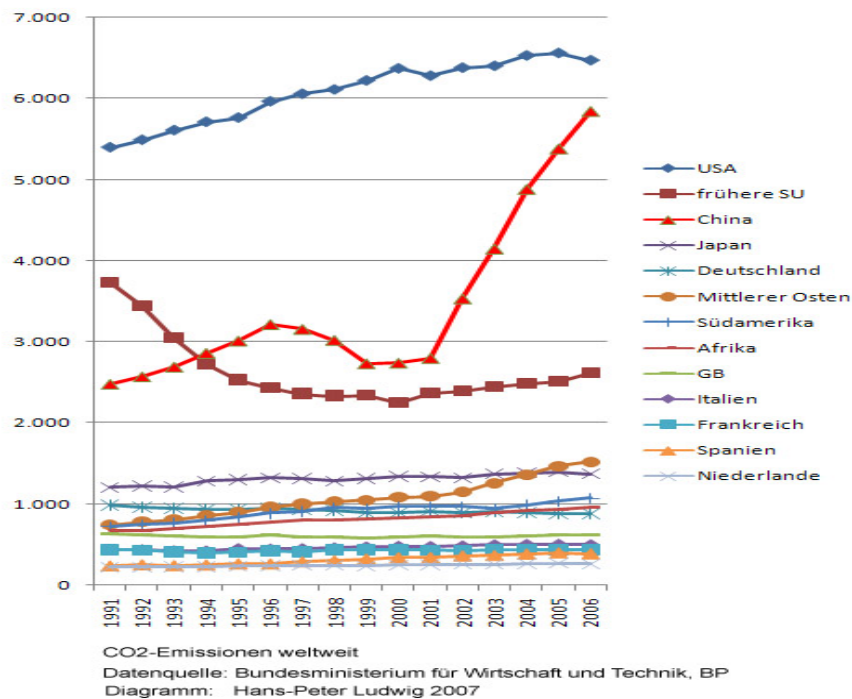


Figure 5 Source⁵ CO₂ in m. ton p.a.

To be able to integrate these elements into the mathematical model it is necessary to define a unit of measure for a given product to show the difference in the threshold values of pollutants. Conversely it is possible to derive the restrictions that have to be met from this data. And from these figures it is possible to calculate what investments will need to be made.

As the objective here is to discover what cost savings can be realised by lower environmental restrictions, research, perhaps in the form of a survey of companies that have already relocated, is a possibility. An additional study would show if comparative data are already available for costs arising from environmental restrictions; if not then these would have to be researched or the assumption would need to be substantiated. The assumption in terms of this point is that a change in emission restrictions, to match German restrictions for example, in the emergent economic regions or even in the USA, would lead to significant additional economic production costs, which in turn would make relocating less attractive. An initial estimate of these effects raises the suspicion that for example the reasons for not ratifying the Kyoto-protocol could have much more to do with the competitiveness of home-based industry than is currently assumed.

6. ENVIRONMENTAL COSTS AS A DETERMINING FACTOR IN THE SELECTION OF A PRODUCTION LOCATION

'Environmental costs' means those costs necessary for repairing environmental damage. This refers to such things as, for example, the renaturation of land, land consumption per se and water purification. The precise nature of the correlation between the environment protection costs set out in Section 3.3 and environmental costs arising from environmental damage can only be ascertained

through an in-depth study and analysis. It is to be hoped that a mathematically definable relationship exists through which the objectification can be expedited. Should it transpire that such a relationship does not exist and that a numerical model cannot be produced, it would be regrettable inasmuch as including the cost of environmental damage would create some political leverage.

The acceptability of buying products from distant regions whilst shutting ones eyes to the environmental consequences, is directly influenced by the cost differential between a product made in China and a European product.

It may be assumed that two main variables exist in terms of countering the trend towards production site relocation. The other main element is the cost differential for production sites. Examples are modern filtering facilities for exhaust air or wastewater. Two factors apply within Europe in this context. A high investment is required in air cleansing and emission avoidance technology in Europe, as a matter of principle, due to the stringent requirements for environmental protection and the high standard of technology required to meet the target values. Further improvements in air or wastewater quality can only be achieved with yet higher expenditure for small improvements.

This situation contrasts with that in the Asian region for example. The wastewater cleansing or air filtration technologies employed there are of a very low standard, whereby significantly greater emission reductions are possible at a much lower cost than in Europe.

07062: Treibhauseffekte der Industrieverlagerung nach China und Indien

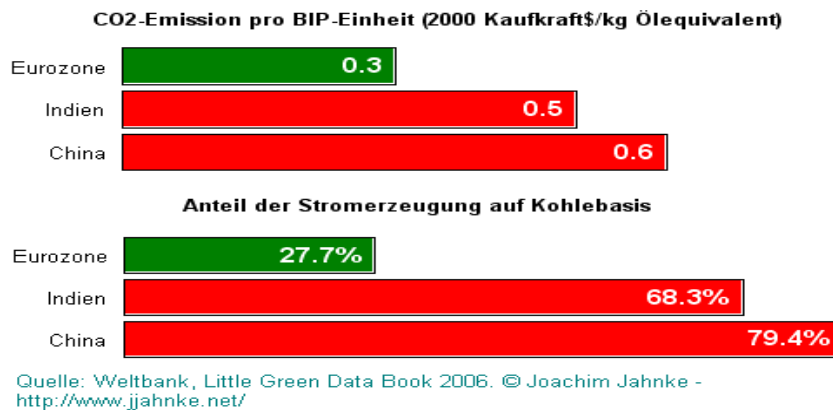


Figure 6 Source⁶

The above diagram clarifies the issues relating to the different restrictions in the context of relocating to China and India.

7. CONCLUSION

Reports about the renunciation of production sites in China are appearing in the press as well as in the publications of various institutes with increasing frequency. This rejection is happening because the cost of labour is increasing and the quality issues associated with Chinese manufacturing are no longer outweighed. These effects demonstrate that the market reacts sensitively to fluctuations in specific factors.

8. OUTLOOK

It can be assumed that relocation cycle times are influenced by wage developments on the one hand but also from the other prevailing conditions in the various countries on the other. Given the increasing cost of labour in the low-wage countries and increasing consumer sensitivity in terms of environmental compatibility in conjunction with increasing energy costs, the degree to which a return to local production may be economically viable should be investigated.

Acknowledgement

This paper was supported by projects APVV-0176-071/0453/08 and KEGA 3/7426/09.

REFERENCES

- [1.] Externe Kosten kennen – Umwelt besser schützen, Umweltbundesamt, April 2007
- [2.] <http://www.tecson.de/poelhist.htm>
- [3.] http://diepresse.com/images/uploads/7/8/8/378760/23s26_Arbeitskosten_Lohnkosten_EU_Vergleich_2007_Kopie2008422205410.jpg
- [4.] http://www.econbiz.de/archiv/myk/whumyk/controlling/loehne_china.pdf, S. S. 48, io new management Nr. 11 | 2005
- [5.] http://www.personalvitality.com/artikel_sterne/ENNEAD_a1_co2_emission_diagram.jp
- [6.] http://www.jjahnke.net/index_files/07062a.gif





¹Ferenc BAGLYAS, ²Gábor SUGATAGI

MULTIVARIATE ANALYSIS IN A WINE MARKET RESEARCH IN HUNGARY

¹. COLLEGE OF KECSKEMÉT, FACULTY OF HORTICULTY, HUNGARY

². GfK HUNGARY MARKET RESEARCH LTD., BUDAPEST, HUNGARY

ABSTRACT:

Marketing managers are faced with numerous difficult tasks directed at assessing future profitability, sales, and market share for new product entries or modifications of existing product or marketing strategies. Each of the identified marketing problems may be addressed and solved using the conjoint analysis methodology. In addition, a conjoint based competitive strategy may be implemented by modifying the marketing mix, i.e., new product/concept identification, pricing, advertising and distribution.

In this article the main steps of the model is shown in a study through the research of the Hungarian wine market.

A set of wine attributes, that were anticipated as the most important factors when buying wine, were offered to respondents. These attributes included growing site, variety, quality and price. Each of the attributes were further divided into levels, e.g. growing site consisted of Kunság, Szekszárd, Eger and Villány, while other attributes had their particular levels according to their characteristics. Twenty out of the total combination of attributes were chosen and so call profile cards were made. Respondents were asked to rank order cards according to their preference, thus simulating a purchase situation. Conjoint analysis calculated the utility of each levels of attribute for all of the respondents.

KEYWORDS:

conjoint analysis, wine attributes, design

1. INTRODUCTION

Customer satisfaction and delight are core values within the quality movement. Achieving these goals in an economic way by finding the quality attributes most valuable to customers has become a key issue in today's design activities. Conjoint analysis is considered an excellent tool for this purpose. This method is included among the seven product planning tools developed by the Union of Japanese Scientists and Engineers (Nótári et.al., 2009).

Conjoint analysis is a set of techniques designed to measure the importance individual consumers attach to each attribute and their degree of preference for each level of each attribute. Respondents are asked to rank the combinations of these factors as they do in the purchasing process (Nótári et.al., 2010).

Further advantages of this model is that customers can not be influenced by the responder's will. Wider spread of this method in the past was due to the lack of high-tech computers. Now the advance of technology and user friendly software (SPSS, SYSTAT etc.) make its use possible.

In this present article the use of this method is illustrated in a wine market research case study. We tried to keep the process as simple as possible to encourage other researchers to make an effort to test the technique themselves. We followed Churchill's suggestion in compiling a research schedule (Gustaffson, 1999).

2. MATERIAL AND METHODS

A. Research problems and objectives

The first task is to identify the specific research problem and objectives. Attributes and their levels should be limited, because a strenuous survey can lead to improper answers. Green &

Srinivasan (1990) suggest to limit the number of attributes to six or fewer. A more knowledgeable or motivated person can be exposed to a larger set of attributes (Ferencz et. al., 2010/a).

The main objective of the conjoint survey is to find the ideal combination of the product attributes and their levels that are most attractive to consumers. It is essential to know before we conduct research how the market is segmented, what the competitive environment is like, and how we wish to position our product (Ferencz et. al, 2010/b).

The basic goal of this study was to reveal the preference of those wine consumers who drink wine regularly and buy bottled wine in an average of two weeks. Social-demographic segmentation was used to further analyze preferences by means of ANOVA. The following questions emerged: What are those attributes that influence purchase decision most? We hope the derived information can cease the limit of knowledge, decision makers always faced.

B. Research population

Sampling procedure can be separated into two categories: probability and non-probability. Probability sampling is more common when dealing with consumer products. When using probability sampling there are different techniques to choose from: simple random, cluster, systematic and stratified sampling.

Non-probability sampling can be applied when the relationship to customer is closer. However, we must be aware of the danger that the desired population is not reached. Non-probability sampling techniques are also available in a wide range e.g. convenience, purposive, quota and snowball sampling (Gustaffson, 1999).

In this study non-probability, purposive sampling method was used. Students of the College of Kecskemet helped to find those respondents who met the above mentioned criteria.

C. The way of communication

Among the communication forms personal interview is the most commonly used. One reason for this is that the collected data will be of higher quality since it is possible to control the situation. This is inevitably important since conjoint analysis can be strenuous and complex. Also, this way of communication generate higher response rates. Another advantage of personal interview is that it reduces the risk of misunderstandings since respondents can be guided through the survey. The down side of personal interview is cost.

The second most frequent means of collecting data is by mail surveys. First, it is cheaper and second, more respondents can be approached. In this case however, scaling method should be as simple as possible. The down side here is the low response rate (Gustaffson, 1999).

In our case students communicated with respondents through questionnaires that reduced the cost of interview to zero.

D. The basic concepts

The attributes and the levels of each attribute should be chosen to be realistic and related to the problem. There are three basic rules that should be take into account (Gustaffson, 1999):

- ❖ Attributes chosen might be important to the respondent (sometimes seemingly no meaningful attributes can be important).
- ❖ Attributes are possible to alter, that is the product is in the earlier stage of design.
- ❖ Attributes included should cover the core competence of the producer.

The first problem is to find the adequate number of levels. Too many levels can confuse respondents. In our case the following attributes and levels were included (Table 1):

Table 1. Wine attributes and their levels

Attribute	Site	Taste	Quality	Variety	Price
Levels	Kunság	Sweet	Table	Chardonnay	269 HUF
	Eger	Semi-sweet	Quality	Lindeblättrige	389 HUF
	Szekszárd	Semi dry		Portugiser	529 HUF
	Villány	Dry		Blaufränkish	799 HUF
				Merlot	

The selection of the above attributes was based on our prior research and the experiences of GfK Hungary Ltd. in market research.

E. Design matrix

A fundamental procedural decision in conjoint analysis is whether to use full profile or pair-wise procedure for data collection. The pair-wise procedure presents the respondents with a set of matrixes representing all possible attribute pairs, with the levels of one attribute appearing on the X axis and the levels of the other attribute appearing on the Y axis. Respondents are asked to rank-order each combination (cell) in each table to reflect their preference or purchase likelihood. The number of possible combination is $N(N-1)/2$, where N indicate an attribute. Although it was initially widely used, the pair-wise approach is rapidly losing favor in applied research studies.

Full profile conjoint, what was applied in our study, involves presenting the respondents with a set of product descriptions such that each description contains information on the level of each attribute. The number of descriptions increases geometrically with the number of attributes. In our case it means $2^{17} = 131\ 072$ combinations. Fortunately, a fractional orthogonal array can be used to simplify the situation. SPSS 9.0 for Windows ORTHOPLAN command selected 25 so called profile cards, five of it were dropped. The 20 cards were marked by letters A, B, C... up to T. Even number of cards makes splitting possible to two groups: preferred and not preferred. Orthogonality was distorted but this did not deteriorate the results. Table 2 contains the descriptions (or cards) included in the survey questionnaire.

Table 2. List of cards used in the full profile conjoint analysis

MARK	SITE	VARIETY	TASTE	QUALITY	PRICE (HUF)
A	Szekszárd	Chardonnay	Sweet	Quality	529
B	Szekszárd	Portugiser	Dry	Quality	269
C	Villány	Chardonnay	Dry	Table	269
D	Kunság	Lindeblättrige	Dry	Quality	389
E	Kunság	Merlot	Sweet	Table	269
F	Eger	Lindeblättrige	Semi-dry	Quality	529
G	Villány	Lindeblättrige	Sweet	Quality	799
H	Villány	Blaufränkish	Semi-dry	Quality	269
I	Kunság	Portugiser	Semi-dry	Quality	269
J	Eger	Portugiser	Sweet	Table	389
K	Eger	Merlot	Dry	Quality	529
L	Eger	Chardonnay	Semi-sweet	Quality	269
M	Kunság	Chardonnay	Dry	Quality	799
N	Eger	Chardonnay	Semi-dry	Table	389
O	Szekszárd	Blaufränkish	Dry	Quality	389
P	Villány	Merlot	Semi-sweet	Quality	389
Q	Szekszárd	Lindeblättrige	Semi-sweet	Table	269
R	Eger	Lindeblättrige	Dry	Table	269
S	Villány	Portugiser	Dry	Quality	529
T	Eger	Portugiser	Semi-sweet	Quality	799

F. The questionnaire

The next step was to design the questionnaire. Our first two questions regarded the frequency of wine consumption and purchase of bottled wine. Only those questionnaires were evaluated that met the criteria. In order to make the selection of cards easier we used pictorial illustration. One card represented one wine description, just like the label of wine bottle does. Respondents were instructed to split the 20 cards into two groups: more favored and less favored. Out of the two 10-piece pack of cards respondents were asked to take the more favored pack and split them in the same way again. Thus, they could easily rank the most preferred five cards. This iteration was going on until the last card was positioned. Separately, the preference of different attributes was measured on a Likert scale. This helped us evaluate the consistency of answers. Finally, basic social-demographic questions followed.

G. Data analysis

There are different ways of analyzing conjoint data: MONANOVA and ordinary least square regression (OLS). Between the two the later is more frequently used.

From a strict statistical point of view OLS is not feasible for analyzing rank ordered data, since rank order scale does not include any measure of distance. This deficiency, however can be mitigated by introducing gaps (“do definitely believe in” etc.). Instead of introducing gaps we checked the consistency of answers as described above.

For each individual respondent the part-worth (also known as “utilities”) or relative preferences among the attributes were estimated. In addition, the part-worths of the sample mean were calculated.

3. RESULTS AND VALIDATION

The sample means part-worths give some indication of the relative importance of the different attributes. The actual magnitude of the part-worths is of little importance. Rather, their relative size is of interest (Figure 1-4).

Calculating part-worths for the sample mean is somewhat dangerous. If, for example, there are distinct segments in the sample with opposite preference regarding one attribute, the effect from each of the segments will be cancelled, giving a false result that the attribute is not considered important. To avoid this danger ANOVA was applied for the social-demographic segments for all part-worths of each attribute levels calculated. Results are shown in Table 3.

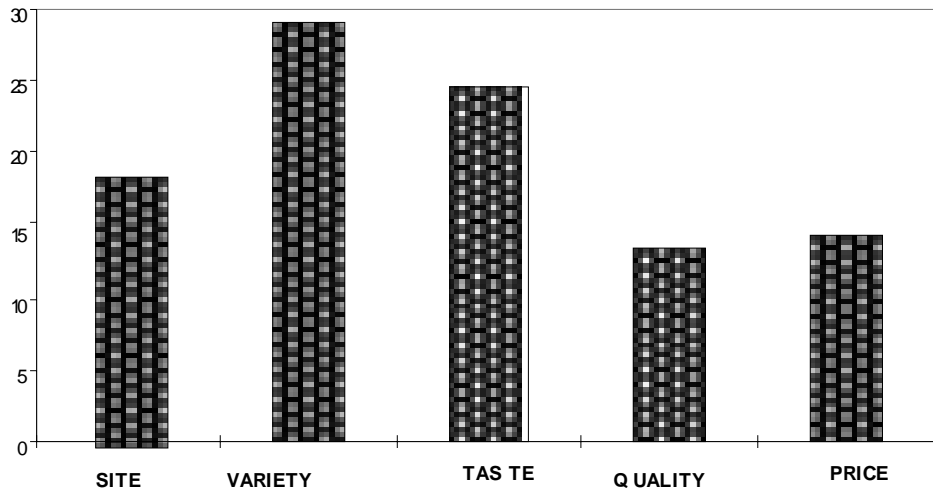


Figure 1. Averaged importance of attributes

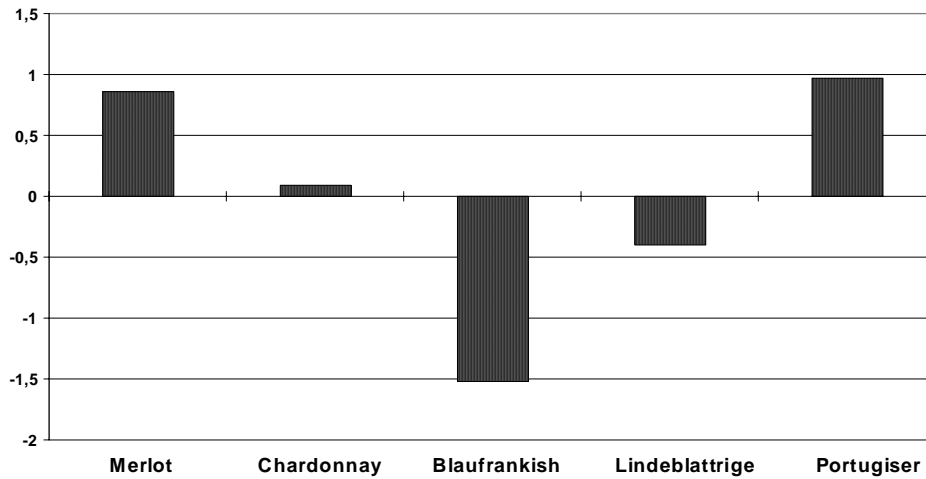


Figure 2. Utility of "variety" in the sample

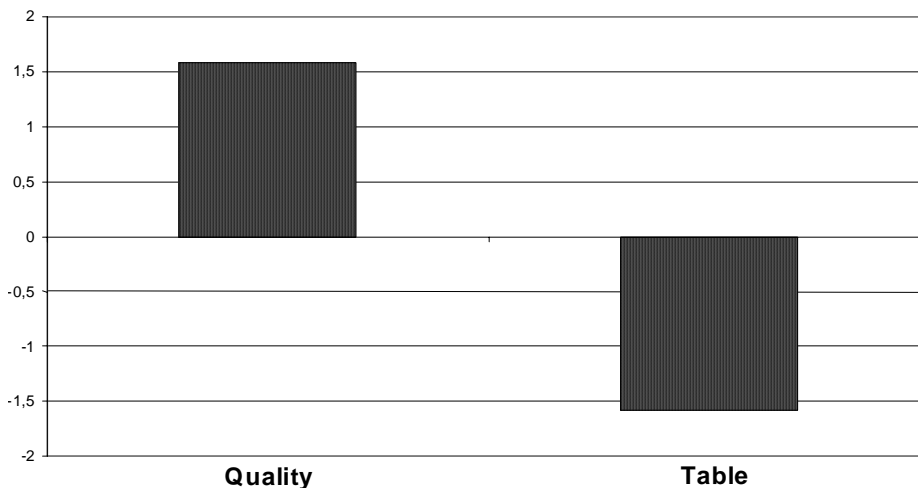


Figure 3. Utility of "quality" in the sample

Apart from semi-dry taste category there are significant differences between sexes. It means, that, as it is seen in the output report, men prefer dry wines to sweeter ones. Women's preference is just the reverse.

As far as varieties are concerned only Portugiser's preference differs significantly between sexes. As it is seen from also the part-worth values, men like this variety better than women.

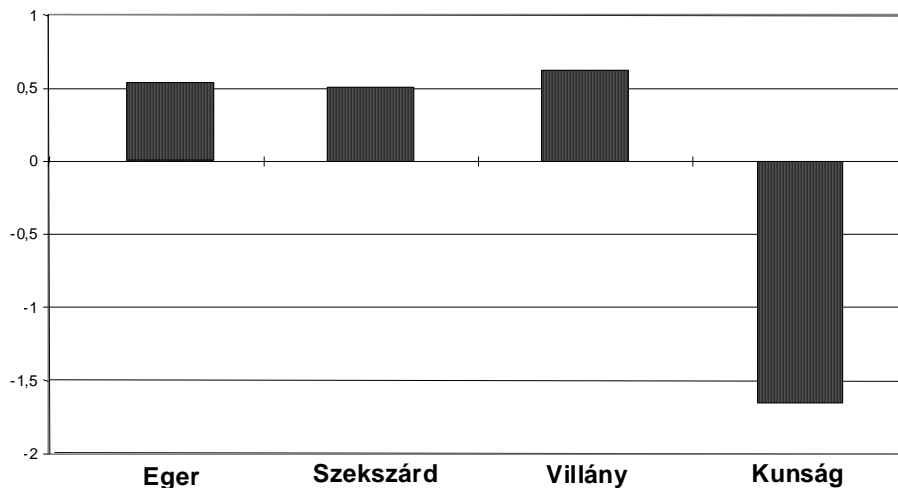


Figure 4. Utility of “growing site” in the sample

As for growing site no significant difference was found in any segments.

Almost unanimously respondents preferred quality wine to table wine regardless of sex, place of living or any other differentiating category.

Table 3. ANOVA Table of wine taste and variety in relation to sexes

Dry*SEX	Sum of Squares	df	Mean Squares	F	Sig.
Between groups	109,69	1	109,69	10,56	0,002
Within groups	1215,21	117	10,39		
Total	1324,90	118			
Semi-dry*SEX					
Between groups	11,77	1	11,77	1,83	0,179
Within groups	753,60	117	6,44		
Total	765,37	118			
Semi-sweet*SEX					
Between groups	50,19	1	50,19	8,18	0,005
Within groups	717,83	117	6,14		
Total	768,02	118			
Sweet*SEX					
Between groups	46,52	1	46,52	4,32	0,04
Within groups	1258,70	117	10,76		
Total	1305,22	118			
Merlot*SEX					
Between groups	2,39	1	2,39	0,321	0,572
Within groups	869,769	117	7,434		
Total	872,159	118			
Chardonnay*SEX					
Between groups	8,387	1	8,387	0,972	0,326
Within groups	1009,66	117	8,63		
Total	1018,048	118			
Blue Frankish*SEX					
Between groups	0,005	1	0,005	0,00	0,983
Within groups	1411,166	117	12,061		
Total	1411,171	118			
Lindeblättrige*SEX					
Between groups	3,886	1	3,886	0,332	0,565
Within groups	1368,597	117	11,697		
Total	137,483	118			
Portugiser*SEX					
Between groups	40,212	1	40,212	6,287	0,014
Within groups	748,358	117	6,396		
Total	788,570	118			

Price was not considered as a differentiating factor.

If we were to design a new wine for both sexes than it would probably be a red, semi-dry, quality wine at the price of 529 HUF a bottle from the Villány region.

REFERENCE

- [1.] Gustaffson, A. - Ekdahl, F. - Bergmann, B. (1999): Conjoint analysis: a useful tool in the design process, *Total Quality Management*, Vol. 16. No. 3. 327-343 p.
- [2.] Ferencz Á. – Berde Cs. - Nótári M. (2010): The Role of Quality Management of Traditional Horticultural Products in Rural Development in Hungary International Society for Horticultural Science 28th International Horticultural Congress Portugal, Lisboa 218. p.
- [3.] Ferencz Á. – Berde Cs. - Nótári M. (2010): The Role of Sales Management of Traditional Horticultural Products in Rural Development in Hungary International Society for Horticultural Science 28th International Horticultural Congress Portugal, Lisboa 219.p.
- [4.] Nótári M. – Ferencz Á. (2009): A hungarikum termékeket fogyasztók életstílusának elemzése. Jelenkori Társadalmi és Gazdasági Folyamatok. Vol. IV. No. 3-4. 69-73. p.
- [5.] Nótári M. – Ferencz Á. (2010): Marketing Possibilities of Functional Food on the Hungarian Market Functional Food Scientific Conference University College Cork, Ireland p. 48





¹ Abdelnaser OMRAN, ² Imre KISS

FACTORS INFLUENCING COST OVERRUNS ON CONSTRUCTION PROJECTS IN LIBYA

¹SCHOOL OF HOUSING, BUILDING AND PLANNING,
UNIVERSITI SAINS MALAYSIA, MINDEN, PULAU PINANG, MALAYSIA

²DEPARTMENT OF ENGINEERING AND MANAGEMENT, FACULTY OF ENGINEERING – HUNEDOARA,
UNIVERSITY OF POLITECHNICA OF TIMISOARA, ROMANIA

ABSTRACT:

Construction industry is considered as one of the most important industries in Libya. It is well known that most construction projects in Benghazi city exposed to cost overrun. These phenomena may affect the progress of construction industry in Libya as well as may expose many institutions of construction to be destroyed. Therefore, the aim of this paper was to identify factors influencing cost overruns on construction projects in Libya. The objective of the study was achieved through a valid questionnaire that was obtained from contracting companies, consultants, and owners in Benghazi city (Libya). As results, it was indicated that "lack of cost planning" occupied the first rank in importance, where "design changes" and "delay in materials delivery to the site" were among the most important affected factors. The study recommended owners, contractors, and consultants to hold their responsibilities to avoid cost overrun which could be achieved by good management of the project and finding new methods for storing the needed materials from the beginning of the project.

KEYWORDS:

1. INTRODUCTION

One of the most important problems in the construction industry is time and cost overruns. Time and cost overruns occur in every construction project and the magnitude of these delays and cost overruns varies considerably from project to project. So it is essential to define the actual causes of time and cost overruns in order to minimize and avoid the delays and increasing cost in any construction project. This chapter reviews literature concerning the major issues of time and cost overruns in order to recognize the related information regard those issues. Cost overrun is defined as excess of actual cost over budget. Cost overrun is also sometimes called "cost escalation", "cost increase" or "budget overrun" (Zhu *et al.*, 2004). Cost overrun is defined as the change in contract amount divided by the original contract award amount. Choudhry (2004) defined the cost overruns as the difference between the original cost estimate of project and actual construction cost on completion of works of a commercial sector construction project.

2. SHORT OVERVIEW ON FACTORS THAT INFLUENCE COST OVERRUNS

Previous research has attempted discover reasons for the disparity between the tender sum the final account. This section identifies the factors that influence cost overruns. Four factors were identified from the existing research findings (Morris *et al.*, 1990; Kaming *et al.*, 1997; Chimwaso, 2001). These are; design changes, inadequate planning, unpredictable weather conditions; and fluctuations in the cost of building materials. To broaden the investigation it was decided to complement the above list of factors with other factors gleaned from the final account reports. These were compared with the factors from the existing research findings, and a final list of 18 factors was prepared. Those were than divided into two groups of seven critical factors and nine other factors, which are usually ignored, but perceived to be of equal significance (Chimwaso, 2001).

2.1 List of critical factors

1. Incomplete design at the time of tender
2. Additional work at owner's request
3. Changes in owner's brief
4. Lack of cost planning/monitoring during pre-and-post contract stages
5. Site/poor soil conditions
6. Adjustment of prime cost and provisional sums.
7. Re measurement of provisional works.
8. Logistics due to site location
9. Lack of cost reports during construction stage.

2.2 List of other factors, which are usually ignored

1. Delays in issuing information to the contractor during construction in delays
2. Technical omissions at design stage
3. Contractual claims, such as, extension of time with cost claims
4. Improvements to standard drawings during construction stage
5. Indecision by the supervising team in dealing with the contractor's queries in delays
6. Delays in costing variations and additional works
7. Omissions and errors in the bills of quantities
8. Ignoring items with abnormal rates during tender evaluation, especially items with provisional quantities.
9. Some tendering maneuvers by contractors, such as front-loading of rates.

The prime variables of cost overruns have been commonly identified as: unpredictable weather, inflationary material cost, inaccurate materials estimates, complexity of project, contractor's lack of geographical experience, contractor's lack of project type experience, and non-familiarity with local regulations (Kaming et al., 1997). Morris (1990) studied the factors influencing cost overruns in public sector projects, he found that Escalation in costs is attributable partly to the fact that the original estimates were prepared at the then current prices, and partly to delays which enhance the effect of inflation and to direct escalation in costs arising out of change in scope, errors etc.

Based on certain assumptions with regard to the pace of expenditure on projects Morris has roughly computed that for the 133 projects which were studied only about 25 to 30% of the cost increase can be attributed to inflation. The remaining 70 to 75% has to be explained in terms of delays, inefficiencies, scope changes, changes in statutory levies, variations in exchange rates and to the combined effect of these factors with inflation. Morris (1990) was mentioned ten factors that influencing cost overruns of construction projects. These factors are: inadequate project preparation, planning and implementation, delay in construction as the first cause of cost overruns. The second factor was supply of raw materials and equipment by contractors. The third one was change in the scope of the project. The fourth factor of cost overruns was resources constraint: funds, foreign exchange, power, associated auxiliaries not ready. The delays in decisions making by government, failure of specific coordinating bodies was the fifth factor. The sixth cause was wrong/inappropriate choice of site. The seventh one was technical incompetence and poor overruns was natural calamities, Indo-Pakistan war and last one was the lack of experience of technical consultants, inadequacy of foreign collaboration agreements, monopoly of technology. Kaming *et al.*, (1997) examined the factors influencing construction cost overruns on high-rise projects in Indonesia. They found that cost overruns occur more frequently and are thus a more severe problem than time overruns on high-rise construction in Indonesia. The predominant factors influencing cost overruns are material cost increases due to inflation, inaccurate materials estimating and degree of project complexity. Chimwaso (2001) evaluated ten projects to assess their cost performance. The results have shown that seven out of ten projects had reported cost overruns. The factors that influence cost overruns have been identified and ranked in order of significance. These factors have further been classified under categories according to the formal of final account reports. By classifying them into categories, helps to deal with them effectively. The four categories arrived at are: variations, measurement of provisional works, contractual claims and fluctuations in the cost of labour and materials, with variations being the most significant. Frimpongs *et al.*, (2002) studied 26 factors that cause cost overruns in construction of ground water projects in Ghana, they sent to 55 questionnaire to owners, 40 to contractors and 30 to consultant. According to the contractors and consultants, monthly payments difficulties from agencies was the most important cost overruns factor, while owners ranked poor contractor management as the most important factor. Despite some difference in viewpoint held by the three groups surveyed, there is a high degree of agreement among them with respect to their ranking of the factors. The overall ranking results indicates that the three groups felt that the major factors

that can cause excessive groundwater project overruns in developing countries are poor contractor management, monthly payment difficulties from agencies, material procurement, poor technical performance, escalation of material prices according to their degree of influence. The amount of cost-increase (overruns), increased with an increase in the total cost of a residential project. However, private residence owners who spent more time on the pre-planning phase spent more money on the design phase; issued less change orders; selected more experienced contracting companies; and hired a supervising engineer to independently supervise the progress of work and ensure the delivery of materials – experienced less and cost – increases during the implementation phase of their residential projects. A major factor contributing to the sample projects and cost-increase was the insufficiency of money and time allocated to its design phase (Koushki *et al.*, 2005).

3. RESEARCH METHODOLOGY

This research consists of seven phases, the first one is the proposal for identifying and defining the problems and establishment of the objectives of the study and development of research plan. The second phase of the research includes literature review. Literatures of cost overruns were reviewed. The third phase of the research included a field survey which included the construction firms located within Benghazi city in Libya. The fourth phase of the research includes the questionnaires design, through distributing the questionnaire to a sample of contractors' firms. The fifth phase of the research was questionnaire distributors. The questionnaire was used to collect the required data in order to achieve the research objective. The sixth phase of the research focused data analysis and discussion. Statistical package for the Social Sciences, (SPSS) was used to perform the required analysis. The last phase of the research includes the conclusions and recommendations.

4. RESULTS AND DISCUSSION

Table 1 shows the ranking of factors that influencing cost overruns amongst fifteen factors which were used in the questionnaire. RII test was used to provide the ranking of these factors according to their importance. The respondents of contractors were ranked the "Lack of experience of project type" in the first position at this table. "Inadequate project preparation, planning and implementation" was ranked as the second important factor of cost overruns. The results as shown in Table 1 illustrate the other ranking of the factors by the contractors.

Table1. Ranking the factors influencing cost overruns

Factors	RII	Rank
Lack of experience of project type	.931	1
Inadequate project preparation, planning and implementation	.902	2
Low commitment of donor to compensate any bad result that may come from the bad economic and political situation	0.898	3
Omissions and errors in the bills of quantities	0.881	4
Lack of coordination at design phase	0.879	5
Delays in costing variations and additional works	0.874	6
Delays in issuing information to the contractor during construction stage	0.854	7
Change in the scope of the project, in Government policies	0.851	8
Absence of managerial programs that help in saving materials inside the site	0.846	9
Re-measurement of provisional works	0.838	10
Delay in project's handing over	0.836	11
Incomplete design at the time of tender	0.827	12
Lack of experience of local regulation	0.794	13
Delays in decisions making by Government, failure of specific coordinating	0.787	14
	0.785	15

5. CONCLUSION

From the results obtained from questionnaire when the researchers carried out the study, it was found that there are a real similarity of the important factors that influencing cost overruns (Table 1) when comparing them to those were found in the previous published studies. The only difference is that the ranking level was differed whereas it noticed that these ranking varied from one city or country to another. In addition, this study was ended by recommending some important strategies or policies to avoid such matter. These strategies are as following:

1. Contractors are recommended to have a time schedule that clarifies their needs for equipments in the site, so it would be ready where needed without delay.
2. Contractors are recommended to set up a computerized system to perform documentation process for all the activities in the site, so they would be able to detect performance in the work and to follow the time schedule continuously within the estimated costs.

REFERENCES

- [1.] Chimwaso, K.D., (2001). An Evaluation of cost performance of public projects; case of Botswana. Department of Architecture and Building Services, Private Bag 0025, Gaborone, Botswana.
- [2.] Choudhury I., and Phatak O., (2004). Correlates of time overrun in commercial construction, ASC proceeding of 4th Annual Conference, Brigham Young University- provo-Utah, April 8-10.
- [3.] Frimpongs Yaw, Oluwoye Jacob, and Crawford Lynn., (2003). Causes of delay and cost overruns in construction of groundwater projects in a developing Countries; Ghana as a case study. International Journal of Project Management, Vol. 21, No.5, pp. 321-326.
- [4.] Kaming Peter, Olomolaiye Paul, Holt gary, and Harris Frank C., (1997). Factors influencing construction time and cost overruns on high-rise projects in Indonesia, Journal of Construction Management and Economic. Vol. 15, No.1, pp. 83-94.
- [5.] Koushki, P.A, AL-Rashid, Khalid and Kartam, Nabil., (2005). Delays and cost increases in the construction of private residential projects in Kuwait, Journal of Construction Management and Economics. Vol. 23, No.3, pp. 285-294.
- [6.] Morris S., (1990). Cost and time overruns in public sector projects. Economic and Political weekly, Nov.24,1990, Vol. xxv, No.47, PP. M 154 to M 168.
- [7.] Zhu. K. and Lin.L., (2004). A stage – by – stage factor control frame work for cost estimation of construction projects, Owners Driving Innovation International Conference. [http:// flybjerg.Plan.aau.dk / JAPAASPUBLISH ED.pelf](http://flybjerg.Plan.aau.dk/JAPAASPUBLISH ED.pelf).





¹. Mohammed Salleh HAMMAD, ².Abdelnaser OMRAN, ³.Abdul Hamid Kadir PAKIR

IDENTIFYING WAYS TO IMPROVE PRODUCTIVITY AT THE CONSTRUCTION INDUSTRY

¹⁻³. SCHOOL OF HOUSING, BUILDING AND PLANNING, MINDEN, UNIVERSITI SAINS MALAYSIA, MALAYSIA

ABSTRACT:

In the current environment, contractors are had pressed to find ways to gain a competitive advantage and improve slim profit margins. In any given geographical area, construction labour, material and equipment costs are essentially the same. One of the few opportunities to improve the bottom line is to increase productivity. This paper is attempted to identify some ways to improve productivity at the construction site in Libya. Interviews were carried with contractors, owners and consultants. The paper has concluded that the consultants understand both best industry practice and the current construction technologies that can improve productivity. Perhaps most important, the consultants can provide the supervisor and crew with the training that will yield the greatest productivity improvements.

KEYWORDS:

Productivity, Improvement, Construction industry, Interviews, Libya

1. INTRODUCTION

Productivity is one of the key components of every company's success and competitiveness in the market. Productivity translates directly into cost savings and profitability (Proverbs et al., 1998). A construction contractor stands to gain or lose, depending on how well his company's productivity responds to competition. Construction companies may gain advantage over their competitors by improving upon productivity to build projects at lower costs; yet, most contractors do not systematically and properly address this strategic issue or evaluate its impact on the project's profit. It is no longer sufficient to outbid a singular, neighboring contractor because many companies compete nationally and/or internationally for construction contracts. Contractors must strive to improve productivity continuously or risk losing important contracts. A company has the ability to increase its competitiveness through enhanced productivity by raising the level of value-added content in products and/or services more rapidly than competitors. The concept of productivity is importantly linked to the quality of input, output, and process. Productivity is also a key to long-term growth (Helander, 1981).

A sustainable improvement in productivity, when associated with economic growth and development, is that productivity generates noninflationary increases in wages and salaries (Banik, 1999; Rojas & Aramvarekul, 2003b). A productive industry also may be profitable, allowing for growth and innovation while having a positive effect on society. For example, productivity improvement in the housing construction market may contribute to the supply of more affordable housing (Haas et al., 1999); however, sometimes the very nature of construction industry makes the productivity concept a complex one, due to such variables as small firm sizes, low profit margins, industry fragmentation, environmental issues, limitations on the supply of skilled labor, and other resources (Bernstein, 2003). Despite the importance of the productivity concept, productivity enhancement in construction has been overlooked for decades. While the manufacturing industry drew benefits from proven production management techniques (Neumann *et al.*, 2003), the construction industry lagged due to insufficient research in the area of productivity.

Methods for improving construction productivity to assist managers in identifying productivity barriers and offer solutions were limited. In contrast, there are few studies of enhanced productivity in the construction industry. In reality, increasing productivity benefits the stakeholders' in several ways:

- ❖ Projects are completed more quickly;
- ❖ Project cost is lowered;
- ❖ The contractor can submit more competitive bids; and
- ❖ The project can be more profitable

Most of the previous studies indicated that workers on a construction project are unproductive for 50 percent of their time on site. Waiting eats up more than half of an employees' unproductive time and about one-third of total project time. It can wreck a schedule and reduce the contractor's profits. Some studies indicated that a third of waiting periods result from factors under managements control. By improving management practices, a construction company can therefore reduce waiting time significantly. Besides long periods of waiting, there are many other drains on productivity at the construction site, including:

- ❖ Poorly planned materials management;
- ❖ Cleaning up the job site;
- ❖ Materials waste and theft;
- ❖ Accidents;
- ❖ Substance abuse;
- ❖ Redoing substandard work and completing client punch lists

Improving site productivity is easy to pose as a strategic objective, but not so easy to achieve given the complexity of the construction process. The study is carried out to identify some effective ways to increase the productivity in a construction company. A quantitative approach has been conducted with 25 project managers, contractors, consultants who are working with in the city of Benghazi in Libya. Based on their opinions and suggestion, the useful effective ways has been discussed briefly in the next section.

2. RESULT FINDINGS

From the interviews, it can said that these are the most effective ways that recommended by the interviewers who are working the construction filed within the city of Benghazi in Libya. They are as following:

2.1 Analyze the entire construction process in detail

A construction company should analyze each phase of its process to determine what the barriers are to improving productivity. It should begin by measuring key factors and setting benchmarks and goals for improvement. For example, the company can carefully observe the percentage of productive and nonproductive time at a site. By comparing project, the company can determine why one project was more productive that the other. For instance, perhaps productivity always slides when a certain piece of equipment is used. The construction company or firm can set a goal for using the equipment more efficiently, and then provide the training the crew needs to reach the goal.

2.2. Providing better planning

There will never be a magic solution that eliminates all work changes, but better planning will mitigate the impact of work changes and also eliminate the unnecessary waits that result from imprecise planning. For example, if contractor do not order material to arrive at the date it is needed, the crew will be forced to wait until the material arrives. Therefore, better planning is essential. There is also need to develop a measurement for determining how accurate the current planning process is, plus develop a realistic benchmark for improvement.

2.3. Train supervisors and the crew

Interviews confirmed that an important key to improving productivity is to train the crew. This is especially for construction supervisors, whose knowledge and skills can make or break a project in sound management principles and techniques. Construction companies rarely hesitate to train employees in specific skills such as how to operate a new piece of equipment. The benefit of training is measurable almost immediately: the employee is more productive as soon as he or she has mastered the new skill. Supervisor training should be specifically related to how to improve productivity at the job site. Supervisors must be trained to look at the job non on a day-to-day basis, but a work process with many discrete steps that must be completed over an extended, if limited period of time.

2.4. Regular meetings

In order to resolve the productivity problems associated with the management, a weekly informational staff meeting is recommended among the project manager, the project superintendent and their assistants. The weekly meeting would benefit productivity and profitability of project through prompt exchange of information. Weekly issues facing the project, information received from the engineer and owner, the project schedule, safety, critical materials and the machinery were among the topics to be discussed in the weekly meetings between the project's key personnel.

2.5. Safety planning

From the interviews, it can be indicated that some of the new workers seemed not to have a clear understanding of safety culture on the project. Some of the new workers did not utilize fall protection (despite the availability of this equipment on site), when standing at the edge of an excavation deeper than six feet. There were some workers who wore no hearing protection when working at different areas of the site that had a high level of noise. There was no orientation program for new hires and no training was performed for hazard identification and elimination. There were no safety incentives in place for recognition of goal directed behavior. Therefore, safety planning is an important element for increasing the productivity at construction sites.

3. CONCLUSION

Productivity is a serious issue for the construction industry, which because of its large size has a dramatic impact on the economy. This research was carried out in the developing economy of Libya. It may be that the issues of the key factors, the model developed and the alternative solutions here can provide guidance to the other economies in transition. Concepts such as practicing productivity in construction sites are not well understood by construction personnel. They often do not realise that there are many alternative ways that can lead to productivity and improve its achievements and values. The 5 identified ways can actually contribute to an increase in the value of construction productivity and could increase the performance level as well.

REFERENCES

- [1.] Banik, G. C. (1999). Construction productivity improvement. ASC Proceedings of the 35th Annual Conference. San Luis Obispo, CA, 165-178.
- [2.] Bernstein, H. M. (2003). Measuring productivity: An industry challenge. *Civil Engineering*, 73 (12), 46-53.
- [3.] Everett, J. G. & Kelly, D. L. (1998). Drywall joint finishing: Productivity and ergonomics. *Journal of Construction Engineering and Management*, 124(5), 347-353.
- [4.] Haas, C.T., Borchering, J. D., Allmon, E., & Goodrum, P. M. (1999). U.S. Construction Labor Productivity Trends 1970-1998. (Rep. No. 7). Center for Construction Industry Studies, University of Texas at Austin.
- [5.] Helander, M. (1981). Human factors/Ergonomics for building and construction. *Construction Management and Engineering*. New York, Wiley.
- [6.] Neumann, W.P., Winkel, J., Magneberg, R., Mathiassen, S.E., Forsman, M., Chaikumarn, M., et al. (2003). Ergonomics and productivity consequences in adopting a line-based production system. Proceedings of the 15th Triennial Congress of the International Ergonomics Association. Seoul, Korea.
- [7.] Proverbs, D.G., Holt, G.D. & Olomolaiye, P.O. (1998). A comparative evaluation of planning engineers' formwork productivity rates in European construction. *Building and Environment*, 33(4), 180-188.
- [8.] Rojas, E. M. & Aramvareekul, P. (2003). Is construction labor productivity really declining? *Journal of Construction Engineering and Management*, 129(1), 41-46.





¹Ferenc BAGLYAS

CONSUMER ATTITUDES TO GLOBAL GRAPE VARIETIES VERSUS HUNGARICUM VARIETIES IN THE SOUTH-ALFÖLD REGION

¹KECSKEMÉT COLLEGE FACULTY OF HORTICULTURE, DEPARTMENT OF VITICULTURE, HUNGARY

ABSTRACT:

In our days markets are segmented and the competition between the producers/suppliers is fierce. The main challenge for the marketing experts is to develop differentiated products that can develop a good market share and are able to keep their marketing share. The number of new products that are introduced to the market developed enormously. Multidimensional scaling is a useful tool in creating perceptual maps that is for positioning. Histograms are useful to “see behind the curtain”.

KEYWORDS:

Consumer, grape varieties, markets

1. INTRODUCTION

Marketing experts are faced with enormous difficulties when they try to estimate income, sale, market share of a new product, or the effect of a marketing strategy (Nótári et. al., 2010/a).

In our days markets are segmented and the competition between the producers/suppliers is fierce. The main challenge for the marketing experts is to develop differentiated products that can develop a good market share and are able to keep their marketing share. The number of new products that are introduced to the market developed enormously (Nótári et. al., 2010/b).

Success of strategic decisions depends on a well-operating marketing information system. Marketing research uses multivariate statistical methods to better understand consumer behavior (Ferencz et.al., 2009/a).

The abundance of measured data supposes statistical methods. As there is a continuous change (evolution) of living organisms the trends can be calculated statistically by computers especially if the available time for decision making is short (Ferencz et.al., 2009/b).

2. MATERIAL AND METHODS

The present study shows the results of a survey done among college students. In order to measure the attitude to wine regions and varieties a 1000 sample size survey was carried out. The data was processed by SPSS 10.0 for Windows statistical program package. The two methods used were multidimensional scaling and histogram of frequencies.

3. RESULTS

Figure 1. shows that, as for the wine producing region, Tokaj-Hegyalja is located in the corner of the map and Kunság Wine Growing district is the farthest from it. Frequencies show that consumers attribute high price for wines from Eger and Tokaj Hegyalja and low price to the wines originated from Kunság Wine Growing Region.

Figure 2. shows that as for the fame of the wine producing consumers regard Tokaj-Hegyalja, Eger and Badacsony the most renowned while Kunság the least one. Not surprisingly Pannonhalma-Sokoróalja is not positioned well which is attributed to its relatively new age.

Figure 3. shows that as for the quality of wine produced, Tokaj, Eger, Badacsony are well positioned while Kunság is again the least positioned. This shows that respondents attribute higher price to a more prestigious wine producing region.

Figure 4. shows the positioning of white varieties. As histograms indicate (Figure 5-6) Furmint, Hárslevelű varieties are favored while Kövidinka was not. Perhaps respondents were orientated by the fame of the region. Kövidinka, a local variety, or hungaricum is well adapted to the Alföld (Kunság) region which gives a light table wine. This variety is takes an important part in the wine strategy of the Alföld (Kunság) region. It is going to be difficult for the marketing experts to reposition this variety.

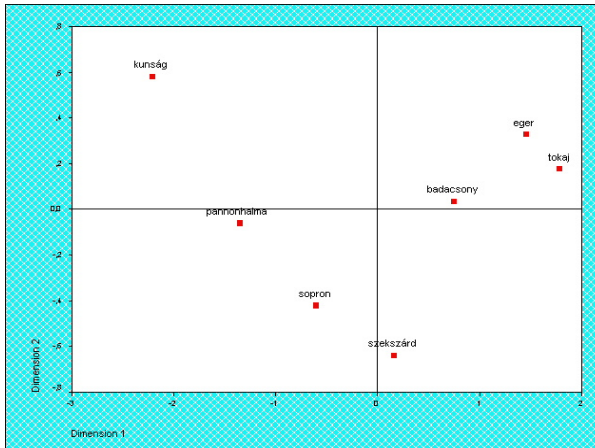


Figure 1.: Positioning according to price of wine

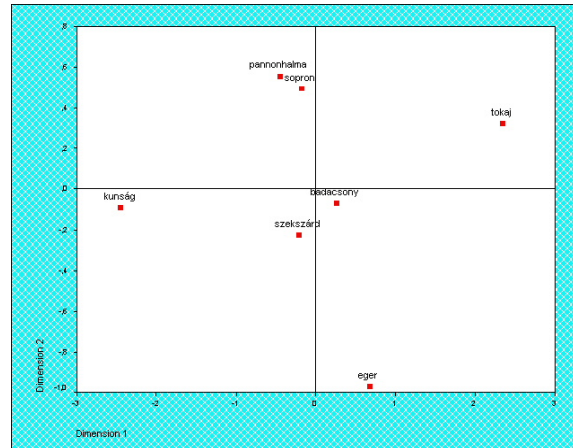


Figure 2.: Positioning according to fame

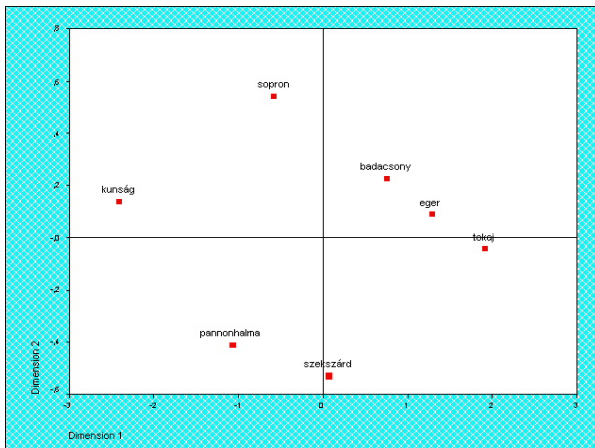


Figure 3.: Positioning according to quality of wine

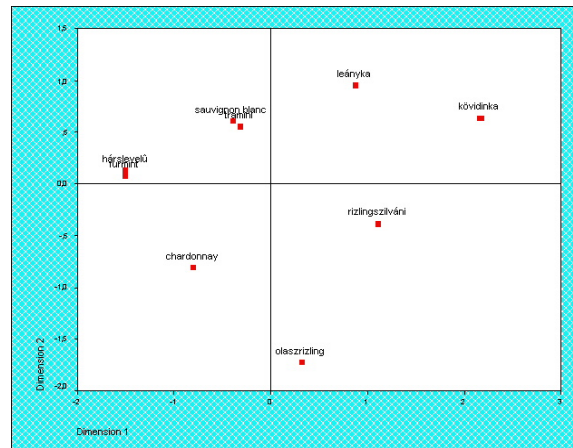


Figure 4.: Positioning of white varieties

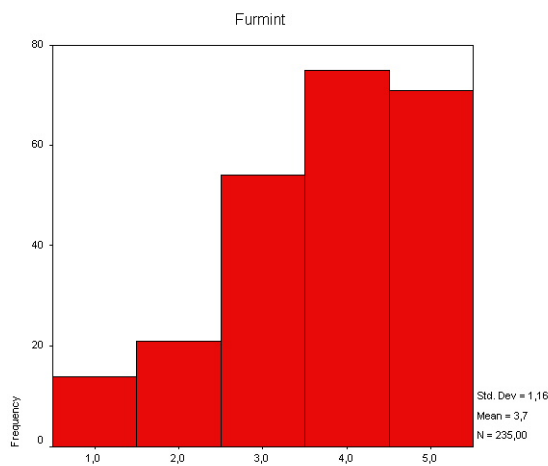


Figure 5.: Histogram of Furmint variety

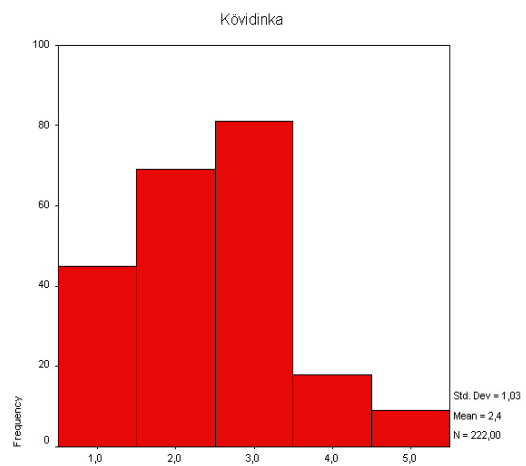


Figure 6.: Histogram of Kövidinka

Among red varieties so called “global” varieties (Merlot, Cabernet sauvignon) are preferred to local wines. Kadarka is the least favored hungaricum variety. Zweigelt is in an intermediate position (*Figure 7*). Histograms help to reveal the inner structure of the relations (*Figure 8-9*).

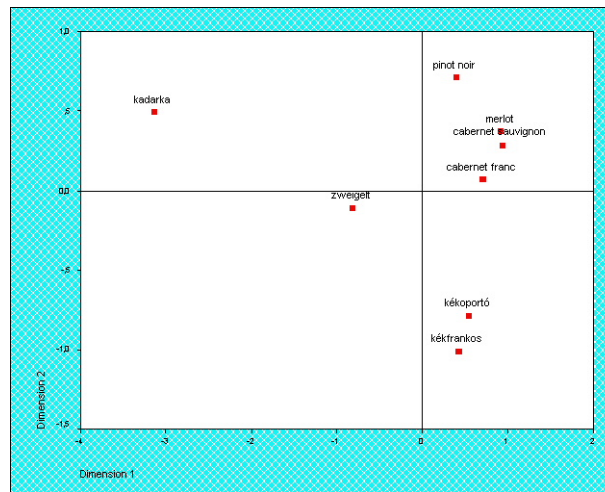


Figure 7.: Positioning of red varieties

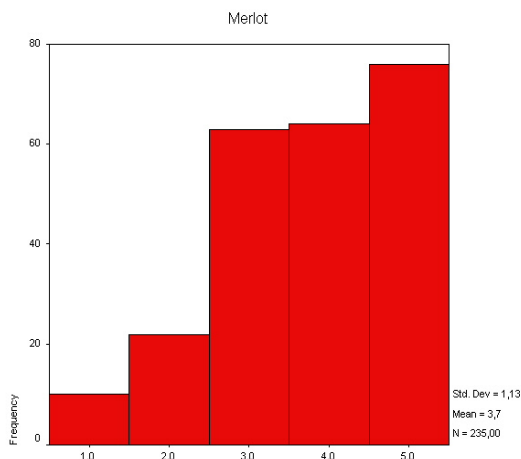


Figure 8.: Histogram of Merlot variety

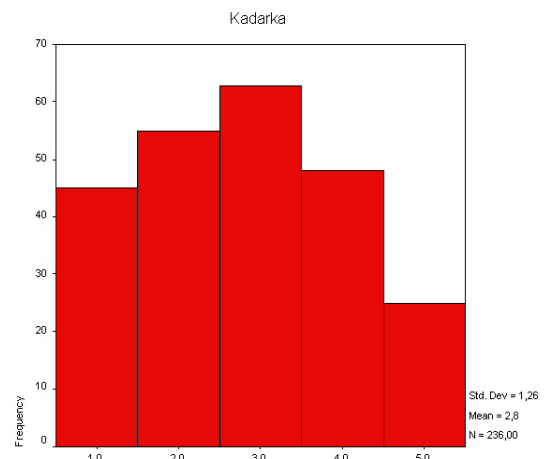


Figure 9.: Histogram of Kadarka variety

4. CONCLUSION

Multidimensional scaling is a useful tool in creating perceptual maps, that is for positioning. Histograms are useful to “see behind the curtain”.

It is seen that the wine producing regions with high reputation is reflected in the positioning, whereas Kunság and Pannonhalma-Sokoróalja are less positioned. This later is a new region therefor it is intermediately positioned. Fame and quality positively price is negatively correlated. Respondents attribute higher price of the wine to more renowned regions.

As far as varieties are concerned, among white varieties Furmint, Hárslevelű varieties are positioned best, because their “Tokaj” image. Kövidinka, a local variety, mostly grown in the Kunság region has a negative reputation even though this is a valuable variety, that has its place on the market. Among the reds, Merlot and Cabernet sauvignon are favored, while Kadarka is not. Kadarka is also associated to Kunság region and produce a light colored table or quality wine. It has a renaissance in the Szekszárd Wine Producing region.

BIBLIOGRAPHY

- [1.] Ferencz, Á - Notari M. (2009/a): Economic and marketing examination of traditional horticultural products among the costumers in Hungary. Annals of the Faculty of Engineering Hunedora. Vol.4. No.VII.145-150.p.

- [2.] Ferencz Á.-Nótári M. (2009/b): Piaci kihívások és lehetőségek a régiós, tradicionális kertészeti termékeknel a dél-alföldi régióban. *Gazdálkodás*. Vol. 53. No. 5. 440-446.p.
- [3.] Nótári M. – Ferencz Á. (2010/a): Examination of the market opportunities of the regional horticultural and food industry products in Hungary International Scientific Symposium Management of Sustainable Rural Development Timisoara Seria I. Vol 2 p. 136-142.
- [4.] Nótári M. – Ferencz Á. (2010/b): Communication Management of Functional Food in Hungary Functional Food Scientific Conference University College Cork, Ireland p. 49





RESEARCH COOPERATION BETWEEN THE UNIVERSITY OF TIMISOARA AND THE UNIVERSITY OF SZEGED

¹⁻³ DEPARTMENT OF PHARMACEUTICAL TECHNOLOGY, UNIVERSITY OF SZEGED, HUNGARY;

⁴ UNIVERSITY OF MEDICINE AND PHARMACY, TIMISOARA, ROMANIA;

⁵ UNIVERSITY OF MEDICINE AND PHARMACY, TARGU-MURES, ROMANIA

ABSTRACT:

In the framework of a friendly scientific cooperation, three talented, young researchers obtained their PhD degree in the Department of Pharmaceutical Technology of the University of Szeged. The first steps and the major results of this cooperation are summarized.

KEYWORDS: Scientific cooperation, mineral complexes with montmorillonite and inclusion complexes of cyclo-dextrins

1. INTRODUCTION

It is evident that excellent possibilities of cooperation are inherent in things which have belonged together naturally – geographically, economically – for centuries. The same is also true for scientific cooperation and for the trilateral relationships among Timisoara (Romania), Novi Sad (Serbia) and Szeged (Hungary) extending over the borders.

In our case, the first steps were taken about ten years ago when *Professor dr. Z. Szabadai* (University of Medicine and Pharmacy, Timisoara, Romania) proposed scientific PhD work carried out by two young researchers (*Codruta Soica* and *Cristina Trandafirescu*) from Timisoara UMF in the Department of Pharmaceutical Technology of the University of Szeged. In Targu-Mures (Romania), *Professor dr. Á. Gyéresi*, Head of the Department of Pharmaceutical Chemistry, UMF, was the scientific coordinator for them. Parallel with this, a third young researcher from Timisoara (*Ildikó Fejér*), also obtained a scholarship and a possibility to do her scientific research at the University of Szeged.

2. INVESTIGATED DRUGS

Investigated drugs in two main fields were the following: a) *inclusion complexes* containing acetazolamide, albendazole, betulinic acid, bifonazole, chlorthalidone, flufenamic acid, furosemide, hydrochlorothiazide, indapamide, mefenamic acid, meloxicam, simvastatin and cyclodextrins, and 2) *mineral complexes* containing benzalkonium chloride, buformin hydrochloride, glibenclamide, promethazine hydrochloride and montmorillonite.

3. STATISTICAL DATA OF COOPERATION

3.1 Publications in edited journals

Languages:

English	13
Hungarian	3
Romanian	9
Total	25.

Character:

Experimental publications	23
Refresher publications	2
Total	25.

Journals in which publications were edited:

Acta Medica Marisiensis, Targu-Mures/Marosvásárhely, Ro
Bulletin of Medical Sciences/Orvostudományi Értesítő, Cluj-Napoca/Kolozsvár, Ro
Colloid and Polymer Science, Springer-Verlag
Farmacia, Bucuresti, Ro
Gyógyszerészet/Pharmacy, Budapest, H
Revista de Chimie, Bucuresti, Ro
Revista de Medicina si Farmacie/Orvosi és Gyógyszerészi Szemle, Targu-Mures, Ro
Timisoara Medical Journal, Timisoara/Temesvár, Ro.

3.2 Presentations

Languages:

English	20
Hungarian	10
Romanian	2
Total	32.

Character: all are experimental presentations.

It must be pointed out that we also held an extra presentation at the 7th International Symposium Interdisciplinary Regional Research (ISIRR 2003), on 25-26 September, 2003, in Hunedoara/ Vajdahunyad, Romania. *M. Kata* and *Á. Gyéresi* were the authors and the title of their presentation was „Trilateral Cooperation in the Fields of University Activities”.

Cities where presentations were held:

Basel, Switzerland
Bristol, UK
Budapest, H
Cluj-Napoca/Kolozsvár, Ro
Dijon, France
Gdansk, Poland
Hunedoara/Vajdahunyad, Ro
Miercurea Ciuc/Csíkszereda, Ro
Oradea/Nagyvárad, Ro
Szeged, H
Targu-Mures/Marosvásárhely, Ro
Targu-Secuiesc/Kézdivásárhely, Ro
Timisoara/Temesvár, Ro
Versailles, France
Würzburg, Germany
Zalau/Zilah, Ro.

3.3 PhD theses

3.3.1 Title of PhD thesis of *Ildikó Fejér*: „Study of Drug-Montmorillonite Organocomplexes as Drug Carrier”, Szeged/Hungary, 2001.

3.3.2 Title of PhD thesis of *Codruta Soica*: „Preparation and Analysis of Inclusion Complexes of Some Diuretics with Cyclodextrins”, Targu-Mures/Marosvásárhely, Romania, 2007.

3.3.3 Title of PhD thesis of *Cristina Trandafirescu*: „Study of Interaction of Cyclodextrins with Azole Derivatives of Therapeutical Use”, Targu-Mures/Marosvásárhely, Romania, 2008.

4. OTHER CO-WORKERS

Rita Ambrus, Cristina Dehelean, Ibolya Fülöp and *Emőke Rédei*.

5. SUMMARY

The geographical proximity, the European approach and the interdependence of the Universities in Timisoara and in Szeged render cooperation possible: in the Department of Pharmaceutical Technology of the University of Szeged, three talented, young researchers prepared their PhD theses and obtained their PhD degree. At present, *Ibolya Fülöp* is conducting her PhD research. The first steps of this cooperation and its results to date are summarized by the authors.

As a result of collaboration for about 10 years, the authors investigated 16 drugs by inclusion and mineral complexations with up-to-date methods, they had 25 publications in quality journals (having *impact factors*), 32 presentations in different cities of Europe and 3 successfully defended PhD theses.



¹Eva BATEŠKOVÁ, ²Martina NOVÁKOVÁ, ³Tibor KRENICKÝ

TRANSFORMATION OF STN STANDARDS TO EN ISO STANDARDS IN THE FIELD OF ENGINEERING

¹⁻³ TECHNICAL UNIVERSITY OF KOSICE, FACULTY OF MANUFACTURING TECHNOLOGIES
WITH A SEAT IN PRESOV, PRESOV, SLOVAKIA

ABSTRACT:

The paper deals with the ISO standards processing. Standardization, being the basic method of documents formatting, is usually utilized to order and define rules which govern editing of the forms and documents. Moreover, ISO standards are widely applied not just for the purposes of the document editing, playing an important role in achieving the goals targeted by the manufacturing process and modelling the role of particular company segments.

KEYWORDS:

standard, ISO standard, STN standard

1. INTRODUCTION

The market of particular countries becomes competitive on international scale following the extent of ISO standards introduction that acts as a factor that affects the fundamental characteristics of manufactured product. This competitiveness is of great benefit to all suppliers. Recently, standardization has become a fundamental cornerstone in the whole industry, introducing innovative approaches to preventing imperfections of production, taking into account the economic advantage. The need for efficiency of production, the production process transparency is a way of the approaching the success for the companies engaged in the production. Nowadays, this issue addresses the introduction of ISO standards in order to define precisely the conditions under which the product is manufactured. But it is not only the production where ISO standards found its application, playing an irreplaceable role in editing of documents and modelling activities and organizational structure of the company.

2. THE STUDY

2.1 Characteristics of a standard

Standard is a document created on the base of agreement and is approved by a recognized institution that provides rules and guidelines for common and repeated use, for activities or their results so as to achieve an optimum degree of organization in a given context [1]. Standards vary according to the nature, scope and method of dissemination. Standards:

- ❖ cover several disciplines; dealing with all technical, economic and social aspects of human activities and cover all the basic disciplines such as language, mathematics, physics, etc.;
- ❖ are coherent and consistent; standards are prepared by technical committees that are coordinated by specialized institutions that guarantee that barriers between different fields of activities and business are overcome;
- ❖ are the result of cooperation; standards reflect the results of the joint work of all interested parts and are confirmed by the agreement by the relevant representatives: manufacturers, users, laboratories, public administration, consumers, etc.;
- ❖ are a living process; standards based on experience and lead to actual results in practice (products and services, test procedures, etc.); standards represent a compromise between current level and economic restrictions at the time;
- ❖ are currently; standards are regularly revised, or if circumstances dictate, standards evolve along with technological and social processes;

- ❖ have the status of reference documents; in commercial contracts and disputes in lawsuits;
- ❖ are recognized nationally and internationally; the standard is a document that is valid - nationally, regionally or internationally;
- ❖ are accessible to everyone; standards can be bought or studied without restrictions.

As a general rule, the standards are not mandatory, but are used voluntarily. In particular, implementation of standard may be required (e.g. safety, electrical installations, etc.) [1] Standard represents a level of know-how and technology, which makes the presence of industry in the process of its preparation inevitable. Standard is never neutral, this is reference document that is used specifically in connection with public contracts or contracts in international trade or for concluding commercial contracts. Moreover, standard is used by industrialists as unquestionable reference, which simplifies and clarifies the contractual relationship between economic partners. Finally, it is a document that is increasingly used in law suits.

2.2 Usage of a standard

Preparation of a standard usually consists of seven main stages depicted in Fig. 1. Then, standards can be used as:

- ❖ the basic standards introducing terminology, metrological concepts, conventions, marks and symbols;
- ❖ methods of testing and standards for analysis, the characteristics are measured;
- ❖ tools for defining the parameters of the product (product standard) or standards with specifications of services and defining the lowest parameters that must be adhered;
- ❖ organizational standards, dealing with the description of the company objective and its relationships, and modelling the activities (management and quality assurance, maintenance, logistics, project management and systems management of production (organization of production), etc. [2].

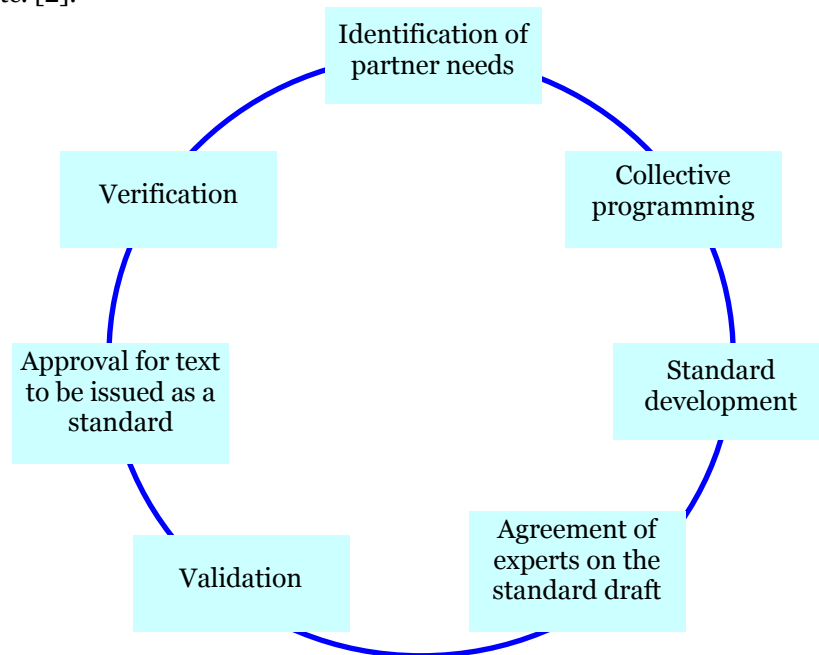


Fig. 1 Main stages of development of a standard [3]

2.3 European standardization institutions

Fig. 2 shows the European institutions for standardization.

SUTN - Slovak Standards Institute - the main activities of SUTN are:

- ❖ development, approval, issuance, distribution and sale of STN standards;
- ❖ development and maintenance of the national fund of STN; fund of European, international and foreign standards;
- ❖ providing searches in databases;
- ❖ organization of international cooperation from the post of official National standardization institution (i.e., participation in the development of international and European standards);
- ❖ providing activities of the National Information Centre (NIS);

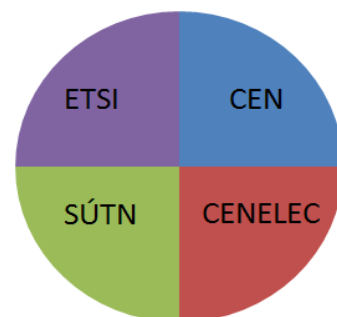


Fig. 2 European institutions for standardization [3]

- ❖ notification of national standards in CEN;
- ❖ issuing of standardization publications and periodicals;
- ❖ providing education for the technical community through seminars and trainings. [1, 4]

ETSI - European organization working in the field of telecommunications

ETSI is the largest developer and publisher of European standards on electronic communications, which prepares and issues with the approval of the European Commission to promote European Union policies. ETSI participates in the decisions on the further development of telecommunications, radio communications, mobile and other data networks, radio and television digital broadcasting, the Internet and other related areas. Moreover, ETSI cooperates mainly with the European organizations for standardization - the European Committee for Standardization (CEN), European Committee for Electrotechnical Standardization (CENELEC) and International Telecommunication Union (ITU). ETSI is a non-profit and non-governmental European organization which associates hundreds of members from various areas.

CENELEC - European Committee for Electrotechnical Standardization.

Its mission is to develop electrotechnical standards that facilitate to develop the European Single Market - European Economic Area for electrical and electronic goods and services, removing barriers to trade; creating new markets and reduce compliance costs.

CEN - European Multi-sectoral Standardisation Organisation acting in all areas except the electrical and telecommunication fields.

The role of CEN is to promote the European economy, social well-being of European citizens and the environment. The main principles of CEN activities can be summarized as following:

- ❖ openness
- ❖ transparency
- ❖ consensus
- ❖ relationship / identity
- ❖ national commitment.

3. ANALYSE OF TYPES OF STANDARDS

3.1 ISO standard

International Standard Organization (ISO) is as the world's largest developer and publisher of international standards. It is a network of national institutes for standardization of 159 countries as displayed in Fig. 3, founded in 1947 with headquarters located in Geneva. ISO covers standardization in all areas except the electrical. [1] ISO acts as the world leader in the development of international standards. ISO standards are dealing with the requirements that products must comply to be introduced to the global market as well as provide a mechanism for evaluating compliance ensuring that these products meet parameters that are specified in the standards. The result is that suppliers from both developed and developing countries can compete in any market under the same conditions. [6]

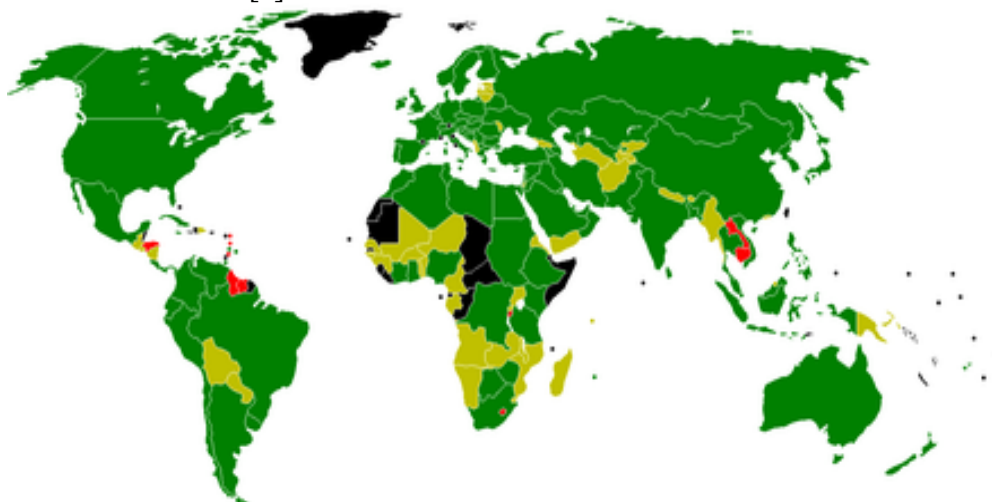


Fig. 3 Map of ISO members: green – members, yellow – correspondent members, red – supporting countries, black – non-members

These standards can be obtained although are rather expensive as they are protected by copyright and are generally prohibited to copy and distribute them. However, they may be implemented through national standards as follows:

- ❖ translated - maintains everything, including a code of international standard;
- ❖ translated with modifications - text and parameters are modified as compared to the source, the structure of international standard is retained;
- ❖ incorporated - text, structure and parameters of international standards are modified;
- ❖ taken original - very rarely (issued without translation for limited use in a defined group of experts).

ISO standard is published in a paper form, in A4 format – it is one of the ISO standard paper size. It may be up to several hundred pages long. ISO standards are also available for download in electronic form and some are available as part of a collection on CD or in manuals. [5]

3.2 STN standards

These standards are valid in the territory of Slovak Republic. Their position in the legal system is defined by the act on technical requirements for products and on conformity assessment and on change and amendment of some Acts in the wording of Act No. 436/2001 Coll. and Act No.254/2003 Coll. (Act No.264/1999 Coll.). [6]

The Act is mainly determining:

- ❖ codification of the method for setting the technical requirements for products;
- ❖ ways of assessment the conformity of product characteristics with these requirements; testing, certification, conformity standardization of products etc.;
- ❖ the rights and obligations for economic subjects (manufacturers, importers, distributors, etc.) in the introducing of products;
- ❖ the rights and obligations of legal subjects and organizations responsible for activities associated with the development, approval and issuance of technical standards.

3.3 EN standards

EN standard is the basic document of CEN and:

- ❖ it is required to be taken at the national level along with cancellation the standards that are inconsistent with it;
- ❖ its use is optional;
- ❖ its validity is unlimited and reviewed every five years.

The European standard is a document which that was adopted by one of the three recognized European organizations for standards: CEN, CENELEC and ETSI. EN is available in the three official CEN languages (English, French and German). European standards are a key part of the European Single Market. These technical documents are essential to facilitate European trade and therefore have high importance among producers from all around the world.

4. TRANSFORMATION OF STN STANDARDS TO EN ISO STANDARDS FOR SELECTED MATERIALS

A standard represents a model for specifications or technical solutions which can be traded in the market. Along with our country implementation into the European Union and with the adoption of technical standards there arose some questions of implementation related to the new standardization of materials.

In Table 1 - Table 3 are given examples providing the comparison of steel standardization under the corresponding original STN standard and current standard EN, respectively EN ISO standard.

Tab. 1 Steel Class 11

STN steel nomenclature	EN or EN ISO steel nomenclature	Material number W. Nr.
11 109	11SMn30	1.0715
11 110	10S20	1.0721
11 120	15SMn13	1.0725
11 140	35S20	1.0726
11 321	DC01	1.0330
11 343	S195T	1.0026
11 373	S235JRG1	1.0036
11 375	S235JR(G2)	1.0038

Tab. 2 Steel Class 12

STN steel nomenclature	EN or EN ISO steel nomenclature	Material number W. Nr.
12 010	C10E	1.1121
12 020	C16E	1.1148
12 024	C22E	1.1151
12 030	C25E	1.1158
12 031	C30E	1.1178
12 040	C35E	1.1181
12 041	C40E	1.1186
12 042	35B2	1.5511
12 050	C45E	1.1191
12 051	C50E	1.1206

Tab. 3 Steel Class 13

STN steel nomenclature	EN or EN ISO steel nomenclature	Material number W. Nr.
13 030	20Mn5	1.1133
13 141	28Mn6	1.1170
13 180	70Mn4	1.1244

5. CONCLUSIONS

In the study, structure of national and international systems of standards and process of transition between them is given. Standards are in frequent use in manufacturing in order to increase efficiency and productivity and are regularly updated. Using of a standard creates conditions for the regular audit of its relevance by the supervising organization and allows determining the time when it is necessary to adapt the standard for new needs. Finally, it should be noted that this analyse of the transition of materials labelling standardization is necessary part of such processes as the EU enlargement, since it facilitates the nonverbal communication within the unified market.

REFERENCES

- [1] <<http://www.sutn.sk/default.aspx?page=81f79981-12c5-491e-87e3-491c73710141>>; [cited 2010-06-12]
- [2] <http://www.tf.uniag.sk/e_sources/katmech/TN/Pr_TN5.pdf>; [cited 2010-06-12]
- [3] Šimočko, M.: Prehľadová štúdia spracovania ISO noriem v oblasti navrhovania technologických konštrukcií. Thesis, FMT TU of Košice, 2010, 47 p. (in Slovak)
- [4] <<http://www.cen.eu/cen/AboutUs/WhatIsCEN/Pages/default.aspx>>; [cited 2010-06-12]
- [5] Medvecký, Š. and al.: Konštruovanie 1. Žilina, EDIS – ŽU, 626 p., 2006, ISBN 978-80-8070-640-1 (in Slovak)
- [6] Leinveber, J., Vávra, P.: Strojnícke tabuľky. Prague, 914 p., 2008, ISBN 978-80-7361-051-7 (in Czech)





IMPLICATION OF NON-COMPLETION PROJECTS IN MALAYSIA

¹⁻²: SCHOOL OF HOUSING, BUILDING AND PLANNING,
UNIVERSITI SAINS MALAYSIA, MINDEN, PULAU PINANG, MALAYSIA

ABSTRACT:

The construction industry continues to occupy an important position in the nation's economy even though it contributes less than the manufacturing or other service industries. The contribution of the construction industry to national economic growth necessitates improved efficiency in the industry by means of cost-effectiveness and timelines and would certainly contribute to cost savings for the country as a whole. A major criticism facing the construction industry is the growing rate of delays in project delivery. Delay is a situation when the contractor and the project owner jointly or severally contribute to the non-completion of the project within the original or the stipulated or agreed contract period. Thus, this paper is investigated the implication of non-completion in construction projects in Malaysia.

KEYWORDS:

Projects, Implications, Non-completion, Delay, Malaysia

1. INTRODUCTION

The construction industry continues to occupy an important position in the nation's economy even though it contributes less than the manufacturing or other service industries. The contribution of the construction industry to national economic growth necessitates improved efficiency in the industry by means of cost-effectiveness and timelines and would certainly contribute to cost savings for the country as a whole. A major criticism facing the construction industry is the growing rate of delays in project delivery. Delay is a situation when the contractor and the project owner jointly or severally contribute to the non-completion of the project within the original or the stipulated or agreed contract period. In countries such as United State of America (USA), United Kingdom (UK) and Western Germany, Mobbs (1982) found that 'construction time' is better. The Construction Sector is one of the important sectors that contribute to Malaysia's economic growth. The sector accounted for nearly 3.3% of GDP in the year 2005 and employed about 600,000 workers including 109,000 foreign workers (MALBEX, 2005). The huge volume and complexity of projects in Malaysia's construction sector pose a great challenge and provide a wealth of opportunities to various companies in the construction industry. In Nigeria, Ajanlekoko (1987) observed that the performance of the construction industry time wise is poor. An investigation by Odeyinka and Yusif (1997) shows that seven out of ten projects surveyed suffered delays in their execution. According to Chan and Kumaraswamy (1993) timely delivery of projects within budget and to the level of quality standard specified by the client is an index of successful project delivery. When projects are delayed, they are either accelerated or have their duration extended beyond the scheduled completion date. These are not without some cost consequences. The conventional approach to managing the extra cost is to include a percentage of the project cost as contingency in the pre-contract budget. According to Akinsola (1996) conventional allocation of contingency is based on judgment. However construction projects are unique; as they may have a distinctive set of objectives, require the application of new technology or technical approaches to achieve the required result. This uniqueness makes the contingency allowance allocation based on assumption

and intuition inadequate and unrealistic. An investigation by the authors revealed that in Nigeria 5–10% of pre-contract estimate is in most cases allowed as contingency. This allowance was found to be inadequate. Inadequate contingency implies extra financial commitments, which in some cases are beyond the capacity of the owner. Clients are in some cases not prepared for such extra cost and so fund inform of loan are sought to offset the unexpected costs.

2. PROJECT NON-COMPLETION/ABANDONMENT AND DELAY

Construction projects have been managed since time immemorial. Traditionally this was the responsibility of the “master of the works” – a concept retained in the modern French. It emerged as industrial societies started to build complex systems such as rail and power networks. Projects are classically defined by the need to complete a task on time, to budget, and with appropriate technical performance/quality. In recent decades, projects have tended to become more time-constrained, and the ability to deliver a project quickly is becoming an increasingly important element in winning a bid. There is an increasing emphasis on tight contracts, using prime contractor ship to pass time-risk onto the contractor.

i. Project Delay

Failure to complete a complete a project either by the original planned time or budget, or both, ultimately results in project delay. The social and economic costs of delay can be staggeringly high and to a certain extent cannot be absorbed by the industry. When a delay can no longer be absorbed by the client, it will result in the project being abandoned. Thus, it is important to predict and identify problems in the early stages of construction and diagnose the main causes and implement the most appropriate and economical solutions to prevent further negative impacts of delay. In construction, delay could be defined as the time over run either beyond completion date specified in a contract, or beyond the date that the parties agreed upon for delivery of a project. It is a project slipping over its planned schedule and is considered as common problem in construction projects. To the owner, delay means loss of revenue through lack of production facilities and rentable space or a dependence on present facilities. In some cases, to the contractor, delay means higher overhead costs because of longer work period, higher material costs through inflation, and due to labor cost increases. Completing projects on time is an indicator of efficiency, but the construction process is subject to many variables and unpredictable factors, which result from many sources. These sources include the performance of parties, resources availability, environmental conditions, involvement of other parties, and contractual relations. However, it is rarely happen that a project is completed within the specified time. Stumpf (2000) defined delay as an act or event that extends the time required to perform the tasks under a contract. It usually shows up as additional days of work or as a delayed start of an activity. He showed, in his article, that delay does matter, and that different methods for analyzing schedule delay lead to different results for the owner and contractor. Construction delays became an integral part of the project's construction life. Even with today's advanced technology, and management understanding of project management techniques, construction projects continue to suffer delays and project completion dates still get pushed back (Stumpf, 2000).

ii. Project non-completion/Abandonment

There are several stages, as defined by the ministry, before a project is declared abandoned. If it has passed its promised delivery date by 10%, it is considered late; if the delay stretches beyond 10%-30%, then it is considered 'sick'; and finally, if no work has been carried out or no workers are on the project site for up to six months, then it is deemed abandoned (The star, 2009). Abandoned housing development means where a licensed housing developer had refused to carry-out or delayed or suspended or stopped or ceased works continuously for a period of six months or more or beyond the stipulated period of completion as agreed under a sales and purchase agreement (Sabah, 2005). A housing project is classified as "abandoned" by the Ministry of Housing and Local Government (MHLG) when there is no activity at the project site, continuously, for more than six months after the expected date of delivery of vacant possession. This is based on the date of the first Sale and Purchase Agreement (SPA) signed between the developer and a purchaser. A project is also classified as abandoned if, within this six month period, the developer has been wound-up and the company taken over by an official receiver or private liquidator recognised or affirmed by the Housing Controller, who is the Secretary-General of MHLG.

3. MALAYSIAN ABANDONED PROJECT

Project delays are known to affect project cost, workers morale, quality of completed works and the industry's reputation. Modern construction techniques and the use of sophisticated ICT tools on their own do no ensure that a project can be delivered on time. The right level of

knowledge, experience, methods and management skills are needed to ensure a greater chance for projects to be completed on or before the deadlines. Delay is a serious problem in the construction industry. It is costly for both owner and contractor. The owner loses by missing out on the potential revenues from the use of the project and by increased overhead cost for contract administration and supervision. The contractor also loses due to increased costs in over-head and tied-up capital. His losses may include lost opportunities for new projects because of diminished financial capabilities. In public projects, the public may also be affected by the delay in the utilization of the facilities and by the extended inconveniences such as traffic disturbances. Delay, therefore, is an important issue to the construction industry. Investigation into this problem area is needed in order to better manage delay situations and to mitigate their consequences. Assessing the frequency of delay, the extent to which delay may occur, and the responsibility for delay can provide insights for early planning to control these factors and improve project performance. Every step prescribed under the Housing Development (Control and Licensing) Act (the Act) is being taken by the Ministry of Housing and Local Government (MHLG) to minimise the number of abandoned housing projects in the country. However, there are unforeseen circumstances beyond the control of the ministry, such as the Asian financial crisis of 1997-98 and increases in the cost of building materials that have hurt many small housing developers and caused project abandonment. The public relies on this legislation and the enforcers to protect them in their quest for homeownership and many are fed-up with the lack or lax enforcement when problems surfaced. In the past, weak enforcement and monitoring had allowed errant developers to flourish. The previous Prime Minister, Abdullah Badawi was on 22.11.2005 quoted as saying: "If the projects have been monitored on a regular basis from the start, any sign of them being abandoned could have been detected and the projects salvaged" (Please see Table 1).

Table 1. Statistic of Abandoned Housing Project

STATISTIK PROJEK-PROJEK PERUMAHAN BERMASALAH (LEWAT, SAKIT & TERBENGKALAI)
 SEHINGGA FEBRUARI 2009

BIL.	NEGERI	PROJEK LEWAT			PROJEK SAKIT			PROJEK TERBENGKALAI			JUMLAH		
		BIL. PROJEK	BIL. UNIT RUMAH	BIL. PEMBELI	BIL. PROJEK	BIL. UNIT RUMAH	BIL. PEMBELI	BIL. PROJEK	BIL. UNIT RUMAH	BIL. PEMBELI	BIL. PROJEK	BIL. UNIT RUMAH	BIL. PEMBELI
1	PERLIS	3	67	52	2	30	27	0	0	0	5	97	79
2	KEDAH	14	1,301	847	14	2,473	1,502	9	1,445	709	37	5,219	3,058
3	PULAU PINANG	32	4,162	2,415	18	4,123	3,607	10	6,517	4,784	60	14,802	10,806
4	PERAK	52	3,182	1,713	43	3,622	1,925	6	822	597	101	7,626	4,235
5	SELANGOR	39	6,130	3,221	68	21,972	17,998	39	21,733	14,642	146	49,835	35,861
6	WP KUALA LUMPUR	10	2,471	896	9	895	564	6	2,408	1,365	25	5,774	2,825
7	NEGERI SEMBILAN	17	2,276	936	10	1,135	948	20	4,743	2,383	47	8,154	4,267
8	MELAKA	9	510	350	6	1,448	1,033	7	1,109	570	22	3,067	1,953
9	JOHOR	15	1,142	508	30	6,958	5,053	32	9,280	5,419	77	17,380	10,980
10	PAHANG	9	779	181	7	1,000	750	11	3,866	1,972	27	5,645	2,903
11	TERENGGANU	3	261	213	3	52	48	1	21	20	7	334	281
12	KELANTAN	5	193	109	6	286	228	3	519	367	14	998	704
13	SABAH	0	0	0	1	455	45	4	326	260	5	781	305
14	SARAWAK	0	0	0	0	0	0	8	406	288	8	406	288
JUMLAH KESELURUHAN		208	22,474	11,441	217	44,449	33,728	156	53,195	33,376	581	120,118	78,545
PERATUS		36	19	15	37	37	43	27	44	42	100	100	100

Source: Ministry of Housing & Local Government

NOTE: These figures do not include unlicensed and 'commercial' project developers.

Between 1990 and December 2005, a total of 261 housing projects were identified as abandoned by MHLG. These projects totaled 88,410 units, involving 58,685 house buyers for properties valued at a total of RM8.04 billion. Of these, 87 projects were revived and completed by white knights and another six by Syarikat Perumahan Negara Bhd (SPNB). Of the 168 remaining, 149 projects were classified as having the potential to be revived. These contained 63,894 units involving 42,706 buyers and a total sales value of RM5.4 billion. Another 10 projects housing 4,191 units, 2,074 buyers and RM426.2 million in sales value have been taken over by new developers, while nine others involving 2,866 units, 1,364 buyers and RM 335.29 million in sales value were classified as "not viable for revival". Of the total 70,960 units abandoned in the 168 projects, 31,276 are high-cost houses, 18,731 medium-cost and 20,953 low-cost units. The total number of abandoned projects makes up only 1.3 per cent of the 13,286 projects implemented between 1990 and December last year. It must be noted that the developers that abandoned the 261 projects

between 1990 and December 2005 had their licenses issued before the housing law was amended on Dec 1, 2002.

4. CAUSES OF NON-COMPLETION PROJECT

There are a number of factors behind the abandonment of a housing project:

- i. Finance
- ii. Poor marketing and sales strategies
- iii. Technical problems faced during construction
- iv. Problems caused by compensation demanded by squatters for resettlement.

The MHLG's findings have shown that 118 or 70 per cent of the 168 projects abandoned were due to the financial problems of developers. Another 23 (14 per cent) arose from poor marketing and sales strategies while 27 (16 per cent) failed over problems arising from squatter resettlement, poor company management and disputes between developers and contractors or with landowners (News Tarikh, 2006). There are financial problems of a developer caused by incidences such as the 1997-98 economic crisis. Crisis within the development company, including disputes between shareholders or embezzlement of progress payment collections, problems involving contractors and even disagreements with landowners are more reasons for abandoned housing projects. There are many reasons why delays occur. They may be due to:

- i. strikes,
- ii. rework,
- iii. poor organization,
- iv. material shortage,
- v. equipment failure,
- vi. change orders,
- vii. Act of God and so on.

In addition, delays are often interconnected, making the situation even more complex (Alkass, 1996). The factors which may give rise to non completion or late completion of projects cannot be exhaustively discussed due to space constraints, so only some are dealt with below. It is the responsibility of the parties to take account of any risk which might distort the completion of the plant, its operation and revenue stream (Dow and Andrews-Speed, 1998). Lenders as well as sponsors need be aware of the events which may endanger the completion of the project and the implication of leaving such factors unabated.

i. Insolvency Of Contractor

The insolvency of a contractor engaged in the construction of housing might mean distortion for the completion schedule. This is particularly an instance where a turn-key contract proves inadequate to mitigate completion risk, unless the contractor's obligation had been guaranteed under a bond by a credit-worthy third party. Although it might not be possible to predict the contractor's state of affairs such as to determine impending insolvency, engaging an experienced, financially responsible and strongly capitalized contractor is a way to mitigate this risk.

ii. Cost Overrun

Cost overrun can arise from so many events which include: an increase in the cost of energy supply for the construction, transportation cost, labour cost and material cost. Cost overrun may also arise from delay which can give room for inflation. Sometimes, design changes initiated by the owners or the government after the commencement of construction could so gravely invite cost overrun. Recently for instance, Multiplex Construction, the contractor in charge of the Wembley National Stadium in the UK has threatened to sue the clients for £150 Million allegedly being overrun cost it has suffered for the over 560 design changes made by the clients (Rogers, 2006). A power project experiencing cost overrun faces the risk of delay in completion pending the determination of the party committed or obliged to make provision for the overrun cost, unless adequate provisions had been made to salvage such eventuality. Sometimes, this determination emerges after a long and heated litigation process. Also, it could lead to outright non completion by frustrating the furtherance of construction work on the project where the party under obligation for the overrun cost is incapable of providing for it. This is especially so because power project sponsors, are often not as hugely capitalized as their oil counterparts, and in oil there is often resort to a great deal of joint ventures which helps to easily absorb such overrun risk.

iii. Currency Fluctuation

Whenever there is mismatch between one currency against another in a single project for loan disbursement and construction cost, there could arise the issue of currency fluctuation. The construction phase for a conventional plant has an average lead time of at least three years (Beck, 1994); thus within this time; cost overrun could set in arising from an unfavourable fluctuation of exchange rate. An example could be a loan denominated in British Pounds Sterling for which

construction contract and machinery accessories are in American Dollars. A devaluation of the Pounds Sterling against the Dollar would mean that more Pounds would be needed to fulfill the completion of the original plan. This was the case in Indelpro polypropylene plant in Mexico, where cost overrun was experienced partly as a result of fluctuation of the Mexican Pesos rate against the American Dollars (IFC, 1999). Thus currency fluctuation is an issue for consideration in mitigating completion risk. Lenders can explore a host of methods, including but not limited to denominating the loan currency in the currency of the technology to be adopted, however where this is not practicable.

iv. Regulatory Changes

There could be delays due to changes in policies, standards and regulations; these could also result in extreme cases of non-completion/cancellation. In the United States (US), majority of the unjustifiable cancellations of nuclear plants were blamed on constraints set in by ever evolving regulatory requirements (Joskow and Schmalensee, 1983). Often, some conditions like requirements to use modern and costly technology, are subsequently imposed which have the effect of eroding the bankability of the project, and for which the lenders would never have advanced capital had they been put in place from the very beginning. The difficulty has always been borne by parties who had no fault, drawn from the change in government regulation of the enterprise. With ever increasing environmental standards, it becomes even worse to predict what environmental compliance would be required of a power plant by the government. This is a potent risk in view of the long lead times of a conventional power plant. Environmental regulation contributed to the California electricity debacle - it was more cumbersome to get sitting and permitting approvals for new plants than in other US states and also the legal system gave the inhabitants and environmental groups the right to substantially delay the construction of new plants leading to inability to complete plants as scheduled.

v. Contractual Disputes

Disputes may be inevitable whenever parties to a contract have duties and obligations. With the several contracts needed to put a housing project into operation (concession, construction, loan, shareholders, interlenders, power purchase agreement and so on), the non existence of well established institutions and processes for dispute resolution, could lead to delay in completion of a housing project. Court proceedings are often presided over by judges who have no special training in the kind of contracts involved; and could also evidence very extensive delays. This is an area that a lender should not ignore in its objective to see the project completed according to schedule. Arbitration is the easy alternative since it gives the parties the flexibility to frame the process to suit their own peculiar circumstance, but even that is not a final solution in itself since arbitration awards will have to be enforced by a regular court. In India for example, a dispute concerning transfer of technology cannot be a subject of arbitration and the courts will not enforce any such award.

5. IMPLICATION OF NON-COMPLETION PROJECT

Abandoned housing projects have certain implications on the affected parties. Losses and difficulties faced by house buyers in servicing the interest on housing loans they have taken while paying house rental as well is one. The revival of an abandoned project involves:

- ❖ High capital injection, either by the developer or by other parties interested in reviving the project. This is due to vandalism at the project site, price increases of raw materials and changes in building requirements.
- ❖ Developers also face non-performing loans and land-owners risk their land being foreclosed.
- ❖ There is also, the possibility that a project may no longer be viable for revival or that no company is interested in reviving it. All these mean a loss to the economy.

Non-completion projects have certain implication on the affected parties. Managing and reviving a non-completion project is a complicated affair involving the developer, purchaser, financier, landowner and other parties. It will take time for all parties to reach a consensus since each parties want to protect their interest. When a single building is faced case of non completion, there is usually a confrontation between these parties. What to do with the project and who has to pay are usually sensitive issues that end up in costly and slow lawsuits. Abandoned buildings also have a significant impact towards socio economics nature and environment. Some closed ended implications are as follows:

i. End user/ house buyers

The consequences of abandoned housing projects are many. Some of them are, first, on part of the purchasers, they surely are unable to occupy the houses on time as promised by the developers in the Sale and Purchase agreement. The construction of the houses are terminated and partly completed which results to the fact that they are useless for occupation for a long duration of

time (mostly), unless they could, expeditiously be revived. Apart from the inability to occupy the houses, the purchasers too have to pay monthly installments to their banks. This is pathetic as the purchasers have to part with their monies but they could not get the houses. There are many side effects to home buyers especially those who still do not have their own homes and are forced to rent a house while waiting for the house is completed. They had to bear interest bank loans in addition pay the cost of rental houses while. This is their burden of middle income and low cost of living due to the increasing. There are not uncommon cases, where banks had made the purchasers bankrupt on the ground that they failed to pay monthly installments.

ii. Developers/ clients

Developer or client who is interested in reviving the project was burdened by the high capital injection. This is due to vandalism at the project site, price increases of raw materials and changes in building requirements. They also face non-performing loans and yet the land being foreclosed. Consequently, there is the possibility that the project may no longer viable for revival or there is no company interested to invest in the project. All these mean a loss to the economy. Private sector failures are sometimes solved by the public administration so the transfer of cost happened between private and public sector.

iii. Illegal activities are conducted

Studies showed that abandoned buildings are magnets for crime. First, they provide centres for the pursuit of a range of criminal activities, including prostitution, the consumption and trafficking of drugs, and crimes against property. Evidence of this is found in Spelman's (1993) study of 59 abandoned residential buildings in a low-income Austin, Texas neighborhood. Of these buildings, 34% were being used for illegal activities. Of the 41% of buildings that were unsecured, some 83% were being used for illegal activities (Spelman, 1993). Greenberg and other's (1990) study of TOADS in the 15 largest American cities finds that vacant buildings are frequently used as crack houses, and cites the use of TOADS as locales for drug dealing as one of the most prominent social ills associated with abandonment. According to Spelman (1993), abandoned buildings are ideal places to trade, conceal, and consume drugs. Activity within them is rarely visible from the street, while police officers are reluctant to enter abandoned buildings for legal reasons, because of general uncertainty and the possibility of danger and because of the low probability of a worthwhile payoff (i.e. slight chance of making an arrest). Evidence of drug use was found in 19% of the abandoned buildings in Spelman's study. Spelman (1993) also finds evidence of sexual activity and prostitution in 20% of the buildings in his study, and evidence of two different types of crimes against property. First, almost all of the unsecured buildings in Spelman's study are found to have been plundered by trespassers. Copper piping and wire, appliances, carpets and furniture are favorite targets. Second, 8% of the buildings in the study are found to be housing goods ranging from wallets to lawn furniture to bicycles stolen elsewhere. Abandoned buildings are not just centres where illegal activities are conducted. They also provide meeting places where offenders who perpetrate crimes elsewhere can gather, meet and plan their activities. Spelman (1993) suggested that abandoned buildings are well suited for this purpose because they physically shield criminals from the attention of outsiders. He even argues that, used as meeting places, abandoned buildings might actually foster and exacerbate criminal tendencies. This occurs as the lack of the usual social surveillance mechanisms erodes the self-control of those who meet there, while promoting group cohesion and the illusion of invulnerability. A clear association between abandoned buildings and neighborhood crime rates emerges from Spelman's (1993) study. City blocks blighted by unsecured abandoned buildings were found to suffer crime rates (including cases of drug, theft, and violent crimes) that were twice as high as those found in "control blocks" characterized by the absence of abandoned residences. Of course, this is not definitive proof that abandonment fosters criminal activity — perhaps the crime pre-dated and actually caused the abandonment, rather than the other way around. This possibility must be taken seriously because of the evidence that crime causes abandonment in Newman (1980). Spelman (1993) argues, however, that the "crime causes abandonment" thesis is not consistent with the qualitative features of the pattern of abandonment observed in Austin, Texas during the later 1980s. For example, abandoning owners were largely absentee landlords not local residents, who were responding to plummeting real estate prices throughout the region, not block specific characteristics such as crime rates. This provides some indication that the association between abandonment and neighborhood crime rates in Spelman's study is, indeed, explained by the notion that abandonment causes crime.

i. Cost overrun and time overrun

Cost overrun and time overrun (elongation of project duration) were the two most frequent effects of delay in the construction industry. Delay had significant effects on actual project duration. The model relating delay and actual project duration provide a benchmark for future

research work in the study of project management in Nigeria and also facilitate comparison with other countries. Loss and expense claims arising from delay and fluctuation claims during the delay period had significant effect on cost overrun. The models provide a benchmark for future research work in the study of project management in Nigeria and also facilitate comparison with other countries. Loss and expense claims arise from ascertained and approved delay caused by the client or his agent. The significant effect of loss and expenses claims on project cost overrun suggests that clients are a significant cause of delay in Nigerian building projects. This corroborates the result of a previous study where client-related delay was found to be significant. Delays in project completion seem to be a perennial problem and the lack of oversight by various ministries and departments in the procurement of goods and services continue to cost the Government hundreds of millions of ringgit. Delays in project completion, work not done in accordance with the original scope of works will increase project costs due to the inclusion of procurement of equipment and assets in the scope of works, unutilised facilities upon completion, improper payments made for works not done and shortage of officers in project supervision. These range from multi-billion ringgit infrastructure projects to the procurement of laptops and maintenance of government assets. For example, Kolej Kemahiran Tinggi Mara Balik Pulau in Penang paid RM84,640 for two laptops or RM42,320 per laptop and spent RM2.08mil on computer software that was not used, among other things. Then, there is the over RM15mil the Perak government spent on new purchases of cars and maintenance over the past four years and still not being able to manage its vehicles properly.

ii. Dispute and Arbitration

Furthermore, associated delay problems can also result in dispute, arbitration, total abandonment and protracted litigation by the parties. To some extent the contract parties through claims usually agree upon the extra cost and time elongation associated with delay. Nevertheless, this has in many cases given rise to heated arguments between the owner and contractor. The question of whether a particular delay to progress of work warrants an extra cost and or extension of project duration is usually the cause of disagreement. Such situations, usually involve questioning the facts, causal factors and contract interpretation, which have been addressed by (Alkass *et al.*, 1995). In specific terms, Odeyinka and Yusuf (1997) have addressed the causes of delays in Nigeria building projects. Another problem that has been identified is the disagreement prevailing among the purchasers, bankers, local authorities and the contractors concerned when it comes to revive the abandoned housing projects. This problem is complex as is evident in many cases. Consequently, the projects could or may not be rehabilitated as there is no common consensus among them.

iii. Rehabilitation Problem

Further to aggravate and worsen the situation, in the event there are plans for rehabilitation, the plans and attempts to rehabilitate are not easy. Many impending problems and difficulties, neither subtle nor obvious, would be awaiting the purchasers and the developers. Among the traumatic problems are the impossibility to revive the projects as the projects have been too long overdue without any prospect of reviving and to rehabilitate them, needing additional and substantial costs and expenditure. Cases show that most of the purchasers are reluctant to take additional money out from their own pockets on the ground, 'that it was not their fault', as the 'fault was squarely due to the developers'. 'Thus, the developers concerned should advance their own money to revive the projects'. Matters would not be settled that easy since most of the developers involved do not have enough money, which may be due to poor management or they had calculatedly siphoning off the company's assets and monies through unreasonable directors' allowances and high overhead operating costs. Worst still and of all, most of them have been wound up and the directors have absconded, unable to be traced and contacted.

iv. Delay on completion Time and Delay on Payment

Delays defer income, while interest keeps accumulating. Long delays may result in projects ending up in the so-called 'interest trap' (Flyberg *et al.*, 2004), where a combination of escalating construction costs, delays and increasing interest payments result in cost overrun. According to Arditti *et al.*, (1985), lengthy delays in inflationary environments increase cost overruns tremendously. The overall lack of finance to complete a project, or delays in the payments for services by the project owners or clients can lead to significant problems. If the costs of a project have increased significantly beyond the original estimate, then work on the project may have to be stopped or be delayed until additional funds can be found. Delays on payment may some times provoke the contractor to claim for interest rates. If the payment by a project owner is slow, the contractor may begin to commit fewer resources to a project, and may even cease work if cash flow becomes a problem.

v. Late Site Hand Over or Change of Location of Construction site

Late hand over of construction sites, some times may happen and substantially increase the cost of construction projects. In most international projects in Ethiopia late site hand over is a common form of claim source for compensation for contractors (Girmay, 2003). For example, the Addis Ababa Bolle International Airport Project has suffered an additional cost of about \$1,000,000.00 USD due to late site hand over (Girmay, 2003). Fortunately, domestic contractors do not ask for compensation due to late site hand over. Sometimes the owner may decide to change the location of the project after the award to the winning contractor. This is a rare phenomenon but it does happen due to sudden and unavoidable circumstances. The change of location of a project might extensively change the entire character of the work that was initially required under the (awarded) contract or the new location of the construction site may have different sub surface condition that may necessitate the structure to be redesigned. In such cases it is rightly alleged that the changes do alter the “general scope of work” and therefore, the final cost of the project might exceed the original contract amount.

vi. Acceleration Costs

Acceleration occurs when a project has been delayed, yet the owner demands that the contractor completes the contracted work before the contract completion date, or agreed upon changed completion date, or when the contractor wants to complete early. When acceleration occur the contractor typically will incur additional direct and indirect costs. While direct costs are relatively easy to quantify, indirect costs are difficult to identify and quantify (William, 2002). If the contractor establishes a valid acceleration claim, it is entitled to recover the costs incurred. These costs may include increased mobilization and demobilization costs due to the need to commit additional resources in terms of labor, equipment and supervision at the project than originally contemplated by the original schedule; specifically, direct labor costs include such items as increased wage costs for additional workers, overtime pay and rental costs for additional equipment. Further, the contractor may incur additional costs for inefficiencies in labor. These inefficiencies may include congestion or fatigue from extensive overtime work. Labor inefficiencies are a hidden but very expensive cost of acceleration. Nevertheless, while labor inefficiencies are a very real part of an acceleration cost, they are extremely difficult to quantify.

vii. Environmental impacts:

Visual impact: View quality is partially dependent on relatively unchanging landscape elements like mountains or valleys; views are also affected by more readily altered landscape features, particularly built structures such as buildings (Miller, 2001). In case of abandoned buildings view quality can be seriously deteriorated, especially if towering over flat coastal areas where the visual field is wide and open. Puntillo Del Sol building (Tenerife) is composed of two enormous unfinished and badly preserved fifteen-storey buildings. Its dilapidated appearance and its location at the top of a cliff generate a huge negative visual impact (CIEM, 2003). Similar visual impact has Azaña Hotel, also in Tenerife, a twenty-storey building seriously deteriorated. In these and other cases, and in accordance with Kearny *et al.*, (2008), the existing regulations do not meaningfully reflect general public attitudes regarding visual impacts.

viii. Landscape modification.

The original topography is significantly changed once urbanisation process starts. Waste soils, gravels and residues, temporary soil piles on construction sites, vegetation elimination and asphalt cover are common actions during urbanisation. These processes change progressively the especially sensitive coastal landscapes. Once the coastal stretch has become superficially indistinguishable from the rest of the hinterland's landscape in terms of vegetation and apparent sedimentary inactivity, development pressures and the absence of strict planning controls leads to encroached urbanisation in a number of prime locations. For instance Costa Esury housing development, in Huelva, consists of 2,184 houses (half of them under construction), two shopping malls, hotels and two golf courses. All of the latter elements are also under construction. The current bankrupt situation of the building company has paralysed the works. Up to date the landscape has changed drastically, and what before was riverside land nowadays is half-built housing development.

ix. Erosion.

At most locations, the occupation of the back-beach by infrastructural work has affected the littoral dynamics in a predictable way. The back-beach, which had previously been effective as a coastal defense feature through the provision of protection in rare severe wave conditions, became fixed by vegetation during relatively long periods of inactivity. In the most highly urbanised sections of the coastal fringe, the complete elimination of the back-beach as a morphological feature has occurred. Also digging and moving of soil and rocks leave abandoned loose earth and residues. Experimental studies and field investigations show that loose silt and earth piles formed

by urban construction can be eroded seriously (Hu *et al.*, 2001). In Lanzarote, the tracks generated thirty years ago during the construction phase of Atlante Del Sol site still remain. These tracks cause severe erosion problems in the area. The vegetation is unable to remain in these conditions as the little forest cover of the soil disappears and the area become more vulnerable to erosion. The deterioration of Puntillo Del Sol Building in Tenerife and its possible collapse are considered serious environmental hazards. It can produce erosive phenomena and affect to the Cabrera precipice and to the inter-tidal space located down the precipice (CIEM, 2003).

x. Biodiversity decrease

As coastal habitat conservation is directly related to species conservation, degradation of coastal areas would end in a decrease of biodiversity. Club Mediterranee de Cadaqués, in Catalonia, is located in the high ecological value area of Cap de Creus, part of the Natura 2000 network and Especial Protected Area. It is the damage to biodiversity and ecological values resulting from the abandoned of the resort what has driven Public Administration to order its demolition (BOE, 2008). Atlante Del Sol is located in an arid area of Lanzarote Island, but despite extreme conditions this area is rich in species of plants (CIEM, 2008). However, due to the fragility of this ecosystem, plants population has decreased in the surroundings areas of the abandoned building due to the erosion process described above.

xi. Pollution

Abandoned buildings usually trigger the creation of uncontrolled and unsupervised garbage disposal. As the case of Arenales Del Sol Hotel, in Alicante, this is dirty, full of garbage, an attraction to rats and a focus for illnesses. Besides garbage, half-built housing development may bring other kind of pollution. In Costa Esuri, Huelva, some people are currently living without sewage treatment plant. The pollution generated is being noticed downstream the Guadiana's river, where organic pollution is increasing. Pollution effects can be summarise as a decrease of water quality for aquatic life and recreational activities, eutrophication, alteration of ecological conditions and increase of illnesses related to water (DHG, 2009).

6. MEASURES TO PREVENT NON-COMPLETION /ABANDONED PROJECT

These are some of the measures MHLG has taken to prevent housing projects from becoming abandoned:

- ❖ Tightening procedures for issuance of housing development licenses and focusing on a developer's financial capacity;
- ❖ Continuous project monitoring through Form 7f;
- ❖ Regular visits to the project site and developer's premises to counter-check information provided in Form 7f;
- ❖ Exercising greater control over the Housing Development Account to ensure compliance with the Housing Development Regulations;
- ❖ Counter-checking all claims made on the Housing Development Account;
- ❖ Ensuring developers submit their annual audited financial reports;
- ❖ Taking legal action against developers for offences; under the Act and its Regulations; and
- ❖ Allowing licensed developers to apply for the minister's permission to revoke SPAs should they be unable to fulfill their obligations to purchasers.

7. EFFORT TO REVIVE ABANDONED PROJECT

Since housing projects are abandoned at various stages of construction for a variety of reasons, MHLG has adopted several approaches in the revival process. However, its main role is to:

- ❖ Act as mediator/facilitator to house buyer committees, financiers and developers to determine the direction of the revival scheme;
- ❖ Act as adviser to project revivers (white knights) and other affected parties to ensure their full co-operation and commitment to revive the scheme;
- ❖ Request SPNB to conduct viability studies to revive and complete a project should no other party want to;
- ❖ Allow for winding up of a developer and placing of a project under an official receiver or applying for a court order to appoint receivers and managers, or a white knight to revive it with the consent of the majority of the buyers;
- ❖ Allow a project financier, as debenture holder, to use its powers to appoint receivers to take control, revive and complete a project;
- ❖ Direct a company to assume, control and carry on the business of a developer vide the minister's powers under Section 11 (1) (c) or to use Section 11 (1) (d) to direct a developer to petition the High Court to wind up its business.

8. STAGES IN REVIVING AN ABANDONED PROJECT

Basically, all abandoned housing projects are first classified as having the "potential for revival". Subsequently, this classification is further stream-lined into four categories.

The first category is for abandoned projects newly identified in a particular year. At this stage, MHLG will focus on information gathering and allow for the appointment of a receiver or private liquidator for the developer, with the winding-up petition being served. **Thereafter** a feasibility study will be conducted on the project. This is normally done one year or more after the project is declared abandoned. It is at this stage that white knights may surface with project revival proposals. The MHLG will act as facilitator, giving advice and guidance to all affected parties.

The third stage in project revival is the selection of a white knight and ensuring all affected parties have reached a consensus on the project revival proposals. At this point, MHLG will act as a coordinator between the white knight and other technical agencies in order to speed up the approval of plans for the project to take off.

The fourth stage is when the contractor is appointed and construction is under way.

9. PROBLEMS REVIVING ABANDONED PROJECTS

Managing and reviving an abandoned project is a complicated affair involving the developer, purchasers, bridging financier, landowner and other parties. It will take time for all parties to reach a consensus, since each wants to protect its interest. Some of the hurdles MHLG faces in reviving abandoned projects include:

1. The involvement of the developer in other business activities or in a company with a diversified business portfolio. Though a Housing Development Account has been opened for the project, the receivers will take stock of all the developer's financial accounts when it goes into receivership. While project revival and debt settlement remain a priority, at times there would be very little left in the account to complete the project and settle liabilities.
2. When a developer is wound-up, the master charge is to get the first priority for debt repayment - and it usually wants the project foreclosed.
3. Developers also impose conditions in their consent for project revival in order to get returns for the effort they have put in from the parties reviving the projects.
4. Some developers don't own the land they are developing, so the rights of the landowners cannot be denied, especially if they have imposed conditions to protect their rights.
5. Consultants of developers who are in possession of detailed or amended building plans often refuse to cooperate with receivers or liquidators until their dues are paid.
6. Purchasers often insist that the late delivery clause in a SPA be honoured, or that no additional payment be imposed on them to revive the scheme.
7. Drawn-out court battles against developers by squatters, landowners, bridging financiers or contractors over contractual matters may further delay the revival of a project.

10. CONCLUSION

The issue of non completion of construction projects is one that has tremendous effects on the industry and economy of the country. From this research, we have identified the implications of non completion of projects from high capital injection, inability to occupy houses on time by the end users, building being subject to crime, cost and time over run, disputes, arbitration and protracted litigation by parties, difficulty in rehabilitation, project delay, increased cost of construction, environmental implications such as altered landscape view, unsightly scenery due to wastes, residues, soils etc, erosion, pollution, biodiversity decrease; socio-economic implications such as unemployment increase, conflicts between the public administration and the private sector, loss of economic value of the project and the area at large, consequential marginalization of the population to unwarranted transfer of cost between private and public sector; and numerous causes of non completion of projects which includes inadequacy of finance, poor marketing and sales strategies, technical problems faced during construction, problems caused by compensations demanded by squatters for resettlement, insolvency of contractor, cost overrun and currency fluctuation amongst others. We have also identified some possible measures towards cropping this problem both from the public and private sector namely: tightening procedures for issuance of housing development licenses and focusing on a developer's financial capacity; continuous project monitoring through Form 7f; regular visits to the project site and developer's premises to counter-check information provided in Form 7f; exercising greater control over the Housing Development Account to ensure compliance with the Housing Development Regulations; counter-checking all

claims made on the Housing Development Account; Ensuring developers submit their annual audited financial reports; taking legal action against developers for offences; under the Act and its Regulations; and allowing licensed developers to apply for the minister's permission to revoke SPAs should they be unable to fulfill their obligations to purchasers.

We observed that there have been efforts made by the government towards reviving abandoned and non completed projects and some problems faced in this course. However, it is important to note that abandoned projects do not benefit the construction industry and has negative effects on the economy of the country and most effectual on the end users. It is therefore, expedient that efforts are made jointly by the public and private sector to crop this problem.

REFERENCES

- [1.] Ajanlekoko JO. (1987). Controlling cost in the construction industry. Lagos QS Digest, Lagos. 1(1):8–12.
- [2.] Akinsola, A.O. (1996). A Neutral network model for predicting Building projects' Contingency. Conference: Proceedings of Association of Researchers in Construction Management, ARCOM 96, Sheffield Hallam University, England, 11–13 September 1996, pp. 507–516.
- [3.] Alkass, S., Mazerolle, M., Tribaldos, E., and Harris, F. (1995). "Computer Aided Construction Delay Analysis and Claims preparation", Construction Management & Economics. 13, 335-352.
- [4.] Ardity, D., Akan, G.T., and Gurdamar, S. (1985). Cost overruns in public projects. International Journal of Project Management, 3, 218–225.
- [5.] Bagué, G. (2004). El Club Mediterraneo de Cadaqués cierra y pretender vender su paraíso natural al estado. El País Online, 1 June 2004.
- [6.] Beck, P. (1994). Prospects and Strategies for Nuclear Power, Global Boon or Dangerous Diversion? 53 (London, UK: Earthscan Publications Ltd, 1994).
- [7.] Chan, D.W.M., & Kumaraswamy, M.M. (1993). A survey of time-cost relationships in Hong Kong construction projects. Building Technology and Management Journal. 20 (2), 54–72.
- [8.] CIEM (Canary Islands Environmental and Territorial Policy Ministry), (2003). Plan Especial Paisaje Protegido Costa de Acentejo.
- [9.] Czamanski, D. (1999). Privatization and Restructuring of Electricity Provision 32 (West Port, US: Praeger Publishers).
- [10.] Bordoli, D.W., and Baldwin, A.N. (1998). A methodology for assessing construction project delays. Construction Management and Economics. 16, 327–337.
- [11.] DHG (Demarcación Hidrográfica del Guadiana), (2009). Contaminación localizada en aguas de transición. Plan Hidrológico 2009, Tema Importante nº 13. Confederación Hidrográfica Guadiana.
- [12.] Dow, R., & Andrews-Speed, P., (1998). China's Electricity Industry under Reform 1996-1998 (Dundee, UK: CEPMLP).
- [13.] Flyvbjerg, B., Holm, M.K.S., and Buhl, S.L. (2003). How common and how large are cost overruns in transport infrastructure projects? Transport Reviews, 23, 71–88.
- [14.] IFC, (1999). Lessons of Experience: Project Finance in Developing Countries 43 (Washington, US).
- [15.] Joskow, L., & Schmalensee, R. (1983). Markets for Power: an Analysis of Electric Utility Deregulation (Massachusetts, US: The MIT Press).
- [16.] Kearny, A.R; Bradley, G.A.; Petrich, C.H; Kaplan, R.; Kaplan, S., and Simpsons-coleman, D., (2008). Public perception as support for scenic quality regulation in a nationally treasured landscape. Landscape and Urban Planning. 87.
- [17.] MALBEX, (2005). Market watch – construction industry, Kuala Lumpur Exhibition Center Report. Pp.1–8.
- [18.] Miller, D. (2001). A method for estimating changes in the visibility of land cover. Landscape and Urban Planning. 54, 91–104.
- [19.] Mobbs, G.N. (1982). Speeding up construction. The Quantity Surveyor. 38(1):2–3.
- [20.] Newman, O. (1980). Community of Interest. New York: Anchor Press/Doubleday.
- [21.] Odeyinka, H.A., & Yusif, A. (1997). The causes and effects of construction delays on completion cost of housing projects in Nigeria. Journal of Financial Management of Property and Construction; 2(3):31–44.

- [22.] Rogers, D. (2006). Multiplex sues Football Chiefs & Wembley Designer next in line for Legal Action, Construction News, April 6, 1–3.
- [23.] Sabah, (2005). Housing Development (Control and Licensing) Enactment 1978 (Amended 2005).
- [24.] Sander, H.A., and Manson, S.M. (2007). Heights and locations of artificial structures in viewshed calculation: How close is close enough?. Landscape and Urban Planning, 82.
- [25.] Spelman, W. (1993) "Abandoned Buildings: Magnets for Crime" Journal of Criminal Justice. 21: 481-95.
- [26.] Stumpf, G. (2000). Schedule delay analysis. Construction Engineering Journal. 42(7):32–45.





¹: Éva MATIJEVICS

APPLICATION OF PROJECT MANAGEMENT METHODOLOGY IN PREPARING OF THESIS

¹: SUBOTICA TECH – COLLEGE OF APPLIED SCIENCES, SERBIA

ABSTRACT:

The final phase of the high school education, is to write a thesis. The student has to do it alone, and use his acquired knowledge, that he studied in the school. He must demonstrate, that he is able to work in this area of speciality. Preparing this work lasts up months, because it includes a lot of work such as going to the library and find a good theme, formulate a task, consulting with the teacher, using simulations, ... Inadequate timing, and inadequate understanding the work schedule can cause the delay of efficient work. The network planning, which is constructed by the project method, helps us to optimize the steps in the work, the length of each phase and relationship to each other.

During the construction of our work, we used successfully the computer and other multimedia tools such as film, projector and interactive whiteboard. We made a network plan under several hours, which shows the process of preparing a thesis. Students worked in a group. We made photos, and videos of the atmosphere of the education in the class, and the result of our work was valued through questionnaires.

KEYWORDS: Project Management Methodology, network plan

1. THE MEANING OF TEAMWORK

To construct a project, it is necessary to work in a team. The activities of such a group will follow-up during the class. A group of students, who work in the classroom, simulates a real environment and want to create a conceptual product. Working in group will develop the division of labor, cooperation, adaption, communication. [2] Meanwhile, students discuss what to do, they use technical terms. They are able to apply knowledge, ideas in experimental situations, so they improve their understanding of knowledge.

2. THE MEANING OF PROJECT

The meaning of a project is defined in 1994, by the standard ISO 8402 with the following terms:

Project: a project is a temporary endeavor undertaken to create a unique product or service. Every project has a definite beginning and a definite end. It has a clear aim. To achieved this aim, the activities of team is co-ordinated and controlled. All this proces is indicated by specific requirements such as constraints of time, cost and resource constraints. [10]

Project can take various forms, where each has its own specific requirements. Each requires a separate project management. Despite the differences, each project has the following properties:

- ❖ the timeframe for the implementation of the project;
- ❖ the product of a project, so the aim, that is intended to be implemented;
- ❖ there is a description of the plan of project implementation;
- ❖ the cost for realization is given;
- ❖ there is a financial plan that is broken on parts of the project time;
- ❖ there are formulated the quality expectations and requirements against the project;
- ❖ the uncertainty project sites and inhibitor facts are signed, and
- ❖ valuation of potential risks and reactions. [10]

In every project we must specify – it`s size (the activities which represents the individual tasks)
– resources that includes: - labor (so called “work”)
- materials
- money
– and its deadline.

After this first phase follows the tracking of implementation.

- a) One of the requirement of tracking systems is to collect continuously (in real time) data about the
- implementation and
- costs.
- b) Another requirement is that the results of an analysis of the data must be submitted as soon as it is possible. For this process it is necessary to have
- appropriate techniques and
- tools. [10]

In order to answer the above requirements, the planned phases are realized by deploying a variety of methods. Finally, the preparation process of the thesis and the steps were drawn up in the network. There are several well-known network planning methods, they are taught in graph theory in operational research.

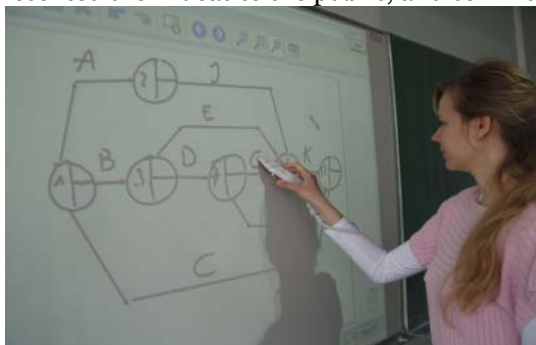
The network planning is a plan of work. That plan contains the optimal project scheduling and analysis, contains the coordination of the timing of certain activities, contains the timing of those activities which can do one after the other or can do in parallel schedule. This helps us to follow through the actual implementation of the workflow, to recognize in time the significant backwardness and delay the plan. If it is necessary, the corrective action can take. The processes of tasks are presented in a network plan. [9]

3. METHODS OF WORKS

Our knowledge - we have – is thanked to older generations. We take their expertise and empirical knowledge, or they teach us. This process is realized mostly through books, magazines, courses, school education. [1]

At the beginning of the work, the team must be educated about thesis requirements, it`s phases and about method how to prepare our work. The knowledge that we use in project management, is partly from studies in the universities, and partly from skills of professionals. [7] Their skills help us to determine the amount of resources and their schedule on tasks. To ask for skills, we prepared some questions, and collected them into interview. The subject of our interview, we choose such persons who have recently graduated, or who are now preparing his thesis. The questions are constructed by students by using the method Brainstorming. These ideas were grouped according to the phases of thesis. The interactive whiteboard was a useful tool for our notes, that was good visible for everybody. We opened new pages for a group of questions, so the ideas we entered on the correct page. Saved the file, and this is our document in our project. Some of the main questions are to be found in the appendix. (A)

During the work in classroom, the atmosphere in a group was friendly. The members easy presented their ideas to the public, and communicated well.



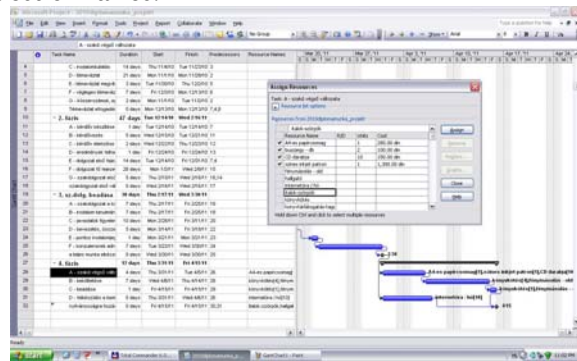
Figures 1 and 2. The teamwork

At the next time a member of the group, reported the results of the interview. Our topic was processed based on these data. We made videos of students work, and we played them back. These play backs are always interesting for students, because it is a time when they can watch themselves as an outsider. Each step has discussed together. The comments were written on the interactive whiteboard. They were saved, and if it was necessary, easily could turn a page back. These notes are also the part of the documentation.



Figure 3, 4, 5 and 6. During our work, the interactive whiteboard was a favorite tool. As a result of our work is a product, that is a network plan, which our students can realize. The tasks from network plan, were entered into the computer. Information of the duration of tasks, and costs of the activities, were collected from questionnaires.

3. fázis:
- A - szakdolgozat a konzulensnél
 - B - irodalom tanulmányozása, összevetése a munkákkal
 - C - javaslatok figyelembevétele - dolgozatunk második változata
 - D - bevezetés - 2 old.
 - E - pontos irodalomjegyzék - 2 old
 - F - a harmadik változat átadása
4. mérőföldkő - a teljes munka elkészülése



Figures 7 and 8. Data on the board, and in the computer

The phase of the follow-up is created during student's actual thesis writing, when he follows up the phases of work, quickly notices any deviations so he can change and modify the additional activities. To construct the working plan, the student can avoid to late of term or not to finish his work on time.

<p>1. milestone – selection the topic:</p> <ul style="list-style-type: none"> A – search for topic B – in the library C – looking for ideas from the literature D – the sketch of the topic – 5 pages E – consulting with the assistant F – the final sketch of the topic G – purchase the writing – materials such as paper, ink....2 <p>2. milestone – accept the sketch of topic</p> <p>2. phase:</p> <ul style="list-style-type: none"> A – construct the questionnaire B – filling the questionnaire C – analysing the questionnaire D – applying the answers E – constructing the first part of the thesis – theory – 10 pages F – constructing the main parts of the thesis – 40 pages G – the first version of the thesis <p>3. milestone – the first version give to assistant</p>	<p>3.phase:</p> <ul style="list-style-type: none"> A – the assistant analysis our thesis B – compare our work with the literature C – accept the suggestions of assistant – the second version of our thesis D – writing the introduction – 2 pages, summary – 3 pages E – correct references – 2 pages F – the assistant analysis the third version of our thesis <p>4. milestone – the whole thesis are finished</p> <p>4. phase:</p> <ul style="list-style-type: none"> A – the final version of the thesis B – bookbinding our thesis C – give it to archives D – preparing the presentation of the work <p>5. milestone – present the work to the public</p>
--	--

Figure 9. Lists of signs of activities and durations

We evaluated our project well. It was succeeded to construct an acceptable timetable. It shows that it is necessary a half year to prepare a thesis, of which about 20% of the study of literature, 10% of the time the work is at assistant, and 60% of the work is it's writing.

In pedagogical education are known the impacts of project method. [2] I presented them to students in the form of a questionnaire. While they filled and formulated the questions, they were thinking about facts by which they became richer.

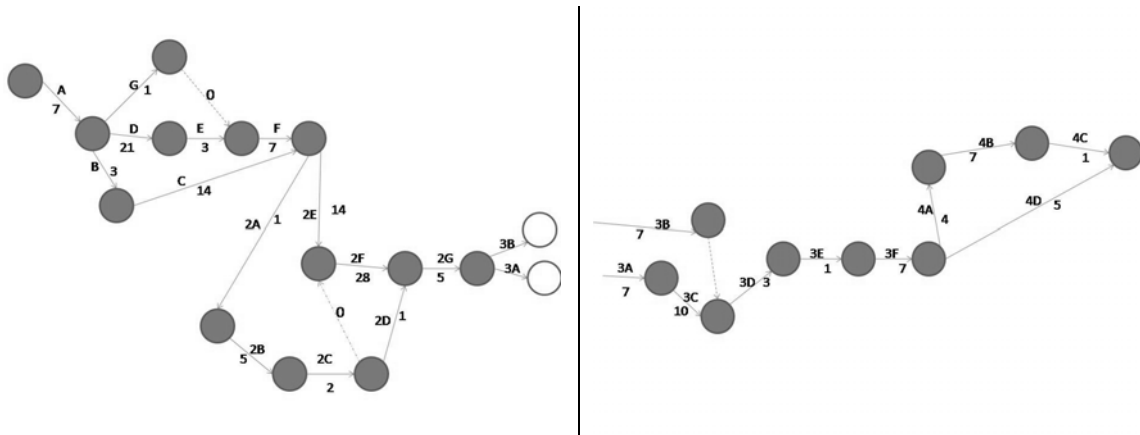


Figure 10. The network plan

The results were discussed by us all together. We made a stand that students in our work became richer in knowledge, in skills and also in experience.

As the final step in our project activities, we summarized our skills, and positively evaluated our work.

4. SUMMARY

The construction of the project must do by the team. The student, through their studies, took part in this kind of work, and applied his knowledge, ideas, and thoughts. Improved the curriculum, and learned the reactions of the group. In this work, a chosen theme is solved by team using the method of project management. The result is a product, which serves the interests of students, i.e. a network plan of tasks for thesis. During solve our task, we used multimedia tools. We analyzed the phases of the project, and wrote our noticed.

APPENDIX (A)

(A) Questionnaire to the students who graduated:

- a) questions related to choice the topic
 - how long did finalize the topic
- b) questions related to planning (how to define aims and tasks):
 - how long did construct the sketch of topic, and what period of time was necessary to work with the assistant
- c) questions about finding literature:
 - how many time did he spend on searching the literature, looking for adequate topic in the books, magazines, and how many time did he spend browsing on websites
 - how much did he spend in the library (by paying membership, photocopying ...)
- d) questions about elaborating the topic:
 - how long did it elaborate each chapters, and how long did it elaborate the chapter which described the main topic
- e) preparing the presentation about production
 - which time was it necessary to construct the versions of the work
- f) questions related to the presentation of the production:
 - what time was it necessary to duplicate, and bookbinding the thesis
 - how much did it cost and how did they be satisfied with it

REFERENCES

- [1.] Orosz Sándor 1987. Korszerű tanítási módszerek. Budapest: Tankönyvkiadó.
- [2.] Radnóti Katalin. Milyen oktatási és értékelési módszereket alkalmaznak a pedagógusok? <http://www.oki.hu/oldal.php?tipus=cikk&kod=Hidak-Milyen>
- [3.] Falus 1998. <http://www.oki.hu/oldal.php?tipus=cikk&kod=Hidak-Milyen>
- [4.] Eva Matijevics, A hálótervezés oktatásának megszervezése korszerű módszertani eszközökkel. Proceedings of the IV. International Scientific Conference of „Modern Methodological Aspects”. September 23-25, 2010. Subotica 1/10 old. ISBN 978-86-87095-08-3, COBISS.SR-ID 255685127
- [5.] piku.freeblog.hu/files/kerdoivkesziteshez3w_0316.doc
- [6.] Project Management Institute 2006. Projekt-menedzsment útmutató PMBOK Guide Budapest: Akadémiai Kiadó.
- [7.] http://www.oki.hu/oldal.php?tipus=cikk&kod=Erettsegi_maskent-Projekt-Kiskate
- [8.] www.georgikon.hu/tanszekek/matek/.../Operaciokutatas09-10.doc
- [9.] K.Lockyer, J.Gordon 2000. Projektmenedzsment a hálós tervezési technikák. Budapest: Kossuth kiadó

¹ Mihaela POPESCU

DIRECTIONS TO APPROACH ERGONOMICS ISSUES IN WELDING

¹UNIVERSITY POLITEHNICA TIMISOARA, FACULTY OF MECHANICAL ENGINEERING, TIMISOARA, ROMANIA

ABSTRACT:

Principles of ergonomics in welding are treated as a whole into the scope and interdisciplinarity of existing connections. The whole approach is oriented to minimizing risk in welding and prevents occupational diseases of the musculoskeletal kind, indicating the possible remedies, as stipulated in international standards.

The applicability in WELDING of these principles, both in manufacturing processes and products, is leading to performance, but also to efficiency.

Insisting on the fundamental directions of approach, but also on specific cases completes the application domain perspective.

KEYWORDS:

Risk, welding, ergonomics

1. INTRODUCTION

Ergonomics relates to the human body behaviour in the working activity, with a view to optimize it considering the corresponding performances. More interdisciplinary sciences and disciplines are involved (figure 1), [12].

The object of ergonomics, which involves man - machine system, , imposes the approach and analyses considering the biomechanical conditions during the work activity and implicitly physical and intellectual repercussions on the human body [3,4].

Occupational medicine, is involved in watching people adapting to their jobs, depending on demands of work, in early detection of morpho - multifunctional changes to appear in the body under the influence of environmental factors, in the analysis of factors to adapt, in causes of morbidity, in diagnosis of deficiencies occurring due to the conditions offered by certain jobs, in psychology. Especially work psychology is concerned with the human in relation to all objective conditions of work [1-14].

Studying the mental mechanisms work and the impact of various factors on these mechanisms, psychology provides items such as: rational and balanced involvement of human psychological function in work tasks. Psychological mechanisms determine the degree of mental application, study and psychological limits of human determination.

Sociology gives information on factors to consider in the way human adapt at work, the way work adapts to the man, respectively.

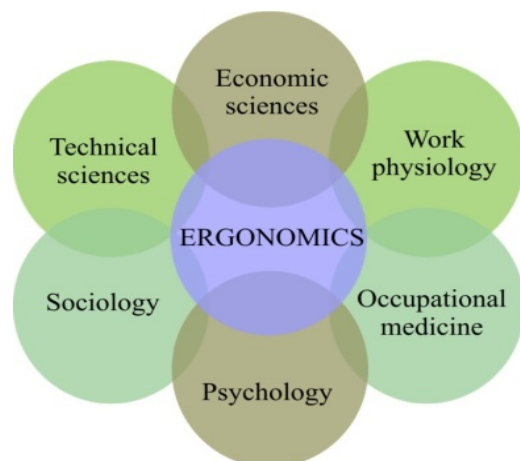


Figure 1. Interdisciplinary sciences and disciplines involved in ergonomics

Technical sciences involves, too when the relation ergonomics - technical sciences appears in two-way. Data and knowledge are used to conceive ergonomic machinery and technology, considering technical issues to be solved, establishing new trends of research in the field [12].

Economics is in a two-way relation with ergonomics. So, ergonomic research provides an optimum organization of work, under the modern production, and economic studies to answer to the efficiency of the concept.

2. PRINCIPLES OF ERGONOMICS IN WELDING

Ergonomics generally describes the possibility of reaction and the limits of the operating personnel in its activity. The adaptability of the personnel working at operating conditions during the service is also one of the objectives.

Welding is a demanding profession it requires safe operation, concentration, routine work, and a lot of skill. Ergonomic principles, lead to performance, economic efficiency and productivity, when applied in the welding activity, under quality assurance conditions.

WELDING also has a strong impact on many sciences, technologies and disciplines (metallurgy physics, heat treatment, physics of welding processes and allied ones, electro technique and electronics, automation, robots, elements of artificial intelligence, design and manufacturing of welded structures, certification, reliability, destructive and non-destructive examination, quality assurance etc [1,2,5,11].

Its preoccupations are on welding technology and on auxiliary devices, too, manipulators with cranes and specialized carriages to support welding, welders clothing, footwear welders, environmental management, environmental protection for vibration and noise etc. related to their adaptability to the ergonomics principles in welding. Research developed in welding ergonomics has a remarkable dynamic having as priority the minimization of risks and occupational illnesses, through secure products and processes, the adaptation to the operator's skill, but also his limits. Two concepts specific to the ergonomics environment: the ergonomics of the process and that of the products, related to activities in the field of welding and allied techniques are widely used. The target is the implementation of measures to avoid physical constraints of welding operators (position - effort) and cognitive constraints (complexity-regularity) [7, 8, and 9].

Within welding processes the aim is to place correctly the equipment in the fabrication flux, corresponding lightning, correct working position, correct ventilation, colour of the ambient etc. For products everything is different.

Nowadays firms offer equipment, welding guns, clothing, and accessories etc, which present ergonomic aspects, too.

In this sense SR EN 13291:2007 "Individual protection equipment. Ergonomic principles" is a guide related to the ergonomic characteristics of such products. This standard as the other standards has to be applied both by certification bodies and by users when identifying the necessary characteristics for individual protection equipment.

Among the factors to be considered when establishing the ergonomic requirements are: integration of ergonomic performances and requirements, factors to determine the optimal provided level of protection, practical use understanding the instructions, to measure the impact of physiological factors of the protection equipment (oxygen consumption, respiratory flow, body temperature changes, sweating, fatigue or muscle contraction) anthropometric factors, biomechanical characteristics (mass distribution, the dynamics of the human body inertial forces, hindering movement, abrasion or compression of the skin and muscles, increased vibration) thermal characteristics of protective equipment (thermal insulation, water vapor permeability, air permeability, water absorption and desorption) effect on the senses (sight, hearing, taste, smell, touch) [5,6,7].

SR EN ISO 10819:2002: "Mechanical vibrations and shocks. Hand arm vibrations." The method of measurement and evaluation of vibration transmission from glove to hand contains requirements that are necessary for anti-vibration gloves. These gloves do not have to amplify the vibrations of the medium frequency range (i.e. between 31.5 Hz and 200 Hz) and must reduce vibration up to 60% of the measured without gloves in high frequency range (between 200 Hz and 1000 Hz).

Checking the characteristics of protective equipment with soft ergonomic includes: technical performance tests conducted at the laboratory level, specific ergonomic tests, but tests on subjects and carriers. These tests should be done before placing on the market, the certification model, in order to apply the CE mark. Simple design accompanying the reliability of welding equipment (light welding guns, allowing access to adjustments in welding for any configuration of the joints, easy to access to a corresponding adjustment), adapted furniture, besides turntables or scissor, furniture, shelves, racks, flexible seating options suitable for operators etc.

Helmet - masks with lens that automatically darkens when arc ignition, its advantage being that it reduces repetitive impact in advancing the neck, gives comfort and protection in place safe. Lumbo-abdominal belts protects back against overload by supporting the spine during lifting operations, muscles of the lower back and abdominal muscles [13,14].

Comfortable clothing [SR EN 340:2004], which ensures freedom of movement, made of safe materials, heat and fire resistant, comfortable footwear [SR EN ISO 20344:2004], pliable gloves, comfortable elastic supports for the wrist and palm [SR EN 420:2004].

Corps of the welding operators must be protected for activities involving great efforts. So they must use: wrist cuffs protection for heavy work, removable instep, lombo-abdominal belts. On the other hand positions sometimes require access to the welding work in the knees. The risk of chronic diseases, including cartilage damage, due to continued pressure on the knees [2, 3, 4, 5, 6, 13 and 14].

International legislation imposes to wear knee having the role of spreading forces on a regular basis and to prevent small hard object to cause injury. Knee can be made of materials highly resistant to abrasion and mechanical shock, eg ABS, rubber compounds, with or without adjustment system / closing. When such activities are long lasting, it is proposed to alternate the position of the knee walking, risks and lancing, compression of objects with sharp edges are important, the design must take into consideration all these factors, exercise equipment including the possible stress on muscles or blood vessels. It is subject to SR EN 14404: 2005 "Knee protection. PPE protection for working in the knees".

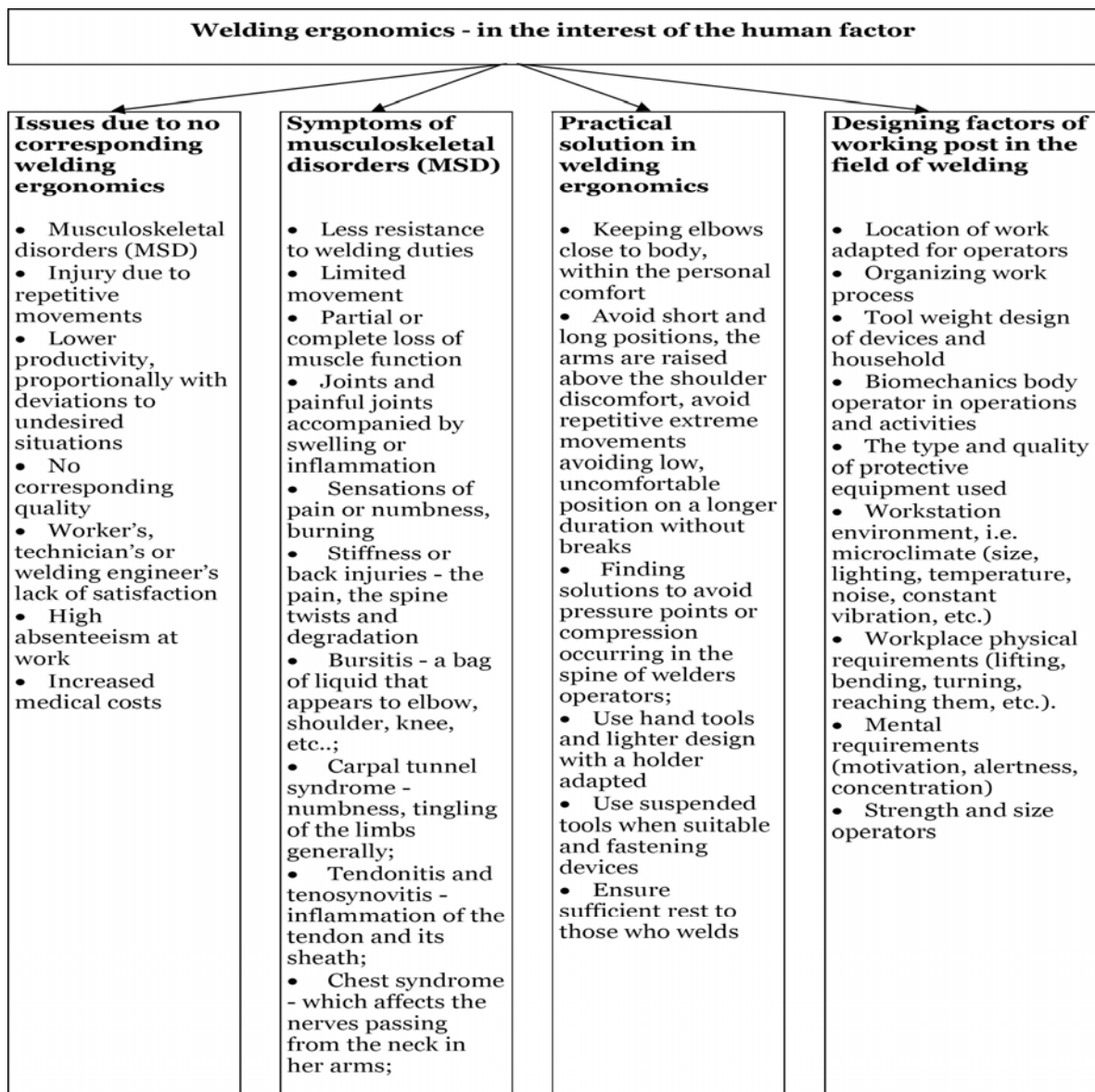


Figure 2. Elements of welding ergonomics - Systematization

Ergonomics is focussing on changing things (instruments, tools, devices, equipment, facilities etc., Figure 2). Healthy welding personnel assure the highest operational training level, and without other professional categories contribute, statistically to a lot of reported accidents.

Many injuries can be developed if the capabilities of the working force and the requirements of welding operator's tasks do not match. These differences are, generally called musculoskeletal disorders, or WMSDs (Work Related Musculoskeletal Disorders).

All these occur due to overstressing the body. Vertebral disc is composed of flexible cartilage and semi-liquid containing gel. Cartilage is ring shaped. When a person performs duties higher than capable, these rings may degrade. If the person continues these activities a long time, everything gets worse and can break down, with many nerve complications.

3. RISK FACTORS DURING THE WELDING OPERATION

Risk assessment in welding represents the way to working places with a healthy and secure climate [12].

Being a dynamic process it gives employers and occupational organizations the possibility to implement a proactive risk management policy at work. Risk assessment approach to welding, is done in stages (Figure 3), established on the bases of a attentive appreciation.

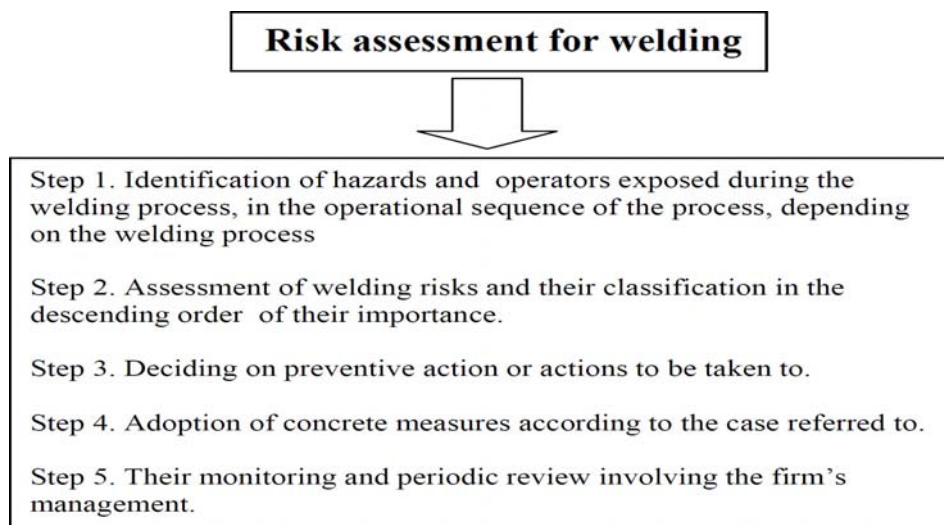


Figure 3. Steps in the assessment of welding risks

4. ANALISES, DISCUSSIONS, APPROACHES AND INTERPRETATIONS

4.1. Welding ergonomics criteria approach

Relevant requirements according to several criteria (Figure 4) addressed to as ergonomics.

"To watching" criterion refers to adapting work to human ergonomics, human adaptation to the work. "Stage" and "implementation phase" refers to the concept and "the purpose of concerns" refers either to production or to the product.

As regards the "content" it is made to ergonomics survey information cognitively involved, based on perception and reasoning and decision topoergonomics, dealing with research and dimensional design of machines, control bodies of working places according to human anthropometric data, and bio ergonomics related to the phenomenon of human body fatigue in relation to elements of work organization.

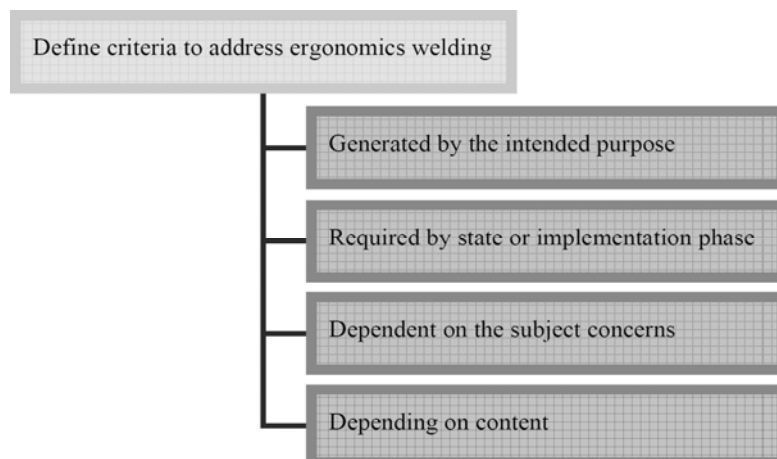


Figure 4. Criteria of ergonomic approach

4.2. Approach specialized bodies

Welding ergonomics is approached by specialized bodies such as the International Institute of Welding (IIS/IIW), which through its Commissions and Working Groups has directed preoccupations (it is the concrete case of Commission VIII), international standardizations forums and the European Welding Federation (EWF), (Figure 5). It is worth mentioning that among the study objectives and preoccupations of Commission VIII of the IIS/IIW, alongside ergonomics there are the effects of fume and welding gas components on the operators, the effect of fire, electro shocking due to noises in the field a.s.o.

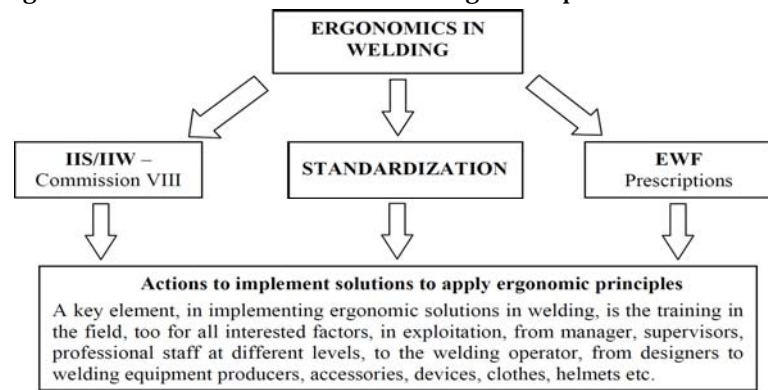


Figure 5. Implications of international organizations IIS/IIW,EWF,ISO

On the other hand the international standardization too is in step with technological developments and related areas of concern and expanding in this direction. The principle of harmonization and standardization of Romanian standards is so aligned in this way. Actions for implementation come considering the results of concerns.

4.3. Professional training in ergonomics

The training in ergonomics represents a key element, in implementing ergonomic solutions in welding from manager, supervisors, professional staff at different levels, to the welding operator, from designers to welding equipment producers, accessories, devices, clothes, helmets etc. Training and continuous watching of changes in legislation and professional directives is compulsory.

New standards are imposed from the quality a point of view, through durable values. The target is to assure a high level of safety during the working activity, man being the most precious resource.

5. CONCLUSIONS

The paper insists on the importance of ergonomics and the interdisciplinary of its field in approaching welding processes and products.

The approaching criteria of welding ergonomics, risk factors and steps in their assessment, as well as the focalization on symptoms of musculoskeletal disorders (MSD), practical solutions and designing factors of working posts in the field of welding complete the data presented. The paper enumerates the possible ergonomic for solutions indicating the requirements according to the in law standards.

The adaptation of the human operator and his skill on the bases of his own limits, with the contribution made by applying the results of ergonomics studies in WELDING complete the data presented.

Preoccupations of the International Institute of Welding (IIS / IIW) are punctually presented, too [1-14].

REFERENCES

- [1.] Colombo, F.(2006). Ergonomia e organizzazione del lavoro, Rivista Italiana de la Saldatura anno LIVII, no.6, pp. 817-822, ISSN 0035-6794
- [2.] Danciu, I. M.; Popescu, M.; Margina, M. R.; Opris, C.: Studii de caz- Aplicatii ergonomice in sudura (Case studies – Ergonomic applications in welding), Buletinul AGIR, 2010, a. XIV, nr.2-3, apr-sept, pp., 73-81, ISSN 1224-9728
- [3.] Draghici, A.: Ergonomie vol.I Noi abordari teoretice si aplicative (New theoretical and applicative approaches), Editura Politehnica, Timisoara, 2006, ISBN 973-625-270-1
- [4.] Draghici, A.:Ergonomie vol. II Aspecte novatoare ale cercetarii ergonomice
- [5.] (Innovative aspects of ergonomic research), Editura Politehnica, Timisoara, 2007, ISBN 978-973-625-349-2
- [6.] Holstein, P.: (2009) How to choose ergonomic hand tools, Welding Journal, vol.88, no.3, pp. 90-91, ISSN 0043-2296

- [7.] Iosif, G.; Marhan, A. M.: Ergonomie cognitivă și interacțiune om-calculator
- [8.] (Cognitive ergonomics and interaction man - computer), Editura Matrix Rom, București, 2005, ISBN 973-685-923-1
- [9.] Irimie, S.: Ergonomie Industrială (Industrial ergonomics), Editura AGIR, București, 2008, ISBN 978-973-720-196-6
- [10.] Kadefors, R. :(2006).Welding and ergonomics, Australasian Welding Journal, vol. 51, no.1, pp.22-23, ISSN 1093-0642
- [11.] Popescu, M.; Marta, C; Radescu, D.; Danciu, I. M.:(2009), Welding and ergonomics. Case studies, RaDMI, 9-th International, Proceedings Conference „Research and Development in Mechanical Industry, 16-19 September, Vrnjacka Banja, Serbia, ISSN 978-86-6075-007-7
- [12.] Popescu, M; Danciu, I. M.; Codrean, C.; Utu, I.: (2009), General principles of ergonomics with direct application in welding engineering, Scientific Bulletin of the POLITEHNICA University of Timisoara, Transaction on Mechanics tom 54(68), fasc.4, pp.70-74, ISSN 1224-6077
- [13.] Popescu, M.; Danciu, I. M.; Opris, C.: Principii de ergonomie in tehnica sudarii
- [14.] (Ergonomics principles in welding technique), Buletinul AGIR, 2010, an.XIV, nr.2-3, apr.-sept., pp. 69-72, ISSN 1224-9728
- [15.] Popescu, M.: WELDING: ERGONOMICS-ELEMENTS, DAAAM International Conference, 2010, vol. 9, pp.351-352, ISSN 1726-9687, ISBN 978-3-901509-74-2
- [16.] xxx: Ergonomics guide for welders
- [17.] xxx: OSHA Guidelines for Shipyards, (2008), ergonomics for the prevention of Musculoskeletal Disorders





¹Mihaela POPA, ²Florin BUCUR

STUDY REGARDING COSTILL METHOD EFFICIENCY IN TRAINING OF SEMI-FUND RUNNERS

¹⁻² FACULTY OF ENGINEERING HUNEDOARA, ROMANIA,

ABSTRACT:

At the current of performance level, the crucial role in guiding and directing the training process it can not have any "intuition" or "stimulus" coach or athlete, but follow the strict methodological approach, previously established for the current year (Puică,I.,1994;Dragnea,A.,1996; Bompa,T.,2001). National results in long-distance race semi fund and fund athletes in the C.S.S. Hunedoara, we have determined, given the scarcity of training, to systematize and rationalize only those methods and means of preparation leading to relatively short time to obtain valuable results by increasing performance.

KEYWORDS:

performance, semi-run, annual planning, methods, means

1. INTRODUCTION

Streamlining and standardizing operations sports training is required by the need to exploit the best biological and psychological potential of the athlete and the coach available time to achieve a stable performance as a branch or sports sample (Cârstea, G.,2000; Bompa, T.,2001).

Methodological guiding sports training require systematic data recording and regular analysis after processing and interpretation (Dragnea,A.,1996; Gârleanu,D.,1996; Bompa,T.,2001).

This analysis reveals an inventory of methods and means most effective in training, recovery and especially in preparation for competition.

2. AIM

It is assumed that the streamlining and standardization of means and methods in sports training, after application of methodological procedures Costilla leading to higher levels in great performance advanced semi-fund of athletics department at CSS. Hunedoara.

3. ASSUMPTIONS

We made the following assumptions:

- ❖ Standardization means and methods of training involve their implementation in all training structures, while targeting training goes to the essence of competition;
- ❖ In training must be identified those means and methods that meet operational performance objectives as specific athletic events;
- ❖ Establishment of training model is achieved by the method of statistical correlation between two variables: the preparatory year (x) and performance competition (y) (Drăgan, I., 1994; Bompa,T.,2001).

Following objectives were separated:

- ❖ Making a summary of the methodological approach of training semi-fund;
- ❖ Highlighting the interdependence of the key parameters of the effort in training volume - duration - intensity;
- ❖ Identifying the most effective ways and means of streamlining and standardizing training from semi-fund group advanced athletes to the CSS. Hunedoara.

4. RESEARCH PLAN

Research has resulted in investigations conducted during the annual cycle of training, the group of advanced level - junior semi-fond of CSS. Hunedoara, following application Costilla method. Costilla method allows two things:

- ❖ Calculation of Indirect VO₂ max;
- ❖ Calculation tempo runs (at 70% of maximum oxygen consumption per kg / body).

5. RESULTS AND DISCUSSIONS

Group of semi-advanced level junior fund being investigated, consists of a total of 6 athletes. Costilla method, emphasizes the consumption of oxygen per kg / body.

Looking at the results summarized in tables which show us what was the average speed that traveled long distances in training and comparing them with average speeds required by coach to browse these distances can be observed:

Coach request:

- ❖ uniform tempo running: 3.40/km;
- ❖ varied terrain running: 3.45/km.

Table 1 The average speed per km from the calculations by the Costilla method

B.F.	- 3:43,8/km = 223,8 sec
A.C.	- 3:46,2/km = 226,2 sec
D.A.	- 3:55,2/km = 235,2 sec
C.A.	- 3:58,2/km = 238,2 sec
D.V.	- 4:15,6/km = 255,6 sec
M.N.	- 4:18,6/km = 258,6 sec

Graph representing, one may note that the first two runners who have close value have run in training duration with appropriate speed.

For other runners, for which we had baseline data to take them into account, the speed required for coach training was superior to their ability.

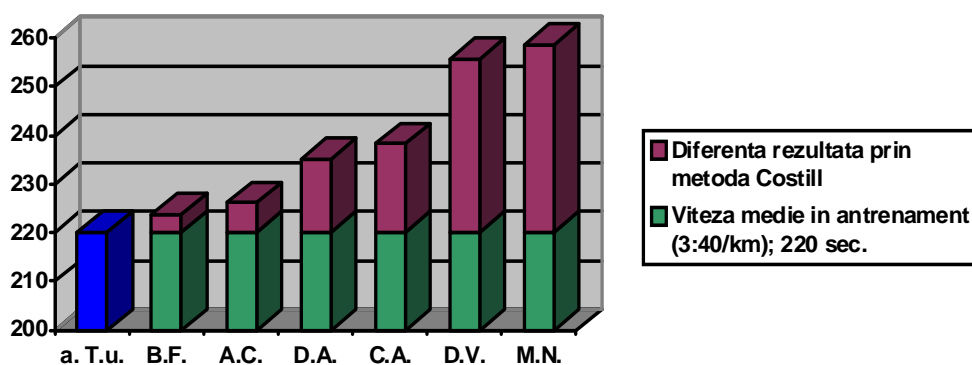


Figure 1 – Uniform tempo running

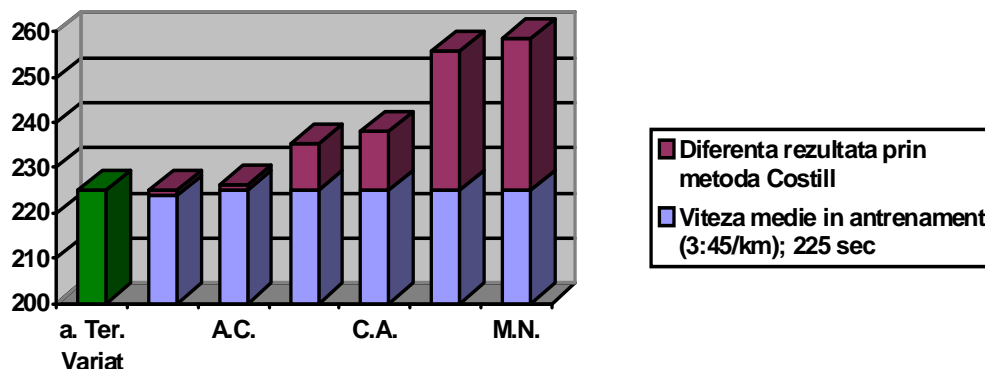


Figure 2 – Varied terrain running

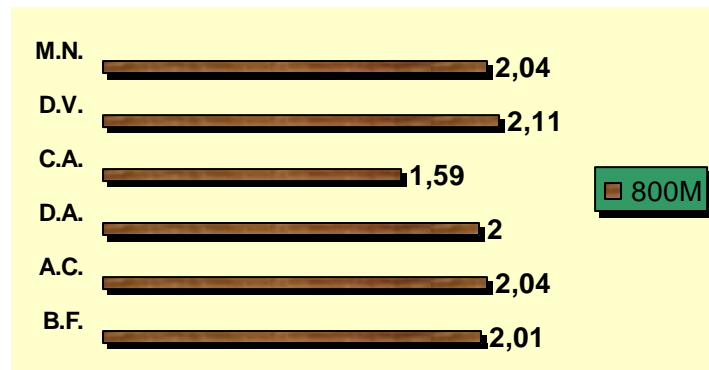


Figure 3. Dynamics of the sample of 800 level performances

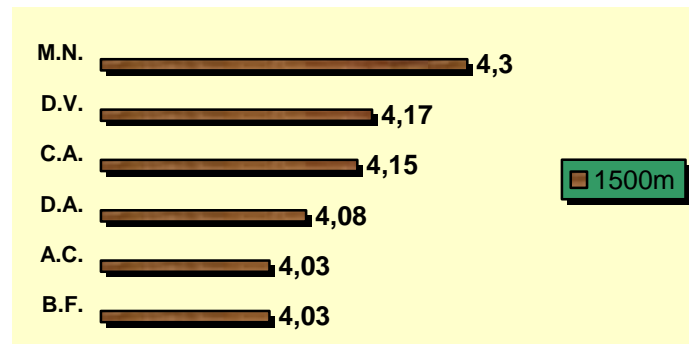


Figure 4. Dynamic of the sample of 1500m level performances

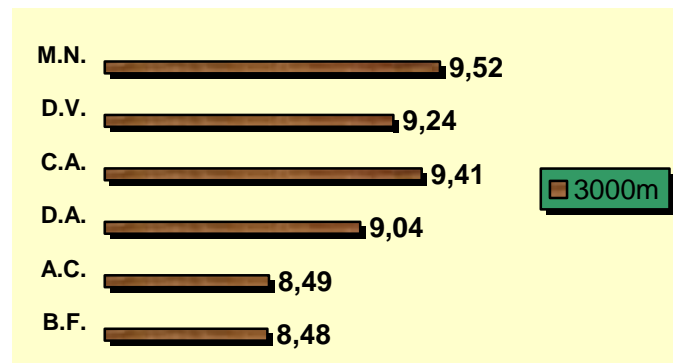


Figure 5. Dynamic of the sample of 3000m level performances

6. CONCLUSIONS

- ❖ The means and methods of training should be structured so that all components have constant values, except for one that will evolve over time. For that, initially, we must standardize the means and methods of training, in order to capture the statistical, mathematical correlation of each mode of training with another variable, which is just the purpose of practice increasing performance level (Gârleanu, D., 1983; Alexei, M., Monea, G., Bogdan, V., 1996);
- ❖ Based on results from major competitions, we tried to find the correlation between the method chosen and the performance level and the impact of orientation and dynamic implications of the main parameters of effort;
- ❖ During the competition we will bring the following operational algorithms:
 - 12 days before the contest: 6 to 8 x 400m launched run; pause: 200m low run;
 - 9 days before the competition: control rules on intermediate distances:
 - 500m + 300m for 800m
 - 1200m + 300m for 1500m
 - 3000m + 1200m for 5000m
 - 4 days before the contest 6x200m; pause 200m low run.

- ❖ If we believe that training is only a systematic repetition of exercises, we can not achieve true understanding of its complexity and depth that involve physical, functional, biochemical and psychological of great complexity, due to processes determined of adaptation (Drăgan,I.,1994);
- ❖ In planning we have to take account, in addition to our experience, that addressing a situation of training can not ignore the social and human dimension of the training process, which determines the interpenetration of scientific thinking with intuitive perception of reality teaching (imagination and creativity)

BIBLIOGRAPHY

- [1.] ALEXEI, M., 2005, Athletics - technical evidence, University Press Publishing House, Cluj-Napoca;
- [2.] ALEXEI, M., MONEA, G., BOGDAN, V., 1996, Athletics course, engineering samples, Publisher UBB Cluj-Napoca;
- [3.] BOMPA, T., 2001, Theory and methodology of sports preparation - Publishing Ex Ponto, Bucharest;
- [4.] BOMPA, T., 2001, All about training young champions – Publishing Ex Ponto, Bucharest;
- [5.] BOGDAN, V., 2005, Biomechanical evidence of Athletics Features, Faculty of Physical Education and Sport, Cluj-Napoca;
- [6.] BOGDAN, V., POP, A., 2005, Initiation into athletics. Athletics School, Faculty of Physical Education and Sport, Cluj-Napoca;
- [7.] CÎRSTEA, GH., 2000, Theory and methodology of physical education and sport, Publishing AN-DA, Bucharest;
- [8.] DRAGNEA, A., 1996, Sports training, Didactic and Pedagogical Publishing House, Bucharest;
- [9.] DRĂGAN, I., 1994, Applied sports medicine, Youth and Sports Publishing EDITIS, Bucharest;
- [10.] GÂRLEANU, D., 1996, Course athletics, Ecological University, Bucharest;
- [11.] GÂRLEANU, D., 1983, Athlete steps training, Bucharest Publishing, Bucharest;
- [12.] PUICĂ, I., 1994, Training of semi fund and fund for girls, Youth and Sports Publishing EDITIS, Bucharest;





¹. Georgeta Emilia MOCUTA, ² Ioana IONEL,
³ Mihaela TILINĂ, ⁴ Luisa Isabela DUNGAN

ENGINEERING TRAINING SUPPORT THROUGH PRACTICE

^{1,2,4} POLITEHNICA UNIVERSITY OF TIMISOARA, ROMANIA

³ FREELANCER CONSULTANT, ROMANIA

ABSTRACT:

Most engineering tasks require teamwork. For a good development in the engineering profession one should cultivate social skills to facilitate group interactions which are a work team or organization with the purpose of production which have to manage the future engineer.

Developing social competence is a necessity of having an impact on individual privacy, the relationships he has with those close to him and even on his professional results.

KEYWORDS:

Teamwork, professional learning and development

1. INTRODUCTION

Besides professional competence, which is imperative for progress and performance, now, requirements are that every young student of engineering profile of any specialization to be prepared so as to intervene promptly in addressing relevant problems of economic and social reality, having positive effects in terms of reaching professional and social performance.

Progress in life, both in school and in a profession largely depends on the power to manage and use our social skills.

These behaviours are founded on successful professional learning and development supported by the ability of social competence, capacity, fitness and personal abilities.

Capacity - conditional ability and degree of maturation of learning and exercise - is our ability to achieve success when performing a task or profession.

Fitness, representing a trait or traits of a young system, mediates its success in an activity and the possibility to act and get performance. The fitness appears as a defining factor of the person that facilitates knowledge, practice, technical development, arts and communication.

Ability differs from capacity by its specificity for a technique that involves and requires learning. Ability is also the trait synonymous with skill, dexterity, skill, dexterity, skill, highlighting the ease, speed, high quality and precision with which a person carries out certain activities, involving self-organization suitable to concrete task, smooth and effective adaptation. You should not confuse ability with skills or aptitudes. Together, they condition the substrate skills. Psychologically and subjectively competence is a result of knowledge, skills, abilities, skills, capacities, skills and temper- character traits that lead to performance in different areas.

Most engineering tasks require teamwork. For a good development in the engineering profession one should cultivate social skills to facilitate group interactions which are a work team or organization with the purpose of production which have to manage the future engineer.

A future engineer who is granted a major role by members of the group in which it manifests professionally and who by interpersonal relationships fulfils a clear role in human resource structure will be provided with a series of attributes as shown below:

- ❖ cognitive experience;
- ❖ communication skills;
- ❖ judgement power and understanding the transmitted message;
- ❖ resolute capacity, creativity in thinking and action;
- ❖ availability to knowledge;
- ❖ availability for cooperation and interpersonal communication within the group;

- ❖ self-confidence and to another;
- ❖ attitude to overcome the obstacles to attaining the proposed profit;
- ❖ flexible style of approach to the task and interaction with its partners to achieve the common goal of the group;
- ❖ honesty, responsibility and empathy in interpersonal relationships;
- ❖ need for cognition, affection and social valuation
- ❖ for relationships, development, acceptance and integration in the work group;
- ❖ satisfaction with participation and individual and group success
- ❖ skills and interpersonal skills.

This actually represents the sequence of factors whose interaction network and networking abilities outline of a sphere of social competence of a responsible individual.

Developing social competence is a necessity of having an impact on individual privacy, the relationships he has with those close to him and even on his professional results.

2. THE STUDY

European Youth Pact focuses on facilitating access of youth on the labour market, combating youth unemployment and increases the quality of education.

The PRACTICOR project co-financed by the European Social Fund through the Human Resources Development Operational Programme 2007-2013 aims establishment of transnational networks regarding the educational guidance, counselling career and practice, coupled with labour market in knowledge society.

We started this project the need for social skills training in the engineering profession.

Development of social skills and recovery in the workplace is a necessity due to multiple effects abilities clearly targeted toward productivity and success.

Of these empathy allows understanding and cooperation within an organizational structure, both vertically and horizontally.

For example, non-empathically managers produce discontent among employees who may become the cause for dissatisfaction, absenteeism and staff rotation.

Assertiveness also provides personal opinions and provides the ability to protect the rights that a person holds, which will lead to gaining authority and respect in front of other employees or supervisors.

Gratuity and conflict resolution skills improve steep lines that may arise at some point in their professional relations.

Along with taking advantage of these abilities, competence in communication is presented as a basic need to achieve professional success.

To prepare students as future engineers aims to train these skills through practical activities carried out in the middle of productive environmental of the economic reality.

The overall objective of the Practicor project was to organize practice to ensure their students a greater chance on graduation, in the labour market and strengthen their training level, in line with socio-economic reality.

In addition, through this project it is also aimed the guidance and advice in career to those who wish to choose a vocational route to embrace a successful career in priority areas of engineering and to improve through practice, correlating and aligning learning and labour market.

To provide initial training anchoring with the labour market demands preparation of engineering as a whole must take the following steps:

Step 1. "Saying" – didactic presentation for information and knowledge skills that are to be trained
- activity that is done in classes and seminars;

Step 2. "Show" - creating opportunities and necessary platform demonstrating behaviour and possible responses - Work carried out under laboratory hours;

Step 3. "Doing" – putting students in a position to perform, to practice the skills - stage made within hours of practical training;

Step 4. "Transfer" – providing logistics and resources to implement the new abilities gained in solving specific production tasks - step resulted in practice in a job at the employer;

Step 5. "Feedback" - ensure awareness and reflective dimension of learning - is an ongoing process rather than a step and takes place through self-evaluation and evaluation of student activity and behavior from peers and the coach / guardian of the level achieved for gained skill;

Step 6. "peer learning" - the participants support each other in developing skills - by solving a common task - again a continuous process integrated in all other stages. To strengthen my skills is a co-drive with a "master" phase in which for example may have involved another student who graduated step four.

Another way to enhance skills through training is done under the supervision of "master." To maintain the skill level is achieved by building "personal training".

3. ANALYSES, DISCUSSIONS, APPROACHES AND INTERPRETATIONS

Bologna strategy is beginning to implement the national and European system of higher education and should be supported. Basically reducing the learning period in the first cycle degree (four years) than the old system of diplomats engineers (5 years) should be compensated through careful use of the time of preparation, particularly related to specific practical and necessary areas of society, especially productive and importance related to the company's energy security and environmental protection.

The Practicor project gives the opportunity to develop skills training and supported the acquisition of skills to help graduates.

The Practicor project helps students to find a job and begin a successful career after graduation.

The Practicor project is an initiative of the Polytechnic University of Timisoara, as coordinator and project partners: University from Pitești, The Institute for Studies and Energetic Design ISPE București and FRAUNHOFER – Gesellschaft zur Förderung der angewandten Forschung, Germany.

On completion of the project in 2013 students must be better prepared not only theoretically but also practically, and their prospects for employment upon graduation to increase significantly.

Our goal is that business people and companies to want to hire our graduates.

Companies agree to have a say in our students' practical training, and project facilities are part of the team with us. So companies conducting practice under the guidance of tutors trained specifically in the project, assisting students trained during practice for the acquisition of specific job skills. These skills will facilitate the integration to the working place of graduates trained in the Practicor project.

Other support activities relate to counselling and career guidance through visits to companies, presentations, panel discussions with representatives of the business world, workshops, simulations (job interviews, job fairs).

Practice partner companies have selected a group of employees to participate in a tutor-training practice to put in dialogue with the teachers of universities and practitioners together to prepare students. This course completes with a certification of the competence recognized by the Ministry of Labour and Ministry of Education;

4. CONCLUSIONS

The Practicor project is relevant because the younger generation has the main subjects of future engineers who will ensure the sustainable development in the context of the ecologic balance change, the need to intensify innovative actions environmental protection and saving energy resources, organization and implementation of sustainable transportation technologies.

The project duration is from October 2010 until October 2013. Trans-national network related to educational guidance, career counselling and practice, coupled with labour market, in the knowledge society formed under the project will work and after completion of the project.

Team of the project is a partnership and homogeneous unit based and complementary, formed community of interests and goals, which aims to provide greater access to opportunities in priority areas that support sustainable development of European society, in areas related to traditional and renewable energy resources, transportation and advanced technology to protect the environment and ensure evolution and harmony in the society's transnational space in the process of sustainable development.

Cohesion of interests, experience and awareness that there is room for improvement are the glue of the partnership.

For Politehnica University from Timisoara the purpose of the project is to ensure performance and financial conditions for the organization of the students' practice in the Department of Mechanical Machinery, Technology and Transportation for a chance to ensure increased and enhanced training, in agreement with the necessity of the labour market.

Related objectives is to develop sustainable partnerships with employers for students in first to four years of study and building a relationship with the business community, developing a guidance system and counselling for career integrated into the practice of students.

Besides establishing a network of tutors to coordinate and guide the students practice in line with the practical needs of society and skills development helps prepare students for future employment.

REFERENCES

- [1.] Gilson Morales, Clarissa Unica Morales, Model for engineering education to development of competences and abilities, International Conference on Engineering Education – ICEE 2007-05-01, available: www.ineer.org/Events/ICEE2007/papers/74.pdf
- [2.] Moti Frank, Knowledge, abilities, cognitive characteristics and behavioural competences of engineers with high capacity for engineering systems thinking (CEST). *Systems Engineering*, Volume 9 , Issue 2 (May 2006) pp. 91 – 103, Publisher John Wiley and Sons Ltd. Chichester, UK ISSN:1098-1241
- [3.] Eileen P. Arnold, Global Systems Engineering Competencies: A Business Advantage, INCOSE 2008 Symposium, available: www.incose.org/.../May_IS2008_Arnold_Global%20SE%20Competency.pdf
- [4.] Gonczi A. 1996, Reconceptualising Competency Based Education and Training, PhD thesis, at <http://epress.lib.uts.edu.au/dspace/bitstream/handle/2100/303/01front.pdf?sequence=1>





¹Reiner KEIL, ²Tamás HARTVÁNYI, ³Péter NÉMETH

RELIABILITY THEORETICAL APPROACHES FOR ORGANIZATION OF RESOURCE-LIMITED INFRASTRUCTURE LOADS

¹ TECHNICAL UNIVERSITY OF DRESDEN, GERMANY

²⁻³ SZÉCHENYI ISTVÁN UNIVERSITY, HUNGARY

ABSTRACT:

The management of mobile systems is essential for optimal management of transport systems to ensure even with the increasing complexity the transportation services in freight transport and passenger transport in terms mobility and safety of traffic flows.

Through the use of mobile devices as a source of traffic data today all the technical possibilities are available to control traffic chaos with the use of LBS and GIS technologies. Actually, it's all about avoiding the chaos from the start.

KEYWORDS:

reliability, transport systems, management, mathematical modelling

1. INTRODUCTION

The current level of traffic telematics solutions brings the following problems that are to be solved:

- Through the active and unconditional use of navigation systems - i.e. the driver uses the navigation system and adheres strictly to its recommended route - a growing number of road users may get the effect that they use together with other road users the same bypass, creating a new traffic jam on this bypass route, especially if the navigation systems use the same or similar routing algorithms and use the same current traffic condition data
- At the current time existing traffic restrictions will be considered even if these on the optimal route, but are at a great distance from the current location are, and thus it is not certain whether this limitation is still present upon arrival of the vehicle,
- Traffic forecasting models, that consider future transport density on the optimum route or at sub-optimal alternative routes are still lacking, its use however promise to optimize traffic flows especially in overload situations,
- The stationary traffic control systems can indeed take with its dynamic signposting the current traffic situation into account and to bypass the traffic around the obstacles encountered, but does not allow individual route to a better utilization of several diversion alternatives
- To monitor the traffic condition traditionally stationary detectors are used: induction loops, video based or infrared technology. These systems are supplemented particularly in city traffic with floating car data systems, the use of the results from this point measurements for prediction of traffic on the road network are possible only with restrictions.

The management of mobile systems is essential for optimal management of transport systems to ensure even with the increasing complexity the transportation services in freight transport and passenger transport in terms mobility and safety of traffic flows [1], [2].

A task of transport telematics is to optimize the path that traffic objects or subjects of traffic through a transport network under given conditions and by setting an objective function. Starting point for such considerations can be the dynamic routing strategies of conventional telecommunications networks. Through the use of mobile devices as a source of traffic data today

all the technical possibilities are available to control traffic chaos with the use of LBS and GIS technologies [1]. Actually, it's all about avoiding the chaos from the start.

To be able to solve the above problems the following theses will be set:

1. The target function for the optimization of traffic flow is to minimize the sum of the lives of travel time of all travel subjects rather than minimizing the travel time of an individual subject's movement, because it does not lead to a global minimum. The following relationship has to be used

$$\left(\sum_i T_{T_i} \right) \rightarrow \min \neq \sum_i (T_{T_i} \rightarrow \min) \quad (1)$$

2. The routing decisions are made so that the travel time for traffic subject reached a local minimum and the network load is too large by the selected route. That means, that not already heavily loaded edges of the network traffic should be driven, even if this means that the travel time for a single subject will be longer.
3. The routing decisions for each transport subjects has to be taken with cooperation of a traffic control centre. An appropriate model for this was presented in [3].
4. For the organization of the transport process, the transportation network is divided in some intervals, the observed surface with a very large number of direct traffic sources (such as a household or a company with a number of vehicles) is divided in clusters, this is according to [4] based on postcode areas proposed and the streets are divided according to [3] in cells of the size of 100 meters. Furthermore, it is carried out according to the calculation of the rush hour for a time clock in 15-minute period.

2. MATHEMATICAL MODEL

2.1. Basic Approach

The starting point of mathematical modelling is the definition of process reliability $Z_{\Pi}(t)$ according to [1], which is split into the following reliabilities:

- $Z_{Tr}(t)$ - Transport reliability
- $Z_V(t)$ - Traffic reliability
- $Z_{Sy\eta}(t)$ - System reliability of the operator,
- $Z_{Sy_v}(t)$ - System reliability of transport vehicles and
- $Z_{Sy_r}(t)$ - System reliability of transport routes (infrastructure reliability).

The transport reliability $Z_{Tr}(t)$ defined as the probability that a transport entity travels in time t from i to j can be characterized by the undisturbed transport process, the transport reliability $Z_V(t) = f(X_q(\tau, w_q), Z_{Tr}(t))$ is considered with the temporal and quantitative stochastic of the arrival process of traffic entities X in the traffic sources w_q , while the other components of the process reliability are accessible of the failure and recovery processes. The process reliability is calculated as

$$Z_{\Pi}(t) = Z_V(t) \cdot Z_{Sy\eta}(t) \cdot Z_{Sy_v}(t) \cdot Z_{Sy_r}(t) \quad (2)$$

The following sections describe some fundamental approaches of the individual part reliabilities.

2.2. Modeling of system reliability

The system reliability $Z_{Sy}(t)$ is according formula (2) will be distinguished as the **equipment reliability** - transport vehicle reliability - the **operator reliability** $Z_{Sy\eta}(t)$ and **infrastructure reliability** $Z_{Sy_r}(t)$.

Infrastructure reliability is influenced by the following events:

- ❖ Accidents
- ❖ Breakdown of vehicles
- ❖ Construction sites,
- ❖ Blocking of traffic lanes for any reason

The operating areas for modelling the infrastructure reliability can be characterized as follows:

- ❖ **Nominal operation:** all lanes are available to the currently available speed limit, which refers to the current state and the state it will be like when the subject travelling through this area, i.e. construction sites that are present with probability $Z_{Sy_r}(t) = 1$ be regarded as nominal operation)

❖ **Downgraded operation:** there are either fewer lanes available and / or the currently permitted maximum speed is temporarily limited, the probabilities should be calculated with the probability of these speeds. Because of the given range of speeds only various speed limits are considered.

❖ **Collapse:** there is no lane by accident, breakdown, weather, etc. available

For accident-related restrictions stationary models can not be used because the probability is of interest to a restriction at the time when the subject's moving in that cluster. One issue is for example "How likely is in the cluster i at time t a traffic jam if at time $t = 0$ there was no traffic jam or if at time $t = 0$ there was a traffic jam."

The infrastructure reliability can be calculated analytically with transient reliability models. The procedure is demonstrated in the following simplified example. There is a lane with the following speed limit areas:

❖ Free traffic = State $Z_{\kappa=0} = Z_{Sy}^{[nenn]}$ = Nominal Operation

❖ Limited Traffic = State $Z_{\kappa=1} = Z_{Sy}^{[stör]}$ = Downgraded operation

❖ Stationary traffic ($v = 0$), i.e. blocking of lane = State $Z_{\kappa=2} = Z^{[koll]}$ = Collapse

The following figure represents the system reliability (Fig.1).

The mathematical model for a cell of a single-lane road has been described by [3] closer.

In the second approximation is the route, i.e. the first edge e_{ij} , regardless of the real net structure in $\hat{\xi}$ into equal-sized cells

divided. In calculating the system reliability of a cell $Z_{Sy_i\xi}^{[\kappa]}(\tilde{x}, \tilde{t})$, the failure rate λ_ξ refers to this area. The parameter \tilde{x} characterizes

the (discrete) place and \tilde{t} the discrete time when the vehicle is in (the center) of the cell. A vehicle must go through all the cells $\xi \in [1, \hat{\xi}]$ of the edge. In reliability-theoretic sense, this can be

modeled by a series circuit. To calculate the non-stationary reliability $Z_{Sy_i\xi}^{[\kappa]}(\tilde{x}, \tilde{t})$ the system state of

all cells $Z_{Sy_i\xi}^{[\kappa]}(\tilde{x}, 0)$ at the time $\tilde{t} = 0$ will be determined. The variation of time in the calculation is

performed in discrete steps determined by the width of a cell Δx and the average velocity $v_m(\rho_m)$. Density-dependent fluctuations should not be considered first. For the nominal operation:

$$Z_{Sy_i}^{[nenn]}(\xi) = \prod_{\xi=1}^{\hat{\xi}} Z_{Sy_i\xi}^{[nenn]} \left(\xi \cdot \Delta x, \frac{\xi \cdot \Delta x}{v_m(\rho_m)} \right) \Big|_{Z_{Sy_i\xi}^{[\kappa]}(\xi \cdot \Delta x, 0)} \quad \kappa \in [nenn \vee stör \vee koll] \quad (3)$$

This is the probability that all cells are passed in nominal operation, under the condition of the current operating range k , $k \in [1, \hat{\xi}]$ at time $t = 0$ (starting time) of each cell $\xi \in [1, \hat{\xi}]$.

For degraded operation:

$$Z_{Sy_i}^{[stör]}(\xi) = \prod_{\xi=1}^{\hat{\xi}} Z_{Sy_i\xi}^{[stör]} \left(\xi \cdot \Delta x, \frac{\xi \cdot \Delta x}{v_m(\rho_m)} \right) \Big|_{Z_{Sy_i\xi}^{[\kappa]}(\xi \cdot \Delta x, 0)} \quad \kappa \in [nenn \vee stör \vee koll]$$

This is the probability that all cells are passed in degraded operation, under the condition of the current operating range k , $k \in [1, \hat{\xi}]$ at time $t = 0$ (starting time) of each cell $\xi \in [1, \hat{\xi}]$. For simplification a valid speed must be defined for all cells.

The calculation of the probability that all cells are passed in collapse state makes no sense and leads to no useful result. An example calculation indicates that (Fig.2).

For the red curve, all cells are in the initial state in the nominal operating range, the blue curves are two cells in the initial state not in nominal operation. This can be clearly seen at the two jumps, the impact on the overall reliability decreases with distance.

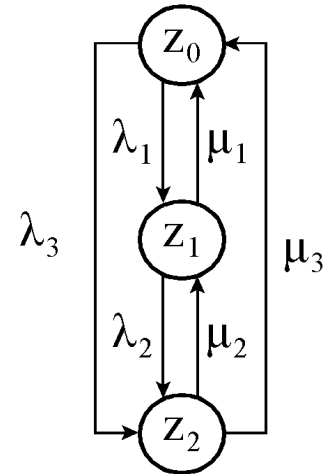


Figure1.: System reliability for a cell of a single track road

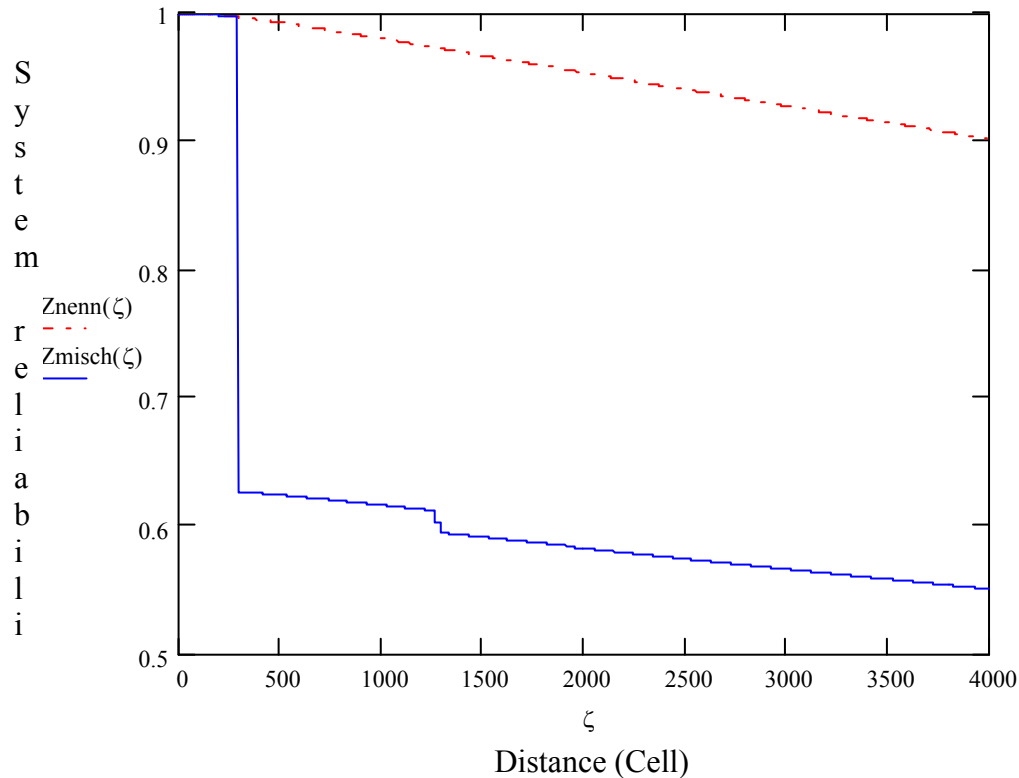


Figure 2.: System reliability - different initial states

The consideration of equipment reliability $Z_{S_{y_v}}(t)$ here the reliability of transport vehicle should be for example the charging the battery of an electric car. As a model, the maintenance theory of planned preventive maintenance to age-related cycle (period t_p) can be used to complete repairs by interference (time t_s) [5]. Preventive maintenance is the scheduled charging of the battery or the exchange of the battery. Disruption maintenance is regarded as the stopping of the vehicle when the battery is depleted. The maximum availability is

$$V_{Sy}^{[nenn]}(\tau_0) = \frac{1}{1 + \lambda(\tau_0)(t_s - t_p)} \quad (5)$$

The operator reliability, i.e. the probability of the driver's failure during the time t is neglected.

2.3. Modeling of transport reliability

Due to the complexity of the transport process for its modeling a multi-stage calculation method is used to the abundance of the factors considered separately. First, the transport reliability is calculated independently of the arrival process.

The transport reliability is the distribution function of the transport time T_{Tr} without consideration of the influence of traffic density, ie it is considered the speed of free traffic v_f . This is dependent on many factors, e.g.

- ❖ Legally fixed limits,
- ❖ Road conditions
- ❖ Traffic conditions
- ❖ use of the utility weight,
- ❖ Specific drive performance,
- ❖ Behavior of drivers.

The transport reliability is calculated for each cell of the transport network in time interval. In [6] for modeling the transport time, normal distribution was used. Using a deterministic transport path by forming a function of stochastic variables according to Richter [7] to estimate the distribution function of the duration of transport can be achieved. It is

$$T_{Tr} \in N\left(\frac{s}{\mu_v}, \frac{\sigma_v^2 s^2}{\mu_v^4}\right) \quad (6)$$

This distribution function corresponds to the transport reliability $Z_{Tr}(t)$.

For the assessment of reliability of traffic is $\rho(\Delta \xi, \Delta \tau)$ used. From the density of traffic, the transport speed is through an approach of Kuehne [8] calculated.

$$v(\rho) = v_f \left[1 - \left(\frac{\rho}{\hat{\rho}} \right)^a \right]^b \quad (7)$$

The transport rate is a function of

- ❖ Road-specific empirical parameters a and b,
- ❖ Assignment of the road (traffic density) ρ
- ❖ Maximum occupancy of the road $\hat{\rho}$ and
- ❖ The speed of free traffic v_f .

Reliability for the traffic is according to [3]:

$$Z_V(t) = \frac{v(\rho(\Delta \xi, \Delta \tau))}{v(0)} = \frac{v(\rho(\Delta \xi, \Delta \tau))}{v_f} = \left[1 - \left(\frac{\rho(\Delta \xi, \Delta \tau)}{\hat{\rho}(\Delta \xi)} \right)^a \right]^b \quad (8)$$

This shows that the speed of free traffic has no effect on the ability to reliability. It is calculated from the ratio of the current to maximum traffic density of the route part (cell). With the help of macroscopic traffic models [8] the variation of traffic density and traffic speed can be - for a limited time horizon - calculated and numerically the time of transport can also be determined. One approach was presented in [3].

In this calculation the composition of the traffic density from the individual relationships $\rho(w_q, w_s)$ between the traffic source and traffic destination does not matter, however these factors should be considered now. Here the following question emerges:

- How many traffic subjects will be on the individual sections of the route, if that section is passed? Or to put it mathematically, the traffic density $\rho(\Delta \tau, \Delta \xi[\psi(w_q, w_s)])$ is sought.

To calculate this traffic, the following parameters could be used:

- Matrix of the traffic density from measured data of the past $\bar{P}(\Delta \tau)$
- Matrix of the objective factors from measured or estimated data of the past $\bar{F}(\Delta \tau)$
- Swelling of the subjects $X_{inp}(w_q(\Delta \tau))$ in the individual road traffic clusters, this data can be measured or estimated by different methods and data acquisition systems (Figure 3)

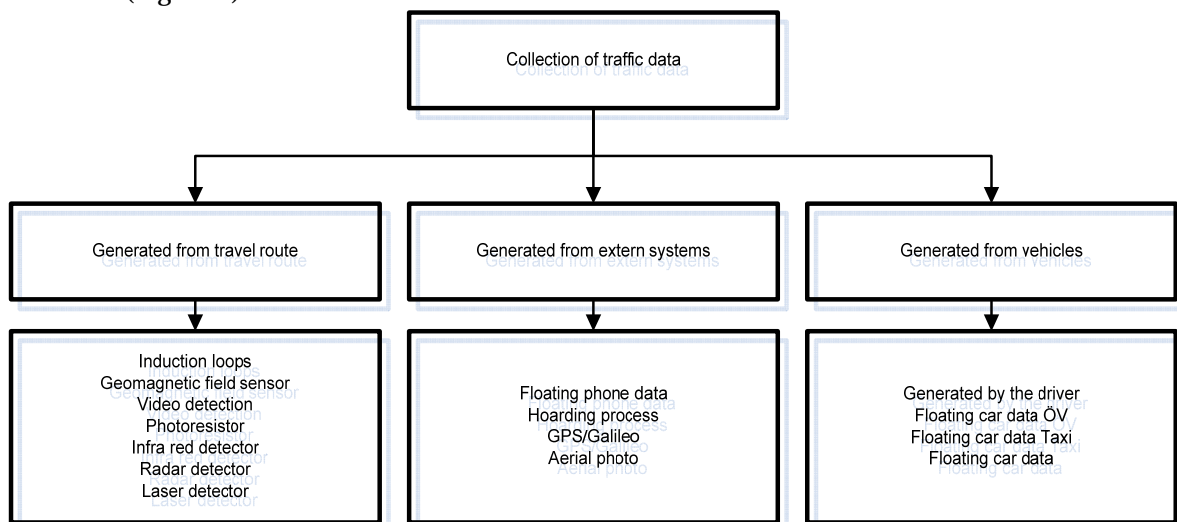


Figure 3.: Classification of traffic data collection

The data acquisition systems are usually suitable for recording the traffic density and speed. Traffic flows can be determined by a number of systems at the time of acquisition, but difficult is the detection of the target cluster w_s of all traffic entities at the time of acquisition. Suitable for this purpose are for example navigation systems with a communication session from the vehicle to a

control centre. To estimate the density of traffic in the future forecasting models of the transport planning can also be used.

3. CONCLUSIONS

If an edge or a node of the network is detected as a critical spot for trouble-free transaction processing in the whole network, so can this fit into a management model. Here, the inflow will be measured, directions of traffic selected, loads for a specific point forecasted, and constrained by the available capacity inflows to this point limited or amended by another traffic control. The detection of an overload condition of an associated site infrastructure at a future date allows an activation of defensive strategies by

- ❖ Inflow reduction,
- ❖ Alternative routing under time restrictions,
- ❖ Temporal effect as speed limits in the form of maximum or minimum speed etc.

REFERENCES

- [1] Bärwald, W., Baumann, S., Keil, R.: Organisation ressourcenbegrenzter prognostizierbarer Infrastrukturbelastungen, Schriftenreihe des Sächsischen Telekommunikationszentrums e.V. Band 09/2010, Dresden 2010, ISSN 1863-1878
- [2] Hrnčiar, M.: Analyse der Content-Management Bedingungen für LBS in der Slowakischen Republik, in Proceedings from workshop "LBS und RFID - Lösungsansätze in Logistik und Verkehr". Győr - Ungarn. 2006. ISSN 1611-8839
- [3] Bärwald, W., Baumann, S., Keil, R.: Managing Infrastructures of Limited Resources, in Acta Technica Jaurinensis, Series Logistica Vol. 2. No. 3 (2009) Faculty of Engineering Sciences, Széchenyi István University Győr, ISSN 1789-6932
- [4] Bärwald, W.; Baumann, S.: LBS- und GIS-gestütztes Hoarding. In: Strobl/Blaschke/Griesebner (Hrsg.) Angewandte Geoinformatik 2008 – Beiträge zum 20. AGIT-Symposium S. 254 - 259, Wichmann Verlag Heidelberg
- [5] Fischer, K.: Zuverlässigkeits- und Instandhaltungstheorie, transpress Verlag für Verkehrswesen Berlin 1990
- [6] Keil, R.: Beschreibung des Zeitverhaltens informationslogistischer Prozesse in Schriftenreihe des Sächsischen Telekommunikationszentrums e.V. Band 02/2006, Dresden 2006, ISSN 1863-1878
- [7] Richter, G.: Zum Verteilungsproblem bei zufälligen linearen Gleichungen, Dissertation B, Hochschule für Verkehrswesen „Friedrich List“ Dresden 1989
- [8] Helbing, D.: Verkehrsdynamik, Neue physikalische Modellierungskonzepte, Springer-Verlag Berlin Heidelberg New York 1997



¹Vasile ALEXA, ²Imre KISS

METHOD FOR CREATING AND MAINTAINING AN HIGHLY PERFORMING SPACE AT THE WORKPLACE

¹⁻². UNIVERSITY "POLITEHNICA" TIMISOARA, FACULTY ENGINEERING HUNEDOARA, ROMANIA

ABSTRACT:

The philosophy of the "5S" focuses on the workplace and standard procedures at the workplace. The "5S" lead to an appropriate working environment, to decreasing the losses and useless activities, to improving quality, efficiency and safety. The workplace problems cannot be observed in due time if there is disorganization. Cleanliness and organization at the workplace help the worker team to discover and solve problems. By making problems visible we step closer to improvement. Maintaining the workplace clean, insuring an appropriate working environment and increasing productivity lead to time economies, time which we can dedicate to research, to cost reduction, to insure safety, loss decrease, and induce in workers the conscience of responsibilities and the pride of belonging to the team of enterprise employees.

The "5S" program helps us create an appropriate environment for the standard work, offers conditions for high quality, encourages visual control, helps identify loss and places great emphasis on safety. The individual implementation technique consists in complying with the "5S". We propose for your attention a short theoretically study in which we will present the five components of the method necessary for a correct implementation in every workplaces.

KEYWORDS:

workplace, performing space, humanized approach, productivity increase, "5S", method

1. INTRODUCTION

The "5S" method represents a method for creating and maintaining an organized, clean and highly performing space at the workplace, or better yet, a conditioned discipline for Kaizen.

Kaizen is a daily activity, whose purpose only exceeds productivity improvement. It is also a process which when performed correctly humanizes the workplace, eliminates excess work and teaches people how to perform experiments regarding their activity by using the scientific method and how to teach them to detect and eliminate waste produced during different processes. This process suggests a humanized approach of workers and of productivity increase: "Te idea is to fuel the company's human resources, as well as to praise and encourage their participation to kaizen activities". Its successful application needs "the participation of workers in the improvement activities".

The philosophy of the "5S" focuses on the workplace and standard procedures at the workplace. The "5S" lead to an appropriate working environment, to decreasing the losses and useless activities, to improving quality,



Fig. 1. The "5S" method

efficiency and safety. The workplace problems cannot be observed in due time if there is disorganization. Cleanliness and organization at the workplace help the worker team to discover and solve problems. By making problems visible we step closer to improvement. Maintaining the workplace clean, insuring an appropriate working environment and increasing productivity lead to time economies, time which we can dedicate to research, to cost reduction, to insure safety, loss decrease, and induce in workers the conscience of responsibilities and the pride of belonging to the team of enterprise employees.

The “5S” program helps us create an appropriate environment for the standard work, offers conditions for high quality, encourages visual control, helps identify loss and places great emphasis on safety. The “5S” are (fig. 1):

- ❖ Seiri (sort) – selection;
- ❖ Seiton (stabilize / straighten) – engagement;
- ❖ Seiso (shine / sweep) – cleanliness;
- ❖ Seiketsu (standardize) – standardization;
- ❖ Shitsuke (sustain) – sustenance.

The individual implementation technique consists in complying with the “5S”.

2. SEIRI – THE SELECTION PHASE

It represents the first “S” of the the “5S” and involves the focus on eliminating what is not necessary and keeping only what is necessary for a certain purpose. Seiri thus involves the separation the useful from the useless, the elimination of what is in excess at the workplace and in its environment. An ABC-type classification system allows the determination of the necessary compulsory stock for the job, but also the removal of what is in excess. In our case the signification of the 3 parameters afferent to the Pareto-type technique is the following:

- ❖ A – daily use;
- ❖ B – weekly or monthly use;
- ❖ C – rare use.

The objective is the saving and recovery of the work space. Table 1 presents the ABC classification.

An efficient visual method to discover all these unused objects is the “red marking”. This marking is placed on all objects that are not used to complete the work. Marked in this manner these objects are moved in a so-called waiting area. Occasionally, the used objects are moved in a more organized area found outside the work area.

Table 1.

Priority	Usage frequency	How it is used
High (type A articles)	Once a day	It is located at the workplace
Medium (type B articles)	At least twice in 6 months Once a month Once a week	It is stored together
Low (type C articles)	Less than once a year	It is disposed of or stored outside the workplace



Fig. 2. Marked spaces in the workplaces – example

As far as the performed mold is concerned, it means the daily use of rubber as a basic material. That is why in the case of sorting materials, it belongs to the A type article group. In the same group is included the portable cone type device which must be available to the worker to perform the wiring.

The tools, apparatuses and devices used to tune the mold, the hydraulic operation of the slider and the preventive and predictive maintenance activities belong to the B type article group.

3. SEITON – THE ENGAGEMENT PHASE

It represents the implementation of a resource organization system so that the resources are easily identifiable. For this, three questions must be answered:

- ❖ what do I need?
- ❖ where do I keep what I need so as to be easily accessible?
- ❖ how much do I need?

The engagement is done as follows: the placement element is defined depending on the usage frequency, the system address with the identification number and the recipient label is determined, and the minimum grade and maximum quantity are decided.

Methods for highlighting and ordering the necessary resources:

- ❖ colored panels;
- ❖ lining the work areas and the location;
- ❖ tools on shelves.

Before improvement (Fig. 3.a) it can be seen that the work table is too wide, the spare parts are too far and situated horizontally, this makes them hard to see and reach. After improvement (Fig. 3.b) it can be seen that the work table has been reduced, the spare parts have been placed so that the worker can reach them and have been sloped slightly to be better grabbed and seen.

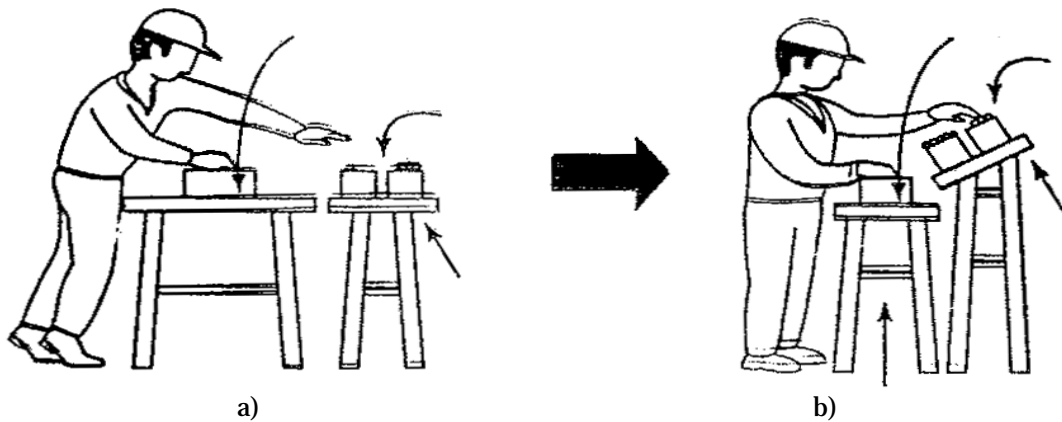


Fig. 3. Manual assembly operations before (a) and after (b) improving the work space

Like the case in Fig. 3, the portable cone type device must be available to the worker to minimize the wiring time. As far as the mold injection process is concerned, the injected material must be close to the under-pressure casting machinery so as to be introduced in the fueling cone.

4. SEISO – THE CLEANLINESS PHASE

It is the third “S”, which helps us understand how to prevent the material contamination and to insure good working conditions.

After all the elements causing problems regarding work start are eliminated (removal of useless objects for the injection process, respectively the wiring one) and after the materials used for work start are established, the next step is to clean the work area thoroughly (fig. 4). Daily cleaning is necessary so that the workers can be proud of their workplace, as well as to ensure an adequate environment for performing different processes, less dirty equipment and better health protection.



Fig. 4. To clean the workplace means quality improvement

If there were no change in the work area of each worker, then this would lead to decreasing production, angry and stressed workers.

The purpose of cleanliness is to maintain a pleasant work environment in which the need for esteem and status of the employees will be protected, and the work relationships will be improved. All these have considerable effects on the company's productivity.

The cleanliness is done for:

- ❖ surface protection in case those sediments alter the physical-chemical properties of that surface;
- ❖ preparing technological operations (reconditioning, disassembling, etc.);
- ❖ maintenance and improvement of the exterior aspect of the installation, which constitutes an element appreciation of the professional culture of the personnel that maintains, respectively services the installation.

In the case of parts molded under pressure inclusions appear in the part material due to the fact that the form basis and cavity have not been adequately cleaned from impurities. Also, the material introduced in the injection installation must have a certain composition, without being mixed with impurities, to obtain the desired physical and mechanical properties.

Taking into consideration the hydraulic operation of the lateral sliding mechanism, there can be spills of hydraulic oil that must be cleaned.

5. SEIKETSU – THE STANDARDIZATION PHASE

The fourth “S” represents the standardization resulting after the fulfillment and maintenance of the other three steps. Seiketsu is necessary because the workplace degenerates very quickly if certain standards are not imposed. The visual control is made based on:

- ❖ warning lights;
- ❖ transparent windows;
- ❖ color codes;
- ❖ tables and marking;
- ❖ periodic inspections.

The rules referring to visual control once implemented the need to select the best practices and their standardization is felt. All these are done more efficiently by involving employees.

The main objectives of standardization and rule appliance regarding the workplace are the following:

- ❖ the workplace design;
- ❖ clear work instructions;
- ❖ well defined work methods;
- ❖ ergonomic work courses;
- ❖ reducing the time cycle;
- ❖ training and documentation.

Referring to the injection installation, we can say that the means to use it is standardized within the enterprise so as to insure the repeatability of the molding process identically, obtaining the desired material characteristics and thus a higher quality of the part obtained.

6. SHITSUKE – THE SUSTENANCE PHASE

It is the fifth “S” and represents one of the hardest stages because people in general show a certain resistance to change and favor status quo (the desire to maintain the existing situation) in the detriment of change. That is why the efforts will be focused on redefining the de facto condition and the lining of new standards. Shitsuke must insure the continuous supervision of rule application, memorization and correction of derivatives.

By establishing a tracking system with indicative display the “5S” are ensured, but the gradual recovery of their initial limits is necessary in a continuous improvement action, respectively the Kaizen. The problems that appear when the 5 points are not insured and mentioned are the following:

- ❖ the materials used begin to reappear at the workplace, creating chaos;
- ❖ after using tools, they are not placed appropriately, encumbering their location when needed;



Fig. 5. Examples of marking for notice

- ❖ the frequent contamination of equipment does not represent a reason not to clean them, but the contrary;
- ❖ the placement of objects in the workers' access area, which can lead to their harm;
- ❖ the dirty machinery does not function appropriately and leads to obtaining faulty goods.

7. SAFETY – THE SIXTH “S”

The implementation of the sixth “S” is recommended, namely SAFETY, which wishes to eliminate all workplace accident risks, ensuring the operator's safety.



Fig. 7. The 6S method

There are many reasons for using the sixth “S”, which depend on:

- ❖ Using adequate tools or adequately marked ones, using the protective equipment where necessary (overalls, gloves, protective glasses, masks, helmets, etc.);
 - ❖ Maintaining the access aisles free;
 - ❖ Storing the protective equipment in predetermined easily-accessible locations;
 - ❖ Non-existence of material spread on the floor, uneven floor, sharp edges, suspended stocks unmarked.
- A three-step approach is used for Safety, namely:
- ❖ preparation (we take into consideration the client's expectations, we build a purpose, define the goals, evaluate if the event makes sense, prepare the people and place for the beginning of the event);
 - ❖ operation (we inform the worker team regarding the purpose, goals and expectations of applying this element, we evaluate the losses, come up with improvement ideas, select the best ideas, improve and measure the improved results);
 - ❖ supervision of the improvements that appear following the application of the “6S”.

In the area of the injection installation the workers must work with protective equipment due to the high temperatures that are involved in the material melting. When taking the part out of the mold the worker must use gloves, the parts being hot.



Fig. 8. The situation before (a) and after (b) improving the 5S (6S) method in the case of office

The “6S” (Fig. 7) is an instrument whose value is easily understandable. An important quality of the “6S” is the fact that it does not allow doubts. It offers people a working area without events that prevent their activity, and this is a marvelous way in which people can be involved in improving their own working conditions.

The “6S” system helps in the daily activity by preventing and the due remedy of deficiencies and lack of compliance noticed. The results of the applied method are seen in the better performing working manner, efficiency, and low number of complaints from clients, giving the employees a real accomplishment feeling and pride, which can create the beginning of a cultural transition.

8. CONCLUSIONS

The “6S” is modeled after the “5S” process improvement system designed to reduce waste and optimize productivity through maintaining an orderly workplace and using visual cues to achieve more consistent operational results. It derives from the belief that, in the daily work of a

company, routines that maintain organization and orderliness are essential to a smooth and efficient flow of activities. Implementation of this method “cleans up” and organizes the workplace basically in its existing configuration. It is typically the starting point for shop-floor transformation. The “5S” pillars provide a methodology for organizing, cleaning, developing, and sustaining a productive work environment. The “6S” uses these five pillars plus an added pillar for Safety. The “6S” encourages workers to improve the physical setting of their work and teaches them to reduce waste, unplanned downtime, and in-process inventory.

When the six pillars have been implemented and organizational and safety procedures are maintained, the workplace becomes a safer and more efficient place to work leading to increased productivity and worker confidence. Although other Lean methods can be used without using “6S”, the “6S” method creates a streamlined workplace and a good base which can often times enhance the results from other Lean processes.

As a general conclusion, we can conclude that the “5S” (and also, the “6S”) represents a strategy to develop and maintain a working environment that is clean and organized. Such an environment almost guarantees a better working environment for workers, a more organized system for tools and equipment, and a safer work environment. Start today to make 5S part of any strategy of bringing greater effectiveness and efficiency to all business.

The “5S” is a visually-oriented system of cleanliness, organization, and arrangement designed to facilitate greater productivity, safety, and quality. It engages all employees and is a foundation for more self-discipline on the job for better work and better products. The teamwork and discipline built through the “5S” improve worker-to-worker and worker-to-manager relationships. When people see that what they do makes a difference, and when they see that they have eliminated wasteful practices, their pride grows. This is perhaps the greatest benefit of the “5S”.

BIBLIOGRAPHY

- [1.] HIRANO, HIROYUKI. 5 Pillars of the Visual Workplace (Portland, Oregon: Productivity Press, 1995).
- [2.] PETERSON, JIM, ROLAND SMITH, Ph.D. The 5S Pocket Guide (Portland, Oregon: Productivity Press, 1998).
- [3.] Productivity Press Development Team. 5S for Operators: 5 Pillars of the Visual Workplace (Portland, Oregon: Productivity Press, 1996).
- [4.] Productivity Press Development Team. 5S for Safety Implementation Toolkit: Creating Safe Conditions Using the 5S System (Portland, Oregon: Productivity Press, 2000).
- [5.] Productivity Press Development Team. 5S for Safety: New Eyes for the Shop Floor (Portland, Oregon: Productivity Press, 1999).
- [6.] SHIGEO SHINGO – „The SMED System”, Productivity Inc., 1985
- [7.] <http://en.wikipedia.org/wiki/Kaizen>
- [8.] http://en.wikipedia.org/wiki/Shift_work
- [9.] <http://en.wikipedia.org/wiki/SMED>
- [10.] http://membres.multimania.fr/hconline/smed3_us.htm
- [11.] MASA AKI IMAI – „Gemba Kaizen”, Productivity Inc., 1997
- [12.] <http://www.theleanman.com/Item-5S-Red-Tags-50-Pak.aspx>
- [13.] <http://www.5stoday.com/>



¹Mihaela POPA, ²Grigore CONSTANTIN

SPORTS MARKETING MIX IN THE CONTEXT OF TRADITIONAL MIX MARKETING

¹⁻²UNIVERSITY POLITEHNICA TIMISOARA, FACULTY OF ENGINEERING HUNEDOARA, ROMANIA

ABSTRACT:

Marketing mix is the central part of an organization's marketing tactics, so when an organization decided development to one specific market, the mix marketing has an important role.

The essential features of sport marketing are determined by:

- ❖ unique nature of sport as a marketing product
- ❖ complexity of consumer and its participation in sport
- ❖ specificity of industry and sport market

The diversity of industry and sporting phenomenon, led to the delineation of two major sports marketing industry, namely:

- ❖ Marketing through sport - which uses sport to promote other types of goods, services or ideas;
- ❖ Marketing of sports - sports goods and services.

In sport industry service, the element *product* should be extended, so it is considered by experts that there are at least five major elements of marketing mix in sport marketing namely: product, price, promotion, public relation and distributions.

KEYWORDS:

marketing mix, sport, product, price, promotion, distribution, public relations

1. INTRODUCTION

The uniqueness of the sport as a product resulting from the following:

- ❖ Sport is a consumer product, industrial product and service;
- ❖ Sport is a subjective, intangible and ephemeral experience, can not be viewed, sent or exhibited before sale;
- ❖ Sport is produced and consumed simultaneously;
- ❖ Sport is often consumed in groups;
- ❖ Sport as a series of mass production is impossible;
- ❖ The product sport has a unsteady character;
- ❖ Sport has a universal magnetism;
- ❖ Sport is a product that is personalized and nationalized;
- ❖ Sport offers a high level of personal identification;

2. PRODUCT SPORT

In the marketing mix context, product means what a market is offering for use or consumption, and can be a physical object or service of any kind.

The life cycle of a product, requires a focus on cosmetic products from when he was placed on the market until it is withdrawn.

Mullin, Hardy and Sutton, identifies the following components, of product sport namely:

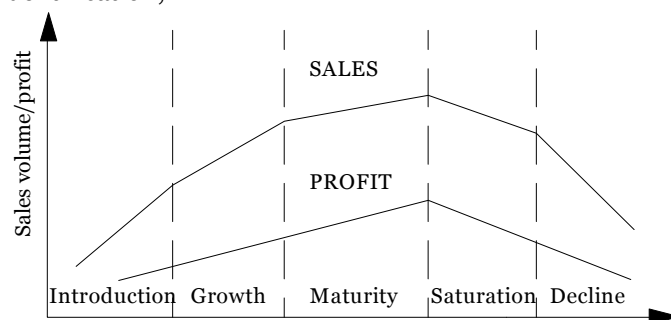


Figure 1 Life cycle of a product

- ❖ *Essential benefits* - related to the satisfaction of some needs or desires;
- ❖ *A generic form of sport* - competition requires rules, equipment, physical abilities and a certain frame (sports facilities);
- ❖ *A specific form of sport* – the specific forms of sport are developed either in a non-institutionalized environment - recreational sports in family, or in one institutionalized environment and sports performance have a proper organizational framework;
- ❖ *A marketing mix* - in a industry based in services such as sport, the element *product* should be extended, so it is considered by experts that there are at least five major elements of marketing mix in sport marketing namely: *product, price, promotion, distribution and public relations*.

3. PRICE

An important element of the marketing mix - price - is the only part of the mix that produces benefits, because all other represent costs.

The satisfaction of the consumer - Benefits - Cost involved

In assessing the overall impact of price to the sports consumer, marketing specialist must take into account the actual cost of the product for the consumer, given the fact that in sports there is not a direct determination between the level of income and the price of participation in sport.

4. COMMUNICATIONAL COMPONENT

The specifics of the communication tools used in sports marketing, is given by the double role which they fulfill, namely: communication and funding.

Mullin, Hardy and Sutton, proposing to use an impact matrix which shows the interaction between the main components of the marketing mix in order to explain the relationship of interdependence between marketing communications and other elements of marketing mix:

- ❖ The impact between product and promotion - product sets appropriate environment which will communicate the message, and in some cases the choice of environments can have a major effect on the product image;
- ❖ The impact between product and public relations - public relations contributes to building a long-term picture, depend on the goodwill of the press and broadcasters and plays a crucial role in consumer responsiveness;
- ❖ The impact between price and promotion - the price of a product determines the environments through the product will be promoted, determines the marginal profit generated by the product, with repercussions on the budget communication, which determines the selection of environments;
- ❖ The impact between price and public relations - the organization's image, created through public relations media will determine receptivity and subsequent consumer attitudes towards a possible change in price;
- ❖ The impact between distribution and promotion – sports complex image is strong and has a direct impact on the image product / service;
- ❖ The impact between distribution and public relations - careful management of the staff of a sports complex can help to maintain a positive global image through public relations.

Table 1. Matrix of the 5 P's of marketing mix (Mullin, Hardy, Sutton)

	Product	Price	Distribution	Promotion	Public Relations
PRODUCT		Price-value	Interaction of images	Position of product	Consumer receptivity
PRICE			Interaction of images	The choice of environment	The sincerity of public relations
DISTRIBUTION				Interaction of images	Interaction of images
PROMOTION					Complete interdependence
PUBLIC RELATION					

5. PROMOTION

5.1 PUBLIC RELATION

The main components of public relations are:

- ❖ Relations with the media - sending and receiving information to the media's and careful receptivity of the feedback;

- ❖ Relations with the community - generate goodwill and understanding from the public.
Strategic planning of public relations in sports involves followings:
- ❖ Identifying targets;
- ❖ Setting goals;
- ❖ Building the image of the organization: setting the content of messages;
- ❖ Choosing the most appropriate techniques: printed materials, contacts records, special events, other manufacturers of photography;
- ❖ Implementer of the public relations program, which involves: qualification of public relations staff in the art to produce and deliver news; make a list of media; drawing up a timetable of specific activities which details the sequence of actions and deadlines for compliance throughout the campaign;
- ❖ Evaluation of results.

5.2 PUBLICITY

5.2.1 Publicity through sport involves:

- ❖ advertising for competition;
- ❖ sports equipment and referees advertising;
- ❖ publicity in sports publications - the choice of publications is based on criteria such as: readers profile, distribution area and circulation, publication timing and selling price of space.

5.2.2 Publicity for sport involves

Sports organizations promote their products / services through the following forms, classical "of advertising:

- ❖ advertising on television and radio - broadcasting;
- ❖ display and outdoor advertising;
- ❖ print advertising - competition schedules, event programs, invitations, admission tickets, stationery;
- ❖ special advertising - through ceremonial objects that accompany athletic performance or souvenirs (shirts, pins, keychains, pens, etc.).
- ❖ public address systems;
- ❖ advertising interactive computer networks – Internet

Personal sales are the most expensive form of promotion and range from simple acquisition of a store orders (or sales office), to create new types of sales over a highly competitive market. Overall sales process has five immediate objectives, and one subsequently as it shows in fig.2.

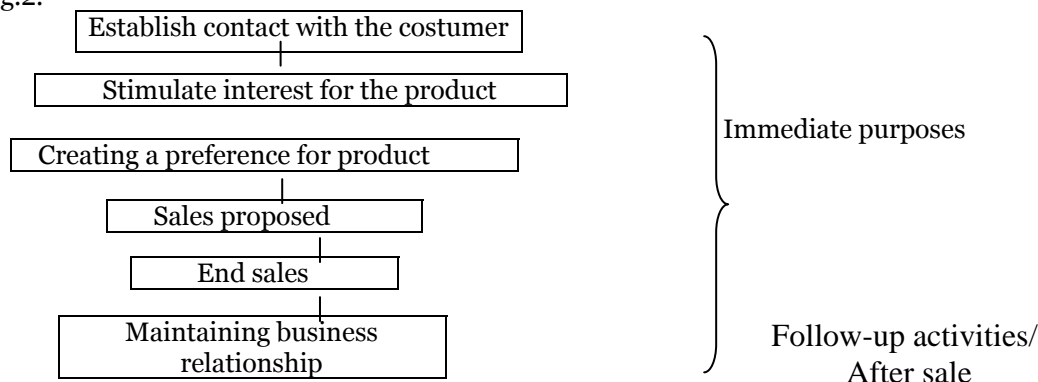


Figure 2 Sales objectives

5.2.3 Sales promotion

For sports, sales promotion may have the following targets:

- ❖ Sales forces : main incentives offered are: public recognition, diplomas, awards, medals, cups, titles, bonuses, gifts, special events;
- ❖ Intermediaries - in sports they can be owners of databases, agencies selling tickets to games, equipment suppliers;
- ❖ Policy makers - people who are recommending through their decision power, participation in sport to other persons: physical education teachers, parents, doctors, dieticians;
- ❖ Sponsors: maintain and improve existing partnerships, expanding forms of cooperation with firms that are already sponsoring and rewarding or expressing gratitude to the partners;
- ❖ Consumers of sport.

Techniques used for sales promotion:

- a) Techniques of promote sustainable by product involves:
 - ❖ temporary price reductions;
 - ❖ grants and gifts;

- ❖ playing techniques: organizing competitions which purpose is to promote a club and its stars; lottery ticket;
- ❖ free trial - providing opportunities to receive individual sports experience through free access to a sports competition or start a free lesson;
- b) Promotion techniques able to attract potential consumer to the product; presenting the most advantageous product marketing at its commercial place.

Types of programs to promote sales:

Mullin, Hardy and Sutton differentiated merchandising programs in sport, in:

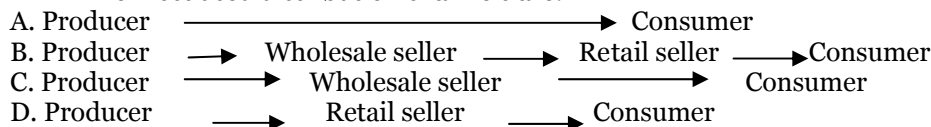
- a) Programs designed to increase the frequency of participation in sports:
 - ❖ programs to increase the frequency of casual consumer participation;
 - ❖ programs to increase the frequency of average users;
 - ❖ programs which maintain the frequency of the active participant.
- b) Programs designed to prevent early supporters or motivating them, like:
 - ❖ providing preferential places to subscription holders;
 - ❖ offering free competition programs at the renew subscriptions;
 - ❖ free parking;
 - ❖ free access to stadium club.

6. DISTRIBUTION

The distribution purpose - transfer the product or service to the consumer named target.

Distribution deals with distribution channels and physical distribution.

The most used distribution channels are:



6.1. Market segmentation

The most common methods of market segmentation have variables of different natures such as geographic, demographic and behavior of the purchaser as listed below:

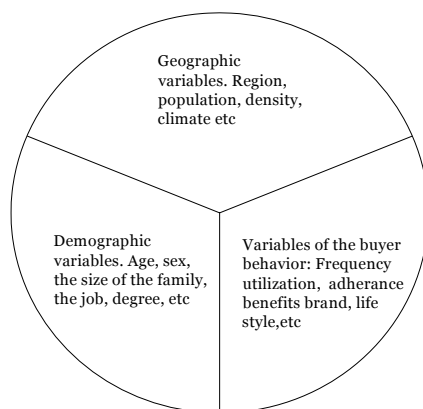


Figure 3 Market segmentation

An important variable in consumer behavior is measurable utilization of purchases volumes.

The main benefits of market segmentation in terms of the seller are:

- ❖ the seller has a better picture of the market as a whole, especially in relation to the marketing opportunities of the market segments;
- ❖ seller can build the marketing mix depending to the needs of specific segments;
- ❖ the seller, familiar with one or more segments can easily evaluate their response, a valuable element in planning.

The main benefit of the consumer's point of view is the fact that they satisfy their needs, taking into account the above variables.

7. CONCLUSIONS

- ❖ To attract, right customer, manufacturers and retailers must vary the marketing mix to the needs of different market segments;
- ❖ Merchandising programs in sport is based on the different stages which consumer engage in sports participation;
- ❖ Objectives which are used in the service of sales promotion techniques, is closely related to age product, regardless of their target hosts, so each phase of the stage of product life cycle corresponds to specific techniques and methods of promotion;
- ❖ The goal of mature sports organizations is not only to attract new customers, but more importantly, to increase the frequency of participation of existing customers and as this is done, increase the profitability of the organization;
- ❖ Image - immaterial component of the sport, is associated with different aspects of life such as: exercise, relaxation, social identification, prestige, self-realization, business, industry, religion becomes, especially in sports performance, the main purpose of marketing;

- ❖ In sports marketing, distribution function focuses on the location and design characteristics of sports and then to establish networks and the sale of tickets for transmission by electronic media (radio, television, Internet), because there is no physical movement of product.

REFERENCES

1. Gerald A.Cole – Management – theory and practice, ed. Știința, 2004;
2. Oprisan, V. – Marketing and communication in sport, Ed. Uranus, 2002;
3. Mullin, B.J., Hardy, S. & Sutton, W.A. – Sport marketing, Ed. A II-a Ed. Human Kinetics, SUA, 2000;





HIGH PRODUCTIVITY INSTALLATION FOR THE RECOVERY OF WASTE BY BRIQUETTING OF POWDER

¹ UNIV. POLITEHNICA OF TIMISOARA, FACULTY OF ENGINEERING FROM HUNEDOARA, ROMANIA

ABSTRACT:

This briquetting method is for obtained spherical, oval or rectangular pieces of ore from dust. Operations of pressing are made on specialized equipment, followed by a drying - roasting process in order to increase their mechanical characteristics. This method is characterized by high productivity and appropriate mechanical characteristic briquette. In other words, paper presents a way for the recovery and reinstates the economic cycle of this pulverous waste.

KEYWORDS:

Pulverous wastes, briquette, pressure, hydraulic press

1. INTRODUCTION

For obtaing of briquette, the raw material can be finely crushed if is necessarily. Milling operation is usually done in ball or bars mills similar to those described in the ores preparation. In the intimate mixture between binder additions and ore are used different types of machines such as scraper mixer with one or two axes.

Regarding of briquetting methods, they can be divided into two categories:

- ❖ briquetting without binder additions;
- ❖ additions briquetting with binders.

Depending on the made pressures in order to obtain, for both briquetting metod, they can be obtained by:

- ❖ low pressure briquetting (50 - 150 kg/cm²)
- ❖ medium pressure briquetting (150-750 kg/cm²)
- ❖ briquetting under high pressure (over 750 kg/cm²).

For briquetting, also can be used several types of machines, some with limited productivity and other with high productivity. For high productivity and low pressures are required for certain types of briquette are use roller press.

Most often, for obtaining the briquette with higher work pressure, but also with considerable productivity is used the ring presses, consisting of an outer ring supported on rollers and a serrated inner cylinder, placed eccentric. Rotation of inner cylinder inside ring presses the dust and results the briquette.

So, in Hunedoara area are greater quantities of this type of wastes, most of them are stored in pounds, but also stored in special places designed for this purpose. In figure 1 is presented these places from a satellite map.

2. THE STUDY

Waste results from the gas treatment plants and industrial wastewater discharged from various steel processes. It is therefore a source of ferrous waste generated by the action of preventing environmental pollution, air and water.

Ring presses can achieve pressures up to 3000 daN/cm², with productivity up to 9 t/h. For drying briquette and their heat treatment are used tunnel furnaces with 35m lengths, 1.2 m wide and 1.8 to 1.9 m high, equipped with track for truck where briquette are drying.



Fig. 1 Distribution of pulverous waste in Hunedoara area

Taking into account sources that generates ferrous waste can be established the following classification of them:

- ❖ ferrous waste from the steel industry
- ❖ iron waste from industrial activities or processes that use steel products
- ❖ ferrous waste from disposal of fixed assets and collected from the population (in households and downgraded objects containing steel or iron).[1,2,4]

Need for a highly productive presses in the briquetting process occurred because of the possibility of processing a large quantity of waste, especially in the area that these types of waste are present in large amounts.

To design this type of press, experimental tests were conducted to determine the optimal compress forces of waste so not destroy the briquette when is extracting from the form.

In figure 1 is presented the experimental test made for obtains the optimal press force.



Fig.2 Experimental briquette made with hydraulic press and manual installation

Figure 2 presents experiments carried out to obtain briquette. Attempts have been made in two versions:

- ❖ pressing the waste at high pressure using a hydraulic press that can develop a maximum pressing force of 41 kN;
- ❖ pressing at low pressures by pressing waste manual with different compression forces 100N, 150N and respectively 300N.

Where are compaction of waste using hydraulic press, the mechanical strength of resulting briquette was large enough to reach up to 450 N/briquette, depending on the of waste recipes mixture pressed at high specific pressures (25 N/mm² for Ø45 mm punch, respectively 84 N/mm² for Ø25 mm punch).

In case of manual pressing, the forces are much smaller, so for Ø45 mm punch specific pressures are small, up to 0.188 N/mm² and due to greater height of mold and lower pressing forces the compactness are smaller on height of briquette.

In variant of use Ø25 mm punch, the results are satisfactory as it was considered that the maximum specific pressure is approximately 0.611 N/mm².

The mechanical strength of briquette is increased, either by chemical hardening (using a binder to do this as bentonite or cement) or by thermal hardening (burning, eventually sintering the briquette in furnace with electric resistors or flame).

Briquette strength was measured in raw state and after burning. In raw state it was used three methods to measure mechanical resistance, as follows:

- ❖ empirical approximate method, when compressive strength of briquette was determined by static progress loading (using the weights) until is observed the cracking of briquette;
- ❖ 2nd method using a specialized mechanical-hydraulic installation to determine the compressive strength of briquette [4].
- ❖ Mechanical resistances are influenced by several factors such as:
- ❖ the quality of the binder and its quantity - the mechanical strength increases with increasing of binder quantity.
- ❖ water content of the mixture - the mechanical strength increases with increasing of water quantity. If it exceeds a certain percentage of, intergranular water shell becomes much thicker, interaction forces between the dipoles of water molecules and crystal lattice forces become weaker and leading to a decrease strength of the mixture
- ❖ the degree of tamping - mechanical strength increases with increasing of tamping degree. A tamping too strong can cause cracking of the briquette;
- ❖ grain size and shape of powdered material – change of the granulation conduct to increasing of mechanical strength. Strength of briquette made from less grain waste will be higher than the mechanical strength of briquettes from more grain waste. Higher mechanical strength values are obtained when are uses a non-uniform waste granulation (large and small granules).

According to the literature are considered best values of compressive strength between 1.2 ... 4.1 N/mm² for raw state and shear resistance between 0.8 ... 2 N/mm² . In case of hand pressing resistance to compression are presented in table 1.

Table 1. Compressive strength for raw briquette in case of hand pressing

Compression forces		Specific pressures	Compressive strength (raw briquette)
kN		N/mm ²	N/mm ²
Punch Ø25 mm	0.1	0.203	11
	0.15	0.407	17
	0.3	0.611	21
Punch Ø45 mm	0.1	0.063	inconsistente briquette
	0.2	0.126	inconsistente briquette
	0.3	0.188	inconsistente briquette

where specific pressures are :
$$P_{sp} = \frac{F_{press}}{S_{transverse\ punch}}$$

3. DISCUSSIONS

Based of these experiments, can be used two models in construction of this ring press, depending on the pressing force:

- ❖ first version, when made of briquette is based on compressing the mixture of waste by roller pressing, due to its own weight;
- ❖ the second option involves a higher clamping force, resulting mainly due to the constructive way (fixing the pressure cylinder in bearing, which allows the development of high clamping forces up to 300N/mm² especially for industrial facilities). [3]

3.1. First constructive version

For this alternative design, when the specific pressures and also the pressure forces are small, for get good briquette the mold from clamping cylinder is small. Pressure cylinder moves freely within the compression ring, being guided left-right, as is presented in figure 3. [3]

In terms of computing elements and design is necessary to determine the weight of entire pressing cylinder. So the design of surfaces where is made compacting the pulverous waste (mold) will be consistent figure 4, where dimension are:

D=25 mm – width; L=50 mm – length.

Outer surfaces are:

$$S_{ext.} = \frac{\pi \cdot D \cdot L}{2};$$

$$S_{ext.} = \frac{3.14 \cdot 50 \cdot 50}{2} = 3925 \text{ mm}^2$$

Necessary compacting forces:

$$F = p_{sp} \cdot S_{ext.} \quad F = 0.4 \cdot 3925 = 1570 \text{ N}$$

where: $p_{sp} = 0.4 \text{ N/mm}^2$

Mass of compacting element:

$$m = \frac{F}{g}; \quad m = \frac{1570}{9.81} = 160.04 \text{ kg}$$

The volume of compacting element, in case of this is made from manganese steel or white cast iron ($\rho_{\text{steel-iron}} = 7.8 - 7.6 \text{ kg/dm}^3$):

$$V = \frac{m}{\rho_{\text{steel-iron}}}; \quad V = \frac{160.04}{7.8} = 20.52 \text{ dm}^3$$

Diameter of compacting element, in case of $g=50 \text{ mm}$ are thickness of compacting element:

$$D_{cp} = \sqrt{\frac{4 \cdot V}{\pi \cdot g}} = \sqrt{\frac{4 \cdot m}{\rho_{\text{fonta}} \cdot \pi \cdot h}}; \quad D_{cp} = \sqrt{\frac{4 \cdot 160.04}{7.8 \cdot 3.14 \cdot 0.5}} = 7.23 \rightarrow dm = 723 \text{ mm}$$

Because is necessary a greater compacting forces, this constructive variant lead to a large diameter of cylinder for pressing the raw material in ring. In order to assure a better stability as it reinforces through a spacer element such two tooth pressure cylinder, design of machinery is similar with the roller press.

3.2. Second constructive version.

This constructive variant allows the development of compression forces much higher and increased stability in the functioning of the press.

The difference with the first possibility is that the design of tooth pressure roller is mounted on bearing and pressing force is developed by the eccentric mounting of the cylinder to the outer ring gear (drums).

The wear both of pressing ring and the tooth compress cylinder is lower than the previous version because these two machine parts do not come into direct contact with each other.

In both cases, to prevent mutual slippage between the ring gear and the pressure cylinder, the peripheral speed of the two components must have the same value.

In fig.5.a the tooth cylinder is fitted with eccentric gear after the two axes of the coordinate system inside the pressure ring, which leads to an appearance of overturning moment of the ring by pressing the roller support. This moment must be balanced by a force, applied through a roller press-balancing 1.

In fig.5.b the tooth pressure cylinder is only fitted with eccentricity of OY the axis of coordinate system, roll 1 may be absent from the construction of press ring, because the press force acting on the ring pressing, keeping it in contact with support rollers 5. [3]

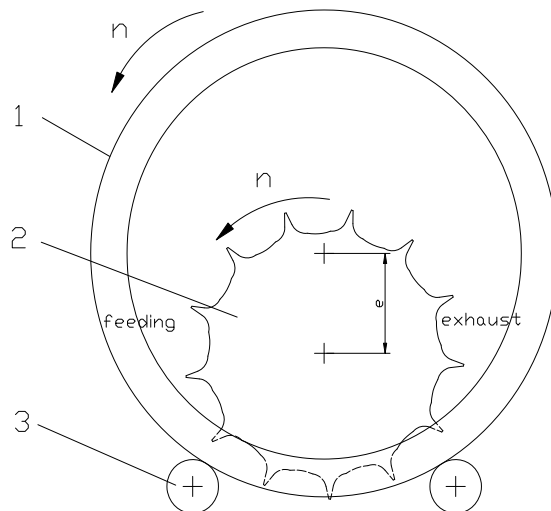


Fig. 3 Design scheme of the ring press, first constructive variant

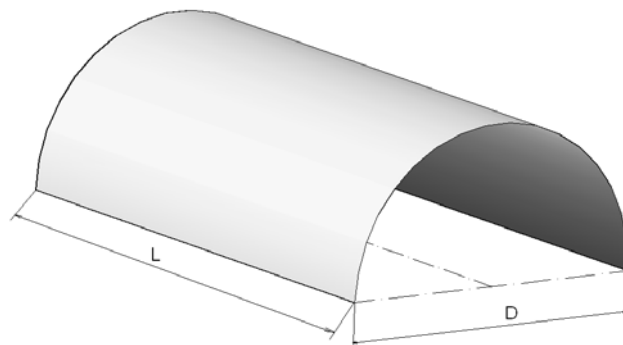


Fig. 4. Dimension of mold

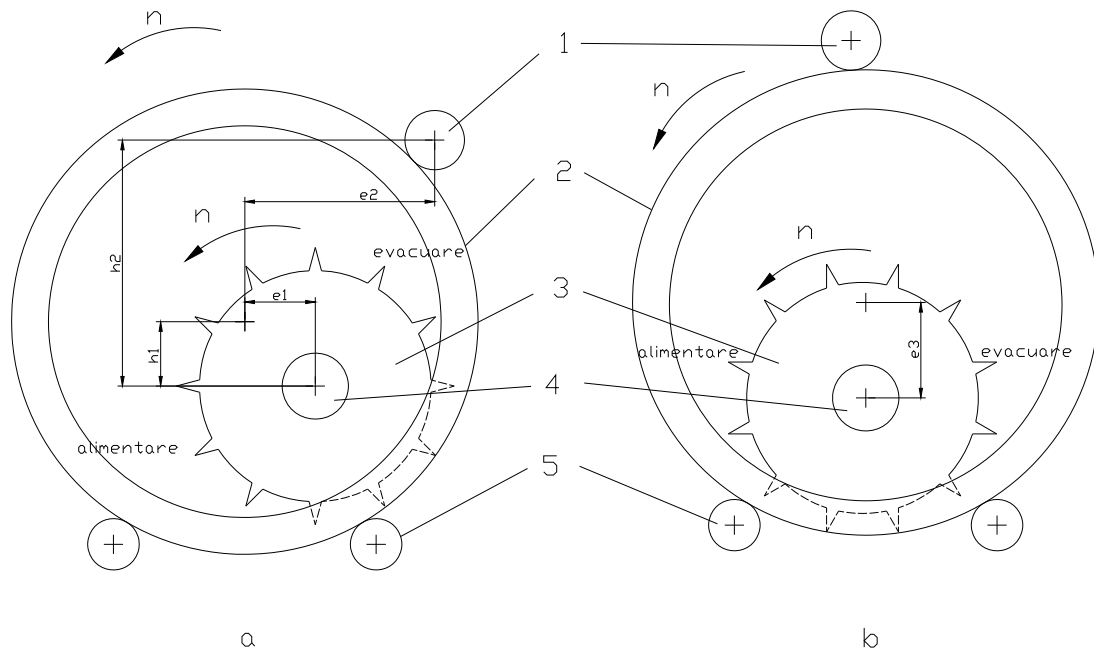


Fig. 5. Ring press
 1- press-balancing roll; 2-pressing ring; 3-tooth press cylinder;
 4 - axle; 5 – support roll.

Because construction from fig. 5.a. complicates the ring press, although it increased the space through which granular material is introduced into the pressing zone, the preferred construction is on fig.5.b By design, is established the specific pressure at the value of 8 N/mm^2 .

Is determined the pressure area formed by summation of the three areas of empty space (mold) between two consecutive teeth of the tooth pressing cylinder, presented in fig.6 , where: $b=60 \text{ mm}$ – width of tooth cylinder; $h=31 \text{ mm}$ – length of inclined part of the tooth; $l_R=62 \text{ mm}$ – length of circular segment with radius $R=150 \text{ mm}$ between two consecutive tooth flanks.

Maximum compacting forces, when this force is distributed evenly throughout the interior surface of mold:

$$F_{\max} = S_p \cdot p_{sp}, \text{ N} ;$$

$$F_{\max} = 7440 \cdot 8 = 59520 \text{ N}$$

Calculate starting at the specific pressure the thickness of material will be briquetting and which will be deposited uniform before the compression cylinder. This calculation will be based on an analogy with the tamping pressure of mixtures with medium pressure.

Degree of tamping:

$$\rho = 1 + C \cdot p_{sp}^{0.25}, \text{ g/cm}^3 ; \rho = 1 + 0.45 \cdot 8^{0.25} = 2.19, \text{ g/cm}^3$$

where: $C=0.4 \dots 0.5$ – coefficient by pressure tamping

Total height of layer a submitted to tamping from at tamping degree of $\rho_0=1\text{g/cm}^3$ to at tamping degree $\rho=2.19 \text{ g/cm}^3$ are:

$$H_t = H \cdot \frac{\rho}{\rho_0}, \text{ mm} , H_t = 30 \cdot \frac{2.19}{1} = 65.88 \text{ mm}$$

Driving is done separately for the outer ring, respectively toothed cylinder. Kinematic scheme is shown in fig.7 for drive of tooth pressing cylinder. Mechanical movement is done using an AC electric motor, worm gear (gear-motor) and an external gear.

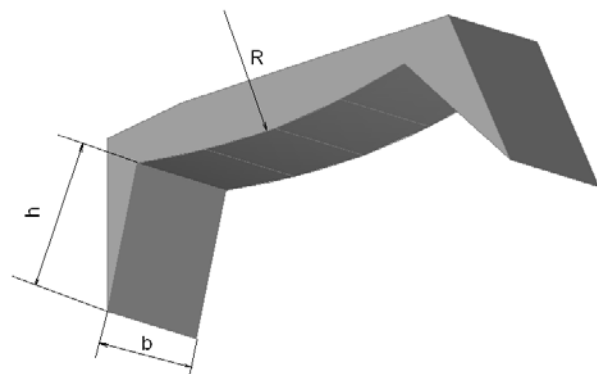


Fig.6. Part of tooth cylinder (mold)

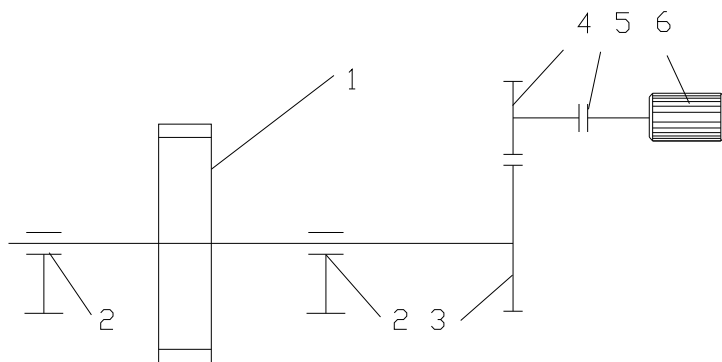


Fig.7. Kinematic scheme of action for tooth press cylinder
 1-tooth cylinder; 2-bearing; 3,4-gears; 5-clutch gear; 6 gear-motor

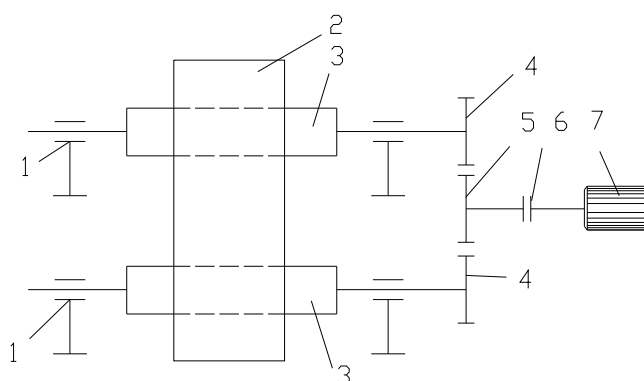


Fig.8. Kinematic scheme of action for press ring
 1-bearings; 2-press ring; 3-suport roll; 4, 5-gears; 6-clutch gear; 7- gear-motor

In fig.8 is presented a schematic diagram of the ring press drive. The ring 2 is pressed through three support rollers, and driving of this is made trough worm gear motor and outdoor gear.

4. CONCLUSIONS

Briquetting, pelletising and agglomeration represents a viable alternatives technology is if you want to reuse small and powdery waste. This type of installation can be used for recovery the large quantities of waste, in industrial equipment. Can reuse the waste stored in ponds and dumps, but can be adapted in steelworks technological flow chart for recovery of electrofilter dust from EAF furnaces.

For this briqueting equipment is characteristic a higher productivity. Also is selected the second constructive variant because the compacting forces not depends of tooth cylinder weight, and this force value resulting from design of press and is determinated in laboratory experiments. This constructive variant allows the

development of compression forces much higher and increased stability in the functioning of the press. In conclusions, using of this press is adequate for recovery of large amounts of waste existing in the Hunedoara area.

ACKNOWLEDGMENT

The researches do the object of Research Project no.31-098/2007, with title Prevention and fighting pollution in the steelmaking, energetic and mining industrial areas through the recycling of small-size and powdery wastes, financed by National Center of Program Management, project managed by Prof.dr.ing. Teodor Heput.

REFERENCES

- [1.] Nicolae, M., ș.a., Dezvoltare durabilă în siderurgie prin valorificarea materialelor secundare, Ed. Printech, București, 2004.
- [2.] Apostol, T., Mărculescu, C., Managementul deșeurilor solide, Editura AGIR, București, 2006.
- [3.] Zubac, V., Utilaje pentru turnătorie, Ed. Didactică și Pedagogică, București 1982.
- [4.] Heput, T., ș.a., Prevenirea și combaterea poluării în zonele industriale siderurgice, energetice și miniere prin reciclarea deșeurilor mărunte și pulverulente, Contract de cercetare nr.31-098/2007, beneficiar: CNMP, parteneri: CEMS București, SC CCPPR SA Alba Iulia.





¹Irina VÎLCIU, ²Maria NICOLAE, ¹Emanuela-Daniela STOICA

DIFFRACTOMETRIC ANALYSE OF STEEL SLAGS VIEWING THEIR USE FOR ROAD CONSTRUCTION

^{1,3} ECOLOGICAL UNIVERSITY OF BUCHAREST, ROMANIA

² POLITEHNICA UNIVERSITY BUCHAREST, ROMANIA

ABSTRACT:

The development of steel industry must provide solutions for environmental protection issues and using of production wastes, thus, aiming mineral resources and energy savings. The slag is the main waste type resulting from metal making and represents a valuable raw material for many industries. Steel slag is a product of much importance for road construction, successfully substituting natural materials. The X-ray diffraction analysis carried out in this paper gives a deeper insight in the mineralogical constitution and behavior of such slags when used for road construction purposes.

KEYWORDS:

steel slag, recycling, road construction

1. INTRODUCTION

The steel slag shows good technical and ecological properties, thus being used for the manufacturing of aggregates required by road construction. The reuse steel making slags for road construction must comply with an essential requirement, namely their volumetric stability. This is a condition to be met especially by steel slag, its composition having free calcium and magnesium oxides. The hydration of these oxides increases its volume, possibly causing important damages [1]. Therefore, these slags need a so-called “ageing” time (6 to 12 months) in order to be reused without creating any problems. The increasing use of the converter slag in application fields which demand high qualities is possible by improving the volumetric stability. Insufficient volumetric stability results from the presence of free CaO and occasionally, MgO in the slag.

2. QUANTITATIVE EVALUATION ON SHORT AND AVERAGE TERM OF STEEL SLAGS FROM ROMANIA

In order to perform a quantitative evaluation of slags from Romania, the following presumptions were made:

- ❖ Converter and electric steel production in 2015 (average term): 5% increase for converter steel production and 10% increase for electric steel production means 9,173 mil. t/year;
- ❖ Steel treated by secondary metallurgy LF type: 7,5 mil. t in 2008 and 8 mil. t in 2015;
- ❖ There is no forecast concerning any progress within the specific slag share in steel industry.

Table 1. Quantitative evaluation of steel slags from Romania [2]

Slag type	2006		2008		2015	
	Production, (steel) mil. t/year	Generated slag mil. t/year	Production, (steel) mil. t/year	Generated slag mil. t/year	Production, (steel) mil. t/year	Generated slag mil. t/year
Converter slag	5,5	0,660	5,745	0,689	6,032	0,724
Electric furnace slag	1,65	0,240	2,855	0,414	3,141	0,455
Secondary metallurgy slag (LF)	5,25	0,150	6,000	0,156	8,000	0,208
Total	Total	1,250	Total	1,759	Total	1,987

Under conditions presented above, Table 1 and Fig.1 present the quantitative evaluation of steel slags.

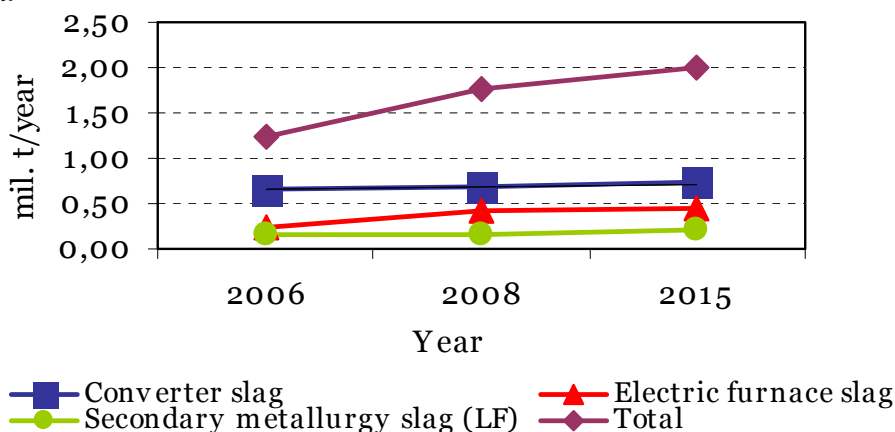


Fig. 1. Quantitative evaluation of steel slag from Romania [2].

Based on the presented evaluation, one considers that on short term the generated total slag amount will increase up to approximately 1,75 mil. t and on average term even to 1,9 mil. t.

2. STEEL SLAG CHARACTERIZATION

The chemical compositions and main performances of analyzed slags as compared with those of crushed stone and pit ballast products most frequently used for road construction are shown in Table 2 and 3.

Steel slag is a dense rock having a raw density > 3,2 g/cm³. Thus, steel slag is successfully used for road construction (e.g. for portant layers or asphalt layers submitted to high loads). Steel slags are resistant to erosion. By providing a granulation distribution determined by technical regulations, one can observe that the manufactured mineral materials mixtures have to resist to repeated frost-defrost cycles.

Steel slags contains pores, which provide a durable adherence if they are used as mineral material for wear resistant layers. Thus, steel slags are recommended to be used in wear resistant asphalt layers as chippings. The high values of polishing strength are tied to the low shock attrition value (less than 18% of the weight), which is concomitantly the precondition of manufacturing asphalt layers having the capability to reduce the level of traffic noise.

Due to the metallurgical technology, steel slags contain only low amounts of CaO not chemically bound and/or free magnesium oxides. Because these mineral constituents retain water by increasing their volume, for road construction one must check the volumetric constancy [3].

Table 2. Chemical compositions for steel slag

Constituent %	Converter slag	Secondary metallurgy slag (LF)	Electric furnace slag – EAF (average)
CaO	40,10	49,56	40,78
SiO ₂	17,80	14,73	17,81
FeO	12,92	0,44	9,25
Fe ₂ O ₃	6,58	0,22	3,97
Fe _{tot}	21,18	0,68	12,51
Fe _{met}	6,55	0,17	2,56
MnO	6,52	0,39	9,79
MgO	6,32	7,88	8,53
P ₂ O ₅	1,13	0,20	0,74
S	0,46	0,80	0,30
Cr ₂ O ₃	0,00	0,00	1,42
Al ₂ O ₃	2,04	25,55	4,23
C	0,45	0,07	0,64
CaO _{liber}	3,90		

Table 3. Main characteristics of steel slags

Characteristics	Slags	Crushed aggregates	Pit ballast aggregates
Apparent density, kg/m ³	3300-3500	2500-2700	2600
Water absorption, mass %	0,7-1,0	<0,5	<0,5
Grain shape – shape factor, %	<10	<10	<10
Crushing degree, mass%	13-17	17	21
Los Angeles test machine, wear %	18-22	12	21
Compression strength, N/mm ²	320-350	260	250
Frost-thaw resistance, mass% - frost cleftness factor	<0,5	<0,5	<1
Bitum adhesivity, %	>90	>80	>80
Polising factor (PSV), %	58-61	48	45

The portant capacity values required by standards for the manufacturing of frost-resistant layers and portant layers consisting in ballast were easily reached and frequently, outstripped due to the 100% crushed stone content, the compact shape of the grains and the harsh surface of steel slag.

These favorable properties give a high deformation resistance to portant asphalt, asphalt binder and wear resistant asphalt layers after placing and compacting.

Due to its chemical and mineralogical composition, the slag desintegrates in free atmosphere (in stockpiles) under the action of atmospheric factors, reaching a quasistatic state after cca. 6 months [4]. This duration can be diminished by watering the fresh slag, the temperature of water ranging from 40 to 50°C. The slag further desintegrated/attrited under the influence of atmospheric factors cause its decay due to the carbonation of the hydrated lime.

3. DIFFRACTOMETRIC ANALYSIS

In order to identify the structural constituents in slags, we have performed phase-analyses on diffractometer DRON 2.0. The working parameters used were:

- ❖ 30 kV tension; anodic current 34 mA;
- ❖ radiation used CoK α ;
- ❖ angular frequency $\omega=1/2^\circ$ min.

The phases identified from the viewpoint of qualitative and quantitative estimation and their specific diffraction parameters (diffraction angles, interplanar distances, Miller indices of crystallographic planes) are presented in Table 4.

Table 4. Phases identified in iron and steel slags

Test code	Identified phases	Proportion of phase [%]	Miller index of planes crystallographic (hkl)	Crystallographic system
OLD	2CaO·Al ₂ O ₃ ·SiO ₂ gehlenite	28,3	(111); (201); (211); (220); (311); (400); (323);	T
	Fe ₂ O ₃	39,0	(101); (112); (101); (102); (202); (123); (103); (224); (134); (204); (235);	R
	CaO	22,5	(111); (200); (220); (222); (331); (400); (420);	C.F.C
	FeO	10,2	(111); (200); (220); (311); (222);	C.F.C
LF	β CaO·SiO ₂ wollastonite	38,0	(400); (310); (501); (203); (710); (313); (631); (322); (314); (223); (205);	Tr
	CaO·Al ₂ O ₃ ·2SiO ₂ anorthite	36,1	(220); (004); (204); (132); (130); (111);	Tr
	CaS	11,3	(111); (200); (220);	C.C.
	α Al ₂ O ₃	14,6	(112); (102); (202); (123); (234); (202); (131); (134); (225);	H
TC	2CaO·Al ₂ O ₃ ·SiO ₂ gehlenite	14,7	(111); (211); (212); (400); (410); (600);	T
	γ Ca ₂ SiO ₄	33,9	(020); (103); (113); (121); (104); (311);	O
	α Al ₂ O ₃	19,0	(112); (102); (202); (134); (231); (204);	H
	CaO	9,4	(200); (220); (332); (222); (400);	C.F.C
	Al ₂ O ₃ ·SiO ₂	23,0	(122); (230); (042);	O
OE	MnO ₂	8,0	(111); (200); (301);	T
	MnO	13,9	(111); (200); (220);	C.F.C.
	Fe ₂ SiO ₄	52,5	(002); (130); (022); (112); (230); (150); (113); (241); (152); (311); (321); (224); (400); (314); (174);	O
	Fe ₇ SiO ₁₀	25,6	(311); (411); (112); (312); (131); (114); (121); (604);	M

Four slag specimens sampled from different zones of the integrated process line and a specimen from the electric furnace process line have been examined. The samples have been codified as follows:

- ❖ Code OLD – slag removed after LD converter steelmaking process;
- ❖ Code LF – slag resulting from treatment on LF installation;
- ❖ Code TC – slag resulting after stirring in the casting ladle;
- ❖ Code OE – slag removed after electric furnace steelmaking process.

After analyzing the results obtained, one can state following:

- ❖ Slag code OLD contains iron oxides as FeO (10,2% quantitative ratio), but also Fe₂O₃ in a higher proportion, 39%;

- ❖ Slag code TC, besides CaO , Al_2O_3 and simple or complex calcium and aluminum silicates *does not contain iron oxides*;
- ❖ Slag code OE contains manganese oxides MnO_2 , MnO and iron silicates of Fe_2SiO_4 , $\text{Fe}_7\text{Si}_{10}$ types;
- ❖ Slag code LF contains Ca, Si and Al oxides.

The graphic of diffractogrammemms is emphasized in Figures 2-5.

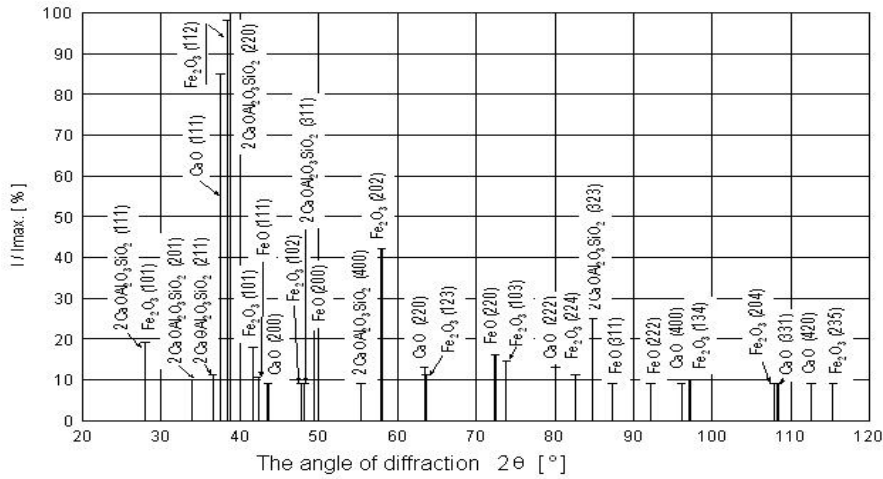


Fig. 2. Relative intensity of the diffraction lines function of the diffraction angle for sample code OLD.

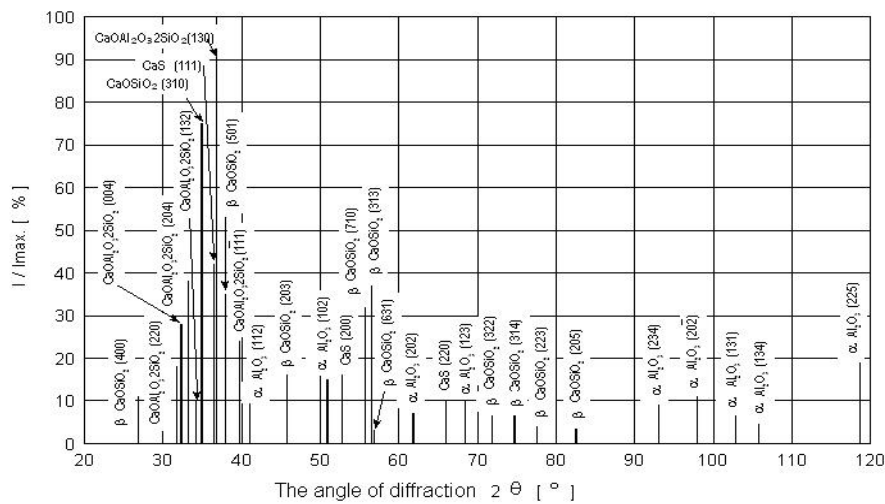


Fig. 3. Relative intensity of the diffraction lines function of the diffraction angle for sample code LF.

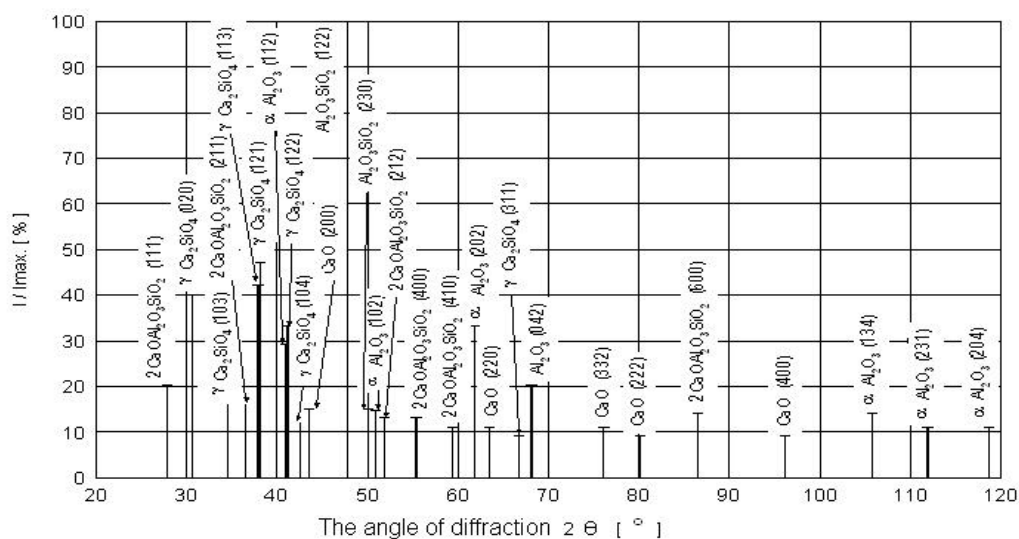


Fig. 4. Relative intensity of the diffraction lines function of the diffraction angle for sample code TC.

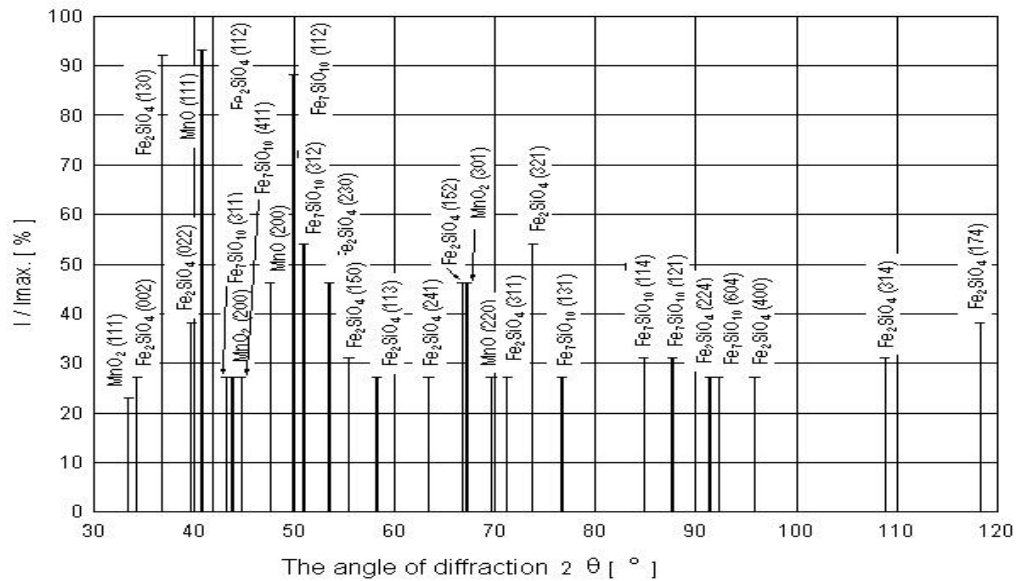


Fig. 5. Relative intensity of the diffraction lines function of the diffraction angle for sample code OE.

4. DISCUSSION

The LF slag comprises mainly CaO. During the cooling process, can be emphasized a beta-gamma structural transformation of dicalcic silicate. Furthermore, it results a pulverized material by the reaction of calcium oxide with carbon dioxide, in the presence of atmospheric humidity (CaO – 50-60%, MgO – 5%, SiO₂ – 5-10% and Al₂O₃ – 5-10%).

After analyzing the converter slag in the CaO-FeO_n-SiO₂ system one can understand how it is possible to avoid this phenomenon (Figure7).

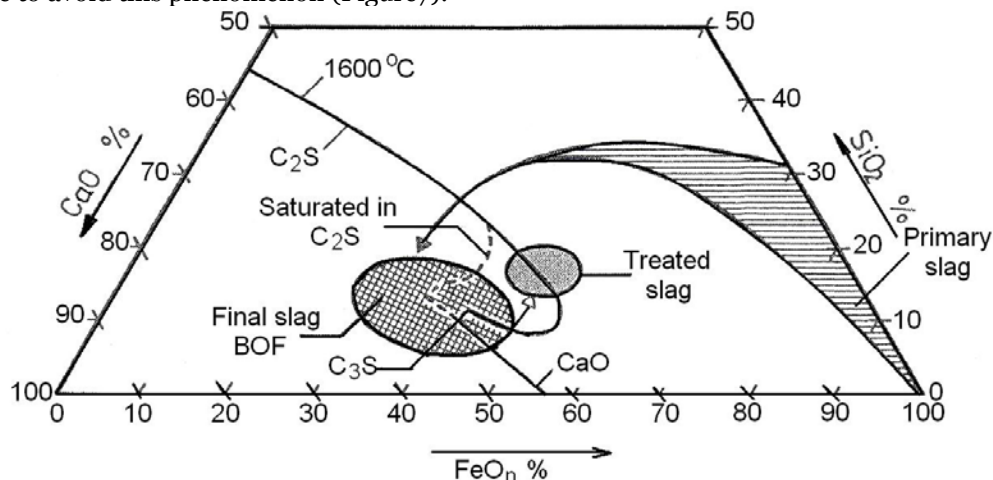


Fig.7. Converter slag location in the system CaO-FeO_n-SiO₂.

Similarly, the converter slag is deficiently as concerns its volumetric stability. The volumetric stability is influenced especially by the free CaO content. During the free air deposition, over time, due to the atmospheric humidity and rain, the major part of free lime is transformed into calcium hydroxide. This reaction is accompanied by a volume increase of almost 100% and an attrition of the slag aggregate structure. This is disadvantageous because of the amount of dust generated that creates dysfunctions.

The primary converter slag belongs rather to the FeO_n-SiO₂ system. The higher is the lime amount, the closer to the final slag, which can be observed in the saturation zone in 2CaOSiO₂, 3CaOSiO₂ and CaO. Therefore, the converter slag contains important amounts of free CaO, which influence the volumetric stability of the solid slag through hydration phenomena. In order to avoid this phenomenon, after the final slag has fulfilled its function in the converter, it is preferred to treat it and to let it migrate into the unsaturated slag zone in CaO and C₂S (eventually by increasing SiO₂ amount).

5. CONCLUSIONS

Due to its raw density, the steel slag is considered a dense rock successfully used in road construction for portant layers or asphalt layers submitted to high loads.

During the cooling of the LF slag, besides the beta-gamma structural transformation of dicalcic silicate, the calcium oxide reacts with carbon dioxide and in humid atmosphere one can obtain a pulverous material (CaO – 50-60%, MgO – 5%, SiO₂ – 5-10% and Al₂O₃ – 5-10%).

The converter slag is volumetrically instable, being influenced by the free CaO content, thus, requiring a free air deposition and due to the atmospheric humidity, the major part of the free lime is transformed into calcium hydroxide.

REFERENCES:

- [1.] Aşmin B., Smirnov L., ş. a., Prelucrarea zgurelor metalurgice - Sinteză Informstal, nr. 20, 1988;
- [2.] Nicolae M., Nicolae A., ş.a., Dezvoltarea durabilă în siderurgie prin valorificarea materialelor secundare, Editura PRINTECH, Bucureşti 2004;
- [3.] Kuehn M., Drissen P., Future development of minimising the residues in EAF steelmaking, Forschungsgemeinschaft eisenhüttenschlachen E.V., Duisburg, Germany;
- [4.] *** Integrated Pollution Prevention and Control (IPPC), Best Available Techniques Reference Document on the Production of Iron and Steel, December 2001;





¹ Adina Milena TATAR

ATMOSPHERIC POLLUTION IN AREA CAREER GARLA

¹ HIGH SCHOOL MUSIC AND ARTS, TG. JIU, ROMANIA

ABSTRACT:

In this paper it is shown activity carried out within the career streams, as the main source of atmospheric pollution, identify all on-site air emissions. Were monitored emissions from combustion processes and direct emissions from processes. Determinations were made in particulate matter sedimentation after puberty comparing them with the permissible limit values, realizing the risk assessment matrix.

KEYWORDS: air emissions, processes, quarrying, mining, pollutants

1. GENERAL CONSIDERATIONS

Garla mining perimeter is located in the county territory Drăguțești municipalities, and city Bilteni Rovinari and is in operation since 1969 through extensive mining days. Activity in the area of operation is the extraction and processing brown coal and lignite NACE code: 1020. From the administrative point of view is part of career Garla Rovinari Energy Complex - EMC ROVINARI.. The mine is located near the city perimeter and Rovinari. Identificate all will be on-site air emissions. This identification should include all aspects of:

- ❖ emissions from combustion processes;
- ❖ processes and direct emissions;
- ❖ emissions of air purification installations, air conditioning systems up to (if any);
- ❖ details on prevailing wind direction.

The amount and nature of air emissions will be detailed as the conditions imposed by permits, analyzing compliance. It will detail the general nature of the emissions data, including data on particulate matter (smoke), toxic emissions, odors, etc.. In the workplace emissions will be monitored according to business rules developed to ensure the accomplishment of work safety and hygiene. This is important for personnel working in confined spaces. Also presented will be examined and air conditioning systems and cooling agent used for them. It should be mentioned any Legionella pneumophila record, found the system of observation.

2. AIR EMISSIONS. RISK ASSESSMENT

Air emissions on site are two ways :

- ❖ emissions from combustion processes
- ❖ direct emissions from processes
- ❖ emissions from combustion processes have two sources:
- ❖ mobile sources
- ❖ stationary sources for equipment

To own equipment and transport their yearly consumption is known, in this case the emissions into the air by exhaust gases and particles mainly driven on the roads of land in the dumps career and estimated CORINAIR program

- ❖ Fuel (consumption) Car > 3,5 tonnes : 230 686
- ❖ Diesel (consumption) 193776 kg / 6 months Content : 0.035%

To produce the heat necessary for heating and sanitary hot water, is used as fuel, lignite career with PCI = 1600 kcal / kg, coal that is burned in boilers PAC15-TubalBuc type, installed thermal electric power boiler is 0 15 Gcal = 174 kW (t) and the installed electrical power boiler (pumps and fans) = 20 kW.

Table 1. Emissions

	Emission factors	M. U.	Emission (kg)
SO ₂		kg/month	135,643
SO _x	15,9	kg/ month	3081,042
dust	3,35	kg/ month	455,375
heavy metals Cd	0,01	kg/ month	1,938

Table 2. Emissions - coal CT November 2007

lignite (fuel quantity)	79	t/month		
Hi. (internal heating-power)	1815	kcal/kg	7599 kJ/kg	7,599 MJ/kg
content S (anhydrous, maf)	0,01			
As (S retention in ashes)	0,6			
ash content (anhydrous , maf)	0.3	kg/kg	600,3243 GJ	
ash content (wet basis)	30	%		

Table 3. Pollutant

Pollutant	Emission factors	UM	Emission (t)
SO	1053	g/Gj	0,632
NO _x	100	g/Gj	0,062
nmvoc	15	g/Gj	0,009
CO	121	g/Gj	0,073
CH ₄	0,7	g/Gj	0,000
CO ₂	100,2	Kg/Gj	60,2
N ₂ O	0,8	g/Gj	0,000
dust	51	Kg/t	4,029
dust	5145,39	g/GJ	3,1

After firing, a process resulting ash (wet basis) 30%, which is stored in a special place near the power station, after which it is discharged to the dump and which, by blending with it is not polluting area. The main components of ash and sulfur coal are silicates, whose concentration is below acceptable limits, according to Order 592/25 June 2002. Gases resulting from combustion of lignite process are discharged into the atmosphere through the chimney, whose height of 15 m, well above the heights of buildings in the area, allowing a good dispersion of pollutants in the atmosphere under normal conditions and safety, without dangerous work area. For thermal power plants the emissions in the atmosphere have been estimated CORINAIR program considering the amount of coal consumed per month.

A potential source of toxic gases is the auto-ignition of coal deposits or strata which outcrop. Because of the incomplete combustion of carbon monoxide emitted into the air and in smaller quantities oxide

and sulfur dioxide, light hydrocarbons, toxic substances at concentrations which did not reach to exceed limits.

At career Garla to prevent auto-ignition of coal layers that outcrop, coal is not leaving out fully covered by a sterile layer of approx. 5-10 cm. Measures to prevent auto-ignition of coal in deposits. Proceed to:

- ❖ regular water sprinkling of coal, and coal
- ❖ loosen periodic continuous movement of stocks during the delivery.

Monitoring of air emissions sources was made in the methodological norms approved by Order no. 592 of 25 June 2002 the Ministry of Waters and Environmental Protection for approval of the standard setting the limit values, threshold values and evaluation criteria and methods of sulfur dioxide, nitrogen dioxide and nitrogen oxides, particulate matter (PM10 and PM2, 5), lead, benzene, carbon monoxide and ozone in ambient air.

Determinations were made:

- ❖ particulate matter (PM10) with aerodynamic diameter 10µm, the tree through a hole selection by size, with a yield of 50% off
- ❖ dust settled

Particulate matter sampling stations aimed at protecting human health were located near equipment distribution of type MAN from:

- ❖ inside career Tismana I
- ❖ inside career Tismana II

So as to provide data on air quality in the area where the greatest concentrations occur in the population may be exposed, directly or indirectly, on a 24 hour averaging period of the value (s) limit.

- ❖ same machines, the same type, there are careers Garla and results analysis of particulate matter can be considered as having the same values.
- ❖ measurement point at 65 m from the node distribution inside the quarry near Tismana I (there certainly could leave for 24 hours to pump suction sampling) value measured = 195.91 mg / m³
- ❖ limit value allowed = 50 mg / m³ - Order 592 / 25 June 2002

Measurement point at 65 m from the node distribution inside next career Tismana II (if it could safely leave for 24 hours to pump suction sampling)

- ❖ Measured value = 185, 49 mg / m³

- ❖ limit value allowed = 50 mg / m³ - Order 592 / 25 June 2002
- ❖ the same machines, same type of construction, there are career Garla and particulate matter analysis results can be considered as having the same values for the same distance. It is necessary to protect personnel serving these plants by watering around the sources of dust
- a. Depositing powders were made by placing containers in the field laboratory in the sampling point more representative of polluted eel on period of 15 days.
Sedimentary points for dust measurements were as follows:
 - ❖ limit Carbesti inhabited village (career Garla)
 - ❖ limit Carbesti inhabited village (career Garla) measured value = 7, 45 g / m² / month according to STAS 12574/87 permissible limit value = 17 g / m² / month
- b. Pollutant emission tests for cars and lorries weighing > 3.5 t
We measured emissions (kg) of SO₂, NO_x, particulates and heavy metals. The amount of gaseous emissions from heating the coal career Garla is calculated based on the calorific value of lignite used, its sulfur content, ash retention, and ash content.
To own equipment and transport their yearly consumption is known, in this case the emissions into the air by exhaust gases and particles mainly driven on the roads of land in the dumps career and estimated CORINAIR program

3. CONCLUSIONS

The activity in the career of Garla lignite surface mining, the main source of air pollution particles in suspension. Find loose rocks excavated mostly with low mechanical resistance, plus low humidity, especially in hot weather, leading to the formation of dust. Air quality is affected mainly by the process of career dump coal deposit, the growth in certain points of the perimeter of the mine, the concentration of dust, gas, turn result from vehicles and combustion processes.

Note that these values are very small, very local effect within the quarry, where there are no provisions of Order no. 592 of 25 June 2002 for approval of the standard setting the limit values, threshold values and evaluation criteria and methods of sulfur dioxide, nitrogen dioxide and nitrogen oxides, particulate matter (PM₁₀ and PM_{2.5}), lead, benzene, carbon monoxide and ozone in ambient air and the impact of emissions from vehicles in the quarry is negligible on the atmosphere of populated areas surrounding career, from the actual business impact of their career.

REFERENCES

- [1.] Huidu E, Sisteme de depozitare a carbunilor, Ed. Tehnica , Bucuresti, 1996
- [2.] STAS 11103/78 Puritatea aerului. Determinarea Pulberilor in suspensie
- [3.] Tatar Adina -Milena, Modelarea proceselor dinamice din atmosfera, Referat nr. 3, Universitatea din Petrosani ,2010
- [4.] Vorduca A., Moldoveanu A.M, Moldoveanu G.A, Poluarea, prevenire si control, Ed. Matrix Rom, Bucuresti, 2002







¹Avram NICOLAE, ²Ionel BORS, ³Cristian PREDESCU, ⁴Maria NICOLAE,
⁵Mirela SOHACIU, ⁶Ecaterina MATEI

ELEMENTS OF METALLURGICAL ECONOLOGY

^{1,3-6} POLITEHNICA UNIVERSITY OF BUCHAREST, ROMANIA

² ARCELOR MITTAL ROMANIA, ROMANIA

ABSTRACT:

A new branch of science called *econology* is being defined and shortly characterized as studying the *economics-ecology-energy* associations (3E or E³ associations). In the future, the ternary must be transformed into *tehnology(T)-economy- energy-ecology*, so that the symbol of the econology shall be TE³.

A new classification of the indexes is put up for approval:

- Indexes, I_e, regarding the *extensive character* of the econological events; these indicators may be characterized as passive-meditative-observing, (*extensive* and *extensity* – antonym for *intensive* and *intensity*);
- Indexes, I_i, regarding the *intensive character* of the econological events; these indicators may be characterized as dynamic-operative-active.

There are defined and characterised the following simple indexes:

- ❖ energetic extensity and energetic intensity of the gross domestic product;
- ❖ energetic extensity and energetic intensity of productivity (hourly production);
- ❖ extensity and intensity of material consumptions;
- ❖ extensity and intensity of pollutant emittance:
 - in metallurgical engineering;
 - in car area.

There are defined and characterised econological-aggregate indexes of 2E and TE levels.

There are defined and characterised an aggregate index of 3E level (economy-energy-ecology).

Special characteristics are assigned to the metallurgical industry.

KEYWORDS:

metallurgical econology, extensity indexes, intensity indexes, econological-aggregate index

1. INTRODUCTION

The approach of the sustainable development concept can be based on two knowledge methodologies.

On one side, especially in the engineering area, specialization plays an important part. This in the reason why, for example, in metallurgy, the environment engineering is based more and more on a new subbranch of science called *ecometallurgy*. Its objective is the theoretical foundation of the knowledge and application of the technologies and techniques of improvement in the metallic material industry in agreement with the objectives of the durable development concept. Under the same terms, some other branches of knowledge can be brought forward: *environment economics* and *environment energetics*.

On the other side, in agreement with the globalization tendency, the inter (trans) disciplinary knowledge becomes more and more a necessity. This instrument allows the analysis of the *metallurgical process – industrial ecology – environment economics* associations as integralist-type modern methodology (Nicolae A., *ș.a.*, 2009).

The above-mentioned have tunder lately into concern to explore (by study and research) the interdisciplinary area related to the *economics – ecology association* under optimization terms of *energetic requirements*. It is the area of the 3 E or, to underline the significance further, the area of

E³. This new field of scientific knowledge has been called *econology*. In the future, this ternary must be transformed into the *technology(T)-economy- energy-ecology* associations, so that the symbol of econology shall be TE³. No special arguments are required to accept that econology deals, in particular cases, also with type 2E (or E²) associations: economics – ecology, economics – energetics or ecology – energetics.

Econology came into being at the end of the XXth century. The etymology of the word is the result of a combination between the prefix *econo* (from *economics*) and the suffix *logy* (from *ecology*).

Considering the above, it is difficult to briefly, but wholly define econology. The authors of the present article mean, by econology, the scientific branch of research - development – innovation and the discipline of study regarding the optimization of the pollution prevention and control strategies and of the natural resource consumption strategies under economic effectiveness and energetic requirement minimization terms. If econology approaches a certain sector of industrial activities, it may get specific forms as *metallurgical econology*. Considering the importance of the environmental conditions to the durable development of the society, for the metallurgical engineer, econology means knowledge with reference to associations in the field of environment economics – econometallurgy – environment energetics – technological processes.

In the metallurgical econology, the 3E correlations have to be studied as interdependences among the following functions:

- ❖ **Energetic performance;** it measures the minimization degree of the energetic consumptions;
- ❖ **Ecological performance;** it refers to the pollution level;
- ❖ **Economic performance;** it is a mixture of:
 - *financial performance* (minimisation of the fabrication costs of the product);
 - *production and productivity performance* (maximization of production, maximization of labour & facility productivity);
 - *quality performance* (social utility degree, whereby the product acquires competitiveness conditions).

From the metallurgical point of view, for the analysis and evaluation of the 3E correlations, it is required to define and use specific ecological indexes and indicators. We propose to classify them into two groups:

- ❖ *Extensity indexes* of the events (processes); there are indexes that refer to the size of the energetic consumptions or to the quantity of exhausted pollutants; because they can be derived by measurements or by calculations, they have a *passive* character (*of finding*); in this paper, they are denoted with I_e;
- ❖ *Intensity indexes* of the events (processes); there are indexes that refer to the economic performance; for the engineer that works in the industry of metallic materials, the performance of production and productivity has a special importance; because these indexes highlight the modalities of increasing the production and productivity in terms of decreased costs and increased quality, we consider they have a *dynamic* character (*of reforming, of intensification*); in this paper, they are denoted with I_i.

One of the basic principles of the metallurgical econology is: *the ecologic performance doesn't have to affect the economic performance*. In other words, the concerns regarding the minimisation of costs and increase of quality, production and productivity have priority. Therefore, we conclude that the econologic indexes must be predominantly from the category of intensity indexes.

2. DEFINITION AND CHARACTERISATION OF SOME SIMPLY INDEXES

Hereinafter, we are going to present some econologic indexes and indicators applicable in the industry of metallic materials.

The extensity and intensity of specific material consumptions

Currently, the specific consumption index is defined by the quantity of materials [tons of materials] consumed to produce one unit of metallurgical product [1 ton of metallic products]. Because it primarily refers to the quantity of consumed materials and not to the production of metallurgical goods (pig iron or steel), it should be the extensity index:

$$I_{e.m.c} = \left[\frac{\text{tons of materials}}{1 \text{ ton of steel}} \right] \quad (1)$$

We propose to replace it with the index that measures the quantity of steel [tons of steel], produced when consuming one unit of materials. Because it primarily refers to the steel production under conditions of restricting the material consumption, it should be the intensity index:

$$I_{i.m.c} = \left[\frac{\text{tons of steel}}{1 \text{ ton of materials}} \right] \quad (2)$$

The energetic extensity and intensity of the C production and p productivity

Currently, the index that characterises the energy consumptions is defined by the P electric power [Mw] of the facility used to realise the C production [tons of steel] with the p productivity [tons of steel/h]. Because it refers to the energy consumptions (power) and not to the productivity or production, it should be the extensity index:

$$I_{e.e.p} = \left[\frac{\text{h} \cdot \text{MW}}{1 \text{ ton of steel}} \right] \quad (3)$$

We propose to replace it with the index that measures the productivity we can get for one unit of power. Because it primarily shows the importance of the productivity, should be the intensity index:

$$I_{e.i.p} = \left[\frac{\text{tons of steel}}{\text{h} \cdot \text{MW}} \right] \quad (4)$$

The analysis of the above mentioned indexes shows that I_{ee} represents, in fact, the specific consumption of electric energy, in [MW·h/t. steel]. This means that the usually-used index called *specific consumption of energy* is an extensity index that has to be waived. It should be replaced with the intensity index $I_{i.e}$ [tons of steel/MW·h], which indicates the production to be obtained when consuming 1 MW·h.

The extensity and intensity of the pollutant emissivity of the metallurgical facilities

Currently, the index of the pollutant emissivity is defined by the quantity of pollutants [kg; m_N^3 pollutants] exhausted when producing one unit of metallurgical products [1 ton of steel]. Because it primarily refers to the quantity of pollutants and not to the metallurgical production, it should be the extensity index:

$$I_{e.e.p.m} = \left[\frac{\text{kg}; m_N^3 \text{ pollutant}}{1 \text{ ton of steel}} \right] \quad (5)$$

We propose to replace it with the index that measures the steel quantity that can be produced when restricting the pollutants to 1 kg; m_N^3 . Because this index highlights the role of the steel production, it should be the intensity index:

$$I_{i.e.p.m} = \left[\frac{\text{tons of steel}}{1 \text{ kg}; m_N^3 \text{ pollutant}} \right] \quad (6)$$

The extensity and intensity of the pollutant emissions of the vehicles used in metallurgy

Currently, the index is defined by the quantity of CO_2 exhausted when running 1 km distance. Because it refers to the quantity of pollutant without any information regarding the dynamic factor (number of kilometres), it should be the extensity index:

$$I_{e.e.p.v} = \left[\frac{\text{g } CO_2}{1 \text{ km}} \right] \quad (7)$$

We propose to replace it with the index that measures the number of kilometres afferent to an imposed quantity of CO_2 . In this case, we refer to the intensity index:

$$I_{i.e.p.v} = \left[\frac{\text{number of kilometres}}{100 \text{ g } CO_2} \right] \quad (8)$$

The above information can be interpreted, for example, as follows:

- ❖ The furnace producing 0.8 tons of steel is more efficient than the furnace producing 0.7 tons, when the same quantity of materials (1 ton) is consumed;
- ❖ The vehicle that exhausts 100 g of CO_2 when running 1.2 km is more efficient than the vehicle that exhausts the same amount of CO_2 when running 0.9 km.

Extensity and intensity of the energetic evaluation of the gross domestic product (GDP). Currently, the energetic value of GDP is calculated by using an indicator that measures the energy consumption [GJ] required to obtain 1 unit of GDP:

$$\text{The current indicator used for the energetic evaluation of PIB} = \frac{[GJ]}{1 \text{ unity GDP}} \quad (9)$$

Defined by this formula, it is an extensity indicator, because it refers to the consumed quantity of energy and not to the PIB to be realised. We propose to replace it with the intensity indicator:

$$I_{i.e.GDP} = \frac{[GDP \text{ units}]}{1GJ} \quad (10)$$

which measures the value of the PIB produced in a country by consuming an energy unit.

Based on the above-mentioned things, the rankings of countries, according to the national energetic consumptions, are as follows (Table 1):

Table 1. Evaluation of the national energetic consumptions (Badea A., 2003)

Sr. no.	Country	Current situation		Proposed situation	
		Extensity index [GJ/1000USD]	Place in the rankings	Intensity index [USD/1 GJ]	Place in the rankings
1.	Austria	5.278	9	189.5	2
2.	France	7.076	6	142.0	5
3.	Italy	5.000	10	200.0	1
4.	Germany	6.700	7	149.0	4
5.	Spain	5.770	8	173.0	3
6.	Hungary	16.000	5	62.5	6
7.	Poland	18.450	4	54.2	7
8.	Czech Republic	23.000	3	43.5	8
9.	Romania	31.260	2	32.0	9
10.	Bulgaria	46.800	1	21.37	10

The information about the econologic indexes is summarized in the table 2.

Tabelul 2. Sistematizarea informațiilor

Target	Defining relations	
	Extensity indexes (current solution)	Intensity indexes (proposed solution)
Specific consumption of materials	$\frac{\text{tons of materials}}{1 \text{ ton of steel}}$	$\frac{\text{tons of steel}}{1 \text{ ton of materials}}$
Energetic characterisation of the productivity	$\frac{h \cdot MW}{1 \text{ ton of steel}}$	$\frac{\text{tons of steel}}{h \cdot MW}$
The pollutant emissivity of the metallurgical facilities	$\frac{\text{kg; } m_N^3 \text{ pollutant}}{1 \text{ ton of steel}}$	$\frac{\text{tons of steel}}{1 \text{ kg; } m_N^3 \text{ pollutant}}$
The pollutant emissions of the vehicles	$\frac{gCO_2}{1 \text{ km}}$	$\frac{\text{number of kilometres}}{100 \text{ g } CO_2}$
The energetic characterisation of the gross domestic product	$\frac{GJ}{1 \text{ unity GDP}}$	$\frac{PIB \text{ units}}{1 \text{ GDP}}$

3. AGGREGATE INDEXES OF 2E AND TE LEVELS

a) The ecological-energetic index, $I_{ecl.en.}$. It is a *2E level index*, which highlights the ecological-energetic correlation. In this paper, it is defined as the ratio between the required energy quantity, as input measure, and the CO_2 quantity emitted in the technological processes:

$$I_{ecl.en.} = \frac{[GJ]}{[1 \text{ ton } CO_2]} \quad (11)$$

The maximisation of this index implies, at the same energy requirement, the minimisation of the energy quantities (heat) obtained by burning materials that contain carbon substances. In this respect, we recommend to act as follows:

- ❖ to use the enthalpy of the secondary energetic resources;
- ❖ to extend the energy making processes (heat) based on hydrogen;
- ❖ to increase the share of the energy supplied by hydro and nuclear stations;
- ❖ to use renewable energy sources.

b) The technological-ecological index, $I_{th.ecl.}$. It is an index used to analyse the influence of the technological factors on CO_2 constants. The $I_{th.ecl.}$ index is a *TE level index*. It is used to analyse the interdependence between the technological factors and the CO_2 conditions. For example, we can define two such indexes:

$$m_{CO_2} = f([\%Si]) \quad (12)$$

$$m_{CO_2} = f(Pg) \quad (13)$$

In the above expressions, [%Si] is the silicon percentage in the pig-iron made in the blast furnace, and Pg is the pressure at the loading aperture.

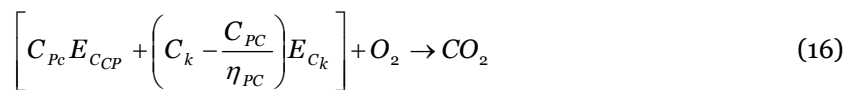
c) The degree of coke replacement by powdery coal, η_{PC} . This index characterises the coke quantity that can be replaced by powdery coal (PC) at making iron in blast furnaces. It is measured in [t.coke/t.coal]. It is also a TE level index (technology-ecology), which characterises the technological role of the coke replacement by powdery coal in the modification of CO₂ quantities. It is also an intensity index, because it firstly refers to the *coke performance*, and secondly to the *coal performance*.

The ecological evaluation of the substitutes for coke and especially of the powdery coal (PC), can be realised by taking into account the comparison of the chemical reactions of the CO₂ emissions. Appealing to the concept of equivalent carbon, the CO₂ emission can be written as follows:

For coke:



For PC and coke:



In the above relations, C_k is the specific consumption of coke, in [t-coke/t-pig iron], C_{PC} is the specific consumption of coal [t-coal/t-pig iron], E_{C_k} is the equivalent in carbon of the coke [t-carbon/t-coal], $E_{C_{PC}}$ is the equivalent in carbon of the PC [t-carbon/t-coal], and η_{PC} is the degree of substitution [t-coke/t-coal].

In making the coal replacement advantageous in terms of CO₂ emission, the following inequality should be satisfied:

$$C_{PC} E_{C_{CP}} + (C_k - \eta_{PC} \cdot C_{PC}) E_{C_k} < C_k \cdot E_{C_k} \quad (17)$$

When solving the inequality, we obtain the *maximum allowable value* of the substitution degree, in terms of CO₂ emission:

$$\eta_{PC} > \frac{E_{C_{PC}}}{E_{C_k}} \quad (18)$$

For instance, to replace the coke with 0.85 C with coal with 0.60% C, the process is allowed in terms of CO₂ emission if $\eta_{PC} > 0.70$.

d) The financial-ecological index $I_{f.ecl.}$. It is a *2E level index*, which analyses the link between the savings to be realised through various technological processes and the quantity of CO₂. It can be expressed as follows:

$$I_{f.ecl.} = \frac{E_c}{1t.CO_2}, \quad \left[\frac{\frac{Euro}{t \cdot (pig\ iron)}}{1t \cdot CO_2} = \frac{Euro}{t(pig\ iron) \cdot t_{CO_2}} \right] \quad (19)$$

where $E_c = (CF_1 - CF_2)$ is the saving [Euro] realised due to the difference between the production costs recorded in two different situations.

4. AGGREGATE INDEX OF 3E LEVEL, FOR ECONOLOGICAL ANALYSES

The evaluation of the efficiency of the econological measures in the *ecology-economy-energy system* requires recourse to specific indexes of *3E level*.

The authors couldn't find this kind of indexes in the iron-steel industry. To define the indexes to be used in the engineering field, we should start from the information found in the economic literature (*Purica I., 2005*). So, for large scale systems (country, geographical area), there are defined indexes resulted from the multiplication of simpler indexes. For example, such index is recommendable:

$$I = \frac{1}{\frac{Energy}{PIB}} \cdot \frac{PIB}{Population} \cdot \frac{1}{CO_2\ emission}; \quad \left[\frac{PIB^2}{Energy \cdot Population \cdot CO_2\ emission} \right]$$

Analysing the above things, we found that the index trend was:

- ❖ inversely proportional to energy consumption;
- ❖ directly proportional to PIB;
- ❖ inversely proportional to the CO₂ emission.

Starting from this idea, we can define for the ecology-economy-energy correlation (e.e.e) an ecological index whose trend is:

- ❖ inversely proportional to material price, p_{mat} ;
- ❖ directly proportional to calorific power, H_i ;
- ❖ inversely proportional to carbon equivalent, E_c .

Therefore, we propose the following ecological index:

$$I_{e.e.e} = \frac{1}{p_{mat}} \cdot H_i \cdot \frac{1}{E_c} \left[\frac{1}{\frac{\text{Euro}}{\text{kg.mat.}}} \cdot \frac{\text{MJ}}{\text{kg.mat.}} \cdot \frac{1}{\frac{\text{kg.carbon}}{\text{kg.mat.}}} = \frac{\text{kg.mat.} \cdot \text{MJ}}{\text{Euro} \cdot \text{kg.carbon}} \right] \quad (20)$$

Applying the above mentioned things when replacing the coke with powdery coal at blast furnaces, and using the *estimative values used in Romania*, we obtain the results presented in Table 3.

Table 3. The values of the $I_{e.e.e}$ index.

Material	Price [Euro/kg]	H_i MJ/kg	E_c [kg,carbon/kg]	$I_{e.e.e} \left[\frac{(\text{kg.mat.}) \cdot (\text{MJ})}{(\text{kg.carbon}) \cdot (\text{Euro})} \right]$
Coke	0.18	31.5	0.85	206.0
Natural gas (98% CH ₄)	0.20	34.0	0.52	327.0
Fuel oil	0.22	42.0	0.87	220.0
Powdery coal	0.10	22.0	0.60	366.0

5. SOME CONCLUSIONS

- ❖ The metallurgical ecology (application of the industrial ecology) is a new field of knowledge to be researched and operationalised at the real conditions of the metallic materials industry.
- ❖ We propose and demonstrate the possibility to use the intensity indicators and indexes of events instead of the current ones, which characterise the extensity of events.
- ❖ Regarding the replacement of coke with powdery coal at blast furnaces, we can affirm that, from the ecological point of view, all the materials proposed as coke replacements have a higher ecological index.
- ❖ The recommended replacement materials are (in descending order):
 - powdery coal;
 - natural gas;
 - fuel oil.
- ❖ From E_c , combined with the other two parameters, we can deduce that, from the point of view of CO₂ emission, the partly replacement with PC is superior to the other two solutions.
- ❖ The above findings are supported by the results of other research areas. So, to improve the thermal performances of the blast furnace, we recommend the following materials (in descending order of importance): low-volatile coal, high-volatile coal, liquid fuel (fuel oil) and natural gases (*Peters K. H., 1995*).

REFERENCES

- [1.] Nicolae A., Borş I., Predescu C., Nicoale M., Şerban V., Predescu Andra, Predescu A., Berbecaru A. – (2009), *Metallurgical Ecology* (In Romanian), Ed. Printech, Bucureşti.
- [2.] Badea, A. – (2003), Proc. *CNND*, Bucureşti.
- [3.] Purica, I. – (2005), Proc. *Sustainable development in Romania*, Ed. Expert, Bucureşti.
- [4.] Peters, K. H. – (1995), *Stahl und Eisen*, 115, p.4-29.



¹: Aleksandar DVORNIC, ²: Maja DJOGO
³: Mirjana VOJINOVIC – MILORADOV, ⁴: Goran VUJIC

BIOLOGICAL AND CHEMICAL OXYGEN DEMAND AS INDICATORS OF ORGANIC POLLUTION OF LEACHATE AND PIEZOMETRIC WATER FROM SEMI CONTROLLED, NON SANITARY LANDFILL IN NOVI SAD, SERBIA

¹⁻⁴: FACULTY OF TECHNICAL SCIENCES, UNIVERSITY OF NOVI SAD, SERBIA

ABSTRACT:

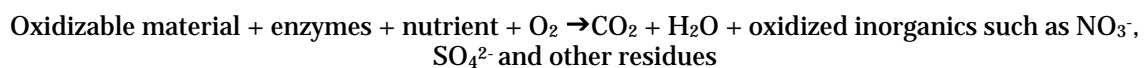
Landfill leachate is one of the most serious problems of municipal solid waste landfills. Leachate is generated as a result of the percolation of water and other liquid through any waste and the squeezing of the waste due to its weight. Since all natural waterways contain bacteria and nutrient, almost any waste compounds introduced into such waterways will initiate biochemical reactions. In August and September of 2008. Research was conducted to determine composition and quantity of waste that is disposed at semi controlled, non sanitary, municipal waste landfill in Novi Sad. The leachate samples and samples from piezometers were collected from collecting channel and 6 piezometers in municipal solid waste landfill in Novi Sad in January and May of 2010.

KEYWORDS:

BOD₅, COD, landfill, leachate, waste

1. INTRODUCTION

Landfill leachate is one of the most complex problems of municipal solid waste landfills. is generated as a result of the percolation of water through landfill body and the squeezing of the waste due to its weight, and it is contaminated with dissolved and suspended organic and inorganic compounds with different characteristics. Any oxidizable material present in a natural waterway or in an industrial wastewater will be oxidized both by biochemical (enzymatic) or chemical processes. The result is that the oxygen content of the water will be decreased. Basically, the reaction for biochemical oxidation may be written as:



Oxygen consumption by reducing chemicals such as sulphides and nitrites is typified as follows:



Since all natural waterways contain nutrients and bacteria, their enzymes will initiate biochemical reactions of almost any waste compounds that are introduced into such waterways. Oxidizable chemicals (such as reducing chemicals) introduced into a natural water will similarly initiate chemical reactions. Both the BOD and COD tests are a measure of the relative oxygen-depletion effect of a waste contaminant.

Non sanitary, semi controlled municipal solid waste landfill in Novi Sad, Serbia was opened in 1964., but systematic land filling with reasonable amount of waste begin in 1980. Landfill size is

56 acres, from which landfill body occupies 22 acres. At the landfill, there is about 2000000 m³ of waste. Landfill is divided into 3 main fields (Figure 1): I, II and III field (III field is divided into two parts: *a* and *b*). Height of waste at some parts of landfill body is in range from 2.5 to 14 meters.



Figure 1. Landfill in Novi Sad

2. METHODOLOGY

In August and September of 2008 research campaign was conducted to determine composition and quantity of waste that is disposed at landfill in Novi Sad. Figure 2 shows composition of municipal solid waste in Novi Sad.

The biggest part of waste from households and commercial sector is biodegradable, organic waste that is decomposed by microbiological and chemical mechanisms in landfill body (Figure 3). Biodegradable waste consists of:

- **Garden waste:** grass, old dirt, flowers, branches, leaves,
- **Waste from food:** bread, meat, fruit, vegetables,
- **Paper:** old newspaper, journals, books, notebooks, letters, receipts...
- **Cardboard:** cardboard boxes, flat cardboard, packages for juices, yoghurt, milk, etc....
- **Textile:** nature fabrics (cotton, wool, ...)

The biggest percentage of waste is biodegradable organic matter (Figure 2).

3. FINAL RESULTS

The leachate samples and samples from piezometers were collected from collecting channel and 6 piezometers in municipal solid waste landfill in Novi Sad (Figure 4) in January and May of 2010. The samples were transported to the laboratory and analyzed immediately.

Biological oxygen demand (BOD₅) was determined using HACH BOD TRAK device. The sample is kept in a sealed container fitted with a pressure sensor. According to manufacturer specifications, lithium hydroxide is added in the container above the sample level as a substance

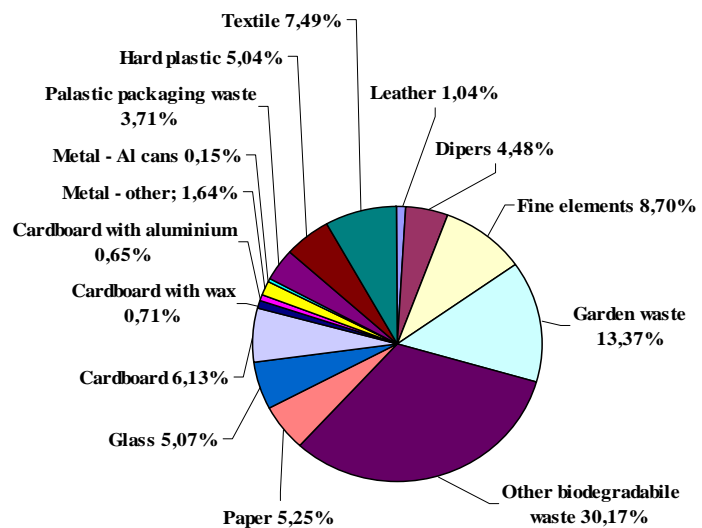


Figure 2. Composition of municipal solid waste in Novi Sad

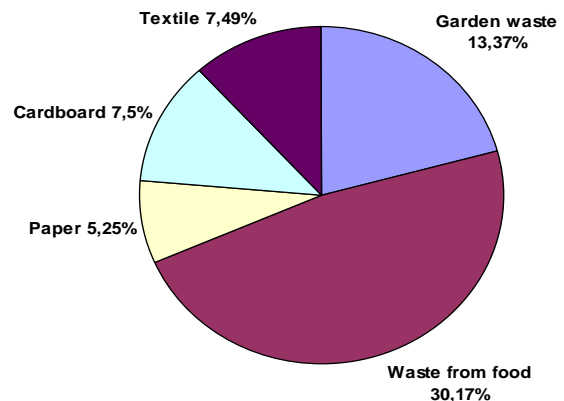


Figure 3. Waste composition of municipal solid waste in Novi Sad

which absorbs carbon dioxide. Oxygen is consumed and, as ammonia oxidation is inhibited, carbon dioxide is released. The total amount of gas, and thus the pressure, decreases because carbon dioxide is absorbed. From the drop of pressure, the sensor electronics computes and displays the consumed quantity of oxygen.



Figure 4. Sampling sites at landfill in Novi Sad

Chemical oxygen demand was determined using reagent test tubes in HACH DR5000 UV visible spectrophotometer. To perform the test, simply pipette water sample to a cuvette and leave it in a heater for 2 hours at 148°C. At the end of this period the intensity of colour in the solution is directly related to the COD value in the sample, and can be measured quickly, accurately and easily.

The results for COD and BOD of the water samples are presented in Table 1.

Table 1. Results for COD and BOD of the water samples

No.	Parameter	Unit	Piezometers						Collecting channel		
			Pz1	Pz2	Pz3	Pz4	Pz5	Pz6	1	2	3
1.	Water temperature	°C	8	12	9	10	8	12	3	3	3
2.	Ambiental air temperature	°C	-1	0	0	-1	-1	-1	0	0	0
3.	BOD ₅	mg/l	8	90	22	80	26	14	86	66	144
4.	COD	mg/l	21.3	443	44.9	88.1	60.2	34.6	429	593	714
Date of analysis: 25.01.2010.											
No.	Parameter	Unit	Piezometers						Collecting channel		
			Pz1	Pz2	Pz3	Pz4	Pz5	Pz6	1	2	3
1.	Water temperature	°C	11	14	12	12	15	12.5	16	16	16
2.	Ambiental air temperature	°C	20	20	20	20	20	19	20	20	20
3.	BOD ₅	mg/l	8	85	23	21	15	9	102	90	120
4.	COD	mg/l	10.2	156	27.1	60.3	42.6	12.9	164	163	155
Date of analysis: 07.05.2010.											

Non sanitary, semi controlled municipal solid waste landfill in Novi Sad doesn't have impermeable barrier so contaminated leachate is leaking into the soil and could cause pollution of soil and groundwater. From Figure 5 and Figure 6 it can be seen that most contaminated piezometer is P2 with BOD values from 85 – 90 mg/l, and COD values from 156 – 443 mg/l. This piezometer is located downstream from landfill body and suffers most of the contamination (Figure 4). Also there is noticeable difference in BOD and COD values obtained in January and May.

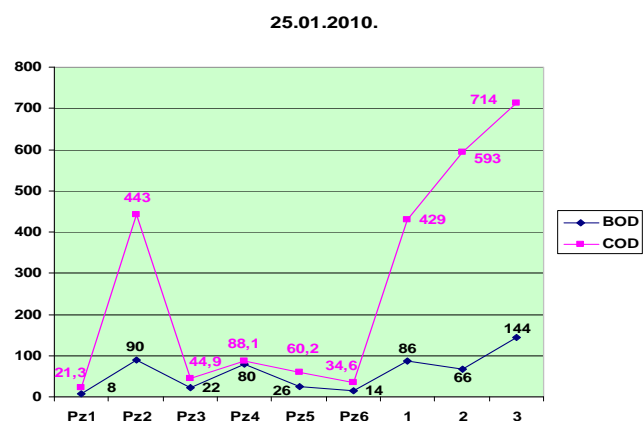


Figure 5. Values for BOD and COD from January 2010

The values for BOD and COD are lower in May than in January. This can be explained as the consequence of seasonal temperature and precipitation variations and hydrological characteristics. Rain and snow melting are causing dilution of leachate and lower BOD and COD values. Also, because there were lot of rain in this period the groundwater level is much higher than in January 2010.

COD values for collecting channels were in range from 155 – 714 mg/l. The collecting channels are located downstream of landfill body and they are collecting leachate water from landfill but also they collect atmospheric water (rain, snow) and groundwater. Having this in mind, the real values for COD and BOD of leachate is much higher than measured values.

BOD values for collecting channels were in range from 66 – 144 mg/l. These high values of BOD show great organic pollution of leachate water with biodegradable organic matter.

4. CONCLUSION

Landfilling is still one of the most used methods for waste disposal. One of the biggest problems with landfills is highly contaminated leachate that is produced in landfill body. In Vojvodina region (northern part of Serbia), there is only one sanitary landfill that has impermeable bottom membrane and leachate collection system (landfill in Kikinda). From obtained results of BOD₅ and COD it can be concluded that the leachate from landfill in Novi Sad is contaminating soil and groundwater *in continuus*. The most contaminated piezometer is P2 that is located downstream from landfill body and suffers most of the contamination. The groundwater level in this part of landfill is very high so there is justified concern for spreading of contamination. Because leachate is very toxic (high content of heavy metals, organic matter and pathogenic microorganisms) it is necessary for landfill to be sanitary (impermeable bottom liner, leachate collection system, on-site wastewater treatment facility...) for prevention of further soil, groundwater and contamination of surrounding environment.

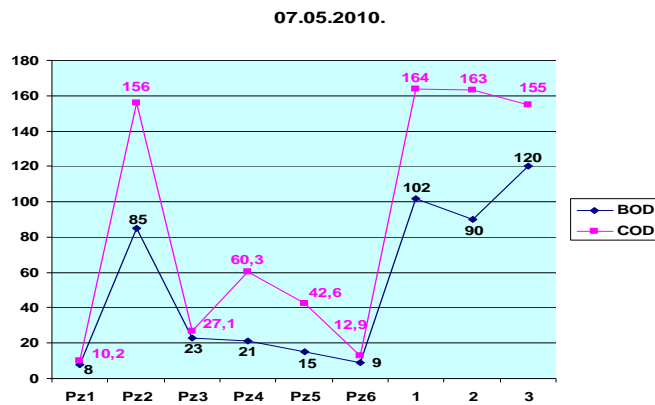


Figure 6. Values for BOD and COD from May 2010

REFERENCES/BIBLIOGRAPHY:

- [1.] STANISAVLJEVIĆ N., BATINIĆ B., MRKAJIĆ V., DVORNIĆ A., UBAVIN D., Calculation of landfill gas quantity on small unsanitary landfills, Association for water technology and sanitary engineering, Conference, Vršac, 2008.
- [2.] VADILLO I, BARTOLOME A, CARRASCO F (2005): Groundwater contamination by landfill leachates in a karstic aquifer. Water, Air, and Soil Pollution
- [3.] VOJINOVIĆ MILORADOV M., VUJIĆ G., RADONIĆ J., DJOGO M., DVORNIĆ A., UBAVIN D., MILOVANOVIC D., A field investigation of the quality of gas and piezometric water from municipal solid waste landfills in Vojvodina area, ISWA Beacon conference, Novi Sad, 2009.
- [4.] VUJIĆ G., VOJINOVIĆ MILORADOV M., RADNOVIĆ D., TURK SEKULIĆ M., RADONIĆ J., UBAVIN D., DJOGO M., DVORNIĆ A., BAČLIĆ S., MAOUDUŠ N., STOČIĆ M., Preliminary qualitative and quantitative analysis of leachate water and gas from the waste landfills for establishment of continuous monitoring - Project, Faculty of Technical Sciences, Department of Environmental Engineering, Novi Sad, 2009.





¹: Zsuzsanna H.HORVÁTH, ²: Cecília HODÚR

ANALYSIS OF COLOUR CHARACTERISTICS OF PAPRIKA POWDER WITH DIFFERENT OIL CONTENT

¹: UNIVERSITY OF SZEGED, FACULTY OF ENGINEERING, HUNGARY

ABSTRACT:

We investigated the several quality Hungarian paprika powders. The oil contents of paprika powders were increased by 1%, 2%, 3%, and 4% relative to the initial sample. The colour, determined by using the CIE L^* , a^* , b^* colour system, was measured with a Minolta CR-300 tristimulus colorimeter. The colour coordinates were evaluated by using variance analysis of one factor. The colour differences (ΔE^*_{ab}) and hue differences (ΔH^*_{ab}) of the initial samples and the samples with various added oil contents were calculated to determine the changes in colour. The lightness coordinate L^* and yellowness coordinate b^* were found to decrease significantly. The redness coordinate a^* did not change significantly. A significant and perceptible change relative to the initial samples is observed at an added oil content of 3%. The changes in the colour characteristics in response to oil content increase can be observed visually, the powder becoming darker and redder.

KEYWORDS: Hungarian paprika powders, quality, colour characteristics, investigations

1. INTRODUCTION

The use of natural food colours is preferred to that of artificial dyestuffs for modern alimentary purposes. Paprika is a spice plant grown and consumed in considerable quantities worldwide, and also used as a natural food colour. Hungarian paprika powder is still regarded as a "Hungaricum" today. Paprika is cultivated in areas of the world such as Spain, South Africa and South America, where the weather is favourable for the growth of this plant and for the development of its red colouring agents. The large number of hours of sunshine allows the paprika to ripen on its stock, so that the basic material reaching the processing mills has high dyestuff content. Hungarian paprika has a unique aroma and a specific smell, but the production of powder with a good red colour is a considerable problem. The colour of paprika powder is very important, because the consumer concludes its colouring powerful based on its colour, although the relation isn't unequivocal between them (H.Horváth, 2005). The colouring powerful is determined by quality and quantity of colouring agent of paprika squarely, but the colour of the powder is influenced by many factors besides the colouring agent content. Various investigations have been made of the connection between the colouring agent content of the powder and the colour characteristics measured by different techniques (Navarro et al., 1993, Nieto- Sandoval et al., 1999). Such investigations have yielded partial results, but there is no formula that describes the correlation between the colouring agent content and the colour characteristics. Since the 1970s a number of papers have been published on measurements of the colour of paprika powders (Horváth&Kaffka, 1973, Drdak et al., 1980, Huszka et al., 1984, Drdak et al., 1989). Measurements have been performed relating to the changes in the colour stimulus components X, Y and Z of powders during mixing (Huszka et al., 1984) and to the correlation between visual sensing and the instrumentally measured colour characteristics (Huszka et al., 1985). The effects of ionizing irradiation on the colour of paprika powder were investigated by Fekete-Halász et al. (1996). Minguez et al. (1997) analysed how the colour of the powder is changed by the ratio of the yellow and red pigments within the total colouring agent content. Chen et al. (1999) investigated the effects of particle size in Korean cultivars and established that the lightness coordinate of the powder was influenced by the particle size. Applying a Hungarian milling technique, Horváth&Halász-Fekete (2005) demonstrated that the particle size exerts a significant influence on

all three colouring characteristics of powders made from Hungarian, South African and South American paprika. Kispéter et al. (2003) investigated the influence exerted on the colour by saturated steam used for germ reduction. In the case of Korean cultivars, no significant change in colour characteristics was detected when the moisture content varied between 10% and 15% (Chen et al., 1999). H.Horváth&Hodúr (2007a) investigated Hungarian paprika powders and depicted, that the colour of the powder was observed to turn into darker and deeper red with increasing moisture content.

The influence of physical and chemical properties of Hungarian paprika powder on its colour was investigated in course of our work. In this paper is presented, how the colour characteristics of Hungarian paprika powders change following increase of the oil content.

2. THE STUDY

2.1. COLOUR MEASUREMENT

Colour measurements were performed with a Minolta CR-300 tristimulus colour measuring instrument. The CIELab colour system was used for colour characterization. In this colour space the colour points are characterized by three colour coordinates. L^* is the lightness coordinate ranging from no reflection for black ($L^*=0$) to perfect diffuse reflection for white ($L^*=100$). The a^* is the redness coordinate ranging from negative values for green to positive values for red. The b^* is the yellowness coordinate ranging from negative values for blue and positive values for yellow.

The total colour change is given by the colour difference (ΔE_{ab}^*), in terms of the spatial distance between two colour points interpreted in the colour space: (Hunter, 1987)

$$\Delta E_{ab}^* = \left[(L_1^* - L_2^*)^2 + (a_1^* - a_2^*)^2 + (b_1^* - b_2^*)^2 \right]^{1/2} \quad (1)$$

If $\Delta E_{ab}^* > 1.5$, then the color difference between two paprika grists can be visually distinguished (H.Horváth, 2007b). The chroma (C_{ab}^*) the hue difference were used to determine the change of color.

$$C_{ab}^* = \left((a^*)^2 + (b^*)^2 \right)^{1/2} \quad (2)$$

The chroma represents colour saturation which varies dull at low chroma values to vivid colour at high chroma values (Hunter,1987). The equations used to describe the hue difference (ΔH_{ab}^*) between two colour points are as follows:

$$\Delta H_{ab}^* = \text{sign}(a_1^* \cdot b_2^* - a_2^* \cdot b_1^*) \cdot \left((\Delta E_{ab}^*)^2 - (\Delta L^*)^2 - (\Delta C_{ab}^*)^2 \right)^{1/2} \quad (3)$$

2.2. PREPARATION AND MEASUREMENT OF THE SAMPLES WITH INCREASED OIL CONTENT

Ten paprika powder samples were prepared from different Hungarian paprika varieties. The oil content of each of the samples was increased by 1%, 2%, 3% and 4% relative to the initial sample. The samples of 10 g of powder were weighed with four-digit accuracy on an analytical balance, after the 0.1 g, 0.2 g, 0.3g and 0.4g of oil was added to samples. After homogenisation the colour coordinates of these samples were measured in 3 parallel measurements. The data were evaluated by using variance analysis of one factor.

3. ANALISES, DISCUSIONS, APPROACHES AND INTERPRETATIONS

Tables 1-3. present the variance analysis results.

Table 1 Variance table for lightness coordinate L^*

Source of variation	SQ	DF	MQ	F-ratio	p
Between groups	20.96	4	5.24	2.871	0.0335
Within groups	82.14	45	1.82		
Total	103.10	49			

Table 2 Variance table for redness coordinate a^*

Source of variation	SQ	DF	MQ	F-ratio	p
Between groups	17.31	4	4.32	1.681	0.1700
Within groups	115.82	45	2.57		
Total	133.13	49			

Table 3 Variance table for yellowness coordinate b^*

Source of variation	SQ	DF	MQ	F-ratio	p
Between groups	48.13	4	12.03	2.22	0.0811
Within groups	243.14	45	5.40		
Total	291.27	49			

The data in Tables 1-3 demonstrate the lightness and yellowness coordinates were significantly influenced by increasing oil content (significant level was $p=0.0335$ and $p=0.0811$), whereas there was no influence on the redness coordinate. As concerns the detailed analysis, the average values of the colour coordinates are presented in Figs 1-3, differences being taken as significant at a level $p = 0.05$.

It can be seen that the lightness coordinate L^* progressively decreased with increasing oil content. An added 3% oil content caused a significant and well-perceptible change. Further added oil did not induce any additional perceptible decrease. The average value of redness coordinate a^* similarly decreased with increasing oil content, as compared with the initial sample, the difference was 1 unit at an added oil content of 4%. The yellowness coordinate b^* changed more strongly. With increasing oil content, the average values of b^* decreased significantly, 2.1 units at added oil contents of 3%.

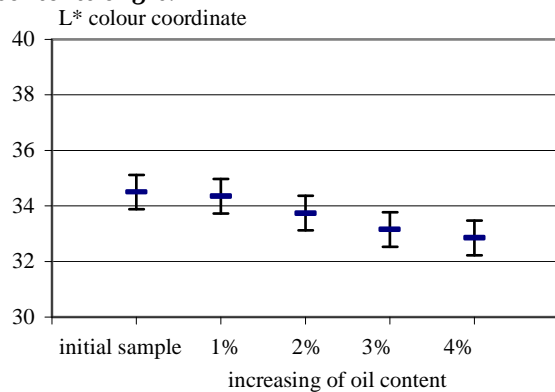


Fig. 1. Result of variance analysis of lightness coordinate (average \pm $SD_{0.05}$)

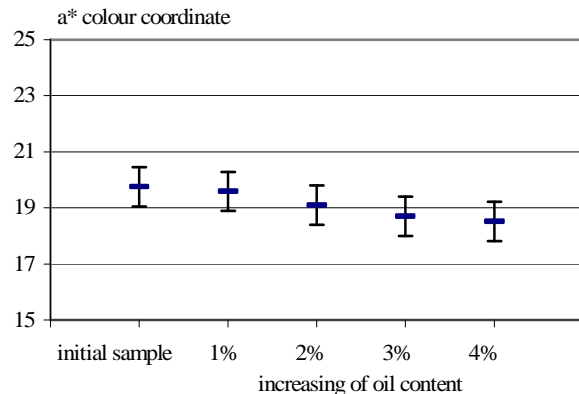


Fig. 2. Result of variance analysis of redness coordinate (average \pm $SD_{0.05}$)

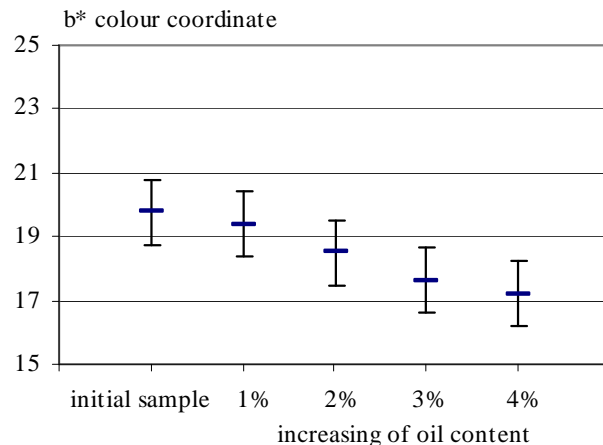


Fig. 3. Result of variance analysis of yellowness coordinate (average \pm $SD_{0.05}$)

The colour (ΔE^*_{ab}) and hue (ΔH^*_{ab}) differences of the initial samples and the samples with various added oil contents were calculated to determine the changes in colour. The values are shown in Table 4.

We can see, that the value of $\Delta E^*_{ab} > 1.5$ for all samples at an added oil content of 3%, therefore an added 3% oil content caused a significant and perceptible change.

The hue difference was negative for all samples at an added oil content of 3%, too. This indicates that the paprika powders became redder.

Table 4. The colour (ΔE^*_{ab}) and hue (ΔH^*_{ab}) differences of the initial samples and the samples with various added oil contents

Sample	Increasing of oil content							
	1 %		2 %		3 %		4 %	
	ΔE^*_{ab}	ΔH^*_{ab}	ΔE^*_{ab}	ΔH^*_{ab}	ΔE^*_{ab}	ΔH^*_{ab}	ΔE^*_{ab}	ΔH^*_{ab}
P1	0,69	-0,36	1,57	-0,15	2,43	-0,82	4,09	-1,08
P2	0,93	0,48	1,09	-0,34	2,44	-0,80	3,42	-1,09
P3	1,10	0,43	2,09	-1,15	1,53	-0,52	2,23	-0,62
P4	1,09	-0,43	3,43	-1,40	3,58	-0,93	4,35	-0,72
P5	0,70	0,03	1,48	0,05	3,10	-0,91	3,70	-1,23
P6	0,33	0,11	1,31	-0,04	2,93	-0,41	3,28	-0,49
P7	0,49	-0,14	2,75	-1,43	3,35	-1,53	3,14	-0,71
P8	2,91	-1,41	2,78	-1,24	4,84	-1,68	5,56	-1,37
P9	0,57	-0,43	2,49	-1,28	1,79	-0,37	2,38	-0,39
P10	1,13	-0,42	1,05	0,01	2,65	-0,71	3,62	-0,72

4. CONCLUSIONS

- ✓ The oil content influenced the lightness coordinate L^* significantly, it decreases with increasing added oil content.
- ✓ The oil content influenced yellowness coordinate b^* significantly, too, gradually decreases with increasing added oil content.
- ✓ The redness coordinate a^* did not change significantly.
- ✓ A perceptible change relative to the initial samples is observed at an added oil content of 3%.
- ✓ The changes in the colour characteristics as the added oil content is increased can be observed visually: the powders became darker and redder.

REFERENCES

- [1.] Chen Q., Hak-kyun-koH., Jae-Bok-Park., (1999): Color evaluation of red pepper powder. Transaction-of-the-ASAE., 42(3), 749-752.
- [2.] Bok-Park (1999): Color evaluation of red pepper powder. Transaction-of-the-ASAE. 42(3), 749-752.
- [3.] DrdaK M., Sorman L., Zemkova M., Schaller A., (1980): Ergebnisse von Studien über den Zusammenhang zwischen Zusammensetzung und Farbe von gemahlenem Gewürzpaprika. Confructa, 25(3/4), 141-146.
- [4.] DrdaK M., Greif G., Kusy P., (1989): Comparasion between the sensory and spectrophotometric method for determination of colour of paprika powder. Nahrung 33(8), 737-742.
- [5.] Fekete-Halász M., Kispéter J., (1996): Effect of irradiation on colour of ground red paprika. Acta Alimentaria 25(2), 189-193.
- [6.] H.Horváth, Zs., Halász-Fekete M., (2005): Instrumental colour measurement of paprika grist.. Annals of the Faculty of Engineering Hunedora, 101-107.
- [7.] Zs., H.Horváth, C. Hodúr (2007a): The colour of paprika powders with different moisture content. International Agrophysics, 21: 67-72 p.
- [8.] Zs., H.Horváth (2007b): Procedure for setting the colour characteristics of paprika grist mixtures. Acta Alimentaria, 36: 75-88. p
- [9.] Horváth L., Kaffka K., (1973): Instrumental Colorimetry of Red-pepperGrist. Mérés és Automatika 21(9) 341-348. (In Hungarian)
- [10.] Hunter R., 1987. The measurement of appearance. Wiley Press, New York
- [11.] Huszka T., Halászné Fekete M., Hováth M. Zs., Lukács Gy., (1984):Számítógépes színrecept számítási eljárás fűszerpaprika őrlémények optimalizált előállítására. Mérés és Automatika, 32(5) 170-177.(In Hungarian)
- [12.] Huszka T., Halász-Fekete M., Lukács Gy., (1985): Colour Tolerance of Red-Pepper Powders. Hungarian Scientific Instruments 60, 43-47.
- [13.] Huszka, T., Horváth, Zs., Halász-Fekete, M., Véha, A., Gyimes, E., (1990): Computer aided quality planning and production control of red-pepper powders. 4th European Seminar of the EOQ Food Section, Berlin, Proceedings, 176-178.
- [14.] Kispéter J., Bajusz-Kabók K., Fekete M., Szabó G., Fodor G., Páli T., (2003): Changes induced in spice paprika powder by treatment with ionizing radiation and saturated steam. Radiation Physics and Chemistry 68, 893-900.
- [15.] Minguez-Mosquera M. I., Perez-Galvez A. (1997): Color quality in paprika oleoresins. Journal of Agricultural and Food Chemistry 46 (12), 5124-5127.
- [16.] Navarro F., Costa J., (1993): Evaluation of Paprika Pepper Color by Tristimulus Colorimerty. Revista Espanola de Ciencia y Tecnología de Alimentos 33(4):427-434.
- [17.] Nieto-Sandoval J. M., Fernandez-Lopez J. A., Almela L., Munoz J. A., (1999): Dependence between apparent color and extractable color in paprika. Color Research and Application 24(2), 93-97.





¹Richard LADANYI

OPTIMISATION OF SELECTIVE WASTE COLLECTION ROUTES ON THE BASIS OF GEOGRAPHICAL INFORMATION SYSTEM (GIS)

¹ BAY ZOLTAN FOUNDATION FOR APPLIED RESEARCH, UNIVERSITY OF MISKOLC, MISKOLC, HUNGARY

ABSTRACT:

The advantages of GIS systems are extended from determining positions into complex route optimisation software. A specialized type of these solutions are applied for elaborating the functions of advanced selective waste collection systems to handle the effects of variable – in some cases non-deterministic – boundary conditions. The aim of this paper is to represent the research activities according to the development of methods towards on one hand the above mentioned application and on the other hand to harmonize them for the sake of economic operation of the collection systems.

KEYWORDS:

optimisation software, waste collection systems, GIS systems

1. INTRODUCTION

Countrywide spreading of selective waste collection systems extends the demand for services which enable the cost -effective operation of these systems. These services are important as the marketing activities regarding the positive environmental effects of the selective collection enhance the amount of waste fractions which became secondary raw material in this way. Accordingly the time period between the unloading procedures of the collection islands have to be shortened to avoid the consumers facing overloaded and contaminated containers. There are several other factors which have influence on the waste amount which is carried to the selective islands (during the periods between the unloading service days) besides this emerging trend. One of these factors is the emerged amount of PET bottles in summer time or another one is the less amount of paper in case of the school organized paper collection actions.

2. THE STUDY

Keeping the regular service level while emerging waste amounts means the continuous revision of the collecting vehicle routes and continuous monitoring of the waste amounts gathered in the collection islands. Collection Service Operators (CSOs) are interested in economic operation accordingly they seek combined collection possibilities of the different waste fractions which ensure the maximal utilization of the collection capacities. My research deals with the effects of various collection conditions and seasonal differences of the waste generation on the vehicle routes. It is possible to answer the following practical questions regarding the operation of collection systems in the base of the research activities:

- ❖ What effects the varying gathered waste amount has
 - on the route of the collection vehicles and on the collection time,
 - and on the number of collecting vehicles and other resources?
- ❖ What influence the varying velocities of the collection vehicles have on the collection time and length of the routes?
- ❖ What kinds of savings are realized (if any) by combined collection?

- ❖ Which recycling facilities have to be chosen in a specific situation?
- ❖ How collection parameters are influenced by relocating the collection islands or by modifying the configuration of the waste fraction containers on the islands?

The only way of answering these questions is to carry out simulation examinations regarding on one hand the different alternatives of measure of the waste generation and on the other hand the alternatives of collection system operation. The broader aims of the examinations are to determine the optimal service method which is in strict correlation with the decision about the mutual or separated collection of the waste fractions, after these the necessary number of routes has to be determined. Spatial modelling the road network of the service area with the island locations and receivable types and container number of waste fractions in each collection islands are preconditions for accomplishing the examinations.

A sample examination on a route optimization for an urban area selective waste collection system will be presented in the followings. The examined system contains 130 collection islands and covers 3 types of waste fractions: paper, plastic (mainly PET) and glass bottles.

The examinations are carried out by simulation activities on the ground of the following thoughts:

- ❖ adequately parameterized (regarding e.g. the fraction types, service locations, vehicle container capacities, vehicle speed, fuel) collection vehicle goes from island to island
- ❖ shifts the waste fractions from the waste bins of the collection islands to the vehicle container (The amounts of the waste quantities are taken into account by average load volumes of the waste bins in the case of every fraction. These averages are applied on every island)
- ❖ searching the treatment facility in case of reaching the vehicle container capacity
- ❖ continuing collection route after bulk unloading at the facility

3. ANALYSES, DISCUSSIONS, APPROACHES AND INTERPRETATIONS

These simulation steps in iteration cycles are continuing until all island containers serviced and minimal collection route length found. The primary topic of this paper is not the calculation of the minimal route length but the interpretation of the effects of the above listed condition changes (e.g. the quantitative change of the waste on the islands between the unloading services) on the routes.

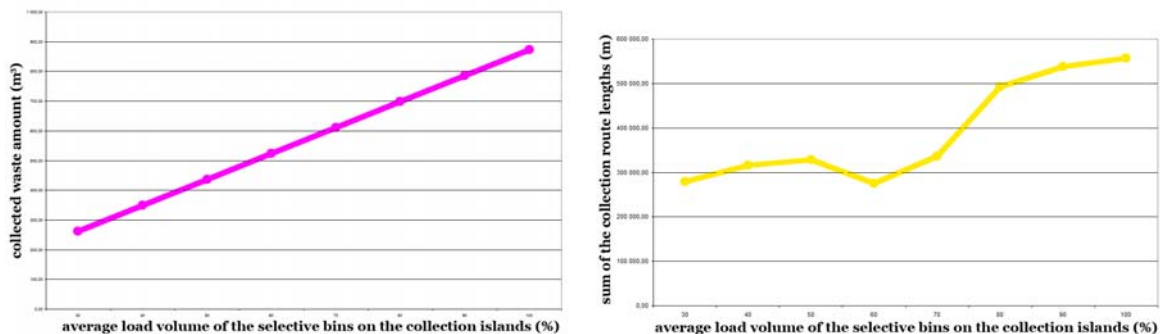


Fig.1.: Collected waste amount and sum of the collection route lengths against the average load volume of the selective bins on the collection islands

Left side of the 1st figure presents the achievement of the examination which regards to the collected waste amount against the average load volume of the selective bins on the collection islands. It shows that the collected waste amount is emerging proportionally with emerging of the average load volumes.

Right side of the 1st figure presents the achievement of the examination which regards to the sum of the collection route lengths against the average load volume of the selective bins on the collection islands. The result shows that the change of the summarized collection length is not proportional with the change of the average load volume. Accordingly higher load volumes of the selective bins will not mean longer collection routes in every case.

This graph shows that higher loads mean shorter routes in some cases. The potential causes to be taken into account for accepting this result are the following:

- ❖ the utilization of the vehicle container capacity (tons/km) is better if the load volumes of the selective bins are higher,
- ❖ the rate of the filling of the vehicle container is different in the cases of the different average load volumes of the selective bins. It means that treatment facility is visited from the different collection islands in these cases.

Since these visits mean different itineraries and in some cases the shorter route lengths for the collection of higher waste amounts are documented in the course of the route optimization processes.

It is necessary to answer the questions regarding the required number of collection vehicles. On one hand this number is an output parameter of the route optimization process and on the other hand this number has similar correlation to the load volumes of the selective bins such as the previous presented parameter (the sum length of collection routes) had. By the side of the collection service providers it is important to determine the increment of the load volumes of the selective bins which requires involvement a new vehicle to the collection fleet.

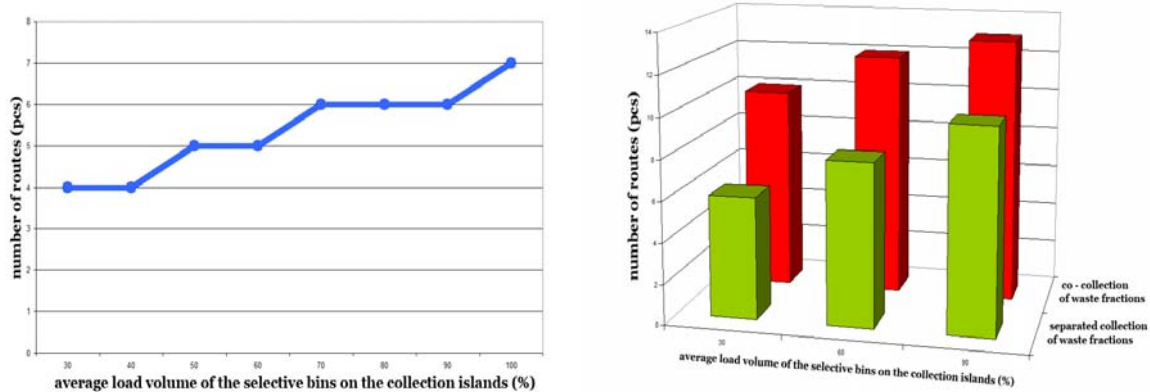


Fig.2.: The number of collection routes against the average load volume of the selective bins on the collection islands and the effects of the different collection methods on the collection routes

Left side of the 2nd figure presents the achievement of the examination which regards the number of collection routes against the average load volume of the selective bins on the collection islands. An important achievement of the examination is that the rising rate of the route numbers is lower than the rising rate of the average load volumes. By means of the previous achievement the reserves of the applied collection fleet are quantifiable by the service providers. E.g. the number of routes which set up for service of waste bins with 70 percent average load volume is able to service waste bins with 90 percent average load volume too.

The right side of the 2nd figure shows that the necessary number of routes in the case of combined collection (when waste collected into separated collection container sections of the same vehicle) is higher than this number of routes in case of separated collection of the waste fractions. The reason is the different loading rate of the vehicle container sections in correlation with the different rate of disposition of the waste fractions on the selective islands.

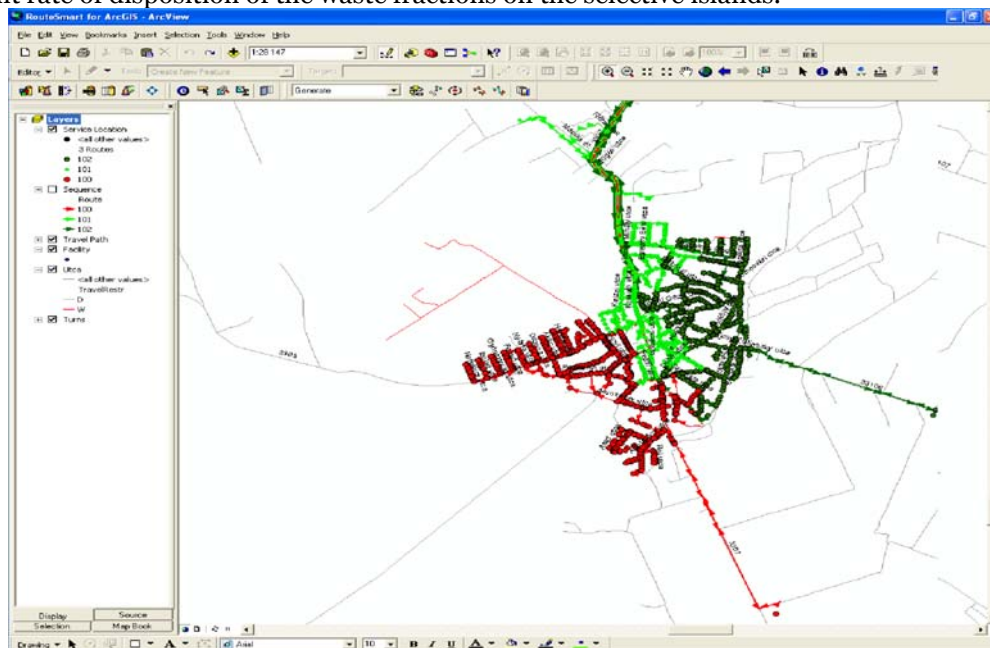


Fig.3.: Service area and collection routes (presented in different colours) in RouteSmart for ARCGIS

The volume of the separated sections are smaller than the volume of the whole vehicle container capacity therefore each of them are filled faster along the collection way. The section of the infrequent waste fraction is filled relatively slower than the section of the other fraction accordingly there will be unused capacity every time after the other section is filled. The collection vehicle visits the treatment facility more often because of this faster filling rate hence the collection route length is emerging.

4. CONCLUSIONS

These statements depend on the examined area however, their application is generalized. Location of the selective collection islands correlated to each other and to the traffic infrastructures and the classification of the actual service area by settlement type (e.g. building estates or bungalow zone) have influence on the quantity of the selective waste fractions to be collected.

An important achievement of these examinations is that the interpretation of a routing system (even the evaluated one) as constantly valid set-up for collective vehicle operation is faulty.

Accordingly the routing system has to be revised and actualised periodically and during these revisions the boundary conditions, economic operation and keeping the desired service level have to be taken into account.

REFERENCES

- [1.] PHAM D.T. and KARABOKA D., "Intelligent Optimization Techniques", Springer-Verlang, London, (2000)
- [2.] BAST, H., FUNKE, S., SANDERS, P., SCHULTES, D.: Fast routing in road networks with transit nodes. Science (2007)
- [3.] CSELÉNYI J., ILLÉS B., NÉMETH J.: Hálózatszerű karbantartás és hálózatépítés készleteinek optimális elhelyezése Projekt orientált működés esetén, Gépgyártás. 2005., XLV. évfolyam 1 szám. pp. 19-26.





¹ Adina Milena TATAR

AIR POLLUTION IN THE AREA OF COAL DEPOSITS OF SE ROVINARI. RISK ASSESSMENT

¹ HIGH SCHOOL MUSIC AND ARTS, TG. JIU, ROMANIA

ABSTRACT:

This paper is analyzed the work carried out on site is Rovinari generators of pollution. It analyzes the level of pollution, making a quantitative and qualitative risk assessment. Qualitative risk assessment aims to identify factors: source, path, receiver location analysis. Quantitative assessment is made based on a classification system of probability and severity.

KEYWORDS: risk assessment, coal deposits, air pollution

1. GENERAL CONSIDERATIONS

Rovinari Central is located approximately 16 km west of the city of Targu-Jiu, in a hilly area at an altitude of 150 m. Central Rovinari works in: - precincts Rovinari CTE - Rosia coal chamber.

CTE Rovinari - is located on the right side of the river Jiu, near the main road connecting the city of Targu-Jiu Filiasi. Rovinari CTE enclosure includes two coal deposits (and deposit Rogojelu crushed) in the extreme western limit Rogojelu the village.

Rosia coal chamber - (Rosia notbreaking coal deposit) is located in the south-east precinct at about 1500 CTE Rovinari I also mention that it also includes CTE Rosia conveyor between CTE and coal deposit, Rosia 1.5 km in length.

SE Rovinari activity covers the production of electricity and heat. This is accomplished by having produced a total of six boilers that are fueled by coal, with an hourly consumption of about 2300t / h, plus secondary fuel oil and natural gas. lignite power plant supply of household coal is the employer or directly from the pits through conveyor belts.

Household coal supply is designed and flow necessary to continue the six steam boilers, running on fuel from the main pit lignite coal basin Oltenia, located nearby. Lignite supply plant on conveyor belts is high capacity buses (type TMC) that collects the coal from the several quarries: Rosia de Jiu Tismana I Tismana II, streams and Rovinari East.

To compensate for variations of supplies of coal no rhythm (higher in warm seasons and lower in winter) and required power generation plant (higher summer and lower in winter) have constructed deposits of coal (raw and crushed) designed to ensure a match between supply and consumption possibilities.

Sources of coal dust in coal deposits are: - conveyor systems - machines and deposit taking bucket wheel - grinding stations

Emissions of coal dust deposits from the raw coal open pits Rovinari ,Tismana Garla and Rosia, equipment that comes into the production process flow of dust emissions during operation. These emissions occur in the formation of coal deposits for cars with combined KSS1; KSS2; M5a, M6a and acquisition of raw coal deposits of cups impeller discharge conveyor belt.

They also place the discharge of dust emissions on cars combined coal belt conveyors leading to the sorting station for sorting, crushing stations was provided an indoor facility for dusting which reduces emissions of dust in these buildings.

Emissions of coal dust in the form of particulate matter are driven by wind to nearby residential areas and ecosystems. Determinations were made of emissions of particulate matter in open areas immediately surrounding the coal deposits, Rogojelu village, Rosia Rovinari and neighborhood blocks. The results highlight determinations exceeding the maximum permissible concentration of protected areas (according to STAS 12574/87 between 1.2 to 2.4 times)

It should be noted that assessment of the deposit was influenced by the synergistic action due to power plant emissions of pollutants, namely particulate emitted by chimneys, dust from the transport, etc..

2. QUALITATIVE RISK ASSESSMENT

Air pollutants, the potential of respiratory disease are dust (or sediment in suspension). In small and medium concentrations, these pollutants can cause pathological changes of the respiratory system by overloading the respiratory defense mechanisms.

Particulate matter with a diameter greater than 10 μm (sediment) are retained in the rate of 90% in supraglottic extrapulmonary airways, their removal is relatively faster. Powders with a diameter less than 10 μm (suspended) in percentage retention extrapulmonary airways is inversely proportional to their size, ranging from 80-90% for close to 10 μm in diameter, until a little more than 5% for those with a diameter of 1 μm.

Particles with diameter less than 3 μm intrapulmonary enter the airways where they propose retained in 1-2%. When particle sizes are very small (less than 0.001 mm) retention processes are similar to those of gas.

The mechanism of action on the lung tissue is to stimulate the production of mucus and impaired movements of cilia vibrations pulmonary macrophage function, bronchial hyper activity, stimulation of fibrogenesis. The effect depends on both the nature and concentration of pollutant agent or combination with other risk factors.

TABLE 1. Relationship analysis matrix for source-path-receiver

Nr. crt.	Pollutant	Danger	Source	Way	Receptors	Achieving the target path of the source	The importance of risk (quantitative risk assessment, MXP)	The need for remedial works
1.	Suspended powders	Pneuxnocniogen	Transport System	air	Human (people living in the area analyzed)	Yes	6 average	Yes
			Submission and answer machines					Yes
2.	Sediment particles	Changing natural environment	Transport System	air	ground	Yes	3 average	Yes
			Submission and answer machines		wells	Yes	3 average	
					vegetation	Yes	3 average	Yes
					material goods	Yes	3 average	
3.	Noise	Effect on body additive and other diseases	Transport System	Airborne acoustic wave	Human (people living in the area analyzed)	Yes	6 average	Yes
			Submission and answer machines					Yes

Risk calculation is based on a classification system where the probability and severity of an event is classified Top randomly assigning them a score.

Classification probabilities: 3 = high probability 2 = average 1 = low

Classification of severity: 3= major 2 = average 1 = slight

The risk factor is calculated by multiplying the probability of gravity, thus obtaining a comparative figure, it will allow for comparisons between different risks. As the result is greater, the greater will be the priority will be given to controlling risk.

$$R = P \times G$$

R :risk of an unpredictable element

P :probability

G:hazard severity

Slacking

Suspended dust

$$P=3 ; G=2 R=3 \times 2=6$$

sediment particles

$$P=3 ; G=1$$

$$R=3 \times 1=3$$

Noise

$p=3$; $G=2$

$R=3 \times 2=6$

Risk assessment can be presented as a matrix.

3. CONCLUSIONS

As a result of risk assessment matrix is presented above suggest the following measures (Measures to reduce dust-generating sources):

- ❖ To reduce dust aerosol spray is proposed to apply water at the point of discharge / charge carriers or components from loading / unloading conveyors.
- ❖ To reduce dust is proposed to apply the dusting installation to the designed parameters, that the designed system components from the crusher. Measures to limit coal dust deposit
- ❖ To reduce dust aerosol spray is proposed to apply water at the point of discharge components from loading / unloading conveyors
- ❖ Measures to limit dust in inhabited areas in order to reduce dust and sediment suspension in private residential areas shall apply dust control measures at the source. Making screensavers (plantations - where Rosia village church and between deposit and adjoining blocks Rovinari the city).
- ❖ Monitoring and surveillance measures to limit dust requires periodic monitoring of concentrations of suspended dust at source and deposit receptors and receptors for tracking the dust settled the efficiency measures implemented.

REFERENCES

- [1.] Tumanov. S, Calitatea aerului , Ed. Tehnică 1989
- [2.] Ataman . E ș.a , Metodologia de analiză a impactului centralelor asupra mediului , București , 1995
- [3.] Tuțuianu . O , Anghel .M , Metodologia de evaluare operativă a emisiilor de SO₂ , NO_x, pulberi , CO₂ din centrale termice și termocentrale , Buc 1994
- [4.] Păsculete . E, Tehnologii moderne pentru îndepărtarea NO_x din gazele de ardere a centralelor care folosesc combustibili solizi , Energetica ,1994
- [5.] Groza .L, Ioana. Ionel, Activități de studii și proiectare necesare încadrării în prevederile Măsurarea emisiilor din gazele de ardere cu ajutorul senzorilor electrochimici, Timișoara , 1994
- [6.] Ataman. E , Considerații asupra reducerii poluării cu NO_x , Energetica 1994







¹Imre DÉKÁNY

TITANIUM DIOXIDE AND GOLD NANOPARICLES FOR ENVIRONMENTAL AND BIOLOGICAL APPLICATION

¹ SUPRAMOLECULAR AND NANOSTRUCTURED MATERIALS RESEARCH GROUP OF THE HUNGARIAN ACADEMY OF SCIENCES, DEPARTMENT OF PHYSICAL CHEMISTRY AND MATERIALS SCIENCES, UNIVERSITY OF SZEGED, HUNGARY

ABSTRACT:

In the work presented here we wished to study the role of clay minerals as environmentally friendly supports of the photocatalyst P 25 TiO₂ in detail. The reason for our interest is that layer silicates are outstandingly efficient adsorbents for organic pollutants, since organic molecules are adsorbed on the surface of clay minerals, which, so to say, accumulate environmentally harmful substances [5,6]. We wish to point out that the layer silicate component has a significant influence on the rate of catalytic degradation and, therefore, TiO₂/montmorillonite nanocomposites are eminently suitable for practical applications such as air and water purification technologies.

In the second part of this work reproducibly size-controlled gold nanoparticles reduced and stabilized by citrate were synthesized in aqueous dispersions. Gold nanorods were grown on functionalized gold surface and the kinetics of growth was studied. The surface of Au nanoparticles was modified by thiol-containing compounds, namely cysteine and glutathione, and the effect of pH and increasing cysteine concentrations on the dispersions was investigated by UV-Vis spectrometry.

KEYWORDS:

Nanocomposites, nanoparticles, gold, application

1. INTRODUCTION

The heterogeneous photocatalysis one of the most dynamically developing fields of high-efficiency oxidative procedures. This method based on irradiation of metal oxide semiconductor nanoparticles using visible light. These procedures show high significance because environmentally hazardous materials can be efficiently degraded by conversion of solar energy into chemical energy [1-3]. Degradation of these toxic substances by photocatalysis in aqueous medium could be the basis of a novel waste treatment method [4-6]. Volatile organic components are widely applied not only in industrial procedures but also in households, which leads to water and air pollution. In the presence of water vapor, the intermediate and final products accumulate on the catalyst surface, causing its deactivation.

In the work presented here we wished to study the role of clay minerals as environmentally friendly supports of the photocatalyst P 25 TiO₂ in detail. The reason for our interest is that layer silicates are outstandingly efficient adsorbents for organic pollutants, since organic molecules are adsorbed on the surface of clay minerals, which, so to say, accumulate environmentally harmful substances [5,6]. We wish to point out that the layer silicate component has a significant influence on the rate of catalytic degradation and, therefore, TiO₂/montmorillonite nanocomposites are eminently suitable for practical applications such as air and water purification technologies.

The preparation and biological applicability of gold nanoparticles are available in the special literature. Reduction of transition metal ions to colloids in aqueous or organic media in the presence of stabilizing agents was first published by M. Faraday in 1857 [7]. The first reproducible method was presented by Turkevich, who synthesized Au nanoparticles with a diameter of 20 nm via reduction of HAuCl₄ by trisodium citrate, while boiling and continuously stirring the reaction mixture [8]. In general, particles of different geometries are obtained depending on the quality of the precursor used [9], whereas the size of the particles obtained depends on the

precursor/reductant ratio.; the plasmon resonance peaks of the gold nanodispersions were between 520 and 530 nm. The color of the Au nanodispersion ranged from reddish orange (520 nm) to reddish purple (530 nm) depending on particle size [10].

The work of Liz-Marzán *et al.* is of fundamental importance in the preparation of nanoparticles of various shapes (spherical and anisometric [rod-like and prism-shaped]) [11, 12]. These authors summarize basic procedures and protocols for the preparation of Au, Ag and Cu nanoparticles and explain their optical properties in the journal *Materials Today* [13]. The resonance wavelength of anisometric particles such as nanorods depends on the orientation of the electric field. Two types of oscillation are possible, namely longitudinal and transverse. The longitudinal and transverse plasmon modes are both found to blue-shift, and the shift is larger for rods with larger aspect ratios. The color changes are visible to the eye for rods with aspect ratios around 2-3 [14].

Zhong *et al.* showed that gold nanoparticles reduced and stabilized by citrate have a negative surface charge and preferentially bind to thiol, amine, cyanide or diphenylphosphine functional groups [15]. They also showed that the reactivity of the amine group of amino acids is pH-dependent. Binding via α -amino groups is preferential at low pH and is suppressed at neutral and high pH, due to electrostatic repulsion between the surface of gold and the charged carboxyl groups.

In the second part of this work reproducibly size-controlled gold nanoparticles reduced and stabilized by citrate were synthesized in aqueous dispersions. Gold nanorods were grown on functionalized gold surface and the kinetics of growth was studied. The surface of Au nanoparticles was modified by thiol-containing compounds, namely cysteine and glutathione, and the effect of pH and increasing cysteine concentrations on the dispersions was investigated by UV-Vis spectrometry.

2. EXPERIMENTAL SECTION

Materials and Methods

Degussa P25 TiO₂ photocatalyst was used ($a^s_{\text{BET}}=50 \text{ m}^2/\text{g}$), Ca-montmorillonite (Siid-Chemie AG, Germany, $a^s_{\text{BET}}=72.95 \text{ m}^2/\text{g}$) and their mixtures with TiO₂ contents of 25%, 50%, 65% and 80%.

Phenol used for degradation was 99% purity (Aldrich). Anhydrous ethanol used in vapor phase degradations was 99.8% (Molar Chemicals Ltd, Hungary), and toluene was 99.94% (Molar Chemicals Ltd, Hungary).

Preparation of the photocatalyst

In each case, 10% suspensions made of Degussa P25 TiO₂ and Ca-montmorillonite were ground in an agate vibration mill (type GIF 3600, Hungary) with agate balls for 30 min. Suspensions were next dried at 110°C and, in order to ensure identical particle size in each experiment, sieved on a 90 μm sieve.

Preparation of gold nanoparticles

Materials used for the preparation of Au nanoparticles were: H₂AuCl₄*3H₂O (Sigma-Aldrich), tri-Na-citrate (Reanal) which served the dual role of a reductant and stabilizer and MQ water. The H₂AuCl₄ was dissolved in deionized water and the result a faintly yellowish solution. It heated until in boils and continued the heating, and while stirring vigorously, was added the sodium citrate solution and kept stirring for the next 30 minutes. The colour of the solution would changed from faint yellowish to clear to grey to purple to deep purple, until setting on wine-red. Added water to the solution was necessary to bring the volume back up to the original volume (to account for evaporation). The identification of prepared gold nanoparticles was performed by their plasmon resonance maximum value.

The formation of Au nanoparticles was followed by Ocean Optics Chem 2000-UV-Vis spectrophotometer at wavelength 200-800 nm. During the preparation, the absorbance spectrum was recorded.

Preparation of gold nanorods

Materials used for the preparation of Au nanorods were: 3-mercaptopropyl-trimethoxysilane (MPTMS, Aldrich), H₂AuCl₄*3H₂O (Sigma-Aldrich), cetyl-trimethyl-ammonium-bromide (CTABr, Reanal), L+ ascorbic acid (Reanal) and MQ water.

For the preparation of nanorods were treated the glass substrates with MPTMS and then with citrate stabilized gold nanoparticle seeds at different concentrations and growth solution which containing cetyl-trimethyl-ammonium- bromide, ascorbic acid and gold ions.

Transmission electron micrographs (TEM) were performed in Philips CM-10 transmission electron microscope with an accelerating voltage of 100 kV. The microscope was equipped with a Megaview II digital camera. TEM grids were prepared by placing one drop of undiluted sols on a

Formwar foil covered copper grid. The size distribution of the particles was determined by using UTHSCSA Image Tool 2.00 software.

The growth of Au nanorodes was also monitored by a Nanoscope III Multimode Atomic Force Microscope (AFM Digital Instruments) using a piezo scanner. Particle size and size distribution was measured by dynamics light scattering (DLS) with a Zetasizer Nano ZS ZEN 4003 (Malvern Instrument, UK).

Degradation of phenol in aqueous TiO₂/Ca-montmorillonite suspensions

An aqueous solution containing 0.5 mM/L phenol was degraded in a thermostatically controllable reactor ($t=25\pm 0.1^\circ\text{C}$) with a submerged lamp (a high-pressure mercury vapor lamp, 150 W, Heraeus TQ 150). The lamp emits predominantly in the range of 250-440 and 540-590 nm. The lamp was surrounded by a quartz shield in order to be able to also utilize high-energy photons ($\lambda < 310\text{ nm}$) of the lamp's UV light. A 280 ml stirred 0.1% TiO₂/Ca-clay suspension was filled into the reactor and flushed with air, ensuring a constant concentration of dissolved oxygen. 30 min adsorption time was allowed before the start of photooxidation reactions. For analysis of 2 ml samples were withdrawn from the illuminated suspensions at 20-min intervals and their total organic carbon (TOC) contents were measured in a Euroglas TOC 1200 (The Netherlands) apparatus. The total carbon contents of the suspensions were measured directly, injecting 100 μl aliquots.

If the adsorption equilibrium of solute is obtain, the original solution concentration c_0 is reduced to c_0' . In the course of the subsequent photooxidation, phenol concentration decreases to various extents depending on irradiation time, making possible the determination of the concentration vs. t function (Fig. 1).

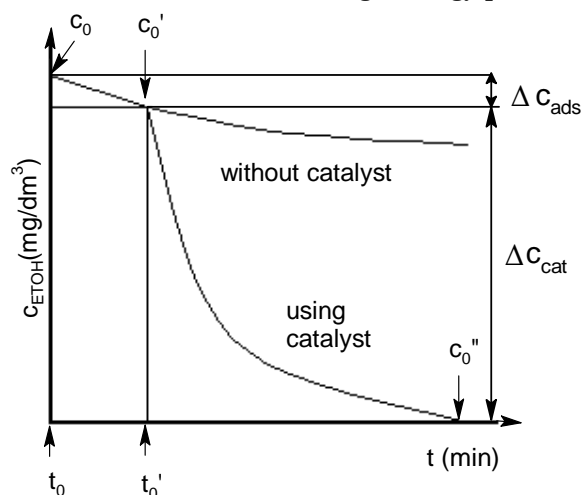


Figure 1. Schematic curve of photooxidation: t_0' is the switching of the light source.

The time difference $t_0 - t_0'$ is the adsorption time

3. RESULTS AND DISCUSSION

Phenol degradation in aqueous TiO₂/Ca-clay suspensions

Studies on the structure of TiO₂/Ca-montmorillonite nanocomposites clearly show that Bragg-reflexions characteristic of TiO₂ and montmorillonite are both present. In other words, no intercalation takes place during the grinding step, since the diameter of the TiO₂ nanoparticles is ca. 50 nm. Particles of such copious size would only be induced by surface charges to interact with the negatively charged lamellae of the clay mineral and to form a heterocoagulation structure.

Photocatalytic degradation of the aromatic phenol molecule was performed in 0.1% aqueous suspensions made of Ca-montmorillonite composites containing 0, 25, 50, 65, 80 or 100% Degussa P25 TiO₂ in a reactor with a submerged lamp, using 2-hour irradiations. The c/c_0 values calculated from the data measured after irradiating the samples, represented as a function of catalyst mixture composition are shown in Fig. 2.

Ca-montmorillonite does not have a significant photoactivity, as demonstrated by a decrease of only 12% in the amount of phenol present after 2 hours of UV irradiation. Photoactivity increases parallel with the increase in the amount of TiO₂: the mixture containing 25% TiO₂ degrades 70% of the phenol present in 60 min, whereas the samples containing 80% TiO₂ and pure P25 TiO₂ break down 95-98% in 40 min. In all cases, the decrease in phenol concentration

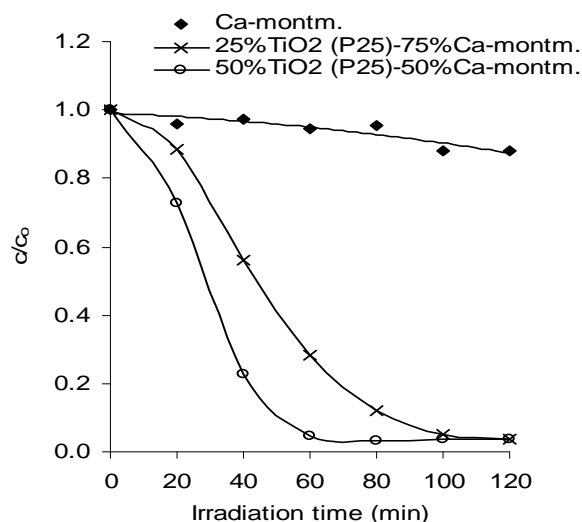


Figure 2. Photooxidation of phenol on Ca-clay and Ca-clay/TiO₂ composites

achieved in 60 min is expressed as ΔTOC . $\Delta\text{TOC} = \text{TOC}(t_0) - \text{TOC}(t_{60\text{min}})$, i.e. ΔTOC means CO_2 production realized in 60 min, starting at the onset of irradiation. When a theoretical phenol consumption is calculated for the TiO_2 -content of composites, taking into account phenol consumption measured in the case of pure TiO_2 (Fig. 3), the degrading capacity of each mixture surpasses the theoretical value. Significant excesses were observed in the case of the mixtures containing 50% and 75% Ca-montmorillonite. When ΔTOC values are normalized to unit weight of TiO_2 and represented as a function of the TiO_2 /clay mineral ratio, the synergistic effect is even more conspicuous.

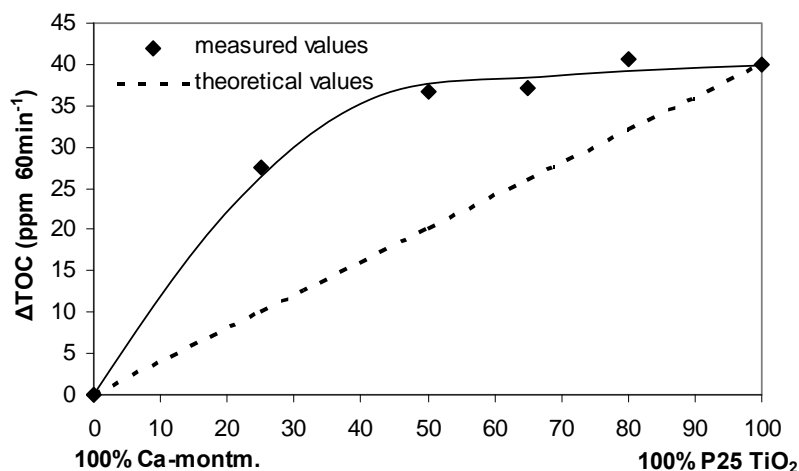


Figure 3. The synergistic effect of photooxidation on Ca-montmorillonite/ TiO_2 composites

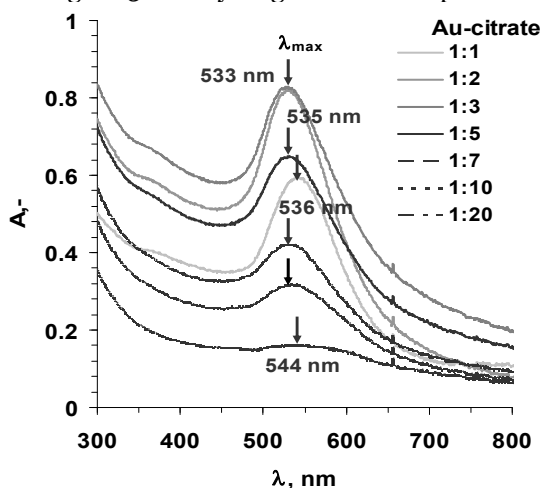


Figure 4. Absorption spectra of gold nanoparticles at ratio of gold/citrate 1:1-1:20 ($c_{\text{citrate}} = 0.2-4\text{mM}$ and $c_{\text{Au}^{3+}} = 0.2\text{mM}$) after 30 min reduction time and 24 hours

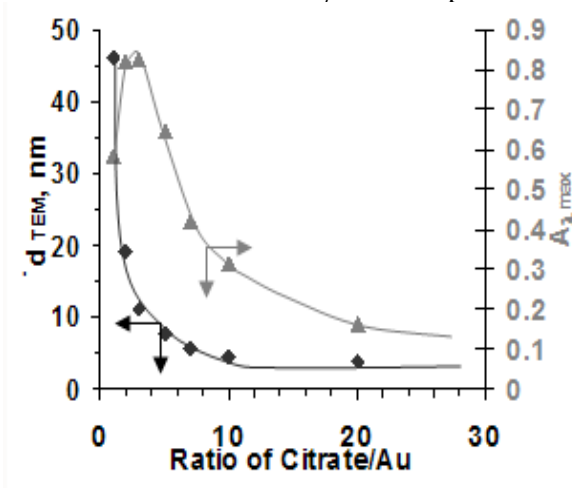


Figure 5. Relation between the maximum absorption values and the diameter at increasing citrate/gold ratio ($c_{\text{Au}^{3+}} = 0.2\text{mM}$) after 30 min reduction time and 24 hours

Interaction of nanostructured gold particles with cysteine

A method was developed for the controlled synthesis of gold nanoparticles in aqueous medium by reduction using trisodium citrate dihydrate at 25°C , and the size and size distribution of the particles formed and the colloid stability of the gold dispersions obtained were studied. The size and size distribution of the particles formed were determined by the analysis of TEM images. The most commonly used preparative method is reduction by trisodium citrate. We studied the effect of variations (i) in the gold:citrate ratio in the composition range of 1:1 - 1:20 (where $c_{\text{Au}^{3+}} = 0.2\text{mM}$ and $c_{\text{citrate}} = 0.2-4\text{mM}$) (Fig. 4) and (ii) in the initial gold concentration (in the range of 0-1 mM, $c_{\text{citrate}} = 2\text{mM}$) on the size of the nascent particles (Fig. 5). It is clearly shown in Fig. 4 that the plasmon resonance maximum of gold nanoparticles varies within the wavelength range of 533-544 nm, depending on citrate concentration. No systematic shift is observed. Maximum absorbance values are seen to increase when the amount of citrate added is increased from a ratio of 1:1 to 1:3 and to decrease in the ratio range of 1:3 - 1:20, which may be due to the formation of particles of different sizes depending on citrate concentration. The more citrate is present, the smaller are the nascent particles owing to the stabilizing effect of citrate. Relatively large gold nanoparticles are

distinguished by narrow, well-defined peaks, whereas smaller particles are characterized by broader, less sharp maxima (Fig. 4). To determine the size of the Au nanoparticles formed in the various gold dispersions on the basis of TEM images, samples were prepared on copper grids. Particle diameters determined in TEM images decrease exponentially with increasing amounts of citrate and absorbance maxima change in a nearly parallel fashion, i.e. an initial maximum is followed by nearly exponential decrease (Fig. 5).

According to Fig. 6 increasing the initial concentration of HAuCl_4 (in the range of 0.1-1 mM) results in a continuous increase in particle size at a constant citrate ion concentration of 2 mM. As precursor concentration is increased, increasingly larger particles (5-18 nm) are obtained by the evidence of the particle size distribution curves based on TEM images. Particle sizes determined by dynamic light scattering (DLS) (10-22 nm) (Fig. 6), however, do not match those determined on the basis of TEM images (5-18 nm), although the two sets of results are within the same order of magnitude. The TEM image of gold nanoparticles formed in the solution containing 0.8 mM HAuCl_4 and their size distribution are shown in Fig. 7. The average diameter of the particles is ~18 nm, whereas in the samples containing 0.2 mM HAuCl_4 particles measuring ~5 nm were formed (Fig.8). Size distribution is more homogeneous in dispersions containing smaller particles than in those containing larger particles. The higher extent of homogeneity is due to the presence of larger amounts of citrate ions. The application of lower citrate/Au ratio (1-5) leads to a decrease in the stability of Au dispersions, resulting in the aggregation of gold nanoparticles.

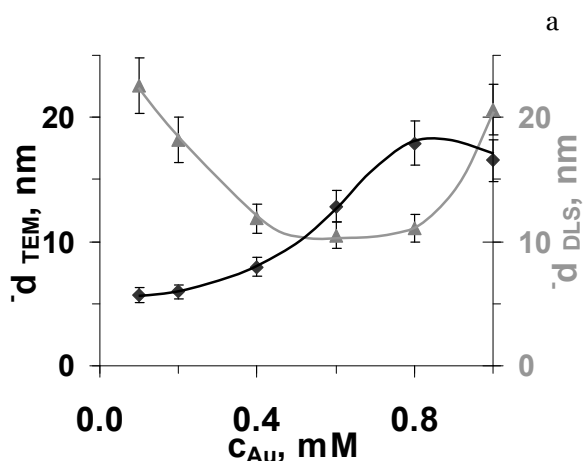


Figure 6. Relation between the particle size measured by TEM and DLS and the original gold concentration ($c_{\text{Au}^{3+}} = 0.1-1$ mM and $c_{\text{citrate}} = 2$ mM).

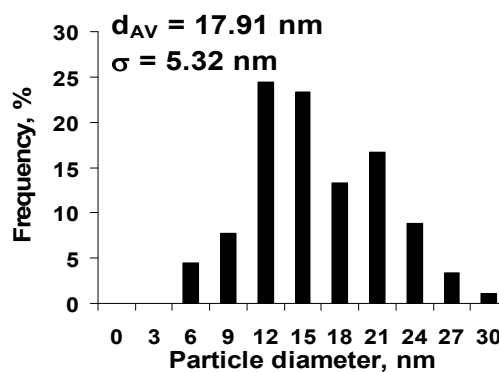
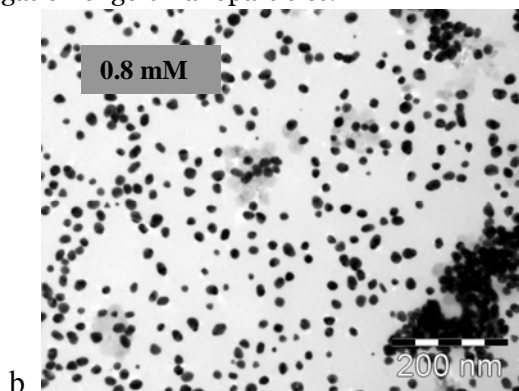


Figure 7. TEM pictures of $c_{\text{Au}} = 0.8$ mM (~18 nm) gold.

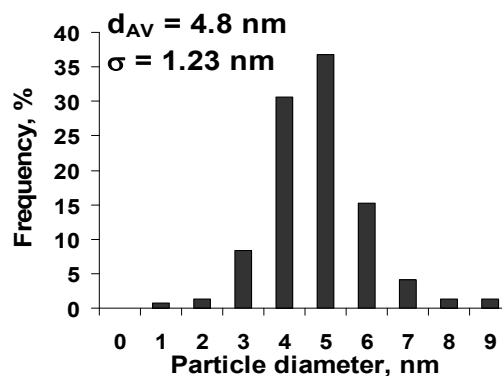
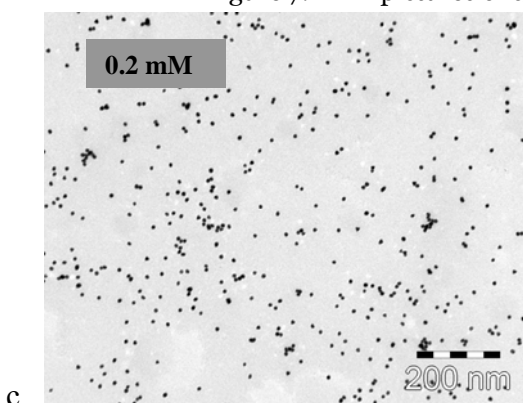


Figure 8. TEM pictures of $c_{\text{Au}} = 0.2$ mM (~5 nm) gold

Gold nanosols reduced and stabilized by citrate were also used for growing gold nanorods, and the kinetics of growth and the detectability of functionalized surfaces by recording UV-Vis spectra were investigated. Nanorods were grown in the following way. Previously synthesized gold nanoparticles were spread on the surface of microscope slides that had been thoroughly cleaned in chromosulfuric acid and functionalized by mercaptopropyl-trimethoxysilane (MPTMS) (Fig. 9). The silanized glass plates were let to stand in the gold sol for 25 min. The surface-modified glass plates carrying the gold nanoparticles were next submerged into the “nanorod growth solution” consisting 0.1 M cetyltrimethylammonium bromide (CTAB), and 0.05 M HAuCl₄ and 0.1 M ascorbic acid. Gold nanoparticles were generated in the growth solution via reduction by ascorbic acid, forming gold nanorods on the surface.

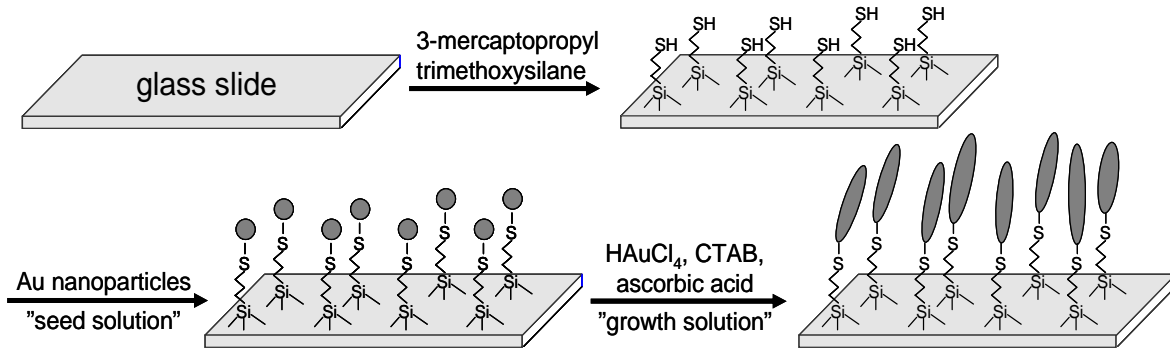
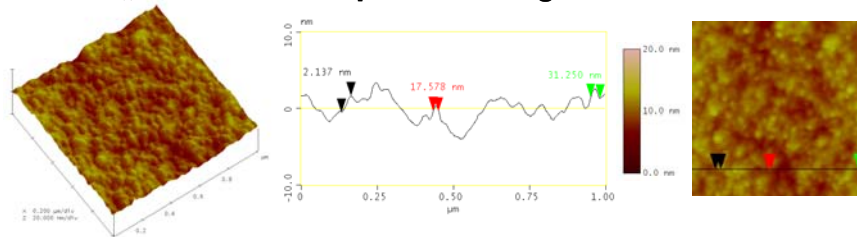
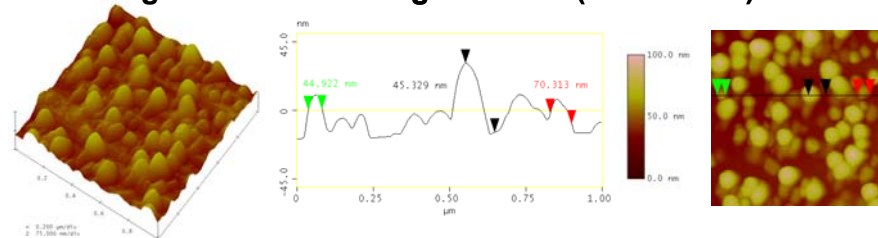


Figure 9. The scheme of the formation of gold nanorods on modified glass surface.

„Seed” Au nanoparticles on glass slide



Growing Au nanorods on glass slide (20 minutes)



Au nanorods on glass slide (40 minutes)

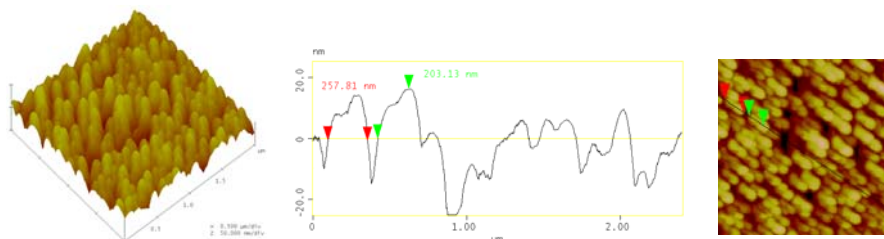


Figure 10. Growing of the gold nanorods on modified glass surface

The nanorod growth process was studied by AFM (Fig. 10). In the course of growth, the difference between rods grown for 0, 20 and 40 min is well discernible in the diameter analysis plot based on the AFM images. The diameter and height of rods grown for 20 min were ~45 nm, whereas the height of rods grown for 40 min was ~200 nm and their diameter was ~120 nm. After growth for 40-45 min the height of rods did not change any more.

4. CONCLUSION

Photocatalytic efficiency of TiO₂/Ca-montmorillonite composite suspensions was studied in liquid phase. We developed a double-walled photoreactor, in which TiO₂-composite thin films are spread on glass surface, for measurements on the solid/liquid interface. It was established that aqueous phenol solution and VOCs are degraded at a significantly higher efficiency on TiO₂/Ca-montmorillonite composites than on pure (Degussa P25) TiO₂.

Size quantized gold nanoparticles reduced and stabilized by citrate were synthesized. The particles were identified on the basis of their plasmon resonance maxima by UV-Vis spectrometry and their sizes were determined by particle size distribution functions calculated from images obtained by transmission electron microscopy. It was demonstrated by UV-Vis spectrometry that the rate of particle formation depends on the gold/citrate ratio: the higher the concentration of reductants and stabilizers in the dispersion, the lower are the apparent rate constants, i.e. the rate of particle formation decreases. The rate of aggregate formation in the liquid phase of dispersions containing gold and cysteine at various ratios was also studied by DLS. These experiments revealed that large aggregates are not formed in samples containing high amounts of cysteine and, due to the stabilizing effect of cysteine, the rate of aggregation is slower. Nanorods were synthesized on silanized glass surfaces and particle growth was followed by AFM. Our experience shows that growth solutions containing relatively high concentrations of HAuCl₄ deposit thicker gold layers on the surface; the thickness of the gold layers was determined as ~200 nm by AFM measurements.

ACKNOWLEDGEMENTS

The authors are very thankful for the financial support of the Hungarian Scientific Research Fund (OTKA) Nr. K 73307.

REFERENCES

- [1.] Hoffmann, M.R., Martin, S.T., Choi, W., Bahnemann, D.W. *Chem. Rev.* 1995, **95**, 69
- [2.] Ilisz, I., Dombi, A., Mogyorósi, K., Farkas, A., Dékány, I. *J. Appl. Catal. B.* 2002, **39**, 247
- [3.] Kőrösi, L., Dékány, I. *Colloid Surface A.* 2006, **280**, 146
- [4.] Kun, R., Mogyorósi, K., Dékány, I. *Appl. Clay Sci.* 2006, **32**, 99
- [5.] Marci, G., Addamo, M., Augugliaro, V., Coluccia, S., Garcia-López, E., Loddó, V., Martra, G., Palmisano, L., Schiavello, M. *J. Photochem. Photobiol. A* 2003, **160**, 105
- [6.] Mogyorósi, K., Dékány, I., Fendler, J.H. *Langmuir* **19**, 2003, 2938
- [7.] J. Turkevich, *Gold Bulletin*, 1985, **18**, 3
- [8.] Y. Luo, *J. of Nanoscience and Nanotechnology*, 2007, **7**, 2, 708
- [9.] D. Andreescu, T. Kumar Sau, D.V. Goia, *J. Colloid and Int. Science*, 2006, **298**, 742
- [10.] J. Pérez-Juste, I. Pastoriza-Santos, L.M. Liz-Marzán, P. Mulvaney, *Coordination Chem. Rev.* 2005, **249**, 1870
- [11.] L.M. Liz-Marzán, *J. Mater. Chem.* 2006, **16**, 3891
- [12.] P. Mulvaney, J. Pérez-Juste, M. Giersig, L.M. Liz-Marzán, Pecharromán C, *Plasmonics*, 2006, **1**, 61
- [13.] L.M. Liz-Marzán, *Materials Today*, 2004, 26
- [14.] K.H. Lee, K.M. Huang, W.L. Tseng, T.C. Chiu, Y.W. Lin and H.T. Chang, *Langmuir*, 2007, **23**, 1435
- [15.] Z. Zhong, S. Patskovsky, P. Bouvrette, H.T. Luong, A. Gedanken, *J. Phys Chem. B.* 2004, **108**, 4046





RESEARCHS REGARDING THE PELETIZING PROCESS OF FERROUS PULVEROUS WASTE

¹⁻⁴ UNIVERSITY POLITEHNICA OF TIMISOARA, FACULTY OF ENGINEERING FROM HUNEDOARA, ROMANIA

ABSTRACT:

This paper summarizes the technologies laboratory experimental phase to determine solutions for material recovery and compatible ferrous powder and small to produce pellets using a series of small and dry waste, from the steel industry, energy and mining, such as electric steelworks dust, dirt (sludge) from agglomeration, blast-scale (the scale slurry) sideritic waste, slag foundries (ferrous fraction), coal dust, coke or graphite, fly ash, dust lime, cement, bentonite.

KEYWORDS:

waste, pellets, recovery, steel, technology

1. INTRODUCTION

Small waste processing and powder technology is all the operations which are processed for use under the conditions required by the user. Technological operations are crucial in the process of recovery (recycling) of secondary materials (waste powder and small).

Reduction process based oxide material, technology solutions that we propose take into account the recovery of secondary materials consisting of waste powder (steelworks dust from sintering, blast furnaces, lime powder, etc.) and small (dross, slag fraction ferrous foundries, etc.).

Approach, resolution and implementation of technology depends:

- ❖ Nature of material submitted for processing in case of waste as secondary materials must Recycling;
- ❖ Form the finished product as these materials are processed.

We felt, based on documentation in the literature [1,2] and based on experiments and their results [3,4], as well as fundamental solutions compatible material after processing these wastes as raw materials in steel, the following: briquetting, pelletizing, congestion, mechanical mixture.

2. METHODOLOGY AND DISCUSSION

In order to achieve phase laboratory experiments, we sampled several powdery waste sections of a steel platform and ponds, storage, representative samples were collected from the following types of waste:

- ❖ Electric steelworks dust;
- ❖ Dump the dross and dross;
- ❖ Dust from sintering-blast (agglomeration slurry-blast)
- ❖ Lime powder.

Each waste sample was subjected to the operation of mixing (the homogenization was processed drum). Evaluating the quality of waste powder, determinations were made of physicochemical characteristics, namely: chemical composition and size.

It was also tested in the reaction pellet heating (combustion). In Fig.1 is presented aspects of these experiments.

The chemical composition of pellets is given in table 1. Fig.2 shows aspects of the pelletizing process (using a flat plate pelletizing machine) and the resulting micro-pellets, observing the technological flux of producing pellets (fig.3).

Pellets that can be used as foaming agent in the final slag smelting electric arc furnace load, which was placed in charge of the final metal tip (possibly together with other auxiliary materials).

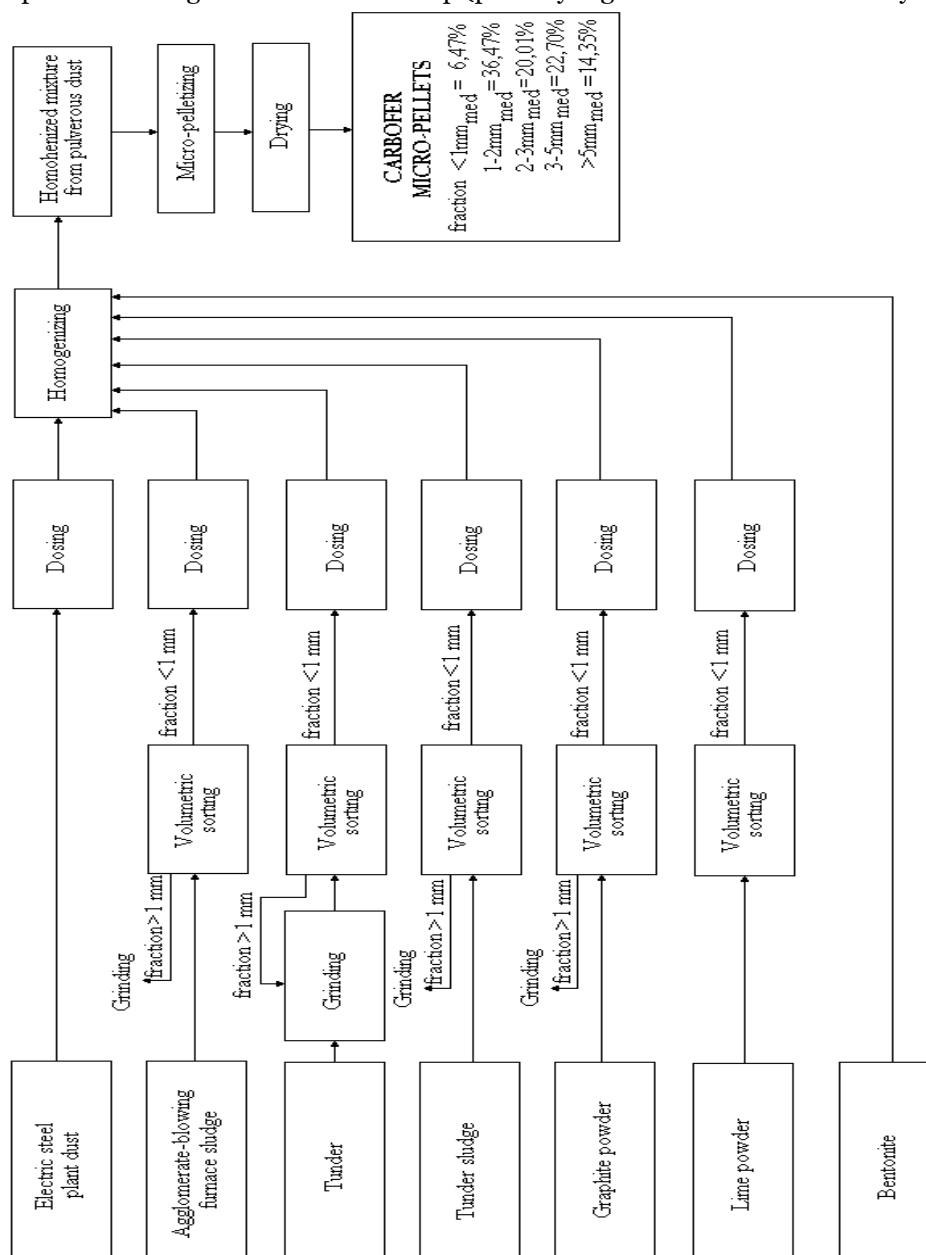


Fig.1. The technological flux of producing pellets

Table 1. The chemical composition of pellets

Recipe no.	Content of recipes [%]										
	SiO ₂	FeO	Fe ₂ O ₃	P ₂ O ₅	S	C	Al ₂ O ₃	CaO	MgO	MnO	other oxide
R1	6,74	3,97	38,32	0,10	0,44	13,94	3,53	20,98	1,14	1,37	9,47
R2	7,45	3,97	38,34	0,10	0,44	14,92	3,65	19,10	1,13	1,36	9,53
R3	9,01	3,83	32,68	0,09	0,47	19,19	4,06	18,38	1,19	1,16	9,93
R4	8,45	4,11	34,94	0,10	0,49	17,59	4,06	17,54	1,20	1,19	10,34
R5	8,15	4,11	40,10	0,10	0,44	14,92	3,76	16,25	1,11	1,37	9,68
R6	8,37	4,19	36,38	0,10	0,48	18,39	3,98	15,53	1,15	1,19	10,24
R7	7,80	4,34	34,19	0,09	0,50	21,69	4,00	14,68	1,16	1,04	10,51
R8	7,89	4,28	33,60	0,09	0,51	22,84	4,08	13,81	1,17	1,07	10,66
R9	8,03	4,41	33,25	0,09	0,53	21,24	4,21	14,93	1,22	1,04	11,04
R10	8,03	4,59	36,79	0,09	0,53	20,26	4,20	12,05	1,19	1,14	11,14

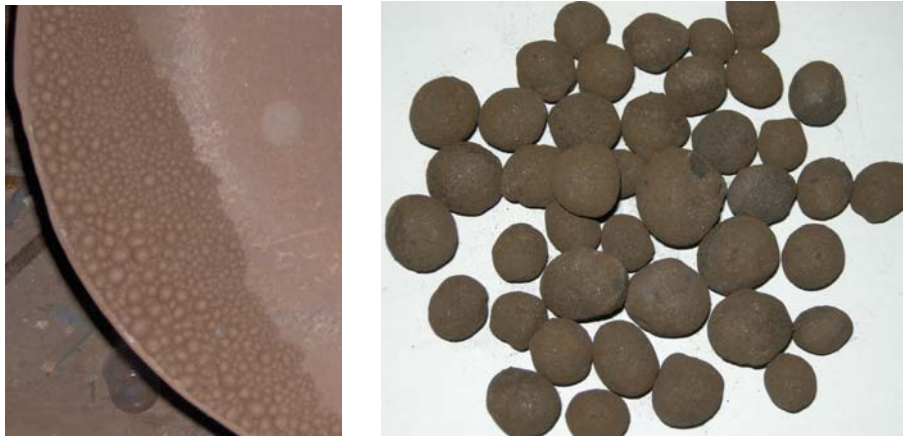


Fig.2. Aspects of the process of producing pellets

Combustion was performed in an oven with forced bars. Was found from the temperatures above 700°C is generated due to intense flames burn carbon monoxide resulting from the combustion of iron oxides.

Burning iron oxide increased the temperature, leading to partial melting pellets (from which came in contact with flame, that top load).



a. pellets heated at a temperature of 1050 °C respectively 1250 °C



b. Burning pellets in volatile release and clearance of carbon monoxide



c. Molten pellets

Fig.3. Aspects of these experiments

3. CONCLUSIONS

The ecological advantages are clear, namely: cutting down the amount of powdery wastes by their continuous recycling, the diminishing of soil pollution with metallurgical waste by reducing the dumping areas, the valorization by recycling of these wastes, without any negative impact upon the environment.

The economical advantages have both an immediate impact, i.e. transferring the depositing costs to other scopes, the obtaining of secondary raw materials, the low costs of processing by

means of this procedure, as compared to others, and also long term advantages, such as cutting down costs by partial replacing of some raw materials. Considering that processing the powdery materials resulting from steel making in view of recycling and/or re-using them represents an issue with real ecological and economical implications we found it appropriate to carry out researches in the field of their superior valorization.

REFERENCES

- [1.] NICOLAE, M., TODOR, P., LICURICI, M., MĂNDRU, C., IOANA, A., SEMENESCU, M., PREDESCU, C., ȘERBAN, V., CALEA, G., SOHACIU, M., PAPPALÀ, D., NICOLAE, A., Sustainable development in steel by secondary material recovery, PRINTECH Publishing House, București, 2004, pg. 3-5.
- [2.] DRISSEN, P., Reciclarea prafului de CAE, La Revue de Metalurgie, April, 2002, pp.341-344.
- [3.] ARDELEAN E., ARDELEAN M., HEPUT T., Research concerning the obtaining from industrial wastes of a cover powder used in steel continuous casting, Advanced Materials Research, vol.23: Materials and Technologies, 2007, pp.329-332.
- [4.] PROJECT no. 31-098/2007: Prevention and fighting pollution in the steel making, energetic and mining industrial areas through the recycling of small-size and powdering wastes, Program PN II.



DETERMINATION OF POROUS MATERIALS' ACOUSTICAL PARAMETERS

¹⁻² TECHNICAL UNIVERSITY IN KOŠICE, FACULTY OF MECHANICAL ENGINEERING,
DEPARTMENT OF ENVIRONMENTAL STUDIES AND INFORMATION ENGINEERING, KOŠICE, SLOVAKIA

ABSTRACT:

One of the most frequent problems faced by noise control engineers is how to design sound absorbers that provide the desirable sound absorption coefficient that minimizes the size and cost, does not introduce any environmental hazards, and stands up to hostile environments. The designers of sound absorbers must know how to choose the proper sound absorbing materials, its geometry and the protective facing. Porous sound-absorbing materials are utilized in almost all areas of noise control engineering. This paper deals with the acoustical parameters of porous materials and their measurement.

KEYWORDS:

porosity, flow resistivity, tortuosity, measurement

1. INTRODUCTION

A small part of the acoustical parameters used to describe the visco-inertial and thermal behavior of acoustical porous materials are directly measurable. This is the case for the open porosity, the static air flow resistivity and the high frequency limit of the dynamic tortuosity.

2. OPEN POROSITY

The open porosity, term commonly reduced to "porosity", refers to the ratio of the fluid volume occupied by the continuous fluid phase to the total volume of porous material. For acoustical materials, its range of values is approximately [0.70 0.99]. The schematic representation of an acoustical porous medium is shown on figure 1. The fluid phase, in white, is made up of a network of connected pores. The closed pores are considered to be a part of the solid phase, in grey. [9].

Open porosity measurement

The porosity can be directly measured and there are several methods to do so [2].

The **gravimetric measurement** of porosity requires the weighing of a known volume of dry material. Shot can be separated from fiber by a centrifuge process. The dry weight can be used together with the sample volume to calculate the bulk density ρ_B . Subsequently an assumed solid density is used to calculate the porosity h from [7]:

$$h = 1 - \frac{\rho_A}{\rho_B} \quad (1)$$

where: h – is the porosity, ρ_A – is the solid density [kg.m⁻³], ρ_B – is the bulk density [kg.m⁻³].

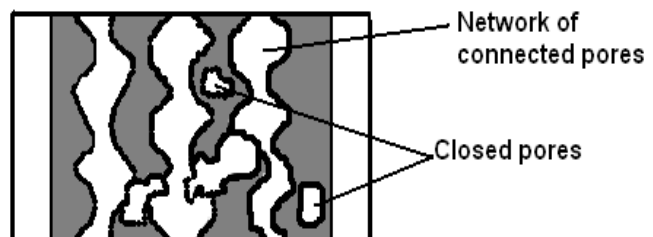


Figure 1 Schematic representation of an acoustical porous medium [9]

A **gravimetric method** may be used with some consolidate granular materials is to saturate the sample with water and deduce the porosity from the relative weights of the saturated and unsaturated samples. Mercury has been used as the pore-filling fluid in some applications, but for many materials the introduction of liquids affects the pores.

The **dry method** of porosity determination has been developed by Champoux et al.[3] is based on the measurements of the change in pressure within a sample container subject to a small known change in volume. The lid of the container is a plunger, which is driven by a precise micrometer. The pressure inside the chamber is monitored by a sensitive pressure transducer and an air reservoir connected to the container through a valve serves to isolate the system from fluctuations in atmospheric pressure. The system has been estimated to deliver values of porosity accurate to within 2%. This method measures the porosity of connected air-filled pores. However the gravimetric methods do not differentiate between sealed pores and connected pores. The open porosity measurement apparatus is shown on figure 2.

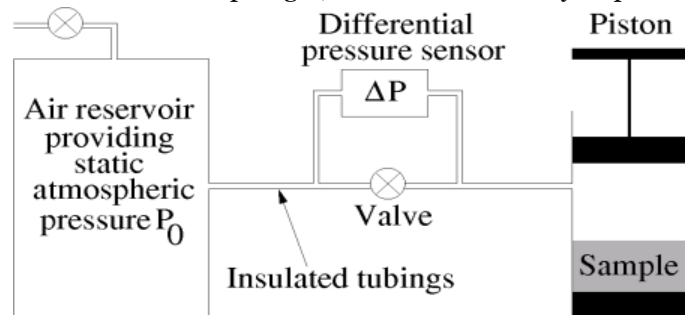


Figure 2 Schematic representations of the open porosity measurement apparatus presented by L. Beranek [9]

An **acoustical (ultrasonic) impulse method** for measuring porosity using the impulse reflected at the first interface of a slab of air-saturated porous material has been proposed and has been shown to give good results for plastic foams.

3. STATIC AIR FLOW RESISTIVITY

The static air flow resistivity, term commonly reduced to "resistivity", is one of the two most known parameters, with the open porosity, used to describe the acoustical behavior of porous materials. It characterizes, partly, the visco-inertial effects at low frequencies. Sound is vibrations in the air, so it is easy to imagine that sound cannot easily propagate through materials which air can hardly pass through [10]. In other word, flow resistivity can represent the difficulties of the propagation of sound (air-borne sound) in the gap in porous materials. A material such as iron and rubber etc. which air cannot pass through easily does not propagate the air-borne sound but propagate only the structure-borne sound (vibration). The models by Delany-Bazley [4] and Delany-Bazley-Miki [6] use only this parameter to describe the behavior of fibrous acoustical materials.

For bulk -, blanket -, or board-type porous materials the flow resistivity R_f is defined as specific flow resistance per unit thickness [7]:

$$R_1 = \frac{R_f}{\Delta x} \quad [\text{N.s.m}^{-4}] \text{ or } [\text{Pa.s.m}^{-2}] \quad (2)$$

where: R_f – is the airflow resistance $[\text{N.s.m}^{-3}]$ or $[\text{Pa.s.m}^{-1}]$,

Δx – is the thickness of the layer $[\text{m}]$.

The flow resistivity is a measure of the resistance per unit thickness inside the material experienced when a steady flow of air moves through the test sample. Flow resistance R_f represents the ratio of the applied pressure gradient to the induced volume flow rate and has unit of pressure divided by velocity. [7]

$$R_f = \frac{\Delta p}{v} \quad [\text{N.s.m}^{-3}] \text{ or } [\text{Pa.s.m}^{-1}] \quad (3)$$

where: Δp – pressure $[\text{N.m}^{-2}]$ or $[\text{Pa}]$,

v – velocity $[\text{m.s}^{-1}]$.

If a material has a high flow resistivity it means that it is difficult for air to flow through the surface. For acoustical materials, its range of values is approximately $[10^3 \text{ } 10^6]$. [9]

4. STATIC AIR FLOW RESISTIVITY MEASUREMENT

The resistivity can be directly measured [5]. The measurement of the flow resistance and flow resistivity of porous building materials has been standardized on a compressed-air apparatus [1]. In this measurement the pressure gradient across the sample in a fixed sample holder is monitored together with various flow rates. Compressed air is passed through a series of regulating valves and very narrow opening into chamber E. This creates an area of low pressure immediately in front of

the three tubes connected to the rest of the system. Air is drawn from the environment through the sample as a result of the pressure differential. The rate of airflow through the system is controlled by three flowmeters, giving a total measurement range between 8.7 and 0.1 L/min. Normally the flow rate must be kept below 3 L/min to avoid structural damage to the sample. The schematic representation of compressed-air apparatus for laboratory measurement of flow resistance is shown on figure 3. [7]

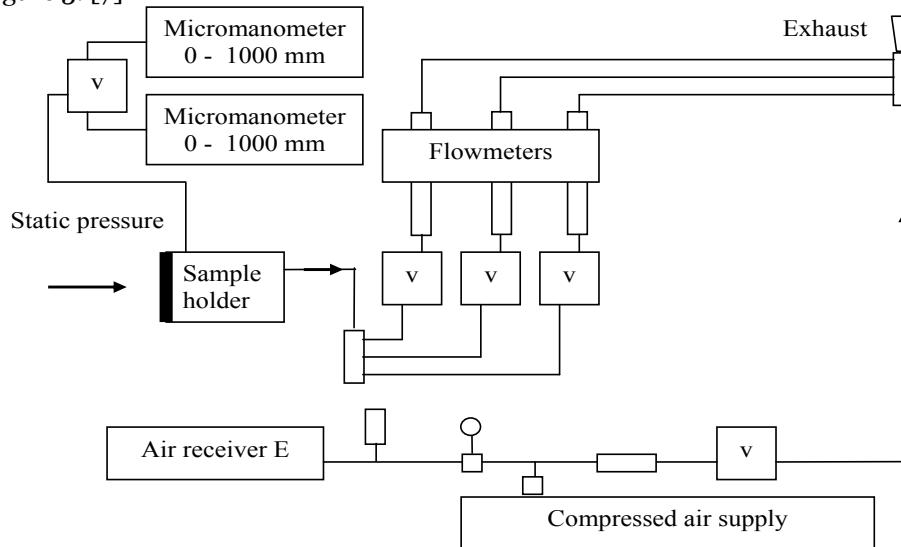


Figure 3 Schematic representation of a compressed-air apparatus for laboratory measurement of flow resistance [7]

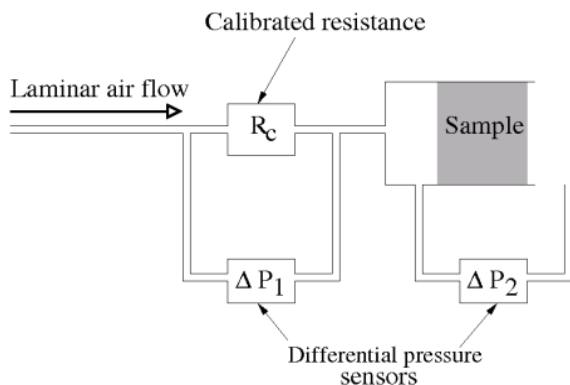


Figure 4. Schematic representation of the static air flow resistivity measurement apparatus presented in [ISO 9053]

A comparative method [8] makes use of a calibrated known resistance placed in series with the test sample. Variable capacitance pressure transducers are used to measure pressure differences across both the test sample and the calibrated resistance. For steady, nonpulsating flow, the ratio of flow resistance equals the ratio of measured pressure differences. The schematic representation of this apparatus is shown on figure 4.

5. TORTUOSITY

The tortuosity or the structural form factor of the material takes into account the curliness of the pores (see figure 5).

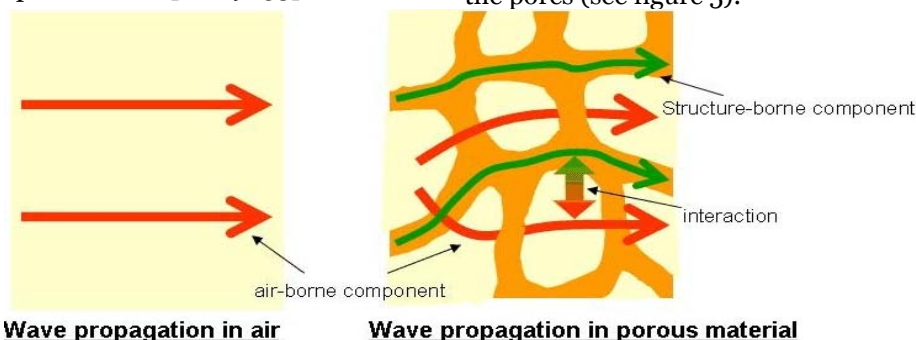


Figure 5. The sound propagation in the air (left) and in a porous material (right)[10]

Tortuosity is responsible for the difference between the speed of sound in air and the speed of sound through a rigid porous material at very high frequencies. Tortuosity is related to the formation factor used to describe the electrical conductivity of a porous solid saturated with conducting fluid. Indeed tortuosity can be measured using an electrical conduction technique in which the electrical resistivity of such a saturated porous sample is compared to the resistivity of the saturating fluid alone. Thus:

$$T = \frac{F}{h} \quad (4)$$

where: h – is the porosity of the sample,

F – is the formation factor defined by $F = \frac{\sigma_s}{\sigma_f}$ where σ_f and σ_s are the electrical conductivities of the fluid and fluid saturated sample, respectively. These in turn are defined by $\sigma = \frac{GL}{A}$ where L is the length of the sample, A is the area of the end of the sample, and G is the ratio of the resulting current to the voltage applied across the sample. [7]

Tortuosity measurement

Tortuosity measurement is based on the measurement of formation factor. To measure the formation factor, first a cylindrical sample of the material is saturated with a conducting fluid. Saturation is achieved by drawing the fluid through the sample after forming a vacuum above it. Agitation of the sample is also required if the pore sizes are small. A voltage is applied across the saturated sample placed between two similarly shaped electrodes at a known separation. The

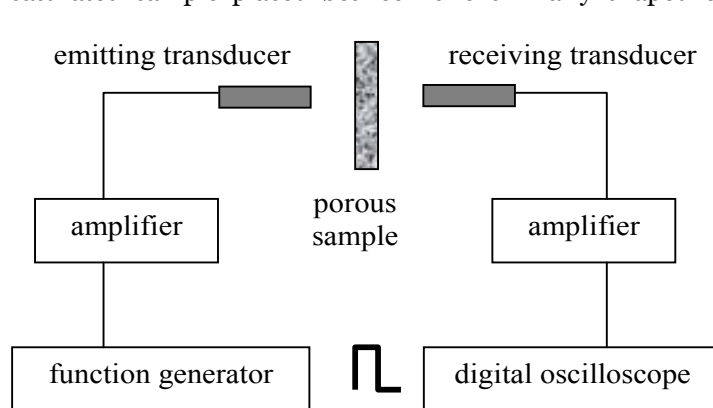


Figure 6. Schematic representation of the tortuosity measurement apparatus [11]

conductivity of the fluid is measured at similar voltages within a separate fluid-tight unit. The use of separate current and voltage probes assures a good contact between the end of the sample and the electrodes, eliminates problems associated with voltage drop at the current electrodes, and allows the simultaneous measurement of the electrical resistivities of the fluid and the saturated porous material. Tortuosity can be measured by measuring the velocity of sound which is transmitted in the fluid

that fills the porous material, in ultrasonic domain. Therefore, the measurement system is composed of sensors for transmitting and receiving ultrasound, power amp and oscilloscope.

6. Conclusion

Acoustical parameters of porous materials give the necessary and important information for noise control engineers. Profound knowledge their physical characteristics enable an effective sound absorber material design. The theory of sound-absorbing materials has progressed considerably during the last decade. A noise control engineer with serious interest in sound absorbing technology is advised to study all this parameters.

Acknowledgement

This paper was supported by projects APVV-0176-071/0453/08 and KEGA 3/7426/09.

REFERENCES

- [1] ASTM C 522-87: Standard Test Method for Airflow Resistance of Acoustical Materials., American Society for Testing and Materials, West Conshohocken, PA, pp 169 – 173
- [2] Beranek L. L., Acoustic impedance of porous materials, J. Acoust. Soc. Am. 13, 1942, pp. 248-260
- [3] Champoux Y.- Stinson M.R. –Daigle G.A.: Air- Based System for the Measurement of Porosity, J. Acoust. Soc. Am, 1991, pp. 910 – 916
- [4] Delany M. E. and Bazley E. N., Acoustical properties of fibrous absorbent materials, Applied Acoustics 3, 1970, pp. 105-116
- [5] [ISO 9053] International Organization for Standardization Acoustics - Materials for acoustical applications - Determination for airflow resistance.
- [6] Miki Y., Acoustical properties of porous materials - Modifications of Delany-Bazley models, J. Acoust. Soc. Jpn (E). 11(1), 1990, pp. 19-24

INHIBITOR MULTIENZYME BIOSENSOR SYSTEM IN DYNAMIC MODE – PHOSPHATE MEASUREMENT

¹ TECHNICAL UNIVERSITY SOFIA – BRANCH PLOVDIV, BULGARIA

²⁻³ TECHNICAL UNIVERSITY SOFIA, BULGARIA

ABSTRACT:

In this paper a multienzyme inhibitor system is investigated. A hybrid inhibitor biosensor for measuring concentration of phosphate is used. Enzymes kinetic of Michaelis-Menten and ping-pong kinetics are accepted. Partial differential equations of that complex system are solved numerically and are received concentration profiles of five reagents. The influence of starting concentration of inhibitor is investigated and influence of reaction rate constant of inhibitor

KEYWORDS:

mathematical modeling, inhibitor biosensor, simulations, phosphate

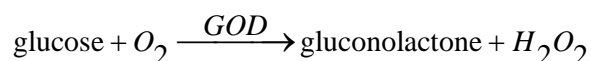
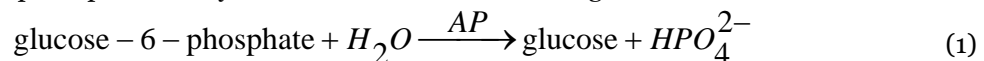
1. INTRODUCTION

Biosensors are analytical devices which tightly combine biorecognition elements and physical transducer for detection of the target compounds. Biosensors useful serve ecological purposes by enabling precision pollutant control [1, 2, 3]. In practice the most important are biosensors that identify water conditions [4, 5, 6, 7, 8] and to a lesser extent air [9, 10] and soil condition [11]. Two main water pollutant are phosphates and fluorides. For determination of phosphate and fluoride ions enzyme, microbial and multienzyme biosensors can be used. Multienzyme biosensors however are very complex devices.

2. DESCRIPTION OF THE MATHEMATICAL MODEL

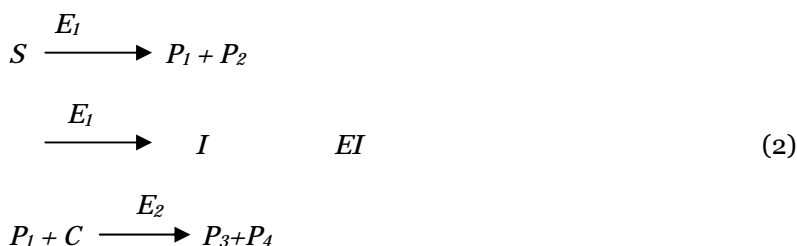
The starting concentrations of substrate, co-substrate and inhibitor in the research medium are denoted with S_0, C_0, I_0 . The concentration profiles for substrate $S(x)$, co-substrate $C(x)$ and inhibitor $I(x)$ are formed in the active membrane. In this paper a hybrid biosensor with two enzymes acid phosphatase (AP) and glucoseoxidase (GOD) is used for the investigation.

Operation principle of the hybrid biosensor is based on the given biochemical reaction:



Under the activity of the enzyme acid phosphatase the glucose-6-phosphate is hydrolyzed to glucose and inorganic phosphate. In the second reaction the oxygen present oxidizes the obtained glucose. The amount of hydrogen peroxide being produced is measured electrochemically. In the presence of phosphate the hydrogen peroxide is produced at a slower rate. This happens because of the inhibitory effect of those element have on the catalytic activity of the acid phosphatase. As a result the glucose production is decreased which leads to more production of H_2O_2 . As the AP is inhibited from the phosphate the substance can be identified with a biosensor according to its ability to support the formation.

The reactions above can be present with following successive enzyme reactions with competitive inhibition



AP is the first enzyme, let denote its reaction velocity with V_1 , GOD is the second enzyme let denote its reaction velocity with V_2 ; P_1 – glucose, first product; P_2 – second product, not informative; S – glucose-6-phosphate, substrate; I – (KH_2PO_4) measured inhibitor, C – oxygen, co-substrate; P_3 – product H_2O_2 and P_4 – galactonic acid.

We admit that indicatory electrode has symmetrical geometry and assume that diffusion is one-dimensional in space and is described with second Fick's law than we can write the system of equations for those bi-substrate sensitive amperometric system

$$\begin{aligned}
 \frac{\partial S}{\partial t} &= Ds \frac{\partial^2 S}{\partial x^2} - \frac{V_1 S}{Ks \left[1 + \frac{I}{k_I} \right] + S}; & \frac{\partial I}{\partial t} &= Ds \frac{\partial^2 S}{\partial x^2} - \frac{V_1 S}{Ks \left[1 + \frac{I}{k_I} \right] + S}; \\
 \frac{\partial C}{\partial t} &= Dc \frac{\partial^2 C}{\partial x^2} - \frac{V_2}{1 + \frac{Kp_1}{P_1} + \frac{Kc}{C}}; & \frac{\partial P_1}{\partial t} &= Dp_1 \frac{\partial^2 P_1}{\partial x^2} + \frac{V_1 S}{Ks \left[1 + \frac{I}{k_I} \right] + S} - \frac{V_2}{1 + \frac{Kp_1}{P_1} + \frac{Kc}{C}}; \\
 & & \frac{\partial P_3}{\partial t} &= Dp_3 \frac{\partial^2 P_3}{\partial x^2} + \frac{V_2}{1 + \frac{Kp_1}{P_1} + \frac{Kc}{C}},
 \end{aligned} \quad (3)$$

where: Ds , Dc , Dp_1 , Dp_2 and Dp_3 are diffusion coefficients for substrate, co-substrate, product 1 and product 3, Ks - reaction constant for substrate, Ki - reaction constant for inhibitor, Kc - reaction constant for co-substrate, Kp_1 - reaction constant for product 1, Kp_3 - reaction constant for product 3. The output current is proportional to gradient of H_2O_2 concentration at the electrode surface

$$I = nFAD_{P_3} \left. \frac{\partial P_3}{\partial x} \right|_{x=d}, [A] \quad (4)$$

where: n is the number of electrons taking part in electrochemical reaction, F is the Faraday's number, A is the electrode surface [m^2].

Let we denote $x = 0$ for the bulk/membrane interface and $x = d$ for the electrode surface. The action in biosensor starts when some quality of substrate is appears into biological recognition element – active membrane. The initial conditions are:

$$t = 0 \quad S(x,0) = S_0 \quad I(x,0) = I_0 \quad C(x,0) = C_0 \quad P_1(x,0) = 0 \quad P_3(x,0) = 0$$

Limiting conditions are:

$$x = 0 \quad S(0,t) = S_0 \quad I(0,t) = I_0 \quad C(0,t) = C_0 \quad P_1(0,t) = 0 \quad P_3(0,t) = 0$$

The substrate, and co-substrate didn't react with the electrode, oxygen and glucose fully exhausted and medium is well stirred and it remain constant at the electrode surface, then the limiting conditions are

$x = d$

$$\left. \frac{\partial S}{\partial x} \right|_{x=d} = 0, \quad C(d,t) = 0 \quad P_1(d,t) = 0 \quad \left. \frac{\partial P_1}{\partial x} \right|_{x=d} = 0, \quad P_3(d,t) = 0$$

3. RESULTS AND DISCUSSIONS

For solving system (4) of non-linear partial differential equations (PDE) we use Matlab solver *pdepe*. It use both finite difference and finite element methods as described in [12]. *pdepe* solve initial-boundary value problems for system of parabolic-elliptic PDEs in the one space variable x and time t . The ordinary differential equations resulting from discretization in space are integrated to obtain approximate solutions at times specified in a time vector. Time vector specifying the points at which a solution is requested for every value in distance vector. The *pdepe*

function returns values of the solution on a mesh provided in a distance vector. Distance vector specifying the points at which a numerical solution is requested for every value in time vector.

Concentration profiles of substrate, co-substrate, inhibitor, product 1 and 3

Because oxygen is consumed during enzymatic conversion output current of biosensor is descending function. Parameters used for simulations are

$n = 2$, $S_0 = 100$ mM, $C_0 = 0,25$ mM, $I_0 = \text{changed}$, $P_{01} = 0,0$ mM, $P_{03} = 0,0$ mM

$F = 96,5$ A.s / mmol - Faraday's number

$A = 7,85 \cdot 10^{-7}$ m² - diameter of cathode is 1mm

$K_s = 80$ mM - reaction rate constant for substrate

$K_c = 0,5$ mM - reaction rate constant for oxygen

$K_i = 0,1$ mM, $K_{p1} = 100$ mM - reaction rate constant for inhibitor and products 1

$D_s = 2,50 \cdot 10^{-10}$ m²/s, $D_c = 2,5 \cdot 10^{-11}$ m²/s, $D_I = 2,50 \cdot 10^{-9}$ m²/s, $D_{p1} = 2,5 \cdot 10^{-10}$ m²/s, $D_{p3} = 2,5 \cdot 10^{-10}$ m²/s,

$d = 60$ μ m

$V_{m1} = 1$ mM/s, $V_{m2} = 20$ mM/s,

At fig.1, 2, 3, 4 and 5 in three dimensional size are given concentration profiles of substrate $S(x,t)$, inhibitor $I(x,t)$, co-substrate $C(x,t)$, product 1 $P_1(x,t)$, product 3 $P_3(x,t)$ in active membrane with thickness $d = 60\mu\text{m}$ for the time $t = 8\text{s}$, for values of reaction velocities $V_1 = 1$ mM/s and $V_2 = 20$ mM/s. The value of inhibitor is $I_0=0.0$ mM and the value of substrate is $S_0=100$ mM.

Figure 7 shows the output current I which is proportional to the concentration of the oxygen. It is seen that oxygen is consumed very rapidly for the case starting concentration $I_0 = 0$, because there is no inhibitor in the research medium. Hydrogen peroxide (product P_3) has value about 0.25 because the oxygen is almost exhausted. The velocity of changing of concentration of co - substrate depends of presence of the inhibitor (eq.3), because now there is no inhibitor oxygen is consumed very rapidly- fig.4.

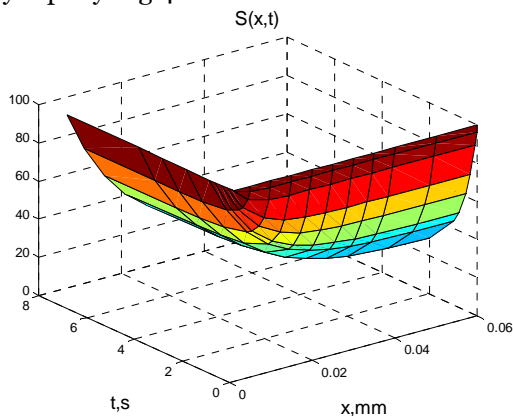


Fig. 2. Concentration profile of substrate.
 $I_0 = 0$ mM.

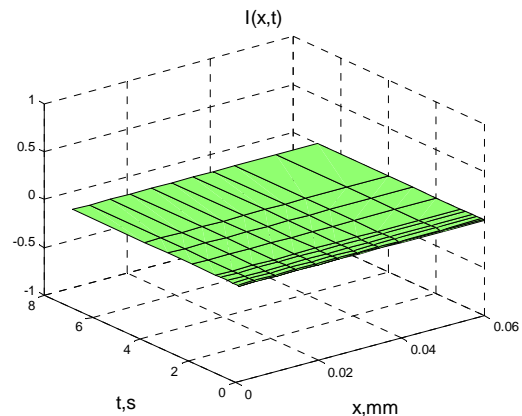


Fig. 3. Concentration profile of inhibitor.
 $I_0 = 0$ mM.

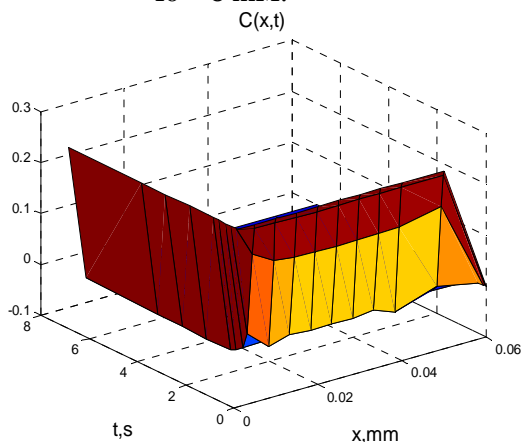


Fig. 4. Concentration profile of co-substrate.
 $I_0 = 0$ mM.

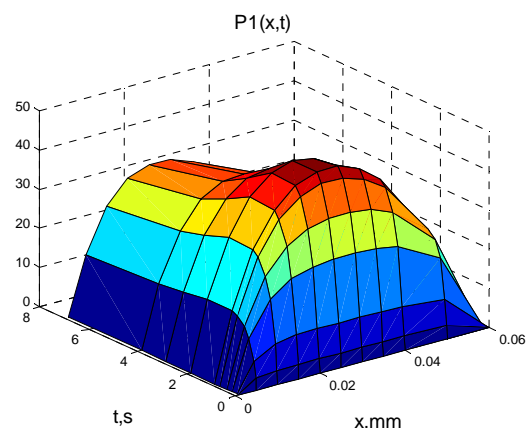


Fig. 5. Concentration profile of Product 1.
 $I_0 = 0$ mM.

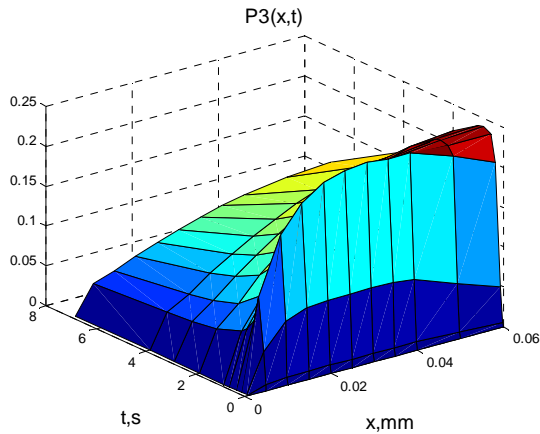


Fig. 6. Concentration profile of Product 3.
 $I_0 = 0$ mM.

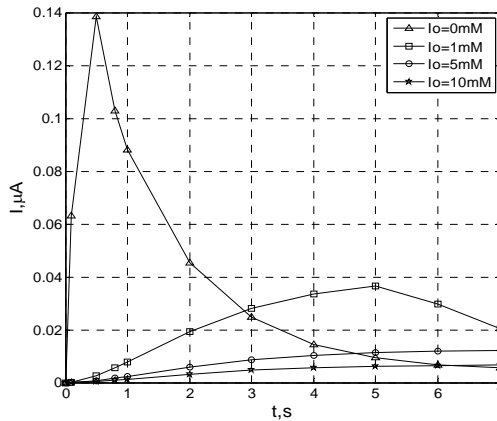


Fig. 7. Output current of the biosensor.

The investigated biosensor is co-substrate sensitive and because of that it is important the analyze of changing of co-substrate C and inhibitor I. At the next pictures are given the dependence of the output current of the biosensor and concentration profiles of substrate, co – substrate, inhibitor and products for the values of $I = 1.0$ mM.

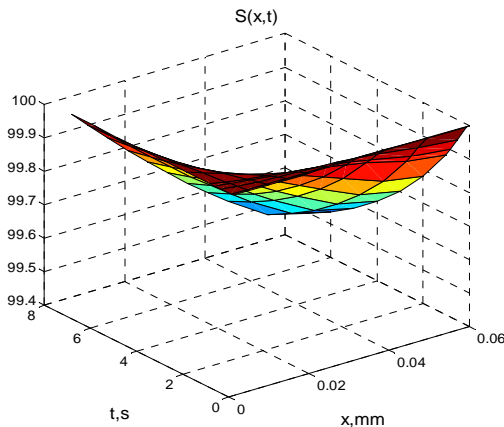


Fig. 8. Concentration profile of substrate.
 $I_0 = 5$ mM.

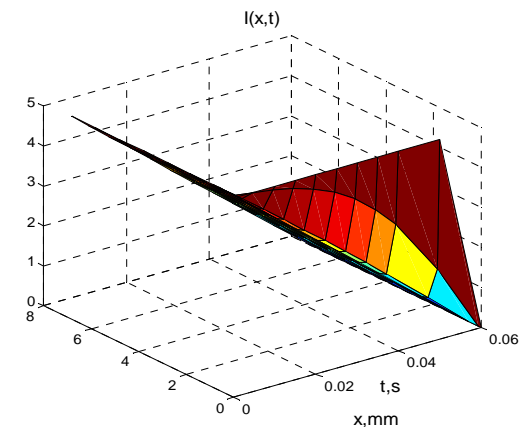


Fig. 9. Concentration profile of inhibitor.
 $I_0 = 15$ mM.

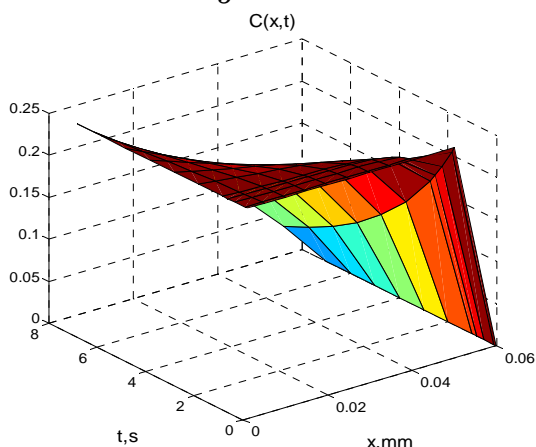


Fig. 10. Concentration profile of co-substrate.
 $I_0 = 5$ mM.

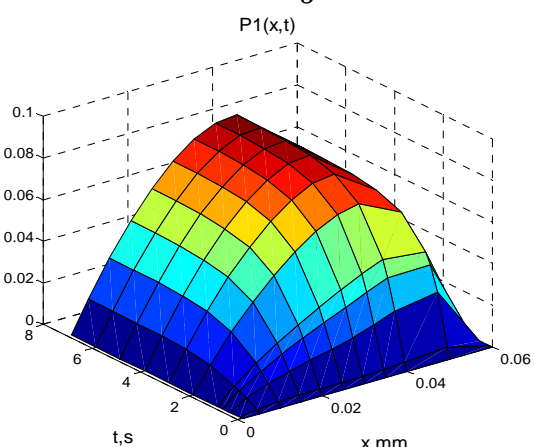


Fig. 11. Concentration profile of Product 1.
 $I_0 = 5$ mM.

At fig.8, 9, 10, 11, and 12 are given concentration profiles of substrate $S(x,t)$, inhibitor $I(x,t)$, co-substrate $C(x,t)$, product 1 $P_1(x,t)$, product 3 $P_3(x,t)$ for the starting value of inhibitor $I_0 = 5.0$ mM. It is seen clearly how the inhibitor effects over the all reagents. Substrate decreasing very little – from 100mM to 98mM, for the difference at figure 2 where the decreasing is from 100mM to 20

mM when there is missing inhibitor in the medium. Consuming of the oxygen is less, product 3 formation is increase (fig.12) with the time for the difference at fig.6 where is poorly.

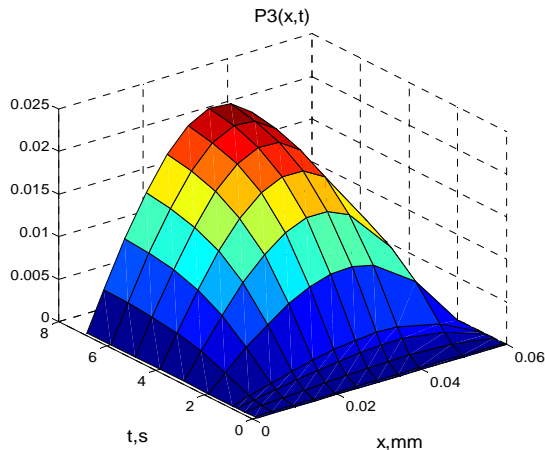


Fig. 12. Concentration profile of Product 3.
 $I_0 = 5 \text{ mM}$.

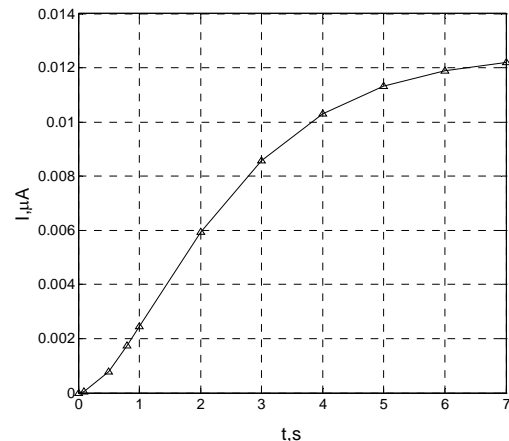


Fig. 13. Output current of the biosensor.
 $I_0 = 5 \text{ mM}$.

At fig. 7 is given the transient process of the output current for the four values of starting concentration of inhibitor $I_0 = 0, 1, 5$ and 10 mM . For the bigger starting concentration of I_0 the value of steady state of the current is increasing (this is the value for the time bigger than 7 s), but it is seen that the dependency is non linear. At fig. 13 it is seen more precise, value of I_0 are $0, 1, 3, 5, 7, 9, 11, 13, 15, 17, 19 \text{ mM}$.

At fig. 14 is investigated the influence of reaction rate constant for inhibitor $K_i = 0,05, 0,1, 0,5, 1, 2, 5 \text{ mM}$ at the constant starting concentration of $I_0 = 5 \text{ mM}$ over substrate concentration profile $S(x,t)$ for $x=d$. With increasing the K_i substrate concentration in active membrane is decreasing.

At fig. 15 is investigated the influence of reaction rate constant for inhibitor $K_i = 0,05, 0,1, 0,5, 1, 2, 5 \text{ mM}$ for the constant starting concentration of $I_0 = 5 \text{ mM}$ over the output current. It is seen that transient processes for the output current strongly depend from K_i . With increasing the reaction rate constant for inhibitor transient process of the current losing its first order system form.

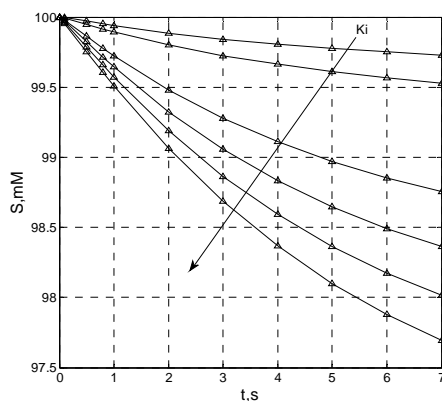


Fig.14. Influence of reaction rate constant over substrate concentration.

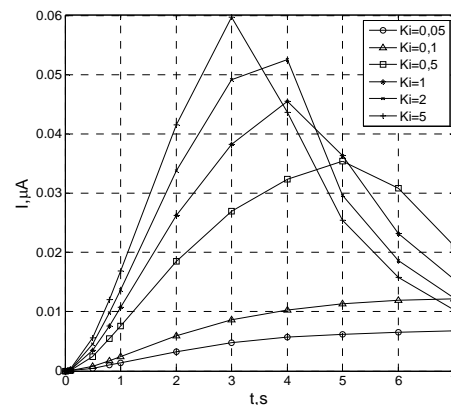


Fig. 15. Influence of reaction rate constant over output current.

4. CONCLUSION

In the paper is investigated the influence of inhibitor starting concentration over biosensor output current for the hybrid biosensor with two enzymes - acid phosphatase and glucoseoxidase in the dynamic mode. Partial differential equations of that complex system are solved numerically and received concentration profiles of five reagents. In the future it will be investigated the influence of enzymes rate over biosensor response and some technical parameters.

REFERENCES

- [1.] Gu M. B., Mitchell R. J., Kim B. C., Whole-cell-based biosensor for environmental biomonitoring and application, *Adv. Biochem. Eng. Biotechnol.* 87, 269-305, 2004.
- [2.] Reshetilov A., Microbial, Enzymatic, and Immune Biosensors for Ecological Monitoring and Control of Biotechnological Processes, *Applied Biochemistry and Microbiology*, 41, 442-449, 2005.
- [3.] D'Souza S. F., Jha S. K., Kumar J., Environmental Biosensors, *Environ. Biotech.* 4, 54-59, 2005.
- [4.] Lei Y., P. Mulchandani, W. Mulchandani, A. Mulchandani, Biosensor for Direct Determination Fenitrothion and EPN Using Recombinant *Pseudomonas putida* JS444 With Expressed Organophosphorous Hydrolase. 2. Modified Carbon Paste Electrode. *Applied Biochemistry and Biotechnology*, 136, 243-250, 2007.
- [5.] Proll G., Tschmelak J., Gauglitz G., 2005, Fully automated biosensors for water analysis, *Anal Bioanal Chem*, 381, 61–63, 2005.
- [6.] Campanella L., Cubadda F., Sammartino M.P., Saoncella A. An algal biosensor for the monitoring of water toxicity in estuarine environments, *Water Research*, 35, 69-76, 2001.
- [7.] Durrieu C., Chouteau C., Barthet L., Chovelon J. M., Tran-Minh C., A Bi-enzymatic Whole-Cell Algal Biosensor for Monitoring Waste Water Pollutants, *Analytical Letters*, 37, 1589-1599, 2004.
- [8.] Rodriguez B. B., Urease-glutamic dehydrogenase biosensor for screening heavy metals in water and soil samples, 380, 284-292, 2004.
- [9.] Sandstrom K. J. M., Newman J., Sunesson A. L., Levin J. O., Turner A. P. F., Amperometric biosensor for formic acid in air, *Sens&Actuators B*, 70, 182-187, 2000.
- [10.] Lanyona Y. H., Ibtisam G. M., Tothilla E., Mascini M., Benzene analysis in workplace air using an FIA-based bacterial biosensor, *Biosen&Bioelectron.* 20, 2089-2096, 2005.
- [11.] Gu M. B., Chang S. T., Soil biosensor for the detection of PAH toxicity using an immobilized recombinant bacterium and a biosurfactant, *Biosen&Bioelectron.* 16, 667-674 , 2001.
- [12.] Skeel, R.D., Berzins, M., A method for the spatial discretization of parabolic equations in one space variable. *SIAM J. Scient. Stat. Comput.* 11, 1–32, 1990.



CAPITALIZATION OF POWDERY WASTE THAT CONTAINING IRON AND BASIC OXIDES UNDER BRIQUETTES FORM

¹⁻⁴ UNIV. POLITEHNICA OF TIMISOARA, FACULTY OF ENGINEERING - HUNEDOARA, ROMANIA

ABSTRACT:

Methods of waste reusing and restoring the economic cycle are a concern both waste generators and those of any processors. From this perspective, the paper presents a possibility of recovery of small and powdery wastes containing iron and basic oxides by produced CARBOFER product used in electric arc furnace as slag foaming agent. Are used waste storage or waste ponds and also waste streams currently on technology: electric steelworks dusts, sludge from agglomeration-blast furnaces, tunder (tunder sludge).

KEYWORDS:

Pulverous wastes, briquette, steel plant dust, agglomeration-blast furnace sludge, lime dust

1. INTRODUCTION

Small and powder waste processing technology is an operations which are processed for use under the conditions required by the user. Technological operations are crucial in the process of recovery (recycling) of secondary materials (waste powder and small). [1,2]

The main methods of processing small and powdery materials, for their reintroduction into the economic circuit, are:

- briquetting;
- pelletizing;
- agglomeration.

Briquetting process has the advantage that allows a variety of wastes containing iron both in terms of chemical composition (primarily Fe content) and granulometric. Thus, in terms of iron content, we consider a limit of 25-60% Fe and granulometry, from dust to about 10mm size (tunder and steelworks slag, ferrous fraction less than 10mm). Therefore, the solution for these materials is the **briquetting process**.

2. THE STUDY

For recovery in the form of briquette to small and pulverous waste from the steel industry, energy and mining, we consider the following wastes: electric steelworks dusts, sludge from agglomeration-blast furnaces, tunder (tunder sludge) and as binder: lime, bentonite, cement. [3]

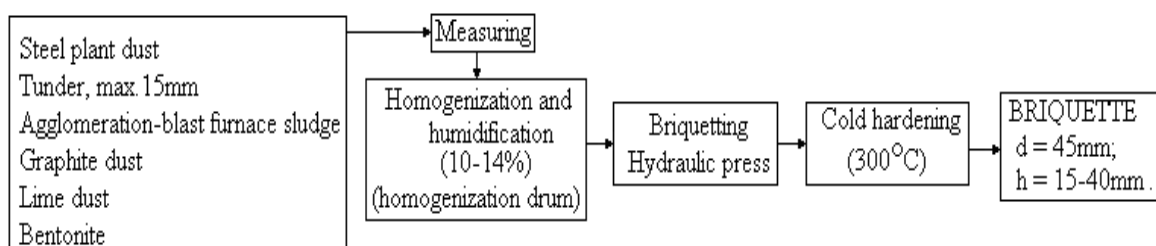


Figure 1. Waste flux processing technology in the form of briquettes



Figure 2. Facilities and equipment used in the experiments.

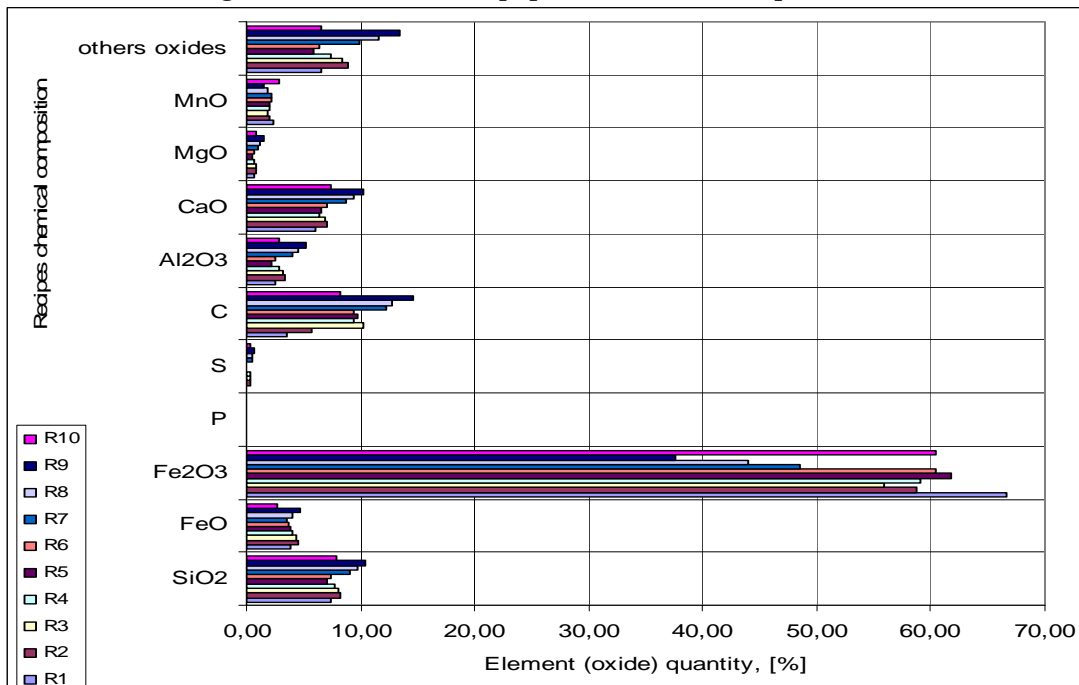


Figure 3. Briquettes chemical composition

Considered waste used in laboratory experiments were processed according to the technological flow shown in Figure 1, using the facilities and equipment existing in the laboratories of the Faculty of Engineering of Hunedoara. Issues during trials and several briquette obtained are presented in Figure 2. In laboratory phase we made a total of 10 recipes briquettes, the recipes chemical composition is presented in graphical form in Figure 3.

3. DISCUSSIONS

Below we presented the results of research on resistance lighters from recyclable materials [3, 4, 5, 6,7], research conducted to know:

- ❖ the changing of the briquette resistance according to the weight (in the preparation recipe) of the steel plant dust particles (EAF), rolling-mill tunder, sludge from agglomeration-blast furnace, lime, bentonite;
- ❖ the influence of some chemical compounds (found in the materials recycled through briquetting) on resistance.

To evaluating the resistance qualitative characteristics during handling and transportation of the briquettes, we determined, through experiments, three technological characteristics:

- Crack resistance: $R_f = \frac{F_f}{A}$, [kN/cm²] (1)

where: F_f – crack force, [kN]; A – area of the sample (briquette) section, [cm²].

The crack force F_f is considered to be the applied force at which we can see the first cracks. After performing a quite large number of preliminary tests, we consider that this force has the value recorded at $\tau = 2$ seconds.

- Crushing resistance: $R_s = \frac{F_s}{A}$, [kN/cm²] (2)

where: F_s – crushing force, [kN]; A – area of the sample (briquette) section, [cm²].

Based on the preliminary observations, we considered that the crushing force has the value recorded at $\tau = 12$ seconds.

- Crushing interval: $\Delta R_{fs} = R_s - R_f$, [kN/cm²] (3)

In case of the studied briquettes (cylindrical), past relations becomes:

$$R_f = \frac{4 \cdot F_f}{\pi \cdot d^2}, \text{ [kN/cm}^2\text{]} \quad (4)$$

$$R_s = \frac{4 \cdot F_s}{\pi \cdot d^2}, \text{ [kN/cm}^2\text{]} \quad (5)$$

A number of correlations carried out for experimental recipes are presented in figure 4, 5 and 6; so we represented the variation of resistance to cracking, breaking and crushing interval according to the proportion of steel plant dust, dust (sludge) from agglomeration - blast furnace and tunder [6].

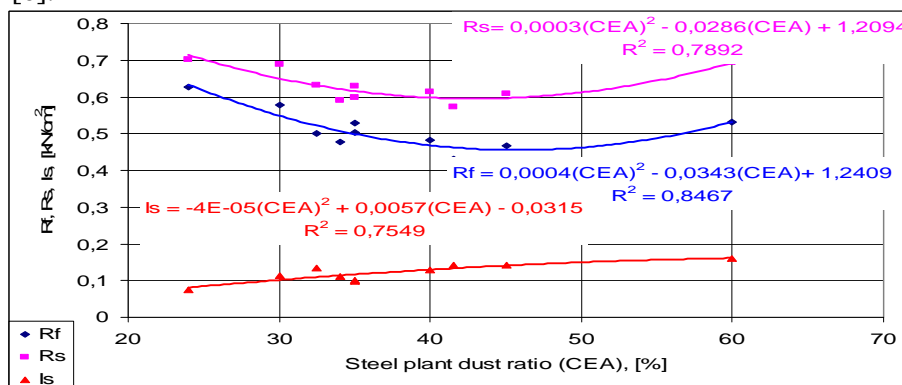


Figure 4. R_f , R_s , I_s according to the proportion of steel plant dust

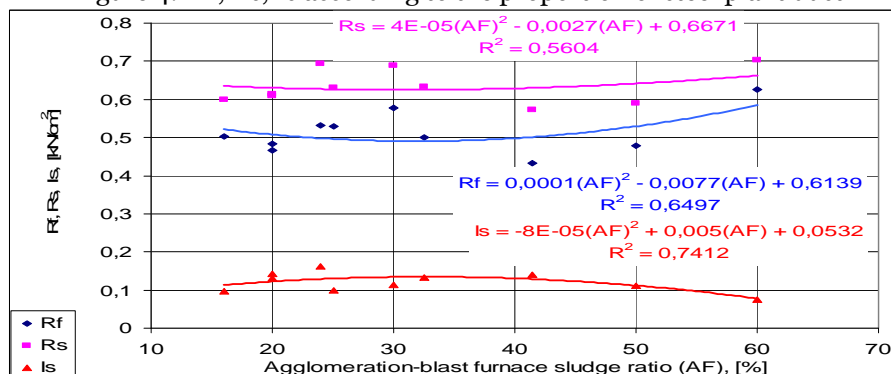


Figure 5. R_f , R_s , I_s according to the proportion of agglomeration-blast furnace sludge

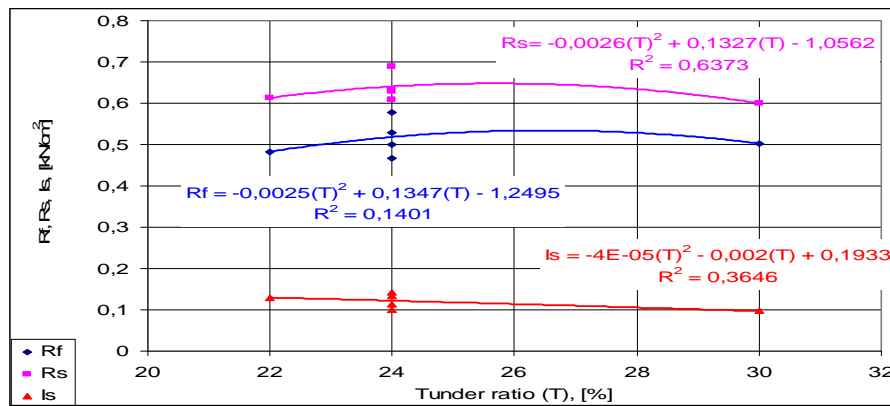


Figure 6. R_f , R_s , I_s according to the proportion of tunder

4. CONCLUSIONS

From analysis of data results in laboratory experiments were obtained the following conclusions:

- ❖ best limits of variation of ferrous waste proportions: 50-60% of steel plant dust, agglomeration-blast furnace sludge from 20-30% and 22-24% tunder;
- ❖ the appropriate behavior was a recipe No. 9, composed of agglomeration-blast furnace sludge, steel plant dust, tunder, bentonite, lime, graphite powder;
- ❖ for this recipe, bulk density was 0.7899 kg/dm³, the degree of reduction of 91.92%. As a result of good mixing of the burden of briquetting and fine grains of agglomeration-blast furnace sludge and graphite respectively, to obtain a contact surface Fe₂O₃ - reducing (C) high, so a large reduction front. In addition, develops CO reduction reaction.

After laboratory testing can be concluded that CARBOFER product under the form of briquettes can be used as a slag foaming agent, especially at lower capacity furnaces or aggregates that not using gaseous oxygen.

ACKNOWLEDGMENT

The researches do the object of Research Project no.31-098/2007, with title Prevention and fighting pollution in the steelmaking, energetic and mining industrial areas through the recycling of small-size and powdery wastes, financed by National Center of Program Management, project managed by Prof.dr.ing. Teodor Heput.

REFERENCES

- [1.] Nicolae, M., ș.a., Dezvoltare durabilă în siderurgie prin valorificarea materialelor secundare, Ed. Printech, București, 2004.
- [2.] Constantin, N., Procedee neconvenționale de obținere a materialelor feroase, Editura Printech București, 2002.
- [3.] Dobrovici, D., Hățărascu, O., Șoit-Vizante I., Intensificarea proceselor din furnal, Ed. Tehnică, București, 1983
- [4.] Ilie, A., Cercetări privind valorificarea superioară a materialelor pulverulente din siderurgie, Teză de doctorat, Conducător științific: Prof.dr.ing. Dragomir I., București, 1999.
- [5.] Borza, I., Popoiu, Ghe., Coican A., Tehnologia elaborării fontei, Litografia Timișoara, 1983.
- [6.] Heput, T., ș.a., Prevenirea și combaterea poluării în zonele industriale siderurgice, energetice și miniere prin reciclarea deșeurilor mărunte și pulverulente, Contract de cercetare nr.31-098/2007, beneficiar: CNMP, parteneri: CEMS București, SC CCPPR SA Alba Iulia.
- [7.] Socalici, A., Heput, T., Ardelean E., Ardelean M., Researches regarding the obtaining of active slag by using reactive admixtures produced from ferrous and basic scrap, The 6th WSEAS International Conference on ENERGY, ENVIRONMENT, ECOSYSTEMS and SUSTAINABLE DEVELOPMENT (EEESD'10), 21-23 octombrie 2010, Timisoara, Romania.





¹Beata HRICOVÁ, ²Henrieta NAKATOVÁ

POSSIBILITIES OF APPLICATIONS OF TOOLS FOR ECODESIGN IN VARIOUS STAGES OF DESIGN PROCESS

¹⁻²TECHNICAL UNIVERSITY IN KOŠICE, FACULTY OF MECHANICAL ENGINEERING,
DEPARTMENT OF ENVIRONMENTAL STUDIES AND INFORMATION ENGINEERING, KOŠICE, SLOVAKIA

ABSTRACT:

Organizations that develop new products need to consider many factors related to the environmental impact of their products, including government regulations, consumer preferences, and corporate environmental objectives. Although this requires more effort than treating emissions and hazardous waste, it not only protects the environment but also reduces life-cycle costs by decreasing energy use, reducing raw material requirements, and avoiding pollution control. Ecodesign tools and strategies have therefore become an important set of activities for product development organizations.

KEYWORDS:

Ecodesign, non-software, tools

1. INTRODUCTION

The current situation may seem at first sight very difficult to comprehend, since the eco-design tools are a large number. Such a situation arose because the development and application of software and non-software tools was done spontaneously and uncoordinated. Any company, enterprise or other institution that has developed tools for their specific conditions. Remarkably, however, that the basic philosophy and methodological basis of these instruments tend to be not very different, since they were subject to the same goal - to improve their level of eco-products in the crucial stages and throughout their life cycle [4].

2. APPLICATION OF SOFTWARE TOOLS OF ECODESIGN

Based on the facts, the usual intermediate targets developers of software tools may be different, which earned their distinction. This is as follows:

- ❖ analysis of existing products and processes and use of recorded information as feedback to improve the environmental performance of the product - **LCA / LCI tools**
- ❖ analysis of existing products and processes and use of information found to improve certain aspects of the product - **DFX tools**
- ❖ comparison of certain materials and processes in order to detect different levels of their impact on the environment - **PP and WP tools**, meaning to prevent pollutants (PP) and waste (WP)
- ❖ application of improvement methodology throughout the design process to improve the entire design process - **I - tools**, while here include tools like EIME and EcoDesign Tool.

The designations of these instruments means:

- LCA** - Life Cycle Assessment,
- LCI** - Life Cycle Inventory,
- DFX** - Design For X, "X" means that area, department, etc.,
- PP** - Pollution Prevention,
- WP** - Waste Prevention,
- I** - Improvement,
- EIME** - Engineering Information Management Executive.

This approach (goals difference) leads to the differentiation of basic eco-design software tools. It should be noted that the amount of applied data and calculation procedures, the use of these tools required is considerable work with a high proportion of routine activities. For these reasons, the rational use of those tools and methodologies they developed in the form of software products. [2] Answers to questions - where, how, when and in which stages of the design process will be advantageous to deploy these tools indicated in table 1.

Table 1 Application of eco-design software tools in various stages of the design process

Stage	Marketing	Schedule of product	Conceptual design	Design group	Detail design	Production
Tools						
LCA/LCI		Past results				
DFX						
PP / WP			Targets	Targets	Targets	Targets
I - TOOLS						

Legends: - **Field of application**

3. APPLICATIONS OF NON-SOFTWARE TOOLS OF ECODSIGN

A feature of the ecodesign tools non-software nature is that their application is possible and often without a rational means of computing. On the other hand, it should be emphasized that these tools and their combinations are usually based software tools based on design requirements. This was more - less forced practice and legislative measures States regarding the protection of environment and promotion of sustainable development at local, regional and global level. It is in the interests of manufacturers that their products throughout their life cycle in the least impair the environment and are compatible with this. Not every company, and also for economic or other reasons (eg, specific peculiarities of manufactured products) can be deployed in the process of designing an environmentally-oriented software tools. In such cases it is preferred and must use the non-software tools of ecodesign. [2,3]

Answers to questions - where, how, when and in which stages of the design process will be advantageous to deploy these instruments provides us with table 2.

Table 2 Application of eco-design non-software tools in various stages of the design process

Stage	Marketing	Schedule of product	Conceptual design	Design group	Detail design	Production
Nástroj						
EDM metod						
EI- 99 metod						
Ecodesign PILOT						
Metod of DfE matrix						
Metod of MET matrix						
Metod of comparator analysis						

Legends: - **Field of application**

4. CONCLUSION

Defining prevention as the primary goal in attempting to avoid the waste and toxic substances is the primary task in taking up so. net generation (clean production). As a next step, which should be pursued to minimize environmental impact? Those efforts should be applied to the entire environmental life cycle of a product, from raw material extraction to final disposal (clean product). The intention is to optimize the socio-economic system of the product and its use in accordance with the criteria of sustainable development in the future. This meets all its meaning and concept of ecodesign principles, which it brings, which is in accordance with progressive prosperity, meaning a reduction in "consumption" of the environment. [1]

The process begins here ecodesign product modeling system, taking into account specific conditions in the company. It draws on environmental parameters and information that are

specific to individual phases of the life cycle of a product as the newly designed products, as well as existing, to be on improving their environmental analysis. These are based on progressive analysis tools and methods, some of which are more or less considered in the EU as a standard.

Ecodesign brings a new dimension to the design and development of new engineering products and processes to improve existing products. The challenge is to provide the most relevant information as soon as possible to continue with the development of this knowledge. Providing external and internal incentives for environmentally responsible design - ecodesign should be part of defining the product and its creative cycle.

Acknowledgement

This paper was supported by projects APVV-0176-071/0453/08 and KEGA 3/7422/09.

REFERENCES

- [1] MIHÓK, J., LIBERKOVÁ, L.: Vyhodnocovanie efektívnosti znižovania miery zaťažnosti ŽP. In: Moderné prístupy k manažmentu podniku, Bratislava, STU, 2005, s. 360-363, ISBN80-227-2284-7
- [2] MURÁNSKY, J., BADIDA, M.: Ekodizajn v strojárstve – základy metodiky. Vydavateľstvo Michala Vaška, TU, Sjf, Košice, 2005, ISBN 80-8073-119-5
- [3] MURÁNSKY, J.: Environmentally Oriented PLM in Mechanical Engineering. In: Transactions of the Universities of Košice, 3 – 4 / 2004, pp.33 – 37
- [4] MYER,KUTZ: Environmentally conscious mechanical design. USA, 2007, ISBN-13 978-0-471-72636-4







¹Marek MORAVEC, ²Ervin LUMNITZER, ³Katarína LUKÁČOVÁ

APPLICATION OF ACOUSTIC CAMERA FOR MACHINE NOISE VISUALISATION AND DIAGNOSTIC

¹⁻³. TECHNICAL UNIVERSITY IN KOŠICE, FACULTY OF MECHANICAL ENGINEERING,
DEPARTMENT OF ENVIRONMENTAL STUDIES AND INFORMATION ENGINEERING, KOŠICE, SLOVAKIA

ABSTRACT:

The Acoustic Camera was the first commercially viable system using beam forming to visually localize acoustic emissions. The tool is now used in a variety of industries and has a growing customer base worldwide. The advantage of the Acoustic Camera: it is a light-weight, modular and therefore flexible system which is rapidly set up and ready to use. After a few minutes only, you get the first acoustic images on your computer screen. The software allows a clear, exact and fast analysis of noise sources. The benefits of the Acoustic Camera are straightforward: Noise sources are visualized, quality problems are detected and development times are reduced.

KEYWORDS:

Acoustic Camera, Measurement, Noise

1. INTRODUCTION

A digital camera is taking an image of the noise emitting object. At the same time an exactly computed array of microphones acquires and records the sound waves emitted by the object. Special developed software calculates a sound map and combines the acoustical and the optical images of the sound source. The Acoustic Camera can extend the time and frequency selectivity and add a location-selective component. With this method the sound signal is shown and also a sequence of acoustic images can be acquired – acoustic films are generated. Nevertheless the Acoustic Camera comprises traditional analysis methods as well, like A-weighting, one-third octave band and narrow band analysis.

With the Acoustic Camera it can be precisely analyzed when, where and which part is occurring the sound emission. The so far used analyses do have an important disadvantage as the location of the emission is limited or not possible. If the sound from several spots of an appliance is to be acquired simultaneously, individual microphones are required for each reading point, and they must be placed very close to the object – a time consuming and costly method.

The whole measurement and subsequent analyses are characterized by:

- ❖ high accuracy,
- ❖ high speed,
- ❖ dynamic operational mode,
- ❖ high effectiveness,
- ❖ transparent result processing (colored acoustic maps, movies, records).

2. APPLICATION OF ACOUSTIC CAMERA

The fields of application are as various as the world of sound and range from measurements in the open field, acoustic labs to the use in automation engineering.

The benefits of the Acoustic Camera are straightforward: Noise sources are visualized, quality problems are detected and development times are reduced.

Application of acoustic camera:

- ❖ localization and identification of noise sources,
- ❖ quantitative and qualitative analyze of noise sources,
- ❖ diagnostic and control measurements of machine and equipment,
- ❖ noise records,
- ❖ acoustic video and picture records,
- ❖ noise reduction.

The acoustic camera comprises traditional analysis methods as well, like A-weighting, one-third octave band analysis and narrow band analysis, filters, and many more. Based on these methods far more detailed research becomes possible. In a spectrogram, for example, sounds can be highlighted in the time and frequency ranges. The acoustic camera then shows the exact origin of this sound. The approach can also be made from the other end: After selection of a spot on the measured object, the sound originating from that spot can be reconstructed, visualized and broken

down into its spectral components. It is also possible to replay the sound via speakers - any time after the measurement is completed.

Acoustic pictures and videos acquired by the acoustic camera is possible also use for quality control and diagnostic different machines and equipment which are producing noise during their activity.

Next acoustic pictures and diagrams presents results of measurement air cooling equipment. First acoustic picture present overall noise emissions of whole equipment.

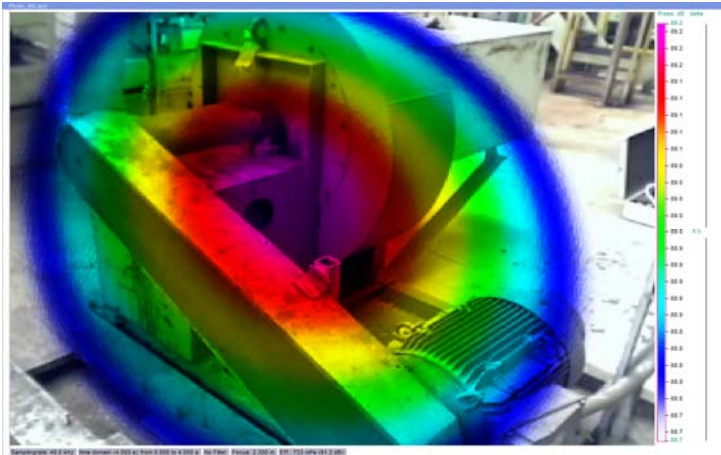


Figure 1 Overall noise emissions

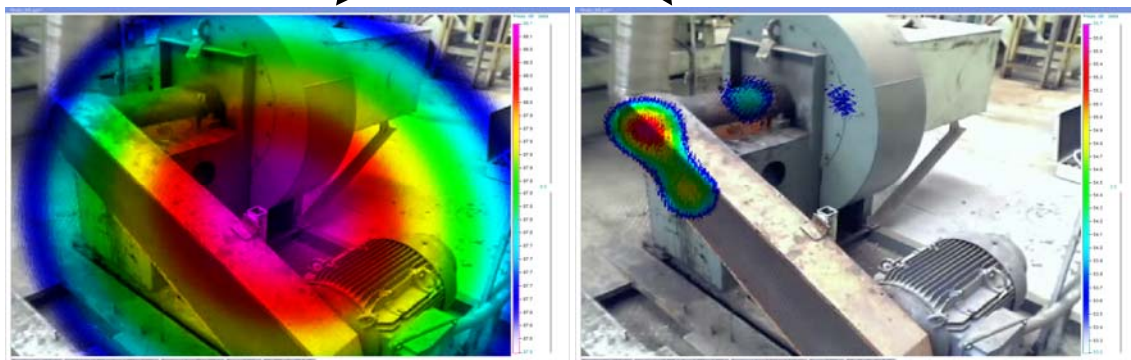
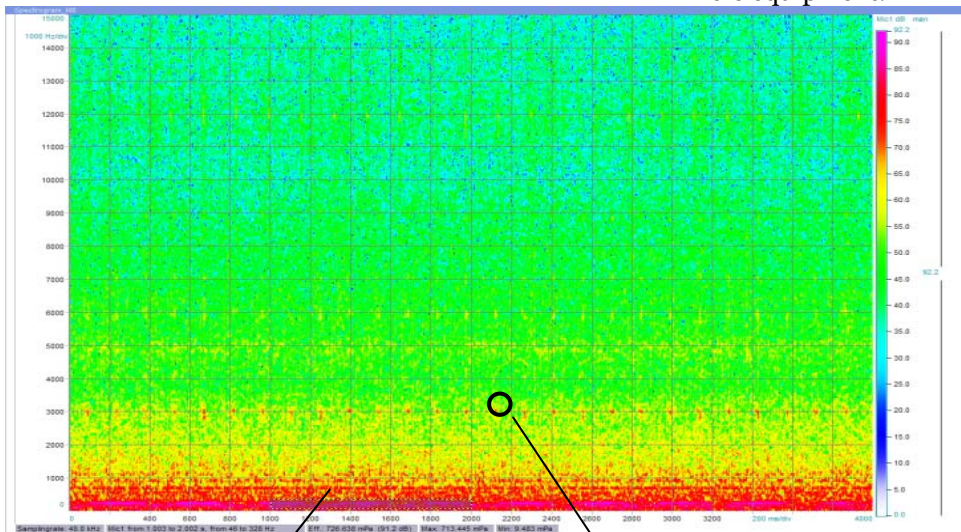


Figure 2 Spectrogram and acoustic pictures

Next picture presents noise spectrogram for this equipment. From this spectrogram was created two different acoustic pictures for two different frequency band. First acoustic picture was created for frequency band 200 – 300 Hz. This frequency band is the most critical and the share of overall noise emissions. Also was created second acoustic for frequency about 3000 Hz where is significant cyclic repeat noise. Creation of acoustic picture clearly show noise source at the field 3000 Hz. This noise was not hearable due the reason of lower noise intensity and was covered by the noise of other parts. Next maintenance discovers wrong seating of driving shaft.

3. CONCLUSION

By the use of Acoustic Camera in field measurements it is possible to localize different sources, even with other dominating sources present. It is possible to cover a large number of measurements per day if one makes proper preparations. The measurements results from the Acoustic Camera shows good correlation with sound level meter measurements, after applying correction. By the use of the various new evaluation possibilities such as Acoustic Photo, Acoustic Movie and Spectral Frames it is quite possible to localize noise sources, also when these do not really dominate the overall levels.

Acknowledgement

This paper was supported by the project VEGA 1/0453/08, KEGA 3/7426/09 and APVV-0176-07.

REFERENCES

- [1] DÖBLER, D., Time-Domain beamforming using zero-padding, Berlin Beamforming Conference (BeBeC), 2008.
- [2] JAECKEL, O. – SCHRÖDER, R.: Beamforming - Zeitbereich versus Frequenzbereich, Gesellschaft zur Förderung angewandter Informatik e.V. (GFaI e.V.), Berlin.
- [3] LIPTAI, P. a kol.: Dynamická vizualizácia emisií hluku pomocou akustickej kamery. In: Environmentálne inžinierstvo a manažérstvo, Zborník príspevkov, Košice 2007, s. 269-276, ISBN 978-80-8073-894-5.
- [4] LUMNITZER, E. a kol.: Vizualizácia hluku prostredníctvom akustickej kamery a jej aplikácia pri riešení problematiky priemyselného hluku. In:9. Banskoštiavnické dni 2007, Zborník prednášok, TU Zvolen 2007, s. 55-59, ISBN 978-80-228-1786-8.
- [5] MORAVEC, M. - LIPTAI, P.: Aplikácia akustickej kamery pri riešení problematiky priemyselného hluku. In: Novus scientia 2007, 10. celoštátna konferencia doktorandov strojníckych fakúlt technických univerzít a vysokých škôl s medzinárodnou účasťou, Košice, SJF TU, 2007, s. 401-405, ISBN 978-80-8073-922-5.







¹Sorina Gabriela ȘERBAN, ²Maria Laura STRUGARIU

RESEARCH ON WATER QUALITY IN THE CITY HATEG

¹⁻² UNIVERSITY POLITEHNICA OF TIMISOARA, FACULTY OF ENGINEERING FROM HUNEDOARA, ROMANIA

ABSTRACT:

Water pollution is a growing challenge in many countries. The choice of modern methods of wastewater treatment, to discharge or recirculation in their natural receptors, leading to the arrest and the formation of large quantities of sludge which includes both raw water polluting materials, and those formed in the process of treatment. The study presents aspects of the qualitative and quantitative levels of water pollution in the area Hațeg.

The study presents qualitative aspects and quantitative assessment of water pollution levels in the area Hațeg. Hațeg City currently has a network of sewerage system divider network in which 49% are domestic, 10% of the storm and 41% in areas without sewer systems. Wastewater volume represents 80% of drinking water distributed by the centralized water population of the city. Mode operation and efficiency of the treatment plant was evaluated by Cole. Samples of ground water, waste and surface water were also evaluated for chemical content of organic and inorganic substances. High levels were observed as indicators of sewage out of the station (pH_{entry} = 6.89, pH_{output} = 6.76; suspension entry = 22.7, suspensions output = 48.6) indicating adequate treatment plant malfunction.

The influences of environmental factors studied were characterized by the location of the pollution index and indices of quality IP-Ic. In a study of IP has values between 0 and 20.0 - which compares with a level of reliability expressed by grades 1 to 10 depending on the value of IP and Ic-quality indices. In a study of IP have values between 0 and 20.0 - which compares with a level of reliability expressed in notes 1 to 10 depending on the value of IP and to reveal the degree of environmental pollution factor analysis and its effects on the environment. Ic values are between -1 and 1 were also compared with the scale of creditworthiness.

Stresses the lack of efficiency results in appropriate handling WWTP discharged water from the city and the need Hațeg reconstruction and rehabilitation of existing stations.

KEYWORDS:

water pollution treatment processes, wastewater treatment Hateg IP pollution index, quality index Ic.

1. INTRODUCTION

Water is an essential element for life and natural processes. Our existence and our economic activities are entirely dependent on this precious resource. It is equally important climatic factor that supports the development of ecosystems and key components of substance and energy exchange in the hydrological cycle. Moreover, globally, water is a scarce resource, which requires addressing it, so to ensure water resources for future generations. The main strategic objective of Romania in the field of water is linked to European integration, which requires the harmonization and implementation of the *acquis communautaire* in the field of water quality protection. Romania's water resources consist in surface waters - rivers, lakes, the Danube River ($\approx 90\%$) - and groundwater ($\approx 10\%$).

For years, the entire world population puts more often the same questions. It is mankind into a state of slow death? The issue of environmental degradation? Natural resources are so indispensable to life? Gradual degradation of the environment in the whole world is mainly due to human action, that the need to improve their living conditions, cause damage to the landscape. Through this work we tried to reveal the problem of the environment, seen from the perspective of pollution and water quality.

Situated at the confluence of the River Great Strei Hațeg depression (310-350 m altitude) is the meeting of three roads linking the main regions of south-western Transylvania. The administrative area of the city covers an area of 61.6 square kilometers and includes the towns Nalatvad, Silvașu Upper Lower Silvașu. The natural environment is hilly, mountainous, like a natural fortress defended by Orastie Mountains to the east, south of Parang, Poiana Rusca Retezat west and north, forming the very core of whether state and Romanian Dacia. There is also a very dense river network

2. THE STATE WATER QUALITY

Water quality status of water pollution is altering the physical, chemical and biological characteristics of water, produced directly or indirectly, natural or man. Polluted water becomes unfit for normal use. Pollution can take place:

- ❖ continuing (permanent), where sewage from a city, or from industry and Fire residues discharged into the waters,
- ❖ batch, at regular intervals or irregular time - temporary (eg temporary colonies)
- ❖ accidentally Fail

Water pollution sources are classified according to several criteria, given their diversity:

- ❖ After source: household activities, industry, agriculture and transport.
- ❖ After the range of pollutants - local sources (sewage pipes, ramps download) - diffuse, when pollutants are spread over a large area. It is sometimes difficult to locate the source or sources of Evolution.
- ❖ After their position: - Fixed sources - mobile (cars, homes and facilities, moving, etc.).

For example, industry chemicals discharged into natural waters, organic and inorganic, vegetable and animal waste, solvents, hydrocarbons, heat, etc. Materials can be solid or liquid, miscible or immiscible with water, light or heavy volatile, more or less toxic. By their nature are pollutants: organic, inorganic, biological, radioactive, thermal aggregation by Status different particulates (insoluble in water) water-soluble pollutants, dispersion colloidal.

Once during natural degradation in water are distinguished: easily biodegradable pollutants, poorly biodegradable (the natural degradation takes less than 30 days), non-biodegradable (degradation in 30 - 60 days), and refractory (with degradation and over two years).

Water self-purification processes are all physical, chemical and biological weapons that discard pollutants contained water without human intervention. Wastewater means all operations carried out to reduce levels of pollutants, so that the remaining concentrations do not cause pollution of receiving waters.

3. WWTP OVERVIEW

Presentation perimeter interested WWTP is located in the east of the city Hațeg at approx. 700-800 downstream of the city on the right bank of the Yellow River, its major riverbed in the distance. 2.5 km from the confluence with the Yellow River Valley High. Within this site perimeter treatment plant is in its Depression-Drastic Hațeg, depression Hațeg compartment in the central part of it.

City wastewater treatment plant was carried Hațeg in two stages:

Stage I - in 1962 started the construction of wastewater treatment plant. The project requires only a mechanical stage technological scheme, with a treatment capacity of 1631 cubic meters per day (19 l / s). The evolution of the city, the emergence of industry and population increase led to the need for an extension of the station.

Phase II - was launched in 1976 an investment to increase capacity from 55 l / s (4741 m³ / day) provided with mechanical and biological. Work on new investment began in 1980 and were discontinued after 1990 due to lack of funds.

Currently, sewage is passed only through the old station, which is obsolete in terms of capacity and efficiency of treatment. In general, operation is "at random" because the station does not have a laboratory to manage daily station output and, accordingly, to have the operation (emptying sludge from settling tanks, fermentation processes, floating sludge, etc.).

4. QUALITATIVE AND QUANTITATIVE ASSESSMENT OF WATER POLLUTION LEVELS IN THE AREA HAȚEG

Hațeg City currently has a network of sewerage system division (separation)

- ❖ about 11,700 m of sewage collectors
- ❖ about 2200 m of rainwater collectors.

For wastewater with high organic load, obtained from the slaughterhouse Hațeg (currently in idle state there are two drains - one for waste water by faces which are run by the city's wastewater treatment plant - one for conventional clean water in Yellow River discharge directly.

In the residential area in the eastern part of the city, sewage is unitary, rainwater, together with domestic wastewater treatment plant being conducted.

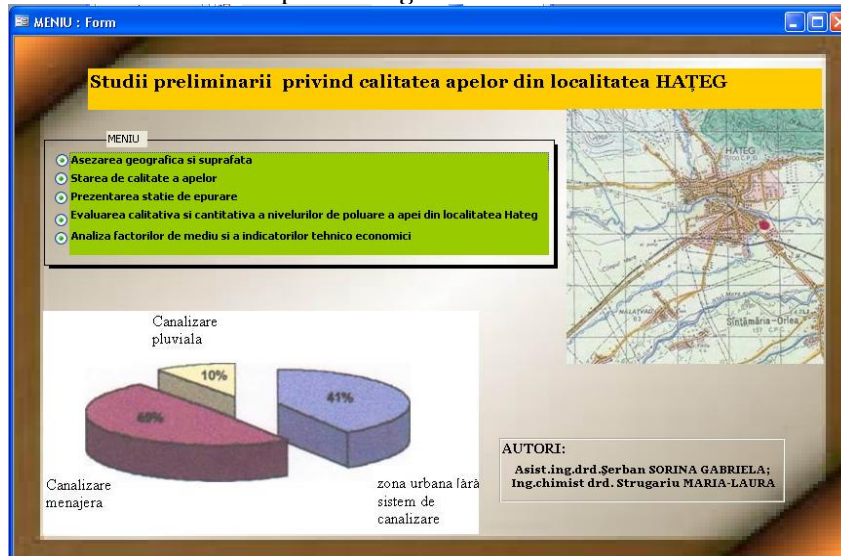


Fig.1 Main menu

Monthly average flow is necessary city:

$Q_{u \max} = 76.000 \text{ m}^3/\text{month}$ of which - 51.000 m^3/month population
 - 25.000 m^3/month operators

Currently, sewage is passed only through the old station which is exceeded in terms of treatment capacity and efficiency.

The existing facility is partially operational, is undergoing a process wastewater treatment mechanical treatment technology does not comply with the characteristic (transition times are much smaller than projected).

In order to determine how and efficiency of operation of the station were collected wastewater samples from the following points: - city station entrance, beer station entrance, exit station emissary. Data from the tests performed are presented in Table 1, and the situation of treatment effectiveness and efficiency station which currently makes only a mechanical treatment, and additional load of the Yellow River after discharge clean effluent is presented in Table 2.

Indicator	UM	Intrare oras	Intrare fabrica	Iesire statie emisar
NH_4	-	6,89	6,77	6,76
suspensii	mg/l	22,7	20,2	48,6
reziduu filtr.	mg/l	278	269	310
CCO-Mn	mg/l	322,5	141,8	335,5
CB05	mg/l	178,6	65	195
NH4	mg/l	7,39	9,78	10,27
detergenti	mg/l	0,5074	0,3974	0,097
extractibile	mg/l	5,3	4,5	4,1
CCO-Cr	mg/l	-	-	3,94

Fig.2. Data collected

Indicator	Intrare ape	Iesire statie	Randament epurare	Pr Galbena amonte	Pr Galbena aval	Incarcare suplimentara
CCO Mn	800	2,00448	640	1,60358	17,6	144%
CB05	414	1,03732	347	869,44	8,93	186%
Azotați	-	-	-	-	2,99	26%
Azotii	-	-	-	-	0,08	33%
P04	452	11,33	2,36	5,91	1,34	
P total	148	3,71	0,769	1,93	-	
NH4	284	71,16	8,95	22,43	6,94	290%
Suspensii	243	608,86	162	405,91	25	79%
Sulfuri	914	22,9	10,02	25,11	6,8	530%

Fig.3. Situation of wastewater treatment plant performance and efficiency

5. ANALYSIS OF ENVIRONMENTAL FACTORS AND ECONOMIC

I Indicators for evaluation of the limits permitted in pollution of the environment in the location studied, Ip pollution index was used that resulted from the ratio of the maximum determined by the physico - chemical on specific pollutants and the maximum permissible concentration. Introducing the first two blocks measured concentration and maximum concentration, we get the third box index

Sampling was done from a point located near considered significant discharges of wastewater (from the grease trap) on the soil unprotected by the downstream flow direction to the phreatic water catchment area of the course. Sample groundwater, in theory, should correspond to specific water quality conditions (STAS 1342/1991). The quality of groundwater was determined taking into account the two regulatory laws MAPPM: Order 184/1997. The test results are presented in Table 3.

Fig.4. Calculation of pollution index

Indicatori	Concentratii masurate	CMA STAS 1342/91
Concentratia ionilor de hidrogen pH	6,7	6,5 - 7,4
Amoniac NH4	7,3	0,0
Azotiti NO2-	0,9	0,0
Azotati NO3-	2,3	45,0
Cloruri Cl-	380,0	250
Fenoli	0,02	0,001
Fosfati PO4-3	1,5	0,1
CCO - Cr	32,5	3,0
Sulfati SO4-2	248,0	200
Sulf S	10,2	0,0
Zinc Zn	97,0	5,0
Plumb Pb	32,5	0,05
Cupru Cu	5,7	0,05
Mangan Mn	29,0	0,05
Magneziu Mg	26,2	50

Fig.5. The test results

Caracteristici	Ip	Nb
Amoniac	-	1
Azotiti	-	1
Azotati	0,05	10
Cloruri	1,52	6
Fenoli	20	2
Fosfati	15	2
CCO-Cr	10,8	3
Sulfati	1,24	6
Sulf	-	1
Zinc	19,4	2
Plumb	650	1
Cupru	114	1
Mangan	580	1
Magneziu	0,52	7

Fig.6. Pollution index

Compared to the results determined physico-chemically, we have interpreted the pollution index and determined the water sample (Table 4). In order to identify the efficiency of municipal wastewater treatment plant and to quantify the effects of water discharges in the area of the Yellow River, and have collected two water samples:

- ❖ A1 - from raw sewage entering the treatment plant;
- ❖ A2 - out of treated water treatment plant

The data collected are presented in tabelul5.

Compared to the results determined physico-chemically, we interpreted and determined discharged effluent pollution index, the limits reported NTPA 001 (tabelul6), and the situation of treatment effectiveness and efficiency station is currently only a sewage mechanical load and further purified effluent after discharge of the Yellow River, are shown in Table 7.

Indicatori	Concentratii masurate A1 influent	Concentratii masurate A2 efluent	NTPA ptr evacuare in Galbena
pH	7,1	7,0	6,5-8,5
CB05	414	347	20,0
CCO - Mn	800	640	-
Fosfor total	1,48	0,76	1,0
Suspensii	243	162	35,0
Amoniac - NH4	28,4	8,95	2,0
Sulfuri	9,14	10,02	0,5
Fosfati - PO4*	4,52	2,36	-

Fig.7.Date taken

Caracteristici	Ip	Nb
CB05	17,35	2
Fosfor total	0,76	7
Suspensii	4,6	4
Amoniac - NH4	4,47	4
Sulfuri	20,04	1

Fig.8. Pollution index

Indicator	Randament epurare	Incarcare suplimentara
CCO Mn	0,20	144%
CBO5	0,16	186%
Azotati	-	26%
Azotiti	-	33%
PO4	0,48	-
P total	0,48	-
NH4	0,68	290%
Suspensii	0,33	79%
Sulfuri	0,10	530%

Fig.9. Statement of effectiveness and efficiency

Two samples were taken from surface water to establish categories of Yellow River water quality before and after evacuation:

- ❖ A3 - upstream water treatment plant discharge,
- ❖ A4 - treatment with the downstream discharge station. 100m (to allow dilution of effluent).

The test results were compared with the Order 1146/27.03.2003 on surface water quality classification, which according to article 2 Order. STAS-4706 repeated the "Surface - categories and quality technical.

Data are presented in tabelul 8.

Indicator	ClsI	ClsII	ClsIII	ClsIV	ClsV	Valori masurate in amonte	Valori masurate in aval
pH	6,5-8,5	6,5-8,5	6,5-8,5	6,5-8,5	6,5-8,5	6,8	7,0
CCO Mn	5	10	20	50	>50	7,2	17,6
CBO5	3	5	10	25	>25	3,12	8,93
Azotati	1	3	6	15	>15	2,37	2,99
Azotiti	0,01	0,06	0,12	0,3	>0,3	0,06	0,08
Fosfati	0,05	0,1	0,2	0,5	>0,5	0,0	1,34
Amoniu	0,2	0,3	0,6	1,5	>1,5	1,78	6,94
Suspensii	-	-	-	-	-	14	25
Sulfuri	-	-	-	-	-	1,08	6,8

Fig.10.Rezultatele obtained

6. CONCLUSIONS

At present, sewage is passed only through the old station which is exceeded in terms of capacity and efficiency of treatment. The existing facility is partially operational, is undergoing a process wastewater treatment plant mechanic who does not comply with treatment technology feature (time crossings are much smaller than projected).

In order to determine how and efficiency of operation of the station were collected wastewater samples from the following points: the city station entrance, beer station entrance, exit station emissary. It is noted high levels of quality indicators out of treatment plant, resulting in the fact that the station is not working properly.

For businesses that discharge wastewater treatment plant in the city, it is proposed the implementation of local stations pre-treatment before discharge into the sewer system. Referring to the garbage coming technology and effluent treatment plant exclusively, we can say that they are insignificant from raw municipal wastewater flow entering the station.

Following this report - resulting values between 0 and 20.0 – IP value to be compared with a level of reliability expressed by grades 1 to 10 depending on the value of IP and to reveal the degree of pollution factor environmental analysis and its effects on the environment.

If the effluent discharged into the yellow surface is observed in almost all indicators exceeded watch (except the total phosphorus and pH). Deviations are explained considering the fact that currently the treatment of municipal wastewater is confined to a mechanical treatment stage, nor properly exploited this.

Note that the average creditworthiness water sample has a value of 3 which corresponds to the average lifetime of lethal effects of exposure, the environment is degraded level, however I have noticed, the depreciation of the Yellow River water quality from discharge of & quot; treated & quot; in treatment plant, the area is classified in Class III the quality on most indicators. limit values in that class are 2-3 times higher than those of targets mean.

To achieve certain calculations we used an application made by Microsoft Access. The results of tests carried out lead to inefficiency & quot; Station municipal wastewater treatment & quot; of the city Hașeg, reconstruction and rehabilitation of existing stations is imperative.

BIBLIOGRAPHY

- [1.] Vișan S.,Angelescu A.,Alpopi C., *"Mediul înconjurător-poluare și protecție"*, Ed.Economică, București, 2000;
- [2.] Angelescu A., Ponoran I., Ciobotaru V., *"Mediul ambiant și dezvoltarea durabilă"*, Ed. A.S.E., București, 1999;
- [3.] Rojanschi V., Bran F., Diaconu Gh., *"Protecția și ingineria mediului"*, Ed.Economică, București, 1997;
- [4.] Negulescu M. ș.a., *"Epurarea apelor uzate industriale"*, vol.2, Ed.Tehnică, București, 1989;
- [5.] Masotti L., *"Depurazione delle acque"*, Ed.Calderini, Bologne, 1993



THE POTENTIAL OF WIND ENERGY AND ITS USAGE IN THE CONDITIONS OF THE SLOVAK REPUBLIC

¹⁻³TECHNICAL UNIVERSITY IN KOŠICE, FACULTY OF MECHANICAL ENGINEERING,
DEPARTMENT OF ENVIRONMENTAL STUDIES AND INFORMATION ENGINEERING, KOŠICE, SLOVAKIA

ABSTRACT:

The main aim of this paper is to bring near wind energy as one of the mostly used renewable energy source.

The article's purpose is to familiarize the reader with the concept of the wind energy usage, its effects on the environment, current status of use and plans how to increase the use of wind energy in the Slovak Republic.

KEYWORDS:

wind energy, wind energy plants, renewable energy sources, environment

1. INTRODUCTION

The energy that we use today in the form of heat, electricity and fuels for motor vehicles, has its origins mostly in fossil fuels (coal, oil, natural gas). These fuels are below the surface, where it originated millions of years after the decomposition of prehistoric plants and animals. Although fossil fuels the action of natural forces (heat and pressure) ever created, its current consumption far outweighs their formation. The fact that they are not replenished nearly as fast as they are being consumed means that in the near future they run out. For this reason, fossil fuels are considered non-renewable energy sources. The main negative consequences of burning fossil fuels is serious damage to the environment and therefore it is today, when rising demand for electricity we must seek alternative sources of energy. Between a so-called renewable, "green", energy sources we include biomass, geothermal, solar, water and wind energy.

2. USAGE OF WIND ENERGY

The exploitation of wind force has been known for a couple of thousand years and it is being linked to the beginning of the human civilization when man decided to make use of this kind of energy.

Since wind energy is being counted into unexhaustible renewable energies without direct impact on the environment and represents a clean form of energy with no waste production, no air pollution and no negative effect on the human health, a tremendous development of wind energy plants, which is the fastest growing branch in energy producing, is being observed.

The currently mostly used forms of wind use are wind energy plants using turbines. They are converting kinetic energy of the air molecules to mechanical work of the turning rotors which, through a geared mechanism, drive electric generators that transform work energy into electricity.



Figure 1 Wind turbines [3]

An effective step in transforming wind energy into electricity is also building wind energy plants/parks where the main concept is to maximize the possibilities of the given location. Therefore, several turbines are built in the same location.

3. EFFECT ON THE ENVIRONMENT

Every form of energy production creates negative effects on the environment, however while using wind energy plants, the negative effects are minimal in comparison with other, traditional electric production. [1]



Figure 2 Wind farm [3]

Replacing the production of electricity from fossil fuels with wind chargers brings positive facts: [2]

1. Saving the fuel that is not renewable
2. Reducing the amount of CO₂ that would be produced while burning this fuel
3. Reduction of gas emission (SO_x, NO_x)
4. Reduction of dust outlet
5. Reduction of liquid and solid waste
6. Reduction of the waste heat leaking into the atmosphere or water systems

4. CURRENT STATUS OF WIND ENERGY UTILIZATION

Although the wind energy is one of the youngest technologies of energy production and does not have such background as other commercial sources of electricity production, with time its usage as a renewable source of energy grows more and more.

Despite the massive development in Europe in the field of wind energy began in the early 90's, many of those managed to establish world leadership in a relatively short time. Wind energy and its usage reached the highest growth from the entire spectrum of renewable energy sources in the EU (tab. 1). Together with solar energy, it is considered to the "second generation" technologies.

Table 1. The development of renewable energy sources in the EU [3]

Order	Energy	Year			
		1990	2000	2010	2020
1	Solar Energy	0.1	0.2	0.9	3.2
2	Wind Energy	0	0.1	0.4	2
3	Geothermal Energy	0.1	0.3	0.5	0.8
4	Modern Biomass	1.4	2.2	3.5	5.1
5	Small water generators	0.2	0.3	0.4	0.6
	Total	1.8	3.1	5.7	11.7

The reduction of electricity prices is a commonly observed trend in the wind energy field. This is tightly bound to the power increase of the new wind turbines. As a side effect, the competitiveness of the wind energy with commercial energy production is growing as well. At the same time it gets less dependent on the state grants reflected mainly in the buying prices of the renewable energies. It is to be expected that the prices of electricity will continue to drop, as well as the competitiveness of wind energy with current energy sources will continue to grow. The development of the equipment is also foreseeable.

5. THE POTENTIAL OF WIND ENERGY UTILIZATION IN SLOVAKIA

Slovakia as an inland country has its potential in utilizing wind energy rather limited as in comparison with the west European countries. It has been estimated to 600GWh/r which, in comparison with other renewable energy sources potential (biomass, water), is very low.

Despite relatively large occurrences of wind during the year, not every region is suitable for electing a wind charger. In our latitude and average altitude of 600m above sea level, the wind speed is averaging to 2-3m/s while the ideal wind speed would be 12m/s. In the mountain terrain that is characteristic for Slovakia, is the wind flow relatively inconsistent. As a result of terrain obstacles the wind intensity and direction is changing and inapt turbulences occur. Therefore multiple year long specific measurements with special analysis needs to take place to estimate the suitability of the locality for wind chargers.

Despite the good wind conditions with speeds over 5,5m/s are certain areas, like the National Parks (High Tatra National Park etc.), excluded from electing wind parks for environmental reasons.

6. BARRIERS IN THE UTILIZATION OF WIND ENERGY IN SLOVAKIA

Among the barriers that are complicating the utilization of wind energy in Slovakia are being counted:

1. lack of knowledge of the wind climate (wind intensity and its temporal and geographic variability)
2. a strong dependence on wind climate
3. lack of knowledge of the effects of a high proportion (approximately over 5%) in electricity production and fluctuations in transmission and distribution system
4. negative impact on power system stability
5. problems in perception, mainly related to changing visual environment
6. restrictions in protected areas
7. lack of awareness of health and environmental impacts of operational wind farms

Another important criterion is the economic return of wind power in the form of electricity generation. The cost of installing 1 kW wind power in Slovakia are from 1500 to 2000 Euros, the price paid for electricity generated from wind power is 94 Eur / MWh. From that follows that the period for the return of total investment is about 17 years.

7. WIND POWER PLANT IN SLOVAKIA

Even though we are not a country with ideal conditions for the use of wind energy, there are currently 9 wind turbines in operation in Slovakia in three operating wind parks located in (Fig.3).

These power plants annually produce about 6 GWh of electricity (as of 2004). Slovakia uses only about 1% of its full potential. The reason is the wide range of economic, legislative and environmental barriers, of which the introduction of fixed prices for electricity generation from renewable sources eliminate at least some. Highly actual issue, which divides the professional community impact assessment, is mainly impact of the construction of wind farms on the environment.



Figure 3 Wind farms in Slovakia [6]

8. VISION OF SR WIND ENERGY UTILIZATION LISTEN

Slovak Republic as a European Union member country is obliged under their obligations to contribute to increased share of renewables in the total resources, thereby reducing negative environmental impacts, the European Union's heavy dependence on imported fossil fuels and vulnerability to fluctuations in energy prices.

Setting targets for the years 2010 and 2015 gives a real opportunity for Slovakia to increase the current 4% share of renewables in total energy consumption to 12% share in 2020.

Basis for setting a binding target for Slovakia in 2020 will be elaborated in a forthcoming material, energy security strategy of the SR, which is an indication of the outlook to 2030.

According to ZVES (Association of wind energy in Slovakia), Slovakia has the potential to increase the current total installed capacity of 5 MW to approximately 600 MW over the next 5-7 years and the prospect to further enhance the technology up to 1000 MW. This objective can be considered as a realistic and feasible in the horizon of 2020.

9. CONCLUSION

If we are to get even closer to achieving the objectives of increased use of wind energy as a renewable energy source and thus avoid possible sanctions from the EU, it is essential to use all available and economically and environmentally sound electricity generation from renewable energy sources, which include the use of wind energy.

Acknowledgement

This paper was supported by projects APVV-0176-071/0453/08 and KEGA 3/7426/09.

REFERENCES

- [1.] RYBÁR, R., KUDELAS, D., FISCHER, G.: Alternatívne zdroje energie III, Edičné stredisko/AMS, 2004 Košice, ISBN 80-8073-144-6
- [2.] KRÁLIKOVÁ, R., BADIDA, M., HALÁSZ, J. :Technika ochrany životného prostredia, Elfa Košice, 2007, ISBN 978-80-8086-062-2
- [3.] Veterná energia [citované 10.10.2008] <http://www.inforse.org/europe/fae/OEZ/index.html>
- [4.] Veterná energia [citované 20.10.2008] <http://www.seps.sk/zp/save/uvod>
- [5.] Veterná energia [citované 10.10.2008] <http://www.inforse.org/europe/fae/OEZ/index.html>
- [6.] OZEPORT veterné turbíny [citované 23.10.2008] <http://www.ozeport.sk/zdroje/veterna.html>





NOISE AND ITS SOURCES FOR THE REDUCTION IN WORK ENVIRONMENT

¹⁻³ TECHNICAL UNIVERSITY IN KOŠICE, FACULTY OF MECHANICAL ENGINEERING,
DEPARTMENT OF ENVIRONMENTAL STUDIES AND INFORMATION ENGINEERING, KOŠICE, SLOVAKIA

ABSTRACT:

This post is dedicated to acoustic waves, which is part of the physical fields that surround the man, acting on the body, affecting his health, behavior, activity, efficiency and wellbeing. Frequency distribution of sound waves, infrasound and ultrasound affecting human biosphere. However, if the rate exceeded the intensity of the initiative, becoming the acoustic load producing a stress event with the following characteristics of nonspecific adaptive responses with normal speech.

KEYWORDS:

Working environment, noise, noise pressure level

1. INTRODUCTION

In terms of interactions between man and environment is characterized by physical factors, several common characteristics: increasing energy consumption (thermal, electromagnetic, acoustic); the man can act as a "field" (acoustic, electromagnetic); in some cases they cannot perceive the senses.

The severity of these factors stems from the fact that usually affects large population groups, and since their effects on health are not visible immediately, the public underestimates their importance. [1]

Physical working environment factors are ionizing radiation, ultraviolet radiation, visible light, infrared radiation, lasers and electric, magnetic and electromagnetic fields. Other physical factors are noise, vibration, and shock and heat-humidity microclimate. [2]

2. NOISE AS PHYSICAL FACTOR OF WORKING ENVIRONMENT

The main source of noise in the workplace are machinery and technological equipment, some of the activities carried out using hand tools and material handling, for example. When using pneumatic tools, noise occurs mostly in the range from 100 to 110 dB, the power tool is 90 to 100 dB, in forging about 130 dB. High noise levels can be observed even in woodworking machines, it's more than 90 dB. [4] A very important and frequent source of excessive noise is powered hand tools. There is serious risk of noise and operating machinery in metallurgy and heavy machinery where sources of noise are both great machines, but also technological processes. In such operations noise often exceeds 100 dB. [5]

As a result of adverse exposure to noise at work on health, many employees become manifest hearing loss. In the last decades of the 20th century the number of newly reported occupational diseases diagnosed with "Noise-induced hearing impairment" repeatedly exceeded 200 cases per year. The principal enforcement of new legislative measures to protect employees from noise for this number decreased significantly in the 47 cases a year. Noise at work determining the noisiest source. In measuring and assessing noise in the workplace is a distinction:

- Noise in the workplace, i.e. in the area where the workers during the work resides
- Noise in the area of work, i.e. in the area where the workers during the work moves

- Noise levels for the individual who expresses an individual's noise exposure during work time. [4]

In assessing the noise in the working environment of man is paramount to determine what sort of traffic goes, what types of machinery and equipment are at work used, as addressed issues of noise, in which technical condition are used machinery and equipment and the like. Measurement and objectivity to determine what the noise exposure a person is working in the service exposed. [5] The work environment is a way of measuring the noise determines the inspection of workplaces. Measurement of jobs is mainly carried out when employees are staying longer in jobs and the nature and noise are different for different jobs. If employees at work often change jobs and noise at different locations do not differ too, measured the noise in the workspace. Measurement of individual noise load is performed if the workers at work places and frequently changing noise levels at individual sites vary greatly. If the worker persists in the workplace throughout the work shift, characterized by data noise in the workplace also virtually noise load of the individual. The measured value of noise at work then, depending on the method of measurement gives the noise burden on staff or noise at work then, depending on the method of measurement gives the noise burden on staff or noise in the workplace.

Way to evaluate noise and maximum values defining the parameters for the noise in the workplace down the provisions on health protection against noise respectively. Technical standards specifically for the current audible sound, infrasound, ultrasound, high frequency sound and low-frequency sound. [4]

3. EFFECTS OF EXCESSIVE NOISE ON THE HUMAN BODY AND DISEASES

Noise can be adapted to subjective, but objectively his action on the human body cannot be avoided. Noise is mainly the effect of harassing, harmful and disruptive activities and welfare of man. These effects of noise depend on several acoustic and human factors, which are listed in Table 1. [3]

Table 1 Health and comfortinteractiv factors of human [3]

Acoustic factors	Non acoustic factors
<ul style="list-style-type: none"> ▪ type of noise and distance from source ▪ intensity, respectively. sound pressure level, ▪ the amount of frequency emitted noise ▪ tonal spectrum of sound components, ▪ frequency spectrum ▪ interval operation and conduct of exposure ▪ interruption frequency noise levels and the difference between the noise source and background noise ▪ vividness and distinctiveness noise and its unexpectedness. 	<ul style="list-style-type: none"> ▪ gender, age and health, ▪ subjective relationship to the noise source, ▪ time perception of noise operators (day, night, seasons) and the immediate disposition of man, ▪ need noise associated with human activities, ▪ social status, ▪ Experience with noise from the past ▪ economic dependence on the noise source, ▪ relaxation and sleep.

The crucial characteristics of noise in terms of its influence on human organism are intensity, frequency and time course. Sounds above 2000 Hz with a narrow frequency range are effective, short and irregular sounds that cause fright response and disruptive. Effects depend on the noise parameters in addition to a large extent on the individual susceptibility of humans, age, lifestyle, legacy disease, current health status, but also with regard to the sound and its source. [2]

The effect of noise level below which there is damage normal healthy ear of habitual noise exposure is known as the criterion of risk of hearing damage. It should be noted that hearing damage is **cumulative result of sound level and time of exposure** and any criterion must take into account the sound level and time of exposure. [3]

Health effects of noise: Noise is not active only on human hearing, but also affects the function of various organs. One-off **short-term** effect of over-intensity sound can cause **acoustic trauma**, which has been considered as an occupational accident. **Long-term** intense noise causes temporary threshold shift and later at noise levels higher than 85 dB, there is the constant increase and the **onset of hearing loss professional**.

Occupational exposure: Acute **acoustic trauma** resulting from rare may occur after heavy sound impulses such as. Shot blast.

The clinical picture of disease: **acoustic trauma** is manifested resound feelings, pressure and pain in the ear and ear subjective tinnitus. Symptoms may take several minutes to days and then the condition usually normalizes. Tinnitus (ringing in the ears) may be permanent. **Hearing loss from noise** there is repeated exposure to excessive noise on the auditory analyzer. It is a symmetrical two-sided type of cochlear sensory disorder.

Diagnosis of the disease: Diagnosis of occupational hearing loss from noise is based on:

- work anamnesis and establish long-term exposure to excessive noise
- typical clinical picture of disease, confirmed by repeated otorhinolaryngological and repeated audiometric testing. In complicated cases, using the method of objective audiometry.

Rate and Importance of damage is rated from liminal tonal audiogram would Upshot of percentage deficit by Fowler. This calculation performed with, that first must calculate hearing loss

Table 2 Hearing loss calculation
in per cent by Fowler [6]

Hearing loss dB	Hearing loss in per cent [Hz]			
	500	1000	2000	4000
10	0,2	0,3	0,4	0,1
15	0,5	0,9	1,3	0,3
20	1,1	2,1	2,9	0,9
25	1,8	3,6	4,9	1,7
30	2,6	5,4	7,2	2,7
35	3,7	7,7	9,8	3,8
40	4,9	10,2	12,9	5
45	6,3	13	17,3	6,4
50	7,9	15,7	22,4	8
55	9,6	19	25,7	9,7
60	11,3	21,5	28	11,2
65	12,8	23,5	30,2	12,5
70	13,8	25,5	32,2	13,5
75	14,6	27,2	34	14,2
80	14,8	28,8	35,8	14,6
85	14,9	29,8	37,5	14,8
90	15	29,9	39,2	14,9
95	15	30	40	15

in% for each ear separately, this is performed, that is recorded each hearing loss on audiogram in dB for tones of 500, 1000, 2000 and 4000 Hz frequencies will assign matching percent of hearing loss from Table 2. Total of those four values gives percentage loss for right and left ear. Total hearing loss in% is Calculated, that a hearing loss less damage ear Expressed in% is added $\frac{1}{4}$ of difference between both ears. [6]

In total hearing loss in 20% of the affected disorder generally unaware of the loss of up to 40% can be offset by increased attention and to higher losses in the communication difficulties. Initially only understand speech in difficult acoustic conditions, and then do not understand even in normal communicative situations and a quiet room. Specifically,

communication difficulties associated with frequency and disability cannot be unreservedly committed to the disability rate in% according to Fowler. [6]

4. LIMIT AND ACTION VALUES OF NOISE EXPOSURE

On the major workplace part of production and introduction sector employee can be exposed by different work and working environment factor. It is very important, that employee health would be protected before negative work and working environment effects, and eventually that bad affects were adjusted, or their rubbish was reduced for the lowest possible rate.

At present according to Parliament European and council directive no. 2003/10/EC are establishing concepts to our legislation:

- **limit value exposure** $L_{AEX,8h,L} = 87$ dB (or $L_{CPk} = 140$ dB at individual impulses),
- **high action value of exposure** $L_{AEX,8h,a} = 85$ dB (or $L_{CPk} = 137$ dB at individual impulses),
- **lower action value of exposure** $L_{AEX,8h,a} = 80$ dB (or $L_{CPk} = 135$ dB at individual impulses).

Action value of exposure is noise value in the work environment, where at going beyond that has to be done precaution for noise decrease.

Limit value exposure is noise value, which **at employee can not be exceeded for any conditions**, even with earmuffs applications. [7]

5. OBJECTIFICATION METHODS

In measuring and assessing noise in the workplace will use 3 types of limit values and biological, emissions and air pollution.

Biological evaluation of noise and its harmful effects is performed when the noise exposure of workers can not accurately assess the physical measurements, when the hearing impairment and other factors involved and there is no known relationship between exposure, the incidence and size of workers' hearing from noise damage. The basis of the **audiometric examination** of the exposed workers in a quiet audiometric chamber, which measures the increase of hearing loss across the group for one year.

Noise emission values of equipment characterized in terms of their ability to radiate acoustic energy. Using these figures, it can calculate the distribution of noise levels in a certain area, thus the ability to characterize the source of a sound the space. This property is expressed in sound power level. Noise emission values are fundamental and technical characteristics of

machines used to assess the quality of machines in terms of noise and efficiency of technical measures taken to reduce their noise.

Imitated noise values are used for ranking noise on workplaces in terms of potential effects on human organism. The basis of the measurement noise nuisance, i.e. the noise in places of residence of workers. We distinguish between direct measurement of noise load, measurement noise in the workplace and measurement noise in the workspace.

Noise on working place is measured when, during the shift workers are mostly working on one place and outside of this place do not enter into area with Massively A higher noise level than on permanent working place.

Measurement noise in the work area is carried out when in a noisy area moves more people, space is filled with a greater number of noise sources of the same type and level of noise in the workspace does not change significantly. Workers are mostly working part time staying in this area and outside it are not exposed to greater noise. Integral part of measuring and assessing noise in the workplace survey is the type of activity and duration of exposure. Evaluation of noise in the workplace is against the measured values of noise, the type of work and duration of exposure to the permissible limits in the legislation. [2]

6. PREVENTIVE MEASURES AGAINST NOISE

Measures used to prevent or reduce the noise in the work environment can be divided into several groups:

- **technical steps** to eliminate potential sources of noise in the manufacture of machinery and technological equipment, selection of equipment with lower noise, acoustic coatings, noise-absorbent wall materials, preventing transmission of the building structure, isolation of man from the noise source (noise cab), acoustic wall tiles,
- **technological measures:** low-noise technology, covers material transport routes,
- **organizational measures:** reducing the number of exposed workers, reducing exposure (e.g. emergency breaks, which they must spend in the so-called. Quiet noisy areas outside the workplace), relief workers, integrating noisy operations to less busy changes, determination of hazardous work, preventive medical examinations,
- **personal Protection:** failing to implement such measures, or they reached the noise below **85 dB**: earplugs, earmuffs, the noise over 95 db: helmets restrict the bone conduction of sound, and used in noise above **100 dB**. [2]

7. EXAMPLE NOISE REDUCTION BY OPTIMIZATION OF TECHNOLOGICAL ELEMENTS OF MECHANICAL SYSTEM

It should be noted that the real structure contains many discontinuities, which can be considered as a kind of insulator, in which the change of intensity of vibro-acoustic waves, respectively power flux and thus reducing the information content signal. Examination of the vibration transmissibility of the structure, such as detecting the transfer function from point B to point C (Figure 1) does not lead to information that would adequately identify the transmission path. When using traditional construction materials, if not in the way of discontinuity, the attenuation per unit length is negligible. It is therefore important to examine the transmission through the discontinuity. [3]

One example of how to reduce vibration in our mechanical system studied is the change of stiffness of elastic pneumatic clutch and changing the pressure in the compression chamber. For measuring and evaluating the effectiveness of coupling, we used acoustic

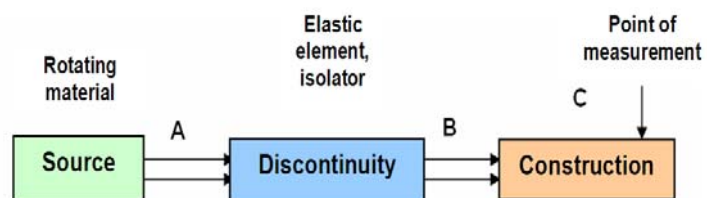


Figure 1 Power flow of mechanical vibration signal [3]



Figure 2 Mechanical system

camera that can record the sound pressure levels throughout the measured frequency spectrum. An example of such mechanical system is shown in Figure 2.

Measurements were carried out in various modes of speed of mechanical systems and various pressures in pneumatic clutch. Also measurements were made when the system elastic clutch was not located; it means that the shafts were combined fast. From the measured data we have in frequency spectrum indicated a frequency of 570 Hz, which is most pronounced in the system. Figure 3.

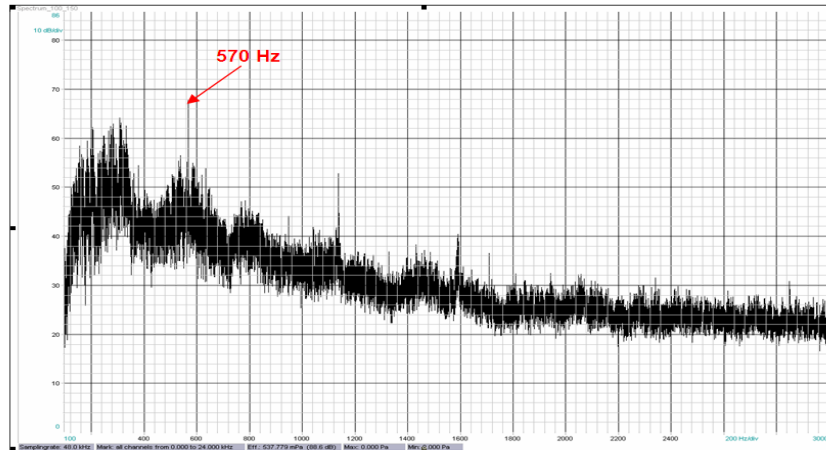


Figure 3 Selection of the frequency in spectrum

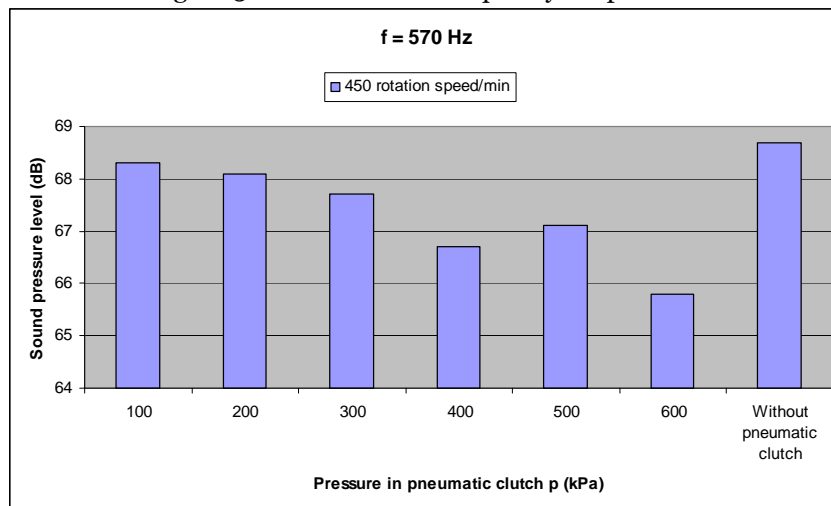


Figure 4 Result measurement and analysis

Evaluation of measurement is presented in the following chart, which is dependent noise pressure level of frequency 570 Hz at mode 450 rpm and different pressure changes in the elastic clutch. Figure 4. With regulation and tuning of rotating mechanical system components the whole mechanism decreasing noise level also occurred following decreasing of sound pressure level in work environment.

8. CONCLUSION

This article provides basic terminology, determinants and physical properties of acoustic wave propagation environment. Discusses the effects of sound waves to a man and an example of noise reduction by optimizing technological elements of the mechanical system.

Acknowledgement

This post was created and is supported by the project **VEGA 1/0453/08** Research of modification possibilities acoustic parameters anti noise systems by application of unique technology of visualization noise Emissions. **KEGA 3/7426/09** Creation of didactic details and publishing of university textbook "Physical factors of environment - valuation and assessment" for main field 2nd and 3rd level of study environmental focused studying programs. **APVV-0176-07** The research of acoustic parameters recycling materials and systems that are applied for protection from industrial and traffic noise.

REFERENCES

- [1] Rovný, I., a kol.: Preventívne lekárstvo, Učebnica pre stredné zdravotnícke školy, Vydavateľstvo Osveta, 1995, Martin, ISBN 80-217-0574-4
- [2] Buchancová, J., a kol.: Pracovné lekárstvo a toxikológia, 1. slovenské vydanie, Vydavateľstvo Osveta, 2003, Martin, ISBN 80-8063-113-1
- [3] Žiaran, S.: Ochrana človeka pred kmitaním a hlukom, Slovenská technická univerzita v Bratislave, 2007, ISBN 978-80-2799-0
- [4] Hatina a kol.: Encyklopedický súbor bezpečnosti a ochrany zdravia pri práci, Bratislava, 2007, Inštitút pre výskum práce a rodiny, ISBN 978-80-7138-124-2
- [5] Lumnitzer, E., Badida, M., Biľová, M.: Hodnotenie kvality prostredia, Elfa s.r.o. Košice, 2007, ISBN 978-80-8073-836-5
- [6] Pelclová, D., a kol.: Nemoci z povolání a intoxikace, Učební texty univerzity Karlovy v Praze, Nakladatelství Karolinum, Praha, 2006, ISBN 80-246-1183-X
- [7] Janoušek, M.: Pravidlá dobrej praxe BOZP, Publikácia 12, Obmedzte hluk! Zásady BOZP pri práci v hluku, 2005, ISBN 80-968834-7-X





¹Sándor BESZÉDES, ²Nora PAP, ³Eva PONGRACZ,
²Riitta L. KEISKKI, ¹Cecília HODÚR

DEVELOPMENT OF MEMBRANE WASTEWATER PURIFICATION PROCESS FOR MEAT INDUSTRY SME'S

¹DEPARTMENT OF PROCESS ENGINEERING, UNIVERSITY OF SZEGED, HUNGARY

²MASS AND HEAT TRANSFER PROCESS LABORATORY, UNIVERSITY OF OULU, FINLAND

³THULE INSTITUTE, NORTECH OULU, FINLAND

ABSTRACT:

Meat processing industries generate a great amount of wastewater. Because of the remote locations of companies in Northern Finland, they face the problem of low efficiency of traditional biological wastewater purification and the need for a decentralized energy supply system. Membrane separation processes integrated in wastewater purification technology could provide an eco-friendly, and economical solution for the small and medium sized meat processing enterprises (SME's). The main aim of our research project was to find technology for the treatment of food industry wastewater, which is suitable for producing recyclable process water, and on the other hand, could provide an economical pre-concentration stage before anaerobic digestion (AD).

KEYWORDS:

membrane technology, wastewater, food industry

1. INTRODUCTION

Food processing companies generate a great amount of wastewater because of the processed high water contented raw materials, dehydration processes, and the high water demand of flushing and cleaning procedures. The level of wastewater pollution and the adaptable purification technology is highly dependent on the characteristics of the processed material and the possibility of a separated process waters collection. The purification technologies should be dynamically fitted to the fluctuated wastewater production and to varied composition. The fluctuating wastewater output is a peculiar problem of small meat processor with periodical operating. One of the possible treatment and utilization methods for food industry wastewater is the irrigation onto land, by which the nitrogen and phosphorus content can be utilizable to increase the biomass production but the cation composition of wastewater is not perfectly suited to the demand of plant cultivating. Luo et al. [1] reported that the long term using of meat processing wastewater damages soil quality due to the varying in exchangeable cations of fertilized soil, and this problem makes uncertain the sustainability of the application of effluents for irrigation.

The membrane technology is known as a flexibly adaptable technique for varying capacity and for the diverse chemical composition of processed water [2]. In RO processes, where the fluid is forced through the porous membrane by the pressure difference, the permeate flow rate depends on the permeability of membranes (L), the physical properties of processed fluid (ρ , η) and the pressure gradient (d_p/d_x). However, the RO process is additionally affected by diffusion through the membrane (D). The mass flux (N) through the membrane pores can be described by Eq. 1. [3]

$$N = \frac{\rho L}{\eta} - D \frac{d_p}{d_x} \quad (1)$$

Based on the solution-diffusion transport model, the mass flux across the membrane depends on the permeability of the membrane for water (L), the transmembrane pressure (Δp) and

the osmotic pressure difference ($\Delta\pi$). The osmotic pressure is in large measure affected by the temperature of the fluid (T) and the concentration difference (ΔC) between the two sides of the membrane. For ideal solutions it can be calculated by Eq. 2. using the ideal gas constant (R):

$$\Delta\pi = \Delta CRT \quad (2)$$

If the thickness of the membrane (l), the solubility (S) and the water partial volume (V) are known, the water flux can be given by the formula of Wijmans and Baker [4]

$$J = \frac{DSV}{RTl} (\Delta p - \Delta\pi) \quad (3)$$

Considering Eq. (1) and Eq. (3), the mass flow through the membrane and the permeate flux are affected by the transmembrane pressure and the temperature. The increasing of the temperature decreases the viscosity of fluids and therefore increases the water and the salt permeability but simultaneously increases the osmotic pressure [5].

The high rejection for organic materials and for detergents makes the RO process suitable for the recycling of food wastewater. Bohdziewicz et al. [6] found that applying RO for meat industrial wastewaters after simultaneous precipitation the organic matter removal efficiency reached the value of 99.8%; the ammonium retention and the total nitrogen retention was 97% and 99%, respectively. In a latter paper of the authors, the performance of RO operation after activated sludge pretreatment was investigated and it was concluded that without chemical precipitation the retention for total nitrogen and total phosphorus was 90% and 97.5%, respectively. The removal of biodegradable materials (expressed by BOD₅) was just 50%, but despite the lower organic matter removal performance the purified wastewater was found suitable for reuse in the production cycle of the plant [7]. In the study of Vourch et al. [8], the efficiency of a one-stage RO, a combined system of nanofiltration (NF) before RO and a two-stage RO+RO operations for dairy process water treatment was compared and it was concluded that there was no significant difference in the retention for electric conductivity and total organic carbon (TOC) between the RO and the NF+RO system.

With RO operations pure water can be obtained and the UF systems are capable of producing clear and transparent wastewater permeate with reduced bacteria content, but the presence of alive microorganisms in the feed solution can assist in depositing the polarization layer on the membrane surface, facilitating membrane fouling [9]. Kornboonraksa et al. [10] found that in membrane bioreactor the total membrane resistance increased by a large scale and the permeate flux decreased because of the released carbohydrates of piggery wastewater which were deposited easily on the membrane surface due to the microbial degradation.

Under high pressure the diffusion rate is reduced due to the more compact (less porous) deposited layer, and the resistance increases with the enhanced local osmotic pressure. This phenomenon is described as biofilm enhanced osmotic pressure (BEOP) [11-12]. During long-time RO concentration operations the membranes can be considered as non-porous materials for the dissolved solids, flocs and colloids and a so-called surface fouling (external fouling) phenomenon is observed on the feed-side surface of the membrane [13]. During the scale formation the salts of feed can crystallize on the surface of a membrane and additionally the rejected solid can form a cake layer [14]. In the formed cake-layer a complex flow pattern can be observed; moreover, the flow direction may even be the reverse of the pressure gradient because of the inter-connectivity of the neighboring pores [15]. Pore blocking with the adsorption of foulants on the pore wall may occur if the foulants' size is comparable with something pore sized or smaller [16]. Internal fouling can also be experienced if the structure of the membrane is irreversibly altered due to the extremely high hydrostatic pressure or chemical degradation.

The effect of fouling can be characterized by the flux decline versus operation time, and to examine the flux behavior and the fouling mechanisms the resistance-in-series model can be used in various membrane processes. In the model the relationship between the permeate flux, transmembrane pressure and the total resistance can be described by the series resistance equation

$$J = \frac{\Delta p}{\eta R_t} \quad (4)$$

where η is the viscosity of the feed fluid and R_t is the total resistance.

The R_t can be defined by the sum of the hydraulic (intrinsic) membrane resistance (R_m), the polarization layer (external fouling) resistance (R_p) and the (internal) fouling resistance (R_f).

$$R_t = R_m + R_f + R_p \quad (5)$$

The model is successfully adopted for the examination of flux behavior during the RO concentration of manure [17] or juice [18], separation of oil in water emulsion [19] and for the control of fouling phenomena in several ultrafiltration processes [20-22].

The traditional concept of the membrane water purification systems, when the concentrate is handled as waste stream, can be changed because the concentrated feed streams with high biodegradable organic matter content are utilizable for anaerobic digestion (AD). Furthermore, in the Northern region the temperature sensitive biological wastewater treatment can be replaced with the membrane processes; hereby the time demand of the purification technology can be reduced and the membrane operation can fulfill the requirements of the periodic and fluctuating wastewater product.

According to the above mentioned concept, the dual aim of our work was to concentrate the organic matter content with membrane processes to get a suitable raw material for AD, and on the other hand to produce pure permeate which can be recyclable or reusable. In our work presented in this paper we examined the effect of transmembrane pressure, recirculation flow rate and the temperature of feed on the permeate flux and resistances concentrating meat industrial wastewater. For the calculation of resistances the resistances-in-series model was used to determine the main influential parameters, and to optimize the conditions for RO operation response, surface methodology was applied.

2. MATERIALS AND METHODOLOGY

2.1. Wastewater sample

The real wastewater samples originated from a medium-sized meat processing company; the sampling point was after the grease tap. The process water originates from meat processing technology, mainly from the flushing and rinsing of equipment (slicing and packaging machines, smoking chambers). To remove grit and other large-sized solids a cloth filter was used. The characteristic of wastewater is shown in Table 1.

Parameter	Mean value	SD
TS (mgL ⁻¹)	3210	296
TOC (mgL ⁻¹)	834.1	35.3
Lipid (mgL ⁻¹)	115.1	21.7
Protein (mgL ⁻¹)	379.4	21.2
pH	6.13	0.23
Conductivity* (μScm ⁻¹)	983.2	14.2
Density* (kgm ⁻³)	1005.3	3.2
Viscosity* (mPas)	0.877	0.009

* at 30°C

2.2. Analytical measurements

During the RO and UF operation the total organic carbon (TOC) content, the fat content and the protein content were assayed. TOC content was measured by a Sievers 900 portable TOC analyzer with a membrane conductometric detector (GE Analytical Instruments, U.S.).

The photometrical protein assay was based on the Lowry method [23] using the bovine serum albumin (BSA) standard. The samples were diluted to avoid interference with lipids, ammonium ions and salts and to minimize the effect of the sample on the pH of the reaction mixture.

The lipid content of wastewater samples was determined by partition-gravimetric procedures after extraction according to the Bligh and Dyer method [24]. For the viscosity measurements of wastewater samples a glass capillary viscometer was used.

2.3. Membrane filtration procedure and calculations

For the pilot-scale filtration test series flow, a B1 module of Paterson Candy International (PCI) was used. The tubular module was equipped by AFC99 polyamide RO (99% nominal retention for NaCl) membranes (ITT PCI Membranes Ltd.). Each 1.2 m long tubular membrane had a 12.5 mm inner diameter, and the total effective membrane area was 0.85 m².

The recirculation flow rate (Q_{rec}) varies between 600 and 1000 Lh⁻¹. Considering the nominal pressure range of the PCI module and the membranes and, furthermore, based on experimental design, the operating pressure for RO tests was 25-35-45 bar, respectively. The temperature of feed was controlled by a coil-type heat exchanger. In each experiment 60 L wastewater was concentrated to reach a 3.75 value of volume reduction ratio (VRR), calculated by Eq. (6)

$$VRR = \frac{V_f}{V_f - V_p} \quad (6)$$

where V_f is the volume of feed, and V_p is the volume of permeate.

The retention for total organic carbon (R_{TOC}), fat (R_{fat}) and proteins (R_{prot}) were calculated using the following equation (Eq. 7)

$$R(\%) = \left(1 - \frac{c_p}{c_0}\right) \times 100 \quad (7)$$

where c_p and c_0 are the concentration of measured components in the permeate and feed, respectively.

The connection between pressure, permeate flux and the resistance components can be described by Eq. 4. From this general expression the hydraulic resistance of the clean membrane (R_m) can be calculated by the data obtained from the permeate flux (J_w , $m^3m^{-2}s^{-1}$) measurement with deionized water at different transmembrane pressures (Δp , Pa) and from the dynamic viscosity (η_w , Pas).

$$R_m = \frac{\Delta p}{\eta J_w} \quad (m^{-1}) \quad (8)$$

During the concentration process the solid and dissolved components build up the polarization layer (cake layer), which can be removed by intensive flushing with water. From the pure water flux measured after flushing (J_f) and using R_m the fouling resistance can be given by Eq. 9.

$$R_f = \frac{\Delta p}{\eta_w J_f} - R_m \quad (m^{-1}) \quad (9)$$

After knowing R_m and R_f and calculating R_t from the permeate flux obtained from the wastewater filtration test the polarization layer resistance can be determined by the combination of Eq. 4. and Eq. 5.

3. RESULTS

3.1. Determination of influential parameters

To examine the possible interactions between the operating conditions and to optimize the influential parameters for membrane purification, central composite face centered (CCF) experimental design and response surface methodology (RSM) was performed using MODDE 8.0 statistical experimental design software (Umetrics, Sweden). RSM is an adequate method to fit a model by a least squares technique when a combination of independent variables and their interactions affect the desired response [25].

For the modeling and optimization the studied factors were the transmembrane pressure (p) of 25 and 45 bar, recirculation flow rate (Q_{rec}) of 600 and 1000 $Lm^{-2}h^{-1}$ and the temperature of 30° and 40°C (Table 2). The values of pressure and the recirculation flow rate were chosen based on the membrane characteristics and considering the specification of the RO unit and the membrane module. The operating temperatures were varied according to the temperature range of produced industrial process water.

The selected responses were the average permeate flux (J), the organic matter retention (R_{TOC}), the total resistance (R_t) and the polarization layer resistance (R_p). To evaluate the reproducibility of the fitted model, five center points were used in the experimental design ($Q_{rec}=800 Lh^{-1}$, $p = 35bar$ at a temperature of 35°C). In order to reduce the systematic error, the runs of the experiments were randomized.

Table 2. The factors and responses of experimental design

Exp. No.	Factors			Responses			
	Q_{rec} (Lh^{-1})	p (bar)	Temp.(°C)	J_{perm} ($Lm^{-2}h^{-1}$)	$R_t \times 10^{14}$ (m^{-1})	$R_p \times 10^{14}$ (m^{-1})	R_{TOC} (%)
1	600	25	30	54.35	2.604	0.716	99.28
2	1000	25	30	55.04	2.556	0.698	99.20
3	600	45	30	71.38	3.211	0.767	97.93
4	1000	45	30	72.27	3.102	0.749	98.04
5	600	25	40	60.21	2.652	1.036	98.77
6	1000	25	40	61.06	2.588	0.998	98.74
7	600	45	40	76.42	3.258	1.057	98.01
8	1000	45	40	78.13	3.189	1.091	97.96
9	600	35	35	69.99	2.954	0.936	98.86
10	1000	35	35	71.51	2.878	0.909	98.71
11	800	25	35	58.25	2.613	0.912	97.21
12	800	45	35	73.21	3.239	0.934	98.99
13	800	35	30	69.40	2.843	0.783	99.09
14	800	35	40	73.65	3.024	1.104	98.51
15	800	35	35	70.87	2.885	0.921	99.05
16	800	35	35	70.95	2.884	0.924	99.12
17	800	35	35	70.85	2.881	0.928	99.06
18	800	35	35	70.93	2.880	0.925	99.15
19	800	35	35	70.96	2.879	0.921	99.17

Retention for TOC, lipids and proteins has not changed significantly with the varying of factors, because the retention of AFC99 membrane for different components is higher than 97%. The calculated value of R_m for the AFC99 membrane was $1.409 \times 10^{14} \text{ m}^{-1}$. In our case the range of R_f was obtained from 8.761×10^{13} to $1.034 \times 10^{14} \text{ m}^{-1}$ but the change was not significant at the 95% confidence interval; therefore, the fouling resistant cannot be used as a response parameter.

To determine which factors have important effects on the response, one factor is varied while the others are kept at the average value. Fig. 1 shows the effects of single parameters and their interactions on the permeate flux (J_p), total resistance (R_t) and polarization layer resistance (R_p).

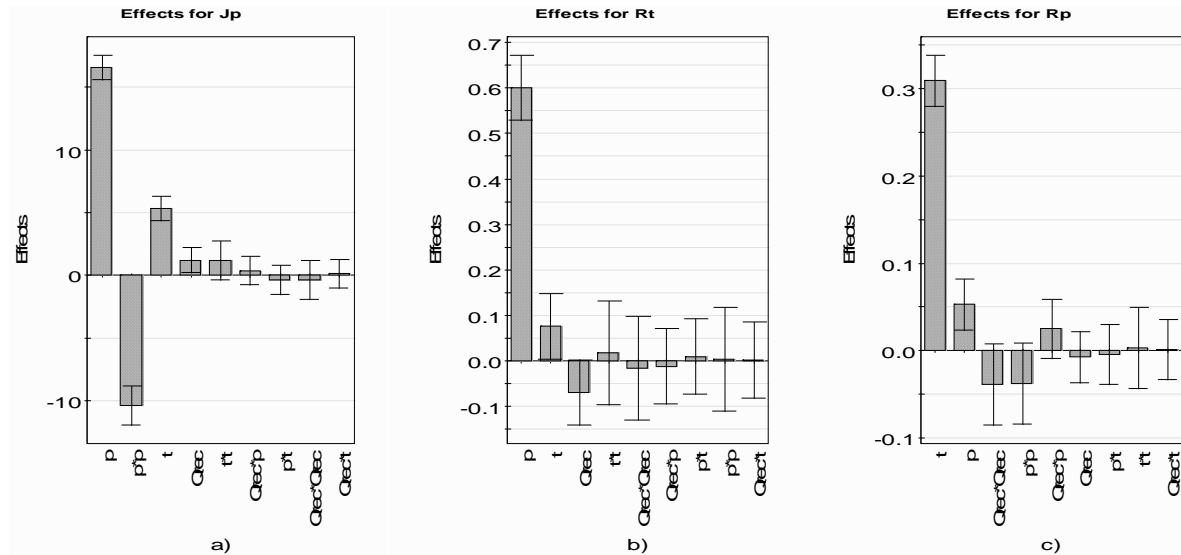


Figure 1. Effects of factors and interactions on the permeate flux (a), Total resistance (b) and polarization layer resistance (c).

Our results show that mainly the pressure and the temperature have an effect on the permeate flux, R_t and R_p ; furthermore, a smaller influence of Q_{rec} was obtained on permeate flux and total resistance. The other factors and the interactions between them have just a negligible effect on response parameters. The significant effect of temperature on flux can be explained by studying Eq. 1 and Eq. 3. With temperature increasing, the permeate diffusivity through the membrane increases and the viscosity decreases simultaneously, which has a positive effect on permeate flux.

Our calculation, based on the resistance in series model, showed that the hydraulic resistance of the membrane (R_m) was in all cases higher than the fouling resistance (R_f) and the ratio of R_m to R_t was from 39.3 to 51.9%, depending on the experimental conditions. The main part of R_m in R_t can be explained by the composition of the wastewater, and the low amount of organic matter could not form a thick polarization layer in the turbulent feed flow; furthermore, the concentration of low molecular size compounds was not high enough to significantly increase the internal fouling.

3.2. Modeling and optimization of RO process

During the refinement the non-significant terms were removed. Since the value of R_t contains the R_p , the change of the two parameters are not independent; therefore, R_p was removed from the responses to obtain a correct statistical model. After refinement a quadratic model was refitted with multiple linear regressions (MLR). The mathematical relationship between the independent variables of pressure (p , bar), recirculation flow rate (Q_{rec} , Lh^{-1}), temperature (t , $^{\circ}\text{C}$) and the response function for permeate flux (J_p , $\text{Lm}^{-2}\text{h}^{-1}$) and total resistance (R_t , m^{-1}) are presented by Eq. (10) and (11), respectively.

$$J_p = 71.0214 + 8.25 p + 0.5659 Q_{rec} + 2.711 t - 4.989 p^2 \quad (10)$$

$$R_t = 2.9009 \times 10^{14} + 2.986 \times 10^{13} p - 3.659 \times 10^{12} Q_{rec} - 3.95 \times 10^{12} t + 3.107 \times 10^{10} p^2 \quad (11)$$

The response function predictions were in good agreement with the experimental data; the R^2 for J_p and R_t was 0.996 and 0.994, respectively (Fig. 2).

In addition, the goodness of fit (Q^2) for J_p and R_t was 0.991 and 0.988, which indicates good predictive power of the models. The reproducibility was over 99.9% and the standard deviations of the fitted models were higher than the standard deviation of the residuals ($R_{adj}^2 > 0.98$ in both cases).

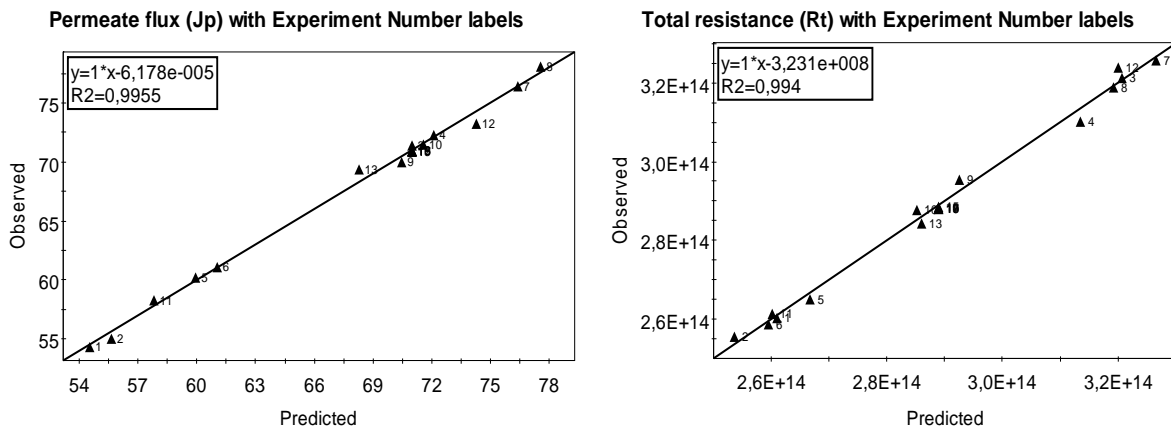


Figure 2. Observed versus predicted values for permeate flux and total resistance

To analyze the effects of factors the characteristic contour plots are shown in Fig. 3. As Fig. 3 shows, the permeate flux is strongly dependent on the pressure and temperature. The difference between operating pressure and osmotic pressure decreased during the concentration and therefore there was a non-linear correlation between the permeate flux and the pressure.

In addition, during the concentration process the deposited cake layer caused a slower diffusion (via longer diffusion path and lower diffusivity) and a higher hydraulic resistance. The temperature increasing caused the viscosity to decrease, which predicted higher permeate flux (Eq. 4), but the higher temperature is also expressed in the higher osmotic pressure, decreasing the driving force of the RO process ($\Delta p - \Delta \pi$). Considering this phenomenon, the relationship between the temperature and permeate flux is also non-linear.

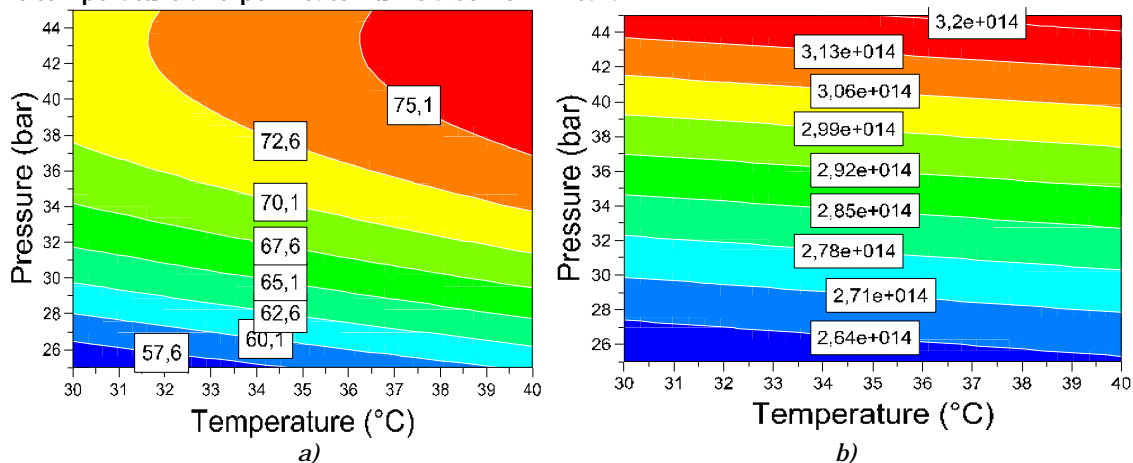


Figure 3. The combined effect of temperature and pressure on permeate flux (a) and r_t total resistance (b)

In our case the highest permeate fluxes can be reached by applying pressure over 37 bar and a temperature over 36.5°C but to achieve the best permeate flux the recirculation flow rate can be set at a value over 750Lh⁻¹ (Re number can be over 20,000). In this region the retention for TOC and protein was higher than 97% and 99%, respectively. On the other hand, the pressure increasing from 25 to 45 bar increased the total resistance by approximately 17% but this effect can be reduced by the application of elevated temperature and/or higher recirculation flow rate.

The antagonist effect of the pressure increasing total resistance and permeate flux can be explained by the altering of the structure of the polarization layer. Under high pressure, the formed cake layer has become less porous, which can increase the hydraulic resistance of the layer [26]. Although Hoek et al. [14] reported that the fouling can improve the selectivity of the membrane; this establishment is acceptable just for removal of larger sized molecules via size-exclusion mechanisms.

Using the refitted model, based on the data obtained from the response surface analysis, the optimal condition of the RO process of meat industrial wastewater was for the highest permeate flux and the lowest total resistance determined at a transmembrane pressure of 38.5 bar and a recirculation flow rate of 1000 Lh⁻¹ at 40°C.

4. CONCLUSIONS

The RO concentration of meat industrial wastewater was carried out in a pilot-scale filtration unit equipped by AFC99 polyamide membranes. For the experimental design and optimization, MODDE 8.0 software was used, investigating the effects of the operation pressure, temperature and recirculation flow rate on the organic matter retention, permeate flux and the resistances calculated from the resistances in the series model.

Our results show that the investigated parameters did not significantly affect the retention but the permeate flux and the total resistance are suitable for the response parameter of modeling. Based on our results, the increasing pressure positively affects the permeate flux but at elevated pressure the total resistance increases as well. The increasing of the temperature and the recirculation flow rate could enhance the permeate flux and decrease the total resistance. The fitted quadratic model was significant at the 95% confidence interval and showed good predictive power as well as high reproducibility.

The optimal conditions for RO concentration of meat industrial wastewater were determined at an operating pressure of 38.5 bar, recirculation flow rate of 1000 Lh⁻¹ and temperature of 40°C. The TOC content and the conductivity of permeate was lower than 5 ppm and 20 µScm⁻¹, respectively, which allows for the recycling and reusing, for example, in cleaning, in the flushing process or for cooling water. The average TS content of RO concentrate was higher than 9% with a TOC content of 2.8 gL⁻¹, protein content of 1.2 gL⁻¹ and fat content of 0.35 gL⁻¹.

ACKNOWLEDGEMENTS

The authors are grateful for support of the work provided by the MicrE project and additionally, Sándor Beszédes acknowledge the financial support of the scholarship of CIMO. Furthermore, the members of the Research Group for Transport Phenomena of the University of Szeged are thankful for the financial support provided by the project GVOP-3.2.1-2004-04/0252/3.0.

REFERENCES

- [1.] Luo, J., Lindsey, S., Xue, J., Irrigation of meat processing wastewater onto lad, Agriculture, Ecosystems and Environment, Vol. 103, pp. 123-148, 2004
- [2.] Van der Bruggen, B., Vandecasteele C, Distillation vs. membrane filtration: overview of process evolutions in seawater desalination, Desalination, Vol. 143(3), pp. 207-218, 2002
- [3.] Bird, R.B., Stewart, W. E., Lightfoot, E.N., Transport phenomena. John Wiley & Sons Inc. New York. 2002
- [4.] Wijmans, J.G., Baker, R.W. The solution-diffusion model: a review, Journal of Membrane Science, Vol. 107, pp. 1–21, 1995
- [5.] Greenlee, L. F., Lawler, D. F., Freeman, B.D., Marrot, B., Moulin P, Reverse osmosis desalination: Water sources, technology, and today's challenges, Water Research, Vol. 43(9), pp. 2317-2348, 2009
- [6.] Bohdziewicz, J., Sroka E, Lobos, E, Application of the system which combines coagulation, activated sludge and reverse osmosis to the treatment of the wastewater produced by the meat industry, Desalination, Vol. 144 (3), pp. 393-398, 1995
- [7.] Bohdziewicz, J., Sroka E, Treatment of wastewater from the meat industry applying integrated membrane systems, Process Biochemistry, Vol. 40(3), pp. 339-346, 2005
- [8.] Vourch, M., Balannec, B., Chaufer, B., Dorange, G, Nanofiltration and reverse osmosis of model process waters from the dairy industry to produce water for reuse, Desalination, Vol. 172(3), pp. 245-256, 2005
- [9.] Saravia, H., Houston, J. E., Toledo, R.T., Nelson, H.M., Economic analysis of recycling chiller water in poultry processing plants using ultrafiltration membrane system, Journal of Food Distribution Research, Vol. 36, pp. 161-166, 2005
- [10.] Kornboonraksa, T., Lee, S.H., Factors affecting the performance of membrane bioreactor for piggery wastewater treatment, Bioresource Technology, Vol. 100(12), pp. 2926-2932, 2009
- [11.] Herzberg, M., Elimelech, M., Biofouling of reverse osmosis membranes: role of biofilm enhanced osmotic pressure, Journal of Membrane Science Vol. 295, pp. 11–20, 2007
- [12.] Chong, T.H., Wong, F.S., Fane, A.G., The effect of imposed flux on biofouling in reverse osmosis: Role of concentration polarisation and biofilm enhanced osmotic pressure phenomena, Journal of Membrane Science Vol. 325(2), pp. 840-850, 2008

- [13.] Amiri M.C., Samiei M. Enhancing permeate flux in a RO plant by controlling membrane fouling, *Desalination* Vol. 207(3), pp. 361-369, 2007
- [14.] Hoek, E.M.W., Allred, J., Knoell, T. Jeong, B-H., Modeling the effects of fouling on full-scale reverse osmosis processes, *Journal of Membrane Science*, Vol. 314(1), pp. 33-49, 2008
- [15.] Yang, Z., Peng, X.F., Chen, M.-Y., Lee, D.-J., Lai, J.Y., Intralayer flow in fouling layer on membranes. *Journal of Membrane Science*, Vol. 287(2), pp. 280–286, 2007
- [16.] Meng, F., Chae, S.R., Drews, A., Kraume, M., Shin, H-S., Yang F., Recent advances in membrane bioreactors (MBRs): Membrane fouling and membrane material, *Water Research*, Vol. 43(6), pp. 1489-1512, 2009
- [17.] Masse L., Massé, D. I., Pellerin, Y., Debreuil, J. Osmotic pressure and substrate resistance during the concentration of manure nutrients by reverse osmosis membrane. *Journal of Membrane Science*, Vol. 348, pp. 28-33, 2010
- [18.] Pap, N., Kertész, Sz., Pongrácz, E., Myllykoski, L., Keiski, R.L. Vatai, Gy., László, Zs., Beszédes, S., Hodúr, C., Concentration of blackcurrant juice by reverse osmosis, *Desalination*, Vol. 241(3), pp. 256-264, 2009
- [19.] T. Mohammadi, M. Kazemimoghadam, M. Saadabadi Modeling of membrane fouling and flux decline in reverse osmosis during separation of oil in water emulsions *Desalination*, Vol. 157, pp. 369-375, 2003
- [20.] Rai, P., Rai, C., Majumdar, G. C., DasGupta, S., De S. Resistance in series model for ultrafiltration of mosambi (*Citrus sinensis* (L.) Osbeck) juice in a stirred continuous mode. *Journal of Membrane Science*, Vol. 283, pp. 116-122, 2006
- [21.] Purkait, M.K., Bhattacharya, P.K., Dem S., Membrane filtration of leather plant effluent: Flux decline mechanism *Journal of Membrane Science*, Vol. 258(1), pp. 85-96, 2005
- [22.] Arora, A., Dien, S., Belyea, R.L., Wang, P., Singh, V., Tumbleson, M. E., Rausch, K.D., Thin stillage fractionation using ultrafiltration: resistance in series model, *Bioprocess Biosystem Engineering*, Vol. 32(2), pp. 225-233, 2009
- [23.] Lowry. O. H., Rosebrough, N.J., Farr, A.L., Randall, R.J., Protein measurement with the folin-phenol reagents, *J. Biol. Chem.* Vol.193, pp. 265-275, 1951
- [24.] Smedes, F., Askland, T., Revisiting the Development of the Bligh and Dyer Total Lipid Determination Method, *Marine Pollution Bulletin*, Vol. 38(3), pp.193-201, 1999
- [25.] Mason, R.L., Gunst, R.F., Hess, J.J., *Statistical Design and Analysis of Experiments with Applications to Engineering and Science*, John Wiley and Sons Inc., Hoboken, NJ, 2003
- [26.] Agashichev, S.P., Modelling the influence of temperature on resistance of concentration layer and transmembrane flux in reverse osmosis system. *Separation Science Technology*, Vol. 39(14), pp. 3215-3236, 2004





¹: Abdelnaser OMRAN, ²: Abdelsalam O. GEBRIL

STUDY OF HOUSEHOLD ATTITUDE TOWARD RECYCLING OF SOLID WASTES: A CASE STUDY

¹⁻². SCHOOL OF HOUSING, BUILDING AND PLANNING, UNIVERSITI SAINS MALAYSIA, MINDEN, PENANG, MALAYSIA

ABSTRACT:

Solid waste management is a growing problem in Malaysia. For this reason the government of Malaysia through The Ministry of Housing and Local Government (MOHLG) have taken various measures to promote recycling amongst its population. Recently, a nationwide campaign was launched to get the people to recycle their wastes. Recycling centers equipped with separate recycling bins for different recyclables have been set up across the country. In addition, publicity drives using the newsprint, the electronics media on top of the other modes of information dissemination such as seminars, workshops and meetings were held on a continuous basis over the years. However, despite the effort little has been achieved due to the lack of participation from the households. This paper identifies the reasons for the failure of the campaign. Data were gathered using a mail-out questionnaire to 400 randomly chosen households. Quantitative analysis made based on 347 responds received indicated that although all of the respondents had a positive attitude towards recycling only a few did recycle. The poor response is largely due to the lack of facilities provided. Many residents are turned down when they are unable to locate the recycling centres and if they are able to locate one, it seems too troublesome to be needed.

KEYWORDS:

Recycling, Solid Wastes, Household Attitude, Malaysia

1. INTRODUCTION

The concept of attitude has played a major role in the history of social psychology. It is undeniable that the concept of "attitude" has become something of a factotum for both psychologists and sociologists (Fishbein, 1976). Nowadays, solid waste recycling is a problem of major relevance for all societies. Moreover, finding acceptable strategies to cope with such a problem is becoming a quite hard task, owing to the increasing awareness of environmental issues by population and authorities. However, Malaysia, with a population of over 24 million in 2005 generates 17,000 tons of domestic waste daily (Noor, 2005). At present, the per capita generation of solid waste in Malaysia varies from 0.45 to 1.44kg/day depending on the economic status of an area, the national average being 0.5 – 0.8 kg/person/day but may increase up to 1.7 kg/person/day in major cities (Agamuthu, 2001). Perak is the second largest state in Peninsular Malaysia. It is bordered on the north by Kedah and Thailand, on the east by Kelantan and Pahang, on the south by Selangor and to the west by the Strait of Malacca. Perak means silver in the Malay language. The name comes most probably from the silvery colour of tin. In the 1890's, Perak, with the richest alluvial deposits of tin in the world was one of the jewels in the crown of the British Empire. However, some say the name comes from the "glimmer of fish in the water" that sparkled like silver. Perak's population is now approximately 2 million. Once Malaysia's most populous state, the decline in the tin mining industry caused an economic slowdown from which it has yet to recover, leading to a massive drain in manpower to higher-growth states such as Penang, Selangor and the Federal Territory of Kuala Lumpur. Modern Perak is divided into 10 administrative divisions, or "Daerah" in Malay.

However, the Executive Council is the highest administrative body in the state. At the local government level, the state has one local authority, namely the Municipal Councils of Ipoh (MCI). The average throw away in Perak is around 0.9 - 1.1 kg of waste/person/day, which is higher than the national average (MOHLG, 2005).

This paper reports on the results of a research study that evaluated attitude of household towards recycling solid wastes. The research aims of shed to light upon the level of environmental awareness of the different household in Perak state at Malaysia concerning recycling of solid wastes and their perception on the success of the recycling campaign. The main objective of the research was to study the attitude of households, their awareness as well as the problems which was related to failure of the recycling campaigns. The findings of this research study may be used in decision making as a measure of attitude of household and should help households to recognize how important the environmental issues of recycling solid wastes recently.

2. THE RECYCLING CAMPAIGN

As mentioned earlier, the Ministry of Housing and Local Government, Malaysia launched a nationwide recycling campaign (Kempen Kitar Semula) in 1993. However, the campaign failed due to lack of response and participation from the people. A bigger and more aggressive campaign was initiated in 2000. Sixty-five (65) drop-off or collection centers, located at schools, gas stations, shopping malls and other convenient public places are opened nationwide.

Table 1: Recycling related activities (January – July 2003). Source: Ministry of Housing & Local Government, Malaysia.

	Type of Activity	Occasions
1	Talks/Speech	13
2	Exhibition	26
3	Meetings	27
4	Actual recycling activity	7
Total		73

Table2: Location of Recycling Collection Centers. Source: Ministry of Housing & Local Government, Malaysia.

	State	Frequency
1	Penang	16
2	Kedah	210
3	Kelantan	0
4	Terengganu	0
5	Perak	180
6	Pahang	138
7	Selangor	177
8	Negeri Sembilan	109
9	Melaka	98
10	Johor	108
11	Sabah	150
12	Sarawak	217
Total		1403

Year round programs aimed at increase awareness and participation of the population were initiated or organized by the Ministry of Housing and Local Government, Non-Governmental Organization's and Consumer groups. These include talks, exhibition and actual recycling activity. (Table 1)

3. METHODOLOGY

The study sought to evaluate the attitude of households in Perak, Malaysia on recycling of solid wastes. Specifically it is aimed to discover reasons why the nationwide recycling campaign organized by the Ministry of Housing and Local Government Malaysia failed to attract households to recycle. Four Hundred (400) questionnaires were distributed within the period of three months beginning the 2nd of February 2006 to 27th of March 2006. To ensure good response, the strategy used was to distribute the questionnaire at randomly selected houses on Perak State. Three Hundred and Forty Seven (347) useable questionnaires (87%) were received and analyzed.

Although, the number of questionnaires received was small, it is sufficient to give some indication of the overall attitude of the households of Perak on recycling of solid wastes and is adequate to enable the findings to be generalized for the whole population of Perak. The descriptive analysis of the data collected is presented below.

4. RESULT AND DISCUSSION

4.1 Awareness of the recycling activities/campaign

A majority (84.7%) of the respondents claimed that they are aware of the ongoing campaign. Most knew it through ads in the newspaper. TV and Radio ads ranked second followed by newsletter and billboards.

4.2 Importance of recycling

Asked on the importance of recycling, all participants (100%) indicated that recycling is important. However, only about 71% (247) of the respondents indicated that they participated in the recycling activity. The main reasons given, ranked in order of importance are i) Concern for the environment; ii) Concern about availability of landfill; iii) Encouragement from their children/others. A small number indicated that they recycled for money.

4.3 Participation in recycling

Amongst those who did not participate in the recycling activity (29% or 100 respondents), the main reasons given are inconvenience and lack of facilities (62%). It is interesting to note that about 18% of the non-participating respondents indicated that they “don’t bother” or find it unimportant (13%). Although the number of respondents within this group is small, particular attention should be taken to ‘convert’ them. Comparing with a Singapore the research by Foo (1997) was found that only 9 % of the respondents practice regular was recycling and another 11 % practice recycling ‘some of the time’, whereas the rest only practice recycling once in a while (64%).

4.4 Facilities provided

Respondents were also asked about the facilities provided for recycling. When asked whether they know the location of the nearest collection point for their area, 61.7% indicated they knew the location. However, more than 52% complained that the location could not be easily located. In term of distance, only 33 % indicated that it was within 1 kilometer from their house, 16 % was within the radius of 2 – 3 kilometer and 44 % indicated that it was more than 5 kilometer radius. Undoubtedly, the farther the location of the collection point, the more discouraged will the householders be. Adenso-Díaz (2005) commented that when citizens who are environmentally concerned have bins near to home, they appear to be willing to recycle more fractions than when they have to walk for a longer time to drop off the waste, due to the inconvenience of carrying the large volumes that this type of waste usually occupies. He concluded that distance and access to the bins is obviously an incentive to recycling. The benefit of facility may bring to local residents can influence attitudes (Lima, 1996). However, citizen’s attitudes depend on knowledge about a facility (Rahardyan, 2004). It was observed that, the farther the location of the collection point was the more discouraged were the householders were to recycling.

4.5 Types of materials recycled

Amongst those who recycled, the type of materials recycled ranked in term of quantity is newspaper, aluminum cans, plastics, cardboards and glass. In response to the question “How often do you recycle”, 46% indicated they sent their recyclables weekly while about 24% indicated they need to recycle more often i.e. twice or three times a week.

4.6 Perception on the success of the recycling campaign

The respondents were asked to give their opinion on the on-going recycling campaign hosted by the Ministry of Housing and Local Government. On the question whether the campaign succeed or failed, a huge 90 % or (311) indicated that it fails and it can be seen in the Figure (1). Asked for the reasons for the failure, their responses can be divided into the following five broad categories:

- i) Little improvement in the surrounding. The surrounding area, public places and rivers are still littered or polluted.
- ii) People continue to throw recyclable items such as papers, glass and aluminum cans in ordinary dustbins. Not many took the effort to separate them before throwing.
- iii) Not enough facilities provided. Many areas are not provided with the facility for recycling. Many people do not know the location of the nearest collection point. Location of collection points is either not good or too far. Easier to throw the recyclables than to bring it to collection point.
- iv) Some people are selfish. They continue to litter and do not bother about the negative effect of their action. Some think of it as a waste of time.
- v) Have very little knowledge about what recycling is. Do not realize the importance of recycling. Never heard of the campaign and never participated.

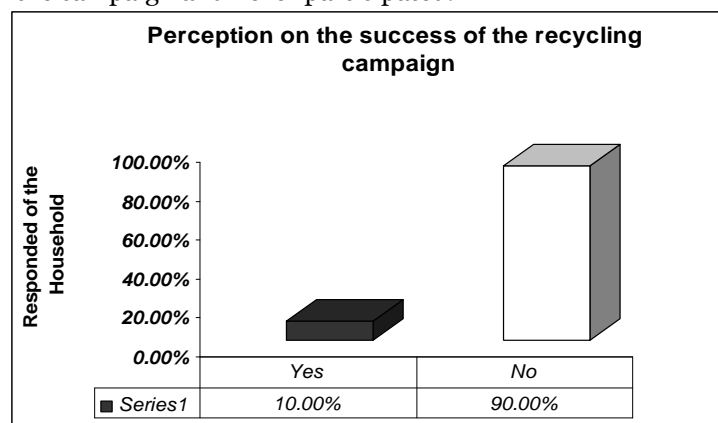


Figure 1: Perception on the success of the recycling campaign

4.7 How can it be improved?

The respondents were also asked of their views on how the situation could be improved. The majority of respondents suggested, “more facilities be provided”. There should be “local collection centers”, which is within easy reach for each community or housing areas. Community or group recycling should be encouraged and more effort is needed to educate the people of the need and importance of recycling. Monetary incentives may also be considered, for example by improving the community facilities in an area as a reward, based on the quantity of recyclables collected. In this regard, it is observed that the high rate of newspaper recycling might be due to the ready market for it. When asked whether they will recycle in the future, if all facilities are provided, all 99 % of the respondents said that they would participate and this will be different comparing with the research by Grodzińska-Jurczak (2003) in Jaslo City, Poland when he asked the same questions to the household whereas got 41 % of 932 interviewed they would to recycle and the rest refused any participation (22%) or did not respond (37%).

5. CONCLUSION

Recycling has become a household word in Malaysia, based on the finding of this study; it is evident that the households in both states are of the opinion that recycling is a very important activity. However, result of the study gave a clear indication that the recycling campaign by the Ministry of Housing and Local Government in Malaysia failed. Even though the households agreed that recycling is important, not many of them did recycle. The quantity of recyclables collected in both states is indeed very small. The main reason, as indicated by the study result, is due to misdirection in the campaign. Although much money was spent on advertisements, there is a clear misinformation. It is observed that advertisement campaigns are focused on informing households to sort their recyclables and place them in separate bins. However, such bins can only be found at designated public places, which are usually at a distant from residential areas. It is therefore not surprising that most of the households find it too troublesome to bring their recyclables to the collection centers. Furthermore, reasons such as “lack of facilities” or “distance of facilities too far from home” are also clear proof that most households are not aware that they can do their bit in recycling by simply putting the recyclables and non recyclables in separate bags and placing them in the ordinary rubbish bins available at home which will then be collected by the council or appointed agents. Therefore, the location of the recycling station is essential and the public attitudes are knowledge about source separation in general and recycling stations in particular are of interest for the functioning of the whole system (Petersen *et. al*, 2004). In the final analysis, it is interesting to note that the actual reason for the failure in terms of recycling, the lack of support and participation of households in Perak on recycling are not due to their negative attitude towards recycling but due to misinformation on the part of the authorities. In order to increase the rate recycling of solid waste and at the same time to reduce the social problem related to solid waste management at the following suggestions were made to the Perak People of Committee as followed:

1. Improving the publics' general knowledge and awareness concerning these issues is of prime importance to the minimization of waste, in general, and harmful effects of landfills on the environment, in particular.
2. Efforts are also needed to involve the public in the policy-formation, development of plans, and implementation of waste management programs and landfill sitting decisions. Public support is essential for the success of such decisions.

REFERENCES

- [1.] Adenso-Díaz (2005). Influence of Distance on the Motivation and Frequency of Household Recycling, *J. of Waste Management*, **25**, 15-23.
- [2.] Agamuthu P., (2001). Solid Waste: Principle and Management, With Malaysian Case Studies, University of Malaya, Kuala Lumpur, Inc.
- [3.] Fishbein M., (1967). Readings in Attitude Theory and Measurement, Department of Psychology, University of Illinois, John Wiley & Sons, Inc.
- [4.] Foo T. S. (1997). Recycling of Domestic Waste: Early Experience in Singapore, *Journal of Waste Management*, **21**, 277-289.
- [5.] Grodzińska-Jurczak M., Marta T. & Read A. D., (2003). Increasing Participation in Rational Municipal Waste Management - A case Study Analysis in Jaslo City (Poland), *J. of Resources, Conservation and Recycling*, **38**, 67-88.
- [6.] Lima M. L. (1996). Individual and Social Determinants of Attitudes towards the Construction of

- waste Incinerator: tow case studies, the 1996 Annual Meeting of the Society for Risk Analysis-Europe. The Centre for Environmental Strategy, University of Surrey, Guildford, Surrey.
- [7.] Noor M. Z. (2005). The Scenario of Solid Waste Management in Malaysia, A case Study, (Pre-Conference) Professional Training Programme on Solid Waste Management in SEA Cities, 4-5 July, Siem Reap, Cambodia.
- [8.] Petersen C. H. M. & P. E. O. Berg, (2004). Use of Recycling Stations in Borlänge, Sweden – Volume Weights and Attitudes, *Journal of Waste Management*, **24**, 911-918.
- [9.] Rahardyan B., T. Matsuto, Y. Kakuto & N. Tanaka, (2004). Resident's Concerns and Attitudes towards Solid Waste Management Facilities, *Journal of Waste Management* 24,437-45, Japan.
- [10.] Read A. D. (1998). Getting the message across: recycling in Kensington and Chelsea. *J. of Education and Information*, **17**, 299-314.
- [11.] Socio-Economic & Environmental Research Institute of Penang 18. 8.2005 via website <http://www.seri.com.my>
- [12.] Teik K. H. (2005). Heading toward Zero Waste in Solid Waste Management, The Penang Experience, (Pre-Conference) Professional Training Programme on Solid Waste Management in SEA Cities, 4-5 July, Siem Reap, Cambodia.
- [13.] Tom E. & A. D. Read, (2001).Local Authority Recycling and Waste Awareness Publicity/Promotion, *J. of Resources, Conservation and Recycling*, **32**. 275-291, UK.







¹ Katarína KORÁLOVÁ

ENVIRONMENTAL ASPECTS SAFETY RISKS

¹ TECHNICAL UNIVERSITY IN KOŠICE, FACULTY OF MECHANICAL ENGINEERING, DEPARTMENT OF ENVIRONMENTAL STUDIES AND INFORMATION ENGINEERING, KOŠICE, SLOVAKIA

ABSTRACT:

This contribution mentions demand for creating a complex definition of safety risks. The aspect of environment is unimproved in last decades, but it makes worse with tendency of accretive trend. For all that is needed to define safety risks on a large scale take into debate safety of environmental community, too. This article commends for answer problems come out mainly from results performed safety audit. These give to real basis and starting – points for exact definition existent concept. Destination of safety audits is analyse risks complex in a concern, treat them, make a proposal and install principles managing of safety so that it didn't peter out to a creation menace and predicamental situations prevented.

KEYWORDS:

safety, environmental risks, menaces, crise, audit of safety

1. INTRODUCTION

1.1. Claim exacter definition concept safety risks

Safety risks are inseparable component all sociable processes. Although this concept like a corpus wasn't till complexly and expressly defined in literature of specialistic. From that argument is needed this problem analyze to specify.

Term dictionary of emergency control, which come out from decree government SR n. 523/2005, define concept of safety like a aspect system of social, nature, technical, technological, or other system, which enable pursuase defined functions and them evolution on the behalf of human and society in concrete inside and outside conditions.[1] For concept of safety is key factor managing of risk, exploration with purpose minimalization. Probably allege, that potential alternative violation safety this system, object or process is risk. From data shown follow that safety is directly pro rata size unadopted risk.

On basis these dates is possible concept safety risks define also as follow: Safety risks indicate alternative interfere with parallel processes, actions and activities in the concrete points depending up inside and outside conditions. Safety risks manifest in corrupted individual factors safety and they activate due level of menace.

En arere were concepts safety, risk, safety risk analyzed in context with defense and safety of state, prevention of citizens and property, eventually work safety. Now get with evolution community into all areas associated with human activities, a savoir technical, economical, information, cultural, but also ambit environment. [2] Change reception and circulation these concepts and create new attitudes, not only to merit rating, but also to answer accrued situations is due to especially social, commercial, perhaps even economical crises, which community hit in last years in world – wide criterion. [4]

1.2. Environmental – healt aspects safety risks

Now big commination represent come-down quality environment. Biggest contaminator environment is industry, and in the view of his massive evolution we suppose that he will be in the future. In commonness global warming, climatic charges, constantly drawings natural resources, falling-off quality water and atmosphere has not effect only on environment, but massive impact

show also in social, economical ambit and over components of environment and on health state population.

From this argument dwell on environmental safety and health risks with that conjoint in a large constant many international organizations tell quel NATO, OSCE, UNEP, UNECE etc. On word levels were accepted follow international contracts:

- ❖ Aarhus Convention (International convention about access to informations, interest community on process of decision and access to justice in rebus environment);
- ❖ Basel Convention about control moves hazardous wastes over border states and them destruct;
- ❖ Framework Convention OSN about climatic changes;
- ❖ Kjots protocol to global convention OSN about climatic changes;
- ❖ Montreal Protocol about materials, that damage ozone layer;
- ❖ Ramar Convention about marshland;
- ❖ Berlin Convention about safety European free living organism's; and more another's;

In conditions SR is environmental safety solution or covered following laws and rules:

- ❖ Law no. 17/1992 codex about environment;
- ❖ Law no. 543/2002 codex about safety natural and country;
- ❖ Laws about safety individual organs environment (safety of water, air, land, etc.);
- ❖ Law no. 24/2006 codex about appraisal effect to environment (EIA), etc.

Zone of environmental safety relating to all regions human activities, that are any way to relationship between human and environment and is partially care more agreements and codex's relevance to environment. Thereupon is necessarily definition of safety risk expand to the territory of environmental aspects, effects and risks.

This definition must come out from extensional and real defined accessions and conditions and must by legislative fixing.

2. ENVIRONMENT – SAFETY AUDIT

Adequate instrument in solution problem of environment safety is also environmental managing (EM). As the largest polluter environment is factory, is advisable the systems, forms and tools environments management, based on principles spontaneity start application on level of business firms and organizations in a broad sense. This tools offer structural and systematic method of incorporation environmental care to the all business activities. Destination of building environmental orientate management systems is not only respect legal enactment and minimalizing risks, but all the time environmental improvement for purpose of expansion economical and environmental safeties. Optimum instrument which is useful make this conditions which a view to been unbroken safeties on all levels of corporation and at the same time been possible detecting eventual hazard this safeties is environmental- safety audit. His object is not only cut down, eventually preventing geneses risk, but also realize activity so that result was perfect and size of risk been lower to minimum. Purposes, which they should by in ambit of company available. is possible bring together to the next steps:

- ❖ Identification low and strong elements system;
- ❖ Creating conditions for controlling risk in company;
- ❖ Proposition of electivity method for activity in zone „complex safeties“;
- ❖ Positive influence other level controlling of company, with purpose push up quality final commodity or service as part of integrate control system;
- ❖ Higher achievement of economical corporation. [3]

Basic elements of environmental-safety audit and progression their realization is visible on image 1.

Environmental-safety audit is assigned company that wants analyzing and controlling environmental-safety risks his company net, handle them and implementate to global (integrated) management organization. Result of environmental-safety audit is report about global

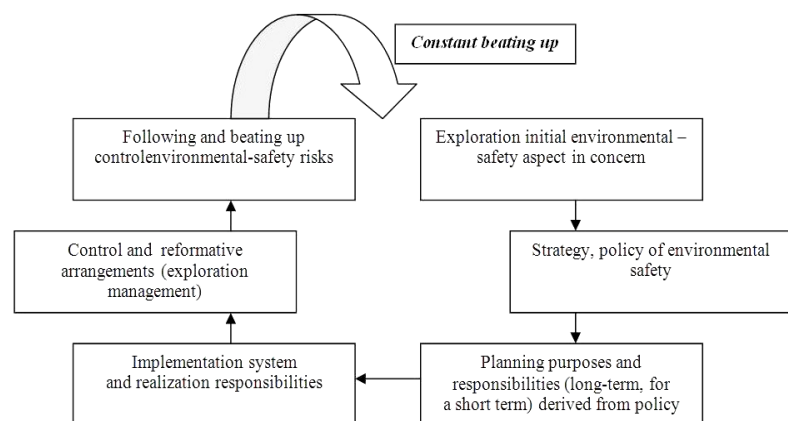


Figure 1. Components environmental – safety audit [2]

reviews in all places of company. This is advisement deuces with relevant standards, legislative and company safety policy.

Managing environmental – safety risks in praxis enable prevent concrete menaces, which invade system of stability and they bring into planned processes, they preclude real prognoses and commercial strategy in the future. [6]

3. CONCLUSION

It is necessary be aware, that neither this complex audit is not absolutely able eliminate all environmental-safety risks. However is applicable instrument for reveals, characterization, analyze and managing safety risks concern complexer. It is necessary show off, that alone audit is only instrument environmental-safety managing. Now Managing of concern risks (his accreditation and certification) is world over coordinated over ISO standards and methodical components. To greates belong: Certification managerial systems environment by ISO 14000; Certification managerial systems BOZP by OHSAS 18001; Certification managerial systems safety of information by ISO 27001 and in ambit SNAS that are e.g.: Methodical regulations MSA CR/01 systems of managing risks ISO/IEC 17 021, ISO/IEC 17011; Systems of environmental managing (EMS)- ISO/IEC GUIDE 66; Systems of managing safety and defense health at work (OH & S MS); Systems of managing safety data's (ISMS); Systems of managing safety foodstuffs(FSMS).

REFERENCES

- [1] ŠIMÁK, L. a kol.: Terminologický slovník krízového riadenia, Fakulta špeciálneho inžinierstva, ŽU, 2005. [citované 10. apríla 2009]. Dostupné na <http://fsi.uniza.sk/kkm/publikacie/tskr.pdf> 2005, ISBN 80-88829-75-5
- [2] MAJERNÍK, M. – BADIDA, M. – LEGÁTH, J.: Systémy environmentálneho manažérstva: Teória a metodika. Košice: Vienaľa, 2002. 303 s. ISBN 80-7099-976-4
- [3] PIATRIK, M.: Environmentálny manažment III. Systém manažérstva kvality a systém manažérstva bezpečnosti práce. Banská Bystrica: Fakulta prírodných vied UMB, 2004. 137 s. ISBN 80-8083-091-6
- [4] MAJERNÍK, M. – BADIDA, M. – MESÁROŠ, M.: Environmentálne manažérstvo: Projektovanie systému. Košice: Vienaľa, 1999. 227 s. ISBN 80-7099-431-2
- [5] ŠIMÁK, L.: Manažment rizík. Žilina, FŠI ŽU, 2006. 116 s.
- [6] LOVEČEK, T. – RISTVEJ, J.: Protection of life and property of strategic infrastructure endangering environment. In: Ecology & Safety Journal. International Scinetific Publications. Vol. 2. Published by Info Invest, Bulgaria. 2008. ISSN 1313-2563







GENERAL PROCESS HOW TO ASSESS EXPOSURE TO SOLID AEROSOL IN WORKING ENVIRONMENT

¹⁻³ TECHNICAL UNIVERSITY IN KOŠICE, FACULTY OF MECHANICAL ENGINEERING, DEPARTMENT OF ENVIRONMENTAL STUDIES AND INFORMATION ENGINEERING, KOŠICE, SLOVAKIA

ABSTRACT:

The paper is focused on solid aerosols and evaluate of their exposure. It describes individual parts of assessment (from identification of potential exposure to concluding). At the end of paper there are described the results of assessment as three possible enclosures. Evaluate exposure of solid aerosol and comparison with limit values is one of the reasons why to do this. In the paper there are noticed other reasons why to do this action.

KEYWORDS:

Exposure, solid aerosol, working environment

1. INTRODUCTION

Solid aerosol can be produced from many sources. Generally, any activity which involves burning of materials or any dust generating activities are sources of solid aerosols. People are exposed to a variety of potentially harmful agents in the air that they have to breathe.

Solid aerosols are very important chemical factor in working environment. It has significant impact on human health. It is also important to know impacts of this factor to human health. This impact depends on exposure to solid aerosol in the working environment.

Measurement or estimation of actual human exposure, coupled with appropriate assumptions about associated health effects or limit values (e.g., acceptable daily intake, tolerable daily intake), is the standard method used for determining whether intervention is necessary to protect and promote human health.

2. ASSESSMENT OF EXPOSURE TO SOLID AEROSOL

Procedure of assessment of exposure to solid aerosol is based on standard EN 689. It is very universal procedure. It can be also modified. The modification depends on many factors for example type of solid aerosol.

Assessment of exposure to solid aerosol consists of three steps:

- ❖ assessment strategy,
- ❖ measurement strategy,
- ❖ measurement procedure,
- ❖ conclusion of assessment.

Assessment of exposure to solid aerosol is realized at the first evaluation and then after every significant change of working conditions, change in technology or change of limit values in legislation.

The figure 1 shows procedure of assessment of exposure to solid aerosol.

3. ASSESSMENT STRATEGY

Assessment strategy is introduction to assessment of exposure to solid aerosol. It consists from three parts. Table 1 describes details of individual parts. There are presented concrete activities.

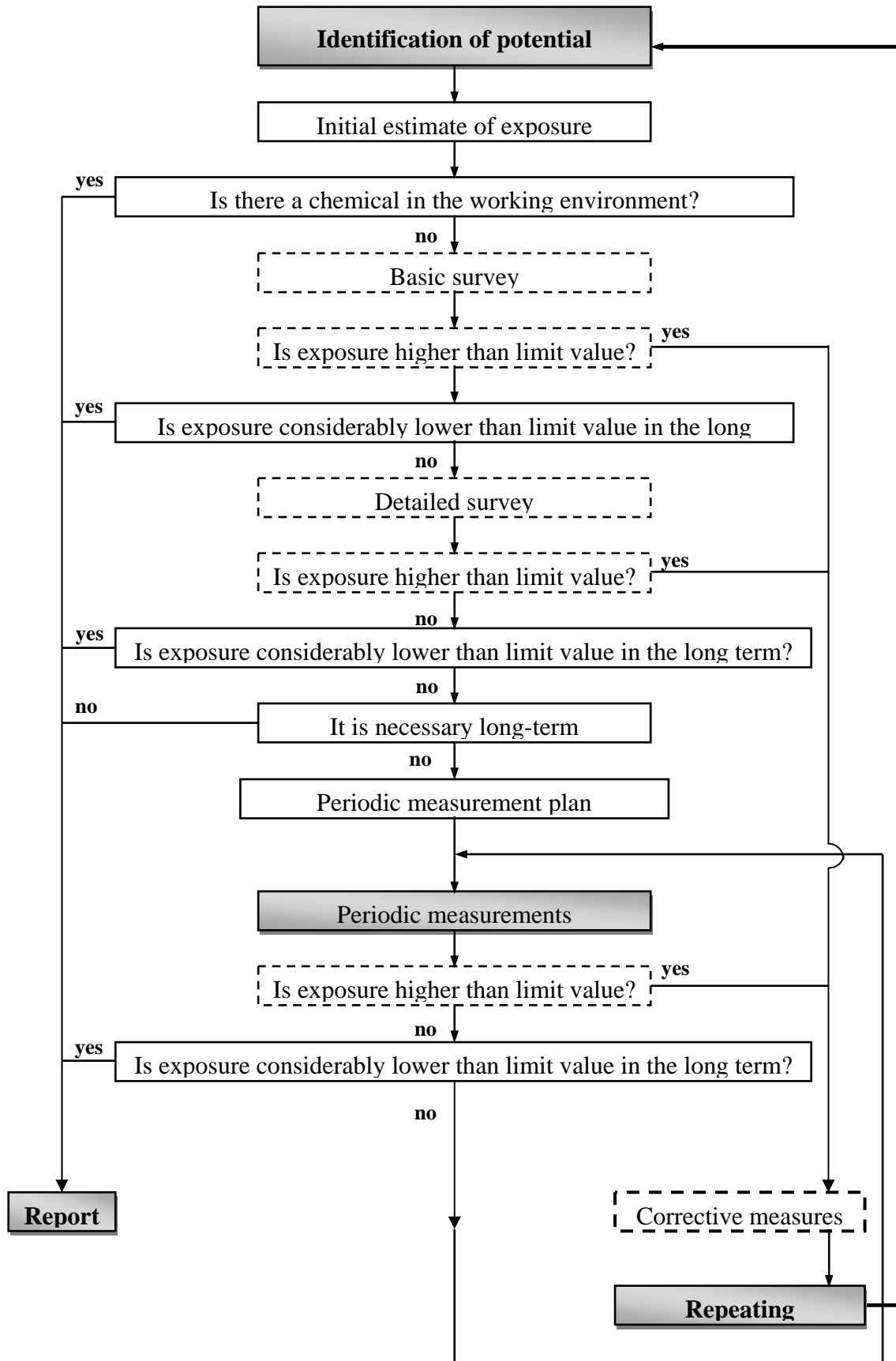


Figure 1 Procedure of assessment of exposure to solid aerosol by EN 689

Table 1 Details of individual steps

step		action
1.	Identification of potential exposure	– preparing the list of chemicals, – determination limit value for chemicals.
2.	Determination of workplace factors	– determination of working process and procedure,
3.	Evaluation of exposure	– initial estimate, – basic survey, – detailed survey.

4. MEASUREMENT STRATEGY

Measurement strategy is selected on the base of the assessment strategy. It includes the following steps:

- ❖ employees selection. It can be: casual, grouping workers into homogeneous groups or based on to the experience.
- ❖ measurement in the fixed point. It can be used only in certain cases. The measurement is realized close to employees' breath area.
- ❖ selection measurement conditions. It depends on kind of measurement.
- ❖ progress of measurement. It can be affected by different conditions: the frequency and duration of work tasks, analytical conditions etc. If conditions during the measurement are without significant changes, sample time could be shorter and minimal number of samples could be lower.

5. MEASUREMENT PROCEDURE

Measurement procedure must offer representative results.

Process of measuring includes:

- ❖ specification chemicals,
- ❖ sampling procedure,
- ❖ analytical procedure,
- ❖ sampling points
- ❖ duration of sampling,
- ❖ timing measurement and interval between measurements,
- ❖ calculations of concentrations of chemicals in the work environment of individual analytical values,
- ❖ other technical instructions for measurement,
- ❖ work activities which should be monitored.

In the case if is possible, it should be used equipment for personal sampling. This equipment is placed directly to the employee's clothes. Sampling head is placed close by employee's breath area. It is the best way how to obtain relevant results.

6. CONCLUSION OF ASSESSMENT

It is necessary to formulate conclusion of assessment irrespective of previous three steps of assessment. This conclusion is formulated based on comparison. It means comparison between calculated results and the limit value – highest permissible exposure limit. These limit values are notice in legislation. Limit values are determined by the whole working time as average value of the overall concentration exposure of solid aerosol or respirable fraction of solid aerosol. There are three possibilities:

- ❖ exposure is higher than limit value – it is necessary to adopt appropriate corrective measures and also periodic measurements are necessary,
- ❖ exposure is considerably lower than limit value – it is not necessary to adopt corrective measures and periodical measurements,
- ❖ exposure is just below the limit value – periodic measurements are required.

The highest permissible exposure limit is for two basic groups of solid aerosols:

- ❖ solid aerosols mostly with toxic effects,
- ❖ solid aerosols without toxic effects.

If there is in working environment more than one substance, they will influence together. Limit value will be calculated by the equations. These equations are notices in legislation. Whole process of assessment exposure to solid aerosol is finished after the elaborating of Report of measurement.

7. FINAL REMARKS

In this paper there was shortly characterized process of assessment exposure to solid aerosol in the working environment.

This process also enables:

- ❖ assessment dustiness in working environment,
- ❖ evaluation effectiveness of the used measures for decreasing dust production,
- ❖ assessment risk of dust or assessment individual dust load,
- ❖ appreciate machines, technological process or working operation,
- ❖ provide background papers for epidemiological research.

The procedure described in this paper can be used for different chemicals (not only solid aerosol).

ACKNOWLEDGEMENT

This paper was supported by the project KEGA 3/7422/09 and KEGA 3/7426/09.

REFERENCES

- [1] EN 689: Workplace atmospheres. Guidance for the assessment of exposure by inhalation to chemical agents for comparison with limit values and measurement strategy.
- [2] <http://www.inchem.org/>
- [3] LUKÁČOVÁ, K.: Prašnosť v pracovnom prostredí a jej vplyv na zdravie človeka. Písomná práca k dizertačnej skúške. Košice, 2009, 90 s.





¹Lenka MAGULÁKOVÁ, ²Lenka RUSINOVA, ³Ladislav BARTKO

POSSIBILITY OF USAGE A NONSTANDARD SOURCES FOR WIND ENERGY

¹⁻³TECHNICAL UNIVERSITY IN KOŠICE, FACULTY OF MECHANICAL ENGINEERING,
DEPARTMENT OF ENVIRONMENTAL STUDIES AND INFORMATION ENGINEERING, KOŠICE, SLOVAKIA

ABSTRACT:

At the present time the usage of alternative source of energy is really actual from the point of view to save the natural sources for the next generations, to decrease the pollution of environment. Energetic economy measure has high influence on decreasing emission of materials as well as green house gasses which are conducive to fulfill state's strategies in environment area and climate changes. This article is focused on the problematic of usage the wind power to produce the electric energy as an alternative source of energy. It also highlight the positive effect of the nonstandard source of wind energy using the M.A.R.S. turbine.

KEYWORDS:

Wind energy, offshore wind energy, turbines M.A.R.S.

1. INTRODUCTION

Offshore Wind Energy (OWT) stations produce clean energy without any emissions, which neither cases any climatic changes nor pollute the air. This kind of electric energy production represents the home source of energy production, that we have not have to pay for it to the foreign companies and we become more self-sustaining and energy independent.

2. OFFSHORE WIND ENERGY

Currently are mostly construct OWT with watts in the range of 1,5 – 2,5 MW. Modern OWT are less noisy than the old one, that's why they are also accepted by vicinetum. The designed life of those OWT is 20 till 25 years. During the designed life, the OWT should work at least 120 thousands of hours.

Suitable areas for an OWT are areas where the average wind speed is at least 6 m/s in the high of 60m above the terrene. The areas with lower average wind speed are not suitable due to lower power of a wind. The best areas are the mountain areas and the lowlands. The construction of an OWT is forbidden in the national parks which decreases the amount of suitable areas with enough wind power. This kind of restriction eliminates a huge part of suitable areas in Slovakia to construction an OWT, nevertheless there are a lot of areas where they can be built the OWT ranches. It is also important to mention, that the enough wind power is just one part of requirements to build an OWT ranch. The other requirements are: ability to connect to the distribution network, area that does not affect the national parks or the diversity of human population in near by areas. Those factors also eliminates a lot of suitable areas [1].

3. MAGENN AIR ROTOR SYSTEM (M.A.R.S.)

The system Magenn air rotor system (M.A.R.S.) is one of the types of OWT. This kind of turbine is lighter than the air. It uses the wind power to produce electric energy. The reason why it is possible to stay in higher level of atmosphere is the Helium that is used to fulfill the turbine. This helps the turbine to be in areas where wind has higher speed, than on the lower levels of atmosphere. The M.A.R.S. spins around the horizontal axis following the wind direction. This way

is produced more energy from the wind power, which is transferred to the surface transformer station using the cables. It has a lot of advantages comparing to the conventional OWT e.g. low cost of produced electric energy, lower noise, turbine is placed in higher location, lower constrains where it can be placed, high mobility level, it is not required to use a heavy duty machines, lower risk to harm a birds or bats.

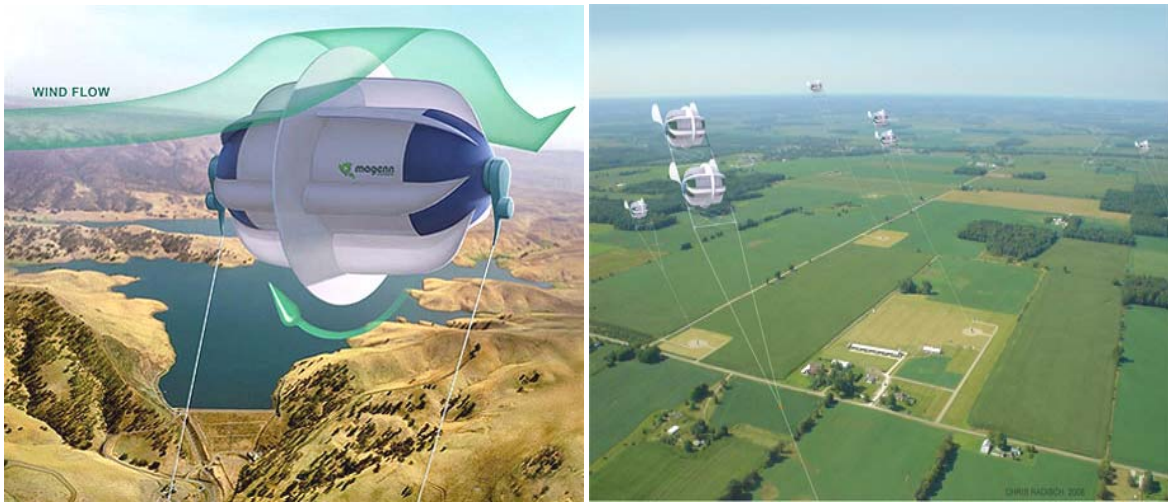


Figure 1 Turbine M.A.R.S. [2]

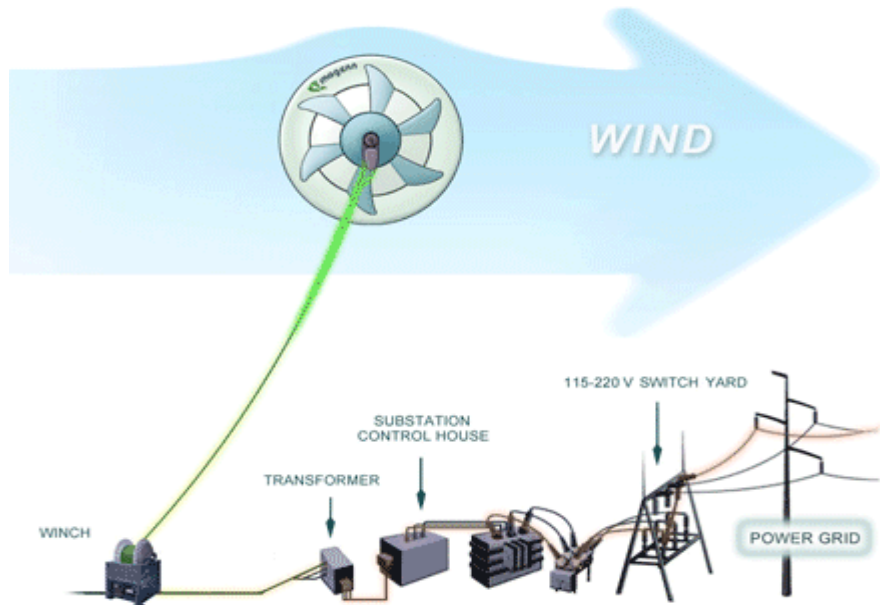


Figure 2 Schema of wiring connection for the M.A.R.S. [2]

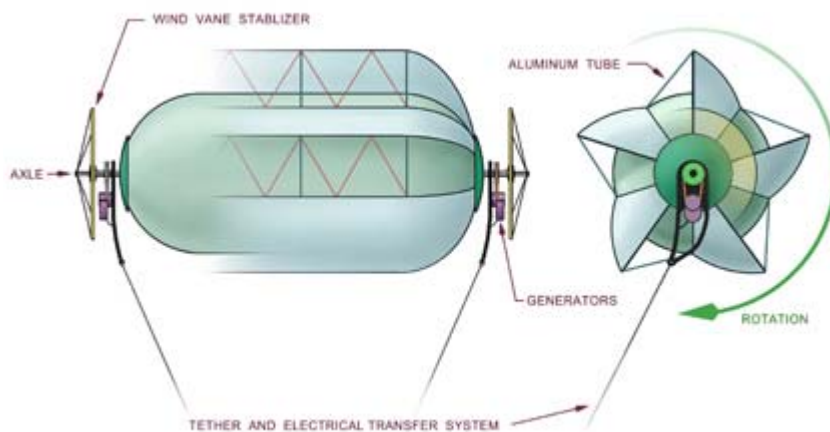


Figure 3 System functioning fundamentals of M.A.R.S. [2]

The OWT M.A.R.S. can be taken out higher over the surface, than the conventional systems, so it can catch more power full wind. The conventional systems are placed in areas where the wind is higher over the surface e.g. coastlines or mountain terrenes. The most suitable areas are in national parks, areas far away from the consumers of the electric energy, which raise up the energy losses during the long-distance power transmission. This mentioned problems are able to be solved using the M.A.R.S..

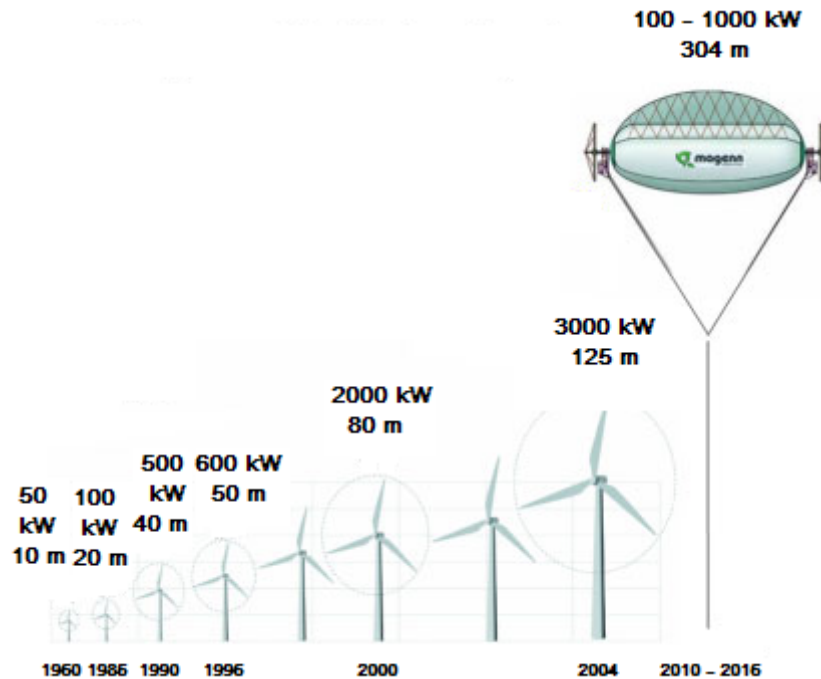


Figure 4 Overview of wind turbines. [2]

The OWT M.A.R.S. cannot be placed in any air-space nor closer than 8km from the airport. The caring balloon contains the reflex material and also radar using the frequency in the range 200 - 2700 MHz. The cover and backband of the M.A.R.S. system is made of material that are lighter and stronger than the steel, has almost no absorbability, abrasively resistance and UV rays.

4. IMPACT OF WIND TURBINES ON THE ENVIRONMENT

The biggest problem of the classical OWT is that there is a direct contact with birds and bats that end by death. The rotors of turbines are moving, which case a lot of problems to avoid for them. The advantage of the M.A.R.S. is that it stays on one place without moving, which allows the birds and bats to easily avoid it.

5. CONCLUSION

The OWT M.A.R.S. is suitable to produce the electric energy due to its ability to use in the developing countries with reduced infrastructure or in the areas of country where is no infrastructure. This approach of energy producing is also able to use on islands, outlying farms, during the nature catastrophes.

ACKNOWLEDGEMENT

This paper was written using project KEGA 3/7426/09 Creation of didactic details and publishing of university textbook "Physical factors of environment - valuation and assessment" for main field 2nd and 3rd level of study environmental focused studying programs.

REFERENCES

- [1] Úrad vlády Slovenskej republiky: Materiál z rokovania vlády SR: Accessible: <http://www.rokovania.sk/appl/material.nsf/0/92AF7F8727FE82ECC12572C30041823C?OpenDocument> (2009-12-15)

- [2] Magenn wind power anywhere: Magenn power air rotor system: Accessible:
<http://www.magenn.com/> (2010-02-01)
- [3] Ubergizmo: High flying wind turbines: Accessible:
http://www.ubergizmo.com/15/archives/2007/04/high_flying_wind_turbines.html (2009-12-15)
- [4] Alternative energy sources information website: Air Turbines: Technology: Accessible:
<http://www.netpilot.ca/aes/at/tech.html> (2009-12-15)





¹Zsuzsa FARKAS, ²Péter LÉVAI

GROWING GREENHOUSE CUT FLOWER IN HYDRO-CULTURE

¹⁻² DEPARTMENT OF FLORICULTURE LANDSCAPE ARCHITECTURE,
FACULTY OF HORTICULTURE, COLLEGE OF KECSKEMET, HUNGARY

ABSTRACT:

The importance of hydro-cultural growing is significantly increasing. We have been dealing with the hydro-cultural growing of cut flowers at the Department of Ornamental Plant Growing and Maintenance of Gardens at the College Faculty of Horticulture at Kecskemét College since 1988. We started our experiments by growing carnation in growing establishment without soil then we introduced other species of cut flowers and potted ornamental plants into our research work (Lévai *et al.*, 2010/b). Our aim was to examine the effect of Grodan and PU-sponge media on the growth, the yield of flowers, the diameter of the flowers and the length of the stem concerning the species of carnation 'Pink Castellaro'. In case of comparing the species our aim was to examine the effect on the development of the plants, the yield and the characteristics of the flowers: the diameter of the flower and the length of the stem.

The Phytomonitor instrument is placed in the French Filclaire greenhouse and we at the Floriculture and Park Maintaining Department measure rose culture parameters in hydroponics. We measure the following factors: air temperature, leaf temperature, radiation, relative humidity of air, stem diameter and soil moisture (Lévai- Turiné, 2009.)

Using Phytomonitor data processing make it possible to use nutriment in an optimal level thus apply a low-cost environmentally friendly technology.

KEYWORDS: hydroculture, carnation, Rose, PU sponge, Grodan, Phytomonitor

1. INTRODUCTION

The effect of the species on the flower diameter of carnation: Most of the species in the experiment reached or exceeded the parameters of 1st class products determined by the standards, minimum was 7.0 except for the values of 6,91 and 6,96 of 'Candy' and 6,87 and 6,89 of 'Ondina' average yearly flower diameter (Lévai *et al.*, 2010).

The largest flower diameters of the red species were experienced in the case of 'Iury' and 'Rodolfo', from the point of flower diameter these species are worth being involved in hydro-cultural growing. In case of the 'Castellaro' species 'Pink Castellaro' produced significantly larger flowers (Lévai – Turiné, 2005).

Experiments with the species:

- ❖ 'Danton' is of high growth, of good yield, with large flowers and long stem
- ❖ 'Gigi' is of high growth, of good yield, with large flowers and long stem
- ❖ 'Iury' is of high growth, of average yield, with large diameter of flower and long stem
- ❖ 'White Castellaro' is of high growth, of good yield, with large diameter of flower and long stem
- ❖ 'Pink Castellaro' is of high growth, of excellent yield, with large flower and long stem
- ❖ 'Candy' is of average growth, of excellent yield, with average size of flowers, with average long stem
- ❖ 'Rimini' is of high growth, of good yield, with large flowers, really long stem
- ❖ 'Rodolfo' is of high growth, of excellent yield, really large flowers, really long stem
- ❖ 'Ondina' is of average growth, of good yield, with average size of flowers, long stem
- ❖ 'Olivia' is of high growth, of excellent yield, with large flowers and long stem

Each of the species in the survey is adequate for hydro-cultural growing (*Lévai – Turiné, 2005a, b; Lévai – Turiné, 2007*).

2. MATERIAL AND METHODS

We made experiments of hydro-cultural growing of carnation with the following species: 'Danton', 'Gigi', 'Iury', 'White Castellaro', 'Pink Castellaro' and 'Candy', 'Rimini', 'Rodolfo', 'Ondina', 'Olivia'.

The experiments of carnation were carried out by the French Filclair growing establishment, growing was arranged in a closed, circular system. The planting of shoots with roots was arranged by 40 pieces/m² at the end of May. We applied PU-sponge as the medium of plantation for the comparative experiments, the length of the growing season was one year. The experiment was carried out by repeating the procedure four times. The supply of nutritional material was made by using complex chemical fertilizer, the pH of the nourishing solution was 5,0-6,5, the conductivity was 2,5-3,5 mS and these parameters were continuously controlled. We measured the quantity of the picked flowers from the beginning of blooming each time. We chose 10-10 of the picked flowers by random choice and measured the characteristics of flower quality: the diameter of the flower and the length of the stem.

A PhyTech company plays a pioneer role in the Phytomonitoring™ system, it detects the plants remotely. It uses advanced methods, collects and analyses the data derived from wireless communication sensors and innovative softwares. The main purpose is the detection of early plant stress, optimal growth and quality of product to increase income.

Results

The effect of the media on the height of the carnation

In case of the hydro-cultural growing of carnation both the polyurethane-ether sponge and Grodan had a good effect on the growth of the plant, both are adequate as a plantation media but the stock grown in the sponge was higher.

The effect of the media on the yield of the carnation

We managed to reach the average flower yield of 7-9 flowers per stem (Figure 1.) characteristic of the traditional chemo-cultural growing in case of hydro-cultural growing in polyurethane-ether sponge and in Grodan that is both are adequate plantation media for hydro-cultural growing.

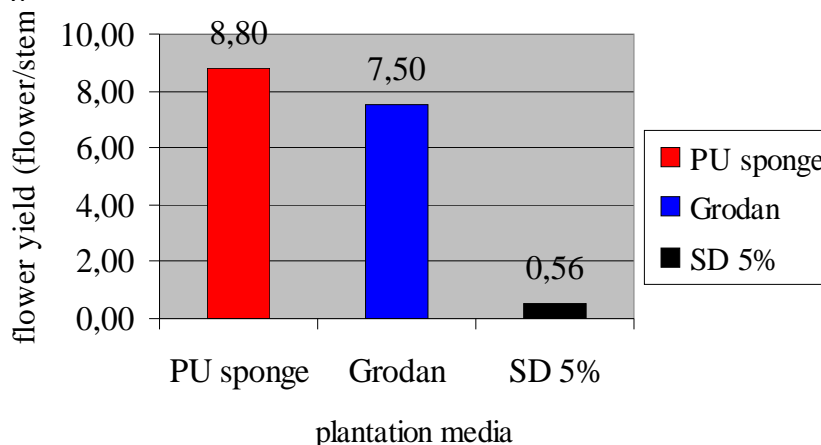


Figure 1. The effect of plantation media on the yearly yield of carnation 'Pink Castellaro' (Kecskemét, 1999-2000.)

The effect of the media on the flower diameter of the carnation

During the two growing seasons of the experiments the average diameter of the flowers planted in polyurethane-ether sponge and in Grodan reached the parameters of 1st class flowers that is 7-cm flower diameter. We did not experience significantly better results in case of the two media so both are adequate for the hydro-cultural growing of carnation.

The effect of the media on the length of the flower stem of carnation

The plantation media influenced neither the yearly nor the monthly length of the stem significantly in the years of research.

Taking the yearly average into consideration we reached the requirement of 1st class quality that is 55-60-cm stem length in case of both media.

Considering all the above both polyurethane-ether sponge and Grodan are adequate media for hydro-cultural growing.

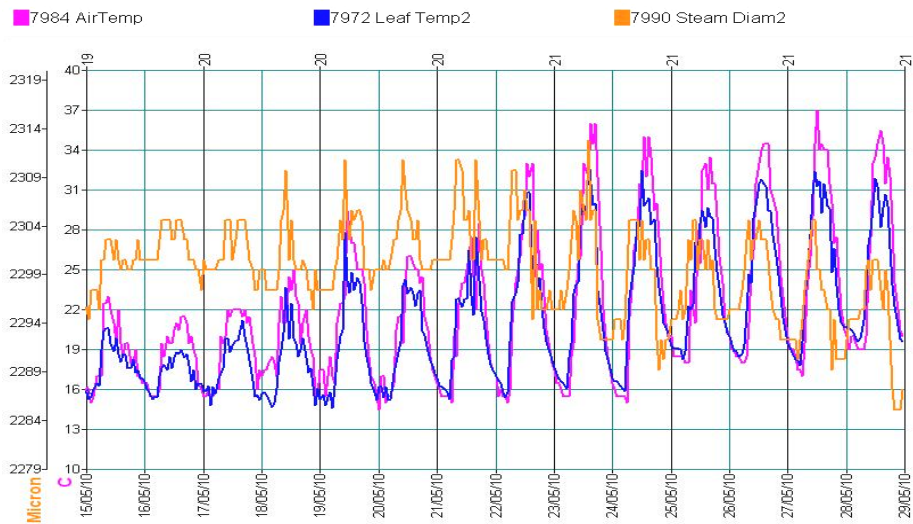


Figure 2: The effect of air temperature on rose leaf temperature and expansion of stem (2010.Kecskemet)

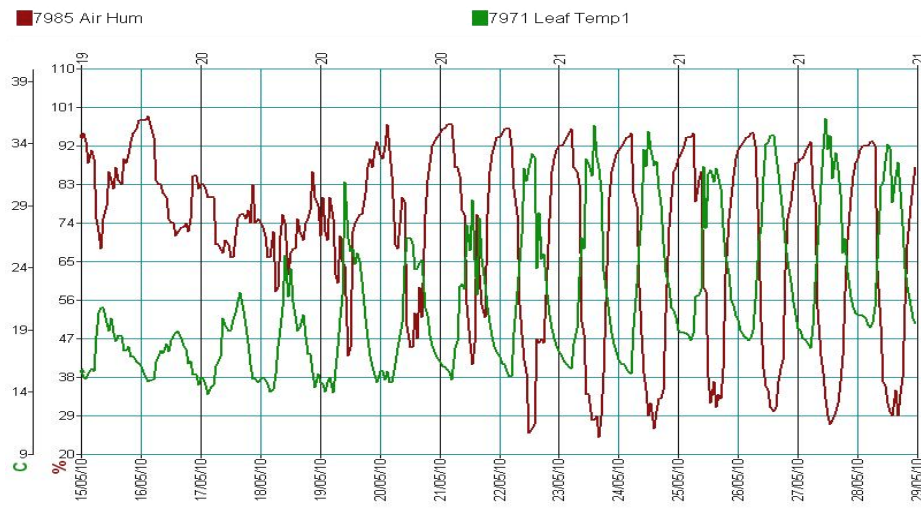


Figure 3.: Rose leaf temperature in relation with the air humidity (2010.Kecskemet)

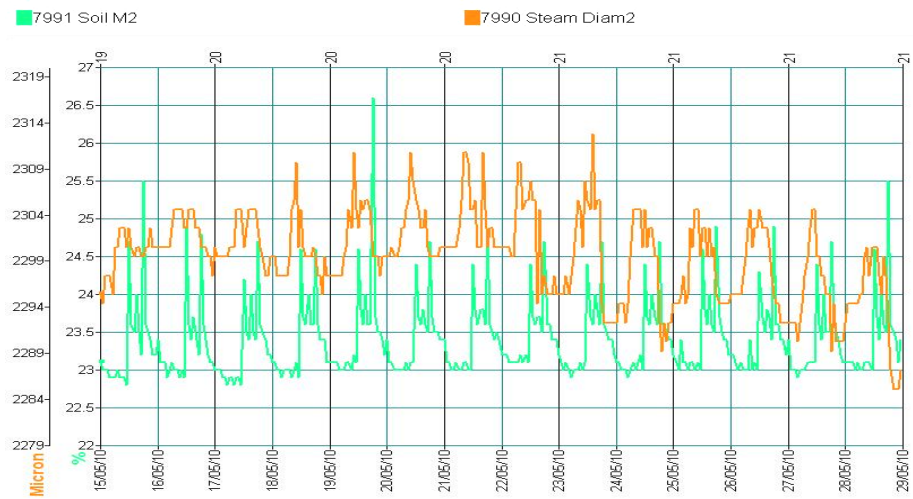


Figure 4: The expansion of rose stem in accordance with soil wetness (2010. Kecskemet)

The fluctuation of air temperature well indicates the change of the phases of the day (Figure 2). The expansion of stem follows this cycle. It was pointed out that the higher was the daily maximum temperature the expansion of stems was more intensive. Respectively the fewer daily fluctuation made the stem expansion more stable. By the increase of daily temperature the

expansion of stems are significant. The temperature of leaves increases parallel with the air temperature.

By the increase of temperature the relative humidity decreases. The temperature change of leaves follows the change of air temperature (Figure 3). According to it the relative humidity is higher in the night and lower in the day.

The wetness of soil indicates the time of irrigation (Figure 4). The expansion of stems well follows the wetness of the soil.

3. DISCUSSIONS

Concerning environmental protection PU sponge is more and more adequate media for growing carnation since it can be used until complete decomposition. Both PU sponge and Grodan have got a favourable effect on the growth of the plant, the yield of the flowers and the flower quality characteristics that is why Grodan is also an adequate media for the hydro-cultural growing of carnation. Phytomonitoring is one of the growing decision support devices which gives fast information about the tendency of plant development. It is an information technology which provides the grower with incredibly valuable information about the plant physiologic stage.

REFERENCES

- [1.] Lévai P. – Turiné Farkas Zs. (2005a):. Development of Hydro-Cultural Carnation Growing. Lippay János – Ormos Imre - Vass Károly Tudományos Ülésszak Budapest, 2005. otóber 19-21. 75 p.
- [2.] Lévai P. – Turiné Farkas Zs. (2005b):. The hydroculture of carnation. 10th International Scientific Conference. 20th April 2005, Nitra 51p.
- [3.] P. Lévai –Zs. Turiné Farkas (2007): The development of hidroponic way of growing in floriculture. "Lippay János – Ormos Imre – Vas Károly" Tudományos Ülésszak 2007. november 7–8. Összefoglalók, Kertészettudomány. Budapesti Corvinus Egyetem, Kertészettudományi Kar, Budapest 63. p.
- [4.] Lévai P. – Turiné Farkas Zs. (2009): Legújabb eredmények a Phytomonitor használatának következtében Erdei Ferenc V. Tudományos Konferencia Kecskemét, 2009. szeptember 3–4.
- [5.] Lévai P. – Ferencz Á. – Nótári M. (2010): The Marketing Analysis of some ornamental Plants in Hungary International Society for Horticultural Science 28th International Horticultural Congress Portugal, Lisboa 220.p.
- [6.] Lévai P. – Ferencz Á. – Nótári M. (2010): Image Profile Analysis of Cut Flowers in Hungary International Society for Horticultural Science 28th International Horticultural Congress Portugal, Lisboa 221.p.





METHODS FOR RECOVERY AND RE-USE OF SLUDGE RESULTED FROM WASTE WATER TREATMENT

¹⁻⁴ UNIVERSITY POLITEHNICA OF BUCHAREST – SCIENCE AND MATERIAL ENGINEERING FACULTY, ROMANIA

ABSTRACT:

Most of the water treatment plants discharge their sludge to the environment without consideration of possible side effects. Since this kind of sludge is generally considered pollutant, the sludge treatment of water industry seems to be an essential task. These sludges from wastewater treatment process must be treated in a safe and effective manner. There are many ways to manage these sludges. One very important is this use on agriculture, as support for different crops, after their pre-treatment thus the content of hazardous pollutants to be reduced and even totally destroyed.

KEYWORDS:

sludge, soil, biodegradable wastes, biogas

1. INTRODUCTION

Sludge originates from the process of treatment of waste water. Due to the physical-chemical processes involved in the treatment, the sludge tends to concentrate heavy metals and poorly biodegradable trace organic compounds as well as potentially pathogenic organisms (viruses, bacteria etc) present in waste waters. Sludge is, however, rich in nutrients such as nitrogen and phosphorous and contains valuable organic matter that is useful when soils are depleted or subject to erosion. The organic matter and nutrients are the two main elements that make the spreading of this kind of waste on land as a fertilizer or an organic soil improver suitable.

2. THE BIODEGRADABLE WASTES

The Sewage Sludge Directive 86/278/EEC seeks to encourage the use of sewage sludge in agriculture and to regulate its use in such a way as to prevent harmful effects on soil, vegetation, animals and man. Treated sludge is defined as having undergone "biological, chemical or heat treatment, long-term storage or any other appropriate process so as significantly to reduce its fermentability and the health hazards resulting from its use". To provide protection against potential health risks from residual pathogens, sludge must not be applied to soil in which fruit and vegetable crops are growing or grown, or less than ten months before fruit and vegetable crops are to be harvested. Grazing animals must not be allowed access to grassland or forage land less than three weeks after the application of sludge. The Directive also requires that sludge should be used in such a way that account is taken of the nutrient requirements of plants and that the quality of the soil and of the surface and groundwater is not impaired.

Within the term "biodegradable waste" we can consider livestock manures, sewage sludge, organic fraction of municipal solid waste and the residues of some industries (food processing, paper, textiles, wood, etc).

It is a difficult task to estimate the industrial and agricultural quantities of bio-waste (waste versus byproducts), the variable or unknown water content and the "in situ" recycling operations. The quantity of sludge has been increasing greatly in Europe after the implementation of Council Directive 91/271/ECC on urban wastewater treatment. Recent official reports coming from a survey financed by EU results in a production of 7,5 millions of tones (dry matter).

In our country, the Council Directive 91/271/ECC is implemented by Order no. 344 / 2004 referring to wastewater sludge requirements in case of their use onto agriculture soils.

The environmental balance of the various options available for the management of this waste can depends on a number of local factors, inter alia collection systems, waste composition and quality, climatic conditions, the potential of use of various waste derived products such as electricity, heat, methane-rich gas or compost. Thus, the objectives followed for managing the wastes are:

- ❖ The promotion of the biological treatment of organic waste by harmonizing the national measures in order to prevent or reduce any negative impact on the environment.
- ❖ The protection of soil and the insurance in the use of bio-waste results in agricultural benefit.
- ❖ The insurance that human, animal and plant health are not affected by the use of bio-waste.

Only treated bio-waste is allowed to be spread on land. High quality standards for compost are required.

In the next graph, the maximum admitted values are given for metals, as mg/kg dry soil, from soil and also from sludges, as comparison.

The main steps for wastes management is the separate collection, composting, anaerobic digestion (biogas recovery), biological treatments and finally uses on land.

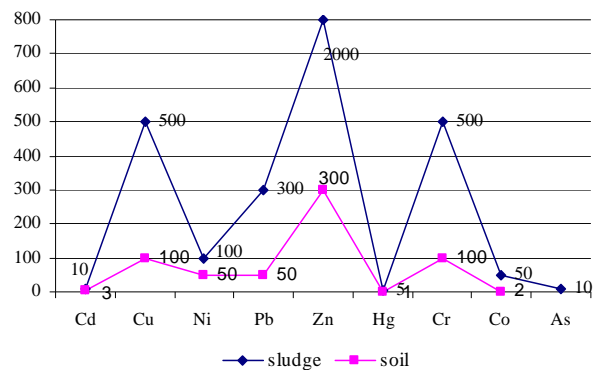


Fig. 1: Maximum admitted values, mg/kg dry soil, for metals from sludge and from soil where the sludge is use

3. Methods for re-use of biodegradable wastes

In wastewater treatment plants, the high quantities of sludges may be *an important source of organic matter for agriculture soil*. This type of sludge contains fertilizing substances, about 50% from nitrogen and potassium being present in fermented sludge. There are also other ways to re-use the sludge.

The agricultural use or land application of organic waste is considered the best environmental option.

One of the alternatives for re-use of biodegradable wastes is the use of these as *road construction materials*, combined with a marine alga. This represents a new re-use alternative in order to preserve natural resources, having in mind the difficulty of choosing a proper method for diminution of environmental impact. Using a proportion of 0, 20, 50, 80 % clay content, it can be obtained palletized aggregates with density between 1,48 and 2,25 g/cm³, in comparison with 2,56 g/cm³ as granite density.

Another re-use option is the obtaining of *biogas*, as a mixture of combustible gasses formed by organic matters decay in wet atmosphere and without oxygen. The main component of biogas is the methane. The process of biogas formation is the anaerobic fermentation between 20 – 45 °C, in the presence of two bacteria species:

- ❖ *Bacilus cellulosa* methanicus, responsible for methane formation and
- ❖ *Bacilus cellulosa* hidrogenicus, responsible for hydrogen formation.

With the help of anaerobic fermentation, the microorganism decomposes the organic matter, releasing some metabolites as carbon dioxide and methane.

Among the chemical components of organic matters, the highest conversion rate belongs to the cellulose, hemicelluloses and fats.

An industrial biogas plant has as components:

- ❖ Wastewater pump station;
- ❖ Settling tank;
- ❖ Sludge dewatering device;
- ❖ Sludge pump station;
- ❖ Anaerobic fermentation chamber for biogas capture.

By help of anaerobic fermentation the high quantities of biogas may result. From anaerobic fermentation is obtained a stabilized sludge which can be valorized into agriculture or used as inert material for disposal.

There are some factors influencing the quality of anaerobic fermentation, from material quality and installation parameters to enzymatic equipment, more difficult, with complex methods for investigation. Some of process factors are presented below:

- ❖ *Solids substances concentration from sludge* chosen to assure water consumption for bacteria; it is important a concentration about 5-10% solids; highest concentration made difficult the pump and homogenized process.
- ❖ *Organic component of the solid phase* is very important parameter for gas production; it is assumed that about 50% from organic component means a relative stability for sludge. The gas composition is influenced by decomposition rate of organic matter. The main groups which influenced the quantity and gas fermentation composition are: carbon hydrates, proteins and fats.

Anaerobic fermentation is suitable for almost organic substances, except lignin and mineral oils.

- ❖ *Mineral components*, especially nitrogen and phosphorous salts, are important for anaerobic fermentation. Some cations (Ca^{2+} , Mg^{2+} , Na^+ , K^+ , NH^+) have an inhibiting action for anaerobic fermentation for concentrations higher than 10 g/l. In table 1, the limits for some substances influencing the fermentation process are presented.

Table 1. The limits for concentrations of some substances with influence on fermentation process

Substance	Conc. (mg/l)	Substance	Conc. (mg/l)
Sulfides	200	Calcium	2000-6000
Soluble heavy metals	1	Magnesium	1200-3500
Sodium	5000-8000	Ammonia	1700-4000
Potassium	4000-10000	Free ammonium	150

- ❖ *Optimum value pH* is situated between 6,8 and 7,6;
- ❖ *Temperature influence*; anaerobic fermentation takes place between 4 and 60°C; the microorganisms are very sensitive with temperature variations even between 2-3°C.
- ❖ *The mixing – recirculation – inoculation* has as objective the mixing of the settled sludge with the upper sludge from surface, obtaining a fast decay of organic substance and in this way a short time for fermentation process.

Aerobic fermentation represents as well as anaerobic fermentation a biochemical decay process of degradable organic compounds. This alternative, it is possible by separately aeration of sludge (primarily, secondary or mixed) in open tanks. This alternative it is recommended when there is not primarily treatment and for high quantity of activated sludge. The equipment for aerobic fermentation is designed for about 8 – 15 days, depending on sludge characteristics.

Comparing the two systems, it is obviously that anaerobic stabilization is more efficiency then aerobic one, especially energetically point of view. These aspects are presented in table 2. In case of high content of hazardous organic and inorganic compounds in sludges, the incineration may be a solution.

The incineration of the sludge lead to the completely oxidation of the organic compounds and metallic compounds may be found as ash. Incineration equipments have to be designed with washing and filter equipments for exhausted gasses and it is very important that the sludge for incineration to be dewatered. Also, the anaerobic and aerobic stabilization is very important because in this way is diminished the caloric value of the waste. The sludge processing before incineration has to lead to auto - combustion.

Table 2. Data referring to aerobic and anaerobic fermentation

Characteristics	Aerobic Fermentation	Anaerobic Fermentation
Retention time (days)	8 - 15	15 - 20
Energy consumption (KWh/m ³ sludge)	5 - 10	0,2 - 0,6
Comments	Low cost for investment; high energy consumption	High cost of investment and exploitation; Low energy consumption; Energy resource by gas production

The usual equipment for sludge incineration consists of circular rotary kilns with multiple hearths or fluidized beds. Also, in case of neutralization of a dewatering sludge, the *disposal* can be an option.

The disposal involves landfills. These may be on public land such as a municipality owned landfill, or on private land. Landfill operators commonly require 15 to 30 % sludge (solids). The minimum concentration required is often determined by local sanitary landfill regulations. For example, for alum sludges, effective landfilling requires the solids concentration to be at least 25%. At lower concentrations, land application is more appropriate.

4. CONCLUSIONS

In Romania, the most wastewater treatment plants use only mechanical and biological treatment stages. The mechanical treatment consists of screening and primarily settling. Biological treatment consists of aeration, secondary settling, and pump station for recirculation of the sludge.

Sludge treatment plant is rarely used or its function is difficult. In case of its operation, this consists of gravitational thickening tanks, fermentation equipments and dewatering platforms.

According to the latest reports regarding the use of sludge in agriculture, it is can be observed that in 2003, the quantity used for agriculture was about 12% and in 2008 was about 14%, for our country.

The first condition for sludge use into agriculture is its anaerobic fermentation, followed by natural or mechanical dewatering and disposal for at least 60 days.

The spreading of the sludge onto agriculture soil is a very well method, with benefits regarding the crops and the soil quality.

Limits of the application are given by inadequate composition of the sludge (heavy metals) and by the difficult option to find a proper site at a covenant distance.

The management of biodegradable wastes may be a tool for the future use of them as soil amendments by help of the neutral obtained compost. For our country, as well as for European Union countries, the limit of these methods is given by metals presented in sludges (especially heavy metals).

Also there appears a difficult situation in funding the proper site not too far from sludge source to spread them.

REFERENCES:

- [1] X X X: "Use of Reclaimed Water and Sludge in Food Crop Production", National Academy Press, Washington D.C., ISBN 0-309-05479-6, 1996
- [2] W. W. Eckenfelder, J. L. Musterman: "Activated Sludge Treatment of Industrial Wastewater", Technomic Publishing Company, Inc., Basel, Switzerland, ISBN 1-56676-302-9, 1995
- [3] N. P. Cherenmisihoff: "Biotechnology for waste and wastewater treatment", Noyes Publications, Westwood, New Jersey, USA, ISBN 0-8155-1409-3, 1996.





¹Siniša BIKIĆ, ²Maša BUKUROV, ³Dušan UZELAC,
⁴Slobodan TAŠIN, ⁵Marko ĐURĐEVIĆ

FILTER NOZZLE TESTING BY THE INSTALATION WITH COLUMN AND MANOMETER

¹⁻⁵. FACULTY OF TECHNICAL SCIENCES NOVI SAD, SERBIA

ABSTRACT:

This paper deals with filter nozzles which are used for water treatment. They are applied in many sectors including drinking water, water demineralization process, urban and industrial waste water treatment, filtration of river or well water for irrigation, water for swimming pools, etc. The filter nozzles are made from the thermoplastic material, with different number and widths of gaps at the head of the nozzles. It is necessary to determine performance curve of filter nozzle before it is installed. The performance curve actually represents the nozzle water gauge head as a function of flow rate. This performance curve has been traditionally determined by measuring of hydrostatic pressure above the nozzle with level meters (graduated scale, ultrasound, capacity etc.). In order to measure a couple of meters water gauge head, a reservoir is necessary. This research is aimed to examine possibility to apply the installation with column and manometer instead of the reservoir, in order to determine filter nozzle performance curve. The water gauge head is measured by manometer and flow rate through the filter nozzle by mass method. Authors are of the opinion that installation with column and manometer could be successfully applied to determine filter nozzle performance curve. In comparison with the reservoir, the installation with column and manometer is more compact and comfortable.

KEYWORDS: Filter nozzle, column, filtration, washing

1. INTRODUCTION

Filter nozzles are placed in:

- ❖ open systems – for preparation of drinking water, industrial waste water treatment, filtration of river or well water for irrigation, water for swimming pools and
- ❖ closed systems – for preparation of feed, technological and cooling water.

The filter nozzles are made from the thermoplastic material, with narrow gaps at the head of the nozzles. They enables preparation of water using ion exchangers. The number and width of the filter nozzle gaps vary by model. Thanks to the installed nozzle, this kind of filter has very fast filtration. Filter nozzle enables collection and drainage of filtrate evenly. In the process of washing, nozzles make possible water and air to be evenly distributed. In this way filter nozzles contribute to fast, stabile and economic exploitation of filter stations.

One of the most important characteristic of filter nozzle is to deliver sufficient volume of water in processes filtration and washing. In order to check filter nozzle it is necessary to conduct test before installation. Also is necessary to determine performance curve of filter nozzle before installation. The performance curve actually represents the nozzle water gauge head vs flow rate. This performance curve has been traditionally determined by measuring of hydrostatic pressure above the nozzle with level meters (graduated scale, ultrasound, capacity etc.). In Fig. 1 is shown performance curve of model with 40 narrow gaps, 0.2 mm in width at the head of the nozzles (producer BRAN & LUBBE) [2]. In order to measure a couple of meters water gauge head with this method, a reservoir is necessary.

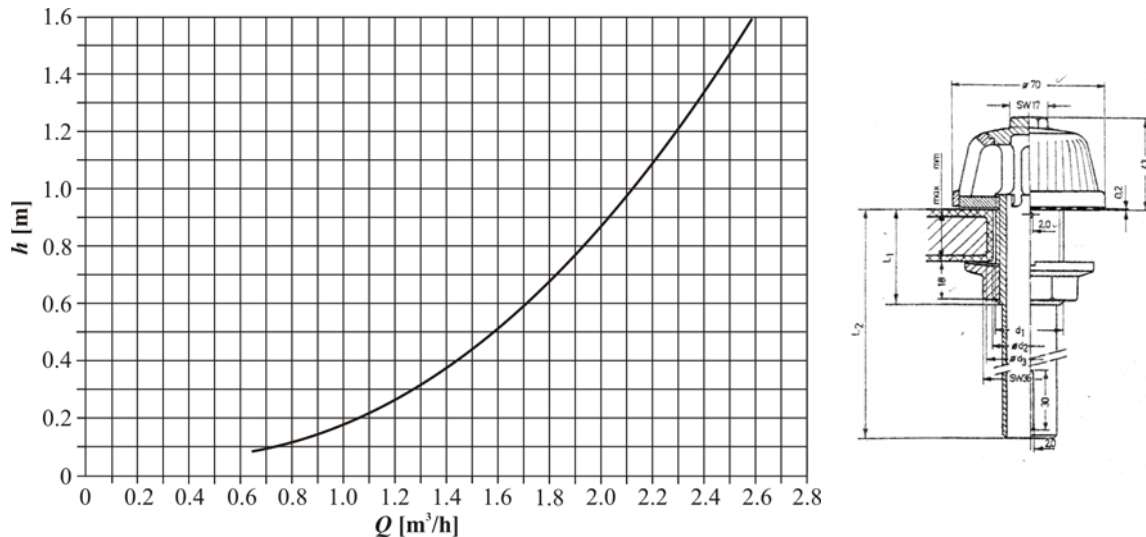


FIGURE 1. The performance curve of filter nozzle of model with 40 narrow gaps, 0.2 mm in width at the head of the nozzles (producer BRAN & LUBBE) [1]

This research is aimed to examine possibility to apply the installation with column and manometer instead of the installation with reservoir, in order to determine filter nozzle performance curve. The hypothesis of work was that installation with column and manometer could be successfully applied to determine filter nozzle performance curve. The report on filter nozzles testing of models RV001/A, RV001/B and RV001/D (producer RAVEX) provides background for this paper [2]. The RAVEX Company from Vrbas, Serbia, is a leader of filter nozzles production in the Balkan region [3].

2. METHODOLOGY OF INVESTIGATION

An installation with column and manometer for filter nozzles testing has been designed at the Faculty of Technical Sciences, Laboratory for Fluid Mechanics. The filter nozzle model RV001/A was tested to verify method with proposed installation. The model RV001/A corresponds to model in Fig. 1, 40 narrow gaps, 0.2 mm in width at the nozzle head [3]. The tests were carried out for two processes: filtration (Fig. 2) and washing (Fig. 3).

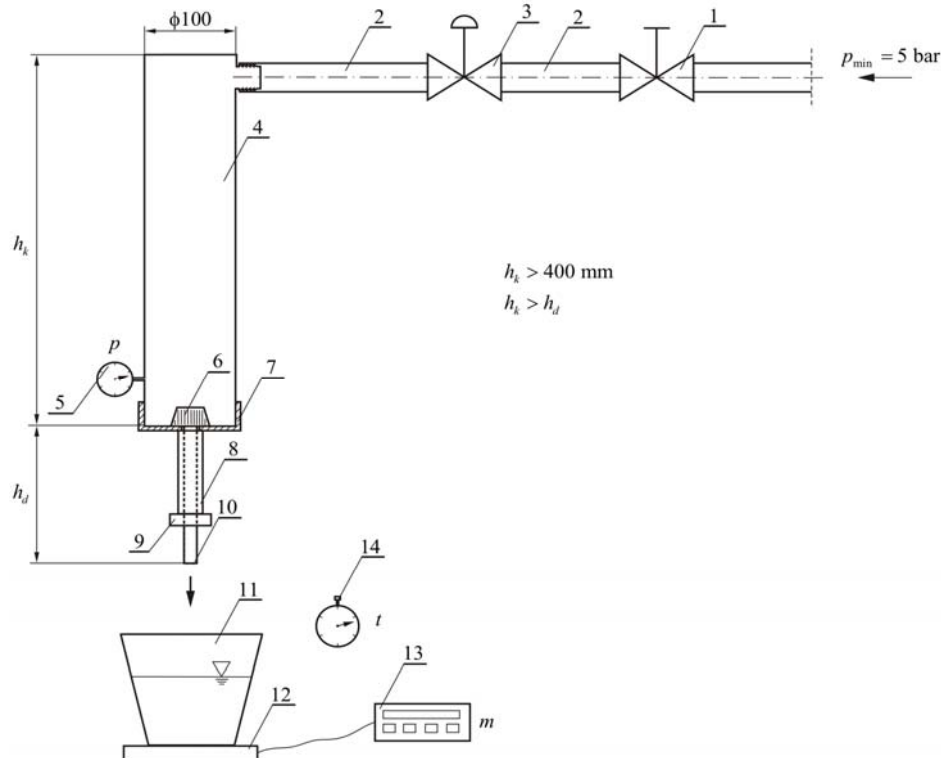


FIGURE 2. Scheme of installation with column and manometer for filtration process

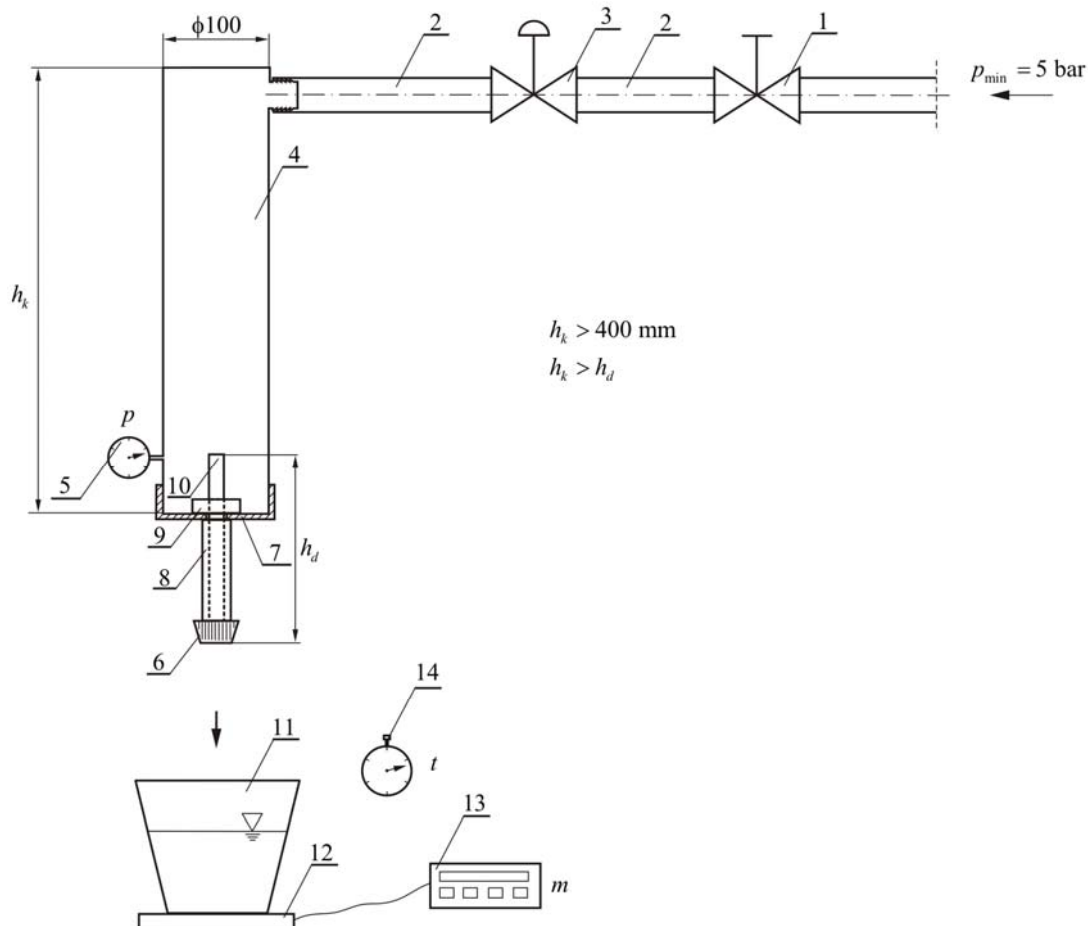


FIGURE 3. Scheme of installation with column and manometer for washing process

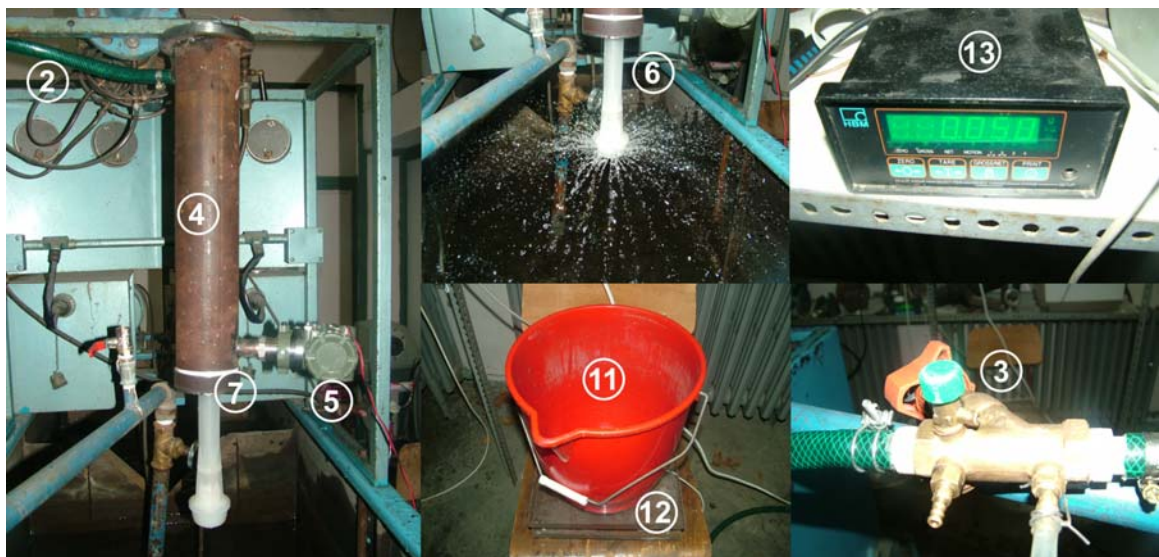


FIGURE 4. View of installation with column and manometer for washing process

In Fig. 2, Fig. 3 and Fig. 4 are: 1-valve, 2-rubber hose, 3-regulator, 4-housing, 5-manometer, 6-filter nozzle, 7-bottom with threaded connection, 8-built in piece, 9-screw nut, 10-nozzle neck, 11-vessel, 12-precision balance, 13-data acquisition and 14-stopwatch.

The length of the housing is $h_k = 550$ mm, which is more than the length of the nozzle neck ($h_d = 400$ mm). Regulation of water flow rate (\dot{m}) was carried out by balance valve (3). The pressure at the position 5 was measured by manometer of producer YOKOGAWA, model EJA530A [4]. The measuring range of manometer is $p = 0 \div 400$ mbar, with uncertainty of $\pm 0,35$ %. The

change of filter nozzle position for two testing processes (filtration in Fig. 2 and washing in Fig. 3) was enabled by bottom with threaded connection 7 and built in piece 8. The mass of water (m) was measured with precision balance (12) with uncertainty of $\pm 0,02\%$, while the time (t) was measured with digital stopwatch (14).

Mass flow rate is as follows: $\dot{m} = \frac{m}{t}$.

Volumetric flow rate is: $Q = \frac{\dot{m}}{\rho}$.

The water gauge head is: $h = \frac{p}{\rho g}$,

where are:

p – preassure [Pa];

ρ – density of water [kg/m^3];

g – earth accelaration [m/s^2].

The water gauge head (h) depends on determined volumetric flow rate (Q). The flow rate was varied by regulator and relation equation $Q = f(h)$ was formed.

3. EXPERIMENTAL RESULTS AND ANALYSIS

The results of filter nozzle testing of producer RAVEX, model RV001/A are shown in Fig. 5 and Fig 6. In the Fig. 5 is shown performance curve for the filtration process and in the Fig. 6 performance curve for the washing process.

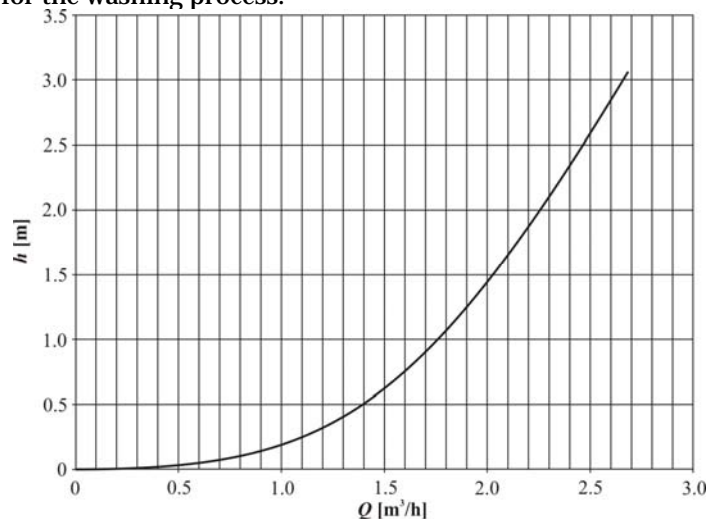


FIGURE 5. The performance curve of filter nozzle model RV001/A for the filtration process

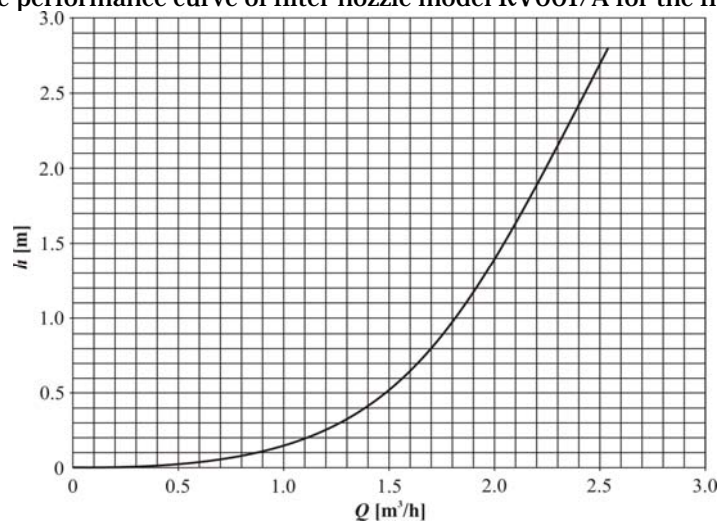


FIGURE 6. The performance curve of filter nozzle model RV001/A for the washing process

The gained performance curves for filtration and washing processes in Fig. 5 and Fig. 6 were expected. These curves thoroughly suit curves for filter nozzles with 40 narrow gaps, 0.2 mm in width at the nozzle head. In this way hypothesis of work was proved and installation with column and manometer could be successfully applied to determine filter nozzle performance curve. In comparison with the reservoir, the installation with column and manometer is more compact and comfortable. The performance curve in filtration process which was determined by installation with the reservoir had up to 1.6 m water head gauge, as shown in Fig.1. It means that maximal level of water in the reservoir is 1.6 m. The performance curve in filtration process which was determined by installation with column and manometer had up to 3 m water head gauge, as shown in Fig. 5. For the same water head gauge, the level of the water in the reservoir should be 3 m. On the other hand the height of column was only 0.5 meter.

4. CONCLUSIONS

The same model of filter nozzles was tested with the help of the installation with reservoir and the installation with column and manometer, respectively. Very good agreement between these two performance curves was obtained. Authors are of the opinion that column could be successfully applied to determine filter nozzle performance curve. In comparison with the reservoir, the installation with column and manometer is more compact and comfortable.

Acknowledgement

This work was supported by Serbian Ministry of Science in the framework of the project TR.20065.B.

REFERENCES

- [1.] <http://www.branluebbe.com/>
- [2.] Bikić, S. (2009) Izveštaj ispitivanja filter dizni proizvođača Ravex d.o.o Vrbas, modeli RV001/A, RV001/B i RV001/D, Fakultet tehničkih nauka u Novom Sadu, februar 2009, broj izveštaja 01-192/55.
- [3.] RV Program filterskih dizni, <http://ravex-vrbas.net/>
- [4.] Model EJA510A and EJA530A Absolute Pressure and Gauge Pressure Transmitters, User's Manual, Yokogawa, <http://www.yokogawa.com/>.





¹Dan CONSTANTINESCU, ²Mirela SOHACIU

ENERGY AND METAL SAVING IN THE HEATING FOURNACES MEANS A CLEANER ENVIRONMENT

^{1, 2} UNIVERSITY POLITEHNICA OF BUCHAREST, ROMANIA

ABSTRACT:

As a major consumer of energy the steel producers are always mentioned as interesting field of investigations. The aim of this paper is to establish the basic relations for a model in order to help to evaluate the parameters of the heat transfer and energy consumption in the case of some metallurgical heating furnaces for billets reheating. Starting from considerations about the burning process of the fuels, the paper establishes connections between the heat exchange coefficients, energy and metallic material saving. Saving energy and lost metal due to the oxidation process, means to have a cleaner environment. A new disposing system of the burners inside the furnace can lead to saving energy and metal. The paper offer also a model to calculate the temperature in the furnace (temperature of the flue gases) taking in consideration the global heat exchange, the technological temperature of the billet in order to evaluate the thermal energy losses.

KEYWORDS:

oxidation, heating, energy, furnace, thermal regime, clean environment

1. INTRODUCTION

1.1 Oxidation and heating process

In the case of the heating process in furnaces using the combustion in view of rolling of the cast billets, the source of energy can be analyzed from two points of view:

- a) as component which can reduce the material losses due to the oxidation process
- b) as component which assure the technological conditions for the heating process

In order to analyze the source of energy as component influencing the steel oxidation process one can use the partial pressures (p) of $H_2O_{(gas)}$, H_2 , CO_2 and CO in the flue gases. So, it is obtained the K_a coefficient:

$$K_a = \frac{P_{H_2O} / P_{H_2}}{P_{CO_2} / P_{CO}} = \frac{K_H}{K_C} \quad (1)$$

In the figure 1 there are presented the influence of type of the fuel, the furnace temperature and the air coefficient φ , on the quantity of the oxides.

In order to analyse how to influence the heat exchange and to assure the thermal technological conditions, one start from the equation of heat exchange between the flue gases, the furnace thermal isolation and the metallic material. It is necessary to considerate that the heat exchange is simultaneously by radiation and convection. So, the thermal energy, Q_{gp} , received by the furnace isolation from the flue gases is:

$$Q_{gp} = S \cdot \alpha_{gp} \cdot \varepsilon_p \cdot (\theta_g - \theta_p) + S \cdot \alpha_c \cdot (\theta_g - \theta_p) \quad [kJ/h] \quad (2)$$

S : internal surface of the thermal isolation, m²

θ_g : temperature of the flue gases, °C

θ_p : temperature of the thermal isolation, inside the furnace, °C

α_{gp} : radiation heat exchange coefficient between the gases and the thermal isolation, kJ·m⁻²·h⁻¹·K⁻¹

α_c : convection heat exchange coefficient between the gases and the thermal isolation, kJ·m⁻²·h⁻¹·K⁻¹

ε_p : emission coefficient of the thermal isolation

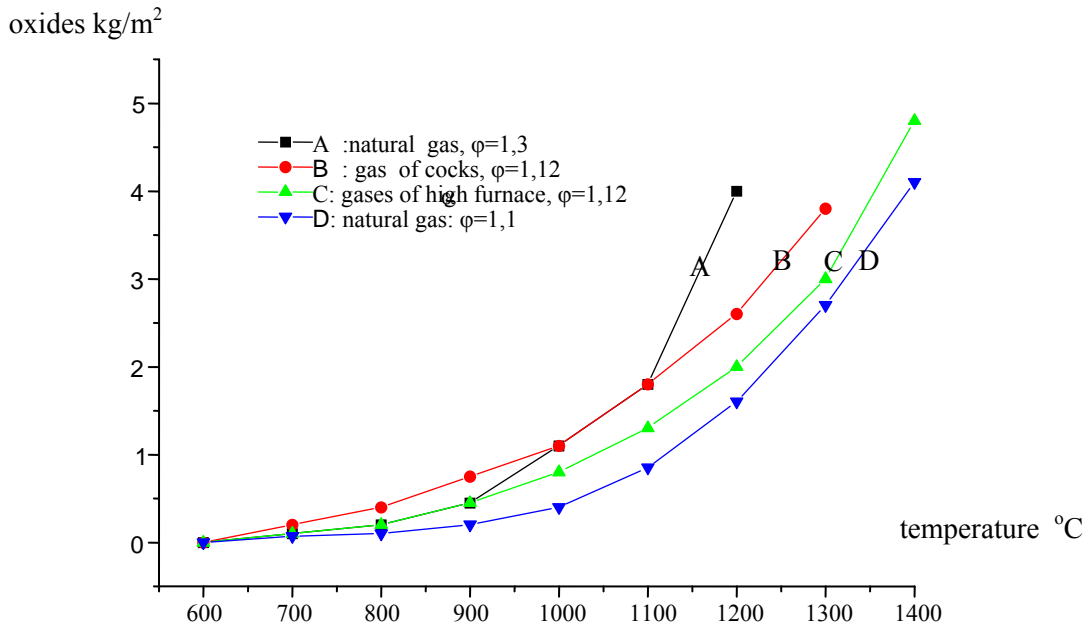


Figure 1 : Dependence of the quantity of the iron oxides, during the heating process of the non alloyed steels on the fuel, temperature and air excess coefficient, ϕ

In the same time:

$$Q_{gp} = Q_{pm} + S \cdot q_{ex} \quad [\text{kJ/h}] \quad (3)$$

Q_{pm} : thermal energy from the isolation of the furnace to the heated billets, $\text{kJ}\cdot\text{h}^{-1}$

q_{ex} : thermal flow thru the furnace's isolation, $\text{kJ}\cdot\text{m}^{-2}\cdot\text{h}^{-1}$

The computation of the heat exchange by radiation between the thermal isolation components can be calculated using the angular coefficient of radiation, [1].

In the case of heating pushing type furnaces and walking type furnaces, [1; 2], it was obtained (4), (figure 2):

$$\beta = \frac{1}{\pi} \left[\frac{1}{B \cdot L} \cdot \ln \frac{(1+B^2)(1+L^2)}{1+B^2+L^2} - \frac{2}{B} \arctg(L) - \frac{2}{L} \arctg(B) + \frac{2}{L} \sqrt{1+L^2} \arctg \frac{B}{\sqrt{1+L^2}} + \frac{2}{B} \sqrt{1+B^2} \arctg \frac{L}{\sqrt{1+B^2}} \right] \quad (4)$$

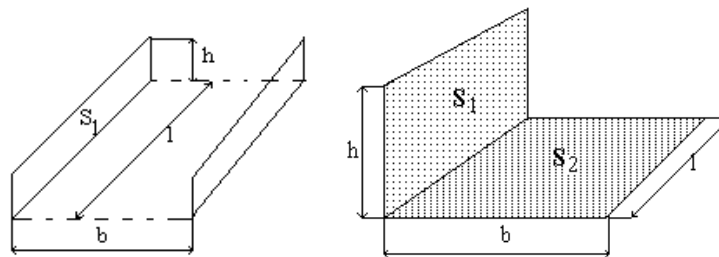


Figure 2: dimensions referring to the continuous furnaces in order to establish the coefficient ϕ [$B=h/b$; $L=l/b$]

In the case of heat exchange between the thermal isolation (figure 3) and the billets, the coefficient β is [2]:

$$\beta = \frac{1}{2\pi} \left(\frac{B}{\sqrt{1+B^2}} \cdot \arcsin \frac{L}{\sqrt{1+B^2+L^2}} + \frac{L}{\sqrt{1+L^2}} \cdot \arcsin \frac{B}{\sqrt{1+B^2+L^2}} \right) \quad (5)$$

1.2 Energy source and material losses during the heating process

Starting from the equation (1) it can be observed that it is necessary to calculate the quantity of oxygen, resulted from the fuel and from the combustion air:

$$O_x = O_{2c} + 0,21 \cdot v_{oa} \cdot \lambda = CO_2 + 0,5CO + 0,5H_2O$$

v_{oa} : specific air volume, necessary for the reaction with 1m^3 of fuel, $\text{m}^3_{\text{N(air)}}\cdot\text{m}^{-3}_{\text{N(fuel)}}$

λ : coefficient of air excess

CO_2 : in flue gazes

It is obtained:

$$H_2O = 2O_x - C \frac{0,5 + K_c}{1 + K_c}$$

where $C = CO + CO_2$

Analysing the oxidation phenomena of the steel in the case of the most usual fuel (the natural gas), it can be deduced that the oxidation process is very fast for the temperatures up to 800°C. In order to reduce the oxidation process, the theoretic burning temperature must be under 1360°C. If the heating temperature of the steel in view of rolling must be 1200...1250°C, this case is not economic from energetic point of view.

The calculation of the temperature of the source of energy starting only from the equation (1) is valid if the oxygen content of the air combustion and of the fuel together can assure the transformation in CO of the carbon resulted from the dissociation of the carbides. If the air excess coefficient is too small to assure this transformation, the flue gases will include particles of black pigment.

Due to the low values of the equilibrium constant $K = (p_{CO_2}/p^2_{CO}) = 10^{-2} \div 10^{-4}$, for the Bell-Boudoir reaction ($CO_2 + C \leftrightarrow 2CO$), the presence of the black particles in the flue gases is of low importance in the case when the coefficient of air excess is over the normal values resulted from the chemical reactions.

2. METHODOLOGY

2.1 The heating furnace temperature and steel oxidation

The theoretical output η_t , indicate the efficiency of the use of the energetic sources (the fuel).

If in the furnace is introduced a quantity of thermal energy, resulted from the fuel combustion:

$$Q_{cb}^t = Q_{cb} \cdot \eta_t + v_{ga} \cdot \theta_{ga} \cdot c_p \quad (6)$$

v_{ga} : the volume of the flue gases related to a thermal unit of the fuel (for example to 1000kJ), [Nm³/10³Kj]

θ_{ga} : temperature of the flue gases at the exit from the furnace, °C

c_p : thermal capacity of the flue gases, kJ·m⁻³·K⁻¹

If Q_{cb} , is a unit of the fuel, it can be written:

$$v_{ga} \cdot \theta_{ga} \cdot c_p = v_{ot} \cdot \theta_{ga} \cdot c_p + (\varphi_a - 1) \cdot v_{oa} \cdot \theta_{ga} \cdot c_a \quad (7)$$

v_{ot} : theoretical volume of the flue gases related to the thermal unit of the fuel, [Nm³/10³kJ]

v_{oa} : theoretical volume of air combustion related to the thermal unit of the fuel, [m³N/10³ kJ]

c_a : air combustion thermal capacity, kJ·m⁻³·K⁻¹

If the fuel and the air combustion are heated and the real air combustion volume is $\varphi_a \cdot v_{oa}$, it results:

$$\eta_t = 1 + \varphi_a \cdot v_{oa} \cdot \frac{\theta_a \cdot c_a}{Q_{cb}} + \frac{\theta_{cb} \cdot c_{cb}}{H_i} - \frac{v_{ot} \cdot \theta_{ga} \cdot c_p}{Q_{cb}} - (\varphi_a - 1) \cdot v_{oa} \cdot \frac{\theta_{ga} \cdot c_a}{Q_{cb}} \quad (8)$$

The equation (8) establishes a correlation between the theoretical output, the nature of the fuel and the air excess coefficient [by the factor $(\varphi_a - 1) \cdot v_{oa} \cdot \frac{\theta_{ga} \cdot c_a}{Q_{cb}}$].

Else, the oxidation process of the metal can be controlled by the air excess coefficient.

If it is defined "the factor of the fuel":

$$K_{cb} = 1 + \frac{\theta_{cb} \cdot c_{cb}}{H_i} \quad (9)$$

it is obtained:

$$\eta_t = K_{cb} + \frac{1}{Q_{cb}} (\lambda_a \cdot v_{oa} \cdot \theta_a \cdot c_a - v_{ot} \cdot \theta_{ga} \cdot c_p - (\varphi_a - 1) \cdot v_{oa} \cdot \theta_{ga} \cdot c_a) \quad (10)$$

The equations (8) and (10) can be used to choose the thermal source (gas fuel) in correlation with the preheating degree of the fuel and the air combustion and with the coefficient of air combustion excess which control the oxidation process in the heating furnace.

2.2 Heat exchange coefficients and the thermal process in the heating furnace

If all the thermal energy radiated by the isolation, Q_{pm} , is receipted by the heated metal, it is possible to write:

$$Q_{pm} = \alpha_{pm} \cdot \varepsilon_{pm} \cdot s \cdot (\theta_p - \theta_m) \quad (11)$$

θ_m : temperature of the metal, °C

α_{pm} : heat exchange coefficient by radiation between the thermal isolation and the metal, $\text{kJ}\cdot\text{m}^{-2}\cdot\text{h}^{-1}\cdot\text{K}^{-1}$

s : heated surface of the metallic material (billets), (reception surface, S_2 , in fig. 3), m^2

But, a part of this radiation is absorbed by the flue gases. The absorption process depends on the partial pressure of CO_2 and H_2O . The absorbed thermal energy by radiation, Q_{abs} , is equal with the quantity of energy which the metal could receive from the flue gases if the temperature of the gases is equal with the temperature of the thermal isolation:

$$Q_{abs} = \alpha_{gpm} \cdot \varepsilon_p \cdot s \cdot (\theta_p - \theta_m) \quad (12)$$

α_{gpm} : heat exchange coefficient from the gases to the metallic material, if it is considerate that the temperature of the gases is the same with the temperature of the thermal isolation, $\text{kJ}\cdot\text{m}^{-2}\cdot\text{h}^{-1}\cdot\text{K}^{-1}$

So, the real value of Q_{pm} is:

$$Q_{pm} = s(\alpha_{pm} \cdot \varepsilon_{pm} - \alpha_{gpm} \cdot \varepsilon_p) \cdot (\theta_p - \theta_m) \quad (13)$$

Replacing, it is obtained:

$$S \cdot (\alpha_{gp} \cdot \varepsilon_p + \alpha_c) \cdot (\theta_g - \theta_p) = s \cdot (\alpha_{pm} \cdot \varepsilon_{pm} - \alpha_{gpm} \cdot \varepsilon_p) \cdot (\theta_p - \theta_m) + S \cdot q_{ex} \quad (14)$$

If $\sigma = s/S$, equation (14) will be:

$$\theta_g \cdot (\alpha_{gp} \cdot \varepsilon_p + \alpha_c) = \theta_p \cdot (\alpha_{gp} \cdot \varepsilon_p + \alpha_c + \sigma \cdot \alpha_{pm} \cdot \varepsilon_{pm} - \sigma \cdot \alpha_{gpm} \cdot \varepsilon_p) - \theta_m \cdot \sigma (\alpha_{pm} \cdot \varepsilon_{pm} - \alpha_{gpm} \cdot \varepsilon_p) + q_{ex} \quad (15)$$

Equation (15) correlates the temperature of the flue gases, temperature of the thermal isolation and the temperature of the billets (θ_m). But, the establishing of the values of the heat exchange coefficients is yet difficult.

The thermal flow sanded to the metallic material (billets) includes:

- radiation thermal flow from the thermal isolation

$$q_{pm} = (\alpha_{pm} \cdot \varepsilon_{pm} - \alpha_{gp} \cdot \varepsilon_p) (\theta_p - \theta_m) \quad [\text{kJ}\cdot\text{m}^{-2}\cdot\text{h}^{-1}] \quad (16)$$

- radiation and convection thermal flow from the flue gases

$$q_{gm} = (\alpha_{gm} \cdot \varepsilon_m + \alpha_c) (\theta_g - \theta_m) \quad (17)$$

The total thermal flow received by the billets is:

$$q = q_{pm} + q_{gm} \quad (18)$$

Starting from the equation (15), it is noted:

$$(\theta_p - \theta_m) + (\theta_g - \theta_p) = (\theta_g - \theta_m) \quad (19)$$

Then, the coefficient of the global heat exchange can be calculated:

$$\begin{aligned} (\alpha_{gp} \cdot \varepsilon_p + \alpha_c) \cdot [(\theta_g - \theta_m) - (\theta_p - \theta_m)] &= \sigma (\alpha_{pm} \cdot \varepsilon_{pm} - \alpha_{gpm} \cdot \varepsilon_p) (\theta_p - \theta_m) + q_{ex} \\ (\theta_p - \theta_m) \cdot [\sigma (\alpha_{pm} \cdot \varepsilon_{pm} - \alpha_{gpm} \cdot \varepsilon_p) + (\alpha_{gp} \cdot \varepsilon_p + \alpha_c)] + q_{ex} &= (\theta_g - \theta_m) (\alpha_{gp} \cdot \varepsilon_p + \alpha_c) \end{aligned} \quad (20)$$

Replacing the expressions of the thermal flows, it is obtained:

$$q = (\alpha_{pm} \cdot \varepsilon_m - \alpha_{gm} \cdot \varepsilon_p) \cdot (\theta_p - \theta_m) + (\alpha_{gm} \cdot \varepsilon_m + \alpha_c) \cdot (\theta_g - \theta_m) \quad (21)$$

Eliminating $(\theta_p - \theta_m)$ and $(\theta_g - \theta_m)$ from the last two expressions, there are obtained the following expressions regarding the complex heat exchange in the analysed furnace:

1. The heat exchange coefficient between the thermal isolation and the billets:

$$\alpha_1 = \frac{\alpha_{gm} \cdot \varepsilon_m + \alpha_c}{\alpha_{gp} \cdot \varepsilon_p + \alpha_c} \cdot \left(\alpha_{gp} \cdot \varepsilon_p + \alpha_c + \sigma \cdot \alpha_{pm} \cdot \varepsilon_{pm} - \sigma \cdot \alpha_{gpm} \cdot \varepsilon_p + \frac{q_{ex}}{\theta_p - \theta_m} \right) \cdot \frac{1}{\theta_p - \theta_m} \quad [\text{kJ}\cdot\text{m}^{-2}\cdot\text{h}^{-1}\cdot\text{K}^{-1}] \quad (22)$$

2. The heat exchange coefficient between the flue gases and the billets:

$$\alpha_2 = \frac{\alpha_{pm} \cdot \varepsilon_{pm} - \alpha_{gpm} \cdot \varepsilon_p}{\alpha_{gp} \cdot \varepsilon_p + \alpha_c + \sigma \cdot (\alpha_{pm} \cdot \varepsilon_{pm} - \alpha_{gpm} \cdot \varepsilon_p)} \cdot \left(\alpha_{gp} \cdot \varepsilon_p + \alpha_c - \frac{q_{ex}}{\theta_g - \theta_m} \right) + \alpha_{gm} \cdot \varepsilon_m + \alpha_c \quad [\text{kJ}\cdot\text{m}^{-2}\cdot\text{h}^{-1}\cdot\text{K}^{-1}] \quad (23)$$

3. RESULTS, DISCUSSIONS, ANALYZIS

A general solution to modeling the thermal regime

Using the ratio $\sigma = s/S$, it can be deduced the temperature of the flue gases:

$$\theta_g = \theta_p \frac{\alpha_{gp} \cdot \varepsilon_p + \alpha_c + \sigma \cdot \alpha_{pm} \cdot \varepsilon_{pm} - \sigma \cdot \alpha_{gpm} \cdot \varepsilon_p}{\alpha_{gp} \cdot \varepsilon_p + \alpha_c} - \theta_m \cdot \sigma \cdot \frac{\alpha_{pm} \cdot \varepsilon_{pm} - \alpha_{gpm} \cdot \varepsilon_p}{\alpha_{gp} \cdot \varepsilon_p + \alpha_c} + \frac{q_{ex}}{\alpha_{gp} \cdot \varepsilon_p + \alpha_c} \quad (24)$$

In the case when heating the billets in view of rolling there are used, in the most of the cases, natural gas, high furnace gas and cocks gas (fig.1). In this case the values of the emissive coefficients are:

$$\varepsilon_p = 0,77\dots 0,8 \quad \varepsilon_m = 0,8\dots 0,88 \quad \varepsilon_{pm} = \frac{1}{\frac{1}{\varepsilon_m} + \sigma \left(\frac{1}{\varepsilon_p} - 1 \right)} = 0,8\dots 0,81 \quad (25)$$

In these conditions it is obtained in (23):

$$\alpha_p = \frac{0,8 \cdot [\alpha_{gp} + \alpha_c + \sigma(\alpha_{pm} - \alpha_{gpm})]}{0,8 \cdot \alpha_{gp} + \alpha_c} \quad [\text{kJ}\cdot\text{m}^{-2}\cdot\text{h}^{-1}\cdot\text{K}^{-1}] \quad (26)$$

$$\alpha_m = \sigma \frac{0,8(\alpha_{pm} - \alpha_{gpm})}{0,8 \cdot \alpha_{gp} + \alpha_c} \quad [\text{kJ}\cdot\text{m}^{-2}\cdot\text{h}^{-1}\cdot\text{K}^{-1}] \quad (27)$$

So, the temperature of the flue gases will be:

$$\theta_g = \alpha_p \cdot \theta_p + \alpha_m \cdot \theta_m + \frac{q_{ex}}{0,8 \cdot \alpha_{gp} + \alpha_c} \quad [^\circ\text{C}] \quad (28)$$

where the conduction thermal flow is:

$$q_{ex} = \frac{\theta_p - \theta_{pex}}{\sum_{i=1}^n \frac{\delta_i}{\lambda_i}} \quad [\text{kJ}\cdot\text{m}^{-2}\cdot\text{h}^{-1}] \quad (29)$$

θ_{pex} : temperature of the outside of the thermal isolation layer, $^\circ\text{C}$

Using practical data from [3], [4], [5], [6], for the steels, thermal isolation materials and chemical composition of the flue gases, there where established the values for the coefficients α_{gp} , α_{pm} , α_{gpm} (figures 4 and 5).

In the equation (25) the temperature of the billets is considerate as “known data” from the technological conditions. So, it is necessary to establish the values for θ_p .

In order to follow, it is necessary to use the equations (20) and (23). For the beginning it is considerate that $\theta_g = \theta_p$, in order to establish the necessary data for the equation (23) (fig. 4 and 5).

The exact value of the temperature of the thermal isolation (inside the furnace) will be:

$$\theta_p = \theta_m - \frac{q_{ex}}{\sigma \cdot (\alpha_{pm} \cdot \varepsilon_{pm} - \alpha_{gpm} \cdot \varepsilon_p)} \quad [^\circ\text{C}] \quad (30)$$

Equation (30) can be in correlation with the particularities of a kind of furnace. For example, in the case of a rotary type furnace for circular billets it can be established the dependence of the flue gases at the exit from the furnace (θ_g), furnace’s productivity (P) and the disposal mode of the burners [7]. It can be deduced using the equation (28):

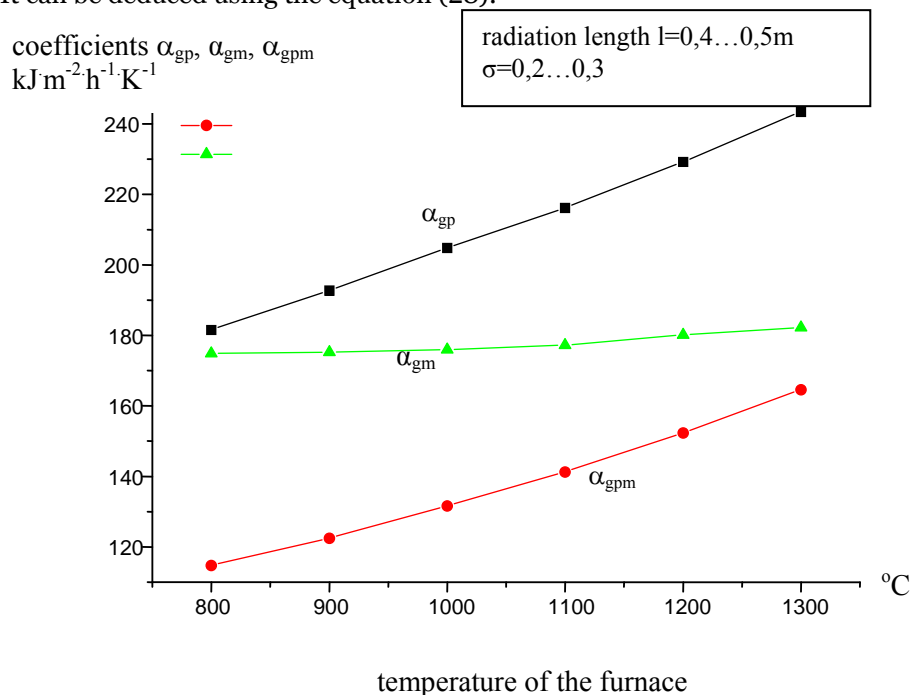


Figure 4: Variation of the coefficients α_{gp} , α_{gm} and α_{gpm} depending on the temperature of the furnace, thermal radiation’s length and the ratio σ

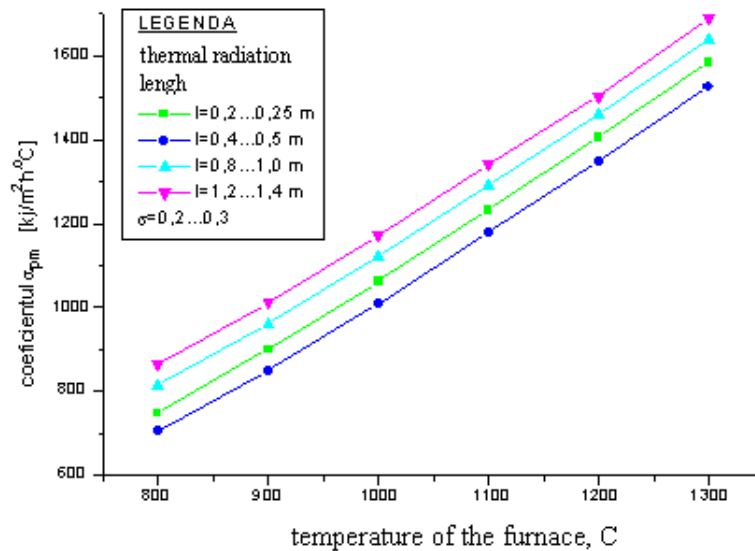


Figure 5: Variation of the coefficient α_{pm} depending on the temperature of the furnace, thermal radiation's length and the ratio σ

$$\theta_g = \alpha_p \cdot \theta_p + \alpha_m \cdot \theta_m + \frac{Q_p}{0,8 \cdot \alpha_{gp} + \alpha_c} = \frac{A}{y} - B \cdot y + C \quad [^{\circ}\text{C}] \quad (31)$$

where: Q_p : total losses due to the heat conduction in the furnace's isolation

$$A = \frac{Q_p}{\pi(D+d) \cdot V_g \cdot c_p} \quad B = \frac{4 \cdot P \cdot c_m \cdot (\theta_2 - \theta_1)}{\pi \cdot K \cdot b \cdot (D+d)} \quad (32)$$

D, d : dimensions of the circular furnace, m

θ_1, θ_2 : final and initial temperature of the billets, $^{\circ}\text{C}$

V_g : flue gases debit, $\text{m}^3 \cdot \text{h}^{-1}$

K : coefficient of the furnace, depending on the design, dimensions, output and working temperature [7]

4. CONCLUSIONS

- ◇ The quantity of the metallic material lost by oxidation during the reheating of the billets depends on the chemistry of the atmosphere in the heating furnace, on the temperature and on the duration of the thermal process.
- ◇ During the reheating process, the soaking duration of the billets at the high temperature must have a minimum value. This is recommended from the points of view of oxidation a decarburising process and for energy saving too. In practice, in most of the cases, the soaking duration of the billets is too long and the temperature is too high. It is necessary to impose that the plastic deformation temperature (the rolling beginning temperature) are reached by the billets moment of the defournement or just a few minutes before. On the other hand, the deformation temperature must be minimum admitted for the category of steel.
- ◇ To reduce the oxidation and decarburising process an important action regards the control of chemical composition of the flue gases. This is possible by the control of the air combustion excess coefficient and the designee of the heating furnace.
- ◇ Using the proposed general solutions for the remodelling of the thermal regime it can be obtained a better control of the temperatures in each heating zone of the furnace and to correlate it with the necessary temperatures of the billets. It is also possible to control the temperature of the thermal isolation, and by this to save thermal energy.
- ◇ Using the above established equations it is possible to control the flue gases temperature in each heating zone of the furnace in correlation with the temperature of the metallic material. It is possible also to control the temperature of the thermal isolation and by this to save important quantities of thermal energy.
- ◇ The coefficients $\alpha_p, \alpha_m, \alpha_{gpm}$ are at the basis of the control process of heat exchange between the flue gases, metallic material and the thermal isolation. The values of this coefficients are established in the present work

- ◇ The basics of the general solution to modeling the thermal regime allowed establishing the disposal mode of the burners in connection with the design of the furnace and the necessary output. The design of the furnace can be also changed having in view the thermal and the dynamic particularities of the flow gases.

REFERENCES

- [1.] Heiligenstaedt, W.: Thermique appliquee aux fours industriels, tom1, Dunot, Paris, 1971
- [2.] Constantinescu, D : Cercetări privind îmbunătățirea parametrilor de funcționare ai agregatelor tehnologice de încălzire a materialelor metalice supuse deformării prin laminare, tesis, UPB, 621.771.06 (043)
- [3.] Rosier , Ch.: Etude sur la valeur d'usage des combustibles; CIT, 6/1990
- [4.] Schack, A. : Strömungsverhältnisse und Wärmebilanz neuzeitlicher Tieföfen; in Wärmestelle der Vereins Deutscher Eisenhütteleute nr.435
- [5.] Constantinescu, D., Nicolae, A., Predescu, C., Sohaciu, M. : Termotehnica metalurgică, Printech, Bucuresti, 2003
- [6.] Constantinescu, D.: A model of the dynamic of the burned gazes in heating furnaces for rolling mills; 4th International Symposium of Croatian Metallurgical Society, June 2000, in "Metalurgija - Metallurgy" vol.39, nr.3/2000 p. 216.
- [7.] Constantinescu, D., Mazankova, M.: Heat exchange and metall saving in the furnaces for billets reheating in view of rolling; pag.53, Metal 2003, Hradec nad Moravici, Czech Republic, May 2003
- [8.] Constantinescu, D., Sîrbu, E., Smical, I. Equipment for Metallurgical Processing and the Environment; Metalurgia International, Special Issue nr.2, February 2009 pag.63, ISSN 1582-2214
- [9.] Constantinescu, D., Application of the mathematical modeling to the dynamic design of the thermal space of the furnaces for rolling mills; METAL2007, 16th Metallurgical and Material Conference, Hradec nad Moravici, Czech Republic, May 2007, pag.51, ISBN 978-80-86840-33-8, <http://www.metal2007.com>







¹ Georgeta Emilia MOCUȚA

PROMOTION OF PASSENGER RAIL TRANSPORT AS A FRIENDLY SOLUTION TO ENVIRONMENT

¹ MECHANICAL ENGINEERING FACULTY, POLYTECHNIC UNIVERSITY OF TIMISOARA, ROMANIA

ABSTRACT:

The paper presents the objectives of the ECORailS project (Energy Efficiency and Environmental Criteria in the Awarding of Regional Rail Transport Vehicles and Services co-financed by IEE – Intelligent Energy Europe program.

The regional passenger rail transport presents advantages from the energetic efficiency point of view and its impact of performance on the environment. However, rail transport has not yet given the full measure of its potential. Under the conditions of growing energy prices and increasing environmental problems, this potential must be exploited.

The ECORailS project relates to improving energy efficiency and reduces environmental impact of rail transport. The target groups are Public Transport Administrations (PTA) currently playing a key role in terms of improving the quality of rail travel and the impact of this performance. Auctions, other types of procurement procedures and Public Service Contracts (PSC) are appropriate tools for optimizing energy and environmental performance of rail services.

ECORailS will provide a Guide so that PTAs include successfully criteria related to the environment in their procurement procedures. The aim of the ECORailS project is to reduce the energy specific consumption of the regional passenger rail transport with 15 % till 2020.

A first version of the Guide ECORailS will be tested in four-point test in Europe: Copenhagen /Oresund (Danemarca), Berlin-Brandenburg (Germania), Timișoara (Romania) and Lombardia (Italia), PTAs in these regions are partners within the project. Experiences resulted after applying tests will be included in the final version in order to provide its utility in the current practice both for diesel functioning and the electric one. The duration of the project: May 2009 – June 2011.

KEYWORDS:

ECORailS project, regional passenger rail transport

